nature
Vol 295 No 5844 7–13 January 1982 £1.60 $4.00

University Colleges of Science & Technology
92, A.P.C. Rd., Cal. 9
LIBRARY COMPLEX
Departments of:
Chemical Engineering
Chemical Technology
Plastics & Rubber Technology

291

14-11-83

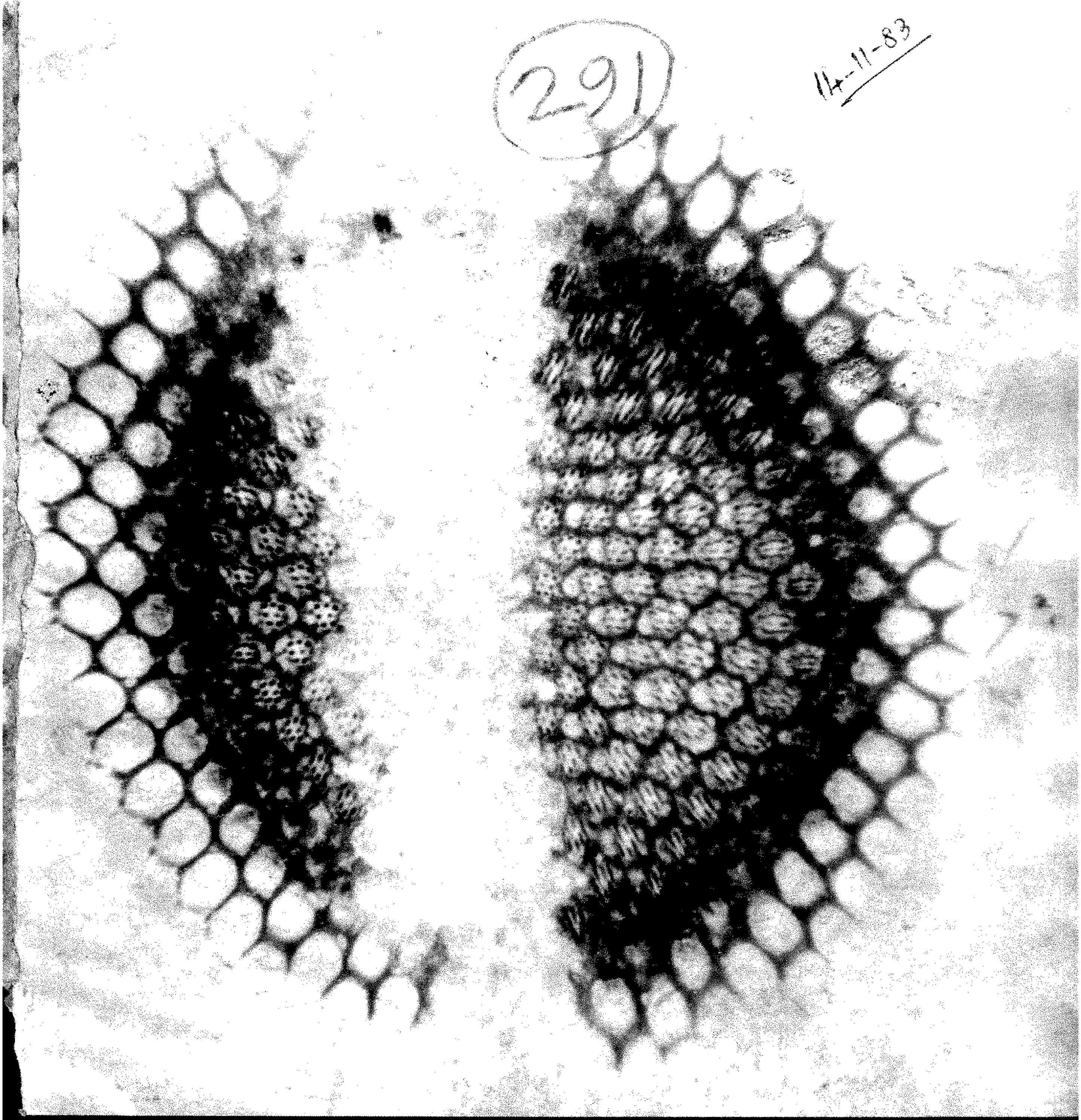

STAINING CELLS TO STUDY DEVELOPMENT

4011

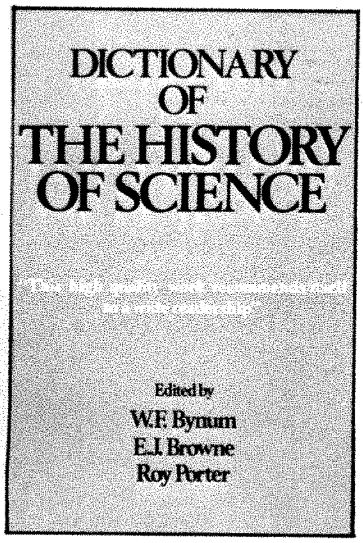

Special offer to subscribers to Nature – Save £3.50 off published price!

Is this the missing link?

Is there a gap in your bookcase? Until now, there hasn't been a dictionary devoted exclusively to the history of scientific ideas. And however you are involved in today's scientific world, you will agree that your present work and scientific attitudes are inevitably influenced by and built on those from the past.

Science and its key doctrines – from quantum theory to genetics – are central to the modern world; yet daily it changes and develops, becomes more technical and diverse. What is needed is a reference book that enables you not only to master the past but also to keep you in touch with the theories underlying the most recent scientific and technological developments.

The Dictionary of the History of Science fills the gap.

Authoritative
It is the work of three editors: W.F. Bynum, E.J. Browne and Roy Porter; of ten subject editors – including Michael Hoskin, Richard Burkhardt, William Brock, Steven Shapin, Roger Smith, Eric Aiton, Roy Bhaskar, John Heilbron – and over 90 contributors, all authorities in their field. It explains the core features of Western science and their development. 700 entries, alphabetically arranged, cover such fields as astronomy, biology, chemistry and earth sciences, the historiography, philosophy and sociology of science; human sciences, mathematics, medicine and physics.

Substantial concepts such as Evolution and Light are given generous entries, while more specialized sub-areas like Neo-Darwinism and Light Velocity are allocated smaller amounts of space. All are cross-referenced back and forth.

Comprehensive
Although the Dictionary is principally concerned with the Western scientific tradition of the last 500 years, it touches, too, on the central scientific ideas of classical and medieval times, and of other cultures. In addition, it features such topics as the development of technology and clinical medicine, and of important scientific instruments like the astrolabe and the thermometer.

Our understanding of the processes of scientific discovery and change is often controversial. But however you view them, it is important that you have easy access to all the ideas you are building on today, in the most scholarly, up-to-date and comprehensive detail.

If you are searching for the missing link, the Dictionary of the History of Science is your natural selection. At this special price to subscribers to Nature, it must be!

Price: £14 (Published price: £17.50)
496 pages: **234** × **156** mm.: **700** entries: bibliographies: biographical index: ISBN 0 333 29316 9

Please supply . . . . . . copy/copies of the Dictionary of the History of Science (ISBN 0 333 29316 9) at the special Nature subscriber price of £14. I understand that I will not be charged for postage and packing. This special offer closes on March 30th 1982.

I enclose a cheque for £________
Please charge to my credit card account:
☐ Access ☐ Visa/Barclaycard ☐ American Express ☐ Diners Club
My credit card number is________ Card Expiry Date____
Signature________
Name (please print)________
Address________
____
Town________
County________ Postcode________
Date________

Please return completed coupon to:
Nature Promotion, 4 Little Essex Street, London WC2R 3LF.

Registered No: 785998 England Registered Office: Macmillan Journals Ltd, 4 Little Essex Street London WC2R 3LF

nature

Vol. 295 No. 5844 7 January 1982

Reagan's mistake on Soviet sanctions 1
More change now due 1

NEWS

Not President perpetual
Anxiety about Reagan's sanctions
Polish academia only partly normal
High-energy physics
Hardly any change
American science
UK director for US Biogen laboratory
Biomedical research
New director chosen for NIH
Molecular biology
Microbial collections
Stanford University 3

CORRESPONDENCE

Space colonies/Baseball/Systems ecology/Fossil record 8

NEWS AND VIEWS

Reservoirs and the triggering of earthquakes (P J Smith)
How eggs breathe while avoiding desiccation and drowning (J M Diamond)
Sexual differentiation and H-Y antigen (P N Goodfellow & P W Andrews)
Electrostatic interactions in proteins (J M Thornton)
Cell-mediated immunity in theileriosis (F E G Cox)
Oddities in the initiation of translation (P Model)
Magnetic messages from the Earth's core (D Gubbins)
Animal disease and conservation (G R Smith) 9

BOOK REVIEWS

Science and Technology Policy: Priorities of Governments (*by* **C A Tisdell**) Eric Ashby; **Bones: Ancient Men and Modern Myths** (*by* **L R Binford**) C K Brain; **Nature's plumbing**: Philip England four books about geothermal systems; **Comparative Ecology, 2nd Edn** (*by* **Y Itô**) John Lawton; **Mechanics and Thermodynamics of Biomembranes** (*by* **E A Evans and R Skalak**) A Silberberg; **Laser Interaction and Related Plasma Phenomena, Vol.5** (**H J Schwarz** *et al., eds*) M H Key 83

Cover

Section through a *Drosophila* eye. The white sector represents a clone of cells lacking genes responsible for the red pigment and blue staining. The clones are both cell viable and normal. A similar technique shows that myoblasts from *Drosophila* wing disk contribute to developing muscles throughout the fly (see page 55)

ARTICLES

Ion-supported tori and the origin of radio jets	M J Rees, M C Begelman, R D Blandford & E S Phinney	17
Structural evolution of a crustal section in the western Himalaya	M P Coward, M Q Jan, D Rex, J Tarney, M Thirlwall & B F Windley	22
Cellular origin and role of mink cell focus-forming viruses in murine thymic lymphomas	S K Chattopadhyay, M W Cloyd, D L Linemeyer, M R Lander, E Rands & D R Lowy	25
The highly polymorphic region near the human insulin gene is composed of simple tandemly repeating sequences	G I Bell, M J Selby & W J Rutter	31
Lysis gene expression of RNA phage MS2 depends on a frameshift during translation of the overlapping coat protein gene	R A Kastelein, E Remaut, W Fiers & J van Duin	35

LETTERS TO NATURE

Particle acceleration at planetary bow shock waves	M M Hoppe & C T Russell	41
Organic and inorganic interpretations of the martian UV–IR reflectance spectrum	K D Pang, S F S Chun, J M Ajello, Z Nansheng & L Minji	43
Chorus-related electrostatic bursts in the Earth's outer magnetosphere	L A Reinleitner, D A Gurnett & D L Gallagher	46
Coordination model for the defect structure of hyperstoichiometric UO^{2+x} and U^4O^9	G C Allen, P A Tempest & J W Tyler	48
Synergistic tellurium–caesium embrittlement of Type 316 stainless steel	M G Adamson, E A Aitken & S Vaidyanathan	49
Carotenoid transformations in coastal marine waters	D J Repeta & R B Gagosian	51
Marine deposits 35,000–25,000 years old in the Chott el Djerid, southern Tunisia	G W Richards & C Vita-Finzi	54
Myoblasts from *Drosophila* wing disks can contribute to developing muscles throughout the fly	P A Lawrence & D L Brower	55
Electrical stimulation of hindlimb increases neuronal cell death in chick embryo	R W Oppenheim & R Núñez	57
Significance of the potassium signal from neurones to glial cells	V W Pentreath & M A Kai-Kai	59
Depletion of substance P-containing axons in substantia gelatinosa of patients with diminished pain sensitivity	J Pearson, L Brandeis & A C Cuello	61

Nature® (ISSN 0028-0836) is published weekly on Thursday, except the last week in December, by Macmillan Journals Ltd and includes the Directory of Biologicals (mailed in December) and Annual Index (mailed in February). Annual subscription for USA and Canada US $198.50 (for subscription prices elsewhere, see next page). Orders (with remittance) and change of address labels to: Macmillan Journals Ltd, Brunel Rd, Basingstoke RG21 2XS, UK. Second class postage paid at New York, NY10010 and additional mailing offices. US Postmaster send form 3579 to: *Nature*, 15 East 26 Street, New York, NY 10010. ©1981 Macmillan Journals Ltd.

0028-0836/82/01000C-02$01.00

Contents continued overleaf

Are you locked in to a ^{32}P-schedule?

Amersham provides the key.

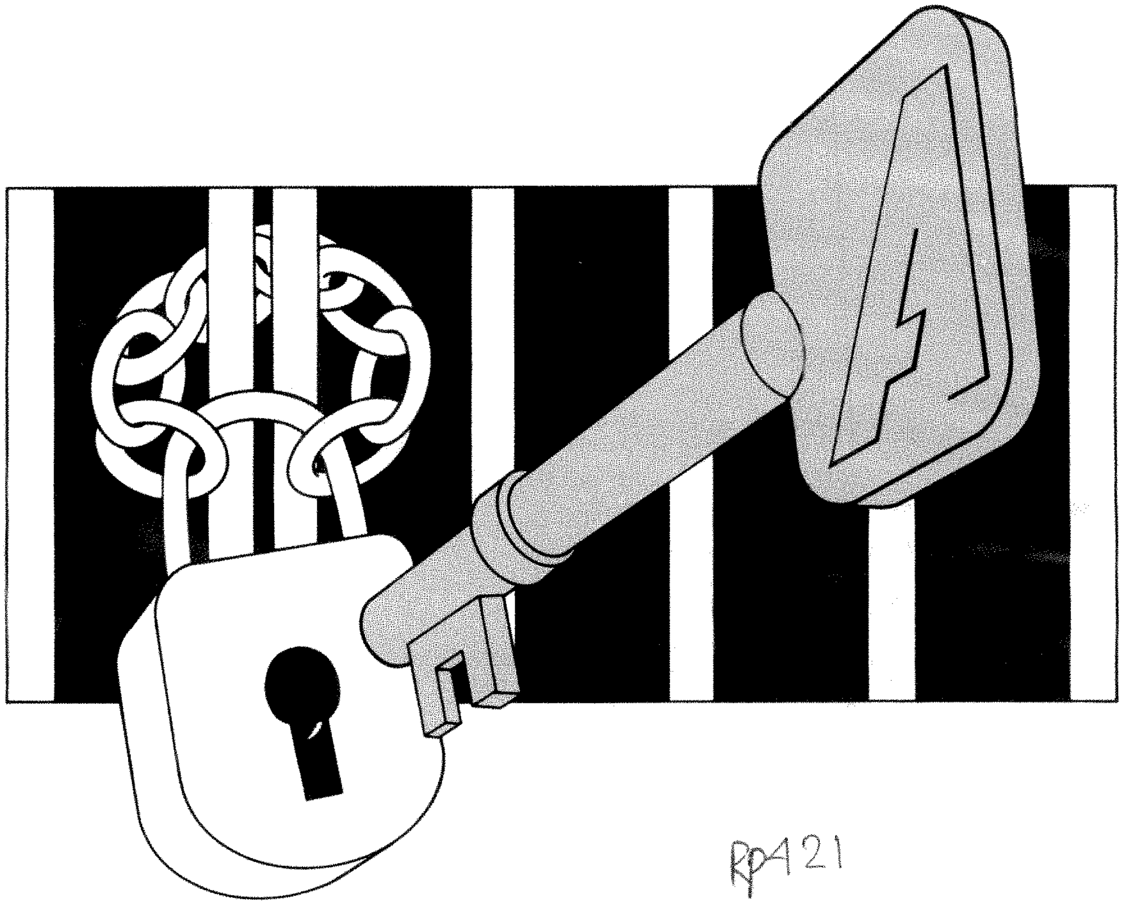

Rp421

New ● All deoxynucleotides at ~3000Ci/mmol available **every week.**

● All deoxynucleotides at ~800Ci/mmol available **every week.**

● All deoxynucleotides at >400Ci/mmol available **every week.**

The reliable supply of the complete range of $[\alpha - {}^{32}P]$ dNTPs every week gives you the convenience of selecting the specific activity most appropriate for your experiments at any time.

Amersham - for products you can trust

Amersham International Limited, Amersham, England Telephone 024-04-4444
In the U.S.A. and Canada, Amersham Corporation, Illinois 60005 Telephone 312-364-7100
and 800-323-9750 (Tollfree)
In W. Germany, Amersham Buchler GmbH & Co KG, Braunschweig Telephone 05307-4691

Circle No. 13 on Reader Enquiry Card.

Amersham

•How Britain runs its Science
•How the US runs its Science

These two new *Nature* wallcharts are now available.

The 2 x 3 ft. guides offer a comprehensive survey of the administration of science in Britain and the US, showing the interlocking relationship between science, engineering and medical establishments.

Designed as fold-out sheets, the wallcharts can be carried easily to meetings or hung as posters for permanent reference.

The new 1981 wallcharts are available at £3.50 or $7.95 each from *Nature's* offices in London, Basingstoke and New York.

Annual Subscription including Index (51 issues)

UK & Eire		£85
USA & Canada		US$198.50
Belgium	Airspeed only	BF7450
West German	Airspeed only	DM450
Netherlands	Airspeed only	G505
Switzerland	Airspeed only	SF395
Rest of Europe	Airspeed only	£100
Rest of World	Surface	£100
Rest of World*	Airmail	£150

**(not USA, Canada & Europe)*

Personal subscription rates are available in some countries to subscribers paying by personal cheque or credit card.

Details can be obtained from:
UK: *Nature* Promotion Department,
Canada Road, Byfleet, Surrey KT14 7JL
Telephone: Jonathan Earl: Byfleet (09323) 41459

USA: *Nature*, 15 East 26 Street, New York, NY 10010
Credit card orders only (in USA & Canada):
Call toll-free: (800) 824-7888 (Operator 246)
In California: (800) 857-7777 (Operator 246)

Back issues: (Post-paid) UK, £2.50; USA & Canada, US$6.00 (surface), US$9.00 (air); Rest of World, £3.00 (surface), £4.00 (air).

***Nature* Binders:**
Single Binders: UK, £4.00; Rest of World, $10.00
Set(s) of 3 Binders: UK, £10.00; Rest of World, $25.00

***Nature* First Issue Facsimile:**
UK, 75p; Rest of World (surface), $1.50, (air), £2.00

***Nature* Annual Indexes (1971-1980):**
Price (post-paid):
UK, £5.00 each; Rest of World, $10.00

***Nature* Directory of Biologicals**
(Hardcover edition) (to be published late 1981)
UK, £20.00; Rest of World, $45.00

***Nature* Wallcharts:**
How Britain Runs its Science; How the US Runs its Science; UK, £3.50; USA, $7.95 each

***Nature* in Microform:**
For Information:
UK: UMI, 18 Bedford Row, London WC2R 4EJ
USA: 300 North Zeeb Road, Ann Arbor, Mi 48106

Orders (with remittance) to:
Nature, Macmillan Journals Ltd.,
Brunel Road, Basingstoke, Hants RG21 2XS, UK
Tel: (0256) 29242 Telex: 858493

M MACMILLAN JOURNALS

S-100 protein in human chondrocytes — K Stefansson, R L Wollmann, B W Moore & B G W Arnason 63

A very small porcine virus with circular single-stranded DNA — I Tischer, H Gelderblom, W Vettermann & M A Koch 64

A monoclonal antibody against human T suppressor lymphocytes binds specifically to the surface of cultured oligodendrocytes — J Oger, S Szuchet, J Antel & B G W Arnason 66

T-cell mitogens cause early changes in cytoplasmic free Ca^{2+} and membrane potential in lymphocytes — R Y Tsien, T Pozzan & T J Rink 68

Lower fidelity of RecA protein catalysed homologous pairing with a superhelical substrate — C DasGupta & C M Radding 71

Three clases of mouse H-2 messenger RNA distinguished by analysis of cDNA clones — D Cosman, G Khoury & G Jay 73

Cloning and analysis of cDNAS encoding plant storage protein precursors — R R D Croy, G W Lycett, J A Gatehouse, J N Yarwood & D Boulter 76

Carboxyl–carboxylate interactions in proteins — L Sawyer & M N G James 79

MISCELLANY

100 years ago 14

Classified advertising xvi

GUIDE TO AUTHORS

Authors should be aware of the diversity of *Nature*'s readership and should strive to be as widely understood as possible.

Review articles should be accessible to the whole readership. Most are commissioned, but unsolicited reviews are welcome (in which case prior consultation with the office is desirable).

Scientific articles are research reports whose conclusions are of general interest or which represent substantial advances of understanding. The text should not exceed 3,000 words and six displayed items (figures plus tables). The article should include an abstract of about 50 words.

Letters to *Nature* are ordinarily 1,000 words long with no more than four displayed items. The first paragraph (not exceeding 150 words) should say what the letter is about, why the study it reports was undertaken and what the conclusions are.

Matters arising are brief comments (up to 500 words) on articles and letters recently published in *Nature*. The originator of a Matters Arising contribution should initially send his manuscript to the author of the original paper and both parties should, wherever possible, agree on what is to be submitted.

Manuscripts may be submitted either to London or New York (decisions being made only in London). Manuscripts should be typed (double spacing) on one side of the paper only. Three copies are required, each accompanied by copies of lettered artwork. No title should exceed 80 characters in length. Reference lists, figure legends, etc. should be on separate sheets, all of which should be numbered. Abbreviations, symbols, units, etc. should be identified on one copy of the manuscript at their first appearance.

References should appear sequentially indicated by superscripts in the text and should be abbreviated according to the *World List of Scientific Periodicals*, fourth edition (Butterworth 1963–65). The first and last page numbers of each reference should be cited. References to books should clearly indicate the publisher and the date and place of publication. Unpublished articles should not be formally referred to unless accepted or submitted for publication, but may be mentioned in the text.

Each piece of artwork should be clearly marked with the author's name and the figure number. Original artwork should be unlettered. Suggestions for cover illustrations are welcome. Original artwork (and one copy of the manuscript) will be returned when manuscripts cannot be published.

Requests for permission to reproduce material from Nature *should be accompanied by a self-addressed (and, in the case of the UK and USA, stamped) envelope.*

Introducing

THE CENTRIFUGAL FORCE MACHINE

To 110,000 x g (25,000 RPM)

Let's face it. A machine that is used to produce force shouldn't communicate only in terms of RPM. It's somewhat like a car without a speedometer or odometer.

That's why we taught the new MICRO-25 to talk RCF. You simply key in the g-force desired, rotor number, acceleration and deceleration characteristics, run time and temperature. The instrument does the rest. You can even specify the force at any given point in your sample tube. And the continuously displayed G × minute parameter gives you a direct readout of the entire centrifugal field applied during the run, enabling straightforward experimental replication.

The MICRO-25's computer and its many operational and computational features are just part of the story. There are significant mechanical innovations as well. Like a speed control system with ± 5 RPM accuracy. And an infrared temperature detector that enables *rotor* temperature control to ± 0.5°C.

If you're considering the purchase of a high speed centrifuge, consider a high force machine instead. Send for complete information.

■ Up to 50 stored programs ■ Multiple segment program capability for stepped centrifugation ■ Continuous display of set and actual run conditions ■ Superior speed control, ± 5 rpm ■ Rotor recognition ■ Infrared rotor temperature detector, ± 0.5°C control ■ Safety cover interlock system ■ Automatic overspeed protection ■ Delayed start feature ■ Absolute containment

INTERNATIONAL EQUIPMENT COMPANY
A DIVISION OF DAMON

300 Second Ave., Needham Hts., MA 02194
Tel: (617) 449-0800. Telex: 92-2499, INTLEQUIP NEDM.
DAMON/IEC (UK) LTD.,
Unit 7, Lawrence Way, Brewers Hill Road, Dunstable, Bedfordshire, LU6 1BD, England. Tel. (0582) 604660

Circle Reader service No. 08 for Salesman to call

nature

Vol. 295 No. 5845 14 January 1982

Creationists and science in schools 85
Selling off telephones 85
How to save a university 86

NEWS

Arkansas verdict against creation science
Creationism judged a religion, not science
University of London
Academic censorship
Relative prosperity
Polish crisis
British medical research
US agricultural aid
Drug regulation in Brazil
UN technical development
Biotechnology
Cold comfort 87

CORRESPONDENCE

Dioxin/Anonymous referees/Specialized journals/Sheldrake/Creationists 92

NEWS AND VIEWS

Europe probes the auroral atmosphere (H Rishbeth)
Do all laboratory mice trace back to a single female? (M F W Festing)
How black is the Universe? (R A Muller)
Islet cell precursors are neurones (A G E Pearse)
The nature of galactic shells (G Gilmore)
Developing synthetic vaccines (A J Zuckerman)
A problem for the theory of biological structure (D Eisenberg)
Spacecraft collisions (D W Hughes) 93

BOOK REVIEWS

The DNA Story: A Documentary History of Gene Cloning (*by* J D Watson and J Tooze) Marie Jahoda; **A Geology of Ireland (C H Holland, *ed.*)** W S McKerrow; **The Papers of Joseph Henry, Vol. 4 (N Reingold, *ed.*)** C Russell; **Geomorphological Techniques (A Goudie, *ed.*)** C Kidson; **Amino Acid Analysis (J M Rattenbury, *ed.*)** A Darbre; **Semiconducting Polymers (*by* M Kryszewski)** H Mark 173

MISCELLANY

Product review: water analysis xxvii
Announcements xix
Classified advertising xx

Cover

The capsid electron density map of polyoma virus viewed down the pentavalent and hexavalent morphological units. White and yellow regions are closest to the viewer while red and magenta are furthest away (graphics by Tim Baker and William Saunders). See page **110.**

Transcription of *Xenopus* 5S ribosomal RNA genes (a review) L J Korn 101

ARTICLES

After the deluge: Mediterranean stagnation and sapropel formation M Rossignol-Strick, W Nesteroff, P Olive & C Vergnaud-Grazzini 105
Polyoma virus capsid structure at 22.5 Å resolution I Rayment, T S Baker, D L D Caspar & W T Murakami 110
Cellular genes analogous to retroviral *onc* genes are transcribed in human tumour cells A Eva, K C Robbins, P R Andersen, A Srinivasan, S R Tronick, E P Reddy, N W Ellmore, A T Galen, J A Lautenberger, T S Papas, E H Westin, F Wong-Staal, R C Gallo & S A Aaronson 116
DNA sequences necessary for transcription of the rabbit β-globin gene *in vivo* G C Grosveld, E de Boer, C K Shewmaker & R A Flavell 120

LETTERS TO NATURE

Nature of the shells of NGC1344 D Carter, D A Allen & D F Malin 126
A possible link between the rotation of Saturn and its ring structure F A Franklin, G Colombo & A F Cook 128
Radiation effects and the leach rates of vitrified radioactive waste W G Burns, A E Hughes, J A C Marples, R S Nelson & A M Stoneham 130
A mesospheric source of nitrous oxide E C Zipf & S S Prasad 133
Auroral effects on power transmission line systems S-I Akasofu & J D Aspnes 136
Acid snow in the Canadian high Arctic R M Koerner & D Fisher 137
Molluscan biostratigraphy of the Koobi Fora hominid-bearing deposits P G Williamson 140
Aneural muscle cell cultures make synaptic basal lamina components L Silberstein, N C Inestrosa & Z W Hall 143
Hypothalamic paraventricular nucleus is a privileged site for brain–pituitary interaction in long-term tissue culture A J Baertschi, J-L Beny & B Gähwiler 145
Vasoactive intestinal polypeptide enhances muscarinic ligand binding in cat submandibular salivary gland J M Lundberg, B Hedlund & T Bartfai 147
Neuronal spread of scrapie agent and targeting of lesions within the retino-tectal pathway H Fraser 149
Immune interferon release when a cloned cytotoxic T-cell line meets its correct influenza-infected target cell A G Morris, Y L Lin & B A Askonas 150

Nature® (ISSN 0028-0836) is published weekly on Thursday, except the last week in December, by Macmillan Journals Ltd and includes the Directory of Biologicals (mailed in December) and Annual Index (mailed in February). Annual subscription for USA and Canada US $198.50 (for subscription prices elsewhere, see next page). Orders (with remittance) and change of address labels to: Macmillan Journals Ltd, Brunel Rd, Basingstoke RG21 2XS, UK. Second class postage paid at New York, NY10010 and additional mailing offices. US Postmaster send form 3579 to: *Nature*, 15 East 26 Street, New York, NY 10010.

0028-0836/82/02000C-02$01.00

Contents continued overleaf

Are you locked in to a ^{32}P-schedule?

Amersham provides the key.

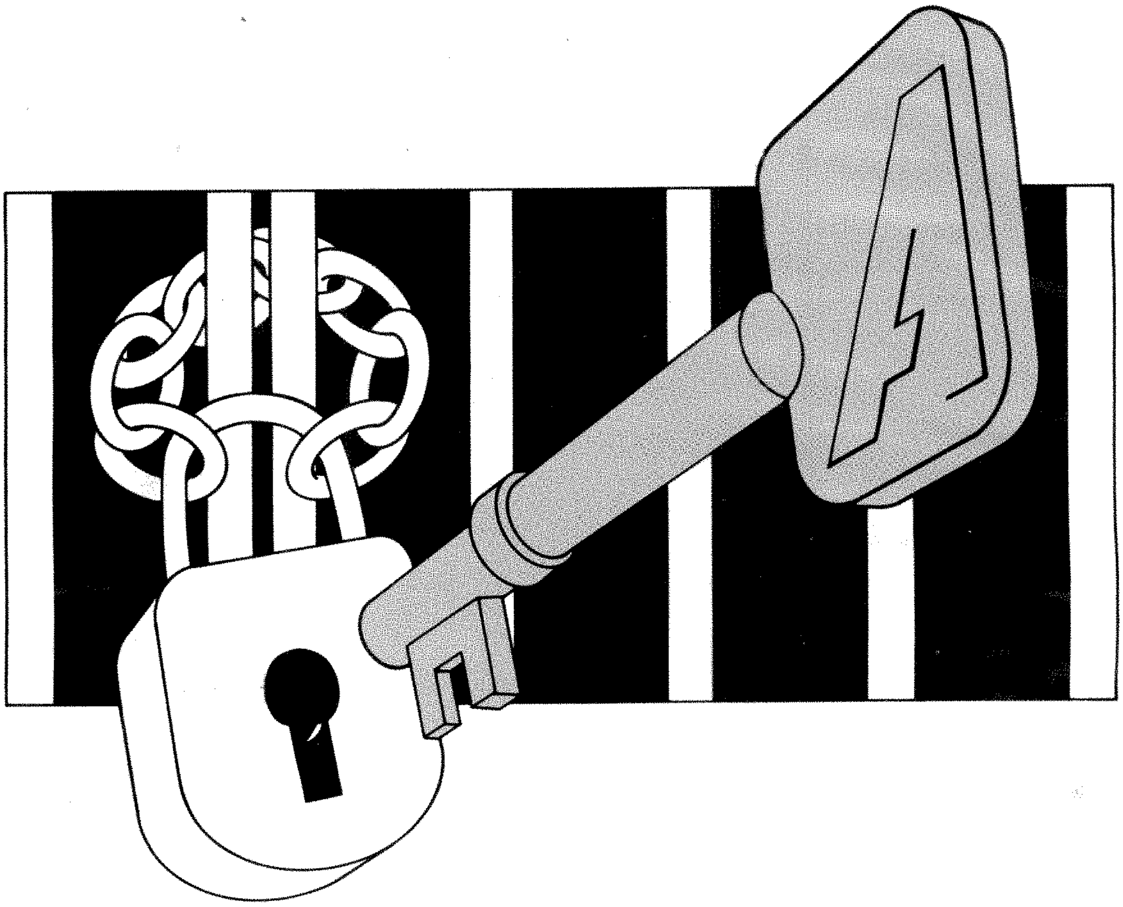

New ● All deoxynucleotides at ~3000Ci/mmol available **every week.**
● All deoxynucleotides at ~800Ci/mmol available **every week.**
● All deoxynucleotides at >400Ci/mmol available **every week.**

The reliable supply of the complete range of [α −^{32}P] dNTPs every week gives you the convenience of selecting the specific activity most appropriate for your experiments at any time.

Amersham - for products you can trust

Amersham International Limited, Amersham, England Telephone 024-04-4444
In the U.S.A. and Canada, Amersham Corporation, Illinois 60005 Telephone 312-364-7100
and 800-323-9750 (Tollfree)
In W. Germany, Amersham Buchler GmbH & Co KG, Braunschweig Telephone 05307-4691
Circle No. 13 on Reader Enquiry Card.

Amersham

• **Voyager 1 at Saturn**

The new results from Voyager 1, which appeared in *Nature* of 20 August 1981 are now available in a glossy, 88-page booklet.

Copies can be ordered from the *Nature* offices in London, Basingstoke and New York at the following prices (including postage):

UK £2.00 each; USA & Canada US $4.00; Rest of World £2.50 (surface), £3.50 (air)

Payment should accompany orders and may be in any currency at the prevailing exchange rate. Cheques should be made payable to *Nature*.

Annual Subscription including Index (51 issues)

UK & Eire		£85
USA & Canada		US$198.50
Belgium	Airspeed only	BF7450
West German	Airspeed only	DM450
Netherlands	Airspeed only	G505
Switzerland	Airspeed only	SF395
Rest of Europe	Airspeed only	£100
Rest of World	Surface	£100
Rest of World*	Airmail	£150

**(not USA, Canada & Europe)*

Personal subscription rates are available in some countries to subscribers paying by personal cheque or credit card.

Details can be obtained from:
UK: *Nature* Promotion Department,
Canada Road, Byfleet, Surrey KT14 7JL
Telephone: Jonathan Earl: Byfleet (09323) 41459

USA: *Nature*, 15 East 26 Street, New York, NY 10010
Credit card orders only (in USA & Canada):
Call toll-free: (800) 824-7888 (Operator 246)
In California: (800) 857-7777 (Operator 246)

Back issues: (Post-paid) UK, £2.50; USA & Canada, US$6.00 (surface), US$9.00 (air); Rest of World, £3.00 (surface), £4.00 (air).

***Nature* Binders:**
Single Binders: UK, £4.00; Rest of World, $10.00
Set(s) of 3 Binders: UK, £10.00; Rest of World, $25.00

***Nature* First Issue Facsimile:**
UK, 75p; Rest of World (surface), $1.50, (air), £2.00

***Nature* Annual Indexes (1971-1980):**
Price (post-paid):
UK, £5.00 each; Rest of World, $10.00

***Nature* Directory of Biologicals**
(Hardcover edition) (to be published late 1981)
UK, £20.00; Rest of World, $45.00

***Nature* Wallcharts:**
How Britain Runs its Science; How the US Runs its Science; UK, £3.50; USA, $7.95 each

***Nature* in Microform:**
For Information:
UK: UMI, 18 Bedford Row, London WC2R 4EJ
USA: 300 North Zeeb Road, Ann Arbor, Mi 48106

Orders (with remittance) to:
Nature, Macmillan Journals Ltd.,
Brunel Road, Basingstoke, Hants RG21 2XS, UK
Tel: (0256) 29242 Telex: 858493

MACMILLAN JOURNALS

Phorbol-12, 13-diester 12-ester hydrolase may prevent tumour promotion by phorbol diesters in skin M Shoyab, T C Warren & G J Todaro 152

Calmodulin confers calcium sensitivity on secretory exocytosis R A Steinhardt & J M Alderton 154

Measurement of changes in cytoplasmic free Ca^{2+} in fused cell hybrids M B Hallett & A K Campbell 155

Antibody to hepatitis B surface antigen after a single inoculation of uncoupled synthetic HBsAg peptides G R Dreesman, Y Sanchez, I Ionescu-Matiu, J T Sparrow, H R Six, D L Peterson, F B Hollinger & J L Melnick 158

New Epstein–Barr virus variants from cellular subclones of P3J-HR-1 Burkitt lymphoma L Heston, M Rabson, N Brown & G Miller 160

Evidence from mtDNA sequences that common laboratory strains of inbred mice are descended from a single female S D Ferris, R D Sage & A C Wilson 163

Recent divergence from a common ancestor of human IFN-α genes T Miyata & H Hayashida 165

***H–2*-like genes in the *Tla* region of mouse chromosome 17** D H Margulies, G A Evans, L Flaherty & J G Seidman 168

MATTERS ARISING

A pitfall in random sampling L M Van Valen 171

Anomalous ^{13}C depletion in Precambrian organic carbon K M Towe 171
Reply: M Schoell & F W Wellmer 172

Are monozygotic twins similar due to genetic factors alone? J L Jinks, C S Haley & K A Last
Reply: K Gärtner & E Baunack 172

GUIDE TO AUTHORS

Authors should be aware of the diversity of *Nature*'s readership and should strive to be as widely understood as possible.

Review articles should be accessible to the whole readership. Most are commissioned, but unsolicited reviews are welcome (in which case prior consultation with the office is desirable).

Scientific articles are research reports whose conclusions are of general interest or which represent substantial advances of understanding. The text should not exceed 3,000 words and six displayed items (figures plus tables). The article should include an abstract of about 50 words.

Letters to *Nature* are ordinarily 1,000 words long with no more than four displayed items. The first paragraph (not exceeding 150 words) should say what the letter is about, why the study it reports was undertaken and what the conclusions are.

Matters arising are brief comments (up to 500 words) on articles and letters recently published in *Nature*. The originator of a Matters Arising contribution should initially send his manuscript to the author of the original paper and both parties should, wherever possible, agree on what is to be submitted.

Manuscripts may be submitted either to London or New York (decisions being made only in London). Manuscripts should be typed (double spacing) on one side of the paper only. Three copies are required, each accompanied by copies of lettered artwork. No title should exceed 80 characters in length. Reference lists, figure legends, etc. should be on separate sheets, all of which should be numbered. Abbreviations, symbols, units, etc. should be identified on one copy of the manuscript at their first appearance.

References should appear sequentially indicated by superscripts in the text and should be abbreviated according to the *World List of Scientific Periodicals*, fourth edition (Butterworth 1963–65). The first and last page numbers of each reference should be cited. References to books should clearly indicate the publisher and the date and place of publication. Unpublished articles should not be formally referred to unless accepted or submitted for publication, but may be mentioned in the text.

Each piece of artwork should be clearly marked with the author's name and the figure number. Original artwork should be unlettered. Suggestions for cover illustrations are welcome. Original artwork (and one copy of the manuscript) will be returned when manuscripts cannot be published.

Requests for permission to reproduce material from Nature *should be accompanied by a self-addressed (and, in the case of the UK and USA, stamped) envelope.*

BRITISH MADE

ULTRA PURE WATER WITHIN YOUR GRASP

Analytical grade water at less than 4.0 pence per litre, in any volume and with the minimum of maintenance. These are a few of the advantages of Elga's extended range of Laboratory Reverse Osmosis units.

Designed to meet the growing demand for organically pure, colloid-free water in HPLC tissue culture etc. LabRO and Spectrum RO are cost-efficient answers to a common laboratory problem.

LabRO is a self-contained unit for either bench mounting or free standing and is the latest product of Elga's reverse osmosis expertise. A LabRO unit can produce up to 1,000 litres per day.

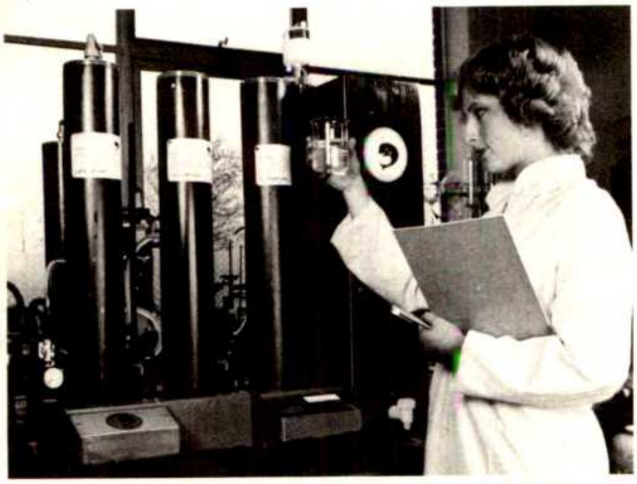

Spectrum RO is an addition to the established Spectrum deioniser range and is ideal for the production of smaller volumes.
There is more, much more, that you should know about these products, so contact Elga today for full information.

Name
Position
Organisation
Address
Telephone
I use .... litres of purified water per ....
N182

The Elga Group
Lane End Buckinghamshire England
HP14 3JH Telephone: High Wycombe
(0494) 881393 Telex: 83516

ELGA
THE ULTRA PURE WATER PEOPLE.

Circle No.18 on Reader Enquiry Card.

nature

Vol. 295 No. 5846 21 January 1982

Can change damage your mental health? 177
Paying the price for coal 177
Ice age or melt-down? 178

NEWS

Mental stress given environmental status
European nuclear safety policy attacked
French colloquium
River of words, mountain of paper
University of London
AT&T pact hits snag
Polish universities
Gentle Polish protest
Finnish–Soviet research
Deep sea mining
Indian agriculture
Bridging the Indian gap 179

CORRESPONDENCE

Anonymous referees/Soviet problem/ DNA policy/etc. 184

NEWS AND VIEWS

Hominoid evolution (P Andrews)
Measuring atmospheric gases and aerosols (D D Davies, W L Chameides & C S Kiang
A hydrothermal plume remobilizes sedimentary organic matter (A S Mackenzie)
Prostaglandins and cancer (P Alexander)
A new British flower (P D Moore)
Analysing atmospheric carbon dioxide levels (M J Rycroft)
Mammary gland as an endocrine organ: implications for mastectomy (J M Diamond)
Exciting Rydberg atoms in cavities (P Knight) 185

BOOK REVIEWS

The Mathematical Papers of Isaac Newton, Vol.VIII, 1697–1722 (*by* **D T Whiteside,** *ed*) Richard S. Westfall; **The Nobel Duel** (*by* **N Wade**) Walter Gratzer; **Zeta Potential in Colloid Science** (*by* **R J Hunter**) John Gregory; **Lower Palaeozoic of the Middle East, Eastern and Southern Africa, and Antarctica** (**C H Holland,** *ed.*) Janet V Watson; **The Lower and Middle Palaeolithic Periods in Britain** (*by* **D A Roe**) Paul Mellars 265

Cover

A new partial skull of *Sivapithecus indicus* from 8-million-year-old rocks in the Potwar Plateau of Pakistan is reported on page 232. (Photo: William Sacco).

ARTICLES

A seasonal signal in ocean currents to abyssal depths	R R Dickson, W J Gould, P A Garbutt & P D Killworth	**193**
Hydrothermal petroleum in mineralized mounds at the seabed of Guaymas Basin	B R T Simoneit & P F Lonsdale	**198**
Cloning and sequence analysis of cDNA for bovine adrenal preproenkephalin	M Noda, Y Furutani, H Takahashi, M Toyosato, T Hirose, S Inayama, S Nakanishi & S Numa	**202**
Molecular cloning establishes proenkephalin as precursor of enkephalin-containing peptides	U Gubler, P Seeburg, B J Hoffman, L P Gage & S Udenfriend	**206**
Multiple arrangements of viral DNA and an activated host oncogene in bursal lymphomas	G S Payne, J M Bishop & H E Varmus	**209**

LETTERS TO NATURE

Occurrence of the 3.3-μm feature in galaxies	T J Lee, D H Beattie, I Gatley, P W J L Brand, T Jones & A R Hyland	**214**
γ-Quanta capture by magnetic field and pair creation suppression in pulsars	A E Shabad & V V Usov	**215**
New evidence for degassing processes during explosive eruptions	R S J Sparks & S Brazier	**218**
Ice core sample measurements give atmospheric CO_2 content during the past 40,000 yr	A Neftel, H Oeschger, J Schwander, B Stauffer & R Zumbrunn	**220**
Steroid hydrocarbons and the thermal history of sediments	A S Mackenzie, N A Lamb & J R Maxwell	**223**
Fine-scale isotopic heterogeneity in the sub-Atlantic mantle	N Machado, J N Ludden, C Brooks & G Thompson	**226**
Fluid evolution and graphite genesis in the deep continental crust	W Glassley	**229**
New hominoid skull material from the Miocene of Pakistan	D Pilbeam	**232**
Body temperature changes during the practice of g Tum-mo yoga	H Benson, J W Lehmann, M S Malhotra, R F Goldman, J Hopkins & M D Epstein	**234**
Preferences for cousins in Japanese quail	P Bateson	**236**
Early auditory experience modifies sound localization in barn owls	E I Knudsen, P F Knudsen & S D Esterly	**238**
Defective T-cell response in beige mutant mice	R K Saxena, Q B Saxena & W H Adler	**240**
Further studies on supposed lamarckian inheritance of immunological tolerance	L Brent, P Chandler, W Fierz, P B Medawar, L S Rayfield & E Simpson	**242**

Nature® (ISSN 0028-0836) is published weekly on Thursday, except the last week in December, by Macmillan Journals Ltd and includes the Directory of Biologicals (mailed in December) and Annual Index (mailed in February). Annual subscription for USA and Canada US $198.50 (for subscription prices elsewhere, see next page). Orders (with remittance) and change of address labels to: Macmillan Journals Ltd, Brunel Rd, Basingstoke RG21 2XS, UK. Second class postage paid at New York, NY10010 and additional mailing offices. US Postmaster send form 3579 to: *Nature,* 15 East 26 Street, New York, NY 10010.

0028-0836/82/03000C-02$01.00

Contents continued overleaf

Are you locked in to a ^{32}P-schedule?
Amersham provides the key.

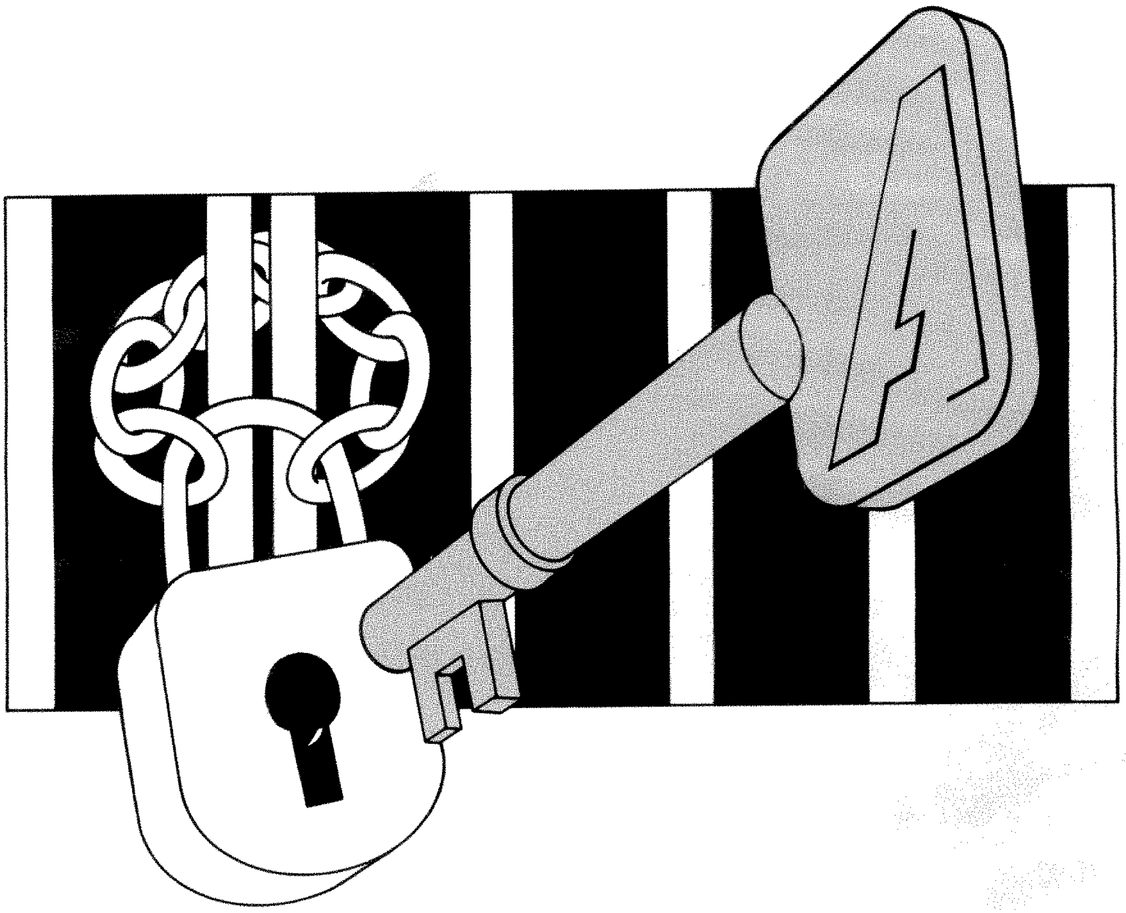

New
- All deoxynucleotides at ~3000Ci/mmol available **every week.**
- All deoxynucleotides at ~800Ci/mmol available **every week.**
- All deoxynucleotides at >400Ci/mmol available **every week.**

The reliable supply of the complete range of [$\alpha - ^{32}$P] dNTPs every week gives you the convenience of selecting the specific activity most appropriate for your experiments at any time.

Amersham - for products you can trust

Amersham International Limited, Amersham, England Telephone 024-04-4444
In the U.S.A. and Canada, Amersham Corporation, Illinois 60005 Telephone 312-364-7100
and 800-323-9750 (Tollfree)
In W. Germany, Amersham Buchler GmbH & Co KG, Braunschweig Telephone 05307-4691

Circle No. 13 on Reader Enquiry Card.

Amersham

Adult haematopoietic cells transplanted to sheep fetuses continue to produce adult globins E D Zanjani, G Lim, P B McGlave, J F Clapp, L I Mann, T H Norwood & G Stamatoyannopoulos **244**

Thrombospondin is the endogenous lectin of human platelets E A Jaffe, L L K Leung, R L Nachman, R I Levin & D F Mosher **246**

A microtubule-associated protein in the mitotic spindle and the interphase nucleus J G Izant, J A Weatherbee & J R McIntosh **248**

Rous sarcoma virus-induced phosphorylation of a 50,000-molecular weight cellular protein J S Brugge & D Darrow **250**

Endogenous MuLV infection does not contribute to onset of radiation- or carcinogen-induced murine thymoma A Mayer & K Dorsch-Häsler **253**

Altered methylation of endogenous viral promoter sequences during mammary carcinogenesis T Breznik & J C Cohen **255**

High frequency of gene transfer after fusion between bacteria and eukaryotic cells M Rassoulzadegan, B Binetruy & F Cuzin **257**

Circular double-stranded RNA in potato spindle tuber viroid-infected tomatoes R C French, M A Price & K S Derrick **259**

A + T-rich linkers define functional domains in eukaryotic DNA J Moreau, L Marcaud, F Maschat, J Kejzlarova-Lepesant, J-A Lepesant & K Scherrer **260**

MATTERS ARISING

Guidance system for pheromone orientation in moths T R Tobin & W J Bell Reply: J S Kennedy, A R Ludlow & C J Sanders **263**

Tilt of the central gas disk of the Galaxy A H Nelson Reply: J W-K Mark & L Blitz **263**

Lipoprotein assembly in *Xenopus* yolk-platelet crystals L J Banaszak & D H Ohlendorf Reply: R H Lange **264**

MISCELLANY

100 years ago **187**
Author index Vol 294 **ix**
Books received **xv**
Announcements **xxi**
Classified advertising **xxiii**

92, A.P.C. Rd. Cal-9
LIBRARY COMPLEX
Chemical Technology
Rubber Technology

• Voyager 1 at Saturn

The new results from Voyager 1, which appeared in *Nature* of 20 August 1981 are now available in a glossy, 88-page booklet.

Copies can be ordered from the *Nature* offices in London, Basingstoke and New York at the following prices (including postage):

UK £2.00 each; USA & Canada US $4.00; Rest of World £2.50 (surface), £3.50 (air)

Payment should accompany orders and may be in any currency at the prevailing exchange rate. Cheques should be made payable to *Nature*.

Annual Subscription including Index (51 issues)

UK & Eire		£85
USA & Canada		US$198.50
Belgium	Airspeed only	BF7450
West German	Airspeed only	DM450
Netherlands	Airspeed only	G505
Switzerland	Airspeed only	SF395
Rest of Europe	Airspeed only	£100
Rest of World	Surface	£100
Rest of World*	Airmail	£150

**(not USA, Canada & Europe)*

Personal subscription rates are available in some countries to subscribers paying by personal cheque or credit card.

Details can be obtained from:
UK: *Nature* Promotion Department,
Canada Road, Byfleet, Surrey KT14 7JL
Telephone: Jonathan Earl: Byfleet (09323) 41459

USA: *Nature*, 15 East 26 Street, New York, NY 10010
Credit card orders only (in USA & Canada):
Call toll-free: (800) 824-7888 (Operator 246)
In California: (800) 857-7777 (Operator 246)

Back issues: (Post-paid) UK, £3.00; USA & Canada, US$8.00 (surface), US$10.00 (air); Rest of World, £4.00 (surface), £5.00 (air).

***Nature* Binders:**
Single Binders: UK, £4.00; Rest of World, $10.00
Set(s) of 3 Binders: UK, £10.00; Rest of World, $25.00

***Nature* First Issue Facsimile:**
UK, 75p; Rest of World (surface), $1.50, (air), £2.00

***Nature* Annual Indexes (1971-1980):**
Price (post-paid):
UK, £5.00 each; Rest of World, $10.00

***Nature* Directory of Biologicals**
(Hardcover edition) (to be published late 1981)
UK, £20.00; Rest of World, $45.00

***Nature* Wallcharts:**
How Britain Runs its Science; How the US Runs its Science; UK, £3.50; USA, $7.95 each

***Nature* in Microform:**
For Information:
UK: UMI, 18 Bedford Row, London WC2R 4EJ
USA: 300 North Zeeb Road, Ann Arbor, Mi 48106

Orders (with remittance) to:
Nature, Macmillan Journals Ltd.,
Brunel Road, Basingstoke, Hants RG21 2XS, UK
Tel: (0256) 29242 Telex: 858493

M MACMILLAN JOURNALS

Ask LKB about High Performance Liquid Chromatography for proteins and peptides

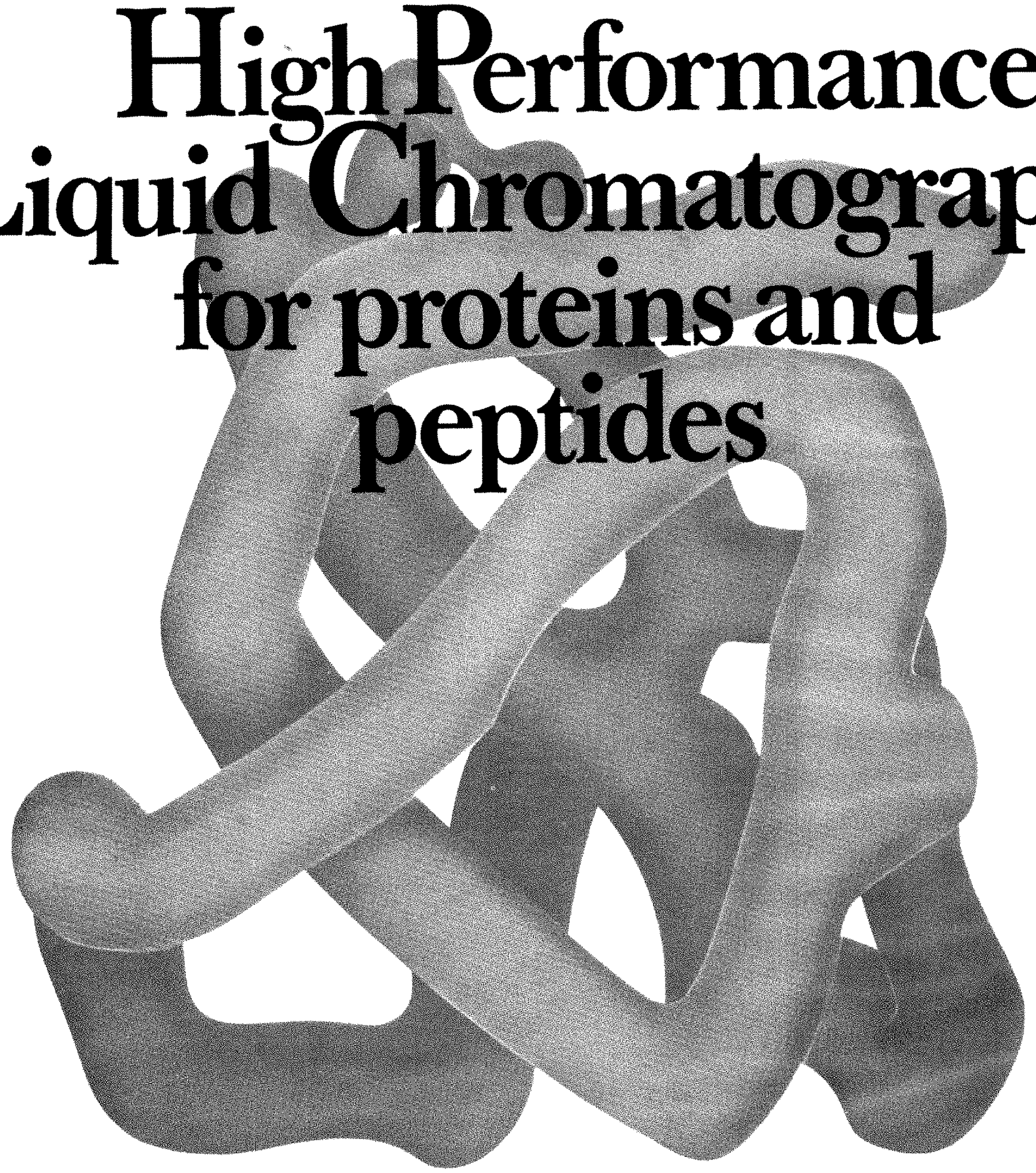

By combining years of experience in biochemical research and the latest advances in HPLC technology, LKB has perfected the first practical HPLC system for life science applications. For more information, just circle our number on the Reader Service Card.

Designed by biochemists for the biochemist.

LKB
BROMMA

Head office: LKB-Produkter AB, Box 305, S-161 26 Bromma, Sweden. Tel. 08-98 00 40, telex 10492
Main US sales office: LKB Instruments, Inc. 12221 Parklawn Drive, Rockville, MD 20852. Tel. 301-881 25 10, telex 230 89 682
UK sales office: LKB Instruments Ltd., 232 Addington Road, S. Croydon, Surrey CR2 8YD, England. Tel. 01-657 8822, telex 264414
Other sales offices in: Athens (for Middle East), Copenhagen, Ghent, The Hague, Hong Kong, Munich, Paris, Rome, Turku, Vienna

Circle No.09 on Reader Enquiry Card.

4011

nature

Vol. 295 No. 5847 28 January 1982

Can even mere knowledge be a threat? 269
Why arms control? 270
Academic freedom and security conflict
Harvard guidelines for avoiding fraud
Polish academics
UK nuclear power
Interferon used at last
US research spending
EEC research and development
Fusion decision awaited
US university funding
Telecommunications
Soviet biotechnology
Pasteur institute 271

CORRESPONDENCE

Creationism in UK/Herbicides in Hungary 276

NEWS AND VIEWS

Mirror-image navigational errors in migrating birds (J M Diamond)
Meteorite erosion and cosmic ray variations (D W Hughes)
Prohormones for vasopressin (B T Pickering)
Is phosphatidylinositol now out of the calcium gate? (J N Hawthorne)
A new model for giant H II shells (J C Raymond)
Fluorescence photobleaching in cell biology (K Jacobson, E Elson, D Koppel & W Webb)
Gravitational lenses (C Alcock) 277

BOOK REVIEWS

Science: Good, Bad and Bogus (*by* M Gardner) P B Medawar; **Towards Understanding Receptors (J W Lamble, *ed.*)** G L E Koch; **The Chemistry of Soil Processes (D J Greenland and M H B Hayes, *eds*)** T S West; **The Earth Generated and Anatomized (*by* W Hobbs, R Porter, *ed.*)** John Sutton; **Symbiosis in Cell Evolution (*by* L Margulis)** T Cavalier-Smith; **The Theory of Magnetism I: Statics and Dynamics (*by* D C Mattis)** D Sherrington; **Ontogeny and Phylogeny of Hormone Receptors (*by* G Csaba)** Eugene R DeSombre 351

IMMUNOLOGY

Developments in non-isotopic immunoassay (J N Miller) xxiii
Product review xxiv

Cover

Two South American species of tropical pasture legume produce sticky secretions which immediately immobilize larvae of the cattle tick, *Boophilus microplus* (see page **320**).

ARTICLES

Crater densities and geological histories of Rhea, Dione, Mimas and Tethys J B Plescia & J M Boyce **285**
The tectonics of Ganymede E M Parmentier, S W Squyres, J W Head & M L Allison **290**
The molecular structure of d(^{i}CpCpGpG), a fragment of right-handed double helical A-DNA B N Conner, T Takano, S Tanaka, K Itakura & R E Dickerson **294**
Nucleotide sequence of cloned cDNA encoding bovine arginine vasopressin–neurophysin II precursor H Land, G Schütz, H Schmale & D Richter **299**

LETTERS TO NATURE

Creation of open universes from de Sitter space J R Gott III **304**
Ionospheric troughs in Antarctica J R Dudeney, M J Jarvis, R I Kressman, M Pinnock, A S Rodger & K H Wright **307**
Two-dimensional modelling of potential ozone perturbation by chlorofluorocarbons J M Steed, A J Owens, C Miller, D L Filkin & J P Jesson **308**
Electromagnetic jet-propulsion in the direction of current flow P Graneau **311**
A composite semiconductor photoanode for water electrolysis Y Nakato, N Takamori & H Tsubomura **312**
Thermoluminescence dating of sand dunes in Rajasthan, India A K Singhvi, Y P Sharma & D P Agrawal **313**
Australian–Antarctic depression from the mid-ocean ridge to adjacent continents J J Veevers **315**
Phylogeny and classification of thecodontian reptiles S Chatterjee **317**
Tropical legumes of the genus *Stylosanthes* immobilize and kill cattle ticks R W Sutherst, R J Jones & H J Schnitzerling **320**
Role of gut flora in the genotoxicity of dinitrotoluene J C Mirsalis, T E Hamm Jr, J M Sherrill & B E Butterworth **322**
Effects of overfeeding on energy balance and brown fat thermogenesis in obese (*ob/ob*) mice P Trayhurn, P M Jones, M M McGuckin & A E Goodbody **323**
Expression of HLA antigens, β-microglobulin and enzymes by human amniotic epithelial cells M Adinolfi, C A Akle, I McColl, A H Fensom, L Tansley, P Connolly, B-L Hsi, W P Faulk, P Travers & W F Bodmer **325**
Leukotriene C_4 affects pulmonary and cardiovascular dynamics in monkey G Smedegård, P Hedqvist, S-E Dahlén, B Revenäs, S Hammarström & B Sameulsson **327**

Nature® (ISSN 0028-0836) is published weekly on Thursday, except the last week in December, by Macmillan Journals Ltd and includes the Directory of Biologicals (mailed in December) and Annual Index (mailed in February). Annual subscription for USA and Canada US $198.50 (for subscription prices elsewhere, see next page). Orders (with remittance) and change of address labels to: Macmillan Journals Ltd, Brunel Rd, Basingstoke RG21 2XS, UK. Second class postage paid at New York, NY10010 and additional mailing offices. US Postmaster send form 3579 to: *Nature*, 15 East 26 Street, New York, NY 10010.

0028-0836/82/04000C-02$01.00

Contents continued overleaf

Are you locked in to a ^{32}P-schedule?

Amersham provides the key.

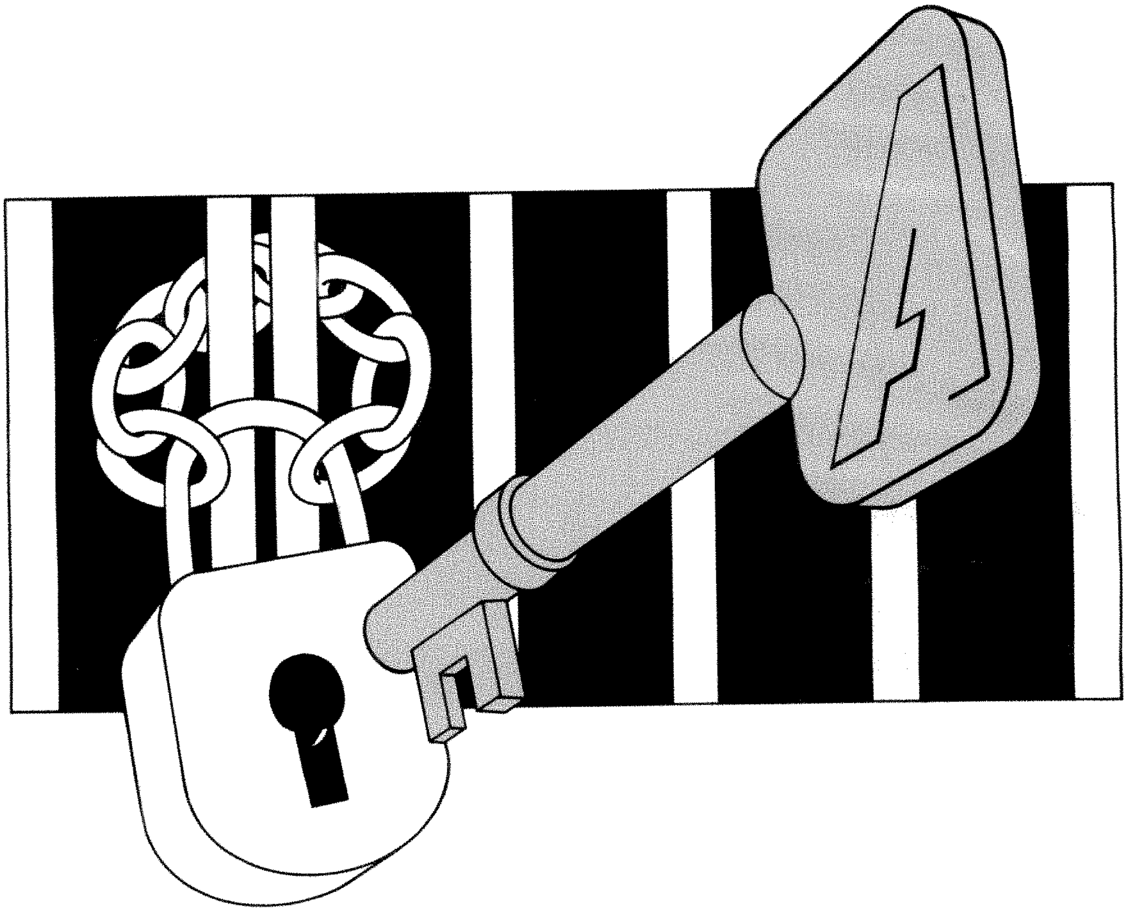

New ● All deoxynucleotides at ~3000Ci/mmol available **every week.**

● All deoxynucleotides at ~800Ci/mmol available **every week.**

● All deoxynucleotides at >400Ci/mmol available **every week.**

The reliable supply of the complete range of [α – ^{32}P] dNTPs every week gives you the convenience of selecting the specific activity most appropriate for your experiments at any time.

Amersham - for products you can trust

Amersham International Limited, Amersham, England Telephone 024-04-4444
In the U.S.A. and Canada, Amersham Corporation, Illinois 60005 Telephone 312-364-7100
and 800-323-9750 (Tollfree)
In W. Germany, Amersham Buchler GmbH & Co KG, Braunschweig Telephone 05307-4691

Circle No.13 on Reader Enquiry Card.

Amersham

• Voyager 1 at Saturn

The new results from Voyager 1, which appeared in *Nature* of 20 August 1981 are now available in a glossy, 88-page booklet.

Copies can be ordered from the *Nature* offices in London, Basingstoke and New York at the following prices (including postage):

UK £2.00 each; USA & Canada US $4.00; Rest of World £2.50 (surface), £3.50 (air)

Payment should accompany orders and may be in any currency at the prevailing exchange rate. Cheques should be made payable to *Nature*.

Annual Subscription including Index (51 issues)

UK & Eire		£85
USA & Canada		US$198.50
Belgium	Airspeed only	BF7450
West German	Airspeed only	DM450
Netherlands	Airspeed only	G505
Switzerland	Airspeed only	SF395
Rest of Europe	Airspeed only	£100
Rest of World	Surface	£100
Rest of World*	Airmail	£150

**(not USA, Canada & Europe)*

Personal subscription rates are available in some countries to subscribers paying by personal cheque or credit card.

Details can be obtained from:
UK: *Nature* Promotion Department,
Canada Road, Byfleet, Surrey KT14 7JL
Telephone: Jonathan Earl: Byfleet (09323) 41459

USA: *Nature*, 15 East 26 Street, New York, NY 10010
Credit card orders only (in USA & Canada):
Call toll-free: (800) 824-7888 (Operator 246)
In California: (800) 857-7777 (Operator 246)

Back issues: (Post-paid) UK, £3.00; USA & Canada, US$8.00 (surface), US$10.00 (air); Rest of World, £4.00 (surface), £5.00 (air).

***Nature* Binders:**
Single Binders: UK, £4.00; Rest of World, $10.00
Set(s) of 3 Binders: UK, £10.00; Rest of World, $25.00

***Nature* First Issue Facsimile:**
UK, 75p; Rest of World (surface), $1.50, (air), £2.00

***Nature* Annual Indexes (1971-1980):**
Price (post-paid):
UK, £5.00 each; Rest of World, $10.00

***Nature* Directory of Biologicals**
(Hardcover edition) (to be published late 1981)
UK, £20.00; Rest of World, $45.00

***Nature* Wallcharts:**
How Britain Runs its Science; How the US Runs its Science; UK, £3.50; USA, $7.95 each

***Nature* in Microform:**
For Information:
UK: UMI, 18 Bedford Row, London WC2R 4EJ
USA: 300 North Zeeb Road, Ann Arbor, Mi 48106

Orders (with remittance) to:
Nature, Macmillan Journals Ltd.,
Brunel Road, Basingstoke, Hants RG21 2XS, UK
Tel: (0256) 29242 Telex: 858493

MACMILLAN JOURNALS

Lack of immune response gene control for induction of epitope-specific suppression by TGAL antigen — L A Herzenberg, T Tokuhisa, K Hayakawa & L A Herzenberg 329

Rapid lateral diffusion of functional ACh receptors in embryonic muscle cell membrane — M-m Poo 332

Reorganization of HeLa cell cytoskeleton induced by an uncoupler of oxidative phosphorylation — B Maro & M Bornens 334

Chromaffin granule membrane–F-actin interactions are calcium sensitive — V M Fowler & H B Pollard 336

Isolation and structure of dynorphin, an opioid peptide, from porcine duodenum — S Tachibana, K Araki, S Ohya & S Yoshida 339

A carboxypeptidase processing enzyme for enkephalin precursors — V Y H Hook, L E Eiden & M J Brownstein 341

RNA synthesis and cytoplasmic polyadenylation in the one-cell mouse embryo — K B Clegg & L Piko 342

Partial nucleotide sequence of human calcitonin precursor mRNA identifies flanking cryptic peptides — R K Craig, L Hall, M R Edbrooke, J Allison & I MacIntyre 345

Heterogeneity of the BALB/c IgM anti-phosphorylcholine antibody response — J A Owen, N H Sigal & N R Klinman 347

Excision of polyoma virus genomes from chromosomal DNA by homologous recombination — L Lania, S Boast & M Fried 349

MISCELLANY

100 years ago 279
Erratum 350
Classified advertising xxvii

GUIDE TO AUTHORS

Authors should be aware of the diversity of *Nature*'s readership and should strive to be as widely understood as possible.

Review articles should be accessible to the whole readership. Most are commissioned, but unsolicited reviews are welcome (in which case prior consultation with the office is desirable).

Scientific articles are research reports whose conclusions are of general interest or which represent substantial advances of understanding. The text should not exceed 3,000 words and six displayed items (figures plus tables). The article should include an abstract of about 50 words.

Letters to *Nature* are ordinarily 1,000 words long with no more than four displayed items. The first paragraph (not exceeding 150 words) should say what the letter is about, why the study it reports was undertaken and what the conclusions are.

Matters arising are brief comments (up to 500 words) on articles and letters recently published in *Nature*. The originator of a Matters Arising contribution should initially send his manuscript to the author of the original paper and both parties should, wherever possible, agree on what is to be submitted.

Manuscripts may be submitted either to London or New York (decisions being made only in London). Manuscripts should be typed (double spacing) on one side of the paper only. Three copies are required, each accompanied by copies of lettered artwork. No title should exceed 80 characters in length. Reference lists, figure legends, etc. should be on separate sheets, all of which should be numbered. Abbreviations, symbols, units, etc. should be identified on one copy of the manuscript at their first appearance.

References should appear sequentially indicated by superscripts in the text and should be abbreviated according to the *World List of Scientific Periodicals*, fourth edition (Butterworth 1963–65). The first and last page numbers of each reference should be cited. References to books should clearly indicate the publisher and the date and place of publication. Unpublished articles should not be formally referred to unless accepted or submitted for publication, but may be mentioned in the text.

Each piece of artwork should be clearly marked with the author's name and the figure number. Original artwork should be unlettered. Suggestions for cover illustrations are welcome. Original artwork (and one copy of the manuscript) will be returned when manuscripts cannot be published.

Requests for permission to reproduce material from Nature *should be accompanied by a self-addressed (and, in the case of the UK and USA, stamped) envelope.*

Miles-Made
Peroxidase Conjugates

High titers...for high dilutions.

Miles offers a broad selection of peroxidase conjugated antisera, each tested for satisfactory immunoassay performance. Some popular products include:

Peroxidase Conjugated	Host	Code No.
Anti-Human IgA (α)	Goat	61-131
Anti-Human IgE (ε)	Goat	61-133
Anti-Human IgG	Goat	61-230
Anti-Human IgM (μ)	Goat	61-132
Anti-Goat IgG	Rabbit	61-201
Anti-Mouse IgG	Rabbit	61-204
Anti-Rabbit IgG	Goat	61-202

For a complete listing of Miles peroxidase conjugated antisera and lectins, call or write:

Miles Laboratories, Inc.
P.O. Box 2000, Elkhart, IN 46515 U.S.A.
Telephone: Toll-free **800-348-7465**
(In Indiana, 219-264-8804;
in Canada, 416-248-0771)

Miles Laboratories, Ltd.
P.O. Box 37, Stoke Poges
Slough SL2 4LY, U.K.
Telephone: Farnham Common 5151

Research Products Division MILES

© 1981 MILES LABORATORIES, INC.

MRP-5147861

Circle No.16 on Reader Enquiry Card.

Miles-Made
Alkaline Phosphatase Conjugates

The Miles label, a quality standard in biochemicals and immunologicals, guarantees consistent quality in antisera.

We offer a wide range of antisera conjugated with labeling-grade alkaline phosphatase that is highly suitable for use in immunoassay procedures.

Alkaline Phosphatase Conjugates

Antigen	Host	Code Number
Goat IgG	Rabbit	61-276
Guinea Pig IgG	Rabbit	61-279
Human IgA (α)	Goat	61-272
Human IgG	Goat	61-270
Human IgM (μ)	Goat	61-271
Mouse IgG	Rabbit	61-278
Rabbit IgG	Goat	61-275
Rat IgG	Rabbit	61-277

Detailed product literature is available on request from:

Miles Laboratories, Inc.
Research Products Division
P.O. Box 2000, Elkhart, IN 46515
Telephone: Toll-free **800-348-7465**
(in Indiana, 219-264-8804)

Miles Laboratories, Ltd.
P.O. Box 37, Stoke Court, Stoke Poges
Slough SL2 4LY, England
Telephone: Farnham Common 5151

Research Products Division MILES

© 1981 MILES LABORATORIES, INC.

MRP-5141851

Circle No.15 on Reader Enquiry Card.

SPEED VAC
- Concentrator
- Concentrer
- Konzentrieren

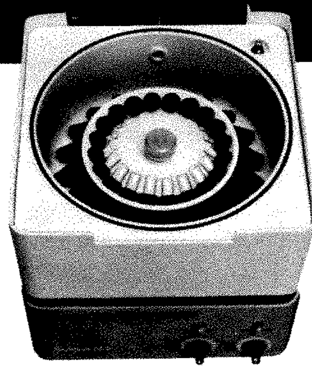

No Bumping	Keine Blasenbildung	Sans Projections
No Smearing	Kein Verschmieren	Sans Mousse
No Washdown	Kein Runterwaschen	Sans Entrainement
No Dilution	Keine Verdunnung	Sans Dillution
No Transfer	Kein Transfer	Sans Contamination
No Losses	Kein Verlust	Sans Pertes

The Speed Vac Concentrator will yield virtually 100% sample recovery with Eluates, Hydrolysates, Extracts and Dialyzed solutions.

Concentrate prior to analysis by Gas Chromatography (GC), High Pressure Liquid Chromatography (HPLC), Electrophoresis, TLE or TLC.

A lab tested, work saving system now widely used in Drug Monitoring, RNA & DNA, Sequencing, Protein Structure Analyses, Isolation of a wide range of organic and biochemical species.

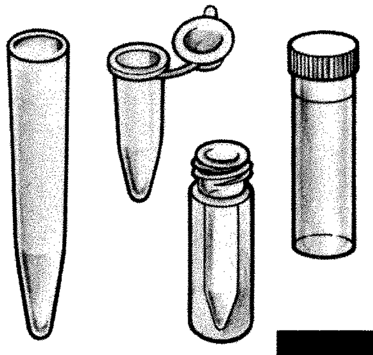

Send for literature today. ***SAVANT INSTRUMENTS, INC.***
221 Park Ave., Hicksville, NY 11801 (516) 935-8774.

U.S. PATENT NO. 4226669

Savant

Circle No.09 on Reader Enquiry Card.

nature

Vol. 295 No. 5848 4 February 1982

Unemployment and the future 355
Goodbye to guidelines 356
Maths without teachers 356

NEWS

Making private interests public
Another French director resigns
Polish higher education
Recombinant DNA guidelines
A letter to Leonid Brezhnev . . .
Lead additives in petrol
Satellite communications
Cashing in now
Technical change in France
Fluoridation in Scotland
Rubik's cube 357

CORRESPONDENCE

Soviet sanctions/Specialist journals/Anthrax/Ease of reading/Repeated sequence 362

NEWS AND VIEWS

Mantle heterogeneity and isotopes in oceanic basalts (W M White & A W Hofmann)
New measurements near the Gulf Stream (W J Gould)
Substorms and the growth phase problem (S W H Cowley)
T cell function: Ly phenotype and the MHC (E Simpson)
Great voids in the Universe (J Silk)
How the malarial parasite enters the red blood cell (R J Wilson)
The mystery of the mouse α-globin pseudogene (R A Flavell) 363

BOOK REVIEWS

Electronic Colonialism (*by* **T L McPhail)** *and* **Global Talk** (*by* **J N Pelton)** Brenda Maddox; **The Foundations of Ethology** (*by* **K Z Lorenz)** Mark Ridley; **Galactic Astronomy: Structure and Kinematics, 2nd Edn** (*by* **D Mihalas and J Binney)** John D Barrow; **Optical Information Processing: Fundamentals (S H Lee, *ed.*)** P W Hawkes; **The Biology of Centipedes** (*by* **J G E Lewis)** John A Wallwork; **Protein Phosphorylation (O M Rosen and E G Krebs, *eds*)** P J England; **Excitons: Their Properties and Uses** (*by* **D C Reynolds and T C Collins)** Dennis Dunn 439

Cover

A complete carrot plant regenerated from roots containing a region of the virulence plasmid of *Agrobacterium rhizogenes*, causative agent for hairy root disease. This Ri plasmid joins the Ti plasmid (causing crown gall disease) as a possible vector for genetic engineering in plants. (See page **432**.)

Grain alignment in the galactic magnetic field (a review) — P E Johnson — 371

ARTICLES

Ultrasonic borehole televiewer investigation of oceanic crustal layer 2A, Costa Rica Rift — M D Zoback & R N Anderson — 375
Resolving the functions of overlapping viral genes by site-specific mutagenesis at a mRNA splice site — C Montell, E F Fisher, M H Caruthers & A J Berk — 380
Unusual physical organization of the *Halobacterium* genome — C Sapienza & W F Doolittle — 384

LETTERS TO NATURE

Detection of $HC_{11}N$ in IRC + 10°216 — M B Bell, P A Feldman, S Kwok & H E Matthews — 389
On the reported detection of sub-GeV antiprotons in galactic cosmic rays — D Eichler — 391
Vortex solitary waves in a rotating, turbulent flow — E J Hopfinger & F K Browand — 393
A suspended sediment front in the Severn Estuary — R Kirby & W R Parker — 396
Successive palaeomagnetic reversal records from Kauai — S W Bogue & R S Coe — 399
Rapid growth of a deep-sea manganese nodule — J L Reyss, V Marchig & T L Ku — 401
Biogenic calcite structures forming in Lake Fryxell, Antarctica — R A Wharton Jr, B C Parker, G M Simmons Jr, K G Seaburg & F G Love — 403
Neural reorganization during metamorphosis of the corpora pedunculata in *Drosophila melanogaster* — G Technau & M Heisenberg — 405
Co-occurrence of substance P-like and Leu-enkephalin-like immunoreactivities in neurones and fibres of avian nervous system — J T Erichsen, A Reiner & H J Karten — 407
Rapid kinetics of single glutamate-receptor channels — S G Cull-Candy & I Parker — 410
T-cell colonies recognize antigen in association with specific epitopes on Ia molecules — R B Clark, J Chiba, S E Zweig & E M Shevach — 412
Progesterone monoclonal antibody blocks pregnancy in mice — L J Wright, A Feinstein, R B Heap, J C Saunders, R C Bennett & M-Y Wang — 415
Isolation from murine sarcoma cells of novel transforming growth factors potentiated by EGF — A B Roberts, M A Anzano, L C Lamb, J M Smith, C A Frolik, H Marquardt, G J Todaro & M B Sporn — 417

Nature® (ISSN 0028-0836) is published weekly on Thursday, except the last week in December, by Macmillan Journals Ltd and includes the Directory of Biologicals (mailed in December) and Annual Index (mailed in February). Annual subscription for USA and Canada US $198.50 (for subscription prices elsewhere, see next page). Orders (with remittance) and change of address labels to: Macmillan Journals Ltd, Brunel Rd, Basingstoke RG21 2XS, UK. Second class postage paid at New York, NY10010 and additional mailing offices. US Postmaster send form 3579 to: *Nature*, 15 East 26 Street, New York, NY 10010.

Contents continued overleaf

Are you locked in to a ^{32}P-schedule?

Amersham provides the key.

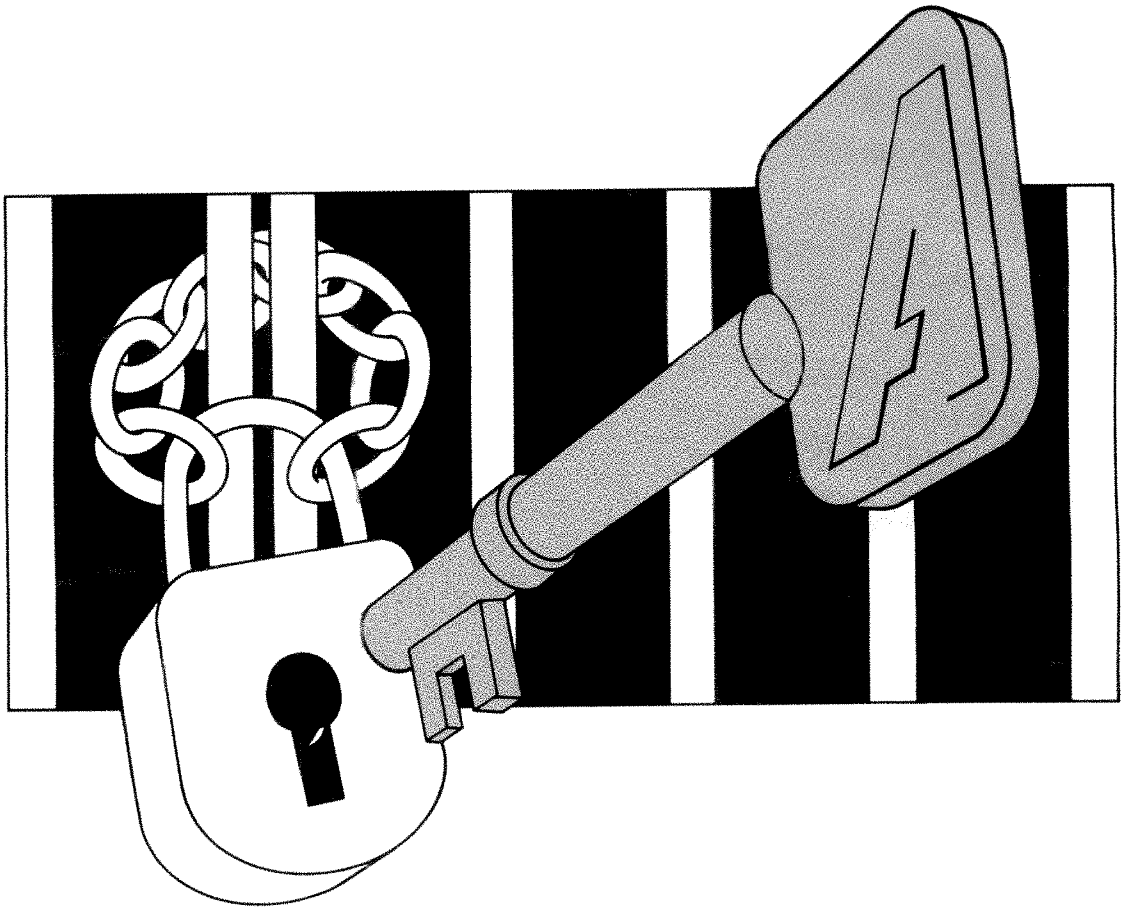

New ● All deoxynucleotides at ~3000Ci/mmol available **every week.**

● All deoxynucleotides at ~800Ci/mmol available **every week.**

● All deoxynucleotides at >400Ci/mmol available **every week.**

The reliable supply of the complete range of [α – ^{32}P] dNTPs every week gives you the convenience of selecting the specific activity most appropriate for your experiments at any time.

Amersham - for products you can trust

Amersham International Limited, Amersham, England Telephone 024-04-4444
In the U.S.A. and Canada, Amersham Corporation, Illinois 60005 Telephone 312-364-7100
and 800-323-9750 (Tollfree)
In W. Germany, Amersham Buchler GmbH & Co KG, Braunschweig Telephone 05307-4691

Circle No.13 on Reader Enquiry Card.

Amersham

• Voyager 1 at Saturn

The new results from Voyager 1, which appeared in *Nature* of 20 August 1981 are now available in a glossy, 88-page booklet.

Copies can be ordered from the *Nature* offices in London, Basingstoke and New York at the following prices (including postage):

UK £2.00 each; USA & Canada US $4.00; Rest of World £2.50 (surface), £3.50 (air)

Payment should accompany orders and may be in any currency at the prevailing exchange rate. Cheques should be made payable to *Nature*.

Annual Subscription including Index (51 issues)

UK & Eire		£85
USA & Canada		US$198.50
Belgium	Airspeed only	BF7450
West German	Airspeed only	DM450
Netherlands	Airspeed only	G505
Switzerland	Airspeed only	SF395
Rest of Europe	Airspeed only	£100
Rest of World	Surface	£100
Rest of World*	Airmail	£150

**(not USA, Canada & Europe)*

Personal subscription rates are available in some countries to subscribers paying by personal cheque or credit card.

Details can be obtained from:
UK: *Nature* Promotion Department,
Canada Road, Byfleet, Surrey KT14 7JL
Telephone: Jonathan Earl: Byfleet (09323) 41459

USA: *Nature*, 15 East 26 Street, New York, NY 10010
Credit card orders only (in USA & Canada):
Call toll-free: (800) 824-7888 (Operator 246)
In California: (800) 857-7777 (Operator 246)

Back issues: (Post-paid) UK, £3.00; USA & Canada, US$8.00 (surface), US$10.00 (air); Rest of World, £4.00 (surface), £5.00 (air).

***Nature* Binders:**
Single Binders: UK, £4.00; Rest of World, $10.00
Set(s) of 3 Binders: UK, £10.00; Rest of World, $25.00

***Nature* First Issue Facsimile:**
UK, 75p; Rest of World (surface), $1.50, (air), £2.00

***Nature* Annual Indexes (1971-1980):**
Price (post-paid):
UK, £5.00 each; Rest of World, $10.00

***Nature* Directory of Biologicals**
(Hardcover edition) (to be published late 1981)
UK, £20.00; Rest of World, $45.00

***Nature* Wallcharts:**
How Britain Runs its Science; How the US Runs its Science; UK, £3.50; USA, $7.95 each

***Nature* in Microform:**
For Information:
UK: UMI, 18 Bedford Row, London WC2R 4EJ
USA: 300 North Zeeb Road, Ann Arbor, Mi 48106

Orders (with remittance) to:
Nature, Macmillan Journals Ltd.,
Brunel Road, Basingstoke, Hants RG21 2XS, UK
Tel: (0256) 29242 Telex: 858493

M MACMILLAN JOURNALS

Stimulation of tyrosine-specific phosphorylation by platelet-derived growth factor — B Ek, B Westermark, Å Wasteson & C-H Heldin — 419

A hypothesis for the initiation of genetic recombination in eukaryotes — P Markham & H L K Whitehouse — 421

Bacterial expression of an enzymatically active protein encoded by RSV *src* gene — J P McGrath & A D Levinson — 423

Association between a transposed α-globin pseudogene and retrovirus-like elements in the BALB/c mouse genome — K Lueders, A Leder, P Leder & E Kuff — 426

Structural alterations in J regions of mouse immunoglobulin λ genes are associated with differential gene expression — J Miller, E Selsing & U Storb — 428

Nucleotide sequence of a macronuclear gene for actin in *Oxytricha fallax* — B P Kaine & B B Spear — 430

***Agrobacterium rhizogenes* inserts T-DNA into the genomes of the host plant root cells** — M-D Chilton, D A Tepfer, A Petit, C David, F Casse-Delbart & J Tempé — 432

Stratification and terminal differentiation of cultured epidermal cells — F M Watt & H Green — 434

Unusual interactions of benzodiazepine receptor antagonists — D J Nutt, P J Cowen & H J Little — 436

MISCELLANY

100 years ago 370
Errata 438
Books received 443
New on the market xiii
Classified advertising xv

GUIDE TO AUTHORS

Authors should be aware of the diversity of *Nature*'s readership and should strive to be as widely understood as possible.

Review articles should be accessible to the whole readership. Most are commissioned, but unsolicited reviews are welcome (in which case prior consultation with the office is desirable).

Scientific articles are research reports whose conclusions are of general interest or which represent substantial advances of understanding. The text should not exceed 3,000 words and six displayed items (figures plus tables). The article should include an abstract of about 50 words.

Letters to *Nature* are ordinarily 1,000 words long with no more than four displayed items. The first paragraph (not exceeding 150 words) should say what the letter is about, why the study it reports was undertaken and what the conclusions are.

Matters arising are brief comments (up to 500 words) on articles and letters recently published in *Nature*. The originator of a Matters Arising contribution should initially send his manuscript to the author of the original paper and both parties should, wherever possible, agree on what is to be submitted.

Manuscripts may be submitted either to London or New York (decisions being made only in London). Manuscripts should be typed (double spacing) on one side of the paper only. Three copies are required, each accompanied by copies of lettered artwork. No title should exceed 80 characters in length. Reference lists, figure legends, etc. should be on separate sheets, all of which should be numbered. Abbreviations, symbols, units, etc. should be identified on one copy of the manuscript at their first appearance.

References should appear sequentially indicated by superscripts in the text and should be abbreviated according to the *World List of Scientific Periodicals*, fourth edition (Butterworth 1963–65). The first and last page numbers of each reference should be cited. References to books should clearly indicate the publisher and the date and place of publication. Unpublished articles should not be formally referred to unless accepted or submitted for publication, but may be mentioned in the text.

Each piece of artwork should be clearly marked with the author's name and the figure number. Original artwork should be unlettered. Suggestions for cover illustrations are welcome. Original artwork (and one copy of the manuscript) will be returned when manuscripts cannot be published.

Requests for permission to reproduce material from Nature *should be accompanied by a self-addressed (and, in the case of the UK and USA, stamped) envelope.*

NIKON VISIONS

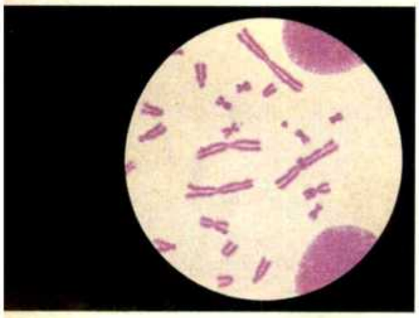

NIKON HIGH-PERFORMANCE CF OPTICS. POSSIBLY THE FINEST EVER AVAILABLE.

CF Plan Apochromat 100x (Oil) N.A. 1.35 Mouse chromosome, gimsa stain

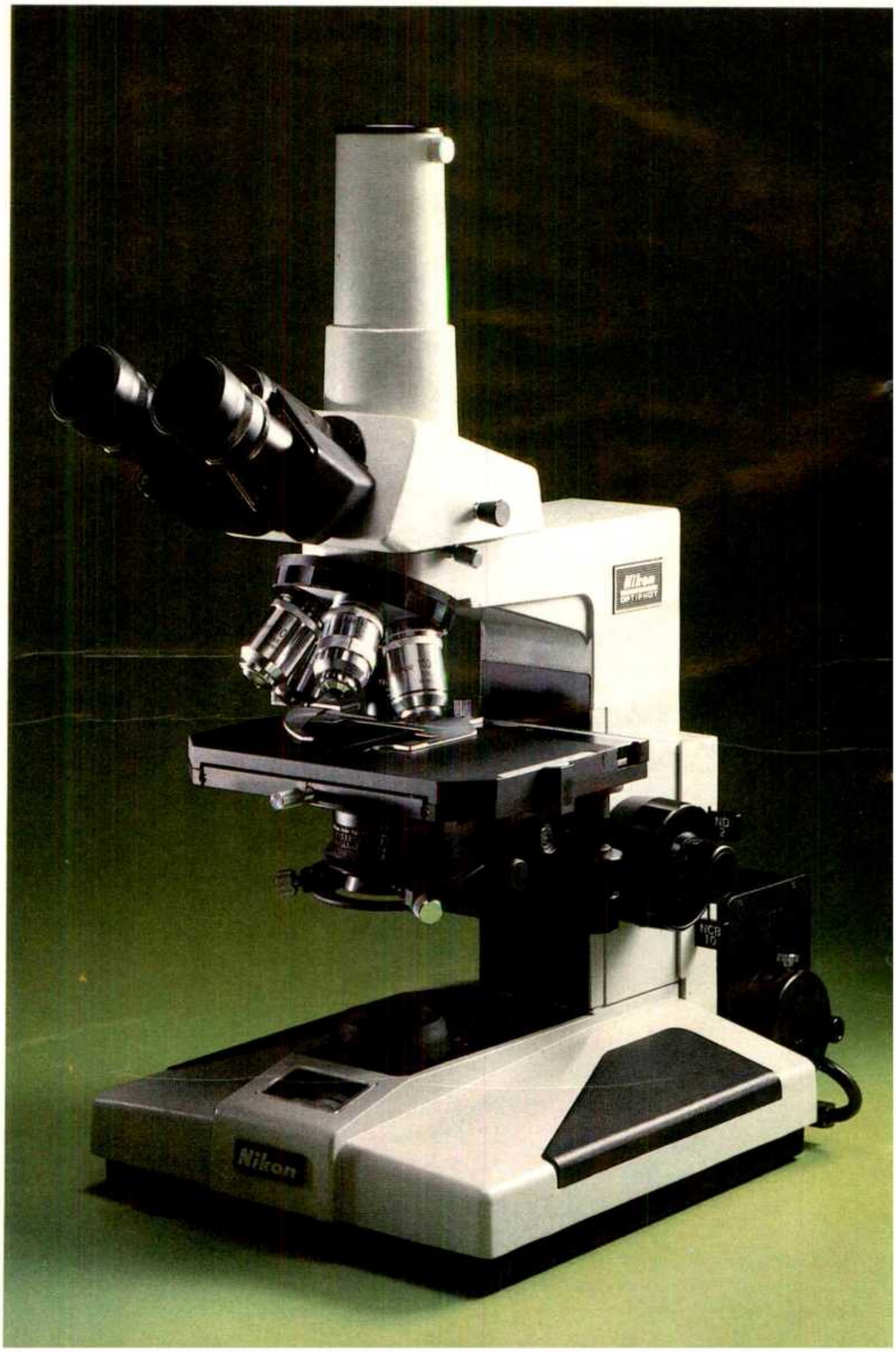

INSTRUMENTATION
Nikon Optiphot microscope with CF objectives.

SIGNIFICANCE
Nikon's revolutionary CF optics virtually eliminate chromatic aberration. Within this series, several high-performance objectives significantly extend observation powers.

SPECIFICS
While all Nikon CF objectives provide a dramatic improvement in resolution, color rendition and contrast over the old compensation system, the following lenses are exceptional. The unique CF 2x plan apochromat has excellent image flatness for low power photography. The CF 40x plan apochromat, N.A. 0.95, dry, produces exceptionally bright, high-contrast images. Nikon's CF 100x NCG plan apochromat is designed to work without a cover glass. Its sharpness must be seen to be believed.

These remarkable optics are matched to a microscope body and illumination system equal to their performance — the Nikon Optiphot. This totally new design is extremely stable. A standard 50-watt halogen Koehler illumination system covers all magnifications without need for adjustment, and the full range of Nikon accessories is available to match any assignment.

Extend *your* vision. Write:
NIPPON KOGAKU K.K.,
Fuji Bldg., 2-3, Marunouchi
3-chome, Chiyoda-ku, Tokyo
100, Japan.

Nikon
Extending Man's Vision

Circle No.32 on Reader Enquiry Card.

nature

Vol. 295 No. 5849 11 February 1982

Test-tube babies pilloried again 445
Down with airline cartel 445
New budget, no change 446

NEWS

DNA panel has second thoughts
Budget protection for US research
US budget described in outline
US defence research
British university crisis
Soviet dissidents
Research growth fund
Polish universities
Euratom treaty
Laboratory animals 447

CORRESPONDENCE

Creationism/Evolution/International Union/Soviet sanctions/Polish appeal/Fossil forelimbs/States of America 452/540

NEWS AND VIEWS

Immune interferon: success, structure and speculation (L B Epstein)
Stem cell regulation in erythropoeisis (P R Harrison)
The nature of immune response gene defects (R H Schwartz)
Making muonium in vacuum (C J Batty & G Marshall)
Is amorphous silicon played out? (J I B Wilson) 453

Cover

Unlike vertebrates, colonial tunicates undergo transplantation in nature. The *Botryllus* histocompatibility system may reflect the original adaptive funtion of the major histocompatibility complex (see page 499). The cover shows a single system from a *Botryllus* colony.

TEXTBOOK SUPPLEMENT

What makes a good textbook? 459
In Dirac's shadow — quantum mechanics for students R B Jones 460
Variations on cosmology and astrophysics — three recent textbooks Joseph Silk 461
High Energy Astrophysics (*by* M S Longair) G T Bath 461
An Introduction to Atmospheric Physics, 2nd Edn (*by* R G Fleagle and J A Businger) *and* An Introduction to Atmospheric Radiation (*by* K-N Liou) J S A Green 462
Mixed diet for students of climatology — traditional and modern approaches to the subject J P Palutikof & T M L Wigley 462
Earthly delights — two new editions of introductory geology textbooks Keith Bell 463
Earthlike Planets (*by* B Murray *et al.*) L Wilson 463
Tectonics as theory, tectonics as history — recent textbooks on aspects of plate tectonics B C Burchfiel 464
Crystallography (*by* E J W Whittaker) *and* Mineralogy for Students, 2nd Edn (*by* M H Battey) R A Howie 464
Mixed sediments — books for students of sedimentary rocks R C Selley 465
Marine Geology (*by* J P Kennett) Peter J Smith 466
Soils: their genesis and physics — facets of soil science David Rimmer & Michael Adey 466
Soils and Landforms (*by* A J Gerrard) M J Kirkby 467
Back to the land — textbooks on the stratigraphy and structure of the British Isles, and on field geology D L Dineley 467
Basalts and Phase Diagrams (*by* S A Morse) K G Cox 468
Paleobotany (*by* T N Taylor) Keith Allen 468
100 Families of Flowering Plants (*by* M Hickey and C King) *and* The Study of Plant Structure (*by* T P O'Brien and M E McCully) Peter D Moore 469
Panglossian botany — approaches to plant ecophysiology J L Harper 470
Growth and Differentiation in Plants, 3rd Edn (*by* P F Wareing and I D J Phillips) James F Sutcliffe 470
Secondary Plant Metabolism (*by* B and M L Vickery) T W Goodwin 471
Biology of Plants, 3rd Edn (*by* P H Raven *et al.*) Ralph S Quatrano 471
Historical Plant Geography (*by* P Stott) Honor C Prentice 472
An Introduction to Behavioural Ecology (*by* J R Krebs and N B Davies) *and* Modern Ethology (*by* S A Barnett) Peter Marler 472

Nature® (ISSN 0028-0836) is published weekly on Thursday, except the last week in December, by Macmillan Journals Ltd and includes the Directory of Biologicals (mailed in December) and Annual Index (mailed in February). Annual subscription for USA and Canada US $198.50 (for subscription prices elsewhere, see next page). Orders (with remittance) and change of address labels to: Macmillan Journals Ltd, Brunel Rd, Basingstoke RG21 2XS, UK. Second class postage paid at New York, NY10010 and additional mailing offices. US Postmaster send form 3579 to: *Nature*, 15 East 26 Street, New York, NY 10010.

0028-0836/82/06000C-03$01.00

Contents continued overleaf

Are you locked in to a ^{32}P-schedule?

Amersham provides the key.

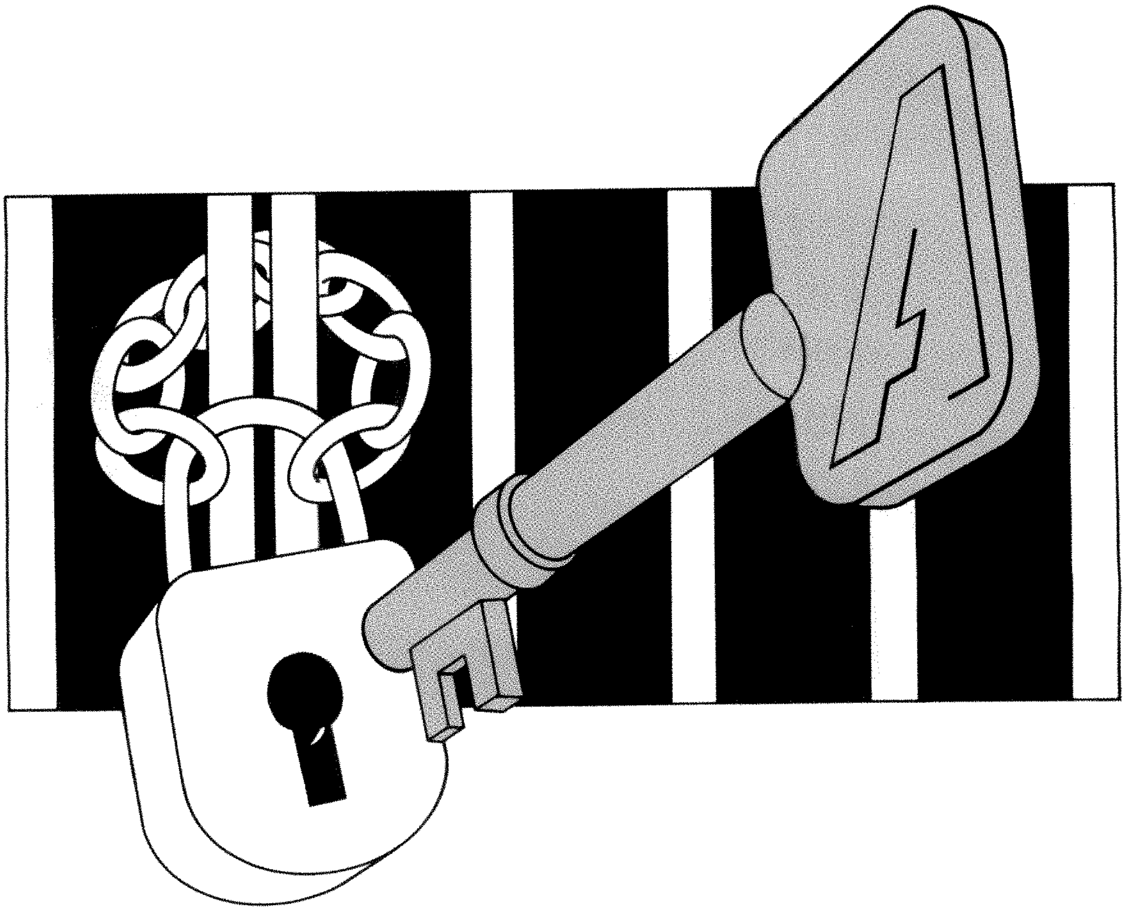

New ● All deoxynucleotides at ~3000Ci/mmol available **every week.**

● All deoxynucleotides at ~800Ci/mmol available **every week.**

● All deoxynucleotides at >400Ci/mmol available **every week.**

The reliable supply of the complete range of [α -^{32}P] dNTPs every week gives you the convenience of selecting the specific activity most appropriate for your experiments at any time.

Amersham - for products you can trust

Amersham International Limited, Amersham, England Telephone 024-04-4444
In the U.S.A. and Canada, Amersham Corporation, Illinois 60005 Telephone 312-364-7100
and 800-323-9750 (Tollfree)
In W. Germany, Amersham Buchler GmbH & Co KG, Braunschweig Telephone 05307-4691

Circle No. 13 on Reader Enquiry Card.

Amersham

Nature Binders

Keep your copies of *Nature* protected in these tough black PVC binders

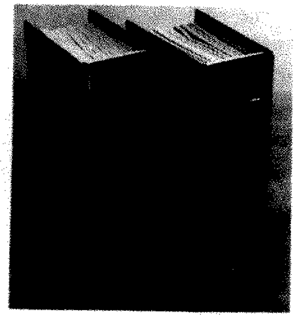

- Each binder is supplied with a set of wires for the easiest possible loading

  Nature logo blocked in gold on spine

  Transparent plastic pocket provided for your own reference
- Each binder takes two volumes of *Nature;* three binders will serve for a year

Prices (including postage):
Single Binders:
UK, £4.00;
Rest of World, $10.00
Set(s) of 3 Binders:
UK, £10.00;
Rest of World, $25.00

Orders (with remittance) to:
Nature,
Macmillan Journals Ltd.,
Brunel Road, Basingstoke,
Hants RG21 2XS, UK

•How Britain runs its Science
•How the US runs its Science

These two new *Nature* wallcharts are now available.

The 2 x 3 ft. guides offer a comprehensive survey of the administration of science in Britain and the US, showing the interlocking relationship between science, engineering and medical establishments.

Designed as fold-out sheets, the wallcharts can be carried easily to meetings or hung as posters for permanent reference.

The new 1981 wallcharts are available at £3.50 or $7.95 each from *Nature's* offices in London, Basingstoke and New York.

Sixty years on? — contrasting views of population biology	Michael B Usher	473
In search of a science — introductory neuroethology	Graham Hoyle	473
Principles of Neural Science (E R Kandel and J H Schwartz, *eds*)	Maria Fitzgerald	474
Foundations of Developmental Psychology (*by* R C LaBarba) *and* Developmental Psychology, 3rd Edn (*by* R M Liebert and R Wicks-Nelson)	Albert Yonas	474
Behavior Genetics and Evolution (*by* L Ehrman and P A Parsons)	B Burnet	475
Basic Population Genetics (*by* Bruce Wallace) *and* Introduction to Quantitative Genetics, 2nd Edn (*by* D S Falconer)	J S Jones	475
Mendel meets DNA: the story continued — introductory genetics textbooks	D J Cove	476
Not quite Wilson — cytogenetics for students	Michael Ashburner	477
The Genetic Basis of Development (*by* A D Stewart and D M Hunt)	P A Lawrence	477
Bacterial and Bacteriophage Genetics (*by* E A Birge)	Neville Symonds	478
Genetics: Human Aspects (*by* A P and E J Mange) *and* Human Chromosomes: Structure, Behavior, Effects (*by* E Therman)	Dorothy A Miller	478
Science or scholarship for students of developmental biology? — four recent textbooks	D R Newth	479
A View of Life (*by* S E Luria *et al.*)	E C Cox & R M May	479
Understanding Evolution (*by* E D Hanson)	Bentley Glass	480
Patterns of Vertebrate Biology (*by* E W Jameson, Jr)	Barry Cox	480
The welcome return of J.Z. Young — textbooks of vertebrate zoology	L Beverly Halstead	481
No bones, but plenty of meat — general, specialized and practical invertebrate zoology	A E Brafield	482
Insects entomed — entomology textbooks	M E G Evans	483
Saline solutions — aspects of marine biology	D J Crisp	483
Functional Adaptations of Marine Organisms (F J and W B Vernberg, *eds*) *and* Animal Osmoregulation (*by* J C Rankin and J Davenport)	J A Riegel	484
Animal Physiology (*by* F R Hainsworth)	Garth Chapman	484
Enzymology: the general and the specific — four new textbooks	R N Perham	485
Biochemistry, 2nd Edn (*by* L Stryer)	Peter H W Butterworth	485
Whole chemistry? — introductory chemistry for students of the life sciences	Peter Garratt	486
Beyond description — quantitative problem-solving for biochemists	H Hassall	486
Physical chemistry: sugar in the medicine — physical chemistry for biologists	S P Spragg	487
Talking of organic chemistry — three recent textbooks	John Mann	487

Contents continued overleaf

SAFE

n the knowledge of Barr & Stroud technology at work

A commonplace scene on a busy road, but safer if Barr & troud fibre optic traffic signs were installed.

Our signs allow virtually no misleading phantom images ven in the most difficult conditions.

We are a leading light in the fibre optics field, where our xperience spans a wide spectrum of equipment, systems nd applications—in computers, process control, medicine, colour detection, automatic inspection, as well as traffic signs.

Barr & Stroud's leadership and innovative skills in today's technologies are at the service of science and industry.

We have proved it in fibre optics; we have proved it in other areas. Because of our serious commitment to research and development, engineers and designers everywhere can rely on our expertise to solve their most complex problems.

Barr & Stroud
make fibre optics work

Barr & Stroud Limited,
Caxton Street, Anniesland, Glasgow G13 1HZ.
Melrose House,
4-6 Savile Row, London W1X 1AF.

PILKINGTON GROUP

Circle No. 05 on Reader Enquiry Card.

● **Voyager 1 at Saturn**

The new results from Voyager 1, which appeared in *Nature* of 20 August 1981 are now available in a glossy, 88-page booklet.

Copies can be ordered from the *Nature* offices in London, Basingstoke and New York at the following prices (including postage):

UK £2.00 each; USA & Canada US $4.00; Rest of World £2.50 (surface), £3.50 (air)

Payment should accompany orders and may be in any currency at the prevailing exchange rate. Cheques should be made payable to *Nature*.

Annual Subscription including Index (51 issues)

UK & Eire		£85
USA & Canada		US$198.50
Belgium	Airspeed only	BF7450
West German	Airspeed only	DM450
Netherlands	Airspeed only	G505
Switzerland	Airspeed only	SF395
Rest of Europe	Airspeed only	£100
Rest of World	Surface	£100
Rest of World*	Airmail	£150

**(not USA, Canada & Europe)*

Personal subscription rates are available in some countries to subscribers paying by personal cheque or credit card.

Details can be obtained from:
UK: *Nature* Promotion Department,
Canada Road, Byfleet, Surrey KT14 7JL
Telephone: Jonathan Earl: Byfleet (09323) 41459

USA: *Nature*, 15 East 26 Street, New York, NY 10010
Credit card orders only (in USA & Canada):
Call toll-free: (800) 824-7888 (Operator 246)
In California: (800) 857-7777 (Operator 246)

Back issues: (Post-paid) UK, £3.00; USA & Canada, US$8.00 (surface), US$10.00 (air); Rest of World, £4.00 (surface), £5.00 (air).

***Nature* Binders:**
Single Binders: UK, £4.00; Rest of World, $10.00
Set(s) of 3 Binders: UK, £10.00; Rest of World, $25.00

***Nature* First Issue Facsimile:**
UK, 75p; Rest of World (surface), $1.50, (air), £2.00

***Nature* Annual Indexes (1971-1980):**
Price (post-paid):
UK, £5.00 each; Rest of World, $10.00

***Nature* Directory of Biologicals**
(Hardcover edition) (to be published late 1981)
UK, £20.00; Rest of World, $45.00

***Nature* Wallcharts:**
How Britain Runs its Science; How the US Runs its Science; UK, £3.50; USA, $7.95 each

***Nature* in Microform:**
For Information:
UK: UMI, 18 Bedford Row, London WC2R 4EJ
USA: 300 North Zeeb Road, Ann Arbor, Mi 48106

Orders (with remittance) to:
Nature, Macmillan Journals Ltd.,
Brunel Road, Basingstoke, Hants RG21 2XS, UK
Tel: (0256) 29242 Telex: 858493

MACMILLAN JOURNALS

Theory guides, but experiment decides — practical organic chemistry Gary O Spessard 488

Physical Chemistry, 2nd Edn (*by* P W Atkins) *and* Physical Chemistry (*by* J P Bromberg) Maurice Rigby 489

Drawings in the Textbook Supplement by Andrew Birch

ARTICLES

Convective growth rates of equatorial features in the jovian atmosphere G E Hunt, J-P Müller & P Gee 491

Glacial to interglacial contrasts in the northern Indian Ocean J C Duplessy 494

Protochordate allorecognition is controlled by a MHC-like gene system V L Scofield, J M Schlumpberger, L A West & I L Weissman 499

Expression of human immune interferon cDNA in *E. coli* and monkey cells P W Gray, D W Leung, D Pennica, E Yelverton, R Najarian, C C Simonsen, R Derynck, P J Sherwood, D M Wallace, S L Berger, A D Levinson & D V Goeddel 503

LETTERS TO NATURE

Is the remnant of SN1006 composed of iron? A C Fabian, G C Stewart & W Brinkmann 508

Asymmetric Balmer line profiles in Seyfert galaxies A Lawrence 509

A molecular interpretation of stress corrosion in silica T A Michalske & S W Freiman 511

Errors and resolution of thermal techniques for obtaining the geomagnetic intensity D Walton 512

Sm–Nd dating and cooling history of Scourian granulites, Sutherland F J Humphries & R A Cliff 515

Asphalt in carbon-14-dated archaeological samples from Terqa, Syria M I Venkatesan, T W Linick, H E Suess & G Buccellati 517

***O*-sulphated Leu-enkephalin in brain** C D Unsworth, J Hughes & J S Morley 519

Molecular size of benzodiazepine receptor in rat brain *in situ*: evidence for a functional dimer? A Doble & L L Iversen 522

Use of carboxyfluorescein diacetate to study formation of permeable channels between mouse blastomeres H Goodall & M H Johnson 524

Crystal structure of a polyfunctional macrocyclic K^+ complex provides a solid-state model of a K^+ channel J-P Behr, J-M Lehn, A-C Dock & D Moras 526

Transient nature of early haematopoietic spleen colonies M C Magli, N N Iscove & N Odartchenko 527

Isolation of membrane components associated with human red cell antigens Rh(D), ($\bar{c}$), (E) and Fy^a S Moore, C F Woodrow & D B L McClelland 529

Absence of *Ir* gene control of T cells recognizing foreign antigen in the context of allogeneic MHC molecules N Ishii, Z A Nagy & J Klein 531

tRNA precursor transcribed from a mutant human gene inserted into a SV40 vector is processed incorrectly M Zasloff, T Santos & D H Hamer 533

Stereochemistry of iron in deoxyhaemoglobin M F Perutz, S S Hasnain, P J Duke, J L Sessler & J E Hahn 535

^{3}H nucleotides that solve a problem with a better solution

^{3}H Nucleotides ready to pipet

To save you the bother of removing or concentrating the packaging solution, we've packaged seven ^{3}H nucleotides in aqueous solution at 2.5mCi/ml.
At the same time we extended their radiochemical stability with 10mM Tricine, a proven stabilizer known to be compatible in research systems.

TTP, [*methyl*-^{3}H]- 50-80Ci/mmol
NET-221A 250µCi 1mCi 5mCi in dry ice
TTP, [*methyl*-1′, 2′-^{3}H]- 90-110Ci/mmol
NET-520A 1mCi 5mCi in dry ice
dATP, [8-^{3}H]- 10-25Ci/mmol
NET-268A 250µCi 1mCi 5mCi in dry ice
dCTP, [5-^{3}H]- 15-30Ci/mmol
NET-369A 250µCi 1mCi 5mCi in dry ice
dCTP, [5, 5′-^{3}H]- 40-60Ci/mmol
NET-601A 1mCi 5mCi in dry ice
dGTP, [8-^{3}H]- 5-15Ci/mmol
NET-429A 250µCi 1mCi 5mCi in dry ice
dGTP, [8, 5′-^{3}H]- 25-50Ci/mmol
NET-448A 1mCi 5mCi in dry ice

Also available in standard ethanol:water packaging by deleting the A from the ordering number.

Circle No.39 on Reader Enquiry Card.

ω-3 Polyunsaturated Fatty Acids

For studies of the metabolic pathways and biological actions of these acids

Linolenic acid, 9, 12, 15-[1-^{14}C]-
40-60mCi/mmol Ethanol under argon, in dry ice
NEC-779 50µCi 250µCi
Docosahexaenoic acid, 4, 7, 10, 13, 16, 19-[^{14}C(U)]-
>100mCi/mmol Ethanol under argon, in dry ice
NEC-784 5µCi 10µCi
Eicosapentaenoic acid, 5, 8, 11, 14, 17-[1-^{14}C]-
40-60mCi/mmol Ethanol under argon, in dry ice
NEC-772 10µCi 50µCi
Eicosapentaenoic acid, 5, 8, 11, 14, 17-[^{14}C(U)]-
50-100mCi/mmol Ethanol under argon, in dry ice
NEC-754 5µCi 10µCi

Circle No.42 on Reader Enquiry Card.

Calmodulin [^{125}I]

Stable. Produced by Bolton-Hunter Reagent conjugation to bovine brain calmodulin
Tested for antibody binding
Calmodulin,[^{125}I]-
50-150µCi/µg
0.05M phosphate buffer, pH 7.4, 0.1M NaCl
0.1% gelatin, 0.05% sodium azide
NEX-172 5µCi 10µCi
Also available . . . Calmodulin,[^{125}I]- RIA Kit

Circle No.43 on Reader Enquiry Card.

Iodocyanopindolol [^{125}I]

Specific to β_1 and β_2 adrenergic receptors
Higher affinity (K_D~27-40pmol) and specificity than iodohydroxybenzylpindolol
Carrier-free~5400µCi/µg
Iodocyanopindolol,[^{125}I]-
2200Ci/mmol
n-Propanol:water:phenol (50:50:1.2), in dry ice
NEX-174 100µCi 500µCi 1mCi

Circle No.44 on Reader Enquiry Card.

FSH, LH [^{125}I]

Follicle Stimulating Hormone,[^{125}I]-
50-100µCi/µg
Lyophilized from sodium phosphate buffer, pH 7.4, containing BSA and a proteolytic enzyme inhibitor
NEX-173 10µCi 25µCi 100µCi
Luteinizing Hormone,[^{125}I]-
50-100µCi/µg
Lyophilized from sodium phosphate buffer, pH 7.4, containing BSA and a proteolytic enzyme inhibitor
NEX-170 10µCi 25µCi 100µCi

Circle No.45 on Reader Enquiry Card.

Not for use in humans or clinical diagnosis.

NEN New England Nuclear®
a Du Pont company

New England Nuclear
549 Albany Street, Boston, MA 02118
Call toll free: 800-225-1572, Telex: 94-0996
Mass and Internat'l: 617-482-9595
Europe: NEN Chemicals GmbH, D-6072, W. Germany
Postfach 401240, Tel. (06103) 803-0, Telex 4-17993 NEN D
NEN Canada: 2453 46th Avenue, Lachine, Que H8T 3C9
Tel. 514-636-4971, Telex 05-821808

nature

Vol. 295 No. 5850 18 February 1982

What universities should aim at 541
Doves in false garb 542
Up and over the top 542

NEWS

Cancer institute withholds grant
Amersham International floats
Polish students
British anti-nuclear campaign
Rights on DNA
Chemical warfare
Deep-sea mining
Small growth fund
German academics
Scientific exchanges
Lister Institute 543

CORRESPONDENCE

Blériot to jumbo/Bibles etc. 548

NEWS AND VIEWS

Breaking the 600 metre barrier (The Scientific Party, DSDP Leg 83)
Ocean floor conductivity measured (T J G Francis)
Fifty years of substance P (T M Jessell)
The unregenerate nervous system (M Robertson)
What role for autologous marrow transplantation in cancer therapy (R Storb)
Quasars resolved? (M G Edmunds) 549

BOOK REVIEWS

Is Science Sexist? And Other Problems in the Biological Sciences (*by* **M Ruse**) Jon Beckwith; **Cultural Transmission and Evolution** (*by* **L L Cavalli-Sforza and M W Feldman**) Lindon J Eaves; **The Brightest Stars** (*by* **C De Jager**) J B Hutchings; **Chemistry in Two Dimensions: Surfaces** (*by* **G A Somorjai**) D H Everett; **Male Reproductive Function and Semen** (*by* **T Mann and C Lutwak-Mann**) R J Aitken; **Manual of Macrophage Methodology** (**H B Herscowitz *et al., eds***) S Gordon; **Potential Energy Surfaces and Dynamics Calculations for Chemical Reactions and Molecular Energy Transfer** (**D G Truhlar, *ed.***) J N Murrell 631

NEW PRODUCTS

Better detectors for HPLC (C Burgess) xxvii

Cover

Colour-graphic display of a computer-simulated ciliary beating of the protozoan *Paramecium*. Upper: top view. Lower: side view. The displayed cilium is white at the beginning of the recovery stroke, changing to red as the ciliary beat proceeds to the end of the effective stroke (see page 609).

ARTICLES

Molecular effects in pion capture in complex materials D F Jackson, C A Lewis, K O'Leary & G K Y Lam 557
How honey bees use landmarks to guide their return to a food source B A Cartwright & T S Collett 560
Rate of turnover of structural variants in the rDNA gene family of *Drosophila melanogaster* E S Coen, J M Thoday & G Dover 564
Activation of SV40 genome by 72-base pair tandem repeats of Moloney sarcoma virus B Levinson, G Khoury, G Vande Woude & P Gruss 568
Intracellular transport of microinjected 5S and small nuclear RNAs E M De Robertis, S Lienhard & R F Parisot 572

LETTERS TO NATURE

Alignment of randomly distributed objects E J Zuiderwijk 577
Oxygen evolution on tantalum–polypyrrole–platinum anodes G Cooper, R Noufi, A J Frank & A J Nozik 578
Penetration of water into hot rock boundaries of magma at Grímsvötn H Björnsson, S. Björnsson & Th. Sigurgeirsson 580
Handling and measurement techniques for anoxic interstitial waters W Davison, C Woof & D R Turner 582
Radiation-induced dissolution of colloidal haematite G V Buxton, T Rhodes & R M Sellers 583
Uranium–lead system in fragments of a single zircon grain U Schärer & C J Allègre 585
Thermal stresses in subducting lithosphere can explain double seismic zones L S House & K H Jacob 587
New dates for the Tata, Hungary archaeological site H P Schwarcz & I Skoflek 590
Proline content does not influence pest and disease susceptibility of barley S W J Bright, P J Lea, J S H Kueh, C Woodcock, D W Hollomon & G C Scott 592
Identification of a β-endorphin-like peptide in cultured human placental cells A S Liotta, R Houghten & D T Krieger 593
Averaged evoked responses and psychometric intelligence S F Blinkhorn & D E Hendrickson 596
Motilin in the Purkinje cell of the cerebellum G Nilaver, R Defendini, E A Zimmerman, M C Beinfeld & T L O'Donohue 597
Closure of membrane channels gated by glutamate receptors may be a two-step process K A F Gration, J J Lambert, R L Ramsey, R P Rand & P N R Usherwood 599
Similar mode of action of pyrethroids and DDT on sodium channel gating in myelinated nerves H P M Vijverberg, J M van der Zalm & J van den Bercken 601

Nature® (ISSN 0028-0836) is published weekly on Thursday, except the last week in December, by Macmillan Journals Ltd and includes the Directory of Biologicals (mailed in December) and Annual Index (mailed in February). Annual subscription for USA and Canada US $198.50 (for subscription prices elsewhere, see next page). Orders (with remittance) and change of address labels to: Macmillan Journals Ltd, Brunel Rd, Basingstoke RG21 2XS, UK. Second class postage paid at New York, NY10010 and additional mailing offices. US Postmaster send form 3579 to: *Nature*, 15 East 26 Street, New York, NY 10010.

0028-0836/82/07000C-02$01.00

Contents continued overleaf

Are you locked in to a ^{32}P-schedule?

Amersham provides the key.

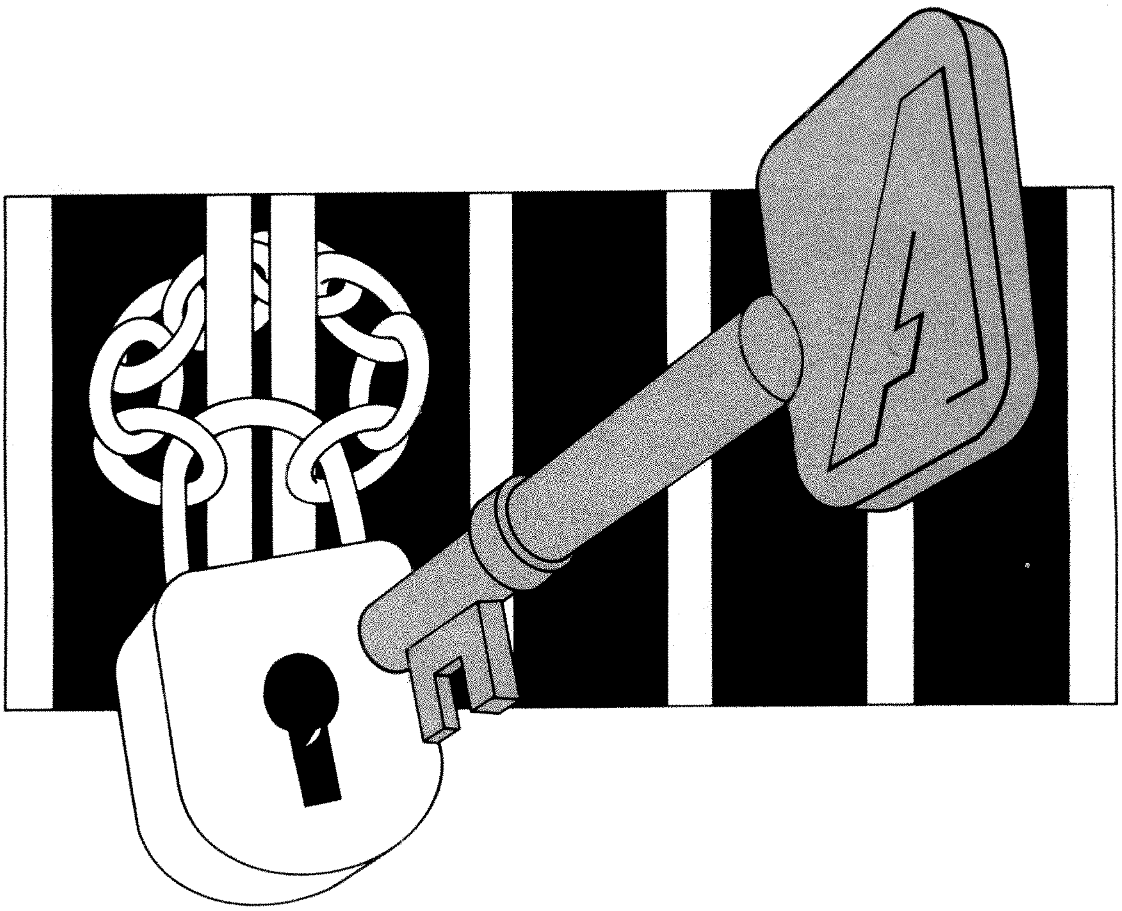

- **New** ● All deoxynucleotides at ~3000Ci/mmol available **every week.**
- ● All deoxynucleotides at ~800Ci/mmol available **every week.**
- ● All deoxynucleotides at >400Ci/mmol available **every week.**

The reliable supply of the complete range of [$\alpha - ^{32}$P] dNTPs every week gives you the convenience of selecting the specific activity most appropriate for your experiments at any time.

Amersham - for products you can trust

Amersham International Limited, Amersham, England Telephone 024-04-4444
In the U.S.A. and Canada, Amersham Corporation, Illinois 60005 Telephone 312-364-7100
and 800-323-9750 (Tollfree)
In W. Germany, Amersham Buchler GmbH & Co KG, Braunschweig Telephone 05307-4691

Circle No.13 on Reader Enquiry Card.

Amersham

•How Britain runs its Science
•How the US runs its Science

These two new *Nature* wallcharts are now available.

The 2 x 3 ft. guides offer a comprehensive survey of the administration of science in Britain and the US, showing the interlocking relationship between science, engineering and medical establishments.

Designed as fold-out sheets, the wallcharts can be carried easily to meetings or hung as posters for permanent reference.

The new 1981 wallcharts are available at £3.50 or $7.95 each from *Nature's* offices in London, Basingstoke and New York.

Annual Subscription including Index (51 issues)

UK & Eire		£85
USA & Canada		US$198.50
Belgium	Airspeed only	BF7450
West Germany	Airspeed only	DM450
Netherlands	Airspeed only	G505
Switzerland	Airspeed only	SF395
Rest of Europe	Airspeed only	£100
Rest of World	Surface	£100
Rest of World*	Airmail	£150

**(not USA, Canada & Europe)*

Personal subscription rates are available in some countries to subscribers paying by personal cheque or credit card.

Details can be obtained from:
UK: *Nature* Promotion Department,
Canada Road, Byfleet, Surrey KT14 7JL.
Telephone: Jonathan Earl: Byfleet (09323) 41459
USA: *Nature*, 15 East 26 Street, New York, NY 10010
Credit card orders only (in USA & Canada):
Call toll-free: (800) 824-7888 (Operator 246)
In California: (800) 857-7777 (Operator 246)

All other circulation enquiries concerning existing subscriptions please contact:
Nature Circulation Department, Macmillan Journals Ltd., Brunel Road, Basingstoke, Hants RG21 2XS, UK
Telephone: (0256) 29242 Telex: 858493

Back issues: (Post-paid) UK, £2.50; USA & Canada, US$6.00 (surface), US$9.00 (air); Rest of World, £3.00 (surface), £4.00 (air).

***Nature* Binders:**
Single Binders: UK, £4.00; Rest of World, $10.00
Set(s) of 3 Binders: UK, £10.00; Rest of World, 25.00

***Nature* First Issue Facsimile:**
UK, 75p; Rest of World (surface), $1.50, (air), £2.00

***Nature* Annual Indexes (1971-1980):**
Price (post-paid):
UK, £5.00 each; Rest of World, $10.00

***Nature* Directory of Biologicals:**
(Hardcover edition)
UK, £22.50; Rest of World, $45.00

***Nature* Wallcharts:**
How Britain Runs its Science; How the US Runs its Science; UK, £3.50; USA, $7.95 each

***Nature* in Microform:**
For Information:
UK: UMI, 18 Bedford Row, London WC2R 4EJ
USA: 300 North Zeeb Road, Ann Arbor, Mi 48106

Orders (with remittance) to:
Nature, Macmillan Journals Ltd.,
Brunel Road, Basingstoke, Hants RG21 2XS, UK
Tel: (0256) 29242 Telex: 858493

MACMILLAN JOURNALS

Selective killing of leukaemia cells by antibody–toxin conjugates: implications for autologous bone marrow transplantation K A Krolick, J W Uhr & E S Vitetta 604

Mitochondrial transformation of mammalian cells M A Clark & J W Shay 605

^{31}P NMR examination of two patients with NADH-CoQ reductase deficiency G K Radda, P J Bore, D G Gadian, B D Ross, P Styles, D J Taylor & J Morgan-Hughes 608

Simulated cross-bridge patterns corresponding to ciliary beating in *Paramecium* K Sugino & Y Naitoh 609

Release of spectrin-free spicules on reoxygenation of sickled erythrocytes D Allan, A R Limbrick, P Thomas & M P Westerman 612

A non-collagenous glycoprotein from elastic tissue acts as substratum for growth of cells *in vitro* P Knox, P Wells & A Serafini-Fracassini 614

A role for mRNA secondary structure in the control of translation initiation M N Hall, J Gabay, M Débarbouillé & M Schwartz 616

Partial sequence of 16S ribosomal RNA and the phylogeny of *Prochloron* E Seewaldt & E Stackebrandt 618

Substrate and sequence specificity of a eukaryotic DNA methylase Y Gruenbaum, H Cedar & A Razin 620

Long terminal repeats of endogenous mouse mammary tumour virus contain a long open reading frame which extends into adjacent sequences N Kennedy, G Knedlitschek, B Groner, N E Hynes, P Herrlich, R Michalides & A J J van Ooyen 622

Expression of human *hprt* gene on the inactive X chromosome after DNA-mediated gene transfer A J R de Jonge, P J Abrahams, A Westerveld & D Bootsma 624

Inter-replicon transposition of Tn*1/3* occurs in two sequential genetically separable steps P A Kitts, A Lamond & D J Sherratt 626

MATTERS ARISING

Two major genes, linked to HLA and Gm, control susceptibility to Graves' disease N R Farid & J C Bear Reply: T Sasazuki & H Uno 629

Positive selection causes purifying selection M Goodman Reply: W-H Li, T Gojobori & M Nei 630

MISCELLANY

100 years ago 551
Classified advertising xxxiii

Confidence, IT COMES FROM QUALITY.

Reproducible high resolution is the result of quality chemicals and equipment. Quality of design and synthesis has been incorporated into isoelectric focusing products from Pharmacia Fine Chemicals, giving you confidence in performance every time.

Some of the new quality design ideas used in construction are: **movable electrodes** (so you can use any gel size you need), **high efficiency aluminum cooling plate** (for faster runs at higher voltages), **larger cooling plate size** (to increase sample number or for preparative work), and our latest response to your requests—a **cooling plate with grid markings** (for fast and accurate set-up).

Our unique synthesis procedures for Pharmalyte® carrier ampholyte and Agarose IEF give you quality chemicals on whose consistent performance you can rely. Each Pharmalyte interval yields a stable and linear pH gradient in either polyacrylamide or agarose. The low and even conductivity of Pharmalyte allows you to focus faster at high voltages confidently—even at 3000V with the Electrophoresis Constant Power Supply ECPS 3000/150.

Agarose IEF is a highly purified, balanced charge agarose making it the matrix of choice for reliable focusing of proteins. Agarose IEF is easy and reliable to use since there is no worry about electroendosmotic effects, various polymerization problems, toxic chemicals or lengthy staining and destaining times.

The use of quality isoelectric focusing equipment and chemicals from Pharmacia Fine Chemicals assures you high resolution IEF results without risking your sample or equipment.

Pharmalyte: Consistent gradients and low, even conductivity continues to be the hallmark of ready-to-use Pharmalyte carrier ampholytes.

ISOELECTRIC FOCUSING EQUIPMENT AND SUPPLIES QUALITY HAS MADE Confidence A REALITY.

Pharmacia Fine Chemicals AB
Box 175
S-75104 Uppsala 1
Sweden

Pharmacia Fine Chemicals

Circle No. 34 on Reader Enquiry Card.

nature

Vol. 295 No. 5851 25 February 1982

What to tell the White House 635
A strategy for coal 636
Mercury handcuffed 636

NEWS

New White House science council
Keyworth irked by national labs
Council's members
Turkish civil rights
European Space Agency
Agricultural Research Council
Spain back to fold
Polish universities
US student loans
Indian Antarctic expedition
Acid rain
Dutch elm disease 637

CORRESPONDENCE

National Coal Board's angle/Beware of commercialism/How many satellites? 642

NEWS AND VIEWS

Whence so much ^{15}N? (J F Kerridge)
The Vredefort structure still not understood (R A F Grieve)
Carbon dioxide and climate: has a signal been observed yet? (S L Thompson & S H Schneider)
Evolution of photosynthetic pathways in flowering plants. (P D Moore)
Dynein in the spindle? (J Hyams)
Intracellular membrane traffic (M J Geisow) 643

BOOK REVIEWS

The Development of Darwin's Theory (*by* **D Ospovat**) David L Hull; **The Biological Aspects of Rare Plant Conservation (H Synge,** *ed.*) H McAllister; **Physiology of the Gastrointestinal Tract (L R Johnson,** *ed.*) G J Dockray; **Phylogenetics** (*by* **E O Wiley**) Alan J Charig; **The Immune System (C M Steinberg and I Lefkovits,** *eds*) J H Humphrey; **Jets of Hadrons** (*by* **W Hofmann**) M G Albrow 719

MISCELLANY

100 years ago 650
Product review:
  Pittsburgh Conference xvii
Announcements xx
Classified advertising xxi

Cover

The Multiple Mirror Telescope operated by the University of Arizona and the Smithsonian Institution. New developments in ground-based astronomical telescopes are reviewed on page 651. (Photo courtesy MMT Observatory.)

Very large ground-based telescopes for optical and IR astronomy (a review) J R P Angel 651

ARTICLES

Simulating silicate structures and the structural chemistry of pyroxenoids C R A Catlow, J M Thomas, S C Parker & D A Jefferson 658
Primary structure of the human Met- and Leu-enkephalin precursor and its mRNA M Comb, P H Seeburg, J Adelman, L Eiden & E Herbert 663
Studies of X chromosome DNA methylation in normal human cells S F Wolf & B R Migeon 667
Vitamin A and pattern formation in the regenerating limb M Maden 672

LETTERS TO NATURE

X-ray observations of the 1980 Cygnus X-1 'high state' Y Ogawara, K Mitsuda, K Masai, J V Vallerga, L R Cominsky, J M Grunsfeld, J S Kruper & G R Ricker 675
Quantum conformal fluctuations in a singular space-time T. Padmanabhan & J V Narlikar 677
Individual electrons detected after the interaction of ionizing radiation with gases O H W Siegmund, J L Culhane, I M Mason & P W Sanford 678
Nonlinear reflectivity of high-power radio waves in the ionosphere H Kopka, P Stubbe, T B Jones & T Robinson 680
Unusual luminescence behaviour of terbium phosphate glasses D J Cronin, D H Blackburn & W K Haller 680
Slope anomaly in the vapour pressure curve of Hg S R Hubbard & R G Ross 682
Factors controlling the acidity of natural rainwater R J Charlson & H Rodhe 683
Mesozoic magnetic anomalies in the southern Natal Valley S W Goodlad, A K Martin & C J H Hartnady 686
Magnetic granulometry results for intrusive rock samples G S Murthy & R R Pätzold 688
Explicit dialogue between left and right half-systems of split brains D M MacKay & V MacKay 690
Somatotopic maps are disorganized in adult rodents treated neonatally with capsaicin P D Wall, M Fitzgerald, J C Nussbaumer, H Van der Loos & M Devor 691
Neural cell adhesion molecule is on embryonic muscle cells and mediates adhesion to nerve cells *in vitro* M Grumet, U Rutishauser & G M Edelman 693
Non-dopaminergic fibres may regulate dopamine-sensitive adenylate cyclase in the prefrontal cortex and nucleus accumbens J P Tassin, H Simon, D Hervé, G Blanc, M Le Moal, J Glowinski & J Bockaert 696

Nature® (ISSN 0028-0836) is published weekly on Thursday, except the last week in December, by Macmillan Journals Ltd and includes the Directory of Biologicals (mailed in December) and Annual Index (mailed in February). Annual subscription for USA and Canada US $198.50 (for subscription prices elsewhere, see next page). Orders (with remittance) and change of address labels to: Macmillan Journals Ltd, Brunel Rd, Basingstoke RG21 2XS, UK. Second class postage paid at New York, NY10010 and additional mailing offices. US Postmaster send form 3579 to: *Nature*, 15 East 26 Street, New York, NY 10010.

0028-0836/82/08000C-02$01.00

Contents continued overleaf

Are you locked in to a ^{32}P-schedule?

Amersham provides the key.

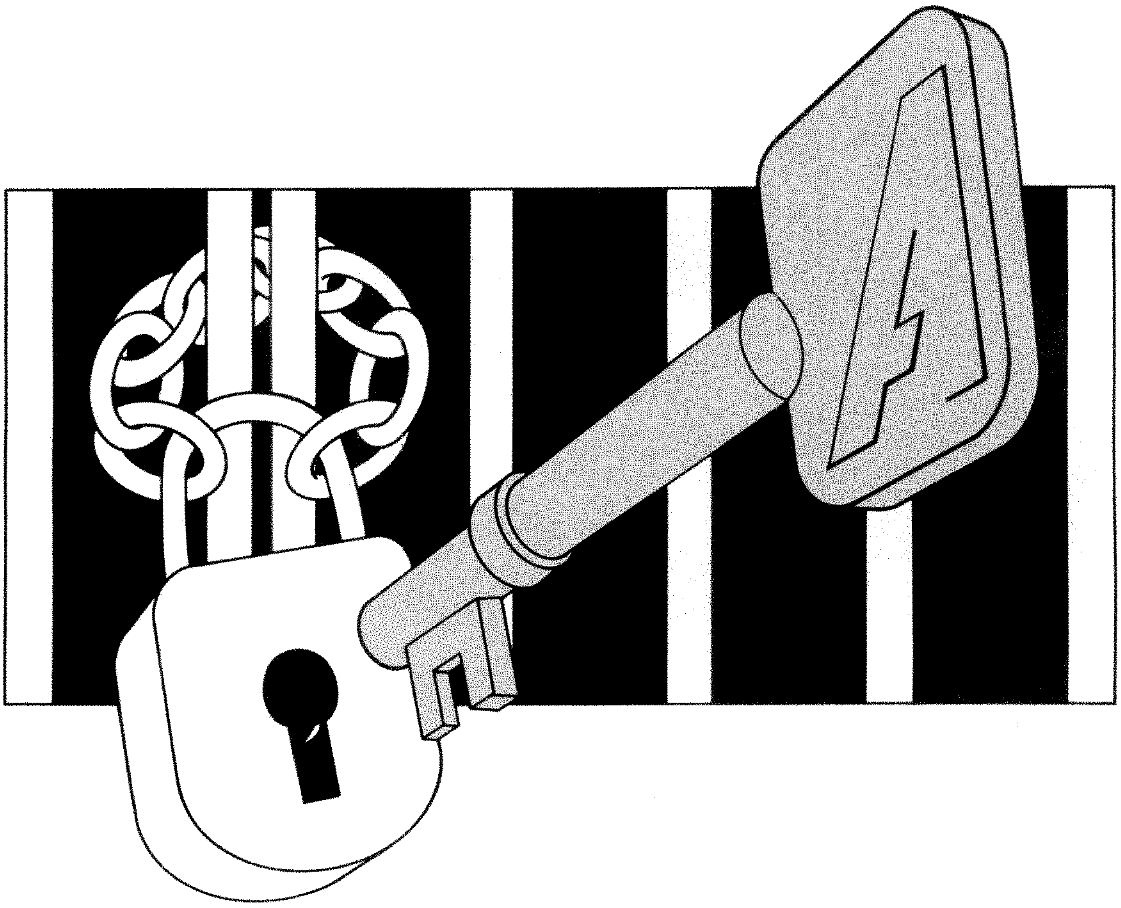

- **New** ● All deoxynucleotides at ~3000Ci/mmol available **every week.**
- ● All deoxynucleotides at ~800Ci/mmol available **every week.**
- ● All deoxynucleotides at >400Ci/mmol available **every week.**

The reliable supply of the complete range of [$\alpha - ^{32}$P] dNTPs every week gives you the convenience of selecting the specific activity most appropriate for your experiments at any time.

Amersham - for products you can trust

Amersham International Limited, Amersham, England Telephone 024-04-4444
In the U.S.A. and Canada, Amersham Corporation, Illinois 60005 Telephone 312-364-7100
and 800-323-9750 (Tollfree)
In W. Germany, Amersham Buchler GmbH & Co KG, Braunschweig Telephone 05307-4691

Circle No. 13 on Reader Enquiry Card.

Amersham

•How Britain runs its Science
•How the US runs its Science

These two new *Nature* wallcharts are now available.

The 2 x 3 ft. guides offer a comprehensive survey of the administration of science in Britain and the US, showing the interlocking relationship between science, engineering and medical establishments.

Designed as fold-out sheets, the wallcharts can be carried easily to meetings or hung as posters for permanent reference.

The new 1981 wallcharts are available at £3.50 or $7.95 each from *Nature's* offices in Basingstoke and New York.

Annual Subscription including Index (51 issues)

UK & Eire		£85
USA & Canada		US$198.50
Belgium	Airspeed only	BF7450
West Germany	Airspeed only	DM450
Netherlands	Airspeed only	G505
Switzerland	Airspeed only	SF395
Rest of Europe	Airspeed only	£100
Rest of World	Surface	£100
Rest of World*	Airmail	£150

**(not USA, Canada & Europe)*

Personal subscription rates are available in some countries to subscribers paying by personal cheque or credit card.

Details can be obtained from:
UK: *Nature* Promotion Department,
Canada Road, Byfleet, Surrey KT14 7JL.
Telephone: Jonathan Earl: Byfleet (09323) 41459
USA: *Nature*, 15 East 26 Street, New York, NY 10010
Credit card orders only (in USA & Canada):
Call toll-free: (800) 824-7888 (Operator 246)
In California: (800) 857-7777 (Operator 246)

All other circulation enquiries concerning existing subscriptions please contact:

Nature Circulation Department, Macmillan Journals Ltd., Brunel Road, Basingstoke, Hants RG21 2XS, UK
Telephone: (0256) 29242 Telex: 858493

Back issues: (Post-paid) UK, £2.50; USA & Canada, US$6.00 (surface), US$9.00 (air); Rest of World, £3.00 (surface), £4.00 (air).

***Nature* Binders:**
Single Binders: UK, £4.00; Rest of World, $10.00
Set(s) of 3 Binders: UK, £10.00; Rest of World, 25.00

***Nature* First Issue Facsimile:**
UK, 75p; Rest of World (surface), $1.50, (air), £2.00

***Nature* Annual Indexes (1971-1980):**
Price (post-paid):
UK, £5.00 each; Rest of World, $10.00

***Nature* Directory of Biologicals:**
(Hardcover edition)
UK, £22.50; Rest of World, $45.00

***Nature* Wallcharts:**
How Britain Runs its Science; How the US Runs its Science; UK, £3.50; USA, $7.95 each

***Nature* in Microform:**
For Information:
UK: UMI, 18 Bedford Row, London WC2R 4EJ
USA: 300 North Zeeb Road, Ann Arbor, Mi 48106

Orders (with remittance) to:
Nature, Macmillan Journals Ltd.,
Brunel Road, Basingstoke, Hants RG21 2XS, UK
Tel: (0256) 29242 Telex: 858493

MACMILLAN JOURNALS

Importance of amino acid uptake and decarboxylation in gastrin release from isolated G cells — L M Lichtenberger, R Delansorne & L A Graziani — 698

Inhibition of spindle elongation in permeabilized mitotic cells by erythro-9-[3-(2-hydroxynonyl)] adenine — W Z Cande — 700

Inhibitors of dynein activity block intracellular transport in erythrophores — M C Beckerle & K R Porter — 701

Cyclic AMP induces maturation of trout sperm axoneme to initiate motility — M Morisawa & M Okuno — 703

Different mRNAs from the transforming region of highly oncogenic and non-oncogenic human adenoviruses — A Virtanen, U Pettersson, J M Le Moullec, P Tiollais & M Perricaudet — 705

Site-specific mutagenesis by error-directed DNA synthesis — R A Zakour & L A Loeb — 708

No evidence for 'stress' α-globin genes in chicken — W Knöchel, B Wittig, S Wittig, M E John, U Grundmann, W Oberthür, J Godovac & G Braunitzer — 710

Univalent antibodies kill tumour cells *in vitro* and *in vivo* — M J Glennie & G T Stevenson — 712

Homocopolymer sequences in the spacer of a sea urchin histone gene repeat are sensitive to S_1 nuclease — C C Hentschel — 714

MATTERS ARISING

Magma chamber profiles from Bay of Islands ophiolite complex — C H Donaldson; Reply: J F Casey & J A Karson — 717

K^+ depletion and Na^+ pump density — J F Lamb, J F Aiton & P Ogden; Reply: A Nørgaard, K Kjeldsen & T Clausen — 717

The active radio galaxy 1413 + 135 — H S Murdoch — 718

GUIDE TO AUTHORS

Authors should be aware of the diversity of *Nature*'s readership and should strive to be as widely understood as possible.

Review articles should be accessible to the whole readership. Most are commissioned, but unsolicited reviews are welcome (in which case prior consultation with the office is desirable).

Scientific articles are research reports whose conclusions are of general interest or which represent substantial advances of understanding. The text should not exceed 3,000 words and six displayed items (figures plus tables). The article should include an abstract of about 50 words.

Letters to *Nature* are ordinarily 1,000 words long with no more than four displayed items. The first paragraph (not exceeding 150 words) should say what the letter is about, why the study it reports was undertaken and what the conclusions are.

Matters arising are brief comments (up to 500 words) on articles and letters recently published in *Nature*. The originator of a Matters Arising contribution should initially send his manuscript to the author of the original paper and both parties should, wherever possible, agree on what is to be submitted.

Manuscripts may be submitted either to London or New York (decisions being made only in London). Manuscripts should be typed (double spacing) on one side of the paper only. Three copies are required, each accompanied by copies of lettered artwork. No title should exceed 80 characters in length. Reference lists, figure legends, etc. should be on separate sheets, all of which should be numbered. Abbreviations, symbols, units, etc. should be identified on one copy of the manuscript at their first appearance.

References should appear sequentially indicated by superscripts in the text and should be abbreviated according to the *World List of Scientific Periodicals*, fourth edition (Butterworth 1963–65). The first and last page numbers of each reference should be cited. References to books should clearly indicate the publisher and the date and place of publication. Unpublished articles should not be formally referred to unless accepted or submitted for publication, but may be mentioned in the text.

Each piece of artwork should be clearly marked with the author's name and the figure number. Original artwork should be unlettered. Suggestions for cover illustrations are welcome. Original artwork (and one copy of the manuscript) will be returned when manuscripts cannot be published.

Requests for permission to reproduce material from Nature *should be accompanied by a self-addressed (and, in the case of the UK and USA, stamped) envelope.*

Nature announces the first wall chart showing how the U.S. runs its science

...shows who makes U.S. science decisions, who gets the money, and how it's spent

If you're involved in making decisions about science, or if you're looking for your share of science funding, you need Nature's new 1981 guide to how the nation spends its science dollars and who controls that money.

Compiled by Nature from literally hundreds of sources, the wall chart offers data on actual dollars spent on science by government agencies, industry, foundations, universities, research and medical centers. The chart lists key U.S. government policy makers, with their addresses and phone numbers.

Most significantly, the chart shows the interlocking relationships within the science, engineering, and medical establishments.

Designed as a fold-out that you can carry to meetings, or for hanging as a 2 x 3 ft. wall poster for permanent reference, the chart enables you to answer questions that might otherwise take weeks of research to dig out. Compact, color-keyed, and handy, it will be an enormous aid to you and your colleagues. We strongly urge you to order sufficient copies to cover the needs of your entire staff or department.

"How the U.S. Runs Its Science"

—another authoritative publication from Nature, for more than 100 years, the world's most respected source of science data.

For credit-card orders only, **call toll-free now, 24 hrs/day, any day: (800) 824-7888. Ask for Operator 130.** In California: (800) 852-7777. Ask for Operator 130.

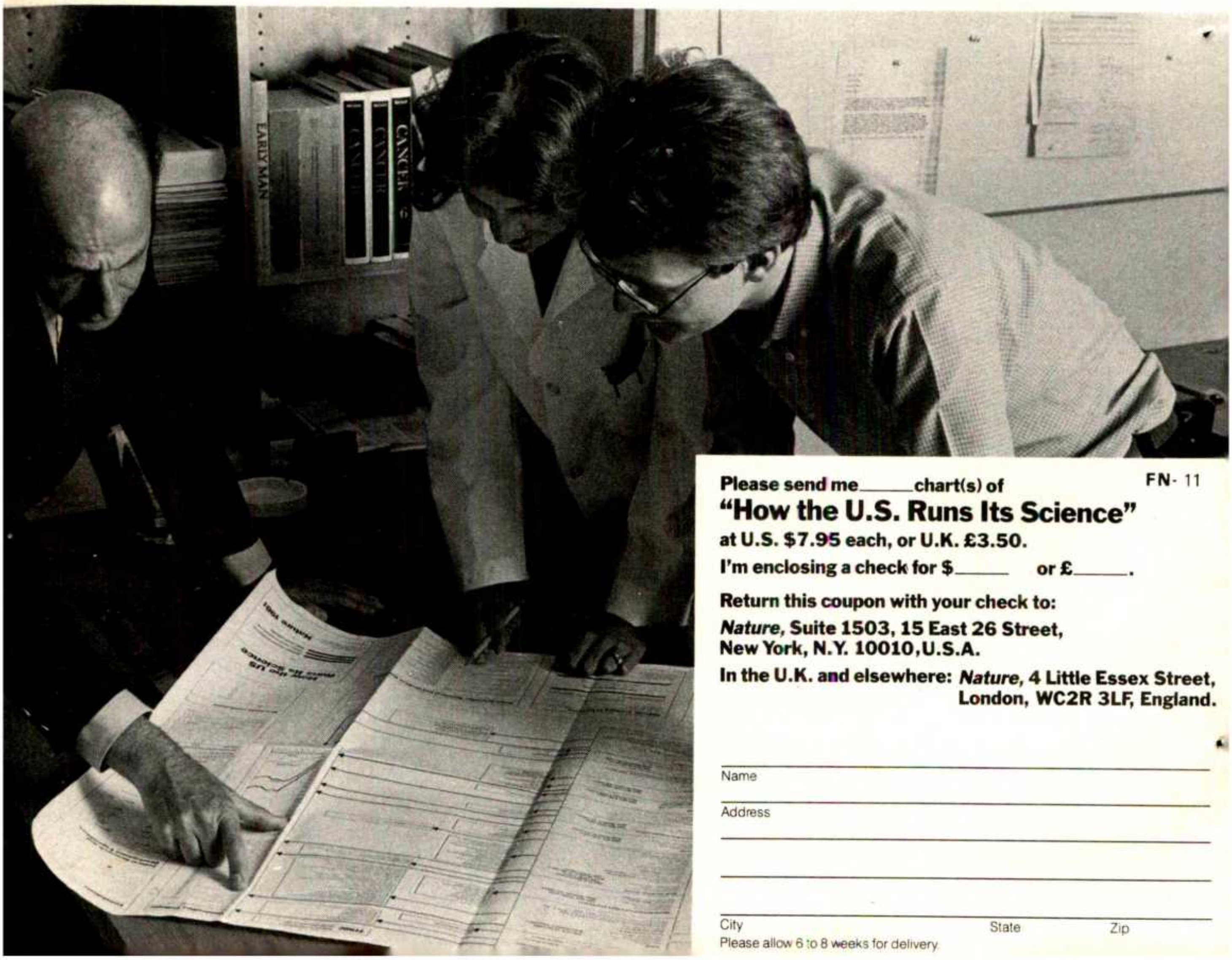

Please send me_____chart(s) of FN- 11

"How the U.S. Runs Its Science"

at U.S. $7.95 each, or U.K. £3.50.

I'm enclosing a check for $_____ or £_____.

Return this coupon with your check to:

***Nature*, Suite 1503, 15 East 26 Street,**
New York, N.Y. 10010, U.S.A.

In the U.K. and elsewhere: *Nature*, 4 Little Essex Street,
London, WC2R 3LF, England.

Name

Address

City State Zip

Please allow 6 to 8 weeks for delivery.

nature

7 January 1982

Reagan's mistake on Soviet sanctions

The US Administration, seeking to punish the Soviet Union for what is happening in Poland by suspending an exchange agreement, has revealed its ignorance of what science is for.

Towards the end of the Napoleonic wars, Sir Humphry Davy went on a journey on the European mainland untrammelled by the circumstance that Britain was literally at war with France (and that most other European states were at war with at least one other) The journey, frequently described as an illustration of how even then the international interests of science took precedence over international politics, is made still more pointed by the knowledge that Davy was combining business with pleasure — his honeymoon Personal travel and national hostilities were, it seems, independent of each other Now all that has changed President Ronald Reagan's suspension last week of the exchange agreement between the United States and the Soviet Union, part of his programme of sanctions against the Soviet Union in response to the supposed Soviet support of martial law in Poland, will effectively put latter-day Davys in their place It is also a stupid and a dangerous move It should be quietly abandoned

Programmes of economic and cultural sanctions have been frequently tested in the years since the Second World War, and have as frequently been found wanting The best thing to be said about them is that they are less damaging than outright warfare They are also, usually, ineffectual, as President Carter found after Afghanistan On this occasion, the difference of opinion between some Western European governments and the United States on the wisdom of sanctions as a means of interdiction will further undermine what President Reagan can hope to achieve — which by all accounts (see page 3) is not in any case very much It is however clear that neither he nor his advisers appreciate the enormity of including within a set of sanctions the suspension of a longstanding programme for the exchange of academic scientists between one country and another

This is why Open warfare is a means by which one nation state can legitimately (*pace* the pacifists) enforce its will on another Even nations that unfashionably declare war on others usually express their hope that in due course all will again be sweetness and light Programmes of sanctions, damage-limiting though they may be, also anticipate the earlier return of normalcy So sanctions should be designed to maximize the short-term damage done but to create as few impediments as possible for the hopefully happy years ahead Denying the Soviet Union the right to buy pipe-laying machines in Texas is unambiguously in the former category, suspending the exchange agreements unfortunately in the latter

That there should have to be formal schemes for enabling scientists from one country to work, if they wish, in laboratories in another is, of course, in itself a mark of failure If Dr X should wish to work in Dr Y's laboratory and Dr Y should be agreeable, and if one or other should be able to find the necessary funds, why should governments be involved? People like Mr Frank Carlucci, Deputy Secretary at the Pentagon, think they know why not if Dr X is a Soviet citizen, he will be part of a "highly orchestrated, centrally directed" effort to pick the brains of unsuspecting American scientists Mr Carlucci is naturally right to say that Soviet participants in the bilateral exchange agreement benefit from their visits to the United States, and are afterwards potentially more useful as applied scientists, sometimes in military programmes But is there any evidence that their American hosts, the Dr Ys of this world, are entirely without benefit? If so, the exchange programme has been maladministered — visitors have been foisted on unwilling hosts If not, Mr Carlucci should embark on what would be called an evaluation of the benefits and disbenefits of the exchange programme He would come to two conclusions — first, that the total benefit from mutually sought exchanges for the research enterprise is greater than the sum of the individual benefits and, second, that his government's proper course of action, as a signatory of the Helsinki accords, is to insist that the then agreement, at least in principle, that people should be more or less free to move to where their inclinations take them, should be honoured

That, unfortunately, will seem too abstract a course to the Reagans and Carluccis of this world The Soviets *are* benefiting, and must be prevented from doing so, they will say And we know that Helsinki doesn't work, don't we? That, of course is true, even if the statement of the truth comes oddly from the inheritors of those who negotiated the agreement But the reasons why Helsinki has failed in respect of scientific exchanges need more careful consideration The objective now should be to restore some semblance of the *laissez-faire* of Humphry Davy's time The only way of doing that is to shift responsibility for the administration of exchanges from the State Department (and the Pentagon) to some convenient halfway house such as the National Academy of Sciences That stratagem has been adopted elsewhere, even in backward Britain Perhaps the time has come when the National Academy of Sciences in Washington should insist that no other body, not even the State Department, can do what is required If necessary, it should be prepared to raise the funds required privately, from the foundations and from industry

More change now due

Reform of the British research council system is overdue. Does the government have time?

The British government has mostly done the decent thing in its dealings with the publicly-supported research councils Broadly speaking, their budgets for the financial year beginning on 1 April are unchanged (see page 4) So the Prime Minister will be able to tell the British electorate at the next general election, some time before 3 May 1984, that she has "protected" publicly-supported civil science from damaging economies On present form, the government may have very little else to boast about at the end of what is almost certainly its last full financial year in office But this is not a vote-catching issue Thus the government's generosity towards the research councils — a curious description of a recipe for continued stagnation, but appropriate in the circumstances — must be taken as deliberate Will it therefore, in the remainder of its time in office, put in hand the structural reforms of the mechanisms for supporting the five research councils that are now long overdue?

The research councils are inevitably a mixed bunch But even those with responsibilities for fostering basic research in fields such as medicine or agriculture are important sources of support for university research The Science and Engineering Research

0028-0836/82/010001-02$01 00

Council, on the other hand, although enjoined to support academic research, has for the past decade been flirting with ways of making university research more directly relevant to British industry. On the grounds that all of the councils have a finger in the university pie, their funds are channelled through the Department of Education and Science, but the total sum available each year has for the past decade been divided between the various councils on the recommendation of the Advisory Board for the Research Councils. Even when this mechanism was established, in the wake of the Rothschild reorganization in 1971, it was feared that the board, on which the executive officers of the research councils are necessarily influential, would become an arid device for sharing out funds in such a way as not to give too much offence. So it has turned out.

The advisory board is thus an obvious candidate for change. But how? There is much to be said for the recipe offered last November by the House of Lords Select Committee on Science and Technology — appoint a full-time chairman, give him (or her) a small staff and require the board to comment on the policy questions that now go largely by default. Under such an arrangement, the chairman of the board would become what the Department of Education and Science now conspicuously lacks — a chief scientist of a kind. These proposals have the advantage that they could be put into effect without much trouble. They would also be improvements. The government should listen to what the House of Lords has said, and quickly.

There are, however, snags. The reform of the Advisory Board for the Research Councils along the lines suggested by the House of Lords committee would leave untouched the habitual secrecy of advisory bodies working for British government departments. The theory is simple, advisory bodies exist to give advice which ministers may, at their pleasure, decline. And, the argument goes, it would be unseemly, cramping and politically irksome if the rejection by a minister of an advisory committee's advice were publicly advertised. But this is precisely what has happened with this year's advice on the research council budgets. The decision that the budget of the Social Science Research Council should be reduced by £1.1 million (just over 5 per cent) was taken by Sir Keith Joseph, the Secretary of State for Education and Science, in flat contradiction of the recommendation of the Advisory Board for the Research Councils. No explanation has been given, so that there is no way of telling whether the minister's fiat reflects the fashionable animus against the social sciences or whether there were — as there might well have been — more substantial grounds for his decision. Whatever the truth, the minister is likely to be more seriously damaged by the gossip that will now flourish than he would have been by an open discussion of his reasons. Secrecy, it seems, hurts even those whom it is intended to protect.

The case of the Social Science Research Council illustrates another weakness of the present system. The council was set up nearly twenty years ago to foster academic research in the social sciences. Throughout that period, it has struggled hard to establish academic centres of excellence in the face of open hostility from its enemies and, more disarming, the wayward kookiness of some of its friends. On the grounds of youth, it was exempted from Lord Rothschild's recommendation in 1971 that government departments should pay for the cost of applied research supported by the research councils. Since then, the Social Science Research Council has been complaining that government departments are too fond of stealing its clothes by commissioning basic research from their own resources. Now, ironically, there is to be another inquiry by Lord Rothschild into the application of the customer–contractor principle in this field, one result may be to reconcile the advisory board with its minister.

What will remain undecided are the questions that the advisory board should have had the wit to take up several years ago — is a research council the best mechanism for fostering the social sciences? what criteria of excellence make sense? and what, in any case, is to be made of the peculiarly British sneer that what are called the social sciences are not science? It is easy to understand why the advisory board would have shrunk from such an investigation, if the precedent were established that the constitution of the newest research council might be questioned, who could then ensure that the well-established councils were free from scrutiny? The advisory board, in other words, is undermined by backscratching which is then strengthened by the convention of secrecy.

The habit of secrecy is not merely damaging to all those concerned but also inappropriate. Over the years, the research councils have (to their credit) established a remarkable sense of trust with their customers in the universities. In Britain as elsewhere, the peer review of research proposals has created a sense that substantial parts of their budgets are spent by the scientific community, not by career officials. Some of the councils have also developed a knack of putting controversial ideas into circulation before they are finally decided. But the questions that the advisory board should be tackling — the place of social science, the health (or sickness) of the dual support system, the success (or otherwise) of the University Grants Committee's designated courses in engineering education and so on — are also questions that cannot be settled convincingly by a small group of people, however appointed.

The lessons for the government are clear. The advisory board should be strengthened along the lines suggested by the House of Lords and, in the process, the dominant influence of the research councils should be deliberately weakened but not abolished. Then, some device must be found for making the advisory board a more public body, able at least to advertise the issues on its agenda and ideally compelled to publish not less than once a year a reasoned account of what it has been doing. There is no substantial danger that in the process the British Constitution would be undermined or the freedom of ministers compromised. On the contrary, ministers would be less at risk than at present of having to make up their minds without the benefit of even half-baked advice.

Not president perpetual

Dr Philip Handler, who died last week served the US National Academy of Sciences well.

Being President of the United States is a relatively simple job, power and patronage help to bring to heel unwilling cabinet colleagues and even members of the Congress. Presidents of the National Academy of Sciences in Washington enjoy no such benefits. Even though elected, they must continually reassert their authority among their electors, many of whom declare that they could do the job just as well if only they chose to spend their time in such a demeaning way. One measure of Dr Philip Handler's achievement in this office is that during his twelve-year stint at the academy, which ended last June, he was twice re-elected.

A large part of the explanation is that he was an articulate man, he could make fine speeches but also talk his way out of trouble. He was also courageous. He fought the extremists among the environmentalists when many others thought it prudent to keep their heads down. He fought Congress on several occasions, not only about the scale of support for research but over occasional threats of interference. Handler's early years at the academy saw the rapid growth of its secular activity — producing reports on topical issues, sometimes important and sometimes trivial — whereafter he had to fight the committees for the right to ensure that their reports were properly reviewed before publication. Not all his battles were successes. The campaign to finance the purchase of Einstein's statue now in the academy's front garden might have been successful if the statue had been better.

Inevitably, continual battles take a toll. Handler, always an iconoclast, occasionally seemed to be oversensitive to criticism. Latterly, he was concerned to know what he would do on leaving the academy and, more recently, was embrittled by his largely secret knowledge of his mortal illness. He will, however, be remembered well, not merely for his wit and eloquence but for having rescued the academy from its earlier spells of idiosyncratic and then indolent leadership — and for ensuring that it is no longer simply an academy.

0028-0836/82/010002-01$01.00

Anxiety about Reagan's sanctions

Two views on the wisdom of suspension

Washington

President Reagan's announcement last week that the United States is suspending its scientific exchanges with the Soviet Union, as part of a package of reprisals aimed at chastising the Soviet Union for its support of the military clampdown in Poland, has provoked concern in the scientific community that the move indicates an increasing willingness to use science for explicit political purposes.

The immediate effect of the President's decision will be to suspend the scientific exchange agreement signed by President Richard Nixon and Soviet President Leonid Brezhnev in 1972. Furthermore, Mr Reagan announced that unless the situation in Poland changes the agreement will not be renewed when it runs out in July.

Similarly, agreements for cooperation in energy and space research will not, at present, be renegotiated when they run out in May. And a number of other agreements which include scientific components are also being suspended and reassessed.

To a large extent, however, Mr Reagan's decision to suspend scientific exchanges is viewed as more symbolic than substantive. In the case of high-technology trade, an area announced for suspension, even the US Department of Commerce accepts that the Soviet Union is little more than a "marginal market" for sophisticated equipment, accounting for less than one per cent of the US electronics industry's annual sales of $200,000 million, and that the Soviets may well be able to meet their needs from other sources.

Officials at the National Science Foundation, which is responsible for nine of the twelve working groups still operating under the terms of the 1972 agreement, argue that as a result of deliberate efforts over the past few years to eliminate exchanges involving a marked imbalance of benefits, those still in effect provide scientific benefit to both sides.

Many — although not all — US scientists fear that if even these exchanges are now halted, the effect could be counter-productive. Not only would it close off an important channel of communication between two intellectual communities, but it would provide a useful propaganda weapon for use against those attempting to separate politics from science.

"I feel that it is very important that these communication channels are kept open because they provide a crucial link between different societies and different peoples during periods of difficulty, and because they can be kept separate from immediate political concerns", Dr Alan Bromley, professor of physics at Yale University and president of the American Association for the Advancement of Science, said on the eve of the association's annual meeting.

At the National Academy of Sciences, which two years ago suspended all bilateral symposia, seminars and workshops with the Soviet Academy of Sciences in protest at the treatment of physicist Dr Andrei Sakharov, but has made no move to interrupt the exchange of individual scientists between the two academies, president Dr Frank Press said he was concerned that if there was no formal scientific agreement at all between the United States and the Soviet Union, it would be difficult to keep channels of communication open.

Even some of the groups which have been most vocal in their protests over the treatment of Dr Sakharov and other dissident scientists have expressed fears that their effectiveness could be severely reduced if scientific exchanges were terminated. Dr Max Gottesman, a member of the Committee of Concerned Scientists, said last week that since Soviet diplomats did not seem to consider the termination of such exchanges to be a major blow to their domestic scientific effort, the United States stood to lose more than it might gain in terms of influence over opinion in the Soviet scientific community.

In contrast, there is less consensus on how far the federal government should go in restricting access by foreign scientists, in particular those from the Soviet Union, to US research laboratories on the grounds that the knowledge they pick up might later be used for military purposes.

Following protests from the scientific community that such restrictions could unnecessarily restrict the flow of scientific information, Mr Frank Carlucci, deputy secretary of the US Defense Department, has provided a detailed list of instances where, he claims, the Soviet Union has achieved significant military or technical benefits through visits to US laboratories made by Soviet scientists on exchange programmes. According to Mr Carlucci, "it is quite apparent the Soviets exploit scientific exchanges as well as a variety of other means in a highly orchestrated, centrally-directed effort aimed at gathering the technical information required to enhance their military posture".

A significant number of scientists are known to be in general agreement with the Defense Department's position. Dr Bromley, for example, said that although he felt restrictions should not be applied to basic science, he was concerned that information of potential military value might have been "given away" through exchange programmes.

The National Academy of Sciences is considering setting up a committee to look at the implications for the scientific community of existing and proposed federal restrictions on the flow of technical data. Dr Richard D. DeLauer, Under-Secretary of Defense for Research and Engineering, is said to be in favour of such a committee, although academy officials fear the government might act before a proper study can be carried out. **David Dickson**

Polish academia only partly normal

Polish academic life formally resumed this week but was, however, only partial. There are reliable reports that only graduate and fifth-year (finals) students have been readmitted to the universities and that all other undergraduate courses have been suspended until next year.

This leaves in doubt the status of the suspended students. A decree of the Military Council, passed on 30 December, obliges all able-bodied males between 18 and 45 years of age to work for the duration of martial law. Students as such are exempt, but it is not clear whether the exemption applies to those who must wait until next autumn to resume their studies.

There are also unconfirmed reports of some first-year students being drafted for military service. University graduates who have not yet found work are obliged to report to plenipotentiaries from the Ministry of Labour, Wages and Social Affairs stationed at their former colleges. Since unemployment among young graduates is considerable — particularly in the humanities and social sciences — there seems little chance that for them the clause in the decree, enjoining the administrators to take professional qualifications into consideration "as far as possible", will be of more than a token significance.

Academic staffs are far from happy with the new situation in Poland. On 23 December, the Prime Minister, General Wojciech Jaruzelski, together with Deputy Prime Minister Mieczyslaw Rakowski and Politburo member Hieronim Kubiak, met 69 leading academics to discuss what Jaruzelski described as "the active role of Polish scientists, intellectuals, writers and artists working for the salvation of the homeland, consolidation of the state and the building of a bridge of special patriotic agreement". Both Kubiak and Rakowski have the reputation of being liberals, and the academics seem to have been selected mainly from those who played little or no active part in the campaign for academic autonomy of the past 16 months.

Even so, no agreement was reached. The official communiqués spoke merely of a "long and frank discussion", with the

0028-0836/82/010003-02$01.00

academics stressing the "urgent need to rebuild trust and calm scientific teaching in Polish universities". According to an unofficial *Solidarity Information Bulletin* now circulating in Warsaw, the seven-hour meeting was deadlocked by the persistent demand of the academics for the release of all detainees and for the participation of the university rectors recently elected under the new democratic procedures in any further negotiations.

The presence at the meeting of Dr Aleksander Gieysztor, president of the Academy of Sciences, must have sharpened the discussion of the detainees. He was himself picked up in one of the early round-ups, although released shortly afterwards.

The unofficial lists of detainees now being compiled reflect just how active a role the academic community played in the Solidarity movement. They include:

- Lecturers from the unofficial Society of Academic Courses (the "Flying University") Stefan Amsterdamski, Wiadyslaw Bartoszewski, Andrzej Celínski, Jerzy Jedlicki and Jan Walc.
- Solidarity advisers from the universities, including Dr Bronislaw Geremek, a Warsaw lecturer in economics, who was a member of the Solidarity delegation to France last October, and Dr Stefan Kurowski who drew up the project for economic renewal discussed at the Solidarity Congress.
- Doctors and medical workers including Grazyna Przybylska-Wendt from the Solidarity presidium.
- Academy or university employees who, until now, have never achieved this type of prominence — among whom Dr Stanislaw Kozlowski, the new rector of Poznan University, is the most eminent so far.

The military rulers seem willing to make some small concessions to the academics — the constitution of the Polish People's Republic (Art.5.3) enjoins them to maintain the "constant progress of science and technology". Academic detainees from the Warsaw area are housed in a government hotel near Drawsko. Earlier reports that Solidarity advisers Jacek Kuron and Adam Michnik had been savagely beaten are unfounded.

The main instigators of the academic turmoil, according to the official statements, were the activists of the Independent Students Union (NZS). These, it is said, had tried to turn NZS into a political organization, rejecting the policy of social accord and "stirring up anti-Soviet sentiments" — a line which suggests that a purge of the student body may be forthcoming.

So far, no mention has been made of the fact that, only a few days before the military take-over, the Conference of University Rectors, meeting in Poznan, had formally endorsed the recent NZS protests as a valuable contribution to the struggle for academic freedom.

Vera Rich

High-energy physics

All change

With approval for its latest accelerator, LEP, under its belt, the European Centre for Nuclear Physics, CERN near Geneva, seems prepared to experiment — not so much with particles but with its governing body. For alongside the announcement of the CERN budget, and the final approval for LEP (see *Nature* 24/31 December, p.685), comes news of the appointment of two active new characters to the CERN Council. Sir Alec Merrison, currently chairman of the UK Advisory Board for the Research Councils and vice-chancellor of the University of Bristol, is to become president of the council; and Umberto Vattani, a high-ranking Italian civil servant who was involved in a disagreement two years ago between Italy and Germany over the appointment of a German (Professor Herwig Schopper) as director-general of CERN, becomes one of the two vice-presidents.

Sir Alec was himself a high-energy physicist, and in fact in 1959 he was co-author of the first experimental paper to come out of CERN. He was also a director of the now defunct Daresbury electron accelerator, NINA, and has defended the place of "big science" in the highly-constrained UK science budget.

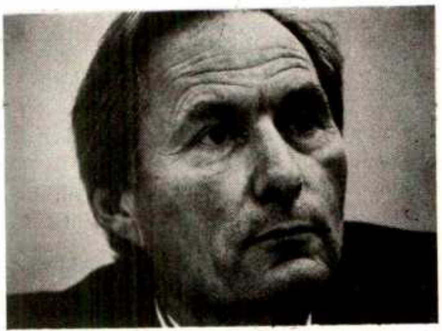

Merrison: chairman everywhere?

On his appointment — which gives him control of the CERN Council's committee and subcommittee work during the next year, as well as presidency at the council itself — Sir Alec said he was delighted at the decision over LEP. "All the delegates are amazed that CERN has been able to pull this thing off," he said, but at the same time the next few years would see CERN taking "a jolly dangerous path".

This is because LEP is to be built out of the current budget only by making massive savings in the present programme. Closing certain facilities entirely would save something, but most of the savings will have to come from running down the experimental work on the CERN 400-GeV super proton synchrotron, the laboratory's biggest machine. There will therefore be a hiatus in research.

Vattani, on the other hand, now reassured that Schopper has proved an "excellent" director, and that Germany will not try to squeeze CERN in favour of its own national accelerators, sees looming problems in personnel and pensions

Other questions which will arise for the council in 1982 are late payment (some members have indicated that they may not be able to pay their subscriptions on time) and the management of the LEP project itself. LEP will span two countries, be 27 km in circumference, cost £275 million, and will still face some environmentalist opposition in the region. Professor Schopper will no doubt welcome all the help that the council can give him in this, the largest ever CERN project.

Robert Walgate

Hardly any change

The arguments put forward by the past and present chairmen of the British Science and Engineering Research Council (SERC) that the council should take a larger slice of the science vote have modestly borne fruit. Although the civil science budget for 1982–83, made public a few days before Christmas, has roughly kept its real value, SERC's budget has been increased by about 1 per cent. Most of the council's extra money will be spent on biotechnology, information technology and on helping universities to maintain the quality of research in spite of cuts in their own budgets.

It is equally no surprise that the council to come off worst in this year's division of the science vote is the Social Science Research Council (SSRC), with a real budget for 1982–83 about 4 per cent less than in 1981–82. SSRC has suffered substantial cuts in the real value of its grant for the past three years, reflecting uncertainties about the role of social science research in Britain.

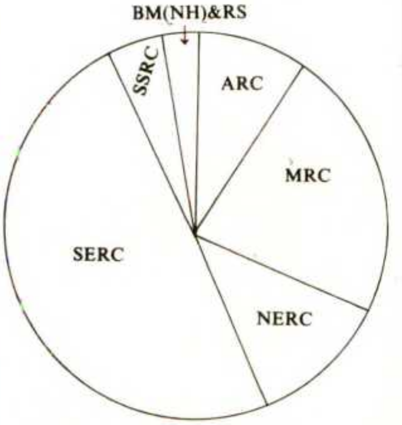

The three other research councils, however, are to receive the same real budget in 1982–83 as in 1981–82. All, however, will be concerned that the government has allowed for only a 4 per cent increase in salaries over the year. If, as last year, the increase in the salary bill is higher, then the amount of research the councils can buy is bound to decrease.

Judy Redfearn

0028-0836/82/010004-02$01.00

American science

Supply-siders now

Washington

"We are now forging a substantially closer relationship with both the legislative and executive branches of Congress", the retiring president of the American Association for the Advancement of Science (AAAS), Dr Alan Bromley of Yale University, said on the opening day of the association's annual meeting in Washington on Monday

Dr Bromley listed various ways in which AAAS was exercising what he described as a "service role" for private and public science decision-makers Such activities range from providing testimony to congressional hearings to preparing regular and widely quoted assessments of the impact of federal policy on the size of the US research and development effort

But if a considerable amount of AAAS's time is now spent helping the government to do its job, there has also been an expansion of effort to compensate for federal actions — for example, the cutting back of support for science education in schools

Following up an initiative launched at last year's annual meeting in Toronto, the chairman of the AAAS board of directors, Dr Frederick Mosteller, announced that the association had just received a $6 5 million grant from Philips Petroleum for a series of television films to complement the work of mathematics teachers in public schools "by making mathematics more lively and significant"

Another educational initiative is the publication of a set of science teacher notes based on articles appearing in AAAS's monthly science magazine *Science 82* The association is also convening two conferences later this year with leaders of various scientific and technical societies, the first dealing with urgent policy issues in science education, the second concentrating on the growing shortage of science and mathematics teachers

Inevitably, a prominent theme of this year's meeting is the impact of the Reagan Administration's cuts in public spending on scientific research In an address on Sunday evening, the President's Science Advisor, Dr George (Jay) Keyworth, emphasized again the Administration's awareness of the importance of basic science, promising that the next "budget submission will clearly reflect that"

He also again warned that there were hard choices to be made In the short term, there was general acceptance at the meeting that such a policy was appropriate Dr Bromley pointed to the Department of Energy's High Energy Physics Advisory Board and the Nuclear Science Advisory Committee as examples of ways that scientists in a particular fields, when finances get tight, have been able to determine their own scientific priorities

But in the longer term, it was said, repeated budget cuts will be severely disruptive Figures produced by AAAS itself last week showed that for the two-year period 1981–82, the result of federal actions will be to reduce the civilian research and development budget by about 16 per cent in real terms (constant dollars), with a 22 2 per cent growth in the military research and development budget over this period

Another issue being hotly debated in the meeting rooms and corridors is the current dispute about creationism and the teaching of evolutionary theory in public schools On Monday morning, the AAAS board unanimously passed a resolution that "creationist groups are imposing beliefs disguised as science upon teachers and students to the detriment and distortion of public education in the United States"

Registration at the 1982 meeting is expected to be about 5,000 which AAAS officials say is approximately the same as the last time the association held its annual meeting in Washington three years ago Next year, in Detroit, they are hoping for something better, by moving the timing of the meeting from January to May

That decision has been partly determined by the weather During last year's meeting, Toronto experienced its coldest winters for almost a century, with temperatures of -30°C The previous year, San Francisco airport had been closed by fog **David Dickson**

UK director for US Biogen laboratory

Dr Richard Flavell, one of Britain's whizz-kids of gene cloning, is to leave the country to become research director of Biogen Inc , the American arm of the international biotechnology firm, Biogen NV

Flavell is currently leader of the only gene cloning group at the National Institute of Medical Research (NIMR), Mill Hill, London, one of the two principal laboratories of the UK Medical Research Council Gene cloning is also done at other laboratories of the council — notably at Hills Road, Cambridge — but there is a strong feeling that application of the technique, central now to the whole of molecular biology, should be more in Britain The loss of Dr Flavell is thus significant, particularly at a time when NIMR is seeking a new director and reconsidering its role within British biology

In fact, Flawell has officially been granted "leave of absence" from Mill Hill for two years, but it seems unlikely that two years hence Flavell will want to leave Cambridge, Massachusetts, where the Biogen laboratory is being set up

Flavell will continue to direct a group at Mill Hill, if at a distance, but he wishes to take some of the more fashionable work with him He expects that half-a-dozen of his Mill Hill team will go with him to Biogen, taking with them expertise on the H-2 regions of the mouse genome These regions code for histocompatibility antigens in the mouse, and it may be speculated that Biogen will now take an interest in the generation of reagents for tissue-typing in man, using the equivalent human HLA regions Flavell will leave at Mill Hill the part of his group which deals with the globin genes, also important in immunology but less at the centre of attention now than H-2 and HLA

At Biogen, Flavell will take over a fledgling staff of 20 scientists, which he will increase to 75 by the end of 1982 He will, of course, be concerned mostly with fostering the commercial interests of Biogen through research, but has been guaranteed the opportunity to pursue his own basic research — largely through the Mill Hill team he takes with him

Flavell cannot say yet what the research interests of his new laboratory will be, but according to Professor Charles Weissmann of Zurich, who is chairman of the scientific council of Biogen, the Cambridge laboratory was originally planned to pay closer attention to the chemical and processing aspects of biotechnology than Biogen's Geneva laboratory which was founded earlier (see *Nature* 27 October 1981, p 599) Whether Flavell will in fact follow this line is open to question

Robert Walgate

Biomedical research

NIH takes a cut

Washington

The National Institutes of Health (NIH) told recipients of biomedical research grants and contracts last week that new and continuation grant awards made in the next three months are likely to be 4 per cent lower than initially proposed by President Reagan in his budget request to Congress last March

It could have been worse A revised budget request, issued in September, demanded a further 12 per cent reduction in all discretionary public spending and many federal agencies have had their activities curtailed significantly in the drive to reduce the federal deficit As it is the NIH budget for 1982 — the fiscal year which started last October — will only increase by 2 2 per cent, considerably less than the current rate of inflation, and the first significant drop in real terms for federal support of biomedical research since the mid-1970s

However, in the short term, no major damage seems to have been inflicted, and

0028-0836/82/010005-02$01 00

NIH's budget strategy of attempting to stabilize the number of new and renewing competitive awards at about 5,000 remains virtually intact Furthermore, Congress has replaced much of the money for research training grants which the Office of Management and Budget wished to cut

Technically, the 4 per cent reduction is only a provisional figure, valid up to March Unable to agree on a detailed appropriations bill, Congress agreed last month to a "continuing resolution" for the next three months In practice, however, since debate on the budget for the 1983 fiscal year begins later in January — and no substantial objection to the provisional 1982 totals are expected from the White House — the 4 per cent reduction is likely to run to September

It has been a confused budget year for NIH Before leaving office in January, President Carter proposed a biomedical budget for the institutes of $3,770 million, a figure left virtually untouched in the Reagan Administration's budget review in March and representing an increase of about 5 6 per cent over 1981 However, realizing that the budget deficit in general was going to be much larger than initially anticipated, the Reagan Administration in September recommended an across-the-board cut of 12 per cent, which would have reduced the NIH budget to $3,310 million

The net result of last month's continuing resolution is that, rather than having to reduce the number of new awards for competing research projects to 4,230, as the proposed September revisions would have required, NIH expects to be able to make almost 4,800 of these during the current financial year This is little short of the 5,000 which was adopted as a goal two years ago, following several years in which the number of such awards, which are provided to support investigator-initiated research projects, had fluctuated widely

The budget resolution procedure thwarted a move supported by several legislators in the House of Representatives to direct additional research funds to three institutes the National Institute of General Medical Sciences, the National Institute of Allergy and Infectious Diseases, and the National Institute of Child Health and Human Development These were felt to be suffering more than the others from the squeeze on research funds, in terms of the quality of the research projects that were being refused funding

NIH officials are optimistic that the 1983 budget which Mr Reagan submits to Congress next month will again contain a small increase for NIH Secretary of Health Mr Richard Schweiker is said to have argued successfully against major cuts in biomedical research that had been proposed by the Office of Management and Budget **David Dickson**

New director chosen for NIH

Washington

Dr James B Wyngaarden, chairman of the department of medicine at Duke University in North Carolina, is expected to be nominated by President Ronald Reagan as the new director of the US National Institutes of Health (NIH) in Bethesda, Maryland

Although yet to be formally announced — and subject to approval by the US Senate — Dr Wyngaarden's appointment is thought to have been unofficially approved by the White House, and the delay in making an announcement is the result of the lengthy security and financial checks which all presidential appointees undergo

Dr Wyngaarden would probably be a popular choice at NIH's headquarters, and with the biomedical research community in general Those who know him say they expect him to provide strong leadership and vigorously to defend the $3,600 million research budget of NIH, the principal source of federal funding for biomedical research in the United States

Dr Wyngaarden has been a close professional colleague of Dr Donald Fredrickson, who resigned as NIH director last July after six years in the post Together with Dr John B Stanbury, the three were co-editors of an influential collection of essays, *The Metabolic Basis of Human Diseases* First published in 1960, the book is about to go into its fifth edition, and is considered by many to be a classic in its field

Dr Fredrickson said last week that he had "no doubt" that Dr Wyngaarden would fill the NIH position extremely well "He is a good physician, an excellent scientist, and understands the institutional aspects of medical research very well, I have every confidence that he will be an excellent director"

A graduate of the University of Michigan, Dr Wyngaarden is no stranger to Washington science policy circles He was a consultant to the Office of Science and Technology Policy between 1966 and 1972, and a member of the President's Science Advisory Committee from 1972 until its abolition in 1973 Before his appointment at Duke, he was professor of medicine and chairman of the department at the University of Pennsylvania from 1965 to 1967

NIH scientists hope that a speedy confirmation of Dr Wyngaarden's appointment will help to accelerate other senior appointments at NIH Six of the twelve institutes lack a permanent director, and approving the new appointments will be one of the first tasks awaiting the new director

David Dickson

Molecular biology

Trimming costs

Molecular biologists who are used to relying on the European Molecular Biology Organisation for providing fellowships and other useful means of mobility within Europe may have to pay closer attention to the politics of its budget next December — for the 1982 budget has seen a 3 per cent fall (in real terms) for the second year running

The secretary of the organization, Dr John Tooze, says that management costs have been trimmed to the absolute minimum, and that for 1982 cuts will have to be undertaken in the EMBO programme itself The 1982 budget will be DM 3 5 million (£825,000), numerically 8 per cent above last year but 3 per cent below EMBO's calculated inflation figure

The EMBO scheme accounts for 400 fellowships in any year, plus 40 courses and workshops and a small lectureship programme — which often takes prominent American and other visiting scientists around Europe on a lecture tour It is this lecture programme which is likely to be cut this year

If the budget were to be cut again for a third year, the fellowships and workshops would be hit, says Tooze Then the smaller countries (of the 17 member states of EMBO) would certainly object These countries are probably the main beneficiaries of the programme, and they in fact constitute a two-thirds majority of states on the council which votes the budget of EMBO each year Decisions can be taken by such a majority but the remaining states — Britain, France, Germany and Italy — contribute nearly 60 per cent of the budget The danger is that if the small countries kick up a fuss, the big four could refuse to pay This year a compromise has been reached It may not be so easy next year

Robert Walgate

Microbial collections

Bugs in hazard

Once again, a British microbial culture collection is threatened by lack of funds At the end of last year the Ministry of Agriculture, Fisheries and Food announced its intention to withdraw support for the National Collection of Industrial Bacteria housed at the Torry Research Station in Aberdeen This is the third time in two years that culture collections have been threatened by withdrawal of funds The Brewery Research Foundation and the agriculture ministry have already stopped supporting the national yeast culture collection and the Commonwealth Mycological Institute and Natural Environment Research Council have said that they wish to cut support for the national fungi collection

Although the problems of the yeast and fungal collections have been at least

0028-0836/82/010006-02$01 00

temporarily solved, the threat to the industrial bacteria collections has stimulated the UK Federation of Culture Collections to urge that a single government agency should take over responsibility for all of Britain's ten national collections. The problem is that the collections currently share seven sponsors, not all of which ascribe high priority to their sponsorship.

In the event, the industrial bacterial collection may also be saved, though not necessarily to the satisfaction of its users. The most likely outcome is that the agriculture ministry, the collection's sole sponsor, will relinquish responsibility to the University of Aberdeen from next April. Negotiations are under way for transferring the collection to the university's company, which handles the commercialization of research relevant to industry. The idea is that the collection should eventually operate as a commercial concern.

Under the arrangements now being discussed the ministry would pay the university for running the collection, although payment would be considerably less than current running costs of about £200,000 a year. Savings would be achieved largely by reducing the number of staff from twelve to about seven. Still to be determined are the university's commission on continuing business, the ministry's initial grant and what should be charged for consultancy and services. Although the proposal would save the collection, the microbiological community, which fears that commercialization could jeopardize some of the services currently on offer and increase costs to users, is glum about the prospects.

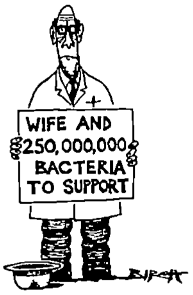

Last year, an inter-research council committee was set up to deal with the funding problems of culture collections as and when they arise. But the UK Federation of Culture Collections now argues that the committee's remit is too narrow. Together with three learned societies, including the Society for General Microbiology, the federation is hoping to persuade one government agency to take over responsibility for all ten microbial collections and to coordinate the formulation of a national policy for genome conservation including plant and animal cell lines as well as microbial cultures. As yet, however, no obvious agency has come forward, although the federation is hopeful that a meeting with the Department of Industry early in the year will be fruitful.

Judy Redfearn

Stanford University

At the helm

Palo Alto

When biologist Donald Kennedy became Stanford University's eighth president in August 1980, he pledged strong support for the humanities. Now, more than a year later, he has delivered. $5.6 million in gifts and grants have helped to create a new Humanities Center. From other contributions, eight professorships have been endowed.

Nevertheless, some faculty members remain sceptical of Kennedy's efforts to make support for the arts and humanities comparable with that for the sciences. One humanist complains that too much time is spent on training and not enough on students' personal development. He thinks that a university should be primarily concerned with values. He is waiting for Kennedy to enunciate his values and to exert intellectual leadership. "You can buy administrative ability", the disgruntled professor believes.

During Kennedy's spell in Washington as Commissioner of the Food and Drug Administration, he won wide respect for his administrative ability. Although he denies rumours about his own political ambitions, he still travels frequently to the capital.

He says that one of his objectives is to improve government understanding of the kinds of problems research universities face and about national science policy. He has the experience and the contacts to talk about these matters in the right places.

And lean, six-foot-one Kennedy believes that Stanford will be able to continue as a first-rate centre of basic research in spite of federal research cutbacks this year of 2 or 3 per cent. He is a self-avowed "relentless optimist". Nevertheless, he worries about reduced support for student financial aid. More than half of Stanford's 12,800 students receive scholarships. Research and training should go hand in hand, a truth not always recognized by the Reagan Administration, Kennedy says.

Kennedy remains doubtful that private support for universities will help to cover the gap created by diminished federal funding. Although private support for research has grown, it amounts to only 3.5 per cent of Stanford's total research budget of $130 million a year.

The success of Stanford's own venture in commerce is necessarily still unclear. Last month, 71 companies signed licences for the gene-splicing and cloning patents developed by Stanford geneticist Dr Stanley Cohen and University of California biochemist Dr Herbert Boyer. Both scientists have made over their share of royalties to their universities. Initially, the licensing will yield $710,000 annually, but the long-term potential could be much higher.

Donald Kennedy keeps ahead

In the face of his campus's burgeoning biotechnology, Kennedy spends much of his time on the ethical questions of proprietary research. He has organized a conference in March with administrators, faculty scientists and representatives of industry to establish possible guidelines for the future. His own interest in science policy stems from his work as a founder of the human biology programme at Stanford. He was chairman of the biology department in 1965–72. His colleagues consider him a brilliant administrator and a fine scientist, able to articulate his views clearly.

Although a member of the National Academy of Sciences, Kennedy does not expect to return to the laboratory. His speciality is the neurophysiology of behaviour. He continues to work on two unpublished papers about how connections among nerve cells are responsible for fixed behavioural acts.

Meanwhile, he enjoys his contact with students and giving guest lectures, as well as advising eight freshmen. He has a reputation as an outstanding and entertaining lecturer. Thus, to illustrate man's evolution from the primitive fish *Amphioxus*, he will sing to the tune of "It's a long way to Tipperary",

Goodbye fins and gill slits,
Hello teeth and hair.
It's a long way from *Amphioxus*,
But we came from there.

Kennedy is blessed with enormous energy. But some of his faculty grumble that he is too enthusiastic, that he is also too generous, and that he resorts too quickly to resolving disagreements with university funds.

Students nevertheless like him. Graduating seniors have repeatedly asked him to address them. He attends more than 24 sherry parties annually in student dormitories.

Will his present enjoyment of his leadership of Stanford last? A close associate suggests that within five years Kennedy will start to think about a new post. It takes that long for the excitement and pleasure of the office to begin to dissipate.

At present it is possible to find Stanford's president at 6.30 a.m. each Tuesday and Friday morning running four miles over hilly terrain. Those who wish to discuss problems or to offer suggestions are welcome to join him. Most of his colleagues agree that one has to be pretty swift to outrun him.

Charlotte K. Beyers

0028-0836/82/010007 01$01.00

CORRESPONDENCE

The ultimate question

SIR — G K O'Neill's statement that we are probably alone in our galaxy (*Nature* **294**, 25, 1981) is based on two different arguments — one about the unlikeliness of the phenomenon of life and the second about the probability of the development of space colonies by any long-lived civilization I show here that there is an unexpected link between the two arguments

It may well be true that the survival of life on Earth is due to an extraordinarily lucky series of accidents by which the surface temperature remained remarkably constant On the other hand, J E Lovelock's suggestion that life itself was and is responsible for the maintenance of a life-friendly temperature, is not without evidence In his book *Gaia, a New Look at Life on Earth,* Lovelock wrote that the fact that the Earth's climate has changed very little since life appeared, despite variations in the output of heat from the Sun, was one of the reasons for developing the Gaia hypothesis This hypothesis proposes that "the entire range of living matter on Earth, from whales to viruses, and from oaks to algae, could be regarded as constituting a single living entity, capable of manipulating the Earth's atmosphere to suit its overall needs and endowed with faculties and powers far beyond those of its constituent parts" In another version of the Gaia-hypothesis Lovelock calls this entity an organism, but he prefers to talk about the "Gaia system" The word "organism" is indeed confusing when used to refer to an entity of which the constituent parts are organisms But I see no reason why this "Earth life system" (having assumed its existence) shouldn't have the property that distinguishes living systems from dead matter, namely the capability to procreate

O'Neill's second argument — "The development of space colonies is a natural and not particularly difficult stage in the development of any intelligent civilization" — can be rephrased, if we are prepared to admit that the human species and its technology is integrated in the whole of living nature, to read "The development of space craft is a natural process in every planetary life system and will lead to the creation of independent descendants (space colonies), so to ensure the pre-existence of the planetary life system"

So — is there an association between the hypothesis of an overall "organism" and the (also hypothetical) development of space colonies? It is a question that goes beyond science, and gives us a choice between heroic antropocentrism and a more objective but difficult to accept biocentrism

ROELAND A DE BIE

Rotterdam, The Netherlands

Base mettle

SIR — I was pleased to note that your editorial staff has at last discovered the greatest of American sports as reported in your column "Shame on New York" (*Nature* 5 November 1981, p 2) While your comments on the competition " quaintly known as the 'World Series" were touching and amusing, I was surprised to note a large number of errors of fact in the column Given *Nature's* reputation as a scientific journal, I am sure you will want to waste no time in correcting these

You suggested that good players are able to hit one fair ball in three Actually, good players will hit about 8 fair balls in 10, with about 3 in 10 resulting in safely reaching the first base A player who could hit only one fair ball in three would shortly be sent packing for another sport where his talents might be more appropriate to the level of play (cricket perhaps?)

You noted that the Yankees were not as skilled in catching and throwing the ball as the Dodgers This is a strange comment on an event in which one member of the Dodgers set the all-time record for most errors (serious mistakes in catching or throwing) in the "World Series" One might also have noted that members of the New York Yankees Baseball Club, once "on base", displayed a remarkable propensity for running directly towards the Dodger player in possession of the ball The only biological parallel I can think for this behaviour is that of certain species of whales running themselves aground and eventually perishing of their own weight In the interests of science, *Nature* might humbly have suggested that representative members of the Yankees should be selected for inner ear examinations or behavioural analysis during the winter I believe that Mr Steinbrenner has made similar suggestions, couched in rather different language

Finally, *Nature's* comments on the random flight of the batted ball are completely innaccurate Every baseball player is aware that while the flight of any individual batted ball is unpredictable, when a large sample of batted balls from any one individual is examined, certain patterns emerge As more and more samples are taken, a pattern of probabilities (not unlike probability patterns in electron orbitals) can be assembled and a definite and nonrandom distribution becomes clear In the case of the Dodgers, these functions fell quite frequently beyond the bounds of the playing surface In the case of the Yankees, the result of swinging the bat was that all too often the probability function for position of the batted ball reached a maximum in the glove of the catcher

KENNETH R MILLER

Brown University,
Providence, Rhode Island, USA

Another contender

SIR — I note the absence of contributions on systems ecology to your debate on evolution

The branching tree is a forceful image of evolution which has proved reasonably compatible with the limited evidence of the fossil record Recently, some palaeontologists engaged on rigorous studies of fossil lineages have come to crave some theoretical innovation which would better model the history of evolutionary progress[1] They may be suspected of trying to induce innovation by creating what they consider to be favourable conditions for an ideological revolution that is, by promoting a theory of "punctuated equilibrium" as an antithesis to "gradualism" So far, the rather unsurprising product gleaned from articles in your journal is that evolution can occur at varying rates[1,2] It also appears that evolutionary progress by punctuation of an equilibrium does not require a qualitatively different type of evolution from that predicted by the genetic theory[2]

Rates of evolution seem to depend largely on the rate of change in selective stress, which results from a changing environment for example, the gradual evolution of a species supposes gradual change in environment However, the range of physical environments has remained fairly uniform through time their geography may change but this is usually accommodated by a mobile biota New forms which evolve in small isolated populations under environmental stress are likely to be shortlived when their isolation breaks down and normal conditions return they are likely to be out-competed by more broadly adapted and numerous "ancestor" species

In contrast, the biological environment has a capacity for accretionary change[3] "Gradualists" should look to the progressive development of biological systems for their selective pressures Proponents of punctuated equilibrium might investigate the instabilities which are likely to be inherent in such systems

GILES MORRELL

Calgary, Alberta, Canada

---

1 Williamson, P G *Nature* **293**, 437-443 (1981)
2 Cronin, J E , Boaz, N T , Stringer, C B & Rak, Y *Nature,* **292**, 113-122 (1981)
3 Sepkoski, J J Jr, Bambach R K , Raup, D M & Valentine, J W *Nature* **293**, 435-437 (1981)

Is this a record?

SIR — A recent paper by Sadler[1] shows that the stratigraphic record of geological time is very incomplete In commenting on this, van Andel[2] notes that contemporary evolutionary theorists ascribe major evolutionary steps to a jump advance or "punctuation" — concentration of major change in a brief time interval

If major change happens rapidly, and rapid events are rarely preserved in the fossil record, it follows that most major evolutionary events are beyond study because they have no stratigraphic record But the actual *evidence* for a punctuational view of evolution depends on literal reading of the fossil record, that is, the assumption that gaps between successive stages of the stratigraphic record are insignificant[3] If gaps represent more time than fossiliferous strata do, gradual transitions between species will necessarily appear punctuated

Sadler himself noted "In their treatment of the fundamental character of biological evolution, Eldredge and Gould (1972) are concerned with the completeness of the record Unfortunately they tackle only the question of the abundance of fossils It is equally important to determine whether the completeness of the sediment accumulation is adequate for the recognition of 'punctuations' in the fossil record that are phyletic in origin rather than indicators of sedimentary lacunae We have attempted to quantify the sedimentary aspect, these numbers need to be matched by estimates of the duration implied by 'punctuations' "

PHILIP D GINGERICH

Museum of Paleontology,
The University of Michigan, USA

---

1 Sadler, P M *J Geol* **89**, 569 (1981)
2 van Andel T H *Nature* **294**, 397 (1981)
3 Eldredge N & Gould, S J in *Models in Paleobiology* (ed Schopf, T J M) (Freeman-Cooper, San Francisco, 1972)

NEWS AND VIEWS

University Colleges of Science & Technology
92 A.P.C Rd Cal.-9
LIBRARY COMPLEX
Departments of :
Chemical Engineering
Chemical Technology
Plastics & Rubber Technology
1982

Reservoirs and the triggering of earthquakes

from Peter J. Smith

In spite of early doubts, it is now well established that large reservoirs can generate earthquakes. When the possibility of reservoir-induced seismicity was first mooted during the mid 1960s, it was greeted with scepticism in some quarters, largely because comparable before-and-after records for the few examples then known were unavailable. Systematic seismic surveys had only been started after impounding was under way or even, in some cases, complete, and so the details of the pre-reservoir seismic background were uncertain at best. A scientifically rigorous presentation of the evidence was therefore impossible, even though in one spectacular case (Koyna, India, 1967) a large reservoir had clearly given a relatively aseismic zone the ability to kill.

But there are no doubts now, for well documented examples of reservoir-induced seismicity are known throughout the inhabited continents. In general terms, what happens is that the huge mass of water in a reservoir changes the stress patterns in the underlying rocks. The water load exerts a simple vertical pressure on the rocks immediately, whilst the pore pressure in them increases gradually as the water infiltrates at a rate that depends on their permeability and prior water content. In addition, the water reduces the rocks' coefficient of initial friction and in the longer term can change their chemical, and hence physical, properties by weathering. Even so, it is widely held that such effects are not by themselves sufficient to generate earthquakes in zones not already subject to tectonic stress. The role of the water is rather to trigger seismic events in a highly stressed system close to break point.

This is clearly the case in the Tadjikistan region of the USSR, where the Nurek reservoir has been generating seismic activity since filling began in the early 1970s. In this, as in a number of other cases, the induced seismicity is not related directly to the absolute amount of water present but to variations in it. Bursts of seismic activity are triggered when the water level changes, the intensity of the activity increasing with the rate of level change. The temporal fluctuations in the seismicity are thus easily related to the fluctuations in the phenomenon inducing it.

The spatial distribution of the seismic activity, by contrast, is less straightforward. Most of the induced earthquakes occur beneath the central part of the reservoir and upstream (southward) from it. The region containing that half of the reservoir immediately behind the dam, on the other hand, is almost completely aseismic. Yet both the seismic and aseismic zones are lithologically similar, consisting largely of Upper Cretaceous to Palaeogene shallow-water limestones interbedded with mixed components of shale and gypsum. What, then, governs the location of the induced seismicity?

The answer, as Leith *et al* have discovered (*Geology* 9, 440; 1981), lies in the varying structure and the different permeability regimes to which it leads. The limestone units in the region beneath the reservoir are highly fractured and thus relatively permeable, whereas the gypsum and shale units have very low permeability. The alternation of permeable and impermeable strata thus gives rise to a strongly directional overall permeability. Normal to the bedding the overall permeability is very low because the largely impermeable layers prevent, or severely restrict, water transport. Parallel to the bedding, however, the permeability is high because the water can easily diffuse along the permeable layers. In other words, in their originally horizontal configuration the strata would have prevented most vertical fluid migration.

The strata beneath the Nurek reservoir are no longer horizontal, although immediately upstream from the dam the effect is little different. Here the alternating layers of limestone and gypsum–shale are folded into a syncline. Any water entering one of the permeable layers could migrate to the bottom of the basin formed by that layer but would be prevented from moving any further in the vertical direction by the impermeable rock layer beneath. In this region, therefore, water cannot enter the vast mass of rock below and cannot thereby change the pore pressure. The reservoir here acts only as a load, which is insufficient to induce seismicity.

Further upstream from the dam, on the other hand, the strata are folded into a moderately plunging open anticline with the dip in the upstream direction. In this region water entering a permeable layer can diffuse along it and thus be carried to various depths without restriction. Here the pore pressure at depths does change and is sufficient to generate seismicity.

What all this amounts to in the end, of course, is yet another version of the old, old story, namely, that general geological processes governed by universal physical laws will nevertheless lead to unique consequences depending on the particular environment in which the processes take place. As far as reservoirs are concerned, it is known that the large masses of water involved can generate earthquakes, but whether and precisely where they will actually do so depends critically on local conditions.

The Nurek case shows that the pattern of induced seismicity rests upon very local conditions indeed. The lithological environment in the Nurek area is not unusually inhomogeneous on a regional scale, yet the distribution of seismic activity varies on a subreservoir scale. The obvious conclusion is that if the environmental effects of future reservoir impounding are to be predicted accurately, it will be necessary to investigate the rocks underlying the sites in no less detail. ☐

Peter J Smith is editor of 'Open Earth' *and is a Reader in the Department of Earth Sciences, The Open University, Milton Keynes MK7 6AA, Buckinghamshire, UK*

0028-0836/82/010009-02$01 00

How eggs breathe while avoiding desiccation and drowning

from Jared M Diamond

An avian egg is an almost self-contained life-support system providing all the nutrients, minerals and water necessary for the embryo's development All that is required from the outside is oxygen and heat The design of an egg involves numerous compromises It must be strong enough to resist accidental breakage, yet fragile enough for the embryo eventually to break out It must lose exactly the right amount of water during incubation neither so much that the embryo dries out, nor so little that it drowns in its own metabolic water The egg must be sufficiently impermeable to prevent drying out, yet sufficiently permeable that the embryo can acquire oxygen and get rid of carbon dioxide The egg's incubation time must be geared to its metabolic rate, size and parents' time budget The egg's size and nutrient content must be geared to the embryo's size and developmental state at birth, and perhaps to the clutch size How is all this possible?

Answers to many of these questions have come from 13 years of work at the State University of New York at Buffalo, by Hermann Rahn, Charles Paganelli, Amos Ar* (of Tel-Aviv University) and their colleagues[1] Their interest in eggs began when a new student innocently asked how eggs breathe As they had never thought about this problem, they began studies which eventually yielded the answer by diffusion The rate-limiting barrier to the egg's gas exchange is the egg shell itself, through which gas transport is diffusive, not convective Oxygen, carbon dioxide and water cross the shell at rates proportional to their gas-phase diffusion coefficients Since these gases follow identical diffusion paths, measurement of the egg's conductance to one (K_{O_2}, K_{CO_2}, or K_{H_2O}) lets one calculate the other two conductances Water flux may be simply measured as the weight loss of an egg kept in a desiccator and egg conductances for 61 species of duck[2] and 84 other species of birds[3] have been measured in this way

Diffusion occurs through microscopic pores arising from imperfect packing of the calcium carbonate crystals that make up the egg shell The pores can be visualized by putting an egg in water in a closed jar connected to a vacuum pump gas bubbles emerging over the whole surface of the egg mark the pores Underneath the shell lie two membranes of protein fibre meshwork, in turn resting on a tissue sheet called the chorioallantois in whose capillaries the avian embryo's gas exchange occurs

Bird eggs vary in size from the 300 mg of a small hummingbird to the 9 kg of the recently extinct elephant bird of Madagascar, and in incubation period from 11 to 80 days It is therefore astonishing[4] that *all* eggs lose 15 ± 2 5 per cent of their initial weight during incubation[1] As Ar and Rahn point out, the fixed water loss ensures that the egg maintains constant relative water content throughout incubation, in the face of metabolic consumption of dry matter (mainly yolk fat) and accompanying production of metabolic water Without water loss, the embryo would drown Yet why is egg water loss so constant among species, when yolk content varies with species from 14 to 67 per cent? One might guess, although it is as yet untested, that the critical variable is constancy of the embryo's tissue osmolarity — for an embryo sealed within its egg, the only means of osmoregulation is water loss

But how do different eggs ensure similar water losses? The explanation, from measurements of egg K_{H_2O} in dozens of species, proves to be that K_{H_2O} increases in direct proportion to egg weight (not to egg surface area) and in inverse proportion to incubation time K_{H_2O} is determined by knA_p/L, where n is the number of pores, A_p the mean area of individual pores, L the pore length or shell thickness and k a constant The shell and its pores are synthesized just before laying and do not change during incubation Bigger eggs have thicker shells and lower pore density but wider pores and greater fractional pore area A 10-fold increase in egg mass is associated with a 2 7-fold increase in shell thickness, an 18-fold increase in total pore area and thus a 18/2 7 = 6 5-fold increase in K_{H_2O}

Eggs of the Wedge-tailed Shearwater (*Puffinus pacificus*) and chicken, for example, are of similar size (58 *vs* 54 g), pore radius (7 6 *vs* 8 0 μm) and shell thickness (0 27 *vs* 0 35 mm), and achieve similar water losses by the time of hatching (14 *vs* 15 per cent), despite the fact that the incubation period is two and a half times longer in the shearwater (52 days) than in the chicken (21 days) This result is achieved through the shearwater having many fewer pores (3,700 *vs* 12,400 per egg), hence lower water conductance[5] (6 1 *vs* 14 4 mg H_2O per day, torr) Chickens and Red-winged Blackbirds living at high altitudes, where water loss would otherwise be high because of low atmospheric pressure and high gas diffusion coefficients, have shells with lower total pore area and lower K_{H_2O} than sea-level populations, and hence have similar water loss during incubation[6]

Regulation of water loss during incubation implies regulation not only of shell K_{H_2O} but also of nest humidity Continual release of water and CO_2 tends to humidify the nest as well as to raise nest P_{CO_2} Water vapour pressure in the nest air is always above ambient, as Rahn, Ackerman and Paganelli[7] documented by an ingenious 'egg hygrometer' This consisted of an egg emptied of its contents, refilled with desiccated silica gel, placed in the nest under the brooding adult, weighed after several days and calibrated by weighing after storage in desiccators at known relative humidities The result all nests were maintained at water vapour pressures of 18–26 torr, although the species studied ranged from Alaskan gulls and Mexican desert island gulls to ducks and songbirds Does the brooding adult measure nest microclimate and then ventilate the nest to maintain the required rate of egg water loss, ventilating more rapidly as ambient humidity rises towards nest humidity? Is the water vapour gradient chronically abolished in species nesting in humid habitats such as moss forest of tropical mountains?

One group of birds violates these patterns the mound-builders (family Megapodiidae) of New Guinea, Australia and adjacent islands Unique among the world's birds, their eggs are not incubated by body heat but by external heat sources, including volcanoes and solar radiation Several species bury their eggs in enormous mounds of rotting vegetation, which they build so that the heat of fermentation maintains a temperature of 37°C (see refs 8–10 and the figure) The humidity in these mounds is saturated The water conductance of eggs of the mound-builder *Alectura lathami* is nearly triple that of a 'normal' egg of the same size and incubation period, due to an unusually thin egg shell[11] The megapode embryo avoids suffocating in the high CO_2 levels (9 per cent CO_2!) and low O_2 levels (14 per cent O_2) in the mound, escapes drowning in its metabolic water, and still musters enough energy on hatching to spend two days digging its way up through a metre of dirt to the surface The eggs of hole-nesting and burrow-nesting birds must also be able to deal with similar problems of gas exchange

As one would expect, the metabolic rate of an egg (rate of O_2 consumption, Q_{O_2}) increases with egg size But metabolic rate also decreases with incubation time, this is because water conductance decreases with incubation time, and as O_2 and H_2O traverse the shell by the same diffusion path, an egg of long incubation time must also have low O_2 conductance Thus eggs of any size and incubation time not only lose a fixed relative amount of water (15 per cent) but also gain a fixed relative amount of O_2, 100 cm^3 per gramme of egg, over the

Jared M Diamond is Professor of Physiology at the University of California Medical School, Los Angeles, California 90024

---

*In recognition of this work Rahn, Paganelli and Ar received the Elliot Coues Award at the 99th annual meeting of the American Ornithologists Union, Alberta, 24-28 August, 1981

0028-0836/82/010010-02$01 00

The Mallee Fowl, one of Australia's mound-builders In April or May, parent birds begin digging a pit that eventually measures 10 feet wide and 3 feet deep, and rake plant litter into it With the early spring rains in August the litter begins to decompose and the birds cover it with a mound of sand up to 3 feet thick The female lays eggs one at a time, in the mound, throughout the spring The male is responsible for regulating the temperature of the eggs during the spring he opens up the mound to let excess heat escape from the compost, in summer he piles more sand onto the mound during the day to insulate the eggs from excessive heat from the Sun, and each morning opens up the mound to dispel any heat remaining from the previous day, by autumn the compost has nearly stopped fermenting and the male opens up the mound each day so the eggs can be heated by the Sun, each evening he covers the eggs with warmed sand By April all the eggs will have hatched

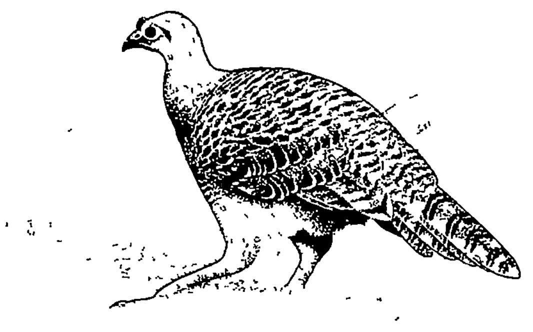

from Tim Halliday *Vanishing Birds* Penguin, 1980

incubation period[12,13] The metabolic rate is geared to the incubation time and delivers a finished chick by hatching time, whether 11 or 80 days after laying time

The energy for this metabolism comes, of course, from the yolk But not all eggs are equally endowed Altricial eggs (ones whose chick hatches in a helpless state, at an early stage of development) contain only 24 per cent yolk, so that the egg is 84 per cent water, only 6 per cent lipid and offers only 1 1 kcal energy per g weight Precocial eggs (whose chicks hatch able to fend for themselves, at an advanced stage of development) contain on the average 40 per cent yolk (67 per cent in a mound-builder), consist of 75 per cent water and 10 per cent lipid, and offer 1 9 kcal energy per g weight[14] A parent can give its chick a head-start either by producing an egg with higher yolk content or just by producing a larger egg Conversely, if a head-start is not important, a typical altricial egg saves its mother 80 per cent of the cost of manufacturing a typical precocial egg, through reduction in egg size and yolk content

The questions posed by eggs seem endless Large birds tend to lay large eggs, but egg size varies fivefold among birds of similar size belonging to different orders[15] Why, among parents weighing 100 g, does a parasitic cuckoo produce a 4 5-g egg, an owl an 11-g egg and a petrel a 21-g egg? Evolutionary biologists debate this question, as well as the puzzle why the variation in incubation time from 11 to 80 days includes a large component independent of egg size, and the question of which variable among egg size, metabolic rate, incubation time and developmental state at hatching ultimately determines the others Bioengineers debate why the relation between total weight and skeletal weight has a similar slope but a different intercept among bird eggs, molluscs, spiders, land mammals and whales[16] Students of insects, reptiles, amphibia, fish and the duck-billed platypus have barely begun to explore for eggs of these animals the questions that Rahn, Paganelli, Ar and colleagues have illuminated for bird eggs □

---

1 Rahn, Ar & Paganelli *Scient Am* 240, 46 (1979), *Am Zool* 20, 325 (1980)
2 Hoyt, Board, Rahn & Paganelli *Physiol Zool* 52, 438 (1979)
3 Ar & Rahn in *Respiratory Function in Birds, Adult and Embryonic* (ed Piper, J) (Springer, Berlin, 1978)
4 Ar & Rahn *Am Zool* 20, 373 (1980)
5 Paganelli *et al Physiologist* 23, 152 (1980)
6 Rahn, Carey, Balmas, Bhatia & Paganelli *Proc natn Acad Sci U S A* 74, 3095 (1977)
7 Rahn, Ackerman & Paganelli *Physiol Zool* 50, 269 (1977)
8 Frith *The Mallee—Fowl* (Angus & Robertson, Sydney, 1962)
9 Baltin *Z Tierpsychol* 26, 524 (1969)
10 Seymour & Ackerman *Am Zool* 20, 437 (1980)
11 Seymour & Rahn in *Respiratory Functions in Birds, Adult and Embryonic* (ed Piper, J) (Springer, Berlin, 1978)
12 Hoyt & Rahn *Respir Physiol* 39, 255 (1980)
13 Rahn & Ar *Am Zool* 20, 477 (1980)
14 Carey, Rahn & Parisi *Condor* 82, 335 (1980)
15 Rahn, Paganelli & Ar *Auk* 92 750 (1975)
16 Anderson, Rahn & Prange *Q Rev Biol* 54 1139 (1979)

Sexual differentiation and H-Y antigen

from P N Goodfellow and P W Andrews

AMONG the many problems still awaiting the application of the new techniques of molecular genetics is that of mammalian sexual differentiation The question can be simply phrased – why are males male and females female? Analysis of individuals with abnormal numbers of sex chromosomes indicates that the presence of the Y chromosome usually correlates with primary male characteristics[1] It has been suggested that this correlation is due to expression of the H-Y antigen controlled by the Y chromosome[2,3]

The study of the 'H-Y antigen' began with the observation that females from inbred strains of mice can reject skin transplanted from male mice of the same strain[4] As the only qualitative genetic differences between the mice is that the Y chromosome is present in males but not in females, the antigen responsible for the graft rejection was termed histocompatibility-Y, or H-Y, antigen[4] Although it is possible to use the transplantation assay to demonstrate that simple hormonal differences are unlikely to be responsible for the expression of H-Y antigens by males[6], detailed investigation is hampered by difficulties in quantification and limitations in the use of transplantation assays in outbred species, such as man

Serological definition of H-Y antigens

An important advance was made when Goldberg and colleagues showed that sera from female mice which had rejected male skin grafts are cytotoxic for sperm in the presence of complement, and that this activity can be absorbed by male but not female mouse cells[7] The antigen(s) recognized serologically in this way is also called H-Y, although it has not been shown whether the same determinant is being detected in the two different assays Indeed, in a mutation experiment Melvold *et al* have observed one male mouse, unfortunately sterile, that appeared H-Y negative by the transplantation assay, but was serologically H-Y positive[8] Unfortunately the only cells that are susceptible to complement-mediated lysis by these anti-H-Y sera are sperm, which are difficult to read-in the usual cytotoxicity assay, and tail skin epidermal cells[9], which are difficult to obtain Nevertheless many other cell types specifically absorb this activity, and by the absorption of syngeneic murine female anti-male sera followed by testing the residual activity on mouse sperm, serologically detected H-Y antigen is found to be strongly conserved and to be expressed on the male cells of all mammalian species tested Conservation of this determinant is also seen in animals other than mammals where H-Y antigen is found to be associated with the heterogametic sex (in mammals, males are heterogametic having X and Y sex chromosomes, whereas in birds the female is heterogametic having the so-called ZW sex chromosome constitution)[10]

This conservation and the association with one or other sex led to the suggestion that H-Y antigen was concerned in directing the organogenesis of the heterogametic gonad[2] Evidence for this has been presented and discussed elsewhere[3] Suffice it to say here that in mammals the presence of testicular tissue has generally been shown to be associated

P N Goodfellow is in the Imperial Cancer Research Fund Laboratories, Lincoln's Inn Fields, London WC2A 3PX, and P W Andrews is in the Wistar Institute, Philadelphia, Pennsylvania 19104

0028-0836/82/010011-03$01 00

with the expression of H-Y antigen, irrespective of genetic (that is, XX or XY chromosomal constitution) or phenotypic sex The converse case – the expression of H-Y antigen being associated with the presence of testicular tissues – is not always true Two explanations for individuals being H-Y antigen positive but without any testicular differentiation have been offered either the H-Y molecule is 'functionally' absent (for example, the functional part of the molecule has been mutated while it remains immunologically active, or the H-Y receptor on the target cell has been inactivated) or testicular differentiation could depend on the quantity of H-Y antigens produced, a critical level required for the induction of testicular differentiation not being reached

Technical difficulties with H-Y serology

The serological description of the H-Y antigen as outlined above is well established but this does not mean that H-Y serology is without difficulties These result from two technical problems The first is due to the sperm cytotoxicity test, which is one of the most difficult serological assays to perform The extreme reactivity of sperm with naturally occurring heterophile antibodies requires careful control not only of the H-Y antisera but also screening and absorption of the serum used as a source of complement Even the scoring of the sperm cytotoxicity test is difficult sperm are mobile and very small and it is not easy to distinguish between dead and live sperm In addition, there is often only a small difference between a positive and a negative result as the maximum kill in the assay is usually only 50–60 per cent, whilst the background kill in absence of any sera may be as high as 30 per cent Unfortunately, the alternative assays used to detect H-Y antigen, which include every imaginable variation of cell surface immunological detection techniques[11], all seem to suffer from similar problems of high backgrounds and low maximum reactions Undoubtedly this is due in part to the low surface density of H-Y antigen on many cells but it is also due to the poor-quality low titre of the anti-H-Y sera Even after repeated immunization many female mice fail to make H-Y antibodies and those mice which do respond produce low titre antisera This leads to the second problem — the small amounts of antisera that are available

The paucity of H-Y antisera has two adverse effects The first is a reduction in the exchange of antisera which is needed to standardize anti-H-Y reagents and to demonstrate that all H-Y assays are recognizing the same antigen(s) The second effect is to produce an understandable reluctance to perform quantitative absorptions (that is, multiple absorptions with varying numbers of cells), rather than the single point absorptions usually performed Quantitative absorptions are essential for the proper quantification of the amounts of H-Y antigen present This is especially important when studying cells with postulated intermediate amounts of antigen, such as has been proposed to explain the recessive inheritance of male sex-determining genes in the polled goat and in humans[12,13].

An additional problem arises with the recently introduced H-Y test based on the complement-mediated killing of Raji cells (a male human, Burkitt's lymphoma line) by antisera from female rats immunized with male rat cells[14] In this xenogeneic system absorption of anti-human heterophile antibodies is essential to ensure meaningful results Furthermore, even if this absorption is carried out satisfactorily, there is no assurance that the antigen detected by the male-specific absorption of the remaining antibodies is the same as the antigen detected by absorption of syngeneic mouse serum tested on sperm, merely because they both appear to be male associated

Conflicting results of H-Y typing

The technical difficulties and differences in methodology described above may explain the apparent contradictory results reported by the group in Freiburg associated with U Wolf and U Muller and by the workers in New York associated with S Wachtel and G Koo The German group has demonstrated that females with Turner's syndrome (those lacking one of the two X chromosomes found in normal females) express H-Y antigen, although at reduced levels compared with males[16] A similar situation has also been described in mice[17] Based on these results Wolf and his colleagues have suggested that the H-Y antigen is coded by a structural gene on an autosome, that this gene is induced by an activator coded by a Y-linked gene, and that it is repressed by the product of another regulator gene located on the short arm of the X chromosome which escapes X-inactivation in normal females They further propose that interaction of these genes can lead to continuously variable levels of H-Y expression, depending on genotype, and that a certain threshold level of H-Y is required to induce testicular differentiation[16,18] One problem is that they would predict that an excessive number of X chromosomes in a Y chromosome-carrying individual would produce sufficient H-Y repressor to overcome the activator produced by the Y chromosome, such an individual should exhibit female characteristics Nevertheless 49 XXXXY individuals with apparently male phenotype have been observed[19]

Contrary to these ideas is the older hypothesis that the H-Y antigen is specified by a gene or genes normally located on the Y chromosome H-Y antigen-positive XX males, such as are caused by the *Sxr* gene in mice, or the *Polled* gene in goats, are explained by a postulated translocation of H-Y genes from the Y chromosome to an autosome, a suggestion which has received support from molecular analysis of sex chromosome-specific DNA sequences in sex-reversed mice[20] Threshold levels for H-Y antigen activity and, perhaps multiple H-Y genes, are needed to explain why the sex-reversal properties of *Sxr* in mice are dominant whereas they are recessive in the case of the *Polled* gene in goats

Consistent with Y-linkage of the H-Y structural gene is the finding that female Turner's syndrome patients with deleted or rearranged Y chromosomes can be either H-Y antigen positive or negative[21] In particular, two patients have been described that have a Y isochromosome of the long arm These patients are H-Y antigen negative[21, 22] It is difficult to understand why XO Turner's syndrome patients are H-Y antigen positive if XYp-Turner's syndrome patients are H-Y antigen negative

Another possible point of contention between the two groups is the recent suggestion by the German group that XY fertile female wood lemmings do express H-Y antigen[23] In this species karyotypic analysis has demonstrated that some fertile females have a Y chromosome and an abnormal X chromosome, designated X* As these individuals are normally fertile, wild populations of wood lemming contain XX, XX* and X*Y females The earlier studies of Wachtel *et al* suggested that X*Y wood lemming females are H-Y antigen negative and that the abnormal X* chromosome carries a suppressor of H-Y antigen expression[24] The recent experiments yielding the opposite results (X*Y females being H-Y antigen positive) have led Wolf and Muller to propose that H-Y antigen affects its target cells via a receptor that is specified by an X-linked gene and that this gene has been deleted from the abnormal X

---

1 Davis, R *J med Genet* **18**, 161 (1981)
2 Wachtel, S S , Ohno, S , Koo, G C & Boyse, E A *Nature* **257**, 235 (1975)
3 Ohno, S *Monogr Endocr* **11**, 1 (1979)
4 Eichwald, E J & Silmser, C R *Transplantn Bull* **2**, 148 (1955)
5 Billingham, R E , Silvers, W K & Wilson, D B *Proc R Soc* **163**, 61 (1965)
6 Silvers, W K , Billingham, R E & Sanford, B H *Nature* **220**, 401 (1968)
7 Goldberg, E , Boyse, E A , Bennett, D , Scheid, M & Carswell, E A *Nature* **232**, 478 (1971)
8 Melvold, R W , Kohn, H I , Yergania, G & Fawcett, D W *Immunogenetics* **5**, 33 (1977)
9 Scheid, M , Boyse, E A , Carswell, E A & Old, C *J exp Med* **135**, 938 (1972)
10 Wachtel, S S , Koo, G C & Boyse, E A *Nature* **254**, 270 (1975)
11 Koo, G C *Hum Genet* **58**, 18 (1981)
12 Wachtel, S S , Basrur, P & Koo, G C *Cell* **15**, 279 (1978)
13 de la Chapelle, A , Koo, G C & Wachtel, S S *Cell* **15**, 837 (1978)
14 Fellous, M *et al J exp Med* **148**, 58 (1978)
15 Wachtel, S S *et al New Engl med J* **293**, 1070 (1975)
16 Wolf, U *et al Hum Genet* **54**, 315 (1980)
17 Engel, W , Klemme, B & Ebrecht, A *Hum Genet* **57**, 68 (1981)
18 Wolf, U *Hum Genet* **58**, 25 (1981)
19 Simpson, J L *Disorders of Sexual Differentiation and Clinical Delineation* (Academic, New York, 1976)
20 Jones, K W & Singh, L *Hum Genet* **58**, 46 (1981)
21 Koo, G C *et al Science* **198**, 940 (1977)
22 Rary, J M , Cummings, D K , Jones H W & Rock J A *J Heredity* **70**, 78 (1979)
23 Wolf, U & Muller, U *Hum Gene Mapping* **6** (in the press)
24 Wachtel, S S *et al Nature* **264**, 638 (1976)
25 Koo, G C , Chaganti, R & Hammerling, U *Hum Genet* **57**, 64 (1981)
26 Koo, G C & Varano, A *Immunogenetics* **14**, 183 (1981)
27 Simpson, E & Matsunaga, T *Transplantation* **27**, 295 (1979)
28 Goodfellow, P N & Tippett, P *Nature* **289**, 404 (1981)

0028-0836/82/010012-02$01 00

chromosome of the wood lemmings[23]

Two explanations may be offered for these opposite results Either there are two populations of wood lemming such that both H-Y$^+$ and H-Y$^-$ X*Y females occur, or, because the authors are using different antisera and different techniques, they are actually studying different antigens

Future prospects

As in many other fields, monoclonal antibodies potentially offer a solution to the many problems of H-Y antigen serology Monoclonal antibodies, which could be freely exchanged between different groups, will undoubtedly form the basis of agreement for the serological definition of the H-Y antigen One such monoclonal antibody has recently been described[25] and attempts have been made to demonstrate identity between the antigen recognized and H-Y defined by cell-mediated cytotoxicity[26], an *in vitro* assay which correlates well with transplantation rejection[27] Other monoclonal antibodies, which apparently recognize products controlled by the Y chromosome, are being studied in several laboratories (ref 28, S Wachtel, personal communication, M Fellous, personal communication) Next year we should know much more about serologically defined antigens controlled by the Y chromosome ☐

Electrostatic interactions in proteins

from Janet M Thornton

PROTEINS are very polar molecules Almost two-thirds of the twenty amino acid side chains are polar and four are charged at neutral *p*H In addition, the arrangement of electrons on the backbone peptide groups gives rise to dipoles which, in the α-helix, align to give a helix macrodipole equivalent to a half unit of charge at each end of the helix (see ref 1 for a review) In analysing protein structure, attention has been focused on the interactions of polar groups with water, a fundamental rule being that polar groups are exposed to solvent, or, where buried, form hydrogen bonds or salt bridges By contrast, interactions between charged groups and dipoles within proteins have received little attention It has been assumed that because all the ionized groups are exposed to water, the electrostatic contribution to free energy will be small, if not zero[2] Two papers[3,4] recently published in *Nature* suggest, however, that the electrostatic interactions between charges and dipoles make important contributions to protein stability and may play a significant part in determining protein structure

Wada and Nakamura[3] consider the relative distribution of positive and negative charges (including the equivalent helix dipole charges) in fourteen proteins For every possible pair of charges e_i, e_j separated by r_{ij} in the protein, they calculate the electrostatic interaction, e_ie_j/r_{ij}, and sum pairwise interactions within a given separation range By comparing the distributions as a function of r for attractive and repulsive interactions they find that there are considerably more attractive, than repulsive, interactions at small separations In other words, a charged group, including the apparent charges of the helix dipole, is on average surrounded by charges of the opposite sign This had already been shown to be true for myoglobin[5] but, surprisingly, it is the first unequivocal proof that charged groups in general are not distributed randomly on the surface of proteins The suggestion is that the charges, including the α-helix dipoles, contribute to the stability of the protein This is an important result because it does not depend on dielectric constant, which is notoriously difficult to evaluate reliably for proteins

The problem of how much energy the charge interactions contribute to the protein is much more difficult Wada and Nakamura evaluate the electrostatic energy of the interactions using the method of Tanford and Kirkwood[6] with the internal dielectric constant set to 4 and the external dielectric constant that of water, at 80 The electrostatic energies they obtain for the fourteen proteins range from +5 kcal mol^{-1} for trypsin to -595 kcal mol^{-1} for liver alcohol dehydrogenase The model does not, however, adequately allow for the different dielectric environments felt by side chains in a complex protein structure Many charged groups are completely exposed to solvent and their electrostatic interactions will be correspondingly decreased Gurd and co-workers[7] have tackled this problem by incorporating a solvent accessibility parameter which reduces electrostatic interactions between exposed groups Their calculation for charge–charge interactions in myoglobin reduces the calculated electrostatic free energy from approximately −400 kcal mol^{-1} to -8 5 kcal mol^{-1} This energy contribution is more reasonable, although the lack of comparable experimental data is a problem

In the hydrophobic interior of the protein electrostatic interactions are much stronger than those between charges exposed to solvent on the surface of the protein Hol *et al*[4] use this argument to suggest that the interactions between the helical dipoles, which are predominantly buried, make a significant contribution to protein stability Their main observation is that a pair of anti-parallel helices is energetically more favourable than a pair of parallel helices, because of the electrostatic interaction between the peptide dipoles The energy difference is evaluated by using the formal charges, assigned to the peptide backbone to mimic the observed dipole moment, and calculating the coulombic interaction e_ie_j/r_{ij} They argue that a macroscopic dielectric constant is inappropriate at the level of atom–atom interactions in the hydrophobic core, and claim their energies are incorrect by no more than a factor of 2 Using this method, the anti-parallel arrangement is more stable, by almost 20 kcal mol^{-1}, than its parallel equivalent They suggest that this electrostatic contribution may have a significant role in determining the observed preference for the anti-parallel arrangement of helices in the all-helical proteins For four of these proteins the dipolar electrostatic stabilizations range from -5 to -23 kcal mol^{-1}

In the α/β proteins with alternating α-helices and β-strands, the α-helices lie approximately parallel, maximizing unfavourable dipolar interactions However, Hol *et al* point out that in parallel β-sheets there is also some alignment of the peptide dipole, which gives a small macrodipole, equivalent to one-fifteenth of a unit of charge at each end of the strand This dipole, together with the fact that the helices are usually tilted because of the twist of the sheet, effectively cancels out the unfavourable interactions

Clearly the helix dipole interactions do contribute to the stability of the anti-parallel helices However, the number of kilocalories involved has yet to be satisfactorily evaluated The figures calculated by Hol *et al* provide the maximum possible stabilization to be derived from dipole interactions Most helices are partially, if not predominantly, exposed, especially in the small all-helical proteins, so presumably some of the peptides will be in contact with solvent However, the closest contacts will be in the hydrophobic core, so although this effect should be considered, perhaps in terms of solvent accessibility, it may not markedly affect the energies

The importance of the electrostatic dipole interactions for determining the anti-parallel alignment of helices and thus protein folding is difficult to assess Many other factors are involved, whose energies may be even more difficult to quantify Topological considerations are one such possibility For every parallel interaction between two sections of chain there must be an anti-parallel connection For example, in the parallel β-barrels, such as in triose phosphate isomerase, the helical connections run approximately anti-parallel to the strands Therefore, we would expect anti-parallel connections to be more common The dipole interactions

---

Janet M Thornton holds an SERC Advanced Fellowship at Birkbeck College, Malet Street, London WC1E 7HX

0028 0836/82/010013 02$01 00

will help stabilize the anti-parallel arrangements, although since the dipoles must be buried to make any significant contribution to energy, they only become important once the hydrophobic core of the protein has been formed

To conclude, both these papers draw our attention to the contribution which charged groups, including the α-helical dipole, make to protein stability The difficulty of assigning an effective dielectric constant, or indeed if a macroscopic dielectric constant is valid for these atom–atom interactions, has yet to be satisfactorily solved and needs urgent attention More experimental data for electrostatic energies or effective dielectric constant, such as that provided by Rees[8], would be of enormous value With high-resolution coordinates now available for many proteins, it should be possible to characterize charge interactions in detail A more exciting possibility is that charged groups, being on the surface of proteins, will be of general importance for recognition between molecules, including protein–DNA interactions Preliminary evidence from the cytochrome *c* peroxidase structure[9] and the assembly of tobacco mosaic virus subunits[10] lends support to this hypothesis Perhaps it is in this context that direct electrostatic interactions may prove most significant ☐

---

1 Wada, A *Adv Biophys* **9**, 1 (1976)
2 Finney, J L , Gellatly, B J , Golton, I C & Goodfellow, J *Biophys J* **32**, 17 (1980)
3 Wada, A & Nakamura, H *Nature* **293**, 757 (1981)
4 Hol, W G J , Halie, L M & Sander, C *Nature* **294**, 532 (1981)
5 Friend, S H & Gurd, F R N *Biochemistry* **18**, 4620 (1979)
6 Tanford, C & Kirkwood, J G *J Am chem Soc* **79**, 5333 (1957)
7 Friend, S H & Gurd, F R N *Biochemistry* **18**, 4612 (1979)
8 Rees, D C *J molec Biol* **141**, 323 (1980)
9 Poulos, T L & Kraut, J *J biol Chem* **255**, 10322 (1980)
10 Bloomer, A C , Champness, J N , Bricogne, G , Staden, R & Klug, A *Nature* **276**, 326 (1978)

100 YEARS AGO

A SPECIAL despatch has been received at St Petersburg from M Sullowsky, dated Irkutsk, December 26 (O S) 1881, which says "At 10 o'clock on the morning of August 9 I parted with the *William Rodgers*, which shaped her course for Herald Island The clipper *Strelok* then returned to the Chinese ports Up to that time the *Strelok* and *William Rodgers* had kept company They were joined in Providence Bay by an American schooner, having on board the captain of a whaler which had stranded This captain narrated that he had seen a boat with dead men on board which had been driven upon Herald Island The boat also contained, besides other articles, some silver spoons with the name *Jeannette* engraved on them In consequence of this narrative the captain of the *William Rodgers* resolved to proceed to Herald Island with the view of wintering there, and, with the aid of dogs purchased in Kamschatka, sending out his crew in small parties to the various sides of the island and its vicinity to search for the lost explorers "

Admiral Mouchez will give his usual annual *soirée* at the Paris Observatory in March He had distributed to the leading Parisian engineering firms the conditons for the construction of the cupola for the great equatorial to be built in the newly-annexed grounds The diameter of the revolving cupola is to be 20 metres The form must be hemispherical The time required for rapid revolution is 10 minutes It is to revolve in the same direction as the heavens, and the mechanism will cause the revolution of a seat for two astronomers

From *Nature* **25**, 249 & 250, January 12, 1882

Cell mediated immunity in theileriosis

from F E G Cox

THERE are strong indications that antibody does not play a major role in the immune responses to parasitic protozoa that inhibit nucleated cells but there is some evidence that antibody-independent cell-mediated mechanisms may play a part in protection and recovery Such mechanisms may involve lymphocyte mediated cytolysis (Class I reaction), soluble lymphocyte products (Class II reaction) or natural killer (NK) cells but these mechanisms, although well characterised in mice, are difficult to implicate in the parasitic diseases of man and domesticated animals It is, however, now clear that cell mediated cytolysis plays a major, if not the major, part in the immune response to one of the most important protozoan diseases of cattle, a form of theileriosis known as East Coast Fever

Theileriosis is caused by several species of *Theileria*, of which *T parva*, in Africa, and *T annulata*, which occurs in North Africa, the Mediterranean area and elsewhere, are the most important Considerable mortality results, particularly in calves Theileriosis is a tick-borne disease and cattle become infected when sporozoites are injected by an infected tick The sporozoites enter lymphocytes in which they grow and undergo nuclear division giving rise first to macroschizonts and later microschizonts, the products of which infect red blood cells and thence ticks once again While in the lymphocytes the parasites cause the host cells to undergo rapid division transforming them into what are effectively lymphoblastic cell lines During the stage of macroschizont production there is an accompanying massive destruction of lymphocytes and the infected animal becomes ill and may die

Theileria sporozoites can also transform lymphocytes *in vitro*[1-2] and the availability of such lymphoid cell lines has provided scientists with an ideal opportunity to study cell mediated immune responses against cells of the same genetic type, for uninfected cells can be taken from an animal before infection, transformed and maintained for subsequent study during the course of an infection[3] Scientists at ILRAD (International Laboratory for Research on Animal Disease, Nairobi) have followed *T parva* infections in groups of cattle that died from theileriosis, recovered naturally from the disease or were protected by being infected and treated at the same time with a long acting tetracycline[4-7] In unprotected cattle, by day 14 after infection there was evidence of nonspecific cytotoxic activity against both infected cells and unrelated cells of a mouse tumour line[5] suggesting a mechanism similar to the natural killer (NK) cell phenomenon seem in mice and humans[8] In immunised cattle, on the other hand, small numbers of macroschizonts were detected during days 15-18 after infection and cytolysis was confined to genetically identical infected cells[5-6] An analysis of the mechanisms involved implicated thymus derived lymphocytes as the effector cells[7] and a restriction mechanism whereby effector cells have to recognise both foreign antigens and self antigens simultaneously[6] This is characteristic of class I cell mediated immune responses such as are seen in virally altered cells[8] Although the details of class I reactions and the nature of restriction in cattle remain to be determined all the evidence suggests that in theileriosis the main component of the immune response is the recognition of theilerial antigens on infected cells and the subsequent destruction of these cells by thymus derived lymphocytes

The significance of this work is that it demonstrates the importance of cell mediated immunity in the natural host of an important protozoal disease and also extends the phenomenon of cytolytic restriction to the protozoa Thus theileriosis joins leishmaniasis[9] as examples of intracellular protozoa that are controlled by cell-mediated immune responses, class I in the case of the former and class II in the latter, giving support to the suggestion that the main function of the major histocompatibility complex (MHC) molecules is to guide T lymphocytes to deliver appropriate responses to diverse kinds of infection[10] The diseases of man caused by *Toxoplasma gondii* and *Trypanosoma cruzi*, which are also intracellular, may soon yield up their secrets ☐

F E G Cox is Professor of Zoology at King's College London

---

1 Brown, C G D *et al* *Nature* **245**, 101 (1973)
2 Pearson, T W *et al* *Nature* **281**, 678 (1979)
3 Emery, D L & Morrison, W I *Immunology* **40**, 229 (1980)
4 Allison, A C & Eugui, E M *Amer J Path* **102**, 114 (1981)
5 Emery, D L *et al* *Immunology* **43**, 323 (1981)
6 Eugui, E M & Emery, D L *Nature* **290**, 251 (1981)
7 Emery, D L , Tenywa, T & Jack, R H *Infect Immunity* **32**, 1301 (1981)
8 Doherty, P C & Zinkernagel, R M *J exp Med* **141**, 502 (1975)
9 Cox, F E G *Nature* **291**, 111 (1981)
10 Mitchison N A *Immunology Today* **1**, 91 (1980)

0028-0836/82/010014-02$01 00

Oddities in the initiation of translation

from Peter Model

A report from Kastelein, Remaut, Fiers and van Duin in this issue of *Nature* (p 35) suggests that we may need to modify some of our ideas on how translation is initiated — at least in the particular case of the lysis gene of bacteriophage MS2 Most researchers have concluded that translation is initiated independently at each gene, even in multi-gene operons It may be that mRNA structure will occlude the initiation site at a particular place, and in such instances translation of a preceding gene may be required for effective initiation at some cistrons, but this has generally been viewed as a secondary, complicating phenomenon which obscures the otherwise fundamentally independent nature of the initiation process

Kastelein and his colleagues now present very persuasive evidence that initiation at the lysis gene requires translation of the preceding coat gene and a shift in the reading frame of at least some of the ribosomes into the +1 frame which, in turn, leads them to terminate at an *ochre* codon three nucleotides before the initiating AUG start codon This termination is required for translation of the lysis gene for if the *ochre* codon is removed, translation is abolished If by suitable manipulation of the cloned gene a frame shift is introduced which forces all or most of the ribosomes into the +1 frame, initiation is enhanced Translation of the lysis gene is strictly dependent on active translation at the coat cistron, supplying coat protein in *trans* does not replce this requirement

These data strongly suggest that there is something special about ribosomes that have just terminated at the *ochre* codon that they are in a state which facilitates initiation at sites which would not normally be translational initiators It is not yet clear what this special property might be, it could be a special state of the ribosome, or retention of the 30S ribosomal subunit on the RNA after termination of synthesis It has been noted previously that termination at various chain-terminating codons within genes facilitates re-initiation at specific distal sites, although here too the mechanism (s) remains undefined

These observations would at first glance seem to run counter to recent *in vitro* results from Kaji's laboratory Ryoji, Berland and Kaji (*Proc natn Acad Sci U S A* **78**, 5973, 1981) report that when they removed the ribosome release factor from *Escherichia coli* ribosomes and then supplied an RNA containing an amber mutation as template, these release factor-depleted ribosomes synthesize two fragments of the relevant protein One starts at the usual initiating methionine and stops at the *amber* codon, while the other starts at the codon immediately after the *amber* codon and ends at the normal C terminus of the protein Ryoji *et al* argue that this result excludes 'special conformation' or 'sterile pass' models of ribosome initiation following termination They conclude that when a ribosome terminates it either dissociates completely or else starts again at the very next codon The characterization of the products of the release factor-depleted ribosomes was careful and thorough, the question that remains is whether there is any relationship between the behaviour of these release factor-depleted ribosomes *in vitro* and the phenomenon described *in vivo* by Kastelein *et al* Kaji and co-workers have carefully characterized an experimental system of their own design which may shed light on the mechanism of termination/initiation, but which may not be relevant to the genesis of the phenomena described by Kastelein *et al* They propose on the basis of their rather specific *in vitro* work that there are only two possible fates for a ribosome when it reaches a stop codon release with no special state, or retention on the mRNA, in which case it will simply start protein synthesis at the next codon The *in vivo* studies from Van Duin's lab suggest that other possibilities are available, and have been exploited by the RNA phages ☐

Peter Model is in the Rockefeller University, 1230 York Avenue, New York, NY 10021

Magnetic messages from the Earth's core

from David Gubbins

OVER the centuries the Earth's magnetic field has shown marked changes This 'secular' variation, known even to the early navigators, almost certainly originates in the core of the Earth and provides one of the few sources of information about the physical processes that occur there Shorter-duration magnetic field changes can also be recorded (on a time scale of a few years) but are hard to interpret because of the difficulty of separating changes in intrinsic magnetism from the short-term influences of the Sun and the upper atmosphere The major problem at present is how best to make use of the information provided by the secular changes

Alldredge[1] has recently proposed a model of intrinsic field fluctuation The fluctuation propagates up through the Earth's mantle, which is a rather poor conductor of electricity, and his model produces surprisingly sharp changes at the surface In consequence, if we are to decipher these signals from the interior of the Earth, we must measure and study even shorter-period wavelength variations than hitherto This important conclusion stands quite independent of Alldredge's specialized and rather arbitrary models, and it is timely coming soon after the MAGSAT mission which has provided the most complete and accurate magnetic chart we have ever had[2] Unfortunately MAGSAT only flew for a few months, not long enough to chart the secular changes with any accuracy At present the best data for this purpose come from permanent magnetic observatories A second MAGSAT, flown about five years hence, would yield vastly more accurate and complete information

The liquid core of the Earth extends out to about one-half the radius, is made mainly of iron, has a viscosity rather like water and is a better electrical conductor than copper The mobility of this liquid causes the magnetic field to change through electromagnetic induction The phenomenon occurs very rapidly in geological terms, the fluid moving at a rate of a few millimetres per second

Secular change was much discussed, even in the earliest days of geophysics Halley, like others of his time, believed the magnetic field to be due to magnetized rocks. The secular changes could not be due to motion of rocks near the surface because the required speed would be too great, so Halley proposed that the interior of the Earth was hollow, and that an inner, magnetized sphere was rotating westwards, generating the slow westward drift of the magnetic field pattern[3] This remarkable theory came 200 years before the discovery of a liquid core by seismology With modern ideas of a 'hot' Earth and a liquid iron core we can now deduce a value of the core radius from magnetic measurements alone[4]

The big snag is that we do not yet fully understand the dynamo theory of the origin of the magnetic field itself, and therefore there are no really satisfactory models of the field changes in the core Alldredge uses a very common mathematical device representation by a distribution of dipole sources These dipoles have no physical meaning whatever, unless one wants to adhere to Halley's ideas of moving magnetized rocks and represent them by little bar magnets in the core, which is not the intention Granted a source of field,

---

David Gubbins is in the Department of Earth Sciences, University of Cambridge, Cambridge CB3 0EZ.

0028-0836/82/010015-02$01 00

there is still a serious theoretical difficulty in propagating magnetic disturbances through a liquid conductor, and in order to make progress Alldredge has been forced into treating the core as a solid, thus substituting the theory of electromagnetic propagation for the much more difficult hydromagnetic theory But the physics of the two situations are very different a liquid, for example, allows propagation of a variety of waves which are impossible in a solid, and these waves will allow magnetic variations to propagate, when in a solid they would be screened due to electrical conduction In fact the core possesses a whole spectrum of free hydromagnetic oscillations[5].

Although hydromagnetic theory is difficult, it is possible to describe the induction process in the core by Maxwell's laws On the time scale over which we have observations, say 10–20 years, the electrical conductivity of the core is so high that resistance effects can be ignored This assertion can, and has been, tested against observation One might hope, therefore, to infer the motion of the fluid at the top of the core from magnetic observations, but this is not possible[6] unless we can confidently make further assumptions about the forces driving the flow However, recent work has shown how to find some general features of the core flow even though a detailed map of the motions may be beyond our grasp For example, upwelling of liquid from deep inside the core can be measured at points where the magnetic field at the core attains a maximum of minimum vertical component Surprisingly, the upwelling is very small at these locations[7], suggesting that the liquid is not convecting strongly, at least near its upper surface

This and other recent proposals[8] suffer from the poor quality of available data Field changes are monitored at only a few Southern Hemisphere sites The field must be projected down onto the core surface before it can be interpreted — a procedure well understood in principle but inherently unstable when the observations are inaccurate or sparse Two recent models of the secular change for 1965 agree quite well at the surface of the Earth but differ by factors of up to two or three at the core The differences are due in part to the methods that are used in computing the models from the observations, and not all to inadequate data, so that while we wait for another MAGSAT there is still hope for improvements in models of past years by new analytical methods. □

1 Alldredge, L R *J geophys Res* **86**, 7957 (1981)
2 Barraclough, D R *Nature* **294**, 14 (1981)
3 Halley, E *Phil Trans R Soc* **17**, 470-478 (1692)
4 Hide, R & Malin, S R C *Proc. R Soc* **A374**, 15 (1981)
5 Hide, R *Phil Trans R Soc* **A259**, 615 (1966)
6 Backus G E *Phil Trans R Soc* **A263**, 239 (1968)
7 Whaler K A *Nature* **287**, 528 (1980)
8 Barton, E R *Phys Earth planet Int* **20**, 111 (1979)

Animal disease and conservation

from Geoffrey R Smith

WHEN the material interests of man and the well-being of wild animals are considered side by side, real conflicts of interest emerge Advances in human medicine lead to the growth of population, an increased demand for land and a corresponding loss in wildlife habitat Environmental pollution is a well recognized side effect of industrial development Less well understood by many is the threat to wild animals from infectious disease Fatal or incapacitating infections may be introduced by domestic animals, and there can also be times when the destruction of wildlife becomes necessary to protect man and domestic animals from disease These matters were considered at a recent symposium* held at the Zoological Society, under the general chairmanship of Sir Andrew Huxley, PRS.

From 1889 to 1898 rinderpest swept from North-east Africa to the west coast and Cape of Good Hope in a 'virgin-ground' panzootic that produced catastrophic losses in cattle and many wild ungulate species (W Plowright, ARC Institute for Research on Animal Diseases) The disease was eliminated from southern Africa, but a focus of mild permanent infection later became established in the Serengeti region Rinderpest disappeared from both cattle and game in that region in about 1964, after cattle had been treated with attenuated tissue-culture vaccine for several years Between 1961 and 1971 the number of buffaloes and wildebeest in the Serengeti more than doubled, probably largely because the young no longer died from rinderpest There are now 1–15 million highly susceptible wild ungulates in the Serengeti. Once again they are under threat of invasion by rinderpest from the north-east Plans need to be made now to meet this threat

Although antigenically very similar, rabies virus strains from vampire bats in South America and foxes in western Europe have characteristic features detectable by monoclonal antibodies Bats and foxes are sometimes killed as a means of controlling rabies When fox population density falls below 0 3 per km^2 the disease disappears An alternative strategy, still experimental but possibly of great significance, is the use of attenuated virus, concealed in chicken-head baits, to immunize foxes The oral-vaccine virus multiplies in the tonsil and so far shows no sign of reversion to virulence (F Steck, Vet.-Bakteriologisches Institut, University of Bern)

The role of animal infections in the origin and spread of human influenza pandemics is still the subject of much speculation (M Kaplan, Pugwash Conferences on Science and World Affairs, Geneva) Inter-species infections can and do occur on occasion, apparently when mutations and recombinations take place The segmental mode of replication of influenza virus favours recombinative encounters between human and animal strains Wild birds, in which infection is mainly intestinal and symptomless, constitute an ineradicable reservoir of the everchanging virus — a reservoir that is a permanent potential threat to man and other animals Recent observations on whales, seals and terns show that influenza in wildlife is not always subclinical, and that high mortality can occur

Botulism kills millions of waterfowl annually on lakes and marshes throughout the world, and no radical control methods are known (G R Smith, Institute of Zoology, The Zoological Society of London) Mud from certain localities, such as the Camargue, inhibits the growth of *Clostridium botulinum* Our knowledge of the inhibitory mechanisms is incomplete, and a deeper understanding might give some hope for control As an adjunct to wetland management, surveys for the causative organism are advocated to distinguish between areas of high and low risk

The evidence that bovine tuberculosis infection is transmitted from badgers to cattle is irrefutable, and the impossibility of separating the two species physically or protecting them adequately by vaccination has necessitated the policy of gassing badgers in the south-west of England (Sir William M Henderson) While research on the problem continues, the present control policy cannot be abandoned without causing suffering for us all — human beings, cattle and, not least, badgers.

It is impossible to generalize about the part played by disease in the control of numbers of wild animals in comparison with that due to water and food supply But what the symposium made absolutely clear is that the whole field of animal disease is now of major importance The subject overlaps at almost every point with that of disease in man and in domesticated animals and offers a great intellectual challenge to the research worker □

---

*The proceedings of the symposium on 'Animal disease in relation to animal conservation', held at the Zoological Society of London on 26 and 27 November 1981, will be published for the Society by Academic Press in the series '*Symposia of The Zoological Society of London*'

Geoffrey R Smith is Head of the Department of Infectious Diseases, The Institute of Zoology, Regent's Park, London NW1 4RY

0028-0836/82/010016 01$01 00

Nature Vol 295 7 January 1982

Ion-supported tori and the origin of radio jets

M. J. Rees*, M. C. Begelman*‡, R. D. Blandford† & E. S. Phinney*

* Institute of Astronomy, Madingley Road, Cambridge CB3 0HA, UK
† Theoretical Astrophysics, California Institute of Technology, Pasadena, California 91125, USA
‡ Department of Astronomy, University of California, Berkeley, California 94720, USA

While apparently supplying tremendous power to their extended radio-emitting regions, the nuclei of most radio galaxies emit little detectable radiation. It is proposed that at the centre of each is a spinning black hole surrounded by a torus of gas too hot and tenuous to radiate efficiently. The torus anchors magnetic fields which extract rotational energy from the hole in the form of two collimated beams of relativistic particles and fields. These in turn drive the observed radio jets and hot spots. A large supply of accreting gas is thus unnecessary and radio galaxies may be interpreted as starved quasars.

ALL extended radio sources seem to be associated with elliptical galaxies or quasars, and the evidence[1] suggests that quasars too are located in ellipticals. As the present number-density of dead quasars is comparable with that of elliptical galaxies[2,3], it is reasonable to suppose that radio sources are powered by $\sim 10^8 M_\odot$ black holes[3] left over from a quasar phase. A long-standing problem in the theory of active galactic nuclei has been that of finding a supply of nuclear gas adequate to 'feed the monster'. Stars in the galactic nucleus cannot provide more than $\sim 10^{-3} M_\odot \text{yr}^{-1}$, unless conditions are so extreme that stellar collisions dominate the evolution[4]. Gas originating further out must dispose of substantial angular momentum to enter the nucleus[5,6], and it must do so before succumbing to galactic winds or star formation.

The observational evidence is less ambiguous: radio sources almost certainly do have low fuelling rates. Low-luminosity double-jet radio sources of the sort being mapped with the VLA generally have no detectable nuclear emission in the optical or X-ray bands; of the more powerful double hot spot radio sources, only a few (such as 3C390.3 with $\sim 2 \times 10^{44} \text{erg s}^{-1}$ in both optical and X-ray bands[7], and Cygnus A with $\sim 2 \times 10^{43} \text{erg s}^{-1}$ in optical continuum[8]) have nuclear luminosities above $10^{42} \text{erg s}^{-1} = 10^{-4} M_8^{-1} L_{\text{Edd}}$ (refs 9, 10). They cannot be produced by any process requiring super-Eddington luminosity, unless the hole mass is very small. This it cannot be because (even aside from the progenitor argument) some low-luminosity radio sources have giant ($\sim$Mpc) extensions with minimum energies[11] of up to $2 \times 10^{60} \text{erg s}^{-1} = 10^6 M_\odot c^2$. Even if we make optimistic estimates of the efficiency of the central 'engine' and of the likely efficiency with which power emitted from the nucleus can accelerate relativistic electrons in the radio lobes, we must conclude that a mass of at least 10^7–$10^8 M_\odot$ is involved (in computing the powers and energies above, we have used a Hubble constant of $H_0 = 50 \text{ km s}^{-1} \text{Mpc}^{-1}$).

Recent VLBI observations[12–17] have corroborated the view that the jets which power extragalactic sources are collimated on scales $\leqslant 1$ pc. These observations reveal small-scale structure which is generally aligned with larger-scale structure. Misalignments of up to ~45°, which have been found in the core-dominated superluminal sources, are probably caused by viewing a slightly curved jet along an almost parallel line of sight. In the case of the cores of extended radio sources, however, the alignment is fairly good. Any mechanism which purports to explain them must, therefore, be capable of producing collimated jets of at least trans-relativistic velocities while radiating as waste heat much less than an Eddington luminosity. Furthermore, it must, at least in some more extreme sources, put orders of magnitude more power into the jet than escapes as (detectable) radiation from the nucleus. These constraints rule out the class of models involving thick disks supported by radiation pressure[18–25].

Sub-critical accretion

To understand radio sources, we should therefore study accretion at very low rates, $\dot{M} \ll \dot{M}_{\text{Edd}} \equiv L_{\text{Edd}}/c^2$. Accreted gas should carry with it some magnetic flux, and shearing motions will maintain the magnetic field energy $B^2/8\pi$ at a significant fraction β^{-1} of the pressure P. The Larmor radius is then, for the applications which interest us, about 10 orders of magnitude smaller than the scale of the flow. Ordinary 'molecular' viscosity will consequently be suppressed, and magnetic (or possibly turbulent) viscosity will probably govern the shear stress. The viscous stress may be written as αP, where estimates of magnetic viscosity suggest $\alpha \geqslant 0.01$ (ref 26). Although this estimate is uncertain, there is no reason why α should diminish as $\dot{M}$ falls: if α is fixed, the torque per unit mass will be independent of $\dot{M}$ (except insofar as the disk structure depends on $\dot{M}$). Thus the inflow time in a disk of half-thickness $h(r)$ around a hole of gravitational radius $r_g = GM/c^2$,

$$t_i = \alpha^{-1}\left(\frac{r}{r_g}\right)^{3/2}\left(\frac{h}{r}\right)^{-2}\left(\frac{r_g}{c}\right) \qquad (1)$$

does not depend explicitly on density. (See refs 27–29 for the standard theory of thin disks with $h \ll r$.) The cooling time, on the other hand, is inversely proportional to the density.

The thickness of the disk depends on how fast it can radiate (or otherwise dispose of, say by a wind) the binding energy liberated by viscous stresses. The major cooling mechanisms available to the accreting matter are illustrated in Fig. 1. Depending on initial conditions and external perturbations the matter may find itself in any of several temperature states. In fact, for $10^{-7} \leqslant (\dot{M}/\dot{M}_{\text{Edd}})\alpha^{-2} \leqslant 50$ there are two self-consistent solutions to the fluid and radiation equations.

One is a thin, dense disk that remains at $\sim 10^4$ K. If matter with well defined angular momentum is fed in steadily (with high angular momentum) at a large radius, and there are no traumatic perturbations, this cold disk should be selected. These disks are, however, subject to instabilities[5,30,31], and if heated up and thickened, they will thereafter be unable to radiate the energy dissipated by viscous stresses, and will inflate to become pressure-supported tori with vortices along the rotation axis (see Fig. 2). The hot torus solution will also be selected if cool matter is preheated by high-frequency non-thermal radiation (for example, from a jet), or if the gas is supplied hot (for example by colliding stellar winds[6] or by tidal disruption of stars[32,33]). Both of these latter examples lead to flows which join naturally onto the ones described here.

0028-0836/82/010017—05$01.00

For an optically thin disk to radiate by bremsstrahlung, the energy dissipated between r and $r/2$, the accretion rate must satisfy

$$m = M/M_{\mathrm{Edd}} \geqslant \alpha_{\mathrm{f}}^{-1}\left(\frac{m_{\mathrm{p}}}{m_{\mathrm{e}}}\,\frac{r_{\mathrm{g}}}{r}\right)^{1/2}\alpha^{2}\left(\frac{h}{r}\right)^{2}, \quad r > \left(\frac{h}{r}\right)^{2}\left(\frac{m_{\mathrm{p}}}{m_{\mathrm{e}}}\right)r_{\mathrm{g}} \qquad (2a)$$

$$m \geqslant \alpha_{\mathrm{f}}^{-1}\alpha^{2}\left(\frac{h}{r}\right)^{3}(\log\gamma_{\mathrm{re}})^{-1}, \quad r < \left(\frac{h}{r}\right)^{2}\left(\frac{m_{\mathrm{p}}}{m_{\mathrm{e}}}\right)r_{\mathrm{g}} \qquad (2b)$$

where $\alpha_{\mathrm{f}} = 1/137$ is the fine structure constant and $\gamma_{\mathrm{re}} = 3\,\mathrm{k}T_{\mathrm{e}}/m_{\mathrm{e}}c^{2}$ Hence at the low accretion rates of interest ($m \simeq 10^{-4}$), a disk once heated to $T \approx T_{\mathrm{virial}} = (m_{\mathrm{p}}c^{2}/3k)(r_{\mathrm{g}}/r)$ will be unable to cool through bremsstrahlung and must remain pressure-supported with $h \approx r$

As the gas moves in, however, it will shear and amplify any seed magnetic field until $B^{2}/8\pi \simeq P_{\mathrm{gas}}$, and the fields begins to rise buoyantly out of the disk (moving perpendicular to the plane of a thin disk, towards the vortex funnel in a thick torus) We thus expect the ratio β to be self-limiting at $\beta \simeq 1$, although β may be $\ll 1$ in a corona if the latter is threaded by field lines anchored to interior (high-pressure) parts of the disk, as in the solar atmosphere The corona may also join onto a wind (M C B *et al* in preparation, and ref 34) This magnetic field provides the torus with a new cooling mechanism for $r < (m_{\mathrm{p}}/m_{\mathrm{e}})r_{\mathrm{g}}$, electrons at the virial temperature of the ions would be relativistic, and each would radiate an energy

$$\Delta E_{\mathrm{r}} \approx kT_{\mathrm{i}}\left(\frac{50r_{\mathrm{g}}}{r}\right)^{31/4} m_{-4}^{1/2}\alpha_{-2}^{-3/2}\beta^{-3/2}M_{8}^{-1/2} \qquad (3)$$

by optically thick synchrotron radiation as it spiralled in from r to $r/2$ (where $m_{-4} = 10^{4}\,m$ and $\alpha_{-2} = 10^{2}\alpha$) The actual cooling rate is considerably higher for

$$r < r_{\mathrm{comp}} \equiv \left(\frac{m_{\mathrm{p}}}{m_{\mathrm{e}}}\right)^{4/5}(m\alpha^{-1})^{2/5} = 65\,m_{-4}^{2/5}\,\alpha_{-2}^{-2/5} \qquad (4)$$

since then the dominant cooling is due to Compton scattering of the synchrotron photons (Fig 1) Thus if the electrons and ions are kept in energy equipartition, a thick torus will cool and deflate to a thin disk for $r \leqslant 50r_{\mathrm{g}}$

The torus will be 'collisionless' inside some large radius (typically ~2,000 r_{g}, but defined more precisely below), in the sense that through two-body collisions alone protons at temperature T_{p} give less than half their energy to electrons (with $T_{\mathrm{e}} < T_{\mathrm{p}}$) on the inflow time scale, if

$$m < \left(\frac{m_{\mathrm{p}}}{m_{\mathrm{e}}}\right)(\ln\Lambda)^{-1}\alpha^{2}\left(\frac{m_{\mathrm{p}}}{m_{\mathrm{e}}}\,\frac{r_{\mathrm{g}}}{r}\,\frac{T_{\mathrm{e}}}{T_{\mathrm{p}}}\right)^{3/2}$$

$$\approx 50\alpha^{2}\left(\left(\frac{2{,}000r_{\mathrm{g}}}{r}\right)\left(\frac{T_{\mathrm{e}}}{T_{\mathrm{p}}}\right)\right)^{3/2} \quad kT_{\mathrm{e}} < \tfrac{2}{3}m_{\mathrm{e}}c^{2} \qquad (5a)$$

$$m < \left(\frac{m_{\mathrm{p}}}{m_{\mathrm{e}}}\right)\left(\frac{\gamma_{\mathrm{re}}}{\ln\Lambda}\right)\alpha^{2} = 50\gamma_{\mathrm{re}}\alpha^{2} \quad kT_{\mathrm{e}} > \tfrac{2}{3}m_{\mathrm{e}}c^{2} \qquad (5b)$$

In these conditions, collective plasma phenomena will determine the particle distribution functions, the radiative efficiency, and thus the pressure and shape of the whole torus/disk In most of what follows we assume that collective processes are unable to transfer more than half the proton's kinetic energy to the electrons [which would in turn quickly radiate it compare with equation (3)] Given the complexity of the plasma physics and the uncertainties in accretion theory, it may be a long time before this assumption can be checked If the collective transfer can take place, the structure is similar to that already familiar from results at high accretion rates If it cannot, one consequence, as already realized in the context of accretion disks around stellar-mass black holes[35 36], is a 'two-temperature' flow

Two-temperature tori

Consider an accretion flow where equation (5) is satisfied for $r < r_{\mathrm{D}}$, and assume that the protons and electrons are then

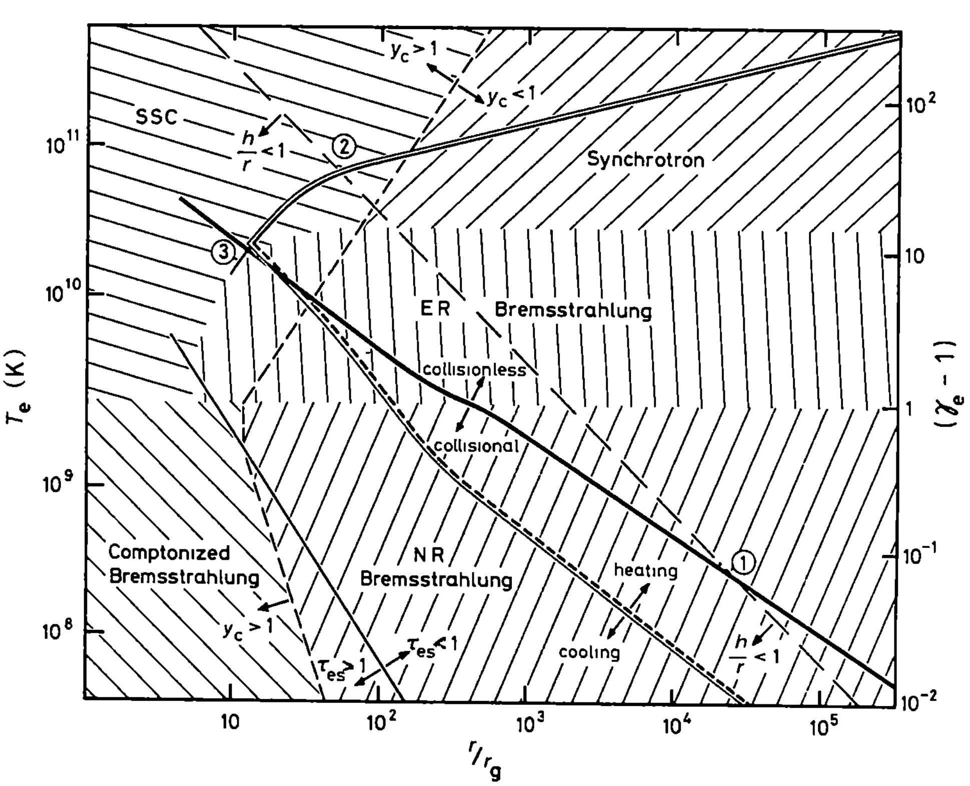

Fig. 1 The dominant local cooling mechanisms for a representative ($\alpha = 10^{-2}$, $\beta = 1$) low-accretion rate ($m \equiv M/M_{\mathrm{Edd}} = 10^{-4}$) flow about a central mass of $10^{8}M_{\odot}$, as a function of distance (measured in units of $r_{\mathrm{g}} \equiv GM/c^{2}$) from the central mass and electron temperature (which also parametrizes disk thickness, a scale of electron kinetic energy in units of $m_{\mathrm{e}}c^{2}$ is at right) We have assumed electron and ion temperature to be everywhere equal, although Coulomb collisions are insufficient to maintain equipartition for disk states above the heavy solid line In the C-shaped region to the left of the double lines the cooling rate exceeds the rate of viscous heating and the disk will collapse To the right of the double lines the rate of heating exceeds that of cooling and the disk will thicken (states above the $h/r = 1$ line are unphysical in the absence of external pressure forces) SSC denotes synchrotron self-Compton cooling ('the Compton catastrophe'), τ_{es} is the optical depth to Thomson scattering

$$y_{\mathrm{e}} = \begin{array}{ll} \tfrac{8}{3}(\gamma_{\mathrm{e}}-1)\tau_{\mathrm{es}}(\tau_{\mathrm{es}}+1) & \text{for } \gamma_{\mathrm{e}}-1 \ll 1 \\ \tfrac{16}{9}\gamma_{\mathrm{e}}^{2}\tau_{\mathrm{es}}(\tau_{\mathrm{es}}+1) & \text{for } \gamma_{\mathrm{e}}-1 > 1 \end{array}$$

is the Compton y-parameter Not included are induced Compton cooling, non-local Compton cooling/heating and losses to winds The disk is everywhere supported by gas pressure Radiation pressure is only important in the inner parts of cold, thin disks for $m > 10^{-3}$ If, for $r \leqslant 10^{7}r_{\mathrm{g}} \simeq 100\,M_{8}$ pc, the disk is heated to a temperature above that at which bremsstrahlung cooling becomes inefficient (double dashed line) it will thicken to a torus, $h \sim r$ For $r < r_{\mathrm{D}} = 2\times10^{4}r_{\mathrm{g}}$ (point 1), Coulomb collisions cannot maintain equipartition If plasma processes take over this job, the disk will begin to cool by SSC at $r \simeq 50r_{\mathrm{g}}$ (point 2) and will gradually thin to $(h/r) \sim \frac{1}{4}$ at $r = 10r_{\mathrm{g}}$, at which point (3) bremsstrahlung will rapidly cool it to a new equilibrium at $T \sim 10^{4}$ K and $(h/r) \sim 10^{-4}$ where it radiates as a black body (optically thick bremsstrahlung and line cooling just balance viscous heating) If, as assumed here, equipartition cannot be maintained, the electrons continue to cool (Fig 3) inside $r = r_{\mathrm{D}}$ (point 1) but the ions remain at the virial temperature The torus will thus remain thick, with the structure shown in Fig 2 indeed thermally decoupled from each other Equation (2) shows that, for $m_{-4} \simeq 1$, the thick ($h \simeq r$) torus is a self-consistent solution even for $r \gg r_R = 2{,}000 r_g$ (see Fig 1) At $r_D \gtrsim r_R$, electrons and ions will decouple, but as neither can cool, they may remain at the same temperature For $r < r_R$, the electrons become relativistic If the heating of both species is adiabatic, then $T_p \propto n^{2/3}$ while $T_e \propto n^{1/3}$, so the ions are preferentially heated Shock heating may likewise favour the ions, as isotropization of the bulk flow velocities will give to each species a thermal energy proportional to its mass Fermi acceleration processes will amplify any temperature difference once it exists Thus the electrons are granted little of the ions' energy, despite their ability to radiate it [equation (3)] The ions remain at the virial temperature, and the two-temperature torus remains thick even inside $r \simeq 50 r_g$ [equations (3) and (4)]

If the torus surrounds a spinning black hole, the Lense–Thirring effect can enforce axisymmetry with respect to the hole's spin axis[37] out to a radius $\sim \alpha^{-2/3}(J/J_{max})^{2/3} r_g$, where J is the hole's angular momentum and $J_{max} = M r_g c$ is the maximum value allowed by the Kerr metric We would expect the holes to have been spun up to $J \approx J_{max}$ during their previous quasar phase[38 39] There may be misalignment outside this radius if the gas is not supplied in the equatorial plane of the hole The isotherms within the torus can then be calculated in the same way as for radiation-supported tori[18 19,22] If the pressure support is due primarily to non-relativistic ions, then the effective specific heat ratio will be about 5/3 If α is independent of radius, then $n \propto r^{-3/2}$, and most of the mass of the torus resides at large radii If both these conditions are fulfilled, then the ions are roughly isentropic

The contours of Fig 2 have been computed by this procedure The results are subject to the same uncertainties as those for radiation-supported tori problems with self-consistency in viscosity (R D.B and M Jarozyński, in preparation), and the absence of a formalism for properly matching one of these inner solutions onto a flow field specified at large radii Magnetic fields will modify the simple structure shown However, essential features, such as the characteristic vortex funnel, which becomes parabolic in the limit of a flow with constant specific angular momentum l and is less collimated than parabolic for a flow with l increasing outwards, are unlikely to be changed (Flows for which l decreases outwards are argued to be unstable, note, however, that l must be constant along the surface if there is no poloidal circulation and we insist that the surfaces have zero energy-at-infinity) In this 'zone of non-stationarity', matter cannot have enough angular momentum to achieve near-equilibrium between centrifugal force, pressure and gravity A fluid flow in the funnel must either fall straight into the hole, or have enough enthalpy to leave the region rapidly Hydromagnetic effects[40] or flares (compare with previous remarks about buoyant fields) on the funnel walls will inject into it particles of positive energy-at-infinity The liberated power will escape along the two funnels, leading to a pair of inertially collimated jets carrying some fraction of $Mc^2 = 10^{42}\, m_{-4} M_8$ erg s^{-1} This may be enough to explain the low-luminosity double-jet radio sources

Electromagnetic extraction of the hole's rotational energy

If the central black hole is near-maximally rotating ($J \simeq J_{max}$), a much greater supply of free energy is available the rotational energy of the hole (up to 29% of Mc^2 for $J = J_{max}$) If an ordered electromagnetic field can be supported around the hole, then it can put particles (which may in fact be inside the horizon if the field threads the latter) systematically on negative energy orbits The negative energy swallowed by the hole appears as positive energy in the external fields and thus drives away from the hole a Poynting flux of luminosity[41–43]

$$L_{EM} \lesssim B_{pH}^2\, r_g^2 (J/J_{max})^2 c \qquad (6)$$

where B_{pH} is the poloidal field in the flux tube that intersects the hole s horizon If $J \simeq J_{max}$, then this power $\lesssim 10^{44} M_8 \alpha_{-2}^{-1} m_{-4} \beta_{pH}^{-1}$ erg s^{-1} (where β_{pH} = (maximum gas pressure in torus)/($B_{pH}^2/8\pi$)) can exceed by $\gtrsim \alpha^{-1}$ the rate of liberation of binding energy by the accreting matter The torus will be able to confine and initially collimate the extracted power, as the associated radiation (or ram) pressure will be less than the gas pressure in the torus if

$$Mc^2/4\alpha > L_{EM} \lesssim Mc^2/(20\alpha\beta_{pH}) \quad (J/J_{max})^2 \qquad (7)$$

Both these inequalities are nearly always satisfied since $\beta_{pH} \gtrsim 1$

To extract power predominantly from the hole, we must have $\beta_{pH} \simeq 1$ and $\alpha \ll 1$ Is this consistent with a physically attainable disk structure? One might naively suppose that the poloidal field could be generated by currents distributed through the torus, and thus be an extension of an ordered field structure within it But if this were the case, the internal fields would transport energy and angular momentum outwards so efficiently that $\alpha \simeq 1$ and L_{EM} would be $\lesssim Mc^2$ Furthermore, in the presence of a magnetosphere any current loop in keplerian rotation around a central mass loses energy from its outer light cylinder at a rate (~vacuum magnetic dipole power) $\simeq (J_{max}/J)^2$ times the rate at

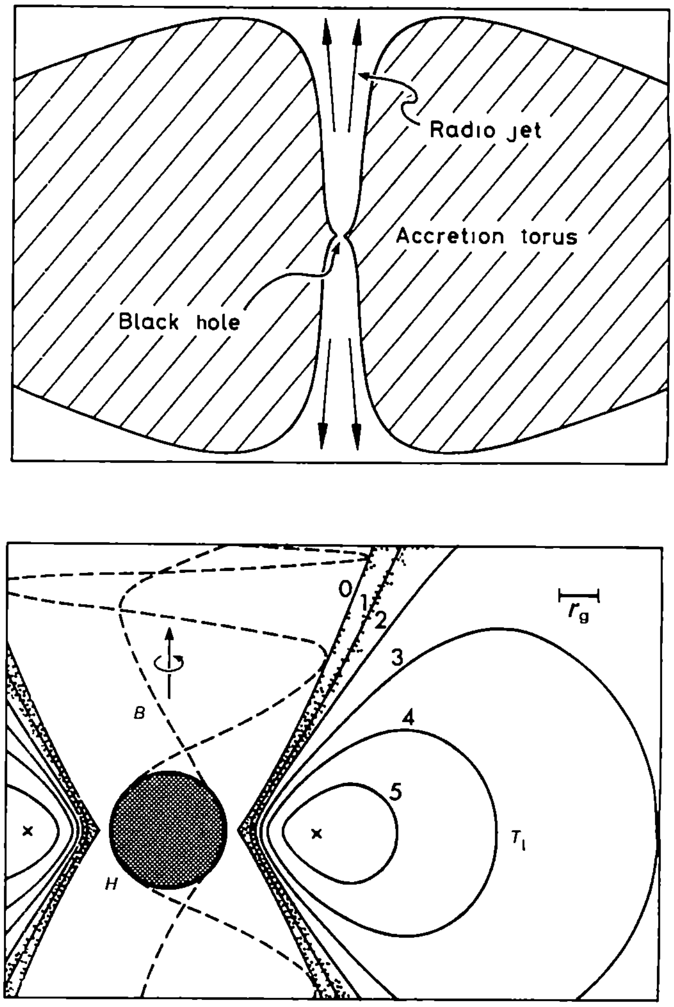

Fig. 2 An accretion torus supported by ion pressure surrounds a spinning black hole The torus defines a pair of funnels capable of collimating a relativistic hydromagnetic flow which ultimately forms the observed radio jets The enlargement shows the inner regions of the torus and displays contours of ion temperature in units of 10^{11} K (solid lines) These have been calculated assuming that the ions are an isentropic gas with constant specific angular momentum and that the hole (horizon H) has $J = 0\ 9\ J_{max}$ (see ref 19) The outer isotherm is also the surface of zero binding energy The dashed lines represent the magnetic field lines in the configuration discussed in the text A poloidal current flows in the funnel Large toroidal currents and the return poloidal currents flow in a thin surface layer (stippled)

which it could extract power were the central mass a black hole of angular momentum J If the current loop runs in an accretion disk, the missing power must be provided by the liberation of binding energy, which again implies $L_{EM} \lesssim Mc^2$ (compare with the thin-disk solution of Blandford and Znajek[42] in which $L_{EM} \simeq 0\ 3\ (J/J_{max})^2\ L_{disk}$)

To understand how a torus could avoid all this energy transport and loss, it is helpful to consider the time evolution of a perfectly conducting torus with a very weak ($\beta_p \gg 1$) magnetic field piercing it at large radii (It may also have internally closed field loops of arbitrary strength) This weak field is convected in with the flow, and by applying Faraday's law to a sufficiently large loop encircling the rotation axis, we find that the magnetic flux through the funnel increases as we carry field in, even though the field lines are causally disconnected from the matter in which they were frozen after the latter has crossed the horizon[43] If the torus behaves like a perfect conductor, it will exclude this increasing external flux by developing surface currents The field and surface currents will increase (perhaps shutting off the accretion altogether) until either some massive plasma-field interchange instability leads to an explosive energy release or, more likely, dissipation in the surface layer destroys piercing field as fast as it is convected in The structure of such a torus is rather different from that of the field-free torus the $\mathbf{J}_T \times \mathbf{B}_p$ force across the surface layer (funnel boundary) must be balanced by a gradient of gas pressure, so that at its base $P_{gas} \simeq B_{pH}^2/8\pi$ If we want $\beta_{pH} \simeq 1$, most of the drop of gas pressure must occur in the surface layer, the inner parts of the torus being at roughly constant pressure

We can imagine the following self-consistent solution for a torus with a jet (Fig 2) toroidal currents in the thin surface layer of the vortex funnel produce a poloidal field which is torqued by the hole, driving an outgoing Poynting flux This will soon become plasma-loaded, toroidal fields will begin to dominate, causing self-collimation[34 44 45] The return poloidal current must also flow in the thin surface layer, pulling material from it into the funnel, but leaving the bulk of the torus unaffected The only forces from the jet transmitted to the body of the torus are those due to the poloidal field (transmitted by the gas pressure in the subcutis), whose pressure drops as (area of funnel)$^{-2}$ and which thus has less effect on the structure of the torus the further out we go Simple solutions ignoring the jet can therefore correctly model the torus, while the jet may collimate itself on the paraboloidal field lines thus defined without exerting much modifying force

The above discussion shows how a torus supported by ion pressure, with a low accretion rate $\dot{M}$ can catalyse the extraction of a hole's spin energy at a rate $\gtrsim \dot{M}c^2$ Moreover, we show below that the luminosity from the torus itself may be $\ll \dot{M}c^2$ Thus if the meagre losses from the torus can be replaced by energy and angular momentum extracted from the hole, there need be no accretion only the inertia of the torus, and the currents in it are needed to confine the magnetic fields that tap the hole's energy

Losses and radiation from the torus

The total power dissipated in the surface layer of thickness s is $\sim (s/r_g) L_{EM} \ll L_{EM}$ Moreover, as only a very weak field need penetrate the torus, transport and losses from the outer light cylinder may also be negligible The radiation emitted by the body of an ion-supported torus will be primarily non-thermal, its magnitude depends sensitively on the efficiency of electron acceleration The torus will generally be optically thin to Thomson scattering, with a total optical depth along a line of sight in the equatorial plane, from the hole to infinity, of $\sim \dot{m}\alpha^{-1}$ Incoherent cyclotron and synchrotron radiation will be self-absorbed (The conditions envisaged resemble those of a so-called 'plasma turbulent reactor'[46], so that a power law spectrum may be set up) The torus will, however, be optically thin to γ radiation produced by relativistic electron bremsstrahlung, and to inverse Compton radiation at frequencies above 10^{13} Hz The relevant relaxation times that go into fixing the electron temperature are plotted in Fig 3, which shows that the electrons will be able to radiate efficiently from the inner part of the torus only if their temperatures exceed 10^{10} K At higher temperatures the power radiated increases very rapidly with temperature the optically thick synchrotron losses vary as T_e^7, and the dependence on T_e is steepened further because repeated Compton scattering of synchrotron photons up to the γ-ray band dominates when $\gamma_e^2 \tau_{es} > 1$ However, as long as equation (5) is satisfied, the electrons can radiate only the small fraction of the total energy which they can drain from the ions (or derive from adiabatic heating) and the ion-supported torus will not collapse For the parameter range of interest, the radiation will be in the far IR or the γ-ray region of the spectrum, according as $\dot{m} \lessgtr 10^{-5} \alpha_{-2}^{3/5} \beta^{-3/5} M_8^{-1/5}$ We cannot exclude the possibility that coherent radiation from fields ~ 100 G may be important But, although this might seem relevant to the phenomenon of low-frequency radio variability[47] it would be subject to electron synchrotron absorption and induced Compton scattering[48 49]

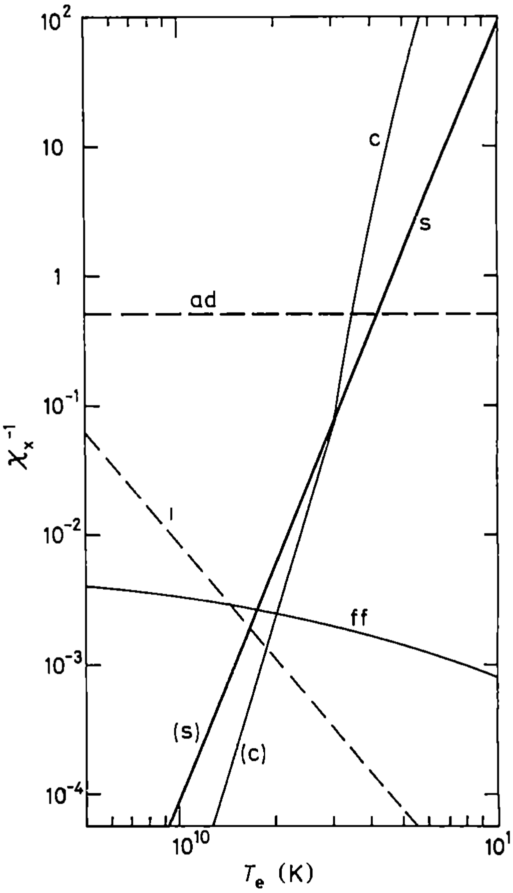

Fig 3 Dimensionless electron relaxation rates χ_x^{-1} as a function of the electron temperature T_e χ_x^{-1} is related to the heating or cooling rate per unit volume ε_x by

$$\chi_x^{-1} = \frac{\varepsilon_x}{3n^2kT_e\sigma_T c}$$

The lines are drawn for $\alpha = 10^{-2}$, $\beta = 8\pi nkT_i/B^2 = 1$, $\dot{m} \equiv \dot{M}/\dot{M}_{Edd} = 10^{-4}$, $r_* = r/r_g = 5$, and $M = 10^8 M_\odot$ The relaxation rates with appropriate scalings are compressional heating, $\chi_{ad}^{-1} \propto \alpha^2 \dot{m}^{-1}$, collisional heating by ions, $\chi_i^{-1} \propto r_*^{-1}$, optically thick synchrotron cooling, $\chi_s^{-1} \propto \alpha^{1/2}\beta^{-3/2} r_*^{-7/4} \dot{m}^{-1/2} M^{-1/2}$, optically thin Compton cooling, $\chi_c^{-1} \propto \alpha^{-2}\beta^{-1} r_*^{-3\ 25} \dot{m}^2$, and relativistic electron bremsstrahlung χ_{ff}^{-1} (no scaling) Self-absorption of the Compton radiation, double-Compton and pion cooling and pair production are unimportant for the range of densities and temperatures under consideration The virial temperature of the ions is 7×10^{11} K $(r_*/5)^{-1}$ (see also Fig 2), while in the absence of losses, compressional heating of electrons transrelativistic at $r_* \simeq 1{,}000$ would give $T_e \simeq 3 \times 10^{10}\ (r_*/5)^{-1/2}$ K

The γ-ray flux from the inner regions of the torus (which may include a redshifted positron annihilation line) would have only a small probability of being reabsorbed near the hole Nevertheless, the small number of interactions that will occur can produce sufficient electron–positron pairs within the funnel to complete the circuit and allow electric current to flow through the hole For example, to support an electromagnetic power of 10^{44} erg s^{-1} in the funnel, a current of 3×10^{17} A must flow, which requires a minimum pair creation rate of $\sim10^{36}$ s^{-1} This can be maintained by γ rays from the torus

If, as assumed above, the electrons and ions are indeed thermally decoupled when equation (5) is satisfied, then the inner part of the torus will radiate much less than $0\ 1\ Mc^2$, and this power is in the far IR or the γ-ray band But if, on the other hand, collective plasma effects couple the ions and electrons at all radii, then (see Fig 1) there will be a thin disk for $r \leqslant 50\ r_g$, radiating $\sim 0\ 1\ Mc^2$ with a spectrum peaking in the optical For $m_{-4} > 50\ \alpha_{-2}^2$, even Coulomb coupling of electrons and ions is efficient enough to cool the ions, and one would expect a thin disk radiating in the near UV When m is low, the predicted emission from galactic nuclei depends so drastically on whether or not the electrons and ions are coupled by plasma effects, that this issue can perhaps be settled observationally more readily than by the efforts of plasma theorists

The maximum power that can be self-consistently extracted from a black hole by a thick ion-supported torus, M being given, is achieved when α has the lowest value consistent with the electron–ion decoupling condition $m < 50\ \alpha^2$ Even if M is a free parameter, the maximum power than can be self-consistently extracted from a black hole by a thick torus supported by ion pressure is $\sim 10^{45}\ \alpha_{-2} M_8$ erg s^{-1} However, if strong magnetic fields are anchored in a dense radiation-pressure-supported torus[18–21], whose thermal luminosity is $\gtrsim L_{\rm Edd}$, there is no clearcut reason why the power extracted electromagnetically from the hole should not be orders of magnitude larger A model along these lines may be relevant to objects such as 3C273 where (in contrast to the radio galaxies) there is a nuclear thermal luminosity $\sim L_{\rm Edd}$, but where there is evidence also for a powerful relativistic jet

Astrophysical context

We have argued that, provided the viscosity parameter α is not too low and the electron–ion coupling is sufficiently weak, a two-temperature, ion-supported torus can be maintained around a massive black hole accreting gas at a very subcritical rate in a galactic nucleus The inner region of such a torus can collimate a pair of relativistic jets comprising electrons, positrons and electromagnetic fields If radio jets originate in the funnels of accretion tori, the latter are likely to be supported by ion pressure rather than radiation pressure in most observed cases The luminosity of the torus would then be far less than the kinetic energy flux in the jets (The scale of the observed jets is, of course, many orders of magnitude larger than the torus itself, so some further collimation process may also be operative)

If most of the power is extracted from a spinning black hole, a fuelling rate of $\sim10^{-3}\ M_\odot$ yr^{-1} suffices for most radio sources A 'baseline' value for M in galactic nuclei would be supplied by debris from stars which pass so close to the hole that they are tidally disrupted[4 32,33] This debris would have an angular momentum appropriate to an orbit at a few times r_g (for $M_8 \simeq 1$) but a specific binding energy of only $\sim10^{-5}\,c^2$ (ref 33) This debris would then form a torus extending out to $\sim10^5\ r_g$, a single disrupted star could then maintain $m \approx 10^{-4}$ for $\sim10^4$ yr

If the energy in radio source jets derives mainly from the spin of the central black hole, then the hole probably underwent a phase of rapid mass accretion at an earlier epoch One can speculate on a possible evolutionary sequence governed by accretion rate If $m > 10$, a radiation-supported torus can be formed. For $50\alpha^2 \leqslant m \leqslant 10$ the situation is less clear, but an ion-supported torus could possibly result, with most of the mass being contained within cool clouds or a thin disk

Disks with $m > 50\alpha^2$ will be strong sources of ionizing radiation, and should be associated with strong line emission from the nucleus Tori with $m < 50\alpha^2$ will be essentially invisible except as γ-ray sources Both may drive the strongest of extended radio sources Recent quasar observations have shown that the majority are radio-quiet, have small percentage polarization, and relatively low X-ray luminosity[50–52] Presumably these do not create large fluxes of relativistic particles, and are perhaps $\sim10^8\ M_\odot$ black holes surrounded by radiation-supported tori without dominant magnetic fields Seyfert galaxies may be similar, but with $\sim10^6\ M_\odot$ black holes The radio loud and (usually) X-ray luminous objects may then be associated with electromagnetically powered tori, the BL Lac and superluminal radio sources perhaps being viewed at small angles to the jet axis

Finally, the physics we have been discussing, with the exception of the detailed radiative properties of the torus, involves no intrinsic mass scale. Indeed, there may be an ion-supported torus around a $\leqslant10^6\ M_\odot$ hole in our galactic centre, and relativistic jets collimated by tori around stellar-mass black holes may exist within our Galaxy

M C B acknowledges partial support under NSF grant AST 79-23243 R D B acknowledges hospitality at the Institute of Astronomy and support under NSF grant AST 80-11752 and from the Alfred P Sloan foundation E S P thanks the Marshall Commission for financial support

Received 28 July, accepted 9 November 1981

1 Wyckoff, S , Wehinger, P & Gehren, T *Astrophys J* **247,** 750 (1981)
2 Schmidt, M *Phys Scr* **17,** 135 (1978)
3 Soltan, A *Mon Not R astr Soc* (in the press)
4 Frank, J *Mon Not R astr Soc* **184,** 87 (1978)
5 Gunn, J E *Active Galactic Nuclei* (eds Hazard, C & Mitton, S) (Cambridge University Press, 1978)
6 Sparke, L S & Shu, F H *Astrophys J Lett* **241,** L65 (1980)
7 Barr, P *et al* *Mon Not R astr Soc* , **193,** 549 (1980)
8 Osterbrock, D E & Miller, J S *Astrophys J* **197,** 535 (1975)
9 Koski, A T *Astrophys J* **223,** 56 (1978)
10 Costero, R & Osterbrock, D E *Astrophys J* **211,** 675 (1977)
11 Waggett, P C , Warner, P J & Baldwin, J E *Mon Not R astr Soc* **181,** 465 (1977)
12 Cohen, M H & Readhead, A C S *Astrophys J Lett* **233,** L101 (1979)
13 Readhead, A C S *et al* *Nature* **276,** 768 (1978)
14 Linfield, R P *Astrophys J* **244,** 436 (1981)
15 Pearson, T J *et al* *Nature* **290,** 365 (1981)
16 Cotton, W D , Shapiro, I I & Wittels, J J *Astrophys J Lett* **244,** L57 (1981)
17 Jones, D L , Sramek, R A & Terzian, V *Astrophys J Lett* **247,** L57 (1981)
18 Abramowicz, M A , Jaroszynski, M & Sikora, M *Astr Astrophys* **63,** 221 (1978)
19 Kozlowski, M , Jaroszynski, M & Abramowicz, M A *Astr Astrophys* **63,** 209 (1978)
20 Abramowicz, M A , Calvani, M & Nobili, L *Astrophys J* **242,** 772 (1980)
21 Paczynski, B & Wiita, P *Astr Astrophys* **88,** 23 (1980)
22 Jaroszynski, M , Abramowicz, M A & Paczynski, B *Acta Astr* **30,** 1 (1980)
23 Abramowicz, M & Piran, T *Astrophys J Lett* **241,** L7 (1980)
24 Sikora, M *Mon Not R astr Soc* **196,** 257 (1981)
25 Sikora, M & Wilson, D B *Mon Not R astr Soc* (in the press)
26 Eardley, D M & Lightman, A P *Astrophys J* **200,** 187 (1975)
27 Shakura, N I & Sunyaev, R A *Astr Astrophys* **24,** 337 (1973)
28 Novikov, I D & Thorne, K S in *Black Holes* (eds DeWitt, C & B S) (Gordon & Breach, New York, 1973)
29 Pringle, J E *Ann Rev Astr Astrophys* **19,** 137 (1981)
30 Pringle, J E *Mon Not R astr Soc* **177,** 65 (1976)
31 Shakura, N I & Sunyaev, R A *Mon Not R astr Soc* **175,** 613 (1976)
32 Hills, J G *Mon Not R astr Soc* **182,** 517 (1978)
33 Frank, J *Mon Not R astr Soc* **187,** 883 (1979)
34 Blandford, R D & Payne, D *Mon Not R astr Soc* (in the press)
35 Shapiro, S L , Lightman, A P & Eardley, D M *Astrophys J* **204,** 187 (1976)
36 Eardley, D M , Lightman, A P , Payne, D G & Shapiro, S L *Astrophys J* **224,** 53 (1978)
37 Bardeen, J M & Petterson, J A *Astrophys J Lett* **195,** L65 (1975)
38 Thorne, K S *Astrophys J* **191,** 507 (1974)
39 Abramowicz, M A & Lasota, J P *Acta Astr* **30,** 35 (1980)
40 Galeev, A A , Rosner, R & Vaiana, G S *Astrophys J* **229,** 318 (1979)
41 Znajek, R L thesis Cambridge Univ (1976)
42 Blandford, R D & Znajek, R L *Mon Not R astr Soc* **179,** 433 (1977)
43 Macdonald, D & Thorne, K S *Mon Not R astr Soc* (in the press)
44 Blandford, R D *Mon Not R astr Soc* **176,** 465 (1976)
45 Chan, K L & Henriksen, R N *Astrophys J* **241,** 534 (1980)
46 Norman, C A & ter Haar, D *Phys Rep* **17,** 307–358 (1975)
47 Condon, J J *et al* *Astr J* **84,** 1 (1979)
48 Levich, E V & Sunyaev, R A *Astrophys Lett* **7,** 69 (1970)
49 Wilson, D B & Rees, M J *Mon Not R astr Soc* **185,** 297 (1978)
50 Condon, J J *et al* *Astrophys J* **244,** 5 (1981)
51 Ku, W H M , Helfand, D J & Lucy, L B *Nature* **288,** 323 (1980)
52 Angel, J R P & Stockman, H S *A Rev Astr Astrophys* **18,** 321 (1980)

R421

4011

Structural evolution of a crustal section in the western Himalaya

M. P. Coward*, M. Q. Jan†, D. Rex*, J. Tarney‡, M. Thirlwall* & B. F. Windley‡

* Department of Earth Sciences, The University, Leeds LS2 9JT, UK
† Department of Geology, University of Peshawar, Peshawar, Pakistan
‡ Department of Geology, The University, Leicester LE1 7RH, UK

Recent field work on the Kohistan complex in the Karakorum Range of North Pakistan has shown its stratigraphy to be repeated by several phases of tight to isoclinal folding. This reveals a close association between igneous activity and a late deformation and complicates the previously proposed island arc model.

AN exciting crustal section has recently been discovered in the Karakorum Range of North Pakistan[1,2] This was considered to be a complete section of an island arc (the Kohistan complex or sequence) thrust over rocks of the Indian plate and turned on end during Himalayan orogeny (for details of the regional setting, see ref 3) The arc was initially interpreted as a stratigraphic sequence from upper crustal sediments and volcanics in the north through tonalites and diorites to lower crustal granulites in the south. Our recent field work has shown a more complex structure, stratigraphy being repeated by several phases of tight to isoclinal folding. The Kohistan sequence forms a major tight syncline whose plunge varies over 90° and this folds a complete section through the crust, the lower crustal rocks having previously been isoclinally folded The Kohistan sequence was thrusted southwards over the gneisses of the Indian plate and the earlier arc structures were steepened to a near-vertical attitude Most of the tonalite–diorite suite was intruded during this deformation sequence, but some outlasted the deformation This close association between igneous activity and late deformation complicates a simple arc model

North–south traverse

Figures 1 and 2 show a simplified map and section of the Kohistan area adapted from refs 3, 4 and a new unpublished map by R A K Tahirkheli We consider here a north to south section from the Karakorum Ranges to the molasse deposits of the Indian plate In the Hunza valley in the north there is a chaotic arrangement of lithologies including limestones, sandstones, conglomerates, basic volcanics and ultrabasic rocks such as serpentinites, meta-harzburgites, talc-carbonate and talc-chlorite schists, all occurring as lenses several kilometres long separated by chloritoid slates These slates increase in grade rapidly northwards to garnet–staurolite mica schists intruded by the granodiorites of the Karakorum batholith The slates and schists contain a well developed schistosity folded around a large-scale, gently dipping synform (see Fig 2) This chaotic pile of lithologies resembles a large-scale tectonic mélange which is situated along the northern suture

To the south there are gabbros, basic volcanics, including spectacular sections of deformed pillow lavas, volcaniclastic sediments and greywackes folded into tight large-scale anticlines and synclines Further south these sediments and volcanics are invaded by tonalites, diorites and large pegmatite swarms, locally constituting 30% of the rock volume Between these intrusions there are screens of graded greywackes and pillow lavas from which younging directions can be obtained (see Fig 1) This sequence extends for ~70 km from the northern suture The dominant structures are large-scale, upright antiforms and synforms, whose hinges plunge steeply NNE parallel to mineral lineations down the dip direction of the cleavage The major structure shown on the map is a westward-facing, steeply plunging anticline at Gilgit and a complementary major syncline with a half wavelength of >50 km together with common smaller-scale parasitic folds These structures bring the major stratigraphy from north of Gilgit southwards to Jaglot, particularly repeating the spectacular pillow lavas seen in the north This same Jaglot syncline probably continues westwards to the central part of Kohistan where it contains the Eocene Kalam volcanics[5] and underlying sediments, in this region the syncline has a more horizontal plunge

On the south limb of the syncline one passes down into a vast stratiform cumulate complex containing chromite-layered dunites, troctolites, gabbros and predominant norites with spectacular phase graded units There are very spectacular and abundant graded units which have allowed numerous younging directions to be obtained In the Chilas area these layers are deformed into large-scale steeply plunging folds, parasitic on the Jaglot syncline However, there are changes in facing direction as shown by the cumulate grading indicating an earlier major isoclinal fold phase The central part of the Chilas complex is composed of a zone of ultramafic rock and this youngs to metanorite at the northern and southern margins The whole Chilas complex is interpreted as one isoclinal anticline refolded by Jaglot syncline age structures. The complex has suffered metamorphism of two pyroxene granulite facies, the minerals of which are aligned in the fabric of Jaglot syncline age

There are two important later stages of deformation which affect both the Chilas complex and the metasediments and igneous rocks to the north A phase of southward dipping, small-scale folds produces crenulation cleavage in the more schistose rocks, possibly related to the nearly recumbent fold in the Hunza valley Later deformation produced a major conjugate set of NW–SE dextral and NE–SW sinistral trending shear zones with dominantly strike-slip sense of displacement these vary from ductile to brittle, and from phyllonites of amphibolite–greenschist facies to pseudotachylites

To the south of the Chilas complex there is a complex sequence of metasediments, amphibolites, gabbros, deformed granites and pegmatites and post-tectonic granites Most rocks show two phases of deformation the dominant second phase deforms early fabrics and folds, and produces steeply-plunging folds parasitic on the Jaglot syncline as shown in Fig 2

At Patan there is the Jijal complex[6] of chromite-layered dunites and granulites, which we interpret as part of the Chilas complex metamorphosed to a high-pressure (garnet–clinopyroxene) granulite grade This interpretation requires a first-phase tight syncline between the Chilas and Jijal complexes The Jijal complex shows two phases of deformation similar to those described above, the first fabric of which is difficult to detect, being largely overgrown by granulite facies assemblages To the south the rocks become intensely sheared and metamorphosed to the amphibolite facies All these structures become more

0028-0836/82/010022–03$01 00

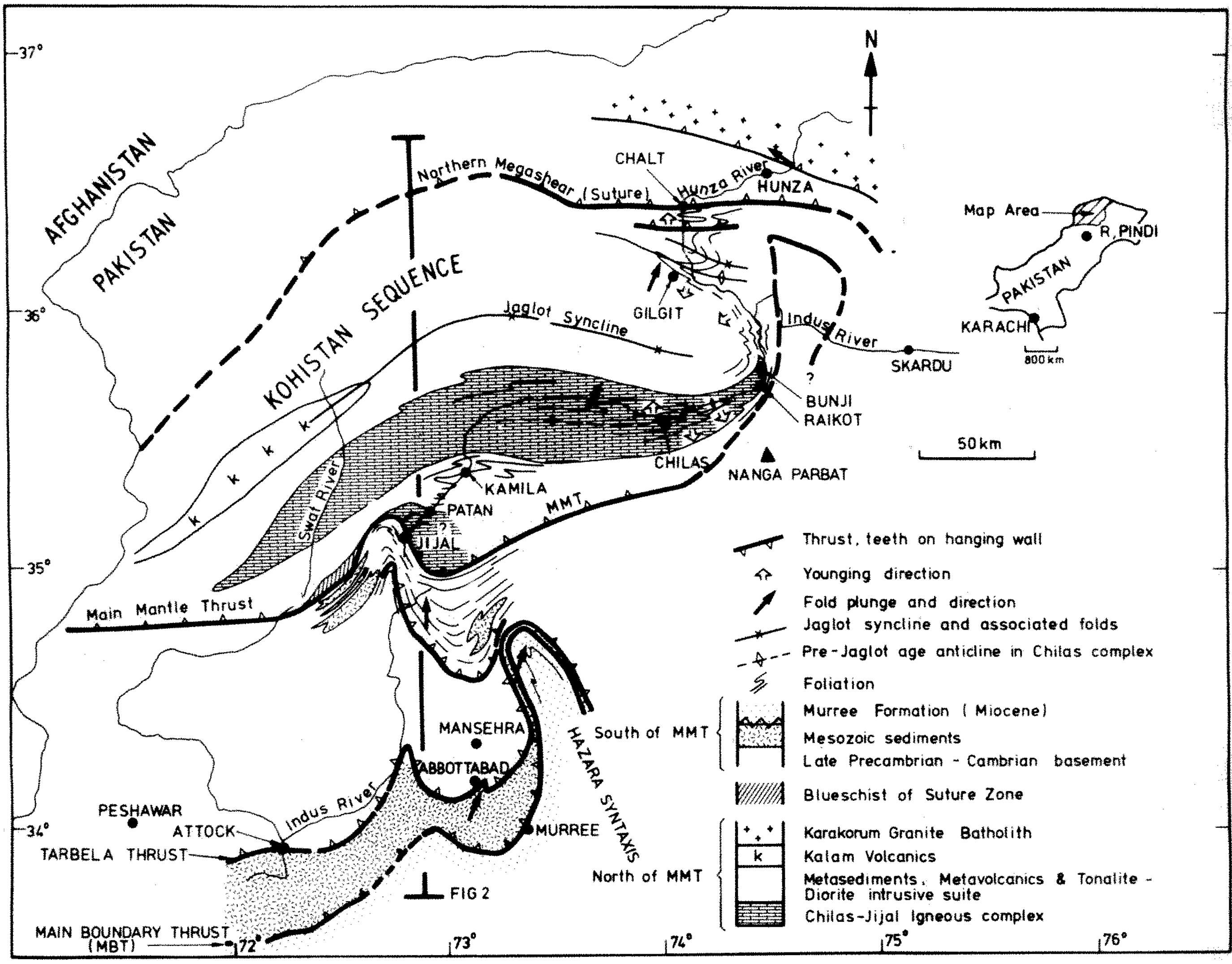

Fig. 1 Map of the Kohistan region showing the main structures (modified from refs 2 and 4).

gently dipping to the south, so that near Jijal the fabrics are flat-lying or dip only gently northwards. Along strike to the south-west there is a 10–15 km wide thrust wedge of blueschists[7] along the Main Mantle Thrust (MMT) (Fig. 1), though to the east, around the Nanga Parbat bulge (Fig. 1), no blueschists occur, the MMT is difficult to detect and the obvious faults and shears are late structures which post-date the folding.

At Jijal a major shear zone, the MMT[1,2], carries the Jijal complex and the Kohistan sequence southwards over quartzo-feldspathic gneisses of the Indian plate containing an intense fabric folded by recumbent, nearly isoclinal folds with hinges plunging to the NNE. Both sets of structures are folded around large-scale upright F_3 folds. The gneisses with intense deformation and isoclinal folds can be followed for 10–20 km south of the MMT and contain infolded synclines of Mesozoic cover rocks (marbles, graphite schists and conglomerate). Further south where deformation decreases, the unconformity can be seen between these sediments and the underlying basement gneiss. Where least deformed by Himalayan shearing, as at Mansehra, this basement appears as a homogeneous porphyritic

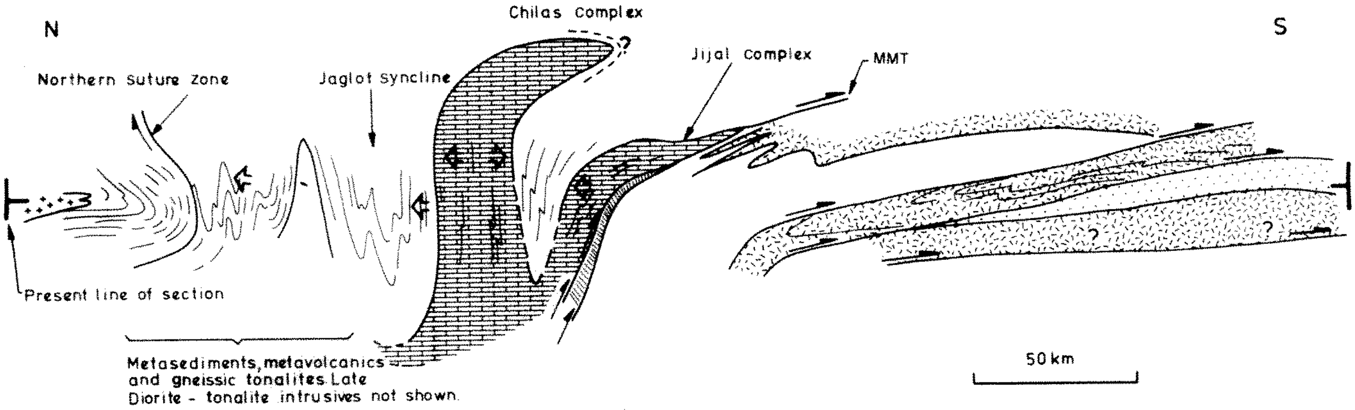
N
S
Chilas complex
Northern suture zone
Jaglot syncline
Jijal complex
MMT
Present line of section
Metasediments, metavolcanics and gneissic tonalites. Late Diorite - tonalite intrusives not shown.
50 km

Fig. 2 Simplified tectonic cross-section of the region. For location and caption see Fig. 1. The dip and position of the major thrusts at depth is uncertain. Evidence for flat-lying thrusts beneath the Indian plate is given in ref. 13. Vertical scale = horizontal scale.

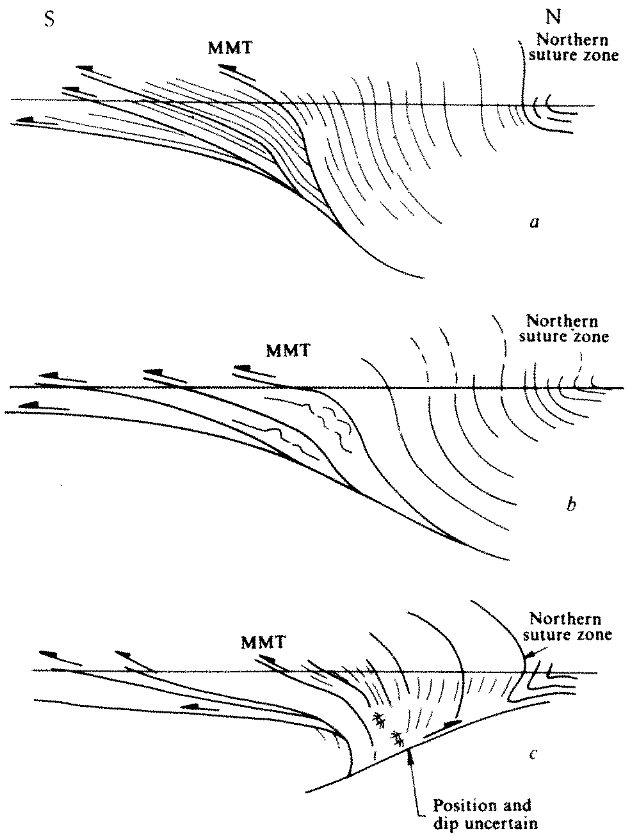

Fig. 3 Model section to show how Kohistan sequence achieved its steep dip: *a*, due to climb and fanning of thrusts to the south; *b*, due to folding above a decoupling horizon[9]; *c*, due to back thrusting. The structure of the Kohistan complex is simplified to show approximate dips of foliation and fold axial planes. Vertical scale = horizontal scale.

granite which has a Rb/Sr whole rock isochron age of 516± 16 Myr (ref. 8). This granite has a contact aureole against pelitic sediments of presumed late Precambrian age. These basement rocks are thrust southwards over Mesozoic sediments near Abbottabad and together with the Mesozoic sediments they are further thrust over mid-Oligocene to mid-Miocene red sandstones and shales (the Murree Formation). All these rocks are folded into a major steeply-plunging tight anticline (Fig. 1) which is a first phase structure in the Miocene and at least a third phase structure in the Mesozoic sediments and their gneissic basement. To the south there are even more thrusts in sediments ranging in age from Palaeocene to Cambrian, flooring in a blind thrust in the sediments above the basement.

Discussion

The MMT clearly separates crustal blocks of two different ages, origin and lithology[1,2]. The gneisses to the south form part of the late Precambrian–early Palaeozoic segment of the Indian plate, while to the north no old basement has been found, but rather deformed sediments and igneous rocks of Mesozoic–Cenozoic age. The Mesozoic–Cenozoic Kohistan sequence was considered to represent an island arc[1,2], but our studies show this to have a more complicated structural history and a compound origin.

The lower crust is made up of the basic–ultrabasic Chilas complex which is >300 km long and >8 km thick, and is thus one of the largest intrusions in the world. Above this there are mainly pillow lavas and greywackes intruded by gabbros, diorites and tonalites. The early isoclines are developed in the lower crustal rocks of the southern Kohistan sequence associated with granulite facies metamorphism. These structures are folded by one of the largest synclines known, which folds the whole upper crust of Kohistan. Its synclinal axis changes from near horizontal in the west to steeply NNE near the Indus River parallel to the Himalayan overthrust direction. This major syncline and related structures seem to be related to the MMT, though the eastern continuation of the MMT is difficult to trace around the Nanga Parbat syntaxis which has the form of a late fold with late faults along its western margin. In Kohistan the MMT marks a major suture bringing granulites against blueschists and amphibolites. The immediately underlying Indian plate contains a 10–20 km wide, gently dipping shear zone with Mesozoic cover tightly infolded into basement gneiss. To the south there are more discrete thrust planes, the floor thrust of which climbs southwards from basement to progressively higher levels of sediment. These structures propagated southwards: the earlier thrusts and folds in the north are refolded by structures developed in the south. The Kohistan sequence north of the MMT has been backfolded to become vertical to southerly dipping west of the Nanga Parbat syntaxis. The origin of this backfold is uncertain: one method of modelling would be to produce the above-described major thrusts in the form of an imbricate fan analogous to that in accretionary wedges[9] (see Fig. 3*a*). Alternatively, the more northern thrusts could be folded into a steep orientation above a low-level decoupling horizon analogous to that suggested for the Swiss Alps (Fig. 3*b*)[10]. In both these models the depth to the decoupling zone would be at least 100 km below the present erosion surface (Fig. 3*a*, *b*). In the Ladakh area, however, 200 km along the strike to the east of Kohistan, there are southward-dipping faults overthrusting to the north[11], and similar thrusts occur along the Indus suture in the central Himalaya[12]. Possibly the backfold is related to uplift on these faults (Fig. 3*c*).

Conclusion

One important conclusion from our study is that the predominant diorite–tonalite igneous activity in northern Kohistan is late to post-tectonic; some of it certainly postdates the Jaglot syncline and may postdate the backfolding. This conclusion is supported by a preliminary study of the Skardu area, east of the Nanga Parbat, where most granites, tonalites and gabbros postdate the intensely deformed metasediments and volcanics. This throws doubt on the contribution of this igneous activity to the development of the island arc. The problem of the origin of these diorites and tonalites may be solved by isotope and trace element geochemistry, at present underway at Cambridge, Leeds and Leicester.

The other exciting feature of the Kohistan area is the size of the structures involved. The Kohistan complex is now up to 150 km thick though this is largely the result of two phases of folding; little evidence has been found for thrust repetition as originally suggested by Bard *et al.*[2]. The Jaglot synform is one of the largest reported structures in the world and involves deformation of the whole crust with decoupling at considerable depth (>100 km) in the mantle. Similar decoupling depths are indicated by the different models to explain the backfolding (Fig. 3).

We thank NERC for research grant GR3/4242, and R. A. K. Tahirkheli for logistical support.

Received 10 August; accepted 5 November 1981.

1. Tahirkheli, R. A. K., Mattauer, M., Proust, F. & Tapponnier, P. in *Geodynamics of Pakistan* (eds Farah, A. & DeJong, K. A.) 125–130 (Geological Survey of Pakistan, 1979).
2. Bard, J. P., Maluski, H., Matte, P. H. & Proust, F. in *Geol. Bull. Univ. Peshawar Spec. Iss.* **13**, 87–94 (1980).
3. Tapponnier, P., Mattauer, M., Proust, F. & Cassaigneau, C. *Earth planet. Sci. Lett.* **52**, 355–371 (1981).
4. Tahirkheli, R. A. K. & Jan, M. Q. *Geol. Bull. Univ. Peshawar Spec. Iss.* **11** (1979).
5. Khan, J. *Geol. Bull. Univ. Peshawar Spec. Iss.* **11**, 153–162 (1979).
6. Jan, M. Q. & Howie, R. A. *J. Petrol.* **22**, 85–126 (1981).
7. Shams, F. A., Jones, G. C. & Kempe, D. R. C. *Miner. Mag.* **43**, 941–942 (1980).
8. Le Fort, P., Debon, F. & Sonet, J. *Geol. Bull. Univ. Peshawar Spec. Iss.* **13**, 51–61 (1980).
9. Moore, J. C. & Karig, D. E. *Bull. geol. Soc. Am.* **87**, 1259–1268 (1976).
10. Hsu, K. J. *Am. J. Sci.* **279**, 353–366 (1979).
11. Frank, W., Gansser, A. & Trommsdorf, V. *Schweiz. miner. petrogr. Mitt.* **57**, 89–113 (1977).
12. Shackleton, R. M. *J. struct. Geol.* **3**, 97–105 (1981).
13. Seeber, L. & Armbruster, J. in *Geodynamics of Pakistan* (eds Farah, A. & DeJong, K. A.) 131–142 (Geological Survey of Pakistan, 1979).

Cellular origin and role of mink cell focus-forming viruses in murine thymic lymphomas

Sisir K. Chattopadhyay[*†‖], **Miles W. Cloyd**[‡], **David L. Linemeyer**[§], **Marilyn R. Lander**[*†], **Elaine Rands**[*] & **Douglas R. Lowy**[*]

[*] Dermatology Branch, † Pediatric Oncology Branch and § Laboratory of Tumour Virus Genetics, National Cancer Institute, Bethesda, Maryland 20205, USA

‡ Rocky Mountain Laboratory, National Institute of Allergy and Infectious Diseases, Hamilton, Montana 59840, USA

Embryo DNA of AKR mice contains several copies of intact mink cell focus-forming (MCF)-like env *gene sequences with a proviral structure. In spontaneous thymic tumours, these MCF-like* env *sequences have regularly recombined with a specific region of the 3′ end of ecotropic* env. *This specific recombination is probably a critical event in the pathogenesis of spontaneous AKR tumours.*

MURINE leukaemia viruses (MuLVs) are endogenous to laboratory mice[1-3]. The MuLVs of these mice have been divided into three related classes on the basis of their host range in tissue culture, which is determined by the viral envelope glycoprotein (gp70) encoded by the viral gene *env*[4]. These classes are: ecotropic, which infect only murine cells; xenotropic, which replicate primarily in heterologous cells; and mink cytopathic focus-forming (MCF) viruses, which grow in both murine and heterologous cells[5-8]. Biochemical studies of viral nucleic acids have suggested that MCF viruses are recombinants between ecotropic MuLV and endogenous *env* sequences related to xenotropic viruses[9,10].

Among laboratory mice, the AKR strain[11] has been intensively studied because of its high incidence of MuLV-associated spontaneous T-cell leukaemias, which originate in the thymus. Some steps leading to the development of this thymic disease have been determined, but many aspects of this complex process remain to be elucidated[12]. Each AKR mouse cell contains in its chromosomal DNA one or more complete copies of an ecotropic MuLV genome (proviral DNA)[13-16]. This viral genome is usually spontaneously activated shortly before birth, leading to high levels of circulating virus throughout the animal's life[17]. This ecotropic virus expression is apparently necessary but not sufficient for tumour development, which occurs only after the animal is at least 6 months old[18]. MCF viruses have been isolated primarily from preleukaemic thymuses and from tumour tissue[5,6], suggesting that MCF viruses may represent a more proximate cause of the tumour.

The origin and role of MCF viruses in tumorigenesis, which we have studied here, are still incompletely understood. The endogenous non-ecotropic viral sequences which presumably participate in the formation of MCF viruses have not been identified in normal cells, but it is known that AKR and other mice contain multiple copies[2,3] of sequences homologous to part of the complete AKR ecotropic viral genome. In addition, only certain MCF viruses are oncogenic[19]. It therefore appears that virological factors in addition to the expanded *in vitro* host range have a significant role in tumorigenesis.

In this study, we have used restriction endonucleases and a viral probe specific for MCF and xenotropic *env* sequences to map the viral sequences in high molecular weight DNA from AKR mouse embryos and from spontaneous and MCF virus-induced tumours. These maps have been compared with those recently developed for the DNAs of MCF viruses[20], where consistent differences were noted between DNAs of pathogenic and non-pathogenic MCF viruses. We have found: (1) AKR embryo DNA contains ~10 copies of apparently complete *env* sequences closely related to those found in MCF viral genomes; (2) these endogenous MCF-like *env* sequences resemble the *env* of the non-pathogenic MCF viruses more closely than they do those of pathogenic MCF viruses; (3) at least some copies of these *env* sequences have the structure of endogenous proviruses; (4) spontaneous AKR tumours are clonal in origin and contain recombinant viral DNA with the same structure as that found in pathogenic MCF viral DNAs. The results suggest that specific recombinational events between the endogenous MCF-like sequences and ecotropic viral sequences are a prerequisite for the establishment of AKR tumours.

Physical maps of ecotropic, xenotropic and MCF viral DNAs

Before analysing the AKR high molecular weight DNA, we will summarize the results of physical mapping studies of unintegrated DNAs of ecotropic, xenotropic and MCF viruses from AKR and other strains so that these maps can be compared with those generated here for endogenous non-ecotropic viral sequences in the high molecular weight DNA (Fig. 1)[20,21]. The viral DNAs, which are 8.8 kilobases (kb), contain three genes: *gag* (spanning 1.0–2.7 kb; map locations are given by their distance from the left (5′) end of the viral DNA), which specifies the virion core proteins, *pol* (2.7–5.8 kb), which encodes the reverse transcriptase, and *env* (5.8–8.2 kb), which codes for the virion envelope proteins gp70 and p15E (see Fig. 1) (refs 22–26 and C. Van Beveran and I. M. Verma, personal communication). The p15E sequences, which begin at ~7.5 kb, are located to the right of those which encode gp70 (refs 24–27 and C. Van Beveran and I. M. Verma, personal communication). The viral DNAs are flanked at each end by 0.6 kb of repeat sequences called the long terminal repeat (LTR).

As predicted from earlier studies of viral RNA oligonucleotides[28], each MCF viral DNA was unique, each was apparently composed of ecotropic and non-ecotropic sequences, and each contained non-ecotropic *env* sequences which shared restriction endonuclease sites with xenotropic *env* sequences (such as *Eco*RI at 6.9 and *Bcl*I at 7.0 kb, Fig. 1). However, some sites (such as *Bam*HI at 6.2 kb) were unique to MCF viruses, suggesting that the non-ecotropic sequences of MCF viruses might not be derived from proviruses of known xenotropic viruses. In addition, a consistent difference between the viral DNAs of non-pathogenic and pathogenic MCF viruses was that pathogenic MCF viral DNAs contained an *Xba*I site in p15E at 7.7 kb which was apparently derived from the ecotropic viral parent, while non-pathogenic MCF viruses did not have this site. Finally, in certain MCF viral DNAs, the span of the inferred segment of non-ecotropic sequences was much greater than only part of the gp70 coding region (Fig. 1). These results suggested

---

[‖] To whom reprint requests should be addressed at: Building 41, Room A114, National Institutes of Health, Bethesda, Maryland 20205, USA.

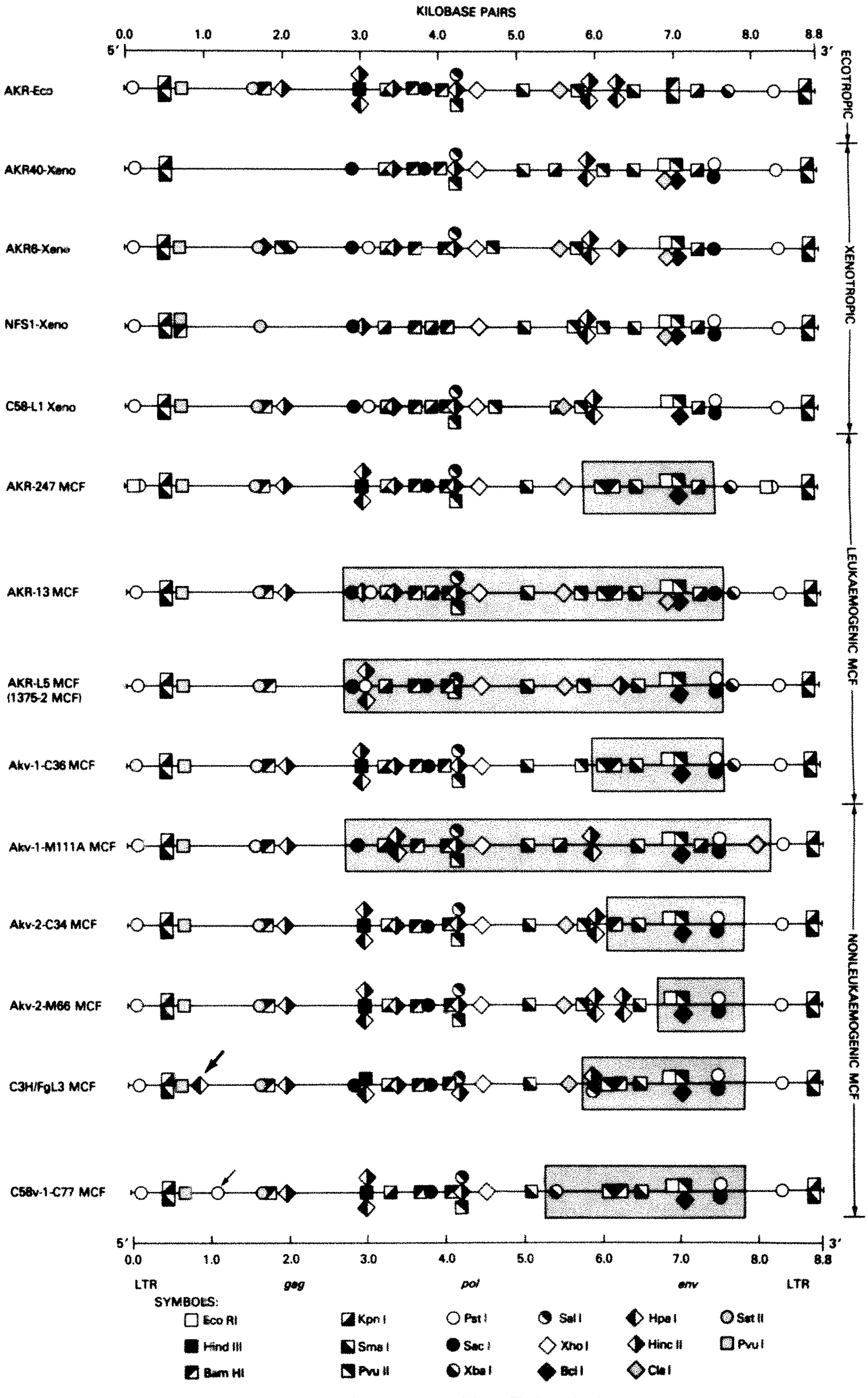

Fig. 1 Comparison of linear restriction endonuclease maps of representative ecotropic, xenotropic and MCF murine leukaemia viral DNAs. The viral DNAs are grouped according to the viral host range and within MCF viruses according to their disease-inducing capability. Each symbol corresponds to an enzyme as indicated in the figure. AKR-eco (ecotropic virus isolated from an AKR mouse) is virtually identical to ecotropic viruses of many inbred strains of mice (the strains and isolates analysed are: *Akv-1*, two isolates; *Akv-2*, two isolates; C58, three isolates; C3H/Fg, three isolates; PL, three isolates; F, one isolate; BALB/c, one isolate) and of *Mus musculus molossinus*[20,21]. Nomenclature and origin of various viruses have been described previously[20,21]. Each MCF DNA has been assumed to contain a continuous insert of non-ecotropic sequences, which may represent oversimplification in some instances. In general, the length of this insert (depicted by the wide bar) represents a minimum estimate, based on the presence of xenotropic or MCF-specific sites and/or the loss of sites common to ecotropic and xenotropic DNAs. The *Hpa*I site at 0.8 kb in C3H/FgL3 MCF and the *Pst*I site at 1.0 kb in C58v-1-C77 MCF (shown by arrows) are not found in ecotropic MuLVs, but have not been considered in the estimated segment of non-ecotropic sequences. These maps were derived from the unintegrated proviral DNAs as described in detail elsewhere[20,21,50]. Briefly, cells were infected with MuLV from chronically infected cells and DNA was extracted from them by the Hirt[51] procedure 18 h after infection. DNA from the Hirt supernatant was used as the starting material for restriction endonuclease digestion. Unintegrated proviral DNAs were digested with various enzymes, electrophoresed, transferred to nitrocellulose filters[52] and hybridized with ^{32}P-cDNA synthesized either from 70S viral RNA or by nick-translation of molecularly cloned viral DNAs. The cleavage products of each enzyme were ordered and oriented for each viral DNA by hybridization of digested DNAs with a 5' probe (the 4.6-kb *Sma*I fragment spanning 0.5–5.1 kb of AKR ecotropic MuLV DNA), a 3' probe (the 1.7-kb *Sma*I fragment spanning 7.0–8.7 kb of the ecotropic DNA) derived from molecular clone AKR MuLV 623 DNA[50] or a full xenotropic or MCF probe after single and/or double digestion of various Hirt DNAs with restriction endonucleases.

that the gp70 (and p15E) of at least some MCF viruses might be derived entirely from non-ecotropic sequences and that the *env* sequences which encode the expanded *in vitro* host range of MCF viruses might be found in high molecular weight DNA of normal cells.

Isolation of a DNA fragment specific for MCF and xenotropic *env*

To probe the high molecular weight DNA for the endogenous sequences which might give rise to the non-ecotropic portion of MCF viruses, we cloned in pBR322 a viral DNA *env* fragment which hybridized to MCF and xenotropic viral DNAs but not to ecotropic viral DNAs. This viral probe, designated BE, is composed of the 0.7 kb between a *Bam*HI and *Eco*RI site in *env* of the Friend spleen focus-forming virus (SFFV) DNA[29], a helper-dependent MuLV whose *env* is closely related to those of MCF viruses[30]. This region in SFFV corresponds exactly to the segment in some MCF viral DNAs between the *Bam*HI site at 6.2 kb and the *Eco*RI site at 6.9 kb (see diagram in Fig. 2). The BE fragment was characterized by radioactively labelling it and incubating it with Hirt supernatants containing ecotropic, xenotropic or MCF viral DNAs: the probe hybridized strongly to MCF DNAs and moderately to xenotropic DNAs, but not to ecotropic DNAs (Fig. 2). Similar results were obtained with the analogous *Bam*HI–*Eco*RI fragment derived from cloned MCF 247 DNA (data not shown).

Embryo DNA contains MCF-like *env* sequences

We then used the BE fragment to probe AKR embryo DNA for the presence of endogenous sequences from which the non-ecotropic *env* sequences of MCF viruses should have been derived (Fig. 3*b*, *c*). Hybridization of the BE probe to *Bam*HI-digested embryo DNA was used to estimate the number of copies of cross-reacting sequences in this DNA, as the BE probe should hybridize to cell–virus DNA junction fragments in high molecular weight DNA digested with this enzyme. *Bam*HI digestion (Fig. 3*b*) yielded $\sim$12–15 fragments, indicating that there are multiple copies in embryo DNA of sequences which cross-hybridize with the BE probe.

We had previously found that *env* of many non-pathogenic MCF viral DNAs had a *Bam*HI site at 6.2 kb, all had an *Eco*RI site at 6.9 kb and a *Bcl*I site at 7.0 kb, some had a *Kpn*I site at 7.3 kb and all had a *Pst*I site at 7.5 kb, a *Kpn*I site at 7.3 kb, a *Pst*I site at 7.5 kb and a *Kpn*I site at 8.7 kb (in the LTR) (see Figs 1, 3). Several copies having these sites were also present in the embryo DNA.

For example, *Eco*RI–*Bcl*I digestion (Fig. 3*b*) shortened each *Bcl*I fragment by 0.1 kb, which indicated that each fragment contained an *Eco*RI site 0.1 kb away from a *Bcl*I site, as was also the case in *env* of every xenotropic and MCF viral DNA. *Bam*HI–*Eco*RI digestion (Fig. 3*c*) gave a more simplified pattern than did *Bam*HI digestion; the intense 0.7-kb fragment corresponded to the *Bam*HI–*Eco*RI fragment spanning 6.2–6.9 kb in many MCF viral DNAs, suggesting the presence of several copies of this fragment in embryo DNA. Endogenous fragments which contained the *Kpn*I site at 7.3 kb should yield a 1.1-kb *Bam*HI–*Kpn*I fragment (6.2–7.3 kb), while those lacking this *Kpn*I site should yield a 2.5-kb *Bam*HI–*Kpn*I fragment (6.2–8.7 kb); these are the two prominent fragments of this double digestion (Fig. 3*c*). The 7.5-, 2.9- and 2.4-kb *Pst*I fragments were apparently all shortened by 0.6 kb when cleaved with *Eco*RI (Fig. 3*b*), which suggests that the right end of these *Pst*I fragments all terminate at 7.5 kb.

It was also important to determine if the *Bam*HI fragments contained an *Xba*I site corresponding to that found in p15E at 7.7 kb in pathogenic MCF viruses. Hybridization of the BE probe to *Bam*HI–*Xba*I-digested AKR embryo DNA (Fig. 3*c*) did not yield a 1.5-kb fragment which would correspond to the *Bam*HI–*Xba*I fragment found in pathogenic MCF viruses such as MCF247. The *Xba*I site at 7.7 kb noted in ecotropic viruses and in pathogenic MCF viruses was therefore not covalently linked to the 6.2-kb *Bam*HI site in the embryo DNA. Taken together, the results described above demonstrated that AKR embryo DNA contained multiple (we estimate $\sim$10) copies of apparently complete *env* sequences with the same restriction sites mapped in non-pathogenic MCF viral DNAs, and at least some of these *env* sequences were linked on their right to an LTR. It is probable that several of these copies can participate in the formation of MCF viruses, as their heterogeneity with respect to the *Bam*HI site at 6.2 kb is correlated with heterogeneity at this site in MCF viruses (Fig. 1).

Endogenous MCF-like *env* sequences are part of proviral DNAs

We have also found evidence that at least some of these MCF-related *env* sequences are part of proviral DNAs, as they are also linked on the left to LTR, *gag* and *pol* sequences. As seen in Fig. 2 and Fig. 3*b*, the BE probe hybridized to a prominent 7.5-kb *Pst*I fragment, which is the expected length of a proviral fragment spanning sequences from a *Pst*I site near the left end of the LTR to a *Pst*I site at 7.5 kb (both of these *Pst*I sites have been found in xenotropic and MCF viral DNAs, see Figs 1, 3). Most of the copies that make up this *Pst*I fragment do extend to 7.5 kb, because, as noted previously, *Eco*RI digestion apparently shortens this fragment by 0.6 kb. In addition, this 7.5-kb *Pst*I fragment hybridizes to probes specific for the 5′ end (5′ probe), middle portion (M probe) and LTR (L probe) of viral DNAs (Fig. 3*a*). (The 8.2-kb *Pst*I fragment which hybridized to each probe except the BE probe represents the endogenous ecotropic proviral DNA cleaved at the *Pst*I site in each LTR[15].) Several *pol*–*env* fragments which corresponded to fragments in MCF viral DNAs in Fig. 1 whose non-ecotropic sequences were inferred to include the *pol* region were also noted in embryo DNA. For example (Fig. 3*b*), the 5.3-kb *Kpn*I fragment corresponded to a fragment in L5 MCF (3.4–8.7 kb) and the 1.8-kb *Kpn*I fragment to a fragment in M111A MCF (5.5–7.3 kb).

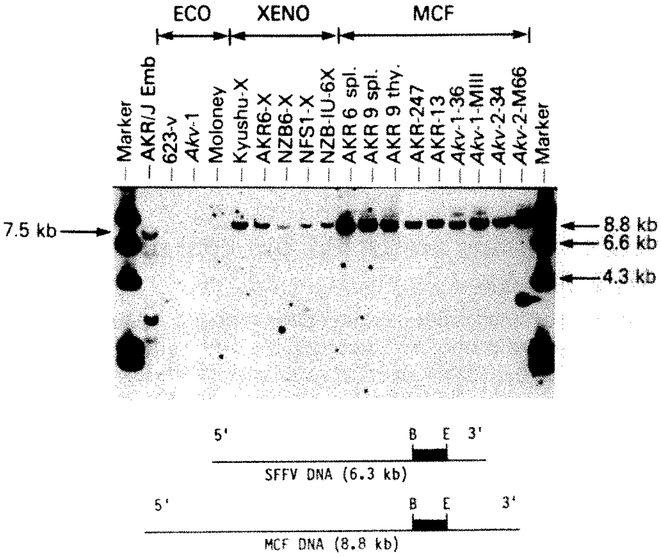

Fig. 2 Southern blot showing selective hybridization of the BE probe to MCF and xenotropic viral DNAs, but not to ecotropic viral DNAs. The BE probe, derived from a 0.7-kb *Bam*HI–*Eco*RI fragment of Friend SFFV DNA[29], was molecularly cloned (by D.L.L.) in pBR322 via the *Bam*HI and *Eco*RI sites. In the upper diagram, the location of the BE probe sequences in SFFV DNA is represented by the heavy line between B (= *Bam*HI) and E (= *Eco*RI). Also shown are the sequences in the BE probe which correspond to the 6.2–6.9-kb region in MCF viruses in *env*, as described in the text. Unintegrated ecotropic (eco), xenotropic (xeno) and MCF viral DNAs were isolated by the Hirt procedure 16–18 h after infection of permissive cells as described in Fig. 1 legend. Hirt supernatant DNAs (5–7 μg each for ecotropic viruses, 15–20 μg of each for xenotropic and MCF viruses) were electrophoresed in horizontal 0.7% agarose gels (35 V, 16 h), transferred to nitrocellulose filters and hybridized with ^{32}P nick-translated 0.7-kb BE probe. The amount of Hirt DNA added for each virus gave an 8.8-kb band of similar intensity when hybridized to its homologous probe (data not shown). *Pst*I-digested high molecular weight AKR/J embryo DNA was electrophoresed in the lane marked AKR/J Emb. 623-v indicates the 623 ecotropic MuLV isolated from NIH3T3 cells transfected with AKR MuLV 623 DNA. The origin of the other viruses has been described previously. Marker was *Hin*dIII-digested ^{32}P-labelled λ DNA. The numbers beside the panels indicate the length of fragments in kb.

The above results therefore indicate that at least some of the endogenous sequences which hybridize to the BE probe are organized as proviral DNAs, as already shown for mouse ecotropic[15,16] and avian leukosis[31] viral genomes in embryo DNA. We have also found multiple copies of similar MCF-like sequences in other mouse strains, including BALB/c and NIH Swiss, and have molecularly cloned from high molecular weight DNA of BALB/c and NIH cells *Eco*RI fragments which hybridize strongly to the BE probe: each clone contains cell sequences linked to 6.9 kb of proviral DNA truncated at the (6.9 kb) *Eco*RI site (unpublished data).

Tryptic analysis of viral gp70s has suggested that this protein in MCF viruses is part ecotropic and part xenotropic, which has led to the hypothesis that the MCF gp70 is invariably a hybrid gene product[32]. However, the finding that the endogenous MCF-like *env* sequences closely resemble those in MCF viruses supports the alternative hypothesis[20,33] that the MCF phenotype assayed in culture may be encoded completely by the endogenous non-ecotropic *env* sequences. The development of MCF-specific gp70 assays[30,34–36] is also consistent with this hypothesis. Further, the MCF gp70 tryptic peptides which resemble ecotropic peptides, which have been localized to the amino terminus of this protein[37], are encoded in the BE probe, and the *env* sequences in the truncated BALB/c and NIH Swiss clones mentioned above resemble the *env* of MCF247 in that they contain the same *Pvu*II, *Bam*HI, *Sma*I and *Eco*RI sites between 6.1 and 6.9 kb (unpublished data). These data suggest that ecotropic-like gp70 peptides of the MCF viruses may be derived from the endogenous MCF-like *env* sequences. However, a direct answer must await biological studies of these endogenous sequences after they have been molecularly cloned intact.

AKR tumours are clonal and contain new MCF DNAs

Having characterized the endogenous sequences which hybridized to the BE probe, we examined the viral sequences in high molecular weight DNA from 19 spontaneous AKR tumours and from 11 tumours induced (accelerated) in AKR mice with MCF247 virus. Other studies with unfractionated probes have found new viral DNA fragments in tumour DNA[38-40]. The DNAs from MCF virus-induced tumours were used principally as controls for the spontaneous tumours, as it is known that the inoculated MCF virus can be recovered intact from these tumours[38].

The tumour DNAs were digested with *Bcl*I-*Xba*I and hybridized to three viral probes: the 5′ probe, to detect new MuLV sequences of any tropism; an ecotropic specific probe (the E probe shown below Fig. 3*a*) to detect viral DNAs with ecotropic gp70 sequences; and the BE probe, to detect viral DNAs with MCF gp70 sequences. As all three probes are composed of sequences located to the left of 7.0 kb, while the only *Bcl*I and *Xba*I sites in AKR MCF or ecotropic viral DNAs were located to the right of 7.0 kb, this digestion should reveal new left-hand cell–virus junction fragments with each probe.

Representative results are presented in Fig. 4. When thymic tumour DNA digested with *Xba*I/*Bcl*I was hybridized with the 5′ probe, novel fragments were detected in all MCF virus-induced tumours (Fig. 4*a*, tumours I 01 and I 02) and in eight of the spontaneous tumours. In Fig. 4*a*, one spontaneous tumour contained a novel fragment (S 02, arrow), while the other spontaneous tumour did not (S 01). Others[39,40] have also found new viral fragments in only some spontaneous AKR tumours, probably because of the high background of multiple endogenous fragments. The tumours induced with MCF247 virus contained several new copies of viral DNA, as denoted by haziness and new distinct bands of 7–9 kb. By contrast, the spontaneous tumours usually contained only a single novel fragment. For each MCF-induced tumour DNA, most of the new viral fragments hybridized to the BE probe (Fig. 4*b*), but other fragments hybridized to the ecotropic probe (Fig. 4*d*), indicating that the tumours were infected with both MCF and ecotropic viruses. By contrast, the new fragment detected with the 5′ probe in spontaneous tumours also hybridized with the BE probe (Fig. 4*b*, tumour S 02, arrow), but no new ecotropic fragments were detected in spontaneous tumours (Fig. 4*d*), despite the small numbers of endogenous ecotropic fragments. These results suggest that ecotropic viruses as such do not usually infect the cells before they become a tumour. (Since submission of this article, Yoshimura and Breda[41] have reported similar observations.) Thymic lymphocytes have been reported to be resistant to infection by ecotropic virus, and our failure to find additional ecotropic viral genomes in the spontaneous tumours is consistent with this observation[42,43].

We also determined that the AKR tumours were, as previously suggested[38,39], probably of clonal origin, as has already been demonstrated for avian leukosis virus-induced bursal tumours in chickens[44,45]. Each new fragment in the DNA of a given thymoma was found to be characteristic of all tumour tissue from a given animal, whether the tumour arose spontaneously or was induced by MCF247 (Fig. 4*c*, arrow). Note also that uninvolved intestinal tissue from leukaemic animals did not contain these new fragments. As the metastatic tumours contained the same new viral fragments as the primary

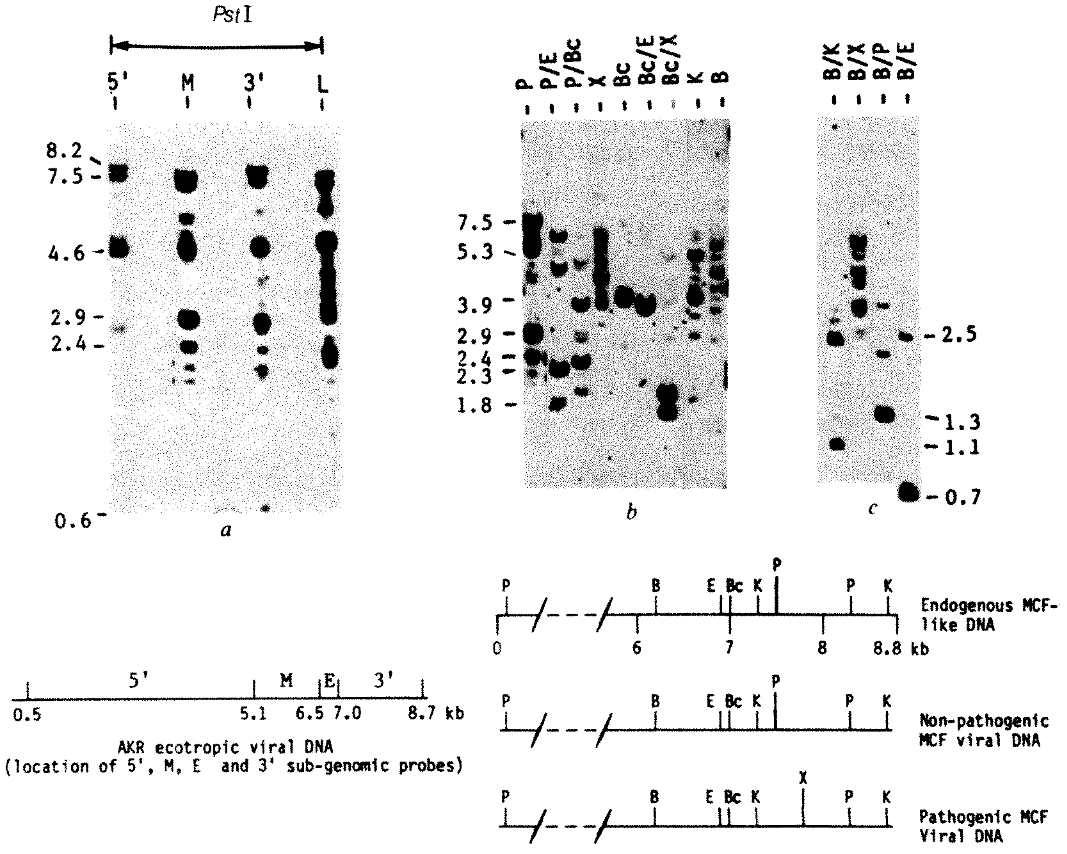

Fig. 3 Blot analysis of nonecotropic sequences of AKR/J embryo DNA. AKR/J embryo DNA was digested with various enzymes as indicated, electrophoresed in 0.5% agarose gels (35 V, 24 h), UV irradiated for 10 min, transferred to nitrocellulose filters and hybridized with various viral probes as described below. Fragment lengths are given in kb. In *a*, each lane contained *Pst*I-digested embryo DNA. The lanes labelled 5′, M and 3′ were hybridized to probes derived from cloned *Sma*I fragments of AKR ecotropic viral DNA as shown in the diagram below *a*. The 5′ probe spans 0.5–5.1 kb, the M probe spans 5.1–6.5 kb and the 3′ probe spans 7.0–8.7 kb. The 3′ includes 0.5 kb of LTR and will therefore hybridize to LTR sequences at the 5′ end of the viral DNAs in addition to hybridizing to sequences at the 3′ end of viral DNAs. The lane in *a* labelled L was hybridized to a probe composed of the LTR sequences of Harvey murine sarcoma viral DNA (provided by E. H. Chang, NCI); this probe also hybridizes to the LTRs of the viruses isolated from AKR mice. In *b* and *c*, the embryo DNA was hybridized to the BE probe, described in Fig. 2 legend. In these two panels and in the diagram below them, K = *Kpn*I, P = *Pst*I, B = *Bam*HI, X = *Xba*I, E = *Eco*RI, Bc = *Bcl*I. The deduced restriction endonuclease map of the non-ecotropic viral sequences in the embryo DNA has been shown in the map labelled 'endogenous MCF-like viral DNA'. These sequences have been compared with those found in non-pathogenic and pathogenic MCF viral DNAs. Viral sequences located rightward from the *Bam*HI site at 6.2 kb have been emphasized here. However, at least some of these endogenous MCF-like DNAs are organized as proviral DNAs (LTR, *gag*, *pol*, *env*, LTR), as noted in the text.

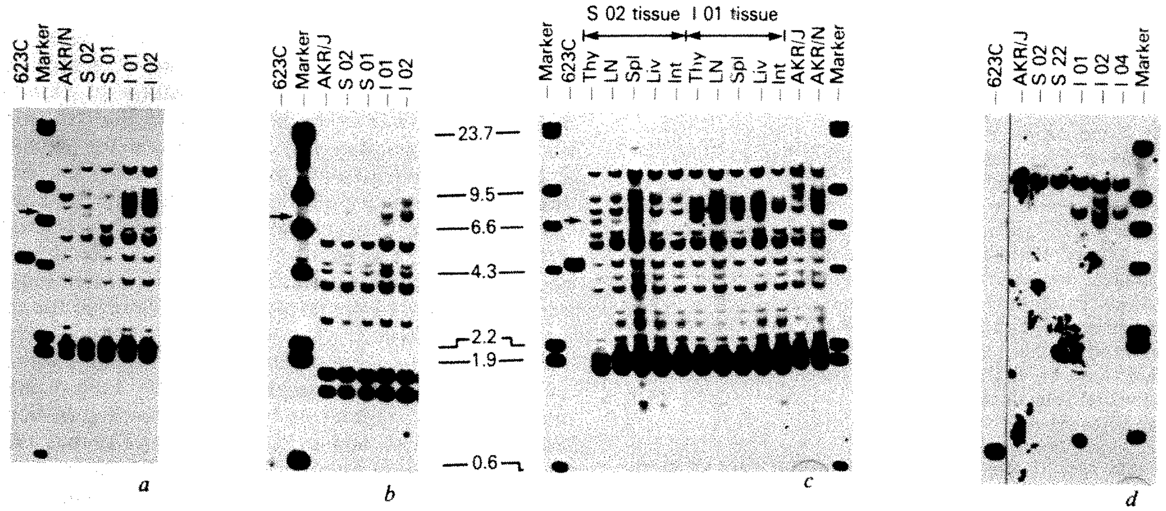

Fig. 4 AKR tumours are clonal in origin, contain new MCF viral DNA, but not new ecotropic viral DNA. *a* Shows that new viral DNA fragments are detected in some spontaneous tumours and all MCF virus-induced tumours; *b* shows that in spontaneous tumours the new fragments hybridize with the BE probe; *c* shows the clonal nature of the tumours; *d* shows that spontaneous tumours do not contain new ecotropic viral DNAs, but that MCF virus-induced tumours do. High molecular weight DNAs isolated from various spontaneous tumours (S) or MCF-induced tumours (I) were digested with *Bcl*I–*Xba*I, electrophoresed in 0.5% agarose gel (35 V, 24 h), UV irradiated for 10 min, transferred to nitrocellulose filters and hybridized with ^{32}P nick-translated viral probes: the 5′ probe (described in Fig. 3 legend) in *a* and *c*, the BE probe (described in Fig. 2 legend) in *b*, or an ecotropic-specific probe spanning 6.6–7.0 kb in AKR ecotropic viral DNA (labelled E in the diagram below Fig. 3*a*) in *d*. *Hin*dIII-digested ^{32}P-labelled λ DNA was used as marker and the number indicates length of the DNA in kb. In *a*, *b* and *d*, DNAs from thymic tumours were used. AKR/J and AKR/N indicates DNAs from embryos of these strains respectively. In *c*, Thy = thymus, LN = lymph nodes, Spl = spleen, Liv = liver, Int = intestine. Thymus, lymph nodes, spleen and liver contained tumours, while intestine did not. In each panel, the lane marked 623C represents *Sma*I-digested clone 623 AKR ecotropic viral DNA as a specificity control. In *d*, the AKR/J embryo DNA contains one more ecotropic fragment than does the DNA from the spontaneous tumours. This additional copy is present only in some AKR/J embryos (M. Martin, personal communication).

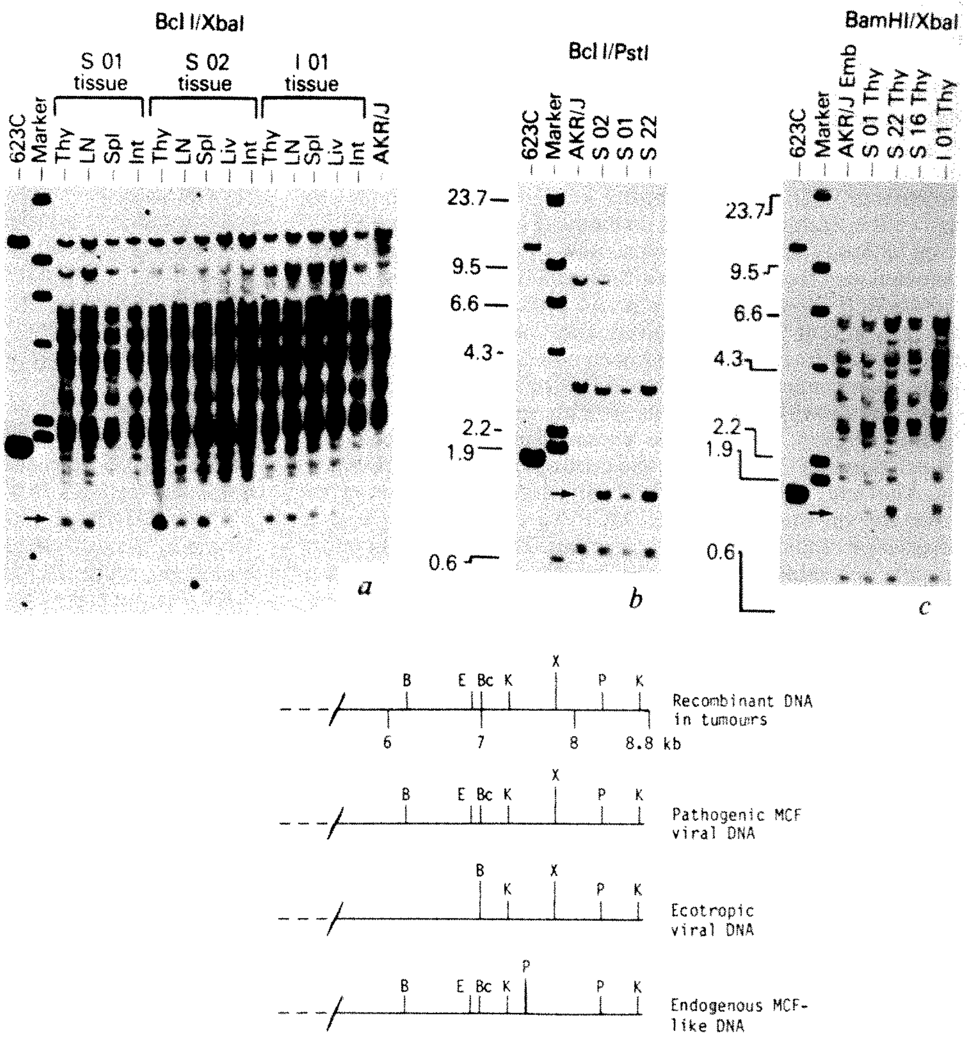

Fig. 5 Blot analysis of tumour DNAs showing that they contain recombinant viral sequences. S = spontaneous; I = induced; Thy = thymus; Spl = spleen; LN = lymph node; Liv = liver; Int = intestine. Thymic tissue was used for tumours in *b*. In each panel, the lane marked 623C contains *Sma*I-digested clone 623 viral DNA as a specificity control. High molecular weight DNAs were digested with various combinations of restriction endonucleases as indicated at the top of each panel, electrophoresed in 0.5% agarose gel (35 V, 24 h), UV irradiated, transferred to nitrocellulose filters and hybridized with a ^{32}P-labelled nick-translated 3′ probe (described in Fig. 3). In the diagram, the restriction enzyme sites of the recombinant viral *env*–LTR are shown on the map labelled 'recombinant DNA in tumours' (the presence of the *Kpn*I sites has not been determined experimentally).

Table 1 MCF virus in AKR thymus

	Infectious centres per 10^7 cells
AKR247 MCF-induced thymomas (19)	10,000–85,000
AKR spontaneous thymomas (7)	Trace, 1,000
Pre-leukaemic AKR (<6 months old) (9)	0*

Mink lung cells (CCL64) were plated at 2×10^5 cells per 60-mm dish in Dulbecco's modified minimal essential medium with 10% fetal calf serum. The following day, serial dilutions of thymus or spleen cells were plated as infectious centres onto the mink cultures in medium containing 16 μg ml^{-1} polybrene. The medium was changed 24 h later and the cultures were scored for characteristic MCF cytopathic foci (mink CPE) after confluence (days 5–7). The numbers in parentheses indicate the number of individual animals tested.

* Thymus and spleen.

thymoma, these results suggest that the tumours are of clonal origin.

Recombinant nature of new MCF DNA in AKR tumours

We also analysed the DNA of spontaneous tumours for recombinant viral DNA sequences, again using the cell DNA of MCF virus-induced tumours as positive controls for specific DNA fragments. In these studies, we hybridized the restriction endonuclease-digested tumour DNAs to the 3′-viral probe shown below Fig. 3*a*; this probe recognizes viral sequences to the right of 7.0 kb and includes the *Xba*I site at 7.7 kb which had been found in the DNA of pathogenic MCF viruses but had not been detected in the non-ecotropic sequences of AKR embryo DNA mapped with the BE probe in Fig. 3.

As noted earlier, all MCF viruses contained a *Bcl*I site at 7.0 kb, as did the endogenous non-ecotropic sequences in embryo DNA. Using the 3′ probe, the lack of linkage in AKR embryo DNA of the *Bcl*I site to an *Xba*I site corresponding to 7.7 kb was confirmed, as embryo DNA digested with *Bcl*I–*Xba*I did not contain the 0.7-kb *Bcl*I–*Xba*I internal viral fragment (Fig. 5*a*, arrow) found in the pathogenic MCF viruses and easily detected in the cell DNA of MCF virus-induced tumours (Fig. 5*a*, tumour I 01). However, the 0.7-kb *Bcl*I–*Xba*I fragment was detected in each spontaneous thymoma (Fig. 5*a*, S 01 and S 02), even in those tumours in which no new viral fragment had been detected with the other probes (tumour S 01). The recombinant 0.7-kb *Bcl*I–*Xba*I fragment was also present in all metastases, but was absent from uninvolved intestinal tissue. This same recombinant fragment has also been noted in thymomas arising in mice congeneic for *Akv-1* or *Akv-2* (ref. 40) and in C58 mice (data not shown). Such results strongly suggest that a recombinational event between the endogenous non-ecotropic *env* (which donated the *Bcl*I site) and ecotropic *env* (which donated the *Xba*I site) generated a hybrid *env* which corresponds to the structure of the pathogenic MCF viruses. The invariable association of this fragment with tumour DNA suggests that this specific recombination may be an important aspect of the oncological process in AKR tumours. (After this article was submitted, we learned that Quint *et al.*[46] and W. Herr and W. Gilbert (personal communication) had independently made similar observations in AKR tumours.)

In attempts to define further the region of recombination, we took advantage of the previously noted finding that many of the endogenous sequences which hybridized with the BE probe contained a *Pst*I site at 7.5 kb, while this site was not present in AKR ecotropic MuLV. If the recombination took place to the left of this *Pst*I site, then *Bcl*I (at 7.0 kb)–*Pst*I (at 8.2 kb), digestion should yield a 1.2-kb fragment; this was the case for all five spontaneous tumours studied (Fig. 5*b*, arrow). This result indicates either that recombination occurred between MCF sequences located to the right of 7.0 kb and ecotropic sequences located to the left of 7.5 kb, or that the recombination involved an unusual non-ecotropic *env* which lacked the *Pst*I site at 7.5 kb.

We also determined that the non-ecotropic sequences extended leftward at least to the *Bam*HI site at 6.2 kb, which had been noted in many endogenous non-ecotropic fragments mapped in embryo DNA. Hybridization of *Bam*HI–*Xba*I-digested tumour DNA to the 3′ probe or the BE probe, which should reveal a novel 1.5-kb fragment if the *Bam*HI site at 6.2 kb were now linked to the *Xba*I site at 7.7 kb, showed that this fragment was present in most (S 01 and S 22) but not all (S 16) spontaneous tumours (Fig. 5*c*, arrow; only 3′ probe results are shown). These results suggested that the non-ecotropic sequences extended leftward at least to 6.2 kb in most of these recombinant DNA fragments, as was also true for the pathogenic MCF viruses.

The mechanism by which the viral recombination has occurred is unknown although it probably follows infection of non-target cells by ecotropic virus. Relatively good homology to the left of 6.2 kb and to the right of 7.3 kb has been noted between ecotropic, xenotropic and MCF viruses, and the non-ecotropic sequences of MCF viruses usually include at least this 1-kb DNA segment[20,47]. It therefore seems reasonable to speculate that the non-ecotropic *env* of MCF virus genomes has been generated by homologous recombination through a double-crossover mechanism.

MCF virus production in tumours

As noted above, tumours induced experimentally by inoculation with MCF virus contained several new MCF viral DNA fragments, whereas the DNA of spontaneous tumours contained few new viral DNA fragments. We therefore sought to determine whether these biochemical differences would be reflected biologically in the frequency of virus-positive cells in MCF virus-induced tumours versus spontaneous tumours. By infectious centre assay (Table 1), no more than 0.01% of the thymoma cells from spontaneous tumours were releasing infectious virus whereas a much higher proportion of the cells from tumours induced by experimental inoculation with an MCF virus released MCF virus. These results therefore correlate with the biochemical data.

The mechanism underlying the low MCF virus production in spontaneous tumours remains to be elucidated. One attractive hypothesis is that the MCF viral sequences in the spontaneous AKR tumour cells is defective for replication. This mechanism has recently been noted in avian leukosis virus-induced bursal tumours[44,45]. Alternatively, the virus may be unable to be expressed efficiently in tumour cells. However, the release of MCF virus from a significant proportion of the cells in tumours induced experimentally by MCF247 does not support this conjecture.

Significance of recombinant viral sequences

The presence in spontaneous tumours of recombinant *env* sequences with a structure similar to that found in pathogenic MCF viral DNAs, combined with the lack of new ecotropic viral DNAs in the tumours, suggests that MCF viruses with recombinant *env* represent a more immediate inducer of spontaneous AKR lymphomas. The consistent association of the tumours with sequences present in pathogenic MCF viruses (and their absence from non-tumour tissue) suggests that this specific rearrangement of endogenous sequences is an important step in the development of the spontaneous tumours, perhaps by altering the differentiation state or the proliferative capacity of the target cell directly[48] or by promoter insertion[49]. The non-pathogenic nature of MCF viruses that have apparently acquired the endogenous MCF-like *env* without also retaining the ecotropic virus-derived sequences around the *Xba*I site at 7.7 kb suggests that activation of those endogenous non-ecotropic sequences is not by itself sufficient for tumour induction. Rather, pathogenicity occurs only after certain specific recombinational events between ecotropic virus and the endogenous MCF-like viral sequences. We presume that the non-ecotropic sequences facilitate adsorption and penetration of the virus into the target tissue. The function of the ecotropic sequences around the *Xba*I site is not known. However, they may also be important for infection of the target tissue, as pathogenic MCF viruses replicate better in the thymus than do the non-pathogenic viruses we have studied[19].

We thank Drs Alan Rein and Michael Potter for a critical reading of the manuscript, Dr Wallace Rowe for tumour tissues from *Akv* congeneic mice, and Mrs Lorraine Shaughnessy and Mr Harry Schaefer for preparation of the manuscript. This research was supported in part by a contract from the National Cancer Institute to Meloy Laboratories.

Received 6 August; accepted 27 October 1981.

1. Gross, L. *Oncogenic Viruses* 2nd edn (Pergamon, Oxford, 1970).
2. Gelb, L. D., Milstein, J. B., Martin, M. A. & Aaronson, S. A. *Nature new Biol.* **244,** 76–79 (1973).
3. Chattopadhyay, S. K., Lowy, D. R., Teich, N. M., Levine, A. S. & Rowe, W. P. *Cold Spring Harb. Symp. quant. Biol.* **39,** 1085–1101 (1974).
4. Stephenson, J. R. in *Molecular Biology of RNA Tumour Viruses* (ed. Stephenson, J. R.) 245–297 (Academic, New York, 1980).
5. Kawashima, K. *et al. Proc. natn. Acad. Sci. U.S.A.* **73,** 4680–4684 (1976).
6. Hartley, J. W., Wolford, N. K., Old, L. J. & Rowe, W. P. *Proc. natn. Acad. Sci. U.S.A.* **74,** 789–792 (1977).
7. Fischinger, P. J., Dunlop, N. M. & Blevins, C. S. *J. Virol.* **26,** 532–535 (1978).
8. Troxler, D. H., Yuan, E., Linemeyer, D., Ruscetti, S. & Scolnick, E. M. *J. exp. Med.* **148,** 639–653 (1978).
9. Troxler, D. H., Lowy, D., Howk, R. R., Young, H. & Scolink, E. M. *Proc. natn. Acad. Sci. U.S.A.* **74,** 4671–4675 (1977).
10. Rommelaere, J., Faller, D. V. & Hopkins, N. *Proc. natn. Acad. Sci. U.S.A.* **75,** 495–499 (1978).
11. Furth, J., Seibold, H. R. & Rathbone, R. R. *Am. J. Cancer* **19,** 521–604 (1933).
12. Rowe, W. P. *Cancer Res.* **33,** 3061–3068 (1973).
13. Rowe, W. P. *J. exp. Med.* **136,** 1272–1285 (1972).
14. Chattopadhyay, S. K., Rowe, W. P., Teich, N. M. & Lowy, D. R. *Proc. natn. Acad. Sci. U.S.A.* **72,** 906–910 (1975).
15. Chattopadhyay, S. K., Lander, M. R., Rands, E. & Lowy, D. R. *Proc. natn. Acad. Sci. U.S.A.* **77,** 5774–5778 (1980).
16. Steffen, D. L., Bird, S. & Weinberg, R. A. *J. Virol.* **35,** 824–835 (1980).
17. Rowe, W. P. & Pincus, T. *J. exp. Med.* **135,** 429–436 (1972).
18. Lilly, F., Duran-Reynals, M. & Rowe, W. P. *J. exp. Med.* **141,** 882–889 (1975).
19. Cloyd, M. W., Hartley, J. W. & Rowe, W. P. *J. exp. Med.* **151,** 542–552 (1980).
20. Chattopadhyay, S. K., Lander, M. R., Gupta, S., Rands, E. & Lowy, D. R. *Virology* **113,** 465–483 (1981).
21. Rands, E., Lowy, D. R., Lander, M. R. & Chattopadhyay, S. K. *Virology* **108,** 445–452 (1981).
22. Stephenson, J. R., Tronick, S. R. & Aaronson, S. A. *Cell* **6,** 543–548 (1975).
23. Jamjoon, C. A., Naso, R. B. & Arlinghaus, R. B. *Virology* **78,** 11–34 (1977).
24. Karshin, W. L., Arcement, L. J., Naso, R. B. & Arlinghaus, R. B. *J. Virol.* **23,** 787–798 (1977).
25. Donoghue, D. J., Rothenberg, E., Hopkins, N., Baltimore, D. & Sharp, P. A. *Cell* **14,** 959–970 (1978).
26. Rothenberg, E., Donoghue, D. J. & Baltimore, D. *Cell* **13,** 435–451 (1978).
27. Sutcliffe, J. G., Shinnick, T. M., Verma, I. M. & Lerner, R. A. *Proc. natn. Acad. Sci. U.S.A.* **77,** 3302–3306 (1980).
28. Lung, M. L., Hering, C., Hartley, J. W., Rowe, W. P. & Hopkins, N. *Cold Spring Harb. Symp. quant. Biol.* **44,** 1269–1279 (1979).
29. Linemeyer, D. L., Ruscetti, S. K., Menke, J. G. & Scolnick, E. M. *J. Virol.* **35,** 710–721 (1980).
30. Ruscetti, S., Linemeyer, D., Feild, J., Troxler, D. & Scolnick, E. *J. exp. Med.* **148,** 654–663 (1978).
31. Astrin, S. M. *et al. Cold Spring Harb. Symp. quant. Biol.* **44,** 1105–1110 (1979).
32. Elder, J. H. *et al. Proc. natn. Acad. Sci. U.S.A.* **74,** 4676–4680 (1977).
33. Green, N. *et al. J. exp. Med.* **152,** 249–264 (1980).
34. Stockert, E., DeLeo, A. B., O'Donnell, P. V., Obata, Y. & Old, L. J. *J. exp. Med.* **149,** 200–215 (1979).
35. Cloyd, M. W., Hartley, J. W. & Rowe, W. P. *J. exp. Med.* **149,** 702–712 (1979).
36. O'Donnell, P. V., Stockert, E., Obata, Y., DeLeo, A. B. & Old, L. J. *Cold Spring Harb. Symp. quant. Biol.* **44,** 1255–1264 (1979).
37. Niman, H. L. & Elder, J. H. *Proc. natn. Acad. Sci. U.S.A.* **77,** 4524–4528 (1980).
38. Pedersen, F. S., Buchhagen, D. L., Chen, C. Y., Hays, E. F. & Haseltine, W. A. *J. Virol.* **35,** 211–218 (1980).
39. Canaani, E. & Aaronson, S. A. *Proc. natn. Acad. Sci. U.S.A.* **76,** 1677–1681 (1979).
40. Steffen, D. L., Bird, S., Rowe, W. P. & Weinberg, R. A. *Proc. natn. Acad. Sci. U.S.A.* **76,** 4554–4558 (1979).
41. Yoshimura, F. K. & Breda, M. *J. Virol.* **39,** 808–815 (1981).
42. Gisselbrecht, S., Blaineau, C., Hurot, M. A., Pozo, F. & Levy, J. P. *Cancer Res.* **38,** 939–941 (1978).
43. Blank, K. J. & Pincus, T. *J. exp. Med.* **152,** 458–462 (1980).
44. Payne, G. S. *et al. Cell* **23,** 311–322 (1981).
45. Neel, B. G., Hayward, W. S., Robinson, H. L., Fang, J. & Astrin, S. M. *Cell* **23,** 323–334 (1981).
46. Quint, W., Quax, W., van der Putten & Berns, A. *J. Virol.* **39,** 1–10 (1981).
47. Chien, Y., Verma, I. M., Shih, T. Y., Scolnick, E. M. & Davidson, N. *J. Virol.* **28,** 352–360 (1978).
48. McGrath, M. S. & Weissman, I. L. *Cell* **17,** 65–75 (1979).
49. Hayward, W. S., Neel, B. G., & Astrin, S. M. *Nature* **290,** 475–480 (1981).
50. Lowy, D. R., Rands, E., Chattopadhyay, S. K., Garon, C. F. & Hager, G. L. *Proc. natn. Acad. Sci. U.S.A.* **77,** 614–618 (1980).
51. Hirt, B. *J. molec. Biol.* **26,** 365–369 (1967).
52. Southern, E. M. *J. molec. Biol.* **98,** 503–517 (1975).

The highly polymorphic region near the human insulin gene is composed of simple tandemly repeating sequences

Graeme I. Bell, Mark J. Selby & William J. Rutter

Department of Biochemistry and Biophysics, University of California, San Francisco, California 94143, USA

The sequence of the highly polymorphic region near the human insulin gene, which begins 363 base pairs before the start of transcription and extends upstream, indicated that it is generated by variation in the number and arrangement of members of a family of tandemly repeating nucleotides whose structure is related to ACAGGGGTGTGGGG. Another 15-base pair sequence, repeated twice near the human gene, is located ~325 base pairs on either side of the polymorphic region. One member is in the transcriptional control region.

THE human insulin gene region of two human chromosome 11 homologues has been isolated and characterized[1–5]. The organization and structure of the 1,430-base pair (bp) segment encoding the insulin mRNA precursor and ~40 kilobases (kb) of the flanking sequence on different chromosomes are similar, but restriction mapping studies of 150 individuals (ref. 6 and G.I.B. and J. Karam, unpublished results) indicated that a highly polymorphic region is located ~500 bp before the point where transcription of insulin mRNA begins[6]. Sixty-three per cent of non-diabetic caucasian individuals examined are heterozygous at this site, and there are two major and one minor class of alleles[6]. However, as there is heterogeneity within each class, there are many different alleles at this locus. Preliminary data also indicate that there may be racial differences in the frequency of alleles, that this polymorphism is inherited in a mendelian fashion in a four-generation pedigree and that the organization of the polymorphic region in DNA prepared from an insulin-secreting adenoma and white blood cells of the same individual is identical (G.I.B., unpublished). However, the molecular events which produce either this highly polymorphic region or one with similar properties that has been described at an unidentified locus[7], have not been determined.

Restriction mapping studies of the insulin gene region suggested that the restriction fragment length polymorphism is generated by the insertion–deletion of DNA sequences, so that fragments of different size are generated when DNA from a heterozygous individual is digested with selected restriction endonucleases. The insertions in this region are primarily of two size classes: 0–600 bp and 1,600–2,200 bp; restriction fragments possessing insertions of 600–1,600 bp are rarely observed. We have sequenced the corresponding polymorphic regions of two chromosomes to determine the basis for this length polymorphism. The sequence comparison indicated that the polymorphism is generated by variation in the redundancy of

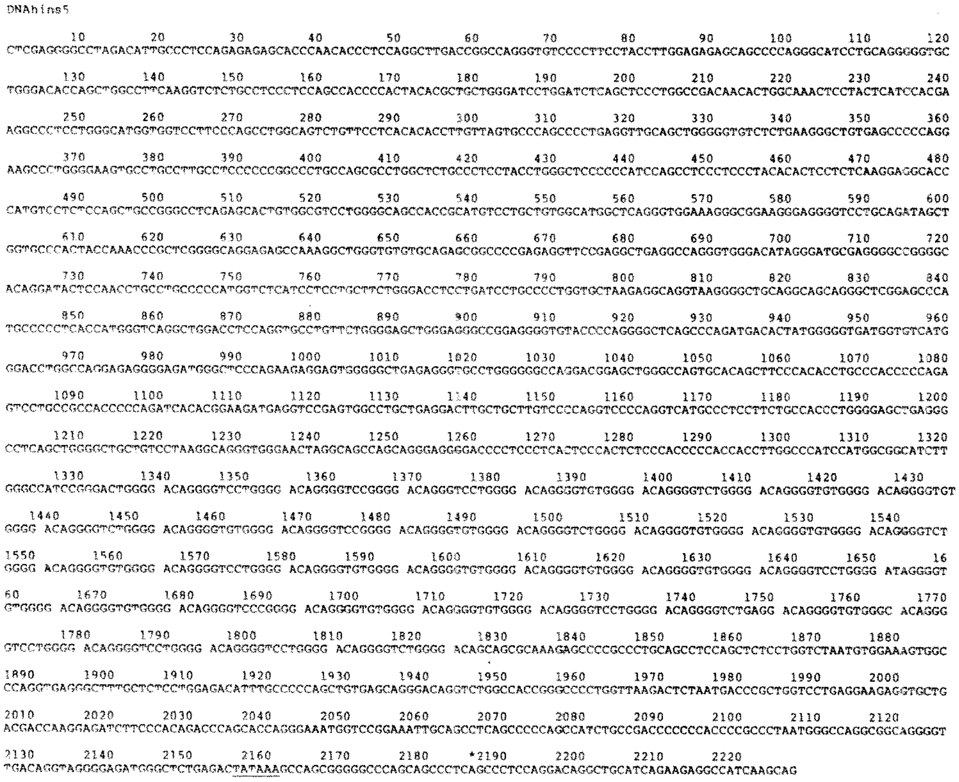

```
DNAhins5

         10        20        30        40        50        60        70        80        90       100       110       120
CTCGAGGGGCCTAGACATTGCCCTCCAGAGAGAGCACCCAACACCCTCCAGGCTTGACCGGCCAGGGTGTCCCCTTCCTACCTTGGAGAGAGCAGCCCCAGGGCATCCTGCAGGGGGTGC

        130       140       150       160       170       180       190       200       210       220       230       240
TGGGACACCAGCTGGCCTTCAAGGTCTCTGCCTCCCTCCAGCCACCCCACTACACGCTGCTGGGATCCTGGATCTCAGCTCCCTGGCCGACAACACTGGCAAACTCCTACTCATCCACGA

        250       260       270       280       290       300       310       320       330       340       350       360
AGGCCCTCCTGGGCATGGTGGTCCTTCCCAGCCTGGCAGTCTGTTCCTCACACACCTTGTTAGTGCCCAGCCCCTGAGGTTGCAGCTGGGGGTGTCTCTGAAGGGCTGTGAGCCCCCAGG

        370       380       390       400       410       420       430       440       450       460       470       480
AAGCCCTGGGGAAGTGCCTGCCTTGCCTCCCCCCGGCCCTGCCAGCGCCTGGCTCTGCCCTCCTACCTGGGCTCCCCCCATCCAGCCTCCCTCCCTACACACTCCTCTCAAGGAGGCACC

        490       500       510       520       530       540       550       560       570       580       590       600
CATGTCCTCTCCAGCTGCCGGGCCTCAGAGCACTGTGGCGTCCTGGGGCAGCCACCGCATGTCCTGCTGTGGCATGGCTCAGGGTGGAAAGGGCGGAAGGGAGGGGTCCTGCAGATAGCT

        610       620       630       640       650       660       670       680       690       700       710       720
GGTGCCCACTACCAAACCCGCTCGGGGCAGGAGAGCCAAAGGCTGGGTGTGTGCAGAGCGGCCCCGAGAGGTTCCGAGGCTGAGGCCAGGGTGGGACATAGGGATGCGAGGGGCCGGGGC

        730       740       750       760       770       780       790       800       810       820       830       840
ACAGGATACTCCAACCTGCCTGCCCCCATGGTCTCATCCTCCTGCTTCTGGGACCTCCTGATCCTGCCCCTGGTGCTAAGAGGCAGGTAAGGGGCTGCAGGCAGCAGGGCTCGGAGCCCA

        850       860       870       880       890       900       910       920       930       940       950       960
TGCCCCCTCACCATGGGTCAGGCTGGACCTCCAGGTGCCTGTTCTGGGGAGCTGGGAGGGCCGGAGGGGTGTACCCCAGGGGCTCAGCCCAGATGACACTATGGGGGTGATGGTGTCATG

        970       980       990      1000      1010      1020      1030      1040      1050      1060      1070      1080
GGACCTGGCCAGGAGAGGGGAGATGGGCTCCCAGAAGAGGAGTGGGGGCTGAGAGGGTGCCTGGGGGGCCAGGACGGAGCTGGGCCAGTGCACAGCTTCCCACACCTGCCCACCCCCAGA

       1090      1100      1110      1120      1130      1140      1150      1160      1170      1180      1190      1200
GTCCTGCCGCCACCCCCAGATCACACGGAAGATGAGGTCCGAGTGGCCTGCTGAGGACTTGCTGCTTGTCCCCAGGTCCCCAGGTCATGCCCTCCTTCTGCCACCCTGGGGAGCTGAGGG

       1210      1220      1230      1240      1250      1260      1270      1280      1290      1300      1310      1320
CCTCAGCTGGGGCTGCTGTCCTAAGGCAGGGTGGGAACTAGGCAGCCAGCAGGGAGGGGACCCCTCCCTCACTCCCACTCTCCCACCCCCACCACCTTGGCCCATCCATGGCGGCATCTT

       1330      1340      1350       1360       1370      1380       1390       1400      1410       1420       1430
GGGCCATCCGGGACTGGGG ACAGGGGTCCTGGGG ACAGGGGTCCGGGG ACAGGGTCCTGGGG ACAGGGGTGTGGGG ACAGGGGTCTGGGG ACAGGGGTGTGGGG ACAGGGGTGT

  1440      1450       1460       1470      1480       1490       1500       1510      1520       1530       1540
GGGG ACAGGGGTCTGGGG ACAGGGGTGTGGGG ACAGGGGTCCGGGG ACAGGGGTGTGGGG ACAGGGGTCTGGGG ACAGGGGTGTGGGG ACAGGGGTGTGGGG ACAGGGGTCT

1550      1560       1570       1580      1590       1600       1610       1620      1630       1640       1650       16
GGGG ACAGGGGTGTGGGG ACAGGGGTCCTGGGG ACAGGGGTGTGGGG ACAGGGGTGTGGGG ACAGGGGTGTGGGG ACAGGGGTGTGGGG ACAGGGGTCCTGGGG ATAGGGGT

60        1670       1680       1690       1700       1710       1720       1730       1740      1750       1760       1770
GTGGGG ACAGGGGTGTGGGG ACAGGGGTCCCGGGG ACAGGGGTGTGGGG ACAGGGGTGTGGGG ACAGGGGTCCTGGGG ACAGGGGTCTGAGG ACAGGGGTGTGGGC ACAGGG

       1780      1790       1800       1810      1820       1830      1840      1850      1860      1870      1880
GTCCTGGGG ACAGGGGTCCTGGGG ACAGGGGTCCTGGGG ACAGGGGTCTGGGG ACAGCAGCGCAAAGAGCCCCGCCCTGCAGCCTCCAGCTCTCCTGGTCTAATGTGGAAAGTGGC

1890      1900      1910      1920      1930      1940      1950      1960      1970      1980      1990      2000
CCAGGTGAGGGCTTTGCTCTCCTGGAGACATTTGCCCCCAGCTGTGAGCAGGGACAGGTCTGGCCACCGGGCCCCTGGTTAAGACTCTAATGACCCGCTGGTCCTGAGGAAGAGGTGCTG

2010      2020      2030      2040      2050      2060      2070      2080      2090      2100      2110      2120
ACGACCAAGGAGATCTTCCCACAGACCCAGCACCAGGGAAATGGTCCGGAAATTGCAGCCTCAGCCCCCAGCCATCTGCCGACCCCCCCACCCCGCCCTAATGGGCCAGGCGGCAGGGGT

2130      2140      2150      2160      2170      2180      *2190     2200      2210      2220
TGACAGGTAGGGGAGATGGGCTCTGAGACTATAAAGCCAGCGGGGGCCCAGCAGCCCTCAGCCCTCCAGGACAGGCTGCATCAGAAGAGGCCATCAAGCAG
```

Fig. 1 Sequence of the 5'-flanking region and first coding region (exon) of the human insulin gene. The sequence of the insulin gene region of allele 1 (recombinant λHi1[1,2,5]) was determined by the procedure of Maxam and Gilbert[26], including the modified G·A reaction described by Cooke *et al.*[27]. The TATAAA sequence (Hogness box) is underlined and the putative 5' end of the mRNA (capping site) indicated by an asterisk. The individual oligonucleotide units in the tandemly repeating array are separated. As described in the text, there are several ways to divide this region into oligonucleotide units. The sequence presented here is part of a 4,992-bp DNA segment which also includes the sequence of the insulin gene and 3'-flanking sequence. This complete sequence, with a list of all restriction sites, is available on request. The sequence includes three changes from that previously published[1] which corrects one clerical and two sequencing errors, but still does not completely agree with that determined by Ullrich *et al.*[5]. The sequences across the *Bam*HI and *Pst*I sites at positions 185 and 817, respectively, were not determined.

a family of G + C-rich oligonucleotides. This family of sequences is only tandemly repeated in this region of the human genome, and as the arrangement of members of this family differs in these two homologous chromosomal regions, this region also shows DNA sequence polymorphism. The highly variable structure of this region contrasts with adjacent regions which are characterized by conservation of size and nucleotide sequence.

Molecular basis for length polymorphism

Restriction mapping studies established that the highly polymorphic region was in a section of the 5'-flanking region of the gene between *Bgl*I and *Pvu*II sites located ~1,300 and 259 bp, respectively, before the insulin mRNA coding region[2,6]. The sequence between and flanking these restriction sites was determined for two allelic DNA segments. The 2,227-bp sequence in this region for allele 1, recombinant λHiI (refs 1, 2) (β (ref. 5)), is shown in Fig. 1. This is a portion of a 4,992-bp segment of known sequence which includes 2,185 bp of 5'-flanking sequence, 1,430 bp encoding insulin mRNA precursor and 1,367 bp of the 3' flanking region.

As we previously noted[1], the insulin gene has a high G+C content (64.8%) and this is maintained in the 5'-flanking region (67.8% G+C). Another unusual feature of the 5'-flanking region occurs in the region 363–846 bp (nucleotides 1,825–1,340, respectively, Fig. 1) before the putative capping site in that it consists of 34 tandem repeats of a family of G+C-rich 14–15-bp oligonucleotides. Other oligonucleotides, ⩾10 bp, are also repeated, both direct and inverted (rc), in this region (Table 1). The most interesting is the 15-bp sequence AGGGGAGATGGGCTC (at nucleotides 976 and 2,135 (Fig. 1)) which is directly repeated 350 and 312 bp, 5' and 3' respectively, on either side of the region of tandemly repeating oligonucleotides. This sequence is not present elsewhere in the 4,992-bp segment. The 15-bp repeated oligonucleotide at nucleotide 2,135 is located between the two putative transcription control sequences[8,9]: the TATAAA sequence (Hogness box), nucleotides 2,156–2,161 (Fig. 1), and the −75 to −90 region (remote control sequence), nucleotides 2,110–2,118. These two 15-bp sequences are 1,159 bp apart in this allele. Examination of the 2,185 bp of 5'-flanking sequence and 1,367 bp of 3'-flanking sequence for additional control sequences, TATA (Hogness box) and AATAAA (polyadenylation signal), showed that the only ones observed were those of the insulin gene. Thus, this sequence does not indicate the position of any adjacent genes nor the presence of any other insulin-like sequences. Moreover, we have not observed by hybridization any insulin-like sequences within 20 kb of the insulin gene. As we previously indicated[1], the sequence including the putative 5' end of insulin mRNA CAGCCCT (nucleotides, 2,185–2,191, Fig. 1) (the A is the residue which is capped), is tandemly repeated upstream at nucleotides 2,178–2,184 (Fig. 1). This sequence is also present within intervening sequence 1, coding region 3 and the region encoding the mature 3' end of the mRNA (CAG$\overset{*}{\mathrm{C}}$CCT) (the asterisk indicates the residue which is polyadenylated). Such repetition of the sequence in the regions encoding the 5' and 3' ends of the mature mRNA is thus far unique to the human insulin gene.

The 1,274-bp sequence in the 5'-flanking region of allele 2, recombinant λHi2 (refs 1, 2) (α (ref. 5)), was determined from a *Pst*I site corresponding to the *Pst*I site at nucleotide 817 of allele 1 (Fig. 1) to the *Pvu*II site at nucleotide 1,927. The sequences of the two alleles were identical at nucleotides 815–1,394 and 1,764–1,930, diverging in the region of the family of tandemly repeating G + C-rich oligonucleotides. There were 45 repeats in the region flanking allele 2. These 11 additional repeating units (158 bp) account for the size difference previously observed by restriction endonuclease mapping and DNA heteroduplex analysis of the two alleles[2]. Thus, variation in the redundancy of the oligonucleotide sequence is responsible for the differences in the length of homologous restriction fragments.

Organization and sequences of the repeating oligonucleotide family

Ten different oligonucleotide sequences have been observed among the 79 repeats analysed (Table 2). The frequency of each member of the family and the organization of the array were different within the two allelic chromosomal DNA segments (Table 2), the most frequent oligonucleotide (46.8%) being the 14-bp ACAGGGGTGTGGGG. (As there is no unit number of repetitions, the sequence description is somewhat arbitrary (Fig. 1).) This 14-bp sequence is also the consensus sequence for members of this family and changes have been observed at 8/14 positions, the most variable portion being that between

GGGGT and GGGG. Both nucleotide substitutions and single nucleotide insertions are observed: G → CC, G → C, GT → CCC. And in addition the boundaries of this region, 5'CTGGGG,ACAG3', are found in the 14-bp sequence.

Although the arrangement of the various oligonucleotide sequences within the polymorphic regions is different (Fig. 2*b*), the composition and order of the three units at the 5' boundary and the four units of the 3' boundary of this region are identical. Moreover, the variant sequence ACAGGGTCCTGGGG (in Table 2) is found only once in both arrays in this conserved 5' boundary region. These data suggest that the molecular processes which generate the divergence within this family operate on the central regions of the array.

Length variation of polymorphic forms

We have previously shown that the polymorphism exists in two major forms[6]. Approximately 75% of all the insulin gene regions analysed have a short polymorphic region (0–600 bp) and ~25% possess a longer polymorphic region (1,600–2,200 bp). Polymorphic regions of intermediate size are rarely observed (6/300 chromosomes examined). The two allelic DNA segments which we have sequenced are of the more frequent shorter form. As the length heterogeneity in this class is essentially due to variation in the number of oligonucleotide repeats, our previous data[6] can be reinterpreted. The shorter polymorphic region is composed of alleles with 26–63 repeating oligonucleotide units, with an average of 38 repeats.

We have examined the nature of the longer polymorphic form by hybridizing an *in vitro* labelled 879-bp *Pvu*II fragment of the flanking region of allele 2 (λHi2, the allelic DNA segment corresponding to the region at nucleotides 1,206–1,927, Fig. 1) to a *Sac*I digest of DNA of nine individuals, four of whom possessed both a short and a long polymorphic region (individuals 019, 025, 035 and 038, Fig. 2). This 879-bp *Pvu*II fragment included 45 repeating units of 641 bp, as well as 134 bp on the 5' end and 105 bp on the 3' end. We reasoned that if the length variation in the larger polymorphic region was due to this same repeating oligonucleotide, we should observe more intense hybridization to DNA fragments containing the longer polymorphic region.

There was more intense hybridization to the larger fragment in four individuals: 019, 025, 035 and 038 (Fig. 2). In contrast, a DNA fragment specific for the insulin gene, which included a 59-bp 5'-flanking sequence, 1,430-bp structurel region and 118-bp 3'-flanking sequence, hybridized with equal intensity to both DNA fragments (data not shown and Fig. 2C in ref. 6). Thus, this differential autoradiographic signal is not due to differential transfer or selective loss of DNA from the filter but is due at least in part to variation in the redundancy of this family of oligonucleotides. However, without cloning and sequencing the longer polymorphic allele or the rare intermediate form, we cannot exclude the possibility that another sequence in the ~100 bp on either side of the repeating oligonucleotides has not been selectively amplified. There are no other tandemly repeated sequences flanking the polymorphic region, so if additional sequence amplification occurred, it is of a non-repeated sequence. However, as we have defined the boundaries of the region of length variation for all forms, *Bgl*I and *Pvu*II sites at nucleotides 1,025 and 1,927 (Fig. 1), respectively[2,6], and more recently between *Pvu*II sites at 1,206 and 1,927 (unpublished)), we believe that the variation in the redundancy of this family of G+C-rich oligonucleotides accounts for all length variation. Thus, the longer polymorphic regions contain 141–209 repeats, with an average of 163. The rare intermediate forms possess ~80 repeats and the short form possesses ~40 repeats. The significance of the arithmetic progression in the number of repeats is unknown.

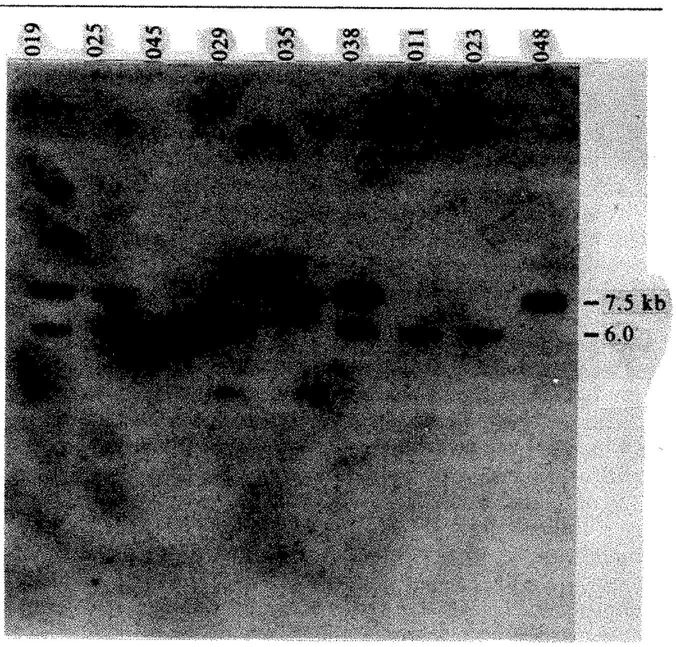

Fig. 2 Hybridization of a DNA fragment containing the region of tandemly repeating oligonucleotides to *Sac*I digests of human DNA. DNA was prepared from white blood cells, digested with *Sac*I, the fragments were separated by electrophoresis in a 1% agarose gel, transferred to nitrocellulose filters and hybridized as described previously[6]. Individuals are indicated by number above the autoradiogram and sizes of hybridizing fragments on the right.

Table 1 Non-tandemly repeated sequences of ≥10 bp in the 5'-flanking region of the human insulin gene

Sequence	Positions*
GGCCAGGGTG	60, 684
AGCAGCCCCAG	91, 1,208 rc
GCCTCCCTCC	150, 445
CTCAGCTCCC	194, 1,189 rc
CAGCTGGGGG	323, 1,921 rc
AGGGAGGGGTCC	578, 1,260 rc
AGGGGTCCTG	582, 1,342, 1,567, 1,638, 1,724, 1,767, 1,782, 1,797
CAGGGTGGGA	687, 1,227
CCCTGGTGCT	788, 2,035 rc
CTGGGGAGCTG	884, 1,186
AGGGGAGATGGGCTC	976, 1,135
TGGGGGCTGAG	1,003, 2,067 rc
CCCACCCCCA	1,069, 1,282
CCACCCCCAGA	1,070, 1,090
TGTCCCCAGG	1,147, 1,348 rc, 1,376 rc, 1,573 rc, 1,730 rc, 1,773 rc, 1,788 rc, 1,803 rc
GCTGCTGTCC	1,212, 1,822 rc
GCTCTCCTGG	1,859, 1,902

* Sequences denoted 'rc' form an inverted repeat.

Presence of the polymorphic region in the genome

We have been unable to detect additional regions of hybridization of the 879-bp *Pvu*II fragment to digests of genomic DNA (Fig. 2) or the ~45 kb of DNA sequence around and including the insulin gene (data now shown). Thus, the sequences within the 879-bp *Pvu*II fragment are restricted to the region flanking the 5' end of the insulin gene or at least they are not tandemly repeated elsewhere in the genome. This confirms our previous results[2]. The redundant oligonucleotide region is therefore a single copy sequence.

Comparison with the rat insulin I gene

We have examined the 5'-flanking region of the rat insulin I gene for a similar polymorphic region and have determined the sequence of this region of the gene from a *Pvu*II site 414 bp from the 5' end to the beginning of the mRNA coding region (Fig. 3). There were no tandemly repeating sequences. If such sequences exist they must be more than 414 bp from the 5' end of the coding region.

A comparison of the extended 5′-flanking sequences of the human and rat I insulin genes (Fig. 3) indicated that the homology is more extensive than suggested by the heteroduplex analysis[2]. In fact, interrupted regions of nucleotide sequence homology extend for ~365 bp from the structural portion of the gene, the homology apparently ending at or near the boundary of the polymorphic region of the human gene without being re-established on its other side. This nucleotide sequence conservation suggests that DNA sequences besides the TATAAA (Hogness box) sequence at −25 to −30 and the remote control sequence at −75 to −90 are involved in the regulation of insulin gene expression.

The regions of homology might represent points of interaction between the DNA and other regulatory molecules. Wu and Gilbert[10] have also suggested that additional sequences in the 5′-flanking region of the insulin gene may be involved in the regulation of insulin gene expression. They observed that a region of the rat insulin II gene, 250–300 bp upstream from the start of transcription, exhibits tissue-specific DNase sensitivity. Lomedico *et al.*[11] also observed that the homology between the rat insulin I and II genes included ~500 bp in the 5′-flanking region.

Discussion

The human insulin gene and its flanking regions exhibit conserved and highly variable sequences. Comparison of 2,357-bp segments from two chromosomes showed only four substitutions (4/2,357, 0.17%; this paper and ref. 5), all within the 1,430-bp portion encoding the mRNA precursor. The 5′-flanking region contains a section of extensive length and sequence heterogeneity which is generated by variation in the number and arrangement of members of a family of G + C-rich oligonucleotides whose consensus sequence is ACAGGGGTGTGGGG. This polymorphic region, although internally repetitious, is a single-copy structure. A comparison of the size of this region in individuals indicates that it can vary from 26 repeat units (364 bp) to 209 units (2,926 bp). The latter generates a DNA segment twice the size of the structural region (1,430 bp) of the human insulin gene. Moreover, the sequence polymorphism suggests that those alleles which cannot be distinguished by size may be distinguished by sequence.

```
1,781 CAGGGGTCCTGGGGACAGGGGTCCTGGGGACAGGGGTCTGGGGACAGCAGCG CAAAGAG
      ***  *  **  * *    * *         *    *          *** * ****** 
    1 CAGCTGAGCTAAGAATCCAGCTATCAATAGAAACTATGAAACAGTTCCAGGGACAAAGAT

1,840 CCCCGCCCTGCAGCCTCCAGCTCTCCTGGTCTAAT   GTGGAAAGTGGCCCAGGTGAGG
       ** *  *  ** *  *     **    *   ***   ***** ** * ***   ***
   61 ACCAGGTCCCCAACAACTGCAACTTTCTGGGAAATGAGGTGGAAAATG CTCAGCCAAGG

1,897 GCTTTGCTCTCCTGGAGACATTTGCCCCCAGCTGTGAGCAGGGACAGG     TCTGGCC
           *    ***       * **   * *    ** ** * **   *      ** ****
  120 AAAAAGAGGGCCTTACCCTCTCTGGGACAATGATTGTGCTGTGAACTGCTTCATCAGGCC

1,952 ACCGGGCCCCTGGTTAAGACTCTAATGACCCGCTGGTCCTGAGGAAGAGGTGCTGACGAC
      * * ***** ** **** * ****** ****   **** * **  **** ** ***** *
  180 ATCTGGCCCTTG TTAATAATCTAATTACCCTA GGTC TAAGT AGAGTTGTTGACGTC

2,012 CAAGGAGATCTTCCCACAGACCCAGCACCAGGGAAATGGTCCGGAAATTGCAGCCTCAGC
      *** ***  *** *  *****  ***** *** ** ** *  ******* **** *****
  236 CAATGAGCGCTTTCTGCAGACTTAGCACTAGGCAAGTG TTTGGAAATTACAGCTTCAGC

2,072 CCCCA  GCCATCTGCCGACCCCCCCACCCC   GCCCT AATGGGCCAGGCGGCAGGGG
      ***    ********** ***  ***  **    ***** *********  *****  * 
  295 CCCTCTCGCCATCTGCCTACCTACCCCTCCTAGAGCCCTTAATGGGCCAAACGGCAAAGT

2,126 TTGACAGGTAGGGGAGATGGGCTCTGAGACTATAAAGCCAGCGGGGGCCCAGCAGCCCTC
            ** ** *  ** * *** ** ******** ** ** * ***** * * * *
  355 CCAGGGGGCAGAGAGGAGGTGCTTTG GACTATAAAGCTAGTGGAGACCCAGTAACTCCC

2,186 AGCCCTCCAGGACAGGCTGCA TCAGAAGAGGCCATCAAGCAG
      * ****    ***  *** ** *** *      ** *******
  414 AACCCTAAGTGACCAGCTACAATCATAGACCATCAGCAAGCAG
```

Fig. 3 Sequence of the 5′ flanking region of the rat insulin gene and homology with the corresponding region of the human insulin gene. The rat I and human insulin gene sequences are indicated. The sequence of coding region 1 is also included. The putative 5′ end of the mRNA is A-414 in the rat I sequence and A-2186 in the human sequence. The isolation and characterization of the rat insulin I gene has been described[28]. The sequence was determined by the procedure of Maxam and Gilbert[10] as described in Fig. 1 legend. The human sequence is from Figure 1. Asterisks indicate homologous nucleotides. Gaps have been used to maximize homology.

Table 2 Organization of the oligonucleotide repeats in two allelic polymorphic regions

Sequence	Occurrences	
	Allele 1 (λHi1)	Allele 2 (λHi2)
a, ACAGGGGTGTGGGG	13 (38.2%)	24 (53.3%)
b, ACAGGGGTCCTGGGG	8 (23.5%)	7 (15.6%)
c, ACAGGGGTCTGGGG	5 (14.7%)	6 (13.3%)
d, ACAGGGGTCCGGGG	2 (5.9%)	1 (2.2%)
e, ATAGGGGTGTGGGG	1 (2.9%)	0
f, ACAGGGGTCCCGGGG	1 (2.9%)	5 (11.1%)
g, ACAGGGGTCTGAGG	1 (2.9%)	0
h, ACAGGGGTGTGGGC	1 (2.9%)	0
i, ACAGGGTCCTGGGG	1 (2.9%)	1 (2.2%)
j, ACAGGGGTGTGAGG	0	1 (2.2%)

Arrangement of oligonucleotides

Allele 1 5′*cdi aba aba dab aab aca aaa cea faa cgh ccc b* 3′ (ref. 45)

Allele 2 5′*cdi jfa faa aba baa aaf aba afa baa aac aaa cac baa afc ccb* 3′ (ref. 34)

Upper panel, sequences of different oligonucleotides and the number of times (and percentage of all repeats) they occur in the two allelic DNA segments. Lower panel, arrangement of oligonucleotides in the polymorphic region. Each oligonucleotide sequence was assigned a letter as indicated in the upper panel.

The insulin polymorphic region can be distinguished from other regions of tandemly repeating oligonucleotides. Its unique chromosomal location and single copy nature distinguish it from the hexanucleotide sequences repeated at the ends of the fragmented, macronuclear DNA molecules of some protozoa[12,13], while its smaller size, greater internal redundancy and sequence simplicity distinguish it from the repeated sequences found at the *ori*-region of SV40 that have been implicated in the regulation of replication and perhaps transcription[14,15]. The insulin polymorphic region is similar to a region in the *Xenopus* 5S rRNA gene nontranscribed spacer which is also polymorphic and possess 2–12 copies of a 15-bp oligonucleotide[16] as well as to simple tandem repetitive sequences in the recombinational switch regions of immunoglobulin heavy chain genes[17]. The highly repetitive satellite DNAs present in eukaryotes are often composed of shorter repeated units (oligonucleotides)[18,19]. However, the insulin polymorphic region is only found at one site in the human genome, in contrast to those in the rRNA genes and satellite DNAs, which are present at many locations.

The sequence simplicity of the polymorphic region suggests that it could be involved in some recombinational process. However, the persistence of the bimodal distribution of insertion sizes[6] suggests that random crossing over within this array does not occur frequently because such exchanges would be expected to produce a unimodal distribution[20]. The insulin polymorphic region is more complex than the repeating T · G dinucleotide region in intervening sequence 2 of the human fetal γ-globin genes which has been implicated in gene conversion[21]. A similar region of repeating C · T dinucleotides has been observed in the sea urchin histone H2A and H1 spacer and it has been proposed that this region is involved in the maintenance of homogeneity of the histone gene repeating unit[22]. The sequence data on the regions flanking the insulin polymorphic region provide no evidence for gene conversion. There are 0/525 nucleotide differences on the 5′ side of the polymorphic region and 4/1,832 on the 3′ side (this paper and ref. 5).

The function of this polymorphic region is unknown. It could be intergenic or spacer DNA. Its location, within 363 bp or 2 nucleosomes from the coding region of the gene, adjacent to the putative transcription control region, suggests that the polymorphic region could have a role in the regulation of human insulin gene expression. However, this region does not seem to affect the transcription of the gene in cell-free extracts prepared from HeLa cells (G.I.B. and O. Laub, unpublished). If similar regions of tandemly repeating sequences have a general role in the regulation of insulin expression, they might be found flanking insulin genes of other species. Our sequence analysis of the rat insulin I gene indicated that it does not possess an homologous region in the same position, and that if present it is more than 50 bp upstream from the corresponding position of the human gene. However, this does not preclude a role for this region, as there are two non-allelic insulin genes in rats and only one in humans and most other organisms[23]. Thus, some elements of regulation of gene expression could be different.

The role of the additional, non-tandemly repeated sequences in the flanking region of the human gene is also unknown. The 15-bp sequence (Table 1) which is directly repeated ~325 bp on either side of the polymorphic region is particularly interesting as one member is located in the control region of the gene. It could be involved in the function of the polymorphic region or define some aspect of expression of the insulin gene. Though far and variably distant in the DNA sequence, these two sites could be contiguous in chromatin. Physical joining of these sites in chromatin could affect insulin gene transcription by regulating access of the RNA polymerase to the control regions.

The analysis of length variation in the 5′-flanking region of the human insulin gene indicated that 63% of the individuals examined were heterozygous at this site[6]. As this region also possesses DNA sequence polymorphism, the extent of heterozygosity was underestimated and it may be possible to distinguish the two parental alleles in most individuals by analysing this region for both length and sequence differences. This polymorphic region is a useful molecular marker for the insulin gene on the short arm of chromosome 11 (refs 4, 24) and may serve as marker for loci up to $10–20 \times 10^6$ bp distant[25].

We thank Dr D. N. Standring for useful discussions and Ms L. Spector and S. Bock for assistance in the preparation of this manuscript. This research was supported by an Elliott P. Joslin Research and Development Award of the American Diabetes Association, Inc., to G.I.B., and NIH grants to W.J.R.

Received 20 August; accepted 3 November 1981.

1. Bell, G. I. *et al. Nature* **284,** 26–32 (1980).
2. Bell, G. I., Pictet, R. L. & Rutter, W. J. *Nucleic Acids Res.* **8,** 4091–4109 (1980).
3. Owerbach, D., Bell, G. I., Rutter, W. J. & Shows, T. B. *Nature* **286,** 82–84 (1980).
4. Owerbach, D., Bell, G. I., Rutter, W. J., Brown, J. A. & Shows, T. B. *Diabetes* **30,** 267–270 (1981).
5. Ullrich, A., Dull, J. J., Gray, A., Brosius, J. & Sures, I. *Science* **209,** 612–615 (1980).
6. Bell, G. I., Karam, J. H. & Rutter, W. J. *Proc. natn. Acad. Sci. U.S.A.* **78,** 5759–5763 (1981).
7. Wyman, A. R. & White, R. *Proc. natn. Acad. Sci. U.S.A.* **77,** 6754–6758 (1980).
8. Corden, J. *et al. Science* **209,** 1406–1414 (1980).
9. Efstratiadis, A. *et al. Cell* **21,** 653–668 (1980).
10. Wu, C. & Gilbert, W. *Proc. natn. Acad. Sci. U.S.A.* **78,** 1577–1580 (1981).
11. Lomedico, P. *et al. Cell* **18,** 545–558 (1979).
12. Klobutcher, L. A., Swanton, M. T., Donini, P. & Prescott, D. M. *Proc. natn. Acad. Sci. U.S.A.* **78,** 3015–3019 (1981).
13. Katzen, A. L., Cann, G. M. & Blackburn, E. H. *Cell* **24,** 313–320 (1981).
14. Benoist, C. & Chambon, P. *Nature* **290,** 304–310 (1981).
15. Gruss, P., Dhar, R. & Khoury, G. *Proc. natn. Acad. Sci. U.S.A.* **78,** 943–947 (1981).
16. Fedoroff, N. *Cell* **16,** 697–710 (1979).
17. Nikaido, T., Nakai, S. & Honjo, T. *Nature* **292,** 845–848 (1981).
18. Brutlag, D. L. *A. Rev. Genet.* **14,** 121–144 (1980).
19. Streeck, R. E. *Science* **213,** 443–445 (1981).
20. Smith, G. P. *Science* **191,** 528–535 (1976).
21. Slightom, J. L., Blechl, A. E. & Smithies, O. *Cell* **21,** 627–638 (1980).
22. Sures, I., Lowry, J. & Kedes, L. H. *Cell* **15,** 1033–1044 (1978).
23. Humbel, R. E., Bosshard, H. R. & Zahn, H. in *Handbook of Physiology* Sect. 7, Vol. 1 (eds Steiner, D. F. & Freinkel, N. 111–132 (American Physiological Society, Washington DC), 1972).
24. Harper, M. E., Ullrich, A. & Saunders, G. F. *Proc. natn. Acad. Sci. U.S.A.* **78,** 4458–4460 (1981).
25. Botstein, D., White, R. L., Skolnick, M. & Davis, R. W. *Am. J. hum. Genet.* **32,** 314–331 (1980).
26. Maxam, A. M. & Gilbert, W. *Meth. Enzym.* **65,** 499–560 (1980).
27. Cooke, N. E., Coit, D., Shine, J., Baxter, J. D. & Martial, J. A. *J. biol. Chem.* **256,** 4007–4016 (1981).
28. Cordell, B. *et al. Cell* **18,** 533–543 (1979).

Lysis gene expression of RNA phage MS2 depends on a frameshift during translation of the overlapping coat protein gene

R. A. Kastelein, E. Remaut*, W. Fiers* & J. van Duin†

Department of Biochemistry, University of Leiden, PO Box 9505, 2300 RA Leiden, The Netherlands
* Laboratory for Molecular Biology, University of Ghent, Ghent, Belgium

Translation of the lysis cistron of MS2 RNA requires a frameshift of ribosomes reading the upstream coat protein mRNA. The out-of-phase fraction of ribosomes terminates at either one of two nonsense codons just preceding the lysis cistron. Termination is followed by initiation at the start codon of the lysis protein message.

THE group I single-stranded RNA bacteriophages (including MS2, f2, R17 and M12) contain the information for at least four proteins[1–5], the order of which is illustrated in Fig. 1. The figure shows that the newly characterized L gene, whose product is involved in lysis of the host, overlaps the coat and synthetase gene in the +1 reading frame. The complete primary sequence of MS2 RNA has been published previously[6].

The timing and efficiency of phage gene expression in the infected cell has been extensively reviewed for the three longer known genes[7]. As for the lysis gene, why has it evolved in its present position, where there is overlap with two other genes? In particular, in what way does this position relate to the level and time of expression? The L protein is made in small amounts and its appearance in the infected cell coincides with that of the coat protein[5]. A relationship between coat and L protein synthesis is suggested by the observation that phage coat ambers do not lyse their (non-permissive) host[8].

The availability of cloned MS2 DNA[9] allowed us to examine how the expression of the L gene is regulated. We used the recombinant DNA approach, which has several advantages over studies using normal phage infection: it allows the site-selected introduction of almost any kind of mutation and the expression of a single gene can be examined.

Our results indicate that the lysis cistron does not possess an independent entry site for ribosomes. Instead its translation depends on the readout of the coat gene. Ribosomes that experience a frameshift when reading the coat gene preceding the lysis cistron, terminate protein synthesis a few codons before

---

† Present address: Thimann Laboratories, University of California, Division of Natural Sciences, Santa Cruz, California 95064, USA.

0028–0836/82/010035—07$01.00

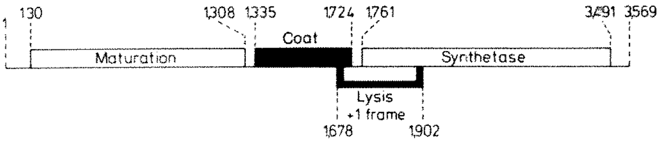

Fig. 1 Genetic map of the RNA phage MS2. Nucleotide numbers are taken from ref. 6. The reading frame of the lysis gene is +1 with respect to the coat and synthetase frame.

this gene due to the presence of two out-of-phase stop codons. Termination of protein synthesis at these positions elicits synthesis of the lysis protein.

Expression of the lysis gene in wild-type MS2 DNA subgenomic regions

In this study, selected regions of the MS2 genome were inserted into plasmid pPLa831, just downstream of the λ leftward promoter pL. The plasmid has been described in detail elsewhere[10]. The promoter pL is closed at 28 °C by a thermosensitive repressor encoded by the host chromosome. At 42 °C the repressor is unstable and the promoter is turned on.

The stringency of temperature control over the promoter in pPLa831-derived plasmids is demonstrated in Fig. 2. (Here, *Escherichia coli* strain M5219 (ref. 10) was transformed with pMS2 (Table 1) and labelled with radioactive amino acids.) At 28 °C, no MS2 coat protein is detected (Fig. 2, lanes 1 and 2), but at 42 °C the coat protein of the phage becomes the major product synthesized (lanes 3–7). Similarly, the presence of the almost complete MS2 DNA genome (nucleotides 103–3,569) in pPLa831 did not interfere with the growth of the transformed cells as long as transcription from pL was blocked by keeping the culture at 28 °C. However, if this particular clone (pMS23) was shifted to 42 °C, complete lysis was observed (Fig. 3*a* and Table 1). Apparently the L gene is expressed in the experimental conditions used. Evidence that cell lysis can indeed be ascribed to the presence of the L gene is provided by a clone containing pMS20. This plasmid carries a 58 nucleotide-long deletion in the L gene (Table 1). As shown in Fig. 3*a*, the deletion abolishes cell lysis, in agreement with the proposed genetic map.

To determine a possible contribution of the other gene products to cell lysis we deleted large parts of the maturation protein gene and the synthetase gene to obtain plasmid pMS16. Cells harbouring this plasmid still lyse on induction of the pL promoter (Fig. 3*a*). Thus neither the maturation (A) protein nor the synthetase appears necessary for cell lysis. The ability of plasmids to lyse the host cell is maintained up to a point where the whole A protein is removed (pMS17; Table 1).

L gene expression requires overlap of coat and L genes

When the MS2 DNA information in pMS17 was trimmed away further to give pMS1 (Table 1), there was no cell lysis at 42 °C (Fig. 3*b*). There are several possible explanations for this and we have considered the two that are more likely. (1) L protein synthesis is under translational polar control of the coat gene. In this case, ribosomes reading the coat message must open up the initiation region of the L cistron to allow independent initiation by another ribosome. The start region of the L cistron is thus thought to be inaccessible to ribosomes in the unperturbed mRNA. In ribosome binding experiments, this region of MS2 RNA has been found to be unprotected against RNase digestion[4,11]. (2) Absence of cell lysis in pMS1 clones could indicate that the coat protein itself is in some way required for cell lysis to occur—involvement of the coat protein has been suggested previously[8].

To test alternative (2), we modified pMS1 by inserting the MS2 DNA region specifying the coat protein behind the L gene, thus uncoupling the gene overlap. Clones carrying this new plasmid (pMS1.9) did not lyse on induction, although the presence of the MS2 coat protein was evident from protein gel analysis of the type shown in Fig. 2. This suggests that L protein synthesis depends on the native gene arrangement and supports a polar control mechanism. Further evidence for the involvement of translational polar control was provided by pMS25. Here we deleted the initiation region of the coat gene and the ability of this plasmid to induce cell lysis was lost (Table 1; and Fig. 3*b*). As before, lysis is not restored when the information for the coat protein is supplied behind the L gene (pMS25.9). Note that in pMS25 the 5′ context of the L gene is kept intact for over 300 nucleotides. This virtually excludes the possibility that the lack of mRNA translation is due to the deletion of translational start signals (in the conventional sense).

Efficiency of coat protein synthesis correlated with onset of cell lysis

During this study we obtained independent evidence that the translation of coat and L protein mRNA sequences is coupled; clones producing large amounts of coat protein also lysed quickly. In contrast, clones synthesizing small amounts of coat protein showed delayed lysis. Variations in coat gene expression can be obtained by varying the length of the MS2 DNA region proximal to the coat gene. For example, after induction of pMS2, coat protein comprised 30% of the newly synthesized proteins after 30 min, as opposed to <5% for pMS17. Cell lysis (as measured by the decrease in turbidity) began after 30 min for pMS2 and only after 75 min for pMS17. The data for several clones are summarized in Table 2. A positive correlation between the rate of MS2 coat protein synthesis and the onset of cell lysis is apparent. Such a relationship is consistent with a polar translational control mechanism.

Fine regulation of polar control

During phage infection, polar control of synthetase translation is observed in coat protein mutants that have a nonsense codon in the position of the sixth amino acid. The control is relieved when the stop codon is found further downstream at amino acid residue 50, 54 or 70 (ref. 12). Based on these data and the MS2 RNA secondary structure model, a molecular basis for this polarity has been proposed[13], the main feature of which is the base-pairing between the synthetase initiation region and a coat cistron coding sequence (see Fig. 4). Ribosomes passing this region are thought to expose the synthetase ribosomal binding site to allow independent initiation of protein synthesis. A similar situation may exist at the start of the L gene. Assuming the validity of the 'coat–lysis polarity control' one would expect that the L gene becomes readable once ribosomes pass over

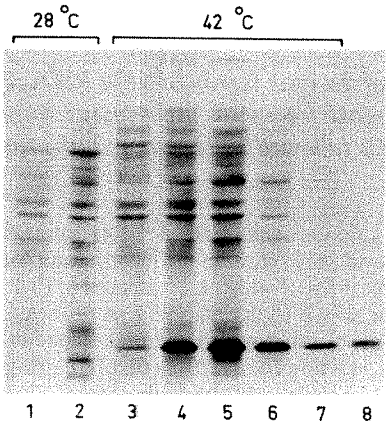

Fig. 2 Expression of MS2 DNA in cells transformed with pMS2. Cultures were grown to 0.2 A_{650}, then labelled with ^{14}C-amino acids for the time intervals indicated below. Proteins were analysed on polyacrylamide gels containing 0.1% SDS. Lanes 1, 2: pattern after labelling at 28 °C for 5–25 and 95–115 min, respectively. Lanes 3–7: labelling at 42 °C for 5–10, 5–25, 35–55, 65–85 and 95–115 min, respectively. Lane 8: *in vitro*-labelled MS2 coat protein.

Table 1 Host cell lysis by pPLa831-derived plasmids after induction at 42 °C

Plasmid no.	MS2 DNA inserted in pPLa831	Cell lysis after induction at 42°C	Schematic representation of MS2 genes present
pMS1	1,628-2,057	-	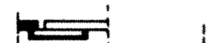
pMS1.9	1,628-2,057. 1,221-1,736	-	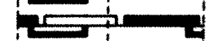
pMS2	103-2,057	+	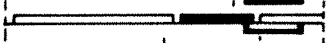
pMS9	1,221-1,736	-	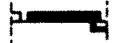
pMS12	1,221-2,057	+	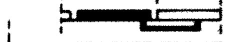
pMS16	869-2,057	+	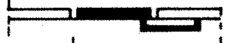
pMS17	1,305-2,057	+	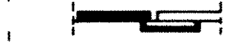
pMS18	869-3,569	+	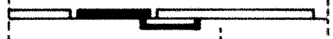
pMS20	869-2,057 (∇ 1,764-1,822)	-	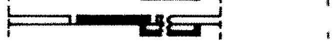
pMS23	103-3,569	+	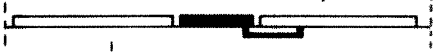
pMS25	869-2,057 (∇ 1,013-1,365)	-	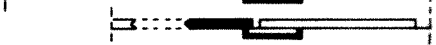
pMS25.9	869-2,057 (∇ 1,013-1,365). 1,221-1,736	-	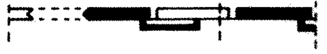
	MS2 DNA inserted in pPLa932		
pMS32.00	1,221-2,057 1,628 1,629	+	
pMS32.04	1,221-2,057 (G.AAT.TAA.TTC.)	-	
pMS32.259	1,221-2,057 (∇ 1,369-1,628) GTC.GAA.ATT.C 1,369 1,629	+	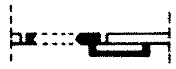

All nucleotide numbers refer to the primary structure of MS2 RNA (Fig. 1; ref. 6). MS2 DNA was inserted in pPLa831 according to standard procedures using either the *Eco*RI site, the *Bam*HI site or both. When the MS2 DNA region of interest did not contain a suitable site, *Eco*RI or *Bam*HI restriction site linker sequences were attached. MS2 DNA sites used were: *Eco*RI (103) (nucleotide number), *Pvu*II (869), *Sal*I (1,013), *Hae*III (1,221), *Xba*I (1,305), *Sal*I (1,366), *Eco*RI (1,628), *Hae*III (1,736), *Bam*HI (2,057). pPLa932 is identical to pPLa831 except that the *Eco*RI site was removed by cutting with *Eco*RI, filling in the single-stranded regions with DNA polymerase I (large fragment) and re-sealing with T4 DNA ligase. Thus, pMS32.00 is equivalent to pMS12 except for the *Eco*RI site in the vector. pMS32.04 was constructed by opening up the *Eco*RI site of pMS32.00 at position 1,628. The resulting sticky ends were filled with DNA polymerase I (large fragment) and the plasmid re-sealed with T4 DNA ligase. The new sequence around 1,628 is shown. The coat reading frame is indicated by dots. The construction of pMS32.259 is described in the text. The distance between the *Sal*I and *Eco*RI positions is 263 nucleotides. As 4 nucleotides are recovered by the action of the polymerase, the final deletion is 259 nucleotides. The reading frame is indicated by broken lines.

nucleotides 1,563–1,570. To test this, we introduced a UAA stop signal in the coat gene beyond this region, that is, at position 1,632. Surprisingly, cells harbouring this new plasmid, pMS32.04, did not lyse the host cell (Fig. 3*c*). The expression of the inserted MS2 DNA was apparent from the synthesis of a protein having the size of the expected coat protein ochre fragment (Fig. 6). The absence of lysis in clone pMS32.04 indicated that for L cistron translation to occur, ribosomes have to move beyond position 1,632 of the MS2 RNA sequence. To achieve this we again modified pMS32.00. The unique *Sal*I and *Eco*RI restriction sites, at positions 1,366 and 1,628 respectively, were used to delete this region of 263 nucleotides. The resulting staggered ends were filled in with DNA polymerase I (large fragment) and the plasmid re-sealed (pMS32.259). A consequence of the deletion was a shift to the +1 reading frame at the junction site. The +1 reading frame allows ribosomes that start at the coat cistron to proceed up to position 1,672, where they encounter an ochre stop codon, three nucleotides before the L cistron start (Fig. 4). Clones containing this plasmid (pMS32.259) lysed quickly on induction. Their growth curve was almost identical to that of pMS32.00 (not shown). From this we make two important conclusions. First, intact coat protein is not required *per se* for the synthesis or activity of the L protein. Second, ribosomes shifting their reading frame to +1 during coat cistron translation, so as to arrive at the ochre stop codon at nucleotide 1,672, trigger synthesis of the L protein.

Reading frameshifts in coat cistron promote synthesis of lysis protein

Results from clone pMS32.259 suggest that synthesis of the lysis protein from wild-type RNA may depend on a ribosomal frameshift to the +1 mode at the appropriate region. To explore this further, we constructed a collection of coat gene deletion mutants that potentially contain all three reading frames. Experimentally, pMS32.00 was opened at its unique *Eco*RI site and the linearized DNA treated with exonuclease *Bal*31 for 15, 30, 60 and 90 s, respectively. The reaction mixtures were pooled, the DNA ligated and used for transformation. Of 250 recombinants obtained, 60 were selected for further restriction analysis and lytic properties. The growth curves obtained were of three general types: quick lysis, delayed lysis and no lysis.

Nine clones, with the general nomenclature pMS32.*N*, where *N* is the number if nucleotides deleted, were selected for sequence analysis of the modified region (Table 3). Clones pMS32.16 and pMS32.28 change the coat reading frame to +1 at the junction. These clones lyse quickly, as does pMS32.259 (Fig. 5). There are three more clones in which the coat reading frame is forced to +1 by the deletion. In two of these, pMS32.55 and pMS32.85, the onset of lysis was delayed with respect to the previous +1 frameshift mutants (Fig. 5), which may be related to deletions in the Shine–Dalgarno sequence, AGGU, around position 1,664 (Table 3). The last +1 frameshift clone is pMS32.88, which lacks the nonsense codon at position 1,672 together with the first 12 codons of the L gene, thus the absence of lysis was not unexpected. The coat protein ochre fragments or fusion peptides coded for by the respective plasmids can be detected in minicells (for examples see Fig. 6). In two clones, pMS32.17 and pMS32.50, the deletion leads to a −1 shift in the reading frame. In pMS32.17 this shift caused ribosomes to terminate at ochre stop codon 1,652. Evidently, termination at this position also allowed translation of the L gene mRNA, albeit with a lower frequency as judged by the delayed lysis of this clone (Fig. 5). Clone pMS32.50 did not lyse but in this case the −1 frame stop codon at position 1,652 had been deleted. It seems, therefore, that the frameshift itself was not signalling lysis protein expression but rather its inevitable consequence, chain termination.

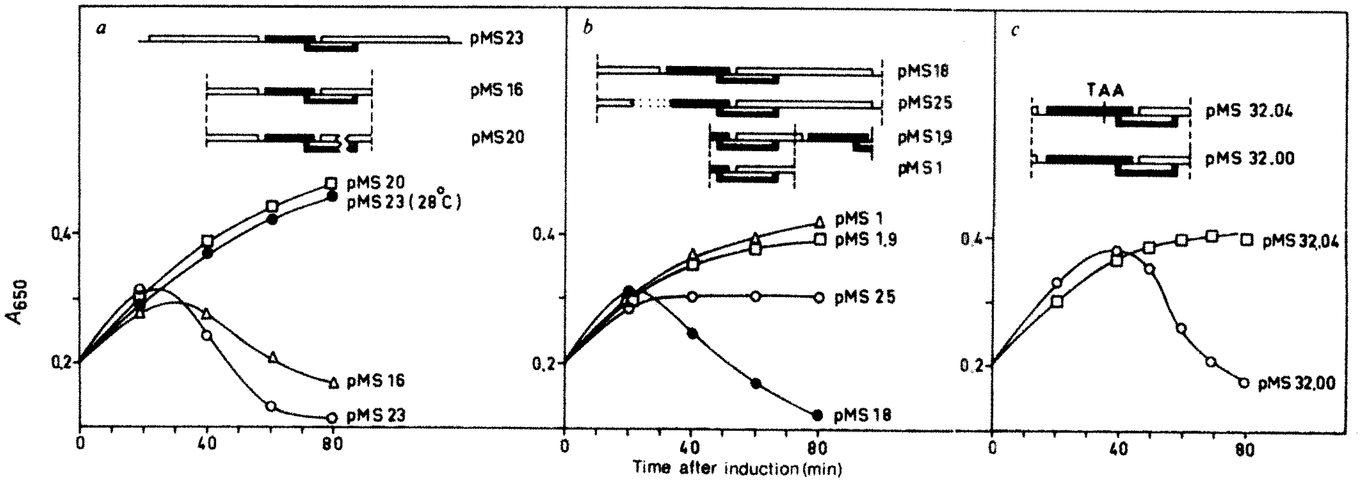

Fig. 3 Lytic properties of clones containing various regions of MS2 DNA inserted in pPLa831 or pPLa932 (see Table 1). Cells were grown at 28 °C to an A_{650} of 0.2. Growth was then continued at 42 °C (except where indicated). MS2 DNA regions present are shown schematically at the top.

Deletions in coat gene that do not change the reading frame

Two clones, pMS32.27 and pMS32.3, have deletions that do not change the reading frame. These two plasmids have lost the property to lyse their host (Fig. 5), which supports the view that expression of the L gene requires a ribosomal frameshift.

Obviously the absence of lysis in 0 frame coat mutants poses a problem as the wild-type sequence is read by definition in the zero frame. It seems, therefore, that the deletion decreases the chances that a phase shift occurs. The frameshift in wild-type MS2 RNA could arise in two ways: (1) interference of coat protein, bound to the start of the synthetase, with the movement of the reading ribosome. Although this involves an unknown mechanism it is formally correct, as the absence of wild-type coat protein distinguishes the 0 frame deletion mutants from the wild type. However, there is one argument that weakens this possibility. We have constructed a 0 frame mutant that carries a deletion of 18 nucleotides at the 5′ end of the coat gene (∇1,365–1,384), which is still able to lyse its host. (2) Frameshift is induced by a specific RNA structure present in or around the deleted region at position 1,628. An interesting sequence CAAUUUUC, present around position 1,620, or its immediate neighbourhood, was found to induce a +1 frameshift in yeast mitochondria[14]. However, the limited number of deletion mutants analysed does not allow a strong conclusion to be made concerning the significance of the 8-base homology. With regard to this, note that a +1 frameshift was observed *in vivo* between nucleotides 1,675 and 1,724, which does not include this particular nucleotide sequence[5].

Translation of overlapping messages

As initiation of protein synthesis is slow compared with elongation, the independent translation of overlapping messages presents a general problem. Frequent readout of the upstream messenger (coat cistron) seems bound to interfere with independent initiation at the downstream message (L gene). At first glance one would therefore expect a regulatory mechanism

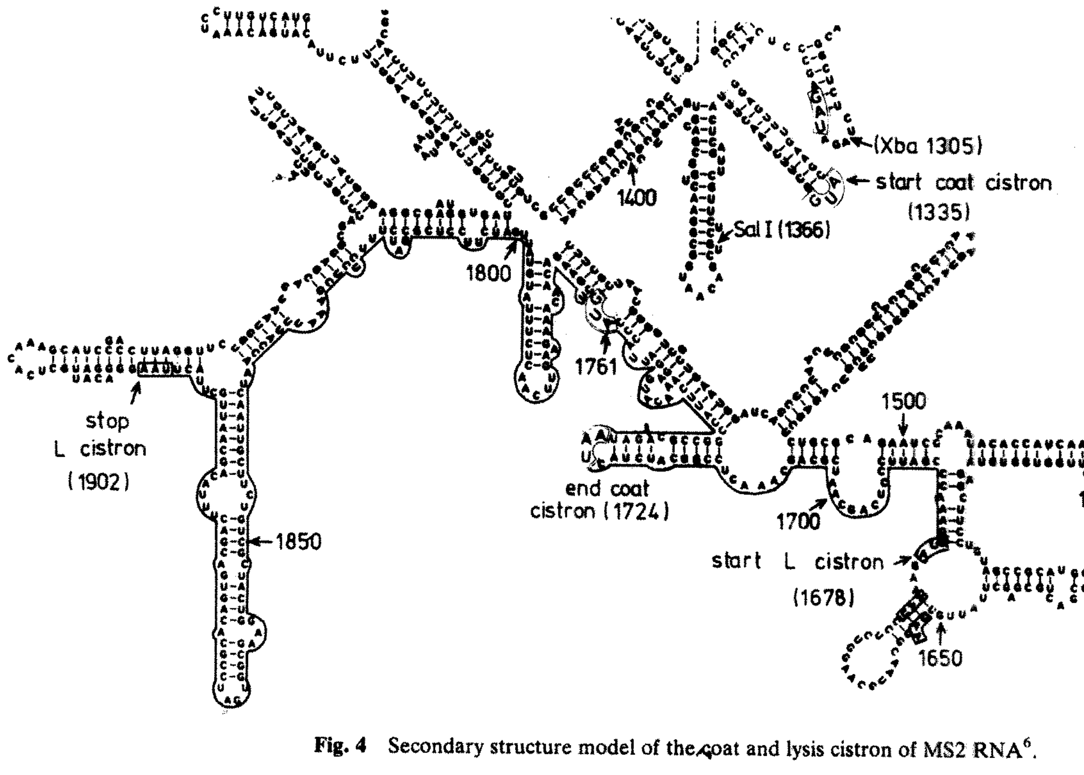

Fig. 4 Secondary structure model of the coat and lysis cistron of MS2 RNA[6].

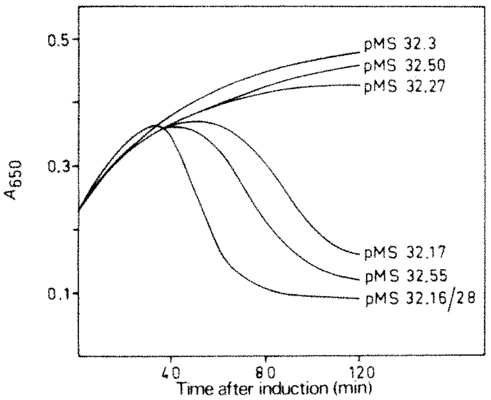

Fig. 5 Effect on cell lysis of reading frameshifts in the coat protein cistron. The MS2 DNA present in the plasmids is shown in Table 3. Growth of the cultures was as described in Fig. 3 legend.

that promotes expression of the downstream gene by interfering with the translational start at the upstream message to clear the template of ribosomes. However, such a solution seems impossible or inappropriate in this case. Instead, phage MS2 has solved the expression of the overlapping genes in an extraordinary way. The clones of the pMS32.*N* series lead us to conclude that translation of the L cistron relies on the fraction of the ribosomes that arrives out of frame at the beginning of this gene. The positions of two ochre codons, respectively in the +1 and −1 frame, just before the L cistron, elicits peptide chain termination, which in turn allows the reinitiation at the start of the L message, a region otherwise inaccessible to ribosomes. It is unlikely that ribosomes leave the RNA at this point as this would again create the problem of independent initiation.

The phenomenon of reinitiation has been recognized for some time in the *lac*I, *lac*Z and the bacteriophage T4 rIIB RNA. It may occur after a polypeptide chain is prematurely terminated at the site of a nonsense mutation[15-18]. Although several translational restarts have been analysed at the nucleotide level, it is not fully understood which features transform a sequence into a potential reinitiation site[19,20]. The presence of a Shine–Dalgarno region seems dispensable for a translational restart[20]. This agrees with the ability of our clones pMS32.55 and pMS32.85, which lack all or part of this region, to express the L gene, although expression is less efficient than when the Shine–Dalgarno sequence is still present (pMS32.16 and pMS32.28).

It is interesting to note that the phage may be able to adjust the level of L gene expression by varying the distance between the AUG start codon and the preceding stop codon. This distance is 47, 23 and 3 nucleotides in pMS32.04, the −1 and the +1 frameshift mutants, respectively. The +1 frameshift mutant lyses quickly, the −1 slowly and pMS32.04 not at all. Although these represent only three cases, we suggest that the shorter the distance between termination and initiation codons, the higher the probability for reinitiation. The present data do not tell us if both or one particular phase shift operates *in vivo*. A recent analysis[21] using *in vitro* translation of MS2 RNA seems to argue for a −1 phase shift in the region of interest. The occurrence of a frameshift polypeptide (peptide 9) terminating at position 1,652 has been reported elsewhere[21].

Table 2 Relationship between rate of MS2 coat protein synthesis and onset of cell lysis in four recombinants

Plasmid no.	MS2 coat protein present 30 min after induction at 42 °C (% of newly synthesized total protein)	Onset of lysis (min)
pMS2	30	30
pMS16	13	35
pMS12	6	40
pMS17	3	75

The relative amount of newly synthesized MS2 coat protein is calculated from protein separation on polyacrylamide gels (see Fig. 2). The coat protein is the major band in most clones and is identified by co-migration with *in vitro*-labelled MS2 coat protein extracted from the phage.

Translational fidelity and expression of the lysis gene

The frameshift model presented here predicts that ribosomes which exhibit extreme fidelity in translation will not (or only barely) synthesize the L protein. This point is implicit in the recent observation of De Mars Cody and Conway[22], that on infection of a particular streptomycin-resistant strain with wild-type f2 phage, virus particles accumulate inside the cell but no lysis follows. Ribosomes from streptomycin-resistant bacteria have a decreased error frequency, both with respect to mis-sense and frameshift[23].

Analogy with ΦX174 and G4?

Whether this model can be applied to other overlapping genes is uncertain. However, note a peculiar similarity between the overlap region in MS2 and that at genes A and B in the DNA

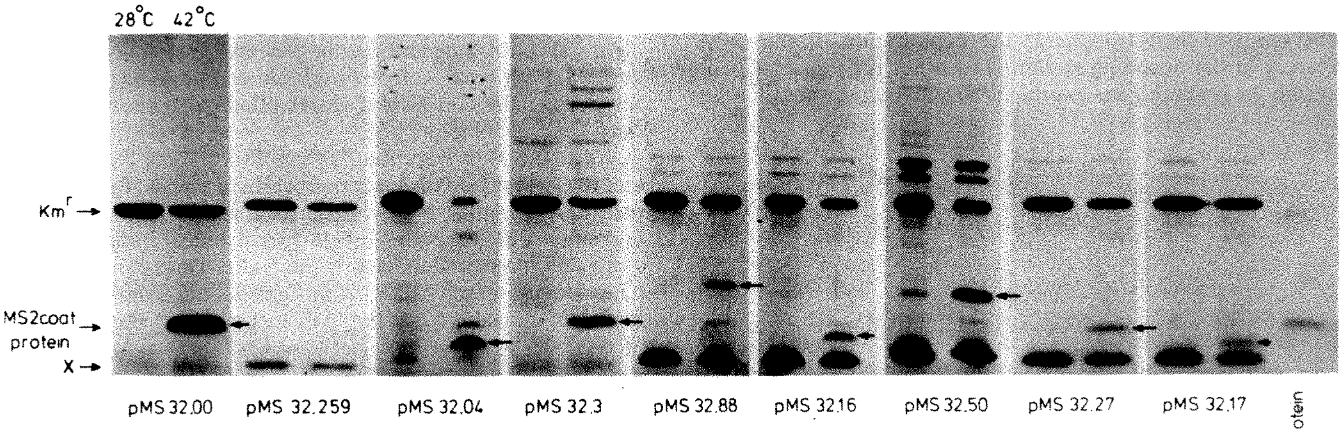

Fig. 6 Proteins synthesized in minicells carrying the indicated plasmids. For each plasmid the protein pattern before (left lane) and after (right lane) induction of the pL promoter is shown. The DNA sequence of pMS32.04, pMS32.16 and pMS32.17 predicts the formation of coat protein nonsense fragments of slightly different sizes. pMS32.50 and pMS32.88 give elongated proteins which, according to the DNA sequence, arise from fusion between the N-terminal region of the coat protein and a C-terminal part derived from a −1 frame (pMS32.50) or from the lysis protein (pMS32.88). Band X derives from a (stable) host mRNA. pMS32.3 and pMS32.27 are expected to yield MS2 coat protein lacking 1 and 9 amino acids, respectively. The protein formed in pMS32.3 cross-reacted with antiserum against MS2 coat protein. The lysis protein is not visible in any of the gels—this is possibly due to the very low level of synthesis of the protein. Translation from the start of the synthetase cistron produced a small amount of fusion protein running at the position of the coat protein (see for example pMS32.88). Arrows facing left indicate the MS2 coat protein or nonsense fragments, and the fusion proteins derived from it.

Table 3 Effect on cell lysis of deletions in the coat protein sequence around nucleotide 1,628

1,610 1,620 1,630 1,640 1,650 1,660 1,670 1,680

CAUUCCAAUUUUCGCCACGAAUUCCGACUGCGAGCUUAUUGU$\boxed{\text{UAA}}$GGCAAUGCAAGGUCUCC$\boxed{\text{UAA}}$AAGAUG

Stop (−1 frame) Stop (+1 frame) Start lysis gene

No. of nucleotides deleted		Reading frame		Cell lysis
3	CAUUCCAAUUUUCGCC	0	AAUUCCGACUGCGAGCUUAUUGUUAAGGCAAUGCAAGGUCUCCUAAAAGAUG	−
16	CAUUCCAAUUUUCGCC	+1	AGCUUAUUGUUAAGGCAAUGCAAGGUCUCC$\boxed{\text{UAA}}$AAGAUG	+
17	CAUUCCAAUUUUCGC	−1	AGCUUAUUGU$\boxed{\text{UAA}}$GGCAAUGCAAGGUCUCCUAAAAGAUG	+
27	CAUUCCAAUUUUCGCC	0	AAGGCAAUGCAAGGUCUCCUAAAAGAUG	−
28	CAUUCCAAUUUUCGCC	+1	AGGCAAUGCAAGGUCUCC$\boxed{\text{UAA}}$AAGAUG	+
50	CAUUCC	−1	GUCUCCUAAAAGAUG	−
55	CAUUCC	+1	C$\boxed{\text{UAA}}$AAGAUG	+
85		+1	← Deleted up to nucleotide 1,580 GUCUCC$\boxed{\text{UAA}}$AAGAUG	+
88	CAUUCCAAUUUUCGCC	+1	Deleted up to nucleotide 1,714 →	−

pMS32.3 was constructed by opening the unique *Eco*RI site of pMS32.00 at position 1,628. The linearized DNA was treated with T4 DNA polymerase and re-sealed with T4 DNA ligase. The other plasmids were constructed by treatment of pMS32.00 with the enzyme *Bal*31 as described in the text. All sequences were determined by the procedure described elsewhere[25]. 0, +1 and −1 in the deleted sequence refer to the change in reading frame at the junction. Stop codons are boxed. In pMS32.*N*, *N* indicates the number of nucleotides deleted. The position of the deleted nucleotides is shown.

phages ΦX174 and G4 (Fig. 7). Strikingly, the nucleotide indicated by an arrow in the out-of-phase ochre codon of ΦX174 is the third base of a codon specifying alanine, thus any other base would do. The corresponding U in G4 specifies asparagine, thus a C here would not change the meaning of the codon. Statistically, the chance of finding a U in the marked position in both phages is thus 1 in 8, if the only purpose is to specify the particular amino acids. This suggests that the U is there to introduce a stop codon.

Why gene overlap?

The design adopted by the phage to control and express the L gene has two aspects. One is the exploitation of the noise inherent in the decoding system. The other is the use of gene overlap. In general, gene overlap is considered as a solution for storing as much information as possible in a limited amount of RNA or DNA. It seems that another aspect of the overlap may be equally important: it allows and enforces the extreme coupling of expression of two genes that may be difficult or impossible to realize were the genes separated. For example, the chosen design guarantees that there will not be lysis of the host unless enough coat protein has been made, that is, until the infection has proven successful[24]. The use of the phase shift siphons off a very small fraction of the ribosomes destined for L protein synthesis. This, together with the position(s) of the nonsense codon(s), sets the balance between the amount of coat and L proteins needed.

The exploitation of reading frame errors represents a novel means of controlling and coupling the expression of overlapping genes. If such errors can be programmed into the base sequence this permits the synthesis of a large number of different proteins from a single template.

We thank Ben Berkhout, Johan Twilt, Kees Ravensbergen and Koos Van der Plas for construction of clones, Rein Dijkema for introducing us to the Maxam–Gilbert sequence technique and Hanny Bakker-Steeneveld for technical assistance. This work was sponsored in part by the Netherlands Foundation for Chemical Research (SON) with financial aid from the Netherlands Organization for the Advancement of Pure Research (ZWO).

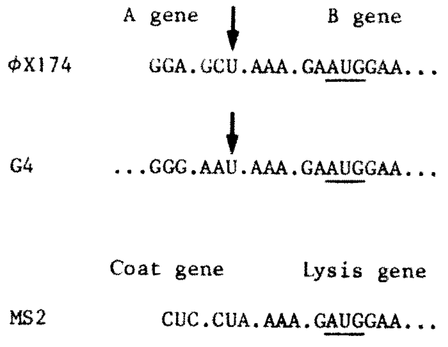

Fig. 7 Nucleotide sequences at the A/B gene overlap of phage ΦX174 and G4. The marked U is nucleotide 5,058 of ΦX174 (ref. 26) and 1,270 of the G4 sequence (ref. 27). Dots indicate the reading frame of the A gene. The coat–lysis overlap of MS2 is given for comparison.

Received 15 July; accepted 13 October 1981.

1. Horiuchi, K. in *RNA Phages* (ed. Zinder, N. D.) 29–50 (Cold Spring Harbor Monogr. Ser., 1975).
2. Jeppesen, P. G. N., Argetsinger-Steitz, J., Gesteland, R. F. & Spahr, P. F. *Nature* **226**, 230–237 (1970).
3. Model, P., Webster, R. E. & Zinder, N. D. *Cell* **18**, 235–246 (1979).
4. Atkins, J. F., Steitz, J. A., Anderson, C. W. & Model, P. *Cell* **18**, 247–256 (1979).
5. Beremand, M. N. & Blumenthal, T. *Cell* **18**, 257–266 (1979).
6. Fiers, W. *et al. Nature* **260**, 500–507 (1976).
7. Robertson, H. D. in *RNA Phages* (ed. Zinder, N. D.) 113–145 (Cold Spring Harbor Monogr. Ser., 1975).
8. Zinder, N. D. & Lyons, L. B. *Science* **159**, 84–86 (1968).

9. Devos, R., Van Emmelo, J., Contreras, R. & Fiers, W. *J. molec. Biol.* **128,** 595–619 (1979).
10. Remaut, E., Stanssens, P. & Fiers, W. *Gene* **15,** 81–93 (1981).
11. Steitz, J. A. in *RNA Phages* (ed. Zinder, N. D.) 319–352 (Cold Spring Harbor Monogr. Ser., 1975).
12. Lodish, H. F. in *RNA Phages* (ed. Zinder, N. D.) 301–318 (Cold Spring Harbor Monogr. Ser., 1975).
13. Min Jou, W., Haegeman, G., Ysebaert, M. & Fiers, W. *Nature* **237,** 82–88 (1972).
14. Fox, T. D. & Weis-Brummer, B. *Nature* **288,** 60–63 (1980).
15. Sarabhai, A. & Brenner, S. *J. molec. Biol.* **27,** 145–162 (1967).
16. Files, J., Weber, K. & Miller, J. *Proc. natn. Acad. Sci. U.S.A.* **71,** 667–670 (1974).
17. Michaels, C. & Zipser, D. *J. molec. Biol.* **41,** 341–347 (1969).
18. Manley, J. L. *J. molec. Biol.* **125,** 449–466 (1978).
19. Steege, D. A. *Proc. natn. Acad. Sci. U.S.A.* **74,** 4163–4167 (1977).
20. Napoli, C., Gold, L. & Swebelius Singer, B. *J. molec. Biol.* **149,** 433–449 (1981).
21. Atkins, J. F., Gesteland, R. F., Reid, B. R. & Anderson, C. W. *Cell* **18,** 1119–1131 (1979).
22. De Mars Cody, J. & Conway, T. W. *J. Virol.* **37,** 813–820 (1981).
23. Gorini, L. in *Ribosomes* (eds. Nomura, M., Tissières, A. & Lengyel, P.) 791–803 (Cold Spring Harbor Monogr. Ser., 1974).
24. Sugyama, T., Stone, H. & Nakada, D. *J. molec. Biol.* **42,** 97 (1969).
25. Maxam, A. & Gilbert, W. *Proc. natn. Acad. Sci. U.S.A.* **74,** 560–564 (1977).
26. Sander, F. *et al. Nature* **265,** 687–695 (1977).
27. Godson, G. N., Barrel, B. G., Staden, R. & Fiddes, J. *Nature* **276,** 236–247 (1978).

LETTERS TO NATURE

Particle acceleration at planetary bow shock waves

M. M. Hoppe & C. T. Russell

Institute of Geophysics and Planetary Physics, University of California, Los Angeles, California 90024, USA

We can extend our understanding of collisionless shocks by comparing their behaviour in a variety of plasma conditions at several different planets. One property of such shocks is the occurrence of upstream magnetohydrodynamic waves associated with particle beams accelerated at these shocks, and flowing back towards the Sun[1]. We report here observations of one of these classes of wave at Mercury, Venus, Earth and Jupiter. First, we show that the empirical relationship between the interplanetary field strength and the frequency of the waves in the observer's rest frame, derived originally from ground-based pulsation studies, and later, *in situ*, is approximately true at all the planets. Second, the observed frequencies are consistent with resonance with beams of ions of essentially the same energy at each of the planets. This observation is consistent with Sonnerup's[2] geometrical model of ion reflection at collisionless shocks. The universality of this ion acceleration mechanism in the Solar System suggests that like acceleration occurs in similar astrophysical systems outside our Solar System and thus may provide a source of acceleration for cosmic rays.

One characteristic feature of the solar wind interaction with the planets is the creation of an upstream bow shock, formed when the supersonic solar wind encounters the planetary atmosphere or magnetic field. Such shocks have been seen at all the planets so far probed by interplanetary spacecraft, and their general character is similar in many ways to that of Earth's bow shock. However, certain facets of shock structure *per se*, such as the associated plasma wave spectra[3] and the magnetic field overshoot[4], do vary between planets. These changes are generally consistent with the evolution of solar wind parameters with heliocentric distance.

We present a complementary comparative study of planetary foreshocks, those regions upstream of, but magnetically connected to, the bow shocks. The varieties of reflected particles and associated waves characteristic of this region at the Earth have been studied in some detail[5]. We focus here on the large-amplitude ($\Delta B/B \sim 1$), low-frequency ($\sim$0.03 Hz) waves and the associated backstreaming ion populations. We now briefly review results of the terrestrial work which are pertinent to the current study and compare them with studies of the upstream regions of Mercury, Venus and Jupiter.

We use primarily magnetic field data because the plasma analysers onboard extraterrestrial missions tend to be configured to measure the solar wind and are not in general appropriate instruments for characterizing the lower-density reflected particles. We focus on the large-amplitude low-frequency waves which have been documented in the upstream regions of Mercury, Venus, Earth and Jupiter, and studied in depth at the Earth[6,7]. It seems likely that these waves are generated through cyclotron resonance with beams of reflected ions[8], although theory does not yet reproduce all the features of the observations[9]. These waves have been of interest for some time, partially because of their role in the foreshock structure, but also because of their apparent connection with geomagnetic pulsations of the same frequency.

The relationships between upstream conditions and pulsation character have been investigated on the hypothesis that the upstream waves may be the ultimate source of at least some classes of pulsations. A linear relationship between pulsation frequency and the magnitude of interplanetary magnetic field has been found[10,11]. Russell and Hoppe[12] recently verified that the same relationship that holds for ground data also holds for the upstream waves. We have found that this same relationship is maintained to a remarkable degree over the orders of magnitude differences in wave frequency and field strength observed during the various planetary encounters. This is shown in Fig. 1 where the frequencies of the upstream waves observed at the different planets are plotted as a function of the associated magnetic field strengths. Data for Mercury represent Fairfield and Behannon's[13] estimate of 5–10 s periods for the 'low-frequency' waves encountered by Mariner 10 on its outbound pass. The Venus data were obtained from the Pioneer Venus magnetometer. The Earth data are from ref. 12 and the two points from Jupiter represent intervals of upstream wave activity, one observed by Pioneer 10 (ref. 14), the other by Voyager 2. The straight line is the empirical relationship between wave frequency and field magnitude found at Earth[12]. Points for all the planets clearly fall along the same linear trend.

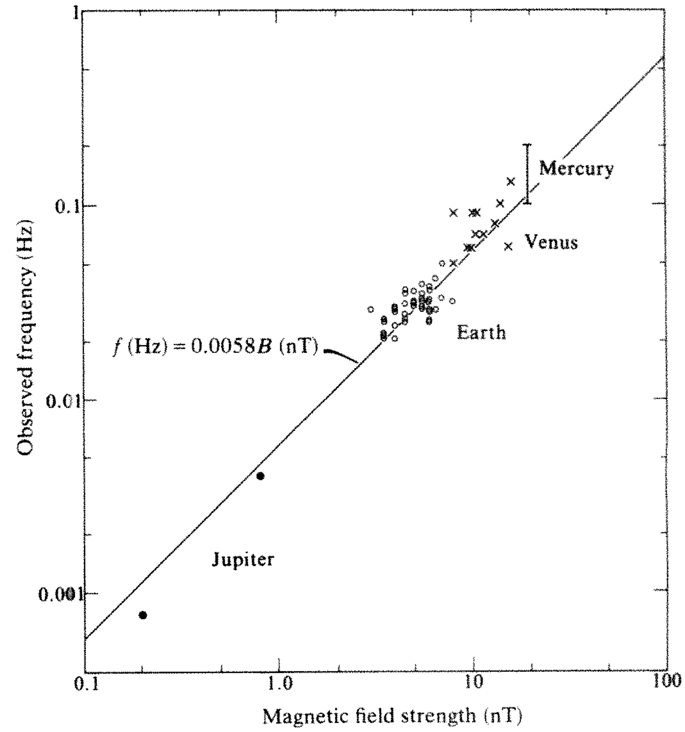

Fig. 1 Upstream wave frequency as observed in the spacecraft frame (f_{obs}) of reference as a function of ambient magnetic field strength.

0028-0836/82/010041—02$01.00

Table 1 Observed and rest-frame frequencies and resonant velocities

Planet	f' (Hz)	f_0/f_{ci}	v_r/v_{sw}
Mercury	0.1–0.2	0.09–0.17	1.2–2.2
Venus	0.06–0.13	0.064, 0.074	1.7, 1.9
Earth	0.02–0.04	0.03–0.08	2.5±0.3
Jupiter	0.0008(P)	0.06	2.3
	0.003(V)	0.02	2.1

Plasma data for Mercury from ref. 21, for Venus from Barnes (personal communication), for Earth from the Los Alamos ISEE team (personal communication) and for the Voyager Jupiter encounter (V) from the MIT plasma group (personal communication). Typical terrestrial values were scaled to provide estimates for the Pioneer Jupiter encounter (P).

This relationship can be understood as a combined effect of ion resonance and Doppler shifting, assuming that the waves are in each case low-frequency magnetosonic waves similar to those observed at the Earth. The terrestrial waves, which are a characteristic feature of the foreshock region, have long been thought to result from instability of ion beams reflected back along the IMF by the bow shock[8,15], although resonance with relativistic electrons has also been recently suggested as a source of the jovian waves[14]. The terrestrial waves are, however, very closely linked with upstream ion distributions[16] and spacecraft studies[17] have demonstrated that their properties are generally consistent with an ion beam generation mechanism. Specifically, it was shown that the terrestrial upstream waves are indeed magnetosonic waves with rest frame frequencies (f_0) of the order of 0.1 the local proton cyclotron frequency (f_{ci}). Because of Doppler shift effects this identification required the use of two point measurements, which for the terrestrial case were provided by the dual ISEE 1 and 2 spacecraft. One cannot ordinarily determine a wave's rest frame frequency using data from a single satellite. This is because even given the observed frequency (f'), solar wind velocity ($\mathbf{v}_{sw}$) and wave propagation direction $\hat{\mathbf{k}}$, there remain two unknowns, the rest frame frequency (f_0) and wavelength (λ) in the Doppler shift equation:

$$f' = f_0 + \frac{\mathbf{v}_{sw} \cdot \hat{\mathbf{k}}}{\lambda} \tag{1}$$

The number of unknowns can be reduced if we assume that the upstream waves at the extraterrestrial planets have rest frame frequencies of the same order as the terrestrial waves, $f_0 \leqslant 0.1 f_{ci}$. Waves in these low-frequency ranges have phase velocities very close to the Alfvén speed, $v_A = B^2/(4\pi n)^{1/2}$, where B is the magnetic field strength and n is the plasma density. Using this fact allows us to substitute $f_0 v_A = \lambda$ for λ equation (1). We can solve for f_0 in terms of the measured parameters f', v_{sw}, k, B and n:

$$f_0 = f' \Big/ \left(1 + \frac{\mathbf{v}_{sw} \cdot \hat{\mathbf{k}}}{B/(4\pi n)^{1/2}}\right) \tag{2}$$

Rest frame frequencies were estimated using this approach for all observations for which solar wind data were available, and wave propagation directions were determined through minimum variance analysis when possible. The 180° ambiguity which results in minimum variance analysis may be resolved by assuming the waves at Mercury, Venus and Jupiter are attempting to propagate upstream, as has been demonstrated to be the case at Earth. The angle between $\mathbf{v}_{sw}$ and $\hat{\mathbf{k}}$ was determined by minimum variance analysis of the Mercury, Earth and Voyager Jupiter data, was estimated from the average field orientation for Pioneer 10, and was assumed to have the same average value (35°) at Venus. Table 1 summarizes rest frame frequencies estimated in this way, normalized to the local proton cyclotron frequency. Estimated rest frame frequencies are of the same order at each planet, averaging about $0.07 f_{ci}$.

Having found results consistent with the hypothesis that the waves are in each case low-frequency magnetosonic waves, we can estimate the proton beam velocities required to generate waves of the observed frequencies. This was done by substituting calculated rest frame frequencies into the formula for the resonant velocity (v_r) of protons interacting with a magnetosonic mode wave[18]:

$$\frac{v_r}{V_A} = \frac{(1 + f_0/f_{ci})^{3/2}}{f_0/f_{ci}} \tag{3}$$

Calculated resonant velocities normalized by the ambient solar wind speeds are also presented in Table 1. Note that the resonant velocity given is the velocity parallel to the magnetic field relative to the component of the solar wind velocity along the field whereas most measurements are of total energy of the particles in the shock frame of reference. The beam energies are remarkably similar in all four cases, suggesting that essentially the same mechanism operates at each bow shock.

The consistency of the relationship between the observed wave frequencies and the magnetic field strength at the various planets derives from this equivalence of the source beam energies. In fact, taking a value of 2 for v_r/v_{sw}, solving for f_0 using equation (3) and substituting this value of f_0 into equation (2) using a nominal $\cos\theta_{kx} = -0.8$ yields the relationship f' (Hz) = 0.006 B (nT), which is in excellent agreement with the empirically determined relationship. Furthermore, the similarity of the inferred beam energies argues that the magnitude of bow shock acceleration must be relatively constant despite differences in shock size and structure. This similarity is consistent with Sonnerup's description of bow shock acceleration through particle displacement along the interplanetary electric field during the reflection process. In this description, which appears to predict accurately reflected beam energies at Earth[19], shock structure and strength have no influence and the amount of ion energization is determined strictly by geometrical effects. On the other hand, it is intriguing to see the smallest energies associated with the small relatively weak bow shock of Venus[20]. In any case, whatever the particle acceleration mechanism, the analysis presented here suggests that ion acceleration is a characteristic feature of planetary bow shocks and furthermore that reflected particle energies are of the same order regardless of shock scale size or structure.

Mariner 10 magnetic field data for Mercury and Voyager magnetic field data for Jupiter were obtained from NSSDC. This work was supported by NASA through contracts NAS 5-25772 and NGL 5-007-190.

Received 28 July; accepted 3 November 1981.

1. Hoppe, M. M. & Russell, C. T. *Adv. Space Res.* **1,** 327–332 (1981).
2. Sonnerup, B. U. Ö. *J. geophys. Res.* **74,** 1301–1304 (1969).
3. Scarf, F. L., Gurnett, D. A. & Kurth, W. S. *Nature* **292,** 747–750 (1981).
4. Russell, C. T., Hoppe, M. M. & Livesey, W. A. *Nature* (in the press).
5. *J. geophys. Res.* **86.** 4519–4536 (1981).
6. Fairfield, D. H. *J. geophys. Res.* **74,** 3541–3553 (1969).
7. Hoppe, M. M., Russell, C. T., Frank, L. A., Eastman, T. E. & Greenstadt, E. W. *J. geophys. Res.* **86,** 4471–4492 (1981).
8. Barnes, A. *Cosmic Electrodyn.* **1,** 90–114 (1970).
9. Gary, S. P., Gosling, J. T. & Forslund, D. W. *J. geophys. Res.* **86,** 6691–6696 (1981).
10. Troitskaya, V. A., Plyasova-Bakovnina, T. A. & Gul'yel'mi, A. V. *Dokl. Akad. Nauk. SSSR* **197,** 1312 (1971).
11. Gul'yel'mi, A. V. & Bol'shakova, O. V. *Geomagn. Aeron.* **13,** 535 (1973).
12. Russell, C. T. & Hoppe, M. M. *Geophys. Res. Lett.* **8,** 615–618 (1981).
13. Fairfield, D. H. & Behannon, K. W. *J. geophys. Res.* **81,** 3897–3906 (1976).
14. Smith, E. J., Tsurutani, B. T., Chenette, D. L., Conlon, T. F. & Simpson, J. A. *J. geophys. Res.* **81,** 65–72 (1976).
15. Gul'yel'mi, A. V. *Space Sci. Rev.* **16,** 331–345 (1974).
16. Paschmann, G. *et al. Geophys. Res. Lett.* **6,** 209–210 (1979).
17. Hoppe, M. M. & Russell, C. T. *EOS* **62,** 363 (1981).
18. Kennel, C. F. & Petschek, H. E. *J. geophys. Res.* **71,** 1–28 (1966).
19. Paschmann, G., Sckopke, N., Asbridge, J. R., Bame, S. J. & Gosling, J. T. *J. geophys. Res.* **85,** 4689–4694 (1980).
20. Russell, C. T., Elphic, R. C. & Slavin, J. A. *Nature* **282,** 815–816 (1979).
21. Ogilvie, K. W. *et al. Science* **185,** 145–151 (1974).

Organic and inorganic interpretations of the martian UV–IR reflectance spectrum

Kevin D. Pang*, Sandy F. S. Chun†, Joseph M. Ajello*, Zhao Nansheng‡, & Liang Minji§

* Jet Propulsion Laboratory, California Institute of Technology, Pasadena, California 91109, USA
† School of Medicine, University of California, San Francisco, California 94143, USA
‡ Beijing Planetarium, China
§ Beijing Glass Institute, China

Although some data from the Viking Lander biology experiments can be interpreted as indicative of biological activity, the existence of organisms in the martian soil samples is considered unlikely because of the non-detection of organic compounds in the sample[1]. Viking gas chromatography–mass spectrometer analysis detected no organic molecules above a concentration of parts per 10^9 (ref. 2). We consider here why no organic molecules were detected at the landing sites, whether the sterility of the two sites is representative of the entire planet and if there are locations on Mars more conducive to the formation and preservation of organics. We first simulate the destruction of organic compounds in Mars-like laboratory conditions, and then examine whether the destructive mechanism would operate planetwide; and second re-examine UV and IR reflectance spectra of Mars for any evidence of organic molecules, and in doing so set an upper limit on the organic carbon content of average martian soil. The results reveal that the average martian soil is organic-poor and makes an unfavourable habitat for life forms based on carbon chemistry. There is no reason to believe that organic molecules are preferentially preserved anywhere on the planet.

Recent observations of the outer Solar System by ground-based and spacecraft UV–IR spectroscopy show an abundance of organic compounds, existing as atmospheric gases and imbedded in carbonaceous chondrites. Because of its proximity to the outer Solar System, Mars should have received a large infall of carbonaceous meteorites[3,4]. The fact that Viking found no organics at the landing sites means that a very efficient process must be operating on Mars to destroy the organic molecules.

Chun *et al.*[3,4] proposed a mechanism for the destruction of organics on Mars: UV-stimulated catalytic oxidation. The degradation process from complex organic ultimately into inorganic compounds is:

$$\begin{array}{c}\text{Complex}\\ \text{organic}\\ \text{compounds}\\ O_2\end{array} \xrightarrow[\text{TiO}_2]{h\nu} \begin{array}{c}\text{Simple}\\ \text{organic}\\ \text{compounds}\\ O_2\end{array} \xrightarrow[\text{TiO}_2]{h\nu} \begin{array}{c}\text{Inorganic}\\ \text{compounds}\end{array}$$

In a controlled laboratory experiment, powders of Murchison meteorite (C2), rich in organics, and TiO_2 were degassed in Pyrex flasks. The flasks were filled with oxygen at approximately martian surface partial pressure, 0.1 torr. These flasks were then irradiated with UV-visible light. Hard UV light that may cause photolysis was first filtered out. The flasks were rotated on a turning wheel to keep the powder constantly agitated, and inhomogeneities in the radiation field averaged out. The flasks were examined for changes in gaseous composition using a mass spectrometer. Samples of the powder were pyrolysed and analysed with a mass spectrometer. According to our proposed mechanism, an evolution of CO_2 in the flasks, and/or a change in distribution of masses from high to low molecular weights in the solids would mean that UV-stimulated catalytic oxidation of organic compounds has taken place.

After irradiation for 4 days a copious supply of CO_2 was observed in flasks where all three ingredients, O_2, TiO_2 and carbonaceous chondrite, were present. The evolution of CO_2 was accompanied by a decrease in O_2 abundance. In flasks where all ingredients, except TiO_2 were present a small but detectable reaction took place. In flasks where all ingredients except O_2 were present, or where the carbonaceous chondrite was replaced by basalt, there was no evolution of CO_2. Also no reaction was observed in flasks with all ingredients present but kept in the dark.

We interpret the results of the controlled experiment to mean that organic compounds in the carbonaceous chondrite are photocatalytically oxidized. Activation energy, provided by energetic photons, is required for the reaction to take place. A catalyst, TiO_2, speeds up the reaction, but is not essential.

Mass spectra of pyrolysed solid samples were difficult to interpret due to the vast number of peaks present. Attempts to identify and trace the breakdown of high-molecular-weight compounds, such as undecane (abundant in C2), into low-molecular-weight compounds, such as acetone (a product generally observed from photocatalytic oxidation of alkanes), were not successful due to obscuration by fragments from the breakdown of many other organic compounds. Instead of trying to trace the breakdown of a mixture of organic compounds present in the carbonaceous chondrite, we decided to trace the breakdown of one compound at a time. An example is the breakdown of naphthalene, an aromatic compound. The naphthalene sample was prepared and irradiated along with O_2 and TiO_2 as its carbonaceous chondrite counterpart. The evolution of CO_2 was again observed, accompanied by the appearance of

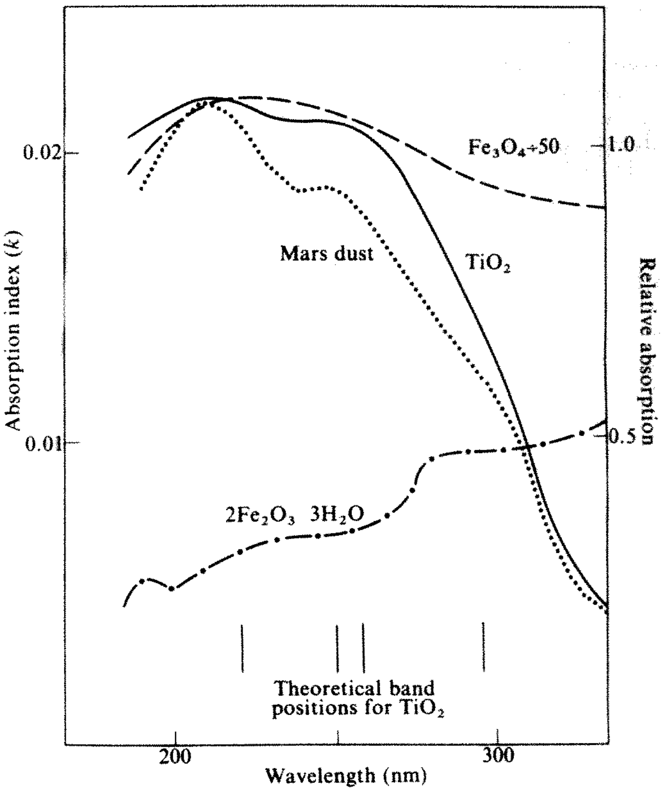

Fig. 1 Dotted curve indicates the absorption index *k* of martian dust (ref. 13). Solid curve is the relative absorption of anatase (an allotrope of TiO_2), normalized to the peak of Mars dust (measured by Zhao and Liang at the Beijing Glass Institute). Molecular orbital calculations for TiO_2 predict bands at the wavelengths indicated by tick marks (ref. 21). Data for magnetite (dashed curve) and limonite (dot-dashed curve) are from refs 23 and 24, respectively.

0028-0836/82/010043—04$01.00

simple organic compounds such as methane. We conclude that the naphthalene has broken down into simpler compounds.

Recently Sancier and Wise[5] found that photocatalytic oxidation is responsible for the degradation of organic compounds in terrestrial sand dunes. The catalyst for the sunlight-assisted reaction can be ordinary sand particles.

Whereas all conditions required for the photocatalytic oxidation of organic compounds: O_2 (ref. 6), sand (the dunes in Viking Lander pictures are evidence), and UV irradiation (as indicated by the darkening of UV-sensitive chips mounted on the Viking Landers, ref. 7) are present at the Viking landing sites, we conclude that the proposed mechanism operates at least at these two locations. To extrapolate this finding to the rest of the planet we need to examine conditions elsewhere to see if the requirements for photocatalytic oxidation are also satisfied.

The polar regions of Mars have been suggested as the most favourable sites for preservation of organics but there is no basis for this speculation. First, Mariner 9 UV spectrometer observations showed that solar radiation of wavelengths as short as 200 nm easily penetrates the martian atmosphere down to the polar cap[8]. Second, sand grains exist in great abundance in the polar regions on Mars—in dunes and laminated between condensates[9]. Third, ozone is found in the martian polar atmosphere, although not in a concentration to attenuate the solar UV significantly[10]. The presence of O_3 requires that O_2 be there also. Therefore, all conditions necessary for the photocatalytic oxidation of organics—UV radiation, oxygen, and sand—are present in the polar regions of Mars, and the destruction of any organic molecules on the polar caps seems almost certain.

Theoretical atmospheric modelling by Hunten[11] showed that the formation of oxidants is planetwide on Mars. Atmospheric radiative transfer calculations by Kuhn and Atreya[12] found that all latitudes on Mars receive lethal annual dosage of solar UV radiation. Sand dunes are common on Mars[9]. Therefore, all conditions required for photocatalytic oxidation of organics seem to be satisfied, and we conclude that there is no basis for optimism for finding organic molecules anywhere on Mars. Organics could be buried undergound, but the fact that Viking found none under a rock does not support this conjecture.

In addition to the above comparative analysis we can use spectral remote sensing data of Mars to extend the Viking findings. UV and IR spectroscopy are very sensitive techniques in quantitative organic analysis. Therefore, UV and IR reflectance spectra of Mars, when properly interpreted with the aid of laboratory 'ground truth' measurements, can yield the surface chemical composition of areas not examined *in situ*.

Most molecules have spectral signatures in the small range of UV wavelengths 120–320 nm. Unfortunately UV observations of the martian surface are usually hampered by Rayleigh scattering (at $\lambda \leqslant 320$ nm) and absorption (at $\lambda \leqslant 180$ nm) due to carbon dioxide molecules in the martian atmosphere[10,13]. However, during dust storms surface material is raised and suspended as dust in the atmosphere. The 1971 global dust storm was particularly favourable for remotely sensing the physical properties of Mars dust particles, and the UV spectrometer on the Mars-orbiting Mariner 9 spacecraft observed the dust clouds as resolutions and phase angles not possible from the Earth. By modelling the observed phase function (intensity as a function of the scattering angle) of the dust particles with theoretical scattering calculations their complex refractive index ($n - ik$) can be determined. The wavelength dependence of the absorption index k of martian dust is shown in Fig. 1. The absorption increases with decreasing wavelength down to ~210 nm, but decreases at still shorter wavelengths. A structural shoulder in the absorption spectrum occurs near 250 nm. A third feature is also present at ~300 nm. Both the absolute value of k and its variation in the UV are consistent with k values in the visible/IR, determined by Viking Lander spectrophotometric observations of martian aerosols[14]. UV observations of the dust-shrouded Mars by the Orbiting Astronomical Observatory (OAO 2) are also consistent with the Mariner 9 measurements[15].

Abadi and Wickramasinghe[16] have suggested that the absorption feature at 210 nm may be a signature of highly complex organic or pre-biotic molecules in martian dust clouds. Their conclusion is based on similarities between the 210 nm martian dust band and bands in the absorption curves of organic materials, including an extract of the Murchison meteorite[17,18]. Although there is a superficial resemblance between the martian dust absorption spectrum and the data in refs 17 and 18, comparisons reveal important differences in both band strength and position. Searching through more than 2,000 UV absorption spectra of organic compounds[19] we could not find any that closely resemble the dotted curve in Fig. 1. A combination of organic compounds or a sample that we did not examine may have had the required spectral characteristics. However, the following inorganic interpretation is more reasonable because of its simplicity, and because it accounts for all the UV features observed in martian dust.

The suggestion that the UV absorption bands in martian dust are due to electronic transitions in titanium dioxide[13] has been experimentally verified at the Beijing Glass Institute. Titanium oxide was vacuum evaporated onto a fused quartz substrate, and then oxidized by heat treatment[20]. X-ray diffraction study revealed the crystalline structure of the TiO_2 to be in the anatase form. The optical density of the sample was measured with a spectrophotometer at a resolution of $\Delta\lambda/\lambda = 0.001$. The solid curve in Fig. 1 shows the relative absorptivity of the anatase sample, normalized to the peak of martian dust absorption. Molecular orbital calculations predict absorption bands at 220, 250, 258, and 296 nm due to metal–ligand transitions in TiO_2 (tick marks in Fig. 1)[21]. We should also consider whether other electronic transitions (Fe^{2+}, Fe^{3+}) that have been suggested to explain the visible/near IR absoprtion features of Mars[22] may also account for the UV absorption features. Absorption spectra of Fe_3O_4 and $2Fe_2O_3 \cdot 3H_2O$ are also shown in Fig. 1. The ferric and ferrous transitions do not fit the Mars dust data as well as TiO_2. In any case, TiO_2 is expected to dominate the UV spectrum of Mars surface material despite its lower abundance, because its band strength is far stronger than that of the iron oxides below about 320 nm (refs 23–25). Our conclusion is

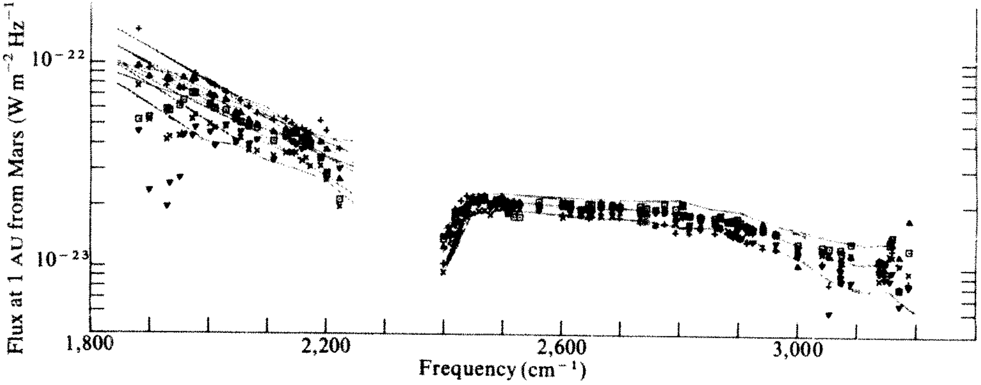

Fig. 2 Observed IR flux of Mars compared with inverse wavelength. Different symbols refer to different observing runs. Different curves were generated by a temperature–albedo model. Reproduced from refs 27, 28, with permission of Reidel, Boston.

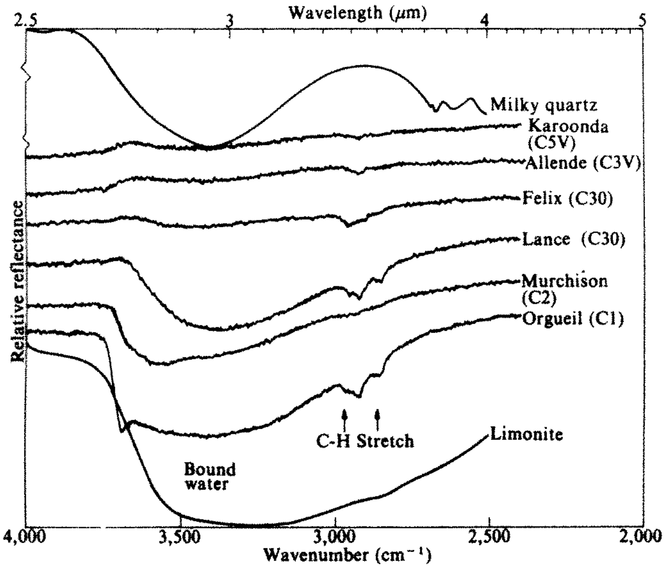

Fig. 3 Relative reflectance of powders (particle sizes between 0 and 74 μm) of quartz, limonite, and carbonaceous chondrites. Petrographical classification in parentheses. Reflectance (relative to MgO) at λ 2.5 μm are: Murchison 7%, Orgueil 9%, Allende 11%, Karoonda 14%, Felix 15%, Lance 17%, limonite 34%, and quartz 82% (see ref. 46). Reflectance measurements of carbonaceous chondrites made by Salisbury are published in part in ref. 39. Quartz and limonite spectra are given in ref. 40.

consistent with the detection of titanium by Viking Lander inorganic analysis[26].

In addition to the UV analysis we may reinterpret IR reflectance spectra of Mars to derive useful upper limits on the organic carbon content of martian soil. Extensive IR spectroscopic studies of Mars have been carried out with sophisticated groundbased, airborne, and spacecraft instrumentation. The martian IR spectrum shows the signatures of atmospheric carbon dioxide, carbon monoxide, water vapour, and oxygen; and of silicates, solid CO_2, bound and frozen water on the surface[22,27–32]. Stringent upper limits have been placed on undetected atmospheric constituents, for example, parts per 10^8 for methane[33–36]. The wavelength interval 3.3–3.6 μm has been especially well scrutinized because nearly all organic compounds containing C and H have absorption bands here due to excitation of the C–H stretching vibration[37,38]. As all gases known to be present in the martian atmosphere[6] are transparent in this spectral region, any absorption feature found superimposed on the wing of the 3-μm water of hydration band may be assigned to organic constituents in Mars surface material. Despite intensive search the C–H absorption bands have never been found on Mars. Figure 2 shows high resolution spectra of Mars taken by Beer[27]. Absorption features due atmospheric CO_2 and water bound in surface material (3,300 cm^{-1} or 3 μm) are clear. However, the C–H bands (2,800–3,000 cm^{-1} or 3.3–3.6 μm) are absent. Observed flux variations in this spectral interval can be adequately accounted for by a simple temperature–albedo model.

Laboratory measurements are useful for quantitative reinterpretations of IR reflectance spectra of Mars. Figure 3 shows laboratory reflectance spectra of quartz, limonite, and representative carbonaceous meteorites[39,40]. The methyl and methylene (symmetric and anti-symmetric) vibration bands are clearly resolved as a doublet on the long wavelength wing of the water of hydration band in the spectra of the carbonaceous chondrites. The strength of the C–H bands correlates with the organic carbon content of the meteorite, for example, Orgueil, 2.5%; Lance and Felix 0.4%; and Allende, 0.2%. The C–H bands are detectable in even in Karoonda, with an organic carbon content of only 0.08%. The 3.3–3.6 μm features are not present in quartz and limonite, representing terrestrial minerals and rocks with organic carbon contents of 0.02–0.06% (ref. 41, 42). Organic carbon content has been estimated to be about 80% of total carbon content by Nagy. The remaining 20% carbon is in carbonates which do not have the C–H bond. Total organic carbon contents of terrestrial rocks are estimated from vaporization-pyrolysis measurements of representative rocks, scaled to that of the Allende meteorite[43]. We conclude that the absence of the fundamental C–H stretching absorption features in the martian reflectance spectra indicates that the organic carbon content of its average surface material is at or below parts per 10^4. The upper limit for organic carbon content pertains to a value averaged over the whole martian planet, as when Mars is observed by low spatial resolution Earth-based IR spectroscopy, or to a value averaged over the field of view (FOV) of spacecraft IR spectrometers, which have best resolution of the order of 100 km. The organic carbon content of an area smaller than the resolution limit might exceed that averaged over the FOV, although Viking GC-MS results make this proposition seem unlikely. Field observations in the dry valleys of Antarctica have shown that soil samples with organic carbon contents <0.1% are generally sterile[44,45]. This implies that Mars in general and areas examined by IR spectroscopy in particular have soil deficient in organic matter, and are unfavourable habitats for life forms based on carbon chemistry.

An inorganic interpretation of Mars' UV reflectance spectrum is, therefore, more plausible than an organic interpretation. The IR reflectance spectrum places a stringent upper limit on the organic carbon content of average martian soil, virtually ruling out biological activities. Laboratory simulation and site comparisons give no reason to believe that organic molecules are preferentially preserved anywhere on Mars. Taken together, the evidence suggests that the sterility of the Viking landing sites is representative of the entire planet.

We thank Drs William H. Pickering and Ta-Jin Kuo for initiating this collaborative effort, and Drs Jack W. Salisbury, Eddie N. Wells, Larry A. Lebofsky, and James L. Gooding for helpful comments. K.D.P. performed part of the research during his tenure as a National Academy of Sciences Senior Resident Research Associate. S.F.S.C.'s participation was made possible through funding from the 1977 Newcomb Cleveland Award, given by the American Association for the Advancement of Science. This research was performed in the People's Republic of China and at JPL. The work carried out at JPL, California Institute of Technology, was sponsored by NASA. The Murchison meteorite specimen used in our research was provided by the Smithsonian Institution.

Received 21 September; accepted 30 October 1981.

1. Klein, H. P. *Rev. Geophys. Space Phys.* **17,** 1655–1662 (1979).
2. Biemann, K. & Lavoie, J. M. Jr *J. geophys. Res.* **84,** 8385–8390 (1979).
3. Chun, S. F. S., Pang, K. D., Cutts, J. A. & Ajello, J. M. *Nature* **274,** 875–876 (1978).
4. Chun, S. F. S., Pang, K. D. & Ajello, J. M. *NASA Conf. Publ.* **2072,** 15 (1979).
5. Sancier, K. M. & Wise, H. *Atmos. Envir.* **15,** 639–640 (1981).
6. Owen, T. *et al. J. geophys. Res.* **82,** 4635–4639 (1977).
7. Arvidson, R. & Jones, K. *NASA Conf. Publ.* **2072,** 3 (1979).
8. Pang, K. & Hord, C. W. *Icarus* **18,** 481–488 (1973).
9. Carr, M. H. *Space Sci. Rev.* **25,** 231–284 (1980).
10. Barth, C. A. & Hord, C. W. *Science* **173,** 197–201 (1971).
11. Hunten, D. M. *J. molec. Evolut.* **14,** 71–78 (1979).
12. Kuhn, W. R. & Atreya, S. K. *J. molec. Evolut.* **14,** 57–64 (1979).
13. Pang, K. & Ajello, J. M. *Icarus* **30,** 63–74 (1977).
14. Pollack, J. B. *et al. J. geophys. Res.* **84,** 2929–2946 (1979).
15. Caldwell, J. *Icarus* **32,** 190–209 (1977).
16. Abadi, H. & Wickramasinghe, N. C. *Nature* **267,** 687–688 (1977).
17. Sakata, A. *et al. Nature* **266,** 241 (1977).
18. Hoyle, F. & Wickramasinghe, N. C. *Nature* **266,** 241–243 (1977).
19. Scott, A. I. *Interpretation of the Ultraviolet Spectra of Natural Products* (Pergamon, Oxford, 1964).
20. Hass, G. *Vacuum* **2,** 331–345 (1952).
21. Loeffler, B. M., Burns, R. G., Tossell, J. A., Vaughan, D. J. & Johnson, K. H. *Proc. 5th Lunar Sci. Conf.* 3007–3016 (1974).
22. Singer, R. B., McCord, T. B., Clark, R. N., Adams, J. B. & Huguenin, R. L. *J. geophys. Res.* **84,** 8415–8426 (1979).
23. Huffman, D. K. & Stapp, J. L. in *Interstellar Dust and Related Topics* (eds Greenberg, M. & van de Hulst, H. C.) 297–301 (Reidel, Boston, 1973).
24. Egan, W. G., Hilgeman, T. & Pang, K. D. *Icarus* **25,** 344–355 (1975).
25. Cardona, M. & Harbeke, G. *Phys. Rev.* **137,** A1467–A1476 (1965).
26. Toulmin, P. III *et al. J. geophys. Res.* **82,** 4625–4634 (1977).
27. Beer, R. in *Exploration of the Solar System* (eds Woszczyk, A. & Iwaneszewska, C.) 229–239 (Reidel, Boston, 1974).

28. Barker, E. S. in *Exploration of the Solar System* (eds Woszczyk, A. & Iwaneszewska, C.) 229–239 (Reidel, Boston, 1974).
29. Noxon, J. F., Traub, W. A., Carleton, N. P. & Connes, P. *Astrophys. J.* **207,** 1025–1035 (1976).
30. Egan, W. G., Hilgeman, T. & Smith, L. L. *Icarus* **35,** 209–226 (1978).
31. Pimentel, G. C., Forney, P. B. & Herr, K. C. *J. geophys. Res.* **79,** 1623–1634 (1974).
32. Hanel, R. *et al. Icarus* **17,** 423–442 (1972).
33. Maguire, W. C. *Icarus* **32,** 85–97 (1977).
34. Beer, R., Norton, R. H. & Martonchik, J. V. *Icarus* **15,** 1–10 (1971).
35. Horn, D., McAfee, J. M., Winer, A. M., Herr, K. C. & Pimentel, G. C. *Icarus* **16,** 543–556 (1972).
36. Owen, T. & Sagan, C. *Icarus* **16,** 557–568 (1972).
37. Duley, W. W. & Williams, D. A. *Nature* **277,** 40–41 (1979).
38. Rea, D. G., O'Leary, B. T. & Sinton, W. M. *Science* **147,** 1286–1288 (1965).
39. Lebofsky, L. A. *Mon. Not. R. astr. Soc.* **182,** 17P–21P (1978).
40. Salisbury, J. W. & Hunt, G. R. *Nature* **222,** 132–136 (1969).
41. Nagy, B. *Carbonaceous Meteorites* (Elsevier, Oxford, 1975).
42. Wiik, H. B. *Commentat. physico.-math.* **34,** 135–145 (1969).
43. Levy, R. M., Grayson, M. A. & Wolf, C. J. *Geochim. cosmochim. Acta* **37,** 467–483 (1973).
44. Cameron, R. E. in *Research in the Antarctica* (eds Quam, L. O. & Porter, H. D.) 137–189 (American Association for the Advancement of Science, Washington DC, 1971).
45. Horowitz, N. H., Cameron, R. E. & Hubbard, J. S. *Science* **176,** 242–245 (1972).

Chorus-related electrostatic bursts in the Earth's outer magnetosphere

L. A. Reinleitner, D. A. Gurnett & D. L. Gallagher

Department of Physics and Astronomy, University of Iowa,
Iowa City, Iowa 52242, USA

We report here recent studies of wideband plasma wave data from the ISEE 1 and ISEE 2 spacecraft which reveal that whistler-mode chorus emissions in the Earth's outer magnetosphere are often accompanied by high-frequency bursts of electrostatic noise. The chorus features that correlate to the electrostatic bursts have a hook-like frequency–time variation in the frequency range 200–400 Hz, and the associated electrostatic bursts have a frequency range of ~4–8 kHz. In some cases these electrostatic bursts have a harmonic frequency structure with a frequency spacing corresponding to the chorus frequency. This harmonic structure apparently results from the fact that the burst intensity is modulated at the chorus frequency.

Selected wideband spectrograms[1] obtained from ISEE 1 of the chorus-related electrostatic bursts are shown in Figs 1–3. Figure 1 indicates some of the general features of the bursts. In this case, the bursts appear to be strongly correlated to discrete hook-like features in the chorus band[2]. In addition to this example, many cases of the electrostatic bursts are observed in conjunction with intense chorus bands without hooks. In such cases the electrostatic bursts are usually merged together in a nearly continuous band similar to the extended burst in Fig. 1 from about 1738:40 to 1738:50 UT. A comprehensive survey of the locations where the bursts (with or without hooks) are observed has not yet been performed. However, all cases observed have been in the outer magnetosphere near the dayside magnetopause boundary from 7.0 to 17.5 magnetic local time (MLT), about 9–12 R_E and within ~30° of the magnetic equator.

The frequent occurrences of the electrostatic bursts, whether accompanied by hooks in the chorus band or not, as well as the rather limited physical region of occurrence, strongly indicate that the bursts are not caused by instrumental effects. To check that the bursts are not due to some cross-modulation effect in the instrument electronics, wideband data from the IMP 6 spacecraft have been examined. (The plasma wave instrumentation on IMP 6 is detailed in refs 3 and 4.) Although IMP 6 was not in the correct wideband mode to observe both frequencies of interest as often as ISEE 1, intense chorus accompanied by electrostatic bursts have, nevertheless, been found in several passes through the outer magnetosphere on the dayside region.

The electrostatic bursts have several characteristics. The bursts typically occur in a frequency band extending from near the electron plasma frequency f_p as determined by the lower edge of the continuum radiation[4], down to approximately half f_p, as in Fig. 1. In the examples shown, the frequency range of the burst does not extend up into the continuum radiation, although bursts extending up into the plasma frequency have been found. In all cases, the bursts occur at frequencies above the electron gyrofrequency ($f_g \sim 1.2$ kHz in Fig. 1).

The bursts have been described as electrostatic because no wave magnetic field can be detected in association with them. Typically the broadband electric field strength of the bursts are about 50 μV m^{-1}. Because the wave magnetic field remains at the instrument noise level in all cases, a limit can be placed on the electric-to- magnetic field ratio of about $E/cB \geqslant 0.25$ (which corresponds to an index of refraction $n \leqslant 4$). Because no electromagnetic plasma wave mode is known to exist with $E/cB \geqslant 0.25$ in the frequency range $f_g < f_{burst} < f_p$, the bursts are almost certainly electrostatic. The typical field strengths of the chorus emissions associated with the electrostatic bursts are about 300 μV m^{-1} and 40×10^{-12} T.

The electrostatic bursts occasionally have narrowband harmonic structure of the type shown in Fig. 2. The harmonic structure should not be confused with the vertical striations due to the rapid time dependence of the bursts. The harmonic structure is only evident when the chorus emission has a narrow bandwidth, such as when the hook-shaped features occur. The frequency spacing of the harmonic structure corresponds exactly with the instantaneous emission frequency of the chorus burst.

When chorus hooks are found to be correlated with the electrostatic bursts, the onset of the electrostatic burst usually coincides with the minimum frequency of the hook. This relationship can be seen most clearly in the first and last hook in the upper panels of Fig. 3. Note that the electrostatic burst usually continues for a time after the hook has disappeared or merged back into the chorus band.

Comparative studies using both ISEE 1 and ISEE 2, were possible because both spacecraft were in nearly identical orbits with a separation of only hundreds of kilometres. Although virtually identical chorus hooks were found in the electric field wideband data, the electrostatic bursts, while correlated, were not identical at the two spacecraft which indicates that the structure of the electrostatic bursts varies significantly on spatial scales of only hundreds of kilometres. To estimate the wavelength of the electrostatic noise, the electric field strength has been compared on ISEE 1 and 2, which have electric antenna lengths of 215 m and 30 m tip-to-tip. For bursts which had similar characteristics at the two spacecraft, the electric field

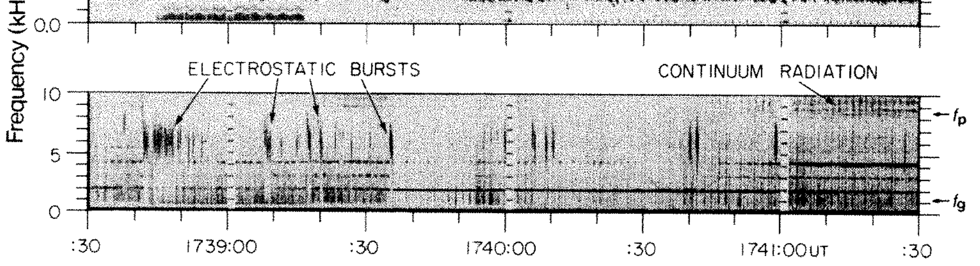

Fig. 1 Frequency versus time wideband plasma wave data for 5 November 1977 showing general features of the chorus related electrostatic bursts. The slight inter-features of the chorus related electrostatic bursts. The slight interference from 1738:45 to 1739:17 UT (also in Fig. 3) is from the ISEE electron density experiment. $R = 11.04 R_E$; magnetic lat. = 21.1°; MLT = 11.6 h.

0028–0836/82/010046—03$01.00

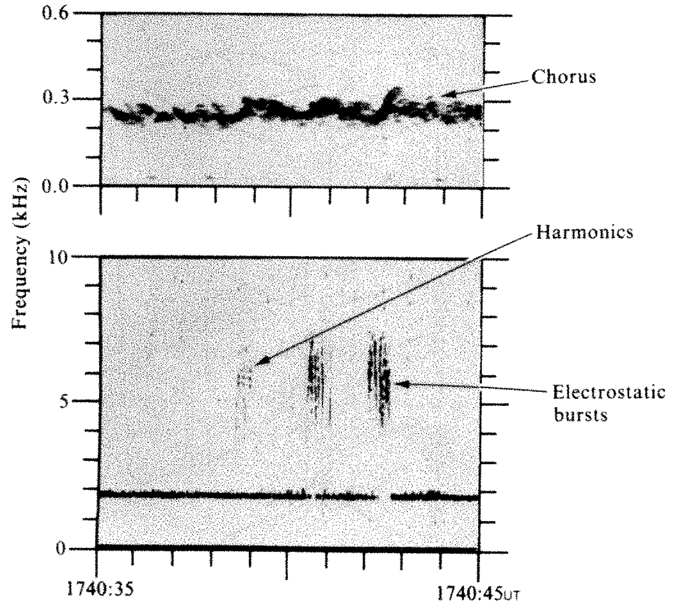

Fig. 2 Wideband plasma wave data showing narrowband harmonic structure for 5 November 1977. $R = 11.01\ R_E$; magnetic lat. = 21.1°; MLT = 11.7 h.

strengths were in good agreement, thereby indicating that the wavelength of the bursts must be longer than both of the antennas, implying a wavelength for the electrostatic bursts of $\lambda_{\text{burst}} > 215$ m.

Comparisons of the waveforms of the chorus and the electrostatic bursts reveal several interesting features. The lower panel of Fig. 3 shows the electric field versus time for both the chorus and the electrostatic burst. The lower signal is that of the chorus while the upper high frequency signal is the associated electrostatic burst. Both signals have been run through bandpass filters to eliminate signals not in the frequency band of interest. Note that the time duration of these waveform data is only 8 ms. The waveform therefore comprises only a small portion of the electrostatic burst from which it was taken. As can be seen, the electrostatic noise is actually composed of many shorter bursts of a high frequency signal which is modulated at the chorus frequency. Thus, the harmonics evident in Fig. 2 are a modulation effect caused by the periodic pulsing of the electrostatic noise at the frequency of the chorus emission. In the cases where the harmonics do not occur, the chorus does not occur as a single frequency but rather as a band of frequencies, which tends to blend harmonics into a broad continuous spectrum.

The correlation between the envelope of the bursts and the chorus waveform is often not as good as the example shown; however, the basic modulation effect in which the intensity of the high frequency emission maximizes at a given phase of the chorus waveform is usually evident. Also, despite the apparently abrupt initial turn-on of the bursts in the usual wideband data, waveform data show a gradual increase in the amplitude of the high frequency bursts, as well as a gradual decrease toward the end of each burst. For the case shown in the lower panel of Fig. 3, the frequency of the electrostatic emission is 6.7 kHz (±0.5 kHz) which is near but below the plasma frequency of 8.5 kHz (±0.5 kHz) as determined by the lower cutoff of the continuum radiation.

The strong correlation between the envelope of the electrostatic bursts and the chorus waveform suggests some strong physical interaction between these two wave modes. We currently believe that the chorus is phase bunching electrons at the phase velocity of the whistler mode and that these resonant electrons are triggering an electrostatic instability through a two-stream (or bump-on-tail) type mechanism[5]. We are not certain of the exact identification of the electrostatic mode involved but the best candiate seems to be a Langmuir wave or related beam mode, because the emission occurs very close to the local electron plasma frequency. The shift in the frequency of the electrostatic emission below the plasma frequency could

Fig. 3 The lower panel shows the oscilloscope waveform pattern taken from the very short burst indicated in the upper panels of wideband data for 5 November 1977. The low frequency signal in the bottom of the lower panel is the chorus waveform, while the high frequency signal bursts at the top of the lower panel are the electrostatic bursts. The phase of the chorus waveform may differ from that shown by a constant (instrumental) phase factor. $R = 11.04\ R_E$; magnetic lat. = 21.1°; MLT = 11.6 h.

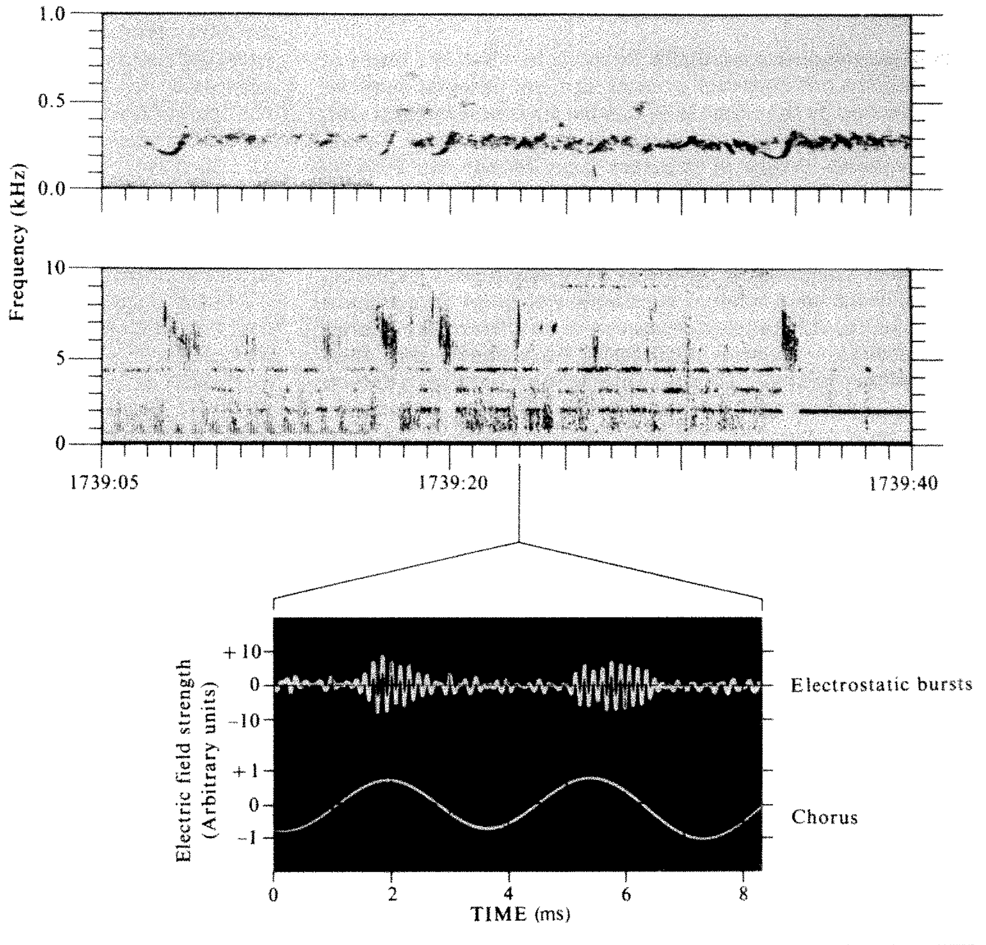

be due to either a Doppler shift or an intrinsic effect related to the two-stream interaction.

We also believe that the correlated whistler and electron plasma oscillation bursts detected in the solar wind by Kennel *et al.*,[6] are probably essentially identical to the chorus related electrostatic bursts described here. Most differences are attributable to differing plasma parameters in the two different regions of interest. The hypothesized interaction between these two wave modes is seen as a better alternative than the secondary impulsive electron heating mechanism proposed by Kennel *et al.*[6].

We thank Dr Alain Roux for valuable suggestions on theory, and Dr Roger R. Anderson for help with analysis of the data. This research was supported by NASA through grant NGL-16-001-043 from NASA Headquarters and contract NAS5-20093 with Goddard Space Flight Center, and the Office of Naval Research.

Received 3 July; accepted 16 October 1981.

1. Gurnett, D. A., Scarf, F. L., Fredricks, R. W. & Smith, E. J. *IEEE Trans. Geosci. Electron.* **GE-16,** 225–230 (1978).
2. Helliwell, R. A. *Whistlers and Related Ionospheric Phenomena* (Stanford University Press, 1965).
3. Shaw, R. R. & Gurnett, D. A. *J. geophys. Res.* **80,** 4259–4271 (1975).
4. Gurnett, D. A. & Shaw, R. R. *J. geophys. Res.* **78,** 8136–8149 (1973).
5. Krall, N. A. & Trivelpiece, A. W. *Principles of Plasma Physics* (McGraw-Hill, New York, 1973).
6. Kennel, C. F. *et al. Geophys. Res. Lett.* **7,** 129–132, (1980).

Coordination model for the defect structure of hyperstoichiometric UO$_{2+x}$ and U$_4$O$_9$

G. C. Allen, P. A. Tempest & J. W. Tyler

Central Electricity Generating Board, Berkeley Nuclear Laboratories, Berkeley, Gloucestershire GL13 9PB, UK

Non-stoichiometric compounds or solids in which the ratios of the amounts of elements present are not integral may be characterized by the formula MX$_x$ where x is non-integral and, in many crystalline compounds, may vary over quite a wide range without change of structure type. Ideally the thermodynamic stability and physical properties of such compounds should be related to the same atomic and electronic model but the ways in which various simple structures adapt to departures from ideal composition have not been adequately explored. Models based on a random distribution of point defects have proved successful but selected area electron diffraction and ultra high resolution electron microscopy have shown that their distribution is not simple. Interaction between defects produces microscopic sub-structures or clusters introducing specific local properties. Although our knowledge of the principal morphological features of sub-structures has advanced, their precise interatomic arrangements are generally unknown. Here we derive a model for non-stoichiometric oxides of uranium.

Some oxides of the lanthanide or actinide elements have fluorite-type structures and a propensity towards deviation from simple stoichiometry. Oxygen can be transferred easily between the MO$_x$ lattice and the ambient gas phase. UO$_2$ is no exception and its stoichiometric form is not easy to obtain. Although some oxidation occurs even at very low temperatures, homogeneous oxidation products are not formed in this way. At room temperature, surface oxidation processes are responsible for the non-stoichiometric nature of UO$_2$ in dry air and further oxidation is controlled by diffusion of oxygen either in the dioxide lattice or through a diphasic surface layer. Only above ~300 °C does the oxidation become so rapid that uniform accessibility of oxygen to the entire sample becomes a factor. In many defect oxides with the fluorite structure non-stoichiometry occurs through untenanted anion sites, the cation sublattice remaining essentially intact. The formation of UO$_{2+x}$ and U$_4$O$_9$, however, occurs by the incorporation of additional oxygen atoms at interstitial sites in the fluorite structure of UO$_2$ rather than the creation of uranium vacancies, and the occupation number of cations again remains the same as in the stoichiometric compound.

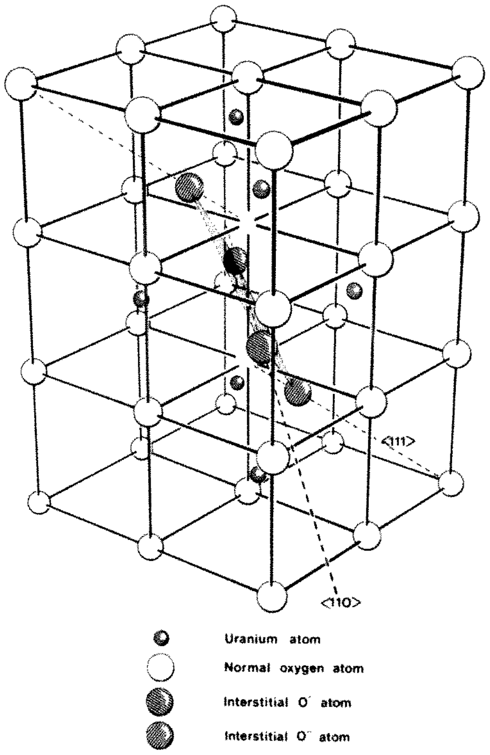

Fig. 1 The oxygen sublattice showing a 2 : 2 : 2 cluster.

The interstitial sites have been identified by Willis[1,2]. These are of two types which are displaced from the cubic-coordinated sites by about 1 Å in the ⟨110⟩ and ⟨111⟩ directions. This aggregate or 'cluster' depicted in Fig. 1 has the 2 : 2 : 2 configuration which contains two oxygen interstitial atoms along ⟨110⟩ identified as 0′, two oxygen interstitial atoms along ⟨111⟩ identified as 0″, and two vacancies in the oxygen sublattice. The formation of these clusters contrasts with the structural defects present in other anion-excess fluorite-related superlattices in which the basic oxygen cube of the fluorite structure changes to a square antiprism[3].

Martin[4] suggested that ordering of defects in fluorite lattices could occur to form chains of coordination defects. For MO$_{2-x}$ phases Martin's recognition of this phenomenon was based on assemblies of vacancy point defects. However, a detailed analysis of the X-ray photoelectron spectrum of UO$_{2+x}$ suggested a defect grouping based on a unique coordination of Willis type clusters in which an individual oxygen atom has a total negative charge less than in the isolated oxygen ion[5]. Thus ordering similar to that suggested by Martin could occur in UO$_{2+x}$ based on oxygen interstitials. Our model for the structure of UO$_{2+x}$ including U$_4$O$_9$, incorporates a chain-like coordination of oxygen defect clusters.

In Fig. 1 the 2 : 2 : 2 cluster bridges two uranium atoms which then become 9-fold rather than 8-fold coordinate. Using neutron diffraction data[6] for this UO$_9$ coordination polyhedron the internuclear separations are; 6(U–O) at 2.37 Å, 2(U–O′) at 2.22 Å, and 1(U–O″) at 2.29 Å emphasizing the higher degree of covalency in the uranium-cluster bonds. These calculations require that the U–U distance be fixed although in practice, this is unlikely. Single crystal X-ray diffraction studies of defect fluorite-type structures reveal consistent lengthening of U–U and shortening of O–O distances around a vacant oxygen site[7] and similar polarization effects would be expected in the vicinity of a cluster. This would shorten the U–U interatomic distance

0028–0836/82/010048—02$01.00

across the cluster and create preferred interstitial oxygen sites along the opposite edge of the oxygen cube containing the original defect grouping. Thus in addition to the tendency for clusters to order under coulombic forces to develop a superstructure, on geometrical grounds we can postulate the formation of a 2:2:2 cluster chain along $\langle 110\rangle$. A $\langle 110\rangle$ chain in the oxygen sublattice is shown in Fig. 2 and its relationship to the conventional UO_2 unit cell is given in Fig. 3.

Within the chain each uranium atom now has the coordination number 10. Most models for the anion excess phase invoke doubly charged intersitials (O_i^{2-}) compensated by singly charged holes (h^+) present as U^{5+} cations[2]. At first sight bond length data seem to support this view. The average U–O separation in most metal uranate (VI) structures is 2.07–2.10 Å but in the eight coordinate $CaUO_4$ structure this distance is 2.21 Å (ref. 8) which approaches the values derived above. Data from measurements of the X-ray photoelectron spectra in the U4f region may also be interpreted in terms of a uranium atom in crystallographically inequivalent sites where it apparently resides in 4+ and 6+ ionic configurations[9,10] so that although ESR measurements on uranates favour the presence of U^{5+} in U^{6+} lattices[11] this may not be the case in the fluorite structure of UO_2.

The length and frequency of chains determines the overall nature of the structure. For low values of x in UO_{2+x} a random distribution of clusters is envisaged. As x increases the probability of oxygen interstitials being influenced by clusters already formed increases. Gradually as x approaches 0.25 cluster chains develop and become ordered. Continuous chains are only allowed in every alternate uranium sublattice layer parallel to $\langle 001\rangle$ because of O″ interference in the oxygen sublattice. At a distance of closest approach of $2\sqrt{2}a_0$ (where a_0 is the lattice parameter of the parent UO_2 fluorite lattice) in the $\langle 110\rangle$ direction only 32 clusters can be accommodated by a unit cell of edge $4a_0$ which yields the composition of U_4O_9 exactly, and is consistent with the superlattice observed by Willis[6]. A chain spacing of $\frac{3}{2}\sqrt{2}a_0$ parallel to $\langle 110\rangle$ yields U_3O_7 but is not consistent with the U_4O_9 superlattice. Any increase in oxygen content above $UO_{2.33}$ would involve severe distortion of the parent fluorite lattice as additional oxygen atoms would have to be accommodated by oxgyen cubes already distorted by O′ or O″ interstitials. Not surprisingly the next characterized oxide phase U_3O_8 has a completely different structure. The increased electrostatic force between uranium atoms separated by a 2:2:2 cluster produces a lattice shrinkage along the unique [110] chain axis. Conversely O′ interstitials along $[1\bar{1}0]$ produce a lattice expansion. Hence in U_4O_9 the presence of one or several preferentially oriented chains will distort the superlattice from cubic symmetry. Indeed distortion from the cubic to rhombohedral structure in the superlattice of U_4O_9 has been observed[12].

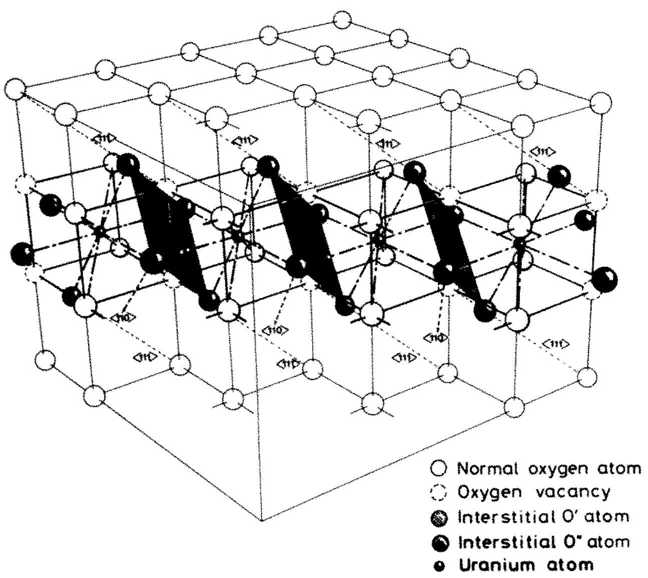

Fig. 2 A chain of 2:2:2 clusters in the oxygen sublattice.

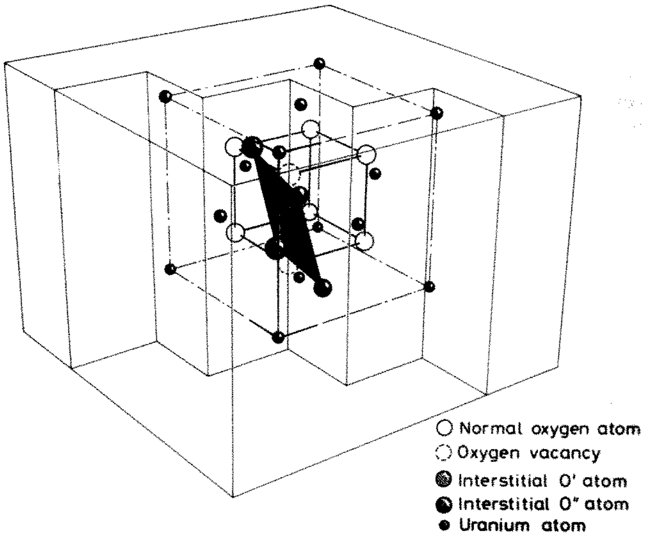

Fig. 3 The relationship between a 2:2:2 cluster and the normal fluorite unit cell.

Although the U_3O_7 composition could be accommodated by the above model no complete experimental determination of its crystal structure exists. Lattice dimensions have been reported in terms of a face-centred tetragonal cell derived from the UO_2 structure but the tetragonal phase may be metastable.

This paper is published by permission of the Central Electricity Generating Board.

Received 3 September; accepted 13 November 1981.

1. Willis, B. T. M. *Nature* **197**, 755–756 (1963).
2. Willis, B. T. M. *Acta crystallogr.* **A34**, 88–90 (1978).
3. Bevan, D. J. M., Greis, O. & Strähle, J. *Acta crystallogr.* **A36**, 889–890 (1980).
4. Martin, R. L. *J. Proc. R. Soc. N.S.W.* **109**, 137–150 (1976).
5. Allen, G. C., Tucker, P. M. & Tyler, J. W. *JCS chem. Commun.* 691–692 (1981).
6. Willis, B. T. M. *J. Phys. Radiat.* **25**, 431–439 (1964).
7. Thornber, M. R. & Bevan, D. J. M. *J. Solid-St. Chem.* **1**, 536–544 (1970).
8. Allen, G. C., Griffiths, A. J. & Lee, B. J. *Transition Metal Chem.* **3** 229–233 (1978).
9. Verbist, J., Riga, J., Pireaux, J. J. & Caudano, R. *J. Electron Spectros. relat. Phenom.* **5**, 193–205 (1974).
10. Allen, G. C., Tucker, P. M. & Tyler, J. W. *J. phys. Chem.* (in the press).
11. Allen, G. C., Griffiths, A. J. & Suckling C. W. *Chem. Phys. Lett.* **53**, 309–312 (1978).
12. Belbeoch, B., Boivineau, J. C. & Perio, P. J. *Phys. Chem. Solids* **28**, 1267–1275 (1967).

Synergistic tellurium–caesium embrittlement of Type 316 stainless steel

M. G. Adamson

General Electric Company, Vallecitos Road, Pleasanton,
California 94566, USA

E. A. Aitken & S. Vaidyanathan

General Electric Company, 310 DeGuigne Drive, Sunnyvale,
California 94086, USA

Austenitic stainless steels have become important high-temperature structural and containment alloys in applications ranging from industrial processes to energy generation and conversion. The AISI Type-300 series of iron–base austenitic stainless steels, in particular, is widely used as a barrier or primary containment material for both nuclear and fossil fuels operation at temperatures as high as 700 and 1,000 °C, respectively. Thus any observed deleterious effect of chemical environment on the alloy mechanical properties such as the 'hot' embrittlement of austenitic stainless steel by liquid zinc[1,2] is very

0028-0836/82/010049—03$01.00

important and, indeed, Old[3] has mentioned that fission products such as caesium, cadmium and tellurium might embrittle the austenitic stainless steel cladding of fast reactor fuel pins in certain conditions. The few investigations of the high temperature mechanical behaviour of iron–base austenitic stainless steels in chemical environments intended to simulate in-reactor conditions have not positively identified any particularly severe chemomechanical degradation, such as that accompanying stress corrosion cracking or liquid metal embrittlement. We now report the observation of rapid, severe embrittlement of AISI 316 stainless steel by liquid tellurium–caesium mixtures in the temperature region 500–700 °C. Our results were obtained using a test technique that involves radially deforming small ring specimens contained inside an environmental chamber by compressive loading at a uniform displacement rate. This ring compression test technique has the advantages of facile control of the chemical environment and ease of adaptation for work with irradiated materials.

AISI 316 is an austenitic iron–base alloy containing by weight about 17% Cr, 13% Ni, 2.5% Mo, 2% Mn, 0.5% Si, 0.06% C and various trace elements. The liquid Te–Cs mixtures, which were applied to the alloy specimens as thin coherent coatings, contained dissolved oxygen at very low activity levels. The ring specimens used in our analyses were short (6.35 mm) lengths of 5.84 mm o.d., 0.381 mm wall AISI 316 seamless tubing with average grain diameters in the range 25–36 μm. Specimens, neutron-irradiated to a fluence of 8×10^{22} neutrons cm^{-2} ($E >$ 0.1 MeV) at 488 °C in the Experimental Breeder Reactor-II at Idaho, were also tested.

Photomicrographs and scanning electron fractographs of unirradiated 20% cold-worked AISI 316 specimens stressed and broken in the presence of equimolar Te–Cs mixtures at 550–625 °C are shown in Figs 1–3. Figure 1 indicates the extreme brittleness of the fracture obtained at 625 °C, as illustrated by the sharp drop in load-bearing capability just past the yield load. The scanning electron micrographs of the 625 °C fracture surface shown in Figs 2*b* and 3*a* indicate the totally intergranular nature of the nonductile fracture. Similar results have been obtained on solution-treated AISI 316 and the fast neutron-irradiated 20% cold-worked materials. The embrittlement appeared to be even more marked in the irradiated material, occurring throughout the temperature range 450–625 °C with a peak load consistently lower than the load corresponding to initial yielding.

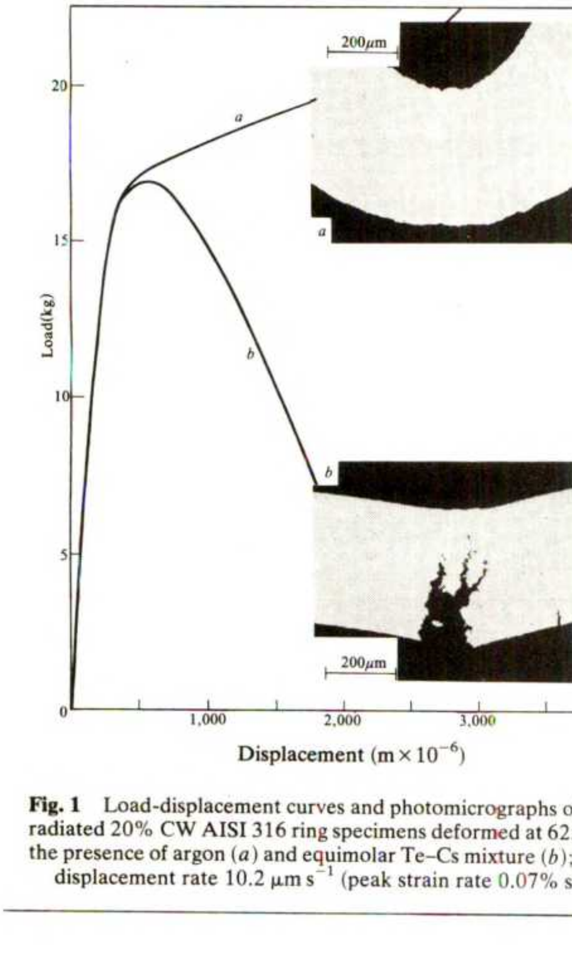

Fig. 1 Load-displacement curves and photomicrographs of unirradiated 20% CW AISI 316 ring specimens deformed at 625 °C in the presence of argon (*a*) and equimolar Te–Cs mixture (*b*); linear displacement rate 10.2 μm s^{-1} (peak strain rate 0.07% s^{-1}).

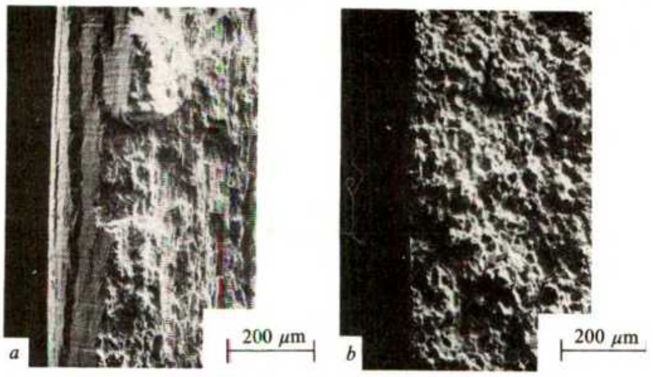

Fig. 2 Low magnification scanning electron fractographs of unirradiated 20% CW AISI 316 specimens stressed and broken in the presence of equimolar Te–Cs at 550 °C (*a*) and 625 °C (*b*); the direction of fracture is left to right for each specimen.

In equivalent test conditions, caesium alone did not embrittle cold-worked AISI 316, neither did simulated fission product mixtures of cadmium, indium, tin, antimony and iodine, with or without (excess) caesium. Liquid tellurium caused some reduction in yield stress at 625 °C, but no observable loss of ductility at either 475 °C or 625 °C. The marked embrittlement caused by liquid Te–Cs mixtures seems to be restricted to compositions lying between Cs_2Te and Te and, due to the absence of any concomitant Cs, Te-assisted oxidation of the alloy specimens, it is assumed to proceed independently of this corrosion process.

The observed 'hot' embrittlement of Type 316 stainless steel by liquid Cs–Te exhibits many features characteristic of 'classical' liquid metal embrittlement[3]. Only small quantities of the embrittling agent are required but it must be liquid and must be in intimate contact with the test specimen during loading. In one test, after initially coating the specimen with the Cs–Te mixture corresponding to the conditions for the test results given in Fig. 1, the coating was removed with successive washes of water and absolute ethanol. The load-deflection pattern for this specimen was found to be identical to the uncoated material, indicating that the embrittlement effect requires the presence of a surface layer of the liquid metal—a typical feature of liquid metal embrittlement. The stressed specimen in all cases exhibits normal elastic deformation up to some critical strain but, once this threshold has been exceeded, nonductile fracture rapidly follows; and, at a given strain rate, embrittlement occurs within a well-defined range of temperature whose lower limit usually coincides with the melting temperature of the embrittling agent.

The unique feature of this particular embrittlement process is the apparent chemical synergism between tellurium and caesium as embrittling agents—a synergism that is manifested by a marked dependence of embrittling agent activity on tellurium chemical potential. On the other hand, the activity of the embrittling agent did not appear to be markedly influenced by oxygen chemical potential, at least within the relatively narrow range of values expected inside a fast breeder reactor oxide fuel pin. The concept of 'inert carriers' in liquid metal embrittlement has been discussed elsewhere[3]; however, in the present case the role of caesium is thought to be more complex, being also possibly related to the manner in which wettability and tellurium activity change as a function of Cs/Te ratio.

We believe that the present results are the first observation of synergistic 'hot' embrittlement of AISI 316 stainless steel by liquid Te–Cs mixtures. This particular chemical synergy parallels the synergy operating in Cs, Te-assisted oxidative corrosion of AISI 316 that sporadically appears inside fast reactor oxide fuel pins[4], however, the mechanisms and consequences seem to be remarkably different.

Our recent results may have important implications for the design and operation of advanced fast reactor fuel pins. The composition and chemical states of fission products deposited on the inside surface of a fast reactor oxide fuel pin cladding are influenced by processes such as transport under thermal gradients, selective chemical reactions between fission products and between fission products and the fuel, and the temperature at a given location. Preliminary thermochemical analyses of the conditions inside operating fast reactor fuel pins indicate that Cs/Te ratios <2 are possible at the fuel-cladding interface. However, for the specific mechanism discussed here to be operative in a particular fuel pin, the loading on the cladding would have to produce the specific threshold strain for liquid metal embrittlement at the same time that the chemical conditions are satisfied. Estimates of the associated probability will have to await the outcome of detailed chemical and mechanical modelling studies.

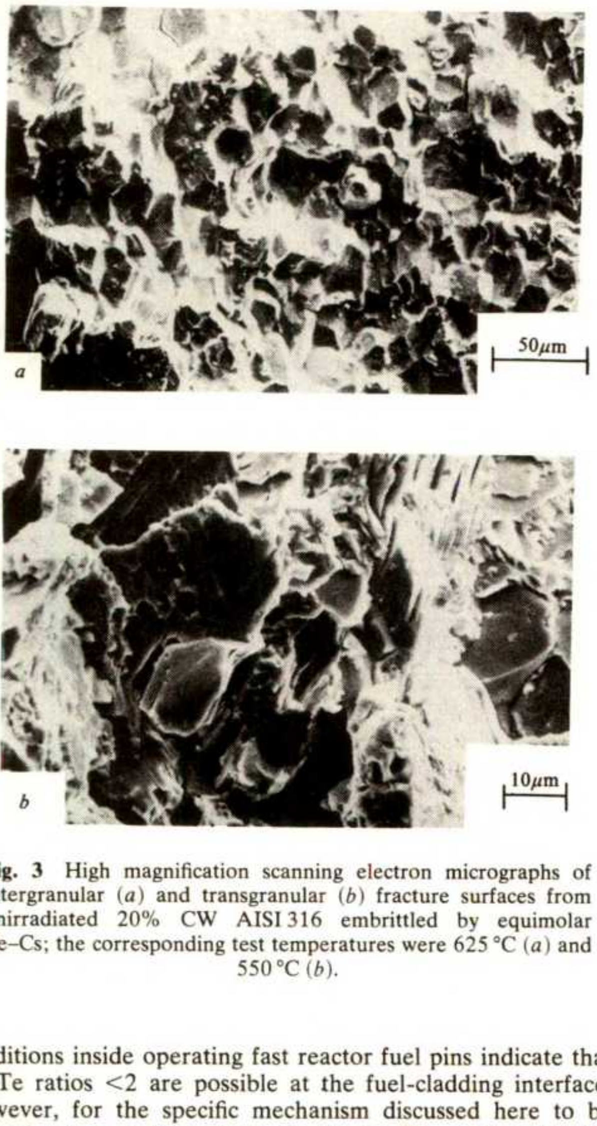

Fig. 3 High magnification scanning electron micrographs of intergranular (*a*) and transgranular (*b*) fracture surfaces from unirradiated 20% CW AISI 316 embrittled by equimolar Te–Cs; the corresponding test temperatures were 625 °C (*a*) and 550 °C (*b*).

We thank T. A. Lauritzen and W. H. Reineking for experimental assistance, the US Department of Energy for financial support, and personnel at the Hanford Engineering Development Laboratory for supplying irradiated stainless steel specimens.

Received 20 July; accepted 30 October 1981.

1. Elliot, D. *Process Engng* 67–71 (July 1976).
2. Cahn, R. W. *Nature* **265**, 11–12 (1977).
3. Old, C. F. *J. nucl. Mater.* **92**, 2–25 (1980).
4. Adamson, M. G. *IAEA Rep. IWGFR/16*, 108–136, 170–189 (1979).

Carotenoid transformations in coastal marine waters

Daniel J. Repeta & Robert B. Gagosian

Department of Chemistry, Woods Hole Oceanographic Institution,
Woods Hole, Massachusetts 02543, USA

Rapidly sinking large particles contribute a major portion of the mass flux from marine surface waters to the sea floor. The recognition that organic matter associated with these particles undergoes major alterations in its chemical composition during vertical transit has raised new questions on the role of rapid transformation processes in carbon and nitrogen cycling, benthic nutrition, and post-depositional degradation[1]. Analysis of specific organic compounds has established some of the compositional changes of these transformations[2–4]. However, most of the changes observed represent the sum of biological production and degradation. For example, bacterial and chemical degradation of fatty acids in the water column may be completely masked by an even greater production of these compounds by zooplankton. Hence it is often difficult to distinguish between competing degradative processes, and to assess the relative significance of each. Carotenoid pigments have characteristics which make them particularly suitable for use as organic tracers to distinguish between short-term degradation processes. Carotenoids are widely distributed in both photosynthetic and nonphotosynthetic organisms; many of them are source specific; they contain diverse functional groups; and they represent one of the more labile biogenic compound classes in the sea. We report here for the first time the isolation and identification of carotenoid transformation products from sediment trap experiments conducted in coastal marine waters, and discuss the source and significance of observed transformation products with respect to a proposed degradation pathway.

Sediment traps were deployed in Buzzards Bay, Massachusetts (41°32′ N, 70°42′ W) for two 30-day periods between 20 May and 23 July 1980. Traps were set 4 m below the surface in a 10-m water column. Collected material was filtered and sonic-extracted with methanol (twice, 20 min each) and dichloromethane (once, 20 min). Extracts were concentrated

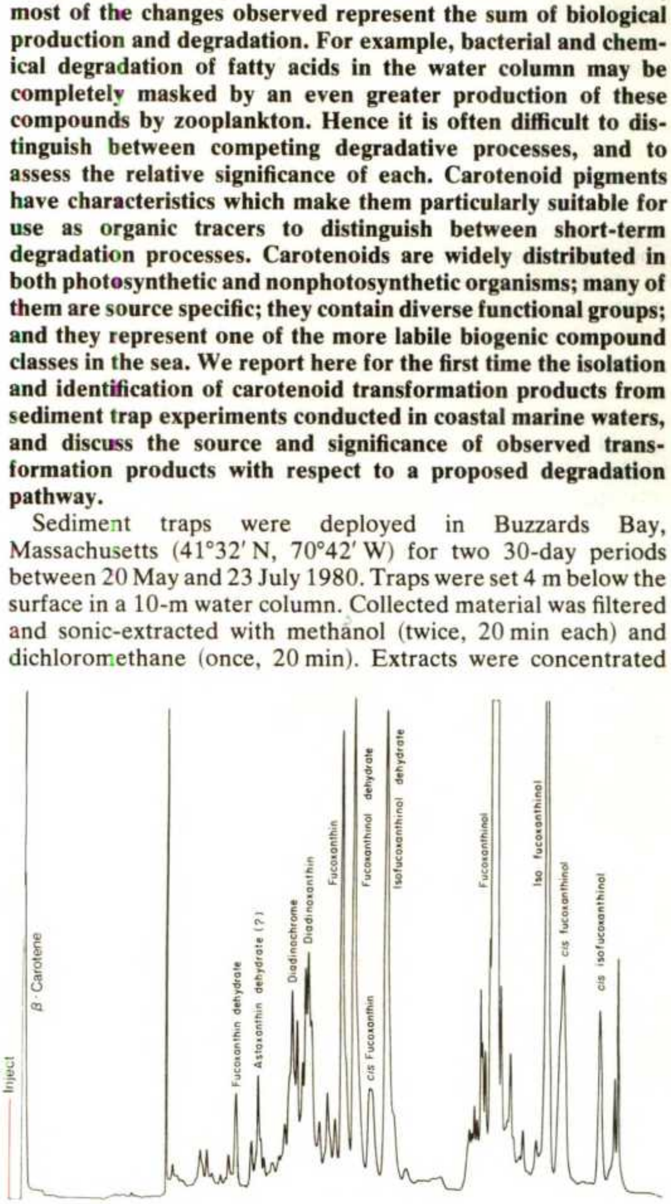

Fig. 1 HPLC trace of Buzzards Bay sediment trap sample no. 3. Conditions are: 30 × 3.9 mm 5 μm amino column, eluted with a linear gradient of 0–13% THF/methanol (80/20, v/v) in hexane at 2 ml min^{-1} for 45 min. After 55 min the eluant was stepped to 30% THF/methanol for an additional 10 min. Detection was at 436 nm.

0028-0836/82/010051—04$01.00

Table 1 Fucoxanthin metabolites in Buzzards Bay sediment trap 3, 21 June–23 July 1980

	% Total*	% Phytoplankton
Fucoxanthin (Ia)	5	100[7]
Fucoxanthinol (Ib)	69	Trace[8]
Isofucoxanthinol (IIb)	12	ND
Fucoxanthin dehydrate (IIIa)	1	ND
Fucoxanthinol dehydrate (IIIb)	6	ND
Isofucoxanthinol dehydrate (IV)	7	ND
	100%	

ND, not detected.

* Total fucoxanthin-derived pigments, relative abundances not corrected for small differences in extinction coefficients (see ref. 9).

under reduced pressure then separated into compound classes by gel permeation chromatography using 100 Å μStyragel (Waters Associates) with dichloromethane as the mobile phase. This procedure removes low-molecular weight lipids and chlorophyll pigments which interfere with subsequent steps in the analysis. The carotenoid fraction was collected, reconcentrated, then separated into individual components by high pressure liquid chromatography (HPLC) using a Spherisorb 5 μm amino column (300 × 3.9 mm) eluted with a linear gradient of hexane and 0–13% THF/methanol (80/20, v/v) at 2 ml min^{-1} (Fig. 1). Carotenoids were detected spectroscopically at 436 nm, collected, and further analysed by visible spectroscopy and mass spectrometry. Mass spectra were collected on a Finnigan 3200 quadrapole spectrometer interfaced with an INCOS (Finnigan) 2300 data system. Conditions are described in Fig. 2 legend. All operations were performed at or below 20 °C and in low light conditions. A more detailed description of the analytical method will be given elsewhere.

The lability of carotenoids has posed severe problems in their analysis[5]. When discussing geochemical transformations in particular, care must be taken to ensure transformation products are not artefacts of the analytical procedure. Analysis of blanks spiked with carotenoid mixtures (astaxanthin, β-carotene, diadinoxanthin, fucoxanthin and lutein), and of cultured phytoplankton (*Peridinium trichoidium*) of known carotenoid composition[6] showed that no degradation other than *cis* ⇄ *trans* isomerization occurs during our analytical work-up.

Fucoxanthin (Ia) is the major carotenoid in diatoms and a few dinoflagellates, often constituting 70–90% of the total carotenoids[7]. In our sediment trap samples, fucoxanthin comprised only 4% of the total carotenoid and 5% of the total fuco-pigments (Table 1, Fig. 1). The remaining 95% of the total fuco-pigments consisted of the fucoxanthin transformation products fucoxanthinol (Ib), isofucoxanthinol (IIb), fucoxanthinol dehydrate (IIIb), isofucoxanthinol dehydrate (IV) and fucoxanthin dehydrate (IIIa). Together these compounds constitute 82% of the total carotenoids with diadinoxanthin (V) and diadinochrome (VI) contributing another 3% and 1%, respectively. Fucoxanthinol (Ib) has been reported as a minor component of some algae, and is thought to be an intermediate in fucoxanthin biosynthesis[8,9]. Isofucoxanthinol (IIb) is known to arise from base-catalysed epoxide opening and is commonly cited as an analytical artefact[10]. For reasons outlined above, we believe that the opened epoxides (iso-compounds) in these samples are not artefacts of the analytical method, but are due to chemical transformations in the water column. We know of no reports of naturally occurring dehydrates (IIIa, b) of either fucoxanthin or fucoxanthinol.

Fucoxanthinol (Ib) (Fig. 2) is the most abundant pigment in the samples (Table 1). Acylation with acetic anhydride in pyridine yields fucoxanthin acetate which co-elutes with standard fucoxanthin acetate synthesized from fucoxanthin (see Fig. 2 legend, which gives mass spectrometry and IUPAC data for all compounds discussed in this paper). Thermal isomerization of fucoxanthin acetate produces an equilibrium mixture of *cis* isomers identical in both chromatographic retention time (HPLC) and relative abundance to those derived from the standard. The ester hydrolysis which converts fucoxanthin to fucoxanthinol can occur by two pathways, a base-catalysed chemically mediated ester hydrolysis, or biochemical metabolism. Base-catalysed ester hydrolysis seems unlikely as epoxide opening should precede ester hydrolysis[10]. In our samples fucoxanthinol, which still contains the epoxide group, predominates over isofucoxanthinol, its open epoxide counterpart. Biochemical metabolism by zooplankton and other higher organisms seems a more likely source. Fucoxanthinol has been found as a major fuco-pigment in the guts of sea urchins[11], thus it is not unreasonable that other higher organisms have the ability to hydrolyse the ester without rearranging the epoxide. As particles collected in sediment traps are thought to represent material which has been extensively reworked by heterotrophic

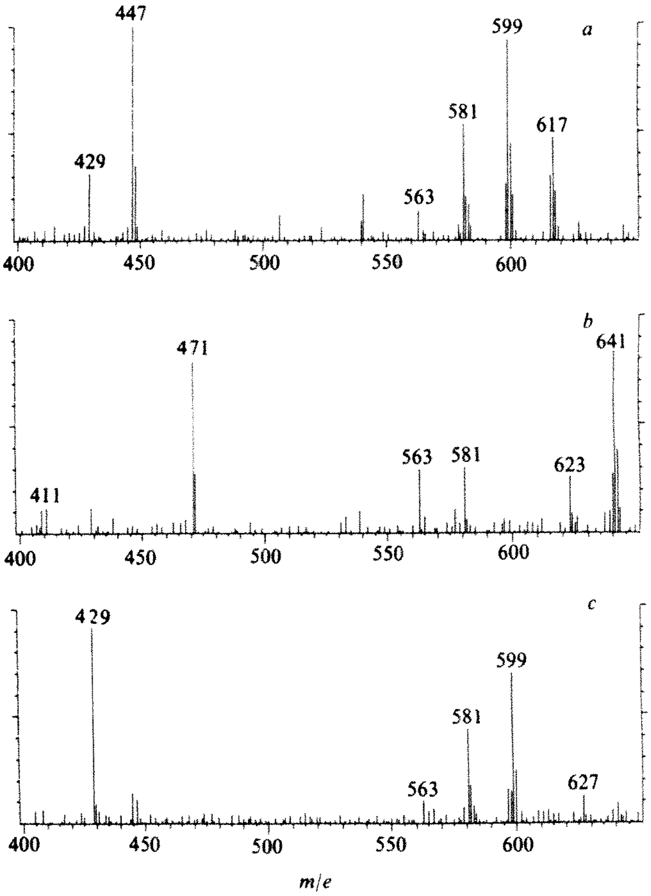

Fig. 2 Chemical ionization mass spectra of *a*, fucoxanthinol (Ib) (M+1 = 617, M+1-18(-H_2O) = 599, M+1-18-18 = 581, M+1-18-18-18 = 563, M+1-170 (cleavage to the 7,8 ketone) = 447, M+1-170-18 = 429); *b*, fucoxanthin dehydrate (IIIa) (M+1 = 641, M+1-18 = 623, M+1-60(-acetate) = 581, M+1-18-60 = 563, M+1-170 = 471); and *c*, fucoxanthinol dehydrate (IIIb) (M+29 = 627, M+1 = 599, M+1-18 = 581m M+1-18-18 = 563, M+1-170 = 429); CH_4 reactant gas 900 μm, ionization voltage 130 eV, ionization current 500 μA. Where: fucoxanthinol (Ib) (5,6-epoxy-3,3′,5′-trihydroxy-6′,7′-didehydro-5,6,7,8,5′,6′-hexahydro-β,β caroten-8-one) (M+1 = 617, M+1-18 = 599, M+1-18-18 = 581, M+1-18-18-18 = 563, M+1-170-18 = 429). Fucoxanthin acetate (5,6-epoxy-3,3′,5′-trihydroxy-6′,7′-didehydro-5,6,7,8,5′,6′-hexahydro-β,β caroten-8-one, 3,3′-diacetate) (M+1 = 701, M+1-18 = 683, M+1-60 = 641, M+1-18-60 = 623). Fucoxanthin dehydrate (IIIa) (5,6-epoxy-3,3′-dihydroxy-4′,6′,7′-tridehydro-5,6,7,8,6′-pentahydro-β,β caroten-8-one 3′-acetate) (M+1 = 641, M+1-18 = 623, M+1-60 = 581, M+1-18-60 = 563, M+1-170 = 471). Fucoxanthinol dehydrate (IIIb) (5,6-epoxy-3,3′-dihydroxy-4′,5′,7′-tridehydro-5,6,7,8,6′-pentahydro-β,β caroten-8-one) (M+1 = 599, M+1-18 = 581, M+1-170 = 429). Dehydro-fucoxanthin diacetate (5,6-epoxy-3,3′-dihydroxy-4′,6′,7′-tridehydro-5,6,7,8,6′-pentahydro-β,β caroten-8-one 3,3′-diacetate) (M+1 = 683, M+1-60 = 623, M+1-212 = 471). Double bond in dehydrates tentatively assigned to the 4′,5′ position. (See ref. 10.)

organisms[1], we propose that fucoxanthinol represents a metabolite of heterotrophic activity. Other studies conducted in our laboratory, concerned with the direct collection of zooplankton faecal pellets from field cultures, verify this hypothesis[12].

The mass spectra of fucoxanthin dehydrate (IIIa) and fucoxanthinol dehydrate (IIIb) (Fig. 2) are both consistent with loss of the tertiary alcohol at the 5′ position (Fig. 3). The mass fragment M + 1-170 arises from a cleavage of the 7,8 bond α to the 8-ketone. The resulting mass fragments (471, 429 AMU) correspond to a loss of a hydroxyl group at either the secondary 3′ or tertiary 5′ position. Acylation of the isolated fucoxanthinol dehydrate (IIIb) yields a diacetate. Acetic anhydride in pyridine acylates only primary and secondary alcohols in the conditions used in our synthesis. The mass increase of 84 AMU for the acylated dehydrate over the underivatized parent is consistent with the esterification of the two hydroxyl groups at the 3 and 3′ position. Therefore, dehydration proceeds with the loss of the 5′ alcohol. Sufficient amounts of fucoxanthin dehydrate (IIIa) could not be isolated to derivatize, hence our conclusion of 5′ hydroxyl loss for this compound rests on mass spectral evidence alone.

Determining the mechanism of dehydration is difficult. There is little evidence in favour of either a biochemically or chemically mediated reaction. Chemically, an acid-catalysed dehydration reaction seems most likely. However, we find substantial amounts of the unrearranged 5,6 epoxide, diadinoxanthin (V) in our samples. In acidic conditions the 5,6 epoxide rapidly rearranges to the 5,8 furanoxide, diadinochrome (VI)[13]. If the acidic conditions necessary to dehydrate fucoxanthin existed in our samples, all the diadinoxanthin should have rearranged to the 5,8 furanoxide. Although some diadinochrome was observed, we believe that dehydration is probably not a result of chemical acid catalysis, but a more site-specific metabolic reaction.

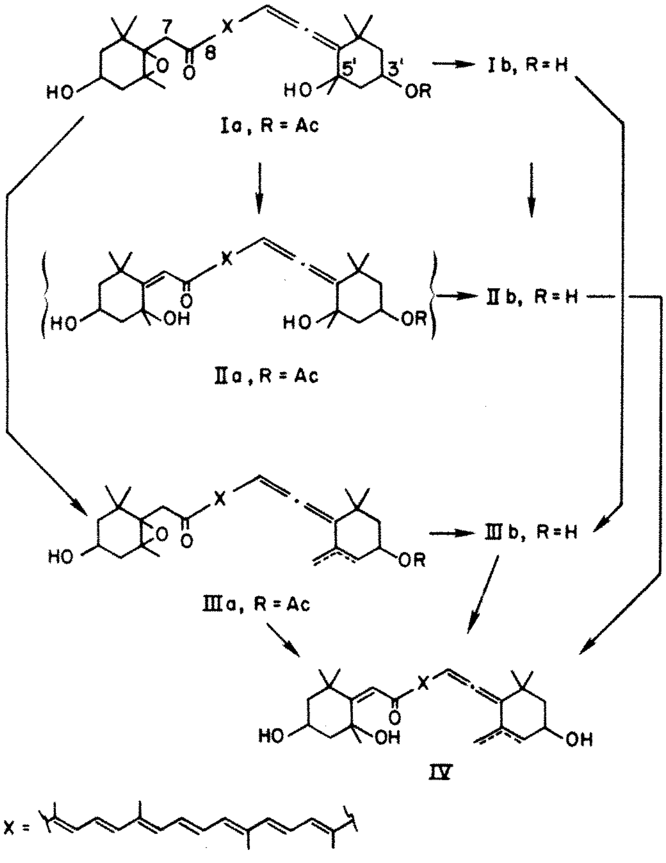

Fig. 3 Proposed pathway showing ester hydrolysis, dehydration and epoxide opening for biochemical and chemical degradation of fucoxanthin. Compound in parentheses was not isolated in this study.

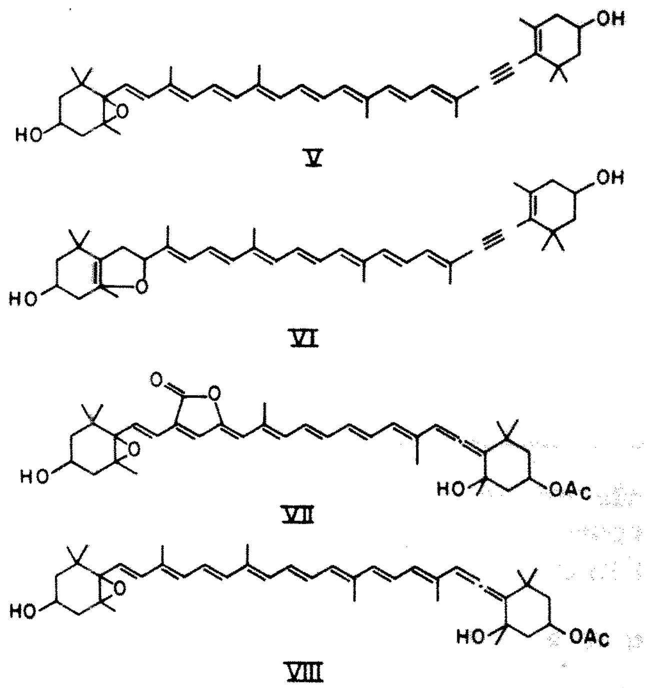

Fig. 4 Molecular structure of diadinoxanthin (V), diadinochrome (VI), peridinin (VII) and dinoxanthin (VIII).

The dehydration of sterols[15,16], amino acids[17], and phytol[18] occurs in a variety of marine environments and both chemical and biochemical mechanisms have been proposed. The dehydration of stanols to sterenes is structurally analogous to the dehydration of the secondary 3 or 3′ hydroxyl of carotenoid alcohols. The dehydration products of fucoxanthin (Fig. 3, IIIa, b) arise from loss of the tertiary 5′ hydroxyl group, with retention of the hydroxyl groups at both the 3 and 3′ positions. This suggests either that different processes exist for the dehydration of stanols and carotenoid alcohols, or there is a general process which displays an order of biochemical reactivity (for example, tertiary alcohols dehydrate faster than secondary alcohols). In the latter case we would expect to observe a sequential dehydration through the 3,5′ (or 3′,5′) didehydro and 3,3′,5′ tridehydro intermediates. The carotenoid mixtures in our samples contain ~100 components, of which only the 20 major components have been identified by our methods. Our analysis does not exclude the existence of more highly dehydrated metabolites in our samples.

In conclusion, we have observed ester hydrolysis and dehydration of fucoxanthin associated with particles collected in sediment traps. We propose a biochemically mediated transformation pathway (Fig. 4) which predicts that other carotenoids structurally similar to fucoxanthin (such as peridinin (VII) and dinoxanthin (VIII) from dinoflagellates) should undergo analogous transformations. We are conducting experiments with both long- and short-term sediment trap deployments, and direct collection of zooplankton faecal pellets to substantiate the proposed mechanisms.

This research was supported by the NSF, Division of Ocean Sciences, grant nos OCE 79-25352 and OCE 81-18436 and by contract no. N00014-74-CO-262 NR083-004 from the Office of Naval Research. D.J.R. thanks the Woods Hole Oceanographic Institution for financial assistance. We thank Drs Nelson M. Frew for mass spectrometric analyses, John W. Farrington, Cindy Lee and John K. Volkman for valuable comments, and Tim Cowles for cultured phytoplankton. Woods Hole Oceanographic Institution contribution no. 4957.

Received 19 August; accepted 3 November 1981.

1. Honjo, S. *J. mar. Res.* **38**, 53–97 (1980).
2. Wakeham, S. G. *et al. Nature* **286**, 798–800 (1980).
3. Lee, C. & Cronin, C. C. *J. mar. Res.* (in the press).

4. Gagosian, R. B., Smith, S. O. & Nigrelli, G. E. *Geochim. cosmochim. Acta* **45,** 2161–2168 (1981).
5. Davies, B. H. in *Chemistry and Biochemistry of Plant Pigments* Vol. 2 (ed. Goodwin, T. W.) 38–165 (Academic, New York, 1971).
6. Johansen, J. E., Svec, W. A. & Liaaen-Jensen, S. *Phytochemistry* **13,** 2261–2271 (1974).
7. Goodwin, T. W. (ed.) in *Aspects of Terpenoid Chemistry and Biochemistry* 315–356 (Academic, New York, 1971).
8. Liaaen-Jensen, S. in *Marine Natural Products* Vol. 2 (ed. Scheuer, P. J.) 2–73 (Academic, New York, 1978).
9. Liaaen-Jensen, S. in *Marine Natural Products Chemistry* (eds Faulkner, D. J. & Fenical, W. H.) 239–260 (Plenum, New York, 1977).
10. Bonnett, R. *et al. J. chem. Soc.* C, 429–454 (1969).
11. Galasko, G. *et al. J. chem. Soc.* C, 1264–1265 (1969).
12. Repeta, D. J. & Gagosian, R. B. in *Advances in Organic Geochemistry* (ed. Bjoroy, M.) (Heyden, London, in the press).
13. Buchecker, R. & Liaaen-Jensen, S. *Phytochemistry* **16,** 729–733 (1977).
14. Gagosian, R. B., Smith, S. O., Lee, C., Farrington, J. W. & Frew, N. M. in *Advances in Organic Geochemistry 1979* (eds Douglas, A. G. & Maxwell, J. R.) 407–419 (Pergamon, Oxford, 1980).
15. Dastillung, M. & Albrecht, P. *Nature* **269,** 678–679 (1977).
16. Bada, J. L. & Hoopes, E. A. *Nature* **282,** 822–823 (1979).
17. Simoneit, B. R. *Init. Rep. DSDP* **21,** 909–923 (1973).

Marine deposits 35,000–25,000 years old in the Chott el Djerid, southern Tunisia

G. W. Richards & C. Vita-Finzi

Department of Geography, University College, Gower Street, London WC1E 6BT, UK

The Chott el Djerid is a large, salt-covered depression in southern Tunisia (Fig. 1). The late nineteenth century idea that the basin had been invaded by the sea[1,2] has been superseded by the view that any Quaternary flooding of the Chott must have resulted from climatic changes, as the fossils found in its sediments are not exclusively marine and there is no indication of the fluctuations in sea level or of the crustal movements that would be required to fill and then empty the basin[2,3]. We report here evidence for a marine connection 35,000–25,000 years ago and show that it implies subsequent uplift by some 80 metres in an area long regarded as either stable[2] or prone to subsidence throughout the Quaternary[4].

Two sets of terraces border the Chott. The earlier terrace dates from Villafranchian (Lower Pleistocene) times. The younger terrace contains numerous shells of the bivalve *Cerastoderma* (= *Cardium*) *glaucum* (Bruguière) and a few of the gastropods *Melania tuberculata* (Müller) and *Hydrobia* sp. In the Tozeur area *Corbicula fluminalis* (Müller) is also present. The microfauna includes 14 species of marine foraminifera, predominantly *Ammonia beccarii* (d'Orb.), and three species of ostracoda (*Cyprideis* sp.)[5].

Radiocarbon ages ranging from 22,000 ± 800 to $32,400^{+4,100}_{-2,800}$ yr BP on shell samples obtained from the younger terrace by Page[6] supported previous estimates[2] of its age and confirmed that it formed at a time when sea level was lower than today. Flooding was thus ascribed to climatic oscillations whether in the guise of reduced evaporation and thence a rise in the water table[3] or of an increase in rainfall effectiveness[6]. The fauna appeared to be consistent with lacustrine conditions. *C. glaucum* can tolerate salinities of 3–60% (ref. 7). *M. tuberculata*, though sometimes washed onto modern beaches (as at Gabes), is essentially a freshwater species. Both species occur together with *Hydrobia* sp., *Corbicula africana* and other freshwater or brackish water organisms as well as Foraminifera in Quaternary lake deposits in Wadi Shati, south Libya[8,9].

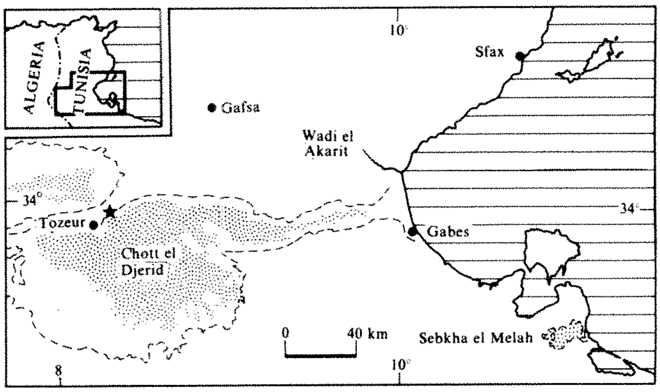

Fig. 1 Location map. Dashed line (after ref. 3) shows former extent of Chott el Djerid. Stipple indicates present-day salt-covered depressions. Star shows location of sites sampled for ^{14}C dating.

In March 1981 we found numerous rolled fragments of the oyster *Ostrea stentina* (Payr.) in one of the two type sections[3] in the younger terrace at Helba, 1.5 km north-east of Tozeur (Fig. 1) and 40 m above sea level. The deposits, which also contained abundant *C. glaucum* and a few specimens of *M. tuberculata*, consisted of a pebbly sand 30-cm thick resting unconformably on a southward-dipping clastic series ascribed to the Plio-Pleistocene[3]. What appears to be a regressive shoreline is exposed 5 m lower and some 200 m to the south-east of the first section. Here *O. stentina* is present within two gravel beds separated by 30 cm of massive sand containing a few *C. glaucum*. The upper bed is 5 cm thick and composed of large pebbles, the lower is a fine gravel at least 20 cm thick (Fig. 2).

Ostrea stentina is now found living in the intertidal zone at Gabes and elsewhere on the Tunisian coast. Unlike *C. glaucum* it has not been recorded from hypersaline or brackish lagoons[10]. Redeposition from older rocks is unlikely because the only oysters hitherto reported from the local Tertiary rocks are *O. multicostata* Desh., *O. punica* Thomas and *O. bellovacina* Lmk[11]. Transport by man cannot be ruled out, but it is improbable in view of the absence of complete shells and of artefacts or other evidence of human occupation at the two sections, and the lack of oyster shells from local prehistoric sites[12].

Radiocarbon ages were determined on oysters from the two exposures (Fig. 2) and also on a sample of *C. glaucum* from the upper exposure. No sample showed evidence of recrystallization when examined in thin section, and X-ray diffraction confirmed that the *C. glaucum* shells had retained their aragonitic composition. The stable isotope measurements (Table 1) and the good agreement with the ^{14}C ages previously reported[6] for the terrace are consistent with this view[13]. If one accepts that ~30,000-yr ago sea level lay 40 m below its present position[14], the beach deposits represent total emergence by 80 m and 75 m respectively, and hence uplift rates of 2.3–3.3 mm yr^{-1}. A sea level of −8 m as indicated by the sedimentary record beneath the Sebkha el Melah[15] (Fig. 1) would yield uplift rates of 1.4–1.7 mm yr^{-1}.

The results conflict with the evidence presented by geomorphologists for local stability[2] and by geologists for local sub-

Table 1 Sample data from the Chott el Djerid

Sample no.	Lab. no.	Lat. and long.	Age* (yr BP)	$\delta^{13}C$ ‰	$\delta^{18}O$ ‰	Species
T81/2o	BETA-2653	33°56′ N, 8°9′ E	35,140 ± 1,190	1.14	−2.67	*Ostrea stentina*
T81/2c	BETA-2615	33°56′ N, 8°9′ E	28,950 ± 280	−0.06	−1.17	*Cerastoderma glaucum*
T81/3	BETA-2654	33°56′ N, 8°9′ E	25,360 ± 270	1.27	−2.51	*Ostrea stentina*

* Normalized to $\delta^{13}C = 0‰$ PDB.

0028–0836/82/010054—02$01.00

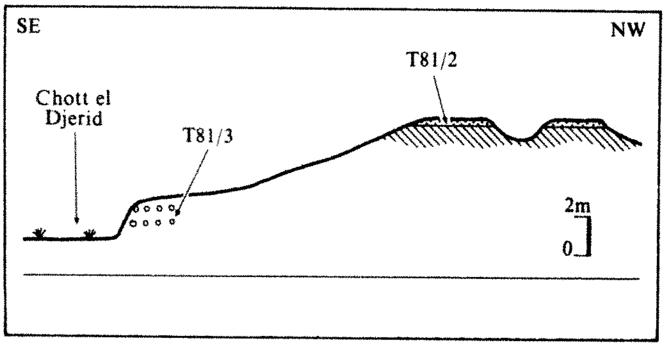

Fig. 2 Section at sample locality. Stipple represents the older of the two dated terraces; open circles denote gravel bands in younger terrace; inclined lines denote Plio-Pleistocene beds. The two sample points are listed in Table 1.

sidence[4], but accords with reports of uplift by 9 m since 9,500 yr BP (equivalent to an average of 3.9 mm yr^{-1}) in the Wadi el Akarit[6] (Fig. 1). It remains to be seen whether other parts of the Chott el Djerid yield a similar record and how it relates to the Pleistocene folding at Gafsa[16] and the slight Holocene uplift detected on the Tunisian coast south-east of Jerba[17].

We thank John Billeter, Solene Morris, Pat Nuttall, Reza Samadian and Brian Walker for their help. G.W.R. holds a NERC studentship.

Received 9 June; accepted 20 November 1981.

1. Lesseps, F. de *Rev. Scient.* **21,** 495–496 (1883).
2. Coque, R. *La Tunisie Présaharienne* (Colin, Paris, 1962).
3. Coque, R. & Jauzein, A. in *Guidebook to the Geology and History of Tunisia*, 227–257 (Petroleum Exploration Society of Libya, Tripoli, 1967).
4. Burollet, P. F. *Annls Mines Géol. Tunis* **18,** 1–345 (1956).
5. Milokhoff, E. *C.r. XIXe Congr. géol. int., Alger* **15,** 337–339 (1954).
6. Page, W. D. thesis, Univ. Colorado (1972).
7. Gaillard, J. M. & Testud, A.-M. in *The Geology of Libya* Vol. 3 (eds Salem, M. J. & Busrewil, M. T.) 809–813 (Academic, London, 1980).
8. Gaven, C., Hillaire-Marcel, C. & Petit-Maire, N. *Nature* **290,** 131–133 (1981).
9. Petit-Maire, N., Casta, L., Delibrias, G., Gaven, C. & Testud, A.-M. in *The Geology of Libya* Vol. 3 (eds Salem, M. J. & Busrewil, M. T.) 797–807 (Academic, London, 1980).
10. Zaouali, J. *Bull. off. natn. Pêch. Tunisie* **3,** 107–140 (1979).
11. Domergue, Ch., Dumon, E., De Lapparent, A. F. & Lossel, P. *C.r. XIXe Congr. géol. int., Alger, Monogr. rég. Tunisie* **7** (1952).
12. Gobert, E. G. *Quaternaria* **6,** 271–307 (1962).
13. Millman, J. D. *Marine Carbonates* (Springer, New York, 1974).
14. Chappell, J. & Veeh, H. H. *Nature* **276,** 602–603 (1978).
15. Fontes, J.-C. & Perthuisot, J.-P. *Nature* **244,** 74–75 (1973); *Rev. géog. Phys. géol. Dyn.* **13,** 299–314 (1971).
16. Castany, G. *Geol. Rdsch.* **43,** 196–203 (1955).
17. Dalongeville, R., Paskoff, R., Sanlaville, P., Thommeret, J. & Thommeret, Y. *C.r. hebd. Séanc. Acad. Sci., Paris* **D290,** 303–306 (1980).

Myoblasts from *Drosophila* wing disks can contribute to developing muscles throughout the fly

Peter A. Lawrence & Danny L. Brower*

MRC Laboratory of Molecular Biology, Hills Road,
Cambridge CB2 2QH, UK

In insect embryos groups of epidermal cells are already determined[1] to form particular compartments of the adult[2–4]. In *Drosophila* this determination is maintained through cell divisions, is stable to experimental interference[1,5,6] and is thought to depend on the activity of a particular class of homoeotic genes[4,7,8]. In contrast to our understanding of the ectoderm, we know little about determination of the mesoderm, which gives rise to the musculature. A recent study of cell lineage in the thorax of adult *Drosophila* has shown that the muscles of each segment are divided precisely into sets (P.A.L., in preparation). The dorsal and ventral muscle sets of the mesothorax probably derive from adepithelial myoblasts[9–11] in the wing and leg imaginal disk, respectively (P.A.L., in preparation). We describe here a new method of marking cells to trace myoblasts from the wing imaginal disk. We show that, when implanted, these mesodermal cells do not develop as they would *in situ* but instead contribute indiscriminately to developing host muscles. This result suggests that, whereas the ectodermal cells of the disk are committed to form a particular region of the adult, the mesodermal cells are not.

Portions of the wing imaginal disk from a wild-type larva were implanted into mature larval hosts. The donor cells carried the wild-type allele (sdh^+) at a locus which affects the enzyme succinate dehydrogenase; the host larvae were mutant (sdh^2/sdh^7) at this locus[12]. After metamorphosis the flies, as well as unimplanted controls of both genotypes, were histochemically stained for enzyme activity (see Fig. 1 legend). In the sdh^+ flies all muscles stained an intense dark blue, the stain being localized in the mitochondria. In the sdh^2/sdh^7 flies most muscles varied between pure white and pale blue in colour; 25 abdomens were examined, and dark blue muscles were seen only in the genital region. For this reason the genital muscles were not studied in the following experiments. Of 25 mutant thoraces sectioned, all muscles were white to pale blue.

A portion of the wild-type wing disk (**02** piece[13]; see Fig. 1) containing muscle precursors, the adepithelial cells, was implanted into 29 adults. In every case where the implant was retrieved it consisted of mesonotum and wing hinge structures, as expected[13], and was usually found in the posterior region of the abdomen. Only occasionally were implants associated with substantial numbers of adventitious muscle fibres and these could not be recognized as being of any particular type. Near the implant, some of the hosts showed abdominal muscles that were frequently (28/29 cases) stained dark blue (Fig. 2). These host muscles appeared normal in every other respect. The intensity of staining varied from fibre to fibre, densely stained fibres often being intermingled with unstained ones (Fig. 3). Further from the implant only occasional muscle fibres were stained, but these were prominent against the pale unstained background of the other fibres. The pleural membrane of the abdomen is covered with a delicate sheet of laterally oriented fibres, and these were also stained blue near the implant. In addition, the thoraces of many of the experimental flies (10/26) contained stained muscle fibres. For example, dark patches of stain were observed in both the direct and indirect flight muscles but were never found in the unimplanted controls (Fig. 4*a*, *b*).

There were three successful implantations of portions of the wing disk which probably do not contain adepithelial cells[14] (**58** pieces, Fig. 1). These implants formed the expected type of cuticle (wing blade and thoracic pleura[13]) and were not associated with any muscle fibres. All the host muscles of the abdomen and thorax were normal in structure and position and none stained dark blue.

Clonal analysis has shown that *sdh* alleles are cell-autonomous markers[12] which can be used in the muscles (P.A.L., in preparation). It is therefore highly unlikely that the succinate dehydrogenase activity was rescued other than by myoblast fusion. This is supported by the absence of staining when pieces of disk (**58**) lacking adepithelial cells are used. The sporadic staining of fibres far from the site of the implant also suggests that the myoblasts migrate and fuse with host muscles. The fact that pale, intermediate or dark fibres are closely intermingled suggests that none, a few or many donor cells may contribute to each fibre. It therefore seems that sdh^+ myoblasts, released from the wing imaginal disk, fuse indiscriminately with host muscles.

---

[*] Present address: Developmental Biology Center, University of California, Irvine, California 92717, USA.

0028–0836/82/010055—03$01.00

The adult muscles vary in many respects including sarcomere length, nuclear shape, mitochondrial size and fibre dimensions. However, when the host muscles of the abdomen and thorax stained blue, and were therefore at least partly composed of donor myoblasts, their structure appeared normal in every detail. There is evidence that the donor myoblasts *in situ* form only the dorsal muscle set of the mesothorax, which includes all the indirect flight muscles and a specific set of the direct flight muscles (P.A.L., in preparation). After implantation, they exhibit no such restriction and can apparently contribute to any host muscles with which they happen to fuse. Thus when removed from their normal environment, the adepithelial cells are not determined with respect to the type and location of the muscles they will form. By contrast, the fate of the epidermal cells is determined; when transplanted into mature larvae they differentiate according to their prospective fate[1,13].

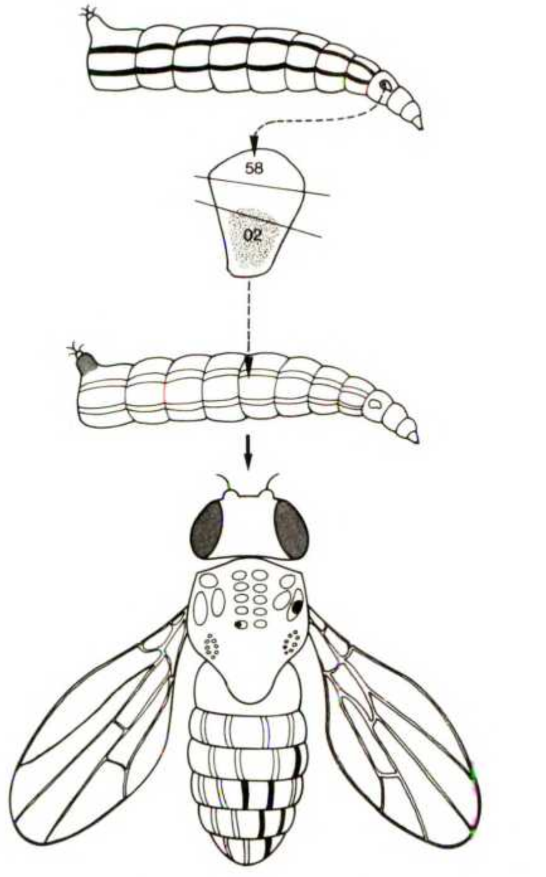

Fig. 1 Summary of the experimental procedure. A wing imaginal disk was dissected from a wild-type larva, and either the **58** or **02** piece[13] was sliced with tungsten needles and transplanted into the abdomen of a mutant host larva. After metamorphosis the host fly was stained for enzyme activity; dark fibres were found sporadically in the muscles, especially near the site of the implant. The shaded area in the disk shows the distribution of adepithelial cells, based on the binding patterns of fluorescent peanut lectin and a monoclonal antibody[14]. For marking the cells we used different alleles at the *sdh* locus[12]. Hosts were $b\ sdh^2/b\ sdh^7$ and therefore contain a thermolabile form of the enzyme succinate dehydrogenase[12]. After careful heating the succinate dehydrogenase activity disappears in sdh^2/sdh^7 muscles but survives in sdh^+ muscles. Donors were from a wild-type (Barton) stock. The *black* (*b*) mutation (see ref. 24) allowed the identification of the sdh^2/sdh^7 host larvae, which could be distinguished from their siblings by the dingy colour of the posterior spiracles. Enzyme activity, which is located in mitochondria, was specifically stained using the reduction of nitrobluetetrazolium[12]. Mature sdh^+ disk fragments were implanted into the abdomen of fully grown sdh^2/sdh^7 larvae by standard methods[25]. After metamorphosis the abdomen was dissected with the implant, heated to 52 °C in Ringer's solution for 15 min then stained for 2 h. The thoraces were heated to 53 °C in Ringer's solution for 15 min, stained for 2–3 days, embedded in paraffin wax and sectioned at 25 μm.

In contrast to earlier studies[15,16] it has been shown that the adepithelial cells do not arise directly from the disk epithelium (refs 17, 18 and P.A.L., in preparation) and fate-mapping studies of the adult flight muscles place their precursors in the mesodermal region of the blastoderm, at some distance from the presumptive epidermis[19]. The adepithelial cells can therefore be designated as mesoderm. Experiments on insect embryos have shown that when pieces of ectoderm are removed or damaged,

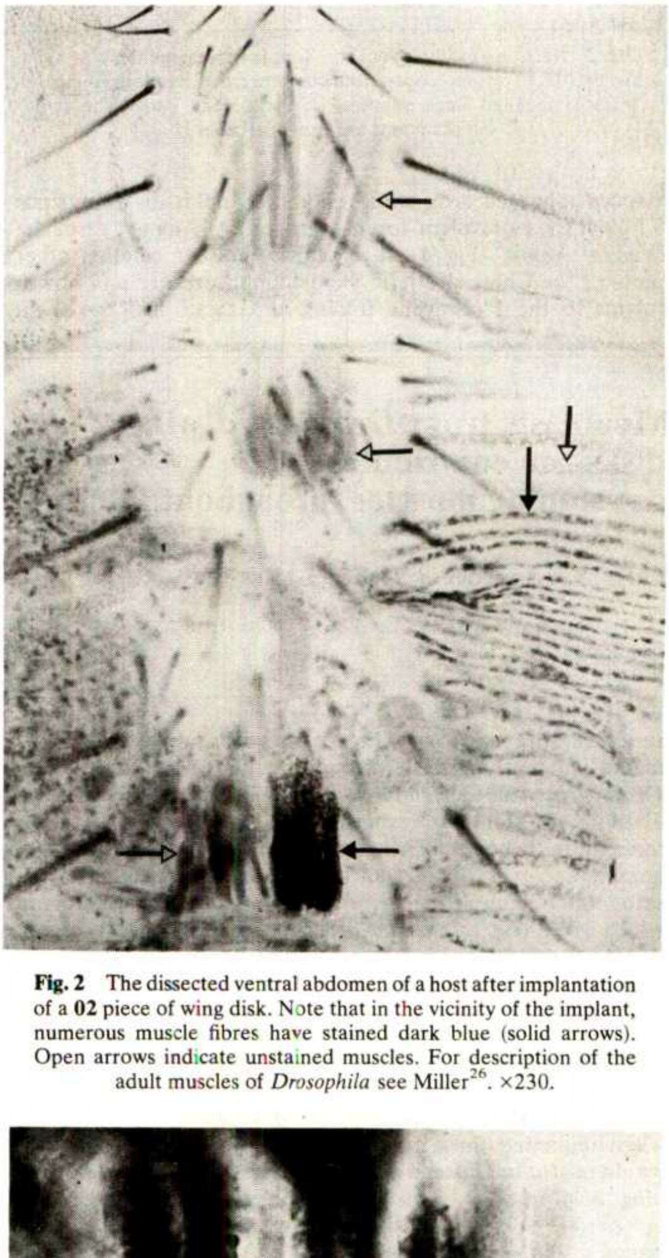

Fig. 2 The dissected ventral abdomen of a host after implantation of a **02** piece of wing disk. Note that in the vicinity of the implant, numerous muscle fibres have stained dark blue (solid arrows). Open arrows indicate unstained muscles. For description of the adult muscles of *Drosophila* see Miller[26]. ×230.

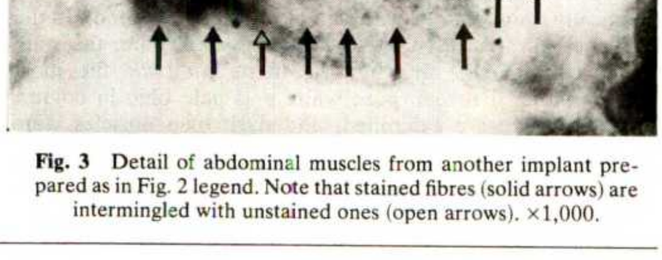

Fig. 3 Detail of abdominal muscles from another implant prepared as in Fig. 2 legend. Note that stained fibres (solid arrows) are intermingled with unstained ones (open arrows). ×1,000.

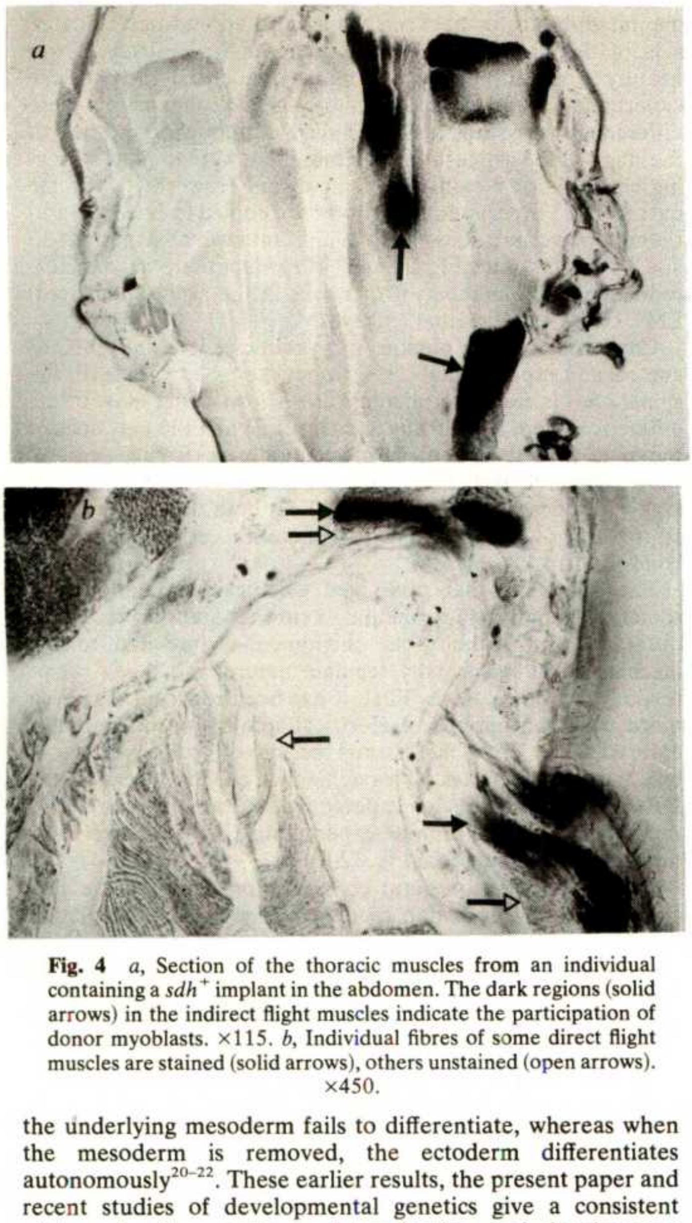

Fig. 4 *a*, Section of the thoracic muscles from an individual containing a *sdh*$^+$ implant in the abdomen. The dark regions (solid arrows) in the indirect flight muscles indicate the participation of donor myoblasts. ×115. *b*, Individual fibres of some direct flight muscles are stained (solid arrows), others unstained (open arrows). ×450.

the underlying mesoderm fails to differentiate, whereas when the mesoderm is removed, the ectoderm differentiates autonomously[20–22]. These earlier results, the present paper and recent studies of developmental genetics give a consistent picture. In the ectoderm, determination and development depend on genetic elements which are locally deployed in segmental and subsegmental compartments[4,7,8,23]. By contrast, the mesodermal cells do not appear to be as precisely determined, their development being at least partly dictated by the neighbouring ectodermal cells. Thus the cellular and genetic mechanisms of control seem to differ for the two germ layers.

We thank Mark Bretscher and Pat Simpson for discussion, Paul Johnston for assistance and Gary Struhl for help with the manuscript.

Received 26 October; accepted 3 December 1981.

1. Hadorn, E. *Brookhaven Symp. Biol.* **18,** 148–161 (1965).
2. Garcia-Bellido, A., Ripoll, P. & Morata, G. *Nature new Biol.* **245,** 251–253 (1973).
3. Lawrence, P. A. *J. Embryol. exp. Morph.* **30,** 681–699 (1973).
4. Morata, G. & Lawrence, P. A. *Nature* **265,** 211–216 (1977).
5. Chan, L.-N. & Gehring, W. *Proc. natn. Acad. Sci. U.S.A.* **68,** 2217–2221 (1971).
6. Illmensee, K. *Symp. R. ent. Soc. Lond.* **8,** 76–96 (1976).
7. Lewis, E. B. in *Role of Chromosomes in Development* (ed. Locke, M.) 231–252 (Academic, New York, 1964); *Nature* **276,** 565–570 (1978).
8. Garcia-Bellido, A. *Ciba Fdn Symp.* **29,** 161–178 (1975).
9. Ursprung, H., Conscience-Egli, M., Fox, D. J. & Walliman, J. *Proc. natn. Acad. Sci. U.S.A.* **69,** 2812–2813 (1972).
10. Reed, C. T., Murphy, C. & Fristrom, D. *Wilhelm Roux's Arch. dev. Biol.* **178,** 285–302 (1975).
11. Poodry, C. A. in *The Genetics and Biology of Drosophila* Vol. 2d (eds Ashburner, M. & Wright, T. R. F.) 407–441 (Academic, New York, 1980).
12. Lawrence, P. A. *J. Embryol. exp. Morph.* **64,** 321–332 (1981).
13. Bryant, P. J. *J. exp. Zool.* **193,** 49–78 (1975).
14. Brower, D. L., Smith, R. J. & Wilcox, M. *J. Embryol. exp. Morph.* (in the press).
15. Vaney, C. *Annls Univ. Lyon* **2,** 1–171 (1902).
16. Schneiderman, H. A. in *Mechanisms of Cell Change* (eds Ebert, J. & Okada, T.) 243–272 (Wiley, New York, 1979).
17. Perez, C. *Archs Zool. exp. gén.* **5,** 1–275 (1910).
18. Brower, D. L., Lawrence, P. A. & Wilcox, M. *Devl Biol.* **86,** 448–455 (1981).
19. Hotta, Y. & Benzer, S. *Nature* **240,** 527–535 (1972).
20. Bock, E. *Wilhelm Roux's Arch. dev. Biol.* **141,** 159–247 (1942).
21. Haget, A. *Biol. Bull. Fr. Belg.* **87,** 123–217 (1953).
22. Sauer, E. *Wilhelm Roux's Arch. dev. Biol.* **147,** 302–354 (1954).
23. Lawrence, P. A. *Cell* **26,** 3–10 (1981).
24. Lindsley, D. & Grell, E. H. *Genetic variations of Drosophila melanogaster* (Carnegie, Washington, 1968).
25. Ephrussi, B. & Beadle, G. W. *Am. Nat.* **70,** 218–225 (1936).
26. Miller, A. in *Biology of Drosophila* (ed. Demerec, M.) 420–534 (Wiley, New York, 1950).

Electrical stimulation of hindlimb increases neuronal cell death in chick embryo

Ronald W. Oppenheim

Neuroembryology Laboratory, Department of Mental Health,
Anderson Hall, Dorothea Dix Hospital, Raleigh,
North Carolina 27611, USA

Ramon Núñez

Biological Sciences Group, University of Connecticut, Storrs,
Connecticut 06268, USA

The daily treatment of chick embryos with neuromuscular blocking agents during the period of massive naturally occurring death of spinal motoneurones (days 5–10) reduces the normal loss of these cells[1,2]. Because both pre- and postsynaptic blocking agents have this effect[3], the cause seems to be related to a reduction in synaptic and/or muscular activity. If this interpretation is correct, an experimentally induced increase in nerve or muscle activity (and/or an increased activation of acetylcholine receptors, AChR), during the normal cell death period should accelerate or enhance the loss of motoneurones. Consistent with this prediction, we have found that daily treatment with the nicotinic receptor agonist, carbachol, or with the anticholinesterase (anti-ChE) agent, eserine, leads to a significant enhancement of cell death of spinal motoneurones[3]. However, because in the same study other related agents (for example nicotine) failed to alter normal cell death, we believed that a different approach might provide a better test of our prediction. We now report that short-term continuous electrical stimulation of the hindlimb (the musculature and nerve trunks) initiated at any time between stages 31 (day 7) and stage 34 (day 8) results in a significant reduction in the number of healthy motoneurones and an increase in the number of pyknotic (degenerating) motoneurones in the lumbar lateral motor column (LMC). As the number of pyknotic cells in the dorsal root ganglia (DRG) is unaltered, this effect seems to be specific to motoneurones.

White Leghorn chick embryos were treated with curare, α-bungarotoxin (α-BTX) or saline as previously described[2]. Briefly, beginning on day 5, 100–200 μl of a curare (2–2.5 mg per embryo), α-BTX (75 μg per embryo) or 0.9% saline solution was injected daily onto the vascularized chorioallantoic membrane (CAM). About half the embryos in each group (saline and curare or α-BTX) were used for electrical stimulation while half were subjected to sham procedures. The curare and α-BTX treatment was associated with a significant reduction in the rate of spontaneous neuromuscular activity (embryonic motility)[1,2]. Data from the curare and α-BTX embryos were pooled (curare/α-BTX). To gain access to the embryo's leg, a relatively large lateral window was made in the shell, and the CAM and amnion were cut, avoiding most blood vessels. In all cases, the right leg was used for both the experimental (stimulation) and sham procedures. Stimulation suction electrodes (2.5 mm tip diameter), made from polyethylene tubing, were filled with a saline solution and held in a micromanipulator for attachment to the thigh region of the leg. The leg of the embryo was stabilized by either pulling it out of the amniotic fluid and placing it on top of the CAM or by securing it with a hair loop which was attached to the shell. Despite these

0028-0836/82/010057—03$01.00

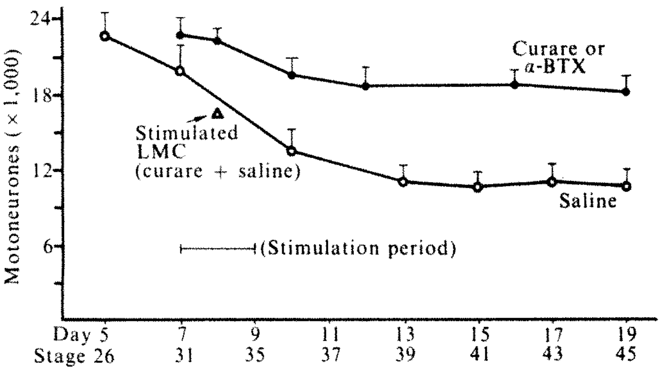

Fig. 1 The average number of motoneurones (±s.d.) in the lumbar LMC of saline (○) and curare/α-BTX (●) treated embryos. Embryos were treated as described by Pittman and Oppenheim[2]. △, The average number of motoneurones in the right LMC of all experimental embryos in the present study (saline plus curare-α-BTX treated, stages 31–35) following electrical stimulation of the right hindlimb at various times during the stimulation period (—) (see text for details).

precautions, the suction electrode occasionally became detached from the leg. Consequently, the embryos were checked every 3–4 h and in those cases where the electrode had lost contact it was re-attached. Following the attachment of the electrode, the window in the egg was closed with Parafilm and the egg placed in a temperature-controlled environment of 33–35 °C. Electrical pulses were delivered via a Grass stimulator (duration 0.6 ms, rate 0.5–1.0 s^{-1}). The stimulus intensity was adjusted to 1.5–2.0 times the minimal intensity required to produce visible contractions of the leg. It was sometimes necessary to readjust the stimulus intensity during the experiment. The sham procedure was similar in all respects to that described above except that the stimulator was not turned on. At the end of the stimulation period, the surviving embryos (<12% of the total) were killed, staged[4], fixed and processed for histological examination. The histological procedures and the methods for counting healthy and pyknotic neurones were as previously described[5,6] (also see Fig. 2*b* legend).

From a total of 210 embryos, 24 survived and were killed after 5–22 h of treatment (mean 12.8 and 14.3 h for experimental and control respectively). Of these, nine (five experimental, four control) were found to have various degrees of limb necrosis caused either by the manipulation involved in attaching the electrodes or by electrolytic damage. Two animals in each group (experimental and control) had extensive necrosis of the leg and were excluded from further analysis. (Compared with the other experimental cases these embryos had more than double the number of pyknotic neurones in both the lumbar DRG and LMC.) The other five embryos (three experimental, two control) had only a small amount of necrosis, limited to the foot region, and thus are included in the data analysis. With these exceptions, based on a preliminary light microscopic analysis of limb musculature, there were no obvious differences in muscle histology between the experimental and control limbs. Most of the experimental embryos used for analysis were still showing visible limb contractions in response to the electrical stimulation at the end of the experiment.

Figure 1 shows an analysis of the changes in motoneurone number during development of the lumbar LMC of control saline and curare/α-BTX treated embryos, together with the pooled data on healthy neurones from the electrically stimulated embryos. It can be seen that both stimulation periods (stages 31–33 and 34–35) fall within the time span of massive naturally occurring cell death.

Because no differences were found in the number of either healthy or pyknotic motoneurones between the right and left LMC of both the saline and curare/α-BTX control (sham) embryos, the data from the two sides were pooled for all subsequent comparisons with the experimental, stimulated embryos. In all comparisons between the control and experimental embryos, or between the stimulated and unstimulated side of the experimental embryos, there were always fewer healthy motoneurones in the right (stimulated) LMC of the experimental cases (Fig. 2*a*). In most of the comparisons these differences were statistically significant, although in the case of the stage 31–33 saline-treated group there were too few surviving embryos for a statistical comparison. However, when the data from all experimental embryos are pooled (saline + curare) the differences are statistically significant both at stages 31–33 and 34–35 ($P < 0.01$, Fig. 2*a*). In both groups there was a ~20% reduction in the number of neurones in the right (stimulated) LMC of the experimental embryos.

Comparison of the number of pyknotic cells in the LMC of control and experimental cases, or between the two sides of the spinal cord in the experimental cases showed that most of the differences were statistically significant. When the two sides of the spinal cord of the pooled experimental cases (saline + curare) were compared statistically, the differences were found to be highly significant ($P < 0.01$, Fig. 2*b*). At both stages there were approximately twice as many degenerating cells in the stimulated (right) LMC.

The possibility that prolonged electrical stimulation may somehow be lethal to developing neurones and that the effect observed is a pathological phenomenon unrelated to the mechanisms that normally regulate natural cell death seems unlikely for two reasons. First, it has been reported that even more polonged periods of electrical stimulation of the chick embryo wing, after the normal period of extensive loss of brachial motoneurones[7], does not induce cell loss[8]. Second, the DRG cells, which are also undergoing natural cell death during the stages examined in these experiments[5], were unaffected by the electrical stimulation (Fig. 2*b*).

An additional procedural consideration concerns the rate and pattern of stimulation used here. The rate of stimulation

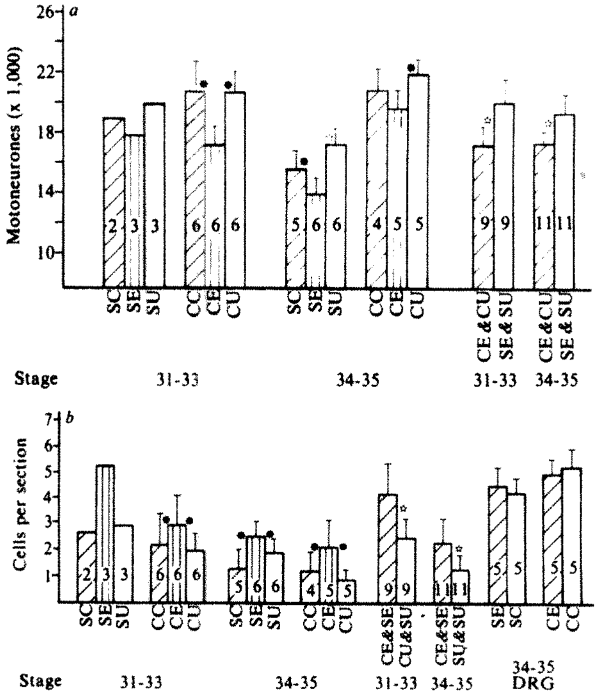

Fig. 2 The number of 'healthy' motoneurones (mean ± s.d.) (*a*) and of dying (pyknotic) motor and sensory neurones (mean ± s.d.) (*b*) in the lumbar LMC following electrical stimulation of the right hindlimb at stages 31–33 or 34–35. SC, saline control; SE, saline experimental (stimulated or right) LMC; SU, saline unstimulated (left) LMC; CC, curare/α-BTX control; CE, curare/α-BTX experimental (stimulated or right) LMC; CU, curare/α-BTX unstimulated (left) LMC. CE & SE and CU & SU represent pooled data from the saline plus the curare/α-BTX treated embryos. ★ $P < 0.05$; ☆, $P < 0.01$, Mann–Whitney tests, one-tailed. All statistical comparisons are relative to the experimental (stimulated) group, SE or CE. Sample size is as indicated in the bars.

(0.5–1.0 s^{-1}) was considerably higher than the normal rates of limb motility at these ages, which is between 6 and 12 per min (ref. 2). Although we chose a high rate of stimulation to increase our chances of finding an effect, we cannot rule out the possibility that the results reflect non-physiological conditions. However, in adult mammals a wide variety of stimulus rates and patterns are effective in maintaining the normal properties of denervated muscle[9]. We are now attempting to determine the effects of differing rates and patterns of stimulation on motoneurone death in the chick embryo.

We have suggested a model for explaining the role of activity in the regulation of neuronal cell death[1,2,10]. Briefly, we proposed that during embryonic development, synaptic and/or muscle activity regulates those events which lead to a reduction in the availability of a trophic substance and/or in the level of AChR in muscle. This reduction would limit the number of synaptic sites that can be formed on a muscle cell, leading, in turn, to competition between neurones for a relatively fixed number of synaptic sites (and/or for a limited supply of trophic substance), in which competition the losers undergo cell death. We suggest that neuromuscular blockade suppresses and electrical stimulation enhances this series of normal events.

Although many questions remain unanswered concerning the specific cellular and molecular events by which neuromuscular interactions regulate the number of motoneurones that survive the cell death period, the present findings provide additional support for our contention that synaptic and/or muscular activity is involved. In view of the increasing evidence that many other properties of the neuromuscular system depend on physiological activity for their normal differentiation and maintenance[10–15], it is perhaps not surprising that motoneurone cell death should now be added to this list.

This work was supported by NSF grant BNS 40397, by a grant from the Amyotrophic Lateral Sclerosis Society (ALS) and by funds provided by the North Carolina Department of Mental Health. Part of this work was done during the tenure of a Muscular Dystrophy Association Fellowship to R.N. We thank R. Jones for technical assistance, and Lanny Haverkamp and Jerome Maderdrut for their helpful comments.

Received 14 August; accepted 26 October 1981.

1. Pittman, R. & Oppenheim, R. W. *Nature* **271,** 364–366 (1978).
2. Pittman, R. & Oppenheim, R. W. *J. comp. Neurol.* **187,** 425–446 (1979).
3. Oppenheim, R. W. & Maderdrut, J. L. *Neurosci. Abstr.* **7,** 291 (1981).
4. Hamburger, V. & Hamilton, H. L. *J. Morph.* **88,** 49–92 (1951).
5. Hamburger, V., Brunso-Bechtold, J. L. & Yip, J. *J. Neurosci.* **1,** 60–71 (1981).
6. Chu-Wang, I. & Oppenheim, R. W. *J. comp. Neurol.* **177,** 33–58 (1978).
7. Oppenheim, R. W. & Majors-Willard, C. *Brain Res.* **154,** 148–152 (1978).
8. Toutant, M. & LeDourain, G. *IRCS med. Sci.* **8,** 408–409 (1980).
9. Lømo, T. & Westgaard, R. H. *J. Physiol., Lond.* **252,** 603–626 (1975).
10. Oppenheim, R. W. in *Studies in Developmental Neurobiology: Essays in Honor of Viktor Hamburger* (ed. Cowan, W. M.) 74–133 (Oxford, New York, 1981).
11. Brown, M. C., Holland, R. L. & Hopkins. W. G. *A. Rev. Neurosci.* **4,** 17–42 (1981).
12. Dennis, M. J. *A. Rev. Neurosci.* **4,** 43–68 (1981).
13. Fambrough, D. M. *Physiol. Rev.* **59,** 165–227 (1979).
14. Lømo, T. *Trends Neurosci.* **3,** 126–129 (1980).
15. Pestronk, A., Drachman, D. B., Stanley, E. F., Price, D. L. & Griffin, J. W. *Expl Neurol.* **70,** 690–696 (1980).

Significance of the potassium signal from neurones to glial cells

V. W. Pentreath & M. A. Kai-Kai

Department of Biology, University of Salford, Salford M5 4WT, UK

Neurones transmit signals to glial cells by releasing potassium into the intercellular spaces during nerve activity, simultaneously depolarizing their membrane potential[1]. It is thought that the glial cells may respond metabolically or trophically to the released K, and that they may also take up excess K, thereby protecting the neurones against perturbations in the extracellular concentration of this ion[2,3]. We have studied metabolic interactions between the two cell types in leech and snail ganglia using a recently discovered application[4,5] of the radioactively labelled 2-deoxyglucose (2-DG) technique[6]. This approach derives from the finding that ^{3}H-2-DG is partially and selectively metabolized into glycogen within nervous tissue, and thus can be used as a sensitive, specific marker for mapping sites of glycogen synthesis and distribution in nervous tissue[4,5]. In the leech and snail ganglia, the large size of the neuronal perikarya, together with the grouping of the glial cells around them and the location of the axonal and dendritic processes in the core of the ganglia, allows the distributions of the labelled glycogen in the different cell types and their processes to be resolved by light and electron microscope autoradiography[7,8]. Here we describe how in both animals, antidromic stimulation of nerves entering the ganglia increased the incorporation of ^{3}H-2-DG into glycogen in glial cells surrounding the activated neurones. Increased extracellular K had a similar effect, which was maximal for a K concentration ~4 mM above normal. We therefore conclude that neuronal activation causes a K-mediated increase in ^{3}H-2-DG uptake and synthesis into glycogen by the satellite glial cells.

In the technique used, incorporation of ^{3}H-2-DG into 2-deoxyglycogen proceeds analogously to the glucosyl transfer from uridine diphosphate glucose (UDPG) into glycogen; the enzymes for glycogen synthesis are relatively nonspecific to the presence or absence of the hydroxyl group at C-2 of the glucose unit. The labelled 2-deoxyglycogen is able to withstand autoradiographic processing with aqueous media, whereas unmetabolized 2-DG and 2-DG-6-PO_4 are washed out. The resulting autoradiographs show the distribution of 2-DG incorporated into glycogen, which corresponds to the amounts of endogenous glycogen.

Isolated abdominal ganglia of the leech, *Haemopis sanguisuga*, and buccal ganglia of the snail, *Planorbis corneus*, were immersed in appropriate salines[9,10] containing 5–10 μM 2-deoxy-D[1-^{3}H]glucose (15.0 Ci $mmol^{-1}$; Radiochemical Centre, Amersham) and incubated at room temperature for 5–60 min. The effects of increased nerve activity were studied by stimulating nerves from the ganglia with suction electrodes, using pulses of 2.5–5.0 ms duration, 1–10 V at 5 Hz for between 10 min and 1 h. The uptake and metabolism of 2-DG in the presence of increased extracellular K were measured by incubating ganglia in saline solutions containing additions of 4 mM and 15 mM K at room temperature for 15 min to 1 h. Following the load periods with ^{3}H-2-DG, all experimental tissues were analysed by three procedures. First, the levels of radioactivity in the ganglia were measured by liquid scintillation counting. Second, the amounts of ^{3}H-2-DG incorporated into glycogen were assessed by the method of Mordoh *et al.*[11] (this method extracts high molecular weight glycogen in a pure form; the glycogen is not degraded and loss of label is minimized). Third, the distributions of labelled glycogen in the ganglia were determined by light and electron microscope autoradiography of tissues fixed with aldehyde and processed with aqueous media for histology[4].

During 15–60 min exposure to ^{3}H-2-DG, the ganglia of *Haemopis* and *Planorbis* progressively accumulated ^{3}H-2-DG at a rate of 0.13 and 0.16 nmol per g nervous tissue per min respectively. After 1 h, 4–5% of the ^{3}H-2-DG was recovered in the high molecular weight glycogen fraction from *Haemopis*, and ~1% in the fraction from *Planorbis* (Fig. 1*b*). The autoradiographic pattern of glycogen labelling observed by light microscopy differed in the two species. In *Haemopis*, small areas of radioactivity were located in a narrow band of the peripheral cytoplasm of most neuronal perikarya, often in clumps of 1.5 μm diameter (Fig. 2*a*); axonal and dendritic processes were unlabelled. The giant glial cells[7,8] surrounding the perikarya were labelled. In *Planorbis*, groups of neurones were selectively and heavily labelled after 1 h exposure to ^{3}H-2-DG (Fig. 2*c*). Serial section analysis revealed that the radioactivity was distributed evenly throughout the axonal and dendritic processes. The glial cells surrounding the neurones were not labelled or only weakly. Electron microscope autoradiography showed that

028-0836/82/010059—03$01.00

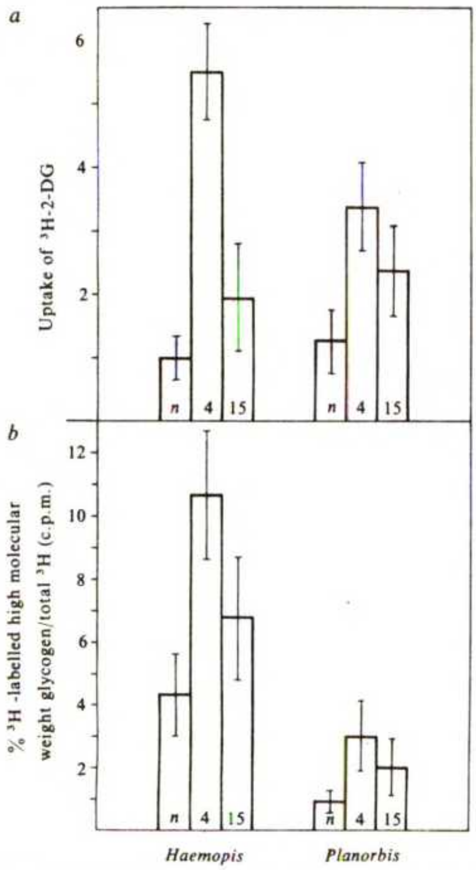

Fig. 1 Stimulation of ^{3}H-2-DG uptake (*a*) and incorporation into high molecular weight glycogen (*b*) in abdominal ganglia of *Haemopis* and buccal ganglia of *Planorbis*. Each set of histograms shows results for normal saline K concentrations, *n* (4.0 mM for *Haemopis*; 1.3 mM for *Planorbis*), and for salines containing additional 4.0 mM and 15.0 mM K, added in the form of sulphate ions. Results are the means of three experiments in each case; bars indicate s.e. *a*, The ganglia were rinsed in saline (1 min) after the load period, homogenized in a tissue solubilizer (NCS; Radiochemical Centre, Amersham) and counted by liquid scintillation. All counts were corrected against blank controls (ganglia processed in parallel but without exposure to radioactive tracer) and for quenching (generally <1% using NCS solubilizer) by conventional methodology. The uptake of radioactivity by a unit weight of ganglia is expressed (in c.p.m.) relative to the uptake by *Haemopis* ganglia in normal saline (unity). *b*, After the load period, high molecular weight undegraded glycogen was separated by a method similar to that described elsewhere[11]. Ganglia were homogenized in ~3 vol 3% $HgCl_2$ and centrifuged at 2,000*g* for 5 min. The supernatant was added to ~2 vol of 95% ethanol, and the resulting precipitate separated by centrifugation (2,000*g* for 5 min). The precipitate was redissolved in water (0.5 ml) and the solution centrifuged again. The resulting supernatant was mixed with 2 vol of ethanol, and the sample was centrifuged at 2,000*g* for 10 min. The final sediment (the high molecular weight glycogen) was dissolved in NCS solubilizer and the radioactivity measured by liquid scintillation counting. Counts are expressed as percentages of the total radioactivity recovered in all the fractions. The lower molecular weight glycogen is not readily extracted by this procedure, thus the total percentages of labelled glycogen are likely to be higher.

the differences in labelling patterns were correlated directly with differences in the distribution of glycogen in the two species[4]. In *Haemopis*, aggregates of glycogen particles were frequently contained within glial processes extending into the neuronal somata (Fig. 3).

Stimulation of nerves (1 h at 5 Hz) entering the ganglia of both species resulted in an approximate fivefold increase in accumulated radioactivity as measured by liquid scintillation. However, the incorporation of ^{3}H-2-DG into glycogen was not proportional to this increase; the levels of labelled high molecular weight glycogen extracted from the tissues were increased 2.3–3.2 times (*Haemopis*, mean increase = 3.2 ± 1.4, 4 experiments; *Planorbis*, mean increase = 2.3 ± 1.1, 4 experiments). When the distribution of labelled glycogen was studied by light microscope autoradiography, it was found that the labelling of the neurones, particularly their perikarya, was increased in both species, but a striking feature was the increased grain density in the glial cells surrounding the perikarya (Fig. 2*b*, *d*). Thus neuronal activation caused an increase in uptake of ^{3}H-2-DG by the nervous tissues, and to a lesser extent its incorporation into high molecular weight glycogen. As the neurones were stimulated via nerves outside the ganglia, the increased levels of glycogen in the glial cells inside the ganglia resulted indirectly from the neuronal activation.

There is evidence that extracellular [K] may normally be increased by 4 mM during maintained nerve activity in leech abdominal ganglia[12], and by 4–8 mM in the cat cortex[13]. Higher experimental levels of extracellular K produce increased depolarization of glial cells, but it is unlikely that such levels are of normal physiological significance[3]. The role of K in mediating the activity-induced increase in ^{3}H-2-DG uptake and incorporation into glycogen was investigated by incubating ganglia in saline containing ^{3}H-2-DG with elevated K levels and measuring the uptake of radioactivity and its conversion to glycogen. Other ganglia incubated in parallel were processed for autoradiography. Exposure of *Haemopis* ganglia to a wide range of extracellular [K] from the normal level (4.0 mM) to 40 mM in 1 mM increments for 1 h revealed a maximal increase in ^{3}H-2-DG uptake (about five times) when the increase was 3–5 mM (Fig. 1*a*). Higher values of extracellular K gave lower increases in 2-DG uptake, which varied between 1.5 and 2.2 times, although increases of up to four times were occasionally ob-

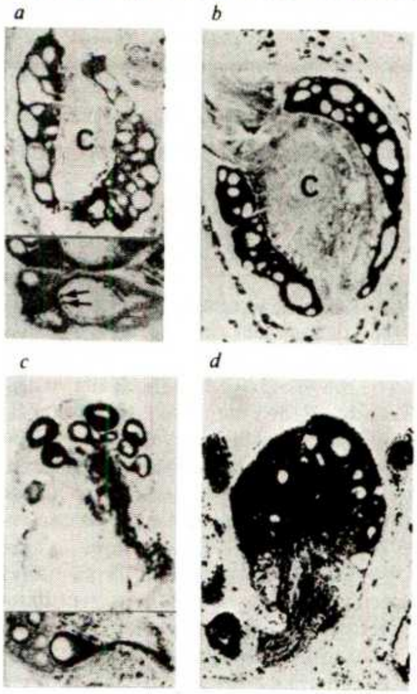

Fig. 2 Distribution of labelled glycogen in the abdominal ganglion of *Haemopis* (*a*, *b*) and the buccal ganglion of *Planorbis* (*c*, *d*). The ganglia were exposed to ^{3}H-2-DG for 1 h, then processed by aldehyde fixation, water–ethanol dehydration and wax sectioning[4]. The autoradiographs were prepared by coating the sections with Kodak AR 10, storing for 2 weeks, and then developing in Kodak D-19. *a*, Top: the labelled glial cells surround the neuronal perikarya which are located in the cortex of the ganglion. The core of the ganglia (C) contains large numbers of axonal and dendritic processes, but few glial cell processes[7]; bottom: at higher magnification grain clumps can be distinguished in the peripheral somatoplasm of some neurones (arrows). Many of these correspond to the glial invaginations visualized by electron microscope autoradiography (Fig. 3). *b*, Section of a ganglion stimulated antidromically via the abdominal connective at 5 Hz for 1 h in the presence of ^{3}H-2-DG. Note the heavy labelling of the glial cells. *c*, Labelled neurones in a buccal ganglion of *Planorbis*: top, a group of labelled neurones which project into the neuropile of the ganglion; bottom, a large neurone cut in section to illustrate the equal distribution of labelled glycogen in the peripheral cytoplasm of the cell body and its axon. The branching patterns of the main axonal processess of the labelled neurones were mapped by comparison with adjacent serial sections. *d*, Section of buccal ganglion stimulated antidromically via the cerebro-buccal connective at 5 Hz for 1 h. Note the intense labelling of the glial cells which surround the neuronal perikarya, and increased labelling of the neurones. In both species the ganglia are avascular, but there are no restrictive barriers to the access of small molecules[1]. All magnifications, ×100, except for *a*, bottom (×320) and *c*, bottom (×175).

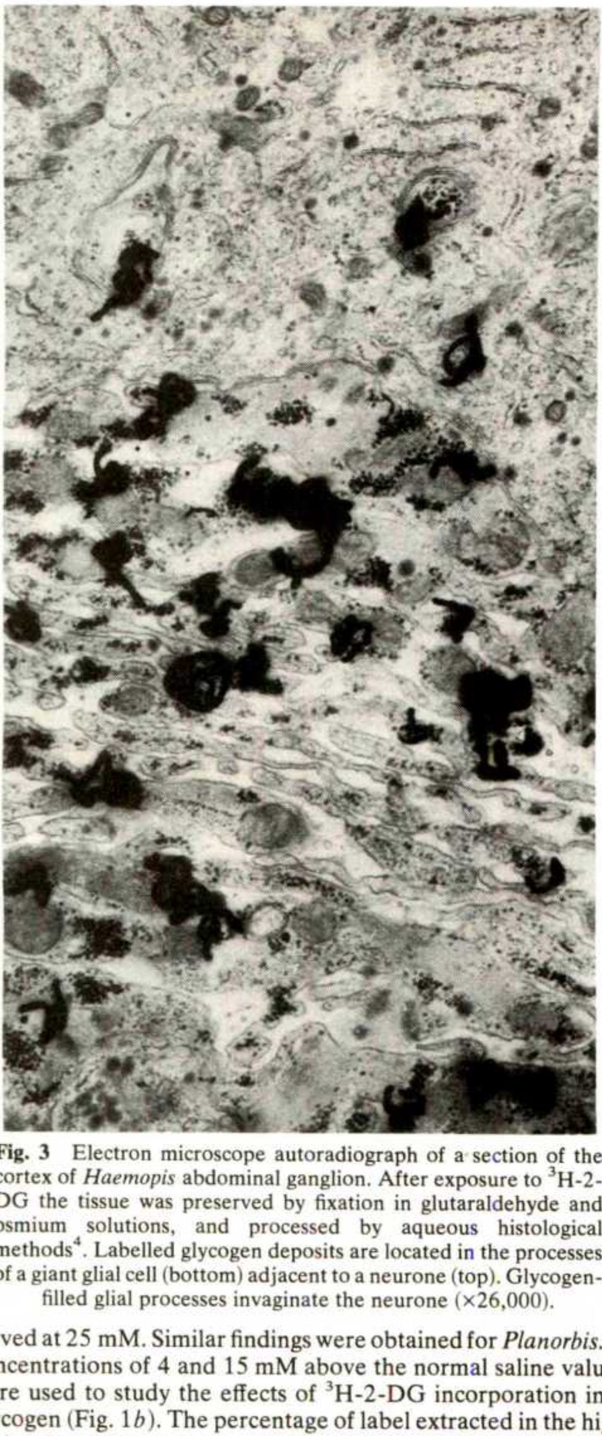

Fig. 3 Electron microscope autoradiograph of a section of the cortex of *Haemopis* abdominal ganglion. After exposure to ^{3}H-2-DG the tissue was preserved by fixation in glutaraldehyde and osmium solutions, and processed by aqueous histological methods[4]. Labelled glycogen deposits are located in the processes of a giant glial cell (bottom) adjacent to a neurone (top). Glycogen-filled glial processes invaginate the neurone (×26,000).

served at 25 mM. Similar findings were obtained for *Planorbis*. K concentrations of 4 and 15 mM above the normal saline values were used to study the effects of ^{3}H-2-DG incorporation into glycogen (Fig. 1*b*). The percentage of label extracted in the high molecular weight glycogen was increased 2.5-fold for *Haemopis*, and 3-fold for *Planorbis* at 4 mM K, and to a lesser extent at 15 mM K. Autoradiographic analysis showed that 4 mM K (1 h exposure) produced labelling of glial cells that was comparable to the effects of electrical stimulation. A concentration of 15 mM caused some increase in the grain density overlying the glial cells, and also over the neurones. Extracellular recording experiments showed that the 4 mM increase in [K] caused no significant increases in the electrical activity of neurones in either species. Activity was initially greatly enhanced, but not maintained, at [K] >12 mM.

These results provide direct evidence that increased neuronal activity causes a significant potassium-mediated increase in ^{3}H-2-DG uptake and incorporation into glycogen by the satellite glial cells. The similarity of the findings in both leech and snail ganglia indicate that this may be a general neurone–glial property. Both electrical stimulation and increased extracellular [K] increased the amounts of ^{3}H-glucose incorporated into glycogen in leech and snail ganglia (our unpublished observations), however the sites could not be resolved accurately by autoradiography as the label was also extensively incorporated into proteins and lipids.

The enzyme systems that synthesize and catabolize glycogen in mammalian brain are the same as those in other tissues[14,15], although they appear to differ in certain kinetic properties and modes of regulation[16]. It is evident that glycogen metabolism within the central nervous system must be controlled locally, because circulating hormones cannot pass the blood–brain barrier. There are no data on possible modulatory roles of K or K-induced depolarization on glycogen metabolism in nervous tissue. However, the selective stimulatory effects of K on glycogen formation in liver are well established [17,18]. Glial cell membranes are selectively permeable to K[1] and the K-mediated promotion of glycogen synthesis in glial cells caused by localized neuronal activity could provide a significant mechanism for ensuring continued energy supplies during any subsequent intense activity if local blood–glucose levels fell or were inadequate.

This work was supported by the SERC.

Received 3 July; accepted 9 November 1981.

1. Kuffler, S. W. & Nicholls, J. G. *Ergebn. Physiol.* **57,** 1–90 (1966).
2. Kuffler, S. W. & Nicholls, J. G. *From Neuron to Brain* (Sinauer, Sunderland, Massachusetts, 1976).
3. Varon, S. S. & Somjen, G. G. *Neurosci. Res. Prog. Bull.* **17,** (1) (1979).
4. Kai-Kai, M. A. & Pentreath, V. W. *J. Neurocytol.* **10,** 693–708 (1981).
5. Pentreath, V. W., Seal, L. H. & Kai-Kai, M. A. *Neuroscience* (in the press).
6. Sokoloff, L. *et al. J. Neurochem.* **28,** 897–916 (1977).
7. Kai-Kai, M. A. & Pentreath, V. W. *J. comp. Neurol.* (in the press).
8. Coggeshall, R. E. & Fawcett, D. W. *J. Neurophysiol.* **27,** 229–289 (1964).
9. Nicholls, J. G. & Kuffler, S. W. *J. Neurophysiol.* **27,** 645–671 (1964).
10. Berry, M. S. *J. exp. Biol.* **56,** 621–637 (1972).
11. Mordoh, J., Krisman, C. R. & Leloir, L. F. *Archs Biochem. Biophys.* **113,** 265–272 (1966).
12. Baylor, D. A. & Nicholls, J. G. *J. Physiol., Lond.* **203,** 555–569 (1969).
13. Somjen, G. *A. Rev. Physiol.* **37,** 163–190 (1975).
14. Coxon, R. V. in *Handbook of Neurochemistry* Vol. 3 (ed. Lajtha, A.) 37–52 (Plenum, New York/London, 1970).
15. Siesjö, B. K. *Brain Energy Metabolism* (Wiley, New York, 1978).
16. Goldberg, N. D. & O'Toole, A. G. *J. biol. Chem.* **244,** 3053–3061 (1969).
17. Buchanan, J. M., Hastings, A. B. & Nesbett, F. B. *J. biol. Chem.* **180,** 435–445 (1949).
18. Hastings, A. B. & Buchanan, J. M. *Proc. natn. Acad. Sci. U.S.A.* **28,** 478–482 (1942).

Depletion of substance P-containing axons in substantia gelatinosa of patients with diminished pain sensitivity

John Pearson*, Leslie Brandeis* & A. Claudio Cuello†

* Department of Pathology, New York University Medical Center,
New York, New York 10016, USA
† Departments of Pharmacology and Human Anatomy,
University of Oxford, Oxford OX1 3QT, UK

Substance P is an undecapeptide which may be involved in transmission of nociceptive information at synapses of primary sensory neurones[1,2]. It occurs in 10–20% of rat dorsal root ganglion neurones[3,4]. Small substance P-immunoreactive (SP-IR) axons from dorsal root ganglia enter the spinal cord and form a dense terminal network in the substantia gelatinosa of the rat dorsal horn[3]; analogous fibres from the trigeminal ganglion terminate in the substantia gelatinosa of the spinal trigeminal tract of the medulla oblongata[4,5], while sensory axons travelling via the petrosal and nodose ganglia terminate in the tractus solitarius of the medulla[5–8]. Substance P is also present in human spinal cord and pallido-nigral system[9–12]. In addition to sympathetic and parasympathetic abnormalities, patients with familial dysautonomia (the Riley–Day syndrome) have severe diminution of temperature and pain sensitivity, reduced populations of primary sensory neurones and small Lissauer's tracts[13]. It was thus postulated that a diminution of primary substance P axons might be demonstrable using immunocytochemistry. We report here the presence of anatomically discrete depletion of substance P immunoreactivity in the substantia gelatinosa of spinal cord and medulla of patients with familial dysautonomia. The results are consistent with the hypothesis that substance P is involved in the transmission of impulses related to pain.

0028-0836/82/010061—03$01.00

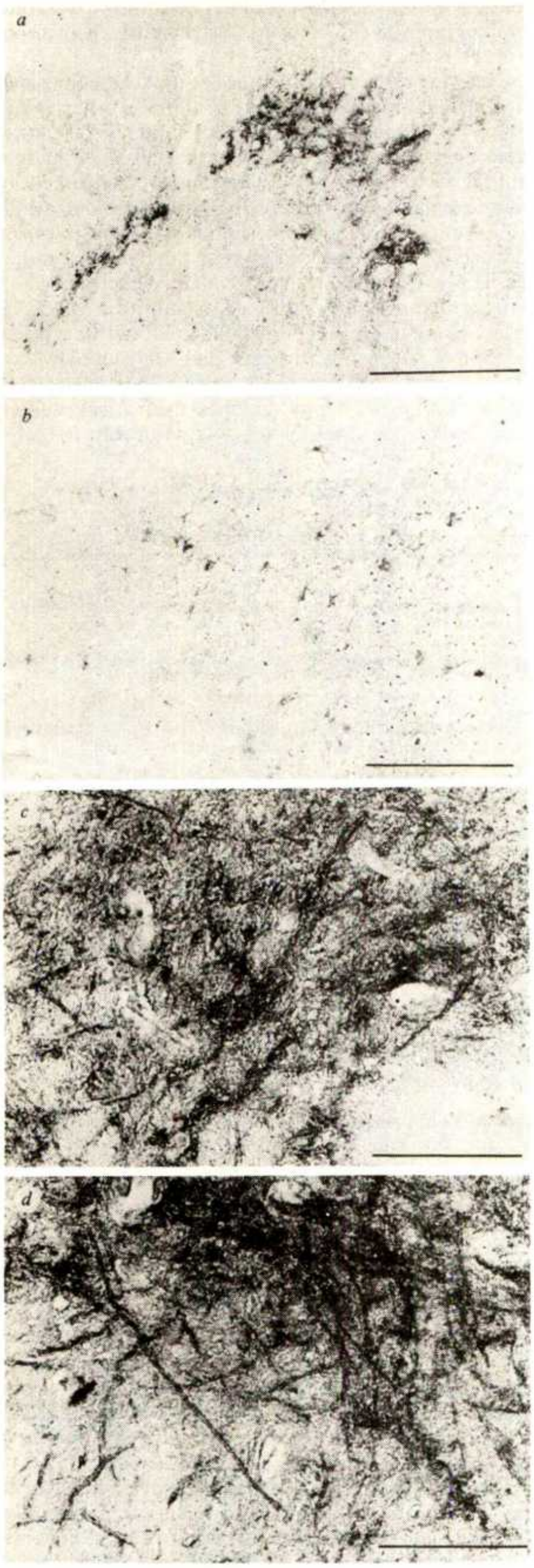

Fig. 1 The substantia gelatinosa of the control spinal cord (*a*) contains multiple substance P-immunoreactive (SP-IR) axons and their terminals, which form a distinct cap over the dorsal grey horn; no such cap is visible in the familial dysautonomia patient's spinal cord (*b*). The substantia nigra of both the control (*c*) and the patient (*d*) contain similar amounts of SP-IR fibres. Scale bars, 100 μm.

The present studies used a well characterized monoclonal antibody (NCI/34HL) to substance P[14]. Thus, it does not cross-react with any other known mammalian neuroactive peptide, stains substance P in brain regions shown to contain the peptide by bioassay, and stains the peptide which accumulates proximal to peripheral nerve ligatures and which can be independently identified on Sephadex columns[14]. The antibody was used with the peroxidase–antiperoxidase (PAP) technique of Sternberger[15]. Staining controls included normal serum and antibody adsorbed with substance P, neither of which gave any positive reaction. Test tissues used were from five patients aged 14, 15, 17, 18 and 22 yr, diagnosed as having Riley–Day syndrome at the Dysautonomia Treatment and Evaluation Center of New York University Medical Center. The diagnosis was confirmed at autopsy by a characteristic combination of defects in the tongue, sympathetic ganglia and dorsal root ganglia. Spinal cord and brain stem sections were made from archival blocks of paraffin-embedded tissue which had been fixed in 10% formalin. Storage times for patient and control tissues were similar.

In contrast to the controls, which showed large concentrations of SP-IR terminals in the substantia gelatinosa of spinal cord and medulla oblongata (Fig. 1*a*), there was almost complete absence of such terminals from these regions in all patients with familial dysautonomia (Fig. 1*b*). Some of the few remaining SP-IR axons observed may have been derived from the brain stem, as studies in other species[1,2] have shown the presence of SP-IR axons in this region. Patients did not differ from controls in the density of SP-IR axons in the substantia nigra (Fig. 1*c*,*d*). Immunoreactive axons were also readily demonstrable in the tractus solitarius of patients. It is not possible to obtain good staining of the small quantities of substance P normally present in the perikarya of primary sensory neurones of monkey or man, and colchicine pretreatment is necessary to cause sufficient accumulation of the peptide in most lower animals. We were therefore unable to demonstrate directly depletion of primary sensory substance P-containing neurones in the patients. Nevertheless, we have previously demonstrated severe losses of sensory axons, especially those of small diameter, in familial dysautonomia and have shown that severe deficits of dorsal root ganglion neurones occur in young patients[13]. Depletion of spinal dorsal horn neurones has not been demonstrated, and the fact that spinal dorsal column fibres only diminish as sensory neuronal loss continues into adulthood[13] indicates that initial deficits are mainly among neurones projecting onto the substantia gelatinosa and other parts of the dorsal grey. Small-calibre sensory axons projecting onto the substantia gelatinosa and containing substance P have been suggested as being involved in processing of pain-related impulses[1,2]. The coincidence of analgesia, loss of sensory neurones and small diameter axons projecting onto the substantia gelatinosa, and severe diminution of dorsal horn substance P immunoreactivity in familial dysautonomia support this idea. However, it does not prove the case because other sensory modalities, notably those related to temperature, are also attenuated in familial dysautonomia; other putative neurotransmitters yet to be examined may be found to be decreased in the disease.

The persistence of some substance P in axons of the tractus solitarius might be attributed to sources within the central nervous system. Alternatively, there might be less sensory neuronal loss in cranial ganglia, some of which are of placodal origin, than in dorsal root ganglia, which are of neural crest origin. No formal neuronal counts have been made of patients' cranial ganglia.

Although immunocytochemistry cannot definitively demonstrate the absence of an antigen, there is no doubt that the amount of substantia gelatinosa axon substance P in the patients was far below normal. That this was not an artefact of autolysis is indicated by comparison with controls in which the postmortem intervals were generally longer than those of the patients but in which substantia gelatinosa SP-IR axons were readily demonstrable. Furthermore, substance P has been demonstrated to have excellent postmortem stability[12,16,17]. Finally, the ready detection of SP-IR axons in the tractus solitarius and substantia nigra of the patients provides excellent internal control both of staining efficacy and postmortem preservation of the peptide. The fact that SP-IR is normal in these structures indicates that familial dysautonomia does not involve a generalized defect in substance P synthesis.

Our data indicate a need for prospective studies of substance P levels in fresh wet tissue from patients. They also demonstrate the usefulness of immunocytochemistry in the microscopic study of human neurobiology and in the detection of deficits in chemically defined neurones in human disease.

This work was supported by the Dysautonomia Foundation (to J.P., L.B.) and the MRC, Wellcome Trust and the Royal Society (to A.C.C.).

Received 4 August; accepted 6 November 1981.

1. Nicoll, R. A., Schenker, C. & Leeman, S. E. *A. Rev. Neurosci.* **3,** 227 (1980).
2. Henry, J. L. *Brain Res.* **114,** 439 (1976).
3. Hokfelt, T. *et al. Neuroscience* **1,** 131 (1976).
4. Cuello, A. C., DelFiacco, M. & Paxinos, G. *Brain Res.* **152,** 499 (1978).
5. Sumal, K. K., Pickel, F. M., Miller, R. J. & Reis, D. J. *Soc. Neurosci.* **6,** 353 (1980).
6. Maley, B. E. & Elde, R. P. *Soc. Neurosci.* **6,** 355 (1980).
7. Helke, C. J., O'Donohue, T. L. & Jacobowitz, D. M. *Peptides* **1,** 1 (1980).
8. Gillis, R. A., Helke, C. J., Hamilton, B. L., Norman, W. P. & Jacobowitz, D. M. *Brain Res.* **181,** 476 (1980).
9. Cuello, A. C., Polak, F. & Pearse, A. G. E. *Lancet* **ii,** 1054 (1976).
10. de Lanerolle, N. C. & LaMotte, C. *Soc. Neurosci.* **6,** 353 (1980).
11. Defendini, R., Nilaver, G., Zimmerman, E. A. & Tennyson, V. M. *Soc. Neurosci.* **6,** 103 (1980).
12. Kanazawa, I., Bird, E., O'Connell, R. & Powell, D. *Brain Res.* **120,** 387 (1977).
13. Pearson, J. *J. autonomic nerv. Syst.* **1,** 119 (1979).
14. Cuello, A. C., Galfre, G. & Milstein, C. in *Receptors for Neurotransmitters and Peptide Hormones* (eds Pepeu, G., Kuhar, M. J. & Enna, S. J.) 349 (Raven, New York, 1980).
15. Sternberger, L. *Immunocytochemistry* (Wiley, New York, 1979).
16. Cooper, P. E., Fernstrom, M. H., Leeman, S. E. & Martin, J. B. *Soc. Neurosci.* **6,** 680 (1980).
17. Emson, P. C., Arregui, A., Clement-Jones, V., Sandberg, B. E. B. & Rossor, M. *Brain Res.* **199,** 147 (1980).

S-100 protein in human chondrocytes

K. Stefansson*, R. L. Wollmann*, B. W. Moore† & B. G. W. Arnason*

* Departments of Pathology and Neurology, University of Chicago,
950 East 59th Street, Chicago, Illinois 60637, USA
† Department of Psychiatry, Washington University School of
Medicine, St Louis, Missouri 63110, USA

Chondrocytes in the fetal skull and visceral cartilage are considered to be of neural crest origin[1] while those found elsewhere in the body are thought to be derived from mesoderm[2,3] (mesodermal chondrocytes). Chondrocytes of pelvic rudiments from chick embryos are the only cells known to respond to nerve growth factor that are not of neuroectodermal origin[4]. In addition, embryonic spinal cord[5] and neural retina[6] of chickens synthesize type II collagen[5,6], originally thought to be confined to cartilage. Here we report the presence of the S-100 protein (S-100) in chondrocytes of skull, vertebrae, ribs, sternum, larynx and long bones of the human fetus, and larynx and xiphoid process of the human adult. Mesodermal chondrocytes are the only cells which contain S-100 and yet are not considered to be of neuroectodermal origin, thus our results indicate that these chondrocytes may be developmentally closer to neuroectoderm than traditionally thought.

S-100, an acidic protein which has been isolated from the central nervous system (CNS) of mammals, has a molecular weight (M_r) of 21,000–24,000 (refs 7–9) and exists in both membrane-bound and soluble forms[10]. It has been shown to increase activity of RNA polymerase in nuclei isolated from brains of immature chickens[11]. S-100 facilitates passage of γ-aminobutyric acid across nerve-cell membranes[12] and undergoes orthodromic axonal transport[13]. In the CNS the concentration of S-100 is low at birth, increasing with age[7,14].

S-100 has been detected by immunological methods in all vertebrates examined[7]. In the CNS, it is located primarily within astrocytes and oligodendrocytes[15–17]. Some investigators have also demonstrated S-100 in CNS neurones[18–20] and in isolated synaptosomes[10]. Outside the CNS, S-100 has so far been demonstrated only in Schwann cells of peripheral nerve and in satellite cells of dorsal root and autonomic ganglia[21].

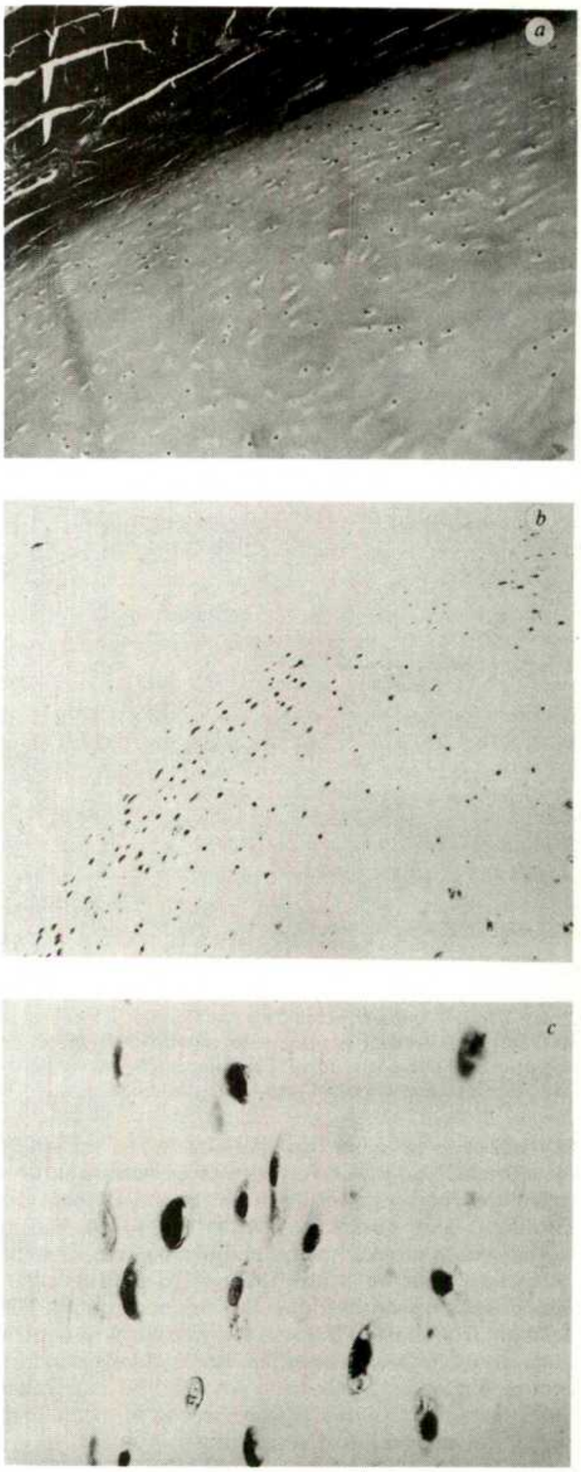

Fig. 1 Serial paraffin sections from the xiphoid process of human adult: *a*, haematoxylin and eosin stain (×90); *b*, immunoperoxidase reaction for S-100 protein, without counterstain (×90). Reaction product is present only within chondrocytes; the extracellular matrix of the cartilage and the surrounding fibrous connective tissue are unstained. *c*, Same section as *b* (×500).

While looking for S-100 in the fetal nervous system we discovered that the protein is present in chondrocytes of the vertebral column and decided to determine its distribution using anti-S-100 antiserum and the peroxidase–antiperoxidase method described elsewhere[22]. Rabbit anti-S-100 antiserum was raised by five or more intradermal injections of bovine

0028–0836/82/010063—02$01.00

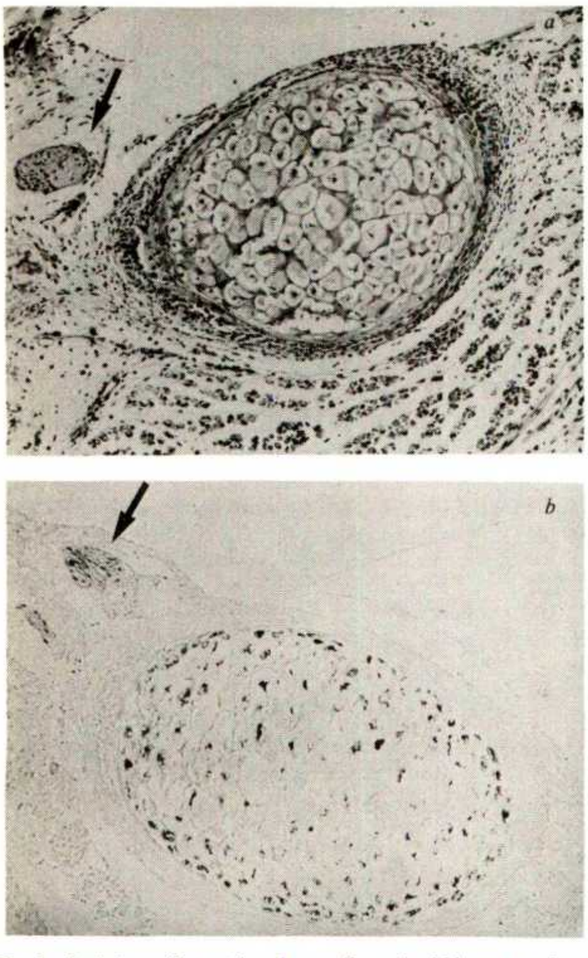

Fig. 2 Serial paraffin sections from a 7-week-old human embryo. *a*, Haematoxylin–eosin stain of a rib and adjacent intercostal nerve (arrow), ×100. *b*, Immunoperoxidase reaction for S-100 protein, ×100. Reaction product is present in chondrocytes of rib and Schwann cells of intercostal nerve. The adjacent fibrous connective tissue and skeletal muscle are unstained.

S-100 (isolated as described previously[7,23]), mixed with complete Freund's adjuvant. As control sera we used anti-S-100 antiserum absorbed with S-100 until it no longer reacted with human brain, and serum from a rabbit which had been immunized with complete Freund's adjuvant alone. The anti-S-100 antiserum and the control sera were used at dilutions containing the same concentration of immunoglobulins. Tissues studied were from human fetuses of various ages and included cranium, larynx, trachea, vertebrae, ribs and lower and upper extremities. Xiphoid processes and laryngeal cartilage of adults were also examined. All tissues were fixed in formalin, embedded in paraffin and cut into 6-μm sections.

Chrondrocytes in all tissues examined were stained with anti-S-100 antiserum. Staining was both cytoplasmic and nuclear; the extracellular matrix was unstained. Control sera did not stain any of the tissues (Figs 1, 2).

Chondrocytes which form the fetal skull as well as the visceral cartilage are said to be of neural crest origin[1] and those found elsewhere are considered to be derived from mesoderm[2,3]. Nevertheless, it is accepted that tissues of neuroectodermal origin can exert a considerable influence on differentiation of mesodermal chondrocytes[3]. Extirpation of the neural tube from chick embryos inhibits formation of axial cartilage, and grafting of spinal cord with or without notochord and neural crest into any region of the somite of tail-bud embryos results in formation of a complete secondary vertebral column[2]. The standard interpretation of these phenomena has been that the spinal cord induces formation of cartilage in the somites[3].

Type II collagen was originally thought to be unique to cartilage but recently it has been demonstrated that neural retina[6] and probably spinal cord[5] of chick embryos also produce type II collagen. In addition, nerve growth factor inhibits chondromucoprotein synthesis by cartilage of pelvic rudiments from chick embryos[4]. Mesodermal chondrocytes are the only cells known to respond to nerve growth factor but not thought to be of neuroectodermal origin.

We have shown that S-100 is present in both mesodermal and neural crest chondrocytes of man. The presence of S-100 in chondrocytes of skull, larynx and trachea is perhaps not unexpected, but the fact that we have found S-100 in chondrocytes of vertebrae, ribs, xiphoid processes and extremities suggests that mesodermal chondrocytes may be developmentally closer to neuroectoderm than was previously believed.

Note added in proof: The S-100 protein has recently also been identified in melanocytes and Langerhans cells of normal human skin by D. Cocchia, F. Michetti and R. Donato (*Nature* **294,** 85–87 (1981)).

Received 20 August; accepted 5 November 1981.

1. LeLivre, C. *J. embryol. exp. Morph.* **31,** 453–477 (1974).
2. Holzer, H. & Detwiler, S. R. *J. exp. Zool.* **123,** 335–369 (1953).
3. Hall, B. K. *Adv. Anat. Embryol. Cell Biol.* **53,** 1–49 (1978).
4. Eisenbarth, G. S., Drezner, M. K. & Lebovitz, H. E. *J. Pharmac. exp. Ther.* **192,** 630–634 (1975).
5. Trelstad, R. L., Kang, A. H., Cohen, A. M. & Hay, E. D. *Science* **179,** 295–297 (1973).
6. Smith, G. N., Leisenmayer, T. F. & Newsome, D. A. *Proc. natn. Acad. Sci. U.S.A.* **73,** 4420–4423 (1976).
7. Moore, B. W. & Perez, V. J. in *Physiological and Biochemical Aspects of Nervous Integration* (ed. Carlson, F. D.) 343–368 (Prentice-Hall, Englewood Cliffs, New Jersey, 1968).
8. Moore, B. W. *Biochem. biophys. Res. Commun.* **19,** 739–744 (1965); *Int. Rev. Neurobiol.* **15,** 215–255 (1972).
9. Dannies, P. S. & Levine, L. *J. biol. Chem.* **246,** 6276–6283 (1971).
10. Donato, R. & Michetti, F. *Experientia* **30,** 511–512 (1974).
11. Miani, N., Michette, F., DeRenzi, G. & Ganiglia, A. *Experientia* **29,** 1499–1501 (1973).
12. Hyden, H., Lange, P. W. & Larson, S. *J. neurol. Sci.* **45,** 303–316 (1980).
13. Miani, N., DeRenzi, G., Michette, F., Sangiacomo, C. O. & Ganiglia, A. *J. Neurochem.* **19,** 1387–1394 (1972).
14. Zuckerman, J. E., Herschmann, H. R. & Levine, L. *J. Neurochem.* **17,** 247–251 (1970).
15. Perez, V. J., Olney, J. W., Cicero, T. J., Moore, B. W. & Bahn, B. A. *J. Neurochem.* **17,** 511–519 (1970).
16. Ludwin, S. K., Kosek, J. C. & Eng, L. F. *J. comp. Neurol.* **165,** 197–208 (1976).
17. Matus, A. & Mughals, S. *Nature* **258,** 746–748 (1975).
18. Sviridou, S. M., Korochkin, L. I., Ivanov, V. N., Maletskaya, E. I. & Bakhtina, T. K. *J. Neurochem.* **19,** 713–718 (1972).
19. Hansson, H. A., Persson, L., Rönnbäck, L. & Haglid, K. G. *Cytobios* **15,** 45–48 (1976).
20. Hyden, H. & McEwen, B. S. *Proc. natn. Acad. Sci. U.S.A.* **55,** 354–358 (1966).
21. Stefansson, K., Wollman, R. L. & Moore, B. W. *Brain Res.* (in the press).
22. Stefansson, K. & Wollmann, R. L. *Acta neuropath.* **52,** 135–140 (1980).
23. Levine, L. & Moore, B. W. *Neurosci. Res. Prog. Bull.* **3,** 18–22 (1965).

A very small porcine virus with circular single-stranded DNA

I. Tischer, H. Gelderblom, W. Vettermann & M. A. Koch

Robert Koch-Institute of the Federal Health Office, Nordufer 20,
1000 Berlin 65, FRG

It was reported previously that cultures of the porcine PK-15 cell line (ATCC-CCL31) were chronically infected with a small virus, supposedly containing RNA[1]. No gross cytopathic effect was seen in these cultures. During the search for an *in vitro* model of persistent virus infections the agent was studied in more detail. These studies showed the virus to have a diameter of 17 nm, and to contain a covalently closed circular single-stranded DNA with a molecular weight of 0.58×10^6 and a main capsid polypeptide with a molecular weight of 36,000. Of the animals tested, only pigs were found to have antibodies. On the basis of these properties the virus appears to be a member of a family of animal viruses so far not encountered. We have named the virus porcine circovirus (PCV).

The virus was obtained from PK-15 cells. It can be propagated in selected PK-15 clones which are free of porcine parvovirus, porcine papovavirus, mycoplasmas and of PCV. Virus was concentrated by ultracentrifugation of Freon-treated cells and supernatants and then purified by two cycles of CsCl-gradient centrifugation. Sucrose gradient centrifugation yielded a sedimentation coefficient for the virion of 52S. On isopycnic centrifugation in CsCl virus particles banded exclusively at a density of 1.37 g cm^{-3}. Electron micrographs (Fig. 1) confirmed that the

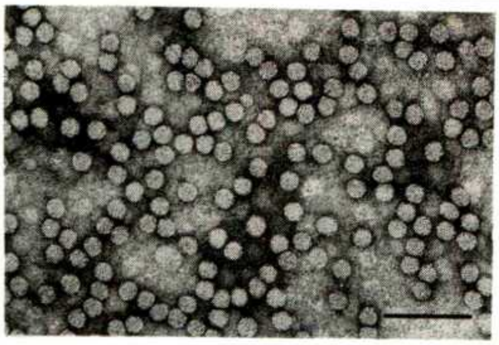

Fig. 1 Electron micrograph of purified PCV particles negatively stained with 1% aqueous uranyl acetate. Scale bar, 100 nm.

virus is an isometric particle with a diameter of 17 ± 1.3 nm. No stain-filled particles were observed.

Purified ^{3}H-leucine-labelled virus was disrupted at 100 °C for 1 min with SDS (1%) and mercaptoethanol and the protein moiety was analysed by polyacrylamide gel electrophoresis[2]. Only a single band containing radioactivity was found. Its position corresponded to that of a polypeptide of molecular weight 36,000 ± 2,300, using bovine serum albumin, ovalbumin and chymotrypsinogen as references.

For isolation and characterization of the nucleic acid, [*Me*-^{3}H]thymidine-labelled virus was lysed with SDS (0.5%) and sodium *N*-lauroyl sarcosinate (1%) for 15 min at room temperature, followed by a digestion with proteinase K (500 μg ml^{-1}) for 4 h at 37 °C. Nucleic acid was purified by centrifugation in a neutral sucrose gradient (5–20% wt/wt; rotor SW 40; 33,000 r.p.m.: 7.5 h; 20 °C), and by precipitation with two parts of ice cold ethanol containing 0.4 M lithium chloride. The pellet was washed with 75% ethanol and then resuspended in 0.1 × SSC. The incorporation of ^{3}H via [*Me*-^{3}H]thymidine, the buoyant densities and the alkali stability demonstrated that the nucleic acid of PCV is DNA. The buoyant densities were found to be 1.718 g cm^{-3} in CsCl using adeno 2 ^{14}C-DNA (1.715 g cm^{-3}) and DNA from *Micrococcus lysodeikticus* (1.731 g cm^{-3}) as markers, and in Cs_2SO_4 to be 1.45 g cm^{-3}. Purified tritium-labelled PCV DNA was kept in 0.3 M NaOH for 20 h at room temperature[3]. The radioactivity in trichloroacetic acid precipitates of treated and untreated nucleic acids was then assayed. While an untreated control yielded of the order of 5,500 c.p.m. the treated sample contained 5,750 c.p.m. The efficacy of this treatment on RNA was tested using 16S and 23S ribosomal RNA.

In transfection experiments[4] native PCV DNA purified as above was shown to be infective (~0.04 μg PCV DNA per 1.5 × 10^6 cells). This infectivity was abolished completely by DNase 1—that is, using DNase-treated PCV DNA for transfection, cells producing virus, as revealed by staining with fluorescein-labelled specific antibodies, were not detectable even after two passages of the cells. In control experiments with untreated PCV DNA, more than 1,000 specifically stained cells per 1.5-cm diameter coverslips with about 2.5 × 10^5 cells were seen.

The sedimentation behaviour of native PCV DNA and of heat- or alkali-treated PCV DNA in neutral sucrose gradients as well as in alkaline gradients (Fig. 2) revealed that the DNA is single stranded[5]. The degradation of PCV DNA by the single-strand-specific nuclease S_1 confirmed this conclusion (Fig. 3). The sedimentation coefficient of PCV DNA determined in 1 M NaCl at *p*H 7.2 was 12.7S, and about 9S at *p*H 12.7. In 1.5% agarose gels the PCV DNA migrated about 2.3 times further than ΦX174 virion DNA.

When PCV DNA was examined by electron microscopy more than 85% of the molecules seen were circular (Fig. 4). To determine the size of the circular DNA, contour length measurements were performed using ΦX174-am-3 virion DNA[6] as an internal marker. From the data for ΦX174

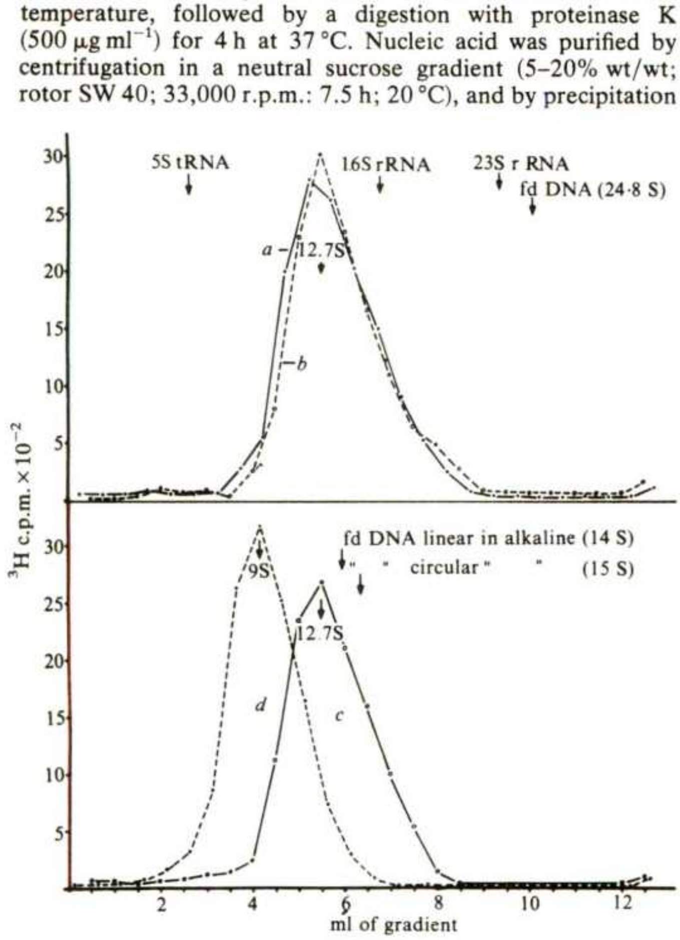

Fig. 2 Sedimentation profiles of [*Me*-^{3}H]thymidine-labelled native, heated and alkali treated PCV DNA in sucrose gradients (5–20% wt/wt). *a*, Native DNA; *b*, heated DNA (10 min; 100 °C) *c*, alkali treated (0.1 M NaOH; 5 min; 22 °C) and subsequently neutralized (with 0.1 M HCl) DNA in neutral gradients (1 M NaCl; 0.01 M Tris; 0.001 M EDTA; *p*H 7.2); *d*, alkali-treated DNA in an alkaline gradient (0.9 M NaCl; 0.1 M NaOH; 0.001 M EDTA; *p*H 12.7). Beckman rotor SW 40; 33,000 r.p.m.; 7.5 h; 20 °C. The sedimentation coefficients of PCV DNA were determined on the basis of the sedimentation of the markers (RNA) in the neutral gradient. For comparison virion fd-DNA was included.

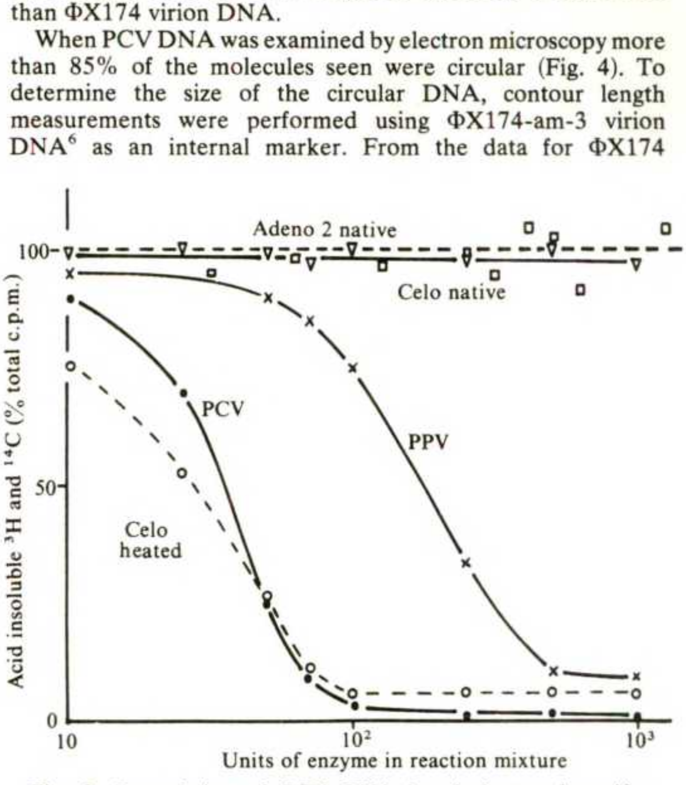

Fig. 3 Degradation of PCV DNA by single-strand-specific nuclease S_1. PCV DNA was treated with nuclease S_1 (buffer: 0.1 M Na-acetate; 0.1 mM $ZnSO_4$; *p*H 4.5) in parallel with the double-stranded ^{14}C-adeno 2-DNA and ^{3}H-Celo-DNA as well as with the single-stranded ^{3}H-DNA from porcine parvovirus (PPV) and denatured (95 °C, 10 min) ^{3}H-Celo DNA. DNA was incubated with nuclease S_1 for 30 min at 37 °C and DNA was precipitated with trichloroacetic acid at a final concentration of 5% in the presence of 100 μg carrier RNA. Degradation is expressed as the relative loss of acid-precipitable radioactivity by increasing amounts of enzyme.

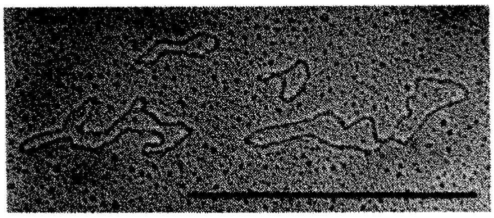

Fig. 4 Electron micrograph of PCV DNA (top) and ΦX174 virion DNA (bottom). A mixture of both species was spread from a hyperphase (carbonate buffer *p*H 10, 0.01% cytochrome *c*, 40% formamide) at room temperature. The specimen was rotary shadowed with Pt/Pd. Scale bar, 1 μm.

($n = 198$, 1.94 ± 0.12 μm) and for PCV ($n = 212$, 0.633 ± 0.05 μm) a genome size of 1.76 kilobases, corresponding to a molecular weight of 0.58×10^6, was calculated for PCV.

The sedimentation behaviour described above (Fig. 2) shows that the configuration of the molecule is unaffected by denaturing conditions, that is, after renaturation molecules of multiple unit length were never detected. This indicates that PCV DNA is a covalently closed circular molecule rather than a closed circle due to self-complementing cohesive ends. This interpretation is supported by the fact that no linearization of PCV DNA was detected when DNA was spread under heat denaturation. As internal controls *Hin*dII, *Hin*dIII restriction fragments of fd-DNA carrying the transposon Tn*5* (ref. 7) were included. These restriction fragments consist of DNA molecules which are circular due to self-complementary ends of 190 and 340 bases respectively which readily opened in the conditions used.

Purified virus was used to raise specific antibodies in rabbits. Such antibodies aggregated PCV, neutralized infectivity and, using indirect immunofluorescence, detected virus producing cells. It was found that in chronically infected cultures only a small, but varying proportion of cells expressed virus antigens. PCV antisera did not inhibit agglutination of human red blood cells by porcine parvovirus. Attempts to demonstrate agglutination by PCV or RBC from man, rhesus monkey, pig, rabbit, guinea pig, mouse and chicken were unsuccessful.

Most probably the agent has its origin in pigs. A serological survey showed that 20 out of 22 randomly collected pig sera contained specific antibodies. Sera from rabbits, mice, calves and man, including sera from laboratory staff working with the agent, were negative. The physicochemical properties of this agent set it apart from all known animal viruses[8]. Similarities exist only with several plant pathogens comprising the group of geminiviruses[9,10].

We thank Renate Rasch, Doris Peters, S. Pociuli, H. Reupke and D. Elsen for technical assistance. Helpful suggestions were made by Professor H. Ludwig, Professor H. Köhler, and Drs Giovanna Morelli, G. Pauli, E. Werner and especially by Professor H. Schaller who also donated the fd derivative fd Km-30 and its restriction fragments.

Received 11 September; accepted 12 November 1981.

1. Tischer, I., Rasch, R. & Tochtermann, G. *Zbl. Bakt. Hyg., I. Abt. Orig.* A**226**, 153–167 (1974).
2. Laemmli, U.K. *Nature* **227**, 680–685 (1970).
3. Munro, H. N. *Meth. biochem. Anal.* **14**, 113–176 (1966).
4. Graham, F. L. & Van der Eb, A. J. *Virology* **52**, 456–467 (1973).
5. Studier, F. W. *J. molec. Biol.* **11**, 373–390 (1965).
6. Sanger, F. *et al. Nature* **265**, 687–696 (1977).
7. Herrmann, R., Neugebauer, K., Zentgraf, H. & Schaller, H. *Molec. gen. Genet.* **159**, 171–178 (1978).
8. *Classification and Nomenclature of Viruses: 3rd Rep. int. Committee on Taxonomy of Viruses* (ed. Matthews, R. E. F.) (Karger, Basle, 1979).
9. Goodman, R. M. *Virology* **83**, 171–179 (1977).
10. Harrison, B. D., Barker, H., Bock, K. R., Guthrie, E. J. & Meredith, G. *Nature* **270**, 760–762 (1977).

A monoclonal antibody against human T suppressor lymphocytes binds specifically to the surface of cultured oligodendrocytes

Joel Oger

INSERM U-49, 35043 Rennes, France

Sara Szuchet, Jack Antel & Barry G. W. Arnason

Department of Neurology and the Brain Research Institute,
University of Chicago, Chicago, Illinois 60637, USA

The cardinal pathological feature of multiple sclerosis (MS) is the presence within brain and spinal cord of regions called plaques, from which myelin has been lost[1]. It has been proposed that autoimmunity may be involved in MS and that oligodendrocytes, the cells responsible for the formation and maintenance of central nervous system myelin, may provide a target for immune attack in this disease. The fact that oligodendrocytes are reduced in number in MS plaques[2] is consistent with this hypothesis. MS is characterized by attacks and remissions. During attacks, a subset of T lymphocytes, known as T suppressor cells, is depleted from the circulation[3–5]. The reason for this depletion is unknown, but the suppressor cells could be destroyed, sequestered, for example in brain, or modulated so that they are no longer detectable by the assays which enumerate them or which measure their functional capacities. Were suppressor cells and oligodendrocytes to share a determinant relevant to MS, both cell types could be targets for immune-mediated killing by the same autoimmune response. Recently, monoclonal antibodies which recognize human monocytes, T lymphocytes and T-cell subsets have become available. We have tested cultured ovine oligodendrocytes with a battery of monoclonal antibodies directed against human lymphocyte and monocyte antigens, seeking evidence for shared determinants, and present here data suggesting that shared determinants exist.

All antibody clones were produced by hybridization of spleen cells from mice sensitized to human T lymphocytes with P3 mouse myeloma. Antibodies were generated by intraperitoneal passage of cloned hybrid cells in mice[6]. Oligodendrocytes were isolated from the white matter of 4–6-month-old lambs as described previously[7,8]. Trypsin was used in the isolation procedure. Cells were plated on glass chamber slides and maintained in culture for up to 40 days (for details see Fig. 1 legend); medium was changed twice weekly. Cultured cells were identified as oligodendrocytes by ultrastructural, biochemical and immunological criteria[9]. Cultured oligodendrocytes were washed free of medium and pre-reacted with normal sheep serum (NSS) as a source of excess sheep IgG. All monoclonal antibodies were screened at a concentration of 5 μg IgG per ml, the cultures were washed, and binding of the monoclonal antibodies was assessed by adding goat anti-mouse IgG labelled with fluorescein isothiocyanate (FITC).

As shown in Fig. 1, cultured oligodendrocytes pretreated with 1:500 NSS, exposed to OKT8 and then to 1:10 goat anti-mouse IgG–FITC, gave distinct membrane-bound fluorescence with scattered irregular dots outlining the cell cytoplasm and processes. This pattern of fluorescence resembles that seen when human suppressor lymphocytes are reacted with OKT8. A similar fluorescence pattern was obtained with OKT3 and OKM1. In contrast, OKT4, OKT5, OKT6, OKT10 or OKI1 showed no fluorescence. Control cultures incubated with goat anti-mouse IgG–FITC alone were negative, as was ascitic fluid (produced by injecting P3 mouse myeloma cells into mice), even at 2 mg ml^{-1} IgG. In dilution experiments, using the same 1:10 dilution of goat anti-mouse FITC, OKT3 became negative at concentrations below 2.5 μg ml^{-1} IgG, but OKT8 and OKM1 remained positive at 1.25 μg ml^{-1} IgG. Table 1 gives the IgG subclasses of the monoclonal antibodies used, their specificities for human cell types, and summarizes the data on membrane-bound fluorescence.

As immunoglobulins can bind nonspecifically to Fc receptors on cells or specifically through their Fab portion, it was possible that monoclonal antibody binding was occurring through the Fc

0028-0836/82/010066—03$01.00

Table 1 Binding of monoclonal antibodies to ovine oligodendrocytes

Monoclonal antibody	IgG class	Human specificity	Ovine oligodendrocyte binding at 5 μg ml^{-1} in the presence of 1:500 NSS	1:10 NSS
OKT3*	IgG2a	T/effector	+	—
OKT4†	IgG2b	T/helper	—	—
OKT5‡	IgG1	T/suppressor	—	ND
OKT6†	IgG1	Thymocytes	—	—
OKT8†	IgG2a	T/suppressor	+ + +	+ +
OKM1*‡	IgG2b	Monocytes	+ +	—
OKI1‡	IgG2a	Anti-Ia	—	—
OKT10‡	IgG1	Anti-thymocyte	—	—

ND, not determined.

* Commercially available from Ortho Laboratories at 25 μg ml^{-1} of mouse IgG. † Commercially available from Ortho Laboratories at 50 μg ml^{-1} of mouse IgG. ‡ Ascitic fluid gift of Dr P. C. Kung obtained at 2 mg ml^{-1} of mouse IgG.

region, particularly as oligodendrocytes have been shown to bear Fc receptors[10,11]. Sheep red blood cells (SRBC) coated with mouse anti-SRBC were shown to form rosettes with our oligodendrocyte population. This Fc rosetting was totally inhibited by preincubating oligodendrocytes with a 1:10 dilution of NSS. Human lymphocytes to which the mouse monoclonal antibody OKT8 had been bound specifically also formed rosettes with oligodendrocytes (Fig. 2). This Fc receptor binding was also blocked by preincubating the oligodendrocytes with a 1:10 dilution of NSS (Fig. 2). Direct binding of OKT3, OKT8 and OKM1 to oligodendrocytes was therefore re-evaluated following a preincubation of the oligodendrocytes in 1:10 NSS. OKT3 and OKM1 binding was no longer seen, indicating that their binding might have occurred through Fc. Although Fc receptor binding is known to depend on IgG subclass when IgG and Fc receptors are from the same species[12], we found no correlation between mouse IgG subclass and monoclonal antibody binding to ovine oligodendrocyte Fc receptor. This might be attributable to species differences, to the presence of aggregates in some of the OKT or to variability in the structure of the Fc regions of the monoclonal antibodies.

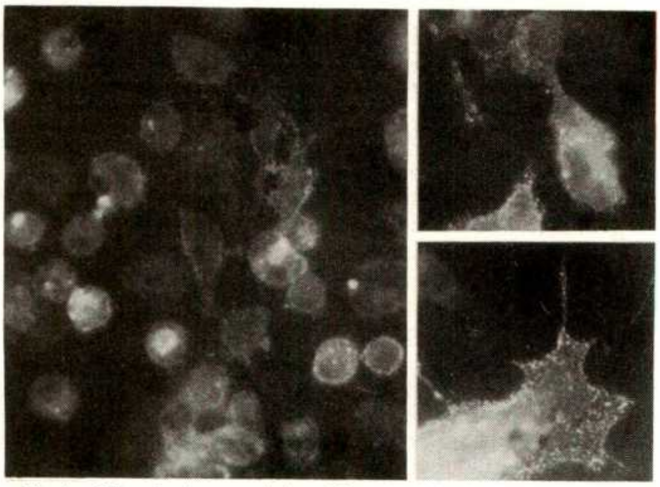

Fig. 1 Oligodendrocytes isolated from lamb brain (as described in ref. 8) were cultured (in multiple-well glass slides) in Dulbecco's modified minimum essential medium (with 20% horse serum added) at 37 °C in humidified air containing 5% CO_2. After 2–3 weeks in culture, the slides were washed three times with Ca^{2+}–Mg^{2+}-free Hanks' balanced salt solution containing 1% bovine serum albumin, *p*H 7.4 (HBSS + 1% BSA). They were incubated for 15 min with a 1:500 dilution of heat-inactivated normal sheep serum in HBSS + 1% BSA. The preincubation solution was then aspirated off and mixed with the monoclonal antibody OKT8 (Ortho) up to a final concentration of 5 μg ml^{-1} of mouse IgG. The mixture was added back to the cells and allowed to react for 30 min at 0 °C. After three washes with HBSS + 1% BSA, a 1:10 dilution of goat anti-mouse IgG–FITC was added for 30 min at 0 °C. The goat anti-mouse IgG–FITC (Cappel) was diluted with one part heat-inactivated normal goat serum and eight parts HBSS + 1% BSA. Slides were then washed four times, fixed with 4% paraformaldehyde in HBSS at 0 °C, mounted and observed under a Leitz Ortholux II UV microscope. Pictures were taken with an Orthomat camera.

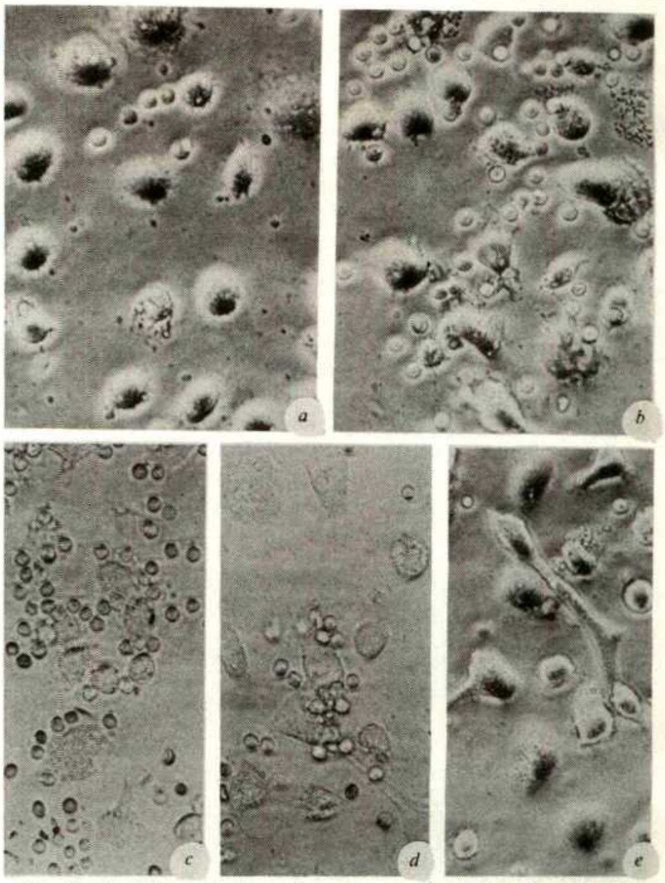

Fig. 2 Blocking effect of sheep serum on Fc binding of the monoclonal antibody OKT8. Human mononuclear cells were separated from peripheral blood by Ficoll–Hypaque flotation[13]. T lymphocytes were then isolated by the nylon wool technique[14]. After washing, T cells were incubated at 4 °C for 30 min with a 5 μg ml^{-1} solution of OKT8 in HBSS + 1% BSA and washed three times in the cold. 20% of the T lymphocytes were shown by immunofluorescence to have bound OKT8. T cells coated with OKT8 were then added to oligodendrocytes in culture. After centrifugation at 200*g* for 5 min, incubation for 30 min and gentle washing, cultures were observed for the presence of T cells bound to oligodendrocytes. In *a*, uncoated lymphocytes have been added and no binding is seen. In *b*, T cells precoated with OKT8 have been added to washed oligodendrocytes; the presence of free Fc receptor is shown by binding of the T cells to the oligodendrocytes. *c*, *d* Demonstrate reduced binding after preincubating oligodendrocytes with 1:500 (*c*) and 1:50 (*d*) NSS. *e* Shows that a 1:10 dilution of NSS in the preincubation step totally blocks binding to Fc receptors.

After preincubation with 1:10 NSS, OKT8 binding was still evident by immunofluorescence (Fig. 3), again in a pattern reminiscent of that seen when human suppressor T cells are reacted with OKT8. Ultracentrifugation of OKT8 at 100,000*g* for 1 h, to remove aggregated IgG, did not affect its binding to oligodendrocytes.

Galactocerebroside is an accepted marker for oligodendrocytes. Double labelling experiments were done using, in a first step, a mixture of OKT8 and rabbit anti-galactocerebroside antiserum and in the second step, goat anti-mouse IgG (FITC labelled) mixed with goat anti-rabbit IgG (rhodamine labelled). Using three-week-old cultures, 75% of cells labelled for galactocerebroside, 86% for the T8 antigen and 68% showed double labelling.

Freshly isolated ovine oligodendrocytes studied in suspension did not exhibit fluorescence with any of the antibodies tested.

Thus, the OKT8 reactive determinant, as well as the Fc binding site, seems to be lost during the isolation procedure and regenerated in culture. Failure of freshly prepared cells to bind could be a consequence of the trypsinization step used during isolation. Indeed, when 0.3 mg ml^{-1} of trypsin was added for 45 min at 37 °C to human mononuclear cells in suspension or to ovine oligodendrocytes which had been maintained in culture, both lost their capacity to bind OKT8, OKT3 and OKM1. Serial experiments performed using OKT8 showed that antibody binding was first evident after 3 days in culture and was invariably present thereafter up to 40 days in culture, the last time point tested. Per cent positive cells varied between cultures but binding was always present in more than 50% of the cells.

We attempted to stain non-trypsinized sheep hepatocytes in suspension and cultured sheep fibroblasts using the same antibodies; neither cell type was positive with any monoclonal antibody. These results indicate that cross-reactivity of the monoclonal antibodies is at least relatively restricted to oligodendrocytes and does not reflect reactivity with globally distributed ovine antigens. Interestingly, sheep splenocytes in suspension did not stain with any of the monoclonal antibodies. It would be of paramount interest to develop methods for maintaining human oligodendrocytes in culture and to test them for reactivity against OKT3, OKM1 and OKT8.

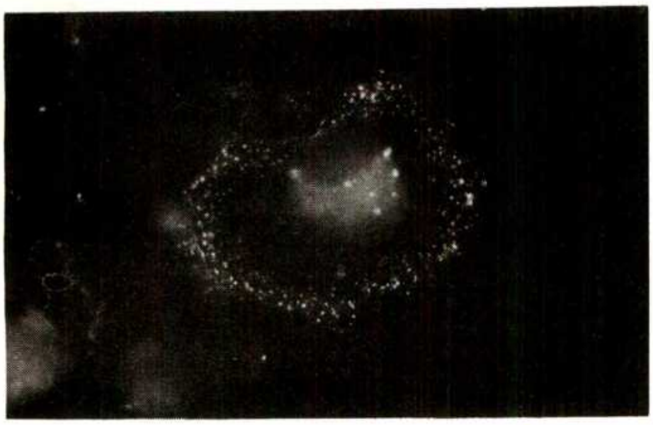

Fig. 3 Immunofluorescence pattern of oligodendrocytes stained with OKT8 in conditions described in Fig. 1 legend, except that a 1 : 10 dilution of normal sheep serum (shown to block Fc receptors) was used in the preincubation step.

If determinants are shared by suppressor lymphocytes and oligodendrocytes, as the present data suggest, this could explain why both suppressor cells and oligodendrocytes disappear in multiple sclerosis. The nature of the putative multiple sclerosis-relevant antigen in brain may even be approachable through study of circulating lymphocytes.

This work was supported by National Multiple Sclerosis Society grants MS:RG 1223-B-3 and MS:RG 1130-C-16. Monoclonal antibodies (in mouse ascites fluid) were purchased from Ortho Laboratories (OKT3, OKT4, OKT6 and OKT8) or were provided by Dr P. C. Kung (OKM1, OKT5, OKT10 and OKI1). Anti-galacto cerebroside antiserum was a gift from Dr R. Lisak.

Received 28 August; accepted 20 October 1981.

1. Charcot, J. M. *Gaz. Hôp. Paris* **41,** 554–566 (1868).
2. McAlpine, D., Compston, N. D. & Lumsden, C. E. (eds) *Multiple Sclerosis* (Livingston, Edinburgh, 1955).
3. Antel, J. P., Arnason, B. G. W. & Medof, M. E. *Ann. Neurol.* **5,** 338–342 (1979).
4. Reinherz, E. L. *et al. New Engl. J. Med.* **303,** 125–129 (1980).
5. Bach, M. A. *et al. Lancet* **ii,** 1221–1222 (1980).
6. Reinherz, E. L., Kung, P. C., Goldstein, G. & Scholossman, S. F. *J. Immun.* **124,** 3, 1301–1307 (1980).
7. Szuchet, S., Arnason, B. G. W. & Polak, P. J. *J. Neurosci. Meth.* **3,** 7–19 (1980).
8. Szuchet, S. & Stefansson, K. *Adv. cell. Neurobiol.* **1,** 313–346 (1980).
9. Szuchet, S., Stefansson, K., Wollmann, R. L., Dawson, G. & Arnason, B. G. W. *Brain Res.* **200,** 151–164 (1980).
10. Goust, J. M., Banik, N., Bethea, A. & Sullivan, L. M. *Trans. Am. Neurol.* A (in the press).
11. Ma, B. I., Joseph, B., Walsh, M., Potuim, P. F. & Tourtellotte, W. W. *Ann. Neurol.* **9,** 371–377 (1981).
12. Diamond, B. & Scharff, M. D. *J. Immun.* **125,** 631–634 (1980).
13. Boyum, A. *Scand. J. clin. Lab. Invest.* **21,** Suppl. 97, 77–89 (1968).
14. Greenwalt, T. S., Gajewski, M. & McKenna, J. L. *Transfusion* **2,** 221–229 (1962).

T-cell mitogens cause early changes in cytoplasmic free Ca^{2+} and membrane potential in lymphocytes

R. Y. Tsien*, T. Pozzan† & T. J. Rink

Physiological Laboratory, University of Cambridge,
Cambridge CB2 3EG, UK
† Istituto di Patologia Generale, Via Loredan 16,
35100 Padova, Italy

One of the best models for studying the control of mammalian cell growth and proliferation is the response of lymphocytes to mitogenic agents[1–4], which stimulate growth, DNA synthesis and division. How mitogens work remains obscure, although it has been hypothesized that they increase cytoplasmic free calcium, $[Ca^{2+}]_i$, as a trigger for the cascade of intracellular processes necessary for proliferation[3–6]. However, lymphocyte $[Ca^{2+}]_i$ has not previously been measurable. A new technique[7] for loading a novel Ca^{2+}-specific indicator[8] into the cytoplasm of intact small cells has now made possible the first direct measurements of $[Ca^{2+}]_i$ in mouse thymocytes and pig node lymphocytes. We show here that lectins known to stimulate T cells raise average $[Ca^{2+}]_i$ approximately twofold within a few minutes. Deprivation of external Ca^{2+} or elevation of cyclic AMP, conditions known to inhibit mitogenesis, prevented the $[Ca^{2+}]_i$ response. Rises in $[Ca^{2+}]_i$ were accompanied by hyperpolarization of the membrane potential, apparently due to a Ca^{2+}-activated K^+ conductance. The co-carcinogen 12-*O*-tetradecanoylphorbol-13-acetate (TPA) seems to stimulate cell functions normally activated by Ca^{2+}.

$[Ca^{2+}]_i$ was measured with a fluorescent indicator (structure 3b of ref. 8, now called 'quin2') which shows a fivefold fluorescence enhancement on binding Ca^{2+}. Quin2 has a 1:1 stoichiometry of Ca^{2+} binding, with an apparent dissociation constant[9] of 115 nM in the presence of 130 mM K^+, 20 mM Na^+, 1 mM free Mg^{2+}, at *p*H 7.05 and 37 °C, conditions chosen to mimic lymphocyte cytoplasm (refs 10, 11 and T.P., T.J.R. and R.Y.T., in preparation). The indicator was trapped inside the cells by incubating them with its membrane-permeant intracellularly hydrolysable acetoxymethyl ester[7]. Available tests suggest that the quin2 is free in the cytoplasm, not significantly contained in organelles such as mitochondria, and neither excluded from nor accumulated in the nucleus, so that its signals can be taken to measure cytoplasmic free calcium[9]. The signals are calibrated by releasing the indicator from the cells with digitonin or Triton X-100 at the end of the experiment and recording the fluorescence at 0% and 100% Ca saturation, that is, <1 nM and 1 mM $[Ca^{2+}]$. From these fluorescence levels, F_{min} and F_{max}, the $[Ca^{2+}]_i$ corresponding to fluorescences F from trapped intracellular dye, are calculated by the equation

$$[Ca^{2+}] = (115\ nM)(F - F_{min})/(F_{max} - F)$$

Parallel measurements of lymphocyte membrane potential (V_m) were made with a potential-sensitive oxonol dye as previously described[12].

Figure 1 shows fluorescence signals from quin2-loaded lymphocytes. The indicated resting $[Ca^{2+}]_i$ had a mean ± s.e. of 123 ± 6 nM ($n = 27$). These levels are consistent with those measured in other cell types[13] and argue against any gross toxicity. Further evidence against toxicity was that (1) loaded cells maintained high (<90%) eosin exclusion; (2) ATP levels[9] remained within 30% of normal with up to 3mM intracellular quin2; (3) capping of surface ligands was unaffected by quin2 (ref. 14); (4) membrane potential responses of quin2-loaded mouse thymocytes were similar to those of normal cells

---

* Present address: Department of Physiology-Anatomy, University of California, Berkeley, California 94720, USA.

0028-0836/82/010068—04$01.00

(compare Figs 2 and 3*b*); and (5) thymocytes and spleen cells loaded with quin2 and then treated with concanavalin A (Con A) at normal optimal doses can undergo mitogenic transformation as assessed by thymidine uptake (T. R. Hesketh, personal communication). All our results pertain to cells washed free from ester hydrolysis products after the loading period; leaving the hydrolysis by-products in the suspension may have long-term deleterious effects.

Although quin2 is a Ca^{2+} chelator, increasing its loading does not affect steady-state $[Ca^{2+}]_i$. Atomic absorption measurement of total Ca shows that during loading, the cells take up sufficient Ca from the medium approximately to half-saturate the trapped quin2 and keep $[Ca^{2+}]_i$ near 120 nM. Loading in Ca^{2+}-free medium does reduce $[Ca^{2+}]_i$ to as low as 16 nM (ref. 9).

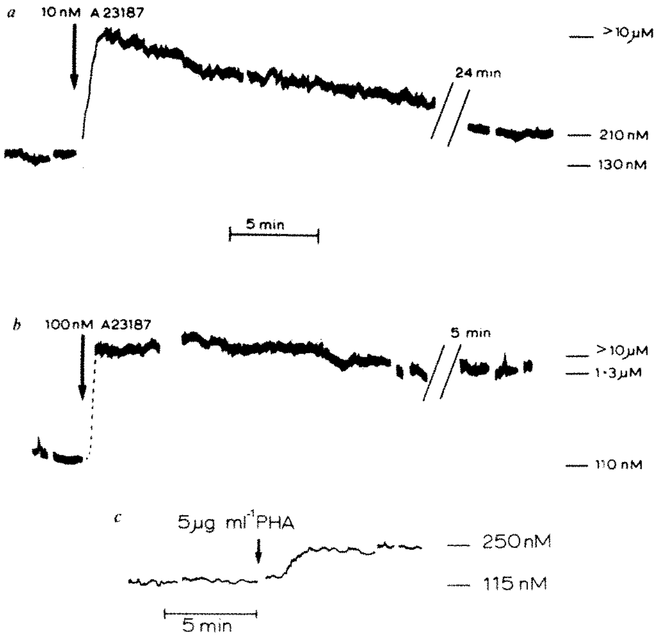

Fig. 1 Resting $[Ca^{2+}]_i$ levels and responses to A23187 and PHA. *a*, *b*, Lymphocytes from the mesenteric nodes of pigs were prepared as previously described[36]. Quin2 acetoxymethyl ester (50 µM) was added to a cell suspension containing about 10^8 cells per ml and incubated for 20 min. The suspension was then diluted 10-fold and incubated for a further 40–60 min. The resulting quin2 loading was typically 2 mmol per litre of cells; higher or lower loadings could be achieved by altering the ester concentration. After loading, the cells were centrifuged at 1,000*g* for 3–4 min and resuspended in fresh RPMI–1640 at $\sim 10^7$ per ml and kept at room temperature. Cells usually lost <5% of their dye per hour. For measurement of fluorescence, 1–2 ml of this stock suspension was centrifuged for a few seconds at 14,000*g* and the cells resuspended in 2 ml of a physiological saline and transferred to the cuvette, the whole resuspension procedure taking about 1 min. Unless otherwise specified, the physiological saline consisted of (mM): NaCl, 145; KCl, 5; Na_2HPO_4, 1; $CaCl_2$, 1; $MgSO_4$, 0.5; glucose, 5; Na HEPES, 10; *p*H 7.40 at 37 °C. This simplified saline was routinely used instead of RPMI–1640 because the latter contains many absorbing and fluorescing substances; however, qualitatively similar $[Ca^{2+}]_i$ signals (see *c*) could be obtained in the full culture medium. Typical measurement conditions, with 2 mM quin2 content in $0.5-1\times10^6$ cells per ml, are equivalent to about 1–2 µmol dye per litre of suspension. Quin2 fluorescences were recorded with Perkin-Elmer MPF-44 spectrofluorimeters in cuvettes thermostatted to 37 °C. Excitation and emission wavelengths were 339 and 492 nm with 4 and 10 nm bandwidths. 10 or 100 nM A23187 added from dimethyl sulphoxide (DMSO) stock solutions as indicated. Final DMSO concentrations were 0.1% (v/v); control experiments showed no effect of DMSO up to 1%. *c*, PHA (Sigma) was added as indicated to mouse thymocytes teased from thymus glands of 5–8-week-old BALB/c mice and loaded with 2 mM quin2 content as in *a*, *b*. This experiment was done in RPMI–1640 medium containing 1 mM free Ca^{2+} and 0.2 mM Ca^{2+}-EGTA. Although PHA is less effective at stimulating thymidine uptake in thymocytes than in mature T cells, it does induce the early metabolic changes characteristic of mitogenesis[37,38]. In this and Figs 2 and 3, fluorescence was calibrated in terms of $[Ca^{2+}]_i$ as described in the text from F_{max} and F_{min} determined after quin2 release by 50 µM digitonin or 0.02% (v/v) Triton X-100. Cells not loaded with quin2 gave no fluorescence responses to ionophores or lectins. Gaps in the trace denote additions to or stirring of the suspension. The synthesis of quin2 is described in ref. 8. Quin2/AM was prepared from quin2 by the general procedure of ref. 7. Some experiments used batches of quin2/AM chromatographically purified and crystallized by Dr G. A. Smith, but with no difference in results from less exhaustively purified material.

Two different mitogenic calcium ionophores, A23187 (ref. 15) and ionomycin[16], each proved very potent in nanomolar concentrations at raising $[Ca^{2+}]_i$. Fig. 1*a* shows that 10 nM A23187, a submitogenic dose, increased $[Ca^{2+}]_i$ to a peak of ≥1 µM, from which it gradually decayed back nearly to resting level during 1 h. The decay may be due to slow disappearance of ionophore from solution[17], and could explain why 10 nM is a submitogenic dose[3]. A second addition of 10 nM A23187 can produce a renewed $[Ca^{2+}]_i$ rise. A single application of 100 nM A23187, the optimal mitogenic concentration[3], is sufficient to keep $[Ca^{2+}]_i$ above 1 µM for at least 40 min (Fig. 1*b*).

T lymphocytes can also be stimulated by the lectins phytohaemagglutinin (PHA) and Con A. At typically mitogenic doses both lectins give similar quin2 responses from thymocytes in 1 mM extracellular Ca^{2+}. A typical PHA response is shown in Fig. 1*c*. After a delay of 30–60 s, the fluorescence rises over 2–3 min by an amount corresponding to a 1.5- to 2.5-fold increase in average $[Ca^{2+}]_i$. Increasing the dye loading has no effect on the final apparent level of $[Ca^{2+}]_i$, which is 200–300 nM, but slows the response slightly. The elevation of $[Ca^{2+}]_i$ is maintained for at least tens of minutes with optimally mitogenic doses of Con A. In nominally Ca^{2+}-free media, Con A gives no increase in $[Ca^{2+}]_i$, which fits with the dependence[3,15,18,19] of lectin mitogenicity on extracellular Ca^{2+}. If Ca^{2+} is then added back to the Con A medium, $[Ca^{2+}]_i$ rises immediately. Agents which raise intracellular cyclic AMP levels are known to prevent or abort mitogenic stimulation[5,20,21]; the $[Ca^{2+}]_i$ response in thymocytes to Con A is antagonized by such agents, for example 100 µM theophylline, 10 mM Ro20/1724 (another phosphodiesterase inhibitor[21]), 0.25 µM dibutyryl cyclic AMP, or preincubation with 1 µg ml^{-1} cholera toxin. By contrast, no effects on $[Ca^{2+}]_i$ of millimolar exogenous cyclic GMP or its dibutyryl or 8-bromo derivatives have yet been detected.

These lectin-induced rises in average $[Ca^{2+}]_i$ may seem small. However, any influence of $[Ca^{2+}]_i$ on cell growth is probably exerted over several hours[3], giving time for a small activation to have a large cumulative effect. Moreover, not all the cells in these unfractionated populations are identically responsive to lectin[3,22–24]. If, say, half the cells remain at resting $[Ca^{2+}]_i$, at which level the quin2 is about 50% saturated with Ca^{2+}, the quin2 in the responsive cells would have to reach 80–90%

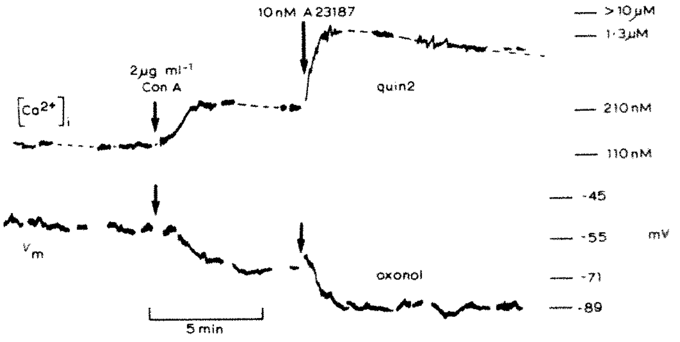

Fig. 2 Effect of Con A (Miles-Yeda, crystallized three times) on $[Ca^{2+}]_i$ and membrane potential, V_m. Mouse thymocytes containing 3 mM quin2 were in the standard physiological saline, to which was added 0.1 µM oxonol. Upper trace shows the quin2 signal, lower trace the oxonol fluorescence (excitation 540 nm, emission 580 nm) from another aliquot of the same batch of quin2-loaded cells. During each recording, the wavelengths were intermittently changed to verify that the other dye was responding normally, hence the large number of gaps in each trace. The V_m calibration was obtained after application of A23187 by adding KCl to raise external K^+ in steps and assuming that the increase in K^+ permselectivity was by then sufficient to bring V_m close to the K^+ equilibrium potential, E_K. The calibration marks relate oxonol fluorescence to E_K for each external K^+ concentration. The value of resting potential, −50 mV, estimated from oxonol fluorescence, is in reasonable agreement with independent assessments using the distribution of triphenylmethylphosphonium cation ($TPMP^+$) in other lymphocyte types[39,40]. However, the lectin-induced hyperpolarizations have not been reported previously. $TPMP^+$ equilibration takes 0.5–1 h and is thus not suitable for following early changes. Cyanine dyes[12] are unsuitable probes because they poison mitochondria, deplete lymphocyte ATP[41] and raise $[Ca^{2+}]_i$ to a point where lectins produce no further increase.

saturation ($[Ca^{2+}]_i = 450$–1,000 nM) to account for the observed average rise to 65–70% saturation. The quin2 response does not come primarily from the $[Ca^{2+}]_i$ of macrophages, since the response was not reduced by depletion of macrophages by adherence to glass, nor was any fluorescence response to Con A observed from macrophages obtained by peritoneal lavage and loaded with quin2.

We have found that lectin-induced $[Ca^{2+}]_i$ rises are sufficient to cause at least one immediate cell response: a negative shift of membrane potential. Figure 2 compares the $[Ca^{2+}]_i$ rise and the hyperpolarization in a single batch of quin2-loaded cells responding to mitogenic doses of Con A. The membrane potential as assessed by oxonol fluorescence changes from its resting level of approximately −50 mV to −70 mV with an initial delay and S-shaped time course similar to the $[Ca^{2+}]_i$ rise. A23187 produces an immediate further increase in $[Ca^{2+}]_i$ and hyperpolarization. The hyperpolarization is likely to be due to a K^+ conductance because it is associated with increased responsiveness of V_m to external $[K^+]$; also, of the main intracellular ions, only K^+ has an equilibrium potential[10,11,25] more negative than the resting potential. The hyperpolarization is also blocked by 0.5 mM quinine, an agent known to block Ca^{2+}-activated K^+ conductances[17]. Stimulation of electrogenic Na^+/K^+ pumping is probably not responsible because the hyperpolarization persists in the presence of 1 mM ouabain with only 1 mM external K^+. The hyperpolarization is a consequence of the $[Ca^{2+}]_i$ rise, not vice versa, as in Ca^{2+}-free solution Con A induces neither a rise in $[Ca^{2+}]_i$ nor hyperpolarization, but when external Ca^{2+} is restored, the $[Ca^{2+}]_i$ rise and V_m hyperpolarization develop in parallel. Conversely, imposed hyperpolarization or depolarization[26] do not affect the Con A-induced $[Ca^{2+}]_i$ rise. The similarity of the V_m responses between cells with and without quin2 (Figs 2 and 3*b*) argues that the indicator does not greatly perturb the $[Ca^{2+}]_i$ response to Con A.

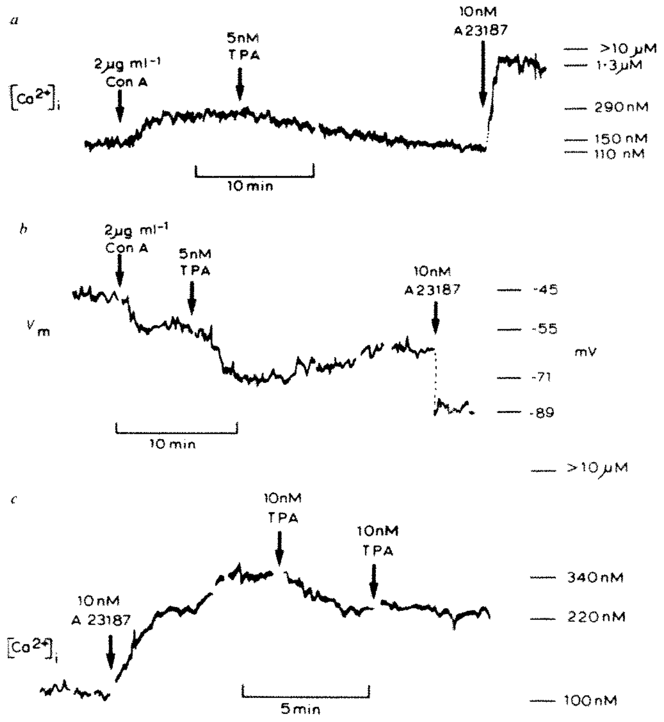

Fig. 3 Effects of TPA (Sigma). *a*, Mouse thymocytes containing 2 mM quin2. After elevation of $[Ca^{2+}]_i$ by Con A, $[Ca^{2+}]_i$ is reduced by 5 nM TPA to below the resting level. Finally 10 nM A23187 raises $[Ca^{2+}]_i$ to above 1 μM. *b*, Mouse thymocytes from the same preparation as *a* but not loaded with quin2. Signal from 0.1 μM oxonol. After a Con A hyperpolarization, 5 nM TPA causes a further, incompletely maintained hyperpolarization. V_m was calibrated as for Fig. 2. *c*, Pig lymphocytes loaded with 2.5 mM quin2. 10 nM TPA partially reversed the rise in $[Ca^{2+}]_i$ caused by A23187. A second addition of 10 nM TPA had no further effect. The smallness of the initial response to 10 nM A23187 may have been due to reduced potency of the particular stock solution used.

A counterexample to the correlations between known mitogenic potency and the ability to raise $[Ca^{2+}]_i$ was found in TPA, a weak mitogen by itself and a potent synergist with ionophores and lectins[16,27–30]. Ten nanomolar TPA gradually lowers resting $[Ca^{2+}]_i$, suppresses Con A-induced rises in $[Ca^{2+}]_i$ (Fig. 3*a*) and can even partly antagonize an ionophore response (Fig. 3*c*). These effects may be due to stimulated Ca^{2+} pumping. Yet TPA hyperpolarizes the cells by itself and enhances a Con A-induced hyperpolarization (Fig. 3*b*). The transience of the TPA hyperpolarization in Fig. 3*b* can be explained by the eventual fall in $[Ca^{2+}]_i$ counteracting the initial direct stimulation or increase in Ca^{2+} sensitivity of the K^+ conductance. All these actions of TPA are detectable in tens of seconds or minutes and are near-maximal at 10 nM, a concentration comparable with the reported dissociation constants for lymphocyte TPA-binding sites[31]. We suggest that TPA fairly directly stimulates a variety of normally $[Ca^{2+}]_i$-dependent processes, such as the Ca pump, K^+ conductance and events leading to mitogenesis. Analogous stimulations might explain many actions of TPA on other cell types[32–34], including the aggregation of platelets while lowering $[Ca^{2+}]_i$ (S. W. Smith, T.J.R. & R.Y.T., unpublished data). Interestingly, the high-affinity binding of phorbol diesters to cellular receptors is enhanced by $[Ca^{2+}]$ in the submicromolar range[35], suggesting that TPA binding may reciprocally increase the Ca^{2+} affinities of those receptors.

These results support the view that $[Ca^{2+}]_i$ is a primary messenger in lymphocyte mitogenesis, although we cannot say whether it is the only initial messenger without further studies such as analysis of lymphocyte heterogeneity and correlation of long-term $[Ca^{2+}]_i$ with mitogenesis. The surprising ability of the co-mitogen TPA to lower $[Ca^{2+}]_i$ can be rationalized by its stimulation of normally Ca^{2+}-dependent processes. Changes in $[Ca^{2+}]_i$ sensitivity of cellular processes, as well as modest sustained rises in $[Ca^{2+}]_i$, may be of more general significance in the control of normal and malignant cell proliferation.

This work was supported by SRC and CNR grants. T.P. held an EMBO Long-term Fellowship. We thank Dr G. A. Smith for samples of specially purified quin2 acetoxymethyl ester ('quin2/AM'), and Dr T. R. Hesketh for permission to cite unpublished results.

Received 15 July; accepted 24 November 1981.

1. Oppenheim, J. J. & Rosenstreich, D. L. *Prog. Allergy* **20**, 65–194 (1976).
2. Wedner, H. J. & Parker, C. W. *Prog. Allergy* **20**, 195–300 (1976).
3. Metcalfe, J. C., Pozzan, T., Smith, G. A. & Hesketh, T. R. *Biochem. Soc. Symp.* **45**, 1–26 (1980).
4. Hume, D. A. & Weidemann, M. J. *Mitogenic Lymphocyte Transformation* (Elsevier, Amsterdam, 1980).
5. Coffey, R. G., Hadden, E. M. & Hadden, J. W. *J. Immun.* **119**, 1387–1394 (1977).
6. Whitfield, J. F. *et al. Ann. N.Y. Acad. Sci.* **339**, 216–240 (1980).
7. Tsien, R. Y. *Nature* **290**, 527–528 (1981).
8. Tsien, R. Y. *Biochemistry* **19**, 2396–2404 (1980).
9. Pozzan, T., Rink, T. J. & Tsien, R. Y. *J. Physiol., Lond.* **318**, 12P–13P (1981); *J. Cell Biol.* (submitted).
10. Lichtman, M. A., Jackson, A. H. & Peck, W. A. *J. cell. Physiol.* **80**, 383–396 (1972).
11. Pozzan, T., Rink, T. J. & Tsien, R. Y. *J. Physiol., Lond.* **319**, 102P (1981).
12. Rink, T. J., Montecucco, C., Hesketh, T. R. & Tsien, R. Y. *Biochim. biophys. Acta* **595**, 15–30 (1980).
13. Alvarez-Leefmans, F. J., Rink, T. J. & Tsien, R. Y. *J. Physiol., Lond.* **315**, 531–548 (1981).
14. Pozzan, T., Arslan, P., Tsien, R. Y. & Rink, T. J. *J. Cell Biol.* (submitted).
15. Maino, V. C., Green, N. M. & Crumpton, M. J. *Nature* **251**, 324–327 (1974).
16. Lyall, R. M., DuBois, J. H. & Crumpton, M. J. *Biochem. Soc. Trans.* **8**, 720–721 (1980).
17. Lew, V. L. & Ferreira, H. G. *Curr. Topics Membranes Transport* **10**, 217–277 1978).
18. Freedman, M. H. in *Cell Biology and Immunology of Leukocyte Function* (ed. Quastel, M.R.) (Academic, New York, 1979).
19. Bard, E., Colwill, R., L'Anglais, R. & Kaplan, J. G. *Can. J. Biochem.* **56**, 900–904 (1978).
20. Watson, J. *J. Immun.* **117**, 1656–1663 (1976).
21. DeRubertis, F. R. & Zenser, T. *Biochim. biophys. Acta* **428**, 91–103 (1976).
22. Whitesell, R. R., Hoffman, L. H. & Regen, D. M. *J. biol. Chem.* **252**, 3533–3537 (1977).
23. Gerhart, S., Mills, G., Monticone, V. & Paetkau, V. *J. Immun.* **117**, 1314–1319 (1976).
24. Wagner, H. *et al. Immun. Rev.* **51**, 215–255 (1980).
25. Iversen, J. G. *J. cell. Physiol.* **89**, 267–276 (1976).
26. Montecucco, C., Rink, T. J., Pozzan, T. & Metcalfe, J. C. *Biochim. biophys. Acta* **595**, 65–70 (1980).
27. Whitfield, J. F., MacManus, J.P. & Gillan, D.J. *J. cell. Physiol.* **82**, 151–156 (1973).
28. Mastro, A. M. & Mueller, G. C. *Expl Cell Res.* **88**, 40–46 (1974).
29. Wang, J. L., McClain, D. A. & Edelman, G. M. *Proc. natn. Acad. Sci. U.S.A.* **72**, 1917–1921 (1975).
30. Rosenstreich, D. L. & Mizel, S. B. *J. Immun.* **123**, 1749–1754 (1979).
31. Estensen, R. D., DeHoogh, D. K. & Cole, C. F. *Cancer Res.* **40**, 1119–1124 (1980).
32. Schleimer, R. P., Gillespie, E. & Lichtenstein, L. M. *J. Immun.* **126**, 570–574 (1981).
33. Estensen, R. D. *et al.* in *Control of Proliferation in Animal Cells* (eds Clarkson, B. & Baserga, R.) (Cold Spring Harbor Press, New York, 1974).
34. Malaisse, W. J. *et al. Cancer Res.* **40**, 3827–3831 (1980).
35. Dunphy, W. G., Kochenburger, R. J., Castagna, M. & Blumberg, P. M. *Cancer Res.* **41**, 2640–2647 (1981).

36. Hesketh, T. R., Smith, G. A., Houslay, M. D., Warren, G. B. & Metcalfe, J. C. *Nature* **267,** 490–494 (1977).
37. Resch, K., Ferber, E., Prester, M. & Gelfand, E. W. *Eur. J. Immun.* **6,** 168–173 (1976).
38. Gron ik, K.-O. & Andersson, J. *Immun. Rev.* **51,** 35–59 (1980).
39. Kiefer, H., Blume, A. J. & Kaback, H. R. *Proc. natn. Acad. Sci. U.S.A.* **77,** 2200–2204 (1980).
40. Deutsch, C. J., Holian, A., Holian, S. K., Daniele, R. P. & Wilson, D. F. *J. cell. Physiol.* **99,** 79–94 (1979).
41. Montecucco, C., Pozzan, T. & Rink, T. J. *Biochim. biophys. Acta* **552,** 552–557 (1979).

Lower fidelity of RecA protein catalysed homologous pairing with a superhelical substrate

Chanchal DasGupta & Charles M. Radding

Departments of Human Genetics and Molecular Biophysics and
Biochemistry, Yale University School of Medicine, New Haven,
Connecticut 06510, USA

The heteroduplex joint, a splice containing paired strands from each of two DNA molecules is a key feature of homologous genetic recombination[1,2]. The formation of such a lap joint ensures that heterologous chromosomes do not recombine; presumably the degree of homology determines the frequency of crossing over between related but non-identical chromosomes. On the other hand, according to the current ideas on recombination, the formation of heteroduplex joints is not a stringent process. Genetic evidence supports the view that the classical phenomena of meiotic gene conversion and aberrant meiotic segregation result in part from the inclusion of mismatched base pairs in heteroduplex joints, and the subsequent correction of some of these mismatched pairs before replication[3–5]. Thus meiotic gene conversion signals one kind of departure from perfectly faithful pairing. The association of increased mutation frequencies with crossing-over is another kind of departure from fidelity in recombination[6–8]. Little is known about the effect of imperfect homology either on the initial pairing of DNA molecules, or on the formation and extension of heteroduplex joints. The nucleotide sequences of phages ΦX174 and G4 are related, but differ by 33% of bases in the coding regions. Here we show using combinations of ΦX174 and G4 DNA, that *Escherichia coli* RecA protein catalyses the formation of joint molecules with many mismatched base pairs, but only if one of the molecules is superhelical. By contrast, in the absence of RecA protein, superhelicity does not cause ΦX174 and G4 DNA to form D-loops spontaneously at any temperature between 37 and 75 °C. These observations focus attention on the role of RecA protein in unwinding DNA, and on superhelicity as a factor that can lessen the fidelity of homologous pairing.

Recent studies of RecA protein, which is essential for genetic recombination of *E. coli*[9,10] have shown that this single purified protein can promote two central steps of genetic recombination *in vitro*, namely synapsis, the pairing of homologous molecules, and strand exchange, which produces long heteroduplex joints[11–13]. Synapsis is experimentally separable from the formation of heteroduplex joints: RecA protein can pair a single strand with homologous duplex DNA in the absence of a free end in any of the strands[11]; and *E. coli* topoisomerase I, acting on these intermediates can interwind a single strand with its complement in duplex DNA[12]. When a free end exists, for example in the combination of linear duplex DNA and circular single-stranded DNA, RecA protein causes the formation of long heteroduplex joints[11] by driving strand exchange in one direction[14–16]. RecA protein can also cause the uptake of a linear single strand by superhelical or non-superhelical DNA to form a particular kind of heteroduplex joint called a D-loop[17,18].

In vivo, both synapsis and heteroduplex formation presumably contribute to the fidelity of homologous pairing. In experiments on the reactions promoted *in vitro* by RecA protein, we have observed effects of imperfect homology on both synapsis and strand exchange[12,15]. RecA protein makes joint

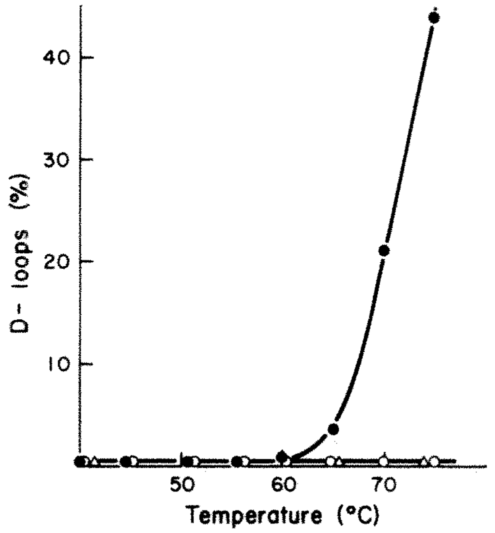

Fig. 1 Spontaneous formation of D-loops plotted against temperature. Superhelical DNA, and fragments of single-stranded DNA, each at 80 μM, were heated for 40 min at the temperature indicated in 20 μl reaction mixtures containing 10 mM Tris (*p*H 7.5), 1 mM EDTA and 200 mM NaCl. D-loops were assayed according to Beattie *et al.*[25]. The superhelical DNA in all reaction mixtures was from ΦX174. ●, ΦX174 single-stranded fragments; ○, G4 single-stranded fragments; △, no single-stranded DNA.

Table 1 Superhelicity promotes the pairing of ΦX174 and G4 DNA by RecA protein

Double-stranded DNA	Single-stranded DNA		Joint molecules (%)
(*a*) Linear	Fragments	Circular	
G4	G4		42
		G4	32
	ΦX		0.1
		ΦX	0.4
ΦX	ΦX		36
		ΦX	12
	G4		0
		G4	0.2
(*b*) Superhelical	Fragments	Circular	
G4	G4		69
		G4	26
	ΦX		**21**
		ΦX	0
ΦX	ΦX		70
		ΦX	31
	G4		**17**
		G4	0
(*c*) Nicked circular	Fragments		
G4	G4		43
	ΦX		6
ΦX	ΦX		38
	G4		6

Duplex DNA, 4.2 μM, and single-stranded DNA, 6.0 μM, were incubated for 30 min at 37 °C in 20 μl reaction mixtures containing 31 mM Tris (*p*H 7.5), 100 μg ml bovine serum albumin, 25 mM $MgCl_2$, 1.2 mM ATP and 3.0 μM RecA protein. When the duplex DNA was superhelical, the reaction was stopped by adding 130 μl of 25 mM EDTA (*p*H 8.5) and 0.5% Sarkosyl. Aliquots of 40 μl were diluted in 2 ml of 1.5 M NaCl/0.15 M Na citrate, held at 41 °C for 4 min, diluted in cold NaCl/Na citrate, and filtered through nitrocellulose[11]. When the duplex DNA was nicked circular or linear DNA, we stopped the reaction by adding 100 μl of 25 mM EDTA (*p*H 8.5) and diluted it in cold 1.5 M NaCl/0.15 M Na citrate before filtration.

0028–0836/82/010071—03$01.00

Table 2 Sequences of the 5′ ends of the viral strand ΦX174 and G4 DNA each beginning at a different *Pst*I site

G4 DNA												
	6			6/12					29			
G	GAA	TT**G**	CT**G**	**T**TG	CT**A**	**AC**T	TAC	GAA	TTA	AAT	CGA	AGT
				9/10								
GGA	CTG	CTG	GTG	GAA	AAT	GAG	**G**AA	ATT	C**A**A	**T**CT	**CAA**	
ΦX 174 DNA												
		15							15/23			
G	AGT	TTT	ATC	GCT	TC**C**	ATG	AC**G**	**CA**G	AA**G**	TTA	ACA	**C**TT
		16										
TCG	GAT	ATT	TCT	GAT	GA**G**	**TCG**	AAA	AA**T**	TAT	CTT	CAT	

Sequences are taken from Godson[21,22]. For G4 DNA, the sequence shown is that of the viral strand, proceeding 5′ to 3′ from the *Pst*I site in gene A; for ΦX174 it is the sequence from a different *Pst*I site in gene A. Letters in bold type represent differences between the corresponding sequences of ΦX174 and G4. The brackets separate continuous runs of homologous bases from regions containing differences, and the numbers above the brackets indicate the number of perfectly matched bases.

molecules from mixed pairs of circular single-stranded DNA and linear duplex DNA of fd and M13, whose nucleotide sequences differ by 3% of bases[19,20]. However, even these relatively sparse mismatches can stop the unidirectional growth of heteroduplex joints[15]. When we did the same experiment with pairs of ΦX174 and G4 DNA, no joint molecules were formed. Neither fragments nor circular single-stranded ΦX174 DNA formed joint molecules with linear duplex G4 DNA, whereas the perfectly homologous combination of single-stranded G4 DNA with duplex G4 DNA yielded joint molecules. Parallel observations were made with single-stranded G4 DNA and duplex ΦX174 DNA (Table 1*a*).

The pairing by RecA protein of circular viral single strands with linear duplex DNA is a precise reaction in which a heteroduplex joint forms preferentially at the 3′ end of the complementary strand and grows in one direction away from the end[11,14,15]. When the linear molecules are produced by restriction cleavage of circular duplex DNA, the formation of heteroduplex DNA begins at a specific sequence. Thus with regard to the pairing of ΦX174 and G4 DNA, the published nucleotide sequences reveal the degree of homology at the sites from which heteroduplex formation begins. The nucleotide sequences of the appropriate ends of linear duplex ΦX174 DNA and G4 DNA are listed in Table 2[21,22]. A short distance from each end, there is a subterminal region in which 1/3 to 1/2 of bases do not match. Experiments reported elsewhere have shown that a density of mismatches as low as 1 base pair in 10 can retard the growth of heteroduplex joints promoted by RecA protein[15]. In the case of relaxed ΦX174 and G4 DNA the greater density of mismatched sequences blocks not only the enlargement of heteroduplex joints, but also the formation of any stable joint molecules by RecA protein. Superhelicity, however, overcomes the inability of RecA protein to pair these partially homologous molecules. When we reacted fragments of single-stranded ΦX174 DNA and superhelical G4 DNA, or vice versa, with RecA protein, we observed the formation of joint molecules (Table 1*b*). The mixed combinations of circular single-stranded DNA with superhelical DNA (Table 1*b*) or of fragments with nicked circular DNA (Table 1*c*) did not yield joint molecules.

Table 3 The size of D-loops made by RecA protein from partially homologous fragments and superhelical DNA

	Superhelical DNA	
Fragments of ssDNA	ΦX174	G4
ΦX174	340±110*	220±120
G4	250±130	320±100

D-loops were made with superhelical DNA and single-stranded fragments as for Table 1. Measurements of the lengths of D-loops by electron microscopy were made as described previously[23].

* 14–19 D-loops were measured in each sample.

The joint molecules made by combinations of ΦX174 and G4 DNA had the electron microscopic appearance of D-loops (data not shown). Measurement showed that the mean lengths of D-loops in the mismatched combinations exceeded 200 base pairs, corresponding to about 2/3 to 4/5 of the lengths of D-loops made in perfectly matched combinations (Table 3). Since the median length of perfectly matched sequences in ΦX174 and G4 is 14 bases and since no perfectly homologous sequence exceeds 30 bases, the D-loops made by ΦX174 and G4 must contain many mismatched base pairs. For example there is a stretch of 30 homologous bases in gene D; in the 200 bases preceding and following this stretch there are 65 and 42 mismatched bases. The other 3 homologous runs of 28–30 bases are flanked by similarly large numbers of mismatched bases[22].

Table 4 Summary of observations on fidelity of homologous pairing promoted by RecA protein

Type of DNA				
	Physical			
Genetic	Single stranded	Duplex	Formation of joint molecules	Ref.
G4+ΦX174	Circular	Linear	−	This paper
	Circular	Superhelical	−	12
	Fragmented	Nicked circular	−	This paper
	Fragmented	Superhelical	+	This paper
fd+M13	Circular	Linear	+	15
	Circular	Superhelical	−	Unpublished

When superhelical DNA containing D-loops is nicked, the D-loops promptly dissociate by spontaneous branch migration[24]. We compared the dissociation of D-loops made from homologous and mixed combinations of ΦX174 and G4 DNA. D-loops made from mixed combinations dissociated more rapidly, as expected for shorter D-loops and for D-loops containing mispaired bases (data not shown).

The experiments described above show that superhelicity promotes the formation by RecA protein of heteroduplex joints that contain many mismatches. No measurable formation of D-loops occurred in 60 min at 37 °C in the absence of RecA protein, even when the DNA was perfectly homologous (Fig. 1). The requirement of RecA protein for the formation of D-loops from ΦX174 plus G4 DNA is further shown by experiments in which we tried to make D-loops from ΦX174 and G4 DNA by annealing[25]. Homologous pairs of DNA formed 21–24% D-loops in 30 min at 75° C, but the mixed combinations G4 superhelical DNA and ΦX174 single-stranded fragments, or vice versa, formed none. In the absence of RecA protein, we did not observe the spontaneous formation of D-loops by ΦX174 superhelical DNA and fragments of G4 DNA at any temperature between 37° and 75 °C (Fig. 1).

Thus observations on the pairing of DNA from related small DNA phages have shown that the basis for discriminating a high degree of relatedness from perfect or nearly perfect homology exists in the mechanism by which RecA protein promotes homologous pairing (summarized in Table 4). We can begin to relate the effects of mispairing to the two steps in the reaction, namely synapsis and heteroduplex formation. The sequences of fd and M13 differ by 3% of bases; whereas ΦX174 and G4 differ by 33% of bases in the coding regions which comprise 95–96% of their genomes[19-22]. These different degrees of potential mismatching have distinguishable effects. According to previous observations on the joint action of RecA protein and *E. coli* topoisomerase I, the imperfect homology of ΦX174 and G4 DNA interferes with synapsis, a step that precedes the formation of an extensive heteroduplex joint[12]. However, if the single-stranded DNA is fragmented, and the duplex DNA is superhelical, then even 33% nonhomology does not bar the formation of joint molecules, although the frequency is reduced relative to completely homologous molecules. The 3% nonhomology of fd relative to M13 permits the formation of joint molecules in non-superhelical DNA, but interferes with the growth of heteroduplex joints that is actively promoted by RecA protein[15]. Nonetheless, many mismatched base pairs are included in the joint molecules formed by fd and M13 DNA, and correspondingly more mismatched base pairs are included in the joint molecules that are formed by ΦX174 and G4 DNA when superhelicity favours the reaction.

Although spontaneous uptake of homologous single-stranded fragments by superhelical DNA is driven by the energy of superhelix formation, additional energy in the form of heat is required to make the reaction go at readily measured rates. On several grounds, we suggested that this energy unwinds the helix at potential nucleation sites and that this unwinding is the rate-limiting step. Following nucleation, the superhelix energy causes the D-loop to grow because it stabilizes the product, which is a less constrained structure than the original superhelix[25]. In the present experiments, the failure of ΦX174 and G4 DNA to form D-loops in the thermal reaction is presumably due to lack of nucleation of imperfectly matched sequences at high temperatures, in other words to instability of a nascent heteroduplex joint. RecA protein may promote the pairing of G4 and ΦX174 because it unwinds the helix at 37 °C (ref. 26) at which temperature even imperfectly paired sequences may form a nucleus that can be enlarged by the energy of superhelix formation. According to this interpretation, RecA protein, using the energy of ATP, replaces the role of thermal energy in unwinding the helix so that nucleation can occur. In the absence of superhelicity, RecA protein fails to pair ΦX174 and G4 DNA because there is a net loss of perfectly paired bases without the offsetting entropic gain that is associated with formation of a D-loop in superhelical DNA[25].

With regard to recombination, and possibly mutagenesis, the significant observation reported here is that RecA protein, using superhelical DNA as the recipient of a strand transfer, can make heteroduplex joints containing many mismatches.

We thank Lynn Osber for technical assistance and John Flory for helpful comments on the manuscript. This research was sponsored by grant NP 90G from the American Cancer Society and grant USPHS CA 16038-07 from the NCI.

Received 10 August; accepted 9 November 1981.

1. Fox, M. S. *A. Rev. Genet.* **12,** 47–68 (1978).
2. Radding, C. M. *A. Rev. Biochem.* **47,** 847–880 (1978).
3. Stadler, D. R. *A. Rev. Genet.* **7,** 113–127 (1973).
4. Fogel, S., Mortimer, R., Lusnak, K. & Tavares, F. *Cold Spring Harb. Symp. quant. Biol.* **43,** 1325–1341 (1978).
5. Rossignol, J-L., Paquette, N. & Nicolas, A. *Cold Spring Harb. Symp. quant. Biol.* **43,** 1343–1352 (1978).
6. Magni, G. E. & Von Borstel, R. C. *Genetics* **47,** 1097–1108 (1962).
7. Magni, G. E. *Proc. natn. Acad. Sci. U.S.A.* **50,** 975–980 (1963).
8. Strigini, P. *Genetics* **52,** 759–776 (1965).
9. Clark, A. J. *A. Rev. Genet.* **7,** 67–86 (1973).
10. Kobayashi, I. & Ikeda, H. *Molec. gen. Genet.* **166,** 25–29 (1978).
11. DasGupta, C., Shibata, T., Cunningham, R. P. & Radding, C. M. *Cell* **22,** 437–446 (1980).
12. Cunningham, R. P., Wu, A. M., Shibata, T., DasGupta, C. & Radding, C. M. *Cell* **24,** 213–223 (1981).
13. DasGupta, C., Wu, A. M., Kahn, R., Cunningham, R. P. & Radding, C. M. *Cell* **25,** 507–516 (1981).
14. Kahn, R., Cunningham, R. P., DasGupta, C. & Radding, C. M. *Proc. natn. Acad. Sci. U.S.A.* **78,** 4786–4790 (1981).
15. DasGupta, C. & Radding, C. M. *Proc. natn. Acad. Sci. U.S.A.* (in the press).
16. Cox, M. M. & Lehman, I. R. *Proc. natn. Acad. Sci. U.S.A.* **78,** 3433–3437 (1981); *Proc. natn. Acad. Sci. U.S.A.* **78,** 6018–6022 (1981).
17. Shibata, T., DasGupta, C., Cunningham, R. P. & Radding, C. M. *Proc. natn. Acad. Sci. U.S.A.* **76,** 1638–1642 (1979).
18. McEntee, K., Weinstock, G. M. & Lehman, I. R. *Proc. natn. Acad. Sci. U.S.A.* **76,** 2615–2619 (1979).
19. Beck, E. *et al. Nucleic Acids Res.* **5,** 4495–4503 (1978).
20. van Wezenbeek, P. M. G. F., Hulsebos, T. J. M. & Schoenmakers, J. G. G. *Gene* **11,** 129–148 (1980).
21. Godson, G. N., Fiddes, J. C., Barrell, B. G. & Sanger, F. in *The Single-Stranded DNA Phages* (eds Denhardt, D. T., Dressler, D. & Ray, D. S.) 51–86 (Cold Spring Harbor Laboratory, New York, 1978).
22. Godson, G. N. in *The Single-Stranded DNA Phages* (eds Denhardt, D. T., Dressler, D. & Ray, D. S.) 671–695 (Cold Spring Harbor Laboratory, New York, 1978).
23. Cunningham, R. P., DasGupta, C., Shibata, T. & Radding, C. M. *Cell* **20,** 223–235 (1980).
24. Radding, C. M., Beattie, K. L., Holloman, W. K. & Wiegand, R. C. *J. molec. Biol.* **116,** 825–839 (1977).
25. Beattie, K. L., Wiegand, R. C. & Radding, C. M. *J. molec. Biol.* **116,** 783–803 (1977).
26. Cunningham, R. P., Shibata, T., DasGupta, C. & Radding, C. M. *Nature* **281,** 191–195 (1979); **282,** 426 (1979).

Three classes of mouse H–2 messenger RNA distinguished by analysis of cDNA clones

David Cosman, George Khoury & Gilbert Jay

Laboratory of Molecular Virology, National Cancer Institute,
National Institutes of Health, Bethesda, Maryland 20205, USA

The major histocompatibility complex (MHC) is composed of a set of linked genes encoding proteins involved in the host's immune response[1]. A subset of these proteins are the classical transplantation antigens, which are responsible for rapid allograft rejection and are involved in the associative recognition of foreign antigens by cytotoxic T cells[1,2]. Three different genetic loci coding for the transplantation antigens in humans (HLA-A, -B and -C) and in mice (H–2K, D and L) have been identified[3,4]; they are highly polymorphic[1]. The recent molecular cloning of HLA[5,6] and H–2[7,8] cDNA sequences provide the basis for detailed characterization of the genetic organization and expression of the MHC. We report here the identification, by analysis of cDNA clones, of at least three distinct classes of H–2 messenger RNAs that can be differentiated on the basis of their disparate 3′-non-translated regions, and describe an unusual sequence arrangement in one class of H–2-like molecule.

An adult liver cDNA library, derived from SWR/J mice (*q* haplotype) and cloned into the *Pst*I site of pBR322 (ref. 9), was screened by hybridization using as a DNA probe the insert from the HLA cDNA clone of Sood *et al.*[6]. Approximately 150,000 colonies were screened and 30 clones isolated. Excision of the DNA inserts from each of the putative H–2 clones, by digestion with *Pst*I, generated multiple fragments which show extensive overlaps between the clones (Fig. 2*a*), suggesting that most of the clones are related to each other.

Clone pH2 was chosen for further analysis. The entire DNA insert at the *Pst*I site of pBR322 is ~1,150 base pairs (bp) long and contains three internal *Pst*I cleavage sites (Fig. 1). The order of the four *Pst*I fragments is C (220 bp), B (250 bp), A (530 bp) and D (170 bp). Nucleotide sequence analysis of each fragment has shown that pH2 is highly homologous to the H–2 cDNA clones isolated by others[7,8] and to the known amino acid sequences of H–2 transplantation antigens[4]. The entire pH2 insert extends from the codon for amino acid 86 (numbered according to the sequence of H–2K$^{\mathrm{b}}$)[4] to the 3′ end of the mRNA, including the presumptive polyadenylation signal, AAUAAA, located 11 nucleotides from the poly(A) tract (data not shown). The sequences determined corresponded to amino acids 86–138 from within fragment C, 198–236 from fragment B and 237–315 from fragment A.

0028–0836/82/010073—04$01.00

Clone pH2 was used as a prototype with which to compare the other cDNA clones. Individual *Pst*I fragments of pH2 DNA were ^{32}P-labelled by nick-translation and hybridized to Southern blots of *Pst*I digests of DNA from the other recombinant plasmids. Figure 1 shows the maps for nine of the cDNA clones obtained by this cross-hybridization. During the mapping experiments, we noted many similarities between the clones. Most of the clones have either a 530- (pH2, 16, 18) or 570- (pH8, 12, 19, 6) bp cross-hybridizing A fragment (Fig. 2*b*), and a common 250-bp B fragment. The A and B fragments are internal fragments in pH2 (see Fig. 1). The clones differ extensively in the size of their 5′ fragments, a presumed artefact of cDNA synthesis, as well as in their 3′ D fragments. In addition, the D fragment of pH2, which contains entirely 3′-non-coding sequences immediately adjacent to the poly(A) tract, did not cross-react to any extent with the 3′-non-coding D fragments of many of the other clones.

To determine whether the 3′-non-coding regions of the various clones may be useful for distinguishing different classes of H-2 molecule, the *Pst*I D fragment (170 bp) from pH2, the D_1 fragment (185 bp) from pH8 and the D_2 fragment (135 bp) from pH12 were purified, labelled by nick-translation and hybridized to Southern blots of *Pst*I digests of the same set of nine plasmid DNAs (Fig. 2*c–e*). Figure 2*c* shows that the D fragments of clones pH2, pH16 and pH18 are indistinguishable on the basis of size or extent of cross-hybridization. The pH2 D fragment did not cross-react with any of the other clones. The pH8 D_1 fragment hybridized to itself (Fig. 2*d*) and pH25, pH26 and pH35 (data not shown). On the other hand, the pH12 D_2 fragment hybridized to a similar-sized fragment from pH19 (Fig. 2*e*) and to pH24 and pH31 (not shown). Thus at least three classes of H-2 mRNA molecule can be defined by differences in their 3′-non-coding regions, represented by clones pH2 (pH16, pH18), pH8 (pH25, pH26, pH35) and pH12 (pH19, pH24, pH31). Although clones pH5, pH6 and pH7 cannot be classified on the basis of this analysis because they lack a D fragment, they are not in the same class as pH2 (see below and Fig. 2*f*).

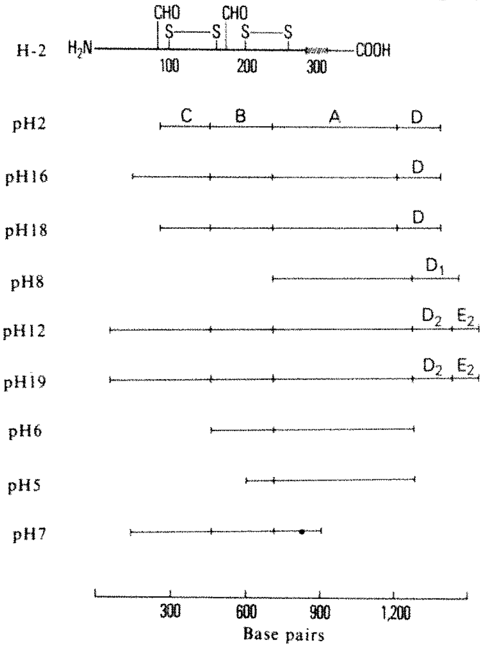

Fig. 1 The *Pst*I restriction maps of nine H-2 cDNA clones. As the recombinant plasmids were constructed by the dG–dC tailing method[9], the cDNA inserts could be excised using *Pst*I. The multiple restriction fragments generated by *Pst*I cleavage were ordered by analysis of partial digestion products. The orientation and location of each fragment derived from clone pH2 DNA relative to the linear structure of the H-2 antigen were determined by DNA sequence analysis. The map for each of the nine clones is presented in alignment with a schematic representation of the linear structure of the H-2 antigen, including the locations of the carbohydrate side chains (CHO), the disulphide bridges (S–S) and the membrane-binding region (hatched).

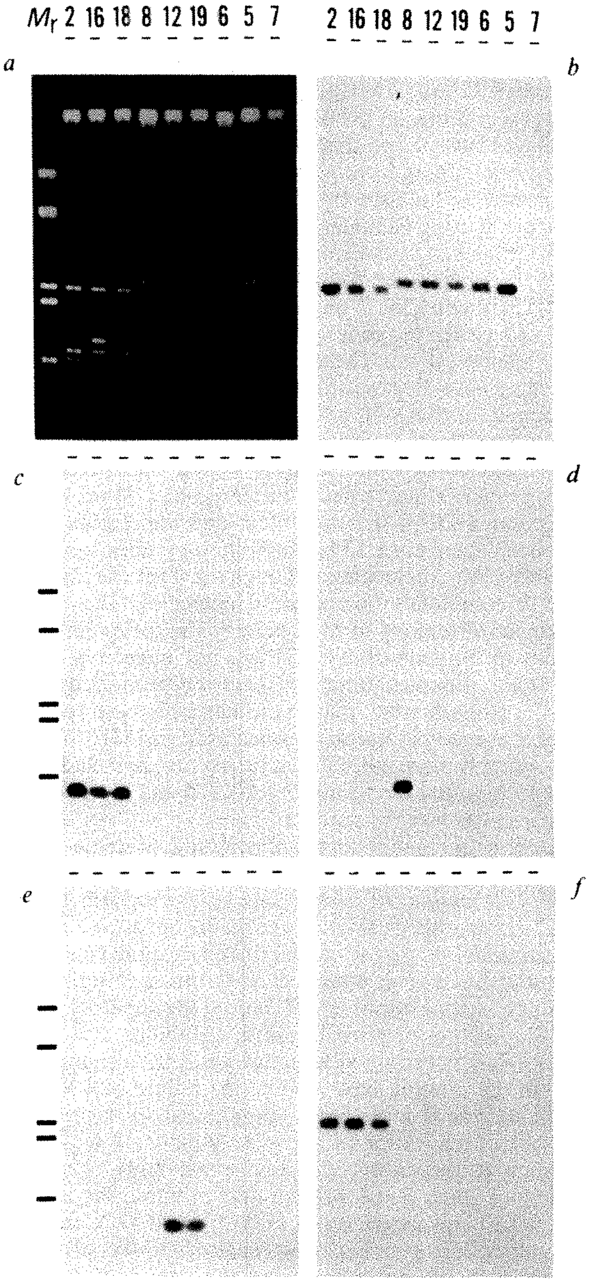

Fig. 2 Identification of different classes of H-2 cDNA clones by cross-hybridization analyses. Nine plasmid DNAs were digested with *Pst*I and fractionated by electrophoresis on 1.6% agarose gels (*a*). The DNA fragments were transferred from the gels to nitrocellulose sheets by the method of Southern[12]. The sheets were prehybridized for 2–3 h at 65 °C in 3×SSC (1×SSC = 0.15 M NaCl, 0.015 M Na citrate), 5×Denhardt's (1× Denhardt's = 0.02% Ficoll, 0.02% polyvinylpyrolidone, 0.02% bovine serum albumin), 0.1% SDS, before hybridization for 16 h in the same conditions with one of several ^{32}P-labelled DNA probes (*b–f*). DNA fragments used as probes were generated by digestion with the appropriate restriction enzymes and fractionated by electrophoresis through 5–8% polyacrylamide gels. The appropriate DNA bands were eluted and ^{32}P-labelled by nick-translation[13] to a specific activity of $0.5\text{–}2\times10^8$ c.p.m. per µg. The 23-bp DNA fragment (*f*) was self-ligated with T4 DNA ligase before nick-translation. Following hybridization, the nitrocellulose sheets were washed extensively in 3×SSC, 0.1% SDS at 65 °C, dried and exposed to Kodak XAR-5 films. The molecular weight markers (M_r), derived from simian virus 40 DNA by *Hin*dIII digestion, were 1,768, 1,169/1,118, 526, 447 and 215 bp long. *a* Is a picture of an ethidium bromide-stained gel; autoradiograms of Southern blots were obtained with the following DNA probes: *b*, pH2 *Pst*I A fragment; *c*, pH2 *Pst*I D fragment; *d*, pH8 *Pst*I D_1 fragment; *e*, pH12 *Pst*I D_2 fragment; and *f*, the 23-bp *Hin*fI–*Sau*3A subfragment from the pH2 *Pst*I A fragment.

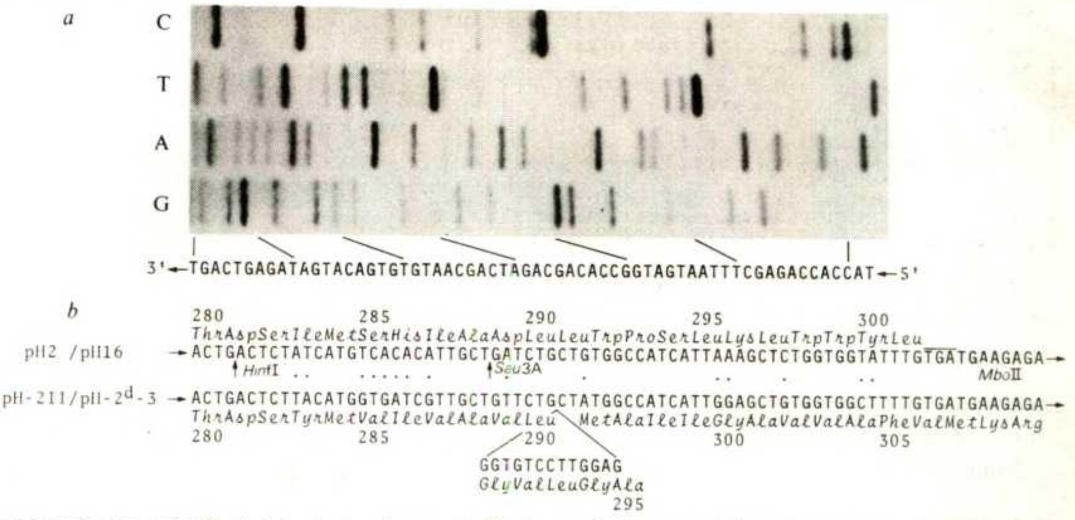
a
C
T
A
G
3'←TGACTGAGATAGTACAGTGTGTAACGACTAGACGACACCGGTAGTAATTTCGAGACCACCAT←5'
b
280 285 290 295 300
ThrAspSerIleMetSerHisIleAlaAspLeuLeuTrpProSerLeuLysLeuTrpTrpTyrLeu
pH2 /pH16
→ACTGACTCTATCATGTCACACATTGCTGATCTGCTGTGGCCATCATTAAAGCTCTGGTGGTATTTGTGATGAAGAGA→
HinfI
Sau3A
MboII
pH-2II/pH-2d-3
→ACTGACTCTTACATGGTGATCGTTGCTGTTCTGCTATGGCCATCATTGGAGCTGTGGTGGCTTTTGTGATGAAGAGA→
ThrAspSerTyrMetValIleValAlaValLeu MetAlaIleIleGlyAlaValValAlaPheValMetLysArg
280 285 290 300 305
GGTGTCCTTGGAG
GlyValLeuGlyAla
295

Fig. 3 Comparison of the amino acid sequence around the transmembrane region of the classical H-2 antigen with the predicted amino acid sequence of the corresponding region from clone pH2. *a*, Autoradiogram of a sequencing gel showing the nucleotide sequence of the antisense strand of pH2 DNA around amino acids 280–300. The *Pst*I A fragment of pH2 DNA was cleaved with *Mbo*II and end-labelled with [γ-^{32}P]ATP by the exchange reaction[14]. A 220-bp fragment was purified by polyacrylamide gel electrophoresis and recleaved with *Rsa*I to give two fragments. The larger of these was subjected to sequence determination by a modification of the Maat–Smith procedure[15,16]. This sequence has been confirmed by analysis of both strands using the Maxam–Gilbert procedure[14]. *b*, Comparison of the pH2 sequence with the corresponding sequence from two previous isolates, pH-2II (ref. 8) and pH-2^d-3 (ref. 10). The sequences are aligned for maximum homology showing the 13-bp deletion of pH2 relative to pH-2II and pH-2^d-3. All differences in nucleotide sequences are indicated by ●. The numbers correspond to the amino acid sequence of H–$2K^b$ (ref. 4).

The pH2 class can be further distinguished from the pH8 and pH12 classes by its slightly faster-migrating A fragment (Fig. 2*a*). DNA sequence analysis of pH2 showed an unusual feature in the part of the A fragment expected to encode the transmembrane portion of the H-2 molecule, from amino acids 284–307 (for reviews on the structure of the H-2 molecule, see refs 3, 4). Comparison of the sequence of the presumed transmembrane region, which is comprised of 25 uncharged and nonpolar amino acids, from two previous isolates from other laboratories, pH-2II (ref. 8) and pH-2^d-3 (ref. 10), showed perfect conservation of hydrophobic residues (Fig. 3). Analysis of the corresponding region in pH2 indicated that (1) there are extensive nucleotide and amino acid substitutions at the beginning of the transmembrane region, between positions 284 and 290, with three out of six hydrophobic residues being replaced by charged or polar amino acids; (2) this is followed by a deletion of 13 bp, which removes the codons for amino acids 291–294, located in the middle of the transmembrane region, and also the first base of the codon for amino acid 295, resulting in a shift in the reading frame; and (3) this frameshift results in the introduction of a termination codon 34 nucleotides downstream at amino acid position 302. Figure 3 shows the nucleotide sequence and predicted amino acid sequence around this region of the pH2 molecule. Note that three charged amino acids (His 286, Asp 289, Lys 296), as well as three polar residues (Ser 285, Ser 294, Pro 293), are now found interspersed throughout that region of the pH2 molecule which is equivalent to the hydrophobic transmembrane region of the classical H-2 antigen.

To determine whether this unusual sequence was present in any other cDNA clones, we purified from pH2 the 23-bp *Hinf*I–*Sau*3A restriction fragment that spans amino acids 281–288. Following self-ligation and ^{32}P-labelling by nick-translation, it was hybridized to Southern blots of *Pst*I-restricted plasmid DNAs (Fig. 1*f*). Only those clones representing the pH2 class, and containing a smaller 530 bp, rather than 570 bp, A fragment, hybridized strongly to this probe. These clones (pH2, pH16 and pH18) also have indistinguishable D fragments (Fig. 2*c*). Direct sequence analysis of pH16 further confirmed its identity to pH2 in this region of the molecule. This unusual pH2-like sequence is not a general feature of the transplantation antigens present in liver cells of mice of the *q* haplotype. In fact, clone pH7 has been found to have a classical hydrophobic transmembrane sequence from amino acids 280 to 293, at which point the clone is terminated by dG-dC tails (Fig. 1). The very weak hybridization of the 23-bp pH2-specific probe to pH8, -12, -19, -6, -5 and -7 (Fig. 2*f*) is probably due to the homology between amino acids 281 and 284 (see Fig. 3).

The 250-nucleotide sequence immediately upstream from this unusual region of pH2 has been determined and contains neither in-frame nonsense codons nor frameshifts (data not shown). This region, between amino acids 198 and 279, shows 88% homology to the H-$2K^b$ amino acid sequence[4]. The presence of this unusual sequence in liver mRNA raises the possibility that the mRNA represented by pH2 encodes a shortened form of the H-2 antigen (301 amino acids) that might have a different biological function. Such a truncated antigen is expected to contain the entire biologically active portion of the H-2 molecule. The absence of a hydrophobic region in this putative polypeptide makes it unlikely that it could be inserted into the plasma membrane. The loss of the C-terminal hydrophilic tail would preclude it from interacting with cytoplasmic components. It is possible that such a molecule could be secreted.

Although an altered form of the H-2 antigen has not previously been described, we have observed a protein of molecular weight 35,000 that can be immunoprecipitated by anti-H-2 antiserum from cell-free translation products of liver mRNA (unpublished results). It remains to be determined whether this protein is the product of the mRNA represented by pH2. Until a protein product of this mRNA is identified, we cannot exclude the possibility that pH2 represents a transcriptionally active H-2-like pseudogene.

This study demonstrates that different classes of H-2 cDNA clones can be identified on the basis of non-homologous 3′-untranslated sequences. The classes cannot yet be assigned to the H-2K, -D or -L loci as complete amino acid sequences from the *q* haplotype are not available. This observation should provide both a method for differentiating between members of a multi-gene family and a clearer understanding of their genomic organization and expression.

After this manuscript had been submitted, Steinmetz *et al.*[11] published the sequence of an H-2-like pseudogene with unusual changes in the transmembrane region that are distinct from those in pH2. It was not determined whether this pseudogene was transcribed.

We acknowledge the generous gifts of the HLA-B cDNA plasmid from Dr Sherman Weissman and the mouse liver cDNA library from Drs John Monahan and Michael Tocci.

Received 25 August; accepted 4 November 1981.

1. Klein, J. *Science* **203,** 516–521 (1979).
2. Zinkernagel, R. M. & Doherty, P. C. *Adv. Immun.* **27,** 51–177 (1979).
3. Ploegh, H. L., Orr, H. T. & Strominger, J. L. *Cell* **24,** 287–299 (1981).
4. Nathenson, S. G. *et al. A. Rev. Biochem.* **50,** 1025–1052 (1981).
5. Ploegh, H. L., Orr, H. T. & Strominger, J. L. *Proc. natn. Acad. Sci. U.S.A.* **77,** 6081–6085 (1980).

6. Sood, A. K., Pereira, D. & Weissman, S. M. *Proc. natn. Acad. Sci. U.S.A.* **78,** 616–620 (1981).
7. Kvist, S. *et al. Proc. natn. Acad. Sci. U.S.A.* **78,** 2772–2776 (1981).
8. Steinmetz, M. *et al. Cell* **24,** 125–134 (1981).
9. Norgard, M. V., Tocci, M. J. & Monahan, J. J. *J. biol. Chem.* **255,** 7665–7672 (1980).
10. Bregegere, F. *et al. Nature* **292,** 78–81 (1981).
11. Steinmetz, M. *et al. Cell* **25,** 683–692 (1981).
12. Southern, E. M. *J. molec. Biol.* **98,** 503–517 (1975).
13. Rigby, P. W. J., Dieckmann, M., Rhodes, C. & Berg, P. *J. molec. Biol.* **113,** 237–251 (1977).
14. Maxam, A. M. & Gilbert, W. *Meth. Enzym.* **65,** 499–560 (1980).
15. Maat, J. & Smith, A. J. H. *Nucleic Acids Res.* **5,** 4537–4545 (1978).
16. Seif, I., Khoury, G. & Dhar, R. *Nucleic Acids Res.* **8,** 2225–2240 (1980).

Cloning and analysis of cDNAs encoding plant storage protein precursors

Ronald R. D. Croy, Grantley W. Lycett, John A. Gatehouse, Jennifer N. Yarwood & Donald Boulter

Department of Botany, University of Durham, Science Laboratories, South Road, Durham DH1 3LE, UK

The major storage protein in many legume seeds is legumin, a hexameric molecule of molecular weight (M_r) 360,000–400,000 consisting of six subunit pairs, each of which comprises a 40,000-M_r, acidic polypeptide linked by disulphide bonds to a 20,000-M_r, basic polypeptide[1]. We have recently shown that these subunit pairs are synthesized, *in vivo* and *in vitro* in *Pisum* and *Vicia*[2,3], as a 60,000-M_r precursor polypeptide, putatively containing one copy each of the acidic and basic subunits covalently linked together. We describe here the cloning and identification of cDNA sequences coding for the legumin precursor. Additionally, we have used these cDNAs to verify that the legumin mRNAs are of sufficient size to code for the precursor and to demonstrate the presence of four single-copy legumin genes in genomic DNA. Possible mechanisms for the processing of the legumin precursor are discussed. Identification of cloned cDNA sequences coding for vicilin, the secondary storage protein of *Pisum sativum*[4], is also reported.

Double-stranded DNA complementary to poly(A)$^+$ RNA from developing seed cotyledons was prepared[43] and cloned in plasmid pBR322[5,6] as described in Fig. 1 legend. Transformed colonies strongly hybridizing to mRNA or cDNA probes were selected as putative legumin and vicilin cDNA clones and plasmid 'minipreps' made according to Klein *et al.*[7]. Southern 'blots' of cDNA inserts, excised from the recombinant plasmids, strongly hybridized mRNA and cDNA probes, further confirming the presence of cDNA inserts. The cDNA inserts were used to prepare and identify complementary mRNAs by hybrid-selected translation[8,9] (Fig. 1).

An initial selection of 12 clones contained 6 cDNAs encoding vicilin 50,000 and 47,000-M_r subunits[4,10–13], two encoding the legumin 60,000-M_r precursor[2,3] and several others coding for unidentified polypeptide products (Fig. 1).

Physical maps of two legumin cDNAs have been constructed from restriction endonuclease analyses and are shown in Fig. 2 together with the sequencing strategies. The legumin cDNA, pRC 2.2.4, identified by hybrid-selected translation, has been completely sequenced and corresponds to a 638-nucleotide sequence from the 3′ end of the legumin mRNA (Fig. 3). There is, in addition, a polyadenylated sequence at the 3′ terminus. The second legumin cDNA (pRC 2.11.7), selected by screening the cDNA clone bank with pRC 2.2.4 cDNA, has been partially sequenced. It is essentially identical to 2.2.4, but is larger by about 150 nucleotides extending towards the 5′ end of the message.

The close agreement of the predicted amino acid composition, tryptic peptide and N-terminal sequence data with published data[1,14,15] unequivocably identifies the nucleotide sequence as that of a legumin cDNA and also locates the basic (20,000 M_r) subunit at the 3′ end of the legumin messenger coding sequence. The additional coding sequence of pRC 2.11.7 shows that the amino acid sequence extends unbroken upstream beyond the N terminus of the basic subunit for at least 30 amino acids, presumably past or approaching the C terminus of the acidic subunit[1,16]. There are no termination or initiation codons in this pre-N-terminal sequence, confirming the legumin precursor theory[3]. The sequence data also show that the legumin mRNA has a significant non-coding sequence between the coding sequence and the poly(A) tail. This 137–nucleotide sequence is A+T rich, in common with many other eukaryotic mRNAs, and contains the hexanucleotide sequence -AATAAA-, about 20 nucleotides upstream from the 3′ end, as also found in other eukaryotic mRNAs[17–22].

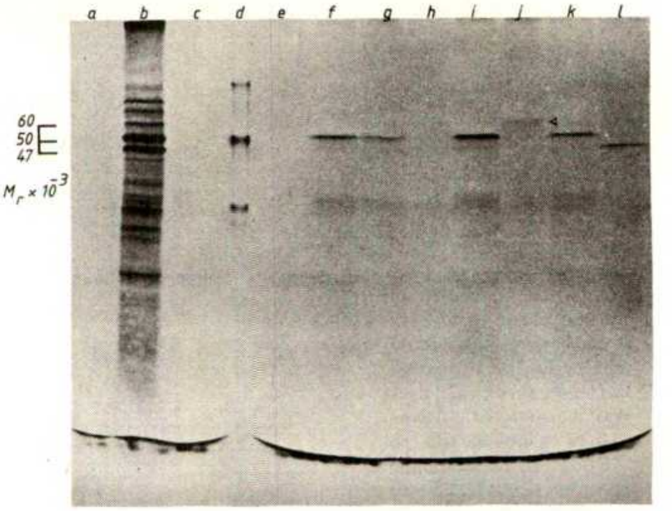

Fig. 1 Identification of recombinant plasmids containing cDNAs by translation of hybrid-selected mRNAs. Polyadenylated RNA, purified from 14-day-old pea cotyledons, was used to synthesize double-stranded cDNA by avian myeloblastosis virus reverse transcriptase and DNA polymerase I as described previously[43]. The double-stranded cDNA was cloned in the *Bam*HI site of pBR322 after attachment of *Bam*HI synthetic oligonucleotide linkers, essentially by the method of Sippel *et al.*[6]. 1 μg of ^{32}P- or ^{3}H-labelled cDNA, blunt-ended with DNA polymerase I, was ligated to 400 pmol of 5′-phosphorylated linkers for 15 h at 12.5 °C (ref. 6). After digestion with an excess of *Bam*HI, the cDNA was fractionated on a Sepharose 6B column (100 mm × 15 mm diameter) and the fractions containing the largest cDNAs were pooled and recovered by alcohol precipitation. pBR322 (5 μg) linearized with *Bam*HI, was treated with alkaline phosphatase to remove the 5′-phosphate groups (to prevent self-ligation and non-recombinant transformations[6,44]) and after extensive phenol extraction the plasmid was passed through a Sephadex G-50 column and recovered by alcohol precipitation. The cDNA was ligated to the plasmid for 48 h at 12.5 °C. 0.5–1.0 μg of the recombinant DNA was used to transform competent cells prepared from RecA$^-$ or BedBC$^-$ strains of *Escherichia coli* K-12, after 24 h incubation in calcium chloride to enhance competence[22]. Transformants were selected on ampicillin plates and screened by colony hybridization on nitrocellulose filters with ^{32}P-labelled cDNA and mRNA[45]. Hybridizations were performed in the presence of polyadenylic acid to prevent any non-specific binding of probes to poly(dT-dA) regions in the clones[44]. Probing with pea ribosomal RNA showed the complete absence of any ribosomal cDNA clones. cDNA containing plasmids, purified by the method of Clewell[4,6] and Katz *et al.*[47], were restricted with *Bam*HI to excise the cDNA inserts, and 20–30 μg aliquots of total DNA were denatured and applied to freshly prepared diazobenzyloxymethyl paper[9] as described by Smith *et al.*[8]. Poly(A)$^+$ mRNA was allowed to hybridize, 5 μg per filter, to the plasmids and specifically bound mRNAs were eluted[8] and translated in the reticulocyte lysate system[3]. Translation products labelled with ^{3}H-leucine were separated and visualized by SDS-polyacrylamide gel electrophoresis followed by fluorography[48]. Track *b* shows the translation products from total poly(A) mRNA: tracks *a* and *c* show, respectively, endogenous translation products from RNA nonspecifically bound to pBR322. Tracks *e*–*l* show the translation products from mRNAs specifically bound to cDNA plasmids. pRC 2.1.7, 2.1.8, 2.1.18, 2.1.20, 2.2.1, 2.2.4 (band indicated with an open arrow), 2.2.5, 2.2.10, respectively. (Track *d* shows a ^{3}H-labelled standard protein preparation.) Legumin 60,000 M_r precursor and vicilin 50,000 and 47,000 M_r precursors were identified as described previously[3,4]. Characterized and ^{32}P-nick translated[28] cDNAs, prepared as described in Fig. 4 legend, were used to rescreen the cDNA clone bank for related but longer cCNA sequences. Clones were arrayed and grown on nitrocellulose filters and subjected to colony hybridization using the legumin cDNA insert from pRC 2.2.4. In this way the complementary and larger legumin cDNA, pRC 2.11.7, was detected and isolated.

As further evidence for synthesis of legumin as a single polypeptide precursor, we have determined the size of the

0028-0836/82/010076—04$01.00

legumin mRNA. Total and polyadenylated RNA preparations from developing cotyledons and leaves were denatured by glyoxylation[23] and size fractionated by agarose electrophoresis, and after transfer to nitrocellulose paper[24], the 'Northern' blots were probed with ^{32}P-labelled legumin cDNAs (Fig. 4). Legumin cDNA hybridized strongly to a single component in both seed RNA preparations corresponding to a 19S mRNA (2.2×10^3 bases), sufficiently long to code for a precursor polypeptide of at least 60,000 M_r. Although hybridization of legumin cDNA to smaller mRNA species was observed in seed polyadenylated RNA (Fig. 4), the binding was never to discrete mRNA sizes and was unique to polyadenylated preparations. No such hybridization was observed in total seed RNA preparations, indicating the absence of small mRNA species which may have coded for the smaller (basic) polypeptide components found in legumin isolated from mature seeds. We conclude from these results that extensive degradation of the 19S legumin mRNA occurs during the preparation of polyadenylated RNA, in agreement with the reports of Dunham *et al.*[25]. There was also no hybridization of the probes to any components in the leaf polyadenylated RNA preparations, verifying the tissue-specific expression of the storage protein genes[26].

We have also used the legumin cDNAs to probe for the homologous sequences in genomic DNA. Pea genomic DNA was prepared from leaf tissue[27] and equal aliquots were digested to completion with *Eco*RI or *Hin*dIII restriction endonucleases (which do not cut within the cDNA sequence) (Fig. 5). After separation on agarose gels, the genomic DNA fragments were blotted on to nitrocellulose paper[24] and then hybridized to an excess of ^{32}P-nick-translated[28] cDNA insert (specific activity $\geq 2 \times 10^7$ c.p.m. per μg) from pRC 2.2.4 (Fig. 5). Various amounts of linearized pRC 2.2.4 corresponding to different gene copy numbers were also included on the gels[29] (Fig. 5). We have only been able to detect four *Eco*RI genomic fragments (excluding any intron sites) hybridizing to legumin cDNA and an estimate of the intensities of hybridization to genomic fragments and cDNA plasmids indicates a single gene copy per fragment and therefore an apparent maximum complement of four legumin genes per haploid genome. This agrees with the recent reports of Spencer and Higgins[30] of a set of at least three legumin precursors found *in vivo*, and of J.A.G. *et al.* (unpublished) of at least three legumin precursors *in vitro*. Other reports have indicated that up to four major legumin species exist in mature pea seeds, depending on the genetic line[16,31–34]. However, there have also been many reports of a greater number of minor legumin species in pea and other legumes, based on polypeptide

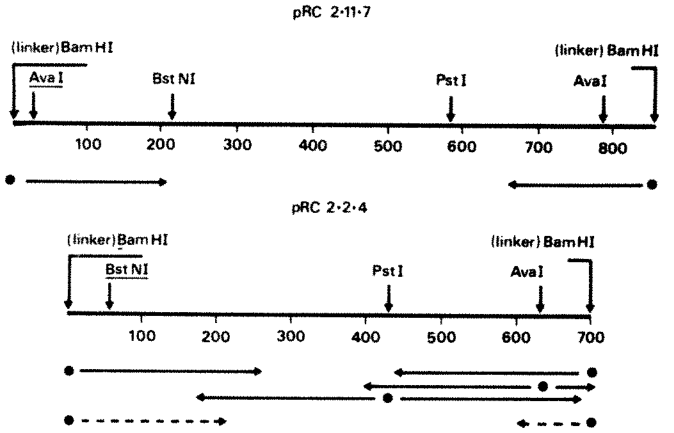

Fig. 2 Restriction maps of cDNAs from plasmids pRC 2.11.7 and pRC 2.2.4 showing the positions of restriction enzyme targets used in the sequencing experiments. The horizontal scales represent nucleotide base pairs from the 5′ end of the coding strand. Numbers of nucleotide base pairs in pRC 2.11.7 correspond to the scale in the nucleotide sequence (Fig. 3). The horizontal arrows indicate the extent of the fragments sequenced and the direction of sequence reading from the 5′-labelled ends (●). Sequencing was by the method of Seif *et al.*[49] (continuous arrows) or that of Maxam and Gilbert[50] (broken arrows).

```
  1                       25  AvaI                 50                      75
a GAAAGGTGGACTCAGGATCATAAGCCCACCCGAGAAGCAAGCGCGCCACCAGAGAGGCAGCCAAAAAGGCAAAAG
b  K  G  G  L  R  I  I  S  P  P  E  K  Q  A  R  H  Q  R  G  S  Q  K  G  K  S

                          100                     125                     150
a CAGAAGGCAAGGAGACAATGGGCTTGAGGAAACAGTTTGCACTGCTAAACTTCGATTGAACATTGGCCCGTCTTC
b [R  R] Q  G  D  N  G  L  E  E  T  V  C  T  A  K  L  R  L  N  I  G  P  S  S
c                    G  L  E  E  T V/I C  T  A  K  L  R L/E N  I A/G P (S)(S)
                    |N terminal

                          175                     200 BstNI               225
a ATCACCAGACATCTACAACCCTGAAGCTGGTAGAATCAAAACTGTTACCAGCCTGGACCTCCCAGTTCTCAGGTG
b  S  P  D  I  Y  N  P  E  A  G  R  I  K  T  V  T  S  L  D  L  P  V  L  R  W
c (A) P  D  L  Y  N  P  E  A  G  X (L) K  T  V  T  S L/I D L/I P  V L/I R

                          250                     275                     300
a GCTCAAACTAAGTGCTGAGCATGGATCTCTCCACAAAAATACTATGTTTGTACCTCACTACAACCTGAATGCAAA
b  L  K  L  S  A  E  H  G  S  L  H  K  N  T  M  F  V  P  H  Y  N  L  N  A  N

                          325                     350                     375
a CAGCATAATATACGCATTGAAGGGACGTGCAAGGCTACAAGTAGTGAACTGCAATGGCAACACCGTGTTTGATGG
b  S  I  I  Y  A  L  K  G  R  A  R  L  Q  V  V  N  C  N  G  N  T  V  F  A  G
c                                    L  Q  V  V  N (P) N  G (N)

                          400                     425                     450
a AAAGCTAGAAGCCGGACGTGCATTGACAGTGCCACAAAACTATGCTGTGGCTGCAAAGTCACTAAACGACAGGTT
b  K  L  E  A  G  R  A  L  T  V  P  Q  N  Y  A  V  A  A  K  S  L  N  D  R  F
c                    A L/I T  V  P  Q  N  Y  A  V  A  A

                          475                     500                     525
a CTCATATGTAGCATTCAAGACCAATGATAGAGCTGGTATTGCAAGACTTGCAGGGACATCATCAGTTATAAATGA
b  S  Y  V  A  F  K  T  N  D  R  A  G  I  A  R  L  A  G  T  S  S  V  I  N  D
                                A  G L/I A  R

                          550         PstI        575                     600
a TCTGCCCTTGGATGTGGTTGCAGCTACATTCAAACTGCAGAGGGATGAGGCAAGGCAGCTCAAGTCCAACAATCC
b  L  P  L  D  V  V  A  A  T  F  K  L  Q  R  D  E  A  R  Q  L  K  S  N  N  P

                          625                     650                     675
a CTTCAAATTTCTAGTTCCAGCTCGTCAGTCTGAGAACAGAGCTTCGGCTTAGATTTCGCACCAAATCAATGAAAG
b  F  K  F  L  V  P  A  R  Q  S  E  N  R  A  S  A Amber
c        F L/I V  P  A  R (Q)

                          700                     725  AvaI               750
a TAATGAATAAGAAAACTAAGGCTTAGATGCCTTTGTTACTTGTGTAAAATAACTCGAGTCATGTACCTTTTTGCG

                          775                     800
a GAAACAGAATAAATAAAAGGTAAAATTTCAGTGCTC*AAAAAAAAAAAAAAAAAAAAAAAAAAAA
```

Fig. 3 Composite cDNA sequence coding for the legumin basic subunit. The figure shows the DNA (mRNA) sequence (line *a*) derived from pRC 2.11.7 and pRC 2.2.4. Numbering in the nucleotide sequence corresponds to that of pRC 2.11.7 in Fig. 3. The asterisk at position 787 indicates the only position at which the two sequences differ, with an adenine residue occurring in 2.2.4 and a thymine residue in 2.11.7. Restriction endonuclease sites are overlined and the termination codon is underlined, as are the overlapping AATAAA hexanucleotide sequences at the 3′ end of the mRNA. DNA sequencing was by the methods of Seif *et al.*[49] or Maxam and Gilbert[50]. Where the method of Seif *et al.*[49] was used, the products of forward and backward reactions were pooled before lyophilization. In both cases, end-labelled DNA fragments were prepared according to Maxam and Gilbert and sequencing gels (6 and 8% polyacrylamide) were prepared as described by Smith[51] and run at 1,500 V. The predicted amino acid sequence (line *b*) was obtained from the DNA sequence by the use of a computer program (provided by Dr M. D. Watson). Line *c* shows peptide amino acid sequences matching the predicted sequence. The N-terminal peptide sequence was obtained from the published data of Casey *et al.*[15] and all other sequences (underlined) were obtained by sequencing purified tryptic peptides from the legumin basic polypeptides (J.N.Y., in preparation). Basic subunits were isolated from total legumin by ion-exchange chromatography in formamide, as described by Gatehouse *et al.*[37]. The separated basic subunits were extensively dialysed against distilled water and lyophilized. Tryptic digestions were carried out for 6 h at 37 °C (100/2 w/w) and the peptide mixture lyophilized before separation by HPLC. The tryptic peptides were separated on a reverse-phase column (C18, 10μ, Varian MCH-10) using a trifluoroacetic acid/acetonitrile gradient (0–70% acetonitrile). Separated peptides were collected and lyophilized before being sequenced by the DABITC method of Chang *et al.*[52].

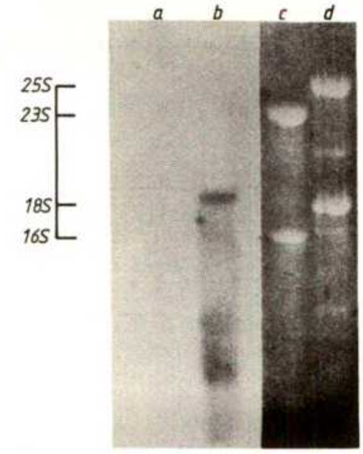

Fig. 4 Identification and sizing of legumin mRNA. Poly(A)$^+$ mRNA (1 μg) or total seed RNA (5 μg), prepared according to the methods of Hall *et al.*[53] and Girard[54], were denatured by glyoxylation and electrophoresed on 1.5% agarose gels by the method of McMaster and Carmichael[23]. The nucleic acids were transferred to nitrocellulose paper according to Thomas[24] and hybridized with ^{32}P-end-labelled or -nick-translated[28] cDNAs (specific activity 10^7 c.p.m. per μg). cDNAs were excised from the plasmids with *Bam*HI and separated on 0.5% agarose gels. The cDNAs were electroeluted from gel slices into dialysis tubing and recovered by alcohol precipitation. After end labelling or nick-translation, the cDNAs were re-electrophoresed through 0.5% agarose into dialysis tubing and used without alcohol precipitation for the hybridizations. Hybridizations were performed in the presence of 100 μg ml^{-1} polyadenylic acid to prevent nonspecific binding[44]. Autoradiographs of the hybridizations are shown as follows: track *a*, poly(A) mRNA from leaves; track *b*, poly(A) mRNA from developing seeds hybridized with ^{32}P-legumin cDNA (pRC 2.2.4). Tracks *c* and *d* show standard ribosomal RNAs, *E. coli* 16S and 23S, and pea 18S and 25S respectively, stained with acridine orange[23].

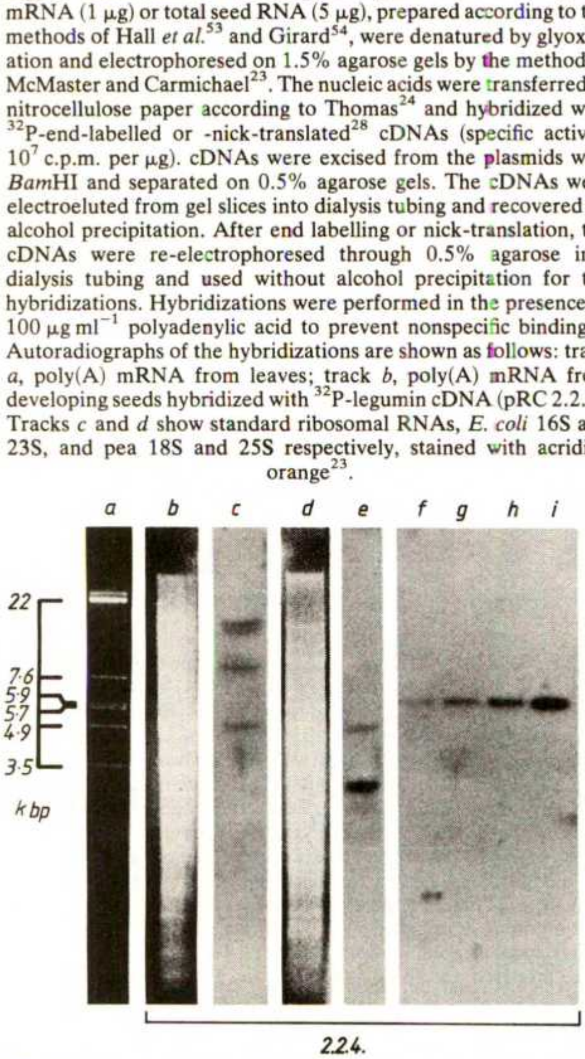

Fig. 5 Use of specific cDNAs to probe for legumin genes. Genomic DNA was isolated from developing pea leaves and purified twice on caesium chloride gradients[27]. Aliquots (5 μg) of the pure DNA were digested to completion with *Eco*RI, or *Hin*dIII. The fragments were then separated by electrophoresis overnight on 0.5% agarose gels and transferred to nitrocellulose paper[24]. The genomic blots were hybridized with ^{32}P-cDNAs prepared as described in Fig. 4 legend (specific activity $\geq 10^7$ c.p.m. per μg). Track *a* shows standard fragments of an *Eco*RI digest of λNM258, stained with ethidium bromide; tracks *b*, *c* show *Eco*RI and tracks *d*, *e* *Hin*dIII digests of pea genomic DNA stained with ethidium bromide (tracks *b*, *d*) and probed with ^{32}P-legumin cDNA (pRC 2.2.4) (tracks *c*, *e*); tracks *f*–*i* show 2.6, 5.3, 10.6, 26.5 pg of linearized plasmid pRC 2.2.4 (corresponding to 0.5, 1, 2 and 5 legumin gene copies in 5 μg of genomic DNA[27]) and hybridized with ^{32}P-legumin cDNA.

analyses and amino acid sequencing of purified acidic and basic polypeptides (refs 16, 31–33, 35 and Nielsen, personal communication)—that is, more than could be specified by four genes (for a review see ref. 36). Some of the additional heterogeneity may be accounted for by post-translational modifications[3,37] or, on the other hand, the probe used here may not have hybridized to all legumin DNA sequences. Similar analysis of genomic DNA isolated from pea seed cotyledons gave no evidence for selective amplification or alteration of the legumin genes in these tissues, supporting previous work[38].

The amino acid sequence deduced from the legumin cDNA nucleotide sequence clearly shows that the coding sequence for the acidic subunit precedes that of the basic subunit in the mRNA. The processing of legumin[1] seems to be analogous to that of animal insulin, where excision of a linking (C) peptide from the precursor proinsulin by proteolytic cleavage at Arg-Arg and Arg-Lys paired basic residues produces two disulphide-linked subunits[39,40]. Such adjacent basic residues have a prominent role as endopeptidase recognition sites in the processing of many animal polypeptide hormones and secretory proteins[21,40,41]. Although a similar linking peptide has not been demonstrated for the legumin precursor, examination of the deduced amino acid sequence upstream from the N terminus of the basic subunit reveals an unusually high content of the basic amino acids and the presence of an Arg-Arg sequence only five residues from the N-terminal amino acid. Although this may be a processing site, clearly further peptidolytic processing would be required to produce the N-terminal glycine. Similar 60,000-M_r legumin precursors have been demonstrated for *Vicia faba*[3] and *Glycine max* (unpublished results), suggesting a common processing mechanism.

The relatively long half life of the legumin precursors established by *in vivo* labelling[3,28] is in accordance with the above suggestions, and implicates a secondary membrane system distinct from the endoplasmic reticulum, such as the Golgi apparatus, in this processing. Harris[42] has suggested that the Golgi apparatus may be involved in the post-translational modifications and internal secretion of seed proteins, and it is known that the processing of proinsulin is carried out in this membrane system.

Results to be published elsewhere suggest that, like legumin, the vicilin polypeptide precursors[4,12] are synthesized only from high molecular weight mRNAs (17S) and these vicilin mRNAs are also derived from genes present in single or low copy number in the pea genome.

We thank Philippa Brown, Dave Bown and Ray Taylor for technical assistance, and Bill Brammar and Dick Flavell for their help and advice on cloning strategy. The financial support of the SRC is acknowledged.

Received 17 August; accepted 13 November 1981.

1. Derbyshire, E., Wright, D. J. & Boulter, D. *Phytochemistry* **15,** 3–24 (1976).
2. Evans, I. M. *et al. Planta* **144,** 455–462 (1979).
3. Croy, R. R. D., Gatehouse, J. A., Evans, I. M. & Boulter, D. *Planta* **148,** 49–56 (1980).
4. Croy, R. R. D., Gatehouse, J. A., Evans, I. M. & Boulter, D. *Planta* **148,** 57–63 (1980).
5. Bolivar, R. *et al. Gene* **2,** 95–113 (1977).
6. Sippel, A. E. *et al. Nucleic Acids Res.* **5,** 3275–3294 (1978).
7. Klein, R. D., Selsing, E. & Wells, R. D. *Plasmid* **3,** 88–91 (1980).
8. Smith, D. F., Searle, P. F. & Williams, J. G. *Nucleic Acids Res.* **6,** 487–506 (1979).
9. Alwine, J. C., Kemp, D. J. & Stark, G. R. *Proc. natn. Acad. Sci. U.S.A.* **74,** 5350–5454 (1977).
10. Gatehouse, J. A., Croy, R. R. D., Morton, H., Tyler, M. & Boulter, D. *Eur. J. Biochem* **118,** 627–633 (1981).
11. Thomson, J. A., Schroeder, H. E. & Dudman, W. F. *Aust. J. Pl. Physiol.* **5,** 263–279 (1978).
12. Higgins, T. J. V. & Spencer, D. *Pl. Physiol.* **67,** 205–211 (1981).
13. Croy, R. R. D., Gatehouse, J. A., Tyler, M. L. & Boulter, D. *Biochem. J.* **191,** 509–516 (1980).
14. Croy, R. R. D., Gatehouse, J. A., Lycett, G. W. & Boulter, D. *Biochem. Soc. Trans.* **9,** 254P, S29–18 (1981).
15. Casey, R., March, J. F. & Sanger, E. *Phytochemistry* **20,** 161–163 (1981).
16. Croy, R. R. D., Derbyshire, E., Krishna, T. G. & Boulter, D. *New Phytol.* **83,** 29–35 (1979).
17. Kafatos, F. C., Efstratiadis, A., Forget, B. G. & Weissman, S. M. *Proc. natn. Acad. Sci. U.S.A.* **74,** 5618–5622 (1977).
18. Bell, G. I. *et al. Nature* **282,** 525–527 (1979).
19. Cheng, C. C. *et al. J. molec. Biol.* **107,** 527–547 (1976).
20. Proudfoot, N. J. & Brownlee, G. G. *Nature* **252,** 359–362 (1974).
21. Hobart, P., Crawford, R., Shen, L., Pictet, R. & Rutter, W. J. *Nature* **288,** 137–141 (1980).
22. Dagert, M. & Ehrlich, S. D. *Gene* **6,** 23–28 (1979).
23. McMaster, G. K. & Carmichael, G. G. *Proc. natn. Acad. Sci. U.S.A.* **74,** 4835–4838 (1977).
24. Thomas, P. S. *Proc. natn. Acad. Sci. U.S.A.* **77,** 5202–5205 (1980).
25. Dunham, S. M., Tenniswood, M. & Tata, J. R. *Biochem. Soc. Trans.* **9,** 202P, S17–18 (1981).
26. Millerd, A. A. *Rev. Pl. Physiol.* **26,** 53–72 (1975).

27. Graham, D. E. *Analyt. Biochem.* **85,** 609–613 (1978).
28. Amersham International *Nick Translation Kit Pamphlet* P1/86/81/4.
29. Young, R. A., Hagenbüchle, O. & Schibler, U. *Cell* **23,** 451–458 (1981).
30. Spencer, D. & Higgins, T. J. V. *Biochem. Int.* **1,** 502–509 (1980).
31. Krishna, T. G., Croy, R. R. D. & Boulter, D. *Phytochemistry* **18,** 1879–1880 (1979).
32. Casey, R. *Biochem. J.* **177,** 509–520 (1979).
33. Matta, N., Gatehouse, J. A. & Boulter, D. *J. exp. Bot.* (in the press).
34. Guldager, P. *Theor. appl. Genet.* **53,** 241–250 (1978).
35. Moreira, M. A., Hermodson, M. A., Larkins, B. A. & Nielsen, N. C. *J. biol. Chem.* **254,** 9921–9926 (1979).
36. Matta, N. thesis, Univ. Durham (1981).
37. Gatehouse, J. A., Croy, R. R. D. & Boulter, D. *Biochem. J.* **185,** 497–503 (1980).
38. Millerd, A. & Whitfeld, P. R. *Pl. Physiol.* **51,** 1005–1010 (1973).
39. Steiner, D. F. *Diabetes* **26,** 322–340 (1977).
40. Steiner, D. F., Quinn, P. S., Chan, S. J., Marsh, J. & Tager, H. S. *Ann. N.Y. Acad. Sci.* **343,** 1–16 (1980).
41. Cohen, S. N. *et al. Ann. N.Y. Acad. Sci.* **343,** 415–423 (1980).
42. Harris, N. *Planta* **146,** 63–69 (1979).
43. Evans, I. M., Croy, R. R. D., Brown, P. & Boulter, D. *Biochim. biophys. Acta* **610,** 81–95 (1980).
44. Bedbrook, J. R., Smith, S. M. & Ellis, R. J. *Nature* **287,** 692–697 (1980).
45. Grunstein, M. & Wallis, J. *Meth. Enzym.* **68,** 379–389 (1979).
46. Clewell, D. B. *J. Bact.* **110,** 667–676 (1972).
47. Katz, L., Williams, P. H., Sato, S., Leavitt, R. W. & Helinski, D. R. *Biochemistry* **16,** 1677–1683 (1977).
48. Bonner, W. M. & Laskey, R. A. *Eur. J. Biochem.* **46,** 83–88 (1974).
49. Seif, I., Khoury, G. & Dhar, R. *Nucleic Acids Res.* **8,** 2225–2240 (1980).
50. Maxam, A. M. & Gilbert, W. *Meth. Enzym.* **65,** 449–560 (1980).
51. Smith, A. J. H. *Meth. Enzym.* **65,** 560–580 (1980).
52. Chang, J. Y., Braver, D. & Wittam-Liebold, B. *FEBS Lett.* **93,** 205–214 (1978).
53. Hall, T. C. *et al. Proc. natn. Acad. Sci. U.S.A.* **75,** 3196–3200 (1978).
54. Girard, M. *Meth. Enzym.* **12A,** 581–588 (1967).

Carboxyl–carboxylate interactions in proteins

Lindsay Sawyer* & Michael N. G. James†

MRC Group in Protein Structure and Function, Department of Biochemistry, University of Alberta, Edmonton, Alberta, Canada T6G 2H7

Much of our present understanding of macromolecular architecture has come from the extrapolation to large molecules of rules derived from analysis of small molecules. This is exemplified by the work of Pauling *et al.*[1] on polypeptide conformation, which depended on the insight afforded by the crystal structures of individual amino acids and some dipeptides. Now that accurate protein crystal structures are available, it appears that most of the hydrogen-bonding patterns that are observed have already been found in the structures of small molecules. Thus we can learn much about weak interactions in proteins by analysing small molecule crystal structures. Here we comment on the existence of hydrogen bonds between two carboxyl groups, forming what amounts to the acid salts of monobasic carboxylic acids. We believe these interactions are more important in stabilizing the structures of protein crystals and multi-subunit complexes at low *p*H than has been realized previously. Furthermore, the interaction contributes to hydrolytic activity and may be involved in inter-subunit recognition.

Speakman[2] has described type A and B monobasic acid salts of general formula MHX_2. Examples of type B, having the formula $M^+X^-.HX$, rubidium hydrogen bisglycollate hydrate[3] and potassium hydrogen di-*p*-nitrobenzoate[4]. On the other hand, type A salts have formally equivalent X units requiring the O...H...O bond to be situated on a symmetry element. For example, the carboxyl groups in the crystals of potassium hydrogen bisphenyl acetate are related by a centre of symmetry[5] and, of more interest here, sodium hydrogen diacetate has a dyad axis relating the acidic groups[6]. Only one proton is involved in the interaction so that the carboxyl groups adopt an offset arrangement which allows a variety of conformations. We have defined these conformations in terms of five angles and the distance of the hydrogen bond (see Table 1). The remaining negative charge in the case of the small molecule is balanced by a nearby cation, M. The structures of many such acid salts have been reported and it is not surprising to find that they exist in proteins. Table 1 shows some typical carboxyl group dimensions for these salts.

'Pronase', a crude extract from cultures of *Streptomyces griseus*, contains several distinct proteolytic enzymes, of which the crystal structures of protease A (SGPA) and protease B (SGPB) have been refined at high resolution. Each has a distinctive carboxyl–carboxylate hydrogen bond as an essential intermolecular interaction. SGPB crystallizes in space group $P2_12_12$ from 1.2 M KH_2PO_4, *p*H 4.2 (ref. 7). Refinement has given an *R* factor of 14.9% for the data to 1.7 Å. From Fig. 1*a*, which shows the region around the crystallographic dyad, it can be seen that the Glu 137 residues (192A) form a close interaction. (Numbers in parentheses refer to alternative numbering schemes[9,10].) This relationship is precisely that found in type A acid salts and the separation is consistent with a very short hydrogen bond (see Table 1). Note that there is no balancing cation as observed in the small molecule structures. O255 could perhaps be considered a cation but the occupancy and temperature factor would be consistent only with H_3O^+. However, in every case where an oxonium ion has been examined in a crystal, there is a pyramidal arrangement with three hydrogen bonds of ~2.6 Å (ref. 8). The hydrogen bond from Glu 137 O^ϵ (192A) to Cys 162 N (220) will partly counteract the extra negative charge because of the peptide dipole. At *p*H ~4, partial protonation of a glutamic acid side chain (pK_a = ~4.3) is expected. Removal of

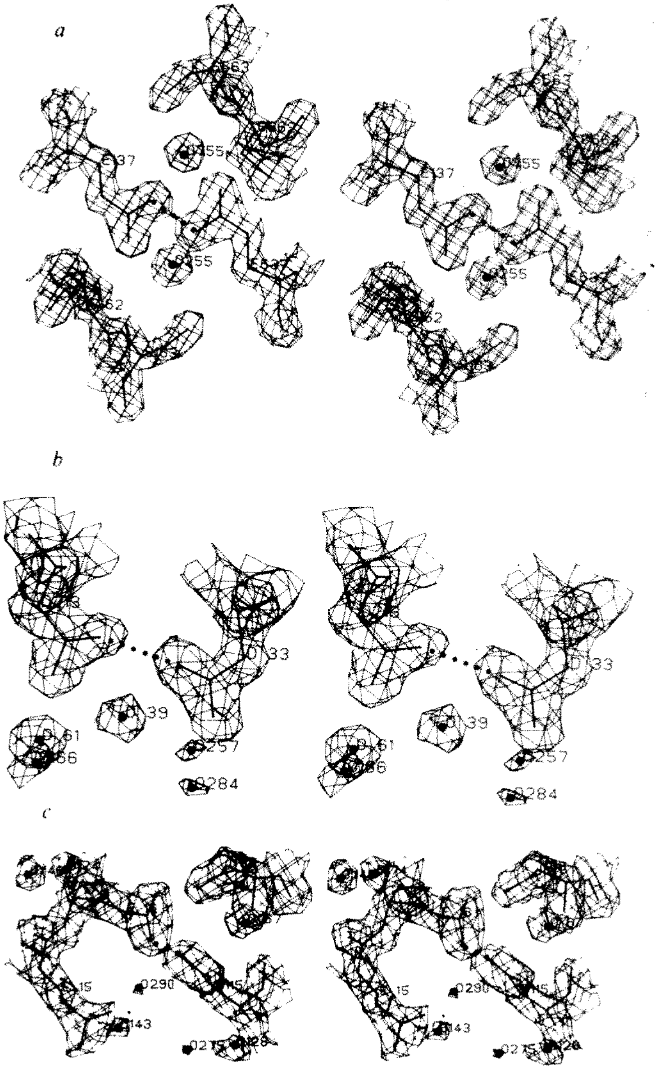

Fig. 1 The carboxyl–carboxylate interactions in *S. griseus* protease B and penicillipepsin. In each case, the hydrogen bond is shown as a dotted line but for clarity the other hydrogen bonds have been omitted. *a*, Type A interaction in SGPB viewed in the direction of the dyad axis parallel to *c*. The contour level is 0.6 e $Å^{-3}$. For ease of identification the residues of the twofold-related molecule have had 500 added to their sequence numbers. *b*, Type B interaction of the two catalytic residues in penicillopepsin, Asp 33(32) and Asp 213(215). The contour level is 0.5 e $Å^{-3}$. *c*, The second type B interaction in penicillopepsin involves Asp 115(114) and Glu 16(13). The contour level is 0.45 e $Å^{-3}$.

---

* Permanent address: Department of Chemistry, Napier College, Edinburgh EH10 5DT, UK.
† To whom correspondence should be addressed.

0028–0836/82/010079—02$01.00

Table 1 Distances and angles for carboxyl–carboxylate interactions

Compound	κ_1	κ_2	κ_3	κ_4	κ_5	d (Å)	Type
Rubidium bisglycolate hydrate	172.6	172.6	57.0	115.7	120.6	2.53	B
Potassium hydrogen di-*p*-nitrobenzoate	175.5	149.0	81.3	109.7	140.4	2.49	B
Potassium hydrogen bisphenyl acetate	177.7	180.0	177.7	113.9	113.9	2.44	A
Sodium hydrogen diacetate	166.8	137.7	166.8	110.8	110.8	2.45	A
Imidazolium hydrogen maleate*	49.8	38.7	49.6	109.6	109.2	2.37	A
SGPA	168.2	130.9	54.9	118.5	116.1	2.51	B
SGPB	173.0	159.5	173.0	112.5	112.5	2.49	A
Penicillopepsin Asp 33–Asp 213	123.8	149.8	147.1	159.0	147.4	2.88	B
Penicillopepsin Glu 16–Asp 115	168.4	134.1	163.7	123.1	113.0	2.75	B
Actinidin†	168.6	174.8	168.0	124.5	119.5	2.51	B

The angles are defined with respect to the carboxyl groups assigned, for type B acid salts, such that subscript numbers 1–4 refer to the —COOH and, for proteins, to the group of lower sequence number.

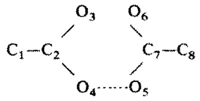

Torsional angles: κ_1, C_1C_2–O_4O_5; κ_2, C_2O_4–O_5C_7; κ_3, O_4O_5–C_7C_8. Bond angles: κ_4, $C_2\hat{O}_4O_5$; κ_5, $O_4\hat{O}_5C_7$. Distance: d, O_4–O_5. Angles are measured in degrees. Standard deviations for the small molecule structures are of the order of 0.01 Å for bond length, 0.1° for bond angle and 0.2° for torsion angle. For the protein structures, the corresponding values are ~0.1 Å, 3.0° and 5.5°. Type A salts exhibit very short, apparently symmetrical hydrogen bonds typified by[22] OH stretching frequency in the 700–1,000 cm^{-1} region and bond strength of ~8 kcal mol^{-1}. * Ref. 21. † Ref. 16.

the proton by raising the *p*H leads to repulsion of the two negative charges, which in turn destabilizes the crystals and at *p*H values >4.5, both SGPB and SGPA crystals dissolve. In a paper describing the refinement of SGPA, Seilecki *et al.*[11] present the interaction between the carboxyl group of Asp 123 and the terminal carboxyl group of Leu 242. This hydrogen-bonded interaction is of type B and includes a charge neutralizing Na^+. The two carboxyl groups arise from separate molecules and thus contribute to the stability of the crystal structure. Parameters for this interaction are also included in Table 1.

The crystal structure of the aspartyl protease, penicillopepsin[12], has recently been refined at 1.8 Å resolution to an *R* factor of 13.6% (to be published). The carboxyl groups of the two catalytic aspartyl residues, Asp 33(32) and Asp 213(215), also share a proton at *p*H 4.4, the *p*H of the native crystals. These carboxyl groups are at the junction of the two large domains of the aspartyl proteases, at the bottom of the substrate-binding cleft. Their spatial arrangement is different from the examples given above (see Fig. 1*b*). As in SGPB, there is no balancing cation for the type B acid salt in penicillopepsin. However, the excess negative charge is in part balanced by the proximity of several peptide dipoles[13]. The carboxyl groups are also arranged so as to provide an electrophilic proton as well as to help stabilize the inter-domain junction. Furthermore, pepsin is reported[14] to have a slightly raised pK_a for Asp 215(213) which is as expected where two carboxyl groups are maintained in close contact. That such a juxtaposition can cause an unfavourable interaction is seen in the structure of *Rhizopus chinensis* pepsin, where the homologous aspartyl residues adopt a totally different disposition to relieve the repulsion evident at *p*H 6.5 (ref. 15).

A further example of this is found in penicillopepsin (Fig. 1*c*), where the juxtaposition of the carboxylate of Asp 115(114) with that of Glu 16(13) demands that they share a proton, but the torsion angles (see Table 1) in this case seem more in keeping with a type A structure, although the small molecule data may not be representative. This seems to be associated with the additional presence of a hydrogen-bonding amide group from Asn 118(117) which donates the proton from Asn 118 $N^{\delta2}$ to the other oxygen $O^{\epsilon1}$ of Glu 16 ($d = 2.91$ Å). It can be seen that the carboxyl group of Glu 15 is not involved directly with these interactions.

The values of torsion angles κ_1–κ_3, bond angles κ_4 and κ_5, and bond length d, for the proteins examined are not unusual when compared with those of the acid salts (Table 1). However, the values of κ_4, κ_5 for the Asp 33(32)–Asp 213(215) interaction in penicillopepsin are appreciably higher and the distance separating the oxygen atoms is slightly longer than in the other examples. This is consistent with the less than ideal arrangement of proton sharing expected if the proton is to take part in catalysis.

The imposition of a restricting, near-neighbour arrangement for two carboxyl groups can lead to an anomalous pK_a. Thus, the *cis*-double bond of maleic acid leads to the high pK_{a2} of 6.1 as compared to that of 4.4 for the *trans*-isomer, fumaric acid. In proteins it seems unlikely that an anomalous pK_a may arise from an analogous restrained environment around two carboxyl groups. Unfortunately the unambiguous assignment of anomalous titration data to particular carboxyls in proteins does not coincide with the highly refined structures available. For example, the actinidin structure at *p*H 5.9 (ref. 16) shows a type B acid salt interaction between glutamic acid residues 50 and 86 but no titration data are available. In the case of tobacco mosaic virus there is ample evidence for anomalous carboxyl groups[17,18] but their interactions, although almost certainly of the type we describe, are not yet known in sufficient detail[19,20].

We may conclude that the carboxyl–carboxylate interaction is an important stabilizing force in protein–protein interactions at low *p*H and, at higher values, may occur more frequently than previously believed in association with an anomalous pK_a. Conversely, the unambiguous detection of an anomalous pK_a for acidic groups in proteins can be, and often is, a sign of carboxyl–carboxylate interactions of the type described here.

We thank W. Anderson for helpful criticism and C. Broughton, C. McPhalen and A. Sielecki for valuable assistance. L.S. thanks the MRC (Canada) for a Visiting Scientist Award and Lothian Regional Council for leave of absence. This work was supported by a MRC (Canada) grant to the Group on Protein Structure and Function, University of Alberta.

Received 30 June; accepted 26 October 1981.

1. Pauling, L., Corey, R. B. & Branson, H. R. *Proc. natn. Acad. Sci. U.S.A.* **37,** 205–211 (1951).
2. Speakman, J. C. *Structure & Bonding* **12,** 141–199 (1972).
3. Golič, L. & Speakman, J. C. *J. chem. Soc.*, 2521–2530 (1965).
4. Shrivastava, H. N. & Speakman, J. C. *J. chem. Soc.*, 1151–1163 (1961).
5. Manojlović, L. & Speakman, J. C. *Acta crystallogr.* **B24,** 323–325 (1968).
6. Speakman, J. C. & Mills, H. H. *J. chem. Soc.*, 1164–1175 (1961).
7. Delbaere, L. T. J., Hutcheon, W. L. B., James, M. N. G. & Thiessen, W. E. *Nature* **257,** 758–763 (1975).
8. Lundgren, L.-O. & Olovsson, I. in *The Hydrogen Bond* Vol. 2 (eds Schuster, P., Zundel, G. & Sandorfy, C.) 471–526 (North-Holland, Amsterdam, 1976).
9. Hartley, B. S. *Nature* **201,** 1284–1287 (1964).
10. Tang, J. *et al.*, *Proc. natn. Acad. Sci. U.S.A.* **70,** 3437–3439 (1973).
11. Sielecki, A. R. *et al.*, *J. molec. Biol.* **134,** 781–804 (1979).
12. Hsu, I.-N., Delbaere, L. T. J., James, M. N. G. & Hofmann, T. *Nature* **266,** 140–145 (1977).
13. James, M. N. G., Hsu, I.-N., Hofmann, T. & Sielecki, A. R. in *Structural Studies on Molecules of Biological Interest* (eds Dodson, G., Glusker, J. P. & Sayre, D.) 350–389 (Oxford University Press, Oxford, 1981).
14. Cornish-Bowden, A. J. & Knowles, J. R. *Biochem. J.* **113,** 353–362 (1969).
15. Subramanian, E., Liu, M., Swan, I. D. A. & Davies, D. R. in *Acid Proteases Structure, Function and Biology* (ed. Tang, J.) 33–60 (Plenum, New York, 1977).
16. Baker, E. N. *J. molec. Biol.* **141,** 441–484 (1980).
17. Caspar, D. L. D. *Adv. Protein Chem.* **18,** 37–121 (1963).
18. Durham, A. C. H. & Kung, A. *Nature new Biol.* **229,** 42–46 (1971).
19. Stubbs, G., Warren, S. & Holmes, K. C. *Nature* **267,** 216–221 (1977).
20. Bloomer, A. C., Champness, J. C., Bricogne, G., Staden, R. & Klug, A. *Nature* **276,** 362–368 (1978).
21. James, M. N. G. & Matsushima, M. *Acta crystallogr.* **B32,** 1708–1713 (1976).
22. Novak, A. *Structure Bonding* **18,** 177–216 (1978).

BOOK REVIEWS

Nationalized science and technology

Eric Ashby

THIS is a sober and sobering book. Professor Tisdell was asked "to prepare an independent background report on the subject of priority assessment in science and technology for the Australian Science and Technology Council". His book is an expansion of this report. Don't assume that it is of interest only to Australians; the prospects for Britain might be less depressing if a number of senior civil servants and members of the present government were to be given three days' leave in order to read the book and ponder its message.

When Queen Victoria came to the throne the pursuit of science, like the pursuit of literature, was a career for the self-employed, often subsidized by payment from some other occupation. T.H. Huxley earned his living at first by teaching; Anthony Trollope by inspecting post-offices. The notion that there was need for a science policy would have been as crazy as the notion that there was a need for a policy among poets and novelists.

By the time Queen Elizabeth came to the throne all this had changed. Poets and novelists could still pursue their stars without deviations caused by governments, but scientists were no longer immune from influence. The critical time was the year when the government grant to universities exceeded 50 per cent of their total income. There was no *dirigisme* at first, of course. The taxpayer had become paymaster and patron of science but initiative was left, still, to individuals. But the seeds of *dirigisme* had been sown. We are now painfully reaping the harvest: a rank growth of policy-documents, technology assessment, predictions about research and development. The public interest is now called a "customer" and the laboratory worker a "contractor": science by mail order.

This is, of course, the inevitable result of the staggering successes of science applied to human needs (though in one sense it would be more accurate to say science applied to human destruction). Governments have realized that research and development is too important to be left to industry alone. More and more scientific research — both pure and applied — is now the "property" of the taxpayer, whose money pays for government research establishments, the grants from research councils and a great deal of the costs of universities. The scientist, provided he is willing to work on problems for which he can get grants, can adapt himself to this situation. It is the customer who is in a dilemma. He has to draw up a shopping list and he hasn't enough money to pay for all the science he would like to have. So he has to decide priorities. And since "he", in a pluralistic democracy, is the social welfare function — the consensus of society — the task of deciding priorities is, on rational criteria, insuperable. The best one can do is to make provisional choices on imperfect evidence.

Science and Technology Policy: Priorities of Governments. By C.A. Tisdell. Pp.222. ISBN 0-412-23320-7. (Chapman and Hall: 1981.) £12, $25.

Tisdell's book is a manual of advice for those who make such choices. His starting points are the lists of research and development objectives published by OECD and the EEC. They are taxonomic lists of no great value. He then discusses an issue of special relevance to countries with small economies (compared with the giants), namely how much science should such countries import and exploit? And to what extent should such countries rely on their own springs of initiative in pure research? There is, he explains, a trade-off between the import of ideas and their local production. The profit to be made out of the exploitation of a new idea will vanish as soon as some (so called) less developed country starts marketing it at a fraction of the manufacturing cost.

The bulk of Tisdell's book is taken up with an analysis, well documented and supported by quantitative data, of the research and development policies of large economies (Germany, Japan, Britain and the USA) and small economies in the OECD (Belgium, Canada, Netherlands, Sweden and Switzerland). In all of these countries there is some formal procedure for setting priorities, sometimes well co-ordinated, sometimes (notably in Britain) fragmented among different government departments. For a while these procedures were conducted by bureaucrats and experts without reference to the public and without canvassing public opinion. This, as Tisdell demonstrates, is no longer practicable or desirable. Not only does the public want to participate through public interest groups — that is proving difficult enough — but also there are surges of pressure to change the order of priorities. Thus in the 1950s the assumption was to use profit and market success as the units for assessing research and development. Then in the 1970s the assumption was challenged; improvement of the quality of life rose higher in the shopping list. Now we are back again to less exalted objectives: in a world depression, the high priority is to survive economically by capturing markets, and this has come to be the short-term aim of research and development.

In a sombre last chapter, Tisdell asks the questions — though of course he cannot supply the answers — that spin round in the policy-maker's mind all the time. Everyone admits that the optimum social welfare function cannot be derived from individual welfare functions; no one has a *politically* practicable alternative except to bring to politics the techniques of the oriental marketplace: haggling, trade-off and bluff. Not everyone, but many thoughtful people, admit that high unemployment among untrained people is a consequence of much modern technology; no one has a remedy for this evil except to repeat platitudes about making education more relevant (hardly a practicable proposal for schools on their present starvation diet).

At one point Tisdell suggests three options open to governments for science and technology: to try to slow down the rate of change; to let change proceed unplanned, in which individual governments and industries pursue their own self interest "with scant regard to the common good"; to establish collective or social priorities (and, I would add, international priorities) for the programme of change in science and technology. The first of these options is as feasible as stemming the tide; the second is an open cheque for chaos; the third is the only tolerable option. But will a nation as pluralistic as the United States, or as socially polarized as Britain is these days, adopt this option? President Carter's call for austerity to cope with "the moral equivalent of war" didn't meet with much response; Britain's attitude to the Brandt Report hasn't provoked a surge of altruism. The question, often asked and not yet answered, is whether human communities can make painful adaptations to avoid a breakdown in economic order before it comes; or whether, like communities of animals and plants, the adaptations will follow only as a response to a harsh environment after its effects have begun to bite. It is a sign of his anxiety that Tisdell turns at the end of his book to Daniel Bell's ominous book on the post-industrial society, with its "lack of an ordering mechanism to make social choices". Tisdell warns: "We may all know that collectively we are heading for tragedy but individual self-interest of nations and of individuals may necessitate the tragedy to be played out". In a sensational pamphlet on doom such a sentence as this might be shrugged off. In an economist's sober report to the Australian Science and Technology Council, the sentence has a ring of integrity and conviction; for Tisdell offers an antidote to despair: "A fall in exports and in living standards *could* be worthwhile from the point of view of achieving more basic ends". ☐

Lord Ashby was formerly Master of Clare College, Cambridge. His most recent book, written with Mary Anderson, is The Politics of Clean Air *(Clarendon/Oxford University Press, 1981.)*

From myth to methodology

C.K. Brain

Bones: Ancient Men and Modern Myths. By Lewis R. Binford. Pp.320. ISBN 0-12-100035-4. (Academic: 1981.) £24.20, $36.50.

IT IS perhaps surprising that a new book by one of the most influential of archaeologists should deal, not with cultural remains, but with bones. By way of explanation, Lewis Binford observes that almost all of our ideas on the behaviour of prehistoric men have been based on interpretations of faunal remains and their depositional context — not, as so many textbooks would lead one to believe, of stone tools. So, in discussing reconstructions based on bones, Binford has significant things to say about the proper conduct of scientific enquiry as well as about the behaviour of early man.

Most of the inferences that have been drawn about the nature and activities of our prehistoric ancestors are seen by Binford as little more than "myths of prominent men". Some of these concepts may well have been accurate, but unless they were the products of a robust and reliable methodology for giving meaning to bones, they remain myths based on the opinions and perhaps even the biases of the investigating archaeologists. In traditional archaeology, Binford believes that concepts about early man have often been judged in accordance with the status of the archaeologist who propounded them. "We desperately need to abandon the technique of evaluating men and adopt the strategy of evaluating ideas", he writes, for in the absence of methodology it is people's reputations that are reshuffled.

The kind of methodology proposed by Binford as an alternative to myth-making is embodied in what he calls "middle-range research". A crucial characteristic of theories resulting from such research is that they are intellectually independent of the arguments about the phenomena they are used to illuminate. As an example, Binford cites the case of carbon-14 analysis, where independent physical research had established a reliable body of theory about the relationships between living organisms, atmospheric ^{14}C and rates of degeneration of the radioactive isotope. Such relationships have been put to good use by archaeologists wishing to date organic remains preserved at their sites.

Apart from philosophical considerations of myths and methodologies, the main aim of the book is to provide a set of objective criteria for the recognition of human influence in the accumulation of a bone assemblage. What are the characteristic patterns of bone modification produced by non-human agents and how can these be distinguished from human modes of bone alteration? In attempting to answer these questions, Binford has drawn on his own extensive observations of Nunamiut Eskimos and their dogs in Alaska, as well as of wolves that inhabit those parts. He has provided a wide-ranging review of relevant work done elsewhere and has set up a convincing array of diagnostic criteria for separating hominid- from non-hominid-built bone accumulations.

Finally, in the third part of the book, Binford applies his methodology to bone assemblages from Olduvai Gorge, making use of data provided by Mary Leakey in Vol. 3 of *Olduvai Gorge.* As Clark Howell has pointed out in the foreword to Binford's book, these data were not collected for this specific purpose and so are not ideal. Nevertheless, some bold conclusions have been reached by Binford, such as that there is no evidence that Olduvai hominids hunted, or that they made use of base camps to which food was carried to be shared. Instead, our hominid ancestors are seen as having been scavengers at discarded carnivore kills where hammerstones were used to break open leg bones to extract marrow.

Binford's book is a major, if controversial, contribution to the rapidly expanding literature on the new science of taphonomy. Already his conclusions are being challenged, for example by H.T. Bunn (*Nature* **291**, 574–577), and it will be interesting to follow the fortunes of his ideas under the impact of the rigorous methodology that he so eloquently advocates. ☐

C.K. Brain is Director of the Transvaal Museum, Pretoria, South Africa.

Nature's plumbing

Philip England

Geysers and Geothermal Energy. By John S. Rinehart. Pp. 223. ISBN 3-540-90489-1. (Springer-Verlag: 1981.) $22.50, DM 38. *Geothermal Resources: An Energy Alternative.* By Harsh K. Gupta. Pp. 227. ISBN 0-444-41865-2. (Elsevier Scientific: 1981.) $61, Dfl. 125. *Geothermal Systems: Principles and Case Histories.* Edited by L. Rybach and L.J.P. Muffler. Pp. 359. ISBN 0-471-27811-4. (Wiley: 1981.) £22, $52.25. *Geothermal Systems.* By John Elder. Pp. 508. ISBN 0-12-236450-3. (Academic: 1981.) £20.60, $49.50.

STATED simply, a geyser is a water system to which mass and/or heat are added until a portion of the column is super-critical. At some stage nucleation of boiling occurs in this region and the consequent expansion partially empties the water column, reducing the pressure within it and leading to further boiling in the decompressed system, with spectacular eruptions of steam and water at the surface. The diversity of style and periodicity of geyser eruptions results from the almost endless variations on this theme which are possible given the multiple recharge–discharge systems occurring in nature.

In *Geysers and Geothermal Energy* John Rinehart has provided a detailed — one might say an affectionate — catalogue of these idiosyncrasies, together with the complex hydrological interpretations of them, when available. He also discusses briefly the geochemical and environmental aspects of geysers. One disappointing aspect of the book is that not enough attention is paid to the central process of geyser eruption: the problems of boiling initiation and bubble nucleation are dealt with in a cursory fashion. In other respects the book provides all the information on geysers that the layman or student could reasonably ask for. There is, in addition, one chapter of 15 pages on geothermal energy.

The remaining three books reviewed here all approach geothermal systems by way of an outline of plate tectonic theory, mantle convection and the present distribution of tectonic activity, and then diverge along lines that are to be expected from their formats. Gupta's *Geothermal Resources* is one of Elsevier's series on Developments in Economic Geology, and attempts to cover every aspect of the subject at the expense of the brevity which a 200-page format imposes on such an approach. The book is a review of the subject, covering everything from Earth structure and the basics of heat transfer (although convection is treated solely in terms of Newton's law of cooling) to production technology and world energy problems. The level and quality, however, are considerably lower than either of the two remaining books. The section on global dynamics is not good, and nothing is dealt with in adequate detail. Further, the material is not particularly up-to-date and for a book of its price and brevity it has been poorly edited.

Geothermal Systems: Principles and Case Histories, a collection of papers edited by Rybach and Muffler, concentrates on specific topics. Following an introduction on geothermal anomalies and global tectonics, there are contributions on heat and mass transfer in hydrothermal systems, geothermal prospecting, heat extraction from reservoirs and resource assessment and environmental aspects, on which lucid and informative reviews (with up-to-date references) have been provided by people active in these particular fields. The reviews fill two-thirds of the book, the remainder consisting of case histories from various geothermal fields. These latter papers provide roughly the same sequence of information — geological framework, history of exploration, present-day exploitation — but are of a more variable quality than the first part of the book. The areas covered are the low enthalpy resource of the Pannonian Basin, the use of steam for electrical power generation from the Krafla field in Iceland, the Takinoue field in Japan and the Ahuachapan field in El Salvador, and the Jemez geothermal field — which contains high- and low-temperature hydrothermal systems as well as hot dry rocks. The book concentrates on the geological and geophysical aspects of geothermal energy extraction, so that there is little information on the engineering problems or the economics of this source of power.

To a greater extent than is usual for a collection of papers, this volume does succeed in giving a coherent picture of the subject. Credit for this must go to the editors who have chosen judiciously the areas to concentrate on and, I suspect, exerted some unifying influence on the contributions in the last one-third of the book.

If the antipodean reader were to feel that the geothermal fields of New Zealand are given unduly little attention in Rybach and Muffler's book, this hole is firmly plugged in Elder's volume of the same title. The book ought more properly to be called *Hydrothermal Systems*, as the possibility of extracting heat from dry rocks is not addressed. Instead, Elder provides a comprehensive survey of the mechanisms of heat and mass transfer within the Earth, at a higher level, but in a style which will be familiar to readers of the *Bowels of the Earth*. I am not referring to the use of anatomical analogies; that aspect is, mercifully, absent from the book (one may imagine the emunctory analogues which could be produced for hydrothermal systems).

The approach Elder adopts is more that of the engineer than of the applied mathematician or physicist; as he explains in the preface, this arises from a natural desire to avoid deducing from first principles a set of results that are inconsistent with our observations of the Earth. It leads him to produce models for each system that he investigates which are characterized by pragmatism and simplicity, and which permit him to estimate order-of-magnitude figures for everything from global partial melting to the motion of steam bubbles in mud. Such an approach can be extremely successful (more so with bubbles than partial melt) but depends on the amount of common ground one shares with Professor Elder; certainly, it beats deriving every aspect of water–rock interaction from the Second Law of Thermodynamics, but it can be carried too far. After 400 pages of models being pulled out of whichever hat Professor Elder is wearing, either one suspends critical faculties and accepts each model at face value (rather than working out the extent to which it matches geological reality), or one starts to feel the need for a more explicit physical base to what is being said. This is more of an error of judgement than a major drawback and there is much to gain from such a refreshing approach to the subject.

My only other criticism is of a similar order: the first 160 pages of this book are devoted to global tectonics and the origin and emplacement of magma bodies: aside from the fact that a newcomer to the subject would gain from it an impression that no geophysicist or geologist has worked on these problems, this is surely an over-long introduction. ☐

Philip England is in the Department of Geological Sciences, Harvard University.

Ecology: a Japanese perspective

John Lawton

Comparative Ecology, 2nd Edn. By Y. Itô. Edited by Jiro Kikkawa. Pp. 436. ISBN hbk 0-521-22977-4; ISBN pbk 0-521-29845-8. (Cambridge University Press: 1981.) Hbk £22.50, $54; pbk £9.95, $19.95.

SCIENCE, like pop music or *haute couture* has fads and cliques, although scientists like to pretend otherwise. Ecology is no exception, with too many groups isolated to a greater or lesser extent by language, geography, tradition and the impossibility of reading even a fraction of the relevant literature. Contact between European, North American and Japanese ecologists has generally been good, but inevitably many papers in Japanese go unread by English-speaking scientists. A major strength of Professor Itô's book is to summarize and publicize work originally published in Japanese — roughly ten per cent of the entries in the long and comprehensive bibliography are in this category.

That said, I have to admit that I found the book heavy going, not because of Jiro Kikkawa's excellent translation, but because of the almost overwhelming mass of detail which Itô compresses between the covers, organized around a single unifying, but in the end not wholly convincing, theme.

For Itô, the animal kingdom is divided into beasts of the two sorts. On the one hand are those opting for high fecundity, living in environments where food for their young is easily procured; and on the other are species whose young enter a more hostile world, displaying low fecundity and parental care as a consequence. The whole of population dynamics, territorial behaviour and animal society are then interpreted within this simple framework.

Itô is at pains to show how his world view differs from the deeply entrenched traditions of "r and K selection" more familiar to European and North American ecologists. Certainly there are differences, albeit rather subtle. More importantly, Itô's view stands or falls on his ability to provide an independent measure of food supply. On this fundamental point his thesis is distinctly shaky. Food supplies are never measured directly; indeed his logic is often

IRCS JOURNALS

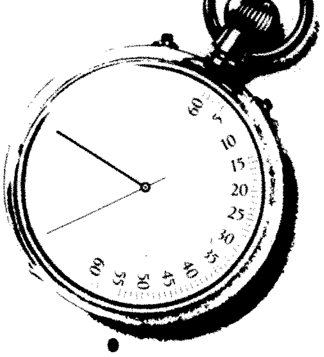

Keeping pace with science

IRCS Medical Science
St. Leonard's House
St. Leonardgate,
Lancaster, U.K.

A member of Elsevier Science Publishers

Circle No. 12 on Reader Enquiry Card.

circular — if an animal displays parental care, its young, by definition, face an impoverished habitat.

To be fair, I suspect that Itô hopes to provoke others into making the necessary measurements, and like all attempts to force the bewildering variety of the living world into a manageable framework, his vision is certainly true in parts. Thus high, or low, fecundities (Chapter 1) do tend to be associated with particular types of survivorship curves (Chapter 2), generating particular patterns of population fluctuations (Chapter 3), and social systems (Chapters 4–6). But there are bound to be numerous exceptions, and in trying to force every example into one mould, the book sometimes makes difficult reading.

European and North American colleagues will also feel uneasy with those parts of the book which fail to incorporate important concepts from their own contemporary literature. I noticed this particularly in Chapter 3, which deals with population fluctuations in a way that fails to reflect major advances of recent years.

I make these criticisms very reluctantly, because any book which increases the flow of ideas and information between groups of ecologists is to be welcomed. Nonetheless it must be said that this is not a good book to use with undergraduates, despite the fact that they may be more receptive to new ideas than teachers! But I do think that anybody interested in animal population dynamics and social behaviour should look at it, particularly for the richness and relative unfamiliarity of many of its principal characters. □

John Lawton is a Senior Lecturer in Ecology in the Department of Biology, University of York.

The inconstant biological membrane

A. Silberberg

Mechanics and Thermodynamics of Biomembranes. By E.A. Evans and R. Skalak. Pp.272. ISBN 0-8493-0127-0. (CRC Press/ Blackwell Scientific: 1981.) $34.95, £26.

MOST material systems are not mechanically simple. The stresses which arise cannot be expressed by the one- or two-parameter relationships which, nevertheless, have scored enormous practical successes. Much of fluid mechanics is based on the Navier–Stokes equations for an incompressible Newtonian fluid, and much of solid state deformation theory on a loss-less, purely elastic material constitutive equation.

The science of rheology has tended to bridge this gap in the engineering world, but in biology such complications are still mostly avoided. This is particularly reprehensible when, as is natural with living systems, movement of components, and indeed chemical reactions, have to be considered alongside any description of the stresses and strains which shape and confine the structural components. In developing the analysis of the chemical potential gradients along which transport of the various distinguishable chemical species will occur, the mechanical contribution is generally represented by a hydrostatic pressure gradient at most. Structural elements are taken out of consideration by being thought of as chemically inert and mechanically rigid.

This book by Evans and Skalak is thus a most welcome newcomer. It contains four main sections which, following an introduction, cover the kinematics, the dynamics and the thermodynamics of membranes; the final section summarizes the experimental situation. Some 100 references are given and a good index is also provided. The authors deal specifically with those membranes which confine cells or sub-cellular compartments, discussing the factors which mechanically govern the shape and thermodynamically will influence the stability of these systems.

This is, to my knowledge, the first systematic attempt to develop the considerations basic to the field in textbook form. The book is thus highly recommended to all workers in physiology and biophysics — to all scientists, in fact, who are dealing with the mechanics and thermodynamics of the interface in systems of heterogeneous and complex structure.

A. Silberberg is the Joseph and Marian Robbins Professor of Biorheology in the Department of Polymer Research, The Weizmann Institute, Rehovoth, Israel.

Electron microscopy

- A new volume in the series *Practical Methods in Electron Microscopy*, edited by Audrey Glauert, has recently been published by Elsevier/North-Holland Biomedical Press. Volume 9, *Dynamic Experiments in the Electron Microscope* by E.P. Butler and K.F. Hale, deals with the study of the response of materials to a change in state, using the transmission electron microscope, and costs hbk Dfl.195, $95; pbk Dfl.92, $45.
- M.A. Hayat's *Principles and Techniques of Electron Microscopy: Biological Applications* has now appeared in a second edition. Like its predecessor, the aim of the new edition is to provide a foundation in the biochemical concepts underlying the preparation of specimens for transmission electron microscopy. Co-published by University Park Press and Edward Arnold, the book costs $34.50, £27.50.

MeV volume

M.H. Key

Laser Interaction and Related Plasma Phenomena, Vol.5. Edited by Helmut J. Schwarz *et al.* Pp.850. ISBN 0-306-40545-8. (Plenum: 1981.) $75, £47.25.

LASER plasma interactions at high levels of irradiance involve a fascinating variety of physical processes and phenomena. Plasma produced in this way has many significant applications, arising mainly from the extreme energy density available. Laser fusion is the major motivation of much of the world-wide activity, but basic physics investigations — for example into X-ray lasers, energy transport in high temperature gradients and the characteristics of matter at extreme pressures — are beneficiaries of the technical developments arising from laser fusion research.

It is difficult to produce books which adequately describe the state of the art in such a wide-ranging and fast-moving field. The well-tried formula of a compilation of contributions from specialist authors has the best possibilities and the present volume is the latest in a series of this genre.

The old editorial team of H.J. Schwarz and H. Hora has been strengthened by M.J. Lubin and B. Yaakobi of the University of Rochester, and the book presents contributions from an internationally representative panel of 37 scientists who lectured at a workshop in 1979. I find that the book provides a better-organized selection of material than some of the earlier volumes; it has a mix of basic reviews and current research topics, and therefore offers something both for those researching in the same field and for those with a more general interest.

There are five major sections, covering lasers and alternative pulsed power sources, interaction experiments, general considerations for fusion, fusion-related experiments and interaction theory, and here the reader is given a fairly good guide to the topical issues of 1979–1980. The review material covers subjects such as new lasers, free electron lasers, light ion beams, new fusion fuels, high-density diagnostics, target manufacture, soliton theory, Rayleigh–Taylor instability, stimulated scattering and Stark broadening of high Z ion lines. It is generally authoritative and up to date. The descriptions of more detailed research activities have inevitably become somewhat dated, though specialists will find them useful as sources of reference to past work.

I feel researchers in the field will want access to this book as a valuable compendium of information, while non-specialists may wish to consult one or more of its review sections. □

M.H. Key is Deputy Head of the Laser Division at the SERC Central Laser Facility, Chilton, Oxfordshire.

nature

Library Company
Chemical Engineering
Chemical Technology
& Rubber Technology

14 January 1982

Creationists and science in schools

Creation science has rightly been denied a licence in Arkansas on the grounds that it is religion in disguise. The educational implications are even more sinister.

The creationists may have lost the battle in Arkansas, but they are unlikely now to abandon the war on which they are engaged. Science educators everywhere, but especially in the South, had better reconcile themselves to that. The United States courts are notoriously a means by which determined if misguided people can refuse to accept the inevitable, creating confusion and widespread nuisance. In the circumstances, it is important that everybody should be clear what the war is about. It is not a war about the validity of Darwinism, however understood and glossed. Nor is it a war between religion and science, for some of the most influential evidence against the creationists in Judge William Overton's court came from religious people anxious to dissociate themselves from the claims of the creationists. The underlying dispute is between a small section of the religious community in the United States to whom the evolutionary view of the world, inanimate and living, is anathema. The claim that "creation science" should be taught alongside orthodox evolution as if it, too, were science is both preposterous and disingenuous.

The richest irony in the creationists' case is the attention that it pays to the supposed flaw in Darwinism, which is alleged to be unfalsifiable experimentally. By what logic can it be held that because Darwinism is unfalsifiable in some technical (and disputed) sense, a set of hypotheses which is in the same sense falsifiable and amply falsified should be given equal time in the curriculum of the public schools of Arkansas and elsewhere? How, in the side-by-side science lessons for which they have been asking, would the creationists deal with questions such as the presence in the Earth's crust of lead isotopes which have apparently accumulated over the past 4,500 million years? By asserting that the technically falsifiable but amply verified explanation of radioactive decay is also false? And in that case, why should the proportions of radiogenic and nonradiogenic lead have been created at some later time in such a way as to mimic the effects of geochemical differentiation? To fool us? Or to show that the Creator was a good geophysicist? Most religious people rightly and consistently dismiss such questions as irrelevant, and and even sacrilegious.

Other educational questions remain. Although the chief basis of Judge Overton's decision was that the state law he struck down was unconstitutional by providing a disguise for religious teaching, in many ways its requirements of science teachers were a more sinister threat to good sense. For teachers who are not allowed to tell what they consider to be the truth and who are required to tell lies are necessarily bad teachers. How are these epitomes of duplicity to be trained? Or is it thought, in Arkansas and elsewhere, that the teaching of science consists of the recitation of facts by teachers and feats of memory by students? Legally, what Arkansas had planned to ask of its teachers was an offence against the First Amendment. The damage that Arkansas had unthinkingly proposed inflicting on the education of its young people would have cast a longer shadow. When the issue of creationism in the schools comes up next, in Louisiana or wherever, the educational folly of giving equal time and place to a literal interpretation of *Genesis* should be given as much attention as its consitutional impropriety.

At the same time, some thought should be given to the way in which an over-literal interpretation of the constitutional interdiction against religious teaching in the public schools is itself an impoverishment of American education. *Genesis* may be a pack of lies, or of allegories, but it is also an important part of the cultural heritage. So, too, is the Koran. Is it necessary that these important topics should be forever ignored, or relegated to "Eng Lit." or fuzzy courses such as "the world about us" simply because school boards fear they may be accused of propagating religious views? For that matter, should the history of the world outside the Americas continue to be considered suitable only for colleges and universities? It is unlikely that the creationists now pushing for creation science would be mollified by concessions along these lines. But school boards throughout the United States should not think that Judge Overton's judgement is an all-round endorsement of the present curriculum.

Selling off telephones

Settlement of the anti-trust suit against AT&T will change the company — and the world

The Justice Department in the United States has followed the only sensible course by agreeing to stop its long-standing action against the world's largest company, American Telephone & Telegraph Company (AT&T). The basis of the complaint, that the dominant telephone company in the United States has used its profits from one kind of service (long-distance telephone calls for example) to subsidize other services (local telephone services) has in any case been overtaken by events. In a long succession of decisions in the past decade, the Federal Communications Commission has balanced a relaxation of the rules restricting regulated telephone companies (such as AT&T) from entering unregulated business (such as data transmission) with increasingly explicit rules against cross-subsidies. If the judgement in the suit had gone against the company, it would have seemed a nonsense in present circumstances — and would have left unresolved the question of what, in any case, should happen to AT&T. Only the lawyers would have profited.

So does last week's settlement presage the most radical transformation of American industry since Standard Oil of New Jersey was broken up in 1911? Not necessarily. AT&T has undertaken to sell off its interests in those local and regional telephone companies across the United States which at present deal directly with local customers. It will retain its long-distance network and will also win the right to compete directly with other companies in the telecommunications business, both domestically and overseas. Perhaps more important in the long run, the company will retain control of the Bell Laboratories (and of its manufacturing subsidiary, Western Electric). This formidable technological enterprise has hitherto functioned partly with one hand tied behind its back. Plainly the company is now gambling on the chance that even though its assets will be reduced by nearly two-thirds, it will be able to grow more quickly when disencumbered of the unprofitable telephone companies. Three uncertainties lie ahead. The process of divestment may be more difficult than foreseen. Congress and the courts may decide that they do not like the settlement, or some parts of it. And the fields that AT&T hopes to enter are already partly occupied by other unregulated telecommunications companies. (There would

0028-0836/82/020085-02$01.00

have been howls of protest if the anti-trust suit against IBM had not also been dropped last week.) So for AT&T the future has the air of being an unaccustomed gamble, but a good one.

The chances are that it will succeed, and that the consequences will be profound, not merely in the United States. First, the emerging public telephone system in the United States will be an invaluable economic model for suggesting how such enterprises can be run on commercial lines. Nowhere else is such a task attempted. United States users of the telephone will most immediately discover that it costs them more to use the local telephone service as if it were unmetered water. Further ahead, however, they will find their habits changing, and telephones will be used increasingly for what they are best suited for in present circumstances — long-distance communications. It will be interesting to see how long telecommunications authorities elsewhere will be able to pretend this model is irrelevant to them.

The liberation of AT&T from the regulatory framework will also help to change the character of telecommunications. For several years it has been clear that technical innovation has outstripped the capital resources of the industry (and the capacity of potential consumers to buy its products). The result is that people who read in the technical literature of novel kinds of office switchboards, facsimile transmission by satellite, electronic mail of various kinds and high-density communications channels, have to put up with the much more rudimentary means of communication already in service. Competition from AT&T should help to bring down the prices at which these novel services are sold. More important, the entry of even a truncated AT&T into such fields should help to speed the exploitation of existing innovations as well as to sustain the pace of discovery.

But why all the bother? Can it really be of such great importance that people who have not yet learned to use pocket-size computers should be more able to install computer terminals in their living rooms? Or that people in Europe should be able to watch American television (and vice versa)? There is a widespread and unhealthy scepticism prompting these and other questions. The common underlying fallacy is to ignore the present importance of the telecommunications industry and to dismiss as unimportant the potential growth. Yet if the industrialized world wishes seriously to find something with which to occupy itself in the decades ahead, can it afford this insouciance?

How to save a university

The University of London is in danger of collapsing. It needs a recipe for survival.

For a quarter of a century, and in spite of a succession of supposed reforms, it has been clear that the University of London could not continue as it had become. The question now is whether it can survive. The request by University College, the university's largest college, to be supported directly by the University Grants Committee and not through the university's own bureaucracy (see page 88) is not intended as a threat to the continued existence of the federal structure. But that is what the effect will be. If University College gets its way, others — the London School of Economics, for example — will want the same, and will not easily be denied. And even though separate financing does not of itself mean separation, what would be left of the university's central administration would be even less able than at present to give the university a sense of coherence.

How, it will be said elsewhere, have the mighty fallen. Within living memory, the University of London was not merely the largest single university in the United Kingdom and the largest source of qualified physicians (which it still is) but a godfather to emerging universities in Britain and elsewhere in the British Commonwealth. The university was then an important source of academic qualifications (by means of its external degrees) for those studying on their own while, almost as a sideshow, it administered school-level examinations in most Commonwealth countries, old and new. In its heyday, the university was imaginative and flexible, setting up a number of internationally important postgraduate institutions. Although always a federation in the sense of being the umbrella beneath which several constitutionally autonomous educational establishments agreed to function, the university appeared as a unified academic institution because its examinations and degree systems were administered centrally. Under the pressure of disparate events, most of these activities have been shed. The emergent universities have emerged, and no longer need an avuncular guiding hand. Countries once eager for London's services as a school-level examiner increasingly prefer to look after themselves. The demand for external degree examinations fell away as access to universities became easier in the 1960s. And, for more than a decade now, the university had delegated to its constituent parts much of the responsibility for setting their own degree examinations, largely in recognition that any common system must inhibit the pursuit of excellence by the stronger colleges. At the centre of the university is now to be found little but an office.

The past year has shown how vulnerable is an entity like this. The federation has become so loose that its vice-chancellor at the time (Lord Annan) was less able than his colleagues elsewhere to protest convincingly at the British government's decree that overseas students' fees must be increased (in 1979) and at the proposed cut in university budgets. Lord Annan did his eloquent best, but since last summer his successor, Professor Randolph Quirk, has had little choice but to hope against hope that the plans for retrenchment at individual colleges will somehow add up to compliance with the instructions of the grants committee for the university as a whole. (The obviously necessary survey of the scale of teaching in various subject areas, put in hand last September, will nevertheless probably come too late to provide individual colleges with timely guidance.) The university has promised to put redundant academics on a central register, and has asked colleges about to hire staff to think first of people being put out of work elsewhere within the university. So far, however, there is little prospect that the university will be able to put together an academic plan for the years ahead. The committee set up to do just that, under Sir Peter Swinnerton-Dyer, has been pre-empted by events. And if a plan should emerge by accident from the work of the subject review committees, the chances are meagre that this would be adopted by the university's senate.

It will, however, be tragic if the university simply withers away because it has no way of deciding what to do or how to do it. But time is so short that almost any plan will be better than none. So it is that it falls to the vice-chancellor to do off his own bat what the university's maze of committees cannot accomplish, and to say what the future will be like. A few simplifying assumptions will help. First, University College (bigger than many other British universities) is, like Imperial College, big enough to look after itself but should pay for its financial independence with unbreakable promises of help for the smaller fry. It is absurd, for example, that research facilities remain as jealously protected as they are, or that colleges wishing to provide specialized teaching must usually provide it for themselves. Second, the London School of Economics merits a similar degree of independence by its success in recruiting students from overseas.

Third, the vice-chancellor's chief concern should be with the rest of the university — seven or eight smaller colleges and a host of postgraduate institutes. The past few months have shown clearly that even willing partners in schemes for collaboration are given pause by the stark truth that collaboration cannot preserve jobs at all the institutions concerned, and may also hurt the academic pride of many of the teaching departments. The moral is that there should be an academic plan for these smaller components of the University of London that will, in due course, make collaboration between them natural and relatively painless. Any plan would enable these small but distinctive parts of the university to know where they are likely to be standing some years from now. No plan is a recipe for the further erosion of the university — or even for an agreement among the rump that it too would like collective independence. In that case, there would be nothing left.

0028-0836/82/020086-01$01 00

Arkansas verdict against creation science

But battle now to move to Louisiana

Washington

Last week's ruling by a federal judge in Little Rock, Arkansas, that a state law requiring equal treatment of "creation science" and Darwinian evolution in public schools is unconstitutional, represented a significant victory for those who have argued that, even without any explicit reference to the Bible, such laws violate the required separation of church and state

Yet if this particular battle has been won, the war against the creationists is far from over Indeed both the publicity given to last month's trial in Arkansas and the apparent reasonableness of the demand for "balanced treatment" have in some ways helped the creationists' case Only minutes after Judge William Overton had announced his verdict, the state Senate in Mississippi passed by a substantial majority a virtually identical bill to the one which had just been declared unconstitutional in Arkansas

Judge Overton was uncompromising in his criticisms of Act 590, passed hurriedly by the state legislature in March during the closing hours of its 1981 session Declaring creation science as having "no scientific merit or educational value", he said that "the conclusion is inescapable that the only real effect of Act 590 is the advancement of religion"

The verdict came on a suit against the state which had been brought by the American Civil Liberties Union (ACLU) on behalf of 23 local religious organizations, biology teachers and school children ACLU had asked that the judge overturn the law on the grounds that the act constitutes an establishment of religion, abridges the academic freedom of both teachers and students, and is impermissibly vague, "all in violation of the constitution and laws of the United States"

During ten days of hearings at the beginning of December, ACLU produced a series of religious and scientific witnesses to support its arguments The former developed the claim that, whatever the wording of the act, they felt its intention to be clearly religious, since the particular set of circumstances which it implied for the origins of the Earth was only compatible, among available descriptions, with the version that appears in the Bible

Scientists called to testify on behalf of ACLU disputed claims made by creationist groups that conventional evolutionary theory is so full of holes that the alternative hypotheses they support are at least sufficiently plausible to deserve a hearing in a public school classroom They also claimed that creation science did not meet the criteria for scientific theories generally accepted by the scientific community, although this was disputed by some of the creationist witnesses produced by state attorney general Steve Clark as part of his defence of the law

In the end Judge Overton — as had been widely expected — agreed with ACLU's position But the strength of his criticisms of the supporters of the bill surprised even those who had been expecting a favourable verdict In a 38-page written opinion, the judge provided a detailed description of the reasons why he found none of the creationists' claims convincing and said that they had admitted that the law was "a religious crusade coupled with a desire to conceal this fact"

The judge criticized the creationists for not taking data and weighing them against alternative scientific data in an empirical way to reach their conclusions Rather, he said, "they take the literal wording of *Genesis* and attempt to find scientific support for it"

The verdict was, predictably, welcomed with relief by the scientific community The American Association for the Advancement of Science, whose annual meeting in Washington last week had spent much time discussing the implications of the creationist controversy, issued a statement saying that, in Arkansas at least, "teachers now can get back to teaching science, and students can get back to learning"

Similarly the National Association of Biology Teachers, co-plaintiffs in the ACLU suit, said that it was "gratified" by

Creationism judged a religion, not science

Washington

In his verdict, Judge William Overton said that the evidence presented during the ten-day trial "established that the definition of 'creation science' has as its unmentioned reference the first 11 chapters of *Genesis*", and that "references to the pervasive nature of religious concepts in creation science texts amply demonstrate why state entanglement with religion is inevitable" under the Arkansas law, referred to as Act 590

"The two-model approach of the creationists is simply a contrived dualism which has no scientific factual basis or legitimate educational purpose", Judge Overton wrote "The emphasis on origins as an aspect of the theory of evolution is peculiar to creationist literature Although the subject of origins of life is within the province of biology, the scientific community does not consider origins of life a part of evolutionary theory "

In line with arguments that had been presented by the American Civil Liberties Union, Judge Overton stated that the essential characteristics of science were (1) that it is guided by natural law, (2) that it has to be explanatory by reference to natural law, (3) that it is testable against the empirical world, (4) that its conclusions are tentative, that is, are not necessarily the final word, and (5) that it is falsifiable Creation science, he said, as defined in the Arkansas act, failed to meet these essential requirements

"Some of the state's witnesses suggested that the scientific community was 'close-minded' on the subject of creationism and that explained the lack of acceptance of the creation science arguments," Judge Overton wrote "Yet no witness produced a scientific article for which publication had been refused Perhaps some members of the scientific community are resistant to new ideas It is, however, inconceivable that such a loose-knit group of independent thinkers in all the varied fields of science could, or would, so effectively censor new scientific thought

"The methodology employed by creationists is another factor which is indicative that their work is not science A scientific theory must be tentative and always subject to revision or abandonment in the light of facts that are inconsistent with, or falsify, a theory A theory that is by its own terms dogmatic, absolutist and never subject to revision is not a scientific theory "

The next biology lesson is taken from the Book of Revelations

As he had indicated during the court proceedings last month, Judge Overton made no direct reference in his ruling to the status of evolutionary theory as a science

David Dickson

0028 0836/82/020087 02$01 00

the ruling, claiming that "school boards can now resist pressure to include creationism in science classes". Indeed, as a result of the Little Rock decision, a school board in Tacoma, Washington, last week stopped requiring the teaching of creationism in biology classes.

However, the dispute is not going to wither away and the next major test will come later this year in Louisiana, which also passed a law requiring equal treatment for creation science and evolution in its public schools last year. Ms Martha Kegel, the executive director for the state's ACLU chapter which is mounting a comparable challenge to that raised in Arkansas, said last week that she was "elated" not only by Judge Overton's verdict, but by the detailed critique of creation science that he had developed on the basis of the testimony delivered during the Little Rock trial.

Yet the Louisiana case is far from clear-cut. In the first place, the local judge is under no legal obligation to take Judge Overton's verdict into account, since it is a separate jurisdiction.

Second, the Louisiana bill omits some of the detailed provisions of the Arkansas law, for example its stipulation that creation science must include the notion that the Universe, energy and life were created "from nothing", a requirement which several religious witnesses said clearly implied the necessary existence of a creator. ACLU claims that this change only exacerbates the extent to which the bill is unconstitutionally vague, the creationists hope that this revision will remove the basis for some of the strongest objections.

Third, leading members of the creationist movement are likely to take a much more active role in the prosecution of the Louisiana case than they were permitted to do in Little Rock.

Meanwhile in Arkansas the state attorney general has yet to decide whether to implement his previous promise that he would appeal against the verdict if it went against him. And in ACLU, contingency plans are being discussed for Mississippi, in case it is decided that the law should be contested there as well. **David Dickson**

University of London

Separatists emerge

The University of London, parts of which already live with the threat of bankruptcy, now faces balkanization as well. Last week, University College, the largest multidisciplinary college in the university (with 6,000 students) formally asked that it should in future be dealt with financially as if it were an independent university, with its own grant allocation from the University Grants Committee.

The demand is more like gauntlet thrown down before the university's management than a unilateral declaration of independence. Sir James Lighthill, Provost of University College, nevertheless says that the college would continue to play a full part in the university even if, like Imperial College, it were directly financed.

Especially since last summer's delayed allocation of funds to the London colleges by the court of the university, University College has been a fierce critic of the court's procedures. Last year, Sir James Lighthill won acceptance of the principle that a college's success in obtaining research grants should count — in its favour — in the annual distribution. The precedent for his latest move is Imperial College, which has been directly financed for the past two decades.

The problem now facing the university court, the ultimate authority which shares out funds among the colleges, is tricky. It is certain to regard financial independence for University College as a dangerous precedent. But the court must also be conscious that with the impending retirement of the principal (its chief officer), Mr J R Stewart, together with some of his more experienced colleagues, its ability to administer its funds intelligibly may be further impaired.

Discontent about the court's procedures has been simmering since the summer, when the court translated the grants committee's targets for 1983–84 into financial allocations for the present academic year and target student numbers for two years ahead. One difficulty for the colleges is that they are required to adjust to reduced budgets without knowing whether their individual plans for the future will add up to what the grants committee expects of the university as a whole. This gap will be bridged only after the publication (expected next week) of the reports of the committees set up in September to consider the balance of teaching in broad subject areas.

Meanwhile, the non-medical parts of the university have made little headway with reorganization. The announced bethrothal of King's College and Bedford College has not led to marriage but to an agreement to associate. The plan for an association between Queen Elizabeth College (the smallest in the university) and Imperial College has been put on ice, partly because Queen Elizabeth College could not accept that the association should be contingent on conditions, such as the provision of new buildings, that could not be satisfied for some time to come.

The late starters have on the whole done best. Chelsea College, faced with starkly reduced numbers and the continuing cost of buying its new site, began the academic year with a draconian plan which entailed the elimination of whole departments, and is now in a position to make substantial economies while softening its plan. And Royal Holloway College, blessed with a huge site 20 miles from central London, is being reluctantly courted by various suitors hopeful that they may be able to turn their city sites into handsome dowries.

Academic censorship

Shadow ahead

Washington

Admiral Bobby Inman, deputy director of the US Central Intelligence Agency, last week dismissed as "somewhat disingenuous" the blanket claims of scientists to scientific freedom in the light of arrangements routinely made with private, corporate sources of funding, and said that the overlap between technical information and national security "inevitably produces tension".

Admiral Inman, who as head of the National Security Agency under the Carter Administration started a dialogue with the scientific community over how to handle potentially sensitive but unclassified research in cryptography, also urged cooperation between scientists and security agencies to find a mutually acceptable relationship "before significant harm does occur which could well prompt the federal government to overreact". He suggested that a potential balance between national security and science "may lie in an agreement to include in the peer review process (prior to the start of research and prior to publication) the question of potential harm to the nation".

The admiral's remarks, delivered to a session forming part of the annual meeting of the American Association for the Advancement of Science (AAAS) in Washington, provoked a strong protest from some of the scientists present.

Professor Peter Denning, for example, professor of computing at Purdue University and president of the Association for Computing Machinery, claimed that efforts to restrict the publication of technical research data reflected a growing protectionist mood in the government which would stifle scientific communication and ultimately prove destructive to the growth of new technologies.

Responding to such concerns, the board of directors of the AAAS later passed unanimously a resolution opposing government restrictions on the dissemination, exchange or availability of unclassified knowledge. Others who took part in the AAAS session, however, accepted that the issue was not clear cut, and that many of the government's concerns were legitimate — even if they had occasionally been executed over-zealously, or had had their legal ambiguity exploited in the past.

Dr Mary Cheh, for example, professor of law at George Washington University, said in a paper on the government control of private ideas that the real question was not whether the government was justified in imposing secrecy on scientific research, but how far its efforts should be permitted to go.

Similarly, Congressman Paul McCloskey presented a paper, read in his absence, describing his legislative efforts to introduce a new bill aimed at clearing up

0028-0836/82/020088-02$01 00

the ambiguities that allowed the government to prosecute *The Progressive* for publishing an article on how the hydrogen-bomb works, even though it was based on material taken from public library shelves

As Admiral Inman and others pointed out, however, the debate over the national security implications of scientific research is no longer purely a military question, linking up directly with concerns about the "export" of commercially valuable information through open publication

"Some of our most carefully nurtured technological advances have suffered from a haemorrhage of foreign technology transfer from international trade — the licit or illicit selling of everything from chips to detailed manuals — to explicit espionage efforts", the session was told by Mr Daniel C Schwarz, an attorney who, as general counsel to the National Security Agency, had helped draw up the proposed prepublication review procedure for cryptography research

Admiral Inman also suggested, though emphasizing that he was expressing a personal opinion only, that there were several other fields such as computer hardware and software, lasers, crop projections and manufacturing procedures where publication of certain technical information "could affect the national security in a harmful way"

He also reacted to the charge that the National Security Agency had not provided public proof of its concerns about the potential damage that could be caused by the publication of the results of cryptography by arguing that such information was often even more sensitive than the basic information itself

"Nowhere in the scientific ethos is there any requirement that restrictions cannot, or should not, when necessary be placed on science", he said "Scientists do not immunize themselves from social responsibility simply because they are engaged in a scientific pursuit "

He quoted several other areas, such as controls on genetic engineering research or on the protection of proprietary data, in arguing that there was nothing inherently wrong with an attempt to impose restrictions on science "Some of these restrictions are common sense, some are federal requirements, some are simply good business and some are good science," Admiral Inman said **David Dickson**

Relative prosperity

A gift of $1 million from Mr Harold McGraw, chairman of McGraw-Hill the publishers, has ensured that work on the Einstein papers can continue to completion But Dr John Stachel, the editor of the project for the past four years, says that although the gift is enough to ensure continuity, more money will be needed if the staff of the project is to be increased from two (at present) to the desired four or five

For the time being, work is concentrated on the early years of Einstein's academic life The intention is to include not merely extant letters and published papers but also ancillary documents Dr Stachel is pleased to have come across already a letter of commendation from Einstein's eventual colleagues at the Eidgenossische Technische Hochschule (ETH), Zurich (where Einstein went from the Patent Office in Berne) saying, in effect, that although Einstein was a Jew, he was "quite a nice Jew, not like the others"

At this stage nobody is prepared to guess how long the project will take, or how many volumes will eventually be published (by Princeton University Press) although there will certainly be a score of them Dr Stachel expects to be working on the project for twenty years

Polish crisis

Exiled students speak

Paris

Poland's "independent student association" was disbanded last week by order of the Ministry of Science, Higher Education and Technology According to this decision, the association was disbanded for continuing militant activity after the declaration of martial law Activists had, it is alleged, continued to distribute leaflets calling for strikes and other protest actions which represented a "flagrant violation of the decree on martial law"

The day after the decree, a group of Polish students, stranded in the West by the declaration of martial law, set up a "coordination group of the independent student association" with a provisional office in Paris The group intends to work mainly for the relief of academics and students interned in Poland under the martial law regulation At a press conference in Paris last week, however, it stressed that the current situation, with the threat that oaths of loyalty must be taken by academics and students who wish to continue working in the universities, will prove disastrous for higher education in Poland

It has therefore asked students throughout the world to press for the liberation of the interned students, and for all intellectuals to take a similar stand concerning intellectual and academic staff In particular, it called for a boycott of scientific, economic and sporting cooperation with "representatives of Jaruzelski, Moscow and the Eastern bloc" until martial law is lifted in Poland

One of the speakers at the conference, Miss Anna Krajewska, a philosophy student from Kracow, said that one of the major "sins" of the independent student association had been its participation in a plan to create a new international student organization independent of all political slant or affiliations

Recent announcements by General Jaruzelski's military government has accused the association of "striving to create a new anti-socialist student international organization and at the same time to break up the existing international students' association" (a reference to the Prague-based and socialist-oriented IUS)

According to official statements in Poland, the Ministry of Science, Higher Education and Technology (which is at present without a minister) feels sure that members of the former independent student association will "judge correctly" the extremist leaders who "abuse the confidence" of rank and file students By taking up studies, says the ministry, and "respecting the law", they can be sure of preserving their student status This is a clear hint that the current process of political "verification" now taking place in Polish industry will be imposed on students before they are allowed to resume their studies A meeting last week between the rectors of medical academies and political leaders suggests that in medical schools the process will be introduced even more rapidly and strictly **Vera Rich**

British medical research

Vacancy filled?

Dr J D ("Dai") Rees, from Unilever, is for the time being the Medical Research Council's preferred appointment as director of its National Institute for Medical Research at Mill Hill, in suburban London An appointment has become necessary because Sir Arnold Burgen, the present director, is leaving in the summer to become the Master of Darwin College, Cambridge A definite proposal has not yet been put to Dr Rees, it is understood

Dr Rees has been connected with the Medical Research Council for the past two years, since his part-time appointment as co-director of the council's Biophysics Unit based at King's College, London Recently he has played an important part in suggesting a new management structure for the National Institute, which has an annual budget of £8 million Part of this proposal, on which senior staff at the institute are being consulted, is that the new director should be advised by a four-member management committee empowered to determine the general pattern of research

Dr Rees, in his early forties, is a carbohydrate chemist by background who has established a dazzling reputation at Unilever by his work leading to the development of polysaccharides capable of lending physical structure to otherwise fluid materials The technique is now used commercially in the manufacture of ice cream and of instant desserts

More recently, Dr Rees has turned to cell biology, including the study of cell movement on surfaces

0028-0836/82/020089 02$01 00

Dr Rees's obvious attractions as director at Mill Hill include his combination of individual experience with his reputation as a scientist and his formidable reputation for getting on well with people

Among the questions to be settled before an appointment can be offered are an appropriate salary — the director of Mill Hill has traditionally been a physician whose salary has been linked with those of medically qualified academics There is also a question of the new director's freedom to make appointments of his own

US agricultural aid

Balance for all

Washington

A report by the General Accounting Office (GAO), the investigative arm of the US Congress, criticizes the ability of US universities to carry out agricultural research and technical assistance relevant to the needs of Third World countries

The report, recently published in Washington, focuses on the impact of legislation passed by Congress in 1975 which directed the Agency for International Development (AID) to find ways of strengthening and improving the involvement of US universities in solving the food problems of the developing nations. The action by Congress was meant to halt the decline in AID research grants to universities which had taken place in the early 1970s and covers projects totalling about $400 million

After a detailed assessment of the various initiatives taken under the new legislation, an amendment to Title XII of the Foreign Assistance Act, known as "Famine Prevention and Freedom from Hunger", the GAO concludes that progress in achieving its goal had been slow and in some cases virtually non-existent

The debate over the relationship between AID, Third World needs and the US research community has considerable significance for US foreign policy Increased assistance for agricultural research was one of the recommendations that won universal endorsement — including that of President Ronald Reagan — at October's summit meeting in Cancun, Mexico

The Reagan-appointed administrators of AID, who see Title XII as providing a firm basis for switching the emphasis of foreign aid towards technical assistance, particularly in agricultural research, claim that parts of the GAO report create an impression "which seriously understates the very substantial progress made during the first five years of Title XII"

However, Mr Herbert L Beckington, the agency's inspector general, commenting on a draft report, said that in general AID accepts its recommendations and intended to carry them out And AID deputy administrator Mr Joseph Wheeler told a recent meeting of the Board for International Food and Agricultural Development that plans were already under way to issue a policy directive clarifying the agency's commitment to the Title XII concept and to make implementation more effective.

AID officials emphasize that the legislation was originally intended to ensure that US universities with a tradition of agricultural research received adequate support to enable them to provide technical assistance to developing nations, a capability which they claim was eroded in the early 1970s as foreign-aid policy switched to commodity and credit agreements They accept many of the criticisms of the way in which technical assistance programmes have worked out in practice The GAO investigators, for example, found that many AID field missions distrusted teams sent out by US universities, claiming that members of such teams often lacked relevant experience of the problems they were meant to tackle.

The GAO report also criticizes the AID contract procedures in universities In some cases, for example, it is claimed that the agency has taken up to two years to approve the award of a contract to a particular university In addition, it says that the resource registry used to identify the best institutions and individual resources is not up to date, contains inadequate information and is cumbersome to use

Supporters of Title XII within AID, who feel that their efforts to implement the legislation effectively received only lukewarm support from the Carter Administration, have generally welcomed the GAO report and hope that the new Administration will prove more sympathetic **David Dickson**

Drug regulation in Brazil

Troubles building

Rio de Janeiro

The inauguration last month of a new headquarters for Brazil's National Institute for Health Quality Control underlines the urgent need to bring order to the chaotic system of marketing pharmaceuticals in Brazil Over the past ten years, Brazil has licensed on average 8,000 new brand names for drugs each year and the country is among the most liberal in the developing world for allowing the exploitation of pharmaceutical products

Brazil now ranks sixth in the world for pharmaceutical sales, and the market is dominated by the multinational companies which lobby in Brasilia against tighter regulatory measures Import licences are issued by the Ministry of Commerce which registered US $5 5 million of "pharmaceutical drug imports" and $300 million under the category "other pharmaceutical additives" during the first three months of 1981 Total sales last year amounted to almost $2,000 million, or six times the amount spent for all public health programmes in the country

Last month Brazil's president, General Figueiredo, opened a new $5 million seven-point star-shaped building for the National Institute for Health Quality Control and its director, Eduardo Peixoto, outlined the institute's main role — that of "moderating the free flow of licensing of pharmaceutical products in Brazil" Such steps are clearly needed, but the institute's predecessor, the National Secretariat for Health Vigilance (SNVS), given the responsibility for registering and controlling drugs six years ago, did not set a good precedent Its Central Control Laboratory functioned for three years with only two technicians, at the end of which time it received its new name — and now after a further three years, a new building

In the absence of effective controls, Brazil's pharmaceutical industry has gone on expanding despite the general economic recession, with the biggest growth area being psychotherapeutic drugs Almost all drugs can be sold over the counter in any pharmacy without a prescription and the average consumption per person is several times greater than in developed countries

One of the most alarming problems is the indiscriminate use of antibiotics Antibiotics are routinely bought to treat colds, and with six of the ten best-selling drug products being antibiotics there have been many examples of falsification by private laboratories and distributors The Maerson Laboratory of São Paulo was providing hospitals with "ziricillin" and "ampicillin" capsules which in fact contained pure starch And in Rio de Janeiro, after a series of complaints from consumers, Roche Laboratories discovered that their Bactrim balsam had been the victim of large-scale falsification by distributors and that several Rio pharmacies were selling an adulterated product diluted to half its normal concentration A further abuse of antibiotics came to light last November when the respected Adolfo Lutz Institute of Biology confirmed the accusation made by the president of the Pharmaceutical Association of São Paulo that the milk sold in São Paulo contained antibiotics used as preservatives

In a recent report, Dr Carlyle Guerra de Macedo, a consultant to the World Health Organization, denounced the "inefficiency of official controls which permits the marketing of many dangerous drugs" Many drugs are still available in Brazil, even with no prescription, long after they have been prohibited in the United States And many of the products on sale contain no warnings about the possible harmful effects of abuse These problems are further complicated by the fact that in many pharmacies the staff are inadequately trained and know little about the products they sell

The list of faults in the Brazilian way of marketing drugs is extensive, and the revitalized National Institute for Health Quality Control faces a daunting task

Maurice Bazin

0028-0836/82/020090 01$01 00

UN technical development

Licence to spend

Washington

The General Assembly of the United Nations has agreed on a new financing system which came into operation at the beginning of the year, aimed at supporting efforts by developing nations to build up their scientific and technological capabilities.

In effect the resolution prolongs for one more year the interim arrangements for carrying out an ambitious plan of action agreed at the UN Conference on Science and Technology for Development (UNCSTD), held in Vienna in 1979. However, the form of the final arrangements is still under discussion.

The money so far received for the plan of action remains far below target. While it was agreed in Vienna, for example, to set up an interim fund under the auspices of the United Nations Development Programme (UNDP) to attract voluntary contributions of at least $250 million during 1980 and 1981, less than $40 million has been formally pledged.

The new resolution talks of setting up a financing system which would raise an annual $200 million over 1983–85. Several UN observers feel that this, too, is wildly optimistic, pointing out that Congress has even deleted the $10 million the United States was to have contributed to the fund from the foreign aid bill signed by President Reagan in November.

Perhaps more significant than the financial targets, however, has been the outcome of a dispute running since before the Vienna conference over who should control the distribution of the funds.

At UNCSTD the interim fund was established under UNDP, but at the same time a new Center for Science and Technology was created within the United Nations, under a new assistant director-general, whose principal responsibility was to provide secretariat services for an Intergovernmental Committee, open to all UN member states. The committee has had broad responsibility for the policy directions taken by the fund, but despite the strong efforts of some of the more militant developing countries, it was not given direct control of the fund.

During recent negotiations in New York on the resolution to set up a financing system that could be approved by the General Assembly, several of the more advanced developing nations again pressed for the Center for Science and Technology to be given greater responsibility for distributing funds.

Other countries opposed this move, however, on the grounds that if the management of the fund became too much an instrument of the more militant members of the Group of 77, this would further reduce the chances of the fund receiving significant resources from the developed nations.

Eventually, the latter view prevailed. The financing system approved by the General Assembly will have transferred to it the projects and personnel that now make up the interim fund, with the Intergovernmental Committee involved primarily through a small subgroup which will negotiate with potential donors. The resolution does not mention the centre.

It is hoped in New York that during the first year of these arrangements, definite procedures can be devised for raising donations from both developed and oil-producing countries along the lines endorsed by 20 developing nations at a meeting in Caracas in early October.

Observers in Washington remain sceptical. Although the State Department has offered moral support for the new initiative, Congress eliminated from the foreign aid bill $38 million which was to have gone to another special fund, the International Fund for Agricultural Development, on the grounds that much of the promised OPEC contribution had failed to materialize. In New York there is more optimism that a pragmatic compromise between political demands and technical needs can eventually be found.

David Dickson

Biotechnology

Going Dutch

Brussels

Dutch biotechnology researchers are awaiting with keen interest a report due early this year which is to define areas deserving future investment. A government-sponsored committee was set up last May under the chairmanship of Professor Schilpoloord of the University of Leiden with the aim of coordinating research in the Netherlands and increasing its emphasis on commercial applications.

The committee, which brings together experts from industry, the governmental applied research organization (TNO) and universities, is a by-product of the Dutch government's drive to stimulate innovation which was launched on the basis of a 1979 white paper which recommended that the government invest in new technologies.

A sum of 4 million guilders (£870,000) a year has been set aside for the biotechnology committee to allocate to selected projects. This is already being spent, with researchers at the University of Groeningen the first to benefit. The committee is expected to make recommendations on priority areas for funding which will include not only commercially viable projects but also related needs for developing, testing and producing genetically engineered microorganisms on a commercial scale.

The construction of a laboratory for work at P3 containment level is in progress under the aegis of TNO, and work should be completed in 1983. Whether the new laboratory will be used as soon as it is ready depends on advice from another committee set up last May — the Committee on the Ethical Implications of Genetic Engineering. This panel includes theologians, a professor of ethics, scientists and doctors, and is chaired by a former politician, Mr Oele.

At present the committee is undecided whether to go ahead with a separate report on research at P3 level followed by a general report or to leave the first issue to the final report even though it may mean the laboratory is unused for a while. Research at P1 and P2 levels is currently subject to authorization by municipal authorities but P3 research will be agreed on at national level. Industry in the Netherlands is at present battling against some decisions by municipal authorities which are alleged to be overcautious and restrictive. As an official of the government's science policy department confessed, "in Holland the whole issue is a political can of worms".

Jasper Becker

Cold comfort

Bombay

India has launched its first scientific expedition to Antarctica. A group of 20 scientists left Goa last month aboard the *Polar Circle*, a 600-tonne ship chartered from Norway. The cruise to Antarctica and back is to last 80 days and should include a total of 15 days actually on the ice doing experiments.

The Indian expedition is being led by Dr S. Z. Qasim, secretary to the Department of Environment and former director of the National Institute of Oceanography in Goa.

The Antarctic expedition, which will cost approximately £1.3 million, is one of several major projects of the newly created Department of Ocean Development, directly under Prime Minister Indira Gandhi. The expedition team consists of scientists from ten organizations including the National Institute of Oceanography, the Indian Meteorological Department, the Geological Survey of India and the Indian Institute of Geomagnetism. Two Norwegian scientists are with the expedition to assist in the operation of specialized equipment from Norway.

As well as collecting oceanographic and weather data, the expedition team will be looking for samples containing evidence that India was part of Antarctica before it broke away some 100 million years ago. During the cruise the ship will survey the ocean bed for nodules.

India becomes the third developing country after Chile and Argentina to reach Antarctica — shortly to be followed by China, which is planning to send its first expedition this year. So far there are no plans for a permanent Indian research station in Antarctica.

K.S. Jayaraman

0028-0836/82/020091-01$01.00

CORRESPONDENCE

Data on dioxin

Sir — In discussing the metabolism of chlorinated dioxins, Alastair Hay[1] reviews the epidemiological evidence for an association between soft tissue sarcomas and phenoxy herbicides

In fact the evidence in favour of an association is much stronger than he suggests He fails to mention that in addition to the findings of the surveys of two different groups of Swedish agricultural and forestry workers exposed to phenoxy acids and chlorophenols[2,3], studies of industrial workers exposed to these substances during manufacture in the United States have also been published A review of four such studies[4] showed that 3 of 105 deaths in the workers under observation had been due to soft tissue sarcomas This compares with 0 07 per cent of deaths in the total population of US males aged 20–84 Since the publication of this review a fourth (non-fatal) case of soft tissue sarcoma has been reported in one of these groups of men[5] A fifth case has been described in an employee of one of the American firms but it is not clear whether he was under observation as part of one of the published cohorts[6]

The Finnish study quoted by Alastair Hay has not followed a sufficient number of men for a long enough period to furnish other than weak negative evidence The study might easily have missed an increased relative risk of five

The epidemiological data cannot at present distinguish between a risk due to 2,4,5-T itself (or to related herbicides) and one which is due to contaminants of these compounds

E D Acheson

MRC Environmental
Epidemiology Unit,
University of Southampton, UK

1 Hay, A *Nature* 294, 514 (1981)
2 Hardell, L & Sandstrom, A *Br J Cancer* 39, 711 (1979)
3 Eriksson, M *et al Br J ind Med* 38, 27 (1981)
4 Honchar, P A & Halperin, W E *Lancet* i, 268 (1981)
5 Cook, R R *Lancet* i, 618 (1981)
6 Moses, M & Selikoff, I J *Lancet* i, 1370 (1981)

Beat the clock

Sir – The anonymity of journals' referees has been much discussed A common nuisance is the tardy referee who sits on papers sometimes for months, and about whom authors can do little I believe these could be dealt with effectively if the anonymity of referees were maintained for say a month from dispatch to them of the manuscript After that the editor would automatically pass on the identity of the offender to the authors who could, and usually would, then take up the cudgels directly on their own behalf

I am sure this simple measure would effect a speedy acceleration of the turnover time of papers in editorial offices Many of us who are sometimes authors, sometimes referees, would, I am sure, accept this constraint on our latter function in the interests of our former

P C Wilkinson

Department of Bacteriology
and Immunology,
University of Glasgow, UK

Niche work

Sir — Concerning H G Pickles' imagined "very small niche indeed" (Pharmacology Issues, *Nature* 1 October 1981, p 355) for *Journal of Ethnopharmacology* compared with *Journal of Cardiovascular Pharmacology*

I propose that more people can certainly be directly involved and interested in what plants they can eat or apply therapeutically or in any other useful way (because anyone may pluck, cultivate or look for plants) than can be directly involved in cardiovascular drugs (because they are not readily available)

All the best to cardiovascular pharmacologists, but please watch out for the relegation to niches (To be honest, I did think I was writing esoterica when I submitted my first article to *Journal of Ethnopharmacology* but there must be a lot of people out there in a lot of very small niches, because I received 48 reprint requests immediately following publication and they are still dribbling in)

Howard H Hirschhorn

Arlesheim, Switzerland

Morphic field sports

Sir — The rather intemperate reaction of *Nature* to Sheldrake's hypotheses (24 September 1981, p 245), against which Josephson has protested (*Nature* 15 October 1981, p 594), is in part the result of Sheldrake's own choice of Bergsonian — or Paracelsan — explanations for the effect he postulates, and in part the result of noncommunication between biology and physics

Had Sheldrake said that the quantum interconnectedness might extend to macrosystems, including biological systems, I do not think that *Nature* would have felt that its virginity was in peril A model of interconnectedness does in fact flow from Bohm s idea of explication The experimental agenda is to see how far beyond the subatomic level this patterning extends If particles correspond to the asteroids and space-ships of a video game, appearing to behave as objects subject to cause–effect, but being in fact virtual displays built up from pulses which bear no translational resemblance to the "display", Darwinian evolution might well be (some would say, "must be") a video game of the same order, appearing to follow simple selection–adaptation principles, as the game-pieces appear to collide, explode and so on — but in fact determined by information from an implicate substrate

The relevance of interconnectedness to middle-order systems looks like a prime candidate for confirmatory research If it were confirmed, Sheldrake would be both right in principle and wrong in his postulated mechanism of "morphic fields" viewed in this way, his suggestion is far from absurd

One awaits with interest *Nature*'s reaction to the first book which points out that Bohm's model also blows up the convention of Helmholtzian mind That suggestion might prove even more alarming than a physics-based neovitalism

Alex Comfort

UCLA Neuropsychiatric Institute,
California, USA

Dead-end theory

Sir — In a recent letter Darnbrough, Goddard and Stevely (*Nature* 2 December 1981, p 302) have argued in support of Creationism They claim that given belief in a God who reveals Himself in the structure of nature they "expect to find evidence consistent with His revelation of Himself" In their view "the fact that all things exist, and show evidence of design and purpose" is the only form of empirical evidence providing support for Creationism

In their arguments, your correspondents have forgotten that evidence which is merely consistent with a theory does not necessarily support that theory An illustration of this is that all possible evidence is consistent with the hypothesis that one minute ago a God created everything in the Universe, including our memories Clearly, for an observation to be consistent with a theory is only a necessary but not sufficient condition for it to provide that theory with evidential support

A fundamental problem with creation theories is that because the mechanisms proposed are supernatural, the theories fail to provide an explanation of natural phenomena which can be further investigated, developed and understood In fact, unlike present evolutionary theory, all theories which invoke a supernatural creator are scientific dead ends, failing to lead to new knowledge

This difference between creation theory and modern evolutionary theory can be illustrated by considering how each handles anomalous evidence Darnbrough, Goddard and Stevely claim that such evidence tends to be put to one side to await future investigations which will either show the evidence to be erroneous or permit its asssimilation into the original theory They neglect to point out that the development of creation theory through time, unlike evolutionary theory, has been one long retreat from the evidence In order to assimilate anomalous evidence, numerous *ad hoc* changes have been made to creation theory Such alterations were made in respect to the age of the Earth, the number of centres of creation, the number of separate creations and catastrophes through time, and the existence of variation within species, to name only the better known examples Meanwhile, evolutionary theory has not been without its own troubles, as the current debate over possible rates of evolution shows However, in the past, anomalies have been assimilated into evolutionary theory in a non *ad hoc* manner, leading to the further articulation and development of the theory This is a major difference between the two theories

What is being claimed here is that evolutionary theory is explanatory and has a heuristic function which helps our understanding of natural phenomena to grow Creation theory, however, is a pseudo-explanation which aids us not at all in our understanding of nature and leads us nowhere Naturally individuals may hold any metaphysical beliefs they wish, but the introduction of the notion of supernatural creation into scientific explanations should be resisted as contributing nothing, or worse, to our understanding of the world

Malcolm Haddon

Department of Zoology,
University of Otago, Dunedin, New Zealand

NEWS AND VIEWS

Europe probes the auroral atmosphere

University Colleges of Science & Technology
92, A.P.C. Rd., Cal.-9
LIBRARY COMPLEX
Departments of :
Chemical Engineering
Chemical Technology
Plastics & Rubber Technology
14 NOV 19

from Henry Rishbeth

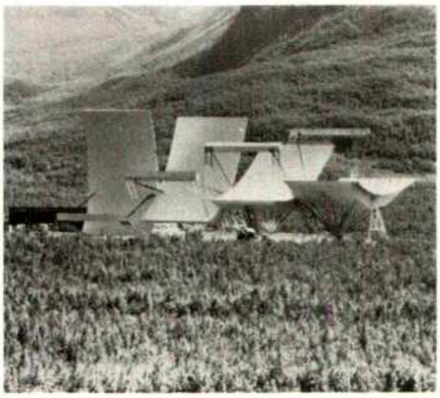

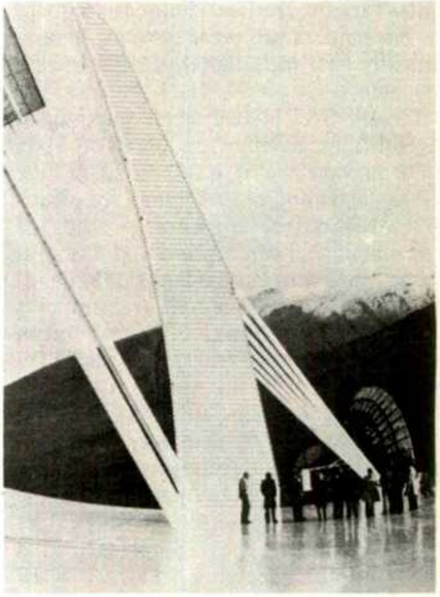

Fig.2 The EISCAT UHF dish and VHF antenna at Tromsø, Norway.

(EISCAT Scientific Association photographs, taken by Henry Rishbeth.)

FORMALLY opened by HM The King of Sweden on 26 August 1981, the European Incoherent Scatter programme (EISCAT) has begun its experimental task of probing the auroral ionosphere with ultrahigh frequency (UHF) radar. Next year, the very high frequency (VHF) transmitter should be commissioned and, after some frustrating delays due to transmitter problems, the system will then approach full operation.

The idea of a high-power radar in northern Scandinavia was mooted at the 1969 General Assembly of URSI, the International Union of Radio Science. Following years of planning and negotiations an agreement between national scientific organizations of six European countries, setting up the EISCAT Scientific Association with headquarters at Kiruna (Sweden), entered into force in December 1975. Three of the associates — CNRS of France, MPG of the German Federal Republic and SRC (now SERC) of the United Kingdom — each contribute one-quarter of the funding, the remainder coming from the 'Nordic' Associates — SA of Finland, NAVF of Norway and NFR of Sweden. Total capital expenditure to date is about £13 million.

The incoherent scatter technique[1], envisaged[2] in 1928 but not seriously proposed[3] until 1958, was demonstrated successfully in the latter year[4], and subsequently exploited at a few sites ranging from the magnetic equator in Peru to the sub-Arctic in Alaska. The technique uses a powerful radio beam at a frequency (between 40 and 230 MHz) much too high to undergo the almost mirror-like reflection from the ionosphere that is used in radio communication. The 'target volume' in the ionosphere is defined either by pulsing the radar beam and sampling the scattered echoes at a selected time delay, or geometrically by using separated, highly directional transmitting and receiving antennas. EISCAT uses both methods in its UHF system, but only the pulse method in its VHF system. Of a peak transmitted power of some megawatts, all but microwatts escape into space and mere picowatts are typically intercepted by the receiving antennas.

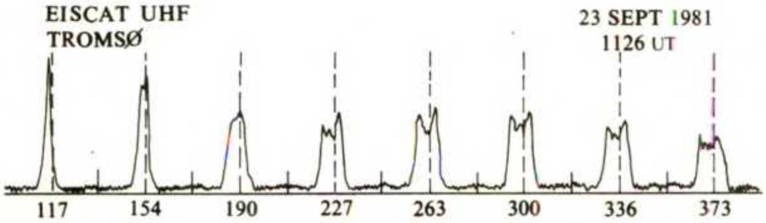

Fig. 1 Early EISCAT data: incoherent scatter spectra taken at eight heights over Tromsö, with approximately 37 km height resolution and 30 s integration. The amplitudes have not been corrected for the inverse-square dependence of scattered power on height. With increasing height, the spectral shape progressively changes from the narrow collision-dominated spectrum in the E region to the broader two-humped spectrum characteristic of the F region. The vertical dashes mark the transmitted frequency, and the vertical bars mark the limits of the 100 KHz passband of each spectrum.

The incoherent scatter spectrum (Fig. 1) depends on the spectrum of random thermal fluctuations of plasma density in the ionosphere. Analysis of the spectrum can yield a variety of parameters which (according to circumstances) may include ion density, composition and drift velocity, ion and electron temperature, and ion–neutral particle collision frequency (see ref. 1 and refs therein). Application of well established theory to these data gives several

---

Henry Rishbeth is at the Rutherford Appleton Laboratory, Chilton, Didcot, Oxfordshire OX11 0QX.

0028-0836/82/020093-02$01.00

other ionospheric and upper atmosphere parameters, such as electrical conductivity and current density, electric field, neutral air temperature and wind velocity. Further information on electron density, temperature and drift velocity may be derived from the 'plasma sidebands' flanking the main spectrum, which are excited by photoelectrons or other low-energy particles[5-7]. In the highly active conditions of an auroral arc, with particle bombardment and large electrical currents, additional spectral features are produced by various plasma waves — the more so in an intensely heated ionosphere such as can be produced by a powerful high-frequency 'heating' transmitter. Incoherent scatter experiments have to be designed within a variety of constraints set by the equipment, the ionosphere and scientific requirements such as height and time resolution. The EISCAT system meets these constraints with a variety of radar techniques: frequency hopping, multi-pulse groups, phase-coded pulses, with digital data processing to match.

The EISCAT UHF system, operating at several frequencies centred at 933.5 MHz (0.32 m wavelength), has three 32 m fully steerable paraboloid antennas, of which that at Tromsó (Norway) is used for transmission and reception and those at Kiruna (Sweden) and Sodankylä (Finland) for reception only. The UHF transmitter is rated at 2 MW peak, 0.25 MW mean power and the VHF transmitter at 5 MW peak, 0.6 MW mean power. The VHF transmitting/receiving antenna at Tromsó (Fig. 2), 120 m × 40 m in size, can scan in the meridian plane by tilting its four panels; its beam can be offset by up to 20° from the meridian plane by inserting phasing cables in the feed system. The USSR plans to build an array for receiving EISCAT VHF signals at a Polar Geophysical Institute site in the Apatiti region.

EISCAT will primarily study the ionosphere, at heights of about 70–2,000 km. The list of measurable parameters shows that the technique can be used to study the upper atmosphere as a whole, not just the ionization. The aim is to build up an integrated picture of the structure, motions and energy sources and sinks of the upper atmosphere. Incoherent scatter observations at low latitudes, complemented by intermittent but more mobile data from satellites, have revealed much about the temperatures, winds and tides — in particular the motions driven by solar UV and X rays.

In addition the upper atmosphere receives a substantial input of energy from the magnetosphere, mainly at high latitudes. This input is very variable, peaking during auroral substorms when the input of electric currents and high-energy auroral particles sets up atmospheric gravity waves and circulatory winds which carry energy to lower latitudes. EISCAT will study such disturbances at their source, and its electric field measurements in the lower magnetosphere should help to elucidate one major outstanding question: the acceleration mechanisms of auroral particles. The auroral input is superimposed on another high-latitude input, not quite so rapidly varying — the input of momentum from the solar wind — probably through the impulsive connection and subsequent disconnection of the interplanetary and terrestrial magnetic fields as the solar wind flows past the Earth. This process sets up a large-scale circulation of plasma in the magnetosphere and ionosphere, which causes a related circulation of the neutral air above 150 km at polar latitudes.

EISCAT is also being used as a plasma diagnostic to study waves and instabilities in nature's vast plasma laboratory in the magnetosphere. This usage involves cooperation with the GEOS 2 satellite, kept in operation for the purpose, and with the West German ionospheric heating experiment at Trosmsø[8]. The 'plasma physics' aspect of EISCAT's work will be boosted when the VHF transmitter becomes operational.

EISCAT's immediate tasks include cooperation with several other programmes: the NASA Dynamics Explorer satellite, the USSR/French ARCAD 3 satellite, rocket experiments at ESRANGE, Kiruna, and optical interferometric measurements of upper atmosphere winds made from Spitzbergen. There are also investigations of small-scale ionospheric structure and (without the transmitter) radio-astronomical studies of interplanetary scintillations. An experiment is proposed in which UHF signals, transmitted from the Chatanika radar in Alaska and incoherently scattered from the polar ionosphere, will be received by EISCAT. EISCAT will also be used as a stratospheric radar. The move of the Chatanika radar to Greenland, planned for 1982, will intensify the scientific probing of the high-latitude ionosphere, particularly the magnetospheric 'polar cleft'. Meanwhile the processed EISCAT data being accumulated at the Rutherford Appleton Laboratory in the UK, and institutions in other EISCAT countries, will receive keen study from scientists. ☐

---

1. Beynon, W.J.G. & Williams, P.J.S. *Rep. Progr. Phys.* **41**, 909 (1978).
2. Fabry, C. *C.r. hebd. Séanc. Acad. Sci., Paris* **87**, 777 (1928).
3. Gordon, W.E. *Proc. IRE* **46**, 1824 (1958).
4. Bowles, K.L. *Phys. Rev. Lett.* **1**, 454 (1958).
5. Yngvesson, K.O. & Perkins, F.W. *J. geophys. Res.* **73**, 97 (1968).
6. Bauer, P., Cole, K.D. & Lejeune, G. *Planet. Space Sci.* **24**, 479 (1976).
7. Hagfors, T. & Lehtinen, M. *J. geophys. Res.* **86**, 119 (1981).
8. Kopka, H., Stubbe, P., Jones, T.N. & Robinson, T. *Nature* (in the press).

Do all laboratory mice trace back to a single female?

from M.F.W. Festing

IN this issue of *Nature*, Ferris, Sage and Wilson suggest that all the 'old' inbred strains of laboratory mice are descendants of one single female who lived some time between 1200 BC and AD 1920 (see p.163). At first sight this is an astonishing claim. Further reflection shows, however, that it is really not so unexpected, and that in view of the maternal mode of inheritance of the mitochondrial DNA (which they analysed) through the egg cytoplasm, the implications for the genetic pool of variation in laboratory mice are not as profound as they would at first appear to be.

What Ferris, Sage and Wilson have done is to study genetic variation in mitochondrial DNA (mtDNA), using eleven restriction enzymes. They sampled wild mice from a wide geographical distribution, as well as nine 'old' inbred strains (for example, BALB/c, C57BL/6 and DBA/2) and five colonies of inbred mice recently derived from wild mice. Among 20 wild mice they found 15 distinct types of mtDNA. All the old inbred mice had identical mtDNA, while four of the five new wild-derived inbred colonies differed from the old inbred strains. They concluded that the most likely explanation is that all the old inbred mice can be traced back to a single female who could have lived as recently as 1920.

Evidence that wild mice differ in many ways from laboratory mice is accumulating rapidly. The two groups differ in cell surface antigens[1], biochemical markers[2] and in some types of behaviour[3]. Several different wild populations have also been shown to carry chromosomal polymorphisms not found in laboratory stocks[4]. Such differences could have arisen as a result of the very different selective pressures on wild and laboratory mice, or as a result of a strong founder effect, or as a result of both these forces. Unfortunately, the historical records are very incomplete and provide little useful information on the domestication of our laboratory mouse stocks.

Mice have been domesticated since at least 1100 BC in China, and our laboratory stocks are believed to be descended from

---

M.F.W. Festing is at the MRC Laboratory Animals Centre, Woodmansterne Road, Carshalton, Surrey SM5 4EF.

0028-0836/82/020094-02$01.00

these mice following their establishment in Japan, and subsequent importation to Europe by traders in the early nineteenth century[5]. However, mice had also been independently domesticated in Europe, where they were frequently used for auguries and for pharmaceutical purposes.

Many of the old inbred strains may be traced back to the mouse colony established by Miss Abbie Lathrop in Grancy, Massachusetts, in the early part of this century. The origins of these mice are not known in detail, but they included fancy mice imported from Europe, as well as wild mice. Potter[6] describes this colony as "the American mouse melting pot", but there is very little information on the extent to which wild mice actually contributed to the gene pool. If there were crosses involving the wild mice, it is likely that wild males would have been crossed with tame females, which are far more likely to rear their young successfully in captivity. Thus, such crosses would not have altered the mtDNA, though they would have altered the nuclear DNA of the tame mice. However, not all the old inbred strains are derived from this colony. Strain SWR, one of the strains studied by Ferris, Sage and Wilson, was established from 'Swiss' mice which were not imported into the US until 1926[7]. This would imply either that the Swiss stock became contaminated by American mice, or that the common ancestral female lived some time before about 1920.

Although pedigree records are not available for our mouse stocks, study of other domestic species in which reliable pedigrees are available shows that a single individual often makes a substantial contribution to the development of a breed. Sewell Wright showed that in 1920 55 per cent of individuals of the Shorthorn breed of cattle could be traced back to a single bull, Favourite, born 20–24 generations previously in 1793. Similar close inbreeding was also found in several other breeds[8]. True, breeds of cattle cannot directly be equated with fancy mice. However, there were probably few tame mouse colonies in Europe during the early part of the nineteenth century, and when mouse fanciers did become organized in England in 1895, they were dominated by Walter Maxey, known as "father of the fancy"[9]. Those that found their way into research may well have been passed from one investigator to another as quite small groups, leading to a number of severe population bottlenecks.

If Ferris, Sage and Wilson's findings are not, therefore, too surprising, what are the scientific implications? First, it must be emphasized that what they have shown is that the *cytoplasm* of the old inbred strains may have come from a single female. Few, if any, of the nuclear genes need have come from that female. Thus, their results do not necessarily imply that laboratory stocks come from a narrow nuclear gene pool, as does the Shorthorn breed of cattle. Infusions of new genetic material from wild males, as may have happened in Miss Lathrop's colonies, would leave the mtDNA unaltered. This study will then be of most significance to developmental biologists who are interested in the relationship between the nucleus and the cytoplasm. In more general terms it also shows that the study of wild mouse populations can be extremely profitable — had Ferris and his colleagues not included wild mice in their studies, they would have concluded that mice are monomorphic for their mtDNA genomes[1]. It is hoped that their work will further stimulate studies of all types of genetic variation in wild mice, with the importation of much more genetic material into the laboratory. This should provide more insight into the genetics and evolution of the mouse, as well as providing many more variants which can be used as tools in the study of all aspects of mammalian biology. □

---

1. Klein, J *et al* in *Origins of Inbred Mice* (ed Morse, H C III) 667 (Academic, New York, 1978)
2. Eicher, E M *Prog clin biol Res* **45**, 7 (1981)
3. Mackintosh, H J *Symp zool Soc Lond* **47**, 337 (1981)
4. Evans, E P *Symp zool Soc Lond* **47**, 127 (1981)
5. Festing, M F W & Lovell, D P *Symp zool Soc Lond* **47**, 43 (1981)
6. Potter, M in *Origins of Inbred Mice* (ed Morse, H C III), 497 (Academic, New York, 1978)
7. Lynch, C J *Lab Anim Care* **19**, 214 (1969)
8. Wright, S *Evolution and the Genetics of Populations* Vol 3 (University of Chicago Press, 1977)
9. Cooke, T *Exhibition and Pet Mice* (Spur, Hindhead, UK, 1977)

How black is the Universe?

from Richard A Muller

ALL but 10^{-9} of the known particles in the Universe are microwave photons of the 3K cosmic background radiation, discovered by Penzias and Wilson in 1965[1], and still the subject of intense study and interest. We believe that these photons are the Doppler-shifted remnant of the thermal radiation from the hot matter of the early Universe. The big bang theory[2] predicted that the photons would have a Planck frequency spectrum similar to that of the thermal emission from a black (that is, totally absorbing) object, hence the microwave signal came to be known as the cosmic blackbody radiation. True justification for this name came only recently, when the measurements of Woody and Richards[3] confirmed that the spectrum followed the general shape of the blackbody predictions.

But the Woody and Richards data also showed a small, statistically significant departure from the perfect blackbody curve. The radiation was slightly more intense than expected at the peak of the spectrum (near 1 mm wavelength) and somewhat less intense in the shorter wavelength region. Woody and Richards were properly cautious about this observation. They state

> "Although there is a statistically significant deviation from a Planck spectrum, there are serious limitations to the statistical analysis where systematic errors are likely. It is clear that another generation of measurement with better accuracy is required before any deviation from a Planck spectrum can be firmly established."

Others have been less cautious. The literature is now full of analysis of the 'observed distortion' by theorists starved for cosmological data. A likely candidate to produce a deviation from the blackbody shape is Compton scattering from free electrons released relatively late in the history of the Universe, during the era of star formation. However, the effect of Compton scattering is to depress the peak of the spectrum and to elevate the low frequency tail[4,5], this signature is opposite to that required. Other possible causes of distortion involve injection of energy in the early Universe, perhaps by early star formation. Unfortunately, most explanations involve so many parameters that one cannot feel confident that a true explanation has been found. Attention is more properly focused on the reality of the distortion.

Measurement of the millimetre region of the microwave radiation is extremely difficult because of interfering thermal emissions from the atmosphere, the Earth and the apparatus itself. Measurements must be made at high altitudes, from rockets, balloons, or satellites. Calibration requires a source with known emissivity and temperature similar to that of the radiation (3K). Accurate calibration is critical, a 27 per cent error could account for the entire distortion reported by Woody and Richards. (The peak would be reduced by the calibration error, the high frequency depression would be accounted for if the temperature of the radiation were 2.7K instead of 2.0K.) Woody and Richards calibrated their balloon-borne instrument on the ground both before and after their flight, and checked the calibration in-flight by observation of atmospheric O_2 emission lines. The check was consistent with the ground calibrations, indeed they have been unable to discover any mechanism which could cause a change in calibration during flight by the amount required to discredit the distortion.

Nonetheless, the in-flight calibration has recently been called into question. H Pickett, E Cohen and D Brinza[6] at the

Richard A Muller is Professor of Physics at the University of California, Berkeley, California 94720 and Faculty Senior Scientist at the Lawrence Berkeley Laboratory

0028-0836/82/020095-02$01 00

California Institute of Technology measured the pressure broadening of the oxygen lines on which the calibration check depends, and found a value larger than that assumed by Woody and Richards Ironically, as the Cal Tech group points out, the result is opposite to that needed to explain away the distortion of the microwave spectrum If we were to use as the primary calibration of the Woody and Richards experiment the oxygen emission measurements with the new widths determined by the Cal Tech group, we would conclude that the distortion in the spectrum is greater than originally reported It is not clear, however, that the in-flight oxygen measurements provide a better calibration than the ground-based measurements

Several experiments are being built which could independently test the existence of the distortion These include not only new spectrum measurements from balloons and satellites, but also high frequency observations of the cosine anisotropy caused by the motion of the Earth, comparison with existing low frequency anisotropy measurements[7-9] allows the shape (but not the overall normalization) of the spectrum to be determined[10] Woody and Richards give sound advice when they urge that we wait for "another generation of measurements" before accepting the deviation from blackness as real □

---

1 Penzias, A & Wilson, R *Astrophys J* **142,** 419 (1965)
2 See, for example, Peebles, P J E *Physical Cosmology* (Princeton University Press, 1971) The microwave radiation was predicted independently by two groups see Alpher, R A , Bethe, H A & Gamov, G *Phys Rev* **73,** 803 (1948), and Dicke, R H , Peebles P J E , Roll, P G & Wilkinson, D T *Astrophys J* **142,** 414 (1965)
3 Woody, P D & Richards, P L *Phys Rev Lett* **42,** 925 (1979), *Astrophys J* **248,** 18 (1981)
4 Zel'dovich, Ya B , Illarionov, A Z & Sunyaev, R A *Zh Eksp Teor Fiz* **35,** 643 (1972), *Soviet Phys JETP* **62,** 1217 (1972)
5 Sunyaev, R A & Zel'dovich, Ya B *A Rev Astr Astrophys* **18,** 537 (1980)
6 Pickett, H M , Cohen, E A & Brinza, D E *Astrophys J Lett* **248,** L49 (1981)
7 Smoot, G F , Gorenstein, M V & Muller, R A *Phys Rev Lett* **39,** 898 (1977)
8 Cheng, E S , Saulson, P R , Wilkinson, D T & Corey, B E J Lett **232,** L139 (1979)
9 For a recent review see Weiss, R *A Rev Astr Astrophys* **18,** 489 (1980)
10 Lubin, P M Lawrence Berkeley Laboratory astrophys Note 411 (unpublished), NASA Cosmic Background Explorer memo COBE 5020 (unpublished), 1980

Islet cell precursors are neurones

from A G E Pearse

In a recent report Teitelman and her colleagues[1] describe parallel immunocytochemical studies on the localization, in mouse embryo pancreas, of the peptide hormone glucagon and the four catecholamine-synthesizing enzymes tyrosine hydroxylase (TH), DOPA decarboxylase, dopamine-β-hydroxylase and phenylethanolamine-*N*-methyltransferase A later study[2] has added insulin to the list The presence in a cell of all four enzymes would signify an adrenergic phenotype, of the first three a noradrenergic and of the first two only, a dopaminergic phenotype With the exception of the decarboxylase, the other three enzymes have been found only in cells of neuroectodermal origin The results of this elegant study once again bring into focus arguments concerning the derivation of the pancreatic islet cells and hence the whole basis of the APUD concept[3], particularly as it concerns the pancreatic and related endocrine cells of the gastrointestinal tract

APUD is an acronym, standing for amino precursor uptake and decarboxylation, that was first attached in 1968[4] to a short list of established or presumptive peptide-secreting cells which were situated either in established endocrine glands or diffusely in other regions of the body These two amino-handling functions were considered to be the most representative ones of seven cytochemical and ultrastructural characteristics possessed in common by the cells designated by the acronym Growth of the original list has brought the number of APUD cells to more than 40, if one includes, as one must, the magno- and parvo-cellular neurosecretory cells of the hypothalamus

Classically the islet cells are regarded as modified intestinal mucosal cells[5,6] For around a hundred years they have been considered to arise from stem cells in the pancreatic ducts[7], thus sharing a common endodermal origin with the cells of the exocrine pancreas[8] A more modern hypothesis, postulating a neural or neural crest origin for the cells, was first proposed in 1966 as part of the original APUD concept[4,9] This view required modification when work with rabbit embryos[10] and avian chimaeras[11] showed that the cells of the definitive crest could not be implicated as ancestors or antecedents of the islets, and the concept was then amended to derive them from committed neuroendocrine-programmed precursors arising in the embryonic ectoblast[12,13]

The real question is whether in the pancreas the four peptide-producing cells of the APUD series, and in the gut a further fourteen, are descendents *seriatim* and from day to day of multipotent endodermal stem cells, capable of differentiation into enterocytes, Paneth, goblet, duct, acinar and endocrine cells, or whether they arise by transformations occurring in committed neuroendocrine cells In the former case the enteropancreatic APUD cells cannot be regarded as sensory effectors, and they cannot be components of the postulated third division of the nervous system which the cells are held to constitute They can only be by-products of an exocrine, mucous, absorptive and duct cell replacement programme The functional characteristic of the cells, demonstrated cytochemically, and their independently long turnover time[14], have been held to support the second possibility and a neuroectodermal origin, or at least neuroendocrine determination, but morphological evidence has continued to support the unitarian (endodermal) hypothesis[15]

Teitelman and her colleagues[1] have now established, in embryonic mice, that the catecholamine-synthesizing enzyme TH appears in a population of cells in the developing (dorsal) pancreas at day 11 From day 12 to day 14 TH and glucagon can be localized, by serial immunocytochemistry, in identical cells and in up to 40 per cent of all cells containing either antigen At 14 5 days some of the TH cells are found to contain immunoreactive insulin rather than glucagon[2]

Expression of the catecholaminergic (dopaminergic) phase is transient, TH is no longer detectable in the glucagon or insulin cells, or in any other cell, after the fifteenth embryonic day It reappears, in a morphologically distinct islet cell, some time after birth This observation parallels the transient APUD facility exhibited by enteroendocrine cells in fish[16] and avian[17] embryos By contrast, the conversion of DOPA to dopamine can be detected in the endocrine cells of the developing mouse pancreas from the eleventh day onwards[18,19], and this function continues into the adult state It may also be observed that Teitelman *et al* have now provided concrete, rather than inferential, evidence of the presence of the decarboxylase in all the islet cells

What conclusions can be drawn from their investigations? Teitleman *et al*[1] formulate their own hypothesis which implies "that all the pancreatic A (glucagon) cells and, conceivably, other pancreatic endocrine cells originate by the transformation of precursors that express catecholamine biosynthetic enzymes" Their current formulation presumably includes the B (insulin) cells as originating in the same manner What, then, are the implications of this view? "All cells in the periphery that express one or more specific catecholamine biosynthetic enzymes are of neuroectodermal origin"[1] Do the pancreatic A and B cells constitute the first exception to this rule? That seems unlikely, to say the least

According to Teitelman *et al*[1] their data

A G E Pearse is Emeritus Professor of Histochemistry in the University of London at the Royal Postgraduate Medical School, Hammersmith Hospital, Ducane Road, London W12 0HS

clearly "tend to support Pearse's hypothesis" but "full validation of the developmental aspect of the APUD concept would require the identification of the germ layer from which the TH cells of the pancreas are derived" But the germ layer theory has probably outlived its usefulness The point at issue is not so much whether the APUD cell precursors are initially of endodermal or ectodermal origin, but rather whether they are an irrevocably neuroendocrine-determined self-replicating entity, needing only to effect relatively facile transformations to express functions clearly shown to be related, such as the co-production of amines and peptides[8] and the switch from one peptide to another, by modification of existing genes (gene splicing)[20] or by transcription of closely related genes in place of the original ones

Significant as they are, the investigations of Teitelman and her colleagues must clearly be extended to include further parallel studies of the association between TH and the other two pancreatic peptides, somatostatin and pancreatic polypeptide (or three if one includes gastrin, which is present in fetal islets) These matters require examination not only in the dorsal pancreatic anlage, where glucagon and then insulin are the first demonstrable peptides, but also in the ventral equivalent where, in the adult, pancreatic polypeptide comes to predominate We need to know which peptide, if any, is expressed by the morphologically distinct TH-positive cells of the adult mouse islet and, on a broader basis, whether the other peripheral and perhaps likewise the central APUD cells of the pituitary gland and hypothalamus express a transient or permanent dopaminergic function.

Conclusive proof of a neuroectodermal origin has now been established for just two of the enteropancreatic endocrine cells Confirmation of neuroendocrine status for the remaining sixteen cells can confidently be expected to follow ☐

1 Teitelman, G , Hoh, T H & Reis, D J *Proc natn Acad Sci U S A* **78**, 5225 (1981)
2 Teitelman, G , Joh, T H & Reis, D J *Neuroscience* (in the press)
3 Pearse, A G E *J Histochem Cytochem* **17**, 303 (1969)
4 Pearse, A G E *Proc R Soc* **B170**, 71 (1968)
5 Barrington E J W *Hormones and Evolution* (English University Press, London, 1964)
6 Steiner, D F *et al Recent Prog Horm Res* **25**, 207 (1969)
7 Laguesse, M E *C r Séanc Soc Biol* **47**, 699 (1895)
8 Pictet, R & Rutter, W J in *The Endocrine Pancreas* Handbook of Physiology, Vol 1 (eds Steiner D F & Freinkel, N) 25 (Williams & Wilkins, Baltimore, 1972)
9 Pearse, A G E *Nature* **211**, 598 (1966)
10 Pictet, R L , Rall, L B , Phelps, P & Rutter, W J *Science* **191**, 191 (1976)
11 Fontaine, J & Le Douarin, N M *J Embryol exp Morph* **41**, 209 (1977)
12 Pearse, A G E *Med Biol* **55**, 115 (1977)
13 Pearse, A G E & Takor, T *Fedn Proc* **38**, 2288 (1979)
14 Bertrand, P & Willems, G *Gastroenterology*, **78**, 918 (1980)
15 Cheng, H & Leblond, C P *Am J Anat* **141**, 537 (1974)
16 Rombout, J H W M , Rademakers, L H P M & van Haes, J P *Cell Tissue Res* **203**, 9 (1979)
17 Andrew, A *Gen comp Endocr* **26**, 485 (1975)
18 Pearse, A G E & Polak, J M *Gut* **12**, 783 (1971)
19 Pearse, A G E , Polak, J M & Heath, C M *Diabetologia* **9**, 120 (1973)
20 Rosenfeld, M G , Amara, S G , Roos, B A , Ong, E S & Evans, R M *Nature* **290**, 63 (1981)

The nature of galactic shells

from Gerard Gilmore

THE outer regions of galaxies are rapidly becoming as mysterious as their nuclei Kinematic studies have shown that the outer regions of disk galaxies like the Milky Way rotate with the same angular velocity as their inner regions, thus requiring the dominant contributor to the total mass of the galaxy (and the Universe) to be dispersed over a much larger volume than the luminous mass The nature and true distribution of this 'missing mass' is still unknown Now it seems that the luminous mass of stars in the outer regions of at least some galaxies is distributed in a much more ordered fashion than expected, with several narrow ripples and shells present at very large distances from the galactic nuclei In this issue of *Nature* (p 126), Carter, Allen and Malin from the Anglo-Australian Observatory present a detailed study of one such shell, which is 180 kpc (roughly twenty times the distance of the Sun from the galactic centre) from the nucleus of the galaxy NGC1344 Their observations show that the shells are probably normal stars with colours a little bluer than those of the more central regions of the galaxy

Why then do they form such dramatically sharp features? If the stars currently in the shells have spent their whole lifetimes in the outer regions of the galaxy without perturbation, their velocity dispersion in the radial direction would long ago have smeared out any sharp features in their spatial distribution The stars must, then, either be young or have had their orbits recently modified The first possibility was discussed by Fabian, Nulsen and Stewart[1], who suggested recent stellar formation from the gas driven from the galaxy by supernovae blast waves While young star formation cannot take place in regions of low gas density, Fabian *et al* showed that shocks can form as the outflowing gas meets the intergalactic medium, thereby producing locally enhanced density and permitting stellar formation These young stars will, however, fall back into the parent galaxy in the free fall time Thin shells will be visible only for times short compared with this, or perhaps 3 x 10^8 years The shells will therefore be populated predominately by luminous young stars, which are very blue — too blue, in fact, for consistency with the observations reported by Carter *et al*, which therefore require another explanation

One likely possibility is that the shells are remnants of galactic cannibalism Mergers of galaxies can produce an amazing variety of shapes and structures, possibly including shells Numerical simulations of the passage of a mass similar to that of a dynamically cool (disk) galaxy through the disk show a strong circular density wave to propagate outwards, possibly followed by lesser waves[2] In a recent simulation by Peter Quinn[3] of the Mount Stromlo Observatory in Canberra, a spherical and a disk galaxy were merged, and attention was focused on those particles ejected to large distances from the central region In all such simulations, dynamical friction causes the galaxies to merge after a bumpy meeting Initially, the disk passes through the main spheroidal component, then falls back in a series of rapidly dying oscillations, each of which ejects some of the disk stars In this way Quinn was able to generate three or four shells at large distances from the galactic centre, which bear some resemblance to those observed The stars in the shells are somewhat bluer than the main galaxy as they are preferentially ejected from the younger disk population, in agreement with observations The shells formed, however, are not as sharp as those seen, nor is it possible to generate the eight to nine separate features seen at different radii in NGC3923 Whether these are fundamental constraints or merely indicate the limitations of the current N-body simulations is not yet clear

Several examples of galaxies with shells are now known[4,5], in some cases with other evidence of anomalous features (loops, jets, active nuclei) which again suggest recent dynamical evolution Other explanations are, however, possible For example, the colour differential between the shells and the main body of the galaxy is also consistent with a mild radial decrease of the abundances of the chemical elements heavier than helium, which would not be surprising The shells would then have to be explained in terms of, for example, internal resonances in the velocity distribution inside the galaxy

A detailed explanation of the properties of the shells will require both a much more detailed numerical study of galactic mergers, and more specific observations of their properties David Carter is currently carrying out detailed surface photometry of several examples, to define their luminosity and colour distributions in more detail While spectroscopy would be highly desirable to define the kinematic properties in detail, it will be extremely difficult No emission lines have been detected from the shells, and the surface brightness is too low for easy absorption line studies (The surface brightness

Gerard Gilmore is at the Royal Observatory, Blackford Hill, Edinburgh EH9 3HJ

1 Fabian, A C , Nulsen, P E J & Stewart, G C *Nature* **287** 613 (1981)
2 Toomre, A *IAU Symp* **79**, 109 (1978)
3 Quinn, P J *Astrophys J Lett* (in the press)
4 Malin, D F *Nature* **277**, 279 (1979)
5 Schweizer, F *Astrophys J* **237**, 303 (1980)

0028-0836/82/020097-02$01 00

reported for the outer shell of NGC1344 corresponds to a photon rate of one per arc second per Angstrom every 3 hours with the IPCS on the 3 9 m AAT) Similarly, no neutral hydrogen 21 cm emission has yet been detected Detailed study of the inner shells of this galaxy, while difficult, is possible, and should provide a fascinating insight into the processes of galactic cannibalism □

Developing synthetic vaccines

from Arie J Zuckerman

In this issue of *Nature* (p 158) Dreesman and his colleagues describe a step towards the production of a synthetic vaccine for hepatitis B infection Using a computer analysis of the amino acid sequence of a major polypeptide portion of the hepatitis B surface antigen they were able to predict hydrophilic regions which would be exposed on the intact 22 nm surface antigen particle and might represent antigenic determinants Two peptides containing one of these regions were synthesized and found to elicit the production of hepatitis B surface antibody in mice after a single injection

In the long term the development of synthetic vaccines is an exciting prospect The ultimate goal is the production of chemically synthesized multivalent vaccines that would replace current bacterial and viral vaccines[1] which can often contain many irrelevant microbial antigenic determinants, proteins and other materials that contaminate the essential immunogen and may cause untoward side effects

Although use of synthetic peptide vaccine may soon be a reality, the urgent need for protective immunization against hepatitis B virus — it is estimated there are 200 million carriers of markers of hepatitis B virus world wide — is likely to be met in the short term by more conventional vaccines Progress in their production and towards the creation of synthetic vaccines is reviewed below

Hepatitis B subunit particle vaccines

The development of a conventional vaccine has been hampered by the failure to grow hepatitis B virus in tissue culture and this has led to attempts to find other preparations which might produce active immunity (see refs 2,3), including the use of inactivated hepatitis B surface antigen purified from plasma of asymptomatic human carriers Guidelines for the preparation of experimental hepatitis B vaccines were suggested by the WHO Expert Committee on Viral Hepatitis[4], and the proposed requirements for hepatitis B vaccine were published by the WHO Expert Committee on Biological Standardisation[5] Progress in the safety and efficacy testing of such vaccines has been rapid The safety, immunogenicity and high protective efficacy of two such preparations have been demonstrated by placebo-controlled, randomized, double-blind trials in susceptible male homosexuals who are known to be at high risk of hepatitis B infection[6] and among healthy volunteer staff from 48 haemodialysis units[7] and in subsequent studies[8,9]

This type of subunit vaccine may, however, suffer from several disadvantages First, pooled plasma, with high titre of hepatitis B surface antigen (often *e* antigen positive), is required in large quantity from persistant carriers, and it is impossible to characterize each carrier donor on an individual basis Second, the supply of such plasma may be difficult to secure in the long term and live virus containment facilities are required for production Third, the manufacturing process is expensive (the reported cost of the vaccine recently licensed is 120–150 US dollars for three doses required for the first course of immunization) and possible extraneous/adventitious agents and other contaminants must be removed Strict safety testing of the vaccine is required, including tests for residual infectivity of hepatitis B virus in susceptible chimpanzees

Polypeptide vaccines

To overcome some of these problems, 'second generation' hepatitis B polypeptide vaccines containing hepatitis B-specific antigenic determinants associated with a nonglycosylated polypeptide with a molecular weight in the range 22,000–24,000 and a glycosylated polypeptide with a molecular weight in the range 26,000–29,000 have been prepared and tested for safety, immunogenicity and protective efficacy in susceptible chimpanzees[10-12] Although the two major polypeptide species of purified hepatitis B surface antigen of molecular weight 22,000 to 25,000 or 26,000 (variation exists between analyses of purified antigen from different sources), and a glycoprotein of molecular weight 28,000–30,000, have been frequently designated p22 or p23 and gp28, Peterson[13] considers that these should more properly be designated p25 and gp30, based on the probable true molecular weight of the protein as deduced from the DNA sequence of the viral gene and the results of amino acid analysis by various techniques

The advantages of polypeptide vaccine, derived from any source[14], include precise biochemical characterization, exclusion of genetic material of viral origin, exclusion of host- or donor-derived substances and potency[15] Disadvantages of polypeptide vaccines include low yield if strong ionic detergents are used for separation, although the yield has been substantially improved by the use of non-ionic detergents[16]

Genetic biosynthesis

Particularly attractive sources of antigenic material would be prokaryotic cells expressing hepatitis B surface antigen proteins Cloning of hepatitis B viral DNA and the production of small amounts of surface antigen have been reported by several groups and in significant amounts by Edman *et al* [17] Expression of hepatitis B proteins in eukaryotic cells has also been achieved in mutant mouse LM cells and in HeLa cells, but sources such as transformed heterotransplantable producer cell lines have not yet been licensed by any National Control Authorities for vaccine production Expression of glycosylated hepatitis B surface antigen in yeast cells has recently been reported by W J Rutter of the University of California, San Francisco, and this is potentially a most important development for large-scale *in vitro* production of an immunogen

Synthetic hepatitis B peptide vaccines

The feasibility[18] of developing synthetic vaccines was first demonstrated by the identification of the amino acid sequences responsible for immunogenic activity of the tobacco mosaic virus Such amino acid moieties can be synthesized and, when coupled to carrier protein, will induce the production of neutralizing antibody in experimental animals In 1976, Langbeheim *et al* [19] accomplished the neutralization of a bacterial virus with antibody elicited by a synthetic antigen The first example of successful active immunization against bacterial toxin — diphtheria toxin — using a synthetic antigen has been published recently[20] Diphtheria toxin is a single polypeptide chain of 62,000 molecular weight with two disulphide bridges The loop of 14 amino acids subtended by the disulphide bridge near the NH_2 terminus has been implicated in the toxicity and immunological specificity of the molecule A synthetic tetradecapeptide linked covalently to two different carriers elicited antibodies in guinea pigs which bind specifically with the toxin and neutralize the dermonecrotic and lethal effects

Induction of type-specific immunity has also been achieved using a synthetic peptide of *Streptococcus pyogenes* M protein containing only 12 amino acid residues[21] The immunogenicity of such small peptides points the way to the development of safe vaccines against streptococcal infections which cause rheu-

---

Arie J Zuckerman is Professor of Microbiology in the University of London at the London School of Hygiene and Tropical Medicine, Keppel Street, London WC1E 7HT, and Director of the WHO Collaborating Centre for Reference and Research on Viral Hepatitis

0028-0836/82/020098-02$01 00

matic heart disease, and the efficacy of very small peptides will permit a large portion of the protein molecule to be disposed of, so reducing the chances of eliciting immunological cross-reactions against host tissues Possible approaches to the development of chemically synthesized hepatitis B vaccines were described a few years ago by several groups of investigators, and current progress suggests that such synthetic peptide vaccines are within reach

Valenzuela *et al* [22], and subsequently others, identified an 892 base pair region along the DNA strand of hepatitis B virus with the *adw* determinants using cloned DNA fragments, and the full sequence of the 226 amino acids coding for the 23,000–25,000 molecular weight polypeptide of hepatitis B surface antigen was predicted The corresponding sequence for the *ayw* subtype suggested that it differed in 16 amino acids[23] Employing an unpublished computer program designed by J E Kyte and R F Doolittle, which has been used to predict the internal and external residues of proteins with known structure, Lerner *et al* [24] chemically synthesized 13 peptides corresponding to amino acid sequences predicted from the nucleotide sequence for hepatitis B surface antigen Seven out of the 13 free or protein carrier-linked synthetic peptides elicited an anti-peptide response in rabbits Where used, the carrier protein was keyhole limpet haemocyanin in complete and subsequently incomplete Freund's adjuvant Antisera against four of the six soluble peptides, ranging from 10 to 34 amino acid residues long, reacted with the native antigen and also precipitated the 23,000 and 28,000 molecular weight major polypeptides of hepatitis B surface antigen Hopp[25] also used a computerized analysis of the amino acid sequences of the surface antigen protein to predict an antigenic site determinant An amino acid sequence of residues 138–149 was synthesized and examined for its ability to bind antibodies to a mixture of the *ad* and *ay* subtypes of hepatitis B virus Although the peptide bound only 9 per cent of the antibodies, the maximum binding capacity was not reached

Dreesman and his colleagues used a similar technique to predict two hydrophilic regions of the surface antigen molecule Two cyclic peptides, containing disulphide bonds in the region between amino acids 117 and 137, were synthesized The two synthetic peptides with amino acids 117–137 and 122–137 were incorporated into several adjuvants including Freund's complete adjuvant, alum, and multilamellar liposomes with and without muramyl dipeptide Groups of BALB/c mice were immunized intraperitoneally with each of the preparations Hepatitis B surface antibody was induced 7–14 days after inoculation in approximately 50 per cent of the mice in each group, and in four or five of six mice when the immunizing preparation of the 117–137 peptide was emulsified with Freund's complete adjuvant On day 21, the peak levels of antibody decreased in most groups of mice It should be noted that the antibody response was elicited in mice after a single injection without covalent linkage to a carrier protein

Thus, synthetic peptides may be used, in due course, as vaccines although mixtures of more than one of the peptides may be required Of the many questions which remain to be answered, the critical issues are whether antibodies induced by synthetic immunogens will be protective in susceptible non-human primates, and whether protective immunity will persist in chimpanzees and subsequently in man Nevertheless, it is clear that we are entering the era of antibody engineering, and the prospect of multivalent synthetic vaccines against a variety of microbial agents may well be within reach □

1 Sela *Adv Immun* **5**, 29 (1966)
2 *Nature* **233**, 92 (1971)
3 *Nature* **246**, 445 (1973)
4 World Health Organization *Tech Rep Ser* No 602 (1977)
5 World Health Organization *Tech Rep Ser* No 658 (1981)
6 Szmuness *et al New Engl J Med* **303**, 833, (1980)
7 Crosnier *et al Lancet* i, 455 (1981)
8 Maupas *et al Lancet* i, 289 (1981)
9 Krugman *et al J med Virol* **8**, 119 (1981)
10 Zuckerman *New Scient* **88**, 167 (1980)
11 Skelly *et al Nature* **290**, 51 (1981)
12 Dreesman *et al Infect Immun* **32**, 62 (1981)
13 Peterson *J biol Chem* **256**, 6975 (1981)
14 Skelly *et al Nature* **282**, 617 (1979)
15 Zuckerman *Nature* **255**, 104 (1975), *Lancet* i, 1396 (1976)
16 Skelly *et al J gen Virol* **44**, 679 (1979), *J Virol Meth* **3**, 51 (1981)
17 Edman *et al Nature* **291**, 503 (1981)
18 Sela *Perspectives in Virology IX* (Academic, London, 1975)
19 Langbeheim *et al Proc natn Acad Sci U S A* **73**, 4636 (1976)
20 Audibert *et al Nature* **289**, 593 (1981)
21 Beachey *et al Nature* **292**, 457 (1981)
22 Valenzuela *et al Nature* **280**, 815 (1979)
23 Galibert *et al Nature* **281**, 646 (1979)
24 Lerner *et al Proc natn Acad Sci U S A* **78**, 3403 (1981)
25 Hopp *Molec Immun* **18**, 869 (1981)

A problem for the theory of biological structure

from David Eisenberg

An unexpected result for the structure of the polyoma virus capsid is presented by Rayment, Baker, Caspar and Murakami on page 110 of this issue of *Nature* It is unexpected because it does not conform to the pattern, proposed by Caspar and Klug in 1962, for the assembly of 'spherical' viruses[1] Their scheme provided a description of highly symmetric structures related to the icosahedron, formed from identical protein subunits, and it seemed able to account for the structure and assembly of a wide variety of structures The central idea was that of quasiequivalent bonding in an icosahedron-like, near-spherical shell, each of many subunits can have an environment nearly equivalent (or quasiequivalent in the terminology of Caspar and Klug) to every other subunit (The importance of this may not seem very great unless you know that it is impossible to arrange more than 60 asymmetric objects in identical environments in a closed shell) The biochemical significance of quasiequivalent bonding is that each subunit forms nearly equivalent bonds to other subunits This equivalence of bonding means that the assembly can be simply encoded in the three-dimensional structure of the subunit It thus becomes easy to imagine how self-assembly of the virus coat might occur, simply through the repeated formation of nearly equivalent, low-free energy contacts

The Caspar–Klug theory has correlated many observations from electron microscopy and X-ray diffraction, and has been welcome in a field where experimental results are emerging at a rate far greater than principles Many previous results on structure and assembly have been consistent with the Caspar–Klug ideas The most striking are the monumental X-ray crystallographic structures of RNA plant viruses from the laboratories of Harrison and Rossmann[2, 3] Both studies revealed virus coats that display quasiequivalent bonding of the sort predicted by Caspar and Klug Thus the new report of decided non-equivalence of bonding of subunits in the polyoma virus coat is particularly startling

Previous analysis of electron micrographs of the polyoma capsid had shown that the sphere-like shell of a surface is built from 72 clumps of subunits, or 72 'capsomeres' Twelve of these are surrounded by five identical capsomeres and are thus termed pentavalent Sixty capsomeres are surrounded by six others and are termed hexavalent In the Caspar–Klug theory such an arrangement is called $T = 7$, where T, the triangulation number, describes the number of subunits and the nature of their quasiequivalence In a $T = 7$ shell, it was expected that there would $7 \times 60 = 420$ subunits, $12 \times 5 = 60$ of these in the pentavalent capsomeres and $60 \times 6 = 360$ of these in the hexavalent capsomeres What would permit nearly equivalent bonding is that each pentavalent capsomere containing five subunits would be surrounded by five other capsomeres, whereas each hexavalent capsomere containing six subunits would be surrounded by six other capsomeres This 'five around five' and 'six around six' arrangement results in each subunit having nearly the same environment as every other, and thus being able to

David Eisenberg is Professor of Molecular Biology in the Department of Chemistry at the University of California, Los Angeles, California 90024

0028 0836/82/020099-02$01 00

form nearly equivalent bonds to neighbours

In their electron density map, Rayment *et al* find unexpectedly that the hexavalent capsomere is a pentamer, as is the pentavalent capsomere Thus there appear to be only $(12\times5)+(60\times5)=360$ subunits of the major coat protein VP1 in the capsid, rather than the expected 420 The authors buttress their observation by citing studies of the molecular weights of the capsid and VP1 protein which suggest that there are indeed fewer than 420 copies

Another consequence of the hexavalent unit being a pentamer is that the bonding among coat protein subunits is distinctly non-equivalent. This is illustrated clearly in Fig 7 on page 114, where the non-equivalence can be seen by comparing panel *c* with panel *d*, and by comparing in panel *d* the various relationships of the five protein subunits of the central capsomere to the six surrounding capsomeres Figure 7*f* illustrates that the observed structure can be accounted for by three types of contact between neighbouring pentamers, a much more complicated pattern than the expected single type of contact

Such an unexpected result, even from the laboratory of a co-author of the Caspar–Klug theory which the result seems to challenge, will no doubt face some scepticism The refinement method used to obtain the phases for the 22 5 Å resolution electron density map is not the thoroughly tested and trusted multiple isomorphous replacement In place of heavy atoms to constrain phases, the refinement is constrained only by the icosahedral symmetry and overall dimensions of the capsid Rayment *et al* present control calculations that suggest the phase refinement procedure leads to a correct and unique result, and they conclude that "the similarity of the hexavalent and pentavalent capsomeres seen in the electron density map is an intrinsic feature of the virus capsid structure rather than some unaccounted artefact of the refinement procedure" The authors go on to suggest that simian virus 40 and other members of the papova family may all have capsids built of pentameric capsomeres Some workers in the field of biological structure, while finding all of this intriguing, may reserve final judgement until the study of polyoma structure has reached higher resolution, presumably with the aid of isomorphous replacement

If the capsomeres of polyoma and related viruses are in fact built all of pentomers, the ideas of Caspar and Klug are in need of some revision They sought to explain why icosahedral shells had been selected for the design of closed containers built from many identical subunits They came up with the elegant idea of quasiequivalence in an icosahedral shell built from 60*T* identical units, each unit can have nearly the same environment and hence form nearly equivalent bonds to neighbours If subunits do not all have similar environments, then the reason for the icosahedral shells is unexplained

The result of Rayment *et al* seems to transfer the problem of virus structure and assembly from the realm of completely symmetric structures, such as the quaternary structures of oligomeric enzymes, for which the principles are obvious, one step towards the realm of asymmetric structures, such as the ribosome and the tertiary structures of enzymes, where the principles still elude us

---

1 Caspar, D L D & Klug, A *Cold Spring Harb Symp quant Biol* **27**, 1 (1962)

2 Harrison, S C, Olson, A J, Schutt, C E, Winkler, F K & Bricogne, G *Nature* **276**, 368 (1978)

3 Abad-Zapatero, C *et al Nature* **286**, 33 (1980)

Spacecraft collisions

from David W Hughes

THE region of near Earth space, extending to about 5,000 km above the Earth's surface, contains many orbiting satellites and bits of satellites Collisions between them are inevitable and an estimate of just how frequently this will occur has now been made by L Schnal and L Pospíšilová of the Astronomical Institute of the Czechoslovak Academy of Sciences Their findings are published in a recent edition of the *Bulletin of the Astronomical Institutes of Czechoslovakia* (**32**, 310, 1981)

First, it was necessary to calculate the number of spacecraft per unit volume of space Satellites are continually tracked by radar systems in the US and the results published in *NASA Satellite Situation Reports* The figure below shows how the number of trackable orbiting bodies in near Earth space has varied in recent years

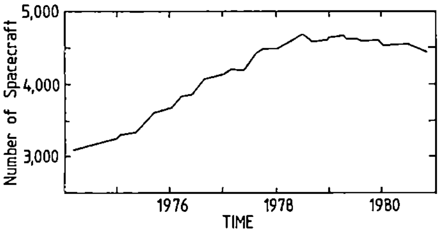

Between 1975 and 1978 the number was increasing at a rate of about 400 per year but more recently it has remained constant at just over 4,500 Radar sensitivity is sufficient to detect a large majority of objects bigger than 10 cm Sensitivity is less at high altitudes and for objects below heights of 500 km The number of small untrackable objects probably exceeds the number of trackable objects by a factor of 2

Orbital perturbations cause the argument of perihelion and the longitude of the orbit's ascending node to change fairly rapidly and this results in a uniform distribution of spatial density as a function of geocentric longitude Analysis of the orbital data leads to a value for the spatial density as a function of distance from the Earth and geocentric latitude The density is highest in the equatorial regions since every satellite must cross the equatorial plane twice per orbit To calculate the number of impacts per unit time one needs to know the relative impact velocity Schnal and Pospíšilova came to the conclusion that 7km s^{-1} was a reasonable overall value in near Earth space, agreeing with the previous estimate made by D J Kessler and B G Cour-Palais (*J. geophys Res* **86**, 2637, 1978) The computed mean is an averaged value resulting from two sets of collision velocities Satellite orbital inclinations are unevenly distributed, the majority being due to satellites moving from west to east One velocity set peaks at about 13 km s^{-1} and is due to head–on collisions between satellites orbiting in opposite directions The other set is peaked around the 1 –3 km s^{-1} region and is due to satellites catching each other up

The authors assume that the mean cross-section of a trackable body is 1 5 m^2 and that the untrackable objects have a mean cross-section of 0 001 m^2 The collision frequency, ΔC, is then given by

$$\Delta C = \tfrac{1}{2} \Sigma A\, V D^2\, \Delta S$$

where A is the assumed average cross-sectional area, V is the relative velocity, D the spatial density and ΔS an element of volume Integrating over all the regions out to a distance of 4,000 km from the Earth's surface results in an average collision frequency per year of 0 017 This is equivalent to around one spacecraft collision per 60 years, the estimated uncertainties being about 50 per cent.

This collision probability has remained reasonably constant over the last few years because the annual number of new launches has remained at about 120 per year Also, the recent solar maximum caused the atmosphere to expand and this has 'cleaned up' the lower regions by enhancing atmospheric drag and causing the small debris to spiral in quickly 'Killer' satellite tests and the accidental explosions of rocket motors have also decreased, thus lowering the number of small objects in near Earth space

A space crash would cause a rapid increase in the number of small orbiting bodies, some of which may be capable of fragmenting another satellite and thus creating even more fragments But still, with a rate of only one collision per 60 years or so, Schnal and Pospíšilová conclude that inner space is relatively safe □

David W Hughes is in the Department of Physics at the University of Sheffield, Sheffield S3 7RH

0028-0836/82/020100-01$01 00

REVIEW ARTICLE

Transcription of *Xenopus* 5S ribosomal RNA genes

Laurence Jay Korn
Department of Genetics, Stanford University School of Medicine, Stanford, California 94305, USA

The accurate transcription of 5S RNA genes when injected into the nucleus of Xenopus *oocytes or when added to an* in vitro *transcription system has allowed identification of the DNA sequences and one of the protein factors required for 5S RNA synthesis. Moreover, 5S RNA genes as part of intact chromosomes maintain a transcriptionally regulated state when injected into* Xenopus *oocyte nuclei. A detailed picture of the developmental regulation of 5S RNA gene expression is now emerging.*

DIFFERENTIAL gene expression underlies many of the differences between cell types. Gene expression in turn is controlled at several levels, with transcription especially subject to cellular regulation. There are two general processes which need to be understood in the transcription of eukaryotic genes: one is the nature of the DNA signals and other macromolecular components required for the initiation and termination of transcription of any gene; the other is how transcription is regulated throughout development, that is, what determines whether a particular gene is transcribed at a specific time and in a specific cell.

In the context of differentiation, the most interesting genes are those encoding proteins, as their products determine the cell phenotype. However, genes specifying a small, untranslated RNA molecule, the 120 nucleotide-long 5S RNA component of ribosomes, have so far yielded perhaps the most detailed picture of eukaryotic gene expression and its regulation. 5S RNA multigene families have been best characterized in the South African clawed toad, *Xenopus*, and are the focus of this review (Fig. 1). (For a more general review of eukaryotic gene transcription see refs 1–4.)

In contrast to most eukaryotic mRNAs, which are modified after transcription by the addition of a 5′ cap structure and a 3′ poly(A)sequence and by the removal of intervening sequences (see refs 4–6 for reviews), *Xenopus* 5S RNA does not undergo post-transcriptional modification[7,8]; the primary transcript is mature 5S RNA. This has facilitated the development of methods for transcribing purified 5S DNA (DNA containing the 5S RNA genes and flanking spacer sequences). When injected into the nucleus of *Xenopus* oocytes[9–11] (immature, unfertilized eggs), or incubated in a cell-free extract[8,12–15], 5S DNA is accurately and efficiently transcribed (Fig. 2). These transcription systems have helped identify the DNA sequences and other macromolecular components required for faithful synthesis of 5S RNA.

Not only are the 5S RNA genes well suited for transcription studies, but they are also amenable to investigations of the regulation of gene expression during development. In amphibians, there are two major classes of 5S RNA genes[16], the 'oocyte type'[17,18] and 'somatic type'[18]. The more abundant class of genes specifies oocyte-type 5S RNA; these genes are transcribed (active) during oogenesis, but are not transcribed in somatic cells[17,18]. In contrast, the somatic-type 5S RNA genes are expressed in somatic cells as well as in oocytes[18]. In the frog *Xenopus laevis*, transcripts from these two types of 5S RNA genes are the same length, but differ in sequence by six nucleotides[18,19], which allows the two types to be distinguished experimentally. The regulation of 5S RNA synthesis during development is discussed below.

Expression of 5S RNA genes in injected oocytes

A method for accurately transcribing purified genes was needed to identify the DNA sequences required for RNA synthesis. The transcription of purified 5S DNA after injection into the nucleus of *Xenopus* oocytes was the first example of faithful transcription of an isolated eukaryotic gene (Fig. 2)[9]. In initial

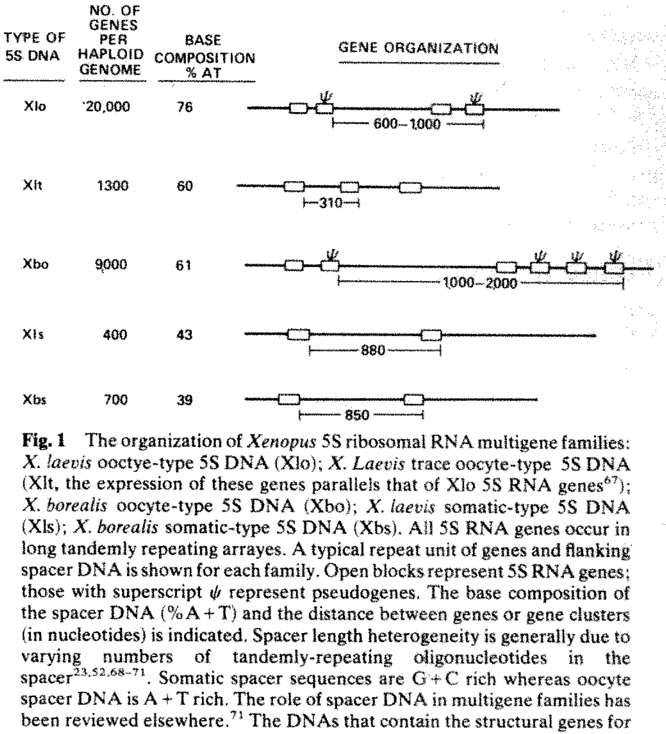

Fig. 1 The organization of *Xenopus* 5S ribosomal RNA multigene families: *X. laevis* ooctye-type 5S DNA (Xlo); *X. Laevis* trace oocyte-type 5S DNA (Xlt, the expression of these genes parallels that of Xlo 5S RNA genes[67]); *X. borealis* oocyte-type 5S DNA (Xbo); *X. laevis* somatic-type 5S DNA (Xls); *X. borealis* somatic-type 5S DNA (Xbs). All 5S RNA genes occur in long tandemly repeating arrayes. A typical repeat unit of genes and flanking spacer DNA is shown for each family. Open blocks represent 5S RNA genes; those with superscript ψ represent pseudogenes. The base composition of the spacer DNA (%A+T) and the distance between genes or gene clusters (in nucleotides) is indicated. Spacer length heterogeneity is generally due to varying numbers of tandemly-repeating oligonucleotides in the spacer[23,52,68–71]. Somatic spacer sequences are G+C rich whereas oocyte spacer DNA is A+T rich. The role of spacer DNA in multigene families has been reviewed elsewhere.[71] The DNAs that contain the structural genes for *Xenopus* oocyte- and somatic-type 5S RNAs have been isolated and cloned[51,52,67,72]. The nucleotide sequence of 5S RNA[17–19,23,73] and the DNA sequence of a complete repeat unit of each type of 5S DNA has been determined[13,23,52,68,74,75]. The dominant 5S RNA sequence of each of the five types of *Xenopus* 5S RNA differs from that of the other types by one to several nucleotides[19]. The nucleotide sequences of 5S RNA from numerous other organisms have recently been reported[76]. A structure resembling the 5S RNA gene, a 5S 'pseudogene', which differs in sequence from the normal 5S RNA gene by ~10%, is present in every repeat unit of *X. laevis* oocyte-type 5S DNA[75,77,78] and in some repeat units of *X. borealis* oocyte-type 5S DNA (ref. 23 and L J. K. and D. D. Brown, unpublished results). In *X. borealis* oocyte-type 5S DNA, the number and relative position of genes and pseudogenes in each cluster is variable (ref. 23 and L. J. K. and D. D. Brown, unpublished results). Pseudogenes can be transcribed by injection into oocytes[79] or by adding them to an *in vitro* system[23,48]. There are no pseudogenes in somatic-type 5S DNA[52]. The structural organization of the *Xenopus* 5S RNA genes has recently been reviewed[80].

0028-0836/82/020101—05$01.00

experiments, the template consisted of 5S DNA containing many tandem-repeat units of 5S RNA genes and surrounding spacer DNA (see Fig. 1 legend). The subsequent finding that a single cloned 5S DNA repeat can support accurate and efficient synthesis of 5S RNA when injected into oocytes (Fig. 2)[10,11] demonstrated that each repeat unit contains all the information necessary for its own transcription. This eliminates the possibility that a site at the beginning of an array of tandemly repeating 5S RNA genes is essential for transcription of all the genes in the array. Further delineation of the specific nucleotide sequences and other factors required for accurate transcription was facilitated by the development of an *in vitro* transcription system.

Expression of 5S RNA genes *in vitro*

As purified RNA polymerase does not faithfully synthesize 5S RNA from naked 5S DNA, but transcribes faithfully chromatin containing 5S DNA[20], it was clear that either certain structural features of chromatin or chromatin-associated components are required for accurate transcription. Unfortunately, chromatin fractionation has not led to the further identification of factors for transcription. Instead, the identification of transcription factors has come primarily from soluble *in vitro* transcription systems using purified 5S DNA and cell extracts.

The first such *in vitro* transcription system consisted of manually isolated oocyte nuclei, disrupted by gentle pipetting and clarified by low-speed centrifugation[8]. The supernatant accurately and efficiently transcribed cloned 5S DNA (Fig. 2). An *in vitro* transcription system capable of synthesizing 5S RNA can also be made from whole oocytes[14] and from extracts derived from cultured somatic cells[15,21,22].

The extracts used in these *in vitro* transcription systems, whether prepared from oocytes[8] or somatic cells[21], support 5S RNA synthesis from both oocyte- or somatic-type 5S RNA genes. Thus, although they efficiently and faithfully transcribe 5S DNA, the *in vitro* systems do not show any developmental control. However, using such systems, significant progress has been made in identifying the DNA sequences and other factors required for accurate transcription of 5S RNA, as reviewed below.

Transcription initiation signals

The minimum DNA sequences required for initiation of 5S RNA transcription as well as the sequences which influence the rate or precise site of initiation have been determined by correlating DNA sequence with transcriptional activity. Specifically, DNA sequences altered *in vitro* and recloned have been tested for their ability to support RNA synthesis.

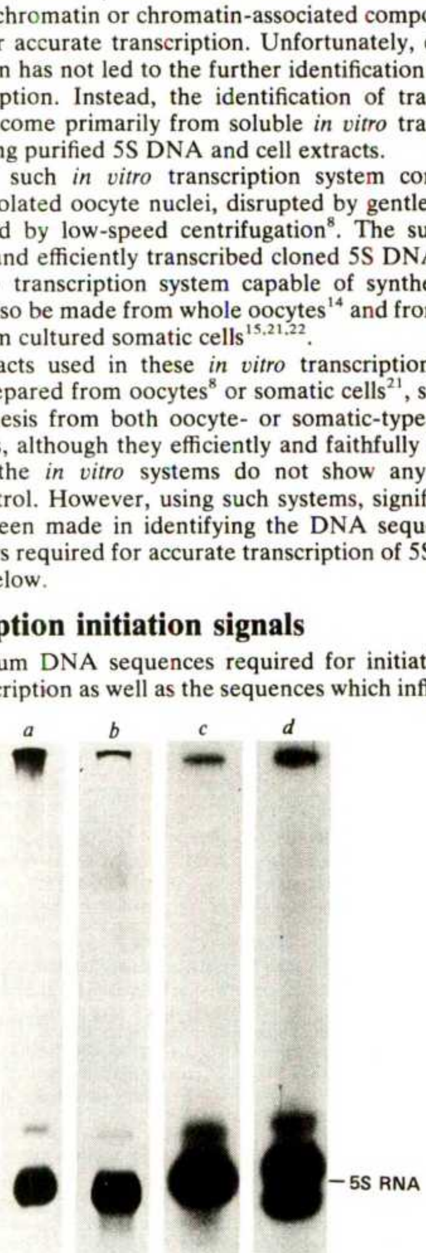

Fig. 2 Polyacrylamide gel electrophoresis of radioactive RNA synthesized after injection of the following types of 5S DNA into *Xenopus* oocytes (*a*, *b*) or after addition of 5S DNA to an *in vitro* transcription system (*c*, *d*). *a*, High-molecular weight genomic Xlo 5S DNA; *b*, plasmid containing Xlo 5S DNA; *c*, plasmid containing Xbs 5S DNA; *d*, plasmid containing Xbo 5S DNA. (Reproduced with permission from Brown and Gurdon[10] and Brown *et al.*[13].)

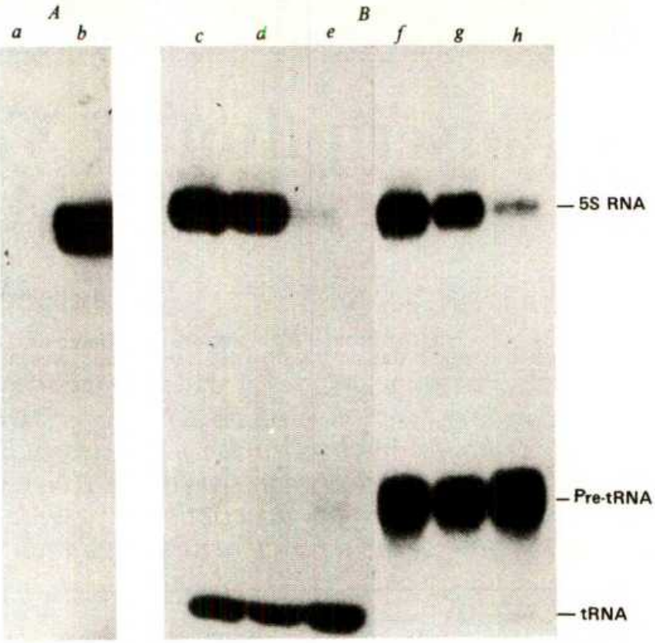

Fig. 3 *A*, polyacrylamide gel analysis of RNA synthesized in an *in vitro* transcription system containing a *Xenopus* egg S100 with no additions (*a*), or supplemented with TF IIIA (*b*). The egg contains very low levels of TF IIIA. This experiment shows that TF IIIA is required for 5S RNA synthesis *in vitro*. (Reproduced by permission from Honda and Roeder[37].) *B*, effect of antibodies against TF IIIA on 5S RNA synthesis. Transcription in an oocyte extract (lanes *c*–*e*) or a somatic cell extract (lanes (*f*–*h*) was performed with a mixture of a cloned 5S RNA gene and a cloned tRNA gene. Lanes *c* and *f*, no additions; lanes *d* and *g*, plus non-immune IgG; (lanes *c*–*e*) or a somatic cell extract (lanes *f*–*h*) was performed with experiments show that TF IIIA is required for 5S RNA synthesis, but not tRNA synthesis. The oocyte, but not the somatic cell extract processes tRNA transcripts. (Reproduced with permission from Pelham *et al.*[21].)

It is known that each repeat unit of 5S DNA contains all the signals required for accurate initiation of 5S RNA synthesis as individual cloned repeat units are transcribed accurately when injected into oocytes[10,11]. Furthermore, deletion of almost all the A+T-rich spacer sequence preceding the 5S RNA gene does not affect transcription[23,24]. In contrast to the situation in bacteria, where promoter sequences are located in the 5′ flanking region[25–28], the minimum sequence required to direct initiation of transcription of 5S DNA has, surprisingly, been shown to lie near the centre of the gene[29,30]. A series of deletions of the *Xenopus borealis* somatic-type 5S RNA gene which extend varying distances into the gene from the 5′ or 3′ ends were constructed. These genes have been characterized by DNA sequence analysis and tested for expression in nuclear extracts. It was found that the entire 5′ flanking sequence can be deleted without loss of 5S RNA gene transcription[13,29]. A transcript of approximately the correct size is still produced even when the first 50 nucleotides of the gene are deleted, although transcription is abolished by deletions extending to nucleotide 55 or beyond[29]. Similarly, initiation is not affected by deleting the 3′ flanking region or by deleting the 3′ end of the gene as far as nucleotide 83, but is abolished in a gene deleted to nucleotide 80 (ref. 30).

The deletions from each end of the 5S RNA gene identify a central region between nucleotides 50 and 83 which specifies transcription initiation. RNA polymerase initiates transcription at an approximately fixed distance upstream from this control region. For example, when a DNA fragment consisting of the central region (nucleotides 41–87) was inserted into plasmid

DNA, it directed initiation at a site ~41 nucleotides upstream[30]. In addition, 5S 'maxigenes' were constructed in which 6 or 20 nucleotides were inserted between the control region and the normal site of transcription initiation. In each case, transcription started within the gene rather than at the usual initiation site[29].

The precise site and rate of transcription initiation is influenced by sequences at or surrounding the start site[29,31–33]. Deletions leaving at least 26 nucleotides preceding the 5S RNA gene are unaltered in their transcriptional efficiency[31]. In contrast, deletion mutants with a shorter 5′ flanking region are transcribed with decreased efficiencies. Furthermore, deletion of 5′ flanking sequences can also allow heterogeneity in the initiation site[29]. These 5′ flanking sequences may include certain oligonucleotides that share homology with the flanking region of other genes transcribed by RNA polymerase III[13,23]. The exact site of initiation may also be influenced by the preference of this enzyme for starting transcription with a purine residue[12,23]. Moreover, an examination of initiation sites of transcription by RNA polymerase III reveals that the initiating purine is generally flanked by pyrimidines (Pyr^{-1}Pur^{+1}Pyr^{+2})[12].

Factors required for accurate transcription initiation

As discussed above, purified RNA polymerase III (the enzyme which transcribes 5S DNA *in vivo*; for review see ref. 34), and 5S DNA are not sufficient for 5S RNA synthesis *in vitro*. To search for other components which might direct accurate initiation, oocyte homogenates have been fractionated. In addition to RNA polymerase III, at least two protein factors are required, one of which has been purified (Fig. 3)[35,36]. Antibodies raised against this purified protein, transcription factor TF IIIA, inhibit 5S RNA synthesis *in vitro* (Fig. 3)[21,37]. When TF IIIA is mixed with 5S DNA, it binds to a region in the centre of both oocyte and somatic 5S RNA genes (nucleotides 45–96)[35]. This region includes that required for initiation of transcription (nucleotides 50–83)[29,30]. Furthermore, the ability of deleted fragments of 5S DNA to bind TF IIIA correlates with their ability to transcribe 5S RNA *in vitro*[38]. These results suggest that the influence of the central region on transcription initiation is mediated by TF IIIA.

A protein that shows immunological cross-reactivity with TF IIIA has been isolated from somatic cells[21]. It is unknown whether this protein, or the small amount of TF IIIA which is also present in somatic cells, is the factor required for 5S RNA synthesis in these cells. However, TF IIIA is not required for the expression of other genes transcribed by RNA polymerase III (Fig. 3)[35].

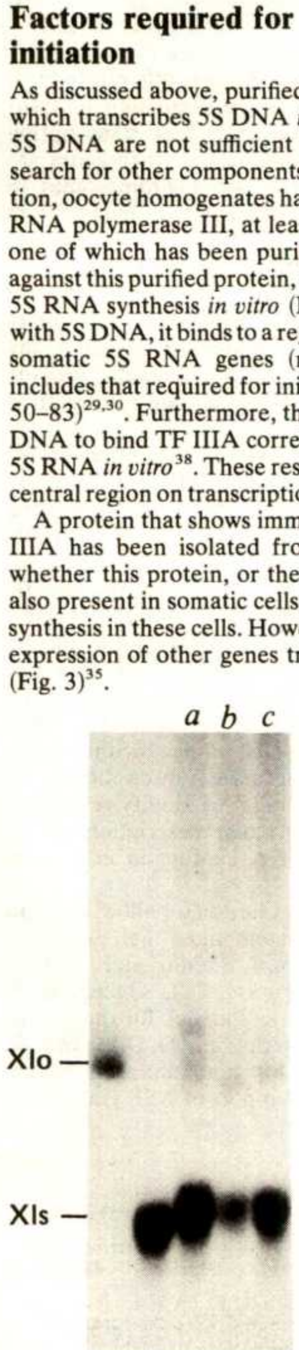

Fig. 4 Polyacrylamide gel analysis of RNA synthesized in *Xenopus* oocytes. 5S RNA genes in somatic nuclei injected into *Xenopus* oocytes continue to transcribe somatic-type 5S RNA, but do not reactivate the oocyte-type 5S RNA genes[64]. Approximately 500 somatic nuclei prepared by lysolecithin treatment of *X. laevis* kidney cells growing in culture[81] were injected into the nucleus of individual oocytes. The RNA from a single oocyte was electrophoresed in each lane of a non-denaturing polyacrylamide gel (lanes *a–c*). Xlo and Xls 5S RNA markers are indicated. The non-denaturing gel system resolves RNA molecules of the same length but which differ in sequence (for example, Xlo and Xls 5S RNA)[64]. (Reproduced with permission from Korn and Gurdon[64].)

Transcription initiation signals for other eukaryotic genes

As reviewed above, the sequence which directs the initiation of transcription of the *Xenopus* 5S RNA genes is contained within the gene. Whether this finding is general remains to be determined, but probably depends on the polymerase responsible for transcribing the gene in question. Experiments analogous to those on the *Xenopus* 5S RNA genes show that an intragenic sequence also controls initiation of transcription of the 5S RNA genes in the newt *Notophthalmus*[39]. Other genes transcribed by RNA polymerase III are controlled in a similar manner to the 5S RNA genes; the control region is within the gene. DNA fragments containing tRNA genes from *Xenopus*[40], *Drosophila*[41] and *Bombyx*[42–44], in which the 5′ flanking sequence has been deleted, can still support accurate transcription initiation when injected into the nucleus of *Xenopus* oocytes or when added to extracts from these nuclei. In contrast, a fragment containing the entire 5′ flanking region and the first 30 nucleotides of the *Xenopus* tRNA$^{\text{Met}}$ gene, but lacking the rest of the gene, cannot support tRNA synthesis[45]. A single base pair change in the middle of the yeast SUP4 tRNA$^{\text{Tyr}}$ gene (position +56) also prevents initiation of transcription[46]. These results suggest that tRNA genes, like 5S RNA genes, contain within the gene a control region which directs transcription. There is also evidence supporting an intragenic control region for the adenovirus VA RNA gene[33]. Sequence homologies have been reported between the 5S RNA gene control region and analogous internal regions of the adenovirus VA RNA gene and tRNA genes[30,33,46].

The other eukaryotic RNA polymerases seem to require different DNA sequences for initiation of transcription. RNA polymerase II transcribes the genes which specify mRNAs for proteins. Deletion of the 5′ flanking sequence of these genes prevents their expression *in vitro* (for review see ref. 4), which implies that DNA signals in the region preceding the gene are essential for transcription by RNA polymerase II. In contrast, the region immediately surrounding the initiation site appears to be critical for gene transcription by RNA polymerase I. Preliminary results indicate that for the *Xenopus* 18S and 28S rRNA genes, the sequence defined by nucleotides −12 to +16 is essential for transcription initiation (B. Sollner-Webb and R. H. Reeder, personal communication).

Transcription termination signals

Termination of *Xenopus* 5S RNA synthesis requires a cluster of four or more T residues in the DNA and is enhanced by an adjacent G+C-rich region[23,47,48]. These requirements have been demonstrated using mutants. A single base change (T → C), in the cluster of four T residues at which termination of 5S RNA synthesis normally occurs, allows RNA synthesis to continue past this site[10,13]. Deletions extending into the gene from the 3′ end, and thus deleting the T cluster at which termination normally occurs, prevent transcription termination, although the 3′ flanking sequence itself can be removed entirely without affecting termination[30,48]. Moreover, two yeast tRNA$^{\text{Tyr}}$ mutations which increase a string of three consecutive T residues in the middle of the gene to five or six T residues, cause premature termination within the T cluster[46]. A similar set of experiments shows that a high G+C content in the region immediately surrounding the termination site increases the efficiency of transcription termination[48]. Prokaryotic termination sequences share with 5S RNA termination sequences T clusters and G+C-rich regions, but also require dyad symmetries that are apparently not needed by the 5S RNA sequences[23,49,50].

Developmental regulation of 5S RNA synthesis

To provide for the massive synthesis of proteins during early development, there are at least 1,000 times more ribosomes in an oocyte than in a somatic cell. Two different mechanisms, selective gene expression and gene amplification, are used by the cell to enhance the rate of synthesis of ribosomal RNA (5S, 18S, 5.8S and 28S RNA) during oogenesis (see ref. 1 for review). Selective gene expression accounts for the synthesis of large amounts of 5S RNA. The 20,000 oocyte-type 5S RNA genes[51,52] per haploid chromosome set in *X. laevis* are present in all cells, but are only expressed in oocytes, where they account for >95% of the 5S RNA[17,18]. In contrast, the 18S, 5.8S and 28S RNA genes use gene amplification to synthesize large amounts of ribosomal RNA during oogenesis. *Xenopus* has 450 copies of the genes encoding these RNAs per haploid chromosome set[53,54]. Disproportionate replication[54-57] of these genes in oocytes provides extra templates for RNA synthesis, which are not used after the end of meiosis[58].

When the oocyte matures into an egg, 5S RNA synthesis stops and remains inactive until blastula formation[19,59,60]. At this point, somatic-type 5S RNA gene transcription resumes; somatic-type genes account for almost all 5S RNA synthesized throughout the rest of development. Thus, both the amount and type of 5S RNA synthesized varies during amphibian development.

Studies *in vitro* have suggested that the amount of 5S RNA gene transcription is regulated by feedback inhibition by the gene product, as 5S RNA specifically inhibits transcription of cloned 5S RNA genes[61]. The mechanism of this inhibition has been determined: 5S RNA binds to TF IIIA to form a 7S ribonucleoprotein particle, thereby competing with 5S DNA for TF IIIA[37,61,62]. As TF IIIA is essential for transcription of 5S RNA, high levels of 5S RNA inhibit its own synthesis[61]. This competition between 5S RNA and 5S DNA for TF IIIA indicates that the amount, but not necessarily the type, of 5S RNA synthesized is determined by TF IIIA.

Several models have been proposed to explain the selective expression of oocyte- and somatic-type 5S RNA genes. In one model an activator, which may be limiting for transcription in somatic cells, has a greater or exclusive affinity for somatic- compared with oocyte-type 5S RNA genes. TF IIIA has certain of the properties of such an activator: for example, it is limiting for 5S RNA synthesis in somatic cell extracts[21,22]. Moreover, the level of TF IIIA and the rate of 5S RNA synthesis are both high in immature oocytes and fall rapidly when the oocyte matures into an egg[21,22,35,37]. However, because TF IIIA has only a fourfold greater affinity for somatic- than oocyte-type 5S RNA genes[63], whereas the ratio of oocyte- to somatic-type 5S RNA changes 1,000-fold during development[64], TF IIIA is unlikely to act alone in regulating transcription. The recent discovery of a factor in somatic cells[21] which has immunological cross-reactivity with TF IIIA raised the possibility that this factor may be involved in regulating 5S RNA synthesis.

Alternatively, chromatin structure may control 5S RNA synthesis. Regions of highly condensed chromatin (heterochromatin) are normally inactive in transcription, perhaps because the DNA is not accessible to certain components of the transcriptional machinery. The 20,000 oocyte-type 5S RNA genes per haploid genome of *X. laevis* are located in blocks of ~1,000 near the telomeres of the long arm of most or all of the 18 chromosomes[65]. The telomeres are thought to be heterochromatic in somatic cells[65]; however, they may not be condensed in oocytes, where the oocyte-type 5S RNA genes are transcribed. This association of the oocyte-type 5S RNA genes with the telomeres therefore offers a possible explanation of their developmental regulation. In support of this model, *X. laevis* liver cells labelled in organ culture or kidney cells in culture, do not normally synthesize oocyte-type 5S RNA[64,66]. However, in one tissue culture cell line some 5S RNA genes are translocated to a novel site adjacent to the nucleolar organizer[65]. In this cell line, 10–20% of the 5S RNA synthesized is oocyte-type[66].

Other models for the developmental control of 5S RNA synthesis include a repressor–operator system analogous to that found in prokaryotes, and changes in the DNA methylation patterns during development. To differentiate between these models, a system is needed that mimics the regulated synthesis of 5S RNA and can be manipulated experimentally. There is no evidence of transcriptional regulation of 5S DNA purified from *Xenopus* or cloned into plasmids. When injected into *Xenopus* oocytes[10,11], or added to an *in vitro* system prepared from either oocytes[8] or somatic cells[21], both oocyte- and somatic-type 5S RNA genes are transcribed. A likely explanation is that the proteins which are normally associated with the DNA in a eukaryotic cell are absent from cloned DNA.

One study of the selective expression of oocyte and somatic 5S RNA genes during development, without using isolated DNA or cloned genes, has involved the transplantation of somatic cell nuclei into *Xenopus* oocytes[64]. When nuclei derived from erythrocytes or tissue culture cells are injected into oocytes from some frogs, they continue to synthesize somatic-type 5S RNA, but do not express the oocyte-type 5S RNA genes (Fig. 4)[64]. This finding leads to two important conclusions. First, 5S RNA genes as part of intact chromosomes behave differently from purified 5S RNA genes with respect to regulation of transcription. Second, the developmentally regulated transcription pattern of 5S RNA genes can be maintained when genes are transferred from one cell to another as part of chromosomes. In specific conditions, including treatment of nuclei with 0.35 M NaCl before injection (a condition which removes some nonhistone chromosomal proteins, but not histones), the oocyte-type genes can be reactivated[64]. Similar results have been obtained using isolated *Xenopus* chromatin[22]. The ability to manipulate 5S RNA genes in chromosomes in such a way as to alter their transcriptional capacity should provide means of identifying factors involved in controlling their expression.

Surprisingly, certain frogs have oocytes in which the oocyte-type 5S RNA genes of injected somatic nuclei are expressed (activating oocytes)[64]. When extracts from such activating oocytes are injected along with somatic nuclei into non-activating oocytes, these genes are then expressed (L.J.K. and J. B. Gurdon, unpublished results). NaCl treatment of somatic nuclei or addition of extracts from activating oocytes may exert their effect by respectively removing or adding specific factors which control 5S RNA transcription[64]. Alternatively, they may act by altering chromatin structure and in so doing influence the ability of factors already present in the cell to regulate 5S RNA synthesis. With our present understanding of the DNA sequences and factors required for accurate transcription of the *Xenopus* 5S RNA genes, and the ability to modify selectively that transcription, a complete molecular description of the developmental regulation of 5S RNA expression may be in sight.

I thank Drs D. D. Brown and J. B. Gurdon for allowing me to study the *Xenopus* 5S RNA gene system under their guidance; Drs D. F. Bogenhagen, D. D. Brown, J. B. Gurdon, F. D. Lee, D. A. Melton, P. Newmark, C. S. Parker, C. L. Queen, M. P. Wickens and R. A. Young and Ms J. Warwick for their comments and suggestions on the manuscript; and D. D. Brown, R. G. Roeder and B. Sollner-Webb for communicating results before publication. I acknowledge support of NSF grant PCM 8104522.

1. Brown, D. D. *Science* **211,** 667–674 (1981).
2. Wickens, M. W. & Laskey, R. A. in *Genetic Engineering* Vol. 1 (ed. Williamson, R.) (Academic , New York, in the press).
3. Gurdon, J. B. & Melton, D. A. *A. Rev. Genet.* **15** (in the press).
4. Breathnach, R. & Chambon, P. *A. Rev. Biochem.* **50,** 349–383 (1981).
5. Banerjee, A. K. *Microbiol. Rev.* **44,** 175–205 (1980).
6. Abelson, J. *A. Rev. Biochem.* **48,** 1035–1069 (1979).
7. Denis, H. & Wegnez, M. *Biochimie* **55**, 1137–1151 (1973).
8. Birkenmeier, E. H., Brown, D. D. & Jordan, E. *Cell* **15,** 1077–1086 (1978).
9. Brown, D. D. & Gurdon, J. B. *Proc. natn. Acad. Sci. U.S.A.* **74,** 2064–2068 (1977).
10. Brown, D. D. & Gurdon, J. B. *Proc. natn. Acad. Sci. U.S.A.* **75,** 2849–2853 (1978).
11. Gurdon, J. B. & Brown, D. D. *Devl Biol.* **67,** 346–356 (1978).
12. Korn, L. J., Birkenmeier, E. H. & Brown, D. D. *Nucleic Acids Res.* **7,** 947–958 (1979).
13. Brown, D. D., Korn, L. J., Birkenmeier, E., Peterson, R. & Sakonju, S. *ICN–UCLA Symp.* **14,** 511–519 (1979).
14. Ng, S. Y., Parker, C. S. & Roeder, R. G. *Proc. natn. Acad. Sci. U.S.A.* **76,** 136–140 (1979).
15. Weil, P. A., Segall, J., Harris, B., Ng, S. Y. & Roeder, R. G. *J. biol. Chem.* **254,** 6163–6173 (1979).

16. Brown, D. D. & Sugimoto, K. *Cold Spring Harb. Symp. quant. Biol.* **38,** 501–505 (1973).
17. Wegnez, M., Monier, R. & Denis, H. *FEBS Lett.* **25,** 13–20 (1972).
18. Ford, P. J. & Southern, E. M. *Nature new Biol.* **241,** 7–12 (1973).
19. Ford, P. J. & Brown, R. D. *Cell* **8,** 485–493 (1976).
20. Parker, C. S. & Roeder, R. G. *Proc. natn. Acad. Sci. U.S.A.* **74,** 44–48 (1977).
21. Pelham, H. R. B., Wormington, W. M. & Brown, D. D. *Proc. natn. Acad. Sci. U.S.A.* **78,** 1760–1764 (1981).
22. Pelham, H. R. B., Bogenhagen, D. F., Sakonju, S., Wormington, W. M. & Brown, D. D. *ICN-UCLA Symp.* (in the press).
23. Korn, L. J. & Brown, D. D. *Cell* **15,** 1145–1156 (1978).
24. Fedoroff, N. V. *Cell* **16,** 551–563 (1979).
25. Pribnow, D. *Proc. natn. Acad. Sci. U.S.A.* **72,** 784–788 (1975).
26. Gilbert, W. in *RNA Polymerase* (eds Losick, R. & Chamberlin, M.) 193–205 (Cold Spring Harbor Laboratory, New York, 1976).
27. Brown, K. D., Bennett, G. N., Lee, F., Schweingruber, M. F. & Yanofsky, C. *J. molec. Biol.* **121,** 153–177 (1978).
28. Rosenberg, M. & Court, D. *A. Rev. Genet.* **13,** 319–353 (1979).
29. Sakonju, S., Bogenhagen, D. F. & Brown, D. D. *Cell* **19,** 13–25 (1980).
30. Bogenhagen, D. F., Sakonju, S. & Brown, D. D. *Cell* **19,** 27–35 (1980).
31. Wormington, W. M., Bogenhagen, D. F., Jordan, E. & Brown, D. D. *Cell* **24,** 809–817 (1981).
32. Thimmappaya, B., Jones, N. & Shenk, T. *Cell* **18,** 947–954 (1979).
33. Fowlkes, D. M. & Shenk, T. *Cell* **22,** 405–413 (1980).
34. Roeder, R. G. in *RNA Polymerase* (eds Losick, R. & Chamberlin, M.) 285–329 (Cold Spring Harbor Laboratory, New York, 1976).
35. Engelke, D. R., Ng, S. Y., Shastry, B. S. & Roeder, R. G. *Cell* **19,** 717–728 (1980).
36. Roeder, R. G. *et al. ICN-UCLA Symp.* **14,** 521–540 (1979).
37. Honda, B. M. & Roeder, R. G. *Cell* **22,** 119–126 (1980).
38. Sakonju, S. *et al. Cell* **23,** 665–669 (1981).
39. Kay, B. K., Schmidt, O. & Gall, J. G. *J. Cell Biol.* **90,** 323–331 (1981).
40. Telford, J. L. *et al. Proc. natn. Acad. Sci. U.S.A.* **76,** 2590–2594 (1979).
41. DeFranco, D., Schmidt, O. & Söll, D. *Proc. natn. Acad. Sci. U.S.A.* **77,** 3365–3368 (1980).
42. Hagenbüchle, O., Larson, D., Hall, G. I. & Sprague, K. U. *Cell* **18,** 1217–1229 (1979).
43. Sprague, K. U., Larson, D. & Morton, D. *Cell* **22,** 171–178 (1980).
44. Garber, R. L. & Gage, L. P. *Cell* **18,** 817–828 (1979).
45. Kressmann, A., Hofstetter, H., DiCapua, E., Grosschedl, R. & Birnstiel, M. L. *Nucleic Acids Res.* **7,** 1749–1763 (1979).
46. Koski, R. A., Clarkson, S. G., Kurjan, J., Hall, B. D. & Smith, M. *Cell* **22,** 415–425 (1980).
47. Brown, R. D. & Brown, D. D. *J. molec. Biol.* **102,** 1–14 (1976).
48. Bogenhagen, D. F. & Brown, D. D. *Cell* **24,** 261–270 (1981).
49. Korn, L. J., Queen, C. L. & Wegman, M. N. *Proc. natn. Acad. Sci. U.S.A.* **74,** 4401–4405 (1977).
50. Adhya, S. & Gottesman, M. *A. Rev. Biochem.* **47,** 967–996 (1978).
51. Brown, D. D. & Sugimoto, K. *J. molec. Biol.* **78,** 397–415 (1973).
52. Peterson, R. C., Doering, J. L. & Brown, D. D. *Cell* **20,** 131–141 (1980).
53. Brown, D. D. & Weber, C. S. *J. molec. Biol.* **34,** 661–680 (1968).
54. Brown, D. D. & Dawid, I. B. *Science* **160,** 272–280 (1968).
55. Dawid, I. B., Brown, D. D. & Reeder, R. H. *J. molec. Biol.* **51,** 341–360 (1970).
56. Gall, J. G. *Proc. natn. Acad. Sci. U.S.A.* **60,** 553–560 (1968).
57. Perkowska, E., MacGregor, H. L. & Birnstiel, M. L. *Nature* **217,** 649–650 (1968).
58. Brown, D. D. & Blackler, A. W. *J. molec. Biol.* **63,** 75–83 (1972).
59. Brown, D. D. & Littna, E. *J. molec. Biol.* **20,** 95–112 (1966).
60. Miller, L. *Cell* **3,** 275–281 (1974).
61. Pelham, H. R. B. & Brown, D. D. *Proc. natn. Acad. Sci. U.S.A.* **77,** 4170–4174 (1980).
62. Picard, B. & Wegnez, M. *Proc. natn. Acad. Sci. U.S.A.* **76,** 241–245 (1979).
63. Sakonju, S. thesis, Johns Hopkins Univ.
64. Korn, L. J. & Gurdon, J. B. *Nature* **289,** 461–465 (1981).
65. Pardue, M. L., Brown, D. D. & Birnstiel, M. L. *Chromosoma* **42,** 191–203 (1973).
66. Ford, P. J. & Mathieson, T. *Nature* **261,** 433–435 (1976).
67. Brown, D. D., Carroll, D. & Brown, R. D. *Cell* **12,** 1045–1056 (1977).
68. Fedoroff, N. V. & Brown, D. D. *Cell* **13,** 701–716 (1978).
69. Carroll, D. & Brown, D. D. *Cell* **7,** 467–475 (1976).
70. Carroll, D. & Brown, D. D. *Cell* **7,** 477–486 (1976).
71. Fedoroff, N. V. *Cell* **16,** 697–710 (1979).
72. Brown, D. D., Wensink, P. C. & Jordan, E. *Proc. natn. Acad. Sci. U.S.A.* **68,** 3175–3179 (1971).
73. Brownlee, G. G., Cartwright, E., McShane, T. & Williamson, R. *FEBS Lett.* **25,** 8–12 (1972).
74. Fedoroff, N. V. & Brown, D. D. *Cold Spring Harbor Symp. quant. Biol.* **42,** 1195–1200 (1977).
75. Miller, J. R., Cartwright, E. M., Brownlee, G. G., Fedoroff, N. V. & Brown, D. D. *Cell* **13,** 717–725 (1978).
76. Erdmann, V. A. *Nucleic Acids Res.* **8,** r31–r47 (1980).
77. Brownlee, G. G., Cartwright, E. M. & Brown, D. D. *J. molec. Biol.* **89,** 703–718 (1974).
78. Jacq, C., Miller, J. R. & Brownlee, G. G. *Cell* **12,** 109–120 (1977).
79. Miller, J. R. & Melton, D. A. *Cell* **24,** 829–835 (1981).
80. Korn, L. J. & Bogenhagen, D. F. in *The Cell Nucleus* (eds Busch, H. & Rothblum, L.) (Academic, New York, in the press).
81. Gurdon, J. B. *J. Embryol. exp. Morph.* **36,** 523–540 (1976).

ARTICLES

After the deluge: Mediterranean stagnation and sapropel formation

Martine Rossignol-Strick

Laboratoire de Palynologie, Muséum National d'Histoire Naturelle, 61 rue de Buffon, 75005 Paris, France

Wladimir Nesteroff, Philippe Olive & Colette Vergnaud-Grazzini

Département de Géologie Dynamique, Université Pierre et Marie Curie, 4 place Jussieu, 75005 Paris, France

In an East Mediterranean marine core, the upper sapropel begins soon after the start of a global event—a very heavy precipitation which occurred in the equatorial latitudes during the late Glacial–early Holocene. This heavy precipitation in Africa, channelled by the Nile River across 35° of latitude, produced a low-salinity surface layer in the East Mediterranean. In this confined basin, with high bottom salinity, the steep salinity gradient stratified the water column. The stagnant bottom waters triggered the sapropel formation. Cretaceous sapropels in the tropical oceans may result from the same chain of events in warm, humid climates, with contrasting wet-and-dry seasonal rhythm.

THE periodic sedimentation of black, pelagic muds rich in marine organic matter (sapropels) has been described extensively in Quaternary and Neogene cores of the East Mediterranean Sea[1–6].

Sapropel formation involves the establishment of a steep vertical salinity gradient in the water column, initiated by highly saline bottom waters[1] and completed by a low salinity surface layer[2,3,5,7,8], which prevents thermohaline convection and triggers a stable density stratification[1,3,4]. Stagnant bottom waters are rapidly depleted of oxygen, and this reducing environment preserves the pelagic organic matter. The epipelagic fauna is unusual in abundance, assemblage[2,7–9] and isotopic composition[5,7,10–12], the mesopelagic fauna is normal and the benthic fauna almost disappears[2,8,9,13]. Sapropels occur mostly during Quaternary warming phases, but also during some cool isotope stages[3,5,7,8,14].

As a key to stagnation control, several hypotheses on the origin of the low salinity surface layer have been formulated. The Eurasian ice-sheet meltwater hypothesis[2,3,5,11,15,16] is rejected by our ^{14}C data of the most recent sapropel, 11,760–7,950 yr BP: its flushing into the Mediterranean, through the Bosphorus, ended too early, around 13,500 yr BP (ref. 17). It may have lowered the sea surface salinity, but that did not trigger stagnation.

The local Mediterranean increased rainfall hypothesis[1,2,5], is not supported by pollen data (Fig. 1): in Greece and south-west Turkey, the warming trend started around 10,600 BP, and was probably accompanied by a small increase in moisture which became significant only after 8,200 yr BP (refs 18–20). Further south, in Crete[21], moisture increased around 9,500 and after 10,000 yr BP in Syria[22], where warming occurred at 11,500 yr BP.

0028–0836/82/020105—06$01.00

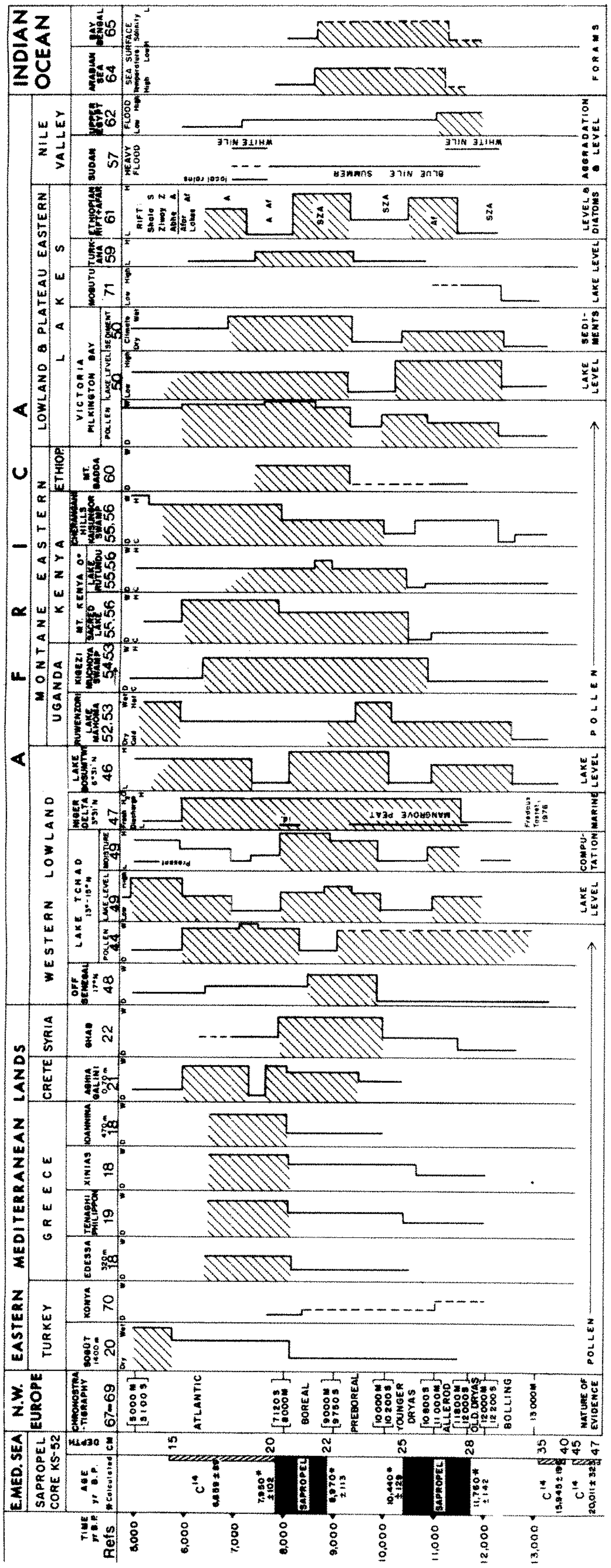

Fig. 1 Chronological setting for sapropel formation, East Mediterranean and African precipitations, Indian Ocean events. Hatched zones indicate the wettest periods.

Around 11,000 yr BP, winters had a very low insolation in the Northern Hemisphere[23], therefore it is unlikely that warmer winter temperatures might have prevented the convective sinking of the Mediterranean surface waters[2]. Downwelling now occurs in winter only in the North Adriatic Sea and around Rhodes[24]. Before stagnation, the marked contrast in seasonal insolation activated the thermohaline convection, with summer evaporation and winter downwelling.

The hydrological isolation of the deep waters in the confined East Mediterranean basin[24] progressively increased their salinity[1]. Stagnation occurred only when the surface water density became appreciably lower than the bottom water[1]. The unusual bottom fauna associated with presapropel layers reflects this increasing bottom salinity as oxygen saturation declines when salinity increases.

Precise dating of the most recent sapropel and isotopic and palynological analysis of its hydrological context suggest that it was the spreading over the sea surface of a low density, low salinity layer of great Nile River floods which triggered total deep-water stagnation. This high-nutrient discharge channelled the precipitation of a very wet period in equatorial Africa into the Mediterranean.

Dating and ^{18}O and ^{13}C isotope analysis

Core Medor 75-KS52 from the Levantine Basin (Fig. 2) (Strabo Trench, south-east of Crete, isolated from Crete by ridges, 34°00′ N–26°19′ E, water depth 3,118 m) displays the upper sapropel from 20 to 28 cm core depth. This is interrupted by a grey nanno-ooze oxygenated layer from 22 to 25 cm (ref. 13). The sapropel overlies a grey hemipelagic nanno-ooze (protosapropel) (40–28 cm) and is topped by a light brown nanno-ooze (20–0 cm).

We have established ^{14}C dates from bulk carbonates above and below the sapropel (Table 1). The absence of detrital material >63 μm does not suggest contamination by older carbonates. Since compensation occurs between the −400 yr apparent age resulting from the ^{14}C 50‰ excess in marine organisms compared with terrestrial vegetals (from the ^{13}C 25‰ enrichment of the former), and the +500 yr apparent age resulting from the ^{14}C 60‰ depletion of marine dissolved C, no correction has been applied to the measured ^{14}C age[25,26]. Assuming a constant sedimentation rate, a linear age–depth regression indicates a mean sedimentation rate between 2.0 and 2.3 cm yr^{-1}. Moreover, the isotopic stratigraphy of this core points to the rapid transition Younger Dryas–Preboreal, which took place sometime between 10,500 and 10,000 yr BP (ref. 27), at core depth 25–24 cm, precisely during the sapropel interruption.

Based on the two bracketing ^{14}C dates and the 10,000 yr BP transition, a linear interpolation yields calculated ages of the two-layered sapropel of 11,760 ± 142 to 10,440 ± 129 yr BP, and 8,970 ± 113 to 7,950 ± 102 yr BP. Although the generally accepted age has been 9,000–7,000 yr BP (refs 3, 14), our chronology is strongly supported by our isotopic stratigraphy.

^{18}O/^{16}O and ^{13}C/^{12}C ratios of the epipelagic foraminifera *Globigerinoides ruber* are presented in an unprecedently tight sampling of 34 levels in 50 cm of core length in Fig. 3. Oxygen isotopic compositions decrease overall by 3.75‰, from about 17,000 yr BP (40 cm core depth), through several large shifts, to minimal values reached between 8,000 and 6,000 yr BP (21–17 cm). This 3.75‰ decrease ought to correspond to the Termination I continental warming and melting of the northern ice sheet. However, it occurs here over 9,000–11,000 yr, which is much too long. Moreover, it displays three main phases:

(1) A stepwise decrease averaging 2‰ between 40 and 28 cm (17,000–11,800 yr BP) before sapropel deposition (at 28 cm) but including several sharp oscillations of about 1‰ amplitude after 14,000 yr BP. The very high, sharp depletion peak at 28 cm, is 1.5‰ higher than the previous average level, immediately before the beginning of sapropel.

(2) From around 11,000 yr BP to around 10,000 yr BP, a return to values slightly higher than at 17,000 yr BP. They

Table 1 Upper sapropel ^{14}C dates in Mediterranean cores

Ref.	Core	Sediment	Depth (cm)	Age (^{14}C yr BP)
72	Alb-194	Sapropel mud	9–17	8,330 ± 130
73	V10-64	Carbonate in sapropel:	23.5–28.5	
		coarse fraction		8,700 ± 1,000
		fine fraction		7,400 ± 200
		organic matter		8,400 ± 250
74	24M067	Sapropel		7,900 ± 170
75	OT 26	Varved layer	174–178	8,210 ± 185
	OT 25	Under finely laminated layer	core basis	9,640 ± 150
14	P6510-4	Organic ooze above sapropel	21–28	6,575 ± 160
		Sapropel (50–63 cm)	51–60	8,215 ± 160
		Hemipelagic mud below	101–110	10,475 ± 140
This work	KS 52	Nanno-ooze above sapropel-S1	15–20	6,659 ± 89 CRG 97
		Nanno-ooze below sapropel-S1	35–40	15,945 ± 196 CRG 98
		Nanno-ooze	45–47	20,011 ± 323 CRG 99

appear during sapropel deposition and precede ~600 yr the deposition of the intercalated oxygenated ooze, during which the maximum $\delta\ ^{18}$O is reached. This interval of high values is synchronous with the Younger Dryas cold event (11,160–10,000 yr BP).

(3) A second large, rapid decrease of 3.75‰ before deposition of the younger part of the sapropel, until minimal values are reached between 8,000 and 6,000 yr BP. A subsequent increase of ~1.4‰ leads to present day (average) values, which appear in the upper 10 cm.

^{13}C depletions correlate with minimal $\delta\ ^{18}$O values at 28.5 and 23.5 cm, but this species displays a rather strong non-equilibrium fractionation[28].

Palaeoclimatic implications

The East Mediterranean basin thus experienced a slow and complicated isotopic transition from glacial stage 2 to postglacial stage 1. The overall 3.75‰ $\delta\ ^{18}$O variation is more than double the 1.7‰ normal difference between glacial stage 2 and present-day values. The 2.05‰ additional difference is too large to signal only a temperature increase, which would be an excessive +10 °C. A 2–3 °C increase is generally accepted in the Mediterranean during Termination I[5,8], accounting for a $\delta\ ^{18}$O of −0.7‰. The remaining 1.35‰ has to be accounted for by fresh water influx forming a low salinity surface layer[5,7,10,11].

Moreover, both ^{13}C and ^{18}O isotope depletions occur rapidly before sapropel deposition. A simple calculation shows that the isotopic composition of the fresh water entering the Mediterranean has to be higher than −10‰. This low estimate suggests that precipitation and river discharge are the dominant source of the surface brackish water layer, and not ice sheet meltwater, which would have an isotopic composition around −30‰. River floods started around 12,500 yr BP (second half of the first decrease), waned around 11,000 yr BP, and reappeared immediately after 10,000 yr BP.

The earliest 2.5‰ $\delta\ ^{18}$O decrease (45–30 cm), dated 20,000–12,600 yr BP, is accounted for by three elements: part of the 1.7‰ global isotopic effect, the 2–3 °C temperature rise, and some salinity decrease due, until 13,500 yr BP, to meltwater influx through the Bosphorus. Partial stagnation developed, resulting in the grey protosapropel layers. Sapropel formation was triggered, after a 230-yr time lag, by the second, sharp, highest 1.5‰ $\delta\ ^{18}$O depletion, (30–28 cm) between 12,600 and 11,700 yr BP, entirely a salinity effect due to heavy floods.

The Nile River is the only contender for such a discharge. Before the Aswan High Dam construction, Nile flood water was partly carried eastward along the Israeli coast, where it flowed as a 15-m thick surface layer, decreasing the salinity from its normal values of 38.8‰ to 31.80‰ in September[29]. Local rainfall from December to March decreases the salinity only to 36‰ (ref. 30). The Nile flood does not seem to exert a temperature effect[30]. Present-day mean weighted isotopic values of precipitation at Entebbe, Uganda, is −2.91‰ (ref. 31). The freshwater discharge becomes brackish when mixed by winds, currents and internal waves with the seawater. The Nile origin of the brackish surface layer accounts for the frequently observed east–west gradient of decreasing stagnation and surface productivity in the sapropels. A 10% decrease (from 38‰ to 34–35‰) of the surface salinity is sufficient to induce water stratification. Today, stable stratification is observed seasonally in the open tropical oceans where the freshwater discharge of large rivers spreads as a brackish surface layer (<50 m deep), sometimes as far as several hundred kilometres. Stratification from monsoonal discharge occurs in the Andaman Sea, caused by the Irrawady[32], off the West Coast of India with the runoff from the Ghats[33], and from non-monsoonal (zenithal) discharge, in the West Equatorial Atlantic under the influence of the enormous Amazon flow, which sends isolated lenses of brackish water as far as Barbados[34]. In all these cases, a 2–4‰ vertical salinity gradient in the upper 50 m is responsible for the density stratification, whereas the generally warm temperature has little effect on the pycnocline.

The present day Amazon discharge (75 times the Nile), would cover the entire Mediterranean Sea with a 3-m deep freshwater layer in one year[34]. If the late Glacial Nile discharge was 2.5 times larger than today, like the present Zambeze, it could have accumulated a 25-m deep freshwater surface layer over the Levantine and Ionian basins in only 15 yr. The lags we see in the core between the two sets of heavy floods and sapropel incipience are 230 and 800 yr.

The very rapid 3‰ $\delta\ ^{18}$O increase from 28 to 26.5 cm (11,000–10,000 yr BP) is a result of the cumulative effects of the Younger Dryas glacial buildup, the colder temperatures, and the dramatic decrease of Nile floods, resulting from the simultaneous period of aridity in equatorial Africa. This arid episode is clearly seen in many African low lake levels and pollen diagrams (Fig. 1). It occurred even though the very high incoming summer insolation[23] could have been expected to promote heavy tropical rainfall. The insolation effect in this case is overrun by the atmospheric cooling of high-latitude origin. Colder temperatures in the Mediterranean area are reflected in the Macedonian pollen diagram (zone Y3)[19].

The sharp 3‰ $\delta\ ^{18}$O depletion from 24.5 to 23.8 cm took place in about 300 yr. It is much too large and rapid to be caused solely by ice melt and warming of the Younger Dryas–Preboreal transition[27]. It signals a salinity lowering due to resumption of heavy Nile floods after 10,000 yr BP. They correlate with the African main rainy period from 10,000 to 8,000 yr BP which builds the highest lake levels around 9,500 yr BP (Fig. 1).

The second half of the sapropel is a consequence of these floods. The time lag between the high floods and sapropel incipience is ~800 yr, which is much longer than the previous one, because the floods discharged over a much more saline sea surface.

In the shallower East Mediterranean core GA32, the bottom-to-surface $\delta\ ^{18}$O gradient increases suddenly at two levels, suggesting a two-step flooding sequence[12]. The isotopic variation related to salinity change is also 1–1.5‰ here.

Although high nutrient input and planktonic productivity are associated today with the arrival in September of the tongue of Nile flood water off the Israeli coast[30,31,35], one should not argue that the low ^{13}C/^{12}C ratios in surface waters are caused by a higher nutrient input. (Each plankton net haul yields 3 cm^3 of

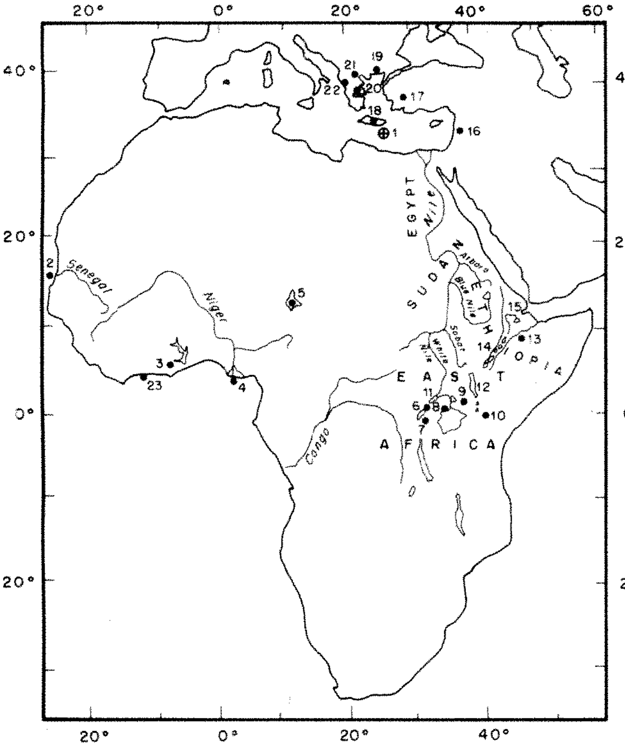

Fig. 2 Location of core and mentioned sites. 1, Core KS52. 2, Core off the Senegal River mouth. 3, Lake Bosumtwi, Ghana. 4, Core off the Niger River mouth. 5, Lake Tchad. 6, Ruwenzori, Lake Mahoma. 7, SW Uganda, Muchoya Swamp. 8, Lake Victoria, Pilkington Bay. 9, Cherangani Hills. 10, Mt Kenya, Sacred Lake, Lake Rutundu. 11, Lake Mobutu Sese Seko (Albert). 12, Lake Turkana (Rudolf). 13, Mt Badda. 14, Ethiopian Rift Lakes. 15, Afar Lakes. 16, Ghab Valley, Syria. 17, Sogüt, Anatolia. 18, Aghia Gallini, Crete. 19, Tenaghi Philippon, Macedonia. 20, Xinias Lake. 21, Edessa. 22, Ioannina. 23, Ivory Coast littoral.

plankton in August, 30–35 cm^3 in September; the yearly average is 4.7 cm^3 and the spring bloom reaches only 12.5 cm^3 (ref. 31).) In the Indian Ocean, the δ ^{13}C of shallow dwelling foraminifera is not related to nutrient supply of upwelling origin[36]. High primary productivity might even be the cause of a higher δ ^{13}C of the ΣCO_2 at the same depths (J. C. Duplessy, personal communication). Thus, the depletion we measure in core KS52 are related to the influx of organic rich freshwaters (with a low ^{13}C/^{12}C ratio of the ΣCO_2) of continental origin. These low surface ratios result in an intense vertical δ ^{13}C gradient in the water column.

Pollen

The upper sapropel pollen spectrum (pollen sum 356) (around 9,500 yr BP) predominantly reflects a Mediterranean (48.2%) and warm temperate (6.5%) vegetation. It is very similar to the earliest Holocene in Macedonia (Zones Z1 and 2, 10,300–9,000 yr BP)[19]. An open (herbaceous: 45.4%) oak (31.1%) pine (15.1%) forest occupied the Greek and Turkish Mediterranean shores, and broad-leaved trees (6.5%) requiring more summer moisture grew higher on the slopes. Littoral or desert halophytes (11.1%) were more abundant here than in Macedonia. The cold steppe *Artemisia* is hardly present (6.0%). The pollen is transported by wind to the sea surface, then dispersed by currents as a pelagic element[37]. Well specified Nilotic pollen[38] is absent: the Nile water does not appear to carry pollen further than its sedimentary load; they are only found in Nile silt[38]. The low density characteristic of the Nile water is thus preserved far beyond the silt and pollen deposition limits. The geological implication is that bottom waters in a deep or shallow basin may become anoxic under the influence of fluvial discharge even if the local climate reflected by pollen cannot feed such rivers, and even where clastic sediments do not reach. In fact, bottom anoxicity may occur whatever the lithology of the depositing sediment, provided distance from the continent is not too great. Moreover, this limiting factor can be enlarged in a globally warm climate like the Cretaceous, during which weak winds and sluggish ocean currents do not enhance water mixing.

Late Glacial–early Holocene equatorial deluge

During the last Glacial maximum (19,000–13,000 yr BP), extreme aridity spread in the tropics. It was immediately followed, during the late Glacial–early Holocene (Alleröd–Preboreal–Boreal), by an equatorial heavy rainfall period of global scale, recorded by pollen, in northern South America (Guantiva Interstadial)[39], the Galapagos[40,41], most probably New Guinea[42], with extensive wet Lower Montane *Nothofagus* forest, Sumatra[43], and the Indian Ocean and Africa. Raised lake levels are also conspicuous. It was the wettest period of the past 20,000 yr.

The formation of the Mediterranean sapropel results from a link (the Nile River) across 35° lat. between this climatic event in equatorial Africa and the marine hydrology. The relevant data are shown in Fig. 1.

In Africa, from west to east, and within 10° N of the Equator, the highest precipitation is recorded between 12,500 and 8,000 yr BP. In West Africa, data are from the southern drainage area of Lake Tchad[44], the Ivory Coast mangrove peat[45], the level of Lake Bosumtwi in Ghana[46], and the Niger River discharge[47]. North of 10° N, the onset of the rainy period is delayed. The mangrove along the Senegal River lower course (17° N) thrives after 9,600 yr BP (ref. 48), and the high level of Lake Tchad (13–15° N)[49] and its wettest vegetation[44] occur after 8,500 yr BP.

In East Africa, where the Nile watershed is situated, reinterpreted pollen data from the mountains, 3 °S–2 °N, correlate aridity before 12,000 yr BP with a cool climate, and moisture thereafter with a warm climate[50,51]. On the Ugandan (Ruwenzori, Kigezi[52–54]) and Kenyan (Mt Kenya, Cherangani Hills[55,56]) mountains, the shift towards a wetter and warmer vegetation

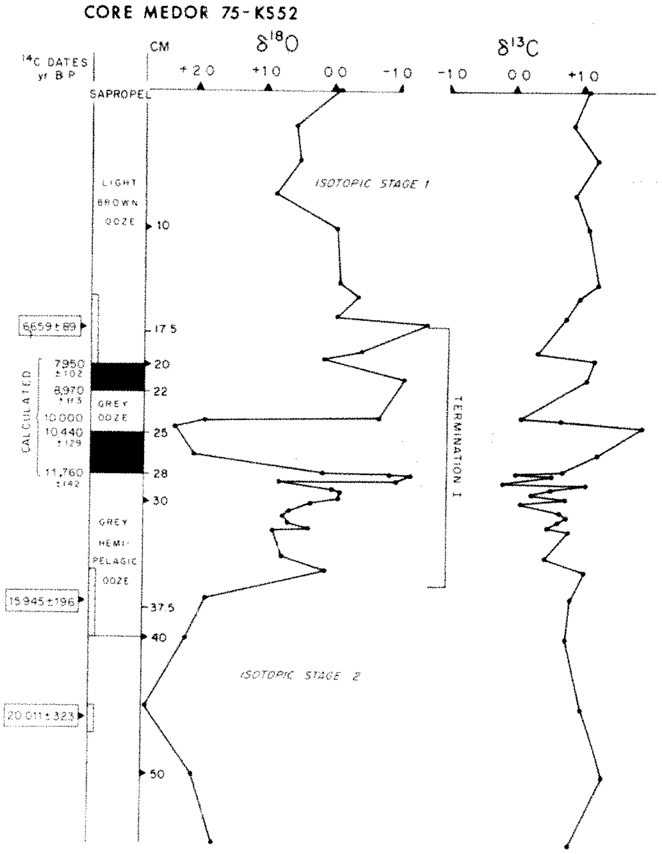

Fig. 3 Sapropel age, ^{18}O and ^{13}C isotopes stratigraphy in core KS52.

belt, of different types according to the altitude of the site, started as early as 12,700 yr BP and developed around 10,800 yr BP. The warmest and wettest local vegetation is usually installed around 8,000 yr BP.

In the lowlands around Lake Victoria, the moisture increased after 12,500 yr BP, and the wettest climate is signalled between 9,500 and 7,000 yr BP by the vegetation, the lake level and its sediments[50]. A widespread dry spell, synchronous with the Younger Dryas, is recorded between 10,800 and 9,500 yr BP in the low levels of Lakes Bosumtwi, Tchad and Victoria, as well as in the vegetation around Lake Victoria and on Mt Kenya.

Before 12,000 yr BP, the Main Nile was dry most of the year, the meagre summer flow fed only by the weak Ethiopian monsoon. After 12,000 yr BP, the East African bi-seasonal rainfall was higher and the White Nile became a very large permanent river, well regulated by the lakes[51,57,58]. Its catchment area was expanded from 9,500 to 7,500 yr BP by the inclusion of the much higher, larger Lake Turkana[59].

Wetter conditions occurred on the southeastern Ethiopian Plateau at Mt Badda, after 11,500 yr BP or possibly only 9,500 yr BP (ref. 60).

Drained by the Blue Nile and the Atbara, the northern Ethiopian Highlands (10–13° N) are inaccessible, but their palaeoclimate is documented by the peripheral Rift and Afar Lakes[61]. The lake levels were highest, much above today, and they merged between 9,500 and 8,500 yr BP. The Ethiopian summer flood of the Nile was therefore much heavier. This seasonal variation accounts for the lamination of the sapropels: the white laminae are formed by coccoliths[14] blooming with the flood, rich in dissolved ions of Ethiopian basalt origin.

The Nile Valley aggradation records these floods mostly from 12,000 to 11,000 yr BP, and from 8,000 to 7,000 yr BP in Sudan and Upper Egypt[57,58,62]. There, aggradation indicates a "wild Nile with aberrant summer floods of a phenomenal volume"[62]. Moreover, higher local Sudanese (15° N) rainfall, which may have reached 550 mm yr^{-1} (163 today)[63], between 8,000 and 7,000 yr BP (ref. 57), suggests decreased evaporation along the course of the Nile. Today, evaporation in the Sudanese swamps heavily reduces the Nile discharge.

The African and Indian monsoons, of equatorial westerlies origin, both controlled by the continental heat trough, displayed the same peak when the summer insolation was higher than today around 11,000 yr BP. At that time, strong monsoonal air flow and high rainfall in India is suggested by low sea-surface summer temperature in the Arabian Sea[64], due to strong upwelling induced by the southwesterly air flow, a mangrove much more extensive than today on the Indian coast near Bombay (E. Van Campo, personal communication), and river discharge higher than today in the Bay of Bengal[65]. The Intertropical Convergence of the tropical easterlies, with its zenithal rains, was reactivated in East equatorial Africa.

From the eastern tropical Atlantic to the Bay of Bengal, along the inner tropics of the African continent and Indian Ocean, and in the other equatorial longitudes, as the summer insolation was highest, the late Glacial–early Holocene was a very wet period, the most humid of the past 20,000 yr. From around 12,500 yr BP, during the Bolling–Alleröd interstadial, the higher rainfall belt migrated progressively from the Equator polewards through the Preboreal and Boreal. The Atlantic was the wettest period in the 50–55° N lat. zone. It was set back by a drier episode which corresponds to the cold Younger Dryas, recorded in the Mediterranean sapropel by the disappearance of the brackish surface layer, thus interrupting the stagnation from 10,400 to 9,000 yr BP.

Conclusion

The Mediterranean two-layered upper sapropel in core KS52 is dated at 11,800–10,400 yr BP and 9,000–8,000 yr BP, the interruption resulting from the Younger Dryas cold/dry event. This is too late to be caused by the influx of Eurasian ice-sheet meltwater. Instead, oxygen and carbon isotope variations in planktonic foraminifera show that the light, low-salinity, organic and nutrient rich sea-surface layer which spread slightly before sapropel deposition and selectively increased the planktonic productivity, originated as rainfall. The pollen record around the eastern Mediterranean does not indicate much increased local rainfall at that time. Meanwhile, in equatorial Africa, very heavy rainfall began at 12,500 yr BP and culminated between 10,000 and 8,000 yr BP. We conclude that this equatorial deluge, channelled by the Nile River over 6,700 km is, as already suggested[58,66], the source of the surface brackish-water layer in the Mediterranean. This layer enhanced the vertical salinity and density gradient, and established stable stratification. Thus bottom stagnation was triggered in this hydrographically restricted deep basin, and sapropel formation resulted. The East Mediterranean behaved as an ectogenic meromictic lake as a stratified estuary and as a fjord during the stagnation events.

The establishment of these climate links have far-reaching geological implications.

(1) The Quaternary climatic chronology of Africa is recorded in the eastern Mediterranean subsurface. Sapropels are formed during all the periods of high summer insolation of the Northern Hemisphere displayed by the Milankovitch curve, which occur even during glacial isotopic stages 3, 4 and 6. The isotope stratigraphy supports these correlations.

(2) Widespread marine stagnation events occurred during certain short and well-defined periods of the Cretaceous. They deposited pelagic laminated sapropels and we suggest that they result from the same chain of events as this recent Mediterranean sapropel. In equatorial West Gondwana around the opening Atlantic, the thick fluvio-deltaic sediments of the Barreirinhas Basin suggest great river discharge in a seasonally very humid tropical climate, with a contrasting dry season enhancing evaporation. These Cretaceous sapropels may be important as possible petroleum generating environments.

Cruise Medor 75 was supported by the Centre National pour l'Exploitation des Oceans, France. The European Economic Community provided research funds. Support was by the CNRS, France. Revision of an earlier version of the manuscript and comments by J. C. Duplessy are acknowledged. We thank L. Burckle, R. Fairbanks, A. Gordon, F. McCoy, A. McIntyre, W. B. F. Ryan for helpful discussions and R. M. Cline for editorial assistance.

Received 8 June; accepted 28 October 1981.

1. Kullenberg, B. *Göteborgs K. Vetensk.-O. Vitterh Samh. Handl.* **B6,** 3–37 (1952).
2. Olausson, E. *Rep. Swedish Deep-Sea Expn 1947–8* **8,** 5, 287–334 (1960); **8,** 6, 337–391 (1961).
3. Ryan, W. B. F. in *The Mediterranean Sea* (ed. Stanley, D. J.) 149–169 (Dowden, Hutchinson & Ross, Stroudsburg, 1972).
4. McCoy, F. W. thesis, Harvard Univ. (1974).
5. Vergnaud-Grazzini, C., Ryan, W. B. F. & Cita M. B. *Mar. Micropaleont.* **2,** 353–370 (1977).
6. Kidd, R. B., Cita, M. B. & Ryan, W. B. F. *Init. Rep. DSDP Leg* **42,** 1, 421–443 (U.S. Govt Print. Off., Washington, 1978).
7. Cita, M. B. *et al. Quat. Res.* **8,** 205–235 (1977).
8. Thunell, R. C., Williams, D. F. & Kennett, J. P. *Mar. Micropaleont.* **2,** 371–388 (1977).
9. Parker, F. L. *Rep. Swedish Deep-Sea Expn. 1947–48* **8,** 2, 217–283 (1958).
10. Vergnaud-Grazzini C. & Herman-Rosenberg Y. *Rev. Geogr. Phys. Geol. Dyn.* **11,** 279–292 (1969).
11. Williams, D. F., Thunell, R. C. & Kennett, J. P. *Science* **201,** 252–254 (1978).
12. Luz, B. *Nature* **278,** 847–848 (1979).
13. Pastouret, L. *Bull. Mus. Anthrop. Prehist.* **16,** 155–171 (Monaco 1970).
14. Stanley, D. J. & Maldonado, A. *Nature* **266,** 129–135 (1977).
15. Ryan, W. B. F. & Cita, M. B. *Mar. Geol.* **23,** 197–215 (1977).
16. Thunell, R. C. & Lohmann, G. P. *Nature* **281,** 211–213 (1979).
17. Grosswald, M. G. *Quat. Res.* **13,** 1–32 (1980).
18. Bottema, S. thesis, Univ. Gröningen (1974); in *The Environmental History of the Near and Middle East since the Last Ice Age* (ed. Brice, W. C.) 15–28. (Academic, New York, 1978).
19. Wijmstra, T. A. *Acta bot. neerl.* **18,** 511–527 (1969).
20. Van Zeist, W., Woldring, H. & Stapert, D. *Palaeohistoria* **17,** 53–143 (1975).
21. Bottema, S. *Rev. Palaeobot. Palynol.* **31,** 193–217 (1980).
22. Niklewski, J. & Van Zeist, W. *Acta bot. Neerl.* **19,** 737–754 (1970).
23. Berger, A. L. *Quat. Res.* **9,** 139–167 (1978).
24. Lacombe H. & Tchernia, P. *Cah. Oceanogr.* **12,** 527–547 (1960).
25. Broecker, W. S. & Gerard, R. *Limnol. Oceanogr.* **14,** 883–888 (1969).
26. Broecker, W. S. *J. geophys. Res.* **84,** 3218–3225 (1979).
27. Lowe, J. J., Gray, J. M. & Robinson, J. E. *Studies in the Late Glacial of North West Europe* (Pergamon, Oxford, 1980).
28. Duplessy, J. C., Bé, A. W. H. & Blanc, P. L. *Palaeogeogr. Palaeoclimatot. Palaeoecol.* **33,** 9–46 (1981).
29. Hecht, A. *Bull. Sea Fish, Res. Sta. Haifa, Israel* **36,** 24 pp (1964).
30. Liebman, E. *Rapp. P.-v. Réun. Comm. int. Explor. scient. Mer Mediterr.* **9,** 181–186 (1935).

31. Statistical Treatment of Environmental Isotope Data in Precipitation *Tech. Rep., Ser.* 206, (IAEA, Vienna, 1981).
32. Ramesh Babu, V. & Sastry, J. S. *Ind. J. mar. Sci.* **5**, 179–189 (1976).
33. Wyrtki, K. *Oceanographic Atlas of the International Indian Ocean Expedition* (National Science Foundation, Washington, 1971).
34. Ryther, J. H., Menzel, D. W. & Corwin, N. *J. mar. Res.* **25**, 69–83 (1967).
35. Halim, Y. *J. Cons. perm. int. Explor. Mer* **26**, 57–67 (1960).
36. Prell, W. L. & Curry, W. B. *Oceanol. Acta* **4**, 91–98 (1981).
37. Rossignol-Strick, M. *Init. Rep. DSDP Leg* **13**, 971–991 (1973).
38. Rossignol, M. *Notes Mém Moyen-Orient* **10**, 1–272 (1969).
39. Van Geel, B. & Van der Hammen, T. *Palaeogeogr. Palaeoclimatol. Palaeoecol.* **14**, 9–92 (1973).
40. Colinvaux, P. A. *Nature* **240**, 17–20 (1972.
41. Colinvaux, P. A. & Schofield, E. K. *J. Ecol.* **64**, 989–1012 (1976).
42. Hope, G. S. *J. Ecol.* **64**, 627–663 (1976).
43. Maloney, B. K. *Nature* **287**, 324–326 (1980).
44. Maley, J. *X INQUA Congr. Suppl. Bull. AFEQ* **1**, 50, 187–197 (1977).
45. Fredoux, A. & Tastet, J. P. *7th Africa Micropaleont. Colloq.* Ile-Ife, Nigeria (1976).
46. Talbot, M. R. & Delibrias, G. *Earth planet. Sci. Lett.* **47**, 336–344 (1980).
47. Pastouret, L., Chamley, H., Delibrias, G., Duplessy, J. C. & Thiede, J. *Oceanol. Acta* **1**, 217–232 (1978).
48. Rossignol-Strick, M. & Duzer D. *Pollen Spores* **21**, 105–134 (1979).
49. Servant M. & Servant-Vildary, S. *Palaeoecol. Afr.* **6**, 87–92 (1972); in *The Sahara and the Nile* (eds Williams, M. A. J. & Faure, H.) 133–172 (Balkema, Rotterdam 1980).
50. Kendall, R. L. *Ecol. Monogr.* **39**, 121–176 (1969).
51. Livingstone, D. A. *A. Rev. Ecol. System.* **6**, 249–280 (1975).
52. Livingstone, D. A. *Ecol. Monogr.* **37**, 25–52 (1967).
53. Hamilton, A. in *East African Vegetation* (eds Lind, E. M. & Morrison, E. S.) 188–209 (Longman, London 1974); *Palaeoecol. Afr.* **7**, 45–149 (1972).
54. Morrison, M. E. S. *Nature* **190**, 483–486 (1961); *J. Ecol.* **56**, 363–384 (1968).
55. Coetzee, J. A. *Nature* **204**, 564–566 (1964); *Palaeoecol. Afr.* **3**, 1–146 (1967).
56. Van Zinderen Bakker, E. M. & Coetzee, J. A. *Palaeoecol. Afr.* **7**, 151–181 (1972).
57. Williams, M. A. J. & Adamson, D. A. *Nature* **248**, 584–586 (1974); in *The Sahara and the Nile* (eds Williams, M. A. J. & Faure, H.) 281–304 (Balkema, Rotterdam, 1980).
58. Adamson, D. A., Gasse, F., Street, F. A. & Williams, M. A. J. *Nature* **288**, 50–55 (1980).
59. Butzer, K. W., Isaac, G. L., Richardson, J. L. & Washbourn-Kamau, C. *Science* **175**, 1069–1076 (1972).
60. Hamilton, A. C. *X INQUA Congr. Abs. Birmingham* 193 (1977).
61. Gasse, F., Street, F. A. *Palaeogeogr. Palaeoclimatol. Palaeoecol.* **24**, 279–325 (1978).
62. Butzer, K. W. in *The Sahara and the Nile* (eds Williams, M. A. J. & Faure, H.) 253–280 (Balkema, Rotterdam 1980).
63. Wickens, G. E. *Boissiera* **24**, 43–65 (1975).
64. Prell, W. L. in *Evolution des Atmosphères planétaires et Climatologie de la Terre*, 149–156 (CNES Colloq. Int., Nice, 1978).
65. Cullen, J. L. *Geol. Soc. Am. San Diego Meet. Abstr.* 408 (1979).
66. Nesteroff, W. D., Olive, P., Rossignol-Strick, M. & Vergnaud-Grazzini, C. *P. V. CIESM-17 Congr. Cagliari* (1980).
67. Shotton, F. W. in *British Quaternary Studies, Recent Advances* (ed. Shotton, F. W.) 17–29 (Clarendon, London 1977).
68. Mangerud, J., Andersen, S. T., Berglund, B. E. & Donner, J. J. *Boreas* **3**, 109–127 (1974).
69. Mangerud, J., Larsen, E., Longva, O. & Sonstegaard, E. *Boreas* **8**, 179–187 (1979).
70. Roberts, N., Erol, O., de Meester, T. & Uerpmann, H. P. *Nature* **281**, 662–664 (1979).
71. Livingstone, D. A. in *The Sahara and the Nile* (eds Williams, M. A. J. & Faure, H.) 339–359 (Balkema, Rotterdam, 1980).
72. Olsson, J. *Am. J. Sci., Radiocarbon Suppl.* **1**, 87–102 (1959).
73. Olson, E. A. & Broecker, W. S. *Am. J. Sci. Radiocarbon Suppl.* **3**, 141–175 (1961).
74. Pastouret, L. *Tethys* **2**, 227–266 (1970).
75. Fabricius, F. H., Von Rad, U., Hesse, R. & Ott, W. *Geol. Rdsch.* **60**, 164–192 (1970).

Polyoma virus capsid structure at 22.5 Å resolution

I. Rayment, T. S. Baker & D. L. D. Caspar

Rosenstiel Basic Medical Sciences Research Center, Brandeis University, Waltham, Massachusetts 02254, USA

W. T. Murakami

Department of Biochemistry, Brandeis University, Waltham, Massachusetts 02254, USA

X-ray diffraction data from polyoma capsid crystals were phased by refinement of low-resolution starting models to obtain a self-consistent structural solution. The unexpected result that the hexavalent morphological unit is a pentamer shows that specificity of bonding is not conserved among the protein subunits in the icosahedrally symmetric capsid.

X-RAY crystallographic studies on polyoma virus were begun to visualize the protein subunit packing in the icosahedral capsid and to explore the way in which the chromatin core of this tumorigenic virus is packaged inside its protein shell[1]. Analysis of electron micrographs has established that the capsid consists of 12 five-coordinated and 60 six-coordinated morphological units[2] (capsomeres) arranged on a $T = 7d$ icosahedral surface lattice[3] (Fig. 1). It has been presumed, based on the principles formulated to account for the morphology and chemical composition of simple icosahedral virus particles[4], that the capsids of the $T = 7$ papova viruses should be constructed from 420 identical protein subunits quasi-equivalently bonded into 12 pentameric and 60 hexameric capsomeres. High-resolution X-ray structure determination of tomato bushy stunt virus[5] and southern bean mosaic virus[6] has established that quasi-equivalence is used to conserve essential bonding specificity among the 180 chemically identical subunits of these $T = 3$ icosahedral capsids. Our 22.5-Å resolution electron density map of the polyoma capsid reveals unexpected substructure in the hexavalent capsomere that is inconsistent with the expectation of quasi-equivalent bonding of identical subunits. (The adjectives 'hexavalent' and 'pentavalent' are introduced to identify the six- and five-coordinated morphological units without prejudging the nature of their substructure.)

The starting point for our analysis of the polyoma capsid diffraction data was a model representing the coarse surface features seen in the three-dimensional image reconstruction from electron micrographs of negatively stained particles[3]. The capsomeres in this image reconstruction appear as hollow, stubby protrusions with no regular substructure, about 50 Å in diameter and separated from their nearest neighbours by 80–90 Å at a radius of 200 Å in the capsid. Pentavalent and hexavalent morphological units appear to be about the same size, which would not be expected if they were composed of pentamers and hexamers of identical protein subunits.

Cells infected with polyoma virus and other papova viruses produce, in addition to intact virions and empty capsids, hollow tubular particles that appear to be polymorphic assemblies of the capsomeres[7]. There are two categories of tube: wide tubes,

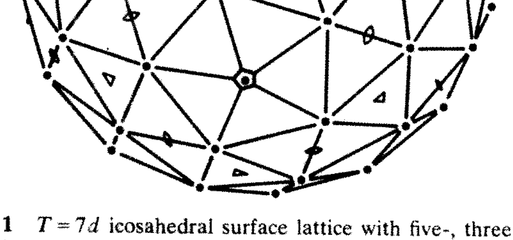

Fig. 1 $T = 7d$ icosahedral surface lattice with five-, three- and two-fold axes marked. The drawing shows one side of the polyhedral surface consisting of 60 six-coordinated and 12 five-coordinated lattice points at the same radius. The location of the six-coordinated point is that determined for the hexavalent morphological unit in the polyoma capsid.

0028-0836/82/020110—06$01.00

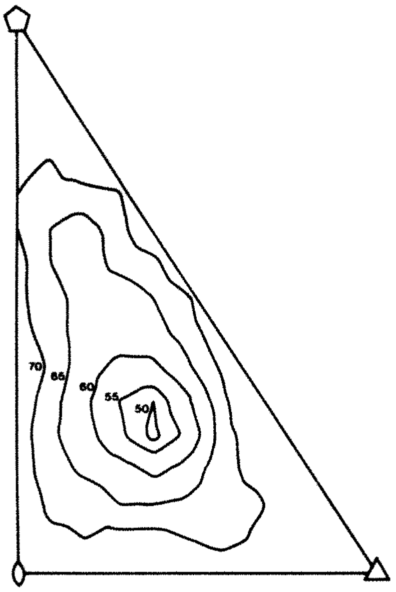

Fig. 2 Location of the hexavalent unit in the icosahedral surface lattice. The R factor comparing the calculated and measured diffraction pattern is plotted as a function of the position of the hexavalent unit in the icosahedral cell defined by the five-, three- and two-fold axes (see Fig. 1). The model giving the smallest R factor is shown in Fig. 3*a*.

about the diameter of the virion, which are built of capsomeres arranged in a hexagonal surface lattice, and narrow tubes, which Kislev and Klug[8] showed to be constructed of pentameric capsomeres arranged in a lattice they called a 'pentagonal tessellation'. The capsomeres of the wide tubes were presumed to be hexamers but the chemical and structural relationships between the morphological units of the 'hexamer' and 'pentamer' tubes could not be established at that time. In the light of our results new questions are raised about the structure of these polymorphic assemblies of the capsid subunits.

Complete virions contain seven different proteins, four of which are cellular histones associated with the DNA, the other three (VP1, VP2 and VP3) being virus coded[9]. VP1 (molecular weight (MW) ~42,000) is the major capsid protein. The function of VP2 and VP3 (MW ~ 35,000 and ~23,000, respectively), which constitute less than 20% of the virion proteins, is not clear. Purified capsids have been prepared that contain only VP1[10] and these particles have normal morphology. Thus, the pentavalent and hexavalent capsomeres seem to be built of identical VP1 subunits.

Crystallography

Polyoma virus capsids of the strain Sp-34 were isolated as previously described[11]. The preparation used for growing crystals consisted predominantly of the major capsid protein, VP1, and only a small amount of VP2 and VP3 compared with the intact virion. Crystals, in the rhombic dodecahedral form[12], were grown by equilibrating a solution of polyoma virus capsids at 4 mg ml^{-1} in 0.02 M Tris *p*H 9.5 and 0.17 M sodium sulphate against 0.55 M sodium sulphate by vapour diffusion. Crystals grew over a period of 1 month at room temperature. These crystals diffracted to a resolution of at least 8 Å. The icosahedral capsids, of packing diameter 495 Å, are located at the centre and corners of the b.c.c. lattice (space group I23, unit cell edge 572 Å) with particle two- and three-fold axes coincident with the crystallographic axes[1]. Diffraction data were collected to 22.5 Å resolution by screened precession photography (crystal-to-film distance 150 mm) with an Elliott GX6 rotating anode X-ray generator using a 0.2-mm focal cup and two perpendicular-focusing mirrors[13]. A total of 11 zero level ($\mu = 2°$) and 4 upper level ($\mu = 1.5°$) photographs were collected, each a 48-h exposure. These gave 1,481 independent reflections between (1/150) and (1/22.5) Å spacing, representing 94% of the data within this resolution range. The individual films were digitized on an Optronics P1000 densitometer at 50 μm scanning raster and processed using a modified version of the Harvard Scan-11 system on a PDP-11/40 computer. The films scaled together with an R factor measuring the mean variation in intensity of symmetry-related reflections of 5.7%.

Models for phase refinement

Trial phases, calculated to 30 Å resolution from models based on information from electron microscopy[3] and small-angle X-ray diffraction[1], were refined and extended to 22.5 Å resolution by imposing the constraints of non-crystallographic symmetry and solvent flattening. This approach is similar to that used to determine the structure of southern bean mosaic virus to 22.5 Å resolution[14]. Our starting model of the polyoma capsid, consisting of 72 morphological units arranged in a $T = 7d$ icosahedral surface lattice (Fig. 1), is a non-centrosymmetric structure. Consequently, calculated trial phases will introduce the non-centric component of the structure factors from the start. This is essential to the quality of the subsequent real-space phase refinement and extension.

Models consisting of 72 hollow cylindrical capsomeres on a spherical shell were formulated with 9 adjustable parameters defining the size and position of the structural elements. Phases from these models were calculated by Fourier transforming a density map generated in a lattice corresponding to the polyoma crystal. The model parameters were adjusted by comparing the calculated and observed structure factor amplitudes. The models which gave the best R factor fit were built from morphological units about 40 Å high and 80 Å in diameter with a 35-Å diameter axial hole, resting on a shell extending from a radius of 180–200 Å. The effect of moving the hexavalent morphological unit in this model is shown in Fig. 2, where the R factor is plotted as a function of position. The position of the minimum is close to the hexavalent capsomere location observed in Finch's image reconstruction from electron micrographs[3]. A projection of this 'best' model down a two-fold axis is shown in Fig. 3*a*. The R factor for this model to 30 Å resolution was 50% where R is defined as

$$R = \frac{\sum ||F_o| - |F_c||}{\sum |F_o|} \times 100$$

where $|F_o|$ and $|F_c|$ are observed and calculated structure factor amplitudes. The R factor as a function of resolution is shown in Fig. 4*a*.

Particle envelope

Flattening the solvent regions of the electron density map places a powerful constraint on the low resolution phases and also provides the basis for phase extension. Thus, the envelope chosen to enclose the virus capsid is critical in the phase refinement and extension. The envelope used was a spherical shell extending from 165 Å to 260 Å truncated by planes perpendicular to the icosahedral three-fold axes 247 Å from the virus centre. These boundary planes bisect the line of contact between virus particles along the crystallographic three-fold axes. The three hexavalent units adjacent to the crystallographic three-fold axis make contact tip to tip with the related set on the neighbouring particle. As there is no discernible interdigitation of the capsomeres at this resolution, the boundary planes perpendicular to the three-fold axes define the volume associated with one virus particle.

Solvent density for both the interior and exterior of the capsid was taken as the average observed density of the shell extending from 160 to 165 Å. This approach was used because omitting unmeasured low-resolution <(1/150) Å reflections in the initial calculations results in spurious electron density ripples inside the capsid. When the average density of the total solvent region defined by the particle envelope was used as suggested by Bricogne[15], the refinement calculation converged more slowly. Nevertheless, both methods of determining the solvent density gave very similar final values.

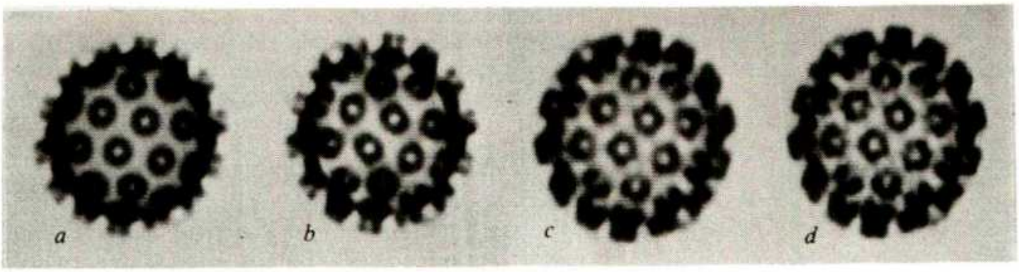

Fig. 3 Density maps of the top half of particles (diameter 495 Å) projected down a two-fold axis (orientation as in Fig. 1). The maps were scaled to have the same total electron density and were photographed directly from a 256 grey scale TV graphics display. *a*, Model map at 30 Å resolution; *b*, map computed using observed data and model phases to 30 Å resolution without refinement; *c*, 30 Å resolution refined map; *d*, refined map at 22.5 Å resolution calculated by phase extension from 30 Å. Note how the substructure in the morphological units develops as the refinement proceeds. Even at 30 Å resolution the hexavalent unit has a pentagonal appearance.

Refinement method

The calculated phases from the model structures were refined to 30 Å resolution against the observed structure factor amplitudes by imposing the constraints of solvent flattening and the five-fold non-crystallographic symmetry[15–17]. An electron density map was calculated to 30 Å resolution using the model phases and observed amplitudes, and averaged over the five non-crystallographic asymmetric units within the particle envelope. The observed amplitudes were weighted according to their fit to those calculated from the model according to the scheme

$$W = \exp\left(-\frac{|F_o| - |F_c|}{|F_o|}\right)$$

This simple weighting scheme gave faster convergence than that suggested by Sim[18], but the final phase set was not sensitive to the weighting procedure used.

The averaged, solvent-flattened density map was Fourier transformed to calculate phases and amplitudes for the first cycle of refinement; the r.m.s. phase difference and R factor comparing initial and refined structure factors were evaluated; refined phases were combined with measured amplitudes to initiate the next cycle of refinement; these calculations were iterated until the calculated phase difference and R factor did not change significantly from one cycle to the next.

There are two possible orientations for the icosahedral five-fold axis in the I23 unit cell. The orientation used was that indicated by the intensity spikes in the diffraction patterns[1]. If the alternative orientation of the five-fold axis was chosen, the R factor between refined and observed structure factors never dropped below 50%. The standard deviation in the density between the five icosahedral units in the crystallographic asymmetric unit for the correct orientation was 1/7th of that calculated for the alternative.

Omission of the unmeasured data below (1/150) Å spacing systematically lowers the calculated amplitudes for the observed structure factors below (1/100) Å spacing. The amplitudes of the innermost observed reflections are the largest in the data set and dominate the scaling of the calculated to the observed structure factors. This effect was mitigated by including the calculated values for the unmeasured data after the fourth cycle with a weight of 0.9. Reduced weighting was applied to avoid divergence of these large terms in the iterative refinement. Various test calculations have established that the low order data can be accurately estimated from the higher resolution data. Without the eight calculated values for the missing low order data, the refinement converged to only 27% as compared with 10.5% with these data after 14 cycles of phase refinement.

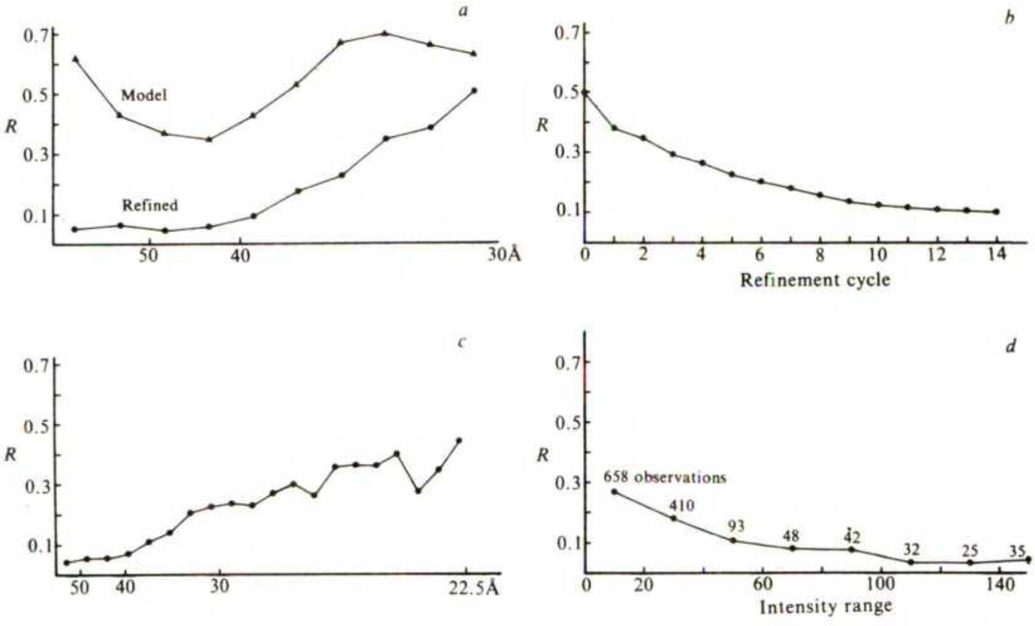

Fig. 4 R factors comparing the agreement between observed and calculated structure factor amplitudes. *a*, As a function of resolution comparing initial model and refined map at 30 Å resolution; *b*, as a function of refinement cycle at 30 Å resolution; *c*, as a function of resolution for the phase extension from 30 to 22.5 Å resolution; *d*, as a function of intensity for the 22.5 Å refined map. For *a* and *c* the points are plotted so that the interval between points corresponds to equal volume increments in reciprocal space. The starting model (Fig. 3*a*) fits the observed data best in the 40–50 Å resolution range where there is a strong modulation in the transform determined by the surface lattice arrangement of the morphological units[1]. After 14 cycles of refinement (*b*) there is a substantial improvement in the fit between the calculated and observed amplitudes at low resolution (*a*). The structure amplitudes phased by extension from 30 to 22.5 Å resolution represent over half of the total data to this resolution. The R factors for these higher resolution data (*c*) are uniformly satisfactory. The phase extension also leads to an improvement in the R factor for the data to 30 Å resolution by reducing series termination effects. Plotting the R factor of the 1,343 non-zero reflections as a function of intensity (*d*) shows that there is a correlation between the R factors and the accuracy of the data which are more precise for the stronger reflections.

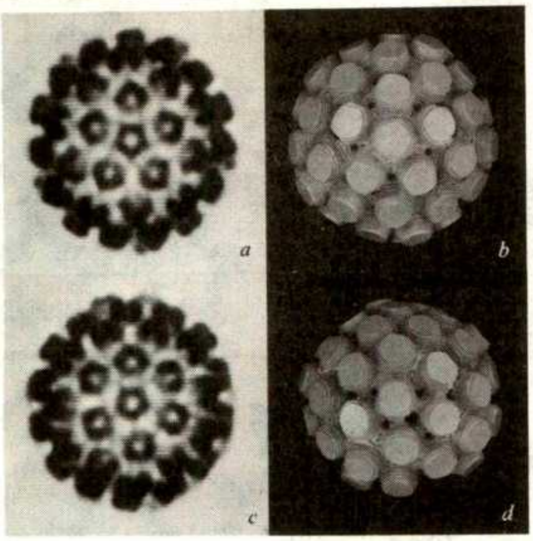

Fig. 5 Views of half the capsid (495 Å diameter) down the five-fold axis (*a*, *b*) and down the axis of the hexavalent unit (*c*, *d*). *a* And *c* are computer graphics projections of the electron density map at 22.5 Å resolution, *b* and *c* are photographs of a model of stacked sections of the map at 30 Å resolution with the external contour level set at 0.2 of the maximum density. The half-model was built symmetric about the five-fold axis (*b*), thus, when it is tilted to view down the hexavalent unit (*d*) the bottom portion of the image is incomplete.

Figures 3*a–c* and 4*b* illustrate the progress of the refinement in real and reciprocal space. Figure 4*b* shows the *R* factors as a function of refinement cycle. Figure 3*a* represents the starting model to 30 Å resolution, Fig. 3*b* the unrefined structure calculated from the observed amplitudes with model phases, and Fig. 3*c* the refined structure at 30 Å resolution.

Tests of refinement method

There is no established criterion for determining the correctness of the electron density map described subsequently. Because the map shows unexpected features, considerable effort was devoted to demonstrate the uniqueness of the refinement. Phases from any model consisting of 72 bumps distributed on the surface of a spherical shell, in a manner consistent with the image from electron microscopy[3], refined to the same solution. Indeed, a starting model which placed 60 hemispheres close to the location of the hexavalent units on a spherical shell with no density protruding on the five-fold axes (initial *R* factor = 65%) refined to the same phase set as the more realistic models, although it took 18 cycles of refinement. Furthermore, phases from elaborate models with hexavalent morphological units containing either five- or six-fold substructure refined to the same final structure.

The reliability of the refinement method was tested by using amplitudes calculated from models in place of observed data. Because the model structure factor calculations give both the amplitude and the phase, it is possible to judge absolutely how well another set of trial phases converges to the correct values. In the test calculations, amplitudes from various $T = 7$ capsid models were combined with phases from models with different morphology; refinement of the phases always converged to the phases of the model from which the amplitudes were taken. For example, refining initial phases from an all-pentamer $T = 7$ model against the amplitudes from a 60 hexmer + 12 pentamer model led back to the phases of the model built with hexamers. Thus, our refinement procedure recovers the correct structure corresponding to the amplitudes of the data even when trial starting phases were chosen to attempt to bias the calculation to produce an incorrect result.

Phase extension

The polyoma diffraction data between 30 and 22.5 Å resolution were phased by extension from the refined 30 Å phases. This was necessary because the model phases are only reliable to ~30 Å resolution. Attempts to refine the data directly to 22.5 Å resolution using trial model phases did not converge satisfactorily.

Phase extension is possible because imposition of the envelope on the electron density generates phase information for reflections just beyond the resolution of those used to calculate the map. The characteristics of phase extension were tested using model structure factors and phases in place of the real polyoma diffraction data. Starting from 30 Å resolution, using calculated amplitudes and phases as test data, it was possible to extend and refine the phases to 22.5 Å resolution. The r.m.s. phase difference between the correct and the refined extended phases were generally less than 30°.

The resolution of the actual data refinement was extended from 30 Å to 22.5 Å over 18 cycles. Predicted phases for structure factors within one reciprocal lattice distance (1/572) Å of the previous resolution were included in alternate cycles. The final *R* factor between observed and calculated structure factor

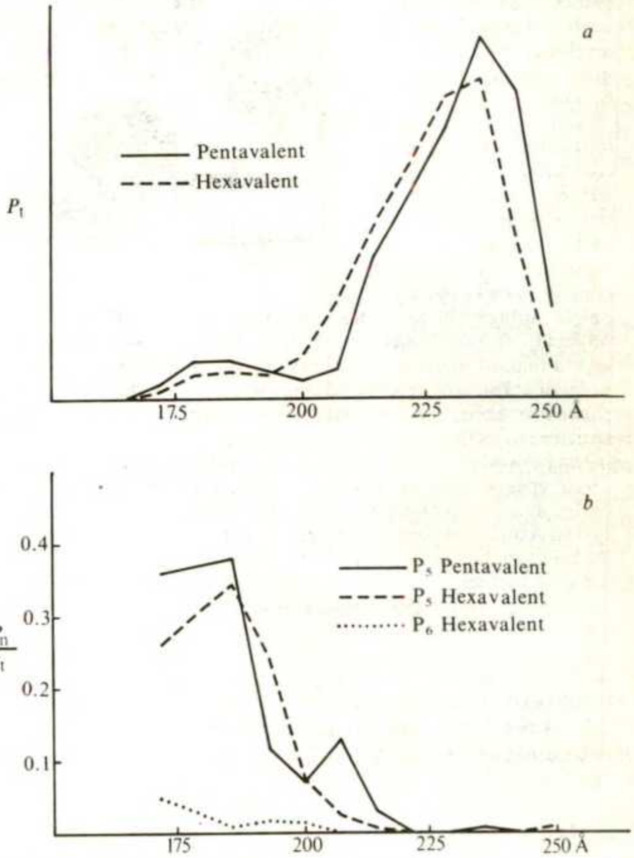

Fig. 6 Rotational power spectra of the pentavalent and hexavalent units. *a*, P_t is the sum of all cylindrical harmonics in sections of the map through the capsomeres normal to the five-fold axis and the 'best' axis of the hexavalent units, plotted as a function of the distance of the section from the centre of the particle. *b*, Relative strength of the five-fold harmonic of the pentavalent unit and the five- and six-fold harmonic of the hexavalent unit. P_t is proportional to the integrated density in each section. At small radii in the capsid a cylindrical boundary of 93 Å diameter was chosen for calculating the power spectrum of the capsomeres. These cylinders touch at a radius of 170 Å. The integrated density of the inner portions of the capsomere may be underestimated by the methods of calculation. The correspondence in the rotational power spectra distribution of the pentavalent and hexavalent units indicates a close similarity in their structures and a small difference in their radial positions. The relative strength of the order 5 harmonic for the outer portion of both the pentavalent and hexavalent capsomere is reduced because the cylindrically symmetric component, which is the dominant term in P_t, is very strong for this part of the structure. The order 5 harmonic for the hexavalent capsomere is always much stronger than that of order 6 (or any other non-zero harmonic).

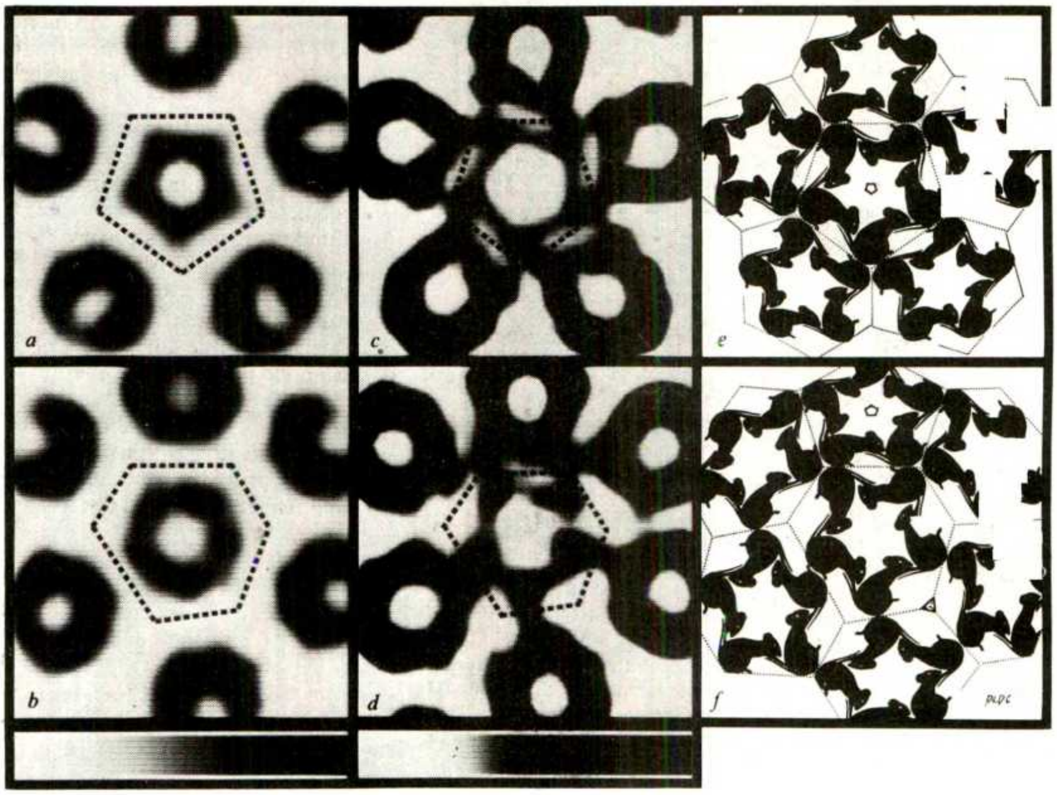

Fig. 7 Sections of the electron density map showing substructure of the capsomeres (*a–d*) and drawings on a polyhedral surface (*e*, *f*) illustrating an inferred packing relation of structure units. Upper row: views down five-fold axis and lower row: views down axis of hexavalent capsomere. Width of sections displayed 215 Å. Orientation as in Fig. 5. Grey scales at the bottom show the relation between darkness in the images and map density that increases uniformly from left to right of the scales. *a*, *b*, Maps of section planes 215 Å above centre of capsid. At this level and above there is little detectable contact between neighbouring capsomeres. *c*, *d*, Maps (displayed with enhanced contrast) of section planes 195 Å above centre. At this level and below five basal parts of the capsomeres splay out and contact basal parts of neighbouring capsomeres. Section planes are perpendicular to the axis of the central capsomere and slice through the neighbouring capsomeres obliquely. In the obliquely sectioned parts the substructure is obscured. Intersections of adjacent planes equidistant from the centre of the capsid that are normal to the axes of the pentavalent and hexavalent capsomeres define 12 equal regular pentagons and 60 equal irregular hexagons. The polygons delineating the domain of the central capsomeres are marked by dotted lines on the density maps. The drawings *e* and *f* (constructed on the polyhedral surface made up of the pentagonal and hexagonal facets) illustrate that bonding specificity among identical structure units (represented by graphically cloned mice) cannot be conserved in all the contacts between capsomeres. Arranging structure units in the hexavalent pentamer (centre of *f*) with quasi-five-fold symmetry resembling the pentagonally symmetric pentamer (centre of *e*) leads to three types of contacts between structure units of neighbouring pentamers: (1) the two structure units at the top of the central pentamer in *f* each contact two neighbours (one from the pentavalent and one from another hexavalent pentamer) related by a quasi-three-fold axis; (2) the two structure units below and right of centre in *f* make quasi-two-fold contacts with neighbours related by an icosahedral three-fold axis; (3) the one structure unit left of centre in *f* makes an intimate dimer contact with a unit equivalently related by an icosahedral two-fold axis. Thus, the six structure units in the icosahedral asymmetric unit can be put into three categories according to their bonding relations: three in the quasi-trimer, two in the quasi-dimer and one in half the strict dimer.

amplitudes was 14.2%. Figure 3*d* shows a projection down a two-fold axis of half a virus particle excised from the refined map at 22.5 Å resolution and an analysis of the *R* factor as a function of resolution and intensity at 22.5 Å resolution is shown in Fig. 4*c*, *d*.

Electron density map

Figure 5, comparing views of half a virus particle down the icosahedral five-fold axis with that down the axis of a hexavalent morphological unit, reveals a striking similarity between the penta- and hexavalent morphological units. Indeed, the hexavalent capsomere shows a distinctive five-fold character, not six-fold as would be expected from a $T=7$ icosahedral surface lattice consisting of $60T$ quasi-equivalent structure units (Fig. 1).

Power spectra of the cylindrical harmonics in sections through the penta- and hexavalent units are shown in Fig. 6. This harmonic analysis demonstrates the structural similarity between the two types of capsomeres as a function of their radial coordinates, in particular, the dominant five-fold substructure of the hexavalent unit. Icosahedral symmetry requires the 12 identical pentavalent units to have five-fold symmetry and the 60 hexavalent units to be identical; but there are no constraints on the size, shape or symmetry of the hexavalent unit. The similarity of the pentavalent and hexavalent capsomeres seen in the electron density map cannot be an artefact of the imposition of the non-crystallographic symmetry in the phase refinement. Thus, our results indicate that all 72 capsomeres are pentameres of identical or very similar subunits.

The electron density map may be divided into two regions: the protruding pentagonal caps and the basal parts connecting capsomeres. The contacts between capsomeres extend inward from ~210 Å radius of the capsid. The protruding caps are ~85 Å in diameter and extend out ~40 Å. The central hole in the capsomere has a diameter of 40 Å at a radius of 210 Å and tapers shut 15 Å from the surface, leaving a dimple on the top of the cap. The basal parts of the capsomeres extend in ~40 Å.

The similarity of the pentavalent and hexavalent morphological units seen in the electron density map, together with the chemical evidence for one kind of protein subunit, indicates that the capsid is built of 360 VP1 molecules. The radial extent of the capsid measured from the electron density map implies a protein subunit ~80 Å long. The dimensions of the wall of the pentagonal cap indicate a subunit diameter in the range 30–40 Å. An ellipsoidal subunit with these dimensions has a volume compatible with that expected for a 42,000-MW protein.

Molecular weight

All the available MW measurements are consistent with a capsid built of 360 VP1 subunits and inconsistent with a 420-subunit structure. The MW of the empty capsid, determined by sedimentation equilibrium[10], is $15 \pm 1 \times 10^6$, which agrees with the total weight of VP1 in the intact virion estimated from its MW and composition. Furthermore, the MW of 221,000 measured for isolated capsomeres[19] corresponds to a 15.9×10^6-MW capsid built of 72 identical capsomeres, in accord with the direct measurement. The calculated MW of VP1 for a $15 \pm 1 \times 10^6$-MW capsid consisting of 420 subunits would be 35,700 ± 7%, or 41,700 ± 7% for 360 copies. The calculated MW of VP1 from the DNA sequence is 42,834 (ref. 20) and 42,458 (ref. 21) for two strains of polyoma virus. These sequence values are upper limits because the protein in the capsid may be smaller due to possible post-transcriptional or post-translational processing. Estimates for the MW of VP1 from SDS-gel electrophoresis range from 42,000 to 50,000 but are not very reliable because of dependence on gel concentration[10]. Measurement by gel exclusion chromatography of VP1 dissociated with guanidine hydrochloride chloride gives a MW of 41,400 (ref. 10). Although there is no definitive MW measurement for the VP1 subunit in the capsid, all measured values are greater than or close to that expected for 360 subunits, and the smallest measured values are at least 15% larger than expected for 420 subunits.

Protein–subunit interactions

The electron density map provides information about subunit interactions even though the protein subunits themselves are not sharply resolved. Figure 7*a* and *b* are sections through the hexavalent and pentavalent capsomeres above the level at which they make contact with each other. It is evident that the projecting portions of the two kinds of capsomeres have very similar pentagonal substructure, indicating that the bonding specificity of the projecting parts of the structure units is conserved. This is analogous to the situation in the tomato bushy stunt virus structure[5] where bonding specificity is conserved within the two types of protruding dimer domains.

Where the polyoma capsomeres contact each other there are significant differences in the bonding as the five subunits of the hexavalent pentamer cannot interact equivalently with subunits of the six neighbouring pentamers. This is seen in Fig. 7*c* and *d*, which are sections at the level of contact between capsomeres. At this resolution, subunit boundaries cannot be distinguished; however, it is possible to suggest the types of interaction which would account for the observed density.

Our results show there are six structure units in the icosahedral asymmetric unit, five from the hexavalent and one from the pentavalent pentamer. Each of these subunits has a symmetrically distinct environment in the capsid. However, these six units can be put into three different classes according to their bonding relations inferred from the electron density map. These relations of the six structure units in the icosahedral asymmetric unit are schematically illustrated in Fig. 7*e* and *f*: three units are connected in one quasi-trimer, two in one quasi-dimer and one in half a strict dimer. The use of the three types of bonds can account for the assembly of the 72 pentamers in the capsid; but we do not know how the bonding specificity of the structure units is switched to control the assembly process.

Conclusion

The electron density map shows a hexavalent capsomere that closely resembles the regular pentameric capsomere in size, shape and substructure. Because the hexavalent capsomere was expected to be a hexamer, the reliability of the refinement method used to solve the structure has been critically examined. In contrast to the isomorphous replacement method in which the phase determination is constrained by measurement of heavy atom positions, and the Fourier refinement method at atomic resolution which is constrained by detailed stereochemical information, our refinement method, starting with trial phases from models representing the coarse particle morphology, is only constrained by the icosahedral symmetry and overall dimensions of the virus capsid. Our tests of the refinement method, applied to Fourier transforms calculated from capsid models to the same resolution as the experimental data, show that the constraints of the particle symmetry and overall size do lead to correct solutions starting with trial phases from any model with approximately related capsomere morphology. We believe, therefore, that the similarity of the hexavalent and pentavalent capsomeres seen in the electron density map is an intrinsic feature of the virus capsid structure rather than some unexplained artefact of the refinement procedure. As chemical analysis indicates that the capsid is built of VP1, it seems that both the hexavalent and pentavalent capsomeres are pentameres of VP1.

The similarities between polyoma virus, SV40 and other members of the papova family suggest that these may all have capsids built of pentameric capsomeres. Polymorphic tube structures are associated with all the papovaviruses. The common occurrence of pentamer tubes is understandable if all the capsomeres are pentameric. We suspect that the hexamer tubes are also made of pentamers. Re-examination of the published electron micrographs[7,8] indicates that this may indeed be the case. We are starting image analysis of electron micrographs to try to understand how the polymorphism of these structures arises.

Quasi-equivalence was conceived to explain why icosahedral symmetry should be selected for the design of closed containers built of a large number of identical structure units with conserved bonding specificity[4]. However, as bonding specificity is not conserved in the polyoma capsid, the reason for its icosahedral symmetry is no longer obvious. Why has an icosahedral capsid design of 72 pentamers been selected for polyoma and presumably other papova viruses? How is the bonding specificity of the structure unit switched to fit into the symmetrically distinct environments? Answers to these questions may be found by solving the capsid structure at higher resolution and by studying the structure of assembly intermediates.

We thank G. N. Phillips Jr, J. P. Fillers, D. J. DeRosier and W. C. Phillips for helpful discussions and technical assistance, J. DeRoy for X-ray unit maintenance, C. Ingersoll for instrument modification, W. Saunders for photography, and the staff of the Brandeis University Computer Center and W. Alexander, in particular, for assistance with the refinement calculations on the PDP-10 computer. The power spectrum analysis programs were provided by L. Amos, the molecular replacement programs by J. E. Johnson and we thank him for his encouragement and helpful suggestions. The film processing and image display instrumentation linked to the PDP-11/40 were provided by NSF grant PCM79-22766. T.S.B. is a Charles A. King Trust Research Fellow. This work was supported by a Young Investigators Research Grant CA27260 to I.R. and NCI grant CA15468 to D.L.D.C.

Received 26 March; accepted 2 November 1981.

1. Adolph, K. W. *et al. Science* **203,** 1117–1119 (1979).
2. Klug, A. *J. molec. Biol.* **11,** 424–431 (1965).
3. Finch, J. T. *Gen. Virol.* **24,** 359–364 (1974).
4. Caspar, D. L. D. & Klug, A. *Cold Spring Harb. Symp. quant. Biol.* **27,** 1–24 (1962).
5. Harrison, S. C., Olson, A. J., Schutt, C. E., Winkler, F. K. & Bricogne, G. *Nature* **276,** 368-373 (1978).
6. Abad-Zapatero, C. *et al. Nature* **286,** 33–39 (1980).
7. Finch, J. T. & Klug, A. *J. molec. Biol.* **13,** 1–12 (1965).
8. Kiselev, N. A. & Klug, A. *J. molec. Biol.* **40,** 155–171 (1969).
9. Tooze, J. (ed.) *DNA Tumour Viruses* (Cold Spring Harbor, New York, 1980).
10. Murakami, W. T. & Schaffhausen, B. S. *25th a. M.D. Anderson Symp.*, 43–62 (Williams & Wilkins, Baltimore, 1974).
11. Murakami, W. T., Fine, R., Harrington, M. R. & Ben Sassan, Z. *J. molec. Biol.* **36,** 153–166 (1968).
12. Murakami, W. T. *Science* **142,** 56–57 (1963).
13. Harrison, S. C. *J. appl. Crystallogr.* **1,** 84–90 (1968).
14. Johnson, J. E., Akimoto, T., Suck, D., Rayment, I. & Rossmann, M. G. *Virology* **75,** 394–400 (1976).
15. Bricogne, G. *Acta crystallogr.* **A32,** 832–847 (1976).
16. Bricogne, G. *Acta crystallogr.* **A30,** 395–405 (1974).
17. Johnson, J. E. *Acta crystallogr.* **B34,** 576–577 (1978).
18. Sim, G. A. *Acta crystallogr.* **12,** 813–815 (1959).
19. Friedmann, T. *Proc. natn. Acad. Sci. U.S.A.* **68,** 2574–2578 (1971).
20. Deininger, P., Esty, A., LaPorte, P. & Friedmann, T. *Cell* **18,** 771–779 (1979).
21. Soeda, E., Arrand, J. R., Smolar, N., Walsh, J. E. & Griffin, B. E. *Nature* **283,** 445–453 (1980).

Cellular genes analogous to retroviral *onc* genes are transcribed in human tumour cells

Alessandra Eva*, Keith C. Robbins*, Philip R. Andersen*, Alagarsamy Srinivasan*, Steven R. Tronick*, E. Premkumar Reddy*, Nelson W. Ellmore*, Angela T. Galen*, James A. Lautenberger†, Takis S. Papas†, Eric H. Westin‡, Flossie Wong-Staal‡, Robert C. Gallo‡ & Stuart A. Aaronson*

Laboratories of *Cellular and Molecular Biology, †Molecular Oncology and ‡Tumor Cell Biology, National Cancer Institute, National Institutes of Health, Bethesda, Maryland 20205, USA

Polyadenylated RNAs of certain human tumour cell lines are shown to contain transcripts related to the cell-derived transforming onc *genes of molecularly cloned primate, murine or avian transforming retrovirus genomes. Thus, analogues of retroviral transforming genes are both present and frequently expressed in human neoplastic cells.*

THE study of RNA tumour viruses, designated transforming retroviruses, has provided a potentially important approach to elucidating mechanisms involved in human malignancy. These agents generally cause sarcomas and haematopoietic malignancies, but in some cases also induce carcinomas (for reviews see refs 1–4). There is convincing evidence that these viruses have arisen by recombination of replication-competent type C RNA viruses with evolutionarily well conserved cellular genes. Moreover, these latter sequences, termed *onc* genes, have been found to be required for the induction and/or maintenance of viral transformation[5–11]. Certain independent sarcoma virus isolates of the same[12–15] and even of different species[16,17] have been found to contain the same or closely related *onc* genes. These findings suggest that only a limited set of distinct cellular genes with transforming potential exists.

Molecular cloning techniques have facilitated the isolation and amplification of transforming retrovirus genomes and their cell-derived *onc* genes for detailed biochemical analysis. To investigate the possible role of *onc*-related genes in human neoplasia, we have analysed whether cellular DNA analogues of these genes are present and actively transcribed in human cancer cells.

Transforming retroviral *onc* genes as probes for detecting related transcripts in human cells

Our study required that the transforming retroviruses should meet certain criteria: (1) They should be capable of inducing a wide range of malignancies. (2) The genes used should be available as well defined genetic segments of molecularly cloned viruses. (3) Such gene segments should possess sufficient homology with human DNA to detect related information at low copy number with reasonably high signal intensity. Molecularly cloned transforming retroviruses meeting these criteria included simian sarcoma virus (SSV)[18–20], BALB murine sarcoma virus (MSV)[21], Abelson murine leukaemia virus (MuLV)[22] and MC-29 virus[23]. SSV and BALB MSV induce sarcomas in susceptible hosts[24,25], whereas Abelson MuLV causes lymphoid tumours[26]. *In vitro* and *in vivo* studies have indicated that other cell types can be targets for transformation by both Abelson MuLV and BALB MSV (refs 27, 28 and J. Hoelzer Pierce and S.A.A., unpublished observations). MC-29 has the widest known range of target cells and has been reported to induce sarcomas, haematopoietic tumours and carcinomas[2].

Infectious DNA clones of each virus were obtained by recombinant DNA techniques and their cell-derived *onc* genes defined by restriction endonuclease and heteroduplex mapping techniques[18–23]. Figure 1 shows the physical maps of the molecular clones and indicates the region of each viral genome used to prepare DNA probes. According to recent convention, the cell-derived *onc* sequences of SSV are designated *sis*, while those of Abelson MuLV, BALB MSV and MC-29 are termed *abl*, *bas* and *myc*, respectively[29].

Nick-translated DNA probes of each viral *onc* gene were first analysed for their ability to detect homologous sequences in human DNA. Normal human cellular DNA was cleaved with *Eco*RI, a restriction enzyme that did not cut within any of the viral *onc* genes (Fig. 1). The DNA was then subjected to agarose gel electrophoresis and Southern Blotting analysis[30]. As shown in Fig. 2, each viral *onc* DNA probe detected one or at most a few DNA fragments. The signal intensity was highest with the SSV *sis* DNA probe, probably reflecting its greater homology with human DNA than that of the other viral *onc* genes analysed. The DNA fragments hybridized by each viral *onc* gene had different molecular weights, indicating that each detected a different homologue within human DNA. Lack of relatedness among the viral *onc* genes was confirmed by experiments in which each nick-translated fragment was hybridized to Southern blots containing the four unlabelled viral *onc* DNAs. Even in relaxed hybridization conditions[31], there was no detectable relatedness among the *onc* genes of SSV, BALB MSV, Abelson MuLV or MC-29 (data not shown).

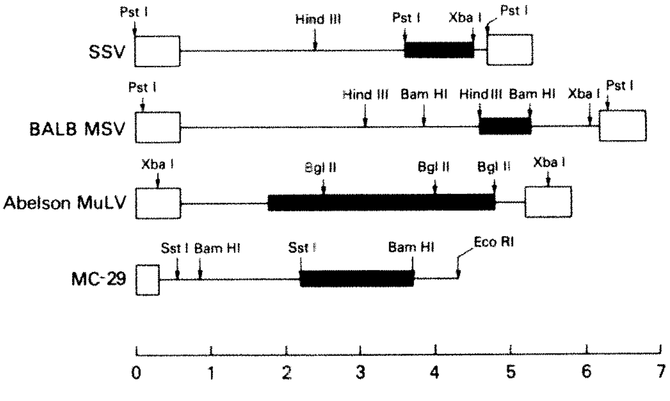

Fig. 1 Restriction maps of transforming retroviral genomes used to detect *onc*-related sequences in human cells. The *onc* genes of each retrovirus are indicated by the solid boxes. The white boxes represent the long terminal direct repeats (LTRs). Pertinent restriction sites are indicated. The integrated biologically active form of each viral genome was cloned in a λ phage vector[18–23]. Host cellular flanking sequences are not shown. DNA probes were derived from subgenomic fragments of each viral *onc* gene as follows: SSV, *Pst*I–*Xba*I fragment; BALB MSV, *Hind*III–*Bam*HI fragment; Abelson MuLV, 5′ *Bgl*II–*Bgl*II fragment; MC-29, *Sst*I–*Bam*HI fragment. With the exception of SSV, each subgenomic DNA fragment was cloned in pBR322.

0028–0836/82/020116—04$01.00

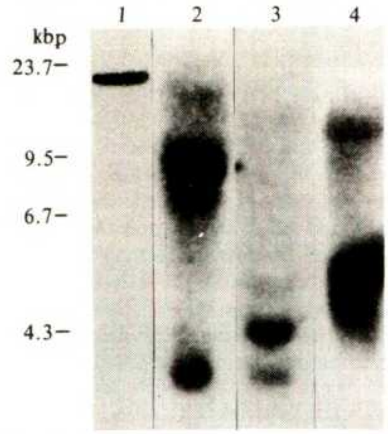

Fig. 2 Detection of human DNA sequences related to transforming retroviral *onc* genes. High-molecular weight human placental DNA was digested with *Eco*RI and electrophoresed on 0.8% agarose gels. Southern blots were prepared and incubated for 24 h with 2×10^6 c.p.m. ml^{-1} nick-translated (2×10^8 c.p.m. per μg) viral *onc* probes prepared from cloned DNAs of SSV (lane 1), BALB MSV (lane 2), Abelson MuLV (lane 3) and MC-29 (lane 4). Hybridization with the SSV *sis* probe was performed at 50 °C in 50% formamide and 5×SSC followed by washing at 50 °C with 6×SSC as described previously[17]. The other probes were hybridized at 65 °C in 6×SSC and washed at 45 °C in 0.1×SSC–0.1% SDS according to Hieter *et al.*[49]. The blot in lane 1 was exposed for 16 h, and those in lanes 2–4 were exposed for 48 h using Kodak XAR-5 film and Dupont Cronex Lightning Plus screens. *Hind*III-generated fragments of bacteriophage λ DNA were used as molecular weight standards: kbp, kilobase pairs.

In our search for transcripts related to viral *onc* genes in human tumours, we selected tumour cell lines representing a diverse spectrum of malignancies, including carcinomas, sarcomas, melanomas and glioblastomas. The establishment and biological characterization of some of these cell lines have been reported previously (Table 1). Each cell line was malignant in athymic nude mice and reproduced the histopathology of the original tumour (refs 32, 33 and S.A.A. and N. W. Ellmore, unpublished observations). These established lines enabled us to conduct a systematic analysis of viral *onc* gene expression in human malignancies.

The approach used to detect *onc*-related transcripts in human tumour cells involved isolation of poly(A)-containing RNAs and analysis by agarose gel electrophoresis and Northern blotting techniques[34–36]. Selection of poly(A)-containing RNAs provided the most sensitive method of detecting transcripts with properties of most known mRNAs, the sensitivity of detection of viral RNA in a typical retrovirus-transformed nonproducer cell being enhanced 30–40 fold by this procedure. This enhancement was consistent with the enrichment expected from the known fraction of poly(A)-containing RNA in total cellular RNA[37] and the percentage of poly(A)-containing RNA recovered by oligo(dT) selection[34]. Human cells were routinely tested for the presence of viral *onc*-related transcripts both as total and poly(A)-selected RNAs. In no case did we detect transcripts in total RNA that were not present in the poly(A) fraction. All cell lines were analysed for transcripts related to each viral *onc* gene. In some experiments, blots were sequentially hybridized with different *onc* probes as an internal control of the level of expression of the different *onc*-related transcripts.

SSV *sis* gene expression specific for certain human tumour cells

Nick-translated SSV *sis* DNA detected a single 4.2-kilobase (kb) transcript in 8 of 23 human tumour cell lines analysed, including 5 of 6 sarcoma cell lines and 3 of 5 glioblastoma lines. As shown in Fig. 3, the signal intensity of this transcript varied, the highest level being detected in a human glioblastoma line, A172 (Fig. 3, lane 1). The transcript was present at somewhat lower level in each of the positive sarcoma cell lines, as indicated for representative osteosarcoma and fibrosarcoma lines (Fig. 3, lanes 2 and 3, respectively). A second RNA species of lower molecular weight and much lower signal intensity was occasionally detected in some of the cell lines showing the 4.2-kb transcript. SSV *sis* gene expression was specific for these tumours as RNA isolated from normal human embryonic fibroblasts did not detectably hybridize (Fig. 3, lane 4). Furthermore, the SSV *sis*-related transcript was not observed in poly(A)-selected RNAs of any carcinoma, melanoma or other tumour cell line analysed. Note that SSV nonproducer cell RNA (Fig. 3, lane 5) exhibited genomic and one subgenomic RNA species containing *sis* sequences, neither of which corresponded in size to that of the 4.2-kb *sis*-related transcript in human sarcomas or glioblastoma cells.

A single MC-29 *myc*-related transcript in human tumour cells of different origins

The MC-29 *myc* probe, like SSV *sis*, detected a single transcript in human tumour cells. As shown in Fig. 4, this 2.7-kb transcript was observed in all cell lines examined, including normal human fibroblasts. Although the Northern blotting technique is not highly quantitative, there seemed to be a striking increase in the levels of *myc*-related RNA in some tumour cell lines analysed. In repeated experiments with the same RNAs or with RNAs independently prepared from the same cell lines, we reproducibly observed a 5–10-fold higher signal intensity of this transcript in lines derived from a sarcoma (A1383) and two carcinomas (A2780 and A549) as well as in the NC37 B-lymphoid line (Fig. 5). NC37 cells were initially established from Epstein–Barr virus (EBV)-positive lymphoid cells of a normal human[38]. However, NC37 cells also possess an abnormal karyotype and are tumorigenic in nude mice (unpublished observations), indicating their malignant phenotype. Notably, there was no correlation between those cell lines demonstrating high levels of the 2.7-kb MC29 *myc*-related RNA and those containing the 4.2-kb SSV *sis*-related transcript.

Table 1 Human tumour cell lines studied

Origin	Cell line	Ref.	Origin	Cell line	Ref.	Origin	Cell line	Ref.
Sarcoma			Carcinoma			Glioblastoma		
rhabdomyo-	A673	32	skin	A388	32		A172	32
osteogenic	HOS	46		A431	32		A1235	–
	A2394	–	lung	A549	32		A1207	–
fibro-	8387	47	GI	A1617	–		A1690	–
	A1383	–	renal	A498	32		A2781	–
synovial	A2095	–	ovarian	A1847	–			
			ovarian	A2780	–			
Melanoma			Teratoma			Other		
	A101D	32		Tera I	33	B lymphoid	NC37	38
	A375	32				normal fibroblast	M413	48
	A1306	–						

In the columns of references, – indicates unpublished work.

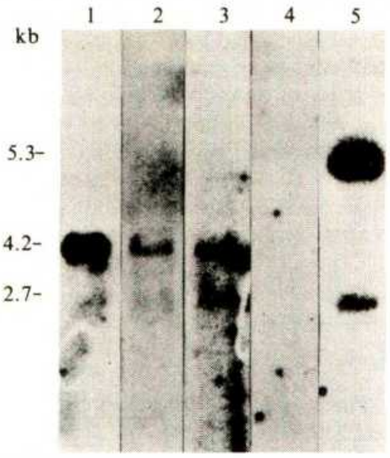

Fig. 3 SSV *sis*-related transcripts in human tumour cell lines. Total cellular RNA was isolated by a modification of the guanidine hydrochloride extraction method[50] as described elsewhere[51]. Poly(A)-containing RNA was selected by one cycle of chromatography on oligo(dT)-cellulose columns[34]. Poly(A)-containing RNAs (5 μg per lane) were denatured in 13 mM methyl mercury hydroxide and size fractionated on 1% agarose gels containing 5 mM methyl mercury[35] and transferred to nitrocellulose filters as described previously[36]. RNAs containing SSV *sis*-related sequences were identified by hybridization with 2.5×10^6 c.p.m. μl^{-1} nick-translated (2×10^8 c.p.m. per μg) *Pst*I–*Xba*I DNA fragment of molecularly cloned integrated SSV DNA[18–20]. Hybridization with the SSV *sis* probe was performed in 20% formamide, 5×SSC at 37 °C for 36–48 h, followed by washing at 42 °C in 0.1×SSC, 0.1% SDS as described previously[36,49]. SSV *sis*-related transcripts were visualized by exposing the blots to X-ray films for 5–7 days with intensifying screens. Poly(A)-selected RNAs included those from: A172 glioblastoma cells (lane 1); HOS and 8387 human sarcoma cells (lanes 2 and 3); M413 normal human fibroblasts (lane 4); SSV nonproducer NRK cells (lane 5).

Multiple transcripts related to mouse *onc* genes in human tumour cells

onc gene probes of two mouse-derived transforming viruses, BALB MSV and Abelson MuLV, each detected related transcripts in all human tumour cell lines analysed. Figure 6 shows the results with representative tumour cell lines. The pattern of BALB MSV *bas*-related transcripts was complex (Fig. 6*a*), showing three distinct bands of 7.0, 5.9 and 1.8 kb, in many tumours. Some tumour cell lines seemed to contain a much lower level of the 1.8-kb transcript whereas in other cells, including normal human fibroblasts, this RNA species was not detected.

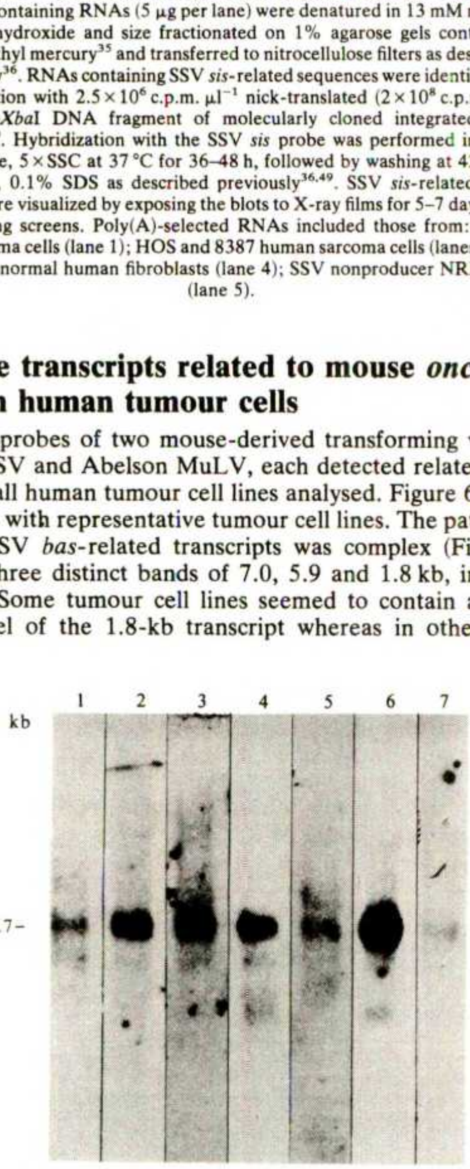

Fig. 4 MC-29 *myc*-related transcripts in human tumour cells. Poly(A)-selected RNAs were prepared and analysed as described in Fig. 3 legend. MC-29 *myc*-related transcripts were identified by hybridization with 2.5×10^6 c.p.m. ml^{-1} nick-translated *Sst*I–*Bam*HI DNA fragment of molecularly cloned integrated MC-29 DNA[23]. Poly(A)-selected RNAs include those from: A2394 and A2095 sarcoma cell lines (lanes 1 and 2); A2780 and A549 carcinoma cell lines (lanes 3 and 4); A375 melanoma cell line (lane 5); NC37 B-lymphoid cell line (lane 6); M413 normal human fibroblasts (lane 7).

An even more complex pattern of transcripts was observed with the Abelson MuLV *abl* probe. At least five RNA species were detected in most of the tumour cell lines analysed (Fig. 6*b*), while normal fibroblasts demonstrated only the two largest *abl*-related transcripts. The widespread presence in tumours and even normal fibroblasts of multiple transcripts related to the *onc* genes of BALB MSV and Abelson MuLV suggests that expression of related human genes may be associated with an important cellular function(s). Whether the multiple RNAs observed with these probes reflect RNA processing or transcription of more than one member of a family of related *onc* genes remains to be determined.

Implications of retroviral *onc* gene expression in human cells

The present report demonstrates that sequences related to the *onc* genes of different transforming retroviruses are not only present in human DNA but can also be actively transcribed. Retroviral *onc* genes have been transduced by type C RNA viruses from the genomes of species as diverse as primates, mice and chickens (for reviews see refs 1–4), and their presence in the DNAs of diverse vertebrate species, including man, indicates that such genes are highly conserved. Our findings that these genes are actively transcribed in human normal and/or neoplastic cells as polyadenylated RNA species provides additional evidence for the functional nature of these well conserved genetic elements.

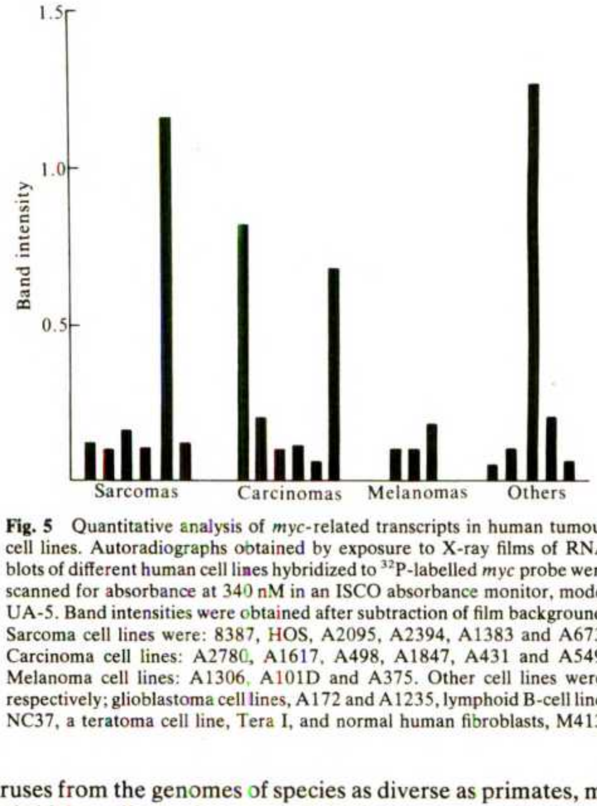

Fig. 5 Quantitative analysis of *myc*-related transcripts in human tumour cell lines. Autoradiographs obtained by exposure to X-ray films of RNA blots of different human cell lines hybridized to ^{32}P-labelled *myc* probe were scanned for absorbance at 340 nM in an ISCO absorbance monitor, model UA-5. Band intensities were obtained after subtraction of film background. Sarcoma cell lines were: 8387, HOS, A2095, A2394, A1383 and A673. Carcinoma cell lines: A2780, A1617, A498, A1847, A431 and A549. Melanoma cell lines: A1306, A101D and A375. Other cell lines were, respectively; glioblastoma cell lines, A172 and A1235, lymphoid B-cell line, NC37, a teratoma cell line, Tera I, and normal human fibroblasts, M413.

It is clearly important to determine whether viral *onc* genes are critical to the transformation process in humans. It has recently been shown that genetic manipulation of a cloned normal mouse cell DNA analogue of one transforming retroviral *onc* gene so as to cause it to be transcriptionally activated, confers on it the ability to transform mouse cells[9,39]. Moreover, other studies have indicated that leukaemia viruses may induce tumours by a mechanism involving 'downstream' promotion and transcriptional activation of cellular gene(s)[40–42]. The markedly elevated levels of single transcripts related to either SSV or MC29 *onc* genes in certain human tumour cells are consistent with the transcriptional derepression of these genes. Thus, if

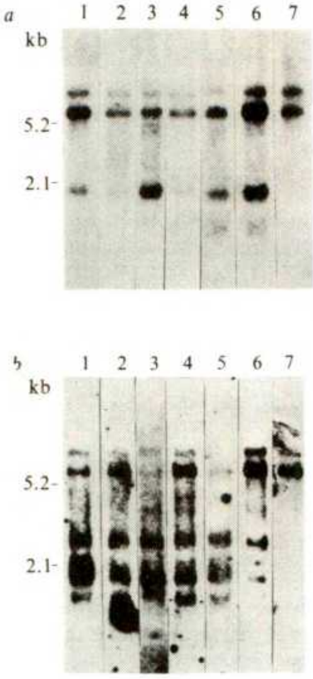

Fig. 6 BALB MSV and Abelson MuLV *onc* gene-related transcripts in human tumour cells. Poly(A)-selected RNAs were prepared and analysed as described in Fig. 3 legend. *a*, BALB MSV *bas*-related transcripts were identified by hybridization with 2.5×10^6 c.p.m. ml^{-1} nick-translated *Hin*dIII–*Bam*HI DNA fragment of molecularly cloned integrated BALB MSV DNA[21]. Poly(A)-selected RNAs include those from: A2095 and HOS sarcoma cell lines (lanes 1 and 2); A549 and A2780 carcinoma cell lines (lanes 3 and 4); A1306 melanoma cell line (lane 5); A1235 astrocytoma cell line (lane 6); M413 normal human fibroblasts (lane 7). *b*, Abelson MuLV *abl*-related transcripts in poly(A)-containing RNAs of cell lines as indicated in *a* were identified by hybridization with 2.5×10^6 c.p.m. ml^{-1} nick-translated 5′ *Bgl*II–*Bgl*II DNA fragment of molecularly cloned integrated Abelson MuLV DNA[22].

their functional products were analogous to those of the SSV and MC29 transforming genes, the specific transcriptional activation of these *onc*-related genes in certain human tumours may be sufficient to explain the transformed state of the cells.

The present studies used human tumour cell lines rather than primary tumours because of technical difficulties in obtaining sufficient amounts of intact RNAs from the latter. In each case, the tumour cell lines used reproduced the histopathology of the primary tumour in nude mice, indicating that each preserved the transformed phenotype of the original tumour. Our findings of marked differences in the levels of expression of SSV *sis* and MC-29 *myc* transcripts among various cell lines further argue that the increased expression of these genes in only some tumour lines is not attributable to tissue culture adaptation. We have recently examined the expression of retroviral *onc*-related RNAs in a variety of human primary tumours and tumour cell lines of haematopoietic origin[52] and found the levels of expression of the different *onc* gene-related transcripts in both fresh and cultured cells to be comparable, with no evidence of alteration associated with tissue culture.

Our demonstration of SSV *sis*-related transcripts in human fibrosarcoma cell lines but not in their normal fibroblast counterparts argues that the expression of this *onc* gene is probably associated with the transformed state of the cells. Moreover, the differences in levels of expression of *sis* or *myc* genes among individual carcinoma or glioblastoma cell lines suggest that the expression of these genes cannot be correlated with a particular tissue type. The more complicated patterns of transcripts related to BALB MSV and Abelson MuLV *onc* genes in human normal and neoplastic cells raise additional questions concerning the mode of processing of such transcripts, and their source from one or more related genes. Nonetheless, the almost universal presence of these transcripts in human cells argues strongly that these viral *onc*-related genes possess some important function(s). Whether they are directly related to the malignant state or to specific stages of cellular differentiation remains to be determined.

Understanding of the mechanisms involved in human neoplastic transformation is still at a very early stage. Recently, Krontiris and Cooper[43] and Weinberg and co-workers[44] provided evidence that cellular transformation can be a consequence of a single dominant genetic change, as transfection with DNA of certain tumours transmitted the transformed phenotype. In other cases, the transformed phenotype has not been transferable[43,44] or has seemed to be recessive in somatic cell hybrids with normal cells[45], arguing that the genetic changes associated with transformation may be *trans*-acting or multiple.

One approach to investigating whether the high levels of expression of human cellular analogues of certain viral *onc* genes are aetiologically linked to the development of the neoplastic state extends from the model for transformation associated with dominant genes. We are now analysing DNAs from some of our tumour cell lines for transforming activity in transfection assays. Should these DNAs possess the ability to transform cells, it will be possible to probe such transformants for expression of transcripts of the type specifically elevated in the original tumour cell lines. By such an approach, it may be possible to establish directly whether the high levels of expression of these genes in some human tumours is causally related to the neoplastic state.

Received 15 June; accepted 10 November 1981.

1. Bishop, J. M. *A. Rev. Biochem.* **47,** 35–88 (1978).
2. Graf, T. & Beug, H. *Biochim. biophys. Acta* **516,** 269–299 (1978).
3. Rosenberg, N. E. & Baltimore, D. in *Viral Oncology* (ed. Klein, G.) 187–203 (Raven, New York, 1980).
4. Shih, T. Y. & Scolnick, E. M. in *Viral Oncology* (ed. Klein, G.) 135–160 (Raven, New York, 1980).
5. Wang, L. -H. & Duesberg, P. H. *J. Virol.* **14,** 1515–1529 (1974).
6. Stehelin, D., Varmus, H. E., Bishop, J. M. & Vogt, P. K. *Nature* **260,** 170–173 (1976).
7. Anderson, P., Goldfarb, N. P. & Weinberg, R. A. *Cell* **16,** 63–75 (1979).
8. Canaani, E., Robbins, K. C. & Aaronson, S. A. *Nature* **282,** 378–383 (1979).
9. Oskarsson, M., McClements, W. L., Blair, D. L., Vande Woude, G. F. & Maizel, J. V. *Science* **207,** 1222–1224 (1980).
10. Rosenberg, N. & Witte, O. N. *J. Virol.* **33,** 340–348 (1980).
11. Wei, C. -M., Lowy, D. R. & Scolnick, E. M. *Proc. natn. Acad. Sci. U.S.A.* **77,** 4674–4678 (1980).
12. Bister, K., Löliger, H.-C. & Duesberg, P. H. *J. Virol.* **32,** 208–219 (1979).
13. Frankel, A. E., Gilbert, J. H., Porzig, K. L., Scolnick, E. M. & Aaronson, S. A. *J. Virol.* **30,** 821–827 (1979).
14. Ellis, R. W. *et al. Nature* **292,** 506–511 (1981).
15. Ghysdael, J., Neil, J. C. & Vogt, P. K. *Proc. natn. Acad. Sci. U.S.A.* **78,** 2611–2615 (1981).
16. Shibuya, M., Hanafusa, T., Hanafusa, H. & Stephenson, J. R. *Proc. natn. Acad. Sci. U.S.A.* **77,** 6536–6540 (1980).
17. Andersen, P. R. *et al. Cell* (in the press).
18. Robbins, K. C., Devare, S. G. & Aaronson, S. A. *Proc. natn. Acad. Sci. U.S.A.* **78,** 2918–2922 (1981).
19. Gelmann, E. P., Wong-Staal, F., Kramer, R. A. & Gallo, R. C. *Proc. natn. Acad. Sci. U.S.A.* **78,** 3373–3377 (1981).
20. Wong-Staal, F., Dalla Favera, R., Franchini, G., Gelmann, E. P. & Gallo, R. C. *Science* **213,** 226–228 (1981).
21. Andersen, P. R., Tronick, S. R. & Aaronson, S. A. *J. Virol.* (in the press).
22. Srinivasan, A., Reddy, E. P. & Aaronson, S. A. *Proc. natn. Acad. Sci. U.S.A.* **78,** 2077–2081 (1981).
23. Lautenberger, J. A., Schultz, R. A., Garon, C. F., Tsichlis, P. N. & Papas, T. S. *Proc. natn. Acad. Sci. U.S.A.* **78,** 1518–1522 (1981).
24. Theilen, G. J., Gould, D., Fowler, M. & Dungworth, D. L. *J. natn. Cancer Inst.* **47,** 881–889 (1971).
25. Peters, R. L. *et al. J. natn. Cancer Inst.* **53,** 1725–1729 (1974).
26. Abelson, H. T. & Rabstein, L. S. *Cancer Res.* **30,** 2208–2212 (1970).
27. Scher, C. D. & Siegler, R. *Nature* **253,** 729–731 (1975).
28. Rosenberg, N. & Baltimore, D. *J. exp. Med.* **143,** 1453–1463 (1976).
29. Coffin, J. M. *et al. J. Virol.* (in the press).
30. Southern, E. M. *J. molec. Biol.* **98,** 503–517 (1975).
31. Howley, P. M., Israel, M. A., Law, M. & Martin, M. A. *J. biol. Chem.* **254,** 4876–4883 (1979).
32. Giard, D. J. *et al. J. natn. Cancer Inst.* **51,** 1417–1423 (1973).
33. Fogh, J., Fogh, J. M. & Orfeo, T. *J. natn. Cancer Inst.* **59,** 221–226 (1977).
34. Aviv, H. & Leder, P. *Proc. natn. Acad. Sci. U.S.A.* **69,** 1408–1412 (1972).
35. Bailey, J. M. & Davidson, N. *Analyt. Biochem.* **70,** 75–85 (1976).
36. Thomas, P. S. *Proc. natn. Acad. Sci. U.S.A.* **77,** 5201–5205 (1980).
37. Adams, J. M. in *Ribonucleic Acids* (eds Stewart, P. R. & Letham, D. S.) 81–128 (Springer, Berlin, 1977).
38. Durr, F. E., Monroe, J. H., Schmitter, R., Traul, K. A. & Hirshaut, Y. *Int. J. Cancer* **6,** 436–449 (1970).
39. Blair, D. G. *et al. Science* **212,** 941–942 (1981).
40. Hayward, W. S., Neel, B. G. & Astrin, S. M. *Nature* **290,** 475–480 (1981).
41. Neel, B. G., Hayward, W. S., Robinson, H. L., Fang, J. & Astrin, S. M. *Cell* **23,** 323–334 (1981).
42. Payne, G. S. *et al. Cell* **23,** 311–322 (1981).
43. Krontiris, T. G. & Cooper, G. M. *Proc. natn. Acad. Sci. U.S.A.* **78,** 1181–1184 (1981).
44. Shih, C., Shilo, B. Z., Goldfarb, M. P., Donnenberg, A. & Weinberg, R. A. *Proc. natn. Acad. Sci. U.S.A.* **76,** 5714–5718 (1979).
45. Stanbridge, E. J. & Wilkinson, J. E. *Int. J. Cancer* **26,** 1–8 (1980).
46. Rhim, J. S., Cho, H. Y. & Huebner, R. J. *Int. J. Cancer* **15,** 23–29 (1975).
47. Aaronson, S. A., Todaro, G. J. & Freeman, A. E. *Expl Cell Res.* **61,** 1–5 (1970).
48. Aaronson, S. A. & Todaro, G. J. *Virology* **36,** 254–261 (1968).
49. Hieter, P. A., Max, E. E., Seidman, J. G., Maizel, J. V. Jr & Leder, P. *Cell* **22,** 197–207 (1980).
50. Cox, R. A. *Meth. Enzym.* **12,** 120–129 (1967).
51. Adams, S. L. *et al. Proc. natn. Acad. Sci. U.S.A.* **74,** 3399–3403 (1980).
52. Westin, E. H. *et al. Proc. natn. Acad. Sci. U.S.A.* (in the press).

DNA sequences necessary for transcription of the rabbit β-globin gene *in vivo*

G. C. Grosveld, E. de Boer, C. K. Shewmaker* & R. A. Flavell

Laboratory of Gene Structure and Expression, National Institute for Medical Research, Mill Hill, London NW7 1AA, UK

The DNA sequences required for the expression of the rabbit β-globin gene in vivo *have been examined. A variety of mutant rabbit β-globin gene templates were linked to a simian virus 40–plasmid recombinant and introduced into HeLa cells; in these conditions the rabbit β-globin gene is expressed from its own promoter. Comparison of the level of β-globin transcripts in a variety of deletion mutants shows that for efficient transcription, both the ATA or Goldberg–Hogness box, and a region between 100 and 58 base pairs in front of the site at which transcription is initiated, are required. Deletion of either of these regions results in a decrease in the level of β-globin transcripts by an order of magnitude; deletion of the ATA box causes an additional loss in the specificity of the site of initiation of RNA synthesis. The DNA sequences downstream from the ATA box, including the natural β-globin mRNA cap site, are dispensable for transcription* in vivo.

ALTHOUGH we have a good understanding of the DNA sequence elements which constitute prokaryotic promoters, their eukaryotic counterparts are poorly defined. Comparison of the DNA sequences in the 5′ extragenic regions of a large number of genes has revealed two conserved sequence elements with a location consistent with a promoter-like role. The first of these is an A+T-rich region with the canonical sequence 5′ TATA$^{T}_{A}$A$^{T}_{A}$ 3′ (the Goldberg–Hogness or ATA box)[1,2] which is located about 30 base pairs (bp) upstream from the site of initiation of RNA synthesis. The second is the CCAAT box[3,4] located about 80 nucleotides upstream from the cap site. Considerable evidence now indicates that RNA synthesis initiates at the cap site (see, for example, refs 5, 6).

In vitro transcription systems have recently been developed that synthesize specific capped transcripts from a variety of viral and cellular gene templates[7,8]—again *in vitro* the site of initiation is the cap site. Using these *in vitro* systems, several groups have shown that the ATA box is required for specific transcription of the adenovirus late[9,10] conalbumin[11] and β-globin[12] genes *in vitro*. Deletion of the CCAAT box has little or no effect on the *in vitro* transcription of the these genes[9–12]. The comparative simplicity of the *in vitro* results is not, however, found *in vivo*. In the case of the simian virus 40 (SV40) early region, deletion of the ATA box does not prevent expression of the early mRNAs, and removal of the DNA sequences containing the 72-bp repeat localized at ∼150 bp (−116 to −188; and −189 to −261) upstream from the site of initiation of RNA synthesis abolishes early gene transcription[13]. A similar picture is seen for polyoma (R. I. Kamen, personal communication). Likewise, a segment of ∼50 nucleotides containing the ATA box is not required for the expression of the sea urchin histone H2A gene when it is injected into *Xenopus* oocytes[14,15]. However, this deletion does alter the specificity of the site of initiation and causes the appearance of at least three transcripts with discrete 5′ ends. This alteration of the specificity of initiation also occurs when the ATA box of the early region of SV40 is deleted[13]. There is also evidence for the role of upstream DNA sequences in the transcription of the histone H$_2$A gene *in vivo*: deletion of a DNA segment containing the sequences from −184 to −524 strongly reduces the level of synthesis from the histone H2A promoter[15].

It is unclear at present to what extent the recent results obtained in the two systems represent the general sequence organization of eukaryotic promoters and to what extent the results are gene specific, or specific to the test system used. There is no obvious sequence homology between the upstream DNA sequences necessary for transcription in SV40 and in the sea urchin H2A gene that would point to a common promoter element. The SV40 72-bp repeat may represent more than a simple promoter element in the sense that this term is used for prokaryotic promoters (see below).

We have recently examined the *in vitro* transcription of a wide range of deletion mutants of the rabbit β-globin gene in HeLa cell extracts[12]. It is important to determine the effects of deletion of these DNA sequences on the expression of this gene *in vivo* and in the same cell type—particulary given the obvious differences recently seen between *in vivo* and *in vitro* transcription in the SV40 and polyma systems. In addition, we would like to know whether there is any evidence for upstream DNA sequences analogous to those of the SV40 and histone genes in the rabbit β-globin gene system.

To date, two approaches have been used to analyse the transcription of globin genes *in vivo* in animal cells. Mantei *et al.*[16] linked the rabbit β-globin gene to the herpes simplex virus (HSV) thymidine kinase (TK) gene and transformed mouse TK$^-$ cells to the TK$^+$ phenotype. Those cells containing the β-globin gene expressed this at a low, but easily detectable, level. Although this method has the advantage that only a few copies of the β-globin gene are present per cell, the comparison of different transformant cell lines is complex, because the exogenous DNA has become integrated and in each case the site of integration appears to differ. Hamer *et al.* have analysed the expression of the mouse α-globin gene, as an SV40–mouse α-globin recombinant after its introduction into monkey cells permissive for SV40 replication[17]. In these conditions the mouse α-globin gene is expressed at a high level from its own promoter. It was recently shown[20] that the rabbit β-globin gene inserted (as a 4.8-kilobase (kb) *Kpn*I fragment; see Fig. 1) in the *Kpn*I site of an SV40–pBR322 recombinant is expressed from its own promoter in HeLa cells which are only semi-permissive for SV40 replication. In the present work, we use this SV40–HeLa system to analyse the transcription *in vivo* of a number of deletion mutants of the rabbit β-globin gene.

To assay for the expression of the rabbit β-globin gene, we used S_1 mapping procedures[18], in most cases using as probe a 221-bp *Bst*NI fragment ^{32}P-labelled at its 5′ end using polynucleotide kinase. When hybridized to this probe, rabbit globin mRNA protects a 139-nucleotide fragment from S_1 nuclease digestion (Fig. 1). This variant of the S_1 mapping protocol permits the determination of the 5′ end of the respective transcripts to within 1–2 nucleotides[19].

We have analysed the expression of the rabbit β-globin gene at two different sites of insertion in the SV40–plasmid recombinant. The first site is the *Kpn*I site of the origin region of SV40 on the plasmid pSVβG*Kpn* (Fig. 1), that is, the original plasmid analysed by Banerji, Rusconi and Schaffner[20]. In this case, the rabbit β-globin gene is inserted in the promoter region of SV40.

---

*Present address: Department of Zoology and Microbiology, Ohio University, Athens, Ohio 45701, USA.

0028-0836/82/020120—07$01.00

In agreement with their original observations, we found that the rabbit β-globin gene is transcribed from its own promoter in these conditions since RNA from HeLa cells infected with this SV40–globin recombinant protects a fragment the same length as that given by normal rabbit β-globin mRNA (Fig. 1).

To investigate whether the rabbit β-globin gene must be present embedded within the SV40 moiety of the recombinant, we first constructed an SV40–pBR328 recombinant by ligating the two respective *Bam*HI–*Eco*RI double digest fragments of SV40 and pBR328 (see Fig. 2). The resultant plasmid, which is analogous to that of Schaffner except that pBR322 is replaced by pBR328, contains the entire early region of SV40, but lacks a 751-bp segment of the late region. We inserted the 2,070-bp *Bgl*II partial digest fragment, which contains the entire rabbit β-globin gene, together with 425 nucleotides of 5′-flanking DNA sequences and 355 nucleotides of the 3′-flanking regions, into the *Bam*HI site of the SV40–pBR328 recombinant. The globin gene segment is therefore interposed between the late region of SV40 and the remaining 3′ segment of the tetracycline gene of pBR328. Since this β-globin gene lacks the DNA regions to the 5′ side of position −425, we shall refer to this recombinant as ∇ 5′ to −425. The rabbit β-globin gene is expressed specifically in both of the two possible orientations (Fig. 1). Clearly then, the globin gene segment does not need to be embedded in the SV40 promoter region. We have estimated the approximate level of β-globin mRNA by standardizing our S_1 mapping procedures with purified rabbit $\alpha + \beta$ globin mRNA (see, for example, Fig. 4). From these data we calculate that ~10,000 molecules of β-globin mRNA are produced assuming that all cells are expressing the β-globin genes. As the real fraction of cells expressing the gene is likely to be significantly lower than this (usually 15–30% of the cells are positive for SV40 antigen), this value is probably an underestimate by a factor of 2–5.

From the above experiments it can be seen that the rabbit β-globin gene is expressed on an SV40 plasmid in at least two different sites with respect to both the SV40 and plasmid sequences; expression is independent of the orientation of the β-globin gene with respect to the SV40 plasmid DNA sequences. We have obtained similar results with the human β-globin gene (C.K.S., N. Moschonas and E. de B., unpublished) derived from both normal and β°-thalassaemic individuals. Although in these cases the early region of SV40 is also present, a functional early region is not required for this expression[20].

Rabbit DNA sequences necessary for expression of the rabbit β-globin gene *in vivo*

To determine which rabbit DNA segments are required for the expression of the rabbit β-globin gene in HeLa cells, we have prepared a series of deleted rabbit β-globin genes and introduced these into the SV40–plasmid recombinant. This insertion was performed as described in Fig. 2 legend, and results in the replacement of the pBR328 moiety of the SV40 recombinant with that of pAT153, another pBR322-derived bacterial plasmid. In the first case examined, the rabbit β-globin gene segment extends from −100 to approximately +1,870; the recombinant therefore contains 100 nucleotides of 5′ extragenic DNA sequences and ~280 nucleotides of 3′ extragenic DNA sequences. The plasmid segment (pAT153) is in the opposite orientation to that described above for ∇ 5′ to −425 and the rabbit DNA segment is interposed between the 3′ segments of the β-lactamase gene of pAT153 and the late region of SV40 DNA (at nucleotide 2,468)[21,22]. Following the same terminology, we shall call this recombinant ∇ 5′ to −100. We have examined the transcripts found in HeLa cells for only one orientation of the β-globin gene (where the 5′ end of the β-globin gene adjoins the plasmid sequences), but here again, a high level of rabbit β-globin mRNA is produced with its 5′ end

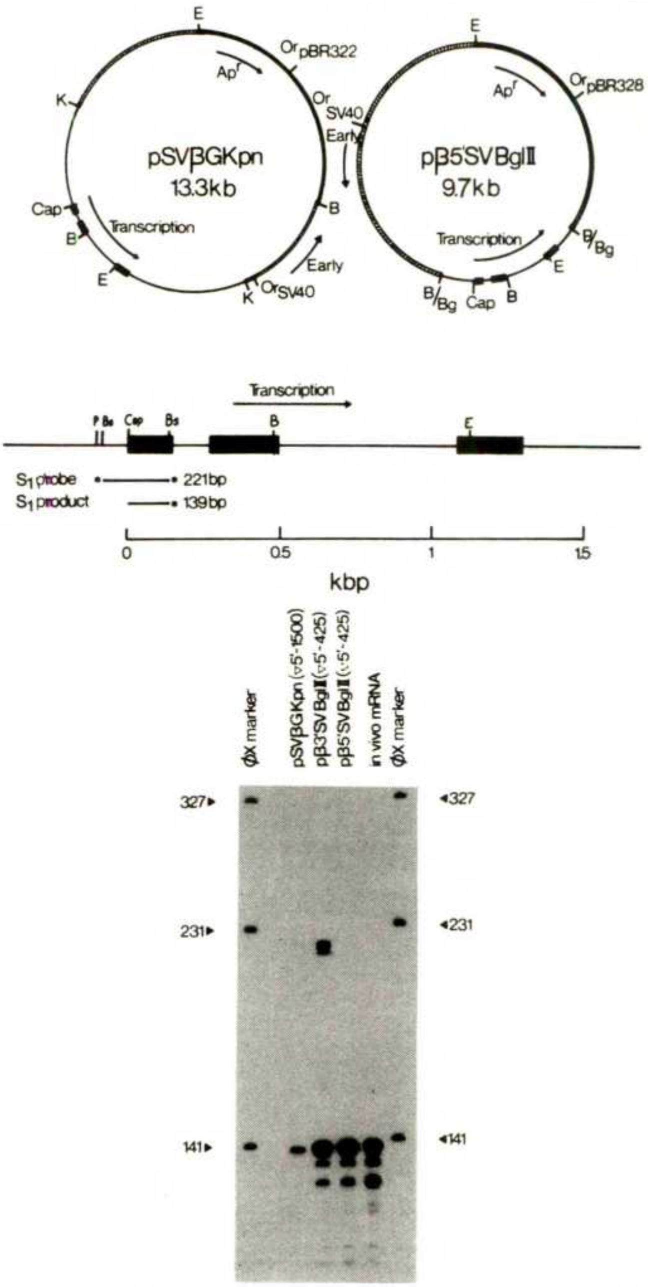

Fig. 1 Transient expression of the rabbit β-globin gene linked to SV40 sequences in HeLa cells. 15 μg DNA from either pSVβG*Kpn*, pβ5′SV*Bgl*II or pB3′SV*Bgl*II (which has the same structure but the β-globin gene segment is in the opposite orientation with respect to the SV40 sequences) were mixed with 25 μg of salmon sperm DNA and used to transform a half-confluent 100-mm dish of HeLa cells using the calcium phosphate method[27]. Three dishes were used for each DNA sample. After 10 h the medium (H21, 10% newborn calf serum) was changed, the cells grown for another 24 h, collected and the RNA isolated by the LiCl–urea method[28]. The upper part of the figure shows schematic restriction maps of pSVβG*Kpn* and pβ3′SV*Bgl*II DNA. pSVβG*Kpn* contains the 3.9-kb *Bam–Eco* fragment of pBR322, the 4.4-kb *Bam–Eco* fragment of SV40 and the 4.8-kb *Kpn*I rabbit β-globin fragment ligated into the *Kpn*I site of SV40 DNA. The construction of pβ3′SV*Bgl* and pβ5′SV*Bgl* DNA is outlined in Fig. 2—they contain the 2-kb rabbit β-globin *Bgl*II partial fragment in two orientations with respect to the SV40 sequences ligated into the *Bam*HI site of the SV40–pBR328 DNA junction. The rabbit β-globin RNAs present in the transformed HeLa cell RNA were detected by S_1 mapping[18] using end-labelled DNA probes[19]. In the centre of the figure is the 221-bp *Bst*NI 5′-labelled fragment used as probe in this experiment, containing 139 nucleotides of the 5′ end of the rabbit β-globin gene, which is protected against S_1 nuclease digestion in the DNA–RNA hybrid. The lower part of the figure shows the S_1 products of globin RNAs from HeLa cells transformed with vector DNA, pSVρG*Kpn* DNA, pβ3′SV*Bgl*II or Pβ5′SV*Bgl*II DNA analysed on a 5% polyacrylamide sequence gel[29] (SVpBR328, see Fig. 2). As a positive control the S_1 product of the *Bst*NI probe with *in vivo* rabbit β-globin mRNA is shown. The labelled marker is ΦX174 × *Hae*III. The numbers on the side are the lengths of the marker fragments in nucleotides. Hatched areas represent SV40 DNA, solid lines plasmid sequences, and thin lines and filled boxes the rabbit β-globin exons.

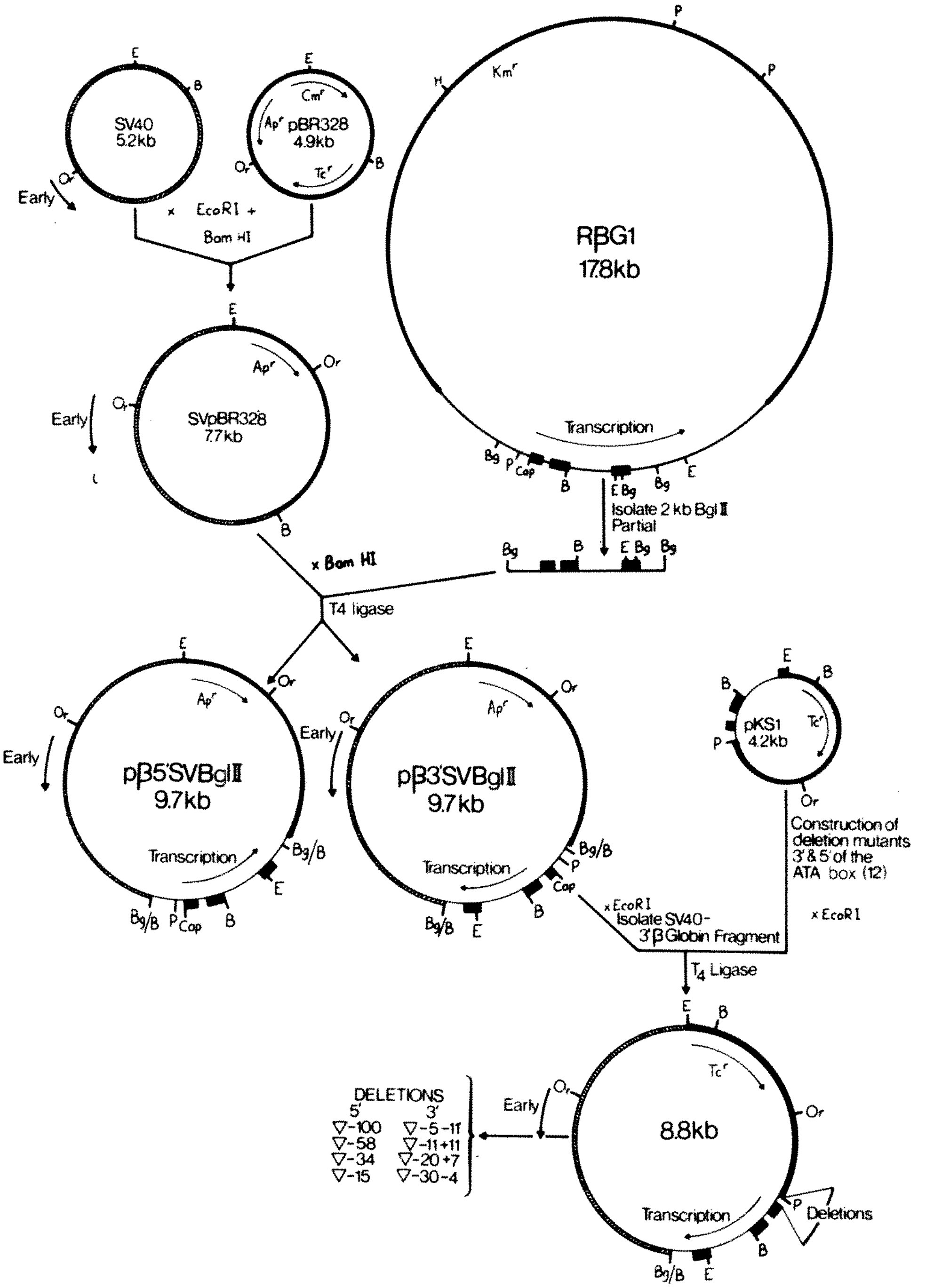

Fig. 2 Construction of SV40 derivatives of β-globin DNAs deleted in the promoter region. To prepare SVpBR328, SV40 DNA and pBR328 DNA (each 5 μg) were digested with *Eco*RI and *Bam*HI, both large *Bam–Eco* fragments were cut out from a 0.5% low melting agarose gel, purified on a DEAE 52 column[19] and ligated for 4 h at 15 °C at a DNA concentration of 20 μg ml^{-1} with T4 ligase and transfected into *Escherichie coli* HB101. From the ampicillin-resistant colonies an SV40–pBR328 recombinant was isolated. To clone the 2-kb *Bgl*II fragment (which contains the rabbit β-globin gene) into this vector, 50 μg RβG-1 DNA were partially digested with *Bgl*II and loaded on a 0.5% low melting agarose gel. The 2,070-bp β-globin *Bgl*II partial band was cut out and the DNA recovered by DEAE cellulose chromatography. This fragment was ligated into the *Bam*HI-linearized pBSV328 DNA at a final concentration of 20 μg DNA per ml. From the ampicillin-resistant colonies both orientations of the globin fragment were isolated with the globin 5′ end facing SV40 (pβ*5′SV Bgl*II) and the globin 3′ end facing SV40 (pβ3′SV*Bgl*II) respectively. pKSI DNA, a plasmid containing the *Pst*I-*Eco*RI rabbit β-globin gene fragment (containing the globin sequences from −100 to +1,120) inserted into *Pst*I-*Eco*RI of PAT153[12], was used to produce deletions in the globin promoter region[12] with end points to the 5′ side of the ATA box (−100, −58, −34, −15) and the 3′ side of the ATA box (−11 −5, −11 +11, −20 + 7, −30 + 4). To clone these DNAs into an SV40-containing vector, 25 μg 5′pβ5′SV *Bgl*II DNA was digested with *Eco*RI and the 4.8-kb SV40–globin band containing *Bam–Eco* SV40 and the 3′ end of the rabbit β-globin gene was recovered from a 0.5% low melting agarose gel. Then *Eco*RI-linearized pKSI DNA or DNA from the derivative deletion clones was ligated (20 μg ml^{-1}) into this fragment. Tetracycline-resistant colonies that hybridized to SV40 DNA were picked and screened by restriction analysis. Hatched area, SV40 DNA; solid lines, plasmid sequences; thin lines, rabbit DNA; filled boxes, the β-globin exons.

coincident with that of natural rabbit β-globin mRNA (Fig. 3.). In addition to this component, however, a number of bands are seen which identify the presence of RNAs with 5′ ends at several sites from +42 to +48. As these bands are seen when a 5′-labelled 221-nucleotide *Bst*NI minus strand probe is used, these components must be transcribed from the same DNA strand as β-globin mRNA. Together these bands amount to about twice the number of RNA molecules formed from the normal rabbit β-globin promoters. These components are also seen in the case of the ∇ 5′ to −425 mutant (that is, the *Bgl*II fragment discussed above), but the abnormal products comprise only about one-third of the total β-globin transcripts. The same abnormal RNAs have been described previously[23,24] as transcripts produced from the rabbit β-globin gene when introduced into mouse L cells and maintained as stable TK⁺ transformants. We have also synthesized cDNA on RNA from HeLa cells transfected with the rabbit β-globin gene using an *Sfa*NI–*Bst*NI fragment (from the 3′ end of the first exon) labelled at its 5′ end. This experiment reveals cDNAs corresponding to natural β-globin mRNA and a second predominant cDNA which derives from an upstream promoter, in addition to several minor shorter cDNA bands which presumably result from early termination of cDNA synthesis. As no cDNA is seen that would correspond to a RNA with a 5′ end at +42 to +48, we conclude that the 5′ ends detected by S_1 mapping do not result from transcriptional initiation events, but probably derive from upstream RNAs which splice to the A-G at position +47 and +48 of the rabbit β-globin gene. In addition, in S_1 mapping experiments we see a low level of transcripts derived from a plasmid or SV40 promoter.

We have introduced a variety of deletion mutants, derived originally from ∇ 5′ to −100, into the SV40–plasmid at the same site, and in the same orientation as the ∇ 5′ to −100 mutant. Thus, each mutant is inserted with the 5′ moiety of the rabbit β-globin gene adjacent to the 3′ regions of the β-lactamase gene. The DNA sequence of each mutant DNA has been determined around the regions spanning the deletion and Fig. 5 shows the relevant areas of sequence.

These DNAs have been introduced into HeLa cells in standard conditions and the 5′ ends of the transcripts produced

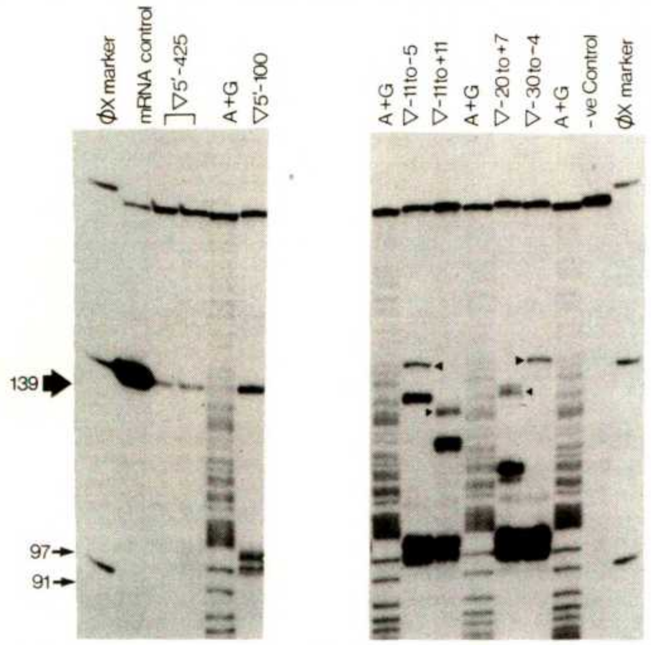

Fig. 3 Transcription of the β-globin gene in mutants at the 3′ boundary of the promoter. HeLa cells were transformed with the 5′ deletion clones ∇ −425 (pβ3′SV*Bgl*II) and ∇ −100 or the 3′ deletion DNA clones ∇ −5 −11, ∇ −11 +11, ∇ −20 +7 and ∇ −30 −4 (see Figs 2, 5) as described in Fig. 1 legend. (See Figs 2 and 5 legends for explanation of the deletions.) The rabbit β-globin mRNAs present in the RNA of those HeLa cells was analysed by S_1 mapping using 5′-end-labelled 221-bp *Bst*NI fragment as indicated in Fig. 1. The S_1 products were loaded onto a 5% polyacrylamide sequence gel and run next to G + A sequence ladders of the 221-nucleotide *Bst*NI minus strand. As an additional size marker, end-labelled ΦX174 × *Rsa*I fragments were used. The numbers on the side indicate products from the natural β-globin 5′ end (139 nucleotides) and RNA products that map within the first exon of the gene (91–97 nucleotides). Besides these two products there are S_1 products labelled with ► in the lanes from the 3′ deletion clones which are derived from an upstream promoter as explained in the scheme of Fig. 4.

determined as above. To orient these 5′ ends with respect to the DNA sequence of the rabbit β-globin gene, a G + A sequence ladder has been run in every third lane on the same gel (Fig. 3).

Sequence requirements for the regions downstream from the ATA box

We have previously analysed *in vitro* transcription using as templates a variety of mutants which lack DNA sequences to the 3′ side of the ATA box. From this we concluded that the DNA sequences downstream from the Goldberg–Hogness box are not necessary for specific *in vitro* transcription because a variety of mutants lacking sequences extending from −20 (or about 4 nucleotides to the 3′ side of the ATA box) to as far as +164 (in the small intron) are transcribed effectively *in vitro*[12]. The *in vivo* cap site is therefore not required; in fact, the RNA polymerase initiates RNA synthesis at about 30 nucleotides downstream from the ATA box, essentially irrespectively of the DNA sequences at the site of initiation. However, extending the deletion to −30, and hence removing the ATA box, eliminates the specificity of *in vitro* transcripts[12]. To determine the effects of the same deletions *in vivo* and in the same cell type, we introduced SV40 recombinants, containing these deletion mutants into HeLa cells. For this purpose we chose the following four mutants: (1) ∇ −11 to −5, which lacks 7 nucleotides between the ATA box and the natural cap site; (2) ∇ −11 to +11 which has the same 5′ break point as the above mutant but which also lacks the natural cap site and a total of 22 nucleotides; (3) ∇ −20 to +7, which lacks 27 nucleotides and all but 4 nucleotides of the 5′ extragenic DNA sequences downstream from the ATA box; and (4) ∇ −30 to −4, which also lacks 27 nucleotides but which, since the deletion is displaced to the 5′ side, lacks the ATA box and retains the natural cap site. All these mutants were constructed in the mutant ∇ 5′ to −100 and therefore lack the DNA sequences upstream of −100.

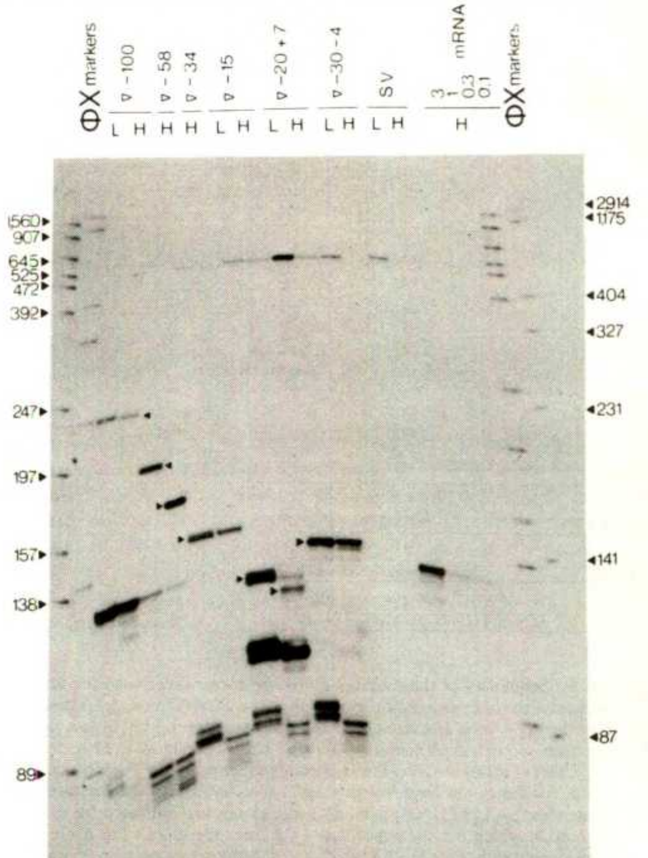

Fig. 4 Transcription of the rabbit β-globin gene from mutant templates lacking DNA sequences at the 5′ and 3′ boundaries of the promoter. HeLa cells were transformed with 5′ deletion clones ∇ −100, ∇ −58, ∇ −34 and ∇ −15 and the 3′ deletion clones ∇ −20 +7 and ∇ −30 −4, as described in Fig. 1 legend. The RNA products from these cells were analysed by S_1 mapping, using a 488-nucleotide 5′-end-labelled *Mbo*II probe that contains 360 bp upstream sequences and the first 128 bp of the 5′ end of the rabbit β-globin gene (−360 to +128). The S_1 reactions were done at 20 °C (L) or 40 °C (H) using 3,000 U S_1 nuclease per sample (0.3 ml). The bands labelled ► are derived from RNA starting at an upstream promoter that is picked up by the *Mbo*II probe, as explained in the lower part of the figure. The bands at +42 to +47 shift at 40 °C lower in the gel because S_1 nuclease attacks the A + T-rich splice junction. To calibrate the hybridization, natural rabbit β-globin mRNA (3.1, 0.3 and 0.1 ng) was hybridized and treated with S_1 nuclease at 40 °C. Relative amounts of rabbit β-globin mRNAs were determined by scanning bands on X-ray film. Numbers are given in Fig. 5. Labelled marker bands on each side of the gel are ΦX174 × *Taq*I (left) and ΦX174 × *Rsa*I (right), respectively. nt, Nucleotides.

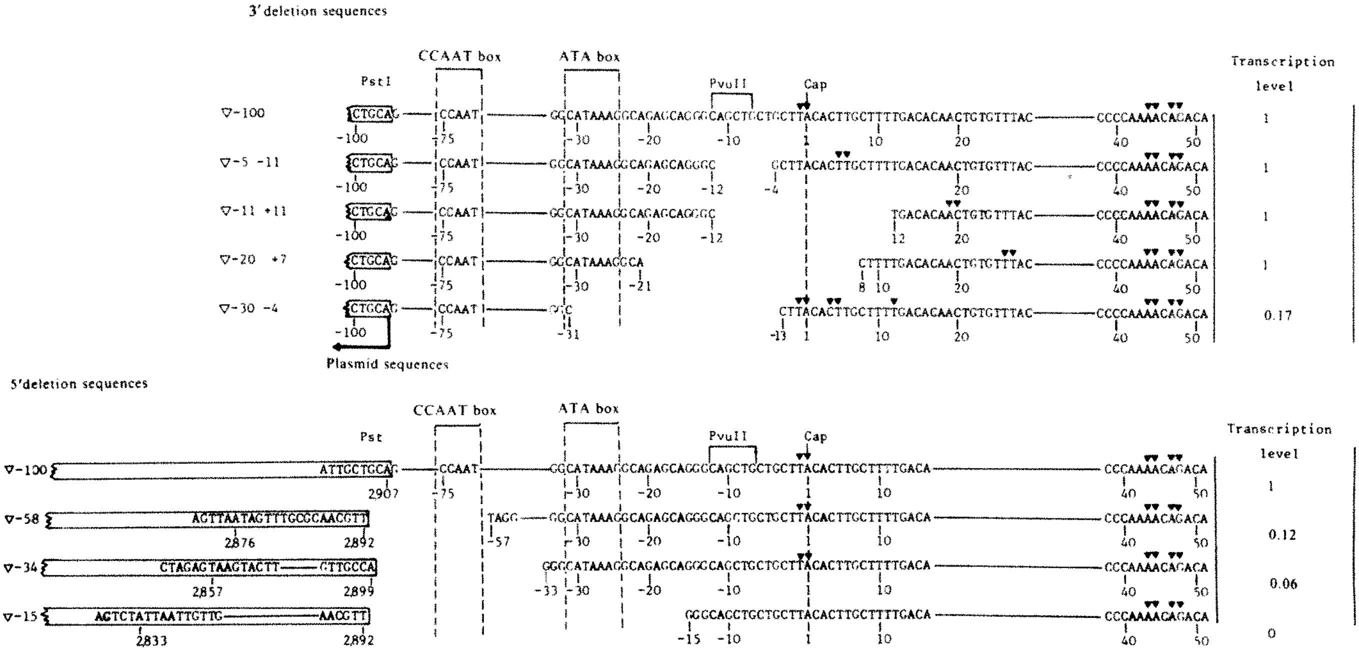

Fig. 5 Sequences of the rabbit β-globin promoter deletions used for SV40-mediated transient expression in HeLa cells. The upper part of the figure gives the relevant areas of DNA (vector–globin junction, CCAAT box, ATA box, cap sequences and start sequences within the gene) of the β-globin clones that have deletions 3' to the ATA box. The size of the deletions are represented by the gap which is left open. As the deletions were constructed from pKSI (Fig. 2), all clones have 5' upstream sequences present to −100 (*PstI* site). The junctions of vector DNA (pAT153) and rabbit β-globin sequences are indicated by the boxed nucleotides. The lower part of the figure gives the important sequences of the β-globin clones that have been deleted 5' to the ATA box. The size of the deletions is again represented by a gap. All the clones have lost the rabbit sequences 5' to the deletion since the construction of these deletions was started from the *BalI* site at −75. The vector sequences (pAT153 DNA) present in the clones are indicated by the sequences in the box. The numbers indicated within the plasmid sequences represent the nucleotide which is now at position −75 from the globin cap nucleotide. The 'transcription level' refers to relative levels of globin mRNA in the HeLa cells transformed with these DNAs, which was determined by scanning the autoradiogram of Fig. 4 with a Joyce—Loebl densitometer. The mRNA signals were compared by assuming that the signal of readthrough RNA starting at an upstream promoter is not influenced by the various deletions in the globin promoter region and was therefore taken as an internal standard signal. ▼ Indicates transcription starts seen in the various clones as concluded from the A + G sequence marker lanes in Fig. 3, and the splice sites located at +44 to +48.

The level of specific transcripts from ∇ −11 to −5, ∇ −11 to +11 and ∇ −20 to +7 is similar to that seen for the control plasmid ∇5' to −100 (Fig. 3). The 5' ends of these mutant transcripts are displaced to the 3' side by essentially the same number of nucleotides as the length of the deletion (Figs 3, 5); we previously found the same result for the transcription of these mutants *in vitro*[12]. The same results have recently been obtained for the SV40 early region *in vivo*[13] and *in vitro*[25]. These data are consistent with the notion that the polymerase is ultimately bound to the ATA box and starts transcription ~30 nucleotides downstream from this site.

The mutant DNA ∇ −30 to −4 which has a deletion of the same size as ∇ −20 to +7, but which lacks the ATA box, shows heterogeneous transcripts, among which is a faint band at the *in vivo* cap site; there are numerous other components. The abnormal RNAs (5' ends at +44 to +48) and 'upstream' plasmid SV40 transcripts are, however, still produced at a similar level to that found for the other mutants. In Fig. 3, a few faint bands are visible in the case of mutant ∇ −30 to −4 that are also visible in the control which contains RNA from HeLa cells transformed with the SV40–pBR328 vector; these are products of incomplete S_1 nuclease digestion which are sometimes obtained from this probe when the S_1 nuclease treatment is performed at 20 °C; note that these products are seen in the lanes from all RNA samples including the RNA from HeLa cells transformed with only the vector.

To eliminate these incomplete digestion products, we treated hybrids formed between a 5'-labelled DNA probe (in this case a 488-bp *Mbo*II fragment; see Fig. 4) and RNA from HeLa cells transformed with the β-globin gene deletion mutants with S_1 nuclease at 20° or 40 °C. Figure 4 shows that the background bands are completely digested at 40 °C in these conditions; in addition however, some cleavage occurs near the 5' end of the perfect hybrids formed with β-globin mRNA and the 5'-labelled probe and these overdigestion products are consequently also seen in the hybrids formed with the transcription products of mutant template ∇ 5' to −100. More important however, the heterogeneous faint bands seen when the mutant template lacking the ATA box, ∇ −30 to −4, is used, are resistant to S_1 nuclease digestion at high temperature and therefore reflect genuine transcripts. As judged from the S_1-resistant DNA fragments, transcriptional starts are found at about five sites on this template (see Fig. 5).

Sequence requirements for the DNA regions upstream from the ATA box

The initial experiments with the SV40–β-globin recombinants showed that the rabbit β-globin gene is transcribed effectively when 1,500, 425 and 100 nucleotides of the 5'-flanking DNA regions are present. There are differences in the level of β-globin transcripts found, but as these three examples have been inserted into different sites on the SV40-plasmids and as the plasmid segments differ, the significance of these differences is not clear. (Note that the template with only 100 nucleotides of 5' upstream sequences is transcribed, if anything, better than the two templates with more 5'-flanking rabbit DNA—there is therefore no compelling evidence at this stage to invoke promoter sequences further upstream than −100.)

To test whether DNA sequences downstream from −100 are required for transcription in this *in vivo* system, we examined the expression of four deletion mutants. A correlation of the transcription efficiency (but see below) with the extent of the 5'-flanking DNA sequences present is justified in these cases as the β-globin gene is present at the same position and in the same orientation with respect to the plasmid and SV40 DNA sequences. The mutant templates we compared are: (1) ∇ 5' to −100, which contains both the CCAAT and ATA boxes; (2) ∇ 5' to −58, which lacks the CCAAT box region but retains the ATA box (together with about 30 nucleotides to the 5' side of this structure); (3) ∇ 5' to −34 which also has the ATA box but only 3 nucleotides upstream from this structure; and (4) ∇ 5' to −15 which lacks both boxes.

As stated above, the mutant template ∇ 5′ to −100 gives a high level of product from the rabbit β-globin gene promoter, together with a high level of abnormal transcripts which give S_1 nuclease-resistant fragments with ends at +44 to +48.

The level of correct product from the ∇ 5′ to −58 mutant is reproducibly reduced when compared with ∇ 5′ to −100 (Fig. 4). As these effects are quantitative, rather than qualitative, we have calibrated the levels of correctly initiated RNA chains within the β-globin gene as a function of the deletion of the 5′ regions of the β-globin gene in two ways. We have first made use of the fact that there is a plasmid or SV40 promoter which initiates RNA synthesis to the 5′ side of the β-globin gene and whose transcripts run into this gene. Since all deletions discussed here are downstream from the promoter, it is reasonable to assume that they will not have a large effect on the frequency of these upstream transcripts. The upstream promoter generates RNAs that form S_1 nuclease-resistant hybrids of a length that in each case reflects the 3′ boundary of the deletion in the DNA template, as explained in Fig. 4. We have therefore used this upstream promoter as an internal control; the S_1 nuclease-resistant bands from the upstream promoter are indicated by a ▼ in Figs 3 and 4. We have compared the levels of products from the two promoters by scanning the autoradiogram; the results are summarized in Fig. 5. Figures 4 and 5 show that the ∇ 5′ to −100 template generates significantly more RNA with the correct 5′ end, relative to the 'plasmid' promoter, than does ∇ 5′ to −58. According to these data, the deletion of the DNA sequences from −100 to −58 caused an eightfold decrease in the level of the correct transcripts. The level of the correct transcripts for the ∇ 5′ to −34 mutant is reduced by another factor of 2. Nonetheless, both these mutant templates produce rabbit β-globin RNA with the correct 5′ terminus, albeit at reduced efficiency. In contrast, ∇ 5′ to −15 shows no detectable product at the correct position. Treatment of hybrids produced with RNA from the HeLa cells transformed with ∇5′ to −15, with S_1 nuclease at both 20 and 40 °C, gives no detectable S_1 nuclease-resistant fragments except the product from the upstream plasmid/SV40 promoter and the abnormal bands at +44 to +48 (Fig. 4). Thus, while the detection of the DNA sequences upstream from the ATA box reduces the level of correct transcripts in the HeLa cells, a deletion that removes the ATA box alters the specificity of transcription. We have confirmed the quantitative difference in the level of β-globin mRNA from the ∇−100, ∇−58 and ∇−34 mutant templates by transfecting HeLa cells with a mixture of the relevant mutant rabbit and the normal human β-globin genes. The result is the same as that in Fig. 4. The correctly initiated rabbit β-globin mRNA is decreased in amount (relative to human β-globin mRNA) when RNA from the ∇−100, ∇−58 and ∇−34 mutant templates is compared; the 'upstream' RNAs referred to above do not vary in amount relative to the human β-globin mRNA (data not shown).

The quantitative effects of deletion of the sequences to the 5′ side of the ATA box may possibly be due to the loss of the CCAAT box region. Inspection of the mutant templates ∇ 5′ to −58 and −34 shows that the plasmid DNA sequences, which replace the sequences deleted, do not contain a recognizable CCAAT structure at the usual 40–50 nucleotides upstream from the ATA box. Similar data have recently been obtained by Dierks *et al.*[24], who analysed the transcription of the rabbit β-globin gene, linked to the HSV TK gene, after the introduction of mutant templates into L cells and the selection of stable TK$^+$ transformats. Their comparison of mutant templates ∇ 5′ to −425, ∇ 5′ to −76 and ∇ 5′ to −68 revealed a high level of the correct β-globin transcripts in the former two cases, but a significantly reduced level in ∇ 5′ to −66, that is, on deletion of a region containing the CCAAT box. The ∇ −66 mutant is adjoined to the plasmid DNA sequences by a dG-dC linker tract that is absent in ∇ −76. It is therefore also possible that the difference between the results obtained with these two mutants is influenced by the dG-dC tract[24]. A requirement for the −80 region for the expression of the human α-globin gene on an SV40 vector has also been demonstrated (P. Mellon, V. Parker, Y. Gluzman and T. Maniatis, personal communication). It seems that the CCAAT box region may be involved in the efficiency of generation of specific transcripts from the rabbit β-globin promoter. Proof of this awaits the specific alteration of the CCAAT sequence by single base deletion or point mutation experiments.

Conclusions

The results obtained with the rabbit β-globin gene (this work and refs 12, 25) have aspects in common with observations made recently on the sea urchin histone genes after microinjection into *Xenopus* oocytes and the SV40 early genes *in vivo*, but there are also significant differences. First, the ATA box is clearly required for the fixing of the transcriptional start sites of the β-globin gene[12] and the SV40 early genes *in vitro*[25] and for all three genes *in vivo* (this work and refs 13, 15). This site of initiation is apparently discrete and is located ∼30 nucleotides downstream from the first nucleotide (CATAAAG) of the box. This precision is not influenced *in vivo* (this work) or *in vitro*[12] by the deletion of essentially all the 5′-extragenic β-globin gene sequences upstream from the ATA box (as in ∇ 5′ to −34) or all the sequences from the ATA box to past the natural cap site. Thus the positioning of the start site is independent of the CCAAT box region *in vivo* and of the presence (as in ∇ −11 to −5) or absence (as in ∇ −11 to +11) of the natural cap site. These results are broadly similar to those obtained for the SV40 early region[13].

Deletion of the ATA box generates RNAs with heterogeneous 5′ ends for the sea urchin histone H2A gene[14], SV40 early genes[13] and the rabbit β-globin gene (this work) if the DNA sequences further upstream from the ATA box are present. In the case of the SV40 early region, the amount of early RNA produced does not seem to be strongly influenced[13], while the ATA box deletion in both the histone[14] and β-globin (this work) genes is a strong down mutation (Figs 3, 5). It is significant that these heterogeneous RNAs are not observed when the β-globin DNA sequences lying between −100 and the ATA box are also deleted, as in mutant ∇ 5′ to −15. It is therefore plausible that the CCAAT box region is involved in the promotion of these heterogeneous RNAs when the ATA box is lacking and that their absence in transcripts derived from ∇ 5′ to −15 results from the absence of the CCAAT box.

The results for the β-globin gene differ significantly from those for the SV40 early region and sea urchin histone genes, as sequences far upstream from the β-globin gene are not required to generate a high level of β-globin mRNA in the SV40-based system. For both the histone H2A gene[16] and the SV40 early region[13], sequences located about 200–300 nucleotides upstream are essential for RNA synthesis. This does not appear to be the case for the rabbit β-globin gene since mutant ∇ 5′ to −100 is transcribed as well as, or better than, ∇ 5′ to −425. There is evidence, however, that DNA sequences near the CCAAT box (which is at −75) are involved in promoting high-efficiency transcription from the rabbit β-globin gene cap site (this work and ref. 25). The SV40 early region contains two putative CCAAT (both (CTAAC) boxes at 80 and 101 nucleotides upstream from the first cap site[21], and deletion of this region causes a decrease in the level of early gene expression. In contrast, the deletion of this region in the sea urchin H2A histone gene stimulates RNA synthesis[14]. When considering the effect of DNA sequences far upstream, note that the results with the β-globin gene have been obtained on templates carrying the SV40 72-bp repeats that are absolutely required for SV40 early gene transcription and which constitute the upstream sequences of the SV40 early region. Note also that a region of SV40 which contains the 72-bp repeat is required to obtain a high level of transcription of the rabbit β-globin gene in HeLa cells[20]. It is therefore possible that this SV40 region is supplanting the requirement for rabbit β-globin upstream sequences; a corollary of this is that these rabbit sequences, if they exist, must not be present on the 4.8-kb genomic *Kpn*I segment which contains the rabbit β-globin gene, since this segment is expressed at a 100-fold level in the absence of the SV40 moiety[20]. We are currently testing whether such modulator sequences exist further from the β-globin gene. If the SV40 sequences do have this role, then it is significant that this function can be provided by SV40 sequences located at variable distance (~3,200–4,400 bp) and in either orientation (at least in 5′ to −1,500 and ∇ 5′ to −425) to the β-globin gene. This is not the type of effect expected from a classical promoter-type sequence. Remember, however, that evidence exists for effects on globin gene expression of deletions far from the genes affected *in vivo* in man (ref. 26 for example). The relevance of these effects to promoter sequences is at present unclear, as is the relevance of the effects observed in the current type of experiment to the problems of promotion of RNA synthesis from the rabbit β-globin gene in its natural chromosomal location in an erythroblast.

Finally, note that in all the systems discussed here (sea urchin histone genes, SV40 and rabbit β-globin genes), several promoters are being utilized on the same DNA template. This might complicate interpretation: for example, transcription from an upstream promoter might influence RNA synthesis from the promoter being studied, in our case the rabbit β-globin gene promoter. At present insufficient data are available to evaluate the extent of these problems.

We thank F. G. Grosveld for helpful suggestions and W. Schaffner for advice on the HeLa cell system. C.K.S. was the recipient of a Jane Coffin Childs Fellowship. This work was supported by the British MRC.

Received 3 July; accepted 16 November 1981.

1. Proudfoot, N. J. *Nature* **279,** 376 (1979).
2. Gannon, F. *et al. Nature* **278,** 428–434 (1979).
3. Benoist, C., O'Hare, K., Breathnach, R. & Chambon, P. *Nucleic Acids Res.* **8,** 127–142 (1980).
4. Efstratiadis, A. *et al. Cell* **21,** 653–668 (1980).
5. Ziff, E. & Evans, R. *Cell* **15,** 1463–1475 (1978).
6. Contreras, R. & Fiers, W. *Nucleic Acids Res.* **9,** 215–236 (1981).
7. Weil, P. A., Luse, D. S., Segall, J. & Roeder, R. G. *Cell* **18,** 469–484 (1979).
8. Manley, J. L., Fire, A., Cano, A., Sharp, P. A. & Gefter, M. L. *Proc. natn. Acad. Sci. U.S.A.* **77,** 3855–3859 (1980).
9. Corden, J. *et al. Science* **209,** 1406–1414 (1980).
10. Hu, S. L. & Manley, J. *Proc. natn. Acad. Sci. U.S.A.* **78,** 820–824 (1981).
11. Wasylyk, B., Kedinger, C., Corden, J., Brison, O. & Chambon, P. *Nature* **285,** 388–390 (1980).
12. Grosveld, G. C., Shewmaker, C. K., Jat, P. & Flavell, R. A. *Cell* **25,** 215–226 (1981).
13. Benoist, C. & Chambon, P. *Nature* **290,** 304–310 (1981).
14. Grosschedl, R. & Birnstiel, M. L. *Proc. natn. Acad. Sci. U.S.A.* **77,** 1432–1436 (1980).
15. Grosschedl, R. & Birnstiel, M. L. *Proc. natn. Acad. Sci. U.S.A.* **77,** 7102 (1980).
16. Mantei, N., Boll, W. & Weissmann, C. *Nature* **281,** 40–46 (1979).
17. Hamer, D. H., Kachler, M. & Leder, P. *Cell* **21,** 697–708 (1980).
18. Berk, A. J. & Sharp, P. A. *Cell* **12,** 721–732 (1977).
19. Weaver, R. F. & Weissmann, C. *Nucleic Acids Res.* **6,** 1175–1193 (1979).
20. Banerji, J., Rusconi, S. & Schaffner, W. *Cell* (in the press).
21. Fiers, W. *et al. Nature* **273,** 113–120 (1978).
22. van Heuverswijn, H. & Fiers, W. *Eur. J. Biochem.* **100,** 51–60 (1979).
23. Wold, B. *et al. Proc. natn. Acad. Sci. U.S.A.* **76,** 5684–5688 (1979).
24. Dierks, P., van Ooyen, A., Mantei, N. & Weissmann, C. *Proc. natn. Acad. Sci. U.S.A.* **78,** 1411–1415 (1981).
25. Mathis, D. J. & Chambon, P. *Nature* **290,** 310–315 (1981).
26. Bernards, R. & Flavell, R. A. *Nucleic Acids Res.* **8,** 1521–1534 (1980).
27. Wigler, M. *et al. Cell* **16,** 777–785 (1979).
28. Auffray, C. & Rougeon, F. *Eur. J. Biochem.* **107,** 303–314 (1980).
29. Maxam, A. M. & Gilbert, W. *Meth. Enzym.* **65,** 499–560 (1980).

LETTERS TO NATURE

Nature of the shells of NGC1344

D. Carter, D. A. Allen & D. F. Malin

Anglo-Australian Observatory, PO Box 296, Epping,
New South Wales 2121, Australia

Various theories have been proposed to account for the origin[1,2] of the low surface brightness features resembling thin shells seen in projection around some otherwise normal elliptical galaxies[3]. It has proved impossible to discriminate between these models owing to the lack of quantitative data on the nature of the shells. Here we present broad-band optical (*B, V, R*) and near-IR (*J, H*) photometry of one of the shells to determine their constitution and place constraints on their mode of formation. The colour indices derived suggest that the shell comprises a population of stars, perhaps bluer than the main body of the galaxy. There is no evidence for recent star formation. Our results favour dynamical models for the formation of the shells, perhaps from recent mergers of disk galaxies with the elliptical.

The shells are visible on high-contrast derivatives of deep IIIaJ plates taken with the UK Schmidt and Anglo-Australian telescopes (AAT). For quantitative photometry we obtained images with a linear panoramic detector. The instrument available was the UCL Image Photon Counting System (IPCS) at the AAT. The large-scale spatial nonuniformities are worse than a conventional photographic plate and, at the time of our observations, were time variable, perhaps because of the effect of ambient temperature variations on the electronics, so that their removal by flat fielding is not perfect. Also, because of the finite frame rate of the IPCS, data arrival rates above about 30 photons arc s^{-2} s^{-1} will cause saturation. This limits the dynamic range of the system, and standard stars must be very faint. These factors limit the precision of the optical photometry; nevertheless, quantitative data can be obtained.

IPCS images of an area 110×90 arc s containing part of the boundary of the outermost shell to the north-west of NGC1344 were obtained with the AAT on the night of November 11 1980. Figure 1 illustrates the position of the IPCS field. Images of the faint globular cluster Hodge 11 were also obtained, this cluster contains faint electronographic sequences by Walker[4] and unpublished photometry by Bessell and Gascoigne. Table 1 lists the observations made.

The data were flat-fielded with a combination of exposures of the inside of the dome and the twilight sky. Residual nonuniformities in sensitivity, at the level of 1% in the line increment direction of the IPCS (corresponding to the declination direction on the sky) were removed by fitting a low-order polynomial to the sky background to improve the cosmetic appearance of the images.

To establish zero points the intensity of several star images in the Hodge 11 field was integrated, in a circle of some 5 arc s diameter, and the background level determined from an annulus around each was subtracted. The resultant intensity was compared with Walker's[4] electronographic magnitudes for *B* and *V*, and in *R* with magnitudes predicted from *V* and $B-V$ using the colours for giants tabulated by Bessell[5]. Hodge 11 was assumed to be unreddened. This procedure yielded zero points internally accurate to ~0.08 in *B* and *V*, and 0.15 in *R*. Extinction coefficients typical for Siding Spring Mountain on a photometric night were adopted. Each of these assumptions will

Table 1 IPCS observations

Object	Filter	Exposure time (s)	Mean wavelength (μm)
NGC1344 shell	*B*	6,000	0.45
	V	6,000	0.55
	R	8,000	0.66
Hodge 11	*B*	300	0.45
	V	300	0.55
	R	500	0.66

Conditions were photometric for the whole night.

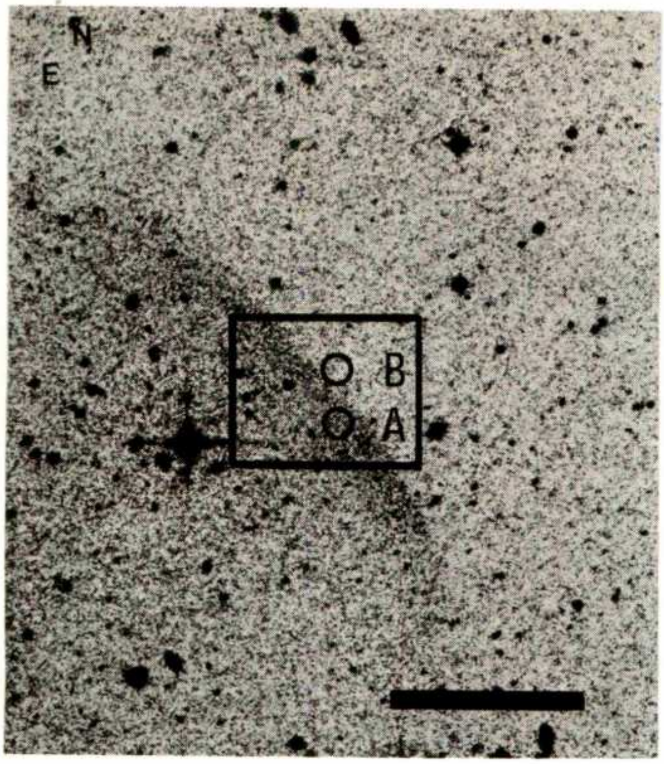

Fig. 1 The north-west shell of NGC1344. IR photometry of the areas indicated by circular apertures A (shell) and B (sky) was obtained. Two-dimensional photometry in B, V, and R was obtained of the area within the rectangle. Scale bar, 2 arc min.

contribute uncertainties of 0.03 mag or less to the derived zero points.

Although the B optical image was much more uniform than V and R, the shell was clearly visible on all three. The shell surface brightness was measured by integrating the intensity in circular apertures of diameters 5–14 arc s on the brighter part of the shell, near the edge, and subtracting from it the intensity in a similar aperture just off the shell, separated from the first aperture in RA only (that is, the direction perpendicular to that along which a polynomial was fitted). This was done at several points along the shell edge, and particularly at the point coincident with the IR aperture (see below and Fig. 1).

Because of the brightness distribution of the shell, conventional IR photometry, using symmetrically placed sky reference beams, is extremely difficult and would, in any case, require a much larger beam throw than was available. We therefore made our observations using the d.c. electronics[6] of the IR photometer spectrometer on the AAT. The telescope was driven back and forth between the shell and a point 36 arc s north on the sky, completing a cycle shell–sky–shell in typically 5.6 s At this frequency we could approach quite closely the expected photon shot noise at J. The stronger and highly variable sky emission at H did not allow such precision. A slight improvement in the precision was obtained by editing from the data any portion where successive measurements (whether of shell or sky) differed by more than 10 times the expected photon shot noise.

Our basic measurements were made with a 14-arc s diameter circular aperture centred at position A in Fig. 1. This and the sky position, B, were chosen to avoid all stars and galaxies visible on a contrast-enhanced Schmidt plate or on the IPCS images. To check that contamination from invisible sources was not influencing our data we made additional observations at J with a 10-arc s aperture, and in a second position with the 14-arc s aperture. The consistency of the measured surface brightnesses gives us confidence that our measurement refers to the shell alone.

At J the shell was 8×10^{-4} of the minimum sky brightness, which occurred near 3 a.m. LT. At H the corresponding value was 1.5×10^{-4}.

Measuring the surface brightness in B, V and R at several points along the shell edge yields:

$B-V=1.1\pm0.25$ mag
$B-R=1.2\pm0.3$ mag

Errors due to sky subtraction uncertainties dominate over zero point errors. Surface brightness measured at position A in Fig. 1 are:

B (0.45 μm) $=26.5\pm0.2$ mag/arc s^{-2}
V (0.55 μm) $=25.1\pm0.2$ mag/arc s^{-2}
J (1.25 μm) $=23.93\pm0.10$ mag arc s^{-2}
H (1.65 μm) $=23.43\pm0.17$ mag/arc s^{-2}

$B-J=2.57\pm0.22$ mag
$B-H=3.07\pm0.27$ mag

Because of the long baseline and the lower errors we would rely more on $B-J$ and $B-H$ than anything else. All of the measured colours are consistent with those of stars of spectral type between G5 and K4. However, if we are sampling a composite system, we will record bluer stars in the optical than in the IR. Persson *et al.*[7] report IR and optical photometry for several composite systems. Most are redder than the colours we observe for the shell of NGC1344. For the nucleus of NGC1344 they obtain:

$B-J=3.13$ (corrected to match our J filter)
$B-H=3.84$

For a small (7 arc s diameter) patch in the galaxy ~50 arc s north of the nucleus we measure:

$B-V=0.85\pm0.15$ mag
$B-R=1.60\pm0.15$ mag

Thus the shell near NGC1344 is bluer than the main body of the galaxy.

What do the shells consist of? Observations at 21 cm by A. E. Wright, D.F.M. and D.C. (unpublished) give an upper limit of $7.7\times10^{8}\ (50/H_0)^2\ M_\odot$ for the neutral hydrogen content of NGC1344 in a 14-arc min beam, which includes the outer shell. Less stringent upper limits were also placed on the H I content of some other shell galaxies. Long slit spectra covering the inner shells of NGC1344 and NGC3923, obtained by P. Quinn and D.C. show no detectable line emission at Hβ or [O III], even after many thousands of seconds integration time. We conclude that the shells consist almost entirely of cool stars. The colours are consistent with a population of stars which is bluer than the main body of a normal elliptical. Of the systems studied by Frogel *et al.*[8], some of the bluer lenticulars, such as NGC404 (ref. 8) and NGC5102 (ref. 7), have similar colours. Quinn[2] shows that features like these can form from mergers of dynamically cool systems, such as disk galaxies, with an elliptical galaxy, so it is perhaps not surprising that the shells have the colours of disk galaxies.

The measured B surface brightness implies a total luminosity of the outer shell of $3\times10^{8}\ (50/H_0)^2\ L_\odot$.

A more remote possibility is that the shells consist of dust, reflecting light from the main body of the galaxy. However, unless the dust grains were abnormally large, their scattering properties would render the shells bluer than the galaxy by at least 1.5 mag over a baseline from B to H. This is ruled out by the data. Also it has been shown[3] that a substantial optical depth would be required to produce the observed shell surface brightnesses, and unless the dust to gas ratio is abnormal, this is not consistent with the limit on the H I content of the galaxy.

In conclusion, the shells apparently consist of stars, probably with the colours of a disk population rather than an elliptical population, but not so blue that they might have been formed very recently, for example in a hot galactic wind. Thus our data support dynamical models for the formation of the shells[2], rather than models in which stars are formed in a galactic wind[3], which would predict colours for the shells some 0.5 mag bluer in $B-V$, and therefore some 1.6 mag bluer in $B-J$, than the main body of the galaxy.

Received 23 October; accepted 17 November 1981.

1. Fabian, A. C., Nulsen, P. E. J. & Stewart, G. C. *Nature* **287**, 613 (1980).
2. Quinn, P. J. *Astrophys. J. Lett.* (in the press).
3. Malin, D. F. & Carter, D. *Nature* **285**, 643 (1980).
4. Walker, M. F. *Mon. Not. R. astr. Soc.* **186**, 767 (1979).
5. Bessell, M. S. *Publ. astr. Soc. Pacif.* **91**, 589 (1979).
6. Barton, J. R. & Allen, D. A. *Publ. astr. Soc. Pacif.* **92**, 368 (1980).
7. Persson, S. E., Frogen, J. A. & Aaronson, M. *Astrophys. J. Suppl.* **39**, 61 (1979).
8. Frogel, J. A., Persson, S. E., Aaronson, M. & Matthews, K. *Astrophys. J.* **220**, 75 (1978).

A possible link between the rotation of Saturn and its ring structure

F. A. Franklin, G. Colombo & A. F. Cook

Harvard-Smithsonian Center for Astrophysics, 60 Garden Street,
Cambridge, Massachusetts 02138, USA

We present here evidence that two previously unidentified, yet conspicuous gaps in Saturn's rings lie at distances corresponding to 2/3 and 4/3 of the planet's rotation period. Gaps such as these can be produced in a ring of large bodies or small uncharged particles only by a non-axisymmetric gravitational field (both of the above can be associated with the $l=m=3$ harmonic), a fact that is relevant to models of planetary interiors.

The 'classical' picture of the radial structure of Saturn's rings explains its narrow gaps and boundaries as the consequence of resonant perturbations with certain satellites, in particular, Mimas, Titan and Iapetus. Thus, for example, the inner part of the prominent Cassini division lies at a distance from Saturn (117,900 km) where the orbital frequency of residual ring particles is essentially twice that of Mimas[1]. Two recent developments have brought a new perspective to the association between certain ring divisions and satellite resonances. The first is a study by Goldreich and Tremaine[2] of a mechanism whereby satellites can produce gaps that may eventually achieve widths of hundreds, possibly thousands, of kilometres, while the second is the data provided by the Voyager mission concerning the locations, dimensions and sheer number of ring features[3]. These new data will require a careful study when more precise positions are provided by Voyager 2. Aspects of this analysis are underway with the preliminary result that many ring features in portions of the ring having low optical thickness ($\tau \lesssim 0.2$) show a clear correspondence with satellite resonances. There are, however, obvious exceptions in which large gaps fail to have any association with moderate-to-strong satellite resonances. We supply here a possible explanation for two divisions, and specifically for the conspicuous gap, some 200 km wide, located in the outer part of ring C, 86,700 ± 700 km from the centre of Saturn. Ring particles at this distance have mean motions one and one-half times the value corresponding to Saturn's 10 h 39.4 min rotation period[4] and the planet can act to produce a gap, several hundred kilometres wide, just as a satellite would, only if its mass distribution is non-axisymmetric. (The ellipticity of the Earth's Equator is one such example.) If we suppose asymmetries to be present in Saturn, then the disturbing potential[5] can be written

$$V_{lm}=\frac{\mu_s a_s^l}{a^{l+1}}\sum_{p=0}^{l}F_{lmp}(i)\sum_{q=-\infty}^{\infty}G_{lpq}(e)S_{lmpq}(\tilde{\omega},\lambda,\Omega,\theta_s) \qquad (1)$$

where l and m are usual subscripts arising in an expansion in spherical harmonics, p and q are introduced by the inclination and eccentricity functions, $F(i)$ and $G(e)$ which allow V to be expressed in terms of orbital elements. The a refers both to the equatorial radius of Saturn, s, and the semimajor axis of a ring particle and $\mu_s \equiv GM_s$. The quantity S_{lmpq} contains the harmonic coefficients, C_{lm} and S_{lm} that are associated with cos and sin terms whose angular argument is

$$[\lambda(l-2p+q)-m\theta_s-q\tilde{\omega}-(l-m-2p)\Omega] \qquad (2)$$

where λ is the mean longitude, $\tilde{\omega}$ and Ω are the longitudes of pericentre and node, respectively, and θ_s is the longitude on Saturn associated with a given harmonic so that $\dot{\theta}_s \equiv \omega_s$ is the spin rate of 810.7601° day^{-1} (ref. 4). At present we consider only orbits in the equatorial plane so that $i=0°$, whence it follows that for $F(i=0°)\neq 0$, $l-m=2p$. The function G is proportional to $e^{|q|}$, where e is the eccentricity of a ring particle. The case $q=0$ corresponds (see equation 2) only to synchronous rotation, that is $\dot{\lambda}\equiv n=\omega_s$, where n is the mean motion. This case—the analogue of the 1:1 resonance of the Trojan asteroids—produces effects that must be analysed differently from those arising at other resonances[5]. Synchronous rotation, presumably not by coincidence, lies in the outer part of ring B where $\tau \gg 1$. The orbital behaviour of (non-colliding) particles near the synchronous distance, d, is well known[5] so that the surface brightness can apparently show an azimuthal dependence over a narrow annular region centred on d.

Table 1 Correspondence of ring features and certain resonances

Resonance		a_{obs}	a_{calc}	Width	n/n_s
		(10^5km)		(km)	
Mimas, 2:1		1.179	1.1754	450	
Titan 'apsidal'		0.773	0.7765	200	
m	q				
2	−1	0.732	0.7201	—	2:1
3	+1	1.361	1.3607	~30	3:4
3	−1	0.867	0.8637	250	3:2

The first, a 2:1 ratio between local mean motion and that of Mimas and the second, equality of local apsidal precession frequency and the mean motion of Titan, provide characteristic values of the positional accuracy of Voyager 1 measurements. Final three (first of these is a boundary, not a gap) are associated with the non-axisymmetric gravitational field of Saturn. n/n_s is the ratio of the orbital frequency at resonance to the planet's rotation rate[4].

The cases, $q=\pm 1$ are the equivalent of the $n/(n+1)$ orbit-orbit resonances. As is evident from the Lagrange planetary equations, forcing terms associated with them contain $e^{|q|-1}$ and are therefore stronger than higher order commensurabilities. We consider only the $|q|=1$ case so that, for $i=0°$, the time derivative of equation (2) yields

$$n=\frac{m\omega_s \pm \dot{\tilde{\omega}}}{m\pm 1} \qquad (3)$$

where, apart from $l-m=2p$, $m\leq l$ is the only remaining restriction on equation (3).

In the saturnian case, the first—and presumably the strongest—nonaxisymmetric term (given by the C_{22} or S_{22} coefficients) produces, apart from the case at the synchronous distance just mentioned, no resonance lying within the ring system. However, the $q=-1$ case, whence $n=1591.70°\ \mathrm{day}^{-1}$ and $a=72{,}010$ km lies just inside the inner boundary of ring C, measured by Voyager 1 at 73,200 ± 700 km. (All these calculations use $a_s=60{,}330$ km, $J(\propto C_{20})=0.0244488$ and $K(\propto C_{40})=0.0034375$ and $\mu_s=3.79209\times 10^{22}$.)[6] Two cases where the identification seems likely arise when $m=3$, that is $n=(3\omega_s-\dot{\tilde{\omega}})/2$ and $n=(3\omega_s+\dot{\tilde{\omega}})/4$. Calculations (Table 1) place the former at 86,370 km, the latter at 136,070 km and, in each case, especially the former, a prominent ring gap is nearby. A caveat remains because systematic errors as large as ±700 km (ref. 7) attend the positional measures made by Voyager 1 and the accurate Voyager 2 results require reductions not yet complete. To offset this uncertainty, we have compiled in Table 1 predicted and measured locations for two strong satellite resonances whose identifications are well-established, together with those, just considered, that we associate with the planet's rotation.

It seems premature to examine evidence linking less conspicuous gaps in ring A with larger values of m. For future efforts

0028–0836/82/020128—03$01.00

and because much 'fine structure' has been detected in the Cassini division[7], we list in Table 2 selected resonance locations arising from non-axisymmetric terms up to $m = 13$. The stellar occultation experiment of Voyager 2 will provide the observational material for comparison.

Using the analysis of Goldreich and Tremaine[2], we can estimate the magnitude of the C_{33} coefficient required to produce the large gap in outer C ring by replacing the disturbing function due to an exterior satellite by one appropriate for the non-axisymmetric mass distribution of Saturn. For the case $i = 0°$ and $|q| = 1$, the disturbing function (1) can be written.

$$V^{lm}_{|q|=1} = (-)^{(l-m)/2} \frac{\mu_s}{\pi^{1/2} a_s} 2^{m-1} \left(\frac{a_s}{a}\right)^{l+1} \Gamma\left(\frac{l+m+1}{2}\right) \times (l - 2qm + 1) e S_{lmpq} \qquad (4)$$

where Γ is the gamma function and S_{lmpq} contains the C_{lm} and S_{lm} coefficients. Equation (4), when combined with the development of Goldreich and Tremaine, shows that a combined harmonic coefficient, $(C^2_{33} + S^2_{33})^{1/2} \gtrsim 2 \times 10^{-10}$ is sufficient to generate the observed gap width is the process[2] can operate essentially for the age of the Solar System. As there is no evidence favouring such long-term operation, it is useful to see if the lower limit can be raised. Values of $(C^2_{33} + S^2_{33})^{1/2}$ must be large enough to ensure that a gap can be cleared, thanks to angular momentum transport, in the presence of continuing viscous diffusion. The relevant equations have been derived by Goldreich and Tremaine[8], whence the most stringent condition is

$$(C^2_{33} + S^2_{33})^{1/2} \gtrsim \frac{1}{3} \left(\frac{\nu}{\Omega_K r^2}\right)^{1/2} \qquad (5)$$

where ν is the kinematic viscosity and Ω_K the local keplerian angular velocity. The former has recently been derived[7] from observations, made by Voyager 1, of the Cassini division, $\nu = 170 \pm 80\ \text{cm}^2\ \text{s}^{-1}$, which approximately accords with theoretical estimates[2]. If we assume that the same value of ν applies in parts of the ring having larger optical thickness, then the right-hand side of equation (5) yields $\sim 3 \times 10^{-8}$ as the appropriate limit.

The gap at 1.361×10^5 km in the outer part of ring A is produced by the same $l = m = 3$ harmonic, with $q = +1$ rather than -1 (although higher harmonics may contribute to both). Equation (4) indicates why it is so much narrower (see Table I). In addition to the difference in the saturnicentric distance of the two, for the outer resonance, the factor $(l - 2qm + 1)$ drops by a factor of 5.

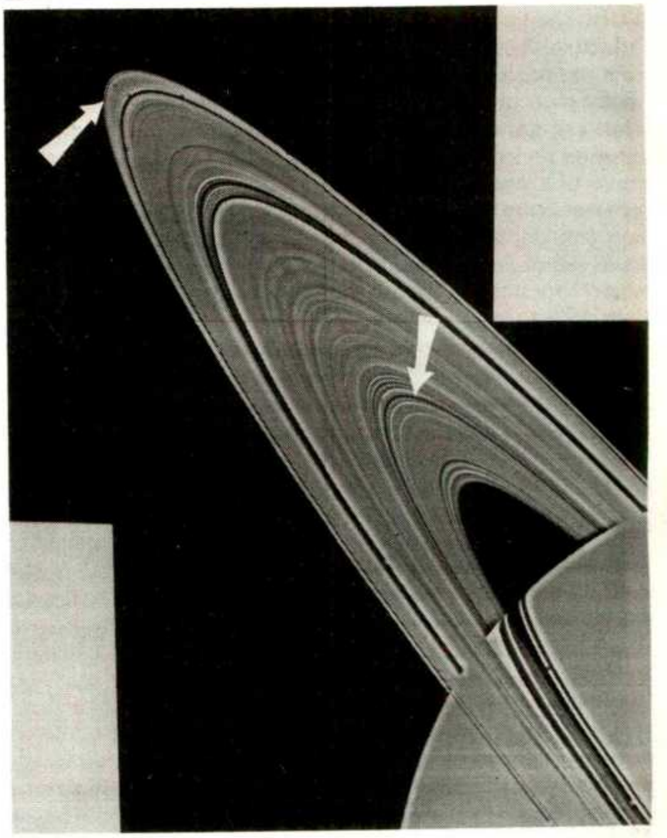

Fig. 1 Ring system from Voyager 1. Arrows mark the two gaps that can be accounted for if Saturn has an $l = m = 3$ harmonic.

Following the Saturn encounter of Voyager 2, a more detailed examination of the positions and widths of all ring features, especially in regions of low optical thickness, is necessary. We shall also need an equally careful review of the mechanism of gap formation to infer more precise values for the harmonic coefficients. There now seems to be some evidence that Saturn's gravitational field does contain at least the (3,3) harmonic. Although it is tempting to suppose that the (2,2) term, with its strong resonance just inside the inner ring C boundary is responsible for the truncation of that ring, how this happens is not clear. If the ring system once did extend closer to Saturn, into the D-ring region, then were the planet to have a substantial (2,2) term, a broad gap near 72,000 km could be produced, with its outer boundary at the observed truncation of the C ring. However, we would apparently still require an additional process[9] to reduce the surface density inside that resonance. In this context, we should note that the effective inner boundary of Jupiter's ring lies at a distance corresponding to the $l = m = 3$ resonance, or, where $2n = 3\omega_J - \dot{\omega}$. Adoption of $\omega_J = 870.5443°\ \text{day}^{-1}$ (corresponding to a period of 9 h 55 min 29.37 s), $J = 0.02208$, $K = 0.00244$ and $R_J = 71430$ km shows this resonance to be located at 1.227×10^5 km, whereas, although the ring can be faintly traced nearly to the jovian cloud tops, measurements place the inner edge of the bright portion (viewed in backscattered light) at $1.228 \pm 0.007 \times 10^5$ km (ref. 10). The influence on particle orbits that we attributed to tesseral harmonics of the gravitational field might instead result from the primary's inclined, displaced magnetic field. As for Saturn, the outer ring boundary seems to be established by a small satellite.

Table 2 Positions (in optically thin regions) of additional strong resonances associated with higher harmonics of Saturn's field

m	q	a_{calc}	n/n_s
4	+1	1.3037	4:5
5	+1	1.2690	5:6
8	+1	1.2159	8:9
9	+1	1.2060	9:10
10	+1	1.1980	10:11
11	+1	1.1915	11:12
12	+1	1.1860	12:13
13	+1	1.1814	13:14

Cassini division, where many narrow gaps appear[7], stretches from ~ 1.177 to $\sim 1.210 \times 10^5$ km. Precise positions from Voyager 2 are necessary for a detailed comparison.

It seems unlikely that harmonic coefficients with $m \neq 0$ refer to the shape of Saturn's (probable) rock–ice core. However, Stevenson[11] has proposed a new interior model with three distinct layers, in addition to the core, that can account both for the planet's unexpectedly weak magnetic field and its excess heat flux. The model's outermost layer consists of an envelope of molecular H_2 and He, with the latter somewhat depleted. The existence of metallic H characterizes the next layer which is inhomogeneous because of the limited solubility (dependent on temperature and pressure) of He in metallic H. Deeper, droplets of He eventually dissolve to form a much more homogeneous layer above the core. The inward migration of He releases gravitational energy and might inhibit convection, but, for our purposes, the vital point is the existence of several distinct layers. The likelihood that various instabilities can exist on the surfaces of these layers such that their interfaces assume a wavy form was suggested by R. Smoluchowski. In a nonlinear regime, denser parts of the fluid will collect near the troughs, while the crests can grow by buoyancy to reinforce the wave. Although diffusion seeks to eliminate such waves, they may, in a poorly convective layer, persist for a long time or be regenerated. If such waves are the source of Saturn's gravitational asymmetries, then concomitant ring features may well vary to some time scale—all of which means that any estimate of $(C_{33}^2+S_{33}^2)^{1/2}$, but perhaps not its existence should be treated cautiously. As an alternative to instabilities at layer interfaces, one might consider an interior model possessing large scale convective cells that develop and sustain non-axisymmetric mass distributions—presumably over extended periods of time.

We thank Drs R. Smoluchowski, I. Shapiro and J. Cuzzi for useful discussions. Aspects of this study were funded by NASA under contract NAS 7-100 with the Jet Propulsion Laboratory.

Received 19 August; accepted 13 November 1981.

1. Collins, S. A. *et al. Nature* **288,** 439–442 (1980).
2. Goldreich, P. & Tremaine, S. *Icarus* **34,** 240 (1978).
3. Smith, B. A. *et al. Science* **212,** 163 (1981).
4. Warwick, J. *et al. Science* **212,** 239 (1981).
5. Kaula, W. M. *Theory of Satellite Geodesy* (Blaisdell, 1966).
6. Null, G. W. *et al. Astr. J.* **86,** 456 (1981).
7. Cuzzi, J. N., Lissauer, J. J. & Shu, F. H. *Nature* **292,** 703–707 (1981).
8. Goldreich, P. & Tremaine, S. *Astrophys. J.* **241,** 425 (1980).
9. Smoluchowski, R. *Nature* **274,** 669 (1978).
10. Jewitt, D. C. & Danielson, G. E. *J. geophys. Res.* (in the press).
11. Stevenson, D. *Science* **208,** 746 (1980).

Radiation effects and the leach rates of vitrified radioactive waste

W. G. Burns, A. E. Hughes, J. A. C. Marples, R. S. Nelson & A. M. Stoneham

Atomic Energy Research Establishment, Harwell, Didcot,
Oxon OX11 0RA, UK

There is much concern that long-lived radioactive elements incorporated in glasses for the disposal of highly active nuclear waste might eventually return to the environment. The most important mechanism begins with leaching of the glass by groundwater and a leach rate, usually based on laboratory tests of simulated vitrified radioactive waste, has been used as the basis of analyses of the radiological safety of a waste repository[1–3]. The possibility that radiation damage to the glass from the products of nuclear decay could change the leach rate has been studied both by the incorporation of active elements in the glass and by irradiation from external sources. The most important contribution to radiation damage comes from the recoil nuclei during α decay[4]. Typically the recoil nucleus has a kinetic energy of ~100 keV and displaces >1,000 atoms in the glass. Experiments which simulate this damage by incorporating short-lived α-emitting isotopes such as ^{238}Pu into the glass have not shown significant increases in leach rate at doses equivalent to $>10^{18}$ α decays g^{-1} (refs 5–9). Figure 1 shows that for wastes considered in the UK this corresponds to a time after vitrification of at least 10^3–10^4 yr. Recent work with ion beams inducing the radiation damage[10–12] has suggested that large increases (up to a factor of just over 50) in leach rate will occur after a critical dose of radiation from the α-decay processes. In addition, experiments in which the leaching solution is irradiated with γ rays[13–15] have shown that radiolysis effects in the water can increase the leach rates of glasses. We present here new data and calculations which relate these studies to the conditions expected in a real waste repository. Our analysis is described in more detail elsewhere[16,17].

Dran *et al.*[10,11] irradiated glasses and crystalline minerals with 200-keV Pb ions and found that an enhanced leach rate occurs above a critical fluence of $\sim 5\times10^{12}$ ions cm^{-2}, which corresponds to the dose at which the individual damage zones (each of lateral extent ~10 nm) produced by the Pb ions overlap. Such effects have been observed before, for example, in ion-irradiated garnets[18]. One expects similar overlap of damage zones to occur in a glass containing α emitters at a dose of $\sim 10^{18}$ decays g^{-1}.

Table 1 Leach tests on samples of glass 189* doped with $^{238}PuO_2$

			Holding temperature (°C)	
		First year	50	170
		Subsequent years	20	20
Date	Dose (α-disintegrations g^{-1})	Equivalent time (yr)	Leach rates (mg cm^{-2} day^{-1})	
November 1975	0.89×10^{18}	7,000	1.6	1.5
February 1977	2.0×10^{18}	250,000	2.3	2.3
March 1977	2.1×10^{18}	300,000	2.4	2.2
November 1977	2.7×10^{18}	500,000	2.3	2.6
July 1978	3.3×10^{18}	700,000	2.3	2.5
January 1981	5.5×10^{18}	1,400,000	3.2	2.7
February 1981	5.6×10^{18}		3.0	

The equivalent times assume 0.5% of the plutonium and 0.25% of the uranium originally present in Magnox fuel go into the waste. The fuel is assumed to be reprocessed after 6 months out of the reactor. Leach rates were measured by the Soxhlet method, in which the sample is in contact with frequently changed distilled water at 100 °C. The initial Soxhlet leach rate expected for undoped glass of this composition is 1.3 ± 0.2 mg cm^{-2} day^{-1}.

* The composition of this glass in wt% is SiO_2: 41.5; B_2O_3: 21.9; Na_2O: 7.7; Li_2O: 3.7; simulated waste product oxides: 25.2.

Each incident 200-keV Pb ion in the ion beam experiments produces $\leq 3{,}000$ displacements. The irradiated region has a depth of 50 nm so that at a critical fluence of 5×10^{12} ions cm^{-2} the average number of displacements is not more than 3×10^{21} cm^{-3}. We calculate that each α decay produces 1,380 displacements so the critical fluence is equivalent to 2.2×10^{18} α decays cm^{-3}. For a typical glass density of 2.6 g cm^{-3} this is 8.5×10^{17} decays g^{-1}. Dran *et al.*[11] quote $\sim 2\times10^{18}$ decays g^{-1} as the equivalent dose to a Pb ion fluence of 5×10^{12} cm^{-2}. Their method is based on an equivalent number of heavy ion tracks crossing unit surface area. However, whichever approach is used the appropriate figure is clearly $\sim 10^{18}$ decays g^{-1}.

Table 1 shows recent results from work at Harwell on samples of UK glass 189 which have been doped with 5 wt% of $^{238}PuO_2$. Regular leach tests of these samples in distilled water using the Soxhlet test have been made since their manufacture in 1975. Only modest increases in leach rate have been observed even after 5.6×10^{18} α decays g^{-1}. The PuO_2 may not be completely homogeneously dispersed in these samples, but it is believed that most of it is in solid solution in the glass as would be the case for the α-emitting isotopes in real vitrified waste. There is no evidence of a large increase in leach rate as found by Dran *et al.* One of these samples has now also been tested in a 250 g l^{-1} NaCl solution at 100 °C as used by Dran *et al.* and showed an increase by a factor of only 1.2 over an unirradiated sample. Furthermore the leach rates were an order of magnitude smaller in the NaCl solution than in distilled water.

We therefore believe that the large effects noted by Dran *et al.* do not occur in the simulations using α emitters, which, of course, are accelerated versions of the effects that will actually occur in practice. In trying to rationalize these results we have considered possible effects of dose rate[16]. Simulations with α emitters are carried out at rates 10^4–10^5 times higher than those pertinent to a real waste repository at times $\gtrsim 100$ yr, whereas the ion beam experiments are accelerated by a factor of 10^{10}–10^{11}. If r cm^{-3} s^{-1} is the rate of damaging events and v cm^3 the volume of a damaged zone created by one event (that is, by a single incident ion or single recoil nucleus), then the time required to reach a stage where the zones overlap is $t_{\text{crit}} \simeq (rv)^{-1}$.

Obviously if an individual zone recovers (anneals) in a time short compared with t_{crit}, overlap of zones is not reached. By extrapolating data obtained at Harwell on the annealing of density change of the glass and the release of irradiation-induced stored energy on heating, we estimate[16] that the mean recovery time of a damaged zone is in the range 10^4–10^7 s between 25 and 200 °C. With $v \sim (10\ \mathrm{nm}^3)$ we estimate that $t_{crit} \sim 10$ s for the ion beam experiments, $\sim 10^8$ s for simulations with α emitters and $\sim 10^{10}$–10^{12} s for a real waste glass. We therefore suggest that the effects observed with ion beams will not occur in simulated or real glasses in which the damage results from α-decays at a relatively low rate.

Our remarks apply more strongly to the work by Hirsch[12] in which the damage is produced by 2-keV Ar ions. These have a range in the glass of only 2.4 nm and accelerate the damage rate by a factor of perhaps 10^{14}. Such low energy ion beams also produce changes in surface composition and (at high fluences) topography[19–21] which may have more influence on chemical attack than the effects of structural changes produced by radiation damage in the bulk of the material.

Some recovery of damage may also occur during laboratory leach tests if these are carried out at 100 °C as in the Soxhlet method. We estimate that up to 15% recovery could have occurred during leach tests for the samples in Table 1. Obviously recovery effects must be considered both during irradiation and during any tests after irradiation; our estimates show that they could be extremely important in the long time, low dose-rate conditions that apply to real vitrified waste.

McVay and co-workers[13–15] have measured the leach rates of US glass 76–68 while the glass and aqueous leachant were being irradiated with ^{60}Co γ rays at a dose rate of 2.4 Mrad h^{-1}. They found increases by a factor of about two in the rate of loss of weight of the glass and larger increases in the leach rate of some individual elements. They showed that these effects are not due to radiation damage to the glass by γ rays, but must be associated with the effects of radiation on the leachant. In those experiments where air was present, some of the effect could be caused by the production of nitric acid when air or nitrogen is irradiated in the presence of water[22,23]. However, the increases in leach rate in a system in which air was removed[15] must be caused by radiolysis of the water.

To relate these experiments to the conditions likely to exist in a waste repository, we have used the methods of radiation chemistry[24,25] to calculate the concentrations of radicals produced by the irradiation of water next to the glass surface. These calculations consider the known yields[26–27] of the primary species H^+, e^-_{aq}, H, OH, HO_2, H_2 and H_2O_2 produced by ionization of water, and known rates of secondary reactions[28] involving these species, water molecules and possible solutes. We have made preliminary calculations for the following irradiation conditions. (*a*) 2.4 Mrad h^{-1} γ radiation, as used by McVay *et al.* (*b*) 4 Mrad h^{-1} α radiation, which represents the situation for leach rate measurements on samples doped with $^{238}PuO_2$ (see Table 1), where simultaneous leaching and irradiation is inevitable. (*c*) The radiation conditions in a repository, assuming pessimistically that the leachant contacts the glass directly at all times. Some typical dose rates at various times after vitrification are given in Table 2.

Table 2 Typical radiation dose rates to the leachant in a waste repository

Time after vitrification (yr)	Dose rates (Mrad h^{-1}) Lightly ionizing radiation (β, γ)	α radiation
4	5.3×10^{-1}	2.72×10^{-2}
50	8×10^{-2}	2.25×10^{-2}
500	~0	1.08×10^{-2}

These figures assume that the leachant is in contact with the radioactive glass and are based on the same data as in Fig. 1.

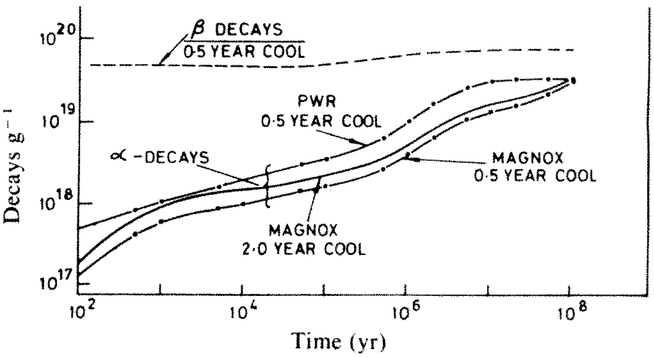

Fig. 1 The number of decays g^{-1} as a function of time for highly active vitrified waste: 12.5% fission products in glass; 0.5% Pu, 0.25% U to highly active vitrified waste. The different curves refer to different reactors and processing conditions as indicated. Each α decay produces over 1,000 atomic displacements whereas each β decay produces ≤ 1 displacement. Long term radiation damage effects are therefore dominated by α decays.

Because dissolved oxygen was removed in McVay and Pederson's experiments[15] and is not expected in an underground repository, most of our calculations are for sealed systems with no gas phase present. However, in case (*b*) we assumed that the water is saturated with dissolved air at the temperature used as was the case in these experiments.

The results are shown graphically in Fig. 2. We note first that in case (*a*) the radicals with highest concentration are OH and O_2^-, suggesting that these are the species responsible for the enhanced leach rates in McVay *et al.*'s experiments (note that McVay and Pederson[15] show that H_2O_2 has no discernible effect). We find small changes (factor of ≤ 2) in the concentrations of H^+ and OH^-. Experiments[29,30] in which leach rate has been measured as a function of *p*H show that such small changes will have a negligible effect on leach rate. The absence of any significant change in initial leach rate for $^{238}PuO_2$-doped glasses when compared with undoped glass (see Table 1) suggests that OH is more active than O_2^- in promoting an increase in leach rate, since we find in Fig. 2 that there is a higher O_2^- concentration in case (*b*) than in case (*a*). Clearly in Fig. 2, in real repository conditions the concentrations of these radicals fall to values low compared with those for the laboratory experiments in case (*a*). We also find that the presence of the solutes NO_3^- and Cl^-, which are found in real waters equilibrated with rocks, can reduce the OH concentration by factors of up to several thousand. We conclude that radiolysis of the leachant will not have a large effect on the leach rate in a real repository.

We have tried to quantify the production of nitric acid when air or nitrogen is irradiated in the presence of water. From experimental data[22,23] we deduce that the nitric acid concentration *N* mol dm^{-3} at time *t* h for irradiation of a sealed air/water system is given by

$$N = 2C_0R[1 - \exp(-1.45 \times 10^{-5}\ GDt)] \qquad (1)$$

where *D* is the dose rate in Mrad h^{-1}, *R* is the ratio of the volume of air to the volume of liquid and the *G* value for the reaction is 1.9. C_0 is the concentration of N_2 in the air in mol dm^{-3}. Equation (1) shows that a *p*H change from 5.7 to 3.3, as observed by McVay and Pederson[15] after 5 days irradiation in the presence of air, would be consistent with a value of *R* of the order unity.

A repository should be free of air pockets soon after burial (N. A. Chapman, personal communication) and the absence of air as a separate phase precludes the formation of nitric acid because this compound is a negligible product of the irradiation of water containing dissolved nitrogen[23,31]. Measurements by Rai *et al.*[32] with particulate suspensions of plutonium compounds suggest that nitric acid could be formed fairly efficiently from dissolved nitrogen, but this interpretation is suspect as air was present in their tubes as a gas, which was probably irradiated by the Pu-containing particles, distributed

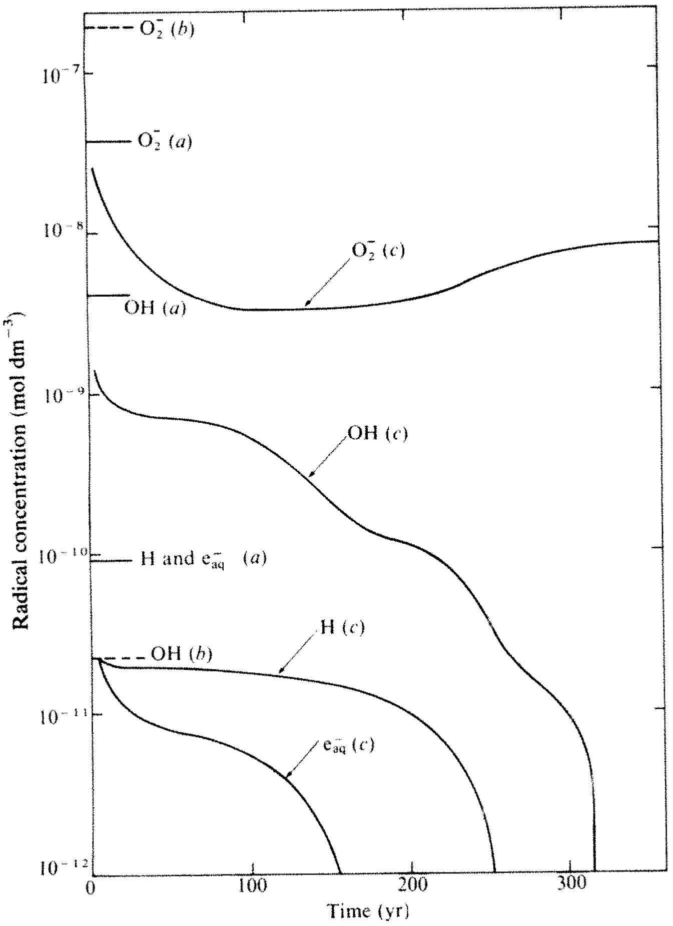

Fig. 2 Concentrations of the radiolytic species H, OH, e_{aq}^- and O_2^- produced by radiolysis of the water next to glass in a repository. The concentrations for irradiation conditions (*a*) and (*b*) described in the text are shown on the left. The H and e_{aq}^- concentrations in case (*b*) are below the scale at 1.1×10^{-13} and 4.1×10^{-14}, respectively. The rise in the O_2^- concentration after ~100 yr is caused by the preponderance of α radiation at long times (see Table 2).

non-uniformly (the greatly increased energy yield found with shaking, and the increase in the rate of acid formation with time support the latter interpretation).

If air were present in a repository the radiation could reach it only through containment and probably a layer of water. At times when the containment may have failed, say after a few hundred years, Table 2 shows that the only significant radiation is from α particles. These have a range of $<4 \times 10^{-2}$ mm in water, so would be completely absorbed in this thickness. The conditions in a repository therefore militate quite strongly against the formation of nitric acid and its consequent contribution to leaching.

The experimental data discussed here all point to leach rates in real repository conditions no more than a few times larger than those of unirradiated glasses. Note, however, that rather wide extrapolations and interpolations in dose rate are involved, and more data are needed over a range of dose rates. Leaching data for specific elements would also be informative because nearly all existing measurements refer to total weight loss. Experiments that have been done suggest that actinide elements dissolve more slowly than the bulk glass structure[14,33].

Note also that the leach rate as usually measured in laboratory tests is unlikely to be the rate-determining factor for the dissolution of glass in a real waste repository, because of the very slow flow rate of water past the glass surface[34-36]. In these conditions the rate of removal of elements from the glass will be controlled by the saturation solubility of the glass in the water, or, in stagnant conditions, by the diffusion of species away from the glass surface[17]. Chapman *et al.*[36] have estimated that the water flow through a (fractured) 1 m^3 block of glass in a repository even without clay backfill would be ~4 ml day^{-1}. If we assume a solubility of 2 g l^{-1}, which is an order of magnitude higher than the solubility of amorphous silica in water at 50 °C (ref. 37), then the rate of mass loss of the block will be 8 mg per day. If the block is fractured into 10-cm cube segments the total surface area is 6×10^5 cm^2 so that the effective leach rate would only be 10^{-8} g cm^{-2} day^{-1}. This can be compared with laboratory values (see Table 1) and the figure of 10^{-7} g cm^{-2} day^{-1} below which radiological analysis gives a clear margin of safety[2]. Backfilling might reduce the flow rate and hence the effective leach rate by a factor[36] of 10^4. A major uncertainty in this argument is the effective solubility of real vitrified waste, but there is evidence that the solubility of actinide species from glasses is extremely low[38]. Radiation damage should not change the solubility by more than a small factor as one is dealing with a situation approaching chemical equilibrium, rather than with a kinetically determined rate process as in a normal surface leach rate measurement.

This work was carried out with the financial support of the Department of the Environment, as part of its radioactive waste management research programme. We thank Drs L. E. J. Roberts, J. Williams, D. Pooley, N. A. Chapman, D. P. Hodgkinson, R. L. F. Kay and Mr D. Savage for valuable comments, and Dr G. L. McVay for discussing his results before publication.

Received 26 August; accepted 17 November 1981.

1. Hill, M. D. & Grimwood, P. D. *NRPB Rep. R-69* (National Radiological Protection Board, 1978).
2. Hill, M. D. *NRPB Rep. R-86* (National Radiological Protection Board, 1979).
3. Hill, M. D. & Lawson, G. *NRPB Rep. R-108* (National Radiological Protection Board, 1980).
4. Permar, P. H. & McDonnell, W. R. in *Proc. 10th Symp. on Effects of Radiation on Materials* (American Society for Testing and Materials, Philadelphia, in the press) (available from National Technical Information Services CONF 800609-5, and as Dupont Report DP-MS-80-27).
5. Marples, J. A. C. (ed.) *European Res. Rep.* No EUR7138 (in the press).
6. Weber, W. J., Turcotte, R. P., Bunnell, L. R., Roberts, F. P. & Westsik, J. H. in *Ceramics in Nuclear Waste Management* (eds Chikalla, T. D. & Mendel, J. E.) 294–299 (Technical Information Center, US Dept of Energy, CONF-790420, 1979).
7. Mendel, J. E. *et al.* in *Management of Radioactive Wastes from the Nuclear Fuel Cycle* Vol. 2, 49–61 (IAEA, Vienna, 1976).
8. Bibler, N. E. & Kelley, J. A. *Dupont Rep. DP-1482* (Dupont Savannah River Laboratory, Aiken, 1978).
9. Scheffler, K. & Riege, U *KfK Rep. 2422* (Kernforschungszentrum, Karlsruhe, 1977).
10. Dran, J. C., Maurette, M. & Petit, J. C. *Science* **209**, 1518–1520 (1980).
11. Dran, J. C., Maurette, M., Petit, J. C. & Vassent, B. in *Scientific Basis for Nuclear Waste Management*, Vol. 3 (ed. Moore, J. G.) 449–456 (Plenum, New York, 1981).
12. Hirsch, E. H. *Science* **209**, 1520–1522 (1980).
13. McVay, G. L., Weber, W. J. & Pederson, L. R. *ORNL Conf. on Leachability of Radioactive Solids*, Gatlinburg (1980).
14. McVay, G. L. & Buckwalter, C. Q. *Nucl. Technol.* **51**, 123–129 (1980).
15. McVay, G. L. & Pederson, L. R. *J. Am. ceram. Soc.* **64**, 154–158 (1981).
16. Burns, W. G., Hughes, A. E., Marples, J. A. C., Nelson, R. S. & Stoneham, A. M. *AERE Rep. R-10189* (AERE, Harwell, 1981).
17. Hughes, A. E., Marples, J. A. C. & Stoneham, A. M. *AERE Rep. R-10190* (AERE, Harwell, 1981).
18. Johnson, W. A., North, J. C. & Wolfe, R. *J. appl. Phys.* **44**, 4753–4757 (1973).
19. Coburn, J. W. *J. Vac. Sci. Technol.* **13**, 1037–1044 (1976).
20. Binkowski, N. J., Heitzenrater, R. F. & Stephenson, D. A. *J. Am. ceram. Soc.* **59**, 153–157 (1976).
21. Stephenson, D. A. & Binkowski, N. J. *J. Non-Cryst. Solids* **22**, 399–421 (1976).
22. Wright, J., Linacre, J. K., Marsh, W. R. & Bates, T. H. *Proc. Int. Conf. on the Peaceful Uses of Atomic Energy* Vol. 7, 560–563 (United Nations, New York, 1956).
23. Linacre, J. K. & Marsh, W. R. *AERE Rep. R-10027* (AERE, Harwell, 1981).
24. Burns, W. G. & Moore, P. B. *Rad. Effects* **30**, 233–242 (1976).
25. Burns, W. G. & Moore, P. B. in *Proc. Conf. on Water Chemistry of Nuclear Reactors*, 281–289 (British Nuclear Energy Society, London, 1978).
26. Anbar, M., in *Fundamental Processes in Radiation Chemistry* (ed. Ausloos, P.) 651–685 (Interscience, New York, 1968).
27. Appleby, A. & Schwarz, H. A. *J. phys. Chem.* **73**, 1937–1941 (1969).
28. Boyd, A. W., Carver, M. B. & Dixon, R. S. *Radiat. phys. Chem.* **15**, 177–185 (1980).
29. Boult, K. A., Dalton, J. T., Hall, A. R., Hough, A. & Marples, J. A. C. *AERE Rep. R-9188* (AERE, Harwell, 1978).
30. Marples, J. A. C., Lutze, W. & Sombret, C. in *Radioactive Waste Management and Disposal* (eds Simon, R. & Orlowski, S.) 307–323 (Harewood Academic, 1980).
31. Dollé, J. & Rosenberg, L. in *Proc. Conf. on Water Chemistry of Nuclear Reactors*, 291–297 (British Nuclear Energy Society, London, 1978).
32. Rai, D., Strickert, R. G. & Ryan, J. L. *Inorg. nucl. Chem. Lett.* **16**, 551–555 (1980).
33. Bradley, D. J., Harvey, C. O. & Turcotte, R. P. *PNL Rep. 3152* (Pacific Northwest Laboratory, 1979).
34. American Physical Society. *Rev. Mod. Phys.* **50**, S1–S186 (1978).
35. Hodgkinson, D. P. *AERE Rep. M-2997* (AERE, Harwell, 1978).
36. Chapman, N. A., McInley, I. G. & Savage, D. *OECD/NEA Workshop on Radionuclide Release Scenarios for Geologic Repositories*, Paris (in the press).
37. Rimstidt, J. D. & Barnes, H. L. *Geochim. cosmochim. Acta* **44**, 1683–1699 (1980).
38. Rai, D. & Strickert, R. G. *Trans. Am. nucl. Soc. Europ. nucl. Soc. 1980 int. Conf. on World Energy: Accomplishments and Perspectives*, 185–186 (American Nuclear Society, La Grange Park, Illinois, 1980).

A mesospheric source of nitrous oxide

Edward C. Zipf

Department of Physics and Astronomy, University of Pittsburgh,
Pittsburgh, Pennsylvania 15260, USA

Sheo S. Prasad

Jet Propulsion Laboratory, California Institute of Technology,
4800 Oak Grove Drive, Pasadena, California 91109, USA

In the terrestrial atmosphere, nitrous oxide (N_2O) has a major role in the chemistry of ozone. Current atmospheric models assume that N_2O is produced only by fixation at the Earth's surface and that there are no local sources in the stratosphere or mesosphere. We point out here that a significant *in situ* N_2O source does exist above 20 km due to the excitation of the metastable $N_2(A^3\Sigma_u^+)$ state by resonance absorption of solar UV photons that penetrate deeply into the atmosphere through the λ1,800–2,200 Å O_2–O_3 window. This source significantly affects the NO altitude distribution in the mesosphere and, in the Earth's prebiological atmosphere, made N_2O an important stratospheric constituent.

Literature estimates of the profile of eddy diffusion coefficients, of the effective lifetime of N_2O in the lower atmosphere and of the magnitude of the role of nitrous oxide in the chemistry of the ozone layer are predicated in part on the assumption that there are no significant *in situ* N_2O sources. Previously, the only aeronomically interesting mechanism known to produce nitrous oxide was the reaction[1]

$$O(^1D)+N_2+M \rightarrow N_2O+M \quad (1)$$

But the rate of this reaction in the gas phase is negligibly slow, so that it is not a factor at stratospheric altitudes and above[2]. However, a recent laboratory experiment found that the reaction[3]

$$N_2(A^3\Sigma_u^+)+O_2 \xrightarrow{k_2} N_2O+O \quad (2)$$

produces nitrous oxide with an efficiency of 0.6 ± 30%. Because reaction (2) is the dominant $N_2(A^3\Sigma_u^+)$ loss mechanism below 90 km, the resulting N_2O production rate in the mesosphere and below will be directly proportional to the local $N_2(A^3\Sigma_u^+)$ excitation rate.

Metastable $N_2(A^3\Sigma_u^+)$ molecules are formed efficiently[4] by electron impact

$$e+N_2(X^1\Sigma_g^+) \rightarrow N_2(A^3\Sigma_u^+)+e \quad (3)$$

with a total cross-section that is quite large ($\sim 1.4\times10^{-16}$ cm^2 at 15 eV). In the upper atmosphere, therefore, these energy-rich molecules will be produced copiously by the secondary electrons resulting from the absorption of relativistic electrons and solar protons in the mesosphere[5] and from the absorption of auroral electrons[6] and solar X rays and EUV in the ionospheric D and E regions.

Processes (2) and (3) may result in N_2O concentrations as high as 10^9 cm^{-3} in the auroral D region during an active substorm[6]. However, energetic particle precipitation is a less important $N_2(A^3\Sigma_u^+)$ source mechanism at mid-latitudes and in the equatorial region and at low altitudes ($z < 50$ km). In these regions, optical pumping of the $A^3\Sigma_u^+$ state by the resonant absorption of solar photons in the λ1,800–2,100 Å wavelength range

$$\begin{aligned} h\nu+N_2(X^1\Sigma_g^+) &\rightarrow N_2(A^3\Sigma_u^+) \\ N_2(A^3\Sigma_u^+)+O_2 &\rightarrow N_2O+O \end{aligned} \quad (4)$$

seems to be an effective nitrous oxide source throughout the mesosphere and to altitudes as low as 20 km in the stratosphere.

At first sight, optical pumping of the $N_2(A^3\Sigma_u^+)$ state by solar UV photons looks unpromising: the $A^3\Sigma_u^+$ state is metastable with an average radiative lifetime of 2 s (ref. 7), so that the cross-sections for resonance absorption will be quite small. Furthermore, the Franck–Condon factors for the $X^1\Sigma_g^+ \rightarrow A^3\Sigma_u^+$ transition favour transitions from high vibrations levels ($v''>4$) of the $X^1\Sigma_u^+$ ground state which are negligibly populated at the low temperatures that prevail in the stratosphere. However, from a stratospheric point of view, these properties could be regarded as an advantage because the solar

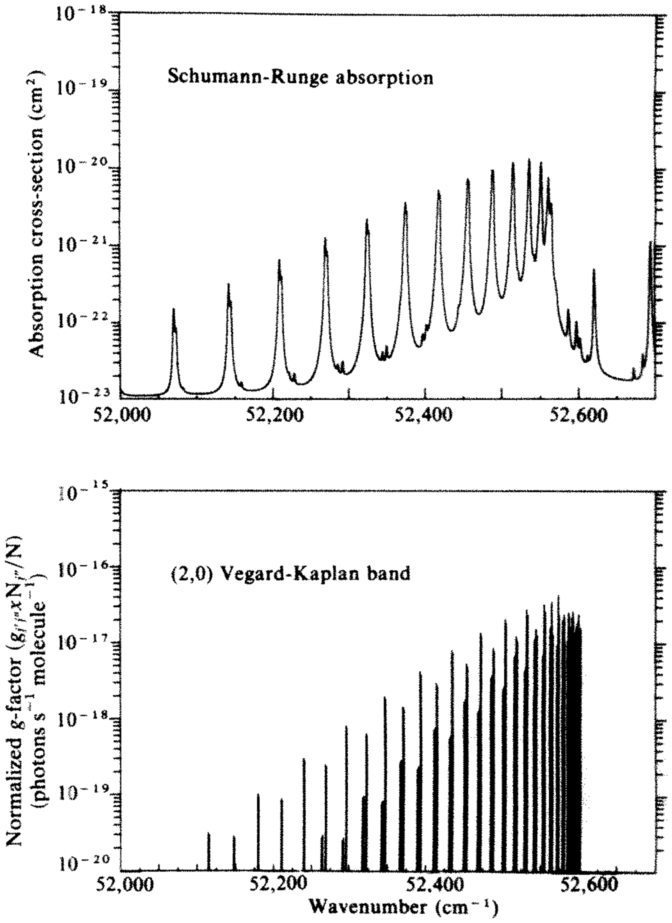

Fig. 1 The normalized g-values $[g_{J'J''}xN_{J''}/N]$ for the (2, 0) Vegard–Kaplan band $[A^3\Sigma_u^+ \leftrightarrows X^1\Sigma_g^+]$ and the absorption cross-sections for the (5, 0), (6, 1), (8, 1) and (9, 1) Schumann–Runge bands of O_2.

Table 1 The $g_{J'J''}$ factors for solar optical pumping of the metastable $N_2[A^3\Sigma_u^+(v', 0)]$ state

$^1\Sigma_g^+$–$^3\Sigma_u^+$	(0, 0)	(1, 0)	(2, 0)	(3, 0)	(4, 0)
$R_2(J'')$	5.04(−18)*R**	2.39(−17)*R**	4.22(−16)*R**	2.03(−15)*R**	5.34(−15)*R**
$Q_1(J'')$	2.52(−18)	1.20(−17)	2.11(−16)	1.01(−15)	2.67(−15)
$Q_3(J'')$	2.52(−18)	1.20(−17)	2.11(−16)	1.01(−15)	2.67(−15)
$P_2(J'')$	5.04(−18)*P*†	2.39(−17)*P*†	4.22(−16)*P*†	2.03(−15)*P*†	5.34(−15)*P*†

* For example, 5.04(−18)*R* = $5.04\times10^{-18}\,[J''/(2J''+3)]$ photons per s per molecule.
† For example, 5.04(−18)*P* = $5.04\times10^{-18}\,[(J''+1)/(2J''-1)]$ photons per s per molecule.

0028-0836/82/020133—03$01.00

photons that optically pump the Vegard–Kaplan band system $[X^1\Sigma_g^+ \leftrightarrows A^3\Sigma_u^+]$ will penetrate deeply into the atmosphere before they are absorbed. Thus, the net $N_2(A^3\Sigma_u^+)$ production in the 20–50 km region of the lower atmosphere will reflect the outcome of the competition between process (4) and the absorption of solar photons by O_2 and ozone.

The Vegard–Kaplan bands that contribute most significantly to nitrous oxide production in the mesosphere and stratosphere are the (0, 0), (1, 0), (2, 0), (3, 0) and (4, 0) transitions (see Table 1) which are located quite favourably in the 1,800–2,100 Å $[O_2–O_3]$ atmospheric window.

We have estimated the magnitude of the local $N_2(A^3\Sigma_u^+)$ production rate due to solar UV absorption as follows. The excitation rate of a specific rotational transition (J', J'') for a $(v', 0)$ Vegard–Kaplan band, η, can be expressed in terms of the g-factor[8]

$$\eta(z; v', 0; J', J'') = g(v', 0; J', J'')N_{J''}(z) \qquad (5)$$

where $N_{J''}(z)$ is the population density of the $N_2(X^1\Sigma_g^+)$ ground state molecules in the $v''=0$ vibrational level and in the J'' rotational level at altitude z, and

$$g(v', 0; J', J'') = \pi F_\nu(z)\frac{\pi e^2}{mc} f(v', 0; J', J'') \qquad (6)$$

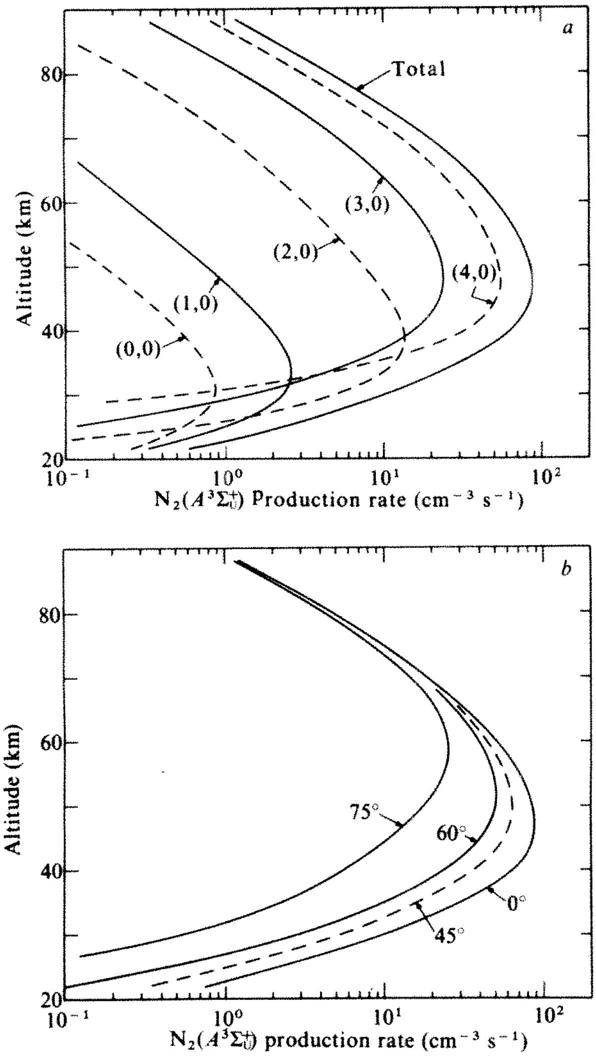

Fig. 2 *a*, Production rates of $N_2(A^3\Sigma_u^+)$ due to solar resonant scattering for overhead Sun conditions. The number in the parentheses denotes the vibrational levels in the $A \leftarrow X$ electron transition. The curve 'total' is obtained by summing the contribution from the various vibrational levels. *b*, Total production rate of $N_2(A^3\Sigma_u^+)$ for various solar zenith angles.

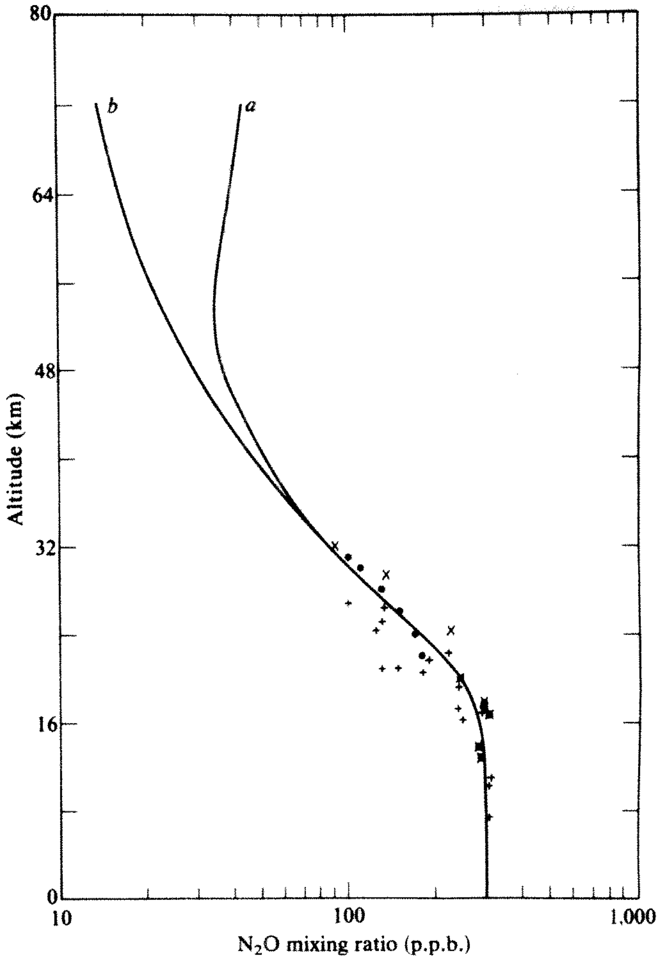

Fig. 3 Mixing ratios of N_2O. Curves *a* and *b* represent theoretical values for two cases: with and without the nitrous oxide production due to the excited $N_2(A^3\Sigma_u^+)$, respectively. Observed values are from Farmer *et al.*[14] (●), Schmeltekopf *et al.*[16] (+) and Ehhalt *et al.*[15] (×).

In this expression, $f(v', 0; J', J'')$ is the optical oscillator strength of the $J'' \rightarrow J'$ rotational transition of the $(v', 0)$ *VK* band, and $\pi F_\nu(z)$ is the incident photon flux at frequency, ν, from the Sun. The local flux can be related to the flux outside the atmosphere, $\pi F_\nu(\infty)$, in units of photons cm^{-2} s^{-1} Hz^{-1} by the expression

$$\pi F_\nu(z) = \pi F_\nu(\infty)\sum_i \exp(-\tau_\nu^i/\mu_0) \qquad (7)$$

where τ_ν^i/μ_0 is the slant optical thickness due to absorption. In this calculation, only O_2 and O_3 were considered as significant absorbers. For modelling purposes, the calculations assumed an effective rotational temperature of 230 K and used the solar flux data published by Nicolet[9].

Values for $f(v', 0; J', J'')$ were derived from the work of Shemansky[7] for the R_2, P_2, Q_1 and Q_3 branches of each of the five *VK* bands $[(v', 0); v' = 0 \rightarrow 4]$ included in this study by using the expression

$$\frac{\pi e^2}{mc} f(v', 0; J', J'') = hc\nu B^{0,v'}_{J'',J'} \qquad (8)$$

The effective optical thickness of the atmosphere due to O_3 absorption was calculated using the cross-section data of Hudson[10] and the ozone profiles given by Nicolet[9]. The effects of O_2 absorption in the Schumann–Runge bands and in the Herzberg continuum were treated in detail. This involved calculating the effective absorption cross-section for each rotational line of the Vegard–Kaplan bands due to the rotational lines of the 14 branches: P_1, P_2, P_3, $^RP_{31}$, $^NP_{13}$, Q_{12}, $^PQ_{23}$, $^RQ_{32}$, $^RQ_{21}$, R_1, R_2, R_3, $^PR_{13}$, $^TR_{31}$. In this computation, the absorption oscillator strengths and line widths given by Lewis *et al.*[11] were used.

Figure 1 shows a representative result for the (5, 0) Schumann–Runge band and the (2, 0) Vegard–Kaplan band. The specific $g(v', 0; J', J'')$ values were then calculated from these results using the solar flux data reviewed by Nicolet[9].

Figure 2*a* shows the production rate for the first five vibrational levels of $A^3\Sigma_u^+$ state due to solar optical pumping for a zenith angle of 0°. At 50 km, the effective N_2O production rate is ~ 51 cm^{-3} s^{-1} assuming a 60% efficiency for reaction (2) (see ref. 3). Based on current one-dimensional photochemical models, the nitrous oxide loss rate due to photodissociation and reactions with $O(^1D)$ atoms would be approximately 79 cm^{-3} s^{-1} and 8 cm^{-3} s^{-1}, respectively, at 50 km. Thus, optical pumping of the $N_2(A^3\Sigma_u^+)$ state by solar UV photons is a significant N_2O source in the mesosphere. Figure 2*b* shows the net $N_2(A^3\Sigma_u^+)$ and N_2O production rates for several solar zenith angles.

To explore the effects of this source, we carried out a globally averaged one-dimensional calculation in which the N_2O photochemistry and transport were treated in detail. The model assumes that N_2O molecules are lost by photodissociation and by reaction with $O(^1D)$ and formed by process (4). The $O(^1D)$ concentration was calculated on the basis of a local chemical equilibrium between its production from O_3 photolysis and loss by quenching collisions with N_2 and O_2. The empirical method of Shimazaki *et al.*[12] was used to determine the absorption of solar UV in the Schumann–Runge bands. We assumed an N_2O mixing ratio of 3×10^{-7} at the lower boundary and a zero flux at the upper boundary at 100 km. Out of the two profiles of eddy diffusion coefficients recommended by Danielson[13], we used the k_1 profile because it gives a better performance in describing the available observations of N_2O. Calculations were done for a solar zenith angle of 30° using the US Standard Atmosphere 1976. Two cases were considered: (*a*) with and (*b*) without the process (4). Results are shown in Fig. 3, together with the observed values of N_2O mixing ratios from Farmer *et al.*[14], Ehhalt *et al.*[15] and Schmeltekopf *et al.*[16]. Because observations of N_2O above 30 km are of low precision they have been omitted. The fact that we reproduce the observed values of N_2O mixing ratios verifies the soundness of our basic model and computational details.

An important point from our analysis is that the new source of N_2O is capable of sustaining significantly increased amounts of N_2O in the upper stratosphere and mesosphere. Compared with the case (*b*), which ignores the process (4), N_2O mixing ratios are increased by 10%, 39%, 102% and 192%, respectively, at 40, 50, 60 and 70 km in the case (*a*). Nitrous oxide is a source of nitric oxide (NO) through the reaction:

$$N_2O + O(^1D) \rightarrow 2NO \qquad (9)$$

Accordingly, increased amounts of N_2O in the upper stratosphere (30–50 km) will lead to increased NO production in this region. In the present calculation, the height-integrated production rate of NO in the 30–50 km region increased by 10%. The observed amounts of NO are less than the predictions of contemporary theories[17] which neglect process (4). Thus, the new source of N_2O (process (4)) magnifies the current discrepancy between the observed and predicted amounts of NO in the upper stratosphere. The key point, however, is that the introduction of this source should lead to a more realistic assessment of this discrepancy and to its satisfactory solution.

Mesospheric NO has been attributed to either the downward transport of NO from the ionospheric E region or to the upward transport from the stratosphere, because there is no *in situ* source of nitric oxide in the mesosphere other than the indirect and weak production by reaction (9). Thus, depending on the transport parameters used, theoretical models had difficulties in accounting for the observed amounts of mesospheric NO (ref. 18), such as those from Tisone's[19] experiments. It is, therefore, significant that the introduction of our new source leads to 100–200% increases in the mesospheric production of NO by reaction (9). Possibly, this increase could alleviate the difficulties of accounting for the observed mesospheric NO.

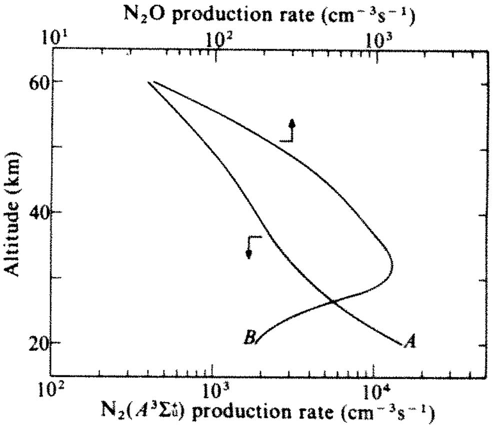

Fig. 4 The $N_2(A^3\Sigma_u^+)$ and N_2O production rate due to solar optical pumping the $A^3\Sigma_u^+$ state 3,500 Myr ago in the Earth's prebiological atmosphere.

Finally, note that the magnitude of the N_2O source due to process (4) is modest in our present-day atmosphere because O_2 and O_3 absorption below 35 km severely attenuates much of the solar flux that would otherwise optically pump the $N_2(A^3\Sigma_u^+)$ state. However, in the Earth's prebiological era ($\sim$3,500 Myr ago), the O_2 and O_3 content of the atmosphere was many orders of magnitude smaller so that copious N_2O production occurred. Figure 4 shows the results of a simplified calculation illustrating the potential magnitude of this source using the prebiological model atmosphere 1 of Kastings and Walker[20].

During this period, the $O(^1D)$ concentration was also very small so that reaction (9) was not a significant N_2O sink; photodissociation and transport were the chief loss mechanisms. In the present-day stratosphere, only solar photons with wavelengths >1,750 Å figure prominently in N_2O photodissociation and result in an effective J_∞ value $\sim 10^{-6}$ s^{-1}. However, with the loss of the O_2–O_3 screening effects in the prebiological atmosphere, more energetic solar photons could reach the upper stratosphere where they would, at first sight, accelerate the N_2O photodissociation. But the absorption by N_2O of most photons with wavelengths $< \lambda$ 1,560 Å leaves the N_2 photofragment in the $B^3\Sigma_g$ or $A^3\Sigma_u^+$ state which subsequently form N_2O through reaction (4), so the effective N_2O photodissociation loss rate at low altitudes is not enhanced much over present-day values. This suggests that the N_2O concentration at 30 km in the Earth's prebiological atmosphere was of the order of 10^9 cm^{-3} during a period well before bacterial action provided a surface source. Ultimately, as the oxygen content of the atmosphere increased, reaction (9) gradually began to provide an atmospheric source of fixed nitrogen (NO) which may have played an important part in the subsequent development of life.

Received 11 June; accepted 30 October 1981.

1. DeMore, W. B. & Raper, O. F. *J. chem. Phys.* **37,** 2048 (1962).
2. Simonaitis, R., Lissi, E. & Heicklen, J. *J. geophys. Res.* **77,** 4248 (1972).
3. Zipf, E. C. *Nature* **287,** 523 (1980).
4. Cartwright, D. C., Chutjian, A. & Trajmar, S. *Phys. Rev.* **A16,** 1041 (1977).
5. Prasad, S. S. & Zipf, E. C. *Nature* **291,** 564 (1981).
6. Zipf, E. C. & Prasad, S. S. *Nature* **287,** 525 (1980).
7. Shemansky, D. E. *J. chem. Phys.* **51,** 689 (1969).
8. Chamberlain, J. W. *Physics of Aurora and Airglow* (Academic, New York, 1961).
9. Nicolet, M. *Rev. Geophys. Space Phys.* **13,** 593 (1975); *Pure Appl. Geophys.* **118,** 3 (1980).
10. Hudson, R. E. *Can. J. Chem.* **52,** 1465 (1974).
11. Lewis, B. R. *et al. J. Quant. Spectrosc. Radiat. Trans.* **20,** 191 (1978); **22,** 312 (1979).
12. Shimazaki, T., Ogawa, T. & Farrel, B. C. *NASA Tech. Not. TND-8399* (National Aeronautics and Space Administration, Washington DC, 1977).
13. Danielson, E. F. in *Stratospheric Ozone Depletion by Halocarbons: Chemistry and Transport* (US National Academy of Sciences, Washington DC, 1979).
14. Farmer, C. B., Raper, O. F., Robbins, B. D., Toth, R. A. & Miller, C. J. *J. geophys. Res.* **85,** 1621 (1980).
15. Ehhalt, D. H., Heidt, L. E., Lueb, R. H. & Pollock, W. *Pageophysics,* **113,** 389 (1975).
16. Schmeltekopf, A. L. *et al. J. atmos. Sci.* **34,** 729 (1977).
17. Hudson, R. E. & Reeds, E. I. (eds) *The Stratosphere: Present and Future,* 55 (NASA Ref. Publ. 149, Washington DC, 1979).
18. Mitra, A. P. *Ionospheric Effects of Solar Flares* (Reidel, Boston, 1974).
19. Tisone, G. C. *J. geophys. Res.* **78,** 746 (1973).
20. Kasting, J. F. & Walker, J. C. G. *J. geophys. Res.* **86,** 1147 (1981).

Auroral effects on power transmission line systems

S.-I. Akasofu

Geophysical Institute, University of Alaska, Fairbanks,
903 Koyukuk Avenue North, Fairbanks, Alaska 99701, USA

J. D. Aspnes

Electrical Engineering Department, University of Alaska, Fairbanks,
Alaska 99701, USA

As human activity advances northwards, its supporting systems, such as power transmission lines and oil/gas pipelines, extend across the auroral zone. As the auroral electrojet, a concentrated ionospheric current along the auroral zone, induces a potential of up to 1 V km^{-1} on the Earth's surface, a significant amount of electric current can be induced in long conductors which are grounded at points separated by a long distance[1-6]. We show here that auroral activity can induce surges in the protective relay system of a power transmission line.

We have previously reported that major fluctuations in a power transmission line (138 kV, 100 A) near Fairbanks are mostly induced by auroral activity. The Healy–Fairbanks power transmission line, which runs approximately in the north–south direction (~166 km), is terminated at an autotransformer at the Gold Hill substation which is located just outside the city of Fairbanks. Aurora-induced current fluctuations in the power line were monitored in terms of the autotransformer 'neutral current' by measuring the voltage developed across a 62.5 μΩ resistor inserted between the autotransformer neutral and substation ground.

Figure 1 shows both the 'Earth current' and the neutral current records which were obtained on 3 October 1981. The former was obtained by recording the voltage developed between two electrodes (separated by 100 m) which are located about 5 km from the autotransformer site. Most of the fluctuations in the Earth current were caused by the simultaneous auroral activity[1-7]. Comparing both records, the earth-current fluctuations are well reproduced in the neutral-current fluctuations, indicating that the latter were mostly induced by auroral activity.

To examine possible damaging effects of the aurora-induced currents on the powerline system, however, we need to determine whether such low-frequency (or quasi-d.c.) fluctuations affect the protective relay system and the autotransformer in the circuit. The autotransformer has an electrically isolated winding which provides a current to drive protective relays. This current is zero in a perfectly balanced three-phase power system and is non-zero if an imbalance (such as a short-circuit or other unbalanced load) occurs. An additional cause of increased relay current is an enhancement of certain current harmonics (third, ninth, fifteenth and so on). Half-cycle saturation of transformers caused by d.c. winding current produces such harmonics.

Figure 1 shows the simultaneous record of the current in the protective relay system. The impulsive changes superimposed on continuous and random fluctuations of the neutral current are indicated by arrows. Those impulses were associated with significant low-frequency (or quasi-d.c.) excursions of the neutral current. Figure 2 shows another example of the simultaneous recordings of the current in the protective relay circuit and the neutral current during a medium intensity geomagnetic storm of 19 December 1980. A series of surges can easily be identified in the relay current. We believe that these results are the first confirmation that auroral activity induces surges in the protective relay system of a power transmission line.

D.c. transformer excitation causes a larger than normal amount of harmonic components to be generated in a trans-

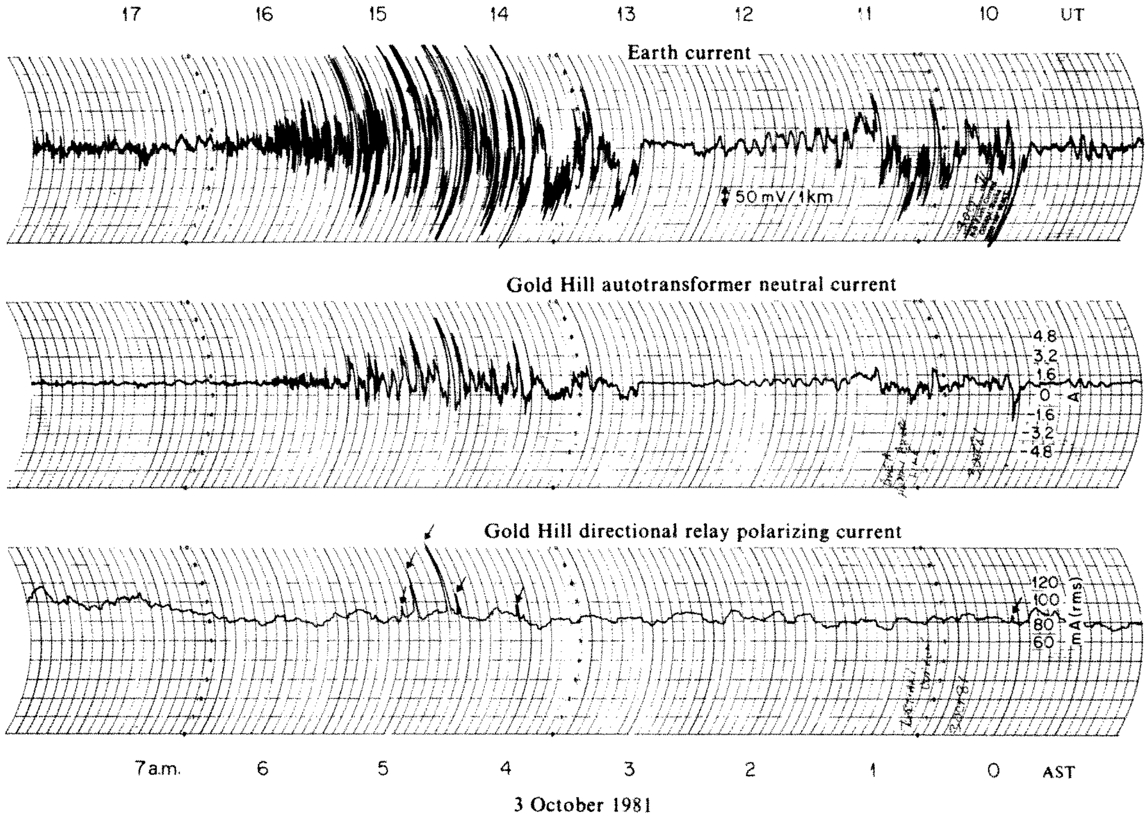

Fig. 1 Simultaneous recordings of Earth current (Earth surface potential), neutral current and protective relay system current (directional relay polarizing current) in the autotransformer located at the Gold Hill substation near Fairbanks on 3 October 1981. Excursions of ±4 A neutral currents represents ±8 A d.c. flowing in the transmission line. AST = Alaska standard time.

0028-0836/82/020136—02$01.00

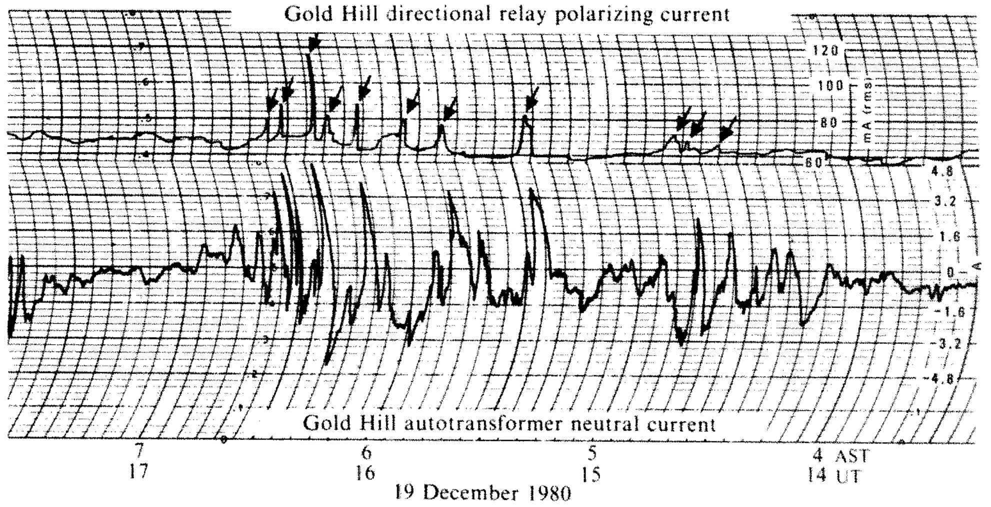

Fig. 2 Simultaneous recordings of aurora-induced surges in a protective relay system (directional relay polarizing current) and the neutral current in the Gold Hill autotransformer on 19 December 1980.

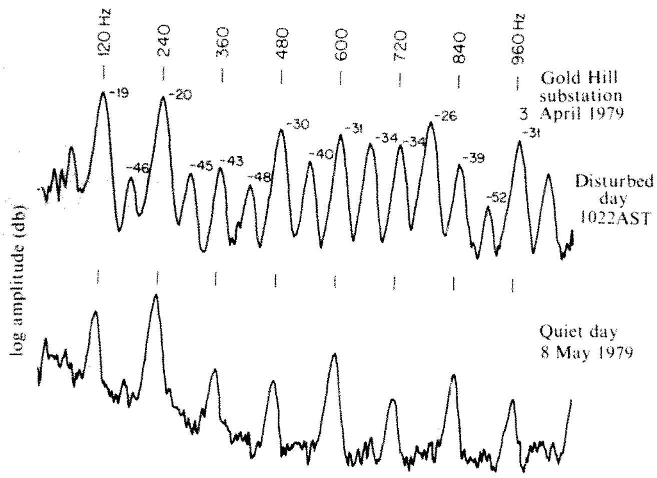

Fig. 3 Transformer sound spectra during a disturbed period (3 April 1979) and a quiet period (8 May 1979).

former[8-10]. Sound spectra were experimentally determined for the autotransformer for periods of both weak and substantial auroral activity at different occasions. This was achieved by a spectrum analyser processing tape-recorded sound measurements. Transformer sound occurs in 60 Hz power systems because ferromagnetic materials change size slightly when magnetized. This change in size (magnetostriction) normally occurs during each half cycle of the 60 Hz fundamental frequency or 120 times s^{-1}. As the magnetostriction process is nonlinear, all harmonics of 120 Hz are also present, contributing to transformer sound output. If d.c. excitation is present, however, the measured transformer sound spectrum contains the 60 Hz fundamental and all harmonics of 60 Hz. This occurs because magnetostriction is no longer symmetrical over successive half cycles of 60 Hz excitation. Figure 3 shows the sound spectrum for a disturbed period and a quiet period, respectively. Note that a large increase of all harmonics of 60 Hz would increase eddy currents in the transformer core and cause possibly destructive transformer overheating.

This work was supported by the Department of Energy, contract DE-AT06-76ER70005.

Received 15 October; accepted 4 November 1981.

1. Angot, A. *The Auroral Borealis* (Appleton, New York, 1897).
2. Chapman, S. & Bartels, J. *Geomagnetism* (Oxford University Press, 1940).
3. Goddard, W. R., & Boerner, W.-M. *Rep. on Study of Solar Induced Currents for the Proposed 500 kV Transmission Line* (University of Manitoba, Winnipeg, 1978).
4. Wait, J. R. *Electromagnetic Waves in Stratified Media* (Pergamon, Oxford, 1962).
5. Albertson, V. D. & Van Baelen, *IEEE Trans. Power Apparatus Systems* **PAS-89**, 578 (1970).
6. Hessler, V. P. & Wescott, E. M. *Sci. Rep.* No. 2 (Geophysical Institute, University of Alaska, 1959).
7. Akasofu, S.-I. & Merritt, R. P. *Nature* **279,** 308 (1979).
8. Aspnes, J. D., Merritt, R. D. & Akasofu, S.-I. *IEEE Trans. Power Apparatus and Systems* **PAS-100,** 1845 (1981).
9. Boerner, W.-M. *et al. Proc. 5th int. Wroclaw Symp. on Electromagnetic Compatibility* (1980).
10. Pirjola, R. *Proc. 5th int. Wroclaw Symp. on Electromagnetic Compatibility* (1980).

Acid snow in the Canadian high Arctic

R. M. Koerner & D. Fisher

Polar Continental Shelf Project, Energy, Mines and Resources
Canada, 880 Wellington Street, Ottawa, Ontario,
Canada K1A 0E4

Increasing levels of acid sulphates in precipitation have recently been discovered in locations as far north as Barrow, Alaska and Bear Island (74° N and 19° E) in the Norwegian Sea[1-4]. The high sulphur concentrations are attributed to mid-latitude Eurasian sources[1]. We present here acid concentrations (each representing several years of snow accumulation) in ice from part of a 337-m surface-to-bedrock core on northern Ellesmere Island (81° N, 73° W) representing the past 5,000 yr and compare these with significantly higher acid concentrations in snow deposited over the past 25 yr at the same location showing seasonal variations in the concentrations which together constitute a significant trend of increasing acid levels over the past 25 yr.

Thermal core samples (Fig. 1) were taken in 1977 with a thermal drill at 1,600 m altitude within 1 km of the top of the Agassiz Ice Cap on northern Ellesmere Island, N.W.T., Canada (81° N 73° W). At this location melting occurs in most summers but affects only 3% of the surface annual layer. Samples from these cores were prepared and analysed in our Ottawa laboratory. The ice was first cleaned thoroughly with warm distilled, deionized and filtered water (10 MΩ). The sample was then allowed to melt partially; this melt was discarded. The final melt was collected for analysis and represented <50% of the original sample. The surface samples (Fig. 2) were collected in 1980 with a stainless-steel hand auger and split into two monthly increments. They were then stored in Whirlpak plastic bags that were free from contaminants. The samples were handled with plastic gloves cleaned by 'vigorous rinsing' in clean snow at the site. As these samples were considered uncontaminated for our purposes no cleaning procedures were used. Both core and surface samples were allowed to stand covered to reach room temperature before pH and conductivity (σ) measurements were taken on site. In addition to these samples 400 snow/firn samples were collected from a 10-m pit in 1977 at the same

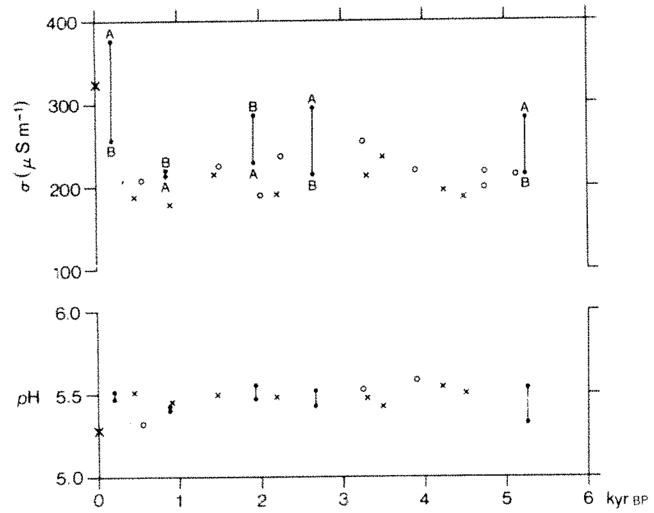

Fig. 1 Electrolytic conductivity (σ, measured with a Radiometer CDM 3m) and acidity (*p*H, measured on an Orion Research Ionanalyser) 0–5,000 yr BP. Agassiz Ice Cap, Canada. A and B represent periods before and after major volcanic eruptions that laid down acid layers on the ice cap. ○, × mean values for samples consisting of five or more years of accumulation. The time scale is based on an analysis of seasonal variations of particulates (measured in a Coulter Counter) and K (measured by graphite furnace AA) at 15 levels in the core.

location. We also measured for Na, Mg, K and Mg using flameless atomic absorption and particulate concentrations.

The reproducibility of the trend of increasing σ with decreasing depth (Table 1) between two sets of samples collected quite differently is strong evidence of the absence of a sampling artefact in the results. However, the most serious 'contaminant' in our samples is CO_2 which appears as H_2CO_3 in our melted samples and increases the acidity. Water at 0 °C (sample just melted) contains about twice as much CO_2 as at the 20 °C at which we measured our samples. We did not ensure complete equilibration with ambient air and therefore some noise from a variable H_2CO_3 background may have affected our results. However, our samples were measured in random order and the trend we discuss later cannot have arisen in this way.

Snow/firn density increases with depth. Therefore, in any one sample the sample-to-air ratio also increases with depth. This lessens the equilibration with air of an enclosed sample with firn depth which, because of lower CO_2 loss from the sample with depth, should increase the acidity in the same direction. Our trend is precisely the opposite and must therefore be reduced by any CO_2 effect.

Our seasonal *p*H cycles agree well in shape and amplitude with the *p*H cycle in snow calculated from sulphate concentration in air over Mould Bay[5] (76° N 120° W). The H^+ noise background due to H_2CO_3 is at most only about a sixth of the magnitude of our seasonal H^+ amplitude and a third of that of the total H^+ change over the past 27 yr and, as we have argued, does not contribute to it. While slightly <70% of the Holocene acid (Fig. 1, Table 1) is calculated to be due to CO_2-associated H^+ ion, the changes above this level, whether they are seasonal cycles or decadal trends, are not due to any variable CO_2 effect.

The Holocene results are shown in Fig. 1 (some results from our investigation of volcanic layers in the ice are included for comparison). The main feature of Fig. 1 is that the present-day (AD 1954–80) acidity ($pH = 5.23$) and σ (311 μS m^{-1}) show the snow is significantly more acid and conductive than snows from the preceding 5,000 yr. Only annual values at the peak of volcanic acid injections into the atmosphere (not shown in Fig. 1) exceed the present-day 25-yr *p*H value. We measured the core samples at our Ottawa laboratory which is some 1,500 m lower in altitude than the field camp where the surface samples were measured. Because of different levels of CO_2 in the air, this makes our Holocene value more acid than the true value (more H_2CO_3 in the sample melt). The 5,000 yr *p*H values for the Agassiz and Devon Island ice caps[6] and Crête, Greenland[7] show a Holocene background value equivalent to ~1.0 μmol non-CO_2 associated H^+ ion kg^{-1}.

The seasonal variation in *p*H and conductivity over the 26-yr period which represents the 'present-day' mean is shown in Fig. 2. The acid and/or conductive peaks are at the surface in May and may be termed a spring peak, although concentrations show an irregular, but overall gradual, increase over the winter. Concentrations of Na, Ca, K, Mg and insoluble particulates are also at maximum in the spring. The ions tend to peak about a month before the insoluble particulates. We do not consider that spring peaking of various elemental constitutents in the snow results from stratospheric injections due to tropopause folding mainly because the particulates increase by a factor of 10 whereas the acid concentration increases by a factor of three. Yet stratospheric chemistry shows a non-volcanic SO_4/Al ratio of 10:1 (ref. 8) (our pre-1963 values cover a volcanically quiet period). As most of the SO_4 ions are present as H_2SO_4 (ref. 8), our spring peak should show a 100-fold and not a 3-fold (4-fold in ref. 5) enhancement of the non-CO_2 associated H^+ ion if we have a 10-fold enhancement of Al (particulates). Over the past 26 yr (where our time scale is based on a knowledge of the surface accumulation rate and the seasonal *p*H and σ variations) the *p*H has shown an overall decrease (Fig. 3 and Table 1) of 0.007 yr^{-1} (or 0.007 μmol H^+ kg^{-1} yr^{-1}). The *p*H and σ trends (3.69 μS m^{-1} yr^{-1}) are compatible with the increase in conductivity being due almost entirely to increasing levels of acid in the snow. If we project this trend backwards we find the acid began to increase from general Holocene values some time in the early 1930s. However, the overall trend may well not be a linear one.

We examine four possible explanations for this trend. First, increasing turbulence in the atmosphere over the past 26 yr might give rise to a longer transport of the H^+ ion without there being any increasing production rate. Second, there may have been decreasing levels of neutralizing components in the atmosphere. Third, there could have been a change in the precipitation or nucleating processes at the cloud level. Finally, we may be seeing a genuine increase in the levels of acid in the atmosphere, generally, or just along a preferred trajectory from a particular source.

Table 1 Particulate, acid, sodium concentrations and electrolytic conductivity of near surface snow and deep ice on Agassiz Ice Cap

Component	Concentration units	Holocene mean	Recent mean pit, 1950–77 (a) core, 1954–80 (b)	Recent trend per yr pit, 1950–77 (a) core, 1954–80 (b)
Particulates $d > 1.0\mu m$	No. × 10^3 l^{-1}	18.2	18.3 (a)	0.6 (a)
Na	p.p.b.	32*	25 (a)	0.47 (a)
Electrical conductivity	μS m^{-1}	201	314 (a) 311 (b)	3.3 (a) 3.7 (b)
Acid	*p*H	5.48	5.28 (a) 5.23 (b)	— −0.007 (b)

* All associated with volcanic episodes.

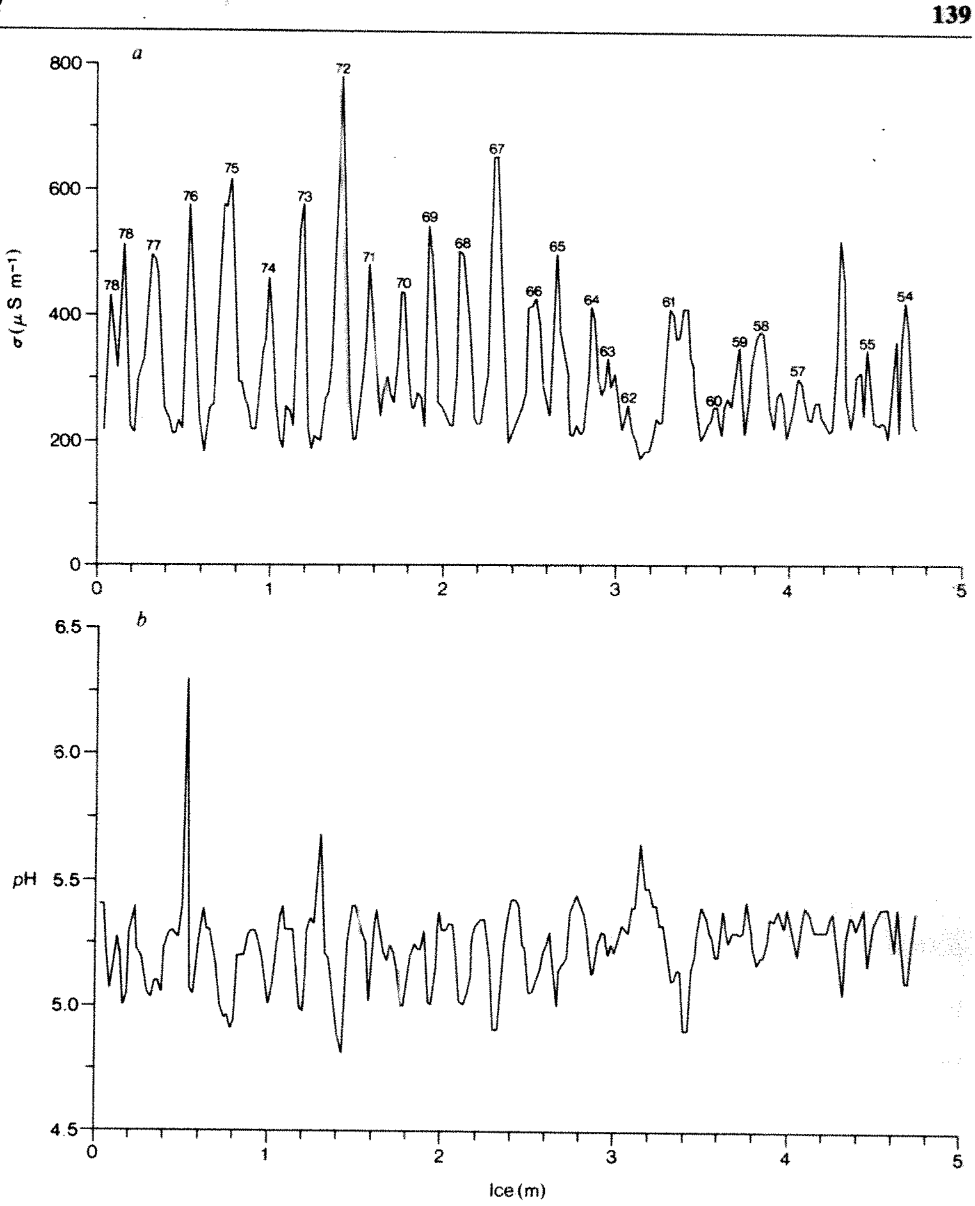

Fig. 2 Seasonal variations of *a*, electrolytic conductivity (σ), and *b*, acidity (*p*H) as measured on a 10 m core from Agassiz Ice Cap, Canada. The numbers refer to the spring in each year according to 72 = 1972.

From our pit results in 1977 we find significant trends of increasing concentrations of sodium and particulate matter in the snow (Table 1). At first sight this could be seen as evidence of increasing turbulence in the high Arctic over the same period. However, present-day particle concentrations (Table 1) are not significantly different to those over the past 5,000 yr. The same is true of our Devon Island core[6] and also of the Crête core in Greenland[7]. This indicates that there have been no major changes in turbulence at the ice cap site or in the high Arctic generally over the same period. The lack of change in particulate concentrations would also suggest that there has been little general change in the neutralizing capacity of aerosols over the high Arctic in the past 5,000 yr.

Junge[9] cautioned against considering that changes in concentrations of elemental components in ice cores represent or are the effect of similar changes in aerosol composition and concentration. He believes changes in the moisture content of precipitating clouds (c) and/or the mass fraction of aerosols used for condensation (ε_m) would cause changes in the concentration of the same aerosols when incorporated in the snow. However, we do not find a significant correlation between the changing acid concentrations and $\delta^{18}O$ in the snow. The $\delta^{18}O$ value is largely determined by the temperature of condensation at the cloud level[10] and temperature at this level is probably the main determinant of c and possibly ε_m.

We are, therefore, left with the most likely explanation that increasing acid levels in the snow are due to similarly increasing acid levels in the atmosphere over the ice cap and that this mutual increase is somehow allied to augmented acid production at its source. The source(s) could be natural (volcanic) or anthropogenic (industrial pollutants). There have not been steadily-increasing levels of volcanic sulphur injections into the atmosphere over the past two decades[11,12] which does not favour a volcanic acid origin. Stratospheric SO_4 concentrations measured in quiet, that is non-volcanic, periods have been increasing by 9% yr^{-1} over the past 20 yr (refs 11, 12). The increase has been assigned an anthropogenic origin[11,12].

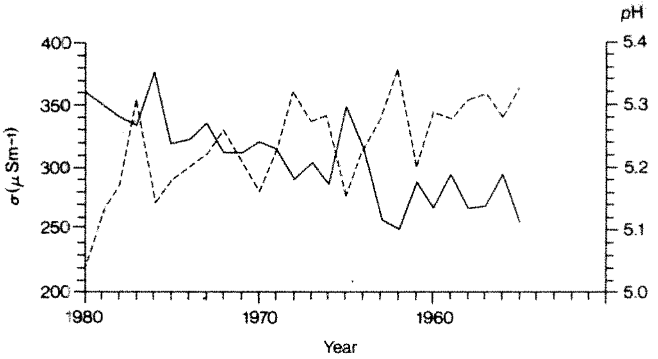

Fig. 3 Annual values (measured from spring to spring) of acidity (*p*H, dashed line) and electrolytic conductivity (σ, solid line) from a 10-m core on Agassiz Ice Cap, Canada.

However, because we do not detect the eruption of the volcano Gonung Agung in 1963 in our work (Fig. 2), we must be measuring a tropospheric acid input to the northern Ellesmere ice cap rather than a stratospheric one (which agrees with our earlier comments on the spring maximum of dust, acid and other ions). In the same tropospheric context high levels of industrial sulphates have already been shown for Barrow, Alaska[1,2,4] Bear Island[3] in the Norwegian Sea and Mould Bay in Arctic Canada[5]. Increases in sulphates have also been declared for Greenland over the past 20 or 30 yr (refs13, 14) and for post-1970 snows compared with pre-1900 snow[15]. However, in recent work there is no evidence for a trend of increasing acid levels in the snow at Crête, Greenland[7]. Similarly, detailed electrolytic conductivity measurements made at the top of the Devon Island ice cap (1,800 m a.s.l.) and spanning more than 30 yr show no conductivity trend between 1942 and 1972. The lack of increasing conductivity in recent snows on the Devon Island Ice Cap, although the present-day value there is significantly higher than the Holocene one, may be due to the fact that the Devon Island Ice Cap has a very strong input of marine aerosols[6] which presents a strong noise background that is swamping the acid trend. However, we cannot ignore the possibility that the proposed acid trajectory across the Arctic Ocean from Eurasian sources[1,2,4] excludes those high Arctic areas distant from the Arctic Ocean thereby favouring northern Ellesmere rather than Devon Island or Crête, Greenland. We should mention that preliminary results from a hand-cored profile at 82° N 77° W also on northern Ellesmere but closer to the Arctic Ocean than the Agassiz Ice Cap show an identical trend to the latter's of increasing acidity over the past 28 yr.

The full implications of increasing acid precipitation in the High Arctic are beyond the scope of this paper. However, the most acid snow is at the snow surface when melt begins in May or June in the high Arctic. Unless this melt refreezes at the base of the snowpack, the first runoff in spring will be the most acid. Acid levels in high Arctic snow, and their effects, should therefore be monitored on a routine basis as in certain areas, for example where lake fish form a source of Inuit income, there could be social implications.

Received 4 May; accepted 28 October 1981.

1. Rahn, K. A. & McCaffrey, R. J. *Nature* **280,** 479–480 (1979).
2. Rahn, K. A. & McCaffrey, R. J. *Ann. N.Y. Acad. Sci.* 486–503 (1980).
3. Rahn, K. A., Joranger, E., Semb, A. & Conway, T. J. *Nature* **287,** 824–826 (1980).
4. Kerr, R. A. *Science* **205,** 290–292 (1979).
5. Barrie, L. A., Hoff, R. M. & Daggupaty, S. M. *Atmos. Envir.* (in the press).
6. Fisher, D. A. & Koerner, R. M. *Quaternary Paleoclimate* (ed. Mahaney, W. C.) 249–272 (Geol. Abstracts, Norwich, 1981).
7. Hammer, C. U. *Nature* **270,** 482–486 (1977).
8. Junge, C. E. *Air Chemistry and Radioactivity*, 1–382 (Academic, New York, 1963).
9. Junge, C. E. *Proc. IUGG Symp. Isotopes and Impurities in Snow and Ice* (IAHS Publ. 118, 63–76, 1977).
10. Dansgaard, W. *Tellus* **16,** 436–468 (1964).
11. Hofmann, D. J. & Rosen, J. M. *Science* **208,** 1368–1370 (1980).
12. Hofmann, D. J. & Rosen, J. M. *On the Background Stratospheric Aerosol Layer* (Rep. AP-56b, University of Wyoming, 1980).
13. Weiss, H. V., Koide, M. & Goldberg, E. D. *Science* **172,** 261–263 (1971).
14. Weiss, H. V., Bertine, K., Koide, M. & Goldberg, E. D. *Geochim. cosmochim. Acta.* **39,** 1–10 (1975).
15. Herron, M. M., Langway, C. C., Weiss, H. V. & Cragin, J. H. *Geochim. cosmochim. Acta* **41,** 915–920 (1977).
16. Hummer, C. U., Clausen, H. B. & Dansgaard, W. *Nature* **288,** 230–235 (1980).

Molluscan biostratigraphy of the Koobi Fora hominid-bearing deposits

Peter G. Williamson

Museum of Comparative Zoology, Harvard University, Cambridge, Massachusetts 02138, USA

Since the discovery[1] of late Cenozoic hominid-bearing deposits in the Koobi Fora area, north Kenya, a variety of studies[2–9] have been undertaken to provide a chronostratigraphical and palaeoenvironmental context for the important palaeoanthropological and early archaeological discoveries[1,10]. Unfortunately, although the exposures are areally extensive (>1,000 km^2), they are broken up into subareas (Fig. 2); these local sections are often difficult to correlate with one another due to intervening bush cover and faulting. Here I summarize a molluscan biostratigraphical analysis which demonstrates serious stratigraphical miscorrelations between certain local sections, including some previously indicated by vertebrate evidence. These miscorrelations require substantial revisions to current stratigraphical interpretation of the Koobi Fora deposits. In particular, both the Suregei and Tulu Bor tuff horizons actually represent different levels. Although the Tulu Bor is considered to overlie the Suregei, some exposures currently attributed to the Tulu Bor are actually older than some units previously mapped as the Suregei. Fortunately, the stratigraphical miscorrelations reported here do not significantly affect the relative placement of the mollusc faunas reported in a previous evolutionary analysis[15]; superpositional relationships in the areas from which these faunas were collected (mainly collecting areas 102, 103, 110, 123, 202 and 203) are unaffected by the miscorrelations reported here.

Lithostratigraphical correlations in the Koobi Fora area have been based on certain tuffaceous horizons which regularly punctuate the late Cenozoic sequence. These tuffs are generally secondarily waterlain[5,6]; their bases have been considered laterally extensive, mappable and essentially isochronous[11,12]. The supposed recognition of these tuffs in geographically-separated local sections has formed the basis of a regional chronostratigraphical scheme[5–7] (Fig. 1*a*); this scheme has provided a framework for palaeontological discoveries and palaeoenvironmental interpretations. The validity of this framework, and of all interpretations based on it, relies entirely on the correct recognition and correlation of the various tuffs in widely separated local sections. But these tuffs are laterally variable in field aspect, and proposed correlations between local sections are therefore often questionable. In addition, vertebrate studies have suggested miscorrelations between certain tuffs[13,14].

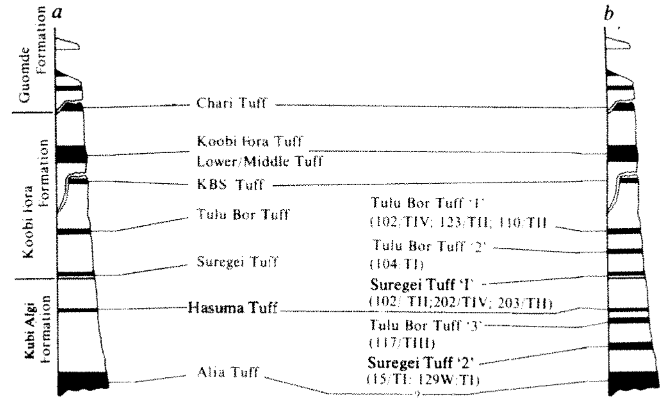
a
b
Guomde Formation
Koobi fora Formation
Kubi Algi Formation
Chari Tuff
Koobi fora Tuff
Lower/Middle Tuff
KBS Tuff
Tulu Bor Tuff
Suregei Tuff
Hasuma Tuff
Alia Tuff
Tulu Bor Tuff '1' (102/TIV; 123/TII; 110/TII
Tulu Bor Tuff '2' (104/TI)
Suregei Tuff 'I' (102/ TII;202/TIV; 203/TII)
Tulu Bor Tuff '3' (117/TIII)
Suregei Tuff '2' (15/TI; 129W/TI)
?

Fig. 1 Stratigraphical relationships of late Cenozoic deposits of the Koobi Fora region. A, Currently accepted stratigraphical framework (after ref. 7). B, Generalized revisions suggested by this report. Note that several tuffs previously allocated to the Suregei and Tulu Bor Tuffs actually represent horizons of widely differing age. These various horizons are designated by the informal terms 'Tulu Bor '1'', 'Tulu Bor '2'', and so on. This terminology, adopted here solely to indicate which horizons were previously considered lateral correlates, has no formal status whatsoever. The different Tuff horizons previously allocated to the Suregei and Tulu Bor Tuff levels are also distinguished by the 'area/succession' scheme suggested by Harris and White[13]; a given tuff exposure is designated by the collecting area in which it occurs, and by its stratigraphical position with respect to other tuffs within the local section of that collecting area. Thus, the designation 102/TI indicates the earliest (lowest) tuff in the local stratigraphical sequence in collecting area 102. Total thickness of the Kubi Algi, Koobi Fora and Guomde Formations is considered to be ~350 m (ref. 7).

0028–0836/82/020140—03$01.00

The profound evolutionary changes recorded in the mollusc faunas of the Koobi Fora area[15] permit the recognition of several events which are time-significant for the basin. Putative correlations between exposures of marker tuffs in various areas were therefore tested using these faunas. Molluscan biostratigraphical type sections were designated in the same general areas as the lithostratigraphical type sections for the three late Cenozoic formations of the area, and on the basis of the evolutionary events recorded in 40 mollusc faunas from these type sections, 10 concurrent range zones were defined (Fig. 3); 112 faunas collected in other areas, away from the type sections, were then allocated to the appropriate biozone. When these latter faunas occur close to local exposures of the various marker tuffs, the position of these tuff exposures relative to the molluscan type section can be more or less accurately determined.

Although the biostratigraphical type sections for each of the three late Cenozoic formations in the area are continuous local sections, these sections are, like the lithostratigraphical type sections, geographically separated (Fig. 2). However, the superpositional relationships of these sections are unambiguous[16]. Together, these three sections exhibit 9 of the 10 proposed molluscan biozones (zones 2–10). Zone 1 is not certainly developed in the lithostratigraphic type section of the area; the type section for this zone is the Karsa Waterhole sequence[17], which appears either immediately to predate the Kubi Algi Formation, or to correspond to some level in the lower half of this unit (I.C. Findlater, personal communication) (no mollusc faunas are known from the lower half of the type section of the Kubi Algi).

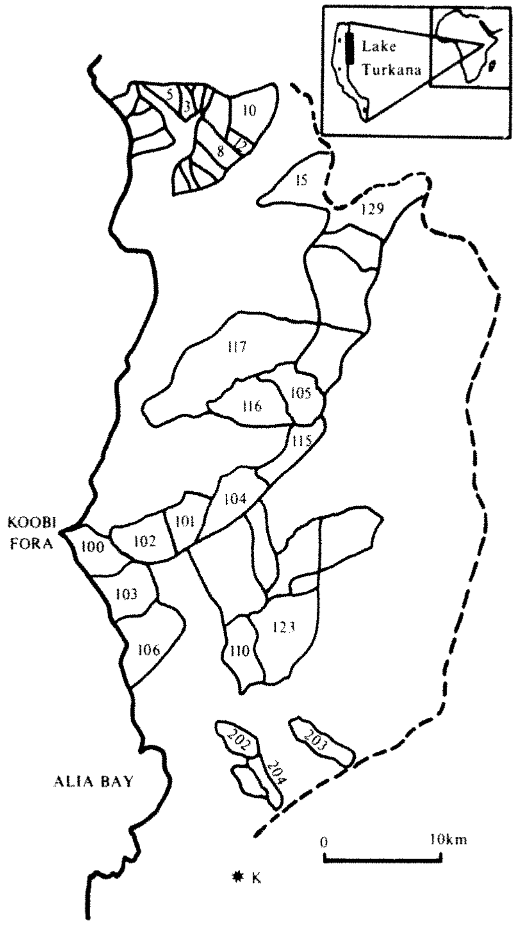

Fig. 2 Principal palaeontological collecting areas designated in the Koobi Fora area, north Kenya. Molluscan biostratigraphical type section for the Kubi Algi Formation is in area 203, that for the Koobi Fora Formation in area 102, and that for the Guomde Formation in area 3. These type sections encompass molluscan biozones 2–10; the type section for zone 1 is the Karsa Waterhole sequence[17] ('K'), to the south of the basin margin (indicated by heavy broken line).

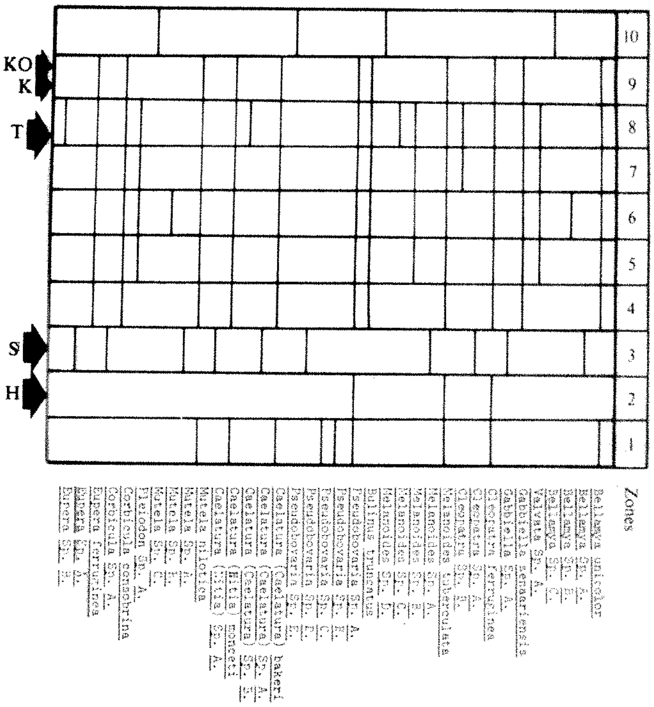

Fig. 3 Range zones of freshwater molluscs from the Plio–Pleistocene deposits of the Koobi Fora area. Zone 1 faunas are characterized by the presence of two distinctive forms of *Pseudobovaria* and by the absence of *Corbicula*. Zone 2 faunas consist of widely distributed and generally still extent taxa, but are taxonomically restricted and dwarfed, reflecting the period of high alkalinity consequent on the marked regressive phase at and above the Hasuma Tuff level[7]. Zone 3 faunas document contemporaneous speciation events in all lineages in the basin during a continuation of this regressive phase, and presumed geographical isolation of faunas[15]. Zone 4 faunas document the elimination of the zone 3 endemics as typical ancestral stocks return to the basin, coincident with a major transgressive phase. Zones 5–8 document a progressive intrabasinal radiation of several of these stocks and the accumulation of certain 'exotic' taxa in the Lower Member of the Koobi Fora Formation. Zone 9 documents a major reduction in faunal diversity; all the endemics and exotics of zones 5–8 were extirpated by the rise in alkalinity[24] in the uppermost Lower Member consequent on a climatically induced[25] regression[6,26]. The zone 10 faunas from the Guomde Formation document a second series of contemporaneous speciation events in the various lineages present in the basin, again coincident with major regression and presumed geographical isolation. Widths of zones as drawn do not reflect their relative stratigraphical thicknesses. Heavy arrows to side of diagram reflect the placement of certain tuff horizons with respect to the molluscan biozones, in the biostratigraphical type section. H, Hasuma Tuff; S, Suregei Tuff; T, Tulu Bor Tuff; K, KBS Tuff; KO, Koobi Fora Tuff.

The evolutionary events previously documented[15] in the mollusc faunas of the Koobi Fora region actually form the basis for the differentiation of zones 2–10 inclusive. The faunas here attributed to zone 1 have not been reported previously; they are characterized by the presence of two distinctive species of *Pseudobovaria* and by the absence of the now extremely widespread and eurytopic genus *Corbicula*. One or other of these forms of *Pseudobovaria* have been previously recognized by Vandamme from either the Kanapoi deposits to the south of the Turkana Basin, or from the lower parts of the Omo Valley sequence to the north[18]. Both forms of *Pseudobovaria* apparently became extinct during the high alkalinity phase documented by the stunted zone 2 faunas; *Corbicula* appears to have been a rather recent Eurasian immigrant into Africa[19]. Zone 1 faunas are also now known from the Warata Formation[20], north-east of the Koobi Fora area.

The stratigraphical positions of various marker tuff horizons relative to the biostratigraphical type section can be determined when the mollusc faunas bracketing them are allocated to the proposed biozones. Clearly, the precision with which a tuff horizon in a given local section can be related to the biostratigraphical type section will be determined by how closely it is bracketed by zonally attributable mollusc faunas. The relative

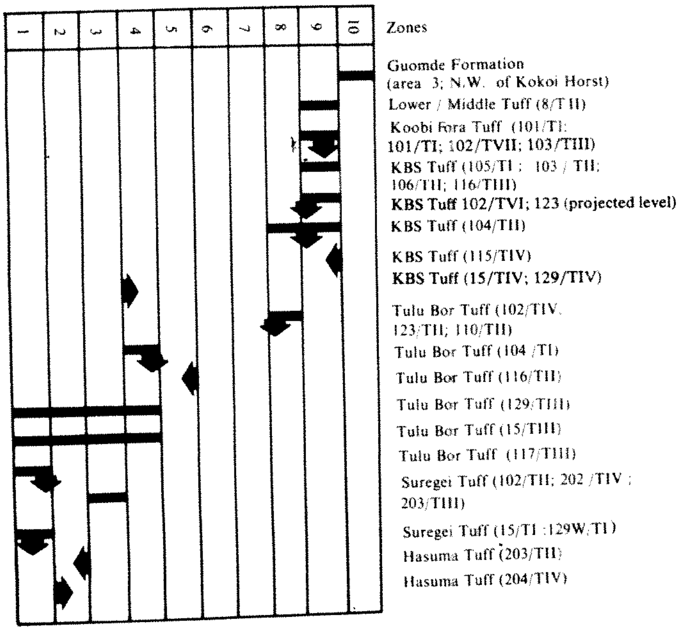

Fig. 4 Positions of various exposures of the major marker tuffs, and of Guomde age sediments, with respect to the various molluscan biozones. Possible range of positions of the tuffs within the zonal scheme indicated by heavy vertical bars. Most probably positions of the various tuffs, suggested by superpositional data and by propinquity to zone boundaries, indicated by horizontal arrows. Upward and downward facing arrows indicate the uppermost and lowermost possible positions, respectively, of poorly bracketed tuffs. Note that horizons attributed to both the Tulu Bor and Suregei levels fall into a wide range of biozones, suggesting the stratigraphical revisions indicated in Fig. 1*b*. Notations after tuff names indicate the geographical and stratigraphical positions of the various tuff horizons according to the scheme suggested by Harris and White[13]; a given tuff exposure is designated by the collecting area in which it occurs, and by its stratigraphical position with respect to other tuffs within the local section of that collecting area. Thus, the designation 102/TI indicates the earliest tuff in the local stratigraphic sequence in collecting area 102. Allocation of the horizon attributed to the Suregei Tuff in areas 15 and 129 to zone 1 assumes the apparently firm short-distance lithostratigraphical correlation between these areas to be correct (this horizon is immediately underlain by zone 1 faunas in area 15, and immediately overlain by zone 1 faunas in area 129).

positions of several important exposures of marker tuffs, determined as accurately as possible by this method, are indicated in Fig. 4. Several serious miscorrelations of tuffs have occurred. In particular, various horizons allocated to the important Suregei and Tulu Bor Tuffs fall, in both cases, into different biozones; both stratigraphical terms therefore encompass several horizons of differing age. (Studies on fossil suids from these deposits have previously suggested that certain exposures assigned to the Tulu Bor Tuff in fact pre-date the Suregei Tuff horizon of the type section of the Koobi Fora and Kubi Algi Formations[13,14]. A generalized and tentative revised stratigraphy suggested by this analysis is indicated in Fig. 1*b*. Only tuffs whose relative positions with respect to the biostratigraphical type section are unambivalent are indicated; the remaining, less securely bracketed tuffs shown in Fig. 4 may or may not be lateral correlates of those shown in Fig. 1*b*. In addition, due to the absence of faunal evidence from the Alia Tuff, its stratigraphical position with respect to the 'Tulu Bor 3' and 'Suregei 2' horizons (see Fig. 1) is unclear.

The present study has three immediate implications:

(1) The Plio–Pleistocene deposits of the Koobi Fora area were originally divided by Bowen and Vondra[21] into two main stratigraphical units, the Kubi Algi and overlying Koobi Fora Formations and the boundary between them was formally defined as the base of the Suregei Tuff[21]. The type locality of the Suregei Tuff lies close to the Suregei escarpment (from which it is named) in area 15 (refs 13, 14) (see Fig. 2). Unfortunately, as demonstrated above (Fig. 4), this tuff exposure is substantially older than its supposed correlate horizon in areas 102, 202 and 203 (Koobi Fora–Alia Bay area). But this latter horizon lies within the formal type sections of both the Kubi Algi and Koobi Fora Formations! Clearly, the terms 'Kubi Algi Formation', 'Koobi Fora Formation' and 'Suregei Tuff' must be either redefined or abandoned.

(2) In terms of the currently accepted stratigraphical scheme, large areas of exposure in areas 117, 129 and 15, previously allocated to the Koobi Fora Formation, are considerably older than the lithostratigraphical type section of this unit, and apparently correspond in age to some part of the type section of the Kubi Algi (see also refs 13, 14).

(3) Hitherto, the apparent restriction of Kubi Algi age sedimentation to the southern part of the Koobi Fora region (Alia Bay area) implied a generally regressive regime in the earlier Plio–Pleistocene[7], succeeded by a major transgression at the (apparently) areally extensive Suregei Tuff level[7]. In contrast, the Mursi, Usno and Lower Shungura Formations in the neighbouring Omo area document intermittently widespread lacustrine conditions throughout this period[22,23]. However, recognition that Kubi Algi age sedimentation occurs throughout the Koobi Fora area, and that the 'Suregei Tuff' level consists of at least two separate horizons and does not represent one extensive depositional event during a single major transgression, implies a similar picture of intermittent lacustrine conditions in the earlier Plio–Pleistocene throughout the Koobi Fora region. These observations bring the depositional histories of these two regions into greater congruence, suggesting that widespread lacustrine conditions pertained intermittently throughout the Turkana Basin in the earlier part of the Plio–Pleistocene depositional cycle.

This project was funded at the University of Bristol by the FROM Foundation, New York. I thank R. J. G. Savage, A. P. Gotto, R. E. F. Leakey, J. M. Harris, G. Ll. Isaac, D. Vandamme, and all members of the Koobi Fora Research Project for assistance.

Received 7 July; accepted 14 October 1981.

1. Leakey, R. E. F. & Leakey, M. *Koobi Fora Research Project Monographs* Vol. 1 (Clarendon, Oxford, 1979).
2. Harris, J. M. in *Koobi Fora Research Project Monographs* Vol. 1 (eds Leakey, R. E. F. & Leakey, M.) (Clarendon, Oxford, 1979).
3. Bonnefille, R. *Nature* **264**, 403–407 (1976).
4. Behrensmeyer, A. K. in *Earliest Man and Environments in the Lake Rudolf Basin* (eds Coppens, Y., Clark Howell, F., Isaac, G. Ll. & Leakey, R. E. F.) (University of Chicago Press, 1976).
5. Vondra, C. F. & Bowen, B. E. in *Geological Background to Fossil Man* (ed. Bishop, W. W.) (Scottish Academic, Edinburgh, 1978).
6. Vondra, C. F. & Bowen, B. E. in *Earliest Man and Environments in the Lake Rudolf Basin* (eds Coppens, Y., Clark Howell, F., Isaac, G. Ll. & Leakey, R. E. F.) (University of Chicago Press, 1976).
7. Findlater, I. E. in *Koobi Fora Research Project Monographs* Vol. 1 (eds Leakey, R. E. F. & Leakey, M.) (Clarendon, Oxford, 1979).
8. Brock, A. & Isaac, G. Ll. in *Earliest Man and Environments in the Lake Rudolf Basin* (eds Coppens, Y., Clark Howell, F., Isaac, G. Ll. & Leakey, R. E. F.) (University of Chicago Press, 1976).
9. Fitch, F. & Miller, J. A. in *Earliest Man and Environments in the Lake Rudolf Basin* (eds Coppens, Y., Clark Howell, F., Isaac, G. Ll. & Leakey, R. E. F.) (University of Chicago Press, 1976).
10. Isaac, G. Ll. in *Koobi Fora Research Project Monographs* Vol. 1 (eds Leakey, R. E. F. & Leakey, M.) (Clarendon, Oxford, 1979).
11. Findlater, I. C. in *Early Man and Environments in the Lake Rudolf Basin* (eds Coppens, Y., Clark Howell, F., Isaac, G. Ll. & Leakey, R. E. F.) (University of Chicago Press, 1976).
12. Findlater, I. C. in *Geological Background to Early Man* (ed. Bishop, W. W.) (Scottish Academic, Edinburgh, 1978).
13. Harris, J. M. & White, T. *Trans. Am. phil. Soc.* **69**, 1–128 (1979).
14. White, T. & Harris, J. M. *Science* **198**, 13–21 (1977).
15. Williamson, P. G. *Nature* **293**, 437–443 (1981).
16. Williamson, P. G. thesis, Univ. Bristol (1980).
17. Fuchs, V. E. *Phil. Trans. R. Soc.* **B229**, 219–274 (1939).
18. Vandamme, D. thesis, Riissuniver. Ghent (1976).
19. Gautier, A. *Annls Mus. r. Afr. cent. Sér. 8vo Geol.* **67**, 1–144 (1970).
20. Watkins, R. & Williamson, P. G. *Proc. 8th Pan African Congr. Prehistory and Quaternary Studies* (1979).
21. Bowen, B. E. & Vondra, C. F. *Nature* **242**, 391–393 (1973).
22. Heinzelin, J. de, Brown, F. H. & Howells, F. C. *Quaternaria* **13**, 247–268 (1970).
23. Heinzelin, J. de, Haeserts, P. & Howell, F. C. in *Early Man and Environments in the Lake Rudolf Basin* (eds Coppens, Y., Clark Howell, F., Isaac, G. Ll. & Leakey, R. E. F.) (University of Chicago Press, 1976).
24. Cerling, T. E. *Palaeogeogr. Palaeoclimatol. Palaeoecol.* **27**, 247–285 (1979).
25. Abell, P. I., Awramik, S. M., Osborne, R. H. & Tomellini, S. *Sedim. Geol.* (in the press).
26. Johnson, G. D. & Raynolds, R. G. H. in *Earliest Man and Environments in the Lake Rudolf Basin* (eds Coppens, Y., Clark Howell, F., Isaac, G. Ll. & Leakey, R. E. F.) (University of Chicago Press, 1976).

Aneural muscle cell cultures make synaptic basal lamina components

Laura Silberstein, Nibaldo C. Inestrosa*
& Zach W. Hall

Division of Neurobiology, Department of Physiology, University of California, San Francisco, San Francisco, California 94143, USA

The basal lamina that runs between the presynaptic and postsynaptic membranes at the neuromuscular junction has distinctive functional properties[1-3] amd differs in molecular composition from the extrasynaptic basal lamina to which it is attached[4,5]. In regenerating muscle, synaptic basal lamina can direct the accumulation both of neuronal transmitter vesicles at specific sites near the presynaptic nerve terminal membrane and of acetylcholine receptors (AChRs) in the postsynaptic muscle membrane[1-3]. Four components that are concentrated in synaptic basal lamina, but are not detectable in extrasynaptic basal lamina, have been recognized. The first is a particular form of acetylcholinesterase (AChE), the A_{12} or 16S species, which is concentrated at the synapse in rats[6,7] and mice[8]; its distinctive feature is thought to be a long collagen-like tail[9] that attaches it to the basal lamina[10]. Three other components of the synaptic basal lamina have been distinguished immunocytochemically using antisera raised against basement membrane extracts or collagen-rich preparations[4]. Although it has been previously reported that aneural muscle cell cultures may make the 16S form of AChE[11,12], the role of the nerve in the synthesis and organization of the synaptic basal lamina is unknown. We report here that cells of a mouse muscle line, in the absence of nerves, have surface accumulations of each of the four synaptic basal lamina components described above: the 16S AChE, and cross-reactive antigens recognized by each of the synapse-specific antisera.

Cells of the C_2 line, derived from regenerating skeletal muscle of adult C3H mice[13], proliferate as myoblasts in high serum medium (Dulbecco's minimal essential (DME) medium containing 0.5% chick embryo extract and 20% fetal calf serum) and fuse into myotubes in low serum medium (DME with 10% horse serum). Within 3 days after the medium is changed, the cultures contain numerous long, cylindrical, multi-nucleated myotubes that contract spontaneously. The synapse-specific basal lamina antigens were detected using three sera described by Sanes and Hall[4]: we refer to the serum produced against solubilized anterior lens capsule as 'junctional-specific I' (JS-I); to the serum raised against muscle basement membrane collagen, and subsequently adsorbed with extrasynaptic muscle basement membrane so as to reveal synapse-specific antigens, as JS-II; and to the serum produced against lens capsule collagen and similarly adsorbed, as JS-III. Some experiments were also performed with the unadsorbed sera, which stain both synaptic and extrasynaptic basal lamina. Immunofluorescence observations were made as described by Sanes and Hall[4]. Methods for detection of AChE are described in detail elsewhere[8,14,15].

C_2 myotubes, cultured without nerve cells, synthesized the synapse-specific A_{12} form of AChE. After 5 days in fusion medium, ~30% of the total AChE activity sedimented at 16S (Fig. 1*a*). Histochemical examination of these fibres showed a patchy distribution of enzyme activity on the myotube surface (Fig. 1*b*). Such focal accumulations of AChE have been observed by others in primary myotube cultures from rat or chick embryonic myoblasts only in the presence of nerves[12,16-18]. Focal accumulations of AChE in such nerve–muscle co-cultures appeared at the same time as the A_{12} form of the enzyme[12,18]. We have demonstrated, and report in detail elsewhere, that the patches of AChE observed in aneural C_2 cultures correspond to the A_{12} form of enzyme and are apparently associated with the extracellular matrix[8,19].

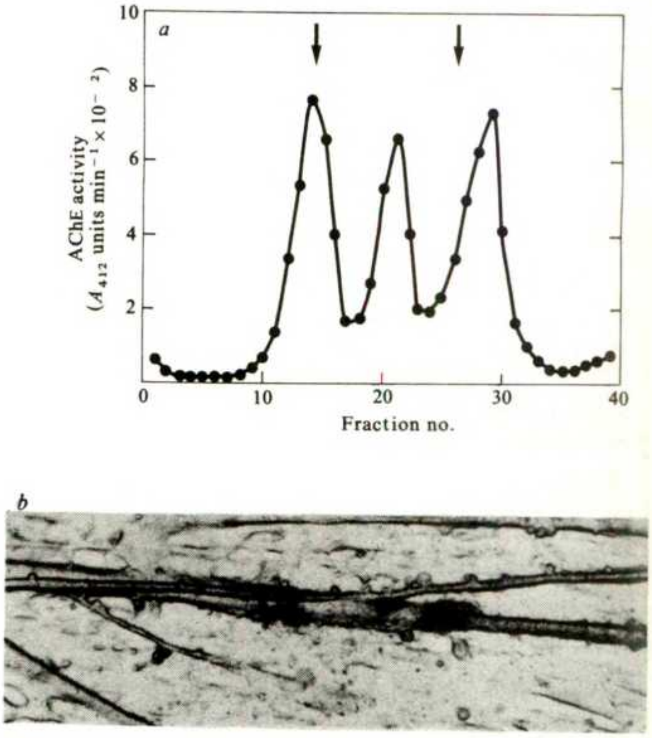

Fig. 1 Molecular forms and focal accumulations of AChE in C_2 myotube cultures. C_2 myotubes were grown for 5 days in fusion medium on a tissue culture plastic substrate and then examined for esterase activity. *a*, AChE was extracted from myotubes in a high ionic strength (1 M NaCl) buffer containing 0.5% Triton X-100, 20 mM EDTA and protease inhibitors[8], and analysed by zone sedimentation on a sucrose gradient[6]. Enzyme activity was measured by the Ellman procedure[14]. The arrows indicate the position of (left) β-galactosidase (16S) and (right) alkaline phosphatase (6.1S). *b*, Esterase activity was localized *in situ* using the histochemical method of Karnovsky and Roots[15] following fixation with 1% paraformaldehyde and 0.8% glutaraldehyde in 0.13 M sucrose buffered with 90 mM sodium phosphate, *p*H 7.4 (ref. 17). ×335.

To visualize the extracellular matrix produced by C_2 myotubes, we used antisera that bind uniformly to synaptic and extrasynaptic basal lamina in rat muscle[4] and mouse muscle (L.S. and Z.W.H., unpublished) (see Fig. 2*a*). The matrix formed a network of fibrils that stretched from cell to cell connecting the unfused myoblasts and myotubes, while an uneven pattern of staining outlined each myotube. Antibodies bound at low density over large areas of the myotube surface; more intense staining was seen in small patches and in long, thin arcs. None of these patterns was observed in control cultures that had been incubated with non-immune serum. These results show that the C_2 cells produce an extensive extracellular matrix.

We observed a more restricted distribution of immunofluorescence following incubation of the cultures with the synapse-specific antisera. In most cases, the antigens appeared as either arcs (Fig. 2*c*) or patches (Fig. 2*b,d*) on the myotube surface. Myotubes stained with the JS-III serum often displayed areas of fluorescent speckles (see Fig. 2*d*), a pattern not seen with the other synapse-specific antisera. Adsorption of each of the synapse-specific sera with C_2 myotubes abolished the staining of endplates in frozen sections of mouse muscle. Thus, the antibodies bound by C_2 myotubes are those recognized by the adult muscle synaptic basal lamina.

The arcs and small patches resembled the distribution of clusters of AChRs seen in separate experiments. Simultaneous labelling of the receptors with rhodamine-conjugated α-bungarotoxin and of the antigens with fluorescein-conjugated

---

* Permanent address: Laboratory of Neurophysiology, Department of Cell Biology, Catholic University of Chile, Santiago, Chile.

0028-0836/82/020143—03$01.00

antibody demonstrated that in many cases the antigens were restricted to areas of the myotube surface containing high concentrations of AChRs. As shown in Fig. 3, the coincidence of the two was often striking. The greatest coincidence of antigens with AChR clusters was observed with the JS-I serum. In cultures examined 3 days after fusion, 30–45% of all receptor clusters coincided with patches of JS-I antigen(s). Similarly, the JS-II antigen(s) sometimes appeared in patches whose distribution was identical to that of AChR clusters. In both cases, however, antigen patches unrelated to receptor clusters were also present. Co-localization of the JS-III antigen(s) with AChR clusters has thus far not been observed in C_2 myotube cultures. Because at least one synaptic basal lamina component, JS-III, seems to be unrelated to receptor clusters whereas the other two sometimes are, the distributions of each of the synaptic basal lamina antigens cannot be completely coincident.

The presence of synaptic basal lamina components in aneural C_2 myotube cultures can perhaps be understood in the context of myoblast maturation. Several studies suggest that the myoblast's potential for gene expression changes through a maturation sequence that is dependent on innervation. For example, Koenig and Vigny[12] observed that myotubes in primary rat muscle cultures could make 16S AChE in the absence of nerves only if derived from embryonic muscles that had already been innervated; myotubes formed by cells from uninnervated muscles could make 16S AChE only if co-cultured with nerves. Similarly, in chick muscle, both the ability of myoblasts to fuse *in vitro* and the morphology of myotubes seem to be regulated by neural contact within the limb bud[20–25]. The ability of C_2 myotubes to express 16S AChE, as well as other synapse-specific components of the basal lamina, is consistent with this scheme, as the cell line is derived from adult muscle; that is, the C_2 cell line may represent an advanced stage of myoblast differentiation that results from *in vivo* exposure to neuronal influences before isolation of the myoblasts.

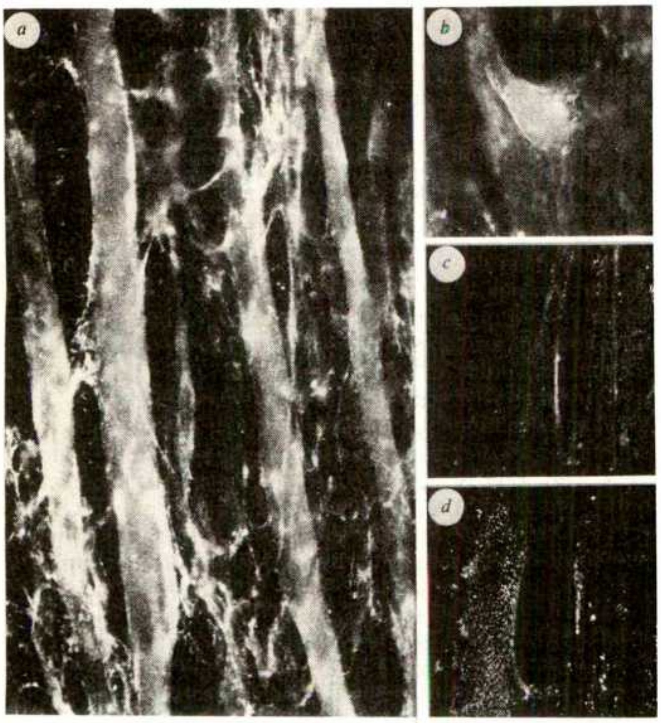

Fig. 2 Fluorescent antibody localization of extracellular matrix in C_2 myotube cultures. Cells were plated on tissue culture plastic and grown for 5 days in fusion medium, then incubated with rabbit antisera directed against the muscle basal lamina[4] at 1/100 dilution in low serum medium (1 h, 37 °C), followed by fluorescein isothiocyanate-conjugated goat anti-rabbit serum (Cappel) at 1/100 dilution in medium (1 h, 37 °C), washed with 0.15 M NaCl, 20 mM sodium phosphate, *p*H 7.2 (PBS) in 1 mM $CaCl_2$, mounted under 10% Gelvatol 20/30 (Monsanto), 20% glycerol in PBS, and examined with a Leitz Ortholux II microscope equipped with L2 (excitation bandpass (BP) 450–490, barrier BP 525/20) and N2 (excitation BP 530–560, barrier BP 580) filters. Reaction with: *a*, anti-muscle basement membrane collagen[4] (similar results were observed after incubation with anti-lens capsule collagen, data not shown); *b*, JS-I; *c*, JS-II; *d*, JS-III. ×236.

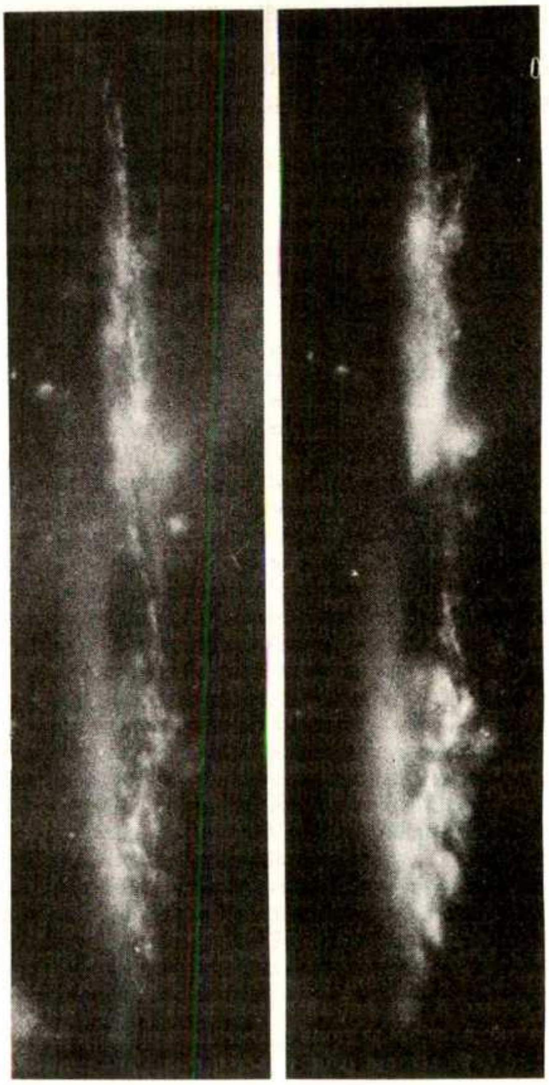

Fig. 3 Simultaneous localization of AChR clusters and basal lamina antigens in C_2 myotube cultures. Cells were plated on plastic coverslips, grown for 5 days in fusion medium and incubated with fluorescent reagents as before. Left, localization of JS-I antigen(s) by labelling with fluorescein-conjugated goat anti-rabbit serum as before. Right, AChR cluster in the same field observed after incubation with 50 nM rhodamine-conjugated α-bungarotoxin. Receptor clusters in control cultures, incubated with non-immune serum and photographed and printed in identical conditions, could be seen with rhodamine, but not fluorescein, filters. No receptor clusters were seen in cultures preincubated with unlabelled α-bungarotoxin (1 μM), followed by rhodamine-conjugated α-bungarotoxin. ×1,564.

In this context, the presence of synapse-specific basal lamina components in aneural C_2 muscle cultures does not imply that nerves are without influence on the normal appearance or localization of synaptic basal lamina components. We have shown previously that nerves can induce the appearance of synapse-specific basal lamina at sites of new endplate formation in adult muscle[26]. It will be of interest to investigate the role of nerves in the organization and production of synaptic basal lamina in myoblast cultures of different developmental ages.

We thank Dr D. Yaffe for the C_2 cell line, Dr Helen Blau for advice in cell culture techniques, Ms Miu Lam and Ms Nicole

Robitaille for technical assistance, Ms Liz Neville and Ms Veronica Oliva for help with the manuscript and Drs R. J. Greenspan, J. B. Miller, C. G. Reiness and J. R. Sanes for their comments on the manuscript. This work was supported by grants from the NIH, Muscular Dystrophy Association (MDA) and the NSF. L.S. is a NIH postdoctoral fellow and N.C.I. is a MDA postdoctoral fellow.

Received 22 June; accepted 11 November 1981.

1. Sanes, J. R., Marshall, L. M. & McMahan, U. J. *J. Cell Biol.* **78,** 176–198 (1978).
2. Burden, S. J., Sargent, P. B. & McMahan, U. J. *J. Cell Biol.* **82,** 412–425 (1979).
3. Bader, D. *J. Cell Biol.* **88,** 338–345 (1981).
4. Sanes, J. R. & Hall, Z. W. *J. Cell Biol.* **83,** 357–370 (1979).
5. Sanes, J. R. *J. supramolec. Struct. cell. Biochem.* Suppl. 5, Abstr. 821 (1981).
6. Hall, Z. W. *J. Neurobiol.* **4,** 343–361 (1973).
7. Vigny, M., Koenig, J. & Rieger, F. *J. Neurochem.* **27,** 1347–1353 (1976).
8. Inestrosa, N. C., Silberstein, L. & Hall, Z. W. (submitted).
9. Bon, S., Vigny, M. & Massoulie, J. *Proc. natn. Acad. Sci. U.S.A.* **76,** 2546–2550 (1979).
10. McMahan, U. J., Sanes, J. R. & Marshall, L. M. *Nature* **271,** 172–174 (1978).
11. Sugiyama, H. *FEBS Lett.* **84,** 257–260 (1977).
12. Koenig, J. & Vigny, M. *Nature* **271,** 75–77 (1978).
13. Yaffe, D. & Saxel, O. *Nature* **270,** 725–727 (1977).
14. Ellman, G. L., Courtney, K. D., Andres, V. & Featherstone, R. M. *Biochem. Pharmac.* **7,** 88–95 (1961).
15. Karnovsky, M. J. & Roots, L. *J. Histochem. Cytochem.* **12,** 219–221 (1969).
16. Koenig, J. *Biol. Cell.* **35,** 147–152 (1979).
17. Rubin, L. L., Schuetze, S. M. & Fischbach, G. D. *Devl Biol.* **69,** 46–58 (1979).
18. Rubin, L. L., Schuetze, S. M., Weill, C. L. & Fischbach, G. D. *Nature* **283,** 264–267 (1980).
19. Inestrosa, N. C., Silberstein, L. & Hall, Z. W. *J. supramolec. Struct. cell. Biochem.* Suppl. 5, Abstr. 812 (1981).
20. White, N. K. & Hauschka, S. D. *Expl Cell Res.* **67,** 479–482 (1971).
21. Hauschka, S. D. & White, N. K. in *Research Concepts in Muscle Development and the Muscle Spindle* (eds Banker, B. Q. *et al.*) 53–71 (Excerpta Medica, Amsterdam, 1971).
22. Bonner, P. H. & Hauschka, S. D. *Devl Biol.* **37,** 317–328 (1974).
23. White, N. K., Bonner, P. H., Nelson, D. R. & Hauschka, S. D. *Devl Biol.* **44,** 346–361 (1975).
24. Bonner, P. H. *Devl Biol.* **66,** 207–219 (1978).
25. Bonner, P. H. *Devl Biol.* **76,** 79–86 (1980).
26. Weinberg, C. B., Sanes, J. R. & Hall, Z. W. *Devl Biol.* **84,** 255–266 (1981).

Hypothalamic paraventricular nucleus is a privileged site for brain–pituitary interaction in long-term tissue culture

Alex J. Baertschi & Jean-Louis Bény

Department of Animal Biology, University of Geneva,
1211 Geneva 4, Switzerland

Beat Gähwiler

Preclinical Research, Sandoz Ltd, CH 4002 Basle, Switzerland

It is generally accepted that hypothalamic factors are released from the median eminence into the hypophysial portal vessels and exert a powerful control on the secretion of anterior pituitary hormones[1]. The brain sites involved in the synthesis of hypothalamic factors—particularly those that control ACTH secretion[2,3]—are, however, not yet established. It is also not known whether these sites are targets for pituitary hormone action, although recent anatomical[4] and physiological studies[5,6] suggest that pituitary hormones may reach the brain. For these reasons, we co-cultured[7,8] various hypothalamic explants from rat brain for 4 weeks with anterior pituitary. We report that during the third and fourth week *in vitro*, there is an approximately 10-fold increase in bioactive ACTH[9,10] in the medium of co-cultures prepared from the paraventricular nucleus and anterior pituitary, and that this increase is highly correlated with an increase (up to 10-fold) in concentrations of immunoreactive[11,12] arginine vasopressin (AVP). Hormone levels did not increase when basal hypothalamus was co-cultured with anterior pituitary, paraventricular nucleus with posterior pituitary, or supraoptic nucleus with anterior pituitary. Thus, we propose a specific interaction between anterior pituitary and paraventricular nucleus that results in a mutual enhancement ofeach other's peptide production.

The hypothalamus of Sprague–Dawley rats aged 6 to 7 days of either sex was cut within the frontal plane into slices about 400 μm thick, starting at the level of the optic chiasm (slice 1) and ending at the level of the posterior median eminence (slice 4). The paraventricular (PV) and supraoptic (SO) nuclei were punched out with a needle of 0.75-mm diameter by the Palkovits method[13] from slice number 1, and the basal hypothalamus (BH) from slice number 3 and 4. The tissues were cultured as explants[7,8] either alone or side by side with one half of an anterior pituitary (AP). Three half APs (three for technical reasons) were cultured alone as a control. The medium was collected and replaced every 7 days. After 28 days, the cultures were inspected by phase-contrast microscopy, and only those paraventricular and supraoptic explant combinations that displayed large size neurones were processed. The tissues were extracted in 0.1 M HCL, and the supernatants and pellets were stored at −20 °C pending hormone[9–12] and protein[14] assays.

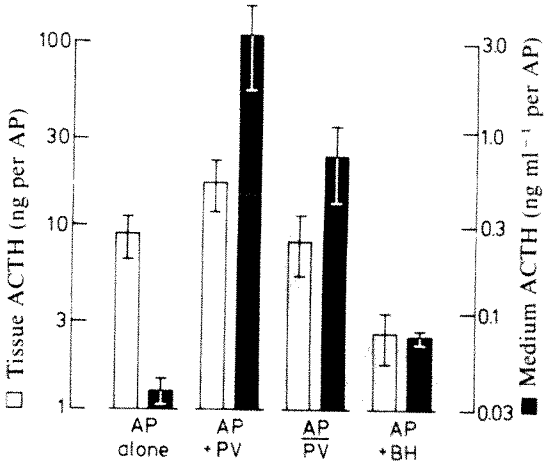

Fig. 1 Bioactive ACTH content (mean ± s.e.m.) of tissue (open bars) and medium (solid bars) from five to six hypothalamo-anterior pituitary cultures (AP, anterior pituitary; PV, paraventricular nucleus; BH, basal hypothalamus). AP+PV denotes a co-culture of the two explants in close apposition, as shown by the example of a AP+SO co-culture in Fig. 4*a*. In contradistinction, AP/PV signifies that the two explants were cultured on separate opposing coverslips within the same culture tube. The explants were embedded in a plasma clot and cultured in Falcon roller tubes. The medium (volume 1 ml) contained 25% horse serum, 25% Hanks' balanced salt solution, 50% basal medium (Eagle) and 6.5 mg ml^{-1} glucose[7,8]. The medium was replaced every week; hormone levels of the fourth week medium only are shown above. The tissue was homogenized in 700 μl of 0.2 M acetic acid and centrifuged at 15,000 r.p.m. and 4 °C for 15 min. The supernatant and the pellet, resuspended in 0.5 ml of 0.2 M NaOH, were frozen at −20 °C pending assays of hormones and proteins. Bioactive ACTH content of the tissues and media was measured by adding 5 or 10 μl of the 700 μl supernatant and 100 μl of the AP culture medium, respectively, to a 1 ml suspension of adrenocortical cells and by measuring the corticosterone secretion[9,10]. Note log display in this and all other figures.

When PV was co-cultured with AP for 28 days, the ACTH content of the medium (Fig. 1, solid bars, AP + PV) was 30 to 50 times larger than that of APs cultured alone or together with BH ($P < 0.025$). This large amount of medium ACTH was not due to a loss of ACTH from the tissue, since the tissue ACTH content (Fig. 1, open bars, AP + PV) was at least twice ($P < 0.05$) that found in any other type of cultures (AP alone, AP + BH). To test whether direct contact between the explants is necessary (see Fig. 4*a*), PV and AP were also cultured on separate opposing coverslips within the same tube. The ACTH content of the medium (Fig. 1, PV/AP) was at least 10 times larger than that of AP cultured alone, demonstrating that a factor released into the medium probably is responsible for the large increase in ACTH secretion induced by co-cultured paraventricular tissue.

The AVP contents of tissue (Fig. 2, open bars) and medium (dark columns) were about six times larger in PV–AP co-cultures than in PV cultures ($P < 0.05$). A trend towards elevated AVP levels was also observed when PV and AP were cultured on separate coverslips (AP/PV). Plotting the medium AVP and ACTH as a function of time in culture (Fig. 3) revealed a remarkable coincidence between the changes of both hormone

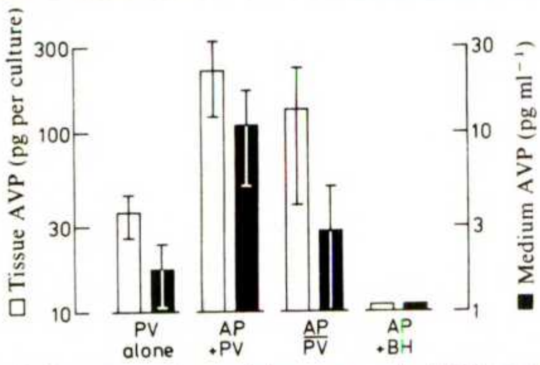

Fig. 2 Immunoreactive arginine vasopressin (AVP) content (mean ± s.e.m.) of tissue (open bars) and medium (solid bars) of the cultures shown in Fig. 1. For abbreviations, see Fig. 1 legend. The AVP content of the tissue was measured without extraction and the AVP content of the medium following vycor extraction by a specific radioimmunoassay[12,13]. AVP in the samples dilutes according to standard curve. The AVP tracer was from NEN, the AVP standard (500 IU mg^{-1}) is a gift of Drs K. Lederis and R. Mathison. The anti-vasopressin antibody, a gift of Dr J. Durr, does not cross-react with oxytocin, DD-AVP, ACTH, α-MSH, β-endorphin or with the enkephalins. The antibody was used at a dilution of 1:200,000. Recoveries were controlled in assay buffer and culture medium and varied from 58% to 70% between assays and ±3.5% within assays. Sensitivity was 0.25 pg per tube, about 0.4 pg per ml medium and 10 pg per culture. AVP was not detectable in AP + BH or BH alone. In AP/PV cultures where the two explants could be extracted separately, only the PV extract contained AVP. Separate experiments (not shown) indicate that co-cultures of PV with either posterior pituitary, hippocampus or cerebellar explants have AVP levels similar to those of PV alone.

levels which is also illustrated by a strong correlation between log(ACTH) and log(AVP) ($=0.91 \pm 0.04$).

In view of the possible role of AVP as a corticotropin releasing factor (CRF) *in vivo* and *in vitro*[10,15,16], we investigated whether the presence of vasopressin or vasopressinergic cells was sufficient to stimulate ACTH release from the anterior pituitary. We therefore added 100 pg of synthetic AVP (Ferring) once every week to anterior pituitaries. Medium ACTH levels were about 30% higher than controls ($P < 0.05$) and AVP levels ranged from 2–20 pg ml^{-1}, demonstrating that, although this increase in ACTH by AVP was far below that induced by co-cultured PV, very low amounts of AVP can exert significant CRF activity in this culture system. In another set of experiments, we determined whether other vasopressinergic cells display similar CRF activity. As illustrated in Fig. 4*b*, a co-cultured SO explant did not influence ACTH content and secretion by AP (Fig. 4*b*), whereas the presence of PV again elicited effects on AP qualitatively similar to those shown in the previous culture series.

This study clearly indicates that the PV region, and most probably not the hypophysiotrophic area, is a site for CRF synthesis. Stimulation[17], lesion[18,19] and histochemical[20–22] studies have previously implicated the PV in adrenocortical control. It remains to be seen if the CRF released from PV is identical with the one recently described[23], and if AVP is a cofactor in the control of ACTH secretion[24] by PV. However, the increased AVP levels in PV–AP co-cultures reveal a remarkable interaction between anterior pituitary and a specific region of the brain, and may have been caused by a known[25–27] or unknown growth factor from the pituitary or hypothalamus.

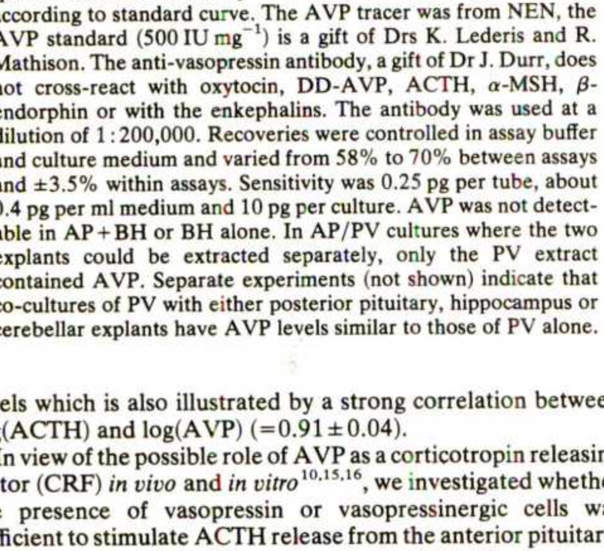

Fig. 3 Bioactive ACTH and immunoreactive AVP content of medium obtained from five individual AP–PV co-cultures as function of time *in vitro*. Tissues are the same as shown in Figs 1 and 2. Each symbol stands for one and the same co-culture. In PV cultures, AVP started to increase in half the cultures during the fourth week *in vitro*, whereas in AP cultures, ACTH gradually decreased from initial levels similar to those observed in AP + PV co-cultures.

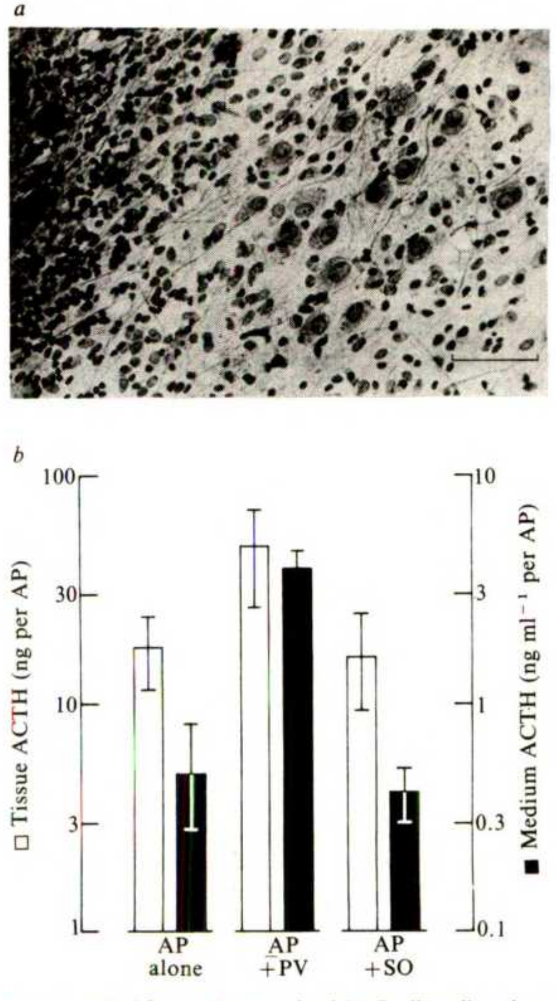

Fig. 4. *a*, AP–SO co-culture stained by Bodian-silver impregnation after 35 days *in vitro*. Note large cells with fine processes on right, and small anterior pituitary cells on left. Morphological aspects are similar in AP–PV co-cultures, although no morphometric analysis has yet been carried out. Scale bar, 60 μm. *b*, Bioactive ACTH content (mean ± s.e.m.) of tissue (open bars) and medium (solid bars) from five cultures (SO, supraoptic nucleus) after 4 week *in vitro*. AVP levels in SO cultures were about half those in PV cultures and, therefore, close to the detection limit. The existence of vasopressin was, however, clearly established by pooling three cultures of SO. The presence of AP had no detectable effect on AVP levels in co-cultures of AP + SO. Protein contents ranged from 180 μg (three half-anterior pituitaries) to 260 μg (hypothalamic cultures and co-cultures), and they are not significantly different in the various groups. Results from the set of experiments illustrated in this figure are presented elsewhere[28].

Our tissue culture approach opens new ways for identifying additional sites involved in the synthesis of CRF and other hypothalamic factors, and for exploring anterior pituitary actions on the brain.

This study was in part supported by Swiss NSF grant 3.581.0.79. We thank Ms L. Rietschin and M. Friedli for technical assistance, Dr J. Durr, Denver, for a sensitive and specific anti-vasopressin antibody, and Professor J.J. Dreifuss for valuable discussions.

Received 23 July; accepted 26 November 1981.

1. Harris, G. W. in *Handbook of Physiology* Vol. 2, Sect. 1, 1007–1038 (American Physiological Society, Washington DC, 1960).
2. Szentágothai, J., Flerkó, B., Mess, B. & Halász, B. *Hypothalamic Control of the Anterior Pituitary* (Akadémiai Kiadó, Budapest, 1968).
3. Makara, G. B., Stark, E., Rappay, G., Kárteszi, M. & Palkovits, M. *J. Endocr.* **83**, 165–173 (1979).
4. Bergland, R. M. & Page, R. B. *Science* **204**, 18–24 (1979).
5. Oliver, C., Mical, R. S. & Porter, J. C. *Endocrinology* **101**, 598–604 (1977).
6. Moldow, R. & Yalow, R. S. *Proc. natn. Acad. Sci. U.S.A.* **75**, 994–998 (1978).
7. Gähwiler, B. J. *Neurosci. Meth.* (in the press).
8. Gähwiler, B., Sandoz, P. & Dreifuss, J. J. *Brain Res.* **151**, 245–253 (1978).
9. Sayers, G. *Ann. N.Y. Acad. Sci.* **297**, 220–241 (1977).
10. Bény, J. L. & Baertschi, A. J. *Neuroendocrinology* **30**, 108–112 (1980).
11. Dogterom, J. thesis, Univ. Utrecht (1977).
12. Baertschi, A. J. & Vallet, P. *J. Physiol., Lond.* **315**, 217–230 (1981).
13. Palkovits, M. *Anatomical Neuroendocrinology* 72–80 (Karger, Basle, 1975).
14. Lowry, O. H., Rosebrough, N. J., Farr, A. L. & Randall, R. J. *J. biol. Chem.* **193**, 265–275 (1951).
15. Baertschi, A. J., Vallet, P., Baumann, J. B. & Girard, J. *Endocrinology* **106**, 878–882 (1980).
16. McCann, S. M. *Neuroendocrinology* **31**, 355–363 (1980).
17. Dornhorst, A., Carlson, D. E., Seif, S. M., Robinson, A. G., Zimmerman, E. A. & Gann, D. S. *Endocrinology* **107**, 1420–1424 (1981).
18. Makara, G. B., Stark, E., Kárteszi, M., Palkovits, M. & Rappay, G. *Am. J. Physiol.* **240**, E441–E446 (1981).
19. Baertschi, A. J., Bény, J. L. & Makara, G. B. *Adv. Physiol. Sci.* **14**, 57–61 (1981).
20. Vandesande, F., Dierickx, K. & De Mey, J. *Cell Tiss. Res.* **180**, 443–452 (1977).
21. Zimmerman, E. A., Stillman, M. A., Recht, L. D., Antunes, J. L. & Carmel, P. W. *Ann. N.Y. Acad. Sci.* **297**, 405–417 (1977).
22. Burlet, A., Chateau, M. & Czernichow, P. *Brain Res.* **168**, 275–286 (1979).
23. Vale, W., Spiess, J., Rivier, C. & Rivier, J. *Science* **213**, 1394–1397 (1981).
24. Gillies, G. & Lowry, P. *Nature* **278**, 463–464 (1979).
25. Noble, R. N., Beer, C. T. & Gout, P. W. *Cancer Res.* **40**, 2437–2440 (1980).
26. Brockes, J. P., Lemke, G. E. & Balzer, D. R. *J. biol. Chem.* **255**, 8374–8377 (1980).
27. Pearson, D. B., Goodman, R. & Sachs, H. *Science* **187**, 1081–1082 (1975).
28. Baertschi, A. J., Bény, J. L., Friedli, M. & Gähwiler, B. *J. Physiol., Lond.* **318**, 67P (1981).

Vasoactive intestinal polypeptide enhances muscarinic ligand binding in cat submandibular salivary gland

Jan M. Lundberg

Department of Pharmacology, Karolinska Institutet, Fack,
S-104 01 Stockholm, Sweden

Britta Hedlund* & Tamas Bartfai

Department of Biochemistry, University of Stockholm,
Arrhenius Laboratory, S-106 91 Stockholm, Sweden

The salivary secretion from the cat submandibular salivary gland induced by parasympathetic nerve stimulation is considered to be due to release of acetylcholine (ACh) which binds to muscarinic receptors and activates secretory elements[1]. Recent evidence suggests that cholinergic neurones in the cat submandibular gland contain and release another neurotransmitter candidate, vasoactive intestinal polypeptide (VIP)[2,3]. Although VIP *per se* does not induce salivary secretion, it potentiates the secretion induced by ACh infusions[2,3]. The present study offers a possible explanation for this potentiation by showing that VIP in physiologically relevant concentrations enhances the binding of muscarinic cholinergic ligands in the cat submandibular gland.

Membranes were prepared from the submandibular salivary gland of adult cats using previously described methods[4].

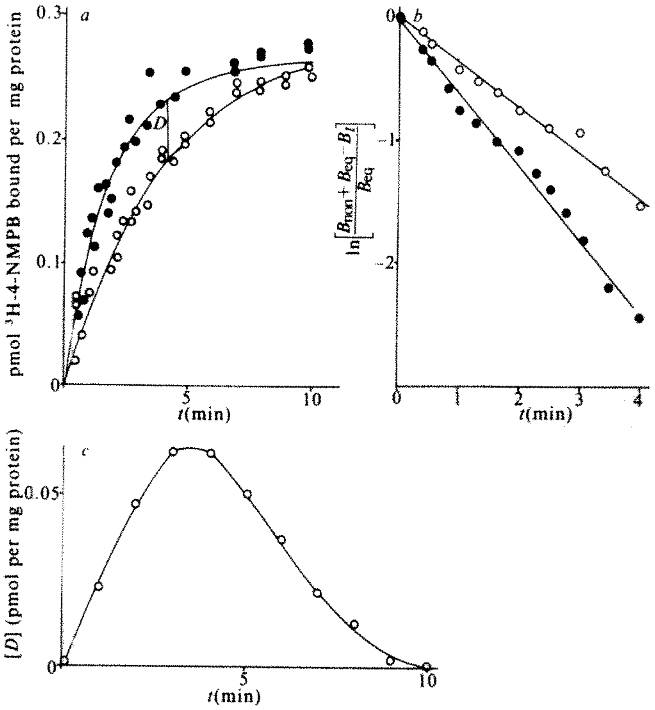

Fig. 1 *a*, Association rate of ^{3}H-4-NMPB (5.6 nM) to membranes from the cat salivary gland in the absence (○) and presence (●) of VIP (5 nM). Using a loose-fitting glass–Teflon homogenizer at 695 r.p.m., a 10% homogenate (w/v) of the glands in 0.32 M sucrose was prepared by 15 up-and-down strokes. After centrifugation at 1,000*g* for 5 min the resulting supernatant was subjected to further centrifugation at 10,000*g* for 40 min. The pellet thus obtained was resuspended in a modified Krebs–Ringer's buffer (137 mM NaCl, 2.68 mM KCl, 1.8 mM $CaCl_2$, 1.05 mM $MgCl_2$, 5 mM HEPES, 10 μM phenylmethylsulphonyl fluoride, 1 g l^{-1} glucose) and used in the binding studies without further treatment. All incubations with muscarinic ligands and VIP were carried out at 37 °C and the incubations were started by addition of VIP and ^{3}H-4-NMPB. Reaction was stopped by filtration through Whatman GF/B glass fibre filters and rinsing of the filters with 10 ml of ice-cold buffer. The filters were counted in a scintillation spectrometer on the next day in toluene/5% diphenyloxazole/0.1% *p*-phenylene phenyloxazole at an efficiency of 45–55%. The experiment was carried out three times with similar results. Data from one representative experiment are shown. Protein was determined according to Lowry *et al.*[17] using bovine serum albumin as standard. The points are the mean (±s.e.m.) of triplicate determinations. *b*, The semilogarithmic plot of the association rate data of *a*. These data were analysed by nonlinear least-square fit of the data to the following equation:

$$B_t = B_{non} + B_{eq}(1.0 - e^{-kt})$$

where B_t is the total amount ^{3}H-4-NMPB bound, B_{non} is the nonspecific binding which is equilibrated within seconds, B_{eq} is the amount of ^{3}H-4-NMPB bound in equilibrium and k is the observed pseudo-first order rate constant. This rate constant is influenced by several factors besides the concentration of ^{3}H-4-NMPB. The effect of VIP is demonstrated here but not analysed in detail because the VIP effect is transient (*c*), probably due to degradation and because the binding rate of VIP to its receptor is not known, only the onset of its effect on muscarinic binding. *c*, The transient effect of VIP (5 nM) on the association rate of ^{3}H-4-NMPB (5.6 nM). The difference (*D*) between the curves (*a*) in the presence and absence of VIP is plotted as a function of time.

Muscarinic receptor binding studies were performed using ^{3}H-*N*-methyl-4-piperidinyl benzilate (^{3}H-4-NMPB) as the labelled ligand[5]. All incubations were carried out at 37 °C immediately after preparation of the membranes. Highly purified porcine VIP was used in all incubations. The biological activity of the VIP solutions were also tested *in vivo* on cats, by measuring potentiation of the ACh-induced salivary secretion[3].

Figure 1*a* and *b* show that the association rate of the muscarinic antagonist ^{3}H-4-NMPB[5] at concentrations of 2–15 nM was increased in the presence of VIP (5 nM). This effect was smaller with 50 nM VIP. The effect of VIP was time dependent, being maximal at 3–4 min, and undetectable after 10 min (see Fig. 1*c*). The observed pseudo-first order rate constants[6] determined for the first 3 min (compare Fig. 1*a* and *b*) were 0.32 ± 0.07 and 0.52 ± 0.11 min^{-1}, respectively, in the absence and presence of VIP (5 nM). The difference was statis-

---

* To whom correspondence should be addressed.

0028–0836/82/020147—03$01.00

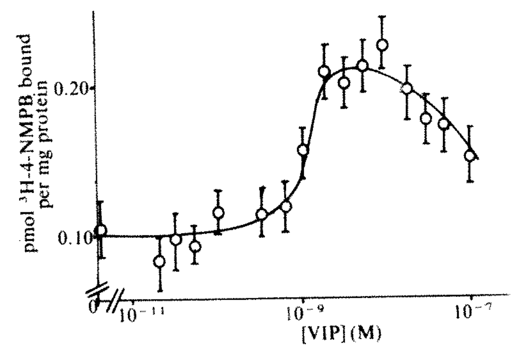

Fig. 2 The effect of VIP on binding to the muscarinic cholinergic receptors. Membranes were incubated with ^{3}H-4-NMPB (14 nM) and different concentrations of VIP (10^{-11}–10^{-7} M) for 2 min at 37 °C. Data shown are the mean (±s.e.m.) of quadruplicate determinations.

tically significant ($P < 0.001$). The dose dependence of the effect of VIP on ^{3}H-4-NMPB binding was then studied in pseudo-first order conditions. Figure 2 shows that at 2 min of incubation a bell-shaped curve of bound ^{3}H-4-NMPB versus VIP concentration was obtained, with a maximum between 3×10^{-9} and 3×10^{-8} M VIP. This curve was shifted to the right at longer incubation times, but the effective VIP concentrations were still in the nanomolar range.

At equilibrium conditions (60 min incubation), 0.30 pmol ^{3}H-4-NMPB per mg protein could be specifically bound both in the absence and presence of VIP, thus suggesting that only the affinity ($K_D = k_{diss}/k_{ass}$) and not the number of receptors is changed. The dissociation rate (k_{diss}) for ^{3}H-4-NMPB from the receptor was determined by starting the measurement after 2 min of incubation with ^{3}H-4-NMPB by addition of carbamylcholine (10 mM). No effect of VIP (1–50 nM) was detected on the dissociation rate of the ^{3}H-4-NMPB–receptor complex. Isoprenaline (10^{-7} M), adrenaline (10^{-5} M) and substance P(10^{-7} M), known to influence the function of the submandibular gland, were also tested, but none affected the association rate of muscarinic ligands with the receptor. To determine the tissue specificity of the effect of VIP on muscarinic ligand binding, rat cardiac membranes were tested in similar experiments (the auricles, which are known to have some VIP innervation, were removed). No effect of VIP on the association rate of ^{3}H-4-NMPB was detected in this preparation.

A 10-nM concentration was chosen from the plateau of the dose–response curve (Fig. 2) to examine the effects of VIP on muscarinic agonist binding. Figure 3*a* shows that in the presence of VIP, carbamylcholine behaved as a 1,000-fold more potent competitor of ^{3}H-4-NMPB binding than in the absence of VIP. Note that the slope of binding curves obtained in non-equilibrium conditions (Fig. 3*a*) is much higher than that in equilibrium conditions (Fig. 3*b*). The higher slopes may indicate cooperative interactions between carbamylcholine binding sites.

In equilibrium conditions (60 min incubation, Fig. 3*b*) VIP had no effect on the displacement of ^{3}H-4-NMPB by carbamylcholine. This 'absence' of effect is probably due to degradation of VIP during the long incubation. Figure 1*c* shows that the effects of VIP after 10 min have already disappeared, either due to degradation or desensitization. Analysis of VIP after exposure to tissue extracts or plasma indicates that the peptide is rapidly degraded ($t_{1/2} = 1$–1.5 min)[7,8], suggesting that degradation may be the major factor in the disappearance of its effects. Until stable VIP analogues are available it is not possible to evaluate the contribution of desensitization to disappearance of the effect. A similar disappearance of the effect of VIP over 10–20 min is observed when displacement of ^{3}H-4-NMPB by another agonist, ACh (10^{-9}–10^{-2} M), is studied. In the presence of VIP at 5 min incubation time but not with 10 and 20 min incubation, ACh behaves as a 10^5 times more potent agonist ($IC_{50} \approx 3\times10^{-9}$ M, Fig. 3*c*) than at equilibrium conditions.

The present findings suggest that VIP increases the affinity of muscarinic ACh receptors in the cat submandibular gland. Under physiological conditions VIP and ACh are probably released simultaneously upon activation of the secretory nerves[3]. Although VIP by itself does not induce salivation[2], the findings offer a possible explanation of the potentiating effect of VIP on ACh-induced saliva secretion[2,3]. Because, in the presence of VIP, the affinity of the muscarinic receptors for ACh increases 10^5-fold (Fig. 3*c*) a large increase can be expected in the secretory response which is governed by occupancy of muscarinic receptors[1]. Although it is early to speculate about the molecular mechanism of the VIP-mediated increase in muscarinic receptor affinity and association rate, it is relevant that equilibrium binding studies with muscarinic agonists suggest the existence of two or three interconvertible receptor populations having high and low affinity, respectively[9]. It is conceivable that occupancy of VIP receptors induces a shift from low- to high-affinity receptor conformation. (However, note that the data showing an effect of VIP on agonist binding (Fig. 3*a*, *c*) were not obtained in equilibrium conditions.)

Some of the muscarinic responses, such as increased cyclic GMP synthesis, seem to be linked to occupancy of low-affinity agonist binding sites, whereas other responses, such as phosphatidylinositol turnover, are apparently linked to both high- and low-affinity binding sites. (See refs 10, 11 for reviews.) Muscarinic responses involved in stimulation of secretion of the lacrimal cells[12], pancreatic cells[13] and parotid gland[14] relate high-affinity ($K_d < 1$ μM) agonist binding to increased Na^+ permeability. Accordingly, in the salivary gland VIP may switch muscarinic receptors to the high-affinity conformer and thereby increase their efficiency in changing Na^+ permeability and secretion.

The present data suggest that VIP receptors and muscarinic receptors interact in the plane of the membrane. Interaction between different receptors in the same membrane has been reported for muscarinic and β-adrenergic receptors in cardiac membranes[15] as well as for opiate receptors and nicotinic receptors[16] in the adrenal medulla.

This study was supported by grants from the Swedish MRC (17X-5438), the Swedish Tobacco Company and grants to T.B. from the National Institute of Mental Health, Bethesda, USA, and from the Swedish MRC (B82-13X-5415-04B). Highly purified porcine VIP was a gift from Professor V. Mutt, Karol-

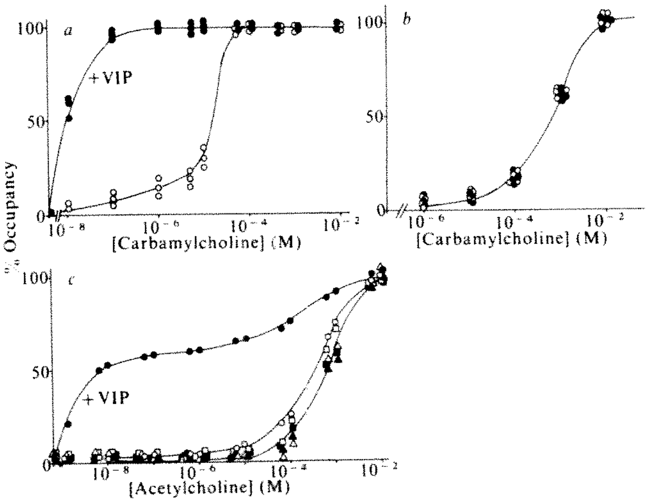

Fig. 3 *a*, The effect of various concentrations of carbamylcholine on binding of ^{3}H-4-NMPB (7 nM) in the absence (○) and presence (●) of VIP (10 nM). The samples were incubated for 2 min at 37 °C. *b*, The effect of various concentrations of carbamylcholine on binding of ^{3}H-4-NMPB (7 nM) in the absence (○) and presence (●) of VIP (10 nM). The samples were incubated for 90 min at 37 °C. *c*, The effect of VIP (10 nM, filled symbols) on diplacement of ^{3}H-4-NMPB (7 nM) by various concentrations of acetylcholine (in the presence of physostigmine, 10 μM). The displacement curves were run with incubation times of 5, 10 and 20 min. The symbols are: ○, no VIP; ●, +VIP (10 nM); 5 min incubation. △, No VIP; ▲, +VIP (10 nM); 10 min incubation. □, No VIP; ■, +VIP (10 nM); 20 min incubation.

inska Institutet and the supply of ^{3}H-4-NMPB by Professor M. Sokolovsky, Tel-Aviv University, is also gratefully acknowledged.

Received 3 June; accepted 6 November 1981.

1. Babkin, B. P. *Secretory Mechanism of the Digestive Glands* 2nd edn (Hoeber, New York, 1950).
2. Lundberg, J. M., Änggård, A., Fahrenkrug, J., Hökfelt, T. & Mutt, V. *Proc. natn. Acad. Sci. U.S.A.* **77**, 1651–1655 (1980).
3. Lundberg, J. M. *Acta physiol. scand.* **112**, Suppl. 496, 1–57 (1981).
4. Hedlund, B. & Bartfai, T. *Molec. Pharmac.* **15**, 531–544 (1979).
5. Kloog, Y. & Sokolovsky, M. *Brain Res.* **144**, 31–48 (1978).
6. Järv, J., Hedlund, B. & Bartfai, T. *J. biol. Chem.* **255**, 5595–5598 (1979).
7. Domschke, S. *et al. Gut* **19**, 1049–1053 (1978).
8. Keltz, T. N., Straus, E. & Yalow, R. S. *Biochem. biophys. Res. Commun.* **92**, 669–674 (1980).
9. Birdsall, N. J. M., Burgen, A. S. V. & Hulme, E. C. *Molec. Pharmac.* **14**, 723–736 (1978).
10. Birdsall, N. J. M. & Hulme, E. C. *J. Neurochem.* **27**, 7–16 (1976).
11. Heilbronn, E. & Bartfai, T. *Prog. Neurobiol.* **11**, 171–188 (1978).
12. Parod, R. J., Leslie, B. A. & Putney, J. W. *Am. J. Physiol.* **239**, G99-G105 (1980).
13. Putney, J. W., Landis, C. A. & van de Walle, C. M. *Pflügers Arch. ges. Physiol.* **385**, 131–138 (1980).
14. Putney, J. W. & Parod, R. J. *J. Pharmac. exp. Ther.* **205**, 449–458 (1978).
15. Watanabe, A. M. *et al. J. biol. Chem.* **253**, 4833–4836 (1978).
16. Kumakura, K., Karoum, F., Guidotti, A. & Costa, E. *Nature* **283**, 489–492 (1980).
17. Lowry, O. H., Rosebrough, N. J., Farr, A. L. & Randall, R. J. *J. biol. Chem.* **193**, 265–275 (1951).

Neuronal spread of scrapie agent and targeting of lesions within the retino-tectal pathway

H. Fraser

ARC and MRC Neuropathogenesis Unit, West Mains Road,
Edinburgh EH9 3JQ, UK

Scrapie is a transmissible encephalopathy of sheep and goats, and a number of mammalian species can be infected experimentally. Various strains of the transmissible agent are distinguishable on pathological and biological grounds in inbred mice[1–3]. The agents replicate in a variety of tissues, such as those of the lympho-reticular systems[1,4,5], but their pathological effects are confined to the central nervous system (CNS). The type, distribution and local intensity of the brain lesions vary, depending mainly on the agent strain, host genotype, route of infection and dose of agent. The principal type of lesion is vacuolar degeneration, typically with a bilaterally symmetrical distribution[6]. (Exceptional reports of its asymmetry can be attributed to 'class III' strains of agent[7], none of which is used in the present study.) Whether spread of infection around the body involves the migration of infected cells, the agent passing from infected to adjacent uninfected cells, or via a possible viraemic phase to cells remote from infected foci[8,9], or transport over considerable distances along nerves, possibly with trans-synaptic infection, is not known. There is evidence that infection spreads in the CNS from the thoracic spinal cord posteriorly and to the brain[10,11], but it is still unknown whether the spread is partly or exclusively via neurones, and which types of cell are infected. The finding that the retina became infected following intracerebral injection[12] has been interpreted as evidence for neural spread but this is not conclusive because it can be shown that tracers, for example, can travel from the subarachnoid space into the perineural space of the optic nerve to the epichoroidal and episcleral tissues of the eyeball[13–15]. I have now investigated whether lesions and infectivity can be targeted into a sensory nucleus following injection into a sense organ on one side of the body with the ipsilateral organ and nucleus acting as controls. The results show that scrapie agent can spread over a considerable distance along a nerve pathway.

The possibility that neural spread of scrapie infectivity could produce targeted lesions was tested by injecting the ME7 strain of scrapie into the right eye of inbred C3H/LacDk mice. Groups of mice were killed for histological examination at intervals of 155–260 days after injection; by 260 days the mice were within 2–3 weeks of the terminal stage of the disease. Haematoxylin- and eosin-stained transverse paraffin sections of their formol-saline-fixed brains were examined, using a standard procedure[16]. In mice killed at the earlier intervals, asymmetrical lesions were confined to the contralateral (left) superior colliculi and no lesions were apparent elsewhere in the brain. This tectal asymmetry continued throughout the series (Fig. 1*a*), becoming less frequent as lesions developed symmetrically in both the tectum and other regions of the brain. By 250 days post-injection only symmetrical lesions were present (Table 1). From about 70% of the way through the incubation period of 265 ± 3 (mean ± s.e.) days, an increasing proportion of cases showed a form of tectal asymmetry having severe degeneration of the contralateral side, but much less involvement of the ipsilateral superior colliculus (Fig. 1*b*), and low-grade symmetrical lesions elsewhere in the brain.

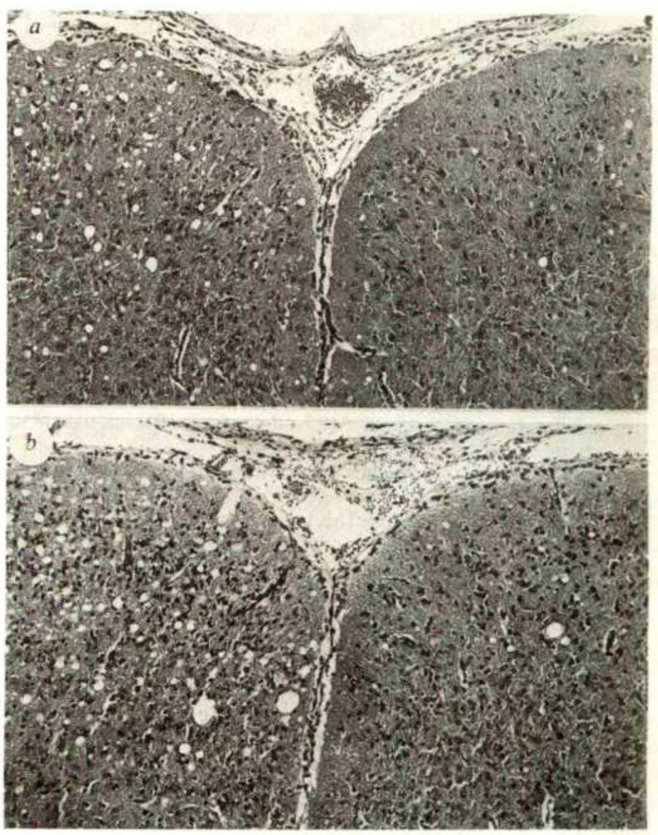

Fig. 1 Asymmetry of vacuolation in the left superior colliculus in C3H mice killed 185 (*a*) and 190 (*b*) days after right intraocular injection of ME7 scrapie agent. Haematoxylin and eosin stains used. ×78.

Retinal ganglion cells are known to project to and synapse with various brain nuclei, including the superior colliculi and lateral geniculate bodies[17]. In a few cases, low-grade vacuolation of the contralateral lateral geniculate nucleus occurred, but never with the consistency or severity seen in the optic tectum. This prominent asymmetry in the superior colliculi but not in the lateral geniculate nuclei is readily explained on several grounds. First, when injection routes which give fully symmetrical lesions (such as intracerebral or intraperitoneal injections) are used the ME7 agent in C3H mice produces severe vacuolation in the superior colliculi but only mild vacuolation in the lateral geniculate nuclei. Second the lateral geniculate is only a small homogeneous structure in rodents compared with its greater importance and complexity in carnivores and primates[17]; and third, there is more decussation to the superior colliculi than to the lateral geniculate nuclei[18]—90% to the latter in the mouse[19].

The observed distribution of infectivity in dissected optic nerves and superior colliculi is entirely in accord with the lesion data. Following injection into the right eye, at 68 days infectivity

Table 1 Numbers of C3H mice with vacuolar degeneration in the superior colliculi, at intervals after intraocular injection into the right eye with ME7 scrapie agent

	Days post-injection								
	155	161	167	185	190	200	216	232	251
Asymmetry of vacuolation in superior colliculus									
Left	2	4	2	2	1	2	0	1	0
Right	0	0	1*	0	0	0	0	0	0
Symmetrical lesions	1	0	1	0	0	1	2	0	2
No lesions	1	1	0	0	0	0	0	0	0
Incidence of asymmetry	2/4	4/5	3/4	2/2	1/1	2/3	0/2	1/1	0/2

Inoculum of scrapie agent was 10^4–10^5 ICLD$_{50}$ units per 0.002 ml of a 500*g* supernatant of terminal ME7-affected C57BL mouse brain homogenate.

* Data are available for 78 mice with asymmetrical vacuolation in the optic tectum following intraocular injection with scrapie from these and other unpublished experiments. This is the only deviant result in terms of sidedness and the possibility that the block was inverted during the preparation of sections cannot be excluded.

is present in its optic nerve and tract, and in the contralateral superior colliculus to which it projects, but absent from the optic nerve and tract from the left eye and from the ipsilateral superior colliculus. At 105 days there is 500 times more infectivity in the contralateral than the ipsilateral superior colliculus. We now have preliminary results from a much wider time series which confirms that these findings are part of a consistent trend and that the infectivity appears in the contralateral superior colliculus several weeks before the lesions.

The results reported here provide clear evidence that orthograde axonal spread can occur in scrapie in the CNS, which could account for the differences in titre found for the peripheral and central nervous systems, all pointing to neural spread[10-12]. This is also consistent with the recent evidence that the sympathetic system is a mode of entry of peripherally replicated scrapie into the thoracic spinal cord[20]. The extensive cross-over of retinal ganglion cell axons which occurs in adult rodents[19,21] would, if neural spread occurred, result in the targeting of the earliest lesions largely in the contralateral superior colliculus, as has been demonstrated with tracers of axoplasmic flow such as ^{35}S-methionine and horseradish peroxidase[22-24]. The alternative possibilities, of spread of infection via cell-to-cell contact in epineural glial cells, or of spread by extension through the subarachnoid space around the optic nerves and tracts, are clearly inconsistent with these results as neither method of spread would produce contralateral asymmetry restricted to the optic tectum. As an analogue of a central nervous pathway[25], the evidence for spread in the retino-tectal projection suggests that spread in the CNS may involve a wider range of central axons than previously thought, but does not rule out the possibility of other modes of spread, such as via the extracellular space and within and between glia.

It is now necessary to extend the observations described here, which are limited to the ME7 strain of scrapie agent, to other agents with different pathological manifestations, such as 79A agent in which white matter vacuolation is prominant[26], compared with 22C, where grey matter is involved exclusively, to test whether the targeting within the optic pathway can be shown to be even more specific.

Received 10 September; accepted 11 November 1981.

1. Dickinson, A. G. & Outram, G. W. in *Slow Transmissible Diseases of the Nervous System* Vol. 2 (eds Prusiner, S. B. & Hadlow, W. J.) 13–31 (Academic, New York, 1979).
2. Dickinson, A. G. & Fraser, H. in *Slow Transmissible Diseases of the Nervous System* Vol. 1 (eds Prusiner, S. B. & Hadlow, W. J.) 367–385 (Academic, New York, 1979).
3. Fraser, H. & Dickinson, A. G. *J. comp. Path.* **83,** 29–40 (1973).
4. Fraser, H. & Dickinson, A. G. *Nature* **226,** 462–463 (1970).
5. Fraser, H. & Dickinson, A. G. *J. comp. Path.* **88,** 563–573 (1978).
6. Fraser, H. in *Slow Transmissible Diseases of the Nervous System* Vol. 1 (eds Prusiner, S. B. & Hadlow, W. J.) 387–406 (Academic, New York, 1979).
7. Bruce, M. E. & Dickinson, A. G. in *Slow Transmissible Diseases of the Nervous System* Vol. 2 (eds Prusiner, S. B. & Hadlow, W. J.) 71–86 (Academic, New York, 1979).
8. Palsson, P. A. in *Slow Transmissible Diseases of the Nervous System* Vol. 1 (eds Prusiner, S. B. & Hadlow, W. J.) 357–366 (Academic, New York, 1979).
9. Manuelidis, E. E., Gorgacz, E. J. & Manuelidis, L. *Science* **200,** 1069–1071 (1978).
10. Kimberlin, R. H. & Walker, C. A. *J. comp. Path.* **89,** 551–562 (1979).
11. Kimberlin, R. H. & Walker, C. A., *J. gen. Virol.* **51,** 183–187 (1980).
12. Buyukmihci, N., Rorvik, M. & Marsh, R. F. *Proc natn. Acad. Sci. U.S.A.* **77,** 1169–1171 (1980).
13. Oemichen, M. in *Mononuclear Phagocytes in the Central Nervous System*, 37 (Springer, Berlin, 1978).
14. Davson, H. in *Physiology of the Cerebro-spinal Fluid*, 27–28 (Churchill, London, 1967).
15. Bradbury, M. W. B. & Cole, D. F. *J. Physiol., Lond.* **299,** 353–365 (1980).
16. Fraser, H. & Dickinson, A. G. *J. comp. Path.* **78,** 301–311 (1968).
17. Masterton, R. B. & Glendenning, K. K. in *Handbook of Behavioural Neurobiology* (ed. Masterton, R. B.) 1–38 (Plenum, New York, 1978).
18. Garey, L. J. & Powell, T. S. *J. Anat.* **102,** 189–322 (1968).
19. LaVail, J. H., Nixon, R. A. & Sidman, R. L. *J. comp. Neurol.* **182,** 399–422 (1978).
20. Kimberlin, R. H. & Walker, C. A. *Jl R. Soc. Med.* (in the press).
21. Lund, R. D. *Expl Eye Res.* **21,** 193–203 (1975).
22. Dräger, U. C. & Hubel, D. H. *J. Neurophysiol.* **38,** 690–713 (1975).
23. Colman, D. R., Scalia, F. & Cabrales, E. *Brain Res.* **102,** 156–163 (1976).
24. Land, P. W. & Lund, R. D. *Science* **205,** 698–700 (1979).
25. Bishop, P. O., Jermemy, D. & Lance, J. W. *J. Physiol., Lond.* **121,** 415–432 (1953).
26. Fraser, H. in *Slow Virus Diseases of Animals and Man* (ed. Kimberlin, R. H.) 268–305 (North-Holland, Amsterdam, 1976).

Immune interferon release when a cloned cytotoxic T-cell line meets its correct influenza-infected target cell

A. G. Morris*, Yun-Lu Lin† & Brigitte A. Askonas‡

* Department of Biological Sciences, University of Warwick, Coventry CV4 7AL, UK
† National Institute for Medical Research, The Ridgeway, Mill Hill, London NW7 1AA, UK

T cells stimulated by mitogens[1], specific antigens[2], including viral antigens[3], and alloantigens[4] have been shown to produce immune interferon (IFN-γ). However, the exact circumstances of induction of IFN-γ in T cells have not yet been established, particularly the precise nature of the cell type producing the interferon. We have recently described[5] the selection and cloning of a BALB/c cytotoxic T(T$_c$)-cell line (L4) which grows in the presence of T-cell growth factor (TCGF), is Lyt-2 positive and kills H-2^d target cells infected with any type A influenza virus. The aim of the present study was to examine whether this cloned cytotoxic T-cell line produced IFN-γ on contact with the appropriate target cell. It was found that small amounts of IFN-γ were produced on co-culture of L4 with target cells, whereas L4 cells on their own released no detectable interferon. The pattern of antigenic specificity by L4 cells for interferon production resembled the requirements for killing in that T$_c$ cell mediated lysis was restricted to H-2^d targets infected with influenza A, but not influenza virus B strains, and interferon production was not prevented by a monoclonal antibody to the virus' haemagglutinin, which does not inhibit cytotoxicity while neutralizing the virus.

L4 T$_c$ cells were maintained in RPM1 1640 medium containing 10% fetal calf serum, ampicillin, kanamycin and 10% RS (supernatant from rat spleen cells activated by concanavalin A)[5]. The cytotoxicity of L4 declined rapidly during *in vitro* passage and regular recloning was necessary to maintain the line. ^{51}Cr-release cytotoxicity assays were carried out at regular intervals to survey cytotoxicity.

To examine interferon production, L4 T$_c$ cells were incubated with A/X31-infected P815 (H-2^d) target cells in the same conditions as the cytotoxicity assay except that the target cells were unlabelled. After 6 h incubation the cells were centrifuged lightly and interferon levels in the supernatant medium determined by titration on C3H10T$\frac{1}{2}$ mouse fibroblasts[6] using the inhibition of nucleic acid synthesis method[7] with Semliki Forest virus as challenge virus. Table 1 shows that L4 T$_c$ cells produce interferon on contact with A/X31-infected P815 cells, but that L4 T_c or infected P815 cells incubated alone for the same time period (6 h) do not. A monoclonal antibody (3/1) to the H3 haemagglutinin of A/Memphis/71, which neutralizes A/X31 virus infectivity[8] but does not block killing[9], does not prevent interferon production. P815 cells coated with UV-irradiated A/X31 virus, which do not act as targets, do not induce interferon. A/X31 virus alone added to L4 T_c cells at the same concentration used to infect P815 cells does not induce interferon in L4 T_c cells. Thus, production of interferon by L4 T_c cells required interaction with infected targets. The presence of free infectious virus was neither necessary nor sufficient for interferon production.

---

‡ To whom correspondence should be addressed.

We next determined whether the production of interferon was related to the recognition of appropriate antigens on the target cells. P815 cells infected with either A/X31 or A/USSR both act as targets for L4 T_c cells[5] and both induce interferon production (Table 2). P815 cells infected with B/HK, on the other hand, neither serve as targets for L4 T_c cells[5] nor induce interferon (Table 3).

Table 1 Cytotoxic T-cell clone L4 releases interferon on contact with targets infected with influenza strain A/X31

L4 T_c cells	P815 targets virus infection	Antiserum to HA*	Interferon production (U ml^{-1})	%Target cell lysis at K/T ratio 5/1	2.5/1
+	A/X31	–	100	29.4	27
+	–	–	<3	–	–
–	A/X31	–	<3	–	–
+	A/31	1/100	120	29	26.5
+	UV A/X31	–	<3	–	–

The cytotoxicity assay was carried out as previously described[17]. In brief, P815 cells infected for 1.5 h with 800 haemagglutinin units of virus and labelled with ^{51}Cr were washed three times and plated out at 10^4 per well in 96 round bottom microtitre plates. After 6 h incubation with L4 T_c cells in 0.2 ml at 37 °C, the plates were centrifuged for 5 min at 1,000 r.p.m; 0.1-ml samples were collected and radioactivity estimated in a γ-counter. % ^{51}Cr release = c.p.m. (experimental) – c.p.m. (spontaneous release)/c.p.m. (total) – c.p.m. (spontaneous release). K/T, killer/target cell ratio. To test the production of interferon, the assay was carried out in the same way in 0.2 ml per well except that the infected target cells were not labelled with ^{51}Cr, and K/T was 10:1 or 5×10^5 Tc cells per ml. The supernatant medium was collected and interferon assayed on C3H10T$\frac{1}{2}$ cells[7] by the INAS$_{50}$ method[7]. Briefly, replicate monolayers of cells were treated overnight with dilutions of interferon. The cells were then challenged with Semliki Forest virus and the extent of virus replication directly assessed by labelling with ^{3}H-uridine in the presence of actinomycin D to suppress cell RNA synthesis. Titres are quoted in units per ml and are approximately equivalent to international units of mouse IFN-$\alpha + \beta$ (there is at present no standard for mouse IFN-γ).

* Monoclonal antibody (3/1) to haemagglutinin of A/X31[8] which does not inhibit T-cell killing, but neutralizes infective virus[9].

We further correlated the production of interferon by L4 T_c cells with their ability to recognize and kill infected H–2^d targets but not infected H–2^b cells or infected H–2^{dm2} cells (B.A.A. and Y-L.L. in preparation). The dm$_2$ mutant lacks H–2L and H–2M molecules in the D region of the major histocompatibility locus. To test the killing of virus-infected cells derived from different mouse strains it was necessary to use lipopolysaccharide-stimulated B lymphoblasts as targets, which are not so efficiently killed by L4 T_c cells as P815 tumour cells. IFN-γ production was therefore low, but the amounts produced paralleled the killing obtained in cytotoxicity assays. Thus, whereas A/X31-infected BALB/c (H–2^d) lymphoblasts were killed by L4 T_c cells and induced interferon production, A/X31-infected lymphoblasts from C57/B16 (H–2^b) or BALB/c dm$_2$ mice (H–2^{dm2}) were neither killed by L4 T_c cells nor induced interferon (data not shown).

The type of interferon produced by L4 T_c cells interacting with A/X31-infected P815 cells was determined by antiserum neutralization and acid lability tests. Two antisera were used: a sheep antiserum to interferon produced by induction of C243 cells, and a rabbit antiserum to interferon produced by induction of mouse L cells (obtained from the NIH). Both antisera neutralize both mouse IFN–α and IFN–β but not IFN–γ. We found that both antisera failed to neutralize significantly the interferon produced by L4 T_c cells in conditions where interferon produced by Newcastle disease virus-induced mouse L cells (a mixture of IFN–α and IFN–β)[10] was completely neutralized. IFN–γ is unstable at pH 2 whereas IFN–α and IFN–β are both stable[11], the interferon produced by L4 T_c cells was completely destroyed by pH 2 treatment. Therefore by both these criteria the interferon produced was IFN–γ.

Table 2 Cytotoxic T-cell clone releases interferon on contact with targets infected with heterologous type A influenza virus

L4 T_c cells	P815 targets virus infection	Interferon production (U ml^{-1})
+	A/X31	45
+	A/USSR	50
–	A/X31	<3
–	A/USSR	<3

Experimental conditions were as described in Table 1 legend. The K/T ratio for interferon production was 8:1. At a K/T of 5:1, L4 cells lysed 17% of A/X31-infected and A/USSR-infected target cells.

Recently Marcucci *et al.*[12] have tested several T-cell clones, growing in TCGF, for IFN–γ production after mitogen stimulation. These clones, derived from AKR mice sensitized with picryl chloride, produced up to 800 units of IFN–γ per 10^6 cells. All the clones were Thy-1.1 antigen positive; but since they lacked detectable Lyt markers it was not possible to determine to which T-cell subpopulation they belonged. Our data indicate that Lyt-2-positive, target-specific T_c cells produce IFN–γ on contact with their target cell. There is a previous report of production of lymphokines by T cells of both Lyt-1- and Lyt-2,3-positive phenotype[13]. The characteristics of IFN-γ production resemble closely the characteristics of killing in viral antigenic specificity and H–2 restriction. As the virus alone does not induce IFN-γ, it seems that for IFN-γ production the L4 T_c cells need to 'see' the viral antigen in the context of cellular antigens. Accessory cells (such as macrophages) seem unnecessary for IFN-γ induction, although it is possible that they may augment interferon production and our data do not exclude the possibility that other T-cell subpopulations also produce interferon on appropriate stimulation. We also cannot exclude the possibility that the interferon is produced by the target cells following specific recognition by the T_c cell, but we think this unlikely because the interferon is type γ.

Table 3 Influenza type B virus-infected target cells do not induce interferon release by L4 cytotoxic T cells

L4T_c cells	Virus infection of P815 targets	Interferon (U ml^{-1})	Target cell lysis at K/T ratio 4:1	2:1
+	A/X31	120	20.3	14.5
–	A/X31	<3	—	–
+	B/HK	<3	2.1	0.8
+	—	<3	–	–
–	B/HK	<3	–	–

Assay conditions as in Table 1. L4 T_c cells ± influenza-infected P815 targets were incubated in a microtitre plate for 6 h at K/T ratio of 9:1 (10^4 target cells per well). Cells were centrifuged and the supernatant analysed for interferon. The data show interferon released by 4.5×10^5 L4 cells per ml over 6 h. A parallel assay was carried out with ^{51}Cr-labelled and A virus-infected target cells to measure the % ^{51}Cr released during a 6 h incubation at K/T ratios as shown.

The ability of T_c cells to produce interferon when they meet their histocompatible virus-infected target cell is of considerable importance. Immune T cells have been shown to protect against influenza virus infection[14], and clone L4 cells have been shown to protect against lethal influenza infection[15] and to reduce the replication of influenza virus in the lungs of infected mice. It was thought that T_c cells protect by killing cells early after virus infection, before virion assembly but after the expression of viral proteins on the cell surface. Our finding that L4 T_c cells produce IFN-γ after contact with their target adds another dimension to the role of T_c cells in preventing spread of virus. The IFN-γ produced would reduce spread of virus released from infected cells before killing occurred, and could also activate other immune effector cells, such as natural killer cells[16], which may be involved in resistance to virus infections. It could also serve to protect the T_c cells themselves from infection.

We acknowledge the technical assistance of Mr M. Drofiak and Miss C. Gillespie for interferon assays. We thank Dr P. Demant for a gift of BALB/c dm$_2$ mutant mice and Dr M. Tovey for sheep anti-IFN antiserum. A.G.M. was supported in part by a grant from the Cancer Research Campaign.

Received 9 September; accepted 24 November 1981.

1. Wheelock, E. F. *Science* **149,** 310–311 (1965).
2. Milstone, L. M. & Waksman, B. H. *J. Immunol.* **105,** 1068–1079 (1970).
3. Babiuk, L. A. & Rouse, B. T. *Infect. Immun.* **13,** 1567–1578 (1971).
4. Gifford, G. E., Tibor, A. & Peavy, D. L. *Infect. Immun.* **3,** 164–171 (1971).
5. Lin, Y. L. & Askonas, B. A. *Nature* **288,** 164–167 (1980).
6. Reznikoff, C. A., Brankow, D. W. & Heidelberger, C. *Cancer Res.* **33,** 3231–3238 (1973).
7. Atkins, G. J., Johnston, M. D., Westmacott, L. M. & Burke, D. C. *J. gen. Virol.* **25,** 381–390 (1974).
8. Webster, R. G. & Laver, W. G. *Virology* **104,** 139–148 (1980).
9. Askonas, B. A. & Webster, R. G. *Eur. J. Immun.* **10,** 151–156 (1980).
10. Havell, F. A. & Carter, W. A. *Virology* **108,** 80–86 (1981).
11. Stewart, W. E. in *The Interferon System*, 145–149 (Springer, New York, 1980).
12. Marcucci, F., Waller, M., Kirchner, H. & Kramer, P. *Nature* **291,** 79–81 (1981).
13. Newman, W., Gordon, S., Haemmerling, U., Senik, A. & Bloom, B. B. *J. Immun.* **120,** 927–931 (1978).
14. Yap, K. L., Ada, G. L. & McKenzie, I. F. C. *Nature* **273,** 238–239 (1978).
15. Lin, Y. L. & Askonas, B. A. *J. exp. Med.* **154,** 225–234 (1981).
16. Einhorn, S., Blomgren, H. & Strander, H. *Int. J. Cancer* **22,** 405–412 (1978).
17. Zweerink, H. J., Courtneidge, S. A., Skehel, J. J., Crumpton, M. J. & Askonas, B. A. *Nature* **267,** 324–356)1977).

Phorbol-12,13-diester 12-ester hydrolase may prevent tumour promotion by phorbol diesters in skin

Mohammed Shoyab, Thomas C. Warren & George J. Todaro

Laboratory of Viral Carcinogenesis, National Cancer Institute,
National Institutes of Health, Frederick, Maryland 21701, USA

Tumour promoters are not themselves carcinogenic but can induce tumours in mice treated previously with an otherwise insufficient dose of certain chemical carcinogens[1–6]. One of the most potent tumour-promoting agents is 12-*O*-tetradecanoyl-phorbol-13-acetate (TPA), initially isolated from croton oil[7]. The effects of tumour promoters are species specific[8]; croton oil, of which TPA is the most active component, does not act as a tumour promoter in rat, rabbit, guinea pig or hamster skin in conditions for which it is a potent tumour promoter in mouse skin[8–12]. Recently, we have purified the enzyme phorbol-12,13-diester 12-ester hydrolase (PDEH) to homogeneity from mouse and human liver cytosol[13]. This enzyme converts biologically active phorbol-12, 13-diesters to the inactive phorbol-13-monoester[13] in a dose-, time- and temperature-dependent manner. PDEH has been partially purified from hamster skin but is not detected in mouse skin, suggesting that the basis for the TPA tumour promotion only in mouse skin is a result of differences between the species in levels of TPA inactivating enzyme (PDEH) in the skin. We demonstrate here that responsiveness to TPA-induced tumour promotion is related to the level of PDEH activity in skin of all animals tested.

TPA elicits various biological and biochemical responses *in vitro* as well as *in vivo*[1–6,14–18]. High-affinity specific receptors for biologically active phorbol and ingenol esters have been reported for a wide variety of cells in culture as well as in animal tissues[19,20]. The lack of responsiveness of certain animal species to two-stage tumorigenesis is apparently not due to the lack of initiating carcinogenic activity because rabbit and hamster are highly susceptible to skin carcinogenesis caused by polycyclic aromatic hydrocarbons[21,22].

Table 1 Distribution of PDBu binding sites in skin of various species

Species	^{3}H-PDBu binding (ng per mg protein)
Mouse (BALB/c)	0.38
Rat (Fisher)	0.52
Guinea pig (N-2)	0.35
Hamster (Syrian)	0.23
Rabbit (NZW)	0.35
Cat	0.41
Dog	0.42
Rhesus monkey	0.37
Human	0.32

The shaved skins from adult animals were minced and suspended in 5 vol of cold phosphate-buffered saline (PBS) and disrupted with a polytron PT-10 (Brinkman) at 21,000 r.p.m. at 4 °C for 180 s. Four 30-s pulses at 30-s intervals were used. The crude homogenate was centrifuged at 105,000*g* for 1 h at 4 °C. Human skin from an autopsy specimen of a 5-yr-old female accident victim was similarly processed. The supernatant was removed and used for PDEH assay. The pellet was resuspended in the original volume of cold PBS. The binding of ^{3}H-PDBu to crude homogenate or pellet suspension was performed in duplicate in 12 × 75 mm disposable glass tubes (Kimax) in the absence or presence of 20 μg ml^{-1} unlabelled PDBu. The binding mixture contained 5 ng ^{3}H-PDBu ($\sim 4 \times 10^4$ c.p.m.), 0.2% final concentration of dimethyl sulphoxide (DMSO) and several concentrations of crude homogenate or pellet suspension in a total volume of 0.25 ml binding buffer (BB) consisting of Dulbecco's minimum essential medium (DMEM) containing bovine serum albumin (BSA, 1 mg ml^{-1}) and *N*,*N*-bis-(2-hydroxyethyl)-2-amine-ethane sulphonic acid (BES, 5 mM), adjusted to *p*H 6.8. After incubation at 23 °C for 30 min, tubes were chilled, 0.25 ml cold 4% calf serum (Colorado Serum Corporation) and 0.7 ml cold 25% polyethylene glycol (PEG 6,000) in 1 mM Tris-HCl *p*H 7.4 were added to each tube, the contents vortexed and the tubes allowed to stand at 4 °C for 15 min before being centrifuged (1,500*g* for 10 min at 4 °C). The supernatant solution was carefully drained off, the pellet resuspended in 2.5 ml of cold 10% PEG in 0.1 M Tris-HCl *p*H 7.4, and the tubes were again centrifuged as described above. The supernatant solution was removed and pellets solubilized in 0.8 ml of lysing buffer (0.01 M Tris-HCl *p*H 7.4, containing 0.5% SDS and 1 mM EDTA). The mixture was transferred to counting vials and 10 ml Aquassure (NEN) added to each vial. The vials were shaken vigorously and radioactivity determined using a Beckman β counter. The radioactivity bound in the presence of 20 μg ml^{-1} (50–200 c.p.m.) unlabelled PDBu was considered to be nonspecific and all data were corrected accordingly. Protein concentration was determined as described elsewhere[27]. The animal strains used are given in parentheses.

The phorbol diester inactivating enzyme (PDEH) is a single-chain, hydrophobic glycoprotein with a molecular weight (MW) of 60,000. It has an isoelectric point (*p*I) of 5, exhibits optimum activity at *p*H 7.5–8.5, and is heat- and acid-labile. Phenylmethylsulphonyl fluoride (PMSF) is a potent inhibitor of the enzyme, as are zinc, cobalt and fluoride ions. The amino acid composition and certain properties of the enzyme are different from purified porcine liver carboxy esterase (EC 3.1.1.1)[23,24]. The natural substrate(s) of PDEH are unknown; however, porcine liver esterase (Sigma) unlike PDEH, does not inactivate phorbol diester.

To investigate the restriction of TPA action in nonresponsive species, we studied the specific receptors for biologically active phorbol esters[19,20] and PDEH activity in skin of various species. Enzyme activity was measured by incubating ^{3}H-PDBu (phorbol-12,13-dibutyrate) and tissue extract at 37 °C for 30 min and then measuring the amount of remaining ^{3}H-PDBu by its binding to mouse brain membranous fraction (BMF), the richest source of receptors[20], for 30 min at 23 °C. We found that skin from all species tested contains TPA receptors, and that PDEH activity is absent from normal mouse skin, but present in very high levels in hamster, rat, guinea pig and rabbit skin. The distribution of PDBu binding sites in skin of various species is given in Table 1. Skin from all species (mouse, rat, guinea pig, hamster, rabbit, cat, dog, monkey and human) bound between 0.32 and 0.52 ng PDBu per mg protein. Thus, responsive and nonresponsive animals have roughly comparable levels of TPA receptors in their skin. Therefore, the lack of responsiveness to TPA characteristic of most rodent species except the mouse, is not due to the absence of specific TPA receptors.

Figure 1 shows that extracts from hamster, rat, guinea pig or

Table 2 Distribution of phorbol diester-12-esterase activity in skin of various species

Skin extract	Activity (^{3}H-PDBu cleaved; ng per mg protein)	TPA responsiveness (skin carcinogenesis)
Mouse (*nu*$^-$/*nu*$^-$)	<0.1	++
Heterozygote mouse (*nu*$^+$/*nu*$^-$)	<0.1	NK
Nude mouse (*nu*$^+$/*nu*$^+$)	1.7	–
Rat	22.7	–
Guinea pig	13.9	–
Hamster	100.8	–
Rabbit	7.8	–
Cat	<0.1	NK
Dog	<0.1	NK
Rhesus monkey	<0.1	NK
Human	0.1	NK

NK, not known. –, With low doses of TPA[15].

rabbit readily inactivated ^{3}H-PDBu, reducing its binding to the specific receptors in a dose-dependent manner. In contrast, extracts from mouse, cat, dog, monkey and human skin do not affect ^{3}H-PDBu binding to receptors. Failure of nude mouse skin to respond to low doses of TPA has been reported elsewhere[25]. Interestingly, nude mouse skin extracts contain small but significant amounts of PDEH whereas heterozygote mouse skin extracts, like wild-type mouse skin extracts, do not express any activity (Fig. 1). The levels of PDEH enzyme activity in skin extracts from various species are shown in Table 2. Hamster, rat, guinea pig, rabbit and nude mouse extracts cleaved, respectively, 100.8, 22.7, 13.9, 7.8 and 1.7 ng PDBu per mg protein, in our assay conditions. Mixing experiments demonstrated that the mouse skin extract contains a low level of a PDEH inhibitor, which can slightly decrease the hamster enzyme activity.

Table 3 summarizes a HPLC analysis of ^{3}H-PDBu treated with skin extract from various species. Extracts from hamster, rat, guinea pig and rabbit skin converted ^{3}H-PDBu to ^{3}H-13-PB (phorbol-13-butyrate) while there was no reduction in ^{3}H-PDBu nor appearance of other metabolites in samples treated with mouse, cat, dog, monkey or human skin extracts. HPLC analysis of ^{3}H-PDBu metabolite(s) (24 h after PDBu application) from mouse, hamster and guinea pig skin *in vivo* revealed that all the radioactivity recovered from mouse skin co-elutes with PDBu, whereas ~80% of the labelled material from hamster and ~96% radioactivity from guinea pig skin co-elutes with 13-PB, the rest remaining as PDBu. Thus, the direct application of PDBu to skin gave the same results as those obtained using skin extracts in an *in vitro* assay.

Table 3 HPLC analysis of ^{3}H-PDBu treated with skin extract from various species

Species	% Radioactivity eluted as PDBu	13-PB
Control	100	0
Mouse	100	0
Rat	0	100
Guinea pig	2.6	97.4
Hamster	0	100
Rabbit	35.2	64.8
Cat	100	0
Dog	100	0
Rhesus monkey	100	0
Human	100	0

^{3}H-PDBu (120 μl; ~16×10^4 c.p.m.) in BB, 0.2% final concentration DMSO and 2 mg of skin extract protein in 0.8 ml PBS were incubated for 1 h at 37 °C. ^{3}H-PDBu and products were extracted with a chloroform–methanol mixture (2 : 1), the organic phase containing almost all radioactivity dried under nitrogen, the material dissolved in 25 μl DMSO. Ten microlitres from each sample were analysed by HPLC using C_{18}-Bondapak/Porasil (Waters Associates)[13].

Our results show a close relationship between levels of PDEH activity in skin and responsiveness to TPA-induced tumour promotion in skin in all cases (mouse, hamster, rabbit, guinea pig and rat) for which data are available. Thus, TPA susceptibility of mouse skin, but not of other animal skin, may be due to the lack of expression of PDEH in this tissue. The high levels of PDEH in a tissue would inactivate TPA or other active phorbol esters, leading to insensitivity of that tissue to TPA-induced tumour promotion. On the basis of this observation, one would predict that TPA and related active diterpene esters would act as tumour promoters in cat, dog, monkey and human skin. An effective inhibitor of PDEH such as PMSF[13] would potentiate the action of TPA in skin and might make TPA-nonresponsive animals become sensitive to TPA. Conversely, inducers of the enzyme might render a responsive animal nonresponsive. Increasing the dose of TPA and/or TPA treatment frequency would probably enhance the susceptibility to TPA-elicited tumour promotion in PDEH-positive tissues. In addition, those tumour promoters which do not contain an ester group, such as dihydroteleocidin B[26], should be refractory to the action of PDEH and concomitantly, should act as promoting agents in PDEH-positive tissues, provided that they are not inactivated by some other enzyme in the tissue. Although PDEH is not expressed in mouse skin, very high amounts of the enzyme can be isolated from mouse liver and kidney. One would expect these tissues, like hamster, rat, rabbit or guinea pig skin, to be refractory to the various actions of the TPA-related tumour promoters.

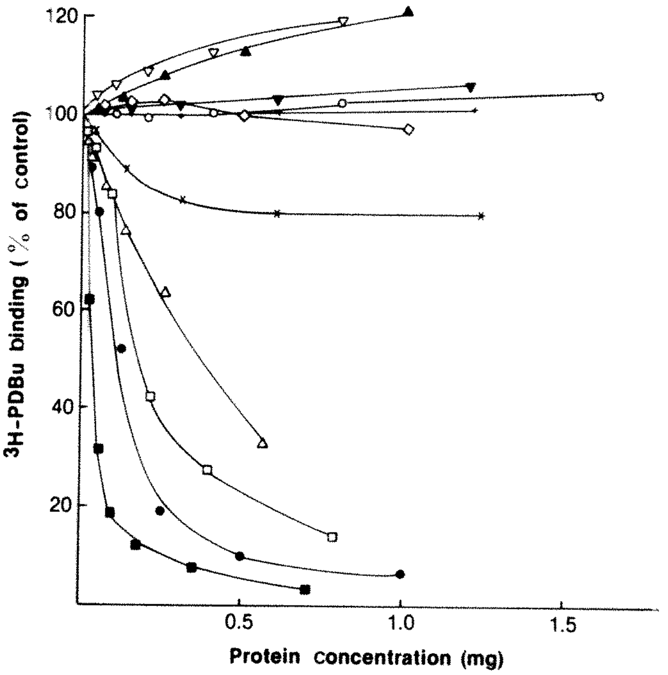

Fig. 1 Effects of protein concentration in skin extracts from various species on ^{3}H-PDBu inactivation. ^{3}H-PDBu (5 ng in 30 μl BB buffer), 0.2% final concentration DMSO and 0–200 μl of skin extract in PBS in a final volume of 0.23 ml were incubated in duplicate at 37 °C for 30 min. Tubes were placed on ice and 20 μl of murine BMF in PBS (50 μg protein) were added to each tube, the contents of the tubes were mixed and incubated at 23 °C for 30 min. After this time PDBu binding was determined as described in Table 1; 100% binding represents ~5,000 c.p.m. ○, Inbred mouse (*nu*$^-$/*nu*$^-$); +, heterozygote mouse (*nu*$^+$/*nu*$^-$); ×, nude mouse (*nu*$^+$/*nu*$^+$); ●, rat; □, guinea pig, ■, hamster; △, rabbit; ▲, cat; ▽, dog; ▼, rhesus monkey; ◇, human.

Received 1 September; accepted 22 October 1981.

1. Van Duuren, B. L. *Prog. exp. Tumour Res.* **11,** 31 (1969).
2. Hecker, E. *Meth. Cancer Res.* **6,** 439 (1971).
3. Boutwell, R. K. *Crit. Rev. Tox.* **2,** 419 (1974).
4. Slaga, T. J., Sivak, A. & Boutwell, R. K. (eds) *Mechanisms of Tumor Promotion and Cocarcinogenesis* (Raven, New York, 1978).

5. Sivak, A. *Biochim. biophys. Acta* **560,** 67 (1979).
6. Diamond, L., O'Brien, T. & Baird, W. M. *Adv. Cancer Res.* **32,** 1 (1980).
7. Hecker, E. *Cancer Res.* **28,** 2338 (1968).
8. Shubik, P. *Cancer Res.* **10,** 13 (1950).
9. Della Porta, G., Rappaport, H., Saffiotti, U. & Shubik, P. *Archs Path.* **61,** 305 (1956).
10. Shubik, P., Pierta, G. & Della Porta, G. *Cancer Res.* **20,** 100 (1960).
11. Saffiotti, U. & Shubik, P. *J. natn. Cancer Inst.* **10,** 489 (1963).
12. Goerttler, K., Loehrke, H., Schweizer, J. & Hesse, B. *Cancer Res.* **40,** 155 (1980).
13. Shoyab, M., Warren, T. C. & Todaro, G. J. *J. biol. Chem.* **256** (in the press).
14. Lee, L. S. & Weinstein, I. B. *Science* **202,** 313 (1978).
15. Shoyab, M., De Larco, J. E. & Todaro, G. J. *Nature* **279,** 387 (1979).
16. Brown, K. D., Dicker, P. & Rozengurt, E. *Biochem. biophys. Res. Commun.* **86,** 1037 (1979).
17. Shoyab, M. & Todaro, G. J. *J. biol. Chem.* **288,** 8735 (1980).
18. Shoyab, M. & Todaro, G. J. *Archs Biochem. Biophys.* **206,** 222 (1981).
19. Driedger, P. E. & Blumberg, P. M. *Proc. natn. Acad. Sci. U.S.A.* **77,** 567 (1980).
20. Shoyab, M. & Todaro, G. J. *Nature* **288,** 451 (1980).
21. Berenblum, I. *J. natn. Cancer Inst.* **10,** 167 (1949).
22. Homberger, F., Hsueh, S. S., Ker, C. S. & Russfield, A. B. *Cancer Res.* **32,** 360 (1972).
23. Heymann, E. & Junge, W. *Eur. J. Biochem.* **95,** 509 (1979).
24. Miller, S. K., Russelmain, A. & Rush, R. S. *J. biol. Chem.* **255,** 7161 (1981).
25. Krueger, G. G., Chambers, D. A. & Shelby, J. *J. exp. Med.* **152,** 1329 (1980).
26. Fujiki, H., Mori, M., Nakayasu, M., Tereda, M. & Sugimura, T. *Biochem. biophys. Res. Commun.* **90,** 976 (1979).
27. Lowry, O. H., Rosebrough, N. J., Farr, A. L. & Randall, R. J. *J. biol. Chem.* **193,** 265 (1951).

Calmodulin confers calcium sensitivity on secretory exocytosis

Richard A. Steinhardt & Janet M. Alderton

Department of Zoology, University of California, Berkeley, California 94720, USA

The cortical reaction at fertilization of a sea urchin egg results in the elevation of the fertilization membrane due to the exocytosis of cortical granules lying directly beneath the plasma membrane. These secretory granules are vesicles ~1 μm in diameter and can be easily observed in phase-contrast optics. Insemination of the egg results in the release of intracellular ionized calcium which acts as the trigger for the fusion of the cortical granules with the plasma membrane and the expulsion of their contents into the extracellular space[1,2]. Although Ca^{2+} is known to be involved in exocytosis, it has not yet been clearly demonstrated how the high sensitivity to calcium is conferred on exocytosis[3,4]. Here we examine the action of antibodies to calmodulin on the secretion of the cortical granules and demonstrate that calmodulin is responsible for the high calcium sensitivity of the cortical reaction and can be localized on the inner plasma membrane surface.

Baker and Whitaker have previously shown that the calcium sensitivity for cortical granule fusion with the plasma membrane is the same for both intact eggs and their *in vitro* preparation of isolated cortical surfaces[5]. Furthermore, they could stabilize the micromolar calcium thresholds for exocytosis by keeping the isolated surfaces in media containing millimolar concentrations of ATP[5]. They also demonstrated a strong inhibition by the antipsychotic drug trifluoroperazine, which suggested that a modulatory calcium-binding protein was involved in exocytosis[6].

Calmodulin is a ubiquitous calcium-binding protein used in many regulatory pathways and has been found in sea urchin eggs where it is known to activate NAD kinase[7-10]. The *in vitro* preparation for exocytosis allowed us to test directly the effects of antibodies to calmodulin without complications from poisoning other enzyme systems. Commercially obtained antibody to electrophoretically homogeneous native rat testis calmodulin was produced in sheep and the calmodulin-specific IgG was purified from other sheep immunoglobins and proteins by affinity chromatography on calmodulin–Sepharose[11]. Isolated cortical surfaces were prepared on poly-lysine-coated glass coverslips in the form of small (5 μl) chambers which could be directly observed with a Zeiss phase microscope while solutions were changed. These chambers were then incubated at 100% humidity and 16 °C in the isolation medium either alone or with calmodulin antibody or preimmune serum or calmodulin antibody plus excess calmodulin (purified from bovine testis)[12]. At the end of the incubation period, each chamber was photographed before and 60 s after testing with a single calcium concentration and the number of reacted cortical granules was counted.

When tested with the isolation medium alone, the calcium sensitivity of exocytosis remained constant for all periods of incubation with >70% discharge of the cortical granules within 60 s at 5 μM Ca^{2+}. Short periods of incubation (45 min) with the calmodulin antibody had no inhibitory effect but inhibition rapidly set in with longer periods, with the calcium threshold rising to 150 μM Ca^{2+} at 65 min and complete block even to 1 mM Ca^{2+} at 75 min. Figure 1 shows the results obtained with 75-min incubations, demonstrating the complete block induced by treatment with calmodulin antibody. In contrast, controls with isolation medium alone, preimmune serum or calmodulin antibody preincubated with excess calmodulin (at a ratio of 7 mol of calmodulin to 1 mol antibody) retain their high sensitivity to Ca^{2+}. A complete reversal of this block could be obtained by a further 10 min of treatment with calmodulin at a concentration of 2×10^{-5} M ($n = 3$). The rapid onset of the block after a delay and the much shorter period required for reversal with calmodulin suggests that a large excess of calmodulin is associated with each cortical granule–plasma membrane complex with only a relatively few calmodulin sites necessary for full calcium sensitivity and discharge at 5 μM Ca^{2+}. If this

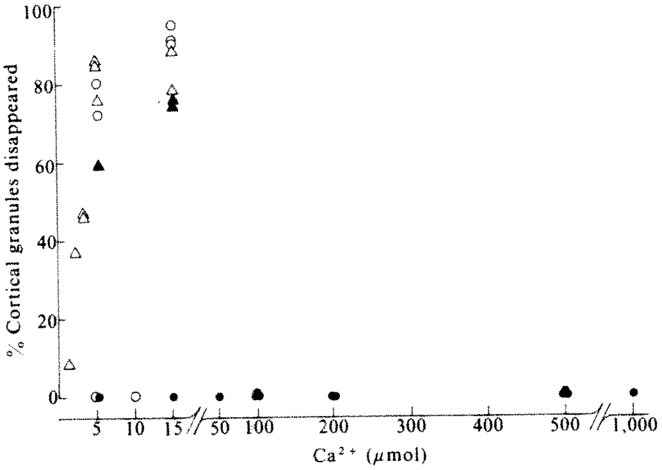

Fig. 1 Influence of antibody to calmodulin on the calcium sensitivity of exocytosis in isolated cortical surfaces. △, Controls in which the cortices were incubated in the isolation medium alone. ▲, Cortices incubated in isolation medium containing 750 μg ml^{-1} protein preimmune serum. ○, Cortices incubated in isolation medium containing 400 μg ml^{-1} sheep antibody to calmodulin plus 2×10^{-5} M bovine testis calmodulin[12]. This represents a molar ratio of 7 calmodulin to 1 sheep IgG. Antibody was preincubated with calmodulin for 1 h before being applied to the cortices. ●, Cortices incubated in isolation medium containing 400 μg ml^{-1} calmodulin antibody. Eggs of the sea urchin *Lytechinus pictus* were obtained as previously described[1]. Isolated cortical surfaces were prepared by the method of Baker and Whitaker[5] by sticking portions of egg cortices on glass coverslips with poly-DL-lysine in the following isolation medium: 250 mM potassium gluconate, 500 mM glycine, 10 mM NaCl, 10 mM HEPES, 10 mM EGTA, 5 mM Mg-ATP, 1 mM free Mg^{2+}, 10^{-7} free Ca^{2+}, pH 6.7. Ionized calcium and magnesium concentrations were calculated from the stability constants for EGTA[14]. The abscissa represents the ionized calcium concentration in the test solutions which were otherwise identical to the isolation medium except that no attempt was made to buffer calcium with EGTA at Ca^{2+} concentrations above 15 μM. Solution changes were made by placing a fragment of filter paper at one open end of the small (5 μl) glass coverslip chamber containing the cortical surfaces and flushing gently 20 μl of new solution through from the other end; this was repeated three times. After a 75-min incubation period at 16 °C, each chamber was viewed with a Zeiss inverted microscope (IM35) using a 63 power oil immersion phase objective. Each cortical preparation was photographed before and 60 s after the introduction of the test solution, with the time being measured from the time of the second flush of new solution. Preimmune serum and antibody to calmodulin were obtained from CAABCO, Houston, Texas. This non-precipitating sheep calmodulin antibody demonstrates cross-reactivity to calmodulin from vertebrates, invertebrates and plants, and exhibits <0.2% cross-reactivity to troponin C and no cross-reactivity to parvalbumin[11].

0028–0836/82/020154—02$01.00

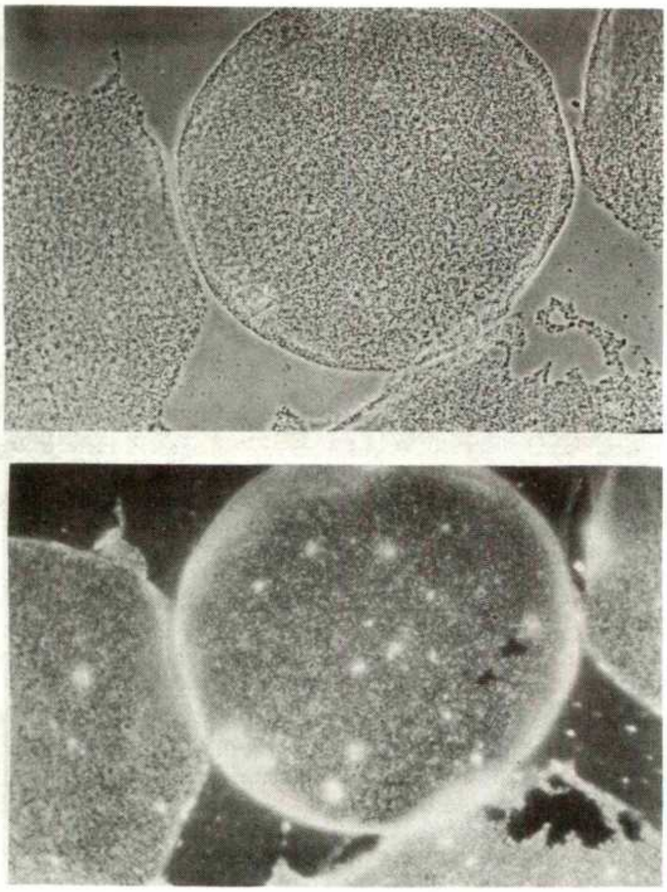

Fig. 2 Indirect immunofluorescent localization of calmodulin on the cytoplasmic side of isolated cortical fragments. Isolated cortical surfaces with only the cytoplasmic side exposed to medium were prepared as described in Fig. 1 legend on poly-lysine-coated glass coverslips. After following the same incubation procedure for 75 min with calmodulin antibody, the cortices were incubated for a further 60 min with fluorescein isothiocyanate-conjugated anti-sheep antibody prepared in rabbit, diluted 16-fold in the isolation medium (Miles). In controls in which the preincubation was with preimmune serum, calmodulin antibody adsorbed with excess calmodulin or isolation medium alone showed little or no staining except for occasional spots where the rabbit fluorescein isothiocyanate-conjugated antibody was trapped in a bit of debris or fold of the cortices. Zeiss epifluorescent microscope, ×63 phase optics. The stuck-down cortical diameter averages 120 μm.

explanation is correct, the delay reflects the time for the lower-affinity components of our heterologous antibody to bind and cover the last sites.

Immunofluorescent localization of calmodulin revealed heavy granular staining in the plane of the plasma membrane just beneath the layer of cortical granules (Fig. 2). During the repeated washes of the immunofluorescent procedure many of the cortical granules were washed away but staining was still found where they had been. Of course we cannot state definitely whether or not calmodulin was associated with the granules as well as the membrane, but it seems most likely that it is associated with both at the region of attachment. Having examined more than 24 samples, we suspect that the pattern of calmodulin staining corresponds to the cortical granule sites since the numbers are consistent with such a logical association; however, this conclusion cannot be convincingly reached using a light microscope and proof would require examination with anti-sheep ferritin-conjugated antibody using an electron microscope.

An important question arises as to whether the isolated fragments can be used as a model for real exocytosis or whether the *in vitro* system operates by some other means of granule discharge. Decker and Lennarz showed that in isolated fragments, a normal vitelline complex with the correct orientation was formed when cortical fragments were exposed to calcium ions[13]. Similar results have been obtained for stuck-down cortical fragments which, when exposed to 3 μM Ca^{2+}, undergo exocytosis, forming the perivitelline space and vitelline membrane (M. J. Whitaker and P. F. Baker, personal communication). Estimates of the peak calcium ion transient at fertilization from aequorin measurements fall in the same range (2.5–4.5 μM)[1]. These results and the identical sensitivity to calcium ions for both intact eggs suddenly lysed in Ca^{2+}-EGTA buffers and stuck-down cortical fragments strongly imply that identical mechanisms of exocytosis are involved[5].

To our knowledge, the results reported here are the strongest evidence to date for direct involvement of a known protein in fusion of a natural biological membrane and exocytosis at physiological concentrations of calcium ions. Our finding implies that calmodulin is bound to the inside surface of the plasma membrane and is integrally involved in the exocytosis of cortical granules, conferring the high sensitivity of calcium on that process. As other exocytotic systems also exhibit a similar dependence on calcium[3,4], we expect that calmodulin or other similar calcium-binding modulatory proteins will be shown to be involved in exocytosis generally.

This work was supported by NSF grant PCM 81-04294 to R.A.S. We thank Dr Joan Egrie for the gift of purified calmodulin and many useful discussions.

Received 22 September; accepted 13 November 1981.

1. Steinhardt, R., Zucker, R. & Schatten, G. *Devl Biol.* **58,** 185–196 (1977).
2. Zucker, R. & Steinhardt, R. *Biochim. biophys. Acta* **541,** 459–468 (1978).
3. Rubin, P. *Calcium and the Secretory Process* (Plenum, New York, 1974).
4. Douglas, W. W. in *Calcium Transport in Contraction and Secretion* (eds Carafoli, E., Clementi, F., Drabiknowski, W. & Margreth, A.) 167–174 (North-Holland, Amsterdam, 1975).
5. Baker, P. F. & Whitaker, M. J. *Nature* **276,** 513–515 (1978).
6. Baker, P. F. & Whitaker, M. J. *J. Physiol., Lond.* **298,** 55P (1979).
7. Means, A. R. & Dedman, J. R. *Nature* **285,** 73–78 (1980).
8. Cheung, W. Y. *Science* **207,** 19–27 (1980).
9. Head, J. F., Mader, S. & Kaminer, B. *J. Cell Biol.* **80,** 211–218 (1979).
10. Epel, D., Patton, C., Wallace, R. W. & Cheung, W. Y. *Cell* **23,** 543–550 (1981).
11. Dedman, J. R., Welsh, M. J. & Means, A. R. *J. biol. Chem.* **253,** 7515–7521 (1978).
12. Dedman, J. R., Welsh, M. J. & Means, A. R. *J. biol. Chem.* **252,** 8415–8422 (1977).
13. Decker, G. L. & Lennarz, W. J. *J. Cell Biol.* **81,** 92–103 (1979).
14. Martell, A. E. & Smith, R. M. *Critical Stability Constants* (Plenum, New York, 1974).

Measurement of changes in cytoplasmic free Ca^{2+} in fused cell hybrids

M. B. Hallett & A. K. Campbell

Department of Medical Biochemistry, Welsh National School of Medicine, Heath Park, Cardiff CF4 4XN, UK

The investigation of many problems in cell biology requires a method for studying chemical 'events' in living cells. For example, the measurement of cytosolic free Ca^{2+}, using Ca^{2+} indicators in giant cells, has provided vital evidence for the role of this ion in the activation of cells by electrical and chemical stimuli[1]. However, the incorporation of Ca^{2+} indicators into small cells (diameter <20 μm), without causing irreversible damage, has proved extremely difficult[1]. Recently, an elegant new technique has been reported[2] for entrapping within small cells a fluorescent Ca^{2+} indicator after hydrolysis within the cell of a membrane-permeant ester of the compound. We have developed a method, using Sendai virus, for fusing cells with erythrocyte ghosts containing photoprotein Ca^{2+} indicators and other membrane-impermeant chemiluminescent-labelled indicators[3,4]. Because of the sensitivity of chemiluminescent analysis, these indicators can be used at concentrations which do not significantly disturb the chemistry of the cells. The ultimate aim was to establish a cell system in which free Ca^{2+}, oxygen radicals and cyclic nucleotides could be directly monitored. Here we report the incorporation of the photoprotein, obelin[5], an indicator of free Ca^{2+}, into small mammalian cell hybrids.

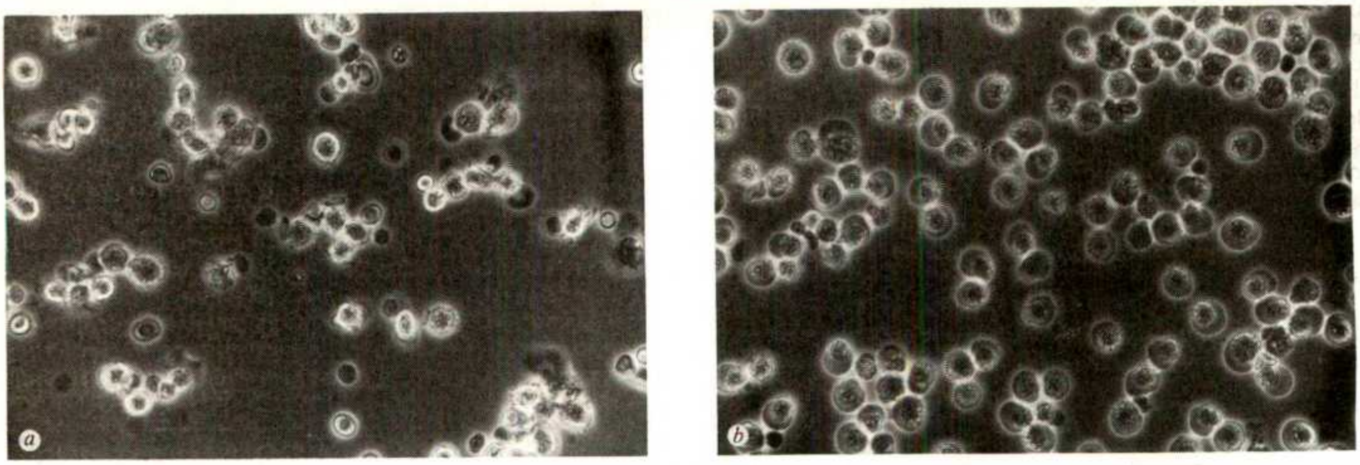

Fig. 1 Phase-contrast microscopy of unfused cells and hybrids. Human erythrocyte ghosts containing obelin were prepared from washed human erythrocytes by lysing preswollen erythrocytes[6] in 10 mM TES (*N*-Tris-(hydroxymethyl)-methyl-2-amino-ethanesulphonic acid, treated with Chelex-100, see ref. 1) and adding obelin (1–10 μl) for 10 min at 0 °C. Isotonicity was restored by addition of KCl (pure) to give a final concentration of 150 mM, and the ghosts were resealed at 37 °C for 30 min. Rat polymorphonuclear leukocytes were isolated from the peritoneal fluid of rats previously injected intraperitoneally with sodium caseinate as previously described[7]. Fusion was achieved by resuspending a mixture of erythrocyte ghosts (5×10^7) and polymorphonuclear leukocytes (5×10^7) in 100 μl of ice-cold medium containing 150 mM NaCl (pure), 10 mM TES–Chelex, 0.25 mM uranyl acetate and 1,500 haemagglutinating units of UV-inactivated Sendai virus, *p*H 7.4. After 10 min at 0 °C, the suspension was incubated at 37 °C for a further 30 min, washed and resuspended in 120 mM NaCl, 4.8 mM KCl, 1.2 mM KH_2PO_4, 1.2 mM $MgSO_4$ and 25 mM HEPES, *p*H 7.4. Unfused polymorphonuclear leukocytes were separated from the hybrids by centrifugation through a preformed Percoll gradient (density 1.05–1.09 g ml^{-1}) at 1,000*g* for 20 min. *a*, Unfused mixture of human erythrocyte ghosts and rat polymorphonuclear leukocytes; *b*, hybrid cells, showing the granules associated with the polymorphonuclear leukocyte portion of the hybrid and the clear cytoplasm associated with the ghosts. Cells and hybrids were stored for 24 h at 4 °C before the photographs were taken.

Human erythrocyte ghosts containing obelin were prepared by a modification of the 'pre-swell' method of Rechsteiner[6]. Rat polymorphonuclear leukocytes were prepared after intraperitoneal injection of sodium caseinate[7]. Fusion was achieved by resuspending a mixture of erythrocyte ghosts and polymorphonuclear leukocytes in a medium containing Sendai virus (Fig. 1). More than 99% of cells in the final preparation were hybrids, as observed by light microscopy (Fig. 1). Oxygen radical formation detected by chemiluminescence was used to monitor a Ca^{2+}-dependent response in the hybrids[8]. A major problem associated with using Sendai virus as a fusogen has been that the virus causes cell lysis. A crucial factor in our method is the use of uranyl acetate in the fusion medium[9], which reduces virus-induced haemolysis of the ghosts from 89% to 2.5%, as measured by haemoglobin release. A second important feature is the absence of extracellular Ca^{2+} during fusion. Although the role of intracellular Ca^{2+} in cell fusion is controversial[10], we have demonstrated that an increase in intracellular free Ca^{2+} is an early event in ghosts exposed to Sendai virus and occurs before fusion (P. Fuchs, M.B.H and A.K.C., unpublished observations). This rise in free Ca^{2+} can cause consumption of >90% of the obelin. However, because this large rise in free Ca^{2+} is not essential for fusion, extracellular Ca^{2+} was omitted from the fusion medium so as to maintain the obelin active in the hybrids. The hybrids were capable of responding to a phagocytic stimulus (latex beads), which induces the production of oxygen radicals, detected by luminol-amplified chemiluminescence[7,8]. The response of the hybrid cells to latex beads was 50–80% of that in the unfused polymorphonuclear leukocytes.

We have developed a method[11,12] for quantifying the extent of fusion between the erythrocyte ghosts and polymorphonuclear leukocytes using the activation of complement by two antisera, one specific for the human erythrocyte ghosts and the other specific for the rat polymorphonuclear leukocytes. Formation of

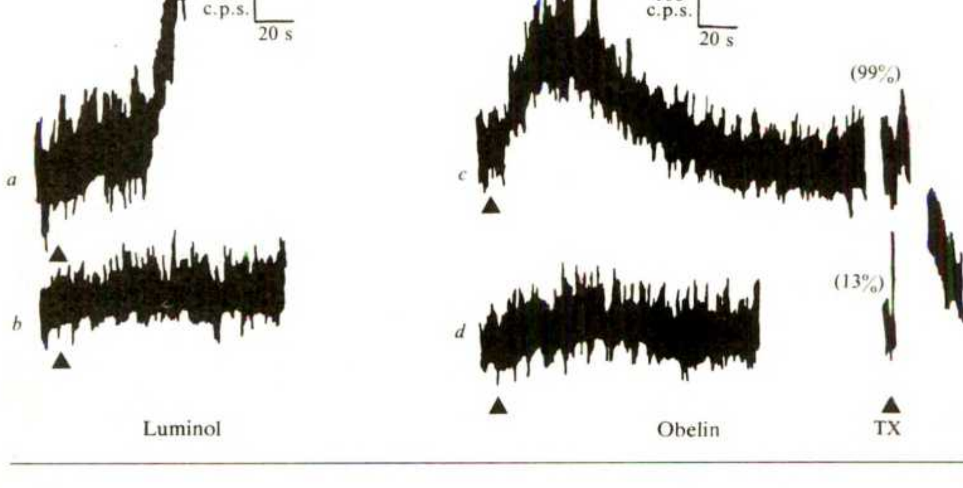

Fig. 2 Obelin luminescence and luminol-amplified chemiluminescence from unfused cells and hybrids. Approximately 5×10^6 hybrids or 10^7 total cells in the unfused mixture were resuspended in 500 μl of Krebs–Ringer HEPES buffer (120 mM NaCl, 4.8 mM KCl, 1.2 mM $MgSO_4$, 1.2 mM KH_2PO_4, 1.3 mM $CaCl_2$, 0.1% bovine serum albumin, (w/v), 25 mM HEPES, *p*H 7.4) and preincubated for 2 min at 37 °C with either anti-human erythrocyte antisera (20 μl) (*a*, *b*) or anti-polymorphonuclear antisera (20 μl anti-rat 5′-nucleotidase antiserum) (*c*, *d*). Oxygen radical formation was monitored after addition of 10 μM luminol to the extracellular medium by chemiluminescence (*a*, *b*). Obelin luminescence was monitored in the absence of luminol and consumption of obelin was demonstrated by addition of Triton X-100 (scintillation grade 2%, w/v) at the end of the time period (TX), allowing all remaining obelin to be stimulated (*c*, *d*). Values in parentheses show the % obelin consumed. *a*, *c* Show responses from hybrids and *b*, *d* responses for unfused cells. At the arrow, human serum (50 μl in 500 μl of Krebs–Ringer HEPES buffer) as a source of complement was added to the suspension. The vertical scale shows luminescent counts per second (c.p.s.) and the horizontal scale shows time.

the complement terminal attack complex on the ghost membrane results in a rapid rise in the intracellular free Ca^{2+} concentration after binding of complement component C9 (ref. 12). Activation of complement by anti-rat polymorphonuclear leukocyte antibody bound to the polymorphonuclear leukocyte surface stimulates oxygen radical formation from the polymorphonuclear leukocyte, and this effect also requires[7] Ca^{2+} and complement component C9. After fusion of the erythrocyte ghosts with polymorphonuclear leukocytes, observed microscopically, complement activation by anti-rat polymorphonuclear leukocyte antibody stimulated obelin luminescence and complement activation by anti-human erythrocyte antibody stimulated oxygen radical formation from the hybrids (Fig. 2). In contrast, no obelin response was detectable from the unfused cell mixture when complement was activated by anti-rat polymorphonuclear leukocyte antibody and no oxygen radical formation was detectable when complement was activated by anti-human erythrocyte antibody (Fig. 2). In the conditions described for Fig. 1, 60–80% of the obelin originally entrapped in the ghosts was transferred to the hybrids.

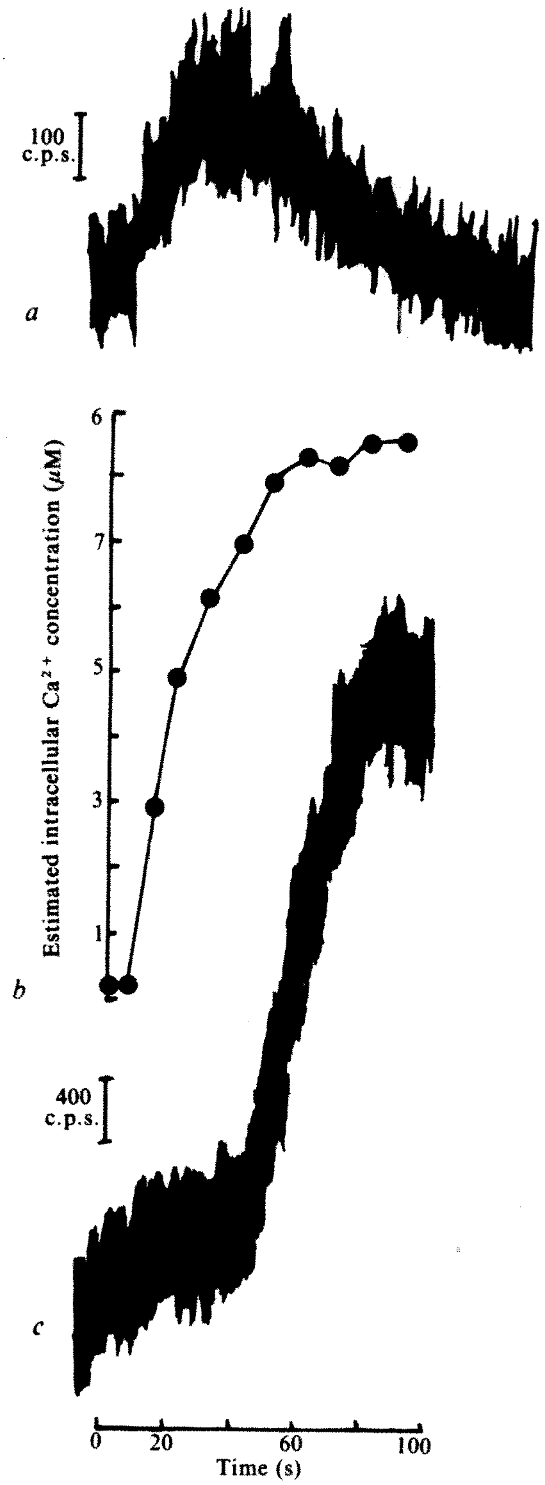

Fig. 3 Relationship between intracellular Ca^{2+} and oxygen radical production from the hybrids. Hybrids were stimulated with anti-polymorphonuclear leukocyte antibody plus complement as described in Fig. 2 legend. *a*, Obelin luminescence; *b*, the cytoplasmic Ca^{2+} estimated from *a*. The rate constant of obelin luminescence was calculated from *a* at various times, and converted to a free Ca^{2+} concentration by reference to a calibration curve relating rate constant to free Ca^{2+} in the presence of 2 mM Mg^{2+} (see ref. 12). *c*, The luminol-amplified chemiluminescence resulting from oxygen radical formation, accompanying stimulation of the hybrids.

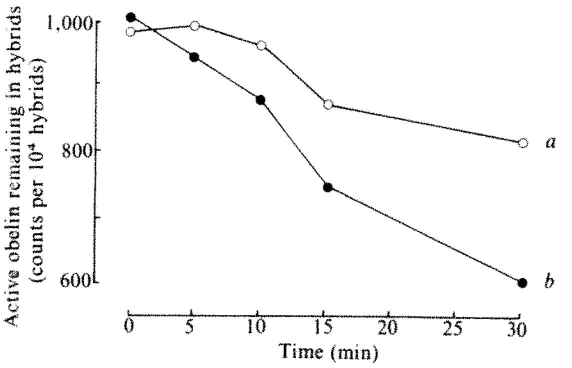

Fig. 4 Consumption of obelin in hybrids stimulated by chemotactic peptide. Total active obelin remaining in the hybrids after various times of incubation was measured by addition of 1% Triton X-100 (scintillation grade) in Krebs–Ringer HEPES buffer to samples of the suspension to stimulate all remaining active obelin. *a*, Incubation at 37 °C with *N*-formyl-L-methionyl-L-leucyl-L-phenylalanine (1 μM dissolved in dimethyl sulphoxide, final concentration 0.1%). *b*, Dimethyl sulphoxide (0.1% v/v) alone. From the curves the mean rate constants of obelin consumption were calculated and compared with calibration curves of obelin luminescence against Ca^{2+} concentration. Assuming the free Mg^{2+} concentration within the hybrid to be ~2 mM, the free Ca^{2+} concentration within the hybrids was estimated to be 0.7 μM (*a*) and 0.3 μM (*b*).

An important application of this fusion technique is the quantification of cytoplasmic free Ca^{2+} in both resting and stimulated cells. The cytoplasmic free Ca^{2+} in the hybrids was estimated by relating the rate constant of obelin to free Ca^{2+} (refs 1, 12). Before fusion, the resting free Ca^{2+} concentration in the ghosts, in the presence of external calcium (1 mM), was ~0.5 μM. However, the estimated resting free Ca^{2+} in the hybrids was lower, ~0.1–0.3 μM assuming an intracellular free Mg^{2+} concentration of 2 mM. Activation of complement by anti-polymorphonuclear leukocyte antibody bound to the hybrid surface resulted in a rise in intracellular free Ca^{2+} which reached a plateau of 8 μM within 1 min (Fig. 3). The initial rise in intracellular free Ca^{2+} preceded that in luminol-dependent chemiluminescence by ~40 s. The chemotactic peptide *N*-formyl-L-methionyl-L-leucyl-L-phenylalanine stimulated oxygen radical formation in the hybrids, detected by luminol-dependent chemiluminescence. It also stimulated a prolonged increase in obelin consumption, the mean free Ca^{2+} concentration over 30 min corresponding to ~0.7 μM, twice the resting cytoplasmic Ca^{2+} concentration (Fig. 4). Phagocytic stimulation of the hybrids produced a low level of endogenous luminescence which was not caused by obelin but was the result of oxygen radicals formed within the cells. No obelin luminescence was observed above this endogenous luminescence, and no increased consumption of obelin was observed. We conclude that this phagocytic stimulus did not cause a prolonged rise in intracellular free Ca^{2+}, despite the fact that oxygen radical formation required extracellular Ca^{2+} and was blocked by the calmodulin inhibitor trifluoperazine[7]. The extent of oxygen radical formation caused by various stimuli did not, therefore, correlate with the length of time of the increase in free Ca^{2+}.

The presented method, although limited to cells which will fuse with erythrocyte ghosts, has applications for incorporating other indicators into the cytoplasm of hybrids which are still capable of responding to a cell stimulus. For example, the chemiluminescent compound luminol, which has been used here extracellularly (Figs 2, 3) to monitor oxygen radicals within the phagosomes, has also been incorporated into the cytoplasm of the hybrids to monitor cytoplasmic oxygen radical formation. Furthermore, macromolecular inhibitors of cell function, such as antibodies, can be incorporated into the hybrids[13]. The uniform distribution of these compounds within our hybrids has been demonstrated by observing fluorescein-labelled albumin and immunoglobulin originally entrapped in the ghosts. This method therefore provides cell biologists with an exciting new tool for studying chemical changes in living cells.

We thank Dr J. P. Luzio for the gift of anti-5′-nucleotidase antiserum, the director and staff of the Marine Biological Association, Plymouth, Professor H. Harris for initial donation of virus, Mr N. Bishop for help in growing the virus, and Dr R. L. Dormer for helpful discussions. This work was funded by the SRC and the Arthritis and Rheumatism Council.

Received 22 September; accepted 20 November 1981.

1. Ashley, C. C. & Campbell, A. K. (eds) *Detection and Measurement of Free Ca^{2+} in Cells* (Elsevier, Amsterdam, 1979).
2. Tsien, R. Y. *Nature* **290,** 527–528 (1981).
3. Campbell, A. K. & Simpson, J. S. A. *Techniques metabolic Res.* **B213,** 1–56 (1979).
4. Campbell, A. K. *et al. J. Physiol., Lond.* **306,** 3P-4P (1980).
5. Campbell, A. K. *Biochem. J.* **143,** 411–418 (1974).
6. Rechsteiner, M. *Expl Cell Res.* **93,** 487–492 (1975).
7. Hallett, M. B., Luzio, J. P. & Campbell, A. K. *Immunology* **44,** 569–576 (1981).
8. Klebanoff, S. J. & Clark, R. A. *The Neutrophil: Function and Clinical Disorders* (North Holland, Amsterdam, 1978).
9. Peretz, H., Toister, Z., Laster, Y. & Loyter, A. *J. Cell Biol.* **63,** 1–11 (1974).
10. Knutton, S. & Pasternak, C. A. *Trends biochem. Sci.* **4,** 220–223 (1979).
11. Hallett, M. B. & Campbell, A. K. *Biochem. J.* **192,** 587–596 (1980).
12. Campbell, A. K., Daw, R. A., Hallett, M. B. & Luzio, J. P. *Biochem. J.* **194,** 551–560 (1981).
13. Heumann, R., Schwab, M. & Thoenen, H. *Nature* **292,** 838–840 (1981).

Antibody to hepatitis B surface antigen after a single inoculation of uncoupled synthetic HBsAg peptides

Gordon R. Dreesman*, Yanuario Sanchez*, Irina Ionescu-Matiu*, James T. Sparrow†, Howard R. Six‡, Darrell L. Peterson§, F. Blaine Hollinger* & Joseph L. Melnick*

Departments of *Virology & Epidemiology, †Medicine and ‡Microbiology & Immunology, Baylor College of Medicine, Houston, Texas 77030, USA
§ Department of Biochemistry, Medical College of Virginia, Richmond, Virginia 23298, USA

A formalin-inactivated hepatitis B virus (HBV) vaccine has been produced in several laboratories (for review, see ref. 1). The sole source of material for these vaccines has been 22-nm lipoprotein particles composed of hepatitis B surface antigen (HBsAg) and derived from plasma of persons chronically infected with HBV. Such a source presents potential hazards in view of unknown factors that may be present in the plasma, and as high-risk populations are immunized, sources of plasma containing large quantities of HBsAg will become scarce. In addition, no tissue culture system has been developed for the propagation of HBV. The possibility of a synthetic peptide vaccine[2,3] for HBV had been suggested[2,3] following studies carried out with tobacco mosaic virus[4,5] and MS-2 coliphage[6]. This possibility recently became a reality when the amino acid sequence for HBsAg was deduced from the nucleotide sequence of the cloned HBV genome (for a review, see ref. 7). More recently a portion of the major polypeptide derived from HBsAg, with a calculated molecular weight of 25,000 (P25), has been sequenced[8]. Lerner *et al.*[9] have described a similar approach towards HBV synthetic peptides. Antibody to HBsAg (anti-HBs) was raised in rabbits inoculated with three or four doses of a series of peptides, each containing 14–15 amino acid residues, but only after covalent linkage of the peptides to a carrier protein. Activity was also found after multiple injections of a peptide containing 34 amino acids. We have now synthesized two cyclic peptides containing disulphide bonds, both unrelated to those prepared by Lerner, from a hydrophilic region of the major viral polypeptide, which elicited an antibody response in mice after a single injection without linkage to a protein carrier.

The first major step in our work was the selection of those amino acid residues containing specific HBsAg determinants using a computer analysis of the amino acid sequence of P25 to predict the secondary structure of the molecule according to the technique of Chou and Fasman[10]. The protein hydrophobicity was estimated using the amino acid assignments of Bull and Breese[11]. HBsAg was found to contain predominantly β structure interrupted with a series of β turns. Three highly hydrophobic regions are located between residues 1 and 42, 66 and 108, and 146 and 226, and two hydrophilic regions between residues 43 and 65, and 109 and 145. The latter hydrophilic regions are probably exposed on the intact particle and, consequently, β turns in these regions would represent potentially exposed antigenic determinants[12].

The region between amino acids 117 and 137 was chosen for our first synthesis because a cyclic disulphide could be formed between Cys 124 and Cys 137 (see Fig. 1). Thus by locking the conformation of the potential β turns at residues 129–132 and 135–137, we expected to obtain a polypeptide more native in structure[7]. A serine was substituted for the cysteine at position 121 in the *ayw* sequence[8] to allow formation of a single cyclic disulphide. Lysine was substituted for Arg 122 to provide a handle for cross-linking to other proteins, if needed, before injection into animals. The selected peptides were synthesized by solid-phase methodology[13] on a Schwarz Bioresearch synthesizer modified for computer control[14]. Butyloxycarbonyl-*S*-*p*-methoxybenzyl-L-cysteine was coupled to *p*-hydroxymethyl-phenylacetamidomethyl polystyrene using dicyclohexylcarbodiimide with a catalytic amount of 4-*N*,*N*-dimethylaminopyridine[15,16]; the loading was 0.09 mM per g of resin. For the synthesis, the α-amino groups were protected with t-butyloxycarbonyl (t-BOC) and the side chain-protecting groups were as follows: benzyl ethers for the hydroxyl of serine and threonine, dichlorobenzyl ether for the phenolic hydroxyl of tyrosine and carbobenzoxy for the ϵ-amino group of lysine. Trifluoroacetic acid (40% in CH_2Cl_2) was used to remove the t-BOC, and the resulting salt was neutralized with *N*,*N*-diisopropylethylamine (5% in CH_2Cl_2). Dicyclohexylcarbodiimide was used to couple the t-BOC amino acids; hydroxybenzotriazole was added to the coupling reaction of glutamine to

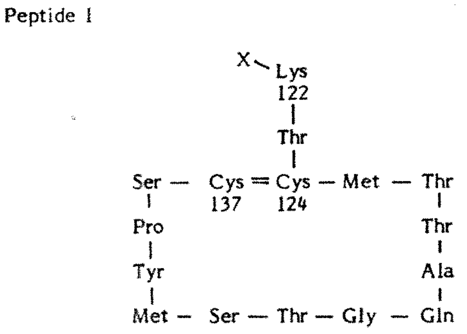

Peptide 2 contains 5 additional amino acid residues:
Ser - Thr - Gly - Pro - Ser - X
117 121

Fig. 1 Amino acid sequences of synthetic peptide 1 (molecular weight 2,219) and peptide 2 (molecular weight 2,739).

0028-0836/82/020158—03$01.00

suppress side chain dehydration. The specific steps of the synthesizer programme have been published elsewhere[15,17].

The protecting groups were removed and the peptide was cleaved from the resin at 0 °C with anhydrous hydrogen fluoride containing 10% anisole and 1% ethanedithiol as scavengers. The HF reagent was removed under vacuum at 0 °C, and then the peptide was precipitated and washed with anhydrous ether. After extraction of the peptide from the resin with trifluoroacetic acid, the solvent was evaporated at 15 °C and the peptide again precipitated with ether. The ether was decanted after centrifugation and the pellet dissolved in 1 M Tris/6 M guanidine hydrochloride; the *p*H of this solution was immediately adjusted to 8. The solution was desalted on a BioGel P-2 column equilibrated in 0.1 M ammonium bicarbonate, and the peptide-containing fractions were pooled and lyophilized.

The cyclic disulphide was formed by oxidation of a dilute solution of the peptide with potassium ferricyanide according to the procedure of Felix *et al.*[18]. The solution was lyophilized and desalted on a BioGel P-2 column, and the peptide further purified by ion-exchange chromatography at 4 °C on a column of SP-Sephadex equilibrated in 0.02 M NaH_2PO_4/6 M urea, *p*H 3.74. The material eluted with a linear gradient of 800 ml of 0.02 M NaH_2PO_4/6 M urea and 800 ml of 0.15 M NaCl/0.02 M NaH_2PO_4/6 M urea, *p*H 3.74. The peptide was located by measuring the absorbance at 275 nm.

After desalting on Bio-Gel P-2 in ammonium bicarbonate and lyophilization, we found that each peptide had the expected amino acid composition by amino acid analysis (Table 1) and eluted as a major peak on C_{18}-reverse-phase HPLC in a linear gradient of 1% triethyl ammonium phosphate, *p*H 3.2, and 2-propanol.

P25 was derived from a purified preparation of HBsAg after solubilization by heating at 100 °C for 2 min in 0.5 M urea/1% SDS/1% 2-mercaptoethanol[19]. The soluble polypeptides were fractionated by cylindrical polyacrylamide gel electrophoresis (PAGE) in 10% gels. (P25 was designated P22 in our previous studies[19,20] based on molecular weight estimations by PAGE.) The SDS-denatured linear P25 polypeptide, which is known to contain 226 amino acid residues, was used as a control for our immunogenicity studies.

The two synthetic peptides (117–137 and 122–137) were incorporated into a series of adjuvant vehicles for immunization of mice. Equal volumes of immunogen and Freund's complete adjuvant (FCA) were emulsified to give a final peptide concentration of 50 μg per 0.4 ml. The alum-absorbed preparations were prepared as described previously[20] with hydrated aluminium potassium sulphate, to give a final suspension containing 50 μg peptide per 0.4 ml. Large multilamellar liposomes were prepared from a mixture of dipalmitoylphosphatidylcholine, cholesterol and dipalmitoylphosphatidic acid in a molar ratio of 2.0 : 1.5 : 0.2 respectively[20]. Dried lipid films were dispersed by vortexing in an aqueous medium at a phospholipid concentration of 20 mM. Liposomes were swollen in solutions containing either 100 μg of peptide per ml or 100 μg of peptide plus 1 mg ml^{-1} muramyl dipeptide (MDP; Sigma). To ensure that comparable doses were given in each case, untrapped antigen was not removed. Previous studies have indicated that ~60% of HBsAg materials were associated with liposomes prepared in these conditions[20]. Final liposome concentrations were adjusted such that each animal received 6 mmol phospholipid and 25 μg peptide with or without 250 μg MDP in a volume of 0.3 ml.

Groups of six female BALB/c mice were immunized intraperitoneally with each of the above preparations. The mice were bled from the tail vein on days 7, 14 and 21. Samples were assayed at a serum dilution of 1 : 4 using a commercial solid-phase radioimmunoassay (Ausab, Abbott, Chicago). Anti-HBs concentrations are expressed as milli-International Units per millilitre (mIU ml^{-1}) based on the international reference preparation of anti-HBs (lot 26.1.77) provided by the International Laboratory for Biological Standards, Central Laboratory of the Netherlands Red Cross Transfusion Service. A computer nonlinear regression program, BMDP3R[21], was used to describe the standard dose–response curve for the WHO international reference preparation from which the potency of each of the samples was obtained[22].

Table 1 Amino acid composition of synthetic peptides

Amino acid	Peptide 122–137	Peptide 117–137 Ser 121
Threonine*	3.75(4)	4.67(5)
Serine*	1.93(2)	3.55(4)
Glutamic acid	1.06(1)	1.06(1)
Proline	0.85(1)	1.92(2)
Glycine	1.00(1)	2.00(2)
Alanine	0.99(1)	1.08(1)
Half cystine†	— (2)	— (2)
Methionine	1.87(2)	1.87(2)
Tyrosine	0.99(1)	0.93(1)
Lysine	0.93(1)	0.92(1)

Analyses were performed on a Beckman model 121 amino acid analyser after hydrolysis *in vacuo* for 24 h at 110 °C in 6 M HCl. The theoretical values are given in parentheses.

* Values are not corrected for destruction during hydrolysis.

† Half cystine was present in the amino acid analysis but was not integrated.

The results given in Table 2 show that (1) approximately 50% of the mice in each group produced detectable levels of antibody 7 days after inoculation of either the synthetic peptides or the P25 polypeptide; (2) the adjuvant vehicle—FCA, alum, liposomes, or liposomes with incorporation of MDP—did not significantly affect the primary antibody response; (3) in several groups the antibody response was greater on day 14, as shown by either the increased anti-HBs concentrations or the number of mice in each group which responded; (4) on day 21, the peak levels of antibody response in most groups of mice decreased; and (5) the antibody response in mice inoculated with purified SDS-denatured P25 was similar to that observed with the synthetic peptides.

When sera from each group of positive mice on days 7, 14 and 21, respectively, were pooled and fractionated by ultracentrifugation in 10–40% (w/v) preformed sucrose gradients[23], IgG antibody was localized in the intermediate fractions and IgM was detected in the rapidly sedimenting fractions. Typical IgM and IgG responses were seen in each group, with one exception: there was no IgG in the group of mice injected with peptide 122–137 emulsified with FCA.

Early work with a plant virus model using tobacco mosaic virus[4,5] and the bacterial virus model using MS-2 coliphage[6] clearly demonstrated the immense potential of preparing immunologically active synthetic peptide analogous to amino acid sequences in an animal virus protein. The present results indicate that amino acid residues localized in the major HBsAg polypeptide, P25, between residues 117 and 137—or more specifically, 122 and 137—contain a determinant that elicits the production of antibody of similar specificity to that produced by immunization with the SDS-denatured linear virus P25 polypeptide[19]. These findings are similar to those reported recently by Lerner *et al.*[9], who prepared a series of synthetic peptides containing segments of the P25 HBsAg polypeptide. Four of their peptides (2–16, 22–35, 48–81 and 95–109) elicited the production of antibody in rabbits which reacted with HBsAg. Synthetic peptides of residues 134–146 and 138–149 (refs 24 and 25 respectively) of P25 have also been prepared. These peptides, which have several amino acids (138–146) in common, were both antigenically active in that each reacted with preparations containing specific anti-HBs activity and they blocked antibody reactivity of sera of animals immunized with intact HBsAg. There have been no reports regarding their immunogenic activity. The amino acid sequences of the six unique immunogenic synthetic peptides included in our study and the above studies have nothing in common except the similarity noted above (residues 138–146) and the overlapping of four carboxyl amino acids of the peptides synthesized in our labora-

Table 2 Anti-HBs concentrations in mice immunized with synthetic HBsAg peptides 117–137 and 122–137

Immunizing preparation	Range of antibody concentrations postinjection (mIU ml^{-1}) Day 7	Day 14	Day 21
117–137–FCA	3.5–8.6(4/6)	3.2–10.3(5/6)	2.6–13.9(5/6)
122–137–FCA	3.6–5.8(3/6)	5.9–11.9(3/6)	17.3–25.9(3/6)
117–137–alum	3.0–7.3(2/6)	2.8–12.6(3/6)	3.4–4.5(2/6)
122–137–alum	2.1–14.5(4/6)	2.5–10.0(3/6)	5.0–6.4(2/6)
117–137–liposomes	2.1–15.4(3/6)	2.0–12.8(4/6)	—
122–137–liposomes	3.6–8.8(3/6)	5.2–12.0(3/6)	5.6–11.8(3/6)
122–137–liposomes +MDP	2.1–23.7(4/6)	2.9–21.0(3/6)	6.8–40.0(2/6)
P25 polypeptide–alum	2.1–17.2(6/6)	2.5–10.5(5/6)	7.1–12.5(2/6)

Only positive antibody values are listed. Numbers in parentheses represent number of mice with an anti-HBs response over total number of mice in each group.

tory with the initial four residues at the amino terminus of the peptide synthesized by Vyas[24]. Thus a number of different amino acid sequences can elicit production of antibody which specifically reacts with HBsAg. It will be essential to immunize susceptible chimpanzees with several of these peptides to ascertain which elicit(s) the production of protective antibody, as we have done with the purified P25 polypeptide[19]. In addition, it will be of interest to learn which sequences contain the cross-reacting 'a' antigenic determinant and which contain the subtype-specific determinants. We selected residues 117–135 because this region is highly hydrophilic, and shows great variation among the published sequences and therefore may contain the subtype-specific determinants[8,24]. It may be found necessary to use more than one of these peptides to produce a highly effective vaccine.

Note that Lerner *et al.*[9] elicited an antibody response to their smaller (14–15 residues) peptides only after repeated inoculation of covalently attached material to a carrier protein. In our study, we observed an antibody response to each peptide (117–137 or 122–137) without using a carrier protein. The greater immunogenicity of our peptides, shown by the detection of antibody activity 7 days after a single injection of peptide, may be because our peptides, consisting of 16 or 21 amino acid residues, contain a determinant which is more immunogenic. Alternatively, disulphide cyclization may be important in locking the secondary structure of a potent immunogen.

The incorporation of various adjuvant vehicles and/or protein carriers should help to increase the immunogenicity of these synthetic peptides. This approach may offer advantages in the production of a vaccine against the hepatitis B virus, since the relative immunogenicity of the HBsAg-derived polypeptides is considerably less than that observed for intact HBsAg 22-nm particles[19].

This work was supported in part by research grant HL-17269 from the National Heart, Lung and Blood Institute, NIH, by research contract DAMD17-81-C-1058 from the US Army Medical Research and Development Command, and by research grant Q-435 from the Robert A. Welch Foundation. J.T.S. is an Established Investigator of the American Heart Association.

Received 28 September; accepted 9 November 1981.

1. McAuliffe, V. J., Purcell, R. H. & Gerin, J. L. *Rev. infect. Dis.* **2**, 470–492 (1980).
2. Rae, K. R. & Vyas, G. N. *Nature new Biol.* **241**, 240–241 (1973).
3. Melnick, J. L., Dreesman, G. R. & Hollinger, F. B. *J. infect. Dis.* **133**, 210–229 (1976).
4. Anderer, F. A. *Biochim. biophys. Acta* **71**, 246–248 (1963).
5. Fearney, F. J., Leung, C. Y., Young, J. D. & Benjamini, E. *Biochim. biophys. Acta* **243**, 509–514 (1971).
6. Langbeheim, H., Arnon, R. & Sela, M. *Proc. natn. Acad. Sci. U.S.A.* **73**, 4636–4640 (1976).
7. Tiollais, P., Charnay, P. & Vyas, G. N. *Science* **213**, 406–411 (1981).
8. Peterson, D. L. *J. biol. Chem.* **256**, 6975–6983 (1981).
9. Lerner, R. A. *et al. Proc. natn. Acad. Sci. U.S.A.* **78**, 3403–3407 (1981).
10. Chou, P. Y. & Fasman, G. D. *Adv. Enzym.* **47**, 45–148 (1978).
11. Bull, H. B. & Breese, K. *Archs Biochem. Biophys.* **161**, 665–670 (1975).
12. Atassi, M. Z. *Immunochemistry* **12**, 423–438 (1975).
13. Merrifield, R. B. *Adv. Enzym.* **32**, 221–296 (1969).
14. Edelstein, M. S., McNair, D. S. & Sparrow, J. T. in *Peptides: Synthesis, Structure, Function* (eds Rich, D. H. & Gross, E.) (Pierce Chemical Co., Rockford, in the press).
15. Sparrow, J. T. *J. org. Chem.* **41**, 1350–1353 (1976).
16. Atherton, E., Woolley, V. & Sheppard, R. C. *JCS chem. Commun.*, 970 (1981).
17. Mao, S. J. T., Sparrow, J. T., Gilliam, E. B., Gotto, A. M. & Jackson, R. L. *Biochemistry* **16**, 4150–4156 (1977).
18. Felix, A. M., Jiminez, M. H., Wang, C. T. & Meienhofer, J. *Int. J. Peptide Protein Res.* **15**, 342–354 (1980).
19. Dreesman, G. R., Hollinger, F. B., Sanchez, Y., Oefinger, P. & Melnick, J. L. *Infect. Immun.* **32**, 62–67 (1981).
20. Sanchez, Y. *et al. Infect. Immun.* **30**, 728–733 (1980).
21. Dixon, W. J. & Brown, M. B. BMDP-79 (University of California Press, Berkeley, 1979).
22. Hollinger, F. B., Adam, E., Heiberg, D. & Melnick, J. L. in *Viral Hepatitis* (eds Alter, H., Maynard, J. & Szmuness, W.) (Franklin Institute Press, Philadelphia, in the press).
23. Fudenberg, H. H. & Kunkel, H. G. *J. exp. Med.* **106**, 689–702 (1957).
24. Vyas, G. N. in *Hepatitis B Vaccine* (eds Maupas, P. & Guesry, P.) (Elsevier, Amsterdam, 1981).
25. Hopp, T. P. & Woods, K. R. *Proc. natn. Acad. Sci. U.S.A.* **78**, 3824–3828 (1981).

New Epstein–Barr virus variants from cellular subclones of P3J-HR-1 Burkitt lymphoma

L. Heston, M. Rabson, N. Brown & G. Miller*

Departments of Pediatrics and Epidemiology and Public Health,
Yale University School of Medicine, New Haven,
Connecticut 06510, USA

The P3J-HR-1 (HR-1) line contains unique Epstein–Barr viruses (EBVs) which fail to immortalize lymphocytes or to induce lymphomas[1–4]. Virus from Jijoye, the parent of the HR-1 clone, retains lymphocyte-immortalizing ability[5,6]. Because the HR-1 virus population is a mixture, it has not been possible to identify conclusively the genomic alterations responsible for the nontransforming phenotype[7]. Submolar fragments produced by restriction enzyme digestion and the variety of patterns found after partial denaturation are evidence for heterogeneity in HR-1 virion DNA[8,9]. To determine whether every cell carried this virus mixture, or whether the line consisted of cells carrying different variants, we separated the mixture by cell subcloning into new variants, which are found to be distinct from parental HR-1 virus both biologically and in genome structure.

HR-1 cells were cloned in agarose with an efficiency of 37% (refs 10, 11). The copy number of EBV genomes in 29 subclones derived in two experiments (FF452, GG68) was determined by nucleic acid spot hybridization[12] (Fig. 1*a*). The parental HR-1 line contained ~300 genomes per cell; all subclones had lower copy numbers, between 3 and 22 genomes per cell. Following treatment with 12-*O*-tetradecanoyl-phorbol-13-acetate (TPA) which induces viral DNA synthesis in the HR-1 line[13], there was an increase, to a minimum of 200 EBV DNA copies per cell, in each of the clones (Fig. 1*b*). However the response to TPA was exaggerated in five clones (GG68 nos 5, 11, 13, 17 and 19) which after treatment contained 3,000–6,000 EBV DNA copies per cell. These clones are called 'superinducible'. The same five clones released large amounts of viral DNA (4×10^7–4×10^8 genomes per ml) into the culture supernatants after treatment with TPA (Fig. 1*c*). Differences in content of viral DNA correlated with levels of viral capsid antigen (VCA). In all clones antigen expression (≤1%) was markedly below the 10% antigen-positive cells found in the HR-1 line. Following treatment with TPA, 50–80% of cells in the five superinducible clones became antigen positive; only slight enhancement of VCA expression was seen in the rest of the clones.

These data indicated heterogeneity among subclones in the extent of viral replication. None of the 29 clones spontaneously released EBV in amounts comparable with the parental line. Cloning of the spontaneous producer may require less stringent conditions. Spontaneous viral particle synthesis in the HR-1 line may involve interaction between different viruses in the line. The superinducible clones will be useful in further studies: as some yield 10–20 times more viral DNA than the parental HR-1 line, they may help in analysis of genome structure and repli-

---

* To whom correspondence should be addressed.

0028-0836/82/020160—04$01.00

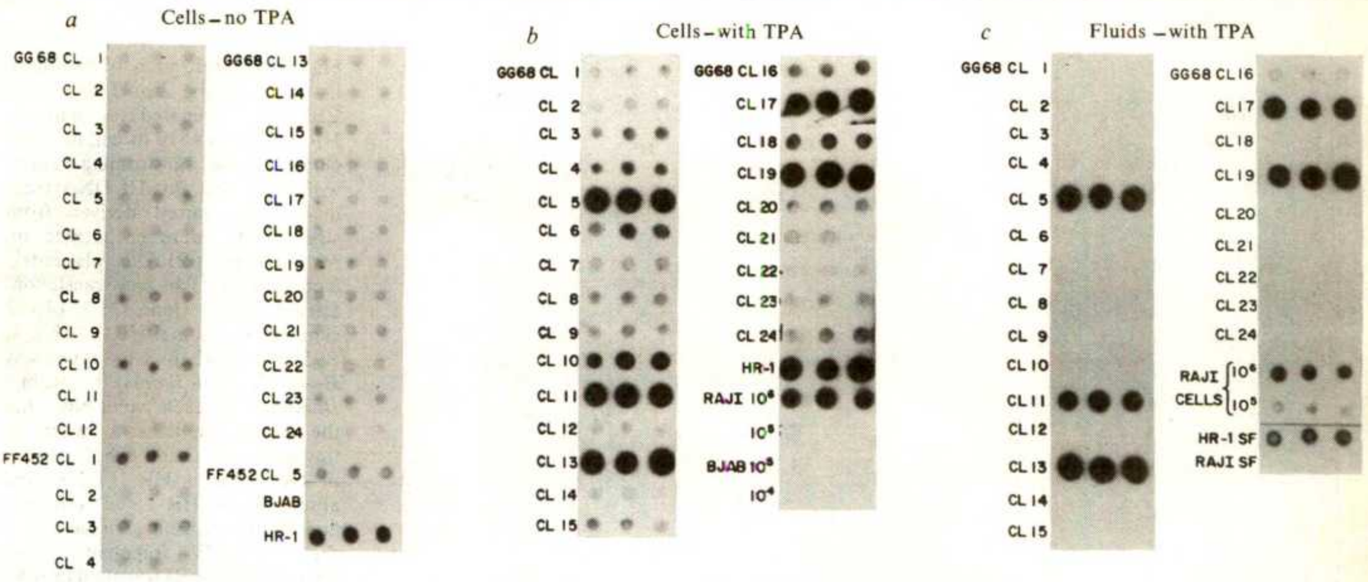

Fig. 1 Estimation of EBV DNA content of the HR-1 line and its subclones by nucleic acid spot hybridization. Each filter was probed with $1\text{-}5\times10^6$ c.p.m. of nick-translated ^{32}P-labelled EBV DNA prepared with 300 ng of HR-1 DNA. *a*, Genome content of 29 subclones and the HR-1 parent without TPA treatment. Each spot contains 10^5 cells collected 6 days after subculture. BJAB cells (EBV genome negative) serve as negative control. Autoradiograph exposed for 18 h. *b*, Genome content of 24 subclones and the HR-1 parent with TPA treatment. Each spot contains 10^5 cells collected 6 days after subculture with 20 ng ml^{-1} TPA. The positive control was 10^6 and 10^5 Raji cells; the negative control was 10^5 and 10^4 BJAB cells. Neither BJAB nor Raji was treated with TPA. *c*, Genome content of supernatant fluids from 24 subclones and the HR-1 parent collected 14 days after subculture in the presence of 20 ng ml^{-1} TPA. 10^6 and 10^5 Raji cells (no TPA treatment) served as positive control. Raji supernatant fluid (SF) which does not contain virions was negative control. High levels of hybridization seen with fluids in *c* are seen in *b* with intracellular EBV DNA from the same cell clones. Autoradiograph exposure in *b* and *c* was 4 h.

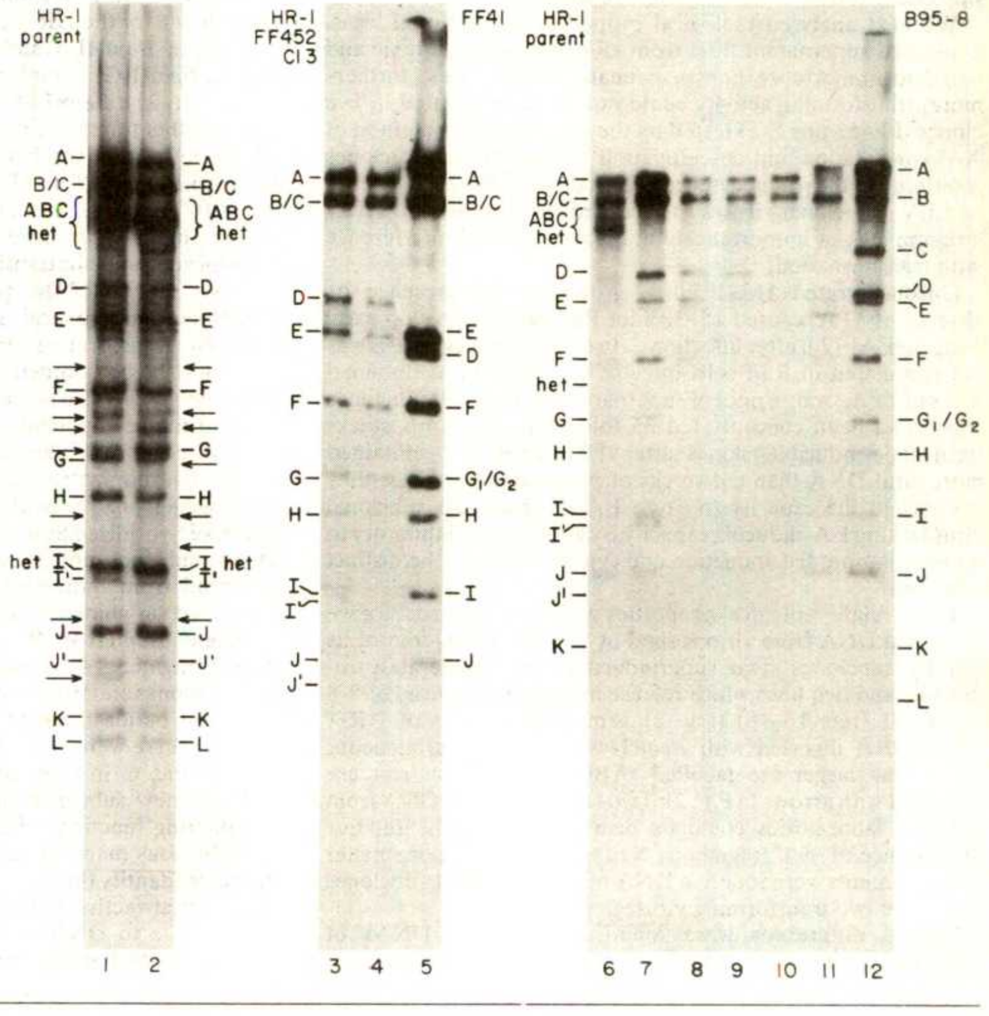

Fig. 2 *Eco*RI digestion of EBV DNA prepared from virions. DNA was extracted from virions shed into 20 l of culture supernatants 14 days after addition of 20 ng ml^{-1} TPA. Lanes 1–5 contained 600 ng of EBV DNA; lanes 6–12 50 ng of DNA. Each panel is an autoradiograph of a Southern blot hybridized with 10^7 c.p.m. of nick-translated ^{32}P-labelled HR-1 DNA. Lane 1, HR-1 parental (LS strain from M. Nonoyama); 2, HR-1 parent (laboratory strain); 3, 4, FF452, clone 3, a 'moderately inducible' HR-1 clone; 5, FF41, a transforming EBV originally from saliva[16]; 6, HR-1 parent (LS strain); 7, GG68 clone 5 'superinducible'; 8, GG68 clone 13 'superinducible'; 9, FF452 clone 3 (this DNA was prepared from the clone passaged for 10 months after preparation of the DNA shown in lanes 3 and 4); 10, FF452 clone 5 moderately inducible; 11, FF41; 12, B95-8, a transforming EBV originally from blood. Note that the bands 'ABC het' and other 'het' bands, indicated by an arrow in the DNA of the HR-1 parent, are not seen in the DNA prepared from the cell clones, and that the *Eco*RI A fragment is smaller in the DNA of the parental HR-1 and all of its subclones than in the DNA of the transforming B95-8 and FF41 strains.

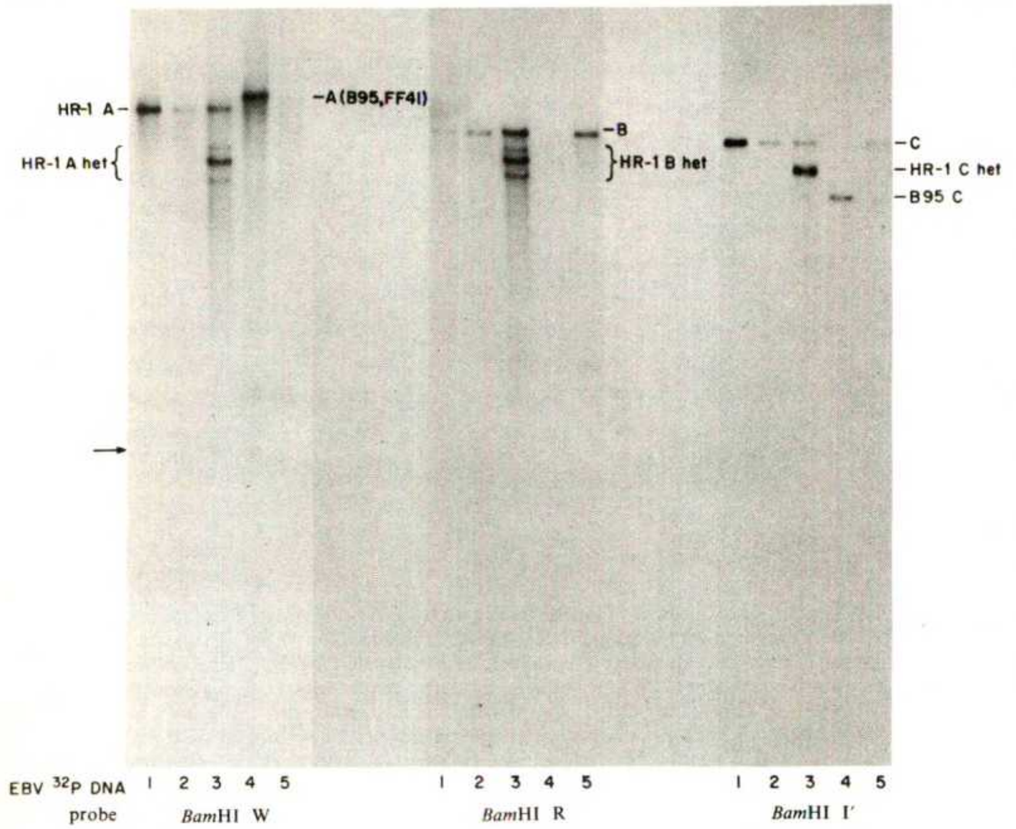

Fig. 3 Hybridization of Southern blots, containing *Eco*RI digests of EBV DNA, prepared from parental HR-1 DNA, two of its cellular subclones and two transforming viruses, with individual *Bam*HI DNA fragments. The latter, derived from strain FF41, were propagated on recombinant pBR322 plasmids[16] labelled with ^{32}P by nick translation. Lane 1, GG68 clone 13; 2, FF452 clone 3; 3, parental HR-1 (lab.); 4, B95-8; 5, FF41. In *a* the probe was *Bam*HI W, in *b* *Bam*HI R, and in *c* *Bam*HI I′. In each panel note that the probe identifies a group of fragments (A, B and C het) present in the parental HR-1 DNA and absent in the HR-1 cell subclones and the transforming viruses. In *a* the *Bam*HI W fragment faintly identifies an *Eco*RI fragment (arrow) of approximate molecular weight 2.4×10^6 in all strains. The genome location of this fragment is not known. *c* Shows the previously described[16,22] deletion in the *Eco*RI C fragment of B95-8.

cation. Studies of transcription of the EBV genome in the absence of productive infection and after TPA induction should ultimately clarify mechanisms by which the cell–virus relationship changes from latency to virus production.

We next analysed biological properties of subclonal virus. Undiluted supernatant fluid from all clones was cytotoxic and failed to immortalize human neonatal lymphocytes; furthermore, transforming activity could not be demonstrated in five clones (FF452 nos 1–5) tested by the more sensitive method of X-ray irradiation and co-cultivation[14]. Virus from two clones interfered with lymphocyte transformation by the B95-8 strain of EBV. Subclonal viruses thus resembled the parental HR-1 strain in lack of immortalization, cytotoxicity and interference with transformation.

Unconcentrated HR-1 virus, grown in the presence or absence of TPA, caused 15–30% of Raji cells to develop early antigen (EA) 72 h after infection[15]. In contrast EA synthesis was not stimulated in Raji cells infected by clonal virus obtained without TPA, or by a pool of supernatants from all 29 subclones which had been concentrated 35-fold. Although virus stocks from superinducible clones after TPA treatment contained more viral DNA than did stocks of parental HR-1 virus, they still lacked the capacity to cause EA synthesis. As subclonal virus lacking EA-inducing capacity is cytotoxic and inhibitory to transformation, EA induction and cytotoxicity must be distinct functions.

To correlate biological properties with genome structure we examined DNA from virions shed by the HR-1 line, four of its cellular subclones (two superinducible, two moderately inducible) and two lines which release immortalizing virus B95-8 and FF41 (refs 16–18) (Fig. 2). Among fragments of HR-1 virion DNA digested with *Eco*RI were many heterogeneous bands (the larger are labelled 'ABC het' and the rest are indicated with arrows in Fig. 2). Two stocks of HR-1 DNA from different laboratories could be distinguished by the relative prominence of 'het' fragments. Neither 'ABC het' nor smaller 'het' fragments were found in DNA of the four HR-1 subclones nor in the two transforming viruses.

Several differences were found between the DNAs of nontransforming viruses (parental HR-1 and its subclones) and the two transforming strains (Fig. 2). These will be described fully elsewhere (M.R. and G.M., in preparation) but briefly: *Eco*RI A is consistently larger in both transforming viruses than in the four nontransforming HR-1 subclones, as has previously been shown for the HR-1 parent[19–21], due to a 1.95 megadalton deletion of *Bam*HI Y and part of *Bam*HI H. In HR-1 and its clones, *Eco*RI G_2 is replaced by two new fragments, *Eco*RI I′ and J′ (ref. 21). *Eco*RI D, the right terminus, is larger in HR-1 than in either transforming virus. In the HR-1 clones there is loss of one restriction site between *Bam*HI B and G and another between *Bam*HI W′ and I′. There is also a deletion in *Bam*HI L ($\sim 5 \times 10^4$ daltons) and an insertion in *Bam*HI P ($\sim 6 \times 10^4$ daltons) in the nontransforming virus. Thus differences between transforming and nontransforming variants are scattered over at least six regions of the genome; however there is extensive homology and general similarity in genome organization between transforming and nontransforming EBVs[20,21]. It remains to be determined which lesions found in the genomes of HR-1 clones are also present in the Jijoye line which retains the transforming component.

Absence of ABC het and smaller het fragments from the *Eco*RI digestion pattern of subclonal viral DNA suggested that heterogeneity had been eliminated by cell cloning. To prove this point we hybridized Southern blots, containing *Eco*RI digests of HR-1, subclone and transforming virion DNA, with probes prepared from individual *Bam*HI fragments of EBV DNA contained on chimaeric plasmids[16] (Fig. 3). The probes were fragments *Bam*HI W, R and I′ which are found, respectively, in *Eco*RI fragments A, B and C[17,18]. Virion DNA from two HR-1 cell subclones and from two transforming viruses each contained only one major fragment with homology to the probes. In contrast there were at least three or four size variants of *Eco*RI 'A', 'B' and 'C' in parental HR-1 DNA.

These new subclonal mutant EB viruses will be useful in deciphering functions of the EBV genome. They could allow unambiguous mapping of the transforming region and should also help identify the genes responsible for EA induction in Raji cells. An attractive hypothesis is that EA induction by HR-1 virus is due to DNA represented by one or more ABC het fragments which were eliminated by cellular cloning.

This work was supported by grants from the NIH and the American Cancer Society. N.B. is a fellow of the Damon Runyon–Walter Winchell Cancer Fund. We thank K. Papov for assistance, and D. M. Horstmann, M. F. Robert and W. C. Summers for reading the manuscript.

Received 27 August; accepted 4 November 1981.

1. Miller, G., Robinson, J., Heston, L. & Lipman, M. *Proc. natn. Acad. Sci. U.S.A.* **71,** 4006–4010 (1974).
2. Menezes, J., Leibold, W. & Klein, G. *Expl Cell Res.* **92,** 478–484 (1975).
3. Frank, A., Andiman, W. & Miller, G. in *Advances in Cancer Research* (eds Klein, G. & Weinhouse, S.) 171–210 (Academic, New York, 1976).
4. Hinuma, Y. *et al. J. Virol.* **1,** 1045–1051 (1967).
5. Sairenji, T. & Hinuma, Y. *Int. J. Cancer* **26,** 337–342 (1980).
6. Ragona, G., Ernberg, I. & Klein, G. *Virology* **101,** 553–557 (1980).
7. Fresen, K. O., Merkt, B., Bornkamm, G. W. & zur Hausen, H. *Int. J. Cancer* **19,** 317–323 (1977).
8. Sugden, B., Summers, W. C. & Klein, G. *J. Virol.* **18,** 765–775 (1976).
9. Delius, H. & Bornkamm, G. W. *J. Virol.* **27,** 81–89 (1978).
10. Yamamoto, N. & Hinuma, Y. *Int. J. Cancer* **17,** 191–196 (1976).
11. Sugden, B. & Mark, W. *J. Virol.* **23,** 503–508 (1977).
12. Brandsma, J. & Miller, G. *Proc. natn. Acad. Sci. U.S.A.* **77,** 6851–6855 (1980).
13. zur Hausen, H., O'Neill, F. J., Freese, U. K. & Hecher, E. *Nature* **272,** 373–375 (1978).
14. Wilson, G. & Miller, G. *Virology* **95,** 351–358 (1979).
15. Henle, W. *et al. Science* **169,** 188–190 (1970).
16. Fischer, D. K. *et al. Cell* **24,** 543–553 (1981).
17. Dambaugh, T. *et al. Proc. natn. Acad. Sci. U.S.A.* **77,** 2999–3003 (1980).
18. Skare, J. & Strominger, J. L. *Proc. natn. Acad. Sci. U.S.A.* **77,** 3860–3864 (1980).
19. Rymo, L., Lindahl, T. & Adams, A. *Proc. natn. Acad. Sci. U.S.A.* **76,** 2794–2798 (1979).
20. Heller, M., Dambaugh, T. & Kieff, E. *J. Virol.* **38,** 632–648 (1981).
21. Bornkamm, G. W., Delius, H., Zimber, U., Hudewentz, J. & Epstein, M. A. *J. Virol.* **35,** 603–618 (1980).
22. Raab-Traub, N., Dambaugh, T. & Kieff, E. *Cell* **22,** 257–269 (1980).

Evidence from mtDNA sequences that common laboratory strains of inbred mice are descended from a single female

Stephen D. Ferris*†, Richard D. Sage‡ & Allan C. Wilson*

* Department of Biochemistry and ‡ Museum of Vertebrate Zoology, University of California, Berkeley, California 94720, USA

The rapid evolution[1] and maternal mode of inheritance[2] of mitochondrial DNA (mtDNA) make it a valuable marker for individuals related by descent from the same female[3]. We report here a study of wild and inbred mice which illustrates this point. We have examined mouse mtDNA from various locales in the Northern Hemisphere using restriction enzymes that cut the molecule at an average of 150 sites and find a high level of restriction-site polymorphism in wild mice but no variation among the 'old' inbred strains. This result is surprising because the nuclear genomes of these strains are known to differ greatly from one another[4]. The old inbred type of mtDNA occurs rarely in wild mice and differs from other types in the wild by an average of 100 nucleotide substitutions. In possible contradiction of published breeding records, these findings indicate that only one female lineage contributed to the formation of all the old inbred lines. In addition, our study of new inbred strains provides genetic markers that will be useful in mouse developmental and cell biology.

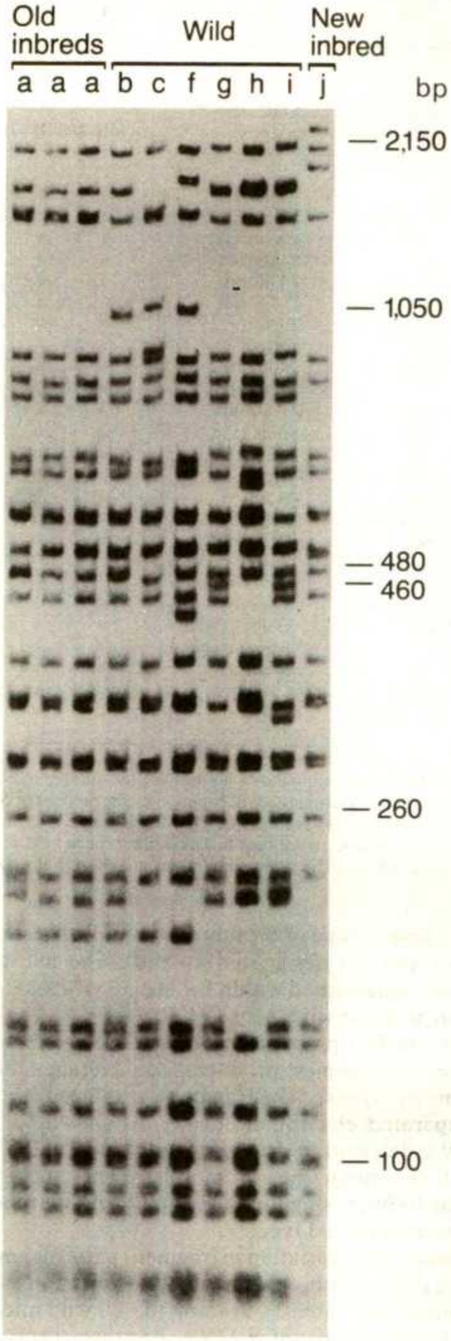

Fig. 1 Electrophoresis of 10 mouse mtDNAs. After purifying mtDNA from tissues of single mice and digesting it with *Mbo*I, the fragments were labelled and separated by electrophoresis as described elsewhere[27]. Lanes 1–3 show the identity of fragment patterns for three old inbred mice, C57BL, BALB/c and SWR. Lanes 4–9 show variation among six wild mice whose fragment patterns correspond to those indicated by small letters in Table 1. The animals are from diverse geographical areas: Maryland (USA), Egypt, Switzerland, Morocco, Yugoslavia and Denmark. Lane 10 shows the fragment pattern of a new inbred strain, SF/Cam, founded from a wild mouse in California. The sizes in base pairs (bp) of the size standards (PM2 phage DNA digested with *Hin*dIII) are indicated on the right.

Thirty-four samples of *Mus domesticus* mtDNA were obtained from 14 inbred strains and 20 wild mice collected in North America, western Europe, North Africa and the Near East. (The name *Mus domesticus* has been coined for a newly recognized species that includes the common laboratory strains and the wild mice populations formerly classified as the subspecies *M. musculus domesticus*, *M. musculus brevirostris* and *M. musculus praetextus*[5]. This species differs substantially from *M. musculus*, the house mouse of eastern Europe (formerly known as the subspecies *M. musculus musculus*), in anatomy, behaviour and protein structure[5,6], as well as in mtDNA structure[7]. Moreover, the two species are almost completely isolated from each other genetically due to geographical and multiple sterility barriers[8].) The sources of the 34 mtDNA samples are

---

† Present address: Department of Genetics, Stanford University Medical School, Stanford, California 94305, USA.

0028-0836/82/020163—03$01.00

Table 1 Fragment patterns of mitochondrial DNA found in wild and inbred mice

	Origin		Fragment pattern											Differences from inbred strain	
Sample no.	Strain or locality	State or country	*Fnu*DII	*Hae*III	*Hin*fI	*Hpa*II	*Mbo*I	*Taq*I	*Ava*II	*Acc*I	*Hinc*II	*Hind*III	*Xba*I	Fragment patterns	Point mutations
Wild mice															
1	Buellton	California	a	a	a	a	a	a	a	a	a	a	a	0	0
2	Vejrumbo	Denmark*	a	a	a	a	a	a	a	a	a	a	a	0	0
3	San Pablo 1	California	a	a	b	a	a	a	b	a	a	a	a	2	23
4	Centerville	Maryland	a	a	a	a	b	a	c	a	a	a	a	2	28
5	San Pablo 2	California	a	a	b	b	a	a	b	a	a	a	a	3	41
6–7	Napa, Orinda	California	a	a	c	a	a	b	a	a	a	b	a	3	66
8	Faiyum	Egypt	a	a	d	a	c	c	c	a	a	b	a	5	198
9	Giza	Egypt	a	a	e	a	d	d	c	a	a	b	a	5	165
10	Erfoud	Morocco	a	a	f	c	e	e	a	a	a	b	a	5	116
11	Viborg	Denmark*	a	b	g	a	a	f	a	b	b	a	a	5	132
12	Petaluma	California	b	a	h	a	c	d	a	a	a	b	a	5	182
13–15	Evansville	Indiana	b	a	h	a	c	d	a	a	a	b	a	5	182
16	Nyon	Switzerland	a	c	i	a	f	d	a	a	c	b	a	6	182
17	Jerusalem	Isreal	a	b	j	a	g	b	c	c	b	b	a	8	182
18	Azrou	Morocco	a	b	j	b	g	g	d	c	b	b	a	9	215
19	Metkovic	Yugoslavia	a	d	k	d	h	b	c	c	b	b	a	9	182
20	Skive	Denmark*	a	b	l	a	i	b	d	b	b	b	b	9	230
Inbred mice															
1–9	Old inbreds	Various	a	a	a	a	a	a	a	a	a	a	a	0	0
10	MOR	Ohio	a	a	a	a	a	a	a	a	a	a	a	0	0
11	PAC	Pennsylvania	a	a	b	a	a	a	a	a	a	a	a	1	12
12	IS/Cam/J	Israel	a	c	m	a	f	d	a	d	a	b	a	6	182
13	SF/Cam/J	California	a	e	n	a	j	h	c	a	b	b	a	7	198
14	SK/Cam/JEi	England	a	e	n	a	j	h	c	a	b	b	a	7	198

Point mutations were estimated by multiplying the number of base pairs (16,295) in mouse mtDNA[10] by the number of base substitutions per base pair (calculated from the fraction of restriction fragments in common by the method of Nei and Li[9]). Old inbreds are BALB/cJ, C57BL/6J, C58/J, DBA/2N, SWR/J, AU/SsJ, C3H, PL/J and AKR/Cu. A cell line (LA9) represented the C3H strain.

* The Danish populations are classified as another species (*M. musculus*) on the basis of morphological and protein evidence[5], but possess *M. domesticus* DNA, probably owing to introgression[7]. The three populations are close to the zone of contact with *M. domesticus*[26].

given in Table 1. Nine of the inbred strains were established over 40 yr ago and are designated as 'old'. The five other inbred strains were established within the last 30 yr[4] from female house mice caught in the wild.

Highly purified preparations of mtDNA were digested with 11 restriction enzymes, producing, on average, 150 restriction fragments per mouse. The fragments produced by each enzyme were separated electrophoretically, as shown for 10 mice in Fig. 1. We detected 58 fragment patterns; Table 1 shows their distribution among the 34 samples. The mice are ordered according to increasing number of pattern differences from the most common inbred type.

We found much variation in fragment patterns among the wild mice and the new inbred strains but no variation among the old inbred mice (see Table 1). Among the 20 wild mice studied we found 15 distinct types of mtDNA; one type corresponds to that found in the old inbred mice. It was found only twice, once in California and once in Denmark. A more recent survey using the enzymes *Hin*fI and *Mbo*I revealed six more mtDNA types in 36 additional wild mice, none of which had the old inbred type (R.D.S., S.D.F. and A.C.W., unpublished observations). The frequency of occurrence of the old inbred type is therefore 0.04 in the wild mice tested.

The extent to which these DNAs differ in nucleotide sequence from the old inbred type may be estimated from the number of fragments they have in common[9]. These estimates are based on the assumption that the differences in fragment pattern are due exclusively to base substitution. There is evidence in support of the assumption that mouse mtDNA evolves almost exclusively by base substitution[7,10]. The old inbred type is estimated to differ from other types of *M. domesticus* mtDNA by 12–230 base substitutions (Table 1). The mean difference of 137 substitutions corresponds to almost a 1% sequence difference, which is typical of the mtDNA diversity found in other mammal species[11–15]. Our result deserves emphasis because earlier surveys using fewer restriction sites[16,17] and fewer mice[18] seemed to indicate a low level of mtDNA polymorphism in wild mice.

The high level of variation in mtDNA of wild *M. domesticus* is consistent with electrophoretic[19,20] and immunological[21] evidence for a high level of nuclear gene variation in this species. However, the absence of mtDNA variation among the old inbred strains contrasts sharply with the presence of large nuclear differences in these strains[4]. To account for this, we suggest that a single female lineage founded all the old inbred strains, the nuclear diversity among these strains being due mainly to the mating of this lineage with diverse males. This hypothesis agrees with the recorded origins of inbred strains of laboratory mice[4,22]. The nine old inbred strains listed in Table 1 are thought to stem from a minimum of five different mothers which founded the primary strains as follows: DBA (in 1909 from a random stock at the Bussey Institute, Cambridge, Massachusetts), BALB/c (in 1913 from an Ohio pet dealer), SWR (before 1920 from a random stock at the Pasteur Institute, Paris), PL (before 1922 from a New Jersey pet dealer), and C57-C58 (in 1921 from a Massachusetts pet mouse dealer). If these five females had been picked at random from the wild, the probability of them all having the old inbred type of mtDNA seems, from our survey, to be extremely low ($\sim 10^{-7}$). It is likely, however, that all were from the pet mouse trade[23,24], in which case the old inbred type of mtDNA could already have been present at high frequency. A high frequency could be the result of a chance event when the pet mouse population was very small. Such an event could have occurred as long ago as 3,200 BP, when the white mouse cult began in the temple of Apollo Smintheus[23].

Selection, rather than chance fixation, could also explain why all the old inbred strains contain the same type of mtDNA and thus appear to be descended from one female. A high frequency of the old inbred type of mtDNA could be attributed to selection for mice bearing this DNA if they were better suited for survival in the pet mouse trade. Selection could act in a second way, by this DNA type giving mice a better chance of surviving laboratory inbreeding. If this were the case, the five primary strains could represent the most successful of many attempts to establish inbred lines. As early publications do not record failures to establish inbred strains, it is uncertain whether such selection need be invoked. However, a selectionist explanation does not account convincingly for the ease with which wild mice give rise to new inbred strains possessing other types of mtDNA, for example, PAC, IS/Cam and SF/Cam (see Table 1). Furthermore, our finding of the SF/Cam type of mtDNA in wild mice of the San Francisco area (R.D.S., S.D.F. and A.C.W., unpublished observations) is evidence against the argument that this inbred type evolved *de novo* in laboratory conditions. Given that an explanation involving chance fixation could account for the data, we think it unnecessary to invoke an additional factor, such as selection.

Contamination of one strain by another also ought to be considered in relation to the hypothesis that all the old inbred strains trace back to one female in the pet mouse population. The five primary strains could have been crossed soon after they were established in the laboratory, which would imply that published reports are inaccurate in describing the early breeding programmes. It is likely that such a mix-up could have occurred between 1919 and 1921 when Strong and Little had the founding stocks of three of the critical strains (DBA, BALB/c and C57-C58)[4,22]. Any inter-strain matings at this time, while the DBA strain was at a low ebb, might reasonably link this strain with at least one of the others.

The reason for suggesting this possibility is that the inadvertent mixing of inbred strains may be a common phenomenon even today. There are four recent cases of apparent contamination. (1) Festing[25] has described contamination of the C3H and AKR strains, based on nuclear evidence. (2) There is the case of the new inbred strain MOR, founded from wild mice in Ohio[4], whose black coat colour is evidence for the presence of nuclear genes from an old inbred strain (probably C57BL/6) in the MOR genome, as this coat colour is rare among wild house mice in North America. Consistent with the idea of contamination, MOR has the old inbred type of mtDNA (see Table 1). (3) Two new inbred strains (SF/Cam and SK/Cam), although founded by wild females in California and England, respectively, have the same rare type of mtDNA (see Table 1). The SK strain examined has probably been mixed with the SF strain because the mtDNA fragment patterns observed for SK/Cam/Ei differ greatly from those reported by Yonekawa *et al.*[17] who used another source of SK/Cam mice. In addition, the SK/Cam/Ei strain carries several protein variants that are diagnostic of the SF/Cam strain (E. Eicher, personal communication). (4) The most spectacular example is provided by two non-inbred strains of the Japanese house mouse, *M. molossinus*[5,6]. One strain, maintained by Potter at NIH, retains the *molossinus* type of mtDNA, which differs by almost 4 per cent in sequence from that of *M. domesticus*[7]. The other strain, KL/oci, is derived from Potter's strain and has been propagated in a series of other laboratories for >10 yr; KL/oci now has the old inbred type of mtDNA, while retaining proteins characteristic of *M. molossinus*. As extensive sampling of wild mice in Japan revealed no *domesticus*-like types of mtDNA[16], this could be the clearest case of laboratory contamination of a strain by *domesticus* mice bearing the old inbred type of mtDNA.

Thus, we propose that the old inbred mouse strains could be descendants of a single female that lived as recently as 1920, in which case she or her daughters cross-bred with the five primary strains of inbred mice. Alternatively, she could have been a member of the pet mouse population possibly as long ago as 3,200 BP. Besides contributing to knowledge of the genealogy of old inbred mice, our mtDNA study draws attention to cases of contamination of other stocks of laboratory mice and provides new genetic markers for use in cell and developmental biology, for example, markers for cells in chimaeras.

This work was supported by the Miller Institute, University of California (S.D.F.), NSF grants DEB 72-02545 (to R.D.S.) and DEB 78-02841 (to A.C.W.) and NIH grant 5 RO1 GM21509-07 (to A.C.W.). We thank R. Cann and E. Zimmer for discussion, V. Chapman, M. Ferris, M. Lieberman, T. Nakada and M. Potter for providing mice, and W. Brown for LA9 mtDNA.

Received 22 May; accepted 9 November 1981.

1. Brown, W. M., George, M. & Wilson, A. C. *Proc. natn. Acad. Sci. U.S.A.* **76,** 1967–1971 (1979).
2. Giles, R. E., Blanc, H., Cann, H. M. & Wallace, D. C. *Proc. natn. Acad. Sci. U.S.A.* **77,** 6715–6719 (1980).
3. Brown, W. M. & Wright, J. W. *Science* **203,** 1247–1249 (1979).
4. Staats, J. *Cancer Res.* **40,** 2083–2128 (1980).
5. Marshall, J. T. & Sage, R. D. in *Biology of the House Mouse* (ed. Berry, R. J.) 15–25 (Academic, London, 1981).
6. Sage, R. D. in *The Mouse in Biomedical Research* Vol. 1 (eds Foster, H. L., Small, J. D. & Fox, J. G.) 39–90 (Academic, New York, 1981).
7. Ferris, S. D., Sage, R. D. & Wilson, A. C. *Genetics* (in the press).
8. Forejt, J. & Iványi, P. *Genet. Res.* **24,** 189–206 (1974).
9. Nei, M. & Li, W.-H. *Proc. natn. Acad. Sci. U.S.A.* **76,** 5269–5273 (1979).
10. Bibb, M. J., Van Etten, R. A., Wright, C. T., Walberg, M. W. & Clayton, D. A. *Cell* **26,** 167–180 (1981).
11. Upholt, W. B. & Dawid, I. B. *Cell* **11,** 571–583 (1977).
12. Avise, J. C., Lansman, R. A. & Shade, R. O. *Genetics* **92,** 279–295 (1979).
13. Avise, J. C., Giblin-Davidson, C., Laerm, J., Patton, J. C. & Lansman, R. A. *Proc. natn. Acad. Sci. U.S.A.* **76,** 6694–6698 (1979).
14. Brown, G. G. & Simpson, M. V. *Genetics* **97,** 125–143 (1981).
15. Ferris, S. D., Brown, W. M., Davidson, W. S. & Wilson, A. C. *Proc. natn. Acad. Sci. U.S.A.* **78,** 6319–6323 (1981).
16. Yonekawa, H. *et al. Genetics* (in the press).
17. Yonekawa, H. *et al. Jap. J. Genet.* **55,** 289–296 (1980).
18. King, B., Shade, R. O. & Lansman, R. A. *Plasmid* **5,** 313–328 (1981).
19. Sage, R. D. in *Origins of Inbred Mice* (ed. Morse, H. C. III) 519–553 (Academic, New York, 1978).
20. Berry, R. J., Sage, R. D., Lidicker, W. Z. & Jackson, W. B. *J. Zool.* **193,** 391–404 (1981).
21. Nadeau, J. H., Wakeland, E. K., Götze, D. & Klein, J. *Genet. Res.* **37,** 17–31 (1981).
22. Morse, H. C. III in *Origins of Inbred Mice* (ed. Morse, H. C. III) 3–21 (Academic, New York, 1978).
23. Keeler, C. E. *The Laboratory Mouse. Its Origin, Heredity, and Culture* (Harvard University Press, Cambridge, 1931).
24. Lynch, C. J. *Lab. Anim. Care* **19,** 214–220 (1969).
25. Festing, M. F. W. *Inbred Strains in Biomedical Research* (Oxford University Press, New York, 1979).
26. Hunt, W. G. & Selander, R. K. *Heredity* **31,** 11–33 (1973).
27. Brown, W. M. *Proc. natn. Acad. Sci. U.S.A.* **77,** 3605–3609 (1980).
28. Thaler, L., Bonhomme, F. & Britton-Davidian, J. in *Biology of the House Mouse* (ed. Berry, R. J.) 27–41 (Academic, London, 1981).

Recent divergence from a common ancestor of human IFN-α genes

Takashi Miyata & Hidenori Hayashida

Department of Biology, Faculty of Science, Kyushu University, Fukuoka 812, Japan

The two major classes of human type I interferons, leukocyte or α-interferon (IFN-α) and fibroblast or β-interferon (IFN-β) are antigenically distinct and encoded by separate structural genes[1]. Recently, genomic hybridization experiments have demonstrated the presence of ~10 or more distinct human IFN-α (Hu IFN-α) genes which code for a family of homologous yet distinct proteins[2,3], and 8 of these have been identified and sequenced[3]. In contrast, no evidence has been found for multiple Hu IFN-β genes[3], although heterogeneity of Hu IFN-β mRNA has been observed[4,5]. The coding sequences of Hu IFN-α and IFN-β genes show weak but appreciable homology, indicating that they were derived from a common ancestor at a remote time[6], whereas Hu IFN-α_1 (a member of class D) and Hu IFN-α_2 (a member of class A) diverged quite recently (~22 Myr ago)[7]. We report here that all eight known IFN-α genes diverged from a common ancestor quite recently, at most ~26 Myr ago. As mammalian divergence is known to have occurred ~75 Myr ago[8], this suggests that the IFN-α multigene family in primates is distinct in organization from that of other mammals. We provide evidence for a much lower rate of evolution for IFN-α G than for other α-interferons, and a rapid evolution of IFN-α E pseudogene similar to that of other pseudogenes[9–11]. A possible evolutionary origin of size heterogeneity in the 3′-noncoding region of IFN-α mRNAs is also discussed.

A single base change in a codon results in either replacement of the encoded amino acid (replacement substitution) or the appearance of a synonymous codon (synonymous substitution). We shall refer to a site where a single base change leads to synonymous (replacement) substitution as a synonymous (replacement) site[12]. At each position in the codon, three

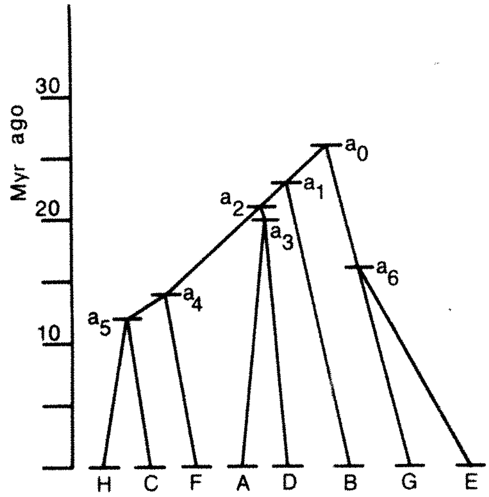

Fig. 1 Evolutionary relationships of eight distinct Hu IFN-α genes. The tree was constructed as follows. Based on the K_S values of pairs of seven functional genes, we first constructed a dendrogram using the clustering method[32]. This method gives an average value of K_S ($\bar{K}_S$) for all pairs of genes between the groups which are derived from a particular node. For example, $\bar{K}_S$ for pairs between groups (H, C) and group (F), which are joined to each other at node a_4, is estimated as 0.127 and that for pairs between groups (H, C, F) and (A, D), which are joined at node a_2, is 0.190, and so on. From $\bar{K}_S$, we have estimated the divergence times of nodes a_0–a_5 as described in the text. The estimated times are 26, 23, 21, 20, 14 and 12 Myr for a_0–a_5, respectively. The date t_6 corresponding to node a_6 was also estimated from K_S as follows. Let O be the common ancestor of G and E; the average difference of synonymous sites between O and G is 0.075 as described in the text. Correcting for multiple hits using $K^c = -(3/4)\ln(1-(4/3)K)$[16,17], and dividing the corrected value by $v_S (= 5.1\times10^{-9}$ per site per yr), the rate of change at the synonymous sites, gives $t_6 = 16$ Myr.

different single base changes are possible, of which a fraction (f) results in synonymous substitutions, while the remainder $1-f$ leads to replacement substitutions. In the codon UUU, for example, the first two positions are replacement sites ($f=0$) whereas for the last position one-third of changes correspond to synonymous sites ($f=1/3$). Thus the codon UUU contains $0.333(=0+0+1/3)$ synonymous sites and $2.667(=1+1+2/3)$ replacement sites.

Previously, on the basis of this definition, we presented a method for estimating mucleotide differences per site at synonymous sites (K_S) and at replacement sites (K_A) by comparing homologous nucleotide sequences of coding regions[12]. Applying the method to several mammalian genes, we showed that the rate of synonymous substitution, v_S, is greater than that of replacement substitution and, more important, is approximately constant among different genes[13]. This is in sharp contrast to the rate of protein evolution, which varies for different proteins[8,14,15]. Thus, because the rate of synonymous substitution for different genes is uniform, it can be used as a 'clock' to show the true evolutionary branching orders of genes in a multigene family, even when the encoded proteins evolve at different rates. For example, if two duplicated genes are compared and the K_S determined, then the time (t) since divergence of the two genes can be estimated from the formula[16,17]

$$t = -(3/4)\ln(1-(4/3)K_S)/2v_S \tag{1}$$

using the value of v_S previously calculated as 5.1×10^{-9} per site per yr[13]. Here, K_S is corrected for the effect of multiple hits (a computer simulation showed that this formula is suited for correcting K_S and K_A at least within a short evolutionary period [unpublished results]). Recently, we have confirmed the uniformity of the synonymous substitution rate by comparing many more sequences of different mammalian genes[18].

From pairwise comparisons of coding sequences of eight distinct Hu IFN-α genes, we have calculated K_S and K_A for each pair of genes (Table 1). Based on the K_S values, phylogenetic relationships among the IFN-α genes, and IFN-α pseudogene, were determined (Fig. 1). The seven functional IFN-α genes were classified into three groups according to the divergence times from ancestors. Surprisingly, all eight Hu IFN-α genes seem to have diverged from a common ancestor quite recently, at most ~26 Myr ago. As mammalian divergence is known to have occurred ~75 Myr ago[8], this result suggests that they have different organization compared with other mammals. This notion is of particular interest in relation to the observation that interferons are often species specific[19]. To test this, IFN-α gene sequences have been compared for different species. A pairwise comparison of the N-terminal 20-amino acid sequence of a mouse IFN-α[20] with the six human α-interferons (A–D, F, H) showed that the latter are much more homologous to each other than to the mouse IFN-α. In fact, of 20 amino acid sites compared, on average 3.8 ± 1.9 sites differ within the six human α-interferons, whereas there are 8.8 ± 1.7 site differences between human and mouse α-interferons. Although the comparison was limited to the N-terminal region, this result in part supports the above argument.

The K_A matrix for seven functional IFN-α genes gives almost the same phylogenetic relationship among the genes as that shown in Fig. 1, except for the IFN-α G gene line. Unusually small K_A values were found for gene pairs with the G gene as a partner. Ratios of K_A/K_S for these pairs are lower (0.26 on average) than those for other pairs (0.43), suggesting that the replacement sites of IFN-α G gene have a low evolutionary rate (note that the ratio for a given pair is insensitive to the divergence time of two compared sequences). Alternatively, the IFN-α G gene may have arisen quite recently, as predicted by K_A values, and accumulated more base substitutions at the synonymous sites than other genes. To resolve this, we compared further the sequences of the 3′-noncoding region (which corresponds to a region upstream of the poly(A) site of the A gene in the aligned sequence[3]) for the seven functional

```
                                                                      50
IFN-α1(3'UF)    aatccattatttgtgttgttcattaaactttactataggaa-cttcctgtat---gtgttcattctttaatat-gaaa
                        ......   .... ...... .........  ..   ... . ...       . ......... ..  ...
B(mRNA)         --------ATTTTGCCATGTTTATTAAATTTTACTATGAAAAAATTCTT-TAT-------TTATTCTTTAAAATTGAA-
F(mRNA)         AATATATTATTTT-CTTTTT--ATTAA-TTTTTACTATTAAAA-CTTCTTATATTATTTGGTTATTCTTTAATAAAGAAA
C(mRNA)         AATATATTAATTT-CCTTTTTCATTAAATTTTTACTATAC(polyA)
H(mRNA)         AATATATTAATTT-CCTTTTTCATTAAATTTTTACTAT(polyA)
E(mRNA)         AATATATTACTTTGCTTTTTTCATTAAATTTTTACTATGG(polyA)


                                   100
IFN-α1(3'UF)    ttcctagcc--tg-actgtgcaacctgattagagaataaagggt
                ...  . ..  .. . ...... ....... ....    . ...
B(mRNA)         CTCCAA-CCCATGAATTGTGCAAACTGATTAAAGAATGGATGGT(polyA)
F(mRNA)         TTCCAAGCCC(polyA)
```

Fig. 2 Alignment of the untranscribed 3′-flanking (3′UF) sequence of IFN-α_1 (ref. 2) (a member of class D)[3] and the terminal sequences of five IFN-α mRNAs[3]. The sequence immediately after the poly(A) site of IFN-α_1 is indicated by lower case letters. Bases that are identical between the IFN-α_1 and B are indicated by dots. The hexanucleotides AATAAA and ATTAAA are underlined. Broken lines indicate gaps introduced to obtain maximum homology.

Table 1 Sequence differences at synonymous sites (K_S) and at replacement sites (K_A) from pairwise comparison of eight distinct Hu IFN-α gene sequences

			K_S							
			I			II			III	
		IFN-α	C	F	H	A	B	D	G	E
K_A	I	C	—	0.128	0.117	0.202	0.216	0.234	0.236	0.286
		F	0.055	—	0.126	0.193	0.193	0.176	0.203	0.256
		H	0.055	0.069	—	0.151	0.191	0.186	0.189	0.232
	II	A	0.078	0.078	0.072	—	0.218	0.176	0.227	0.304
		B	0.094	0.091	0.075	0.075	—	0.202	0.254	0.265
		D	0.079	0.069	0.079	0.072	0.098	—	0.230	0.298
	III	G	0.062	0.046	0.056	0.052	0.071	0.057	—	0.200
		E	0.116	0.098	0.098	0.105	0.121	0.109	0.072	—

K_S (upper half) and K_A (lower half) were calculated by a method described elsewhere[12]. Only the sequence encoding the C-terminal 133 amino acids is available for the coding region of the IFN-α G gene[3]. To make equivalent comparisons of all the gene sequences, only differences in this region were considered for all the genes (even when coding sequences corresponding to mature IFN-α are compared, similar values are obtained for K_S and K_A, although in this case, only the fragment-length sequence is considered in pairwise comparisons involving IFN-α G). IFN-α B gene contains frameshift mutations at codons 98 and 101 (ref. 3), thus this segment was excluded from the comparisons. IFN-α E gene contains a single base insertion[3]; to restore the original reading frame, this insertion was deleted. Functional genes were classified into three groups, I(IFN-α C, F and H), II(A, B and D) and III(G), as the ancestral nodes leading to the present-day genes within each group appear to be in clusters with respect to the divergence time (see Fig. 1).

genes, and obtained a phylogenetic tree (data not shown) essentially identical to that shown in Fig. 1. In addition, the extent of sequence divergence in the noncoding region was similar to K_S in value. These results support the former interpretation.

Using the deduced divergence time, we estimated the rate of evolution at the replacement sites of the G gene (v'_A) and that of other functional genes (v_A). For all pairs between groups which were derived from a particular node in Fig. 1, except for a_0 and a_6, the K_A values of the pairs were averaged ($\bar{K}_A$) and then the v_A calculated as $v_A = \bar{K}^c_A/2t$, where t is the divergence time corresponding to the node and $K^c = -(3/4)\ln[1-(4/3)K]$. For example, two groups, the one containing H and C and the other containing F, were derived from node a_4, and thus the pair F–H and F–C have the same divergence time ($t = 14$ Myr) corresponding to the node. The average difference $\bar{K}_A$ is 0.062, which gives $v_A = 2.3\times10^{-9}$ per site per yr, and so on (Table 1). The average value of v_A, estimated for the five different nodes, is 2.1×10^{-9} per site per yr, which, when converted into rate (v_{aa}) defined at the protein level, corresponds to $\sim5.0\times10^{-9}$ per residue per yr (as the number of replacement sites per codon was estimated to be $\sim$2.4 on average, $v_{aa} = 2.4\ v_A$). This rate is high, almost comparable with that of immunoglobulin[8]. To estimate v'_A, two different speeds of evolution were assumed: one (v'_A) in the line from a_0 to G in Fig. 1; the other (v_A) in the line from a_0 to functional genes (X) other than the G gene. This gives the equation

$$v_A t_0 + v'_A t_0 = K^c_A(\mathrm{G{-}X}) \qquad (2)$$

where t_0 is the date of node a_0 and K(G–X) is the sequence difference between G and X. Solving this for each functional gene and averaging the resulting values of v'_A, we obtain $v'_A = 0.17\times10^{-9}$ per site per yr or $v'_{aa} = 0.41\times10^{-9}$ per residue per yr, which is similar to the rate for insulin, a slowly evolving molecule[8]. It is remarkable that the IFN-α G gene, a direct descendant of the common ancestor of all the eight distinct classes, accumulates far fewer base substitutions at the replacement sites than other IFN-α genes, at a rate of about one-tenth that of the other genes, suggesting the presence of strong selective pressure depending on the unique function of the encoded protein.

The Hu IFN-α multigene family contains a pseudogene (IFN-α E) which shows close sequence homology to the IFN-α G gene, suggesting that it was derived from the G gene during evolution. This represents the first evidence of a pseudogene transcribed into mRNA[3]. Thus it is interesting to determine whether or not the IFN-α E gene shows strong sequence divergence similar to that of other pseudogenes[21–26]. We have calculated differences between gene sequences from their joint node (a_6 of Fig. 1). Designating 'O' for node a_6 and X for any one of IFN-α A, B, C, D, F and H genes, we have a set of equations: $K(\mathrm{X{-}G}) = K(\mathrm{O{-}X}) + K(\mathrm{O{-}G})$, $K(\mathrm{X{-}E}) = K(\mathrm{O{-}X}) + K(\mathrm{O{-}E})$ and $K(\mathrm{G{-}E}) = K(\mathrm{O{-}G}) + K(\mathrm{O{-}E})$, where K(O–G), for example, represents the sequence difference between O and G. Solving this, we obtain $K(\mathrm{O{-}G}) = [K(\mathrm{X{-}G}) + K(\mathrm{G{-}E}) - K(\mathrm{X{-}E})]/2$, $K(\mathrm{O{-}E}) = [K(\mathrm{X{-}E}) + K(\mathrm{G{-}E}) - K(\mathrm{X{-}G})]/2$ and $K(\mathrm{O{-}X}) = [K(\mathrm{X{-}G}) + K(\mathrm{X{-}E}) - K(\mathrm{G{-}E})]/2$. Using the K_S values in Table 1, we calculated the three differences for each X. The mean values (±s.e.) of the three differences were $K_S(\mathrm{O{-}G}) = 0.075(\pm0.031)$, $K_S(\mathrm{O{-}E}) = 0.126(\pm0.040)$ and $K_S(\mathrm{O{-}X}) = 0.149(\pm0.044)$. Similarly, $K_A(\mathrm{O{-}G}) = 0.011(\pm0.006)$, $K_A(\mathrm{O{-}E}) = 0.061(\pm0.014)$ and $K_A(\mathrm{O{-}X}) = 0.047(\pm0.012)$ (the standard errors were calculated by assuming a Poisson distribution for the total number of base changes and by considering, on average, 308.6 replacement sites and 78.4 synonymous sites in the sequences compared). This result suggests that the E gene accumulated more substitutions than the functional genes at both the synonymous and replacement sites, although the standard errors seem rather large. In addition, the rate of change at the replacement sites of the pseudogene, relative to the standard genes, increases more than the rate of change at the synonymous sites: the mean values are $K_A(\mathrm{O{-}E})/K_A(\mathrm{O{-}G})(=5.6) > K_A(\mathrm{O{-}E})/K_A(\mathrm{O{-}X'})(=2.9) > K_S(\mathrm{O{-}E})/K_S(\mathrm{O{-}G})(=1.7) \sim K_S(\mathrm{O{-}E})/K_S(\mathrm{O{-}X'})(=1.9) > 1$, where $K(\mathrm{O{-}X'})$ is $K(\mathrm{O{-}X})/2.25$, as, according to the phylogenetic tree of Fig. 1, the time interval between O and X is estimated to 2.25 times longer than that between O and G. These relationships are the same for each of the six different X genes. These patterns of base substitutions are similar to those of other pseudogenes analysed previously, including α-globin pseudogenes of man and mouse, β-globin pseudogenes of rabbit and mouse and immunoglobulin V_κ pseudogene of man[10], suggesting that pseudogenes show strong sequence divergence compared with functional genes, regardless of whether the mRNAs are transcribed.

A possible interpretation of these results is that in most functional genes, the replacement sites are more constrained than the synonymous sites. However, in pseudogenes the loss of functions frees the gene from several selective constraints, thereby allowing accumulation of substitutions almost uniformly over all the regions at rate higher than the rate of change at the synonymous sites of functional genes, the most rapidly evolving component (see refs in ref. 13). The fact that $K_S(\mathrm{O{-}E}) > K_S(\mathrm{O{-}G})$ suggests that even synonymous sites of functional genes are constrained, although presumably only weakly[10]. The suggestion that the IFN-α E pseudogene has evolved faster than functional genes may support the neutral theory[27], its rate of evolution may approximate to a limiting rate predicted by the neutral theory[9-11,28].

In human α- and β-globin, and rabbit and mouse β-globin gene clusters, pseudogenes are found between functionally distinct genes, that is, between the embryonic or fetal and adult genes[23-25,29]. The suggestion that the IFN-α E pseudogene was derived from the IFN-α G gene is of interest in this regard. The fact that the v_A of the G gene is smaller than that of other genes suggests that the functions of the proteins encoded by them differ. Although the complete linkage arrangement of the Hu IFN-α multigene family has not been established, this suggests that the E pseudogene may be located between the G gene and the other groups of genes. Furthermore, IFN-α C, F and H genes (group I) show close sequence homology, suggesting that they are closely linked. It would be interesting to determine whether further pseudogenes reside between this group and group II (A, B and D) or III (G). This would provide further insights into the mechanisms by which pseudogenes arise during evolution.

Goeddel *et al.*[3] found size heterogeneity in the 3'-noncoding regions of the eight distinct Hu IFN-α mRNA sequences. To trace the evolutionary origin of such heterogeneity, we have compared the untranscribed 3'-flanking sequences of Hu IFN-α_1 (a member of class D)[2] with the IFN-α B, C, E, F and H mRNA sequences in the region corresponding to that immediately after the poly(A) sites of IFN-α A, D and G mRNAs, the shortest mRNAs. We found remarkable homology: the untranscribed 3'-flanking sequence of IFN-α_1 is 74% homologous to the longest B mRNA sequence in the corresponding region. In the IFN-α_1 sequence, the hexanucleotide AATAAA, which is thought to be involved in mRNA polyadenylation and processing[30], and its variant ATTAAA were found at positions 37–42 and 115–120, respectively (see Fig. 2). Presumably the IFN-α A and G genes also contain such hexanucleotides in this region. It seems likely that the presence of multiple hexanucleotides allowed the extension of the 3'-noncoding regions of the IFN-α genes during evolution, and thus gave rise to size heterogeneity of the mRNAs. Interestingly, two hexanucleotides precede the poly(A) sites in the B and F mRNAs, suggesting that the multiple hexanucleotides in each mRNA are recognized with varying efficiency, giving rise to mRNAs having 3'-noncoding regions of different sizes from a single gene[31].

We thank Drs T. Taniguchi and T. Yasunaga for discussions and comments. This work was supported in part by grants from the Ministry of Education, Science and Culture of Japan.

Received 27 July; accepted 18 November 1981.

1. Cavalieri, R. L., Havell, G. A., Vilcek, J. & Pestka, S. *Proc. natn. Acad. Sci. U.S.A.* **74,** 3287–3291 (1977).
2. Nagata, S., Mantei, N. & Weissmann, C. *Nature* **287,** 401–408 (1980).
3. Goeddel, D. V. *et al. Nature* **290,** 20–26 (1981).
4. Sehgal, P. B. & Sagar, A. D. *Nature* **288,** 95–97 (1980).
5. Weissenbach, J. *et al. Proc. natn. Acad. Sci. U.S.A.* **77,** 7152–7156 (1980).
6. Taniguchi, T. *et al. Nature* **285,** 547–549 (1980).
7. Streuli, M., Nagata, S. & Weissmann, C. *Science* **209,** 1343–1347 (1980).
8. Dayhoff, M. O. *Atlas of Protein Sequence and Structure* Vol. 5, suppl. 3 (ed. Dayhoff, M. O.) (National Biochemical Research Foundation, Maryland, 1978).
9. Miyata, T. & Yasunaga, T. *Proc. natn. Acad. Sci. U.S.A.* **78,** 450–453 (1981).
10. Miyata, T. & Hayashida, H. *Proc. natn. Acad. Sci. U.S.A.* **78,** 5739–5743 (1981).
11. Kimura, M. *J. molec. Evol.* **16,** 111–120 (1980).
12. Miyata, T. & Yasunaga, T. *J. molec. Evol.* **16,** 23–36 (1980).
13. Miyata, T., Yasunaga, T. & Nishida, T. *Proc. natn. Acad. Sci. U.S.A.* **77,** 7328–7332 (1980).
14. Wilson, A. C., Carlson, S. S. & White, T. J. *A. Rev. Biochem.* **46,** 573–639 (1977).
15. Kimura, M. & Ohta, T. *Proc. natn. Acad. Sci. U.S.A.* **71,** 2848–2852 (1974).
16. Jukes, T. H. & Cantor, C. R. *Mammalian Protein Metabolism II* (ed. Munro, H. N.) (Academic, New York, 1969).
17. Kimura, M. & Ohta, T. *J. molec. Evol.* **2,** 87–90 (172).
18. Miyata, T. *et al. J. molec. Evol.* (submitted).
19. Stewart, W. E. II *The Interferon System* (Springer, New York, 1979).
20. Taira, H., Broeze, R. J., Jayram, B. M. & Lengyel, P. *Science* **207,** 528–529 (1980).
21. Nishioka, Y. & Leder, P. *Proc. natn. Acad. Sci. U.S.A.* **77,** 2806–2809 (1980).
22. Vanin, E. F., Goldberg, G. I., Tucker, P. W. & Smithies, O. *Nature* **286,** 222–226 (1980).
23. Jahn, C. L. *et al. Cell* **21,** 159–168 (1980).
24. Lacy, E. & Maniatis, T. *Cell* **21,** 545–553 (1980).
25. Proundfoot, N. J. & Maniatis, T. *Cell* **21,** 537–544 (1980).
26. Bentley, D. L. & Rabbitts, T. H. *Nature* **288,** 730–733 (1980).
27. Kimura, M. *Nature* **217,** 624–626 (1968).
28. Kimura, M. *Nature* **267,** 275–276 (1977).
29. Fritsch, E. F., Lawn, R. M. & Maniatis, T. *Cell* **19,** 959–972 (1980).
30. Proundfoot, N. J. & Brownless, G. G. *Nature* **263,** 211–214 (1976).
31. Setzer, D. R., McGrogan, M., Nunberg, J. H. & Schimke, R. T. *Cell* **22,** 361–370 (1980).
32. Sokal, R. R. & Sneath, P. H. A. *Principles of Numerical Taxonomy* (Freeman, San Francisco, 1963).

H-2-like genes in the *Tla* region of mouse chromosome 17

David H. Margulies, Glen A. Evans, Lorraine Flaherty* & J. G. Seidman

Laboratory of Molecular Genetics, National Institute of Child Health and Human Development, National Institutes of Health, Bethesda, Maryland 20205, USA
* Kidney Disease Institute, Division of Laboratories and Research, New York State Department of Health, Albany, New York 12201, USA

H-2K, H-2D, H-2L, Qa-2 and TL are all members of a closely related family of cell-surface glycoproteins. The H-2 molecules (major histocompatibility antigens) are extremely polymorphic, expressed on almost all cell types and play an important part in graft rejection[1-4]. In contrast, Qa-2 and TL are much less polymorphic, and have a limited tissue distribution[4,5]. Nevertheless, all these molecules are similar in that they consist of two chains, one of which is the invariant β_2-microglobulin (molecular weight (MW) 11,500), the other a 45,000-MW glycopolypeptide[2,6-10]. The 45,000-MW H-2K and H-2D map within 0.3 centimorgans of each other in the major histocompatibility complex (MHC) on chromosome 17 (ref. 1). The Qa-2 and TL chains are encoded by genes in the closely linked *Tla* region. Recently, recombinant DNA techniques have been used to study the family of genes encoding H-2-like molecules[11-14]. The finding that cloned *H-2* cDNA hybridizes to 10–20 restriction fragments of genomic DNA has led to the conclusion that there are 10–20 *H-2*-like genes in the murine genome[11,12]. Here we present evidence that most of these genes are encoded on chromosome 17 and that at least three *H-2*-like genes map outside the MHC in the *Tla* region. We also confirm and provide further evidence that there are 10 to 15 *H-2*-like genes in the mouse genome.

Initial studies of the number of genes in the *H-2* family[11,12] used cDNA probes complementary to portions of the *H-2*-like mRNA. Thus, the precise relationship between the structure of the probe and the sequences detected in Southern blotting experiments is uncertain. If these probes span intervening sequences that contain relevant restriction sites, they would be expected to hybridize to several genomic DNA fragments from the same gene, thus overestimating the number of genes. To avoid this we used probes from the cloned genomic DNA to identify *Bam*HI restriction fragments of BALB/cN myeloma DNA that encode *H-2*-like genes (Fig. 1*a*). The 3' probe (Fig. 1*d*) and a probe that encodes amino acids 194–283 (and intervening sequence) identify similar sets of restriction fragments (D.H.M. and J.G.S., unpublished observations). In contrast, the 5' (Fig. 1*d*) and 3' probes do not identify the same fragments of *Bam*HI-digested BALB/c myeloma DNA (Fig. 1*a*). Thus, the 5' and 3' portions of some *H-2*-like genes lie on different *Bam*HI restriction fragments. However, each probe identifies 10–15 fragments. This is a minimum estimate of the gene number as we cannot be certain that our probe detects all the *H-2* genes in the hybridization conditions used and because some of the larger fragments contain two *H-2*-like genes (unpublished observation). These fragments may represent inactive or pseudogenes, and there may be other MHC transplantation genes that are not recognized by the probes. Kourilsky *et al.*[11] detected a similar pattern of *Bam*HI restriction fragments in BALB/c DNA using a probe ~85% homologous to the 3' probe used here.

The fact that the *H-2L*, *H-2D* and *H-2K* genes are all closely linked on chromosome 17 in the MHC does not mean that all *H-2*-like genes are necessarily encoded on this chromosome. To determine which *H-2*-like genes are encoded on chromosome 17, we have analysed the DNA of the cloned somatic cell hybrid, R4 4.1 (ref. 15), which contains a full complement of Chinese hamster chromosomes but only chromosome 17 derived from

0028-0836/82/020168—03$01.00

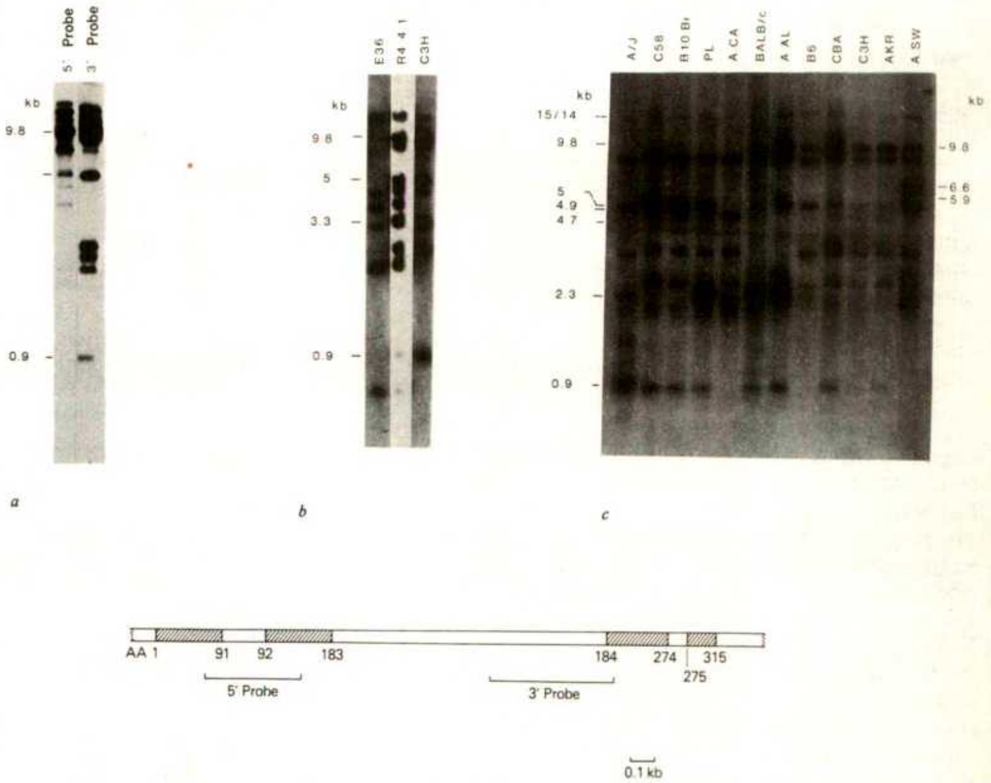

Fig. 1 Southern blot analysis of genomic DNA probed with fragments derived from an *H–2*-like gene. The structure of the *H–2*-like genomic clone and the 5′ and 3′ probe fragments derived from it are shown in *d*. This clone was isolated from the MOPC 41 (BALB/c) Charon 4A library using a fragment of a human HLA genomic clone as probe (G.A.E. and J.G.S., in preparation). This cloned genomic DNA fragment encodes a protein that is 70–90% homologous to H–2K^d, H–2D^d and H–2K^b. The indicated *Sau*3A fragments were cloned in M13mp7 as described elsewhere[18]. The subcloned fragment was separated from the replicative form (double-stranded DNA) by digestion with *Eco*RI, and purified on disulphide-linked polyacrylamide gels[19]. DNA was prepared from: BALB/c myeloma (NP-2) DNA; E36 and R4 4.1 from cultured cells; and C58 from the R1.1 cultured cell line[10]. All other DNA was extracted from livers of mice obtained from either Dr I. Egorov (BALB/cBy) or Dr J. Berzofsky (B10.Br), Jackson Laboratories, or *Tla* and *Qa* recombinant strains[4,5]. Digestion of the DNA *Bam*HI endonuclease, electrophoresis in 0.8% or 1.0% agarose gels (*a*), blotting to nitrocellulose filters, hybridization to the nick-translated probes (specific activity between 2.0 and 4.0×10^8 c.p.m. per μg), washing in 0.015 M NaCl, 0.0015 M Na citrate at 50 °C, and autoradiography were all as described elsewhere[21–23]. Sizes of fragments (in kilobases) are indicated. *a*, BALB/c DNA (NP-2) probed with 5′ and 3′ probes; *b*, Chinese hamster E36, mouse × hamster hybrid clone R4 4.1, and C3H DNAs probed with the 3′ probe; *c*, genomic DNA from the indicated strains (BALB/c, BALB/cBy liver; B6, C57BL/6); *d*, structure of the *H–2*-like genomic clone and derivation of its probes. Shaded areas indicate coding blocks and adjacent amino acids are indicated.

the mouse L cell parent. The *Bam*HI restriction fragments identified in digests of genomic DNA from E36 (Chinese hamster cell), R4 4.1 and C3H (parent of the L cell) are indicated in Fig. 1*b*. Fragments derived from R4 4.1 DNA but not E36 DNA must be encoded on chromosome 17. There are many genes encoded in the hamster genome that hybridize to the H–2 probe. However, the chromosomal location of mouse-derived restriction fragments that co-migrate with hamster-derived restriction fragments cannot be determined from this experiment. Nevertheless, there are at least seven murine-derived restriction fragments in the R4 4.1 DNA digests. Thus at least seven of the 10–15 *H–2*-like genes are encoded on murine chromosome 17.

A unique feature of the H–2 antigens is their extreme polymorphism among inbred mice. Using the 3′ probe to examine the *Bam*HI-derived restriction fragments from a series of inbred mouse strains (Fig. 1*c*), we found that these patterns are similar overall. The number of restriction fragments encoding *H–2*-like genes was similar in the different strains. Thus, the number of *H–2*-like genes does not vary widely among the inbred strains examined. In addition, many fragments (~50%) were common to different mouse strains both in the *Bam*HI digest shown here, and in digests using other enzymes (*Xba*I and *Eco*RI) (unpublished observations). However, comparison of the H–2K and H–2D types (Table 1) of these strains and their restriction fragment pattern (Fig. 1*c*) suggests that there are only a few fragments specific to a *H–2* haplotype. For example, A.SW has two unique fragments of 6.6 and 5.9 kilobases (kb) not found in other strains. These *H–2*-specific fragments may reflect differences in the major histocompatibility antigens of these mice.

There are differences in three restriction fragments between these mouse strains that have a distinct pattern, but which do not reflect the H–2 type of a particular strain. For these cases, if a strain lacks a particular restriction fragment, it is replaced by another, compensating fragment. The surprising feature is that the replacement fragment is the same in several strains. For example, five strains have a 2.3-kb fragment (A/J, PL, BALB/c, A.AL, B6) while the strains that lack this fragment (C58, B10.Br, A.CA, CBA, C3H and AKR) have a 4.7-kb fragment. A.SW is an exception to this rule, lacking both fragments. There are two further examples of this type of compensatory polymorphism: (1) nine strains (A/J, C58, B10.Br, PL, BALB/c, A.AL, CBA, C3H and AKR) have 0.9-kb and 14-kb fragments, while three strains (A.CA, B6, A.SW) replace these with a 15-kb fragment. (2) A 9.8-kb fragment is found in BALB/c, A.AL, B/6, CBA, C3H, AKR and A.SW and is replaced by a 4.9-kb fragment in A/J, C58, B10.Br and PL. A.CA appears to lack the compensatory 4.9-kb fragment. From these patterns we make the following conclusions: (1) Each of these fragments, and their compensatory fragments, represents a single mutational event that affects a single *H–2*-like gene or its flanking sequence. (2) Apparently, each band identified in the Southern

Table 1 Phenotypes of mouse strains

Strain	H–2K	H–2D	Qa-2,3	Tla
A	k	d	a	a
C58	k	k	b	a
B10.Br	k	k	b	a
PL	u	d	ND	a
A.CA	f	f	b	d
BALB/c	d	d	a*	c
A.AL	k	d	ND	c
B6	b	b	a	b
CBA	k	k	b	b
C3H	k	k	b	b
AKR	k	k	b	b
A.SW	s	s	a	b

The phenotypes for the inbred mouse strains are taken from Klein *et al.*[17]. ND, phenotype not determined.

* The phenotype of BALB/cJ is indicated here; the BALB/cBy (*Qa-2,3^b*) analysed in Fig. 1*c* apparently is an exception to the correlation of the presence of the 2,3-kb fragment with *Qa-2,3^a*. However, as it is likely that this is an independent mutation that occurred in a subline of BALB/c, one would not expect it to have the same restriction fragment pattern as other *Qa-2,3^b* strains. (Based on the genomic blot analysis, we can make tentative assignments of the *Qa-2,3* and *Tla* types of the unassigned strains as follows: PL, *Qa-2,3^a*; A.AL, *Qa-2,3^a*.)

blot corresponds to a single fragment in the mouse genome. Presumably, identical multiple mutations would not occur in different genes. (3) Each of these mutations must have occurred before the inbred lines were separated from each other. As several strains (for example, BALB/c, AKR and PL) have distinct origins, we suggest that these mutations occurred in the wild mouse population. The fact that these patterns do not correlate with the H–2 type of the strains suggests that either the mutations segregated independently of the H–2 type during evolution, or the *H–2* haplotypes have been generated by independent mutation since the original mutations occurred.

To test the hypothesis that these polymorphisms segregate with other known genes encoded in chromosome 17, we compared the Qa-2,3 and Tla phenotypes of these strains (Table 1) with their restriction fragment patterns (Fig. 1*c*). The 4.7-kb fragment was found in the $Qa\text{-}2^b$ strains while the 2.3-kb fragment was found in $Qa\text{-}2^a$. The 9.8-kb fragment was found in all Tla^b and Tla^c strains and the 4.9-kb in all Tla^a strains. Furthermore, A.CA, the only strain of the Tla^d haplotype examined, lacks the 9.8-kb as well as the 4.9-kb fragment. This suggests that the mutation separating Tla^b from Tla^c occurred more recently than the mutation distinguishing them from Tla^a. The presence of the 0.9-kb fragment does not correlate with the H-2, Qa-2,3 or Tla phenotypes.

The correlations suggested by examination of polymorphisms in inbred strains of mice might be misleading: the finding of a fragment in one inbred line and its replacement in another might reflect the history of these strains or the chance co-migration of several restriction fragments. Fortunately, several congeneic strains of mice have been isolated which have undergone recombination in the vicinity of the *Qa-2,3* and *Tla* genes[3,9]. We have examined the DNAs of these strains to determine the map location of the restriction fragment polymorphisms (Figs 2, 3). Again, the 2.3-kb/4.7-kb polymorphism maps with the Qa-2,3 phenotype, and the 9.8-kb/4.9-kb fragments with the Tla phenotype. Recently, Steinmetz *et al.* have mapped a 2.7-kb *Bam*HI fragment to the *Qa-2,3* region[16]. The 0.9-kb polymorphism does not segregate with either the Qa-2,3 or the Tla phenotype. However, these recombinant strains allow us to map this polymorphic *H–2*-like gene to the left of the *Tla* gene (as the fragment is found in $A.Tla^b$, but not in B6) but to the right of *H–2D* (as the fragment is found in B6.K1 but not in $B6.Tla^a$).

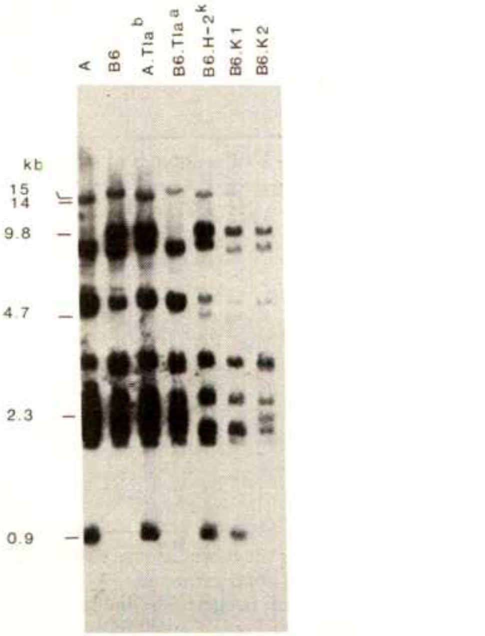

Fig. 2 Restriction fragment analysis of DNA from *Tla* and *Qa* region of congeneic mouse strains. DNA from the indicated strains was analysed as described in Fig. 1 legend. Band intensity is a complex function of various factors. The greater intensity of the 2.5-kb fragment in strain A is a more usual result than the faint intensity of the same DNA seen in Fig. 1.

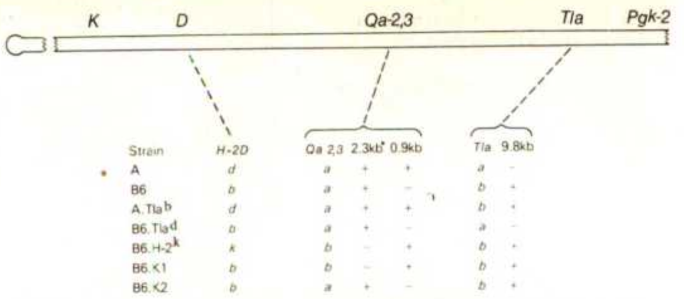

Strain	H-2D	Qa 2,3	2.3kb*	0.9kb	Tla	9.8kb
A	d	a	+	+	a	-
B6	b	a	+	-	b	+
A.Tla b	d	a	+	+	b	+
B6.Tla d	b	a	+	-	a	-
B6.H-2k	k	b	-	+	b	+
B6.K1	b	b	-	+	b	+
B6.K2	b	a	+	-	b	+

Fig. 3 Mapping of the *Tla* region polymorphism on chromosome 17. A schematic map of the relevant region on chromosome 17 is drawn to scale after Klein[1]. The distance from *K* to *D* is 0.33 cm, and from *D* to *Tla* 1.3 cm. *Qa-2,3* maps between *D* and *Tla* but its precise location is unknown. * Size of fragment indicated in Figs 1*c* and 2.

The presence of a 14-kb fragment that moves to 15 kb in the strains lacking the 0.9-kb fragment suggests that either this polymorphism contains a *Bam*HI site or that there are two *H–2*-like genes within 15 kb of each other. Thus, there are at least three *H–2*-like genes encoded in the *Tla* region, although these genes may not be *Qa-2,3* and *Tla*.

These studies, using cloned genomic fragments from an H–2-like molecule as a molecular probe demonstrate that: (1) there are at least 10–15 *H–2*-like genes encoded in the mouse genome; (2) at least seven of these are encoded on chromosome 17; and (3) there are at least three *H–2*-like genes encoded outside the MHC which map to the *Tla* region. Future analysis of cloned *H–2*-like genes will permit a comparison of genes from the MHC with the *Tla*-encoded genes defined here. The basis for differences in the polymorphism and expression of the MHC and *Tla*-encoded genes may be reflected in their nucleotide sequences.

We thank Drs J. Strominger and S. Weissman for providing HLA cDNA clones needed in the early stages of this work, Dr I. Egorov and J. Berzofsky for mouse strains, Dr P. d'Eustachio for the somatic cell hybrid line and Dr J. Michaelson for stimulating discussions of *Qa* and *Tla*. We also thank Ms Terri Broderick for editorial and secretarial assistance. This work was supported in part by NIH grant AI12603 awarded by the onal Institute of Allergy and Infectious Disease (PHS DHHS).

Note added in proof: Subsequent studies have demonstrated that the molecular probes used in these experiments are derived from the $H\text{-}2L^d$ gene[24].

Received 18 September; accepted 20 November 1981.

1. Klein, J. *Biology of the Mouse Histocompatibility Complex*, 1–620 (Springer, Berlin, 1975).
2. Snell, G. D., Dausset, J. & Nathenson, S. *Histocompatibility*, 1–401 (Academic, New York, 1976).
3. Klein, J. *Science* **203**, 516–521 (1979).
4. Flaherty, L. in *The Role of the Major Histocompatibility Complex in Immunobiology* (ed. Dorf, M. E.) 33–58 (Garland STPM, New York, 1980).
5. Flaherty, L. in *Origins of Inbred Mice* (ed. Morse, H. C. III) 409–422 (Academic, New York, 1980).
6. Michaelson, J., Flaherty, L., Vitetta, E. & Poulik, M. *J. exp. Med.* **145**, 1066–1070 (1977).
7. Stanton, T. H. & Hood, L. *Immunogenetics* **11**, 309–318 (1980).
8. Michaelson, J. *Immunogenetics* **13**, 167–171 (1981).
9. Silver, J. & Hood, L. *Nature* **249**, 764–765 (1974).
10. Rask, L., Lindblom, J. B. & Peterson, P. A. *Nature* **249**, 833–834 (1974).
11. Cami, B., Bregegere, F., Abastado, J. P. & Kourilsky, P. *Nature* **291**, 673–675 (1981).
12. Steinmetz, M. *et al. Cell* **24**, 125–134 (1981).
13. Ploegh, H. L., Orr, H. T. & Strominger, J. L. *Proc. natn. Acad. Sci. U.S.A.* **77**, 6081–6085 (1980).
14. Sood, A. K., Pereira, D. & Weissman, S. M. *Proc. natn. Acad. Sci. U.S.A.* **78**, 616–620 (1981).
15. Smiley, J. R., Steege, D. A., Juricek, D. K., Summers, W. P. & Ruddle, F. H. *Cell* **15**, 455–468 (1978).
16. Steinmetz, M. *et al. Cell* **25**, 683–692 (1981).
17. Klein, J., Flaherty, L., VandeBerg, J. L. & Shreffler, D. C. *Immunogenetics* **6**, 459–512 (1978).
18. Messing, J., Crea, R. & Seeburg, P. H. *Nucleic Acids Res.* **9**, 309–321 (1981).
19. Hansen, J. N., Pheiffer, B. H. & Boehnert, J. A. *Analyt. Biochem.* **105**, 192–201 (1980).
20. Ralph, P. *J. Immun.* **110**, 1470–1475 (1973).
21. Southern, E. M. *J. molec. Biol.* **8**, 503–517 (1975).
22. Seidman, J. G., Leder, A., Nau, M., Norman, B. & Leder, P. *Science* **202**, 11–17 (1978).
23. Wahl, G. M., Stern, M. & Stark, G. R. *Proc. natn. Acad. Sci. U.S.A.* **76**, 3683–3687 (1979).
24. Evans, G. A., Margulies, D. H., Ozato, K., Camerini-Otero, R. D. & Seidman, J. G. *Proc. natn. Acad. Sci. U.S.A.* (in the press).

MATTERS ARISING

A pitfall in random sampling

MANY statistical tests depend on random samples. A random sample can be defined[1] as a sample from a distribution (for a univariate distribution this is an area) in which each point or neighbourhood has the same probability of being chosen. It is therefore necessary to pay close attention not merely to the process of sampling, but also to the nature of the distribution itself. It is sometimes easy to misinterpret a distribution and thereby invalidate the resulting test. For example, one can treat as stationary a distribution which may change over time. So stated the trap is obvious, but it can be subtle and occasionally catches excellent biologists. The question is totally different from estimating the shape or position of an average distribution determined *post facto* from a non-stationary process. Such an average distribution exists statistically but may have no causal meaning; an obvious example is the joint distribution of annual income of all residents of London since 1800.

Cole[2] criticizes the work of Evans and Murdoch[3], who showed that herbivorous insect species in a community are a roughly constant proportion of all insect species over a season, despite much turnover. They therefore showed that the distribution is stationary, an important result. Cole not surprisingly found that Evans and Murdoch's data are not significantly different from what they would be if they were random samples of the same size from the total species pool. He then concluded that the data are irrelevant to ecological processes.

The fallacy is in assuming that there is a uniform pre-existing population from which samples are drawn (commonly without replacement, which affects the statistics in a subsidiary way). However, the very existence of such a stationary population is the interesting question, because it implicitly assumes that the relevant properties (here, diet) of the species sampled at different times are the same. Otherwise there would be no overall distribution which could be sampled randomly, and no reason to expect approximate constancy over time in the proportion of herbivores.

Thus, the results of Evans and Murdoch[3] do add support for the idea of a dynamically maintained balance in trophic structure. This balance also has other aspects, notably in energy flow, and its control remains a central problem in ecology[4].

LEIGH M. VAN VALEN

Department of Biology (Whitman),
University of Chicago,
915 East 57th Street,
Chicago, Illinois 60637, USA

1. Van Valen, L. M. in *Conceptual Issues in Ecology* (ed. Saarinen, E.) (Reidel, Dordrecht, in the press).
2. Cole, B. J. *Nature* **288**, 76–77 (1980).
3. Evans, F. C. & Murdoch, W. W. *J. anim. Ecol.* **37**, 259–273 (1968).
4. Van Valen, L. M. *Evol. Theory* **1**, 31–49 (1973).

Anomalous ^{13}C depletion in Precambrian organic carbon

SOME isotopic analyses of Precambrian reduced carbon which is strongly depleted in the heavier ^{13}C isotope have been reported by Schoell and Wellmer[1]. They have argued that these anomalous graphitic carbons might be isotopically light as the result of a fractionation related to methane bacterial action in the Precambrian. This argument is quite reasonable insofar as it assumes that the organic carbon in most Precambrian and early Phanerozoic sediments is itself normal. However, the average isotopic value of such reduced carbon is normal only from the experimental standpoint. When placed in context with the algal biota presumed to have been responsible for its origin and overall composition, it is also anomalously depleted of ^{13}C.

In Fig. 1 of ref. 1, and in other similar compilations[2–5], the mean values for δ^{13}C(PDB) cluster around −24 to −28‰. Such values appear quite normal when compared with the reduced carbon of modern C_3 terrestrial plants[3,4,6,7]. However, a substantial land plant community did not develop until the Silurian, so that when compared with the reduced carbon from modern marine algae and algal mats, these 'normal' Precambrian isotopic ratios become disturbingly anomalous, and are especially so for the carbonate stromatolites[5,8]. Present-day marine algal organic carbon is significantly heavier isotopically, with mean values ranging from −18 to −20‰ (refs 3, 4). Modern marine algal mats are even heavier[8–12], with values ranging from −8 to −19‰. This difference between the average terrestrial isotopic values and the average marine values of reduced carbon is so striking that it has been used to evaluate the impact of land-derived organic matter in modern marine sediments[13,14].

In the absence of a significant terrestrial biota in the Precambrian, how can average values ranging from −24 to −28‰ be explained? Those who have discussed this problem (see refs 3, 8, 10, 12, 15) have variously concluded that the depletion might be the results of: preferential diagenetic enrichment of isotopically light (lipid) fractions; a higher CO_2 partial pressure in the Precambrian environment; or perhaps different primitive metabolic fractionations.

When compared with data on ancient organic matter having both carbon isotopic and H/C atomic ratios[2,16,17], recent laboratory-simulated thermal maturation experiments on algal mat kerogen[11] do not support the diagenetic argument. In these experiments only the most immature algal mat kerogens showed any tendency towards ^{13}C depletion; all mature kerogens (H/C atomic ratios <1.0) were enriched in ^{13}C.

Some laboratory experiments with marine algae grown under elevated CO_2 (1.5 to 3.5%) have produced carbon isotope ratios consistent with the idea of an increased level of CO_2 in the Precambrian[10,15]. But the low cell densities involved and the absence of a potential for bicarbonate-derived CO_2 in these experiments makes them doubtfully applicable to the conditions in which the carbonate stromatolite mats of the Precambrian thrived.

While the very depleted values reported by Schoell and Wellmer[1] and others[2] are certainly anomalous in their own right, and may be the result of Precambrian biogenic methane, a more important anomaly remains. Until the average isotopic composition of organic carbon in a variety of Precambrian and Phanerozoic marine deposits can be explained in a consistent fashion, interpretations of the data to infer the physiology of the organisms involved, or the environments in which they were living, must be considered as tentative. This is especially important to timing the onset of oxygenic photosynthesis in the early history of life[18].

KENNETH M. TOWE

Department of Paleobiology,
Smithsonian Institution,
Washington DC 20560, USA

1. Schoell, M. & Wellmer, F.-W. *Nature* **290**, 696–699 (1981).
2. Hayes, J. M., Kaplan, I. R. & Wedeking, K. W. in *Origin and Evolution of Earth's Earliest Biosphere* (ed. Schopf, J. W.) (Princeton University Press, in the press).
3. Degens, E. T. in *Organic Geochemistry* (eds Eglinton, G. & Murphy, M. T. J.) 304–329 (Springer, New York, 1969).
4. Craig, H. *Geochim. cosmochim. Acta* **3**, 53–92 (1953).
5. Eichmann, R. & Schidlowski, M. *Geochim. cosmochim. Acta* **39**, 585–595 (1975).
6. Smith, B. N. *Bioscience* **22**, 226–231 (1972).
7. Park, R. & Epstein, S. *Geochim. cosmochim. Acta* **21**, 110–126 (1960).
8. Calder, J. A. & Parker, P. L. *Geochim. cosmochim. Acta* **37**, 133–140 (1973).
9. Behrens, E. W. & Frishman, S. A. *J. Geol.* **79**, 94–100 (1971).
10. Pardue, J. W., Scalan, R. S., Van Baalen, C. & Parker, P. L. *Geochim. cosmochim. Acta* **40**, 309–312 (1976).
11. Peters, K. E., Rohrback, B. G. & Kaplan, I. R. *Bull. Am. Ass. Petrol. Geol.* **65**, 501–508 (1981).
12. Barghoorn, E. S., Knoll, A. H., Dembicki, H. & Meinschein, W. G. *Geochim. cosmochim. Acta* **41**, 425–430 (1977).
13. Hedges, J. I. & Parker, P. L. *Geochim. cosmochim. Acta* **40**, 1019–1029 (1976).
14. Sackett, W. M. *Mar. Geol.* **2**, 173–185 (1964).
15. Seckbach, J. & Kaplan, I. R. *Chem. Geol.* **12**, 161–169 (1973).
16. McKirdy, D. M. & Powell, T. G. *Geology* **2**, 591–595 (1974).
17. Leventhal, J., Suess, S. E. & Cloud, P. *Proc. natn. Acad. Sci. U.S.A.* **72**, 4706–4710 (1975).
18. Schidlowski, M., Appel, P. W. U., Eichmann, R. & Junge, C. E. *Geochim. cosmochim. Acta* **43**, 189–199 (1979).

0028-0836/82/010171—02$01.00

SCHOELL AND WELLMER REPLY— Towe has raised some often repeated questions which, however, are not directly relevant to our paper. We aimed to explain why some Precambrian graphites are depleted in ^{13}C compared with the bulk of all other Precambrian graphites. We offered an explanation by suggesting local phenomena such as CO$_2$ from oxidized methane as a food source for the original biota, rather than worldwide phenomena or completely different geochemical processes. However, Towe's comment indirectly bears on our argument and deserves a brief reply.

Two questions have been raised: why some organisms, specifically marine algae, are enriched in ^{13}C compared with common kerogens; and why Precambrian and early Phanerozoic kerogens are isotopically more enriched in ^{13}C as compared with modern marine algae and algal mats.

These problems have already been discussed by previous workers[1,2], who concluded in part that marine algae as found today could not have been the predominant precursor of Precambrian reduced organic matter. Recent work on the Precambrian argues for an establishment of a flourishing yet primitive life already 3,500 Myr ago[3,4]. Detailed work on marine phytoplankton[5] revealed a range of carbon isotope fractionation between HCO$_3^-$ and organisms ranging from −22 to −35‰ (the mean of which interestingly is −27.5‰). The carbon isotopic composition was found to depend on the species and on local conditions (pool size effect). The above figures easily explain the range of 'normal' Precambrian reduced organic matter.

The observation of relatively heavy carbon in less than half a dozen modern algal mats hitherto investigated does not justify the general statement of Precambrian organic matter as being 'disturbingly anomalous'. On the contrary, we emphasize the isotopic similarity of Precambrian, Phanerozoic and recent organic matter and consider this similarity as an argument for the early establishment of biological carbon fixation based on the presently operating enzymatic pathways, that is as proof for (1) the extreme antiquity of CO$_2$ fixation (notably by the RuBP carboxylase reaction) and (2) the constancy of the isotopic composition of the Earth's pool of inorganic carbon (atmospheric CO$_2$ and marine bicarbonate).

We thank M. Schidlowski for careful reading of this manuscript.

M. SCHOELL

Bundesanstalt für
Geowissenschaften und Rohstoffe,
Stilleweg 2, 3000 Hannover 51, FRG

F. W. WELLMER

c/o Bundesminister für Wirtschaft,
Villemombler Straße, 5300 Bonn 1, FRG

1. Calder, J. A. & Parker, P. L. *Geochim. cosmochim. Acta* **37,** 133–140 (1973).
2. Eichmann, R. & Schidlowski, M. *Geochim. cosmochim. Acta* **39,** 585 (1975).
3. Schidlowski, M., Hayes, J. M., Kaplan, I. R. in *Origin and Evolution of Earth's Earliest Biosphere* (ed. Schopf, J. W.) (Princeton University Press, in the press).
4. Schidlowski, M., Appel, P. W. U., Eichmann, R. & Junge, C. E. *Geochim. cosmochim. Acta* **43,** 189–199 (1979).
5. Wong, W. W. & Sackett, W. M. *Geochim. cosmochim. Acta* **42,** 1809–1815 (1978).

Are monozygotic twins similar due to genetic factors alone?

THE number of errors and inconsistencies in the paper by Gärtner *et al.*[1] raises doubts about the validity of their conclusions. In Table 1, the mean and standard deviation of 51-day-old monozygotic (MZ) males are incorrect and differ from the mean and standard deviation for the same data given in Table 2. For 51-day-old dizygotic (DZ) males the authors estimate the between-pairs component of variance as +1.18 when the correct value is either zero, since it is not significant, or negative. This error is repeated for the same data in Table 2 where in addition, the same error is made for body weight of DZ males, aged 61 days. Also in Table 2, the *F* ratios between estimates of the variance components s_b^2 for MZ and DZ twins are incorrect. The ratios are not *F* tests; the degrees of freedom attributed to them are incorrect as are, therefore, the probabilities. Furthermore, for reasons which are not discussed in the text and which are not obvious, these probabilities appear to be one-tail. Even if the between-pairs items had been compared using correct tests, it is difficult to see what conclusions could have been drawn for the many characters for which, according to Table 2, MS$_w$s differ significantly between MZs and DZs.

Incidentally, the estimates of MS$_w$ cannot take the extremely small values that are given in Table 2 unless their true values are zero and the values given are rounding-off errors or arbitrary. The assumption of "random effects" is superfluous for the analysis used, and an explanation is required for pooling males and females for some characters and omitting females for others when the authors say that all statistics were calculated separately for males and females.

Finally, there are features of the data which are difficult to reconcile with the explanation given by the authors. For example, examination of body weight in females from 31 to 61 days shows that the DZs, as expected, retain their initial level of variability as reflected in the total variance. Indeed, this variance increases slightly with age. In complete contrast, on the same criterion the MZs are as variable as the DZs at day 31, but lose their variability as they age. Indeed at day 61, they display almost no variability at all. Since the main conclusion of this paper is that there is a lower level of variation within the MZs than the DZs and that this can be attributed to events that occur early in life, it is difficult to see why these MZ females reached their maximum variability early in life and their minimum as adults.

J. L. JINKS
C. S. HALEY
K. A. LAST

Department of Genetics,
The University of Birmingham,
PO Box 363,
Birmingham B15 2TT, UK

1. Gärtner, K. & Baunack, E. *Nature* **292,** 646–647 (1981).

GÄRTNER AND BAUNACK REPLY— Our results[1] show that pairs of sexually concordant isogeneic DZ twins differ more than pairs of MZ twins because of a non-genetic mechanism which modifies each zygote differently before the third cell division. We thank Jinks and his coworkers for drawing attention to a few errors in our paper. However, these errors do not affect our conclusion as the similarity within the pairs of MZ is clearly much greater than that within DZ twins of inbred mice whatever the method of statistical analysis. Therefore the valid criticism of Jinks *et al.* of the *F* values for testing the between variance components (s_b^2) does not influence our main conclusion. Nor do the two regrettable errors they mentioned in printing different numbers in Tables 1 and 2 for the 51-day MZ body weights and the absence of the minus sign for the DZ 51 and DZ 61 variance components.

Further discussion of the statistical procedure helps only to a very small degree. To shorten this discussion we are prepared to send to any interested scientist our original data for statistical analysis by a method of his/her own choice.

We do not accept the other criticisms. The first three variables of Table 2 (appearance of the hair, eye opening, ear opening) are data measured in whole days. All the MZ pairs exhibited the event on the same day. It seems unrealistic to compare the alteration of the variance in the MZ female twins as Jinks *et al.* suggest, because of the very small numbers of female MZ twins.

Further confirmation can only come from the results of similar experiments in other laboratories. However, further experiments in our own laboratory using twins produced since our original paper, together with many additional characters, support our conclusions.

K. GÄRTNER
E. BAUNACK

Laboratory Animal Science Unit,
Medical School Hannover,
3000 Hannover 61, FRG

0028-0836/82/020172—01$01.00

BOOK REVIEWS

Once a jackass...

Marie Jahoda

IN July 1974, James Watson of *Double Helix* fame was one of the 11 eminent scientists who asked publicly for a voluntary moratorium on two types of experiment involving genetic manipulation. In 1979 Watson described the signatories as "jackasses" who displayed a complete lack of scientific judgement in asking for the moratorium. What happened in between, before and after these dates forms an extraordinary episode in the history of science. Confirming all one's prejudices about national character, events unfolded as a mixture of drama, confrontations, public soul-searching and farce, with the participation of a large and excited lay public in the United States; the issues were the same in England, but working parties rather than public meetings wrestled with them and lay participation was limited to a few individuals on GMAG, the Genetic Manipulation Advisory Group (of which I was one). Lest this contrast between the phlegmatic English and the excitable Americans foster unwarranted interpretations, it should be said immediately that it was the American response that crystallized the questions and dilemmas that the marvellous advances in genetic manipulation present.

The DNA Story: A Documentary History of Gene Cloning. By James D. Watson and John Tooze. Pp.605. ISBN 0-7167-1292-X. (W.H. Freeman: 1981.) $24.95, £17.30.

In this beautifully produced and illustrated volume consisting largely of facsimile documents, Watson and Tooze leave it to the reader to infer the basic questions but emerge with only one clear answer: leave genetic manipulation to the scientists; no special foreseeable hazards are involved, hence no special regulations are required. Apparently the vast majority of the biological establishment in the United States now agrees; but not all, and some Nobel Prize winners are among the dissenters. That scientists disagree among themselves and change their minds is not news. Watson's recantation confirms that even great scientists are only human. Robert Sinsheimer, however, changed his mind in the opposite direction. Everybody's right to be a "jackass" once in a while admitted, how can one decide who is one when? Only the future will tell, but if the Sinsheimers are right, the answer may come too late.

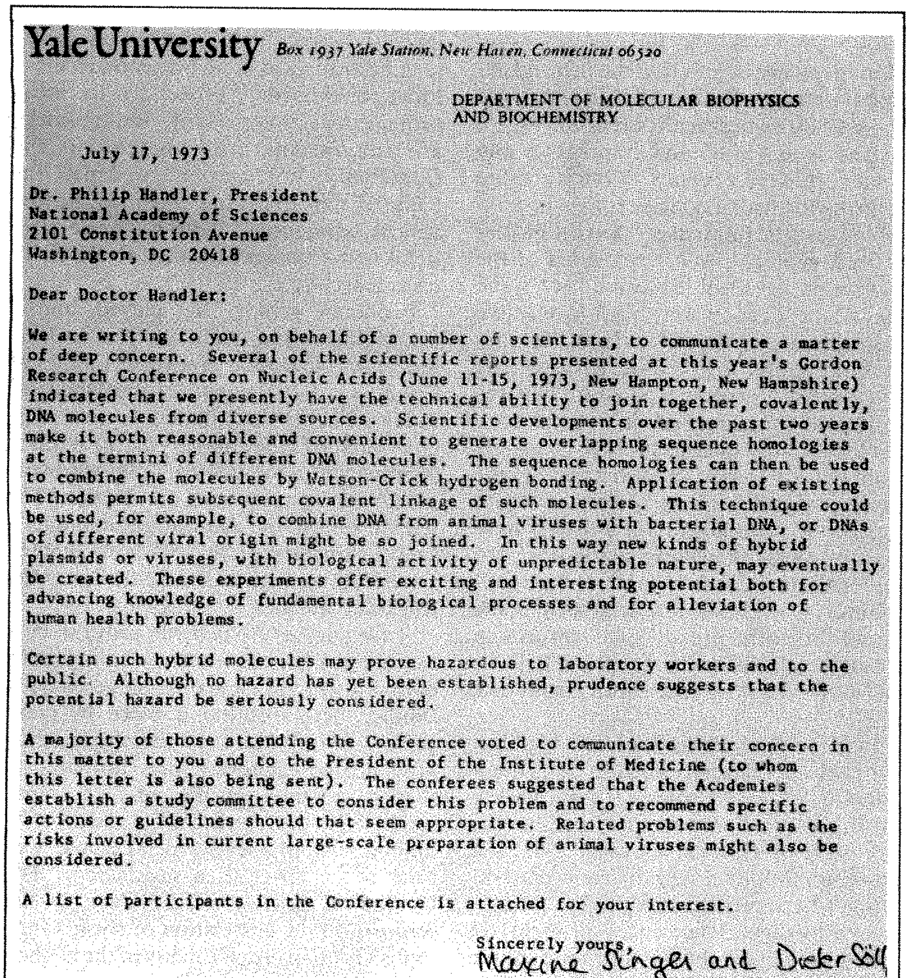

Yale University Box 1937 Yale Station, New Haven, Connecticut 06520

DEPARTMENT OF MOLECULAR BIOPHYSICS
AND BIOCHEMISTRY

July 17, 1973

Dr. Philip Handler, President
National Academy of Sciences
2101 Constitution Avenue
Washington, DC 20418

Dear Doctor Handler:

We are writing to you, on behalf of a number of scientists, to communicate a matter of deep concern. Several of the scientific reports presented at this year's Gordon Research Conference on Nucleic Acids (June 11-15, 1973, New Hampton, New Hampshire) indicated that we presently have the technical ability to join together, covalently, DNA molecules from diverse sources. Scientific developments over the past two years make it both reasonable and convenient to generate overlapping sequence homologies at the termini of different DNA molecules. The sequence homologies can then be used to combine the molecules by Watson-Crick hydrogen bonding. Application of existing methods permits subsequent covalent linkage of such molecules. This technique could be used, for example, to combine DNA from animal viruses with bacterial DNA, or DNAs of different viral origin might be so joined. In this way new kinds of hybrid plasmids or viruses, with biological activity of unpredictable nature, may eventually be created. These experiments offer exciting and interesting potential both for advancing knowledge of fundamental biological processes and for alleviation of human health problems.

Certain such hybrid molecules may prove hazardous to laboratory workers and to the public. Although no hazard has yet been established, prudence suggests that the potential hazard be seriously considered.

A majority of those attending the Conference voted to communicate their concern in this matter to you and to the President of the Institute of Medicine (to whom this letter is also being sent). The conferees suggested that the Academies establish a study committee to consider this problem and to recommend specific actions or guidelines should that seem appropriate. Related problems such as the risks involved in current large-scale preparation of animal viruses might also be considered.

A list of participants in the Conference is attached for your interest.

Sincerely yours,
Maxine Singer and Dieter Söll

The debate widens: the letter expressing concern over aspects of recombinant DNA research written by Maxine Singer of NIH and Dieter Söll of Yale to Philip Handler, President of the National Academy of Sciences. This letter, and another to *Science*, were the upshot of the 1973 Gordon Conference on Nucleic Acids, a private meeting attended by some 130 molecular biologists.

In less colourful terms than Watson uses in his pungent and engagingly informal prose, the question is whether those at the very forefront of science can foresee the consequences of their achievements. The answer is an unqualified no. One remembers Rutherford on splitting the atom. Even Watson himself, talking about the double helix, says ". . . we did not foresee any immediate practical consequences for the world about us . . ." (p.vii), yet his and Crick's discovery was the *sine qua non* of genetic manipulation. When the consequences became clear shortly after, the scientists themselves stopped in their tracks. Why? At the risk of being laughed out of court by these superior rational minds, I suggest that they were overcome by a metaphysical awe at their own power to fiddle with the very building blocks of life. Watson's self-derogatory explanation that he acted originally in a fit of liberal conscience is a bit superficial — conscience in scientists and others had better come not just in occasional fits. That metaphysical awe was akin to Oppenheimer's experience in witnessing the first atomic bomb explosion, and when it communicated itself to the public all hell broke loose. The unforgettable Mayor Velucci of Cambridge, Massachusetts, asked the Academy of Sciences to investigate whether the reported sighting of a monster could be due to genetic manipulation. Not the monster but the "sighting" revealed one theme underlying the debate that preoccupied not only Velucci but also some scientists and many others: the fear of the power of science that could deliberately, not accidentally, change the very nature of living creatures. The other theme, inherent in the position of Watson and his friends, concerned technicalities, not metaphysics, the avoidance of accidents, not the unforeseeable outcome of their deliberate efforts. That the technical theme won in the end is due not only to the greater sophistication of its proponents but also to the fact that the metaphysical question is unanswerable — which does not, however, eliminate it. Fears and hopes were vastly exaggerated and opinions about the unforeseeable polarized. Scientists on both sides of the public debate spent for years large proportions of their time not in research but in lobbying Congress and state governments, and in writing and speaking for the public media. Unused though they were to political manoeuvrings, those on Watson's side did pretty well. The NIH guidelines were significantly relaxed, as were GMAG's procedures, and the scientists, bruised but relieved, could return to their work. The issues raised by the episode remain, however.

During these eventful years some suggested that all genetic manipulation should be stopped. Even if it were desirable, this cannot be done. Short of nuclear catastrophe the acquisition of scientific knowledge is an irreversible process; for better or worse we have to live with it. The question is how? Watson is against all regulations, as is Norton Zinder who believes that recombinant DNA research is ". . . as safe as most other biological research and safer than that dealing with a number of very dangerous microorganisms . . ." (p.201). These scientists defend their wish to be left alone by pointing to other uncontrolled hazards and regard the good sense of the scientific community as sufficient guarantee of safety. Such arguments are suspect because they are so clearly interwoven with self-interest. Richard Novick expressed this best when he declared himself unable to distinguish between the following two statements as bases for his belief that the experiments were safe:

> 1. I am convinced they are not dangerous, and therefore it is ok to do them; or 2. I have convinced myself they are safe precisely because I want to do them! [p.149].

If the whole episode demonstrates one thing it is that there is no harmonious scientific community interested only in the advancement of knowledge and its benefits for mankind. Yes, there is passionate commitment to driving forward their breath-taking discoveries; but there is also ambition, jealousy, lack of foresight, moral ambiguity and arrogance in these scientists, and there is absolutely no reason to assume that they are any better in these matters than we of a lesser breed. It seems reasonable to require that some people whose self-interest is not vested in genetic manipulation should be involved in monitoring these experiments.

This, of course, is easier said than done. Lay participation, as in the United States at the height of the controversy, may only have strengthened the irrational and anti-science trends in society. It has not bridged the enormous gap in knowledge between the scientists and the general public. Lay participation as in England is token participation, symbolic rather than real. What can a lay person do, when scientists disagree about the containment category of a given experiment, but side with the one with the bluer eyes? Perhaps such frustration about one's technical incompetence will be mitigated when issues arise about which we all are equally competent or incompetent. One such issue, though not restricted to genetic manipulation, arises over the possibility of cloning human beings. Sir Peter Medawar (p.246) considers this well nigh impossible but reports that Jacques Monod did not. John Maynard Smith agrees with Monod.

The great merit of Watson and Tooze's book is that it displays the arguments on all sides. It offers only personal, not general solutions to fundamental questions. The worst sequel to this whole exciting episode would be if young scientists decided to withdraw into their ivory towers; the best if it were regarded as a rehearsal for things to come, from which to learn how ill-prepared scientists and the public still are to face the issues that confront them jointly and how to improve their relations while there is time. ☐

Marie Jahoda is Professor Emeritus of Social Psychology and Consultant to the Science Policy Research Unit, University of Sussex. For two years she was a member of GMAG, representing the public interest.

Irish rocks reviewed

W.S. McKerrow

A Geology of Ireland. Edited by C.H. Holland. Pp.335. Hbk ISBN UK 0-7073-0269-2, ISBN US 0-470-27247-3; pbk ISBN 0-7073-0308-7. (Scottish Academic Press/ Halsted: 1981.) Hbk £27.50, $49.95; pbk £15.

MOST geologists know that the British Isles contain rocks of unusually diverse types and ages for such a small part of the world. Ireland is as varied and complex as any other part of these islands; thus it is good to be provided with a concise review of Irish geology. In the final chapter (on the history of Irish geology) we are reminded of the lean years between 1914 and 1947 when significant advances were made in only two branches of geology in Ireland: Tertiary igneous petrology, and Pleistocene stratigraphy and geomorphology. This was followed by a revival in which both academic and economic geologists, mainly from outside Ireland, played a part. In the past two decades Irish geologists (living in Ireland, if not all of Irish descent) have performed an increasing amount of the geological research in Ireland. The ten contributors to the book have each spent much or all of their professional careers in Ireland, eight in Dublin and two in Belfast, and each of them is an authority in his own field.

In the preface, Professor Holland points out that a lot has happened in our understanding of Irish geology since Charlesworth's *Historical Geology of Ireland* was published by Oliver & Boyd in 1963, but this book follows a very different pattern. While Charlesworth attempted to refer to every paper (good, bad and indifferent) on Irish geology, and thus is still a good source for the older literature, Holland has been much more selective; and while Charlesworth covered the whole country single-handed, Holland has gathered a team for the task. The authors each possess an individual style and range of expertise, but the editor has clearly stamped his authority on the book. Each chapter is a very readable, well-illustrated, resumé of our knowledge and understanding of Irish geology today. (Or is it yesterday? Most chapters make little reference to work later than 1976, and most fail to include references later than 1978).

In addition to the chapters on stratigraphy, there are sections on tectonics, igneous activity and geophysics, which might be expected in such a general review. More unexpected, especially to those geologists who regard drift as a nuisance, are the fascinating chapters on the Quaternary, which extend well past the 5,000 BP date of the first Irishmen, and are almost continuous, with no more than small non-sequence, through to the final, historical chapter.

Economic geology has played, and is continuing to play, a major part in Irish life, from the Bronze Age copper mines of County Cork to the search for offshore oil today. The review includes clear descriptions of the major metal mines, together with a summary of opinions on the possible origins of the ore bodies. The section on oil and natural gas contains a useful summary of the offshore geology around Ireland, from the Celtic Sea to the Rockall Plateau.

A Geology of Ireland will prove to be a useful book for the student who wishes to obtain a general view of Irish geology; it should therefore find a place in every geology library. But the research geologist, academic or economic, may not find all that he requires in the text, or, more seriously, in the references — the editor has limited them to a level which I would consider to be lower than satisfactory. The Geological Society of London *Special Reports* on the correlation of rocks in the British Isles do provide many of the missing references, but some of these are now even more out of date than the references listed in the book. ☐

W.S. McKerrow is a Lecturer in the Department of Geology at the University of Oxford.

Joseph Henry: letters from America

Colin Russell

The Papers of Joseph Henry, Vol. 4: January 1838–December 1840, The Princeton Years. Edited by Nathan Reingold. Pp.475. ISBN 0-87474-792-9. (Smithsonian Institution Press, Washington DC: 1981.) $30.

JOSEPH Henry (1797–1878) was an American physicist and a researcher in electricity and magnetism. He had the misfortune to be a contemporary of Faraday by whom he has been considerably overshadowed; even when he emerges from the penumbra of the great Englishman he is not seen as a major luminary in science, and one may wonder at the colossal expenditure of labour in this reprinting of his papers. If it may not be justified in terms of Henry's inherent scientific stature, the rationale would appear to lie in his position within the community of early nineteenth-century science, particularly in America. He knew almost everyone of importance on both sides of the Atlantic, and such people flit effortlessly in and out of his correspondence. To read his papers is to gain a richer understanding of the social milieu in which Henry lived and much of modern physics took shape.

During most of the period covered by this book (1838–1840) Henry's life was fairly uneventful, concerned mainly with his family at home or seriously fulfilling his calling as Professor of Natural Philosophy at Princeton. For this reason the present volume lacks something of the punch and zest of its predecessor (for review see *Nature* **286,** 311; 1980), which dealt mainly with his grand tour of Europe. However there are compensations, and a large proportion of the book is concerned with his "records of experiments" from manuscript material. Some of his work was over-hasty as he wished to establish priority over Faraday, but here is an unselfconscious record of one man working under great pressure to unravel the complex phenomena of electromagnetism. Amongst his most significant discoveries of this time was that of electric induction across great distances, leading him to take the side of those who advocated an all-pervasive ether, thus anticipating in certain respects the more comprehensive theories of Maxwell.

In the correspondence a note that constantly reappears is that American science must at all costs be protected from the quacks and the charlatans (amongst whom he numbers the egregious Samuel Morse). In this respect New York was worse than Philadelphia, but the danger was endemic in a small beleaguered community of science that lacked the checks and balances of its older European counterparts. Much could be learned from Europe, of course, and America had its English-sounding Society for the Promotion of Useful Arts, while the American Association for the Advancement of Science was consciously modelled on the British equivalent. But Henry (who had been unfairly savaged at a BAAS meeting a few months earlier) very much preferred a meritocracy of science to the arrangements in Britain, in which "wisdom" and "ignorance" were mixed and where the Society was "quite as aristocratical as the government of the nation". Thus we are offered a view of British science which is rather different from that purveyed by the popularizers and promoters in Britain itself.

As in previous volumes of this series there is a short introduction, very full footnotes (which include indications of variant readings) and an excellent index. Diagrams are reproduced in facsimile and there are several pages of portraits and illustrations. One or two editorial statements raise an eyebrow here and there (for example that the preparation of magnesium was "first reported" in 1831) and on p.310 two lines have been transposed. However, as we have come to expect, the standard of production is generally superb, with the luxury of footnotes at the bottom of the page or at the end of each document. When several publishers are charging twice as much for shorter works, with much less lavish presentation, this book is a rare bargain for all concerned with history of nineteenth-century physical science. ☐

Colin Russell is Professor of History of Science and Technology at the Open University. His most recent book, Science and Social Change, *will be published by Macmillan, London, later this year.*

Standard methods in geomorphology

C. Kidson

Geomorphological Techniques. Edited by Andrew Goudie. Pp.416. Hbk ISBN 0-004-551022-3; pbk ISBN 0-004-551043-1. (George Allen & Unwin: 1981.) Hbk £25, $60; pbk £12.95, $29.95.

GEOMORPHOLOGY, the science which seeks to understand the processes which shape the surface of the Earth, lies in the borderland between geography and geology. In the United States it is firmly based in geology. In Europe, however, most of the recent major developments in the subject have, by and large, been the work of physical geographers. The British Geomorphological Research Group, for whom this volume is edited, have, as a subject group of the Institute of British Geographers, been in the forefront of research in this field. Thus it is entirely appropriate that an attempt to bring together those techniques, both field and laboratory, most appropriate to the discipline should emanate from this active and distinguished group of geographers. In a sense, the book is a natural development from their successful series of *Technical Bulletins,* two-thirds of which are referred to in the text. It does, however, go well beyond the scope of that series.

A prime objective of a "manual of useful techniques" should be to provide a work of reference for those who wish to improve their technical repertoire. Kummel and Raup's *Handbook of Palaeontological Techniques* (W.H. Freeman, 1965) is an example of what can be achieved. In its better sections, *Geomorphological Techniques* matches the high standards set in that volume — Parts 3 (*Material Properties*) and 4 (*Process*) are as useful and authoritative summaries as the readers of the book could hope to find. In others, however, notably the first two parts on form and time, the techniques are enclosed in a matrix of theory and philosophy which suggest a textbook rather than a manual. In falling between two stools the value of these parts is reduced.

Inevitably, in a volume arranged on the basis of form, materials, process and time, and written by more than 30 authors, there are some techniques which have been inadequately dealt with or even omitted. Topographic survey methods such as levelling are superficially treated. Plane tabling, which one would have thought to be basic to students of landforms, is totally omitted. The collection of samples with the aid of augers, corers and drills is scarcely mentioned, with the notable exception of the section on glacial processes and that on peats and lake sediments. In addition, the coverage of tracer techniques is woefully inadequate.

Surprisingly, for a work of this calibre, there are some remarkably superficial statements. On p.8, for example, it is asserted that "During the predominance of denudation chronology, data acquisition was dominated largely by qualitative field observations and subjective map analysis". No one who had been in the field with Wooldridge or Cotton, or who had attended a class in cartographic analysis with Hollingsworth, could conceivably have made such such a meaningless generalization.

Despite its imperfections this is a useful contribution to this vigorously growing science. It is the best available comprehensive treatment of the subject and is destined to be the standard work for some time to come. ☐

C. Kidson is Professor of Physical Geography and Head of the Department of Geography at the University College of Wales, Aberystwyth.

Amino acids in clinical studies

A. Darbre

Amino Acid Analysis. Edited by J.M. Rattenbury. Pp.380. ISBN UK 0-85312-194-X; ISBN US 0-470-27141-8. (Ellis Horwood/Halsted: 1981.) £27.50, $89.95.

WITH the appearance of the automated ion exchange column method of Spackman, Stein and Moore in 1958, amino acid analysis became one of the most important analytical techniques in biochemistry. Since that date there has been much research effort put into obtaining both faster and more sensitive analyses, and this has enabled the study of proteins, peptides and amino acids to be extended into many fields.

Proteins having unusual properties (e.g. anti-freeze protein) or specialized functions (e.g. receptor proteins on cell membranes) are being continually discovered and isolated, as are peptides and non-protein amino acids with important physiological and pharmacological properties.

This volume consists mainly of the papers given at a symposium, "Amino Acid Analysis in Clinical Chemistry and Medical Research", held in Edinburgh in June 1979. Thus the short title of the book is misleading — this is not a book for the reader whose primary interest is in protein analysis or in methodology. The volume consists of 24 chapters and is divided into four parts. The first, on technical developments, contains 9 chapters which deal with analysis *per se* and review briefly the history of amino acid analysis, fluorimetric detection techniques, gas chromatographic methods, mass spectrometry, derivative spectroscopy and chemiluminescent nitrogen analysis. (The brief contribution on phenylthiohydantoin amino acids, however, does not have a logical place in this book.) The reader who may have accepted at face value widely disseminated statements that "today, it is possible to analyse picomole levels of amino acids in protein hydrolysates in 1h with the automatic loading of up to 80 samples" (p.138), with complete computation and print out of the results to an accuracy of 3 per cent (see p.132), should read the chapters on standards and accuracy (R. P. Ambler) and collaborative trials (A. P. Williams). These should induce in the researcher a much more critical approach to the "print-out" of results obtained from the computing integrator!

The *raison d'être* for this volume lies in the last 15 chapters, which have been divided into separate parts under the headings of amino acid analysis in, respectively, physiological processes, systemic disease and congenital disorders. There is much of interest here, presented in easily readable form, but the emphasis is on results obtained in a physiological and clinical context, and not on the methods used. Thus there are chapters related to protein digestion and absorption (our knowledge here is still very inadequate), the effect of protein quality on plasma amino acid levels in low birthweight babies and plasma amino acids following parenteral nutrition of the newborn, and in chronic renal failure, acute liver failure and alcoholism. The specific analysis of 3-methylhistidine and hydroxyproline as a measure of protein breakdown, and amino acids as neurotransmitters are also discussed. Two contributions give generalized accounts of amino acid analysis in the study of inborn errors of metabolism, whilst others are devoted to homocystinuria, Wilson's disease and spina bifida.

All chapters include adequate references for further reading. But it should be noted that a new word — "exteriorisable" — (p.153) has crept into the English language: this inborn error of grammar should be quickly eliminated. □

A. Darbre is Senior Lecturer in Biochemistry at King's College, University of London.

Circle No.04 on Reader Enquiry Card.

Bring Your Library Up-To-Date With This ANS Edition...

Paul Cohen
MONOGRAPH

Water Coolant Technology of Power Reactors

456 pages — 6″ × 9″
Hardbound $27.90

American Nuclear Society
555 North Kensington Avenue
La Grange Park, IL 60525 USA

Please take my order for ____ book(s).
☐ Payment in full enclosed.
☐ Bill me and I accept postage and handling charges.

Name ____________
Organization ____________
Street ____________
City ____________
State ____________ **Zip** ________

Synmetals: a new branch to polymerization

Herman Mark

Semiconducting Polymers. By Marian Kryszewski. Pp.710. ISBN 83-01-00818-0. (Polish Scientific Publishers, Warsaw: 1981.) $35.

FOR many years synthetic organic polymers have been of considerable interest and value for their mechanical and thermal properties such as rigidity, strength, elasticity, high softening range and chemical stability. With these properties they have been very useful in a variety of industries, textiles, films, sheets and plastics, for example. Several years ago, however, these materials underwent a surprisingly rapid development as "synmetals", that is, systems which can act as conductors or semiconductors. Their preparation and tailoring for the second application has now grown into a science and technology of considerable proportions.

Marian Kryszewski's *Semiconducting Polymers* is the first comprehensive treatment of this new field. It serves a two-fold purpose: first, it familiarizes the reader briefly with the basic principles of semiconduction, and then it describes how this intriguing property can be obtained with organic polymers.

There are two principles which serve to establish semiconductivity in such systems: the presence of polyconjugated chains and the availability of charge transfer complexes. The largest part of the book is reasonably devoted to the description of polyacetylene because this has been more closely investigated and has already led to semiconductors of wide potential application — f.i. in the construction of new types of photovoltaic cells, pacemakers and thin electrical batteries. Also included in the account of their preparation and behaviour are descriptions of their photoconductivity, magnetic characteristics and catalytic activity.

The author has been through his topic with great assiduity and diligence. For the generally interested reader he has provided a lucid and attractive story; the expert, too, will be grateful to him for the 3,000 or so references which constitute a comprehensive bibliography.

This is a remarkable book and, as the new field grows and unfolds, it may well one day be seen as a classic. □

Herman Mark is Dean Emeritus of the Polytechnic Institute of New York.

nature

21 January 1982

Can change damage your mental health?

The US Court of Appeals says that environmental impact statements should cover psychological factors, giving environmental pressure groups a licence for mayhem.

The United States Appeals Court in Washington has put a pistol, perhaps even a bazooka, into the hands of opponents of new developments of any kind. The court has now ruled (see page 179) that electricity cannot be generated at the undamaged reactor at the Three Mile Island site on the Susquehanna River in Pennsylvania until its luckless owner has shown that the mental health of the local population will not as a result be damaged. The decision is important not merely because it may be the straw that breaks the back of Metropolitan Edison but because it can in principle apply to any project caught by the Natural Environmental Policy Act, 1970.

So far, impact statements have been attempts to anticipate physical, biological and social consequences of new developments. In many ways, they have been interesting and even important documents. The impact statement on the Alaskan pipeline may even now be the handiest source of information on the migration of caribou, for example.

Impact statements as they are suffer from a common imbalance. The most tangible and easily anticipated consequences of some new development are covered in great detail. The species of flora and fauna within striking distance of a development site are usually catalogued in detail, as are the volumes of traffic expected on the highway system. (Farseeing developers do their best to recruit the help of the local university in carrying out this kind of work.) The less tangible but usually more important issues raised by new development projects are, perhaps inevitably, given less close attention. While it may be possible to estimate the long-term consequences of a new development for the economic development of a neighbourhood, even that kind of calculation is necessarily shot through with sources of error. And so far, those responsible for preparing impact statements — itself a kind of growth industry — have shrunk from trying to estimate whether a development will make the local population happier. The importance of last week's decision is that it requires not merely the owners of the Three Mile Island nuclear site, but in principle all other managers of public works in the United States, to show that their proposals will not bring psychological damage.

The objective is laudable but the task which it implies is both impossible and, on grounds of principle, irrelevant. What has happened around Three Mile Island since the accident in March 1979 should have given the Appeals Court pause. The population in the neighbourhood of the reactor has understandably been a focus of interest for social scientists seeking evidence of the minor psychological consequences of such an occurrence. Most accounts of these investigations appear to agree that during the immediate crisis, people living within fifteen miles or so of the damaged reactor consumed more sleeping pills than those living further off. Some of these habits persisted for as much as nine months, but Dr Peter Houts of Pennsylvania State University, the author of one of the most through investigations of this kind, says that his latest survey, in October last year, shows no residual measurable consequences of the reactor accident. Other studies, reported by the Kemeny Commission, suggest that at no stage were the signs of stress reported by the local population sufficient in frequency and intensity to qualify as psychiatric illness.

Against this background, it is inconceivable that environmental impact statements purporting to describe the psychological impact of some new project can be more than fanciful fiction. It is just conceivable that, as at Three Mile Island, it might be possible to measure something tangible. But how, in the absence of a range of studies in the neighbourhood of sites capable of generating serious accidents will it be possible to predict the psychological stress caused by some new development? Will the federal government be expected now to sponsor essential baseline investigations of the incidence of minor symptoms of anxiety among people living near, say, Titan missile silos, or projected missile sites as well as nuclear reactors? What is the chance that the results will be statistically significant? And what use will they be to the drafters of future environmental impact statements?

Even if the measurements the court supposes could be made were made, however, they would be irrelevant. Provided that development projects are not so awesome that they topple people over into frank psychiatric illness, the all-important question becomes that of whether there should be a moratorium on all development projects likely to increase the general level of anxiety in the population. Presumably hydroelectric schemes of all kinds would quickly be stopped, however necessary their output of energy. So too would most defence projects and all nuclear projects. The result would be a nonsense, so that the court's decision must be changed. But that will take time. Meanwhile, environmentalists have a licence to do irreparable damage.

Paying the price for coal

The British coal industry, again in crisis, should be either closed or administered logically.

In February 1974, the then Conservative government called a general election in the wake of a damaging strike about pay by British coal miners. The central issue at the election was the government's question "Who governs Britain?" — the elected government or the miners. The rhetorical question was never answered, although Mr Edward Heath, prime minister at the time, was clearly told that it should not thereafter be him. A similar tangle with workers in nationalized industries among whom the coal miners were again conspicuous put paid to the government which succeeded his, in the spring of 1979, and paved the way for the present administration. It is therefore inevitable that Mrs Thatcher and her colleagues should be nervous about the outcome this week of the ballot among the miners, who are being

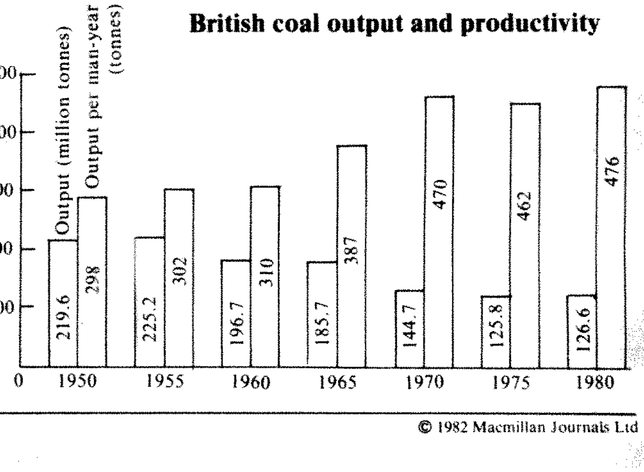
British coal output and productivity

0028-0836/82/0300177-02$01.00

asked by their leaders to agree that there should be another strike, again over pay, if one should "be necessary". Pollsters and soothsayers guess that, this time, the voting will be so close that there will not be a clear mandate for a strike, in which case the government will claim a victory for good sense and for its policies of the past two years, miners' pay will increase by 9.3 per cent and everybody will forget about the issue until next year. That would be a serious mistake. What the British government should now be asking is whether Britain needs a coal-mining industry, or can afford one.

On strictly economic grounds, the mining of coal in Britain should be stopped. The cost of producing and distributing British coal within the United Kingdom is more than that of importing it from the United States and even from Australia. For several years, the nationalized National Coal Board's chief customers, the nationalized Central Electricity Generating Board and British Steel Corporation, have been muttering about the advantages of importing coal, and did indeed buy 5 million tons of coal from overseas in 1980–81. Given encouragement, these two customers for domestic coal production (which take well over three-quarters of total output) could profitably import more. In reality, they are being pushed in the other direction by the National Coal Board and by the miners, chiefly by being offered British coal at prices well below the average cost of production. The British government provides a modest subsidy to this end, but not nearly enough to make good what the coal board loses on the transactions. Two consequences follow inexorably. By hanging on to its chief domestic customers, the coal board is forced to charge others more than would strictly be necessary. But, even so, the coal board's accounts are perennially in deficit. The British government, although perpetually preaching economic realism, and the coal board are in collusion to make water run uphill.

Although this curious state of affairs has arisen because of the determination of British coal miners not to let production fall still further — it has halved in a quarter of a century — it should have been no surprise. More than a century has passed since W. Stanley Jevons argued in *The Question of Coal* that British industry as a whole was vulnerable to competition from abroad because of its dependence on deep-mined coal, inherently more costly than the coal from thick near-surface deposits such as those in the plains states of North America. (Forgivably, Jevons did not anticipate the phenomenon of Japan, industrially competitive with hardly any indigenous fossil fuel.) The British coal industry, like the more heavily subsidized coal industries of Belgium, France and West Germany, is victim to the geology of all extractive industries. The British coal board would be more competitive if it were more free to concentrate production on those coal fields in which seams are thicker and more accessible, but its employees will not let that happen. The board's plan to shut twenty uneconomic coal mines during 1981 was modified after a series of strikes, and in the event only ten were shut. Given that failure, economic logic would suggest that British users of coal should be encouraged to meet their needs from abroad, and that the British coal-mining industry should find its own presumably shrunken level at which costs and prices are in some kind of balance.

There is no prospect of this happening. For half a century, the politics of coal mining have overridden economics and common sense. In present circumstances, the coal board has a minor point in its arguments that the cost of imported coal is now lower than it would be in normal times because the cost of shipping is depressed by the world recession. The board and the government are, however, united in their belief that the British coal-mining industry is strategically necessary — a hedge against the emergence of an Organization of Coal-Exporting Countries or some other improbable development of that kind. The argument would be more convincing if it were made explicit, and if its implications were followed consistently. First, there is no reason why strategic considerations should require 100 per cent self-sufficiency. Why not 80 per cent, or 70 per cent, or some other proportion of present consumption? Second, if the high cost of domestically produced coal is politically and financially an embarrassment, the British government should become the active sponsor it once promised to be of the only other substantial source of indigenous energy — nuclear power stations. Third, and most immediate, if the case for keeping alive the British coal industry is strategic, should the government continue to insist that the substantial hidden costs of that policy should fall primarily on those who use it? The result is that the coal board has to sell its product at too high a price to unwilling customers, thus ironically undermining the objectives of keeping some kind of coal-mining industry in good shape — and needlessly increasing industrial costs at the same time. The British government, which has enthusiastically embraced its predecessor's policy of charging the international price for oil from the North Sea, should now do the same for coal. Then at least the cost of the present policy would be explicit in the government's accounts and not hidden in those of the coal board.

Ice age or melt-down?

Recent winter mid-latitude weather has been awful. But it is a fluctuation, not a cataclysm.

After a couple of weeks of unexpected but seasonal cold weather in Western Europe and North America, the public rumour mills are grinding out news that there may be another glaciation around the corner. A host of people who should know better, many of them professional earth scientists, have been engaged in grave televised discussions about the chances that a few days of snow and slush either presage the return of the ice sheets (this time without bison and mammoth) or are paradoxical accompaniments of the general increase of atmospheric temperature to be expected from the accumulation of carbon dioxide in the atmosphere. Television interviewers have been visibly discomfited by this apparent assault on common sense, and have usually chosen to leave their audiences with a reminder that the ways of science are incomprehensible, and that if a suitable qualified gentleman has said that it has been devilishly cold because the earth is getting warmer, he must be right.

The truth, of course, is that none of this rambling is relevant to the past weeks' weather, in Western Europe, North America or anywhere else. The meteorology of Western Europe's admittedly wretched weather is easily described and is even familiar. The usual stream of depressions across the Atlantic was diverted from course by an apparently stationary centre of high pressure over Scandinavia. As a result, relatively warm southwesterlies were replaced by cold northeasterly winds. Closely similar stationary high-pressures centres occur most winters inland of the western seaboard of Eurasia, but not always at the same longitude. The intriguing question is why such high-pressure centres should be stationary. The simple answer is that nobody knows. The more complicated answer is that many people are trying to find out. Whether the frequency or durability of such high-pressure centres are positively correlated with the atmospheric concentration of carbon dioxide is plainly an unanswerable question, and will remain so until the mechanism of what the meteorologists call blocking is understood.

So is there no choice but to regard the past few weeks' weather as a statistical fluctuation on the usual pattern? None. Are the climatic consequences of all that extra carbon dioxide still in doubt? Yes. And is there a prospect of being able to walk once more from Britain to France as at the peak of the most recent glaciation 18,000 years ago? No, too little is known. That, when the next season of blizzards (or of droughts) comes round, is the public message that the professionals should seek to put into circulation. It is something of a triumph, for the public understanding of the world we occupy, that people's imaginations have been caught by knowing that there is no way of distinguishing between the present period and one of the earlier Pleistocene interglacials. It serves no purpose to corrupt that state of affairs with over-sharp predictions of what the future holds. One swallow does not make a summer, nor one blizzard a glaciation.

0028-0836/82/030178-01$01.00

Mental stress given environmental status

Court delays start at Three Mile Island

Washington

In a precedent-setting decision, the US Court of Appeals in Washington has decided not to allow the Metropolitan Edison Company of Pennsylvania to switch on the undamaged power plant at Three Mile Island, near Harrisburg, until it can demonstrate that such a move would not adversely affect the mental health of people living in the area.

The immediate impact of the decision, which reverses a ruling by the Nuclear Regulatory Commission (NRC) that psychological factors do not necessarily have to be taken into account in deciding whether to allow nuclear plants to start operating, will be to delay for several more months the start up of "Unit One" at Three Mile Island. The reactor was undamaged in the accident which occured to its twin, Unit Two, in March 1979, and since then has been considerably modified to improve safety.

The ruling, however, which was made by two of the three members of the appeals court, could have a significantly wider impact. For the first time it means that although the powerful Natural Environmental Policy Act of 1970 does not require psychological factors to be taken into account when the social impact of a federal decision is being assessed, the act can be interpreted as allowing such factors to be included.

The Three Mile Island accident resulted in a small amount of radioactivity being discharged into the environment but no significant extra radiation exposure to individuals, so nobody suffered physical health damage as a result. The principal focus of interest, therefore, has been on the psychological implications of the accident.

Arguments about the psychological impact of the accident have been continuous since it occurred. Civic leaders warned NRC that thousands of people might be driven from their homes by fear of radiation if krypton gas was allowed to be vented from the crippled plant. Some claimed that "riots" might result as a possible manifestation of the population's nervousness.

Such arguments have, until now, fitted uneasily into the institutional mechanisms set up to cope with the social consequences of major technological actions. Thus when Metropolitan Edison applied to NRC to be allowed to start up the undamaged plant, the commission rejected claims from a local citizens' group, the People Against Nuclear Energy (PANE) of Middletown, Pennsylvania, that such a move would have sufficient psychological effects to make it necessary to take these into account.

The request from PANE had been supported by the members of NRC's own Atomic Safety and Licensing Board — partly on the grounds that taking such factors into account while the licensing decision was being reached could head off later conflict — but was rejected by NRC.

The Appeals Court has now told NRC that it was wrong, and has directed the commissioners to conduct a broad assessment of the effects that starting up Three Mile Island's Unit One will have on "the psychological health of neighbouring residents and on the well-being of surrounding communities". After that, the commission will have to decide whether the National Environmental Policy Act requires a more detailed analysis of the social and environmental impact — possibly including a public hearing — before the decision to restart the undamaged reactor could be taken.

The court's decision was not unanimous. In a strongly-worded dissent, Judge Malcolm Wilkey argued that by establishing psychological stress as a factor which had to be taken into account by NRC, the court was defining "an 'impact' which has never before been considered as covered by the National Environmental Policy Act", a move which, he said, had "enormous consequences".

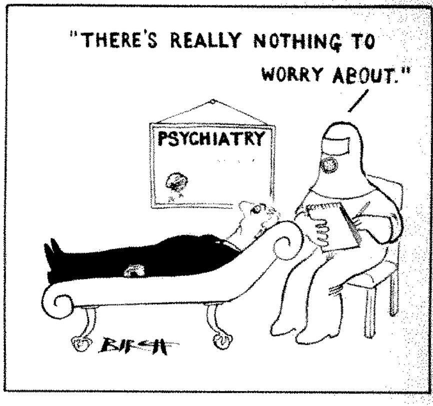
"THERE'S REALLY NOTHING TO WORRY ABOUT."
PSYCHIATRY

The decision was greeted with gloom at Metropolitan Edison, which had been hoping to start up Unit One within the next few days, and which was depending on revenues the reactor would produce from the sale of electricity to help cover some of the costs of the clean-up at Unit Two which are already threatening to force the utility into bankruptcy.

Predictably, the appeal court's decision was welcomed by members of PANE. The group had argued that the inclusion of psychological factors should be part of the responsibility of licensing institutions to protect the public health and safety, as defined in the Atomic Energy Act of 1954.

David Dickson

European nuclear safety policy attacked

Brussels

Has the Euratom treaty, which binds the European Community's nuclear energy policies together, been properly interpreted and applied? A lengthy report by the leading Belgian socialist member of the European Parliament, Anne-Marie Lizin, suggests not and attacks the lack of progress towards achieving the aim of a European zone of unified nuclear safety standards.

Lizin's report was the subject of heated debate in the European Parliament's Committee on Research and Energy, where 91 amendments were proposed. Having looked in detail at EEC's activities in the fields of radiation protection, reactor safety, decommissioning, safety of the fuel cycle and the national nuclear inspection services, Lizin concluded that the Euratom treaty is outdated and vague and that the European Commission has made too little use of its powers under the treaty.

Lizin alleges that when the treaty was first drawn up, more than 20 years ago, too little consideration was given in the nuclear energy development plans to reactor safety and worker protection. Since then, the member states have proved reluctant to provide the European Commission with effective consultation procedures for all decisions concerning the location and operation of nuclear power stations. In Lizin's native country, Belgium, the licence to build a nuclear power station is granted independently of the initial safety analysis, and given the fact that too many nuclear power stations are built close to frontiers or use shared river systems, the report complains that there is too little consultation on measures to protect workers and local populations.

The report goes on to say that although the Community has been efficient at listing methodologies, standards and safety criteria, work on listing similarities and differences among the member states has been too slow and the Community has yet to go on to the third stage of putting forward its own regulations. This work has largely been left to other international bodies such as the Organization for Economic Cooperation and Development and the International Atomic Energy Agency. Lizin attributes particular importance to the Super-Sara project but calls for more studies into the safety of gas-cooled and heavy water reactors. The problems of waste management and recycling are given particular attention because the report considers that this field requires intense supervision by an independent public

0028-0836/82/030179-02$01.00

authority.

The role of the Community in the decommissioning of nuclear plants is reassessed. Lizin suggests that EEC's financial instruments, such as the regional fund, could help and that electricity companies or utilities should be asked to pass on decommissioning costs directly to the consumer. Lizin's lengthy list of recommendations also tries to sting the Commission into providing stricter surveillance of the work carried out by national supervisory authorities.

Undoubtedly something akin to the steel crisis, which made many realize the immense emergency powers invested in the Commission by the treaty of the European Steel and Coal Community, will be necessary to bring the strength of the Euratom treaty into play. But Lizin's awareness of this possibility has been heightened by the controversy surrounding the enlargement of the French nuclear power site at Chooz, a few kilometres from the border with Belgium. Notwithstanding local and national protests from Belgians, and the French socialist party's preelection promises, the French Prime Minister, François Mitterrand, still seems set on increasing the number of nuclear reactors there. **Jasper Becker**

French colloquium

Science passion

Paris

The great national colloquium last week on the state of science in France was sometimes like a high mass, sometimes more like a giant committee meeting. And although, after six months preparation, the colloquium (which was strictly advisory) displayed few radical disagreements, the test of its success will come only with the publication of a new law to be put to the French Parliament in the next few weeks.

The theme running through the four-day meeting was uplifiting. M. Jean-Pierre Chevènement, Minister of State for Science and Technology, told the closing session that "the highest authorities of the state" have decided that scientific research is vital "for the successful change and future of our country". The highest authority himself, President François Mitterrand, had set the ball rolling with a declaration that "only a gigantic effort in research" will allow France to master its technology and thus make certain of its independence.

Both the President and his Prime Minister, M. Pierre Mauroy, were, however, anxious that the forthcoming expansion of science in France should follow the "wishes of society". Mauroy also wishes to reintegrate science into the wider culture of France from which he thinks it has been too long isolated. But to Chevènement himself, "science is a passion and France needs passion". Since the election in May 1981, he said, hostility to science and technology had been turned back.

Inevitably, on what could not fail to be a patriotic occasion, the minister also developed his theme that French science must increasingly be seen to be French. He promised data banks and scientific books in French and that the great international science journals would be translated. Meanwhile, the French cabinet has agreed that the volume of government spending on science should increase by 17.8 per cent a year over the next three years and that private industry should be encouraged to increase research and development investment by 8 per cent a year. This should bring French research and development expenditure to 2.5 per cent of the Gross National Product by 1985. Jobs will be created at the rate of 4.5 per cent a year over the same period.

All this has given the minister for science more spending power and more influence. He already controls almost all the forward-looking agencies of the Ministry of Industry and is thought to be lobbying for the merger of that ministry with his own.

Chevènement is nothing if not visionary and ambitious. The politics of health depend on research, he said, as do the politics of labour and employment. Science and technology could increase French independence while the creation of a "French pattern" for the organization of science could be a model in fields other than science and technology.

The new law, to be prepared in the next few weeks, will define new contracts of employment for researchers, set financial targets for institutions and set the "French pattern" of research for 1983–85. The expectations are that the law will leave most institutions unchanged except for the introduction of union representatives on certain committees. But the law will provide for new small-scale technical enterprises and regional centres of development in certain fields.

Under the promised arrangements, there is to a new high-level advisory council together with regional advisory committees. Social science, Chevènement said, needs to be impelled forward. And what is it all for? "To spread knowledge, to push back anti-scientific prejudice, to assure the progress of the sciences of man and society, to maintain or re-establish French." **Robert Walgate**

River of words, mountain of paper

Paris

There were no *bateaux mouches*, the "firefly boats" with glass roofs, on the Seine last week. The river was a torrent almost filling the arches of the bridges and menacing the city. It was much the same with *la vague Chevènement* (the Chevènement wave) as one paper dubbed it. The Minister of State for Science and Technology, Jean-Pierre Chevènement had organized all the tributaries of science in France, and in its overseas territories and departments, to converge on Paris.

The organizers of this national colloquium for science and technology estimated that there had been nearly 200,000 pages of written contributions to the colloquium and its regional predecessors (held in October and November last year). This is almost a page for each of the 280,000–300,000 scientists and technologists in France. There were almost 10,000 individual documents, all of them arguing over which points needed to be changed, modified or amplified in the politics and organization of science and technology.

A torrent of words, a torrent of ideas and clearly an historic moment for French science: Chevènement certainly hopes so, for his ambitions go beyond science and technology. Last week, he did his best to take strict control of the colloquium. The 200,000 pages were reduced to 950 reviews, written largely by people chosen by the ministry. Then 200 of these reviews were placed before 12 colloquium committees, also hand-picked. And the committees reduced these to 40-page summaries, which were then discussed.

Neither colloquium nor committees were empowered to take decisions. And even the most apparently practical committee, that on finance, was required to discuss only principles: such sordid matters as actual figures and percentages were set aside.

Nevertheless, there had been attempts to make the composition of the committees representative. There were more than 100 people in each committee, making 1,500 in all, drawn from three categories — 200 were directly involved in preparing the national colloquium and the regional summaries, 500 were from institutions, such as industries, the principal science funding bodies, ministries, universities and unions. **Robert Walgate**

0028-0836/82/030180-02$01.00

University of London

All change now

Of the central functions of the University of London, only the students' union is wholeheartedly applauded for its efficiency in the final report of the Committee on Academic Organization, published last week. The committee, set up in March 1980, was originally intended to recommend a new organization for the university. After last summer's financial cuts, the committee's terms of reference were redrafted to exclude the main teaching institutions.

One conspicuous recommendation in the report is that the university's Nuclear Reactor Centre (at Silwood Park in Berkshire) should either be closed or, preferably, transferred to Imperial College. The committee says that the centre's chief function is research, and that it should be possible for the centre to find at least half its total cost of £220,000 a year in research grants.

Among other recommendations are the continuation of the Marine Biological Station on the Clyde (administered jointly with the University of Glasgow) and the Institute of Archaeology. The report also suggests that the university could save £100,000 a year by closing its Botanical Supply Unit.

The most serious criticisms are of the central administrative machinery. The court department (which shares out the university's public grant) is too secretive, and urgently in need of computer techniques, the examinations department is overstaffed and the university's network of academic committees has outlived the time when "the need and even the opportunity for taking genuine decisions . . . has ebbed away".

In general, the committee comes down in favour of a university in which its colleges function autonomously, taking more control from the centre. But it is also against the proposal that University College should be financed separately.

These proposals are for change within the existing framework. The committees set up last September to recommend new patterns of teaching in broad subject areas appear to be following an orthogonal track. The first of their reports, published this week and dealing with the physical sciences, starts from the assumption that only large departments can be successful in research.

Most of its recommendations are that the teaching of science subjects should continue at four colleges (Imperial, King's, Queen Mary and University) and at most one other site within the university. A total of 58 academic posts in the physical sciences would be lost.

Both sets of recommendations will excite opposition. In each case, the next step is discussion by the university's academic committees and the senate.

AT&T pact hits snag

Washington

A federal judge in Washington has injected an element of uncertainty into plans to reorganize the giant American Telephone and Telegraph Company (AT&T) by announcing that, although the federal government and the company have agreed on terms for suspending the anti-trust suit filed by the Department of Justice, he is unwilling to dismiss the suit without further study of the agreement.

The Reagan Administration announced the settlement with AT&T, the largest company in the world, on 8 January. Under the terms of the agreement, AT&T has agreed to sell off 22 local telephone companies, with assets worth around $80,000 million, in return for being allowed to enter other fields of telecommunications, such as electronic data processing, from which it had previously been excluded.

US District Court Judge Harold H. Greene, who has been hearing evidence in the government's case against the company since 1978, said last Tuesday that he was "delighted that a settlement had been reached". At the same time, however, apparently concerned at the secrecy and speed of the negotiations between the company and the Justice Department, he has refused to dismiss the case without further scrutiny of the terms of the agreement. Judge Greene said that the case was "too important to the judicial process, to the public and to the country" to be closed as a result of a "haphazard process".

Judge Greene's actions are in line with a law passed by Congress in 1974 giving the public an opportunity to comment on anti-trust agreements between the government and a private company before these are concluded. The law was passed in partial protest at the secrecy which had surrounded negotiations between the government and AT&T leading to a previous consent agreement in 1956.

David Dickson

Polish universities

Wings clipped

Polish universities will resume work by mid-February, according to a communiqué issued on 10 January by the ruling Military Council of National Self-Defence. Tertiary education establishments, it says, will function "taking into account regulations deriving from the decrees on the state of martial law" and special rules have been laid down governing the running of full-time courses during the state of emergency. Moreover, resumption of university activities each term will be approved on the basis of recommendations from the Provincial Defence Committee — on the basis of how, in the previous term, the university complied with the emergency regulations.

The communiqué effectively abrogates the liberalization of academic life which followed the signing of the Gdansk accords in August 1980. In particular: academic and scholarly work is to be censored. The abolition of the censorship of learned publications was one of the first demands of the Academy of Sciences and the universities in autumn 1980, and was embodied in the censorship law which came into force on 1 October 1981.

University autonomy concerning syllabuses will be restricted. All students will have to attend courses in two foreign languages. This means a return to compulsory Russian, which was abolished by the Lodz accords that ended the students' sit-in last February. New courses and subjects will require ministerial approval, which will presumably not be forthcoming for courses reflecting the "plurality of outlook" promised at Lodz.

University rectors will now be responsible for maintaining order on campus and in students' hostels. No student may remain on campus outside tuition and library hours, and all staff must leave as soon as their working day is over. This reverses the spirit of the Lodz accords which left law and order on university premises firmly to the university authorities and banned civil police from campuses.

Attendance at lectures and classes will be obligatory, and absence without sufficient excuse may result in expulsion. Students may also be expelled for infringing Article 46 of the decree of martial law, which bans union activity and the organization of strikes and protests. Special classes are to be held at the start of the new session, explaining to the students the demands of martial law, and particularly of the new oath of loyalty.

University senates and faculty councils will be reduced to advisory status, and will have a composition "determined by the regulations of the law in force". This provision is ambiguous, since the communiqué also says that the universities will operate on the basis of the 1958 law on tertiary education — which would mean an end to the 30 per cent student participation in senates and faculty councils introduced after Lodz.

The rectors are instructed to appoint special plenipotentiaries to deal with the welfare problems formerly the province of students' unions and self-governance bodies, and will have the right to order their employees to carry out tasks hitherto not considered part of their duties. They may also order students to carry out "socially useful work" for the university or the national economy.

During the past year, all Polish university and technical college rectors have been democratically elected — except in Radom Engineering College, where an attempt to impose a rector who was not so

0028-0836/82/030181-02$01.00

Gentle Polish protest

The Royal Society and the British Academy last week sent a message of "sympathy and support" to the Polish Academy of Sciences. The message, signed by the presidents of the two academies, regrets "the interruption of normal relationships" between Britain and Poland and hopes "that they will soon be resumed". The message is to be sent to other academies which are members of the International Academic Union and the International Council of Scientific Unions.

elected led to nationwide student protests and a virtual shut-down of academic life. At least three rectors have been reported to have been interned: Dr Henryk Samsonowicz of Warsaw, Dr Jozef Gierowski of the Jagiellonian University of Krakow and chairman of the unofficial rectors' conference and Dr Janusz Ziolkowski of Poznan. How far other rectors will comply with regulations which seem aimed at reducing them simply to disciplinarians is unknown. **Vera Rich**

Finnish–Soviet research

Arctic collaboration

A new Finnish–Soviet Arctic research committee will meet for the first time next month, to work out a new joint programme for the development of the Soviet Arctic. The formation of the committee comes at a critical point in Finnish–Soviet relations: the retirement from politics of President Urno Kekkonen, the chief architect of Finland's policy of neutrality coupled with close economic cooperation with the Soviets.

Earlier this month, Mr Ahti Karjalainen, head of the Bank of Finland and chairman of the Finnish–Soviet economic committee, was in Moscow for talks on future deals including an icebreaker to be built for the Soviets in a Finnish shipyard and a contract, worth up to £125 million, for the third stage of the paper mills and urban development being built by Finnish expertise at Svetogorsk, just inside the Soviet frontier.

The new Arctic research committee, though essentially a research and development body, will to a certain extent overlap the economic agreements. For example, Mr Karjalainen has been discussing a joint off-shore geological survey for oil and gas in the Barents Sea. Accordingly, one of the major joint research projects on the agenda of the new committee will be devising the technology necessary to construct an oil and gas drilling rig on an ice floe.

Finland has considerable expertise to offer its partner. One participant in the new committee is the University of Oulu, which under the recent policy of decentralized and regionalized higher education runs a programme of research into the economic and development problems of northern Finland, much of which can be immediately applied to work in Arctic Siberia. In particular, Oulu will contribute a new technique for surveying terrain with up to 2 metres of snow cover. Oulu is also the seat of the Research Council for Arctic Medicine, and has a special laboratory for the study of the physiological hazards of work in a cold climate.

The main workload of the cooperation will be undertaken by the Technical Research Centre (Valtion Tekniken Tutkimuskestus, VTT), a government-sponsored body whose mandate includes research (at cost price) on behalf of those who wish to exploit the results but who do not have the facilities to carry out basic investigations themselves. VTT has 31 laboratories (26 in the Helsinki area, 3 in Tampere and 2 in Oulu). Fifteen of these laboratories will be involved in the cooperation programme, and it is estimated that participation will allow VTT to double its research staff in the next few years. Finland, with a population of 4.7 million, has no less than 18 universities, an escalation from two over the past 25 years resulting from "regionalization" policies, and employment for graduates who wish to remain within the Finnish academic/research structure is a perennial problem. A strong swing of public opinion away from science in the mid-1970s was by no means fully reversed by the then President Kekkonen's call for a reassessment of research and development investments in his New Year message to the nation in 1979. (This was the first time that science had been officially boosted since 1964.)

The new Soviet–Finnish Arctic research programme, the details of which will be worked out next month, is already being regarded by Finnish economists and business experts as a major shot in the arm. Its effect on graduate employment should prove equally beneficial. **Vera Rich**

Deep-sea mining

United States re-think

Washington

United States policy on deep-sea mining is again in the melting pot. The recent discovery of large ocean-bed deposits of polymetallic sulphides in various parts of the world has significantly raised the stakes in the continuing disputes over what form of international regulation should be introduced to deep-sea mining.

In the United States, plans are already being discussed to amend the Deep Sea Mining Act, passed by Congress only two years ago. The act provides a mechanism for issuing licences to US companies wishing to collect manganese nodules from the sea bed but could, as it now stands, exclude retrieval of the sulphides.

A different problem exists with the UN Law of the Sea Treaty, negotiations on which are nearing completion after eight years. The current draft of the law is sufficiently flexible to include polymetallic sulphides but US mining companies, backed by the State Department, are concerned that in its present form with no explicit attention to the sulphides, the whole question could be put on hold indefinitely.

Although chemical geologists have long predicted the existence of sulphide deposits associated with rift phenomena on the ocean bed, the first discovery was made as late as 1978 on the sea floor of the East Pacific Rise, near the coast of Mexico. Since then, several similar sites have been discovered off the Pacific coast of the United States, for example in the Juan de Fuca ridge off the state of Oregon. The minerals involved include cobalt, manganese, platinum, zinc and tin.

The most dramatic discovery so far, however, was announced last October by scientists from the National Oceanographic and Atmospheric Administration (NOAA) of the US Department of Commerce. The NOAA geologists have found several mineralized zones between the Galapagos Islands and Ecuador, in the Pacific, which they estimate to contain 25 million tons of polymetallic sulphides. The high concentration of copper and iron in the sulphides is calculated at about 10 per cent each. Also present are lead, molybdenum, vanadium and zinc (0.1 per cent each), and silver and tin (0.3 per cent), with trace amounts of cadmium, gold and platinum.

Whether the minerals in the sulphide deposits are sufficiently accessible to be worth mining is yet to be determined. The NOAA geologists estimate that the total value of the metals in the latest find is about $3,000 million, and new mining and processing technqiues would have to be developed to retrieve them.

Several large companies such as the consortium headed by Lockheed Missiles and Space, are already turning their attention to the commercial potential of the sulphides and are carrying out preliminary exploratory surveys.

Whatever is discovered, mining of the sulphides will inevitably be affected by the negotiations that have taken place within the United Nations since the resources of the high seas were declared, by an unanimous resolution passed in 1970, to form part of the "common heritage of mankind", whose exploitation should be regulated in a way that would result in the most equitable distribution of benefits.

Deposits relatively close to national coast lines are unlikely to be covered by international legislation. In line with provisions contained in the draft Law of the Sea, the US Congress is expected soon to begin debating a bill which would create a 200-mile exclusive economic zone off the US coast. The discovery of the polymetallic sulphides will add to the political attractions of this bill, since several of the known deposits — such as those in the Juan de Fuca ridge — lie wholly or partially within this distance of the shore. And if the bill passes, as seems likely given the expected support of the Administration, the companies could begin mining the

0028-0836/82/030182-02$01.00

deposits free of international regulation.

The deeper deposits, such as those off the Galapagos Islands, will create more of a problem. The deep sea mining bill passed by Congress two years ago was designed to provide US mining companies with certain rights that would have to be recognized in so-called "grandfather clauses" in any international treaty, since the latter would require ratification by the US Senate.

This law would require amendment in several places. For example, "hard mineral resources" are defined as any deposit or accretion of "nodules" lying "on, or just below, the surface of the deep sea-bed". Similarly the deep sea-bed is defined as including the subsoil "to a depth of 10 metres", while polymetallic sulphide mineral deposits may extend considerably further.

State Department officials are confident that, with the amendment of certain key definitional provisions, the act can be extended to cover the sulphides. There is much less confidence about the implications of the Law of the Sea negotiations, which Mr Otho Eskin of the department's Office of Oceans Law and Policy says raises "a very serious question".

Accepting that fundamental changes are unlikely to be agreed by the negotiators when they meet again in New York in March, and that a treaty in some form is likely to be adopted by the end of the year, the United States has two main alternatives. Either it could sign the treaty (which would be taken as a symbolic victory by the developing countries, for whom the treaty represents the first concrete mainifestation of the "New International Economic Order"); or it could refuse to sign (which could jeopardize the chances of United States-based mining consortia obtaining the necessary loans from the multinational banks).

David Dickson

Indian agriculture

Cattle go West

Bombay

India's ambitious programme of crossbreeding its cows with foreign bulls is endangering the country's agriculture by creating a shortage of draught animal power — the mainstay of farming and rural transport in India. This is the finding of a survey covering the cross-breeding programme in 18 of the 22 Indian states carried out by the Bombay-based All-India Agriculture and Cow Protection Society (AIACPS) founded by Mahatma Gandhi 40 years ago.

A five-member team of veterinarians headed by Dr M. Y. Mangrulekar contacted over 1,600 cattle breeders and government crossbreeding farms for the survey. Their report just published says that the craze for "westernization" of Indian cows has resulted in the neglect of indigenous milch strains of cattle and has led to shortage of good, sturdy bulls for farming operations.

The survey has revealed that exotic crossbreeding has mostly produced bullocks which are uneconomical. The exotic animals need special grade grass and oil cakefeeds and are unsuitable for the rigours of Indian agriculture: they get easily tired and are unable to walk in the sun or plough in wet fields, unlike the docile native bulls which live on paddy straw and are at ease in dry and irrigated fields. More importantly, the exotic crossbred males have no hump and the traditional ploughs do not fit on them. Thus the crossbred bullocks have been left to starve and die or been sent straight to the slaughter house. The AIACPS report says the crossbreeding programme, mostly financed by international agencies, is actually preparing India to become the world's leading exporter of beef to the meat hungry West. The slaughter of male calves is leading to a shortage of bullocks particularly in Bihar state where, the report says, thefts of bullocks are increasing.

In states such as Karnataka, crossbreeding has been in vogue since the 1950s but other states have taken to crossbreeding in the past two decades and the programme was vastly expanded in the early 1970s under the World Bank financed "Operation (milk) Flood". According to the survey, the high pitched crossbreeding programme is weaning the countryside away from indigenous cattle in favour of Holstein–Friesians, Jerseys and Red Danes, and good Indian breeds are being replaced with unproductive crossbreeds.

The programme has led to the import of bulls, semen, vaccines and insemination equipment but has failed to increase milk production. The hybrid cows after second calving yield less milk than the high-yielding native breeds such as Kankrej, Sahiwal, Gir and Haryana. The survey also revealed that exotic crossbreeds are more susceptible to disease than native stocks, which has led to increased import of vaccines.

However, government officials maintain that the survey findings are at variance with their own evaluation. According to Dr R.M. Acharya, deputy director general of the Indian Council of Agricultural Research, Indian cows are not being westernized wholesale. "Only five per cent of the cattle population is exotic", he says and, the humpless crossbred bullocks are gradually becoming adapted to Indian conditions and their number in farming operations is steadily increasing. According to Dr Acharya the crossbreeding is not new to India where all the military farms have been using exotic breeds for several decades. While India has indeed some good breeds, according to Dr Acharya, only a small per cent of them are really high milk yielders. Despite the controversy officials maintain there is no alternative to exotic cross-breeding for increasing India's milk production, which is currently estimated to be 23 million tonnes annually.

K.S. Jayaraman

Bridging the Indian gap

New Delhi

Mrs Indira Gandhi, the Prime Minister, announed last week a substantial increase of support for science and technology. The increase will amount to more than 50 per cent in this next five years. Mrs Gandhi, always sympathetic to science, has accepted a proposal put to her by Dr M. S. Swaminathan which is intended to strengthen government and university laboratories and to improve the quality of research.

Two new technology boards set up by the Indian government could ease the problem of high unemployment among India's scientific and technical personnel and give a new thrust to biotechnology research in the country.

A National Science and Technology Entrepreneurship Board is to be set up which will seek institutional credit for the 300,000 such unemployed persons to enable them to set up self-employed units. Surveys will be conducted to identify the areas in the country with development potential requiring scientific and technical support.

While some areas have a surplus in scientific and technical manpower (mainly due to unemployed polytechnic graduates or postgraduates) other areas are experiencing critical shortages. For instance, although there are about 4,000 vacancies for teachers in polytechnics in the country, suitable candidates are not available.

The Indian government has also decided to set up a biotechnology board to coordinate the functioning of biotechnology organizations in the country. Its purpose will be to utilize new concepts in biotechnology in agriculture, industry and medicine.

Mrs Gandhi said at the National Science Congress, India's biggest annual gathering of scientists, held in the southern city of Mysore on 3 January, that biotechnology was a frontier area of science, and that the country must take advantage of the latest technologies which could enable India to bridge the intermediate stages.

Sunil Saraf

0028-0836/82/030183-01$01.00

CORRESPONDENCE

Referees unmasked?

SIR — The present climate of open decision-making in science has been reflected in the printing of signed editorials in *British Medical Journal* (3 October 1981). Surely now is the time to consider alternatives to the traditional policy of anonymity for the referees of learned journals.

The problems which can arise from such a policy have disturbed authors for many years. Recently (*Nature* 25 June 1981, p.608), it has been suggested that the disclosure of the names of the referees to authors would avoid corruption and injustices. The alternative, that the names of authors and institutions be withheld from referees (*Nature* 30 July 1981, p.402), has obvious flaws and double-blind evaluation (*Nature* 17 September 1981, p.293) is unlikely to be attained.

The publication of the names of the referees would give recognition to their responsibility and we feel would lead to an improvement in the standard of published work. At best, a referee can make a valuable contribution to a manuscript, which deserves open acknowledgement in the published paper. Conversely the cursory examination of research work has resulted in the growth in number of papers of dubious merit, despite editorial vigilance. Responsibility for the appearance of such publications should be shared by the referees and their names no longer concealed.

D.J. LEA
H. SHEPPARD

Robert Jones & Agnes Hunt Orthopaedic Hospital,
Oswestry, UK

Migration fund?

SIR — What practical steps are we going to take to aid our Russian colleagues who are not allowed to leave their country (see letter from Dikii *et al., Nature* 24/31 December 1981, p.688)? Perhaps we should look more closely at why the Soviet government refuses to let them leave; one feels that there must be some governmental reason for the actions that are taken — it cannot, one hopes, be simply a whim of some highly placed individual.

The Soviet government could argue that it has invested heavily in the education of scientists and cannot afford to waste this investment. But the response to an application to emigrate is the withdrawal of scientific employment and the investment is lost anyway. Perhaps the Soviet government sees the use of this scientific education in another country as a double loss, and opts for what it sees as the better of two bad choices.

Interested governments, involved in scientific migrations, might press UNESCO or some similar body (the International Council of Scientific Unions perhaps) to set up a "Migrant Scientists Fund". This hard currency fund would be used to alleviate some of the injustices caused by scientific migration. For example, a country which loses a scientist could receive monetary compensation; the country to which he goes, which at the moment receives a gift of all that expensive education and training, would pay into the fund. This would benefit many countries, in particular the poorer countries which scientists tend to leave, and should prove no hardship to the rich countries to which they go. New Zealand attracts qualified people, but also loses quite a number; on balance we would probably be drawing from the fund. Australia would contribute.

In the case of the Soviet Union the flow is essentially one way, immigration to the country is on a very small scale. The fund could recompense the Soviet government for its lost educational investment and this might be a welcome source of hard currency. Countries which wish to encourage the movement of scientists could actually donate to the fund.

IAN SMALLEY

New Zealand Soil Bureau,
Lower Hutt, New Zealand

Vide the Latin

SIR — In the leading article, page 389 in your issue of 3 December 1981, entitled "Tolerance but not quarter for creationists", it is asserted that "creationism is not a part of science but an alternative to it".

As the word science is derived from the Latin *scire*, to know, would it not have been nearer the truth to apply this statement to the theory of evolution? While making no claim to vast knowledge of things existing, as I consider such known things as the cochlea, or the lens of the eye, or three-dimensional perception, I find creationism truly essential to science. A great mind expressed this in *Romans* Ch. 1 v. 20:- "The invisible things of God from the creation of the world are clearly seen, being understood by the things that are made, even his eternal power and Godhead."

D.H.T. CONWAY

Weymouth, Dorset, UK

Areas of neglect

SIR — I have been following with great and increasing interest the profound cogitations on creationism in your respected columns.

However, it is a pity that these discussions have been restricted to a particular field of biology. Surely there are many other sciences that need a thorough overhaul to put them into agreement with divine revelation. Take astronomy for example. It is high time that the godless Newtonian theories should be expelled and the Earth returned to its lawful place at the centre of the Universe.

Another science that is singularly deficient is psychology. Modern textbooks never mention the well-documented scientific facts of manipulation of the human mind by devils. Surely some enlightened state administrators should provide the necessary funds for an experimental investigation of these important phenomena. In this respect we have fallen far behind what was known in the Middle Ages, when at least a number of practical and efficient methods were in use for dealing with Satanic influences.

As a final example one could cite acoustics. The most important application of this branch of physics — the demolition of city walls by sound waves — is no longer a fashionable subject of study, although new findings in the field of surface acoustic waves could provide a solution to this problem. It is a sad reflection on the state of present-day science that students never hear of it, except through a well-known negro spiritual.

S.V. VAECK

Brussels, Belgium

DNA and Europe

SIR — The article by Jasper Becker on the EEC safety dispute concerning recombinant DNA (*Nature* 24/31 December 1981, p.686) gives a quite correct picture of the situation. But Jasper Becker states that the socialists are in favour of a community directive. This is not quite correct. The socialist group in the European parliament has never voted on this question. Only the socialist members of the environment committee have given their opinion. Other members of the group, like me, have a different position for a multitude of reasons. In my view, only industrial and agricultural applications of recombinant DNA work should be regulated at an EEC level.

FRITZ GAUTIER (MEP)

Socialist Group,
Braunschweig/Brussels, Belgium

Brief encounter

SIR — In your summary "Hoyle on Evolution" (*Nature* 12 November 1981, p.105) you cite Hoyle as saying that for higher life forms to have emerged by chance is comparable to the chance that a tornado sweeping through a junk-yard will assemble the material into a Boeing 747.

This reminds me of a debate I had some years ago with Dr Douane Gish of the San Diego Institute of Creation Research. The occasion was a symposium in Utrecht organized by the Evangelische Omroep, the Dutch Evangelical Broadcasting Company. This company broadcasts the creationist message for several hours per week to Dutch audiences via television and radio. At the symposium in Utrecht I defended the theory of biological evolution, and Dr Gish defended the biological aspects of creationism. During the discussion Dr Gish remarked that the chance that amino acids would spontaneously form biologically active protein molecules was practically zero. I then said: "Dr Gish, if somebody had asked me on the day of my birth to calculate the chance that one day I would have a debate in Utrecht with Dr Gish from San Diego, I would have answered that this chance was practically zero. Am I therefore to understand that you are not Dr Gish from San Diego?" But my opponent had the perfect answer to that one. He said: "I am not here by chance, I was invited!"

MELS SLUYSER

The Netherlands Cancer Institute,
Amsterdam, The Netherlands

NEWS AND VIEWS

...ersity Colleges of Science & Technology
92, A.P.C. Rd., Cal.-9
LIBRARY COMPLEX
...rtments of
...ical Engineering
...mical Technology
...ics & Rubber Technology.
1983

Hominoid evolution

from Peter Andrews

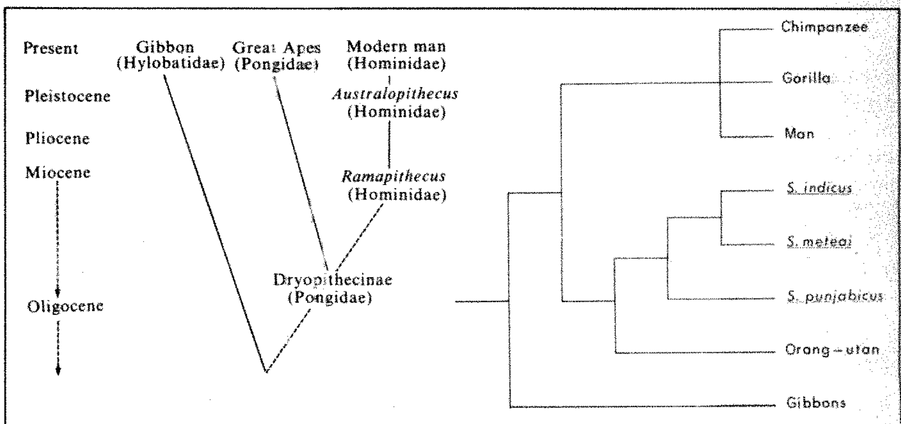

The figure on the left shows the traditional phylogeny of the Hominoidea, with the Great Apes (including chimpanzees, gorilla and orang-utan) separate from the human lineage: the pongids and the hominids. The hominids generally include Pleistocene fossil australopithecines and *Ramapithecus* from the Miocene. The pongids include the living Great Apes and the fossil dryopithecines from the Miocene. The cladogram on the right shows the relationships among the Hominoidea that are proposed here. The Great Apes are split between the orang-utan on the one hand and chimpanzee and gorilla on the other. *Ramapithecus* (= *Sivapithecus*) is held to be related more closely to the orang-utan than to man, chimpanzee and gorilla, and cannot be considered to be a direct human ancestor. One of the consequences of this is that the presence of *Sivapithecus* in deposits 8–12 Myr old suggests a divergence of time of 11–12 Myr for the orang-utan. The divergence of the African apes and man would therefore have been later than this and probably around 6–7 Myr.

In the debate over human origins it has become the traditional view that *Ramapithecus* is the earliest known hominid. Set against this is the opinion, held by a minority, that *Ramapithecus* is more closely related to the orang-utan and is not thus directly connected with the evolutionary line leading to humans. The latter view receives fresh support in this issue of *Nature* (p.232) with the description of a new skull of *Sivapithecus* from Pakistan by David Pilbeam. The specimen is by far the most complete *Sivapithecus* yet found, and it provides information that was previously either unknown or based on reconstructions from less complete material. It will be examined here in relation to two important issues — the position of the orang-utan in relation to other living hominoids and the relevance of fossil primates, in particular *Sivapithecus* and *Ramapithecus*, to hominoid evolution.

The relationships of the living hominoid primates — apes and man — have been greatly clarified by the biomolecular work initiated nearly twenty years ago by Morris Goodman. Three cladogenic events in hominoid evolution have been recognized: the divergence of the gibbon from the common hominoid stock; the subsequent divergence of the orang-utan from the Great Apes and man stock; and the most recent divergence between man and the African apes. As well as defining the sequence of events, molecular anthropology has also been used to date these events, using the so-called 'molecular clock'. Many uses of the clock have been naive, but present estimates for the three events are: gibbon divergence 12 ± 3 Myr; orang-utan divergence 10 ± 3 Myr; and man - African ape divergence 6 ± 3 Myr (Andrews and Cronin, in preparation).

Two consequences arise from these results. First, there is no 'missing link' between apes and man. Man and African apes share a common ancestor, and the man–chimpanzee–gorilla clade shares a common ancestor with the orang-utan. The similarities in grade (mostly from shared primitive characters) between the orang-utan and the African apes means that they are superficially similar and that their ancestral states would also be rather similar. They would therefore be correspondingly hard to identify in the fossil record, and a fossil like *Ramapithecus* might have similarities with either or both. Second, the molecular evidence suggests that the cladogenic events in hominoid evolution occurred later than many palaeontologists have expected. With *Ramapithecus* and *Sivapithecus* thought to be alive between 8 and 12 Myr ago, for example, the fossil taxa would appear to have arisen too early to be ancestral to humans.

The relationships of *Ramapithecus* and *Sivapithecus* can now be examined in more detail to see where their affinities lie. It is becoming apparent that the differences between the two genera are not as great as had formerly been thought. Greenfield (*Am. J. phys. Anthrop.* **50**, 527; 1979) recently proposed that *Ramapithecus* is the same as *Sivapithecus*, and although his systematic procedure is suspect, there is a very high degree of similarity between *Sivapithecus* and *Ramapithecus*. Kay (*Int. J. Primat.*, in the press) has now made a much better case and suggests that *Ramapithecus punjabicus* become *Sivapithecus sivalensis*. Another alternative, which I prefer, is to retain *punjabicus* as a species of *Sivapithecus*. Therefore, in considering the relationships of what was formerly *Ramapithecus* or *Sivapithecus*, the whole complex of *Sivapithecus* species must be considered. At the most conservative estimate there are at least four species of *Sivapithecus* found from 8 to 12 Myr and occurring from Greece and Turkey in the west to southern China in the east.

The specimen of *Sivapithecus* described in this issue of *Nature* is an adult *Sivapithecus indicus* with large parts of the face and palate preserved. It was badly broken when it was found, and Horace French and Rizwana Raza of Yale University have done a magnificent job in restoring it to its present condition. The specimen is the outcome of years of painstaking collecting in Pakistan by the Yale research project, directed by David Pilbeam, now at Harvard, and S.M.I. Shah in Pakistan.

Pilbeam has been very cautious in his assessment of the similarities his new specimen shows with the orang-utan. I will be less cautious and will list some of them: orbits higher than broad, poor development of the supra-orbital torus, narrow interorbital distance, smooth and unstepped floor of the nasal cavity, large zygomatic foramina set above the lower rim of the orbit, extremely small incisive foramina, narrow and slit-like palatine foramina, thick enamel and low cusp

---

Peter Andrews is in the Department of Palaeontology, British Museum (Natural History), Cromwell Road, London SW7 5BD.

0028-0836/82/030185-02$01.00

profile on the molars and very large incisors in comparison with the lateral incisors. All these characters are present on the *S. indicus* skull, and some at least are known to be present on other species such as *Sivapithecus meteai* and *Sivapithecus punjabicus*. They are all interpreted as being derived from the primitive hominoid condition and are thus specializations shared with the orang-utan. There are also many primitive characters shared with the orang-utan, such as the poor development of the supraorbital torus and the slope of the nose, and other characters like the great depth of the zygomatic bone that show greatest ressemblance to the orang-utan but are within the limits of variation of other hominoid species. Set against this list of characters are a few which show similarities with man. Of particular importance are the robustly built jaws, the lateral rotation of the canines and possibly low canine sexual dimorphism. Another similarity with man, the thick enamel and low cusp relief of the molars, is also shared with the orang-utan and cannot be considered diagnostic. The similarities with man are fewer in number and more strongly inter-related with each other than are the similarities with the orang-utan, and it is my belief that *Sivapithecus* must be seen as a relative of the orang-utan. It is shown thus on the accompanying cladogram.

It thus appears that *Sivapithecus* (including *'Ramapithecus'*) is part of the orang-utan clade, and both are more distantly related to man than are the African apes. In other words *'Ramapithecus'* can no longer be considered as part of the human lineage but as part of the orang-utan lineage. The recognition of this relationship provides fossil evidence for the divergence date of the orang-utan, and the time span of 8–12 Myr for the species of *Sivapithecus* is certainly compatible with the molecular date of 10 ± 3 Myr. □

Measuring atmospheric gases and aerosols

from D.D. Davis, W.L. Chameides and C.S. Kiang

SOME nine months ago several of the findings of the National Science Foundation-supported Global Atmospheric Measurements on Tropospheric Aerosols and Gases programmme (GAMETAG) were critically reviewed in these columns[1]. As part of the planning group for this field sampling programme, we welcome efforts to bring GAMETAG results before a larger spectrum of the scientific community. We would now like to go on to clarify some points that were made earlier and to add new information from the most recently available results.

The first point involves the NO/HNO_3 GAMETAG measurements. Before the GAMETAG flights, the little information available on NO_X in remote regions of the troposphere[2–6] suggested that NO levels were in the 100–1,000 p.p.t.v. (parts per 10^{12} by volume) range. The GAMETAG NO instrument, which had a lower detection limit of 50–60 p.p.t.v., gave readings which indicated that over thousands of miles of continental wilderness area and over large stretches of the open Pacific Ocean, NO levels were typically below that lower detection limit. The observations[7] are the first to indicate that NO_X levels in remote marine and northern continental troposheric air are much lower than previously believed. Subsequently, MacFarland *et al.*[8] reported that NO levels in a limited region of the equatorial Pacific were in the 1–10 p.p.t.v. range but the GAMETAG HNO_3 observations were the first extensive remote-global tropospheric data base for this species. Of particular importance is the observation that lower levels of HNO_3 are found in the marine boundary layer than in the middle free troposphere over extensive regions of the open Pacific Ocean. The results are in direct contradiction with all earlier predictions of NO_X/NO_Y altitude profiles and show the need for significant revisions in the tropospheric nitrogen budget.

D.D. Davis, W.L. Chameides and C.S. Kiang are in the School of Geophysical Sciences, Georgia Institute of Technology, Atlanta, Georgia 30332.

A second point involves new data now available on the question of photochemical activity over tropical and sub-tropical marine areas. Since Penkett wrote[1], the data have been released in manuscript form and are shortly to appear in print. Direct OH observations show tropical mid-day marine boundary layer OH levels ranging from $\sim 2 \times 10^6$ up to a high of 1.5×10^7 molecules per cm^3. It is argued by some that the absolute accuracy of the OH system may be in error by as much as a factor of two (the authors think this unlikely) but even if this were so and OH levels were assigned a value a factor of two lower, the conclusion that OH levels in the tropical marine boundary layer are typically quite high would still be clearly justified. It is estimated that the above observations imply a diurnally and seasonally averaged OH value of $\sim 2 \times 10^6$ molecules per cm^3 for the tropical marine boundary layer. For spring and summer conditions, at sub-tropical latitudes, a similar diurnally averaged OH value of 2×10^6 molecules per cm^3 is estimated from our measurements. Mid free-tropospheric (that is, 5–6 km) values over the above latitude range were typically a factor of two to three lower than those observed in the marine boundary layer. These OH values are significantly higher than the globally averaged value estimated by several investigators based on Northern/Southern Hemisphere CH_3CCl_3 measurements[9–11]. This result is consistent, however, with the higher than average levels of H_2O and UV actinic radiation that normally characterize the above latitude zones. They further suggest that in the tropical marine boundary layer, OH radicals are very likely to be responsible for initiating the oxidation of numerous compounds released into the atmosphere in reduced oxidation states. Approximate photochemical lifetimes based on oxidation by OH at a level of 2×10^6 molecules per cm^3 are SO_2 (3.5 days), CH_3SCH_3 (1 day), H_2S (1 day), NO_2 (0.7 day), C_2H_4 (0.7 day), C_3H_8 (0.2 day), CO (20 days) and CH_3Cl (124 days). Virtually all these lifetimes are much shorter than those predicted from washout/rainout or dry deposition.

A final point concerns tropical marine tropospheric-photochemical activity and its relation to the GAMETAG observations which showed no direct evidence of any photochemical generation of O_3. In spite of this observation, it is important to understand that the absence of O_3 generation cannot be equated with the absence of free radical chemistry or the lack of importance of photochemistry, in general. It instead suggests that of the possible HO_2 loss reactions (1)–(3):

$$HO_2 + HO_2 \rightarrow H_2O_2 + O_2 \qquad (1)$$

$$HO_2 + NO \rightarrow OH + NO_2 \qquad (2)$$

$$HO_2 + CH_3O_2 \rightarrow CH_3OOH + O_2 \qquad (3)$$

reaction (2), under tropical marine boundary layer conditions, is unsuccessful in competing with reactions (1) and (3). This result is a direct consequence of the previously described low levels of NO in the tropical marine boundary layer. It should be stressed, however, that the absence of O_3 production does not preclude the use of marine tropical areas of the world as future field sampling sites for studying free-radical tropospheric chemistry. In fact, the simplified chemistry of this region, resulting from highly reduced levels of hydrocarbons and their oxygenated analogues, should present the best opportunity for unravelling many key aspects of tropospheric chemistry. □

---

1. Penkett, S.A. *Nature* **290**, 631 (1981).
2. Noxon, J.F. *Science*, **189**, 549 (1975).
3. Lodge, J.P. & Pate, J.B. *Science* **153**, 408 (1966).
4. Georgii, I.H.W., & Jost, D. *Pure appl. Geophys.* **59**, 217 (1964).
5. Moore, H. *Tellus* **26**, 169 (1974).
6. Cox, R.A. *Tellus* **29**, 356 (1977).
7. Schiff, H.I., Pepper, D & Ridley, B.A. *J. geophys. Res.* **84**, 7895 (1979).
8. MacFarland, M. *et al. Geophys. Res. Lett.* **6**, 1605 (1979).
9. Singh, H.B. *Geophys. Res. Lett.* **4**, 453 (1977).
10. Crutzen, P.J. & Fishman, J. *Geophys. Res. Lett.* **4**, 321 (1977).
11. Chameides, W.L. & Tan, A. *J. geophys. Res.* **86**, 5209 (1981).

0028-0836/82/030186-01$01.00

A hydrothermal plume remobilizes sedimentary organic matter

from Andrew S. Mackenzie

IN this issue of *Nature*, Simoneit and Lonsdale[1] describe petroleum found in dredge samples containing hydrothermal minerals, taken near a hydrothermal vent in the Guayamas Basin, Gulf of California. This 'hydrothermal petroleum' has a quite different composition from 'commercial petroleum' and its distinctive features are related to the rather special circumstances of its generation and migration. There is no evidence that the hydrothermal petroleum has a deep-seated origin and has emanated directly from the vent. Instead, the results suggest that part of the biologically derived organic matter of sediments in the neighbourhood of the vent can be remobilized and transported by the hydrothermal plume.

The most striking feature of the hydrothermal petroleum is its chemical resemblance to the organic matter which can be extracted, with common organic solvents, from relatively immature sedimentary rocks. Indeed, in one sample, a number of organic molecules, whose carbon skeletons have unambiguous links with known biological molecules, are still present as their less stable forms. Within this immaturity, the authors have detected certain components whose continued presence in large relative abundances is best explained by a relatively short-lived heating at temperatures well above those normally found in connection with petroleum formation. The evidence can best be accomodated in a model where the immature organic matter of the Quaternary sediments around the hydrothermal vent has come into contact with a hot hydrothermal plume and has then rapidly cooled as a result of migration in the hydrothermal flow and condensed at the seabed.

Organic geochemistry is much concerned with specific problems of petroleum geology, particularly those associated with thermal maturation[2]. The present paper[1] and others from the same laboratory[3] show some of the advantages of being able to study Earth processes at a specific organic molecular level and perhaps indicate the further contributions the field is poised to make in many other areas of the Earth sciences. Although a tremendous amount has been achieved in cataloguing a large number of specific but previously unknown chemical structures of the organic compounds occurring in sediments and petroleums[4], most of the applications to date have been very empirical. Simoneit and Lonsdale have made use of the sciences of chemical kinetics and thermodynamics in a descriptive sense to predict how the hydrothermal petroleum was formed. Large relative abundances of peri-condensed aromatic hydrocarbons and steroidal alkanes are said to reflect relatively short-lived contact with high temperatures (certainly greater than 250°C), because other reactions, which destroy the aromatic hydrocarbons[5], add hydrogen to triterpenoid alkenes[6] and isomerize triterpenoid and steroid alkanes[7-9], have been promoted to a lesser extent. This observation implies that the rates of the former types of reaction are accelerated to a greater extent by a major increase in temperature than those of the latter reaction types, and stems from the principles of chemical kinetics.

The chemical composition of the migrated hydrothermal petroleum also shows specific differences from organic matter found close to igneous sills[3]. Unsaturated hydrocarbons (alkenes) with carbon–carbon double bonds in the middle of the carbon chains occur in both environments, whilst those with double bonds at the end of the carbon chains are restricted to the organic matter next to sills. Simoneit and Lonsdale argue that the mid-chain alkenes can survive the migration in hot fluids, because of their higher thermodynamic stability, whereas the less stable terminal alkenes are completely destroyed.

Such descriptive integrations of physical chemistry into molecular organic geochemistry are welcome and valid. In the future, attempts will be made to derive more mathematical expressions for organic geochemical processes, particularly for those which can now be studied at a molecular level. Universally applicable expressions are more likely to emerge from the relatively simple interconversions between two known molecular structures than from the complex physicochemical processes which generate petroleum. These expressions will permit a more quantitative evaluation (what temperature and for how long) of the past geological events which have affected the organic mixtures being studied. In such a form molecular organic geochemistry will provide a new set of tools to Earth scientists. ☐

Andrew S. Mackenzie is at the Institut für Chemie, KFA Jülich, Postfach 1913, D-5170 Jülich 1, FRG.

1. Simoneit, B.R.T. & Lonsdale, P. *Nature* **295**, 198 (1982).
2. Tissot, B. & Welte, D.H. *Petroleum Formation and Occurrence* (Springer, Berlin, 1978).
3. Simoneit, B.R.T., Brenner, S., Peters, K.E. & Kaplan, I.R. *Geochim. cosmochim. Acta* **45**, 1581 (1981).
4. For a recent example see McEvoy, J., Eglinton, G. & Maxwell, J.R. *Init. Rep. DSDP* Leg **63**, 763 (1981).
5. Brassell, S.C. *et al. Init. Rep. DSDP* Leg **56**, 57 pt 1 (1980).
6. Ensminger, A. thesis, Univ. Louis Pasteur (1977).
7. Ensminger, A., Van Dorsselaer, A., Spyckerelle, C., Albrecht, P. & Ourisson, G. in *Advances in Organic Geochemistry 1975* (eds Tissot B. & Bienner F.) 245 (Editions Technip, Paris, 1974).
8. Seifert, W.K. & Moldowan, J.M. *Geochim. cosmochim. Acta* **43**, 111 (1979).
9. Mackenzie, A.S., Patience, R.L., Maxwell, J.R., Vandenbroucke, M. & Durand, B. *Geochim. cosmochim. Acta* **44**, 1709 (1980).

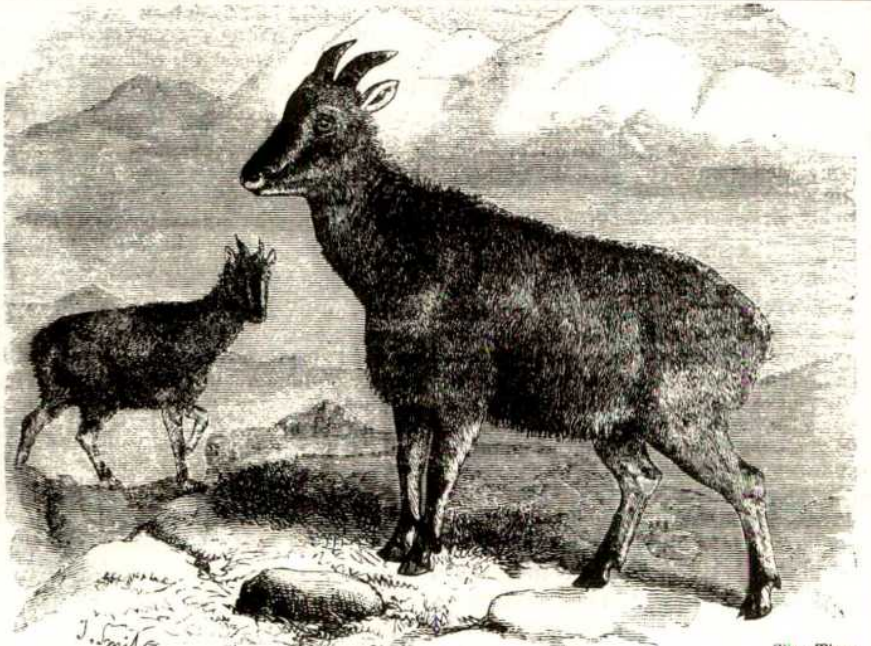

The Thar.

100 years ago From *Nature* 25, 26 January, 297, 1882.

THE THAR (*Capra jemlaica*). — The peculiar Himalayan Goat, known to the Indian sportsmen as the Têhr, Thar, or Tahir, was first described in 1828 by Hamilton Smith, and named *Capra jemlaica*, from the district of Jemlab, to the north of Nepaul, in which his specimen was procured. It is found, however, as Dr Jerden tells us, throughout "the whole extent of the Himalayas at great elevations, generally above the limits of forest and not far from the snow. It frequents rocky valleys and very steep and precipitous ground, and is often seen perched on what appear to be inaccessible crags. If alarmed whilst feeding, these animals all go off at full speed with a clattering sound, but soon halt and turn to gaze on the intruder."

0028-0836/82/030187-01$01.00

Prostaglandins and cancer

from Peter Alexander

PROSTAGLANDINS, thromboxanes, prostacyclins and leukotrienes are produced by most tissues of the body by oxidation of arachidonic acid (AA). Their possible importance in cancer, at levels including carcinogenesis, the rate of proliferation of the tumours and the interaction between the tumour and the host, was the subject of a recent conference*.

Their significance can be seen in relation to the possibility that cancer may be prevented not only by withdrawing carcinogenic stimuli but also by intervening in the complex sequence of events between exposure to a carcinogen and the occurrence of a malignant neoplasm. Prostaglandin (PG) synthetase inhibitors, like aspirin, may be candidates for the 'chemoprevention' of cancer. Most chemical carcinogens need to be converted by metabolic processes into a reactive carcinogenic substance which can combine in a covalent chemical reaction with intracellular nucleophilic constituents. This metabolic activation can occur by reduction and by hydrolysis but most commonly requires oxidation. The cytochrome P450 monooxygenase systems have been shown to be an important oxidative pathway for the production of proximate carcinogens, and evidence is now accumulating that such oxidation can also occur during prostaglandin synthesis.

L. Marnett (Wayne State University, Detroit) showed that in the reactions involving benzopyrene, the conversion of the pro- to the proximate carcinogen was brought about by by-products (free radicals) produced during the synthesis of prostaglandins, although a direct role of lipoxygenase could not be totally excluded. With some tissue preparations, like ribosomes from ram seminal vesicles, an aspirin-like drug totally blocked the production of the proximate carcinogen, whereas with intact epithelial cells the active metabolite was produced via both the P450 and the prostaglandin pathway (T. Eling, National Institute of Environmental Research, North Carolina). Before inhibitors of AA metabolism can be seriously considered for chemoprevention, the relative contribution of prostaglandin-related oxidations in the formation of carcinogens must be determined in different organs. T. Zenzer (V.A. Medical Center, St Louis) presented early results from continuing *in vivo* studies with the potent bladder carcinogen FANFT (a 5-NO_2 furan derivative), the oxidative metabolite of which binds to DNA *in vivo*. Co-administration of aspirin prevents both binding to DNA and the appearance of early hyperplastic and possibly pre-cancerous lesions in the bladder. It will be another 12 months or so before it is known whether the incidence of bladder carcinomas in rodents has been reduced.

In many experimental systems carcinogenesis can be separated into two processes — initiation by the chemical reactive carcinogens and promotion. The most effective and widely studied promoting agents are phorbol esters such as TPA. The biochemical basis of promotion remains unclear because these agents induce a great many changes in cells and tissues. Prostaglandins and related substances could be involved as TPA increases release of their precursor, AA, from cell membranes and this produces an increase in cellular prostaglandins (E. Bresnick, University of Vermont). Indeed, this may contribute to the intense inflammation produced by all the phorbol esters that are active as promoters. R. Boutwell (University of Wisconsin) considers that elevation in ornithine decarboxylase activity is a key event in promotion and this is reduced if inhibitors of PG synthetase are given at the same time as TPA. The decisive test, however, is whether tumour promotion by TPA can be prevented *in vivo* by modulating prostaglandins. G. Fürstenberger finds that indomethacin, a potent prostaglandin synthesis inhibitor, prevents promotion by TPA of skin tumours following initiation with a polycyclic hydrocarbon and that administration of $PGF_{2\alpha}$ reverses this inhibition. But S. Fischer (Oak Ridge National Laboratory) is cautious about simplistic interpretations because she finds that low doses of indomethacin actually enhance promotion and that interference with promotion by high doses may not be due to inhibition of prostaglandin synthesis. She considers, however, that products from AA obtained by the lipoxygenase pathway may be concerned with promotion.

There is mounting evidence for a role of products of the AA cascade in the growth and spread of tumours once they have arisen. *In vitro* there are correlations between growth rate and intracellular prostaglandin concentrations which are not easy to interpret. Certain prostaglandins, notably PGE, slow cell division (B. Jaffe, State University of New York, Brooklyn, and S. Hammarstrom, Karolinska Institute), while L.J. de Asua (Friedrich Miescher Institut) demonstrated that $PGF_{2\alpha}$ is highly specific in causing cells rendered quiescent, for example by serum deprivation, to initiate DNA synthesis, probably by causing changes in the cytoskeleton. It is not, therefore, surprising that experiments in which inhibitors of prostaglandin synthesis are added to cell cultures or given *in vivo* to tumour-bearing animals give rise to conflicting results. In many respects the most impressive effects of prostaglandins on the growth of cells *in vitro* is the induction of maturation and their possible involvement in retinoid-induced differentiation. PGE, probably produced by monocytes, regulates proliferation and differentiation of stem cells in the bone marrow both *in vivo* and *in vitro* (R. Bockman, Memorial Sloan Kettering Cancer Center, New York). The observation that, *in vitro*, certain prostaglandins, notably PGA and PGI_2, can induce differentiation of myeloid (T. Breitman, NIH) and erythroid (G. Santarro, Ospedale Ruiniti, Rome) leukaemia cells as well as of mouse mammary carcinoma (P. Rudland, Ludwig Institute, UK) and neuroblastoma (K. Prasad, University of Colorado Medical Center) cells, constitutes the best reason for persevering with attempts to inhibit the growth of tumours using prostaglandins.

It is also possible that prostaglandins may influence the interplay between the host and the tumour. A popular concept is that some prostaglandins depress immune responses and that inhibition of prostaglandin synthesis will enhance a putative immune reaction of the host to the tumour. As yet, there is little hard *in vivo* data in support for immunotherapy based on prostaglandins. However, there are non-immunological interactions between the tumour and the host in which prostaglandins are involved and which might be manipulated in a therapeutically beneficial manner. Investigation into the control of metastases to bone and of the hypercalcaemia associated with malignancy using inhibitors of prostaglandin synthesis has been motivated by the finding that some prostaglandins cause osteolysis and calcium release from bone *in vitro* and that in two animal models, hypercalcaemia is induced by tumours that make large amounts of prostaglandin and can be stopped by aspirin-like drugs. Unfortunately, in man there is no consistent correlation between serum levels of prostaglandin and hypercalcaemia nor will inhibition of prostaglandin synthesis effect bone metastases or hypercalcaemia (T. Powles, Institute of Cancer Research, Sutton, UK).

Of considerable interest are experiments by K.V. Honn (Wayne State University, Detroit) which are based on the premise that platelet aggregation favours the spread of tumours. Accordingly, he tested

---

Peter Alexander is Professor and Head of the Division of Tumour Immunology at the Institute of Cancer Research, Sutton SM2 5PX, UK.

---

*An international conference on 'Prostaglandins and Cancer' was held from August 30 to September 2 1981, in Washington DC, under the chairmanship of T.J. Powles (Royal Marsden Hospital, Surrey), R. Beckmann (Memorial Sloan-Kettering Cancer Center, New York), K.V. Honn (Wayne State University, Detroit) and P. Ramwell (Georgetown University School of Medicine, Washington DC).

0028-0836/82/030188-02$01.00

in an animal tumour system selective inhibitors of Tx, which promotes platelet aggregation, and the administration of PGI_2 (or of substances which facilitate vascular PGI_2 synthesis), which prevents the formation of platelet emboli. Both procedures reduced the incidence of lung metastasis and in addition slowed the growth of the tumour growing at the site of injection. This latter effect is unlikely to involve interference with platelet aggregation and is thought to be a direct effect on the rate of proliferation of the tumour cells by increasing cyclic AMP.

The meeting was successful in bringing together cancer research workers and many of the leaders in the area of prostaglandins. It was encouraging to both groups that manipulation of the AA cascade may have a role in both prevention and treatment of cancer although the key experiments remain to be performed. □

A new British flower

from Peter D. Moore

BOTANISTS in the tropics will probably throw up their hands in horror but the fact remains that the discovery of a new species of flowering plant in the British Isles (and probably a native one at that) is news. Rix and Woods[1] have now officially recorded the finding of *Gagea bohemica* at Stanner Rocks, near Kington, mid Wales. Its inconspicuous leaves and flower undoubtedly contributed to its success in eluding detection until recently and to its initial misidentification. But the find also has some interesting biogeographical implications, for *G. bohemica* is a species of continental distribution, reaching its northwestern European limits in central Germany and the Seine Valley in France, and extending into central, eastern and southern parts of the European mainland. Stanner Rocks is a site far-removed from the remainder of its range.

One must consider the possibility that the plant has arrived at this location by chance dispersal but, as Carlquist[2] has recently emphasized, it is very difficult to study freak phenomena of this kind. *G. bohemica* reproduces by seed (though at Stanner Rocks only one per cent of the population flowers and no capsules have been observed) and by bulbils. Unlike some lake and seashore sites, a rock outcrop is an unlikely spot for the concentration of a bird migration route, making bird transport an unlikely explanation of its presence.

It is important to consider that Stanner Rocks boasts an unusual assemblage of rare plants currently exhibiting disjunct distributions, including *Lychnis viscaria, Veronica spicata* and *Scleranthus perennis.* Also, on some neighbouring outcrops in mid Wales, is *Potentilla rupestris*[3]. All of these have continental distributions, though *L. viscaria* and *S. perennis* extend further north than the others.

All these species are plants of low growth habit and demand light. Pigott and Walters[4] proposed that plant assemblages having a number of open habitat species of generally disjunct distribution were often associated with disturbed or unstable sites in which the forest cover had remained incomplete throughout post-glacial time. The plants now isolated in such sites may represent relicts of the vegetation of late-glacial or early post-glacial times, which have been extinguished over the bulk of their former range by forest expansion and consequent shading. In the case of Stanner Rocks, such an explanation is supported by the sub-fossil record of certain of the plants concerned. *S. perennis* pollen has been found in late-glacial sediments of mid Wales[5] and a seed of *L. viscaria* was found by Dickson, Dickson and Mitchell[6] in late-Devensian material from the Isle of Man. Unfortunately, no sub-fossil records are available for *V. spicata, P. rupestris* or *G. bohemica* in Britain, but their current, rather southerly, continental distributions do not make them likely candidates for late-glacial relicts.

Gagea bohemica

Peter D. Moore is Senior Lecturer in the Department of Plant Sciences, University of London King's College, 68 Half Moon Lane, London SE24 9JF.

Lamb[7] has constructed global maps of probable atmospheric pressure systems during winter and summer at several stages of post-glacial history, and he concludes that the early part of the post-glacial in north-west Europe (pre 7,000 BP) was characterized by a vigorous circulation of air masses which would have brought dry, anticyclonic conditions to the area both in winter and summer. It may well be that many southern continental plant species were able to migrate into what are now oceanic regions in the north and west during those times. This would have brought into contact a variety of continental species of somewhat southerly and northerly affinities; it is interesting to note that all five of the species under discussion here are currently found together in central Poland, which may give some indication of the climatic conditions during the period of mixing. Rix and Woods[1] note that the Stanner Rocks specimens of *G. bohemica* are morphologically most akin to the western French populations on the continent, which may suggest a west European origin for the British population of this species.

The subsequent history of the mid Wales area has involved forest spread and increasing oceanicity of climate, both of which will have operated against the survival of all these species; but the rock outcrops, such as Stanner, have evidently acted as refuges. Such outcrops would not only have provided steep, unstable slopes keeping the woodland and canopy open and discontinuous, but may also have created microclimatic conditions appropriate for the survival of continental species of plant. *G. bohemica* on Stanner Rocks is currently restricted to shallow soils on southern and eastern aspects. These locations would be well insolated in summer, providing a 'micro-continental' climate, rather analogous to some of the present-day East Anglian breckland habitats of *S. perennis* and *V. spicata.* The importance of aspect for survival of a species at the edge of its climatic range is well documented for such plants as *Cirsium acaule*[8] which reaches its northern British limit in Derbyshire but survives there mainly on southerly aspects. Even under these conditions fruiting is poor and experiments involving daily spraying of the developing fruit with water, thus lowering overall temperatures, reduced success even further. *G. bohemica* fails to fruit at Stanner, but persists by vegetative propagation.

The record of *G. bohemica* from Stanner Rocks is thus more than just one more species on our list — it may also provide important evidence of the climatic and vegetational history of the British Isles. □

---

1. Rix & Woods *Watsonia* **13**, 265 (1981).
2. Carlquist *Am. Scient.* **69**, 509 (1981).
3. Sinker in *Welsh Wildlife in Trust* (ed. Lacey, W.S.) 129 (North Wales Naturalists Trust, 1970).
4. Pigott & Walters *J. Ecol.* **42**, 95 (1954).
5. Moore *New Phytol.* **69**, 363 (1970).
6. Dickson, Dickson & Mitchell *Phil. Trans. R. Soc.* **B258**, 31 (1970).
7. Lamb in *Climate: Present, Past and Future* Vol. 2, 382 (Methuen, London, 1977).
8. Pigott in *Flora of a Changing Britain* (ed. Perring, F.) 32 (Classey, Hampton, Middlesex, 1970).

0028-0836/82/030189-01$01.00

Analysing atmospheric carbon dioxide levels

from Michael J. Rycroft

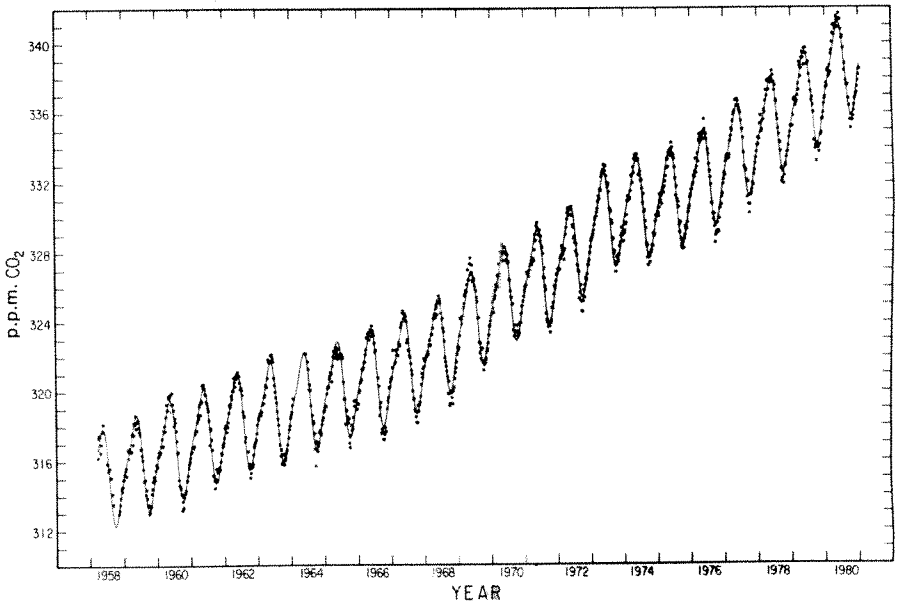

Fig. 1 Atmospheric CO_2 concentrations (weekly averages) measured at Mauna Loa, Hawaii (courtesy of C. D. Keeling). The curve is a spline fit assuming an annual variation of constant amplitude superposed on a long-term trend.

THE possibility that changes in climate may be brought about by increasing levels of carbon dioxide in the atmosphere made a recent conference* devoted to the analysis and interpretation of atmospheric CO_2 data of particular significance. The CO_2 increase is caused primarily by the burning of fossil fuels and secondarily by deforestation in the tropics and changing agricultural practices. Very recently such problems have been put in context by Bach *et al.*[1] and Kellogg and Schware[2], and discussed by Kandel[3]. Following the pioneering work of Manabe and Wetherald[4], several complicated model calculations[5-10] have been performed; these have been reviewed by Schiff[11].

For a doubling of the CO_2 content of the atmosphere, these models calculate that the global mean surface air temperature would rise by 2–4 deg, but with a larger increase at high latitudes[12]. It has been suggested that this could lead, within a thousand years, to deglaciation of the West Antarctic ice sheet[13,14]. The consequent rise of the mean sea level[15,16] would have a profound effect as population is concentrated in low-lying areas of the world. Associated with the temperature rise would be changes of atmospheric circulation and the spatial distribution of rainfall. The changed soil moisture patterns could have serious implications for agriculture and food production. The study of atmospheric CO_2 is thus closely linked with other biospheric processes, studies of carbon budgets and the global carbon cycle[17], the biogeochemical cycles of nitrogen, phosphorus and sulphur, and their mutual interactions[18] in the atmosphere and oceans[19].

R. M. Rotty (Institute for Energy Analysis, Oak Ridge Associated Universities, US) has shown earlier that the global production of anthropogenic CO_2 by fossil fuel burning (98%) and cement manufacture (2%) has increased exponentially between 1860 and 1914 and since 1945. Simple exponential growth, with an *e*-folding time of 24 years, corresponds to compound interest at 4.3% per year from a pre-Industrial Revolution value of at most 290 parts per million (p.p.m.) by volume. However, the situation is not so simple. From 1950 to 1973, the growth rate of CO_2 emission into the atmosphere was 4.6%, and since 1973, when OPEC increased oil prices dramatically, the growth rate halved to 2.3%. At present, 5.3 Gigatonnes (5.3×10^{12} kg) of carbon are being released per year into the atmosphere as CO_2 (19.4 Gt per year). As this adds to the 700 Gt of carbon already present in the atmosphere as CO_2, it would seem that the CO_2 content of the atmosphere should, at the present time, simply increase by 0.76% per year. With a typical atmospheric CO_2 concentration of 335 p.p.m., it might be expected that the concentration of atmospheric CO_2 should increase by 2.5 p.p.m. per year.

However, C. D. Keeling (Scripps Institution of Oceanography) presented measurements of atmospheric CO_2 concentrations made since 1958 using a non-dispersive IR absorption spectrometer at Mauna Loa Observatory, Hawaii, at 20°N. Each point in Fig. 1 is a weekly average; the annual variation is explained by seasonal changes of the rates of photosynthesis and respiration by plants and the soil. Last year, the 340 p.p.m. value was exceeded for the first time. Also evident in the figure is the long-term, quasi-exponential increase of CO_2 concentration, at a rate of 1.3 p.p.m. per year, or 0.40% per year. Thus only 53% of the increased CO_2 is retained in the atmosphere; this is termed the airborne fraction. The remaining 47%, or excess fraction, is taken up mainly by the oceans at middle and high latitudes. Quantitative studies of the air–sea interaction are difficult; comparisons between modelled and observed results are complicated by the fact that the time scales of oceanic CO_2 uptake are between 10 and 100 years (at lesser to greater depths), and are of the same order as the 24 year time constant of the atmospheric CO_2 increase.

Of the CO_2 production, R. M. Rotty showed that 91% occurs at latitudes between 30 and 60°N, primarily over land. This fact accounts, in part, for the CO_2 latitudinal gradient, shown as differences from the Mauna Loa mean in Fig. 2, and derived from measurements made at different observatories and aboard ships and aircraft. Additional factors are the CO_2 source associated with the warm sea surface in equatorial regions and the relatively slow interhemispheric mixing of atmospheric CO_2 across the Inter-Tropical Convergence Zone. CO_2 concentration differences of 1 p.p.m. can be accounted for by the interhemispheric CO_2 fluxes of

Michael J. Rycroft is Head of the Atmospheric Sciences Division of the British Antarctic Survey (Natural Environment Research Council), High Cross, Madingley Road, Cambridge, CB3 0ET.

---

* The joint World Meterological Organization, International Council for Scientific Unions and United Nations Environment Programme sponsored conference on 'Analysis and Interpretation of Atmospheric CO2 Data' was held at the University of Bern, Switzerland, from 14 to 18 September 1981, with support from the International Association of Meteorology and Atmospheric Physics and the US Department of Energy, and was attended by seventy scientists from twenty countries. A book containing abstracts and some papers has been published by the WMO; it is planned that the complete set of papers presented at the conference will be published in the *Journal of Geophysical Research*.

1. Bach, W., Pankrath, J. & Williams, J. (eds) *Interactions of Energy and Climate* (Reidel, Dordrecht, 1980).
2. Kellogg, W.W. & Schware, R. *Climate Change and Society* (Westview Press, Boulder, Colorado, 1981).
3. Kandel, R.S. *Nature* **293**, 634 (1981).
4. Manabe, S. & Wetherald, R.T. *J. atmos. Sci.* **32**, 3 (1975).
5. Hansen, J. *et al. Science* **213**, 957 (1981).
6. Lacis, A., Hansen, J., Lee, P., Mitchell, T. & Lebedeff, S. *Geophys. Res. Lett.* **8**, 1035 (1981).
7. Manabe, S. & Stouffer, R.J. *J. geophys. Res.* **85**, 5529 (1980).
8. Manabe, S. & Wetherald, R.T. *J. atmos. Sci.* **37**, 99 (1980).
9. Mitchell, C.S., Potter, G.L., Ellsaesser, H.W. & Walton, J.J. *J. atmos. Sci.* **38**, 1906 (1981).
10. Ramanathan, V., Lian, M.S. & Cess, R.D. *J. geophys. Res.* **84**, 4949 (1979).
11. Schiff, H.I. *Planet. Space Sci.* **29**, 935 (1981).
12. Kukla, G. & Gavin, J. *Science* **214**, 497 (1981).
13. Mercer, J.H. *Nature* **271**, 321 (1978).
14. Weertman, J. & Peel, D.A. *Nature* **294**, 210 (1981).
15. Thomas, R.H. Sanderson, T.J.O. & Rose, K.E. *Nature* **277**, 355 (1979).
16. Oerlemans, J. *Nature* **290**, 770 (1981).
17. Bolin, B. (ed.) *Carbon Cycle Modelling* SCOPE Rep. 16 (Wiley, Chichester, England, 1981)
18. Bolin, B. *Nature* **293**, 434 (1981).
19. Thompson, S.L. & Schneider, S.H. *Nature* **290**, 1 (1981).
20. Keeling, C.D., Mook, W.G. & Tans, P.P. *Nature* **277**, 121 (1979).

0028-0836/82/030190-02$01.00

about 1 Gt per year

The largest annual variations of CO_2 concentration, with a difference of 15 p p m between maximum and minimum values, occur between 50 and 70°N, there being a 6 p p m difference at Mauna Loa and no annual variation between 10 and 20°S There is also some evidence of two and four year periodicities R B Bacastow and C D Keeling (Scripps Institution of Oceanography) have associated large increases in the CO_2 concentration with a minimum value of the Index of the Southern Oscillation of the atmosphere and with El Nino occurrences These latter events — the presence of 2 deg warmer, nutrient-poor water in a region off the Peruvian coast at 80°W and out to 180°W, which is associated with a reduction, or even cessation, of the upwelling of colder, nutrient-rich water — are of great significance to the region's fishermen

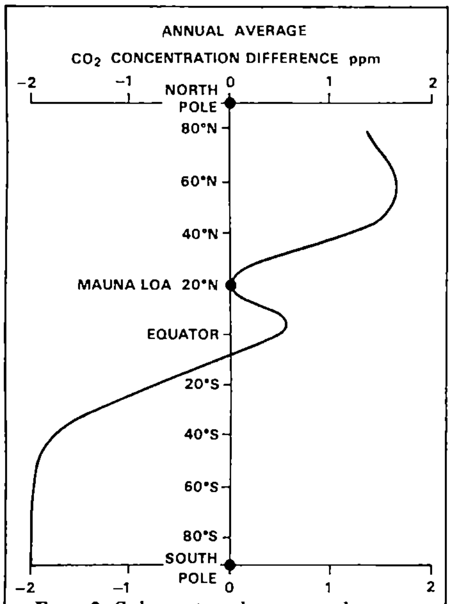

Fig 2 Schematic diagram showing latitudinal differences of annual mean atmospheric CO_2 concentrations from the annual mean value at Mauna Loa, based on observations reported at the 1981 Bern conference by P Hyson and G I Pearman (CSIRO, Australia), C D Keeling (Scripps Institution of Oceanography) and W D Komhyr (NOAA, Boulder, Colorado)

Evidence for slight decreases in the atmospheric $^{13}C/^{12}C$ ratio has been obtained from mass spectrometer analyses[20] Both $^{13}C/^{12}C$ and $^{14}C/^{12}C$ ratios in the cellulose of tree rings similarly reflect the ratios' atmospheric values during successive year's growing seasons It is concluded that biospheric processes, both soil and plant, acted as a net source of atmospheric CO_2 from 1860 until about 1950, since then, biospheric sources and sinks of CO_2 have cancelled each other out For example, the present deforestation in the tropics could be balanced by reforestation at middle latitudes Also, ^{14}C in corals gives information on CO_2 uptake by the surface water of the oceans and on surface water circulation Of course, the radiocarbon concentrations of the atmosphere and ocean have risen considerably since the thermonuclear bomb tests of the 1950s

To identify new trends, continuing and uninterrupted measurements of atmospheric CO_2 concentrations are required at up to 20 well distributed sites around the globe The required absolute accuracy is ±0 1 p p m , this is achievable only by performing very careful intercalibrations, using standard gases, between the different experimental groups Further, there is a pressing need for additional observational studies of seasonal and annual variations of atmospheric CO_2 at particularly interesting sites Such observations, required to a relative accuracy of ±0 1 p p m , can be interpreted in terms of sources and sinks of CO_2, and should lead to an improved understanding of the carbon budget With improved observational knowledge, and with the further development and validation of climate models, better predictions may then be made of the environment in which mankind will find itself in the coming decades and centuries □

Mammary gland as an endocrine organ: implications for mastectomy

from Jared M Diamond

THE traditional view of the mammary gland is that it receives many hormonal signals but sends none Oxytocin acts on it to trigger milk ejection, prolactin to stimulate milk secretion, and oestrogens, progesterone, prolactin and growth hormone to stimulate gland growth during pregnancy The only direct signals that the mammary gland sends to the rest of the body have been thought to be concerned with its own regulation — nerve impulses (the suckling reflex) cause prolactin and oxytocin release from the pituitary and reflexly control milk production This traditional view has determined the assessment of the costs and benefits of mastectomy, an operation that has often been used to deal with mammary tumours Although mastectomy has been increasingly criticized for its psychological consequences, it has at least been thought that the operation is without physiological consequences since the mammary gland has no role outside of lactation

This dogma has been undermined by important recent studies[1-4] of Peaker (Hannah Research Institute, Ayr) and Maule Walker (ARC Institute of Animal Physiology, Babraham), demonstrating that, in goats, the mammary gland releases hormones into the general circulation and mastectomy causes major disturbances of other reproductive functions besides lactation These observations clearly indicate the need for the study of possible physiological consequences of mastectomy in humans

The roots of the new observations go back at least 75 years In 1906 Marshall and Kirkness[5], studying urinary sugars in mastectomized guinea pigs, briefly commented "Considerable difficulty was experienced in inducing the guinea pigs to breed after the removal of the [mammary] glands, some of them failing to do so although kept for over eight months in company with males, and in an apparently perfectly healthy condition" Four of these mastectomized guinea pigs did eventually become pregnant, resulting in one premature still-birth, one abortion and four normal births In the late 1950s Linzell worked out procedures for autotransplanting mammary glands of goats, and in the following 20 years he used the improved experimental access provided by this preparation to answer many problems of mammary physiology Early in these studies he noted[6], in the course of a long paper on milk secretion, that loss of mammary tissue in goats was associated with increased incidence of several reproductive disorders infertility, mastitis, abortion and maternal death at parturition Peaker and Maule Walker have now followed up these observations by studying mastectomized goats, four of which have been followed through three pregnancies The reproductive consequences of mastectomy in the first breeding season were a lengthened first oestrus (115 h vs 30 h in controls), shortened oestrous cycles (8–17 days vs 22–24 days in controls), reduced fertility and slightly shortened pregnancy In the second pregnancy, and even more in the third pregnancy, there was peripheral oedema before term, premature onset of labour and prolonged labour with weak cervical contractions and no cervical dilation

How does removal of the mammary gland lead to these reproductive disturbances? Several possible mechanisms involve disruption of lactation, which is known to have systemic effects Nerve impulses from the mammary gland to brain during lactation stimulate reflex release of pituitary hormones that control not only milk production in mammals generally but also embryonic development in

---

Jared M Diamond is Professor of Physiology at the University of California Medical School, Los Angeles, California 90024

0028-0836/82/030191-02$01 00

marsupials[7] Lactational amenorrhoea may similarly involve mammary reflex control of pituitary hormones, in this case inhibition of follicle-stimulating hormone and luteinizing hormone release Withdrawal of large quantities of glucose and other substrates for milk synthesis from the bloodstream leads to changes in levels of hormones that regulate blood concentration of these solutes, such as insulin and glucagon

However, Peaker and Maule Walker observed no difference between lactating and non-lactating non-mastectomized goats in fertility or in oestrous cycle periodicity Furthermore, the mastectomized goats exhibited oestrous disorders and impaired fertility before they had ever become pregnant or lactated These facts suggest that interruption of lactation is not responsible for the reproductive disorders associated with mastectomy A more likely explanation comes from new evidence that non-lactating mammary gland releases hormones into the systemic circulation, in addition to producing local hormones such as prostaglandins during lactation From earlier observations by Linzell and colleagues[8-10] that the mammary gland of goat can metabolize steroid hormones, Maule Walker and Peaker[1] have gone on to find that the rise in plasma concentration of oestradiol-17β during the last four days before term is due almost entirely to increased production of the hormone by mammary gland

It remains to be seen whether reproductive disorders in mastectomized goats are related to this mammary production of oestradiol-17β, or of other known steroid, peptide, or protein hormones, or of 'new hormones', or else to a non-hormonal mammary signal The great variability among mammals in the control of reproduction suggests that the goat is not necessarily a universal model and studies on other mammalian species, especially on humans, are now urgently needed ☐

---

1 Maule Walker & Peaker *J Physiol , Lond* **284,** 71 (1978)
2 Peaker & Maule Walker *Nature* **284,** 165 (1980)
3 Maule Walker & Peaker *J Physiol , Lond* **312,** 63 (1980)
4 Peaker in *Hormones and Metabolism in Ruminants* (eds Forbes & Lomax) 122 (Agricultural Research Council, London, 1981)
5 Marshall & Kirkness *Biochem J* **2,** 1 (1907)
6 Linzell *Q Jl exp Physiol* **48,** 34 (1963)
7 Renfree *Nature* **278,** 549 (1979)
8 Slotkin *et al Nature* **225,** 385 (1970)
9 Challis & Linzell *J Endocr* **57,** 451 (1973)
10 Heap *et al J Endocr* **64,** 485 (1975)

Exciting Rydberg atoms in cavities

from Peter Knight

HIGHLY excited atoms with one electron orbiting at large distances from an unexcited core are termed Rydberg atoms and have remarkable properties Their size gives them a large polarizability, and they are easy to ionize in weak electric fields If they possess a large angular momentum they do not return rapidly to their ground state by radiative decay simply because decay photons cannot easily carry away all that excess angular momentum Rydberg atoms provide a unique vehicle for studying radiative processes over long times In mid 1981, Kleppner (*Phys Rev Lett* **47,** 233, 1981) proposed using such atoms to study the effects of cavity mode confinement in partially 'freezing out' spontaneous decay rates (*Nature* **293,** 514, 1981) A recent experiment by Vaidyanathan, Spencer and Kleppner (*Phys Rev Lett* **47,** 1592, 1981) reports the observation of such waveguide effects, not on spontaneous transitions but on transitions induced in the Rydberg atoms by thermal blackbody radiation

Rydberg atoms have been used before as detectors of far-IR and microwave blackbody radiation (*Nature* **279,** 476, 1979) but only in effectively unbounded space Kleppner's new experiment reports a sudden increase in the induced lifetime of a Rydberg atomic transition between two conducting plates when the resonant wavelength is increased beyond the waveguide cut-off (twice the plate separation *d*) The conducting plates are unable to support field modes of wavelength less than 2*d* in the direction normal to the plates In addition, those modes parallel to the plates have their density altered but not turned off Thermal radiation can only be supported on these modes so that transitions induced by blackbody radiation inside the plates are sensitive to the confining geometry

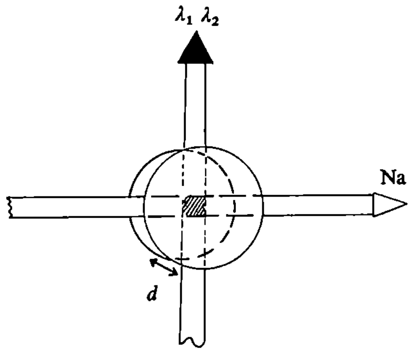

Fig 1 Schematic outline of experiment in which a sodium atomic beam is excited by lasers of wavelength λ_1, λ_2 to the 29d state between two conducting plates

The technique used to observe these waveguide effects by Kleppner and his group is particularly ingenious and is outlined schematically in Fig 1 The sodium 29d Rydberg state is populated by stepwise absorption from two pulsed lasers of wavelengths λ_1 and λ_2 which drive the transitions 3s to 3p to 29d in an atomic beam travelling between two conducting plates separated by 1/3 cm The whole apparatus is placed in a shielded box at 180K so that the photon occupation number at wavelength $\lambda \sim 2d$ is approximately 86 All polarizations in the transition are possible The transition 29d to 30p at a wavelength of 2/3 cm ($\sim 2d$) is chosen for study and is excited by the thermal field at a rate of 300 per second Transitions to other levels at $\lambda \neq 2d$ are of course also induced and contribute to a *d*-insensitive background

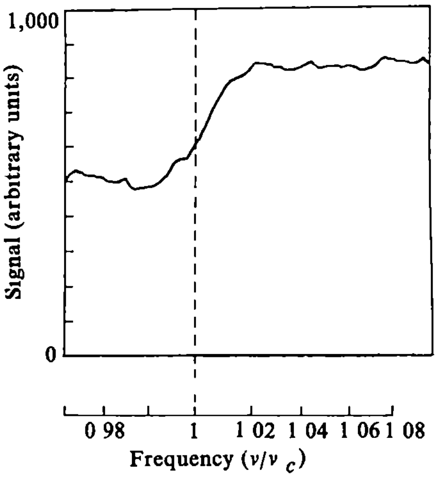

Fig.2 Blackbody radiative transfer signals 29d–30p in sodium between parallel conducting plates as the transition frequency ν is Stark tuned through the cut-off frequency $\nu_c = c/2d$ (from Vaidyanathan *et al*)

The plate separation is kept fixed but the transition wavelength is varied by exploiting the large polarizability of Rydberg states to Stark-shift energy levels in a small d c voltage across the plates The cut-off frequency $\nu_c = c/2d$ is 1 48 cm^{-1} As the electric field across the plates is varied from 0 7 to 5 7 V cm^{-1}, the transition frequency varies from 0 97 ν_c to 1 11 ν_c The transition rate for the production of 30p atoms is measured by selectively ionizing only those 30p atoms making the transition, and counting the ions As the transition frequency ν approaches the waveguide cutoff frequency ν_c, the rate of transition suddenly changes (Fig 2) on the right-hand side, blackbody photons can fit between the plates, and on the left-hand side they cannot, decreasing the 30p production rate As ν increases beyond ν_c, the modes normal to the plate surface are switched on The Einstein relationships between stimulated and spontaneous transition rates imply that spontaneous decay was similarly affected in this experiment The experiment of Vaidyanathan *et al* is a beautiful example of how Rydberg atoms are sensitive to their immediate environment, making them the perfect testbed for what would otherwise be minute and unmeasurable effects ☐

Peter Knight is in the Optics Section, The Blackett Laboratory, Imperial College, Prince Consort Road, London SW7 2BZ

0028-0836/82/030192 01$01 00

ARTICLES

A seasonal signal in ocean currents to abyssal depths

R. R. Dickson*, W. J. Gould†, P. A. Gurbutt* & P. D. Killworth‡

* Ministry of Agriculture Fisheries and Food, Directorate of Fisheries Research, Fisheries Laboratory, Lowestoft, Suffolk NR33 0HT, UK
† Institute of Oceanographic Sciences, Wormley, Godalming, Surrey GU8 5UB, UK
‡ University of Cambridge, Department of Applied Mathematics and Theoretical Physics, Silver Street, Cambridge CB3 9EW, UK

Long-term (9–32 month) current meter records from the eastern North Atlantic (41° N–59° N) suggest that, remote from the influence of the Western Boundary Current, eddy kinetic energy (K_E) at all depths is principally a function of wind stress and stratification, generated during the winter and early spring, propagating to abyssal depths and decaying to a minimum in late summer. Although this seasonal variation in K_E has not previously been described from the midlatitude ocean, some theoretical basis for it is presented

IN their analysis of long-term (644 days) current meter records from the northern Rockall Trough (IOS Mooring I4, 58°50′ N 11°40′ W, Fig 1), Gould and Cutler[1] report a well-defined seasonal signal in eddy kinetic energy estimated at depths of 200, 1,000 and 1,500 m in 1,800 m water depth Each record was first low-pass filtered using a gaussian filter similar to that described by Schmitz[2] with a high frequency cutoff around 0 5 cycles per day (c p d) Finding clear evidence of energetic winter fluctuations in the filtered time series, see for example, Fig 2*a*, each record was then divided into 60-day pieces each overlapping by half their length, and for each piece the eddy kinetic energy (K_E) over a selected band of periods (2 92–40 days) was estimated using spectral analysis techniques similar to those defined by Schmitz and Hogg[3] From this the seasonal nature of the fluctuations is obvious (Fig 2*b*)

We extend this analysis to a widely-scattered range of sites in the eastern North Atlantic and to water depths >4,700 m using long-term (9–32 month) records obtained by the Ministry of

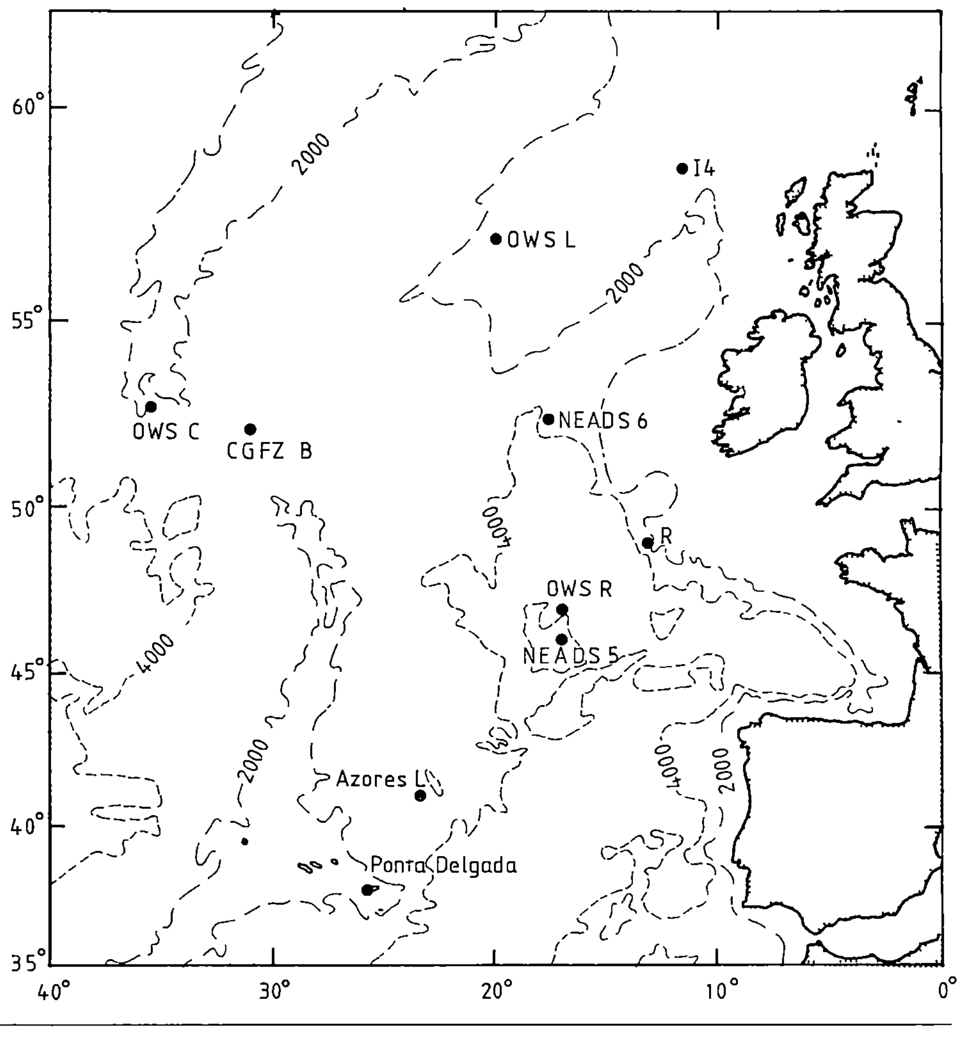

Fig. 1 Location of six current-meter moorings and three Ocean Weather Stations The 2,000-m and 4,000-m isobaths are also shown

Agriculture, Fisheries and Food (MAFF), Fisheries Laboratory, Lowestoft and the Institute of Oceanographic Sciences (IOS), Wormley The 60-day piece-length and low-pass filtering techniques are standard throughout, however, the period bands used vary, to accommodate records of different spectral characteristics and because of differences in the spectral analysis procedures at the two laboratories By the Blackman–Tukey method[4] (MAFF) spectral estimates are derived for frequencies which are fractions of the number of lags ($L = 20$ throughout) while the FFT method[5] (IOS) obtains estimates at frequencies corresponding to fractions of the length of record ($t = 60$ days) Thus generally,

$$K_E(\nu_1\nu_2) = \Delta \sum_{\nu_1}^{\nu_2} K_E(\nu)$$

where $K_E(\nu_1\nu_2)$ is the fluctuation (eddy) kinetic energy between frequencies ν_1 and ν_2, and Δ is the bandwidth of the spectrum ($1/2L$ or $1/t$ according to method) In practice, K_E estimates are reported below for two bands of periods, K_E(3–27) covering periods from 3 to 26 7 days and K_E(3–80) covering those from 3 to 80 days Where the earlier results of Gould and Cutler are described, K_E(3–40) denotes periods from 2 92 to 40 days K_E(Rec) denotes the total kinetic energy per unit mass associated with the entire range of 'eddy' frequencies accessible in the full low-passed record ($\nu = 1/2t$ to 1/2 c p d], that is $K_E(\text{Rec}) = 1/2[\text{var } u + \text{var } v]$, where var u and var v are the variances of the east and north velocity components respectively

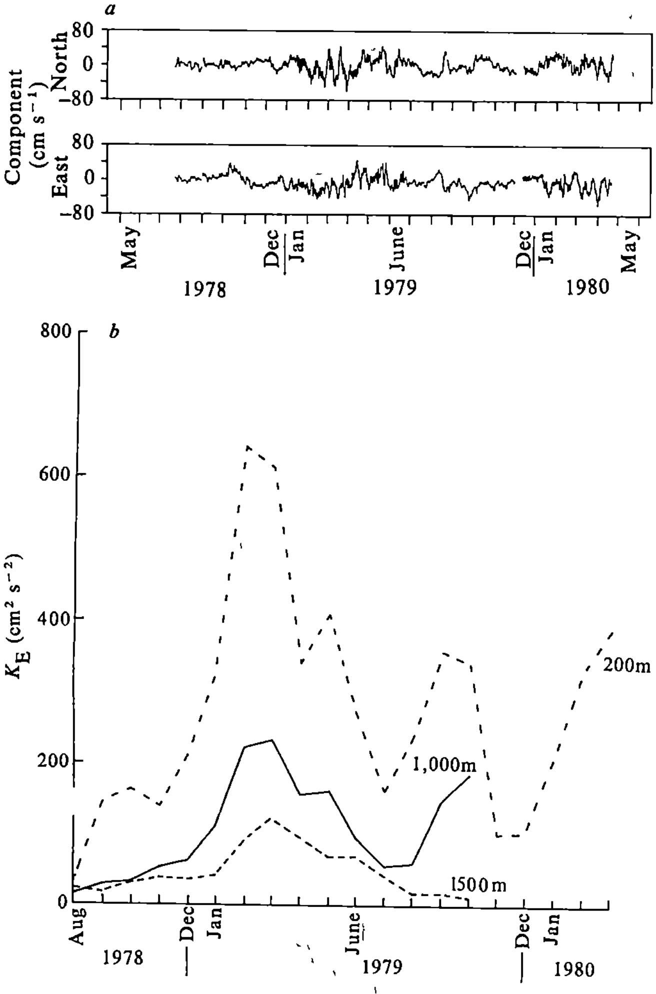

Fig. 2 *a*, Low-pass filtered time-series of north and east current components at Mooring I4 (Rockall Trough, 58°50′ N 11°40′ W), 200 m depth, July 1978–April 1980 *b*, Estimates of eddy kinetic energy in the period band 3–40 days [K_E(3–40)] at 200-, 1,000- and 1,500-m depth, Mooring I4 (Rockall Trough) Individual estimates are for 60-day pieces of record, each overlapping by half their length

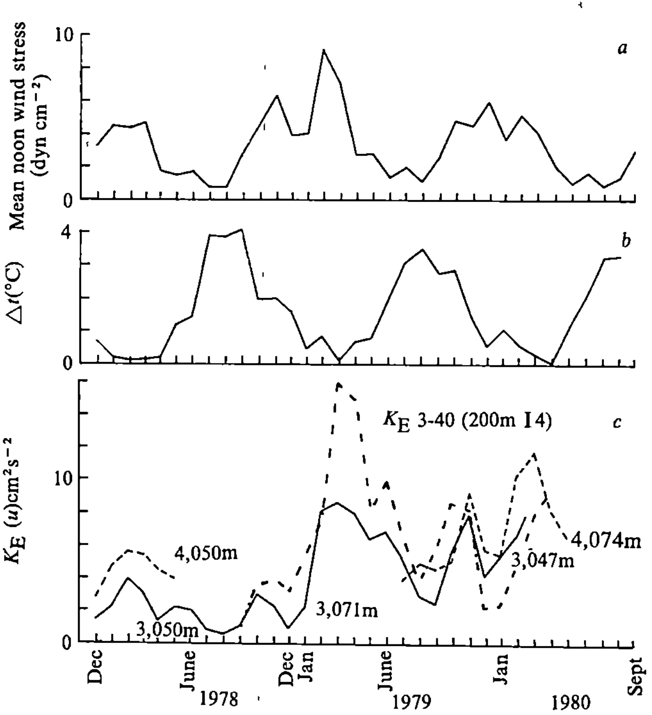

Fig. 3 *a*, Mean noon wind stress at OWS LIMA [57° N 20° W], December 1978–September 1980 *b*, 0–450 m temperature difference at OWS LIMA, from XBT observations *c*, Time-variation of eddy kinetic energy [K_E(3–27)] in the east-west current component at 3,050-m (——) and 4,050 m-depth (– – –), NEADS-6 mooring [52°30′ N 17°45′ W] The 200-m curve of K_E(3–40) from Mooring I4 (Rockall Trough) has been superimposed with a 1-month lag (- - -) to show the close correlation and the apparent 1-month delay in the deep water

Seasonal signal in eddy kinetic energy

The records from the Rockall Trough (Fig 2*b*) appeared to show three characteristics, apart from the obvious seasonality of K_E(3–40) First, the amplitude of the seasonal peak is markedly depth dependent, varying from ~640 cm^2 s^{-2} at 200 m to ~120 cm^2 s^{-2} at 1,500 m Second, the curves seem to lag in time with increasing depth, from 200 m to 1,500 m for example the primary winter peak is delayed by ~1 month Third, there are signs that the main winter peak centred on February–March is preceded by a secondary peak of smaller amplitude in September–October at the time of the equinoctial gales (but before the complete eradication of the seasonal thermocline)

Figure 3 extends this analysis to greater depths using the multiyear records from the NEADS-6 site [52°30′ N 17°45′ W, North-east Atlantic Dynamics Study] on the continental rise at the mouth of the Rockall Trough (see Fig 1) This mooring has been operated continuously by MAFF since October 1977 From 60 day overlapping pieces of the low-passed records, Fig 3*c* illustrates the time-variation of eddy kinetic energy [(K_E(3–27)] in the east–west (along isobath) current component for the 830 day record at 3,050 m and for the discontinuous 602 day record at 4,050 m Water depth is ~4,100 m On the same time-base, Fig 3 *a* describes the mean noon wind stress for each month at OWS LIMA [57° N 20° W] calculated using a quadratic wind stress law with variable drag coefficient as defined by Heaps[6], and Fig 3*b* shows the 0–450 m temperature difference at LIMA from XBT observations

Figure 3 confirms many of the features found in the Rockall Trough, though in this case at abyssal depths roughly coincident with the winter windstress peak and with the eradication of the seasonal thermocline, there is evidence for a February–March peak in the *u* contribution to K_E(3–27) in each of the 3 years, preceded by a lesser peak in October–November (at the time of the equinoctial gales but when some residual stratification remains in the upper water column)

Figure 3 also gives some indication as to the scale of the forcing and on the phase lag with depth In Fig 3*c* the 200 m curve of $K_E(3\text{–}40)$ at I4 (Rockall Trough) has been superimposed on the NEADS-6 time series with a 1-month lag to show both the close correlation and the apparent 1 month delay in the deep water Despite a horizontal separation of >800 km between I4 and NEADS-6, the correlation is sufficiently close between the 200 m (I4) and 3,050 m (NEADS-6) records at 1-month lag to suggest a common broad-scale forcing (over the 19-month overlap period $r = 0\ 76$ though with independent estimates only every 2 months) Note that although the I4 mooring had its main buoyancy close to the surface (150 m), the tidal constituents of the records are constant from season to season, suggesting that the records are free from wave-induced contamination[7] In the case of the NEADS-6 mooring there is no possibility that the observed variation in 'eddy' energy could be due to wave action or to mooring motion arising from it as the uppermost part of the mooring lay at 3,000 m depth throughout the 32-month period of record (The same is true for all other MAFF moorings described below, whose main subsurface buoyancy varied from 1,000 to 4,000 m depth) Depth-modified Aanderaa RCM-4 instruments were used throughout

The 3,050 m time-series in Fig 3*c* was used to investigate the spectral composition of the additional 'winter' eddy kinetic energy The 343 day series from the second deployment at this depth was halved to provide two records of 172 day representing the quiescent 'summer' half year (1 July 1978–19 December 1978) and the energetic 'winter' half year (19 December 1978–8 June 1979) Figure 4*a* shows the winter minus summer spectral energy density for both the u and v spectra At the lowest and highest frequencies of the spectrum there is little difference in energy between summer and winter, but each component shows a sharp winter excess of energy at (different) intermediate frequencies The winter excess in the u (along isobath) component is of greater amplitude and peaks at a longer period (25 days) than the v component (12 5 days) in this particular pair of half-years It is also the more conservative in time Of the three possible (overlapping) adjacent pairs of winter–summer periods in the 3,050 m record, and in the single (discontinuous) winter–summer pairing of the 4,050 m record, the winter excess of eddy energy peaked at 33, 25, 25 and 25 days respectively in the u component while the corresponding peaks in the v component were much more variable and ill-defined (except for the pairing shown in Fig 4*a*)

Figure 5 examines records from four additional sites between January 1977 and May 1980 to test whether the seasonal signal in eddy energy is restricted merely to the Rockall area or is a more widespread and general characteristic of the eastern North Atlantic In most cases, estimates of $K_E(3\text{–}27)$ and $K_E(3\text{–}80)$ are superimposed Locations of the moorings and of the three Ocean Weather Stations discussed are shown in Fig 1

Figure 5 *a–e* displays results from the NEADS-5 site at ~46° N 17° W, in the foothills of the Mid Atlantic Ridge close to its junction with the Porcupine Abyssal Plain Figure 5*a*, *b* shows IOS records (452 and 425 days respectively) from 600 and 3,000 m depth, while Fig 5*c–e* (the deepest records discussed here) is from a later 1-yr reoccupation of the site by MAFF Of Fig 5*f–i* (all MAFF) Fig 5*f*, *g* shows 253 day records at 2,977 and 3,977 m depth from the lower north wall of the Charlie Gibbs Fracture Zone, Southern Trench, at 52°09′ N 31°00′ W[8], Fig 5*h* is a 340 day record from 4,046 m depth on the hilly eastern flanks of the Mid Atlantic Ridge, north-east of the Azores [41°00′ N 23°18′ W] and Fig 5*i* is a 1-yr record at 2,049 m depth from the European Continental Slope (48°59′ N 12°53′ W)

Coupling these results with the earlier discussion of I4 and NEADS-6 we find

(1) At all six sites, ranging in latitude from 41° N to 59° N, ranging in sampling depth from 200 to 4,710 m and with records ranging in total eddy kinetic energy [K_E(Rec)] from the highest values yet encountered in the eastern basin [$K_E(\text{Rec}) = 196\ \text{cm}^2\,\text{s}^{-2}$ at 200 m, I4] to very nearly the lowest [K_E(Rec) =

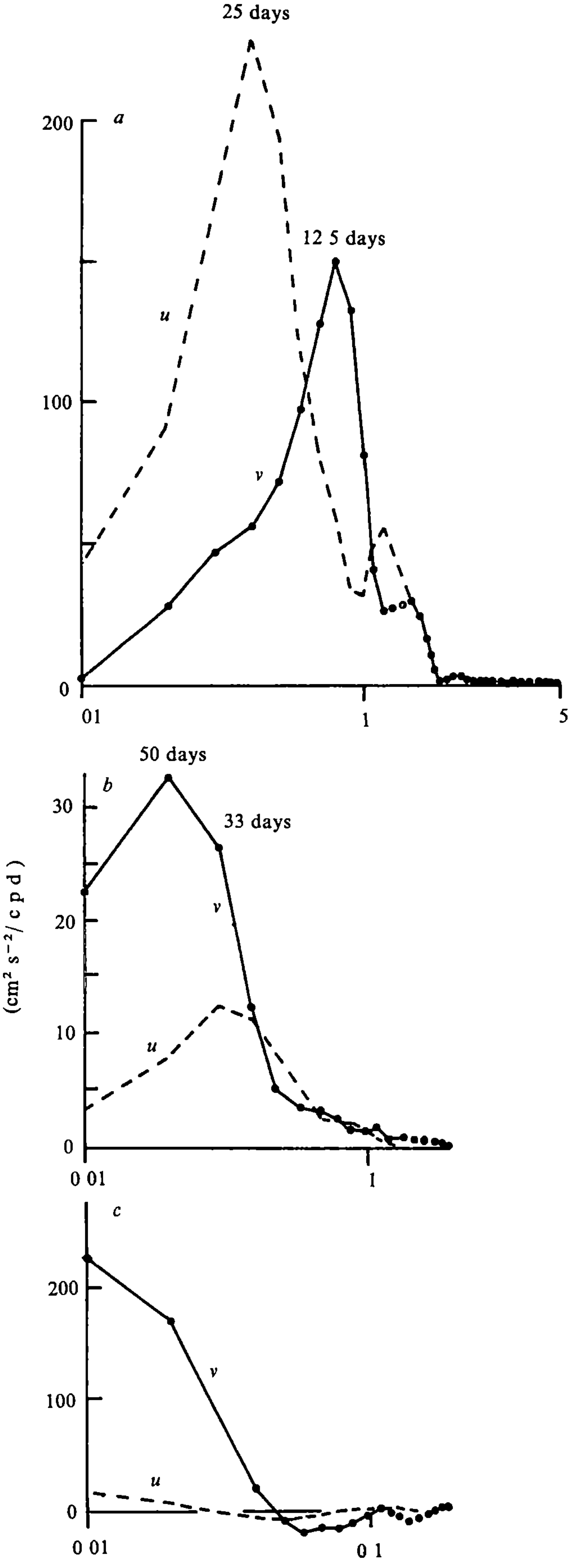

Fig. 4 Winter minus summer spectral energy density for both the zonal (u) and meridional (v) current components at *a*, 3,050-m depth NEADS-6 (52°30′ N 17°45′ W), *b*, 4,050 m depth, NEADS-5 (46° N 17° W), *c*, 2,049-m depth, mooring R (48°59′ N, 12°53′ W, European continental slope)

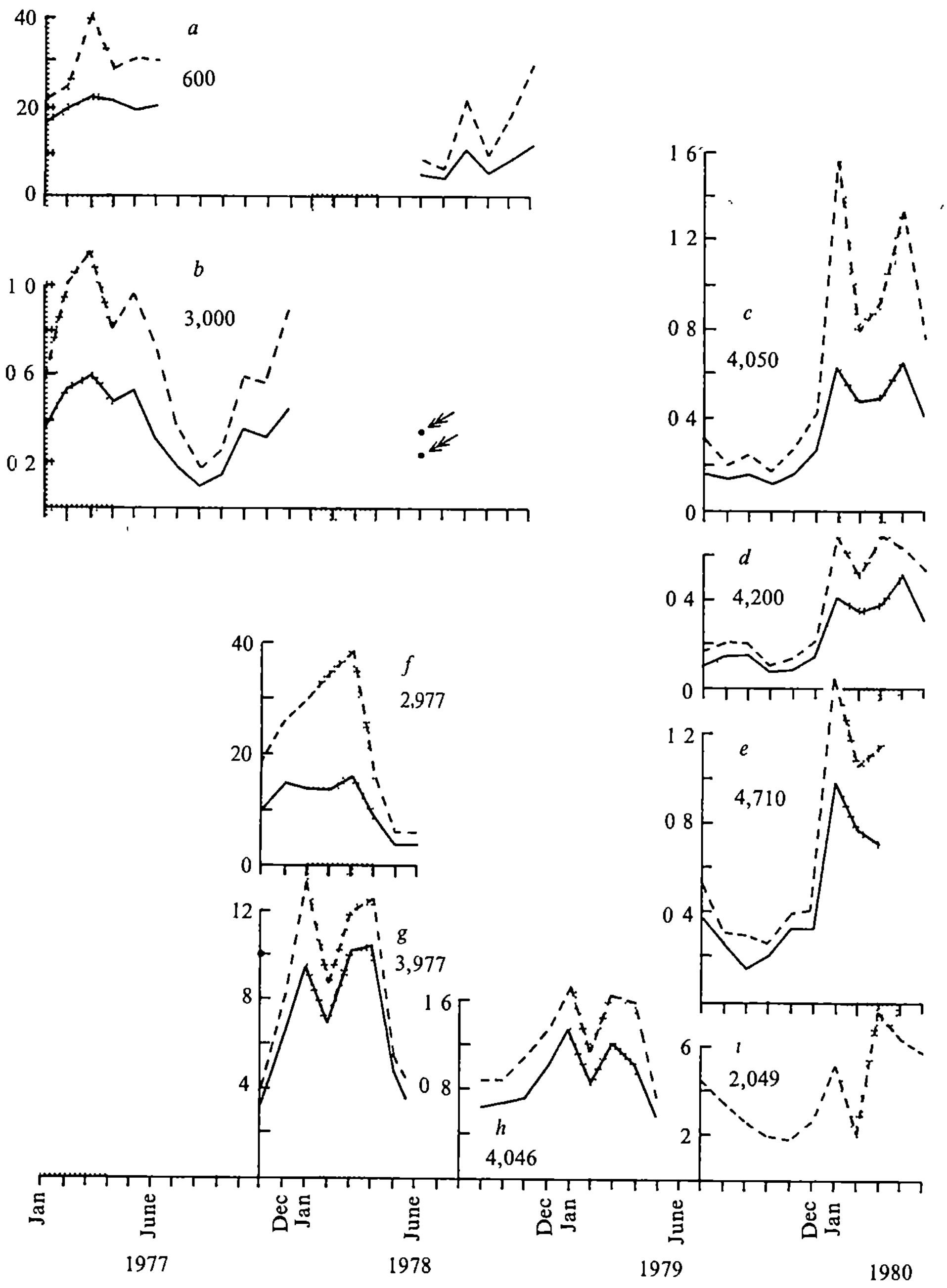

Fig. 5 Time series of eddy kinetic energy estimates in the period bands 3–27 days (——) and 3–80 days (– – –) at *a*, 600-m depth, NEADS-5 [46° N 17° W], *b*, 3,000-m depth, NEADS-5, *c*, 4,050-m depth, NEADS-5, *d*, 4,200-m depth, NEADS-5, *e*, 4,710-m depth, NEADS-5, *f*, 2,977-m depth, mooring B, Charlie–Gibbs Fracture Zone, southern trench [52°09′ N 31°00′ W], *g*, 3,977-m depth, mooring B, Charlie–Gibbs Fracture Zone, southern trench, *h*, 4,046-m depth, mooring L, Azores Array [41°00′ N 23°18′ W], *i*, 2,049-m depth, mooring R, European continental slope [48°59′ N 12°53′ W]

0 6 at 4,200 m, NEADS-5 (ref 9)], there is a clearly-defined seasonal variation in K_E(3–27) or K_E(3–80)

(2) All these sites are characterized by some degree of bottom slope, with either gently-sloping, hilly or abrupt topography Conversely (though not shown here), no clear seasonal variation in K_E could be detected at sites on the flat abyssal plains, for example, at MAFF sites N, O or P on the Porcupine Abyssal Plain[9] (within the NEADS-6–NEADS-5–R triangle) or at the NEADS-3 site on the Iberian Abyssal Plain (42° N 14° W)

(3) The dominant period of the 'excess' winter energy has been examined for four records only (two at NEADS-6) but seems to be highly variable between sites The 25-day and 12 5-day dominant peaks of excess winter energy in the u and v spectra at NEADS-6 (3,050 m) have already been described (Fig 4*a*) At 4,050-m depth on the NEADS-5 site the corresponding peaks are at 33 days and 50 days (Fig 4*b*) while at 2,049 m at mooring 'R' the excess winter energy is still increasing at the longest periods of the spectrum ($\geq$100 days, Fig 4*c*)

(4) In each case the dominant winter excess of energy occurs in the along-isobath component (u for NEADS-6, v for NEADS-5 and 'R') and although any association with topography may be coincidental the dominance of one component over the other appears least on the gentle slope of the continental rise (Fig 4*a*) and greatest on the steep continental slope In the latter case the winter excess of energy is almost solely in the along-slope component (Fig 4*c*)

(5) The apparent ~1-month phase-lag between the time variations of K_E in the upper layer and the deep water is supported in Fig 5, provided that the supposed link with wind stress is a valid (causal) one During July 1979–May 1980 deep current measurements to 4,710-m depth at NEADS-5 can be matched with wind stress at the neighbouring OWS ROMEO site (see Fig 1) At OWS ROMEO the winter wind stress peaked sharply in December 1979, 1 month before the K_E at depth rose to its winter maximum (Fig 5*c*–*e*)

(6) The supposed link between eddy kinetic energy and wind stress is given some credence by the general 'shape' of the curves in Fig 5 At all sites, depths and sampling periods shown, the time variation of K_E is surprisingly similar, following a broad summer minimum centred on September, the subsequent winter peak from January to April is characteristically bimodal, interrupted by a secondary minimum in February Curves of monthly mean noon windstress for the relevant years at OWS CHARLIE, LIMA and ROMEO and at Ponta Delgada, Azores (Fig 6) show that this midwinter 'dip' is also a characteristic feature of the windstress field in January/February

(7) To obtain some estimate of the seasonal contribution to the total kinetic energy of the long-term record, 1-yr records from the second deployment at NEADS-6 (3,050 m) and from 4,050 m at NEADS-5 were split into equal ~6-month periods representative of the quiescent summer and energetic winter periods. The total eddy kinetic energy per unit mass of the summer, winter and full-record time series was then calculated. At 3,050 m, NEADS-6, K_E(Rec)summer = 3.72 cm^2 s^{-2}, K_E(Rec) winter = 15.64 cm^2 s^{-2} and K_E(Rec) for the full record = 9.72 cm^2 s^{-2}, for 4,050 m, NEADS-5, the corresponding figures are 0.48, 1.39 and 1.02 cm^2 s^{-2} respectively. Thus the summer:winter eddy energy is in the ratio of 1:4.2 for the NEADS-6 record and 1:2.9 for that at NEADS-5. The corresponding ratios of summer:winter mean wind stress for 6-month periods, 1 month in advance of the current meter data, are 1:2.2 (LIMA) and 1:1.9 (ROMEO).

Theoretical mechanism

From reviews[10,11] of the known properties of linear wave propagation in a rotating stratified ocean we can identify possible driving forces for the seasonally-varying low-frequency oscillations that we have observed. Candidate mechanisms include (1) a response to local and/or remote forcing at the surface by wind and buoyancy effects, (2) instabilities and/or eddy-shedding over topography in a seasonally-varying mean flow, (3) instabilities of large-scale wave motions (such as planetary waves) driven by surface forcing, (4) propagation from equatorial regions of coastal or Kelvin waves on the eastern boundary which then propagate to the interior either directly as planetary waves or indirectly by following depth (h) or dynamical (f/h) contours as topographic or edge waves ($f = 2\Omega \sin \phi$, where Ω is the Earth's angular rate of rotation and ϕ is the latitude), (5) wave trapping by closed (f/h) contours.

Many of these theoretical mechanisms have been observed in the ocean but mechanism (1) appears be the most relevant in view of the close association with wind stress and stratification in our results. This mechanism was explored using an idealized model[12] which includes a crude representation of stratification, rotation, topography, coastal boundaries and surface wind forcing.

It is important to decide whether the observed waves are likely to be forced or free. The maximum frequency ($\omega_{\max}$) of a free planetary wave is

$$\omega_{\max} = -\tfrac{1}{2}\beta a$$

where β is the northward gradient of the Coriolis parameter and a is the local radius of deformation (that is the distance over which gravitational and rotational forces are balanced). Using baroclinic/barotropic to refer to depth dependent/independent behaviour, we find that for barotropic modes a is ~2,000 km at midlatitudes so that $\omega_{\max}$ corresponds to a period of 3.6 days. Thus barotropic waves could contribute to the observed oscillations but have no vertical dependence and so cannot account for the observed vertical structure. For a first baroclinic mode a is ~30 km and $\omega_{\max}$ corresponds to a minimum period of ~8 months. Thus the oscillations observed at 12–50-day periods cannot be free baroclinic planetary waves (similar calculations for other wave modes are more difficult to make without additional data). Therefore it was assumed that the observed oscillations are not free and we now discuss the forced response to wind. In the present model, the ocean is considered to have two layers of mean depth H_1 and H_2, ($H_1 \ll H_2$) with mean densities ρ_1 and ρ_2 ($\rho_1 < \rho_2$). The stratification is stable but unvarying. Rigid boundaries run north–south but none east-west. Any topography (of height T) is shallower than the lower layer thickness and does not vary north–south. The ocean is driven by an eastward windstress acting on the upper layer such that the response is periodic north–south. A full description of the model is given elsewhere[12].

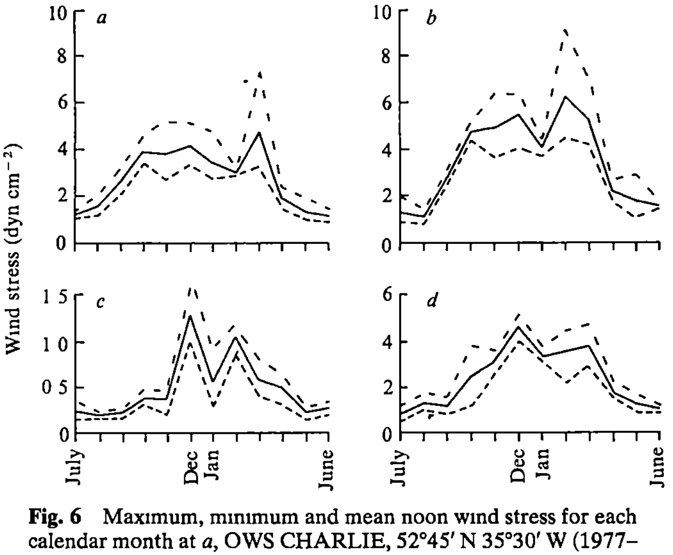

Fig. 6 Maximum, minimum and mean noon wind stress for each calendar month at *a*, OWS CHARLIE, 52°45′ N 35°30′ W (1977–79), *b*, OWS LIMA, 57° N 20° W (1978–80), *c*, Ponta Delgada, Azores (1977–79), *d*, OWS ROMEO, 47° N 17° W (1977–79).

In view of the depth-dependence of the observed oscillations our attention is focused on the equation in ref. 12 describing the baroclinic component of zonal flow. Initial runs using realistic input parameters but flat topography confirm that for the seasonal cycle the planetary wave can propagate, with a rapidly oscillating solution across the basin, but at the (lower) 'eddy' frequencies observed no propagation is possible and $|\hat{u}|$ (the magnitude of the zonal baroclinic component) is small away from the boundaries. The solution is almost purely barotropic as anticipated.

To see if topography orientated north–south can produce a distinct baroclinic signal, the calculation was repeated with topography varying sinusoidally east-west, with amplitude 1,500 m (in an ocean of depth 5,400 m) and wavelength 1,250 km. The results in ref. 12 show that in these circumstances the topographic effect must be unrealistically large to overcome the time-dependence effect and yield a sizeable baroclinic signal. The ratio of the topographic to time-dependent terms is dimensionally $g'Txl(H_1H_2^{-1})^2\omega^{-1}f^{-1}$, where g' is the reduced gravity, $[g(\rho_2-\rho_1)\rho_2^{-1}]$, Tx the topographic slope, and l the north–south wave number of the forcing. For the above parameters, this ratio is about 5×10^{-3}. However, the ratio can easily be increased, by steeper topography, a shorter north–south length scale, or by increasing H_1. All three of these effects are probably relevant in the eastern North Atlantic: the topographical variations can be quite rapid, the confused topography may well induce shorter north–south scales in the oceanic response, and, most encouragingly, the increase in eddy kinetic energy at depth does not occur until a seasonally-strengthening wind stress is accompanied by the breakdown of the seasonal thermocline (that is a rapid increase in H_1). Thus preliminary results from this simple model seem capable of reproducing a baroclinic signal at depth and at the observed eddy frequencies.

Discussion

There are many potential sources of error in the above type of analysis. The spectral analysis techniques are strictly valid only for stationary time series which is not the case in the 60-day pieces of record that were used. The current meter records themselves are relatively short, sparse or discontinuous and rarely provide concurrent full-depth coverage. On the link with wind stress, there is an obvious need for caution in exploring causality between time-series that are dominated by one narrow-band signal such as the seasonal cycle. With one exception, moorings are remote from the Ocean Weather Stations which provide the wind stress data, and although the degree of thermal stratification is thought to be important to the input of eddy energy to the deep ocean, time series of temperature in the upper ocean which define the breakdown and re-establishment of the stratification are very rare.

Nevertheless, the seasonal signal in fluctuation kinetic energy is plainly visible in time series which have been subjected to no more sophisticated processing than the application of a low-pass filter (for example, Fig 2*a*), and where spectral analysis has been used, the seasonal signal in K_E is so consistently shown over a wide range of sites, years and sampling depths as to suggest that it is both real and widespread, not merely an artefact of the analysis We conclude therefore that in the eastern North Atlantic, remote from the influence of the Western Boundary Current, eddy kinetic energy at all depths is principally some function of wind stress and stratification, generated during the winter and early spring, propagating to abyssal depths and decaying to a minimum in late summer If so a similar seasonal signal will probably be found to dominate other records from the eastern midlatitude oceans and may even be detectable within the fields of influence of the western boundary currents or further afield in the equatorial zone (A significant correlation between wind stress and deep ocean currents has recently been observed in the Atlantic North Equatorial Current, east of Barbados, at week to month time scales[13]) Note that the suggested mechanism seems to require some degree of bottom slope, a point which is apparently confirmed in the observations

The above conclusion is not meant to imply that mesoscale eddies as conventionally understood do not exist in the north-east Atlantic Plainly they do, as demonstrated by much direct and indirect evidence[14-16], but equally these random and presumably non-seasonal features are sufficiently sparse (or weak or shallow) to be undetectable against the dominant 'eddy' signal arising from wind stress. To paraphrase the conclusion of Bernstein and White for the north-east Pacific[17], the north-east Atlantic appears to be a 'near void' for mesoscale eddies This is a rather different conclusion to that of Wyrtki *et al*[18] who suggest, from their analysis of ship drift data "that the eddy motion in the ocean is generated in areas of strong mean shear flow and is subsequently distributed over the whole ocean with much less decay than the mean flow". The difference is important, however If the eddy climate of the eastern midlatitude ocean really is more properly described as a function of windstress and stratification than as the synthesis of random mesoscale events, then the problem of its parameterization in general circulation models should be simplified

Received 10 August, accepted 11 November 1981

1 Gould, W J & Cutler, A N *ICES Hydrography Committee*, CM 1980/C 30 (1980)
2 Schmitz, W J Jr *J mar Res* **32**, 233-251 (1974)
3 Schmitz, W J Jr & Hogg, N G *J mar Res* **36**, 725-734 1978)
4 Blackman, R B & Tukey, J W *The Measurement of Power Spectra* (Dover, 1959)
5 Bingham, C, Godfrey, H D & Tukey, J W *IEEE Trans Audio-electroacoust* **AU-15** 56-66 (1967)
6 Heaps, N S *Phil Trans R Soc* **A257**, 351-383 (1965)
7 Gould, W J & Sambuco, E *Deep-Sea Res* **22**, 55-62 (1975)
8 Dickson, R R, Gurbutt, P A & Medler, K J *J mar Res* **38**, 571-583 (1980)
9 Dickson, R R in *Eddies in Marine Science* (ed Robinson, A R) Ch 15 (in the press)
10 Philander, S G H *Rev Geophys Space Phys* **16**, 15-46 (1978)
11 Rhines, P B in *The Sea Ideas and Observations on Progress in the Study of the Seas* Vol 6, (ed Goldberg E D) Ch 7 (Wiley, New York, 1977)
12 Anderson, D L T & Killworth, P D *Deep-Sea Res* **24**, 709-732 (1977)
13 Koblinsky, C J & Niiler, P P *J phys Oceanogr* (submitted)
14 Madelain, F & Kerut, E G *Oceanol Acta* **1**, 159-168 (1978)
15 Dickson, R R & Hughes, D G *Oceanol Acta* **4**, 43-46 (1980)
16 Swallow, J C *Deep-Sea Res Suppl* **16**, 285-296 (1969)
17 Bernstein, R L & White, W B *J phys Oceanogr* **7**, 123-126 (1977)
18 Wyrtki, K, Magaard, L & Hager, J *J geophys Res* **81**, 2641-2646 (1976)

Hydrothermal petroleum in mineralized mounds at the seabed of Guaymas Basin

Bernd R. T. Simoneit*

Institute of Geophysics and Planetary Physics, University of California, Los Angeles, California 90024, USA

Peter F. Lonsdale

Marine Physical Laboratory, Scripps Institution of Oceanography, University of California at San Diego, La Jolla, California 92093, USA

Petroleum has been dredged from an active hydrothermal mound area in the southern rift of Guaymas Basin, Gulf of California This organic matter is composed of gasoline-range aliphatic and aromatic hydrocarbons and predominantly residual polar asphaltic material The aliphatic hydrocarbons of two bitumen samples have very different boiling range and composition Both samples contain polynuclear aromatic hydrocarbons and olefins, which indicate formation at pyrolytic temperatures. The overall compositional data indicate an origin from biological detritus by thermal alteration and rapid quenching by hydrothermal removal, followed by condensation at the seabed.

THE Guaymas Basin is an actively spreading oceanic basin, part of the system of spreading axes and transform faults that extend from the East Pacific Rise to the San Andreas fault system[1,2] The basin is tectonically very active and consists of two rift valleys, the northern and southern troughs, separated by a 20-km transform fault area The sediment blanket accumulates at a high rate (>1 m kyr^{-1}), keeping the basin floor covered, while the ocean plate accretion process occurs by dyke and sill intrusions into the unconsolidated muds[1,3] Both rifts have high conductive heat flow (locally exceeding 1 2 W m^{-2})[4,5]

Petroliferous gasoline-range hydrocarbons were reported in a gravity core from the northern trough and interpreted to be of a thermogenic origin[6] Interstitial gas, bitumen and kerogen analyses of samples from Deep Sea Drilling Project Sites 477 and 481 confirm the alteration of the indigenous organic matter by hydrothermal stress[3,7-10]

The samples discussed here are derived from a deep-tow plus heatflow survey cruise by Scripps Institution of Oceanography in 1980 Numerous hydrothermal mounds rising 20-30 m above the rift floor (water depth ~2,000 m) were mapped in the southern trough (Fig 1) and some had active hydrothermal plumes[11] Photographs showed encrusted mounds and columns covered with tubeworms and other fauna A dredge haul (7D, Fig 1) across a 50 m-wide patch of sinter deposits which form a mound recovered claystones, massive sulphides, barite, talc and other hydrothermal minerals, together with tubeworm specimens Many of the fragments in the dredge were stained with a petroleum-like oil and had a strong odour similar to diesel fuel

Several hand-specimens of these odorous, oil-stained samples were sealed in foil and glass jars, then analysed some months later to determine the nature, composition and source of the petroliferous material One specimen (7D-2B) is a massive sulphide with approximately equal proportions of sphalerite, chalcopyrite and pyrrhotite, and interstitial barite, the others are claystones

---

* Present address School of Oceanography, Oregon State University, Corvallis, Oregon 97331, USA

0028-0836/82/030198—05$01 00

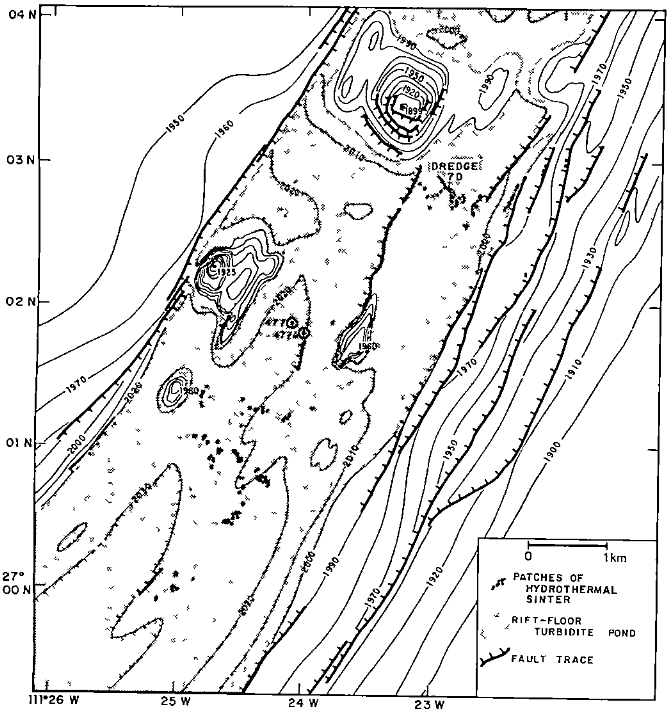

Fig. 1 Location map showing the dredge site (7D) and DSDP Site 477 in the southern rift of Guaymas Basin.

Experimental

Two of the dredge sub-samples (7D-3B and -5A, Fig. 1) were canned under water for analysis of the gasoline-range hydrocarbons as described[6]. A packed column (stainless-steel, 2 m × 2 mm i.d., 0.3% Carbowax 20M on Carbopac C) was used for the analytical gas chromatography (Hewlett–Packard Model 5830A). The injector temperature was at 200 °C and the temperature programme was 30 °C (1 min), 30–225 °C (5 min). The headspace in the cans was 150 cm^3 and the concentrations of the hydrocarbons are reported as ng cm^{-3} of headspace.

Two other dredge sub-samples (7D-2B and -4A, B, Fig. 1) were first extracted as received with methanol and methylene chloride (CH_2Cl_2). The aqueous phase was re-extracted with CH_2Cl_2 and the extracts were combined. The residue was subsequently crushed and extracted further with CH_2Cl_2, which was also combined with the initial extract. The total extracts were concentrated and aliquots were subjected to column chromatography on silica gel (column 1 × 17.5 cm). The samples were separated by elution with hexane (15 ml as F1), hexane/benzene (3:2, 25 ml as F2) and then methanol (20 ml as F3) into the respective fractions, which were analysed by capillary gas chromatography (GC) and gas chromatography–mass spectrometry (GC–MS). The total extracts were also quantified by weighing aliquots of dried extract (or fraction) on a microbalance.

The capillary GC analyses were carried out on a Hewlett–Packard Model 5830 GC with a fused silica capillary column (25 m × 0.20 mm i.d.) wall-coated with SP-2100. The operating conditions were as reported earlier[6]. The GC–MS analyses were conducted on a Finnigan Model 4000 quadrupole mass spectrometer interfaced directly with a Finnigan Model 9620 GC and equipped with a 30 m × 0.25 mm i.d. fused silica capillary column (wall-coated with SE-54). The operating conditions were as reported earlier[6]. The MS data were acquired and processed with a Finnigan-Incos Model 2300 data system. Compound assignments were made from individual mass spectra and GC retention times, with comparison to authentic standards where possible.

Results and discussion

The relative amounts of the major gasoline-range hydrocarbons of two dredge samples are listed in Table 1. Sample 7D-5A has a much greater amount of C_5–C_{10} hydrocarbons than sample 7D-3B and in both cases the concentrations of branched and cyclic compounds (possibly also olefins) far exceed the abundance of the normal hydrocarbons. The approximate total concentration of C_2–C_{10} hydrocarbons for sample 7D-5A is about 10 times greater than for the other sample. The relative distributions of all hydrocarbons are very similar for both samples in the range of C_5–C_{10}, but sample 7D-3B has only minor components from C_2 to C_5 (Table 1). The large amounts of C_2–C_{10} hydrocarbons and their structural diversity confirm their origin by thermal generation from the sedimentary organic matter[7].

The total bitumen (lipid) extract of sample 7D-2B is light amber in colour and black for sample 7D-4A, B, both extracts of the samples exhibit blue fluorescence in solution (Table 2). This colour is typical for (naphtha) heavy condensates and the concentrated extract for sample 7D-4A, B does exhibit a yellow fluorescence, indicating a major amount of heavier oil components. The total yield of bitumen is highest for sample 7D-4A, B and it contains only traces of elemental or organic sulphur. The 'light' bitumen (7D-2B), however, has a major proportion of elemental sulphur and also organic sulphur compounds (the minerals of this sample are massive sulphides). These two bitumens are clearly different, which is further substantiated by the following data. The hydrocarbon yields are found in Table 2, where the aliphatic fraction (F1) is lowest for both samples and most of the bitumen is comprised of asphaltic (F3) and then aromatic/naphthenic (F2) material. The aromatic-to-aliphatic ratio for sample 7D-2B is 9.3 and it is 4.7 for sample 7D-4A, B, typical for many crude oils[12].

The GC traces of the aliphatic hydrocarbons are given in Fig. 2 and they are dramatically different. Sample 7D-2B (Fig. 2*a*) exhibits a pattern typical of a petroleum, where the dominant *n*-alkanes, C_nH_{2n+2}, range from $n = 12$ to 33, with no carbon number predominance ($CPI_{12-33} = 1.03$) and a maximum at *n*-C_{21}. Carbon preference index (CPI) = odd carbon number *n*-alkanes/even over the range indicated for example,

$$CPI_H = \frac{2\Sigma \text{ odd } C_{13}\text{–}C_{33}}{\Sigma \text{ even } C_{12}\text{–}C_{30} + \Sigma \text{ even } C_{14}\text{–}C_{32}}$$

Pristane and phytane are about equal (Pr/Ph = 1.06). The complex, unresolved mixture of branched and cyclic hydrocarbons (that is, hump) ranges from C_{11} to C_{31}, also typical of petroleum. On the other hand, sample 7D-4A, B (Fig. 2*b*) exhibits a much narrower GC profile, skewed to lower carbon

Table 1 Volatile hydrocarbons in dredge samples from Guaymas Basin

Compound*	Retention time (min)	Approximate concentration (ng cm^{-3} of headspace—150 cm^3 total) 7D-3B	7D-5A
2-Methylbutane	5.1	2.6	14
n-pentane	5.4	1.4	39
Cyclohexane	7.3	0.5	6
4-Methyl-2-pentene	8.0	0.8	6.3
3-Methylpentane	8.3	1.4	11
2-Methylpentane + benzene	8.6	0.9	44
n-Hexane	9.7	9.2	260
C_2-Cyclopentane	10.3	3.3	46
Methylcyclohexane	10.7	14	1,050
3-Methylhexane	12.1	3.3	—
2-Methylhexane	12.4	5.8	210
n-Heptane + toluene	13.5	>130	950
n-Octane	16.4	24	29
n-Nonane	19.2	48	26
n-Decane	22.2	17	40
Total C_2–C_{10} hydrocarbons (μg)		80	875

* Identifications based on GC retention time only

Table 2 Yields and composition of bitumen from dredge samples in Guaymas Basin

Sample	Colour	Total bitumen extract Fluorescence (UV)	Total yield (mg)	Total yield (μg per g)	Sulphur (μg S° per g)	Aliphatic HC (F1) (μg per g)	Aliphatic HC (F1) (% of total bitumen)	Aromatic/naphthenic hydrocarbons (F2) (μg per g)	Aromatic/naphthenic hydrocarbons (F2) (% of total bitumen)	Asphaltic (NSO) compounds (F3) (μg per g)	Asphaltic (NSO) compounds (F3) (% of total bitumen)
7D-2B	Light amber	Sky blue	110	1,075	~450	27	2 5	250	23 2	315	29 3
7D-4A, B	Black	Dark blue (yellow on sample matrix)	8,730	70,400	Traces	4,850	6 9	22,700	32 0	42,900	61 0

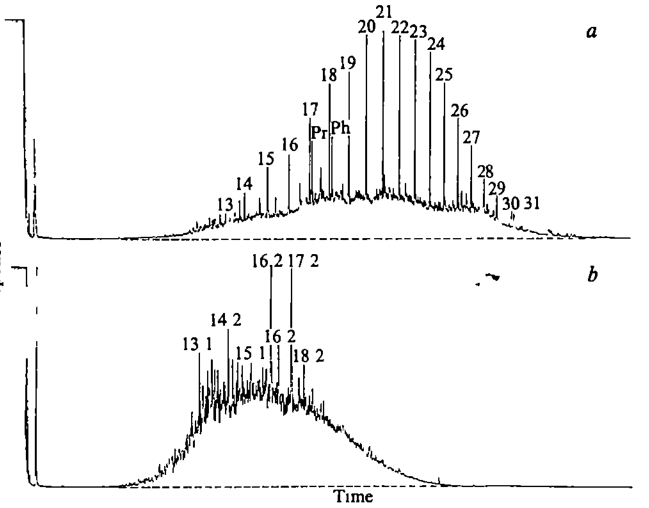

Fig. 2 Gas chromatograms of the aliphatic hydrocarbon fractions (F1) for *a*, sample 7D-2B, and *b*, sample 7D-4A, B The carbon chain length of the *n*-alkanes is indicated by the arabic numerals, olefins are indicated by chain length double bond equivalent, Pr = pristane, Ph = phytane GC conditions as cited in the text

numbers The dominant resolved peaks are various mono- and di-olefins ranging from C_{12} to C_{19} and the hump ranges from C_9 to about C_{21} This is very unlike typical petroleum, as olefins are not found in mature crudes[12,13] Olefinic hydrocarbons have been identified in a crude oil from Bradford, Pennsylvania[14] and they were found to consist of mid-chain normal, branched and cyclic analogues with the double bonds mainly in the *trans* configuration The presence of these olefins was accounted for by a process of natural thermal cracking followed by the rapid disappearance of *cis* and terminal olefins[14] The *n*-alkanes of sample 7D-4A, B are present as minor components and range from C_{10} to C_{23}, with essentially no carbon number predominance (CPI_{10-23} = 1 20) and a maximum at C_{15} Pristane is more abundant than phytane (Pr/Ph = 1 6)

The GC–MS data for sample 7D-2B (F1) confirmed the minor presence of a similar range of mono- and di-olefins ranging from C_{12} to C_{19} These compounds are not terminal olefins as were identified near the sills of DSDP site 481A (ref 9) They are slightly more stable 'in-chain' olefins with methyl branching, similar to those described by Hoering[14]

The major diagnostic molecular markers in this fraction consist of triterpenoids, extended diterpanes and steranes with their rearranged analogs (diasteranes) Their relative distributions are given in Fig 3 with an example of the corresponding compounds in unaltered lipids of shallow sediment from Guaymas Basin[6] The extended diterpanes (Fig 3*a*) range from C_{20} to C_{29} in a similar distribution pattern as observed for other mature petroleum samples[15] They are, however, not present in the unaltered surface sediments (for example, Fig 3*b*)[6,9] The triterpenoids (Fig 3*a*) are surprisingly 'mature', they are for the most part in their thermodynamically more stable form, completely different from unaltered lipids of surface sediments (for example, Fig. 3*b*) The triterpenoids are comprised primarily of the 17α(H), 21β(H)-hopane series ranging from C_{27} (no C_{28}) to C_{35} and the homologues from C_{31} to C_{35} are present as 22-S and R diastereomeric pairs in a ratio of about unity This series constitutes the stable mature form of these compounds[15–18] and seems to have been generated by the hydrothermal activity These compounds are not found in the unaltered sediments (for example, Fig 3*b*)[6,9] where the biogenic markers with the 17β(H), 21β(H) stereochemistry and various triterpenes predominate Minor amounts of 17β(H), 21α(H)-moretanes (C_{29}, C_{30} and C_{31}), 17β(H), 21β(H)-hopanes (C_{27} and C_{30}), *iso*-hop-13(18)-ene and 17β(H)-moret-22(29)-ene are also present in sample 7D-2B These are precursor relics and intermediates from the thermal conversion process

The steroidal markers consist of primarily 5α(H), 14α(H), 17α(H)-steranes (20 R), with lesser amounts of 5β(H), 14α(H),17α(H)-steranes (20 R) and diasteranes [mainly the 13β(H), 17α(H)-20 R or S series][17,19–21] The steranes ranged from C_{26} to C_{30}, with cholestane as the major homologue (Fig 3*c*) The distribution pattern indicates a marine autochthonous origin and fits best with similar data for DSDP Site 477 (ref 9) The large 5α(H)-sterane concentration is a result of the elevated thermal stress which probably converted other steroidal compounds to these hydrocarbons[9]

The extended diterpenoidal, triterpenoidal and steroidal indicator compounds are not detectable by GC–MS in the hydrocarbon fraction of sample 7D-4A, B This fraction is composed of more volatile, lower molecular weight compounds

The GC traces of the aromatic/naphthenic fractions (F2) of both samples are given in Fig 4 Again, the hump of unresolved material is skewed to the lower molecular weight region in the case of sample 7D-4A, B The GC–MS data indicate that the major resolved peaks are polynuclear aromatic hydrocarbons

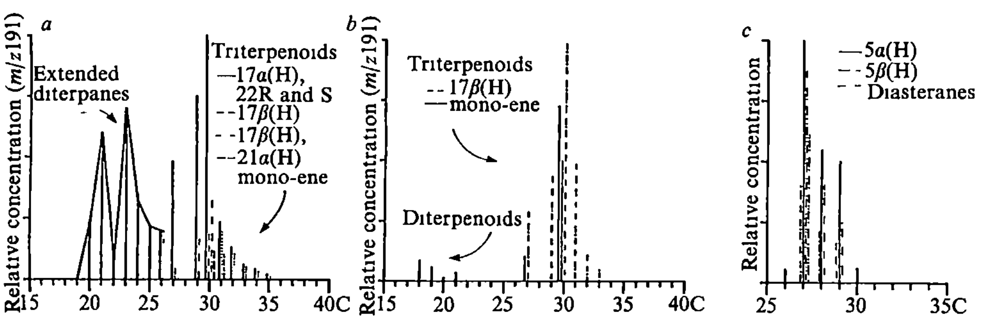

Fig. 3 Relative distribution diagrams for triterpenoids in *a*, sample 7D-2B, and *b*, an unaltered sample, station 30G, 3 5 m subbottom[6], and steranes in *c*, sample 7D-2B Relative concentrations are based upon GC responses and *m*/*z* 191 and 217 mass chromatograms

Table 3 Polynuclear aromatic hydrocarbons in dredge samples from Guaymas Basin

Compound	No *	Formula	MW	7D-2B (ng per g bitumen)	7D-4A, B (ng per g bitumen)
Indane		C_9H_{10}	118	0 5	0 4
Tetramethylbenzene	1	$C_{10}H_{14}$	134	0 6	4 5
Naphthalene		$C_{10}H_8$	128	4	12
2-Methylnaphthalene		$C_{11}H_{10}$	142	8	6
1-Methylnaphthalene		$C_{11}H_{10}$	142	6	4
Biphenyl		$C_{12}H_{10}$	154	3	1 2
Dimethylnaphthalene		$C_{12}H_{12}$	156	50	8
Acenaphthene		$C_{12}H_{10}$	154	0 8	2 8
Trimethylnaphthalene		$C_{13}H_{14}$	170	16	40
Fluorene		$C_{13}H_{10}$	166	5	0 8
Dibenzothiophene		$C_{12}H_8S$	184	12	8
Phenanthrene	2	$C_{14}H_{10}$	178	27	8
Anthracene		$C_{14}H_{10}$	178	5	10
Fluoranthene		$C_{16}H_{10}$	202	40	34
Pyrene	3	$C_{16}H_{10}$	202	200	178
2,3-Dibenzofluorene		$C_{17}H_{12}$	216	40	40
Benz(*a*)anthracene	4	$C_{18}H_{12}$	228	15	16
Chrysene (triphenylene)	5	$C_{18}H_{12}$	228	42	38
Benzo(*b*)fluoranthene		$C_{20}H_{12}$	252	40	28
Benzo(*k*)fluoranthene		$C_{20}H_{12}$	252	10	6
Benzo(*e*)pyrene	7	$C_{20}H_{12}$	252	62	45
Benzo(*a*)pyrene	8	$C_{20}H_{12}$	252	25	16
Perylene	9	$C_{20}H_{12}$	252	45	40
1,2,5,6-Dibenz-anthracene		$C_{22}H_{14}$	278	3	2 4
Benzo(*g,h,i*)perylene	10	$C_{22}H_{12}$	276	100	24
Coronene	11	$C_{24}H_{12}$	300	64	5

* See Fig 4

(PAH), another group of compounds uncommon in petroleums but ubiquitous in higher temperature pyrolysis residues (for example, smoke or from *in situ* organic matter)[12,22 23]

The major components that were identified and resolved are listed in Table 3 The concentrations (μg per g of total oil) of the major analogues are of the same order of magnitude for both samples The dominant analogues for both samples are the peri-condensed aromatic series as for example pyrene, benzopyrenes, perylene, benzoperylene and coronene These peri-condensed structures are more reactive than their angularly condensed analogues[22] Thus, they must have been expelled rapidly after genesis to the seabed for their preservation A further indication for a pyrolytic origin is the presence of five-membered alicyclic rings (such as acenaphthene, fluorene, and fluoranthene, Table 3) which are found in all pyrolysates from organic matter, because once formed they do not easily revert to peri-condensed aromatic hydrocarbons[22 23] Note also that this fraction contains significant amounts of toxic PAH The benzopyrenes are major components and the highly toxic benzo(*a*)pyrene is present at levels of 25 and 16 ng per g of total bitumen Perylene is present in these fractions and is also the dominant PAH in the unaltered sedimentary lipids of samples deposited in the Gulf from oxygen-minimum environments[9 24] Thus, the chemical composition of this fraction indicates a source from pyrolysis with rapid quenching by hydrothermal removal and subsequent condensation at the seabed

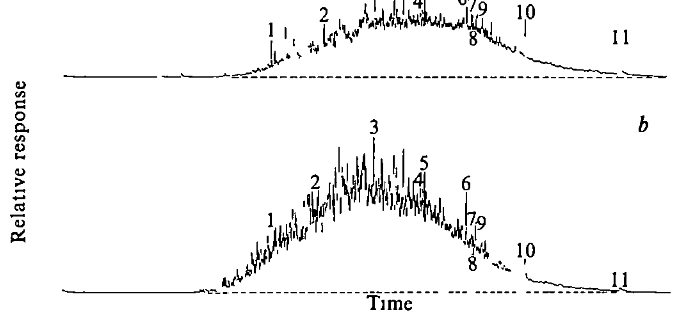

Fig. 4 Gas chromatograms of the aromatic/naphthenic hydrocarbon fractions (F2) for *a*, sample 7D-2B, and *b*, sample 7D-4A, B GC conditions as cited in the text 1, tetramethylbenzene, 2, phenanthrene, 3, pyrene, 4, benz(*a*)anthracene, 5, chrysene, 6, benzofluoranthenes, 7, benzo(*e*)pyrene, 8, benzo(*a*)pyrene, 9, perylene, 10, benzoperylene, 11, coronene

Conclusions

The thermogenic origin of the petroleum-like organic matter in the dredge samples has been confirmed This is based on the following chemical parameters (1) presence of gasoline range hydrocarbons (also the odorous compounds) (2) broad distribution of hydrocarbons (hump, C_{13}–C_{33}) and presence of pristane and phytane, and (3) the relative amounts of aromatic/naphthenic (F2) and asphaltic (F3) material versus the aliphatic hydrocarbons (F1)

The indications that these oils are derived from a higher temperature pyrolysis process rather than the normal petroleum genesis window (maximum ~ 150 °C)[12] are as follows first, the presence of peri-condensed PAH, and second, a large amount of asphaltic material and possibly the presence of various branched and in-chain olefins

Hydrothermal migration is suggested by the following data (1) the virtual absence of primary olefins (they were dominant components near sills at depth in for example DSDP Site 481A)[9], which are highly reactive and are not expected to survive migration in hot fluids, and (2) the same molecular marker fingerprint as *in situ* thermogenic bitumen at DSDP Sites 477 and 477A (ref 9) This is not a case of migration of mature petroleum from geologically old formations (>Quaternary) through the younger sequences, where it could have dissolved the indicators just discussed Such an explanation is inconsistent with the dramatic differences in boiling range for both the aliphatic and aromatic hydrocarbon fractions (F1 and F2) of the two samples It is more likely that a temperature gradient exists at the seabed away from the hydrothermal vent, which controls condensation and solution into ambient cold seawater of the emanating organic matter (oil) This needs further sampling in more controlled conditions

Another indication that these oils are derived from thermal alteration of the immature organic matter (Quaternary) in the basin is found in the minor biogenic marker residues Traces of 17β(H), 21β(H)-hopanes and triterpenes are present in sample 7D-2B and these compounds are not found in mature petroleum The distribution patterns of these molecular markers are very similar to examples from samples at depth (DSDP Sites 477 and 481)[9]

The sediments at depth (DSDP Sites 477, 478 and 481) contain large amounts of thermogenic (admixed with some original biogenic) interstitial gas[8 10], and also thermally derived bitumen[0] Thus, the presence of petroliferous condensate at the seabed indicates that the plume water must contain large amounts of methane and higher molecular weight organic matter This organic matter can represent a carbon source to microbes at the vent site, which in turn can be food for the higher fauna

We thank Captain A Phinney, the crew and scientific party of R/V *Melville* for their skill in collecting the samples, Mr E Ruth for GC–MS data acquisition, Mr Cary Jackson for the hydrocarbon gas analyses, and Ms Dara Blumfield and Ms Dana Blumfield for technical assistance Funding from the NSF (grant OCE 79-08811) is gratefully acknowledged

Contribution no 2177 Institute of Geophysics and Planetary Physics, University of California at Los Angeles, contribution of the Scripps Institution of Oceanography, new series

Received 4 September, accepted 25 November 1981

1 Curray, J R *et al* *Geotimes* **24**, 18–20 (1979)
2 Moore, D G *Bull geol Soc Am* **84**, 1883–1906 (1973)
3 Einsele, G *Nature* **283**, 441–445 (1980)
4 Lawver, L A, Williams, D L & van Herzen, R P *Nature* **257**, 23–28 (1975)
5 Williams, D L, Becker, K, Lawver, L A & von Herzen, R P *J geophys Res* **84**, 6757–6769 (1979)
6 Simoneit, B R T, Mazurek, M A, Brenner, S, Crisp, P T & Kaplan, I R *Deep-Sea Res* **26A**, 879–891 (1979)
7 Whelan, J K & Hunt, J M *Init Rep DSDP* Leg **64** (in the press)
8 Galimov, E M & Simoneit, B R T *Init Rep DSDP* Leg **64** (in the press)
9 Simoneit, B R T & Philp, R P *Init Rep DSDP* Leg **64** (in the press)
10 Simoneit, B R T *Init Rep DSDP* Leg **64** (in the press)
11 Lonsdale, P *EOS* **61**, 995 (1980)
12 Hunt, J M *Petroleum Geochemistry and Geology* (Freeman, San Francisco, 1979)
13 Tissot, B P & Welte, D H *Petroleum Formation and Occurrence, A New Approach to Oil and Gas Exploration* (Springer, Berlin, 1978)
14 Hoering, T C *Chem Geol* **20**, 1–8 (1977)
15 Simoneit, B R T & Kaplan, I R *Mar envir Res* **3**, 113–128 (1980)
16 Dastillung, M & Albrecht, P *Mar Pollut Bull* **7**, 13–15 (1976)
17 Seifert, W K & Moldowan, J M *Geoch m cosmochim Acta* **42**, 77–95 (1978)
18 Ensminger, A, Van Dorsselaer, A, Spyckerelle, C, Albrecht, P & Ourisson, G in *Advances in Organic Geochemistry 1973* (eds Tissot, B & Bienner, F) 235–260 (Technip, Paris, 1974)
19 Mackenzie, A S, Patience, R L, Maxwell, J R, Vandenbroucke, M & Durand, B *Geochim cosmochim Acta* **44**, 1709–1721 (1980)
20 Ensminger, A, Joly, G & Albrecht, P *Tetrahedron Lett* 1575–1578 (1978)
21 Seifert, W K & Moldowan, J M *Geochim cosmochim Acta* **43**, 111–126 (1979)
22 Blumer, M *Chem Geol* **16**, 245–256 (1975)
23 LaFlamme, R E & Hites, R A *Geochim cosmochim Acta* **42**, 289–304 (1978)
24 Simoneit, B R T *Init Rep DSDP* Leg **64** (in the press)

Cloning and sequence analysis of cDNA for bovine adrenal preproenkephalin

Masaharu Noda*, Yasuji Furutani*, Hideo Takahashi*, Mitsuyoshi Toyosato*, Tadaaki Hirose†, Seiichi Inayama†, Shigetada Nakanishi‡ & Shosaku Numa*

* Department of Medical Chemistry and ‡ Institute for Immunology, Kyoto University Faculty of Medicine, Kyoto 606, Japan
† Pharmaceutical Institute, Keio University School of Medicine, Tokyo 160, Japan

The nucleotide sequence of cloned cDNA for preproenkephalin from bovine adrenal medulla indicates that the precursor protein contains four copies of Met-enkephalin and one copy each of Leu-enkephalin, Met-enkephalin-Arg^6-Phe^7 and Met-enkephalin-Arg^6-Gly^7-Leu^8, a previously undetected opioid peptide. The enkephalin and extended enkephalin sequences are each bounded by paired basic amino acid residues. Preproenkephalin may represent a multi-hormone precursor, like the corticotropin–β-lipotropin precursor

METHIONINE-enkephalin (Met-enkephalin) and leucine-enkephalin (Leu-enkephalin) are endogenous pentapeptides with opiate-like activity which were originally discovered in the brain[1] The Met-enkephalin sequence is contained in the structure of β-lipotropin (β-LPH), which is regarded as a pituitary hormone We have previously purified the bovine mRNA coding for the common precursor of β-LPH and corticotropin (ACTH)[2] and have elucidated the primary structure of this precursor protein by determining the nucleotide sequence of cloned DNA complementary to the mRNA[3] Although β-endorphin, a 31-amino acid opioid peptide, which contains the Met-enkephalin sequence, has been shown to be produced from the ACTH-β-LPH precursor (alternatively designated preproopiomelanocortin) by post-translational processing, accumulating evidence indicates that Met-enkephalin itself is not derived from the same precursor (see ref 4 for review) Furthermore, several polypeptides containing Met-enkephalin and/or Leu-enkephalin sequences, and which are not related to β-endorphin, have recently been isolated from bovine adrenal medulla[5–11] Thus, these polypeptides have been suggested as intermediates in the biosynthesis of the opioid pentapeptides

In an attempt to elucidate the primary structure of the initial enkephalin precursor (hereafter referred to as preproenkephalin), we have now cloned DNA sequences complementary to the bovine mRNA coding for the precursor protein Nucleotide sequence analysis of the cloned cDNA has revealed the whole amino acid sequence of bovine preproenkephalin

Isolation of cDNA clones and strategy of DNA sequencing

The initial approach used to clone DNA sequences complementary to preproenkephalin mRNA was to screen a library of cDNA clones by hybridization with a mixture of synthetic oligodeoxyribonucleotides, the sequences of which represented all possible sequences predicted from a known partial amino acid sequence of an enkephalin-containing polypeptide The choice of appropriate hybridization conditions including temperature virtually eliminates the formation of mismatched duplexes without affecting the formation of perfectly matched ones, thus ensuring the selection of desired clones (Such a screening principle[12] would be useful for isolating cDNA clones that carry mRNA sequences present in low abundance) After isolating cDNA clones carrying a partial mRNA sequence and determining the nucleotide sequence of the cDNA, a synthetic oligodeoxyribonucleotide primer complementary to a portion of the determined mRNA sequence was elongated by reverse transcription of preproenkephalin mRNA The cDNA transcripts thus formed were cloned and screened by hybridization with an appropriate restriction fragment derived from initially isolated cDNA clones to yield clones carrying mRNA sequences upstream from the site corresponding to the synthetic primer used

Poly (A)-containing RNA was isolated from bovine adrenal medullas, and double-stranded cDNA was synthesized by reverse transcription of this RNA template using oligo (dT) as primer A cloned cDNA library was constructed by inserting the total cDNA population into the *Pst*I endonuclease cleavage site of the bacterial plasmid pBR322 with the use of poly(dG) poly(dC) homopolymeric extensions Two oligodeoxyribonucleotides, 5′-TCCATCCACCATTC-3′ and 5′-TCCATCCACCACTC-3′ (Fig 1*a*), were synthesized by the modified triester method[13] These tetradecamers represent the only two possible cDNA sequences corresponding to the unique pentapeptide sequence Glu-Trp-Trp-Met-Asp (excluding the

a

Glu Trp Trp Met Asp

5′-GA$^{A}_{G}$ UGG UGG AUG GA$^{U}_{C}$-3′

3′-CT$^{T}_{C}$ ACC ACC TAC CT -5′

b

Tyr Gly Gly Phe Met

5′-UA$^{U}_{C}$ GGG GGC UUC AUG-3′

3′- T$^{A}_{G}$ CCC CCG AAG TAC-5′

Fig. 1 Synthetic oligodeoxyribonucleotides used for priming the reverse transcription of preproenkephalin mRNA and/or for probing cloned cDNA for preproenkephalin In *a*, all possible coding sequences and the corresponding tetradecamers used are given for the unique pentapeptide sequence in peptide I (amino acids 217–221 of preproenkephalin) In *b*, the coding sequences actually found and a mixture of the corresponding tetradecamers used are shown for the four Met-enkephalin sequences composed of amino acids 97–101, 104–108, 133–137 and 182–186 of preproenkephalin For the numbering of amino acid residues, see Fig 3

0028–0836/82/030202—05$01 00

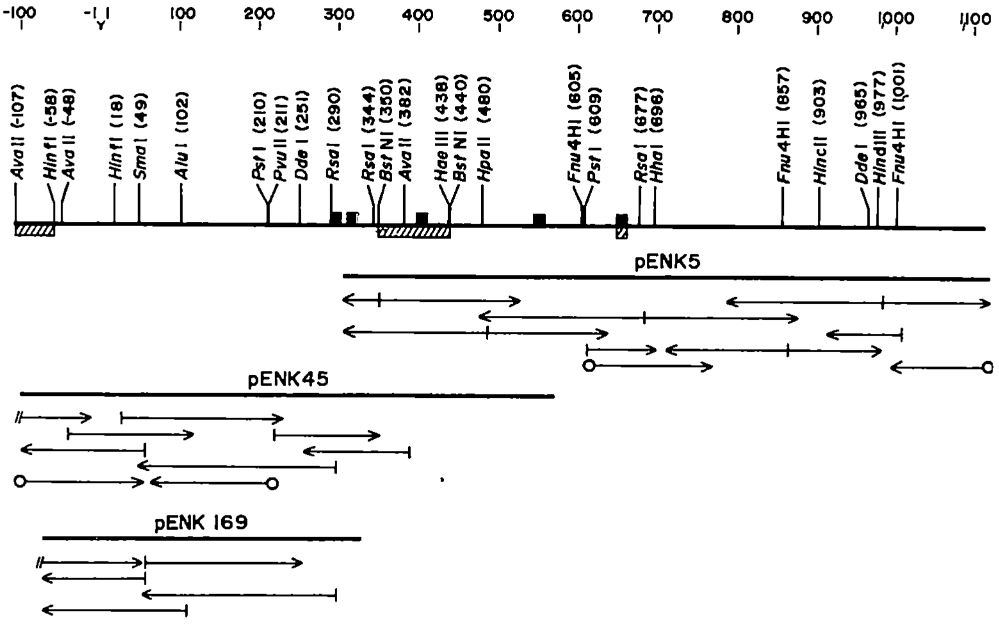

Fig. 2 Strategy for sequencing the cDNA inserts in the plasmids pENK5, pENK45 and pENK169 The clone pENK5 was isolated as follows Total RNA was extracted from bovine adrenal medullas, and poly(A)-containing RNA was isolated by oligo(dT)-cellulose chromatography according to the procedure used previously for the isolating of rat liver RNA[31] Single-stranded cDNA was synthesized by avian myeloblastosis virus reverse transcriptase (provided by Dr S W Beard), using 100 μg of poly(A)-containing RNA as described previously[32] The product was treated with alkali to remove the RNA template[33], and the second DNA strand was synthesized with *Escherichia coli* DNA polymerase I (Klenow fragment)[34] After treatment of the double-stranded cDNA with *Aspergillus oryzae* S_1 nuclease[35], homopolymeric poly(dC) tails were added to its 3′ ends by calf thymus terminal deoxynucleotidyltransferase[35] The poly(dC)-tailed cDNA was annealed to poly(dG)-tailed *Pst*I-cleaved pBR322 plasmid DNA[36] *E Coli* $\chi1776$[37] or HB101[38] was transformed with recombinant plasmids[39], and tetracycline-resistant transformants were screened by hybridization with the probe specified in the text[40], hybridization was carried out at 42 °C To isolate clones pENK45 and pENK169, single-stranded cDNA was synthesized with the specific oligodeoxyribonucleotide primers mentioned in the text as described by Houghton *et al*[41] The subsequent procedures were the same as described above, except that hybridization for selecting clones was conducted at 65 °C (pENK45) or 60 °C (pENK169) with the probes specified in the text The restriction map displays only relevant restriction endonuclease sites, which are identified by numbers indicating the 5′-terminal nucleotide generated by cleavage, for the nucleotide numbers, see Fig 3 The poly(dA) poly(dT) tract and the poly(dG) poly(dC) tails are not included in the restriction map, except the poly(dG) poly(dC) tails at the 3′ termini of pENK45 and pENK169, the location of these termini are approximate The sequences used for specific priming of reverse transcriptase are indicated by closed boxes, and those used as hybridization probes for selecting clones by shaded boxes DNA sequencing was carried out by the procedure of Maxam and Gilbert[14], 3′-end-labelling was conducted as described elsewhere[43] The direction and extend of sequence determinations are shown by horizontal arrows under each clone used The sites of 5′-end-labelling are indicated by short vertical lines at the end of arrows, and those of 3′-end-labelling (*Pst*I sites) by open circles at the end of arrows The slash marks at the end of arrows indicate that the site of 5′-end-labelling was the *Alu*I site on pBR322 plasmid DNA 56 bp from the *Pst*I site flanking the cDNA insert[43] Further details of the sequencing procedures have been described previously[3]

third nucleotide residue of the Asp codon), which is known to be a partial sequence of the enkephalin-containing polypeptides from bovine adrenal medulla, BAM-22P (ref 8), BAM-20P (ref 8) and peptide I (ref 10) An equimolar mixture of the two oligodeoxyribonucleotides was labelled with ^{32}P at the 5′ end and used as a hybridization probe to screen for recombinant plasmids carrying DNA sequences complementary to preproenkephalin mRNA Nineteen hybridization-positive clones were isolated from about 190,000 transformants On restriction endonuclease analysis, at least six of them exhibited a common restriction fragment of 68 base pairs (bp) which corresponded to the *Pst*I(609)-*Rsa*I(677) fragment containing the coding region for Glu-Trp-Trp-Met-Asp (Fig 2), as inferred from possible coding sequences for the known amino acid sequence of peptide I[10] Clone pENK5, which carried the largest cDNA insert, was subjected to nucleotide sequence analysis by the procedure of Maxam and Gilbert[14] according to the strategy indicated in Fig 2 (see Fig 2 legend for experimental details of cloning)

Because clone pENK5 (carrying nucleotide residues 297-1,113 given in Fig 3) evidently did not contain the entire protein-coding sequence, a further attempt was made to isolate cDNA clones carrying the remaining mRNA sequence For this purpose, one of the above-mentioned synthetic oligodeoxyribonucleotides, 5′-TCCATCCACCACTC-3′, the sequence of which was shown by DNA sequencing of the clone pENK5 to encode the amino acid sequence Glu-Trp-Trp-Met-Asp, was used for specific priming of the reverse transcription of preproenkephalin mRNA, poly(A)-containing RNA from bovine adrenal medulla served as a template The transcripts formed by elongation of the primer were converted to double-stranded cDNA, which was cloned in plasmid pBR322 and screened by hybridization with the *Bst*NI(350)-*Bst*NI(440) fragment (Fig 2) ^{32}P-labelled by nick translation[15] Out of ~1,200 transformants, two hybridization-positive clones were isolated which shared an internal *Pst*I site (position 210) located upstream of the other internal *Pst*I site (position 609) present in pENK5 (Fig 2) One of these clones, pENK45, which carried a larger cDNA insert, was subjected to DNA sequencing according to the

Table 1 Codon usage in bovine preproenkephalin mRNA

Phe	UUU	2	Ser	UCU	1	Tyr	UAU	3	Cys	UGU	1
	UUC	8		UCC	4		UAC	8		UGC	6
Leu	UUA	1		UCA	0	Ter	UAA	1	Ter	UGA	0
	UUG	0		UCG	0		UAG	0	Trp	UGG	4
Leu	CUU	4	Pro	CCU	3	His	CAU	0	Arg	CGU	1
	CUC	9		CCC	5		CAC	3		CGC	3
	CUA	4		CCA	2	Gln	CAA	0		CGA	2
	CUG	17		CCG	2		CAG	7		CGG	2
Ile	AUU	0	Thr	ACU	3	Asn	AAU	1	Ser	AGU	3
	AUC	0		ACC	6		AAC	3		AGC	7
	AUA	0		ACA	0	Lys	AAA	7	Arg	AGA	8
Met	AUG	10		ACG	1		AAG	15		AGG	2
Val	GUU	1	Ala	GCU	3	Asp	GAU	6	Gly	GGU	4
	GUC	2		GCC	5		GAC	6		GGC	12
	GUA	0		GCA	3	Glu	GAA	17 (16)		GGA	5
	GUG	3		GCG	4		GAG	15 (16)		GGG	9

Numbers next to codons indicate the numbers of amino acids using particular codons The different numbers given for the Glu codons are due to the difference in residue 267 between the clones pENK45 and pENK169 strategy shown in Fig 2, it contained a sequence of at least 85 bp identical to that present in clone pENK5

To confirm the nucleotide sequence in the region upstream of that encoding enkephalins, we attempted to isolate additional clones carrying sequences in the 5′-terminal region, using cDNA species synthesized with another oligodeoxyribonucleotide primer which corresponded to sequences encoding Met-enkephalin Analysis of the nucleotide sequences determined for clones pENK5 and pENK45 had shown that the coding sequences for the four Met-enkephalin sequences located on the amino-terminal side of the deduced preproenkephalin structure are complementary to either oligodeoxyribonucleotide 5′-CATGAAGCCCCCAT-3′ or 5′-CATGAAGCCCCCGT-3′ (Fig 1*b*) Therefore, we used a mixture of these two oligodeoxyribonucleotides synthesized simultaneously[13] as a specific primer for reverse transcription of preproenkephalin mRNA The cDNA transcripts thus formed were cloned in the plasmid pBR322 as described above From ~100,000 transformants, one clone (pENK169) hybridizing with the *Ava*II(−107)-*Hin*fI (−58) fragment (5′-end-labelled at the *Hin*fI site) was isolated and subjected to DNA sequencing (Fig 2) Clone pENK169 shared a sequence of at least 371 bp with clone pENK45, except that the residues at positions −44 and 267 in pENK169 were C and G, respectively, instead of G and A in pENK45, the latter substitution in the protein-coding region leads to a synonymous codon The observed nucleotide differences may be due to possible polymorphism in the bovine preproenkephalin gene or to possible errors occurring during *in vitro* cDNA synthesis or DNA cloning

Nucleotide sequence of preproenkephalin mRNA and assignment of protein sequence

The primary structure of bovine preproenkephalin mRNA (Fig 3) was deduced from the 1,222-nucleotide sequence (excluding the poly(dA) poly(dT) tract and poly(dG)·poly(dC) tails) determined for the cloned cDNA inserts in the plasmids pENK5, pENK45 and pENK169 The nucleotide sequence was determined on both strands of the cDNA for all but 113 residues in the 3′-terminal region The sequences of nucleotide residues 310–411 and 574–690 correspond precisely to the amino acid sequences determined for peptide F[9] and peptide I[10], respectively, provided that the third (Thr) and the eighth (His) residues of peptide I are interchanged Furthermore, the sequences of nucleotide residues 697–729 and 763–789 match the partial amino acid sequences determined for peptide B[10] The codon for the phenylalanine residue at the carboxyl terminus of peptide B is followed by the translational termination codon UAA Thus the 3′-untranslated region of the mRNA is 324 nucleotides long (excluding the poly(A) tract) All three polypeptide sequences mentioned above, as well as the sequences of Met-enkephalin, Leu-enkephalin and Met-enkephalin with a carboxyl extension of Arg-Phe (Met-enkephalin-Arg^6-Phe^7), are each bounded by paired basic amino acid residues (except at the carboxyl terminus of preproenkephalin)

In assigning the amino acid sequence of the cryptic portion of preproenkephalin, the reading frame of amino acid codons was determined by the frame corresponding to the amino acid sequences of the known polypeptides Thus, an as yet unknown polypeptide of 50 amino acids containing the opioid octapeptide Tyr-Gly-Gly-Phe-Met-Arg-Gly-Leu (Met-enkephalin-Arg^6-Gly^7-Leu^8) at its carboxyl end was identified between peptides F and I Both the polypeptide and octapeptide within are bounded by paired basic amino acid residues Peptide F is connected by Lys-Arg with the preceding polypeptide which contains a Met-enkephalin sequence at its carboxyl end This Met-enkephalin sequence is also flanked by paired basic residues

The translational initiation site was assigned to the methionine codon AUG at positions 1–3 because this is the first AUG triplet that appears downstream from the nonsense codon UGA (residues −96 to −94) found in frame This assignment seems plausible because the sizes of the specific cDNA transcripts formed by reverse transcriptase-mediated elongation of

```
5'--------AGGACCGCGAGAGUGAGGCCCGCCCGCUUUCCUGGCUCUCCCCLCGCCGAGAGUCCCCCGGACCGGGUUUCCACGACCGACCUGCGUGCCCCGAACAGCGGCAACCCC
                  -100                -80                 -60                 -40                 -20                -1

1                                  10                                      20                                      30
Met Ala Arg Phe Leu Gly Leu Cys Thr Trp Leu Leu Ala Leu Gly Pro Gly Leu Leu Ala Thr Val Arg Ala Glu Cys Ser Gln Asp Cys
AUG GCG CGG UUC CUG GGA CUC UGC ACU UGG CUG CUG GCG CUC GGC CCC GGG CUC CUG GCG ACC GUC AGG GCA GAA UGC AGC CAG GAC UGC
1                        20                         40                        60                         80

                                    40                                      50                                      60
Ala Thr Cys Ser Tyr Arg Leu Ala Arg Pro Thr Asp Leu Asn Pro Leu Ala Cys Thr Leu Glu Cys Glu Gly Lys Leu Pro Ser Leu Lys
GCC ACG UGC AGC UAC CGC CUG GCG CGC CCG ACU GAC CUC AAC CCG CUG GCU UGC ACU CUG GAA UGU GAG GGG AAA CUA CCU UCU CUC AAC
            100                       120                        140                        160                       180

                                    70                                      80                                      90
Thr Trp Glu Thr Cys Lys Glu Leu Leu Gln Leu Thr Lys Leu Glu Leu Pro Pro Asp Ala Thr Ser Ala Leu Ser Lys Gln Glu Glu Ser
ACC UGG GAA ACC UGC AAG GAG CUU CUG CAG CUG ACC AAA CUA GAA CUU CCU CCA GAU GCC ACC AGU GCC CUC AGC AAA CAG GAG GAA ACC
                         200                        220                       240                        260

                                    100                                     110                                     120
His Leu Leu Ala Lys Lys Tyr Gly Gly Phe Met Lys Arg Tyr Gly Gly Phe Met Lys Lys Met Asp Glu Leu Tyr Pro Leu Glu Val Glu
CAC CUG CUU GCU AAG AAG UAC GGG GGC UUC AUG AAG CGG UAU GGG GGC UUC AUG AAG AAA AUG GAU GAG CUG UAC CCC CUG GAA GUG GAA
            280                       300                        320                        340                       360

                                    130                                     140                                     150
Glu Glu Ala Asn Gly Gly Glu Val Leu Gly Lys Arg Tyr Gly Gly Phe Met Lys Lys Asp Ala Glu Glu Asp Asp Gly Leu Gly Asn Ser
GAA GAG GCA AAU GGA GGU GAG CUC CUU GGC AAG AGA UAU GGG GGC UUC AUG AAG AAG GAU GCA GAG GAA GAU GAC GGC CUG GGC AAC UCC
                         380                        400                       420                        440

                                    160                                     170                                     180
Ser Asn Leu Leu Lys Glu Leu Leu Gly Ala Gly Asp Gln Arg Glu Gly Ser Leu His Gln Glu Gly Ser Asp Ala Glu Asp Val Ser Lys
UCC AAC CUG CUC AAG GAG CUG CUG GGA GCC GGG GAC CAG CGA GAG GGG AGC CUC CAC CAG GAG GGC AGU GAU GCU GAA GAC GUG AGC AAG
            460                       480                        500                        520                       540

                                    190                                     200                                     210
Arg Tyr Gly Gly Phe Met Arg Gly Leu Lys Arg Ser Pro His Leu Glu Asp Glu Thr Lys Glu Leu Gln Lys Arg Tyr Gly Gly Phe Met
AGA UAC GGG GGC UUC AUG AGA GGC UUA AAG AGA AGC CCC CAC CUA GAA GAU GAA ACC AAA GAG CUG CAG AAG CGA UAC GGG GGU UUC AUG
                         560                        580                       600                        620

                                    220                                     230                                     240
Arg Arg Val Gly Arg Pro Glu Trp Trp Met Asp Tyr Gln Lys Arg Tyr Gly Gly Phe Leu Lys Arg Phe Ala Glu Pro Leu Pro Ser Glu
AGA AGA GUG GGU CGU CCA GAG UGG UGG AUG GAC UAC CAG AAA AGG UAC CGU GGC UUC CUC AAG CGC UUC GCC GAG CCC CUA CCC UCC GAG
            640                       660                        680                        700                       720

                                    250                                     260
Glu Glu Gly Glu Ser Tyr Ser Lys Glu Val Pro Glu Met Glu Lys Arg Tyr Gly Gly Phe Met Arg Phe
GAA GAA GGC GAA AGU UAC UCC AAG GAA GUU CCU GAA AUG GAG AAA AGA UAU GGA GGA UUU AUG AGA UUU UAA UCCCCUUUCCCAUCAGUGACCUG
                         740                        760                       780                      800

AAGCCCCAGCAAGCCUUCCUCUGCCCCCAGUGAAAGACUGCUGCGCUGGUGUGUUGUAUUGUCCCGUGUCGCUUGCAUUAUAUAGUUGACUUGAGAGUCCAGAUAAUUAACUAUACAAC
    820                 840                 860                 880                 900                 920

CUGAAAGCUGUGAUCCCAGGUUCUGUGUUCUGAGAAUCUUUAAGCUUUUAAAUAUUGGUCUGUUGCAGCUGUCUUGUUUCCAUGCUCAGUUUUGUUAUCACUUUGUCCUUUAUUUUUG
    940                 960                 980                 1000                1020                1040

ACACAAUGCCAAUAAAUGCCUACUUGUGUGUAGAUAUAAUAAACCCAUUACCCCAACUGC--------3'
    1060                1080                1100
```

Fig 3 Primary structure of bovine preproenkephalin mRNA The nucleotide sequence of the mRNA was deduced from those of the cDNA inserts in the plasmids pENK5, pENK45 and pENK169, the nucleotide residues −44 and 267 given have been taken from pENK45, whereas those of pENK169 are C and G respectively (see the text) Nucleotide residues are numbered in the 5′ to 3′ direction, beginning with the first residue of the AUG triplet encoding the initiative methionine, and the nucleotides on the 5′ side of residue 1 are indicated by negative numbers The 5′-terminal sequence presented does not extend to the 5′ end of the mRNA (see the text), whereas the 3′-terminal sequence shown is followed by a poly(A) tract of 12 nucleotides, thus apparently representing the complete sequence of this region The predicted amino acid sequence is displayed above the nucleotide sequence, and amino acid residues are numbered beginning with the initiative methionine The sequences of Met-enkephalin, Leu-enkephalin and Met-enkephalin with a carboxyl extension, which are each bounded by paired basic amino acid residues (or by the carboxyl terminus of preproenkephalin), are boxed

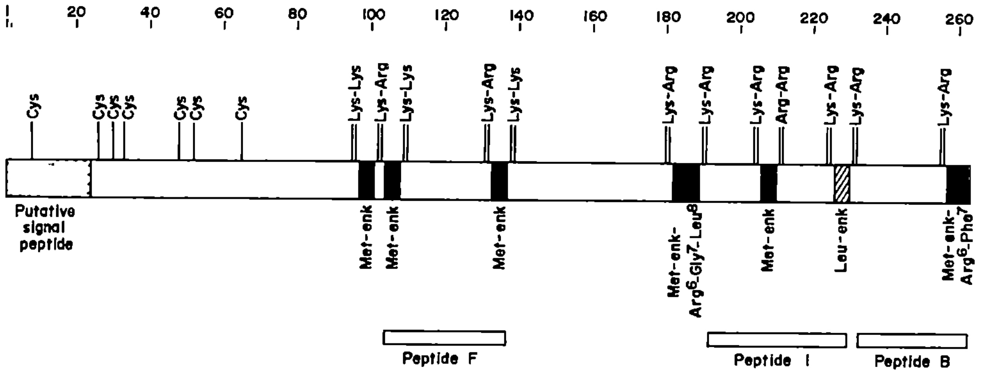

Fig 4 Schematic representation of the structure of bovine preproenkephalin The sequences of Met-enkephalin, Met-enkephalin-Arg^{6}-Phe^{7} and Met-enkephalin-Arg^{6}-Gly^{7}-Leu^{8} are indicated by closed boxes, the sequence of Leu-enkephalin by a shaded box and the putative signal peptide by a stippled box All the paired basic amino acid residues and cysteine residues are shown Amino acid numbers (see Fig 3) are given above The known peptide structures, peptide F (residues 104–137), peptide I (residues 192–230) and peptide B (residues 233–263), are displayed underneath by open bars, the known peptides representing partial sequences of peptide I—peptide E (residues 206–230), BAM-22P (residues 206–227), BAM-20P (residues 206–225) and BAM-12P (residues 206–217)—are not shown

the *Ava*II(−107)–*Hin*fI(−58) and *Ava*II(−48)–*Hin*fI(18) fragments (Fig 2) derived from the 5′-terminal region of the clone pENK45 suggest that no more than ~65 nucleotides are missing from the cloned sequence shown in Fig 3 Furthermore, the first 24 residues starting with the putative initiative methionine (residue 1) include many hydrophobic amino acids (19 nonpolar residues including 7 leucines) Because the signal peptide characteristic of secretory proteins[16] generally contains a region rich in hydrophobic amino acids with large side chains in its central portion and terminates in a residue with a small neutral side chain[17] (for example, alanine, glycine or serine), a possible site for cleavage of the signal peptide of preproenkephalin seems to be after the alanine at position 24 Assuming that the cysteine residue at position 8 is eliminated with the signal peptide, the remaining prohormone would contain six cysteine residues, all of which are located in its amino-terminal region Other peptide hormones, such as insulin and growth hormone, contain an even number of cysteine residues which form disulphide bonds[18]

The structure of bovine preproenkephalin is schematically illustrated in Fig 4 The precursor protein is composed of 263 amino acid residues, having a calculated molecular weight of 29,786 It contains four copies of Met-enkephalin and one copy each of Leu-enkephalin, Met-enkephalin-Arg^{6}-Phe^{7} and Met-enkephalin-Arg^{6}-Gly^{7}-Leu^{8} The amino-terminal region of the prohormone contains cysteine residues and is preceded by a putative signal peptide There is no structure corresponding to α-neo-endorphin[19] or dynorphin[20], both of which contain a Leu-enkephalin sequence The sequences of Met-enkephalin, Leu-enkephalin, Met-enkephalin-Arg^{6}-Phe^{7} and Met-enkephalin-Arg^{6}-Gly^{7}-Leu^{8} are each bounded by paired basic residues, Lys-Arg, Lys-Lys or Arg-Arg (except at the carboxyl terminus of preproenkephalin), implying that these enkephalins with and without a carboxyl extension can be formed by proteolytic processing of the precursor molecule[17] It is also possible that larger enkephalin-containing peptides do not merely represent intermediates in the formation of the opioid peptides of 5–8 amino acids, but possess specific physiological functions[7 8 10 11] A survey of various prohormones suggests that the Lys-Arg pair may be a primary site of proteolytic cleavage[3 17 21–23] Assuming that this is valid for proenkephalin and that the signal peptide is cleaved after the alanine residue at position 24, the primary products formed by proteolytic processing of proenkephalin would be peptides composed of residues 25–101, 104–130, 133–179, 182–189, 192–203, 206–223, 226–230, 233–254 and 257–263, it is possible that the glycine residue at position 130 is eliminated to amidate the preceding leucine residue[3 24] These products include Leu-enkephalin, Met-enkephalin-Arg^{6}-Phe^{7} and Met-enkephalin-Arg^{6}-Gly^{7}-Leu^{8} All the remaining Met-enkephalin-containing polypeptides, except the amino-terminal peptide, would have an enkephalin sequence at their amino-terminal end, as is the case for β-endorphin, α-neo-endorphin and dynorphin This processing pattern seems to be consistent with the known opioid activities of the larger enkephalin-containing peptides[7 8 11] Those with an enkephalin sequence at their amino-terminal end, such as peptide E[11], BAM-22P[8] and BAM-20P[8], but not peptide F[9], exhibit potent opioid activity It is conceivable that the peptide sequence next to the enkephalin portion of a large opioid peptide may modify the latter's physiological activity by conferring additional specificity for recognition of cell surface receptors, by increasing the binding affinity or by affecting its stability *in vivo* Furthermore, the activity of a large opioid peptide may be modified by glycosylation, the sequence Asn-Ser-Ser at positions 149–151 is a possible glycosylation site[25]

Note that the structural organization of preproenkephalin resembles that of the ACTH–β-LPH precursor[3] Both precursor proteins are composed of multiple repetitive units connected with a cysteine-containing amino-terminal sequence preceded by a signal peptide We have previously proposed that the different component peptides of the ACTH–β-LPH precursor, acting coordinately in the central nervous system as well as in peripheral tissues, may be involved in the defence mechanism of the living organism and that the biological significance of a multi-hormone precursor may be to produce multiple peptides with coordinate functions[3 26] Assuming that the enkephalin-containing component peptides of preproenkephalin perform relatea but different physiological functions, their coexistence with catecholamines in the chromaffin granules of adrenal medullary cells[5 27] seems to support the view that they are involved in conditions of acute stress Thus, preproenkephalin may represent another multi-hormone precursor from which different peptides are elaborated by proteolytic processing to function coordinately in the central nervous system and in peripheral tissues

Characteristic features of preproenkephalin mRNA

Computer analysis of the nucleotide sequence of preproenkephalin mRNA reveals that there are, in addition to the coding regions for the enkephalin sequences, many segments that seem to represent direct duplications (for example, residues 29–43 and 50–64, 121–136 and 807–822, 195–207, 462–474 and 597–609, 237–253 and 800–816, 352–367 and 421–436) This suggests that the structural gene for preproenkephalin has evolved by a series of direct duplications of certain common ancestral DNA segments followed by substitution, addition or deletion of some regions A large number of direct duplications was also observed for mRNA coding for the ACTH–β-LPH precursor[3]

Codon utilization for preproenkephalin mRNA, like other eukaryotic mRNAs[28], occurs nonrandomly (Table 1) Specific codon choices are preferred for some amino acids, generally reflecting a preference for G or C in the third position of the codons

The translational termination codon UAA is followed by eight in-frame nonsense codons (residues 814–816, 898–900, 907–909, 919–921, 1,066–1,068, 1,084–1,086, 1,090–1,092 and 1,093–1,095) Two copies of the sequence AAUAAA (residues 1,064–1,069 and 1,091–1,096) are present in the 3′-untranslated region, the latter being located about 20 nucleotides upstream from the poly(A) tract This sequence, which commonly occurs at the equivalent position of eukaryotic mRNAs[29], is probably involved in poly(A) addition after transcription

After completion of this work, Gubler *et al*[30] published the sequence of 45 nucleotides of bovine adrenal preproenkephalin mRNA (residues 613–657) encoding a partial sequence of peptide I Their data, which were obtained by sequencing a cDNA transcript formed by reverse transcriptase-mediated elongation of a specific oligonucleotide primer corresponding to the sequence Trp-Trp-Met-Asp-Tyr-Gln, differ from ours in two residues (G for residue 648 and T for residue 627)

We thank Dr Tatsuo Ooi for his help in computer analysis of the nucleotide sequence, and Miss Michiko Asai for assistance in the synthesis of oligodeoxyribonucleotides This investigation was supported in part by research grants from the Ministry of Education, Science and Culture of Japan, the Mitsubishi Foundation and the Japanese Foundation of Metabolism and Diseases

Received 29 October, accepted 13 November 1981

1 Hughes, J *et al* *Nature* **258,** 577–579 (1975)
2 Kita, T, Inoue, A, Nakanishi, S & Numa, S *Eur J Biochem* **93,** 213–220 (1979)
3 Nakanishi, S *et al* *Nature* **278,** 423–427 (1979)
4 Hughes, J *Nature* **278,** 394–395 (1979)
5 Kimura, S *et al* *Proc natn Acad Sci USA* **77,** 1681–1685 (1980)
6 Lewis, R V *et al* *Science* **208,** 1459–1461 (1980)
7 Mizuno, K, Minamino, N, Kangawa, K & Matsuo, H *Biochem biophys Res Commun* **95,** 1482–1488 (1980)
8 Mizuno, K, Minammo, N, Kangawa, K & Matsuo, H *Biochem biophys Res Commun* **97,** 1283–1290 (1980)
9 Jones, B N *et al* *Archs Biochem Biophys* **204,** 392–395 (1980)
10 Stern, A S, Jones, B N, Shively, J E, Stein, S & Udenfriend, S *Proc natn Acad Sci USA* **78,** 1962–1966 (1981)
11 Kilpatrick, D L *et al* *Proc natn Acad Sci USA* **78,** 3265–3268 (1981)
12 Wallace, R B *et al* *Nucleic Acids Res* **9,** 879–894 (1981)
13 Hirose, T, Crea, R & Itakura, K *Tetrahedron Lett* **28,** 2449–2452 (1978)
14 Maxam, A M & Gilbert, W *Meth Enzym* **65,** 499–560 (1980)
15 Weinstock, R, Sweet, R, Weiss, M, Cedar, H & Axel, R *Proc natn Acad Sci USA* **75,** 1299–1303 (1978)
16 Blobel, G & Dobberstein, B *J Cell Biol* **67,** 852–862 (1975)
17 Steiner, D F, Quinn, P S, Chan, S J, Marsh, J & Tager, H S *Ann N Y Acad Sci* **343,** 1–16 (1980)
18 Dayhoff, M D in *Atlas of Protein Sequence and Structure* Vol 5, 173–227 (National Biomedical Research Foundation, Washington DC, 1972)
19 Kangawa, K, Minammo, N, Chino, N, Sakakibara S & Matsuo, H *Biochem biophys Res Commun* **99,** 871–878 (1981)
20 Goldstein, A, Tachibana, S, Lowney, L I, Hunkapiller, M & Hood, L *Proc natn Acad Sci USA* **76,** 6666–6670 (1979)
21 Herbert, E *et al* in *Frontiers in Neuroendocrinology* Vol 6 (eds Ganong, W F & Martini, L) 67–101 (Raven, New York, 1980)
22 Kronenberg, H M *et al* *Proc natn Acad Sci USA* **76,** 4981–4985 (1979)
23 Lund, P K, Goodman, R H & Habener, J F *J biol Chem* **256,** 6515–6518 (1981)
24 Suchanek, G & Kreil, G *Proc natn Acad Sci USA* **74,** 975–978 (1977)
25 Marshall, R D *Biochem Soc Symp* **40,** 17–26 (1974)
26 Numa, S & Nakanishi, S *Trends biochem Sci* **6,** 274–277 (1981)
27 Schultzberg, M *et al* *Neuroscience* **3,** 1169–1186 (1978)
28 Grantham, R, Gautier, C, Gouy M, Mercier, R & Pave, A *Nucleic Acids Res* **8,** r49–r62 (1980)
29 Proudfoot, N J & Brownlee, G G *Nature* **263,** 211–214 (1976)
30 Gubler, U, Kilpatrick, D L, Seeburg, P H, Gage, P & Udenfriend, S *Proc natn Acad Sci USA* **78,** 5484–5487 (198
31 Taii, S, Nakanishi, S & Numa, S *Eur J Biochem* **93,** 205–212 (1979)
32 Norgard, M V, Tocci, M J & Monahan, J J *J biol Chem* **255,** 7665–7672 (1980)
33 McReynolds, L A *et al* *J biol Chem* **252,** 1840–1843 (1977)
34 Wickens, M P, Buell, G N & Schimke, R T *J biol Chem* **253,** 2483–2495 (1978)
35 Hoeijmakers, J H J, Borst, P, van den Burg, J, Weissmann, C & Cross, G A M *Gene* **8,** 391–417 (1980)
36 Chang, A C Y *et al* *Nature* **275,** 617–624 (1978)
37 Curtiss, R III *et al* in *Recombinant Molecules, Impact on Science and Society* (eds Beers, R F & Bassett, E G) 45–56 (Raven, New York, 1977)
38 Boyer, H W & Roulland-Dussoix, D *J molec Biol* **41,** 459–472 (1969)
39 Wahl, G M, Padgett, R A & Stark, G R *J biol Chem* **254,** 8679–8689 (1979)
40 Hanahan, D & Meselson, M *Gene* **10,** 63–67 (1980)
41 Houghton, M *et al* *Nucleic Acids Res* **8,** 2885–2894 (1980)
42 Tu, C-P D & Cohen, S N *Gene* **10,** 177–183 (1980)
43 Sutcliffe, J G *Nucleic Acids Res* **5,** 2721–2728 (1978)

Molecular cloning establishes proenkephalin as precursor of enkephalin-containing peptides

Ueli Gubler[*], Peter Seeburg[†], Beth J. Hoffman[*], L. Patrick Gage[*] & Sidney Udenfriend[‡]

[*] Department of Molecular Genetics, Hoffmann-La Roche Inc, Nutley, New Jersey 07110, USA
[†] Division of Molecular Biology, Genentech Inc, South San Francisco, California 94080, USA
[‡] Roche Institute of Molecular Biology, Nutley, New Jersey 07110, USA

Molecular cloning and DNA sequencing have yielded considerable structural information about proenkephalin All previously characterized intermediate peptides of the enkephalin pathway in bovine adrenal medulla have now been aligned into an unambiguous primary structure Two basic amino acid residues serve as processing signals for release of each of the different components

ADRENAL medulla, brain and intestinal mucosa from a variety of animal species possess enkephalin-containing polypeptides (ECPs) in addition to free enkephalin[1–3] Ten to twelve ECPs, ranging in molecular weight (M_r) from ~500 (0 5K) to 12K, have been purified to homogeneity from beef adrenal medulla, many of these have been completely sequenced, others only partially[3–8] It has been suggested that these peptides are intermediates in a biosynthetic pathway starting with 'proenkephalin'[9] This protein has not yet been purified to homogeneity, but is known to have a M_r of 40–50K and to contain one Leu- and six or seven Met-enkephalin sequences[9] Such a protein precursor is a likely candidate for the primary translation product in the enkephalin biosynthetic pathway To avoid the problem of purification and sequencing of such a large and scarce protein, we cloned and sequenced proenkephalin mRNA and deduced the primary structure of the protein from its DNA sequence A previous report[10] of the partial characterization of proenkephalin mRNA included a limited nucleotide sequence analysis which clearly established the presence of mRNA sequences encoding a previously described Met-enkephalin-

0028-0836/82/030206–03$01 00

```
 I              5                 10                   15                  20
Ser-Pro-His-Leu-Glu-Asp-Glu-Thr-Lys-Glu-Leu-Gln-Lys-Arg-Tyr-Gly-Gly-Phe-Met-Arg
                                                                                 Peptide I
                25                30                   35              39
Arg-Val-Gly-Arg-Pro-Glu-Trp-Trp-Met-Asp-Tyr-Gln-Lys-Arg-Tyr-Gly-Gly-Phe-Leu

                         5'  UGG UGG AUG GAU UAU G                               mRNA
                                            C    C
                          3' ACC ACC TAC CTG ATG G 5'                            DNA primer
```

Fig. 1 The amino acid sequence and corresponding mRNA nucleotide sequence of one of the bovine adrenal ECPs (peptide I) that was used to derive the synthetic decahexamer described in ref 10 Note that DNA sequencing has allowed us to correct two errors in the published[4] amino acid sequence of peptide I residue 3 has been changed to a histidine, residue 8 to a threonine The top line shows the structure of peptide I and the middle line shows the derived mRNA sequence for the region of interest Note the extremely low degeneracy of the codons The synthetic decahexamer is shown at the bottom

containing polypeptide The mRNA was estimated to be 1,400–1,500 nucleotides long (consistent with a protein of 40–50K) and to represent 0 1% of the total poly(A^+)RNA in beef adrenal medulla

We now report the primary structure of most of the proenkephalin molecule as deduced from nucleotide sequences of cDNA clones These data show unequivocally that a proenkephalin containing at least six Met-enkephalins and one Leu-enkephalin is indeed the initial product of translation in the enkephalin biosynthetic pathway

Cloning and sequencing strategy

Total poly(A^+)RNA from bovine adrenal medulla was transcribed into double-stranded cDNA and molecules >8S were inserted into the *Sph*I restriction site of the plasmid pBR322 by the GC-tailing technique[11] Recombinant plasmids containing ~300 ng of cDNA were then introduced into *Escherichia coli* RR1 by transformation, resulting in ~70,000 clones[11] Clones were screened by the Hanahan–Meselson colony hybridization procedure[12] A synthetic decahexanucleotide was used as the radioactive probe The sequence of this probe was predicted from the available amino acid sequence of one of the characterized ECPs (Fig 1) This probe has also been used in the partial characterization of proenkephalin mRNA as described elsewhere[10] The conditions for hybridizing the decahexamer directly to colony-bearing filters were identical to those used for probing RNA blots[10] Twelve positive clones were obtained after initial screening of ~15,000 recombinants The plasmid DNA of each of these recombinants was analysed and the largest cDNA insert (1 kilobase (kb)) was sequenced using the technique developed by Messing *et al*[13] This cDNA insert proved to be a copy of proenkephalin mRNA incomplete with respect to the 3′ and 5′ ends Knowledge of its sequence, however, allowed us to select another of the recombinants that contained the complete 3′ end and its sequence was established as above The cloning and sequencing of the rest of the mRNA is in progress and will be reported in detail elsewhere

Structure of proenkephalin deduced from DNA sequencing

We used recombinant DNA technology in conjunction with microprotein chemistry to establish the structure of the major part of proenkephalin Several of the ECPs comprising proenkephalin have been isolated and their amino acid sequences determined[3–8] The nucleotide sequence of the partial cDNA clones has now allowed the alignment of these ECPs into an unambiguous primary structure and elucidated the amino acid sequences that link them (Fig 2) All the ECPs previously reported from the adrenal gland are represented in the cloned DNA sequences, which clearly establishes that proenkephalin is their common precursor (Fig 3) The largest ECP found (12 6K, Fig 3) actually extends beyond the 5′ terminus of the largest cDNA analysed The total size of the proenkephalin segment characterized in these combined studies is 27 3K, the initial translation product is certainly larger Earlier experiments[10] estimated proenkephalin mRNA to be 1,400–1,500 nucleotides long and we have accounted for ~1,000 of these in the sequence described here Therefore, we can estimate proenkephalin to be no larger than ~40K Cloning and sequencing of the 5′-terminal region of the mRNA should resolve this issue and also determine whether proenkephalin contains additional enkephalin sequences

The sequence of the proenkephalin cDNA indicates that each isolated ECP is flanked by two basic amino acid residues (Lys-Lys, Lys-Arg, Arg-Arg), demonstrating that the ECPs purified from the bovine adrenal medulla are immediate products of proenkephalin processing rather than artefacts of isolation The arrangement of two basic amino acid residues is known to be a typical prohormone processing signal[14] Moreover, each of the seven enkephalins in the precursor is preceded immediately by these processing signals, thus the N-terminal tyrosine of each of

```
                                                            Glu Cys

Ser Gln Asp Cys Ala Thr Cys Ser Tyr Arg Leu Ala Arg Pro Thr Asp Leu

Asp Pro Leu Ala Cys Thr Leu Glu Cys Glu Gly Lys Leu Pro Ser Leu Lys
----| |---- GCT TGC ACT CTG GAA TGT GAG GGG AAA CTA CCT TCT CTC AAG

Thr Trp Glu Thr Cys Lys Glu Leu Leu Gln Leu Thr Lys Leu Glu Leu Pro
ACC TGG GAA ACC TGC AAG GAG CTT CTG CAG CTG ACC AAA CTA GAA CTT CCT

Pro Asp Ala Thr Ser Ala Leu Ser Lys Gln Glu Glu Ser His Leu Leu Ala
CCA GAT GCC ACC AGT GCC CTC AGC AAA CAG GAG GAG AGC CAC CTG CTT GCT

Lys Lys Tyr Gly Gly Phe Met Lys Arg Tyr Gly Gly Phe Met Lys Lys Met
AAG AAG TAC GGG GGC TTC ATG AAG CGG TAT GGG GGC TTC ATG AAG AAA ATG

Asp Glu Leu Tyr Pro Leu Glu Val Glu Glu Glu Ala Asn Gly Gly Glu Val
GAT GAG CTG TAC CCC CTG GAA GTG GAA GAA GAG GCA AAT GGA GGT GAG GTC

Leu Gly Lys Arg Tyr Gly Gly Phe Met Lys Lys Asp Ala Glu Glu Asp Asp
CTT GGC AAG AGA TAT GGG GGC TTC ATG AAG AAG GAT GCA GAG GAA GAT GAC

Gly Leu Gly Asn Ser Ser Asn Leu Leu Lys Glu Leu Leu Gly Ala Gly Asp
GGC CTG GGC AAC TCC TCC AAC CTG CTC AAG GAG CTG CTG GGA GCC GGG GAC

Gln Arg Glu Gly Ser Leu His Gln Glu Gly Ser Asp Ala Glu Asp Val Ser
CAG CGA GAG GGG AGC CTC CAC CAG GAG GGC AGT GAT GCT GAA GAC GTG AGC
                                     *
Lys Arg Tyr Gly Gly Phe Met Arg Gly Leu Lys Arg Ser Pro His Leu Glu
AAG AGA TAC GGG GGC TTC ATG AGA GGC TTA AAG AGA AGC CCC CAC CTA GAA

Asp Glu Thr Lys Glu Leu Gln Lys Arg Tyr Gly Gly Phe Met Arg Arg Val
GAT GAA ACC AAA GAG CTG CAG AAG CGA TAC GGG GGT TTC ATG AGA AGA GTG

Gly Arg Pro Glu Trp Trp Met Asp Tyr Gln Lys Arg Tyr Gly Gly Phe Leu
GGT CGT CCA GAG TGG TGG ATG GAC TAC CAG AAA AGG TAC GGT GGC TTC CTC

Lys Arg Phe Ala Glu Pro Leu Pro Ser Glu Glu Glu Gly Glu Ser Tyr Ser
AAG CGC TTC GCC GAG CCC CTA CCC TCC GAG GAA GAA GGC GAA AGT TAC TCC
                                                        **
Lys Glu Val Pro Glu Met Glu Lys Arg Tyr Gly Gly Phe Met Arg Phe
AAG GAA GTT CCT GAA ATG GAG AAA AGA TAT GGA GGA TTT ATG AGA TTTTAAT

CCCCTTTCCCATCAGTGACCTGAAGCCCCAGCAAGCCTTCCTCTGCCCCCAGTGAAAGACTGCTGCG

CTGGTGTGTTGTATTGTCCCGAGTCGCTTGCATTATATAGTTGACTTGAGAGTCCAGATAATTAACT

ATACAACCTGAAAGCTGTGATCCCAGGTTCTGTGTTCTGAGAATCTTTAAGCTTTTAAATATTGGTC

TGTTGCAGCTGTCTTGTTTCCATGCTCAGTTTTTTGTTATCACTTTGTCCTTTATTTTTGACATAAT

GCCAATAAATGCCTACTTGTGTGTAGATATAACTAAAA-3'
```

Fig. 2 Complete nucleotide sequence and derived amino acid sequence for the 27 3K ECP The enkephalins are underlined, with the flanking basic amino acids boxed * Octapeptide, Met-enkephalin-Arg^6-Gly^7-Leu^8, ** heptapeptide, Met-enkephalin-Arg^6-Phe^7 (see text) Note that the DNA sequence obtained from the clone does not cover the entire amino acid sequence of the largest ECP The stop codon is underlined, as is the sequence AATAAA in the 3′-untranslated region of the mRNA

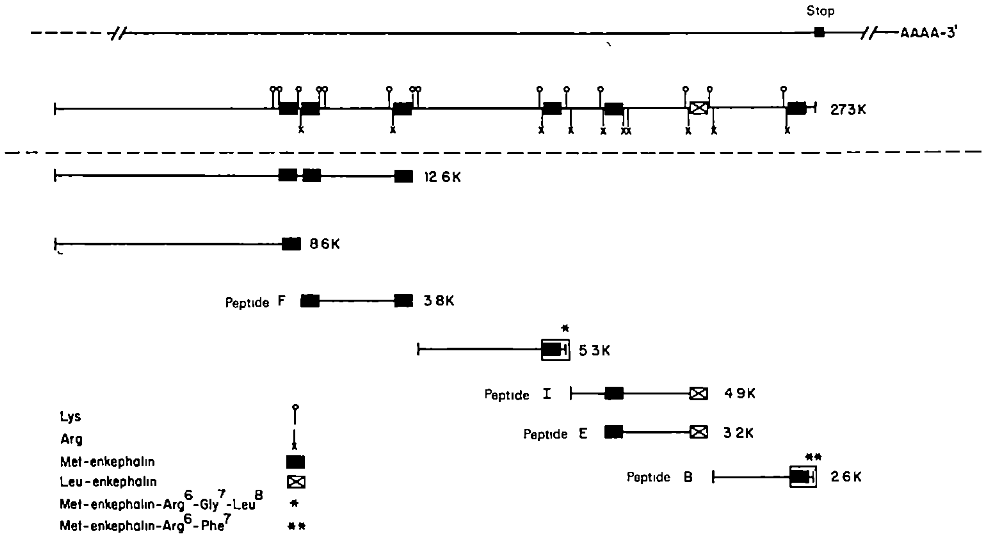

Fig. 3 Partial structure of proenkephalin and its processing At the top is shown schematically the cDNA clone, the next line represents the deduced primary structure of the 27 3K length of proenkephalin Below the broken line are shown the various ECPs whose structures are known K represents M_r of 1,000

the enkephalins, which is required for opioid activity[15], is exposed in these partially processed ECPs

Five of the enkephalins (four Met- and one Leu-enkephalin) are also immediately bounded on the C-terminal side by two basic amino acid residues, indicating that they are ultimately destined to be released as pentapeptides As mentioned above, however, they have also been isolated as parts of large ECPs from adrenal medulla (Fig 3) This observation indicates that, differential processing of proenkephalin and ECPs may occur in the tissue

Two of the Met-enkephalin peptides in proenkephalin are probably not processed to pentapeptides This is indicated by the presence of additional amino acid residues between the C-terminus of the enkephalin and the dibasic amino acid processing sites, for example, the heptapeptide Met-enkephalin-Arg^6-Phe^7, which occurs at the carboxy-terminus of the precursor This heptapeptide is found in the adrenal medulla evidently as a result of processing from proenkephalin at the Lys-Arg signal preceding the peptide It had previously been placed at the carboxy-terminus of proenkephalin because a chymotrypsinlike cleavage at the phenylalanine seemed an unlikely processing event[4] In certain assays, Met-enkephalin-Arg^6-Phe^7 has higher biological activity than free enkephalin[16], as does peptide E[7] Processing of proenkephalin also releases a Met-enkephalin Arg^6-Gly^7-Leu^8 peptide The presence of this octapeptide in adrenal medulla[8] reinforces the validity of this processing mechanism These data suggest that intermediates in the enkephalin pathway may be physiologically important and that proenkephalin yields more than free enkephalins alone

Two technical points need further comment We have not been able to substantiate the previous findings of a compound Leu-enkephalin-Arg^6 (ref 2) Due to low yields after isolation, however, this particular hexapeptide was never purified to homogeneity[2] DNA sequencing now clearly establishes that the Leu-enkephalin sequence is followed by a lysine Comparison of the partial sequence from proenkephalin mRNA reported earlier[10] with the sequence given here shows two discrepancies, but these do not alter the deduced amino acid sequence The earlier sequencing was performed on cDNA transcripts of total adrenal mRNA from several animals, the cDNA clone used here is a copy of only a single mRNA molecule Therefore, these discrepancies could reflect some polymorphism in the proenkephalin gene among the bovine population or the presence of multiple proenkephalin genes per genome

Two other ECPs found in hog tissue, dynorphin[17] and α-neo-endorphin[18], are also extensions of enkephalin at its carboxy terminus and are known to have much greater biological activity than the free enkephalins These peptides are probably products of a different ECP processing pathway as they show no apparent homology with any region of proenkephalin analysed so far except in the enkephalin sequences which they have in common However, the adrenal heptapeptide Met-enkephalin-Arg^6-Phe^7 is found in brain and intestine as well as in guinea pig adrenal gland[19] The tissue distribution of proenkephalin biosynthesis has yet to be determined, as is the origin of this heptapeptide in tissues other than the adrenal gland

β-Endorphin represents another ECP, produced in the anterior pituitary gland[20], that has enhanced biological activity relative to free Met-enkephalin, like peptide E and the heptapeptide from proenkephalin Indeed, the carboxyl extensions that distinguish these molecules may serve several roles, including that of stabilizing them against degradation, or in targeting

Proenkephalin is a unique precursor in that it contains several copies of a biologically active peptide, each in a different amino acid sequence context Complete processing of the precursor yields several enkephalins and larger ECPs The isolation of larger ECPs that are partial products of proenkephalin processing indicates that the full potential of a multivalent precursor of this kind to yield a diversity of ECPs is probably realized *in vivo*

Received 26 November, accepted 11 December 1981

1 Lewis, R V, Stern, A S, Rossier, J, Stein, S & Udenfriend, S *Biochem biophys Res Commun* **89,** 822–829 (1979)
2 Stern, A S *et al Archs Biochem Biophys* **205,** 606–613 (1980)
3 Jones, B N *et al Archs Biochem Biophys* **204,** 392–395 (1980)
4 Stern, A S, Jones, B N, Shively, J E, Stein, S & Udenfriend, S *Proc natn Acad Sci USA* **78,** 1962–1966 (1981)
5 Mizuno, K, Minamino, N, Kangawa, K & Matsuo, H *Biochem biophys Res Commun* **95,** 1482–1488 (1980)
6 Jones, B N, Shively, J E, Kilpatrick, D L, Kojima, K & Udenfriend, S *Proc natn Acad Sci USA* (in the press)
7 Kilpatrick, D L *et al Proc natn Acad Sci USA* **78,** 3265–3268 (1981)
8 Kilpatrick, D L, Jones, B N, Kojima, K & Udenfriend, S *Biochem biophys Res Commun* (in the press)
9 Lewis, R V *et al Science* **208,** 1459–1461 (1980)
10 Gubler, U, Kilpatrick, D L, Seeburg, P H, Gage, L P & Udenfriend, S *Proc natn Acad Sci USA* **78,** 5484–5487 (1981)
11 Norgard, M V, Tocci, M J & Monahan, J J *J biol Chem* **255,** 7665–7672 (1980)
12 Hanahan, D & Meselson, M *Gene* **10,** 63–67 (1980)
13 Messing, J, Crea, R & Seeburg, P H *Nucleic Acids Res* **9,** 309–321 (1981)
14 Steiner, D F, Quinn, P S, Chan, S J, Marsh, J & Tager, H *Ann N Y Acad Sci* **343,** 1–16 (1980)
15 Fredrickson, R C A Nickander, R, Smithwick, E L, Shuman, R & Norris F H *Opiates and Endogeneous Opioid Peptides,* 239–246 (Elsevier/North-Holland Biomedical, Amsterdam, 1976)
16 Inturrisi, C E *et al Proc natn Acad Sci USA* **77,** 5512–5514 (1980)
17 Goldstein, A, Tachibana, S, Lowney, L I, Hunkapiller, M & Hood, L *Proc natn Acad Sci USA* **76,** 6666–6670 (1979)
18 Kangawa, K, Matsuo, H & Igarashi, M *Biochem biophys Res Commun* **86,** 153–160 (1979)
19 Stern, A S *et al Archs Biochem Biophys* **205,** 606–613 (1980)
20 Nakanishi, S *et al Nature* **278,** 423–427 (1979)

Multiple arrangements of viral DNA and an activated host oncogene in bursal lymphomas

Gregory S. Payne*, J. Michael Bishop† & Harold E. Varmus†

Department of Biochemistry and Biophysics* and Department of Microbiology and Immunology†, University of California, San Francisco, California 94143, USA

Proviruses of avian leukosis virus (ALV) are located in the vicinity of a putative cellular oncogene (c-myc) *in ALV-induced bursal lymphomas. Enhanced expression of* c-myc *occurs in association with proviruses found in any of three configurations: (I) on the 5′ side ('upstream') of* c-myc *in the same transcriptional orientation; (II) on the 3′ side ('downstream') of* c-myc *in the same orientation; (III) upstream, in the transcriptional orientation opposite to that of* c-myc. *Thus, activation of adjacent cellular genes by retroviral DNA can involve mechanisms other than provision of a transcriptional promoter.*

AVIAN leukosis viruses (ALVs) are replication-competent retroviruses which lack transforming genes but cause tumours, most commonly bursal (B lymphocyte) lymphomas, after a lengthy latent period[1,2]. Three recent observations indicate that tumour induction by ALVs may depend on activation of cellular genes by proviral DNA, rather than on expression of viral genes. First, all bursal lymphomas are clonal populations of tumour cells containing at least one ALV provirus[3–6], but solitary proviruses are often defective and many tumours are devoid of normal virus-specific mRNAs[4,5]. Second, in most ALV-induced bursal lymphomas, proviral DNA is found in the same region of the host genome[4,5]; Hayward *et al.* have identified this locus as *c-myc*[7], the cellular homologue of the putative transforming gene (*v-myc*) of myelocytomatosis virus-29 (MC-29)[8,9]. Third, many tumours contain unusual species of polyadenylated RNA which anneal with cDNA specific for the U5 domain of the long terminal repeat (LTR) in proviral DNA (cDNA$_{5'}$, see Fig. 1*c*), but not with other viral probes[4,5]. These novel RNAs, presumed to be initiated in proviral LTRs and extended into flanking cellular DNA, appear to contain *c-myc* sequences and are many times more abundant than the usual transcriptional product of the *c-myc* locus[7].

Hayward *et al.*[7] reported that 31 of 37 lymphomas contained proviral DNA linked to *c-myc*, and the structures of proviral DNA and RNA in many of these tumours were consistent with a model in which the abundant *c-myc* transcripts were initiated within a proviral LTR positioned upstream from *c-myc* in the same transcriptional orientation. Six tumours did not show enhanced expression of *c-myc*. On the basis of these findings, it was proposed that a 'promoter insertion' mechanism operates to enhance expression of cellular oncogenes such as *c-myc* during ALV tumorigenesis.

In our previous study of four defective ALV proviruses in bursal lymphomas[4], all seemed to be located in the same region of the host genome, but two (from tumours LL1 and LL4) were in one orientation with respect to flanking DNA and two (from tumours LL2 and LL3) were in the opposite orientation. Further analysis of the tumour DNAs with probes for *c-myc* has shown that all four proviruses are located in or near the *c-myc* locus, upstream from sequences homologous to *v-myc*. The two proviruses (in LL1 and LL4) which conform to the promoter insertion model were associated, as predicted, with RNA species detectable with cDNA$_{5'}$, but similar species were not observed in LL2 or LL3 in which the proviruses and *c-myc* had opposite transcriptional orientations.

The findings with LL2 and LL3 were thus inconsistent with a promoter insertion mechanism and suggested that other kinds of regulatory events might occur in the apparent oncogenic collaboration between proviral DNA and *c-myc*. We have therefore surveyed additional ALV-induced lymphomas for the disposition of proviral DNA with respect to *c-myc* and for the composition of ALV and *c-myc*-related RNA. Our results demonstrate that at least three arrangements of proviral DNA in the *c-myc* locus are associated with enhanced levels of *c-myc* RNA: one of these arrangements is consonant with a promoter insertion mechanism but the other two—viral DNA downstream from *c-myc* in the same orientation and viral DNA upstream from *c-myc* in the opposite orientation—imply that hypotheses other than promoter insertion are required to account for the enhancement phenomena.

Strategies for studying *c-myc* activation

We have used restriction mapping procedures described by us previously[4] (see Fig. 1*c*) to characterize the structure of ALV proviruses and their integration sites in 12 chicken bursal lymphomas and 4 lymphoid cell lines. Cloned restriction fragments from the *v-myc* region of MC-29 viral DNA (see Fig. 1*b*) served as additional hybridization reagents for determining the location and transcriptional orientation of ALV proviruses with respect to at least part of the coding domain of *c-myc*. In each case examined, an ALV provirus was situated at the *c-myc* locus. Physical maps of the interrupted *c-myc* loci from lymphoma DNA were compared with a map of the normal *c-myc* locus generated from restriction endonuclease digests of chicken DNA and from digests of a cloned fragment of chicken DNA containing most or all of the *c-myc* locus (Fig. 1*a*). With these methods, we have identified seven tumours and one cell line with proviruses positioned on the 5′ side of *c-myc* in the same transcriptional orientation (configuration I), one tumour with a provirus on the 3′ side of *c-myc* in the same orientation (configuration II), and four tumours with proviruses on the 5′ side of *c-myc* but in the opposite transcriptional orientation (configuration III). We are unsure of the proviral orientation in the remaining three cell lines, each with multiple proviruses, although there is a provirus upstream from *c-myc* in every case.

We have explored the functional consequences of these arrangements of proviral and *c-myc* DNA by identifying species of polyadenylated RNA from representative tumours with hybridization probes for *myc* and for ALV sequences (particularly U3 and U5, see Fig. 1*c*). In some cases we also determined whether multiple hybridization reagents were annealing with separately co-migrating RNA species or with a single species. Below we present analyses of tumour DNA and RNA from samples illustrating the three arrangements of viral and *c-myc* sequences.

Configuration I: promoter insertion

*Eco*RI digestion of DNA from uninfected chicken cells produces a 14-kilobase pair (kbp) fragment detected by the *Pst*I fragment

0028-0836/82/030209—06$01.00

of cloned MC-29 DNA which served as our *v-myc* probe (referred to hereafter as *myc* probe, see Fig. 1*b* and Fig. 2*b*, lane 2). *myc* probe anneals with two fragments from *Eco*RI digests of DNA from tumour LL4—a new fragment of 3.1 kbp and the normal 14-kbp fragment (Fig. 2*b*, lane 1). The 3.1-kbp fragment was apparently generated by an *Eco*RI site in an ALV LTR adjacent to *c-myc*, as coincident bands were produced by hybridization to either $cDNA_{3'}$ or $cDNA_{5'}$ (Fig. 2*b*, lanes 3, 5). (Fragments of other sizes observed after hybridization of $cDNA_{5'}$ and $cDNA_{3}$, to parallel digests of control DNA (lanes 4, 6) contain sequences from ALV-related endogenous provirus[10,11].) The *Eco*RI site in the ALV LTR is known to be in the U3 domain[4,12]; if the same *Eco*RI restriction fragment anneals to probes for *myc*, U3 and U5, the provirus must be oriented so that it is transcribed in the same direction as *c-myc*. We have previously shown that the single ALV provirus in LL4 is highly defective, composed mostly, if not entirely, of a single LTR; hence, only two new ALV-related *Eco*RI fragments were detected with $cDNA_{3'}$ and only one with $cDNA_{5'}$ (Fig. 2*b*, lanes 3–6). Tests with several additional endonucleases have confirmed the conclusions drawn from the *Eco*RI data and have located the integration site of the defective provirus in LL4 ~0.5 kbp to the left of a *Sac*I site near the 5′ end of the *c-myc* sequences detectable with our *myc* probe (data not shown). Figure 2*a* shows schematically the arrangement of this provirus with respect to *c-myc*.

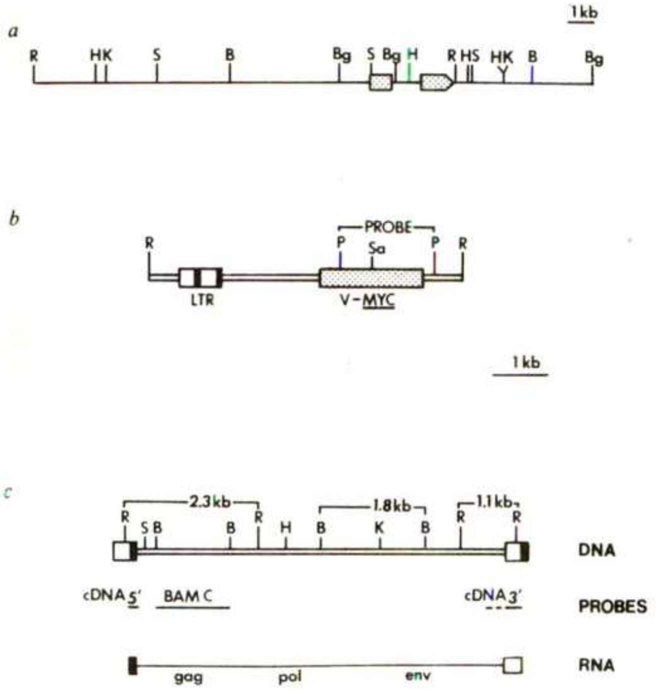

Fig. 1 *a*, Map of restriction endonuclease sites in the region of the chicken genome containing *c-myc*. The physical map of *c-myc* was generated using restriction endonuclease digests of chicken DNA. An identical map has been obtained from a cloned DNA fragment isolated from a recombinant phage library of chicken DNA (B. Vennstrom, manuscript in preparation). The domains homologous to *v-myc* are shown as shaded boxes and were determined using as probe a *Pst*I fragment of cloned MC-29 viral DNA[30], which was subcloned in pBR322. This *Pst*I fragment, as shown schematically in *b*, is 1.5 kbp long and contains, in addition to *v-myc* sequences, a short (<0.3 kbp) sequence from the *env* region of MC-29. As a result, the *v-myc* probe anneals weakly to restriction fragments of ALV-related proviral DNA containing *env* sequences, but the signal is too weak to interfere with our analyses (see Figs 2*b*, 3*b*, 4*b*). The *Pst*I site which marks the 5′ end of the *v-myc* fragment cleaves within the *v-myc* sequences (compare with *b*); thus, a small segment (probably <200 bp) of *v-myc*-specific nucleotides are not represented in the probe, and the shaded boxes may not represent all the *c-myc* coding sequences. The *v-myc* sequences in MC-29 are joined to *gag* sequences encoding viral structure protein[31] generating, on translation, a fusion protein, $P110^{gag\text{-}myc}$ (ref. 32). Thus, the structure of the *c-myc* locus is still incompletely defined, and the map does not indicate transcriptional or translational boundaries for the cellular gene. The direction of transcription of *c-myc* is indicated by the arrow-like shape of the right-hand exon and was determined by preparing restriction fragments from a *Sal*I digest of the *Pst*I *v-myc* fragment as probes specific for the 5′ and 3′ domains of *v-myc*. The length of the intervening sequence was determined by heteroduplex analysis of the cloned *c-myc* DNA fragment and MC-29 viral DNA (B. Vennstrom *et al.* in preparation). (This analysis also confirmed the transcriptional polarity of *c-myc*.) R, *Eco*RI; B, *Bam*HI; S, *Sac*I; K, *Kpn*I; H, *Hin*dIII; Bg, *Bgl*I. *b*, A diagram of cloned MC-29 viral DNA. The MC-29 DNA was cloned by linearizing circular MC-29 viral DNA with *Eco*RI and inserting the DNA into λgtWES · λB (ref. 35). The *Pst*I sites (P) and *Sal* site (Sa) used to generate *v-myc*-specific probes are shown. The *v-myc* region is shown as a shaded box. *c*, Maps of restriction endonuclease sites in RAV-2 DNA. This map was generated as described by Payne *et al.*[4]. The LTRs, ~330 bp, are drawn as boxes at the ends of the DNA. The open box represents sequences specific to the 3′ end of the viral RNA (U3) and the shaded boxes sequences specific to the 5′ end of viral RNA (U5). The approximate location of viral genes are indicated on the diagram of viral RNA. 'Signature fragments', which distinguish RAV-2 DNA from proviruses endogenous to the chickens used in the present study, are marked by lines connecting the two restriction sites. Some of the probes used in our studies represent regions delineated by the labelled lines between the diagrams of viral RNA and DNA. Descriptions of each probe are included in the text and by Payne *et al.*[4].

The configuration of the ALV provirus in LL4 suggests that transcription originating in the proviral LTR could proceed into *c-myc*, in the manner proposed by the promoter insertion model[4,5,7]. The data presented in Fig. 2*c* substantiate this prediction. A single poly(A)$^+$ RNA species of 2.5 kb was detected with $cDNA_{5'}$ (Fig. 2*c*, lane 7). No other species of RNA were observed with probes for other regions of the viral genome, including U3 (Fig. 2*c*, lane 8), a result compatible with the truncated structure of the LL4 provirus. The *myc* probe also anneals to a 2.5-kb species of RNA from LL4 (Fig. 2*c*, lane 9), suggesting that the transcripts observed with $cDNA_{5'}$ also carry *myc* sequences. Uninfected chick embryo fibroblasts also contain 2.5-kb transcripts which anneal with *myc* probe and presumably represent the normal transcription products of *c-myc*[13] (Fig. 2*c*, lane 10); *c-myc* RNA of the same size and

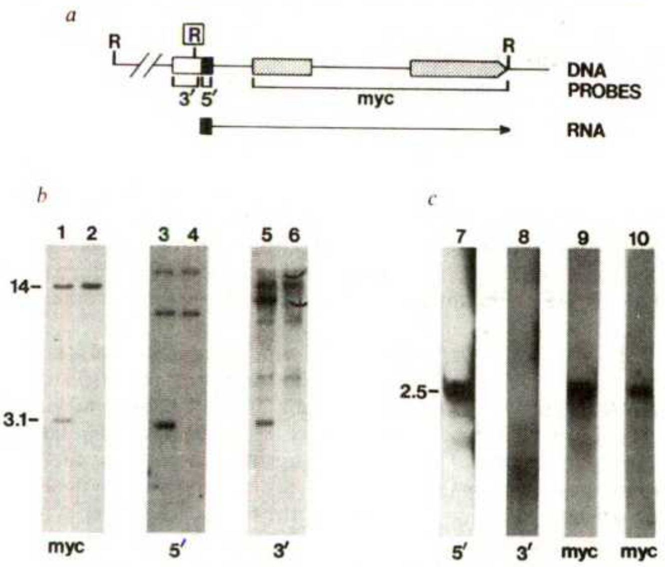

Fig. 2 Configuration I: ALV and *c-myc* DNA and RNA in tumour LL4. *a*, Diagram of the structure of the single ALV provirus in tumour LL4[4] and its position and transcriptional orientation relative to *c-myc*. The symbols for the proviral LTR and *c-myc* DNA are as described in Fig. 1 legend. Cell DNA is represented as a single line. The proviral *Eco*RI site responsible for the 3.1-kbp fragment detected in *b* is enclosed in a box. The sequences detected by the probes used in *b* and *c* are delineated under the diagram of the DNA. The virus-specific RNA in this tumour is shown schematically below the probes. (As these transcripts are equivalent in size to normal *c-myc* transcripts, we presume the hybrid RNA is processed but we are unsure of its precise composition.) *b*, 5 µg each of LL4 tumour (odd-numbered lanes) and DNA from uninfected tissue (even-numbered lanes) from the same bird were digested with *Eco*RI, electrophoresed through 0.8% agarose, transferred to nitrocellulose and annealed sequentially to the probes indicated beneath the lanes[4]. Sizes in kilobases are shown beside the lanes. *c*, Lanes 7–9, poly(A)$^+$ RNA was prepared from the tumour as described by Varmus *et al.*[17] except that frozen tissue was homogenized using a tissumizer (Tekmar) and 20-µg samples were electrophoresed through 1.2% methyl mercury agarose, transferred to diazobenzylmethoxy(DBM)-cellulose paper[33] and annealed sequentially to the designated probes[34]. Lane 10, 50 µg poly(A)$^+$ RNA from uninfected chick embryo fibroblasts was prepared and analysed as described above. The autoradiogram of lane 10 was exposed 8.7 times as long as the autoradiogram of lane 9.

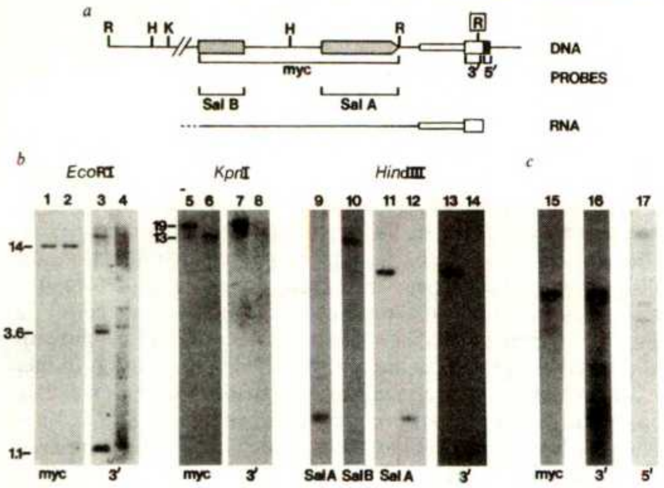

Fig. 3 Configuration II: ALV and *c-myc* DNA and RNA in tumour LL6. *a*, Diagram of the provirus and *c-myc* and the resulting transcripts in LL6 as revealed using the indicated probes in analyses shown in *b* and *c*. The symbols and the preparation of the *Sal* A and *Sal* B probes are described in Fig. 1 legend. Proviral DNA is represented as two parallel lines, cell DNA as one line. The *Eco*RI site introduced by the provirus is boxed. As explained in the text, a large deletion of cellular DNA has occurred on the 3' side of *c-myc* but the precise position and size of the deleted DNA are unknown. The *Hin*dIII, *Kpn*I and *Eco*RI sites on the right-hand side of the provirus lie beyond the region depicted and have been omitted here. *b*, Lanes 1–8, 11–14, tumour DNA (odd-numbered lanes) and uninfected DNA (even-numbered lanes) were analysed with *Eco*RI, *Kpn*I and *Hin*dIII using methods described in the legend to Fig. 2*b*. Lanes 9, 10, uninfected chicken embryo DNA analysed as for Fig. 2*b*. *c*, tumour RNA was analysed as for Fig. 2*c*.

abundance is present in normal bursal tissue (D. Sheiness and T. Gonda, personal communication). The concentration of *c-myc* RNA in LL4 was $\sim$70-fold greater than in normal tissues as determined by densitometry, with adjustments for the amounts of RNA and the autoradiographic exposure times for lanes 9 and 10 (see Fig. 2 legend). Although the transcripts revealed in lanes 9 and 10 are similar in size, we do not know the precise composition of the stable species. It is likely that the transcripts in tumour LL4 have been initiated at a novel promoter provided by the ALV LTR, elongated through the *c-myc* locus and processed to remove at least some intervening sequences.

Configuration II: proviral insertion downstream from *c-myc*

*Eco*RI digests of DNA from tumour LL6 do not contain a novel *c-myc* fragment (Fig. 3*b*, lanes 1, 2). Hybridization with cDNA$_{3'}$ (Fig. 3*b*, lanes 3, 4) confirmed that *c-myc* and ALV proviral sequences are not present in the same *Eco*RI restriction fragment. However, *Kpn*I digestion of tumour DNA produced a new *myc*-specific fragment of $\sim$19 kbp in addition to the normal *c-myc* 13-kbp fragment (Fig. 3*b*, lanes 5, 6). The relative intensity of the bands representing the two *Kpn*I fragments implies that the uninterrupted *c-myc* allele is less abundant than the normal locus. This finding has been confirmed with other enzymes (see, for example, the analysis with *Hin*dIII in lane 11) and observed with several other tumours in our collection; we presume that the tumour cells in these cases are aneuploid for the chromosome bearing *c-myc*.

The annealing of cDNA$_{3'}$ to the 19-kbp *Kpn*I fragment (Fig. 3*b*, lane 7) provides evidence for an ALV provirus between the *Eco*RI site at the 3' end of *c-myc* and a *Kpn*I site positioned further to the right. Confirmatory data for an insertion on the 3' side of *c-myc* were derived from *Bam*HI, *Bgl*I, and *Hin*dIII digests (not shown). Further support was obtained using *Sal*I–*Pst*I fragments of *v-myc* as probes to distinguish between the 5' and 3' exons of *c-myc*. When uninfected chicken DNA is digested with an enzyme (for example, *Hin*dIII) which cleaves within the only identified *c-myc* intron (B. Vennstrom *et al.*, manuscript in preparation), the *Sal* A probe (from the 3' end of *v-myc*) detects a 1.8-kbp *Hin*dIII fragment in digests of normal chicken DNA, whereas the *Sal* B probe (from the 5' end of *v-myc*) detects a 10-kbp *Hin*dIII fragment (Fig. 3*b*, lanes 9, 10). Using the *Sal* A probe to analyse digests of LL6 DNA, we identified a new *Hin*dIII fragment (6.6 kb) that also contains ALV sequences (Fig. 3*b*, lanes 11–14), confirming the position of the ALV provirus near the 3' end of *c-myc*. Further data (not presented here) show that the ALV provirus in LL6 has incurred a large deletion, leaving only the 3' LTR and $\sim$0.7 kb of adjacent viral DNA. Furthermore, a large deletion spanning at least 15 kb of cellular DNA on the 3' side of *c-myc* has occurred in this tumour, removing the *Hin*dIII, *Kpn*I and *Sac*I sites normally proximal to the 3' exon of *c-myc* (compare with Fig. 1*a*). (This deletion explains why the apparent increments in size of *Kpn*I and *Hin*dIII fragments in LL6 greatly exceed the size of the proviral insert.) Additional mapping results (not shown) place the defective provirus within 500 bp of the *Eco*RI site on the 3' side of the *v-myc*-related sequences in the same transcriptional orientation (Fig. 3*a*).

LL6 contains polyadenylated RNA of 3.7 kb which anneals to *myc* probe and cDNA$_{3'}$ but not to cDNA$_{5'}$ (Fig. 3*c*, lanes 15–17). The increase in transcript size over the size of normal *c-myc* transcripts may be partly due to ALV sequences; a probe homologous to the 3' end of *env* also hybridizes to the 3.7-kb transcripts (not shown). The concentration of this RNA was estimated to be 20 times greater than that of *c-myc* RNA in normal bursa or fibroblasts. The arrangement of the template and the size and content of the RNA suggest that transcription of *c-myc* in LL6 originates upstream from *c-myc*, perhaps at the normal initiation site, and proceeds into the ALV provirus, with termination or polyadenylation occurring in or near the end of U3 (see Fig. 3*a*). The ALV provirus has therefore altered the normal biogenesis of *c-myc* RNA, probably by replacing the *c-myc* sequences normally recognized as signals for transcript termination or polyadenylation.

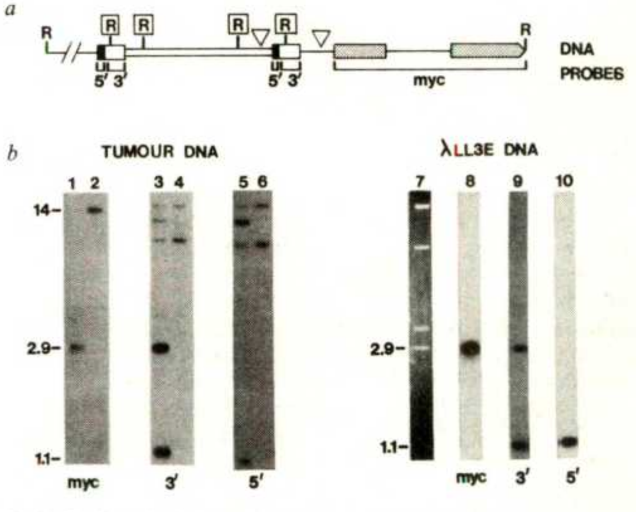

Fig. 4 Configuration III: ALV and *c-myc* DNA in tumour LL3. *a*, Diagram of the ALV provirus and *c-myc* in tumour LL3; the triangles represent deletions. The provirus in the primary tumour LL7 and its liver metastasis have a similar configuration to those in LL3 except there is no deletion in the cell DNA and the deletion within the ALV provirus is smaller. *b*, Lanes 1–6 represent analysis of *Eco*RI digests of tumour DNA (odd-numbered lanes) and uninfected tissue DNA (even-numbered lanes) using probes for *myc*, U3 and U5 as described in the legends to previous figures. Lanes 7–10 contain DNA from λLL3E, a recombinant bacteriophage carrying *c-myc* and part of the ALV provirus from LL3 tumour DNA. Lane 7, a photograph of the ethidium bromide-stained *Eco*RI digest of λLL3E DNA visualized by transillumination with UV light; lanes 8–10, autoradiograms of the results of sequential hybridizations with *myc* probe, cDNA$_{3'}$ and cDNA$_{5'}$ to cloned DNA transferred to nitrocellulose. λLL3E and two others containing different DNA fragments from the *c-myc* region of LL3 tumour DNA were isolated from a recombinant DNA library of partial products of *Sau*3A digestion of tumour DNA cloned in the bacteriophage vector λ1059[14]. Size-fractionated DNA, $\sim$20 kb long, was selected by preparative electrophoresis of 200 μg of digested DNA through low-melting agarose (Seaplaque)[4]. After recombinant molecules had been packaged *in vitro*[35] and used to infect *Escherichia coli* Q359[14], recombinant phage carrying the ALV provirus were detected using cDNA$_{3'}$ (ref. 36).

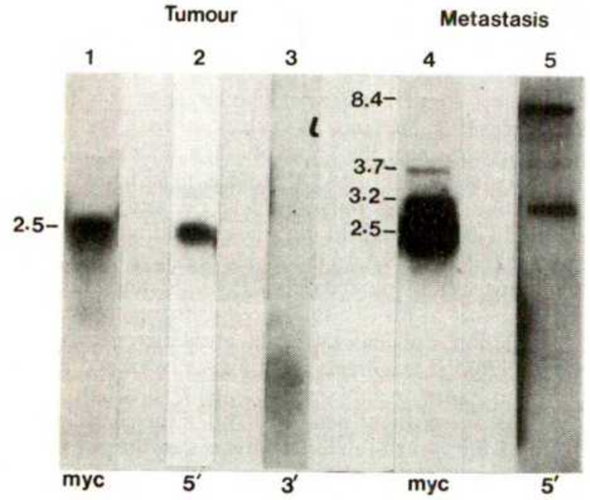

Fig. 5 Configuration III; ALV and *c-myc* RNA in tumour LL7 and its metastasis. Lanes 1–3, analysis of virus-specific RNA from bursal tumour LL7 was performed as in Fig. 2*c*. Lanes 4 and 5 represent an analysis of RNA from a liver metastasis from tumour LL7. 5 μg of poly(A)$^+$ RNA was electrophoresed through 1.2% formaldehyde agarose and transferred to nitrocellulose[37]. The sequential hybridizations using the indicated probes were performed as with the DBM-filter bound RNA.

Configuration III: proviral insertion upstream from *c-myc* in the 'opposite' orientation

Hybridization of *Eco*RI-digested LL3 DNA with *myc* probe reveals a 2.9-kbp fragment in addition to the normal 14-kbp fragment (Fig. 4*b*, lanes 1, 2). Unlike the new *Eco*RI fragment seen in digests of LL4 DNA (see Fig. 2*b*), the 2.9-kbp fragment from LL3 DNA anneals with cDNA$_{3'}$ but not cDNA$_{5'}$ (Fig. 4*b*, lanes 3–6). The most likely interpretation of these data (Fig. 4*a*) is that the LTR adjacent to *c-myc* has assumed a transcriptional orientation opposite to that of *c-myc*. Digestion of LL3 tumour DNA with *Kpn*I and *Hin*dIII followed by sequential annealings with *Bam* C probe and *myc* probe confirmed the proposed orientation (data not shown). Our conclusion is further supported by previously reported evidence that the ALV proviruses in LL3 and LL4 are in opposite orientations within the same chromosomal context[4].

We have constructed a recombinant DNA library of LL3 DNA by inserting tumour DNA partially digested with *Sau*3A into the bacteriophage vector λ1059 (ref. 14). Three recombinant phage containing the ALV provirus and flanking cell sequences were isolated from the library. Figure 4*c* shows ethidium bromide-stained, *Eco*RI-digested DNA from one of our isolates (lane 7) and the results after Southern transfer and hybridization with *myc* probe, cDNA$_{3'}$ and cDNA$_{5'}$ (lanes 8–10). The 2.9-kbp fragment derived from the cloned DNA anneals to cDNA$_{3'}$ and *myc* probe but not to cDNA$_{5'}$. These data and a more detailed analysis of our three isolates (not shown) are in complete agreement with the results obtained using tumour DNA.

Three other bursal tumours (LL2 (ref. 4), LL5 and LL7) have an arrangement of ALV DNA and *c-myc* similar to that described for LL3. We previously reported that LL2 and LL3 lack polyadenylated RNA detectable with cDNA$_{\mathrm{rep}}$ or cDNA$_{5'}$. These results, together with the conclusions from restriction mapping, imply that if the *c-myc* locus is activated by the adjacent ALV DNA in these tumours, a viral promoter is not directly responsible. To address this issue with reagents specific for *c-myc* as well as ALV sequences, we examined RNA from the primary tumour and a large hepatic metastasis of LL7. *myc* probe reveals a species of RNA in the LL7 bursal tumour migrating at 2.5 kb (Fig. 5, lane 1). Surprisingly, this RNA also seemed to react with cDNA$_{5'}$ (Fig. 5, lane 2) but not with probes for other regions of the genome, including cDNA$_{3'}$ (Fig. 5, lane 3). Because our cDNA$_{5'}$ probe is strand specific (it only detects RNA with the same polarity as the viral RNA genome), the orientation of the ALV provirus and *c-myc* in tumour LL7 precludes the possibility that ALV U5 sequences from this provirus are physically joined to a transcript of the *c-myc* coding strand (see Fig. 4*a*). This type of transcript might be produced by a subset of cells in LL7 containing a provirus upstream from *c-myc* in the same orientation. These cells could produce high levels of transcripts with U5 sequences joined to *c-myc* sequences and remain undetected in our DNA analyses if they represented <10% of the total tumour cell population.

In an attempt to isolate a homogeneous population of tumour cells, we examined a liver metastasis from the LL7 tumour. Metastases are often clonal expansions of single tumour cells[4,15]; restriction enzyme analyses of the metastasis DNA (not shown) indicated that the arrangement of ALV and *c-myc* DNA in the LL7 metastasis was identical to that in the predominant cell population in the primary tumour. However, the major 2.5-kb species of RNA from the metastasis which annealed to the *myc* probe did not react with cDNA$_{5'}$ (Fig. 5, lane 5) or anneal to probes for other regions of the ALV genome (data not shown).

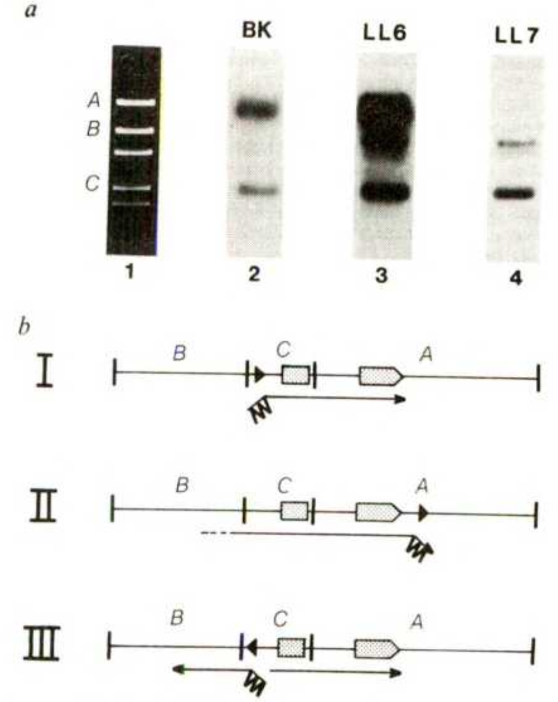

Fig. 6 Tests for linkage of ALV and *myc* sequences in tumour RNAs. The sandwich blot procedure of Dunn and Hassell[16], modified as described below, was used to assess physical linkage of ALV sequences and *myc* sequences in RNA prepared from BK 4484A cell line RNA (lane 2), LL6 RNA (lane 3) and LL7 liver metastasis RNA (lane 4). The 10-kbp *Bam*HI fragment containing *c-myc* (see Fig. 1*a*), obtained from a digest of the recombinant DNA described in Fig. 1*a* legend, was subcloned into pBR322 (D. Sheiness, unpublished). 1 μg of this plasmid, pCMC-2, was digested with *Bam*HI and *Bgl*I and electrophoresed through 1.2% agarose. The DNA was detected as described in Fig. 4 legend, then transferred to nitrocellulose. 5 μg of poly-(A)$^+$ RNA was resuspended in 200 μl of an annealing mix consisting of 50% formamide, 0.5 M NaCl, 20 mM PIPES *p*H 6.8, 5 mM Na$_2$EDTA, 0.4% SDS, 250 μg ml^{-1} poly(A), 2 × Denhardt's solution[38], 200 μg ml^{-1} carrier yeast RNA. This solution was applied to the filter-bound DNA and incubated for 24 h at 41 °C. The filter was washed twice at 53 °C for 15 min, each with 0.1 × SSC, 0.1% SDS. The filter was blotted dry and annealed to cDNA$_{5'}$ or cDNA$_{3'}$ as described by Quintrell *et al.*[34]. This filter was washed twice for 1 h each time at 37 °C with 0.1 × SSC, 0.1% SDS, dried and autoradiographed. Lane 1, photograph of ethidium bromide-stained *Bgl*I–*Bam*HI digest of pCMC-2 DNA. The bands labelled *A*, *B* and *C* result from the *c-myc* insert and are shown schematically in *b*. The other bands consist of pBR322 DNA sequences. Lanes 2, 4, filters annealed to cDNA$_{5'}$. Lane 3, filter annealed to cDNA$_{3'}$. *b*, Diagrams of transcriptional patterns in configurations I, II and III based on sandwich blots shown in *a* and analyses of tumour RNA from BK cell line (not shown), LL6 (Fig. 3*c*) and LL7 (Fig. 5, lanes 4, 5). The restriction sites are labelled as in Fig. 1*a* and the fragments designated *A*, *B* and *C* in *a* are shown. The arrowhead marks the position of the ALV provirus and indicates its transcriptional orientation. The transcriptional pattern of each configuration is shown as an arrow below the diagram. The inclined tail of an arrow marked with a serrated line indicates ALV U5 sequences detected with cDNA$_{5'}$ in configurations I and III, and ALV U3 sequences detected with cDNA$_{3'}$ in configuration II.

Thus, the metastatic process seemed to isolate a population of tumour cells with an ALV provirus upstream from *c-myc* in the opposite orientation and with enhanced expression of *c-myc* in the absence of a fused transcript. The analysis of metastasis RNA in Fig. 5 revealed minor transcripts (3.7 and 3.2 kb in lane 4; 8.4 and 3.2 kb in lane 5) which were apparently absent from the primary tumour. However, long autoradiographic exposures of the filters carrying primary tumour RNA revealed faint bands corresponding to these species (not shown). The 8.4- and 3.2-kb transcripts revealed by cDNA$_{5'}$ represent normal ALV mRNAs and imply the presence of a few cells which harbour non-defective ALV proviruses, either superinfected metastatic lymphocytes or infected normal liver cells. The coincidence of the 3.2-kb transcript detected by the probes in Fig. 5, lanes 4 and 5, can be attributed to co-migrating transcripts (see below).

The *myc* and ALV sequences are covalently joined in RNA from tumours with configurations I and II but not III

Using the 'sandwich blot' procedure of Dunn and Hassell[16] (Fig. 6), we assessed whether ALV U5 sequences were physically linked to *myc* sequences in tumour transcripts. *Bam*HI–*Bgl*I double digests of cloned chicken *c-myc* DNA were electrophoresed (Fig. 6*a*, lane 1) and transferred to nitrocellulose. Unlabelled tumour RNA was annealed to the filter-bound DNA, the filters were washed, and RNA containing ALV U5 or U3 sequences detected by hybridization to labelled cDNA$_{5'}$ or cDNA$_{3'}$. An autoradiographic signal in a position corresponding to one of the *Bam*HI–*Bgl*I restriction fragments indicates physical linkage in RNA of sequences homologous to both the restriction fragment and the ALV LTR. When we used RNA from a tumour cell line (BK 4484A) containing an ALV provirus upstream from *c-myc* in a parallel orientation (configuration I), we observed bands corresponding to fragments *A* and *C* but not *B* when cDNA$_{5'}$ was used as a radioactive probe (Fig. 6*a*, lane 2). This result proves that these cells contain transcripts consisting of ALV U5 sequences physically linked to the *c-myc* sequences in fragments *C* and *A*. This conclusion is shown schematically in configuration I of Fig. 6*b* and conforms to the promoter insertion model.

Figure 6*a*, lane 3, demonstrates that ALV U3 sequences and *myc* sequences are physically linked in RNA from tumour LL6. The signal observed with cDNA$_{3'}$ at the position of fragment *B* locates the 5′ end of these transcripts at least 1 kb upstream from the *Sac*I site marking the 5′ end of the *c-myc* sequences detected by our probe (see Figs 1*a*, 6*b*). If these transcripts originate at the normal *c-myc* promoter, these data place that promoter to the left of the *Bgl*I site which defines the right end of fragment *B* (see configuration II in Fig. 6*b*). Studies of three tumours (LL4, LL5 and LL7) and one cell line (BK 4484A) showed that each provirus is integrated to the right of this *Bgl*I site. Thus, proviruses integrated 5′ to *c-myc* in configurations I and III (see below) would be positioned between the normal promoter and the *myc* sequences that we have detected at increased concentrations in tumour RNA; this could mean that a secondary initiation site is used for *myc* RNA in these cases. We cannot, however, exclude other possibilities; for example, the transcripts in tumour LL6 may be initiated aberrantly, thus obscuring the location of the true *c-myc* promoter, or viral sequences could be transcribed in configuration III and removed from RNA by splicing.

RNA from the LL7 metastasis contains transcripts with U5 joined to sequences in fragments *C* and *B* but not *A* (Fig. 6*a*, lane 4). Because restriction mapping data (not shown) place the ALV provirus in LL7 5′ to the *c-myc* sequences detected by our probe, the sandwich blot indicates that transcription probably originates in the proviral LTR and proceeds through the region represented in fragment *C* and into that contained in fragment *B*. It also confirms that ALV U5 sequences are not joined to the identified *c-myc* coding sequences in transcripts (Fig. 5). Thus, the 3.2-kb RNA species revealed in Fig. 5, lanes 4 and 5, probably represents co-migration of *env* mRNA and a minor *c-myc* transcript containing no ALV sequences.

The ALV provirus can act as an insertional mutagen

We have assessed the relative configurations of ALV proviruses and *c-myc* in 12 ALV-induced bursal lymphomas and 4 cell lines derived from ALV-induced tumours. Each tumour or cell line harboured an ALV provirus situated in the region of *c-myc*, and, in every case examined (five tumours and four cell lines), this insertion was associated with levels of *myc*-containing transcripts elevated 20–100-fold over levels of *c-myc* transcripts in uninfected bursa. These data further support the proposal[7] that ALV exerts its oncogenic effects by increasing the expression of *c-myc*.

Based on the structures of *c-myc* DNA and RNA in their tumours, Hayward *et al.*[7] have argued that the increased level of *c-myc* transcription is uniformly due to the insertion of an ALV promoter upstream from the gene, thus subverting the expression of *c-myc* by supplying a promoter more efficient than its own. In contrast, we have shown that ALV proviruses can assume three different configurations with respect to *c-myc*, and that each configuration is associated with increased transcription of *c-myc*. We have been unable to identify a significant divergence in experimental protocol that might explain the differences between our results and those of Hayward *et al.* In view of our results, we propose that the ALV provirus (specifically the LTR) can act as an insertional mutagen capable of enhancing the expression of a cellular gene, *c-myc*, by as yet unknown mechanisms, one aspect of which may be reflected in promoter insertion.

The belief that these phenomena are instrumental in lymphomagenesis is founded primarily on the extraordinary frequency with which proviral insertions in the *c-myc* locus and high levels of *c-myc* RNA are encountered in ALV-induced bursal tumours. However, the techniques used thus far have not identified the stage of tumour induction at which *c-myc* is affected, nor have they fully assessed the possibility that sequential rearrangements have occurred at the proviral integration sites within the *c-myc* locus. (In fact, deletions affecting proviral or flanking cellular sequences have been encountered at a much greater frequency in this experimental context[4–6] than in others (see ref. 17).) In addition, transformation experiments with DNA from bursal lymphomas indicate that oncogenic loci devoid of viral or *c-myc* sequences may also be activated during the neoplastic process[18,19].

The transcriptional enhancement exerted by the ALV provirus during leukaemogenesis constitutes one of two possible mutagenic effects on the host genome following retroviral DNA insertion: proviruses can also inactivate host genes. The abolition of *v-src* expression due to the insertion of Moloney murine leukaemia virus (Mo-MLV) DNA into a Rous sarcoma virus provirus has recently been observed in culture[17]. Also, the mouse genotype *dilute* may be due to an endogenous MLV provirus inserted at a coat colour-determining locus[20]. The mutagenic properties of retroviral proviruses, as well as structural features[21], are shared with transposable elements found in bacteria and yeast. Although transposable elements have usually been reported to inactivate genes when they induce mutations[22], this probably reflects the genetic selection used; IS*2* in bacteria[23] and Ty*1* in yeast[24,25] also alter the expression of adjacent genes in a positive manner by mechanisms still incompletely defined.

The mechanism of transcriptional enhancement

The mechanism of ALV-induced enhancement of *c-myc* expression also remains obscure. However, two general, non-exclusive proposals can be considered. First, the increase of *c-myc* expression in each of the three observed configurations may reflect properties of *c-myc*. *c-myc* could be under the control of *cis*-acting regulatory elements either 5′ or 3′ to the gene. Integration of ALV DNA into these sequences could then release *c-myc* from their influence. Experiments of Cooper *et al.*[26] suggest that *cis*-acting sequences regulate expression of endogenous chicken proviruses, and *cis*-acting regulators on the 3′ side of a gene have been reported for the mating type locus in yeast[27] and the fetal globin genes in humans[28]. A second, more likely proposal postulates that enhancement reflects a distinctive property of the provirus rather than a property of *c-myc*. For example, the provirus could increase the accessibility of *c-myc* to the host cell's transcriptional machinery by altering the nucleosome positions in the region of *c-myc*. This could account for increased *c-myc* expression in each configuration. Alternatively, the mechanism of enhancement could be unique for each configuration. The proviral LTR could act as a *c-myc* promoter if inserted in the correct orientation upstream from *c-myc*. If inserted in the proper orientation downstream from *c-myc*, the provirus could act to stabilize the *c-myc* transcripts. If inserted upstream from *c-myc* but in an opposite orientation, it could affect chromatin structure or bind accessory transcriptional factors in ways which might increase transcription in both directions.

The hypothesis that a retroviral LTR can enhance the expression of a linked gene may find support in experiments which introduce selectable genes into cultured cells either as a calcium phosphate precipitate or by microinjection. The Moloney murine sarcoma virus LTR markedly augments the frequency of morphological transformation of NIH-3T3 cells by a restriction fragment containing the putative transforming gene of murine sarcoma virus (*v-mos*). This augmentation occurs when the LTR is positioned on either the 5′ or 3′ side of the viral oncogene[29]. When the LTR has been positioned downstream from *v-mos* with the same transcriptional polarity, transcripts which proceed through *v-mos* and terminate in the U3 region are observed in the transformed cells (T. Wood and G. Vande Woude, personal communication). This situation is analogous to the transcriptional pattern found in tumour LL6. Placement of the Rous sarcoma virus LTR at either the 5′ or 3′ end of a complete herpes simplex virus thymidine kinase (HSV-*tk*) gene, including the true HSV-*tk* promoter, enhances the number of HSV-*tk*-positive colonies after microinjection into tk^- mouse L cells (P. Luciw and M. Capecchi, personal communication). It is unclear whether the effect of the retroviral LTR in these cell culture experiments is to increase transcription of the adjacent genes.

In conclusion, we have proposed that the ALV provirus contains a previously unknown ability, independent of its configuration, to affect the transcriptional activity of adjacent cellular DNA. The transcriptional enhancement provided by the ALV provirus suggests that novel mechanisms may control the expression of eukaryotic genes.

We thank Bjorn Vennstrom, Diana Sheiness and Ron Swanstrom for provision of cloned DNA, Lyman Crittenden for supervising the induction of the tumours, W. Hayward for communicating results before publication, S. Courtneidge and H. Hihara for providing the tumour cell lines, J. Migneault for typing the manuscript, and our colleagues, particularly Steve Hughes, Ron Swanstrom, Richard Parker and John Majors, for advice and discussion. This work was supported by grants from the American Cancer Society and the NIH; G.P. is supported by an NIH training grant.

Received 7 August; accepted 2 November 1981.

1. Purchase, H. R. & Burmester, B. R. in *Diseases of Poultry* (eds Hofsad, M. S., Calneck, B. W., Helmboldt, D. F., Reid, W. M. & Yoder, H. M.) 418–468 (Iowa State University Press, 1978).
2. Vogt, P. K. in *Comprehensive Virology* Vol. 9 (eds Fraenkel-Conrat, H. & Wagner, R. R.) 341–455 (Plenum, New York, 1977).
3. Neiman, P., Payne, L. M. & Weiss, R. A. *J. Virol.* **34,** 178–186 (1980).
4. Payne, G. S. *et al. Cell* **23,** 311–322 (1981).
5. Neel, B. G., Hayward, W. S., Robinson, H. L., Fang, J. & Astrin, S. M. *Cell* **23,** 323–334 (1981).
6. Fung, Y. K., Fadly, A., Crittendon, L. B. & Kung, H. J. *Proc. natn. Acad. Sci. U.S.A.* **78,** 3418–3422 (1981).
7. Hayward, W. S., Neel, B. G. & Astrin, S. M. *Nature* **290,** 475–480 (1981).
8. Roussel, M. *et al. Nature* **281,** 452–455 (1979).
9. Sheiness, D. K. & Bishop, J. M. *J. Virol.* **31,** 514–521 (1979).
10. Astrin, S. M. *et al. Cold Spring Harb. Symp. quant. Biol.* **44,** 1105–1110 (1979).
11. Hughes, S. H., Toyoshima, K., Bishop, J. M. & Varmus, H. E. *Virology* **108,** 189–207 (1981).
12. Shank, P. R. *et al. Cell* **15,** 1383–1395 (1978).
13. Sheiness, D. K., Hughes, S. H., Varmus, H. E., Stubblefield, E. & Bishop, J. M. *Virology* **105,** 415–424 (1980).
14. Karn, J., Brenner, S., Barnett, L. & Cesarini, G. *Proc. natn. Acad. Sci. U.S.A.* **77,** 5172–5176 (1980).
15. Poste, G. & Fidler, I. J. *Nature* **283,** 139–146 (1980).
16. Dunn, A. R. & Hassell, J. A. *Cell* **12,** 23–36 (1977).
17. Varmus, H. E., Quintrell, N. & Ortiz, S. *Cell* **25,** 23–35 (1981).
18. Cooper, G. M. & Neiman, P. E. *Nature* **287,** 656–658 (1980).
19. Cooper, G. M. & Neiman, P. E. *Nature* **292,** 857–859 (1981).
20. Jenkins, N. A., Copeland, N. G., Taylor, B. A. & Lee, B. K. *Nature* **293,** 370–374 (1981).
21. Majors, J. E. *et al. Cold Spring Harb. Symp. quant. Biol.* **45,** 731–738 (1980).
22. Kleckner, N. *Cell* **11,** 11–23 (1977).
23. Saedler, H., Reif, J. H., Hu, S. & Davidson, N. *Molec. gen. Genet.* **132,** 265–289 (1974).
24. Errede, B. *et al. Cell* **22,** 427–436 (1980).
25. Williamson, V. M., Young, E. T. & Ciriacy, M. *Cell* **23,** 605–614 (1981).
26. Cooper, G. M. & Silverman, L. *Cell* **15,** 573–577 (1978).
27. Nasmyth, K. A., Tatchell, K., Hall, B. D., Astell, C. & Smith, M. *Nature* **289,** 244–250 (1981).
28. Maniatis, T., Fritsch, E. F., Lauer, J. & Lawn, R. M. *A. Rev. Genet.* **14,** 145–178 (1980).
29. Oskarsson, M., McClements, W. L., Blair, D. G., Maizel, J. V. & Vande Woude, G. F. *Science* **207,** 1222–1223 (1980).
30. Vennstrom, B., Moscovici, C., Goodman, H. M. & Bishop, J. M. *J. Virol.* **39,** 625–631 (1981).
31. Hu, S. F., Lai, M. M. C. & Vogt, P. K. *Proc. natn. Acad. Sci. U.S.A.* **76,** 1265–1268 (1979).
32. Bister, K., Hayman, M. J. & Vogt, P. K. *Virology* **82,** 431–448 (1977).
33. Alwine, J. C., Kemp, J. & Stark, G. *Proc. natn. Acad. Sci. U.S.A.* **74,** 5350–5354 (1977).
34. Quintrell, N., Hughes, S. H., Varmus, H. E. & Bishop, J. M. *J. molec. Biol.* **143,** 363–393 (1980).
35. Blattner, F. R. *et al. Science* **202,** 1279–1288 (1978).
36. Benton, W. D. & Davis, R. W. *Science* **196,** 180–181 (1977).
37. Thomas, P. S. *Proc. natn. Acad. Sci. U.S.A.* **77,** 5201–5205 (1980).
38. Denhardt, D. T. *Biochem. biophys. Res. Commun.* **23,** 641–646 (1966).

LETTERS TO NATURE

Occurrence of the 3.3-μm feature in galaxies

T. J. Lee*, D. H. Beattie*, Ian Gatley*,
P. W. J. L. Brand†, T. Jones‡ & A. R. Hyland‡

* UK Infrared Telescope, 900 Leilani Street, Hilo, Hawaii 96720, USA
† Department of Astronomy, University of Edinburgh, Edinburgh EH9 3HJ, UK
‡ Australian National University, Canberra ACT, Australia

Many emission features have been discovered, in dusty ionized regions such as planetary nebulae or H II regions, with wavelengths longer than 2 μm (ref. 1). Some are gaseous emission lines but many that are too broad to be due to single atoms are attributed to emission from dust grains in or near the ionized gas. The feature at 3.28 μm ('the 3.3-μm feature') has been observed in H II regions[2,3] in planetary nebulae[4] and in particular, in the following extragalactic objects: 3C273 (ref. 5) (quasar), NGC4151 (ref. 6), M82 (ref. 7), NGC253 (ref. 8), NGC2903 (ref. 9), NGC5195 (ref. 9) and NGC6946 (ref. 9). We report here new measurements which contradict some of these results. In particular, we find the feature in the late-type galaxy M83 but do not observe it in either the Seyfert galaxy NGC4151 or the quasar 3C273.

The mechanism that produces the line is thought to be due either to fluorescence of the grains in a UV radiation field[10] (but this requires very high efficiencies) or to the heating of very small grains to high temperatures (several hundred degrees)[11]. The presence of the feature in extragalactic objects such as late-type galaxies is not surprising because these objects contain many H II regions. Measures of equivalent width of the feature will indicate the chemical composition, once studies of galactic objects have established the exact nature of the mechanism. In objects such as Seyfert galaxies and quasars, however, the presence or absence of the 3.3μm feature is important as it is one

0028–0836/82/030214—02$01.00

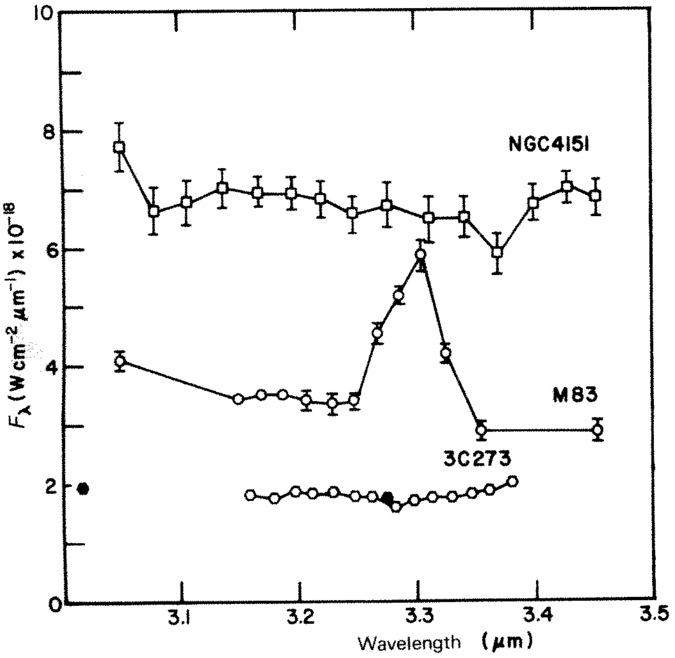

Fig. 1 The circular variable filter spectra of the three objects: NGC4151, M83 and 3C273. The wavelengths are rest wavelengths and broad-band filter measurements are also plotted for the quasar 3C273 as solid symbols. The error bars are ±1 s.d.

of the few unambiguous dust indicators available to settle the question of the presence of dust grains in the nuclei of active galaxies.

As part of a programme to observe a larger number of objects, we have measured the spectra of 3C273, M83 and NGC4151 in the region of the local rest wavelength of the 3.3-μm feature. This was carried out on the nights of 21, 22 and 23 May (UT) 1981, one object being measured each night. In addition, NGC4151 had been observed on 12 April 1981. During these nights the sky was clear above Mauna Kea summit and the visibility good. The telescope and instrumentation used were the UK Infrared Telescope (3.8 m) with an InSb CVF spectrophotometer (1% resolution). Apertures and chopper throws respectively were 7.3 and 13 arc s for 3C273, 10.8 and 18 arc s for M83, and 14.4 and 18 arc s for NGC4151. The wavelengths at which measurements were taken were spaced at 0.02-μm intervals near to the position of the feature and a few more widely spaced points were also measured. In addition broadband data were obtained. At each observed point several 10-s integrations were made and total integration times were 5,600 s for 3C273,4,820 s for M83 and 5,640 s for NGC4151. The spectra are shown in Fig. 1, where the flux density F_λ is plotted against the rest wavelength. For both 3C273 and M83 two spectra were averaged, while for NGC4151 the April data are shown.

The April data on NGC4151 are the more extensive in wavelength and of better signal-to-noise ratio. These data set a 3σ upper limit of 8% of continuum on line height above the continuum (while the May data set a poorer upper limit of 23%). For 3C273, the corresponding limit is 9% of continuum. These limits are conservative, being based on the assumption of a flat baseline, and the spectral profile of the CVF. If the continuum outside the region of the line were to be slightly curved this would reduce the upper limits by a factor of ~2. These limits should be compared with previously[5,6] suggested values of 30% and 40% respectively. Although both 3C273 and NGC4151 are variable by a few tens of per cent, our continuum levels are sufficiently close to, and also fainter than, the previously measured continuum levels, and this cannot cause such a discrepancy.

In M83, a late-type galaxy with H II regions in its nuclear region[12], the 3.3-μm feature is clearly seen in Fig. 1. Equally clearly, at the levels discussed above, the feature is not present in either the Seyfert galaxy NGC4151 or the quasar 3C273. The excellent transparency in the 3-μm region at the summit of Mauna Kea and high instrumental instantaneous signal-to-noise ratios mean that previous detection of the 3.3-μm feature must be considered suspect. This experiment shows no evidence for dust in the Seyfert galaxy NGC4151 or the quasar 3C273, but clearly demonstrates that the dust in M83 and in H II regions in our Galaxy share similar properties.

Received 7 October; accepted 30 November 1981.

1. Aitken, D. K. *IAU Symp. No.* **96,** (1980).
2. Grasdalen, G. L. & Joyce, R. R. *Astrophys. J. Lett.* **205,** L11 (1976).
3. Aitken, D. K., Roche, P. F., Spencer, P. M. & Jones, B. *Astr. Astrophys.* **76,** 60. (1979).
4. Merrill, K. M., Soifer, B. T. & Russell, R. W. *Astrophys. J. Lett.* **200,** L37 (1975).
5. Allen, D. A. *Nature* **284,** 323–324 (1980).
6. Cutri, R. M. & Rudy, R. J. *Astrophys. J. Lett.* **241,** L141–144 (1980).
7. Willner, S. P., Soifer, B. T., Russell, R. W. Gillett, F. C. & Joyce, R. R. *Astrophys. J. Lett.* **217,** L121 (1977).
8. Russell, R. W., Soifer, B. T. & Willner, S. P. *Astrophys. J. Lett.* **217,** L148 (1977).
9. Lebofsky, M. J. & Rieke, G. H. *Astrophys. J.* **229,** 111 (1979).
10. Allamandola, L. J., Greenberg, J. M. & Norman, C. A. *Astro. Astrophys.* **77,** 66 (1979).
11. Dwek, E., Sellgren, K., Soifer, B. T. & Werner, M. W. *Astrophys. J. Lett.* **238,** L140 (1980).
12. Dufour, R. J., Talbot, R. J. & Jensen, E. B. *Astrophys. J.* **236,** 119 (1980).

γ-Quanta capture by magnetic field and pair creation suppression in pulsars

A. E. Shabad

P. N. Lebedev Physical Institute, Leninskiy prospect 53,
Moscow, USSR

V. V. Usov

Space Research Institute, Profsoyusnaya 88, Moscow, USSR

The theory[1] that electron–positron pairs in magnetospheres of pulsars are created by the interaction of γ-quanta with the magnetic field B is the basis of the modern theory of pulsars[2,3]. When considering the process $\gamma + B \rightarrow e^+ + e^- + B$ in pulsars it is usually accepted that the γ-quanta produced by the curvature irradiation of the primary particles are emitted tangentially to the curved line of force of magnetic field and propagate directly. As they do so the pitch angle between the photon wave vector K and the magnetic field B increases until a certain value ψ_1 when the absorption of the photon through pair creation becomes possible. We emphasize here that if the resonant behaviour characteristic of the vacuum polarization in a magnetic field[4,5] is considered this picture changes considerably. Namely, the trajectories of γ-quanta are strongly bent towards the direction of the magnetic field if the latter is sufficiently intense and at the same time the creation is suppressed. We also discuss the effect this may have on the energy yield of pulsars.

In a medium possessing a space-non-uniform refraction index, to which a strong magnetic field with curved lines of force in a vacuum is an example, a photon must propagate along a curved path. However, in this case the path would be curved negligibly as long as the traditional expression[6] for the refraction index is used which differs from unity only by $\sim 10^{-5}$ (for the fields $B \sim 10^{12}$ G). The expressions given in ref. 6, as well as those in later publications, however, do not cover the resonant situation which occurs in the vicinity of the pair creation threshold. This resonant situation has been examined[4,5] on the basis of the first off-mass-shell calculation of the polarization operator in an external magnetic (with electric, as well) field outlined in ref. 7 for arbitrarily strong fields. It was found that the dispersion curve deflects from its conventional shape $\omega/c = |\mathbf{K}|$ which survives only in the region far away from the resonance (ω is the frequency). The resonant dependence of the component $K_\parallel$ of the photon wave vector parallel to the

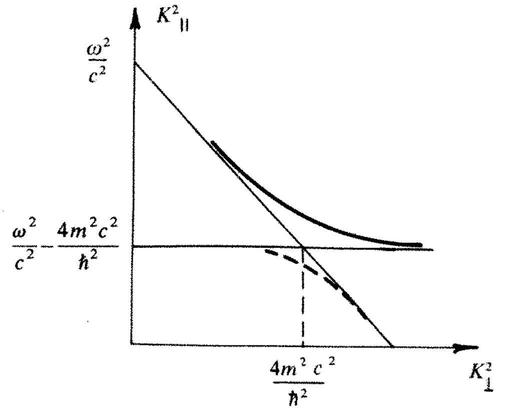

Fig. 1 Two disconnected branches of the dispersion curve of the photon in a magnetic field.

magnetic field **B** on its component $K_\perp$ across **B** with ω kept fixed is shown in Fig. 1. Part of the dispersion curve near the first threshold

$$(K^2_\parallel)_{\text{thr}}=\frac{\omega^2}{c^2}-\frac{4m^2c^2}{\hbar^2} \tag{1}$$

is shown as the solid line in Fig. 1. For $K^2_\parallel \leqslant (K^2_\parallel)_{\text{thr}}$ electrons and positrons are virtually created. Other thresholds, if the value of ω is large enough, are located between the lines $K^2_\parallel = (K^2_\parallel)_{\text{thr}}$ and $K^2_\parallel = 0$. The solid dispersion curve near the threshold is given by the relation

$$K^2_\parallel=\frac{\omega^2}{c^2}+f(K^2_\perp) \tag{2}$$

where

$$f(K^2_\perp)=-\frac{4m^2c^2}{\hbar^2}-\frac{2}{3}\left(K^2_\perp-\frac{4m^2c^2}{\hbar^2}\right)+[((\phi^2+g^3)^{1/2}+\phi)^{2/3}+((\phi^2+g^3)^{1/2}-\phi)^{2/3}]\frac{m^2c^2}{\hbar^2} \tag{3}$$

Here

$$g=\frac{1}{3}\left(\frac{\hbar^2K^2_\perp}{m^2c^2}-4\right), \qquad \phi=\alpha\frac{B}{B_{\text{cr}}}\exp\left(-\frac{K^2_\perp c\hbar}{2eB}\right)$$

where

$$\alpha=1/137, \qquad B_{\text{cr}}=\frac{m^2c^3}{e\hbar}\simeq 4\times10^{13}\text{ G}$$

Near the threshold (1) both $K^2_\perp$ and the refraction index tend to infinity. This singularity may be traced back to the fact that the spectra of electron and positron in magnetic field are partially discrete. The infinite behaviour of $K^2_\perp$ is just what we described as the resonance. Away from the threshold the dispersion curve in Fig. 1 approaches the sloping line $\omega^2/c^2=K^2_\perp+K^2_\parallel=\mathbf{K}^2$. The dashed line in Fig. 1 shows the real part of the dispersion curve in the region of absorption. The frequency here has an imaginary part which is responsible for pair creation. The analytical expressions for the real and imaginary parts of the dispersion curve in this region are given elsewhere[5]. Note that above the horizontal threshold line in Fig. 1 no pair creation by the photon is possible. Figure 1 relates to the case when the magnetic field is constant in magnitude and direction. The stronger the field, the larger is the gap between the two branches of the dispersion curves in Fig. 1:

$$\Delta K_\parallel\sim\left(\frac{\alpha B}{B_{\text{cr}}}\right)^{2/3}\frac{mc}{\hbar}\exp\left(-\frac{4B_{\text{cr}}}{3B}\right)$$

The flattening of the dispersion curve (2) near the threshold causes the group velocity component across the field $\nu_\perp = d\omega/dK_\perp$ to tend to zero when $K^2_\parallel \to (K^2_\parallel)_{\text{thr}}$ from inside the region $K^2_\parallel > (K^2_\parallel)_{\text{thr}}$, the energy of the photon thus being carried along the magnetic field. Previously a constantly-directed magnetic field was considered and this chanelling effect discussed as a refraction on its edge.[4,5]. With the present knowledge of the pulsar phenomena, however, it is more reasonable to consider a constant magnetic field B, but with curved lines of force, and a photon which appears inside it and is directed under a certain initial pitch angle

$$\psi_0=\tan^{-1}\frac{K_\perp(0)}{K_\parallel(0)}<\psi_1$$

with respect to the line of force. Assuming that the curvature radius of the line of force is much greater than the wavelength and other characteristic length parameters, we may also apply the above dispersion pattern to the present case of non-uniform magnetic field. Because the dispersive properties of the 'medium' are directionally non-uniform but constant in time, the frequency of the photon is conserved whereas its wave-vector components are not, and the photon 'travels' along its dispersion curve in Fig. 1. Classically one allows for the possibility that the photon may travel along the sloped straight line in Fig. 1, which is the empty space dispersion law. In this case the path of the photon in space is also straight. After the photon reaches the threshold line in Fig. 1 (when the pitch angle reaches the value $\tan\psi_1=(2mc/\hbar)(\omega^2/c^2-4m^2c^2/\hbar^2)^{-1/2}$, and crosses it) the pair creation becomes allowed kinematically.

However, as long as the dispersion law (2) may be taken seriously (restrictions will be discussed below), the photon travels along the true dispersion curve (solid line in Fig. 1) and never crosses the threshold. Its frequency remains real and the pair cannot be created in the experiment under consideration. This does not stop a photon creating a pair if the former has been prepared below the threshold line, for example, has appeared with the pitch angle exceeding ψ_1. The present situation is analogous to that known in the theory of polaritons[8]. Instead of creating the pair, the photon, in accordance with the above comment on the vanishing of $\nu_\perp$, should turn in the space along the magnetic field when approaching the threshold.

To describe the trajectory of the photon we restrict ourselves to the case of magnetic field whose strength is constant and lines of force are concentric circles. These simplifying assumptions allow us to solve the refraction problem analytically and produce a model sufficiently representative to allow the situation in the more realistic dipole magnetic field to be assessed. Within geometrical optics, the law of refraction may be derived using the fact that the photon travels in a medium whose refraction index is different in each spatial point depending on the direction of the magnetic field in it. For the special case under consideration and the photon moving away from the centre the infinitesimal form of the refraction law is $dK_\perp = K_\parallel\, d\alpha$ where $K_\parallel$ is understood as the function of $K_\perp$ given by equation (2). Taken in conjunction with the equations $dr=\nu_\perp\, dt$, $r\, d\alpha=\nu_\parallel\, dt$ which describe the motion of the centre of the wave packet, with **v**

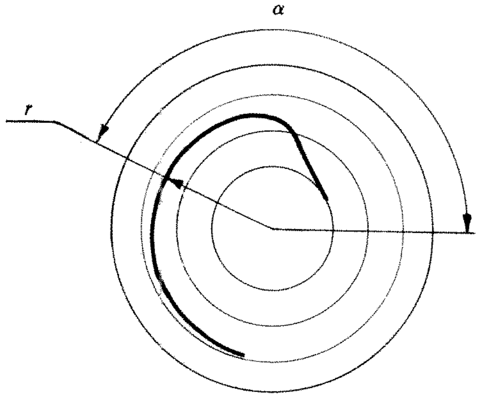

Fig. 2 The photon trajectory in a constant concentrical magnetic field (the solid line). The circles denote the lines of force.

being the group velocity

$$\nu_\perp = \frac{\mathrm{d}\omega}{\mathrm{d}K_\perp} = -\frac{c^2}{\omega}\frac{\mathrm{d}f}{\mathrm{d}K_\perp^2}K_\perp, \qquad \nu_\parallel = \frac{\mathrm{d}\omega}{\mathrm{d}K_\parallel} = \frac{c^2}{\omega}K_\parallel \tag{4}$$

this leads to the law of motion of the γ-quanta

$$t = \frac{\omega r(0)K_\parallel(0)}{c^2}\int_{K_\perp(0)}^{K_\perp}\frac{\mathrm{d}x}{K_\parallel^3(x^2)}$$

$$r = r(0)\frac{K_\parallel(0)}{K_\parallel(K_\perp^2)}, \tag{5}$$

$$\alpha = \int_{K_\perp(0)}^{K_\perp}\frac{\mathrm{d}x}{K_\parallel(x^2)}$$

Here the polar coordinates of the photon r, α and the time t are expressed as depending on the unique parameter $K_\perp$ which gives the corresponding position of the photon on the dispersion curve. The function $K_\parallel^2(x^2)$ is equation (2) using x^2 in place of $K_\perp^2$.

If the traditional dispersion law $K_\parallel^2 = \omega^2/c^2 - K_\perp^2$ is substituted into equations (5) the latter describe the photon propagating along a straight path with the constant speed c. If we approximate the dispersion law (2) by the broken line: $f(K_\perp^2) = -K_\perp^2$ for $K_\perp^2 < 4m^2c^2/\hbar^2$ and $f(K_\perp^2) = -4m^2c^2/\hbar^2$ for $K_\perp^2 > 4m^2c^2/\hbar^2$ we find that the photon moves directly until it gains the pitch angle ψ_1 (which happens at $r(t_1) = r_1 \equiv r_0[\omega^2/c^2 - K_\perp^2(0)]^{1/2}[\omega^2/c^2 - (4m^2c^2)/\hbar^2]^{-1/2}$), it then bends abruptly and propagates along the magnetic field (as now $\nu_\perp = 0$) with the constant angular velocity $(\mathrm{d}\alpha/\mathrm{d}t) = (c^2/\omega r_1)(\omega^2/c^2 - (4m^2c^2)/\hbar^2)^{1/2}$. For the very energetic γ-quantum $\hbar\omega \gg 4mc^2$, the group velocity $\nu_\parallel = c$ and $(\mathrm{d}\alpha/\mathrm{d}t) = (c/r_1)$. With the more exact function $f(K_\perp^2)$ (3) used in equation (5) the bending is less steep (see Fig. 2), the centre of the packet travels along a spiral which approaches asymptotically (from inside) the limiting circle, whose radius is

$$r(\infty) = r(0)\frac{K_\parallel(0)}{K_\parallel(\infty)} \equiv r_1$$

We call this phenomenon the capturing of γ-quantum by magnetic field.

Previously, we have been dealing with photons of only one polarization mode—that which has its electric field lying in the plane containing the magnetic field **B** and the direction of propagation K. The other mode whose electric field is orthogonal to this plane, has its first virtual pair creation threshold at

$$\frac{\omega^2}{c^2} - K_\parallel^2 = \frac{2m^2c^2}{\hbar^2} + \frac{2eB}{c\hbar} + \frac{2mc}{\hbar}\left(\frac{m^2c^2}{\hbar^2} + \frac{2eB}{\hbar c}\right)^{1/2}$$

and not at threshold (1), because the two particles created by the photon of this mode cannot both be in the ground state—one of them must occupy the first excited Landau level[5]. This level being unstable, the threshold level also acquires some width. However, this does not affect the above conclusions about capture. As for the pair creation it does occur but only through tunnelling and is suppressed to this extent.

Consider now the restrictions on the magnetic field necessary for the above treatment. As already noted, the direction of the group velocity changes abruptly in the bending point if one uses the broken-line approximation for the dispersion curve. It follows from equations (2), (3) and (5) that the time r during which this change occurs is about

$$r \sim \left(\frac{\alpha B}{B_{\mathrm{cr}}}\right)^{2/3}\frac{mc^2}{\hbar\omega}\frac{r}{c}\exp\left(-\frac{4B_{\mathrm{cr}}}{3B}\right)$$

The geometrical optics used above is justified if $rc \gg \lambda$, where λ is the photon wavelength. This is only if the magnetic field exceeds $\sim 0.1B_{\mathrm{cr}}$. Other restrictions on the magnitude of the magnetic field are supplied by the following consideration. The derivation of dispersion law (2) was based on calculations which formally treated the magnetic field as external, that is, one which does not undergo any recoil. This approximation should be subjected to an *a posteriori* verification. This reduces to checking whether a given magnetic field can indeed provide the momentum transfer necessary to make the photon follow the law of motion (5). The corresponding analysis indicates that approximately the same condition as above is sufficient to provide the capturing, whereas a lesser field is required to keep the photon on the trajectory along the field once it has been captured.

We now discuss the consequences of the capturing of the γ-quanta in the magnetospheres of pulsars. According to Sturrock's model[1] of pulsars there is a gap near their magnetic poles wherein the component of the electric field $E_\parallel$ parallel to **B** is nonzero and equal to $(\Omega h_{\max}/c)B_{\mathrm{P}} \simeq (\Omega R/c)^{3/2}B_{\mathrm{P}}$, where $\Omega = 2\pi/\mathrm{P}$ is the angular velocity of the pulsar, B_{P} is the magnetic field at its pole, R is the radius of the neutron star and $h_{\max}$ the length of the gap equal to $h_{\max} = (\Omega R/c)^{1/2}R$. Using this model one could explain the energy yield of the system: the pulsar NP0532–Crab Nebula[1,9]. A quantitative theory was also proposed which explains rather well the radiation spectrum of NP0532 and Crab Nebula[10,11]. However, the length of the gap[2] cannot in fact exceed the free path l_γ, which the γ-quantum of the curvature irradiation passes before converting into the e^+e^--pair, as the pairs created screen $E_\parallel$ and the length of the gap decreases to the value l_γ. For old (slowly rotating $P = 1$ s) pulsars, $l_\gamma \sim h_{\max} \sim 10^4$ cm, that is the pair creation does not affect the gap in this case. For fast rotating pulsars the path l_γ, when evaluated using the assumption of the straight-line propagation of the photons, is essentially $< h_{\max}$ for most of the γ-quanta of the curvature irradiation. For example, for NP0532 ($P = 0.033$ s) l_γ is less than $h_{\max}$ by ~ 1.5 orders. Consequently, in the framework of the existing theory of pulsars one cannot explain either the luminosity of Crab Nebula or that of the pulsar NP0532. The analogous difficulty is encountered, although to a lesser extent, with the pulsar PSR0833 − 45 in the remnant of Vela.

The effect considered here may overcome this difficulty. At $B \geqslant 0.1B_{\mathrm{cr}}$ the γ-quanta of curvature radiation generated by the primary particles are captured by the magnetic field and leave the gap region without having created pairs at the ratio sufficient for its screening. Later the γ-quanta leave the domain of strong field. As the field becomes insufficient to keep them in its orbit we go beyond the range in which the above consideration is valid. One may assume, however, that the γ-quanta are released and may create pairs; this would occur at the distance of several radii of the neutron star.

We thank Professor V. L. Ginzburg for helpful discussion.

Received 29 June; accepted 26 October 1981.

1. Sturrock, P. *Astrophys. J.* **164,** 529 (1971).
2. Ruderman, M. & Sutherland P. *Astrophys. J.* **196,** 51 (1975).
3. Arons, J. & Scharlemann, E. T. *Astrophys. J.* **231,** 854 (1979).
4. Shabad, A. E. *Nuovo Cim. Lett.* **3,** 457 (1972).
5. Shabad, A. E. *Ann. Phys. N.Y.* **90,** 166 (1975).
6. Erber, T. *Rev. Mod. Phys.* **38,** 626 (1966).
7. Batalin, I. A. & Shabad, A. E. *Zh. Eksp. Teor. Fiz.* **60,** 894 (1971); *Soviet Phys. JETP* **33,** 483 (1971).
8. Agranovitch, V. M. & Ginzburg, V. L. *Optics of Crystals with the Spatial Dispersion Taken into Account and the Theory of Excitons* (Nauka, Moscow, 1979).
9. Tademaru, E. *Astrophys. J.* **183,** 625 (1973).
10. Machabeli, G. Z. & Usov, V. V. *Soviet Astro. Lett.* **5,** 238 (1979).
11. Lominadze, J. G., Machabeli, G. Z. & Usov, V. V. *Astrophys. J.* (in the press).

New evidence for degassing processes during explosive eruptions

R. S. J. Sparks & S. Brazier

Department of Earth Sciences, University of Cambridge, Downing Street, Cambridge CB2 3EQ, UK

Measurements of pore size distribution in five samples of pumice, formed during explosive eruptions of plinian type, show three distinct sizes of vesicle. The characteristics of the three pore size populations are similar in the samples although they were collected from plinian deposits of five different volcanoes. We interpret the pore size populations as representing the degassing of silicic magma on three very different time scales. The coarse population (≫60 μm) represents slow vesiculation within the magma chamber over periods of weeks, months or years at small levels of gas supersaturation. The medium-sized population (50–5 μm) represents rapid vesiculation of magma on ascent to the surface during the plinian eruption over periods of minutes to hours. The fine population (5–0.5 μm) represents bubbles formed during explosive disruption of magma and rapid ejection into the atmosphere, involving short time scales (a few seconds), but large decompression rates.

The pore size distribution of five individual samples of pumice collected from plinian deposits was measured using mercury porosimetry[1,2] (a detailed description of the technique is given in ref. 2). The porosimetry method involves the forcing of mercury into a porous material under increasing pressure. The technique is based on the principle that when mercury is forced under pressure into a pore of characteristic dimension r and length l, an amount of work W is required which is proportional to the increased surface area exposed by the mercury at the pore wall. Theory[1] shows that the pressure P is related to the pore size, the surface tension of mercury γ and contact angle θ as follows:

$$P = (2\gamma \cos \theta)/r$$

The method allows the determination of pore size distribution from 300 to 0.003 μm, surface area per unit weight of sample for pores greater than any specified value, and an approximate estimate of density. The method strictly measures the dimensions of entrances to pores rather than the internal dimensions. Duplicate runs on the same material using this method typically show a standard deviation of mean pore size of only 2–3%. The actual shapes and dimensions of pores have been examined by scanning electron microscopy (SEM) for comparison. The present results are preliminary but are the first measurements of the detailed pore size characteristics of volcanic ejecta.

The five samples studied were collected from the 18 May plinian deposit of the 1980 eruption of Mount St Helens (STH15), the Avellino plinian deposit of Vesuvius (IT540), the 1975 plinian deposit of Askja volcano, Iceland (AS10), the plinian deposit of the Tierra Blanca tephra, Lago de Ilopango, El Salvador (TBJ) and the plinian deposit of the Bronze Age Minoan eruption of Santorini, Greece (MIN). Table 1 lists some relevant properties of the pumice samples and results of density and surface area determinations.

Figure 1 shows differential pore volume plotted against pore diameter. The most striking feature of the data is that three discrete ranges of pore size are observed in all five samples despite the different localities. The Vesuvius sample shows the same pattern although the glass composition is trachytic whereas the other four samples are rhyolitic. The relative volumetric proportions of the three populations differ from sample to sample. For example, the finest-size population is dominant in the Vesuvius and Tierra Blanca samples, but is subsidiary in the Minoan sample. However, measurements on two other samples of Askja pumice clasts show considerable variation in the amplitude of the three peaks. This implies that many more analyses would be required to demonstrate significant differences in the overall size population distribution of the five pumice deposits. From the distributions in Fig. 1 we separated each pore size population and plotted the data on a graph of log pore diameter against cumulative volume per cent. The range of pore sizes in each population, as measured by the diameters at the 16th, 50th and 84th percentiles on the cumulative plot, is strikingly similar

Table 1 Properties of pumice samples and results of density and surface area determinations

Sample	Locality	Composition	Density ($g\,cm^{-3}$)	Surface area ($cm^2\,g^{-1}$)
STH15	3 km east of Mount St Helens	Dacite with rhyolite glass	0.91	8.47×10^4
MIN	Thera Quarry, Santorini	Rhyodacite with rhyolite glass	0.81	0.79×10^4
IT540	Ottaviano Village, Vesuvius	Trachyte	0.62	8.04×10^4
TBJ	Lago di Ilopango, Nicaragua	Rhyolite	1.03	0.54×10^4
AS10	15 km east of Oskjuvatn Caldera, Askja	Rhyolite	0.69	5.57×10^4

The measurements of surface area are for all pores down to a nominal diameter of 0.003 μm.

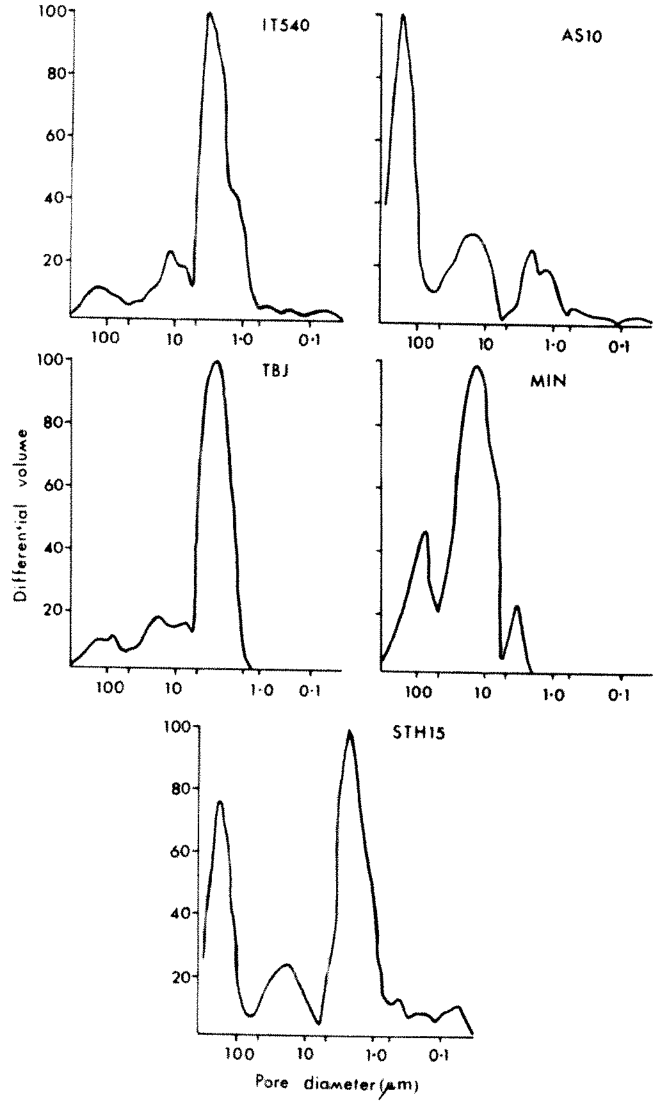

Fig. 1 Plots of differential volume against pore diameter for five pumice samples.

0028-0836/82/030218—03$01.00

for the five samples. Table 2 lists the median pore diameter, pore size range and pore volume per gramme of sample for each population. In three samples (IT540, STH15 and AS10) significant proportions of pore sizes are observed down to 0.02 μm (Fig. 1) whereas in samples MIN and TBJ there are no significant proportions of pore sizes beneath 1.0 μm. The porosimetry method only measures pores <300 μm across. Much larger vesicles are observed in all our samples. Consequently the coarsest population cannot be completely determined.

Examination of the pumice samples by SEM establishes that the pore dimensions determined by porosimetry are representative of the true sizes of vesicles. Furthermore the different size populations of vesicles are also apparent. Figure 2 shows micrographs of sample IT540. Figure 2*a* shows a group of vesicles in the approximate size range 10–20 μm surrounded by areas characterized by much smaller vesicles. Figure 2*b* illustrates an area of the smaller-sized vesicles which are typically in the size range 1–4 μm. The size ranges of the two groups of vesicles observed with the SEM are comparable with the middle-sized and fine-sized pore size populations (Table 2).

The three populations of pore sizes provide intriguing new evidence on the processes of degassing during major explosive volcanic eruptions. The occurrence of essentially the same pore size populations in samples from five different plinian deposits suggests a coherent pattern of degassing in this style of volcanic activity.

Models of explosive volcanic eruptions[3] involving high viscosity magmas recognize three stages of vesiculation. Before an eruption magma oversaturated in volatile components will form bubbles within the chamber. Bubbles can reach substantial dimensions because the time scale for growth can be large (weeks, months, years, even centuries), although the oversaturation pressure causing gas to diffuse into the bubbles may be small[4]. We suggest that the population of coarse pore sizes represents vesiculation of gas within the chamber before eruption.

The second stage of vesiculation occurs as magma ascends to the surface just before and during the eruption. Plinian eruptions typically last a few hours to a couple of days with discharge rates of magma in the range 10^3–10^5 $m^3 s^{-1}$ [ref. 3]. During this period magma is transported from depths of a few kilometres to near the surface where explosive disruption occurs. Models of this process[3,4] suggest that explosive disruption occurs at pressures of a few tens of bars. Thus the magma decompresses from a few kilobars to a few tens of bars in typical periods of many minutes to a few hours. We propose that the medium-sized population of pores are nucleated at this stage. We note that although decompression is rapid in this period, the loss of gas (assumed to be largely H_2O) from silicic magma causes a sharp increase in viscosity. For viscosities $>10^8$ poise bubble growth will be significantly retarded[4]. During this second stage the bubbles that had formed in the chamber will continue to grow by diffusion and decompression resulting in the clear separation of the two generations of bubbles observed in Fig. 1.

Table 2 Data on three pore size populations

Pore population	Sample	Median pore diameter (μm)	Pore volume ($cm^3 g^{-1}$)	Pore size range (μm)
	STH15	166	0.11	234–110
	MIN	98	0.14	173– 60
Coarse	IT540	119	0.07	202– 46
	TBJ	117	0.04	202– 71
	AS10	174	0.38	245–119
	STH15	20.1	0.09	37.0–10.5
	MIN	14.4	0.60	28.1– 7.8
Medium	IT540	12.3	0.21	27.9– 6.6
	TBJ	13.8	0.11	28.8– 6.3
	AS10	20.1	0.30	34.7–10.2
	STH15	2.04	0.37	3.05–1.10
	MIN	3.80	0.05	4.90–3.02
Fine	IT540	2.69	0.77	4.17–1.45
	TBJ	2.88	0.40	3.98–1.80
	AS10	1.91	0.25	2.91–1.17

The pore size range shows the 16th and 84th percentiles of each log normal distribution on a plot of cumulative volume versus pore diameter (see Fig. 1). The pore volume values are approximate estimates of the volume of each population group per gramme of sample.

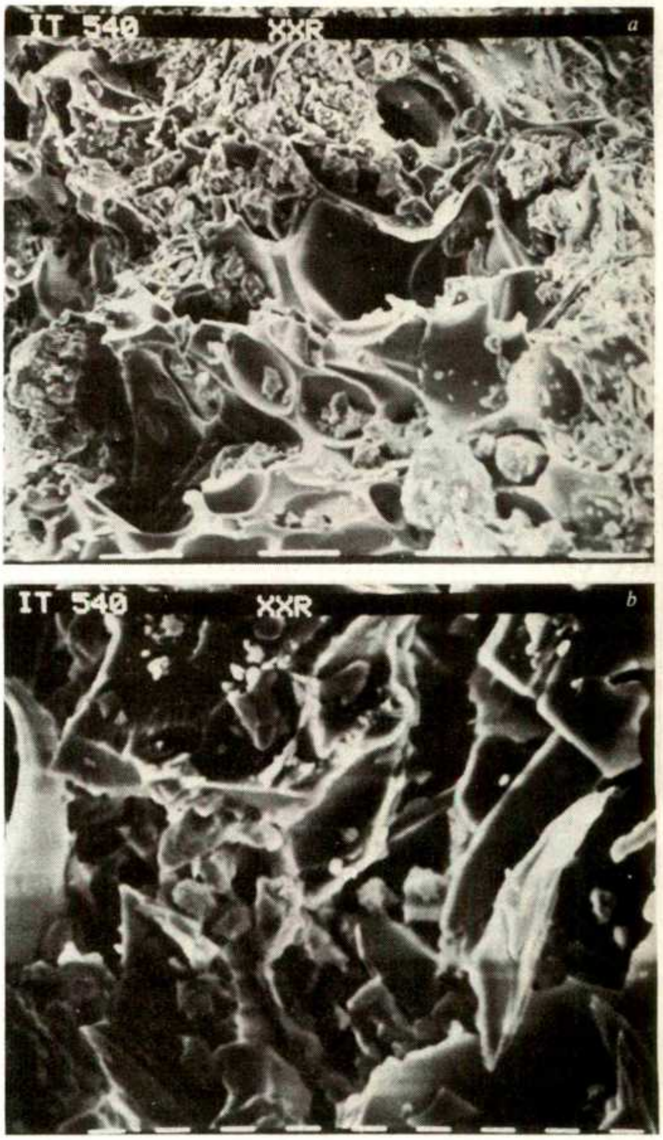

Fig. 2 Scanning electron micrographs of Avellino pumice sample (IT540). *a* Shows a group of large vesicles in the centre which correspond to the middle-sized pore pupulation and areas of small vesicles which correspond to the fine-sized pore population. Scale bars, 10 μm. *b* Shows an area of small vesicles which are prominent in the upper left-hand part of *a*. Scale bars, 1 μm.

The final stage of vesiculation occurs during explosive disruption of the magma into the atmosphere. Velocities of the order 300–600 m s^{-1} and decompressions of the order of a few tens of bars are attained during plinian eruptions[3]. Rapid quenching of disrupted magma (pumice and ash) occurs as cold atmospheric air is mixed turbulently into the explosion column. Time for bubble nucleation and growth is restricted to a few seconds. However, we propose that the large pressure drop nucleates a large number of small bubbles and that the population of fine pores forms at this stage.

The data reveal an unexpected and distinctive pattern of three pore size populations in plinian pumice clasts. The three periods of vesiculation proposed to explain these populations seem to be the most obvious explanation. However, much further work is required to confirm this hypothesis. If our interpretations of the data are correct, the degassing history of magma can be traced back into the chamber. We suggest that studies of pore sizes and surface area in volcanic ejecta may prove a fruitful way of studying the processes of volcanism. Studies of ejecta from different types of volcanic activity could provide new insights into volcanic mechanisms.

Measurements of pore size distribution were made on the Micromeritics Mercury Penetration Porosimeter Model MIC 9200 at Coulter Electronics Laboratory, UK. We thank R. Wenham for advice on the method and its interpretation. This research was carried out under NERC grant 6234.

Received 21 August; accepted 16 November 1981.

1. Washburn, E. W. *Proc. natn. Acad. Sci. U.S.A.* **7,** 115 (1921).
2. Lowell, S. *Introduction to Powder Surface Area* (Wiley, New York, 1979).
3. Wilson, L., Sparks, R. S. J. & Walker, G. P. L. *Geophys. J. R. astr. Soc.* **63,** 117–148 (1980).
4. Sparks, R. S. J. *J. Volcan. geotherm. Res.* **3,** 1–37 (1978).

Ice core sample measurements give atmospheric CO$_2$ content during the past 40,000 yr

A. Neftel, H. Oeschger, J. Schwander, B. Stauffer & R. Zumbrunn

Physics Institute, University of Bern, CH-3012 Bern, Switzerland

Recent measurements[1,2] on ice samples from Camp Century (Greenland, 77°10′ N, 61°08′ W), Byrd Station (Antarctica, 80°01′ S, 110°31′ W) and Dome C (74°40′ S, 125°10′ E) suggest that during the late part of the last glaciation the atmospheric CO$_2$ concentration was significantly lower than during the Holocene. Further investigation of this natural increase of the atmospheric CO$_2$ concentration in the past should aid our understanding of the climatic implications of the man-made CO$_2$ increase since the beginning of industrialization[3]. Here we report new and precise measurements of the CO$_2$ concentration of the air occluded in bubbles of ice samples from Camp Century and Byrd Station, using a new dry extraction technique. The extracted gases were analysed with an IR–laser spectrometer (IRLS). Samples from 22 different depths were analysed from each core. The samples are distributed over a depth interval corresponding approximately to the past 40,000 yr. In addition results for ice samples from selected depth horizons from a colder region (North Central, Greenland 74°37′ N, 39°36′ W) and from a warmer region (Dye-3, Greenland 65°11′ N, 43°50′ W) are given. Based on these results we estimate the trend of the atmospheric CO$_2$ concentration during the past 40,000 yr.

Samples of ~1 g were cut from the ice core with a band saw. The sample was placed into a cooled (−20 °C) container between two needle matrices. The system was then evacuated and the ice cube crushed by pressing the needle matrices against each other. The gas originally trapped in the bubbles of the ice escaped and flowed into an absorption cell, where the CO$_2$ concentration was determined using an IRLS. The crushing process was very quick and the absorption peak was measured repeatedly for a few minutes. The fast extraction and the continuous monitoring of the CO$_2$ concentration of the escaped gas allowed us to check whether the measurement was affected, for example, by a small leak or CO$_2$ contamination from the surface of the container (R. Z., A. N. and H. O., in preparation). The precision of the measurements was 1.5%. Between two and eight samples were measured at each depth.

To determine the total inorganic carbon content, ice samples of 300 g were melted in an evacuated glass container and the gases extracted for 7 h. The samples were analysed with a gas chromatograph[4]. If the melt water was alkaline, CO$_2$-free phosphoric acid was added to complete the extraction of CO$_2$. The total inorganic carbon content consisted of the CO$_2$ in the bubbles, the CO$_2$ dissolved in the ice matrix, the carbonates from dust incorporated in the ice and carbonates from the surface of the ice. Both the IRLS and the gas chromatograph were calibrated with three standard gases prepared by the Scripps Institution of Oceanography[5].

Figure 1 shows the measured CO$_2$ concentrations plotted against depth, together with a simplified $^{18}O/^{16}O$ ratio curve derived from the detailed curve given by Johnsen *et al.*[6]. The originally recovered Camp Century and Byrd Station cores are generally of poor quality between the 400 and 1,200 m depths and the ice is heavily fractured. In these depth intervals the measured CO$_2$ values exhibit large scattering. This might be due to contamination by drilling fluid, a mixture of diesel fuel (88%) and trychlorethylene (12%), penetrating through small cracks into the ice. In these fractured ice zones, we measured several samples at each sample depth. Its small size meant that the sample was probably uncontaminated and we conclude that the lowest CO$_2$ values best represent the CO$_2$ concentrations of the originally trapped air of these depth intervals. In the larger samples (300 g) contamination is almost inevitable and the measured CO$_2$ concentrations tend to be higher than the air originally occluded in the ice. This is one reason for the high CO$_2$ values obtained during the climatic optimum given by Berner *et al.*[1] for the Camp Century core.

The CO$_2$ concentrations measured on 22 samples spaced over 11 cm from the 103-m depth, from North Central (Greenland), a colder location than Byrd Station and Camp Century, have a mean value of 271 p.p.m. The standard deviation of the measurements is only 9 p.p.m. This depth horizon corresponds to an age of ~680 yr. The gas enclosure occurs between 60 and 80 m corresponding to an age interval of 350–500 yr.

Figure 2 shows the CO$_2$ concentration variations measured on a 13-cm long ice core segment drilled in 1979 at Dye 3 (Greenland)—a location that is subject to frequent summer melt at the surface. Figure 2 thus shows the increased CO$_2$ concentrations that are usually associated with a melt feature.

Cold ice which forms by diagenetic processes and sintering of cold dry snow contains samples of atmospheric air in the bubbles. (This has also been shown for N$_2$, O$_2$ and Ar (ref. 7).) The results of the samples from North Central show that reproducible values are obtained for the CO$_2$ content using our improved extraction technique.

Due to atmospheric mixing, the CO$_2$ concentration in the Northern and the Southern Hemispheres should not differ by more than a few p.p.m. (ref. 8). For corresponding times one would expect the same CO$_2$ concentration in the bubbles in very cold ice from Antarctica and Greenland. Indeed, the CO$_2$ results of Camp Century and Byrd Station agree qualitatively. In both cores the decrease of the CO$_2$ content corresponds to the $\delta^{18}O$ decrease which marks the transition from the Wisconsin to the Holocene.

However, there are differences between the Byrd Station and the Camp Century values which exceed the analytical errors. The higher CO$_2$ values in the Camp Century core during the Holocene may be due to the influence of melt water during the ice formation. In fact many melt layers have been observed in the Camp Century core (C. Langway and H. Clausen, personal communication). If meltwater is involved during the ice formation, the CO$_2$ concentration in the bubbles increases as shown by the results from the Dye 3 sample (Fig. 2). Although a detailed stratigraphical examination for the melt features was not made in the Byrd ice core the overall melt in this core is substantially less than recorded in the Camp Century core (C. Langway, personal communication). Therefore, for the Byrd core this effect should be negligible. At the end of last glaciation, when the CO$_2$ concentration was at a minimum, the Camp Century CO$_2$ concentration in the bubbles was slightly lower than those from the Byrd core. During this time the impurity content in the Camp Century core is an order of magnitude higher than in the

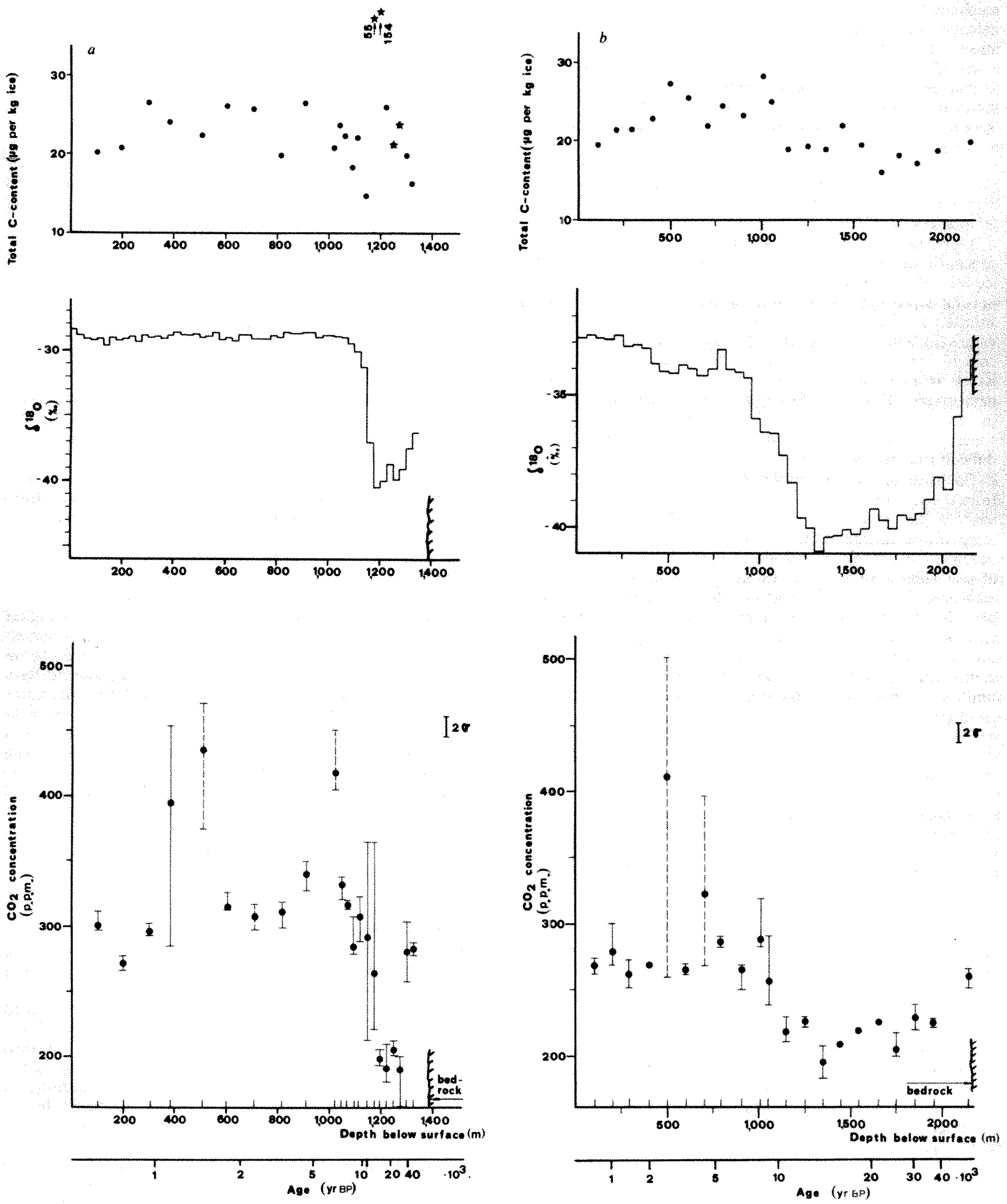

Fig. 1 CO_2 concentrations in the bubbles and total carbonate content of: *a*, the Camp Century core; *b*, the Byrd core. The CO_2 concentrations are presented with the lowest, highest and median values for each depth. The dashed lines indicate depths where drill fluid was observed in the large samples. All samples marked by a star were alkaline and acid was added during the wet extraction.

Holocene[9] and the melted ice samples are alkaline. At present, we cannot rule out the possibility that the alkaline ice matrix absorbs a minor fraction of the CO_2 in the bubbles. Such a mechanism would explain the slightly lower Camp Century values for this period. While the carbonate content is an order of magnitude higher in Camp Century ice at the end of last glaciation than during the Holocene (Fig. 1), it remains almost unchanged in the Byrd core. The qualitative agreement between the two CO_2 concentration time series rules out the possibility of large interaction between CO_2 in the bubbles and the carbonates in the ice.

Note that the oldest samples in the Byrd Station and Camp Century cores (near the bottom of the ice sheets) again exhibit higher CO_2 values which are of the same magnitude as the Holocene values.

A generalized estimate of the history of atmospheric CO_2 concentration is shown in Fig. 3. The age of the Camp Century ice was calculated according to the method of Hammer *et al.*[10]. Several depth–age relationships for the Byrd core are given by Johnsen *et al.*[6]. We selected the time scale for Byrd Station, where the $\delta^{18}O$ decrease from the Holocene to the Glaciation coincides with the $\delta^{18}O$ decrease in the Camp Century core, that is, we assume the climatic events to be synchronous in both hemispheres. Due to the low data density and the uncertainties in the age calculations the estimate of the atmospheric CO_2 range in the oldest sections of the ice cores are more difficult to ascertain.

The increase of the atmospheric CO_2 content at the transition from the Ice Age to the Holocene and its climatic implications has to be discussed with regard to the global carbon system. The temperature change of the sea surface water and the change of ocean volume at this transition accounts for only a 5% increase of atmospheric CO_2 concentration[11]. Both cannot explain the measured CO_2 increase of a factor 1.2–1.4 between the two time periods. The atmospheric CO_2 level depends on the carbonate chemistry of the surface ocean water, especially on the concentration of dissolved inorganic carbon (DIC) which in turn is controlled by biological productivity. Biological activity is limited by the amount of phosphorus available. Broecker links the atmospheric CO_2 increase at the Glacial/Holocene transition with a change in the phosphorus available[12]. He considers the following sequence of events. At the transition a higher sedimentation rate of organic material decreases the amount of phosphorus in the seawater. This leads to less biological productivity and therefore the difference in DIC between surface water and deep water decreases. This leads to a higher concentration of DIC in the surface layer and a higher atmospheric CO_2 concentration. The difference in DIC concentration between surface water and deep water is accompanied by a difference in $\delta^{13}C$ of the DIC. Simultaneous $\delta^{13}C$ measurements on foraminifera living at the surface and at the sea floor do indicate a higher vertical $\delta^{13}C$ gradient during the Glacial than during the Holocene, which agrees with Broecker', theory. The measurements of $\delta^{13}C$ values in the CO_2 gas extracted from ice samples could help us to understand the mechanisms which lead to the atmospheric CO_2 variations during climatic change.

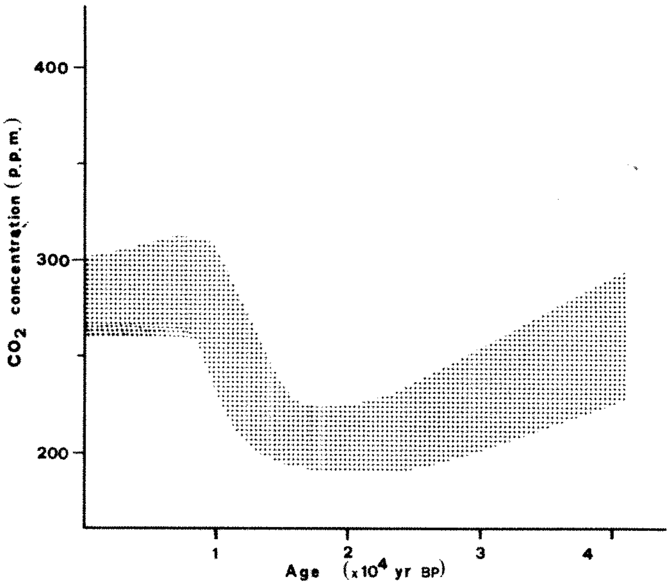

Fig. 3 Estimate range of atmospheric CO_2 during the past 40,000 yr.

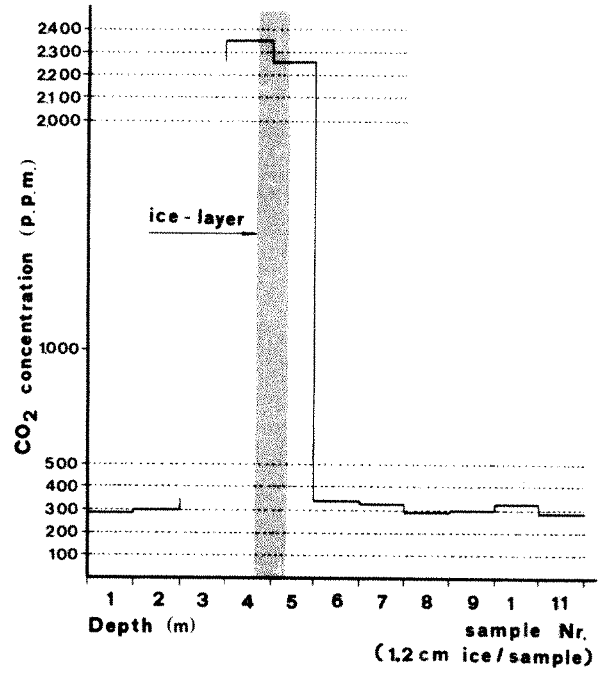

Fig. 2 CO_2 concentration in the bubbles of a 13-cm piece at a depth of 124 m of the Dye 3 core (southern Greenland).

Because CO_2 absorbs IR radiation, it is an important gas in the global radiation budget. Climatic models predict a global warming of between 1.5 and 4 °C for a doubling of CO_2 concentration in the atmosphere[13]. The relationship between the global temperature change and the CO_2 concentration change is approximately logarithmic[14]. A change in the atmospheric CO_2 concentration of 30% would lead to a global warming of $0.9 \pm 0.5°$. It has been reported that the global warming at the Glacial to Holocene transition was at least 2.3 °C (ref. 15). It therefore seems that the CO_2 increase alone was not large enough to explain all this global warming. Considering part of the temperature increase is due to an albedo change by a diminished ice or snow covered surface, the increased CO_2 level in the atmosphere contributes significantly to the global warming at the transition from the last glaciation to the Holocene. In this context it would be interesting to know whether the CO_2 increase preceeded or followed the temperature change. Our data suggest that the time lag between the CO_2 increase and the climatic change cannot have been more than ±2,000 yr.

More accurate estimates of the atmospheric CO_2 history will be possible when samples from very cold locations, such as the South Pole, become available.

We thank Drs C.C. Langway, B.L. Hansen, H. Clausen and Professor W. Dansgaard who envisaged the potential of ice cores for studies of this kind and made them available for the present investigation, also Dr U. Siegenthaler for valuable discussions. This work was supported by the Swiss NSF the

Department of Polar Programs of the US NSF and the US Department of Energy

Received 14 September, accepted 24 November 1981

1 Berner, W , Oeschger, H & Stauffer, B *Radiocarbon* **22,** 227–235 (1980)
2 Delmas, R J , Ascencio, J -M & Legrand, M *Nature* **284,** 155–157 (1980)
3 Keeling, C D & Bacastow, R B in *Energy and Climate* 72–75 (National Academy of Sciences, Washington DC, 1977)
4 Stauffer, B , Berner, W , Oeschger, H & Schwander, J *Zeitschrift fur Gletscherk Glazialgeol* **16,** (in the press)
5 Zumbrunn, R thesis, Univ Bern (1981)
6 Johnsen, S J , Dansgaard, W , Clausen, H B & Langway, C C Jr *Nature* **235,** 429–434 (1972)
7 Raynaud, D , Delmas, D & Lourius, C *Actes du Colloque de Grenoble,* 77–81 (IAHS-AISH Publ no 118, 1977)
8 Bolin, B & Keeling, C D *J geophys Res* **68** (1963)
9 Cragin, J H , Herron, M M , Langway, C C Jr & Klauda, G *SCOR/SCAR Polar Oceans Conf* (McGill University, Montreal, 1974)
10 Hammer, C U *et al J Glaciol* **20,** 3–26 (1978)
11 Siegenthaler, U , Heimann, M & Oeschger, H *Radiocarbon* **22,** 177–191 (1980)
12 Broecker, W S *CIMAS Symp* (ed Kraus, E) (University of Miami, 1980)
13 *Conf Carbon Dioxide and Climate A Scientific Assessment* (U S National Academy of Sciences, Washington DC 1979)
14 Schneider, S H *J Atmos Sci* **32,** 2060–2066 (1975)
15 CLIMAP *Science* **191,** 1131–1137 (1976)

Steroid hydrocarbons and the thermal history of sediments

A. S. Mackenzie*, N. A. Lamb & J. R. Maxwell

Organic Geochemistry Unit, University of Bristol,
School of Chemistry, Cantock's Close, Bristol BS8 1TS, UK

Assessment of the extents to which certain organic chemical reactions have occurred in sedimentary rocks with increasing burial depth and the associated temperature rise, can distinguish differences in the extent of their thermal maturation[1–10]. Heating experiments with sediments have suggested that these different reaction types have different kinetic constants[11]. Therefore, a measurement of the extent to which one reaction type has occurred might be expected to correspond to different values of a measurement based on a different reaction type, depending, for example, on the average sedimentary heating rate (°C Myr^{-1})[12] of the sample. We use here two reaction types to investigate this hypothesis: (1) configurational isomerization in steroid alkanes, represented by the conversion of the biologically inherited configuration, 5α(H), 14α(H), 17α(H), 20R, in a C_{29} sterane to an approximately equal mixture of itself and the corresponding 20S configuration formed in the sediment[6,13]; and (2) apparent aromatization of two C_{29} monoaromatic steroid hydrocarbons (Fig. 2) assumed to be isomeric at C-5 (refs 14–21), based on retention time comparisons with synthesized C-27 analogues, to a presumed product, the C_{28} triaromatic steroid hydrocarbon[9,14]. Comparison of the extents to which these two reactions have occurred in suites of sediment samples has allowed three basins [Pannonian Basin (Pliocene), Mahakam Delta (Miocene), Paris Basin (Toarcian)] with different thermal histories to be distinguished. Extension of the hypothesis to two other sedimentary sequences suggests a higher average heating rate for the Oligocene of the Zhanhua Depression (north-east China) than for the Cretaceous of the Wyoming Overthrust Belt.

The thermal history of a sediment, that is, the temperature versus time profile since deposition, is important for estimating the time at which the sediment was capable of generating petroleum[22] A simple means of describing thermal history is the average heating rate, defined as the product of average sedimentation rate (km Myr^{-1}) and geothermal gradient (°C km^{-1})[12] Table 1 lists the rates (based on present depth/age) for three sample suites (1) 12 Pliocene shales from a borehole in the Pannonian Basin in south-east Hungary[23], (2) three shales and six coals from boreholes around the Handil oilfield of the Mahakam Delta, Kalimantan, Indonesia[24], and (3) 14 Toarcian shales sampled from outcrops and boreholes across the Paris Basin[6 25] Although different types of organic matter occur in the sequences[23–25], the present comparison is valid because the carbon skeletons of the products of the reactions are only formed by thermal maturation and not by biological processes. Where there has been a period of erosion [(2) and (3)] corresponding heating rate values are given in Table 1, which do not include the periods of erosion In either case there are major differences in heating rates over the three sample suites

All the samples contain complex mixtures of stereoisomers of steroid alkanes with both a non-rearranged and a rearranged carbon skeleton, covering a range of carbon numbers[2 5,6,26], and can be partly separated by combined gas chromatography–mass spectrometry (GC–MS)[5 6] The complexity of the mixture increases with increasing thermal maturation due to isomerization at various chiral centres in skeletons[6] Using non-polar GC columns the ratio (%) of the unresolved mixture[26] of the 24R and 24S isomers of (20S)-24-ethyl-5α(H), 14α(H), 17α(H)-cholestane to itself and the corresponding 20R mixture can be measured from the appropriate peak areas in GC–MS fragmentograms of the ion *m/z* 217 (refs 5, 6) (Fig 1) The value of this measurement rises from zero in very immature sediments to a maximum of ~50–55% in mature sediments[5 6], that is the equilibrium constant is ~1, although it may vary slightly with temperature

The samples also contain complex mixtures of monoaromatic and triaromatic steroid hydrocarbons The latter are thought to derive from the monoaromatics as a result of thermal maturation[9 14] The ratio (%) of the C_{28} triaromatic component in Fig 2 to itself and two presumed precursors, thought to be the 5α and 5β(H) isomers of the C_{29} component in Fig 2, can be measured from mass fragmentograms of the ions *m/z* 231 and 253 respectively[9] The two C_{29} monoaromatic components are suggested to be the 5α and 5β(H) isomers of the structure in Fig 2, the assignment being based on 400 MHz ^1H NMR analysis of a 1 1 mixture (GC analysis) of two stereoisomeric ring C monoaromatics isolated from acidic treatment[27] of cholesta-3,5-diene Comparison of chemical shifts with literature compounds[14–19] in conjunction with decoupling and n O e experiments indicates (1) ring C is aromatic (confirming the *m/z* 253 base peak in the mass spectra[15]), (2) there is a methyl group at C-17, consistent with the structures in the triaromatic series[9 14,16], and at C-10, (3) the A/B ring junction is *trans* with the 10β(CH_3), 5α(H) stereochemistry, (4) the 1 1 mixture results from isomerism at C-17 or C-20, that the latter is the case is suggested both by the structures and distribution of the low-molecular weight triaromatics[9] and by the method of preparation[27] The two isomers coeluted (GC–MS) on OV-1 and Carbowax 20M with two major C-27 monoaromatics in the aromatic fraction of Semécourt shale (Paris Basin, see Fig 3*a*) The other two major C-27 monoaromatics in this fraction are inferred to be the 5β(H), 20R and 20S isomers Comparison of elution orders of the C-27 and C-29 monoaromatic components suggests that the two C-29 components used in the measurement are those in Fig 2 [before completion of this work it came to our attention that certain monoaromatic hydrocarbons of this structural type had been assigned and found to occur in sedimentary rocks and petroleum (W K Seifert and J M Moldowan, personal communication). The above conclusions are also consistent with structual assignments reported

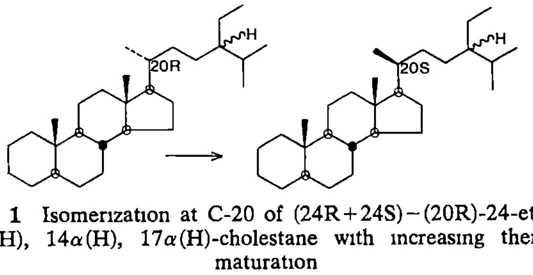

Fig. 1 Isomerization at C-20 of (24R+24S)–(20R)-24-ethyl-5α(H), 14α(H), 17α(H)-cholestane with increasing thermal maturation

---

* Present address KFA-Julich ICH-5 Erdol und Organische Geochemie, Postfach 1913, D-5170 Julich-1, FRG

0028-0836/82/030223—04$01 00

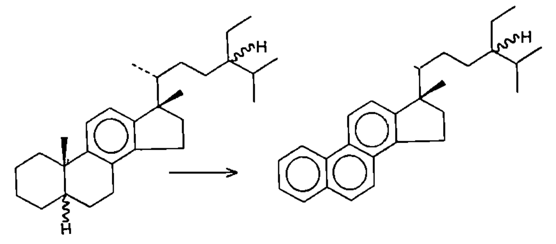

Fig. 2 Proposed aromatization of the 5α(H) and 5β(H) isomers of (24R+24S)-(20R)-24-ethyl-17β-methyl-18-norcholesta-8, 11,13-triene to (24R+24S)-(20R)-24-ethyl-17β-methyl-18,19-dinorcholesta-1,3,5(10),6,8,11,13-heptaene (numbering based on steroid skeleton)

recently[20,21]] Again the 24R and 24S isomers are not resolved on non-polar columns in the conditions used The maximum value of the measurement is ~100% (ref 11), and values as low as zero can occur in immature sediments[9]

Figure 3*a* shows the isomerization measurement plotted against the aromatization measurement for the three sample suites In the Paris Basin Toarcian shales, whose values and maximum burial depths have been reported previously[6 9], there is a steady increase, with some scatter, in both measurements with increasing burial depth such that the presumed end points of both reactions are approached in the two deepest shales Heating an immature Toarcian shale at elevated temperatures in the laboratory resulted in aromatization values approaching the deepest shales, whereas only minor changes were observed in the extent of isomerization at C-20 in the steranes[11] It has been suggested that the rate of aromatization of the monoaromatic steroid hydrocarbons is more temperature dependent than the rate of isomerization of 5α(H), 14α(H), 17α(H)-steranes at C-20 (ref 11)

Although the two reactions seem to have similar average rates at the lower temperatures (<100 °C) experienced by the Toarcian shales (Fig 3*a*), comparison with the laboratory experiments (201, 257 °C) suggests that the aromatization reaction occurs at a faster relative rate at higher temperatures If the reactions follow pseudo first-order kinetics, then according to the Arrhenius equation, the rate constant for the aromatization of steroid hydrocarbons would appear to have higher values of activation energy and pre-exponential factor than the isomerization at C-20 in 5α(H), 14α(H), 17α(H)-steranes ($\log_e k = \log_e k_0 - E/RT$, where k = reaction rate, k_0 = pre-exponential factor, E = activation energy, T = absolute temperature and R = gas constant)

This hypothesis has been examined by comparing the extents of the two reactions in the Toarcian shales with the sample suites from the Pannonian Basin and Mahakam Delta (Fig 3*a*) The Pliocene of the Pannonian Basin has average heating rates at least 20 times higher than the Paris Basin Toarcian shales (Table 1) Details of aspects of the sedimentation and petroleum geochemistry of the Pannonian borehole have been reported elsewhere[23] The four shallowest samples (between 2,051 and 2,500m) show a trend (Fig 3*a*) of enhanced aromatization relative to isomerization akin to that seen in the laboratory heating experiments[11], the aromatization (more temperature dependent) reaction is effectively complete by sample 4 (2,500m, ~105 °C present temperature) At this depth the isomerization (less temperature dependent, and more time dependent) has reached a value of only 16% of the 20S isomer as a proportion of the C_{29} 5α(H), 14α(H), 17α(H)-steranes (Fig 3*a*) High values (~50–55%) in the curve are not reached until a further depth increase of ~800m (3,328m, sample 15, 137 °C) The coal and shale samples from the Mahakam Delta derive from boreholes around the Handil oilfield Detailed information about the geology and geochemistry is given elsewhere[24 28] The heating rate represents an intermediate situation between the Paris and Pannonian Basins (M Vandenbroucke, personal communication) The path followed by the Mahakam Delta samples seems to reflect this intermediacy, although the Der sample from the Paris Basin has similar values to Mahakam samples 3, 9 and 10 The apparently anomalous behaviour of Der (and perhaps Colombotte) may relate to the fact that the Paris Basin samples derive from a wide geographical area[6] and that Der (and Colombotte) may have experienced a period of higher sedimentation[29] not apparent from a study of the present record of sedimentation[30]

Average sedimentary heating rates can only reflect the overall thermal history of a sequence It might be expected, however, that the molecular measurements could also reflect variation in the heating rate at a later stage If the heating rate declines markedly, or even if cooling occurs, the decrease in the rate of the isomerization reaction (less temperature dependent) would be less than the decrease in the rate of the aromatization reaction (more temperature dependent) During such a period, a trend reflecting a high heating rate such as in the Pannonian Basin (Fig 3*a*) would be displaced towards the Paris Basin trend In the case of the Mahakam Delta suite, the samples have experienced heating rates of at least 30 °C Myr^{-1} (M Vandenbroucke, personal communication) during the late Miocene, which are much greater than the average values for the Pannonian Pliocene Since then, they declined such that they never exceeded 3 °C Myr^{-1} during the late Pliocene and subsequent cooling of the samples has occurred during the past 3 Myr, because ~300m has been eroded from the sequence studied (M Vandenbroucke, personal communication). These events explain both the occurrence of samples of late Miocene age at the same depths as late Pliocene Pannonian samples, and the proximity of the Paris Basin and Mahakam Delta trends (Fig 3*a*) which are not obvious from the heating rate differences (Table 1)

Figure 3*b* includes the two measurements plotted for (1) six Cretaceous shales from the Wyoming Overthrust Belt[13], all but one are shallow (20–40m) core samples and derive from a sequence of increasing age within a single thrust slice Calculation of average heating rates is difficult because of the structural complexity of the area[31], (2) six Oligocene (Shaheji) cored shale samples from the Zhanhua Depression in north-east China, of varying burial depth and location[32] Because the area

Table 1 Average heating rates for sample sequences

Sequence	Ref	Age*(Myr)	Geothermal gradient (°C km^{-1})	Average sedimentation rate (m Myr^{-1})†	Average heating rate‡ (°C Myr^{-1})
Pannonian Basin	16	Pliocene (5–7)	38	360–420	14–16
Mahakam Delta‖	17	Miocene (12–14)	34	160–200 (250–290)§	6–8 (8 5–10)§
Paris Basin	6, 9, 25	Toarcian (180)	33	0–15 (5–15)§	0–0 5 (0 2–0 5)§
Overthrust Belt	13	Cretaceous (80–130)	NK	NK	–
Zhanhua Depression	32	Oligocene (25–40)	36	NK	–

NK, not known

* Age of samples for which changes in one or both of the two molecular measurements are seen

† Depth/age

‡ Assuming constant geothermal gradient

§ Excluding erosion phases

‖ M Vandenbroucke, personal communication Data for Handil field

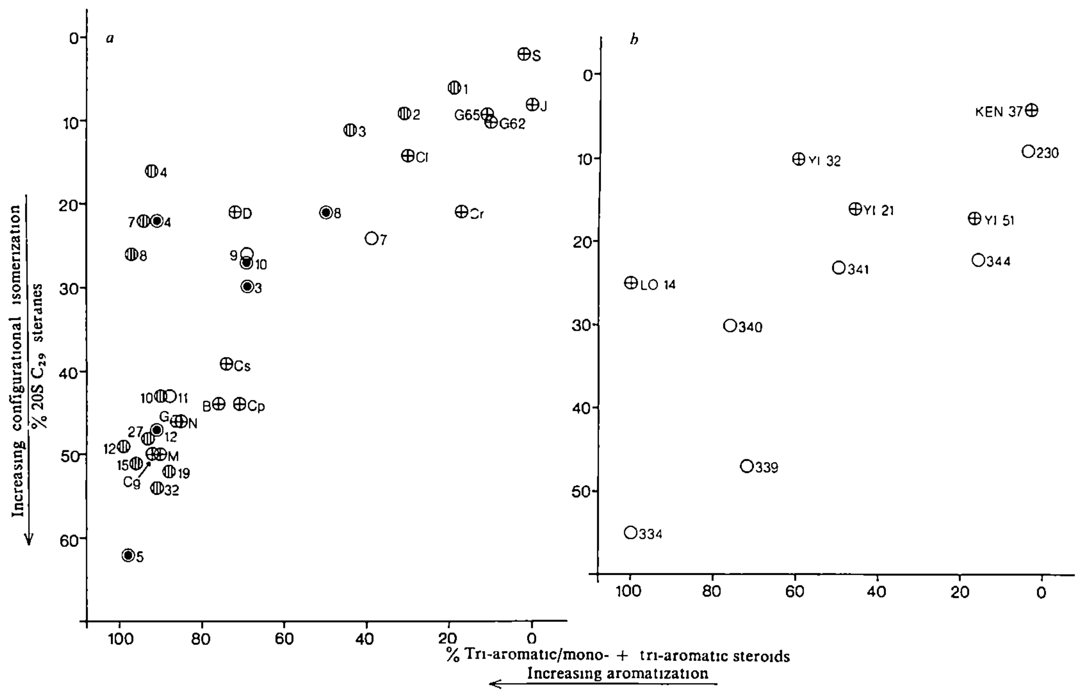

Fig. 3 Plots of the extent of isomerization at C-20 in C_{29} steranes (Fig 1) against the extent of aromatization of C_{29} monoaromatic to C_{28} triaromatic steroid hydrocarbons (Fig 2) for *a*, (maximum burial depths in brackets, where available) Toarcian shales of the Paris Basin (⊕) where S, Semécourt (700m), J, Jouy (700m, G62, G6-2-2 (600m), G65, G6-5-6 (600m), CI, Colombotte (500m), Cr Creveney (500m), D, Der (1,280m), Cs, Cesarville (2,040m), Cp, Coupvray (2,100m), G, Grandville (2,100m), N, Nangis (2,130m), B, Belou (2,207m), M, Montmirail (2,433m), Cg, Courgivaux (2,460m) Miocene coals (●) and shales (○) from the Mahakam Delta (Handil field except 3,4,5) where 7 (2,285m), 8 (2,283m), 9 (2,538m), 10 (2,537m), 11 (2,903m), 12 (2,905m) For samples 3, 4, 5 only T_{max} values[39] are available and are 430, 440 and 448 °C respectively (M Vandenbroucke, personal communication) Pliocene shales and siltstones from a borehole in the Pannonian Basin (⦶) where 1 (2,051m), 2 (2,291m), 3 (2,386m), 4 (2,500m), 7 (2,702m), 8 (2,759m), 10 (2,953m), 12 (3,098m), 15 (3,328m), 19 (3,548m), 27 (4,269m), 32 (4,888m) *b*, (Present depths) Cretaceous shales (○) from Wyoming Overthrust Belt (all shallow core samples (20-40m) except 334, present depth 2,760m) Oligocene (Shahejie) shales from the Zhanjua Depression (⊕), present burial depths in brackets), Ken 37 (1,850-1,860m), YI 51 (2,339m), YI 21 (2,758m), YI 32 (2,899m), LO 14 (2,978m) The isomerization for LO 14 is an average of the C_{29} measurement and the corresponding measurement for the C_{27} skeleton, because there is a reworked component in the steranes with a very high relative abundance of C_{29} steranes[32]

which was sampled has been affected by faults active till the Quaternary, and the samples are from separate boreholes of different location separated by up to 15 km, they presumably have some differences in their average heating rates, the range of which is difficult to estimate Although the sample coverage is less extensive than in the other sequences (Fig 3*a*), measurements suggest that the Overthrust Belt shales (Fig 3*b*) have a similar average heating rate to the Paris Basin samples (Fig 3*a*), whereas the Zhanhua Depression shales seem to have had a recent heating experience of a similar order to that which has affected the shallow Pannonian Pliocene samples Such observations are consistent with available geological information for the two areas[31 32]

Comparison of proposed maximum temperatures for the Pannonian[23] and Paris[33 34] Basins provides further evidence that the aromatization has the greater temperature dependence For a given aromatization value the maximum temperature difference in samples from the two basins is of the order of 10 °C, whereas for a given isomerization value differences of up to 60 °C are apparent

Confirmation and extension of the hypothesis requires (1) determination of the appropriate activation energies and pre-exponential factors, both from laboratory heating experiments[11] (with consideration of the difficulties involved[35]) and from integration with mathematical models for the evolution of sedimentary basins[36 37], which include temporal variations in sedimentation rate and heat flux Preliminary studies of the latter type, using estimated kinetic constants for the reactions, suggest that the trends (Fig 3) follow S-shaped curves (A S M amd D P McKenzie, unpublished results) (2) An examination of the effect which extreme differences in lithology could have on the measurements In the present study, all the samples are shales or silt-stones except for the six coal samples from the Mahakam Delta in which little significant variation was observed between the coals and shales from comparable depths (Fig 3*a*) (3) A search for other measurements which might preserve a record of earlier high heating rate events, although subsequent lower heating rates and/or cooling result in a trend which suggests an overall low average heating rate (see Mahakam)

Care should be taken with the measurements the mixtures are complex and overlap with other components can occur Attention should be paid to peak shapes in various diagnostic fragmentograms, to examination of full mass spectra when required, and to the potential presence of migrated components

This approach has not been extended to a study of crude oils, where migration and subsequent thermal effects in the reservoir (as opposed to those in the source rock) could affect the measurements Preliminary studies[13 32 38] suggest that the configuration at C-20 is not altered significantly by either process, although the proportion of triaromatic to monoaromatic steroid hydrocarbons can decrease in certain cases with increasing distance of secondary migration (unpublished results on Mahakam Delta oils)

If the hypothesis is correct there are other implications For example, there is no reason why variation in the reflectance of vitrinite, commonly used to determine the onset of petroleum generation in sediments, should follow the same kinetic behaviour as the petroleum generation process Reflectance values are different for the threshold of petroleum generation from different types of organic matter[22], but the hypothesis suggests that there may also be differences within a single type of organic matter, depending on heating rate differences

We thank the following for providing samples, geological information and/or GC–MS measurements (recorded in this laboratory in similar conditions and in identical conditions within each suite) Drs B Durand and M. Vandenbroucke (Paris Basin), Drs J M Moldowan and W K Seifert (Overthrust belt), Dr J Oudin (Mahakam Delta), Dr Cs Sajgo (Pannonian Basin), and Dr Shi Ji-yang (Zhanua Depression) We also thank the NERC (GR3/2951 and GR3/3758) for GC–MS facilities and for a fellowship (A S M), the SRC for a Studentship (N A L), Mrs A P Gowar for technical assistance, and Mr C F Hoffman for synthesizing certain triaromatic steroid hydrocarbons and Mr T A Carpenter for 400-MHz data and valuable discussions

Received 10 August, accepted 10 November 1981

1 Ensminger, A, Van Dorsselaer, A, Spyckerelle, C, Albrecht, P & Ourisson, G in *Advances in Organic Geochemistry 1973* (eds Tissot, B & Bienner, F) 245–260 (Editions Technip, Paris, 1974)
2 Mulheirn, L J & Ryback, G *Nature* **256,** 301–302 (1975)
3 Ensminger, A, Albrecht, P, Ourisson, G & Tissot, B in *Advances in Organic Geochemistry 1975* (eds Campos, R & Goni, J) 45–52 (ENADIMSA, 1977)
4 Patience, R L, Rowland, S J & Maxwell, J R *Geochim cosmochim Acta* **42,** 1871–1875 (1978)
5 Seifert, W K & Moldowan, J M *Geochim cosmochim Acta* **43,** 111–126 (1979)
6. Mackenzie, A S, Patience, R L, Maxwell, J R, Vandenbroucke, M & Durand, B *Geochim cosmochim Acta* **44,** 1709–1721 (1980)
7 Mackenzie, A S, Quirke, J M E & Maxwell, J R in *Advances in Organic Geochemistry 1979* (eds Douglas, A G & Maxwell, J R) 239–248 (Pergamon, Oxford, 1980)
8 Seifert, W K & Moldowan, J M in *Advances in Organic Geochemistry 1979* (eds Douglas, A G & Maxwell, J R) 229–237 (Pergamon, Oxford, 1980)
9 Mackenzie, A S, Hoffman, C F & Maxwell, J R *Geochim cosmochim Acta* **45,** 1345–1355 (1981)
10 Mackenzie, A S, Patience, R L, Yon, D A & Maxwell, J R *Geochim cosmochim Acta* (in the press)
11 Mackenzie, A S, Lewis, C A & Maxwell, J R *Geochim cosmochim Acta* (in the press)
12 Wright, N J R *J petrol Geol* **2,** 411–425 (1980)
13 Seifert, W K & Moldowan, J M *Geochim cosmochim Acta* **45,** 783–794 (1981)
14 Ludwig, B, Hussler, G, Wehrung, P & Albrecht, P *Tetrahedron Lett* **22,** 3313–3316 (1981)
15 Schaefle, J, Ludwig, B, Albrecht, P & Ourisson, G *Tetrahedron Lett* **43,** 4163–4166 (1978)
16 Dannenberg, H, Neumann, H G & Dannenberg-von Dresler, D *Liebigs Ann Chem* **674,** 152–167 (1964)
17 Turner, A B *Chemy Ind* **13,** 932–933 (1972)
18 Nagata, W, Terasawa, T & Tori, K *J Am chem Soc* **86,** 3746–3749 (1964)
19 Hewett, C L *et al JCS Perkin I,* 336–340 (1975)
20 Ludwig, B, Hussler, G, Wehrung, P & Albrecht, P in *Advances in Organic Geochemistry 1981* (eds Bjorøy M *et al*) (Heyden, London, in the press)
21 Seifert, W K, Carlson, R M & Moldowan, J M in *Advances in Organic Geochemistry 1981* (eds Bjorøy, M *et al*) (Heyden, London, in the press)
22 Tissot, B & Welte, D H *Petroleum Formation and Occurrence* (Springer, Berlin, 1978)
23 Sajgo, Cs in *Advances in Organic Geochemistry 1979* (eds Douglas, A G & Maxwell, J R) 103–113 (Pergamon, Oxford, 1980)
24 Durand, B & Oudin, J L *Proc 10th World Petrol Congr* **2,** 3–11 (1981)
25 Tissot, B, Durand, B, Espitalie J & Combaz, A *Bull Am Ass petrol Geol* **58,** 499–506 (1974)
26 Maxwell, J R, Mackenzie, A S & Volkman, J K *Nature* **286,** 694–697 (1980)
27 Kirk, D N & Shaw, P M *Chem Commun* 806 (1970)
28 Magnier, Ph, Oki, T & Witoelar Kartaadipoetra, L *Proc 9th Wond Petrol Congr* **2,** 239–250 (1975)
29 Goy, G thesis, Univ Pierre et Marie Curie (1979)
30 Deroo, G *Internal Rep* No 14427 (Inst Fr Petrol, 1967)
31 Powers, R B *Oil Gas J* 180–186 (1977)
32 Shi Ji-yang, *et al Chem Geol* (in the press)
33 Tissot, B, Califert-Debyser, Y, Deroo, G & Oudin, J L *Bull Am Ass petrol Geol* **55,** 2177–2193 (1971)
34 Tissot, B & Espitalie, J *J Rev Inst Fr Petrol* **30,** 743–777 (1975)
35 Snowdon, L R *Bull Am Ass petrol Geol* **63,** 1128–1138 (1979)
36 McKenzie, D P *Earth planet Sci Lett* **40,** 25–32 (1978)
37 Beaumont, C *Geophys, J R astr Soc* **65,** 291–329 (1981)
38 Seifert, W K & Moldowan, J M *Geochim cosmochim Acta* **43,** 77–92 (1978)
39 Espitalie, J *et al J Rev Inst Fr Petrol.* **32,** 23–42 (1977)

Fine-scale isotopic heterogeneity in the sub-Atlantic mantle

N. Machado, J. N. Ludden & C. Brooks

Département de Géologie, Université de Montréal, Montréal,
Québec, Canada H3C 3J7

G. Thompson

Woods Hole Oceanographic Institution, Woods Hole,
Massachusetts 02543, USA

The isotopic composition of Sr and Nd in oceanic basalts reflects the character and chemical evolution of their source regions with respect to Rb/Sr and Sm/Nd. Combined studies of the Sr, Nd and Pb isotopic systems in mid-oceanic ridge basalts (MORB)[1,2] have confirmed previously recognized heterogeneities on a relatively large scale for the oceanic mantle. These heterogeneities have been ascribed to both long- and short-lived mantle processes and to mixing between enriched and depleted mantle sources (for example, see refs 1–4). However, data for the mid-Atlantic ridge (MAR) remote from known hot spots are available for only 14 samples of which only 3 are basaltic glass, the most 'reliable' sample type. Thus, attempts to explain MORB mantle heterogeneities are founded on limited data and remain largely speculative. The extent of variation in isotopic composition of 'normal MORB' over a limited area of the MAR is critical to any isotopic model for the oceanic mantle. Using high resolution seafloor mapping and sampling techniques, we can evaluate isotopic composition on a fine scale both within a ridge segment and across the fracture zones terminating that segment. We report here studies of a series of basaltic glass samples from the MAR intersection with the Kane Fracture Zone located at 22°–24° N (Fig. 1) which have implications for the dynamics of mantle melt segregation and the role of a major transform in mantle convection.

The Kane Fracture Zone is particularly interesting as it is one of the few areas of the MAR where the basalts are interpreted to represent 'normal MORB' and for which geochemical data indicate a relatively simple history of fractional crystallization and partial melting[5] The basalts of the Kane Fracture Zone do not display geochemical complications such as crossing rare-earth element patterns and complex mixing relationships that have been identified for the MAR axis north of 30° N (refs 6, 7) In addition, phase relations and geochemical models[5] indicate that, in many cases, the magma batches that erupted in the 22°–24° N region have evolved independently, and mixed only over a limited geographical area This minimizes the likelihood that large magma chambers or extensive melt segregation and mixing in the upper mantle have homogenized the isotopic systems, and this in turn, enhances the possibility of exposing and resolving fine-scale mantle heterogeneity

All analyses were performed on glass samples to minimize the problem of seawater contamination After separation by hand picking, the glasses were washed in acetone and leached in 6 2 HCl Sr and Nd were isolated by ion exchange following the techniques of Hart and Brooks[8] and Richard *et al*[9] respectively All samples were analysed on a modified, automated NBS 12-inch mass spectrometer at the Université de Montréal Nd and Sm were analysed on a double Ta–Re filament arrangement, whilst all other elements were run on a single Ta filament The data for the glass samples plus Sm, Nd and ^{143}Nd/^{144}Nd data for the rock standard BCR-1 and Nd oxide JMC-321 are given in Table 1 The sample identification conforms to the usual Woods Hole Oceanographic Institution's designation where G104-25-1 indicates sample number 1 from station 25 of RV Gilles Cruise 104

When all the data from 22°–24° are considered, the compositions fall at the low ^{87}Sr/^{86}Sr and high ^{143}Nd/^{144}Nd end of the Sr–Nd correlation[1 2 9–11] and extend the range for oceanic basalts to the most depleted values yet reported from the sea floor Figure 2 shows that the fracture zone clearly marks a barrier to isotopic domains The compositions of the samples from the ridge axis and from the fracture zone walls from the northern section are isotopically distinct from those of the southern section. The range in variation in ^{143}Nd/^{144}Nd isotopic composition exceeds that of ^{87}Sr/^{86}Sr, resulting in a vertical distribution across the oceanic trend similar to that observed for Iceland[12] and for the Marianas[13]

The abundances of the most lithophile elements show

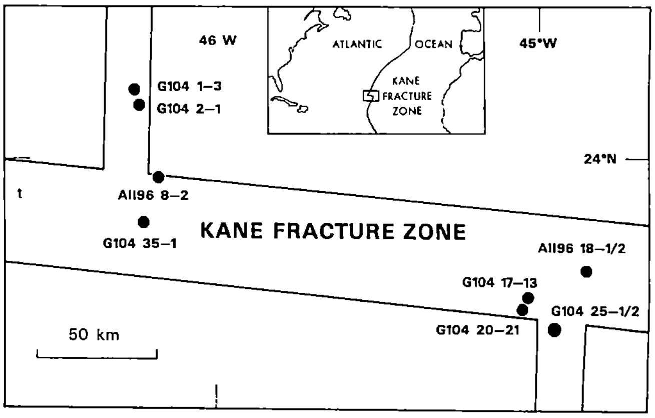

Fig. 1 Sample location map for the Kane Fracture Zone

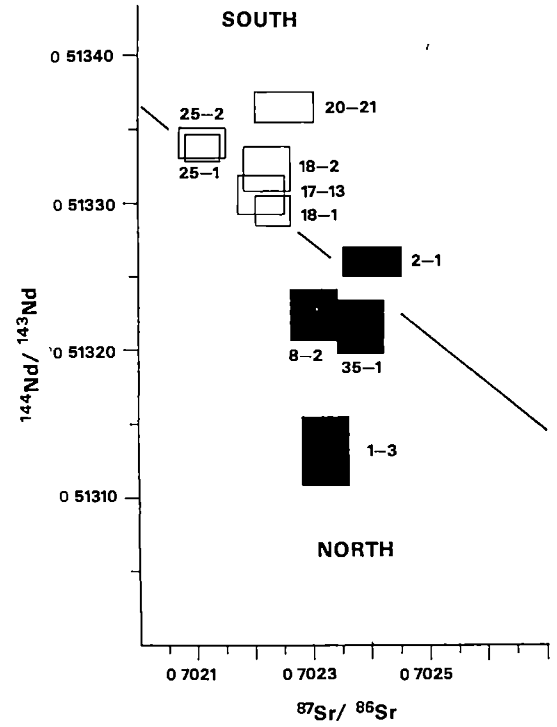

Fig. 2 ^{143}Nd/^{144}Sr and ^{87}Sr/^{86}Sr data for the Kane Fracture Zone basalt glasses (open symbols, southern intersection, solid symbols, northern intersection)

considerable variation both within a ridge section and between the northern and southern sections K/Rb varies from 1,250 to 1,820 in the southern ridge section relative to a variation of 680–760 in the northern section, whilst K/Ba values are of the order of 165 and 65 respectively Both K/Rb and K/Ba exhibit an inverse correlation with ^{87}Sr/^{86}Sr Although there is some overlap between the northern and southern sections, the samples define a positive correlation on the Rb/Sr isochron diagram (Fig 3*a*) which if interpreted as an age corresponds to 805 Myr (with an ^{87}Sr/^{86}Sr $R_{\rm i}$ = 0 70205). In contrast, the samples have similar Sm/Nd in both data sets with the exception of sample G104-2-1 which has a higher ratio This sample and others from this site are anomalous in having high Sr abundance relative to those samples from the northern section (Fig 3*c*)

The most significant geochemical property of the glass samples is their extreme trace element depletion in the southern section (as manifest in K/Rb, K/Ba and Rb/Sr ratios), and the correlation of that depletion with isotopic depletion Possible mechanisms by which these data can be explained include (1) long-lived mantle heterogeneity developed during the evolution of the sub-oceanic mantle, (2) a recent mixing event involving an enriched component added to and mixed incompletely with the oceanic mantle (such as a plume source and lateral transfer away from the plume), (3) transfer of volatile elements from the lower to the upper mantle

The geographical constraints, in which the samples from the northern section are enriched relative to those from the southern section are fundamental in appraising these models For instance, we see no plausible mechanism by which a superficial (lithospheric) structure such as a transform fault could control the observed distribution in isotopic ratios that would arise during voltaile transfer of variably enriched fluids from the lower to the upper mantle Such geographical control requires either a lateral transfer of relatively enriched material in the upper mantle, or mantle heterogeneity developed before or during the initial opening of the Atlantic Ocean The fracture zone is thus controlling or is controlled by the heterogeneity

Two lines of isotopic evidence can be used to support a mixing model First, samples from the northern section are more radiogenic than those from the southern section and may thus represent mixing of enriched and depleted material along a N–S axis Second, there are correlations defined by the samples from the southern section (Fig 3*c*, *d*), which on first examination could be interpreted as mixing lines Bryan *et al*[5] cite trace element data that support magma mixing over limited regions for the southern section However, data such as K/Rb, which confirm the more enriched character of the mantle in the northern section, are inconsistent with a simple mixing model For instance, K/Rb for site 20 is higher than that in the more depleted samples of site 17 When the 1/Sr and 1/Nd diagrams

Table 1 Isotopic and trace element analysis (p p m) of basaltic glasses

Sample	Lat N	Long W	$^{87/86}$Sr	$^{143/144}$Nd	K	Rb	Sr	Ba	Sm	Nd	K/Rb	K/Ba	Rb/Sr	Sm/Nd
G104 1-3	24°11 0′	46°16 9′	0 70242 ±4*	0 513132±23*	806	1 11	126 2		3 45	9 78	729	—	0 009	0 353
G104 2-1	24°09 4′	46°16 1′	0 70250±5	0 513260±19	1,233	1 77	140 5	19 81	3 47	7 58	696	62	0 013	0 458
AII96 8-2	24°00 7′	46°11 2′	0 70240±4	0 513224±17	—	—	—	—	—	—	—	—	—	—
G104 35-1	23°51 2′	46°13 4′	0 70248±4	0 513216±18	812	1 07	127 9	11 28	3 59	10 20	757	72	0 008	0 352
AII96 18-1	23°31 5′	44°49 1′	0 70233±3	0 513295±10	—	—	—	—	—	—	—	—	—	—
AII96 18-2	23°31 5′	44°49 1′	0 70232±4	0 523323±15	—	—	—	—	—	—	—	—	—	—
G104 17-13	23°37 2′	45°02 1′	0 70231±4	0 513306±13	1,509	1 21	138 5	—	8 68	25 61	1,249	—	0 009	0 339
G104 20-21	23°37 1′	45°02 3′	0 70235±5	0 513365±10	1,488	0 92	138 1	—	4 31	12 51	1,619	—	0 007	0 345
G104 25-1	23°32 0′	44°57 4′	0 70221±4	0 513341±10	1,401	0 60	139 5	6 41	4 93	13 78	1,735	162	0 004	0 357
G104 25-2	23°32 0′	44°57 4′	0 70221±3	0 513338±9	1,135	0 62	140 8	6 56	5 05	14 42	1,821	173	0 004	0 348
BCR-1			—	0 512679±20	14,278	46 91	330 0	702	6 71	28 65	—	—	—	—
JMC321				0 511921±12										
Total blank	(ng per g)				9	0 063	0 2	3	0 1	0 2				

* s e at 2σ

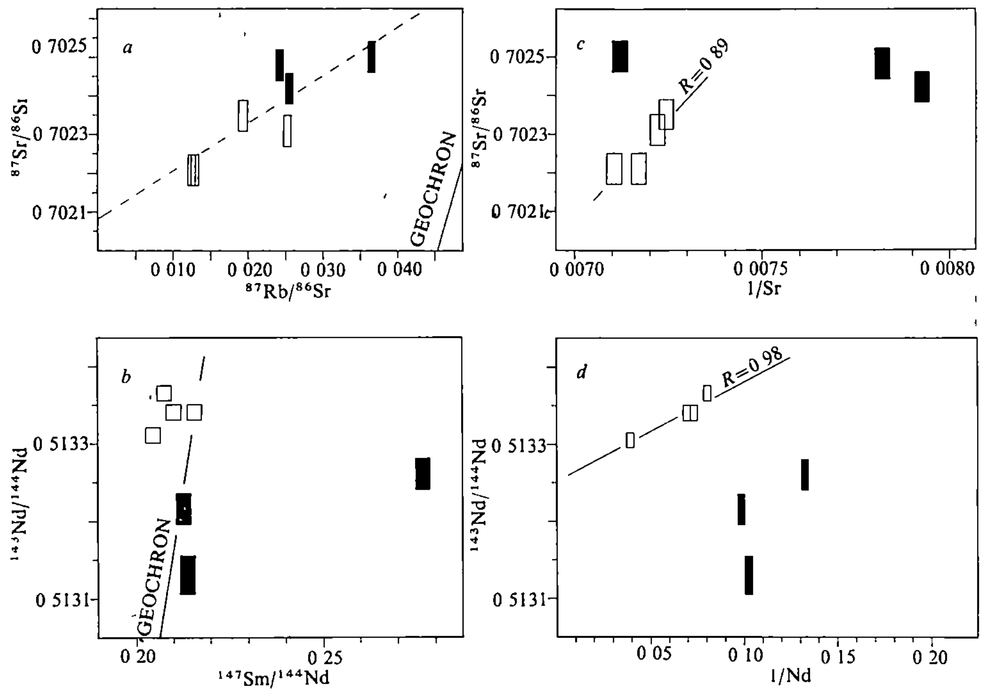

Fig. 3 *a*, Rb–Sr isocron diagram, *b*, Sm–Nd isochron diagram, *c*, $^{87}Sr/^{86}Sr$ against 1/Sr, and *d*, $^{143}Nd/^{144}Nd$ against 1/Nd for the Kane Fracture Zone basalt glasses

are compared they reveal similar inconsistencies For example, one of the end members of the southern section on the 1/Sr diagram plots between the end members on the 1/Nd diagram Although there is no positive confirmation of mixing based on the isotopic data, we cannot discount the possibility that on a small scale (that is between adjacent sites or within a single site, see ref 5) mixing may have occurred

The isochron diagrams (Fig 3*a*, *b*) reveal that whilst the samples define a 'reasonable' age on the Rb/Sr isochron plot, they define ages older than Earth on the Sm/Nd diagram This decoupling of parent–daughter isotopes in the Sm/Nd system is interpreted to be a result of recent petrogenetic processes involving garnet and clinopyroxene[14] Despite these complications, which, for example, result in a vertical distribution on the Sm/Nd isochron plot, we distinguish three subsets on the Sr/Nd correlation diagram (Fig 2) and the Rb/Sr isochron diagram (site 25, sites 1, 2, 8, 35 and sites 17, 18, 20) These subsets may reflect heterogeneities that developed during either a single event[15] or an extended period of mantle differentiation[16] However, the correlation of these subsets on the Rb/Sr isochron diagram implies that, even on a small scale, the mantle has remained heterogeneous over a considerable period

Trace element data for the MAR between the Kane Fracture Zone and 37° N (ref 17) indicate that major transforms such as the Hayes Fracture Zone delineate mantle regimes No isotopic data are available for the MAR between the Kane Fracture Zone and the FAMOUS region (36° N) and we cannot evaluate isotopic heterogeneity across the Hayes transform However, due to the lack of simple mixing relationships between the northern and southern sections of the MAR at the Kane Fracture Zone we speculate that, in some cases, a transform may act as a barrier to different mantle domains Support for this model comes from $^{87}Sr/^{86}Sr$ data for the Gibbs Fracture Zone[4] for which the values vary from $\simeq 0\ 70285$ in the northern section (60°–53° N) to 0 70225 in the southern section (53°–49° N) Furthermore, White and Schilling[4] indicate a sharp increase in $^{87}Sr/^{86}Sr$ initial in the region 49°–43° N which supports our contention that lateral flow away from an enriched mantle source is limited geographically Thus it seems that individual ridge segments bounded by transforms, could sample isolated mantle domains

The recognition of mantle heterogeneity over a limited region of the MAR characterized by 'normal MORB' places constraints on the scale of the heterogeneities and the extent of melt segregation in a convecting mantle Allègre *et al*[16] recognized that the oceanic mantle is heterogeneous on the mineralogical scale and Zindler *et al*[18] identified long-lived mantle heterogeneity on a kilometre scale Our data reveal that the mantle source for MAR is heterogeneous on a scale of tens of kilometres Magma batches of a similar major and trace element geochemistry may thus be characterized by significantly different isotopic ratios. However, our data and other published data[1–4] suggest that this mantle source is heterogeneous on the scale of tens to hundreds of kilometres, and that portions of the MAR are sampling long-lived heterogeneities that predate or coincide with the opening of the Atlantic Ocean Evidence from the Kane Fracture Zone and other Atlantic Ocean fracture zones indicate that these domains may be segmented by major transforms

The existence of isotopic heterogeneities in oceanic basalt glasses from adjacent sites implies that large scale magma chambers and regions of melt segregation do not exist in the upper mantle below the Kane Fracture Zone We envisage that melting, in a convecting upper mantle, results in the separation of liquid from discrete pods and hence basalts from adjacent sites may display totally different pre-eruptive histories

We thank S Hart and A Zindler who helped N M in the French to English to French translation of the Paris Sm/Nd technique, and also to C Gariépy for helpful discussions This work was supported by NSERC of Canada, grants A6096 to J L and A5581 to C B and NSF, grants OCE 77–09195 and OCE 77–26842 to G T

Received 12 August, accepted 4 November 1981

1 Cohen, R S *Nature* **283**, 149–153 (1980)
2 Dupre, B Allegre, C *Nature* **286**, 17–22 (1980)
3 Sun, S -S & Jahn, B -M *Nature* **255**, 527–530 (1975)
4 White, W M & Schilling, J -G *Geochim cosmochim Acta* **42**, 1501–1516 (1978)
5 Bryan, W B *et al. J geophys Res* (in the press)
6 Langmuir, C H *et al Earth planet Sci Lett* **73**, 5925–5941 (1977)
7 Dungan, M A & Rhodes, J M *Contr Miner Petrol.* **67**, 417–431 (1978)
8 Hart, S R & Brooks, C *Contr Miner Petrol* **61**, 109–128 (1977)
9 Richard, P *et al. Earth planet Sci Lett* **31**, 269 (1976)
10 O'Nions R K *et al Earth planet Sci Lett* **34**, 13–22 (1977)
11 De Paolo, D J & Wasserburg, G T *Geophys Res Lett* **3**, 743–746 (1976)
12 Zindler, A *et al Earth planet Sci Lett* **45**, 249–262 (1979)
13 Stern, R J & Bibee, L D *Yb Carnegie Instn Wash* **79**, 465–472 (1980)
14 Hart, S R & Brooks, C *Basaltic Volcanism*, Ch 7 (Pergamon, in the press)
15 Brooks, C & Hart, S R *Earth planet Sci Lett* **32**, 51–61 (1976)
16 Allegre, C J *et al Phil Trans R Soc* **297**, 313–343 (1980)
17 Bougault, H & Treuil, M *Nature* **286**, 209–212 (1980)
18 Zindler, A *et al. EOS* **62**, 424 (1981)

Fluid evolution and graphite genesis in the deep continental crust

William Glassley

Department of Geology, Middlebury College, Middlebury, Vermont 05753, USA

Metamorphism in deep continental crust is often accompanied by carbon-rich, H_2O-poor fluids[1–5], and is characterized by the development of granulite facies mineral assemblages[3–5]. Graphite, a minor phase in many high-grade metamorphic rocks[6–17], has also been recognized in recent xenoliths of deep crustal material[18], demonstrating its presence in modern deep continental crust. Although graphite is most common in biotite schists, it has also been recorded in pyroxene gneisses, two feldspar-quartz pegmatites, marbles and quartzo-feldspathic gneisses[11,15–19]. The presence of supracrustal sequences in granulite facies regions[6–19] suggests that the latter developed through progressive metamorphism and dehydration of shallow level crustal material. Much of this material must have experienced a metamorphic recrystallization in the amphibolite facies, accompanied by the development of hornblende. Although graphite in the high-grade rock may develop from oxidation of organic material, this may not be the most common means for graphite genesis. In much of West Greenland[14] and in southern Norway[12] the low-grade, hornblende-bearing material does not contain significant quantities of organic compounds, although graphite is found in higher-grade metamorphic equivalents. This strongly suggests that introducing CO_2 into deep crustal material leads to fluid evolution and graphite formation. I outline here the evolution of fluid composition in the C–O–H system which is in equilibrium with common crustal mineral assemblages. Thermodynamic data for CO_2–H_2O mixtures[20] and mineral components[21] are used to model the chemical changes in fluid composition which accompany introduction of CO_2 into various types of rock. The results demonstrate that graphite genesis is a direct consequence of deep crustal metamorphism in the presence of a CO_2-rich fluid phase. In addition, the calculations demonstrate that the deep continental crust will not be a reservoir for large volumes of methane-rich gas.

Although the behaviour of fluids in deep continental crust is unknown, fluid inclusion studies imply that carbon-rich fluids may migrate through the crust over large distances (tens of kilometres)[4] Here it is assumed that the fluid migration is accompanied by mixing of introduced CO_2 with *in situ* H_2O Continuous addition (flow) of CO_2 ultimately removes H_2O from the deep crust Thus, H_2O and CO_2 only mix along a migrating front of CO_2-rich fluid Below I examine fluid and mineral behaviour as this front migrates through biotite–magnetite–potassium feldspar (BMK) rocks

Rocks at deep crustal levels experience temperatures >600 °C and pressures >7 kbar In such conditions rocks are unlikely to possess any significant intrinsic pore space Consequently, introduced or *in situ* fluids create pore space sufficient for their volume Thus, fluid pressures are considered equal to lithostatic pressures, and no volume constraints are placed on the fluid

Thermodynamic properties of CO_2–H_2O mixtures were calculated from a modified Redlich-Kwong equation of state (MRK)[20] For the pure gases the derived fugacity coefficients are similar to those derived by Flowers[22], but differ substantially from those presented by Ryzhenko and Volkov[23] H_2, O_2, CO and CH_4 fugacity coefficients were obtained from ref 23

Calculations were carried out to determine in what fluid compositions the BMK assemblage would be stable These compositions were then compared with those for which graphite is stable This comparison determines whether graphite formation could result as a C–O–H fluid evolves in the presence of BMK

The BMK assemblage was considered because it is common in granulite facies rocks This assemblage defines hydrogen fugacity (f_{H_2}) through the equilibrium

$$\underset{\text{Annite}}{KFe_3AlSi_3O_{10}(OH)_2} = \underset{\text{Magnetite}}{Fe_3O_4} + \underset{\text{K-spar}}{KAlSi_3O_8} + H_2 \qquad (1)$$

The equilibrium constant for equation (1) (K_1), derived from the thermodynamic data and SUPCRT computer program of Helgeson *et al*[21], yields

$$\log f_{H_2} = \log\left(\frac{a^{bi}_{ann}}{a^{sp}_{mag}\ a^{feld}_{K\text{-spar}}}\right) - 21\ 68 + 8\ 176 \log (T\ °C) \qquad (2)$$

where a^j_i is the activity of i in phase j (bi, biotite, ann, annite, sp, spinel, mag, magnetite, K-spar, potassium feldspar, feld, alkali feldspar)

Equation (2) was derived by fitting a logarithmic function to log k_1 values which had been calculated at specified pressures and temperatures along chosen geothermal gradients The small volume change of equation (1) at pressures >5 kbar and temperatures >500 °C ($\Delta V_s < 0\ 88$ cm^3) means that no pressure terms are needed in equation (2)

Solution of

$$H_2 + \tfrac{1}{2}O_2 = H_2O \qquad (3)$$

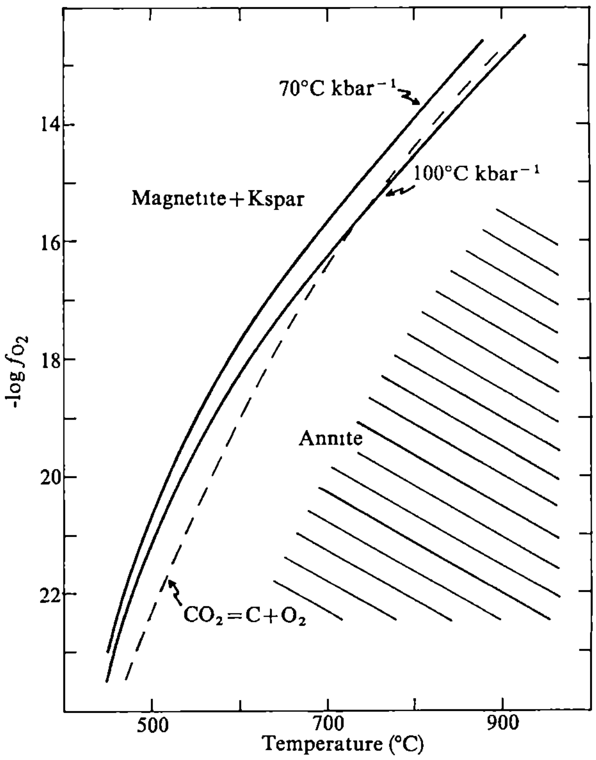

Fig. 1 Log f_{O_2} plotted against T for the BMK assemblage at geothermal gradients of 70 °C kbar^{-1} and 100 °C kbar^{-1} Note the small pressure effect implicit in the curve location The solid curves represent the case where $X_{H_2O} = 1\ 0$ and $X^{bi}_{ann} = 1\ 0$ The graphite–oxygen–carbon dioxide buffer curve is shown for reference (100 °C kbar^{-1}, $P_f = P_{CO_2}$) The ruled region shows the CH_4-dominated portion of the plane where $P_f = P_{CO_2} + P_{H_2O} + P_{CO} + P_{H_2} + P_{O_2} + P_{CH_4}$

0028–0836/82/030229—03\$01 00

allows calculation of f_{O_2} in a BMK assemblage at a specified P, T (degrees kelvin) and X_{H_2O} Solving log k_3 for log f_{O_2}, and substituting equation (2) for log f_{H_2} results in

$$\log f_{O_2} = 2\Big[\log (X_{H_2O}\cdot \gamma_{H_2O}\ P_f) + 21\ 20 - 8\ 176 \log (T-273)$$

$$-\left(\log \frac{a^{bi}_{ann}}{a^{sp}_{mag}\cdot a^{feld}_{K\text{-}spar}}\right) - \frac{12{,}510}{T\ \mathrm{K}} + 0\ 979 \log (T)\Big] \qquad (4)$$

X_{H_2O} is the mole fraction of H_2O in the fluid phase, γ_{H_2O} is the H_2O fugacity coefficient and P_f is the fluid pressure Equation (4) allows f_{O_2} to be calculated in the presence of a fluid of variable composition which is dominated by H_2O and CO_2

$$C + O_2 = CO_2 \qquad (5)$$

allows calculation of f_{O_2} in the presence of graphite at a specified X_{CO_2} Comparison of f_{O_2} values derived from equations (4) and (5), as a function of X_{H_2O}, provides a basis for outlining fluid evolution, graphite genesis and phase composition changes in the BMK assemblage

All calculations were carried out along geothermal gradients For comparison the results for the 100 °C kbar^{-1} and 70 °C kbar^{-1} geotherms are presented.

In the log $f_{O_2} - T^*$ plane, equation (1) exhibits a positive slope similar to that of other oxygen buffers (Fig 1) (Note that T^* represents specified pressure as well as temperature since all calculations are carried out along defined geothermal gradients.) However, the BMK assemblage is not an oxygen buffer because the solid and fluid phases are solutions, the location of the curve in the plane is specified only because the geothermal gradient and phase compositions are specified

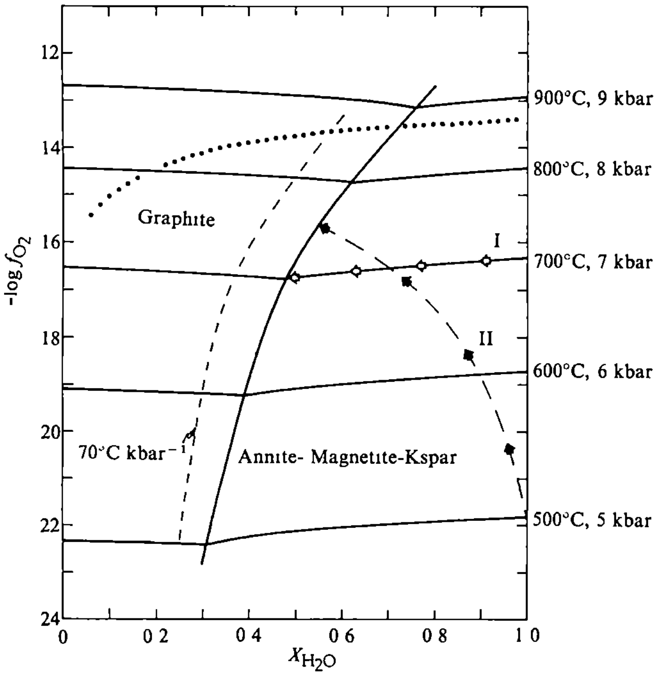

Fig. 2 Projection of BMK–fluid and graphite–fluid surfaces onto the log f_{O_2}/X_{H_2O} plane, from log f_{O_2}–X_{H_2O}–T^* space The solid lines labelled in P and T are contours on the two surfaces (100 °C kbar^{-1}), the intersection of the surfaces being represented by the solid line which cuts the contours at a high angle The intersection at a geothermal gradient of 70 °C kbar^{-1} is shown by the labelled dashed line These contours and intersection are drawn for the case where $X^{bi}_{ann} = 1\ 0$ and assumes $X_{H_2O} + X_{CO_2} \cong 1\ 0$ The effect of lowered iron concentration in the mica is shown by the dotted line, which represents the contour for 700 °C, 7 kbar, $X^{bi}_{ann} = 0\ 3$ Metamorphic pathways (I) (open arrows) and (II) (solid arrows) are discussed in the text

In log f_{O_2}–X_{H_2O}–T^* space, two surfaces can be drawn which represent the temperature-dependent, equilibrium fluid compositions for equations (1) and (5) Figure 2 shows these surfaces projected on to the log f_{O_2}–X_{H_2O} plane, and contoured for T^* In this projection, the isothermic contours for the BMK surface trend to lower log f_{O_2} values as X_{H_2O} decreases In contrast, the isothermic contours for the surface for equation (5) are at high log f_{O_2} values at low X_{H_2O}, and trend to low log f_{O_2} values at high X_{H_2O} Because of the contrast in curvature, these fluid composition surfaces intersect to form a low log f_{O_2} trough in the log f_{O_2}–X_{H_2O}–T^* space, which is represented in Fig 2 by the steeply sloping line To the right of the intersection, the contoured surface represents the fluid composition in equilibrium with BMK assemblages lacking graphite, to the left of the intersection the surface represents the fluid composition in equilibrium with graphite–magnetite–potassium feldspar The assemblage annite–magnetite–graphite–potassium feldspar can occur only along the intersection

Additional components in the biotite will diminish annite activity and the BMK surface (Fig 2) to higher log f_{O_2} values, and will displace the intersection to lower X_{H_2O} values For an $X_{ann} = 0\ 3$, intersection of the surfaces occurs at X_{H_2O} of $<0\ 1$, at 700 °C, where X_{ann} was computed assuming $a^{bi}_{ann} = (X^{bi}_{Fe})^3$, after Wones[24] Addition of other components to magnetite and potassium feldspar shifts the BMK surface such that the intersection occurs at higher X_{H_2O}

Two metamorphic pathways are possible in BMK-bearing deep crustal rocks into which CO_2 is being introduced In the treatment below it is assumed that a geothermal gradient of 100 °C kbar^{-1} is present.

In case (I), CO_2 introduction takes place in isothermal and isobaric conditions If the mica is pure annite, the log f_{O_2}–X_{H_2O} pathway will be that indicated by the open arrows in Fig 2 As CO_2 is added to the system the modal abundance of mica will decrease, as will the oxygen fugacity, until the intersection trough is attained At this point, graphite will precipitate from the fluid and annite will continue to react out until it has been eliminated from the assemblage. Once annite is removed, migration of the fluid composition along the isotherm will resume, increasing log f_{O_2} and X_{CO_2} until all H_2O is removed from the fluid

Case (I) will be complicated if the mica is a mixed annite–phlogopite phase. then the mica composition and its modal abundance become critical equilibrium parameters As CO_2 is added to the fluid the annite component in the mica reacts through equation (1), thus decreasing the activity of annite in the mica As a result, the log f_{O_2}–X_{H_2O} pathway may differ substantially from the pure annite case as the BMK isotherms migrate to higher log f_{O_2} values as the activity of annite in the mica drops (Fig 2) If the number of moles of annite per unit volume is small relative to the number of moles of CO_2 introduced at a given X_{CO_2}, the intersection of the two surfaces will rapidly migrate to very low X_{H_2O} values In such conditions, graphite will probably not precipitate as the annite component will be removed from the mica before the fluid composition reaches the intersection trough Such a system will have a phlogopite-rich mica coexisting with a CO_2-rich fluid phase If the number of moles of annite per unit volume is large relative to the number of introduced moles of CO_2 (a situation likely to occur when the pore volume is low), fluid evolution will approach that for the pure Fe-system where fluid migration can be traced along isotherms fixed in the log f_{O_2}–X_{H_2O} plane Such a system will necessarily produce graphite coexisting with an Fe–Mg biotite

Metamorphic pathway (II) considers the case in which CO_2 is introduced during increasing P and T This case, for the pure Fe-system, is depicted by the dashed, solid-arrowed pathway in

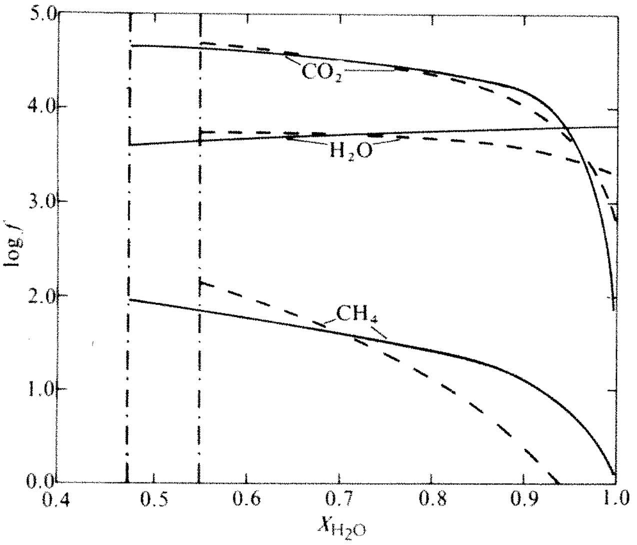

Fig. 3 Fluid evolution along metamorphic pathways (I) (isothermal, solid line) and (II) (polythermal, dashed line). Only H_2O, CO_2 and CH_4 are shown. O_2 can be deduced from Fig. 2; CO is slightly more abundant than CH_4, H_2 slightly less abundant than CH_4 along both pathways. The vertical dash-dot lines mark the point of graphite precipitation from the fluid phase. Both pathways are calculated along the 100 °C kbar^{-1} geotherm, and are represented in Fig. 2.

Fig. 2. For a mixed Fe–Mg biotite the pathway would be much steeper than that depicted, as annite would be progressively removed from mica and the BMK surface would migrate to higher log f_{O_2} values. Whether or not graphite is produced in the Fe–Mg system would again depend on the relative volumes of annite and introduced CO_2.

A comparison of the fluid species fugacities for these two metamorphic pathways (Fig. 3) demonstrates that in both cases a very rapid rise in f_{CO_2} occurs over an X_{H_2O} range of 1.0–0.90. Methane, in both cases, also shows a significant rise, but it never becomes a dominant fluid species. However, the behaviour of H_2O and O_2 are dramatically different for the two cases. In case (I) both these fluid species exhibit a small but significant decrease in fugacity values before graphite precipitation. In case (II), however, both fluid species significantly increase their fugacity values as CO_2 introduction proceeds. In case (I), the H_2O behaviour will lead to progressive dessication of the enclosing rock as dehydration reactions occur in response to the lowering of f_{H_2O}. In case (II), increasing f_{O_2} may result in noticeable oxidation of the mineral assemblage. Solid-phase compositions will change in response to this increase in f_{O_2} through continuous reactions. The exact nature of the phase composition changes will be a function of the appropriate exchange equilibria at *P* and *T*, and can be evaluated from the log *K* expressions for the equilibria.

The BMK-graphite assemblage is not a fluid buffer because biotite composition changes in response to changes in fluid composition. Nevertheless, the assemblage forces fluid composition to lie along the C–CO_2–O_2 surface, placing severe constraints on fluid abundances, at *P* and *T*. If mineral compositions are known, fluid species abundances can be precisely determined. In typical deep crustal conditions (700 °C, 7 kbar), the maximum possible X_{H_2O} is 0.46 for the pure Fe system, although typical mineral compositions (for example, $X^{\text{bi}}_{\text{ann}} < 0.3$, $a^{\text{feld}}_{\text{Kspar}} > 0.7$, $a^{\text{sp}}_{\text{mag}} > 0.7$) allow a maximum X_{H_2O} of 0.15. Log f_{O_2} values are tightly constrained as they must fall on the C–CO_2–O_2 surface which exhibits little variation in log f_{O_2} at a specified *P* and *T*. If either biotite or graphite is missing from an assemblage, fluid composition cannot be quantitatively determined. However, the possible f_{O_2} and X_{H_2O} values can be restricted to specific ranges, at *P* and *T* and specified mineral compositions, because these values must lie along the appropriate isotherm on either the C–CO_2–O_2 surface (biotite absent) or on the BMK surface (graphite absent).

None of the explanations proposed for the genesis of abiotic graphite for a wide range of occurrences[8,25–31] provides a means to develop graphite as a direct consequence of deep crustal metamorphism. The process outlined here, however, demonstrates that graphite will commonly develop in deep crustal settings as a result of CO_2 addition to mineral assemblages in which one of the O–H system fluid species fugacities is mineralogically controlled.

Biotic and abiotic graphite can be distinguished unambiguously by field criteria. In a terrain which has experienced a regional metamorphic event the presence of graphite in high-grade rocks, and the absence of carbon-bearing phases in lower-grade equivalents, for example, in southern Norway[12], is unequivocal evidence for an abiotic origin for the graphite.

The fluid evolution to be expected in such a setting (Fig. 3) is characterized by a very rapid rise in f_{CO_2}. Methane exhibits an increase in abundance, but never becomes a dominant fluid species, in the conditions examined here. Such considerations disprove suggestions[32,33] that intermediate or deep-level continental crust may act as large reservoirs for methane-rich gases.

Although the fluid evolution outlined here relied on the features of only the BMK assemblage, similar observations can be expected from any mineral assemblage which specifies fugacity of a fluid species in the O–H system. Thus, most assemblages containing hydroxyl-bearing minerals and oxides will lead to graphite genesis, provided that the stability limits for these minerals are not exceeded at the X_{H_2O} values compatible with graphite. The particular phase compositions which will be stable with graphite will depend on the geothermal gradient and the modal abundance of the solid phases, as well as on the total fluid volume affecting the rock.

The research reported here was supported by NSF grant DPP-7823305, while I was on leave at the University of California, Berkeley. I thank David Bridgwater, Richard Sack, Kai Sørensen and John K. Winter for helpful discussions, and R. Sack, J. R. Holloway and V. J. Wall for helpful comments and reviews.

Received 22 May; accepted 13 November 1981.

1. Touret, J. *Lithos* **4,** 423–436 (1971).
2. Goldsmith, J. R. *Bull. geol. Soc. Am.* **87,** 161–168 (1976).
3. Hollister, L. S. *Can. J. Earth Sci.* **12,** 1953–1955 (1975).
4. Newton, R. C., Smith, J. V. & Windley, B. *Nature* **288,** 45–52 (1980).
5. Glassley, W. E. & Sørensen, K. *J. Petrol.* **21,** 69–105 (1980).
6. Rao, J. S. R. K. & Rao, V. M. *Econ. Geol.* **60,** 1046–1051 (1965).
7. Katz, M. B. *Int. geol. Congr.* **24,** 43–50 (1972).
8. Dobner, A., Graf, W., Hahn-Weinheiner, P. & Hirner, A. *Lithos* **11,** 251–255 (1978).
9. Bessaire, H. in *The Precambrian* Vol. 3, 133–142 (Wiley, New York, 1967).
10. Dougan, T. W. *Contr. Miner. Petrol.* **46,** 169–188 (1974).
11. Heier, K. S. *Norg. geol. Unders.* **207** (1960).
12. Andreae, M. O. *Contr. Miner. Petrol.* **47,** 299–316 (1974).
13. Barejee, P. K. & Ghosh, S. *Econ. Geol.* **67,** 55–62 (1972).
14. Escher, A., Sørensen, K. & Zeck, H. P. *The Geology of Greenland*, 76–103 (Geological Survey of Greenland, Copenhagen, 1976).
15. Alling, H. G. *Bull. N.Y.S. Mus.* **199,** 1–150 (1917).
16. Cameron, E. N. & Weiss, P. L. *Bull. U.S. geol. Surv.* 1082-E (1962).
17. Wynne-Edwards, H. R. *Geol. Surv. Can. Mem.* **346** (1967).
18. Padovani, E. & Carter, N. *Am. geophys. Un. Monogr.* Ser. **20,** 19–55 (1977).
19. Glassley, W. E. & Winter, J. K. *EOS* **61,** 384 (1980).
20. Kerrick, D. M. & Jacobs, G. K. *Am. J. Sci.* **281,** 735–767 (1981).
21. Helgeson, H. C., Delaney, J. M., Nesbitt, H. W. & Bird, D. K. *Am. J. Sci.* **278A,** 229 p. (1978).
22. Flowers, G. *Contr. Miner. Petrol.* **69,** 315–318 (1979).
23. Ryzhenko, B. N. & Volkov, V. P. *Geochem. Int.* 1971, 468–481 (1971).
24. Wones, D. R. *Am. Miner.* **57,** 316–317 (1972).
25. Winchell, A. N. *Econ. Geol.* **6,** 218–230 (1911).
26. Ford, R. B. *Econ. Geol.* **49,** 31–43 (1954).
27. Mueller, R. F. & Condie, K. C. *J. Geol.* **72,** 400–411 (1964).
28. Strens, R. G. J. *Geol. Mag.* **102,** 393–406 (1965).
29. Salotti, C. A., Heinrich, E.-W. & Giardini, A. A. *Econ. Geol.* **66,** 929–932 (1971).
30. Nagy, B., Zumberge, J. E. & Nagy, L. A. *Proc. natn. Acad. Sci. U.S.A.* **72,** 1206–1209 (1975).
31. Wada, H. *Geochem. J.* **11,** 183–197 (1977).
32. Gold, T. *J. petrol. Geol.* **1,** 3–19 (1979).
33. Soter, S. & Gold, T. *Scient. Am.* **243,** 154–170 (1980).

New hominoid skull material from the Miocene of Pakistan

David Pilbeam

Peabody Museum, Harvard University, Cambridge,
Massachusetts 02138, USA

Neogene hominoid cranial material is regrettably scarce, especially from the middle and late Miocene. Between the 18-Myr-old virtually complete early Miocene *Proconsul africanus* skull from Rusinga[1] and the 3–4-Myr-old Hadar hominoid cranial material[2], the only significant large (non-hylobatid) hominoid facial or cranial specimens are those from the late Miocene Salonika in Greece[3], Yassiören in Turkey[4], Lufeng in China[5], the possibly middle Miocene site of Moroto in Uganda[6] and the new facial-mandibular piece from late Miocene deposits in Pakistan reported here. The specimen is a *Sivapithecus indicus*[7] adult, probably male, and consists of most of the left side of the face including a small portion of the frontal bone, the zygomatic arch and temporo-mandibular joint, the maxilla, a virtually entire mandible and the complete dentition. The fossil, catalogued as GSP 15000, is the property of the Government of Pakistan and is at present on loan for study at Harvard University.

The face was found during the 1979–80 field season of the Geological Survey of Pakistan–Harvard (then Yale) Peabody Museum Siwalik (GSP-HPM) research project on the Neogene of the Potwar Plateau of Pakistan (co-directed by Dr S. M. Ibrahim Shah and myself). The fossil was discovered by Mark Solomon and Dr John Barry and prepared at Yale by Horace French and Rizwana Raza. It comes from GSP-HPM locality 410 near the village of Kaulial in the Potwar Plateau[8]. Locality 410 is in the Dhok Pathan Formation[9], the locality itself being composed predominantly of red silts, representing overbank deposits[10]. The partial skull was probably not transported far after the animal's death, and was probably scavenged after death. The only other directly associated fossils are a few small mammals—murids, a flying squirrel and a dormouse. However, we have an abundant mammal fauna from many localities at the same stratigraphic level as the face, the so-called U sandstone level, after a prominent marker horizon[8].

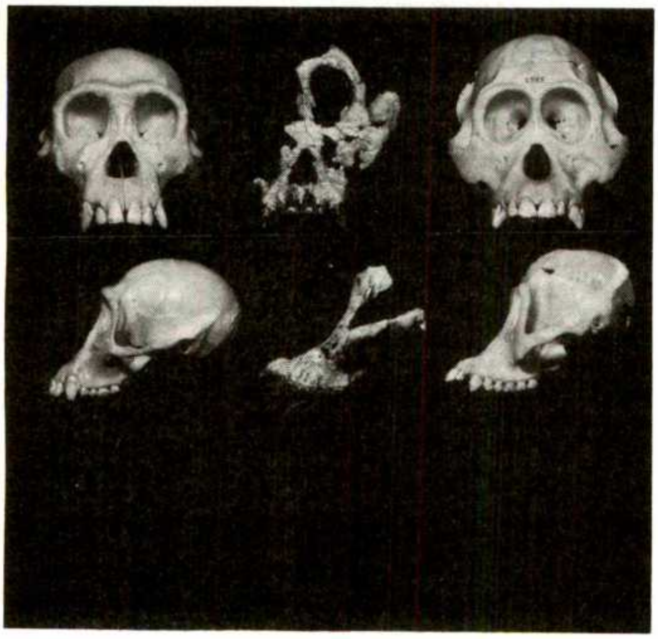

Fig. 1 Crania of *Pan* (left), GSP 15000 and *Pongo* (right).

Table 1 Facial, maxillary and mandibular measurements

Nasal height			84.0
Bizygomatic breadth		est.	75.0
Alveolare to nasospinale			26.0
Nasal aperture height		est.	29.0
Nasal aperture breadth			21.0
Nasal bone length		est.	58.0
Orbital height		est.	43.0
Orbital breadth			34.5
Zygomatic depth		est.	43.0
Orbito-alveolar height		est.	63.0
Minimum biorbital breadth		est.	9.5
Biorbital breadth across lacrymal crests		est.	10.5
Palatal length			83.0
Palatal breadth at C			31.0
Palatal breadth at M^2			32.5
Incisive foramen breadth		est.	2
Palatal depth at C		est.	8
Palatal depth at M^2		est.	17
Alveolar breadth at C			59.0
Alveolar breadth at M^2			59.0
Symphysis	Depth	est.	42
	Thickness	est.	20
Corpus at P_4	Depth		37.0
	Thickness		16.0
Corpus at M_3	Depth		34.0
	Thickness		28.5
Ramus	Notch height	est.	88.0
	Condylar height	est.	108.0
	Length	est.	60.0

For definitions of parameters measured, see refs 4, 6, 17.

The U level is ~8 Myr old, based mainly on magnetostratigraphic correlations[11,12]. A brief period representing perhaps less than 0.1 Myr has been sampled intensively at that level[13]. No significant plant remains are known, but we have tentatively reconstructed palaeography, habitats and faunal communities by a variety of geological and faunal techniques[8,10,13]. The late Miocene sediments were laid down by two major aggrading river systems, with many associated smaller streams, in an area of predominantly low relief. The habitat was probably a complex mosaic of forest, woodland and grassland, probably with a rich shrub layer. This would explain the abundance of browsing mammals, along with grazers, in the community[8,14].

Sivapithecus indicus is well represented at the U level by jaws and teeth, and a few unassociated postcranial elements probably also represent the same species[7]. If these assignments are correct the species was approximately chimpanzee-sized and more hominoid-like than cercopithecoid-like in overall anatomy; it was probably predominantly arboreal.

The new specimen is unusually complete for this range of time, comprising an upper face, palate, and mandible with a complete adult dentition (Figs 1, 2)[15]. The maxilla above the palate is preserved bilaterally and completely outlines the nasal aperture. Most of the remainder of the right side of the face is missing, except for the base of the malar process and a wedge of nasal process extending almost up to the frontal bone. In the midline and on the left side of the face, the specimen includes the nasal bones, almost complete orbital margin including the lower portion of the frontal bone, and the lateral edge of the face marking the anterior border of the temporalis muscle. The zygomatic bone is well preserved on the left and articulates with a segment of the zygomatic process of the temporal bone. A large fragment is missing from the midface on the left in the area of the zygomatico-maxillary suture. A separate fragment of the left temporal bone includes a complete articular fossa with a prominent postglenoid process. The lateral extent of the articular fossa is complete while medially the piece ends just beyond the articular surface. The mandibular corpus is bilaterally preserved back to the third molars, with a buccinator line well preserved on the right but mostly missing on the left. The specimen is broken and somewhat crushed on the left of the midline. Most of the left ramus is present, including a fragment of condyle, and the right ramus is also relatively complete.

0028-0836/82/030232—03$01.00

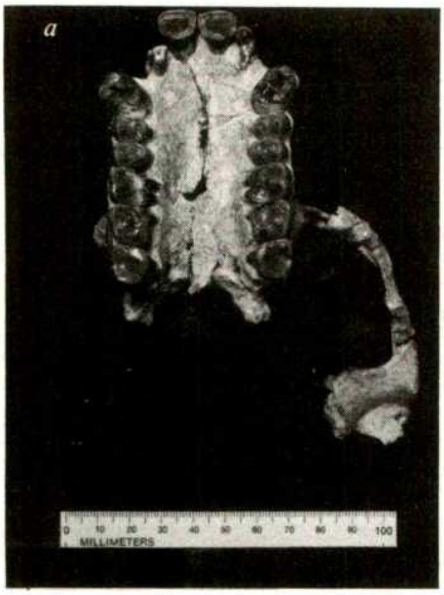

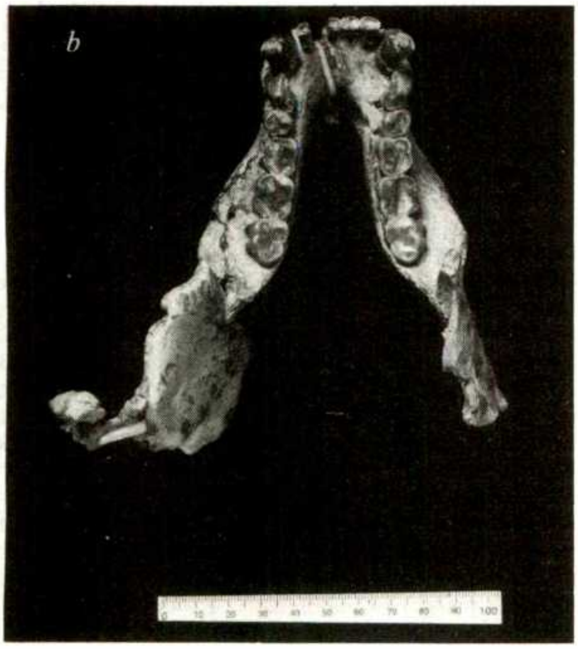

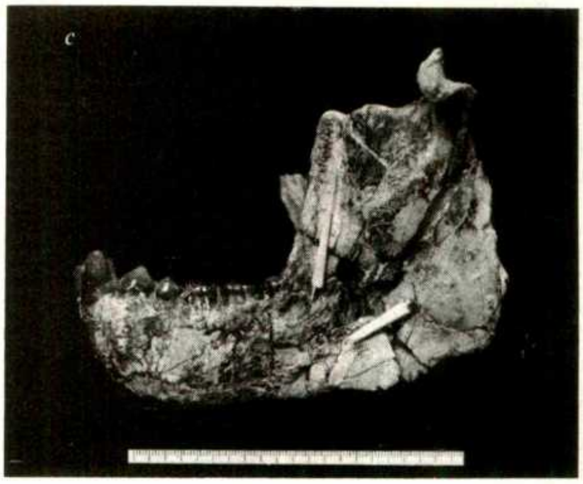

Fig. 2 *a*, Palatal view of GSP 15000; *b*, occlusal mandibular view of GSP 1500; *c*, lateral mandibular view of GSP 15000.

The overall impression is of a delicate face combined with robust jaws and teeth (see Table 1 for measurements). The face is deep from frontal to tooth row and concave in profile. The supraorbital tori are small and the frontal profile steep; there is no frontal sinus. The orbits are ovoid, with their longest dimension vertical, and are separated by a narrow interorbital region. The midfacial length from orbit to nose is greater than that in *Pan* or *Pongo*. The premaxillary region is prow-like and curved, and the incisors quite strongly procumbent. The zygomatic is gracile, and the temporo-mandibular joint shallow and crescentic, with the convexity facing anteriorly; it is ape-like, and similar to that of *Pongo*. The mandible is robust and deep, with well developed posterior symphyseal buttressing; the rami are high and vertical to the corpus.

Table 2 gives dental measurements of GSP 15000. Judging from canine size this is a male. Overall wear on the dentition is very heavy and most occlusal detail is therefore lost; in some cases dentine is extensively exposed. Unworn *Sivapithecus indicus* cheek teeth are high crowned and low cusped, with few occlusal wrinkles, and have thicker enamel than almost all Neogene hominoids with the exception of *Australopithecus*[7]. Wear on the incisors and canines of GSP 15000 is heavy; canines are blunted, and the small upper lateral incisors oddly worn, presumably by occlusion with the lower canines. This suggests extensive anterior tooth use in non-masticatory activity. The maxillary sinus floors descend mostly to the root tips, although posteriorly sinus pockets extend between the roots.

Sufficient frontal bone is preserved and enough known of the position of temporo-mandibular joint and adjacent temporal bone to reconstruct tentatively the anterior half of the brain

Table 2 Dental measurements

		Left	Right			Left	Right
I^1	MD	12.3	12.4		LaLi	—	7.2
	LaLi	9.0	9.1	I_2	MD	—	6.5
I^2	MD	est. 6.0	—		Lali	8.7	8.8
	LaLi	—	—	C̄	Max	13.7	13.8
Ç	Max	16.0	15.5		Tr	9.8	9.3
	Tr	12.3	11.6	P_3	Max	13.9	14.1
P^3	MD	8.6	8.7		Tr	7.9	7.9
	BuLi	11.8	12.1	P_4	MD	8.8	8.9
P^4	MD	8.0	8.4		BuLi	10.4	10.0
	BuLi	12.0	12.3	M_1	MD	12.4	12.6
M^1	MD	12.5	12.4		BuLi	11.3	11.4
	BuLi	13.0	—	M_2	MD	14.3	14.7
M^2	MD	12.8	12.8		BuLi	12.9	13.4
	BuLi	14.4	14.0	M_3	MD	14.3	14.8
M^3	MD	12.4	12.6		BuLi	12.7	12.4
	BuLi	13.4	14.0		Talonid	11.5	11.2
I_1	MD	—	5.7				

For definitions, see ref. 6. Note that all lengths are estimates, and greatly affected by wear.

case. This was hafted high on the face, as in *Pongo* but unlike *Pan*; brain volume was probably in the ape range. In this feature, and in facial profile, jaw joint morphology, malar morphology, orbital shape and disposition, and overall palatal shape, the specimen is quite orang-like. In other features the two species differ; for example, in tooth morphology and wear, and in the considerable fossil midfacial length and ramus height.

Compared with the few other Miocene facial or cranial specimens known, GSP 15000 differs from *Proconsul africanus*[1] and *Proconsul nyanzae*[16] in being more like living pongids, and also differs from the possibly middle Miocene palate and face from Moroto in Uganda[6]. Among other late Miocene hominoids, it is most like the *Sivapithecus* face from Yassiören[4] and less like *Ouranopithecus* from Ravin de la Pluie[3]. However, detailed comparisons with all these specimens, and with those from Lufeng[5] in China and from the Pliocene deposits at Hadar, Ethiopia[2], have not yet been completed.

As reconstruction and analysis of GSP 15000 continues, attention is being paid to the biomechanical meaning and potential functional significance of facial, mandibular and dental features; this involves detailed understanding of equivalent parts in modern systems. As these studies proceed it should be possible to develop a clearer understanding of the significance of the attributes frequently used in taxonomic and phylogenetic analyses. In particular, this will help evaluate the 'primitive' or 'derived' nature of character states.

Meanwhile, there are several similarities between GSP 15000 and *Pongo* that may turn out to be shared derived features. I doubt that *S. indicus* itself is ancestral to *Pongo*; however, I consider it likely that a similar late Miocene species, probably an Asian one, was. To what extent *S. indicus* resembles the last common ancestor of all living pongids and hominids is unclear. There are a few resemblances in mandibular and dental morphology (thick enamel, megadonty, mandibular robusticity) between Pliocene *Australopithecus* and *Sivapithecus* and similar late Miocene species, which may be primitive retentions. If so, in those features at least, the African pongids would be derived rather than primitive, which would have important consequences for the interpretation of hominid origins. However, it would be better to wait until more complete late Miocene hominoid material is recovered, especially from Africa, before constructing evolutionary stories.

This research was supported by NSF grant BNS-8007338 and SFCP grant 908817. I thank Mr Asrarullah the Director General, Geological Survey of Pakistan; all members of the joint project, particularly Ibrahim Shah, Mahmood Raza, Kay Behrensmeyer, John Barry, Catherine Badgley, Horace French and Rizwana Raza; and Richard Smith, Todd Preuss and Steven Ward. Photographs are by William Sacco.

Received 13 October; accepted 26 November 1981.

1. Le Gros Clark, W. E. & Leakey, L. S. B. *The Miocene Hominoidea of East Africa* (British Museum (Natural History), London, 1951).
2. Johanson, D. C. & White, T. D. *Science* **202,** 321 (1979).
3. de Bonis, L. & Melentis, J. *Annls Paléont.* **64,** 185 (1978).
4. Andrews, P. & Tekkaya, I. *Palaeontology* **23,** 85 (1980).
5. Qingwu, L., Q., Xu & L. Zheng, *Vert. PalAsiat.* **19,** 101 (1981).
6. Pilbeam, D. R. *Bull. Peabody Mus. nat. Hist.* **31** (1969).
7. Pilbeam, D. R., Rose, M. D., Badgley, C. & Lipschutz, B. *Postilla* **181** (1980).
8. Pilbeam, D. R., Behrensmeyer, A. K., Barry, J. C. & Shah, S. M. I. *Postilla* **179** (1979).
9. Barry, J. C., Behrensmeyer, A. K. & Monaghan, M. *Postilla* **183** (1980).
10. Badgley, C. & Behrensmeyer, A. K. *Palaeogeogr. Palaeoclimat. Palaeoecol.* **30,** 133 (1980).
11. Tauxe, L. *Nature* **282,** 399 (1979).
12. Lindsay, E. H., Johnson, N. M. & Opdyke, N. D. in *Aspects of Vertebrate History: Essays in Honor of Edwin Harris Colbert* (ed. Jacobs, L. L.) (Museum of Northern Arizona Press, 1980).
13. Behrensmeyer, A. K. & Tauxe, L. *Sedimentology* (in the press).
14. Barry, J. C., Lindsay, E. H. & Jabocs, L. L. *Palaeogeogr. Palaeoclimat. Palaeoecol.* (in the press).
15. Pilbeam, D. R. & Smith, R. *Geol. Surv. Pakistan Mem.* (in the press).
16. Whybrow, P. J. & Andrews, P. *Folia Primatol.* **30,** 115 (1978).
17. Corruccini, R. S. & Henderson, A. M. *Primates* **19,** 35 (1978).

Body temperature changes during the practice of g Tum-mo yoga

Herbert Benson*, John W. Lehmann*,
M. S. Malhotra†, Ralph F. Goldman‡,
Jeffrey Hopkins§ & Mark D. Epstein‖

* Division of Behavioral Medicine, Department of Medicine, Harvard Medical School, Charles A. Dana Research Institute, Harvard Thorndike Laboratory, Beth Israel Hospital, Boston, Massachusetts 02215, USA
† Netaji Subhas National Institute of Sports, Patiala 147001, India
‡ US Army Research Institute of Environmental Medicine, Natick, Massachusetts 01760, USA
§ Center for South Asian Studies, Cocke Hall, University of Virginia, Charlottesville, Virginia 22903, USA
‖ Harvard Medical School, Boston, Massachusetts 02115, USA

Since meditative practices are associated with changes that are consistent with decreased activity of the sympathetic nervous system[1–7], it is conceivable that measurable body temperature changes accompany advanced meditative states. With the help of H.H. the Dalai Lama, we have investigated such a possibility on three practitioners of the advanced Tibetan Buddhist meditational practice known as g Tum-mo (heat) yoga living in Upper Dharamsala, India. We report here that in a study performed there in February 1981, we found that these subjects exhibited the capacity to increase the temperature of their fingers and toes by as much as 8.3 °C.

g Tum-mo yoga is a form of meditation which allegedly allows its practitioners to alter body temperature. Previously, only subjective descriptions of this phenomenon existed: "The neophytes sit on the ground, cross-legged and naked. Sheets are dipped in icy water, each man wraps himself in one of them and must dry it on his body. As soon as the sheet has become dry, it is again dipped in the water and placed on the novice's body to be dried as before. The operation goes on in that way until daybreak. Then he who has dried the largest number of sheets is declared the winner of the competition"[8].

During the practice of g Tum-mo yoga, '*prāna*' (literally, 'wind' or 'air') is withdrawn from the scattered condition of normal consciousness and is made to enter into the 'central channel' inside the body. Then, through the alleged dissolution of these winds in the central channel, the 'internal heat' is ignited. The physiological changes are, therefore, a by-product of a religious practice.

Each of the three monks in the present investigation had spent more than 6 years practising g Tum-mo daily and had lived most of the past 10 years in near-isolation in unheated, uninsulated stone huts $\sim 4\times 7$ m. The floors were earthen and the roofs made of large slate slabs or flattened tin cans. The huts were in isolated locales in the foothills of the Himalayan Mountains at altitudes of 1,800–2,800 m, outside the town of Upper Dharamsala. The first two subjects were studied in their hermitages while the third was studied in a hotel room in Upper Dharamsala. Each participated in the investigation after being asked to do so by H. H. the Dalai Lama. Verbal informed consent was obtained from the three subjects through our translator (J.H.).

Skin temperature was measured in the area of the navel and lumbar region, the chest (nipple), left forearm, left fifth finger nailbed, left calf, left fifth toe nailbed and forehead using small disk thermistors (Yellow Springs Instrument Corporation (YSI), model 427) that were attached to the skin with plastic tape. Rectal temperature was monitored by means of a YSI rectal catheter probe inserted 10 cm beyond the anal sphincter. Air temperature was measured by YSI thermistor air probe (model 405) as well as with a conventional sling psychrometer which was used to measure psychrometric wet bulb temperature to calculate relative humidity. All wires were connected to a multichannel (YSI) switch box (model 4002) and connected to a YSI wide-range Telethermometer (model 42) with a 60 °C range. Heart rate was monitored with a San-EI (model 2D16) Pulse-

0028-0836/82/030234—03$01.00

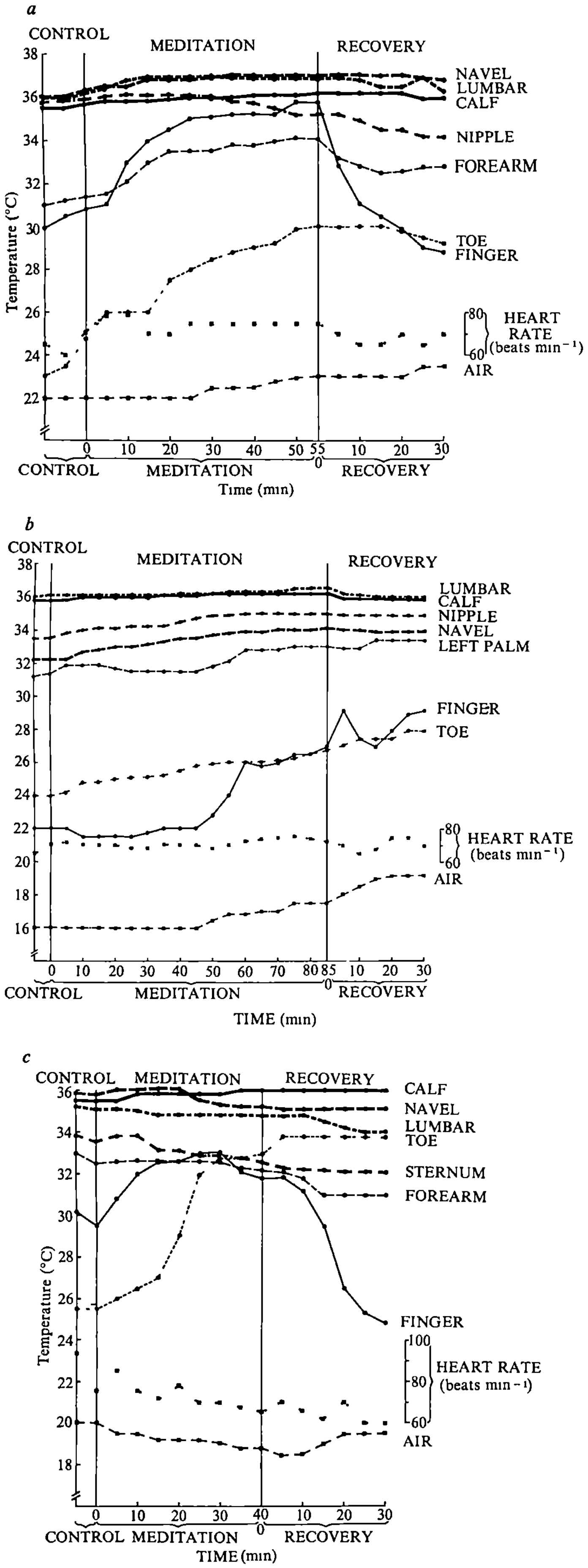

Fig. 1 Skin and air temperature and heart rate changes before, during and after the practice of g Tum-mo meditation in subjects G J (*a*), J T (*b*) and L T (*c*)

meter monitor which used a digital probe to sense each pulse of blood flowing into the thumb Measurements were taken sequentially and tabulated every 5 min during control, meditation and recovery periods

The first subject, Ven G J , aged 59 yr, sat in the cross-legged 'Lotus' posture During a 55-min period of g Tum-mo meditation, his finger temperature increased 5 9 °C and his toe temperature 7 0 °C (Fig 1*a*) In the recovery period, finger temperature returned to baseline levels, while toe temperature, with the toes protected against heat loss by the lotus position, remained elevated Navel and lumbar temperatures increased by 1 °C during the meditative period Rectal temperature was unchanged Air temperature slowly increased from 22 0 to 23 5 °C during the hour Heart rate increased slightly, by 2 beats per min, during the meditative period and then returned to baseline levels

Finger temperature in the second subject, Ven J T , aged 46 yr, increased 7 2 °C, the highest levels being recorded in the recovery period at a time when the subject claimed that, although he had stopped meditating, the subjective experience of g Tum-mo heat had continued (Fig 1*b*) A similar pattern with a 4 0 °C increase was noted in the toe temperature Navel temperature increased 1 9 °C and nipple temperature 1 5 °C Rectal temperature was unchanged Air temperature slowly increased within the hut from 16 °C to 19 2 °C, the most marked changes occurring late in the recovery period Heart rate was essentially unchanged throughout

The third subject, Ven L T , was 50 yr old Because his g Tum-mo changes started any time he was in a sitting posture, baseline measurements were taken in the upright posture We first performed measurements on this subject outside his hut However, high radiant heat temperatures hampered skin temperature measurements and since our visit coincided with the celebration of the Tibetan New Year, when the monk walked to Upper Dharamsala to listen to a lecture given by H H the Dalai Lama, we studied him again in a cool hotel room His finger temperature rose 3 15 °C while toe temperature increased 8 3 °C (Fig 1*c*) There were no other large changes in skin temperature Rectal temperature was unchanged Air temperature within the hotel room decreased during the meditation period from 20 to 18 5 °C, and then rose to 19 5 °C in the recovery period Heart rate decreased after assuming the sitting position and continued to fall slowly throughout the experiment

The subjects in the current experiment exhibited a greater capacity to warm fingers than has been previously recorded during hypnosis and after biofeedback training[9-15] Although it is possible that the practitioners had learned to increase their metabolism to produce more body heat, this seems unlikely Even though they were all lean, the monks claimed not to require more than a 'normal' amount of food Furthermore, their resting heart rates were within normal limits The most likely mechanism to account for the increase in finger and toe temperature is vasodilation Although no direct measurements of peripheral blood flow were made, others have calculated that during the simple meditative process of transcendental meditation, there is a 44% increase in nonhepatic, nonrenal blood flow[16] and they hypothesized an increase in skin or cerebral blood flow or both

We thank H H the Dalai Lama and other members of the Tibetan community of Dharamsala, India, notably Ven Doboom Tulku and Tendzin Choegyal, for their support We also thank Wendy L Wornham, M.D , Irene L Goodale and Nancy E MacKinnon for their assistance This work was supported by grants from the National Science Foundation (NSF INT 8016982), the American Institute of Indian Studies, the National Institutes of Health (HL 22727 and HL 07374), the Fleischmann Foundation and the Fetzer Foundation

Received 22 May, accepted 26 October 1981

1 Wallace, R K , Benson, H & Wilson, A F *Am J Physiol* **221**, 795–799 (1971)
2 Wallace, R K & Benson, H *Scient Am* **226**, 84–90 (1972)
3 Benson, H , Beary, J F & Carol, M P *Psychiatry* **37**, 37–46 (1974)

4 Beary, J F & Benson, H *Psychosom Med* **36,** 115–120 (1974)
5 Benson, H, Steinert, R F, Greenwood, M M, Klemchuk, H M & Peterson, N H *J hum Stress* **1,** 37–44 (1975)
6 Benson, H *The Relaxation Response* (Collins, London, 1976)
7 Hoffman, J W *et al Science* **215,** 190–192 (1982)
8 David-Neel, A *Magic and Mystery in Tibet,* 227 (Dover, New York, 1932)
9 Maslack, C, Marshall, G & Zimbardo, P G *Psychophysiology* **9,** 600–605 (1972)
10 Roberts, A H, Kewman, D G & MacDonald, H *J abnorm Psychol* **82,** 163–168 (1973).
11 Newman, R W *Am ind Hyg Ass J* **36,** 610–617 (1975)
12 Lynch, W C, Hama, H, Kohn, S & Miller, N E *Psychophysiology* **13,** 219–221 (1976)
13 Taub, E & Emurian, C S *Biofeedback Self-Regulation* **1,** 147–168 (1976)
14 Jacobson, A M, Manschreck, T C & Silverberg, E *Am J Psychiat* **136,** 844–846 (1979)
15 Hatfield, J A *Lancet* **ii,** 68–69 (1917)
16 Jevning, R, Wilson, A F, Smith, W R & Morton, M E *Am J Physiol* **235,** R89-92 (1978)

Preferences for cousins in Japanese quail

Patrick Bateson

Sub-Department of Animal Behaviour, University of Cambridge, Madingley, Cambridge CB3 8AA, UK

Early experience affects the mating preferences of many birds and mammals[1,2]. The plasticity of behaviour is such that individuals reared with a member of another species may subsequently choose to mate with that species[3–6]. Recent evidence suggests that the most strongly preferred mates are slightly different from individuals that are familiar from early life[7–9]. The implication of these findings is that an individual is able to strike an optimal balance between inbreeding and outbreeding by learning about its immediate kin and mating with a member of the opposite sex that is slightly different from its immediate kin[1,10]. What such a balance might amount to in practice has previously been uncertain. I report here that Japanese quail of both sexes, having been reared with their siblings, subsequently prefer a first cousin of the opposite sex.

The Japanese quail (22 males and 13 females) tested in this experiment were obtained from eggs laid by four different pairs in our laboratory colony. Eggs from a given pair were collected over 2-week periods and placed simultaneously in a separate compartment in an incubator. When transferred 13 days after the start of incubation to a hatching incubator, eggs were again kept in separate families and hatched separately. Within a day of hatching in the dark, the chicks were transferred to rearing pens and kept in true families in the same conditions as those used in previous experiments[7,9]. The birds were isolated 30 days after hatching. Testing started at 60 days, when the quail were sexually mature.

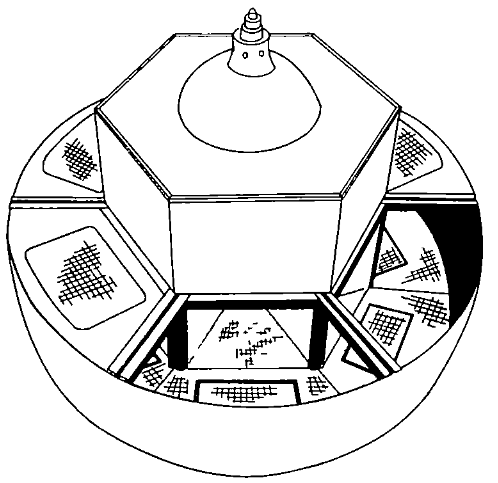

Fig. 1 Apparatus used for testing preferences of adult Japanese quail. Stimulus birds were put singly in the inner compartments, which were painted white and lit from above. The outward-facing windows were fitted with one-way screens. A test bird could move freely round the black unlit outer part of the apparatus. A pedal in front of each window operated a microswitch.

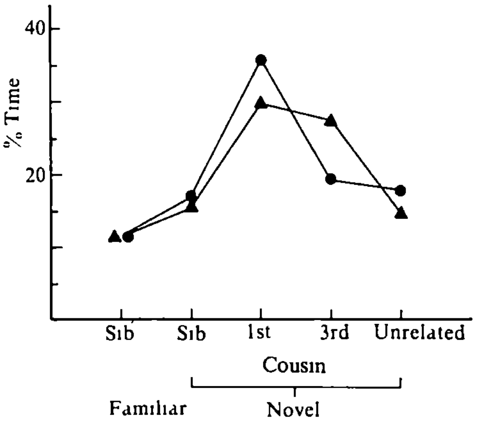

Fig. 2 The mean percentage time spent by adult Japanese quail near members of the opposite sex that were either familiar siblings (Sib), novel siblings, novel first cousins, novel third cousins, or novel unrelated individuals. The chance level is 20%. ▲, Males ($n = 22$), ●, females ($n = 13$).

The pedigrees of the quail in the colony were known for at least four generations and pairings had been carefully arranged. It was possible, therefore, to test all birds with a variety of members of the opposite sex that were of different degrees of relationship but of the same age. In addition, some true siblings were reared separately so that when the birds were tested, they were given choices between familiar and novel siblings, novel first and third cousins, and novel unrelated members of the opposite sex.

The apparatus used for testing the adult quail is shown in Fig. 1. The compartments in which the stimulus birds were placed faced outwards from the centre of the apparatus. The inside walls were painted white and the outside wall consisted of a one-way screen. The outward-facing windows were used so that the test bird was not visible to the stimulus birds. The outer runway was painted black and the test bird could move freely from one window to the next. To eliminate possible bias, when a test bird was initially introduced into the apparatus, it was placed in front of a compartment containing a different stimulus bird from the one tested previously. Furthermore, food and water for the test bird were placed on the outside wall opposite the compartment of every stimulus bird. Each test session lasted 30 min. Pedals which triggered microswitches were placed in front of the compartment of each stimulus bird. The time spent in front of each of these stimulus birds was recorded automatically and expressed as a percentage of the total time spent in front of all five types of stimulus bird.

Figure 2 shows the mean percentage duration spent in front of each category of stimulus bird by both adult males and females. Table 1 gives the scores for each individual. The males were slightly more ready than females to spend time near a third cousin of the opposite sex. However, in this sample at least, the behaviour of the two sexes were statistically indistinguishable and, for the purpose of the analysis, these data were pooled. First, all the data were examined using the Friedman test and the overall deviation from chance was found to be statistically significant ($\chi^2 = 10.07$, $P < 0.05$). Second, the time spent near each category of stimulus bird was compared with the time spent near each other category of stimulus bird using the Wilcoxon matched-pairs test. The time spent near novel first cousins was significantly greater than that spent near both familiar and novel siblings ($z = 3.02$, $P < 0.01$ and $z = 2.23$, $P < 0.05$, respectively). The time spent near novel first cousins was also

0028-0836/82/030236—02$01.00

Table 1 Percentage time spent by adult Japanese quail near members of the opposite sex

Sex	Subject	Familiar sibling	Novel sibling	Novel first cousin	Novel third cousin	Novel unrelated
Male	1	2.3	29.4	41.7	22.5	4.0
	2	42.4	0.0	49.6	0.0	8.0
	3	0.0	4.0	11.8	3.4	80.8
	4	11.7	33.7	23.2	9.6	21.7
	5	14.5	19.1	32.8	33.6	0.0
	6	0.3	43.6	2.1	30.5	23.5
	7	3.4	0.1	26.7	50.8	19.1
	8	0.0	0.4	87.4	0.0	12.1
	9	0.0	0.0	0.1	97.2	2.7
	10	52.4	0.0	1.6	46.1	0.0
	11	3.9	88.3	7.6	0.0	0.2
	12	0.0	0.2	24.8	75.1	0.0
	13	1.0	3.3	30.9	63.8	1.0
	14	0.0	1.3	0.0	94.4	4.3
	15	59.2	0.0	0.0	35.2	5.7
	16	8.5	52.4	13.5	15.5	10.1
	17	17.1	4.5	78.4	0.0	0.0
	18	23.0	14.3	17.8	12.7	32.2
	19	0.0	72.5	26.3	1.2	0.0
	20	10.1	0.0	89.9	0.0	0.0
	21	0.0	5.9	52.2	8.9	33.0
	22	2.9	0.1	34.2	0.1	62.7
Female	23	20.6	6.0	0.3	67.8	5.4
	24	12.8	25.6	43.3	11.8	6.6
	25	0.0	3.4	96.6	0.0	0.0
	26	55.9	26.3	7.3	3.2	7.2
	27	9.6	5.5	13.6	49.1	22.2
	28	0.5	0.0	63.6	0.1	35.8
	29	0.0	23.0	42.6	10.5	23.9
	30	0.0	0.0	7.7	82.0	10.2
	31	30.9	13.4	20.0	8.2	27.4
	32	4.6	61.3	4.3	7.9	22.0
	33	0.0	17.2	77.2	2.8	2.8
	34	14.0	20.2	2.9	9.0	53.9
	35	0.0	0.0	86.1	0.0	13.9
No showing strongest preference for category		4	6	12	9	4

significantly greater than the time spent near unrelated individuals ($z = 2.18$, $P < 0.05$).

Of course, remaining near a member of the opposite sex is not the same as attempting to mate with it. However, other experiments have shown that, in adult male Japanese quail, the time spent near a female in a choice test is strongly linked to the copulation preference[7]. Furthermore, the males in the present experiment were observed to court the females in the choice tests. Finally, I have found in other experiments that birds show no consistent preferences for members of the same sex.

Despite the clear overall preference for first cousins, the data were highly variable and only 12 of the 35 birds spent most time near a first cousin (see Table 1). The variability was expected as the degree of relationship between two individuals only indicates the probability that the two share heritable characters. I have confirmed this by direct measurement of the quails' plumage. Although, for example, first cousins are on average more like each other than unrelated individuals, unrelated birds may resemble each other more closely than some first cousins. Knowledge by a bird of a sibling's appearance must necessarily be an imperfect guide to what a first cousin will look like.

The most preferred category of relations will probably depend on the degree of outbreeding of the population[9]. The quail used here were relatively inbred and 'unrelated' birds were physically rather similar to each other. In populations that are physically more variable than our laboratory quail, the most preferred member of the opposite sex might be more closely related than a first cousin. In contrast, the effect of restricted experience in a laboratory experiment might have meant that the birds were more ready to escape from novelty than would be the case for quail growing up in a natural environment. Therefore, in a free-living population, the effects on sexual preferences of greater variation in the plumage of the population may cancel out those of more varied experience.

In many human societies, marriage to a first cousin is common[11]. This apparent similarity between the behaviour of humans and quail should be noted. Humans may strike a balance between the costs of inbreeding and those of outbreeding[10,12] and in doing so, may rely on their early experience in a way similar to quail. Clearly, many factors deriving from culture and individual experience affect human mating preferences, but one influence may well be an attraction towards a member of the opposite sex who differs, but not to a large extent, from well known, closely-related members of the family.

I thank Mr John Owen for assistance in the care and testing of the animals, and Mr Tom Goss and Mr Brian Maltby for building the apparatus. The research was supported by a SERC grant.

Received 25 September, accepted 27 November 1981.

1. Bateson, P. P. G. in *Biological Determinants of Sexual Behaviour* (ed. Hutchison, J. B.) 29–53 (Wiley, Chichester, 1978).
2. Immelmann, K. & Suomi, S. J. in *Behavioral Development* (eds Immelmann, K., Barlow, G., Petrinovich, L. & Main, M.) (Cambridge University Press, New York, 395–431).
3. Lorenz, K. *J. Orn., Lpz.* **83,** 137–213, 289–413 (1935).
4. Schutz, F. *Z. Tierpsychol.* **22,** 50–103 (1965).
5. Immelmann, K. *Z. Tierpsychol.* **26,** 677–691 (1969).
6. Roy, M. A. *Species Identity and Attachment. A Phylogenetic Evaluation* (Garland, New York, 1980).
7. Bateson, P. *Nature* **273,** 659–660 (1978).
8. Gilder, P. M. & Slater, P. J. B. *Nature* **274,** 364–365 (1978).
9. Bateson, P. *Z. Tierpsychol.* **53,** 231–244 (1980).
10. Bateson, P. *Anim. Behav.* **27,** 470–486 (1979).
11. Fox, R. *Kinship and Marriage* (Penguin, Middlesex, 1967).
12. Bischof, N. *Soc. sci. Inf.* **11,** 7–36 (1972).

Early auditory experience modifies sound localization in barn owls

Eric I. Knudsen, Phyllis F. Knudsen & Steven D. Esterly

Department of Neurobiology, Stanford University School of Medicine, Stanford, California 94305, USA

The auditory system localizes sounds by comparing the timing and intensity of sounds arriving at the two ears, and associating specific binaural differences with directions of sounds in space. Thus, location for the auditory system, like stereoscopic depth for the visual system, is a percept created in the brain by a comparison of inputs from two receivers. We considered whether the neural mechanism underlying sound localization is determined entirely genetically, or if it is modified and regulated by auditory experience. The influence of experience on sound localization has been examined previously in various species, including man, with contradictory results[1-9]. For our study we used the barn owl (*Tyto alba*) as an experimental model because it localizes sounds with extreme accuracy[10,11]. By placing a plug in one ear, we disrupted the owl's binaural localization cues and induced large errors in sound localization. We report here that young owls adjusted to the altered cues and regained normal localization accuracy over a period of weeks. However, as the owls aged, their rate of adjustment slowed, and beyond 6–7 months of age, their capacity to adjust was lost or greatly reduced. This plasticity of the sound localization mechanism early in life thus enables the auditory system to establish precise correlations between binaural cues (which vary between individuals) and directions of sounds in space.

The localization cues used by the barn owl are those used by man—interaural differences in intensity and time[12-14]. However, because of a vertical asymmetry in the positions of the owl's ears, high frequency sounds are loudest in the right ear when they originate above and to the right, and loudest in the left ear when they come from below and to the left[15]. Behavioural and physiological studies demonstrate that owls use interaural intensity cues to localize the elevation of sounds, and both interaural time and intensity cues to localize the azimuth[13,14].

In our experiments, we occluded ears by suturing a foam rubber plug into the auditory canal. The effect of such a plug on the auditory signal was determined in one bird by measuring the sensitivity and phase of cochlear microphonic responses before and after the treatment. The plug attenuated the signal by 30–55 dB from 1 to 10 kHz depending on frequency, and altered the phase of each frequency. Thus, both interaural intensity and timing cues were severely disrupted by this procedure.

The experiments were done in a darkened anechoic chamber with the owl perched in the centre. Sound stimuli were generated by a 4-cm speaker that could be moved to any position around the owl by remote control. Travelling with the speaker and centred in its cone was a 3-mm light bulb that provided a light stimulus. The behavioural paradigm for measuring sound localization error took advantage of a natural head orienting response: on hearing a sound the owl turns its head in a rapid flick or saccade, bringing the source of the sound into a frontal region of maximum spatial acuity for the auditory system[10]. This movement also brings the visual axes of the eyes, which are immobile in their sockets, in line with the target. A normal owl orients its head almost identically to either a sound or a light stimulus. In these experiments, a difference in the orientation of the head to sound as opposed to light was taken as an error in sound localization (Fig 1). The behavioural paradigm simply required the owl to orient its head in response to either the sound or light stimulus, for which it received a food reward. The reward was not contingent on the accuracy of the response, only on its crispness and appropriate latency. To quantify the position of the head, a small mirror was attached to a clip cemented to the skull, and a collimated source of IR light was directed at the bird. The mirror reflected the IR beam onto a grid of 0.5° increments in a horizontal polar coordinate system. The location of the beam on the grid was monitored using a video camera and stored on video tape for subsequent analysis.

The sound target consisted of repetitive noise bursts of variable duration, the light target was a constant dim glow of the bulb. In both cases the stimulus was presented for up to 2 s. If the owl did not respond, the stimulus was turned off, followed by a waiting period of 30 s. Typically, however, the owl responded immediately with a saccadic head movement and sustained fixation. The stimuli were maintained long enough to allow the owl to maximize its accuracy. The coordinates of the head orientation were then recorded, a reward light activated, and a food reward delivered. After every trial the speaker (with light bulb) was moved to a new location. The owl received no feedback regarding the accuracy of its responses during these tests.

Five baby owls were used, four as experimental subjects and one as a control. All were kept in identical holding cages and allowed out daily for training and exercise. The auditory experience they received consisted of self-generated noises when active in their cages, and the sounds in the laboratory when allowed out for exercise. At 4 weeks of age we occluded the left ear of owl 1 and the right ears of owls 2 and 3, the right ear of owl 4 was occluded only at 27 weeks. Owl 5, which served as a control and was never plugged, demonstrated the accuracy and precision that can be expected from a normal owl under our experimental conditions. From four measurements made at 18 weeks of age, the mean error of owl 5 ranged in magnitude from 0.8° to 1.4° in azimuth and from 0.4° to 1.7° in elevation, with respective standard deviations of 1.4–2.3° and 1.3–2.7°. These values are almost identical to the localization accuracies of two adult owls that were studied intensively in previous behavioural experiments, using a different measuring technique[10].

From these results, we defined normal localization accuracy as an error of ≤2° in azimuth and elevation (indicated by broken

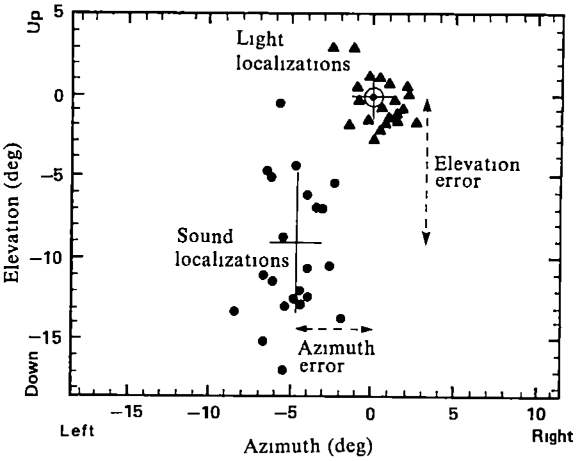

Fig. 1 The distribution of head orientations to sound and light stimuli recorded in a single test session. Each symbol represents a fixation point in response to a sound (●) or light (▲) stimulus. The data were normalized for the location of the stimulus by subtracting the coordinates of the speaker or light bulb from the coordinates of the elicited head orientation. This gave two sets of data points, one for sound and the other for light localizations. The mean and standard deviation of each distribution is indicated by the crossed lines. Sound localization error was defined as the difference in azimuth and elevation of these means. The scatter (standard deviation) of the responses served as a measure of the precision of localization. These data were taken from owl 1 at 120 days old, 1 week after its plug had been removed. In a fully adjusted owl, these point distributions would superimpose almost perfectly.

0028-0836/82/030238—03$01.00

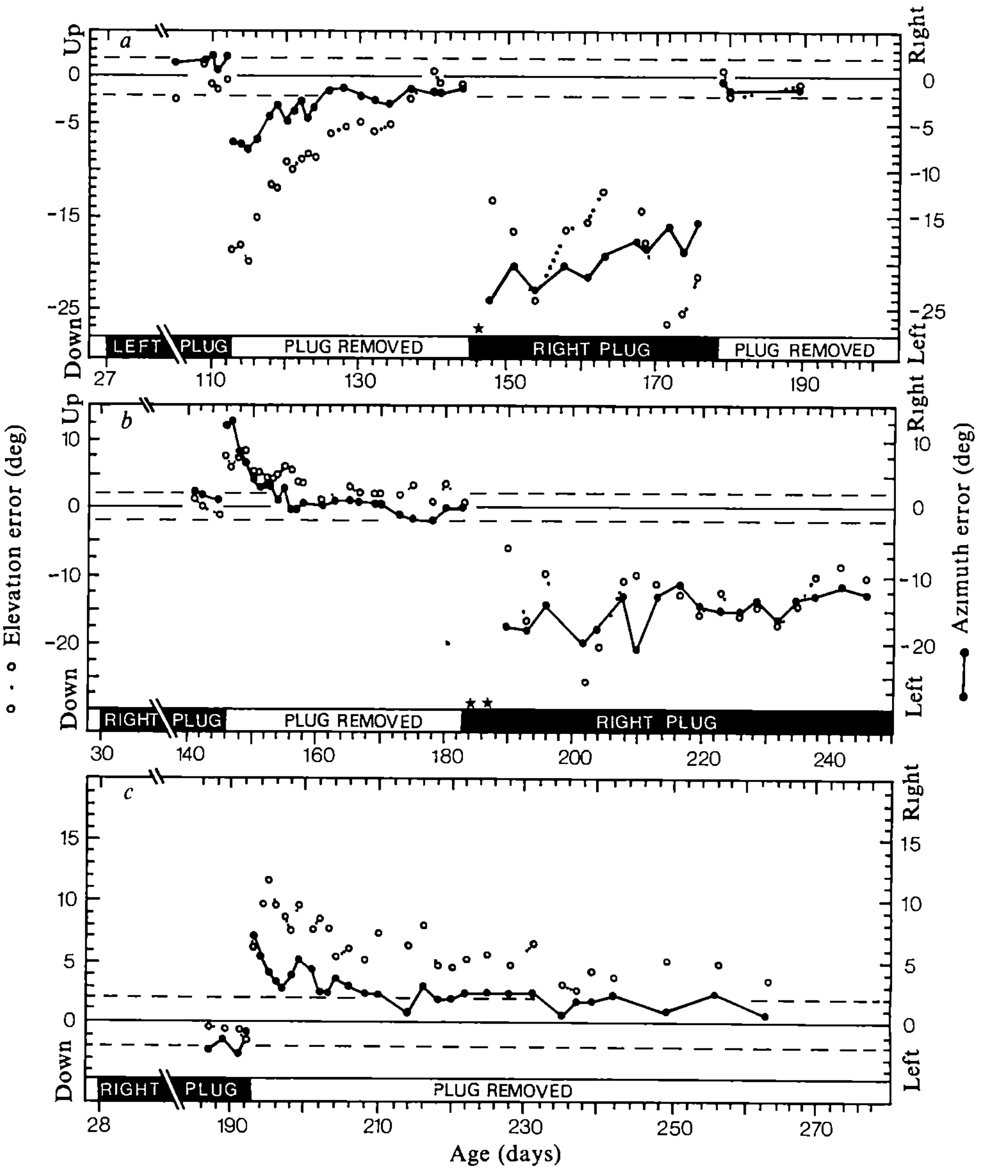

Fig. 2 Adjustment of sound localization accuracy after inserting and removing monaural plugs in three owls *a–c* are owls 1–3, respectively The localization error of each owl is plotted as a function of its age The azimuth (●) and elevation (○) components of the error, derived as shown in Fig 1, are plotted separately The bar at the bottom of each graph shows the auditory history of the owl The limits of what we considered to be normal accuracy are indicated by the broken lines The asterisks on day 146 for owl 1 and on days 184 and 187 for owl 2 represent sessions in which the owls were unable to localize the sound target

lines in Fig 2) An owl was considered to have reached normal accuracy when its error fell within these limits on two consecutive days (In presenting these data, R signifies a localization error to the right of the source, L to the left, + above and − below) Owl 1 (left plug) was the youngest bird to be trained and tested At 16 weeks old, having been plugged for 12 weeks, the median error (±s d) of this owl was R 2 0°±3.1° in azimuth and −1 3°±3 5° in elevation (Fig 2*a*) Apparently, owl 1 had learned to localize with normal accuracy despite the severe monaural impairment caused by the plug At 113 days old the plug was removed, thereby restoring a strong (normal) binaural signal We tested owl 1 immediately and found its localization error had altered dramatically to L 6 7°±4 4° and down to −18 4°±4 1° The error not only remained large for the next 4 days, but increased slightly on the third day to L 7 8°±1 7° and −19 7°±4 7° On the fifth day, azimuth and elevation errors began to decrease sharply The azimuth and elevation errors returned to normal after 15 and 28 days, respectively

The pattern of auditory adjustments exhibited by owl 1 was mirrored by owl 2, in which the right ear was plugged (Fig 2*b*) By the first week of testing, at 21 weeks old, owl 2 had adjusted to the monaural occlusion its error was R 1 1°±4 0° and −1 0°±4 0° Just after removing the plug on day 146, its error changed to R 12 4°±4 6°, and +7 6°±4 5°, again, the largest localization errors occurred 2–4 days after the plug had been removed Azimuth errors declined rapidly after the second day and fell to within normal limits by day 11 Elevation errors peaked on the fourth day and returned to normal after 17 days

The performance patterns of owl 3 were different from those of the first two birds (Fig 2*c*) Owl 3 was 27 5 weeks old and had fully adjusted to the monaural impairment when its right plug was removed its localization error was L 1 9°±2 5° and −0 8°±4 1° After removing the plug its error changed to R 6 9°±3 3° and +6 2°±6 1° However, in this case adjustment to the unplugged condition was exceptionally slow the azimuth error took 25 days to correct and elevation error was still +3 7° after 70 days of normal experience The difference between owl 3 and the first two birds was the age at plug removal whereas owl 3 was 27 5 weeks old, owls 2 and 1 were 21 and 16 weeks old, respectively The data suggest that in the older bird the localization mechanism had become resistant to modification by experience before complete readjustment could occur

The implication that the localization mechanism becomes less plastic with age is supported by the results from owl 4 The right ear of owl 4 was occluded at 27 weeks of age (188 days) and kept occluded for the next 23 weeks, with no sign of adjustment Before the plug was removed the owl's error was still L 7 6°±2 1° and −12 4°±4 1°, and on the day after plug removal its localization accuracy was normal (R 0 7°±2 1° and 0 0°±1 8°) Thus, whereas the owls occluded at 4 weeks of age adjusted completely to the monaural impairment after only 12 weeks, owl 4 did not seem to adjust at all after 23 weeks

A second set of plugging experiments performed on owls 1 and 2 at 21 and 26 weeks of age, respectively, corroborate the results from owl 4 (Fig 2) We plugged the right ear of both owls, that is, the opposite ear for owl 1 and the same ear for owl 2 as were plugged the first time. Neither owl corrected for the induced localization error. Initially the data from owl 1 suggested some adjustment (Fig. 2*a*), but when the plug was removed after 33 days, the owl immediately localized with normal accuracy (0.0°±2.7° and +1.7°±2.5°). Similarly, owl 2, whose ear plug was still in place after 77 days, showed no sign of adjusting its error, which remained at L 10.8°±2.5° and −9.3°±3.7°. The lack of adjustment by owl 2 is particularly revealing because the induced hearing impairment was the same in the first and second experiments (right plug). The owl corrected its error the first time, but not the second. Hence the processes responsible for the adjustment in the first plugging experiment were inoperative in the second, again suggesting that plasticity in the localization mechanism disappears or decreases significantly with age.

During normal growth and development, this capacity for adjustment enables the owl to fine-tune its localization mechanism during the period in life when binaural cues are changing rapidly. After the owl reaches adult size and these cues stabilize, the calibration of the localization mechanism begins to crystallize and finally becomes resistant, if not immune, to further modification by experience.

We thank Carla Shatz, Masakazu Konishi, Earl Schubert, Andy Moiseff and Jim McCasland for reviewing the manuscript. This work was supported by grants from the March of Dimes Foundation (5-285), NIH (5 R01 NS 16099-02), W. M. Hume and Biomedical Research support grant NIH 5S07 RR 5353-18.

Received 3 September, accepted 25 November 1981.

1. Young, P. T. *J. exp. Psychol.* **11,** 399–429 (1928).
2. Held, R. *Am. J. Psychol.* **68,** 526–548 (1955).
3. Bauer, R. W., Matuza, J. L. & Blackmer, R. F. *J. acoust. Soc. Am.* **40,** 441–444 (1966).
4. Willey, C. F., Inglis, E. & Pearce, C. H. *J. exp. Psychol.* **20,** 114–130 (1937).
5. Viehweg, R. & Campbell, R. A. *Trans. Am. otol. Soc.* **48,** 339–350 (1960).
6. Beggs, W. D. A. & Forman, D. L. *Br. J. Audiol.* **14,** 41–48 (1980).
7. Humes, L. E., Allen, S. K. & Bess, F. H. *Audiology* **19,** 508–518 (1980).
8. Clements, M. & Kelly, J. B. *J. comp. Physiol. Psychol.* **92,** 34–44 (1978).
9. Judge, P. W. & Kelly, J. B. *J. acoust. Soc. Am.* **Abstr. 69,** 64 (1981).
10. Knudsen, E. I., Blasdel, G. G. & Konishi, M. *J. comp. Physiol.* **133,** 1–12 (1979).
11. Konishi, M. *Am. Scient.* **61,** 414–424 (1973).
12. Mills, A. W. in *Foundations of Modern Auditory Theory* Vol. II (ed. Tobias, J. V.) 303–348 (Academic, New York, 1972).
13. Knudsen, E. I. & Konishi, M. *J. comp. Physiol.* **133,** 13–21 (1979).
14. Moiseff, A. & Konishi, M. *J. Neurosci.* **1,** 40–48 (1981).
15. Payne, R. S. *J. exp. Biol.* **54,** 535–573 (1971).

Defective T-cell response in beige mutant mice

Rajiv K. Saxena, Queen B. Saxena & William H. Adler

Immunology Section, National Institute on Aging, National Institutes of Health, 4940 Eastern Avenue, Baltimore, Maryland 21224, USA

A role for T cells in immune surveillance has long been suggested[1], but the lack of high tumour incidence in T cell-deficient nude mice represented a challenge to this hypothesis. The discovery of natural killer (NK) cells, which can lyse tumour cells without any previous sensitization, and high NK levels in nude mice, suggested that these cells may constitute a first line of defence against spontaneously arising tumours *in vivo*[2]. Reports[3–5] of a selective NK deficiency and normal T-cell function in C57BL/6 mice carrying the beige mutation (*bg/bg*) suggested that these mice might be useful for assessing the relative importance of T-cell and NK-cell systems in immune surveillance. However we report here that the deficiency of beige mice is not restricted to NK cells. The generation of cytotoxic T lymphocytes (CTLs) in response to alloimmune challenge *in vivo* or *in vitro* was markedly impaired in beige mutants. Thus our results do not support the suggestion[3,5] that beige mice might be useful as a model of a selective NK deficiency.

To examine the generation of alloimmune CTLs in beige mice, 50 mutant (*bg/bg*) and heterozygous control (*bg/+*) mice (H-2^b) were immunized with a single intraperitoneal (i.p.) injection of P815 (H-2^d) tumour cells. Five mice from each group were killed at different time intervals after immunization and the anti-P815 cytotoxic activities of individual spleen cell preparations were determined at various effector/target ratios in a 4-h ^{51}Cr release assay[6]. Lytic units (LU) of alloimmune CTL activity were determined from the dose–response curves[7]. The P815 subline used in these experiments was not significantly susceptible to lysis by mouse NK cells, target lysis being 0.8–2.8% (effector/target = 100:1) by normal spleen cells from unimmunized mice and 2.5–5.4% by interferon-activated mouse spleen cells[7]. Results (see Fig. 1) indicate that the CTL activity in *bg/+* mice increased rapidly from day 5 and reached a peak value of 33 LU per 10^6 spleen cells on day 11. CTL response was specific to P815 target cells and was not observed against syngeneic EL-4 cells (results not shown). By day 17, the activity had declined considerably but a secondary challenge *in vivo* with 2.5×10^6 P815 cells increased the level of CTLs in *bg/+* mice observed 1 week after the second challenge. At all time points, anti-P815 CTL reactivity was markedly lower in *bg/bg* mice; the peak level of CTLs on day 11 was 11 LU per 10^6 spleen cells. Moreover, a secondary immunization did not increase CTL activity in *bg/bg* spleens. Lytic units in individual spleen cell suspensions indicated considerable variation between animals (Table 1). However, analysis of variance showed that the difference in generation of CTL activity

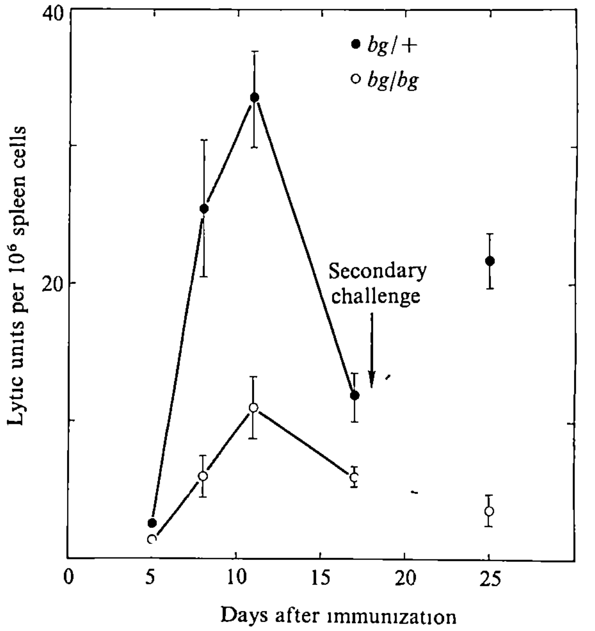

Fig. 1 On day 0, 6-week-old female *bg/bg* or *bg/+* mice were immunized by i.p. injection of 0.2 ml of a P815 tumour cell suspension containing 1×10^7 cells. Tissue-cultured P815 cells used for immunization were washed five times with normal saline before use. On days 5, 8, 11 and 17, five mice each from *bg/bg* and *bg/+* groups were killed and the anti-P815 immune T-cell reactivities of individual spleen cell preparations tested in a 4-h ^{51}Cr release assay at effector/target ratios of 100:1, 50:1, 25:1, 12:1, 12:1 and 6:1 as described previously[6]. Lytic units were calculated from the linear portion of semilog dose–response curves[7]. Each lytic unit represents a target cell lysis of 10% in the test system. Each point in the curve represents the mean ± s.e.m. of lytic units obtained from five spleen cell preparations. On day 18 mice were reinjected with another i.p. dose of P815 tumour cells (2.5×10^6 cells in 0.1 ml saline) and spleen T-cell cytotoxicity was examined on day 25. Spleen cells from unimmunized control mice had no detectable anti-P815 cytotoxic activity.

0028-0836/82/030240—02$01.00

Table 1 Analysis of variance for data in Fig 1

Mice	Lytic units per 10^6 spleen cells*				
	Day 5	Day 8	Day 11	Day 17	Day 25
bg/+	1 86	21 68	32 48	15 44	25 65
	2 46	9 28	38 16	12 48	14 98
	2 32	21 92	36 00	15 12	18 20
	2 68	31 76	41 12	6 64	22 86
	3 56	42 08	20 88	9 68	25 22
bg/*bg*	1 14	6 28	13 04	2 80	1 69
	1 46	1 36	15 20	4 20	6 46
	0 98	9 96	20 88	6 88	4 28
	1 78	8 56	10 64	5 92	1 43
	1 28	3 86	7 28	5 88	3 87

Source of variation	d f	Sum of squares	Mean squares	*F*
Days after immunization	4	2,597 8	649 5	
Beige mutation	1	2,144 2	2,144 2	49 4 ($P<0$ 001)
Error (includes animal-to-animal variation)	44	1,911 3	43 4	
Total	49	6,653 3		

* Each lytic unit represents 10% target lysis in the assay system and was computed from the linear parts of individual dose–response curves as described elsewhere[7]

between *bg*/*bg* and control mice was highly significant ($P<$ 0 001, Table 1)

Administration of tumour cells may induce two types of lymphocyte-mediated cytotoxic activity in mice An early augmentation of spleen NK activity peaks on the third day after tumour administration and falls rapidly thereafter to baseline levels by day 6 or 7 (ref 8) A second peak of specific alloimmune CTL activity occurs later, between days 10 and 11 after immunization[9] In our experiments, anti-P815 cytotoxic activity of spleen cells was first determined 5 days after immunization and the peak of cytotoxic activity occurred on day 11—a typical CTL response Treatment of spleen cells with monoclonal anti-Thy-1 antibodies and complement completely abolished their cytotoxicity for P815 target cells, confirming the T-cell nature of the effector cells (results not shown) The monoclonal anti-Thy-1 antibody used has previously been shown to abrogate completely immune T-cell reactivity with no significant effect on the levels of anti-YAC NK activity in spleen cells[10]

Table 2 Generation of cytotoxic T cells in a mixed lymphocyte reaction by *bg*/*bg* or +/+ mouse spleen responder cells

Source of spleen cells	Anti-P815 cytotoxicity generated in mixed lymphocyte culture (I U per 10^6 spleen cells)
+/+	132 4±13 7
bg/*bg*	39 2±5 4 ($P<0$ 001)

Responder spleen cells were derived from 11-week-old female *bg*/*bg* or +/+ mice (C57BL/6) In each experiment, 50×10^6 responder cells were incubated with 10×10^6 X-ray irradiated (1,000 rad) DBA/2 (12-week-old, female) spleen cells for 5 days in conditions described elsewhere[5] At the end of incubation, cells were washed and tested for cytotoxicity against ^{51}Cr-labelled P815 cells in a 3-h ^{51}Cr release assay at effector/target ratios of 100 1, 50 1, 25 1, 12 1, 6 1 and 3 1 Lytic units were calculated from the linear portion of the dose–response curve as described elsewhere[7] No significant cytotoxicity was detected in cultures without DBA/2 stimulator cells Each value is the mean± s e m of four experiments

Generation of alloimmune CTLs was also studied in a mixed lymphocyte culture system using a method described elsewhere[5], except that, instead of mitomycin treatment, the DBA/2 stimulator spleen cells were X-ray irradiated (1,000 rad) Results of four experiments (summarized in Table 2) indicate that the levels of cytotoxicity generated by *bg*/*bg* spleen cells in 5-day MLC were only 30% of control levels Cytotoxic activity generated in MLC experiments could also be totally abrogated by treatment with anti-Thy-1+complement (results not shown)

Thus, we could not confirm the presence of a normal T-cell function in *bg*/*bg* mice, the reason for the discrepancy between our data and those of Roder[3–5] is unclear The source of *bg*/*bg* and control mice (Jackson Laboratories) was the same for both studies A possible explanation is the considerable variation between animals in levels of alloimmune T cells generated in some beige mice, which can approach the lower limits of a normal response (Table 1) This variation was not reported in the previous study[3–5] and could have contributed to the apparent normality of T-cell function observed in *bg*/*bg* mice, in addition, cells from different mice were pooled and the immune T-cell activity of the pooled spleen cells determined In certain cases the results of assays using pooled spleen cells may not represent the mean of activities of individual spleen cell preparations[11] Finally, the data presented by Roder *et al* [3–5] did indicate a lower than normal level of concanavalin A-induced T cell-dependent cytotoxicity in *bg*/*bg* spleen cells (Figs 6, 8 of ref 5)

To compare the magnitude of the CTL induction defect in *bg*/*bg* mice with the NK cell defect, we attempted to quantify the NK activity in spleen cell preparations derived from *bg*/*bg* and *bg*/+ mice Anti-YAK NK lytic units per 10^6 spleen cells in *bg*/+ spleen cell preparations were 6 26±1 0 (mean ±s e m of eight mice) compared with <0 5 LU in *bg*/*bg* mouse spleen cells These results confirmed the previously reported NK defect in *bg*/*bg* mice[3–5]

Thus we have demonstrated a marked defect in beige mice in the generation of alloimmune T cells both *in vivo* and *in vitro* Whether the defect in T-cell response in *bg*/*bg* mice is generalized is unknown Significantly lower than normal CTL response to lymphocytic choriomeningitis virus infection has been demonstrated in *bg*/*bg* mice[12], whereas the response to vesicular stomatitis virus was approximately normal[13] It is therefore possible that a normal or a subnormal CTL response in *bg*/*bg* mice may depend on the antigen used Our preliminary findings stress the need for caution when using *bg*/*bg* mice as a model for a selective NK deficiency with normal T-cell function Small but significant differences in resistance to certain leukaemias between *bg*/*bg* and *bg*/+ mice[14] could result from a NK-cell defect or T-cell defect or both

We thank Ms Eleanor Wielechowski for secretarial help and Ms Charlotte Adler for preparing the figure

Received 1 September, accepted 11 November 1981

1 Burnet, F M *Prog exp Tumor Res* **13,** 1–27 (1970)

2 Herberman, R B & Holden, H T *Adv Cancer Res* **27,** 305–377 (1978)

3 Roder, J & Duwe, A *Nature* **278,** 451–453 (1979)

4 Roder, J C *J Immun* **123,** 2168–2173 (1979)

5 Roder, J C, Lohmann-Matthes, M-L, Domzig, W & Wigzell, H *J Immun* **123,** 2174–2181 (1979)

6 Saxena R K & Adler, W H *J Immun* **123,** 846–851 (1979)

7 Saxena R K, Adler, W H & Nordin, A A *Cell Immun* **63,** 28–41 (1981)

8 Herberman, R B, Nunn, M E, Holden, H T, Staal, S & Djeu, J Y *Int J Cancer* **19,** 555–564 (1977)

9 Cerottini, J-C & Brunner, K T *Adv Immun* **18,** 67–152 (1974)

10 Saxena, R K., Adler, W H & Nordin, A A *Immun Commun* **9,** 371–378 (1980)

11 Nordin, A A. & Adler, W H in *Developmental Immunobiology* (eds Siskind, G W, Litwin, S D & Weksler, M L) 215–229 (Grune & Stratton, New York, 1979)

12 Welsh, R M & Kiessling, R W *Scand J Immun* **11,** 363–367 (1980)

13 McKinnon, K P, Hale, A H & Ruebush, M J *Infect Immunity* **32,** 204–210 (1981)

14 Karre, K, Klein, G O, Kiessling, R M & Roder, J C *Int J Cancer* **26,** 78–79 (1980)

Further studies on supposed lamarckian inheritance of immunological tolerance

L. Brent*, P. Chandler†, W. Fierz†, P. B. Medawar†, L. S. Rayfield* & E. Simpson†

*Department of Immunology, St Mary's Hospital Medical School, London W2 1PG, UK
†Transplantation Biology Section, Clinical Research Centre, Harrow, Middlesex HA1 3UJ, UK

We have previously reported[1] an unsuccessful attempt to confirm the claim of Gorczynski and Steele[2,3] that tolerance to alloantigens, induced by the inoculation of F_1 hybrid spleen and bone marrow cells in newborn mice, can be transmitted by males to their offspring. Our study had been designed to reproduce the *in vitro* data of Gorczynski and Steele and to extend them by the transplantation of F_1 hybrid skin allografts. It followed that of Gorczynski and Steele[2] very closely but differed from it in two respects: the number of semi-allogeneic lymphoid cells in the inoculum used to establish tolerance in the fathers was 5×10^7 instead of 10^8 and the ratio of spleen cells to bone marrow cells was 9:1 rather than 1:1. Although we argued[1] that it is improbable that these differences of execution could have significantly affected the outcome of the experiments, our departure from the original protocol was nevertheless open to criticism[4] and the purpose of the present further study was to repeat the experiments by following Gorczynski and Steele[2] in every respect. We also report an attempt to confirm the work of Guttman's group[5,6], who claimed that a single CBA male made tolerant to A/J histocompatibility antigens, and mated with normal (CBA × A)F_1 females, produced offspring with a higher incidence of hypo- or unresponsiveness to A/J skin or tumour allografts than the offspring derived from normal males. We have again failed to confirm the work of Gorczynski and Steele and, like Steinmuller[7], we have been equally unsuccessful in confirming the observations of Guttman *et al.*

Five newborn CBA/Ca ($H\text{-}2^k$) males from two litters were made tolerant to A/J ($H\text{-}2^a$) histocompatibility antigens by the intraperitoneal (i.p.) inoculation of 10^8 adult male (CBA × A)F_1 hybrid spleen and bone marrow cells, mixed at a ratio of 1:1. These mice received 5×10^7 cells of the same cell mixture i.p. every 2 weeks throughout the breeding programme. Strain A tail skin allografts were transplanted to them soon after completion of breeding and 4 weeks after their splenic cells (obtained by partial splenectomy) had been tested in the cell-mediated lympholysis assay (CML). The mice were then ~4 months old, all accepted their grafts and were clearly fully tolerant whereas the six normal age-matched control fathers rejected their grafts in the expected manner at ~11 days.

Both tolerant and normal males were mated with groups of three normal CBA females of the same age and, when these had become pregnant, with a further group. Of the five tolerant males, one was sterile, as was one of the six controls. A total of 87 offspring from tolerant fathers ('experimental progeny') and 94 from normal fathers ('control progeny') were raised. Splenic CML data were obtained for 81 (93%) experimental and 79 (84%) control mice and all, with the exception of 4 experimental and 3 control mice that died as a result of partial splenectomy or after skin transplantation, were assessed for reactivity to (CBA × A)F_1 hybrid skin allografts. Skin grafting and assessment of graft survival, splenectomy, the splenic CML technique and the statistical analysis were exactly as described previously[1].

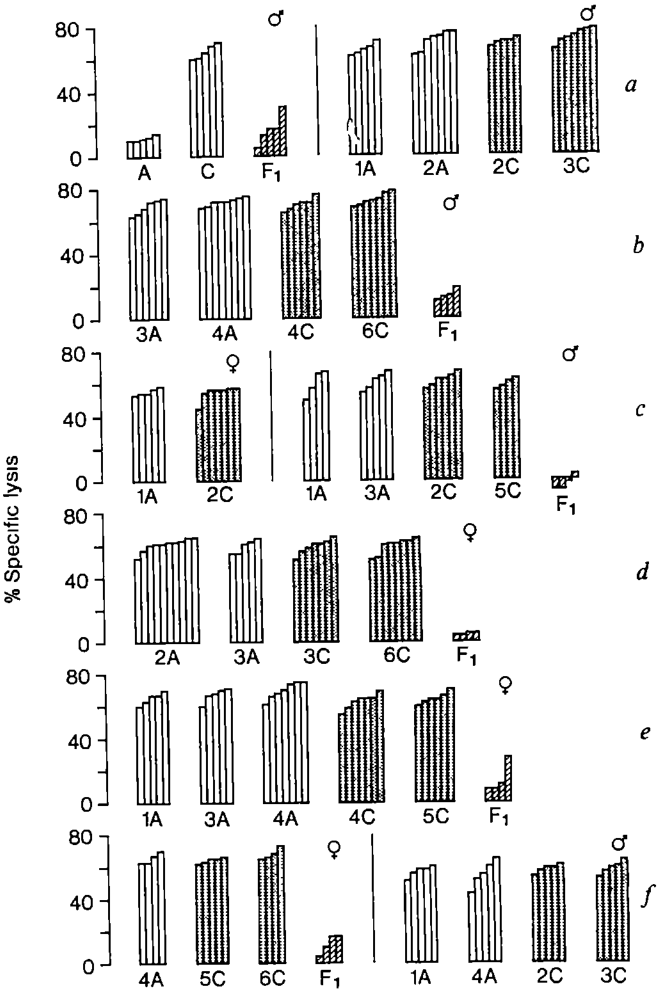

Fig. 1 Anti-A cytotoxic responses of spleen cells from tolerant fathers (A), normal control fathers (C), (CBA × A)F_1 hybrid mice (F_1) and progeny which are identified by the number of the father followed by A or C. Each panel represents the data from a separate experiment, the sex of the responders is indicated. The height of the bars, which represent responses of individual animals, is the % specific lysis at a killer/target ratio (K/T) of 5:1 derived from a 12-point log regression analysis. Groups 1A and 2C included in *a* were retested as shown in *f* (see text). Conditions of culture[1]: 4-ml Linbro wells were set up with 10^7 responder spleen cells and 10^7 irradiated (2,000 rad) strain A stimulator spleen cells per well in bicarbonate-buffered RPMI with 5% fetal calf serum, 5×10^{-5} M 2-mercaptoethanol, penicillin and streptomycin, glutamine and 10 mM HEPES. The assay was carried out on day 5 of culture. Cells were collected from wells, counted and serially diluted (two-fold) in round-bottomed 0.2-ml microtitre wells to which were added a constant number of ^{51}Cr-labelled target cells (24-h concanavalin A blast cells) to give K/T ratios starting at ~10:1. Supernatants were collected after 3 h incubation. Per cent specific lysis was taken as $(E-C)/(M-C)\times100$, where E was the c.p.m. for the experimental supernatant, C the c.p.m. for the medium control supernatant and M the c.p.m. of target cells lysed with 5% Triton.

All spleen suspensions were tested for their ability to respond following mixed lymphocyte culture not only against A antigens but also against 'third-party' C57Bl/10 antigens. The latter acted as a positive control to safeguard against technical failure and in all cases a good response was obtained, they are therefore not included in Fig. 1, which illustrates CML reactivity against the specific A antigens only. This time we confined ourselves entirely to the use of spleen cells for *in vitro* testing, as Gorczynski and Steele[2] had done in their original study, instead of using peripheral blood lymphocytes as well as spleen cells. Two changes were made to our previous protocol: first, the fathers were tested for CML reactivity at 4 months instead of 10 months and, second, (CBA × A)F_1 hybrid control mice were included in each of the major experiments to provide a baseline

Table 1 Survival of (CBA×A)F_1 hybrid skin allografts transplanted to the progeny of tolerant or control CBA males mated with normal CBA females

		Graft survival time (days)	
Father	Sex	Experimental progeny	Control progeny
1	♂	<11 <11 <11 <11 <11 <11 15 15	
	♀	<11 <11 <11 <11 <11 <11 <11 <11	NA
2	♂	<11 <11 <11 <11 <11 <11 <13 15 16	<11 <11 <11 <11 <11 <11 <11 <11 15 16
	♀	<11 <11 <11 <11 <11 <11 <11<11 <11 <11 <11 <11 <11	<11 <11 <11 <11 <11 <11 12 14
3	♂	<11 <11 <11 <11 <11 <11 <11<11 <11 13 13	<11 <11 <11 <11 <11 <11 <11 <11 <11 12 12 13 13 14 16 16
	♀	<11 <11 <11 <11 <11 <11 <11 14 14 14	<11 <11 <11 <11 <11 <11 13
4	♂	<11 <11 <11 <11 <11 <11 <11 <11 <11 12 13 13 15 15 15	<11 <11 12 12 13 14
	♀	<11 <11 <11 <11 <11 <11 <11 <11 <11	<11 <11 <11 <11 <11 13 13
5	♂	NA	<11 <11 12 17
	♀		<11 <11 <11 <11 <11 <11 <11 <11 <11 <11
6	♂	NA	<11 <11 <11 <11 <11 12 13 15 17
	♀		<11 <11 <11 <11 <11 <11 <11 <11 <11 <11 <11 12 12 15
Totals	♂	43	45
	♀	40	46
Median survival times		<11	<11

The sex of the graft donors and recipients was the same NA, not applicable

for the CML data Both changes must be regarded as improvements

Figure 1*a* shows that the experimental fathers (A) were indeed fully tolerant, thus confirming the skin graft data Not only do their responses show a highly significant difference when compared with the controls (C), but it is clear that they did not exceed the baseline provided by the F_1 controls The experimental males were, therefore, as tolerant as the F_1 controls The low level of cytoxicity in the F_1 mice is in agreement with the F_1 anti-parental cytotoxic responses described for other strain combinations[8] Because the tolerant fathers would be expected to be chimaeric for F_1 hybrid lymphoid cells it is possible that the presence of F_1 cells contributed to the low level of responsiveness shown by the tolerant fathers

As for the progeny, Fig 1*a–f* indicates that there were no differences of any interest between experimental and control progeny The differences between the control progeny and the F_1 mice were always highly significant ($P = 0$ 007–0 003) Only two experimental groups deserve special mention First, group 1A (Fig 1*a*) showed a borderline hyporesponsiveness compared with the male controls ($P = 0$ 04), but a repeat experiment some weeks later did not confirm this (included in Fig 1*f*) Second, group 4A (Fig 1*e*) was marginally hyper-responsive compared with all controls ($P = 0$ 01) and there was a slight hyper-responsiveness when all experimental and control mice of panel *e* were compared ($P = 0$ 02) No importance whatever is attached to this, especially as the anti-C57Bl/10 response by this group was also slightly greater than that of the controls ($P = 0$ 01) The conclusion is inescapable that the experimental progeny did not display the hypo- or non-responsiveness described by Gorczynski and Steele

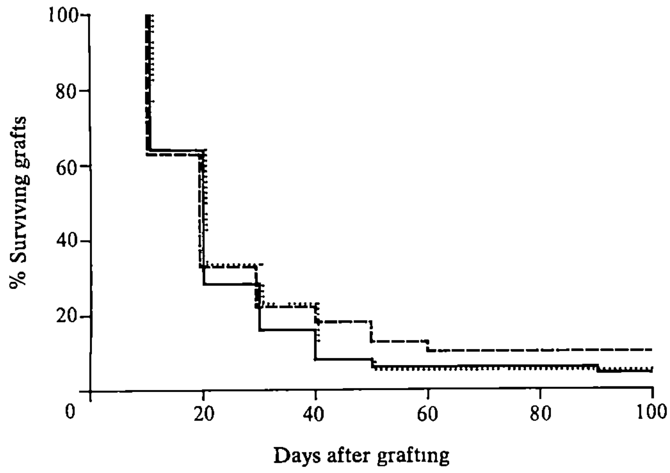

Fig. 2 Survival of female (CBA×A)F_1 tail skin grafts transplanted to the female progeny of tolerant and normal control CBA males mated with normal (CBA×A)F_1 females —— Tolerant, fathers received F_1 lymphoid cells at birth and every 2 weeks thereafter (79 mice), tolerant, fathers received F_1 cells at birth only (39 mice), --- normal fathers (40 mice)

The skin graft data again fully support this Table 1 lists the survival times of individual (CBA×A)F_1 hybrid grafts in experimental and control offspring It will be seen that they do not differ, and this is borne out by statistical analysis (males, $P > 0$ 3, females, $P > 0$ 2) Because F_1 grafts were used, a few were rejected a little more slowly than the majority, especially by male recipients, but this applied equally to the experimental and control progeny

We have therefore confirmed our previous study and failed to substantiate the claim that acquired immunological tolerance can be transmitted to offspring by tolerant male mice Other workers have experienced similar difficulties in a variety of models involving immunological tolerance, from neonatally induced tolerance[9–11], the tolerance of tetraparental[12 13] or adult parabiont[13] mice, to the natural tolerance that characterizes F_1 hybrids[14]

We are again unable to explain the discrepancy between our latest negative results and the original findings of Gorczynski and Steele Our study was, as before, conducted 'double-blind' in that those of us performing the *in vitro* test were presented with the splenic biopsies in coded form and the code was not broken until the data had been fully computed Care was taken to ensure that both skin grafting and graft assessment was carried out without bias We feel we have gone as far as is possible to repeat the precise conditions of the original study as reported by Gorczynski and Steele[2] and we must conclude that the phenomenon described by them was due to some special conditions prevailing in their laboratory Although that might still be of some interest it is unlikely that the lamarckian inheritance they postulate is of any importance in the evolutionary process, if indeed it exists

We have also failed in our attempt to confirm the observation by Guttman's group[5 6] that the offspring produced from a mating between a C3H male, made tolerant at birth by the inoculation of strain A spleen cells, and normal (C3H×A)F_1 hybrid females, accepted A strain skin allografts more readily than controls Two kinds of functionally tolerant males were used in our

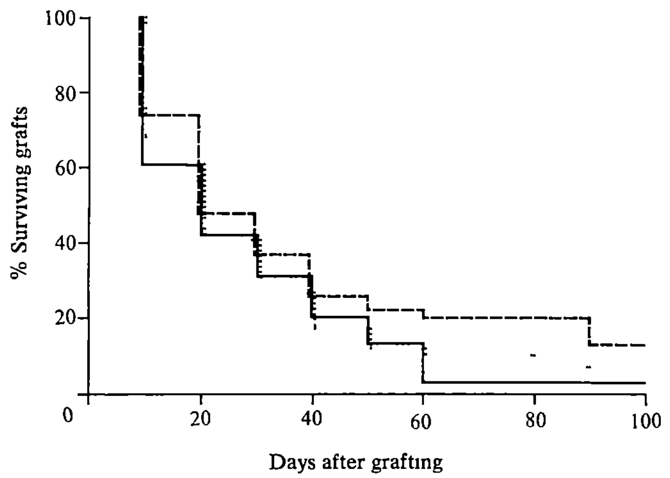

Fig. 3 Survival of male $(CBA\times A)F_1$ tail skin grafts transplanted to the male progeny of tolerant and normal control CBA males mated with normal $(CBA\times A)F_1$ females —— Tolerant, fathers received F_1 lymphoid cells at birth and every 2 weeks thereafter (64 mice), tolerant, fathers received F_1 cells at birth only (41 mice), - - - normal fathers (46 mice)

investigation 10 that had received 5×10^7 spleen and bone marrow cells at birth (in a ratio of 9:1) and the same number every 2 weeks until completion of the breeding programme (designated A), and 4 that had been injected at birth only (designated B). Controls (designated C) were provided by normal age-matched males. All offspring were grafted with $(CBA\times A)F_1$ skin 2–3 months after birth. The only ways in which our protocol differed (because it was carried out during another study[1]) were in the use of CBA mice in place of C3H, although these are compatible for H-2 antigens and similar to C3H mice, and in the use of a mixture of spleen and bone marrow cells. The mice were grafted in five batches over several months, with all groups represented in most batches, and it was sometimes difficult to assess with complete accuracy the end point of survival for grafts that had undergone a slow, insidious form of rejection.

Figures 2 and 3 show that there was no substantial difference between the progeny of groups A, B and C when comparing males with males and females with females. There is no statistically significant difference in the numbers surviving beyond 100 days between any of the groups. If the evaluation is made at 50 days, only the comparison between the male progeny of groups B and C shows a marginal but not significant difference, though in an unexpected direction in that the number of experimental B progeny with surviving grafts is lower than in the control group, using a one-tailed test (χ^2 2×2 test with Yates' correction for continuity, $P<0.05$). Like Steinmuller[7] we are therefore unable to confirm the claim by Guttman and his colleagues in the strain combination used by us.

All advocates of Lamarckism have insisted that the only valid test of whether or not it occurs is that based on the inheritance of specific adaptive changes acquired during an organism's lifetime. The immune response and its specific diminishment (tolerance) are admirably well suited to make the basis of a test for Lamarckism. In their original paper on tolerance, Billingham *et al*[15] (see also ref 9) found that the progeny of CBA parents both tolerant to A strain grafts reacted normally to such grafts, but they might have been mistaken because it was not at that time possible to measure alloimmunity as precisely as may be done today. The results reported here indicate that they were probably right and that in this experimental system acquired tolerance is not inherited.

All examples of supposedly lamarckian inheritance proposed so far[16] have been mistaken or open to more plausible explanations, especially in terms of selection. On the basis of our new evidence we can say with confidence that in respect of the systems we have been investigating, lamarckian inheritance does not obtain.

We thank Miss M Gaffiero and Mr D Conway for their technical assistance and the MRC and Joint Standing Research Committee of St Mary's Hospital for their support.

Received 2 November, accepted 2 December 1981

1 Brent L *et al* *Nature* **290**, 508–512 (1981)
2 Gorczynski, R M & Steele, E J *Proc natn Acad Sci USA* **77**, 2871–2875 (1980)
3 Gorczynski, R M & Steele, E J *Nature* **289**, 678–681 (1981)
4 Howard, J C *Nature* **290**, 441–442 (1981)
5 Guttman, R D & Aust, J B *Nature* **197**, 1220–1221 (1963)
6 Guttman, R D, Vosika, G J & Aust, J B *J natn Cancer Inst* **33**, 1–5 (1964)
7 Steinmuller, D *J natn. Cancer Inst* **39**, 1247–1251 (1967)
8 Nakano, K, Nakamura, I & Cudkowicz, G *Nature* **289**, 559–563 (1981)
9 Billingham, R E, Brent, L & Medawar, P B *Phil Trans R Soc* **B239**, 357–414 (1956)
10 Smith, R N *Nature* **292**, 767–768 (1981)
11 Hašek, M, Holáň, V & Kousalová, M *Folia biol, Praha* **27**, 427–430 (1981)
12 McLaren, A, Chandler, P, Buehr, M, Fierz, W & Simpson, E *Nature* **290**, 513–514 (1981)
13 Nisbet-Brown, E & Wegmann, T G *Proc natn Acad Sci USA* **78**, 5826–5828 (1981)
14 Hašek, M, Holáň, V & Chutná, J in *Cellular and Molecular Mechanisms of Immunological Tolerance* (Dekker, New York, in the press)
15 Billingham, R E, Brent, L & Medawar, P B *Nature* **172**, 603–606 (1953)
16 Medawar, P B in *The Uniqueness of the Individual* (Methuen, London, 1957)

Adult haematopoietic cells transplanted to sheep fetuses continue to produce adult globins

Esmail D. Zanjani*, Giat Lim†, Philip B. McGlave*, James F. Clapp‡, Leon I. Mann‡, Thomas H. Norwood† & George Stamatoyannopoulos†

* Department of Medicine, University of Minnesota and Veterans Administration Hospital, Minneapolis, Minnesota 55417, USA
† Division of Medical Genetics, Departments of Medicine and Pathology, University of Washington, Seattle, Washington 98195, USA
‡ Departments of Obstetrics and Gynecology, University of Vermont College of Medicine, Burlington, Vermont 05401, USA

In man, several primates, sheep and goats, fetal haemoglobin (Hb F: $\alpha_2\gamma_2$) is synthesized during the intra-uterine life, with a switch to adult haemoglobin (Hb A: $\alpha_2\beta_2$) production around birth. The mechanisms underlying the switches in globin gene expression are unknown. Studies of erythroid cell cultures suggest that haemoglobin switching is controlled at the level of haematopoietic progenitor cells[1,2]. To test whether interactions between the haematopoietic environment and the haematopoietic progenitor cells have a role in the haemoglobin switch, we transplanted adult cells into unrelated sheep fetuses at a time of gestation when only fetal haemoglobin was being produced in the recipient cells. We report here that there was engraftment of the donor cells and bone marrow chimaeras were formed. The donor cells, proliferating and differentiating in the fetal environment, continued to produce adult haemoglobin. These results suggest that the fetal environment does not contain elements capable of switching the adult haematopoietic cells to a fetal programme of haemoglobin synthesis.

In the sheep, gestation lasts ~145 days and the switch from fetal to adult globin formation usually starts at ~120–130 days and is completed shortly afterwards[3]. Fetuses younger than 110 gestational days typically have 100% fetal haemoglobin in their red cells (by chemical analysis). In the adult sheep there is a genetic polymorphism at the β locus of the adult haemoglobin[4] with two alleles β^B, providing chains for Hb B ($\alpha_2\beta_2^B$), and β^A, directing the synthesis of Hb A($\alpha_2\beta_2^A$). The existence of this genetic polymorphism allowed us to use haematopoietic cell transplantations to determine the regulation *in vivo* of haemoglobin switching[5] as follows. Bone marrow cells of an adult,

0028-0836/82/030244—03$01 00

homozygous Hb B donor were transplanted to fetuses produced by AA × AA crosses (and hence genetically homozygous for Hb A) that were at a gestational age when they produced only fetal haemoglobin We tested the red cells of the recipient for the presence of Hb B, to obtain information about (1) the fate of the transplanted cells, that is, whether or not, there was engraftment and (2) the globin synthesized by the cells after transplantation to the fetal environment For example, if after transplantation, there was no production of donor Hb B in fetal red blood cells but a chimaeric A/B sheep was born we could deduce that the donor cells were engrafted but had switched during fetal life to fetal globin formation Synthesis of Hb B during gestation and the birth of a chimaeric A/B animal would be evidence that the donor cells were engrafted but did not switch to fetal haemoglobin formation

We used pregnant ewes having confirmed dates of gestation Two heparin-filled polyvinyl catheters (0-9 mm o d) were inserted into the femoral artery and vein of the fetus Direct access to the fetal circulation was gained through a single midline incision of maternal skin and body wall, incision of the uterus, delivery of the fetal hind leg and placement of one catheter each into the fetal femoral artery and vein All incisions were then closed around the catheters, which were secured to the maternal skin, 48 h after surgery, each fetus received the donor bone marrow cells (4×10^8 nucleated cells per estimated kg fetal body weight), via the venous catheter, which was removed immediately after the bone marrow infusion Fetal blood samples were obtained via the arterial catheter for haemoglobin analysis before and at various intervals after infusion To minimize the risk of infection, the catheter was removed 3 weeks after the transplantation and the pregnancy allowed to go to term Blood sampling was resumed in the newborn in the case of successful deliveries

All the fetuses were at day 85–105 of gestation As the donors and recipients were unrelated, in the initial studies we attempted to suppress the haematopoiesis of the recipient fetus before transplantation The fetuses were irradiated or immunosuppressed but all the recipients died within 1–6 days after these manipulations Subsequently, we simply transfused the adult bone marrow cells into untreated fetuses Eleven AA fetuses were given bone marrow cells from the same unrelated female BB donor Six of these were aborted after this treatment, as autopsies were not done, the reason for these losses is unknown The haemoglobins of the five surviving fetuses were analysed by globin chain isoelectric focusing No β^B (donor) or β^A (recipient) globin chains were detected in any of the fetuses on days 1 and 4 post-transplantation, indicating that the minor contamination of the donor's buffy coat cells by red cells did not influence the haemoglobin phenotype of the fetus Two fetuses which were given infusions, respectively, on days 92 and 105 of gestation, failed to exhibit β^B chains (donor) both throughout the 3 weeks of post-transplantation intra-uterine blood-sampling and during postnatal sampling (up to 41 and 53 days, respectively, after birth)

Three fetuses were chimaeric A/B at birth One was studied only at birth and postnatally, a problem with the catheters did not allow intra-uterine sampling in this case This animal remained healthy and was A/B chimaeric throughout the period of sampling Two of the chimaeric fetuses were sampled *in utero* for 21 days post-transplantation One of them died after birth, but the second developed into a healthy animal which remained chimaeric Figures 1 and 2 show the results of haemoglobin analyses The adult haemoglobin of the donor was clearly detectable by day 7 post-transplantation and comprised 41% of the fetal haemoglobin by day 21 post-transplantation

The two living chimaeric lambs (a male and a female) produced both Hb B and Hb A at a ratio of 40 60 As the bone marrow donor was female, chromosomal studies were made of cells from the sole male chimaeric survivor Both donor (XX) and recipient (XY) karyotypes were noted for 50 cells, 58% of the lymphocytes were of the donor (XX) karyotype

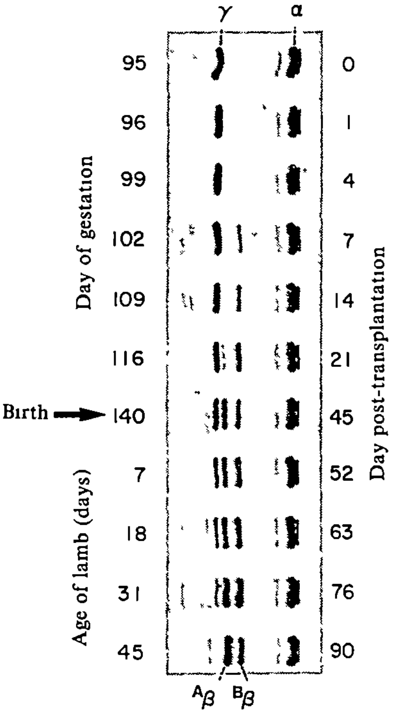

Fig 1 Globin-chain isoelectric focusing of lysates of blood samples obtained from a fetus pre- and post-transplantation Note the absence of detectable β-chains before transplantation and on days 1 and 4 post-transplantation The donor's β^B chains were detectable by day 7 and the intensity of the β^B zone increased thereafter Note also the appearance of significant amounts of β^A chains at birth and that the animal remained β^B/β^A chimaeric With the globin-chain isoelectric focusing method used[6], we achieved clear separation of the globin subunits Subunit β^C (from the inducible haemoglobin C $\alpha_2\beta^C_2$) migrates between subunits β^A and β^B We did not observe β^C-chain synthesis during the intra-uterine sampling of the animals with or without evidence of engraftment The AA fetuses were given cells from the same 2 4-yr old female donor (see text)

Donor bone marrow cells were obtained by multiple aspirations from different sites on the posterior iliac crest The heparinized bone marrow samples were filtered through a screen mesh to remove large particles, the filtrate was allowed to settle at room temperature for 15 min and the supernatant and buffy-coat layers were removed and passed through needles of progressively smaller pore sizes to achieve a single-cell suspension The cells were resuspended in Hanks' balanced salt solution containing the recipient's own plasma (5% v/v) at a concentration of 4–7×10^7 nucleated cells ml^{-1} In all cases the cells were infused into the fetus within 1–2 h of aspiration

These results raise questions for cell immunology and transplantation biology Successful grafts were observed in three of the five animals surviving to birth and all the donor–recipient pairs were unrelated The data suggest that in adult fetus transplantation, conditions may exist which both allow tolerance of the donor cells and diminish the possibility of severe graft-versus-host disease Confirmation of the findings of our experiments and similar studies in primates may have practical relevance If untreated primate fetuses are infused with bone marrow cells from unrelated donors a chimaeric primate may be formed Thus, intra-uterine transplantation of adult bone marrow cells could be considered as an alternative to abortion, when, on prenatal diagnosis, a human fetus is found to be homozygous for a β-chain haemoglobinopathy (such as β-thalassaemia or a Hb S syndrome)

The cellular mechanisms involved in the haemoglobin switch during ontogeny are unknown The question remains as to whether the switch from fetal to adult globin formation is intrinsic to the cell (that is, due to the operation of a developmental clock which informs the cells when or after how many divisions the switch will occur) or whether it is the result of haematopoietic cell–environment interactions If such interactions are involved, are there specific factors present during fetal life or produced during and after the switch-over period which influence the programme of the progenitor cells?

To test the possibility of environment–cell interactions we have previously transplanted haematopoietic cells from pre-switch sheep fetuses into lethally irradiated adult recipients We used the A and B polymorphism of the sheep and in one successful experiment, found that the fetal cells switched to adult globin expression when grafted in to the adult environment[5] There are two possible interpretations of these results (1) the adult environment influenced the programme of the transplanted haematopoietic cells and accelerated the switching process, (2) the transplanted cells were intrinsically programmed to switch and did so in their new environment In the

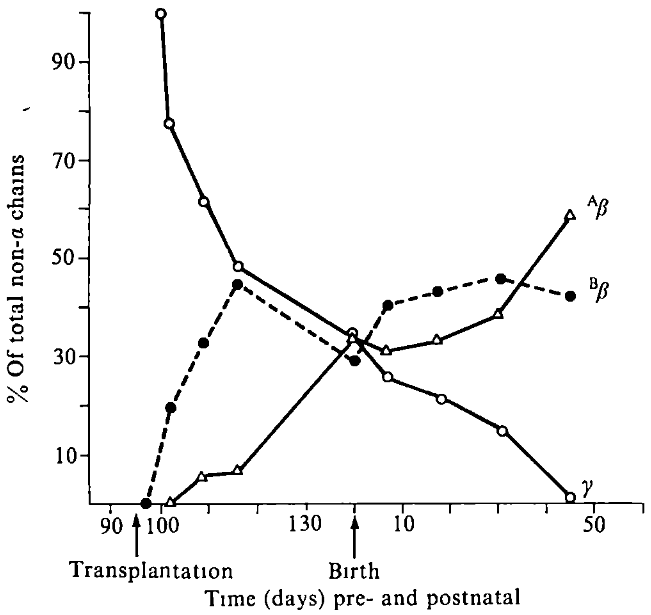

Fig. 2 Proportion of γ, β^A (recipient) and β^B (donor) chains in the haemolysates of blood samples periodically drawn from a fetus (gel shown in Fig 1) Note the striking prenatal increment in the donor's β^B chains, and the lower proportions of β^B chains at birth compared with the prenatal maximal value After the γ- → β-chain switch was complete, the level of β^A chains (derived from the recipient's cells) exceeded the level of β^B chains (originating from the donor cells) A remarkable aspect of these quantitative analyses is the pre- and post-natal proportion of the donor β^B chain The findings are compatible with two peaks of β^B synthesis, one ~20 days post-transplantation and the second 20–30 days after birth A plausible interpretation is as follows The first peak of β^B chain synthesis derives from red cells which have been formed by transplanted committed erythroid stem cells These progenitors have amplified, differentiated, been committed to erythroblastic maturation and have provided the fast rising level in donor haemoglobin after infusion of the donor bone marrow cells The postnatal peak, on the other hand, is derived from red cells produced by the engrafted pluripotent stem cells from the donor

adult → fetal transplantation experiments reported here, we found that the adult donor cells produced large amounts of adult haemoglobin at a time when the cells of the fetuses had not switched to adult haemoglobin synthesis, this suggests that the donor cells continued to follow their adult globin programme even under the influence of the fetal environment The adult → fetal transplantations results are consistent with the mechanisms suggested by the findings of the fetal → adult haematopoietic cell transplantations If the switch from Hb F to Hb A formation is intrinsically controlled, the adult cells did not switch to fetal globin expression because their programme of differentiation had already been intrinsically changed If environment–cell interactions control the switch, both the fetus → adult and adult → fetus transplantations point to the establishment of an 'adult' haematopoietic environment as an underlying cause of the changes in haematopoietic cells effecting haemoglobin switching

Although further experiments are required to assess individually the programmes of the various classes of donor progenitor cells that were transplanted to these fetuses, the data presented here provide evidence against the possibility that there existed at the developmental time of these transplantations, an environment able to switch adult cells to typical fetal haemoglobin synthesis

This work was supported by NIH grants HL20899, GM15253, AM24029 and CA23021 and by Veterans Administration Research Funds

Received 20 August, accepted 13 November 1981

1 Papayannopoulou, Th , Brice, M & Stamatoyannopoulos, G *Proc natn Acad Sci U S A* **74,** 2923–2927 (1977)
2 Stamatoyannopoulos, G & Papayannopoulou, Th in *Cellular and Molecular Regulation of Haemoglobin Switching* (eds Stamatoyannopoulos, G & Nienhuis, A W) 323 (Liss, New York, 1979)
3 Wood, W G *et al Nature* **264,** 799–801 (1976)
4 Blunt, M H & Huisman, T H J in *The Blood of Sheep, Composition and Function* (ed Huisman, T H J) 155 (Springer, New York, 1975)
5 Zanjani, E D , McGlave, P B , Bhakthavathsalan, A & Stamatoyannopoulos, G *Nature* **280,** 495–496 (1979)
6 Righetti, P G *et al J biochem biophys Meth* **1,** 45–46 (1979)

Thrombospondin is the endogenous lectin of human platelets

Eric A. Jaffe*, Lawrence L. K. Leung*, Ralph L. Nachman*, Richard I. Levin* & Deane F. Mosher†

* Department of Medicine, Cornell University Medical College, New York, New York 10021, USA
† Department of Medicine, University of Wisconsin, Madison, Wisconsin 53706, USA

Platelets activated by α-thrombin change shape from disks to spheres and aggregate. During this sequence of activation, platelets develop a membrane-bound lectin activity[1,2] which is expressed after the secretion of intracellular granule contents[3]. This lectin activity seems to be important in mediating platelet aggregation by binding to a specific receptor on other platelets. Gartner *et al.*[4] have recently shown that fibrinogen is the receptor for the endogenous lectin secreted by activated platelets. Thrombospondin[5] (also called glycoprotein G[6] and thrombin-sensitive protein[7,8]) is an α-granule constituent which has a molecular weight (MW) of 450,000 and is a disulphide-linked trimer of 160,000 MW subunits[5,9,10]. Secreted thrombospondin[5–14] binds to platelet membranes in a calcium-dependent manner[12]. We show here that thrombospondin is the endogenous lectin of human platelets.

Thrombospondin and other proteins were tested for lectin activity using minor modifications of the haemagglutination system described by Gartner *et al* [1–4] If thrombospondin is the endogenous lectin of platelets, it may act directly as a haemagglutinin Because thrombin-treated but not native platelets have lectin activity[2 4], we used fixed (formaldehyde-treated) native platelets and fixed thrombin-treated platelets as controls in the haemagglutination assay As expected, fixed native platelets had no lectin activity (Table 1) whereas fixed thrombin-treated platelets had lectin activity and agglutinated fixed trypsin-treated sheep erythrocytes at a dilution of 1 16 (a titre of 16) This haemagglutination was blocked by α-D-mannosamine or α-D-glucosamine but not by *N*-acetylmannosamine or *N*-acetylglucosamine These same inhibitors have previously been shown to block both platelet plasma membrane lectin activity detected using bovine erythrocytes[1] and thrombin-induced platelet agglutination[4] When tested in the same system, thrombospondin purified from human platelets had strong lectin activity (haemagglutinin titre of 256, Table 1) This lectin activity was blocked by glucosamine and mannosamine but not by *N*-acetylglucosamine or *N*-acetylmannosamine In contrast, purified human serum albumin, fibronectin, factor VIII, fibrinogen and plasminogen tested as controls had no lectin activity

If thrombospondin is the endogenous platelet lectin, excess exogenous thrombospondin may also inhibit the haemagglutinating activity of thrombin-treated platelets by blocking thrombospondin receptors To test this hypothesis, proteins were serially diluted, sheep erythrocytes and fixed thrombin-treated platelets then added and haemagglutination was assessed A buffer control did not block haemagglutination (Table 2)

0028-0836/82/030246—03$01 00

Table 1 Lectin activity of thrombospondin

Diluted material	Titre
Fixed native platelets	0
Fixed thrombin-treated platelets	16*
Thrombospondin	256*
Human serum albumin	0
Fibronectin	0
Factor VIII	0
Fibrinogen	0
Plasminogen	0

Haemagglutination of sheep erythrocytes was assayed in microtitre 'V' plates (Cooke Engineering Laboratory Products) as described by Gartner *et al.*[1–4] 25 μl of Tris-buffered saline containing calcium (TCS buffer: 10 mM Tris-HCl, 2 mM CaCl$_2$, 150 mM NaCl, *p*H 7.4) was added to each well, then 25 μl of the diluted material was added to the first well in a row of 12 wells and was serially diluted twice in duplicate series of 11 wells. The remaining well in each series contained no diluted material and served as control. Finally, 25 μl of a 2.5% suspension of trypsin-treated, formalinized sheep erythrocytes in TCS buffer prepared as described by Gartner *et al.*[1–4] was added to each well. The wells were agitated gently and evaluated for haemagglutination after standing overnight at room temperature. The titre of diluted material is defined as the reciprocal of the end point dilution (greatest dilution that gives agglutination). Fixed thrombin-treated platelets were prepared as follows. The platelets in 200 ml of fresh platelet-rich plasma were pelleted, washed once with 120 mM KCl, 75 mM Tris-HCl, 12 mM sodium citrate, *p*H 6.3, twice with 150 mM NaCl, 10 mM Tris HCl, 1 mM EDTA, *p*H 7.4 (ETS), and then resuspended in 5 ml ETS. The resuspended platelets were treated for 2 min at room temperature with human α-thrombin (3 units ml^{-1}, a gift of Dr John Fenton II) and washed once with ETS and once with 0.15 M NaCl, 10 mM Tris HCl, *p*H 7.4 (TS buffer). The resulting pellet was resuspended in 2% paraformaldehyde in phosphate-buffered saline and incubated overnight at 4 °C. The fixed platelets were washed four times with phosphate-buffered saline and resuspended in TS buffer at a concentration of 350,000 μl^{-1} and stored at 4 °C until use. Fixed native platelets were prepared by mixing fresh platelet-rich plasma with an equal volume of 4% paraformaldehyde in phosphate-buffered saline and incubating overnight at 4 °C. These platelets were washed as above, resuspended in TS at a concentration of 350,000 μl^{-1} and stored at 4 °C until used. Thrombospondin was prepared from 4 units of platelets by the method of Lawler[5]. The thrombospondin was >95% pure and contained no fibrinogen when analysed by SDS-polyacrylamide gel electrophoresis (SDS-PAGE). The human serum albumin was obtained from Behring. The purified peak I human fibrinogen was provided by Dr M. Mosesson[32] and was >96% clottable and homogeneous on SDS-PAGE. The human plasma factor VIII was prepared from plasma by methods previously described[33] and did not contain fibronectin or plasminogen when analysed for these proteins by enzyme-linked immunosorbent assay. The purified human plasminogen[34] and fibronectin[35] were gifts from Dr P. Harpel. The factor VIII, plasminogen and fibronectin were absorbed with insolubilized anti-human fibrinogen and were negative for fibrinogen by an enzyme-linked immunosorbent assay. All proteins were added to the first well as 25 μl of a solution of 0.2 mg ml^{-1}.

* This agglutination was inhibited by a 57 mM final concentration of either α-D-mannosamine or α-D-glucosamine but not by 57 mM *N*-acetylmannosamine or *N*-acetylglucosamine.

whereas thrombospondin blocked haemagglutination with an inhibitory titre of 8 (final concentration of thrombospondin in last inhibited well is 6.3 μg ml^{-1}). Human serum albumin and fibronectin inhibited haemagglutination only weakly. Fibrinogen also strongly inhibited haemagglutination with an inhibitory titre of 16 in the presence or absence of calcium. These latter results are at variance with those of Gartner *et al.*[4], who found that fibrinogen inhibited haemagglutination only in the absence of calcium. The discrepancy may be due to the fact that the platelets used in our studies were fixed in formaldehyde after thrombin treatment.

Table 2 Thrombospondin blocks haemagglutination by fixed, thrombin-treated platelets

Diluted material	Inhibitory titre
Buffer	0
Thrombospondin	8
Human serum albumin	2
Fibronectin	2
Fibrinogen	16

The materials listed were added as 25 μl of a solution of 0.2 mg ml^{-1} to 25 μl of TCS buffer and serially diluted as in Table 1. 5 μl of a 12.5% suspension of trypsin-treated, formalinized sheep erythrocytes and 25 μl of fixed thrombin-treated platelets diluted 1:4 with TSC buffer (haemagglutination titre of undiluted fixed thrombin-treated platelets was 16, see Table 1) were then added and the microtitre plates agitated, incubated overnight at room temperature, and read. The inhibitory titre of a diluted material is defined as the reciprocal of the greatest dilution which inhibited haemagglutination compared with a control without any diluted material. Other details are as in Table 1 legend.

Table 3 Thrombospondin blocks the agglutination of fixed, thrombin-treated platelets

Diluted material	Inhibitory titre
Buffer	0
Thrombospondin	16
Factor VIII	0
Human serum albumin	1
Fibonectin	2
Plasminogen	2
Fibrinogen	16

The materials listed were serially diluted as in Tables 1 and 2. 25 μl of fixed thrombin-treated platelets diluted 1:4 with TCS buffer were then added and the microtitre plates agitated, incubated overnight at room temperature and read. The inhibitory titre of a diluted material is defined as the reciprocal of the greatest dilution which inhibited agglutination compared with a control without any diluted material. Other details as in Table 1 legend.

Fixed thrombin-treated platelets also agglutinate when tested alone in a microtitre assay system (titre of 32). If thrombospondin is the endogenous lectin of platelets, excess exogenous thrombospondin may also inhibit the agglutination of fixed thrombin-treated platelets by blocking thrombospondin receptors. To test this possibility, proteins were serially diluted, fixed thrombin-treated platelets added and agglutination assessed (Table 3). Buffer did not inhibit agglutination whereas thrombospondin strongly inhibited agglutination. Factor VIII, human serum albumin, fibronectin and plasminogen inhibited agglutination only very slightly or not at all. Fibrinogen, however, strongly inhibited agglutination.

Of the proteins tested, only thrombospondin had lectin activity (Table 1), blocked haemagglutination by fixed thrombin-treated platelets (Table 2) and blocked the agglutination of fixed thrombin-treated platelets (Table 3). None of the other platelet granule proteins tested had lectin activity and only fibrinogen blocked haemagglutination or platelet agglutination. Studies of other α-granule proteins have shown that neither β-thromboglobulin nor platelet growth factor has lectin activity[15]. Further, although platelet factor 4 was shown to have agglutinating activity[15], it differed from the lectin activity of thrombin-stimulated platelets[2] or thrombospondin in that it was not blocked by mannosamine or glucosamine and was not trypsin sensitive[15]. These observations thus support our conclusion that thrombospondin is the platelet lectin.

The observations that thrombospondin has lectin activity, is a multimer and by itself causes haemagglutination (Table 1) suggest that thrombospondin is a multivalent molecule. The ability of thrombospondin to block haemagglutination and platelet agglutination at low concentrations (6.3 and 3.1 μg ml^{-1}, respectively) suggests that thrombospondin binds with high affinity to its receptor. The blocking effect of fibrinogen is compatible with the recent observation of Gartner *et al.*[4] that fibrinogen is the receptor for the endogenous lectin of platelets. If platelets interact with each other during aggregation via intercellular bridges of thrombospondin anchored to platelet-bound fibrinogen, excess free fibrinogen in an agglutination or haemagglutination assay would react with thrombospondin and block the reaction. The same reasoning applies to the blocking effect of thrombospondin. Our data are also compatible with the recent observation that the platelets from patients with the grey platelet syndrome (which lack α-granules and their constituents, including thrombospondin) are deficient in thrombin, ADP and collagen induced aggregation[16].

Other proteins in platelet granules—for example, factor VIII/von Willebrand factor[17–19], factor Va[20–22], fibrinogen[23–25] and fibronectin[26]—also have major roles in platelet function. Furthermore, it is interesting that endothelial cells, which synthesize von Willebrand factor[27,28] and fibronectin[29], also synthesize thrombospondin[30,31]. Although the level of thrombospondin in plasma as measured by radioimmunoassay is quite low (D.F.M. and E.A.J., unpublished results), endothelial cells in certain conditions may release thrombospondin in a local microenvironment and thus support platelet function

This work was supported by grants from USPHS (HL 18828) and the Arnold R Krakower Hematology Foundation E A J is the recipient of an NIH Research Career Development Award (5 KO4 HL00237) L L is the recipient of NHLBI Individual National Research Service Award HL 06161 R I L is the recipient of an NIH Clinical Investigator Award (1 K08 HL 00748) The work was done while D F M had an AHA Established Investigatorship

Received 6 July, accepted 30 November 1981

1 Gartner, T K, Williams, D C & Phillips, D R *Biochem biophys Res Commun* **79,** 592–599 (1977)
2 Gartner, T K, Williams, D C, Minion, F C & Phillips, D R *Science* **200,** 1281–1283 (1978)
3 Gartner, T K, Phillips, D R & Williams, D C *FEBS Lett* **113,** 196–200 (1980)
4 Gartner, T K, Gerrard, J M, White, J G & Williams, D C *Nature* **289,** 688–690 (1981)
5 Lawler, J W, Slayter, H S & Coligan, J E *J biol Chem* **253,** 8609–8616 (1978)
6 George, J N *J Lab clin Med* **92,** 430–446 (1978)
7 Baenziger, N D, Brodie, G N & Majerus, P W *Proc natn Acad Sci U S A* **68,** 240–243 (1971)
8 Baenziger, N L, Brodie, G N & Majerus, P W *J biol Chem* **247,** 2723–2731 (1972)
9 Hagen, I *Biochim biophys Acta* **392,** 242–254 (1975)
10 Phillips, D R & Agin, P P *J biol Chem* **252,** 2121–2126 (1977)
11 Lawler, J W, Chao, F C & Fang, P H *Thromb Haemostasis* **37,** 355–357 (1977)
12 Phillips, D R, Jennings, L K & Prasanna, H R *J biol Chem* **255,** 11629–11632 (1980)
13 George, J N, Lyons, R M & Morgan, R K *J clin Invest* **66,** 1–9 (1980)
14 Hagen, I, Olsen, T & Solum, N O *Biochim biophys Acta* **455,** 214–225 (1976)
15 Phillips, D R & Gartner, T K in *Receptors and Recognition* Ser B, Vol 6 (ed Beachey, E H) 399–438 (Chapman & Hall, London, 1980)
16 Gerrard, J M *et al J clin Invest* **66,** 102–109 (1980)
17 Hawiger, J, Fujimoto, T & Ohara, S *Fedn Proc* **40,** 833 (1981)
18 Tschopp, T, Weiss, H J & Baumgartner, H *J Lab clin Med* **83,** 296–300 (1974)
19 Weiss, H J, Baumgartner, H R, Tschopp, T B, Turitto, V T & Cohen, D *Blood* **51,** 267–279 (1978)
20 Miletich, J P, Jackson, C M & Majerus, P W *J biol Chem* **253,** 6908–6916 (1978)
21 Tracy, P B, Peterson, J M, Nesheim, M E, McDuffie, F C & Mann, K G *J biol Chem* **254,** 10354–10361 (1979)
22 Kane, W H, Lindhout, M J, Jackson, C M & Majerus, P W *J biol Chem* **255,** 1170–1174 (1980)
23 Mustard, J F, Packham, M A, Kinlough-Rathbone, R L, Perry, D W & Regoeczi, E *Blood* **52,** 453–466 (1978)
24 Marguerie, G A, Plow, E F & Edgington, T S *J biol Chem* **254,** 5357–5363 (1979)
25 Bennett, J S & Vilaire, G *J clin Invest* **65,** 1393–1401 (1979)
26 Plow, E F & Ginsberg, M H *J biol Chem* **256,** 9477–9482 (1981)
27 Jaffe, E A, Hoyer, L W & Nachman, R L *J clin Invest* **52,** 2757–2764 (1973)
28 Jaffe, E A, Hoyer, L W & Nachman, R L *Proc natn Acad Sci U S A* **71,** 1906–1909 (1974)
29 Jaffe, E A & Mosher, D F *J exp Med* **147,** 1779–1791 (1978)
30 Doyle, M J, Mosher, D F & Jaffe, E A *J Cell Biol* **87,** 306a (1980)
31 Mosher, D F, Doyle, M J & Jaffe, E A *J Cell Biol* (in the press)
32 Wolfenstein-Todel, C & Mosesson, M W *Proc natn Acad Sci U S A* **77,** 5069–5073 (1980)
33 Jaffe, E A & Nachman, R L *J clin Invest* **56,** 698–702 (1975)
34 Deutsch, D G & Mertz, E T *Science* **170,** 1095–1096 (1970)
35 Engvall, E & Ruoslahti, E *Int J Cancer* **20,** 1–5 (1977)

A microtubule-associated protein in the mitotic spindle and the interphase nucleus

Jonathan G. Izant*, James A. Weatherbee† & J. Richard McIntosh*

* Department of Molecular, Cellular and Developmental Biology, University of Colorado at Boulder, Boulder, Colorado 80309, USA
† Worcester Foundation for Experimental Biology, Shrewsbury, Massachusetts 01545, USA

Accurate chromosome segregation during mitosis is contingent on the controlled polymerization and function of spindle microtubules. Assembly-promoting polypeptides that co-sediment with microtubules during cycles of polymerization *in vitro* are attractive candidates for regulators of the formation and function of the mitotic apparatus *in vivo*. However, previous work has shown that the major species of microtubule-associated proteins (MAPs) from mammalian brain or tissue culture cells are either not associated with the mitotic spindle[1] or are associated with both mitotic and interphase cytoplasmic microtubules[2–4]. We have therefore sought a novel way to identify spindle regulatory factors. In the study reported here, monoclonal antibodies have been prepared against a MAP fraction from HeLa cells. One of the resulting hybridoma clones produces IgG that binds to a polypeptide of molecular weight ~200,000. During cell division this antigen is associated with fibres in the mitotic apparatus, but in interphase it is located primarily in the nucleus. Surprisingly, the antigen is also detectable on the plasma membrane of circulating human erythrocytes. This spindle component is distinct from previously characterized MAPs and may represent a regulatory factor in the assembly and function of the mitotic apparatus.

The molecular factors controlling the assembly and function of the mitotic spindle are largely unknown Interphase microtubules in lysed cell models display a calcium lability that is modulated by MAPs[5], suggesting that the polypeptides which co-purify with cytoplasmic microtubules may have important regulatory functions Other potential regulatory proteins, such as calmodulin[6] and cyclic nucleotide-dependent kinase[7], have been localized in the mitotic spindle, but although this suggests several models for spindle regulation, the actual functions of these enzymes during chromosome separation remain speculative

We have been studying MAPs from cultured cells using the lymphocyte hybridoma methodology to identify specific mitotic spindle components. Using a crude mixture of HeLa cell MAPs purified by cycles of co-assembly with HeLa tubulin and by ion-exchange chromotography[8] as initial innoculum, we have screened for spindle antigens by radioimmunoassay and immunofluorescence microscopy The antibody produced by hybridoma clone 0-2D5 3 1 binds a polypeptide from HeLa cells with an approximate molecular weight of 200,000 (Fig 1) The 0-2D5 antigen is sensitive to endogenous protease both in purified microtubule protein preparations and in whole-cell homogenates[9], as are the high-molecular weight MAPs from brain[10] The 0-2D5 antibody preparation produces a distinctive punctate nuclear immunofluorescent staining pattern in interphase human cells and stains mitotic spindle fibres intensely (Fig 2) The interphase microtubule array stains only faintly (Fig 2*a*, *b*) The fluorescent nuclear dots range in number from

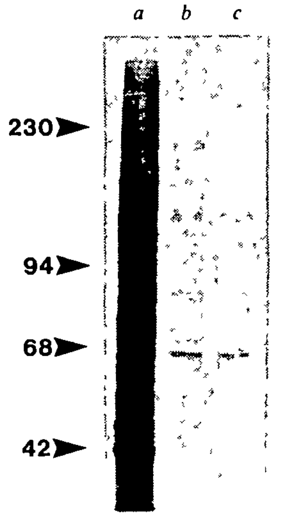

Fig. 1 Immunoprecipitation of HeLa cell MAP Autoradiograph of ^{35}S-methionine-labelled HeLa cell homogenate (*a*) and *Staphylococcus aureus* immunoprecipitates[-7] using 0-2D5 3 1 antibody (*b*) and a control monoclonal antibody (*c*) run on a 7 5% SDS-polyacrylamide gel[18] The 0-2D5 antibody specifically precipitates a protein of molecular weight ~200,000, while there are several additional polypeptides that bind nonspecifically to both immune complexes Molecular weight markers were fibronectin (230,000), phosphorylase *a* (94,000), bovine serum albumin (68,000) and ovalbumin (44,000) The MAP fraction used as antigen was prepared by ion-exchange chromatography of four times-cycled HeLa cell microtubule protein as described elsewhere[8] BALB/c mice were immunized intraperitoneally with 100 μg of SDS-denatured HeLa MAPs emulsified in an equal volume of Freund's complete adjuvant Twenty-one days later the mice were boosted intravenously with 50 μg of MAPs in saline After another 4 days splenic lymphocytes were collected and fused with SP2/0 myeloma cells as previously described[1] Hybridomas were screened by a solid-phase radioimmunoassay, and cells producing specific antibody were cloned twice in soft agar Immunoglobulin from 1 0 l suspension cultures was concentrated 100-fold by 40% ammonium sulphate fractionation and the IgG purified by chromatography on Affi-gel Blue CM (Biorad), followed by another ammonium sulphate precipitation

0028–0836/82/030248—03$01 00

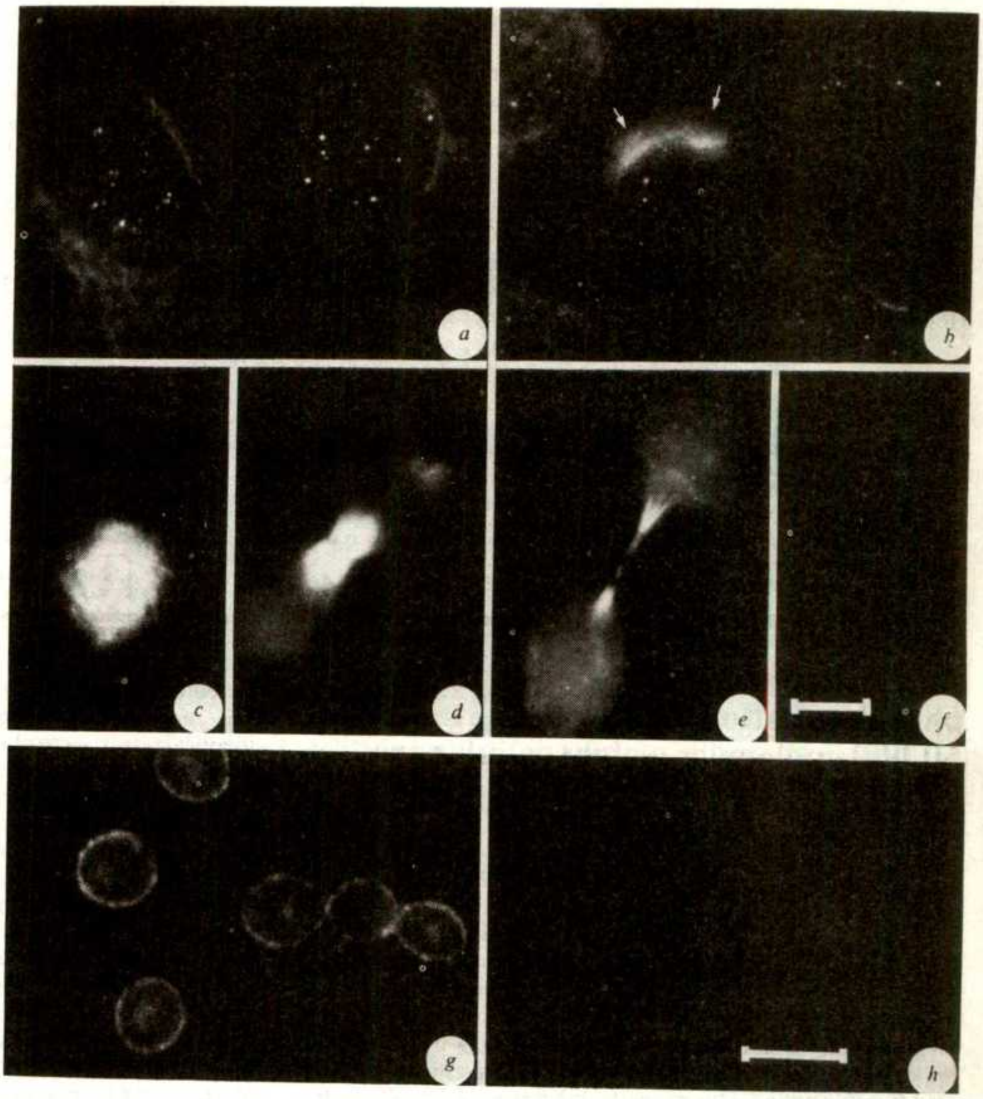

Fig. 2 Indirect immunofluorescent staining pattern of HeLa (*a*, *b*, *d–f*) and Va90 (*c*) cells and human erythrocytes (*g*, *h*). Cells were stained with anti-MAP antibody secreted by hybridoma 0-2D5.3.1 (*a–e*, *g*) or with a control mouse monoclonal preparation (*f*, *h*). The 0-2D5 antibody stained the interphase nucleus (*a*, *b*) and the enlarging prophase asters (*b*, arrows) in human cells. The mitotic spindle stained intensely (*c–e*) with the punctate pattern reappearing during telophase (*e*). The antibody also stained the plasma membrane of circulating erythrocytes (*g*). Tissue culture cells were grown on coverslips in minimal essential medium supplemented with 10% calf serum, rinsed in saline, fixed in 100% methanol at −20 °C for 4 min, postfixed in acetone at −20 °C for 1 min, rehydrated in saline and then processed for immunofluorescence microscopy as previously described[1]. Human erythrocytes were diluted in saline, settled on coverslips and fixed with 2% paraformaldehyde before being permeabilized and stained as above. The secondary antibody was tetramethylrhodamine-labelled goat anti-mouse immunoglobulin (USA Biochemicals) at a 1:50 dilution in 20% goat serum. Specimens were examined on a Zeiss photoscope III equipped with epifluorescence optics, and fluorescent images were recorded on Plus-X film. Scale bar, 5 μm.

14 to 43 and appear to be randomly intranuclear; they are not associated with the nuclear envelope as judged by through-focus examination at high magnification. The punctate pattern of antibody staining disappears during prophase and reappears in association with the decondensing chromatin during telophase (Fig. 2*b*, *d*). There is no evidence of fluorescent dots in metaphase or anaphase cells (Fig. 2*c*, *d*). The spindle fibre staining is apparent even during early prophase when the antibody stains the nascent asters (Fig. 2*b*). No concomitant increase in the staining of the residual interphase microtubule network is observed during this stage. Similarly, the 0-2D5 anti-MAP antibody stains the spindle remnant (midbody) during telophase (Fig. 2*e*), again without significant staining of the arrays of interphase microtubules assembling in the daughter cells. The 0-2D5 antibody does not cross-react with cultured cells of non-human primate, rodent, or marsupial origin, but it does stain the plasma membrane of human erythrocytes (Fig. 2*g*, *h*). No surface staining has been observed in any other cell type tested.

The origin, molecular weight and cellular distribution of the 0-2D5 MAP distinguish it from the major MAPs of brain microtubule protein. The differences between previously published micrographs[4] of anti-MAP staining and the punctate nuclear immunofluorescent images shown here suggest that the set of high-molecular weight HeLa MAPs contains structurally and functionally distinct protein species. The 0-2D5 antigen is also distinct from nuclear mitotic apparatus protein (NuMA), another high-molecular weight antigen found in the interphase nucleus and in association with the mitotic spindle of human cells[11]. The electrophoretic mobility of NuMA and the staining pattern of anti-NuMA monoclonal antibodies (S. E. Winston and D. E. Pettijohn, personal communication) clearly differ from those of 0-2D5 antigen. NuMA was originally isolated as a non-histone chromatin-associated protein and may be involved in the organization or expression of DNA. At present there is insufficient data to determine whether the foci stained by 0-2D5 have structural or enzymatic activity associated with chromatin or the nuclear matrix.

There are striking similarities between a spectrin-binding protein in human erythrocyte membranes called ankyrin or syndein and the 0-2D5 antigen. Both are easily proteolized proteins of molecular weight 200,000 which associate with structural polypeptide polymers (ref. 12; Fig. 1). Antiserum against ankyrin produces spotted nuclear immunofluorescent images and stains the mitotic apparatus in tissue culture cells (V. Bennett, personal communication). Nucleated erythrocytes from birds and amphibians have characteristic circumferential bands of microtubules which contain MAPs[13]; thus the similar distribution of ankyrin and the 0-2D5 MAP raises the intriguing possibility that these antigens have common antecedents as well as similar functional characteristics.

There is no indication, as yet, whether the 0-2D5 antigen, ankyrin or NuMA are necessary spindle components which are sequestered in the nucleus during interphase, or if the antigens function primarily in the interphase nucleus and bind to spindle fibres simply to assure partition into the daughter cells. The rather surprising similarity between an erythrocyte membrane component and a cultured cell MAP suggests that these proteins, or different oligomers of which they are a subunit, may have distinct functions depending on the cellular environment. They may be members of a family of multifunctional molecules like tubulin that are used in different ways according to the stage of the cell cycle or the programme of cellular differentiation.

The data presented here are consistent with the hypothesis that a subset of mitotic spindle components is sequestered in the nucleus during interphase and that nuclear envelope breakdown initiates or augments spindle assembly by releasing important factors into the cytoplasm[14,15]. Detergent-lysed cell models do show an increased ability to nucleate aster microtubules after the breakdown of the nuclear envelope[16]. Generalizing this theory is difficult in view of the variety of organisms that do not dissolve or fenestrate their nuclear envelopes during mitosis. However, the 0-2D5 antigen appears on early prophase asters, suggesting that additional mechanisms may be working to allow or promote the association of this antigen with a specific subset of cytoplasmic structures. The preferential association of the 0-2D5 MAP with mitotic apparatus microtubules supports its identification as a spindle MAP and strengthens its candidacy for a mitotic spindle regulatory factor. Microinjection studies are being done to elucidate the role of the 0-2D5 MAP during spindle formation and chromosome separation.

We thank Bill Wood for making available his epifluorescence microscope and Susan Strome for helpful criticism of the manuscript. This research was supported by grant CD-8D from the American Cancer Society and USPHS award CA-28078 from the NCI.

Received 29 May; accepted 17 November 1981.

1. Izant, J. G. & McIntosh, J. R. *Proc. natn. Acad. Sci. U.S.A.* **77,** 4741–4745 (1980).
2. Connally, J., Kalnins, V. I., Cleveland, D. W. & Kirschner, M. W. *Proc. natn. Acad. Sci. U.S.A.* **74,** 2437–2440 (1977).
3. Lockwood, A. H. *Cell* **13,** 613–627 (1978).
4. Bulinsky, J. C. & Borisy, G. G. *J. Cell Biol.* **87,** 792–801 (1980).
5. Schliwa, M., Euteneuer, U., Bulinsky, J. C. & Izant, J. G. *Proc. natn. Acad. Sci. U.S.A.* **78,** 1037–1041 (1981).
6. Welsh, M. J., Dedman, J. R., Brinkley, B. R. & Means, A. R. *Proc. natn. Acad. Sci. U.S.A.* **75,** 1867–1871 (1978).
7. Browne, C. L., Lockwood, A. H., Su, J.-L., Beavo, J. A. & Steiner, A. L. *J. Cell Biol.* **87,** 336–345 (1980).
8. Weatherbee, J. A., Luftig, R. B. & Weihing, R. R. *Biochemistry* **19,** 4116–4123 (1980).
9. Izant, J. G. thesis, Univ. Colorado (1981).
10. Slaboda, R. D., Dentler, W. L. & Rosenbaum, J. L. *Bioihemistry* **15m** 449784505 (1974).
11. Lydersen, Bj Kj & Pettijth , D. E. *Cell* **22,** 489–499 (1980).
12. Bennett, V. & Stenbuck, P. J. *Nature* **280,** 468–473 (1979).
13. Slaboda, R. D. & Dickersin, K. *J. Cell Ziol.* **87,** 170–179 (1980).
14. Roth, L. E. & Daniels, E. W. *J. Cell Biol.* **12,** 57–78 (1962).
15. Wilson, E. B. *The Cell in Development and Heredity* (Macmillan, New York, 1925).
16. Snyder, J. A. & McIntosh, J. R. *J. Cell Biol.* **67,** 744–760 (1975).
17. Kessler, S. W. *J. Immun.* **115,** 1617–1624 (1975).
18. Laemmli, U. K. *Nature* **277,** 680–685 (1970).

Rous sarcoma virus-induced phosphorylation of a 50,000-molecular weight cellular protein

Joan S. Brugge & Diane Darrow

Department of Microbiology, State University of New York at
Stony Brook, Stony Brook, New York 11794, USA

Transformation by Rous sarcoma virus (RSV) is mediated by a single virus-encoded polypeptide, pp60$^{\mathrm{src}}$ (refs 1–3), which has protein kinase activity specific for tyrosine residues[4–7]. The identification of the proteins phosphorylated by pp60$^{\mathrm{src}}$ is important in understanding the events involved in RSV-mediated transformation. One potential substrate is a 50,000-molecular weight (MW) phosphotyrosine-containing protein (pp50) which is associated in a complex with pp60$^{\mathrm{src}}$ and a cellular 90,000-MW protein (pp90; ref. 8) and thus is immunoprecipitated by antibody to pp60$^{\mathrm{src}}$ (refs 6, 9, 10). We have performed further studies to determine whether this 50,000-MW protein (pp50) is present in uninfected cells and whether its phosphorylation at tyrosine depends on RSV-induced transformation. Here we demonstrate that a phosphoserine-containing form of pp50 is present in uninfected chicken cells and that on transformation by RSV, a second form of pp50, detectable by two-dimensional analysis of ^{32}P-labelled proteins, contains phosphotyrosine as well as phosphoserine. This phosphorylation of pp50 at tyrosine is not temperature sensitive (ts) in cells infected with mutant viruses containing a ts defect in the *src* gene. Previous results[8] have suggested that the temperature stability of this phosphorylation might be a result of the strong interaction between the mutant pp60$^{\mathrm{src}}$ protein and pp50.

To identify pp50 on two-dimensional gels of ^{32}P-labelled chicken cell lysates, a mixing experiment was performed (Fig. 1). First, using serum from tumour-bearing rabbits (TBR), pp50 was immunoprecipitated from ^{32}P-labelled chicken cells transformed by the SR-A strain of RSV. Two-dimensional gel electrophoresis of this immunoprecipitate using ampholytes enriched in the *p*H 5–7 range resolved pp50 ($pI = 5.4$; Fig. 1*a*). Comparison of the two-dimensional gel patterns of uninfected cell phosphoproteins (Fig. 1*b*) with a mixture of the TBR immunoprecipitate and uninfected cell phosphoproteins (Fig. 1*c*) indicated that the pp50 which is bound to pp60$^{\mathrm{src}}$ and precipitated from RSV-transformed cells (pp50A) migrates just to the acidic side of a 50,000-MW phosphoprotein present in uninfected cells (pp50). Although pp50A is not found in uninfected cells (Fig. 1*b*), cells transformed by the SR-A strain of RSV appear to contain both pp50A and pp50B (Fig 1*d*). Identical results were obtained using the Prague, B77 and Bryan strains of RSV; transformation-defective deletion mutant virus-infected cell lysates contained pp50B alone. These observations suggest that pp50A might arise by RSV-induced phosphorylation of pp50B. Indeed, charge calibration of these gels by forced carbamylation[11] indicated a difference of one charge unit between pp50A and pp50B, which at this *p*H could be accounted for by a difference of one phosphate group.

To investigate further the possible relationship between pp50A and pp50B, these ^{32}P-labelled proteins were excized from two-dimensional gels and analysed by partial proteolysis with chymotrypsin, using the method of Cleveland *et al.*[12] (Fig. 2). Several other 50,000-MW phosphoproteins migrating at more basic *p*H than pp50B were also analysed (Fig. 2, upper panel; pp50C, D and E). pp50B from uninfected cells or cells transformed by the SR-A or Bryan strains of RSV had the same cleavage pattern, consisting of two major phosphopeptides (Fig. 2, lower panel). pp50A from cells transformed by either strain of RSV, and isolated by either two-dimensional gel electrophoresis or immunoprecipitation with TBR serum, yielded two phosphopeptides co-migrating with those of pp50B plus two new phosphopeptides (indicated in Fig. 2 by asterisks). The pp50C, D and E spots do not seem to be related to pp50A and B by this type of analysis, although we have not rigorously ruled out such a relationship. These data suggest that pp50A and B represent different phosphorylated forms of the same protein, pp50A being formed by the transformation-dependent phosphorylation of pp50B at a new site(s).

To determine whether phosphorylation of pp50 on tyrosine[6] is transformation dependent, the phosphoamino acid contents of pp50A and B were analysed (Fig. 3). The pp50B species from either uninfected (lane 1) or RSV-transformed (lane 2) cells contains only phosphoserine. The transformation-specific pp50A species contains phosphotyrosine in addition to phosphoserine (lane 3). This observation, combined with the phosphopeptide analysis described above, suggests that the difference in migration of the pp50A and B species during isoelectric focusing is due to an additional phosphate group bound to a tyrosine residue on pp50A.

The observation that pp50 is present in both uninfected and RSV-transformed cells, but is phosphorylated on tyrosine only in the latter, suggested that pp50 may be a substrate for pp60$^{\mathrm{src}}$. To test this hypothesis further, we examined whether the tyrosyl phosphorylation of pp50 was temperature sensitive in chicken cells infected with the NY68 strain of RSV[13], which contains a ts

0028-0836/82/030250—04$01.00

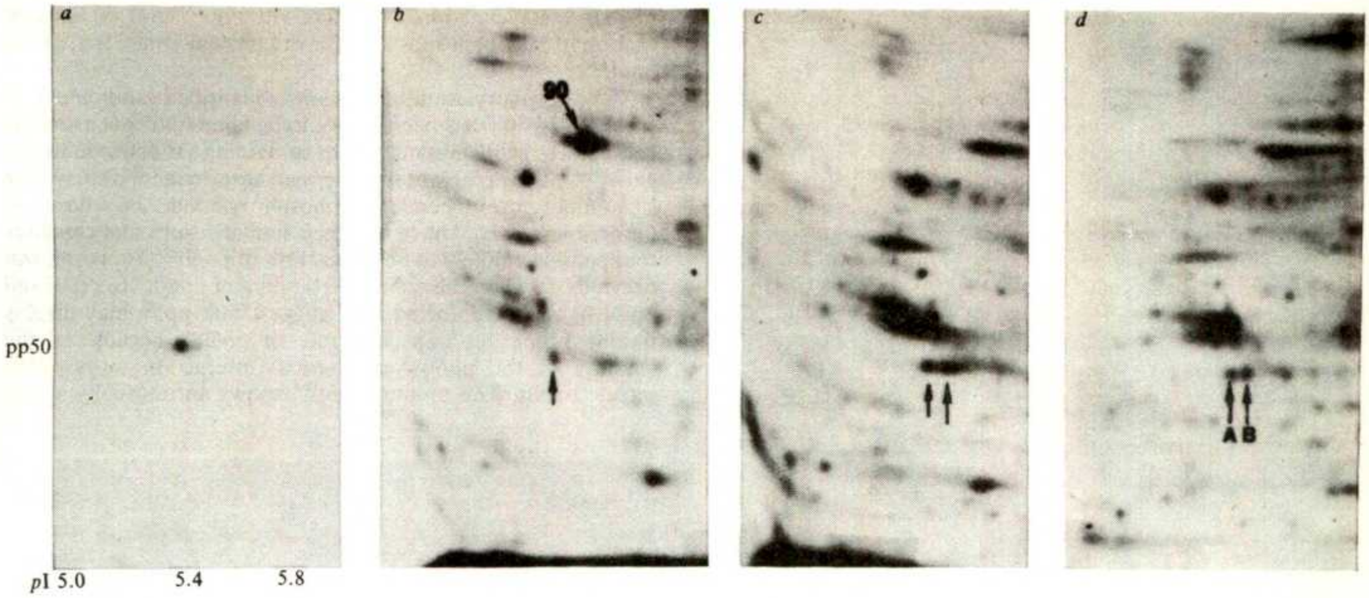

Fig. 1 Two-dimensional analysis of phosphoproteins from normal and RSV-transformed chicken cells. Samples for analysis on two-dimensional gels were prepared as described below. Immunoprecipitated proteins. Chicken cells (1×10^6) transformed by the SR-A strain of RSV were labelled for 4 h with 1 mCi ml^{-1} ^{32}P-orthophosphate in phosphate-free medium. Cell lysates were prepared as described previously[1] using RIPA buffer (150 mM NaCl, 1% Triton X-100, 1% sodium deoxycholate, 0.1% SDS, 10 mM Tris-HCl *p*H 7.2) with 5 mM EDTA. The clarified lysates were incubated with 30 μl of TBR serum for 20 min and then formalin-fixed *Staphylococcus* bacteria[21] were added for 10 min. The washed bacteria were incubated with 30 μl of OFLB (9.5 M urea, 2% NP-40, 5% β-mercaptoethanol, 0.4% ampholytes (LKB) (*p*H 3.5–10), 1.6% ampholytes (LKB) (*p*H 5–7) at 22 °C for 10 min. The bacteria were then removed by centrifugation and the supernatant frozen until ready for use. Total cell lysates. Normal or RSV-transformed (SRA strain) cells (1×10^6) were labelled for 4 h with 1 mCi ml^{-1} ^{32}P in phosphate-free medium. The cells were washed three times with STE (150 mM NaCl, 50 mM Tris-HCl *p*H 7.2, 1 mM EDTA) prepared according to a modification[22] of the O'Farrel method[23] for two-dimensional gel analysis of proteins. Briefly, the cells were incubated for 5 min in 300 μl of 2 mM CaCl, 20 mM Tris-HCl (*p*H 8.8) and 50 μg ml^{-1} *Staphylococcus* nuclease buffer (Boehringer-Mannheim). The cells were then forced through a 25 ga. needle, made up to 0.2% SDS, and 0.1 vol of DNase/RNase buffer (1 mg ml^{-1} DNase I (Sigma), 0.5 μg ml^{-1} RNase A (Sigma), 50 mM $MgCl_2$ and 0.5 M Tris-HCl *p*H 7.0) was added. The sample was quick-frozen, lyophilized and immediately resuspended in 180 μl of OFLB. Two-dimensional gels. Samples (15 μl) were loaded on to 0.2×16 cm cylindrical gels prepared as described elsewhere[23] with a 4:1 ratio of *p*H 5–7/*p*H 3.5–10 ampholytes (LKB). After prefocusing, the gels were run at 400 V, for 17 h, followed 800 V for 1.5 h. The gels were then removed from the tube and the gel section from 2–9 cm was equilibrated for 5 min in 2.5% SDS, 5% β-mercaptoethanol, 10% glycerol and 62.5 mM Tris *p*H 6.8, layered on to a 7.5% Laemmli[24] SDS-polyacrylamide gel and electrophoresed until the bromophenol blue reached the bottom of the gel. The gels were dried immediately and exposed to film for 16–24 h using a Lightning-plus (Kodak) intensifying screen. *a*, Phosphoproteins immunoprecipitated with TBR serum. (The pp60^{src} protein does not focus in this *p*H range and the faint spot around *p*I 5.6 is pp90). *b*, Phosphoproteins from normal chicken cells. (The spot designated 90 represents the protein which co-migrates with the pp90 immunoprecipitated protein). *c*, Phosphoproteins shown in *b* mixed with the proteins shown in *a*. *d*, Phosphoproteins from RSV-transformed chicken cells.

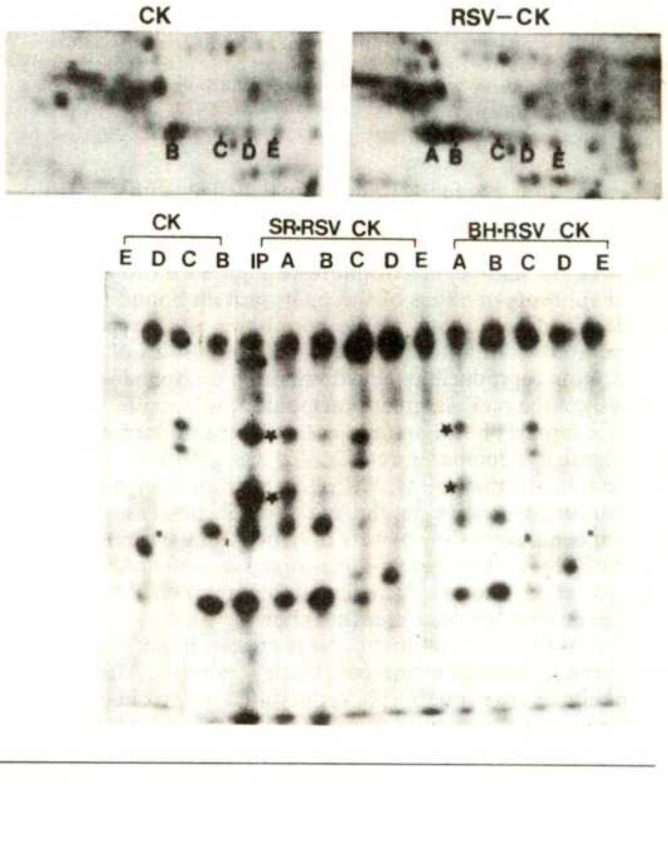

Fig. 2 Partial proteolytic digestion of the 50,000-MW proteins excized from two-dimensional gels. The gels of normal and RSV-transformed (SRA and BH strain) chicken cells were prepared as described in Fig. 1 legend. The upper panel identifies the ^{32}P-labelled RSV-transformed chicken cells (RSV-CK) re-electrophoresed (lower panel) on a 12.5% SDS-polyacrylamide gel with 500 μg ml^{-1} chymotrypsin (Sigma) according to the method of Cleveland *et al.*[12]. The gel was exposed for 1 week using intensification as described in Fig. 1 legend. The two-dimensional gel pattern of cells transformed by the Bryan (BH) strain of RSV was essentially identical to that of the SR-A strain shown in the upper panels. The lane designated IP contains the pp50 protein immunoprecipitated from ^{32}P-labelled RSV (SRA)-transformed cell lysates by TBR serum.

University Colleges of Science & Technology
92, A.P.C. Rd., Cal.-9
LIBRARY COMPLEX
Departments of:
Chemical Engineering
Chemical Technology
Plastics & Rubber Technology

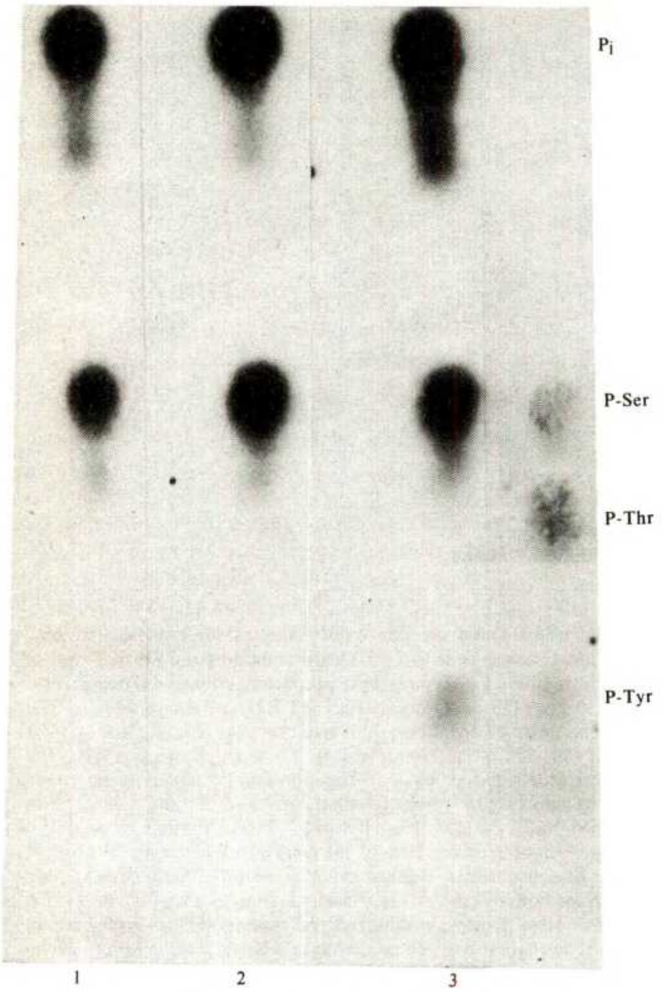

Fig. 3 Analyses of the phosphorylated amino acids associated with the pp50 proteins from normal and RSV-transformed chicken cells. The pp50A and B species were eluted from 12 two-dimensional gels of ^{32}P-labelled proteins from normal and RSV (SR-A) transformed cells prepared as described in Fig. 1 legend. The proteins were TCA-precipitated, acid-hydrolysed and electrophoresed at 4,000 V for 1.75 h in *p*H 3.5 buffer (pyridine/acetic acid/H_2O = 1 : 10 : 189) as described previously[25]. Lane 1, pp50B from normal chicken cells; lane 2, pp50B from RSV-transformed chicken cells; lane 3, pp50A from RSV-transformed chicken cells. Phosphoamino acid markers were co-electrophoresed with each radioactive sample. A representative ninhydrin-stained track is shown adjacent to the autoradiogram at the right of the figure for visualization of the marker amino acids (P-Ser, phosphoserine; P-Thr, phosphothreonine; P-Tyr, phosphotyrosine).

defect in the *src* gene. Cells were labelled with ^{32}P-orthophosphate at either 35 °C or 41 °C and the pp50 bound to pp60^{src} was isolated by immunoprecipitation with TBR serum followed by SDS-gel electrophoresis. Figure 4*a* shows that the tryptic phosphopeptides of the pp50 protein bound to pp60^{src} cannot be distinguished at the permissive and nonpermissive temperatures. Minor differences in the intensities of the spots were not reproducible. Furthermore, phosphoamino acid analysis of the pp50 immunoprecipitated with pp60^{src} indicated that the tyrosyl phosphorylation of pp50 was not reduced at the nonpermissive temperature (Fig. 4*b*). As a positive control, it was confirmed that the tyrosyl phosphorylation of pp60^{src} was temperature sensitive in the NY68-infected cells (Fig. 4*b*). Similar results (not shown) were obtained using the ts *src* mutant LA90[14]. In addition, two-dimensional gel analysis of cells labelled at 35 °C or 41 °C indicated the presence of the pp50A species at both temperatures (not shown).

Thus, we have found that pp50 is present in normal chicken cells as a phosphoserine-containing protein. After transformation by RSV, pp50 is phosphorylated on tyrosine as well as on serine. These results, coupled with the evidence that the protein is associated in a complex with pp60^{src} (ref. 8), suggest that pp50 may be a substrate for the protein kinase activity of pp60^{src}.

The phosphorylation of previously identified candidate substrates of pp60^{src} has been shown to be temperature sensitive in cells infected with mutant viruses containing a ts defect in the *src* gene[15–17]. The pp50 protein described here does not display such a temperature-dependent phosphorylation of tyrosine. Oppermann *et al.*[10] have obtained similar results and conclude that pp50 is unlikely to be a substrate of pp60^{src}. However, our previous data[8] on the enhanced binding of pp60^{src} to pp50 and pp90 in ts virus-infected cells suggest that pp50 may display unique properties as a substrate of pp60^{src} because of the stability of the pp60^{src}–pp90–pp50 interaction in ts virus-infected cells. The mutant pp60^{src} shows an unusually strong

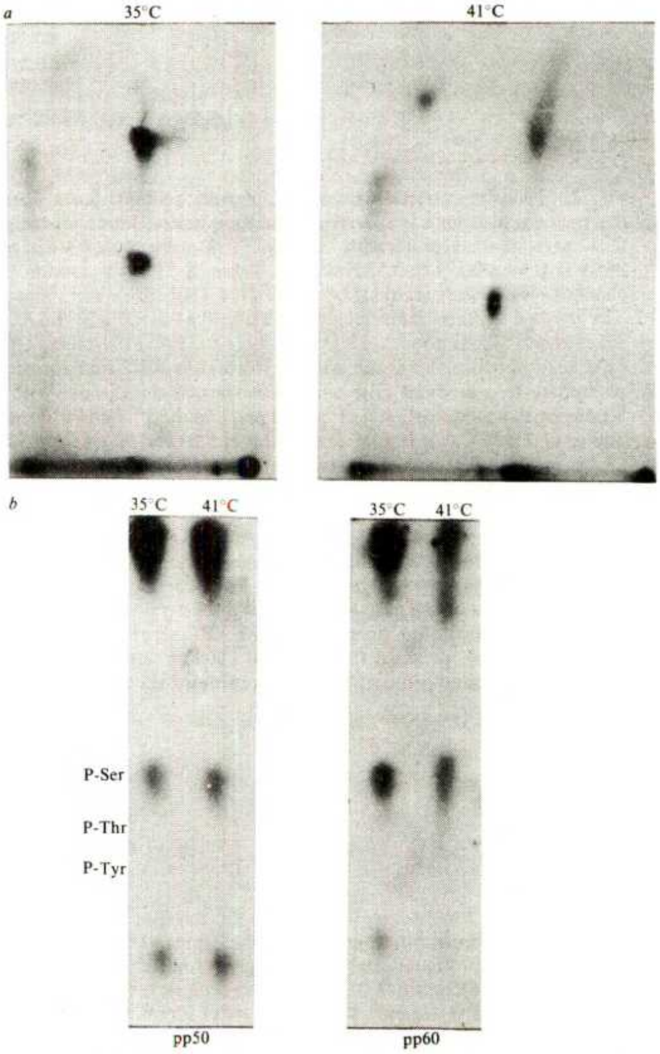

Fig. 4 Phosphopeptide and phosphoamino acid analysis of pp50 associated with pp60^{src} from cells transformed by a ts mutant RSV. Cells transformed by the RSV mutant, NY68 (ref. 13) were incubated at 35 °C or 41 °C for 24 h and subsequently labelled with ^{32}P (1 mCi ml^{-1} in phosphate-free medium) for 4 h. Cell lysates were prepared using RIPA and 5 mM EDTA, then clarified and immunoprecipitated with TBR serum as described in Fig. 1 legend. The immunoprecipitated proteins were electrophoresed on a 7.5% SDS-polyacrylamide gel and the pp50 and pp60 proteins eluted by incubation in 0.05 M ammonium bicarbonate and 0.1% SDS for 16 h. The proteins were then precipitated three times with 20% TCA, acetone-washed and split into two fractions. One half of the pp50 sample was oxidized with performic acid, trypsinized and electrophoresed at *p*H 6.0 as described previously[26]; the other half was hydrolysed in 6M HCl at 110 °C for 2 h, lyophilyzed and electrophoresed as described in Fig. 3 legend. *a*, Phosphopeptide analysis of pp50 from cells grown at 35 °C (left panel) and 41 °C (right panel). Chromatography was performed from right to left and electrophoresis, from bottom to top. The origin is in the lower right-hand corner of each autoradiogram. *b*, Phosphoamino acid analysis of pp50 (left panel) and pp60^{src} (right panel) from cells incubated at 35 °C and 41 °C. Marker phosphoamino acids were co-electrophoresed in each lane and visualized with ninhydrin.

interaction with pp50; up to 90% of mutant pp60^{src} is bound in a complex with pp50 and pp90, while at most 5% of wild-type pp60^{src} is found in this complex[8]. Furthermore, unlike the pp50–pp60^{src}–pp90 complex containing wild-type pp60^{src}, which turns over fairly rapidly, the complex containing mutant pp60^{src} is extremely stable; pulse-chase experiments indicate no detectable dissociation over a 5-h period (our unpublished data). The temperature insensitivity of pp50 phosphorylation might be explained by our previous observation that the binding of ts mutant pp60^{src} to pp50 is very stable at the nonpermissive temperature; thus, it is possible that pp60^{src} is able to phosphorylate pp50 in these conditions, although its ability to phosphorylate other substrates required for transformation is impaired[15–17].

The detection of the pp50A species after RSV infection does not seem to result from pp60^{src} binding to an unstable phosphotyrosine-containing form of pp50 present in the uninfected cell as variations in the amount of the pp50–pp60^{src}–pp90 complex in cells transformed by different strains of RSV were not reflected in the levels of the transformation-specific pp50A species. Although the pp50–pp60^{src}–pp90 complex was only minimally detectable in lysates of cells transformed by the Prague strain of RSV[8], the amount of pp50A species found in these lysates was similar to that found in lysates of cells, transformed by the SR-RSV strain, which contained at least 10-fold greater amounts of pp60^{src} bound to pp50 and pp90. These results suggest that formation of a stable complex between pp50 and pp60^{src} is not required for the detection of the phosphotyrosine-containing form of pp50. It also seems unlikely that pp50 is phosphorylated by a pp60^{src}-activated tyrosine-specific protein kinase as activation of other kinases would be expected to be temperature sensitive in cells infected with ts mutant viruses of RSV. Thus, we conclude tentatively that pp50 is a substrate for pp60^{src}; further testing of this hypothesis, by examining the ability of purified pp60^{src} to phosphorylate pp50 *in vitro*, awaits the purification of the pp50 species containing only phosphoserine (unpublished data).

We have recently obtained evidence that pp50 and pp90 are physically associated with the unrelated transforming proteins of Fujinami sarcoma[18,19] and Y73[20] viruses. Furthermore, we have found that the phosphotyrosine, phosphoserine-containing form of pp50 is detectable on two-dimensional gels of ^{32}P-labelled lysates from cells transformed by these viruses. This suggests that pp50 and pp90 may have a common interaction with transforming proteins which function as tyrosine-specific protein kinases.

During this study we learned that T. Gilmore, K. Radke and G. S. Martin have also demonstrated the presence of phosphoserine-containing forms of pp50 in uninfected chicken cells.

We thank Eileen White for assistance with gels and Mike Chinkers and David Gates for comments on the manuscript. We also thank Jean Altwein and Sandi Donaldson for secretarial help. This work was supported by NIH grant CA27951-01.

Received 17 July; accepted 8 November 1981.

1. Brugge, J. S. & Erikson, R. L. *Nature* **269,** 346–348 (1977).
2. Purchio, A. F., Erikson, E., Brugge, J. S. & Erikson, R. L. *Proc. natn. Acad. Sci. U.S.A.* **75,** 1567–1571 (1978).
3. Brugge, M. S., Erikson, E., Collett, M. S. & Erikson, R. L. *J. Virol.* **26,** 773–782 (1978).
4. Collett, M. S. & Erikson, R. L. *Proc. natn. Acad. Sci. U.S.A.* **75,** 2021–2024 (1978).
5. Levinson, A. D., Oppermann, H., Levintow, L., Varmus, H. E. & Bishop, J. M. *Cell* **15,** 561–572 (1978).
6. Hunter, J. & Sefton, B. *Proc. natn. Acad. Sci. U.S.A.* **77,** 1311–1315 (1980).
7. Sefton, B. M., Hunter, T., Berman, K. & Eckart, W. *Cell* **20,** 807–816 (1980).
8. Brugge, J. S., Erikson, E. & Erikson, R. L. *Cell* **25,** 363–372 (1981).
9. Oppermann, H., Levinson, W. & Bishop, J. M. *Proc. natn. Acad. Sci. U.S.A.* **78,** 1067–1071 (1981).
10. Oppermann, H., Levinson, A., Varmus, H., Bishop, J. M. & Sadaaki, K. J. *Proc. natn. Acad. Sci. U.S.A.* **78,** 1067–1071 (1981).
11. Bobb, D. & Hofstee, B. H. J. *Analyt. Biochem.* **40,** 202–217 (1971).
12. Cleveland, D. W., Fisher, S. G., Kirshner, M. W. & Laemmli, U. K. *J. biol. Chem.* **252,** 1102–1106 (1977).
13. Kawai, S. & Hanafusa, H. *Virology* **46,** 470–479 (1971).
14. Chen, Y. C., Hayman, M. J. & Vogt, P. K. *Cell* **11,** 513–521 (1977).
15. Radke, K., Gilmore, T. & Martin, G. S. *Cell* **21,** 821–828 (1980).
16. Erikson, E. & Erikson, R. L. *Cell* **21,** 829–836 (1980).
17. Sefton, B. M., Hunter, T., Ball, E. H. & Singer, S. J. *Cell* **24,** 165–174 (1981).
18. Feldman, R. & Hanafusa, H. *Cell* **22,** 757–765 (1980).
19. Pawson, T. *et al. Cell* **22,** 767–775 (1980).
20. Kawai, S. *et al. Proc. natn. Acad. Sci. U.S.A.* **77,** 6199–6203 (1980).
21. Kessler, S. W. *J. Immun.* **115,** 1617–1624 (1975).
22. Garrels, J. I. *J. biol. Chem.* **254,** 61–77 (1979).
23. O'Farrel, P. H. *J. biol. Chem.* **250,** 4007–4021 (1975).
24. Laemmli, V. K. *Nature* **227,** 680–685 (1970).
25. Collett, M. S., Erikson, E. & Erikson, R. L. *Virology* **80,** 177–185 (1977).

Endogenous MuLV infection does not contribute to onset of radiation- or carcinogen-induced murine thymoma

Allen Mayer & Karoline Dorsch-Häsler

Department of Pathology, New York University School of Medicine,
550 First Avenue, New York, New York 10016, USA

T-cell lymphoma can be induced in mice by experimental infection with certain strains of murine leukaemia virus (MuLV) or by the action of germ-line transmitted endogenous MuLV[1]. B-cell lymphomas are induced in chickens by inoculation with certain strains of exogenous avian leukosis virus[2]. These systems have two common features: a requirement for actively replicating retrovirus, and a long latency period between introduction or appearance of the virus and development of the tumour. Such features are consistent with models of transformation that require multiple rounds of infection either to activate cellular oncogenes by promoter insertion[3] or to generate recombinant retrovirus genomes that have novel leukaemogenic activity[4]. The development of T-cell lymphoma in mice exposed to radiation or chemical carcinogens is also marked by a lengthy latency period between exposure to radiation or carcinogen and outgrowth of the tumour, and leukaemogenic MuLV is frequently isolated from tumour tissue[5,6]. We show here, however, that active infection of cells by endogenous MuLV is not essential to the development of thymic lymphoma in the mouse following exposure to radiation or chemical carcinogens.

The germ lines of all inbred mouse strains contain multiple copies of MuLV sequences, hence the designation endogenous MuLV[1,7]. A subset of these sequences can be expressed as infectious virus with an ecotropic (mouse-infectious) host range. Relative susceptibility to infection of mouse cells by ecotropic MuLV is regulated by alleles at the cellular *Fv-1* locus[8]. Differing alleles at the *Fv-1* locus, designated *n* and *b*, divide inbred mouse strains into two groups, N-type mice and B-type mice, cells of N-type mice being more susceptible to infection by N-tropic MuLV and those of B-type mice more susceptible to B-tropic MuLV infection. As *Fv-1*-mediated restriction to infection is a dominant phenotype, mice carrying both an *Fv-1*^{n} and an *Fv-1*^{b} allele are relatively restrictive for infection by both N-tropic and B-tropic MuLV[8].

Genetic analysis of the effect of the *Fv-1*^{b} allele on the incidence of lymphoma in the high incidence AKR inbred mouse strain showed that active infection of somatic cells by endogenous MuLV was required for the development of spontaneous thymic lymphoma[9]. AKR mice carry an *Fv-1*^{n} allele, and express N-tropic MuLV to high titres. When AKR mice were crossed to mice of the low lymphoma incidence BALB/c strain (homozygous for the *Fv-1*^{b} allele), both lymphoma incidence and infectious MuLV titre were much lower in F_1 hybrids than in the AKR parent. Suppression of both MuLV expression and spontaneous thymic lymphoma was associated in mice of the (BALB/c × AKR)F_1 × AKR backcross, indicating that the segregating *Fv-1*^{b} allele coordinately suppressed both traits in a genetically dominant fashion.

A similar experiment described here tested the effect of *Fv-1* on the development of radiation-induced thymic lymphoma, to determine whether this form of induced thymoma also requires active MuLV infection. As shown in Fig. 1*a*, both the RF/J and BALB/cJ strains are highly susceptible to radiation induction of

0028–0836/82/030253—03$01.00

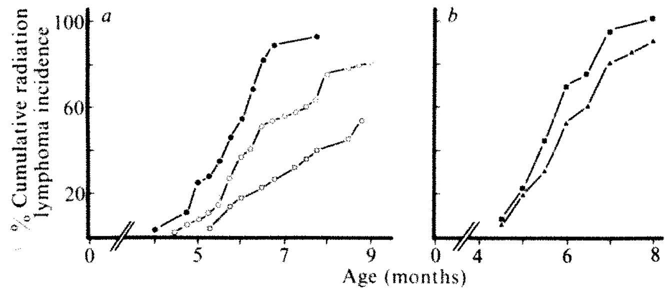

Fig. 1 Cumulative radiation-induced thymic lymphoma incidences in various populations of mice. Female mice were exposed to four weekly doses of 160 rad of γ-ray irradiation[5] (Gammator M ^{137}Cs source, Radiation Machinery Corporation, 530 rad min^{-1}), beginning at 33 ± 3 days old. Mice were checked daily for signs of lymphoma, including laboured breathing and enlarged peripheral lymph nodes. Mice displaying these symptoms were killed so as to detect the grossly enlarged thymus characteristic of this neoplasia. *a*, Populations of 28 RF/J mice (●—●), 22 BALB/cJ mice (□—□) and 52 (BALB/c × RF)F$_1$ hybrid mice (○—○); *b*, two subpopulations of (BALB/c × RF)F$_1$ × RF backcross mice, according to *Fv-1* type. 48 *Fv-1*^{n} homozygous mice (■—■) and 35 *Fv-1*^{n}/*Fv-1*^{b} heterozygous mice (▲—▲). *Fv-1* typing was accomplished by typing individual mice for their alleles at the closely linked *Gpd-1* locus[11], according to the procedure of Ruddle *et al.*[12].

thymoma, but RF mice display a shorter latency of tumour development. RF mice carry an *Fv-1*^{n} allele and express N-tropic MuLV, whereas BALB/c mice carry the *Fv-1*^{b} allele and can express both N-tropic and B-tropic MuLV[10]. If infectious spread of these MuLVs promotes development of radiation-induced thymoma in their respective strains, the (BALB/c × RF)F$_1$ hybrid would be expected to show a lower incidence of radiation-induced thymoma than either parental strain, because the RF-derived *Fv-1*^{n} allele will restrict infection of F$_1$ cells by the BALB/c B-tropic MuLV, while the BALB/c-derived *Fv-1*^{b} allele will restrict infection of F$_1$ cells by the RF N-tropic MuLV. Despite this genetic restriction on virus infection, F$_1$ hybrids showed a high incidence of radiation-induced thymoma, with a latency intermediate between that of the two parental strains (Fig. 1*a*), thus indicating that restrictive *Fv-1* alleles do not suppress development of radiation-induced thymoma.

To measure the effect of *Fv-1* in this cross more directly, the incidence of radiation-induced thymoma was determined in (BALB/c × RF)F$_1$ × RF backcross mice typed for the alleles they carried at the *Fv-1* locus. *Fv-1*^{n} homozygous and *Fv-1*^{n}/*Fv-1*^{b} heterozygous backcross mice were identified by typing each backcross mouse for its phenotype at the *Gpd-1* locus, which is closely linked to the *Fv-1* locus (<1% recombination between the two loci)[11]. The differing electrophoretic mobilities of the glucose-6-phosphate dehydrogenases specified by the *Gpd-1*^{a} and *Gpd-1*^{b} alleles (of RF and BALB/c, respectively)[12] served to distinguish *Gpd-1*^{a} homozygotes (*Fv-1*^{n} mice) from *Gpd-1*^{a}/*Gpd-1*^{b} heterozygotes (*Fv-1*^{n}/*Fv-1*^{b} mice) in the backcross. Figure 1*b* shows that these two subpopulations of the backcross did not differ substantially in their radiation-induced thymoma incidences, confirming that *Fv-1* does not suppress the incidence of this lymphoma.

These findings are not consistent with a requirement for active infection by endogenous MuLV in the development of radiation-induced thymoma. Cellular infection by both ecotropic[8] and dualtropic MCF-type MuLVs[13] are sensitive to *Fv-1* restriction, and the leukaemogenic activity of endogenous MuLV is strongly inhibited by a restrictive *Fv-1* genotype[9] yet here no corresponding strong suppression of radiation lymphoma by *Fv-1* was observed.

When the backcross mice were typed for their haplotype at *H-2*, the major histocompatibility complex of the mouse, no *H-2*-associated effect was observed to influence relative resistance to radiation-induced thymoma. An absence of *Fv-1* and *H-2* influences on thymoma incidence as induced by the chemical carcinogen 3-methylcholanthrene has previously been reported in the I/LnJ × RF cross[14].

We further assessed the contribution of endogenous mouse-infectious MuLV to the development of radiation- and carcinogen-induced thymoma. If infectious MuLV is indeed aetiologically involved in these induced lymphomas, one would expect to observe association between susceptibility to induced thymoma development and the segregation in appropriate genetic crosses of those murine genes that code for mouse-infectious MuLV. The 129 × RF cross was chosen for study because RF mice express endogenous ecotropic MuLV[15] but 129 mice have never been observed to do so[16]. Although 129 mice contain multiple copies of endogenous MuLV genes[7], and indeed express virus-coded antigens *in vivo*[17], their DNA lacks a specific portion of the endogenous ecotropic MuLV genome[16] and hence complete infectious ecotropic MuLV is not elaborated in 129 tissue. Furthermore, we have observed that RF mice contain a single locus governing iododeoxyuridine (IUdR)-induction of XC-detectable ecotropic MuLV. Such loci are thought to represent structural genomes of endogenous MuLV[18]. The conclusion that RF mice carry a single replication-competent ecotropic MuLV genome was reached by *in vitro* IUdR treatment of cultures of tail explant fibroblasts obtained from individual mice of the (129 × RF)F$_1$ × 129 backcross, followed by detection of MuLV production by these cells using

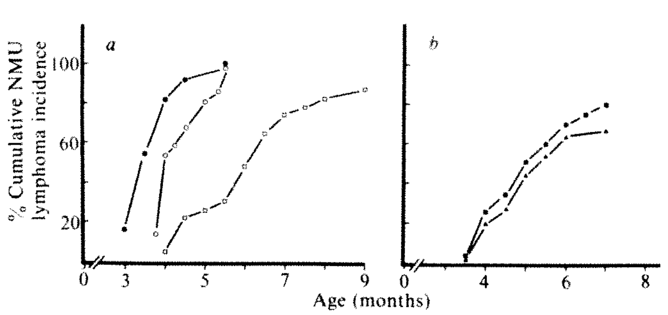

Fig. 2 Cumulative nitrosomethylurea-induced thymic lymphoma incidences in various populations of mice. Female mice were injected weekly with NMU (2 mg ml^{-1} in SSC, 30 mg per kg body weight) intraperitoneally for 5 consecutive weeks, beginning at 5 weeks of age[23]. Development of lymphoma was monitored as described in Fig. 1 legend. *a*, Populations of 39 RF/J mice (●—●), 23 129/J mice (□—□), and 23 (129 × RF)F$_1$ hybrid mice (○—○); *b*, two subpopulations of the (129 × RF)F$_1$ × 129 backcross, 71 mice containing an IUdR-inducible, XC-detectable ecotropic MuLV genome (■—■), and 61 mice lacking this MuLV genome (▲—▲).

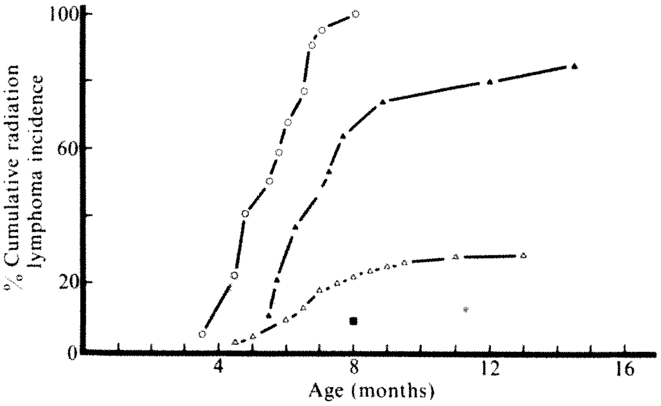

Fig. 3 Cumulative radiation-induced thymic lymphoma incidences in various populations of mice. Female mice were exposed to γ-ray irradiation and monitored for development of thymic lymphoma as described in Fig. 1. legend. 22 RF/J mice (○—○), 11 129/J mice (■—■), 19 (129 × RF)F$_1$ hybrid mice (▲—▲) and 197 (129 × RF)F$_1$ × 129 backcross mice (△—△). Only one of the eleven 129/J mice developed thymoma, and thus this result is presented as a single point.

the XC assay[19]. This procedure has been described by Lander *et al.*[20], and detects the presence of ecotropic MuLV in all RF and $(129 \times RF)F_1$ mice, but not in 129 mice. In a population of $(129 \times RF)F_1 \times 129$ backcross mice, tail cultures from 72 of 132 mice tested were virus-positive, demonstrating the segregation of a single RF-derived ecotropic MuLV locus in the cross. Note that this assay says nothing about the manner or quantity of expression *in vivo* of ecotropic MuLV in the mice tested. It merely detects the presence of a replication-competent ecotropic MuLV genome while allowing individual mice to be tested concomitantly for radiation and carcinogen-induced thymoma development. In contrast to the BALB/c × RF cross described above, RF and 129 mice do not differ with respect to their *Fv-1* genotype[8], and RF ecotropic MuLV expression will not be restricted in this cross as compared with the parental RF strain.

Figure 2*a* shows that both RF and 129 mice are highly sensitive to induction of thymoma by the chemical carcinogen *N*-nitrosomethylurea (NMU), and that RF mice display a shorter latency of tumour development than do 129. F_1 hybrid mice have an intermediate latency. The high incidence of NMU-induced thymic lymphoma in the 129 strain, albeit at later ages than RF, in itself demonstrates that cellular infection by ecotropic MuLV is not required for the development of this induced lymphoma, because, as mentioned above, 129 mice lack this viral activity. When the incidence of NMU-induced thymoma was compared in $(129 \times RF)F_1 \times 129$ backcross mice either carrying or lacking a replication-competent ecotropic MuLV genome, as typed by IUdR induction of tail explant fibroblast cultures followed by detection of MuLV expression using the XC plaque assay[20], the two subpopulations of the backcross showed virtually identical incidences (Fig. 2*b*). This indicates that the RF ecotropic MuLV locus detected here does not seem to be a major determinant in the short latency of NMU-induced thymic lymphoma in RF mice.

Figure 3 shows that RF mice are much more sensitive to radiation-induced thymoma than are 129 mice, and that F_1 hybrid mice also develop a high incidence of this tumour. A population of $(129 \times RF)F_1 \times 129$ backcross mice was exposed to radiation (Fig. 3), and backcross mice that developed thymic lymphoma were randomly tested for the presence of the RF IUdR-inducible ecotropic MuLV locus. Only 22 out of 37 lymphomatous backcross mice tested were seen to carry the RF ecotropic MuLV locus, a result not significantly different from that expected from random segregation of this locus in the lymphomatous population, and indicating that the locus is not a major factor in determining susceptibility to radiation-induced lymphoma.

These findings point to a basic difference between the aetiologies of spontaneous and carcinogen- or radiation-induced thymoma. The spontaneous occurrence of this tumour is associated with expression of endogenous mouse-infectious MuLV activities, including both XC-positive[9] and XC-negative[21] ecotropic MuLVs and dualtropic MCF MuLV[13]. The present data indicate that both carcinogen- and radiation-induced thymoma develop in the absence of replication-competent XC-positive ecotropic MuLV activity. The dependence of spontaneous thymoma development on actual infectious events has been previously indicated by its marked susceptibility to suppression by a restrictive *Fv-1* allele[9]. In contrast, neither carcinogen- nor radiation-induced thymoma development is sensitive to suppression by *Fv-1*. This indicates that those infectious viral events that are aetiologically involved in development of spontaneous thymomas are not required for the development of induced thymomas. Finally, note that the possible importance to the development of induced thymomas of endogenous MuLV antigen expression in the absence of infectious virion production[22] has not been addressed here, and remains a viable hypothesis.

Many discussions with Drs Frank Lilly and Maria L. Duran-Reynals of the Albert Einstein College of Medicine are gratefully acknowledged. This work was supported by NCI grant CA 23834 and CA 16239. A.M. is a Scholar of the Leukemia Society of America and an Irma T. Hirschl Career Scientist Awardee.

Received 28 July; accepted 1 December 1981.

1. Rowe, W. P. *Cancer Res.* **33,** 3061–3068 (1973).
2. Crittenden, L. B., Hayward, W. S., Hanafusa, H. & Fadly, A. M. *J. Virol.* **33,** 915–919 (1980).
3. Hayward, W. S., Neel, B. G. & Astrin, S. M. *Nature* **290,** 475–48 (1981).
4. Cloyd, M. W., Hartley, J. W. & Rowe, W. D. *J. exp. Med.* **151,** 542–552 (1980).
5. Kaplan, H. S. *Cancer Res.* **27,** 1325–1340 (1967).
6. Ball, J. K. & McCarter, J. A. *J. natn. Cancer Inst.* **46,** 751–762 (1971).
7. Lowy, D. R., Chattopadhyay, S. K., Teich, N. M., Rowe, W. P. & Levine, A. S. *Proc. natn. Acad. Sci. U.S.A.* **71,** 3555–3559 (1974).
8. Pincus, T., Hartley, J. W. & Rowe, W. P. *J. exp. Med.* **133,** 1219–1233 (1971).
9. Lilly, F., Duran-Reynals, M. L. & Rowe, W. P. *J. exp. Med.* **141,** 882–889 (1975).
10. Peters, R. L., Spahn, G. J., Rabstein, L. S., Kelloff, G. J. & Huebner, R. J. *Science* **181,** 665–667 (1973).
11. Rowe, W. P. & Sato, H. *Science* **180,** 640–641 (1973).
12. Ruddle, F. H., Shows, T. B. & Roderick, T. H. *Genetics* **58,** 599–606 (1968).
13. Hartley, J. W., Wolford, N. K., Old, L. J. & Rowe, W. P. *Proc. natn. Acad. Sci. U.S.A.* **74,** 789–792 (1977).
14. Mayer, A., Lilly, F. & Duran-Reynals, M. L. *Proc. natn. Acad. Sci. U.S.A.* **77,** 2960–2963 (1980).
15. Mayer, A., Duran Struuck, F., Duran-Reynals, M. L. & Lilly, F. *Cell* **19,** 431–436 (1980).
16. Chattopadhyay, S. K., Lander, M. R., Rands, E. & Lowy, D. R. *Proc. natn. Acad. U.S.A.* **77,** 5774–5778 (1980).
17. Stockert, E., Old, L. J. & Boyse, E. A. *J. exp. Med.* **133,** 1334–1355 (1971).
18. Chattopadhyay, S. K., Rowe, W. P., Teich, N. M. & Lowy, D. R. *Proc. natn. Acad. Sci. U.S.A.* **72,** 906–910 (1975).
19. Rowe, W. P., Pugh, W. E. & Hartley, J. W. *Virology* **42,** 1136–1139 (1970).
20. Lander, M. R., Moll, B. & Rowe, W. P. *J. natn. Cancer Inst.* **60,** 477–478 (1978).
21. Nowinski, R. C. & Hays, E. F. *Virology* **27,** 13–18 (1978).
22. Fischinger, P. J., Jurgen Thiel, H., Ihle, J. N., Lee, J. C. & Elder, J. H. *Proc. natn. Acad. Sci. U.S.A.* **78,** 1920–1924 (1981).
23. Joshi, V. V. & Frei, J. V. *J. natn. Cancer Inst.* **45,** 335–339 (1970).

Altered methylation of endogenous viral promoter sequences during mammary carcinogenesis

Trudy Breznik & J. Craig Cohen

Department of Microbiology and Immunology, Tulane University,
School of Medicine, New Orleans, Louisiana 70112, USA

Mouse mammary tumour virus (MMTV) is a type B retrovirus that may be transmitted either by somatic cell infection via infectious virus borne in mother's milk or vertically by passage of virus-specific sequences in the germ line. Endogenous viral sequences act as stable genetic loci[1] and are found in all inbred mouse strains studied. Available data suggest that, in general, strains exhibiting only endogenous virus have a low tumour incidence whereas a high tumour incidence occurs in strains carrying milk-borne MMTV, in addition to germ-line sequences. However, as removal of the milk-borne virus does not completely eliminate tumours, endogenous proviral sequences may also be involved in tumorigenesis[2–4]. Recent results have shown that proviral sequences acquired from milk are undermethylated (low 5-methylcytosine content), whereas endogenous MMTV sequences are highly methylated. An inverse relationship between proviral methylation and transcriptional activity has also been demonstrated[5,6]. This model suggests that an important mechanism of MMTV-induced tumorigenesis in uninfected mice (those lacking milk-borne MMTV) may involve derepression of endogenous proviruses, possibly through demethylation of these sequences. Here we show that the methylation pattern of endogenous virus sequences is specifically altered during tumorigenesis in uninfected mice.

Several tumours occurring in BALB/c mice were studied both for the acquisition of new MMTV proviral sequences and for demethylation of endogenous viral sequences. As tumours occur infrequently in this strain, those derived from the D1 series of hyperplastic outgrowth lines developed by Medina[7] were used. These tissues (supplied by R. Cardiff) are transplantable and are analogous to the pre-neoplastic nodules commonly seen in the mammary gland. Outgrowth lines are

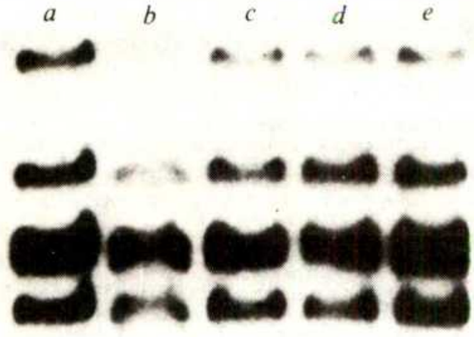

Fig. 1 *Eco*RI digestion of DNA for liver and mammary tumours of the BALB/c mouse strain. DNA was extracted by placing tissue in DNA extraction buffer (0.2 M Tris-HCl *p*H 8.1, 0.01 M EDTA *p*H 7.0, and 0.1 M NaCl) and homogenized using a motor driven, Teflon-glass Dounce homogenizer. Protein was removed by incubation at 37 °C for 12 h with proteinase K (100 g ml^{-1}) and SDS (1%) followed by phenol–chloroform (2 : 1) extraction. DNA was spooled on to a glass rod by addition of 0.2 M sodium acetate and two volumes of cold ethanol. DNA was resuspended in 0.005 M Tris-HCl *p*H 7.4 and 0.1 mM EDTA *p*H 7.0 and concentration determined by UV absorption. Each sample (10 μg) was digested to completion by *Eco*RI (12-fold excess) as determined by using λ bacteriophage DNA as an external control. Samples were electrophoresed in 0.8% agarose in a buffer containing 0.02 M sodium acetate *p*H 7.0, 0.018 M NaCl and 0.002 M EDTA. Bromophenol blue was used as a tracking dye which was electrophoresed 20 cm. ^{32}P-labelled, *Hin*dIII-digested λ bacteriophage DNA was run in parallel as a molecular weight marker. Following electrophoresis DNA was transferred to nitrocellulose sheets (Schleicher & Schuell) by the method of Southern[11] using modifications as described previously[5]. Virus-specific bands were detected by hybridization with ^{32}P-labelled, representative, complementary DNA (cDNArep) synthesized using calf thymus primers to initiate DNA synthesis by reverse transcriptase on a cloned MMTV DNA template. The hybridization buffer included 50% formamide, Denhardt's buffer[11], 20 g ml^{-1} salmon sperm DNA, 0.05 M HEPES buffer *p*H 7.0, and 3 × SSC (SSC = 0.15 M NaCl, 0.015 M Na citrate). After hybridization at 41 °C for 48 h, filters were washed as described previously[5] and bands detected by autoradiography using Kodak XAR-5 X-ray film with Cronex Lightning Plus intensifying screens at −70 °C. *Eco*RI was used to digest DNA from BALB/c liver (lane *a*), D1 mammary tumours 997, 968 and 599 (lanes *b–d*, respectively) and the transplanted mammary tumour 1247 (lane *e*). Molecular weight in kilobases was determined by inclusion of *Hin*dIII-digested λ bacteriophage DNA (not shown).

transplanted into young females along with pituitary isografts to facilitate tumour development.

Virus-specific sequences were detected using the method of Southern[8] following digestion of DNA with *Eco*RI, which has a single restriction site within the full-length MMTV genome. Therefore, cleavage by this enzyme generates from each provirus two virus-specific fragments whose sizes depend on the integration site of the virus in the host genome (thus, fragment length is determined by the nearest *Eco*RI site in cellular DNA). Using this technique we determined that BALB/c mice contain three endogenous MMTV proviruses, designated units I, II and III; units II and III are full length and unit I is subgenomic.

Figure 1*a* is an *Eco*RI digest of uninfected liver[9] DNA, showing the five previously mapped endogenous virus-specific fragments which range in size from 6.7 to 16.7 kilobases (kb). Unit I is included in the 16.7-kb fragment, unit II in fragments of 8.5 and 7.0 kb and unit III in the 10.0- and 7.8-kb fragments. Examination of DNA from BALB/c tumours (Fig. 1*b–e*) reveals virus-specific fragments identical to those found in liver DNA. Because mammary tumours are clonal[10] and acquisition of MMTV proviruses is known to be a random event in the mouse genome[1], the failure to find additional *Eco*RI fragments whose size is dependent on site of integration (see above and ref. 11) indicates that only the genetically transmitted viral sequences are present. Therefore, infection and re-integration of MMTV DNA, although facilitating mammary carcinogenesis, is not essential.

The level of 5-methylcytosine in virus-specific sequences was probed using the restriction enzymes *Msp*I and *Hpa*II, isoschizomers which recognize the sequence 5′CCGG. Because *Msp*I will cleave this sequence regardless of methylation of the internal cytosine residue, while *Hpa*II is inhibited by methylation at this site[5,12], digestion of cellular DNA with these enzymes differentiates methylated from non-methylated sites. Figure 2 shows *Msp*I and *Hpa*II digestion of BALB/c liver and D1 tumour DNAs. *Msp*I digestion of liver DNA (Fig. 2*a*) generates a series of virus-specific fragments of 0.2–8.4 kb (ref. 5). *Hpa*II-cleaved BALB/c liver DNA, on the other hand, demonstrates extensive methylation of all viral fragments, as evidenced by the single high molecular weight (>15 kb) virus-specific fragment. *Hpa*II digestion of D1 tumour DNAs (Fig. 2*d*, *f*, *h*), however, generates two virus-specific bands of 2.1 and 1.4 kb. Therefore, sites in MMTV proviruses methylated in DNA from both uninfected liver and lactating mammary gland (Fig. 2*b*, and ref. 5) are demethylated during mammary carcinogenesis in the BALB/c mouse strain.

We determined the origin of the 2.1- and 1.4-kb *Hpa*II fragments by comparing *Msp*I digests from various inbred mouse strains, as MMTV proviral units vary between different strains[1]. Comparison of the previously published[5] *Msp*I digestion of DNA from the CBA/CaJ mouse strain (which includes units II and III) with that obtained with DNA from BALB/c (which includes units I, II and III), indicated that the 2.1- and 1.4-kb *Msp*I–*Hpa*II fragments are derived from the subgenomic unit I.

*Hpa*II digestion of DNA from BALB/c mammary tumour 1247 (not shown) produced several virus-specific fragments in addition to those derived from unit I, indicating that demethylation of other endogenous proviruses has occurred in this tumour. The origin of these additional sites of demethylation in tumour 1247 was identified by *Eco*RI–*Hpa*II double digestions. By determining which *Eco*RI bands are sensitive to further cleavage by *Hpa*II, one can ascertain the proviral units being demethylated during tumorigenesis (Fig. 3). This is possible in the BALB/c strain because all *Eco*RI fragments are mapped to specific units of MMTV proviral DNA[9].

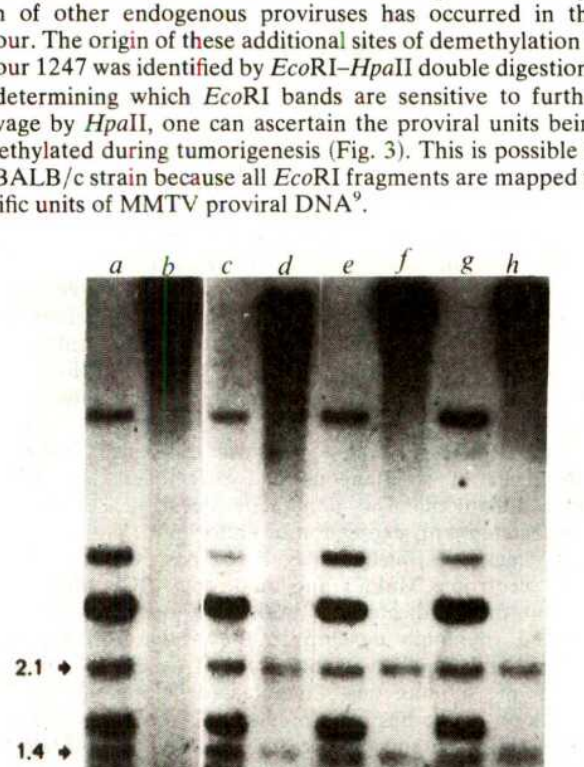

Fig. 2 Methylation of MMTV sequences in BALB/c liver and mammary tumours. DNA from either liver (lanes *a*, *b*) or D1 mammary tumours (lanes *c–h*) were digested with either the methyl-insensitive isoschizomer *Msp*I (lanes *a*, *c*, *e*, *g*) or methyl-sensitive *Hpa*II (lanes *b*, *d*, *f*, *h*) and virus-specific bands analysed as described in Fig. 1. legend.

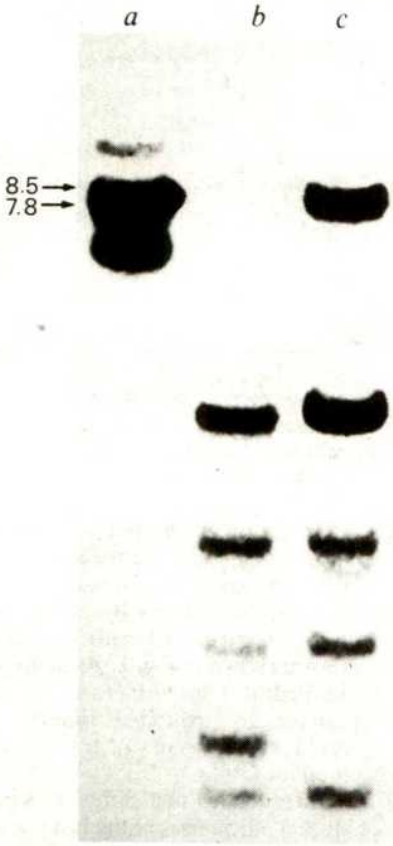

Fig. 3 Characterization of demethylated sequences in mammary tumour 1247. DNA from tumour 1247 was digested with either *Eco*RI (lane *a*) or sequentially with *Eco*RI and either *Msp*I (lane *b*) or *Hpa*II (lane *c*) and virus-specific fragments were detected as described in Fig. 1. legend.

Cleavage of MMTV-specific *Eco*RI fragments by the methyl-insensitive isoschizomer *Msp*I (Fig. 3*b*) indicates the presence of *Msp*I–*Hpa*II sites in all fragments. Double digestion with *Eco*RI and *Hpa*II (Fig. 3*c*) reveals demethylation of specific proviral sequences. The 8.5- and 7.8-kb fragments remain methylated as evidenced by their presence in the *Eco*RI–*Hpa*II double digestion. The 16.7, 10.0- and 6.7-kb *Eco*RI fragments, however, are demethylated because, whereas *Msp*I–*Hpa*II sites in BALB/c liver are highly methylated, resulting in no cleavage of any *Eco*RI fragments by *Hpa*II (data not shown), tumour 1247 showed a specific loss of methylated bases from these three fragments. Previous data[9] mapping restriction endonuclease sites on the endogenous MMTV proviruses of BALB/c mice revealed that the 8.5- and 7.8-kb *Eco*RI fragments are derived from the 5′ ends of units III and II, respectively. Two of the remaining three *Eco*RI fragments (10.0 and 6.7 kb) which are cleaved by the methyl-sensitive *Hpa*II are derived from the 3′ ends of units II and III. The 16.7-kb *Eco*RI fragment is obtained from the subgenomic, 3′ sequence containing unit I. Thus, spontaneous BALB/c tumours studied show the specific demethylation of virus-specific sequences derived from the 3′ region of the viral genome. Recent sequencing data[13] indicate the presence of *Hpa*II cleavage sites in the long terminal repeats (LTRs) of several MMTV proviruses which seem to be identical to units II and III. The demethylation event occurring in tumour 1247 is thus extremely specific, as it distinguishes between two direct repeats occurring at each end of these two proviruses[9]. The significance of these additional demethylation events in tumorigenesis of this particular tumour is unclear, because in other tumours demethylation of only unit I was observed.

Previous studies[14–16] have indicated that, at each end of retroviral DNA, sequences from the 3′ end of the viral genome are repeated along with a short sequence from the 5′ region. In MMTV this LTR is 1,200 base pairs long and contains an open reading frame capable of encoding[13] a protein of molecular weight 38,000. As hypomethylation correlates with gene expression, the demethylation observed in these spontaneous BALB/c tumours may represent activation of this gene. However, no protein derived from this open reading frame has been identified.

Another possible explanation for the specific demethylation of these sequences during mammary carcinogenesis involves promoter activation. The promoter for transcription of the retroviral genes apparently resides in the 3′ sequences of the LTR[17,18], and it has been suggested that carcinogenesis occurs through a mechanism of cell transformation referred to as oncogenesis by promoter insertion, that is, that the introduction of the viral promoter (in the LTR) allows transcription of cellular sequences associated with the 3′ end of the provirus. The present results suggest that in addition to transformation by promoter insertion that may occur during exogenous MMTV infection, carcinogenesis by promoter derepression may occur. This is supported by the observed demethylation of either the defective MMTV sequence (unit I) or specifically the 3′ half of the nondefective proviruses (units II and III), as decreased levels of methylation are known to correlate with increased transcriptional activity of MMTV[5,6] and other eukaryotic genes[19,20].

This work was supported by American Cancer Society grant MV-65.

Received 5 October; accepted 10 November 1981.

1. Cohen, J. C. & Varmus, H. E. *Nature* **278**, 418–423 (1979).
2. Moore, D. in *Cancer: A Comprehensive Treatise* (ed. Becker, F. F.) 131–167 (Plenum, New York, 1976).
3. Benvelzen, P. *Biochim. biophys. Acta* **335**, 236–251 (1974).
4. Nandi, S. & McGrath, C. C. *Adv. Cancer Res.* **17**, 353–414 (1973).
5. Cohen, J. C. *Cell* **19**, 653–662 (1980).
6. Cohen, J. C. *et al.* in *Animal Virus Genetics* Vol. 18 (eds Field, B. *et al.*) 401–409 (Academic, New York, 1980).
7. Medina, D. *Meth. Cancer Res.* **7**, 3–53 (1973).
8. Southern, E. M. *J. molec. Biol.* **98**, 502–517 (1975).
9. Cohen, J. C. *et al. J. Virol.* **32**, 483–496 (1979).
10. Cohen, J. C. *et al. Cell* **16**, 333–345 (1979).
11. Denhardt, D. T. *Biochem. biophys. Res. Commun.* **23**, 641–646 (1966).
12. Waalwijk, C. & Flavell, R. A. *Nucleic Acids Res.* **5**, 4631–4641 (1978).
13. Dickson, C., Smith, R. & Peters, G. *Nature* **291**, 511–513 (1981).
14. Hsu, T. W. *et al. J. Virol.* **28**, 810–818 (1978).
15. Shank, P. R. *et al. Cell* **15**, 1383–1396 (1978).
16. Gilboa, E. *et al. Cell* **16**, 863–874 (1979).
17. Payne, G. S. *et al. Cell* **23**, 311–322 (1981).
18. Neel, B. G. *et al. Cell* **23**, 323–334 (1981).
19. Sutter, D. & Doerfler, W. *Proc. natn. Acad. Sci. U.S.A.* **77**, 253–256 (1980).
20. Desrosiers, R. C. *et al. Proc. natn. Acad. Sci. U.S.A.* **77**, 253–256 (1980).

High frequency of gene transfer after fusion between bacteria and eukaryotic cells

Minoo Rassoulzadegan, Bernard Binetruy & François Cuzin

Centre de Biochimie du CNRS, Université de Nice, Parc Valrose,
06034 Nice, France

Recent studies[1] have demonstrated that eukaryotic simian virus 40 (SV40) genes carried in a bacterial plasmid can be directly transferred into mammalian cells in culture; after polyethylene glycol (PEG)-induced fusion with bacterial protoplasts, a fraction of the recipient cells yielded infectious virus. We have now investigated whether this procedure can also produce stable transformants. We report here that the efficiency of focus formation after transfer of either polyoma virus or SV40 early genes was at least equal to that observed after infection with virions. At high ratios of bacteria/recipient cells, all the cells were observed to express the early viral proteins 48 h after fusion. In optimal conditions, transfer by fusion thus seems to be 10- to 20-fold more efficient than DNA transfection by the Ca^{2+} co-precipitation technique[2] for the introduction of foreign genes into eukaryotic recipients.

0028-0836/82/030257—03$01.00

Escherichia coli (strain 1106; ref. 3) carrying one of the plasmids listed in Table 1 were grown to a density of 2×10^8 cells per ml. Chloramphenicol was added at a final concentration of 200 μg ml^{-1} and the cultures were aerated overnight. Aliquots (10 ml) were centrifuged and the bacteria resuspended at 0 °C in 100 μl of 50 mM Tris-HCl buffer, *p*H 8.0, containing 20% sucrose; 20 μl of a freshly made solution of lysozyme (10 mg ml^{-1}; Boehringer) were added and the suspension incubated at 0 °C for 10 min. After addition of 50 μl of 0.25 M EDTA, the suspension was diluted by progressive addition of 1.3 ml of 50 mM Tris-HCl buffer, pH 8.0, containing 9% sucrose. Microscopic examination indicated that >90% of the bacteria were converted into protoplasts. The recipient cells were grown in Dulbecco's modified Eagle's medium (DMEM, Gibco) in 35-mm Petri dishes to a density of 2×10^5 cells per plate. The medium was removed and the cells were washed once with 2 ml of Tris-buffered saline solution, 2 ml of the protoplast suspension were added to the plates and centrifuged onto the cell layer (1,500 r.p.m. for 3 min). The supernatant was removed and 0.5 ml of a 48% solution of PEG 1,000 in DMEM (48 g PEG dissolved in 52 g DMEM) was added. After 1 min at room temperature, the cells were washed carefully five times with Tris-buffered saline before being returned to the growth medium (DMEM supplemented with 10% newborn calf serum (Gibco)). The medium was changed on alternate days and the cultures were checked after 10 days for the appearance of foci.

As shown in Fig. 1, transformed foci were observed after fusion of FR3T3 rat cells[4] with bacteria carrying plasmid pPY-1. This plasmid includes a full-size wild-type polyoma virus genome recombined with pBR322 at the *Bam*HI site in the late viral region. No foci were produced after fusion with bacteria carrying an intact pBR322 plasmid, and results obtained with recombinants carrying various polyoma virus mutants were always in agreement with the known transforming ability of the viral genes present in the plasmid (Table 1): cleavage of polyoma virus DNA by recombination at the *Eco*RI site in the early region did not interfere with its transforming ability (plasmid pTS25E), as previously demonstrated after DNA transfection[5-7], whereas no transformants were produced using the cloned genome (pNG-1) of a transformation-defective *hrt* mutant[8]. The efficiency of focus induction was ~40 transformants per 2×10^5 cells at an input ratio of 10^4 protoplasts per cell (Fig. 1). Identical efficiencies were observed (data not shown) after fusion of protoplasts carrying either polyoma or SV40 early genes in pBR322 plasmid (plasmids pPY-1 and pSV-1; see Table 1) with both mouse and rat embryo fibroblasts in primary cultures, suggesting an equally high frequency of gene transfer. These values are comparable with those observed after infection of the same cells with high multiplicities of viral particles[4].

As 90–100% of the cells expressed the early proteins (T antigens) after virion infection, the relatively high efficiency of focus formation after fusion suggested a comparable high frequency of gene transfer. This frequency was measured directly by immunofluorescence determination on fixed cells after transfer of the early region of SV40 (plasmid pSV-1; see Table 1) into either permissive CV1 cells or non-permissive FR3T3 cells. Results are shown in Fig. 2. As many as 100% of CV1 nuclei were stained at a bacteria/recipient cell ratio of ~10^4. The dose–response curve exhibited a different slope in the case of FR3T3 rat cells, the efficiency of transfer being about one-half that observed for CV1.

Further studies are needed, as such differences between cell lines may reflect different efficiencies of the fusion process; they may reflect different efficiencies of expression after transfer of a given gene (for example, FR3T3 cells are non-permissive whereas CV1 cells are fully permissive for the development of SV40 virus). Frequencies of T-positive cells >50% were observed in FR3T3 cells at an input ratio of 3×10^4 bacteria per cell. It may be technically difficult to increase this ratio further, because a significant fraction of the cells are killed at very high bacteria/cell ratios.

The transfer frequencies observed were at least one order of magnitude higher than those after DNA transfection, which is

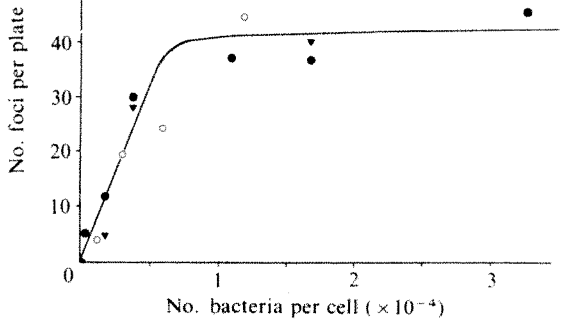

Fig. 1 Efficiency of focus formation after fusion of FR3T3 cells with bacteria carrying genomic polyoma virus DNA inserted in pBR322. Focus formation was measured as described in ref. 4. Abscissa, ratio of number of bacterial protoplasts to number of cells. Ordinate, number of foci per 35-mm Petri dish (2×10^5 cells). The different symbols represent results obtained in three separate experiments.

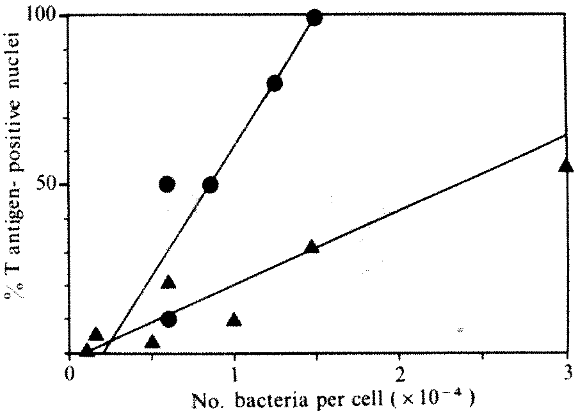

Fig. 2 Expression of the early viral antigens after fusion of FR3T3 (▲) and CV1 (●) cells with bacteria carrying SV40 early genes inserted in pBR322.

Table 1 Efficiency of focus formation after fusion with recipient cells of protoplasts carrying various viral DNA fragments in different plasmids

Plasmid	Viral DNA fragment	Insertion site in pBR322	Focus formation (foci per 2×10^5 cells)*
pBR322	None	—	0
pPY-1	Genomic polyoma DNA (wild-type A2 strain) cleaved at the *Bam*HI site	*Bam*HI	40
pTS25E	Genomic *tsa25E* polyoma DNA cleaved at the *Eco*RI site	*Eco*RI	25
pNG-1	Genomic polyoma *hrt* NG 18 mutant cleaved at the *Bam*HI site	*Bam*HI	0
pMC-2	Wild-type polyoma A2 sequences from *Bam*HI to *Eco*RI sites (distal parts of early and late genes)	*Eco*RI, *Bam*HI	0
pSV-1	Wild-type SV40 sequences from *Bam*HI to *Hpa*II sites (complete early region)	*Eco*RI	32

Plasmids pPY-1, pTS25E, pNG-1 and pMC-2 were constructed in our laboratory by the usual procedures (P. Clertant and M. Canning, unpublished results); plasmid pSV-1 is described in ref. 10 and was obtained from Dr C. Benoist. A2 strain polyoma DNA, see ref. 11; mutant *tsa25E*, ref. 12; mutant *hrt* NG 18, ref. 8.

* FR3T3 cells were fused with bacterial protoplasts as described in the text.

restricted to only a few 'competent' cells[9]. In our experiments, transfer of either polyoma or SV40 virus early genes by the Ca^{2+} co-precipitation technique produced 5–10% T antigen-positive cells at high doses of DNA (10 μg per 10^5 cells).

The frequency of T-positive CV1 cells after fusion was also 15- to 20-fold higher than that reported in comparable experiments[1]. A systematic analysis of the parameters involved (data not shown) indicated that the extent of lysozyme treatment was critical. As expected, incomplete conversion into protoplasts led to reduced frequencies of transformation. The same result was also observed, however, for prolonged lysozyme attacks which led to the lysis of a fraction of the protoplasts, apparent from the increased viscosity of the suspension. On the other hand, the chloramphenicol amplification step seems to be essential: in several cases where this step was omitted, using either pBR322 or pAT153 plasmid, no transformants were produced after fusion (data not shown). However, as these points were checked in previous experiments (W. Schaffner, personal communication), another important parameter that must be considered is the choice of bacterial strain. Although we cannot provide comparative data, it is possible that the strain used here (*E. coli* 1106) is more efficient than others, for example, *E. coli* HB101 (ref. 1), in producing stable protoplasts.

Biohazards associated with the experiments described here have been examined previously by the French National Committee and the experiments were carried out according to the rules established by this Committee.

We thank L. Carbone, F. Tillier and M. L. Varani for technical assistance. This work was supported by grants from the CNRS (ATP "Biologie Moléculaire du Gène") and the Institut National de la Santé et de la Recherche Médicale (AT 79-104, PRC "Génie Génétique").

Received 17 August; accepted 13 November 1981.

1. Schaffner, W. *Proc. natn. Acad. Sci. U.S.A.* **77,** 2163–2167 (1980).
2. Graham, F. L. & Van der Eb, A. J. *Virology* **52,** 456–467 (1973).
3. Murry, N. E., Brammar, W. J. & Murray, K. *Molec. gen. Genet.* **150,** 53–61 (1976).
4. Seif, R. & Cuzin, F. *J. Virol.* **24,** 721–728 (1977).
5. Israel, M. A., Simmons, D. T., Hourihan, S. L., Rowe, W. P. & Martin, M. A. *Proc. natn. Acad. Sci. U.S.A.* **76,** 3713–3716 (1980).
6. Hassell, J. A., Topp, W. C., Rifkin, D. B. & Moreau, P. E. *Proc. natn. Acad. Sci. U.S.A.* **77,** 3978–3982 (1980).
7. Novak, U., Dilworth, S. M. & Griffin, B. E. *Proc. natn. Acad. Sci. U.S.A.* **77,** 3278–3282 (1980).
8. Benjamin, T. L., Carmichael, G. G. & Schaffhausen, B. S. *Cold Spring Harb. Symp. quant. Biol.* **44,** 263–270 (1980).
9. Wigler, M. *et al. Cell* **16,** 777–785 (1979).
10. Benoist, C. & Chambon, P. *Nature* **290,** 304–310 (1981).
11. Soeda, E., Arrand, J. R., Smolar, N., Walsh, J. E. & Griffin, B. E. *Nature* **283,** 445–453 (1980).
12. Eckhart, W. *Virology* **38,** 120–125 (1969).

Circular double-stranded RNA in potato spindle tuber viroid-infected tomatoes

R. C. French, M. A. Price & K. S. Derrick

Department of Plant Pathology and Crop Physiology,
Louisiana State University Agricultural Experiment Station,
Baton Rouge, Louisiana 70803, USA

Viroids are circular molecules of single-stranded RNA consisting of ~360 nucleotides[1,2], and the mechanism by which these smallest of all known infectious agents replicate in host cells has been extensively studied. Earlier work suggested that viroids replicate using DNA intermediates[3], but rigorous hybridization experiments[4,5] failed to detect DNA complementary to potato spindle tuber viroid (PSTV) in infected plants, and there is no specific inhibition of viroid synthesis[6] by actinomycin D. There is strong evidence that the replication of viroids involves RNA intermediates. *Citrus exocortis* viroid (CEV)[7,8]-infected and PSTV-infected[4,9,10] tissues have been shown to contain RNA that is complementary to the infecting viroid, and recently it was shown that DNA-dependent RNA polymerase II, isolated from tomato, will produce full-length complementary copies of purified viroids *in vitro*[11]. Because much of the RNA complementary to CEV was shown to be double stranded, it could be anticipated that viroid-infected tissue contains unique species of double-stranded RNA (dsRNA). Using serologically specific electron microscopy[12], we have now detected molecules of circular dsRNA in crude extracts of PSTV-infected tomato. These molecules have contour lengths that would be expected for a double-stranded intermediate of PSTV.

Using antiserum to dsRNA, serologically specific electron microscopy was used to demonstrate the involvement of dsRNA in the replication of tobacco mosaic virus[13]. Similar assays of PSTV-infected tomato tissue revealed several linear and relaxed circular molecules of dsRNA, whereas extracts of healthy tomato tissue contained a similar number of linear molecules of dsRNA but approximately 10 times fewer circular molecules.

Tomato (*Lycopersicon esculentum* cv. Rutgers) leaves were powdered with liquid nitrogen and ground with 0.1 M Tris-HCl *p*H 8.0, containing 10 mM Na_2EDTA (Tris) (1 ml per g of tissue). The following steps were done at room temperature. Electron microscope grids with carbon-reinforced Formvar films were floated on antiserum to dsRNA, diluted 1/500 with Tris, for 30 min. After washing with Tris the grids were placed on drops of extract for 2.5 h. The grids were washed with Tris and distilled water, dipped in 95% ethanol for 30 s, rinsed with distilled water and placed on drops of 0.1 mg ml^{-1} cytochrome *c* in Tris for 15 min. The grids were washed with distilled water and placed on drops of 0.01 M phosphate *p*H 7.2 for 15 min, then removed from the phosphate and held for 30 s in a stream of drops of 1% aqueous uranyl acetate from a motor-driven syringe equipped with a 0.2-μm filter. They were rinsed by touching to a drop of distilled water for 1 s and blotted dry, then examined under the electron microscope.

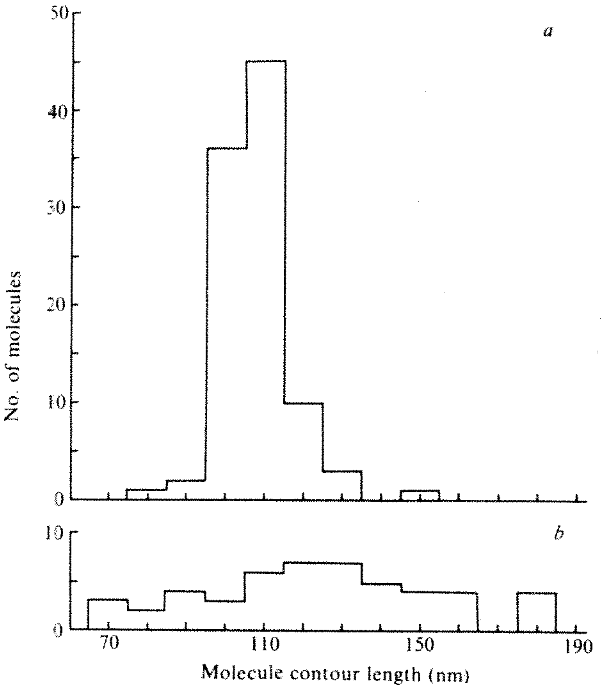

Fig. 1 Histograms of the circumference of circular dsRNA found in extracts of PSTV-infected (*a*) and healthy (*b*) tomato tissue. Electron micrograph negatives of grids prepared as described in the text were projected and the circular forms were traced and measured. We measured a total of 50 molecules from 18 negatives of healthy and 100 molecules from 3 negatives of PSTV-infected tissue extracts.

The assay was specific for dsRNA: neither circular nor linear forms were seen when normal serum or antiserum to a DNA–RNA hybrid were used in the assays. Moreover, the anti-dsRNA serum used (provided by R. M. Lister) does not react

0028-0836/82/030259—02$01.00

with DNA or single-stranded RNA[14]. Assays of PSTV preparations purified by polyacrylamide electrophoresis[15] were negative, confirming an earlier report that PSTV does not react with antiserum to dsRNA[16].

The length of denatured PSTV has been shown to be 100 nm (ref. 17) and 110 nm (ref. 18). Using a linear density of 2.4×10^6 daltons μm^{-1} for dsRNA and a mass of 250,000 daltons, the calculated length of a dsRNA intermediate of PSTV is 104 nm. These lengths compare well with the modal circumference of 110 nm found for the circular dsRNA from PSTV-infected tissue (Fig. 1*a*). The random distribution of sizes of the circular molecules of dsRNA found in healthy tissue suggests they may be closures of linear dsRNA (Fig. 1*b*).

With spherical viruses, the detection limits of serologically specific electron microscopy have been shown to be 10^9 virions per ml (ref. 19). As the number of circular forms attaching to grids decreases rapidly on dilution, the concentration of circular dsRNA in viroid-infected tissue must be of similar magnitude, which is consistent with the low rate of viroid accumulation[15] in the plant.

Received 27 July; accepted 20 November 1981.

1. Sanger, H. L., Klotz, G., Riesner, D., Gross, H. J. & Kleinschmidt, A. K. *Proc. natn. Acad. Sci. U.S.A.* **73,** 3852–3856 (1976).
2. Gross, H. J., Domdey, H., Lossow, C., Jank, P., Raba, M. & Alberty, H. *Nature* **273,** 203–208 (1978).
3. Diener, T. O. & Hadidi, A. *Comprehensive Virol.* **11,** 285–335 (1977).
4. Zaitlin, M., Niblett, C. L., Dickson, E. & Goldberg, R. B. *Virology* **104,** 1–9 (1980).
5. Branch, A. D. & Dickson, E. *Virology* **104,** 10–26 (1980).
6. Grill, L. K. & Semancik, J. S. *Proc. natn. Acad. Sci. U.S.A.* **75,** 896–900 (1978).
7. Grill, L. K. & Semancik, J. S. *Nature* **283,** 399–400 (1980).
8. Grill, L. K., Negruk, V. I. & Semancik, J. S. *Virology* **107,** 24–33 (1980).
9. Hadidi, A. *Phytopathology* **71,** 222 (1981).
10. Rohde, W. & Sanger, H. L. *Biosci. Rep.* **1,** 327–336 (1981).
11. Rachwitz, H. R., Rohde, W. & Sanger, H. L. *Nature* **291,** 297–301 (1981).
12. Derrick, K. S. & Brlansky, R. H. *Phytopathology* **66,** 815–820 (1976).
13. Derrick, K. S. *Science* **199,** 538–539 (1978).
14. Moffit, E. M. & Lister, R. M. *Phytopathology* **65,** 851–859 (1975).
15. Morris, T. J. & Smith, E. M. *Phytopathology* **67,** 145–150 (1977).
16. Stollar, B. D. & Diener, T. O. *Virology* **46,** 168–170 (1971).
17. Riesner, D. *et al. J. molec. Biol.* **133,** 85–115 (1979).
18. McClements, W. L. & Kaesberg, P. *Virology* **76,** 477–484 (1977).
19. Beier, H. & Shepherd, R. J. *Phytopathology* **68,** 533–539 (1978).

A + T-rich linkers define functional domains in eukaryotic DNA

J. Moreau, L. Marcaud, F. Maschat, J. Kejzlarova-Lepesant, J-A. Lepesant & K. Scherrer*

Institut de Recherche en Biologie Moleculaire (CNRS), Université Paris VII, Tour, 432 place Jussieu, 75251 Paris Cédex 05, France

Although an increasing number of detailed DNA sequence studies are being carried out, little is known about the long-range organization of the eukaryotic genome in relation to chromosomal organization and to functional units of transcription, replication, meiotic crossing-over and nuclear architecture. Based on electron microscope (EM) observations of partially denatured DNA of duck, mouse and rat, we have recently reported a systematic punctuation of DNA by early melting zones ('A + T-rich linkers')[1] ~800 base pairs (bp) long which are either clustered or at intervals of 10–40 kbp. In an attempt to correlate this feature with the organization of specific genes, we examined cloned genomic DNA from chick and *Drosophila*, including the globin gene family, and an isolated high-molecular-weight mRNA. We show here that the chick α-globin gene cluster is framed by a cluster of A + T-rich linkers at the 5′ end and by an isolated linker at the 3′ end which maps close to the sites of transcription termination and DNase hypersensitivity. The resulting frame of ~15 kbp correlates well with the maximum size of globin gene transcripts found at the pre-mRNA level. The β-globin gene cluster is also framed, 5′ by a single A + T-rich linker and 3′ a cluster of four linkers. In *Drosophila*, the single mRNA sequence of ~3.3 kbp for the ecdysone-inducible P1 protein is similarly delimited by A + T-rich linkers. A + T-rich linkers thus seem to define domains of the eukaryotic genome which may correlate with putative functional units. The specific organization observed in total DNA of duck, mouse, rat, man, chicken and *Drosophila* is confirmed in gene-specific cloned genomic DNA.

Cloned genomic recombinants including the α- and β-globin gene clusters were taken from the chicken 'library' of Dodgson *et al.*[2]. The globin genomic maps shown in Fig. 1 are based on recent publications[3-5] and unpublished data (J. Dodgson, personal communication). Justification of the experimental approach and general methods of partial DNA denaturation and spreading for EM have been reported previously[1]. Briefly, individual recombinant DNA cloned in λ Charon 4A, was denatured at a concentration of 0.5–0.8 $\mu g\, ml^{-1}$ by 85% formamide (24.5 °C), spread by the Kleinschmitt technique, taken up on collodium-coated grids, shadow-casted with palladium/platinum and observed in a Siemens Elmiscope 101 at a primary magnification of ×10,000. The length of the DNA molecules and the positions of melted regions were measured and statistically analysed by a digitizer branched on a HP 9830 calculator. Figure 2 shows two examples of the original micrographs of such partially denatured DNA molecules.

To determine the 5′–3′ orientation with respect to the mRNA sequences and to begin compilation of denatured regions, we used the characteristic denatured regions in the short arm of the λ vector DNA serving also as a very precise 'internal thermometer'. Out of hundreds of molecules observed, a random sample of 20–30 full-length recombinants was measured for any one clone. The data were then realigned with one of the denaturations observed in the chicken DNA inserts so that the position of the melted regions could be plotted precisely. The accuracy of the measurements was of the order of 0.03 nm or ~100 bp. For both α- and β-globin, three recombinants covering all the known chicken globin genes were analysed. In the case of α-globin, the recombinant DNA available comprised the whole gene domain, whereas in the case of β-globin an interruption of 2.1–4.5 kbp (see below) in between $^{\mathrm{H}}\beta$ and $^{\mathrm{A}}\beta$ escaped cloning (J. Dodgson, personal communication).

Figure 1 shows the results of this analysis. The α-gene-type clones, $\lambda C\alpha G2$, $\alpha G5$ and $\alpha G6$, all contain A + T-rich linkers. Starting from the 5′ end (to the left) of the messenger strand, the map starts with a cluster of three denatured regions of lengths 2,040 (possibly originating from two closely placed linkers), 1,050 and 1,350 bp, separated by 520 and 350 bp respectively of undenatured DNA. The next A + T-rich linker of 1,140 bp is found after the 15.0 kbp of DNA spanning all of the α-globin genes; another A + T-rich linker of 650 bp is located after a further 7.5 kbp of DNA, which includes an unknown region. The cluster of A + T-rich linkers occurs 6.5 kbp upstream from the embryonic π gene; this area includes π', a further unmapped α-type gene (J. Dodgson, personal communication). In the 3′ direction, the single linker bordering the α-globin gene domain is 4.0 kbp downstream from the most 3′ $^{\mathrm{A}}\alpha$ gene. Immediately 5′ to the π gene we detected another mildly denaturing sequence of ~890 bp; however, in view of its low frequency of denaturation it seems to be qualitatively different from the 800±200 bp A + T-rich linkers defined previously[1].

The gap in the β-gene domain for which no cloned recombinants were available was determined to be 2.1 kbp in the White Leghorn chicken[3] and 4.5 kbp in the Brown Leghorn chicken (L.M., unpublished); as we found a value of 2.1 kbp for this region in a further stock of chicken, this area seems to be one of genomic variability. Nevertheless, it is unlikely to contain another β-type globin gene.

Partial denaturation of the DNA of three β-globin recombinants gave the following result. Starting at the 5′ end, a single

---

* To whom correspondence should be addressed.

0028-0836/82/030260—03$01.00

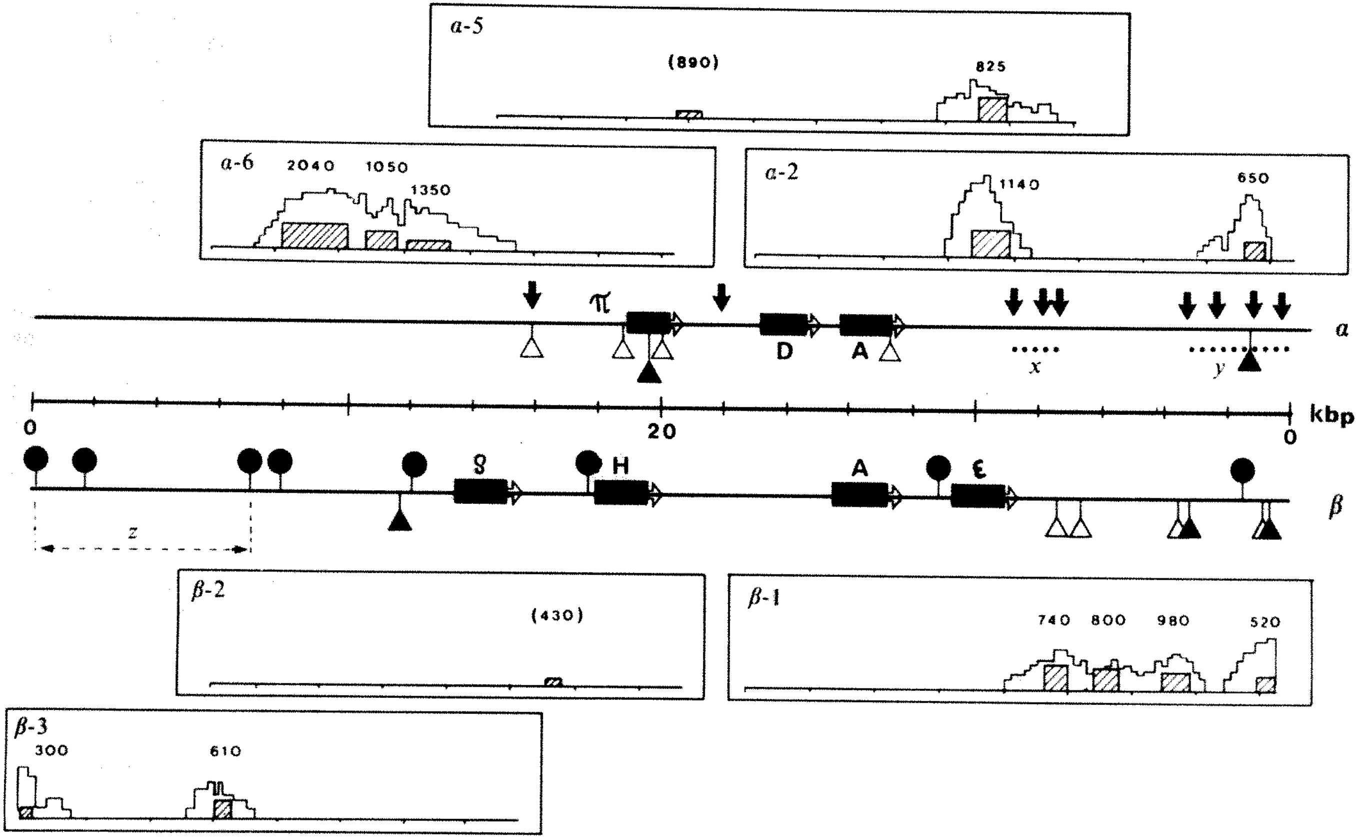

Fig. 1 Globin gene map showing the genomic positions of A + T-rich linkers determined by partial denaturation of cloned recombinant DNA. Insets α-2, α-5, α-6, β-1, β-2 and β-3 show the histograms of frequency of denaturated areas observed plotted against their map position in the cloned DNA, oriented in relation to the long/short arms of the phage DNA. These measurements were realigned against one of the internal denatured zones; means of frequency of occurrence and size of the A + T-rich zones were calculated and represented in the figure by hatched areas and the bp numbers for any one linker. The genomic maps are taken from refs 4 and 5; from the latter came the positions in the globin domain of an area highly resistant to DNase I (*z*) and of hypersensitive areas in the α-globin gene domain (*x*, *y*). Solid arrows mark the positions of methylated *Msp* sites; other restriction enzyme sites used to align the various cloned recombinant DNA: △, *Hin*dIII; ▲, *Eco*RI; ●, *Bam*HI). Recombinants from the chick genomic library were λCαG2, -G5, -G6 and λCβG1, -G2, -G3 (refs 3, 4).

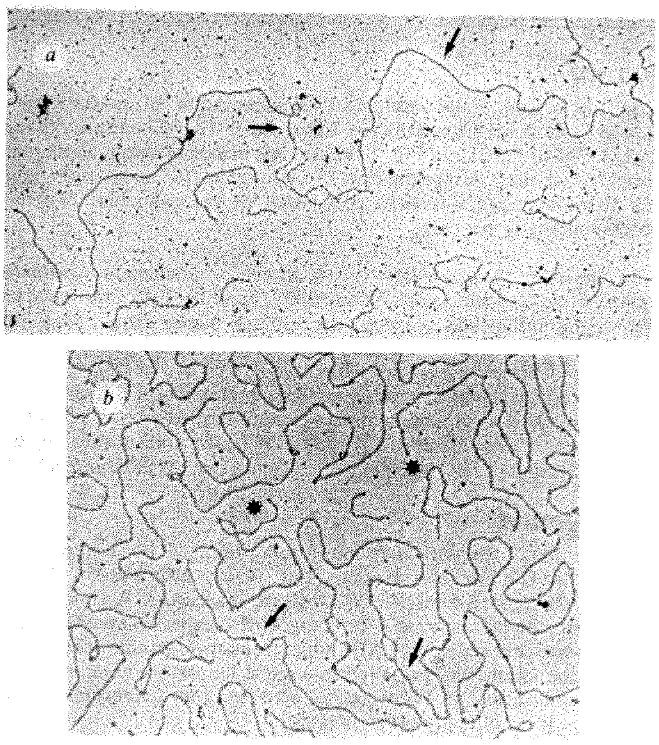

Fig. 2 Partial denaturation of chicken DNA including globin genes cloned in phage λ Charon 4A. DNA was denatured and spread for electron microscopy as described previously[1] and in the text. Arrows indicate the approximate limits of the chicken DNA inserts. *a*, One molecule of clone α-6; the loops include 2,840, 1,290, 1,185 bp; *b*, one molecule of clone (α-2); the loops measure 1,590 and 1,210 bp. The small molecules correspond to pBR322 used as length standard.

610-bp linker was observed, which may be part of a cluster placed further upstream, outside the cloned area. With the possible exception of a very rarely denaturing site 430 bp long, there is no other A+T-rich linker in the 14.0-kbp domain covering the embryonic ρ and $^{H}\beta$ genes, which is limited to 5′ by the interruption. Beyond this gap there is another 9.0-kbp undenatured stretch covering the adult $^{A}\beta$ and embryonic ε-globin genes before a cluster of four consecutive linkers of 740, 800, 980 and 520 bp, separated by 0.94, 1.6 and 2.3 kbp respectively.

In a second approach we analysed a *Drosophila* gene which does not belong to a gene family comparable with that of the globins and which codes for the fairly high-molecular-weight (110,000) ecdysone-inducible P1 protein of the fat body. Its ~3.5-kbp mRNA has been mapped on cloned genomic DNA to the 70 D1-3 region (H. Brock, personal communication) of the 3L polytene chromosome; the gene contains no intervening sequence[6–8].

Partial melting of genomic DNA cloned in phage λ Charon 4, carried out as in the experiments reported above, shows that this area is particularly rich in clusters of A+T-rich linkers (not shown); total embryonic *Drosophila* DNA shows melting patterns generally analogous to those of birds and mammals (ref. 1 and J.M., in preparation). The P1 gene maps in the middle of the phage λ Charon 4 recombinant λDm 117; the central fragment delimited by *Hin*dIII restriction sites was recloned in pBR322 (ref. 8). Figure 3 shows that the P1 mRNA sequence of clone pDmP 1 originates within an A+T-rich linker and runs into a relatively G+C-rich area delimited at a distance of ~5.5 kbp by another A+T-rich linker. The pattern shown in Fig. 3 is typical of several other *Drosophila* genes on the same or other chromosomes—LSP-1β, LSP-1γ and the P6 genes[7]; in each case the mRNA sequence is in a non-denaturing area framed by A+T-rich linkers (J.M. *et al.*, in preparation).

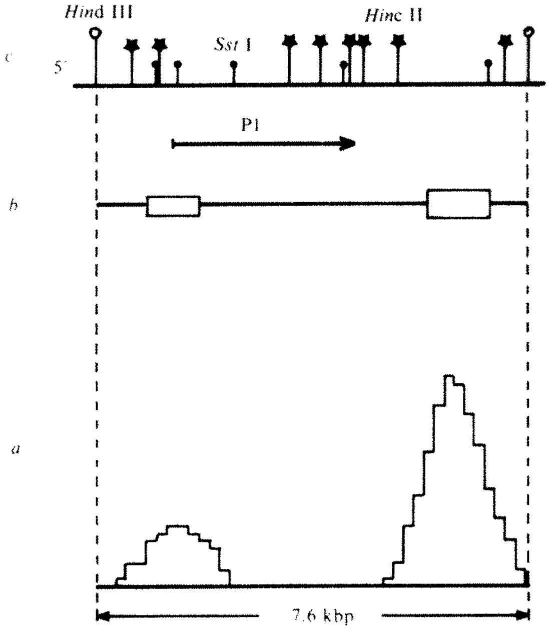

Fig. 3 Partial denaturation of cloned *Drosophila* DNA including the gene for the P1 protein. The DNA of the pBR322 recombinant pDm P1 (ref. 8) was linearized with the *Eco*RI restriction enzyme, denatured as explained in the text in 80% formamide at 24.5 °C, spread for electron microscopy and visualized as explained elsewhere[1]. *a*, Histogram of relative frequency of denaturation of any given segment of DNA, in relation to the ends of the molecule including pBR322 DNA. For higher precision the same measurements were realigned with respect to one of the denaturations in the *Drosophila* DNA and recorded as boxes with a length proportional to the average size of the denatured segment and a width porportional to the frequency of denaturation (*b*). *c*, A partial restriction map taken from refs 7, 8 of the cloned fragment used to position the P1 mRNA sequence.

Three main conclusions may be drawn from this analysis. (1) The fundamental features of A+T-rich linkers as observed in total DNA of chicken, duck, rat, mouse, man and *Drosophila* are found in specific cloned DNA fragments as well. In particular, the average size of the A+T-rich zones, and of the domains separating them, falls within the limits defined previously[1]. Furthermore, the characteristic homogeneous size of isolated linkers on the one hand and clusters of linkers, including A+T-rich linkers of more variable size on the other was also the case in the cloned DNA. (2) The most striking observation may be the clear-cut framing of both the α- and β-globin gene domains by the A+T-rich linkers. (3) The data on *Drosophila* show that A+T-rich linkers may frame individual genes and thus define putative units of gene function. Furthermore, considering recent sequence data of actin[9] and histone[10] genes, it may be the general case that genes or gene domains are placed between A+T-rich zones of the type described here.

Two correlations are of interest. First, the ~15 kbp of the chicken α-globin gene domain, as defined by the A+T-rich linkers, correspond to the maximal size of the transcriptional units found at pre-mRNA level for both the α- and β-globin genes in duck[11]. Recent data[5,12] have confirmed that in mouse and chick, pre-mRNA exists beyond the CAP-poly(A) boundaries. At the 3′ end of the chick $^{A}\alpha$-globin mRNA sequence a further 3 kbp of genomic DNA are co-transcribed[5]; this is about the distance separating, for example, the $^{A}\alpha$ gene from the next A+T-rich linker in the 3′ direction (compare with Fig. 1). Placing the largest (15 kbp) α-globin pre-mRNA reported[11] upstream from this termination point shows that the promoters for these maximal-size transcripts must be in or close to the 5′-framing A+T-rich linker. Second, the mapping of DNase hypersensitive sites, methylation sites and areas of transcriptional activity[5] also reveals correlations with the A+T-rich linker map given in Fig. 1 (see dotted lines and bold arrows). In the α-gene domain, the 3′-hypersensitive sites almost coincide with the corresponding A+T-rich linkers, and most of the methylated *Msp*I sites map within the same A+T-rich linker areas. A region of high DNase resistance correlates with the area immediately to the left of the A+T-rich linker which borders the 5′ end of the β-globin gene domain (dashed line in Fig. 1).

The present data confirm that the A+T-rich linkers are general elements of long-range DNA organization. Furthermore, the clearcut definition of the α- and β-globin gene domains and of the *Drosophila* P1 gene by these linkers suggests that they may have a role as organizational features defining domains of gene function. It is evident that DNA serves multiple functions, not all of which are directly involved in protein synthesis or transcription. The A+T-rich linkers, occurring outside the coding and transcribed areas, might also be involved in DNA functional organization at the chromosome/genome level.

We thank Drs J. Dodgson and D. Engel for their library of cloned chicken DNA and the globin gene-containing clones, Helene Grimal for technical assistance, and members of our team and of the staff of the EM laboratory at the IRBM (director Dr L. Benedetti). We particularly thank Mrs Chantal Cuisinier and R. Schwartzmann for help in preparation of this manuscript. This work was supported by the French CNRS, Délégation Générale à la Recherche Scientifique et Technique, Fondation pour la Recherche Médicale Française and Institut National de la Santé et de la Recherche Médicale.

Received 31 July; accepted 1 December 1981.

1. Moreau, J., Matyash-Smirniaguina, L. & Scherrer, K. *Proc. natn. Acad. Sci. U.S.A.* **78,** 1341–1345 (1981).
2. Dodgson, J. B., Strommer, J. & Engel, J. D. *Cell* **17,** 879–887 (1979).
3. Dolan, M., Sugamman, B. J., Dodgson, J. B. & Engel, J. D. *Cell* **24,** 667–677 (1981).
4. Engel, J. D. & Dodgson, J. B. *Proc. natn. Acad. Sci. U.S.A.* **77,** 2596–2600 (1980).
5. Weintraub, M., Larsen, A. & Groudine, M. *Cell* **24,** 333–344 (1981).
6. Lepesant, J.-A., Garen, A., Kejzlarova-Lepesant, J., Maschat, F. & Rat, L. *ICN-UCLA Symp.* Vol. 14 (eds Maniatis, T. & Axel, R.) (Academic, New York, 1979).
7. Lepesant, J.-A. *et al. Molec. appl. Genet.* (in the press).
8. Maschat, F. thesis, Univ. Paris VII (1981).
9. Firtel, R. A., Timm, R., Kimmel, A. R. & McKeow, M. *Proc. natn. Acad. Sci. U.S.A.* **76,** 6206–6210 (1979).
10. Grosschedl, R. & Birnstiel, M. L. *Proc. natn. Acad. Sci. U.S.A.* **77,** 7102–7106 (1981).
11. Reynaud, C.-A., Imaizumi-Scherrer, M.-T. & Scherrer, K. *J. molec. Biol.* **140,** 481–504 (1980).
12. Hofer, E. & Darnell, J. E. Jr *Cell* **23,** 585–593 (1981).

Errata

In the article 'Palaeontological documentation of speciation in Cenozoic molluscs from Turkana Basin' by P. G. Williamson, *Nature* **293,** 437–443 (1981), in Fig. 3 the top left principal components plot should be labelled '*A*', the top right '*B*', bottom left '*C*' and bottom right '*D*'. In the legend references to parts *a–d* of the figure should refer to the corresponding upper case.

In the letter 'Autoregulation of androgen production in a primary culture of rat testicular cells', *Nature* **293,** 737–738 (1981), the name of the second author was misspelt; the authors' names should read 'Eli Y. Adashi & Aaron J. W. Hsueh'.

In the article 'Glucocorticoids regulate expression of dihydrofolate reductase cDNA in mouse mammary tumour virus chimaeric plasmids' by F. Lee *et al., Nature* **294,** 228–232 (1981), the first sub-heading on page 232 should read 'Mapping the 5′ end(s) of MMTV-*dhfr* RNA'.

Corrigenda

In the letter 'Immune (γ) interferon produced by a human T-lymphoblast cell line' by I. Nathan *et al., Nature* **292,** 842–84 (1981), some of the reported interferon titres are inaccurate. A commercial interferon standard was used in many of the experiments. This preparation was checked against NIH human leukocyte standard; however, some of the commercial preparations used as laboratory standards were subsequently found to be defective, leading to an overestimation of interferon titres of approximately tenfold.

In the letter 'Expression of a human gene for interferon in yeast' by R. A. Hitzman *et al., Nature* **293,** 717–722 (1981), refs 10 and 18 should read:

10. Faye, G., Leung, D. W., Tatchell, K., Hall, B. D. & Smith, M. *Proc. natn. Acad. Sci. U.S.A.* **78,** 2258–2262 (1981).
18. Staehelin, T., Hobbs, D. S., Kung, H., Lai, C. & Pestka, S. *J. biol. Chem.* **256,** 9750–9754 (1981).

MATTERS ARISING

Guidance system for pheromone orientation in moths

THE explanation proposed by Kennedy and co-workers[1] of a new guidance system for pheromone orientation contains several conclusions inconsistent with previous publications: (1) the conclusion that "persistent upwind flight requires decreases as well as increases in the pheromone stimulus" conflicts with the behaviour reported for another moth *Anagasta kühniella*[2], and the persistent upwind orientation of flying *Drosophila*[3], walking silk moths[4], cockroaches[5] and grasshoppers[6] to uniform and constant odours. Possibly the sustained upwind flight could not be elicited in *Adoxophyes orana* because the concentration in the cloud was too low: "at least 30 times lower than the average concentration in the plume".

(2) The hypothesis that zig-zagging and casting flight is a programmed function of pheromone concentration and that "the amplitude of these cross-wind movements change(s) inversely with the strength of the pheromone stimulus" cannot be supported critically by only the anecdotal comparison of *A. orana* flight without pheromone against that in a single pheromone concentration. Alternatively these observations might only be associated with the presence or absence of pheromone.

(3) That "zig-zagging and casting flight is not a response to loss of pheromone" is not adequately supported by noting "frequent track reversals inside the pheromone corridor". An alternative conclusion is that not all turns are elicited by the same mechanism. Reversal turns not related to a plume boundary have previously been reported in other insects[4,5], but this does not imply that turns made specifically at the boundary or after a change in the pheromone concentration are not elicited as a stimulus response. For example, cockroaches turn both at the plume boundary and at irregular points within the plume[7].

An integrated orientation system rather than the models discussed by Kennedy and co-workers[1] would be more consistent with present information. In an integrated system, several factors contribute to the control of the rate and patterns of turning, including compensatory turns made to correct deviations from the preferred wind angle, reversal turns made at the plume boundaries, stochastic turns, and turns initiated internally at a regulated frequency if a turn has not yet been elicited by one of the previous factors. In addition, the concentration of pheromone must also regulate the flight speed and the preferred wind angle.

THOMAS R. TOBIN
WILLIAM J. BELL
Department of Entomology,
University of Kansas,
Lawrence, Kansas 66045, USA

1. Kennedy, J. S., Ludlow, A. R. & Sanders, C. J. *Nature* **288,** 475–477 (1980).
2. Traynier, R. M. M. *Can. Ent.* **100,** 5–10 (1968).
3. Kellog, F. E., Frizel, D. E. & Wright, R. H. *Can. Ent.* **94,** 884–888 (1962).
4. Kramer, E. in *Olfaction and Taste* Vol. 5 (eds Denton, D. & Coghlan, J. D.) 329–335 (Academic, New York, 1975).
5. Bell, W. J. & Kramer, E. *J. chem. Ecol.* **6,** 287–295 (1980).
6. Kennedy, J. S. & Moorhouse, J. E. *Ent. exp. appl.* **12,** 487–503 (1969).
7. Tobin, T. R. *XVI int. Cong. Ent.* Kyoto, Japan (1980); *Science* (in the press).

KENNEDY *ET AL.* REPLY—The new guidance system we proposed is admittedly inconsistent with earlier publications, not least our own, and was therefore not lightly arrived at. Tobin and Bell's numbered points are discussed briefly below but reference should also be made to the full account of this work which appears elsewhere[1].

(1) In the long run some inconsistencies will surely turn out to reflect real differences between cases. However, for the moment note that the only two published examples[2,3] of persistent upwind flying—as distinct from walking—in uniform odour are anecdotal. Our reason for mentioning the non-persistent upwind flights in the very low concentration of our tunnel-filling pheromone cloud, was existing evidence from other moths[4,5] that upwind flight is retarded by high rather than low pheromone plume concentrations. However, we also mentioned non-persistence in our side 'corridor' pheromone cloud, and the concentration in that was higher than the average in the broken pheromone plume where upwind flight was persistent[1]. Thus we concluded that the non-persistence recorded was due to the continuity of stimulation in the unbroken pheromone clouds, not the concentration.

(2) The quoted remark did refer only to the presence or absence of pheromone, but it rested on the non-anecdotal[1] finding that onset of the pheromone stimulus reduced the amplitude of cross-wind movements while cessation of the stimulus increased it; and, in another flying moth, changing the concentration of pheromone present has likewise been shown to produce an opposite change in amplitude[4].

(3) We expected, but did not find, some evidence of pheromone loss inducing cross-wind reversal of the flight track by *Adoxophyes orana*. Of course, we cannot say it never happens, but we can say that the probability of such a reversal increases significantly on entering pheromone[1]; and in another moth cross-wind movements had already been shown to lengthen on leaving pheromone[5].

Like Tobin and Bell, we regard this guidance system as a highly integrated one[5,6] but go further in regarding the stochastic reversal turns, not as a separate class of turn, but as turns initiated internally at a frequency that is regulated stochastically by the pheromone inputs.

J. S. KENNEDY
A. R. LUDLOW
C. J. SANDERS
ARC Insect Physiology Group,
Imperial College at Silwood Park,
Ashurst Lodge, Ascot,
Berkshire SL5 7DE, UK

1. Kennedy, J. S., Ludlow, A. R. & Sanders, C. J. *Physiol. Ent.* (in the press).
2. Kellogg, F. E., Frizel, D. E. & Wright, R. H. *Can. Ent.* **94,** 884–888 (1962).
3. Traynier, R. M. M. *Can. Ent.* **100,** 5–10 (1968).
4. Cardé, R. T. & Hagaman, T. E. *Envir. Ent.* **8,** 475–484 (1979).
5. Marsh, D., Kennedy, J. S. & Ludlow, A. R. *Physiol. Ent.* **3,** 221–240 (1978); **6,** 225 (1981).
6. Kennedy, J. S. *Physiol. Ent.* **3,** 91–98 (1978).

Tilt of the central gas disk of the Galaxy

BLITZ *ET AL.*[1] have suggested that the tilt of the central galactic gas disk might be explained by a bending wave instability due to a gravitational interaction between the thin gas disk and the central stellar bulge. However, the instability theory due to Bertin and Mark[2] on which this suggestion is based, is inapplicable in the case of the central gas disk. For the theory to apply, the vertical gravitational forces on the gas disk must be due largely to its own self gravity with only a small contribution from the bulge. The frequency of the bending waves of a thin self-gravitating disk is then given by[2,3] $(2\pi G\Sigma k)^{1/2}$ where Σ is the surface mass density and k is the radial wavenumber of the bending wave, yielding the group velocity used by Blitz *et al.*[1] to predict the scaling law for the height of the bend (h) as a function of radial distance from the galactic centre (r).

However, the gravitational force experienced by the gas disk between $r =$ 300 pc and 2 kpc is dominated by the stellar potential. The central stellar bulge is in fact significantly flattened[4] (major and minor semi-axes are 2.5 and 1.3 kpc), while the stellar disk component (thickness ~500 kpc) is not completely negligible in the central region[4]. The magnitude of the vertical gravitational acceleration at height h due to the stellar potential is therefore approximately that of an oblate spheroid with mass density ρ_* and eccentricity close to unity[5], that is, $4\pi G\rho_* h$. Whilst the magnitude of the vertical acceleration due to the self gravity of the bent disk can be estimated[2] to be $2\pi Gk\Sigma h$. Using $\rho_* = 6M_\odot \text{pc}^{-3}$ (ref. 6) and $\Sigma = 6M_\odot \text{pc}^{-2}$ (ref. 7) at $r = 1$ kcp, the ratio of the stellar field acceleration to that of the gas self gravity is λ/π, where λ is the wavelength of the bending wave in parsecs. Because $\lambda \sim r$ for the tilt, the

0028-0836/82/030263/01$01.00

stellar force dominates by a factor $\sim 10^2$–10^3, and hence the self gravity of the disk is negligible. Therefore it is invalid to use the Bertin and Mark theory.

A more appropriate approximation would be to consider the bending modes of a gas disk due to motion in the stellar potential alone. The modes obtained from such an analysis[8] which are most closely analogous to the bending wave of Bertin and Mark have a frequency of $\sim(4\pi G\rho_*)^{1/2}$ yielding a very small group velocity in comparison with the phase velocity.

A. H. NELSON
Department of Applied Mathematics and Astronomy,
University College,
Cardiff CF1 1XL, UK

1. Blitz, L., Mark, J.W.-K. & Sinha, R. P. *Nature* **290**, 120–121 (1980).
2. Bertin, G. & Mark, J.W.-K. *Astr. Astrophys.* **88**, 289–297 (1980).
3. Hunter, C. & Toomre, A. *Astrophys. J.* **155**, 747–776 (1969).
4. Maihara, T., Naoki, O., Sugiyama, T. & Okuda, H. *Publ. astr. Soc. Jap.* **30**, 1–19 (1978).
5. Mihalas, D. & Routly, P. M. *Galactic Astronomy* 196 (Freeman, San Francisco, 1968).
6. Oort, J. H. *A. Rev. Astr. Astrophys.* **15**, 295–362 (1977).
7. Gordon, M. A. & Burton, W. B. *Astrophys. J.* **208**, 346–353 (1976).
8. Nelson, A. H. *Mon. Not. R. astr. Soc.* **177**, 265–274 (1976).

BLITZ AND MARK REPLY—Nelson's suggestion that the Bertin and Mark[1] bending wave theory is inapplicable to the dynamics of the gaseous disk at the galactic centre seems to be based on an incomplete analysis of the singular perturbation problem involved when a disk of small (but not altogether negligible) mass is immersed in a larger spheroidal component.

For disk mass much smaller than spheroidal masses, it is not appropriate to omit the disk mass terms. The 'kinematic waves' resulting from this omission (see equation (D7) of (ref. 1) dominated by v_z^2 on the right-hand side) dissipates on the rather short differential rotation shearing time scale $|d\Omega/d\ln r|^{-1}$. On the other hand, including the dynamical effects of the small disk mass results in self-gravitating waves with the much longer group propagation dissipation time, $\sim 2Rdk/d\omega$, which has the dispersion relation (D7) of (ref. 1). The neglect of similar terms in Nelson's[2] formalism for modes symmetric about the galactic plane would fail to produce the familiar Jeans instability (the bending waves are the antisymmetric disturbances about the galactic plane). By contrast, Bertin and Mark have included terms of the 'sound wave' type included by Nelson, but within the context of galaxy warps, stellar dispersive speeds squared are much larger than the corresponding terms in the gas.

In any case, Bertin and Mark have included terms which reflect more completely the dynamics of the disk. The conclusion with or without these additional terms is that the scaling law ($r\Sigma^2h \sim$ constant) used by us is consistent with the observations of the inner disk of the Galaxy as well as the warps of the outer region of several galaxies as shown by Lake and Mark[3].

JAMES W.-K. MARK
LEO BLITZ
Astronomy Department,
University of California,
Berkeley, California 94720, USA

1. Bertin, G. & Mark, J.W.-K. *Astr. Astrophys.* **88**, 289–297 (1980).
2. Nelson, A. H. *Mon. Not. R. astr. Soc.* **177**, 265–274 (1976).
3. Lake, G. & Mark, J.W.-K. *Nature* **287**, 705–706 (1980).

Lipoprotein assembly in *Xenopus* yolk-platelet crystals

FROM his determination of the space group of yolk-platelet crystals from several new species, Lange[1] has questioned earlier data of ours for similar lipoprotein crystals from *Xenopus*[2]. The new data are based entirely on electron micrographs from fixed sectioned specimens, a procedure we intentionally avoided during our studies. This evidence as well as a few other statements made in the paper need to be scrutinized.

The first data shown (Fig. 1 of ref. 1) are three 'tracings' of electron diffraction patterns from yolk crystals of the species *Triturus*. It is unfortunate that Lange did not publish the patterns themselves because frequently the high noise level from such poorly diffracting specimens makes interpretation of the patterns difficult. Furthermore, a more analytical description including the averages and standard deviations of the observed lattice spacings would have been useful. It is, after all, the unit cell spacings which we and now Lange, have used to identify specific projections[1,3].

In further criticism of the data presentation, the space group determination using Figs 2 and 3 of ref. 1 is confusing because no optical diffraction patterns are shown and the micrographs were obtained from two different species. Lange's Fig. 3, for example, bears a strong resemblance to the *hol* zone from lipoprotein crystals of *Xenopus*[3]. Lange describes this as the *hko* zone, suggesting that simple relabelling of the *b* and *c* axes would make the results consistent with the earlier work[3]. Indeed, we agree that the projection shown in Fig. 3 should have *pgg* symmetry. As the *b* and *c* axes in the unit cell for *Xenopus* are roughly the same length, they may equally well be similar in other species and could easily be interchanged. Unit cell dimensions can be precisely obtained for wet and dry crystals by using X-ray powder methods[3].

In image reconstruction studies, the best way to determine the symmetry of a given projection is to examine the phases of strong symmetry-related reflections[4]. In the studies of the lipoprotein complex from *Xenopus*, phases of each centric projection were calculated and were then shifted to minimize the difference between that calculated and the nearest real value[2,5]. Two pairs of strong reflections on the 001 projection ($1, 3, 0$ and $1, \bar{3}, 0$; $2, 3, 0$ and $2, \bar{3}, 0$) had phase relationships consistent with only *pmg* symmetry[5]. Six pairs of reflections had phase relationships consistent with *pgg* symmetry for the view we assigned to the *hol* projection. Many of the projections used in the image reconstruction were studied earlier by optical filtering methods. Even on such filtered images, both the number of molecules and the symmetry can be difficult to ascertain[6].

Furthermore we take issue with Lange's discussion of the reliability of positive versus negative staining[1] in special reference to our image reconstruction results. Certainly the appearance of lattice micrographs will be different when one is positively stained and the other negatively stained. However, the immobilization of stain (positive staining effects) adjacent to solvent channels filled with stain (negative staining), is unlikely to produce major artefactual results. Thus, we emphasize the importance of negative stain as well as the lack of chemical fixation in the earlier study[2].

Finally, we note that although the work on *Xenopus* was severely limited by the chance finding of different crystal fragments, it still contained data from 10 different views selected from several hundred electron micrographs[2,3].

LEONARD J. BANASZAK
Department of Biological Chemistry,
Washington University,
School of Medicine,
St Louis, Missouri 63110, USA

DOUGLAS H. OHLENDORF
Institute of Molecular Biology,
University of Oregon,
Eugen, Oregon 97403, USA

1 Lange, R. H. *Nature* **289**, 329–330 (1981).
2. Ohlendorf, D. H., Wrenn, R. F. & Banaszak, L. J. *Nature* **272**, 28–32 (1978).
3. Ohlendorf, D. H., Collins, M. L., Puronen, E. D., Banaszak, L. J. & Harrison, S. C. *J. molec. Biol.* **99**, 153–165 (1975).
4. Unwin, P. N. T. *J. molec. Biol.* **98**, 235–242 (1975).
5. Ohlendorf, D. H. thesis, Washington Univ. (1978).
6. Ohlendorf, D. H., Wrenn, R. F., Collins, M. L. & Banaszak, L. J. in *Cellular Function and Molecular Structure* (eds Agris, P. & Sykes, B.) 159–164 (Academic, New York, 1978).

LANGE REPLIES—If the symmetric lipoprotein aggregates in yolk platelets of higher anamniotes are orthorhombic crystals as reported for *Xenopus laevis*[1], their space group is $P2_12_12_1$, as documented by symmetry *pgg* of their axial projections[2] at usual electron microscope resolution in eight different species above the cyclostome level (among them *X. laevis*).

R. H. LANGE
Institute for Anatomy and Cytobiology,
Aulweg 123,
D-6300 Giessen, FRG

1. Ohlendorf, D. H., Wrenn, R. F. & Banaszak, L. J. *Nature* **272**, 28–32 (1978).
2. Lange, R. H. *Nature* **289**, 329–330 (1981).

0028–0836/82/030264—01$01.00

BOOK REVIEWS

Newton's achievements: from rumour to fact

Richard S. Westfall

The Mathematical Papers of Isaac Newton Vol.VIII, 1697–1722. Edited by D.T. Whiteside. Pp.704. ISBN 0-521-20103-9. (Cambridge University Press: 1981.) £85, $195.

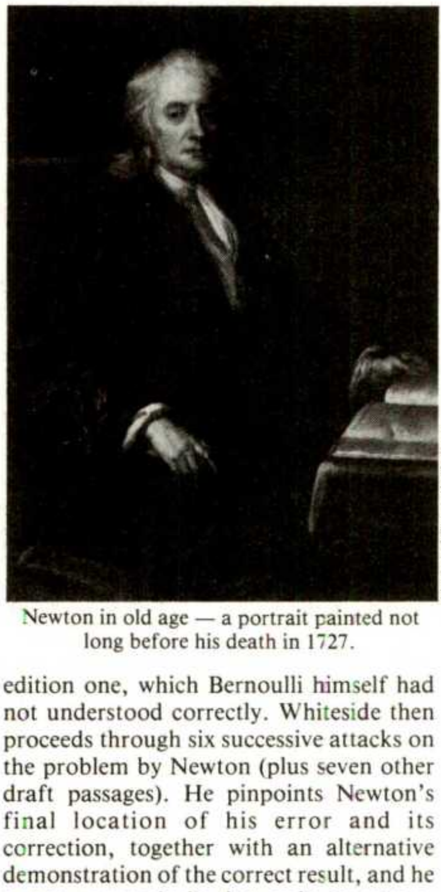

Newton in old age — a portrait painted not long before his death in 1727.

National Portrait Gallery

VOLUME VIII, which, except for a promised volume of indexes, concludes D.T. Whiteside's monumental edition of *The Mathematical Papers of Isaac Newton*, is more of biographical than of mathematical interest. It takes up the final desultory efforts of a man who had recently celebrated his fifty-fourth birthday when the volume commences and had also chosen to fill his life with the administrative minutiae of the Royal Mint instead of the labours of a Lucasian Professor of Mathematics. The volume contains very little original mathematics; almost all of the mathematical activity it displays was provoked by the immediate demands of the battle with Leibniz over priority in the invention of the calculus. Fittingly, it concludes with a draft of an intended preface for the 1722 edition of *Commercium epistolicum*, the volume of letters and papers that Newton himself had secretly compiled and edited and that the Royal Society had published in 1712 as the report of an "impartial" committee appointed to investigate Leibniz's complaint. When he wrote that preface, Newton was approaching 80 years of age. As he himself once said, no old men (excepting Dr Wallis) love mathematics, and it is not surprising that Whiteside finds nothing to include from his remaining five years of life.

Do not mistake the paragraph above as criticism of Vol.VIII. A complete edition of Newton's mathematical papers could not neglect these manuscripts, and to say that they are more of biographical than of mathematical interest is in no way to suggest that they have no interest at all. It is part of the editor's achievement that he infuses into their publication learning equal to that which he devoted to Newton's earlier creative endeavours in mathematics. Thus he conducts us through Newton's responses to the two challenge problems posed by Bernoulli, the initial publication during the first decade of the eighteenth century of various papers written earlier, relevant aspects of the second edition of the *Principia*, and the venomous exchange with Leibniz and his followers on the issue of priority which spread out over a full decade. Whiteside's presentation of the correction of Proposition X, Book II, for the *Principia*'s second edition is a *tour de force* in the full sense of the phrase. From Newton's papers he has assembled the sheets on which Newton confirmed the validity of Bernoulli's objection, and he shows in detail the exact nature of the error in edition one, which Bernoulli himself had not understood correctly. Whiteside then proceeds through six successive attacks on the problem by Newton (plus seven other draft passages). He pinpoints Newton's final location of his error and its correction, together with an alternative demonstration of the correct result, and he argues persuasively that only an unperceived computational error prevented Newton from realizing that he could have amended the proposition within the framework of the original demonstration without the complete redrafting that he finally inserted (to his embarrassment) in edition two.

Whiteside concludes the volume and the edition with 160 pages of documents from Newton's own extended effort to defend his right as true inventor of the calculus. Not long ago, in Vols VI and VII of Newton's *Correspondence*, an extensive documentary history of the priority dispute was published. Naturally the focus was on correspondence, including many hitherto unpublished letters from the Continent. The drafts of Newton's defence of his priority that Whiteside publishes thus supplement, rather than repeat, the *Correspondence*. His lengthy introduction, the valuable account of the priority dispute by the man who knows more about the subject than anyone ever has or is likely to again, likewise complements the masterful *Philosophers at War* by A.R. Hall, the editor of those volumes of the *Correspondence*.

It is fitting now, with the completion of Vol.VIII, to assess the entire edition. Before Whiteside began, we knew comparatively little about Newton's work in mathematics. As Whiteside states in the preface to the present volume, Newton failed to impress the fact, as distinct from the hearsay, of his mathematical achievement on his contemporaries. The period of more than two centuries that followed Newton's death did not amend that state of affairs. Furthermore, Newton did not arrange his papers to facilitate an editor's work. Only Newton scholars who have worked on the manuscripts themselves can appreciate the initial stage of Whiteside's labour, finding his way through what he aptly describes as "the disordered limbo of Newton's private papers".

Volume VIII offers two striking displays of the extent to which he has mastered these difficult manuscripts, though one could find similar examples in every volume. He has identified an unlabelled page of miscellaneous calculations as Newton's demonstration of the essence of Fatio de Duillier's novel solution of Bernoulli's problem on the line of quickest descent (pp.86–91). And from sheets dispersed in both the Portsmouth Papers in the Cambridge University Library and the Macclesfield Papers in Shirburn Castle he has reassembled much of the manuscript for a treatise on fluxional analysis that Newton composed to append to the *Principia*'s second edition. The papers were separated soon after he dropped the idea; thus Whiteside has resurrected an essay which has not existed as a single entity since its composition nearly 270 years ago (pp.258–296).

Impressive as his achievement in arranging the manuscripts is, it pales in comparison to the real work of infusing them with understanding so that the invention of the calculus and a great deal more once again spring to life. In effect Whiteside has done for Newton what Newton failed to do for himself; he has transposed his mathematical achievement from the realm of rumour to the realm of fact. Because of the inherent difficulty of the material, there is no way in which such a work can be made easy for the reader, and

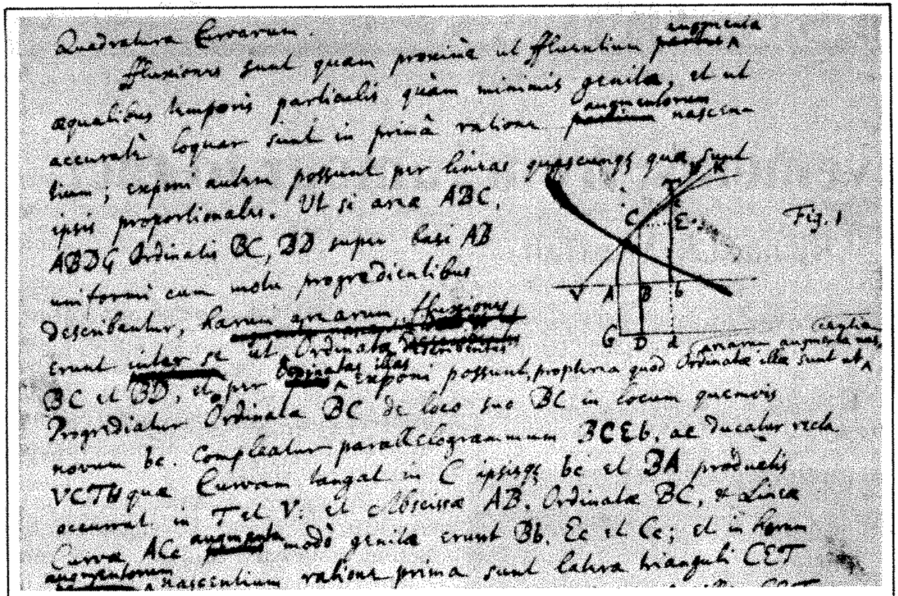

In his own hand — part of the marked-up first page of the printer's copy for the 1704 *De Quadratura Curvarum.*

because Whiteside has brought a high level of mathematical expertise to his task, the edition is doubly difficult. I myself have criticized earlier volumes on this score, arguing that the technical level of the edition effectively closes it to all but a tiny handful of readers. I have come to the conclusion that this criticism was ill-considered, and I take this occasion to apologize to Whiteside. Nonetheless, I still hold the idea that animated it: that it will be a tragedy if the knowledge the edition makes available of Newton's achievement in mathematics, one of the supreme triumphs of the human spirit, does not reach beyond the confined circle of professional historians of mathematics. As it now appears to me, Whiteside has done quite right in treating the papers with a level of sophistication that matches their own. It belongs to others, including Newton scholars such as myself, to translate the achievement into a broader idiom without vulgarizing it. If we fail in the task, we, rather than Whiteside, should be the object of criticism. With this magnificent edition, we cannot complain of an inadequate source.

In a work of such magnitude, there are bound to be — I will not say errors — but a few things that seem to me to be misjudgements. In Vol. VII, annoyed by Newton's apparent revulsion from modern analysis in the 1690s and by his preference for classical geometry, Whiteside has put together a work on *Geometria* in two books, which seems to show that Newton reversed himself once more to embrace analysis anew at the end of his active career in mathematics. By comparing the original manuscripts, I have convinced myself that in this case Whiteside has created an artificial work that never existed, joining a manuscript from the 1680s to a totally separate one from the 1690s in order to portray Newton as he would prefer him to have been. It seems to me, further, that he made a serious mistake in not including the two *epistolae* written in 1676 for Leibniz, even if their texts (though not Whiteside's commentary) are readily available in the *Correspondence*. In an edition notable for its completeness, their absence is the only major omission. Third, I think he erred in substituting the form $\dot{x}$, $\dot{y}$ and $\dot{z}$ for Newton's *m*, *n* and *r* in his translation of *De methodis* of 1671. "Pricked letters", as Newton called the distinctive notation he later devised, assumed some significance in the priority dispute. Readers tend always to use an available translation, and they are apt to be misled by it in the present case. I could list a few more possible defects; but if I have reached this level of triviality with my third, it should be obvious how few and how small I take them to be.

A few years ago I hailed Whiteside's work as the finest edition of scientific papers ever published. I now think that judgement was inaccurate. It erred in being too restrained. I am convinced that *The Mathematical Papers of Isaac Newton* is one of the outstanding scholarly achievements of the twentieth century. Where other editorial projects concerned with less difficult materials have created veritable factories, Whiteside has equipped himself primarily with a writing pad, a pencil and, to restrict himself more fully to his study, a stack of xeroxes. Upon the latter he has exercised an extraordinary level of technical expertise joined to an extraordinary level of devotion. How seldom do the two qualities, raised to such a degree, come together. With them, Whiteside has built what every true scholar dreams of constructing, a monument which will endure through the centuries as part of mankind's precious legacy of learning. ☐

Richard S. Westfall is Professor of History and Philosophy of Science at Indiana University, Bloomington, and author of Never at Rest: A Biography of Isaac Newton *(Cambridge University Press, 1981).*

Iron in the soul

Walter Gratzer

The Nobel Duel. By Nicholas Wade. Pp.321. ISBN 0-385-14981-6. (Anchor Press/Doubleday, New York: 1981.) $15.95.

ONE of the elders of modern biochemistry once recounted how, in the days before peer-review was invented, his benefactor would from time to time visit the laboratory to see what use was being made of his largesse. He inquired on one such occasion whether he could be of any further help and, being told that ten dollars for the purchase of frogs would be welcome, he drew out his wallet, laid two five-dollar notes on the laboratory bench and took his leave.

Well, the past, it has been said, is another country, where they order their affairs differently. The pursuit of the pituitary releasing factors, which is the subject of Nicholas Wade's book, consumed many millions of dollars, the undivided efforts of postdoctoral research fellows, students and technicians in something approaching battalion strength and, according to one estimate, the brains of five million sheep in the isolation of thyrotropin releasing factor alone. The investment was all but wasted: in 1969 the Study Section of the NIH that had supported the two duellists of this story, Guillemin and Schally, through many years of seemingly unproductive toil, came close to deciding that enough was enough. In the words of a member of the committee, the programme was "within an eyelash of being abandoned". The releasing factors had been compared by a respected endocrinologist to the Loch Ness Monster, and Guillemin and Schally had brought ridicule on themselves by an obsessive antagonism that regularly expressed itself in public brawls at conferences.

Sustained by the manic intensity that distinguishes the barons of science from the cannon-fodder in their campaigns, both survived. Each, on the testimony of this account, has an ego like a raging ulcer, as much sensitivity or remorse as a runaway locomotive and awesome reserves of single-mindedness, tenacity and courage. They have in superabundance what Noel Coward defined as the secret of success — the capacity to survive failure. But, in the words of a discarded collaborator of Schally's, such men "are not lovable types". Whether on balance they serve science well, the reader will have to decide for himself.

Nicholas Wade has an engrossing tale to tell and does it in masterly fashion. He does not allow the interplay of personalities that provides much of the drama to obscure the science, which he handles with enviable assurance. No less remarkable is the way in which he has made his cast of characters speak for themselves and has drawn from their mouths reflections of marvellous candour

In the beginning was Geoffrey Harris, the English physiologist, who first postulated that the brain directs the release of pituitary hormones by despatching chemical messages from the hypothalamus to the pituitary Guillemin and the Canadian endocrinologist, Murray Saffran, with whom Schally was then working as a technician, obtained early and independent evidence of the existence of such factors, and there ensued an uneasy collaboration between Schally and Guillemin that soon gave place to an ungovernable rivalry According to *The Devil's Dictionary* calamities are of two kinds, misfortune to ourselves and good fortune to others. Guillemin and Schally dogged each others' footsteps through success and failure, each cast down by the other's victories and elated at his defeats, when, for example, Schally's group took for a releasing factor a proteolytic fragment of myoglobin, which they laboriously isolated and sequenced after processing a quarter of a million brains, Guillemin did not conceal his pleasure

In the laboratory it seems that both Guillemin and Schally (though both had proved their ability as young men) made only minor contributions to the work of their groups, but it was they who kept their groups in being The burden of the science was borne by a superlatively capable corps of young men — Burgus and Vale, Ward and Brazeau for Guillemin, the Japanese, Arimura, Matsuo and Baba, together with Radding, Carter and Nair for Schally Their efforts were ill-rewarded — indeed, on the evidence here, it is small wonder that a postdoctoral liberation movement of a kind appears to be emerging in the United States

Both teams had remarkable achievements One that stands out is a dazzling feat of peptide chemistry by the Japanese visitor, Matsuo, who determined the sequence of LRF by simultaneous analysis of unfractionated, overlapping proteolytic fragments on 50µg of material, and so won the race for Schally

The Nobel Duel is a hugely entertaining read, but it is also much more, for it lays bare the mechanics of Big Science (into which biology is being increasingly assimilated), and exposes its virtues and blemishes to public view Whether the process of discovery feeds on such ferocious competitiveness as is here on display is an interesting and indeed important question Wade opines that other highly regarded workers in the field, such as Saffran and Hearn, had too much of a sense of humour and of the fitness of things to engage in such destructive proceedings, this fastidiousness, just as a classical education has been alleged to do, enabled them perhaps to despise the success that it prevented them from achieving Nonetheless, it is remarkable how close other laboratories with vastly smaller commitments and funds, such as that of Harris, came to a solution of the problem

A piquant footnote to the history of the long haul to the structure and function of the releasing factors is the reaction of an early adversary of Harris's, that most entrenched of all the illuminati of the scientific establishment, Lord (Solly) Zuckerman He, it seems, remains adamant that Harris was wrong from the outset and that the pituitary hormone releasing factors are, after all, no more than a mirage □

Walter Gratzer is in the MRC Cell Biophysics Unit, King's College, University of London

The second volume of Colin Ronan's *The Shorter Science & Civilisation in China* has just been published by Cambridge University Press The book is an abridgement of the material in Vols III and IV/I (for reviews see *Nature* **186**, 36 and **196**, 844) of Joseph Needham's original text, and costs £15

Mysteries of the zeta potential examined

John Gregory

Zeta Potential in Colloid Science. Theory and Application By Robert J Hunter Pp 386 ISBN 0-12-361960-2 (Academic Press 1981) £35, $84

ELECTROKINETIC phenomena, such as streaming potential and electrophoresis, have been known for over a century They arise whenever there is relative motion between a charged interface and a liquid and are usually interpreted in terms of the zeta potential, which is conventionally defined as the electric potential at the plane of shear There has always been an air of mystery surrounding the concept of zeta potential, partly because of theoretical problems concerning the structure of the electrical double layer and the precise location of the shear plane within it, and partly because of difficulties in obtaining reliable experimental values Although there have been several books on electrokinetic phenomena generally, Professor Hunter's is the only one, to my knowledge, which is devoted to the enigmatic zeta potential itself

To a large extent, the book is successful in drawing together and rationalizing a vast amount of material covering many aspects of the subject It should be essential reading for those embarking on research in the area and most established practitioners will want to have a copy within reach, or at least in the library of their institution

After a brief, scene-setting introduction, the author first deals with the distribution of charge and potential at interfaces Most of this material is readily available elsewhere and the treatment here offers no new insights However, since it forms the basis of much of what follows, it could not reasonably have been left out

By far the most useful chapters are those concerned with experimental techniques and the calculation of zeta potentials There is an exceptionally clear and up-to-date exposition of the procedures for obtaining zeta potentials from electrophoretic mobilities The experimental chapter includes a wealth of practical detail, such as the design of electrophoresis cells, and even advice on how to avoid leakage problems with platinum streaming potential electrodes

The chapter on electroviscous and viscoelectric effects is an admirable survey, a task which does not seem to have been previously attempted Hunter's conclusion from the discussion of viscoelectric effects is that the electrokinetic plane of shear cannot lie too far from the outer Helmholtz plane and that the zeta potential must be nearly equal to the potential just inside the diffuse layer This will comfort the many colloid scientists who have been making similar assumptions for years, but those who have advocated comparatively thick layers of structured water at interfaces may still remain unconvinced

The remainder of the book is concerned with applications of zeta potential and the effect of simple inorganic ions and more complex adsorbates The discussion of oxide surfaces raises the important question of the distinction between points of zero charge and isoelectric points, but, unfortunately, in an uncharacteristic lapse from his usually clear style, the author creates some confusion, especially with regard to the role of specifically adsorbed ions There are mentions of applications in such areas as colloid stability, flotation and electrophoretic deposition, but they are too brief to do justice to these various subjects

It becomes evident from the final chapters that there are still major uncertainties concerning the nature of the electrical double layer at solid–liquid interfaces In some cases, experimental values of charge density and zeta potential can only be reconciled with current models by making rather unrealistic assumptions, as the author readily admits Perhaps it is time for a thorough reappraisal of concepts such as the Stern layer and molecular capacitors, bearing in mind that on this scale (c 1 nm) water is not a structureless medium and that real surfaces are almost never smooth □

John Gregory is Reader in Water Chemistry in the Department of Civil Engineering, University College, University of London, and Secretary of the Colloid and Surface Chemistry Group, Society of Chemical Industry

Single-system geology after Arkell

Janet V. Watson

Lower Palaeozoic of the Middle East, Eastern and Southern Africa, and Antarctica With Essays on Lower Palaeozoic Trace Fossils of Africa and Lower Palaeozoic Palaeoclimatology
Edited by C H Holland Pp 331 ISBN 0-471-27945-5 (Wiley 1981) £38, $84

"It has been my personal experience that anyone seeking to understand a single geological system must flounder in the literature for some twenty years   Users of this book will be saved some twenty years work" This wry statement comes from the preface to W J Arkell's *Jurassic Rocks of the World* (Oliver & Boyd, 1956), the first general synthesis of a single system on a world-wide basis During the quarter-century since its publication the need for regional or global syntheses has increased, and the volume under review is therefore sure of a welcome It is the third of an ambitious series focused principally on the Cambrian, but taking in Ordovician and Silurian rocks where the nature of the evidence makes precise chronostratigraphy difficult The regions covered in this volume — the Middle East, north-eastern and southern Africa and Antarctica — are as difficult as any and the decision to cover all of the Lower Palaeozoic systems seems wise

In introducing his now classic volume on the Jurassic, Arkell outlined two objectives

> to present a unified description as a reference work and   to enquire what can be deduced as to faunal realms, climate, palaeogeography, volcanic and plutonic activity and earth movements   during one reasonably circumscribed period of geological activity

Accepting these as the true objectives of any comparable work, one must say immediately that the principal authors here (R Wolfart, E Klitzsch, I C Rust and M G Laird) have dealt nobly with the reference aspect They have brought together details of successions in some of the least-visited and least hospitable terrains on Earth and have provided valuable correlation tables and palaeogeographic maps Their chapters will remain the standard references for the Middle East, Libya and adjacent territories, southern Africa and the Ross geosyncline for years to come As a bonus, there are interesting chapters on Lower Palaeozoic trace-fossils in Africa (T P Crimes) and palaeoclimatology (N Spjeldnaes)

But what about Arkell's second objective? The unity of outlook and stylistic grace which he brought to the Jurassic are perhaps unlikely to be achieved in a volume with many authors one could, however, justly look for a broad treatment of geological events in Lower Palaeozoic times A four-page introduction by R M Shackleton reminds us that the areas dealt with are linked by and partially coincide with one of the world's major systems of mobile belts — the Pan-African — which was active immediately before and sometimes during the Cambrian period Scarcely a mention of this relationship is to be found in the rest of the book, with the honourable exception of the Antarctic chapter An opportunity seems to have been lost here, though the long-suffering editor (C H Holland) whose frustrations are outlined in the preface, may well protest that to have asked for a broader treatment would have made his labours impossible

Nonetheless, a fuller introduction or a final review chapter might have made all the difference Stratigraphy is the senior branch of historical geology, but can it any longer afford to close the door on tectonics, metamorphism and magmatism? □

Janet V Watson is a Professor in the Department of Geology at Imperial College, University of London

Landmark of early man in Britain

Paul Mellars

The Lower and Middle Palaeolithic Periods in Britain By Derek A Roe Pp 340 ISBN 0-7100-0600-4 (Routledge & Kegan Paul 1981) £35, $95

No one is better qualified to write a book on the earliest stages of human occupation in Britain than Derek Roe For the past 20 years he has been involved in detailed first-hand work on the sites of this period, and has produced not only the authoritative gazetteer of the major Palaeolithic localities in Britain, but also the most exhaustive typological analysis of the archaeological assemblages themselves The appearance of this general survey of the earlier Palaeolithic material must therefore be regarded as a major landmark in studies of the period in Britain

Two features of the book are particularly impressive its evident authority in dealing with the difficult interpretative issues involved and its readability Dr Roe writes with a degree of clarity, style and fluency which is all too rare in archaeological literature Some might say that the book is over-written in places, but this kind of judgement must depend to a large extent on the kind of readership which is anticipated Dr Roe has clearly aimed at an audience which includes not only the specialist prehistorian but also the "interested layman", and for this mixed readership his style of presentation is probably ideal

To pick out particular features of interest in a book of this scope is an almost impossible task Perhaps the most significant single feature which emerges from the discussion is the rapidly increasing evidence for the occupation of southern Britain by hand-axe-using communities at some point substantially prior to the Hoxnian interglacial Roe's arguments for believing that sites such as Fordwich (Kent) and Kent's Cavern (Devon) belong to this early phase are to my mind almost conclusive, and for these sites an age of at least 350–400,000 years would, from several lines of evidence, seem reasonable Equally interesting from a somewhat different standpoint is the rather curious dichotomy between hand-axe and non-hand-axe ("Clactonian") industries which has been documented for the Hoxnian interglacial itself This dichotomy — probably clearer in Britain than anywhere else in Europe — remains one of the most intriguing problems in Palaeolithic archaeology, for which a really convincing explanation still remains to be found

Evidence for the later stages of Lower and Middle Palaeolithic occupation is still infuriatingly vague Uncertainties of stratigraphic correlation, coupled with the lack of any reliable technique of absolute dating, renders any analysis of occupation during the Wolstonian and Ipswichian periods exceptionally difficult As Roe points out, there is a wide variety of industrial variants which must belong at some point within this time range, but in the absence of reliable dating any discussion of the meaning of this variation (chronological? cultural? functional?) must remain largely hypothetical and the question of interpretation open

One criticism that might perhaps be levelled at the book is that at some points it verges on the parochial, paying only limited attention to contemporaneous developments in other parts of Europe In the assessment of the earliest Palaeolithic industries this kind of comparison would certainly have been useful, and perhaps even more so in the discussion of the Middle Palaeolithic sites But this is at most a minor criticism and can hardly detract from the overall value of the book Dr Roe's major achievement is to have brought together a remarkably wide-ranging and diverse body of data, and to have presented it in a clear, well-integrated and easily accessible form By performing this task, he has produced what is clearly a classic of British prehistory that will serve as the definitive account of this period for many years to come □

Paul Mellars is a Lecturer in Archaeology at the University of Cambridge

nature

28 January 1982

Can even mere knowledge be a threat?

Academic freedom in the United States has come into conflict with national security. The Administration does not know what to do. The National Academy of Sciences should instruct it.

Stanford University has created an awkward problem for the National Academy of Sciences and, ultimately, for the State Department and the United States Administration Faced with an apparently routine communication from the academy relaying a new set of guidelines for restricting the access of overseas visitors to unpublished research, the university told the academy that the conditions were unacceptable They are that (see p 271) and unworkable as well The suggestion that overseas visitors should be kept in ignorance of unpublished research, for example, betrays ignorance of what university departments are like What else do these people talk about except what they are about to publish?

So, temporarily, the academy is embarrassed at having uncritically passed on a set of unpalatable instructions But it now has no choice but to decide where it stands on the question of national security and academic freedom, an increasing preoccupation of the Administration on which the academy's advice should long since have been sought The trouble is that there is nothing simple for the academy to say A ringing declaration of faith in academic freedom will not suffice, for there is more to the Administration's anxiety than mere xenophobia The academy must begin by teaching the Administration what American universities are for

Scholarship, while one of the chief custodians of tradition, is notoriously subversive of conventional wisdom, so that all scholars are potentially traitors to the establishment that supports them These simple truths, first learned at the Universities of Bologna and Paris, have been known for centuries They are now the basis of the accommodation which has been reached between universities and the rest of society in states confident enough of their political stability to indulge pretensions of liberality and civility Academics are licensed to teach and research as they choose, even when they are technically public servants (as in most European states) Governments, with varying degrees of reluctance, put up with the annoyance and inconvenience inevitably caused by the doctrine of academic freedom for two reasons — young people will otherwise be badly educated, while the new knowledge generated by scholarship is both enlightening and useful

The liberal accommodation between scholarship and society is, however, fragile In Poland in the past few weeks, the military government has evidently decided that academic freedom is more dangerous than benign the short-term benefits of compliance are judged to outweigh the long-term benefits of normality The Polish government's calculation may be accurate, if misguided The emergence of similar tendencies in the United States is not as easily explained

The analogy with Poland is merely superficial Nobody in the United States suggests that the government should decide which academics should teach what — and that unacceptable academics should lose their jobs Nor is it suggested that even students should pass tests of loyalty as well as examinations Indeed, the huffing and puffing there has so far been from agencies in Washington, the State Department and the Pentagon in particular, does not add up to a coherent policy, let alone a decisive break with the liberal habits of the past two decades Rather, it seems as if the Administration is going through one of its periodic attempts to make up its collective mind Senior officials make speeches, less exalted officials distribute circulars and members of Congress introduce bills that will never be debated.

The Administration's fears that free scholarship may be subversive of national security were put most clearly at the beginning of this year by Admiral "Bobby" Inman, now deputy-director of the Central Intelligence Agency but previously director of the National Security Agency (see *Nature* 14 January, p 88) The free publication of research may assist potential enemies, as may the traditional hospitality and liberality of American university departments But, the argument goes, the danger is not exclusively military The economic well-being of the United States may be as seriously damaged by the premature disclosure of commercially valuable high technology to a friendly but competing state So American universities, many of them among the engines of technical innovation, must be more circumspect Advance review of papers intended for publication may be necessary Restrictions on foreign visitors (some of which are permitted by existing legislation) may have to be made tighter And even general education may be suspect — Mr Frank Carlucci from the Pentagon was saying earlier this year (see *Nature* 7 January, p 3) that many visitors to American universities had gone on to posts in Soviet military establishments.

The Administration's case would be more convincing if there were not ample evidence that it is unsure of where it stands in its relationship with the outside world In its innocence — perhaps ignorance is the word — it habitually first sees the dark side of every international issue Yet all the fears that academic liberality may endanger the security of the United States are in reality double-sided questions Thus it is no surprise that foreign visitors to American universities benefit from their experience, or that they are afterwards promoted rapidly, the process by which they are selected would probably ensure that But indirectly, the American university system also benefits, as does scholarship as a whole This is why the Administration's decision to suspend the exchange agreement with the Soviet Union is a mistake

Admiral Inman's fears must be dealt with differently Again, however, it is true that the traditions of liberality benefit others than American taxpayers This is why there has been a running battle since the beginning of the Carter Administration about the prudence of open research on cryptography The ingenious development of the technique of what is called public-key cryptography was fully described in the open literature before the National Security Agency fully appreciated that an unbreakable code would benefit others than itself Much the same happened in 1938, but even more spectacularly, when Hahn and Strassman working in Germany published their first account of the neutron-induced fission of uranium The Admiral Inmans of this world must acknowledge that such accidents must happen repeatedly, and that they cannot be prevented without bringing academic research as such more or less to a halt They have three comforts In each case, the chances are high that similar discoveries would independently have been made elsewhere, while publication has ensured (at least where cryptography is concerned) that valuable commercial use can now be made of unbreakable codes The authorities must learn to live with this hard consequence of liberality, but may further comfort themselves with the knowledge that less liberal university systems have historically

0028-0836/82/040269-02$01 00

been less productive of good ideas and that on many occasions they can rely on the good sense of working scientists to anticipate trouble

There will be few complaints in the United States if the defence authorities now seek to build on this goodwill It would be entirely proper that they should remind people in laboratories that even seemingly academic developments may have defence implications Equally, it would be proper that university administrations should take a continuing interest in the problem It would, however, be a mistake for the military authorities to set up central machinery for supervising academic papers before publication Such a system could prevent the publication of sensitive material only by holding up a great deal of innocuous material Even then, it would make mistakes It would be far preferable that responsibility for deciding how the publication of potentially sensitive material should be arranged should rest with researchers and their universities The proposed arrangements for supervising research in cryptography, designed to shut the stable door after the bolted horse, should be abandoned

The general run of military research proper is more easily handled Since 1940, the Defense Department has learned to rely on American universities for a substantial part of its research and development Academics are well used to this kind of collaboration, and are apparently able without too much difficulty to marry their obligations to liberal teaching with their obligations of confidentiality to the Pentagon Whether the topic is formally registered as secret, or "classified", seems not to matter A more important consideration is that there are limits to the degree to which the university system can be laden with responsibilities for defence research without being compromised The irony is that, in the present economic climate, the universities are more willing collaborators and that the Pentagon seems glad of the welcome it now seems to enjoy from the universities

The issue of commercially important research is novel and fuzzier During the past decade, government agencies have been increasingly anxious that publicly supported research should have some practical relevance while, more cautiously, corporations have begun to recognize the potential of the academic research enterprise What seems not to have been appreciated is that many of those who help to carry through these unclassified programmes are nationals of countries other than the United States

But what is so strange about that? For even the most "relevant" of externally supported research programmes are not — and should not be — programmes of development Most of them are projects intended to gather basic information in some obvious field The fear that foreign visitors may carry off unique information in fields such as the molecular biology of genetic engineering or the development of techniques for making Very Large Integrated circuits is predicated on the assumption that nobody else knows about these important industrial goals That conceit is almost always an illusion It should not be allowed to compromise the civility and freedom of academic research In any case, the agencies and the corporations have the remedy in their own hands They decide what research contracts should be let

Why arms control?

Will arms control fall foul of too literal an interpretation of Kissinger détente?

This has been a bad week for arms control Mr Alexander Haig's long-arranged meeting with Mr Andrei Gromyko in Geneva was being advertised in advance, in Washington at least, as a discussion exclusively about recent events in Poland The promised resumption of bilateral negotiations on strategic arms are apparently to be postponed indefinitely At the same time, there have been mutterings in Washington that the talks now under way in Geneva on the control of weapons in Central Europe may be reduced to one session a week unless there is some sign of let-up in martial law from Warsaw Both developments are consistent with the case argued forcefully last week by Dr Henry Kissinger, previously United States Secretary of State and the architect both of the concept of *détente* and of several arms control agreements between the Soviet Union and the United States In two pungent articles, Dr Kissinger restated his familiar argument that peace is indivisible, and that a succession of agreements on arms control is in itself insufficient, even insubstantial The present Administration has obviously been angered by much of what he said Its responses this week suggest that it is nevertheless prepared to listen

Can this be wise? The Kissinger doctrine of "linkage" is politically and tactically impeccable In making an accommodation with an adversary, and on the assumption that neither side will abandon what it considers to be its essential interests overnight, it is prudent to seek agreements which provide each side with incentives to toe the line and deterrents (not necessarily nuclear) against backsliding The essence of the Kissinger–Nixon theory of *détente* is that the United States would offer the carrot of high technology and trade, gaining in return the relatively insubstantial benefits of the Helsinki agreements and of *détente* itself The corresponding deterrents were ultimately supposed to be what they have been ever since 1946 One essential element in Dr Kissinger's argument, not restated but substantially unchanged, is that it should be possible to withdraw the carrots quickly, making the sticks loom larger Dr Kissinger last week was scornful of the growing United States dependence on the international trade with the Soviet Union in foodstuffs His articles appeared before France had followed West Germany in agreeing to buy substantial quantities of natural gas from the Soviet Union but his arguments do not apply, as seems to be supposed, to the process of negotiating, as distinct from ratifying, agreements on arms control

That conclusion can be reached without much difficulty The experience of the past few years has shown that the parties most acutely embarrassed in negotiations are those who feel bound to reject sensible proposals The United States Administration has turned up at Geneva with an in-built advantage — President Reagan's declaration in November that he (but not necessarily Congress) would settle for the "zero option" — no nuclear missiles (as distinct from aircraft) of any kind in Europe The general opinion, borne out by such official Soviet statements as there have since been, is that Mr Reagan was offering a clever bargain, as much a stick as a carrot Does it make sense, having raised such a possibility, to allow the discussion of this proposal to slip into the background noise, like the continuing negotiations in Vienna on the reduction of conventional forces in Europe? For that matter, can it make sense, if the United States seriously believes it has a moral advantage because of Poland, that Mr Haig should so ostentatiously fail to raise with Mr Gromyko the matter of how far the Soviet Union might be prepared to go on a replacement treaty for Salt II?

The underlying difficulty is that, on arms control, while the more important negotiations are bilateral between the United States and the Soviet Union, neither party is as free as it supposes Paradoxically, the negotiators must constantly have in mind the electorates of countries other than their own Or they should The willingness of the government of France to contract for a decade's supply of natural gas from the Soviet Union should be a reminder that France is a European state The nervousness of the Bonn government about the future of Central Europe is also a measure of the more general concern that alternative governments would pose more complicated problems And who supposes that all members of the Soviet government have slept soundly at nights during the past momentous eighteen months? Mr Haig should talk, not sulk

The moral is, or should be, simple Talking about arms control is better than sulking Talking about arms control to a potential partner at a moral disadvantage may be especially productive Not to talk at all, or to talk only one day a week, is silly And is there not always a chance that the process will itself be worthwhile? In short, the United States should feel free to speak up at Geneva and elsewhere without fear of selling itself short — or of offending Dr Kissinger

0028-0836/82/040270-01$01 00

Academic freedom and security conflict

Challenge to access rule from Stanford

Washington

The National Academy of Sciences (NAS) moved quickly last week to disengage itself from efforts by the US State Department to restrict ideas that American university research workers are allowed to discuss with visiting Soviet scientists

The academy was responding to complaints that, in administering the exchange programme between scientists from the two countries, NAS officials have been routinely passing on instructions from the State Department about limitations to be placed on particular individuals

Scientists at Stanford University in California objected earlier this month to the academy when such a letter was received covering the proposed visit of Dr Nikolay V Umnov, an expert in robotics and walking machines, to the university's department of mechanical engineering It was to be one of a series of visits which the Soviet scientist had requested to universities throughout the country

NAS officials told the university that Dr Umnov's visit had been approved by the State Department, but only under certain conditions He was not to be allowed access to data about programming techniques for robots, nor was he to make any industrial visits to companies with Defense Department contracts The State Department has said that, unless waivers were negotiated with the Department of Defense, Dr Umnov was not to be allowed access to unpublished results of Department of Defense sponsored research even if this was unclassified The academy passed these instructions on to the five universities Dr Umnov was to visit

Following a complaint from Dr Bernard Roth, a professor in the department of engineering the university's dean of research, Dr Gerald J Lieberman, wrote back saying that Stanford was prepared to sponsor Dr Umnov's visit, but refused to accept the conditions imposed by the State Department

"We are not willing to accept responsibility for Dr Umnov's actions — either on or off the campus — during his visit to Stanford," Dr Lieberman wrote He added that the NAS memorandum was a surprise, saying that "we believe that the best interests of American science and technology are served by open exchanges of university research activities and hope that the academy will visibly support universities' position on this critical issue"

A spokesman for the academy said last week that it had been decided to suspend the simple transmission of restrictions required by the State Department until the governing board of the National Research Council and the council of the academy "has had a chance to examine the whole thing from the policy point of view" Both bodies meet next month

As efforts have been made to tighten restrictions on visiting scientists, concern about the implications have been growing on US campuses A year ago, Stanford sent a letter on behalf of the presidents of five major research universities to the Department of Defense, Commerce and State, complaining that such a tightening could seriously hamper the work of the scientific community The president of the academy, Dr Frank Press, has also expressed publicly his concern about suggestions from the deputy director of the Central Intelligence Agency, about the need for greater caution in the publication of research results in fields such as lasers and computer software

Last year a group set up jointly by the National Security Agency and the American Council on Education agreed to establish a system by which research results in cryptography could be voluntarily submitted to a review committee before publication, to determine whether the data should be withheld on national security grounds The academy has to agree to accept a request that it nominate two members of the review committee, a move which could be taken as endorsing the idea

Harvard guidelines for avoiding fraud

Washington

A national conference involving both the National Institutes of Health (NIH) and the nation's research universities should be convened to consider a number of "unanswered questions" about dealing with suspicions of falsified research data, according to a committee of inquiry set up by Harvard Medical School to investigate the circumstances surrounding the admitted fabrication of data by a scientist studying the prevention of heart attacks (see *Nature* 24/31 December 1981, p 584)

The committee, chaired by Dr Richard S Ross, dean of Johns Hopkins Medical School, has given its general approval of steps taken by the medical school after colleagues discovered that Dr John R Darsee was faking some of the raw data in an experiment in May 1981

In its report, which was published in Boston on Monday, the committee describes how Dr Darsee was stripped of his position as a research fellow, as well as being removed from staff positions at the Brigham and Women's Hospital, as soon as the fabrication of data had been confirmed, and that his NIH research fellowship was removed at the same time The medical school denied on Monday that it had been wrong to keep Dr Darsee involved in research at another laboratory in Harvard, or that it had been slow to raise public warning signals about his research, claiming that it had been some time before an internal investigation revealed just how extensive the fabrication of data may have been, and that up to that point Dr Darsee had gained a reputation as a talented and hard-working research worker

The report of the review committee, which was set up at the invitation of the dean of Harvard Medical School, Dr Daniel Tosteson, says that it considers the medical school's response to have been appropriate for what was known at the time

The committee makes two specific recommendations to the medical school First, it should establish a committee of senior faculty members that can be called upon to investigate any suspicion of fraudulent data gathering And second, the medical school should improve the internal communication system, so that people can be informed confidentially if a research worker under suspicion in another department has any connection with their own research In the case of Dr Darsee, colleagues in the laboratory in which he was allowed to continue working were not aware of the charges made against him elsewhere in the medical school

The committee also makes some general suggestions about how the scientific community might take steps to make it harder for an individual to publish false results For example, it criticizes the practice of publishing small batches of research findings in a number of different publications, rather than concentrating them in a single, major publication, more likely to receive close scrutiny from the scientific community

The committee also suggests that laboratories should agree on explicit procedures for data gathering, storage and analysis, and that these should be written up and be generally available to research workers In Dr Darsee's case, he was unable to produce much of the raw data on which some of his research results were based, although the committee found that it was general practice in the laboratory that such data should be preserved

Finally, the review committee suggests a national conference to look at the whole area of the falsification of research Topics which it says a conference might address would include what the responsibility of an institution discovering dishonesty among its research staff should be with respect to other institutions, the scientific and medical community and the general public

David Dickson

0028 0836/82/040271-02$01 00

of pre-publication review in selected areas of research

Despite several meetings with government agencies held over the past year, university officials report little indication that the government is prepared to relax its restrictions, in view of the prevailing political climate in Washington

Last Friday, the State Department said that Stanford University would not be included in Dr Umnov's visit since it had refused to recognize the department's restrictions on what he should be allowed to do Scientists at the University of Wisconsin also said they were withdrawing their offer to host a visit from Dr Umnov in the light of the department's actions

The Soviet scientist's trip will still include one week at Aubrun University in Alabama, and "two or three days" at Ohio State University Professor Robert McGhee of Ohio State has said that, although Dr Umnov was originally to spend six weeks at the university, he was only prepared to accept the State Department restrictions for the shorter length of time **David Dickson**

Polish academics

More pressure

There are unconfirmed reports from Poland that Dr Henryk Samsonowicz, rector of the University of Warsaw, has been dismissed for refusing to accept the new rules for the conduct of institutions of higher education laid down by the ruling Military Council for National Salvation Earlier, Dr Samsonowicz was reported to have been among the many academics interned under martial law regulations, while other reports indicate that he has been expelled from the Communist Party

According to Mr Artur Swiergiel, a member of the Mazowsze (Warsaw and home counties) regional executive of Solidarity, who is at present working on animal nutrition in Cambridge (England), the reported dismissal is only the tip of the iceberg He expects a wave of dismissals among the university rectors elected in the past 18 months according to the new democratic procedures, but predicts that the expected purge will be far more sharply felt among junior academics and research students, as it was in 1968 He stresses that Western scientists who wish to campaign on behalf of their Polish colleagues should not concentrate only on the most eminent Current lists include Dr Grzegorz Bialkowski, vice-president of the Polish Physical Society, and Dr Antoni Stawikowski, vice-president of the Polish Astronomical Society, but also their junior colleagues

So far, Western scientists who have approached their local Polish consulates or embassies with requests for further information about interned colleagues have been met with suggestions that if the scientist in question could arrange a job for his colleague in some university or laboratory outside Poland, the authorities would be quite willing to grant an exit visa.

Such an arrangement, Mr Swiergiel stresses, should not be accepted unless there is clear evidence that the scholar concerned definitely wishes to leave Poland, since the army newspaper *Zolnierz Wolnosci* has indicated that Solidarity would have to shed "35,000 intellectual advisers" before it could be allowed to resume "purely trade union" activities This theme has been reiterated by Stanislaw Ciosek, the Minister for Trade Union Affairs, in a recent meeting with "representative workers" from Lodz, who stressed that trade unionism in Poland must return to its "class basis"

Under martial law, scientific exchanges between Poland and the rest of the world have come to a halt In London, the Royal Society has no news of Wieslaw Stanczyk, who was expected to arrive in January to take up an exchange scholarship From Finland it is reported that exchange fellows due in early December failed to arrive, although martial law was not declared until a few days after their expected arrival

Scientific exchanges are based on two types of agreement — the purely academic negotiated with the Royal Society or British Academy and those which form part of the bilateral agreement on trade and technology The financial mainstays of the latter are the various economic agreements negotiated over the past decade These include a licensing agreement between Massey-Ferguson tractors in the United Kingdom and the Ursus motor works in the suburbs of Warsaw In one of the latest moves in "solidarity with Solidarity", workers at the British plant have voted to "black" all spare parts and components from Ursus until martial law is lifted

Vera Rich

UK nuclear power

At last, a plan

At long last the British nuclear industry has a timetable that can be believed in The "wide-ranging" public inquiry into the design and siting of a pressurized water reactor (PWR) at Sizewell in Suffolk will begin in January 1982 The "task force" set up under Dr Walter Marshall, chairman of the United Kingdom Atomic Energy Authority, to speed up the design of the PWR last week reported that its pre-construction safety report was complete and in the hands of the customer for the reactor, the Central Electricity Generating Board This is in line with the timetable set by Marshall last July, as is the date set by the board for the publication of its full safety review — the end of April

The only fly in the ointment seems to be the Nuclear Installations Inspectorate, whose lack of inspectors appears to be putting back the publication of its own, independent safety report The inspectors will now produce a summary review of the generating board's own safety documents in June this year, expressing their reservations (if any), but may produce nothing further before the public inquiry The inspectorate's safety assessment is "an iterative process" says the chief inspector, Mr Ron Anthony. There can be no particular point at which it is best to hold a public inquiry too early, and the inspectorate would have too little time to study the design, too late and it would not be possible to take the inquiry's findings into account without disrupting the project

The task force report will not be published, but Dr Marshall last week outlined its main features His study concentrated on the safety standards and the systems demanded by both the inspectors and the electricity board which — before the task force was set up in July last year — were estimated to imply that the British PWR would cost 50 per cent more than the American Westinghouse/Bechtel Corporation system Marshall estimates that the extra cost will now be only 20 per cent A quarter of that is attributable to measures intended to minimize loss-of-coolant accidents, a quarter to reduce the radiation exposure of workers and the remaining half to the use of two rather than one turbine for converting steam power into electricity.

The emergency core cooling systems will contain four separate high-pressure pumps (twice as many as in French and American PWRs) each feeding one of the four primary coolant loops and backed up by diesel generators, and the outer containment will be a four-foot thick concrete and steel shell, not the double wall originally planned Radiation levels have influenced the British design because the electricity generating board is anxious that exposure at its projected plant should not exceed that at its existing nine plants Thus the task force has attempted to reduce exposure by providing more space within the containment building (150 feet in diameter compared with 140 feet) and by the use of remote maintenance equipment.

The board thus hopes to bring individual operating exposures down to the level of the 0 25 rem per year or so experienced in the old Magnox plants The key factors seem to be good chemical management of the plant, particularly of the primary coolant water, and efficient and fast maintenance procedures Thus the emphasis is now less on the design (the original version of which called for nearly twice as much concrete shielding as the American baseline) than on the efficient operation of the reactor

The eventual cost will be within the target Marshall set himself six months ago — no more than 70 per cent of the cost of an advanced gas-cooled reactor At 1981 prices, this works out at about £1,000 million for 1,200 MW Nevertheless, this is some four times the price of a PWR as estimated by the French, and the National

0028-0836/82/040272-02$01 00

© 1982

Nuclear Corporation (which would build the reactor) and the Central Electricity Generating Board (which would buy it) are now putting their heads together to see how the French do it — and whether the British price might be brought down The generating board intends to announce its final estimate of the cost of the station, and the price of the electricity that it will produce, at the end of February

Robert Walgate

Interferon used at last

The Medical Research Council's Common Cold Unit in Salisbury, England, has resumed its trials of interferon as a preventative of rhinovirus infection — one of the causes of the common cold

Ten years ago, the centre proved the effectiveness of leukocyte interferon, prepared from human blood by Dr Kari Cantell in Finland, against rhinovirus — but abandoned further work because of the high cost of the material Trials have been resumed in the belief that genetically engineered interferon will eventually be so cheap that interferon might one day be used to prevent coughs and sniffles

"TAKE THREE TIMES A YEAR, AFTER WAGE INCREASES"

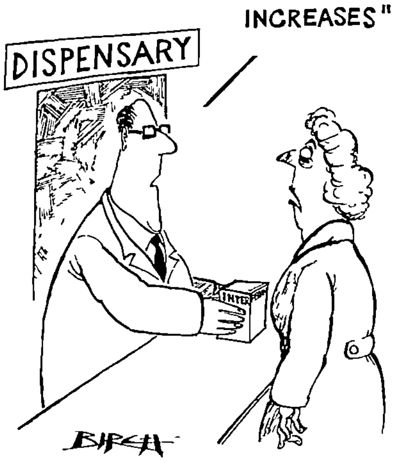

The resumed trials utilize interferon which is much purer than before It is obtained either from white blood cells or from genetically engineered bacteria Both forms are effective at high dosage and the next step at Salisbury will be to test how far the dosage of interferon can be reduced and how late in the course of infection it can be administered Then it will be up to the manufacturers to reduce prices to the level of common palliatives such as aspirin — a tall order, no doubt, but one which may eventually be met The aim is to do better than the Soviets who currently sell, for about $1 a time, interferon of such low dosage as to be useless **Robert Walgate**

US research spending

Problems in public

Washington

Efforts by the Reagan Administration to shift significant responsibility for research from the public to the private sector have produced a new crisis of identity in some national laboratories funded by the US Department of Energy

Established in the early 1950s largely as a means of supporting the research needed for both the military and the civilian uses of nuclear energy, the laboratories expanded the scope of their activities considerably in the 1970s as they were given additional responsibilities

Many of the areas of expansion, however, such as solar energy and conservation, are precisely those whose research budget is being most heavily cut by the Reagan Administration Furthermore, some powerful Republicans are questioning whether it is appropriate for the government to be involved at all in areas which, they claim, should properly be left to the private sector

Budget figures alone tell a significant part of the story For the twelve "multi-programme" laboratories run by independent contractors for the Department of Energy, the total budget for the current fiscal year is $2,803 million, $60 million less than for 1981

Given an expected inflation rate of about 10 per cent, the result will be a significant reduction in overall effort The reductions, however, will not be shared equally, with the two major weapons laboratories, Los Alamos National Laboratory and the Lawrence Livermore National Laboratory, receiving budget increases of 11 per cent and 16 per cent respectively

Laboratories hit harder by cuts include Argonne National Laboratory near Chicago, with a budget reduction of more than 25 per cent, while a reduction of similar magnitude has been absorbed at Oak Ridge National Laboratory, Tennessee In both instances, the major decreases are in programmes of research into fossil energy, conservation technologies and "other energy supplies"

A decision last year by the Department of Energy, in light of its expected budget cuts, to decrease the energy-related programmes by 10 per cent from 1980 levels, has already markedly affected staffing Some laboratories have been able to absorb most of the technical and scientific staff who have been displaced in weapons-related projects, at Oak Ridge, for example, many have moved to nuclear-warhead production Others have not been so lucky Brookhaven National Laboratory in Long Island has already had to lay off 270 out of its total of 3,600 staff At Argonne, the reduction so far has been 600 out of about 4,400

The prospects for next year do not look much better Although precise budget proposals will not be known until they are presented to Congress by President Reagan on 8 February, it is widely expected that the Administration will suggest similar reductions for 1983, after that, the laboratories can expect level funding at best for the next three to five years

A significant change in policy direction was already indicated in a memorandum last May to laboratory directors from Acting Under-Secretary of Energy, Dr Raymond Romatowski Under this regime, Dr Romatowski said that in principle the multi-programme laboratories should be restricted to two main functions The first was to conduct basic and applied research comprising important "technology-base" activities that the private sector is ill-equipped or not motivated to pursue, the second was to undertake development work in promising areas "beyond the private sector's capability and interest"

Several review committees are now looking at how to put these two principles into practice The main review, being carried out by the Office of Science and Technology Policy, will take some time to complete In the shorter term, a panel of the Department of Energy's Energy Research Advisory Board has been asked by the Deputy Energy Secretary, Mr W Kenneth Davis, to carry out its own review of the multi-programme laboratories, and a final report is due by September

Meeting in Washington last week, the members of the advisory board panel agreed to offer various strategies as possible options for action in their interim report, due at the beginning of March

In the course of preparing its full report, the panel will be looking at the experience of other countries in running government laboratories to see if they may provide a model for new institutional arrangements in the United States

Whatever proposals are finally accepted by the Administration, attempts significantly to change the current status of the laboratories is guaranteed to meet an uphill struggle in Congress, where many have powerful political supporters

David Dickson

EEC research and development

Time for success

Brussels

Vicomte Etienne Davignon, European Commissioner for Research and Development in Brussels, set alight a rather quiet meeting on the evaluation of Community research and development on Monday with a sharp attack on previous Community policies There is a "great deal of scepticism" about Brussels-sponsored research and development, he said, and it was time for some successes

Davignon singled out the seven-year gestation of the bioengineering programme, recently agreed at the Council of Ministers, as an example "We came out with a mouse," he said. If anyone believed the Commission should go through that kind of agony again, he was mistaken, said the Commissioner. The Commission should scuttle programmes far sooner when member states do not agree.

Not that Davignon is against Community support for biotechnology — far from it. Rather, he appears to detest the national bickering which delayed the programme so long. His policy now is to set up a "framework for research", a broad structure of ministerial agreement on Brussels research and development policy. The framework would stretch over, say, five years, leaving the Commission room to develop detailed programmes within the guidelines and giving nation states the chance to see a fair return on Community investment in a much wider context.

This framework is to be thrashed out in the next two meetings of the Council of Ministers for research, one in March and the next in June. If nothing happens in 1982, the momentum will be lost, says Davignon. But the transition from the present structure to the new one will be gradual. Some heads have already rolled at the Directorate-General for Research, but Davignon's cabinet insists that the night of the long knives will not last long. The objective is to use existing staff in new ways, Davignon claims — although some Commission staff remain nervous.

And to what end? To revitalize European industry. Davignon, whose commission also covers energy and industry affairs, says Brussels research and development has a way of redirecting European economic development, to fill gaps — such as in telematics and computers — in relation to the Japanese and United States competition. To achieve this, Davignon is prepared to be surprisingly flexible, and sees a role for the Commission even in helping to set up bilateral research and development projects among member states, and in giving international promotion to national centres of excellence. Davignon hopes member states will agree to his ambitious programme because of the economic risks involved in not doing so.

Robert Walgate

Fusion decision awaited

Brussels

The next EEC research council on 8 March is now likely to approve the next five-year programme on controlled thermonuclear fusion. The fear that there might be a gap in the sliding programmes, between the last budgetary allocation and this, was further reduced with the release last week of a favourable opinion from the Consultative Committee for the Fusion Programme, which considers the planned financial envelope — 1,500 million European Currency Units (£750 million) has been allowed.

Continued membership by Sweden, one of the two non-EEC countries participating, is, however, in jeopardy. The committee observes that Sweden finds the cost excessive. One difficulty is that neither Sweden nor Switzerland participates in the EEC's annual budgetary procedure, when the amount of money devoted to a programme can be adjusted. National contributions are assessed on the basis of a percentage of gross national product, and for Sweden more money for the EEC programme means less for national research.

The Commission's thermonuclear research strategy, which is to concentrate effort on the tokamak line while retaining an interest in magnetic confinement, reverse field pinch and stellerators, wins the approval of the committee, which nevertheless recommends a periodic assessment of the relevance of these side-lines to reactor development.

The committee is, however, more cautious in its views on the step to be taken after JET, the Joint European Torus now nearing completion at Culham in Britain. It recommends that plans for the next large thermonuclear machine, called NET (for Next European Torus), should be reviewed again before a decision is made in 1984. Likewise the committee is noncommittal on the need for the proposed tritium laboratory.

Jasper Becker

US university funding

Tax act fails

Washington

Universities in the United States are complaining that so far they have benefited little from the Reagan Administration's attempts to augment spending on research by tax cuts rather than direct support.

On the one hand, the tax cuts were structured in such a way that it has been equally, if not more, tempting to a company to increase its internal research efforts rather than contract work to outside groups. On the other, there is a feeling that the new incentives will have little effect on some of the largest companies which already have relatively low tax liabilities.

Two parts of the Economic Tax Recovery Act signed by President Reagan last summer were supposed to help universities, one a tax credit designed to increase industry support for basic research at universities, the other a new deduction for industries contributing research equipment to universities.

"Neither appears to hold significant promise," Dr John C Crowley of the Association of American Universities (AAU), which follows legislative affairs for the major US research universities, told a recent meeting of the American Association for the Advancement of Science.

Dr Crowley quoted a letter from Mr B J McKelvain, an analyst with General Electric Company, which has been among the most aggressive companies seeking tax incentives to boost spending on research and development. Mr McKelvain presents the company's estimate that the research tax credit will result in an increase of less than two per cent in industry-funded research.

The difference in the incentive for increased support of university research compared with in-house work is probably "negligible", Mr McKelvain had written. And although he says that the incentive for equipment donations should result in some increased giving, "we would not expect the response to have a significant impact on the critical shortage of state-of-the-art equipment available for university research".

The principal reason for this pessimistic assessment is based on the narrow scope of the tax provisions. For example, any equipment donated by a company must have been manufactured by that company and cannot contain purchased parts accounting for more than 50 per cent of the tax costs.

"Despite these limitations, the equipment donation provision is a start in the right direction. If broadened somewhat, it could have a considerable impact on the problem", said Dr Crowley, one of the co-authors of a report prepared by AAU for the National Science Foundation two years ago. This formed the basis for the Carter Administration's proposal to provide an additional $7 million in the foundation's budget for university research equipment, but was one of the first items to be cut by the Reagan Administration when it came to power last January.

As for the broader impact of the new tax laws, Dr Crowley concludes that the 1981 Tax Act offers "only token incentives for research support and donations of research equipment by industry".

This view is confirmed by officials from several major universities. Mr Stuart H Cowen, for example, vice-president for financial arrangements at the Massachusetts Institute of Technology, said that, so far, the institute had "not seen much effect of the new tax law", although speculating that companies may be holding back until the Treasury Department publishes detailed guidelines on how the law will be interpreted.

Although disappointed, few university officials are surprised at the apparent failure of the bill. Whereas they had pushed hard for inclusion in the tax legislation of a clause allowing companies to write off all contributions to university basic research against tax, the Treasury Department was not convinced that the value of this move would outweigh the costs in terms of lost revenue, the bill as finally passed by Congress merely allows for tax relief on the amount that support for such research is increased by a company.

Several congressmen are hoping to

0028 0836/82/040274 02$01 00

introduce legislation that would reinstate the original objective.

The universities are also worried about a new bill passing through Congress which could require that up to three per cent of the federal government expenditure on research and development should go to small businesses. **David Dickson**

Telecommunications

Gear on sale at last

Users of the British telephone network can now legally buy handsets from retail shops. This is the first tangible effect of the Telecommunications Act, passed last November to liberalize part of British Telecom's business. Users may, however, be disappointed that the choice of telephones on the market has not yet increased. So far, only four types of handset have been certified for sale through general retail outlets, all of which British Telecom also markets itself. Twenty-five further requests for certification are waiting in the wings.

The aim of the act is to encourage open competition between manufacturers of equipment for connection to the public network. British Telecom will still retain control of the network but will have the right to connect only the first instrument. The liberalization is to be phased over three years, starting with handsets and discrete modems (digital analog interfaces, as they are known in the trade), followed by integral modems this spring, equipment not using call switching or loudspeakers in July, simple telex-teleprinters in October and, finally, private automatic branch exchanges (PABXs) in July 1983.

The British Standards Institution (BSI) has been charged with the task of drawing up compatibility standards for each type of equipment. Certification of individual items will be taken over by a newly-created subsidiary of the British Electrotechnical Approval Board (BEAB) later in the year.

So far, the liberalization seems to be going according to plan. But users and manufacturers have been concerned that it may be too slow. The system cannot get into full swing until BSI, which must follow lengthy procedures under its charter, has drawn up standards and BEAB has set up the machinery required for certification. Moves by BSI, however, to reorganize existing staff and appoint more and to reduce the time taken for public comment on draft standards to one month seem to have quelled some fears. First drafts for seven standards including plugs, handsets, modems, teleprinters and appliances to be connected to private circuits leased from British Telecom, are due to be published within a few months. Earlier wrangles over the terms under which BEAB would operate also seem to have been resolved. It is now hoped that an independent subsidiary will go into business in July.

Meanwhile, manufacturers have little alternative than to accept the role of British Telecom, one of their competitors, as the approval agency and that of the Department of Industry in selecting applications for consideration. These interim arrangements, however, do not seem to have been a deterrent. The department has already received applications for many types of equipment, the latest being for PABXs from Ferranti, GTE, Harris Systems, Mitel Telecommunications, ITT Business Systems, Philips Business Systems, and Plessey Office Systems. One company, International Business Machines, is planning to be use the liberalization to introduce equipment new to the British market. It is installing an Integrated Networking System, which allows separate telephone switchboards to operate as one, at the American Express International Banking Corporation.

On terminal equipment at least, there seems to be continued optimism that the liberalization will work without destroying too many manufacturers' hopes.

Judy Redfearn

Soviet biotechnology

Keeping a secret

Last month's annual general meeting of the Soviet Academy of Sciences placed a special stress on the development of Soviet biotechnology. Academician Ovchinnikov stressed especially the achievements of biotechnology. Soviet scientists, he said, were now leading the world in "a number of very important branches of biology".

Ovchinnikov's summing-up covers a major confrontation during the past year among scientists involved in biotechnology. There appears to have been a power struggle between Ovchinnikov and his supporters from the physical chemical wing and Academician Dubinin representing the biologists. After some manoeuvring, Ovchinnikov emerged victorious and Dubinin retired from active scientific life. At the same time, there was considerable criticism in the Soviet press of the management of molecular biology research which, since May 1974, has had "top priority" status.

Another and more interesting confrontation has apparently been going on between the academy's biologists and the military scientific sector. This began two years ago when Professor David Goldfarb, a Jewish biologist, applied to emigrate to Israel. Professor Goldfarb had previously been involved in work on bacterial plasmids, and therefore, according to the emigration authorities, his work could be classified as secret. Several Western scientists wrote to Academician Ovchinnikov on Professor Goldfarb's behalf, but received only noncommittal answers. According to the latest information, however, certain academicians have spoken out clearly to say that in their opinion Professor Goldfarb's work was not secret. This accords with the fact that Professor Goldfarb was never cleared by the security authorities for access to secret information. The whole matter appears to reflect not merely the usual blocking of a Jewish scientist wishing to emigrate but a genuine conflict between the academy and the security establishment over what is and is not secret information in the field of biotechnology. **Vera Rich**

Pasteur institute

Rien ne change pas

Paris

François Gros, science adviser to the prime minister of France, has thrown in his lot with politics. He has resigned as director of the Institut Pasteur in Paris, one of the most famous of laboratories. The laboratory was founded in 1888 by Louis Pasteur, and since then it has been directed by a series of well-known biologists. Gros, a Nobel laureate himself, took over from Jacques Monod. The call of the new politics in France must be great!

The new incumbent — who took up his job this month — is Raymond Dedonder, 60, previously director of the Institute of Molecular Biology of the University of Paris. Dedonder is a microbiologist with a strong inclination towards the application of his work to the economy and to medicine — something already well-established in the tradition of the Pasteur. He has worked with *Bacillus subtilis*, of interest to industrial genetic engineering, and with *Bacillus thuringiensis*, contributing to the development of a bacterial toxin against certain insects.

It is unlikely that Dedonder will much change directions at the Pasteur. He spent a large part of his early career there and so is a "Pasteur man" — and Gros himself is likely to continue to take a fatherly interest from the prime minister's office.

So plans made under Gros's directorship — and, in fact, under the previous government — will not change. A new laboratory of immunology has been established and a laboratory of biotechnology will be set up, to come into operation in 1984. The independent management of the Pasteur is likely to continue, despite the fact that half the institute's money comes from government. Dedonder believes that far from wanting to nationalize the Pasteur — as some have suggested — the government wishes to take it as a model of fruitful symbiosis between basic and applied research.

The one change that may come with the new directorship — and new government — is a greater emphasis on the overseas laboratories of the Pasteur, particularly those in Third World countries, such as the Instituts Pasteur in Tunis, Algier, Casablanca, Dakar and so on, in line with the government's foreign policy. Dedonder will be encouraging that development. **Robert Walgate**

0028-0836/82/040275-01$01 00

CORRESPONDENCE

All in The Book

SIR — Creationism is on the march again, not only in the United States, but, as the letter from the Glasgow creationists shows (*Nature* 26 November 1981, p. 302), in the United Kingdom as well. For a concept as theoretically and scientifically destitute as creationism, it is surprising to many that the idea keeps coming back. It seems to have the resilience of herpes.

It is neither easy nor much fun to argue with such grass-roots ignorance in a calm and civil manner. Consequently, lest the following comments be construed as arrogant, condescending, and supercilious, I trust that the Glasgow group will take them with good spirits. The Scots are, after all, renowned for their spirits.

Why do these people channel their vast intellectual energies against the innocuous theory of evolution? Why not against the pernicious satanic forces of quantum mechanics or particle physics? Why do they insist upon biblical literalism only in this specific case? After all, *Leviticus* **11** 19 classifies the well-known mammal, the bat, as a bird. Jesus Christ (in *Luke* **23** 43) says to his friends on the cross, "Today you will be with me in paradise," but everybody knows he did not show up in paradise himself until three days later. Why should anyone want to take *Genesis* **1** more literally?

Nineteen centuries ago, Josephus wrote that Moses "speaks some things wisely, yet enigmatically, and others allegorically" (*Antiquities of the Jews*, Preface, 4). Slightly later, the early Church father Origen wrote in his *De Principiis* (IV,i,5) "Who that has understanding will regard the statement as truthful that the first three days existed without Sun, Moon, and stars, and the first day without even a sky? And who is so ignorant as to suppose that God, as if a husbandman, planted a real tree in Eden such that anyone eating of it with bodily teeth should obtain life, and, eating of another tree, should come to the knowledge of good and evil? … No one, I think, can doubt that (these things) are related figuratively, not literally, in Scripture, and some mystical meaning may be indicated by it."

A single millennium after that (and before now) Maimonides concluded (*Guide for the Perplexed*, II, xxv) "If we accepted the Eternity of the Universe … and assumed, with Plato, that the heavens are likewise transient, we should not be in opposition to the fundamental principles of our religion." If the Bible was taken figuratively by scholars tens of centuries ago, who presumes to assert that it must now be taken at face value? What new information affirms the inerrancy of the Bible more now than in the time of Christ or Aquinas?

As a work of mythology and moral precepts, the Bible is probably as good as anybody's … except, of course, where Jael kills Sisera by nailing his head to the floor, Dinah is raped by Shechem and Lot is seduced by his own daughters. However, the Bible is neither among the most original nor imaginative of such works, as a glance through the mythology of nearly any culture on Earth will quickly reveal.

Nevertheless, those fatuous enough to require a biblical justification for everything, including evolution, might turn to *Ecclesiastes* 3 19 — "For that which befalleth the sons of men befalleth beasts … As the one dieth, so dieth the other, yea, they have all one breath, so that man hath no pre-eminence above a beast, for all is vanity. All go unto one place, all are of the dust, and all return to dust."

The creationists claim that we may come to know the Creator by deducing Him from his work on Earth. Well, we know that there are 750,000 species of insect now alive. Anyone who has ever had a conversation with an entomologist knows what a deadly dull lot those fascinated by insects can be. To envision the Creator expending his divine energy on three-quarters of a million different, meticulously crafted bugs necessitates an image of Him as a dismal, insufferable, cosmic bore!

The patterns of the history of life also argue eloquently about the Creator's revelation of himself. As Haldane put it half a century ago "Most lines of descent end in extinction, and commonly the end is reached by a number of different lines evolving in parallel. This does not suggest the work of an intelligent designer, still less of an almighty one."

Similarly, the fact that humans and chimpanzees hold more than 97 per cent of their genetic material in common should suggest that either they have evolved from a recent common progenitor, or that they were zapped into existence independently by Someone lacking a great deal of imagination.

The belief in such an Omnipotent Simpleton is certainly a matter of personal choice, but his existence (or lack thereof) is completely independent of the reality of evolution. For the natural world all but cries out for us to acknowledge phylogenetic relationships, and these relationships will be equally real to science whether or not deities exist.

Thus, evolution is not atheistic, it is agnostic. The existence of deities is not denied by evolution — it is ignored, because it is irrelevant. The study of evolution is the study of the diversity and unity of known life, the existence of God is as relevant to evolution as the existence of giant boll weevils on the planet Antares. Either things have evolved, or they are designed to appear to have evolved — either way, science leads to the conclusion of evolution, the only paths to non-evolution are fraud and obscurantism.

Finally, one need only compare the last page of the first and sixth editions of *The Origin of Species* to see that even Darwin never completely ruled God out.

Well, everybody makes mistakes.

JON MARKS
Department of Anthropology,
University of Arizona,
Tucson, Arizona, USA

Safe as 2,4,5-T?

SIR — One of us (H.F.T.) reported last year on 2,4,5-T use and congenital abnormality rates in Hungary[1]. Since that report more information has become available on the herbicide used and on congenital abnormality and spontaneous abortion rates.

The Hungarian herbicide is applied either as Klorinol, the 2,4,5-T precursor, 2,4,5-trichlorphenoxyethanol (2,4,5-TE), or as Buvinol, a combination of 2,4,5-TE with *S*-triazine. Buvinol is one of the most important products of the Budapest Chemical Works, which marked its 100th anniversary by publishing a book about it entitled *The Development of a Pesticide as a Complex Scientific Task*[2]. This monograph was published "as a tribute to the skill and many years of painstaking work performed by the research team and to reflect the standard and modern conditions of Hungarian pesticide research"[2]. The editor suggests that the development of Buvinol "may be considered a real — even if not ideal — model of modern pesticide research"[2].

Development of the chlorinated phenoxy alkanols was conducted between 1962 and 1975. In 1969 contamination of 2,4,5-TE by dioxin (TCDD, 2,3,7,8-tetrachlorodibenzo-*p*-dioxin) was discovered. The level of TCDD contaminant until mid-1972 was up to 1.6 p.p.m. After that date improvements in the formulated product reduced the TCDD contaminant to levels below 0.1 p.p.m. The extensive animal testing of 2,4,5-TE and Buvinol included studies of acute toxicology, neurotoxicology, teratogenicity and carcinogenicity[2]. Chromosomal studies were also undertaken of workers manufacturing 2,4,5-TE and Buvinol[2]. The general conclusion reached on the basis of all these studies was that if proper labour safety measures were taken and the relevant regulations for residues observed, no health hazard would arise. The production and consumption of 2,4,5-TE in Hungary has therefore continued to rise. In 1976, 1977 and 1978 consumption of 2,4,5-TE (total product) was 1,278, 1,533 and 1,753 tonnes respectively[3]. Trends in congenital anomalies and stillbirths have continued as described previously[1] despite rising herbicide consumption.

Between 1970 and 1980, there has also been a consistent fall in the national spontaneous abortion rate (16.3 to 11.8 per cent of all recorded conceptions, excluding those terminated by induced abortion). The highest rates of fetal deaths occur in Budapest and the lowest in the country areas. There have been no reports in Hungary linking congenital abnormalities or spontaneous abortions with the use of 2,4,5-TE. Furthermore, a study of female agricultural workers exposed to 2,4,5-TE found no evidence that their offspring had a higher rate of congenital abnormalities[4].

H. F. THOMAS
MRC Epidemiology Unit,
Cardiff, UK

A. CZEIZEL
Department of Human Genetics,
National Institute of Hygiene,
Budapest, Hungary

1. Thomas, H. F. *Lancet* ii, 214-215 (1980).
2. Banki, L. (ed.) *The Development of a Pesticide as a Complex Scientific Task* (Budapest Chemical Works, Medicina, 1976).
3. *Food and Agricultural Organisation. Production Yearbook 1979* (FAO, Rome, 1979).
4. Szabuka, M. *et al. Magy Noorv Lap* 43, 527-534 (1980).

NEWS AND VIEWS

Mirror-image navigational errors in migrating birds

from Jared M. Diamond

EXAMPLES of the navigational accuracy of migrating or homing birds are plentiful the Arctic Tern commutes 18,000 km between its Arctic breeding grounds and sub-Antarctic wintering grounds, the Laysan Albatross is born on Midway Atoll and wanders the ocean for about eight years before returning to Midway to breed, the first year young of New Zealand's Long-tailed Cuckoo head out over the Pacific, unaccompanied by adults, to find and winter on tiny islands up to 8,000 km away But there are also examples of navigational 'failure' These could be of special significance because they may give us some insight into how navigation normally occurs

Particularly interesting are examples[1–5] of mirror-image navigational error The phenomenon was first observed in western North America by David DeSante (Point Reyes Bird Observatory, Stinson Beach, California) He found that some out-of-place birds appearing on the California coast in autumn were following a westerly bearing which was a mirror image of their normal migration path, that is, they were taking the correct bearing with respect to the north–south axis, but choosing the wrong east-west (right–left) sense of that angle He made map comparisons of the aberrant and normal migration tracks and their timings and carried out behavioural tests which proved the captured vagrants unable to tell left from right in the test context[6–10]

The story starts in the 1960s, when growing numbers of bird-watchers on the coast of California began searching for rare birds It turned out that, in the autumn, rare individuals of almost every species of New World warbler (Parulidae) typical of eastern North America appeared on the west coast[11, 12] However, different warbler species were very differently represented among these rare vagrants, two species (Blackpoll and Palm Warblers) accounting for nearly as many records as the other 28 species These vagrants could not be just wind-blown birds, as had been previously suggested[13,14], for then warblers starting from the same breeding grounds would reach California simply in proportion to their breeding abundance Relative abundances combined with small deviations from the normal migration route can account for some of the differences among species[12] but big unexplained anomalies are left

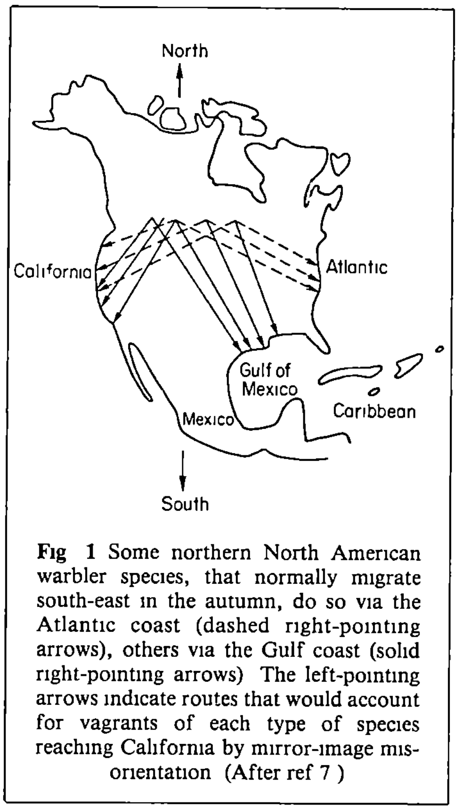

Fig 1 Some northern North American warbler species, that normally migrate south-east in the autumn, do so via the Atlantic coast (dashed right-pointing arrows), others via the Gulf coast (solid right-pointing arrows) The left-pointing arrows indicate routes that would account for vagrants of each type of species reaching California by mirror-image misorientation (After ref 7)

Parulid warblers normally set out from their breeding grounds and fly overland in a series of single night flights, covering about 300 km in a night and resting about four days between flights to feed and replenish fat reserves They then make a long overwater flight across the Gulf of Mexico, Caribbean, or west Atlantic to reach their wintering grounds in Central or South America or the West Indies During the overwater flight landmarks are absent, and it is thought that immature birds, on their first autumn flight south, follow a given (genetically specified) compass direction for a given distance or time[15] They thus need an inherited knowledge of the correct compass bearing, plus the ability to determine a compass reference point (for example, by circumpolar stars[16]) to follow the correct migration route Adults, on the other hand, have already made one round trip and are thought to have knowledge of the map coordinates of the breeding and wintering grounds plus an ability to determine their present location Over ninety per cent of the vagrant autumn parulids on the California coast are immatures, presumably dependent on 'distance-and-direction' navigation

Misorientation and disorientation

Timing of west coast arrival makes it possible to distinguish errors of *mis*orientation from errors of *dis*orientation, that is, an inability to follow *any* consistent direction For each species DeSante tabulated the mean arrival date of normal (easterly) migrants at stations on the US Atlantic or Gulf coasts and, measuring distances from the centre of the breeding range, predicted a date of west coast arrival assuming a direct great-circle flight path and one 300 km night flight every four days (see Fig 1) The predicted arrival dates for each species agreed, on average, with the observed ones to within one day, even though the arrival time of different species differed by nearly a month and the west and east coast arrivals of the same species also differed by up to a month because of the different distances from the breeding grounds The vagrants are thus not *disoriented* but *misoriented* they are covering distance at the same rate as normal migrants, but on the wrong bearing

What type of misorientation error might the vagrants be making? One simple possibility, that the birds were following a reversed (180° out) bearing that would be appropriate for the return to the breeding grounds in the spring can be ruled out by a glance at the map — the commonest vagrant species breed entirely north of California Are the vagrants following an actual mirror image of their normal orientation path or are they simply mis-

---

Jared M Diamond is Professor of Physiology at the University of California Medical School, Los Angeles, California 90024

0028-0836/82/040277-02$01 00

oriented in the sense of having inherited the wrong bearing or a wrong reference point?

Most of the vagrants can be assigned to two groups those that normally bear far east from their breeding grounds to the Atlantic coast, then fly over the western Atlantic to the West Indies or South America, and those that normally bear closer to south to the Gulf Coast, then across the Gulf of Mexico to Central America The two possibilities above make quite different predictions when one compares the Atlantic and the Gulf migrants with respect to their frequency and time of arrival in different parts of California Mirror-image misorientation would, for instance, cause the northern California contribution to all Californian records to be higher for Atlantic than for Gulf migrants, while simple misorientation would not

Examination of the data consistently indicated mirror-image misorientation This conclusion is consistent with the different frequencies of different species or vagrants the two most frequent vagrants are Atlantic migrants, although they are much further off-course than Gulf migrants in California

Mirror-image misorientation in the laboratory

It is no easy task to demonstrate mirror-image misorientation in the laboratory because it is, after all, rare even to *see* the vagrants in California, let alone catch them All Californian bird-watchers combined saw only about 150 individuals per year in the decade 1962-72

De Sante went to the isolated Southeast Farallon Island off the California coast, where lost overwater migrants concentrate, and succeeded in catching alive, in three years' autumn operations, 24 individuals of the commonest vagrant, the Blackpoll Warbler Under a clear moonless sky he tested them individually in an Emlen cage, an inverted paper cone with an ink pad at the bottom, such that the bird fluttering up the cone (about 80 times per hour) marks its direction with inked footprints To analyse the inkmarks, DeSante devised optical scanning techniques and new statistical methods for recognizing multiple modes in a circular distribution, these are important and deserve to be more widely known

The vagrants oriented not just in the expected mirror-image direction (WSW), but in four preferred directions (Fig 2)[1] One mode was about 125° (ESE), the angle of the normal migratory track The second was its mirror image, about 235° (WSW), the angle expected for a mirror-image misorientation flight from Canada to the California coast The other two modes were about 305° (WNW) and 55° (ENE), the 180° reverse tracks of the other two modes

The 180° reverse modes are easy to explain most autumn migrants on the Farallon Islands arrive from the south-west, having overshot the California coast and the islands in their southwesterly flight at night, and doubled back north-east on their track in the morning Orientations cage studies on normal migrants have also noted 180°-reversed modes along with normal modes A reasonable interpretation is that the best strategy for a nocturnal migrant finding itself at dawn over ocean or unsuitable habitat is to fly back up its track until it regains the coast or suitable habitat.

But why did the migrants orient ESE and WSW with equal frequency, when only a WSW track could account for their appearance in California and an alternating ESE/WSW track would have taken them in a zigzag south? In the cage experiment they could not tell left from right, whereas on migration they systematically chose right In both humans and animals, left and right reflex responses are often encoded together, and subsequent success at left/right discrimination depends on available motor and sensory cues[17] It seems likely that both normal and vagrant warblers inherit a knowledge of the correct angle with respect to the north–south axis, that the normal warbler can also use sensory cues to choose the correct east–west sense, but that the vagrant initially chooses the sense at random on the first night and then maintains that sense on subsequent nights

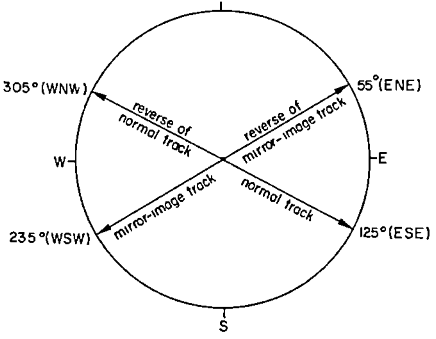

Fig. 2 The four preferred orientations of caged Blackpoll Warblers caught as autumn vagrants in California (After ref 7)

Evolutionary origins

Parulid warblers have extended their breeding ranges far to the north-west since the retreat of the Pleistocene glaciers and may still be sorting out the new navigational techiques needed, including left–right discrimination Most of the mirror-image vagrants probably end up far offshore in the Pacific and die There are, however, several cases of banded mirror-image vagrants returning to the same California location in three consecutive winters Two warbler species, the Townsend's Warbler and 'Myrtle' race of the Yellow-rumped Warbler, have regular west coast winter ranges isolated from their main winter ranges to the south and east, at locations consistent with mirror-image migration Hence mirror-image misorientation may occasionally lead to the evolution of new winter ranges

A worldwide phenomenon?

Observations suggestive of mirror-image misorientation have been described from three other parts of the world First, MacLaren[4] noted the occurrence of western warblers in eastern North America They may have taken the mirror image (NE) of their normal (NW) migration path from their Mexican wintering grounds up the axis of Mexico Second, the Old World warbler species *Phylloscopus proregulus, P inornatus, P trochiloides* and *P borealis* (Sylviidae) breed in Siberia and normally migrate due east in the autumn before heading south, but regularly appear in low numbers as autumn migrants in western Europe[1,18] Other species whose autumn vagrancies in western Europe suggest mirror-image misorientation include the pipits *Anthus novaeseelandiae* and *A gustavi*, and the warbler *Phylloscopus fascatus* Third, several races of the wagtail *Motacilla flava* that breed in Siberia and normally migrate south-west in the autumn occasionally winter in Australia and New Guinea, suggesting a mirror-image flight to the south-east[2,3] Finally, vagrants of numerous species that breed in north-east Asia and normally migrate south-west follow a mirror-image course south-east to western Alaska and the Aleutian Islands, and rarely down the North American coast as far as California[5] Systematic re-examination of off-course migrant records elsewhere in the world, especially Europe, could yield further examples of mirror-image misorientation

Finally, we might speculate that De Sante's work will be linked to the neuropsychological literature on left–right discrimination in humans and other animals Humans with impaired left–right discrimination[19-22] often prove to have lesions in particular parts of the cerebral cortex and other associated sensory and motor problems Behavioural and neuroanatomical studies of captured mirror-image migrants may indicate whether birds and humans with impaired left–right discrimination share similar defects □

---

1 Rabøl *Dansk orn Foren Tidsskr* 70, 5 (1976)
2 Blackwell & Yates *Aust Birds* 14, 35 (1979)
3 Moffatt *Emu* 81, 47 (1981)
4 MacLaren *Auk* 98, 243 (1981)
5 Roberson *Rare Birds of the West Coast* (Woodcock, Pacific Grove, California, 1980)
6 DeSante *et al Am Birds* 26, 112 (1972)
7 DeSante thesis, Stanford Univ (1973)
8 DeSante & Remsen *Am Birds* 27, 110 (1973)
9 Stallcup *et al Am Birds* 29, 112 (1975)
10 DeSante & Ainley *Studies in Avian Biology* No 4 (1980)
11 McCaskie *Calif Birds* 1, 95 (1970)
12 DeBenedictis *Calif Birds* 2, 111 (1971)
13 Bagg *Audubon Field Notes* 24, 4 (1970)
14 Able *Am Birds* 26, 25 (1972)
15 Gwinner *A Rev Ecol Syst* 8, 381 (1977)
16 Emlen *Auk* 84, 309 (1967)
17 Corballis & Beale *Scient Am* 224, 96 (1971)
18 Rabøl *Br Birds* 62, 89 (1969)
19 Gerstmann *Neurology* 7 866 (1957)
20 Sauguet *et al J Neurol Neurosurg Psychiat* 34, 496 (1971)
21 Lezak *Neuropsychological Assessment* (Oxford University Press, New York, 1976)
22 Heilman & Valenstein *Clinical Neuropsychology* (Oxford University Press, New York, 1979)

0028-0836/82/040278-02$01 00

Meteorite erosion and cosmic ray variations

from David W. Hughes

A METEORITE has had a chequered career before it finally ends up in a museum store room. It seems that meteorites were formed about 4.6×10^9 yr ago, but spend a great deal of their time buried in some larger body; each type is exposed to the space environment for a different length of time, although a typical value is 10^7 yr.

The length of the exposure can be estimated by looking at the damage inflicted on the meteorite by cosmic ray bombardment. Nuclear reactions are induced in the elements in the surface regions, and leave behind tracks of radiation-damaged material analogous to the tracks produced by nuclear fission. The tracks extend tens of centimetres into meteorites retrieved from the Earth's surface. If the abundance of the reaction products can be measured and their production rate in space is known, then the exposure age can be simply calculated. Measurements of the rate at which the track density varies as a function of depth can lead to an accurate estimation of the amount of material ablated from the meteorite during its passage through the atmosphere.

A problem remains, however. The exposure ages given by measuring the nuclide ^{40}K (half life 1.3×10^9 yr) are systematically 45 per cent longer than those obtained by measuring relatively short-lived nuclides such as ^{39}Ar, ^{36}Cl, ^{26}Al and ^{10}Be which have half lives of 270, 3×10^5, 7×10^5 and 1.5×10^6 yr respectively. The difference may be caused by a temporal variation of the intensity of galactic cosmic rays. If the intensity was 45 per cent higher over the last 10^6 yr than it had been over the previous 10^9 yr, then the anomaly would be resolved. A second solution is possible if variations in exposure ages are due to some mechanical process such as multiple collisions in the Solar System or the erosion of the meteorite surface. The problem has now been tackled by O.A. Schaeffer, K. Nagel, H. Fechtig and G. Neukum at the Max-Planck-Institut für Kernphysik, Heidelberg, and their findings have been published in *Planetary and Space Science* (**29**, 1109; 1981).

Multiple collisions

A specific meteorite could have spent a considerable time shielded from the cosmic ray flux below the surface of a larger body. If the larger body was then fragmented in a collision the meteorite could find itself in a less shielded position. If the less shielded exposure lasts longer than a few times the half life of the relatively short-lived nuclides (that is, longer than a few million years), the ^{10}Be, ^{36}Cl and ^{39}Ar will be in equilibrium with the high flux whereas the ^{40}K will still register the low flux. Unless the change in shielding is always the same — something that is highly unlikely — the ratio of the two exposure ages will vary from meteorite to meteorite. That ratio has been measured accurately in only twelve meteorites. Eight of them have the ^{40}K exposure age 1.45 ± 0.10 times the short-lived nuclide exposure age. The authors conclude that it is most unlikely that such a large fraction of meteorites has suffered collisions which produce the same exposure age ratio; so the cause of this discrepancy must be something other than their collision history.

Space erosion

An exposed meteorite is continually being cratered by collisions with cosmic dust particles at planetary velocities. As the surface is eroded, over time the cosmic ray intensity at a given depth inside the meteorite increases. Schaeffer, Nagel, Fechtig and Neukum calculate the expected erosion rate in some detail.

Only three meteorites, Přibram, Lost City and Innisfree, have known 'out of atmosphere' orbits. Comparing these orbits with those obtained for the meteoroids responsible for very bright fireballs seen by the camera networks gives a mean aphelion distance of 2.8 AU for the average meteorite.

Using satellite and lunar microcrater data the authors estimate how the flux of microparticles (diameters 1 μm to 1 cm) striking the meteorite surface varies as a function of particle size and distance from the Sun. The collisional velocities of these microparticles have also been calculated as a function of heliocentric distance. It is found that the impact velocity of the 1 – 10 μm particles varies between 15 and 5 km s^{-1} as the meteorite moves between points 1.25 and 3.75 AU from the Sun. Larger particles, with diameters between 100 μm and 1 cm, seem to have a relatively constant impact velocity of around 9 km s^{-1}.

From laboratory experiments, where silicate surfaces were exposed to collisions with small particles, the authors found that the volume, V, excavated by an impacting particle of diameter d is given by $V = 7.94\ d^{3.236}$. Integrating over particle sizes, the meteorite orbit produces a mean erosion rate for stoney meteorites of 650 μm per million years.

Dust particles hitting iron meteorites excavate less material, and laboratory experiments using a light gas gun to accelerate particles indicated that the eroded volume of iron was a factor of 30

100 years ago

ILLUSTRATIONS OF NEW OR RARE ANIMALS IN THE ZOOLOGICAL SOCIETY'S LIVING COLLECTION

THE Beatrix Antelope (*Oryx Beatrix*). — The antelopes of the genus *Oryx* constitute a well-defined and most beautiful group of the Bovine Family. In 1857, the late Dr. Gray described a new *Oryx* species based upon an animal received from Bombay, but supposed to have been originally brought from some port on the Red Sea. The Beatrix Antelope, as it was named by Dr. Gray after the Royal Princess of that name, remained a somewhat obscure species until 1872, when, singularly enough, a second living example was received from Colonel Pelly, H.B.M. Resident at Bushire, and deposited in the Society's collection. In 1878 a third example of the same antelope was received by the Society from Commander Burke, of the S.S. *Arcot*. This animal was obtained at Jedda, but was stated to have been originally captured in the Hedjez passes, some 150 miles in the interior of Arabia. The fourth example of this antelope, lately presented to the Society by Lord Lilford, comes from a still more definite locality, the great desert behind the mountainous district of Oman. It is now therefore abundantly evident from these four examples, which agree in all material points, that the Beatrix Antelope is a good and well-defined species, and that its native home is the interior of the Arabian peninsula, where it replaces the Beisa of the Abyssinian plateau.

From *Nature*, 26 January, 295, 1882.

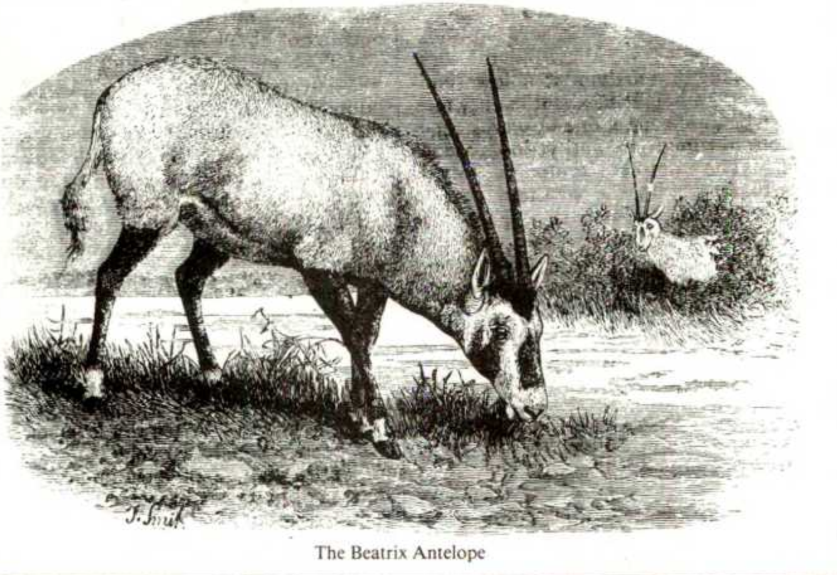

The Beatrix Antelope

David W. Hughes is in the Department of Physics, University of Sheffield, Sheffield S3 7RH.

0028-0836/82/040279-02$01.00

smaller than that for silicate rocks. So the erosion rate for iron meteorites is about 22 μm per million years.

The authors investigated the possibility that the dust particle flux had varied as a function of time. Microcraters on lunar rocks indicate that the flux has remained constant within a factor of 2 for the last 20 million years. There is no information about the small particle flux before this time. As regards large craters, however, it can be concluded that the flux of objects responsible for craters with diameters between 0.01 and 100 km has remained constant to within a factor of 50 per cent for the last 850 million years. By comparing craters on Mars with those on the Moon the authors concluded that there has been no change for nearly 10^9 years in all regions of the Solar System between 1 and 4 AU from the Sun.

The discrepancy between the ^{40}K exposure ages and the ^{39}Ar, ^{10}Be and ^{36}Cl exposure ages could be explained if the erosion rate of iron meteorites was 200 μm per million years, but it has been found to be nine times less; or if the flux of small particles had increased, but it has been found to be constant for about the last 10^9 yr; or if meteorites had had the same collision history, but this is highly unlikely. So one is left with the conclusion that there has been a real change in the cosmic ray flux in the inner Solar System during the last 10^9 yr. And the meteorites indicate that the present flux, the one active over the last 10^6 yr, is about 45 per cent higher than the average flux over the previous 10^9 yr. The next problem, needless to say, is to find out why the cosmic ray flux changed. □

Prohormones for vasopressin

from B. T. Pickering

"STUDIES on the distribution and biosynthesis of neurophysin within the neurones of the [hypothalamo-neurohypophysial complex] suggest the interesting possibilities that either neurophysin and vasopressin share a common precursor or that there is a common genetic unit that controls the synthesis of the major components of the neurosecretory substance." Thus wrote Howard Sachs in 1969[1] and, during the past 12 years, more and more evidence has accumulated in favour of such a common precursor (see, for example, ref.2). The final vindication of Sachs's suggestion is reached today with the publication, by Richter and his colleagues, of the complete amino acid sequence of the bovine vasopressin–neurophysin precursor (see this issue of *Nature*, p.299).

This sequence, deduced from cDNA prepared from hypothalamic mRNA, reveals no surprises, being composed of a leader (or signal) peptide separated by a pair of basic residues from the sequence of arginine vasopressin which is followed by a glycyl residue and a further pair of basic amino acids and then the 97 residue sequence of bovine neurophysin II. The 17.3K precursor is completed with a carboxy-terminal 39 residue polypeptide which represents the glycopeptide known to coexist with vasopressin and neurophysin in the secretory granules of the neurohypophysis[3,4]. Such a sequence had already been predicted in several laboratories, both from isolation of putative precursors labelled *in vivo* and from the nature of the polypeptides synthesized in cell-free systems directed by hypothalamic mRNA. This is not to detract from the latest work of the Richter group, which has not only substantiated the size of the vasopressin precursor but established the order of the component polypeptides within the sequence. It will be interesting to see the nature of the carbohydrate side chain, the biological importance of which is unknown. Even more so because there is no evidence for such glycosylation of the oxytocin precursor which is considerably smaller than the vasopressin one. No doubt the Richter group will soon provide the cDNA, and hence the sequence, of this precursor too.

The successful elucidation of the nature of this vasopressin precursor, while concluding a chapter, does not end the story. As discussed in these columns last year[5], Paul Cohen and his group in Paris have drawn attention to the presence in bovine posterior pituitary extracts of much larger molecules (140K) containing the immunodeterminants of neurophysin and vasopressin and thus qualifying for consideration as putative precursors. This work has now been extended[6] and the 140K species has been shown to behave as one of 80K if examined under denaturing conditions. Moreover, this material appeared to consist of two components, linked by both a labile peptide bond and a disulphide linkage, which could be dissociated to give a 10K polypeptide that showed sequence homology with neurophysin and a 68K one which lacked the immunodeterminant for neurophysin. Rosenior *et al.*[7] also have evidence for immunoreactive vasopressin and neurophysin species of about 80K and 40K in rat hypothalamic extracts, and consider them to be putative precursors.

Arguments against such precursors come from the failure of extracted mRNA to direct the synthesis of products larger than 20–25K and, now, from the apparent completeness of this message with start and stop codons. The French group has argued that the 80K molecule might be directed by a different mRNA than the one preferentially extracted. However, in none of the *in vivo* studies has there been indications of incorporation of tracer amino acid into immunoreactive neurophysin or vasopressin species larger than 25K so that such a message would necessarily be present in minute amounts — much smaller than would be suggested from the relative proportions of larger vasopressin components found by Rosenior *et al.*

Very recently the 80K vasopressin/neurophysin putative precursor has taken on even more significance. Cohen and his colleagues have shown[8] that its 68K fragment contains immunoreactive sequences for both ACTH and β-endorphin, and that biologically active ACTH can be released from it by limited proteolysis. They interpret their data to suggest the existence of a pluripotent molecule which is a common precursor for all, or many, of the neuropeptides found in the posterior pituitary and which they term neurohypophysial coenophorin.

Quite apart from the rigorous criteria necessary to ascertain that large molecules, especially those rich in disulphides, do not arise from self-association of smaller ones (criteria which have been applied by Cohen and his associates), it should perhaps be questioned whether a large polypeptide containing within it the sequence of a smaller one is necessarily a precursor of the latter rather than vice versa. As part of the secretory process a newly synthesized polypeptide is packaged into secretory granules and, in every system which has been studied, there is evidence for a proportion of the secretory product being bound to the granule membrane. Could the large molecules discussed above represent such membrane-bound components which are in fact covalently linked to membrane proteins? Certainly a membrane-associated component from the ACTH system might share many of the properties of a similar component from the neurohypophysial system. Its presence in neurohypophysial extracts might arise from the close association of the pars intermedia and the pars nervosa in the pituitary gland.

Whatever their origin, these large molecules do present a fascinating problem, the solution of which will tell us much more about the nature of the secretory process in the polypeptide-producing cell. □

B.T. Pickering is Professor of Anatomy and Head of the Department of Anatomy at The Medical School, University of Bristol, University Walk, Bristol BS8 1TD.

1. Sachs *Adv. Enzym.* **32**, 327 (1969).
2. Russell *et al. Endocrinology* **107**, 1880 (1980).
3. Jones & Swann *J. Physiol., Lond.* **245**, 45P (1975).
4. Béguin *et al. J. biol. Chem.* **256**, 9289 (1981).
5. Pickering *Nature* **288**, 177 (1980).
6. Béguin *et al. J. biol. Chem.* **256**, 9289 (1981).
7. Rosenior *et al. Endocrinology* **109**, 1067 (1981).
8. Lauber *et al. Proc. natn. Acad. Sci. U.S.A.* **78**, 6086 (1981).

0028-0836/82/040280-01$01.00

Is phosphatidylinositol now out of the calcium gate?

from J.N. Hawthorne

PHOSPHATIDYLINOSITOL (PI) is a minor phospholipid constituent of most mammalian cell membranes and has attracted attention because of its response to the activation of a wide variety of surface receptors. Most of the receptors concerned mobilize calcium as a second messenger and Michell[1] suggested in 1975 that PI hydrolysis opened cell surface Ca^{2+} channels. His hypothesis has been particularly fruitful but recent results make it untenable as a general explanation of the PI response.

The original observation of Hokin and Hokin[2] illustrates the PI response. When treated with acetylcholine, slices of pigeon pancreas secreted amylase. If the incubation medium contained ^{32}P-labelled inorganic phosphate, secretion was accompanied by increased labelling of phospholipids which were later identified as PI and its precursor, phosphatidic acid. It is now generally believed that receptor activation causes hydrolysis of PI to diacylglycerol and inositol phosphates and that the labelling seen in the Hokin experiment reflects subsequent resynthesis of PI. The proposed cycle of events and Michell's suggested link with calcium gating are outlined in the figure.

As a mechanism for controlling Ca^{2+} influx, breakdown and resynthesis of PI seems rather cumbersome. The initial hydrolysis is presumed to be at the plasma membrane, though there is little clear evidence of this. A kinase producing phosphatidate from the resulting diacylglycerol may occur in the same membrane, but the remaining enzymes for PI resynthesis are located on endoplasmic reticulum, so that there are transport problems. Another difficulty is that the phospholipase hydrolysing PI in response to receptor activation is located in the cytoplasm, rather than in the plasma membrane as required. Resynthesis is also costly to the cell, because it involves the loss of three high-energy phosphate bonds. This seems an expensive way to move calcium ions down a concentration gradient.

The cytoplasmic phospholipase just mentioned is activated by Ca^{2+}, suggesting that PI breakdown might be a consequence rather than a cause of Ca^{2+} mobilization. However, the PI effect usually seemed to be independent of extracellular Ca^{2+} and this provided an important argument in favour of the calcium gating theory[1,3]. Further support came from the fact that in several systems calcium entry in response to an ionophore did not cause hydrolysis of cellular PI. However in a number of tissues studied more recently, PI hydrolysis appears to depend on external Ca^{2+}. Some of these results, and their implications, have been reviewed by Cockroft[4]. Furthermore, reinvestigations of pancreas and adrenal medulla, which originally provided support for the gating theory, now provide results contrary to it.

Farese *et al.*[5] repeated the original Hokin experiment, showing that cholinergic release of amylase from rat pancreatic fragments was accompanied by a chemically measured loss of PI. Removal of calcium abolished both effects and the calcium ionophore A23187 itself caused PI breakdown in a medium containing 2.5 mM Ca^{2+}. This implies that the PI loss follows calcium mobilization. Work with rabbit neutrophils led to a similar conclusion[6]. Stimulation of these cells with the peptide fMet-Leu-Phe in the presence of cytochalasin B caused secretion of lysosomal enzymes and breakdown of PI. Extracellular Ca^{2+} was essential for the PI breakdown, which could be produced in response to the calcium-carrying ionophore ionomycin, as well as to the peptide agonist. In platelets also, hydrolysis of PI can be promoted by either thrombin activation or a calcium ionophore[7].

Bovine adrenal medulla presents a different picture. The PI response is to muscarinic but not nicotinic activation, and it is certainly independent of external Ca^{2+}. However, the physiological response, catecholamine secretion, is mediated by nicotinic receptors and associated with an influx of Ca^{2+}. Muscarinic receptors probably modulate the secretory process and their activation[8] causes no measurable entry of Ca^{2+}. Cholinergic muscarinic receptors present a more general difficulty in understanding the PI effect. The post-synaptic ones produce secretory effects by opening calcium gates but the pre-synaptic muscarinic receptors usually inhibit secretion. The mechanism by which they act is not understood, but it is likely that they decrease calcium availability. Yet activation of both pre- and post-synaptic receptors produces breakdown of PI.

Results from some tissues in which receptors control Ca^{2+} mobilization still provide support for Michell's hypothesis. One of the most impressive comes from the blowfly salivary gland[9]. This gland secretes iso-osmotic KCl when stimulated by 5-hydroxytryptamine, a process involving PI breakdown and entry of calcium into the epithelial cells. Continued treatment with the agonist causes loss of a small pool of PI and a fall in Ca^{2+} transport. Incubation of the washed glands with inositol restores both PI sensitivity to 5-hydroxytryptamine and transport, indicating close links between receptor activation, PI hydrolysis and calcium influx. In spite of this, there are so many systems in which the receptor-linked PI loss requires external calcium that a universal role for PI in Ca^{2+} mobilization cannot be upheld.

Michell's insistence on a link with Ca^{2+} should not be lightly set aside and in this respect triphosphoinositide and diphosphoinositide, the phosphorylated derivatives of PI, are of interest. They are highly labile, have considerable affinity for

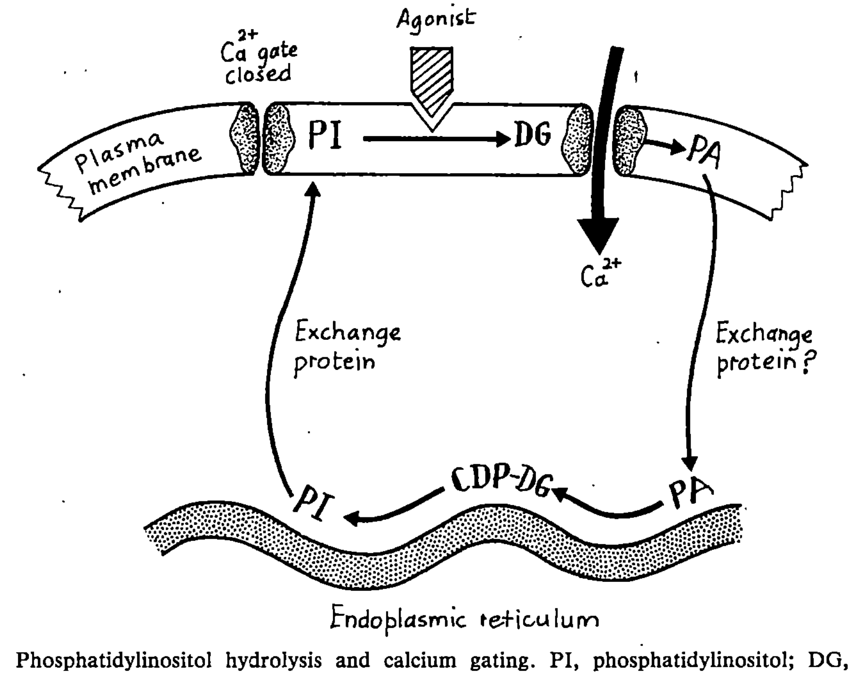

Phosphatidylinositol hydrolysis and calcium gating. PI, phosphatidylinositol; DG, diacylglycerol; PA, phosphatidate.

J.N. Hawthorne is Professor in the Department of Biochemistry, University Hospital and Medical School, Clifton Boulevard, Nottingham NG7 2UH.

0028-0836/82/040281-02$01.00

Ca^{2+} and are usually found in plasma membranes. Both adrenergic and cholinergic stimuli cause breakdown of these lipids[10,11] which would be followed by a loss of PI for their resynthesis. Whether this could explain the PI response generally remains to be seen, since the polyphosphoinositides occur in such low concentrations in most tissues. Polyphosphoinositides are unlikely to replace PI in a calcium gating theory, because their hydrolysis seems to require calcium[11,12]. Nevertheless, on the basis that there is a less obvious calcium requirement for the vasopressin-induced breakdown of triphosphoinositide in hepatocytes[13], Michell now seems prepared to shift his ground from PI to this lipid.

What are PI and polyphosphoinositides doing if not Ca^{2+} gating? There is no shortage of suggestions but none provides a convincing general explanation. Conversion of PI to diacylglycerol, for example, could produce a localized increase in membrane fluidity. This in turn could facilitate exocytosis or protein–protein interactions in a membrane. Recent work suggests that polyphosphoinositides and PI may control protein kinases[14,15]. Activation of some receptors leads to protein phosphorylation, so the possible involvement of inositol lipids deserves further study.

The inositol lipids are rich in arachidonic acid and another theory of the PI response is that receptor-linked hydrolysis supplies this fatty acid for prostaglandin synthesis[16]. Since many systems showing the PI effect do not require prostaglandins for the physiological response, this theory cannot apply generally.

It would be tedious to continue the list of inadequate answers to the puzzle of PI. If this is goodbye to the calcium gating theory, we shall miss it, at least until we have a better explanation. □

1. Michell, R.H. *Biochim. biophys. Acta* **415**, 81 (1975).
2. Hokin, M.R. & Hokin, L.E. *J. biol. Chem.* **203**, 967 (1953).
3. Michell, R.H. & Kirk, C.J. *Trends pharmac. Sci.* **2**, 86 (1981).
4. Cockroft, S. *Trends pharmac. Sci.* **2**, 340 (1981).
5. Farese, R.V., Larson, R.E. & Sabir, M.A. *Biochim. biophys. Acta* **633**, 479 (1980).
6. Cockroft, S., Bennett, J.P. & Gomperts, B.D. *Nature* **288**, 275 (1980).
7. Bell, R.J. & Majerus, P.W. *J. biol. Chem.* **255**, 1790 (1980).
8. Fisher, S.K., Holz, R.W. & Agranoff, B.W. *J. Neurochem.* **37**, 491 (1981).
9. Berridge, M.W. & Fain, J.N. *Biochem. J.* **178**, 59 (1979).
10. Abdel-Latif, A.A., Akhtar, R.A. & Hawthorne, J.N. *Biochem. J.* **162**, 61 (1977).
11. Fisher, S.K. & Agranoff, B.W. *J. Neurochem.* **37**, 968 (1981).
12. Akhtar, R.A. & Abdel-Latif, A.A. *Biochem. J.* **192**, 783 (1980).
13. Kirk, C.J., Creba, J.A., Downes, C.P. & Michell, R.H. *Biochem. Soc. Trans.* **9**, 377 (1981).
14. Kishimoto, A., Takai, Y., Mori, T., Kikkawa, U. & Nishizuka, Y. *J. biol. Chem.* **255**, 2273 (1980).
15. Jolles, J., Zwiers, H., Dekker, A., Wirtz, K.W.A. & Gispen, W.H. *Biochem. J.* **194**, 283 (1981).
16. Marshall, P.J., Dixon, J.F. & Hokin, L.E. *Proc. natn. Acad. Sci. U.S.A.* **77**, 3292 (1980).

A new model for giant H II shells

from J.C. Raymond

SEVERAL years ago it was realized that the energy injected by supernovae can determine the overall structure of the interstellar medium[1,2]. When it is considered that the energy flux of the wind of an early-type star is roughly one per cent of the stellar luminosity it is also apparent that over its short lifetime of a few million years, an O star transfers more energy to the interstellar gas through its powerful wind than it does in its supernova demise. (O stars are massive and very hot blue objects often associated with dust clouds.) Theoretical models of the bubble created by such a wind in the surrounding H II region have been available for more than a decade[3,4] and nebulae having very low densities near the centre, such as the Rosette Nebula, have been considered examples of the phenomenon. Since O stars are generally formed in groups, it is expected that the winds of the stars in a group, together with any supernovae resulting from the rapid evolution of these massive stars, will act together to produce a larger bubble[5]. It is only quite recently that observations of young star clusters and the associated shells have become sufficiently precise for a detailed comparison with the theories.

One such investigation has found excellent agreement between observations of the Cygnus Superbubble and the expanding bubble model[6], but a second, by M. Dopita and colleagues, argues against the straightforward expansion model for an object in the Large Magellanic Cloud[7]. The latter group favours a model in which the stellar winds balance the collapse of the neutral hydrogen cloud from which the stars were formed[8]. In this model, the star cluster is offset from the centre of the collapsing cloud with the result that the standing shock wave created in the stellar wind is oblique. The normal component of the wind velocity is thermalized, providing the pressure to balance the collapsing cloud, while the tangential component becomes a flow along the inner surface of the shell. This flow produces velocity shifts which are largest close to two opposite sides of the bubble, with a band of nearly zero doppler shift (purely tangential velocity) across the middle. The model is similar to one recently proposed for the origin of Herbig-Haro objects from the winds of T Tauri stars[9].

Dopita *et al.* have made a wide variety of observations of N70, a giant filamentary shell in the Large Magellanic Cloud. It is a hollow shell 110 pc in diameter containing the O association Lucke 114. Spectra of nine stars in the cluster and spectra and surface photometry of the shell itself, along with radio observations, demonstrate that photoionization by the stars accounts for the observed emission in the optical lines. Neither radio nor optical evidence supports the earlier suggestions that the shell is an old supernova remnant.

There are two arguments against the model of the standard expanding bubble created by the stellar winds — the age of the cluster, about 6×10^6 years based on the stellar spectra, and the pattern of velocities in the shell, with doppler splittings up to 90 km s^{-1}. While the inferred mass loss rates of the cluster stars are adequate to produce a bubble of the observed size with an expansion velocity of 40–50 km s^{-1}, its age would be less than one million years. Unless something like the effect of mass loss on the evolution of the cluster stars caused an order of magnitude overestimate of the age of the cluster, the observed doppler velocities of the shell are not due to overall expansion.

The second argument against the expansion picture is the pattern of velocity splittings. A nice correlation is found between the observed velocity splittings and those predicted by a model which fits the slightly non-circular shape of the nebula. The primary evidence against expansion comes from several points close to the centre of the nebula which show very little velocity splitting, though the splitting should be largest near the nebula centre if the shell is expanding. In the model of flow along the bubble surface, this is the region where the flow is almost entirely transverse to our line of sight. To rescue the expansion hypothesis it is necessary to place a high density cloud in this section of the shell to inhibit the acceleration. Such a cloud might be consistent with the high surface brightness observed in that region.

If the new model of flow along the inner boundary of the shell is correct, a reinterpretation of observations of many giant and supergiant shells in the Large Magellanic Cloud and other galaxies will be required. □

J.C. Raymond is at the Harvard-Smithsonian Center for Astrophysics, 60 Garden Street, Cambridge, Massachusetts 02138.

1. Cox, D.P. & Smith, B.W. *Astrophys. J. Lett.* **189**, L105 (1974).
2. McKee, C.F. & Ostriker, J.P. *Astrophys. J.* **218**, 148 (1977).
3. Pikelner, S.B. & Shcheglov, P.V. *Sov. Astr.* **12**, 757 (1969).
4. Castor, J., McCray, R. & Weaver, R. *Astrophys. J. Lett.* **200**, L107 (1975).
5. Bruhweiler, F.C., Gull, T.R., Kafatos, M. & Sofia, S. *Astrophys. J. Lett.* **238**, L27 (1980).
6. Abbott, D.C., Beiging, J.H. & Chruchwell, E. *Astrophys. J.* **250**, 645 (1981).
7. Dopita, M.A., Ford, V.L., MacGregor, P.J., Mathewson, D.S. & Wilson, I.R. *Astrophys. J.* **250**, 103 (1981).
8. Dopita, M.A. *Astrophys. J.* **246**, 65 (1981).
9. Canto, J. & Rodriguez, L.F. *Astrophys. J.* **239**, 982 (1980).

0028-0836/82/040282-01$01.00

Fluorescence photobleaching in cell biology

from Ken Jacobson, Elliot Elson, Dennis Koppel and Watt Webb

In the past few years, new techniques have emerged to measure the translational mobility of fluorescence-labelled molecules within microscopic specimens, including living cells. The methods are based on the photobleaching of discrete regions of the samples bearing fluorescent molecules, thereby destroying their emission, and the subsequent observation of the recovery of fluorescence due to the diffusion or flow of unbleached fluorophores from the surrounding region into the irradiated area. The speed of recovery is directly related to the diffusion coefficient or flow velocity of the labelled molecule while the degree to which the fluorescence regains the prebleach value gives the mobile fraction of the measured population of probe molecules.

The techniques have become known as fluorescence recovery (or redistribution) after photobleaching (FRAP), fluorescence photobleaching recovery (FPR), or fluorescence microphotolysis (FM). In most instruments a continuous wave laser is focused by the microscope objective on either a micron-sized spot or lined pattern on the specimen. The simplicity of the techniques has promoted their rapid application to measurements of translational diffusion in natural and artificial membranes, the diffusion of biopolymers in solution and, most recently, molecular diffusion in the cytoplasm of living cells.

The potential importance of such measurements is twofold: first, the measured molecular mobility rates may be related to cell physiological functions; second, by characterizing the structural interactions which limit the translational mobility of the labelled components, a dynamic view of the molecular environment immediately surrounding the diffusant should be obtained. At this juncture, no other methods give comparable information about the translational mobility of molecules in defined regions of individual living cells and their organelles. Advances that have been made using the photobleaching techniques were discussed at a recent meeting*.

Valuable structural information concerning cell surface membranes is beginning to emerge from comparative studies largely based on the well characterized red blood cell membrane and artificial lipid bilayers. In the latter membrane model, photobleaching and magnetic resonance techniques have yielded diffusion coefficients for lipids, peptides and proteins ranging from 10^{-8} to 10^{-7} cm^2 s^{-1}; this range of diffusion coefficients means that the molecules can wander from their starting point a net average of several microns in one second. In sharp contrast to the protein mobility values in artificial bilayers, cell surface (glyco-) proteins, in general, diffuse much more slowly, with some fraction of each population not being observed to move at all on the time scale of the measurement.

Now, experiments on the red cell and tissue culture cells are beginning to resolve this difference. Groups at the University of Connecticut and Harvard have shown that agents (for example, polyphosphates) and conditions (for example, low ionic strength and high temperature) which destabilize the submembranous spectrin–actin protein matrix of normal erythrocytes also increase the lateral mobility of the band 3 integral membrane proteins, while the lateral diffusion rates of membrane lipids remains largely unchanged. Moreover, band 3 diffusion rates are some 50 times higher in spectrin-deficient spherocytic mouse erythrocytes than in normal mouse red cells. In the red cell, therefore, the spectrin network on the cytoplasmic aspect of the plasma membrane is definitely implicated in the control of band 3 lateral mobility. A remaining question is whether the mobility constraints are provided by specific binding interactions of the band 3 proteins' cytoplasmic domain with the spectrin network or whether diffusion is simply hindered by the projection of the cytoplasmic domain of the membrane protein into a subjacent polymer matrix. In a separate attempt to determine constraints on lateral mobility, workers at Cornell University have studied induced membrane blebs on lymphocytes, fibroblasts and myoblasts. Protein diffusion in these blebs is greatly increased compared with mobility in the unperturbed cell surface membranes. As actin-specific fluorescent labels show that the blebs are largely devoid of membrane-associated cytoskeletal elements, structures peripheral to the plasma membrane are again implicated in determining the rates of lateral diffusion of surface membrane glycoproteins.

So far, however, it has not been easy to relate the lateral diffusion coefficients of membrane molecules to biological function. These rates, while undoubtedly obligatory in many reactions, have not been demonstrated to be limiting except perhaps in a few cases where metabolic reactions occur within intracellular membranes, such as the inner membrane of the mitochondrion or the endoplasmic reticulum. In the future, it seems likely that precise relationships between lateral diffusion and function will be characterized in such intracellular membranes.

The validity of the photobleaching techniques has been questioned because of the possible harmful effects of the photobleaching light pulse (M.S. Bretscher *Trends biochem. Sci.* **5**, 6; 1980). The potential for membrane photodamage (that is, protein cross-linking) has been demonstrated in conventional photochemical experiments carried out under conditions different from the photobleaching measurements. Several important experiments suggesting there is no appreciable photodamage artefact in the measurement of lateral mobility have been performed at The Johns Hopkins University. When two spectrally distinguishable fluorescent labels were directed towards the same cell surface determinant, extensive photobleaching of one of the surface labels over the entire cell did not alter lateral diffusion coefficients subsequently determined by spot photobleaching of the second label. Also, measurements of the membrane diffusion coefficient of rhodopsin in the visual receptor membrane both by fluorescence photobleaching and by a photobleaching method which uses the natural photochemistry of rhodopsin yield the same values within experimental error. Finally, a careful comparison shows that lateral diffusion coefficients inferred from rates of antigen intermixing on heterokaryons and obtained independently by photobleaching are consistent.

This latter point has been elegantly extended by workers at the University of Connecticut who have shown that diffusion coefficients derived from membrane protein intermixing following red cell–red cell fusion agree with those obtained by subsequently photobleaching the identical fused cell pair. However, at least one puzzling discrepancy remains to be resolved.

In this issue of *Nature* (see p.332), M-m. Poo gives an estimate of the rate of acetylcholine receptor lateral diffusion in the plasma membrane of embryonic muscle cells from observations of the recovery of sensitivity to acetylcholine following local inactivation of receptors by α-bungarotoxin. Poo finds that the recovery kinetics are consistent with a receptor lateral diffusion coefficient of $\sim 3\times10^{-9}$ cm^2 s^{-1}. This is 50-fold faster than that determined by Axelrod *et al.* (*Proc. natn. Acad. Sci. U.S.A.* **12**, 4594; 1976) using the spot photobleaching technique, which requires that the receptor be labelled with fluorescent α-bungarotoxin. Furthermore, according

---

Ken Jacobson is in the Laboratories for Cell Biology, Department of Anatomy, School of Medicine, University of North Carolina, Chapel Hill, North Carolina 27514; Elliot Elson in the Department of Biological Chemistry, Washington University School of Medicine, St Louis, Missouri 63110; Dennis Koppel in the Department of Biochemistry, University of Connecticut Health Center, Farmington, Connecticut 06032; and Watt Webb in the School of Applied and Engineering Physics, Cornell University, Ithaca, New York 14853.

---

*The 'International Workshop on the Biological Applications of Photobleaching Techniques' was held by the Department of Anatomy and the Laboratories for Cell Biology at the University of North Carolina, Chapel Hill from 25 to 28 October 1981. Abstracts of the talks and a full list of speakers can be obtained from K. Jacobson.

0028-0836/82/040283-02$01.00

to the photobleaching measurements, some 25 per cent of the bungarotoxin–acetylcholine receptor complexes were immobile on the time scale of the measurement, another finding not confirmed by Poo's new experiments. These discordant results raise the possibility that the macromolecular ligand, α-bungarotoxin, has retarded the lateral mobility of the native receptor either by direct interaction with other cell surface components or, indirectly, by enhancing the ability of the receptor to interact with other cellular components. Alternatively, the rate of diffusion might be reduced by a photochemical process unique to this labelled ligand–receptor combination in the muscle cell membrane.

While photobleaching techniques have so far been largely directed towards problems in membrane biology, an exciting development has been their application to the study of macromolecules in solution and within the cytoplasm of living cells. At Syracuse University, photobleaching techniques are being used to study the polymerization of actin monomers in solution by monitoring the growth of the immobile fraction with time and should provide a useful alternative to conventional viscometric techniques. Further, the association of fluorescently derivitized actin with existing fibres in live cells is being examined at the Weizmann Institute using a combination of microinjection and photobleaching techniques. In another novel application, investigators at the University of North Carolina and Penn State University have shown that the diffusion of macromolecules, such as IgG and bovine serum albumin, microinjected into the cytoplasm of living fibroblasts is retarded 70-fold compared with aqueous buffer values; these results suggest that the cytoplasmic matrix hinders the free diffusion of such molecules sterically and/or through binding interactions between the diffusant and the matrix.

These emerging applications of the photobleaching techniques to the study of molecular movement both within cell membranes and within the cytoplasm suggest a great potential for this approach to provide unique dynamic information on cellular structures, particularly when these measurements can be interpreted in the context of available biochemical and ultrastructural data. □

Gravitational lenses

from Charles Alcock

ONE of the most exciting recent developments in astronomy has been the discovery of multiple imaging of quasars. There are three confirmed examples[1-3] of this phenomenon, and in one case, the gravitational lens responsible for the multiple imaging has been detected[4]. It is a large elliptical galaxy near the centre of a cluster of galaxies.

The great virtue of the phenomenon is that, by the standards of extragalactic astronomy, it can be fairly unambiguously interpreted. In each case the optical emission line spectra of the different images are essentially the same and have identical redshifts.

The general properties of gravitational lenses are easy to understand. A galaxy or cluster of galaxies will bend light rays through small angles, producing (in general) an odd number of images of a background quasar. Usually there will be only one image, but fortuitous projection of a quasar behind a galaxy can result in three or more images. The image brightnesses differ from the brightnesses that would be observed if the lens was absent because the beams are focused.

Three papers in a recent issue of the *Astrophysical Journal* explore some more speculative suggestions involving gravitational lenses. In the first, Tyson[5] revives an old suggestion of Barnothy and Barnothy that quasars may be the nuclei of Seyfert galaxies and appear very luminous because an intervening gravitational lens has amplified the flux from the nucleus. The apparent increase in the density of quasars with increasing redshift can then be accounted for by the larger probability that amplification will occur if the Seyfert galaxy is at a greater distance. What is new in Tyson's approach is that he uses his own data (obtained using automated pattern recognition techniques) on the number density of galaxies on the surface of the celestial sphere as a function of measured flux to calculate the logarithmic slope of the number density of quasars as a function of measured flux. The answer, d log $N_{\mathrm{Q}}/\mathrm{d}m_{\mathrm{Q}} = 0.9$ (where $m_{\mathrm{Q}} = 2.5 \log \mathrm{flux}$) is within the range of observed slopes (0.86–0.95).

The primary difficulty with this model is that the large (>15 times) amplification required is difficult to obtain with gravitational lenses. Furthermore, high amplification should be accompanied by multiple imaging but multiple images have only been detected in three cases out of the nearly 1,000 known quasars. In addition there would need to be a large number of distant galaxies, at present undetected, capable of producing amplification to explain the observed surface density of quasars. Since only a minority of the galaxies we see locally appear capable of producing large amplifications, the mean density of the Universe has to be very high if the model is to work. Success in predicting d log $N_{\mathrm{Q}}/\mathrm{d}m_{\mathrm{Q}}$ is not sufficient to remove these doubts.

In the second of the papers Avni[6] addresses a closely related point. He discusses Turner's suggestion that amplification by gravitational lenses may significantly perturb the measured statistics of quasars, perhaps accounting for the apparent increase in the number density of quasars with increasing redshift. Quasar analyses are customarily performed on flux-limited samples, which will preferentially include quasars whose flux has been amplified by an intervening gravitational lens. Avni's improvement on Turner's model is to require average flux conservation, which implies that the mean amplification has to be unity. This is an important, obvious requirement which considerably reduces the effect of lenses on the quasar statistics below that computed by Turner. Avni correctly concludes that it is unlikely that the gravitational lens effect can account for the apparent evolution of the density of quasar with redshift.

The third paper takes a different direction. Paczyński and Górski[7] suggest that a cluster of quasars[8] at redshift 2.05 may be another example of multiple imaging by a gravitational lens. However, there are some difficulties — the objects have a large separation (minutes, rather than seconds, of arc) and their redshifts are different (by about 10^3 km s^{-1}). The authors produce model lenses consisting of two large clusters of galaxies which can account for the large angular separations. The model cannot account for the redshift differences but the time delays between the three images are 10^2–10^3 years, and it is suggested that the quasar's redshift might change during this time interval.

The velocity dispersions of the two clusters of galaxies in the models of Paczyński and Górski are large (>1,500 km s^{-1}). They point out that if there is a positive cosmological constant the necessary velocity dispersion decreases. This suggests that, should the clusters be discovered and their velocity dispersion measured, one could then estimate the cosmological constant.

It is clear that gravitational lenses can in principle do many remarkable things. The studies described here are very speculative, and definitive answers await further work.

Charles Alcock is Associate Professor in the Department of Physics, 6-207, Massachusetts Institute of Technology, Cambridge, Massachusetts 02139.

1. Walsh, D., Carswell, R.F. & Weymann, R.R. *Nature* **279**, 381 (1979).
2. Weymann, R.T. *et al. Nature* **285**, 643 (1980).
3. Weedman, D.W., Green, R.F. & Weymann, R.J. *Nature* (submitted).
4. Young, P.J., Gunn, J.E., Kristian, J., Oke, J.B. & Westphall, J.A. *Astrophys J.* **241**, 507 (1980).
5. Tyson, J.A. *Astrophys. J. Lett.* **248**, L89 (1981).
6. Avni, Y. *Astrophys. J. Lett.* **248**, L95 (1981).
7. Paczyński, B. & Górski, K. *Astrophys. J. Lett.* **248**, L101 (1981).
8. Burbidge, E.M. *et al. Astrophys. J. Lett.* **242**, L55 (1980).

0028-0836/82/040284-01$01.00

ARTICLES

Crater densities and geological histories of Rhea, Dione, Mimas and Tethys

J. B. Plescia

Jet Propulsion Laboratory, California Institute of Technology, Pasadena, California 91109 and Department of Geological Sciences, University of Southern California, Los Angeles, California 90007, USA

J. M. Boyce

Planetary Geology Program, Office of Solar System Exploration, National Aeronautics and Space Administration, Washington DC 20546, USA

Crater density determinations for parts of the surfaces of several of Saturn's icy satellites including Rhea, Dione, Mimas, Tethys and 1980S3 reveal significant variations. These data, combined with observations of surface morphology, indicate that each satellite has undergone extensive post heavy bombardment geological evolution.

THE Voyager 1 encounter with the Saturn system provided the first close view of icy satellites intermediate in size between asteroids and the large icy galilean satellites[1]. The saturnian satellites have surfaces much more diverse than had been anticipated for bodies of such a small mass and low density.

Several of the satellites (Rhea, Dione, Mimas and Tethys) were imaged by Voyager 1 with resolution sufficient to allow crater counts on at least part of their surfaces. These counts were made to determine the character and magnitude of crater density variations and the relative ages of the different terrain types. Enceladus and Hyperion have been viewed at high resolution by Voyager 2 (ref. 2) and will be discussed elsewhere.

Our data indicate that the surfaces of the saturnian satellites are not uniformly cratered and hence not of uniform age. Significant variations in density occur at all diameters but are most noticeably in the distribution of large diameter (>50 km) craters. The differing surface ages and tectonic features argues that these satellites have evolved significantly beyond their post-accretional state. The range in surface age suggests that the duration and degree of evolution varies between satellites. Such extensive post-accretional activity seems remarkable in view of the small size and mass of the saturnian satellites[3].

Rhea

Rhea, the largest of Saturn's airless satellites, is heavily cratered, with bright whispy planetary scale markings. Rhea's surface shows areas of significantly different crater density. Two of the clearest examples occur in the north polar region and in the equatorial region near 30° longitude.

The north polar region (Fig. 22 in ref. 1) can be divided into two zones based on crater size distributions[1], with the boundary occurring at ~0° long. Westward from 0° longitude numerous craters in the diameter range 40–130 km occur, while to the east of that line craters are generally <20 km and all are <30 km diameter. Smith *et al.*[1] suggested that this difference in crater size distribution was correlated with albedo variations observed in far encounter images of Rhea (Fig. 20 in ref. 1)—that the region of low albedo correlated with the area in which the large craters were present while the brighter area correlated with the area in which they were absent. This conclusion, however, is not supported by our analysis.

The crater size boundary, at ~0° long., is sharp compared with the more diffuse albedo boundary lying ~45° to the east, at 315° long. As the two areas do not coincide, it argues against a common origin. The albedo patterns observed in far encounter images of both Rhea and Dione have been attributed to the uneven distribution of micrometeor impacts[1]. The cumulative size–frequency distribution for areas of the north pole shown in Fig. 1 reveal that while the two areas differ markedly at large diameters, they are statistically indistinguishable at small diameters. The distributions have a 10-km crater density of 1,300±300 at 315° long. and 950±150 at 45° long.

The absence of large craters in parts of the polar regions suggests a major resurfacing event[1]. Large craters are generally lacking in the equatorial areas, but are again found at the south pole. Such a distribution could be explained by an internally generated thermal pulse that lowered the viscosity of some parts of the crust and hence preferentially removed the larger craters. This viscous relaxation would have been less effective near the poles perhaps because of the lower surface temperature.

If the crater size frequency distribution for the polar area near 315° is extrapolated from large to small diameters, it indicates a density far in excess of that observed. While a thermal event might be capable of removing large craters it cannot account for the deficiency of small craters. The low density of small craters might best be explained by a blanketting or flooding event that

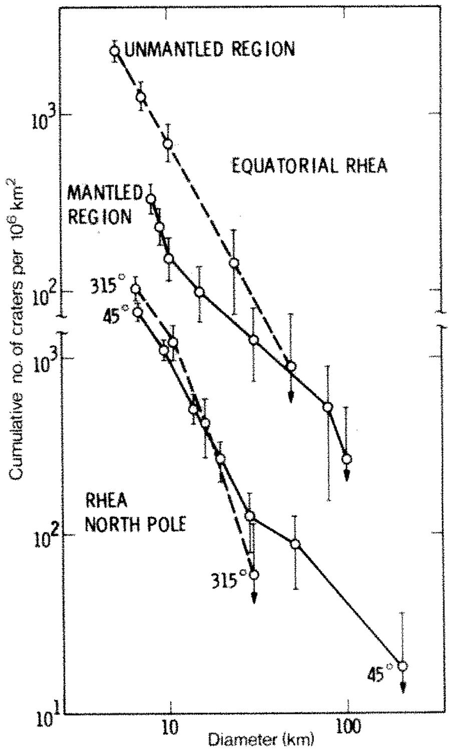

Fig. 1 Cumulative size–frequency distribution for Rhea. Upper distributions indicate crater for the mantled and unmantled equatorial areas. Lower curves illustrate the densities for the north pole.

0028–0836/82/040285—06$01.00

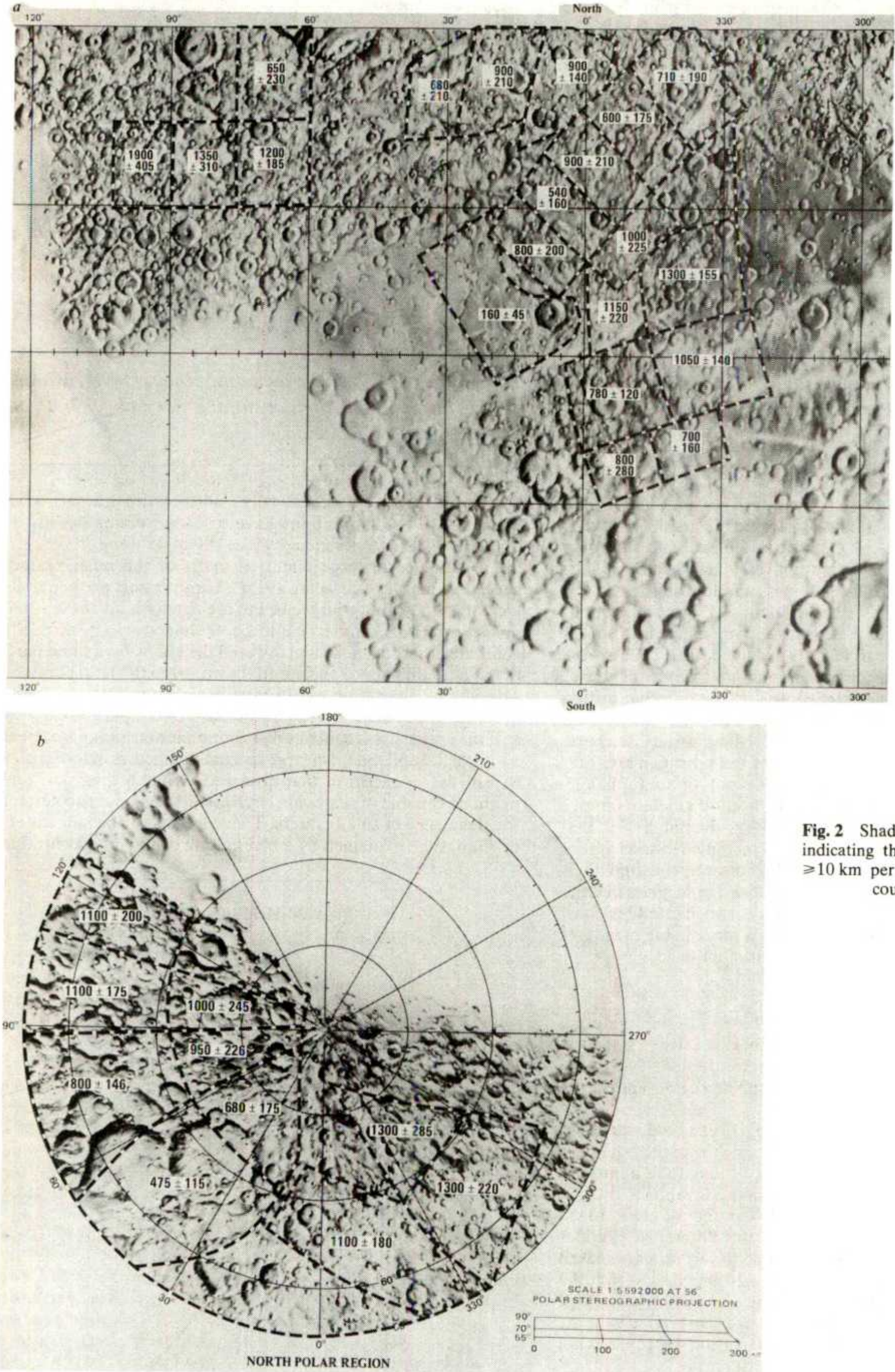

Fig. 2 Shaded relief map of Rhea indicating the number of craters ⩾10 km per 10^6 km^2 for various counting areas.

buried the small craters, and subdued the larger ones. Such an event would also be consistent with the shape of the cumulative size–frequency distribution for the eastern polar area.

Regions near the equator exhibit subdued surface texture when compared with other areas and an absence of small craters suggesting that the area has been mantled (Fig. 21 in ref. 1). This region was imaged only at high Sun angle which may account for some muting of the topography, however, the sharp and irregular shape of the boundary indicates that the mantle is real and not simply a lighting effect. Cumulative size–frequency distributions of craters for the mantled area is shown in Fig. 1. The shape of this curve is suggestive of complete burial of small craters and only partial burial of larger ones. The slope of the curve for the mantled area decreases at diameters <10 km, suggesting that the thickness of the blanket is sufficient to bury 10-km craters or ~2 km deep. A curve for the adjacent unmantled region is also shown and has a 10-km density of 700 ± 150, consistent with the density observed over a large part of the equatorial area. The mantled region has close to a factor of 5 fewer 10-km craters, at 160 ± 45, than does the unmantled region.

Figure 2 shows the extent of the variation of 10-km crater densities observed on Rhea's surface. The most densely cratered regions occur in the mid-northern latitudes west of 60° long. and in the north polar area between long. 300° and 330°. A zone of lower crater density extends from the north pole along the 30° meridian. The area east of 0° long. is heavily cratered but with some variation. Near the equator and extending westward for ~15° is the mantled area. The lack of a clear global crater density pattern suggests that local rather than global processes produced the observed differences. The variations in density and distribution of 10-km and larger craters suggest that Rhea has undergone extensive crustal resurfacing. Processes, most probably endogenic, have operated that are capable of complete erasure of large craters over vast areas of the surface. The absence of large craters suggests that this internal activity extended past the time of post-accretional heavy bombardment when large impacts accumulate.

Mimas

Mimas, the innermost of the major saturnian satellites, is heavily cratered on all areas viewed by Voyager 1. Mimas is heavily, though not uniformly, cratered and has areas of significantly different crater density. On the leading hemisphere (Fig. 14 in ref. 1), west of the crater Herschel, the surface is covered with numerous craters >40 km. The south polar and adjacent areas (Fig. 14 in ref. 1), by comparison, generally lack craters >20 km and are devoid of craters >30 km.

Figure 3 illustrates the cumulative size–frequency distribution for the two areas. Curve E is the distribution for the equatorial area near Herschel (a projected 10-km density in excess of 7,500). Curve SP is the distribution for the south pole (a 10-km crater density of 1,250 ± 490). The density of small craters in the equatorial region could not be determined because of the low resolution of the images. The roughness, at the limit of resolution, caused by 10-km craters seems far less than indicated by the extrapolation, with the surface fairly smooth even near the terminator where subtle relief should be enhanced. Hence the density at 10 km could be the same in both areas. The region 180°–240°, which lies between the equatorial and polar areas, appears to be transitional in terms of size–frequency distribution of craters (curve TC in Fig. 3). An inflection between 15 and 40 km suggests a mixing of two populations of craters, perhaps the result of resurfacing. The small diameter segment is similar to the density for the south pole, while the large diameter segment is comparable to the density in the heavily cratered equatorial area.

The surface of Mimas has apparently been affected by some process which has removed all of the large craters from the south polar region. It had been suggested that numerous impacts of small bodies might have caused destruction of larger craters but there is no evidence that the flux of impacting debris was higher at the south pole than at the equator[1]. The process seems to have been gradational in that progressively smaller craters were spared removal at progressively larger distances from the pole. The distribution of small craters appears to have been reduced over the entire surface of Mimas. This rather uniform and low density of small craters and the absence of large craters at the south pole may reflect at least two episodes of resurfacing.

Dione

Dione exhibits terrain types of distinctly different morphology, ranging from rough heavily cratered areas to smooth lightly cratered plains (Fig. 18 in ref. 1). Planetary scale patterns of bright whispy material stretch across the trailing hemisphere and appear superimposed on the various terrain types and surface features.

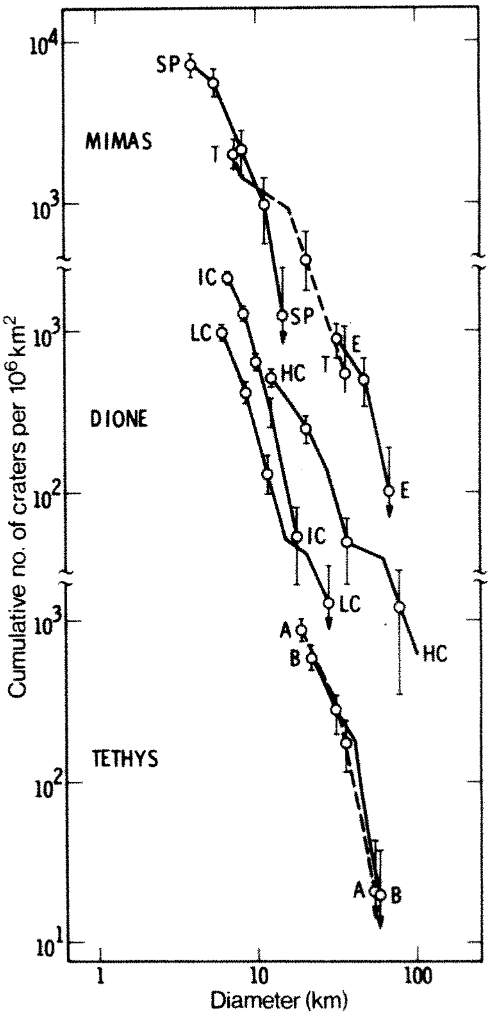

Fig. 3 Cumulative size–frequency distributions for Mimas, Dione and Tethys. Letters refer to locations on the satellites discussed in text.

Three terrain types observed in the highest resolution frames were singled out for preliminary analysis of crater densities: (1) a rough terrain with numerous large craters, centred at ~15° S, 20° long.; (2) a plains unit with intermediate crater density which is elongate in the north–south direction and centred on the equator at 50° long., and (3) a smooth plains unit with low crater density centred on the equator and 65° long. Cumulative size–frequency distributions for these terrains are shown in Fig. 3.

Crater densities for the plains units are considerably less than that for the heavily cratered terrain, indicating a younger age for the plains. At 20 km the heavily cratered area (curve HC) has a crater density of 270 ± 50, compared with ~45 ± 25 for the plains (curves IC and LC). The least cratered plains unit (LC) has a 10-km density of 260 ± 50 compared with 750 ± 100 for the intermediately cratered plains (IC). Figure 3 shows that the heavily cratered distribution has a slope of −2.0, while the younger units have a slope closer to −4.0. This difference in slope, coupled with the apparent age difference, suggests that the two surfaces may reflect different populations of impacting bodies.

These plains units and the structure of the cumulative frequency distribution for the heavily cratered terrain suggest extensive post-accretional alteration of the surface of Dione. It has been suggested that the material responsible for resurfacing parts of the satellite was extruded from the branching trough which extends from the north pole through the plains units. E. Shoemaker (personal communication) and Owen[4] suggested methane snow eruptions from these troughs which would bury surrounding areas and form a smooth young surface. However, the sharp boundary between terrain types suggests a process that totally obliterated all topography up to the boundary which is inconsistent with a snow hypothesis. In such a case topography farther from the vent would receive a thinner blanket of snow than nearer the vent. While the exact nature of the mechanism remains speculative, Dione has clearly undergone some type of endogenic process which has reshaped its surface. The distinct variations in crater density suggests that the process has acted repeatedly beyond the cessation of heavy bombardment.

Tethys

Only one image of Tethys obtained by Voyager 1 in far encounter sequences had resolution sufficient to allow detailed crater density determinations (Fig. 12 in ref. 1). This permitted counting of three regions within a band along the west side of the terminator, between 30° and 60° long.: the cumulative frequency distributions for two regions are shown in Fig. 3. These are statistically indistinguishable from each other (the third region is omitted for simplicity). The size-frequency distributions indicate that this area of Tethys is relatively uniformly and heavily cratered at all diameters investigated. Resolution of $\sim$10 km per line pair prevented determination of densities of smaller size craters. The distributions indicate a 30-km crater density of $\sim 280 \pm 70$ and, by extrapolation, a 10-km density of $2{,}800 \pm 300$.

Voyager 1 images of Tethys' trailing hemisphere show circular features suggestive of large (50–100 km) craters, which would indicate that the trailing hemisphere, like the leading, is heavily cratered. Tethys clearly has undergone post-accretional evolution as reflected in surficial albedo variations and the large canyon-like feature on the sub-Saturn hemisphere. Whether these features were induced by endogenic or exogenic processes and their effect on crater densities is uncertain.

Discussion

Shoemaker and Wolfe[5] have suggested that each saturnian satellite, like the galilean satellites[6], should record a gradient in the cratering rate across their surfaces. The rate should be highest at the apex of motion on the leading hemisphere (equator and 0° long.) and decrease sinusoidally in all directions until the low point is reached at the antapex of motion (equator and 270° long.). Such gradients should occur for impacts generated by extra-saturnian bodies as a result of the high orbital velocity of the satellite compared with the velocity of the impacting body. The ratio of the cratering rate between the apex and antapex for long period comets and Saturn family comets is 6 and 35 respectively for Rhea and 18 and 35 respectively for Mimas[5]. While such a gradient seems to explain the distribution of surfical albedo markings on Rhea and Dione[1] it does not explain the observed distributions of 10-km and larger diameter craters on Rhea, Mimas and Dione.

Figure 4 plots the 10-km crater densities for several counting areas on Rhea as a function of their angular distance from the apex of motion. The data do not follow the predictions of Shoemaker and Wolfe[5]. Crater density determinations for Rhea cover an angular distance of 30°–120° and hence the gradient, if present, should be observable.

A similar analysis for Mimas indicates that the crater densities do not follow the expected distribution, while significant variations occur they are not correlated with distance from the apex. This presents a serious problem in that images of the leading hemisphere have low resolution and hence small diameter (<20–30 km) craters are not observed, while in the southern hemisphere there are no craters larger than 30 km to use for such a comparison. Within the southern hemisphere an angular distance of 80°–140° was observed with no significant variation in density of 10- and 20-km craters.

For such a gradient in crater density to be fully developed the satellite must have remained tidally locked to its parent body during its history, particularly during the period of heavy bombardment. Also comparison between surfaces of the same absolute age must be made to observe the effect.

McKinnon[7] has examined the energy requirements for unlocking Ganymede and Callisto without reorienting the pole of rotation and found that appropriately oriented large impacts, could spin up those satellites. Similar analysis of the saturnian satellites indicates that because of their relatively small size and mass, small and hence frequent impacts could supply sufficient energy for reorientation. Impacts of $\sim 2 \times 10^{27}$ erg for Rhea and 5×10^{25} erg for Mimas would be sufficient to break their tidal lock. Those energies correspond to the formation of a 40-km crater on Rhea and a 15-km crater on Mimas. Because the momentum required must be tangentially oriented, these are minimum crater sizes. Impacts oriented closer to normal would have a smaller tangential component. Thus relatively small impacts, if appropriately oriented, could impart sufficient energy to unlock the satellite. As such craters are relatively abundant, we conclude that each saturnian satellite has been repeatedly unlocked with a frequency that is proportional to the cratering history. This process would effectively prevent the recording of the gradient.

To compare the crater densities between satellites a cumulative frequency distribution for each body is shown in Fig. 5. One of the co-orbital satellites, 1980S3, has a 10-km crater density of $1{,}450 \pm 610$ for the small region which was countable (see Fig. 29 in ref. 1). Except for 1980S3, the curves in Fig. 5 approximate the size-frequency distribution of craters on the sub-saturnian hemisphere at 0° long. to remove any effects which might result from gradients in crater density.

The distributions indicate that the satellites are dominated by two populations of craters. These two groups correlate with populations I and II of Smith *et al.*[1]. The first group, the large diameter craters, represents population I which is exposed on the more densely cratered surfaces of Rhea, Dione, Tethys and Mimas. Population II would correspond to the small diameter segments of the distributions. Craters of population II are found on the younger parts of all of the satellites. The cumulative size-frequency distributions observed on the saturnian satellites are steeper than those observed on the dark terrain of Ganymede and also indicate higher crater densities. At 10 km the densities are at least a factor of 4 higher for the saturnian satellites than for Ganymede's dark terrain. Differences in the slope of the size-frequency distributions suggests that the two systems may have been bombarded by different populations of objects. This difference in density between the two systems may not be a direct function of age in view of the possibly different

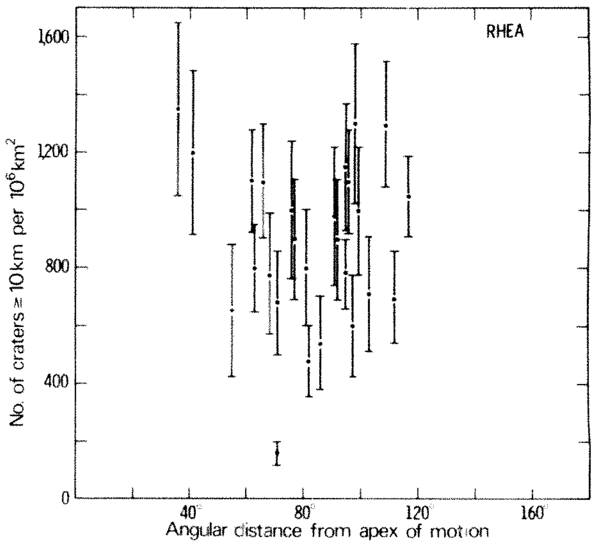

Fig. 4 Plot of crater density at 10 km as a function of angular distance in degrees from the apex of motion of Rhea.

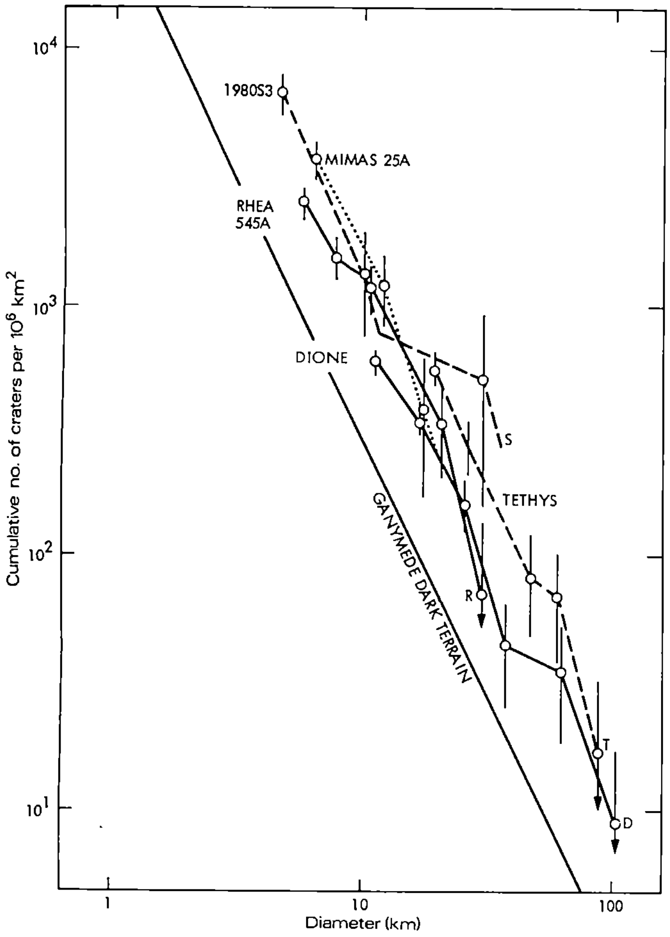

Fig. 5 Cumulative size-frequency distribution for Rhea, Dione, Tethys, Mimas and 1980S3. Average distribution for the dark terrain of Ganymede included for comparison.

impact histories. Alternatively, the steepness in slope of the small crater segment of the distribution may result from numerous secondary impacts produced by projectiles originally lost during larger impacts on these bodies. These secondary materials which would subsequently be swept up and enhance the small crater population have been termed population III (ref. 1).

The crater densities in Fig. 5 can be interpreted as representing two major geological events, which may record several episodes, in the history of the satellites. The higher-density large-diameter distribution reflects the period of late heavy bombardment, characterized by the population I distribution of many large (>50 km) diameter craters, many of which are now subdued and degraded. The second, lower-density population II occurred at a time to record episodes of resurfacing, plains formation and tectonic activity. This has occurred on all the satellites, and may date back to the end of the post-accretion heavy bombardment. The nonuniformity of crater densities on the satellites indicates that modification of their surfaces has been variable in terms of both duration and areal extent. Rhea, Dione and Mimas all exhibit distinctly different crater densities indicative of multiple resurfacing episodes.

The geological history of the saturnian satellites can be deduced from their crater densities. The areas of Dione, Rhea and Tethys, characterized by the presence of population I craters, being the most densely cratered surfaces, are the oldest regions, thought to date from the period of heavy bombardment. Regions of Dione and the leading hemisphere of Mimas which are characterized by high crater densities, combinations of populations I and II craters, suggest partial resurfacing of these areas and represent the next youngest surfaces. These surfaces probably formed during the later part of the heavy bombardment and were subsequently modified. Thereafter, episodes of more localized resurfacing occurred during which the southern hemisphere of Mimas and the north pole and equatorial areas of Rhea were altered. Larger population I craters were obliterated in these areas, and greatly subdued in others. Resurfacing continued on Rhea in more localized areas reducing crater densities. The most recent activity on the satellites discussed here seems to have been the formation of the smooth lightly cratered plains of Dione and the blanketing of parts of Rhea's equator.

The vast range of surfaces observed indicates that surface forming processes were active beyond the period of heavy bombardment. The tectonic features such as lineaments, troughs and great canyons, and the removal of large craters over vast areas indicate prolonged post-accretional activity, all reflecting the operation of internal process. Large impacts, the only major exogenic event likely to occur after the formation of the satellite, might cause extensive local morphological changes, but such events could not cause all of the diversity of ages and surface morphology. This is similar to the general conclusion drawn for the galilean satellites and the terrestrial planets.

Whether generated by core formation or decay of radioactive nuclides, heat is the basic driving mechanism for the internal dynamics of most bodies. Tidal heating seems to be important in only a few cases. Peale *et al.*[8] showed that tidal heating could have contributed only small amounts of energy to the saturnian satellites. Models[3] of the thermal evolution of small icy satellites indicate that such bodies would experience little internal activity after formation. Based on chondritic abundances of radionuclides and a 40% rock and 60% water-ice mixture, no melting would have occurred in the smaller satellites. In the slightly larger bodies such as Rhea and Iapetus a small liquid core might have formed early, however, 90% of the satellite would still have remained frozen. The addition of 10% ammonia as a hydrate would enhance additional limited melting and differentiation which could have had important consequences for the larger icy satellites, but not for those with radii <700 km. An additional mechanism, solid-state convection of ice I, might prove to be important in causing changes in the surface of the small icy satellites where that ice would be the dominant phase[3]. Such a mechanism would transmit heat to the surface allowing the largest craters to be removed by viscous relaxation[9]. Additionally the convective activity may have tectonically disturbed the surface and obliterated craters. However, formation of plains units as on Dione and blanketting on Rhea or giant tectonic features of Tethys would require a more energetic process.

The problem then is the source of the energy responsible for evolutionary processes. One possibility might be inhomogeneous accretion. Smith *et al.*[1] suggested that the saturnian satellites might be of the size where the stochastic nature of accreting compositionally different planetesimals might produce noticeable effects on the satellites' history. Perhaps concentrations of the rocky component exist beneath areas where internal activity seems to have occurred. Such local concentrations might supply sufficient radiogenic heat over a limited area to drive surface modifications. Additional energy could be provided if the local concentration 'melted' its way to the core of the satellite and hence released gravitational energy or by structural disruptions caused by the migration of the concentration.

The small icy satellites of Saturn are therefore a diverse group of bodies with a variety of surface ages and morphologies. These satellites, despite their small size and mass and low density, have evolved beyond their original accretionary state. The alteration processes seem to have been active beyond the period of heavy bombardment as reflected in the crater density determinations. The energy source for the evolution of these bodies remains unknown.

We thank Gary Ransford, Rich Terrile and Doug Nash for discussions and suggestions, and Larry Soderblom for a review.

This paper, Planetology Program publication no. 326-81-72, represents one phase of research carried out at the Jet Propulsion Laboratory, California Institute of Technology under contract with NASA.

Received 10 August; accepted 26 November 1981.

1. Smith, B. A. *et al. Science* **212,** 163–191 (1981).
2. Smith, B. A. *et al. Science* (in the press).
3. Consolmagno G. & Lewis, H. *Icarus* **34,** 280–293 (1978).
4. Owen, T. (in preparation).
5. Shoemaker, E. & Wolfe, R. *Abstr. 12th Lunar planet. Sci. Conf.* Suppl. A, 1–3 (1981).
6. Shoemaker, E. & Wolfe, R. in *The Satellites of Jupiter* (ed. Morrison, D.) (University of Arizona Press, in the press).
7. McKinnon, W. B. *EOS* **62,** 318 (1981).
8. Peale, S. J., Cassen, P. & Reynolds, R. T. *Icarus* **43,** 65–72 (1980).
9. Johnson, T. V. & McGetchin, T. R. *Icarus* **18,** 612–620 (1973).

The tectonics of Ganymede

E. M. Parmentier*, S. W. Squyres†‡, J. W. Head* & M. L. Allison*‡

* Department of Geological Sciences, Brown University, Providence, Rhode Island 02912, USA
† Laboratory for Planetary Studies, Cornell University, Ithaca, New York 14853, USA

The surface of Ganymede, the largest icy jovian satellite, is composed of two distinct terrain types showing abundant evidence of global-scale tectonics. There is geological evidence consistent with the formation of younger bright terrain by the emplacement of relatively clean ice into rift zones developed in the more silicate-rich dark terrain.

GANYMEDE, Jupiter's largest moon, is the largest known icy object in the Solar System. Voyager images of its surface show a complex and unique geology with widespread evidence for tectonic activity[1,2]. For silicate bodies on which significant lateral motion of the lithosphere does not occur, global volume change is an important cause of surface tectonism[3,4]. As a result of internal phase changes, large icy bodies can undergo a substantial volume increase. The transition of dense ice polymorphs in the deep interior to less dense polymorphs or liquid water at shallow depths as internal differentiation and formation of a silicate core occurs could increase Ganymede's surface area by as much as 7% (ref. 5). A temperature increase of several thousand degrees centigrade would be required for a silicate body to undergo an equivalent amount of volume change due to thermal expansion. We examine here evidence concerning the nature of the tectonic processes that have operated on Ganymede. We conclude that a variety of geological evidence is consistent with the progressive rifting of Ganymede's lithosphere possibly in response to planetary expansion.

Style of global tectonics

The two principal geological units present on Ganymede are most simply termed 'dark' terrain and 'bright' terrain. Each unit covers approximately half of the surface. The density of impact craters is substantially higher in the dark terrain, indicating that it is older than the bright terrain[1,2]. The dark terrain is generally present in polygonal regions that are separated by bright terrain (Fig. 1). The bright terrain forms both broad curvilinear bands that separate the dark polygons, and narrow wedge-shaped regions that penetrate and partially divide dark polygons. In some areas bands and wedges of bright terrain appear to coalesce forming broad, irregularly shaped bright regions. Small blocks of dark terrain are frequently interspersed through such regions. The dark terrain is composed of an ice–silicate mixture, and the bright terrain is composed of relatively silicate-free ice. Bright terrain contains many linear topographical depressions called grooves[1,2]. Where it is free of grooves and impact craters, the bright terrain appears smooth at the highest Voyager resolution (600 m per picture element).

The emplacement of the bright terrain by the extrusion of a relatively water-rich magma in regions of lithospheric extension is geologically reasonable and is supported by various geological data. We examine three different styles of extensional tectonics that could be associated with the emplacement of bands of bright terrain between polygons of dark terrain. As shown in Fig. 2, lithospheric spreading (*a*) may be analogous to the formation of new ocean floor at terrestrial mid-oceanic ridges; finite lithospheric extension (*b*) may be analogous to terrestrial rift zones such as the Basin and Range Province of North America or the East African rifts; and finally, flooding of older dark terrain (*c*) may occur by the extrusion of silicate-poor material through fissures or extension fractures. These models clearly involve significantly different amounts of relative lateral motion between adjacent blocks of dark terrain. Lithospheric spreading implies lateral movement of coherent blocks of dark terrain over distances comparable to the width of areas of bright terrain. At the opposite exteme, tension fracturing and flooding would only require small lateral movements of the dark terrain sufficient to provide bright material access to the surface. The simple models provide a conceptual framework within which to interpret various geological data.

The nature of boundaries between the two terrain types provides a basis for determining whether the two surface units have a tectonic or a stratigraphical relationship. Contacts between bright and dark terrain are usually gently curving and

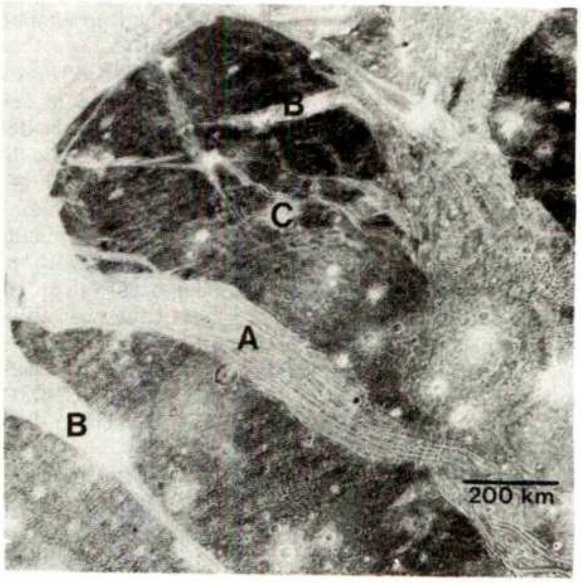

Fig. 1 Bands (A) and wedge-shaped regions (B) of bright terrain separating polygons of dark terrain. Also note single grooves and groove pairs within the dark terrain (C, see discussion of tectonic features). Voyager image 370J2-001.

---

‡ Present addresses: NASA Ames Research Center, Moffett Field, California 94035, USA (S.W.S.); Department of Geology and Geography, University of Massachusetts, Amherst, Massachusetts 01002, USA (M.L.A.).

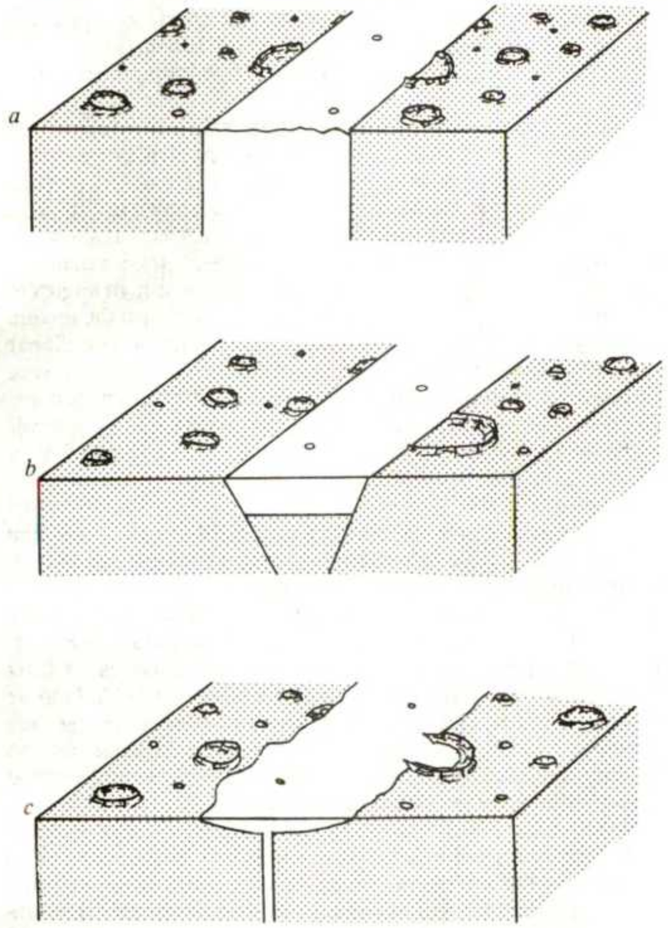

Fig. 2 Three schematic models of extensional deformation associated with the emplacement of the bright terrain: *a*, lithospheric spreading; *b*, rifting due to finite lithospheric extension; and *c*, flooding of older, dark terrain.

sharply defined. Craters and other topographical features in the dark terrain are sharply truncated at such contacts. These characteristics argue for the structural confinement of bright material at many bright terrain–dark terrain boundaries. In irregular areas of bright terrain, the contacts between bright and dark terrain are diffuse, and truncated craters occasionally appear to be filled with bright material. In some areas the bright terrain has a distinctive dark mottling suggestive of a thin layer of bright material overlying dark material. In such areas, bright material appears to have flooded dark terrain. In most cases, however, the bright material was structurally confined, arguing against flooding of dark terrain (*c*) as the main mechanism for the emplacement of the bright terrain.

Several types of observations distinguish between lithospheric spreading (*a*) and finite lithospheric extension (*b*). If lithospheric spreading has occurred, the two parts of a crater transected by a band of bright terrain should appear on opposite sides of the band. This is not observed. Another basis for distinguishing between these two tectonic styles is the degree to which adjacent dark polygons can be fit back together. The boundaries of some adjacent polygons are roughly parallel, creating the superficial impression that they were once joined, and have since drifted apart. Detailed examination shows, however, that this parallelism is only approximate, and that they cannot be fit together[6,7].

Lithospheric spreading would require relative lateral motion between adjacent regions of dark terrain comparable with the width of regions of bright terrain. Although there is evidence that crustal shear has occurred on Ganymede[8], large lateral displacements have not yet been demonstrated. The clearest evidence of shear displacement is provided by a few crater rims that are offset across linear features. The largest offset recognized in these cases is several kilometres[8]. Some bands of bright terrain also appear to be offset across transecting linear features. If these bands were offset after their formation, as much as 100 km of strike-slip dispacement would be indicated[8]. There is no evidence, however, that such bands did not form with an offset across a pre-existing fault. Therefore, post-formation strike-slip displacement is not required to explain their offset appearance. The non-concentricity of arcuate furrows in the dark terrain has also been cited as evidence for large lateral displacement between adjacent regions of dark terrain[8]. These furrows, which are 5–10 km wide flat-floored depressions predating almost all craters in the dark terrain, are thought to be ring graben formed during the viscous collapse of an early impact basin[9]. If the forrows are assumed to have formed an initially circular pattern, their present pattern suggests a lateral displacement between adjacent regions of dark terrain; however, no detailed study of this hypothesis has been reported. There is no evidence that furrows did form an initially circular pattern.

Because bright terrain covers about half of the surface of Ganymede, the formation of this terrain by the complete separation of older blocks of dark terrain cannot be explained by planetary expansion alone. Lithospheric spreading would require large-scale destruction of crustal materials and possible associated compressional deformation. Tectonic features that can be related to compressional deformation have not yet been recognized in the dark terrain. If all the bright terrain were emplaced by lithospheric spreading, it is difficult to reconcile the large area of this terrain with the absence of compressional features in the dark terrain.

All the above observations are consistent with the formation of the bright terrain by the flooding of rift zones formed due to finite lithospheric extension. Although individual tectonic features in the dark terrain, described later, strongly suggest that normal faulting has occurred on Ganymede, the structure of rift zones is not yet clearly defined. Dark terrain may have subsided along normal faults forming graben, as in terrestrial rift zones, or may have stoped[10] or foundered[4] into the deeper interior. The occurrence of small, isolated regions of dark terrain in irregular areas of bright terrain argues against stoping. A piecemeal style of stoping is difficult to reconcile with the continuity and linearity of the contact between bright and dark terrain at the edges of the bright bands.

The thickness of bright deposits place important constraints on the structure of rift zones and, if they are formed by normal faulting, on the amount of lithospheric extension. The burial of pre-existing topography on underlying dark terrain may be one indicator of this thickness. Crater rims, which are the highest topographical features in the dark terrain, are never clearly evident through the bright deposits, even where craters are truncated at a bright terrain–dark terrain boundary. Impact

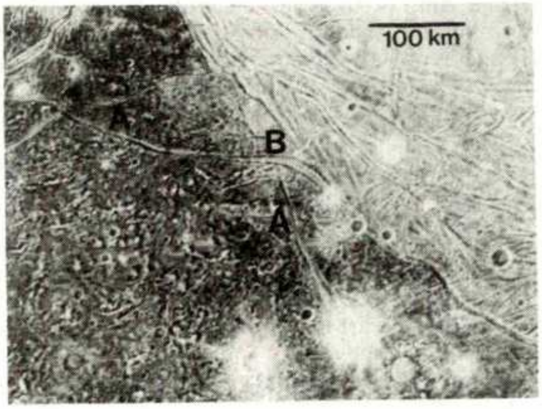

Fig. 3 Single grooves (A) and a groove pair (B) in the dark terrain. The groove pair merges along strike to form a single groove. For part of its length the groove pair forms a bright terrain–dark terrain boundary. Voyager image 382J2-001.

craters excavate crustal material at depth and therefore may be useful indicators of subsurface composition. Craters on the dark terrain with a diameter of <50 km exhibit no bright rim deposits. Larger craters, now highly degraded due to viscous flow, are brighter than the surface on which they formed. If the bright material is not solely impact melt, then the larger craters may have excavated silicate-free material from depth while the smaller craters did not. Although more detailed study is required, this suggests that relatively silicate-free ice occurs below a depth of ~ 10 km beneath the dark terrain[10]. Craters with a diameter $\geqslant 50$ km are virtually absent on the younger bright terrain. However, the floors of smaller craters have an albedo similar to that of the surrounding bright terrain suggesting that they did not excavate silicate-rich material. Thus the thickness of the icy material in some areas of bright terrain may be at least 10 km (ref. 10). Also, craters with bright ray systems are preferentially concentrated in the bright terrain[10,11]. Because there should be no significant difference in retention time of rays on the two terrains[11], this may also indicate the presence of a thick icy layer in the bright terrain. If bands of bright terrain were rift zones bounded by normal faults dipping 60° and containing a 10 km thickness of bright material, a relatively modest volume increase of 1% would produce about five such rift zones perpendicular to any great circle on the planet.

The above observations suggest the bright terrain was formed by extension of an ice-silicate crust which led to normal faulting and creation of broad rift zones[6]. Due to the presence of silicates, the crust could be slightly more dense than liquid water or relatively clean ice, causing this underlying material to be extruded[4] into the structurally defined depressions and in some areas overflowing onto surrounding dark terrain. Solidification of the water-rich magma would form bright curvilinear bands of relatively clean ice. The boundaries of the bands would be sharp where the bright material was confined within a rift zone, but would be diffuse where it overflowed onto adjacent dark terrain. The intersection and coalescence of bright bands could form the complex, irregularly shaped areas of bright terrain. Bright terrain emplacement may thus be analogous to terrestrial rifting and the flooding of rift zones with basaltic magma.

Tectonic features

Further evidence for distinguishing the style of tectonism on Ganymede is provided by structural features. The dominant topographical features on Ganymede, other than impact craters, are long, narrow depressions collectively called grooves[1,2] which we assume are the topographical expression of structural features. Although strongly concentrated in the bright terrain, grooves occur in both types of terrain. There are numerous smooth, groove-free regions of bright terrain, and many grooves in the dark terrain.

Some of the simplest examples of grooves are found in the dark terrain. They occur as single curvilinear depressions or as nearly parallel pairs of depressions with lengths of several tens to several hundreds of kilometers, and widths from a few kilometres down to the resolution limit of Voyager images. Examples of single grooves and groove pairs in the dark terrain are shown in Fig. 3. Groove pairs occur with up to ~ 10 km spacing between the individual grooves. Grooves in a groove pair commonly merge along strike to form what appears to be a single groove. In some cases single grooves or groove pairs in the dark terrain merge with dark terrain–bright terrain boundaries.

Grooves are more abundant in the bright terrain, where they occur as single grooves, groove pairs and groove sets. Single grooves and groove pairs in the bright terrain resemble those in the dark terrain. Groove sets contain many nearly parallel grooves. These sets may be up to several hundred kilometres wide and hundreds of kilometres long. The spacing between parallel grooves in a set is typically in the range of 3–10 km, but often appears more nearly constant within any particular set. Individual grooves within a given set merge or bifurcate along strike, but seldom cross. Topographical relief of grooves in groove sets, as determined by photoclinometric analysis[12], is typically 300–400 m, but does not exceed 700 m. The groove sets show no pronounced or consistent topographical asymmetry.

The pattern of grooves in the bright terrain is most regular in narrow bands of this terrain, either those that divide or partially divide dark polygons. In these areas grooves are nearly parallel to the edges of the bands of bright terrain as shown in Fig. 1. In irregularly shaped areas of bright terrain, such as that shown in Fig. 4, groove sets commonly form irregular, intersecting patterns. Some groove sets in such areas strike at high angles to dark terrain–bright terrain boundaries terminating at the terrain boundary. Grooves crosscut and are crosscut by curvilinear regions of smooth bright terrain indicating that grooves were forming concurrently with the emplacement of bright terrain. Relatively few examples of impact craters disrupted by grooves have been observed which indicates that grooves formed at or very near the time of emplacement of the bright terrain on which they occur.

In considering possible tectonic origins of grooves, it is first important to decide whether they may be of extensional or compressional origin. The topographical symmetry of most grooves argues against their being thrust fault scarps. Folds are not likely to form single grooves in which the surface is consistently depressed below surrounding terrain. Grooves, at least where they occur singly or as groove pairs, are more likely to be extensional features, either tension fractures or graben developed in a brittle surface layer. In the dark terrain, no tectonic features that can be associated with compressional deformation have yet been recognized.

Because the interpretation of the tectonic origin of grooves rests largely on their present morphology, it is important to understand the effects of processes that could have modified their topography. Although various processes can degrade topography, viscous relaxation is important in the modification of impact craters on icy surfaces[13,14]. Unlike the grooves, impact craters provide topography of known initial form. On Ganymede, impact craters are frequently shallower than those on silicate bodies and typically have domical floors. Both of these characteristics can be explained by viscous relaxation of topography on a layer of icy crustal material in which the viscosity is uniform or decreases with depth[13].

To examine the effect of viscous relaxation on tectonically produced topography, experiments have been carried out in

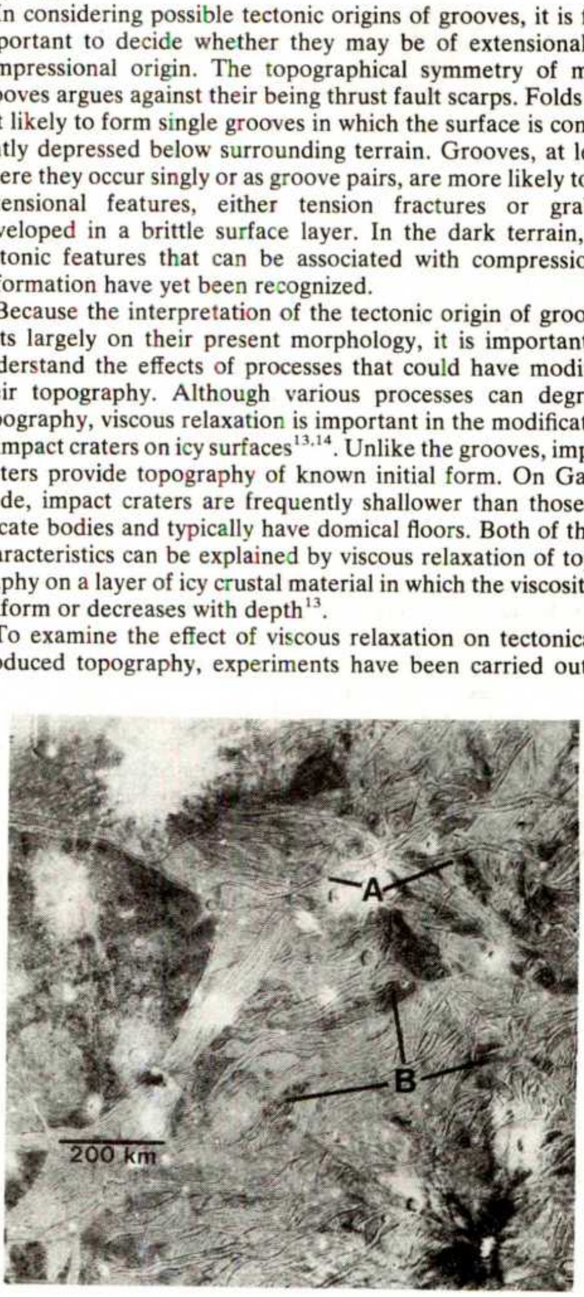

Fig. 4 Complex sets of subparallel grooves in a broad region of bright terrain. Note several well developed groove pairs (A) in the bright terrain, and some small, isolated blocks of dark terrain (B) interspersed through the bright terrain. Voyager image 955J1—000.

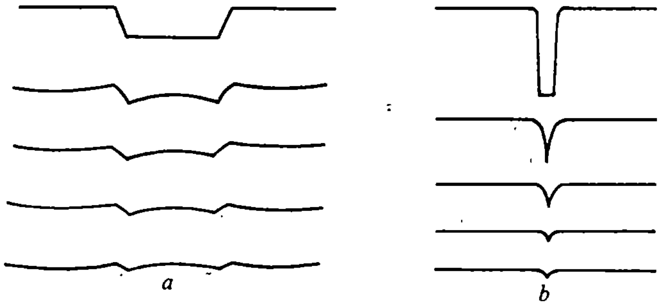

Fig. 5 Experimental relaxation of a graben (*a*) and an extension fracture (*b*) in a thick viscous layer.

which topography is impressed on the surface of a layer of viscous material and allowed to relax. The material used was polyisobutylene, a straight-chain hydrocarbon polymer with a viscosity of about 7×10^5 P at 25 °C. Relaxation was thus slow and could be easily monitored. The form of the relaxing topography at various times was measured with a contour gauge. The relaxation of both graben and tension fractures was studied in this way: typical results are shown in Fig. 5. The form of graben relaxing on a viscous layer with a thickness about twice the graben width is shown in Fig. 5*a*. The relaxing graben develop raised rims and domed floors, much like the morphology of relaxing impact craters. Graben relax to two parallel depressions which appear morphologically similar to groove pairs observed on Ganymede.

Tension cracks relax, as shown in Fig. 5*b*, to form single linear depressions with a width that gradually decreases relative to the initial width of the crack. Because deviatoric stresses are highest near the bottom, the crack closes progressively upwards resulting in a sharp-bottomed depression that shallows with time. The detailed morphology of single grooves on Ganymede cannot be determined, even at the best resolution of available images. These features could be either tension cracks or narrow graben. Relatively low lithostatic stresses on Ganymede would favour the formation of tension cracks in a thin brittle surface layer. However, the recognition of groove pairs as relaxed graben suggests that normal faults have formed. Because many groove pairs, particularly in the dark terrain, narrow along strike to form single grooves, at least some single grooves may be graben.

Another process that could modify the initial topography of grooves is impact erosion and mass-wasting. The steep walls of open extension fractures and fresh graben fault scarps would be especially susceptible to this process. Its general effect would be to widen and partially to fill initially narrow and deep topographical features. This process may thus be important in modifying steep-sided, narrow extension fractures to the broader, more gently sloping features observed. While mass-wasting is expected, Voyager images are of insufficient resolution to identify possible mass-wasting deposits within grooves. We thus cannot yet quantify the degree to which mass-wasting has altered groove topography.

Groove sets in the bright terrain are more complex than single grooves or groove pairs and are therefore more difficult to interpret. They may be a direct consequence of surface fracturing and faulting, or an expression of continuing movement on faults in underlying dark terrain. Alternatively, if the viscosity decreases with depth as indicated by impact crater morphology[13], groove sets may be formed by the folding or boudinage of a high viscocity, near-surface layer. As such, they could reflect either extensional or compressional deformation.

Photoclinometric analysis[12] indicates that in some cases the topography of groove sets is roughly sinusoidal, with groove widths nearly equal to their spacing. In other cases grooves are narrow relative to their spacing and are separated by broad, flat divides. Given the apparent diversity in groove set morphology, a variety of tectonic forms may occur. However, many groove sets could be constructed by placing simple extensional tectonic elements, single grooves or groove pairs, side by side. Given this continuity in form from single grooves and groove pairs to groove sets, it is possible that even in these complex sets the grooves are extensional. This argument is strengthened by the observation that groove sets both crosscut and are crosscut by bands of smooth, ungrooved bright terrain, indicating that the resurfacing and the groove formation must have taken place concurrently in at least some areas. If the resurfacing is a consequence of extensional tectonics, the creation of most groove sets may also be simply explained by this mechanism.

Discussion

At the resolution of available images, the association of extensional deformation with the formation of the bright terrain and the pattern of this terrain on the surface provide a basis for distinguishing the style of global tectonic evolution on Ganymede. As discussed earlier and as shown in Fig. 1, some regions of dark terrain are disrupted by wedge-shaped regions of bright terrain extending inwards from surrounding bright terrain. This pattern of failure would be expected due to membrane stresses[15] in an isolated portion of the lithospheric shell on an expanding planetary body. The continued growth of such wedge-shaped regions of bright terrain would divide a dark region into smaller regions separated by bands of bright terrain. The intersection of bands would form complex, irregular regions of bright terrain. The present pattern of bright terrain could thus be produced by the progressive fragmentation of the lithosphere.

The membrane stress in any unbroken segment of lithospheric shell will depend on its size and the stress acting on its boundary. The boundary stress would arise due to the stress transmitted across areas of bright terrain between adjacent unbroken regions of dark terrain. If the boundary stresses are small or relatively uniform, larger unbroken areas of dark terrain should experience larger membrane stresses for a given amount of planetary expansion. Progressive fragmentation of an initially uniform lithosphere should thus produce unbroken dark areas of roughly comparable size at any stage of fragmentation. This seems to be contradicted by the observation that large regions of dark terrain remain unbroken while smaller regions have undergone fragmentation. Thus, if the tectonic evolution of Ganymede is to be described by progressive fragmentation of an initially uniform lithosphere in response to planetary expansion, the stress transmitted across different areas of bright terrain must differ significantly. Alternatively, lithospheric thickness variations or other mechanisms such as tidal distortion or stresses due to convection beneath the lithosphere may have been important. Additional mapping and analysis based on Voyager images should help resolve many remaining questions about the tectonic evolution of Ganymede.

This research was supported by NASA grant NSG-7605. We thank E.M. Shoemaker for a helpful review of an earlier version of this manuscript and for a preprint describing work on Ganymede geology, and W. B. McKinnon for helpful comments.

Received 13 July; accepted 17 November 1981.

1. Smith, B. A. *et al. Science* **204,** 951–972 (1979).
2. Smith, B. A. *et al. Science* **206,** 927–950 (1979).
3. Solomon, S. C. *Geophys. Res. Lett.* **5,** 461–464 (1978).
4. Parmentier, E. M. & Head, J. W. *J. geophys. Res.* **84,** 6263–6276 (1979).
5. Squyres, S. W. *Geophys. Res. Lett.* **7,** 593–596 (1980).
6. Allison, M. L., Head, J. W. & Parmentier, E. M. *IAU Colloq.* No. **57,** 6–7 (1980).
7. Janke, D. R., Head, J. W. & Parmentier, E. M. *EOS,* **62,** 317 (1981).
8. Lucchitta, B. K. *Icarus* **44,** 481–501 (1980).
9. McKinnon, W. B. & Melosh, H. J. *Icarus,* **44,** 454–471 (1980).
10. Shoemaker, E. M. Lucchitta, B. K., Plescia, J. B., Squyres, S. W. & Wilhelms, D. E. in *The Satellites of Jupiter* (ed. Morrison, D.) (University of Arizona Press, in the press).
11. Squyres, S. W. *Icarus* **44,** 502–510 (1980).
12. Squyres, S. W. *Icarus* **46,** 156–168 (1981).
13. Parmentier, E. M. & Head, J. W. *Icarus* **47,** 100–111 (1981).
14. Passey, Q. R. & Shoemaker, E. M. in *The Satellites of Jupiter* ((ed. Morrison, D.) (University of Arizona Press, in the press).
15. Turcotte, D. L. *Geophys J. R. astr. Soc.* **36,** 33–42 (1974).

The molecular structure of d(^{I}CpCpGpG), a fragment of right-handed double helical A-DNA

Benjamin N. Conner*, Tsunehiro Takano*, Shoji Tanaka*, Keiichi Itakura† & Richard E. Dickerson*

Division of Chemistry and Chemical Engineering, California Institute of Technology, Pasadena, California 91125, USA
† City of Hope National Medical Center, Duarte, California 91010, USA

The DNA tetramer d(^{I}CpCpGpG) or ^{I}CCGG crystallizes as a double-stranded 4-base pair (bp) segment of an A helix. Two such tetramer helices are packed together in the crystal with local helix axes nearly coincident, simulating an 8-bp helix, and four such octamers make up the tetragonal unit cell. Restrained energy and reciprocal space refinement has led to an R factor of 20.5% at 2.1 Å resolution. The ^{I}CCGG helix has a twist corresponding to 10.7 bp per turn, a 19° base tilt and a 2.3 Å rise per base pair along the helix axis. The mean propeller twist of 18° is comparable with, and has the same rotational sense as that observed in the B-DNA dodecamer CGCGAATTCGCG at similarly high alcohol concentration. Backbone phosphate groups in A-DNA are extensively hydrated, including a network across the opening of the major groove, whereas base edge N and O groups in major and minor grooves are less hydrated than in B-DNA. The minor groove spine of hydration observed in B-DNA is totally absent. These observations of relative hydration confirm and extend the model for the B-to-A helix transition proposed earlier on the basis of the B helix structure.

THE first double-helical DNA structures were proposed on the evidence of X-ray diffraction data from drawn fibres obtained from natural sources, supplemented by spectroscopic and chemical information, and model building from the known stereochemistry of component parts[1-7]. Two major families of helix were proposed, A and B, differentiated by sugar puckering, base tilt relative to the helix axis, rise per residue along the axis, distance of base pairs from the centre of the helix and relative dimensions of major and minor grooves (Table 1). A-DNA is characterized by a deep and narrow major groove, a shallow minor groove and base pairs tilted by roughly 19° to the helix axis. In various members of the B family, the bases are more nearly perpendicular to the helix axis and the grooves are of comparable depth, although the major groove is wider.

Fibre diffraction patterns can give the overall average helix parameters for DNA of known composition or repeating sequence, but cannot reveal local variations in helix structure that might be produced by that sequence. This kind of information can only come from single-crystal structure analyses of discrete, homogeneous DNA oligomers. The development of triester and related methods has made the synthesis of such oligomers possible[8]. Structure analyses have been carried out for both a 12-base pair (bp) B helix[9,10] and a totally unexpected new family, the left-handed Z helix[11-13]. We describe here the first single-crystal structure analysis of a member of the A-DNA family, the self-complementary tetramer d(iodo-CpCpGpG) or ^{I}CCGG. It is also the first example of a nucleic acid structure analysis carried out without isomorphous heavy atom derivatives, using initial phasing derived from anomalous scattering as was done for the proteins haemerythrin and crambin (ref. 14 and W. A. Hendrickson and J. Smith, personal communication). (In another structure analysis of an RNA dimer, r(ApU), complexed with 9-aminoacridine, anomalous scattering was used to locate positions of phosphorus atoms, which then became the starting point for non-anomalous phase analysis[15].)

Structure analysis

To find an isomorphous pair of crystal forms, the native CCGG tetramer and four variants with 5-bromocytosine or 5-idocytosine in the first or second position along the chain were synthesized independently by the triester method. Four of these compounds were crystallized, but no two adopted the same space group. Having discussed with W. Hendrickson his experiences with haemerythrin and crambin, we decided to try to solve the better crystal form of the two iodo derivatives, ^{I}CCGG, using anomalous scattering from iodine atoms.

Crystals of the 1-iodo derivative were grown at 2 °C by vapour diffusion against isopropanol, from concentrated aqueous solution of ^{I}CCGG containing spermine hydrochloride buffered at pH 7.5 with sodium cacodylate. The cacodylate buffer was later found to be unnecessary for crystal growth. Crystals began appearing at around 40% isopropanol, and crystal growth was continued to 80% alcohol. The space group of ^{I}CCGG crystals is $P4_32_12$, with cell dimensions $a = b = 41.1$ Å, $c = 26.7$ Å and two tetramer strands (one double helix) per asymmetric unit. A measured density of 1.50 g cm^{-3} and a calculated molecular weight of 1,298 per strand indicate that the crystals are 51.0% DNA by weight.

Data were collected on a Syntex $P\bar{1}$ automatic diffractometer with graphite monochromator, and corrected for X-ray decay and absorption[16]. The pattern was quite strong to 3.5 Å resolution, but declined rapidly beyond that point. One anomalous data set to 2.1 Å resolution contained 1,486 Friedel pairs. Multiple data sets were collected on different crystals for accuracy, so that each reflection within the 3.0 Å sphere was measured at least three times. Mean R factors between independent data sets were ~5% in F.

Patterson and anomalous difference Patterson maps[17] were employed to locate the two iodine positions per asymmetric unit (16 per cell), using the 472 pairs of reflections above the 2σ confidence level within the 3.0 Å sphere. Approximately 36% of these reflections were centric and hence gave no anomalous contribution, but the iodine anomalous scattering factor of $\Delta f'' = 7.2$ electrons for CuKα radiation produced an average difference between Friedel pairs of 11% in F among acentric reflections. The location of iodine atoms was complicated by two factors: the iodine of cytosine C1 was accidentally situated

---

* Present addresses: Molecular Biology Institute, University of California at Los Angeles, Los Angeles, California 90024, USA (B.N.C., R.E.D.); Institute of Protein Research, Osaka University, Osaka, Japan (T.T.); Laboratory of Microbiology, Suntory Institute for Biomedical Research, Mishima-gun, Osaka 618, Japan (S.T.).

0028-0836/82/040294—06$01.00

Table 1 Structural parameters in double-helical DNA

		Fibre diffraction results					
			B family			Z family	
	^{I}CCGG crystal structure	A	B	C	D	Z	Z′
Helix sense	Right	Right	←	Right	→	Left	Left
Sugar pucker	C-3′-*endo*	C-3′-*endo*	←	C-2′-*endo*	→	Alternating	
Glycosyl angle	Anti	Anti	←	Anti	→	Syn(G)/anti(C)	
Twist per base pair	33.6°	32.7°	36°	38.6°	45°	−60°/2	−60°/2
Bases per turn	10.7	11	10	$9\frac{1}{3}$	8	12	12
Rise per base pair (Å)	2.3	2.6	3.4	3.3	3.0	3.7	3.8
Base tilt	19°	19°	−6°	−8°	−16°	−7°	−9°
Groove width (Å)							
Minor	8.8	11.0	5.7	4.8	1.3		
Major	2.0	2.7	11.7	10.5	8.9		
Groove depth (Å)							
Minor	3.7	2.8	7.5	7.9	6.7		
Major	13.8	13.5	8.5	7.5	5.8		
Refs	This work	4	4	4,5	4,5	11	13

Groove width is the perpendicular separation of ideal helix strands drawn through the phosphate groups, decreased by 5.8 Å to represent van der Waals radii of two phosphate groups. Groove depth is defined precisely in ref. 4, but again is based on van der Waals radii, as though measured from a space-filling model.

directly above a 2-fold axis, with coordinates close to $(\frac{1}{4}, \frac{1}{4}, \frac{1}{4})$, and that on cytosine C5 of the other strand of the double helix was nearly just one-quarter of the cell away from it along the *a* axis. Each of these two coincidences introduced false centrosymmetry that decreased the iodine anomalous contribution to many of the acentric reflections. Thus the simple $(\Delta F_{\text{ano}})^2 = (F_{hkl} - F_{\bar{h}\bar{k}\bar{l}})^2$ anomalous difference Patterson map was not interpretable. Iodine positions were ultimately found by comparing F^2 Patterson maps using both centric and acentric reflections, with F^2 Patterson maps using only acentric data. As we suspected that our difficulties arose because the iodines sat on or near symmetry elements, those Patterson peaks which were deleted by the removal of centric data were reinforced in the simple anomalous difference Patterson map, and the composite map was then interpretable in terms of a self-consistent set of iodine–iodine vectors.

Once the iodines were located, electron density maps were calculated using Sim-weighted heavy atom phases[18] for centric reflections, and Sim-weighted anomalous phases[19,20] for acentric reflections. Of the two possible enantiomorphic maps, one was uninterpretable, while the other gave a clear and clean image of the tetramer double helix. The helix obtained from this map was subjected to 28 cycles of simultaneous energy and reciprocal space refinement[21], using the same energy constraints as for the B-DNA dodecamer[10]. Refinement progress was monitored periodically by Fourier and difference Fourier electron density maps. During this process, the *R* factor fell from 39% at 3.0 Å resolution (2σ data) to the current 20.5% at 2.1 Å. The model contains 29 solvent molecules at present and refinement is continuing.

Tetramer structure

The complete unit cell contains eight identical double-helical tetramers, one of which is shown in Fig. 1. The tetramer is a fragment of an A-DNA double helix. A helix-generating program provided by J. Rosenberg enabled us to use the relationships between base pairs within one tetramer to define the parameters of an ideal continuous helix (see Fig. 1). The helix twist angle is 33.6° per base, corresponding to 10.7 bp per turn, and the rise per base pair along the the axis is 2.3 Å. Bases are tilted by 19° from perpendicularity to the helix axis. Sugar rings are all in the C-3′-*endo* conformation with the exception of the 3′-terminal sugar of guanine G4, which is C-2′-*endo*. (See upper left of Fig. 1*b*, or lower left of Fig. 1*c*.) However, as the G4 sugar has no chain continuation to force it into a regular geometry, it is not surprising that it adopts an anomalous conformation. Table 1 compares observed CCGG helix parameters with idealized A-DNA values derived from fibre data and with those of other types of helix.

The base pairs have large propeller twists: 19°, 18°, 18° and 23° for C1–G8, C2–G7, G3–C6 and G4–C5 respectively. The large propeller twist was visible early in the analysis of the anomalously phased electron density map, and hence is not a consequence of the refinement process. The last value is perturbed by the same intermolecular crystal packing that produces the tilted C5 plane visible in Fig. 1, but the other three values are quite consistent. They are larger than the 13° average propeller twist observed for B-DNA in the low-alcohol crystals (35% methylpentanediol, MPD) of CGCGAATTCGCG[10], and more like the 19° observed in the higher alcohol (60% MPD) crystals of CGCGAATT$^{\text{Br}}$CGCG (M. L. Kopka, A. V. Fratini, H. R. Drew and R.E.D., in preparation). The sense of the propeller rotation in A-helical CCGG is the same as that in these B helices: clockwise rotation of the nearer base plane when the base pair is viewed along its long axis, defined here as the positive rotational sense for propeller twist. In contrast, the published coordinates for a model A-DNA structure derived from fibre diffraction data[22] yield an opposite rotation, with a propeller twist angle of −12°. (A recent unpublished set of new fibre-derived A-DNA coordinates supplied by S. Arnott has positive propeller twist angles of +7.5°.) Two RNA dimers are known which are fragments of an A helix: r(ApU) and r(GpC)[23,24]. In these molecules the propeller twist is smaller and of variable sign: +12.5° (average) for r(ApU) and −7.2° for r(GpC). It seems likely that a substantial propeller twist is a consequence of efficient base stacking at successive steps along one strand of a continuous double helix, and hence reasonable that the full twist typical of an infinite helix would not be generated in helices shorter than 3 or 4 bp. Indeed, one unexpected feature apparent from the single-crystal analyses of oligomers of A- and B-DNA has been the large propeller twist angles, which were not anticipated from fibre and dimer studies.

A-helical octamers in the crystal

The most apparent distortion of the tetramer in Fig. 1 is the pushing of the iodine on cytosine C5 towards the centre of the molecule, with a resultant bending of the C5 plane away from that of G4. This is simply explained in terms of the way in which tetramers are packed within the crystal. Two tetramers are stacked with their C1–G8 base planes in contact, their helix axes nearly coincident and a rotation between tetramers that closely approximates a continuous 8-bp A helix (Fig. 2). Four of these octamers are then packed around the 4-fold screw axes of the

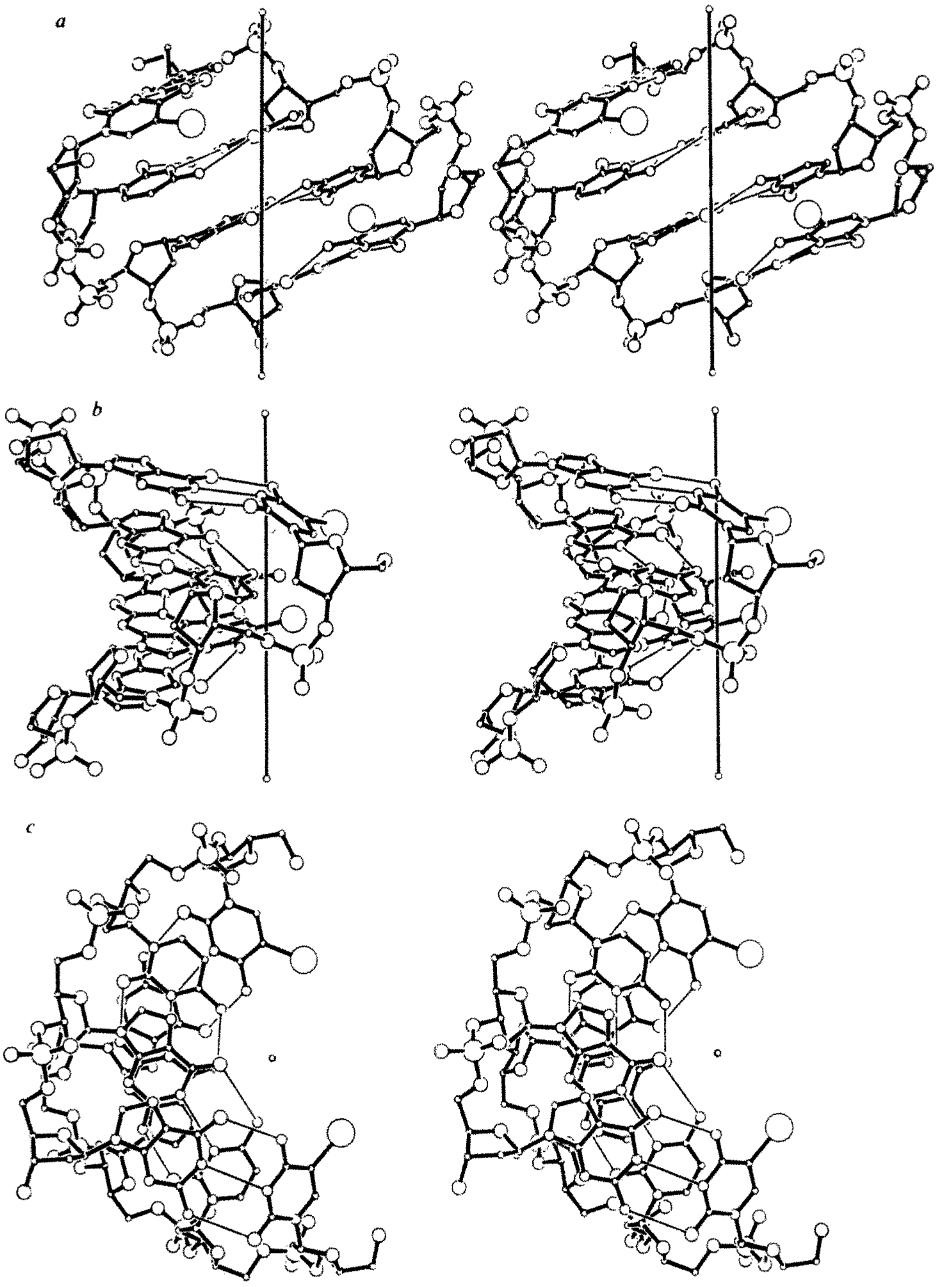

Fig. 1 Stereo views of the ^{I}CCGG double-helical A-DNA molecule. *a*, View into the major groove with helix axis vertical. Bases are numbered: 5′-C1-C2-G3-G4-3′ in one strand and 5′-C5-C6-G7-G8-3′ along the other. The two largest atoms are iodines on cytosines C1 (lower right) and C5 (upper left), and other atoms in order of decreasing size are P, O, N and C. Hydrogen bonds between base pairs are shown as thin lines. Base pair C1–G8 is at the bottom and G4–C5 at the top. *b*, View 90° to the left of *a*, showing the shallow minor groove in profile at left, and the large propeller twist of base planes. *c*, Top view looking directly down the helix axis onto base pair G4–C5. The iodocytosine base planes are tilted away from the planes of their hydrogen-bonded partners, C5 more so than C1, because of intermolecular contacts within the crystal.

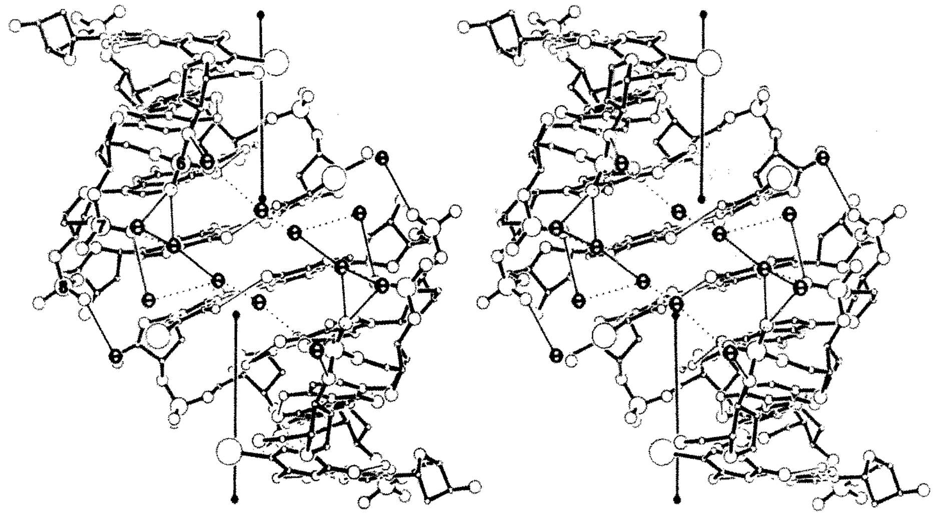

Fig. 2 Two ^{I}CCGG tetramers stacked around a 2-fold axis (normal to the page through the centre of the drawing) as they are observed in the crystal. Their C1–G8 base pairs are in contact, and have very nearly the correct displacement to continue the A helix for 8 bp. Local helix axes, as determined independently for the two tetramers, are shown by vertical lines, and are almost coincident. This view is directly into the major groove, lined by phosphates 6, 7 and 8 (numbered on one strand). After the missing phosphate between tetramers, a continuous helix would use phosphates 2, 3 and 4 around the back of the drawing on the other tetramer. Seven water molecules and their symmetry-related partners are shown spanning the major groove (⊖). Distances of ≤ 3.4 Å are shown by thin solid lines, and distances up to 3.8 Å by dotted lines. As discussed in the text, in a continuous A-DNA helix the major groove would be narrower than shown here, and the bridging network of hydration would be different in detail although similar in character.

$P4_32_12$ cell. The iodocytosine ring C5 at each end of an octamer (top and bottom of Fig. 2) is packed against the minor groove of a neighbouring octamer, between bases C2 and G3. Although the C5 iodine atom is pushed back towards the centre of the octamer, it still is in tight van der Waals contact with the C-2′ sugar atom of cytosine C2 and the C-5′ atom of guanine G3 on a neighbouring octamer.

At the centre of each octamer (deep inside the major groove in Fig. 2), the iodine of cytosine C1 on one tetramer is displaced slightly because of a close contact with the five-membered ring of G8 on the other tetramer (the next base step along the helix), but the effect on its cytosine orientation is small. The two local helix axes as viewed in Fig. 2 are displaced sideways by 1.5 Å, which serves to lessen the overlap between each iodine and its facing G8 ring. The extreme top and bottom of the two axes in Fig. 2 are tipped down into the plane of the page so the axes make an angle of 8° to one another, which also lessens the iodine/guanine clash. The absence of phosphate groups to connect the tetramers allows a degree of adjustment that might not be present in a true double-stranded octamer.

Four octamers as shown are packed into the tetragonal unit cell of the crystal in helical arrays around water channels with elliptical cross-sections, parallel to the *z* axis. Each octamer uses its relatively flat minor groove side to define a long side of one elliptical channel, and its more concave major groove to make the sharp bend at the short side of a different elliptical channel. The individual octamers are hydrated as described below, and networks of localized solvent molecules extend across the channels.

The idealized extended A helix

The octamer in Fig. 2 does not provide a true impression of a continuous A-DNA helix with this helix geometry. Figure 3 shows two views of a full turn of helix, constructed by stacking three identical tetramers on top of one another with their local helix axes coincident. The very deep major groove is particularly striking in stereo (Fig. 3*a*). The groove is narrower in the continuous helix (Fig. 3) than in the crystal structure octamer (Fig. 2) because of the 8° angle between local helix axes in the octamer. If this angle were straightened out to 0°, then the major groove in the octamer would appear as in Fig. 3*a*, with phosphorus–phosphorus separations across the groove of 7.8 Å rather than 10.9 Å, the P6–P6 separation in Fig. 2. This factor will become important in the following discussion of hydration.

The shallow minor groove is hardly a groove at all in comparison with its structure in B-DNA. Figure 3*b* shows the hollow channel down the centre of the helix, a feature peculiar to A-DNA. In a sense the A helix is more a twisted, double-edged ribbon than a cylinder of stacked base pairs. The major groove is only one-quarter as wide as the minor one, but is four times as deep (Table 1).

Hydration and contrast with B-DNA

The A-DNA structure itself has been completely refined;

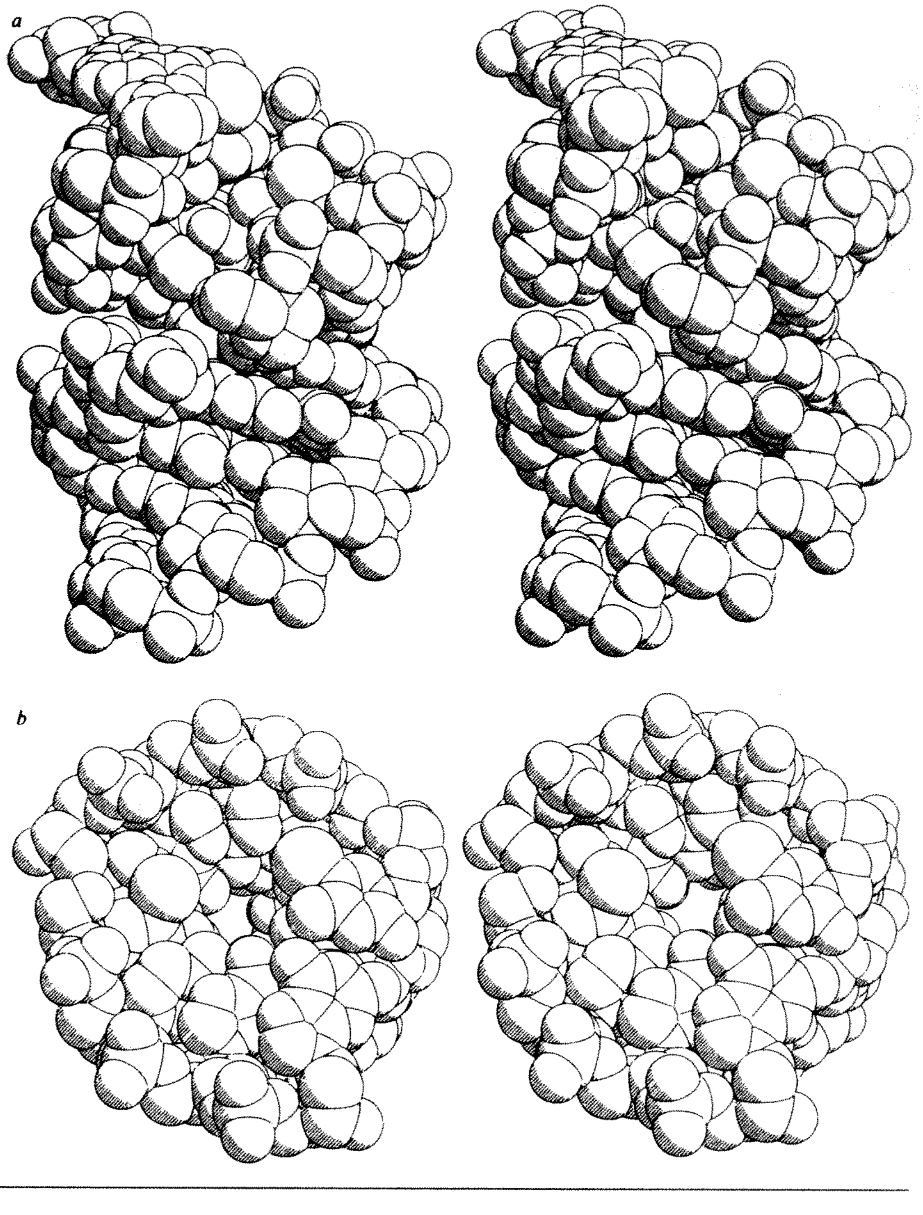

Fig. 3 PLUTO space-filling drawings of three $^{\mathrm{I}}$CCGG tetramers stacked atop one another along their helix axes to form a complete turn of A-DNA helix. In the actual octamer found in the crystal (Fig. 2), one tetramer is inverted before being stacked on the other, with equivalent base pairs in contact. In contrast, in this simulation of a complete turn of helix, all three tetramers are stacked upright in the sense of Fig. 1, with base pair G4–C5 at the top and C1–G8 at the bottom. No attempt has been made to idealize or regularize individual molecules, or to fill in the missing phosphate groups that would connect tetramers in a continuous helix; each tetramer is exactly as observed in the crystal. *a*, Side view looking into the cavernous major groove at the top, with the shallow minor groove in profile at right. *b*, Top view down the helix axis, showing the 'spiral staircase' arrangement of base pairs and the hollow centre.

remaining refinement will be concerned principally with adding more solvent peaks until the difference electron density map has no significant residual features. The 29 solvent peaks added so far give a good impression of the hydration state of the A helix, since most of the peaks that have yet to be incorporated lie in the open solvent channels between molecules. A detailed analysis of intermolecular water networks, and comparison with other results (refs 25, 26 and M. L. Kopka, A. V. Fratini, H. R. Drew and R.E.D., in preparation) will be described elsewhere (B.N.C. and R.E.D., in preparation). The helical octamers are long enough to establish true major and minor groove solvent environments, even though the chemically unique unit is only four bases long.

The hydration state of A-DNA in CCGG is significantly different from that of B-DNA in CGCGAATTCGCG. In the 35% MPD crystals of B-DNA[26], all the N and O groups on the edges of base pairs in the major groove are hydrated by a monolayer of solvent molecules, but the bulk water within the major groove appears disordered. Similarly, except for three examples where a water molecule is trapped in a clathrate-like manner between a phosphate group and a thymine methyl, hydration of B-DNA along the phosphate backbone also is unlocalized, without clearly defined peaks. But taking the B-DNA dodecamer to the higher alcohol concentration of 60% MPD produces a more extensive second- and third-shell hydration within the major groove, and a more extensive and ordered hydration along the phosphate backbone (M. L. Kopka, A. V. Fratini, H. R. Drew and R.E.D., in preparation). Almost every free phosphate oxygen has a solvent ligand, and another solvent molecule frequently bridges the two oxygens. The most striking and unvarying aspect of B-DNA hydration, however, is a zigzag spine of water molecules running down the narrow minor groove, bridging purine N-3 and pyrimidine O-2 atoms on adjacent base pair steps, where not interrupted by N-2 amino groups on guanines. This feature is identical in low and high MPD crystals, though slightly more extensive in the latter. It has been proposed that the breakup of this minor groove spine of hydration is the crucial first step in the cooperative transition from the B to the A form[26,27].

With respect to the phosphate backbone, CCGG in 80% isopropanol resembles CGCGAATT$^{\mathrm{Br}}$CGCG in 60% MPD: a chain of localized water molecules follows each tetramer backbone strand, bonding to the two unesterified oxygens on each phosphorus. Eighteen well defined solvent peaks are associated with the phosphate backbone, and many of these first hydration shell ligands are themselves bridged by other solvent molecules (see Fig. 4). In the view of the octamer in Fig. 2, a network of six solvent molecules (and their six symmetry-related partners) arches across the opening of the major groove, connecting phosphates P-6 and P-7 on opposite sides. This octamer is so short that the two edges of the major groove are in opposition only at P-6 and P-7. In a continuous A helix, such as in Fig. 3, one would expect the opening of the major groove to be crossed by a continuous network of solvent molecules, especially as the actual A-DNA groove would be 3 Å narrower than that in the octamer of the crystal structure. This network of solvent molecules stitching together the two edges of the major groove may be a distinctive feature of the A helix.

In contrast, fewer ordered water molecules seem to be located deep in the major groove of A-DNA, or in the very shallow minor groove, even though the major groove is more accessible in this crystal structure analysis than it would be in continuous A-DNA. Only one-third of the N and O atoms on base edges have clearly defined full-occupancy ligands, five in the major groove and three in the minor one. Another one-quarter has small nearby peaks that may represent partial occupancy sites (three each in major and minor), but hydration within the grooves is less impressive than in either of the grooves of B-DNA, even at comparable alcohol concentrations.

Water structure and the B-to-A transition

In summary, in A-DNA there is no trace of the minor groove spine of hydration that is so prominent in B-DNA, nor does there appear to be as uniform a monolayer of ordered solvent lining the major groove. The extensive solvation of phosphate backbone observed in B-DNA at 60% MPD reappears in A-DNA, where it seems to lace together the two edges of the major groove.

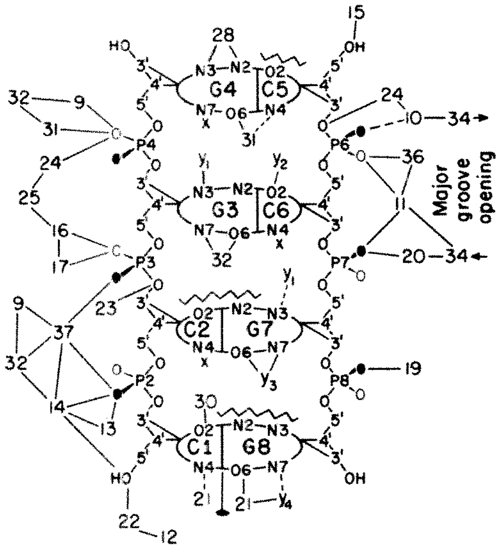

Fig. 4 Schematic drawing of hydration in the immediate vicinity of the CCGG double helix in the crystal. The four central ovals represent purine–pyrimidine base pairs identified by base numbers, as 'G4/C5' at the top. Base ring nitrogen and oxygen atoms are shown by N3, N2, O2 and so on around the perimeter of each oval. The upper edge of each oval faces the minor groove, and the lower edge faces the major. The two sugar–phosphate chains run vertically at either side of the base pair ovals, with C-3', C-4' and C-5' atoms indicated merely by 3', 4' and 5'. (Atoms C-1', C-2' and O-1' are omitted for clarity.) Phosphates are numbered P2–P4 and P6–P8 according to the base to which they are linked via C-5' atoms. Solid black oxygen atoms on phosphates are those facing the major groove. Large numbers identify the most prominent solvent molecules in the immediate vicinity of the double helix. x Indicates that a peak was specifically looked for in the electron density map but not found. y_1–y_4 Are lesser peaks not included in the original hydration search, but found in the map when specifically examined for base edge coordination. ⁓ Indicates that base edge atoms are blocked by neighbouring DNA substituents, and hence unavailable for hydration. The region of the major groove opening depicted in Fig. 2 appears at the upper right edge. A chain of five solvent molecules (24-10-34-11-36) runs diagonally downwards to the right from phosphate P-6 in Fig. 2, with the parallel symmetry-related chain (36-11-34-10-24) just below it. Solvent molecules 19 and 20 in two symmetry-related pairs lie just below and above these two strands in Fig. 2. The solvent network shown at the left of the diagram is necessarily incomplete and distorted because a three-dimensional network cannot easily be flattened into a planar diagram. Solvent atom 32 at the lower left, for example, is part of a network connecting phosphate P-2 with phosphate P-4 on a different double helix (upper left). It also is coordinated directly to major groove atoms N-7 and O-6 on base G3 of the same helix. However, the figure does provide an accurate depiction of the first hydration shell of the helix.

These observations permit the ideas proposed in ref. 26 on the B-to-A helix transition to be carried one step further. The backbone phosphate groups are more polar, and have a greater attraction for water molecules, than do the N and O groups on the edges of base pairs within the grooves. In conditions where the activity coefficient of water is high (conditions favouring B-DNA), all these polar groups should be solvated; but when the water activity is decreased, either by dehydration or by addition of alcohol, then the groove N and O groups should lose their solvation shells before the phosphates do. When the spine of hydration in the minor groove is disrupted, the integrity of the B structure is destroyed and the helix slips into the A form, in which the still hydrated phosphate groups participate in a network of solvation that laces together the two edges of the now quite narrow major groove. The phosphate-associated lacing across the major groove in A-DNA may have a stabilizing role comparable with that of the base-associated spine within the minor groove in B-DNA. When the water activity around an A helix is increased again, rehydration of base edge N and O groups, including re-establishment of the minor groove spine, shifts the equilibrium in favour of B-DNA, because the number of molecules solvating the phosphate backbone is not altered, but only their disposition.

Since submission of this manuscript, O. Kennard and co-workers at Cambridge have solved the structure of another A-DNA helix, of sequence: GGTATACC (personal communication).

We thank Al Fratini, Mary Kopka and Horace Drew for permission to quote their dodecamer results in 60% MPD before publication, and Lillian Casler for assistance with the figures. This work was supported by NIH grant GM-12121 and NSF grant PCM79-13959. B.N.C. was the recipient of an NIH predoctoral traineeship. This is contribution no. 6482 from the Division of Chemistry and Chemical Engineering.

Received 27 July; accepted 27 October 1981.

1. Watson, J. D. & Crick, F. H. C. *Nature* **171,** 737–738 (1953).
2. Langridge, R., Wilson, H. R., Hooper, C. W., Wilkins, M. H. F. & Hamilton, L. D. *J. molec. Biol.* **2,** 19–37 (1960).
3. Fuller, W., Wilkins, M. H. F., Wilson, H. R., Hamilton, L. D. & Arnott, S. *J. molec. Biol.* **12,** 60–80 (1965).
4. Arnott, S. in *Organization and Expression of Chromosomes* (eds Allfrey, V. G., Bautz, E. K. F., McCarthy, B. J., Schimke, R. T. & Tissieres, A.) 209–222 (Dahlem Konferenzen, Berlin, 1976).
5. Arnott, S. & Selsing, E. *J. molec. Biol.* **98,** 265–269 (1975).
6. Marvin, D. A., Spencer, M., Wilkins, M. H. F. & Hamilton, L. D. *J. molec. Biol.* **3,** 547–565 (1961).
7. Davies, D. R. & Baldwin, R. L. *J. molec. Biol.* **6,** 251–255 (1963).
8. Itakura, K. & Riggs, A. D. *Science* **209,** 1401–1405 (1980).
9. Wing, R. M. *et al. Nature* **287,** 755–758 (1980).
10. Drew, H. R. *et al. Proc. natn. Acad. Sci. U.S.A.* **78,** 2179–2183 (1981).
11. Wang. A. H.-J. *et al. Nature* **282,** 680–686 (1979).
12. Arnott, S., Chandrasekaran, R., Birdsall, D. L., Leslie, A. G. W. & Ratliff, R. L. *Nature* **283,** 743–745 (1980).
13. Drew, H., Takano, T., Tanaka, S., Itakura, K. & Dickerson, R. E. *Nature* **286,** 567-573 (1980).
14. Hendrickson, W. A. & Teeter, M. M. *Nature* **290,** 107–113 (1981).
15. Seeman, N. C., Day, R. O. & Rich, A. *Nature* **253,** 324–326 (1975).
16. North, A. C. T., Phillips, D. C. & Mathews, F. S. *Acta crystallogr.* **A24,** 351–359 (1968).
17. Rossman, M. G. *Acta crystallogr.* **14,** 383–388 (1961).
18. Sim, G. A. *Acta crystallogr.* **13,** 511–512 (1960).
19. Sim, G. A. *Acta crystallogr.* **17,** 1072–1073 (1964).
20. Ramachandran, G. N & Raman, S. *Curr. Sci.* **11,** 348–351 (1956).
21. Jack, A. & Levitt, M. *Acta crystallogr.* **A34,** 931–935 (1976).
22. Arnott, S. & Hukins, D. W. L. *Biochem. biophys. Res. Commun.* **47,** 1504–1509 (1972).
23. Seeman, N. C., Rosenberg, J. M., Suddath, F. L., Kim, J. J. P. & Rich, A. *J. molec. Biol.* **104,** 109–144 (1976).
24. Rosenberg, J. M., Seeman, N. C., Day, R. O. & Rich, A. *J. molec. Biol.* **104,** 145–167 (1976).
25. Neidel, S., Berman, H. M. & Shieh, H. S. *Nature* **288,** 129–133 (1980).
26. Drew, H. R. & Dickerson, R. E. *J. molec. Biol.* **151,** 535–556 (1981).
27. Dickerson, R. E., Drew, H. R. & Conner, B. N. in *Biomolecular Stereodynamics* Vol. 1 (ed. Sarma, R. H.) 1–34 (Adenine, New York, 1981).

Nucleotide sequence of cloned cDNA encoding bovine arginine vasopressin–neurophysin II precursor

Hartmut Land*, Günther Schütz*, Hartwig Schmale† & Dietmar Richter†

* Institut für Zell- und Tumorbiologie, Deutsches Krebsforschungszentrum, Im Neuenheimer Feld 280, D-6900 Heidelberg, FRG
† Institut für Physiologische Chemie, Abteilung Zellbiochemie, Universität Hamburg, Martinistrasse 52, D-2000 Hamburg 20, FRG

The sequence of a cDNA encoding the nonapeptide arginine vasopressin (AVP) and its carrier protein, neurophysin II (NpII) from bovine hypothalamus, proves that the 166-amino acid precursor molecule contains a signal peptide of 19 amino acids followed directly by AVP connected to NpII by a Gly-Lys-Arg sequence. The carboxy-terminal region of the precursor contains a naturally occurring glycopolypeptide of 39 amino acids which is separated from NpII by a single arginine residue.

THE nonapeptide hormones arginine vasopressin and oxytocin are synthesized in the supraoptic and paraventricular nuclei of the hypothalamus together with their respective 'carrier' proteins, the neurophysins (for reviews see refs 1–4). Arginine vasopressin and oxytocin are produced by separate populations of magnocellular neurones in both nuclei[5,6]. Together with the neurophysins they are packaged into neurosecretory vesicles and transported axonally to the nerve endings located in the neurohypophysis, where they are either stored or secreted into the bloodstream. More than a decade ago, Sachs and co-workers[7,8] suggested that arginine vasopressin and its corresponding neurophysin (molecular weight M_r) 10,000 are synthesized in the form of a common precursor which is cleaved by proteolysis to yield the biologically functional peptides. This hypothesis is supported by the finding that rats with hereditary diabetes insipidus are deficient in synthesis of arginine vasopressin[9] and one species of neurophysin[10–13]. Further evidence in support of this model of a cellular polyprotein[14] was obtained by the isolation from the hypothalamus of rats[15,16] and mice[17] of precursor polypeptides with apparent M_r of 20,000 and 17,000, respectively. These polypeptides cross-reacted with antibodies directed against neurophysin[17,18] and were found to be processed *in vivo* to polypeptides of neurophysin size[15]. One of the precursors gave rise to an arginine vasopressin-like peptide after trypsinization[16]. Neurophysin precursors were also demonstrated after *in vitro* translation of hypothalamic mRNA[19–21]. Recently, an *in vitro* synthesized common precursor to arginine vasopressin and bovine neurophysin II (AVP-NpII) has been identified both immunologically[22,23] and by tryptic fingerprint analysis[24]. The latter showed that authentic AVP$_{1-8}$ and the expected oligopeptides specific for NpII can be released from the *in vitro* synthesized precursor[24]. Furthermore, comparison of the tryptic peptides obtained from the pre-proform, the glycosylated proform and a 14,000-M_r intermediate of the AVP-NpII precursor indicated that AVP should be directly connected to the signal peptide and that AVP and NpII should be close neighbours within the precursor[24]. However, proof of the intramolecular organization of the AVP–NpII precursor awaits elucidation of its amino acid sequence.

The construction of bacterial plasmids containing the mRNA sequence for the AVP–NpII precursor is a direct approach to analysing the amino acid sequence, the mRNA and the gene for the hypothalamic polyprotein. Here we present the nucleotide sequence of the mRNA which allows us to predict the primary structure of the AVP–NpII precursor synthesized in the bovine hypothalamus.

Cloning of cDNA encoding the AVP–NpII precursor

Poly(A)-containing RNA from bovine hypothalamus was isolated as described in Fig. 1 legend. To estimate the relative proportion of mRNA coding for the AVP–NpII precursor, the RNA was translated *in vitro* using a rabbit reticulocyte lysate in

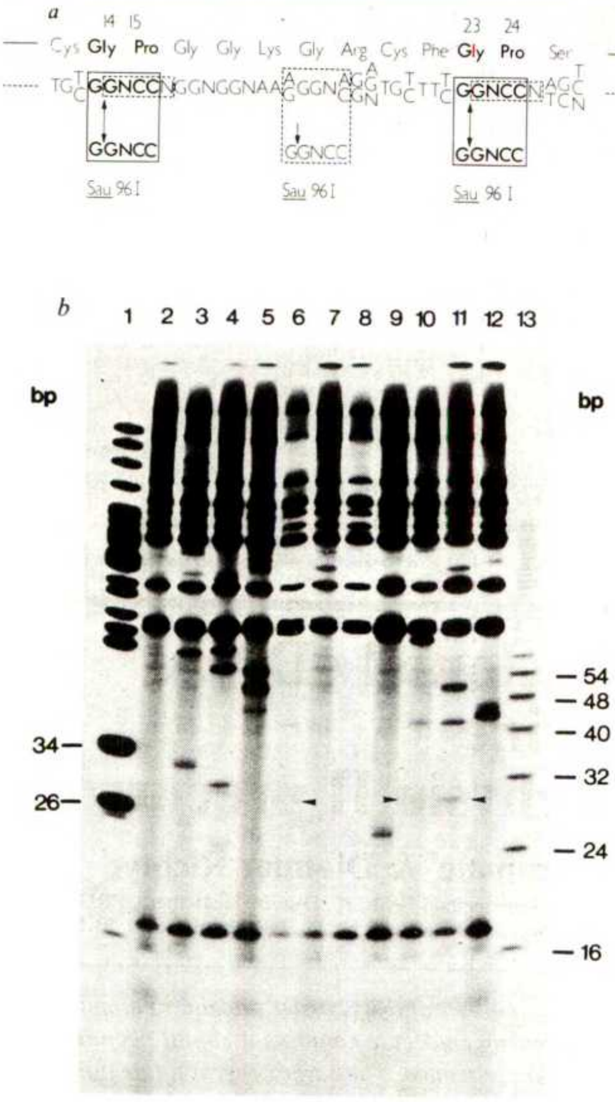
a
14 15
23 24
Cys Gly Pro Gly Gly Lys Gly Arg Cys Phe Gly Pro Ser
TG T/C GGNCCN GGNGGNAA A/G GGN AG/CGN A/G TG T/C TT T/C GGNCCN AGC/TCN T
GGNCC
GGNCC
GGNCC
Sau 96I
Sau 96I
Sau 96I
b
1 2 3 4 5 6 7 8 9 10 11 12 13
bp
bp
34
26
54
48
40
32
24
16

Fig. 1 Cloning of cDNA specific for bovine hypothalamic mRNA and selection of plasmids carrying sequences encoding the AVP–NpII precursor. Membrane-bound polysomes were isolated from bovine hypothalami and the RNA extracted with SDS/phenol/chloroform[27]. Polyadenylated RNA was purified by oligo (dT)-cellulose affinity chromatography. The yield was 0.4–0.5 μg poly(A)-containing RNA per g of tissue[27]; 1.2 μg of single-stranded cDNA was constructed from 10 μg poly(A)-containing RNA with AMV reverse transcriptase[26]. To generate double-stranded cDNA (ds cDNA), the cDNA was dC-tailed at its 3′ end with terminal deoxyribonucleotidyl transferase (TdT). The synthesis of the second cDNA strand was primed by oligo(dG) hybridized to the 3′ tail[26]. The cDNA was extracted with chloroform/isoamylalcohol and ethanol-precipitated twice, then hybridized to oligo(dG). Reverse transcriptase (60 units) was added to the incubation mixture to catalyse synthesis of the complementary cDNA strand. The reaction was stopped as described above. Ds cDNA (0.8 μg) was run on a 2% agarose gel in Tris-acetate buffer *p*H 8.0 and molecules in the range 500–1,500 bp were recovered from the gel by the glass binding method[62], with a yield of 0.2 μg. Ds cDNA was tailed, and ~10 dC residues were added to each 3′ end[63]. The dC-tailed ds cDNA was then annealed to an equimolar amount of *Pst*I-cut (Renner) dG-tailed pBR322. Ten microlitres of annealing solution (2.5 ng vector) were taken for 100 μl of competent cells. Transformation of *E. coli* 5K (ref. 64) was carried out as described elsewhere[65] in L3/B1 conditions as specified by the Zentrale Kommission für Biologische Sicherheit of the FRG. Screening for tetracycline-resistant cells yielded ~200 colonies per ng of ds cDNA with a background of 10% ampicillin-resistant clones. To screen the recombinant colonies, plasmid DNAs from 550 clones were individually prepared according to a minipreparation protocol[66] and spotted on to nitrocellulose filters[67]. The filters were hybridized to a ^{32}P-labelled poly(A)$^+$ RNA probe[68] which was enriched for mRNA coding for the common AVP–NpII precursor by two subsequent separations on isokinetic sucrose gradients[27]. Desired fractions were selected by an *in vitro* translation assay[27]. Plasmid DNAs from 55 colonies giving a hybridization signal markedly above background were collected into 11 groups, RNase A-treated, restricted with *Sau*961 (BLR) and labelled at their 3′ ends with *Escherichia coli* DNA polymerase I Klenow fragment (BRL). Unincorporated radioactivity was removed by centrifuging the reaction mixture through a syringe packed with Sephadex LH-60 (Pharmacia). The excluded material was ethanol-precipitated and run on a 15% polyacrylamide gel (*b*, lanes 2–12). DNA M_r standards: Lane 1, pBR322 was digested with *Hpa*II and the 3′ ends were labelled with [α-^{32}P]dCTP as described above. Lane 13, molecular *Cla*I linkers (Collaborative Research) were phosphorylated with [γ-^{32}P]ATP and ligated. Numbers indicate the size of the DNA marker bands in base pairs (bp). The gel was dried and autoradiographed. *a*, *Sau*961 cleavage sites predicted from the amino acid sequence of neurophysin. Definite sites are framed by solid lines, possible sites by broken lines (for further explanation see text).

the presence of five ^{3}H-labelled amino acids. About 1% of the trichloroacetic acid-precipitable radioactivity was found in material that was immunoprecipitated with antibodies against bovine neurophysin II[25].

Double-stranded cDNA was synthesized from the poly(A)-containing RNA by a method that reduces the loss of the 5′-terminal mRNA sequences in the steps following cDNA synthesis[26]. This approach avoids the self-priming step for generation of double-stranded cDNA. Therefore, no S_1-nuclease digestion step is required. Instead, the cDNA is tailed with dC residues at its 3′ end using terminal deoxynucleotidyl transferase. The synthesis of the second strand was primed by oligo(dG) hybridized to the 3′ tail. dC-tailed double-stranded cDNA was then annealed to the plasmid pBR322 that had been previously linearized by restriction endonuclease *Pst*I and dG-tailed. Tetracycline-resistant transformants were screened for ampicillin sensitivity (for details see Fig. 1 legend).

To identify plasmids carrying the more frequent mRNA sequences, plasmid DNAs from 550 colonies were hybridized to *in vitro* ^{32}P-labelled poly(A)-containing RNA from bovine hypothalamus that was ~10-fold enriched for AVP–NpII mRNA by fractionation after passage through two consecutive sucrose gradients[27]; 55 plasmids gave a positive hybridization signal. Because the yields of mRNA isolated from bovine hypothalami were very low, the RNA-consuming positive hydrid selection assay[28] could not be used for clone identification. To identify clones specific for AVP–NpII precursor sequences, we adopted a strategy whereby restriction endonuclease cleavage sites in an unknown DNA sequence can be predicted unambiguously from a known amino acid sequence. Only a few restriction endonucleases have recognition sequences that fulfil the necessary requirements. *Fnu*4HI (GCNGC)[29] cuts the DNA at any position corresponding to the amino acid sequence Ala-Ala (GCNGCN), *Sau*96I (GGNCC)[30] cuts at all positions coding for Gly-Pro (GGNCCN). The neurophysins exhibit Gly-Pro sequences at positions 14–15 and 23–24. If a DNA sequence coding for neurophysin is digested with *Sau*96I, a 27-base pair (bp) fragment should be generated by cuts at the predicted cleavage sites. Computer analysis revealed the possible existence of an additional restriction site for *Sau*96I within this 27-bp fragment which, if it were present, would lead to cleavage of the 27-bp fragment into fragments of 14 and 13 bp (Fig. 1*a*). To detect clones carrying the 27-bp fragment, the 55 positively hybridizing plasmid DNAs were pooled into 11 groups, cut with *Sau*96I, ^{32}P-labelled at their 3′ ends and run on a polyacrylamide gel (Fig. 1*b*, lanes 2–12). Plasmids revealing fragments of between 25 and 30 bp were identified individually and a partial nucleotide sequence of the inserted cDNA was determined[31]. Neurophysin and arginine vasopressin amino acid sequences were compared with the cDNA sequences using a suitable computer program[32]. Of the eight plasmids giving rise to a *Sau*96I fragment 25–30 bp long, three were found to carry cDNA sequences corresponding to NpII amino acid sequences. The 27-bp fragments in lanes 6, 10 and 11 of Fig. 1 (arrows) represent this type of cDNA sequence. The bands in lanes 6 and 10 are clearly visible on longer exposures.

Rescreening of the 550 recombinant plasmids by hybridization with ^{32}P-labelled cloned cDNA for the AVP–NpII pre-

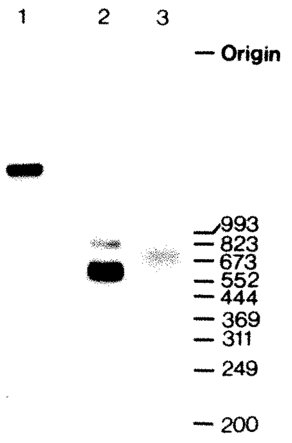

Fig. 2 Size determination of the mRNA encoding the common bovine AVP–NpII precursor. Bovine hypothalamic poly(A)-containing RNA which previously had been separated on a 2% agarose formaldehyde gel and transferred to a nitrocellulose filter[69] was hybridized to ^{32}P-labelled pVNpII-1 DNA. After washing, the dried filter was autoradiographed at −70 °C using an X-ray intensifying screen. Lane 3, bovine hypothalamic poly(A)-containing RNA (~1 μg) hybridized to ^{32}P-labelled pVNpII-1 DNA. Lane 1, chick oviduct poly(A)$^+$ RNA (120 ng) hybridized to ^{32}P-labelled poa-1210 DNA, an ovalbumin cDNA-carrying plasmid (H.L., unpublished results). Lane 2, hybridization of chick oviduct poly(A)$^+$ RNA (1.2 μg) to ^{32}P-labelled pom-48 DNA[70] and pls-1 DNA[71]; pom-48 carries ovomucoid cDNA sequences, pls-1 carries chicken lysozyme cDNA sequences. Assuming a length for the poly(A) tail of ~40 residues, the bands corresponding to the mRNAs represent sizes of 1,900[72], 860[73] and 630[74] nucleotides, respectively. Numbers indicate the lengths of ^{32}P-labelled DNA fragments obtained after *Hin*fI cleavage of SV40 DNA.

cursor identified seven positive clones, all of which were present in the 55 preselected clones; five carried sequences homologous to the bovine AVP–NpII precursor, and two had sequences specific for the oxytocin–nurophysin I precursor. Both cDNAs cross-hybridized because of the high degree of sequence conservation between NpII and NpI.

To correlate the sizes of the inserted cDNAs with the length of the mRNA for the bovine AVP–NpII precursor, poly(A)-containing RNA from bovine hypothalamus was run on a denaturing agarose gel, blotted on to a nitrocellulose filter and hybridized to ^{32}P-labelled cloned cDNA for the AVP–NpII precursor (Fig. 2, lane 3). One band was observed corresponding to a length for the mRNA of 700–750 nucleotides. Because of the sequence homology and the different size (M_r 16,500)[22] of the oxytocin–neurophysin I precursor one might expect to find an additional faster migrating band corresponding to the oxytocin–neurophysin I precursor mRNA. Both mRNAs may be of similar molecular size and may therefore not be separated in this gel system.

The plasmid pVNpII-1, which carries the largest cDNA insert specific for bovine AVP–NpII precursor (~750 bp) was selected for further studies. Its nucleotide sequence was determined using the strategy shown in Fig. 3.

cDNA sequence defines primary structure of AVP–NpII precursor

Figure 4 shows the nucleotide sequence of the bovine AVP–NpII precursor mRNA. AVP is encoded by nucleotides 1–27. Nucleotides 37–321 correspond precisely to the amino acid sequence determined for bovine neurophysin II; nucleotides 301–303 code for valine, a position known to be heterogeneous (Ile/Val) in bovine NpII[33]. The polypeptide carrying the carbohydrate moiety of the precursor[16,17,21,22,34] can be deduced from nucleotides 325–441 and is followed by a stop codon. The predicted sequence is completely homologous to the amino acid sequence previously reported for a glycoprotein of 39 amino acids isolated from bovine pituitary[35].

An open reading frame is found in the cDNA sequence upstream from nucleotide +1. Assuming that the methionine codon AUG at positions −55 to −57 is the location of the translational initiation site, the following 19 mainly hydrophobic amino acid residues would represent the leader or signal peptide similar to that of other secreted proteins[36]. This is in close agreement with the *in vitro* identified prepro- and proforms to AVP–NpII which differ in size by ~15–20 amino acids[23]. The bovine AVP–NpII precursor consists of 166 amino acid residues, with a calculated molecular weight of 17,310, which is smaller than that estimated for the non-glycosylated preproform (M_r ~21,000)[19,21,22] synthesized *in vitro*. This may, however, be explained in a way similar to that of the mature neurophysins, the molecular weights of which are overestimated by SDS-polyacrylamide gel electrophoresis[37]. There is no evidence for the existence of a larger AVP–NpII precursor[38].

The cDNA sequence cloned in pVNpII-1 terminates nine nucleotides upstream from the AUG codon. To determine the sequence of the 5′-terminal portion of the AVP–NpII precursor mRNA which is missing in the cDNA clone, primer extension sequencing experiments[39] were done. The results are shown in Fig. 4: nucleotides −106 to −67 (in parentheses). As this sequence has been obtained for one strand only, it is not yet firmly established; however, these experiments map the 5′ end of the mRNA sequence 40 nucleotides upstream from position −66 (not shown). This implies a length of ~610 nucleotides for the mRNA body. Taking into account the long poly(A) tails cloned in pVNpII-1 and pVNp-2 (~150 A residues), this estimate corresponds well with the size of the AVP–NpII precursor mRNA determined by Northern blotting (Fig. 2).

The codon usage is non-random and very similar to that in other eukaryotic mRNAs (not shown)[40–43]. Particularly, it reflects a high preference for C or G in the third position of the codons: 93 codons (56%) terminate in C, 61 (36%) in G, 7 (4%) in A and 6 (4%) in T. Thus, as in the adrenocorticotropic

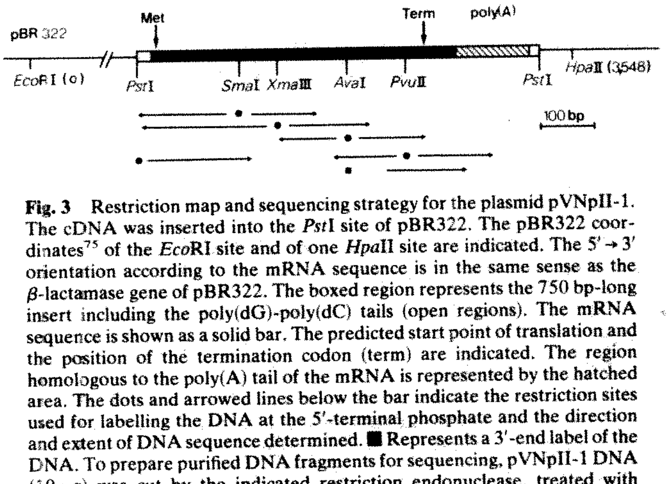

Fig. 3 Restriction map and sequencing strategy for the plasmid pVNpII-1. The cDNA was inserted into the *Pst*I site of pBR322. The pBR322 coordinates[75] of the *Eco*RI site and of one *Hpa*II site are indicated. The 5′→3′ orientation according to the mRNA sequence is in the same sense as the β-lactamase gene of pBR322. The boxed region represents the 750 bp-long insert including the poly(dG)-poly(dC) tails (open regions). The mRNA sequence is shown as a solid bar. The predicted start point of translation and the position of the termination codon (term) are indicated. The region homologous to the poly(A) tail of the mRNA is represented by the hatched area. The dots and arrowed lines below the bar indicate the restriction sites used for labelling the DNA at the 5′-terminal phosphate and the direction and extent of DNA sequence determined. ■ Represents a 3′-end label of the DNA. To prepare purified DNA fragments for sequencing, pVNpII-1 DNA (10 μg) was cut by the indicated restriction endonuclease, treated with alkaline phosphatase from calf intestine (Boehringer) at 37 °C for 30 min in 50 mM Tris-HCl *p*H 8, heated at 70 °C for 10 min in the presence of 6 mM EGTA and then phenol-extracted. DNA was labelled with 10 units of T4 polynucleotide (BRL) at 37 °C for 30 min in a 10 μl volume of 50 mM Tris-HCl *p*H 7.5, 10 mM $MgCl_2$, 5 mM dithiothreitol (DTT), 0.1 mM spermidine, and 50 μCi [γ-^{32}P]ATP (>5,000 Ci mmol^{-1}; Amersham). 3′ Labelling was performed with T4 DNA polymerase (BRL) in 10 μM of 20 mM Tris-HCl *p*H 7.5, 10 mM $MgCl_2$, 1 mM DTT and 50 μCi [α-^{32}P]dTTP (2,000–3,000 Ci mmol^{-1}; Amersham). The labelled DNA was subsequently cut with *Pst*I (BRL), then separated by gel electrophoresis through 5% polyacrylamide in 50 mM Tris-borate *p*H 8.1, 1 mM EDTA. The appropriate fragments were eluted, purified on DE52 (Whatman) and ethanol-precipitated. The *Sma*I$^+$–*Ava*I$^+$ fragment was purified by gel electrophoresis before cutting with *Xma*III. The crosses represent the position of the [γ-^{32}P] label. Sequence reactions were carried out as described elsewhere[31].

```
5'   -100                                                  -50
(NGCACAGUCUACAGAGCAGCACUGCGCACGUGUGCCCACG)CGUGCCAGG  AUG CCC GAC GCC ACA CUG CCC GCC UGC UUC CUC AGC
                                                     MET PRO ASP ALA THR LEU PRO ALA CYS PHE LEU SER
                                                     -19

                        -1  1                                                           50
CUG CUG GCC UUC ACC UCU GCU UGC UAC UUC CAG AAC UGC CCA AGG GGC GGC AAG AGG GCC AUG UCC GAC CUG GAG
LEU LEU ALA PHE THR SER ALA CYS TYR PHE GLN ASN CYS PRO ARG GLY GLY LYS ARG ALA MET SER ASP LEU GLU
                        -1  1                                   10

                                                            100
CUG AGA CAG UGU CUC CCC UGC GGC CCC GGG GGC AAA GGC CGC UGC UUC GGG CCC AGC AUC UGC UGC GGG GAC GAG
LEU ARG GLN CYS LEU PRO CYS GLY PRO GLY GLY LYS GLY ARG CYS PHE GLY PRO SER ILE CYS CYS GLY ASP GLU
    20                                                                              40

                        150                                                             200
CUG GGC UGC UUC GUG GGC ACG GCC GAG GCG CUG CGC UGC CAA GAG GAG AAC UAC CUG CCG UCG CCC UGC CAG UCC
LEU GLY CYS PHE VAL GLY THR ALA GLU ALA LEU ARG CYS GLN GLU GLU ASN TYR LEU PRO SER PRO CYS GLN SER
                                                                60

                                                            250
GGC CAG AAG CCC UGC GGG AGC GGG GGC CGC UGC GCC GCC GCC GGC AUC UGC UGC AAC GAU GAG AGC UGC GUG ACC
GLY GLN LYS PRO CYS GLY SER GLY GLY ARG CYS ALA ALA ALA GLY ILE CYS CYS ASN ASP GLU SER CYS VAL THR
                                            80

                        300                                                             350
GAG CCC GAG UGC CGG GAA GGU GUC GGC UUC CCC CGC CGC GUU CGC GCC AAC GAC CGG AGC AAC GCG ACC CUG CUG
GLU PRO GLU CYS ARG GLU GLY VAL GLY PHE PRO ARG ARG VAL ARG ALA ASN ASP ARG SER ASN ALA THR LEU LEU
                        100

                                                            400
GAC GGG CCG AGC GGG GCC UUG UUG CUG CGG CUG GUG CAG CUG GCG GGG GCG CCG GAG CCC GCG GAG CCC GCC CAG
ASP GLY PRO SER GLY ALA LEU LEU LEU ARG LEU VAL GLN LEU ALA GLY ALA PRO GLU PRO ALA GLU PRO ALA GLN
    120                                                                             140

                        450                                                  500         3'
CCC GGC GUC UAC UGA GGCGCGCCCCCCCCCUCCCCACCCCUGCCCUCGCAGCACGAAAAAUAAACGUUUUAAAGGC(A)~150
PRO GLY VAL TYR ***
            147
```

Fig. 4 Nucleotide sequence of AVP–NpII precursor mRNA from bovine hypothalamus, and deduced amino acid sequence. The nucleotide numbers are shown above the sequence. Nucleotide residues are numbered in the direction $5' \rightarrow 3'$ in the mRNA strand, beginning with the first residue in the coding region for arginine vasopressin. The nucleotides upstream from residue 1 are indicated by negative numbers. The predicted amino acid sequence is numbered by designating as 1 the first residue (Cys) of arginine vasopressin. The amino acids constituting the putative signal peptide are indicated by negative numbers, those towards the carboxy terminus of the precursor have positive numbers. The untranslated sequence at the 5′ terminus, shown in parentheses is derived from primer extension sequencing of the mRNA[39] and has not been confirmed by sequencing of cloned DNA. The ^{32}P-labelled DNA fragments *Bst*NI(−58)–*Sau* 96I(+39)$^+$ and *Dde*I(−23)–*Sau*96I(+39)$^+$ were used as primers. Asterisks indicate the position of the [γ-^{32}P] label.

hormone (ACTH) β-lipotropin hormone (β-LPH) precursor mRNA[43], the AVP–NpII precursor mRNA has a high G+C content (70%) markedly exceeding that of total bovine DNA (39%)[44]. The occurrence of 48 C–G dinucleotides within 610 nucleotides is in contrast to the relatively low abundance of this dinucleotide in other eukaryotic mRNAs[40–42] as well as in total bovine DNA[45]. The sequence AAUAAA commonly found near the 3′ end of eukaryotic mRNAs[40–43] is present in the AVP–NpII precursor mRNA 12 nucleotides upstream from the poly(A) tail.

Structural and functional implications of AVP–NpII precursor

The mRNA sequence presented here proves conclusively that the hypothalamic peptide hormone arginine vasopressin and its carrier protein neurophysin II are synthesized via a common precursor. This precursor is one of the class of cellular polyproteins which have the uncommon feature of being processed into several functionally distinct oligo- or polypeptides[14]. Members of this class include the hypophyseal precursor to corticotropin, melanotropic hormones and endorphins[43] and the precursor containing the Met- as well as the Leu-enkephalins from the adrenal medulla[46]. The precursors to somatostatin[47] and calcitonin[48] may also contain biologically active peptides in addition to the hormones but this has not been proved. Compared with these polypeptides, the AVP–NpII precursor seems to be the only example where the sequence information is entirely represented within the *in vivo* identified cleavage products (Fig. 5). AVP immediately follows the assumed signal peptide, and as indicated by the nucleotide sequence, has a glycine residue (amino acid 10) adjacent to its carboxy-terminus. As with other polypeptide precursors[43,49–52], the gly-

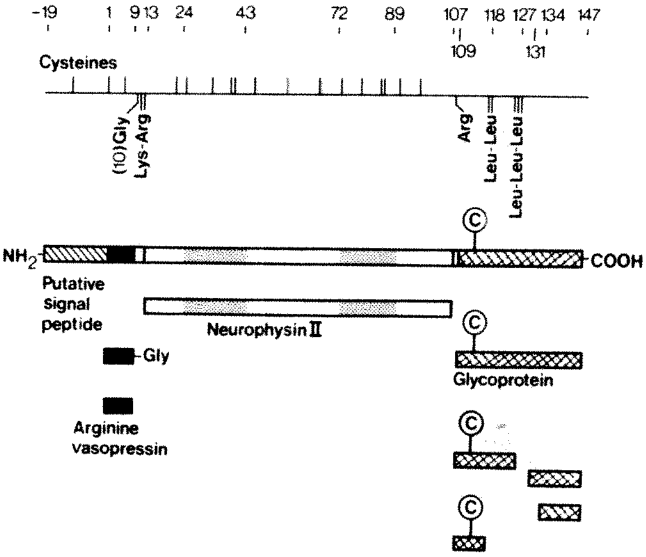

Fig. 5 Schematic representation of the structure of bovine AVP–NpII precursor. Characteristic amino acids are shown: the arrangement of cysteines (marks above the line), and glycine (residue 10) necessary for amidation of AVP and amino acid signals for proteolysis. Numbering of the amino acid residues is as in Fig. 4. The putative signal peptide (−19 to −1) is represented by the hatched bar. Vasopressin (closed bar) extends from amino acid residue 1 to 9. Neurophysin II (13–107), shown as a shaded bar, exhibits areas of internal homology (dark shading) located between amino acid residues 24–43 and 72–89 (ref. 57). The glycoprotein part of the precursor (109–147; cross-hatched bar) carrying a carbohydrate chain (C) at position 114 is further cleaved into several peptides of 10 (109–118), 18 (109–127), 17 (131–147) and 14 (134–147) amino acid residues[35].

cine residue may serve as a signal and amino donor to the preceding amino acid at the C-terminus of AVP. The glycine residue is followed by a pair of basic amino acids suggesting a trypsin- and carboxypeptidase-like cleavage site. For cleavage between neurophysin II and the glycopolypeptide, only one arginine residue (amino acid 108) seems sufficient, whereas the neighbouring arginyl-arginine dipeptide (amino acids 105–106) remains uncut.

A glycoprotein of 39 amino acid residues (109–147) is located at the carboxy terminus of the precursor and contains a typical glycosylation site, Asn-X-Thr (114–116)[53]. This glycopolypeptide has also been isolated from the pituitaries of several species[35,54] and contains a glucosamine-rich side chain at the corresponding asparagine residues[35,54,55]. Microinjection of *Xenopus laevis* oocytes with bovine hypothalamic mRNA gives rise to a glycosylated AVP–NpII precursor containing glucosamine as well as fucose and mannose residues[34]. Smyth and Massey[35] isolated four different naturally occurring subfragments of the glycopolypeptide (see Fig. 5). Two fragments, comprising amino acids 109–118 and 109–127, may be evidence for the existence of an alternative processing activity which cleaves at the carboxyl side of consecutive leucine residues; a similar fragment has been described by Holwerda[55]. The two other fragments extend from residues 131 and 134, respectively, to the carboxy-terminal tyrosine (amino acid 147).

There have been no studies made of the subcellular localization of the glycoprotein and its fragments, nor is anything known about a possible biological function which may be inferred from its remarkable sequence conservation during evolution[54]. However, it is of interest that six consecutive residues (131–136) of the glycopolypeptide show close homology to the amino-terminal region of procine β-LPH (amino acids 1–6, Glu-Leu-Ala-Gly-Ala-Pro)[35,56].

The internal amino acid sequence homology described for neurophysin II between residues 24–43 and 72–89 may represent directly duplicated segments of an ancestral gene[57] as reflected by the repeated arrangement of cysteine residues (Fig. 5). The sequence of the entire precursor does not reveal any additional homologies as observed for the melanotropic hormones in proopiocortin[43].

It is unknown whether the neurophysins have any biological role other than their carrier function. Proteins immunologically related to the neurophysins have been found in the target organs (kidney, uterus and mammary gland) of vasopressin and oxytocin, and it has been suggested that these proteins may act as receptors for the nonapeptides[58]. A cDNA clone encoding lactoglandin, a neurophysin-like protein, has recently been isolated from a lactating mouse mammary gland specific cDNA library. The relationship of this protein to the neurophysins is reflected by a similar pattern of cysteine residues[59].

The functional significance of the components of the AVP–NpII precursor remains to be determined. Although various factors are known to regulate the metabolism of AVP or oxytocin and their corresponding neurophysins[8,60,61], the nature of the control of its synthesis is poorly understood. The cloned cDNA provides the basis for a detailed study of the regulation of arginine vasopressin and neurophysin biosynthesis in the peptidergic neurone.

We thank C. Schmidt and C. M. Strange for technical assistance; Dr J. W. Beard for providing reverse transcriptase; Drs G. Osterburg and J. Collins for help in computer analysis; L. Henninghausen for stimulating discussion; Drs R. Ivell, W. Keller, M. Grez, G. Scherer and A. Scott for critical comments on the manuscript; and U. Joa for secretarial assistance. This work was supported by the Deutsche Forschungsgemeinschaft 192/14 to D.R.

Received 18 November; accepted 1 December 1981.

1. Walter, R. *Ann. N.Y. Acad. Sci.* **248,** 1–512 (1975).
2. Pickering, B. T. & Jones, C. W. in *Hormonal Proteins and Peptides* Vol 5 (ed. Li, C. H) 103–158 (Academic, New York, 1978).
3. Breslow, E. *A. Rev. Biochem.* **48,** 251–274 (1979).
4. Brownstein, M. J., Russell, J. T. & Gainer, H. *Science* **207,** 373–378 (1980).
5. Sokol, H. W., Zimmermann, E. A., Sawyer, W. H. & Robinson, A. G. *Endocrinology* **98,** 1176–1188 (1976).
6. Zimmermann, E. A. & Defendini, R. in *Neurohypophysis* (eds Moses, A. M. & Share, L.) 22–29 (Karger, Basel, 1977).
7. Sachs, H. & Takabatake, Y. *Endocrinology* **75,** 943–948 (1964).
8. Sachs, H., Fawcett, P., Takabatake, Y. & Portanova, R. *Recent Prog. Horm. Res.* **25,** 447–491 (1969).
9. Valtin, H., Sawyer, W. H. & Sokol, H. W. *Endocrinology* **77,** 701–706 (1965).
10. Friesen, H. G. & Astwood, E. B. *Endocrinology* **80,** 278–287 (1967).
11. Burford, G. D., Jones, C. W. & Pickering, B. T. *Biochem. J.* **124,** 809–813 (1971).
12. Pickering, B. T. *et al. Ann. N.Y. Acad. Sci.* **248,** 15–35 (1975).
13. Sunde, D. A. & Sokol, H. W. *Ann. N.Y. Acad. Sci.* **248,** 345–364 (1975).
14. Richter, D., Ivell, R. & Schmale, H. in *Biosynthesis, Modification and Processing of Cellular and Viral Polyproteins* (eds Koch, G. & Richter, D.) 5–13 (Academic, New York, 1980).
15. Brownstein, M. J. & Gainer, H. *Proc. natn. Acad. Sci. U.S.A.* **74,** 4046–4049 (1977).
16. Russell, J. T., Brownstein, M. J. & Gainer, H. *Proc. natn. Acad. Sci. U.S.A.* **76,** 6086–6090 (1979).
17. Lauber, M., Camier, M. & Cohen, P. *FEBS Lett.* **97,** 343–347 (1979).
18. Brownstein, M. J., Robinson, A. G. & Gainer, H. *Nature* **269,** 259–261 (1977).
19. Giudice, L. C. & Chaiken, J. M. *Proc. natn. Acad. Sci. U.S.A.* **76,** 3800–3804 (1979).
20. Lin, C., Joseph-Bravo, P., Sherman, T., Chan, L. & McKelvy, J. F. *Biochem. biophys. Res. Commun.* **89,** 943–950 (1979).
21. Schmale, H., Leipold, B. & Richter, D. *FEBS Lett.* **108,** 311–316 (1979).
22. Schmale, H. & Richter, D. *FEBS Lett.* **121,** 358–362 (1980).
23. Schmale, H. & Richter, D. *Proc. natn. Acad. Sci. U.S.A.* **78,** 766–769 (1981).
24. Schmale, H. & Richter, D. *Neuropeptides* **2,** 47–52 (1981).
25. Richter, D., Schmale, H., Ivell, R. & Kalthoff, H. in *Hormonally Active Brain Peptides* (ed. McKerns, K. W.) (Plenum, New York, in the press).
26. Land, H., Grez, M., Hausser, H., Lindenmaier, W. & Schütz, G. *Nucleic Acids Res.* **9,** 2251–2266 (1981).
27. Richter, D., Schmale, H., Ivell, R. & Schmidt, C. in *Biosynthesis, Modification and Processing of Cellular and Viral Polyproteins* (eds Koch, G. & Richter, D.) 43–66 (Academic, New York, 1980).
28. Ricciardi, R. P., Miller, J. S. & Roberts, B. E. *Proc. natn. Acad. Sci. U.S.A.* **76,** 4928–4931 (1979).
29. Leung, D. W., Lui, A. C. P., Meriless, H., McBride, B. C. & Smith, M. *Nucleic Acids Res.* **6,** 17–25 (1979).
30. Sussenbach, J. S., Steenbergh, P. H., Rost, J. A., Van Leeuwen, W. J. & Van Embden, J. D. A. *Nucleic Acids Res.* **5,** 1153–1163 (1978).
31. Maxam, A. & Gilbert, W. *Proc. natn. Acad. Sci. U.S.A.* **74,** 560–564 (1977).
32. Osterburg, G., Glatting, K. H. & Sommer, R. *Nucleic Acids Res.* (in the press).
33. Chauvet, M. T., Chauvet, J. & Acher, R. *Eur. J. Biochem.* **69,** 475–485 (1976).
34. Ivell, R., Schmale, H. & Richter, D. *Biochem. biophys. Res. Commun.* **102,** 1230–1236 (1981).
35. Smyth, D. G. & Massey, D. E. *Biochem. biophys. Res. Commun.* **87,** 1006–1010 (1979).
36. Lingappa, V. R. & Blobel, G. *Recent Prog. Horm. Res.* **36,** 451–475 (1980).
37. Acher, R. *Angew. Chem.* **91,** 905–919 (1979).
38. Nicolas, P. *et al. Proc. natn. Acad. Sci. U.S.A.* **77,** 2587–2591 (1980).
39. Schreier, P. H. & Cortese, R. *J. molec. Biol.* **129,** 169–172 (1979).
40. Efstratiadis, A., Kafatos, F. C. & Maniatis, T. *Cell* **10,** 571–585 (1977).
41. Ullrich, A. *et al. Science* **196,** 1313–1318 (1977).
42. Seeburg, P. H., Shine, J., Martial, J. A., Baxter, J. D. & Goodman, H. M. *Nature* **270,** 486–494 (1977).
43. Nakanishi, S. *et al. Nature* **278,** 423–427 (1979).
44. Szybalski, W. *Meth. Enzym.* **12B,** 330–360 (1968).
45. Swartz, M. N., Trautner, T. A. & Kornberg, A. *J. biol. Chem.* **237,** 1961–1967 (1962).
46. Stern, A. S., Jones, B. N., Shirely, J. E., Stein, S. & Udenfriend, S. *Proc. natn. Acad. Sci. U.S.A.* **78,** 1962–1966 (1981).
47. Hobart, P., Crawford, R., Shen, L. P., Pictet, R. & Rutter, W. J. *Nature* **288,** 137–141 (1980).
48. Jacobs, J. W. *et al. Science* **213,** 457–459 (1981).
49. Suchanek, G. & Kreil, G. *Proc. natn. Acad. Sci. U.S.A.* **74,** 975–978 (1977).
50. Amara, S. G., David, D. N., Rosenfeld, M. G., Roos, B. A. & Evans, R. M. *Proc. natn. Acad. Sci. U.S.A.* **77,** 4444–4448 (1980).
51. Shibasaki, T., Ling, N. & Guillemin, R. *Biochem. biophys. Res. Commun.* **96,** 1393–1399 (1980).
52. Seidah, N. G., Rochemont, J., Hamelin, J., Benjannet, S. & Chrétien, M. *Biochem. biophys. Res. Commun.* **102,** 710–716 (1981).
53. Pless, D. D. & Lennarz, W. J. *Proc. natn. Acad. Sci. U.S.A.* **74,** 134–138 (1977).
54. Seidah, N. G., Benjannet, S. & Chrétien, M. *Biochem. biophys. Res. Commun.* **100,** 901–907 (1981).
55. Holwerda, D. A. *Eur. J. Biochem.* **28,** 340–346 (1972).
56. Hunt, L. T., Ledley, F. D. & Dayhoff, M. O. in *Atlas of Protein Sequence and Structure* Vol. 5, Suppl. 3 (ed. Dayhoff, M. O.) 145–164 (National Biomedical Research Foundation, Washington DC, 1979).
57. Capra, J. D., Kehoe, J. M., Kotelchuck, D., Walter, R. & Breslow, E. *Proc. natn. Acad. Sci. U.S.A.* **69,** 431–434 (1972).
58. Legros, J. J., Louis, F., Grötschel-Stewart, U. & Tranchimont, P. *Ann. N.Y. Acad. Sci.* **248,** 157–171 (1975).
59. Henninghausen, L. & Sippel, A. E. (in preparation).
60. Robinson, A. G. *Ann. N.Y. Acad. Sci.* **248,** 246–256 (1975).
61. Pearson, D. B., Goodman, R. & Sachs, H. *Science* **187,** 1081–1082 (1975).
62. Gillespie, D. & Vogelstein, B. *Proc. natn. Acad. Sci. U.S.A.* **76,** 615–619 (1979).
63. Roewekamp, W. & Firtel, R. A. *Devl Biol.* **79,** 409–418 (1980).
64. Hubatek, J. & Glover, S. W. *J. molec. Biol.* **50,** 111–127 (1970).
65. Dagert, M. & Ehrilch, S. D. *Gene* **6,** 23–28 (1979).
66. Klein, R. D., Selsing, E. & Wells, R. D. *Plasmid* **3,** 88–91 (1980).
67. Kafatos, F. C., Jones, C. W. & Efstratiadis, A. *Nucleic Acids Res.* **7,** 1542–1552 (1979).
68. Maizels, N. *Cell* **9,** 431–438 (1976).
69. Dobner, P. R., Kawasaki, E. S., Yu, L. Y. & Bancroft, F. C. *Proc. natn. Acad. Sci. U.S.A.* **78,** 2230–2234 (1981).
70. Lindenmaier, W. *et al. Nucleic Acids Res.* **5,** 1221–1232 (1979).
71. Sippel, A. E. *et al. Nucleic Acids Res.* **5,** 3275–3294 (1978).
72. McReynolds, L. *et al. Nature* **273,** 723–728 (1978).
73. Catterall, J. F., Stein, J. P., Kristo, P., Means, A. R. & O'Malley, B. W. *J. Cell Biol.* **87,** 480–487 (1980).
74. Jung, A., Sippel, A. E., Grez, M. & Schütz, G. *Proc. natn. Acad. Sci. U.S.A.* **77,** 5759–5763 (1980).
75. Sutcliffe, J. G. *Nucleic Acids Res.* **5,** 2721–2728 (1978).

LETTERS TO NATURE

Creation of open universes from de Sitter space

J. Richard Gott III

Department of Astrophysical Sciences, Princeton University,
Peyton Hall, Princeton, New Jersey 08544, USA

Hawking[1,2] has shown that event horizons produce thermal radiation. I propose here a new cosmological model which has an early event horizon and in which the observed[3] cosmic microwave background radiation is Hawking radiation. The model starts with de Sitter space—a space-time of constant curvature which is a solution to Einstein's vacuum field equations with a positive cosmological constant. Associated with an event E in de Sitter space there is a quantum barrier penetration tunnelling which leads to an open, negatively curved ($k=-1$) cosmology. This has an early exponential expansion phase but turns into a standard big-bang solution at late times. The geometry and quantum mechanical treatment within the future light cone of E are similar to that found in the Brout, Englert and Spindel (BES) theory[4,5]. This model has the following advantages: (1) It has no singularities. (2) The observed isotropy of the cosmic microwave background is explained because the different regions we observe have all been in causal contact. (3) The temperature at early epochs ($T_0 \sim 10^{19}$ GeV) is high enough to allow grand unified theories (GUTs) to produce the observed baryon excess from an initial thermal distribution through CP violations[6,7]. (4) T_0 is correct to make the BES scenario work. (5) The early exponential expansion phase can naturally account for the observed large number $n_0 \sim 10^{88}$ of particles within a volume a^3 (where a is the radius of curvature) and the Guth[8] flatness problem. (6) It predicts that our Universe is an open $k=-1, \Omega<1$ cosmology consistent with the amount of mass detected in the universe so far[9-11]. (7) The existence of the event horizon makes it possible to create from the original de Sitter space other $k=-1$ universes (perhaps an infinite number) which are entirely disjoint from our own and from each other.

The BES model starts with Minkowski space. At an event E there occurs a spontaneous phase transition from an $m=0$ vacuum (Minkowski space) to an $m \neq 0$ vacuum, the appearance of mass being the signature of a broken symmetry. The metric inside the future light cone of E may be written as

$$ds^2 = -d\tau^2 + a^2(\tau)[d\chi'^2 + \sinh^2 \chi'(d\theta^2 + \sin^2 \theta \, d\phi^2)]$$

(Planck units $G=\hbar=c=k=1$ are used throughout). This is a $k=-1$ cosmological metric. There is a brief transition phase $0 \leq \tau \leq \tau_0$, $\tau_0 \sim 0(1/m)$, $a(\tau) \sim \tau$, followed by a particle creation phase $\tau_0 < \tau < \tau_1$ during which the matter being produced approaches a constant energy density $\rho = \lambda/8\pi$, $P=-\lambda/8\pi$, $\lambda=$ constant. During this period $a(\tau) \propto \exp(\tau/\tau_\lambda)$, $\tau_\lambda = (3/\lambda)^{1/2}$, $T_{\mu\nu} = -\lambda \, g_{\mu\nu}/8\pi$ and the space approximates a piece of de Sitter space. After a time τ_1, incoherence develops, particle production stops and the model enters the conventional radiation dominated regime of a standard $k=-1$ big-bang model. A detailed quantum-mechanical treatment[4] shows that a self-consistent exponential expansion phase is possible only if the mass of the created particles (and anti-particles) is of the order of the Planck mass ($m \sim 0(1)$. τ_λ could be as short as $1/m \sim 0(1)$. τ_1 will be of the order of a relaxation time which is expected to be comparable with the decay time of the particles (say $\sim 10^2 \text{ m}^{-1}$). The BES model has no singularity, and all the regions we see today have been in causal contact (with the event E) explaining the observed isotropy of the cosmic microwave background radiation.

While the BES model has attractive features its overall spacetime can be conformally mapped onto Minkowski space and has no event horizons. In the model proposed here the 'future of E' part of the BES model will be essentially transplanted from its original Minkowski space to a complete de Sitter space with $T_{\mu\nu} = -\lambda g_{\mu\nu}/8\pi$ equal to that found in the exponentially expanding part of the BES solution.

If $T_{\mu\nu} = -\lambda g_{\mu\nu}/8\pi$ and the cosmological constant $\Lambda = 0$, then the solution to Einstein's field equations $G_{\mu\nu} = R_{\mu\nu} - 1/2 \, g_{\mu\nu}R + \Lambda g_{\mu\nu} = 8\pi T_{\mu\nu}$ is de Sitter space. (Note that one usually encounters de Sitter space as the solution to the vacuum field equation with positive cosmological constant: $T_{\mu\nu} = 0$ and $\Lambda = \lambda$). De Sitter space may be embedded as a hyperboloid[12].

$$-V^2 + W^2 + X^2 + Y^2 + Z^2 = r_o^2 = 3/\lambda \tag{2}$$

in a flat five-dimensional space R^5 with a metric

$$ds^2 = -dV^2 + dW^2 + dX^2 + dY^2 + dZ^2 \tag{3}$$

Introduce coordinates $(\eta, \chi, \theta, \phi)$ where $\eta = 2\tan^{-1}[\exp(t/r_0)]$ and $r_0 \sinh(t/r_0) = V$, $r_0 \cosh(t/r_0) \cos\chi = W$, $r_0 \cosh(t/r_0) \sin\chi \cos\theta = X$, $r_0 \cosh(t/r_0) \sin\chi \sin\theta \cos\phi = Y$, $r_0 \cosh(t/r_0) \sin\chi \sin\theta \sin\phi = Z$, then the metric is

$$ds^2 = r_o^2 \cosh^2(t/r_0)[-d\eta^2 + d\chi^2 + \sin^2\chi(d\theta^2 + \sin^2\theta \, d\phi^2)] \tag{4}$$

This can be mapped conformally onto the Einstein static universe $S^3 \times R$ (a static three-sphere existing in time) with $0 < \eta < \pi$.

The event horizon of a black hole in an asymptotically flat space time is usually defined[12] as the boundary of the causal past of future null infinity $\mathscr{I}^+$. Alternatively it can be defined as the boundary of the past of a timelike world-line which has a future endpoint at future timelike infinity i^+. (In an asymptotically flat region $\mathscr{I}^+$ and i^+ are the places where photons and matter particles respectively go as $t \to \infty$). De Sitter space has event horizons satisfying this second definition[13]. An observer whose world-line is $\chi = 0$, $0 < \eta < \pi$, has an event horizon at $\chi = \pi - \eta$. Every timelike geodesic world-line has an event horizon of radius $r_0 = (3/\lambda)^{1/2}$. Gibbons and Hawking[13] have shown that each geodesic observer in de Sitter space detects Hawking radiation from these event horizons with a temperature

$$T = (12)^{-1/2} \pi^{-1} \lambda^{1/2} \tag{5}$$

A thermal radiation field with temperature T equal to the observed Hawking temperature has a classical energy density:

$$\rho_{\text{HAW}} = \frac{\pi^2}{30} N(T) T^4 = \frac{N(T)\lambda^2}{4{,}320\pi^2} \tag{6}$$

where $N(T)$ is equal to the number of helicity states of all particle species ($\times 7/8$ for fermions) with mass less than T. For standard GUTs $N(T) \sim 10^2$ in the high temperature limit[6]. Each geodesic observer observes a total energy density $\rho_{\text{obs}} = \lambda/8\pi$.

In de Sitter space different geodesic observers have different event horizons so the Hawking radiation is observer dependent. This prompted Gibbons and Hawking to argue that it should not contribute to the observed $T_{\mu\nu}$. Press[14] on the other hand has argued that the Hawking radiation should contribute to $T_{\mu\nu}$. Thus the question of whether the Hawking radiation contributes to $T_{\mu\nu}$ is controversial. However, if the Hawking radiation does contribute to $T_{\mu\nu}$ then the symmetries of de Sitter space seem to demand that its contribution be of the de Sitter invariant form $(T_{\mu\nu})_{\text{HAW}} = -\lambda' g_{\mu\nu}/8\pi$ where λ' is a constant. If the Hawking radiation is the only source of $T_{\mu\nu}$ then $\lambda = \lambda'$ and $\rho_{\text{obs}} = \rho_{\text{HAW}}$. The required $P = -\rho$ equation of state for the thermal Hawking radiation may be a natural result of trace anomalies produced by

0028-0836/82/040304—04$01.00

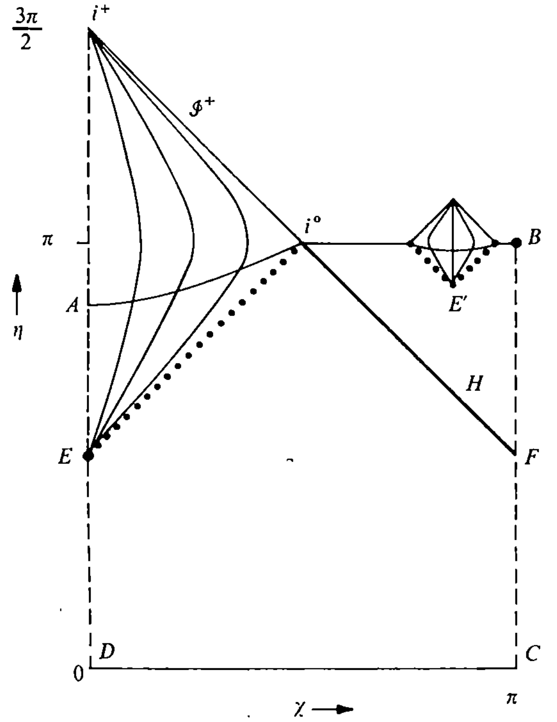

Fig. 1 Penrose diagram of the proposed cosmological model. η is a timelike coordinate and χ is a radial spacelike coordinate. This is a conformal map in which light travels always at ±45° to the vertical. The region $EAi^\circ E'BCD$ has the metric of de Sitter space. At the spacelike hypersurface Ai° there is a phase transition from $P=-\rho$ to $P=\rho/3$. The region $Ai^\circ i^+$ is a standard $k=-1$ Robertson Walker big-bang cosmology from the Planck time onwards. The curved lines connecting E and i^+ are world-lines of co-moving observers in the big-bang universe. This big-bang universe has $\Omega<1$ and expands forever, the fact that the curved lines coverage at i^+ is an artefact of the conformal mapping. There is an event horizon H. Observers in the Robertson-Walker big-bang cosmology never see any photons from events inside the region $Fi^\circ B$. At E' another $k=-1$ universe is created which is entirely disjoint from the E universe. Note, $\eta(A)=2\tan^{-1}[\exp(\tau_1/\tau_\lambda)]$, see text.

the space-time curvature of de Sitter space itself. For example, classically, a massless conformally invariant scalar field ϕ is traceless ($P=\rho/3$). However, DeWitt[15] has shown that in de Sitter space with radius r_0, quantum mechanical effects in the one-loop approximation produce for this field a renormalized $\langle T_{\text{ren}\,\mu\nu}\rangle=-g_{\mu\nu}/960\pi^2r_0^4$ which is de Sitter invariant and has $P=-\rho$. If $\langle T_{\text{ren}\,\mu\nu}\rangle$ is to be the source term producing the de Sitter solution then $\langle T_{\text{ren}\,\mu\nu}\rangle=-3g_{\mu\nu}/8\pi r_0^2$, so $r_0=(360\pi)^{1/2}$ and $\rho=135$ for the self consistent false vacuum state. This density is just a factor of 2 larger than we would obtain from setting $\rho_{\text{obs}}=\rho_{\text{HAW}}$ with $N(T)=1$ for a single scalar field (compare with equation (9)). Trace anomalies become significant when the radius of curvature becomes comparable with the wavelength of the thermal radiation (at the Planck epoch). De Witt's work supports the contention that a self consistent de Sitter false vacuum occurs at an epoch when $\rho_{\text{HAW}}\sim\rho_{\text{obs}}\sim 0(1)$ and $T\sim 0(1)\sim 10^{19}$ GeV rather than at 10^{14-15}GeV as proposed by Guth[8]. There is another reason for equating $\rho_{\text{obs}}=\rho_{\text{HAW}}$ which is independent of whether or not the Hawking radiation contributes to the de Sitter $T_{\mu\nu}$. If the de Sitter false vacuum decays, dumping its energy density ρ_{obs} in the form of thermal radiation there will be no instantaneous change in temperature across the phase transition if $\rho_{\text{obs}}=\rho_{\text{HAW}}$. Such a phase transition (see Fig. 1) leads to formation of an observer-independent event horizon (boundary of the past of $\mathscr{I}^+$). As in the black hole case we expect this to lead to observer-independent Hawking radiation. Setting $\rho_{\text{obs}}=\rho_{\text{HAW}}$ ensures a smooth transition from the observer-dependent Hawking radiation to the observer-independent ($P=\rho/3$) Hawking radiation.

For the above reasons, I adopt $\rho_{\text{obs}}=\rho_{\text{HAW}}$. This gives:

$$T_0=\left[\frac{45}{\pi N(T_0)}\right]^{1/2} \tag{7}$$

$$\lambda=540\pi/N(T_0) \tag{8}$$

$$\rho=135/2N(T_0) \tag{9}$$

Thus, T_0, λ and ρ are all of the order of unity in Planck units.

The BES model with $\lambda=540\pi/N(T_0)$ is now transplanted into this space. Pick an event E in the de Sitter space and choose coordinates so that $\eta(E)=\pi/2$, $\chi(E)=0$ ($W=r_0$, $V=X=Y=Z=0$). Adopt coordinates (τ, χ', θ, ϕ): $W=r_0.\cosh(\tau/r_0)$, $V=r_0\sinh(\tau/r_0)\cosh\chi'$, $X=r_0\sinh(\tau/r_0)\sinh\chi'\cos\theta$, $Y=r_0\sinh(\tau/r_0)\sinh\chi'\sin\theta\cos\phi$; $z=r_0\sinh(\tau/r_0)\sinh\chi'\sin\theta\sin\phi$; then the metric for the future of E, ($W>r_0$, $V>0$) $\tau>0$ is that of equation (1) with $a(\tau)=\tau_\lambda\sinh(\tau/\tau_\lambda)$ and $\tau_\lambda=r_0=(3/\lambda)^{1/2}$. This is a $k=-1$ cosmology. This is equivalent to the BES solution particle production phase and the need for the transition period $0<\tau<\tau_0$ is eliminated. The de Sitter metric applies then for $0<\tau<\tau_1$. As in the BES theory we require that the particle creation halts by the epoch τ_1, causing a transition in the equation of state from $P=-\rho$ to $P=\rho/3$ in the Robertson–Walker frame. At τ_1 each observer with world-line χ', θ, $\phi=$ constant sees Hawking radiation with $T\sim[45/\pi N(T)]^{1/2}$. After τ_1, $P=\rho/3$ with the Hawking radiation observed at τ_1 providing the observed energy density and redshifting in the usual way. Equation (7) gives $T_0\sim 0(1)$. The BES model requires that the created particles in the de Sitter phase have $m\sim 0(1)$ and these particles will be produced in a thermal distribution only if $T_0\sim 0(1)$.

If currently $\Omega_0\sim 0.1$, $H_0\sim 50\text{ km s}^{-1}\text{ Mpc}^{-1}$, $T=2.7$ K, and $N(T_0)\sim 10^2$, the standard big bang model implies $\Omega_1\sim 1-2.5\times 10^{-60}$ at the epoch when ρ is that given by equation (9). This nearness of the initial Ω to unity is the Guth[8] flatness problem. Now for $0<\tau<\tau_1$, $\Omega=8\pi\rho/3H^2=8\pi\rho a^2/3\dot{a}^2=1-[\cosh(\tau/\tau_\lambda)]^{-2}$ so if $\tau_1\sim 69\ \tau_\lambda$ we have approximately the correct initial value of Ω for the big bang phase. Let N_0 be the number of particles in a volume a^3 in present Universe: $N_0\sim 6\times 10^{87}$. The number density of particles in the de Sitter phase is roughly[16] $n_1\sim 1.2N'(T_0)T_o^3/\pi^2\sim 0.66$ where $N'(T_0)\sim 10^2$ is the number of spin states (×3/4 for fermions) (compare with equation 7). If the number of decay products per particle present at τ_1 is of the order of unity the model predicts $N_0\sim 0.66\ a^3(\tau_1)=0.66\ \tau_\lambda^3\sinh^3(\tau_1/\tau_\lambda)$ which gives the correct order of magnitude for $\tau_1\sim 69\tau_\lambda$. With this value of τ_1 we get reasonable initial values for both Ω_1 and N_0 (details will be presented elsewhere). This result shows that the work of Guth[8] on Ω_1 and BES[4] on N_0 as the result of an exponential expansion phase can be combined.

One expects non-conformally invariant massive fields to be present (as in the BES model) in which case the de Sitter exponential expansion will cause particle creation. Adler[17] has formulated a model in which the cosmological constant Λ is fixed by the particle physics at early times and leads to a de Sitter phase. The resulting particle creation acts back on Λ lowering it to zero. This eventually stops the particle creation at $\tau\sim\tau_1$ leading to a standard big bang phase. The Adler[17] model gives a specific mechanism for a slow phase transition at τ_1 and is functionally equivalent to the late stages of BES model.

A Penrose diagram of the entire spacetime is shown in Fig. 1 and represents a mapping onto $S^3\times R$. The dashed lines represent coordinate singularities at $\chi=0$ and $\chi=\pi$. The original de Sitter space would be plotted in the square $0<\chi<\pi$, $0<\eta<\pi$. The event E is shown. The region $0<\tau<\tau_1$ is mapped into the triangular region EAi°. The Robertson–Walker phase $\tau>\tau_1$ is mapped into Ai^+i°. At late epochs this looks like a standard $k=-1$ open cosmological model. The co-moving timelike world-lines of particles in our Universe are indicated by curved lines connecting E and i^+. The region $DEAi^\circ FC$ has the metric of de Sitter space. The causal past of each event in this region includes only unperturbed de Sitter space, therefore each observer in this region sees Hawking radiation with temperature $T \sim 0(1)$. The spacetime has a classical event horizon (boundary of the past of future null infinity $\mathscr{I}^+$) indicated by the heavy diagonal line H. The horizon originates at the event F and increases in area until its area is infinite at i°. This would indicate an infinite entropy[18] and that an infinite amount of information is lost about what happens beyond the horizon. The existence of an event horizon means that there is a region (in this case $i^\circ BF$) of which we can never have any knowledge. Figure 1 shows how an event E' in this region can produce another $k=-1$ universe like our own but entirely disjoint from it. The E' universe also has an event horizon and our Universe lies beyond it. Neither universe can communicate with the other in any way. In fact an infinite number of universes can be created all disjoint from each other. The original de Sitter space is mapped onto $S^3 \times R$. Each universe E_i cuts out of S^3 a sphere of radius $\chi_i = \pi - \eta(E_i)$. An infinite number of such non-intersecting spheres can be constructed. The ability to make an infinite number of universes in the region $i^\circ BF$ goes with the infinite loss of information about this region suggested by the area of the event horizon.

Coleman[19] has shown that because the Minkowski vacuum is of lower density than the de Sitter vacuum, bubbles of ordinary Minkowski vacuum can form in a de Sitter false vacuum by quantum barrier penetration tunnelling. This leads to a causal structure exactly like that in Fig. 1 and provides a simplified case where we can make an exact semi-classical calculation of the Hawking radiation seen at late times in the future light cone of E. Coleman expects each bubble to have an 0(3, 1) Lorentz invariance about some event E. The bubble wall has a space-like separation σ from the event E where $\sigma \leq r_0$. The material that would have been inside the bubble is re-located in a thin bubble wall so that there is energy conservation and outside the bubble wall the metric is that of de Sitter space; inside, the metric is minkowskian. The spacetime can be embedded in the five-dimensional space of equations 2 and 3. The wall boundary is given by $X^2+Y^2+Z^2-V^2=\sigma^2$ and $W^2=r_0^2-\sigma^2$. For $W<(r_0^2-\sigma^2)^{1/2}$, equation (2) is satisfied. The inside of the bubble is embedded as the surface $W=(r_0^2-\sigma^2)^{1/2}$, so that inside V, X, Y, Z are normal Minkowski coordinates. The material in the bubble wall undergoes a proper acceleration $g=1/\sigma$. Inside the future light cone of E the metric is that of an empty $k=-1$ cosmology with $\Omega=0$ and $a(\tau)=\tau$. Coleman does not notice that his bubble formation mechanism produces an event horizon in the spacetime nor does he treat the resulting Hawking radiation. The causal structure is like that in Fig. 1: the bubble wall is a timelike hyperboloid that has a spacelike separation from E, stays just outside the dotted future light cone of E and ends at the point i_0. The positions of i^+, $\mathscr{I}^+$ and the horizon H are unchanged. The wall has an event horizon (boundary of its past) which consists of two parts, the future light cones of E and F. Unruh[20] has shown that accelerated observers in Minkowski space see Rindler–Hawking photons with a temperature $T=g/2\pi=1/2\pi\sigma$. For each timelike world-line moving with the wall material one can find a de Sitter static coordinate system[13] $ds^2 = -(1-\lambda r^2/3)\,dt^2+dr^2(1-\lambda r^2/3)^{-1}+r^2(d\theta^2+\sin^2\theta\, d\phi^2)$ such that the world-line is a line of constant θ, ϕ and $r=(r_0^2-\sigma^2)^{1/2}$. Such an observer sees Hawking photons with temperature[13] $T=1/2\pi\sigma$. So the wall sees a thermal bath with this temperature both inside and outside and to be in thermal equilibrium must be at a temperature of $T_{\text{wall}}=1/2\pi\sigma$. An observer within the future light cone of E will see thermal radiation from the wall with a temperature $T=T_{\text{wall}}\sigma/a$ where a is the Robertson–Walker expansion factor. Thus $T=1/2\pi a$ independent of the bubble size. The temperature decreases with a because at late epochs the observer is seeing portions of the wall that are receding from him more rapidly. (Details of this calculation will be presented elsewhere.) The only thing inside the future light core of E is the Hawking radiation which makes a $k=-1$ cosmology and redshifts in the usual way with $T\alpha 1/a$. The only thing that makes this universe different from our own is that $\Omega=0$ and $N_0 \sim 0(1)$. These deficiencies are due to the fact that the self-gravity of the Hawking radiation has been neglected. If the self gravity curvature effects cause the thermal radiation to have $P \sim -\rho$ then its density will not decrease appreciably in the initial expansion phase and particle creation will exponentially increase N_0. The radiation from the walls will fill the hole and lead to a solution similar to the BES solution. The phase transition simply occurs effectively at a timelike separation τ_1 from E rather than at a spacelike separation σ, the property of 0(3, 1) invariance of the bubble about E preserved. Thus we can see the formation of our Universe as a quantum tunnelling event; our Universe is one of the normal vacuum bubbles.

The causal structure of Fig. 1 at late times occurs regardless of how the de Sitter phase arises. In the Guth model the universe begins with a singularity and a Friedmann phase ($P=\rho/3$) until $\rho=\rho_c$ when a de Sitter phase is reached. The de Sitter false vacuum decays as Coleman type bubbles form; a $k=+1$ Guth model would look much like Fig. 1 except that there would be a singularity at $\eta \simeq 0$. Guth[8] wanted the bubbles to coalesce and fill space so as to eventually lead to a single Friedmann cosmology. He found that the bubbles would not in general fill the space. Press[14] has tried using the Gibbons and Hawking radiation to remedy this. Neither of these models have classical event horizons (boundary of past of $\mathscr{I}^+$). In contrast I propose that each bubble produces a $k=-1$ cosmology and it is an advantage if the bubbles do not bump into each other. Guth cosmologies with $k=+1, 0, -1$ can each produce in principle an infinite number of disjoint $k=-1$ (bubble) cosmologies. Each will have a cosmological event horizon and if the Guth epoch ρ_c occurs at the Planck epoch then all results concerning Hawking radiation will remain intact.

A self-consistent bubble formation process may require that the entire pase of the bubble ($DEi^\circ FC$) is a pure de Sitter state. If this is the case, an infinite number of disjoint $k=-1$ universes can be created. On the other hand bubbles may form randomly with a probability independent of position. For an event E to exist in the de Sitter phase there must not exist another event like E in the past light cone of E (and at a proper time at least τ_1 before E). The four-volume of this region which must be clear of events like E is infinite. For there to be a finite probability of this occurring, the probability of randomly forming an event like E per unit four-volume must be infinitesimal. Several bubbles may form, however, because the four-volume of de Sitter space is infinite. If the bubbles form randomly, they may bump into each other. There is only a 50% chance that two randomly formed E and E' universes will be disjoint as shown in Fig. 1. (E' cannot lie in the past or future light cones of E and the past and future light cones of F dominate the rest of the four-volume of de Sitter space). Such a model would make the creation of more than a few disjoint $k=-1$ universes unlikely. If the de Sitter state, however, is reached from singular or chaotic initial conditions as in the Guth model, even if the bubbles formed randomly, an arbitrarily large but finite number of disjoint universes could be created (the ratio of the four-volume of the future light cone of F to that of region $Ei^\circ F$ is infinite).

In conclusion, $k=-1$ universes may be created naturally from a de Sitter false vacuum state. These universes will have cosmological event horizons and should be filled with Hawking radiation.

This work was supported in part by an Albert P. Sloan Fellowship and by NSF grant AST76-24481.

Received 13 April; accepted 27 November 1981.

1. Hawking, S. W. *Nature* **248,** 30 (1974).
2. Hawking, S. W. *Comm. math. Phys.* **43,** 199 (1975).
3. Penzias, A. A. & Wilson, R. W. *Astrophys. J.* **142,** 419 (1965).
4. Brout, R., Englert, F. & Spindel, P. *Phys. Rev. Lett.* **43,** 417 (1979).
5. Englert, F. *Physical Cosmology*, Les Houches Session XXXII (North-Holland, Amsterdam, 1980).
6. Weinberg, S. *Phys. Rev. Lett.* **42,** 850 (1979).
7. Touissant, D., Treimane, S. B., Wilczek, F. & Zee, A. *Phys. Rev.* **D19,** 1036 (1979).
8. Guth, A. H. *Phys. Rev.* **D23,** 347 (1981).
9. Gott, J. R., Gunn, J. E., Schramm, D. N. & Tinsley, B. M. *Astrophys. J.* **194,** 543 (1974).
10. Davis, M., Tonry, J., Huchra, J. & Latham, *Astrophys. J. Lett.* **238,** L113 (1980).
11. Schramm, D. N. & Steigman, G. *Astrophys. J.* **243,** 1 (1981).

12. Hawking, S. W. & Ellis, G. F. R. *The Large Scale Structure of Space-Time* (Cambridge University Press, 1973).
13. Gibbons, G. W. & Hawking, S. W. *Phys. Rev.* **D15**, 2738 (1977).
14. Press, W. H. *Proc. Moriond Astrophysics Meet.* (in the press).
15. De Witt, B. S. *Quantum Gravity: The New Synthesis, Einstein Centennial* (eds Israel, W. & Hawking, S. W.) (Cambridge University Press, in the press).
16. Wagoner, R. V. *Physical Cosmology*, Les Houches Session XXXII (North-Holland, Amsterdam, 1980).
17. Adler, S. *Rev. mod. Phys.* (in the press).
18. Bekenstein, J. D. *Phys. Rev.* **D7**, 2333 (1973).
19. Coleman, S. *Phys. Rev.* **D15**, 2929 (1977).
20. Unruh, W. G. *Phys. Rev.* **D14**, 870 (1976).

Ionospheric troughs in Antarctica

J. R. Dudeney, M. J. Jarvis, R. I. Kressman,
M. Pinnock*, A. S. Rodger & K. H. Wright*

Natural Environment Research Council, British Antarctic Survey,
High Cross, Madingley Road, Cambridge CB3 0ET, UK

We report here the first observations of the dynamics of both the mid-latitude and high-latitude troughs made by the Advanced Ionospheric Sounder (AIS) at Halley Station, Antarctica (76° S, 27° W; invariant lat. 61°). This experiment is part of a major international project[1] to study the sub-auroral ionosphere and its associations with the magnetosphere. Our analysis provides an accurate quantitative description of the latitudinal movements of these features and the first results delineating the orientation of the poleward edge of the mid-latitude trough. These results show that the AIS has a much greater potential for monitoring large scale ionospheric structures and for tracking their motions than more conventional radio wave experiments.

The AIS[2] uses radio waves in the frequency range 0.1–30 MHz for remote sounding of the ionosphere. It provides a complete vector description of the ionospheric echoes obtained from each transmitted pulse, giving considerable advantage over the ionosonde. This, together with powerful online computing facilities, provides a very flexible tool for radiowave studies of the ionosphere. We concentrate on the ability of the AIS to locate the echoing region in range, azimuth and elevation, and thus to track the motions of large scale ionospheric features. The azimuth and elevation are determined from the spatial change of echo phase measured across an array of receiving antennas[3], whilst range is determined from the echo travel time.

The mid-latitude trough[4] is a major, but incompletely understood, feature of the sub-auroral ionosphere, which has very significant effects on radio wave propagation[5]. It consists of a circumpolar depletion of the night-time plasma concentration (the 'trough minimum') which extends over several degrees of latitude. It is bounded on the high latitude side by a 'wall' of ionization, the 'poleward edge', created primarily by soft (<1 keV) electron precipitation from the magnetosphere[6]. The low latitude boundary (the equatorial edge) is highly variable and is an extension of the mid-latitude ionosphere[7]. The trough is most pronounced at the peak of the F2 layer[8], but has been detected up to 2,500 km (ref. 9). The mean position of the trough is at about 60° invariant latitude, but moves equatorwards through the night as a function of geomagnetic activity[10]. It is statistically associated with the mean position of the plasmapause, although correspondence does not necessarily occur[11,12].

The processes responsible for trough information and their relative importance have yet to be confirmed. However, a very complex dynamic interaction clearly occurs involving the redistribution of plasma under the action of electric fields of magnetospheric origin[13,14] and thermospheric winds[15]; plasma production due to particle precipitation[6] and solar UV radiation; and plasma loss through charge exchange and recombination processes[16,17].

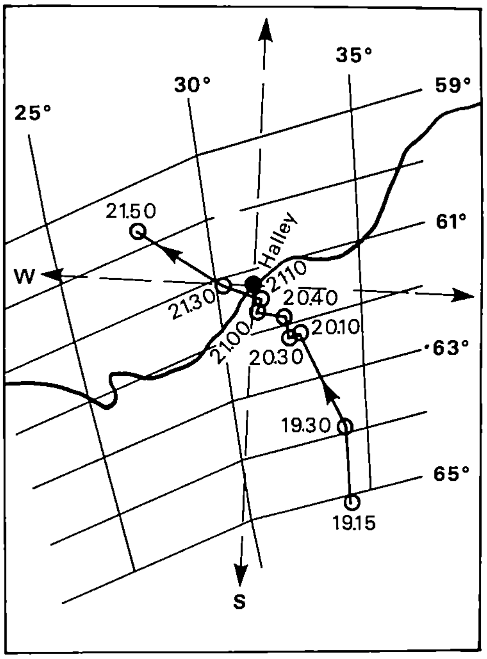

Fig. 1 The ground track of the reflection from the mid-latitude trough observed on the magnetically active night of 22 April 1981 in relation to the shelf ice coast line and Halley. The data come from tracking the poleward edge of the trough; and the numbers by each data point give the local times of the observations. The graticule represents invariant latitude and longitude at 100 km altitude[21].

Halley is an ideal location for ground-based studies of the sub-auroral ionosphere and its associations with the magnetosphere[7]. It is particularly well suited to studies of the mid-latitude trough because this is observed in the vicinity of Halley on most winter nights, over a wide range of geomagnetic activity[18].

The transit of the trough and its associated boundaries produces a characteristic signature on a sequence of ionograms recorded at a particular location[7,19,20]. Normally, echoes from both the trough minimum and the poleward edge can be distinguished. The AIS allows the positions of these features relative to the observing point to be determined and their temporal evolutions to be studied.

The full data from the current Antarctic winter will not be available until May 1982 when RRS Bransfield returns to the UK. However, we have used the local computing power provided with the AIS to analyse data for two nights when the trough was observed. The study periods were selected to provide a contrast between magnetically quiet (9–10 April 1981, $K_p = 1$) and active (22 April 1981, $K_p = 5$) conditions.

Turning first to the magnetically active night, Fig. 1 gives the ground track of the reflection from the poleward edge in relation

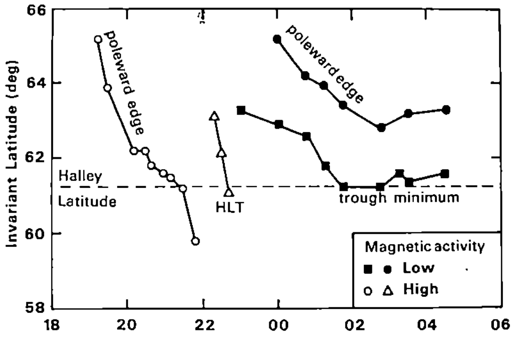

Fig. 2 The temporal evolution of the mid-latitude trough (MLT) and high-latitude trough (HLT) observed at Halley on the night of 22 April 1981 constructed from a combination of the AIS observations and contemporary knowledge of trough structure.

---

* Present address: Halley Station, Antarctica.

0028-0836/82/040307—02$01.00

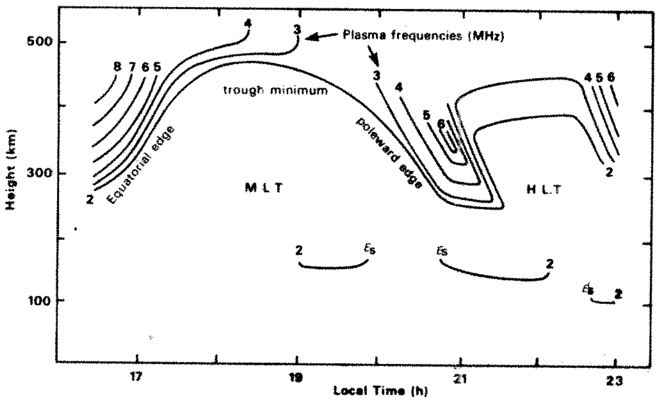

Fig. 3 Comparison of the trough event of 22 April 1981 ($K_p = 5$) with that on the 9–10 April 1981 ($K_p = 1$). The positions of various features identified in Fig. 2 are plotted in terms of their southern range of the reflection point (expressed in invariant latitude) as a function of local time. Local magnetic midnight occurs at 01.30 LT.

to Halley and an invariant coordinate grid[21]. It was first possible to locate the reflection point at 19.15 LT when it was 4° of invariant latitude to the south. It subsequently moved to lower latitudes, passing over Halley at approximately 21.20 LT.

The westward motion of the reflection point, evident in Fig. 1 as the trough moves equatorward, is expected because of the geometry of the trough in Sun–Earth coordinates. However, the actual displacement shown is greater than would be expected from the published statistical relationships[10] linking the invariant latitude of the trough to local time for a fixed level of geomagnetic activity. In fact, this deviation becomes progressively more marked as the event progresses. However, the location of the reflection point moves within the trough structure as the latter transits Halley equatorwards. Thus although firm conclusions cannot be drawn from this one example it will be worthwhile to use a larger data set to investigate the discrepancy and test whether a longitude term should be included in statistical relationships.

The echoes from the trough minimum showed no clear temporal evolution, suggesting that there was considerable fine structure within it; consequently, no single feature was consistently tracked. Following the passage of the poleward edge, a further trough was detected and tracked. This 'high latitude trough' ultimately passed to the north of Halley at about 22.00 LT.

The measured range, maximum plasma frequency and bearing information for the features have been combined with contemporary knowledge[4,6,18,19] of trough structure to give a schematic view of the event as seen from Halley. This is shown in Fig. 2, in which the major assumption is in the choice of the true height of maximum plasma frequency and consequently of the higher frequency iso-ionic contours. Note that in Fig. 1 there is an apparent tendency for the poleward edge reflection point to dwell in the vicinity of Halley between 20.10 and 21.30 LT. We interpret this as that between 19.15 and 20.10 echoes are being returned from the steeply sloping contours of the poleward edge and, although the reflection point moves slightly down in height as the feature approaches, the sequence represents the bulk movement. However, as the feature nears Halley, the reflection point moves relatively rapidly around the lower edge of the poleward edge, causing an apparent reduction in the rate of approach. Subsequently, as the poleward edge goes north of the station the echoes are from the high latitude trough minimum. This hypothesis is consistent with the observed variations in the slant ranges and matches well with structures observed by the Chatanika radar[22].

The patches of sporadic-E ionization (E_s) indicated in Fig. 2 are of a type normally associated with particle precipitation. The decrease in virtual height of the patches with local time suggests a hardening of the particle spectra.

The differences in behaviour between the geomagnetically quiet and disturbed nights are summarized in Fig. 3 which shows the southern component of the range for several trough features plotted as a function of local time. There is a local time difference of 5 h between the onset of the two events, with the active night leading. The rate of movement on the active night is much greater than on the quiet one and the trough moves to considerably lower latitudes. These findings confirm our previous results using more approximate techniques[18]. The trough minimum is apparently unstructured when the magnetic activity is low, and follows the behaviour of the poleward edge closely. Also on this occasion the mid-latitude trough appears to drift slowly poleward after magnetic midnight. A very well defined high latitude trough is observed in active conditions, but is too far south to be seen on the quiet night.

We have demonstrated one of the capabilities of the AIS at Halley to make observations of the sub-auroral ionosphere. We now plan to make detailed studies of the morphology of the trough using this and other sensors at Halley; and then test contemporary theoretical ideas.

We thank many members of BAS, and in particular the base personnel at Halley, for assistance.

Received 8 October; accepted 3 December 1981.

1. Dudeney, J. R. *New Scient.* **91,** 714–717 (1981).
2. Grubb, R. N. *NOAA Tech. Mem.* ERL SEL-55 (1979).
3. Wright, J. W. & Pitteway, M. L. V. *Radio Sci.* **14,** 827–835 (1979).
4. Wrenn, G. L. & Raitt, W. J. *Ann. Geophys.* **31,** 17–28 (1975).
5. Halcrow, B. W. & Nisbet, J. S. *Radio Sci.* **12,** 815–820 (1977).
6. Pike, C. P., Whalen, J. A. & Buchau, J. *J. Geophys. Res.* **82,** 3547–3556 (1977).
7. Dudeney, J. R. & Piggott, W. R. *AGU Antarctic Res. Ser.* **29,** 200–235 (1978).
8. Mendillo, M. & Chacko, C. C. *J. Geophys. Res.* **82,** 5129–5137 (1977).
9. Mahajan, K. K. & Brace, L. H. *J. geophys. Res.* **74,** 5099–5112 (1977).
10. Köhnlein, W. & Raitt, W. J. *Planet. Space Sci.* **25,** 600–602 (1977).
11. Titheridge, J. E. *J. geophys. Res.* **81,** 3227–3233 (1976).
12. Grebowsky, J. M., Hoffman, J. H. & Maynard, N. C. *Planet. Space Sci.* **26,** 651–660 (1978).
13. Knudsen, W. C. *J. geophys. Res.* **79,** 1046–1055 (1974).
14. Spiro, R. W., Heelis, R. A. & Hanson, W. B. *J. geophys. Res.* **83,** 4255–4264 (1978).
15. Fuller-Rowell, T. J. Rees, D. *J. atmos. terr. Phys.* **43,** 701–722 (1981).
16. Banks, P. M., Schunk, R. W. & Raitt, W. J. *Geophys. Res. Lett.* **1,** 239–242 (1974).
17. Schunk, R. W., Banks, P. M. & Raitt, W. J. *J. geophys. Res.* **81,** 3271–3281 (1976).
18. Rodger, A. S. & Pinnock, M. in *Exploration of the Polar Upper Atmosphere* (eds Deehr, C. S. & Holtet, J. A.) 463–469 (Reidel, Dordrecht, 1980).
19. Bowman, G. G. *Planet. Space Sci.* **17,** 777–796 (1969).
20. Nygren, T. *J. atmos. terr. Phys.* **39,** 733–740 (1970).
21. Evans, J. E., Newkirk, L. L. & McCormac, B. M. *Lockheed Palo Alto Laboratory Rep.* DASA 2347 (1969).
22. Vickerey, J. F., Rino, C. L. & Potemra, T. A. *Geophys. Res. Lett.* **7,** 789–792 (1980).

Two-dimensional modelling of potential ozone perturbation by chlorofluorocarbons

J. M. Steed, A. J. Owens, C. Miller, D. L. Filkin & J. P. Jesson

E. I. du Pont de Nemours and Company, Experimental Station, Wilmington, Delaware 19898, USA

The possible adverse effect of man-made chlorine compounds, particularly chlorofluorocarbons (CFCs), on the stratospheric ozone layer has been studied intensely in the past few years[1,2], with assessments being based primarily on one-dimensional (1-D) mathematical models of atmospheric transport and chemistry. Two-dimensional (2-D) models now permit a more realistic comparison of model predictions with observational data over the full range of latitudinal and seasonal variations in many of the important atmospheric trace species[3–8]. We report here 2-D model calculations of the hypothetical steady state arising from constant CFC releases continuing indefinitely into the future. Latitudinal and seasonal variations in the calculated reduction of stratospheric ozone are discussed and contrasted with the calculated perturbation up to 1980. The global average is compared with the corresponding 1-D model. Several changes in the vertical structure of the ozone perturbation are found to result from recent revisions in chemical reaction rates.

The important chlorofluorocarbons FC-11 (CCl_3F) and FC-12 (CCl_2F_2) had historically been released in rapidly increasing quantities until 1974. Since then, global production and release rates have declined by ~20%. These compounds are currently believed to have long atmospheric lifetimes (40–150 yr). For constant release, a 'steady state' would be reached within several hundred years.

The 2-D model used for the present calculations has been described elsewhere[5,6]. Its principal features include a chemical scheme as complete as that in advanced 1-D models and a transport representation based on a parameterization of the lagrangian mean circulation[9,10]. The chemical reaction rate set used is that recommended at the joint meeting of the CODATA Panel and the NASA Panel for Data Evaluation[11] (March 1981). The 1-D model results discussed below use the same rate set and the model described in ref. 12.

Model calculated species concentrations have been compared elsewhere[5] with measurements, for most species of current interest. The model calculated variation of total ozone with latitude and season is given in Fig. 1. The qualitative features of the observed ozone distribution[13] are quite well reproduced, including the spring maximum and the Equator-to-pole gradient. In what follows changes in total ozone are referred to this calculated ambient distribution.

The calculated change in local ozone concentrations arising from the release of FC-11, FC-12 and CH_3CCl_3 up to July 1980 is shown in Fig. 2. Except near the poles, latitudinal variations are small. Maximum depletion for all latitudes is near 6% at ~42 km. A major consequence of recent revisions in chemistry is the local increase in ozone between 10 and 25 km from 30° N to 30° S, and over part of that range at other latitudes. The increase exceeds 1% between 18 and 22 km in the tropics. This net local ozone increase is associated both with increased vertical penetration of solar UV light due to ozone depletion at higher altitudes (the 'self-healing effect') and with interactions of chlorine species with HO_x and NO_x, reducing the efficiency of natural odd oxygen recombination cycles.

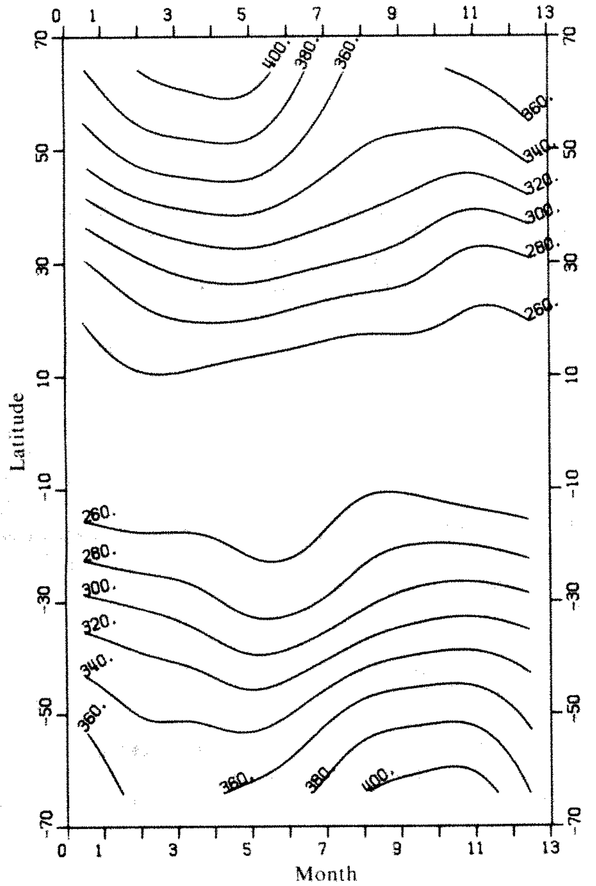

Fig. 1 Latitude–time contour plots of the calculated ambient ozone distribution, in Dobson units. Positive latitudes are North. 1 January corresponds to month 0.0.

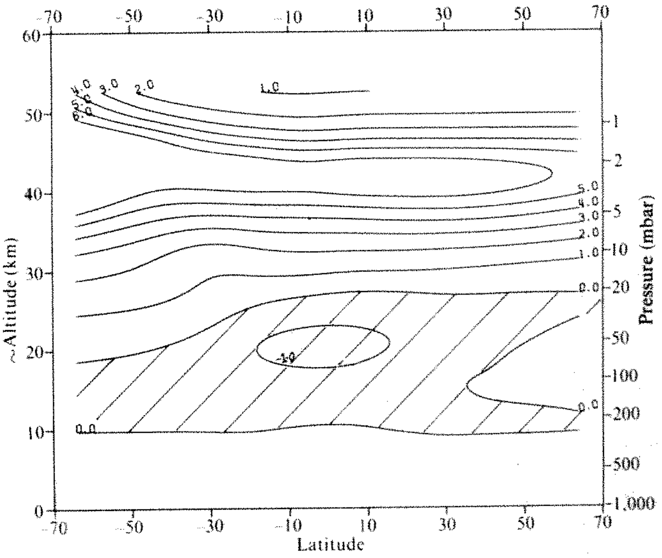

Fig. 2 Calculated latitude–altitude cross-section of percentage ozone decrease up to July 1980 arising from historical releases of FC-11, FC-12 and methyl chloroform. Striped region corresponds to ozone increase.

The calculated latitude–season cross-section of percentage total ozone column depletion for 1980 is shown in Fig. 3*a*. In contrast to the calculations of Pyle and Derwent[4] made with earlier chemical rate recommendations, the annual mean depletion is nearly constant with latitude at ~0.9%. Calculated depletion in the region 30° N–30° S remains in the range 0.90 ± 0.15% throughout the year, whereas the calculated ozone change in polar regions is twice as large (~1.2%) during local winter as in summer (~0.6%). The reduction in polar depletion relative to that in the tropics since the work by Pyle and Derwent[4] arises primarily from an increase in the recommended rate constants for reactions (1) and (2).

$$OH + HNO_3 \rightarrow H_2O + NO_3 \qquad (1)$$

$$OH + HNO_4 \rightarrow H_2O + O_2 + NO_2 \qquad (2)$$

These reactions serve as sinks for OH and are expected to be most important where calculated local HNO_3 and HNO_4 concentrations are large, that is at higher latitudes, especially in winter. Reduced OH slows conversion of HCl to Cl by reaction (3), and thereby increases the effectiveness of HCl as a sink for chlorine.

$$OH + HCl \rightarrow H_2O + Cl \qquad (3)$$

In absolute terms, the calculated change in column ozone up to 1980 is between 2 and 3 Dobson units throughout midlatitude

Table 1 Calculated atmospheric changes due to constant CFC release-initial to steady state

	2-D model				
	5° N	30° N	65° N	Global mean	1-D model
$-\Delta O_3$ (column) (%)	6.1	6.0	6.5	6.2	7.0
ΔClX (at 50 km) (p.p.b.)				7.2	8.4
$\lvert \Delta O_3/\Delta ClX \rvert$ (%/p.p.b.)				0.87	0.84
ΔUV (DNA weighted) (%)	16.5	16.2	15.8	16.2	20
$\lvert \Delta UV/\Delta O_3 \rvert$				2.6	2.8

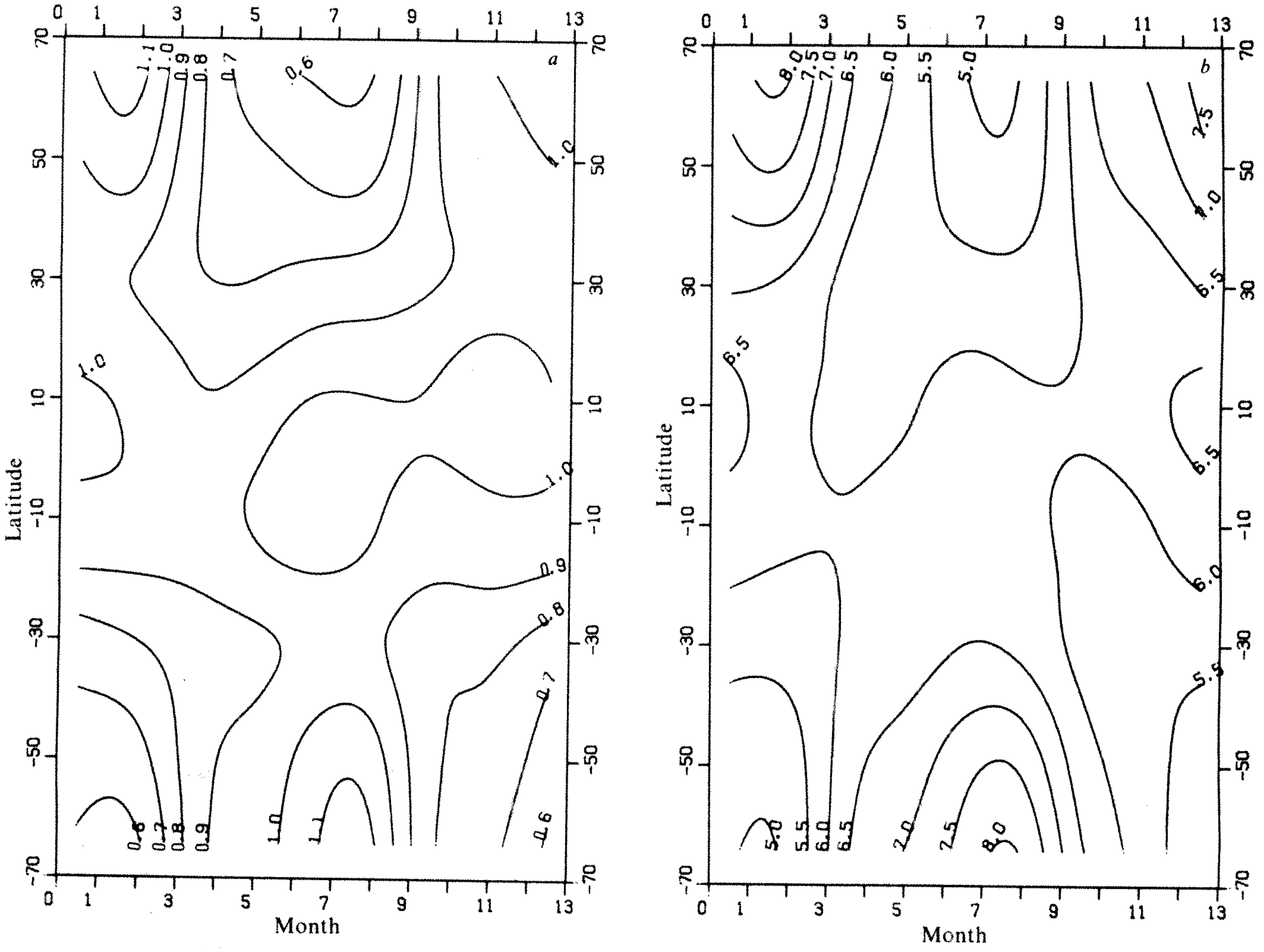

Fig. 3 *a*, Latitude–season contours of percentage ozone depletion up to 1980 relative to the ambient atmosphere based on historical releases of FC-11, FC-12 and methyl chloroform. *b*, Latitude–season contour plot of calculated steady-state percentage ozone depletion due to continued release of FC-11 and FC-12 at mid-1970s release rates.

regions and polar summer, and increases to more than 4 Dobson units during the ozone maximum in polar winter.

Pyle and Derwent[4] noted the expense of calculating a time-dependent approach to steady-state CFC perturbations with a 2-D model. For the present calculations, a method of rapid convergence has been developed which allows an accurate, economical calculation of the steady-state results. The method takes advantage of the slow transport and photolysis of CFCs and relatively fast subsequent photochemistry, by alternating long time-dependent runs retaining CFCs as the only active species (~300 yr of problem time) with short runs in which all species are active.

Assuming the continued release of FC-11 and FC-12 at rates characteristic of the mid-1970s (340×10^3 and 410×10^3 tonnes yr^{-1}, respectively), the calculated global average column ozone depletion at steady state is 6.2%, with a ClX increase at ~50 km of 7.2 p.p.b. (parts per 10^9) over the unperturbed atmosphere. This is compared in Table 1 with the corresponding values of 7.0% and 8.4 p.p.b. obtained with the 1-D model using identical chemistry. Note that $\Delta O_3(\%)/\Delta ClX(p.p.b.)$ is quite similar in the two models, so that the difference in calculated ozone depletion may be partly due to different effective rates of vertical transport in the two models. The 1-D model also neglects the latitudinal covariance between fluorocarbon concentration and photolysis rate, both of which reach maxima near the Equator, so it underestimates the rate of CFC destruction in the lower stratosphere. The neglect of the latitudinal covariance by the 1-D model thus contributes to a longer lifetime for CFCs and more ClX at high altitudes in the steady state.

Figure 3*b* shows the steady-state 2-D calculations of the seasonal and latitudinal variations in column ozone. The calculated depletion for latitudes from 30° N to 30° S varies by <1% for all seasons. The largest ozone change (~8%) occurs in the polar winter, at the time of the ozone maximum. Seasonal variations of nearly a factor of two persist near the poles.

Several interesting features are evident when Fig. 3*a* (for 1980) is compared with Fig. 3*b* (for the steady state). By 1980, the CFCs had not yet reached steady state in the atmosphere. They are more heavily concentrated near their Northern Hemisphere, ground-level sources. As the upward transport of tropospheric trace species is most rapid in the tropics, the CFC and the reactive Cl concentrations in the tropical stratosphere for 1980 are enhanced. This leads to a larger calculated ozone depletion near the Equator (~1.0%) than at higher latitudes (~0.8%). In the steady state, once the CFCs have had time to be transported more effectively to the polar regions, this latitudinal effect is reduced and the yearly-averaged ozone depletion remains essentially constant (~6.2%) for all latitudes. Also note a slight hemispheric asymmetry for 1980 (as shown in Fig. 3*a*), with the ozone depletion in the Northern Hemisphere being slightly higher. The almost perfect north–south symmetry in the steady state (Fig. 3*b*) is due to the input transport data base, which is symmetric about the Equator except for a 6-month seasonal time lag.

An important characteristic of the calculated ozone change is its rate of increase with time. Consistent with the effectively shorter lifetime for CFCs in the 2-D model, the calculated global-mean present day (1980) depletion (0.89%) exceeds that from the corresponding 1-D model (0.50%). However, both are small compared with calculations made over the past few years[1–4]. The currently calculated rate of change in global ozone is between −0.05 and −0.09% yr^{-1}, beginning in about 1970. This is, of course, for CFCs alone. Effects of opposite sign arising from the CO_2 increase and jet aircraft exhausts result in a combined effect on total ozone which is not significantly different from zero in recent 1-D model calculations[14].

The use of 2-D models to calculate potential ozone perturbations due to chemical releases of manmade origin provides a more detailed simulation of the real atmosphere than is possible with 1-D models. Various statistical techniques have been applied[15–18] to the analysis of ground-based ozone measurements made over the past 20 or more years in an attempt to detect trends suggested by 1-D models. Use of 2-D models allows the trend appropriate to a latitude region to be calculated, and information on changes in the seasonal variations as well as long-term trends can be used in the analysis. As noted above (Fig. 3*a*), the latitudinal variation in the present calculations of annual average ozone depletion is small, but the magnitude of the seasonal component increases towards the poles. Incorporating this additional information into analyses of ozone measurements may permit a better identification of any observed trend.

Accompanying a decrease in the amount of atmospheric ozone is an increase in the UV radiation reaching the Earth's surface. We have selected for a UV weighting function the action spectrum for DNA damage[19], which is one of the most sensitive to ozone changes. In general, changes in UV reaching the ground follow the total ozone column. In the steady state, for example, the yearly-averaged DNA-weighted UV dose is calculated to increase by 16%, essentially independent of latitude (Table 1). The largest percentage change occurs during the polar winter when the UV dose is smallest. The 2-D model gives an 'amplification factor', $\Delta UV/\Delta O_3 = 2.6$, while in the corresponding 1-D model this factor is 10% larger (2.8). Unlike calculations performed with previous chemical rate sets[4], we do not find a large variation of this amplification factor with latitude.

In the real atmosphere, more is changing than just the CFC concentrations. Prime examples are the CO_2 concentration, NO_x arising from conventional jet exhausts, and N_2O arising from the application of manmade fertilizers. While it is important to study the potential CFC effect in isolation as we have done here, 2-D models are approaching a degree of refinement where the estimation of multiple perturbations may become feasible. This type of investigation will be reported later.

Received 2 September; accepted 9 November 1981.

1. Hudson, R. D. & Reed, E. I. (eds) *The Stratosphere: Present and Future* (NASA RP-1049, 1979).
2. Panel on Stratospheric Chemistry and Transport *Stratospheric Ozone Depletion by Halocarbons: Chemistry and Transport* (National Academy of Sciences, Washington DC, 1979).
3. UK Department of the Environment *Chlorofluorocarbons and Their Effect on Stratospheric Ozone* (Pollution Paper No. 15, 1979).
4. Pyle, J. A. & Derwent, R. G. *Nature* **286**, 373–375 (1980).
5. Miller, C., Filkin, D. L., Owens, A. J., Steed, J. M. & Jesson, J. P. *J. geophys. Res.* **86** (in the press).
6. Miller, C., Steed, J. M., Filkin, D. L. & Jesson, J. P. *Nature* **288**, 461–464 (1980).
7. Ko, M. K. W., Livshits, M., Ryan, P. B. & Sze, N. D. *Status Report to Chemical Manufacturers Association for A.E.R. 2-D Model Project*, April (1981).
8. Pyle, J. A. & Rogers, C. F. *Nature* **287**, 711–714 (1980).
9. Andrews, D. G. & McIntyre, M. E. *J. Fluid Mech.* **89**, 609–646 (1978).
10. Dunkerton, T. *J. atmos. Sci.* **35**, 2325–2333 (1978).
11. Hudson, R. D., Reed, E. I. & Bojkov, R. D. (eds) *The Stratosphere 1981: Theory and Measurements* Appendix 1 (WMO/NASA, 1981).
12. Miller, C., Steed, J. M., Filkin, D. L. & Jesson, J. P. *Atmos. Envir.* **15**, 729–742 (1981).
13. Dutsch, H. *Adv. Geophys.* **15**, 219–322 (1971).
14. Penner, J. E. *Am. Geophys. Un. Fall Meet.*, San Francisco (1980); *IAMAP 3rd Scient. Assembly, Hamburg* (1981).
15. Hill, W. J., Sheldon, P. N. & Tiede, J. J. *Geophys. Res. Lett.* **4**, 21–24 (1977).
16. St John, D. S., Bailey, S. P., Fellner, W. H., Minor, J. M. & Snee, R. D. *J. geophys. Res.* **86**, 7299–7311 (1981).
17. Reinsel, G., Tiao, G. C., Wary, M. N., Lewis, R. & Nychka, D. *Atmos. Envir.* **15**, 1569–1577 (1981).
18. Bloomfield, P., Thompson, M. L., Watson, G. S. & Zeger, S. *Tech. Rep.* No. 182, Ser. 2 (Department of Statistics, Princeton University, 1981).
19. Setlow, R. B. *Proc. natn. Acad. Sci. USA* **71**, 3363–3366 (1974).

Electromagnetic jet-propulsion in the direction of current flow

Peter Graneau

MIT Francis Bitter National Magnet Laboratory, Cambridge, Massachusetts 02139, USA

Two simple experiments are reported here which demonstrate jet-propulsion in the direction of current flow between liquid and solid conductors. The observed effects seem to conform with Ampere's force-law, but no qualitative nor quantitative explanation has so far been found in terms of lorentzian forces and associated magnetohydrodynamics (MHD) phenomena. This research forms part of a wider investigation of the Ampere–Neumann electrodynamics and its relationship to modern science and technology.

In a classical experiment (Fig. 1) Ampere[1] claimed to have shown that, in addition to transverse forces on the conductor, the electric current creates repulsion between adjacent current-elements on the same straight line. He incorporated both transverse and longitudinal forces in his force-law (equation (1)). The longitudinal forces should place wires in tension and create relative motion between liquid and solid portions of a circuit. In Ampere's experiment the insulated or bare copper hairpin *cdefg* of Fig. 1, floating on two liquid mercury troughs *ab* and *a′b′*, will move towards *bb′* when sufficient current flows in and out of terminals *t* and *t′* connected with copper bars to the *a* and *a′* ends of the troughs. A transverse lorentzian force acts on the upturned hairpin bend *e*, but this should have its reaction force in the legs *cd* and *fg* of the hairpin, because the legs contain the source of the magnetic field at *e*. With action and reaction in the same rigid body, the Lorentz force at *e* should not be able to produce relative motion between hairpin and mercury. This point relating to Newton's third law has been argued strongly elsewhere[2–7].

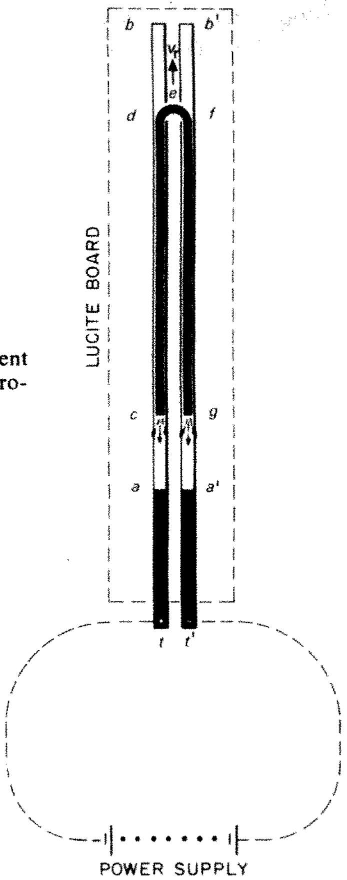

Fig. 1 Ampere's experiment demonstrating longitudinal propulsion.

0028-0836/82/040311—02$01.00

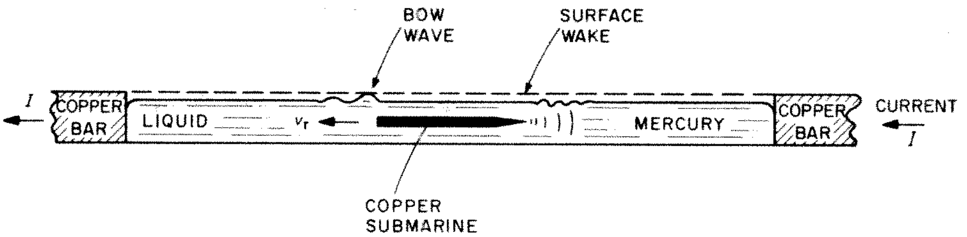

Fig. 2 Copper submarine experiment. Mercury trough length = 30 cm; cross-section 0.5×0.5 inch. Copper extension of troughs 30 cm long, 0.5×0.5 inch cross-section. Remote return circuit. $I = 400$ A. Copper submarine; 5 cm long, 3 mm diameter, 1 cm long taper. $v_r = 15$ cm s^{-1}.

Ampere did not mention that close to *c* and *g* liquid mercury moves relative to the trough walls and away from the ends of the hairpin. This motion confirms longitudinal propulsion, independent of any recourse to Newton's third law. The observation of this motion and the discovery of another longitudinal propulsion effect is now reported. While repeating Ampere's experiment, but mechanically blocking the forward motion of the hairpin, it was found that a wake formed in the liquid as though jets were mounted on the ends of the hairpin. A depression was detected in the liquid level close to *c* and *g*. When the hairpin ends were placed near to *a* and *a'*, liquid would well up on the copper walls and could be made to overflow. Short pieces of copper and stainless-steel wire laid on the mercury next to the hairpin ends were pushed away from *c* and *g*. Finally, a thin dielectric rod driven into the mercury near *c* or *g* and pivoted vertically above the point of immersion moved towards *a* or *a'*. These experimental facts leave little doubt that the longitudinal propulsion forces suggested by Ampere do exist. In showing that the net force of all amperian components on a rectangular circuit is zero, Cleveland[3] proved that longitudinal forces are of the same order of magnitude as transverse forces.

While trying to modify Neumann's[8] demonstration of longitudinal forces, I discovered another, even more remarkable propulsion arrangement. Figure 2 gives the details of this experiment. A copper 'submarine' consisting of a short piece of straight wire, squared off at one end and pointed at the other, has to be placed on the surface of a straight-through mercury trough conductor. When current is forced to flow along the trough, the transverse forces submerge the wire and longitudinal forces drive it along the centre of the trough until it strikes the solid copper bar. The wire travels with its blunt end forward. Its velocity is apparent from the bow wave on the liquid surface. The direction of travel does not depend on the direction of current flow and the experiment works equally well with 60-Hz alternating current.

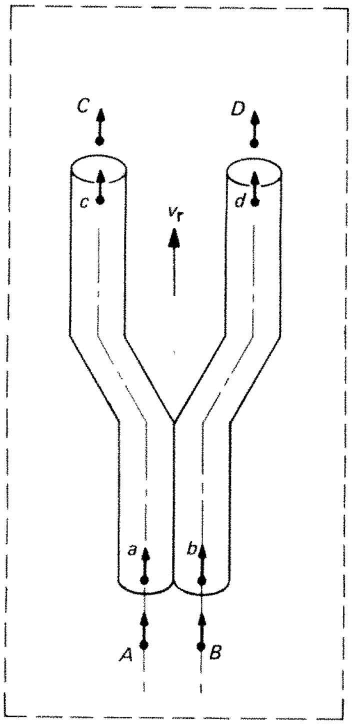

Fig. 3 Two-filament copper wishbone in liquid mercury bath.

Figure 3 explains the amperian submarine propulsion mechanism. This simplified representation shows a wishbone made of two solid current filaments immersed in liquid metal. Only two sets of four current-elements are considered. One set is *a*, *b*, *c* and *d* located in the ends of the wishbone filaments. The other four, *A*, *B*, *C* and *D* are adjacent in-line elements in the liquid. The Ampere force $\Delta F_{m,n}$ in dyn between two current-elements at points *m* and *n* of lengths d*m* and d*n* and separated by the distance $r_{m,n}$ is given by

$$\Delta F_{m,n} = -i_m i_n (\mathrm{d}m \cdot \mathrm{d}n / r_{m,n}^2)(2 \cos \varepsilon - 3 \cos \alpha \cos \beta) \quad (1)$$

where i_m and i_n are the element currents in absolute ampere, ε is the angle of inclination between the elements, and α and β are the angles which the elements make with the distance vector $\mathbf{r}_{m,n}$. When the force is positive it represents repulsion and when negative it represents attraction. Using this law to compute the repulsion between solid and liquid elements at one end of the wishbone and then at the other, it can easily be shown that the solid object is being pushed relative to the liquid in the direction of the velocity v_r indicated on Fig. 3. According to Ampere's law, therefore, it is the current concentration in the pointed end of the wire which is responsible for the propulsion of the copper submarine of Fig. 2.

So far the longitudinal propulsion mechanism has not been explained in terms of relativistic field theory and associated MHD effects. In view of the widespread acceptance of Ampere's force law during the nineteenth century and its implications with regard to solid-state physics and MHD technology, I urge others to repeat these simple experiments and comment on their observations.

This research was sponsored by NSF.

Received 27 October; accepted 26 November 1981.

1. Ampere, A. M. *Memoires sur l'Electrodynamic* Vol. 1, 25 (Gauthier-Villars, Paris, 1885).
2. Bush, V. *J. Math. Phys.* **5,** 129 (1926).
3. Cleveland, F. F. *Phil. Mag.* **25,** 416 (1936).
4. O'Rahilly, A. *Electromagnetic Theory* Vol. 1, 102 (Dover, New York, 1965).
5. Whittaker, E. *History of the Theories of Aether and Electricity* Vol. 1, 84 (Thomas Nelson, London, 1951).
6. Robertson, I. A. *Phil. Mag.* **36,** 32 (1945).
7. Rosser, W. G. V. *Contemp. Phys.* **3,** 28 (1961).
8. Neumann, F. E. *Vorlesungen ueber Elektrische Stroeme*, 102 (Teubner, Leipzig, 1884).

A composite semiconductor photoanode for water electrolysis

Yoshihiro Nakato, Nobuyuki Takamori & Hiroshi Tsubomura

Department of Chemistry, Faculty of Engineering Science,
Osaka University, Toyonaka, Osaka 560, Japan

Photoelectrolysis of water by means of semiconductor photoelectrochemical cells has attracted much attention from the point of view of solar energy conversion[1-5]. Metal oxides such as TiO_2, WO_3, or Fe_2O_3 act as stable photoanodes, but they need an external bias for the photodecomposition of water to compensate for their too low surface band energies. We report here that water can be photodecomposed effectively without external bias by using a semiconductor/redox electrolyte/semiconductor junction (SES) as the photoanode.

The structure of the SES is indicated in Fig. 1. It consists of single crystal wafers of n-CdS and n-TiO_2 (0.3–0.7 mm thick) separated by ~0.2 mm by an aqueous solution containing 1 M NaOH, 1 M Na_2S and 1.5 gram atom l^{-1} S which dissolves in a concentrated sulphide solution. The inside wall of TiO_2 is coated with palladium (<5 nm thick) by vacuum evaporation to mediate electron transfer between n-TiO_2 and the sulphide–polysulphide couples.

As shown in Fig. 2, the onset potential of the anodic photocurrent of the SES electrode in a 1.0 M NaOH aqueous solution lies much more negative than that of an n-TiO_2 electrode. It is ~0.5 V more negative than the onset potential of dark cathodic current in a platinum electrode (Fig. 2). This means that water can be photodecomposed efficiently by a photocell equipped with a SES photoanode, a platinum counter electrode and a 1.0 M NaOH aqueous solution. Such a photocell showed steady photocurrent of ~2 mA cm^{-2} for more than 1 h under illumination with a 250-W mercury lamp. Considerable gas evolution was observed at both electrodes. The current was generated by illumination with polychromatic light containing the wavelengths 300–520 nm. The current was also generated with two monochromatic light beams, one in the range <410 nm and the other in the range 450–520 nm, but not with either of them alone. These results suggest that the current flows only if both n-TiO_2 and n-CdS are excited. The light in the range of 410–450 nm seems to be absorbed mostly by the sulphide–polysulphide solution.

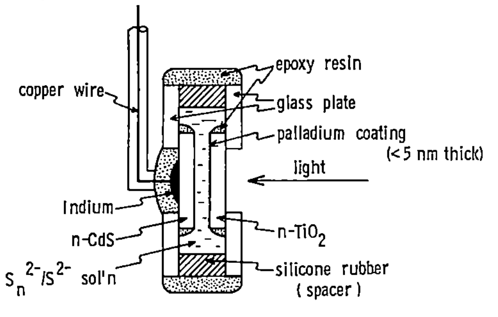

Fig. 1 Schematic diagram of an n-CdS-S_n^{2-}/S^{2-} solution–n-TiO_2 junction (SES) electrode.

The above results can be explained by an energy level diagram for the photocell (Fig. 3), drawn on the basis of the reported flat-band potentials[6,7]. It is known that n-CdS is stable in a solution of the sulphide–polysulphide couple[3–6]. Because the inner sulphide-polysulphide solution and the solution outside the SES electrode have nearly the same *p*H (~14), the energies of the conduction band edges of n-TiO_2 in the dark at both inner and outer surfaces must be equal. However, the accumulation of positive charges in the sulphide–polysulphide solution by injection of holes from the n-CdS under illumination will press down the conduction band energy at the inner surface of n-TiO_2. A stationary state will be attained by balancing the hole injection from n-CdS with the electron injection from n-TiO_2. The electrons are excited twice in the SES, reaching a level high enough to reduce water at the counter platinum electrode.

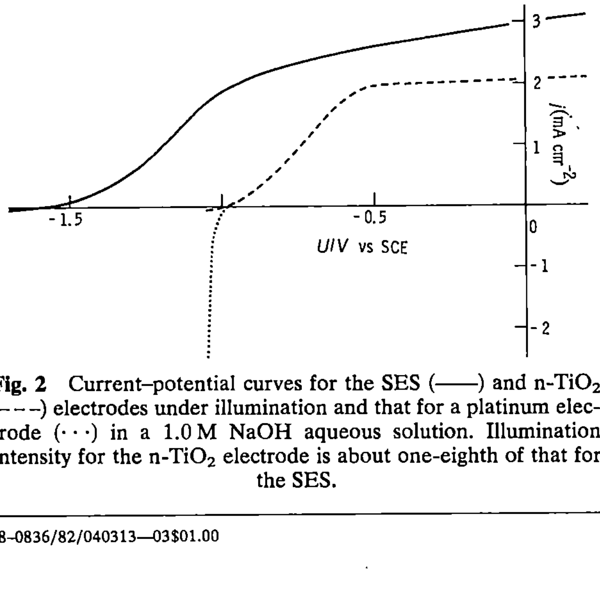

Fig. 2 Current–potential curves for the SES (——) and n-TiO_2 (– – –) electrodes under illumination and that for a platinum electrode (· · ·) in a 1.0 M NaOH aqueous solution. Illumination intensity for the n-TiO_2 electrode is about one-eighth of that for the SES.

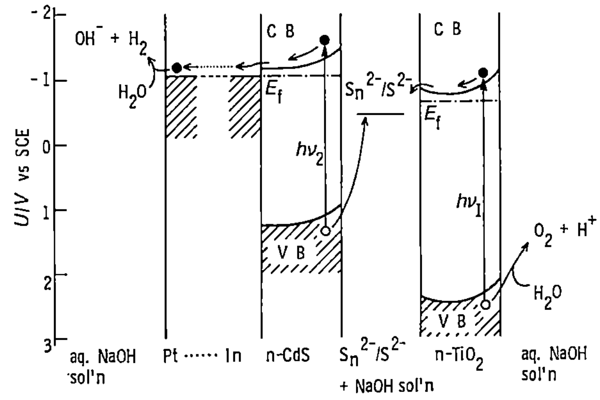

Fig. 3 An energy level diagram for a photocell made of SES and Pt electrodes.

The present SES electrode uses n-TiO_2 which is sensitive to the UV light only. A semiconductor with a narrower bandgap is more desirable for the efficient utilization of solar energy. With such a material the SES electrodes can in principle utilize solar energy of wide spectral range effectively, the shorter wavelength part by the front semiconductor and the longer wavelength part by the rear one. Photoelectrodes with solid n–n (ref. 8) or n–p–n (ref. 9) heterojunctions have been reported to have the same function. Note that the construction of a SES electrode has the advantage that the two semiconductors are prepared separately at their best conditions before they are combined.

Received 14 July; accepted 12 November 1981.

1. Maruska, H. P. & Ghosh, A. K. *Solar Energy* **20,** 443–458 (1978).
2. Scaife, D. E. *Solar Energy* **25,** 41–54 (1980).
3. Gerischer, H. *Topics Appl. Phys.* **31,** 115–172 (1979).
4. Bard, A. J. *J. Photochem.* **10,** 59–75 (1979).
5. Wrighton, M. S. *Accts chem. Res.* **12,** 303–310 (1979).
6. Minoura, H., Tsuiki, M. & Oki, T. *Ber. Bunsenges. Phys. Chem.* **81,** 588–592 (1977).
7. Tomkiewicz, M. *J. electrochem. Soc.* **126,** 1505–1510 (1979).
8. Wagner, S. & Shay, J. L. *Appl. Phys. Lett.* **31,** 446–447 (1977).
9. Morisaki, H., Watanabe, T., Iwase, M. & Yazawa, K. *Appl. Phys. Lett.* **29,** 338–340 (1976).

Thermoluminescence dating of sand dunes in Rajasthan, India

A. K. Singhvi, Y. P. Sharma* & D. P. Agrawal

Physical Research Laboratory, Ahmedabad 380009, India

We report here a new application of thermoluminescence (TL) for dating sand dunes. This application assumes that exposure to sunlight causes bleaching of the geological TL of a sediment to a residual value and that TL accumulation starts again when the sediment is buried under fresh deposit and is thus shielded from the Sun. Although the TL method has been applied to loess[1,2] and ocean sediments[3,4], the application of this technique to sand dunes provides the first reliable dating control for dune dynamics, palaeoclimatology and spread of deserts.

Samples were collected from the stabilized sand dunes that had archaeological association, so that an independent dating control on the TL dates obtained was available. The location of the dunes are: (1) Langhnaj (23°29′ N, 72°26′ E); (2) Amarpura (27°23′ N, 74°37′ E); and (3) Bagor (25°21′ N, 74°23′ E), all in Rajasthan. The fine grain technique[5] was used for the TL analysis. Grains 1–8 μm in size were extracted after pretreatment of the sample with 1M HCl to remove the carbonate fraction which could be post-depositional. The apparatus has been described elsewhere[6]. Glow curves were recorded in an

---

* Permanent address: Department of Physics, Kurukshetra University, Kurukshetra, India.

0028–0836/82/040313—03$01.00

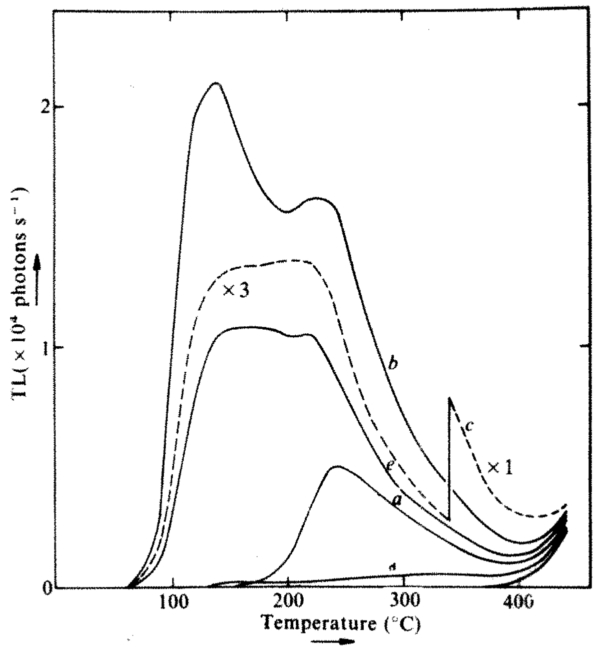

Fig. 1 TL glow curve for a typical sand dune sample: *a*, natural TL; *b*, natural TL+6 h α irradiation; *c*, natural +10.5 krad β exposure; *d*, natural+1,000-min sunlamp bleach; *e*, natural+1,000-min sunlamp bleach+3.5 krad β exposure.

ambient atmosphere of ultra-pure nitrogen (5 l min^{-1}) at a heating rate of 5 °C s^{-1}. Photon counting was used and the optics channel comprised a EMI 9635QA photomultiplier tube coupled with Chance Pilkington HA3 and Corning 7-59+5-58 blue filters. β irradiations were carried out using ^{90}Sr/^{90}Y β plaque and α irradiations were made in vacuum using ^{241}Am foils. A 300 W ultra vitalux 'WOTAN' sunlamp[7], kept 30 cm from the samples, was used.

Although sunlamps are richer in UV than sunlight, we consider that adverse effects would be small and would not upset any of the present conclusions. Typical natural, β, α and post-sunlamp exposure glow curves are given in Fig. 1. Thick source ZnS(Ag) counting was used to estimate the uranium and thorium series α activity, and γ spectrometry was used to estimate potassium. The dose rate was estimated assuming the equilibrium of ^{238}U and ^{232}Th series. No wetness correction was considered necessary as the average water content in stabilized sand dunes does not exceed 1–2% (ref. 8). Typical component dose rates are α dose (U, Th) ~ 40–45%, β dose (U, Th) ~ 10–20%, β dose (K) ~ 10–20%, γ dose (U, Th) ~ 15–20%, γ dose (K) ~ 5%. Cosmic-ray dose rate was taken to be 15 mrad yr^{-1} for all the samples. All the samples were checked for anomalous fading for a storage period of 14 days. No loss of signal was seen within experimental reproducibility limits of ~5%. In addition, TL-S-7 showed no loss of signal for a storage period of 57 days. As a further precaution, all the sample disks were read only 15 days after an irradiation.

The observed TL (I_{nat}) in the sample comprises[3]: (1) the unbleachable TL that was already present in the sample at the time of deposition (I_0); and (2) the TL acquired by the sample since deposition as a buried sediment (I_d)

$$I_{\text{nat}} = I_0 + I_d$$

or equivalently

$$D(I_{\text{nat}}) = D(I_0) + D(I_d)$$

where $D(I)$ refers to the equivalent β radiation dose required to give TL of intensity I. $D(I_d)$ divided by the appropriate dose rate gives the date of depositional event. Thus the estimation of I_d requires determination of I_0 and I_{nat}. A clue to the estimation of I_0 is provided by Fig. 2, which gives the bleaching behaviour of two samples with Sun/sunlamp exposures. The bleaching curve quickly approaches an asymptotic value indicating that TL cannot be bleached beyond a finite residual value by any length of Sun/sunlamp exposure. Taking this residual TL level to represent I_0 and expressing it as a fraction R of I_{nat} we have:

$$I_0 = RI_{\text{nat}}$$

or

$$D(I_d) = (1-R)D(I_{\text{nat}})$$

In the above, $D(I_{\text{nat}})$ can be determined by the additive β dose procedure[9], which implicitly assumes a linearity of the TL growth curve. However, in view of the low equivalent doses, we consider that the assumption of a linear growth applies for the samples reported here. R was estimated from the residual TL level after a prolonged (1,000-min) sunlamp bleach. The 1,000-min exposure was considered to be long enough to approach the asymptotic value (Fig. 2). Indeed, for samples TL-S-9 and TL-S-14, for example, the residual TL after a 250-h Sun exposure was within 20% of the values obtained after a 1,000-min sunlamp bleach. Thus this estimation of $D(I_d)$ is not only

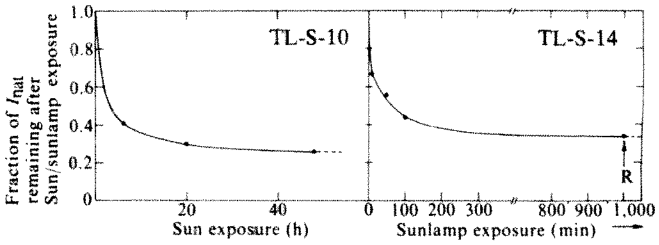

Fig. 2 Effect of Sun/sunlamp exposure on TL. The glow curve temperature is 320 °C. R corresponding to a 1,000-min sunlamp is also indicated.

Table 1 Thermoluminescence data and age estimates for sand dune samples*

Sample no.	Site	Depth (cm)	Plateau region (°C)	$D(I_{\text{nat}})$ (rad)	R	$D(I_d)$ (rad)	a	Dose rate (rad yr^{-1})	Age (yr)	Comments
PRL:TL:S-9	Amarpura	25	300–380	5,885	0.23	4,530	0.16	0.756	6,140	
PRL:TL:S-8	Amarpura	70	300–360	10,330	0.20	8,265	0.14	0.586	14,610	
PRL:TL:S-7	Amarpura	110	300–380	16,860	0.21	13,320	0.13	0.846	16,190	
PRL:TL:S-12	Langhnaj	80	300–360	4,070	0.29	2,890	0.14	0.544	5,180	
PRL:TL:S-11	Langhnaj	160	320–400	4,820	0.37	3,040	0.15	0.361	8,630	3,990 ± 110†
PRL:TL:S-10	Langhnaj	240	300–360	9,610	0.32	6,535	0.17	0.332	20,280	
PRL:TL:S-13	Bagor	50	300–380	3,400	0.29	2,420	0.12	1.172	2,100	2,060 ± 210‡
PRL:TL:S-14	Bagor	80	300–380	4,890	0.27	3,570	0.12	1.070	3,420	3,945 ± 90§ 4,585 ± 105‖

* All the estimates are in yr BP and refer to 1980 as the base year.
† TF-744, radiocarbon date on bone carbonate of associated bone fragments.
‡ PRL-TL-42, TL date on *in situ* pottery.
§ TF-1005 and TF-1006, radiocarbon date on charred bone, depth 73–78 cm.
‖ TF-1009, radiocarbon date on charred bone, depth 89–98 cm.

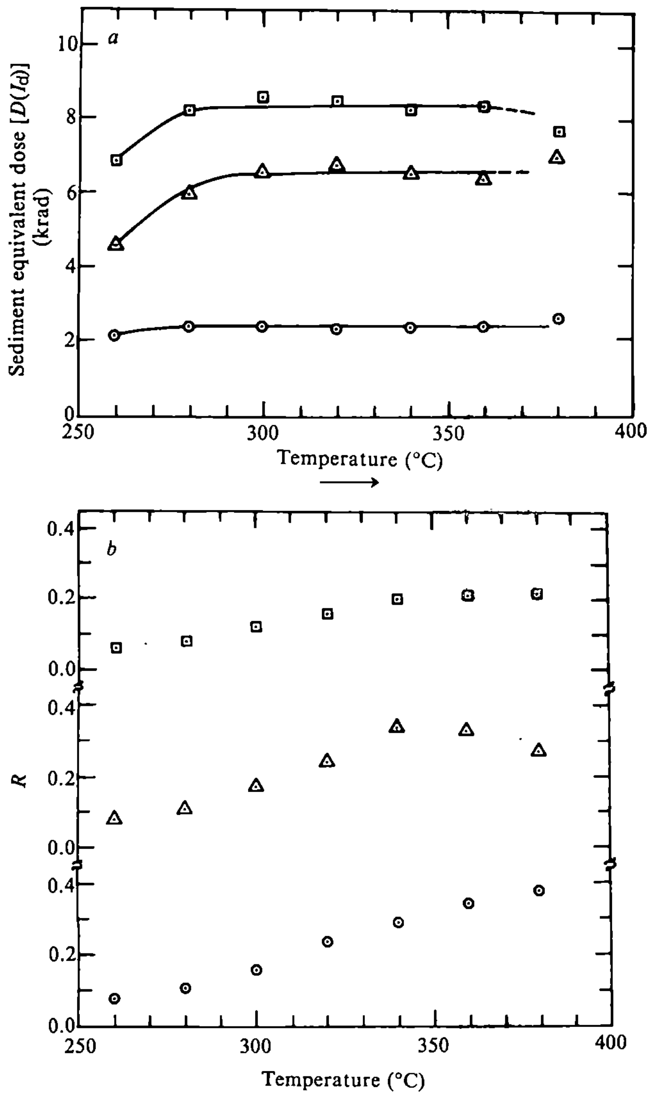

Fig. 3 *a*, Plots of $D(I_d)$ against glow curve temperature. □, TL-S-8; △, TL-S-10; ○, TL-S-13. *b*, Plots of R against glow curve temperature. Same symbols as in *a*.

simple, but has the advantage of circumventing any error due to sensitivity changes following a sunlamp exposure. The method therefore avoids any β exposure that is post-sunlamp bleach[4].

Table 1 summarizes the experimental data and Fig. 3 shows, for three of the samples, the dependence of $D(I_d)$ and R on the glow curve temperature. In most cases a good plateau (~80 °C) began at ~300 °C, as shown in Table 1. Because a glow curve is generally a composite of many glow peaks, the α efficiency (a), $D(I_{nat})$, $D(I_d)$ and R, were all estimated at regular intervals (10 °C) on the glow curves, and an age was estimated for each glow curve temperature. The estimates presented in Table 1 refer to a particular glow curve temperature (340 °C) and the final date is an average over the region where $D(I_d)$ showed a plateau.

A plateau behaviour of $D(I_d)$ in these samples also implies an age plateau as the α efficiency remains practically constant (a change of <10%) over the plateau region. Typical experimental errors are estimated to be 15%.

Note that the equivalent doses corresponding to both I_{nat} and I_d are only a few krads, indicating that the TL in the sample reflects a recent depositional event and not a geological dose. Also in all the cases the TL ages increase with depth; the average sand accretion rates are different for different periods; and the accretion rates are very small, suggesting a gradual buildup of dunes. Multiple exposures, in view of a very easy TL bleachability and very intense Sun exposures available in desert regimes, should not cause any significant errors in the estimates (dates) arrived at using TL. After all, only the last Sun-bleaching event is being dated.

In the Bagor sequence, the TL date of ~2,100 BP on S-13 agrees well with the TL date of ~2,060±210 yr BP on *in situ* pottery (PRL: TL: 42). The TL date of ~3,420 yr BP on S-14 also agrees reasonably well with the radiocarbon dates of 3,945±90 and 4,585±105 yr BP on adjacent coeval stratum. For S-11 a radiocarbon date of 3,990±100 yr BP for the associated bone (on carbonate) and the TL date of ~8,630 yr BP for dune sand from the same stratum seems sensible in view of the possible contamination of bone carbonate by modern carbon.

The agreement between these results confirms the applicability of the TL method in dating sand-dune deposits. The results also indicate that the formula used for estimation of $D(I_d)$, although simple, does provide sensible estimates.

We thank Professors M. J. Aitken, D. Lal and R. M. Walker for help and discussions, Drs V. N. Misra, S. N. Rajaguru and R. J. Wasson for samples and discussion. Y.P.S. acknowledges the grant of a fellowship by the Indian Department of Science and Technology.

Received 23 September; accepted 27 November 1981.

1. Shelkoplyas, V. N. in *Chronology of the Glacial Age* (eds Zubakov, V. A. & Kochegura, V. V.) 155–160 (Geographical Society USSR, Leningrad, 1971).
2. Wintle, A. G. *Nature* **289**, 479–480 (1981).
3. Wintle, A. G. & Huntley, D. J. *Nature* **279**, 710–712 (1979).
4. Wintle, A. G. & Huntley, D. J. *Can. J. Earth Sci.* **17**, 348–360 (1980).
5. Zimmerman, D. W. *Archaeometry* **13**, 29–52 (1971).
6. Agrawal, D. P., Bhandari, N., Lal, B. B. & Singhvi, A. K. *Proc. Ind. Acad. Sci.* (*E*) **90**, 161–172 (1981).
7. *Wotan Sunlamp* (Osram Gesellschaft, Berlin).
8. Gupta, J. P. *J. Hydrol.* **41**, 153–156 (1979).
9. Aitken, M. J. *Physics and Archaeology* 2nd edn (Oxford University Press, London, 1974).

Australian–Antarctic depression from the mid-ocean ridge to adjacent continents

J. J. Veevers

Australian Plate Research Group, School of Earth Sciences,
Macquarie University, North Ryde, New South Wales 2113,
Australia

A morphotectonic depression, some 15×10^6 km^2 in area and centred on the Australia–Antarctic discordance[1], extends across the southern half of Australia through the south-east Indian Ocean to Wilkes Land in Antarctica (Fig. 1*a*, *b*). The depression is co-extensive with a negative satellite free-air gravity anomaly[2] which suggests that the region is underlain by downward convecting asthenosphere. Here I outline the depression and explore its age. In a pre-breakup (>55 Myr) reconstruction (Fig. 1*c*), the Eastern Highlands of Australia and the Transantarctic Mountains are colinear; because the Eastern Highlands were notably high during the late Cretaceous, and shared with the Transantarctic Mountains a history of volcanism in the Jurassic, both highlands probably constituted the eastern flank of the past depression, in the centre of which thick (>8 km) late Cretaceous sediment in the Ceduna Saddle[3], and a possible mirror-image in offshore Antarctica, mark its depocentre. A broad area of late Carboniferous marine sediments in southern Australia[4] may represent the earliest sign of the depression.

The modern morphology of southern Australia and the opposite part of Antarctica (Fig. 1*a*) is dominated by a sinuous depression. A median morphological axis may be drawn through Lake Eyre (12 m below sea level) across the Australian–Antarctic discordance, where the south-east Indian Ocean Ridge (SEIR) has an anomalously low depth of 3.4 km, 1 km deeper than expected[5], to Adelie Land. Two parallel subsidiary axes can be defined: one from the Nullarbor Plain through the ocean to the Budd Coast and thence across an area of poorly-known sub-glacial bedrock topography into the sub-ice Aurora

0028-0836/82/040315—03$01.00

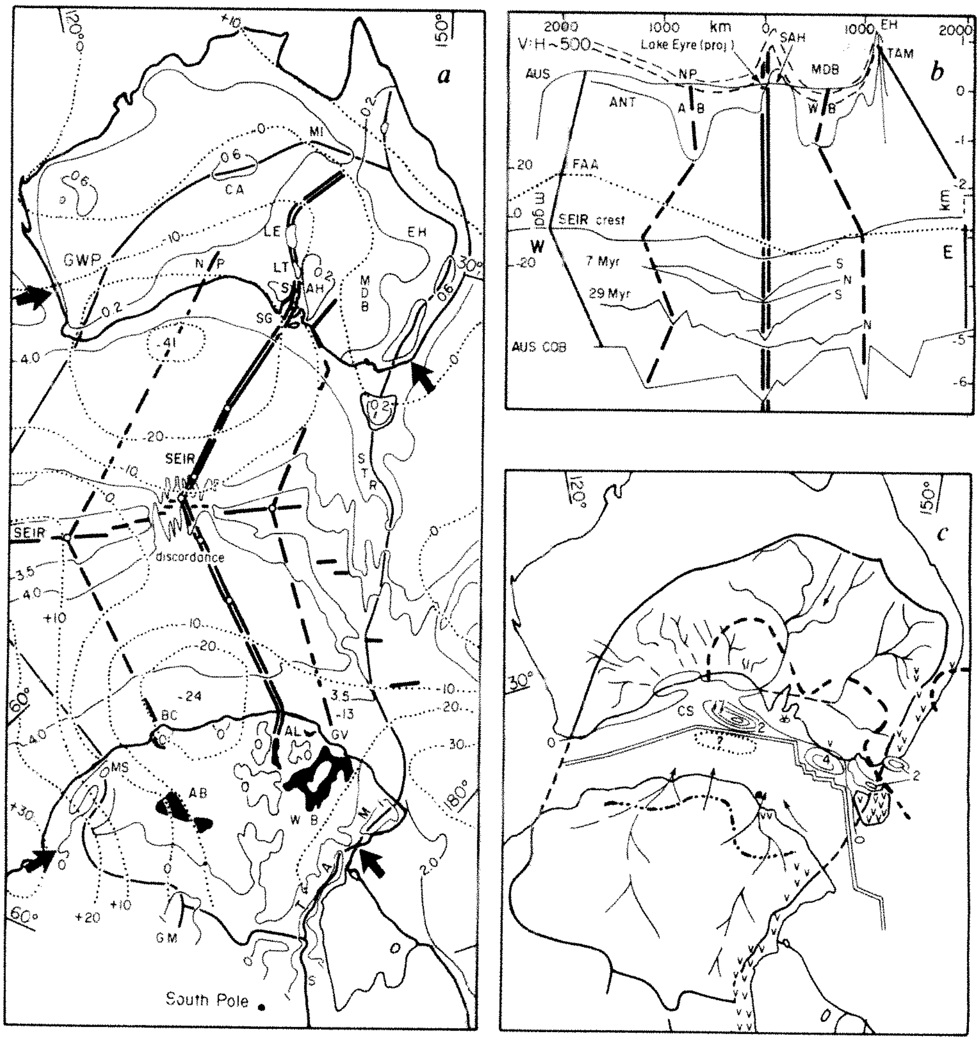

Fig. 1 *a*, Morphology of Australia (contours in km of 1° × 1° area mean rock altitude[21]), the south-east Indian Ocean[22], and Wilkes Land, Antarctica (sub-ice contours in km, < −1 km in black, refs 23–25), and satellite free-air gravity anomalies (in mGals, ref. 2) shown by dotted lines. The Australian–Antarctic depression is outlined (solid line) on the east by the crest of the Eastern Highlands (EH), Tasmania, the South Tasman Rise (STR), a high point on the crest of the south-east Indian Ocean Ridge (SEIR) at long. 150° E, and the Transantarctic Mountains (TAM); on the south by the sub-ice Gamburtsev Mountains (GM); on the west by Mt Sandow (MS), a high point on the crest of the SEIR at long. 95° E (not shown), and the Great Western Plateau (GWP); and on the north by central Australia (CA) and the Mt Isa block (MI). The median morphological axis of the depression (a double line) extends from Lakes Eyre (LE) and Torrens (LT) and Spencer Gulf (SG) within the South Australian Highlands (SAH) through the SEIR discordance[1] to Adelie Land (AL). Subsidiary lowland axes (broken lines) that lie on either side of the continental axial highlands extend on the west from the Nullarbor Plain (NP) to the Budd Coast (BC) and Aurora sub-ice basin (AB), and on the east from the Murray–Darling Basin (MDB) to George V Land (GV) and the Wilkes sub-ice basin (WB). Ends of arcuate continental profiles of *b* shown by arrow tips. Lambert equal-area projection. *b*, Profiles, from top downward, of southern Australia (with the Lake Eyre axis projected southward), Wilkes Land (sub-ice bedrock surface)—the broken lines above show the limits of the profile isostatically adjusted on an ice-free basis according to the method of Brotchie and Silvester[7]—, the crest of the south-east Indian Ocean Ridge (SEIR) and the satellite free-air gravity anomaly[2], the 7- and 29-Myr isochrons[1] on either flank of the SEIR, and the Australian continent–ocean boundary (COB)[3]. As in *a*, the axis is shown by a double line, subsidiary axes by broken lines, and the bounding ridges by a single line. *c*, Pre-breakup reconstruction of Australia and Antarctica (from B. D. Johnson and J.J.V, in preparation) with suture marked by the COB (double line). Present-day outlines of Australian–Antarctic depression, inferred to mark the Mesozoic position, shown by a heavy line, isopachs (km) of late Cretaceous sediments[12,26] by solid lines, direction of post-Cenomanian–late Cretaceous sediment transport[12,13] by arrows, post-Cenomanian–late Cretaceous drainage (a modified modern drainage in Australia, speculative in Antarctica) shown by networks, the single *in situ* occurrence of Mesozoic (Aptian) sediment in East Antarctica[16] by a dot, early and middle Jurassic (185–165 Myr) volcanic rocks[27–30] by Vs, and late Carboniferous (300 Myr) shorelines[4] by heavy broken lines. –·–·– Indicates the approximate position of the shoreline today on an ice-free basis. Note that the Eastern Highlands of Australia and the Transantarctic Mountains are colinear in this and previous reconstructions[31,32]. Lambert equal-area projection; grid applies to present-day Australia only.

basin; the other from the Murray–Darling drainage basin across the ocean to George V Land and thence into the sub-ice Wilkes basin. The profiles (Fig. 1*b*) have a gross symmetry about the median axis. The continental profiles differ from those of the ocean in having the median axis enclosed by highlands. The amplitude of the Antarctic profile is much greater than that of the others, but without its load of 4 km of ice, which has appeared only since the mid-Tertiary[6], the Antarctic profile would rebound by as much as 1 km, according to the method of Brotchie and Silvester[7], and the difference would be greatly reduced, although the great relief of the highlands about the axis would remain (broken lines in Fig. 1*b*).

The correspondence of topography with the satellite free-air anomaly at the discordance led Weissel and Hayes[1] to infer downward convecting currents in the asthenosphere, and the continuation of this correspondence both to the north and south leads me to infer that the entire depression is held down dynamically. How long has the depression existed, and hence how long has this dynamic state applied?

Stratigraphical[8], fission-track age[9], and palaeomagnetic[10] evidence indicate that the Southeast Highlands of Australia date back to the mid-Cretaceous. Voluminous coarse detritus shed into the rift-valley system along south-west Australia during most of the Mesozoic, and in particular during the late Jurassic and early Cretaceous[11], indicates late Mesozoic highlands in the west of Australia. Conclusive evidence of substantial relief in the late Cretaceous is provided by the depocentre of the Ceduna Saddle (Fig. 1*c*), which contains 0.5×10^6 km^3 of post-Cenomanian late Cretaceous sediment, and dwarfs the adjacent south-east Australian basins. If this were an extra-arch basin that formed in a saddle between major uplifts[3], all of its sediment would be derived from north of the suture, which, being marked by a rifted arch, constituted a dam across the centripetal drainage from the highland perimeter. Seismic profiles across the Ceduna Plateau[12] show that this sediment prograded into the sea towards the south. Barely any sediment lodged on the land, which consequently must have had higher stream gradients than at present. And the only known sediment of this post-Cenomanian–late Cretaceous age onshore is fluvial sandstone north-east of Lake Eyre with a southwestward direction of transport[13]. I speculate that the bulk of the sediment in the Ceduna Saddle came from the Eastern Highlands, and that the ancestral Murray–Darling drainage system crossed the site of the South Australian Highlands. With the subsequent uplift of these highlands in the Palaeocene, the Murray–Darling system was impeded, except perhaps for short intervals in the Eocene and Miocene[14], and as a result Cenozoic sediment was deposited to form the Murray Basin[8].

Little direct evidence of the age of the geomorphic elements is available in Antarctica. The Transantarctic Mountains in the Scott Glacier area (S in Fig. 1*a*) existed 18 Myr ago[15], and Drewry[6] argues for uplift in the late Eocene ($\sim$40 Myr ago) but their earlier history is unknown. The late Mesozoic existence of the eastern flank of the Australian–Antarctic Depression is postulated (Fig. 1*c*) because the terrains of the Transantarctic Mountains and the Eastern Highlands are linked today; were colinear before break-up; were the locus of Jurassic volcanism; and the Eastern Highlands stood high during the late Cretaceous. This speculation could be tested by palaeomagnetic and fission-track dating in Antarctica.

The single known *in situ* occurrence of Cretaceous sediment[16] in East Antarctica is Aptian and non-marine. Sediments of this age on the southern margin of Australia, which are also non-marine, in contrast to the widespread marine sediment of this age to the north, reflect the uplift about the suture before and during breakup. Symmetry with Australia about a presumed rift-valley arch[3] suggests a mirror-image of the Ceduna Saddle on offshore Antarctica, a speculation that could be tested by aeromagnetic and seismic surveys. Of the few published thicknesses of sediment off Antarctica[17], this area (at long. 127° E) contains $\sim$5 km of sediment, but how much of this predates break-up is unknown. This postulated depocentre presupposes feeding by an extensive drainage system; the low relief of the South Australian Highlands contrasts with the high Antarctic highlands that today rim the main axis of the depression, so that in the late Cretaceous the Antarctic part of the depression might have been drained by two centripetal networks. As in Australia, so in Antarctica the flanks of the depression may have had sufficient slope to prevent any large accumulation of sediment outside the depocentre, and the shoreline, which on an ice-free basis would now lie some distance inland, as outlined in Fig. 1*c*, probably lay at least as far north as the present coast, and sediment, as in the Ceduna depocentre, reached the postulated depocentre by marine progradation. In this view, the remotely sensed sediment at the axis of the Wilkes sub-ice basin[18] would be either Cenozoic (as in the Murray Basin) but pre-glacial (Palaeogene), or older than late Cretaceous.

The near-restriction of the late Carboniferous sea[4,19] to the southern part of Australia, and the inferred relief at this time of the South Australian Highlands[20] suggest that the morphology of the depression as it is today, with subsidiary lowland axes on either side of a median axis through a highland, is a repeat of that in the late Carboniferous.

I conclude that the morphological depression that extends from southern Australia through the south-east Indian Ocean to Wilkes Land, Antarctica, coincides with a negative gravity anomaly, suggesting that the depression is determined tectonically by downward convection in the asthenosphere. In Australia, the depression can be traced back to the late Cretaceous through a thick pile of sediment deposited in the offshore Ceduna Saddle midway across the southern margin between flanking highlands, and possibly to the late Carboniferous through a broad area of marine sediments in the central and eastern parts of southern Australia. In a pre-breakup ($>$55 Myr) reconstruction of Australia and Antarctica, the eastern flanks of the present depression, comprising the Eastern Highlands of Australia and the Transantarctic Mountains, are colinear; they are also linked by their common history of widespread volcanism in the Jurassic, so that like the Eastern Highlands, the Transantarctic Mountains were highlands during the late Cretaceous. It then follows that a mirror-image of the Ceduna Saddle, with a thick pile of late Cretaceous sediment, may exist in offshore Antarctica.

I thank P. G. Quilty and R. J. Tingey for help with references, J. G. Jones for valuable discussion, B. D. Johnson for comments, and the Australian Research Grants Committee for support.

Received 27 August; accepted 20 November 1981.

1. Weissel, J. K. & Hayes, D. E. *J. geophys. Res.* **79**, 2579–2587 (1974).
2. Anderson, R. N., McKenzie, D. & Sclater, J. G. *Earth planet. Sci. Lett.* **18**, 391–407 (1973).
3. Veevers, J. J. *J. Geol.* **89**, 57–82 (1981).
4. Veevers, J. J. & Evans, P. R. in *Gondwana Geology* (ed. Campbell, K. S. W.) 579–607 (ANU, Canberra, 1975).
5. Veevers, J. J. *Earth planet. Sci. Lett.* **34**, 100–106 (1977).
6. Drewry, D. J. *J. geol. Soc. Lond.* **131**, 255–273 (1975).
7. Brotchie, J. F. & Silvester, R. *J. geophys. Res.* **74**, 5240–5252 (1969).
8. Jones, J. G. & Veevers, J. J. *J. geol. Soc. Aust.* (in the press).
9. Morley, M. E., Gleadow, A. J. W. & Lovering, J. F. in *Gondwana Five* (eds Cresswell, M. M. & Vella, P.) 289–293 (Balkema, Rotterdam, 1981).
10. Embleton, B. J. J. & Schmidt, P. *J. geophys. Res.* **86**, 3998–4008 (1981).
11. Johnstone, M. H., Lowry, D. C. & Quilty, P. G. *J. R. Soc. W. Aust.* **96**, 5–15 (1973).
12. Fraser, A. R. & Tilbury, L. A. *Aust. Petrol. Explor. Ass. J.* **19**, 53–65 (1979).
13. Wopfner, H. *Trans. R. Soc. S. Aust.* **86**, 247–253 (1963).
14. Williams, G. E. & Goode, A. D. T. *Search* **9**, 442–447 (1978).
15. Stump, E., Sheridan, M. F., Borg, S. G. & Sutter, J. F. *Science* **207**, 757–759 (1980).
16. Domack, E. W., Fairchild, W. W. & Anderson, J. B. *Nature* **287**, 625–626 (1980).
17. Houtz, R. E. & Markl, R. G. *Am. geophys. Un. Antarctic Res. Ser.* **19**, 147–164 (1972).
18. Drewry, D. J. *Tectonophysics* **36**, 301–314 (1976).
19. McGowran, B. *Science* **180**, 759–761 (1973).
20. Wopfner, H. in *Gondwana Five* (eds Cresswell, M. M. & Vella, P.) 185–190 (Balkema, Rotterdam, 1981).
21. Wellman, P. *BMR J. Geol. Geophys.* **4**, 373–382 (1979).
22. *Bathymetric Chart of Antarctica* (in Russian) (Main Administration of Geodesy and Cartography, Moscow, 1974).
23. *General Bathymetric Chart of the Oceans* (GEBCO) 5.18 (Canad. Hydro. Serv., Ottawa, 1980).
24. Drewry, D. J. *Pol. Rec.* **17**, 359–374 (1975).
25. Masolov, V. N., Kurinin, R. G. & Grikurov, G. E. in *Gondwana Five* (eds Cresswell, M. M. & Vella, P.) 303–309 (Balkema, Rotterdam, 1981).
26. Richards, K. A. & Hopkins, B. M. *ECAFE Natural Resources Symp.* (Canberra, 1969).
27. Kyle, P. R., Elliot, D. H. & Sutter, J. F. in *Gondwana Five* (eds Cresswell, M. M. & Vella, P.) 283–287 (Balkema, Rotterdam, 1981).
28. Dulhunty, J. A. *J. R. Soc. N.S.W.* **105**, 71–76 (1972).
29. McDougall, I. & Wellman, P. *J. geol. Soc. Aust.* **23**, 1–9 (1976).
30. Schmidt, P. W. & McDougall, I. *J. geol. Soc. Aust.* **25**, 321–328 (1977).
31. Griffiths, J. R. *Nature* **249**, 336–337 (1974).
32. Weissel, J. K., Hayes, D. E. & Herron, E. M. *Mar. Geol.* **25**, 231–277 (1977).

Phylogeny and classification of thecodontian reptiles

Sankar Chatterjee

Department of Geosciences, Texas Tech University, Lubbock, Texas 79409, USA

Thecodontians have long been recognized as the basal stock from which all other archosaurs were derived, but their phylogeny and classification are very confused, and the origin and evolution of archosaurs are consequently still poorly understood. The skull and skeletal morphology of thecodontians is confusingly uniform, and many palaeontologists feel that the ankle joint may provide a more useful clue to the phylogeny and classification of these groups[1,2]. I attempt here to trace some of the thecodontian lineages on the basis of tarsal anatomy. The major structural changes from thecodontian to dinosaurs are most clearly visible in the pelvis and hind-limbs, associated with improvement of gait from the 'sprawler' through the 'semi-improved' to the 'fully-improved' condition[3,4]. As a result, the function of the ankle joint was modified from a simple flexible base for the leg to the more advanced role of a lever. For this reason, an understanding of thecodontian tarsi is necessary if we are to understand the evolution of the later archosaurs.

Existing classifications[5-7] recognize four suborders within Thecodontia: (1) Proterosuchia, primitive quadrupeds with no armour, such as *Proterosuchus* and *Erythrosuchus*; (2) Aetosauria, armoured, herbivorous quadrupeds, such as *Stagonolepis* and *Typothorax*; (3) Parasuchia, long-snouted parasuchids (phytosaurs); (4) Pseudosuchia, various unrelated groups such as ornithosuchids, sphenosuchids, rauisuchids and euparkeriids. Pseudosuchia constitutes the largest and most heterogeneous group and may be regarded as the 'catch all' suborder into which it has been customary to place all thecodontians other than the Proterosuchia. Although these four categories are accepted by most workers, opinions differ greatly concerning the classification and grouping of the lower ranks; many of the genera are known only from fragmentary and incomplete material, and the interrelationships among them are obscure.

The thecodontian tarsus, where adequately known, consists of two large proximal elements, the astragalus and calcaneum, and two smaller distal tarsals, usually identified as the third and

0028-0836/82/040317—04$01.00

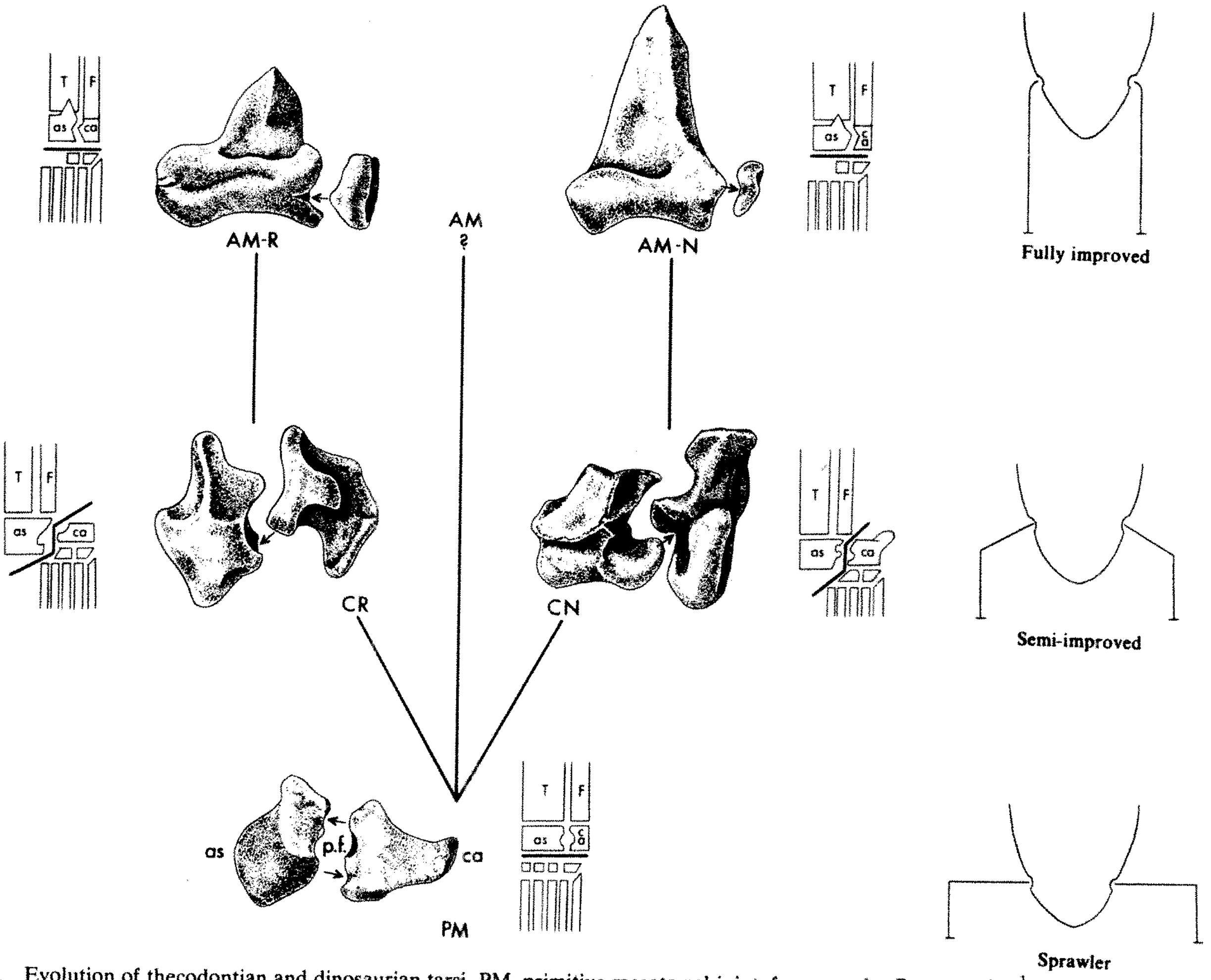

Fig. 1 Evolution of thecodontian and dinosaurian tarsi. PM, primitive mesotarsal joint, for example, *Proterosuchus*[1]; CN, crocodile-normal joint, for example, poposaurid (TTU 9001); CR, crocodile-reverse joint, for example, *Riojasuchus*, drawn from the cast MCZ 4894 (reversed); AM, advanced mesotarsal joint as seen in dinosaurs; AM-R, advanced mesotarsal-reverse joint, for example, *Allosaurus*[20]; AM-N, advanced mesotarsal-normal joint, for example, *Albertosaurus*[21]. All views of the tarsal structure are left anterior; arrow indicates the position of the socket opposite to the corresponding peg; the postures associated with corresponding ankle structures are shown in the right column[3]. Abbreviations: as, astragalus; ca, calcaneum; p.f., perforating foramen; T, tibia; F, fibula. Institutional acronyms: MCZ, Museum of Comparative Zoology, Harvard University; TTU, Texas Tech University.

fourth. Primitive forms also retain free centrale and distal tarsals I and II. The way in which the astragalus and calcaneum articulate with each other and function in relation to the crus and pes is the major characteristic used to classify Thecodontia.

A survey of the thecodontian tarsi reveals that four basic types of ankle joint have evolved in this group of reptiles (Fig. 1):

(1) Primitive mesotarsal (PM) joint: This is the most primitive ankle joint, exemplified by *Proterosuchus*[1], where the astragalus and calcaneum are firmly articulated with the crus, and the hinge of the ankle runs transversely between the proximal and distal rows of the tarsi. The astragalus and calcaneum articulate with each other by means of double convex–concave complementary facets, with a perforating foramen between them. Proximal to the foramen, a concavo–convex joint is present, with the concavity on the astragalus, whereas distal to the foramen the reverse is the case. The calcaneum has a laterally extending tuber. This type of joint occurs in various eosuchians and rhynchosaurs exhibiting a sprawling gait[8]. The arrangement is a precursor to the crocodilian pivot joint[1,2].

Although erythrosuchid tarsi[1] have a perforating foramen between the astragalus and calcaneum similar to that seen in the PM joint, and could therefore be derived from this joint, poor ossification obscures the details of the astragalo–calcanear joint. Cruickshank[9] maintained that such a specialized ankle (highly abbreviated astragalus and calcaneum) indicates that erythrosuchids are a 'dead-end line' that could not have given rise to any other group. The tarsus of *Erythrosuchus* is best considered as a poorly ossified PM joint, and the reduction of ossification may reflect the animal's aquatic habitat.

(2) Crocodile-normal (CN) joint: This pivotal joint between astragalus and calcaneum is found in extant crocodilians[10] and in many thecodontians[11,12]. It differs structurally from the PM joint in that: the calcaneal tuber is extended posteriorly and the perforating foramen has been eliminated; the lower convexo–concave joint is highly elaborated so that the astragalus forms a peg which fits into a deep socket of the calcaneum, allowing rotational movement about a horizontal axis; the calcaneum has developed a rolling convex surface proximally for sliding on the fibula. Functionally the tarsus differs from the PM joint in that the astragalus forms part of the crus, but the calcaneum, distal tarsals and the combined metatarsals move as a unit on the astragalus and fibula. The modification of the CN joint from the PM joint is associated with an improvement in gait from the sprawler to the semi-improved condition[3]. The CN joint occurs in rauisuchids[12,13], stagonolepidids[14,15], parasuchids[16], sphenosuchids[17], *Gracilisuchus*[18] and in poposaurids. Parasuchian tarsi[16] show an intermediate stage between PM and CN joints, where the perforating foramen is highly reduced or lost, the peg and socket joint are not pronounced, and the calcaneum has developed a rolling convex surface for sliding on the fibula, which indicates that some rotational movement was possible at this joint. However, the calcanear tuber is directed laterally, as in the PM joint.

(3) Crocodile-reverse (CR) joint: Bonaparte[5] first recognized this type of pivot joint in ornithosuchids, in which the peg is on the calcaneum and the socket on the astragalus, the opposite condition to that in the CN joint. The calcaneum has a sliding convex surface for the fibula and the perforating foramen

Table 1 Classification of Thecodontia

Nature of ankle joint	Order Thecodontia Owen, 1859
PM joint	1. Suborder Proterosuchia Family Proterosuchidae Broom, 1906 Family Erythrosuchidae Watson, 1917
CN joint	2. Suborder Pseudosuchia a. Infraorder Parasuchia Family Parasuchidae Lydekker, 1885 b. Infraorder Aetosauria Family Stagonolepididae Lydekker, 1887 c. Infraorder Rauisuchia Family Rauisuchidae von Huene, 1942 Family Poposauridae Nopsca, 1928
CR joint	3. Suborder Ornithosuchia Family Ornithosuchidae von Huene, 1908 Family Euparkeriidae von Huene, 1920
AM joint	4. Suborder Lagosuchia Family Lagosuchidae Bonaparte, 1975
Unknown	Thecodontia incertae sedis Family Proterochampsidae Sill, 1967 Family Scleromochlidae von Huene, 1914 Family Dosweliidae Weems, 1980 Family Longisquamidae Sharov, 1970

between the two elements is lost. Cruickshank[1] suggested that the CR joint is present in *Chanaresuchus* (Proterochampsidae), but the critical region of the astragalo–calcanear articulation in available specimens is badly damaged, and thus obscures the nature of ankle joint.

Cruickshank[1] showed that the PM joint is an excellent structural ancestor to both CN and CR joints. The major changes involved in such a transition would be the re-orientation of the calcaneal tuber posteriorly, with the development of the convex sliding surface of the fibula on the calcaneum and the elimination of the perforating foramen. According to Cruickshank, in the CN joint, the lower convexo–concave joint below the perforating foramen was elaborated so that the astragalus formed the peg and the calcaneum the socket. In the CR joint, he believes, the proximal concavo–convex joint was elaborated.

Although the evolution of the CN joint from the PM joint seems straightforward, closer scrutiny reveals that this may not be the situation for the CR joint. Rather, the peg on the calcaneum can be interpreted as being homologous to the whole medioventral process of the calcaneum of the CN or PM type. As a result, the peg of the astragalus below the articulation remains free and wraps around the undersurface of the calcaneum. This indicates that the CR joint might have evolved from the PM joint, not by the elaboration of the upper concavo–convex facets as Cruickshank envisaged, but by the upward migration of the calcaneum above the level of the astragalar peg (Fig. 1).

Both CN and CR joints are associated with the presence of a semi-improved gait, but they differ functionally in that the CN joint is more flexible and allows a greater degree of rotation between the astragalus and calcaneum than does the CR joint. In the CN joint, the peg is directed horizontally, whereas in the CR joint it is projected almost downward. As a result, the CR joint is a better locking and stabilizing device, and is better adapted to withstand the body weight than is the CN joint.

(4) Advanced mesotarsal (AM) joint: Functionally this is similar to the PM joint in that the hinge movement occurs between the proximal and distal rows of the tarsi. However, the astragalus is a mediolaterally elongated hemi-cylinder with an ascending dorsal process for locking the tibia; the calcaneum is reduced and lacks the 'heel'; the perforating foramen is absent. The joint is found in *Lagosuchus*[18] among thecodontians, and in all dinosaurs.

The AM joint could have evolved not only from the PM joint, but also from the CN and CR joints. There are vestiges of the peg and socket in many forms, and accordingly two subtypes of AM joint (AM-normal (N) and AM-reverse (R)) have been distinguished. In *Lagosuchus*[18], the calcaneum shows a rudimentary peg which fits into a corresponding socket of the astragalus, exhibiting the AM-R type. In *Pisanosaurus*[19], the earliest ornithischian dinosaur, the ankle retains the rudimentary peg and socket, but their relationships are not known. Cruickshank[1] remarks that in coelurosaurs, ornithischians and prosauropods, the joint may be of the AM-N type, whereas it may be of the AM-R type in sauropods and carnosaurs. At present, the dinosaur tarsi need very careful analysis before any such generalizations can be made. In most sauropods, the

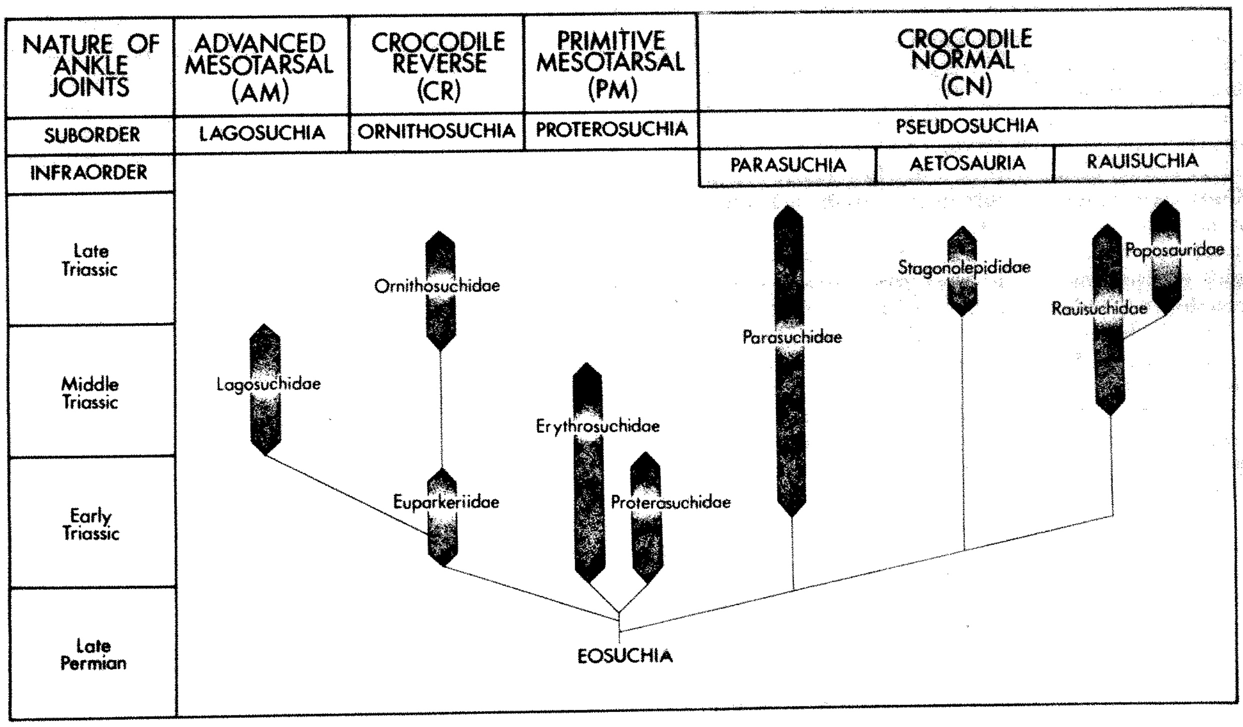

Fig. 2 The phylogeny and classification of Thecodontia.

structure of the calcaneum remains unknown, and the astragalus shows no distinct articular surface for the calcaneum. Among carnosaurs two distinct varieties can be seen. Walker[11] has suggested that two phyletic lines exist within carnosaurs, Megalosauroidea and Tyrannosauroidea, the former showing an AM-R joint and the latter an AM-N joint (Fig. 1)[20,21]. The diversity of AM joints suggests several origins of this type of ankle from different thecodontian lineages, and supports the concept of dinosaur polyphyly[14,22], not the converse[18,23].

The interpretation of the structural evolution of the thecodontian tarsus presented here implies the relationships shown in Fig. 2. This is translated into a classification (see Table 1) which differs from the existing classifications[5-7] in the following points: (1) each suborder is defined by a distinctive pattern of ankle joint. (2) Suborder Pseudosuchia is restricted to those taxa showing a CN joint. Parasuchia (*nom. transl. ex.* Suborder Parasuchia Huxley, 1875) and Aetosauria (*nom. transl. ex.* Suborder Aetosauria Lydekker, 1889) are considered herein as infraorders within Pseudosuchia. Infraorder Rauisuchia (*nom. transl. ex.* Rauisuchidae von Huene, 1942) is shown here to include the two closely related families Rauisuchidae and Poposauridae. Rauisuchia is regarded as a sister group of Aetosauria, and the two together as sister groups of Parasuchia. (3) Ornithosuchidae and Euparkeriidae are removed from Pseudosuchia and grouped into a new Suborder Ornithosuchia (*nom. transl. ex.* Infraorder Ornithosuchia Bonaparte, 1971). (4) *Sphenosuchus*, *Saltoposuchus* and *Hesperosuchus* are considered as Paracrocodylia[17]. (5) Lagosuchidae is removed from Pseudosuchia and promoted to a separate subordinal status Lagosuchia (*nom. transl. ex.* Lagosuchidae Bonaparte, 1975). (6) Proterochampsidae, Scleromochlidae, Dosweliidae and Longisquamidae are regarded as Thecodontia incertae sedis.

I thank Drs A. R. I. Cruickshank, A. D. Walker, P. M. Galton, Nicholas Hotton, Donald Brinkman and Mike Parrish for critically appraising the manuscript and for constructive suggestions, Dr Brinkman for access to *Riojasuchus* material and Mr Mike Nickell for illustrations. The research was supported by the National Geographic Society and Texas Tech University.

Received 20 July; accepted 9 December 1981.

1. Cruickshank, A. R. I. *S. Afr. J. Sci.* **75,** 168 (1979).
2. Thulborn, R. A. *Alcheringa* **4,** 241 (1980).
3. Charig, A. J. in *Studies in Vertebrate Evolution* (eds Joysey, K. A. & Kemp, T. S.) 708 (Oliver & Boyd, Edinburgh, 1972).
4. Bakker, R. T. *Evolution* **25,** 363 (1971).
5. Bonaparte, J. F. *Op. lilloana* **22,** 1 (1971).
6. Romer, A. S. *Breviora* **395,** 1 (1972).
7. Charig, A. S. in *Handbuch der Paläoherpetologie* Vol. 13 (ed. Kuhn, O.) 7 (Gustav Fischer, Stuttgart, 1976).
8. Carroll, R. L. *Ann. S. Afr. Mus.* **72,** 37 (1976).
9. Cruickshank, A. R. I. *Zool. J. Linn. Soc.* **62**(2), 161 (1978).
10. Schaeffer, B. *Bull. Am. Mus. nat. Hist.* **78,** 395 (1941).
11. Walker, A. D. *Phil. Trans. R. Soc.* **B248,** 53 (1964).
12. Krebs, B. *Schweiz. palaeont. Abh.* **81,** 1 (1965).
13. Sill, W. D. *Bull. Mus. comp. Zool. Harvard* **146,** 317 (1974).
14. Sawin, H. J. *J. Paleont.* **21,** 201 (1947).
15. Walker, A. D. *Phil. Trans. R. Soc.* **B244,** 103 (1961).
16. Chatterjee, S. *Palaeontology* **21,** 83 (1978).
17. Walker, A. D. *Phil. Trans. R. Soc.* **B257,** 323 (1970).
18. Bonaparte, J. F. *Acta geol. lilloana* **13,** 5 (1975).
19. Bonaparte, J. F. *J. Paleont.* **50,** 808 (1976).
20. Madsen, J. H. Jr *Utah geol. min. Surv.* **109,** 1 (1976).
21. Lambe, L. M. *Mem. geol. Surv. Can.* **100,** 1 (1917).
22. Charig, A. S. *Linn. Soc. Lond. Symp.* Ser. 3, 65 (1976).
23. Bakker, R. T. & Galton, P. M. *Nature* **248,** 168 (1974).

Tropical legumes of the genus *Stylosanthes* immobilize and kill cattle ticks

Robert W. Sutherst*, Raymond J. Jones† & Herbert J. Schnitzerling*

* CSIRO Division of Entomology, Long Pocket Laboratories,
PMB 3, Indooroopilly, Queensland 4068, Australia
* CSIRO Division of Tropical Crops and Pastures,
Davies Laboratory, PMB, PO Aitkenvale, Townsville,
Queensland 4814, Australia

Ticks affect 800 million cattle and a similar number of sheep worldwide[1] and their control by chemical 'dipping' is expensive and threatened by the widespread development of resistance[2]. Resistant varieties of crops have been used widely to control phytophagous insects[3], but larvae of all species of hard ticks (Ixodidae) ascend plants only in order to transfer to a passing host. Contacts with hosts are infrequent thus the ticks must often wait in the pasture for several weeks[4]. A substantial reduction in the life expectancy of such larvae would lower populations of the damaging parasitic stages. Molasses grass *Melinis minutiflora*, has been shown to reduce tick survival but the effect is small and slow[5]. Some highly productive, nutritious varieties of the tropical pasture legume *Stylosanthes*[6,7], are covered in glandular trichomes or hairs which secrete a viscous fluid. Such trichomes are well known for their role in defence against a variety of plant-feeding insects[3,8]. We report here that two South American species of *Stylosanthes* produce sticky secretions which immediately immobilize larvae of the cattle tick, *Boophilus microplus*. The larvae are poisoned within 24 hours by an unidentified vapour from the secretions. The legumes appear to have the potential to substantially reduce populations of all species of ticks in the extensive tropical and subtropical areas in which *Stylosanthes* sp. can be grown in pasture.

Following preliminary observations, pots were set up, each containing six to eight plants of each species or cultivar of the perennial legumes: *Stylosanthes hamata* cv. Verano; *Stylosanthes scabra* cv. Fitzroy or Seca, CPI 34925 (Commonwealth Plant Introduction number); and *Stylosanthes viscosa*, CPI 34904 and these were grown until near first flowering.

We released tick larvae onto each type of legume and compared survival per pot with that on a control pot made up of a narrow-leafed grass (*Eragrostic tenuifolia*) and one of a broad-leafed grass (*Panicum maximum*). On each occasion, two pots containing the legume of interest were used to make comparisons. Tick larvae (10,000; the progeny of 4–5 female ticks) were released on to the base of the plants in each pot at 20–24 °C. The pots were placed in trays of water to prevent any ticks escaping. On days 1 and 6 after release, live and dead larvae adhering to the trichomes were counted by destructive sampling of the plants.

Differences in larval survival rates between the various treatments were such that statistical analysis was unnecessary (Fig. 1). No larvae reached the tips of untrimmed plants of *S. scabra* and *S. viscosa*. Larvae were immobilized and killed on the glandular hairs of both species within 24 h (Fig. 2) while most of their siblings which had established themselves on grass or on *S. hamata* were alive. The viscous secretion had no repellent properties so that the ticks, which are negatively geotropic, did not attempt to retreat and seek alternative plants. Despite the very large numbers of larvae trapped, each plant was capable of trapping many more.

Table 1 Model predictions of the percentage reductions in numbers of *B. microplus* after trapping of larvae by pubescent *Stylosanthes* for different periods each year

% *Stylosanthes* in pasture	Duration of trapping period (months) 4	6	9
20	48	65	75
40	77	90	96
60	93	98	99+

We investigated the mechanism by which larvae were killed; larvae placed on adhesive tape were still alive after being held for 48 h, whereas others that had been trapped *in situ* on *S. scabra* were all dead after 24 h. We therefore concluded that physical restraint of the larvae was not alone responsible for

0028-0836/82/040320—02$01.00

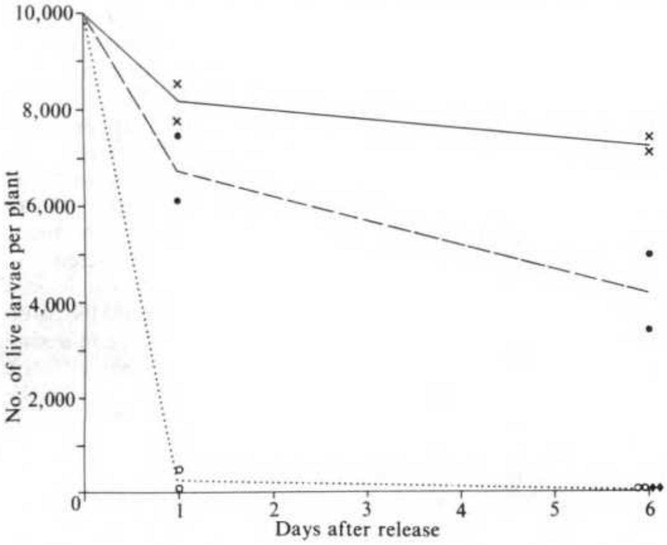

Fig. 1 Numbers of live *B. microplus* larvae recovered from pots containing different types of pasture plants onto which 10,000 larvae had been released. ×, Grass; ●, *S. hamata*; ○, *S. scabra*; ◆, *S. viscosa*.

their death, although in practice it would be adequate to prevent them attaching to a host. The contact toxicity of the secretion was tested by removing it from the trichomes with a small wad of cotton wool which was then extracted with hot methanol. The methanol was evaporated and the residue dissolved in ethanol containing 2% Triton X-100. This was then added to water to give a colloidal suspension. Larvae were dipped for 4 min in suspensions of the extract as described elsewhere[9]. The extract suspension concentrations up to 0.3% w/v failed to kill larvae within 48 h. As conventional acaricides in similar conditions are toxic at concentrations below 0.001% w/v (ref. 9 and H.J.S., unpublished data) we considered the extract to be non-toxic.

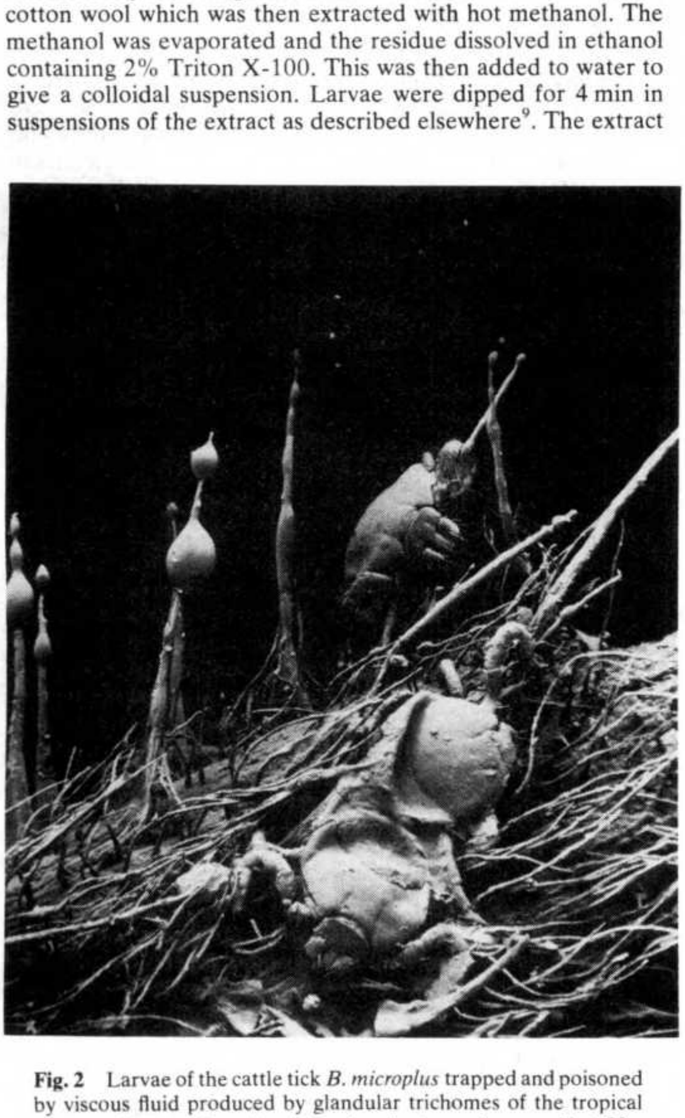

Fig. 2 Larvae of the cattle tick *B. microplus* trapped and poisoned by viscous fluid produced by glandular trichomes of the tropical pasture legume *S. scabra* (scanning electron micrograph). ×50.

The secretion had a characteristic odour, suggesting that the toxic agent might be volatile. If so it would have evaporated during preparation of the extract. The possibility of fumigant action was tested by collecting the secretion from three stems of *S. scabra*, ~15 cm long, using three pieces (16 cm^2) of fine nylon gauze. The gauze was crumpled and placed inside a larva-proof stainless steel gauze cylinder (1 cm × 1 cm). The cylinder was securely capped and held firmly in the middle of a 5 × 1.2 cm glass vial. Approximately 200 larvae were brushed on to the inside of the glass vial which was then secured at the open end with larva-proof nylon gauze. Vials were incubated at 30 °C and 85–100% relative humidity. The larvae in the vials, while being exposed to any volatile component, were not in direct contact with the secretion. This experiment was repeated three times. After 36 h, 94% of the larvae were dead while all control larvae in glass tubes without the viscous fluid were alive. Investigations are under way to isolate and characterize the toxicant.

The results demonstrate that those *Stylosanthes* species that possess glandular hairs have an extremely severe and rapid effect on tick larvae. Preliminary observations on *Stylosanthes guianensis* have shown that some accessions to the Australian collection have comparable effects on ticks to those reported here for *S. scabra* and *S. viscosa*. The effect greatly exceeds that reported for molasses grass, on which there were still 15–20% as many larvae as on other grasses 14 days after infestation[5]. If these results for *Stylosanthes* are reproducible in the field, it may be possible substantially to reduce tick populations throughout much of the tropics and subtropics. The legumes not only trap larval ticks but also improve cattle nutrition, which should enhance their resistance to ticks[10]. This effect will depend on the percentage cover of legume in a pasture and on the duration of the secretory period. Computer simulations using a model of *B. microplus* populations[11], with four generations per year, showed that the legumes are likely to reduce substantially equilibrium tick populations (Table 1). The effect may be enhanced by the observed accumulation of the secretions, especially of *S. viscosa*, on the legs and heads of grazing cattle. The exploitation of pasture plants that are detrimental to ticks is an attractive notion, particularly if the plants also improve the productivity of grazing animals.

The genus *Stylosanthes* will grow in a wide range of climates and soils[7], and it is likely that the legumes will be equally effective against all tropical and subtropical ticks which use pasture plants as a support while host-seeking. The specialized behaviour of tick larvae makes them particularly vulnerable to such a trap.

We thank Mr J. Darley (James Cook University of North Queensland) for photography, Mr D. A. Stegeman and Ms J. Everson for technical assistance, and the Australian Meat Research Committee for contributing funding. Dr J. Nolan and D. P. Sands provided helpful support and several colleagues gave helpful criticisms of the manuscript.

Received 21 October; accepted 14 December 1981.

1. Snelson, J. T. *Pl. Prot. Bull. F.A.O.* **23,** 103–114 (1975).
2. Wharton, R. H. & Norris, K. R. *Vet. parasit.* **6,** 135–164 (1980).
3. Norris, D. M. & Kogan, M. in *Breeding Plants Resistant to Insects* (eds Maxwell, F. G. & Jennings, P. R.) 24–61 (Wiley, New York, 1980).
4. Sutherst, R. W., Dallwitz, M. J., Utech, K. B. W. & Kerr, J. D. *Aust. J. Zool.* **26,** 159–174 (1978).
5. Thompson, K. C., Roa, J. & Romero, T. *Trop. anim. Hlth Prod.* **10,** 179–182 (1978).
6. Burt, R. L., Reid, R. & Williams, W. T. *Agro-Ecosystems* **2,** 293–307 (1976).
7. Edye, L. A. & Grof, B. in *Genetic Resources of Forage Plants* (eds McIvor, J. G. & Bray, R. A.) (CSIRO, Melbourne, in the press).
8. Levin, D. A. *Q. Rev. Biol.* **48,** 3–15 (1973).
9. Schnitzerling, H. J., Schuntner, C. A., Roulston, W. J. & Wilson, J. T. *Aust. J. biol. Sci.* **27,** 397–408 (1974).
10. Sutherst, R. W. & Utech, K. B. W. in *CRC Handbook of Pest Management in Agriculture* Vol 2 (ed. Pimentel, D.) 385–407 (CRC Press, Boca Raton, Florida, 1981).
11. Sutherst, R. W., Norton, G. A. & Maywald, G. F. in *Ticks and Tick-borne Diseases* (eds Johnston, L. A. Y. & Cooper, M. G.) 46–51 (Australian Veterinary Association, Sydney, 1980).

Role of gut flora in the genotoxicity of dinitrotoluene

Jon C. Mirsalis*, Thomas E. Hamm Jr, J. Michael Sherrill & Byron E. Butterworth

Chemical Industry Institute of Toxicology, PO Box 12137,
Research Triangle Park, North Carolina 27709, USA

Dinitrotoluene (DNT), an important industrial nitroaromatic compound, is a potent hepatocarcinogen in rats. Male Fischer-344 rats fed technical-grade DNT in the diet for 12 months showed a 100% incidence of hepatocellular carcinomas[1]. However, various *in vitro* and *in vivo* short-term tests using several genotoxic end points have failed to show activity with DNT or purified DNT isomers[2-6], including unscheduled DNA synthesis (UDS) in primary hepatocytes *in vitro*[7]. In the *in vivo–in vitro* hepatocyte DNA repair assay, which measures chemically induced UDS in hepatocytes isolated from rats treated *in vivo*[8], DNT was found to be a potent UDS inducer[9] having a peak of activity 12 h after a single dose. A possible explanation for the discrepancy between the *in vivo* and *in vitro* results is that metabolism by gut flora may be required for formation of the proximate or ultimate carcinogenic metabolites of DNT. The importance of biotransformation of toxicants by intestinal microflora has been demonstrated for cycasin[10,11] and other xenobiotics[12]. We have used the *in vivo–in vitro* hepatocyte DNA repair assay to study the role of intestinal microflora in DNT genotoxicity. We report here extensive DNT-induced DNA repair in rats having the normal complement of gut flora, but not in rats which have no gut flora. These results indicate that metabolism of DNT by gut flora is a necessary step in the genotoxicity of this compound and illustrate the value of the *in vivo–in vitro* hepatocyte DNA repair assay in assessing the carcinogenic potential of nitroaromatic compounds.

Germ-free (axenic) male Fischer-344 rats (CDF (F-344)/CrlGN) were obtained in sterile isolators from Charles River Breeding Laboratories. Two weeks previously, one group was associated with Charles River Altered Schaedler Flora (CRASF), a mixture of eight anaerobic bacterial strains similar to the normal gut microflora of rats (R. P. Orcutt, personal communication). Rats were maintained on Agway 7RF Autoclavable Rodent Diet while in transit and after arrival. Both the non-associated and associated groups of rats were given 100 mg per kg sterile DNT by gavage in sterile corn oil. (DNT was sterilized by dissolving in absolute ethanol, filter sterilizing (0.45 μm filter) and recrystallizing. Using gas chromatographic analysis, the isomeric proportions were found to be essentially unchanged.) Primary hepatocyte cultures were prepared 12 h later, cultured with ^{3}H-thymidine and UDS measured by quantitative autoradiography as previously described[8]. Cells were scored for net grains per nucleus, calculated as the silver grains overlying the nucleus minus the highest of the grain counts overlying three adjacent nucleus-sized areas of the cytoplasm; 50 cells were scored for each of three slides per animal. A cell with ≥ 5 net grains per nucleus was considered to be in repair.

Rats associated with CRASF showed a marked increase in UDS after DNT treatment (Table 1), whereas axenic rats showed no increase in UDS. Dimethylnitrosamine (DMN), used as a positive control, gave a large increase in UDS, confirming the ability of axenic animals to carry out excision repair of DNA after exposure to a genotoxic agent. This is consistent with the response induced by DMN in conventional animals[8].

The caecal contents of each rat were cultured to confirm its bacterial status; those of the associated animals contained the complete CRASF flora. Several of the non-associated animals were found to be contaminated with one or two bacterial strains. These animals, however, showed only low bacterial counts compared with those found in the CRASF-associated rats. Non-associated rats contaminated with *Streptococcus faecalis* showed a small increase in UDS after DNT treatment while non-associated rats contaminated with *Clostridium perfringens* showed no increase (Table 1). None of the contaminants were CRASF constituents, although *S. faecalis* and *C. perfringens* are frequently found in the normal gut flora of man and conventional laboratory animals. Thus, the level of DNT-induced UDS in the rats that did not have the normal complement of gut flora was significantly lower ($P < 0.01$) than that seen in rats having the complete complement.

The absence of UDS in axenic animals clearly demonstrates a requirement for metabolism by gut flora in order for DNT to be genotoxic. Other studies have indicated that intestinal flora play a part in DNT metabolism. Following treatment of axenic rats with 2,4-DNT, two of the four major urinary metabolites seen in conventional rats were substantially decreased[13]. Metabolism of 2,4-DNT by rat intestinal flora *in vitro* showed reduction of 2,4-DNT to 2-amino-4-nitrotoluene (2-A-4-NT), 2-nitro-4-aminotoluene (2-N-4-AT) and 2,4-diaminotoluene (2,4-DAT)[14]. Isolated rat hepatocytes were unable to produce 2,4-DAT, 2-A-4-NT or 4-A-2-NT at physiological oxygen concentrations[15]. The results of our DNA repair studies combined with metabolism studies provide strong evidence that reductive metabolism in the gut is necessary for formation of a genotoxic metabolite of DNT.

Short-term *in vitro* tests for genotoxicity are widely used as supportive data in the evaluation of the potential carcinogenicity of chemicals[16]. However, these assays do not reflect the species,

Table 1 Induction of UDS in CRASF-associated and non-associated rats 12 h after DNT treatment

Bacterial status	Chemical	Dose (mg per kg)	(*n*)	Net grains per nucleus	% In repair
Associated animals					
Complete CRASF	Control	–	2	−4.2 ± 0.5	7 ± 2
Complete CRASF	DNT	100	4	18.7 ± 1.3	87 ± 3
Non-associated animals					
Axenic	Control	–	1	−3.6	3
Bacillus licheniformis + Clostridium perfringens	Control	–	1	−4.3	1
Total control			**2**	**−4.0 ± 0.4**	**2 ± 1**
Axenic	DNT	100	2	−0.8 ± 0.2	14 ± 2
Streptococcus faecalis	DNT	100	2	2.9 ± 0.7	34 ± 4
Clostridum perfringens	DNT	100	2	−3.5 ± 0.2	4 ± 2
Total DNT		**100**	**6**	**−0.5 ± 1.2**	**18 ± 6**
Axenic	DMN	10	1	43.7	97

Dimethylnitrosamine (DMN) was administered 2 h before killing as a positive control. Controls received corn oil only. *n*, Number of treated animals. The bacterial content of each animal was determined from caecal contents at killing. Axenic means that caecal contents were sterile. Low levels of bacteria found in the non-associated group were adventitious contaminants. Standard errors shown represent animal-to-animal variation. The per cent in repair is the per cent of cells with ≥ 5 net grains per nucleus.

0028–0836/82/040322—02$01.00

sex and organ specificities commonly observed in chemical carcinogenesis. Existing or future systems which will allow the evaluation of chemically induced genotoxic effects in the whole animal should provide a more realistic means of evaluating the potential hazards of be appropriate for evaluating genotoxicity of nitroaromatic and, perhaps, other compounds. In addition, the *in vivo* assays which measure genotoxicity in a target tissue that does not develop cancer[6] may also be inappropriate. The *in vivo–in vitro* hepatocyte DNA repair assay has been demonstrated to be extremely useful for the study of DNT genotoxicity and should, therefore, be one of the primary tests chosen to examine the genotoxicity of nitroaromatic compounds.

* To whom correspondence should be addressed at: SRI International, Biochemical Genetics Department, 333 Ravenswood Avenue, Menlo Park, California 94025, USA.

Received 17 September; accepted 26 November 1981.

1. Chemical Industry Institute of Toxicology, Docket 3278 (1978).
2. Abernethy, D. J. & Couch, D. B. *Mutat. Res.* (in the press).
3. Chiu, C. W., Lee, L. H., Wang, C. Y. & Bryan, G. T. *Mutat. Res.* **58,** 11–22 (1978).
4. Dougherty, R. W., Simon, G. S., Campbell, F. I. & Borzelleca, J. F. *Pharmacologist* **20,** 155 (1978).
5. Simmon, V. F., Eckford, S. L., Griffin, A. F., Spanggord, R. & Newell, G. W. *Toxic. appl. Pharmac.* **41,** 197 (1977).
6. Soares, E. R. & Lock, L. F. *Envir. Mutagen.* **2,** 111–124 (1980).
7. Bermudez, E., Tillery, D. & Butterworth, B. E. *Envir. Mutagen.* **1,** 391–398 (1979).
8. Mirsalis, J. C. & Butterworth, B. E. *Carcinogenesis* **1,** 621–625 (1980).
9. Mirsalis, J. C. & Butterworth, B. E. *Envir. Mutagen.* **3,** 316 (1981).
10. Hill, M. J. *J. hum. Nutr.* **33,** 416–426 (1979).
11. Canvanna, M. *et al. Br. J. Cancer* **39,** 383–390 (1979).
12. Williams, R. T. *Toxic appl. Pharmac.* **23,** 769–781 (1972).
13. Rickert, D. E., Long, R. M., Krakowka, S. & Dent, J. G. *Toxic. appl. Pharmac.* **59,** 574–579 (1981).
14. Guest, D., Schnell, S. R. & Dent, J. G. *The Toxicologist* **1,** 110 (1981).
15. Bond, J. A. & Rickert, D. E. *Drug Metab. Disposit.* **9,** 10–14 (1981).
16. Hollstein, M., McCann, J., Angelosanto, F. A. & Nichols, W. W. *Mutat. Res.* **65,** 133 (1979).

Effects of overfeeding on energy balance and brown fat thermogenesis in obese (*ob/ob*) mice

Paul Trayhurn, Pauline M. Jones,
Martina M. McGuckin & Anne E. Goodbody

Dunn Nutrition Laboratory, University of Cambridge and Medical
Research Council, Milton Road, Cambridge CB4 1XJ, UK

The genetically obese (*ob/ob*) mouse has been used extensively in experimental studies on obesity and to determine the mechanisms involved in regulating energy balance[1]. Excess energy begins to accumulate in the *ob/ob* mouse from ~12 days of age[2], but food intake during the suckling period and up to 4 weeks of age is no greater than in lean siblings[3–5]. This indicates that the initial development of obesity in the *ob/ob* mutant is entirely due to a low energy expenditure, and this has been attributed to a reduction in thermoregulatory non-shivering thermogenesis[6–8], particularly that mediated by brown adipose tissue[9,10]. Hyperphagia does, however, play an important part in the later development of obesity in *ob/ob* mice. Recent studies with young rats of the Sprague–Dawley strain fed a 'cafeteria diet' have suggested that an adaptive diet-induced thermogenesis, also mediated by brown adipose tissue, has a major role in minimizing the accumulation of energy during voluntary overfeeding[11–13]. We now report the effects of overfeeding young lean and obese mice with a cafeteria-type diet, and show that while the lean animals retain little of their excess energy intake, most of the extra intake of the obese mice is deposited. This suggests that the capacity for diet-induced thermogenesis is reduced in the obese compared with the lean mice. We also show that the energy balance measurements are paralleled by different adaptive changes in brown adipose tissue in the two genotypes.

The animals used in this study were male lean (*ob/+* or *+/+*) and obese (*ob/ob*) mice of the 'Aston' variety[2], between 23 and 28 days old at the start of the experiments. They were kept singly in wire-mesh cages in an animal room at 23±1 °C, with a 12-h light/12-h dark cycle (light period from 07.00). Half the animals were fed a standard low-fat commercial diet (Spillers–Spratts Rodent Breeding Diet 1), while the remaining animals from each group were fed a cafeteria diet. The cafeteria diet consisted of two different food items (for example, chocolate and cheese) given each day, in addition to the stock diet. All animals were weighed daily and energy intake was determined each day for the cafeteria mice and every 2–3 days for the stock-fed groups.

The energy balance results for lean and obese mice obtained over 3 weeks are shown in Table 1. The lean mice fed the cafeteria diet had a digestible energy intake that was 69% higher than that of lean animals fed the stock diet alone; thus mice, like rats, can be induced to over-eat on a cafeteria diet. Despite their increased energy intake, the cafeteria-fed lean mice did not show a significantly greater weight gain than the stock-fed controls, and although the total energy gain on the cafeteria diet was 19% greater than that on the stock diet, the increase was not statistically significant. Gross efficiency (energy deposited divided by digestible energy intake) was significantly lower on the cafeteria diet than on the stock diet.

The absolute increase in energy deposition of lean mice fed the cafeteria diet was 36 kJ and this accounted for a mere 4% of the increase in digestible energy intake which occurred during cafeteria feeding. The apparent energy expenditure of the cafeteria-fed lean mice, calculated as the difference between the digestible energy intake and the gain in body energy, was 899 kJ (or 76%) more than the control lean mice. This suggests that young lean mice of the Aston variety exhibit the same diet-induced thermogenesis during overfeeding as has been reported for Sprague–Dawley rats[11]. It is possible that greater physical activity also made some contribution to the increased energy expenditure of the cafeteria-fed mice. Note that energy expenditure in this study has been overestimated because the energy loss in urine was not taken into account. However, as the animals showed no glycosuria, urinary energy losses are unlikely to affect markedly the calculated difference in energy expenditure between stock and cafeteria-fed animals.

The obese mice also increased their energy intake on the cafeteria diet, despite the fact that on the stock diet they were already hyperphagic relative to the lean animals. The digestible energy intake of the cafeteria-fed obese mice was 49% more than in those fed the stock diet alone. In contrast to the lean mice, the obese animals gained significantly more weight and deposited substantially more energy on the cafeteria than on the stock diet. The gain in carcass energy on the cafeteria diet was 88% more than on the control diet, and the gross efficiency of the cafeteria-fed obese animals was higher, rather than lower, than the stock-fed group. The absolute increase in energy deposition (572 kJ) on the cafeteria diet amounted to 55% of the extra energy intake; thus, in the obese mice, unlike the lean, most of the extra energy intake was deposited. The apparent energy expenditure did, of course, rise in the cafeteria-fed obese animals, but it is unlikely that much of the increase was due to the energy cost of fat deposition as high-fat cafeteria diets lead to a suppression of fatty acid synthesis (N. J. Rothwell, M. J. Stock and P. T., unpublished observations), presumably because dietary fatty acids are used directly for triacylglycerol synthesis, at little energy cost.

It has recently been argued[14,15] that cumulative errors occur in energy balance experiments, necessitating the measurement of all three components—intake, output and storage—of the energy balance equation. There is no evidence, however, that the errors involved are large, and they are certainly too small to have more than a minor impact on the conclusions drawn here. Furthermore, in the present study, any cumulative errors will presumably occur for both the lean and obese animals, which showed quite different responses to overfeeding with regard to energy deposition and apparent energy expenditure.

Evidence has been presented that the main effector of diet-induced thermogenesis in rats is brown adipose tissue[11–13],

0028-0836/82/040323—03$01.00

Table 1 Energy balance in lean and genetically obese mice fed control or cafeteria diets for 3 weeks

	Lean		Obese	
	Control	Cafeteria	Control	Cafeteria
Digestible energy intake (kJ)	1,363±45	2,298±95*	2,181±80	3,242±55*
Initial body weight (g)	19.4±1.0	19.5±0.5 (NS)	20.0±1.3	21.8±0.6 (NS)
Final body weight (g)	36.1±1.1	37.3±1.9 (NS)	49.4±1.5	59.0±1.1*
Body weight gain (g)	16.7±0.8	17.8±1.4 (NS)	29.4±0.6	37.2±0.9*
Initial body energy (kJ)	155.5±9.8	156.3±4.6 (NS)	238.6±20.3	265.6±8.4 (NS)
Final body energy (kJ)	341.4±20.2	378.2±36.0 (NS)	887.7±39.4	1,486.5±111.6*
Gain in body energy (kJ)	185.9±16.6	221.9±33.2 (NS)	649.1±25.4	1,220.9±104.9*
Gross efficiency (%)	13.6±1.0	9.7±1.0†	29.9±0.9	37.7±3.1†
Apparent energy expenditure (kJ)	1,177±32	2,076±70*	1,531±64	2,021±107‡

Mice 23–28 days old were fed stock or cafeteria diets for 3 weeks; the lean and obese animals received the same cafeteria foods. The energy content of all food items, carcasses and faeces was determined by bomb calorimetry using a Gallenkamp adiabatic calorimeter (model CB-100), calibrated with dry benzoic acid standards[7]. Energy intake measurements were corrected for any changes in water content of the foods. Faeces were collected throughout the experiment and their energy content measured for the determination of digestible energy intake. At the end of the experiment the mice were killed by ether anaesthesia, the gut contents removed, and the carcasses chopped into small pieces. The carcasses were then autoclaved, homogenized, and finally freeze-dried before measurement of their energy content[7]. Initial carcass energy was estimated from body weight by reference to a baseline group of 10 lean and 10 obese mice of the same age and weight range as the experimental groups[7]. Gross efficiency and the apparent energy expenditure were calculated as described in the text. Results are given as mean values ±s.e.m. for eight animals per group, except for the lean cafeteria group where seven animals were used.

† $P<0.05$; ‡ $P<0.01$; * $P<0.001$ compared with control animals of the same genotype. NS, not significant ($P>0.05$).

which is traditionally associated with non-shivering thermogenesis in many newborn and hibernating mammals[16,17]. We therefore examined brown adipose tissue from the interscapular region of both lean and obese mice fed the stock or cafeteria diets (for results see Table 2). The total amount of interscapular brown adipose tissue was increased by 26% in lean mice after cafeteria feeding, but there was no increase in the total protein content of the tissue. The activity of cytochrome oxidase (E.C. 1.9.3.1.) was, however, increased by 53%, indicating that the total oxidative capacity of brown adipose tissue was augmented by overfeeding in lean mice. In contrast, the obese mice fed the cafeteria diet did not show any increase in the amount of interscapular brown adipose tissue, or in the cytochrome oxidase activity or total protein content of the tissue.

The primary mechanism for thermogenesis in brown adipose tissue is considered to be through a proton conductance pathway across the inner mitochondrial membrane[18], a pathway which can be inhibited by purine nucleotides that bind to a protein of molecular weight 32,000 (refs 19, 20). The extent to which purine nucleotides (for example, GDP) bind to brown adipose tissue mitochondria seems to reflect the activity of the proton conductance pathway, and this has formed the basis of an assay for the 'thermogenic state' of the tissue[21–24]. We therefore measured GDP binding to brown adipose tissue mitochondria from lean and obese animals fed control or cafeteria diets; there was a ~50% increase in binding in the cafeteria-fed animals of both genotypes, which indicates an augmentation of thermogenesis (Table 2). However, for each diet binding was lower in the obese than in the lean animals.

Cafeteria feeding, therefore, seems to result in changes in the proton conductance pathway, as well as in the total oxidative capacity, of brown adipose tissue of lean mice, changes that are similar to the changes reported in Sprague–Dawley rats[12]. Obese mice show less of a response to overfeeding, however, in that only the proton conductance pathway is increased. These different adaptive responses to overfeeding in brown adipose tissue of lean and obese mice parallel the different responses of the two genotypes with respect to whole-body energy balance.

Pair-feeding studies using the *ob/ob* mutant on a normal diet generally involve restricting the intake of the obese to the *ad libitum* intake of the lean, but in the present experiments the digestible energy intake of the cafeteria-fed lean mice proved similar to that of the obese fed the stock diet alone; 'pair-feeding' was therefore achieved with the obese eating *ad libitum*. Note that in this situation the stock-fed obese animals deposited nearly three times as much energy as the cafeteria-fed lean mice, and this was associated with substantial differences between the two groups in cytochrome oxidase activity and GDP binding in brown adipose tissue.

In conclusion, the present results demonstrate a clear difference between the lean and obese genotypes in the metabolic response to voluntary overfeeding, results consistent with the view that a regulatory diet-induced thermogenesis mediated by brown adipose tissue plays an important part in

Table 2 Properties of interscapular brown adipose tissue in lean and genetically obese mice fed control or cafeteria diets

	Lean		Obese	
	Control	Cafeteria	Control	Cafeteria
Brown adipose tissue weight (mg)	80.5±3.4 (16)	101.6±7.7* (16)	343.5±33.2 (8)	315.3±47.2 (NS) (10)
Total brown adipose tissue protein (mg)	10.6±0.8 (13)	11.0±0.6 (NS) (8)	8.6±0.3 (8)	9.7±0.5 (NS) (8)
Total cytochrome oxidase activity (μmol cytochrome *c* oxidized per min)	22.1±1.6 (13)	33.8±1.7† (8)	13.4±1.5 (8)	13.4±1.2 (NS) (8)
GDP binding (pmol GDP per mg mitochondrial protein)	345.3±13.5 (7)	502.2±30.3† (8)	272.2±12.5 (7)	421.7±136.4* (6)

Mice similar to those in Table 1 were fed stock or cafeteria diets for 3 weeks, after which they were killed by cervical dislocation, and interscapular brown adipose tissue rapidly removed, trimmed free of contaminating tissues, and weighed. The cytochrome oxidase activity of the tissue was measured spectrophotometrically[26], and the total protein content measured by a modified Lowry method[27] using bovine serum albumin as standard. For the purine nucleotide (GDP) binding assay, mitochondria were prepared as described elsewhere[28] from brown adipose tissue pooled from the interscapular, subscapular and dorsocervical sites. GDP binding was measured by incubating the mitochondria at 20 °C, *p*H 7.1 for 7 min, with 10 μM ^{3}H-GDP, essentially according to Nicholls[19], as described previously[29]. ^{3}H-GDP and ^{14}C-sucrose were obtained from Amersham. The results are mean values ±s.e.m.; numbers of observations are shown in parentheses.

* $P<0.05$; † $P<0.001$ compared with control animals of the same genotype. NS, not significant ($P>0.05$).

energy balance[11]. The results also demonstrate directly the importance of a reduced capacity for diet-induced thermogenesis in the development of obesity[25]. Obesity in the *ob/ob* mouse, in particular, may be viewed as a consequence of a reduction in both non-shivering and diet-induced thermogenesis in brown adipose tissue; reduced non-shivering thermogenesis leads to a low maintenance requirement and excessive energy gain on a 'normal' energy intake, while a reduction in the capacity for diet-induced thermogenesis leads to an impairment in the ability to dissipate excess energy intake once hyperphagia is established soon after weaning.

We thank Dr W. P. T. James for his helpful comments and the MRC for a studentship (A.E.G.). P.M.J. was a visiting student from the University of Surrey.

Received 7 October; accepted 10 December 1981.

1. Bray, G. A. & York, D. A. *Physiol. Rev.* **59,** 719–809 (1979).
2. Thurlby, P. L. & Trayhurn, P. *Br. J. Nutr.* **39,** 397–402 (1978).
3. Lin, P.-Y., Romsos, D. R. & Leveille, G. A. *J. Nutr.* **107,** 1715–1723 (1977).
4. Rath, E. A. & Thenen, S. W. *J. Nutr.* **109,** 840–847 (1979).
5. Contaldo, F., Gerber, H., Coward, W. A. & Trayhurn, P. in *Obesity: Pathogenesis and Treatment* (eds Enzi, G., Crepaldi, G., Pozza, G. & Renold, A. E.) 319–322 (Academic, London, 1981).
6. Trayhurn, P. & James, W. P. T. *Pflügers Arch. ges. Physiol.* **373,** 189–193 (1978).
7. Thurlby, P. L. & Trayhurn, P. *Br. J. Nutr.* **42,** 377–385 (1979).
8. Vander Tuig, J. G., Romsos, D. R. & Leveille, G. A. *J. Nutr.* **110,** 35–41 (1980).
9. Himms-Hagen, J. & Desautels, M. *Biochem. biophys. Res. Commun.* **83,** 628–634 (1978).
10. Thurlby, P. L. & Trayhurn, P. *Pflügers Arch. ges. Physiol.* **385,** 193–201 (1980).
11. Rothwell, N. J. & Stock, M. J. *Nature* **281,** 31–35 (1979).
12. Brooks, S. L., Rothwell, N. J., Stock, M. J., Goodbody, A. E. & Trayhurn, P. *Nature* **286,** 274–276 (1980).
13. Rothwell, N. J. & Stock, M. J. *Pflügers Arch. ges. Physiol.* **389,** 237–241 (1981).
14. Hervey, G. R. & Tobin, G. *Nature* **289,** 699 (1981).
15. Armitage, G., Harris, R. B. S., Hervey, G. R. & Tobin, G. in *The Body Weight Regulatory System: Normal and Disturbed Mechanisms* (eds Cioffi, L. A., James, W. P. T. & Van Itallie, T. B.) 137–141 (Raven, New York, 1981).
16. Smith, R. E. & Horwitz, B. A. *Physiol. Rev.* **49,** 330–425 (1969).
17. Jansky, L. *Biol. Rev.* **48,** 85–132 (1973).
18. Nicholls, D. G. *Biochim. biophys. Acta* **549,** 1–29 (1979).
19. Nicholls, D. G. *Eur. J. Biochem.* **62,** 223–228 (1976).
20. Heaton, G. M., Wagenvoord, R. J., Kemp, A. & Nicholls, D. G. *Eur. J. Biochem.* **82,** 515–521 (1978).
21. Rafael, J. & Heldt, H. W. *FEBS Lett.* **63,** 304–308 (1976).
22. Desautels, M., Zaror-Behrens, G. & Himms-Hagen, J. *Can. J. Biochem.* **56,** 378–383 (1978).
23. Desautels, M. & Himms-Hagen, J. *Can. J. Biochem.* **57,** 968–976 (1979).
24. Sundin, U. & Cannon, B. *Comp. Biochem. Physiol.* **65B,** 463–471 (1980).
25. Miller, D. S. in *Obesity in Perspective* DHEW Publ. No. 75–108 (ed. Bray, G. A.) 137–143 (1973).
26. Yonetani, T. & Ray, G. S. *J. biol. Chem.* **240,** 3392–3398 (1965).
27. Schacterle, G. R. & Pollack, R. L. *Analyt. Biochem.* **51,** 654–655 (1973).
28. Cannon, B. & Lindberg, O. *Meth. Enzym.* **55,** 65–78 (1979).
29. Goodbody, A. E. & Trayhurn, P. *Biochem. J.* **194,** 1019–1022 (1981).

Expression of HLA antigens, β_2-microglobulin and enzymes by human amniotic epithelial cells

M. Adinolfi*, C. A. Akle†, I. McColl†, A. H. Fensom*, Linda Tansley*, P. Connolly*, B.-L. Hsi‡, W. P. Faulk‡, P. Travers§ & W. F. Bodmer§

* Paediatric Research Unit and † Department of Surgery,
Guy's Hospital Medical School, London SE1 9RT, UK
‡ Blond McIndoe Centre for Transplantation Biology,
Queen Victoria Hospital, East Grinstead, Sussex RH19 3DZ, UK
§ Imperial Cancer Research Fund, Lincoln's Inn Fields,
London WC2A 3PX, UK

A monolayer of epithelial cells, endowed with unique secretory properties, lines the human amniochorion[1,2]. It has been shown that transplantation of these membranes into allogeneic hosts does not result in overt acute graft rejection[3–6]. We demonstrate here that HLA-A, -B, -C and -DR antigens and β_2 microglobulin (β_2m) cannot be detected by immunofluorescence on freshly collected or *in vitro* cultured amniotic epithelial cells, although small quantities of such antigens were detected when more sensitive radiobiological techniques were used. We also show that these cells, cultured *in vitro*, produce large quantities of enzymes absent in patients with lysosomal storage diseases and that their supernatants can correct glycosaminoglycan accumulation in cultured fibroblasts from patients with Hurler's and Hunter's syndromes.

Cryostat sections of human amniotic membranes were studied by immunofluorescence techniques either immediately after collection or following 24 h incubation in RPMI 1640 medium (Flow)[7]. When these sections were independently stained in three laboratories, β_2m could not be detected by immunofluorescence techniques using monoclonal antibodies and rabbit immune sera. The few fibroblasts present in the connective tissue showed intense staining. Using the same methods, β_2m molecules were not detected on the surface of amniotic epithelial cells which had been cultured *in vitro* for over 3 weeks. The expression of HLA-A, -B, -C and -DR antigens was investigated by immunofluorescence using two monomorphic monoclonal antibodies, one (W6/32) reacting with the native HLA-A, -B and -C molecules and the other (DA2) with HLA-DR antigen[8,9]. The amniotic epithelial cells were not stained by these antibodies while cells in the underlying connective tissue, predominantly fibroblasts, were positive with W6/32; another population of these cells, presumably macrophages, were positive with the DA2 antibody.

Although these results suggested the absence or poor expression of HLA-A, -B, -C and -DR antigens and β_2m on the surface of the human amniotic epithelial cells, small quantities of β_2m could be detected in the serum-free media collected from 20 samples of the cells cultured *in vitro*. In fact, 24 h incubation of the cells in a serum-free medium following culture in RPMI 1640 medium supplemented with 20% fetal calf serum for >3 weeks, revealed levels of β_2m of 1.7–14.7 mg l^{-1} (mean 5.8 mg l^{-1}) in the supernatants, using a radioimmunoassay technique (Phadebas β_2 microtest, Pharmacia Diagnostic). However, the amount of β_2m in the supernatants of the amniotic epithelial cells was less than that detected in the supernatants of adult fibroblasts (7.6–18.4 mg l^{-1}; mean 13.2), while fetal fibroblasts appeared to produce much more β_2m than adult fibroblasts (49–68 mg l^{-1}; mean 56).

The synthesis of β_2m and HLA-A, -B and -C antigens was further investigated by labelling the amniotic epithelial cells *in vitro* with ^{35}S-methionine for 4 h. Fibroblasts from adult donors were also labelled and analysed as positive controls. Detergent lysates of these cells were analysed by immunoprecipitation and SDS polyacrylamide gel electrophoresis. Faint bands corresponding to the 43,000 molecular weight HLA-A, -B and -C chain and 12,000 molecular weight β_2m were precipitated from the lysates by antibodies directed against these antigens. None of the antigens was precipitated from the medium in which the cells were grown. Newly synthesized HLA-A, -B and -C chains and β_2m were detected in both extracts and supernatants of adult fibroblasts.

Although it is possible that the few contaminating fetal fibroblasts present in the cultures have contributed to the detection of HLA chains and β_2m by the radiobiological assays, very few fibroblasts were observed in the cultures, and the epithelial cells could be subcultured several times without overgrowth of the fibroblasts.

Amniotic epithelial cells were also strongly reactive with a rabbit antiserum prepared against human amniotic epithelium (Fig. 1)[10]. This antibody reacted with amniotic epithelial cells that had been cultured *in vitro* for several weeks but did not react with fetal skin, adult epithelial cells or fetal fibroblasts.

To establish whether the production of HLA antigens detected by the radiobiological techniques could affect the possible use of these cells in transplantation, seven normal individuals were transplanted subcutaneously with a piece of amniotic epithelial membrane[6]. The results of these experiments will be published in detail elsewhere; briefly, none of the volunteers showed any signs of acute rejection after 6 weeks; four were

0028–0836/82/040325—03$01.00

Table 1 Lysosomal enzyme activities of human amniotic epithelial cells

Enzyme	Amniotic epithelial cells	Normal fibroblasts	Cells from amniotic fluids	Lysosomal storage disease
α-iduronidase	49; 56	21–72	26–136	Hurler's disease
β-galactosidase	556; 1183	394–1,443	345–885	GM_1-gangliosidosis
α-galactosidase A	33	40–120	30–51	Fabry's disease
β-glucosidase	916	350–1,110	320–1,054	Gaucher's disease
α-glucosidase	138	40–90	11–45	Pompe's disease
Sphingomyelinase	251	227–775	305–602	Niemann–Pick disease
Arylsulphatase A	649; 686	325–2,000	146–600	Metachromatic leucodystrophy

Levels are expressed as nmole per h per mg protein. The values for the different enzymes are reported as ranges or individual levels, and are those obtained in the Paediatric Research Unit, Guy's Hospital Medical School.

studied serologically and found not to produce anti-HLA response. Although the implanted tissues were not left long enough to be certain that they were not chronically rejected, the results suggest that amniotic epithelial cells are not immunogenic and can be transplanted to correct certain enzyme deficiencies.

Evidence that the amniotic epithelial cells produce enzymes deficient in some lysosomal storage diseases was obtained as follows. Human amniotic membranes were collected in sterile conditions from caesarian sections and incubated for 24 h in RPMI 1640 medium. The epithelial cells were isolated by trypsinization with 0.25% (w/v) trypsin (Wellcome) and cultured in RPMI 1640 medium supplemented with 20% fetal calf serum in a humidified incubator containing an atmosphere of 5% CO_2 in air. The cells could be maintained in culture for over 20 weeks and several passages (Fig. 2).

The enzyme estimations were performed simultaneously on the amniotic epithelial cells, fibroblasts from adult individuals and cells collected from amniotic fluids (Table 1). The cultured cells were collected, suspended in 0.01% Triton X-100 and disrupted by sonication. The activities of α-iduronidase, β-galactosidase, α-galactosidase A, α- and β-glucosidase, sphingomyelinase and arylsulphatase A were estimated on the supernatants obtained after centrifugation of the disrupted cells using minor modifications of the methods previously described[11–15]. As shown in Table 1, all the enzymes assayed were detected in the extracts from the cultured cells. The levels of all enzymes tested, expressed as nmol per h per mg protein, were similar to those produced by cultured normal fibroblasts and by the cells obtained from amniotic fluids. Figure 3 shows the rates of $Na_2{}^{35}SO_4$ uptake by fibroblasts from a patient with Hurler's disease grown in inorganic sulphate-free medium (Dulbecco's modified Eagle's medium; Flow Laboratories), with and without amnion culture supernatant from cells grown in similar medium[16], as compared with normal fibroblasts. It is clear that within 1 week the amniotic epithelial cell supernatant was able to correct the abnormal accumulation by the Hurler cells. Similar results were obtained using the fibroblasts from a patient with Hunter's syndrome.

The present results uphold the suggestion that the amniotic epithelial cells may be used for transplantation in patients with selected enzyme deficiencies, as they produce substantial quan-

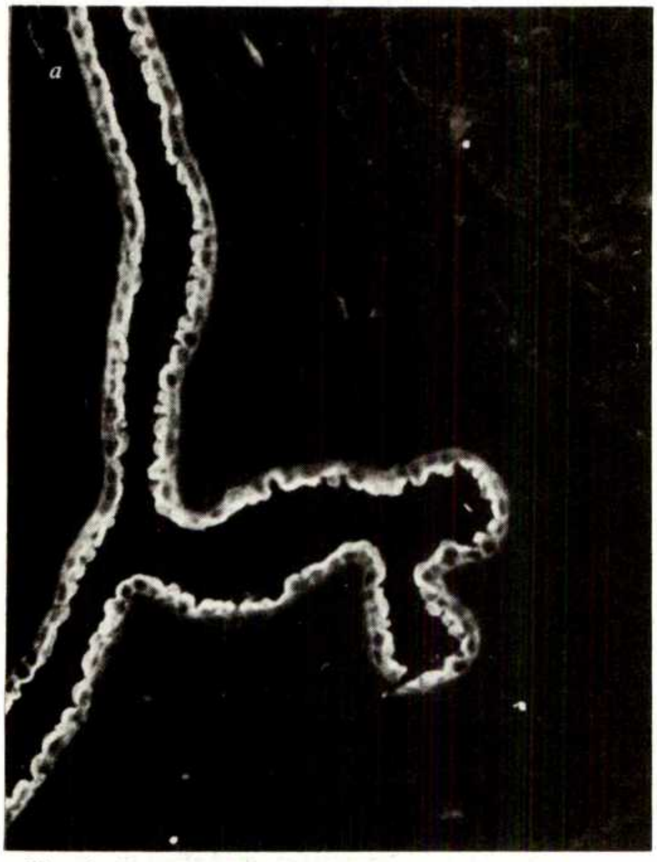

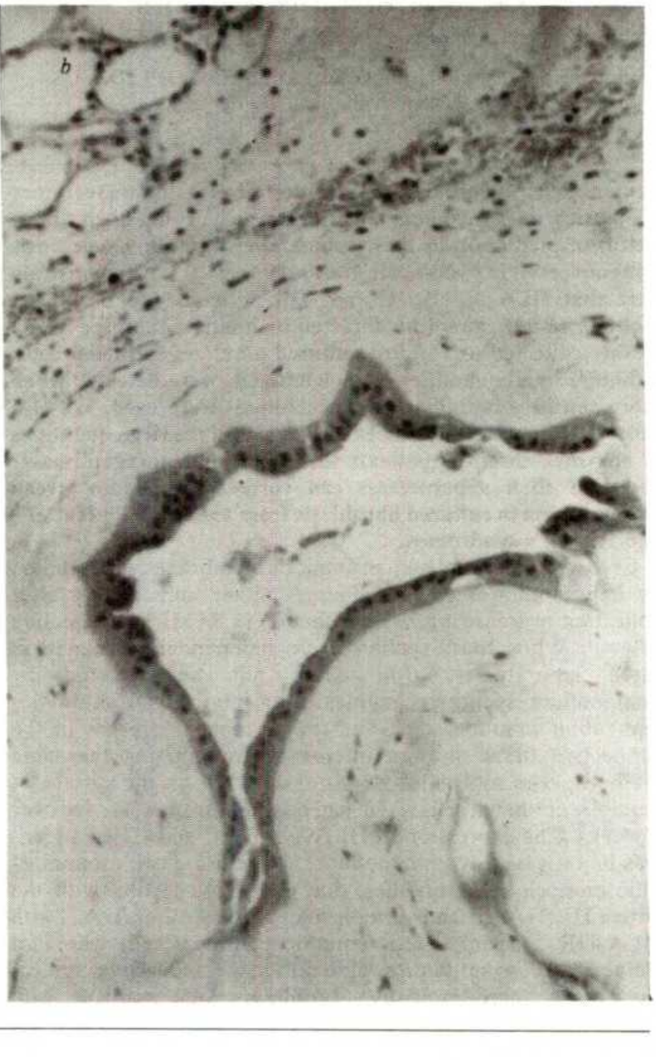

Fig. 1 Human amniotic epithelial cells: *a*, stained by immunofluorescence and a specific rabbit immune serum; the same cells did not stain when monoclonal antisera against HLA antigens or β_2m were used; *b*, in the biopsy taken from a volunteer implanted with cells 32 days previously. There is no evidence of acute rejection.

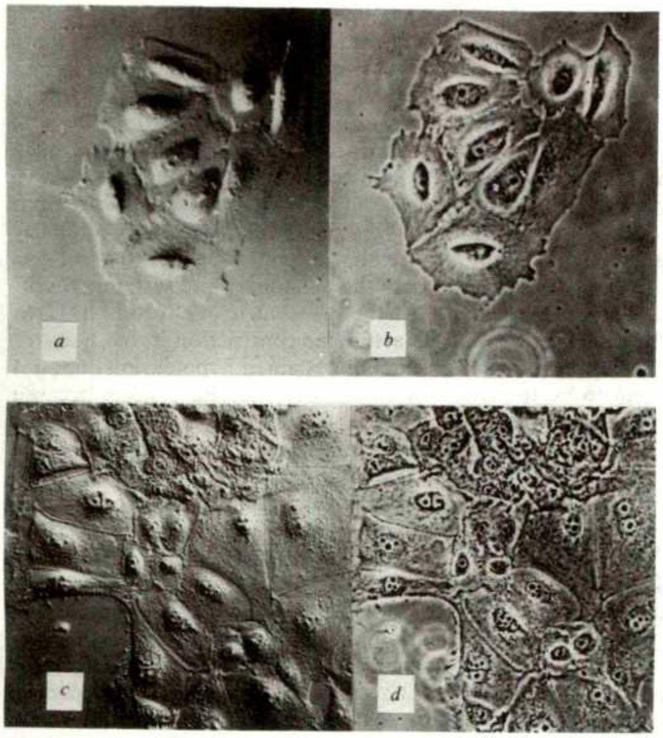

Fig. 2 Photomicrographs of human amniotic epithelial cells in tissue culture taken using Nomarski (*a*, *c*) and phase contrast (*b*, *d*) techniques (×125). *a*, *b*, Cells in culture for 4 days; *c*, *d*, cells in culture for 3 weeks.

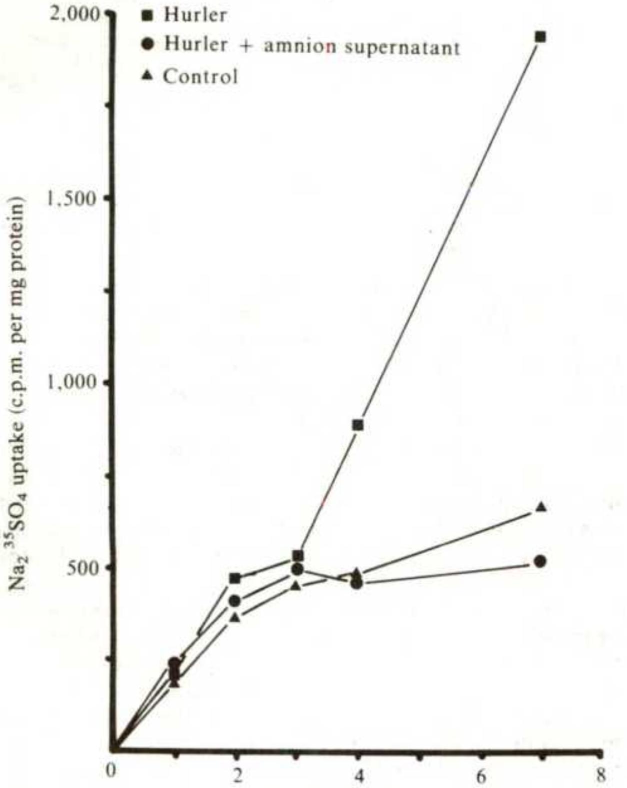

Fig. 3 Rate of Na$_2$^{35}SO$_4$ uptake by fibroblasts. All three groups of cells accumulate label for the first 3 days because of pre-culture in inorganic sulphate-free medium. Subsequently, the Hurler cells (■) continue to accumulate the label, whereas in the presence of amniotic cell supernatant (●) they equilibrate, as do normal fibroblasts (▲).

tities of enzymes lacking in some of the more common enzyme disorders[17]. Work is in progress to see if the cells produce other enzymes, such as adenosine deaminase, of diagnostic and therapeutic value.

The implantation of either sheets of amniotic epithelial cells or cells cultured *in vitro* has many advantages over the use of bone marrow or fibroblast transplants: there should be no risk of graft-versus-host reaction and probably no need to use immunosuppressive therapy with all its attendant complications. Furthermore, the availability of an immune serum which reacts specifically with the amniotic epithelial cells without cross-reacting with fetal or adult skin epithelial cells makes it feasible to identify the transplanted amniotic cells in biopsy material. Another advantage would be that supplies of these cells are readily available from any obstetric unit.

A thorough search of the literature has revealed no evidence of malignant change originating in the amniotic epithelial cells. Whether our suggestion is valid, and whether these cells may be used for transplantation following further genetic engineering remains to be proved by transplanting these cells into patients with selected inborn errors of metabolism.

We thank Dr Michael Joseph for useful discussions and Miss Carolyn Beech for her patience in the preparation of the manuscript.

Received 10 August; accepted 9 December 1981.

1. Bourne, G. *The Human Amnion and Chorion* (Lloyd-Luke, London, 1962).
2. Hoyes, A. D. *Obstet. Gynec. A* **4,** 1 (1975).
3. Trelford, J. D. & Trelford-Sander, M. *Am. J. Obstet. Gynec.* **134,** 835 (1977).
4. Bennett, J. P., Matthews, R. N. & Faulk, W. P. *Lancet* **i,** 1153 (1980).
5. Faulk, W. P. *et al. Lancet* **i,** 1156 (1980).
6. Akle, C., Adinolfi, M., Welsh, K. I., Leibowitz, S. & McColl, I. *Lancet* **ii,** 1003, 1005 (1981).
7. Burgos, H. & Faulk, W. P. *Br. J. Obstet. Gynaec.* **88,** 294 (1981).
8. Trowsdale, J., Travers, P., Bodmer, W. F. & Patillo, R. A. *J. exp. Med.* **152,** 115 (1980).
9. Brodsky, F. M., Perham, P. & Bodmer, W. F. *Eur. J. Immun.* **9,** 536 (1979).
10. Hsi, B.-L., Yeh, G. C. J. & Faulk, W. P. *Placenta* (in the press).
11. Fensom, A. H., Benson, P. F., Babarik, A. W., Grant, A. R. & Jacobs, L. *Biochem. biophys. Res. Commun.* **74,** 877 (1977).
12. Stirling, J. L. *et al. Lancet* **ii,** 37 (1979).
13. Fensom, A. H., Benson, P. F., Grant, A. R. & Jacobs, L. *J. inherited metab. Dis.* **2,** 9 (1979).
14. Baum, H., Dodgson, K. S. & Spencer, B. *Clinica chim. Acta* **4,** 453 (1959).
15. Vanier, M. T. *Adv. exp. Med. Biol.* **101,** 731 (1978).
16. Fratantoni, J. C., Hall, C. W. & Neufeld, E. F. *Proc. natn. Acad. Sci. U.S.A.* **64,** 360 (1969).
17. Akle, C., Adinolfi, M. & McColl, I. *Biol. Res. Pregnancy* **2,** 23 (1981).

Leukotriene C$_4$ affects pulmonary and cardiovascular dynamics in monkey

**Göran Smedegård*†, Per Hedqvist‡,
Sven-Erik Dahlén‡, Björn Revenäs*,
Sven Hammarström§ & Bengt Samuelsson§**

Departments of Experimental Medicine* and Experimental Allergy Research†, Pharmacia AB, Uppsala, Sweden and Departments of Physiology‡ and Chemistry§, Karolinska Institutet, Stockholm, Sweden

Leukotriene C$_4$ (LTC$_4$) and its metabolites LTD$_4$ and LTE$_4$ (Fig. 1) have been identified as the major active constituents of slow-reacting substance of anaphylaxis (SRS-A)[1–3]. Leukotrienes C$_4$, D$_4$ and E$_4$ have rapidly gained recognition as bronchoconstrictors of hitherto unsurpassed potency in the guinea pig *in vivo* and *in vitro*[4–7] as well as acting as oedema-forming substances in guinea pig[3,5,7] and hamster[8]. Here we report that LTC$_4$ is also a prominent bronchoconstrictor in the monkey; it increases transpulmonary pressure in the anaesthetized animal, mainly by decreasing pulmonary dynamic compliance, and it contracts isolated tracheal spiral tissue. Furthermore, LTC$_4$ causes transient pulmonary and systemic hypertension, followed by a prolonged hypotensive period associated with decreased cardiac output, haemoconcentration and reduction in the number of circulating leukocytes. These *in vivo* findings in a primate imply that leukotrienes may also cause important alterations of cardiovascular and pulmonary function in man.

Male monkeys (*Macaca irus*) weighing 2.8–3.2 kg were anaesthetized with ketamine HCl, and ventilated artificially through a tracheostomy. Pressure-monitoring catheters were inserted in the aorta, pulmonary artery and right and left atrium, as described elsewhere[9]. Transpulmonary pressure was measured as the difference between tracheal and intrapleural pressures. Pulmonary dynamic compliance and pulmonary resistance were calculated from simultaneous recordings of tracheal air flow, tidal volume and transpulmonary pressure[10].

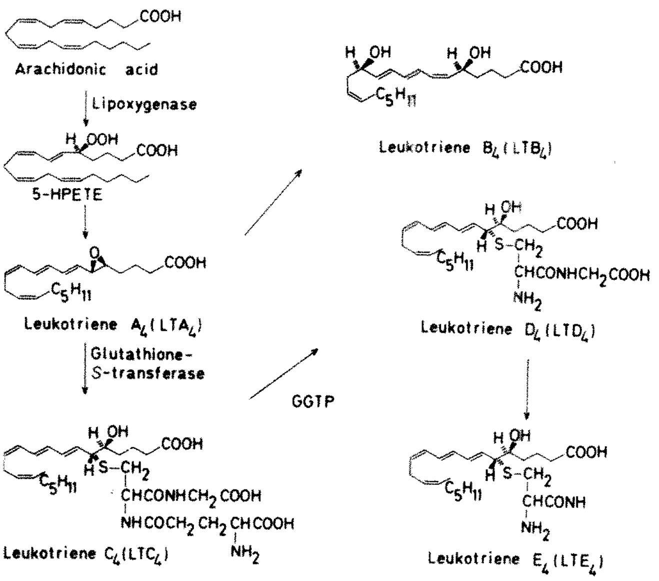

Fig. 1 Leukotrienes biosynthesized from arachidonic acid via an initial lipoxygenase-catalysed formation of 5(*S*)-hydroperoxy-7,9,11,14-eicosatetraenoic acid (5-HPETE). 5-HPETE is transformed into an unstable epoxide intermediate, leukotriene A_4 (5,6-oxido-7,9,11,14-eicosatetraenoic acid, LTA_4), which has the characteristic conjugated triene structure present in all leukotrienes. LTA_4 may form the leukotactic principle leukotriene B_4 (5(*S*),12(*R*)-dihydroxy-6-*cis*-8,10-*trans*,14-*cis*-eicosatetraenoic acid, LTB_4). Addition of glutathione yields the primary SRS-A, LTC_4 (5(*S*)-hydroxy-6(*R*)-*S*-glutathionyl-7,9-*trans*,11,14-*cis*-eicosatetraenoic acid). Successive enzymatic removal of glutamic acid by γ-glutamyl transpeptidase and glycine by a dipeptidase, converts LTC_4 into LTD_4 (5(*S*)-hydroxy-6(*R*)-*S*-cystenylglycyl-7,9-*trans*,11,14-*cis*-eicosatetraenoic acid), and LTE_4 (5(*S*)-hydroxy-6(*R*)-*S*-cysteinyl-7,9-*trans*,11,14-*cis*-eicosatetraenoic acid), respectively. (For details of biosynthesis and nomenclature, see refs 1, 2.)

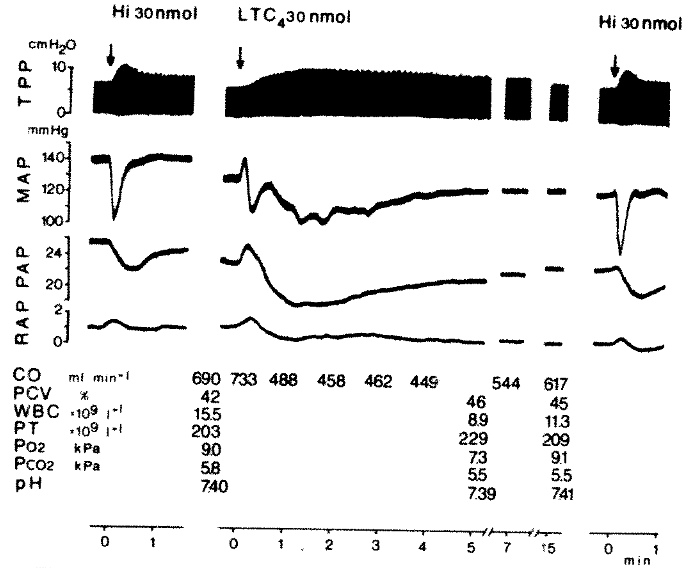

Fig. 2 Effects of systemic administration (injection through catheter placed in right atrium) of histamine (Hi) and LTC_4 in the artificially ventilated monkey. TPP, transpulmonary pressure; MAP, mean systemic arterial pressure; PAP, pulmonary arterial pressure; RAP, right atrial pressure. Cardiac output (CO) was determined by the thermodilution technique. Blood samples for analysis of haematocrit (PCV), white blood cell count (WBC), platelets (PT) and arterial P_{O_2}, P_{CO_2} and pH were drawn before and 5 and 15 min after injection of LTC_4.

Injection of biosynthetically generated[11] LTC_4 (0.5–30 nmol) into the right atrium caused a prompt and transient rise in mean arterial pressure (MAP), followed by a long-lasting hypotensive period (Fig. 2). Pulmonary arterial (PAP), right atrial (RAP) and left atrial (LAP, not shown in figure) pressures were similarly affected. The initial pressor response apparently reflects increased resistance in both the pulmonary and systemic vascular beds, in agreement with the vasocontrictor effects of LTC_4 in the guinea pig[5,7] and its arteriolar constriction in the hamster cheek pouch[8]. The subsequent sustained hypotension does not seem to be the result of changes in vascular calibre, because calculated total peripheral resistance increased during this period; for example, in the experiment shown in Fig. 2 the increase was 25 and 45% at 2 and 4 min respectively. Rather, LTC_4 seems to affect cardiac dynamics, as cardiac output was markedly decreased during the hypotension (in Fig. 2 by 35% at 2 and 4 min), concomitant with little or no change in heart rate. The reduction of cardiac output may be due to a negative inotropic effect of LTC_4 (refs 12, 13), possibly in conjunction with a decrease in plasma volume secondary to increased vascular permeability, as documented in other species[3–5,8]. Plasma leakage induced by LTC_4 could explain the haemoconcentration, which was indicated in the present experiment by a rise in haematocrit. Furthermore, the observed reduction of RAP and LAP after LTC_4 could also be consistent with a peripheral contribution to the decline in cardiac output.

Table 1 Effect of LTC_4 aerosol on transpulmonary pressure in the anaesthetized monkey

Animal	LTC_4 dose (nmol)	Response (% increase)	Equipotent dose of histamine* (nmol)	Ratio equipotent doses (dose histamine/dose LTC_4)
1	2	31	63	31.5
2	10	92	1,490	149
3	10	53	562	56.2
4	20	163	1,480	74.0
		Mean ratio (±s.e.m.) histamine/LTC_4:		77.8±25.3

* Calculated from dose–response relationships established for aerosolized histamine in the same experiment.

Compared with LTC_4, histamine (5–100 nmol, Sigma, injected into the right atrium) had short-lived cardiovascular effects related to its well known vasodilatory properties. Mean systemic and pulmonary arterial pressures were transiently decreased, while heart rate was simultaneously increased, presumably by reflex activation (Fig. 2).

Interestingly, injection of LTC_4 caused a marked but reversible drop in white blood cell count, while platelet count was unaffected (Fig. 2). The reason for this decrease is unclear, but it is possible that LTC_4 induces leukocyte trapping in various microvascular beds, as has recently been reported for leukotriene B_4 (LTB_4) in the hamster cheek pouch[8]. Accordingly, when LTB_4 (6 nmol) was injected systemically into one monkey, white blood cell count decreased from 14.5 to 5.0 × 10^9 per l in 5 min, and had returned to 15.5 × 10^9 per l 30 min later.

Leukotriene C_4 and histamine, when injected into the right atrium, increased transpulmonary pressure. They were virtually equipotent in this respect (Fig. 2), although the time course for their actions differed: the histamine effect peaked after 10–15 s and terminated within 1 min, whereas LTC_4 elicited maximal increase in transpulmonary pressure only after 2 min. The response to LTC_4 then remained at this level for several more minutes before it slowly subsided.

When LTC_4 and histamine were administered as aerosols, both effectively increased transpulmonary pressure (Fig. 3). However, the ratios of doses required to elicit responses of equal magnitude revealed that by this route of administration LTC_4

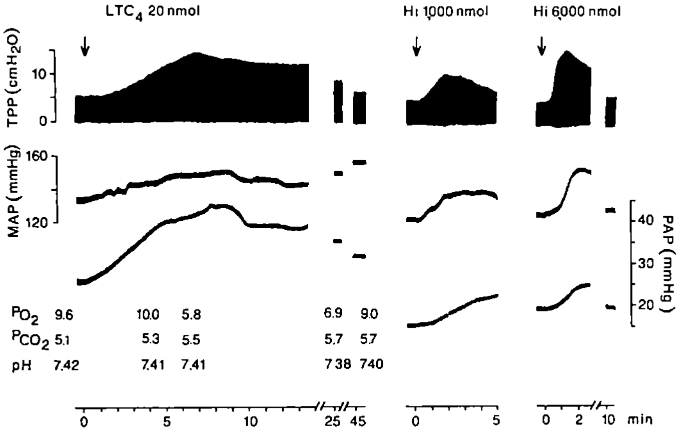

Fig. 3 Effects of aerosol administration (solution containing indicated amounts of substances nebulized into inspired air) of histamine (Hi) and LTC$_4$ in the artificially ventilated anaesthetized monkey. TPP, transpulmonary pressure; MAP, mean systemic arterial pressure; PAP, pulmonary arterial pressure. P_{O_2}, P_{CO_2} and *p*H were determined in arterial blood samples before, and 4, 7, 25 and 45 min after nebulization of LTC$_4$.

was ~100 times more potent than histamine (Table 1). In contrast, LTC$_4$ and histamine were equipotent when injected. This may be at least partly due to LTC$_4$ being rapidly metabolized and eliminated from the circulation, as was recently observed when ^{3}H-LTC$_3$ was injected systemically in monkeys in identical conditions[14]. On the other hand, nebulized LTC$_4$ might be inactivated at a considerably slower rate, as indicated from experiments where ^{3}H-LTC$_3$ was incubated with lung tissue *in vitro*[15,16].

The airway reaction to nebulized LTC$_4$ and histamine differed markedly in several important respects. Histamine caused a reversible increase of transpulmonary pressure, lasting for less than 10 min (Fig. 3), and reflected only by minor transient changes in PAP and arterial P_{O_2}. On the other hand, LTC$_4$ aerosols evoked long-lasting changes of pulmonary function (see Fig. 3). When the response to LTC$_4$ was maximal in this experiment, transpulmonary pressure had increased by 163%, while arterial P_{O_2} had decreased from 9.6 to 5.8 kPa. The hypoxaemia was accompanied by a severe pulmonary hypertension, PAP increasing by almost 100%. Induced changes of transpulmonary pressure, PAP and P_{O_2} only slowly returned to normal values over 45 min, even though the animals were subjected to positive end expiratory pressure to combat the formation of atelectases. Finally, the increase in transpulmonary pressure induced by nebulized as well as injected LTC$_4$ was mainly caused by a reduction of pulmonary dynamic compliance, whereas pulmonary resistance was only slightly affected. Histamine, on the other hand, had relatively little effect on compliance, but caused a marked rise in resistance. This observation is compatible with the view that LTC$_4$ affects peripheral airways, as previously suggested for crude SRS-A[17].

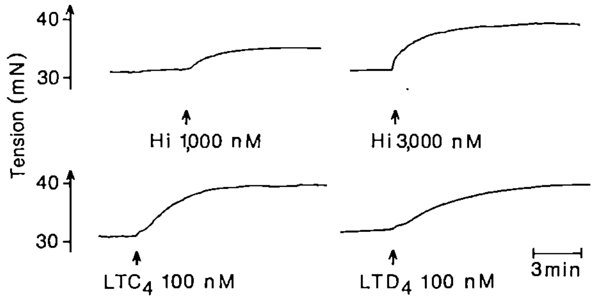

Fig. 4 Isometric recordings of basal tone and contraction responses to histamine (Hi), LTC$_4$ and LTD$_4$ in isolated helical strips of monkey trachea. Drugs were added at arrows to the indicated final concentration in a Tyrode-containing organ bath, and washed away when bath fluid was changed (end of tracing).

The view that LTC$_4$ is a bronchoconstrictor in the monkey gains further support from experiments with isolated tracheal strips. Leukotriene C$_4$ and its immediate metabolite LTD$_4$ potently contracted the monkey trachea (Fig. 4). Note that this species was less reactive to leukotrienes, as well as to histamine, than are corresponding preparations from guinea pig and man[16,18,19]. Nevertheless, the leukotrienes were ~100 times as potent as histamine.

The finding that LTC$_4$ elicits pronounced cardiovascular and bronchial reactions in the monkey *in vivo*, and that systemic injection of LTC$_4$ is accompanied by a reversible drop in circulating leukocytes suggests that these effects are also applicable in man, especially as leukotrienes are active in isolated human tissues[19,20]. Endogenous leukotrienes may contribute to the symptoms of bronchial asthma in man; and the pharmacological actions[7,16] exerted by these substances suggest leukotriene involvement in a number of other hypersensitivity states, as well as in the inflammatory reaction.

We thank Ms G Fredrickson for technical assistance, Mr R. Bentin for animal care and Ms A Lindbom for secretarial help. The work was supported by grants from the Swedish MRC (04X-4342, 03X-217, 03X-5914), the Karolinska Institutet and the Swedish National Association Against Chest and Heart Diseases.

Received 10 September; accepted 13 November 1981.

1. Samuelsson, B., Hammarström, S., Murphy, R. C. & Borgeat, P. *Allergy* **35**, 375–381 (1980).
2. Samuelsson, B. & Hammarström, S. *Prostaglandins* **19**, 645–648 (1980).
3. Lewis, R. A., Drazen, J. M., Austen, K. F., Clark, D. A. & Corey, E. J. *Biochem. biophys. Res. Commun.* **96**, 271–277 (1980).
4. Hedqvist, P., Dahlén, S.-E., Gustafsson, L., Hammarström, S. & Samuelsson, B. *Acta physiol. scand.* **110**, 331–333 (1980).
5. Drazen, J. M. *et al. Proc. natn. Acad. Sci. U.S.A.* **77**, 4354–4358 (1980).
6. Welton, A. F., Crowley, H. J., Miller, D. A. & Yaremko, B. *Prostaglandins* **21**, 287–296 (1981).
7. Piper, P. J. *et al.* in *SRS-A and Leukotrienes* (ed. Piper, P. J.) 81–99 (Wiley, Chichester, 1981).
8. Dahlén, S.-E. *et al. Proc. natn. Acad. Sci. U.S.A.* **78**, 3887–3891 (1981).
9. Smedegård, G., Revenäs, B., Lundberg, C. & Arfors, K.-E. *Acta physiol. scand.* **111**, 239–247 (1981).
10. Revenäs, B., Smedegård, G. & Arfors, K.-E. *Acta anaesth. scand.* **23**, 278–284 (1979).
11. Murphy, R. C., Hammarström, S. & Samuelsson, B. *Proc. natn. Acad. Sci. U.S.A.* **76**, 4275–4279 (1979).
12. Levi, R. in *Advances in Prostaglandin and Thromboxane Research* (eds Samuelsson, B. & Paoletti, R.) (Raven, New York, in the press).
13. Piper, P. J. in *Advances in Prostaglandin and Thromboxane Research* (eds Samuelsson, B. & Paoletti, R.) (Raven, New York, in the press).
14. Hammarström, S. *et al. Biochem. biophys. Res. Commun.* **101**, 1109–1115 (1981).
15. Hammarström, S. in *Advances in Prostaglandin and Thromboxane Research* (eds Samuelsson, B. & Paoletti, R.) (Raven, New York, in the press).
16. Hedqvist, P., Dahlén, S.-E. & Björk, J. in *Advances in Prostaglandin and Thromboxane Research* (eds Samuelsson, B. & Paoletti, R.) (Raven, New York, in the press).
17. Drazen, J. M. & Austen, K. F. *J. clin. Invest.* **53**, 1679–1685 (1974).
18. Dahlén, S.-E., Hedqvist, P. & Hammarström, S. *Acta physiol. scand.* (in the press).
19. Dahlén, S.-E., Hedqvist, P., Hammarström, S. & Samuelsson, B. *Nature* **288**, 484–486 (1980).
20. Hanna, C. J., Bach, M. K., Pare, P. D. & Schellenberg, R. R. *Nature* **290**, 343–344 (1981).

Lack of immune response gene control for induction of epitope-specific suppression by TGAL antigen

Leonore A. Herzenberg, Takeshi Tokuhisa*, Kyoko Hayakawa & Leonard A. Herzenberg

Department of Genetics, Stanford University School of Medicine, Stanford, California 94305, USA

Immune response genes in the *I* region of the mouse major histocompatibility complex (MHC) have been divided operationally according to whether they control responses to antigens which do or do not induce active suppression in non-responder animals (IS and IR genes respectively)[1,2]. Studies presented here, however, show that the synthetic terpolymer poly-L-(tyrosine, glutamic acid)-poly-DL-alanine-poly-L-lysine

---

* Present address: Laboratories for Immunology, School of Medicine, Chiba University, 1-8-1 Inohana, Chiba, Japan 280.

0028-0836/82/040329—03$01.00

Table 1 C3H (Ir-1a) mice are 'non-responders' to TGAL

Strain	TGAL immunizations*		Anti-TGAL response (normalized)* IgM	IgG1	IgG2a	IgG3
C3H	Primary	TGAL	18	2	<3	5
	Primary	TNP–TGAL	7	1	<3	2
	Secondary	TNP–TGAL, TNP–TGAL	7	1	<3	2
C3H.SW	Primary	TGAL	100	100	100	100
	Primary	TNP–TGAL	93	113	65	102
	Secondary	TNP–TGAL, TNP–TGAL	51	319	74	115
	Secondary	TGAL/TNP–TGAL	40	409	85	116

Responses measured by radioimmunoassay (RIA)[20,21] 2 weeks after the last indicated immunization are reported relative to the anti-TGAL primary response of each isotype obtained in C3H.SW mice.

* See Table 4 legend for antigen dosage and immunization schedule.

(TGAL)[3,4], commonly considered the prototype of antigens which do not induce suppression, actually serves as a potent inducer of epitope-specific suppression for antibody responses in non-responder mice.

The induction of epitope-specific suppression is a general (albeit recently recognized) immunoregulatory process readily demonstrable by sequential immunizations with carrier proteins and hapten–carrier conjugates[5–7]. Primary immunization with a carrier protein induces the delayed appearance of carrier-specific suppressor T cells (CTS)[8,9] which persist and induce specific suppression for IgG antibody responses to 'new' epitopes presented subsequently on the priming carrier. The 'epitope-specific' mechanism responsible for this suppression also persists (once induced) and continues to suppress antibody responses to the 'new' epitope, whether presented subsequently on the priming carrier or on a second, unrelated carrier molecule. (We have previously referred to this system as hapten specific, using the term 'hapten' in its more general sense (synonymous with epitope) to indicate a relatively small structure which induces antibody production when presented on a larger (carrier) molecule. The term 'hapten', however, is also commonly used to distinguish artificially added structures, such as the dinitrophenyl group (DNP), from the native epitopes on a carrier molecule (antigen). Therefore, to avoid ambiguity, we have now substituted the term 'epitope-specific' for the previous nomenclature.)

For example, priming with keyhole limpet haemocyanin (KLH) and subsequent immunization with the DNP–KLH (dinitrophenyl hapten conjugated to KLH) induces specific suppression for IgG anti-DNP antibody production[5–9]. This KLH/DNP–KLH-induced suppression then serves with equal effectiveness to prevent antibody responses to DNP presented either on KLH or on chicken γ-globulin (CGG). It does not, however, interfere with antibody production to either carrier molecule.

Table 2 Anti-TNP responses to TNP–TGAL are suppressed in C3H.SW ('responder') mice preimmunized with TGAL and fail entirely in C3H ('non-responder') mice

Strain	Immunization(s)*	Anti-TNP response IgM (U)	IgG1 (μg ml^{-1})	Ig2a (μg ml^{-1})	IgG3 (U)
C3H	TNP–TGAL	144	<3	<1	10
	TNP–TGAL/ TNP–TGAL	191	<15	<3	11
	TGAL/TNP–TGAL	106	<3	<1	8
C3H.SW	TNP–TGAL	125	35	13	63
	TNP–TGAL/ TNP–TGAL	86	95	16	76
	TGAL/TNP–TGAL	96	<3	<9	12

Anti-TNP responses were measured by RIA 2 weeks after last indicated immunization. IgG1 and IgG2a responses are presented as μg antibody per ml serum; IgG3 and IgM responses as percentage of response obtained in an adoptive secondary 'standard' antiserum.

* See Table 4 legend for antigen dosage and immunization schedule.

Reversing the carriers in the immunization sequence yields similar results, that is, CGG/DNP–CGG-induced suppression also prevents subsequent anti-DNP responses to either DNP–KLH or DNP–CGG. Mismatching carriers (such as KLH/DNP–CGG immunization) results, however, in anti-DNP antibody production rather than suppression (ref. 6 and L.A.H. and T.T., in preparation). Thus epitope-specific suppression is induced by carrier-specific interactions but is mediated by an effector mechanism that operates without reference to the carrier on which a hapten (epitope) is presented.

Further selectivity displayed by this effector mechanism generates a characteristic anti-DNP response pattern in suppressed animals: high-affinity anti-DNP antibody production is preferentially suppressed; IgM anti-DNP responses are unaffected; IgG1 responses are usually suppressed initially and generally 'escape' suppression after a second or third stimulation with DNP; and the remaining IgG isotypes (IgG2a, IgG2b, IgG3) are universally suppressed at first and generally require three or four sequential stimulations with DNP to induce substantial escape from suppression (ref. 6 and L.A.H. and T.T., in preparation). Therefore, epitope-specific suppression is recognizable by both its specificity for the inducing hapten and its differential effects on the various immunoglobulin isotype responses produced to that hapten.

Table 3 TGAL/TNP–TGAL immunization induces persistent epitope-specific suppression for IgG anti-TNP antibody production in C3H ('non-responder') mice

Strain	Pre-immunization*	Serum IgG2a anti-TNP (μg ml^{-1}) Subsequent immunizations* (first) TNP–KLH	(second) TNP–KLH	(third) TNP–CGG
C3H	None	35 (2)	68 (60)	85 (40)
	TNP–TGAL	28 (7)	82 (60)	70 (30)
	TGAL/TNP–TGAL	<3	9 (<1)	16 (6)
C3H.SW	None	24 (7)	110 (50)	150 (50)
	TNP–TGAL	250 (140)	370 (220)	160 (50)
	TGAL/TNP–TGAL	14 (<1)	180 (70)	160 (50)

Anti-TNP levels in serum were measured by RIA[20,21] 2 weeks after each indicated immunization. Relative affinity (shown in parentheses) is calculated from ratios of antibody bound to differently substituted TNP conjugates (TNP7–BSA/TNP24–BSA) based on a standard curve developed for absolute measurements of anti-DNP binding affinities (K_a)[21].

* Antibody responses to TGAL and TNP–TGAL in these animals are shown in Tables 1 and 2 respectively. See Table 4 legend for antigen dosage and immunization schedule.

We have now used similar immunization sequences and response criteria in MHC congenic mice to investigate the influence of IR genes on epitope-specific suppression induction by TGAL. The C3H (Ir-1a) mice used are typically 'non-responsive' to the TGAL antigen[3,4] in that they produce no detectable IgG anti-TGAL responses and only a small IgM anti-TGAL response, even when stimulated twice with 100 μg TGAL on alum. The congenic C3H.SW (Ir-1b) mice, in contrast, produce both IgM and IgG anti-TGAL primary antibody responses and show a strong IgG secondary response to this antigen (see Table 1). Similarly, C3H mice do not produce detectable amounts of IgG antibody to the trinitrophenyl (TNP) hapten presented on TGAL whereas C3H.SW mice stimulated with TNP–TGAL produce typical primary and secondary anti-TNP responses (see Table 2).

Surprisingly, this classical difference in responsiveness to TGAL disappears when response is measured in terms of epitope-specific suppression induction by TGAL/TNP–TGAL immunization. Both the 'non-responder' and 'responder' mice respond strongly to this immunization sequence by developing a persistent suppression for IgG antibody production to TNP (see Tables 3 and 4). In fact, the 'non-responder' strain (C3H) responds even more vigorously than the 'responder' in that its

Table 4 Epitope-specific suppression in C3H mice shows typical isotype selectivity

Strain	Immunizations				% Of control anti-TNP response* IgM	IgG1	IgG2a	IgG3
C3H	TGAL	TNP–TGA	TNP–KLH		110	19	<11	10
	TGAL	TNP–TGAL	TNP–KLH	TNP–KLH	86	120	11	25
	TGAL	TNP–TGAL	TNP–KLH	TNP–CGG	53	200	23	10
C3H.SW	TGAL	TNP–TGAL	TNP–KLH		120	16	6	50
	TGAL	TNP–TGAL	TNP–KLH	TNP–KLH	94	100	47	20
	TGAL	TNP–TGAL	TNP–KLH	TNP–CGG	44	70	100	13

Immunizations of 100 μg each antigen were given intraperitoneally on alum at 0, 5, 7, 10 and 14 weeks respectively.

* Serum anti-TNP levels were measured by RIA[20,21] 2 weeks after last indicated immunization. Data are presented as the percentage of the anti-TNP response obtained in corresponding control groups immunized initially with TNP–TGAL (once) rather than with the TGAL/TNP–TGAL sequence. Absolute control responses for IgG2a are shown in Table 3.

IgG2a and IgG3 anti-TNP responses generally remain suppressed following repeated stimulation with TNP (on CGG and KLH) whereas these isotype responses escape suppression in typical fashion in the 'responder' (C3H.SW) strain (see Table 4). Thus 'non-responder' animals clearly recognize TGAL in an immunological context and can use this antigen as a carrier for presenting haptens to initiate the induction of epitope-specific suppression.

These findings suggest that TGAL is capable of generating functional carrier (TGAL)-specific suppressor T cells which induce epitope-specific suppression for TNP on TGAL (as KLH-specific suppressor T cells initiate the induction of epitope-specific suppression in KLH-primed mice)[8,9]. Thus although the IR gene controlling responses to TGAL largely prevents TGAL-dependent stimulation of T-cell proliferation and IgG antibody production, it does not seem to interfere with the full set of (TGAL-dependent) T-cell interactions involved in the development of carrier-specific suppressor T cells[10–15].

Therefore, in addition to demonstrating that both IR and IS genes permit suppression induction, our results indicate that certain TGAL-specific T-cell pathways (not readily demonstrable by T-cell proliferation assays) remain intact in 'non-responder' mice, thereby suggesting several possible roles for the apparently functionless TGAL-specific T-cell clones recently isolated from 'non-responder' mice[16].

Finally, the unhampered induction of epitope-specific suppression in 'non-responder' mice suggests that the epitope-specific system may provide a versatile effector mechanism which permits *I*-region genes to exert a selective, long-term influence on the magnitude and heterogeneity of antibody responses. This would explain how certain of these genes can modify the composition of antibody responses to epitopes on antigens that induce some antibody production in 'non-responder' animals[17,18]. The restricted heterogeneity of these antibody responses, the tendency towards production of IgG1 rather than IgG2a antibodies and the apparent involvement of suppressor T cells in the regulatory process clearly point to epitope-specific regulation. Thus we suspect that diagnostic sequential immunization protocols similar to those used here would reveal the induction of epitope-specific suppression in these partially responsive mice.

TGAL and TNP–TGAL, unlike the antigens discussed above, do not induce substantial IgG antibody production in non-responder mice (see Tables 1, 2). Furthermore, a single initial immunization with TNP–TGAL does not appear to affect subsequent anti-TNP responses to TNP on other carriers (see Table 3). At face value, therefore, the evidence presented here suggests that epitope-specific suppression induction by antigens like TNP–TGAL requires prior TGAL priming (or perhaps two sequential immunizations with the TNP–TGAL conjugate). However, should TNP–TGAL immunization prove to induce B-cell memory for TNP in 'non-responders' (work in progress), this conclusion would have to be modified since the presence of such memory B cells in TNP–TGAL-primed animals would indicate that the primary level anti-TNP response observed to TNP–KLH in these animals actually represents the weak suppression of a potential secondary anti-TNP response.

That the epitope-specific regulatory system may serve to maintain antibody response characteristics dictated initially by *I*-region-defined mechanisms is consistent with evidence from studies showing that this system maintains suppression for responses prevented initially by the allotype suppression mechanism[19] and mediates suppression initiated by carrier-specific suppressor T-cell interactions[8,9]. These data suggest that the epitope-specific system provides a common effector mechanism through which non-responsiveness, whatever its genesis, can be maintained.

Furthermore, because the epitope-specific system suppresses responses to individual epitopes regardless of the carrier on which the epitope is subsequently presented, it offers a general mechanism through which undesirable antibody responses (such as to self) can be controlled should an epitope to which non-responsiveness has been induced be encountered later on an immunogenic carrier. Thus this previously unrecognized regulatory system introduces a novel immunological memory mechanism capable of being 'educated' selectively to suppress antibody production to individual epitopes according to conditions in the regulatory environment when the epitope is first introduced.

We thank Dr A. Singer for preparing the TNP–TGAL hapten–carrier conjugate and for supplying both conjugated and 'native' TGAL. We also thank Mr Timothy Gadus for technical assistance. This work was supported in part by NIH grants HD-01287 and AI-08917.

Received 17 August; accepted 24 November 1981.

1. Debre, P., Kapp, J. A., Dorf, M. E. & Benacerraf, B. *J. exp. Med.* **142,** 1447 (1975).
2. Benacerraf, B. & Germain, R. N. *Immun. Rev.* **38,** 71 (1978).
3. McDevitt, H. O. & Sela, M. *J. exp. Med.* **122,** 517 (1965).
4. McDevitt, H. O. & Benacerraf, B. *Adv. Immun.* **11,** 31 (1969).
5. Herzenberg, L. A., Tokuhisa, T. & Herzenberg, L. A. *Nature* **285,** 664–666 (1980).
6. Herzenberg, L. A. thesis, Univ. Paris VI (1981).
7. Herzenberg, L. A., Tokuhisa, T. & Herzenberg, L. A. in *The Immune System* (ed. Karger, S.) (AG Publications, Basel, in the press).
8. Herzenberg, L. A. & Tokuhisa, T. *ICN–UCLA Symp. on molec. cell. Biol.* Suppl. 5, 8 (1981).
9. Herzenberg, L. A., Tokuhisa, T. & Herzenberg, L. A. *Immun. Today* **2,** 40–46 (1981).
10. Gershon, R. K. in *Contemporary Topics in Immunobiology* Vol. 3 (eds Cooper, M. & Warner, N. L.) (Plenum, New York, 1974).
11. Tada, T., Taniguchi, M. & Takemori, T. *Transplantn Rev.* **26,** 106 (1975).
12. Tada, T. & Okumura, K. *Adv. Immun.* **28,** 1 (1979).
13. Benacerraf, B., Kapp, J. A. & Pierce, C. W. in *Immunological Tolerance* (eds Katz, D. H. & Benacerraf, B.) 507 (Academic, New York, 1974).
14. Basten, A., Miller, J. F. A. P. & Johnson, P. *Transplantn Rev.* **26,** 130 (1975).
15. Sercarz, E. E. *et al. Immun. Rev.* **39,** 108 (1978).
16. Kimoto, M., Krenz, T. J. & Fathman, C. G. *J. exp. Med.* (in the press).
17. Kipps, T. J., Benacerraf, B. & Dorf, M. E. *Eur. J. Immun.* **8,** 415 (1978).
18. Kipps, T. J., Benacerraf, B. & Dorf, M. E. *Proc. natn. Acad. Sci. U.S.A.* **175,** 2914 (1978).
19. Herzenberg, L. A., Tokuhisa, T., Parks, D. R. & Herzenberg, L. A. *Immun. Today* (in the press).
20. Tsu, T. T. & Herzenberg, L. A. in *Selected Methods in Cellular Immunology* (eds Mishell, B. B. & Shiigi, S. M.) 373–397 (Freeman, San Francisco, 1980).
21. Herzenberg, L. A., Black, S. J., Tokuhisa, T. & Herzenberg, L. A. *J. exp. Med.* **141,** 1071–1087 (1980).

Rapid lateral diffusion of functional ACh receptors in embryonic muscle cell membrane

Mu-ming Poo

Department of Physiology and Biophysics, University of California, Irvine, California 92717, USA

During synaptogenesis of the skeletal neuromuscular junction, the acetylcholine (ACh) receptors dispersed over the surface of the embryonic muscle become highly concentrated at the subsynaptic membrane[1,2]. The mechanism by which a nerve induces such a modulation of ACh receptor topography is unknown. Of various possibilities[3], the simplest explanation is that the ACh receptors, freely diffusing in the plane of the muscle membrane, are trapped at the site of nerve contact[4,5]. This 'diffusion-trap' mechanism is plausible only if the diffusion distance covered by the ACh receptors within its lifetime on the cell surface is at least comparable with the dimension of the embryonic muscle fibre (see also discussion in ref. 1). Photobleaching studies had suggested that this was not the case. In the present study, an electrophysiological method was used to measure the lateral diffusion of the dispersed, functional ACh receptors in the plasma membrane of cultured *Xenopus* embryonic muscle cells. The results suggest that these ACh receptors undergo rapid lateral diffusion with a diffusion coefficient of 2.6×10^{-9} cm^2 s^{-1} at 22 °C. This rapid diffusion of the dispersed ACh receptors strongly supports a passive diffusion-trap mechanism for the localization of ACh receptors at the site of nerve–muscle contact.

The experimental strategy used in this study was to inactivate ACh receptors locally on the muscle surface using α-bungarotoxin (α-BTX), a snake toxin that binds irreversibly to the ACh receptor. The recovery of ACh sensitivity at the site of inactivation was mapped by an iontophoretic method[6] to reveal the lateral diffusion of the functional, toxin-free ACh receptors in the membrane. In the first series of experiments using a spindle-shaped muscle cell, ACh sensitivity was monitored continuously by intracellular recording of the membrane depolarizations following repetitive ejection of constant ACh pulses from an iontophoretic pipette. Local inactivation of ACh receptors was achieved by applying a small pulse of α-BTX (50 μg ml^{-1}) through a micropipette, the tip of which was positioned within 1 μm of the site of iontophoretic mapping (Fig. 1*a*). As shown in Fig. 1*b–d*, the local pulse-inactivation resulted in a rapid drop in ACh sensitivity, followed by a return of sensitivity to the original level with a time course of the order of minutes. Recovery of ACh sensitivity was observed in 15 out of 19 cells successfully studied. However, the rate as well as the extent of the recovery varied considerably: the greater the extent (or the wider the spread) of inactivation, the slower and less complete was the recovery.

The return of ACh sensitivity was not due to functional recovery of the inactivated receptors or insertion of newly synthesized receptors into the membrane, as (1) it is known that α-BTX binding to the ACh receptors is irreversible in the time scale of these experiments, and (2) no detectable recovery of ACh sensitivity was observed within 10 h when these cells were inactivated uniformly by bathing them with α-BTX and then extensively washing them with fresh saline. It was not the result of some unknown effect of local pressure application during the pulse-inactivation, as the same local pressure applied through a saline-filled pipette had no effect on the ACh sensitivity. Finally, this recovery of ACh sensitivity was blocked by preincubation of the cells with saline containing concanavalin A (Con A) (100 μg ml^{-1}; Sigma) for 8 min before inactivation experiments (for all 10 cells studied in two separate cultures). Con A, a tetrameric lectin that binds specifically to α-D-glucose or α-D-mannose residues of the cell surface carbohydrates, binds and immobilizes ACh receptors[7–9]. Taken together, these findings strongly suggest that the recovery of ACh sensitivity after local

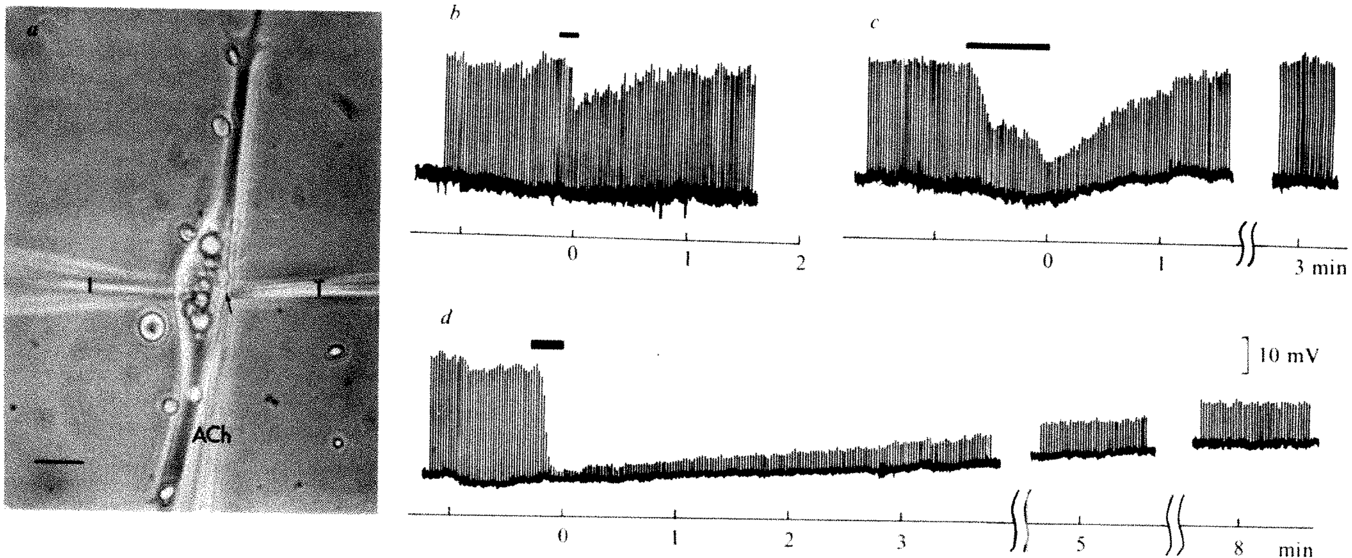

Fig. 1 Recovery of ACh sensitivity after local irreversible inactivation of ACh receptors. Spindle-shaped embryonic *Xenopus* muscle cells in $1\frac{1}{2}$-day-old cultures were used in these experiments (for culture methods, see ref. 8). ACh sensitivity at a local spot on the muscle surface was monitored by an iontophoretic method[6]. Intracellular recordings were made using a glass microelectrode filled with 3 M potassium acetate (resistance 80–150 MΩ). Microelectrodes (resistance 200–350 MΩ) for iontophoretic application of ACh were filled with 3 M acetylcholine chloride (Sigma) and required braking currents of 1.0–2.0 nA to prevent ACh leakage from the pipette and depolarization of the cells. Constant iontophoretic current pulses of amplitude 5–10 nA and 1 ms duration were delivered through a microelectrode preamplifier (Getting) to the ACh pipette near the cell surface. A third glass micropipette having a tip opening of ~2 μm was filled with α-BTX (50 μg ml^{-1}) and positioned near the iontophoretic pipette. A small negative (sucking) pressure was applied using a micrometer-controlled syringe during the positioning of the pipette, and after the local inactivation. Local inactivation of the ACh receptor was achieved by applying a positive pressure through the toxin pipette. *a*, Phase-contrast micrograph showing representative morphology of spindle-shaped *Xenopus* muscle cells, together with the positioning of the pipettes for intracellular recording (I), iontophoresis (ACh) and toxin application (T). Scale bar 20 μm. *b–d*, Continuous d.c. recording of membrane potentials and ACh-induced potentials of three different myotomal cells during the local-inactivation experiments. Solid bars indicate the duration of positive-pressure application through the toxin pipette. The constant amplitudes of membrane depolarizations resulting from constant ACh current pulses before toxin application suggest that no desensitization of the ACh receptor occurred at the frequency of stimulation (~1 Hz) used in these experiments. The rate and extent of recovery of ACh-induced response was reduced from *c* to *d*, as more ACh receptors were inactivated by the toxin. At the start of recording, the membrane potentials of the cells were 96, 92 and 105 mV for the cells in *b*, *c* and *d*, respectively.

0028-0836/82/040332—03$01.00

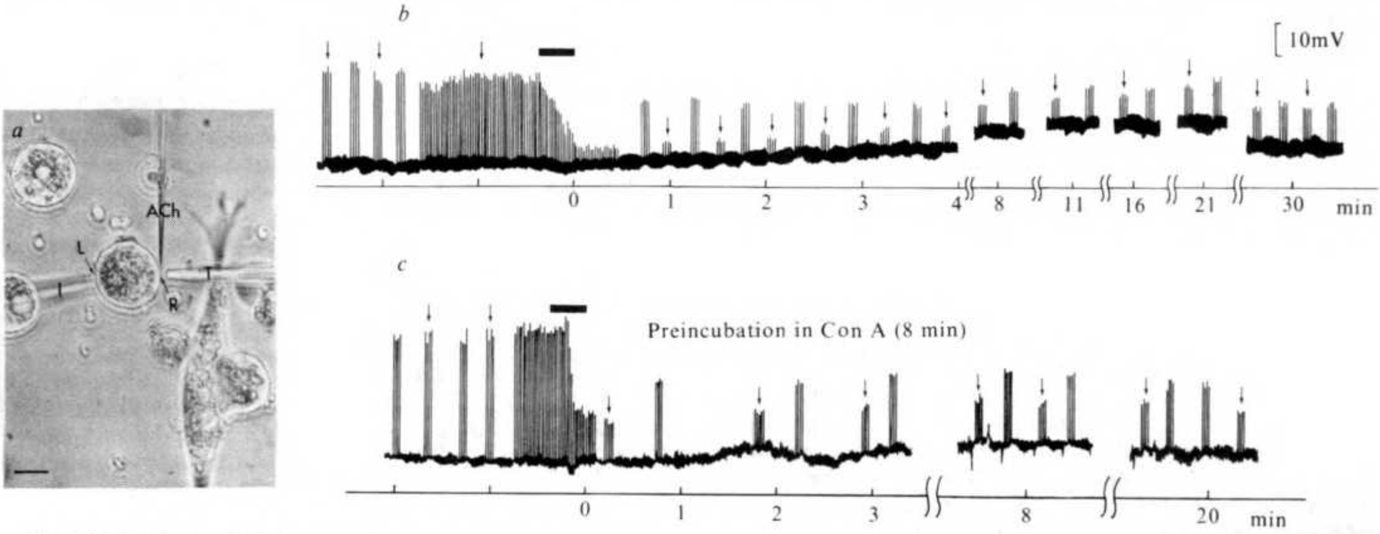

Fig. 2 Redistribution of ACh sensitivity after asymmetric inactivation of ACh receptors on two sides of spherical-shaped *Xenopus* muscle cells in $1\frac{1}{2}$-day-old culture. The electrophysiological method used was the same as that described in Fig. 1 legend, except that the toxin pipette was positioned 2–4 μm away from the cell surface, and the ACh sensitivity was monitored alternately at two opposite poles of the cell, where maximum (R) and minimum (L) inactivation was produced. *a*, Phase-contrast micrograph of a representative spherical muscle cell, showing the positions of the pipettes used for intracellular recording (I), ionotophoresis (ACh) and toxin application (T). Scale bar 20 μm. *b*, Alternating recordings of membrane depolarization responses for ACh ejected at two opposite poles of the spherical muscle cell in a typical experiment. Before preferential inactivation, the responses were almost identical. After pulse-inactivation with α-BTX, the right side (arrow) of the cell was much less sensitive to ACh than the left side (without arrow). This sensitivity asymmetry decayed with time over ~30 min after pulse-inactivation. Solid bar represents the duration of positive-pressure application through the toxin pipette. The membrane potential at the start of recording was 102 mV, and it varied by <15 mV during the 30-min period. Note the concurrent drop in ACh sensitivity on the left side as that of the right side increased. *c*, Typical recording of preferential inactivation experiments on cells pretreated with Con A. Note the absence of any significant redistribution of ACh sensitivity over a period of 20 min after asymmetric receptor inactivation.

pulse-inactivation represents a redistribution of pre-existing functional ACh receptors in the plane of the plasma membrane.

In the experiments described above, it was difficult to estimate quantitatively the diffusion coefficient of the ACh receptors from the rate of sensitivity recovery, as the extent and pattern of inactivation varied from cell to cell. To resolve this, spherical-shaped *Xenopus* muscle cells (Fig. 2*a*) were used in a second series of experiments, in which an asymmetric inactivation of the ACh receptors was produced across the entire surface of the cell. The redistribution of functional ACh receptors across the cells was then monitored by repetitive comparison of ACh sensitivity on the two sides of the cell. The diffusion coefficient of the receptors was estimated from the rate of decay of the sensitivity asymmetry, which, for a first-order approximation, is determined entirely by the size of the cell[10]. Representative results are shown in Fig. 2*b*. Depolarizations of the muscle membrane in response to identical pulses of ACh ejected at two opposite poles of the cells were monitored alternately. As seen in the initial few measurements in Fig. 2*b*, almost identical ACh sensitivity was detected on the opposite sides of the cell. A pipette containing α-BTX was then positioned ~2–4 μm from one side of the cell and used to pulse-inactivate the ACh receptors on the muscle surface, resulting in asymmetric ACh sensitivity on the two sides of the cell. Subsequent comparison of ACh-induced responses on the two sides of the cell indicated that the sensitivity asymmetry decayed with time, suggesting a redistribution of the functional ACh receptors across the cell surface.

The redistribution of ACh sensitivity was determined quantitatively by plotting sensitivity asymmetry index against time after asymmetric inactivation. The asymmetry index (A) is defined by $A=(V_A-V_B)/(V_A+V_B)$, where V_A and V_B are average peak amplitudes of membrane depolarization induced by identical iontophoretic ACh pulses on the minimally and maximally inactivated sides of the cell, respectively. The use of peak amplitude of ACh potential as a simple representation of ACh sensitivity in this formula was considered satisfactory, as these indices differed by <5% (average of three comparisons) from those calculated using ACh sensitivity determined by the conventional method in terms of mV/nC (see for example, ref. 5). Assuming the surface concentration of ACh receptors to be linearly proportional to the ACh sensitivity, the rate of decay of the asymmetry indices can be used to calculate the diffusion coefficient of the ACh receptors in the membrane. Previous analyses of the diffusion process on the surface of a spherical cell[9–11] indicated that the diffusion coefficient (D) of the diffusing molecule is related to the radius (r_o) of the cell by $D=r_o^2/2t_d$, where t_d is the characteristic $1/e$ decay time of the asymmetry in the surface distribution. In a $1\frac{1}{2}$-day-old culture, the average diffusion coefficient of the ACh receptors determined by this method was $2.6\ (\pm 1.6)\times 10^{-9}\ \text{cm}^2\ \text{s}^{-1}$ at 22 °C (±s.d., 14 cells from four separate cultures). Figure 3 shows an analysis of the decay of ACh sensitivity asymmetry in three different cells. Note that the ACh receptor density may be related nonlinearly to the ACh sensitivity[12]. However, because the time course of the decay in sensitivity asymmetry agreed

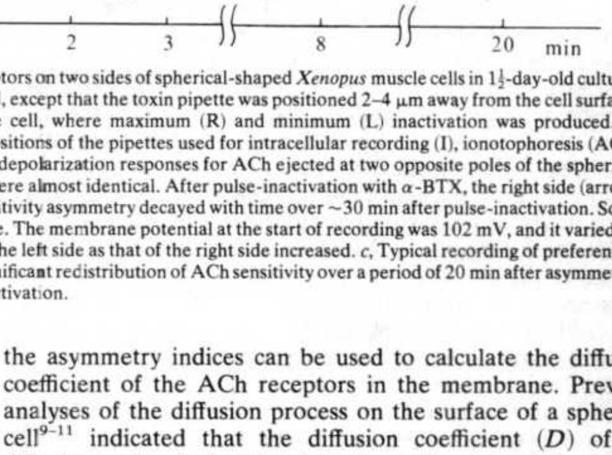

Fig. 3 Asymmetry in ACh sensitivity at two opposite poles of the spherical *Xenopus* muscle cells, plotted against the time after pulse-inactivation with α-BTX of ACh receptors at one pole. Asymmetry was determined as described in the text. Open symbols represent recordings from three different cells of a $1\frac{1}{2}$-day-old culture. Solid curves represent the best least-squares fit to these three sets of data with first-order decay kinetics, including points beyond 20 min. The characteristic $1/e$ times for the decay were 11.0, 12.8 and 11.8 min, respectively, for cells of radius 23, 20 and 20 μm. These decay rates suggest a diffusion coefficient for the ACh receptors of 4.0, 2.5 and $2.7\times 10^{-9}\ \text{cm}^2\ \text{s}^{-1}$, respectively. Solid symbols represent two sets of recordings from cells pretreated with Con A (100 μg ml^{-1}, 8-min preincubation).

satisfactorily with first-order decay kinetics (see Fig. 3), the nonlinearity of the receptor–sensitivity relationship is probably negligible in the present analysis.

The diffusion coefficient of ACh receptors in the embryonic *Xenopus* muscle observed here is surprisingly similar to that found for rhodopsin in the photoreceptor disk membrane[13], for surface antigens on cultured muscle fibres[14] and for several lectin receptors[9,10] in the same *Xenopus* muscle cells as used in the present study. However, the diffusion coefficient is 50-fold higher than that found for ACh receptor–toxin complexes in rat myotube culture by the fluorescence photobleaching method[15]. In addition, whereas 25% of the dispersed receptors were found to be immobile in photobleaching studies[15], I found no evidence of immobile fractions of the dispersed ACh receptors in these cultured muscle cells. The asymmetry in ACh sensitivity (resulting from asymmetric inactivation) always decays to a level close to zero, regardless of the extent of inactivation. For example, in the experiment represented by open circles in Fig. 3, asymmetric inactivation resulted in $\sim$93% and 12% inactivation on the two sides of the cell, respectively (asymmetry index $= 0.85$). If 25% of the ACh receptors are immobile in the membrane, there should be a persistent asymmetry of $\sim$0.2, whereas the data indicate that the asymmetry had decayed to <0.06 within 30 min. The reason for the discrepancy between my results and those from photobleaching studies is unknown. In addition to the possibility of species difference, the binding of α-BTX, a prerequisite for the photobleaching method, may greatly affect the rate of lateral diffusion of the ACh receptors. Diffusion measurements of ACh receptors by both methods using the same cell type are now being made.

Recent studies have shown a rapid accumulation of ACh receptors at nerve–muscle contacts in culture[16–19]. Extensive rearrangement of ACh receptor topography over a distance of $\sim 50\ \mu$m was observed within 6 h after the nerve contact[18,19]. The rate of lateral diffusion ($D = 2.6 \times 10^{-9}\ \mathrm{cm}^2\ \mathrm{s}^{-1}$) of ACh receptors reported here indicates that within 6 h (t), an ACh receptor is capable of diffusing laterally over an average distance ($\bar{s}$) of 150 µm ($\bar{s}^2 = 4Dt$). A simple passive diffusion-trap mechanism could thus account for the lateral rearrangement of ACh receptor topography induced by the nerve contact. By assuming that the nerve terminal region serves as a 'sticky zone' for trapping diffusing extrajunctional ACh receptors, Edwards and Frisch[4] also concluded that a diffusion-trap mechanism could account for the localization of ACh receptors at mature muscle endplates if the diffusion coefficient of the extrajunctional ACh receptors is $2 \times 10^{-9}\ \mathrm{cm}^2\ \mathrm{s}^{-1}$ or higher.

Various cellular processes could provide a trapping mechanism at the site of nerve contact. The surface of the nerve terminal may contain molecular groups that bind specifically to the ACh receptors in the muscle membrane. The nerve terminal may release locally trophic substances[20–22] which promote aggregation of the ACh receptors near the site of release. Alternatively, contact by the nerve terminal may alter the surface properties of the muscle membrane in a way that favours electrodynamic (van der Waals') attraction[23] among the ACh receptors, leading to formation of receptor aggregates at the site of contact. This last process seems the most likely mechanism for the induction of ACh receptor aggregates by nonspecific means, for example, contact with the culture substratum[24], with pieces of thread[25] or with positively charged latex beads[26] placed on top of the cell.

I have demonstrated a rapid diffusional movement of a specific, functional membrane protein/ionic channel in the plane of the plasma membrane which, together with a previous report[6], completes the description of both electrophoretic and diffusional mobilities of a defined membrane protein *in situ*. The rapidity of the lateral diffusion of the ACh receptor in the embryonic muscle membrane supports the notion that an efficient localization of the receptor can be achieved during synapotogenesis by a passive diffusion-trap mechanism. Finally, the asymmetric inactivation method reported here may also prove useful in examining the diffusional mobility of other membrane receptors/ionic channels, for which inhibitory ligands of relatively high affinity are available.

I thank Drs S. E. Fraser, D. Petersen, S. Young and I. Chow for helpful discussion and comments. This work was supported by grants from the NSF and NIH.

Received 14 August; accepted 27 November 1981.

1. Fambrough, D. M. *Physiol. Rev.* **59,** 165–227 (1979).
2. Lømo, T. & Jansen, J. K. S. *Curr. Topics dev. Biol.* **16,** 253–281 (1980).
3. Fraser, S. E. & Poo, M-m. *Curr. Topics dev. Biol.* **17** (in the press).
4. Edwards, C. & Frisch, H. L. *J. Neurobiol.* **7,** 377–381 (1976).
5. Chao, N. M., Young, S. H. & Poo, M-m. *Biophys. J.* **36,** 139–153 (1981).
6. Orida, N. & Poo, M-m. *Nature* **275,** 31–35 (1978).
7. Brockes, J. P. & Hall, Z. W. *Biochemistry* **14,** 2100–2106 (1975).
8. Poo, M-m., Poo, W-j. H. & Lam, J. *J. Cell Biol.* **76,** 483–501 (1978).
9. Poo, M-m., Lam, J., Orida, N. & Chao, A. W. *Biophys. J.* **26,** 1–22 (1979).
10. Poo, M-m. *A. Rev. Biophys. Bioengng* **10,** 245–276 (1981).
11. Huang, N. W. *J. theor. Biol.* **40,** 11–16 (1973).
12. Hartzell, M. C. & Fambrough, D. M. *J. gen. Physiol.* **60,** 248–262 (1972).
13. Poo, M-m. & Cone, R. A. *Nature* **247,** 438–444 (1974).
14. Edidin, M. & Fambrough, D. *J. Cell Biol.* **57,** 27–53 (1973).
15. Axelrod, D. *et al. Proc. natn. Acad. Sci. U.S.A.* **12,** 4594–4598 (1976).
16. Anderson, M. J. & Cohen, M. W. *J. Physiol., Lond.* **268,** 757–773 (1977).
17. Anderson, M. J., Cohen, M. W. & Zorychta, E. *J. Physiol., Lond.* **268,** 731–756 (1977).
18. Frank, E. & Fishbach, G. D. *J. Cell Biol.* **83,** 143–158 (1979).
19. Cohen, M. W., Anderson, M. J., Zorychta, E. & Weldon, P. R. *Prog. Brain Res.* **49,** 335–349 (1979).
20. Christian, C. N. *et al. Proc. natn. Acad. Sci. U.S.A.* **75,** 4011–4015 (1978).
21. Podleski, T. R. *et al. Proc. natn. Acad. Sci. U.S.A.* **75,** 2035–2039 (1978).
22. Jessell, T. M., Siegal, R. E. & Fischbach, G. D. *Proc. natn. Acad. Sci. U.S.A.* **75,** 4011–4015 (1979).
23. Gingell, D. in *Mammalian Cell Membranes* (eds Jamieson, G. A. & Robinson, D. M.) 198–223 (Butterworth, London, 1976).
24. Bloch, R. J. & Geiger, B. *Cell* **21.** 25–35 (1980).
25. Jones, R. & Vrbova, G. *J. Physiol., Lond.* **236,** 517–538 (1974).
26. Peng, H. B., Cheng, P. C. & Luther, P. W. *Nature* **292,** 831–834 (1981).

Reorganization of HeLa cell cytoskeleton induced by an uncoupler of oxidative phosphorylation

Bernard Maro* & Michel Bornens*

Departement de Biologie Moléculaire, Institut Pasteur,
75724 Paris Cedex 15, France

An association between mitochondria and microtubules has been suggested from microscopic studies[1,2] and by the cellular redistribution of mitochondria that is induced by colcemid, which disrupts microtubules[1]. Intermediate filaments have also been proposed to interact with mitochondria[1]. To investigate this association further, we have now studied the effect on the cytoskeleton of impairment of mitochondrial functions induced by three metabolic inhibitors: sodium azide, which inhibits electron transport; oligomycin, which inhibits ATP synthetase; and carbonylcyanide *p*-trifluoromethoxyphenylhydrazone (FCCP), a proton ionophore which uncouples electron transport from ATP synthesis. We have found that treatment of cells with FCCP leads to a disruption of microtubules and an aggregation of vimentin filaments. This effect is not provoked by mitochondrial ATP depletion, but could be linked to another event related to the rapid dissipation of the mitochondrial electrochemical gradient.

FCCP induced a disruption of HeLa cell microtubules (Fig. 1*c* and Table 1) which was complete after 1 h. The only tubulin-positive structures observed were midbodies and juxtanuclear microtubule-organizing centres (MTOC). After 6 h treatment, short microtubules were seen regrowing from the MTOC. However, this might be linked to the inactivation of FCCP because it was correlated with the reappearance of mitochondrion-specific staining by rhodamine-123, which requires a high transmembrane potential[3]. This staining was totally absent during the first hours of FCCP treatment (data not shown).

FCCP had a slower effect on vimentin filaments. The filaments began to aggregate after 1 h treatment and had gathered as

---

* Present address: Centre de Cytologie Experimentale du CNRS, 67 rue Maurice Gunsbourg, 94200 Ivry s/Seine, France.

0028–0836/82/040334—03$01.00

perinuclear bundles after 6 h (Fig. 1*d*). The distribution of actin, which in our culture conditions was seen mainly as a pericellular network, with numerous microspikes and few stress fibres, was apparently unchanged. The effects of FCCP on cytoskeletal components were absent with doses below 10^{-5}M, detectable at 2×10^{-5}M and complete at $\geqslant 3\times10^{-5}$M.

We have established that the doses of FCCP used were non-toxic for the cells. The normal microtubule pattern returned about 6 h after removal of the drug. 2,4-dinitrophenol (DNP) showed a similar but weaker effect compared with FCCP. The highest DNP dose we could use without provoking an effect due to the solvent (ethanol) was 2.5×10^{-3} M. In such conditions many of the microtubules disappeared, and MTOC could be easily identified. Loose bundles of vimentin filaments were observed around the nuclei, distributed in a different pattern from that seen in control cells (data not shown). The effects of FCCP were similar to those obtained with 10^{-6} M nocodazole (Fig. 1*g*,*h*), which inhibits microtubule polymerization[4], the only difference being that MTOC were more easily identified after FCCP treatment than after nocodazole treatment. To control for the method used, we applied cold treatment[5] to verify that the collapse of vimentin filaments did not occur during cell extraction with Triton X-100 in the absence of a normal microtubule network (Fig. 1*i*, *k*). In this latter case MTOC were particularly well detected. Furthermore, the collapse of vimentin filaments was also observed in human lymphoblastoid cells (KE 37 cell line) after only 30 min treatment with FCCP (data not shown).

Table 1 Effects of various treatments on the pattern of cytoskeletal elements in HeLa cells

Treatment (1–6 h at 37 °C)	Action on mitochondrial metabolism*	Action on the pattern of: Tubulin	Vimentin	Actin
FCCP 3×10^{-5} M	H^+ ionophore uncoupler (10^{-6} M)	Disruption	Collapse	None
DNP 2.5×10^{-3} M	H^+ ionophore uncoupler (10^{-3} M)	Disruption (weak)	Collapse (weak)	None
NaN_3 10^{-2} M	Inhibition of electron transport (10^{-2} M)	None	None	None
Oligomycin 2.5×10^{-4} M	Inhibition of ATP synthetase (10^{-5} M)	None	None	None

These effects were judged by immunocytochemistry as described in Fig. 1 legend, using purified anti-tubulin, anti-vimentin and anti-actin antibodies.

* Values in parentheses are the minimal dose decreasing the transmembrane potential[3].

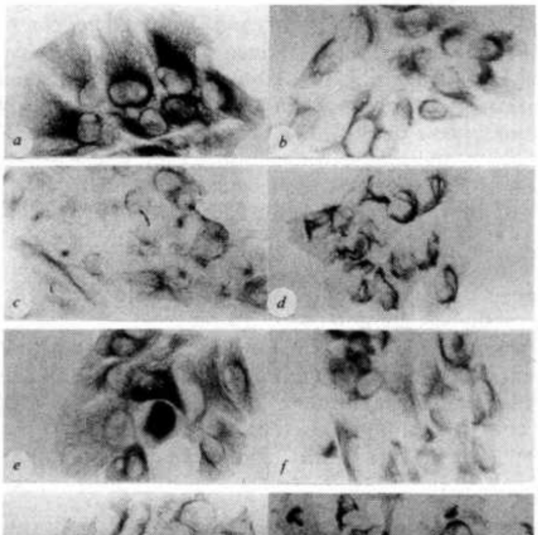

Fig. 1 Immunocytochemical staining of HeLa cells cultivated in Eagle's minimal essential medium (modified) supplemented with 10% fetal calf serum. Cells cultured for 48 h on glass coverslips were washed for 5 s at room temperature with an extraction buffer, *p*H 6.9, modified from Schliwa *et al.*[11], containing 45 mM PIPES, 45 mM HEPES, 5 mM $MgCl_2$, 10 mM EGTA, 1 mM sodium tetrathionate and 1 mM phenylmethylsulphonyl fluoride. They were lysed in extraction buffer supplemented with 1% Titron X-100 for 30 s, washed in extraction buffer, then fixed with 2% glutaraldehyde in the same buffer for 10 min at 20 °C. After three washes in 10 mM Tris-HCl *p*H 7.4, 100 mM NaCl (TBS), glutaraldehyde was neutralized with 1% bovine serum albumin in TBS for 1 h at 20 °C. Immunocytochemical staining of the cells was accomplished using purified sheep anti-tubulin antibodies or purified sheep anti-vimentin antibodies followed by peroxidase-labelled purified rabbit anti-sheep immunoglobulin antibodies as described previously[13] except that all incubations and washes were performed in the presence of 0.1% Tween-20. *a*, *b*, Control cultures; *c*, *d*, cultures treated with 4×10^{-5} M FCCP; *e*, *f*, cultures treated with 10^{-2} M sodium azide; *g*, *h*, cultures treated with 10^{-6} M nocodazole; *i*, *k*, cold-treated cultures. *a*, *c*, *e*, *g*, *i*, Anti-tubulin staining after 2 h treatment; *b*, *d*, *f*, *h*, *k*, anti-vimentin staining after 6 h treatment. ×240.

An energy requirement has been demonstrated for microtubule growth from MTOC in living cells[6,7], although in one case with very high doses of metabolic inhibitors[6]. However as reported by others for microtubule network[7,8], sodium azide (10^{-2} M, Fig. 1*e*,*f*) and oligomycin (2.5×10^{-4} M, data not shown) had no detectable effect on any of the three cytoskeletal components, indicating that FCCP was not acting via mitochondrial ATP depletion.

It is known[3] that FCCP is causing rapid dissipation of the mitochondrial electrochemical gradient; this could modify the local environment of the mitochondria and thus of the microtubules and so affect the stability of the latter. For example, a *p*H dependency of microtubule stability has been reported[9]. It is also known that a calcium efflux from mitochondria is correlated with membrane potential collapse[10]. Schliwa *et al.*[11] have recently shown that 10^{-6} M calcium induces disassembly of the microtubule network. Such effects could occur through a modulation of the activity of microtubule-associated proteins. In this connection it has been reported[8] that the colcemid-induced depolymerization of microtubules in cells is controlled by an ATP-dependent reaction probably a phosphorylation of some of the microtubule proteins. Although a direct effect of FCCP on microtubules cannot be ruled out, we have observed only a slight effect of FCCP on *in vitro* polymerization of rat brain tubulin over a wide range of drug concentrations (work in progress). Moreover, electron microscopic observation of microtubules polymerized in the presence of 4×10^{-5} M FCCP showed no detectable effect on either microtubule number or length relative to control conditions. An effect on nucleating centres is another possibility, and centrioles, which are the primary MTOC, have also been proposed to be involved in the organization of the vimentin network[12]. These possibilities are now being investigated.

We thank Dr D. Paulin for the gift of the anti-vimentin antibodies and Dr E. Karsenti for the gift of the anti-actin antibodies. This work was supported by DGRST grant 80.7.0155.

Received 20 July; accepted 30 November 1981.

1. Heggeness, M. H., Simon, M. & Singer, J. *Proc. natn. Acad. Sci. U.S.A.* **75**, 3863–3866 (1978).
2. Smith, D. S., Jarlfors, U. & Cayer, M. L. *J. Cell Sci.* **27**, 255–272 (1977).
3. Johnson, L. V., Walsh, M. L., Bockus, B. J. & Chen, L. B. *J. Cell Biol.* **88**, 526–535 (1981).
4. Hoebeke, J., Van Nigen, G. & De Brabander, M. *Biochem. biophys. Res. Commun.* **69**, 319–324 (1976).

5. Virtanen, I., Lehto, V. P., Lehtonen, E. & Bradley, R. A. *Eur. J. Cell Biol.* **23**, 80–84 (1980).
6. De Brabander, M., Geuens, G., Nuydens, R., Willebrords, R. & De Mey, J. *Cold Spring Harb. Lab. Conf. on Forms of Microtubule Organization in Cells,* May (1980).
7. Frankel, F. R. *Proc. natn. Acad. Sci. U.S.A.* **73,** 2798–2802 (1976).
8. Bershadsky, A. D. & Gelfand, V. I. *Proc. natn. Acad. Sci. U.S.A.* **78,** 3610–3613 (1981).
9. Regula, C. S., Pfeiffer, J. R. & Berlin, R. D. *J. Cell Biol.* **89**, 45–53 (1981).
10. Nicholls, D. G. & Brand, M. *Biochem. J.* **188**, 113–118 (1980).
11. Schliwa, M., Euteneuer, U., Bulinski, J. C. & Izant, J. G. *Proc. natn. Acad. Sci. U.S.A.* **78,** 1037–1041 (1981).
12. Goldman, R. D., Zackroff, R. V., Starger, J. M. & Whitman, M. *J. Cell Biol.* **83,** 343a (1979).
13. Maro, B. & Bornens, M. *Biol. Cell.* **39,** 287–290 (1980).

Chromaffin granule membrane–F-actin interactions are calcium sensitive

Velia M. Fowler* & Harvey B. Pollard

Cell Biology and Biochemistry Section, Clinical Hematology Branch,
National Institute of Arthritis, Diabetes, and Digestive and Kidney
Diseases, National Institutes of Health, Bethesda,
Maryland 20205, USA

Exocytosis of neurotransmitters, hormones and other secretory products from many cell types is initiated by a rise in the intracellular free calcium ion concentration[1]. By analogy with excitation–contraction coupling in muscle[2], calcium-triggered acto–myosin interactions have been postulated to push or pull the secretory granule to the plasma membrane[1,3–6]. Indeed, there have been several reports of actin interacting with membranes of secretory vesicles from the adrenal medulla (chromaffin granules)[7–12]. Using sedimentation techniques and a novel application[13,14] of falling ball viscometry[15,16] to measure actin binding to membranes, we show here that purified chromaffin granule membranes bind and cause large increases in the viscosity of F-actin. The actin-binding activity of the membranes is trypsin sensitive and thermolabile and interactions between membranes and actin are reversibly inhibited by raising the free calcium ion concentration, $[Ca^{2+}]_{free}$, above 10^{-7} M. We propose that regulation of actin–chromaffin granule membrane interactions may be critical for organelle movement to the plasma membrane during calcium-mediated exocytosis in the chromaffin cell.

Intracellular organelles such as chromaffin granules are particularly suitable for studying interactions between membranes and filamentous cytoskeletal elements such as actin because the cytoplasmic surface of these organelles is immediately accessible experimentally. We have used a low-shear viscometric technique[15,16] to study these interactions partly because it is a sensitive and convenient method to measure F-actin binding to membranes[13,14] but also because it may indicate how interactions between F-actin and chromaffin granules might contribute to cytoplasmic structure and consistency[17]. This approach is thus an extension of that used previously to study gelation of actin-containing cytoplasmic extracts[15,16,18].

Purified chromaffin granule membranes cause large increases in the apparent viscosity of purified rabbit skeletal muscle F-actin (Fig. 1*a*) in conditions that may approximate the resting intracellular environment (*p*H 6.8, 20 mM KCl, 1–2 mM $MgCl_2$, $[Ca^{2+}]_{free} < 10^{-7}$ M, 30 °C). (The effect of *p*H, KCl, $MgCl_2$ and ATP on membrane–actin interactions is described in ref. 17.) Increasing the membrane protein added to the F-actin to >2.5 mg ml^{-1} results in the formation of a solid gel through which the ball does not fall. The ability of membranes to induce increases in the apparent viscosity of F-actin is almost completely abolished by prior heating of the membranes at 60 °C for 15 min (not shown) or at 100 °C for 2 min (Fig. 1*a*), and chromaffin granule membranes alone have a viscosity equivalent to that of the buffer (~1 cP), at all concentrations of membrane protein tested. The ability of membranes to bind (see below) and cause increases in the apparent viscosity of F-actin (Fig. 1*a*) is not an artefact of the lysis and purification procedure, as intact chromaffin granules prepared by centrifugation through a 1.8 M sucrose shelf also bind and induce increases in the viscosity of F-actin[17].

Pelleting of F-actin with chromaffin granule membranes in conditions that do not pellet F-actin alone (Fig. 1*b*) confirms that these increases in apparent viscosity do, in fact, represent actin binding to the membrane[13,14]. Moreover, the amount of F-actin pelleting with membranes is reduced by ~75% after heat treatment of the membranes (Fig. 1*b*), as determined by quantitative densitometry of the Coomassie blue-stained gels. However, note that because the membrane-induced increases in apparent viscosity of actin are not linearly related to the number of F-actin binding sites on the membranes (Fig. 1*a*), and because membranes may bind actin in ways that do not lead to increases in viscosity[13,14], the low-shear viscometric assay cannot be compared quantitatively with the pelleting assay.

The effect of previous heating of membranes on their interactions with actin suggests that the actin-binding components on the membrane are proteinaceous. Indeed, treatment of membranes with trypsin selectively proteolyses certain of the membrane polypeptides (Fig. 2*a*) and also abolishes completely the ability of membranes to induce increases in the apparent viscosity of F-actin (Fig. 2*b*). Controls using trypsin that had been pretreated with soybean trypsin inhibitor, or soybean trypsin inhibitor alone (Fig. 2), demonstrated that the effect of trypsin is not due to a spurious, non-proteolytic action on the membranes. The effect of trypsin was also not due to an effect on the actin itself, as trypsin pretreated with soybean trypsin inhibitor had no effect on the apparent viscosity of actin in the absence of membranes, and SDS-polyacrylamide gel electrophoresis of trypsin-treated membranes plus actin revealed that the actin was not detectably proteolysed.

The actin-binding site(s) may differ from the α-actinin-like actin-binding component reported to be present on the chromaffin granule membrane[10,12], inasmuch as we prepared membranes in conditions (low ionic strength, no Mg^{2+}) that have been reported to elute this α-actinin-like component from the membrane[10]. In contrast to the actin-binding activity of chromaffin granule membranes described by Burridge and Phillips[8], we have also observed no differences between membranes prepared in 150 mM KCl or in isosmotic sucrose media. Finally, Wilkins and Lin[11] recently suggested that exogenous actin may bind to chromaffin granule membranes by polymerizing off pre-existing actin seeds on the membrane. However, in contrast to our results[17], actin binding to membranes in their experiments was strictly dependent on the presence of $MgCl_2$.

The calcium dependence of exocytosis[1] led us to examine the effect of calcium on interactions between chromaffin granule membranes and F-actin. We found that raising the free calcium ion concentration to micromolar levels inhibited the increases in apparent viscosity of F-actin induced by purified chromaffin granule membranes, while having no detectable effect on the apparent viscosity of F-actin alone (Fig. 3*a*). The small increases in viscosity of F-actin caused by heat-treated membranes were unaffected by changes in the $[Ca^{2+}]_{free}$ (not shown). Although it is uncertain why the increases in apparent viscosity were inhibited more in some experiments than in others (compare different symbols in Fig. 3*a*), this may, for example, have been due to variable amounts of a calcium-regulatory factor present in different preparations of chromaffin granule membranes.

If the changes in viscosity as a fraction of the maximal viscosity observed in each experiment are averaged for each *p*Ca ($-\log [Ca^{2+}]_{free}$), we obtain the graph shown in Fig. 3*b*. The $[Ca^{2+}]_{free}$ at which the increases in apparent viscosity are half-maximally inhibited is $\sim 2.6 \times 10^{-7}$ M, which is comparable to free Ca^{2+} concentrations which cause half-maximal inhibition of actin gelation in cytoplasmic extracts from non-muscle cells[15,16,18,19], and inhibition of actin cross-linking and gelation by various purified proteins[16,20,21], but rather less than the micromolar levels that induce release of granule contents from chromaffin

---

* Present address: Department of Cell Biology and Anatomy, The Johns Hopkins University School of Medicine, 725 North Wolfe Street, Baltimore, Maryland 21205, USA.

0028-0836/82/040336—03$01.00

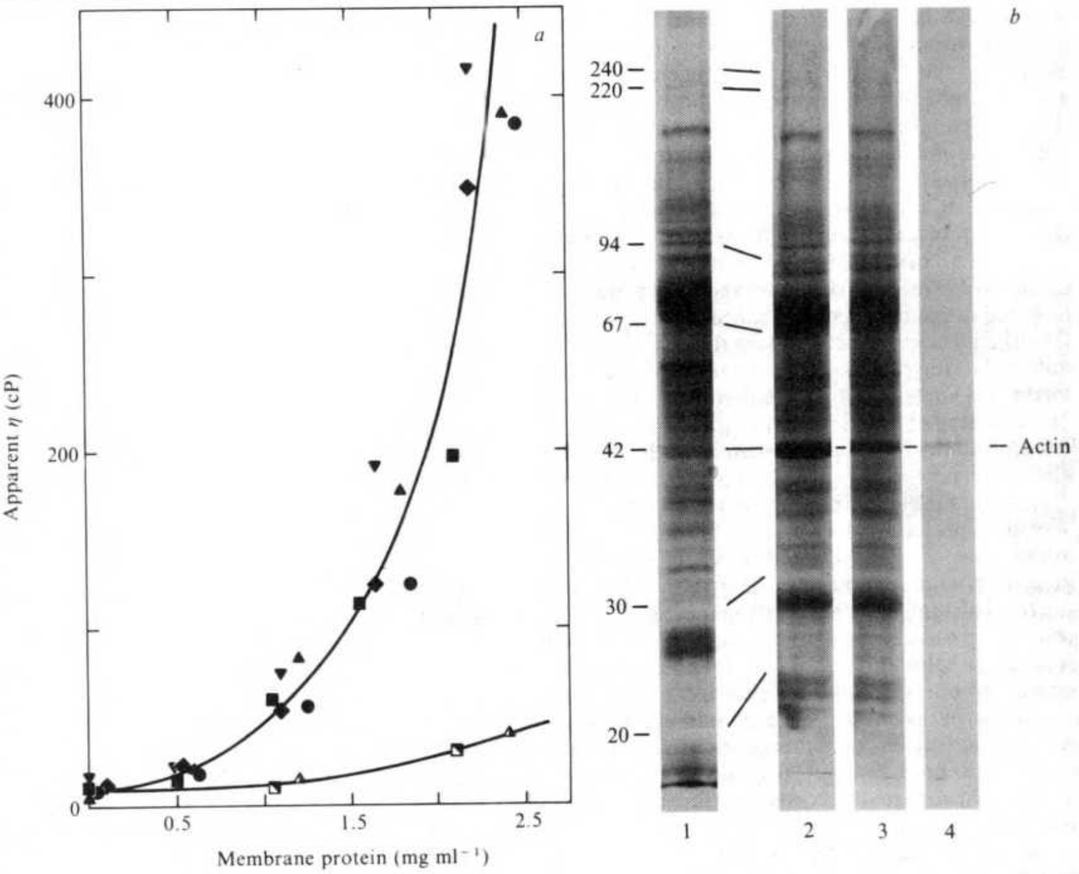

Fig. 1 *a*, Apparent viscosity (η cP) plotted against concentration of membrane protein for chromaffin granule membranes plus F-actin (●, ■, ▲, ▼, ◆) or heat-treated membranes (2 min, 100 °C) plus F-actin (□, △). Each symbol represents a separate experiment using a different membrane preparation. Membranes were mixed with 0.8 mg ml^{-1} F-actin and incubated at 30 °C for 1 h in a buffer containing 40 mM PIPES *p*H 6.8, 20 mM KCl, 1 mM $MgCl_2$ and $[Ca^{2+}]_{free}$ buffered to $\sim 4 \times 10^{-8}$ M with 5 mM EGTA (see Fig. 3). Viscosity was measured using a low-shear falling ball viscometer[15,16] as previously described[13,16,17]. *b*, SDS-polyacrylamide gels of pellets obtained from the centrifugation of (1) chromaffin granule membranes, (2) membranes plus F-actin, (3) heat-treated membranes (60 °C, 15 min) plus F-actin, and (4) F-actin alone. Membranes (0.5 mg ml^{-1}) with or without 0.4 mg ml^{-1} F-actin were incubated as described above and centrifuged through a 15% sucrose shelf to separate membrane-bound from unbound actin[14]. After solubilization of pellets in electrophoresis sample buffer[14], 25 μl of each sample were electrophoresed on 7.5–15% linear gradient polyacrylamide slab gels using the discontinuous buffer system of Laemmli[29]. Chromaffin granules were prepared from bovine adrenal medullae essentially as described by Bartlett and Smith[30], except that the sucrose solutions were buffered to *p*H 7.6–7.8 with 40 mM HEPES, and contained 1 mM EDTA, 1 mM phenylmethylsulphonyl fluoride (PMSF), 1 mM dithiothreitol (DTT) and 0.87% ethanol[17]. Membranes were prepared by lysis of granules at 0 °C in 5 mM HEPES *p*H 7.6–7.8, 1 mM EDTA, 1 mM PMSF, 1 mM DTT, 0.87% ethanol and separated from contaminating mitochondria, lysosomes and other cellular debris[17,31–33] by centrifugation over a 1.0 M sucrose shelf made up in the same buffer (26,000 r.p.m. in Beckman SW 27 rotor at 2–4 °C for 60 min)[17]. The chromaffin granule membranes accumulated as an intense salmon-pink layer on top of the 1.0 M sucrose and were collected, washed twice, then resuspended in a small volume of the 5 mM HEPES lysis buffer to give ~4–5 mg ml^{-1} membrane protein. Membranes were stored on ice for up to 10 days with no loss of actin binding activity. Actin was prepared from an acetone powder of rabbit skeletal muscle with one or two cycles of polymerization and sedimentation from 0.8 M KCl (ref. 34), and was depolymerized and stored as previously described[13]. F-actin was polymerized at 5–7 mg ml^{-1} in 100 mM KCl, 2 mM MgATP at 30 °C for 30–60 min before mixing with chromaffin granule membranes.

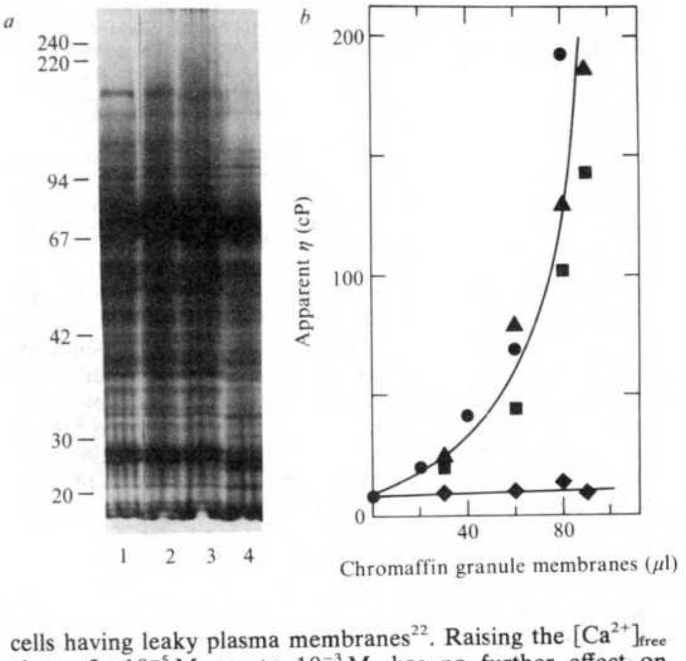

Fig. 2 Effect of trypsin treatment on *a*, 7.5–15% SDS-polyacrylamide gel profiles of chromaffin granule membrane proteins and *b*, the apparent viscosity, η (cP) of chromaffin granule membranes plus F-actin. Lane 1 (●), untreated chromaffin granule membranes; lane 2 (■), control membranes treated with soybean trypsin inhibitor; lane 3 (▲), control membranes treated with trypsin that had been preincubated with soybean trypsin inhibitor; and lane 4 (◆), trypsin-treated membranes. Chromaffin granule membranes were incubated with 100 μg ml^{-1} trypsin (Worthington) at 30 °C for 15 min, followed by an additional 15 min in the presence of 200 μg ml^{-1} soybean trypsin inhibitor (SBTI; Sigma), and then washed by centrifugation (20,000 r.p.m. in a Sorvall SS-34 rotor for 45 min) through a 5% sucrose shelf. As controls, membranes were incubated with SBTI alone at 30 °C for 15 min or with trypsin that had been pretreated with SBTI at 30 °C for 15 min, before washing. Samples were resuspended to equivalent volumes in the 5 mM HEPES buffer (see Fig. 1 legend) by homogenization and then solubilized for SDS-polyacrylamide gel electrophoresis or tested for their ability to induce increases in the apparent viscosity of F-actin. As trypsin treatment released ~35% of the total membrane protein into the supernatant, the apparent viscosity is plotted as a function of the volume (μl) of membranes added to the 150-μl assay mixture instead of as a function of the membrane protein concentration. 10 μl of untreated membranes correspond to 0.26 mg ml^{-1} membrane protein in this experiment.

cells having leaky plasma membranes[22]. Raising the $[Ca^{2+}]_{free}$ above 5×10^{-5} M, up to 10^{-3} M, has no further effect on membrane–actin interactions.

The mechanism by which micromolar free calcium ion concentrations inhibit membrane-induced increases in the apparent viscosity of F-actin is unclear. Calcium may reduce the affinity of actin for (some of) its binding sites, thus resulting in fewer actin filaments bound to the membrane and hence lower viscosities. Alternatively, a calcium-dependent influence of some membrane component on actin filament length, analogous to the calcium-mediated action of gelsolin[20], or possibly a membrane-mediated effect on the degree of actin polymerization, could also account for the reductions in apparent viscosity. However, we demonstrated that the effects of varying the free calcium ion concentration on membrane–actin interactions are reversible, and ruled out the possibility that a calcium-activated protease causes the inhibition of the membrane-induced increases in apparent viscosity of F-actin. The apparent viscosity of membranes plus actin preincubated at a high free calcium ion concentration ($\sim 10^{-6}$ M) returns to twice the original viscosity on reducing the free calcium ion concentration to $\sim 10^{-7}$ M (Fig. 4*b*). Conversely, the apparent viscosity of membranes plus actin preincubated at a low free calcium ion concentration recovers to only ~50% of the original viscosity after raising the $[Ca^{2+}]_{free}$ to $\sim 10^{-6}$ M (Fig. 4*a*). If the free calcium ion concentration is unchanged, but the mixture is vortexed, the viscosity of the membranes plus actin preincubated at low (Fig. 4*a*) or high (Fig. 4*b*) free calcium ion concentrations recovers completely to the premixing viscosity, albeit at a slower rate. Thus, these mixtures are thixotropic.

Additional evidence against involvement of a calcium-activated protease in calcium inhibition of membrane–actin interactions is that SDS-polyacrylamide gels of membranes incubated with actin are not detectably affected by increasing the free calcium ion concentration (not shown). The component conferring calcium sensitivity on these interactions does not seem to be calmodulin as up to 100 μM trifluoperazine (a drug which inhibits calmodulin function[23]) does not reverse the inhibition by calcium. Minor contaminants which have been reported in conventional preparations of rabbit skeletal muscle actin[24] are probably not responsible as membrane-induced increases in apparent viscosity of actin purified by gel filtration[24] were also calcium sensitive.

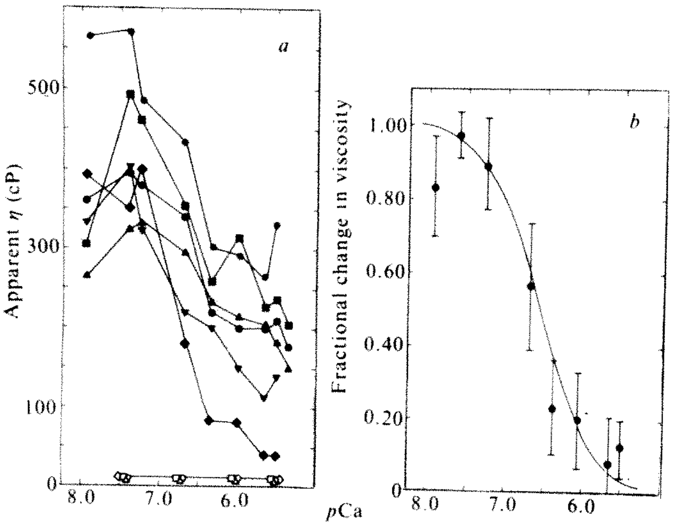

Fig. 3 *a*, Effect of the free calcium ion concentration (expressed as −log $[Ca^{2+}]_{free} = p\mathrm{Ca}$) on the apparent viscosity of chromaffin granule membranes plus F-actin (●, ■, ▲, ◆, ▼, *) and on F-actin alone (○, □, △, ◇). Each symbol represents a separate experiment using a different membrane preparation. *b*, Fractional change in viscosity of membranes plus actin as a function of *p*Ca. The lowest viscosity measured in each experiment was subtracted from the other measured values to give the change in viscosity for each free calcium ion concentration. These values were then divided by the maximum viscosity (which always occurred at *p*Ca 7.58 or 7.26) to compare results from separate experiments. The points represents means ± s.d. (error bars). The curve was drawn (ignoring the two extremes) using a least-squares fit to the Hill equation. The *y*-intercept of this line = −7.3, the slope = 1.1 and correlation coefficient, *r* = 0.92. For these experiments, membranes were dialysed overnight at 0 °C against a large volume of the 5 mM HEPES buffer (Fig. 1) containing 1 mM EGTA instead of EDTA. Chromaffin granule membranes (final concentrations 2.18 (●), 2.44 (■), 2.44 (▲), 2.16 (▼), 2.70 (◆) and 2.50 (*) mg ml^{-1}) were mixed with 0.8 mg ml^{-1} F-actin for viscosity measurements as described in Fig. 2 legend. The $[Ca^{2+}]_{free}$ was adjusted by addition of an appropriate stock to give calcium–EGTA buffer (*p*H 6.8) final concentrations of 5 mM EGTA and 0.095–4.975 mM $CaCl_2$; the free calcium ion concentration for each data point was calculated according to Caldwell[35] using a K_{app} of 1.95×10^6. Other conditions were as in Fig. 1.

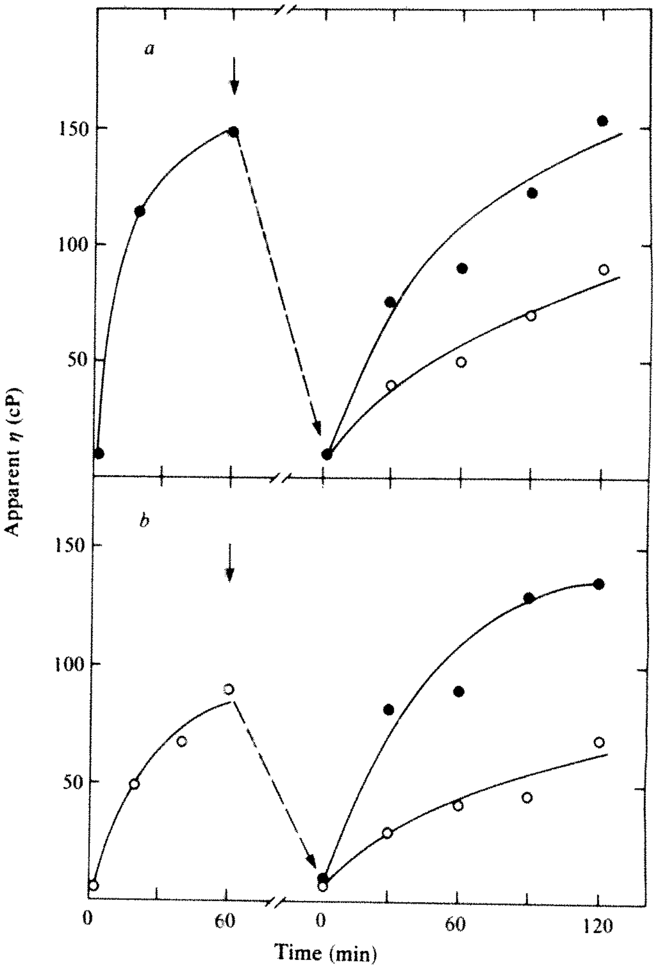

Fig. 4 *a*, Effect of preincubation at 2.7×10^{-8} M $[Ca^{2+}]_{free}$ on the apparent viscosity of chromaffin granule membranes plus F-actin incubated subsequently at 2.7×10^{-8} M (●) or 1.6×10^{-6} M (○) $[Ca^{2+}]_{free}$. *b*, Effect of preincubation at 1.5×10^{-6} M $[Ca^{2+}]_{free}$ on the apparent viscosity of chromaffin granule membranes plus F-actin incubated subsequently at 1.0×10^{-7} M (●) or 3.4×10^{-6} M (○) $[Ca^{2+}]_{free}$. Duplicate samples of chromaffin granule membranes (final concentration 2.14 mg ml^{-1}) were mixed with 0.8 mg ml^{-1} F-actin in assay buffer at low or high $[Ca^{2+}]_{free}$ as indicated above, using 2.0 mM EGTA buffer. For viscosity measurements, one set of samples was incubated in micropipettes at 30 °C for the indicated times. Parallel samples were incubated in test tubes at 30 °C for 1 h. At the time indicated by the arrow, the $[Ca^{2+}]_{free}$ was readjusted by addition of a small volume of an appropriate stock Ca^{2+}/EGTA buffer, the sample was mixed by vortexing (broken line) and then drawn up into micropipettes and incubated at 30 °C for the indicated times before measuring the viscosities. The total calcium and EGTA concentrations during the incubations after the vortexing were (*a*, ●) 0.51 and 10.40, (*a*, ○) 9.10 and 12.07, (*b*, ●) 2.01 and 12.07, (*b*, ○) 9.02 and 10.4 mM, respectively. The free calcium ion concentrations were calculated as described in Fig. 3 legend.

The ability of purified chromaffin granule membranes to bind and cause large increases in the apparent viscosity of F-actin suggests that the membrane vesicles may bind more than one actin filament and, vice versa, that an actin filament may associate with more than one membrane vesicle so as to generate an extensive cross-linked network or gel[13,14]. It is possible that such interactions may have a significant role in the maintenance of cytoplasmic structure and consistency in the chromaffin cell, as chromaffin granules comprise ~13.5% of the total cells cytoplasmic volume[25]. This corresponds to a concentration of ~30 mg ml^{-1} membrane protein (assuming the density of the granule to be 1.12 g ml^{-1} and the membrane protein to be 20% of the total granule protein[26]), which would be expected to generate an apparent viscosity much greater than that measured in our assay (Fig. 1*a*). Moreover, we measured increases in apparent viscosity of only 0.8 mg ml^{-1} F-actin, whereas the cytoplasmic actin concentration is likely to be nearer 3–4 mg ml^{-1} (ref. 27). Thus, chromaffin granules could be securely embedded within and attached to a cytoskeletal actin filament network *in vivo*.

Inhibition of chromaffin granule membrane–actin interactions by free calcium ion concentrations that are thought to activate exocytosis and other cellular movements *in vivo*[4 18 22,28] leads us to propose that dissociation of the chromaffin granules from a cytoskeletal actin filament network may be necessary for their movement to the plasma membrane during exocytosis In addition, regulation of the association of chromaffin granules with an actin network by changes in the free calcium ion concentration, or by other factors[17], could potentially control membrane recovery processes following exocytosis, as well as intracellular translocation of the secretory vesicles from their sites of synthesis and assembly to a more peripheral location in the cell in preparation for exocytosis

V M F is a Fellow of the Jane Coffin Childs Memorial Fund for Medical Research

Received 2 November, accepted 20 November 1981

1 Douglas, W W *Biochem Soc Symp* **39,** 1–28 (1974)
2 Ebashi, S *A Rev Physiol* **38,** 293–313 (1976)
3 Allison, A C *Ciba Fdn Symp* **14,** 109–148 (1973)
4 Durham, A C H *Cell* **2,** 123–136 (1974)
5 Trifaro, J M *Neuroscience* **3,** 1–24 (1978).
6 Malaisse, W J & Orci, L *Meth Achieve exp Path* **9,** 112–136 (1979)
7 Gabbiam, G , DaPrada, M , Richards, G & Pletscher, A *Proc Soc exp Biol Med* **152,** 135–138 (1976)
8 Burridge, K & Phillips, J H *Nature* **254,** 526–529 (1975)
9 Meyer, D I & Burger, M M *FEBS Lett* **101,** 129–133 (1979)
10 Aunis, D , Guerold, B , Bader, M F & Cieselski-Treska, J *Neuroscience* **5,** 2261–2277 (1980)
11 Wilkins, J A & Lin, S *Biochim biophys Acta* **642,** 55–66 (1981)
12 Jockusch, B M *et al Nature* **270,** 628–629 (1977)
13 Fowler, V M , Luna, E J , Hargreaves, W R , Taylor, D L & Branton, D *J Cell Biol* **88,** 388–395 (1981)
14 Luna, E J , Fowler, V M , Swanson, J , Branton, D & Taylor, D L *J Cell Biol* **88,** 396–409 (1981)
15 MacLean-Fletcher, S D & Pollard, T D *J Cell Biol* **85,** 414–428 (1980)
16 Fowler, V M & Taylor, D L *J Cell Biol* **85,** 361–376 (1980)
17 Fowler, V M & Pollard, H B *J supramolec Struct Cell Biochem* (in the press)
18 Taylor, D L & Condeelis, J C *Int Rev Cytol* **56,** 57–144 (1979)
19 Ishiura, M & Okada, M *J Cell Biol* **80,** 465–480 (1979)
20 Yin, H L , Zaner, K S & Stossel, T P *J biol Chem* **255,** 9494–9500 (1980)
21 Mimura, N & Asano, A *Nature* **282,** 44–48 (1979)
22 Baker, P F & Knight, D E *Nature* **276,** 620–622 (1978)
23 Weiss, R & Levin, R M *Adv Cyclic Nucleotide Res* **9,** 285–303 (1978)
24 MacLean-Fletcher, S & Pollard, T D *Biochem biophys Res Commun* **96,** 18–27 (1980)
25 Kryvir, H , Flatmark, T & Terland, O *Eur J Cell Biol* **20,** 76–82 (1979)
26 Pollard, H B , Zinder, O & Hoffman, P G *Cell Biology* 1 (eds Altman, P L & Katz, D D) 358–362 (Fedn Am Soc exp Biol Med , 1976)
27 Gordon, D J , Boyer, J L & Korn, E D *J biol Chem* **252,** 8300–8309 (1977)
28 Stossel, T P *A Rev Med* **29,** 427–457 (1978)
29 Laemmli, U K *Nature* **227,** 680–685 (1970)
30 Bartlett, S F & Smith A D *Meth Enzym* 31, 379–389 (1974)
31 Apps, D K & Schatz, G *Eur J Biochem* **100,** 411–419 (1979)
32 Terland, O & Flatmark, T *Biochim biophys Acta* **597,** 318–330 (1980)
33 Zinder, O , Hoffman, P G , Bonner, W M & Pollard, H B *Cell Tissue Res* **188,** 153–170 (1978)
34 Spudich, J A & Watt, S *J biol Chem* **246,** 4866–4871 (1971)
35 Caldwell, P C *Calcium and Cellular Function* (ed Cuthbert, A W) 10–16 (Macmillan, London, 1970)

Isolation and structure of dynorphin, an opioid peptide, from porcine duodenum

S. Tachibana, K. Araki, S. Ohya & S. Yoshida

Research Laboratory of Biochemistry, Eisai Co Ltd, 4 Koishikawa, Bunkyo-Ku, Tokyo 112, Japan

The presence of endogenous ligands of opiate receptors in gastrointestinal organs has been demonstrated by both bioassay and immunoassay but so far no ligand has been precisely identified. We report here the purification from porcine duodenum of an opioid peptide whose structure coincides with that of the pituitary opioid, dynorphin[1]. Only the N-terminal tridecapeptide of pituitary dynorphin has been published; we have now determined the complete sequence of duodenal dynorphin, and measured its content in the duodenum by radioimmunoassay[2]. We report here that the complete heptadecapeptide has almost the same potency as dynorphin$_{1-13}$ in two bioassays.

Figure 1 shows an outline of the purification procedure We used as starting material the vasoactive intestinal peptide (VIP) fraction (1 kg) obtained from 200,000 porcine duodena[3] The crude material was purified by CM-cellulose and CM-Sephadex column chromatography using a linear gradient of sodium phosphate (20 mM, *p*H 10 to 100 mM, *p*H 12) The active material thus obtained was then applied in succession to two Bio-Gel P6 columns When the column was developed with a basic solvent (0 1 M NH_4HCO_3, *p*H 8), opioid activities emerged coincidently with the salt peak, the column was then eluted with an acidic solvent (0 1 M acetic acid), which gave one major peak of activity eluting immediately after the salt peak The strong affinity of the opioid peptide for Bio-Gel allowed its effective separation from large amounts of inactive material Further purification was achieved by HPLC first using Nucleosil C18 and then Phenyl (Macherly-Nagel) columns Opioid activities were determined using bioassays on guinea pig ileum preparations[4] and dynorphin-like immunoactivities were estimated by the method of Ghazarossian *et al*[2]

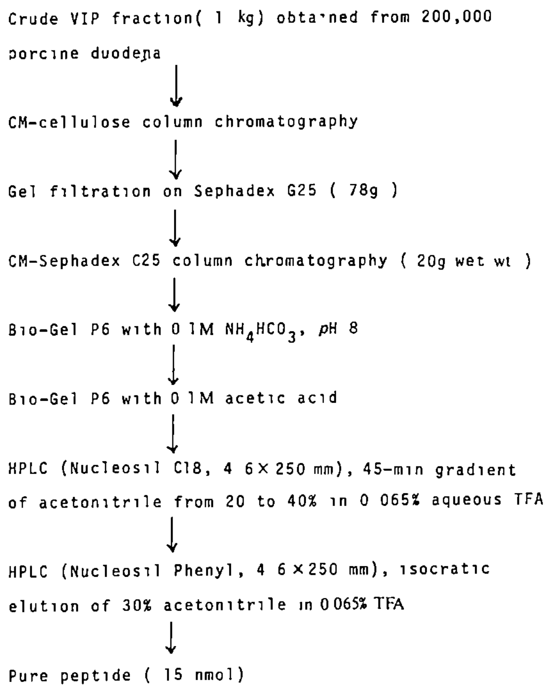
Crude VIP fraction(1 kg) obtained from 200,000 porcine duodena
CM-cellulose column chromatography
Gel filtration on Sephadex G25 (78g)
CM-Sephadex C25 column chromatography (20g wet wt)
Bio-Gel P6 with 0 1M NH4HCO3, pH 8
Bio-Gel P6 with 0 1M acetic acid
HPLC (Nucleosil C18, 4 6×250 mm), 45-min gradient of acetonitrile from 20 to 40% in 0 065% aqueous TFA
HPLC (Nucleosil Phenyl, 4 6×250 mm), isocratic elution of 30% acetonitrile in 0 065% TFA
Pure peptide (15 nmol)

Fig. 1 Procedure used to purify the heptadecapeptide

Homogeneity of the purified peptide was confirmed by determining the N-terminal amino acids using dansyl (DNS) techniques In addition to ε-DNS-Lys, only *O,N*-diDNS-Tyr was detected An amino acid analyser (model 835, Hitachi) linked to an ammonia trapping column was used for amino acid analysis of peptide samples hydrolysed with 3 M mercaptoethanesulphonic acid (Pierce)[5] The peptide was found to consist of 17 amino acids Asp 2, Glu 1, Pro 1, Gly 2, Ile 1, Leu 2, Tyr 1, Phe 1, Lys 2, Trp 1 and Arg 3 The biological characteristics of the peptide, such as slow-reversing activity and high potency on guinea pig ileum preparations[1], as well as immunoreactivity with anti-dynorphin$_{1-13}$ antiserum, suggested that the structure of the newly isolated peptide is similar to that of dynorphin

The peptide was digested with diphenyl carbamyl chloride (DPCC)-treated trypsin (Sigma) and the resultant fragments (T-1, -2, -3, -4 and -5) separated by HPLC as shown in Fig 2 To determine the amino acid sequence of these tryptic peptides, synthetic dynorphin$_{1-13}$ (Protein Research Foundation, Osaka, Japan) was also treated with trypsin and the tryptic fragments

0028-0836/82/040339—03$01 00

separated As expected from the specificity of trypsin for dynorphin$_{1-13}$, reverse-phase HPLC yielded five tryptic peptides whose sequences were easily deduced from their amino acid compositions The amino acid compositions and retention times on HPLC of each of these tryptic peptides were compared with those of the corresponding tryptic fragments from dynorphin$_{1-13}$, four of the five peptides (T-1, -2, -4 and -5) were identical to the corresponding dynorphin$_{1-13}$ fragments

From these data, we estimated that the new heptadecapeptide contained a hexapeptide extension at the C-terminus of the dynorphin$_{1-11}$ sequence We used a manual Edman sequencing method described elsewhere[6] to degrade the tryptic peptide T-3 and the resultant phenylthiohydantoin-amino acids were identified by HPLC[7] The partial sequence Leu-Lys-Trp-Asp(Asx, Glx) was determined by microsequencing at the less than nanomolar level, we were unable to complete the sequencing due to the limited amount of material available We digested the original peptide (1 nmol) with carboxypeptidase A (Sigma) and the amino acids thus released were analysed after 2, 16 and 40 h incubation Carboxypeptidase A first released Gln, followed by the same amounts of Asn and Asp, thus the penultimate residue could not be determined clearly However, the sequencing results combined with the results of carboxypeptidase digestion allowed us to assign the following sequence to the tryptic peptide T-3 Leu-Lys-Trp-Asp-Asn-Gln

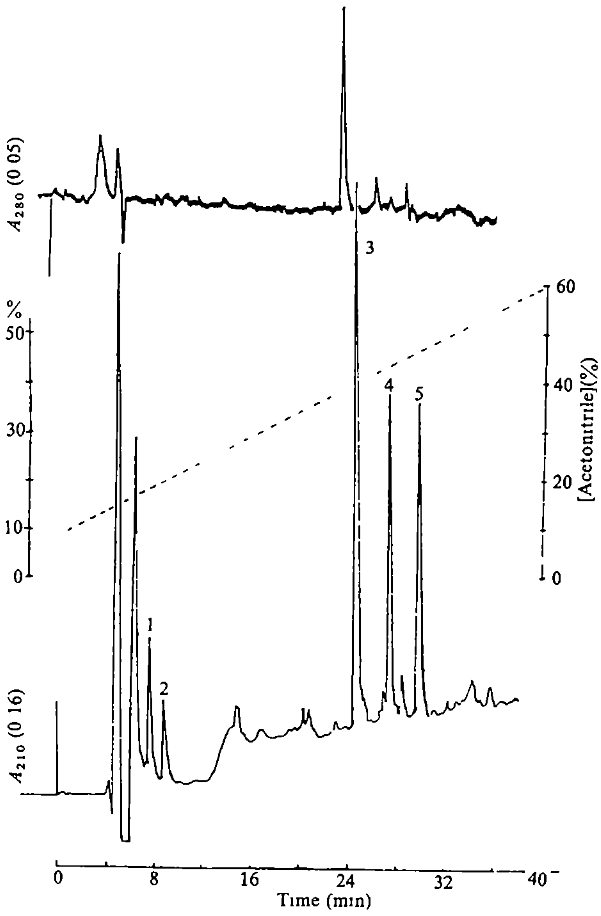

Fig. 2 Reverse-phase HPLC of the tryptic fragments of the newly isolated peptide The peptide (5 nmol) was digested with 300 ng of DPCC-treated trypsin (Sigma) dissolved in 130 µl of 100 mM sodium phosphate, *p*H 7 6, at 37 °C for 1 5 h After acidification with 50 µl of 2M HCl, the enzyme solution was directly loaded onto a Nucleosil column (5 µm, 4 6×250 mm) divided in two We applied to the column a 45-min linear gradient of acetonitrile from 10 to 60% in 0 065% TFA aqueous solution with a flow rate of 1 ml min^{-1} Column effluents were monitored by absorbance at 280 and 210 nm The numbers in parentheses on the abscissa, corresponding to 15 cm space, show the full scale unit of absorption in the detector used

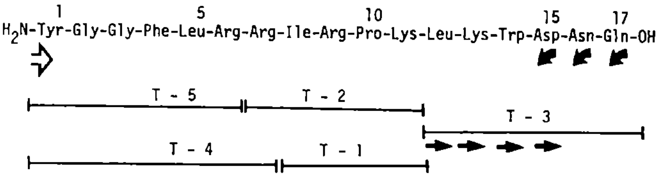
1
5
10
15
17
H$_2$N-Tyr-Gly-Gly-Phe-Leu-Arg-Arg-Ile-Arg-Pro-Lys-Leu-Lys-Trp-Asp-Asn-Gln-OH
T - 5
T - 2
T - 3
T - 4
T - 1

Fig. 3 Amino acid sequence of the heptadecapeptide ⇒ represents DNS method, ↙, carboxypeptidase A digestion, ➡, manual Edman sequencing

The entire sequence of the heptadecapeptide and the strategy used for structural analyses are summarized in Fig. 3 We have confirmed this structure by comparing the retention times of the natural peptide on two HPLC systems with those of the peptide synthesized by the Protein Research Foundation. The HPLC pattern produced by the tryptic fragments of the synthetic peptide was identical to that of natural dynorphin The opioid potencies of the synthetic tri- and heptadecapeptides were compared in *in vitro* bioassays[2 8] The concentration of the heptadecapeptide required for 50% inhibition of the contractile twitch was 199±84 pM (mean±s d , *n* = 9) in guinea pig ileum and 4 4±1 6 nM (*n* = 8) in the mouse vas deferens assay, while the respective IC$_{50}$s of dynorphin$_{1-13}$ were 181±67 pM (*n* = 9) and 6 5±3 4 nM (*n* = 8) Therefore the C-terminal tetrapeptide has little or no influence on potency

To estimate the content of dynorphin in porcine duodenum, five fresh upper intestines (~60 cm long) were extracted individually and concentrated to give crude extracts as described previously[9] Radioimmunoassay studies revealed that porcine duodenum contained 620±120 pg (*n* = 5) of immunoreactive dynorphin and 1 82±0 49 ng (*n* = 5) of β-endorphin[10] per g wet tissue The value for dynorphin is one-tenth that of methionine-enkephalin reported for human duodenum[11] while the concentration of β-endorphin is comparable with that reported in normal rat duodenum[12] Further studies, however, are needed to determine the absolute concentrations of endorphins in gut because estimates tend to vary with the antisera and the extraction procedures used

As opiate has been used for centuries to provide relief from diarrhoea and dysentery as well as for its analgesic actions, we hope that gut dynorphin will prove valuable for clarifying physiological roles of endorphins and pharmacological actions of opiate in the gastrointestinal tract. Since submission of this paper, Goldstein has reported[13] that dynorphin extracted from porcine pituitaries has the same sequence as that determined here

We thank Dr A Goldstein for the gift of anti-dynorphin$_{1-13}$ antiserum and Dr T Suda for his cooperation in the radioimmunoassay studies

Received 14 September, accepted 2 December 1981

1. Goldstein, A , Tachibana, S , Lowney, L I , Hunkapiller, M & Hood L *Proc natn Acad Sci USA* **76**, 6666–6670 (1979)
2 Ghazarossian, V E , Chavkin, C & Goldstein, A *Life Sci* **27**, 75–86 (1980)
3 Suzuki, S , Araki, K & Tachibana, S *Yakugakuzasshi* **99**, 172–179 (1979)
4 Kosterlitz, H W & Waterfield, A A *A Rev. Pharmac* **15**, 29–47 (1975)
5 Penke, B , Ferenczi, R & Kovacs, K *Analyt Biochem* **60**, 45–50 (1974)
6 Tarr, G E *Analyt Biochem* **63**, 361–370 (1975)
7 Fohlman, J , Rask, L & Peterson, P A *Analyt Biochem* **106**, 22–26 (1974)
8 Hughes, J , Kosterlitz, H W & Leslie, F M *Br J Pharmac* **53**, 371–381 (1975)
9 Tachibana, S in *Gastro-Entero-Pancreatic Endocrine System* (ed Fujita, T) 174–192 (Igaku-Shoin Ltd, Tokyo, 1973)
10 Liotta, A S , Suda, T & Krieger, D T *Proc natn Acad Sci USA* **75**, 2950–2954 (1978)
11 Polak, J M , Sullivan, S N , Bloom, S R , Facer, P & Pearse, A G E *Lancet* **i**, 972–974 (1977)
12 Orwoll, E S & Kendall, J W *Endocrinology* **107**, 438–442 (1980)
13 Goldstein, A , Fischti, W , Lowney, L I , Hunkapiller, M & Hood, L *Proc natn Acad Sci USA* **78**, 7219–7223 (1981)

A carboxypeptidase processing enzyme for enkephalin precursors

Vivian Y. H. Hook

Section on Pharmacology, Laboratory of Clinical Science, National Institute of Mental Health, Bethesda, Maryland 20205, USA

Lee E. Eiden & Michael J. Brownstein

Unit on Neuroendocrinology, Laboratory of Clinical Science,
National Institute of Mental Health, Bethesda,
Maryland 20205, USA

Recent studies[1,2] have shown that adrenal medullary chromaffin granules contain relatively large amounts of Met- and Leu-enkephalin and several large enkephalin-containing peptides ranging in molecular weight (M_r) from 3,200 to 50,000. The large, biologically inactive enkephalin-containing molecules can be broken down *in vitro* to give active enkephalins by two enzymes, trypsin and carboxypeptidase B[1]: trypsin liberates enkephalins (for example, Met-enkephalin-Arg^6, Met-enkephalin-Arg^6-Arg^7, Met-enkephalin-Lys^6, Leu-enkephalin-Arg^6) that are extended at their C-terminus by Lys or Arg. These C-terminal residues can be trimmed off by carboxypeptidase B, an exopeptidase that specifically removes C-terminal basic amino acid residues. Presumably, the enkephalin precursor is processed *in vivo* by trypsin-like and carboxypeptidase B-like enzymes[1,3]; it seems reasonable that these enzymes co-exist with the precursor in chromaffin granules. We describe here a carboxypeptidase obtained from bovine chromaffin granules that converts ^{125}I-labelled Met-enkephalin-Arg^6 to ^{125}I-Met-enkephalin. Fulfilment of certain criteria expected of a processing enzyme suggests that this peptidase may be involved in enkephalin precursor processing.

Chromaffin granules were isolated from fresh bovine adrenal glands and kept on ice The medulla was separated from the cortex and the granules purified by differential and discontinuous sucrose density centrifugation (for methods see Fig 2 legend)[4]

Carboxypeptidase activity was assayed by adding 10 μl of the enzyme or tissue homogenate to 25 μl of 1–5 × 10^{-5} M ^{125}I-Met-enkephalin-Arg^6 (1 μCi per tube) (for iodination procedure see Fig 1 legend) in 50 mM potassium phosphate buffer *p*H 6 0, 100 mM NaCl The samples were incubated at 37 °C for 30 min and the reaction stopped by addition of 10 μl ice-cold 95% ethanol After 30 min at 4 °C the samples were centrifuged in a Beckman microfuge for 5 min The ^{125}I-Met-enkephalin-Arg^6 and ^{125}I-Met-enkephalin were separated by TLC Radioactivity was measured along each lane using a BID System 100 radiogram imaging system (Bioscan) The two peptides were resolved on silica gel TLC plates using as solvent pyridine/ethyl acetate/H_2O/acetic acid (33 53 9 4 4 3) (Fig 1) Commercial porcine pancreatic carboxypeptidase B, having a reported *p*H optimum of 7 0–9 0 (ref 5) converted ^{125}I-Met-enkephalin-Arg^6 into a radioactive molecule that co-chromatographed with ^{125}I-Met-enkephalin in thin layer and reverse-phase high performance systems

Purified chromaffin granules were lysed by suspending them in 0 015 M KCl at 4 °C for 30 min The soluble and particulate components of the lysed granules were separated by centrifugation at 100,000*g* for 30 min in a Beckman type 40 rotor (40,000 r p m) Incubation of an aliquot of the soluble fraction with ^{125}I-Met-enkephalin-Arg^6 resulted in the appearance of a radioactive species that co-migrated with ^{125}I-Met-enkephalin (New England Nuclear) (Fig 1*d*) The new peak was not seen if the soluble fraction was boiled for 30 min before being added to the reaction mixture or if the incubation was carried out at 0 °C The behaviour of the ^{125}I-Met-enkephalin-like reaction product was the same as that of ^{125}I-Met-enkephalin when subjected to HPLC [reverse-phase C18 column eluted with 15–20% acetonitrile in TEAP (triethylamine–0 25 M phosphoric acid *p*H 3 0)]

The amount of ^{125}I-Met-enkephalin produced was linearly related to the amount of granule supernatant added The enzyme activity was optimal at ~*p*H 6 0 (Fig 2), with considerable activity being observed in the *p*H range 5 5–6 5 While the soluble fraction derived from chromaffin granules was relatively rich in carboxypeptidase B activity, the membrane fraction contained only low enzyme activity Similarly, other subcellular fractions (Fig 1) containing cytosol (S1, S2, S3), nuclei (P1), mitochondria and lysosomes showed very little carboxypeptidase activity, but these fractions did exhibit other peptidase activities as indicated by the production of a labelled substance other than ^{125}I-Met-enkephalin (Fig 1) The crude granule fraction (P3) not only displayed considerable carboxypeptidase activity, but also contained other peptidase(s) Thus the purified granules are unique in containing only carboxypeptidase B activity and in their apparent inability to cleave

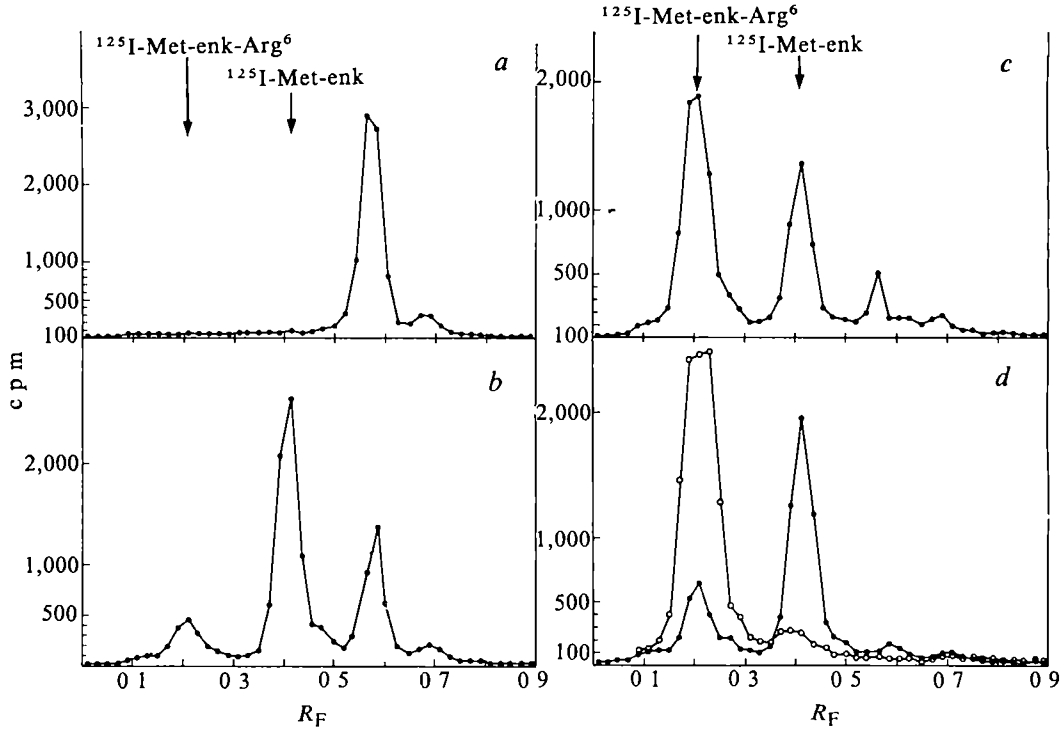

Fig 1 Carboxypeptidase activity in subcellular fractions of bovine adrenal medulla Met-enkephalin-Arg^6 (Peninsula Laboratories) was iodinated by the chloramine-T method[18] Free ^{125}I was removed with a C18 Sep-Pak (Waters Associates) and ^{125}I-Met-enkephalin-Arg^6 eluted off using 30% acetonitrile/70% H_2O Each subcellular fraction (for method see Fig 2 legend) was incubated with ^{125}I-Met-enkephalin-Arg^6 and chromatographed by TLC on silica gel G Arrows indicate the migration position of standard samples of ^{125}I-Met-enkephalin-Arg^6 and ^{125}I-Met-enkephalin *a*, Typical peptidase activity in fractions containing nuclei and large debris (P1) and cytosol (S2 and S3) *b*, Activity in crude chromaffin granules (P3) *c*, Activity in lysosomal and mitochondrial fraction obtained from sucrose gradient *d*, Activity in purified granules (supernatant of lysed granules) (●) and in boiled supernatant granule fraction (○)

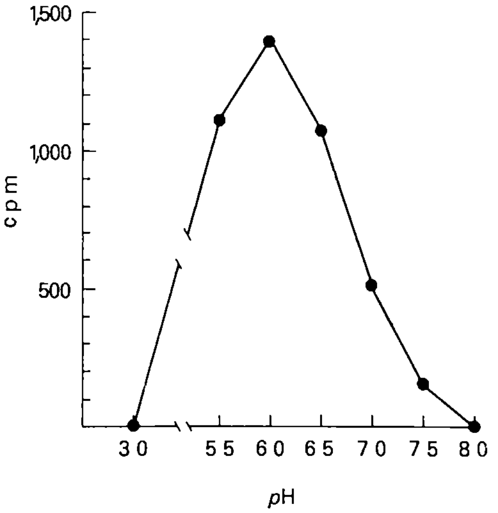

Fig 2 *p*H dependence of carboxypeptidase activity in supernatant of lysed chromaffin granules At *p*H 5–8, 50 mM potassium phosphate was used, TEAP was used for *p*H 3 0 Purified chromaffin granules were obtained by centrifuging adrenal medulla homogenate in 0 32 M sucrose at 1,500 r p m for 20 min (GS-4 rotor, Sorvall centrifuge) to give a pellet (P1) and supernatant (S1) fraction S1 was centrifuged at 8,800 r p m for 20 min (same rotor as above), yielding a pellet containing the crude granule fraction and supernatant (S2) The pellet was washed once (8,800 r p m , 20 min) and taken as the crude granule fraction (P3) Purified chromaffin granules were obtained by applying a suspension of P3 in 0 32 M sucrose on 1 6 M sucrose, and centrifuging at 25,000 r p m for 120 min (Beckman ultracentrifuge, SW-27 rotor) The pellet containing the purified chromaffin granules has been shown to be relatively free from mitochondria and lysosomes which were collected at the interface of the 0 32–1 6 M sucrose gradient[19] The membrane fraction from lysed chromaffin granules displayed a *p*H optimum of 6 0, which is similar to that of carboxypeptidase in the supernatant However, the *p*H optimum of porcine pancreatic carboxypeptidase B has been reported[5] to be in the range 7 0–9 0

^{125}I-Met-enkephalin-Arg^6 into labelled species other than ^{125}I-Met-enkephalin

To determine whether the carboxypeptidase in the soluble fraction of chromaffin granules is similar to other known carboxypeptidases, the effects of various inhibitors were examined Inhibitors of zinc metallopeptidases such as guanidinopropylsuccinic acid, aminopropylmercaptosuccinic acid, benzylsuccinic acid and 2-mercaptomethyl-3-guanidinoethylthiopropanoic acid[6–8] (provided by Dr T H Plummer, New York Department of Public Health) were found to inhibit porcine pancreatic carboxypeptidase B dramatically at concentrations of $2\ 8\times10^{-5}$ M, none of these inhibited chromaffin granule carboxypeptidase, however Similarly, the potato carboxypeptidase inhibitor[9] (given by Dr M Hass, University of Idaho) at 10^{-5} M inhibited the pancreatic but not the adrenal medullary enzyme Other inhibitors of metalloenzymes such as EDTA (10^{-3} M) and 1,10-phenanthroline (10^{-3} M)[10] also had little effect on the chromaffin granule carboxypeptidase In contrast, $HgCl_2$ (10^{-6} M), $CuCl_2$ (10^{-4} M) and *p*-chloromercuriphenyl sulphonic acid (10^{-5} M), which react with thiol groups[11 12], inhibited the carboxypeptidase Leupeptin ($3\ 7\times10^{-3}$ M) and antipain ($1\ 6\times10^{-3}$ M), which inhibit arginyl proteases[12], inhibited completely the chromaffin granule enzyme, whereas the serine protease inhibitors phenylmethylsulphonyl fluoride (10^{-4} M), aprotinin (0 017 trypsin inhibitor units ml^{-1}), and tosyllysine chloromethyl ketone (10^{-4} M)[13] and the lysosomal cathepsin B inhibitor[14], chloroquine (10^{-4} M), had no effect

The carboxypeptidase described here appears to be a unique and novel enzyme, showing a *p*H optimum and a spectrum of inhibitors different from that of other carboxypeptidases (for example, carboxypeptidases A, B and N)[6–9 15] This carboxypeptidase satisfies several criteria for it to be involved in processing the enkephalin precursor (1) it is concentrated in chromaffin granules where the precursors are found, (2) it is active at the intragranular *p*H of 5 7 (refs 16, 17), (3) it removes the basic (arginyl) residue from the C-terminus of Tyr-Gly-Gly-Phe-Met-Arg without degrading the pentapeptide itself It is not clear whether the removal of basic residues to yield the enkephalin pentapeptides is important in enhancing (or diminishing) the action of enkephalin at its physiological receptors Further studies of processing enzymes should elucidate the mechanisms by which extracellular and intracellular changes alter the synthesis of opioid peptides in the adrenal gland, and may lead to the development of drugs that specifically affect these processes

We thank Dr Julius Axelrod for his encouragement and support V Y H H and L E E are research associates in the Pharmacology-Toxicology Program, NIGMS

Received 1 October, accepted 7 December 1981

1 Stern, A S *et al* in *Biosynthesis, Modification, and Processing of Cellular and Viral Polypeptides* (eds Blough, H A & Tiffany, J M) 99–100 (Academic, New York, 1980)
2 Schultzberg, M *et al* *Acta physiol scand* **103**, 475–477 (1978)
3 Brownstein, M *Nature* **287**, 678–679 (1980)
4 Smith, A D & Winkler, H *Biochem J* **103**, 483–492 (1967)
5 Folk, J E & Gladner, J A *J biol Chem* **231**, 379–391 (1958)
6 McKay, T J & Plummer, T H *Biochemistry* **17**, 401–405 (1978)
7 McKay, T J , Phelan, A W & Plummer, T H *Archs Biochem Biophys* **197**, 487–492 (1979)
8 Plummer, T H & Hurwitz, M Y *J biol Chem* **253**, 3907–3912 (1978)
9 Ryan, C A , Hass, G M & Kuhn, R W *J biol Chem* **249**, 5495–5499 (1974)
10 Barrett, A J in *Proteases and Biological Control* (eds Reich, E , Rifkin, D B & Shaw, E) 475 (Cold Spring Harbor Laboratory, New York, 1975)
11 Snellman, O in *Tissue Proteinases* (eds Barrett, A J & Dingle, J T) 29–44 (North Holland, New York, 1971)
12 Aoyagi, T & Umezawa, H in *Proteases and Biological Control* (eds Reich, E , Rifkin, D B & Shaw, E) 431–435 (Cold Spring Harbor Laboratory, New York, 1975)
13 Walsh, K A in *Proteases and Biological Control* (eds Reich, E , Rifkin, D B & Shaw, E) 1–12 (Cold Spring Harbor Laboratory, New York, 1975)
14 Wibo, M & Poole, B *J Cell Biol* **63**, 430–440 (1974)
15 Plummer, T H & Ryan, T J *Biochem biophys Res Commun* **98**, 448–454 (1981)
16 Pollard, H B , Shindo, H , Creutz, C E , Pazoles, C J & Cohen, J S *J biol Chem* **254**, 1170–1177 (1979)
17 Casey, R P , Njus, D , Radda, G K & Sehr, P A *Biochemistry* **16**, 972–977 (1977)
18 Parker, C W *Radioimmunoassay of Biologically Active Compounds*, 71–75 (Prentice-Hall, New Jersey, 1976)
19 Smith, A D & Winkler, H *J Physiol, Lond* **183**, 179–188 (1966)

RNA synthesis and cytoplasmic polyadenylation in the one-cell mouse embryo

Kerry B. Clegg & Lajos Pikó

Developmental Biology Laboratory, Veterans Administration
Medical Center, Sepulveda, California 91343, USA
Division of Biology, California Institute of Technology, Pasadena,
California 91125, USA

The time of onset of transcriptional activity in the early mammalian embryo is unclear. RNA synthesis has been shown to occur at the two-cell stage in the mouse[1–4] and at the two- to four-cell stage in the rabbit[5], but the period immediately following fertilization has proved largely inaccessible to biochemical characterization of transcription because of the low permeability of early embryos to exogenous precursors such as ^{3}H-uridine[1–7]. This difficulty, and the failure to detect RNA polymerase activity in the pronuclei of one-cell mouse embryos[8], suggested that the embryonic genome was transcriptionally inactive until some time after the first cleavage. To investigate this issue further, we have now incubated one-cell pronuclear embryos with ^{3}H-adenosine, which is taken up about 1,000 times faster than uridine[3]. Three labelled RNA species could be identified. The major product is large, heterodisperse, poly(A)$^-$ RNA. High-molecular-weight poly(A)$^+$ RNA is also heavily labelled but this is mostly due to cytoplasmic polyadenylation of previously non-polyadenylated, stored RNA. A significant amount of label is incorporated into the -CCA termini of transfer RNA but some new synthesis of tRNA also takes place. No label was found in ribosomal RNA at the one-cell stage but synthesis of mature rRNA species was evident in the two-cell embryo.

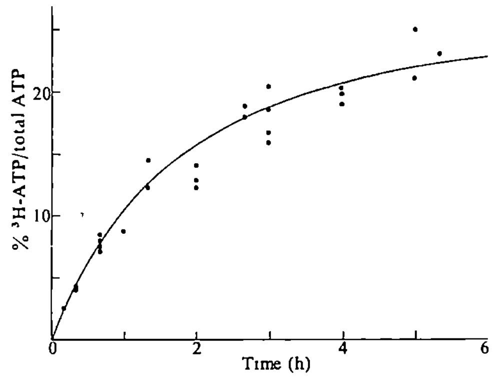

Fig. 1 Specific activity of the ^{3}H-ATP pool in one-cell mouse embryos. Fertilized ova were isolated from superovulated Swiss mice 22–24 h after injection of human chorionic gonadotropin and cultured in a pyruvate–lactate medium (PLM) containing 50 μM [2,8-^{3}H]adenosine (30–40 Ci mmol^{-1}, Amersham) as described previously[3]. At the indicated times 5–10 embryos were removed, the nucleotides extracted with 0.5 M $HClO_4$ at 0 °C, and the extract neutralized and chromatographed on polyethyleneimine (PEI) cellulose[3]. The ATP spot was cut out of the plate, solubilized with NCS tissue solubilizer (Amersham) and counted in OCS scintillant (Amersham). The specific activity of the labelled ATP pool in the mouse embryos was calculated by adding the amount of radioactive ATP to the internal ATP pool (1.1 pmol per embryo[3]) and using this value to derive the fraction of radioactive ATP—pmol ^{3}H-ATP/(1.1 pmol+pmol ^{3}H-ATP). To verify this calculation, pool specific activity measurements were sometimes made in parallel using an isotopic RNA polymerase assay[3]. The results of these assays were within 10% of the calculated value.

Figure 1 illustrates the changes in the specific activity of the total ATP pool in one-cell embryos in the labelling conditions used. The specific activity rises approximately linearly during the first 80 min and increases at a much slower rate during the succeeding 4 h, reaching about 80% of the final specific activity at the midpoint of the labelling period. We used the midpoint specific activity of the ATP pool for estimating the rates of accumulation of the labelled RNA species described below.

The labelled embryo lysates were processed as follows. After extraction with phenol–chloroform, the water phase was made 2 M in LiCl to isolate LiCl-precipitable (large molecular weight) and LiCl-soluble RNA fractions[9]. The latter was freed of labelled nucleotides by precipitation with cetyltrimethylammonium bromide[10]. The LiCl-precipitable RNA was subdivided further into poly(A)$^+$ and poly(A)$^-$ fractions by binding to poly(U)-Sepharose. The individual fractions were analysed as to electrophoretic mobility, sensitivity to RNase and distribution of labelled nucleotides, as described in the figure legends. Special care was taken to denude the eggs of any follicle cells by successive treatments with hyaluronidase and subtilisin[3]. In

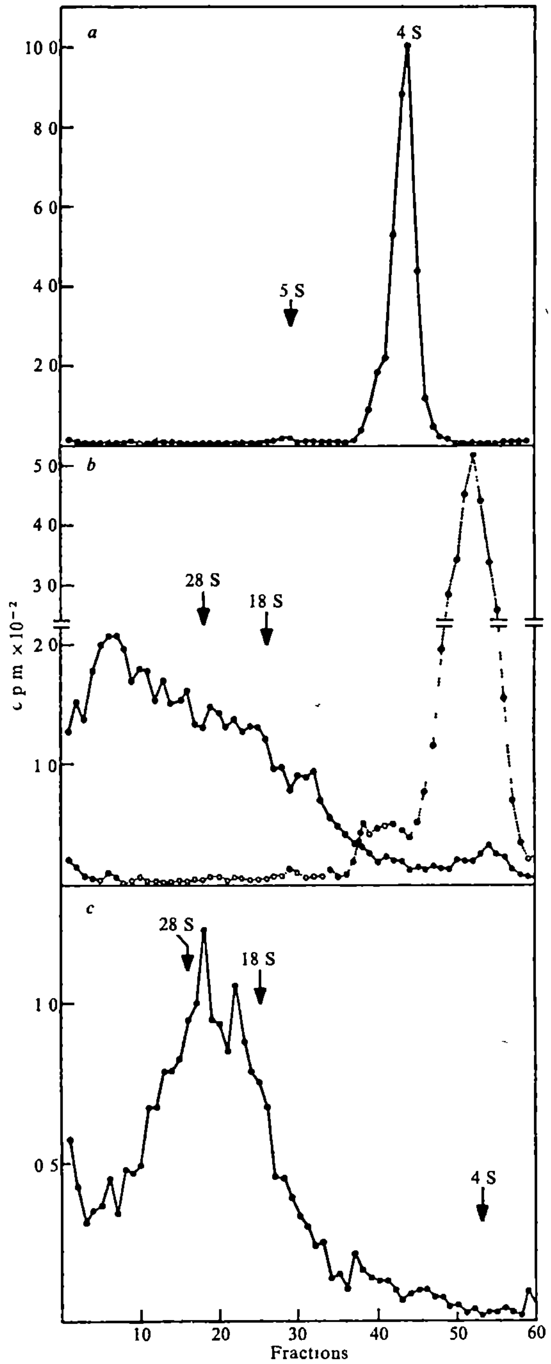

Fig. 2 Electrophoretic patterns of ^{3}H-adenosine-labelled RNAs isolated from one-cell mouse embryos. Fertilized eggs were labelled *in vitro* in PLM containing 50 μM ^{3}H-adenosine for 5–6 h, washed five or six times in HEPES-buffered saline and digested for 30 min at 37 °C in 300 μl extraction buffer (100 mM NaCl, 50 mM Tris-HCl, *p*H 7.5, 5 mM EDTA, 0.5% SDS, 100 μg ml^{-1} proteinase K) containing 10 μg mouse rRNA and 10 μg yeast sRNA (4 S and 5 S) as carriers. The digest was adjusted to 2 M in LiCl and kept at 0 °C for 18 h to precipitate high-molecular-weight RNA[9]. The precipitate was collected and washed three times with ice-cold 2 M LiCl by centrifugation at 70,000*g* for 20 min. The supernatants were pooled and used for the isolation of 4 S and 5 S RNAs. The LiCl-precipitable RNAs were dissolved in 300 μl poly(U)-binding buffer (500 mM NaCl, 10 mM Tris-HCl, *p*H 7.5, 1 mM EDTA, 0.05% SDS) and bound to 30 mg freshly rehydrated poly(U)–Sepharose (Pharmacia) at 37 °C, 15 min in a conical microfuge tube vortexed gently to keep the beads suspended. The unbound poly(A)$^-$ RNA was washed from the beads by centrifugation and resuspension six times in 0.5 ml binding buffer. The washes were pooled and the RNA precipitated with 2–3 vol 100% ethanol at −20 °C. Poly(A)$^+$ RNA was eluted from the poly(U)–Sepharose at 45 °C by six changes of 90% deionized formamide/10% eluting buffer (10 mM Tris-HCl, *p*H 7.5, 1 mM EDTA, 0.05% SDS). The eluate was adjusted to 0.1 M in NaCl, 10 μg of mouse rRNA added and the RNA ethanol-precipitated. The 4 S RNA was collected from the LiCl-soluble fraction by ethanol precipitation and further purified by dissolution in 0.1 M NaOAC, *p*H 5, and reprecipitation with 0.5% cetyltrimethylammonium bromide (CTAB)[10]. The CTAB precipitate was washed extensively with 0.1% CTAB in 0.1 M NaOAc, *p*H 5, to remove soluble nucleotides and the CTAB was removed by washing three times with 70% ethanol/30% 0.1 M NaOAc, *p*H 5. The RNAs were redissolved in Loening's E-buffer[26] (36 mM Tris base, 30 mM NaH_2PO_4, 1 mM EDTA, 0.1% SDS) for electrophoresis. *a*, Pattern of LiCl-soluble RNA from 400 one-cell embryos after electrophoresis in 10% polyacrylamide gel in E-buffer at 5 mA per gel for 3 h, the radioactive peak coincides with the 4 S absorbance marker. *b*, Pattern of LiCl-precipitable, poly(A)$^-$ RNA from 1,000 one-cell embryos after electrophoresis in 2.25% acrylamide–0.5% agarose gels at 5 mA per gel for 2.5 h in E-buffer containing 6 M urea. One-half of the sample was electrophoresed intact (solid line) and the other half after digestion with 100 μg ml^{-1} RNase A + 50 U ml^{-1} RNase T_1 in E-buffer at 37 °C for 30 min (dotted line). Before electrophoresis, the samples were brought to 6 M in urea, heated at 85 °C for 5 min, allowed to cool and layered on the gel. *c*, Pattern of poly(A)$^+$ RNA from 700 one-cell embryos after electrophoresis in 6 M urea as in *b*. All gels were scanned at 260 nm using a Gilford linear transport, sliced in 1.5-mm slices, dissolved in 0.5 ml 90% NCS/10% water at 50 °C for 2 h and counted in OCS scintillant (Amersham) at 30% efficiency.

some experiments, the zona pellucida was completely digested by subtilisin and the polar bodies removed by repeated pipetting of the eggs through a small-bore pipette The amount and distribution of label in the three major classes of RNA was the same in these eggs, suggesting that no significant RNA synthesis occurs in the polar body nuclei The possibility that the egg mitochondria may contribute to the labelling pattern is remote because mitochondrial RNA synthesis has not been detected until the eight-cell stage[11] and we observed no 12S or 16S mitochondrial ribosomal RNA species in the present study

Figure 2*a* shows the electrophoretic pattern of the LiCl-soluble labelled material The large 4 S peak was sensitive to RNase and assumed to be tRNA It was eluted from the gel and analysed further by base hydrolysis and PEI cellulose chromatography of the nucleotides[3] About 83% of the label migrated with the adenosine marker and only about 17% migrated as AMP. Although this indicates that some ^{3}H-adenosine label is incorporated into internal positions, suggesting the synthesis of a small amount of tRNA, it is clear that most of the label is localized in the -CCA terminus, about 60 tRNA molecules being terminally labelled for each newly synthesized tRNA (assuming an average of 14 adenosine residues per tRNA[12]) Terminal labelling presumably reflects the turnover of 3′-terminal adenosine residues[13]

Figure 2*b* shows the electrophoretic pattern of the LiCl-precipitable, poly(A)$^-$ fraction This fraction, which is completely sensitive to RNase, consists of large, heterodisperse RNA with a number-average size[14] of about 2 5 kilobases (kb) The amount of heterodisperse RNA accumulated over a 5-h labelling period was estimated to be ~3 pg per embryo (assuming a 25% adenosine content) However, preliminary studies on the time course of incorporation of ^{3}H-adenosine into this fraction suggest that most of the newly synthesized RNA is turning over rapidly and probably represents heterogeneous nuclear RNA (K B C and L P , unpublished observations) None of the poly(A)$^-$ RNA appears to be ribosomal, as an analysis of the gel pattern of several RNA preparations (as in Fig 2*b*) failed to reveal any evidence of 18 S and 28 S rRNA From the specific activity of the ATP pool, we estimate that the synthesis of as little as 0 03 pg rRNA per embryo during 6 h labelling would have been detected As the rate of synthesis of mature rRNA in the morula is ~2 5 pg per cell per h (ref 15), we conclude that rRNA synthesis in the one-cell embryo, if it occurs at all, is <0 2% of that in the morula on a per cell basis

The LiCl-precipitable, poly(A)$^+$ RNA fraction consists of high-molecular-weight RNA with a number-average size of 1 7 kb (Fig 2*c*) The poly(A)$^+$ RNA peak was completely abolished by digestion with RNase (data not shown) To analyse the distribution of label in this RNA, purified poly(A)$^+$ RNA was digested with RNase A+T$_1$ in conditions which leave the poly(A) tracts intact, and the digest chromatographed on a PEI plate (Fig 3) About one-third of the total label migrated with the AMP marker, suggesting that it was released from an internal location, and about two-thirds remained at the origin, suggesting localization in poly(A) tracts of about (A)$_{20}$ or larger It is unlikely that the label in the AMP peak derived from random cleavage of labelled poly(A) tracts because of the low background between the AMP peak and the origin (where partially digested fragments would appear) and the repeatability of the chromatographic pattern in three separate experiments The number-average size of the labelled poly(A) tracts was (A)$_{50}$, as determined by polyacrylamide gel electrophoresis in relation to poly(A) markers of known length (not shown) To determine what portion of the poly(A) tracts was newly synthesized, we measured the distribution of label between A and AMP by PEI cellulose chromatography of the alkaline hydrolysate of purified poly(A) This procedure gave a ratio of A/AMP of 1 42, or an average length of (A)$_{43}$, suggesting that the labelled poly(A) tracts had arisen mostly, if not entirely, from new synthesis rather than from the elongation of pre-existing tracts From the average size of the labelled poly(A)$^+$ RNA, 1,700 nucleotides, the number of adenosine nucleotides in the non-poly(A) portion of the molecule can be estimated at about 425 (assuming a 25% content in adenosine), about 10-fold higher than the average length of (A)$_{43}$ for newly synthesized poly(A) However, the observed ratio of label in the non-poly(A) portion of the molecule is one-half that in the poly(A) tail, suggesting that only about 5% of the labelled poly(A)$^+$ RNA molecules are newly synthesized, the remainder representing pre-existing maternal mRNA having undergone cytoplasmic polyadenylation As there is about a 20% increase in total poly(A) between fertilization and the late one-cell stage[15] but no increase in the average size of poly(A) tracts (K B C and L P , in preparation), it seems likely that the newly synthesized tracts are added, at least in part, to previously non-polyadenylated RNA Both turnover (and lengthening) of poly(A) and the addition of poly(A) sequences to previously non-polyadenylated RNA occur in fertilized sea urchin eggs and result in a doubling of poly(A) content[16–19] In *Urechis* eggs, total poly(A) increases severalfold as a result of polyadenylation of new RNA sequences on fertilization[20] The present findings suggest that cytoplasmic polyadenylation is an important feature of early mouse development as well A less extensive adenylation, consisting of the terminal addition of short oligo(A) segments to pre-existing poly(A) tracts, has been reported in mouse eggs 1–3 h after fertilization[21] As we used late one-cell embyros for labelling, about 11–17 h after fertilization, the difference may be due to developmental stage-specific changes in cytoplasmic adenylation

Because of the high specific activity that can be attained with the ATP pool, we have re-examined the question of rRNA synthesis by the two-cell mouse embryo Nucleolus organizing activity has been detected by cytochemical (silver) staining at the two-cell stage[22,23], and there is biochemical evidence of a low level of rRNA synthesis (with ^{3}H-uridine labelling)[2] Figure 4 shows the pattern of LiCl-precipitable, poly(A)$^-$ RNA isolated from late two-cell embryos labelled for 6 h with ^{3}H-adenosine Although most of the incorporation is in large heterodisperse RNA, distinct 18 S and 28 S peaks, as well as rRNA precursor peaks, are also evident From the amount of radioactivity under the 18 S and 28 S peaks (~25% of the total), the specific activity of the ATP pool (19%) and the base composition of rRNA (18% adenosine), the rate of synthesis of rRNA at this stage can be estimated at about 0 3 pg per embryo per h On a per cell basis,

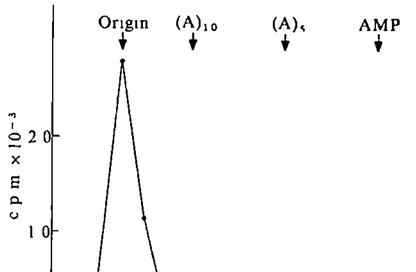

Fig. 3 PEI cellulose chromatography of RNAse A+T$_1$ digest of ^{3}H-adenosine-labelled poly(A)$^+$ RNA from one-cell mouse embryos For labelling conditions and the isolation of poly(A)$^+$ RNA, see Fig 2 legend The ethanol-precipitated RNA was dissolved in 25 μl of 5 μg ml^{-1} RNase A, 10 U ml^{-1} RNase T$_1$ in 300 mM NaCl, 10 mM Tris-HCl, 1 mM EDTA, *p*H 7 5, and incubated at 37 °C for 1 h The digest was mixed with 2–3 μmol each of AMP and the oligomers (A)$_5$, (A)$_{10}$ and (A)$_{33}$ (Miles) and chromatographed on a 2×20 cm PEI plate successively in 100% methanol, distilled water and 1 25 M Tris-HCl *p*H 8 4, to fractionate oligo(A) sequences according to size[27] The plate was cut into 1-cm pieces, digested in 1 ml 90% NCS for 30 min at 22 °C and counted in OCS at 35% efficiency The recovery of labelled nucleotides was better than 90% The position of the markers on the plate was visualized by UV

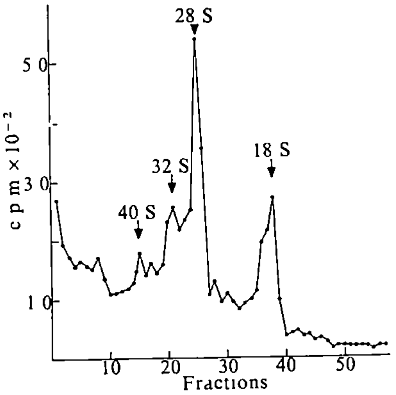

Fig. 4 Electrophoretic pattern of LiCl-precipitable poly(A)$^-$ RNA from 600 two-cell mouse embryos incubated for 6 h (46–52 h post-human chorionic gonadotropin) in the presence of 50 μM ^{3}H-adenosine Any three- to four-cell embryos at the end of the labelling period were removed Electrophoresis was in 2 25% acrylamide–0 5% agarose gels in the presence of 6 M urea For details, see Fig 2 legend

this rate is about one-sixteenth of that in the morula[15] The 4 S RNA peak is also heavily labelled in the two-cell embryo, the distribution of label between the -CCA terminus and internal locations in tRNA being very similar to that observed in the zygote (data not shown), and synthesis of poly(A)$^+$ RNA in the two-cell embryo has been reported previously[4] Therefore all the major classes of RNA seem to be synthesized by the two-cell mouse embryo RNA synthesis intensifies from the eight-cell stage onwards[3], resulting in a sixfold increase in total RNA content between the two-cell stage and early blastocyst[15] As about 40% of the bulk maternal RNA is eliminated by the two-cell stage and at most 30% persists until the early blastocyst[24], a nearly complete shift from the use of maternal to embryo-derived RNA components must take place by the early blastocyst stage The results presented here indicate that transcription has already started in the pronuclei of the zygote The role of the RNA products and the significance of cytoplasmic polyadenylation in the one-cell embryo remain to be elucidated An interesting possibility is that cytoplasmic adenylation may be involved in the selective activation of subpopulations of maternal mRNA which has been reported to take place around the late one-cell to early two-cell stage[25]

This work was supported by the Medical Research Service of the Veterans Administration and by PHS research grant CA24989 from the NCI

Received 3 August, accepted 11 November 1981

1 Woodland, H R & Graham, C F *Nature* **221,** 327–332 (1969)
2 Knowland, J & Graham, C *J Embryol exp Morph* **27,** 167–176 (1972)
3 Clegg, K B & Pikó, L *Devl Biol* **58,** 76–95 (1977)
4 Levey, I L, Stull, G B & Brinster, R L *Devl Biol* **64,** 140–148 (1978)
5 Cotton, R W, Manes, C & Hamkalo, B A *Chromosoma* **79,** 169–178 (1980)
6 Daentl, D L & Epstein, C J *Devl Biol* **24,** 428–442 (1971)
7 Young, R J, Sweeney, K & Bedford, J M *J Embryol exp Morph* **44,** 133–148 (1978)
8 Moore G P M *J Embryol exp Morph* **34,** 291–298 (1975)
9 Barlow, J J, Mathias, A P, Williamson, R & Gammack, D B *Biochem biophys Res Commun* **13,** 61–66 (1963)
10 Bellamy, A R & Ralph, R K *Meth Enzym* **12A,** 156–160 (1968)
11 Pikó, L & Chase, D G *J Cell Biol* **58,** 357–378 (1973)
12 Randerath, E, Chia, L S Y, Morris, A P & Randerath, K *Cancer Res* **34,** 643–653 (1974)
13 Deutscher, M P *Prog Nucleic Acid Res molec Biol* **13,** 51–92 (1973)
14 Vournakis, J N, Gelinas, R E & Kafatos, F C *Cell* **3,** 265–273 (1974)
15 Pikó, L & Clegg, K B *Devl Biol* **89,** 362–378 (1982)
16 Slater, I, Gillespie, D & Slater, D W *Proc natn Acad Sci U S A* **70,** 406–411 (1973)
17 Wilt, F H *Proc natn Acad Sci U S A* **70,** 2345–2349 (1973)
18 Wilt, F H *Cell* **11,** 673–681 (1977)
19 Dolecki, G J, Duncan, R F & Humphreys, T *Cell* **11,** 339–344 (1977)
20 Davis, F C & Davis, R W *Devl Biol* **66,** 86–96 (1978)
21 Young, R J & Sweeney, K *J Embryol exp Morph* **49,** 139–152 (19791)
22 Engel, W, Zenzes, M T & Schmid, M *Hum Genet* **38,** 57–63 (1977)
23 Hansmann, I, Gebauer, J, Bihl, L & Grimm, T *Expl Cell Res* **114,** 263–268 (1978)
24 Bachvarova, R & De Leon, V *Devl Biol* **74,** 1–8 (1980)
25 Braude, P, Pelham, H, Flach, G & Lobatto, R *Nature* **282,** 102–105 (1979)
26 Loening, U E *Biochem J* **113,** 131–138 (1969)
27 Randerath, K & Randerath, E *Meth Enzym* **12A,** 323–347 (1967)

Partial nucleotide sequence of human calcitonin precursor mRNA identifies flanking cryptic peptides

Roger K. Craig*†, Len Hall*, Mark R. Edbrooke‡, Janette Allison* & Iain MacIntyre‡

* Courtauld Institute of Biochemistry, Middlesex Hospital Medical School, Mortimer Street, London W1P 7PN, UK
‡ Endocrine Unit, Royal Postgraduate Medical School, Hammersmith Hospital, Du Cane Road, London W12 0HS, UK

Calcitonin is a small peptide hormone (molecular weight (MW) 3,500) synthesized and secreted in mammals by the C-cells of the thyroid[1,2]. In man a major role of calcitonin is to protect the skeleton during periods of calcium stress such as growth, pregnancy and lactation[3]. Excessive calcitonin levels are associated with familial and sporadic medullary carcinoma of the thyroid[4], and in some cases with ectopic synthesis often by small oat-cell carcinoma of the lung[5]. Evidence from mRNA-directed cell-free protein synthesis suggests that in common with other small peptide hormones[6], human calcitonin is synthesized as a high-molecular-weight precursor protein[7–9]. Recently, we described the construction and partial characterization of recombinant plasmids containing human calcitonin cDNA sequences[9]. Here we demonstrate by nucleotide sequence analysis of these cloned cDNA sequences that human calcitonin resides towards the carboxy terminal of a precursor polyprotein, and is flanked at the amino and carboxy termini by cryptic peptide sequences of unknown biological significance. The cryptic peptide present at the carboxy terminus differs significantly in amino acid sequence from that present in the rat calcitonin precursor polyprotein[10–12].

We have previously described the identification and partial characterization of two cDNA clones (phT-B3 and phT-B6) containing in total an estimated 60% of a mRNA 1,000±100 nucleotides long This mRNA, isolated from a human medullary carcinoma of the thyroid, directed the synthesis in a wheat-germ cell-free system of a 21,000-MW calcitonin precursor protein, as judged by immunoprecipitation and SDS polyacrylamide gel electrophoresis[9] Nucleotide sequence analysis[13] of both cloned cDNA sequences revealed that the larger cloned fragment (phT-B3) contained most of the 3′-untranslated region of the mRNA and a sequence encoding 93 amino acids The smaller cloned fragment (phT-B6) contained the complete 3′-untranslated region, and a sequence encoding 37 amino acids No differences were detected in the nucleotide sequence of cDNA that was common to both plasmids Examination of the 93 amino acids encoded within the cloned 5′ portion of the mRNA (Fig 1) revealed a tract of 33 amino acids comprising the expected sequence of human calcitonin[14 15], with an additional glycine next to the carboxy-terminal proline This sequence is located towards the carboxy end of the precursor protein, and is separated from the adjacent cryptic peptide sequences by basic amino acid residues, presumably sites for proteolytic cleavage[16] The presence of a glycine residue immediately adjacent to the carboxy-terminal proline in the calcitonin precursor reflects the requirement of an amidated carboxy-terminal proline in the fully processed calcitonin, in common with other peptides including rat calcitonin, which contain carboxy-terminal amidated amino acid residues and are synthesized as larger precursor proteins[10–12 17]

Comparative analysis of nucleotide sequence homologies in the coding region of the human and rat[10–12] calcitonin mRNAs (Fig 1) and in deduced amino acid sequences (but excluding gap

---

† To whom correspondence should be addressed

```
       -36 -35 -34 -33 -32 -31 -30 -29 -28 -27 -26 -25 -24 -23 -22 -21 -20 -19         -18 -17 -16 -15 -14 -13 -12 -11
       Val Leu Leu Ala Ala Leu Val Gln Asp Tyr Val Gln Met Lys Ala Ser Glu Leu         Glu Gln Glu Gln Glu Arg Glu Gly

       578                                 550
Human 5'GTC CTG CTG CCT GCA CTG GTG CAG GAC TAT GTG CAG ATG AAG GCC AGT GAG CTG---------GAG CAG GAG CAA GAG AGA GAC GGC
Rat     CGC CTA CTG GCT GCA CTG GTG CAG AAC TAT ATG CAG ATG AAA CTC AGG GAG CTG GAG CAG GAG GAG GAA CAG GAG GCT GAC GGC

       Arg                             Asn     Met             Val Arg         Glu Gln     Glu             Ala

      -10 -9  -8  -7  -6  -5  -4  -3 |-2  -1 | 1   2   3   4   5   6   7   8   9   10  11  12  13  14  15  16  17  18  19
      Ser Ser Leu Asp Ser Pro Arg Ser|Lys Arg|Cys Gly Asn Leu Ser Thr Cys Met Leu Gly Thr Tyr Thr Gln Asp Phe Asn Lys Phe

      500                                                        450
Human TCC AGC CTG GAC AGC CCC AGA TCT|AAG CGG|TGC GCT AAT CTG AGT ACT TGC ATG CTG GGC ACA TAC ACG CAG GAC TTC AAC AAG TTT
Rat   TCT AGC TTG GAC AGC CCC AGA TCT|AAG CGG|TGT GGG AAT CTG ACT ACC TGC ATG CTG GGC ACG TAC ACA CAA GAC CTC AAC AAG TTT

                                                                                                          Leu

      20  21  22  23  24  25  26  27  28  29  30  31  32 |+1 |+2  +3  +4 |+5  +6  +7  +8  +9  +10 +11 +12 +13 +14 +15 +16
      His Thr Phe Pro Gln Thr Ala Ile Gly Val Gly Ala Pro|Gly|Lys Lys Arg|Asp Met Ser Ser Asp Leu Glu Arg Asp His Arg Pro

                      400                                                          350
Human CAC ACC TTC CCC CAA ACT GCA ATT GGG GTT GGA GCA CCT|GGA|AAG AAA ACG|GAT ATG TCC AGC GAC TTG GAG AGA GAC CAT CGC CCT
Rat   CAC ACC TTC CCC CAA ACT TCA ATT GGG GTT GGA GCA CCT|GGC|AAG AAA AGG|GAT ATG GCC AAC GAC TTG GAG ACA AAC CAC CAC CCC

                              Ser                                                  Ala Lys             Thr Asn     His

      +17 +18 +19 +20 +21 +22 +23 +24 +25
      His Val Ser Met Pro Gln Asn Ala Asn term                 term                          term

                                      300                                                   250
Human CAT GTT AGC ATG CCC CAG AAT GCC AAC TAA ACT CCT CCC TTT CCT TCC TAATTTCCCTTCTTGCATCCTTCCTATAACTTGATGCATGTGGTTTGGTTCC
Rat   TAT TTT GGC-----------------------AAC TAG GTC CCT CCT CTC CTT TCC---AGTTTCCATCTTGCTTTCTTCCTATAACTTGATGCATGTACT-----TCC

      Tyr Phe Gly

                              200                                                 150
Human TCTCTGGTGGCTCTTTGGGCTGGTATTGGTGGCTTTCCTTGTGGCAGAGGATGTCTCAAACTTCAAGATGGGAGGAAAGAGAGCAGGACTCACAGGTTGGAAGAGAATCACCTGGG
Rat   TCTCTGGCTGTTCTCTGGGCTATTATGGCTTACTTTCATGA

                 100  term      term                               50                      term     term
Human |AAAATACCAGAAAA|TGAGGGCCGCTTTGAGTCCCCCAGAGATGTCATCAGAGCTCCTCTGTCCTGCTTCTGAATGTGCTGATCATTTGAGC|AATAAA|ATTATTTTTCCCCpoly(A)
```

Fig. 1 Nucleotide sequence of human calcitonin precursor polyprotein mRNA cloned into phT-B3 and phT-B6 The figure compares the known common nucleotide sequence of human and rat[10–12] calcitonin precursor polyprotein mRNA sequences, as determined by DNA sequence analysis of the cloned cDNA sequences, with gaps introduced to maximize homologies Numbers immediately above the human nucleotide sequence denote the relative number of nucleotides from the poly(A) tail Numbers above the human protein sequence refer to amino acid position amino-terminal cryptic peptide −1 to −36, calcitonin, 1–32, carboxy-terminal cryptic peptide, +1 to +25 Base substitutions are indicated by dots Where replacement base substitutions have occurred or the human nucleotide sequence is not present, the alternative or additional amino acid(s) present within the rat precursor polyprotein have been shown immediately below the codon(s) in question Boxed sections of the amino acid and nucleotide sequences indicate regions discussed in the text DNA sequence determination was performed on both strands of the cloned cDNA sequences (phT-B3 and phT-B6) using the procedure of Maxam and Gilbert[13]

sequences introduced to maximize homology) revealed greater nucleotide (85 0%) than amino acid (80 7%) sequence homology Of the 88 codons considered, we found one or more base substitutions within 32 of the codons (36 4%), and of these, 17 (53 1%) represent replacement substitutions The distribution of the replacement and silent substitutions differs, however, between those regions encoding the amino- and carboxy-terminal cryptic peptides and those encoding calcitonin, a situation reflected in the variation in amino acid sequence in the three peptide domains Thus the nucleotide sequence encoding human calcitonin (amino acids 1–32) contains seven silent and two replacement substitutions In contrast, comparison of the nucleotide sequences encoding the flanking cryptic peptides (amino acids −1 to −36, and +1 to +25), particularly the carboxy-terminal peptide, shows a preponderance of replacement substitutions Furthermore, the relative difference in amino acid sequence between human and rat flanking peptides is exaggerated by the presence of an additional dipeptide in the rat amino-terminal cryptic peptide (between positions −19 and −18 of the human sequence) and of a pentapeptide sequence immediately preceding the terminal asparagine of the human carboxy-terminal cryptic peptide which is absent from the corresponding rat peptide A computer search for homologies within established protein sequences failed to reveal homology between the human cryptic peptides and other structural or biologically active peptides Moreover, there seems to be no significant nucleotide homology between the sequence encoding human calcitonin and that present in the human pro-opiocortin mRNA, thought to encode a calcitonin-like peptide[18 19]

The 3′-untranslated region of the human calcitonin mRNA consists of 299 nucleotides including the termination codon UAA Two potential termination codons closely follow the authentic codon The first of these (UAA) remains in phase, while the second is not in phase In common with other eukaryotic mRNAs, the supposed polyadenylation enzyme recognition sequence AAUAA is present 13 nucleotides from the site of poly(A) addition[20] A palindromic-type sequence (5′ AAAAUACCAGAAAA 3′) is also present 100 nucleotides from the poly(A) tail

Although we have yet to identify and sequence cDNA clones that contain the remaining 300–400 nucleotides comprising the 5′ end of the human calcitonin mRNA, and which encode the remainder of the amino-terminal cryptic peptide sequence and presumably an amino-terminal leader sequence, our observations are important for various reasons. Human calcitonin is another of the increasing number of small peptide hormones now known to be synthesized as higher-molecular-weight precursor proteins and subsequently processed to yield one or more biologically active peptides[6] Whether the human calcitonin precursor proves to be a true polyprotein, in the sense that two or more secreted biologically active peptides are specifically processed from a common precursor, remains to be established Our comparative analysis of the nucleotide sequences encoding the human and rat calcitonin peptides implies that both have evolved from a common ancestral gene, and that selection pressures have eliminated base substitutions which might result in adverse alteration of codon specificity The accumulation of silent or supposedly neutral substitutions presumably reflects evolutionary divergence as a result of genetic drift[21] In contrast, the amino- and carboxy-terminal cryptic peptide sequences have diverged to the extent that the latter, in particular, may have acquired different functions in rat and man Equally it might be argued that such extreme sequence divergence implies that the flanking peptides do not have a significant biological role, but are present merely to ensure that the calcitonin precursor protein is in the correct conformation for processing within the secretory pathway Chemical synthesis of the human cryptic peptide sequences should resolve questions related to biological function, antibodies raised against each peptide may be used to investigate the processing of the calcitonin precursor polyprotein, and to determine the presence and levels of the circulating cryptic peptides in subjects of different age, and in varying conditions of calcium stress[3] The antibodies may also be used to characterize high-molecular-weight circulating variants of human calcitonin often associated with ectopic synthesis and secretion[5]

The availability of a cloned human calcitonin cDNA probe will allow comparisons to be made between human calcitonin gene structure and expression in normal thyroid tissue, and in familial and sporadic medullary carcinoma of the thyroid cDNA probes could also be used to investigate linked DNA polymorphisms, thereby providing a quick and reliable means of distinguishing between familial and sporadic medullary carcinoma of the thyroid, avoiding extensive and often invasive investigations[22,23] Finally, the probes may be used for definitive studies of the molecular mechanisms involved in ectopic synthesis of calcitonin

We thank Professor P N Campbell for his continued support and encouragement and Dr M O Dayhoff of the National Biomedical Research Foundation for the computer search for homologies within the cryptic flanking peptides

Received 6 October, accepted 27 November 1981

1 Foster, G V , MacIntyre, I & Pearse, A G E *Nature* **203,** 1029–1030 (1964)
2 Foster, G V *et al* *Nature* **202,** 1303–1305 (1964)
3 Stevenson, J C , Hillyard, C J , MacIntyre, I , Cooper, H & Whitehead, M I *Lancet* ii, 769–770 (1979)
4 Stevenson, J C & Hillyard, C J in *Recent Results in Cancer Research* (ed Duncan, W) 60–67 (Springer, Heidelberg, 1980)
5 Schwartz, K E , Wolfsen, A R , Forster, B & Odell, W D *J clin Endocr Metab* **49,** 438–444 (1979)
6 Herbert, E *Trends biochem Sci* **6,** 184–188 (1981)
7 Desplan, C *et al* *FEBS Lett* **117,** 89–92 (1980)
8 Goodman, R H , Jacobs, J W & Habener, J F *Biochem biophys Res Commun* **91,** 932–938 (1979)
9 Allison, J , Hall, L , MacIntyre, I & Craig, R K *Biochem J* **199,** 725–731 (1981)
10 Amara, S G , David, D N , Rosenfeld, M G , Roos, B A & Evans, R M *Proc natn Acad Sci U S A* **77,** 4444–4448 (1980)
11 Jacobs, J W *et al* *Science* **213,** 457–459 (1981)
12 Jacobs, J W , Potts, J T , Bell, N H & Habener, J F in *Calcitonin 1980* (ed Pecile, A) 25–34 (Excerpta Medica, Amsterdam, 1981)
13 Maxam, A M & Gilbert, W *Proc natn Acad Sci U S A* **74,** 560–564 (1977)
14 Riniker, B *et al* *Helv chim Acta* **51,** 1738–42 (1968)
15 Neher, R , Riniker, B , Rittel, W & Zuber, H *Helv chim Acta* **51,** 1900–1905 (1968)
16 Steiner, D F , Quinn, P S , Chan, S J , Marsh, J & Tager, H S *Ann N Y Acad Sci* **343,** 1–16 (1980)
17 Kreil, G , Suchanek, G & Kindas-Mugge, I *Fedn Proc* **36,** 2081–2086 (1977)
18 Chang, A C Y , Cochet, M & Cohen, S N *Proc natn Acad Sci U S A* **77,** 4890–4894 (1980)
19 Seidah, N G , Rochmont, J , Hamelin, J , Lis, M & Chretien, M *J biol Chem* **256,** 7977–7984 (1981)
20 Proudfoot, N J & Brownlee, G G *Nature* **252,** 359–362 (1974)
21 Jeffreys, A J in *Genetic Engineering* Vol 2 (ed Williamson, R) 1–48 (Academic, New York, 1981)
22 Botstein, D , White, P L , Skolnick, M & Davis, R W *Am J hum Genet* **32,** 314–331 (1980)
23 Stevenson, J C *et al* *Post-grad med J* **57,** 104–108 (1981)

Heterogeneity of the BALB/c IgM anti-phosphorylcholine antibody response

Judith A. Owen*, Nolan H. Sigal† & Norman R. Klinman‡

*Department of Biology, Haverford College, Haverford, Pennsylvania 19104, USA
† Division of Immunology, Research Institute, Hospital for Sick Children, Toronto, Ontario, Canada M5G 1XB
‡ Department of Immunopathology, Scripps Clinic and Research Foundation, La Jolla, California 92037, USA

Although recent advances in the study of the molecular genetics of the antibody system have greatly increased our understanding of the generation of immunological diversity[1–7], the state of B-cell differentiation at which diversification and specificity commitment occur has yet to be determined. In particular, it is unclear whether the entire repertoire of antibody specificities in an individual is expressed in the absence of selective forces, such as antigenic stimulation or network regulation. It has recently been suggested that some elements of variable region diversification, particularly somatic mutations, may accompany the shift from the IgM to IgG isotype[8–10]. These findings support the view that much of B-cell repertoire diversity is the result of antigen-driven somatic events, because isotype shifts normally occur after antigenic stimulation[11–13]. As these experiments used antibodies obtained after at least one *in vivo* antigenic stimulation, they do not address the possibility that the selection occurring during clonal expansion and subsequent IgG synthesis may favour the use of clones expressing unique antibody specificities (clonotypes) far removed from the innate or frequently occurring germ-line sequences. To test whether B-cell diversification may precede IgM expression, we have now determined the range of diversity available in the primary IgM antibody repertoire by studying the clonal heterogeneity of monoclonal IgM antibodies expressed by BALB/c mice in response to phosphorylcholine (PC). Our results indicate that the repertoire of IgM antibodies in an inbred murine strain exceeds 10^7 clonotypes. This diversity is sufficiently large to preclude meaningful comparisons between the IgM and IgG repertoires and suggests that antibody diversification may occur early in B-cell differentiation.

Spleen cells from non-immune adult BALB/c mice were injected intravenously into irradiated (1,300 rad) BALB/c recipients that had been immunized with 0 1 mg of *Limulus polyphemus* haemocyanin (Hy) 1–2 months previously Splenic fragment cultues were established as described elsewhere[14 15] and stimulated with 3-*p*-azophenyl-phosphorylcholine-*N*-acetyl-L-tyrosyl-glycylglycine-BOC-hydrazide–Hy to obtain monoclonal anti-PC responses[15] A radioimmunoassay (RIA) was used to identify fragment cultures containing monoclonal anti-PC antibodies and to determine the immunoglobulin isotype[16] Similar to previous results[15], one B cell in 8×10^4 produced monoclonal anti-PC antibodies which were idiotypically indistinguishable from the TEPC-15 (T15) myeloma protein by either purified rabbit anti-T15 idiotype antibody or anti-idiotypic antisera raised in A/J mice using assay methods and reagents which have been previously described[15] An additional 1 in 10^5 B cells yielded non-T15 anti-PC monoclonal

Table 1 Classification of monoclonal antibodies into indistinguishable groups by the criterion of hapten inhibition of antibody binding

Monoclonal antibody	IC_{50}PC	IC_{50}GPC	IC_{50}C	No of foci in group
5581	0 020	0 40	15	1
5552	0 025	1 6	25	1
5431	0 032	0 20	3 2	3
5265	0 032	0 50	10	3
5527	0 04	0 10	2 5	1
5446	0 04	0 20	10	1
5635	0 05	0 13	5 0	1
5388	0 05	0 40	16	11
5603	0 05	0 50	50	1
5347	0 05	0 79	25	1
5112	0 13	0 79	25	45
5293	0 20	2 0	50	1
5349	0 32	0 20	50	1
5254	0 32	1 0	32	2
5144	0 32	1 6	32	1
5358	0 32	2 5	100	1
5599	0 40	0 063	0 50	1
5292	0 40	1 0	25	25
5315	0 50	0 40	5 0	4
5386	0 50	1 3	7 9	1
5276	1 0	0 40	20	1
5337	3 2	3 2	16	1
5275	3 4	3 8	2 8	1

Monoclonal antibodies had hapten inhibition profiles which were unique or representative of several antibodies The haptens PC, α-glycerophosphorylcholine (GPC) and choline (C) were used to inhibit binding by monoclonal antibodies to polyvinyl plates coated with the antigen PC–BSA by a method reported previously[17] 0 1 ml of the appropriate hapten in phosphate-buffered saline (PBS) was added individually to each well The plates were incubated for 2 h at room temperature and then washed and labelled with ^{125}I-labelled anti-μ antibody After incubation at 4 °C overnight and washing, each well was counted in a γ-counter Each culture fluid was run in triplicate for each hapten concentration and controls in quadruplicate with PBS The percentage of control binding which remained in the presence of each hapten concentration tested was then calculated IC_{50} is expressed here as the concentration of hapten (in mmol) giving 50% inhibition of binding

0028–0836/82/040347—02$01 00

antibodies and 109 of these, derived from 14 donors, produced sufficient IgM antibody (> 100 ng) to permit a comprehensive analysis

The fine specificity of the non-T15 IgM anti-PC monoclonal antibodies was assessed by hapten inhibition (HI) of their binding to phosphorylcholine–bovine serum albumin (PC–BSA)[17] Using the standard errors derived from replicate assays of both T15-positive and T15-negative IgM foci, we estimate that two antibodies can be distinguished from one another if their IC_{50} values differ by greater than twofold for any of the three haptens Table 1 gives the IC_{50} values of all 109 non-T15 IgM antibodies Twenty-three HI patterns were observed The reactivity patterns of focus 5112 and those of 44 other non-T15 antibodies are indistinguishable from that of the T15 myeloma protein and 26 tested IgM monoclonal antibodies bearing the T15 idiotype The single focus (5275) reactive with a rabbit anti-MOPC 167 idiotypic serum is also indistinguishable from MOPC 167 by reactivity pattern analysis Insofar as hapten inhibition of binding can be used as a measure of affinity of antibody for antigen[18], it is clear that non-T15 IgM monoclonal antibodies exist which possess both higher and lower affinity for PC than does the T15 myeloma protein

To discriminate further between the antibodies with indistinguishable HI patterns, the isoelectric points (*p*I) of all 109 antibodies were determined by sucrose gradient isoelectric focusing (IEF)[19] The *p*Is of the 45 antibodies which shared HI properties with the T15 myeloma protein ranged from *p*H 3 35 to *p*H 6 05 Similarly, the *p*Is of antibodies indistinguishable by HI analysis from foci 5292 and 5388 were *p*H3 7–6 4 and *p*H 3 9–5 95 respectively Since antibodies that focus at isoelectric points > 0.2 *p*H units apart can be unambiguously distinguished from one another, each group of antibodies defined by HI criteria could be subdivided on this basis

As a final criterion for discriminating antibodies not clearly distinguishable by HI or IEF, each IgM monoclonal antibody was assessed for partial reactivity with rabbit or mouse anti-T15 idiotype specific antisera Of the 109 non-T15 antibodies, 42 displayed partial cross-reactivity with the mouse anti-T15 idiotype Of these, 23 displayed no reactivity with the rabbit anti-T15 reagent, 3 reacted with the rabbit anti-T15 on a 1 1 weight basis and 16 showed partial reactivity One other antibody reacted with the rabbit anti-T15 reagent 1 1 by wt but showed no cross-reactivity with mouse anti-T15 None of the four antibodies showing complete reactivity with rabbit anti-T15 shared HI characteristics with the T15 protein (for example, antibodies 5358 and 5635, Table 1) However, of the 42 antibodies displaying partial reactivity with mouse anti-T15, 24 (57%) shared the HI pattern of the T15 protein, which may imply a preferential, but not absolute, association of partial mouse anti-T15 reactivity with T15 HI characteristics

Because the distinguishing criteria for each method were set well within their discriminatory limits, some groups of antibodies classified as indistinguishable by our criteria may not be identical by amino acid sequencing On the other hand, differences among antibodies detected by the identification techniques used are unambiguous

By combining all three methods, monoclonal antibodies displaying 60 distinct sets of properties could be discerned among the sample of 109 splenic foci tested Statistical treatment of single (42) versus recurrent (18) clonotypes (counting clonotypes which recur in an individual only once to avoid the effects of clonal expansion[20]) gives a minimum extrapolated value for total IgM anti-PC clonotypes in BALB/c mice of $>10^2$ (ref 21) Note that the vast majority of B cells responding in these conditions can be classified as primary by several criteria[22]

By far the most important implications of the present study relate to the question of the degree of diversity in the primary IgM repertoire Several recent findings have been interpreted as demonstrating that the IgM repertoire is far more restricted in clonotype heterogeneity than the IgG repertoire and that diversification may occur at the clonal level in conjunction with the switch from IgM to IgG production[8–10] Gearhart and colleagues have sequenced a set of hybridoma IgM and IgG anti-PC antibodies, both positive and negative for the T15 idiotype[8], and find that the variable region amino acid sequences of all the IgM antibodies are identical to that of a germ line-encoded variable region gene, whereas the sequence of the IgGs differ considerably from their germ-line counterparts As IgG is known to eventuate from clones which also express IgM[11–13], the finding that IgG diversity may exceed IgM diversity is consistent with the postulate that both diversification and IgG commitment are consequences of antigenic stimulation

An alternative possibility is that all diversification occurs at the stem cell stage before surface immunoglobulin expression by expanded B-cell clones[23] If this were the case, then the apparently greater diversity of the IgG, compared with the IgM, repertoire would be the result of differential selection and expansion of particular pre-existing clones from an already vast repertoire, rather than a consequence of *de novo* antigen-induced diversification Indeed, that a MOPC 167-like specificity is expressed in the IgM repertoire suggests that a clone which is a likely somatic variant of the T15 germ-line V_H[6] and V_L[7] sequences can be triggered in the primary IgM immune response given the appropriate stimulatory conditions However, this possibility could be verified only by analysis of the relevant antibody or nucleotide sequences

The findings reported here demonstrate the extreme diversity of the IgM primary B-cell repertoire Non-T15 B cells represent 1 in 10^5 of all responsive B cells and display at least 10^2 IgM clonotypes, including one which is indistinguishable by idiotypic and HI characteristics from MOPC 167, a known somatic variant[6,7] If such clonotypes are representative of the repertoire as a whole, then an inbred murine strain can synthesize $>10^7$ different IgM antibodies Such diversity effectively precludes accurate comparisons between repertoires of individuals or repertoires expressed in one isotype compared with another These data do not prove that the IgM repertoire is as diverse as the IgG repertoire, but do suggest that conclusions concerning the diversity of the IgM and IgG repertoires may be premature, as the apparent restriction observed in the IgM repertoires may be an artefact of the sampling techniques Conclusive proof that diversification accompanies isotype switch will come only from amino acid sequence analysis of antibodies of two isotypes derived from a single B-cell clone.

This work was supported by the USPHS grant AI 15797 from the NIH and MRC of Canada N H S is a Scholar of the MRC of Canada

Received 10 August, accepted 1 December 1981

1 Sakano, H , Huppi, K., Henrich, G & Tonegawa, S *Nature* **280,** 288–294 (1979)
2 Max, E , Seidman, T & Leder, P *Proc natn Acad Sci U S A* **76,** 3450–3454 (1979)
3 Weigert, M , Gatmaitan, M , Loh, E , Shilling, J & Hood, L *Nature* **276,** 785–790 (1978)
4 Rabbitts, T H , Matthyssens, G & Hamlyn, P H *Nature* **284,** 238–243 (1980)
5 Corey, S & Adams, J M *Cell* **19,** 37–51 (1980)
6 Crews, S , Griffin, J , Huang, H , Calame, K & Hood, L *Cell* **25,** 59–60 (1981)
7 Selsing, E & Storb, U *Cell* **25,** 47–58 (1981)
8 Gearhart, P , Johnson, N D , Douglas, R & Hood, L *Nature* **291,** 29–34 (1981)
9 Rodwell, J D & Karush, F *Molec Immun* **17,** 1553–1561 (1980)
10 Chang, S P & Rittenberg, M B *J Immun* **126,** 975–980 (1981)
11 Gearhart, P J & Cebra, J J *J exp Med* **149,** 216–227 (1979)
12 Okumura, K , Julius, M H , Psu, T , Hertzenberg, L A & Hertzenberg, L A *Eur J Immun* **6,** 467–472 (1976)
13 Teale, J M , Lafrenz, D , Klinman, N R & Strober, S *J Immun* **126,** 1952–1957 (1981)
14 Klinman, N R *J exp Med* **136,** 241–260 (1972)
15 Gearhart, P J , Sigal, N H & Klinman, N R *J exp Med* **145,** 876–891 (1977)
16 Gearhart, P J , Sigal, N H & Klinman, N R *Proc natn Acad Sci U S A* **72,** 1707–1711 (1975)
17 Stashenko, P & Klinman, N R *J Immun* **125,** 531–537 (1980)
18 Karjalainen, K Bang B & Makela, O *J Immun* **125,** 313–317 (1980)
19 Press, J L & Klinman, N R *Immunochemistry* **10,** 621–627 (1973)
20 Klinman, N R & Press, J L *J exp Med* **141,** 1133–1146 (1975)
21 Briles, D E & Carroll, R J *Molec Immun* **18,** 29–38 (1981)
22 Pierce, S K & Klinman, N R *J exp Med* **142,** 1165–1179 (1975)
23 Klinman, N R , Wylie, D E & Cancro, M P in *Immunology 1980—Progress in Immunology* Vol 4 (eds Fougereau, M & Dausset, J) 123–135 (Academic, London, 1980)

Excision of polyoma virus genomes from chromosomal DNA by homologous recombination

Luigi Lania*, Sharon Boast & Mike Fried

Imperial Cancer Research Fund, Lincoln's Inn Fields,
London WC2A 3PX, UK
*Istituto di Biologia Generale e Genetica, Università di Napoli, Italy

Head-to-tail tandem duplications of DNA sequences have been observed to occur naturally in chromosomal DNA of mammalian cells[1,2] and head-to-tail tandem arrays of DNA sequences can be induced upon gene amplification[3,4]. In these cases such sequences have not been detected as free or plasmid forms. After transformation by the two papovaviruses, polyoma and simian virus 40 (SV40), the viral DNA sequences integrated into the host chromosome are often found in head-to-tail tandem arrays[5-11]. When either a partially permissive environment for viral DNA replication exists (polyoma-rat or SV40-human cells) or after fusion of non-permissive transformed cells with permissive cells (polyoma-mouse or SV40-monkey cells), free viral forms are induced provided that a functional viral replication protein and a competent viral origin of DNA replication are present[12]. These results have led to the hypothesis that excision of integrated sequences occurs by viral DNA replication within the chromosomal DNA[6,13]. We show here that free polyoma molecules can be excised from partial head-to-tail duplications of integrated viral sequences in the absence of a functional viral replication protein (large T antigen [T-Ag]) after fusion of transformed rat cells (partially permissive) to permissive mouse cells. The amount of free viral forms produced appears to be proportional to the extent of duplicated integrated viral sequences.

Table 1 gives some properties of the five polyoma-transformed rat cell lines used One cell line, polyoma-rat, contains multiple inserts of integrated viral sequences, free viral genomes and at least one complete early region containing an intact coding region for the polyoma large T-Ag The maps of the single inserts of the integrated viral sequences of the other four lines are shown in Fig 1 These lines do not contain free viral forms or an intact coding region for the polyoma large T-Ag All five lines contain intact coding regions for, and produce, the polyoma small and middle T-Ag species, one or both of which are involved in polyoma-mediated transformation[7 14-19] Only the polyoma-rat cells contain functional polyoma large T-Ag of molecular weight 100,000 (ref 7), whereas the 2b-C2, 2b-C3 (ref 20) and 7axT (ref 14) lines contain other anti-T-Ag immunoreactive proteins which may be truncated forms of the large T-Ag (Table 1) No anti-T-Ag immunoreactive proteins other than the polyoma small and middle T-Ags are detectable in the 53-rat cells[7]

The 53-rat and 2b-C3 inserts contain partial head-to-tail tandem duplications of viral sequences which are respectively 1 17-1 34 and 1 05-1 32 genomes long[7 20] These two lines are able to form an intact coding region for the polyoma large T-Ag as a result of homologous recombination within the duplicated sequences Duplicated viral sequences are not found in either the 7axT (0 79 genome) or the 2b-C2 (0 97-1 0 genome) inserts[14 20]

All five lines were fused either to themselves or to mouse cells and the fused cells were assayed for free viral forms (at varying times) or the production of infectious virus (after 5 days) In the self-fused cells, free viral forms were found only in the polyoma-rat cells (also present in the unfused polyoma-rat cells), no virus was detected (<50 plaque-forming units (PFU) per 10^6 cells) in the self fusion of the polyoma-rat cells The production of both free viral genomes and infectious virus was detected after fusion to mouse cells of polyoma-rat and the two lines, 2b-C3 and 53-rat, containing partial duplications of viral sequences (Table 1, Fig 2) Free viral DNA could be detected as early as 12 h after fusion of 53-rat or 2b-C3 to mouse cells (data not shown) In the two lines that did not contain partial duplications of viral sequences, 2b-C2 and 7axT, no free viral forms or infectious virus could be detected after fusion to mouse cells (Table 1, Fig 2) In the fusions of 2b-C3 and 53-rat with mouse cells, the amount of viral DNA and infectious virus produced (Table 1, Fig 2) seems to be related to the amount of duplicated viral sequences present (more in 53-rat than in 2b-C3), suggesting that excision may be a function of the target size for possible recombination events as has been observed in other systems[21-24]

The production of detectable levels of free viral DNA from 2b-C3 and 53-rat after fusion to mouse cells presumably occurs in two steps The first step would be the excision of a complete viral genome by homologous recombination in the duplicated sequences forming a viral molecule, with an intact coding region for the viral replication protein (large T-Ag) The second step would be amplification of the complete viral genomes by large T-Ag-dependent replication in the permissive environment supplied by the mouse cells As no large T-Ag was detectable before fusion, we conclude that the excision event does not depend on replication at a viral origin as a result of a virus-encoded replication protein as has been postulated for SV40[13] We cannot rule out the possibility that replication in either the

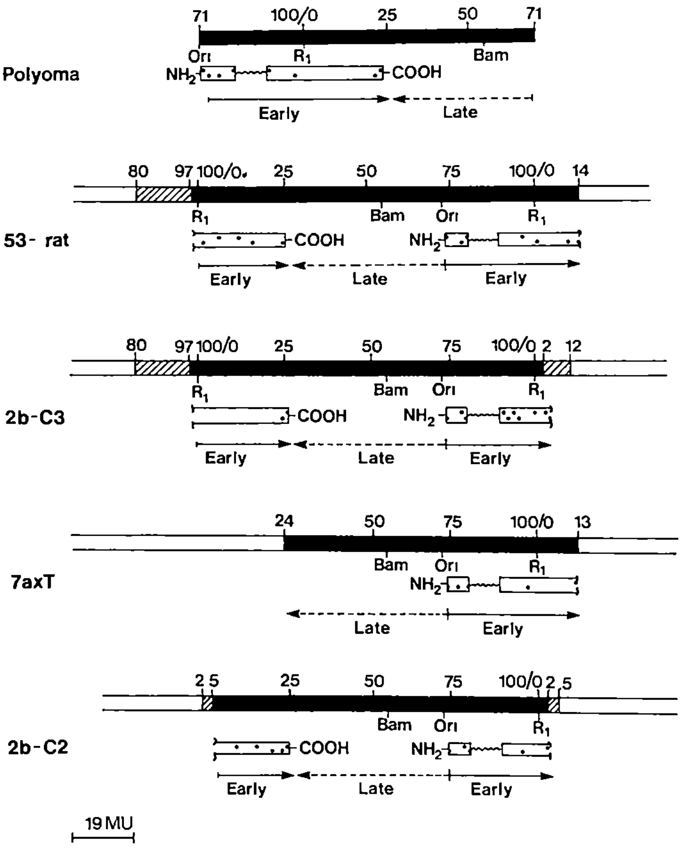

Fig. 1 Maps of the integrated viral DNA sequences in 53-rat, 2b-C3, 7axT and 2b-C2 cell lines as determined by Southern blot hybridization[7 14 20] and molecular cloning (A Hayday, E Ruley, L L and M F, in preparation) The heavy lines represent integrated polyoma DNA sequences The hatched boxes define the regions in which the viral and cellular DNA sequences are joined The positions of the cleavage sites for *Eco*RI and *Bam*HI, the coding region for large T-Ag and the direction of the viral early and late transcription units are indicated Ori represents the origin of the viral DNA replication The region of the DNA not represented in the mRNA for large T-Ag (spliced-out) is indicated by a wavy line The map of polyoma DNA (top) is linearized at the Ori position The numbers above the map of each line are map units (MU) as defined by Griffin *et al*[29]

0028-0836/82/040349—02$01 00

Table 1 Properties of the five polyoma-transformed rat cell lines used

	Viral DNA state		T-antigen species				After fusion with mouse cell	
Cell lines	Free	Integrated	Large-T (100,000)	Middle-T (55,000)	Small-T (22,000)	Others	Free DNA*	PFU per 10^6 cells fused†
Polyoma–rat	+	Multiple inserts tandem duplication	+	+	+	None	+++	2×10^8
53-rat	−	Single insert tandem duplication (1 17–1 34 genome)	−	+	+	None	++	5×10^6
2b-C3	−	Single insert tandem duplication (1 05–1 32 genome)	−	+	+	(50,000)	+	2×10^5
7axT	−	Single insert (0 79 genome)	−	+	+	(75,000)	−	<50
2b-C2	−	Single insert (0 97–1 genome)	−	+	+	(78,000)	−	<50

The organization and expression of the polyoma DNA sequences of the cell lines used have been reported previously polyoma–rat and 53-rat (ref 7), 7axT (ref 20), 2b-C2 and 2b-C3 (ref 14) Numbers in parentheses are molecular weights

* The presence of free viral DNA was determined as described in Fig 2 legend + Indicates the relative abundance of polyoma DNA in the Hirt supernatants

† 10^6 transformed cells were seeded together with 5×10^6 mouse embryo cells in 90 mm Petri dishes After 24 h at 37 °C the cells were fused using the polyethylene glycol procedure described by Pontecorvo[28] The cells were then incubated at 37 °C for 5 days, then collected and assayed for the presence of infectious virus The average value of six independent experiments is shown

integrated viral sequences or the adjacent host DNA sequences was not induced by fusion with the mouse cells It is also possible that the fusion event itself enhances homologous recombination, resulting in the excision of complete viral genomes Although we could not detect free viral genomes before fusion it is possible that homologous recombination was occurring at a low level in the 2b-C3 and 53-rat cells but the amount of excised genomes, which do not replicate efficiently in the rat cells, was below our detection level unless amplified by replication in the permissive environment supplied by the mouse cells Recently, Varmus *et al*[25] have also reported the excision of Moloney murine leukaemia virus DNA from cellular DNA apparently by homologous recombination between repeated sequences at the ends of the provirus

Our results may have implications for cellular DNA A mechanism of rearrangement of genetic information may involve homologous recombination in head-to-tail tandemly duplicated cellular DNA sequences, with the excised circular DNA becoming inserted in another region of cellular genome It would be interesting to know whether the 'minicircles' observed by others[26 27] in many cell types are actually derived from duplicated cellular sequences

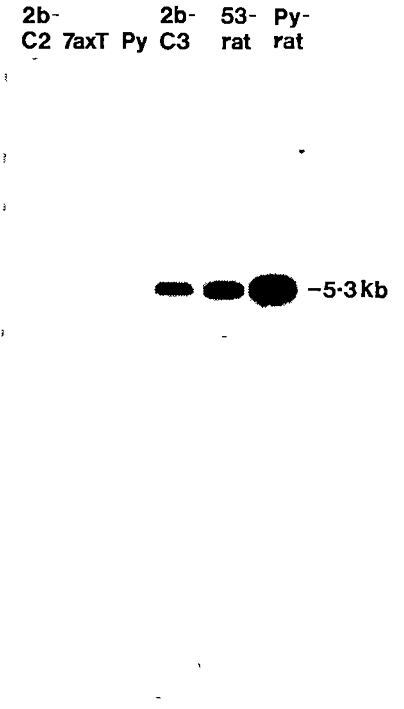

Fig 2 Detection of free viral DNA 24 h after fusion of the transformed cell lines with mouse cells Transformed cells from each of the five cell lines were fused with mouse cells as described in Table 1 legend The presence of free viral DNA was determined after fractionation of the cellular DNA using the SDS-salt precipitation method of Hirt[30] The Hirt supernatant DNAs were extracted with phenol, ethanol-precipitated, then treated with RNase (50 μg ml^{-1} for 3 h at 37 °C), extracted with phenol and ethanol-precipitated For each sample, 5 μg of Hirt supernatant DNA were cleaved with *Eco*RI and the resulting fragments analysed by electrophoresis through a 1% agarose gel The DNA in agarose gel was transferred to nitrocellulose paper according to the procedure of Southern[31] After transfer the filters were hybridized as described previously[7 20] with a polyoma DNA probe The polyoma DNA was labelled *in vitro* by nick-translation[32] to a specific activity of 2×10^8 c p m μg^{-1} After hybridization the filters were washed in 0 6% SSC, 0 1% SDS for 2–3 h at 68 °C The filters were then exposed to Fuji Rx film in the presence of intensifying screen Fuji Mach II at −80 °C for 16 h Lane Py contains 50 pg of the linear form (*Eco*RI cleaved) of polyoma DNA Long exposure (1 week) of the filter does not reveal any other bands When the *Eco*RI digestion was omitted, the Hirt supernatants of the heterokaryons of 2b-C3, 53-rat and Py–rat showed only the presence of free viral molecules as forms I and II kb, Kilobase

Received 19 October, accepted 4 December 1981

1 Long, E O & David, I B *A Rev Biochem* **49,** 727–763 (1980)
2 Davidson, E H & Britten R J *Science* **204,** 1052–1059 (1979)
3 Humberg, J H, Kaufman, R J, Chang, A C Y; Cohen, S M & Schimke, R T *Cell* **19,** 355–364 (1980)
4 Wahl, G M, Padgett, R A & Stark, G R *J biol Chem* **254,** 8679–8689 (1979)
5 Birg, F, Dulbecco, R, Fried, M & Kamen, R *J Virol* **29,** 633–648 (1979)
6 Basilico, C, Gattoni, S, Zouzias, D & Della Valle, G *Cell* **17,** 645–659 (1979)
7 Lania, L *et al* *Virology* **101,** 217–232 (1980)
8 Botchan, M, Topp, W & Sambrook, J *Cell* **9,** 269–287 (1976)
9 Campo, M S, Cameron, I R & Rodgers, M E *Cell* **15,** 1411–1426 (1978)
10 Ketner, G & Kelly, T J Jr *J molec Biol* **144,** 163–182 (1980)
11 Clayton, C E & Rigby, W J *Cell* **25,** 547–559 (1981)
12 Tooze, J *DNA Tumour Viruses Molecular Biology of Tumour Viruses* Pt 2 (Cold Spring Harbor Laboratory, New York, 1980)
13 Botcham, M, Topp, W & Sambrook, J *Cold Spring Harb Symp quant Biol* **43,** 709–719 (1979)
14 Lania, L, Hayday, A, Bjursell, G, Gardini-Attardi, D & Fried, M *Cold Spring Harb Symp quant Biol* **44,** 597–603 (1980)
15 Lania, L, Griffiths, M, Cooke, B Ito, Y & Fried, M *Cell* **18,** 793–802 (1978)
16 Hassell, J W, Topp, D, Rifkin, D & Moreau, P *Proc natn Acad Sci U S A* **77,** 3978–3982 (1980)
17 Novak, U, Dilworth, S & Griffin, B E *Proc natn Acad Sci U S A* **77,** 525–532 (1980)
18 Israel, M A, Vanderryn, D F, Meltzer, M L & Martin, M *J biol Chem* **255,** 3798–3805 (1980)
19 Triesman, R, Novak, U, Favaloro, J & Kamen, R *Nature* **292,** 595–600 (1981)
20 Lania, L, Hayday, A & Fried, M *J Virol* **39,** 422–431 (1981)
21 Fried, M *et al* *Nature* **279,** 811–816 (1979)
22 Kelly, T J, Lewis, A M., Levine, A S & Siegel, S *J molec Biol* **89,** 113–126 (1974)
23 Israel, M A, Chan, H W, Rowe, W P & Martin, M A *Science* **203,** 883–887 (1979)
24 Jaenish, R & Levine, A *Virology* **44,** 480–493 (1971)
25 Varmus, H E, Quintrell, M & Ortiz, S *Cell* **25,** 23–36 (1981)
26 Smith, C A & Vinograd, J *J molec Biol* **69,** 163–178 (1972)
27 Stonfield, S & Helinski, D R *Cell* **9,** 333–345 (1976)
28 Pontecorvo, G *Somatic Cell Genet* **1,** 397–400 (1975)
29 Griffin, B E, Fried, M & Cowie, A *Proc natn Acad Sci U S A* **71,** 2077–2081 (1974)
30 Hirt, B *J molec Biol* **26,** 365–369 (1967)
31 Southern, E *J molec Biol* **98,** 503–515 (1975)
32 Rigby, P W J Dieckmann, M Rhodes C & Berg, P *J molec Biol* **113,** 237–252 (1977)

Erratum

In the letter 'Tumour promoters induce mitotic aneuploidy in yeast' by J M Parry *et al*, *Nature* **294**, 263–265 (1981), Figs 2 and 3 should be transposed, and in column 3 of Fig 1 the lower chromosome should read

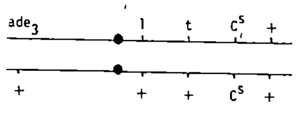

BOOK REVIEWS

Intellectual underworld

P.B. Medawar

Science: Good, Bad and Bogus. By Martin Gardner. Pp.408. ISBN 0-87975-144-4. (Prometheus: 1981.) $18.95.

Martin Gardner — urbane, amused and even-tempered.

THIS is a timely book for a number of reasons. Some simple people — canny, they imagine themselves to be — ever on their guard against being imposed upon by scientific and medical "establishments" are still willing to believe in those brilliant lone geniuses whose work was ridiculed by the establishment before being triumphantly vindicated. Such people have a natural taste for fringe medicine, spoon bending and such. A sharp corrective was needed and this book supplies it. Even if it will not be read by those most urgently in need of the lessons it teaches, it will be read delightedly by scientists. Gardner warns those with paranoid views on the establishment not to "forget that for every example of a crank who later became a hero there were thousands of cranks who forever remained cranks". He is rightly indignant at the way in which TV programmes have sometimes disparaged the establishment to support fringes: when a responsible watchdog committee reproached a number of NBC officials for that network's "outrageous pseudodocumentaries about the marvels of occultism one official shouted in anger 'I'll produce anything that gets high ratings!'."

Gardner's book is made specially readable by his deliberate avoidance of detailed analytic criticisms of the exhibits in his museum — believing it not worth while to explain just why he himself does not believe Venus to have been a rogue satellite of Jupiter that passed by the Earth en route to its present orbit — nor does he stoop to criticize the idea that the Earth is pancake shaped. No: Gardner's technique is to allow his subjects to speak for themselves and condemn themselves out of their own mouths. Thus of a work on *dianetics* ("the science of mental health") he simply invites us to share his consternation at its authors' having said "The creation of dianetics is a milestone for man comparable to his discovery of fire and superior to his invention of the wheel and arch". Examples then follow.

Perhaps because of President Reagan's well-known predilection for creationism, Gardner relaxes his self-imposed ordinance against analytic criticism when he turns to the opponents of evolution who hold the at one time popular view that existing fossils are relics of life before the flood. An old view, this (was it not Cuvier who named a fossil ichthyosaur as *Homo diluvii testis* — man-witness-of-the-flood?). We need not wonder that much of Gardner's copy comes from the United States because the USA is so enormous, and so numerous are its schools, colleges and religious seminaries, many devoted to special religious beliefs ranging from the unorthodox to the dotty, that we can hardly wonder at its yielding a more bounteous harvest of gobbledegook than the rest of the world put together. Gardner devotes special attention to the anti-evolutionary views of a retired professor of geology at the Walla Walla College in Washington who was cited as an authority by William Jennings Bryan during the famous Scopes trial.

Some of the best passages in the book deal with that genuinely sad figure, the hermit scientist, a paranoic who is driven into the occupation of a tiny little world of his own to protect himself from what he thinks of as the uncomprehending enmity of orthodox scientists who reject his views out of jealousy or frank ignorance. Sometimes

> around the Master will cluster a group of ardent admirers — either disciples whose own psychological demands find identification with those of the Master, or simply naive cultists who lack the knowledge to penetrate the Master's self deceptions.

Some of Martin Gardner's marvels of pseudoscience are effectively frauds, though they may have begun in good faith: thus of the discredited cancer cure Krebiozen he says that it consists of "nothing more than creatine" — an inexpensive chemical already present in the body. Though retailing at about 30 cents a gram, a dose containing a fraction of a milligram was meted out in return for a "donation" of $9.50 and its backers quoted the Government a price of $170,000 per gram. Another such bogus medicament was safflower oil prepared from the flowers of *Carthamus tinctorius* L. and sold in conjunction with a "worthless best-seller" *Calories Don't Count*; it provoked the FDA into impounding both book and capsules though the book still sells as a paperback, doubtless because of the welcome message its title brings. As Gardner says:

> It will be a long time until the average citizen is well enough informed about science to make the promotion of popularly written pseudo-scientific books unprofitable. And as long as they are profitable you can be sure they will be written and printed.

Gardner's book adds special weight to a distinction I myself am fond of drawing between natural science and unnatural science. The unnatural sciences ape the manners and the outward appearance of real science. They are especially distinguished by the belief that the use of the computer is a sign of scientific manhood and almost a guarantee of authenticity. The outward appearances to which I refer are the use of long and impressive-sounding words, the profligate invention of abstract concepts and above all the use of a literary style that obfuscates more often than it makes clear.

Generally speaking Gardner is urbane, amused and even-tempered in his condemnations of the bogus, but there is one subject that can be relied upon to bring him out of his corner with arms already flailing: this is occultism, written to pander to a public with a genuine predilection for the mysterious. Horoscopes for dogs, the infiltration of the human mind by thought waves from dolphins arouse his genuine indignation.

Not all scientific nonsense is written by cranks though: quite a lot of it is the work of scientists themselves, very often of scientists who, not content with the research upon which they can speak with some authority, asseverate upon difficult subjects of which they have no deep understanding. Such are electrician–eugenicists, astronomer–microbiologists and all scientists hungry for the recognition or applause their fellow scientists have so far withheld from them. Sometimes, too, to make a good story, inexperienced scientists are cajoled by interviewers into making presumptuous claims for their work, after which instead of withdrawing as gracefully as the situation allows they feel honour bound to stand by their ideas. ☐

Sir Peter Medawar is Head of the Transplantation Biology Section at the Medical Research Council's Clinical Research Centre, Harrow, Middlesex.

Collected receptors

G.L.E. Koch

Towards Understanding Receptors. Current Reviews in Biomedicine, 1. Edited by John W. Lamble. Pp.233. ISBN 0-444-80339-4. (Elsevier/North-Holland Biomedical: 1981.) $25, £7.

RECEPTORS participate in a wide variety of cellular processes, ranging from intercellular communication to the absorption of nutrients from the environment. Indeed, the term "receptor" is used so widely that a universally acceptable definition is not possible, and perhaps the only necessary criterion is that the receptor should be a cellular constituent capable of binding a ligand and generating a response. However, even this leaves open the questions relating to natural and unnatural ligands and responses, and illustrates the importance of emphasizing the context in which the word is used.

In this book, it refers to the receptors which have interested pharmacologists for many decades, that is, those involved in the actions of hormones, transmitters, drugs and toxins. The book consists of over 30 relatively short articles which appeared originally in *Trends in Pharmacological Sciences*, and which relate to the role of receptors for such ligands as acetylcholine, noradrenaline, dopamine and opiates.

The brevity of the contributions permits a wide range of subjects to be covered, but it does mean that there is a tendency towards dogmatism and polemic. However, if one approaches the book as an introduction to the current status of a variety of subjects on receptors, one cannot fail to find it an enjoyable and profitable read. It is likely that with the ever-growing information explosion on specialized subjects, there will be an increasingly important role for books such as this, which serve as a halfway house between the popular *New Scientist* and the more weighty *Annual Reviews*. ☐

Gordon Koch is at the MRC Laboratory of Molecular Biology, Cambridge.

Soil chemistry: an open book

T.S. West

The Chemistry of Soil Processes. Edited by D.J. Greenland and M.H.B. Hayes. Pp.714. ISBN 0-471-27693-6. (Wiley: 1981.) £37.85, $89.85.

The Chemistry of Soil Processes is the companion volume to *The Chemistry of Soil Constituents*, published by Wiley in 1978 and edited by the same two distinguished soil scientists. These two volumes bear a close resemblance to Russell's definitive treatise, *Soil Conditions and Plant Growth* (10th Edn, Longmans, 1974), though as an edited work they cannot present the same comprehensive yet unified view. On the other hand I feel, like many others, that soil science is such a diverse subject and one that has expanded its boundaries to such an extent in recent years that no single author can really cover all of the topics involved. These days it is necessary to involve specialists who can treat each aspect in depth, as Greenland and Hayes have done.

A knowledge of the chemistry of soils is of importance to many scientists other than those entirely involved in soil work and, therefore, I find it particularly encouraging that the present volume is one that may readily be comprehended and appreciated by all chemists who have some knowledge of or interest in the biological sciences. The chemistry, too, is treated in such a way that it should be easily assimilated by specialists in other disciplines such as microbiology and geology. To most readers, therefore, this will be a fairly open book with easily recognized concepts and aims. It is well written and neatly illustrated, and I particularly applaud the avoidance of excessive use of mathematical manipulation by all of the authors.

The opening chapter — written, most appropriately, by the editors — is an excellent scene-setter for the following contributions. It traces the historical development of soil science through an overview of the subjects of pedology, soil chemistry, soil biology and soil physics. The following two chapters treat the movement of mobile components within the soil profile and precipitation phenomena, for example, the deposition of carbonates, sulphates, phosphates and aluminosilicates which all play an important role in most considerations of soil chemistry. Cation and anion exchange phenomena, which are so important in plant nutrition, and the fixation of added fertilizers are then considered separately by different authors, and this is followed by an extensive review of the adsorption of nutrients etc. by soil components such as clays and humic substances. A particularly well written account of redox phenomena describes the profound effect these have on soil chemistry and reactivity. These chapters lead on logically to four separate treatments of the translocation of metal ions in soils, the fate of plant and animal residues, fertilizers and heavy metals in soils; finally, there is an account of the behaviour of pesticides in soils. The book is provided with excellent indexes of subject matter and authors.

The 13 contributors are all recognizably expert in their individual subjects and, whether or not it has arisen by careful planning or by happy coincidence, a rather unique, synoptic view of soil chemistry has emerged which is most unusual in a book with so many authors. The depth and treatment is entirely satisfactory and there appear to be few if any serious inconsistencies.

There is no doubt in my mind that this well-written book will be of the utmost value to all junior, and senior, students of soil science, and an invaluable aid to all who have to refer periodically to matters relating to soil chemistry. ☐

T.S. West is Director of The Macaulay Institute for Soil Research, Aberdeen.

An animated Earth

John Sutton

The Earth Generated and Anatomized: An Early Eighteenth Century Theory of the Earth. **By William Hobbs. Edited by Roy Porter. Pp.158. ISBN 0-8014-1366-4. (British Museum (Natural History)/ Cornell University Press: 1981.) £24.50, $35. Paperback available from the BM(NH), £8.**

WHEN opening a university geology department, Stanley Baldwin once compared geological research with the writing of detective stories. Bow Street runners played little part in the development of geology, but excise men certainly did, the most famous being members of the Peach family whose watch over a whisky-filled wreck off northern Scotland led to the discovery of fossils which first demonstrated the Palaeozoic connection of Scotland and North America. That discovery was made in the nineteenth century. Now Dr Porter brings to light a geologically-minded excise man from the early eighteenth century. His name is William Hobbs. He recorded the tides

●A paperback edition of *Somatic Selection and Adaptive Evolution* by Ted Steele (reviewed in *Nature* **288**, 306; 1980) has recently become available in the USA. The book is published by the University of Chicago Press and costs $5.95.

around Weymouth and more remarkably noted the fossiliferous rocks of the Dorset coast None of his work has been previously published, who he was or what else he did still remains obscure despite Dr Porter's careful enquiry

The main part of this book, which forms a welcome addition to the Historical Series of the Natural History Museum, is a manuscript which Hobbs completed in 1715 Its history is obscure, it emerged in 1825 when it was sold in Southwark and surfaced again in a London sale room some 150 years later, when the Natural History Museum acquired it With his knowledge of eighteenth century geology, Dr Porter is just the person to edit it and he has done a thorough job He provides an introduction, identifying Hobbs as far as this is possible — a detective story in itself — and adds extensive notes on the milieu in which this solitary observer had to work With little formal education Hobbs appears to have spent years in observation along the Dorset coast in a singlehanded enterprise

He had the good judgement to pick on two phenomena which that coast shows well In recording the tides he was doing something that others had done before, but in understanding the significance of the stratification of the fossiliferous Mesozoic rocks he entered new territory Reflecting on his evidence, however, he came to a wholly erroneous explanation Hobbs himself describes his flash of inspiration "I had (at a place well remembered) clearly discovered the Body of the Earth to be an Animal" He supposed the tides were due to movements within the Earth and explained the fossiliferous sediments as dating from a time when the outer parts of the Earth were plastic He linked these two explanations and supposed that pulsations within the Earth could account for them Some years before he wrote the manuscript published here, he had sent a paper covering much the same ground to the Royal Society, which rejected it The referee's comments have survived

> I find him to have a Clear Head, and to be a person of great Diligence and pretty good Judgment considering his Want of Learning, but his Philosophy is much inferior to his Observations of Matters of Fact

That comment could equally be applied to what is now published Although the explanations are nonsensical one cannot help but admire Hobbs's ability to observe and record This manuscript was well worth bringing to light, not only does it show what a solitary individual was able to do, but it illuminates a wider question Dr Porter has considered on earlier occasions, the extent to which nineteenth century geologists drew on eighteenth century thinking, erroneous as that sometimes was □

John Sutton is Pro Rector and Professor of Geology at Imperial College, University of London

---

Symbiosis and the origin of cell organelles

T Cavalier-Smith

Symbiosis in Cell Evolution Life and its Environment on the Early Earth By Lynn Margulis ISBN hbk 0-7167-1255-5, ISBN pbk 0-7167-1256-3 (W H Freeman 1981) Hbk $24 50, £18 20, pbk $14 95, £10 40

Few sights are more fascinating than the teeming microbes from the hind-gut of termites and wood-eating cockroaches To Professor Margulis they also hold the clue to our own origins By 1960 electron microscopy had shown that the prokaryotic cells of bacteria and cyanophytes differ fundamentally from the eukaryotic cells of plants, animals, fungi and protozoa This, and the discovery of chloroplast and mitochondrial DNA, led Ris to revive Mereschkowsky's old idea that chloroplasts evolved from endosymbiotic cyanophytes and Margulis to revive Wallin's theory of mitochondrial origin from symbiotic bacteria. Stimulated by Cleveland's discovery that the termite-gut symbiont *Mixotricha* is propelled by thousands of ectosymbiotic spirochaetes, Margulis also suggested that cilia evolved from such ectosymbionts

The central thesis of her *Origin of Eukaryotic Cells* (Yale University Press, 1970) was that eukaryotic cells originated by the symbiotic uptake of an aerobic bacterium by a wall-less, mycoplasma-like prokaryote to form mitochondria, followed by the conversion of ectosymbiotic spirochaetes into cilia and of cilia into the mitotic spindle In that book she also discussed the symbiotic origin of plastids and the interplay between biological and geochemical evolution *Symbiosis in Cell Evolution* is very similar, but sadly takes little account of the extensive new electron microscopic and biochemical evidence accumulated over the past decade, or of published criticism of many of her ideas Written as a readable elementary textbook, it is avowedly a one-sided point of view which ignores conflicting evidence or arguments that might distract the reader from her message

The author has missed the opportunity to elaborate what should have been her strongest suit the symbiotic origins of plastids *Cyanophora*, the eukaryote possessing a blue-green plastid with peptidoglycan in its envelope but with DNA the same size as chloroplast DNA, is dismissed as a "unique, dead-end symbiotic complex" merely serving as a model of how plastids might have originated But if one compares the cell structure of *Cyanophora*, the other non-peptidoglycan-containing Glaucophyceae and the red algae, it is evident that they form a continuous spectrum which strongly suggests that the *Cyanophora* plastid is a "living fossil" directly descended from the same endosymbiotic cyanophyte that was ancestral to all eukaryote plastids

Margulis's entire treatment of the diversity of plastid types is minimal and inaccurate The origin of the three membranes of the plastid envelopes in *Euglena* and the dinoflagellates is not discussed (*Euglena* is incorrectly drawn with two membranes) Nor is the origin of the plastid endoplasmic reticulum, which others have well explained in terms of a second symbiotic event involving a eukaryotic symbiont (she incorrectly states that chrysophyte and phaeophyte envelopes are triple)

The author's diagram of eukaryote phylogeny shows 15 separate symbiotic origins for plastids, but no justification is given for this — it is not obviously deducible from her apparently unilinear scheme of mitotic evolution — or for the assertion that several independent symbiotic events produced the chlorophytes The scheme itself is essentially her 1967 one (*J Theor Biol* **14**, 225-275), based largely on half-a-century-old light microscopy and her symbiotic theory of ciliary origin, rather than modern ultrastructural data The latter enter the book only in the ten pages devoted to part of Heath's splendid tabulation of protist mitotic variation (fungi are oddly omitted as irrelevant)

Margulis's attachment to her five-step scheme of mitotic evolution makes her say (incorrectly) that "no animal cell that bears undulipodia [a cumbersome neologism for 9+2 cilia] can ever divide" And it is hard to see how her step II, the permanent loss of cilia, could lead to steps III - V which are ciliated Step I — organisms with cilia but lacking mitosis — is based on her theory that spindles evolved from cilia rather than on concrete evidence *Prorocentrum* does have mitosis, and *Pelomyxa palustris* has not been clearly shown to lack it, both contrary to what is stated She barely mentions the conventional view that spindles evolved from cytoplasmic microtubules, and erects as the sole alternative to her view the Aunt Sally that they originated as episomes, which no one has suggested It is also a mistake to call the autogenous origin of cilia "compartmentalization", or to tie their autogenous origin indissolubly to the autogenous origin of plastids She seems not to conceive that anyone could accept the symbiotic origin of plastids and reject the symbiotic origin of cilia, yet most biologists do just this

For mitochondria, Margulis assumes rather than debates a symbiotic origin A reasonably strong case for this theory can be made by supposing that the host was already fully eukaryotic and capable of phagocytosis (for example the mitochondrion-less flagellate protozoa) But she makes her task almost impossible by supposing that symbiotic uptake preceded the origin of the eukaryotic cell and phagocytosis Because prokaryotes lack phagocytosis and never contain cellular endosymbionts she supposes that the symbiont bored its way in, like a predatory *Bdellovibrio* The problem with this is that *Bdellovibrio* bores only through the cell wall, not the plasma membrane, and so never even enters the cell, which it also kills Moreover, the hypothetical wall-less host would have no wall to bore through[1] She now favours *Thermoplasma* rather than mycoplasmas as potential hosts, despite the fact that *Thermoplasma* have branched ether-linked membrane lipids, not phospholipids, and so could not be ancestors of eukaryotes Further, she fails to realize that the resemblances between the respiratory system of purple non-sulphur bacteria and eukaryotes could be explained non-symbiotically by the conversion of a purple non-sulphur bacterium autogenously into nucleus, cytoplasm and mitochondria, and gives only one out-of-date reference to Mahler's extensive arguments for such an origin Her description of which mitochondrial molecules are coded by mitochondrial DNA is inaccurate, incomplete and misleading

The treatment of mitochondrial origins is inadequate, split-genes and RNA splicing receive only three lines and the unique mitochondrial code but half a line The origin of the different cristal morphologies that some see as evidence for multiple symbiosis is totally ignored, as is the evolution of mechanisms to transfer nuclear gene products into mitochondria The problem of gene transfer to the nucleus is barely mentioned

Her classification of living organisms is better than most, but has several inconsistencies for example, acceptance in the text of the basic distinction between Archaebacteria and Eubacteria is not reflected in the appendix Her prokaryote phylogeny ignores the important data from 16S RNA sequences A major defect of the book is the absence of critical phylogenetic analysis, upon which the testing of symbiotic ideas largely depends

The book contains many errors, for example non-Mendelian heredity in *Chlamydomonas* is not a consequence of uniparental transmission of chloroplasts, the gene for the ribulose biphosphate carboxylase large subunit is in the chloroplast not the nucleus, and *Cyanophora* has a pellicle not a cell wall Such an important idea as the role of symbiosis in cell evolution, which Professor Margulis has done much to promote, deserves more thorough and more careful treatment than this □

T Cavalier-Smith is a Lecturer in Biophysics at King's College, University of London

---

Attractive rigour

D. Sherrington

The Theory of Magnetism I Statics and Dynamics By Daniel C Mattis Pp 295 ISBN 3-540-10611-1/0-387-10611-1 (Springer-Verlag 1981) DM 72, $32 80

THE study of magnetism has been one of the growth areas of the past decade It has interest not only in its own right, but also as a testing ground for the quantum-mechanical theory of interacting electrons and as a convenient example for illustrating and probing important questions in statistical mechanics Practical applications are legion, but mainly confined to ferro- and ferrimagnetism The fundamental interest lies more in the intellectual challenge which the subject offers to pure physicists, indeed, this challenge has even attracted the attention of elementary-particle theorists

There are two extreme approaches to the theory of magnetism, the phenomenological and the strictly fundamental At an intermediate level lies the study of idealized models, but with wide variations in emphasis on rigour or qualitative conception Most books on magnetism treat the basics in a fairly cavalier fashion and tend towards a semi-quantitive treatment of models Mattis is a welcome exception His inclinations are towards full rigour, eschewing sleights-of-hand or glossing-over of difficulties

The book is the first of a two-part set This volume is divided almost equally between a detailed analysis of the quantum-mechanical basis of magnetism and an incisive study of several of the intermediate models Subjects discussed include such modern ones as solitons, the Kondo effect, Bethe's ansatz and vortices in the XY model

Mattis's relentless approach will not be to everyone's taste, but his book will be a useful addition to the library of anyone deeply interested in the origins of magnetism and the careful study of mathematical models The statistical mechanician, or the particle theorist looking for hints on how to solve the lattice gauge theory problem, may, however, prefer to wait for the second volume which will cover thermodynamics and statistical mechanics

Finally, praise must be given for the introductory chapter, 38 pages long, which spells out the history of magnetism from the earliest days to the present, places it in the perspective of the general evolution of physics and the development of Western thought, and is backed up by marvellous quotations and an impressive bibliography This chapter can be strongly recommended to anyone interested in the history of science and, almost alone, would justify purchase of the book □

D Sherrington is Reader in Theoretical Solid State Physics at Imperial College, University of London

---

Receptor development

Eugene R. DeSombre

Ontogeny and Phylogeny of Hormone Receptors By G Csaba Pp 172 ISBN 3-8055-2174-X (Karger 1981) DM 172, $86 25

WHILE Professor Csaba does not entirely accomplish the awesome task of providing a synthesis and critical evaluation of our current knowledge of the ontogeny and phylogeny of hormone receptors, in this book he does provide a useful introduction to the subject Most valuable for those who may not have closely followed Csaba's work, the monograph includes extensive data (72 figures and 18 tables) from his contributions on the interactions and biological effects of various hormones of higher organisms in Tetrahymena and Planaria It starts from first principles on the basic concepts of cybernetics and information transfer related to hormone–receptor function and gives a general summary of our understanding of hormone–receptor interactions, paying especial attention to hormones active at the plasma membrane

The subject of the phylogeny of receptors is presented almost exclusively using examples from studies with Tetrahymena and Planaria, with only occasional reference to other species And while the section on ontogeny deals to a limited degree with higher animals — specifically, developmental aspects of receptors in the neonatal chick and rat — as well as with data from Tetrahymena and Planaria, neither of the two parts can be considered to be a definitive review of the topics

Nonetheless, because of the excellent documentation of a variety of studies in these lower species, the useful introductory comments and a substantial concluding discussion, the book is more than a simple summary of Csaba's own experiments His account of various possible developmental routes which could give rise to observed hormone and receptor patterns in different phyla is certainly valuable Unfortunately, the rich literature on steroid hormones, the action of which is mediated through cytosolic receptors, is less well integrated into the presentation The speculation that cytosolic receptors for steroid hormones may have evolved from membrane receptors, an interesting concept, is not well-developed in the book and the entire steroid hormone area is represented only by a few selected references

More appropriately entitled *Selected Topics on the Ontogeny and Phylogeny of Membrane Active Hormone Receptors*, this monograph provides an interesting, if limited, entree to the developmental aspects of hormone receptors □

Eugene R DeSombre is a Professor in the Ben May Laboratory for Cancer Research and Director of the Biomedical Computation Facilities at the University of Chicago

nature

4 February 1982

Unemployment and the future

Most Western governments are seeking separate solutions for unemployment. They should do more to prove to the jobless that there will be a future, and should agree how to bring it about.

The long recession in the industrialized West has now brought its most daunting and predictable consequence: unemployment. In Britain, the total now out of work exceeds 3 million, or close on 10 per cent of the potential workforce. In West Germany, after several resilient years, the jobless rate is now pushing 7 per cent. In the United States, the growth of unemployment has been even sharper. Even Japan has not escaped unscathed. So it is inevitable that there should be great cries of protest at this state of affairs, and that governments everywhere should be under pressure to modify their monetary policies, devised with varying degrees of good sense to counter rapid inflation. (Reagonomics, devised in Washington with the different objective of unshackling industrial production, has had the same effect because the hard-headed New York money markets have agreed to let the Administration and others borrow money only at deflationary interest rates.) Politically, such pressures cannot indefinitely be resisted. In Britain, it is well remembered that the Heath government embarked in 1973 on its ultimately disastrous policy of reflation because unemployment had exceeded the daunting figure of one million. Although all governments except the French say they will continue to regard unemployment as a kind of lesser evil, the danger is that they will hurriedly change course for the wrong reasons, and at the wrong time.

Unemployment at the rates now customary is naturally hard for even those still at work to stomach. For those without jobs, a large proportion of the younger of whom have never worked, unemployment is a personal tragedy that is only inadequately offset by programmes of social security devised to avoid the improverishment of the 1930s. So much is commonly accepted, as is the proposition that a high degree of unemployment is a social waste of people's capacity and willingness to work. Yet the present plight of a substantial proportion of the working population in advanced societies is not merely an inevitable but an intended consequence of economic policies now in force, which have in turn been forced on governments by events in the past decade and in particular by the substantial increase of the international price of oil in 1973 and 1979. To pretend otherwise is to suppose that the rules of simple arithmetic can be suspended at will — which is not to say that there is nothing that can be done.

The first need, however, is to be clear where the present trouble has come from. Compared with the happy years before 1973, oil consumers are now paying more than $200 extra for each tonne of oil they use. For many, this entails a straight transfer of resources to the oil-producing states, which may either decide to convert their funds into a claim on the resources of the oil consumers or, alternatively, may choose to lend back the money through the banking system. Either way, customers for oil on the international markets can have hoped to weather these storms without impoverishment only by increasing their production and therefore their productivity. Japan and West Germany honourably followed that principle for several years. Elsewhere, governments chose to follow their voters' wish that the truth should be concealed from them, inflation gathered pace and had then to be countered by deflationary policies which reduced people's capacity to buy what they think they need and which in turn have now cast their shadow on the economic stalwarts of the West. This argument applies even to Britain, outwardly self-sufficient in oil, because the once cheap oil from the Middle East has been replaced by expensive oil from the North Sea, won only by capital and resources that might otherwise be used for more productive purposes.

For those who would cure unemployment quickly, the snag is that increased productivity is the enemy of job creation. The dilemma for Western governments is that the continuation of the recession will improve the former — even in Britain, productivity in manufacturing industry increased by more than 7 per cent last year — but will increase the unemployment queues. And the opposite is true — reflation would reduce the immediate misery of unemployment but jeopardize the long-term health of the economy. So are governments irretrievably boxed in? Not necessarily. Those most seriously afflicted are right to resist demands that jobs should be "created" in uneconomic pursuits but, on recent form, cruelly indifferent to the need to explain how the unemployment problem may eventually be solved. People who have just lost their jobs are understandably unwilling to accept that their misfortune must wait while inflation is contained. So what should governments attempt to do?

First, domestically, there is an urgent need that people displaced from jobs that have disappeared should be given a tangible and imaginative opportunity to prepare for the more productive world in which they may yet have the good fortune to live. Although the British government, for example, now plans to spend more generously on training programmes, and is in particular planning to offer every school-leaver who fails to find a job some structured opportunity for training at work, there is nothing to suggest that the results will generally be to make people more employable in the years ahead. By the same tests, all governments must recognize that the key to long-term prosperity — production, productivity and employment all high — is a more effective international division of labour than at present. Here too, unfortunately, the omens are not cheerful. Protectionist tendencies are increasing, with governments seeking to shield from overseas competitors industries that will never make economic sense. Is there a chance that the folly of these policies will be openly acknowledged, as it should be, at the "economic summit" advertised for June?

While they are about it, the governments in June should tackle the still more tricky question of how collectively to manage the transition from where we are to where we hope to be. What criteria will be used for telling when it will again be safe to let up in the battle against inflation? By what common criteria should governments decide that the time has come to invest in public works, or to allow commercial companies to borrow money at more modest interest rates? And by what agreed rules should the value of national currencies be determined and then adjusted? Putting these questions to many of the more orthodox turning up in June will be a little like asking a gathering of churchmen to define the circumstances in which sin is acceptable. In reality, the challenge is not so great. For the agreements negotiated towards the end of the Second World War at Bretton Woods in the United States, which were the basis of international financial relations until they collapsed between 1969 and 1971, were themselves an awkward adjustment between financial probity and an imperfect world. What is needed now is an open recognition that the world is far from perfect, that the governments that inhabit it are even less so and that, nevertheless, they must agree to act in concert.

0028-0836/82/050355-02$01 00

Goodbye to guidelines

Recombinant DNA guidelines are on the way out. What should be learned from them?

This week's meeting of the Recombinant DNA Advisory Committee at the National Institutes of Health in the United States will be seen as not so much a landmark as a milestone in the brief but eventful history of the most elaborate attempt so far to regulate scientific research. After two years of agonizing in the wake of the Asilomar conference of 1974, government agencies produced rules for research with recombinant DNA which, once promulgated, were almost as quickly dismantled. Already, the guidelines in force are a pale shadow of the tough regulations that caused many professional people to protest that governments were planning to interfere with research — and many members of the lay public to complain that the controls were entirely inadequate. But on present form, the whole apparatus of regulation will have all but disappeared within a decade of being proposed. Has the whole exercise been a waste of busy people's time? What can be learned from it?

That busy people's time has been occupied is of course beyond dispute. People who might have been cloning some gene, or setting up some new biotechnology company, have instead been required to turn up at meetings of advisory and safety committees. There is probably also something in the complaint that important experiments were delayed by the lack of facilities necessary for compliance with the guidelines, or by the diversion of creative people's talents to the development of organisms even less capable of survival in the human gut than the standard laboratory strains of *E. coli* K12. So, now, there are two commonplace appraisals of the experience of the past few years. Some workers in the field claim that they have said from the beginning that the potential dangers of recombinant DNA research were exaggerated, and that the regulations were pointless and a needless interference with free research. Others, more circumspect but also more cynical, say that the guidelines were an unfortunate necessity, an exercise in public relations whose value is attested by the way in which the public clamour about the hazards of genetic manipulation has died down. The truth, however, lies with the smaller company of professionals who acknowledge that the guidelines were both necessary and valuable, that experience of their operation has been instructive and that the history of the recent past should be remembered well.

The argument is simple and straightforward. At Asilomar and in the months that followed, many people in a good position to know the truth held that the hazards for the general population of the construction of novel organisms could be serious. The hazards were always hypothetical, involving processes not then (or since) demonstrated in the real world. Those who claim to have known all along that the guidelines were unnecessary did at the time argue that organisms encumbered artificially with foreign genes were unlikely to be effective competitors in tissues which they happened to infect, but were too scornful of the now common difficulty of deciding how to assess a large danger which has only a very small probability. In the event, the erosion of the guidelines promulgated by the National Institutes of Health (and analogues elsewhere) has been made possible by scientific rather than philosophical developments — the discovery that the replication of genes in eukaryotic cells is more complicated than in bacteria for example. In 1976, the decision that there should be guidelines of some sort was not merely prudent but responsible. So, now, is the general agreement that the guidelines may be further attenuated without risk.

For the most part, the guidelines have also been well kept, even by the sceptics. The few know transgressions, in the United States and elsewhere, appear to have been engendered as much by frustration at the differences in guidelines applying to competing laboratories as to deliberate attempts at cheating. In the United States, the dominant role of the National Institutes of Health in supporting research must have been a powerful deterrent — which is why, in the history of this period, the failure of successive Administrations to apply to industrial laboratories the sanctions applicable to academic laboratories will seem odd, to say the least. Where guidelines have been backed by legislation, as in the United Kingdom, the courts have not been packed with recalcitrant molecular biologists. The scientific community can claim credit on this score.

So what should happen now? Should the guidelines simply be torn up, and the accompanying bureaucratic apparatus dismantled? That would be to go too far. To the extent that the foreseeable hazards of recombinant DNA research have become no more than coextensive with the risks of working with whatever naturally occurring organisms are involved, the existing rules for research with pathogenic organisms are sufficient. Separate rules for recombinant DNA research are therefore unnecessary, while voluntary compliance with further attenuated regulations will be meaningless. Yet the issues which have been raised in the past several years are interesting and have also made a mark on the public mind. What is needed, now, is a periodic and public reassessment of the risks, hypothetical though they may still be.

For laboratories, the most important procedural discovery since Asilomar is that local safety committees have not turned out to be the interfering busybodies they were feared to be. Even when (as required by the National Institutes of Health) lay members were appointed, the outcome has more often been public enlightenment than outside intrusion into the conduct of research. Indeed, the precedent of local safety committees including members from the nearby community is one that should be more widely adopted in other fields, for example where laboratories have an interest that they should be known to care for their experimental animals — and that the general public should be sensible of their dilemma. It would be no harm if this institution were the chief monument to the guidelines period.

Maths without teachers

British schoolteachers cannot teach mathematics properly, but nobody is surprised.

How should mathematics be taught? And by whom? These questions have perplexed the British educational system ever since it acknowledged, in the 1950s, that everybody profits from education, of which mathematics is an essential ingredient. In despair at not knowing how the questions should be answered, in September 1978, the then British government set up a committee under Dr W. H. Cockcroft, Vice-chancellor of the New University of Ulster in Coleraine, to suggest what might be done. The committee's report now published (*Mathematics Counts*, HMSO, £5.75) is as well polished as the time it has taken to prepare requires in decency that it should be. It is also full of sensible suggestions for the better organization of mathematics teaching in British schools. But on the main issues, the report is muffled.

The trouble with mathematics teaching is that the shortcomings of one part of the educational system are visited upon all others. University courses in mathematics, notoriously arid, are also the chief source of teachers in secondary schools who are saddled with responsibility for teaching mathematics to intending teachers in primary schools. Hitherto (and, indeed, until 1983) it has been possible for young people to embark on careers as teachers without having a formal qualification in mathematics at secondary school, even though they will be required to teach mathematics to young children. The result is that mathematics teaching is everywhere tentative — experts in graph theory teach elementary algebra to thirteen-year-olds, inexpert people wrestle with seven-year-olds on the conundrum of proportionality. The underlying fault, which Cockcroft does not tackle, is that the British educational system makes a fetish of specialization too early, and pays too little regard to general education at all levels. Paying some good mathematics teachers more, and the other stratagems he advocates, may help in the short run. Changing the way the British educate their young is the only long-term remedy.

0028-0836/82/050356 01$01.00

Making private interests public

California may ask academics to declare all

Washington

Under new regulations proposed by the state's Fair Political Practices Committee (FPPC), research scientists at the University of California will no longer be given a blanket exemption from conflict-of-interest regulations covering other state employees

Until now, scientists have argued that academic freedom protects them from being required to disclose their personal stake in outside companies with which they may be involved These ground-rules are now being shifted, largely as the result of several well-publicized cases in which faculty members have profited substantially from such linkages

Last month, at a meeting in Sacramento, the state capital, the members of FPPC voted by three votes to two to require that any scientist who accepts a research contract from a private corporation must declare to the university whether he or she has a financial interest in that corporation

The University of California had previously volunteered to introduce an internal system requiring scientists to report potential conflicts of interest to their heads of department The regulations being proposed by FCCP would not only formalize this arrangement, giving the state the authority to check that such reporting is being carried out, but would also require the university to set up internal review panels at each campus to which conflict-of-interest problems would be referred

The commission's proposal has been published for public comment before its formal adoption, expected early next month It does not go as far as some of the university's critics would have liked, in particular, a legal aid group known as California Rural Legal Assistance, which has been leading a campaign against research into labour-saving agricultural machinery at the university's Davis campus, had petitioned the commission to require research scientists to declare all their interests in outside corporations

In their present form, the regulations would permit a scientist to keep confidential his or her stakes in a private company interested in the same area of research if the research were funded by a public agency The regulations would therefore be more liberal than the full disclosure required of other state officials

However, if the regulations are approved — and are subsequently accepted by the state's Office of Administrative Law — it would mean that faculty members on all nine campuses of the University of California could no longer use academic freedom as a reason for exemption from the conflict-of-interest rules

The law which covers the regulations was passed in the early 1970s as part of a nationwide movement to "clean up" the actions of state and federal officials in the wake of the Watergate scandals Its main purpose is to ensure that state officials are not in a position to gain financially through links with outside contractors and other corporations in which they may have a personal interest

Soon after the law was passed, its application to the state university was challenged by the university's board of regents on the grounds that it infringed the academic freedom of faculty members At the time FPPC, which was set up to administer the regulations, accepted this argument and allowed an exemption

Since then, pressure on research workers to establish closer links with the private sector has increased as both state and federal funding has decreased The consequent growth of linkages between faculty scientists and outside corporations has been particularly noteworthy in the development and exploitation of recombinant DNA techniques and genetic engineering Frequently, however, this has led to tensions between academic and commercial pressures

One campus of the university is already involved in a law suit over the ownership of a cell line passed to research workers in the private sector and subsequently patented, another has told an agricultural scientist working on nitrogen fixation that he cannot both remain principal investigator

Another French director resigns

Molecular biologists in France are sleeping a little less easily this week, following the spectacular resignation of one of their more important political friends, Professor Philippe Laudat, from his post as director-general of the Institut National de la Santé et de la Recherche Médicale (INSERM)

Laudat waited until after the National Colloquium on Science and Technology (see *Nature* 21 January, p 180) before sending his letter of resignation to the Minister of Health, M Jack Ralite, and the Minister of Science and Technology, M Jean-Pierre Chevènement It was against his own "personal ethics", he wrote, after working energetically for the policies of the previous government, to work now for "noticeably different policies"

The ministries appeared surprised Laudat's resignation was neither desired nor solicited, said a spokesman for the Minister of Health "All we did was to ask Laudat to take account of the conclusions of the National Colloquium and the regional assizes [which preceded it] "

INSERM will certainly do that now — for the new director-general will be M Philippe Lazar, who was chief rapporteur for the colloquium Lazar is 45, studied at the Ecole Polytechnique and is an epidemiologist interested in the social and economic aspects of health His star rose with the new government, and his appointment may shift INSERM away from its present strong emphasis on basic biology towards the clinical and softer sciences

The issues are complex, however Clinical science in France is generally thought to be weak Those who work in university hospital clinics are supposed to teach, care for patients and somehow also find time for research The research suffers Clinicians are sore that the last government increased INSERM's effort in molecular biology (with an eye on its application in industry) whilst neglecting sciences closer to medicine There is thus a battle for resources within INSERM between the clinical scientists and the pure scientists, a phenomenon not unknown elsewhere

However, the matter was complicated by Laudat's creation of international panels of experts, which doled out money for certain priority projects These panels were outside the normal semi-democratic control of INSERM's partially-elected review committees, and inevitably they tended to favour the successful (usually basic) laboratories, to the neglect of the ailing clinical research system

The strong French scientific trade unions have long demanded that the international committees should be advisory to, and vetted by, INSERM's elected committees — a procedure which Laudat clearly felt would destroy their effectiveness Since the unions now have much greater leverage on the government, the fear now is that this kind of democratic reform will go ahead — with the result that INSERM resources will be spread more evenly and thinly — exactly what Laudat was trying to avoid

But the government — and Lazar — are unlikely merely to capitulate to union pressure Chevenement, in particular, is well aware of the ineffectiveness of many university hospital clinics, but he puts it down to inefficient structures, in particular the overbearing power of the "grands patrons", the "gerontocracy" that rules French medical laboratories and — according to some — stifles research This view, together with the minister's determination to boost biotechnology and its base in molecular biology, may in the end refresh French biology rather than set it back **Robert Walgate**

0028-0836/82/050357-02$01 00

on a university project sponsored by a large fertilizer corporation and help run a private research company in which the same corporation has invested considerable capital (see *Nature* 8 October 1981, p. 417).

A representative of the university said last week that the new regulations proposed by FPPC represented an acknowledgement of some of the recent scientific developments affecting university–industry relations "particularly in genetic engineering, which were not foreseen when we went into this business".

The precise form in which scientists will be required to disclose either their own financial interests, or those of their spouse or children, in companies financing their research has still to be worked out by the university. Also under discussion is the way that the new reporting requirements would be policed. Here the conventional procedure at the university is that, although faculty members are under no legal obligation to make details of their outside interests available to the university, they can be barred from promotion or salary upgrading — both of which must be approved by the state — if they do not do as required.

So far, the university has reacted cautiously to the proposed regulations, recognizing that they have considerable support in the political community. One official on the Berkeley campus claimed that, although many faculty members felt they were being unnecessarily penalized for the excessive actions of a few, the general reaction was a reluctant acceptance.

But the debate may not be over. Some faculty members have apparently indicated informally that they may challenge the new regulations in court on the grounds that they constitute an infringement of constitutional rights. California Rural Legal Assistance in turn is suggesting that it, too, may sue the state if it feels that the regulations are not tight enough.

David Dickson

Polish higher education

Whose pigeon?

Academic freedom cannot be used to combat socialism and to reduce life to anarchy, General Wojciech Jaruzelski told the Sejm (Polish parliament) last week. This was the first meeting of the Sejm since the introduction of martial law. The two-hour speech was intended to justify the drastic measures of 13 December.

On the universities, he noted that the "political tensions" of the past year had involved most of the higher education system, and "weakened the pace" of academic work, creating "painful gaps" in study. The "reinstatement of law and order", however, was now creating conditions for normal work in the universities. "We want to continue the democratization of academic life, to ensure the self-government and autonomy of the colleges", he said. The new higher education bill should, he said, go ahead.

In spite of his professed support for autonomy, the general suggested that more government control over research would be necessary. In many institutes, he said, the practical results of research are nugatory, and the "discipline of scientific research" must be increased. In this respect he criticized all three sectors of Polish science — the universities, the Academy of Sciences and the "departmental" institutes belonging to the production ministries. Hitherto the "departmental" sector has been given financial priority and better fringe benefits. A main plank of Solidarity's programme for science and culture had been parity between the three sectors. Now, it appears, the three sectors may at least attain parity in the degree of government control. The state, said Jaruzelski, must reserve for itself the supervision of the cost-effectiveness of expensive research, and there should be no repetition in the future of "misguided specialist advice".

This last remark appears to refer to the grandiose investment projects envisaged by the Poland-2000 programme of the Gierek regime — although for the past 18 months the major criticism aimed by the scientists at Gierek was that he commissioned expert reports, and then went ahead with his plans for political reasons in spite of economic and technical indications to the contrary.

The form that the Polish research structure will now take is unclear from the general's speech, although clearly Solidarity's hopes of block-grants for academic research, with autonomy for the universities in the allocation of available resources seem unlikely to materialize. One possibility much discussed during the past 18 months had been the dissolution of the existing Ministry of Science, Higher Education and Technology, and the combination of the higher education sector with the Ministry of Education and Upbringing to form a single education ministry, as existed in Poland before 1972. In that event, a Ministry of Science and Technology would be created with responsibility for all the "departmental" institutes now belonging to the various production ministries, while the Academy of Sciences would continue with its present quasi-ministerial status.

It is not yet certain that these plans will be frustrated. The combination of science, higher education and technology in a single ministry has so far favoured the appointment of a scientist as minister. The new minister, however, appointed last week to replace Dr Jerzy Nawrocki who resigned soon after the declaration of martial law, is Professor Benon Miskiewicz, a military historian, who, until 1981, was rector of the Adam Mickiewicz University of Poznan. The appointment of a minister from the humanities could be the first step towards the eventual reorganization of the ministry. **Vera Rich**

Recombinant DNA guidelines

Only formality

Washington

The Recombinant DNA Advisory Committee (RAC) of the US National Institutes of Health (NIH) is to meet in Bethesda, Maryland, next Monday to decide whether to recommend the *coup de grâce* for federal regulations introduced six years ago to cover research using recombinant DNA techniques.

Many scientists are urging the committee to support a proposal that, as a final step in dismantling regulations initially introduced as protection against potential hazards from such research, would transform them into a voluntary code of practice. Several state and city legislatures, however — most recently the health committee of the California State Assembly — say that if this happens, they may adopt their own stringent regulations.

Judging by past experience, the most likely outcome is that a compromise formula will be worked out by NIH. While reducing the overall stringency of the regulations, this will probably stop short of making them voluntary in the hope of heading off local, more restrictive controls.

Two proposals have been put to RAC as possible major revisions to the NIH guidelines. The more radical suggestion was originally put forward by Dr David Baltimore of Massachusetts Institute of Technology and Dr Allan M. Campbell of Stanford University.

In its current form, which committee members agreed at their last meeting in October should be published for public comment, this revision would reduce the recommended containment level for almost all experiments to P1 physical containment, eliminate all current prohibitions on certain experiments (though retaining two as "admonishments") and abolish the mandatory aspects of the guidelines (see *Nature* 17 December 1981, p. 606, for full details).

A less severe revision has been proposed by RAC member Dr Susan Gottesman, of the National Cancer Institute's Laboratory of Molecular Biology. This would also revise and relax the containment requirements, but the guidelines would remain mandatory, and it would still be necessary for universities and research institutions to operate Institutional Biosafety Committees.

Officials at NIH report that, although both proposals have been widely distributed to the scientific community, the response has been much less than that to previous proposals to liberalize the guidelines made when the public debate about the safety of recombinant DNA techniques was at its height.

Some of those on both sides of the debate are clearly coming to an end of their stamina. "I cannot think of any letter that I

0028-0836/82/050358-02$01.00

A letter to Leonid Brezhnev. . .

Secretary General of the Communist Party
and President of the Council of the Supreme Soviet,
Leonid Brezhnev, Moscow, Kremlin

Sir,

We have followed with great interest your remarks in the press and on television, on the occasion of your latest visit to Bonn, expressing your concern for the maintenance of world peace This concern is shared by all responsible and thinking people throughout the world, independently of their ideological differences, and we stand with you in your desire to preserve humanity from destruction

At the time of your visit, however, we were shaken by the news that your country's Nobel Peace Prizewinner, Prof Andrei Sakharov, and his wife, Yelena Bonner, had embarked on a hunger strike of unlimited duration The ensuing response of the Soviet government, averting the danger to the Sakharovs' lives, was seen by the entire world as an act of humanitarianism Indeed, we recognize in your government's action an important contribution to detente, a regard for human rights being basic to and inseparable from the search for peace

The awarding of the Nobel Peace Prize to Andrei Sakharov acknowledges that he engaged himself unequivocally in the interests of world peace independently of his successes in physics This recognition of Prof Sakharov is a tribute also to all your countrymen who, like our own, are filled with the sincere desire for the peaceful coexistence of all nations following the dreadful sacrifices of the Second World War

In January 1980, Prof Sakharov was exiled to Gorky, without benefit of a court trial or having been sentenced

As members of the international scientific community, we feel we cannot ignore the circumstance that Prof Sakharov, in his two years of exile, has been unable to carry out his scientific work We see here a clear threat to the freedom of scientific endeavour, and indeed to the freedom of the human spirit

We therefore appeal to you to accede to Sakharov's repeated request for a full trial, or to allow him to return to his work at the Soviet Academy of Sciences

Prof Dr Gabriele Taugner

An English translation of a letter which was sent on 29 December last year to Soviet leader Leonid Brezhnev and signed by 136 scientists at the University of Heidelberg, West Germany

have written that has had any effect at all, those of us who think NIH has been dismantling the guidelines too fast still feel as strongly as ever, but we see no evidence that anyone listened to what we were saying", says Dr Susan Wright of the University of Michigan

Most of the letters received by NIH's Office of Recombinant DNA Activities from individual members of the scientific community, commenting on the two published proposals, support the more radical revision, which would make the guidelines voluntary This support, the apparent waning of public concern over the potential hazards of recombinant DNA research, legislative efforts to spur the commercial application of genetic engineering, and the anti-regulatory leaning of the Reagan Administration appear to favour a move towards less control

The single factor which could prevent this, however, is a resurgent militancy in communities in different parts of the country, particularly where new debates about the safety of the research have been triggered by the ambitious plans of the genetic engineering industry

Both the Boston Biohazards Committee and the Cambridge Biosafety Committee, for example, have written to NIH expressing their opposition to any move that would make the guidelines voluntary

In California, the state assembly's health committee has recently held two hearings on the growth of biotechnology companies in the state and the current status of federal safety regulations The chairman of the committee, Mr Art Torres, says he would consider introducing legislation enforcing the guidelines if NIH made them voluntary

With a large proportion of the nation's genetic engineering research taking place in California, threats of state legislation are not being treated idly by NIH In the past, university scientists have made strenuous efforts to prevent Congress from enacting legislation that would turn the NIH guidelines into broad legal requirements, indeed, this has frequently been the motivation behind NIH's agreement to accept tougher restrictions on the research than it would have liked **David Dickson**

Lead additives in petrol

New offensive

A well-organized campaign to persuade the British government to ban lead in petrol was launched in London last week The Campaign for Lead-free Air, or CLEAR, claims already to have 130 Members of Parliament, 8 national organizations concerned with environmental and health matters and 21 scientists and clinicians who are convinced by epidemiological studies or their own clinical experience that low blood lead levels harm the mental health of children The chairman of the campaign, Mr Des Wilson, is a seasoned campaigner whose organization to put forward the case of homeless people, SHELTER, was prominent in the late 1960s

Lead in petrol has been in and out of British politics since 1980 when a working party under Professor Patrick Lawther found no conclusive evidence that low concentrations of lead in the blood are detrimental to health or that lead in air is a major contributor to increased blood lead concentrations In the light of the Lawther report, the government's decision last May to reduce the lead content of petrol from 0 4 to 0 15 grammes per litre by 1985 was a surprise

CLEAR's objectives are to persuade the government to introduce the reduction earlier than planned and to pass legislation requiring all new cars sold in Britain after 1985 to run on lead-free petrol The pressure group will also be pressing for a lower excise tax on lead-free petrol and for it to be on general sale by 1985 at the latest

The campaign, which has received some money from its trustees, hopes to raise £250,000 mainly from public donations Some of the money will be spent on public education and monitoring the government's programme to reduce lead pollution The plan is to send out teams to investigate, for example, the effectiveness of the government's programme to increase public awareness of the hazards of lead in old paint and whether can manufacturers are following government instructions to reduce the amount of lead in solder CLEAR also hopes to support academic research on the effects of low lead levels in the body and to monitor the level of lead in air

At the launch last week, the organizers described two recent studies implicating low levels of lead in the body as harmful to health D A Otto and colleagues in California, whose study was published in *Electroencephalography and Clinical Neurophysiology* **52**, pp 229–239, claim to have found a link between abnormalities in the electroencephalograms of sensory stimulated children aged 1-6 years with blood lead levels as low as 150 microgrammes per litre Dr Fraser Alexander, a paediatrician from Newcastle and a member of CLEAR's scientific and medical advisory committee, reported his as yet unpublished study implicating low blood lead levels in pregnant women with malformation of the fetus **Judy Redfearn**

Satellite communications

Up for grabs

Washington

It seemed a good idea at the time, the RCA Corporation, besieged by more than 50 potential customers eager to lease space on its latest telecommunications satellite, Satcom-IV, successfully launched last month, had previously held a public auction for bids to lease seven separate transponders (frequency-shifted radio relays) The response was even better this time With the auction being held in the Manhattan Galleries of Sotheby Parke Bernet, it attracted a flood of national publicity, the transponders were sold at between $10 7 and 14 4 million for leases that run until 1988, resulting in a total sale of more than $90 million dollars

It was a bit too good to last On Thursday the Federal Communications Commission (FCC) ruled that the auction was illegal, since it resulted in different prices for leases being paid by different buyers, in violation of federal regulations which require no discrimination As a result, negotiations with the seven successful bidders have been suspended

0028-0836/82/050359-02$01 00

until a new way of allocating the leases has been worked out

However, FCC did not rule out the auction idea completely, and has invited the company to make alternative proposals for selecting bidders that would not contravene federal regulations One is that sealed bids should be invited, and leases awarded to the seven highest bidders at the price offered by the lowest of the seven

The dispute between RCA and FCC over how to allocate the leases reflects a gradual shift in attitudes towards the regulation of access to telecommunications satellites In the early 1970s, when the satellites were first coming into service, the federal government introduced strict regulations to prevent manipulation of the market

In practice, this goal has been achieved through classifying companies such as RCA which launch the satellites as "common carriers" which are required to offer leases on their transponders on a first-come, first-served basis at prices that are strictly regulated by FCC The procedure has been effective in protecting smaller users from being squeezed out of the satellite communications market, it has also made it difficult for companies to stockpile transponders, even if they have no immediate need for them, in order to exclude their competitors

Recently, however, concern has been growing about speculators who have bought leases at the regulated prices and resold them at a considerable profit In addition, the growth of available space on satellites has lead the industry to argue that tight federal regulation is no longer needed The cause of deregulation of the telecommunications satellite industry has also been embraced by the members of FCC, which in a 7–0 vote last week agreed to publish for public comment new rules which would allow companies operating satellites to negotiate sales directly with private customers

Satcom IIIR, launched successfully from Kennedy Space Center in November, contains 24 transponders, eight of which were reserved for those who had bought space on the ill-fated Satcom III which failed to go into orbit after its launch in December 1979

Both Satcom IIIR and Satcom IV are dedicated to use by cable television companies The satellites are intended to transmit programmes to local television operators, which would then distribute them to individual homes Since an antenna can only pick up signals from a single satellite at any one time, the companies have been keen to band together rather than lease space on other commercial satellites, such as Westar 1 and Comstar D2

Among the companies which will have to renegotiate the transponder leases with RCA is RCTV, a joint venture of RCA and the Rockefeller Center Inc , which has announced ambitious plans to distribute entertainment programmes through cable television The company has already agreed to buy the first rights of British Broadcasting Corporation programmes for transmission in the United States

Meanwhile, in a separate move illustrating the social and political possibilities being opened up by satellite telecommunications technology, four labour unions have joined with the American Federation of Labor/Council of Industrial Organizations to arrange for the broadcast over public television of two films on safety and health whose distribution had been suspended by the Department of Labor's Occupational Safety and Health Administration The unions have made use of a 1978 amendment to the 1934 Communications Act which allows groups outside public broadcasting to rent time on one of the four transponders which the Public Broadcasting Station (PBS) leases on the satellite **David Dickson**

Cashing in now

British Telecom, exercising its right under last year's Telecommunications Act to form partnerships with commercial enterprises, has launched a company to exploit spin-off from research at its laboratories at Martlesham Heath, Suffolk

The plan is to set up small venture companies to exploit ideas, although patents may be available under licence to existing manufacturers The new company, Martlesham Enterprises, has been set up with £250,000 of issued ordinary share capital, the shareholders being British Telecom (30 per cent), Electra Investment Trust (25 per cent), Lazard Brothers (20 per cent), Raeburn Investment Trust (managed by Lazards) (20 per cent) and Thompson Clive and Partners (5 per cent)

Research at the Martlesham Heath laboratories covers optical fibres, semiconductors, video-phones, slow-scan TV, speech synthesis and public viewdata systems Martlesham Enterprises has already identified five ideas which could form the basis for new manufacturing companies, but so far only one of them, a new materials process for semiconductors, has been developed to any significant extent

Martlesham Enterprises plans to hold a financial interest in new operating companies, giving its shareholders first option to put up new capital Attractive terms are to be offered to inventors who leave the laboratories to help set up new companies Interest on profits will, as normal, return to the shareholders It is hoped that the operating companies will grow to the point where they can be launched publicly, when Martlesham Enterprises will decide whether to retain a financial interest or dispose of them

Judy Redfearn

Technical change in France

Central theme

The French government is to set up a centre for social and systems research on science and technology, inspired to some extent by the Brookings Institution of Washington and, in Britain, the Technical Change Centre in London and the Science Policy Research Unit (SPRU) in Sussex But in the Paris institution there will be a difference it will be strictly linked to, and under the direction of, the Ministry for Research and Technology, and will thus lack the political independence of its models

The Center for Advanced Technological Systems Study (CATSS), to use its Americanized name, (CESTA, Centre d'etudes des systemes et des technologies avancées, in French) should be in full swing by 1984 with a budget of around 40 million francs and a staff of 40 "scientists and engineers"

The creation of CATSS is the immediate result of a report to Prime Minister Pierre Mauroy by Dr Joel de Rosnay, director for research applications at the Institut Pasteur (where François Gros, science adviser to the Prime Minister, was until recently director) De Rosnay recommended that a centre like CATSS be established "to study the industrial, social and cultural change induced by advanced technological systems (such as microelectronics, biotechnology, robotics and solar energy)"

The questions are political and involved, the report notes, and it claims that in France "there are traditional difficulties" in thinking in terms of complex systems and networks CATSS must overcome these difficulties

As a government agency in a government devoted to industrial development through technology, CATSS may find its emphasis lying more frequently on innovation strategy in key industries than on social impact *per se* The emphasis of the report is on missed, or botched, industrial opportunities Concorde, an "indisputable technical success" marred by a failure to anticipate economics, competition and environmental impact, microelectronics, insufficient in France because opportunities to develop liquid crystals and integrated circuits were not taken up, and biotechnology, limited by the lack of researchers and engineers trained in the life sciences

Despite its government links, the centre will be open to scientists, industrialists, union leaders, parliamentarians and local politicians It will also collaborate with outside institutions (including, perhaps, Brookings SPRU and the Technical Change Centre)

CATSS will have a strong training function as well as undertaking research, experimenting with new educational technology and communications systems,

0028-0836/82/050360-02$01 00

and helping to "diffuse" new technology Thus the concept appears to be of an intellectually and politically sophisticated institution to assist the country's technological development one which will be able to help industry to make its forecasts and plans, but will, at the same time, take into account likely social impacts and obstacles CATSS's first programmes begin next month — training programmes in biotechnology and microelectronics A director for the centre is expected to be appointed before the summer **Robert Walgate**

Fluoridation in Scotland

Days in court

A legal trial that will decide whether Strathclyde Regional Council becomes the first Scottish water authority to add fluoride to its water supply has now passed its 130th day, making the record books as the longest ever court case to be heard in Scotland The Edinburgh Court of Session, Scotland's High Court, has become a battleground for fluoridation and anti-fluoridation interests

The case, *McColl v Strathclyde Regional Council*, opened on 23 September 1980, and was originally expected to last twelve weeks The eventual cost is estimated at £1 million, which would make it the most expensive civil case in Scottish legal history The costs of Strathclyde Regional Council will be met by its four area health boards The expense of an expert witness can be as much as £450 a day and many have come from as far away as the United States and Australia If the case lasts for 150 days, as it may well do, lawyers' costs alone could exceed £60,000

The issue at stake is twofold — the legal right of the council to add a trace of fluoride to the water supply and the medical effects of fluoride In 1977, the council voted by a majority of 43 to 42 to build a £2 million plant to introduce fluoride into the water supply Mrs Catherine McColl is contesting the decision, claiming the right of herself and her grandchildren to drink unfluoridated water on the grounds that fluoride is not only useless but can cause cancer and other diseases The hearing is before Lord Jauncey

The evidence has been intricate and technical Mrs McColl appeared in the box only on the first day The medical issues have focused on the contention that fluoride can cause cancer Sir Richard Doll for example, has so far given evidence for two weeks It is expected that Lord Jauncey will take months to reach a judgement

Evidence against fluoridation has been given by Dr John Yiamouyiannis, formerly of the National Health Federation organization and a member of the US National Health Action Committee, and Dr Dean Burk, a retired National Cancer Institute laboratory scientist In some ways the Scottish trial is a re-run of the hearing in West View, Pennsylvania in November 1978, when Drs Yiamouyiannis and Burk also argued that there is a link between fluoride and increased cancer mortality rate Dr Burk has separately told the US House of Representatives that fluoridation is "socially imposed murder"

In Pennsylvania, Judge Flaherty, then a lower court judge, issued an injunction ordering West View Water Authority to cease water fluoridation His decision, however, was appealed against on grounds of jurisdiction In January 1979, after a review of the evidence by the Department of Environmental Resources, the water authority was ordered to continue to fluoridate The Minnesota Governor's Commission, appointed in 1978 to study the health effects of water fluoridation, examined the same body of evidence as Judge Flaherty and concluded that "an association between fluoridation and cancer has not yet been shown"

Fluoride has been added to water supplies in Britain since 1957, and 10 per cent of the population drinks artificially fluoridated water (in the United States 44 per cent of the population drinks treated water) The 1972 Water Act enjoins the water authorities to provide "wholesome water", but although 87 out of 90 area health authorities are in favour of fluoridation, in the past 7 years few schemes have been implemented The water authorities seem reluctant to proceed in the absence of parliamentary legislation

The decision in Scotland could thus be influential, particularly as a similar case is being prepared in Calderdale, Yorkshire If Lord Jauncey decides in favour of Strathclyde, the issue of further legal aid for an appeal will arise If the case goes to the House of Lords, it may take several years for a final decision And neither side may be able to claim a victory — if, for example, the judgement is that fluoride is beneficial to dental health but that water authorities do not have full jurisdiction to determine what goes into the water supply

In Strathclyde, the irony is that local elections early this year could render any judgement nugatory a new council could vote to reverse the fluoridation policy

Jane Wynn

Rubik's cube

Puzzles galore

A decision is expected this week from the British high court hearing of a copyright and passing-off suit brought by the Politehnika Industrial Corporation of Budapest, manufacturers of the original Rubik's cube, against Dallas Print Transfers of London, importers of an alleged copy known as the "Wonderful Puzzler", produced in Taiwan

The case, initiated by an injunction from Politehnika last March, has turned on two main issues As far as copyright is concerned, the emphasis has been on the internal structure of the cube, involving comparison of production blueprints, while the passing-off charge is based on claims that the puzzler has on occasion been marketed as the Rubik cube

The dual nature of the case corresponds appropriately to Dr Erno Rubik's own dual interest in the cube — structure and concept A lecturer in architecture at the Budapest Academy of Applied Arts, he was, he says, originally interested primarily in the internal mechanism of the cube which allows each face, consisting of a 3 × 3 array of cubelets, freely to rotate either clockwise or anticlockwise Only later did he decide to communicate his pleasure in the new device to others by offering it for commercial construction

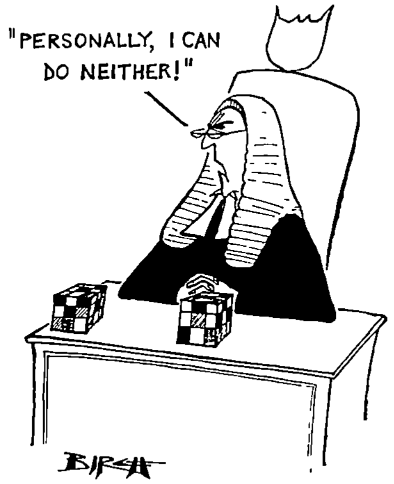
"PERSONALLY, I CAN DO NEITHER!"

Rubik says that other international contributions to the booming market in logic toys — pyramids, spheres and the like — embody essentially the same principle as the cube, since the various sections are displaced without changing the over-all shape of the assemblage The one major exception, known as the "tower", which exists in two contending Hungarian versions, is, in his opinion, simply the old "15 puzzle" invented in the 1880s, rolled up into cylindrical form, since it incorporates a vacant parking spot into which an element can be moved during the transfer process

The popularity of the cube, which Rubik himself cannot adequately explain, has made him reputedly the seventh richest man in Hungary and won for him a "Gold Medal of Labour" for his services to Hungarian industry, and has had a number of unexpected spin-offs The possible and impossible configurations of the cube, Rubik said last December, were attracting attention from physicists as a means of modelling the properties of quarks

In Hungary, the unprecedented boom in the toy industry generated by the cube has highlighted a number of defects in the New Economic Mechanism, and seems to have been in part responsible for the recent relaxation of the rules governing small enterprises **Vera Rich**

0028-0836/82/050361 01$01 00

CORRESPONDENCE

Soviet sanctions

Sir — I welcome your leading article of 7 January (p 1) and in particular your criticism of the suspension of the exchange agreement between the United States and the Soviet Union

Such a suspension must surely weaken world peace The merits and demerits of unilateral nuclear disarmament are much debated but the prior need is for a better understanding between peoples of different cultures — in this case the United States/United Kingdom and the Soviet Union The risk of scientists "having their brains picked" surely matters less than the potential benefits from better knowledge of human beings of the "other" culture — their hopes, fears and hang-ups

As a first line of defence for international understanding and peace, scientific and other exchanges can be good investments and should be fostered, not reduced Their costs, if prohibitive to self-financing individuals, are infinitesimal compared with those of armaments

H J Killick

Abingdon, UK

Ethnic journal

Sir — H H Hirschhorn (*Nature* 14 January, p 92) appears to have misunderstood the "small niche" to which *Journal of Ethnopharmacology* is trying to lay claim, even though my review quoted the aims of the journal in full Rather than being another journal of pharmacognosy, which I would accept could appear to be of greater importance than all the drugs for the cardiovascular system, *J Ethnopharmacology* specializes in the use of drugs by ethnic cultures How does the importance of "ceramic use for prehistoric Datura use in N America" compare with a typical paper from *Journal of Cardiovascular Pharmacology*?

The number of reprint requests might reflect more accurately the obscurity of the journal and difficulty in finding it in a library, than the importance of the subject

Hilary G Pickles

St Bartholomew's Hospital,
London, UK

Anthrax island

Sir — The paper by Manchee *et al* [1] provides the first published quantitative information about the the contamination of Gruinard Island with anthrax spores In view of the public interest and concern that have been expressed, this is welcome Nevertheless, the information given is meagre and the main tentative conclusion questionable

Since no accurate viable counts of spores were made on samples taken before those reported on in the paper, it is impossible to estimate the time course of the contamination The authors consider that its present extent warrants their taking seriously van Ness's assumption[2] that significant multiplication of anthrax bacilli may occur in the soil However, neither in that paper, nor in a series of earlier papers, does van Ness cite experimental evidence to justify this assumption In support, he quotes a paper by Minett and Dhanda[3] But those authors actually come to the *opposite* conclusion — that the anthrax bacillus does *not* behave as a saprophyte in nature

In the past, I have exhumed and examined cadavers of cattle that have died of anthrax, but I failed to isolate anthax from any, even from one buried as little as three months previously The conditions — high ambient temperatures and the availability of blood and tissues from the cadavers for the nutrition of the anthrax bacilli — resembled those postulated by Manchee *et al* [1] as being likely to promote an increase of bacilli and spores in the soil However, those familiar with the epizootiology of anthrax tend rather to regard such conditions as favourable to the increase of soil microflora inimical to anthrax organisms, a view which practical experience reinforces

There is little experimental evidence to support either van Ness's view or the more conventional opinion that anthrax does not behave as a saprophyte Unfortunately, incentives to investigate the ecology of the anthrax bacillus have diminished — despite its intrinsic interest — because of the ease with which anthrax can be controlled by the vaccine I developed[4]

Attention should be paid to studying factors which could be responsible for the exceptionally long survival of the contamination of Gruinard Island Is this related, for example, to the form in which the spores were distributed, to their number, to the character of the soil or of the soil microflora, to the lack of husbandry, or to climatic conditions? It would be deplorable if the special circumstances on Gruinard Island were not used to provide answers to these neglected ecological questions, and particularly to the question as to whether the anthrax bacillus can multiply sufficiently in the soil for this to be a significant factor in the epizootiology of anthrax Practical experience in the control of anthrax does not support this view

M Sterne

Sarisbury Green,
Hants, UK

1 Manchee, R J , Broster, M G , Melling, J , Henstridge, R M & Stagg, A J *Nature* **294**, 254-255 (1981)
2 Van Ness, G B *Science* **72**, 1303-1307 (1971)
3 Minett, F C & Dhanda, M R *Indian J vet Sci* **11**, 308-328 (1941)
4 Sterne, M *Onderstepoorte J vet Sci Anim Ind* **21**, 41-43 (1946)

No change in RE

Sir — D B Jack and M R Gregg (*Nature* 22 October 1981, p 602) have used Flesch's index of reading ease (RE) to suggest that letters to *Nature* became harder to read at some time between 1940 and 1950 Using the first hundred words in each letter as the criterion, the papers analysed from the years 1950 to 1980 were, on average, 15 44 index points more difficult (the harder to read the lower the index)

This conclusion obscures a difference of style between earlier and more recent letters to *Nature*, that of the way in which the opening paragraph is used by authors Current practice demands that the opening paragraph shall serve two functions, both as introduction and as a summary of the main conclusions In its latter function it must often be laden with a burden of latinate technical terms and exactitudes, for those readers who choose to go further The earlier style demanded simply that the opening paragraph served to whet the appetite and to lead the reader gently to the nub of the matter, eschewing difficulties at first

I have therefore computed Flesch's RE for the first and second paragraphs of two samples of 20 letters each, culled from *Nature* of October 1981 and of October 1931 If the second paragraph contained less than a hundred words the third paragraph was lumped with it

	Reading ease		
	Para 1	Para 2	Total text
1931	29 8 ± 4 3	23 7 ± 4 1	26 3
1981	15 1 ± 2 1	21 0 ± 2 4	18 5

This analysis confirms Jack and Gregg's conclusion that the opening sentences today are more difficult than they were 50 years ago In my sample the difference is 14 7 RE points The 50 year difference for the second paragraph, however, is a mere 2 7 points which is not statistically significant In 1931 the second paragraph was on average 6 1 points more difficult than the introduction, today it is 5 9 points easier

Authors today seem not to be cloaking their findings in obscure language significantly more than they did 50 years ago, except in the introduction

D B Carlisle

Environment Canada,
Ottawa, Canada

More repeats

Sir — There appear to be two homologous sequences in a single exon of the collagen $\alpha2(1)$ sequences reported by Wozney *et al* in *Nature* of 12 November 1981[1]

The sequences occur in a single polypeptide and are apparent in the nucleotide sequence but not the amino acid sequence A span of 36 nucleotides is repeated with six differences (marked with ×)

```
1242                                1278
GlyAlaAlaGlyProProGlyProProGlyProSer
GGTGCTGCTGGCCCCCCTGGCCCTCCTGGTCCAAGT
  XX     X                X     X   X
GGCTCTGCTGGTCCCCCTGGCCCTGCTGGTCTAAGA
GlySerAlaGlyProProGlyProAlaGlyLeuArg
1315                                1351
```

The differences are probably due to post duplication mutations

The sequences lie 4 collagen units, $(\mathrm{Gly}\text{-}X_1\text{-}Y)_4$, from each other and contain 4 collagen units each, which makes a 54 base pair (bp) repeat hard to credit I cannot think of a plausible scheme to yield 36 bp repeats from 54 bp units Apparently 36 bp were extracted by double unequal crossover and re-appended 36 bp further down the molecule leading to the internal homology

Michael P Finerty

Tucson, Arizona, USA

1 Wozney, J , Hanahan, D Tate, V , Boedtker, H & Doty, P *Nature* **294**, 129 135 (1981)

Mantle heterogeneity and isotopes in oceanic basalts

from W M. White and A W Hofmann

THE chemistry of volcanic rocks is strongly influenced by processes which occur during magma genesis and evolution and it is generally difficult to relate it to the chemistry of the rocks' sources One exception is the isotopic composition of radiogenic elements such as Sr, Pb and Nd, which are thought to be unaffected by most magmatic processes and provide a means of 'fingerprinting' volumes of source materials in the Earth's mantle It has been known for nearly two decades that the mantle is isotopically and chemically heterogeneous but the interpretation of the geochemical data is not easy because the kinematics of mantle convection remains elusive Now isotope geochemists and mantle convectionists are beginning to interact and collaborate in order to overcome this difficulty Two issues remain unresolved — the size of the domains of mantle heterogeneity and their spatial arrangement — is the mantle layered or irregularly heterogeneous?

On the geochemical side, it is well established that volcanic rocks erupted on oceanic islands are apparently derived from a type of mantle fundamentally different from that which supplies magma to most of the mid-ocean ridge system Second, all of the mantle now involved in mid-ocean ridge volcanism has previously been depleted in incompatible elements (that is, elements having a strong affinity for a melt phase as opposed to the solid) Further, heterogeneity in the mantle is long-lived Pb isotope data suggest that the various reservoirs have remained separate for a time of the order of 2×10^9 yr, demonstrating that mantle convection does not stir the mantle sufficiently to eliminate the heterogeneity Thus, and because of the hope that the isotopic data will somehow give clues about mantle kinematics and dynamics, geochemists continue to gather isotopic data on mantle-derived volcanic rocks

Systematic studies of basalts from the Mid-Atlantic Ridge in the 1970s revealed that, as islands such as Iceland and the Azores are approached, isotopic compositions of Sr and Pb change gradually from those typical of mid-ocean ridge basalts to compositions characteristic of island basalts, providing evidence of geographically correlated variation in mantle chemistry on a scale of the order of 100–1,000 km Two recent papers in *Nature* deal with mantle heterogeneity on a local scale Dupré and co-workers (*Nature* **294**, 552, 1981) report Pb and Sr isotopic data for two well studied areas of the mid-ocean ridge system the FAMOUS area in the North Atlantic and the CYAMEX area of the East Pacific Rise Basalts erupted in these two areas have nearly uniform Sr isotopic compositions and though Pb isotope variations exist, they are much smaller than variations observed on larger scales Earlier studies of Sr and Nd isotopes in basalts from the FAMOUS region also revealed virtual isotopic uniformity

Machado and his colleagues (*Nature* **295**, 226, 1982) report Sr and Nd data on basalts from the vicinity of the Kane Fracture in the North Atlantic, some 200 km from the ridge Measurable variations occur in both Sr and Nd, with basalts from the western ridge segment having systematically higher ^{87}Sr/^{86}Sr and lower ^{143}Nd/^{144}Nd ratios than those from the eastern ridge segment The total range of Sr isotopic compositions (^{87}Sr/^{86}Sr = 0 7022–0 7025) is small compared with what is normally found in mid-ocean ridge basalts, but the range of Nd isotope ratio is relatively large (^{143}Nd/^{144}ND = 0 51337–0 51313) The Fracture Zone apparently forms a boundary between two geochemical domains in the mantle

Yet another recent study bearing on the question of the scale of mantle heterogeneity has been reported by Zindler and co-workers (*EOS* **62**, 424, 1981) They find that seamounts in the vicinity of the East Pacific Rise have ^{87}Sr/^{86}Sr and ^{143}Nd/^{144}Nd ratios varying between 0 7027 and 0 7032 and 0 5132 and 0 5130 respectively, and basalts from a single small seamount span this entire range

Local isotopic variations have been reported from oceanic islands in earlier studies For example, on the island of Sao Miguel (Azores), 60 km in its longest dimension, reported ^{87}Sr/^{86}Sr ratios range from 0 703 to 0 705, while ^{143}Nd/^{144}Nd ranges from 0 51300 to 0 51276 On Iceland's Rekjanes Peninsula, ^{143}Nd/^{144}Nd ratios vary from 0 51317 to 0 51299 on a scale of a few tens of kilometres and less, although ^{87}Sr/^{86}Sr is nearly uniform Although it is often assumed that Sr and Nd isotopic variations are closely related, these studies, and that of Machado and his colleagues, demonstrate that these ratios, and by inference variations in Rb/Sr and Sm/Nd, may occasionally become decoupled

The conclusions that may be drawn from the data accumulated so far are (1) in most regions, especially along the mid-ocean ridge but also on many oceanic islands, isotopic compositions can be mapped, and it is found that the regional variations are larger than the local ones (2) Nevertheless a few regions, such as 45°N on the Mid-Atlantic Ridge, the island of Sao Miguel and the small seamounts off the East Pacific Rise, do show significant local variability and cannot be characterized by a single isotopic ratio (3) The local variations generally have greater amplitudes on oceanic islands than on the mid-ocean ridge (4) The regional variations are also larger for oceanic islands than for ocean floor basalts

The question of scale is intimately related to the question of origin A view widely held by geochemists and geophysicists, but by no means universally accepted, is that oceanic islands result from mantle plumes arising from the deeper mantle, while the upper mantle, depleted in incompatible elements through repeated episodes of melt extraction, is the source of mid-ocean ridge basalts The lower mantle source of mantle plumes may be either primitive, undepleted mantle or subducted oceanic crust An alternative view is that mantle heterogeneity is created by fluids rich in incompatible elements percolating upwards and metasomatizing the upper mantle, this is supported by evidence from mantle xenoliths in alkali basalts and kimberlites In this model there is a large potential for creating small-scale heterogeneity if fluid pathways are not uniformly distributed The plume

---

W M White is in the Geochemistry Department, Max-Planck-Institut fur Chemie, D 6500 Mainz, FRG, of which A W Hofmann is Director

0028-0836/82/050363-02$01 00

hypothesis predicts that oceanic islands are created at quasi-stationary locations and that large quantities of material are advected to the surface in excess of the volume needed to create normal oceanic crust. The existence of isotopic anomalies of large wavelengths and large amplitudes is certainly consistent with this hypothesis, and we have long favoured this idea. However, the hypothesis that isotopic variations are produced by more local phenomena possibly involving metasomatism does not really conflict with this view, rather, it may be the appropriate explanation for many or all of the small-scale isotopic variations observed. Indeed, it seems unlikely that the mantle plumes can explain everything. Surely not all seamounts are former or present sites of mantle plumes, nor is it clear, for example, how the isotopic variations near the Kane Fracture Zone could be related to a mantle plume.

We believe, perhaps unimaginatively, that in order to improve our understanding of mantle heterogeneity we do need to accumulate a lot more isotopic data on more oceanic basalts rather than wait until evidence of a different kind or insight provides a new impetus. Further study of the mid-ocean ridge system will be essential if the questions about the chemical structure of the mantle are to be resolved. Is the well studied North Atlantic Ocean anomalous because of the presence of the very large Iceland and Azores anomalies? Do other areas similar to 45°N exist or is the mid-ocean ridge system more nearly uniform away from oceanic islands? What is the total volume of isotopically anomalous basalts? Do all postulated plumes have large-scale isotopic gradients associated with them? Can the apparently randomly distributed small-scale variations also be mapped with improved coverage? Do major fracture zones, such as the Kane, form boundaries between geochemical domains in the mantle? To reconstruct the distribution of source materials and their movement in the mantle, we still need much more complete isotopic maps of the ocean floor and the oceanic islands than those so far compiled.

What is required is a programme of intensive mid-ocean ridge 'geochemical mapping' similar to that already carried out in the North Atlantic. We believe this would most profitably be accomplished through dredging rather than drilling because of the higher sample quality and the substantially lower costs. Drilling of seamounts and similar anomalous features, already begun by the International Phase of Ocean Drilling (IPOD), should continue. We think of this 'fingerprinting' of source materials in the Earth's mantle using isotopes as perhaps being similar to fingerprinting the oceanic crust using magnetic anomalies, the meaning of which remained obscure until there were enough data for them to be interpreted by simple visual inspection. ☐

New measurements near the Gulf Stream

from W J Gould

THE Gulf Stream is, to the layman, a well known ocean circulation feature responsible for the temperate climate of Western Europe. It would therefore seem surprising that oceanographers should be in any doubt about the structure and dynamics of the Gulf Stream in view of studies that have been made over many years[1–3]. However, until recently, progress in the field has been restricted by the difficulty of measuring directly the current in the strongest parts of the Gulf Stream. Now this problem has been overcome and a recent paper[4] sheds light on the relationship of the Stream to its recirculation and on the Gulf Stream's inherent variability.

The Gulf Stream is the intense (surface currents of 3 knots (150 cm s^{-1}) or more) narrow current that flows northwards along the eastern seaboard of the North American continent from the Florida Straits to south of the Newfoundland Grand Banks. North of Cape Hatteras the Stream begins to meander, with the envelope of the stream tracks spreading like a fan as it turns eastwards away from the continental slope and past the New England seamounts. The intense current is associated with the boundary of the warm Sargasso Sea water, which fills much of the western North Atlantic, and the colder 'slope water' adjacent to the continental slope. (The current axis is often defined as the locus of positions at which the temperature at 200 m depth is 15°C.)

East of the Grand Banks the current and its associated temperature structure rapidly lose their identity and the course of the Gulf Stream becomes diffuse. It is at this point that the current is considered to form two main branches, the North Atlantic current which heads northeastwards towards Europe, and the Gulf Stream recirculation which turns south and eventually westwards to rejoin the Gulf Stream and complete the subtropical Gulf Stream gyre.

Until comparatively recently the view of the Gulf Stream system (Gulf Stream, North Atlantic current and recirculation) has been derived solely from observations of the density field (from temperature and salinity observations) which are then used to derive the geostrophic flow field (based by definition on the assumption of a balance between the horizontal pressure gradients and the Coriolis force). A typical view[5] shows a Gulf Stream system confined almost entirely west of the Mid-Atlantic Ridge and characterized by two anticyclonic (clockwise) gyres penetrating throughout the entire water column. The main gyre is that of the Gulf Stream and its recirculation and the secondary one lies to the east of the Newfoundland Grand Banks. But the interpretation of the temperature and salinity data in terms of two gyres is controversial[6]. The calculation of geostrophic currents provides only a current profile relative to some arbitrary reference level, usually at depth, and thus while the near-surface circulation may be adequately described the deep current field may not.

A possible explanation of the exact nature of the circulation may come from direct observations of currents either by moored current meters (eulerian measurements) or by the tracking of drifters (lagrangian measurements) at the surface or at depth. The strength of the Gulf Stream has so far precluded the use of moored current meters in the upper part of the water column near the Gulf Stream axis although they have been used extensively north and south of the Stream and in the deep ocean below it. Lagrangian measurements do not have the same restriction and recent technology presents new possibilities for investigating the Gulf Stream system.

Neutrally buoyant floats are instrument packages designed to be less compressible than seawater. Thus, as they sink, they gain buoyancy relative to the surrounding water until by suitable ballasting they may be made neutrally buoyant at some pressure level. For many years since their development in the 1950s these floats were tracked acoustically from attendant ships[7,8] but their use was restricted to the duration of a typical research cruise (a few tens of days). In the late sixties and early seventies a series of neutrally buoyant floats with lifetimes of two or three years were tracked in the southern Sargasso Sea[9,10] using low-frequency sound signals (400 Hz) received at shore-based listening stations in the Caribbean. The necessary acoustic propagation over distances of the order of 1,000 km is achieved by means of a minimum near 1,000 m depth in the vertical profile of sound speed in the ocean which acts as a wave guide. This is known as the SOFAR (SOund Fixing And Ranging) channel and the long-range floats as SOFAR floats.

The technique was initially restricted to areas within range of the fixed receivers but the development of moored autonomous listening stations (ALS) in which signals from the SOFAR floats are received, processed and stored has raised the possibility of deploying SOFAR floats almost anywhere in the ocean.

A recent paper by Schmitz *et al*[4] provides some of the first direct measurements of currents in the strongest parts of the Gulf Stream and helps explain the nature of its circulation. The float tracks described are from depths of

---

W J Gould is at the Institute of Oceanographic Sciences, Brook Road, Wormley, Godalming, Surrey GU8 5UB

0028-0836/82/050364-02$01 00

700–2,000 m and have been considered to provide eulerian estimates of current from the areas through which they passed These have been compared with eulerian measurements of currents from either side of the Gulf Stream (There are some fundamental difficulties in the interpretation of the float tracks Since they depend for their neutral buoyancy on the ambient pressure they tend to follow isobaric surfaces and so do not stay with a particular body of water, that is, they are not truly lagrangian)

The float tracks reported exhibit similar complexity in space and time to synoptic views of the Gulf Stream from temperature field maps and from previous current meter records The kinetic energy of the floats is consistent with an extrapolation of known meridional variations of kinetic energy[11] into the region of the Gulf Stream axis The deeper float tracks do not, however, support the view of a vertically coherent Gulf Stream, floats close to the Gulf Stream axis exhibiting both westward and eastward motions The tracks of floats in and above the thermocline (depth of greatest current shear) support previously held views of the circulation

New measurements in the vicinity of the Gulf Stream at both thermocline and abyssal depths raise the possibility of connecting the known (from eulerian measurements) time scales of variability south of the Gulf Steam in the Sargasso Sea recirculation and north of it on the continental slope[12] Subject to the only quasi-lagrangian nature of the float tracks there may also be evidence of the geographical distribution of the recirculation of the Gulf Stream system and a possible resolution of the two gyre controversy

There are now plans for a wider use of SOFAR float technology In particular, the next two years should see measurements taken by US, UK and French laboratories near and to the east of the Mid-Atlantic Ridge in an effort to study the paths taken by the North Atlantic current on its eastward path and long-term dispersion in the deep ocean These projects will use SOFAR floats in areas of more complex sound velocity structure than are found in the western North Atlantic and at much greater depths than previously explored ☐

---

1 Richardson, P L in *Oceanography in the Past* (eds Sears, M & Merriman, D) 703 (Springer, New York, 1980)
2 Fuglister, F C *Prog Oceanogr* **1**, 265 (1963)
3 Stommel, H *The Gulf Stream A Physical and Dynamical Decription* 2nd edn (University of California and Cambridge University Press, 1965)
4 Schmitz, W J Jr *et al J phys Oceanogr* **11**, 1194 (1981)
5 Worthington, L V *On the North Atlantic Circulation* (The Johns Hopkins Oceanographic Studies 1976)
6 Clarke, R A , Hill, H W , Reiniger, R F & Warren, B A *J phys Oceanogr* **10**, 25 (1980)
7 Swallow J C *Deep Sea Res* **3**, 74 (1955)
8 Swallow, J C & Worthington, L V *Deep-Sea Res* **8**, 1 (1961)
9 Rossby, H T & Webb, D *Deep-Sea Res* **17**, 359 (1970)
10 Freeland, H F , Rhines, P B & Rossby, H T *J mar Res* **33**, 383 (1975)
11 Schmitz, W J Jr *J mar Res* **36**, 295 (1978)
12 Luyten, J R *J mar Res* **35**, 49 (1977)

0028-0836/82/050365 02$01 00

Substorms and the growth phase problem

from S W H Cowley

SPACECRAFT observations over the past decade have clearly demonstrated that large-scale dynamic changes in the magnetic field and plasma populations take place periodically inside the Earth's magnetosphere These disturbances are termed magnetospheric substorms They last for 1–2 hours and it is not unusual for several to occur in one day At the Earth, substorms are associated with brilliant auroral displays resulting from bombardment of the upper atmosphere by kilo-electron volt magnetospheric electrons, and with intense ionospheric electric currents flowing at high latitudes

It is generally agreed that substorms tend to occur when the coupling between the magnetosphere and the surrounding solar wind is strong Magnetospheric coupling to the solar wind causes a large-scale circulation of plasma and embedded magnetic field lines within it (see the figure) When the solar wind magnetic field points south, as shown, magnetic 'reconnection' can occur across the dayside boundary so that the solar wind magnetic field becomes directly connected into the Earth's polar magnetic field These terrestrial 'open' field lines are then swept downstream by the solar wind flow and are stretched out into a long magnetic tail typically extending to ~ 1,000 Earth radii (R_E) on the nightside of the Earth A similar 'reconnection' process then occurs (at least eventually) in the tail, returning 'closed' field lines to the Earth and thence to the dayside boundary where the process can repeat, as originally described by Dungey in 1961 The important point is that the strength of the cyclic flow depends primarily on the direction of the solar wind magnetic field Magnetospheric substorms occur preferentially when the field points south and dayside reconnection and the flows reach a maximum As the solar wind field turns northwards, both the flows and the occurrence of substorms decrease

There is broad agreement that once a substorm begins it can be described in terms of auroral brightening and 'break-up', the sharp intensification of ionospheric currents and the disturbances which occur in the magnetic field and plasma in the nightside magnetosphere However, there are two important and opposing views on the events which lead up to substorms the 'growth phase' model of McPherron[1] and the 'directly driven' model discussed most recently by Akasofu[2]

The 'growth phase' picture assumes that the increased magnetic flux transfer from the dayside to the tail which follows a southward turning of the solar wind magnetic field is not immediately matched by increased flux return from the tail to the dayside As a result, magnetic energy is stored in the increasing field in the tail for perhaps 1 hour or more before substorm onset (the 'growth phase') At a certain point, however, an instability occurs (substorm onset), resulting in the formation of a new reconnection region about 15 R_E down-tail from the Earth The rapid tail reconnection which then occurs dissipates the stored magnetic energy, feeding it over periods of about 1 hour into plasma energy (the substorm expansion phase) The substorm subsides when the reservoir of available magnetic energy in the tail is depleted, but a new substorm cycle can then start if the solar wind field remains southerly directed

The 'directly driven' substorm model is based primarily on the close correlation

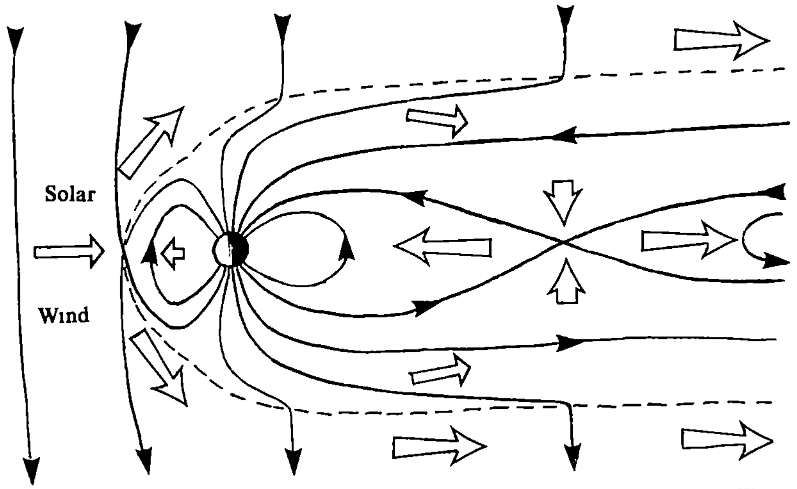

Cross-section of the Earth's magnetosphere in the noon–midnight meridian plane The solid lines are magnetic field lines, and the dashed line is the magnetosphere–solar wind boundary which on the dayside of the Earth lies typically at a geocentric distance of 10 R_E Solid arrows indicate the flow of plasma and embedded magnetic field lines, and snow the convection system set up inside the magnetosphere by the magnetic 'reconnection' which occurs between the Earth's field and the solar wind magnetic field across the dayside magnetopause when the latter is southerly directed observed between substorm and solar wind conditions and postulates that the state of the magnetosphere is determined solely by the solar wind, with a magnetospheric response delay of perhaps a few tens of minutes The correlation is described in terms of a function of solar wind variables termed the 'ε parameter', whose value depends principally on the solar wind field direction, being maximum for southward fields and zero for northwards Substorms are postulated to begin whenever ε exceeds a certain critical value such that an instability occurs in the magnetosphere, and to be continuously maintained so long as ε remains above this value Akasofu suggests that the instability occurs in the current system connecting the magnetic tail with the nightside auroral ionosphere

One important difference between the 'growth phase' and the 'direct' models is the expected magnetospheric response to intervals of steady southward solar wind magnetic fields The 'direct' model would predict steady substorm-like conditions, while the 'growth phase' model suggests that a sequence of substorms would occur, whose time scale is determined by magnetospheric time constants Another important difference concerns the expected behaviour of the tail field at substorm onset In the 'direct' model the tail field may indeed often increase in strength before substorm onset, due to increasing ε and increasing solar wind ionosphere coupling However, onset is not associated with dissipation of the increased tail energy as in the 'growth phase' model Rather, since ε will generally continue to increase as it passes the critical value the tail field strength may also be expected to continue to increase Thus in the 'direct' model the tail field is expected to develop and decay in concert with ε and with the expansion and recovery of substorms, while in the 'growth phase' model the tail field is expected to grow before the substorm and generally to decay after the onset

Recently, Baker *et al*[3] have assembled a variety of observations of a large isolated substorm whose expansion phase onset occurred at about 0100 UT on 29 December 1976, which bears directly on the above question The nightside magnetosphere was monitored by two spacecraft, one directly measuring the tail magnetic field at a distance of $\sim 30 R_E$, the other detecting the changes in the energetic charged particle environment at $\sim 6\ 6\ R_E$ which directly result from the growth and decay of the tail field These data show that for ~ 1 5 hours before the substorm (determined from ground magnetic records) the tail field continuously increased in strength In itself this result is compatible with both substorm models — it can be regarded as a good example of a 'growth phase' or, in terms of the 'direct' model, it can be argued that ε was increasing during this period but remained below the critical value required for substorm onset Unfortunately, solar wind magnetic field data are not available during this interval to test this interpretation The critical observation, however, is that shortly after substorm onset the tail field started to decline, reaching initial values ~ 40 min after onset This result argues strongly in favour of the 'growth phase' model in which stored tail energy is dissipated after onset

An important objection to this conclusion may be made by asserting that while the tail field was increasing, substorms could indeed have been occurring (with ε above critical value), but at sufficiently high latitude that they were not observed at standard auroral zone observatories (about 65°–70° magnetic latitude) Baker *et al* rule out this possibility by examining data obtained from a widespread network of riometers The riometers indicate when energetic electrons are precipitating into the upper atmosphere by measuring the attenuation of cosmic radio noise at 20–40 MHz resulting from the production of D region ionization They gave no indication of substorm-associated precipitation for at least 7 hours before the observed substorm onset The result is confirmed by a 'snapshot' taken of the aurorae ~ 10 min before substorm onset near the height of the growth of the tail field by a US Air Force DMSP weather satellite, which shows the presence of quiet nightside auroral arcs, but no dynamic substorm features such as are plainly evident in the subsequent 'snapshot' taken by the same spacecraft ~ 100 min (one orbit) later

Taken together, the data presented by Baker *et al* clearly argue strongly for the 'growth phase' model of substorm onset One feature of the data does, however, strike a somewhat discordant note It is found that while the decline in the tail field is essentially complete ~ 40 min after substorm onset, the ground data and DMSP observations clearly indicate that intense substorm activity continued for at least another hour This behaviour is reminiscent of Akasofu's 'direct' model, although the suggestion cannot be directly tested in this case due to the lack of simultaneous solar wind magnetic field data It seems reasonable to suggest that, in future, thought might be given to an intermediate substorm picture in which the expansion onset is as described by the 'growth phase' model, as demonstrated by Baker *et al* 's results, but where substorm-like conditions may be maintained after the stored energy has been largely dissipated by a sufficiently large direct energy input from the solar wind □

S W H Cowley is a SERC Advanced Fellow in the Blackett Laboratory, Imperial College, Prince Consort Road, London SW7 2BZ

---

1 McPherron *J geophys Res* **75**, 5592 (1970)
2 Akasofu *Planet Space Sci* **28**, 495 (1980)
3 Baker *et al.* *J geophys Res* **86**, 8941 (1981)

T cell function: Ly phenotype and the MHC

from Elizabeth Simpson

THE lymphocytes of the immune system comprise a heterogeneous collection of subpopulations of cells performing different functions The main distinction is between B cells, which produce antibodies and can be recognized by the antibody molecules on their surfaces, and T cells, which subserve almost all the other functions of the immune system and can be distinguished from B cells by the Thy-1 antigen on their surfaces T cells themselves, however, are functionally heterogeneous, and cell surface markers reliably identifying different functional subsets have been more difficult to find

One of the earliest T lymphocyte marker systems to be described was that of the Ly markers, Ly 1, Ly 2 and Ly 3, first described by Boyse *et al*[1] The importance of these markers lay in their differential expression on T cell subsets[2,3] and it was soon shown that they could be used to distinguish between helper T cells (Ly 1^+ 2^-) and cytotoxic T cells (Ly $1^\pm$ 2^+)[4,5]

At about the same time it became evident that T cells used self major histocompatability (MHC) antigens as guides during recognition of extrinsic antigens[6] For cytotoxic T cells, the self-restricting or guiding elements were class I MHC antigens H–2 K and D in the mouse, HLA-B and -C in man, whilst for helper cells the appropriate self determinants were class II MHC antigens H–2 I in mouse, HLA-D in man[7]

Thus two sets of correlations seemed to be apparent first, cytotoxic T cell function was attributable to Ly $1^\pm$ 2^+ cells and directed towards class I and class I-associated antigens Second, helper cells were Ly 1^+ 2^- and directed towards class II or class II-associated antigens As a result of some recent experiments by Swain, however, the correlation between help and class II antigens and cytotoxicity and class I antigens has now broken down Instead, she proposes that Ly phenotype correlates primarily with the class of MHC antigen rather than with function The basis for this proposition is that, under certain con-

Elizabeth Simpson is in the Transplantation Biology section of the Clinical Research Centre, Watford Road, Harrow, Middlesex HA1 3UJ ditions, (1) T help can be found in populations of T cells responding to class I allo-H-2 antigens, and this help is mediated by Ly 1^+ 2^+ cells, and (2) cytotoxic T cells directed towards class II allo-H-2 antigens can have the Ly 1^+ $2^{\pm}$ phenotype This analysis was made using monoclonal anti-Ly 2 antibodies so that the ambiguities inherent in results from polyclonal antisera were eliminated

It had previously been reported that Ly 2 antibodies would block killing by cytotoxic T cells Swain therefore added anti-Ly 2 antibody to cultures in which T cell help was generated by an allogeneic response against allo-MHC antigens, either class I alone, class II alone or class I plus class II The induction of helper cells against class I antigen alone was blocked by anti-Ly 2 antibody In all other cases, anti-Ly 2 antibody failed to block help This result is concordant with a previous report[10] that helper T cells stimulated with class I allo-MHC antigens had the phenotype Ly 1^+ 2^+ In a second series of experiments Swain tested the effect of anti-Ly 2 antibodies on cytotoxic cells generated against either class I plus class II, class I alone or class II alone MHC alloantigens Cytotoxicity directed against class I alloantigens was inhibited whilst that against class II alloantigens was unaffected This finding is consistent with recent results of both Glasebrook and Pierres[11], using cytotoxic T cell clones directed against class II MHC antigens These clones were phenotypically Ly 1^+ 2^+ or Ly 1^+ $2^{\pm}$ (Swain's bulk culture activity was mediated by Ly 1^+ $2^{\pm}$ cells cells with a reduced expression of Ly 2 surface antigen) but the cytotoxic activity of these cloned lines could not be abrogated by Ly 2 antiserum in the assay Swain's conclusions are that T cells directed towards class II MHC antigens express Ly 1 and (at low levels) Ly 2 and can have helper or cytotoxic function neither of which is blocked by anti-Ly 2 antibody However the presence of at least some Ly 2 antigen on the surface of the cytotoxic cells distinguishes them from the normal Ly 1^+ 2^- helper cells generated in response to class II antigens She also concludes that the helper cells directed against class I antigens have a Ly 1^+ 2^+ phenotype and can be blocked by anti-Ly 2 antibody This last conclusion, however, is perhaps open to one objection it is possible that the helper activity could be mediated by cytotoxic cells making lymphokines — in particular, interleukin-2 which could substitute for helper T cells in the culture This possibility is suggested by the recent discovery of cytotoxic T cell clones directed against class I antigens and producing interleukin-2[11,12] It is also in line with recent evidence that T cell clones with either helper or cytotoxic function can elicit delayed-type hypersensitivity — a T cell-mediated response — when injected into the footpad of a mouse[13,14]

Nevertheless the unifying hypothesis put forward by Swain, that the Ly phenotype of a T cell and its MHC guiding antigen are the primary correlates, while function depends on the nature of the stimulation, is an attractive one, which puts into perspective a certain amount of apparently conflicting data recently accumulated □

---

1 Boyse, E A *et al Proc R Soc* **B178**, 175 (1968)
2 Kisielow, P *et al Nature* **253**, 219 (1975)
3 Cantor, H & Boyse, E A *J exp Med* **141**, 1376 (1975)
4 See Medawar, P B & Simpson, E *Nature* **258**, 106 (1975)
5 See Simpson, E & Beverley, P C L *Prog Immun* **3**, 206 (1977)
6 Zinhernagel, R M & Doherty, P *Nature* **251**, 547 (1974)
7 See Klein, J *et al Nature* **291**, 455 (1981)
8 Swain, S L *Proc natn Acad Sci U S A* **78**, 7101 (1981)
9 Hollander, N *et al J exp Med* **152**, 674 (1980)
10 Swain, S L *et al Eur J Immun* **11**, 175 (1981)
11 See Simpson, E *Nature* **293**, 702 (1981)
12 Widmer & Bach, F H *Nature* **294**, 750 (1981)
13 Bianchi A T J *et al Nature* **290**, 62 (1981)
14 Lim, Y L & Askonos, B A *J exp Med* **154**, 225 (1981)

Great voids in the Universe

from Joseph Silk

ONCE astronomers were content to point to the distribution of galaxies in the sky and infer that the Universe is relatively uniform in appearance More recently, the cosmic microwave background radiation, which samples the Universe at great depth, has provided dramatic confirmation of this homogeneity It is uniform to at least three-hundredths of a per cent, apart from the dipole anisotropy over 180 degrees that is associated with the motion of our Galaxy Our local region of space is obviously inhomogeneous, but this can easily be accounted for because the microwave background radiation is seen as being emitted from a very early phase in the history of the cosmos before structure fully developed One can think of this epoch as corresponding to a cosmic 'surface' or photosphere where the radiation was last scattered, somewhat analogous to the photosphere layer of the Sun below which we cannot see Before this moment of last scattering, which also coincides with the epoch of 'decoupling' of matter and radiation, the radiation was strongly scattered by ionized particles As the Universe expanded, the electrons and protons cooled eventually to combine into hydrogen atoms, which are highly transparent to the radiation, and little scattering subsequently occurred

Since then, small density fluctuations have grown, unimpeded by the drag of the radiation and driven by their own slight increase in gravitational attraction, and have gradually accreted more and more surrounding matter Such primordial fluctuations eventually formed galaxies, clusters and even superclusters of galaxies The smoothness of the radiation provides a measure of the degree of inhomogeneity of the Universe at the decoupling epoch, and a strong constraint on theories of galaxy formation

The larger the structure that is observed, the greater is the challenge to any theory for the origin of large-scale structure The recent discovery of a great void extending over some 10^6 cubic megaparsecs in the direction of the constellation Boötes has therefore attracted considerable attention (R P Kirshner, A Oemler, P L Schechter and S A Schectman *Astrophys J. Lett* **248**, L57, 1981) Several smaller regions containing no luminous galaxies were discovered during the course of galaxy surveys in the vicinities of great clusters, but the Bootes void is considerably greater than these regions It had previously been noted that galaxies surrounding the Coma cluster formed a great supercluster But if galaxies were sprinkled at random locations in space, many of them should have possessed redshifts appropriate to distances intermediate between the Coma cluster and the Virgo supercluster, of which our own Galaxy is an outlying member Instead, great gaps were found in the redshift distribution, and as redshift is a direct measure of distance, this was indicative of an almost complete absence of bright galaxies in the vast space between Coma and Virgo

The void in Boötes was discovered by looking deep into three small regions of sky separated by up to 30 degrees, and measuring the redshifts (and hence the distances) of all galaxies brighter than 16th magnitude In this way, a region of the Universe extending well beyond the Coma cluster was probed When Kirshner and his colleagues analysed the data in each of the three windows, they found a surprising coincidence — there was a similar gap in the redshift distribution in all three data sets In effect, they had surveyed three cone-shaped regions that passed through the same great hole in the distribution of galaxies The only plausible explanation was that the width of the hole spanned at least the 30 degrees they had sampled, and this led to the estimate that it encompassed a roughly cubical volume some 100 Mpc on the side

The absence of bright galaxies in such a volume can be interpreted in several ways Perhaps the region is truly devoid of matter, and is a genuine void in space Galaxy clustering permits the formation of holes, just as in some regions, great aggregations develop This explanation runs into one possible difficulty, since small inhomogeneities should have been

---

Joseph Silk is Professor of Astronomy at the University of California, Berkeley, California 94720

0028-0836/82/050367-02$01 00

present in the matter at the epoch of last scattering of the radiation The inferred amplitude of the associated radiation fluctuations from which this hole and other similar structures grew must have been at least one part in 10^3, and the fluctuations would extend over an angle of about 2° One would expect to see traces of these fluctuations in the microwave background radiation, however recent observations suggest that they are probably absent These primordial fluctuations could, in principle, be smoothed out if the intergalactic medium stayed ionized because of heating from some unknown process, which would rescatter the radiation However, the scale on which such smoothing effects could operate is limited by the distance travelled by light at a time when the density was high enough to permit rescattering of the radiation and amounts to few degrees If the implied radiation fluctuations are definitely not seen, the great void in Bootes cannot be a true hole but must contain matter in some form

This leads to the intriguing implication that there is an underlying dark component of the matter distribution One could imagine it to be distributed uniformly on scales of tens of megaparsecs Only a modest fraction need be clumped to account for the galaxy haloes and clusters which most astronomers believe are bound by such dark matter It is a sobering reflection on our role in the Universe that most of its contents are hidden from view The nature of the pervasive dark matter may, however, soon be resolved Two experiments tentatively reported in 1980 that the neutrino has a finite rest mass Neutrinos are predicted by the big bang theory to fill space in numbers comparable with those of the photons of the microwave background, and several experiments are underway to confirm this result If the neutrino mass ultimately is found to exceed even one-millionth of an electron mass, neutrinos would dominate the mass density of the Universe

Why should the voids contain neutrinos but lack the atoms from which galaxies formed? Adjacent to the voids are huge superclusters of galaxies Evidently galaxies accumulated in great sheet-like or filamentary structures, occupying a small fraction of the volume of space The galaxies could not have simply participated in the collapse of the superclusters, otherwise they would have acquired extremely high random velocities that would grossly violate observational constraints A more plausible possibility is that the matter originally collapsed while still in gaseous form into great sheet-like condensations that subsequently fragmented into galaxies Gaseous matter can radiate away the kinetic energy acquired during free-fall collapse, and so the newly formed galaxies need not develop large random motions This idea is the basis of the pancake (or blini) theory of galaxy formation advanced by Ya B Zel'dovich and his colleagues in Moscow A serious but not necessarily fatal objection to the blini theory is that all galaxies are predicted to form at a relatively late epoch Astronomers have been searching for the luminous protogalaxies predicted by this scenario, but have had little success

A final possibility is that the galaxy formation process has somehow been modified or even suppressed in the great voids between the luminous galaxies Perhaps the voids simply lack bright galaxies but contain vast numbers of faint, low luminosity galaxies or, alternatively, enormous amounts of very diffuse hot gas that has failed to condense into galaxies Existing searches have not been sufficiently sensitive to test either of these hypotheses One can only conclude, as with so many other astronomical problems, that improved observations are urgently needed □

How the malarial parasite enters the red blood cell

from R J Wilson

MALARIOLOGISTS have been thrown into a state of excitement by the expectation that the question of how the malarial parasite interacts with and deforms the erythrocyte membrane in order to gain entry may soon be answered The excitement stems from the rapid accumulation of information about the composition and structure of the erythrocyte membrane and its associated cytoskeleton, as well as the experimental identification of separate stages in the parasite's (merozoite) invasion sequence The stages can be categorized simply as recognition, attachment, junction formation and entry

Recognition

Both the resistance and the susceptibility of animal species to particular malarial parasites correlate with surface interactions between the parasite and the host red cell More specifically, Miller and his colleagues have shown there is an association between 'receptors' for malarial parasites and red cell surface antigens[1] Human erythrocytes lacking the Duffy blood group antigens are resistant to invasion by merozoites of the simian parasite *Plasmodium knowlesi* — an observation which may explain the striking absence of *P vivax* (a human malarial parasite) in West Africa where most of the population is Duffy negative Unfortunately, continuous cultivation of *P vivax* has not been accomplished *in vitro*, so it is not possible to test this hypothesis directly Nevertheless, much data has been gathered to support the hypothesis, culminating in the observation that although *P knowlesi* is, after all, able to recognize and attach to Duffy-negative human red cells, it is not able to enter them. It is the internalization process rather than recognition of an appropriate red cell that is defective

A good case can be made that on human red cells glycophorin acts as a receptor for the major human malarial parasite *P falciparum*[2] Erythrocytes (so-called En(a-) cells) deficient in glycophorin A, the main sialoglycoprotein of the human red cell membrane, are less susceptible to parasite invasion *in vitro* Furthermore, antibodies to glycophorin A block invasion, and the addition of purified glycophorin A to cultures can inhibit parasite invasion *in vitro* Erythrocytes deficient in glycophorin B (S-s-u cells), which are relatively resistant to invasion, become almost completely resistant when trypsinized so as to remove the oligosaccharide-rich N-terminal region of glycophorin A Interestingly, merozoites of *P falciparum* are unable to distinguish between erythrocytes bearing MM, NN or MN antigens As these antigenic structures are determined by the configuration of the five N-terminal amino acids of glycophorin A and the three associated oligosaccharides, the terminal region of glycophorin A seems not to be specifically involved in recognition and attachment

Attachment

Adhesion of a merozoite to an appropriate erythrocyte has no immediate consequences unless the merozoite is oriented with its apical end (which contains various micro-organelles) to the erythrocyte membrane This orientation results in a rapid spasmodic 'flinching' movement involving as much as one-third of the erythrocyte membrane[3] The membrane then appears to relax with the merozoite still attached but largely external to it Next, the parasite is drawn relatively slowly into a tightly localized invagination of the host cell membrane After entry, sealing of the pore is accompanied by irregular but widespread movements of the erythrocyte membrane and slight swelling of the host cell

The changes involved in this dynamic process take about 20 seconds to complete and can be deciphered by drawing on the static structural evidence of transmission electron microscope and freeze-fracture

R J Wilson is at the National Institute for Medical Research, The Ridgeway, Mill Hill, London NW7 1AA

studies, as well as models of the structure of the erythrocyte membrane and its associated cytoskeleton. Transmission electron micrographs indicate that the plasma membranes of the host erythrocyte and parasite do not fuse but the merozoite seems to be attached by its apical tip to the red cell membrane and contents discharged from the merozoite's rhoptry organelles may be implicated in adhesion.

Junction formation

The subsequent invasion process is characterized by the development of a discrete junctional zone — an electron-dense thickening of the erythrocyte membrane closely applied (10 nm) to the parasite's surface coat in the apical region[4]. Electron micrographs indicate that the inner leaflet of the red cell membrane bilayer is thickened and Aikawa and his colleagues[5] have demonstrated by freeze-fracture that in this zone in the protoplasmic or P-face of the membrane, there is an array of tightly packed intramembranous particles (IMPs). Both this and an earlier freeze-fracture study by McLaren *et al.*[6] concur in describing IMP-free vesicles (or sections through a tortuous membranous channel) extending from the parasite's point of attachment deep into the erythrocyte's interior. All the changes just described still occur when merozoites treated with cytochalasin B interact with erythrocytes, even though the merozoites cannot complete the invasion process. Clearly attachment, which may involve recognition sites (receptors) and the formation of an IMP-rich junction area of host cell membrane, needs to be followed by further steps to allow invasion.

One of these is the translocation of the junctional zone as a narrow ring-like structure along the longitudinal axis of the merozoite until it encloses it and forms part of the parasitophorous vacuole surrounding the internalized parasite. Aikawa *et al.*[5] have confirmed the earlier important observation by McLaren *et al.* that the P-face of the invaginated membrane, which ultimately forms the parasitophorous vacuole, has a grossly reduced number of IMPs compared with the intact membrane. Unlike Aikawa, McLaren *et al.* reported few particles in the external or E-face of the invaginated membrane.

Entry into the red cell

During internalization, the surface coat of the merozoite is modified and can no longer be detected within the invagination by electron microscopy. Earlier suggestions that the surface coat accumulates outside the invagination and is eventually sloughed off have been challenged. Aikawa *et al.* maintain that the surface coat is unaltered external to the invagination and that a process akin to capping cannot be invoked to explain the parasite's internalization.

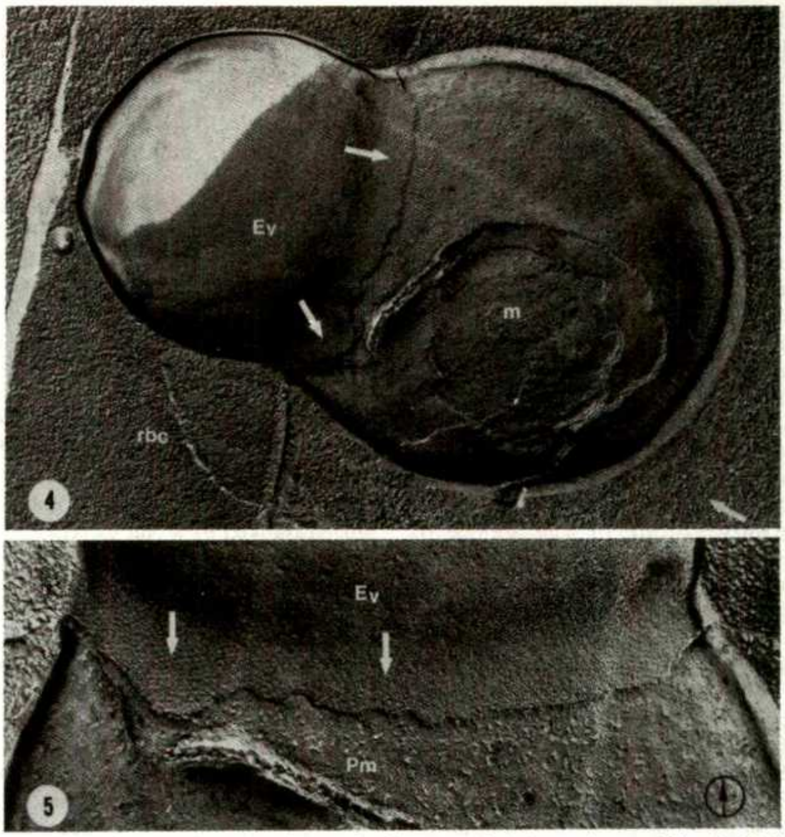

Above, freeze-fracture electron micrograph of a merozoite(m) entering a red blood cell (rbc). The arrows indicate the E-face of the erythrocyte membrane. Ev is the E-face of the vacuole membrane. x37,000. Below, high-power electron micrograph of the neck of the invagination. The E-face of the vacuole (Ev) shows few IMPs. Pm, P-face of the merozoite membrane. x68,700. (From ref. 5.)

The motive forces responsible for invagination of the parasitophorous vacuole membrane and internalization of the attached parasite can only be guessed. Membrane flow past the junctional zone might cause its apparent lateral displacement. The formation of an IMP-rich patch around the initial attachment site and the subsequent invagination of a large IMP-depleted vacuole (commensurate with about 3 per cent of the erythrocyte's surface area) suggest that peripheral membrane proteins such as spectrin and actin are dissociated from the cytosol surface of the erythrocyte membrane to allow lateral redistribution of IMPs. In intact erythrocytes there is evidence that IMPs represent the integral membrane proteins, band 3 and glycophorin. These have restricted lateral movement because of interaction with the cytoskeletal network[7]. It is still unclear whether a histidine-rich (73 per cent) parasite protein is released during invasion and acts like other polyanionic substances to disrupt the cytoskeletal network[8], and whether the IMPs aggregated in the junction zone by the malarial parasite actually correspond to erythrocyte proteins.

So far there have been few studies of the invasion of erythrocytes with modified cytoskeletons. Recently, it was reported that ovalocytic erythrocytes from Melanesions are resistant to invasion by *P. falciparum*[9]. This could be due to an alteration in the erythrocyte's cytoskeleton that reduces the physical deformability of the membrane or prevents the redistribution of IMPs required for junction formation. Alternatively, there may be a defect in the distribution of surface receptor sites. Access to the cytoskeleton for specific reactions with antibodies and other reagents has been achieved by the formation of resealed erythrocyte ghosts which retain their susceptibility to parasite invasion[10]. Preliminary studies (Dluzewski, personal communication) with resealed erythrocyte ghosts containing antibodies to spectrin indicate that parasite invasion is markedly reduced. This approach promises to help clarify the rearrangement of peripheral and integral erythrocyte membrane proteins during invasion. Clearly, many challenging problems remain to be solved at the molecular level before we can claim to understand how the major haemotropic pathogen of man makes its temporary escape from the extracellular environment by invading red cells. □

---

1. Miller, L.H., McAuliffe, F.M. & Mason, S.J. *Am. J. trop. Med. Hyg.* **26**, 204 (1977).
2. Perkings, M. *J. Cell Biol.* **90**, 563 (1981).
3. Dvorak, J.A., Miller, L.H., Whitehouse, W.C. & Shiroishi, T. *Science* **187**, 748 (1975).
4. Aikawa, M., Miller, L.H., Johnson, J. & Rabbege, J. *J. Cell Biol.* **77**, 72 (1978).
5. Aikawa, M., Miller, L.H., Rabbege, J.R. & Epstein, N. *J. Cell Biol.* **91**, 55 (1981).
6. McLaren, D.J., Bannister, L.H., Trigg, P.I. & Butcher, G.A. *Parasitology* **79**, 125 (1979).
7. Fowler, V. & Branton, D. *Nature* **268**, 23 (1977).
8. Kilejian, A. *J. biol. Chem.* **249**, 4650 (1974).
9. Kidson, C., Lamont, G., Saul, A. & Nurse, G.T. *Proc. natn. Acad. Sci. U.S.A.* **78**, 5829 (1981).
10. Dluzewski, A.R., Rangachari, K., Wilson, R.J.M. & Gratzer, W.B. *Br. J. Haemat.* **49**, 97 (1981).

The mystery of the mouse α-globin pseudogene

from R.A. Flavell

THE chromosomes of multicellular organisms seem to be full of a wide variety of DNA sequences which are of no apparent use to their hosts. Some of these sequences, termed pseudogenes, are defective copies of functional genes. The laboratory mouse has two such crippled genes — the α-globin pseudogenes. However, one of them, $\alpha\psi3$, is different from other pseudogenes described to date. It has precisely (to the nucleotide) lost the intervening sequences (or introns) which are present in the functional α-globin genes[1,2]. It is not known why introns are commonly found in the genes of vertebrates — they are removed from the primary RNA transcript during production of a functional messenger RNA and it seems a complicated method of encoding genetic information when intronless genes work well in prokaryotes (for speculations on this subject see ref.3). But whatever the reasons why the insertions are present in the normal α-globin genes; the question of how $\alpha\psi3$ lost its introns is a riddle of great interest.

One possible origin of $\alpha\psi3$ is that an intronless α-globin mRNA altered a duplicated normal α-globin gene to an exact copy of itself by gene conversion[1]. However, although gene conversion between homologous DNA sequences is well characterized, gene conversion by a RNA has not been seen. Another, perhaps more plausible possibility is that $\alpha\psi3$ somehow derived from the copying of an α-globin mRNA into a DNA molecule by the retrovirus-encoded enzyme reverse transcriptase. Such a DNA might also alter a duplicate α-globin gene by gene conversion.

The most exciting proposal is, however, that an α-globin mRNA actually became incorporated into the RNA genome of a retrovirus. Retroviruses are equally at home as either RNA-containing viruses or DNA copies of this RNA (called proviruses) which are integrated into the host cell DNA. Therefore, provided that one accepts that an α-globin mRNA could gain entry into the retrovirus genome, it is only necessary to invoke the normal infectious cycle of the virus to explain the presence of $\alpha\psi3$. Retroviruses are certainly capable of incorporating cellular genes into their RNA genomes[4] and, significantly, comparisons between the cellular and viral genes show that the RNA copies of these cellular genes have sometimes lost the introns which characterize the parent genes[5]. So far the only genes known to have been 'captured' by a retrovirus are those conferring an easily scored phenotype on infected cells (tumorigenic transformation), but it is reasonable to suppose that a retrovirus might incorporate any piece of the cells' transcribed DNA, such as the α-globin gene. Of course, such an event would have to occur in the germ line of the mouse to survive the eventual death of its host.

Such a model demands that the newly integrated α-globin gene be accompanied by a retrovirus provirus. In this issue of *Nature* (p.426), Lueders *et al.* describe their analysis of the flanking DNA of both α-globin pseudogenes and the α-globin genes of mouse. They show that $\alpha\psi3$ is indeed flanked by a pair of retrovirus-like elements whereas the other α-globin genes are not. The elements, which are present in about 1,000 copies per mouse genome, encode a class of virus-like entities called intracisternal type A particles (IAPs) which share close similarities with the commonly studied type B and type C retroviruses. Unfortunately, it is by no means clear whether IAP elements are responsible for the creation of $\alpha\psi3$, as the pseudogene is flanked on either side by about 4 kilobases of cellular DNA before the IAP elements are reached, whereas the model demands that $\alpha\psi3$ be actually connected to the retroviral sequences. It is at this point that the real problem in determining the origin of this pseudogene raises its head.

The pseudogene emerged roughly 20 million years ago, since when there may have been numerous alterations to the gene and its immediate environment, perhaps because $\alpha\psi3$ was probably superfluous to the metabolic requirements of its host. Deletion or insertion of other DNA sequences may have masked its original configuration. The authors point out that a way around this problem may be to study the same pseudogene in related mouse species and in the rat. By looking for alterations which have cropped up during the evolution of these species, the original configuration of $\alpha\psi3$ may be revealed. Two of the authors are accumulating more data on mouse genes flanked by other IAP elements which should show whether the $\alpha\psi3$–IAP complex is particularly unusual. Doubtless, the sequences between the pseudogene and the IAP elements are also being scrutinized for clues to the origin of the arrangement.

If IAPs do turn out to have a role in the creation of the α-globin pseudogene, could such a phenomenon affect genome evolution by inducing the migration of functional DNA sequences to new sites? Or are we looking at a way of creating merely new 'junk' DNA? □

---

1. Nishioka, Y., Leder, A. & Leder, P. *Proc. natn. Acad. Sci. U.S.A.* **77**, 2806 (1980).
2. Vanin, E.F., Goldberg, G.I., Tucker, P.W. & Smithies, O. *Nature* **286**, 222 (1980).
3. Gilbert, W. *Nature* **271**, 501 (1978).
4. Bishop, J.M. *Cell* **23**, 5 (1981).
5. Goff, S.P., Gilboa, E., Witte, O.N. & Baltimore, D. *Cell* **22**, 777 (1980).

R.A. Flavell is at the Imperial Cancer Research Fund Laboratories, Burton Hole Lane, London NW7 1AD.

100 years ago

THE INDIAN DARTER

The Darters form a very peculiar type of birds of the order Steganopodes, allied to the Cormorants in structure, but very Heron-like in gait and gesture. The Darter in its normal position sits erect upon a branch or stump overlooking the water. When proceeding to fish it dives head foremost into the stream, and swimming entirely under water, transfixes its finny prey with the rapidity of lightning. Emerging from the water with the fish speared upon its long slender beak, the Darter chucks the fish into the air, and catching it head foremost with unerring aim, swallows it whole.

The Indian Darter

The Darters usually exhibited in the Royal Society's Gardens are of the South American species (*Plotus anhinga*), but in 1878 an example of the African form Le Vaillant's Darter (*Plotus levaillanti*)[1] was received. In April last an example of a third species of this genus — the Indian Darter (*Plotus melangaster*) was obtained in exchange from the Zoological Gardens of Calcutta.

"In a state of nature," as Dr. Jerden tells us, "this beautiful diver is found throughout all India, Ceylon, Burmah, and Malayana. It is exceedingly numerous in some parts of the country, especially in Bengal; hundreds are often to be seen on a single jheel. They hunt singly in general, or in scattered parties, but often roost in company, both at night and in the middle of the day, when numbers may be seen perched on the trees overhanging some tank or river. They float low on the water, often with nothing but the head and neck visible, and swim and dive with rapidity. After feeding for some time they perch on the bough of a tree or on a pole or stone, and spread their wings out to dry as the Cormorants do."

From *Nature* **25**, 24 January, 297, 1882.

0028-0836/82/050370-01$01.00

REVIEW ARTICLE

Grain alignment in the galactic magnetic field

Paul E. Johnson

Wyoming Infrared Observatory, Department of Physics and Astronomy, University of Wyoming, Laramie, Wyoming 82071, USA

The linear polarization of light observed in many distant stars, presumably an effect of absorption of starlight by elongated interstellar dust grains, provides a means of mapping the magnetic field lines in our own Galaxy as well as probing the properties of the intervening dust. Processes for grain alignment in the galactic magnetic field are reviewed: evidence is examined for grains being spun up to extremely high (10^9 Hz) angular frequencies by the recoil of hydrogen recombination on grains, as an essential part of the alignment process. Grain alignment would then be inhibited in regions of grain growth and would be most effective where grain growth is inhibited or reaches saturation.

WHEN the light from stars close to the galactic plane is analysed, it is found to be both reddened and polarized, with the angle of polarization most often lying in the galactic plane. Both are presumed to be effects of absorption of starlight by a medium containing clouds of elongated dust grains (accompanied by neutral hydrogen), spinning so that their major axes tend to be transverse to the plane of the galaxy. The starlight transmitted through such a medium would appear reddened and linearly polarized in a direction parallel to the galactic plane.

The typical interstellar grain is usually found in diffuse clouds composed of a relatively high density of dust ($\sim 8\times10^{-11}$ grains cm^{-3}) and neutral hydrogen gas ($\sim$20 atoms cm^{-3})[1]. Inside such denser clouds grains are shielded from the destructive effects of stellar UV radiation and can therefore grow by the accretion of volatiles such as H_2O, CH_4 and NH_3. Grain cores are expected to be composed of more refractory materials, such as silicates, SiC and graphite. The observed optical properties of grains indicate overall grain diameters of 0.02 to 0.15 μm (ref. 2).

Martin[3] pointed out that a rotating, charged grain will precess about a magnetic field, regardless of the mechanism aligning the grain. The result of such a precession is that, on a time average, the distribution of grain axes will be symmetric about the magnetic field, if the period of precession is adequately short. Dolginov and Mytrophanov[4] suggested that the Barnett effect, the spontaneous alignment of atomic dipoles in a rotating body, will produce a rapid precession in a magnetic field, even for an uncharged grain. For physical conditions in the interstellar medium the period of either type of precession is much shorter than the time constant for any previously proposed alignment mechanism. Therefore, the polarization of starlight should either be parallel or perpendicular to the magnetic field.

Figure 1 shows that the most orderly regions of polarization are those near the galactic plane exhibiting a polarization parallel to that plane. Therefore, it is reasonable to conclude that the general galactic magnetic field probably runs either parallel or perpendicular to the galactic plane[5].

The increase in the amount of Faraday rotation (which gives $n_e B_\parallel$ integrated along the line of sight, where n_e is the electron number density in the interstellar medium and $B_\parallel$ is the component of the magnetic field directed along the line of sight) with decrease in galactic latitude, as measured in several hundred extragalactic radio sources, is consistent with radiative transfer through a general galactic magnetic field[6]. Uncertain-

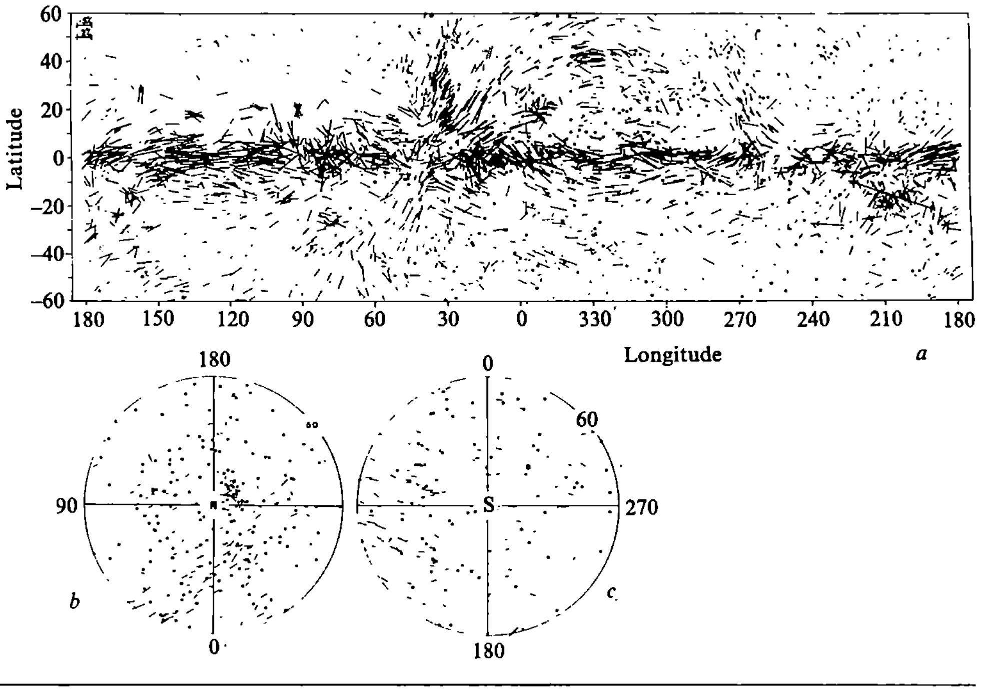

Fig. 1 Interstellar polarization. The direction and degree of linear polarization of nearly 7,000 stars is shown with respect to galactic coordinates. The length of each line is proportional to the linear polarization. Stars with a polarization <0.08% are represented by small circles. (After ref. 5. With the permission of the Royal Astronomical Society.)

0028-0836/82/050371—05$01.00

ties in the electron density and variations in the magnetic field, B, over long pathlengths prevent an accurate determination of the galactic magnetic field from these data[1]. Measurement of the dispersion of pulsar signals (which gives n_e integrated along the line of sight) and their Faraday rotation allows an accurate determination of both the electron density and magnetic field in the solar neighbourhood. The uniform component of the magnetic field in the solar neighbourhood has been measured at $2.2 \pm 0.4 \times 10^{-6}$ G in this way[7]. The variation of the magnetic field with galactic longitude indicates that B runs roughly parallel to the galactic plane. The polarization of starlight has been one of the chief tools with which to investigate the large-scale structure of the galactic magnetic field. I review here the two most viable theories of grain alignment and assess the evidence bearing on them.

Davis–Greenstein grain alignment

It has been generally assumed that interstellar grains are aligned with respect to the interstellar magnetic field by paramagnetic relaxation of thermally rotating grains, as originally proposed by Davis and Greenstein[8] (DG alignment). In this process a paramagnetic grain is set spinning by impacts with the interstellar gas. When such a grain is immersed in an external magnetic field an internal field is induced such that its direction is coincident with the external field. It is impossible for the alignment of the internal and external fields to be achieved instantaneously. Because the grain is spinning there is always a slight misalignment between the two fields. The external field attempts to enforce alignment with a drag torque opposing the angular velocity of the grain about an axis perpendicular to the direction of the magnetic field. This results in grain alignment. DG alignment of aspherical particles was modelled by Purcell[9] and Purcell and Spitzer[10] using a Monte Carlo analysis of the entire process. Their analyses confirmed the theoretical results of Jones and Spitzer[11] that alignment of grains adequate to explain the interstellar polarization of starlight would require a magnetic field $>10^{-5}$ G, much larger than what has been found empirically.

To achieve effective DG alignment, the collisional damping time of grains (due to gas–grain collisions) t_d, must be less than or equal to the paramagnetic relaxation time (the time scale for alignment) t_r (refs 10–12). In a H I cloud one must have

$$\delta \equiv \frac{t_d}{t_r} \approx \frac{B^2 \chi''}{\omega n_H m_H \bar{v}_H a} \leqslant 1 \qquad (1)$$

where χ'' is the complex part of the magnetic susceptibility of the grain material, ω the angular frequency of the grain, n_H the number density of hydrogen atoms, $\bar{v}_H$ the r.m.s. velocity of hydrogen atoms, and a the mean radius of an interstellar grain. For the conditions in a 'typical' H I cloud (the neutral hydrogen density, $n_H = 20$ cm^{-3}, $T_g = 80$ K, $T_d = 15$ K, and paramagnetic grains with $a = 0.3$ μm (ref. 1)) B must be greater than 8×10^{-6} G. So large a magnetic field in H I clouds is inconsistent with the upper limit of 3×10^{-6} G from Zeeman measurements[13].

This problem can be circumvented by assuming that the grains responsible for interstellar polarization are weakly ferromagnetic or superparamagnetic. The latter occurs when isolated clusters of iron atoms, less than 100 Å in size, behave as single, giant magnetic moments[14]. Duley[15] has suggested the existence of weak ferromagnetism or superparamagnetism in grains of mixed MgO FeO SiO. According to this theory, if the cores (100–200 Å in size) of 0.1–0.3 μm grains are composed of such material and covered with ice, then they can be aligned in a field of only 1×10^{-6} G. If the cores are weakly ferromagnetic, relaxation is caused by the spin-lattice relaxation of paramagnetic spins in a mantle of icy material. If, on the other hand, the grains are superparamagnetic, relaxation proceeds as in the case of paramagnetic relaxation, but with fields $<1 \times 10^{-6}$ G. However, it is not certain that this latter process is effective in cores 100–200 Å in size.

In any case, such mixed oxide grains would reproduce the spectral resonances at 3.1 μm and 10 μm seen in such sources as the Becklin–Neugebauer Object (BN) in Orion[16]. Other ferromagnetic materials, such as magnetite[17], used in explaining interstellar polarization cannot easily reproduce these spectral features.

Most other alignment mechanisms are greatly inferior to DG in explaining grain alignment in the galactic magnetic field[14]. For example, Gold's streaming mechanism (in which grains present their smallest cross-section to a stream of rapidly moving gas) falls short of DG by an order of magnitude in explaining the general interstellar polarization[9].

Purcell pinwheel alignment

Purcell's[18,19] pinwheel alignment mechanism seems to be viable for the physical conditions in the interstellar medium. In this theory, a grain spins-up to high angular velocities when inhomogeneities on the surface of the grain result in a mean torque with respect to an axis fixed in the grain. Such torques arise, for example, when hydrogen atoms collide with a grain and stick to it, diffusing over the surface of the grain until they combine with another hydrogen atom at an 'active' site. Hollenbach and Salpeter[20] suggest that a limited number of active sites exist on a grain and are simple impurities or surface defects that serve to catalyse the formation of molecular hydrogen. Such a molecule is subsequently ejected with a linear momentum p_0, resulting in a relatively large torque being imparted to the grain. For ν active sites randomly distributed over the surface of a grain, the mean torque applied by such a collision is about $ap_0/\nu^{1/2}$. A torque can also be the result of a variation in the photoelectric emissivity or the accommodation coefficient (the fraction of gas atom kinetic energy transferred to the grain in a gas–grain collision) over the surface of a grain.

All of these processes will produce relatively strong systematic torques, leading to rotational frequencies as high as 10^9 s^{-1}, corresponding to a rotational velocity, (ωa), of 10^4 cm s^{-1} for a grain of radius 0.1 μm. In comparison, the mean velocity of a gas atom for $T_g = 80$ K is 1.3×10^5 cm s^{-1}. Purcell[19] shows that in the presence of dissipative processes, such as anisotropic elasticity, the grain's angular momentum direction will lie along the principal moment of inertia. Note that almost nothing is known about the shape of grains other than that elongated grains are required to generate the observed polarization of starlight.

Of the above processes, the hydrogen recombination pinwheel should be the most effective in the interstellar medium by several orders of magnitude where hydrogen is mainly in the atomic form.

Effect of grain resurfacing on alignment

The Purcell pinwheel mechanism possesses quantitative difficulties in explaining grain alignment[1,19,21]. These problems arise because we previously assumed that the net torque due to anisotropies on the surface of a grain does not change with time. Here only the case of hydrogen recombination driving the grains suprathermally, the strongest of the processes suggested by Purcell, will be considered, although the results are quite general. Both the theory of grain growth and the measurement of the increase of λ_{max}, the wavelength of maximum linear polarization, with distance into a dark cloud indicate that grains are growing[1]. Therefore, over a period of time, t_L, old active sites will be covered up, leaving new ones. Whether or not the locations of the new sites are correlated with those of the old sites is unknown. It is reasonable to assume that the new torque on a grain would be entirely altered when the radius of a grain is increased by a single monomolecular layer.

Spitzer[1] gives the rate of increase of the radius of a grain due to the accretion of atoms, excluding H and the noble gases, with cosmic composition as

$$\frac{da}{dt} \cong 2 \times 10^{-13} \xi \text{ cm yr}^{-1} \qquad (2)$$

where ξ is the effective sticking coefficient, $T_g = 80$ K, and

$n_H = 20\ \text{cm}^{-3}$. Most growth in dust clouds should be due to the accretion of oxygen and the resulting formation of ice. In 2.4×10^5 yr, the collisional damping time in these conditions, the radius of a grain changes by about 6×10^{-8} cm, exceeding the thickness of a monomolecular layer.

Just as serious as grain growth is the constraint put on Purcell alignment by grain denudation due to UV radiation in unshielded nebulae as well as in dust clouds where there has been a burst of UV radiation during star formation. Such denudation would resurface grains just as effectively as grain growth.

Purcell[19] and Spitzer and McGlynn[21] treat the effect of the alteration of a grain surface on pinwheel alignment in some detail. Let us assume that after a time t_L the torque on a grain, in body coordinates, will have been completely altered. Unfortunately, the effectiveness of paramagnetic relaxation on grain alignment depends critically on t_L, which is uncertain at best. If $t_L \gg t_r$ grains will spin-up to an equilibrium angular velocity in a time t_d, and will then become aligned. However, if t_L is small, the torque about the principal moment of inertia will occasionally change sign and the angular velocity of the grain about the axis will 'cross-over' through zero. The extent to which alignment is affected depends on the magnitude of the change in grain orientation during cross-over and the cross-over frequency. Purcell[19] shows that the mean time between cross-overs is t_x, where

$$t_x = 1.3(t_L + 0.6t_m) \qquad (3)$$

t_m is the time required for a grain to collide with a mass of gas equal to its own mass. If $t_x \sim t_m$ and a grain loses all memory of its orientation during a cross-over, then the Purcell mechanism falls short by at least an order of magnitude in explaining the observed polarization of starlight.

Spitzer and McGlynn[21] used a Monte-Carlo analysis to determine how much orientation a grain loses during cross-over. They were only able to strengthen marginally the ability of the Purcell mechanism to align grains. Some of the physical parameters affecting their model (such as grain size and density) are rather poorly known, however, so that the outcome is not certain.

There are at least two sets of conditions in which pinwheel alignment is still viable. If the grains are superparamagnetic or ferromagnetic χ'' can be larger by up to a factor of 10^5 (ref. 1). Then (t_m/t_r) is small enough so that appreciable alignment is likely, even with fields of 10^{-7} G. Another possibility is the inhibition of grain resurfacing.

Grain growth and destruction in the interstellar medium

Observations of the wavelength dependence of the polarization of the stars obscured by the R Coronae Australis dark cloud has led Vrba *et al.*[22] to conclude that there is an evolution of grain size distribution with age and changing environment (Fig. 2). R CrA is a young cloud ($\leq 10^6$ yr)[23] with its high density and low internal stellar luminosity favouring the formation of large grains. The large variation in grain size (as reflected in the large dispersion in λ_{max}) is likely to be caused by individual grains being formed and growing in different conditions in different parts of the cloud. Stars near the edge of the cloud, for example, would be less shielded than grains in the interior and would therefore experience a slower rate of growth and a smaller mean size.

The α Persei cluster (an analogue of the R CrA cloud with an age of 2×10^7 yr) has a smaller mean grain size, close to that of the general interstellar medium[22]. Coyne *et al.*[24] show that in $\sim 10^7$ yr large grains can be destroyed by photodesorption during a phase of extremely luminous pre-main-sequence evolution, which the α Per cluster has apparently experienced and to which the R CrA cloud has not yet evolved. Stellar winds and radiation pressure may have dispersed large grains, and, of course, UV radiation would be expected to dissipate the mantles of grains, thus reducing their size.

We will assume that grains in the diffuse interstellar medium are cores denuded of their mantles and are strongly growth inhibited by UV desorption. Such grains, almost regardless of their composition, will experience efficient alignment by the Purcell pinwheel alignment process due to the non-existence of an efficient grain resurfacing mechanism in these conditions.

The rate at which an interstellar grain accretes material by gas–grain collisions is given by $\pi a^2 n_a \bar{v}_a \xi$, where n_a is the number density of atoms in the gas other than hydrogen and the noble gases and $\bar{v}_a$ is the r.m.s. velocity of these atoms. The rate at which atoms are desorbed from a grain is given by $\pi a^2 Y_{pd} G_0 \exp(-\tau_{uv})$, where Y_{pd} is the photodesorption yield of a grain, G_0 is the integrated diffuse interstellar photon flux between 912 (the Lyman limit) and 1,900 Å (longward of which photodesorption is rather ineffective[25]), and τ_{uv} is the effective extinction in the UV to the region under consideration[25]. One would expect that even if there is no net grain growth, accretion and photodesorption will redistribute active sites more rapidly

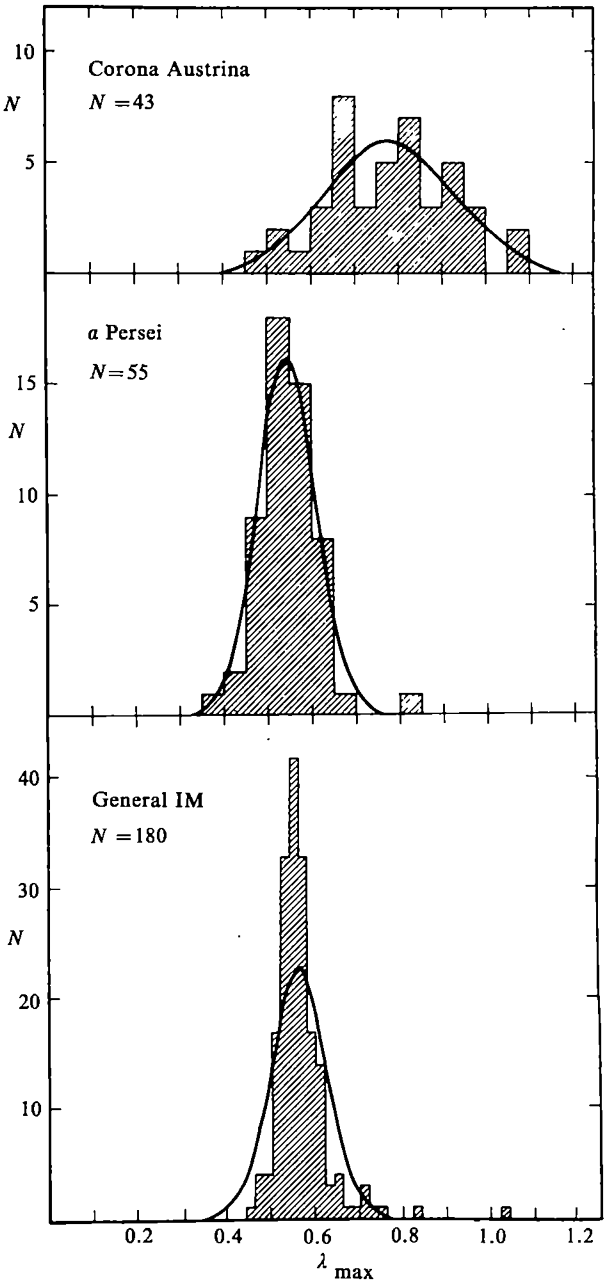

Fig. 2 Histograms of the grain size distribution (as measured by the wavelength of maximum polarization, λ_{max}, for an obscured source) for the diffuse interstellar medium (IM) and the α Per and R CrA dark clouds. The solid curves represent normal distributions fitted to the data. (After ref. 22. With the permission of the University of Chicago Press.)

than accretion alone. For the activation of the Purcell pinwheel mechanism by photodesorption it is then necessary that grains are completely stripped of volatiles, or

$$n_a \bar{v}_a \xi < Y_{pd} G_0 \exp(-\tau_{uv}) \qquad (4)$$

In the interstellar medium nominally we have $\xi \cong 1$, $Y_{pd} \sim 5 \times 10^{-3}$, $G_0 \sim 1.7 \times 10^8$ cm^{-2} s^{-1}, and $\bar{v}_a \sim 8.0 \times 10^3$ cm s^{-1} (corresponding to the r.m.s. velocity of oxygen atoms at 80 K)[25]. Therefore $n_a \exp(\tau_{uv}) \leqslant 8 \times 10^4$ cm^{-3} in order for grain resurfacing to be effectively halted[25]. This criterion would in general be met in the diffuse interstellar medium, but not necessarily in the interiors of dense molecular clouds.

In the above model, grains shielded from photodesorption in the dense interiors of dark clouds would be less susceptible to alignment than unshielded grains. Indeed, it has been observed in both the ρ Ophiuchus dark cloud[26] and in R CrA (ref. 22) that the polarization efficiency of grains (as measured by p/A_v where p is the linear polarization of an obscured object and A_v is its visual extinction) decreases dramatically with the mean size of grains in a particular region (as measured by λ_{max} and the ratio of total to selective extinction, R). This may be due to the anti-correlation between grain alignment and rate of growth in the Purcell model. Such results are also consistent with DG alignment, which is most effective with small particles.

The major difficulty with our model is the efficient grain alignment in regions of dense clouds having large λ_{max}, such as the Orion Molecular Cloud (OMC-1) (ref. 27) and M17 (ref. 28). I suggest that the solution to this apparent dilemma is to dissociate large λ_{max} from a high growth rate. The rate at which the radii of grains can grow due to atomic accretion, in the absence of photodesorption, is given by equation (2). It then follows that the time scale for the adsorption of a molecule or atom by a grain is $5 \times 10^{15}\ a/T_g^{1/2} n_a$ yr (refs 22 and 29), for a in cm, T in K, and n_a in cm^{-3}. The shortness of this time scale (of the order of 10^6 yr for a typical dark cloud) implies two things:

(1) In the regions of dark clouds adequately shielded from UV radiation, grain growth due to molecular accretion will rapidly saturate. The saturation of R in the ρ Oph cloud with $A_v \gtrsim 3.5$ has been shown to be consistent with all heavy elements having been accreted onto grain mantles[30–32]. The correlation between the column density of ^{13}CO versus A_v in the dark cloud L134 up to $A_v \sim 3$–5 can be interpreted as being caused by all C and O being deposited on grain mantles when $A_v \gtrsim 4$ (refs 30, 33).

(2) Grain growth in dense clouds, as indicated by the increase in λ_{max} with extinction is probably caused by coagulation of individual grains and not by accretion of atoms and molecules onto grain surfaces[34]. Accretion can only increase the mean grain size by a factor of ~2, corresponding to the exhaustion of all condensable species in the gas[35].

In these conditions, I suggest that the time scale for grain–grain coagulation from systematic collisions between grains, when acted on by an external force such as gravity or radiation pressure[22,29] is, the limit to spin-up (due to resurfacing) through the Purcell pinwheel alignment mechanism. This is given by

$$t_{gg} \cong 8 \times 10^{17}\ a/n_d V_d\ (\text{yr}) \qquad (5)$$

V_d is the drift velocity of grains with respect to the gas and n_d is the number density of dust grains. V_d, a and n_d are in cgs units. For the inner regions of OMC-1 we estimate t_{gg} (using the formulae in refs 22, 29) at ~10^9 yr. This limit is weak enough to place no constraint whatsoever on Purcell alignment. For Purcell alignment to be effective the alignment time, t_r, must be significantly smaller than the time scale for resurfacing, t_{gg} in this case, or

$$\left(\frac{t_r}{t_{gg}}\right) = 4 \times 10^{-14} \frac{a \rho T_d n_d V_d}{B^2} \ll 1 \qquad (6)$$

with ρ the grain density. For our typical H I cloud with $\rho = 1$ g cm^{-3}, $n_d = 7.6 \times 10^{-11}$ cm^{-3}, and $B = 2.5 \times 10^{-6}$ G we have $t_r/t_{gg} \cong 4 \times 10^{-11}\ V_d$ which is much less than unity for any reasonable choice of V_d.

Grain alignment in star formation regions

Until recently there has been no empirical evidence for pinwheel alignment. Johnson *et al.*[27] have demonstrated the quantitative inadequacies of DG alignment in the OMC-1 quite independent of grain composition. The high density of the nebula means that the temperatures of the dust and molecular gas are expected to be tightly coupled. This has been seen in H$_2$CO maps[36] and 91-μm photometry[37] of the nebula (indicating the temperature of the gas and dust, respectively). DG alignment is driven by differences in the dust and gas temperatures and therefore cannot operate in a region where $T_d \cong T_g$ (ref. 38). Johnson *et al.* hypothesize that grain alignment in OMC-1 is due to pinwheeling, the only viable alternative to DG alignment. The atomic hydrogen abundance necessary to excite hydrogen recombination pinwheeling would be provided by atomic hydrogen left in the wake of a shock propagating through the nebula. Evidence for a shock in OMC-1 has been found[39] from a broad velocity feature ($\Delta v \cong 49$ km s^{-1}) in CO and detection of H$_2$ vibrational emission. Alignment would occur in OMC-1 with a relatively weak (milligauss) magnetic field.

Dyck and Capps[40] have measured the IR linear polarization of 15 compact sources associated with H II regions and molecular clouds. They find a clear correlation such that strong interstellar polarization is associated with the youngest prestellar objects. Dyck and Capps hypothesize that as these objects evolve, the conditions for producing polarization can no longer be maintained. This is the situation that shock-induced grain alignment would predict. Strong shocks in molecular clouds, due to stellar winds accompanying star formation, would produce grain alignment (and thus linear polarization) in the same way that Johnson *et al.*[27] suggest for OMC-1. As prestellar objects evolve onto the main sequence and produce H II regions, shocks in the surrounding molecular cloud will dissipate resulting in the decay of linear polarization of sources embedded in the cloud as all of the atomic hydrogen is consumed. Another possibility is that as a number of luminous pre-main-sequence stars 'turn-on' in the dust cloud, resurfacing of grains by photodesorption begins, thus inhibiting grain alignment.

Conclusions

Both the Purcell alignment mechanism and DG alignment can quantitatively explain interstellar polarization. However, both theories have apparent drawbacks. DG alignment requires invoking ferromagnetic or superparamagnetic grains, thus placing rather stringent requirements on grain composition. DG alignment also seems to fail to explain grain alignment in OMC-1. Although the Purcell theory seems to be equally viable for almost any grain composition, it does require rather small grain resurfacing rates.

In any case, it seems that the typical interstellar grain is suprathermally rotating, and any grain alignment theory must deal with this. The Purcell mechanism would predict that grain alignment is most effective where: (1) grain growth has been inhibited either due to UV photodesorption or depletion of accretable material; and (2) there is a significant atomic hydrogen abundance or an adequate ambient radiation field.

These two conditions seem to be met not only in the unshielded regions exterior to dark clouds but also in regions where pre-main-sequence stars are undergoing a burst of luminosity. Significant progress can be made in this field by checking the predictions above against a detailed set of measurements of the polarization of sources found in or behind a number of clouds exhibiting a wide variety of conditions.

I thank Professors E. M. Purcell and D. W. Smith, and Drs D. Wickramasinghe and R. Wolstencroft for comments. During part of the research I was supported through a fellowship from SERC. Funds were also provided by the NSF through grants AST 76-24242 and AST 77-3187.

1. Spitzer, L. in *Physical Processes in the Interstellar Medium* (Wiley, New York, 1978).
2. Gilra, D. P. *Nature* **229,** 237 (1971).
3. Martin, P. G. *Mon. Not. R. astr. Soc.* **153,** 279 (1971).
4. Dolginov, A. Z. & Mytrophanov, I. G. *Astr. Astrophys.* **69,** 421 (1978).
5. Mathewson, D. S. & Ford, V. L. *Mem. R. astr. Soc.* **74,** 139 (1970).
6. Gardner, F. F., Morris, D. & Whiteoak, J. B. *Aust. J. Phys.* **22,** 813 (1969).
7. Manchester, R. N. *Astrophys. J.* **188,** 637 (1974).
8. Davis, L. & Greenstein, J. L. *Astrophys. J.* **114,** 206 (1951).
9. Purcell, E. M. *Physica* **41,** 100 (1969).
10. Purcell, E. M. & Spitzer, L. *Astrophys. J.* **167,** 31 (1971).
11. Jones, R. V. & Spitzer, L. *Astrophys. J.* **147,** 943 (1967).
12. Cugnon, P. *Astr. Astrophys.* **12,** 398 (1971).
13. Verschuur, G. L. *IAU Symp.* No. 39 (1969).
14. Aannestad, Per A. & Purcell, E. M. *A. Rev. Astr. Astrophys.* **11,** 309 (1973).
15. Duley, W. W. *Astrophys. J. Lett.* **219,** L129 (1978).
16. Millar, T. J. & Duley, W. W. *Mon. Not. R. astr. Soc.* **183,** 177 (1978).
17. Shapiro, P. R. *Astrophys J.* **201,** 151 (1975).
18. Purcell, E. M. in *The Dusty Universe* (eds Field, G. B. & Cameron, A. G. W.) (Watson, New York, 1975).
19. Purcell, E. M. *Astrophys. J.* **231,** 404 (1979).
20. Hollenbach, D. & Salpeter, E. E. *Astrophys. J.* **163,** 155 (1971).
21. Spitzer, L. & McGlynn, T. A. *Astrophys. J.* **231,** 417 (1979).
22. Vrba, F., Coyne, G. V. & Tapia, S. *Astrophys. J.* **243,** 489 (1981).
23. Knacke, R. F., Strom, S. E., Strom, K. M., Young, E. & Kunkel, W. *Astrophys. J.* **179,** 847 (1973).
24. Coyne, G. V., Tapia, S. & Vrba, F. *Astr. J.* **84,** 356 (1979).
25. Barlow, M. J. *Mon. Not. R. astr. Soc.* **183,** 397 (1978).
26. Wilking, B. A., Lebofsky, M. J., Martin, P. G., Rieke, G. H. & Kemp, J. C. *Astrophys. J.* **235,** 905 (1980).
27. Johnson, P. E., Rieke, G. H., Lebofsky, M. J. & Kemp, J. C. *Astrophys. J.* **245,** 871 (1981).
28. Schultz, A., Lenzen, R., Schmidt, Th. & Proetel, K. *Astr. Astrophys.* **95,** 94 (1981).
29. Scalo, J. M. *Astr. Astrophys.* **55,** 253 (1977).
30. Barlow, M. J. *Mon. Not. R. astr. Soc.* **183,** 417 (1978).
31. Carrasco, L., Strom, S. E. & Strom, K. M. *Astrophys. J.* **182,** 95 (1973).
32. Whittet, D. C. B. & van Breda, I. G. *Astrophys. Space Sci.* **38,** L3 (1975).
33. Tucker, K. D., Dickman, R. L., Encrenaz, P. J. & Kutner, M. L. *Astrophys. J.* **210,** 679 (1976).
34. Jura, M. *Astrophys. J.* **235,** 63 (1980).
35. Mezaros, P. *Astrophys. J.* **180,** 381 (1973).
36. Evans, N. J., II, Zuckerman, B., Sato, T. & Morris, G. *Astrophys. J.* **199,** 383 (1975).
37. Harper, D. A. *Astrophys. J.* **192,** 557 (1974).
38. Greenberg, J. M. in *Nebulae and Interstellar Matter* (eds Middlehurst, B. M. & Aller, L. H.) (University of Chicago Press, 1968).
39. Scoville, N. Z. in *Giant Molecular Clouds in the Galaxy* (eds Solomon, P. M. & Edmunds, M. G.) (Pergamon, Oxford, 1980).
40. Dyck, H. M. & Capps, R. W. *Astrophys. J. Lett.* **220,** L49 (1978).

ARTICLES

Ultrasonic borehole televiewer investigation of oceanic crustal layer 2A, Costa Rica Rift

Mark D. Zoback

United States Geological Survey, Menlo Park, California 94025, USA

Roger N. Anderson

Lamont-Doherty Geological Observatory, and Department of Geological Sciences, Columbia University, Palisades, New York 10964, USA

In situ *lithostratigraphy and the distribution of fracture and void zones in oceanic layer 2A were examined with an ultrasonic borehole televiewer at IPOD sites 501 and 504B on the south flank of the Costa Rica Rift. These records indicate a decrease in the size of basalt pillows with depth and a corresponding increase in fracture and void density. The observed increase in P-wave velocity with depth in this hole, as layer 2A merges into 2B, is best explained by an increase in the degree to which clays and zeolites fill fractures and voids. This also explains the order-of-magnitude drop in permeability observed in hole 504B. An increase in alteration-filling with age could explain the transition from convective to conductive heat flow and the correlative disappearance of layer 2A on the flanks of oceanic spreading centres.*

HEAT flow measurements on the flanks of mid-ocean ridges show a transition from primarily convective heat flow near ridge axes to predominantly conductive heat flow in old ocean basins[1]. Coinciding with the change in heat transfer mechanism, oceanic crustal layer 2A essentially 'disappears' with age on the flanks of mid-ocean ridges (Fig. 1; ref. 2). Layer 2A is defined as a seismic transition zone in which a section with anomalously low P-wave velocity ($V_P \sim 2$–$3\ \mathrm{km\ s^{-1}}$) overlies high-velocity layer 2 basalts ($V_P \geq 5\ \mathrm{km\ s^{-1}}$). This transition occurs within the interlayered pillow, flow and rubble zones of the upper 1 km of oceanic crust. To investigate the interrelationship between these thermal and acoustic phenomena and other physical properties of the oceanic crust, we participated in an integrated suite of *in situ* downhole experiments at IPOD sites 501–504B on the south flank of the Costa Rica Rift of the Galapagos Spreading Centre (Fig. 2). The experiments included *in situ* permeability and pore-pressure measurements[3], sonic velocity logging[4] and formation fluid sampling[5]. Here we describe ultrasonic borehole televiewer imagery that was conducted to examine in detail the lithostratigraphy and fracture and void variation with depth, and compare these data with the change in P-wave velocity with depth.

A primary difficulty with interpreting lithostratigraphy of the oceanic crust from core samples recovered by the DV *Glomar Challenger* has been the low percentage of core recovery. Drilling operations crush and wash away an average of 70% of all oceanic crust drilled through. The only measurements capable of recording information over the entire wellbore are geophysical logs, but it has been extremely difficult to interpret these logs in detail because of a lack of comparable examples on land for cross-correlations (see ref. 6).

A borehole televiewer (BHTV) was used to provide the type of continuous data needed to interpret more fully the structure and stratigraphy of the ocean crust. The BHTV is a seldom-used oil-field logging tool developed by the Mobil Oil Corporation for the study of fractures in wellbores and casing (see ref. 7). The downhole tool contains an ultrasonic transducer which rotates three times per second and emits a 1 mHz pulse 180 times per second as the tool is moving vertically in the hole at a speed of $1.5\ \mathrm{m\ min^{-1}}$. By displaying the amplitude of the acoustic pulse that is reflected off the borehole wall as brightness on a three-axis oscilloscope, the BHTV produces an image of the reflectivity and smoothness of the wellbore referenced to magnetic north. Hard, smooth surfaces produce strong reflections (or 'bright zones' on photographs of the data displayed on the oscilloscope) whereas fractures and voids greatly diminish the reflected signal and produce 'dark zones' on the records. Similarly, where the hole reaches great width, or very soft clays are encountered, no appreciable reflection is returned, and dark zones again appear. The result is a complete

0028-0836/82/050375—05$01.00

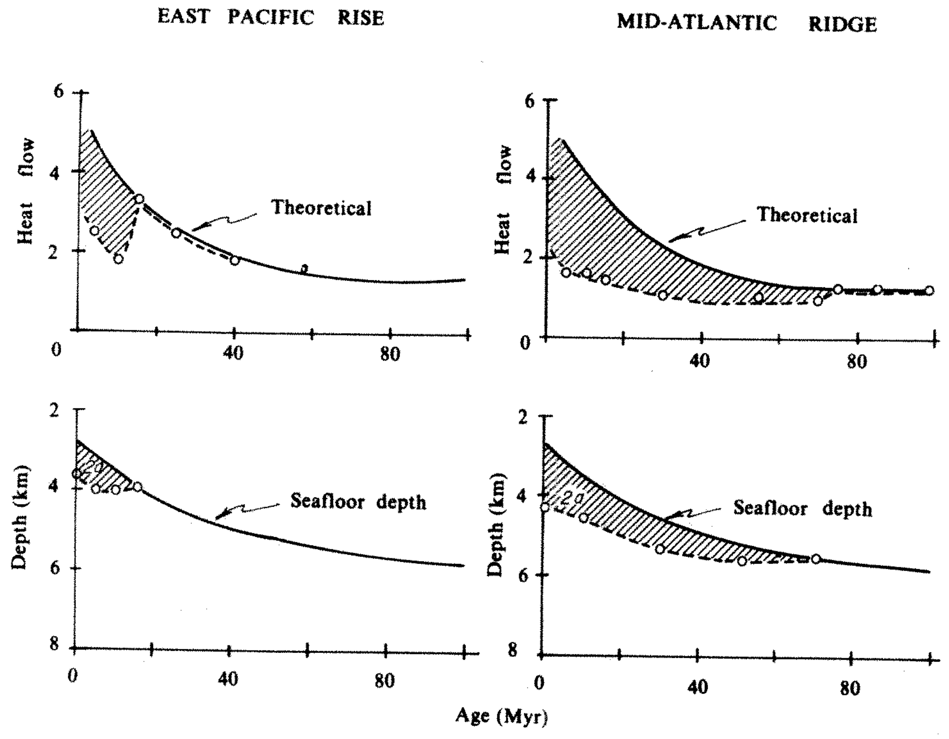

Fig. 1 Heat flow and thickness of seismic layer 2A as they vary with age in the Atlantic and eastern Pacific oceans[1,2]. In the upper plots, ○ represents mean observed heat flow for corresponding age; theoretical curve is prediction of lithospheric cooling model; hatching is heat believed to be carried away by convection through the sea floor. In the lower plots are layer 2A thickness, ○ represents observations from sonobuoy data; hatching is thickness of layer 2A below sediment–rock interface.

north–east–south–west–north 'picture' of the reflectivity of the wellbore.

The setting

We deployed a borehole televiewer at sites 501 and 504B on IPOD Legs 68A and 69 in 6-Myr-old crust on the south flank of the Costa Rica Rift, the easternmost segment of the Galapagos Spreading Centre (Fig. 2). The sites were chosen to penetrate into young oceanic crust with high surface heat flow. The two sites are only about 1 km apart. Because they lie near the Equator where there is rapid productivity of pelagic sediment, a 280 m sedimentary section has formed a thick impermeable lid over a hydrothermal circulation system active in the oceanic crust[3]. Pore pressure measurements[3] and temperature logs[8] indicate oceanic bottom water being drawn naturally into an underpressured aquifer with a permeability of about 200 millidarcies (md) located 50–100 m below the top of layer 2A [8]. Flow tests in hole 504B show that the average permeability of layer 2A drops from 20–40 md in the upper 100 m to 2–4 md about 200 m below the sediment–basalt contact[3]. Sonic logs indicate an increase in velocity of layer 2A from 2.5 to >5 km s^{-1} in the upper 200 m of the oceanic crust.

The BHTV tests conducted in these wells have contributed to our understanding of why the sedimentary layer forms a hydraulic lid, why the permeability drops by an order of magnitude with depth and why the seismic velocity increases with depth. It also gave the first complete glimpse of the lithostratigraphy of the upper oceanic crust.

Structure at site 501

Using the BHTV we logged the entire sedimentary column and 25 m below the sediment–basalt contact in hole 501 of DSDP Leg 68A (Fig. 3). In much of the sedimentary section the record is quite dark (that is, there is no significant reflection from much of the circumferential sweep of the trace). This is due to pronounced 'washing out' and ellipticity of the hole; the problem is most severe at ~3,710 m depth (Fig. 3).

The youngest chert yet encountered by the *Glomar Challenger*[9] was found over the lower 30 m of the sediment column of hole 501. The BHTV records show that the first chert encountered is a solid layer ~5 m thick. Drilling results indicated that within this layer there are interlayered lenses of chert and silicified limestone. The chert, being harder and more resistant to 'washing out', shows up as bright, high-reflectance bands between the darker limestone layers. Although we do not know the horizontal extent of these chert layers, all holes drilled at the 501–504B sites encountered chert over the lower 30 m of the sedimentary section.

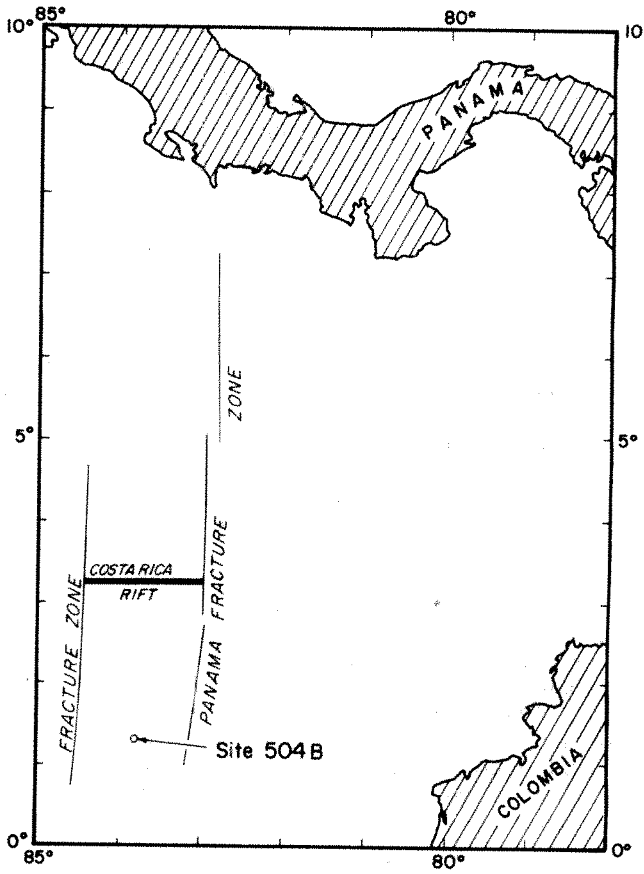

Fig. 2 Index map showing location of DSDP site 504B. 501 is 1 km to the west of 504B. The Costa Rica Rift is the easternmost segment of the Galapagos Spreading Centre.

Pillow basalts recorded by the BHTV appear as bright spots within dark ellipses. These dark ellipses probably represent the pillow's glass and alteration rims that are fractured and washed-out during drilling (Fig. 3). The pillow units as seen in the wellbore also seem to contain large voids where virtually no signal is reflected back to the transducer (for example, at 3,735 m in Fig. 3). Several massive flow units are seen at the top of the oceanic crust interlayered with the pillow basalt units. Because of the poor core recovery, the interrelationship between these stratigraphical units was not previously known. Note the 8 m thick massive flow unit that extends from 3,747 to 3,755 m.

Structure at site 504B

At site 504B on Leg 69, a BHTV was used to log 196 m below the casing which was set 2 m into basalt. Unfortunately, the factory-equipped transducer was destroyed on the first lowering of the tool by a pressure-compensation failure. The hole was then logged using a 600 kHz transducer array taken from an acoustic reentry tool as a replacement televiewer transducer. Sixty-cycle noise (apparently caused by a faulty logging cable) further obscured the BHTV image. Because the noise has proved difficult to remove from the data, we present only line drawings (Fig. 4) rather than the original records. Nevertheless, distinct pillow and flow units were discernible and contacts between distinct eruptive events were often seen (for example, 3,855 m, Fig. 4). Fracture resolution is several millimetres and several fractures this small were seen (for example, 3,860 m, Fig. 4).

The interpretative line drawing of the BHTV records allows us to reconstruct the lithostratigraphy of hole 504B (Fig. 4). We observe that thick flow units dominate the upper 50 m of layer 2A. These flows have numerous fractures which are predominantly horizontal to subhorizontal. Thin interlayers (~1 m thick) of large diameter pillow units are seen at 3,757, 3,765, 3,773–3,778 and 3,782 m. The 8 m thick massive flow unit of hole 501 (at 3,747–3,755 m of Fig. 3) may be correlative with a thick flow encountered at 504B at depths of 3,753–3,758 where it is more broken-up. Another thick massive flow is in 504B seen at 3,785–3,795 m depth.

The percentage of pillow units gradually increases down-section and the average size of the pillows decreases from 20 to 30 cm near the basalt–sediment contact to only a few centimetres (Fig. 4). For example, from 3,838 to 3,851 m a suite of pillow units has a range in sizes up to ~30 cm whereas the pillow units from 3,890 to 3,897 are all <10 cm in size. In addition, the massive flow units become thinner down-section. The entire lower 55 m of the recorded section appears as discrete pillow units <1 m in thickness. Fractures often seem to be concentrated at the borders of separate pillow flows but some zones are uniformly fractured. As in hole 501, most of the fractures observed in hole 504B are horizontal to subhorizontal.

From 3,805 to 3,825 m an anomalously low reflectance zone exists. While some structure can be seen within this zone, the amplitude of reflectance is much lower than zones directly above and below it. The general level of reflectance also drops from flows to pillows and towards the bottom of the hole. The lowered reflectance may be due to the increased occurrence of clay and zeolite which was clearly observed in the cores[9].

Increase in seismic velocity with depth

A primary aim of this project is to interpret the BHTV records in terms of the change in the physical properties of the ocean crust. Specifically, we wish to relate variations observed in the sonic velocity log over the BHTV-logged section of 504B to the stratigraphic variations seen with the BHTV. Although the velocity log from hole 504B is extremely noisy, a marked increase in average P-wave velocity with depth can still be clearly seen (Fig. 5*a*, after ref. 4). The average basement velocity just below the casing begins at ~2.5 km^{-1} and increases over the next 200 m to ~5 km s^{-1} (values typical of layer 2A). Although most of the large-amplitude high-frequency velocity variations in Fig. 5*a* are spurious and due to the effect that changes in the shape of the hole have on the seismic waveforms being transmitted by the velocity tool, the high-velocity interval from 3,785 to 3,795 m correlates with a massive flow unit which contains few fractures or voids at that depth.

Fracture and void counts

The BHTV record of hole 504B allows us to test various hypotheses for the increase in seismic velocity with depth within layer 2A because we can correlate the observed change in character and structure of fracture and void zones down the hole

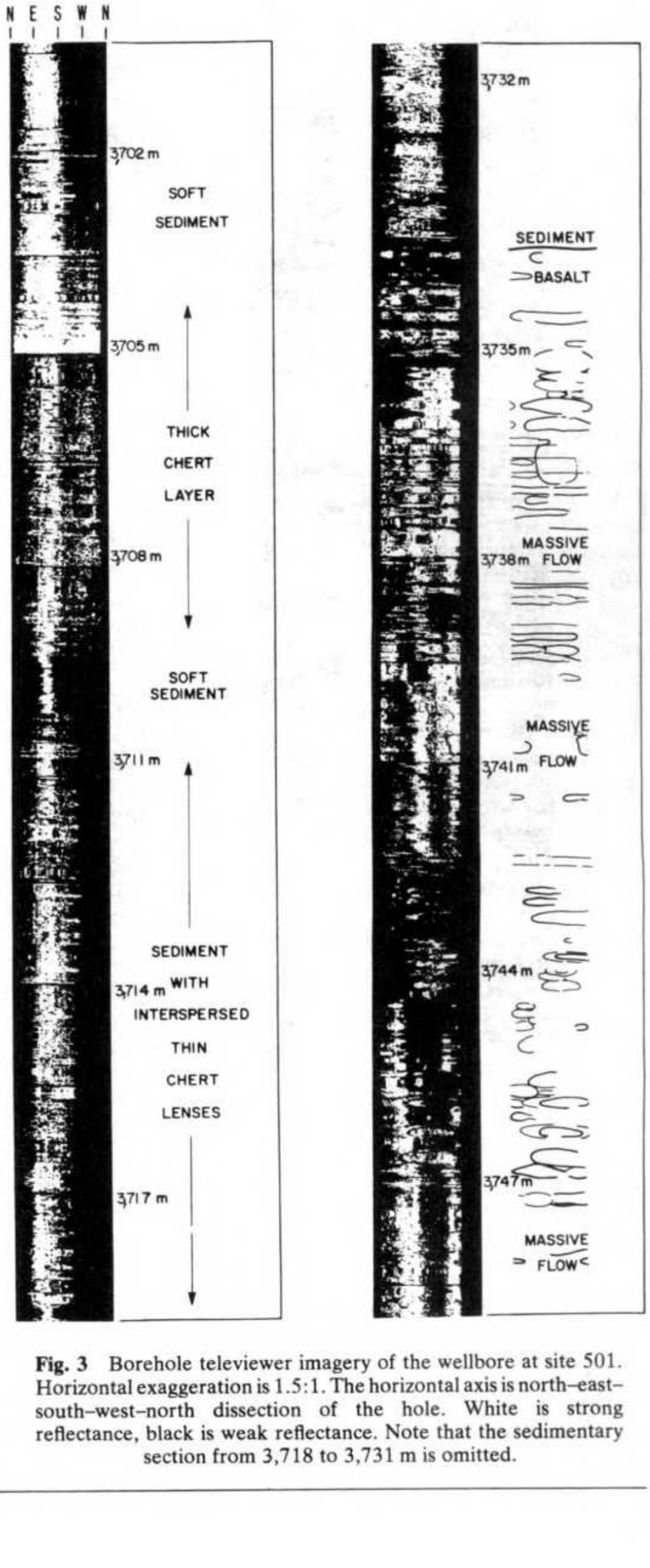

Fig. 3 Borehole televiewer imagery of the wellbore at site 501. Horizontal exaggeration is 1.5:1. The horizontal axis is north–east–south–west–north dissection of the hole. White is strong reflectance, black is weak reflectance. Note that the sedimentary section from 3,718 to 3,731 m is omitted.

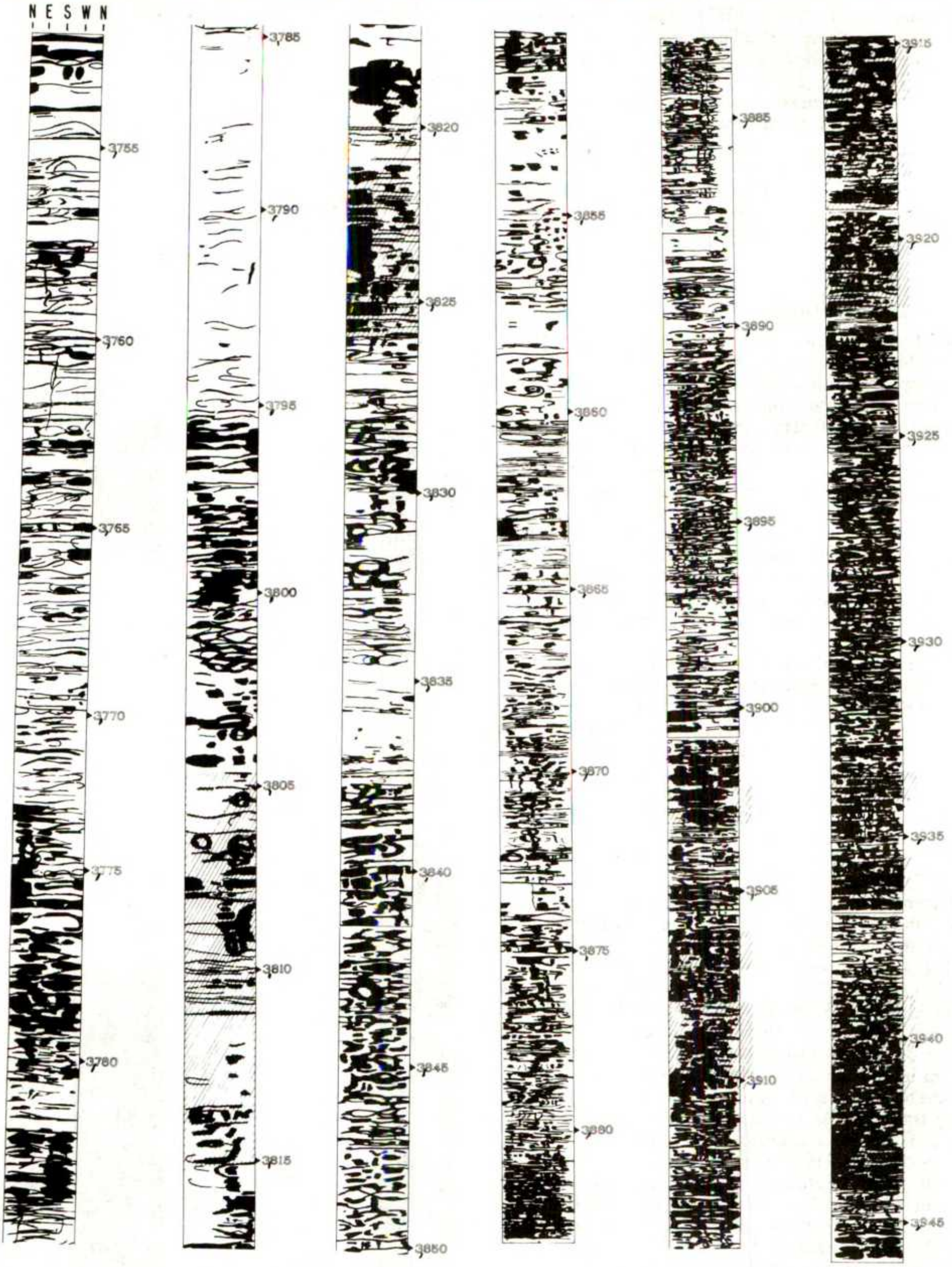

Fig. 4 Line drawing of borehole televiewer imagery of site 504B drillhole. Horizontal exaggeration is 1.5:1. Black-rimmed elliptical images are pillow lavas. Solid white segments are massive flow basalts. Thin lines are cracks and fractures. Hatched areas are of anomalously low reflectance. Depths in metres below sea level. Casing ends at 3,753 m.

with changes in seismic velocity. To this end, we counted the number of fractures observed on the BHTV records from hole 504B (Fig. 5*b*). As can be seen in both Figs 4 and 5*b*, the fracture density actually increases with depth in hole 504B. As laboratory studies show, this would be expected to decrease the velocity if the degree of fracturing alone were controlling V_P in layer 2A. Instead, a marked velocity increase with depth is observed in hole 504B that is typical of layer 2A (Fig. 5*a*).

As voids between pillows might be expected to have a similar effect on velocity as fractures, a plot of the percentage of voids in the wellbore (percentage of black versus white in Fig. 4) is presented in Fig. 5*c*. In the pillow units, this 'void ratio' (Fig. 5*c*) measured the per cent of pillow rims, glassy rind and rubble surrounding the solid basaltic core of each pillow. We observe an increase of voids with depth in the hole because of the decrease in the diameter of the individual pillows with depth. Presumably,

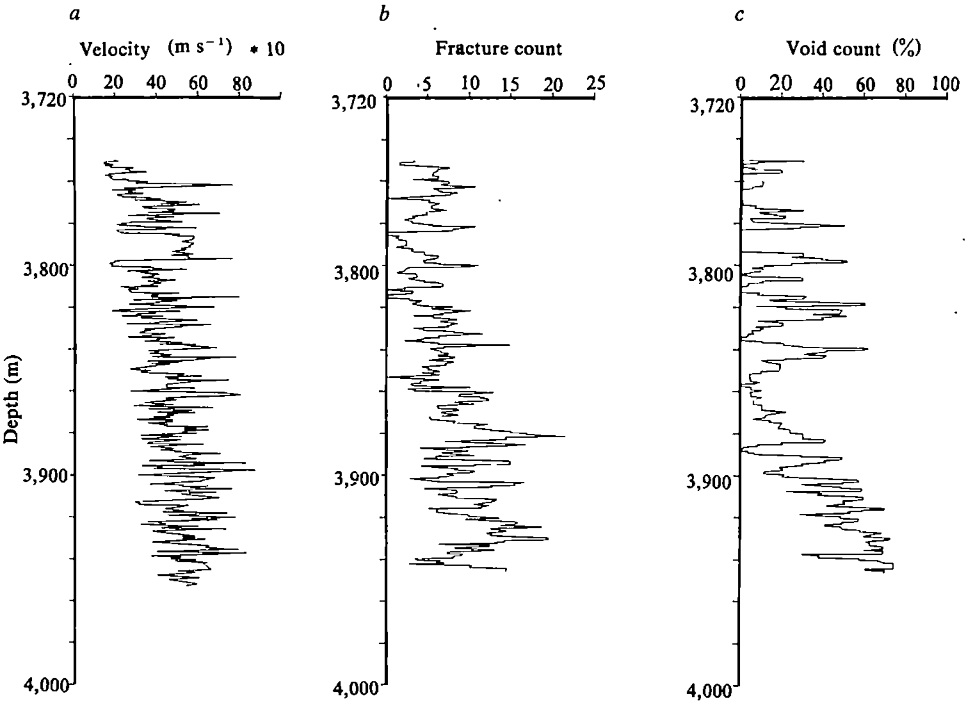

Fig. 5 *a*, Sonic velocity logs of site 504B upper 200 m of basalt corresponding to interval of BHTV log in Fig. 4. Spurious data points with $V_P < 1.5$ and >8 km s^{-1} were excluded from digitization of original analog record. Note that despite the noisy character of the log a clear increase in V_P with depth can be observed in hole. *b*, Histogram of the number of fractures per 50 cm of hole. *c*, Void percentage based on an estimation of the per cent black versus white in Fig. 4 per 50 cm of hole.

a lower seismic velocity might be expected to correlate with the higher void count, but again, an inverse correlation is seen in hole 504B.

Discussion

To explain the variation of velocity in the upper oceanic crust three basic questions must be answered. Why is the velocity of the upper portion of layer 2A so low? Why does the velocity increase so rapidly with depth within layer 2A? And why does layer 2A disappear with age at about the time of the transition in the mode of heat transfer along ridge flanks? It has been argued[10-13] that the low seismic velocity of the upper portion of layer 2A results from the highly fractured and porous nature of the shallow oceanic crust. This explanation seems quite reasonable from the nature of the basalt encountered in holes 501 and 504B. However, what causes the velocity to increase so rapidly with depth? Velocity is expected to increase with depth due to the closure of fractures with pressure, but the increase in effective pressure over only a few hundred metres depth is quite small (only about 15–20 bar per 100 m), and mechanically closing enough fractures and voids to account for the velocity increase over the depth range of interest is highly unlikely[12]. Spudich and Orcutt[14] suggested that the increase in velocity is caused by a decrease in porosity with depth. But why should a decrease in porosity occur in a regular manner on the flanks of many ridges, and how could this account for the disappearance of layer 2A with age?

Schreiber and Fox[12] have proposed a model that seems to explain the seemingly inconsistent seismic velocity and borehole televiewer data in holes 501 and 504B, as well as several of the questions posed above. They suggested that as voids and fractures are filled by alteration minerals like chlorite, zeolite and smectite (with characteristic seismic velocities of ~4 km s^{-1}) the alteration minerals replace seawater (with a seismic velocity of ~1.5 km s^{-1}). Thus, the seismic velocity of layer 2A would be expected to rise rapidly as the degree of alteration increased. Increased alteration in layer 2A would be expected with both depth (due to increased temperature) and age. Geophysical logging data[6] also suggests that an increase in alteration-filling occurs with age on ridge flanks. The alteration-filling hypothesis seems capable of explaining the rapid increase of layer 2A velocity with depth despite an apparent increase in fractures and voids and the eventual disappearance of layer 2A with age. The increased occurrence of clays and zeolites with depth was well noted in the core descriptions of holes 501 and 504B [9] and the rapid decrease in permeability with depth in hole 504B [3] also indicates the filling of fractures and voids with alteration minerals. We do not now understand the cause of the decrease in the size of the pillows encountered in 504B and the related increase in the number of voids. This may be a localized phenomena which is of no general significance. However, the observation of a marked increase in velocity despite an apparent increase in fractures and voids demonstrates that the replacement of seawater by alteration minerals is more important in controlling the increase in velocity than the change in fracture or void density. If this is correct, it suggests that on the flanks of oceanic spreading centres a marked decrease in the permeability of the 'crustal plumbing system' can be expected to correspond to the change in seismic velocity. This would explain the correlation between the transition from conductive to convective heat flow and the disappearance of layer 2A with age.

We thank Bob Broding and the Amoco Oil Field Research Co. of Tulsa, Oklahoma, for loaning us the borehole televiewer used on Leg 68 (hole 501) and for invaluable support, Joseph Svitek Jr, Larry May and the Global Marine drilling crew for making this project successful, and Robin Newmark for help in the preparation of Fig. 4. This work was supported by the NSF under grant OCE-78-27026 and the US Geological Survey.

Received 11 September; accepted 2 December 1981.

1. Anderson, R. N., Langseth, M. G. & Sclater, J. G. *J. geophys. Res.* **92,** 3391–3409 (1977).
2. Houtz, R. E. & Ewing, J. *J. geophys. Res.* **81,** 4060 (1976).
3. Anderson, R. N. & Zoback, M. D. *J. geophys. Res.* (in the press).
4. Cann J. *Init. Rep. DSDP* Legs 69–70 (in the press).
5. Mottl, M. *Init. Rep. DSDP* Legs 69–70 (in the press).
6. Kirkpatrick, J. R. *J. geophys. Res.* **84,** 178–188 (1979).
7. Zemanek, J. *et al. Geophysics* **35,** 254–269 (1970).
8. Becker, K., Langseth, M. G. & Von Herzen, R. P. *Init. Rep. DSDP* Legs 69–70 (in the press).
9. CRRUST *Bull. geol. Soc. Am.* (submitted).
10. Hyndman, R. D. & Drury, M. J. *J. geophys. Res.* **81,** 4042–4059 (1976).
11. Schreiber, E. & Fox, P. J. *J. geophys. Res.* **81,** 4071–4076 (1976).
12. Schreiber, E. & Fox, P. J. *Bull. geol. Soc. Am.* **88,** 600–608 (1977).
13. Fox, P. J. & Stroup, J. B. *The Sea* Vol. 7 (ed. Emiliani, C.) (Interscience, New York, 1981).
14. Spudich, P. & Orcutt, J. *J. geophys. Res.* **85,** 1409–1419 (1979).

Resolving the functions of overlapping viral genes by site-specific mutagenesis at a mRNA splice site

Craig Montell*, Eric F. Fisher†, Marvin H. Caruthers† & Arnold J. Berk*

* Department of Microbiology and Molecular Biology Institute, University of California, Los Angeles, California 90024, USA
† Department of Chemistry, Campus Box 215, University of Colorado, Boulder, Colorado 80309, USA

Early region IA of human adenoviruses encodes a function required for normal induction of early viral genes and virus-induced cell transformation. The region is expressed at early times as two overlapping spliced mRNAs, 12S and 13S, which encode closely related proteins. To distinguish between the functions of these proteins, a single T → G transversion was constructed which prevents splicing of the 12S mRNA. This transversion, in the second base of the 12S mRNA intron, does not alter the protein encoded by the 13S mRNA due to degeneracy in the genetic code. Studies with this mutant demonstrated that only the 13S mRNA encodes the regulatory protein required for normal early gene expression.

MANY eukaryotic genes are interrupted by introns removed from mRNA precursors by RNA splicing. Sequences encompassing splice sites share considerable homology and variants of the following sequence are found at the 5′ end of every intron analysed: 5′-(exon)-AG/GUAAGUA-(intron)-3′ (refs 1–3). Although specific 5′ splice sites differ from this consensus sequence to a greater or lesser degree, the underlined GU dinucleotide which begins the intron is virtually invariant. To determine whether the integrity of this dinucleotide is required for efficient RNA splicing, we constructed an adenovirus mutant with a T → G transversion in the second base of the intron in an early region IA (EIA) gene. We believed that this transversion would eliminate RNA splicing, allowing us to ascribe specific functions to the two overlapping early adenovirus mRNAs transcribed from this region[4]. Animal viruses frequently encode overlapping spliced mRNAs in a common region of the viral genome. Such compact gene organization enables the small viral genomes to encode several related proteins in the same region by splicing a single mRNA precursor in two or more alternative ways.

EIA of adenovirus 2 (Ad2) has attracted considerable interest because it encodes a function required for both normal expression of the other early viral genes[5,6] and virus-induced cell transformation[7,8]. The two overlapping early mRNAs transcribed from this region, 12S and 13S, share identical 5′ and 3′ termini and vary by 138 nucleotides due to the differing sizes of the introns removed by RNA splicing (refs 9, 10; Fig. 1). Assuming translation is initiated at the first AUG, the 12S and 13S messages encode proteins of 243 and 289 amino acids respectively. The 12S and 13S mRNAs are spliced such that they continue in the same reading frame[9]; therefore, the larger protein has the same amino acid sequence as the smaller protein except for an additional internal 46 amino acids encoded by the 138 nucleotides unique to the 13S mRNA. One EIA mutant, Ad5 hr1 (ref. 11), has a single base deletion in the portion of viral genome encoding the unique region of the 13S mRNA[12]. This mutation leads to premature chain termination during translation of the 13S mRNA, but does not affect translation of the 12S mRNA[12]. Ad5 hr1 is deficient in both early viral gene expression[5] and inducing cell transformation[7], demonstrating that the 289 amino acid protein at least is required for these processes.

The question of the role of the 243 amino acid protein in regulating early viral gene expression or virus-induced cell transformation has not previously been addressed. It cannot be investigated using mutants of the 243 amino acid protein as random or directed mutagenesis intended specifically to alter the 243 amino acid protein encoded by the 12S mRNA, without affecting the 289 amino acid protein specified by the 13S mRNA, would be futile since every amino acid in the smaller polypeptide is included in the larger one. To overcome this

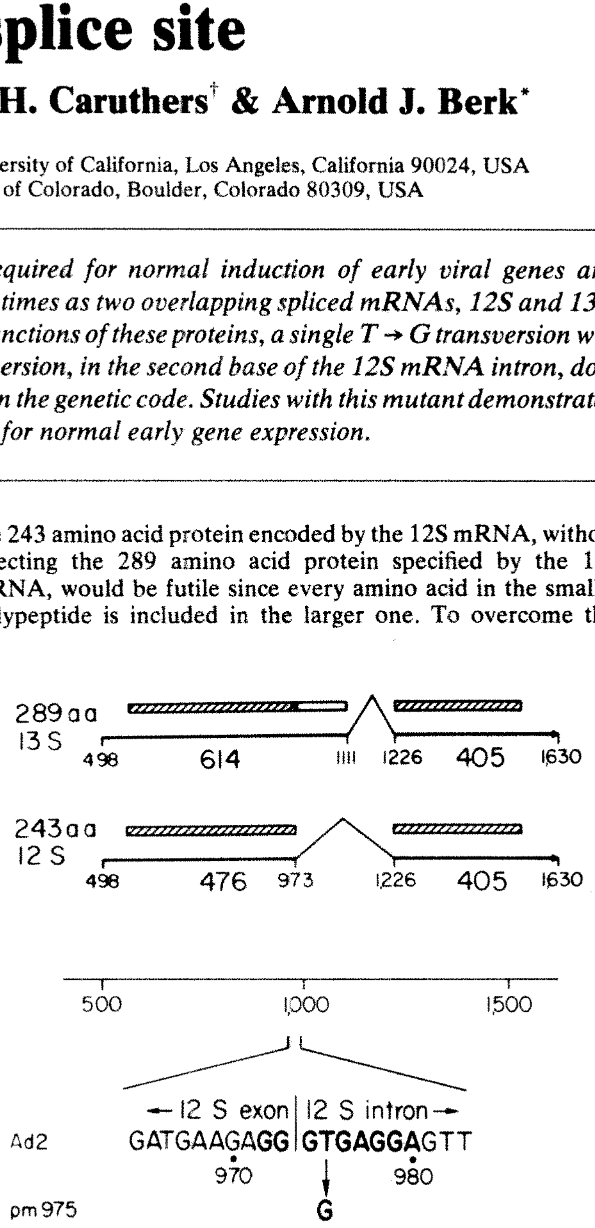

Fig. 1 Structures of EIA gene products at early times. The EIA portion of the Ad2 genome is represented as a line at the centre of the figure marked off in base pairs from the left end of the genome. The horizontal lines joined by carot symbols represent exons of the 12S and 13S mRNAs; the total lengths of exons are indicated in nucleotides below the lines with the end points identified in the Ad2 sequence; arrowheads indicate the 3′ ends of the mRNAs. Boxes above the exons demarcate the translated regions. The lengths of the polypeptides are given as the number of amino acids (aa). The portions of the 289 and 243 amino acid proteins with identical sequences are indicated with hatches; the open box refers to the 46 amino acids unique to the larger polypeptide. The sequence of the L strand of Ad2 in the vicinity of the 12S mRNA 5′ splice site between nucleotides 964 and 983 is shown below the line representing the genome. Those nucleotides included in the 5′ consensus sequence are highlighted. The vertical line identifies the splice junction separating the 5′ 12S exon from the intron and the T → G transversion at nucleotide 975 is indicated. The Ad2 EIA sequence is >99% homologous with the corresponding region in Ad5 (ref. 36). To align the Ad2 with the Ad5 EIA sequence, add one to the Ad2 sequence to account for an additional base pair in the Ad5 inverted terminal repeat.

0028-0836/82/050380—05$01.00

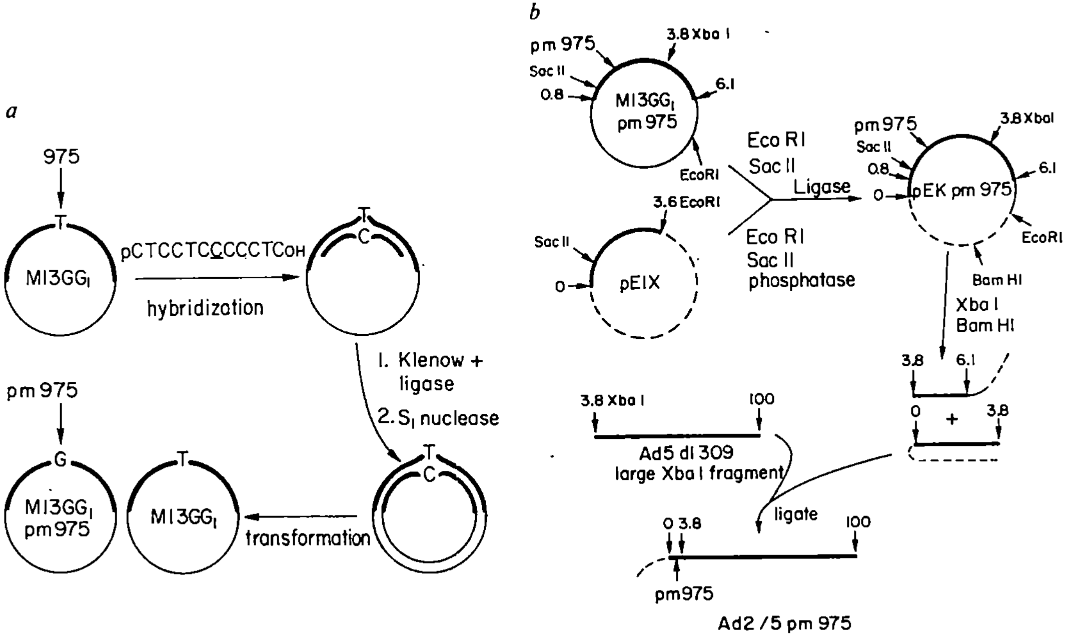

Fig. 2 Construction of Ad2/5 pm975. *a*, Oligonucleotide-directed mutagenesis. The bold portion of the circles represents the Ad2 component. T refers to nucleotide 975 in the Ad2 sequence and the underlined C to the corresponding mismatch in the dodecanucleotide. M13GG1 was constructed (by R. Gaynor) by transferring the Ad2 *Kpn*I fragment from pSB2 (ref. 37) into the *Kpn*I site of M13G*ori*1 (ref. 38) producing a clone of the Ad2 L strand extending from nucleotides 269 to 2,049. Oligonucleotide-directed mutagenesis was performed as described elsewhere[15] with M13GG1 as the single-stranded template and *E. coli* K12 JM101 (ref. 39) as host, except for the following modification. After 4 h of DNA synthesis, the specified amounts[15] of DNA polymerase I large fragment (Klenow) and T4 DNA ligase were added again and incubation continued for 3 h. Transfection was into $CaCl_2$ treated cells[38] rather than spheroplasts. We found that single-stranded viral DNA had an infectivity of $\sim 10^3$ plaque-forming units (PFU) per μg compared with $\sim 10^6$ PFU per μg for double-stranded DNA in $CaCl_2$-treated JM101. The dodecanucleotide primer was synthesized as described in ref. 16 with the following modifications. The support was prepared by coupling 5′-*O*-(dimethoxytrityl)-3′-(-4-*p*-nitrophenyl succinyl)-*N*-benzoyldeoxycytosine to silica treated with 3′-(triethoxysilyl)propylamine. The activated nucleoside was prepared at room temperature and used immediately. Synthesis was carried out in a modified Merrifield apparatus using 150 mg of derivatized support (46 μmol g^{-1}). At each condensation 90 μmol of activated nucleoside was used. Fifty mg of the resulting silica covalently attached to the deoxyoligonucleotide was treated for 90 min with thiophenol/triethylamine/dioxane (1:1:2). The silica was isolated by centrifugation and washed four times with dioxane, three times with methanol and once with diethylether. 400 μl of concentrated ammonium hydroxide were added to the silica. The sealed tube was shaken for 3 h at room temperature followed by centrifugation. The supernatant was transferred to another tube, sealed and heated to 50 °C for 22 h. The sample was dried *in vacuo* and 250 μl of 80% acetic acid were added. After 60 min, the sample was dried *in vacuo* and applied to a 1.5 cm × 50 cm G50/40 column in 0.01 M triethylammonium bicarbonate. Fractions (1.2 ml) were taken and the first three fractions containing UV-absorbing material ($\sim 10A_{260}$) were pooled, lyophylized to dryness, dissolved in 150 μl of 80% formamide and applied to a 20 cm × 20 cm 20% polyacrylamide/7 M urea gel. After electrophoresis the band containing the desired oligodeoxynucleotide was excised, eluted and desalted on a Bio-Gel P 2 column (3 cm × 60 cm). The 2.5-ml fractions were monitored by UV absorption. The fractions containing the compound were pooled (4.4 A_{260}). The sequence of the oligonucleotides was verified by two-dimensional TLC as described previously[40] using Homomix V. *b*, Insertion of pm975 into the complete adenovirus genome. Bold lines represent adenovirus sequences, light lines M13G*ori*1 DNA and broken lines pBR322 sequences. Small numbers refer to Ad2 map units; one map unit is equal to 1% of the Ad2 genome—~350 nucleotides. A derivative of pBE5, pEIX[19], which contains Ad2 sequence from 0 to 3.6 map units inserted between the *Pst*I and *Eco*RI sites of pBR322 (ref. 41), was prepared. The mutation in M13GG1 pm975 was introduced into pEIX by digesting 0.5 μg pEIX with *Sac*II, *Eco*RI and calf intestinal phosphatase; ligating the products of these reactions to 5 μg *Sac*II, *Eco*RI-digested double-stranded M13GG1 pm975; and using the reaction products to transform *E. coli* C600 to Tc^r all as described in ref. 37. Plasmids from transformed colonies were screened by size and restriction endonuclease analysis to identify the desired construct, pEK pm975, which includes the entire left terminus of Ad2. The presence in this plasmid of the T → G transversion at 975 in the Ad2 sequence was confirmed by DNA sequencing[17,18]. 4.5 μg pEK pm975 were digested with *Xba*I and *Bam*HI (to minimize recircularization) and ligated to 1 μg of the large *Xba*I fragment of Ad5 d1309 isolated as described in ref. 19. Ad5 d1309 is a phenotypically wild-type variant of Ad5 containing a single *Xba*I site at 3.8 map units. The ligation creates complete 35 kilobase infectious adenovirus genomes, which include the T → G transversion at base pair 975. The ligation products were transfected into 293 cells by the calcium phosphate technique[42]. Ad2/5 pm975 was collected from a well isolated plaque and the plaque was purified a second time on 293 cells.

problem we used oligonucleotide mutagenesis to create a T → G transversion at position 975 in the Ad2 sequence (Fig. 1). This nucleotide, which is the second base in the 12S mRNA intron, is also the third base of the GGU codon specifying glycine in the overlapping 13S mRNA. Because there is degeneracy in the genetic code, the new codon, GGG, created by this mutation also specifies glycine, thereby leaving the 289 amino acid protein completely unaltered.

We find that the single base change prevents efficient RNA splicing and specifically eliminates the 12S mRNA. Studies with this mutant, Ad2/5 pm975 (pm = point mutation), demonstrate that the 13S mRNA encodes all the early EIA functions required for normal early gene regulation and virus replication in human cells.

Construction of the specific adenovirus point mutant

The T → G transversion was introduced into a bacteriophage M13 clone of EIA by oligonucleotide-directed mutagenesis[13,14]. Conditions for this site-specific mutagenesis have been optimized by Gillam *et al.*[15] for isolating a mutant with a single point mutation at high efficiency without biological selection. The method (Fig. 2*a*) entails hybridization of a synthetic oligonucleotide to a single-stranded circular bacteriophage genome. The oligonucleotide is complementary to the phage DNA except at a single predetermined nucleotide. The hybridized oligonucleotide is used as a primer for DNA polymerase, and the resulting duplex molecules are ligated to form infectious covalently closed circles. In this work, the mutating oligonucleotide was a dodecanucleotide (12 mer) synthesized on a solid support by a modification of the phosphite coupling method of Mattucci and Caruthers[16]. The 12 mer is complementary to the L strand of EIA encompassing the 12S mRNA 5′ splice site except for a mismatch at nucleotide 975 in the Ad2 sequence. The heteroduplexes were transfected into *Escherichia coli* giving rise to a mixed population of mutant and wild-type

Table 1 Host range analysis of pm975

Virus	293	PFU per ml HeLa	HeLa/293
Wild-type Ad2	6.63×10^9	8.71×10^9	1.3
Ad2/5 pm975	1.38×10^9	1.76×10^9	1.3
Virus	HEK	HeLa	HEK/HeLa
Wild-type Ad2	1.17×10^{10}	1.46×10^{10}	0.80
Ad2/5 pm975	1.96×10^9	3.03×10^9	0.65

Stocks of Ad2 and plaque-purified pm975 prepared on 293 cells were serially diluted and assayed in duplicate by plaque formation on 293 and HeLa cells, and HEK and HeLa cells. Titres are based on the average of duplicate plates yielding 30–300 plaques.

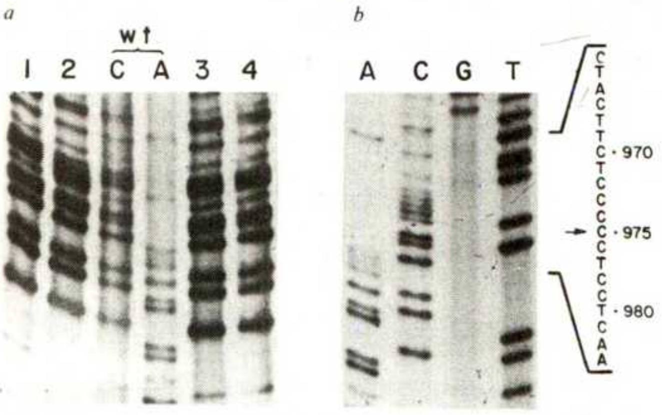

Fig. 3 Identification of M13GG1 pm975 and Ad2/5 pm975 by dideoxy sequencing. *a*, Following the second cycle of enrichment[15], bacteriophage were collected from eight plaques and amplified overnight in 25-ml cultures of JM101; phage were precipitated with polyethylene glycol[38], and viral DNA was isolated as described previously[43]. Purified DNAs were screened for the mutation by reverse transcriptase dideoxy sequencing using dideoxy CTP. The primer was a 31-base *Hpa*II fragment extending from nucleotides 1,009 to 1,040 in the Ad2 sequence. The sequences of four of the eight phage DNAs screened are shown in tracks 1, 2, 3 and 4 adjacent to the wild-type C and A lanes. Sequences shown are of the R strand of Ad2 in the vicinity of the 12S mRNA 5′ splice site. The DNA in track 2 contained the desired mutation at nucleotide 975. *b*, Identification of Ad2/5 pm975. Adenovirus DNA was prepared as described elsewhere[37] from 293 cells infected with virus from well isolated plaques picked from a transfected 293 plate (see Fig. 2 legend). The DNA was digested with exonuclease III creating single-stranded termini ~1,500 nucleotides long[44]. Sequence analysis was by the dideoxy method using the same primer as for *a*. The 20 nucleotide sequence in the vicinity of the 12S mRNA 5′ splice site is listed and the positions of nucleotides 970, 975 and 980 are indicated.

clones. The heterogeneous population of DNA molecules was subjected to two cycles of enrichment by performing the oligonucleotide hybridization in conditions favouring hybridization to the mutant sequence[15]. Potential mutant clones were screened by DNA sequencing by the dideoxy chain termination method using dideoxy CTP[17,18]. Of eight phage plaques thus screened, seven were wild type and one (Fig. 3*a*, lane 2) had the desired point mutation at base pair 975 (M13GG1 pm975). The mutation was introduced into a phenotypically wild-type adenovirus genome, Ad5 d1309, by the method of Stow (ref. 19; Fig. 2*b*).

Unable to predict whether the mutation at base pair 975 would eliminate an essential function, we transfected the reconstructed mutant genome into 293 cells which are capable of complementing all essential EIA functions[8,20]. 293 cells are a line of Ad5-transformed human embryonic kidney cells containing an integrated copy of the left 12% of the Ad5 genome[21] which constitutively express EIA and EIB mRNAs[5] and proteins[22]. DNA sequence analysis showed that three out of four plaques screened contained the point mutation (Fig. 3*b*). The mutant, Ad2/5 pm975, was plaque-purified a second time on 293 cells and sequenced again to confirm the desired base pair change.

12S mRNA is eliminated

EIA mRNAs were assayed by the hybridization/S_1 nuclease technique[23]. Early cytoplasmic RNAs were isolated 6 h post infection from HeLa cells infected with Ad2 or Ad2/5 pm975 and hybridized in DNA excess to a ^{32}P-labelled single-stranded M13 clone of the coding strand of EIA and the 5′ 350 nucleotides of EIB. The hybridization products were digested with S_1 nuclease and the protected fragments were resolved by electrophoresis on a denaturing polyacrylamide gel and detected by autoradiography.

Figure 4*a* displays the DNA fragments protected by hybridization to the wild-type EIA and EIB mRNAs. The 614 nucleotide fragment corresponds to the 5′ exon of the 13S mRNA, the 476 base band to the 5′ exon of the 12S mRNA, the 405 nucleotide fragment to the 3′ exon common to both the 12S and 13S mRNAs and the 350 nucleotide protected fragment to the terminal portion of the 5′ exons of EIB mRNAs. An additional but minor band of 750 nucleotides is protected by RNA species identical to the 13S mRNA except for a ~140 nucleotide extension at the 5′ end[24].

S_1 analysis with RNA prepared from pm975-infected cells reveals bands co-migrating with each of the wild-type Ad2 bands except for the 476 nucleotide protected fragment corresponding to the 5′ exon of the 12S mRNA (Fig. 4*a*). To enhance the sensitivity for detecting the 12S mRNA, poly(A)$^+$ RNA isolated from cells during the late stage of infection was analysed (Fig. 4*b*). The level of 12S and 13S mRNA is increased approximately twofold during the late phase in cells infected with wild-type virus. In addition, a new 9S spliced mRNA having the same 3′ exon as the 12S and 13S mRNAs and a still shorter 5′ exon becomes the predominant form of EIA message[25,26]. This gives rise to the increase in the proportion of protected DNA in the 405 nucleotide fragment and may account for the S_1 protected fragment of ~250 nucleotides. The level of EIB mRNAs is also increased several fold during the late phase[25]. Despite these changes in the pattern of S_1-resistant

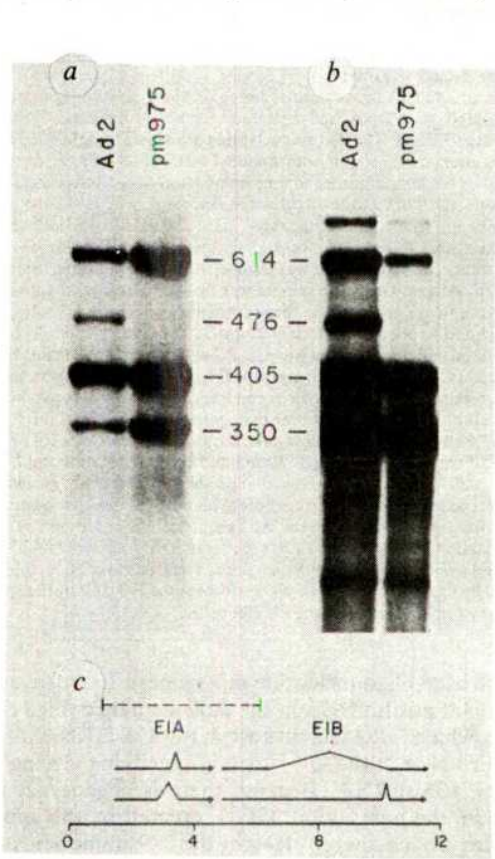

Fig. 4 Hybridization/S_1 nuclease analyses of EIA and EIB mRNAs from pm975 and Ad2. *a*, EIA and EIB early mRNAs. Cytoplasmic RNA was collected as described previously[5] from 500-ml suspension cultures of log phase HeLa cells 6 h after infection with pm975 or Ad2 at 20 PFU per cell. 350 μg cytoplasmic RNA was hybridized to 0.028 μg M13-EIA single-stranded DNA labelled with ^{32}P to a specific activity of 3×10^6 d.p.m. μg^{-1} (ref. 45) for 30 min at 68 °C in 50 μl 1.0 M NaCl, 10 mM Tris *p*H 7.4, 1 mM EDTA. S_1 nuclease digestions in 500 μl were as described previously[23] except that digestions were with 15 Vogt units[46] per reaction at 37 °C for 30 min. Protected fragments were denatured, fractionated by electrophoresis on 14-cm 8 M urea–5% polyacrylamide gels for 15 h at 60 V, dried and visualized by autoradiography with an intensifying screen. The sizes of the predominant bands are indicated in nucleotides. *b*, Analysis of late poly(A)$^+$ EIA and EIB cytoplasmic RNAs. Poly(A)$^+$cytoplasmic RNA (20 μg) isolated from late infected cells[47] was analysed as described in *a*. The autoradiogram was exposed for 17 days with an intensifying screen. *c*, M13 EIA single-stranded DNA probe (R. B. Gaynor and A.J.B., in preparation). The M13 EIA probe is similar to M13GG1 except that the R strand of Ad2 is cloned into the viral strand of M13G*ori*1. The long solid line represents a portion of the adenovirus genome marked off in map units. The horizontal lines joined by carot symbols refer to the exons of the major mRNAs transcribed from EIA and EIB at early times. Arrowheads indicate the 3′ ends of mRNAs. The broken line delineates the adenovirus sequence included in the M13 EIA single-stranded probe.

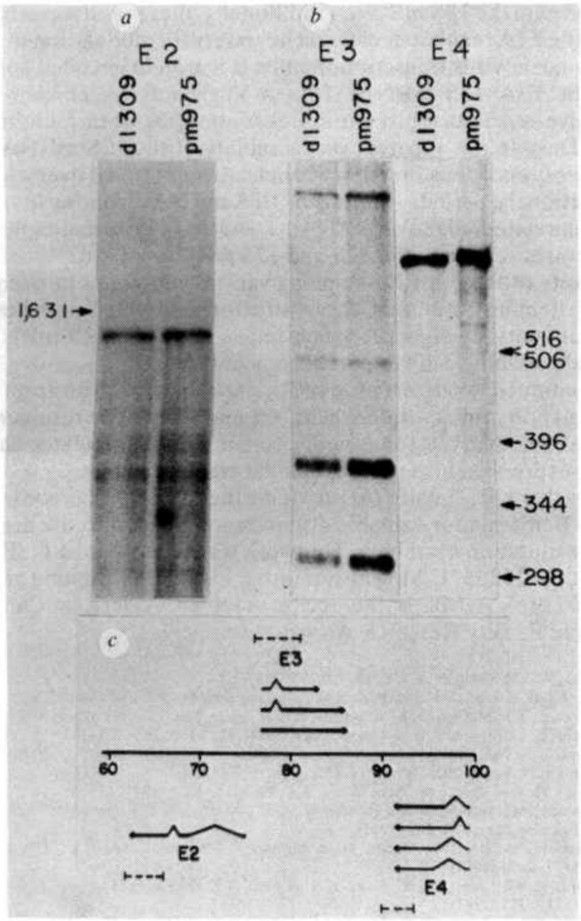

Fig. 5 Hybridization/S_1 nuclease analysis of mRNAs from early regions 2, 3 and 4. Five μg of early poly(A)$^+$ cytoplasmic RNA, prepared from HeLa cells 6 h post-infection with pm975 or d1309, were hybridized to M13 E2, E3 or E4 probes equivalent to 0.2 μg of the complete adenovirus genome. S_1 digestion and gel electrophoresis were as described for Fig. 4*a*. *a*, Early region 2 mRNA. S_1-protected fragments were electrophoresed for 18 h at 120 V. The position of the 1,631 nucleotide *Hin*fI pBR322 marker is indicated. *b*, Early region 3 and 4 mRNAs. The protected fragments were fractionated by electrophoresis for 18 h at 50 V. Although the patterns of protected fragments are identical for d1309 and pm975, the structures of the E3 mRNAs differ from wild-type Ad5 due to a substitution and deletion in the E3 DNA sequence of d1309 (ref. 8). The positions of *Hin*fI pBR322 fragments are included to the right. *c*, M13 E2, E3 and E4 single-stranded probes (R. B. Gaynor and A.J.B., in preparation). The M13 E2 probe was constructed by inserting a *Kpn*I–*Xho*I fragment of Ad2 DNA (61.3–66.0 map units) between the *Kpn*I and *Xho*I sites of M13G*ori*1. The E3 probe was prepared by cloning an *Eco*RI–*Kpn*I fragment of Ad5 DNA (75.9–81.0 map units) between the *Eco*RI and *Kpn*I sites of M13G*ori*1. To construct the E4 probe an *Eco*RI–*Bal*I fragment of Ad2 DNA (89.7–93.2 map units) was cloned between the *Eco*RI and *Pvu*II sites of M13G*ori*1. The Ad5 genome and major E2, E3, and E4 early mRNAs are diagrammed as in Fig. 4*c*. Abundant mRNAs are represented by the bold lines with minor mRNA species indicated by light lines. Broken lines identify the adenovirus sequence included in each of the probes.

fragments at late times, no evidence of the 476 nucleotide S_1 protected fragment is observed in the experiment with pm975 (Fig. 4*b*). Thus, within the sensitivity of the S_1 analysis, the 12S mRNA is eliminated. Based on quantitative densitometry of these autoradiograms, we estimate that it would be possible to detect the 12S mRNA in pm975-infected cells if it were above 2% the level observed in infected wild-type cells.

These results (Fig. 4) prove that substitution of a G for U in the second base of the EIA 12S mRNA intron inhibits RNA splicing at least 50-fold. As the 13S EIA mRNA is produced in pm975-infected cells, the apparent elimination of the 12S mRNA must have been due to interference with RNA splicing. Interference with any other step in RNA processing would have eliminated the 13S mRNA as well, because it is processed from the same mRNA precursor.

13S mRNA encodes all pre-early functions required for normal growth on HeLa cells

Characterization of the functions encoded in EIA and EIB has been facilitated by adenovirus host range mutants selected for their diminished capacity to grow on HeLa cells relative to 293 cells[11]. These mutants fall into two complementation groups (I and II) which map to EIA and EIB respectively[27]. Host range mutants were used to show that EIA encodes a regulatory element[5,6] and that functions encoded in EIA and EIB are required for viral transformation on primary rodent cells[7,8]. One of the motivations for creating pm975 was to define whether one or both of the overlapping EIA mRNAs encode the functions required for virus replication in HeLa cells.

Plaque assays of pm975 and a wild-type control on HeLa and 293 cells (Table 1) establish that pm975 is not host range, and therefore the 12S mRNA is not required for plaque formation on HeLa cells. These data, together with studies of Ad5 hr1 discussed previously, show that only the 289 amino acid, and not the 243 amino acid, polypeptide is required for efficient replication of adenovirus 2 or 5 in HeLa cells.

Because HeLa cells are a continuous cell line, it was considered possible that a requirement for the 243 amino acid protein was masked by the transformed phenotype of these cells. Therefore, plaque assays were repeated with pm975 on HEK cells, a secondary cell culture of human origin, and compared with titres on HeLa cells. The results (Table 1) show that the 12S mRNA is not required for virus replication on HEK cells either.

13S mRNA encodes all pre-early viral regulatory proteins

The pattern and levels of mRNA induced by pm975 and a phenotypically wild-type control (either d1309 or Ad2) were compared using the hybridization/S_1 nuclease technique. The hybridizations were performed between M13G*ori*1 single-stranded DNAs containing portions of the coding strand of each of the early transcription units and early cytoplasmic RNAs extracted from infected HeLa cells. Analysis of the fragment bands protected from S_1 digestion reveals no quantitative or qualitative differences between the early mRNAs induced by pm975 and Ad2 or Ad5 d1309 (see Fig. 4*a* for EIB, Fig. 5 for E2, E3 and E4). These results prove that the EIA regulatory elements that modulate early transcription are not encoded by the 12S mRNA and therefore must be specified by the 13S mRNA only.

Conclusions

A single U → G transversion introduced into the ubiquitous G-U at the 5′ splice site succeeded in eliminating the 12S mRNA in EIA, leaving the overlapping 13S mRNA intact. This demonstrates that a single nucleotide alteration in the 5′ consensus sequence is sufficient to interfere with the RNA splicing apparatus.

The fastidious nature of the splicing apparatus for an unaltered 5′ consensus sequence has also been demonstrated in studies with a nitrous acid-derived Ad5 mutant, Ad5 hr440, which similarly fails to express the 12S EIA mRNA[28]. This mutant has two alterations in the 5′ consensus sequence, at positions five and six of the 12S intron (nucleotides 978 and 979 in the Ad2 sequence). One of these base pair changes creates a termination codon in the 13S mRNA, disrupting translation of the EIA 289 amino acid protein. Therefore, Ad5 hr440 is not useful in discriminating between the functions encoded in the two overlapping early EIA mRNAs.

Analysis of naturally occurring mutations in the β-globin gene from patients with β-thalassaemia has provided evidence that the integrity of the consensus sequence is also required for efficient splicing of cellular mRNAs. Restriction endonuclease[29] and sequence[30] analyses of these mutant β-globin genes have revealed nucleotide alterations only within the 5′ consensus sequence of some of these genes. It is probable that these

β-thalassaemias are associated with disruption of RNA splicing, although this has not been confirmed experimentally.

Models have been advanced suggesting mechanisms for splicing based on hybridizations between small nuclear RNAs and the consensus sequences at the 5′ and 3′ splice sites of mRNA precursors[1-3,31]. These proposals are supported by recent evidence that a small nuclear ribonucleoprotein particle is required for splicing of adenovirus early RNAs[32]. They suggest that failure to splice the pm975 12S mRNA may result from instability of a precursor–small nuclear RNA hybrid. Alternatively, the enzyme(s) involved in the cutting and ligating steps of RNA splicing[33] may have a high degree of specificity for a U in the second position of the intron.

We selected the specific point mutation on the basis of its likelihood to disrupt the 12S mRNA splicing event while leaving the 289 amino acid protein encoded by the 13S mRNA unaltered because of degeneracy in the genetic code. This represents an effective approach with general applicability for ascribing specific functions to individual messages in a series of overlapping spliced RNAs.

Despite the absence of the 12S mRNA, the phenotype of Ad2/5 pm975 on HeLa and HEK cells is indistinguishable from wild-type Ad2 or Ad5, indicating that the only early region 1A function necessary for virus replication in human cells is encoded in the 13S mRNA. Additionally, these results establish that the EIA regulatory element necessary for modulation of the early adenovirus transcription units is a protein encoded solely by the EIA 13S mRNA. Thus a single mRNA encoding a positive regulatory protein in eukaryotes has been identified.

Despite the apparent dispensability of the 12S mRNA, it probably encodes a function which has been selected over a long evolutionary period. Analysis of EIA mRNAs from serotypically unrelated adenoviruses (Ad 7 and Ad 12) reveals spliced structures similar to the 12S and 13S mRNAs of Ad2[34,35]. The ubiquity of these mRNAs among various subgroups of adenovirus demonstrates that these structures survived significant evolutionary divergence, which implies that *the 12S mRNAs* encode a biologically important function *in situ.*

Continued analyses of pm975, including its transforming capacity on primary rodent cells, are underway. The results will reveal whether the same viral protein which modulates early gene expression also induces cellular transformation.

We thank R. Gaynor for providing the M13 DNA probes and Tom Benjamin for valuable discussions which led to the design of the mutational strategy. This work was supported by USPHS grant CA25235. C.M. was supported by USPHS training grant A1 07116. A.J.B. is the recipient of an American Cancer Society Faculty Research Award.

Received 26 October; accepted 20 November 1981.

1. Breathnach, R., Benoist, C., O'Hare, K., Gannon, F. & Chambon, P. *Proc. natn. Acad. Sci. U.S.A.* **75,** 4853–4857 (1978).
2. Lerner, M. R., Boyle, J. A., Mount, S. M., Wolin, S. L. & Steitz, J. A. *Nature* **283,** 220–224 (1980).
3. Rogers, J. & Wall, R. *Proc. natn. Acad. Sci. U.S.A.* **77,** 1877–1879 (1980).
4. Berk, A. J. & Sharp, P. A. *Cell* **14,** 695–711 (1978).
5. Berk, A. J., Lee, F., Harrison, T., Williams, J. & Sharp, P. A. *Cell* **17,** 935–944 (1979).
6. Jones, N. & Shenk, T. *Proc. natn. Acad. Sci. U.S.A.* **76,** 3665–3669 (1979).
7. Graham, F. L., Harrison, T. & Williams, J. *Virology* **86,** 10–21 (1978).
8. Jones, N. & Shenk, T. *Cell* **17,** 683–689 (1979).
9. Perricaudet, M., Akusjarvi, G., Virtanen, A. & Petterson, U. *Nature* **281,** 694–696 (1979).
10. Baker, C. C. & Ziff, E. B. *J. molec. Biol.* **149,** 189–221 (1981).
11. Harrison, T., Graham, F. & Williams, J. *Virology* **77,** 319–329 (1977).
12. Ricciardi, R. P., Jones, R. L., Cepko, C. L., Sharp, P. A. & Roberts, B. E. *Proc. natn. Acad. Sci. U.S.A.* **78,** 6121–6125 (1981).
13. Razin, A., Hirose, T., Itakura, K. & Riggs, A. *Proc. natn. Acad. Sci. U.S.A.* **75,** 4268–4270 (1978).
14. Hutchison, C. A. *et al. J. biol. Chem.* **253,** 6551–6560 (1978).
15. Gillam, S., Astell, C. R. & Smith, M. *Gene* **12,** 129–137 (1980).
16. Matteucci, M. D. & Caruthers, M. H. *J. Am. chem. Soc.* **103,** 3185–3191 (1981).
17. Sanger, F., Nicklen, S. & Coulson, A. R. *Proc. natn. Acad. Sci. U.S.A.* **74,** 5463–5467 (1977).
18. Smith, A. J. H. *Meth. Enzym.* **65,** 560–580 (1980).
19. Stow, N. D. *J. Virol.* **37,** 171–180 (1981).
20. Graham, F. L., Smiley, J., Russell, W. C. & Nairn, R. *J. gen. Virol.* **36,** 59–72 (1977).
21. Aiello, L., Huebner, K. & Weinmann, R. *Virology* **94,** 460–469 (1979).
22. Lassam, N. J., Bayley, S. T. & Graham, F. L. *Cold Spring Harb. Symp. quant. Biol.* **44,** 477–491 (1980).
23. Berk, A. J. & Sharp, P. A. *Cell* **12,** 721–732 (1977).
24. Sambrook, J. *et al. Cold Spring Harb. Symp. quant. Biol.* **44,** 569–584 (1980).
25. Spector, D. J., McGrogan, M. & Raskas, H. J. *J. molec. Biol.* **126,** 395–414 (1978).
26. Chow, L. T., Broker, T. R. & Lewis, J. B. *J. molec. Biol.* **134,** 265–303 (1979).
27. Frost, E. & Williams, J. *Virology* **91,** 39–50 (1978).
28. Solnick, D. *Nature* **291,** 508–510 (1981).
29. Baird, M. *et al. Proc. natn. Acad. Sci. U.S.A.* **78,** 4218–4221 (1981).
30. Shander, M., Woude, S. V., Proudfoot, N. & Maniatis, T. *J. supramolec. Struct. Cell Biochem.* (Suppl.) **5,** 229 (1981).
31. Ohshima, Y., Itoh, M., Okada, N. & Miyata, T. *Proc. natn. Acad. Sci. U.S.A.* **78,** 4471–4474 (1981).
32. Yang, V. W., Lerner, M. R., Steitz, J. A. & Flint, S. J. *Proc. natn. Acad. Sci. U.S.A.* **78,** 1371–1375 (1981).
33. Peebles, C. L., Ogden, R. C., Knapp, G. & Abelson, J. *Cell* **18,** 27–37 (1979).
34. Dijkema, R. *et al. Gene* **12,** 287–299 (1980).
35. Sawada, Y. & Fujinaga, K. *J. Virol.* **36,** 639–651 (1980).
36. van Ormondt, H., Maat, J., De Waard, A. & van der Eb, A. J. *Gene* **4,** 309–328 (1978).
37. Osborne, T. F., Schell, R. E., Burch-Jaffe, E., Berget, S. J. & Berk, A. J. *Proc. natn. Acad. Sci. U.S.A.* **78,** 1381–1385 (1981).
38. Hines, J. C. & Ray, D. S. *Gene* **11,** 207–218 (1980).
39. Messing, J. *Recombinant DNA tech. Bull.* **2,** 43–48 (1979).
40. Jay, E., Bambara, R., Padmanabham, R. & Wu, R. *Nucleic Acids Res.* **1,** 331–353 (1973).
41. Bolivar, F. *et al. Gene* **2,** 95–113 (1977).
42. van der Eb, A. J. & Graham, F. L. *Meth. Enzym.* **65,** 826–839 (1980).
43. Anderson, S. *Nucleic Acids Res.* **9,** 3015–3027 (1981).
44. Dunsworth-Browne, M., Schell, R. E. & Berk, A. J. *Nucleic Acids Res.* **8,** 543–554 (1980).
45. Nomura, N. & Ray, D. A. *Proc. natn. Acad. Sci. U.S.A.* **77,** 6566–6570 (1980).
46. Vogt, V. M. *Eur. J. Biochem.* **33,** 192–200 (1973).
47. Aviv, H. & Leder, P. *Proc. natn. Acad. Sci. U.S.A.* **69,** 1408–1412 (1972).

Unusual physical organization of the *Halobacterium* genome

Carmen Sapienza & W. Ford Doolittle

Department of Biochemistry, Faculty of Medicine, Dalhousie University, Halifax, Nova Scotia, Canada B3H 4H7

The genomes of the extremely halophilic bacteria, Halobacterium halobium *and* Halobacterium volcanii, *contain many repeated sequences. These sequences comprise many families, seem to be highly mobile and are arranged in both clustered and dispersed fashions within these genomes. At least some repeated sequences are more strongly conserved between the two species than are unique sequence DNAs.*

THE archaebacteria (halobacteria, methanogens and certain thermophiles) are thought to have diverged from eubacteria, and from the lineage which gave rise to the nucleus and cytoplasm of eukaryotic cells, at a very early stage in cellular evolution[1-3]. The metabolism, physiology and molecular biology of archaebacteria exhibit some traits which are unique and others which may be considered either 'eubacterial' or 'eukaryotic' in nature[1-4]. Virtually nothing is known about archaebacterial genomes except their genetic complexities. That of *Methanobacterium thermoautotrophicum* has a molecular weight of $\sim 1.1 \times 10^9$ (ref. 5), that of *Thermoplasma acidophilum*[6] $\sim 0.8 \times 10^9$ and those of several halobacteria[7,8] have molecular weights of 2.5×10^9.

The DNA of *Halobacterium halobium* and related species can be separated into components of 66–68 and 57–60 mol % $G+C$ (refs 7, 8). Much, but not all, of the latter fraction comprises a

0028-0836/82/050384—06$01.00

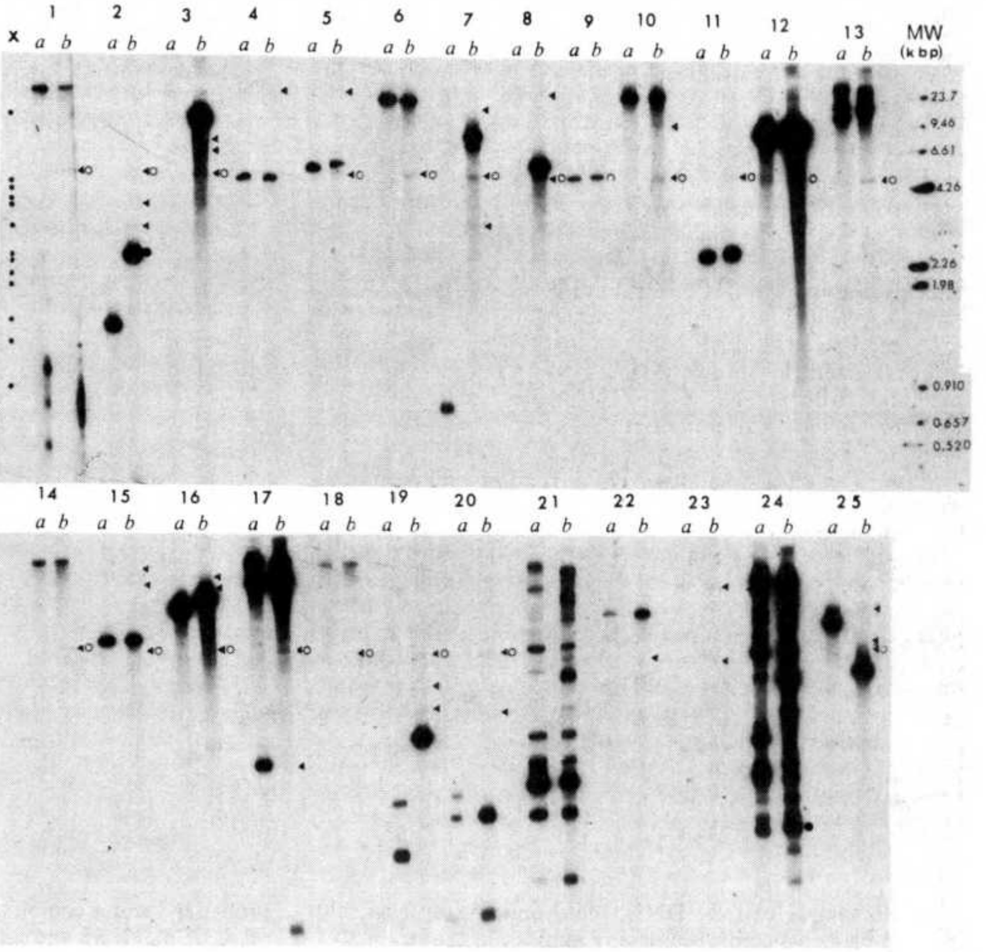

Fig. 1 Autoradiogram showing hybridization of individual ^{32}P-labelled recombinant plasmid DNAs from a genomic library of *H. halobium* R-1 to total DNA from *H. halobium* NRC-1 (tracks *a*) and *H. halobium* R-1 (tracks *b*). ◄, Position of faint bands of hybridization; ○, position of an ~5 kbp band probed by many of the cloned DNAs. Large closed circles in tracks 2*b* and 24*b* indicate hybridization to plasmid DNA fragments. Small closed circles in track X indicate the positions of *Eco*RI fragments of strain R-1 plasmid DNA. The genomic library was constructed by ligating *Bam*HI–*Eco*RI restriction endonuclease (Boehringer) double-digested *H. halobium* R-1 DNA to similarly cleaved pBR322 using T4 DNA ligase[15] (Boehringer). *E. coli* JF1754 (obtained from J. Friesen) was transformed[16] with the ligation mixture and plasmid DNA isolated[17] from 35 Amp^r Tet^s colonies. The recombinant plasmid DNAs were labelled with [α-^{32}P]dCTP (NEN) by nick-translation[11]. *H. halobium* R-1 and NRC-1 DNA was prepared as described elsewhere[18], cleaved with *Eco*RI and subjected to electrophoresis in a 1.2% agarose gel (Sigma). DNA was transferred to a sheet of nitrocellulose filter paper[12] (Millipore) and 0.5 cm strips cut from the sheet. Each probe was hybridized to one 'blot' of each of NRC-1 and R-1 DNA and washed in stringent conditions[19]. Molecular weight markers were λc1857 Sam7 DNA digested with *Hin*dIII and plasmid pBR322 DNA digested with *Alu*I.

150 kilobase pair (kbp) plasmid, four to five copies of which are present in *H. halobium* (ref. 9 and F. Pfeifer, personal communication). Changes in plasmid DNA restriction endonuclease digestion patterns, which can be interpreted as resulting from complex and multiple insertion and deletion events, are associated with easily detectable phenotypic alterations in gas vacuole and pigment production[10]. Such alterations occur with astonishing frequency, suggesting that the *Halobacterium* genome may contain many transposable elements or regions of sequence homology promoting recombination in and between chromosomal and plasmid DNAs.

Renaturation kinetic analyses show no substantial rapidly reannealing fraction which might represent the DNAs of a few, high copy number, repeat sequence families[7,8]. Data presented here, however, do show that (1) the genomes of halobacteria harbour many different, and perhaps rather small, families of repeated sequences whose members are probably both dispersed and clustered in both plasmid and chromosomal DNAs, (2) some repetitive DNAs are more highly conserved in sequence between two distantly related halobacterial species than are unique sequence DNAs, and (3) genomic rearrangements affecting the location of repetitive sequences are frequent and not necessarily associated with detectable phenotypic alterations.

Repeated sequences in a *Bam*HI–*Eco*RI library of *H. halobium* R-1 genomic clones

H. halobium strain R-1 was isolated as a spontaneously occurring, gas vacuole-deficient variant of the 'wild-type' strain NRC-1 in 1969 (W. Stoeckenius, personal communication). It harbours a plasmid of ~50 kbp. Total R-1 DNA doubly digested with *Bam*HI and *Eco*RI was ligated into similarly digested pBR322 and used to transform *Escherichia coli* JF1754. Thirty-five Amp^r Tet^s transformants were randomly selected, and their recombinant DNAs were labelled by nick-translation[11] with ^{32}P-dCTP and used to probe *Eco*RI-digested strain NRC-1 or strain R-1 DNAs bound to nitrocellulose paper strips[12]. Thirty-one of the labelled DNAs probed more than one *Eco*RI fragment of NRC-1 or R-1 DNA; thus each probe contained at least one sequence present more than once in these genomes. Figure 1 shows results for 25 of these cloned probes (faint bands detectable on the original autoradiograph are indicated by ◄). All but clone 9 probe *Eco*RI fragments in addition to those corresponding to the fragment cloned. Sixty to seventy such 'extra fragments' are probed in strain R-1 DNA (tracks *b*); slightly fewer strain NRC-1 DNA fragments (tracks *a*) are probed, and many of these have mobilities different from the probed R-1 fragments. Clones 2 and 24 each probe single and different fragments (indicated by large closed circles) with similar mobilities to *Eco*RI fragments of strain R-1 plasmid DNA (data not shown, but positions of plasmid bands indicated by ● in track X); most of the remaining probed fragments are of chromosomal origin. Although no clones seem to show identical probing patterns (considering patterns obtained with both NRC-1 and R-1), all but clones 4, 21, 22, 23 and possibly 24 probe, with varying intensities, a common ~5 kbp chromosomal fragment in R-1 DNA (○) which is not probed in NRC-1 DNA. For four of these clones probing this fragment (clones 6, 11, 14 and 18), it is the only fragment probed in addition to that cloned; the remaining 15 probing this common 5 kbp fragment probe fragments in addition to this and the fragment cloned (except clone 9, which may contain only the 5 kbp fragment). Thus the 5 kbp common fragment must contain copies of many (>10) different elements which are present in one or two locations elsewhere in the genome. This cluster must either have been created in strain R-1, or disrupted in strain NRC-1, since their divergence 12 yr ago.

The 25 clones used for Fig. 1 and the remaining 10 (not shown) contain in total 250 kbp of *H. halobium* DNA, or 6% of the genome, and contain a minimum of 31 different elements present at least once elsewhere in the genome. If they represent

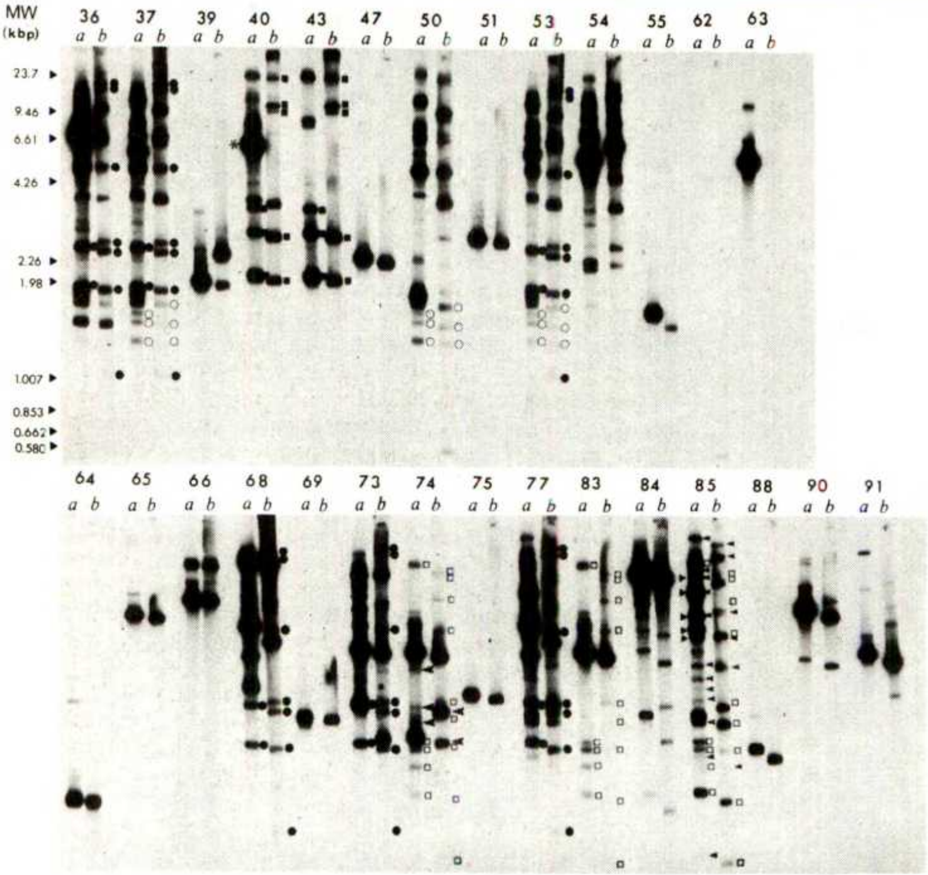

Fig. 2 Autoradiogram showing hybridization of individual ^{32}P-labelled recombinant plasmid DNAs from a genomic library of *H. halobium* NRC-1 to *Eco*RI-digested total DNA from *H. halobium* NRC-1 (tracks *a*) and *H. halobium* R-1 (tracks *b*). The library was constructed by ligating *Eco*RI-digested NRC-1 DNA into *Eco*RI-digested pBR322. All experimental procedures were as described in Fig. 1 legend except that both [α-^{32}P]dCTP and [α-^{32}P]dATP were included in the nick-translation reaction. Open and closed circles and squares indicate shared subpatterns probed by some of the cloned fragments. Small and large arrowheads indicate fragments which distinguish clones 74 and 85 from each other and from clone 83. Closed triangles adjacent to clone 85 (track *a*) indicate *Eco*RI fragments of *H. halobium* NRC-1 DNA which are also probed by several *H. volcanii* cloned DNAs (see Fig. 3*b*).

a random sample of total DNA, there must be at least 500 repeated elements comprising many families in the strain R-1 genome. Some elements must be clustered on cloned DNA, or present in copy numbers >10 in the genome, because clones 21 and 24 alone probe more than one-third of the 'extra' fragments. Variations in intensity of hybridization signals (most obvious with clones 17, 21 and 24) could mean that the fragment probed contains divergent copies of the elements present on the probe, or varying numbers of copies of such elements, or that the probes themselves contain several different repeated elements. The latter interpretation is favoured by data discussed below.

Repeated sequences in an *Eco*RI library of *H. halobium* NRC-1 genomic clones

Strain R-1 is a mutant, and the unknown event which created it may have resulted in the dispersal of repeated sequences within the genome. We constructed a library of wild-type (NRC-1) *Eco*RI fragments cloned into *Eco*RI-digested pBR322 and used 28 of the resulting labelled recombinant DNAs to probe NRC-1 and R-1 DNAs digested with *Eco*-RI (Fig. 2). One of these (clone 62) probed only a single fragment of NRC-1 and R-1 DNAs; the rest probed multiple fragments of either NRC-1 or R-1 DNA. As the NRC-1 plasmid is large (150 kbp), not easily isolated and gives a complex *Eco*RI digestion pattern, it is difficult to say how many probed fragments are of plasmid origin. Most of the fragments probed by at least one of these clones (clone 37) are, however, not of plasmid origin, as judged by comparisons of mobilities of probed *Eco*RI-, *Hin*dIII-, *Sal*I-, *Sst*I- and *Sst*II-generated fragments to plasmid fragments produced by these enzymes (data not shown). All cloned fragments produced different Southern hybridization patterns with DNAs of strains NRC-1 (Fig. 2 tracks *a*) and R-1 (Fig. 2 tracks *b*), and all (except for clones 37 and 53, which may be identical) produced different, probe-specific patterns with each of these DNAs. However several fragments are jointly probed, in different combinations, by different cloned fragments, and can be used to identify at least four shared 'subpatterns' (indicated by open and closed circles and squares in Fig. 2) which are probed in various combinations by clones 36, 37, 40, 43, 50, 53, 68, 73, 74, 77, 83 and 85 (◄ identifies some fragments which distinguish clones 74 and 85 from each other and from clone 83, which otherwise probe common fragments). These 'subpatterns' are also apparent when the same clones are used to probe *Pst*I-digested NRC-1 DNA; those probing various sets of *Eco*RI fragments in different characteristic combinations also probe different sets of *Pst*I fragments in different characteristic combinations (data not shown). The remaining clones produce hybridization patterns with *Eco*RI-digested NRC-1 DNA which appear unique (and also produce unique patterns with *Pst*I-digested DNA). It is not clear whether these patterns too are composed of 'subpatterns', but intensity variations suggest they are. In any case, at least 21 different repetitive sequences are present among these 28 clones (some several times), and most or all of these are different (because they produce different probing patterns) from the repetitive sequences present in clones of the *Bam*HI–*Eco*RI strain RI library. Note that clones 40 and 43 probe common fragments and thus must contain a common element(s), and yet the NRC-1 DNA insert in clone 40 (indicated by an * in Fig. 2) is not itself detectably probed by clone 43. Also, some identical fragments probed by clones 50 and 53 (or 83 and 85) produce hybridization signals of different intensities.

Many of the cloned fragments in the *Eco*RI strain NRC-1 library bear copies of different repetitive elements, some of which must lie close to each other in the genome. Cloned fragments which unquestionably bear two different elements (clones 36, 37, 40, 50, 53, 74, 77 and 85) have an average length of only 3.3 kbp (range 1.75–4.6 kbp). We suspect that the differing intensities with which individual fragments are probed by different cloned DNAs reflect the presence of different numbers of copies, on both probed and cloned fragments, of shared sequences.

There should be (on the basis of its G+C content) ~300 *Eco*RI fragments in the *H. halobium* genome. Elements indicated by symbols in Fig. 2 appear to be present on 10 or fewer *Eco*RI fragments, and yet one of these elements appears five or six times and two of them two or three times in our 28 clones. There are two possible explanations for this apparent statistical improbability. (1) Such elements are present in many copies on the few *Eco*RI fragments which are detected as probed, and also present on a much larger number of other *Eco*RI fragments, but in too few copies to give detectable hybridization signals. Clones bearing *Eco*RI fragments of the latter type would then only probe strongly fragments of the former type. The results with clones 40 and 43 noted above might be consistent with this interpretation. (2) The repetitive sequences represented in Fig. 2 are preferentially located in A+T-rich regions of the genome which are more frequently attacked by *Eco*RI. Indeed, most of the cloned fragments are smaller (average length 3 kbp) than the expected distance between *Eco*RI sites (12 kbp). We may be repeatedly sampling only a small portion of the genome.

To test the latter possibility, we constructed a small library of *Pst*I fragments of NRC-1 DNA inserted into *Pst*I-digested pBR322. The *Pst*I recognition site is similar in G+C content to the *H. halobium* genome. Thirteen such cloned DNAs were used to probe *Pst*I digests of total DNA of strain NRC-1. None probed fragments other than that corresponding in mobility to the fragment cloned, and yet the 13 clones contained in total 48.7 kbp of *H. halobium* NRC-1 DNA, or 51% of the 94.7 kbp represented by *Eco*RI clones shown in Fig. 2, in which there are at least 30 repetitive elements of at least 21 different families.

Repeated sequences in *H. volcanii* genome

16S ribosomal RNA (rRNA) catalogue analyses show *H. volcanii* to be as remote phylogenetically from *H. halobium* as *Pasteurella* or *Aeromonas* species are from *E. coli*[2]. To determine whether *H. volcanii* also contains families of repeated elements and shares any of these with *H. halobium*, we constructed an *Eco*RI library of *H. volcanii* total DNA and used cloned fragments to probe *Eco*RI-digested *H. volcanii* and *H. halobium* NRC-1 DNAs (Figs 3*a*, *b*). Of 30 randomly selected clones, 10 (v71, v82, v86, v107, v110, v113, v118, v123, v144 and v146) contained unique sequence DNA and only probed fragments identical in mobility to the fragment cloned; none of these probed any fragment of NRC-1 DNA. The remaining 20 cloned DNAs probed multiple fragments of *H. volcanii* DNA (the faintest of which are marked by ▲ in Fig. 3*a*). Five different cloned DNAs (v7, v33, v50, v60 and v97) probed an identical large set of *H. volcanii* fragments (some are indicated by ● in Fig. 3*a*). Clone v147 probed the same set, plus several additional fragments. The remaining multiply probing cloned fragments produced hybridization patterns which appear unique, although only two of these (v88 and v122) probed more than three or four fragments in addition to that representing the cloned insert. Only those *H. volcanii* clones probing more than three or four *H. volcanii* DNA fragments probed *H. halobium* NRC-1 DNA but each of these probed multiple fragments (Fig. 3*b*). Thus some repeated sequences are more highly conserved than are unique sequence DNAs.

The clones probing *H. volcanii* fragments indicated by closed circles in Fig. 3*a* probed multiple and similar fragments of *Eco*RI-digested *H. halobium* NRC-1 DNA. Clone v147, which

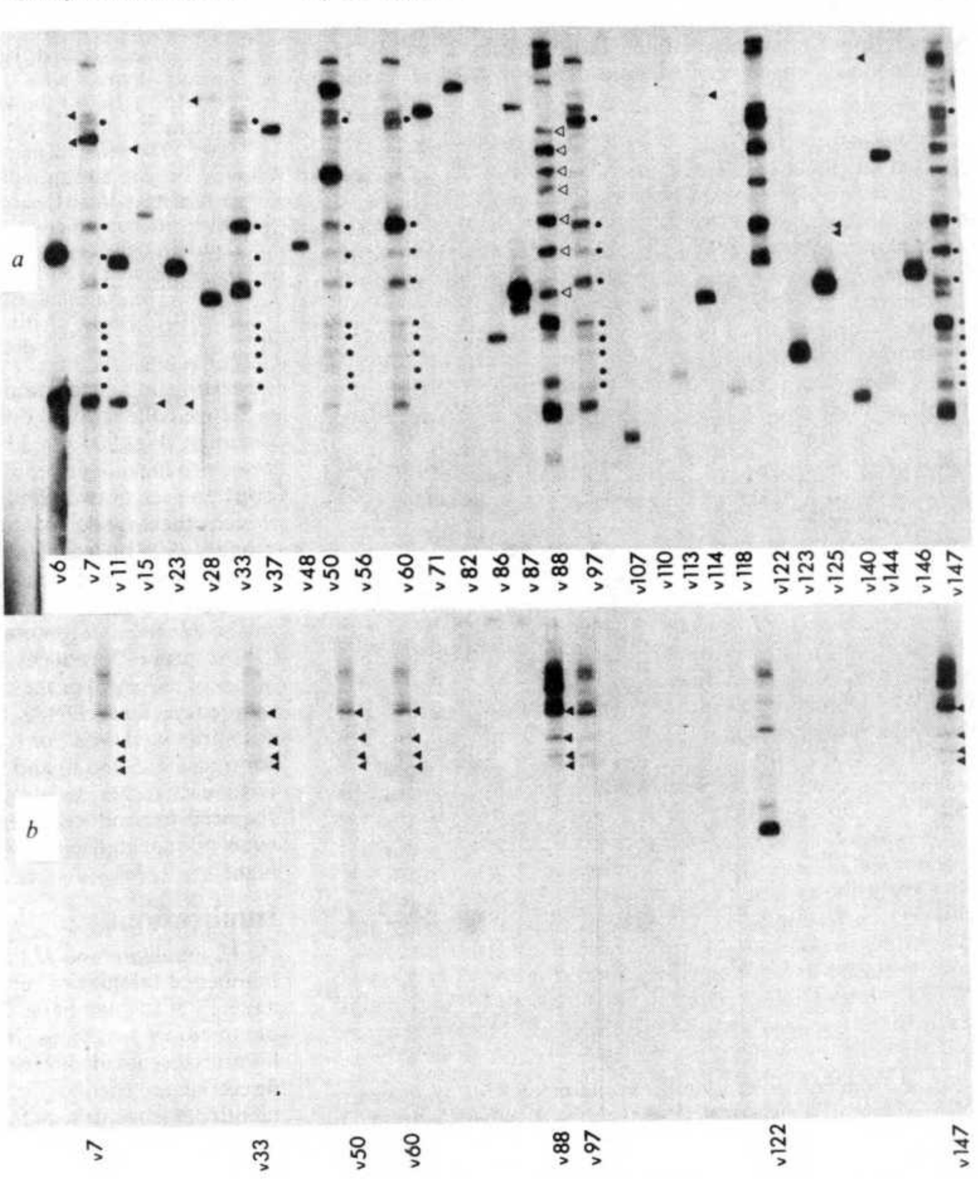

Fig. 3 Autoradiogram showing hybridization of individual ^{32}P-labelled recombinant plasmid DNAs of a genomic library of *H. volcanii* to *Eco*RI-digested total DNA from *H. volcanii* (*a*) or *H. halobium* NRC-1 (*b*). The library was constructed by ligating *Eco*RI-digested total *H. volcanii* DNA to similarly digested pBR322. Both [α-^{32}P]dCTP and [α-^{32}P]dATP were included in the nick-translation reaction. All other experimental procedures were as for Fig. 1. In *a*, ◄ indicates faint bands detected on the original autoradiogram; ●, *Eco*RI fragments of *H. volcanii* DNA hybridized by several *H. volcanii* cloned DNAs and by two *H. halobium* cloned DNAs (see Fig. 4); ◁ adjacent to clone v88 indicates *Eco*RI fragments of *H. volcanii* DNA also hybridized by three *H. halobium* cloned DNAs (see Fig. 4). In *b*, ◄ indicates *Eco*RI fragments of *H. halobium* DNA probed by several *H. volcanii* cloned DNAs and probed by *H. halobium* clone 85 (see Fig. 2).

must contain two different repetitive elements, probed the same fragments and one or two others. Clone v122 probed a unique set of *H. halobium* NRC-1 fragments. More unexpectedly, clone v88 probed the same set of *H. halobium* NRC-1 fragments as did clones v7, v33, v50, v60, v97 and v147, although it does not probe the same set of *H. volcanii* fragments. Thus, repeated elements which are usually separated in *H. volcanii* DNA are usually associated in *H. halobium*.

In a reciprocal experiment (Fig. 4), selected *Eco*RI clones of *H. halobium* NRC-1 DNA which probed multiple *Eco*RI fragments of that DNA were used to probe *Eco*RI-digested *H. volcanii* DNA. Clones 54 and 85 (Fig. 2) probed identical sets of *H. volcanii* DNA fragments, which seem to include all the fragments probed by *H. volcanii* clones v88 and v97 (or others like it), plus some additional high-molecular-weight fragments. This provides reciprocal confirmation of the conclusion reached above. These clones contain inserts of only 3.3 and 1.75 kbp, respectively. However, *H. halobium* NRC-1 clone 84 probes only those fragments probed by *H. volcanii* clone v88, so this clustering is not obligatory in *H. halobium*. Of the remaining seven *H. halobium* NRC-1 clones tested, four (37, 40, 51 and 91) probed unique sets of *H. volcanii Eco*RI fragments and three probed no *H. volcanii* fragments.

Rearrangements affecting *H. halobium* repetitive sequences

Figure 5 shows results obtained by probing *Eco*RI (*a*) or *Sal*I (*b*) digested DNAs from strain NRC-1 (track 1), two NRC-1 single-colony isolates out of 20 picked from a single plate as phenotypically indistinguishable from NRC-1 (tracks 2 and 3), two spontaneously arising gas vacuole-deficient NRC-1 variants (tracks 4 and 5) and strain R-1 (track 6) with two DNAs bearing what we believe to be different and single repetitive elements. The first (Fig. 5*a*) is a 330 bp *Alu*I fragment which appears to comprise most of an ~500 bp repetitive element present in one copy on each of two *Hin*dIII–*Eco*RI fragments of NRC-1 DNA which otherwise do not cross-hybridize. The second (Fig. 5*b*) is a cloned ~900 bp fragment containing an element present on one of two otherwise identical *Hin*dIII fragments of the *H. halobium* R-1 plasmid. (This element is also present at least a dozen times in the *H. volcanii* genome; data not shown.) None of the six DNAs probed produces identical hybridization patterns with either of these two probes, even though the cell populations used to prepare these DNAs derive from phenotypically identical colonies ('wild type' for tracks 1, 2 and 3; gas vacuole-deficient for tracks 4, 5 and 6) and were (except for strain R1) separated from each other by only the number of generations (~30) required to produce enough cells to prepare DNA. Mobility, even of repeated elements selected randomly, is remarkably high.

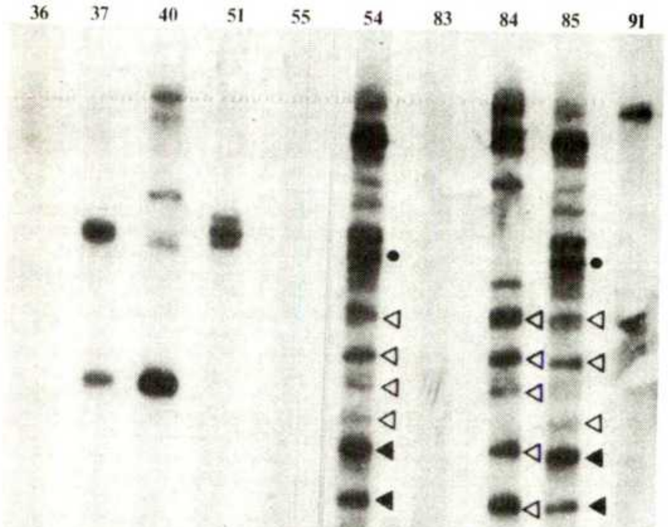

Fig. 4 Autoradiogram showing hybridization of *H. halobium* NRC-1 recombinant plasmid DNAs (see Fig. 2) to *Eco*RI-digested *H. volcanii* DNA. ●, ◁, Fragments also hybridized by *H. volcanii* cloned DNAs (see Fig. 3). ◀, Superimposed symbols ● and △.

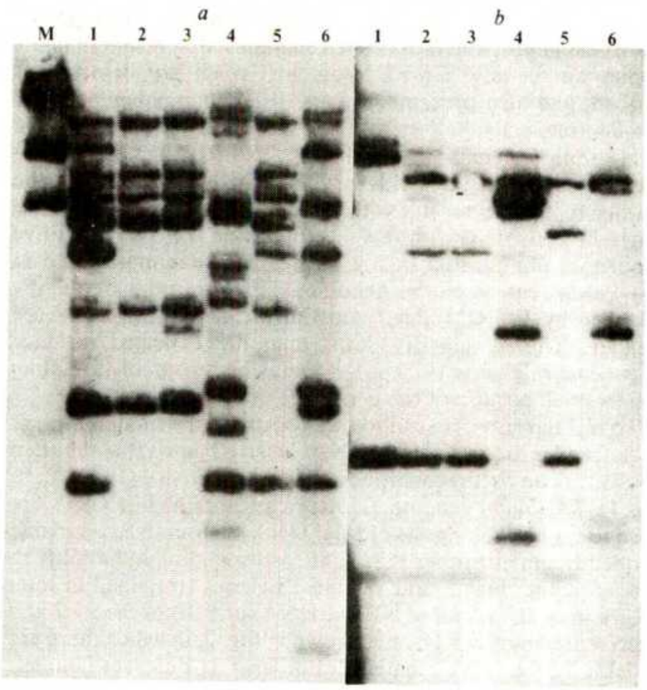

Fig. 5 *a*, Autoradiogram showing hybridization of a ^{32}P-labelled 330 bp *Alu*I fragment of *H. halobium* NRC-1 DNA to *Eco*RI-cleaved total DNA from *H. halobium* NRC-1 (lane 1), two apparently wild-type colonies of strain NRC-1 selected from 20 such isolates (see text; lanes 2 and 3), two gas vacuole-deficient mutants of strain NRC-1 (such mutants arise at a frequency of $1\text{–}3\times10^{-2}$) (lanes 4 and 5), and *H. halobium* R-1 (lane 6). Lane *M* contains ^{32}P-labelled λc1857 Sam7 DNA cleaved with *Hin*dIII. The 330 bp *Alu*I fragment used as a probe appears to comprise most of an ~500 bp repetitive element present in one copy on each of two *Hin*dIII–*Eco*RI cloned fragments of NRC-1 DNA which do not otherwise cross-hybridize (data not shown). *b*, Hybridization of a ^{32}P-labelled 900 bp *Pst*I–*Sal*I strain R-1 cloned DNA fragment to *Sal*I-cleaved DNAs from different *H. halobium* strains. This fragment was discovered as a 900 bp insertion in a *Hin*dIII fragment of strain R-1 plasmid DNA (see text). Lane designations as in *a*.

Implications

(1) *H. halobium* and *H. volcanii* genomes each contain a large number of families of repeated sequences, each of which may have 2–>20 members. The different hybridization patterns obtained when clones from each of the two *H. halobium* libraries discussed above, and a third *Hin*dIII–*Eco*RI library not discussed, are used to probe *Eco*RI-digested *H. halobium* DNA identify at least 50 such families, and there may be many more. The possession of multiple repetitive sequence families is not typical of all archaebacteria; comparable cloning and hybri-

dization experiments with the DNA of the much smaller genome of *T. acidophilum* (not shown) revealed no repetitive sequences. (2) Repetitive elements are often clustered together with other repetitive elements of other families within small genomic regions. Elements of a given family may be clustered with elements of different families in different regions. Some clusters may themselves comprise repeat sequence families, but we cannot be certain of this. (3) Some clusters, such as the 5 kbp fragment identified in Fig. 1, may contain quite large numbers of different elements. (4) Rearrangements which affect the disposition of repeated sequences occur very frequently, and are not obligatorily coupled with any detectable phenotypic alteration, although such alterations are themselves very frequent. The high frequencies of both types of event make it difficult to relate them causally[10]. (5) Sequences which are repeated in the genome of *H. halobium* are frequently present and repeated in the genome of *H. volcanii* and vice versa. They may often be clustered with elements of different repeat sequences in different ways in the two genomes. Most unique sequence DNAs are not conserved between the two genomes. (6) The genome may contain regions of non-random variation in G+C content, in which elements of different families are mostly clustered, because libraries prepared with restriction endonucleases recognizing targets of different per cent G+C contain different numbers and kinds of repeated elements. Although the *H. halobium* chromosome and plasmid are of different G+C contents, they do not contain mutually exclusive sets of repetitive elements (Figs 1, 2 and data not shown). Such compartmentalization, if it exists, is a property of the whole genome.

We know of no other data on prokaryotic genomes which reveal the complexity of repeat sequence composition, arrangement and rearrangement demonstrated here. The only detailed body of data of comparable complexity is that bearing on repeated sequences in the genomes of plants[13] and sea urchins[14], but we hesitate to suggest, on this basis alone, that the halobacterial genome resembles the genomes of eukaryotes more than those of eubacteria. This issue deserves more intensive scrutiny.

This research was supported by a grant from the MRC of Canada. We thank Annalee Cohen for technical assistance.

Received 15 June; accepted 2 December 1981.

1. Woese, C. R. *Scient. Am.* **244**(6), 94–106 (1981).
2. Fox, G. E. *et al. Science* **209**, 457–463 (1980).
3. Doolittle, W. F. *Trends biochem. Sci.* **5**, 146–149 (1980).
4. Bayley, S. T. & Morton, R. A. *CRC crit. Rev. Microbiol.* **6**, 151–205 (1978).
5. Mitchell, R. M., Loeblich, L. A., Klotz, L. C. & Loeblich, A. R. III *Science* **204**, 1082–1084 (1979).
6. Searcy, D. G. & Doyle, E. K. *Int. J. Syst. Bact.* **25**, 286–289 (1975).
7. Moore, R. L. & McCarthy, B. J. *J. Bact.* **99**, 248–254 (1969).
8. Moore, R. L. & McCarthy, B. J. *J. Bact.* **99**, 255–262 (1969).
9. Weidinger, G., Klotz, G. & Goebel, W. *Plasmid* **2**, 377–386 (1979).
10. Pfeifer, F., Weidinger, G. & Goebel, W. *J. Bact.* **145**, 375–381 (1981).
11. Rigby, P. W. J., Dieckmann, M., Rhodes, C. & Berg, P. *J. molec. Biol.* **113**, 237–251 (1977).
12. Southern, E. M. *J. molec. Biol.* **98**, 503–517 (1975).
13. Bedbrook, J., Jones, J. & Flavell, R. *Cold Spring Harb. Symp. quant. Biol.* **45**, 755–760 (1981).
14. Scheller, R. H. *et al. J. molec. Biol.* **149**, 15–39 (1981).
15. Graf, H. *Biochim. biophys. Acta* **564**, 225–234 (1979).
16. Norgard, M. V., Keem, K. & Monahan, J. J. *Gene* **3**, 279–292 (1978).
17. Birnboim, H. C. & Doly, J. *Nucleic Acids Res.* **7**, 1513–1523 (1979).
18. Hofman, J. D., Lau, R. H. & Doolittle, W. F. *Nucleic Acids Res.* **7**, 1331–1334 (1979).
19. Jeffreys, A. J. & Flavell, R. A. *Cell* **12**, 429–439 (1977).

LETTERS TO NATURE

Detection of $HC_{11}N$ in IRC+10°216

M. B. Bell, P. A. Feldman, Sun Kwok & H. E. Matthews

Herzberg Institute of Astrophysics,
National Research Council of Canada,
Ottawa, Canada K1A 0R6

The observations of three rotational transitions ($J = 70 \rightarrow 69$, $71 \rightarrow 70$, and $72 \rightarrow 71$) of $HC_{11}N$ (cyano-deca-penta-yne) in the microwave emission spectrum of the circumstellar envelope of the cool carbon star IRC+10°216 are reported here. The abundances relative to molecular hydrogen and HC_7N are estimated to be $\sim 7 \times 10^{-8}$ and ~ 0.7, respectively. With these observations, taken during March and May 1981 at the Haystack Observatory, $HC_{11}N$ becomes the largest and heaviest molecule yet detected outside the Earth's atmosphere.

The cool carbon star IRC+10°216 (=CW Leo) is believed to be undergoing extensive mass loss and its dense circumstellar envelope is known to be rich in neutral molecules and free radicals. Its comparative proximity to the Earth (~200 pc) and correspondingly large angular diameter (~2.5 arc min as measured in the emission of the CO molecule[1]) have made it especially rewarding in this respect.

Observations of the microwave inversion lines of ammonia in the envelope of IRC+10°216 have shown the presence of a weak feature (U23.698) close to the $NH_3(1,1)$ line. The feature appears in observations made at both the 46-m telescope of the Algonquin Radio Observatory[2] and the 37-m telescope of the Haystack Observatory[3]. After these observations we tentatively identified U23.698 as the $J = 70 \rightarrow 69$ transition of the linear carbon-chain (cyanopolyyne) molecule $HC_{11}N$ (cyano-deca-penta-yne) on the following grounds:

(1) Of the 17 known molecules in the envelope of IRC+10°216, seven have carbon–carbon bonds and 10 have appended CN radicals.

(2) The derived rotational constant ($B_0 \simeq 169.27$ MHz) would be only ~210 kHz greater than the value predicted by Oka[4] on the basis of a simple numerical extrapolation from lower cyanopolyyne chains. The magnitude (~0.1%) and direction of this discrepancy could be readily explained in terms of a slight molecular non-rigidity which is expected on the basis of the extended vibrational satellite patterns found for carbon-chain molecules[5].

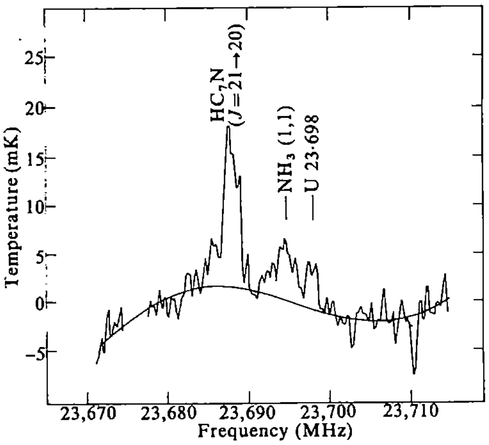

Fig. 1 The spectrum of IRC+10°216 in the region of the $NH_3(1,1)$ line, before baseline removal. Features due to HC_7N ($J = 21 \rightarrow 20$) and the proposed $J = 70 \rightarrow 69$ transition of $HC_{11}N$ (U23.698) also appear in the window. The ordinate is antenna temperature corrected for zenith-angle variations of gain and atmospheric absorption. The gap in the spectrum omits a feature of instrumental origin.

0028-0836/82/050389—03$01.00

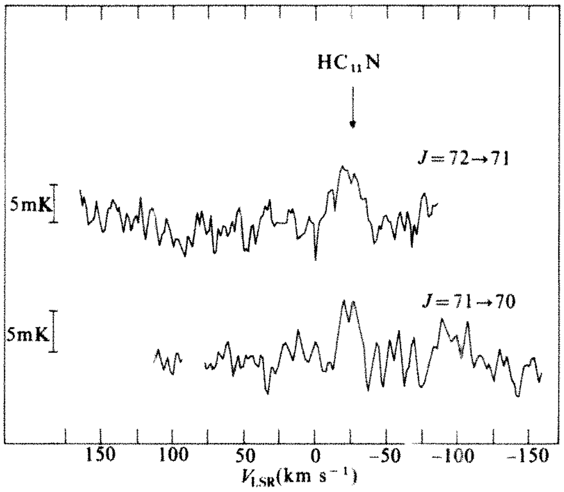

Fig. 2 Two adjacent transitions of HC$_{11}$N in the spectrum of IRC+10°216. The features have been aligned on a common velocity scale using the rest frequencies given in Table 1. The antenna-temperature scales are indicated on the left of the figure. Other details are as for Fig. 1.

(3) Long-chain cyanopolyynes, such as HC$_7$N, are relatively abundant in IRC+10°216. An extrapolation from the lower members of the molecular series[6] suggested that $[HC_{11}N]/[HC_7N] \geq 0.1$. The direct comparison afforded by the presence of both U23.698 and the $J = 21 \rightarrow 20$ transition of HC$_7$N in the NH$_3$(1,1) spectrum[3] is consistent with this expectation.

We have detected two further microwave transitions of HC$_{11}$N (H—C≡C—C≡C—C≡C—C≡C—C≡C—C≡N) using frequencies derived from the above result. This suggests that the identification of HC$_{11}$N is fairly secure and now represents the heaviest (147 AMU) and largest (~15 Å) extraterrestrial molecule known.

At the frequencies employed (close to 24 GHz) the 37-m telescope of the Haystack Observatory has a peak aperture efficiency of 22% at 45° elevation and a beam efficiency of 25%, including radome losses. The half-power beamwidth is 1.4 arc min. The observations were carried out with a maser receiver and an autocorrelation spectrometer of total bandwidth 40 MHz and an effective resolution of 4.9 km s^{-1}.

The observations in March were used to search for the $J = 72 \rightarrow 71$ transition of HC$_{11}$N, expected at ~24,374 MHz. The total-power observing method was used; ~25 h of on-source integration time were accumulated, of which about 30% were affected by adverse weather and were discarded. A further 33 h of on-source time was obtained in May when observations were made of the $J = 71 \rightarrow 70$ transition, predicted to be close to 24,037 MHz. On this occasion, measurements were made using a modified 'double-Dicke' mode[7] when the weather deteriorated, and no data editing was necessary.

Figure 1 shows the spectrum of IRC+10°216 in the region of the NH$_3$(1,1) line as obtained at Haystack[3]. Our new observations of spectral windows containing the proposed $J = 71 \rightarrow 70$ and $J = 72 \rightarrow 71$ transitions of HC$_{11}$N are shown in Fig. 2. The arrow indicates the expected position of the line as predicted from the $J = 70 \rightarrow 69$ transition first detected at ARO ($B_0 = 169.275$ MHz).

Table 1 Transitions of HC$_{11}$N in IRC+10°216

Date	Telescope	Transition $J_u \rightarrow J_l$	Measured rest frequency (MHz)*	Derived B_0 (MHz)†
April 1979 May 1979 February 1980	ARO ARO ARO	70 → 69	23,698.2±0.3‡	169.275±0.002
November 1980	Haystack	70 → 69	23,697.9±0.4‡	169.273±0.003
March 1981	Haystack	72 → 71	24,375.2±0.2§	169.274±0.001
May 1981	Haystack	71 → 70	24,037.1±0.1§	169.277±0.001

* Peculiar velocity −26.0 km s^{-1} assumed.

† Based on $D_0 = 0.22$ Hz; see text.

‡ Line may be confused with NH$_3$(1,1); error quoted includes estimate of possible systematic effects.

§ 1σ formal errors.

Including the earliest measurement[2] of the $J = 70 \rightarrow 69$ transition with the 46-m telescope, four independent observations of microwave rotational transitions of HC$_{11}$N have been made: the results are summarized in Table 1. The rest frequency has been determined for each case from the data assuming a peculiar velocity for IRC+10°216 with respect to the local standard of rest of −26.0 km s^{-1} (see ref. 1). The $J = 70 \rightarrow 69$ transition is confused with the NH$_3$(1,1) line and we take the error in determining the rest frequency in this case to be about three times greater than the formal value. The rotational constant B_0 was calculated for each transition using a centrifugal distortion constant $D_0 = 0.22$ Hz. The latter was estimated from the semi-empirical relation $D_0(HC_nN) \propto [B_0(HC_nN)]^{2.37}$, which provides a good fit to the measured values of the rotational constants of HCN, HC$_3$N, HC$_5$N, and HC$_7$N, and which is consistent with the published transitions of HC$_9$N in TMC 1 (refs 8, 9).

The weighted average of B_0 for all four observations is 169.275±0.001 MHz. This result is unchanged if we omit the poorer-quality 46-m observations of the $J = 70 \rightarrow 69$ line, or if we neglect all the $J = 70 \rightarrow 69$ data on the grounds of its possible confusion with the NH$_3$(1,1) line.

For better estimates of the line parameters we have averaged together the $J = 71 \rightarrow 70$ and $J = 72 \rightarrow 71$ observations on a common velocity scale (see Fig. 3). The line profile thus obtained may show an indication of the non-gaussian (relatively flat-topped) shape found for other molecules in this source[1,10]. We derive a full width at half maximum for the line of 25±2 km s^{-1} and a peak antenna temperature of 6±1 mK.

We have detected three lines in the circumstellar envelope of IRC+10°216, which we believe to be adjacent rotational transitions of the long carbon-chain molecule HC$_{11}$N. While we are confident of the correctness of this assignment, we must still consider whether there are viable alternatives.

The exact agreement in the frequency intervals between the two pairs of lines, and the fact that all three lines have the same intensity leaves little doubt that a single linear species is responsible. If the transitions we detect are not in fact adjacent, but still belong to a single species, that species must have a molecular weight in excess of ~200 AMU. We can argue on abundance grounds that this is much less likely than HC$_{11}$N.

Certain other linear carbon-chain molecules whose exact line frequencies are not known are expected to have a B_0 of the same order; for example, C$_{12}$H and C$_{11}$N. Since C$_4$H and C$_3$N are the longest C$_n$H and C$_n$N carbon chains of their respective types that have yet been found, and because the derived abundance of HC$_{11}$N (see below) is in rough agreement with that extrapolated from lower-order cyanopolyynes, we are led to identify HC$_{11}$N as the source of the detected lines.

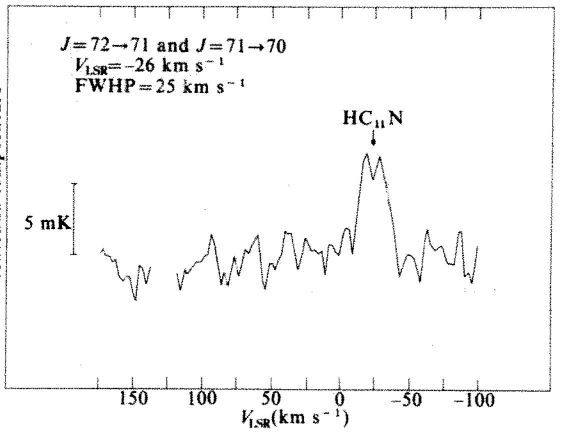

Fig. 3 The average of the $J = 72 \rightarrow 71$ and $J = 71 \rightarrow 70$ transitions of HC$_{11}$N in the spectrum of IRC+10°216. Other details are as for Fig. 1.

Table 2 Cyanopolyyne abundances in IRC + 10°216

Molecule	Observed transition $J_u \rightarrow J_l$	Observed T_A^* (mK)†	Abundance relative to H_2 $\beta = 0.6$	$\beta = 0.8$
HC_5N‡	9 → 8	400 ± 80	7.3×10^{-7}	5.2×10^{-7}
HC_7N	21 → 20	56 ± 8	1.0×10^{-7}	1.0×10^{-7}
$HC_{11}N$	71 → 70 72 → 71	24 ± 4	7.0×10^{-8}	8.0×10^{-8}

See text for details of model used.

† Main-beam brightness temperature corrected for atmospheric absorption and telescope gain-zenith angle efficiency variation.

‡ Measured during May 1981 session.

Molecular line excitation in a circumstellar environment has to be treated differently from that in interstellar dust clouds. Not only does the gas density (and thus also collisional excitation) decrease radially outward from the star, but so also does the IR radiation field responsible for the vibrational excitation. Previous radiative transfer models for the CO and NH_3 molecules[2,11] in the circumstellar envelope of IRC + 10°216 show that the excitation temperature gradient can be approximated by a power law of the form $T_{ex}(r) = T_0(r_0/r)^{\beta}$ where $T_0 = 350$ K at $r_0 = 2 \times 10^{15}$ cm, and $0.6 \leq \beta \leq 0.8$. A gradient of this type, while unimportant for the low rotational states normally observed in the lower-order cyanopolyynes, becomes a significant factor for higher-order members of the series. In the present case, the observed transitions occur between states of rotational energy equivalent to 40 K. The lower excitation temperature in the outer parts of the circumstellar envelope thus leads to a non-uniform distribution of level populations across the molecular gas within the telescope beam.

Model calculations for the circumstellar envelope of IRC + 10°216 have been performed assuming the lines are optically thin and the population distribution at each radius to be in LTE at a temperature $T_{ex}(r)$. We further assume that there is neither significant formation nor destruction of the molecules beyond several stellar atmospheric scale heights[12].

The line brightness temperature over the envelope surface is then computed and the results convolved with the telescope beam. Scaling the results to the observed values leads to the molecular abundances (n_{mol}/n_{H_2}) given in Table 2. Note that the derived abundances scale as (distance/200 pc)^2 × (mass-loss rate/$2 \times 10^{-5}\, M_{\odot}\, yr^{-1})^{-1}$ and are uncertain due to the lack of precise values for these parameters. Table 2 also includes results for the $J = 9 \rightarrow 8$ transition of HC_5N, a short observation of which was made in the May 1981 session at Haystack Observatory for comparison purposes. In addition, although we did not observe a transition of HC_9N, we can predict that in IRC + 10°216 the HC_9N $J = 41 \rightarrow 40$ line should be approximately twice as strong as the lines of $HC_{11}N$ reported here if $n_{HC_9N}/n_{H_2} = 10^{-7}$.

Thus the abundance of $HC_{11}N$ is ~0.7 of that of HC_7N (independent of distance and mass-loss rate). This is interesting in that it is rather higher than would have been expected from an extrapolation from lower-order members of the series. The decrease in abundance as a function of cyanopolyyne molecular weight in the envelope of IRC + 10°216 also seems to be less steep than in TMC 1 (ref. 8) and other interstellar molecular clouds[13]. Moreover, the cyanopolyyne relative abundances compared with molecular hydrogen in IRC + 10°216 are much higher than those found in dark molecular clouds. For example, MacLeod *et al.*[14] reported an abundance ratio $[HC_5N]/[H_2] \approx 10^{-8}$ in TMC 1. We find that this ratio is ≈60 times higher in the case of IRC + 10°216. In fact, relative to H_2, $HC_{11}N$ is ≈7 times more abundant in the envelope of IRC + 10°216 than HC_5N is in TMC 1.

Although the exact mechanism for the formation of long-chain carbon molecules in interstellar space is still in controversy[15–18], we now have evidence that large numbers of such molecules can be produced in the atmospheres of carbon stars like IRC + 10°216 where activation energies can be overcome[19]. Formation of dust grains will quickly lead to momentum grain-gas coupling which will eject the molecules[20].

The current rate of mass returned to the interstellar medium by late-type stars is $6 \times 10^{-10}\, M_{\odot}\, pc^{-2}\, yr^{-1}$ (ref. 21). Assuming 10% of all late-type stars are capable of manufacturing long-chain carbon molecules, our derived abundances for $HC_{11}N$ implies an ejection rate of 10^{39} $HC_{11}N$ molecules $pc^{-2}\, yr^{-1}$ into the interstellar medium alone. While most of these molecules will probably be destroyed by interstellar EUV radiation, clearly the molecular production by stars can be an important ingredient in chemical models of the interstellar medium.

We thank the staff of Haystack Observatory, in particular A. Haschick and B. Leslie, for hospitality and assistance, also L. W. Avery, N. W. Broten, and J. M. MacLeod for encouragement and advice. The Algonquin Radio Observatory is operated by the National Research Council of Canada, Ottawa, as a national radio astronomy facility. Radio astronomy at the Haystack Observatory of the Northeast Radio Observatory Corporation is supported by the NSF.

Received 19 October; accepted 18 December 1981.

1. Wannier, P. G. *et al. Astrophys. J.* **230,** 149 (1979).
2. Kwok, S., Bell, M. B. & Feldman, P. A. *Astrophys. J.* **247,** 125 (1981).
3. Bell, M. B., Kwok, S., Matthews, H. E. & Feldman, P. A. *Astr. J.* (in the press).
4. Oka, T. *J. molec. Spectr.* **72,** 172 (1978).
5. Alexander, A. J., Kroto, H. W. & Walton, D. R. M. *J. molec. Spectr.* **62,** 175 (1976).
6. Winnewisser, G. & Walmsley, C. M. *Astr. Astrophys.* **70,** L137 (1979).
7. Bell, M. B. & Seaquist, E. R. *Astrophys. J.* **238,** 818 (1980).
8. Broten, N. W., Oka, T., Avery, L. W., MacLeod, J. M. & Kroto, H. W. *Astrophys. J. Lett.* **223,** L105 (1978).
9. Avery, L. W. *Proc. IAU Symp.* No. 87, p. 47 (1980).
10. Morris, M. *Astrophys. J.* **197,** 603 (1975).
11. Kwan, J. & Hill, F. *Astrophys. J.* **215,** 781 (1977).
12. McCabe, E. M., Smith, R. C. & Clegg, R. E. S. *Nature* **281,** 263 (1979).
13. Bujarrabal, V., Guélin, M., Morris, M. & Thaddeus, P. *Astr. Astrophys.* **99,** 239 (1981).
14. MacLeod, J. M., Avery, L. W. & Broten, N. W. *Astrophys. J.* **233,** 584 (1979).
15. Schiff, H. I. & Böhme, D. K. *Astrophys. J.* **232,** 740 (1979).
16. Mitchell, G. F., Huntress, W. T. & Prasad, S. S. *Astrophys. J.* **233,** 102 (1979).
17. Churchwell, E., Winnewisser, G. & Walmsley, C. M. *Astr. Astrophys.* **67,** 139 (1978).
18. Allen, M. & Robinson, G. W. *Astrophys. J.* **212,** 396 (1977).
19. Tsuji, T. *Ann. Tokyo. astr. Obs.* **9,** 1 (1964).
20. Kwok, S. *Astrophys. J.* **198,** 583 (1975).
21. Osterbrock, D. E. *Astrophysics of Gaseous Nebulae,* 228 (Freeman, San Francisco, 1974).

On the reported detection of sub-GeV antiprotons in galactic cosmic rays

David Eichler

Astronomy Program, University of Maryland,
Maryland 20742, USA

Buffington *et al.*[1] claim to have detected a $\bar{p}/p$ ratio of $2.2 \pm 0.6 \times 10^{-4}$ at energies between 130 and 320 MeV. This is several orders of magnitude above theoretical predictions[2–4] at these lower energies for $\bar{p}$ fluxes resulting from collisions of primary cosmic rays with the interstellar gas. Measurements at higher energies by Golden *et al.*[5] show a $\bar{p}/p$ ratio of $5.2 \pm 1.5 \times 10^{-4}$, in excess, by a factor of about 3, of the expected values if $\bar{p}$s are of secondary origin in the standard model of galactic cosmic rays. The reported $\overline{He}/He$ ratio[1] is significantly lower than the reported $\bar{p}/p$ ratio, raising difficulties with some scenarios[6] in which the $\bar{p}$s are primary cosmic rays from anti-galaxies. Kiraly *et al.*[7] suggest black hole evaporation as a $\bar{p}$ source. I discuss here scenarios in which the reported sub-GeV $\bar{p}$ excess might be produced as secondaries in high energy collisions. Such production must take place in compact, optically thick sources.

It is assumed that the low energy $\bar{p}$s have lost a few hundred MeV due to modulation by the solar wind. However, while modulation effects may enhance the $\bar{p}$ excess at low energies, they are not nearly strong enough to account for the claimed value (ref. 7 and R. Jokipii, personal communication) (though such considerations could ease the demands on any model of low energy $\bar{p}$ production). In addition to decelerating cosmic rays,

---

Present address: Department of Nuclear Physics, Weizmann Institute of Science, Rehovot, Israel.

0028–0836/82/050391—03$01.00

solar modulation lowers their spatial density so that the low energy p̄ flux is significantly greater outside the heliosphere than in the Earth's vicinity.

Kiraly *et al.*[7] have shown, using Liouville's theorem, that the inferred p̄ flux beyond the heliosphere depends very weakly on the assumptions made about modulation. To infer the interstellar number density, N_{Buf}, implied by Buffington *et al.* I assume that the p̄/p ratio they report ($R_{\mathrm{Buf}} = 2.2 \times 10^{-4}$ at ~ 200 MeV) is reached at 600 MeV ($p = 1.2\, m_{\mathrm{p}}c$) beyond the heliosphere, and that the integral interstellar momentum spectrum of primaries goes as $p^{-1.7}$. The p̄/p ratio R_{Gol} reported by Golden *et al.* at 7 GeV ($p \approx 8m_{\mathrm{p}}c$) is 5.2×10^{-4}. Hence, N_{Buf} is given by

$$N_{\mathrm{Buf}} \simeq \left(\frac{8}{1.2}\right)^{1.7} \left(\frac{R_{\mathrm{Buf}}}{R_{\mathrm{Gol}}}\right) N_{\mathrm{Gol}} \simeq 10\, N_{\mathrm{Gol}} \tag{1}$$

N_{Gol} exceeds the p̄ number density N_{s} predicted by the standard leaky box model of galactic cosmic rays[2-4] by a factor of 3 or so, hence N_{Buf} exceeds that prediction by about one and a half orders of magnitude.

If the p̄ excess is real, and if the p̄s are secondaries, they are apparently decelerated outside the heliosphere from their production energy ($\gtrsim 3$ GeV) down to 600 MeV or so. Scenarios for decelerating secondary p̄s can be broken down into two categories: (1) the p̄s are produced at large cosmological redshift, and are decelerated by the expansion of the Universe; (2) the p̄s are produced and decelerated within the Galaxy. Such scenarios have difficulties with overproduction of secondary products which leads to a model in which the p̄s are produced in dense, optically thick environments—perhaps the galactic centre.

If the p̄s were produced at high redshift, their present cosmic energy density (which would then equal that inside our Galaxy) implied by Buffington *et al.* would be $\sim 10^{-4}$ eV cm^{-3}. As the $\bar{\mathrm{p}}/\nu$ ratio in high energy collisions is $< 10^{-2}$, the implied energy density in high energy νs would exceed 10^{-2} eV cm^{-3}. (The low γ-ray background immediately constrains the p̄s to be produced in dense compact regions where γ rays would be stopped by collisions with other photons.) The Reines experiment[8] limits the cosmic neutrino background at $E > 0.5$ GeV to $< 3 \times 10^{-3}$ eV cm^{-3}, (ref. 9), apparently ruling out the cosmological deceleration scenario.

Stochastic diffusion in momentum space is one possible mechanism[1] for generating low-energy p̄s. However, such a process would cause the cosmic ray spectrum to approach the equipartition differential momentum spectrum $N(p)dp \propto p^2 dp$, which differs vastly from the observed spectrum $N(p) \propto p^{-2.7}$.

We henceforth consider only adiabatic expansion as a deceleration mechanism. Assume that there is some 'new' cosmic ray population that traverses much matter within a compact expanding region. To produce the reported p̄ flux without adding significantly to the observed secondary to primary ratio, (1) the product of the galactic power output P_{N} of the new population and the traversed grammage g_{n} must be at most comparable with that of the 'standard' CR population $P_{\mathrm{s}}g_{\mathrm{s}}$ or (2) the new population must traverse enough grammage near the production site for the secondaries to be thoroughly broken down. 50 g cm^{-2}, roughly 5 destruction pathlengths for L, Be and B, suffices[10]. Note, however, that at grammage larger than 50 g cm^{-2}, the p̄s begin to annihilate before escaping the compact region. Hence this means of avoiding too much secondary production requires 'fine tuning' of the traversed grammage.

A more general constraint is the γ-ray emission from the galaxy above 100 MeV, 8×10^{38} erg s^{-1}. To within a factor of 2, this is what is expected from the standard CR population interacting with 5 g cm^{-2} of matter before escape[11]. It would seem, then, that the total collision rate involving galactic cosmic ray protons and the resulting p̄ production rate cannot be much greater, in optically thin regions, than expected from the standard cosmic population aside from 'factor of 2' uncertainties. If $N_{\mathrm{Buf}} \gg N_{\mathrm{S}}$, this poses difficulties for models that would produce the p̄ excess claimed by Buffington *et al.* in regions from which γ rays escape.

The γ-ray constraint could be circumvented by postulating p̄ production in very young supernova remnants ($T < 10$ yr), for then the associated γ-ray production is sporadic, and could presently be in an 'off' stage. (In any case, in order that primaries produced within the young remnant traverse many g cm^{-2}, it is easy to show that they must do so when the remnant is younger than 10 yr.) This, however, implies that the p̄s suffer enormous adiabatic losses before being deposited in the interstellar medium, and in turn raises the total cosmic ray power and time averaged γ-ray luminosity required to account for the observed p̄ flux by an enormous factor. It can be shown that young supernova remnants in nearby galaxies would then be bright γ-ray sources, contrary to observation.

Another constraint on p̄-production comes from the e$^+$ flux. This constraint is independent of extensive galactic parameters as the p̄/e$^+$ yield depends only on the physics of the high energy collisions. While the results of Buffington *et al.* and Golden *et al.*, given the experimental numbers and other uncertainties, do not necessarily imply too large a p̄/e$^+$ yield in the galaxy, it should be noted that a very large high energy collision rate in the galaxy must be arranged without affecting the observed e$^+$ flux appreciably. (Possibly, the e$^+$s can be disposed of at $E > 1$ GeV by synchrotron radiation in the enhanced magnetic field of a dense environment, if they are produced there.)

In view of the indications that the galactic $\bar{\mathrm{p}}/\gamma$ production ratio (and possibly the p̄/e$^+$ ratio) is higher in our Galaxy than expected from cosmic ray collisions, it is worth considering p̄ production scenarios that yield such high p̄/e$^+$ and $\bar{\mathrm{p}}/\gamma$ ratios. In particular, suppose the anti-protons are produced in dense, compact regions where the radiation density is sufficiently high to block γ-ray escape through photon–photon collisions and to degrade e$^+$s through inverse-Compton reactions at a faster rate than p̄ annihilation. If the p̄s are produced within ejected fluid, they can be adiabatically cooled, and ultimately deposited into the interstellar medium unaccompanied by π^0-decay γ rays or $\pi^{\pm}$-decay e$^+$s.

γ rays at $E_\gamma \simeq 100$ MeV are blocked most effectively by X rays at $10 < E_{\mathrm{x}} < 100$ keV. In any compact source the number density n_{ph} of photons of energy E_{ph} is at least $L/4\pi R^2 c E_{\mathrm{ph}}$, where L is the luminosity in these photons and R is the source radius. The source interior is then opaque to γ rays ($\sigma_{\gamma\gamma} n_{\mathrm{ph}} R > 1$) if

$$(L/L_{\mathrm{ed}})(R_{\mathrm{s}}/R)(\sigma_{\gamma\gamma}/\sigma_{\mathrm{T}})(m_{\mathrm{p}}c^2/E_{\mathrm{ph}}) > 1 \tag{2}$$

Here σ_{T} and $\sigma_{\gamma\gamma}$ are the cross-sections for Thompson scattering and pair production, R_{s} is the Schwarzschild radius, and L_{ed} is the Eddington luminosity defined by $L_{\mathrm{ed}} = 4\pi G M m_{\mathrm{p}} c/\sigma_{\mathrm{T}}$, where M is the mass of the compact object and m_{p} is the proton mass. For $E_\gamma > 100$ MeV, $10 \lesssim E_{\mathrm{ph}} \lesssim 100$ keV, this condition is satisfied by accreting compact X-ray sources by a very large margin. (The X rays need not escape; even if they are eventually blocked and converted into fluid motion, they can still block γ rays close to the compact object.) Indeed, high-energy collisions can be postulated to exist near any compact object where $L/L_{\mathrm{ed}} \gtrsim 1$, independent of its mass, without running into the difficulty of overproducing γ rays. Primary high energy ps can be produced (say, by collisionless shocks) within the accretion or ejection flow near the object, but the particular mechanism for producing them is not crucial to the model.

The column density in Eddington-limited flow onto any compact object is known, by familiar dimensional arguments, to be of the order of 1 g cm^{-2} or more, independent of mass: $L \approx L_{\mathrm{ed}}$, $L \approx \varepsilon \dot{M} c^2$, where $\dot{M}$ is the mass accretion rate, $\varepsilon \lesssim R_{\mathrm{s}}/R$, $\dot{M} \lesssim 4\pi n m_{\mathrm{p}} R^2 \beta c$ where n is the number density of the accreting material and βc is the radial infall velocity, all of which imply that the column density $n m_{\mathrm{p}} R \gtrsim m_{\mathrm{p}}/\beta\sigma_{\mathrm{T}} > 1$ g cm^{-2}. Hence any high energy particles produced in the vicinity of compact objects are likely to have a substantial amount of target matter to interact with.

Finally, if the object ejects matter in the manner of active galactic nuclei or SS433, it can adiabatically decelerate p̄s produced in its vicinity and deposit them into the interstellar medium.

The above scenario also predicts low energy e^+–e^- pairs and photons with $E_{ph} \geqslant 100$ keV from the electromagnetic cascade, and has been proposed[12] to account for the pair production at the galactic centre that is implied by the observed e^+–e^- annihilation radiation[13]. The variable 0.51-MeV line emission from the galactic centre requires $\sim 10^{38}$ erg s^{-1} in pair production if the pairs each have a few MeV in energy, and, according to this scenario, probably requires more than $\sim 10^{39}$ erg s^{-1} in relativistic primary production. Within an optically thick medium, the p̄/p ratio can approach 2×10^{-3}, so a p̄ output of 2×10^{36} erg s^{-1} or more is reasonable for such a source. This compares favourably with the product of the galactic primary output, 3×10^{40} erg s^{-1}, and the p̄/p ratio measured by Buffington *et al.* of $\sim 2 \times 10^{-4}$. A single source of the sort postulated here, or a few of them, could readily account for the galactic p̄ output on energetic grounds. (Note that a necessary condition for producing an e^+–e^- annihilation line is the presence of enough ambient matter so that any e^+s produced within annihilate. It has been suggested[14] that the clouds near the galactic centre are good candidate sites for the annihilation that separates the observed line. Thus, even if the galactic centre, where the ambient density is very high, proves to be a unique source of e^+–e^- annihilation radiation, the phenomenon that produces the e^+s may be a common one. Other hard X-ray sources, for example, remain possible e^+ and p̄ sources through the cascade mechanism even if they display no annihilation line.)

10^{36} erg s^{-1} in high energy neutrinos at a distance of 10 kpc is detectable by DUMAND, so neutrino astronomy might eventually provide independent evidence for such a p̄ scenario.

While the results of Buffington *et al.* may be explainable, they are surprising nonetheless, and independent experimental confirmation is needed. I have also emphasized that the p̄/e^+ and p̄/γ flux ratios are more important than the p̄ flux itself in setting constraints on models of p̄ origin.

I thank Drs T. Gaisser and D. Ellison for useful discussions. This research was supported by NSF grant AST800 2673 and by the Alfred P. Sloan Foundation.

Received 19 August; accepted 3 December 1981.

1. Buffington, A., Schindler, S. M. & Penypacker, C. R. *Astrophys. J.* **248,** 1179 (1981).
2. Gaisser, T. K. & Maurer, R. H. *Phys. Rev. Lett.* **30,** 1264 (1973).
3. Stephens, S. A. *Nature* **289,** 267 (1981).
4. Szabalski, J., Wdowczyk, J. & Wolfendale, A. W. *Nature* **285,** 386 (1980).
5. Golden, R. L. *et al. Phys. Rev. Lett.* **43,** 1196 (1979).
6. Stecker, F. W. *NASA Tech. Mem.* No. 82083 (1981).
7. Kiraly, P., Szabalski, J., Wdowczyk, J. & Wolfendale, A. W. *Nature* **293,** 126 (1981).
8. Crouch, M. F. *et al. Phys. Rev.* D (1978).
9. Eichler, D. *Astrophys. J.* **229,** 39 (1979).
10. Cowsik, R. & Gaisser, T. K. *Proc. 17th Int. Cosmic Ray Conf.*, Paris OG 3.1–16.
11. Stecker, F. *Phys. Rev. Lett.* **35,** 188 (1975).
12. Eichler, D. *Astrophys. J.* (submitted).
13. Riegler, G. R., Mahony, W. A., Ling, J. C., Prince, T. & Jacobson, A. S. *Conf. on Cosmic Ray Astrophysics and Low Energy γ-Ray Astronomy*, Minnesota (1980).
14. Ramaty, R. & Lingenfelter, R. E. *Phil. Trans. R. Soc.* (in the press).

Vortex solitary waves in a rotating, turbulent flow

E. J. Hopfinger

Institut de Mécanique (associé au CNRS) Université de Grenoble,
Grenoble, 38041 France

F. K. Browand

Department of Aerospace Engineering, University of Southern
California, Los Angeles, California 90007, USA

Turbulent flow in a rotating container has been widely studied[1–5], but here we consider an experiment in which the axis of rotation is vertical, the tank deep and a vigorous turbulence is produced near the bottom by a horizontal grid oscillating in the vertical direction. The flow within the rotating container can be envisioned to result from: (1) the disorganized, turbulent motion produced by the grid which, in the absence of rotation, would yield a random field with turbulent intensity decreasing upwards (away from the grid) and turbulent length scale increasing upwards[6]; (2) the organizing influence of rotation which, in the absence of turbulence, would generate a (trivial) flow having a single vertical component of vorticity, 2Ω (Ω is the tank rotation rate), uniform throughout the tank. These two competing effects combined produce a flow field which is surprisingly complex. The major feature of the flow consists of a collection of regions of highly concentrated vorticity, or vortices. These vortices extend coherently throughout the depth of the container. Waves having the form of compact, helical distortions propagate along the vortex cores. We show that the waves are well described by the vortex soliton theory of Hasimoto[7].

The Rossby number, $Ro = u/2\Omega l$, measures the local importance of inertia to rotation in the flow field. Both u, the turbulent velocity, and l, the turbulent length scale, can be assumed constant in planes perpendicular to the axis of rotation but, of course, vary with depth. The Rossby number at the grid location is fixed by the motion of the grid itself, and is given by $Ro_g = n/2\Omega$, where n is the grid oscillation frequency. In our

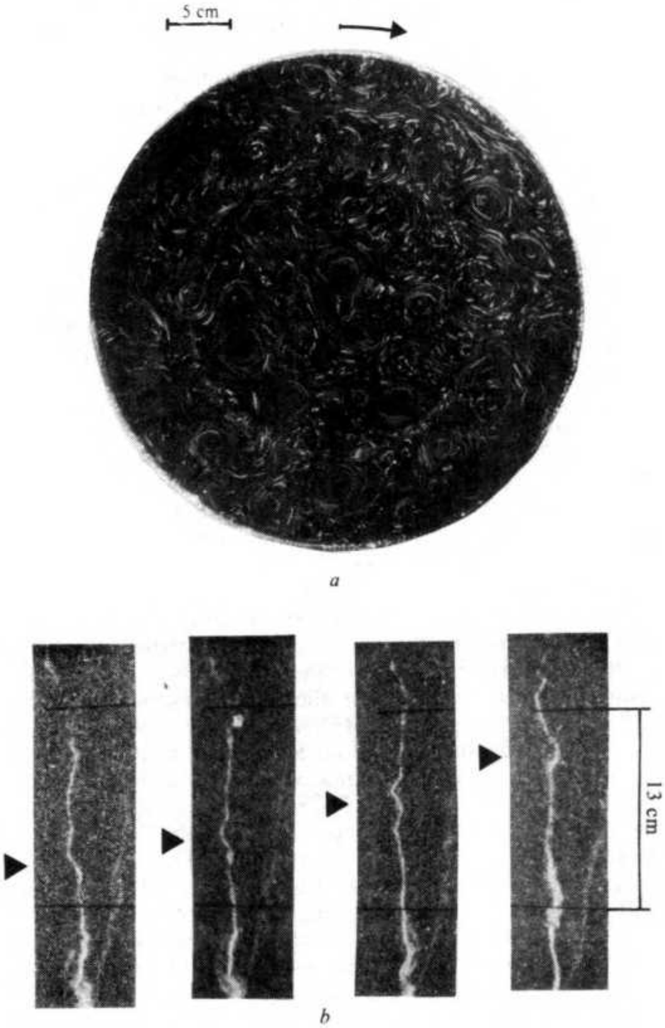

Fig. 1 *a*, Streak photograph illustrating flow in a horizontal plane, $Ro_g = 3.32$. Exposure time is 0.25 s. *b*, Vertical plane visualization of a typical vortex core, utilizing small gas bubbles for illumination. A travelling vortex core wave is marked by arrows.

0028-0836/82/050393—03$01.00

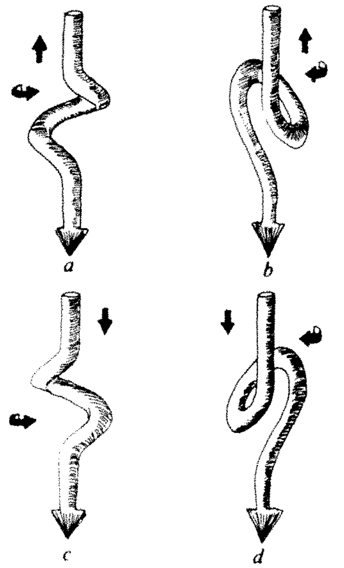

Fig. 2 Schematic representation of possible vortex core wave types. Core vorticity is clockwise, and arrows indicate propagation/rotation of wave patterns.

experiment Ro_g is large, 0(3–30), and the turbulent flow near the grid is relatively unaffected by rotation. Away from the grid the influence of rotation becomes more important, and at some well defined height the flow changes character completely. A collection of concentrated vortices fill the remainder of the tank depth. These vortices are seen in Fig. 1*a* for a grid Rossby number of 3.32. Here the flow in horizontal planes is visualized by passing a light sheet through the tank and observing the trajectories of small wood particles. The local Rossby number associated with the transition height (and with the vortices above) has a constant value of about 0.20 for the range of grid Rossby numbers investigated. Above the transition, there is almost no additional vertical variation of average turbulence quantities.

For a better visualization of these regions of concentrated vorticity, a vertical light sheet is utilized. Small gas bubbles introduced at the bottom of the tank collect in the core regions to provide the ilumination seen in Fig. 1*b*. (The bubbles themselves do not affect the flow significantly, as the same motions are observed when bubble densities are very low.) Only a fraction of the tank depth is shown, but the vortex cores extend to the top of the tank. The lower ends of the cores terminate in the strongly three-dimensional region near the grid. Quantitative estimates show that a typical vortex has a vorticity 40 times the tank vorticity (2Ω), and a core radius $\varepsilon = 0.1$–0.15 cm—a remarkable and unexpected result. A complete description of experimental results can be found in ref. 8. Here we concentrate on one interesting consequence of the presence of these vortex regions—the existence of travelling wave disturbances.

A wave disturbance (marked by arrows) can be seen on the vortex core in Fig. 1*b*. The wave disturbance has the form of a helical distortion of the core. A straight vortex induces no motion on itself, but the wave-distorted core produces a self-induced velocity field which allows propatation of the disturbance. (The propagation of a smoke ring is a simpler example of self-induced motion. The induced velocity field is analogous to the magnetic field which would be produced were the vortex a current-carrying conductor.) The possibility of such vortex core motions was discussed in general by Batchelor[9] and by Hasimoto[7]. Simple dynamical arguments suggest four possible wave types, as outlined in Fig. 2. Waves *a* and *b* are a left-handed kink and anti-kink, respectively, and propagate in a direction opposite to the core vorticity vector. The kink pattern rotates oppositely to the rotation of the core, while the anti-kink rotates in the same sense as core rotation. Waves *c* and *d* are mirror images of *a* and *b*. All these wave types were observed in our experiment.

The waves appear to propagate as single entities and to travel many times their length without appreciable change in shape. This suggests the possibility of a solitary wave (soliton) description for the phenomenon. Hasimoto[7] has demonstrated analytically that solitons can exist on a single, isolated vortex core in an irrotational flow. Wave properties are governed by a non-linear Schroedinger equation for a model which assumes constant circulation and no vortex stretching. The induced motion is calculated as if the vortex filament were a circular ring having the same curvature as the actual filament. For a filament which is straight at infinity, there is a particular solution giving a soliton of constant torsion and varying curvature (torsion is the rate of change of bi-normal direction along the filament).

The assumptions of the theory are not precisely appropriate to the present experiment. There are many cores in the experiment, not just a single core; the outer flow is not irrotational; and there is rotation of the container as a whole. These complications seem to be relatively unimportant, however. Individual vortex cores are often far from neighbouring cores, and the concentration of core vorticity by a factor of 40 above the tank vorticity may qualify them approximately as 'isolated' vortices. Finally, Rossby numbers associated with the wave-induced motions are moderately large, that is, $Ro = \text{(group velocity)}/2\Omega\text{(wave amplitude)} > 1$. Rotation, then, is responsible for the regions of concentrated vorticity, but has little direct effect on the waves themselves.

The wave chosen for detailed comparison is shown sequentially in Fig. 1*b*, travelling upwards with anticlockwise rotation (a left kink). The wave length is ~5 cm, and the total lateral excursion of the core is ~0.6 cm. The corresponding tank rotation rate is 1 revolution per second and the grid oscillation frequency is 6.63 Hz. Two simple comparisons with theory are possible—wave shape and the ratio of propagation speed along the core to the rotation speed of the pattern. The theoretical wave shape predicted by Hasimoto (in suitably non-dimensionalized coordinates) depends on a single parameter,

$$T = \frac{2\text{(Wave torsion)}}{\text{(Maximum wave curvature)}}$$

The quantity used to non-dimensionalize the physical lengths is

$$\nu = \tfrac{1}{2}\text{ (Maximum wave curvature)}$$

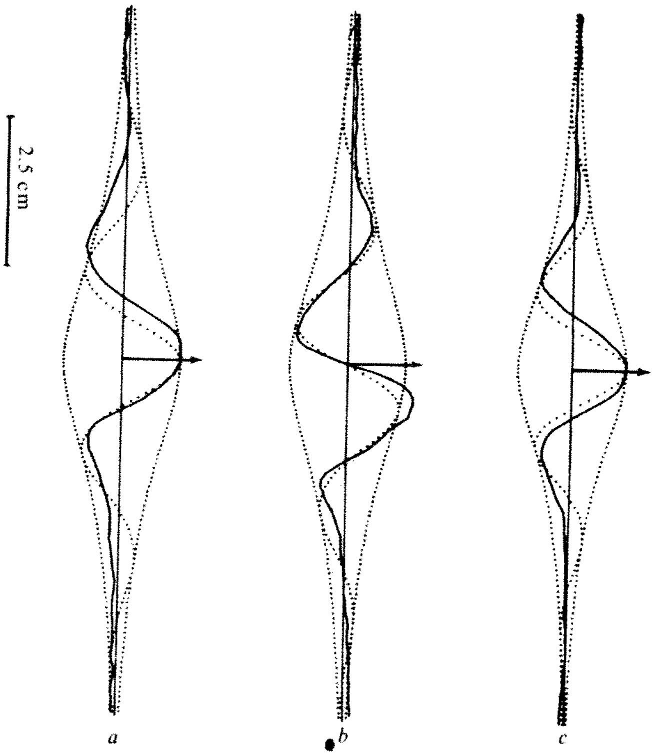

Fig. 3 Comparison of experimental (——) and theoretical (· · ·) soliton wave shapes. *a*, $t = 0$; *b*, t = one-quarter period; *c*, t = one-half period. Lateral scale has been doubled.

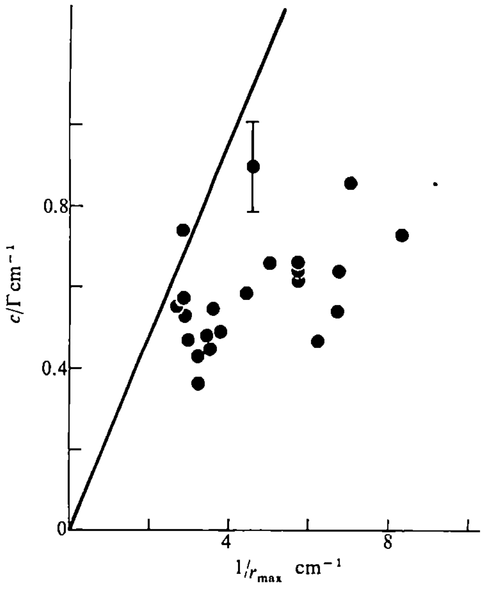

Fig. 4 Observations of group velocity as a function of the inverse of maximum wave radius (taken from film). Solid line is the theoretical upper bound. Error bar indicates relative level of confidence.

In practice, T and ν are chosen to best fit the overall wave shape at three instances of time. The three waves shapes are spaced in time at precisely one-quarter of the pattern revolution, and together represent one-half revolution of the wave. The result of the comparison is shown in Fig. 3. Best overall fit for the three shapes yields the values $T = 3.125$, $\nu = 0.64\,\mathrm{cm}^{-1}$. The wave torsion and maximum curvature are then computed to be, respectively, $2.00\,\mathrm{cm}^{-1}$ and $1.28\,\mathrm{cm}^{-1}$. The theoretical envelope is a hyperbolic secant, and the wave shape is a sinusoidal function within the envelope. Theory predicts additional oscillations at the ends of the wave which are not observed experimentally, and this is the most noticeable discrepancy. However, these oscillations are extremely small—<0.1 cm—and are probably below the resolution of our visual measurements. Overall, the match between experiment and theory is exceedingly good.

The wave envelope travels upwards with group velocity $c = 15.7\,\mathrm{cm\,s}^{-1}$ $\pm 10\%$, and has a rotation rate $\omega = 13.2\,\mathrm{rad\,s}^{-1}$ $\pm 10\%$. Using the observed maximum radius of 0.29 cm, the ratio

$$\frac{\text{Wave envelope speed}}{\text{Maximum rotation speed}} = \frac{c}{\omega r_{max}} \cong 4.05 \pm 0.7$$

The theoretical prediction is

$$\left|\frac{c}{\omega r_{max}}\right| = \left|\frac{T(T^2+1)}{(T^2-1)}\right| = 3.84$$

for $T = 3.125$. Thus, the theoretical estimate agrees with measurement within the accuracy of the measurement. The tentative conclusion is that these isolated waves are indeed solitons and are well described by the theory of Hasimoto.

The theory can be used to draw several additional conclusions in qualitative agreement with experimental observation. The theoretical prediction for the group velocity is

$$c = K\left[\frac{2T}{(T^2+1)}\frac{1}{r_{max}}\right]\Gamma$$

The quantity in parentheses is the wave torsion, here given in terms of T and the maximum wave excursion (or amplitude), r_{max}. Γ is the vortex circulation and K is a constant related to the asymptotic, local-induction approximation. The wave properties just determined, together with an estimated value for the vortex circulation, allow a rough estimate for the constant K. Thus

$$c \cong 0.48 \frac{T}{(T^2+1)}\frac{\Gamma}{r_{max}}$$

The conclusion is that waves of fixed amplitude, on cores of fixed circulation, travel at different speeds depending on wave shape. Furthermore, waves of fixed shape and fixed circulation travel at a speed inversely proportional to wave amplitude. The reason is that the group velocity is proportional to wave torsion (not to wave amplitude); and for fixed shape, a wave of smaller amplitude has the greater torsion. An approximate upper bound on group velocity is obtained by noting that the quantity $T/(1+T^2)$ has a maximum value equal to 1/2 at the value $T = 1$. This value gives

$$c \leqslant 0.24 \frac{\Gamma}{r_{max}}$$

for waves on a core of circulation Γ, and having a maximum radial excursion r_{max}. All group velocity measurements should lie below this estimate. Group velocities taken from films are shown in Fig. 4, divided by the estimated value of vortex circulation, $\Gamma = 32.7\,\mathrm{cm}^2\,\mathrm{s}^{-1}$, and plotted against the inverse of the observed maximum wave radius. There is an indication that smaller waves travel faster, but the data are far from conclusive. The upper bound estimate is reasonable for the larger waves, but much too high for waves of smaller amplitude. Possibly other effects limit the propagation velocities of the smallest waves. Note also the relatively small range of wave amplitudes observed. In terms of estimates of the core radius, the largest waves have $r_{max} = (3\text{–}4)\varepsilon$ and the smallest waves $r_{max} \cong \varepsilon$.

Our rotating turbulent flow thus consists of a three-dimensional turbulent region near the forcing grid, and a quasi two-dimensional field of strong vortices farther away. Non-linear solitary waves provide the connecting link, and carry energy upwards from the strongly turbulent region. However, waves are also produced along the entire length of the vortex core. This local wave production may provide the vertical stretching and the concomitant horizontal flow convergence necessary to maintain the regions of high vorticity.

Concentrated vortices occur in external flows over wing surfaces and internally in rotating machinery and combustors. Solitary waves are present in these flows and can be seen, for example, during the break-up of wing tip vortices in the wakes of high flying aircraft. The most highly concentrated vortex found in nature is the tornado. Pulsations in core size, rapid vertical motions within the core region and various travelling (wave-like) core deformations have been observed over many years (see refs 10,11). It is plausible that some of these effects are manifestations of vortex core solitons. Solitary waves may indeed be a ubiquitous feature of most turbulent flows which contain concentrated vorticity. The contribution these waves make to turbulent vortex dynamics in complex flows would be a fascinating topic for future study.

We thank Professeur Uriel Frisch and P.-L. Sulem for bringing the paper by Hasimoto to our attention, Yves Gagne for helpful discussions and Serge Layat for experimental assistance. Financial support from the Centre National pour l'Exploitation des Oceans under contract no. 80/2345 is acknowledged.

Received 1 September; accepted 20 November 1981.

1. Gough, D. O. & Lynden-Bell, D. *J. Fluid Mech.* **32,** 437–447 (1968).
2. Bretherton, F. P. & Turner, J. S. *J. Fluid Mech.* **32,** 449–464 (1968).
3. Ibbetson, A. & Tritton, D. J. *J. Fluid Mech.* **68,** 639–672 (1975).
4. McEwan, A. D. *Nature* **260,** 126–128 (1976).
5. Colin de Verdiere, A. *Geophys. Astrophys. Fluid Dyn.* **15,** 213–251 (1980).
6. Hopfinger, E. J. & Toly, J. A. *J. Fluid Mech.* **78,** 155–175 (1976).
7. Hasimoto, H. *J. Fluid Mech.* **51,** 477–485 (1972).
8. Hopfinger, E. J. & Browand, F. K. *Proc. IUTAM/IUGG Symp. on Concentrated Atmospheric Vortices*, Reading (1981).
9. Batchelor, G. K. *An Introduction to Fluid Dynamics* (Cambridge University Press, 1967).
10. Reber, C. *Bull. Am. met. Soc.* **35,** 191–197 (1954).
11. Golden, J. H. & Purcell, D. *Mon. Weath. Rev.* **106,** 3–11 (1978).

A suspended sediment front in the Severn Estuary

R. Kirby & W. R. Parker

Institute of Oceanographic Sciences, Crossway, Taunton,
Somerset TA1 2DW, UK

A zone of marked local gradient in the regional suspended solids field has been located along the axis of the Severn Estuary. This front occupies virtually the same position on ebb and flood and on spring and neap tides, although the amplitude of the gradient fluctuates. Thermohaline fronts have been described in coastal waters[1,2] suspended sediment fronts associated with the discharge of major rivers into the sea are common[3–5] whilst fronts caused by convergence of secondary circulations within estuaries have also been reported[6,7]. The previous work describes features with significant differences in the salinity or temperature fields in which any suspended sediment contrasts present are incidental and do not, of themselves, produce large horizontal density variations. In contrast, in the Severn, strong thermohaline gradients in the vicinity of the suspended solids front have not been detected. The mechanisms for the formation and maintenance of the front are not yet known.

The Severn Estuary (Fig. 1) has a large and variable tidal range (12.3 m mean spring range and 6.5 m mean neap range at Avonmouth). It is well mixed with regard to salinity and temperature[8] but commonly stratified with respect to suspended solids concentration[9]. The suspended load over the greater part of the water column ranges between 0.25 and $>10\ \mathrm{g\,l^{-1}}$ and its vertical distribution is controlled by the semi-diurnal and spring–neap tidal energy cycles. At maximum flow on spring tides the suspended load is mixed throughout the water column, whereas near slack water on springs and throughout the neap tides, considerable stratification is apparent with concentration levels in the lower layers well in excess of $10.0\ \mathrm{g\,l^{-1}}$ (ref. 9).

The structure of the suspended solids field was observed using a free-fall array consisting of two narrow-gap optical turbidity meters, a pressure (depth) sensor and, occasionally, a continuously recording conductivity meter, allowing continuous and rapid ($1\ \mathrm{m\,s^{-1}}$) vertical profiles to be made from drifting or anchored vessels. Laboratory calibrations using indigenous material in the range $0–20\ \mathrm{g\,l^{-1}}$ were later corrected with field samples. Performance curves for the turbidity meters were prepared and they were only used within the ranges where errors were $<10\%$. Over the range of concentration values for which the instruments were calibrated they were known to respond to changes in mass concentration and to be insignificantly affected by changes in the state of aggregation of the solids (T. J. Smith personal communication).

Measurements from anchored vessels have been placed in a regional context during wide ranging surveys of the suspended solids field in the area, resulting in 3,500 vertical profiles from 210 stations based on 17 estuary cross-sections, (standard lines), extending from Watchet to The Shoots (Fig. 1). The regional measurements were made chiefly between 1973 and 1979 on all ranges of tide from spring to neap and during most seasons.

Most of the data have been obtained as time series of cross-sections in which the survey vessel repeatedly traversed a standard line stopping at each station to measure a vertical profile. Between stations the array was towed 2–3 m below the surface and a continuous horizontal traverse was recorded. One complete traverse can be made in approximately 1–1.5 h, in a time series continuing over a 12.5-h semi-diurnal tidal cycle.

The regional surface and bed suspended solids distributions on spring and neap tides was studied by grouping the analogue records into spring (all data >9.0 m range) and neap (all data <9.0 m range) tides. For most stations this resulted in a minimum of 10 profiles but the limited accessibility of shallow areas resulted in a poor coverage. The surface and bed concentration values for these groups were averaged. The regional spring surface and spring bed distributions (Fig. 2) show the front as a zone of marked gradient (from <0.5 to $>4.0\ \mathrm{g\,l^{-1}}$ at the bed in 2 km or less) approximately along the axis of the estuary between The Shoots and the Holm Islands, and extending across the inner Bristol Channel to the English coast in the region of Watchet, in Bridgwater Bay. The more turbid water mass lies on the English side of the estuary. On neap tides the regional distribution is similar, although the contrast between surface and bed concentration values is greater.

For more detailed analyses, data from each cross-section have been grouped into spring ebb and flood and neap ebb and flood conditions and the average concentration calculated for each

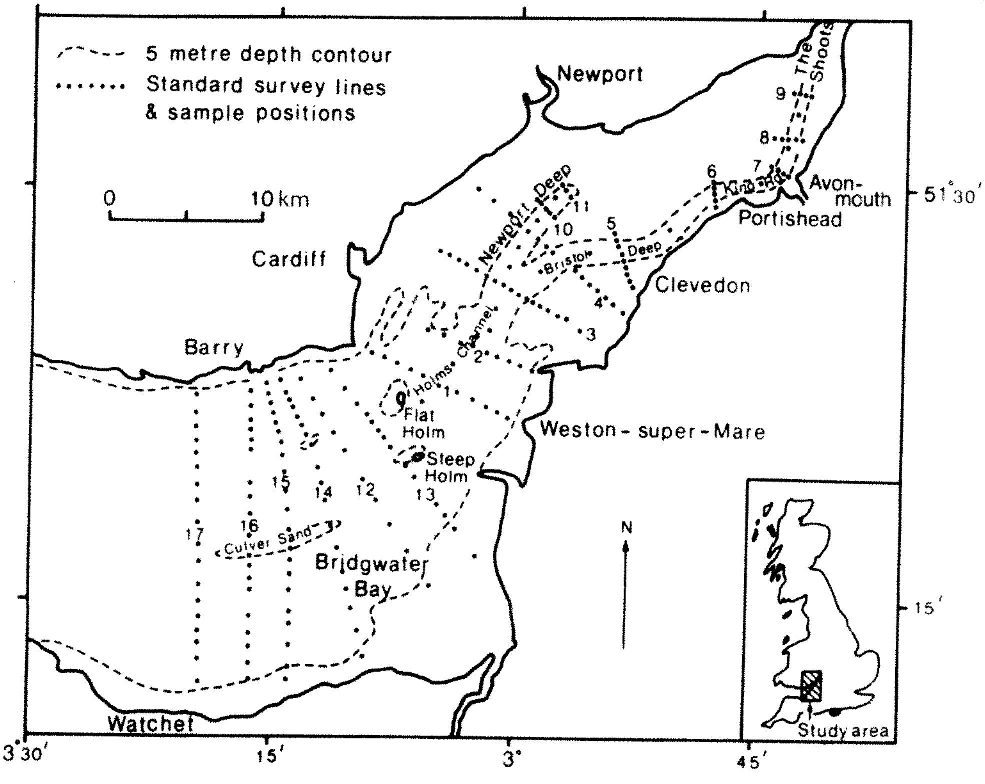

Fig. 1 Location of standard stations used in surveys of suspended solids distribution.

0028–0836/82/050396—04$01.00

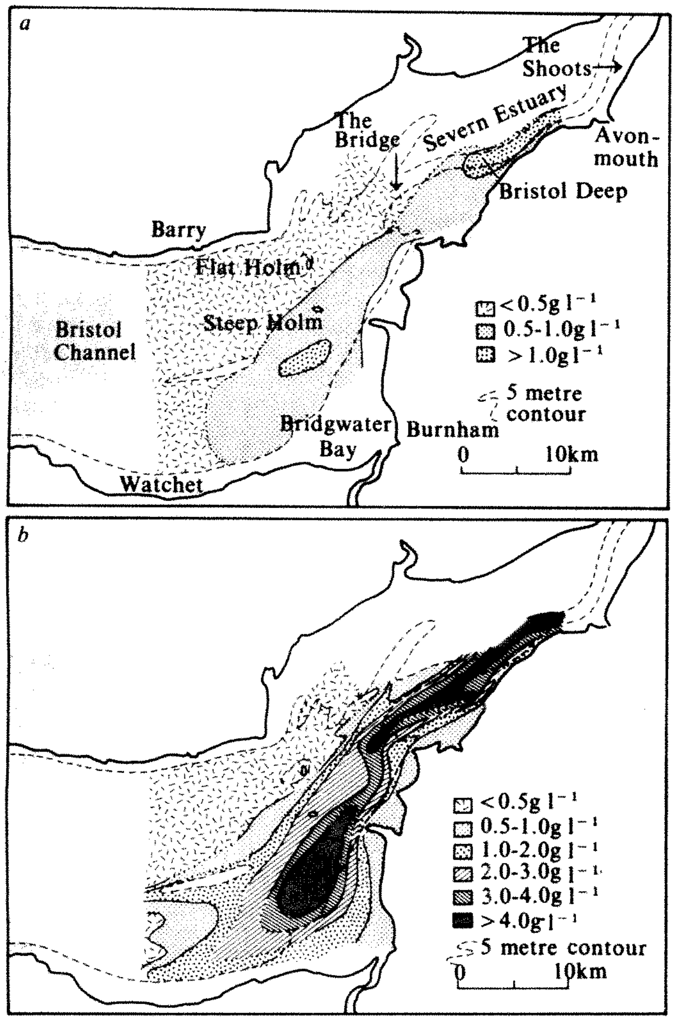

Fig. 2 Plan distributions of spring surface average (*a*) and spring bed average (*b*) suspended solids concentration based on vertical profile data.

tenth percentile of the depth at every station on the cross-section. Plots of average concentration for each sub-group of data in every cross-section were arranged in sequence along the estuary to show the mean position and structure of the front in three dimensions. These plots show that the front is more prominent on spring than on neap tides and on ebb rather than flood tides. An average of all spring ebb data, Fig. 3, shows steeply inclined concentration contours across the gradient zone in the region between The Bridge and a line joining Barry and Burnham. Upstream from The Bridge, in the Bristol Deep, the front is duplicated by a similar, but smaller front on the Welsh side, whilst downstream from the Barry to Burnham line the concentration contours assume a more horizontal attitude.

Figure 3 illustrates the location and nature of the front in the study area but obscures the sequence of development and stability on a semi-diurnal time scale. In Fig. 4, the time series of cross-section plots represents individual traverses along standard line 1 during a spring tidal cycle of ~12.0 m range. The apparent slopes of the water surface are due to the rise and fall of the tide during the period taken by the vessel to steam along the line and have no dynamic significance. Figure 4 shows the effects of mixing of the sediment into the water column during accelerating phases of the tide and settling towards the sea bed on decelerating phases. Although well displayed at times when the tide is running in either direction, settling causes the front to be less evident at the surface and enhanced near the bed at slack water. However, the approximate position of the front remains constant on this time scale, although the concentration differences across it vary. Virtually the same sequence of changes was observed during time series at other ranges of tide at line 1 and also at the other standard lines.

Despite the averaging processes the position of the front remains well defined throughout spring tides (Figs 2, 3), most markedly at the bed during neap tides and during most of the semi-diurnal cycle (Fig. 4). These plan distributions and cross-sections suggest that, although the front is a marked feature on a regional scale, the gradient extends over 2 or more kilometres. In fact, from upstream of The Shoots to the Holm Islands the front can occasionally be seen at the sea surface in calm weather as a sharp interface separating 'blue' and 'brown' water. Continuous horizontal traverses made near the surface show that the front may be as little as 2-m wide at the upper end of the estuary (Fig. 5).

Unpublished data from IOS horizontal suspended solids traverses suggests that the front is not a passive feature associated with some controlling salinity and temperature structure

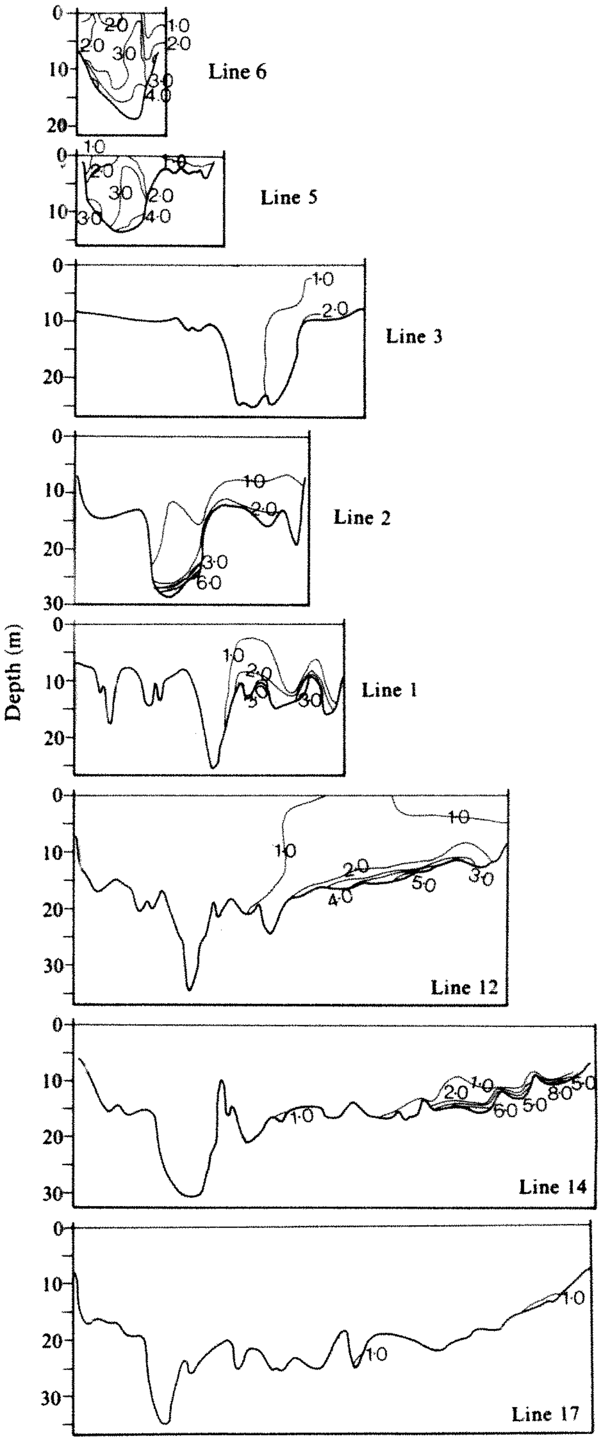

Fig. 3 Spring ebb average suspended solids distributions for cross-sections of the Severn Estuary and Inner Bristol Channel between Avonmouth and Watchet, concentration in g l^{-1}.

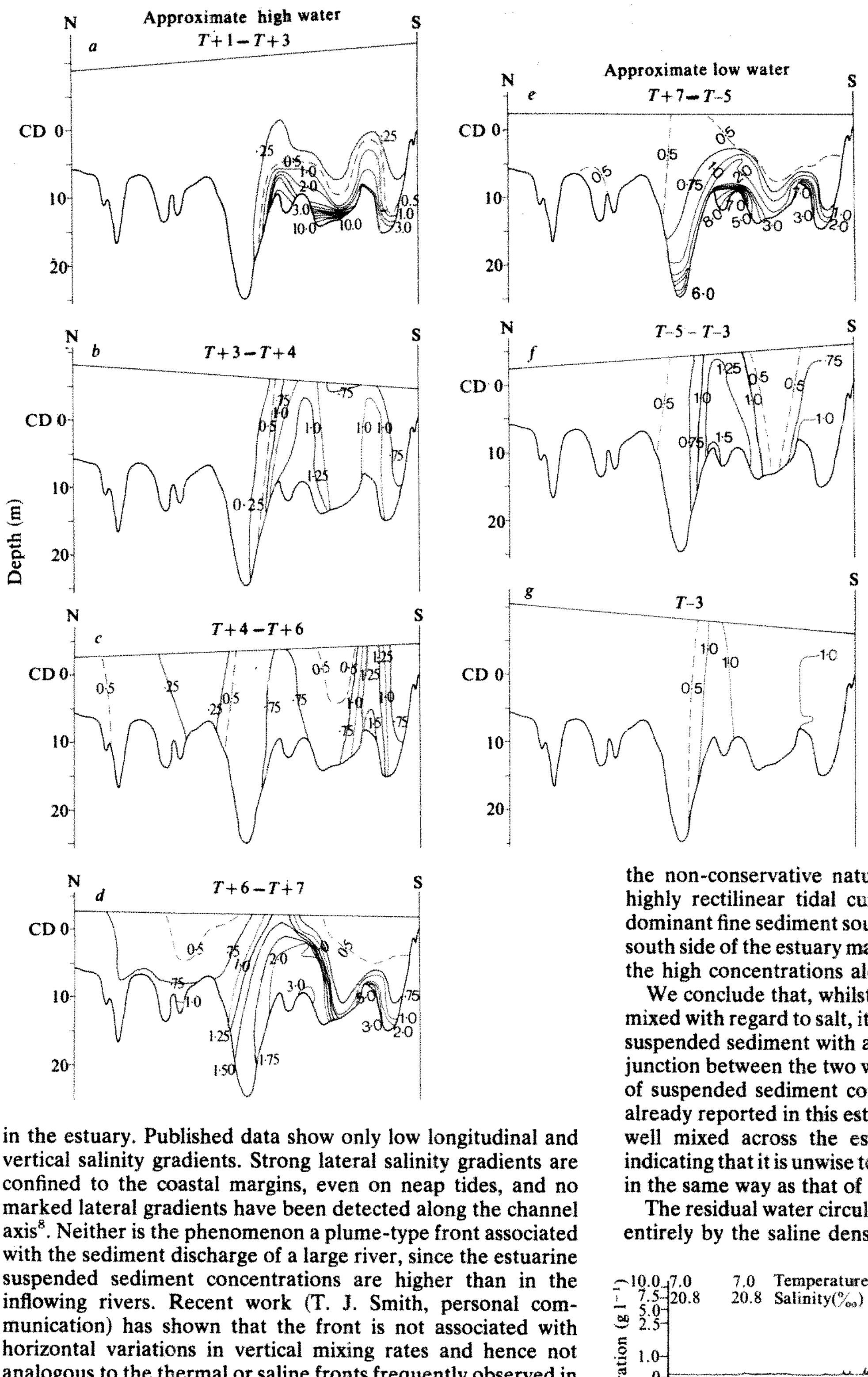

Fig. 4 Time series of cross-sections at Line 1 during a spring tide showing close association of front and main channel. Suspended sediment concentration in g l^{-1}. T numbers are GMT in hours + or − predicted HW at Avonmouth. CD, Chart Datum. *a–d*, Ebb tide sequence; *e–g*, flood tide sequence.

in the estuary. Published data show only low longitudinal and vertical salinity gradients. Strong lateral salinity gradients are confined to the coastal margins, even on neap tides, and no marked lateral gradients have been detected along the channel axis[8]. Neither is the phenomenon a plume-type front associated with the sediment discharge of a large river, since the estuarine suspended sediment concentrations are higher than in the inflowing rivers. Recent work (T. J. Smith, personal communication) has shown that the front is not associated with horizontal variations in vertical mixing rates and hence not analogous to the thermal or saline fronts frequently observed in British coastal waters[10].

The front may be due to an interaction between the regional and local topography, Coriolis effects and lateral phase differences in tidal elevation across the estuary, which set up secondary water circulation cells in the plane of the cross-section, leading to convergence along the main channel axis. Velocity measurements over several tidal cycles made from an anchored vessel in the Holms Channel may be interpreted in support of this secondary circulation hypothesis. The vertical distribution of the lateral component of tidal mean velocity obtained from these measurements indicates a north-west going residual at the bed and a south-east going residual at the surface, in agreement with earlier data[11], placing the survey vessel on the Welsh side of a convergence. Such a circulation, combined with the non-conservative nature of the suspended sediment, the highly rectilinear tidal current regime and the fact that the dominant fine sediment source area, Bridgwater Bay, lies on the south side of the estuary may be the main factors which maintain the high concentrations along the English side of the estuary.

We conclude that, whilst the Severn estuary is generally well mixed with regard to salt, it shows marked lateral partitioning of suspended sediment with a stably positioned front forming the junction between the two water masses. This lateral disposition of suspended sediment compliments the vertical stratification already reported in this estuary[9]. Evidently, whilst salt does get well mixed across the estuary the fine sediment does not, indicating that it is unwise to treat the dispersion of fine sediment in the same way as that of salt.

The residual water circulation in the estuary cannot be driven entirely by the saline density field because comparison of the

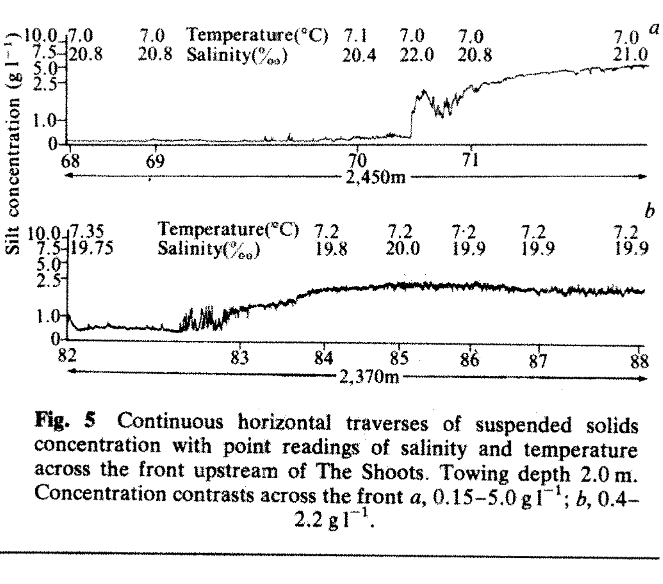

Fig. 5 Continuous horizontal traverses of suspended solids concentration with point readings of salinity and temperature across the front upstream of The Shoots. Towing depth 2.0 m. Concentration contrasts across the front *a*, 0.15–5.0 g l^{-1}; *b*, 0.4–2.2 g l^{-1}.

lateral and longitudinal density fields due to depth average salinity and depth average salinity plus suspended solids, shows that density differences due to suspended solids are at least equal to those due to salt[12]. This comparison was achieved by calculating and comparing the depth mean density of the water column at individual stations across the estuary and along the estuary from Avonmouth to 3°30′ W. Density differences computed using the actual suspended solids vertical profiles, as opposed to depth average values, show the suspended sediment density field to dominate.

As the suspended sediment load is strongly laterally partitioned and vertically stratified, sediment erosion and transport models should take account of the fact that any sediment entrained cannot be assumed to mix completely in lateral and vertical directions since the discontinuities represent a barrier to dispersion. Similarly, the presence of persistent lateral and vertical discontinuities within the suspended sediment concentration field also has an influence on the dispersion of those pollutants which travel with the sediment.

We thank Dr T. J. Smith for advice and encouragement.

Received 26 May; accepted 30 November 1981.

1. Pingree, R. D. in *The North-West European Shelf Seas: The Sea Bed and the Sea in Motion II Physical and Chemical Oceanography and Physical Resources* (eds Banner, F. T., Collins, M. B. & Massie, K. S.) 415–462 (Elsevier, Amsterdam, 1980).
2. Simpson, J. H. & Hunter, J. R. *Nature* **250**, 404–406 (1974).
3. Officer, C. B. *Mar. Geol.* **40**, 1–14 (1981).
4. Castaing, P. & Allen, G. P. *Mar. Geol.* **40**, 101–118 (1981).
5. Oertel, G. F. & Dunstan, W. M. *Mar. Geol.* **40**, 171–198 (1981).
6. Koske, P. H. *Can. J. Fish. Aquat. Sci.* (in the press).
7. Bowman, M. J. & Iverson, R. L. in *Oceanic Fronts in Coastal Processes* (eds Bowman, M. J. & Esaias, W. E.) 87–104 (Springer, Berlin, 1978).
8. Severn Estuary—Survey and Systems Panel *Severn Estuary Joint Committee* (in the press).
9. Kirby, R. & Parker, W. R. *Can. J. Fish. Aquat. Sci.* (in the press).
10. Simpson, J. H. & Pingree, R. D. in *Oceanic Fronts in Coastal Processes* (eds Bowman, M. J. & Esaias, W. E.) 29–42 (Springer, Berlin, 1978).
11. Uncles, R. J. & Jordan, M. B. *Estuar. Coast. mar. Sci.* **9**, 287–302 (1979).
12. Parker, W. R. Smith, T. J. & Kirby, R. *2nd int. Symp. on Stratified Flows* 955–966 (IAHR, Trondheim, 1980).

Successive palaeomagnetic reversal records from Kauai

Scott W. Bogue & Robert S. Coe

Earth Sciences Board, University of California, Santa Cruz,
California 95064, USA

Geomagnetic field reversal is a rapid phenomenon[1,2], perhaps taking only a few thousand years. Knowledge of how the field behaves during these brief and active periods may eventually help to constrain theories of the geodynamo and thus inform us about conditions in the Earth's core. Unfortunately, reliable and detailed palaeomagnetic records of transitional field behaviour are few, almost entirely from Northern Hemisphere sites, and heavily biased toward reversals of the reverse–normal (R–N) sense. We report here new data from basalts on the island of Kauai, Hawaii, which have recorded successive R–N and N–R field reversals. The sequences of changing field directions for the two reversals are very similar, as would be expected if a standing nondipole component controlled the transitional field. The data are also consistent with zonal flooding models in which the reversal process depends on the sign of the field. Other reversal records, however, cannot be explained by these same models unless the standing field or flooding process changes between some reversals.

Two simple models of the reversing field have been proposed in the past 5 years[3,4]. The two involve conceptually different source mechanisms and, in their purest forms, make distinct predictions of transitional field behaviour. Although it is possible that no single process controls transitional fields, we will treat these two models as alternative explanations of palaeomagnetic records of field reversals.

Hoffman's model[3,5] of the reversing field is based on the notion that the reversal process 'floods' through the fluid core from a localized zone or point of initiation. The entire dipole source remains active, but normal and reverse flux is produced simultaneously in different regions. The resulting transitional field depends on how the reversal process propagates through the dipole source. If the reversal initiates at either of the poles or the equatorial zone of the core, essentially axial quadrupolar or octupolar fields, respectively, will predominate during the middle stages of the reversal process. In these purely axisymmetric cases, reversal of the field vector at the Earth's surface occurs by rotation in the north–south vertical plane; the equivalent virtual geomagnetic pole (VGP) moves along the great cricle defined by the geographical poles and the observer's site. Depending on the sense of the reversal, where in the core source region the reversal process initiates, and the hemisphere of the observer, the VGP path for the reversal will be 'near sided' (same longitude as the site) or 'far sided' (180° away)[6].

In contrast to the model of Hoffman, which we will refer to as the flooding model to emphasize its active character, is the standing field model[4]. The latter is a special case of the long held idea[7] that, during reversals, the main dipole field diminishes greatly while at least parts of the nondipole field do not. In particular, the standing field model requires a stationary component of the nondipole field to persist unchanged through dipole reversals. Palaeomagnetic evidence suggests that the dominant part of the nondipole field changes sign with the dipole field[8,9]. Thus, the postulated standing field would have to be in some sense independent of both the dipole and the rest of the nondipole fields.

In the standing field model, the transitional field at any site is the sum of a steady nondipole component plus an axial dipole component that changes only in magnitude and sign. As with simple cases of the flooding model, the equivalent VGP paths are longitudinal great circles. There is, however, no site dependence of path longitude unless the standing nondipole field direction everywhere lies in the north–south vertical plane.

Hoffman[10] has recently proposed a test to distinguish between the flooding and standing field models. The former model predicts that, as long as a reversal is initiated at the same zone in the core each time, successive reversals will be characterized by transitional VGP paths that differ in longitude by 180°. The latter predicts identical VGP paths for successive reversals. Records of back-to-back reversals thus directly test the two models.

On the island of Kauai, Hawaii (22° N), we have collected samples through R–N and N–R transition zones. The thin, shield-building basalt flows of the Napali Formation (Fig. 1), which record the R–N reversal, have yielded K–Ar ages ranging from 4.5 to 5.6 Myr (ref. 11). The thicker, caldera-filling flows of the Olokele Formation (Fig. 1) have not been dated, but can be shown on geological grounds[12] to be synchronous with the upper portion of the Napali sequence. The transition zones in the Napali and Olokele Formations, however, are at nearly the same elevation. In addition, extensive reconnaissance with a portable fluxgate magnetometer has shown that all Napali flows exposed above the R–N horizon and all Olokele flows below the N–R horizon are normally magnetized. It is thus very likely that the two transition zones record a back-to-back, R–N–R reversal pair from the early Pliocene.

Equal-area plots of the flow-averaged palaeomagnetic directions from the two transition zones are shown in Fig. 2. Seven samples per flow were collected, and alternating fields of 100–200 Oe reduced substantially any secondary components of magnetization that were present. We sampled the R–N transition at three widely separated localities (Fig. 1), and the sequence shown in Fig. 2*a* is based on the simplest correlation of directions from the three sections. We sampled only a single section of the N–R transition because of the thick, horizontal character of the caldera basalts.

Neither transition zone displays an abundance of intermediate field directions. This lack of detail may be interpreted as the result of ill-timed lulls in volcanic activity both times the field was reversing. An alternative hypothesis is that the duration of

0028–0836/82/050399—03$01.00

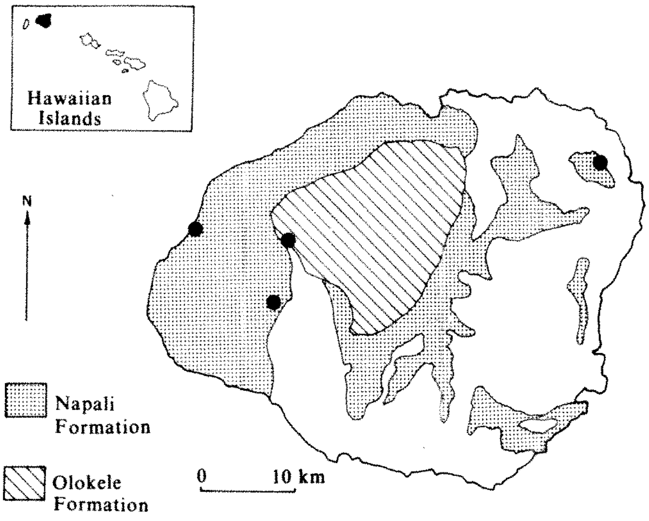

Fig. 1 Map showing outcrop extent of Napali and Olokele Formations on Kauai. Dots indicate locations of palaeomagnetic sampling sites.

intermediate field directions was very short. Our observation that contacts between flows were almost never marked by weathered zones or soil horizons supports the latter idea. In addition, the palaeomagnetic results show clearly that the three sections across the Napali reversal horizon are not identical, and thus that lavas on the flanks of the ancient Kauai volcano were of rather local extent. This pattern is entirely consistent with the modern eruptive style on the big island of Hawaii. Including the Olokele site, therefore, there are a total of four widely separated and essentially independent transitional sections that show this paucity of distinct intermediate directions. These two lines of evidence are mutually consistent, and we tentatively infer that the major change in direction occurred extremely rapidly during both reversals.

In spite of the lack of detail, and regardless of its cause, the pattern of change in field directions is clear for both transitions and is sufficient to apply Hoffman's[10] test. In the R–N transition, the field direction remains southerly while shallowing to nearly horizontal. A single layer with normal polarity occurs among these lower flows. We have examined the anomalous unit and are convinced that it is a flow and not a sill; examples of the latter are easily recognized on Kauai by their distinctive jointing and much greater resistance to weathering. Thus the ancient field apparently underwent a rapid 'flip' in direction during the transition much like those observed in several other detailed records[13–15]. The shallow southerly directions are followed by a steeply downward directed field vector which subsequently shallows to the expected normal field direction. In the N–R reversal, the same sequence is seen except in reverse; a steep northerly field direction precedes shallow southerly directions. Thus, both reversals are characterized by transitional directions that lie near the north–south vertical plane or, equivalently, by VGP paths that pass near the site.

At first glance, this site dependence is most naturally explained by the zonal flooding model. An awkward complication arises, however, because the R–N and N–R paths are so nearly identical. Their similarity requires the presumed flooding processes for the two reversals to have initiated in opposite regions of the core[6]. More specifically, if the transitional field was predominantly octupolar, as is consistent with the very low field intensities that have been inferred from other transition zones[16–18], then flooding for the R–N reversal would have begun at the equator. For the N–R reversal, one is forced to conclude that the reversal somehow initiated simultaneously at both poles. Similarly, quadrupolar transitional fields require initiation at the south pole for R–N reversals and at the north pole for N–R reversals.

If generally true, systematic behaviour such as just described would mean that the postulated flooding mechanism, and hence the reversal process, depends on the sign of the field. Global palaeomagnetic data suggest that statistically significant and long-term differences do exist between the morphology and stability of normal and reversed geomagnetic fields[19], and thus that asymmetry in the reversal process might be allowed. Such asymmetry, however, is intuitively unappealing and cannot arise directly from the basic dynamo equations[6,19].

Theoretical considerations aside, it is important to ask whether the regularities predicted by the flooding models are discernible in the rest of the palaeomagnetic record. Near-sided VGP paths seem to predominate in the R–N reversal records presently available from Northern Hemisphere sites[3,20]. This characteristic is evident in the R–N reversal from Kauai, supporting the general observation. A pattern in the N–R records, on the other hand, is not yet apparent. Several N–R transition zones from Iceland have been reported[21–23]; shallow directions with easterly or westerly declinations are common, so that VGP paths are not strongly near or far sided. Shallow westerly directions are also found in a detailed N–R transition in volcanic rocks of the Shigarami Formation, Japan[24]. Overall, however, this record shows the field tending towards far-sided behaviour. Two N–R records from California[25,26], which we will discuss in more detail with respect to the standing field model, are characterized by intermediate directions which are shallow and easterly. The equivalent VGP paths are slightly near sided. A pair of VGP paths from Russian sites[27,28], the only N–R data considered in detail in a recent review, are not longitudinally confined, but are generally far sided.

More convincing evidence of far-sided N–R behaviour has been found in back-to-back transition zones of Miocene age from Crete[29]. The VGP path for the N–R reversal follows a longitudinal path almost exactly 180° from the site. This record and that from the Olokele Formation on Kauai represent our best examples of site-dependent N–R paths, yet the former is far sided and the latter near sided. Thus, the N–R data as a whole display no coherent trend and, moreover, the two most clearcut records conflict directly. This evidence suggests that, at least for the N–R transitions, the flooding mechanism varies considerably from one reversal to the next.

The similarity of the N–R and R–N reversal records from Kauai is easily explained by the standing field model. Reversals in the early Pliocene were quite frequent[30], and the Kauai data require a standing field that persisted for only a few hundred thousand years. Results from two California localities suggest that a standing field may persist for a much longer period.

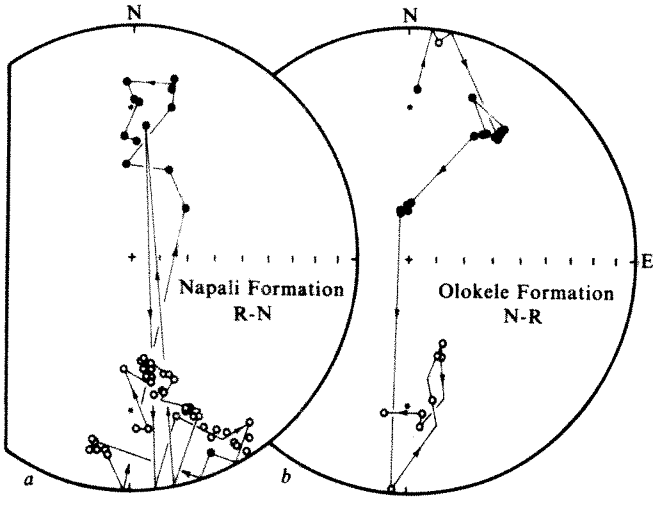

Fig. 2 *a*, Equal-area plot of flow-averaged directions from the R–N transition zone. Results from three sites in the Napali Formation are combined. ● (○) indicate downward (upward) directed magnetization vectors. Connecting lines and arrows show the stratigraphic order from oldest to youngest flows. Centre of plot marked by a plus sign, and ticks indicate 10° intervals. The axial dipole direction (asterisk) is shown for comparison. *b*, Directions from the N–R transition zone in the Olokele Formation.

Volcanic rocks from Clear Lake, California[25], record intermediate directions from two N–R reversals that occurred several hundred thousand years before the Matuyama–Brunhes transition. The VGP's equivalent to these directions fall right on the Matuyama–Brunhes R–N transition path that Hillhouse and Cox[4] found at Lake Tecopa, also in California. Even more remarkable is a detailed record of the Gauss–Matuyama transition in dry lake sediments from Searles Valley, California[26]. This reversal, 1.6 Myr earlier still and N–R, also repeats the Lake Tecopa path. Note that these three VGP paths are not strongly near or far sided, the VGPs passing almost 90° to the east of the site. Such grossly nonaxisymmetric field behaviour, nearly identical for reversals of both senses, can arise only in very special cases of the generalized flooding model[5]. Thus, the California results more strongly support the standing field model than do the Kauai data. More significantly, the ages of the three sites in California imply that the standing field, if that is what controlled the transitional fields, remained unchanged for several millions of years.

The back-to-back reversal records from Crete[29] again provide conflicting evidence. The VGP paths from these two reversals differ from one another by 135°. Marine sediments such as those now exposed on Crete may not record changing field directions as faithfully as rapidly deposited lake sediments or volcanic rocks. Nevertheless, it is difficult to dismiss the general features of these reversal records, especially the significant longitudinal separation of the VGP paths. Unless the standing field can occasionally change between reversals or be masked by other effects (flooding processes?), the results from Crete cannot be reconciled with the standing field model.

An additional problem is that the concept of standing fields has no clear independent basis. Yukutake and Tachinaka[31] mathematically divided the historic nondipole field into standing and drifting parts. The analysis provided a better description of secular variation, but the separation of the field into two parts is arbitrary; it allows but is not strong evidence for an actual standing field. Moreover, analysis of historical field behaviour is not sufficient to demonstrate that a field component can last for millions of years as required by the model; such evidence must come from palaeomagnetism. The 'standing fields' that emerge from analyses of global palaeomagnetic data[19] are by definition statistical; that is, they represent long-term properties of the time-averaged geomagnetic field. Standing fields of the sort needed for the reversal model are again allowed, but in no way proven, by analysis of the time-averaged field. In short, no standing nondipole field capable of controlling transitional fields has been observed, palaeomagnetically or otherwise, except by inference in some of the transition zone data.

In conclusion, the similarity of VGP paths in back-to-back reversal records from Kauai and in several records from California favours the standing field model, according to the test proposed by Hoffman[10]. Conversely, the large latitudinal separation of VGP paths in back-to-back reversal records from Crete and the predominance of near-sided VGP paths in the available R–N records from the Northern Hemisphere favour the zonal flooding model. However, unless the standing field or flooding process can change, at least occasionally, from reversal to reversal, neither model can explain all of the available transition data. It may thus be too simple to assume that a single type of transitional field is always present during reversals. Furthermore, palaeointensity data we are currently analysing for the Kauai R–N reversal suggests that more complex versions of these mechanisms may be required to model even a single reversal. These results will be discussed elsewhere.

We thank C. S. Grommé, J. C. Liddicoat and R. T. Merrill for helpful comments. This work was supported by NSF grant EAR78-12951.

Received 23 September; accepted 3 December 1981.

1. Cox, A. & Dalrymple, G. B. *J. geophys. Res.* **72,** 2603–2614 (1967).
2. Ninkovich, D., Opdyke, N., Heezen, B. C. & Foster, J. H. *Earth planet. Sci. Lett.* **1,** 476–492 (1966).
3. Hoffman, K. *Science* **196,** 1329–1332 (1977).
4. Hillhouse, J. & Cox, A. *Earth planet. Sci. Lett.* **29,** 51–64 (1976).
5. Hoffman, K. *Earth planet. Sci. Lett.* **44,** 7–17 (1979).
6. Hoffman, K. & Fuller, M. *Nature* **273,** 715–718 (1978).
7. Sigurgeirsson, T. *Adv. Phys.* **6,** 240–246 (1957).
8. Cox, A. *Rev. Geophys. Space Phys.* **13,** 35–51 (1975).
9. Merrill, R. T. & McElhinny, M. W. *Rev. Geophys. Space Phys.* **15,** 309–323 (1977).
10. Hoffman, K. *Phys. Earth planet. Inter.* **24,** 229–235 (1981).
11. McDougall, I. *Bull. geol. Soc. Am.* **75,** 107–128 (1964).
12. MacDonald, G. A., Davis, D. A. & Cox, D. C. *Bull. Haw. Div. Hydrogr.* **13,** 1–212 (1960).
13. Watkins, N. D. *Geophys. J. R. astr. Soc.* **17,** 121–149 (1969).
14. Dodson, R. *et al. Geophys. J. R. astr. Soc.* **53,** 373–412 (1978).
15. Niitsuma, N. *Tohuku Univ. Sci. Rep. 2nd Ser.* **43,** 1–39 (1971).
16. Coe, R. S., Mankinen, E. A., Prévot, M. & Grommé, C. S. *I.A.G.A. Bull.* **45,** 200 (1981).
17. Shaw, J. *Geophys. J. R. astr. Soc.* **48,** 263–269 (1977).
18. Van Zijl, J. S. V., Graham, K. W. T. & Hales, A. L. *Geophys. J. R. astr. Soc.* **7,** 169–182 (1962).
19. Merrill, R. T., McElhinny, M. W. & Stevenson, D. J. *Phys. Earth planet. Inter.* **20,** 75–82 (1979).
20. Fuller, M., Williams, I. & Hoffman, K. *Rev. Geophys. Space Phys.* **17,** 179–203 (1979).
21. Dagley, P. & Lawley, E. *Geophys. J. R. astr. Soc.* **36,** 577–598 (1974).
22. Watkins, N. D., McDougall, I. & Kristjansson, L. *Geophys. J. R. astr. Soc.* **49,** 609–632 (1977).
23. Kristjansson, L., Fridleifsson, I. B. & Watkins, N. D. *J. Geophys.* **47,** 31–42 (1980).
24. Momose, K. *Bull. Earthquake Res. Inst.* **41,** 487–534 (1963).
25. Mankinen, E. A., Donnelly-Nolan, J. M., Grommé, C. S. & Hearn, B. C. Jr *U.S. geol. Surv. Prof. Pap.* 1141, 67–82 (1981).
26. Liddicoat, J. C. *EOS* **62,** 263 (1981).
27. Burakov, K. S. *et al. J. Geomagn. Geoelectr.* **28,** 295–307 (1976).
28. Petrova, G. N. *et al. Phys. Solid Earth* **6,** 369–384 (1972).
29. Valet, J.-P. & Laj, C. *Earth planet. Sci. Lett.* **54,** 53–63 (1981).
30. Ness, G., Levi, S. & Couch, R. *Rev. Geophys. Space Phys.* **18,** 753–770 (1980).
31. Yukutake, T. & Tachinaka, H. *Bull. Earthquake Res. Inst.* **47,** 1027–1074 (1969).

Rapid growth of a deep-sea manganese nodule

J. L. Reyss*, V. Marchig† & T. L. Ku‡

* Centre des Faibles Radioactivités, Laboratoire mixte CNRS–CEA,
Avenue de la Terrasse, 91190 Gif-sur-Yvette, France
† Bundesanstalt für Geowissenschaft und Rohstoffe, Hannover, FRG
‡ University of Southern California, Los Angeles, California 90007, USA

Recent studies on marine ferromanganese nodules have suggested a relationship between their growth rate and their chemical composition[1–3]. The suggestion is based on the hypothesis that the metals in nodules have two sources of supply: bottom seawater (hydrogenous) and sediment pore water (diagenetic)[4–7]. The diagenetic source calls for upward diffusion of Mn mobilized in a deeper, low *Eh* zone of the sediment column and its subsequent precipitation in an oxidized surface zone[8]. Addition of the remobilized Mn to surface nodules would augment their accretion rate. It would also render the oxide layers to contain higher Mn/Fe ratios than layers resulting from hydrogenous precipitation. We report here a radiometrically determined accretion rate of 168 ± 24 mm Myr^{-1} for a deep-sea manganese nodule from the Peru Basin in the Pacific. This rate is about two orders of magnitude higher than that frequently found in nodules of deep-sea origin, and emphasizes the importance of sediment diagenetic processes on the growth of manganese concretions.

When compared with their open-ocean counterparts, manganese deposits from shallow-water, continental margin environments commonly show growth rates that are three or more orders of magnitude faster ($1\text{–}10^3$ mm kyr^{-1} compared with 1–10 mm Myr^{-1}), and Mn/Fe ratios that are generally higher, although with large variations (0.5–50 compared with $\simeq 1$) (refs 5–9). Aside from the distance involved in the continental runoff supply of metals, such contrasts have generally been held to reflect the preponderance of the aforementioned one source of Mn over the other. That is, nearshore nodules are principally of diagenetic origin whereas pelagic nodules are hydrogenous[5,10–12]. However, we intend to assert here that the above is not meant to be a dichotomy between nodule growth in shallow marine and in deep abyssal sedimentation regimes. Although the *Eh*-controlled diagenetic reactions should depend geographically on surface productivity and sedimentation rate, nodules of deep-ocean occurrence may

0028–0836/82/050401—03$01.00

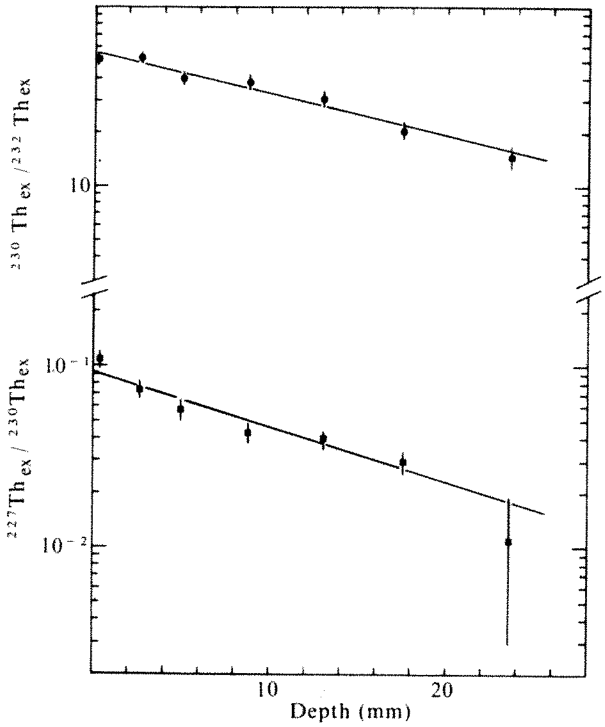

Fig. 1 Plots of ^{230}Th/^{232}Th and ^{227}Th (as ^{231}Pa)/^{230}Th activity ratios as a function of depth in nodule 278 DK. The mean accretion rates (●, $V = 173 \pm 25$ mm Myr^{-1}, ■, $V = 162 \pm 40$ mm Myr^{-1}) shown are determined from the weighted least-square fits (solid lines). Half lives used are 75,200 yr and 34,300 yr for ^{230}Th and ^{231}Pa, respectively.

themselves exhibit, as manifestations of regional variations in diagenetic influence, a range of Mn/Fe and accretion rate values.

As Halbach and his co-workers pointed out [7,13], there is a south-to-north increasing trend in the Mn/Fe ratio of nodules in the Peru Basin, south-east Pacific (the 'Sonne Basin') suggestive of a rising influence of diagenetic supply of Mn towards the north, which lies near the equatorial region of high surface biological productivity. Halbach *et al.*[7] estimated that nodules in this northern region grow at a rate of >60 mm Myr^{-1}, as opposed to rates of a few mm Myr^{-1} in the south. However, these estimates are very uncertain as they are based on extrapolation of the crude relationship between Mn/Fe and growth rate obtained by Heye and Marchig[2].

We have determined the accretion rate of a nodule from the northern part of the basin using U and Th series isotopes. The specimen (sample 278 DK) is a large, spheroidal nodule ~15 cm in diameter. It was retrieved from 4,240 m water depth at 7°40.0′ S and 91°59.5′ W during cruise SO 11/1 of the german RV Sonne. Its high Mn/Fe ratio ≈60 (Table 1) and its botryoidal, highly-mammillated constitution conform with the Halbach[13,14] Ac type nodule, the formation of which they describe as being largely influenced by sediment diagenesis near the sea floor. Each mammillae consists of alternate compact and porous laminations ranging in thickness from 1 to 7 mm.

We have measured U and Th series isotopes in nine oxide layers from surface to 25.5 mm inward, and in sediments attached to the nodule surface. After total acid dissolution of the samples, we measured ^{238}U, ^{234}U, ^{232}Th and ^{230}Th using procedures similar to those of Ku and Broecker[15]. The isotope ^{231}Pa was measured through its granddaughter ^{227}Th, assuming the two are in secular equilibrium. Results are presented in Table 1.

The isotopes found in nodule layers have three possible sources: seawater, pore water and detrital sediment included in the oxides. (No active volcanic activity exists in this part of the ocean floor; thus direct precipitation from hydrothermal solution as a source can be discounted.) From their Al-Si contents (Al <0.8%, Si <3%), the oxide layers seem to include <10% by weight of detrital sediment.

The nodule material contains two to three times more U than the associated sediment, indicating that most of their U isotopes come from seawater and/or pore water. Data on the ^{234}U/^{238}U ratio (Table 1) are consistent with this assessment. This ratio in seawater, pore water and deep-sea sediment has been reported as, respectively, 1.14, 1.17–1.23, and <1.00 (refs 16–19). For the other isotopes: ^{232}Th, ^{230}Th, and ^{231}Pa (^{227}Th), all three sources may have contributed to their presence in the oxide layers. Unlike U, evidence for the possible contribution of the Th isotopes from detrital sediment source includes that ^{232}Th in the sediment is about an order of magnitude higher than in the oxides, and that ^{230}Th/^{232}Th ratios in the surface layers and in the sediment are similar (Table 2). Although little is known about the Th and Pa isotopes in pore fluid, Moore *et al.*[20] have shown the supply of ^{231}Pa and ^{230}Th from this source to the bottom face of a nodule. According to them, a preferential loss of ^{231}Pa relative to ^{230}Th from the sediment to its pore fluid may occur. The ^{227}Th/^{230}Th ratio of 0.11 measured for the outermost layer of nodule 278 DK as compared with the ratio of 0.07 for the associated sediment (Table 2) accords with this possibility.

The accretion rate of 278 DK can be estimated from the rate of decrease of excess ^{230}Th (^{230}Th$_{ex}$) $T_{1/2} = 75.2$ kyr and/or ^{231}Pa (^{231}Pa$_{ex}$) $t_{1/2} = 34.3$ kyr in the nodule. The use of ^{230}Th$_{ex}$/^{232}Th and ^{231}Pa$_{ex}$/^{230}Th$_{ex}$ activity ratios is preferred to the use of specific activities (for example, d.p.m. ^{230}Th$_{ex}$ per gramme of nodule material), in view of the nodule's textural variations. Indeed, the considerable variation of the ^{230}Th specific activities with depth (Table 1) is largely removed when normalized against those of ^{232}Th and ^{227}Th (^{231}Pa) (Table 2).

The sedimentary source for U is unimportant and the uranium precipitated from seawater or pore water is assumed to carry little or no ^{230}Th and ^{231}Pa. Thus the U-supported ^{230}Th and ^{231}Pa should be nil when deposited and increase towards secular equilibrium with uranium at depth. The rate of increase of these U-supported ^{230}Th and ^{231}Pa, as well as the rate of decrease of ^{230}Th$_{ex}$ and ^{231}Pa$_{ex}$ mentioned above, depends on the accretion rate and the decay constants involved. Using an iterative procedure analogous to that of Koide *et al.*[21] for the sediment ^{226}Ra geochronology, we calculate the ^{230}Th$_{ex}$/^{232}Th and

Table 1 Chemical and radiochemical data for nodule 278 DK and associated sediment

Depth interval (mm)	^{234}U (d.p.m. g^{-1})	^{234}U/^{238}U	^{232}Th (d.p.m. g^{-1})	^{230}Th (d.p.m. g^{-1})	^{227}Th (d.p.m. g^{-1})	Fe* (%)	Mn* (%)
0–0.5	3.32±0.16	1.09±0.05	0.280±0.017	14.5±0.7	1.60±0.13	0.58	41.1
1.3–4.0	4.35±0.21	1.14±0.06	0.240±0.012	12.9±0.6	0.97±0.08	0.72	41.6
4.9–5.0	4.35±0.25	1.08±0.06	0.350±0.024	15.0±0.9	0.90±0.09	0.64	45.0
5.0–12.5	4.97±0.24	1.08±0.05	0.427±0.021	18.0±0.9	0.84±0.06	0.56	55.2
12.5–13.5	2.90±0.13	1.17±0.06	0.700±0.042	23.1±1.3	0.97±0.08	1.58	39.1
15.5–19.5	2.87±0.14	1.12±0.06	0.384±0.022	9.8±0.5	0.35±0.03	0.64	42.4
21.5–25.5	3.32±0.16	1.12±0.06	0.190±0.013	5.2±0.3	0.16±0.02	0.72	36.2
Sediment	1.27±0.08	1.04±0.06	2.01±0.12	105±6	7.0±0.6		

Errors quoted are based on counting statistics.
* Atomic absorption.

Table 2 $^{230}Th_{ex}/^{232}Th$, $^{227}Th_{ex}$ (as $^{231}Pa_{ex}/^{232}Th$, and $^{227}Th_{ex}$ (as $^{231}Pa_{ex}/^{230}Th_{ex}$ ratios

Depth interval (mm)	$^{230}Th_{ex}/^{232}Th$	$^{227}Th_{ex}/^{232}Th_{ex}$	$^{227}Th_{ex}/^{230}Th_{ex}$
0–0.5	51.6 ± 3.1	5.69 ± 0.47	0.110 ± 0.011
1.3–4.0	51.4 ± 2.7	3.84 ± 0.35	0.075 ± 0.008
4.9–5.0	40.0 ± 2.9	2.33 ± 0.28	0.058 ± 0.008
5.0–12.5	37.8 ± 2.1	1.64 ± 0.15	0.043 ± 0.005
12.5–13.5	30.9 ± 2.0	1.25 ± 0.12	0.040 ± 0.005
15.5–19.5	21.0 ± 1.5	0.64 ± 0.08	0.030 ± 0.004
21.5–25.5	14.9 ± 2.2	0.16 ± 0.12	0.011 ± 0.008
Sediment	51.6 ± 3.2	3.45 ± 0.32	0.067 ± 0.009

Ratios were calculated using an iterative procedure analogous to that of Koide *et al.*[21] for nodule 278 DK and associated sediment.

$^{227}Th_{ex}/^{230}Th_{ex}$ values corresponding to their respective least-squares fits for an exponentially decreasing function with depth. These values are listed in Table 2 and plotted in Fig. 1. The slopes of the fits give accretion rates estimated for the nodule: 173 ± 25 mm Myr^{-1} from the $^{230}Th_{ex}/^{232}Th$ plots and 162 ± 40 mm Myr^{-1} from the $^{227}Th_{ex}/^{230}Th_{ex}$ plots.

Such rapid accumulation rates have been radiometrically determined for the ridge-hydrothermal and shallow-water manganese deposits[9,22–24]. This is the first determination for a manganese nodule of deep-water origin. Our results support the concept that diagnetic remobilization of Mn in sediment column could significantly affect the growth of manganese nodules at the sediment–water interface[3,7].

Preliminary results on a nodule from the southern part of the basin show a slow growth rate of 4.5 mm Myr^{-1} and a ratio Mn/Fe of about 3. The trend is that nodules largely have a diagenetic origin (278 DK type) in the north and are hydrogenous in the south as deduced from their Mn/Fe ratio[7], the two processes may occur concurrently in intermediate areas. From these data we could expect slow precipitation from bottom sea water, plus, depending on the ambient oxidation potential, or thickness of the surface oxic layer of the sediment, a more or less important diagenetic contribution, resulting in variable growth rates ranging from millimetres to hundred of millimetres per million years. Work in progress should elucidate the relationships between the growth rate and composition of nodules and the oxidative characteristics of their sediment substrates in the Peru Basin.

We thank Dr R. Fellerer, Chief scientist of the cruise SOII in the Peru Basin, J. Labeyrie for his encouragement, C. Lalou for helpful discussions, C. A. Huh for assistance in the computer calculation, and J. Devineau for technical assistance. Laboratory studies were funded by the French CEA, CNRS and the NSF grant OCE81.00662.

Received 7 October; accepted 3 December 1981.

1. Piper, D. Z. & Williamson, M. E. *Mar. Geol.* **23,** 285–303 (1977).
2. Heye, D. & Marchig, V. *Mar. Geol.* **23,** M19–M25 (1977).
3. Lyle, M. *Geol. Soc. Am. Mem.* **154,** (in the press).
4. Murray, J. & Irvin, R. *R. Soc. Edinb.* **37,** 721–742 (1894).
5. Manheim, F. T. *Symp. Marine Geochemistry* 217–276 Univ. Rhode Island (1965).
6. Calvert, S. E. & Price, N. B. *Mar. Chem.* **5,** 43–74 (1977).
7. Halbach, P., Marchig, V. & Scherhag, C. *Mar. Geol.* **38,** M1–M9 (1980).
8. Lynn, D. C. & Bonatti, E. *Mar. Geol.* **3,** 457–474 (1965).
9. Ku, T. L. & Glasby, G. P. *Geochim. cosmochim. Acta* **36,** 699–703 (1972).
10. Price, N. B. *Mar. Geol.* **5,** 511–538 (1967).
11. Glasby, G. P. *Mar. Geol.* **13,** 57–72 (1972).
12. Renard, D. Thesis, Univ. Paris (1980).
13. Halbach, P., Scherhag, C., Hebisch, U. & Marchig, V. *Miner. Deposita* **16,** 59–84 (1981).
14. Halbach, P. & Ozkara, M. *Colloq. Int. C.N.R.S.* No. 289, 77–88 (1979).
15. Ku, T. L. & Broecker, W. S. *Deep-Sea Res.* **16,** 625–627 (1969).
16. Ku, T. L. *J. geophys. Res.* **70,** 3457–3474 (1965).
17. Somayajulu, B. L. K. & Church, T. M. *J. geophys. Res.* **78,** 4529–4531 (1973).
18. Ku, T. L., Knauss, K. G. & Mathieu, G. G. *Deep-Sea Res.* **24,** 1005–1007 (1977).
19. Cochran, J. K. & Krishnaswami, S. *Am. J. Sci.* **280,** 849–899 (1980).
20. Moore, W. S. *et al. Earth planet. Sci. Lett.* **52,** 151–171 (1981).
21. Koide, M., Bruland, K. & Goldberg, E. D. *Earth planet. Sci. Lett.* **31,** 31–36 (1976).
22. Scott, M. R., Scott, R. B., Rona, P. A., Butler, L. W. & Nalwalk, A. J. *Geophys. Res. Lett.* **1,** 355–358 (1974).
23. Burnett, W. C. & Piper, D. Z. *Nature* **265,** 596–600 (1977).
24. Lalou, C., Brichet, E. , Ku, T. L. & Jehanno, C. *Mar. Geol.* **24,** 245–258 (1977).

Biogenic calcite structures forming in Lake Fryxell, Antarctica

Robert A. Wharton Jr*, Bruce C. Parker*, George M. Simmons Jr*, Kenneth G. Seaburg* & F. Gordon Love†

* Department of Biology and † Department of Geological Sciences, Virginia Polytechnic Institute and State University, Blacksburg, Virginia 24061, USA

Stromatolites are organosedimentary structures produced by microorganisms which have been used extensively in the interpretation of Precambrian and, to a lesser extent, Phanerozoic history[1–5]. Modern stromatolites are generally restricted to hot springs or warm, hypersaline and/or alkaline aquatic environments[3]. Recently, however, we documented[6] the presence of modern stromatolites in several cold, perennially ice-covered Antarctic dry valley lakes. Here, we report a finding in Lake Fryxell, Antarctica, of biogenic calcite structures not observed in our previous study of other Antarctic lakes. These structures were laminated, indurate, unbranched, and had either a vertical or horizontal orientation. We infer that these calcite structures are biogenic in origin, and hence stromatolitic based on the following evidence: (1) the presence of an actively metabolizing algal mat on their surface; and (2) an internal composition of filamentous blue-green algal cell wall fragments, diatom frustules and calcite crystals.

Lake Fryxell (77°37′ S, 163°07′ E) is located at the eastern end of Taylor Valley in southern Victoria Land, Antarctica (see Table 1 for physicochemical features). It is 16 m above sea level, 20 m deep, 5.2 km long, 1.7 km wide and has a surface area of 5.4 km^2. This latitude receives approximately 4 months each of sunlight, twilight and darkness. The perennial 4–5-m thick ice-cover of Lake Fryxell overlies ~15 m of water <4°C and allows penetration of <2% of the incident photosynthetically

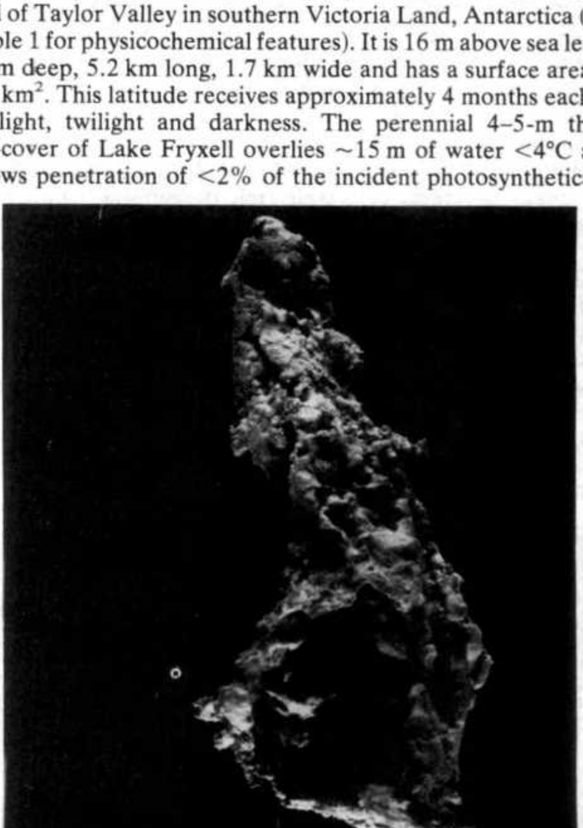

Fig. 1 Typical vertical calcite (determined by X-ray diffraction) structure collected from beneath 0.2–1.0 cm of actively metabolizing algal mat at a depth of ~7 m, Lake Fryxell, Antarctica.

0028–0836/82/050403—03$01.00

Table 1 Selection of physical and chemical variables of Lake Fryxell on 28 December 1980

Depth (m)	Temperature (°C)	% Transmission*	O_2 (mg l^{-1})	CO_2 (mg l^{-1})	Alkalinity (mequiv. l^{-1})	Ca (mg l^{-1})	Mg (mg l^{-1})	pH	Specific conductance (μS cm^{-1})
5	1.1	1.41	23.5	14.1	6.74	29	17	7.5	1,200
6	2.0	1.31				21, 77	40, 129		1,370
7	2.8	0.81	37.0	19.4				7.7	2,520
8	3.2	0.62	10.7	66.0		31	124	7.3	3,320
8.5	3.6	0.46	4.1	91.5	19.52			7.3	3,720
8.75	3.7	0.41	2.3	88.9				7.4	3,930
9	3.8	0.30		86.2	25.84			7.4	4,280
10	3.8	0.08	0	135.5		35	184	7.4	4,300
11	3.8	0.02							5,200
12	3.7	0.01	0	207.7		31, 33	284, 229	7.4	5,800
13	3.7	0.005							6,300
14	3.7	0.003							6,900
15	3.4	0	0	240.2		43	311	7.3	7,200
16	3.2	0				27	331		7,400
17	3.0	0							7,700
18	2.8	0							7,900

Calcium and magnesium data are from ref. 16, first no. and ref. 17, second no.

* Per cent transmission of surface photosynthetically active radiation (400–700 nm wavelength light) through ice and water at depth indicated.

active radiation (400–700 nm wavelength) during the austral summer. The ice cover also prevents free exchange of gases with the atmosphere, wind-generated turbulence and internal mixing of the lake water. This is exemplified by oxygen supersaturation in the upper few metres of the water column, descending to anaerobic conditions below 10 m. The lake lacks outflowing streams, and receives sediment, salts and nutrients from glacial meltstreams during the austral summer.

During the 1980–81 austral summer we melted two dive holes through the ice-cover of Lake Fryxell and SCUBA divers observed and photographed the sub-ice environment. Benthic cores collected at a water depth of 7–9 m revealed that the upper mat layer (0.2–1.0 cm thick) contained actively metabolizing organisms. Metabolic activity was inferred from microscopic examination of motile blue-green algal filaments and diatoms in the mat, isolation of viable microorganisms, and from measurements of photosynthetic pigments, ATP and ^{14}C primary productivity. This top layer of mat consisted primarily of the blue-green alga *Phormidium frigidum* Fritsch, pennate diatoms (for example, *Navicula* sp., *Caloneis* sp.) and heterotrophic bacteria. Below this layer were alternating bands of organic-rich and sediment-rich layers to a depth of ~50 cm. Five organic layers, isolated from 7–32 cm in the sediment, had an average organic matter content of 8.7%. These organic and sediment laminations are similar to the Antarctic stromatolites previously reported by Parker *et al.*[6]. Embedded within these sediments were discrete structures composed of calcite (Fig. 1). These calcite structures were laminated, indurate and unbranched and had developed either a vertical or horizontal orientation. The vertical structures (1–5 cm in diameter, 1–10 cm long) were usually hollow, terete and covered by a 0.2–1.0-cm thick layer of algal mat (Fig. 2). At a depth of ≥ 50 cm in the sediment was a stratiform layer of calcite ~5 mm thick. Microscopic examination of these structures revealed diatom frustules and filamentous blue-green algal cell wall fragments ~1–2 μm diameter, the latter resembling filaments of *Phormidium*.

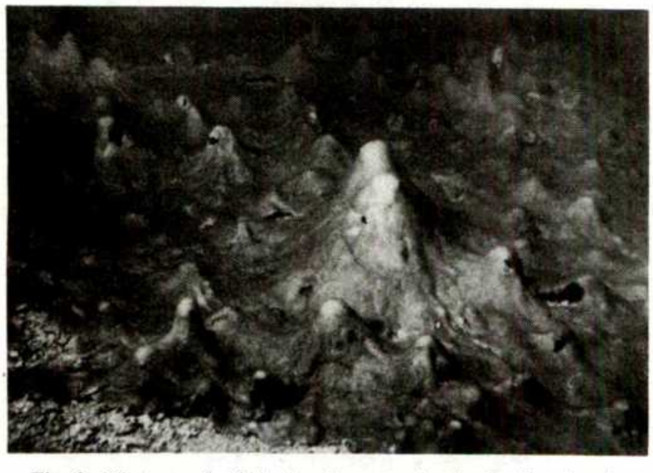

Fig. 2 Photograph of the benthos at a depth of ~7 m showing surface morphology of living algal mat in which trapped photosynthetically produced oxygen has induced lift-off from the substrate (maximum vertical relief, ~10 cm).

The vertical calcite structures in Lake Fryxell apparently result from the growth of the algal mat in dimly-lit, shallow, non-turbulent water. Austral summer photosynthetic production of O_2 causes gas bubbles to be trapped within the sticky mucilaginous algal mat matrix and initiates a vertical growth habit[6–10]. In other Antarctic lakes observed, buoyant forces sometimes tear the mat matrix, and the algal mat detaches completely from the substrate[6–13]. However, in Lake Fryxell, much of the gas-charged mat is stabilized by the precipitated calcite and does not tear loose from the substrate. The hollow nature of the structures suggests that calcite precipitation follows the orientation of the growing mat.

The vertical structures in Lake Fryxell closely resemble some of the calcite-impregnated defluidization structures recently reported from Mono Lake, California[14]. However, in contrast to the Mono Lake structures, which were considered to be formed by physicochemical carbonate deposition, the Antarctic structures seem to be primarily the result of algal activity. The horizontal structures are formed either at greater depth in the sediment where no light is available for photosynthesis or at depths where photosynthetic activity is insufficient to accumulate trapped oxygen, which results in a flat mat growth habit.

Several unique biological, physical and chemical features of Lake Fryxell produce and preserve these stromatolitic structures[6]. (1) While a few tardigrades, rotifers and nematodes inhabit the algal mats in the shallow peripheral margins of the lake, major burrowing and browsing organisms (such as cladocerans, copepods, annelids, gastropods, insect larvae and fish) are entirely absent[15], leaving these mats essentially undisturbed by metazoans. (2) Sediment influx to the lake consists of periodic influxes of glacial meltstreams which flow at most 10–12 weeks of the austral summer, contributing insufficient sediment to obliterate the mats. (3) Except for localized mixing of lake water near glacial meltstream deltas, no internal mixing of lake water occurs which prevents disturbance of existing sediments. (4) Low temperatures and a paucity of metabolically active bacteria possibly slow the decomposition of organic matter. (5) Sufficient calcium and dissolved carbonate[16,17] are available for the biogenic calcite precipitation[18].

These Antarctic stromatolites may resemble ancient permanently submerged stromatolites of the Precambrian era[6,7,9]. Because of low light intensities, lack of water turbulence and absence of burrowing and/or grazing metazoans, the benthos of Lake Fryxell may simulate some of the conditions that occurred in Precambrian deep subtidal marine or lacustrine environments which were dominated by stromatolite-forming microorganisms[5]. Thus, Lake Fryxell is an unusual habitat where modern stromatolites are forming, and further investigation may provide insight into the palaeoecology of Precambrian stromatolites.

This research was supported by the NSF's Division of Polar Programs grant DPP-80-12988. We thank D. Andersen and A. Vass for their diving efforts, I. Farrance and D. Griffiths for field assistance, Drs S. Awramik, S. Golubic, A. Knoll, M. Potts and S. Scheckler for preliminary reviews and helpful suggestions, and Dr J. Craig for X-ray crystallographic analyses.

Received 2 September; accepted 3 December 1981.

1. Awramik, S. M. Margulis, L. & Barghoorn, E. S. in *Stromatolites* (ed. Walter, M. R.) 149–162 (Elsevier, Amsterdam, 1976).
2. Walter, M. R. in *Stromatolites* (ed. Walter, M. R.) 1–3 (Elsevier, Amsterdam, 1976).
3. Awramik, S. M., Gebelein, C. D. & Cloud, P. in *Environmental Biogeochemistry and Geomicrobiology* (ed. Krumbein, W. E.) 165–173 (Ann Arbor Science, 1977).
4. Walter, M. R. *Am. Scient.* **65,** 563–571 (1977).
5. Awramik, S. M. in *Biotic Crises in Ecological and Evolutionary Time* (ed. Nitecki, M. H.) 83–102 (Academic, New York, 1981).
6. Parker, B. C., Simmons, G. M. Jr, Love, F. G., Wharton, R. A. Jr & Seaburg, K. G. *BioScience* **31,** 656–661 (1981).
7. Simmons, G. M. Jr, Parker, B. C., Wharton, R. A. Jr, Love, F. G. & Seaburg, K. G. *Antarct. J. U.S.A.* (in the press).
8. Parker, B. C., Simmons, G. M. Jr, Seaburg, K. G. & Wharton, R. A. Jr *Antarct. J. U.S.A.* **15,** 167–170 (1980).
9. Parker, B. C. & Simmons, G. M. Jr *Trends biochem. Sci.* **6,** III–IV (1981).
10. Parker, B. C., Simmons, G. M. Jr, Wharton, R. A. Jr, Seaburg, K. G. & Love, F. G. *J. Phycol.* (in the press).
11. Golubic, S. in *The Biology of Blue-Green Algae* (eds Carr, N. G. & Whitton, B. A.) 434–472 (Blackwell, Oxford, 1973).
12. Wilson, A. T. *Ecology* **46,** 376 (1965).
13. Komarek, J. & Ruzicka, J. *Preslia* **38,** 237–244 (1966).
14. Cloud, P. & Lajoie, K. R. *Science* **210,** 1009–1012 (1980).
15. Cathey, D. D., Simmons, G. M. Jr, Parker, B. C. & Youngue, W. H. *Hydrobiologia* (in the press).
16. Torii, T. *et al.* in *Geochemical and Geophysical Studies of Dry Valleys, Victoria Land in Antarctica*, 5–21 (Memoirs of National Institute of Polar Research No. 4, Tokyo, 1975).
17. Angino, E. E., Armitage, K. B. & Tash, J. C. *Science* **138,** 34–36 (1962).
18. Jones, B. F. & Bowser, C. J. in *Lakes: Geology, Chemistry, and Physics* (ed. Lerman, A.) 179–235 (Springer, New York, 1978).

Neural reorganization during metamorphosis of the corpora pedunculata in *Drosophila melanogaster*

Gerhard Technau & Martin Heisenberg

Institut für Genetik und Mikrobiologie, 87 Würzburg, FRG

Adult fruit flies and *Drosophila* larvae have very different bodies and behaviour patterns. The question therefore arises: how much reorganization does the brain undergo during pupation? Some apparent shape changes have been documented, for example, the growth of the optic lobes and the separation of the prothoracic and suboesophageal ganglia[1,2]. In the central brain, the issue is less clear. Most neurone cell bodies persist through metamorphosis[3], and the general shape of certain neuropil regions is conserved. However an identified motoneurone in another holometabolous insect (*Manduca*) has been shown to change its dendritic arborization patterns during pupation[4]. Here we report that the mushroom body, a major neuropil area in the insect brain, is extensively reorganized during pupation (that is, many of the intrinsic fibres are broken down and made anew). This reorganization is cryptic—the overall morphology of the mushroom body is apparently constant throughout pupation. We have now studied this reorganization by examining two mutations (*mbd, mud*) which cause derangement of this structure during metamorphosis, and we report that this reorganization is one of the most extensive yet found in insect metamorphosis.

As in most arthropods, the mushroom bodies of *Drosophila* are two conspicuous substructures of the median protocerebrum arranged in mirror symmetry to the saggital midplane. The numerous, relatively small cell bodies of their intrinsic neurones (Kenyon cells) are situated in the posterior dorsal cortex. The calyx is formed by postsynaptic glomerulus-like arborizations of the Kenyon cell fibres and by collaterals of the antennal glomerular tract (AGT) as presynaptic elements. From there, the Kenyon cell axons grow as a large bundle—the peduncle—from back to front through the whole brain on either side of the central complex. Near the anterior margin of the neuropil, most of the axons divide, sending one branch towards the midplane (β-, γ-lobes), the other one upwards (α-lobe). Thus the whole stalk system consists of three arms (peduncle, α-lobe, β-, γ-lobes) oriented roughly parallel to the three main axes of the fly[5–7]. It is this bizarre shape which makes the mushroom bodies already well discernible in the brain of the early first instar larva, where they are found in the same position and orientation as in the imago. Thus, at first sight, mushroom body development seems to imply no more than the addition of Kenyon cells and the elongation of their axons with the growth of the surrounding central brain neuropil.

Recently several mutants altering the morphology of the mushroom bodies have been described[6]. In two of them (*mushroom bodies deranged*^{KS65}, *mbd* and *mushroom body defect*^{KS63}, *mud*) the lobe and stalk system of the mushroom bodies is missing (not always completely in the case of *mbd*) and the calyces are enlarged. We noticed, to our surprise, that these mutant phenotypes occur only in the imago (Fig. 2). In the late third instar mutant larvae, the mushroom bodies have the same shape as in wild-type flies (Fig. 3). Twenty hours after puparium formation their neuropil is more or less completely degraded. Apparently, the newly growing 'imaginal' Kenyon cell axons fail to find their normal way through the central brain neuropil and remain at the site of the calyces, causing abnormal enlargement of these structures. Cell proliferation in the mushroom body cortex still seems to be normal in *mbd* (increased in *mud*). In these mutants, as in wild-type flies, neuroblasts are no longer detectable 3 days after puparium formation.

Replacement of larval Kenyon cell fibres is not a peculiarity of the mutants. A similar process occurs in wild-type individuals as well; apparently, only the course of newly growing 'imaginal' fibres is altered in the mutants. This reorganization of the wild-type mushroom body neuropil is documented by the following data.

Figure 1 shows for wild-type *Berlin* flies the number of Kenyon cell axons in the caudal peduncle, as a function of time measured from egg hatching. Counts were taken from electron micrographs of cross-sections through the peduncle, a few micrometres anterior to the calyx. The number of axons increases from about 300 in the first instar larva to about 2,100 in the late third instar larva. At the time of puparium formation, the number of axons drops abruptly. Already 12 h later, it is reduced by about 40%. From then on, it increases again until it reaches the imaginal level (2,200 fibres). From Golgi preparations of adult *Drosophila*, we know that Kenyon cell axons in the caudal peduncle have no ramifications, which could have contributed to the total cross-sectional count (K. F. Fischbach, personal communication). In electron micrographs of a series of longitudinal sections through the late larval peduncle, we found few ramifications (possibly belonging to extrinsic elements), implying that among the larval Kenyon cells as well, collaterals must be rare or even missing in this part of the mushroom bodies. Therefore we believe that the decrease of fibres in the peduncle of the early wild-type pupa reflects degeneration of whole larval axons rather than collaterals. The fact that Kenyon cell axons degenerate in the mutants supports this conclusion. Note that this is contrary to the situation of the motoneurone in *Manduca*[4] where the axon is maintained.

We have no data on whether extrinsic elements are included in this process. However, we assume that, in the peduncle, these constitute only a small minority of the profiles. In the late larval

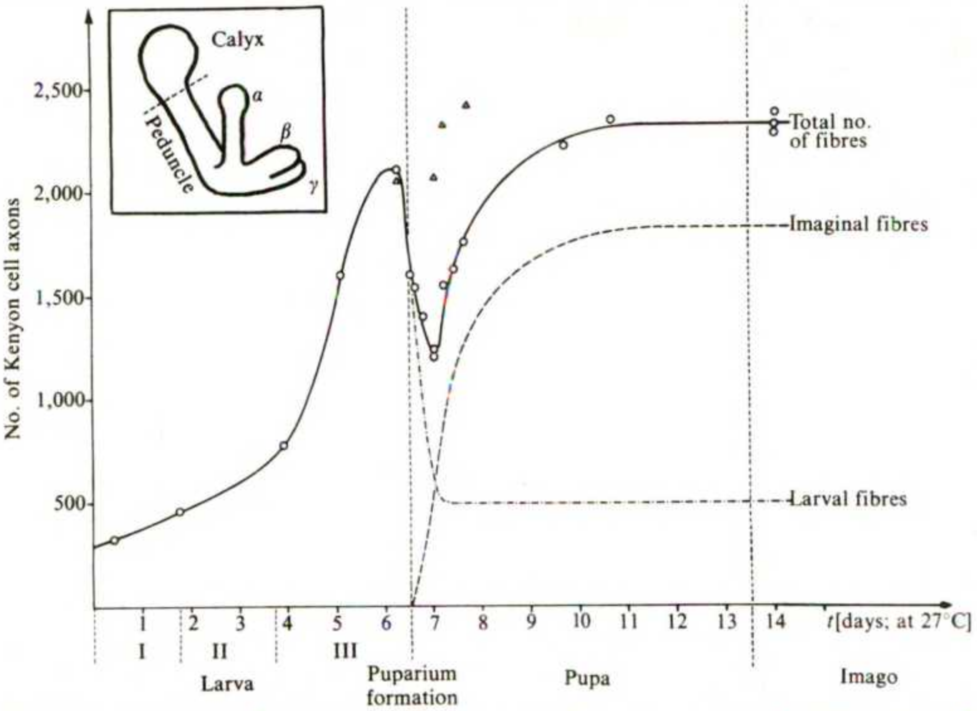

Fig. 1 Total number of Kenyon cell axons (including extrinsic elements) in the caudal peduncle of wild-type *Drosophila* (for plane of section see inset) as a function of developmental time starting at eclosion (zero time). Cell fibres are shown as open circles and cell bodies (relative counts) as triangles. Whereas the fibres of larval Kenyon cells degenerate within the first hours of pupal life, their cell bodies remain alive. The dash and dash-dot lines represent the hypothetical larval and imaginal fibre portions. The curves are based on the assumption that the bundle of (~500) thin fibres positioned centrally in the stalk system contains the only larval fibres which remain throughout metamorphosis.

stage the total number of profiles in the caudal peduncle is very close to that of Kenyon cell bodies. Hardly any tangential elements are observed which could be interpreted as penetrating extrinsic fibres or ramifications of them. Golgi preparations from adult flies rarely show extrinsic elements or specializations of intrinsic fibres in this part of the mushroom bodies. Finally, in the larva as well as the adult, cross-sections from different levels of the peduncle (except for the part close to the lobes) do not vary by more than 5–10% in their total number of profiles. Thus extrinsic elements appear to contribute little to the effect observed.

The cell bodies of the larval Kenyon cells remain alive: a staining procedure which clearly marks degenerated material (Mallory's solution of azur II and methylene blue applied to 1 μm plastic sections) shows no sign of degeneration in the mushroom body cortex at any developmental stage in either wild type or the mutant *mbd*. This is confirmed by the fact that the number of Kenyon cell bodies does not decrease during the time of fibre reduction (Fig. 1). In the pupal stage, addition of new cells to the mushroom body cortex is much less than the number of new 'imaginal' fibres, implying that at least part of these fibres belong to regenerating Kenyon cells. Presumably, sprouting of new fibres continues while larval fibres are degenerating. In fact, scattered profiles of groups of extremely thin fibres, which may represent filipodia of growing axons are found throughout the degeneration period. Thus, loss of larval Kenyon cell axons probably by far exceeds 40% (Fig. 1).

The degenerating neuropil shows typical histological alterations[8] (Fig. 4) in all parts of the mushroom bodies. Axons have short, swollen segments containing electron-dense granules (presumably glycogen), lamellar bodies and an increased number of vesicular components (Fig. 4*c*). Ramifications of glial cells in this area are drastically enlarged. They are filled with osmiophilic material and axon fragments, which suggests their active role in the degeneration process (Fig. 4*b*). Twenty hours after puparium formation, the histological signs of degeneration have already disappeared.

The misrouting of the mutant Kenyon cell axons during metamorphosis is not yet understood. In larvae and early pupae of wild-type flies we find a bundle of very thin fibres located centrally in the peduncle and β-lobe which never shows any histological signs of degeneration (Figs 3*a*, 4*a*). In the mutant *mbd* this bundle is frequently missing. If the frequency of this larval defect correlates with the expressivity of the *mbd* phenotype in the adult, the role of this bundle may be seen as a guide for the ingrowing 'imaginal' fibres. (In the mutant *mud*, cross-sectional profiles in the larval peduncle are doubled in number and are small and uniform in diameter. No special bundle can be detected.)

Since experiments with the mutant *mbd* strongly suggest that the mushroom bodies participate in the evaluation of odors (M. Heisenberg, unpublished), it is tempting to speculate about the

Fig. 2 Cross-section through the peduncle of *a*, 7-day-old wild-type imago; *b*, an imago of the mutant *mushroom bodies deranged*^{KS65}. In flies of this mutant, the number of Kenyon cell fibres (here ~250) forming the peduncle is variable, while in most flies of the mutant *mushroom body defect*^{KS63} peduncles are not detectable. ×3,599.

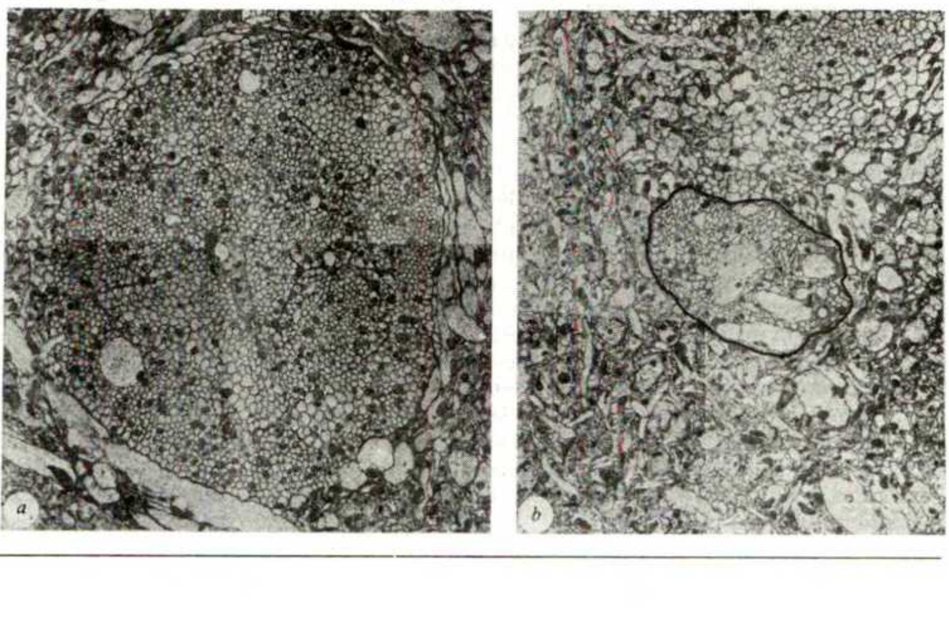

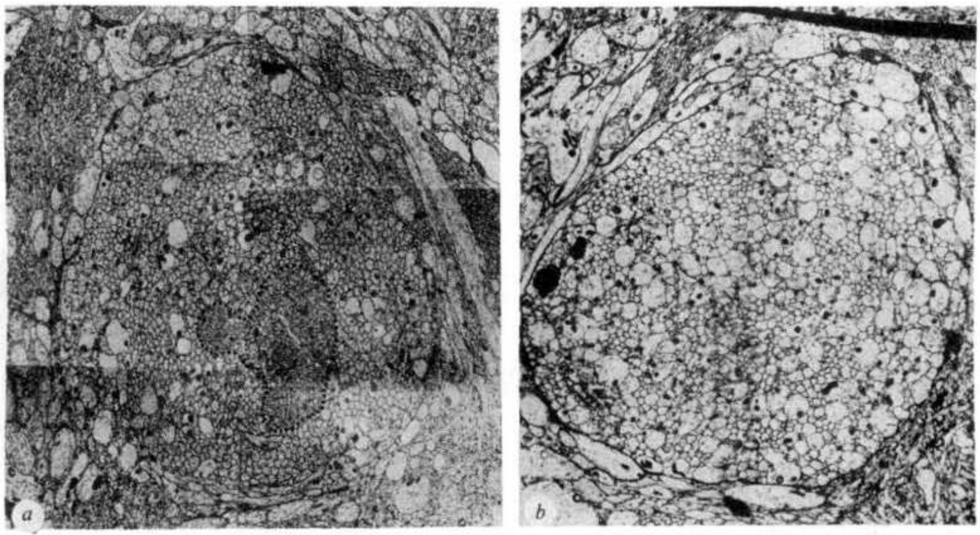

Fig. 3 Cross-section through the caudal peduncle of *a*, late third instar larva of wild type. Note centrally positioned bundle of very thin fibres (encircled by dotted line); *b*, late third instar larva of mutant *mushroom bodies deranged*^{KS65}. During larval life the mushroom bodies have the normal shape. However, in many peduncles, the bundle of thin fibres is missing. ×3,245.

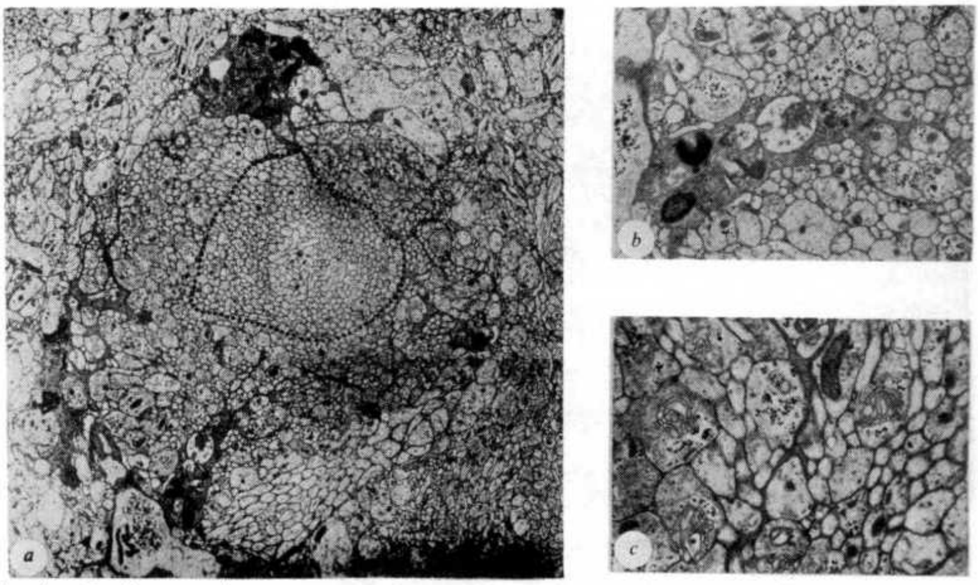

Fig. 4 *a*, Cross-section through the caudal peduncle of wild-type fly 12 h after puparium formation. ×3,658. With the exception of the centrally positioned bundle of small fibres (encircled by dotted line), mushroom body neuropil shows typical signs of degeneration. *b*, Enlarged active glial element enclosing osmiophilic material and axon fragments. ×8,184. *c*, Swollen axons with lamellar bodies, dark granules (possibly glycogen) and an increased amount of membrane-bound vesicles. ×8,184.

functional implications of the reorganization. During pupation, olfactory sense organs are completely demolished and replaced. The AGT fibres must form new connections with the antennal olfactory fibres and this possibly requires new connections between AGT fibres and Kenyon cells as well. Thus, the reorganization of the mushroom bodies may be directly related to the reorganization in the periphery. On the other hand, the presumed different synaptic contacts of the Kenyon cells may also be related to the different 'meaning' some odours have for larva and imago[9].

The reorganization of the mushroom bodies is the most extensive neuronal rewiring during metamorphosis found to date. We do not yet know whether it is characteristic of mushroom bodies in other insects, or whether other insect brain areas are also reorganized in such a wholesale manner.

We thank N. J. Strausfeld, J. R. Wolff and F.-W. Schürmann for valuable suggestions, W. G. Quinn and K. F. Fischbach for critical comments on the manuscript, and Mrs S. Newkirk for correcting the English. This work was supported by a grant from Deutsche Forschungsgemeinschaft to M.H.

Received 21 July; accepted 18 November 1981.

1. Power, M. E. *J. Morph.* **91,** 389–411 (1952).
2. Hertweck, H. *Zeitschr. wiss. Zool.* **139,** 559–663 (1931).
3. White, K. & Kankel, D. R. *Devl Biol.* **65,** 296–321 (1978).
4. Truman, J. W. & Reiss, S. E. *Science* **192,** 477–479 (1976).
5. Power, M. E. *J. Morph.* **72,** 517–559 (1943).
6. Heisenberg, M. in *Development and Neurobiology of Drosophila* (eds Siddiqi, O. *et al.*) 373–390 (Plenum, New York, 1980).
7. Strausfeld, N. J. *Atlas of an Insect Brain* (Springer, Berlin, 1976).
8. Schürmann, F. W. in *Neuroanatomical Technics* (eds Strausfeld, N. J. & Miller, T. A.) 265–284 (Springer, Berlin, 1980).
9. Rodrigues, V. in *Development and Neurobiology of Drosophila* (eds Siddiqi, O. *et al.*) 361–371 (Plenum, New York, 1980).

Co-occurrence of substance P-like and Leu-enkephalin-like immunoreactivities in neurones and fibres of avian nervous system

Jonathan T. Erichsen, Anton Reiner & Harvey J. Karten

Department of Neurobiology and Behavior, State University of New York at Stony Brook, Stony Brook, New York 11794, USA

Neuropeptides are frequently found in neurones that also contain another putative transmitter substance such as a biogenic amine or acetylcholine[1–5]. Such co-existence has led to the suggestion that the roles of neuropeptides in the nervous system may be diverse and may in some systems include a part in conventional neurotransmission as well as an ancillary, or modulatory, role. Recently, several studies have noted the co-occurrence of two peptides within individual neurones of localized regions of the mammalian nervous system[6–9]. Here, we present the first evidence, based on an indirect immunofluorescence technique allowing the simultaneous visualization of separate tissue antigens, that substance P (SP) and Leu-enkephalin (L-Enk) co-occur within individual neurones of widespread regions of the avian central nervous system.

0028-0836/82/050407—04$01.00

The most widely used[3,4,10] immunohistochemical technique for double-label experiments has been the elution technique of Tramu *et al.*[10]. However, this technique requires comparisons of the photographic record of individual neurones following staining for each antigen (according to the indirect immunofluorescence method of Coons[11]) to determine whether any neurone has stained for the presence of both antigens. (An alternative technique involves the comparison of individual neurones in adjacent thin sections (10 μm) which have been processed separately for the presence of the two given substances[1,2,6,7].) In the present approach, immunoreactivity of two separate tissue antigens was visualized simultaneously by using non-cross-reactive primary antisera for SP and L-Enk and two distinct secondary antisera, each of which was specific for only one of the two primary antisera (see Fig. 1 legend). Furthermore, because the terminal fluorescent markers for each tissue antigen were distinct fluorophores, fluorescein isothiocyanate (FITC) and tetramethylrhodamine isothiocyanate (TRITC), the location of each antigen could be readily determined. The tissue was examined for the two fluorophores using a Leitz epi-illumina-

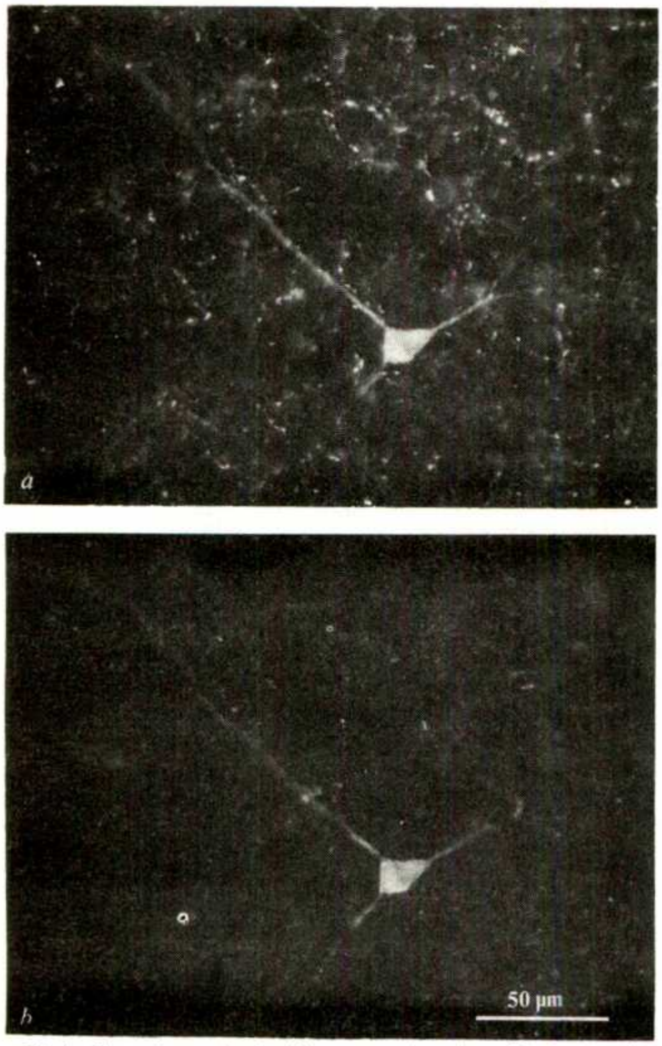

Fig. 1 Photomicrographs of an ICo neurone taken using an N cube (*a*) and an I cube (*b*) (note that different labelled fibres are seen through the two different cubes). This neurone showed TRITC (*a*) and FITC (*b*) fluorescence, indicating that the neurone stained for the presence of both a L-Enk-like substance (*a*) and a SP-like substance (*b*). The L-Enk antiserum (supplied by Dr K.-J. Chang, Wellcome) used was raised in rabbit while the monoclonal SP antiserum (Sera-Lab) used was raised in tissue culture from rat spleen hybridoma. To stain for the presence of the L-Enk and SP antisera, respectively, a goat anti-rabbit IgG conjugated to TRITC (Cappel) and a goat anti-rat IgG conjugated to FITC (Cappel) were used. As neither primary antiserum cross-reacts with either the other primary antiserum or the antigen against which the other primary antiserum is directed and as neither secondary antiserum cross-reacts with either the other secondary antiserum or the primary antigen against which the other secondary antiserum is directed, it proved possible to stain neural tissue simultaneously for the presence of both antigens.

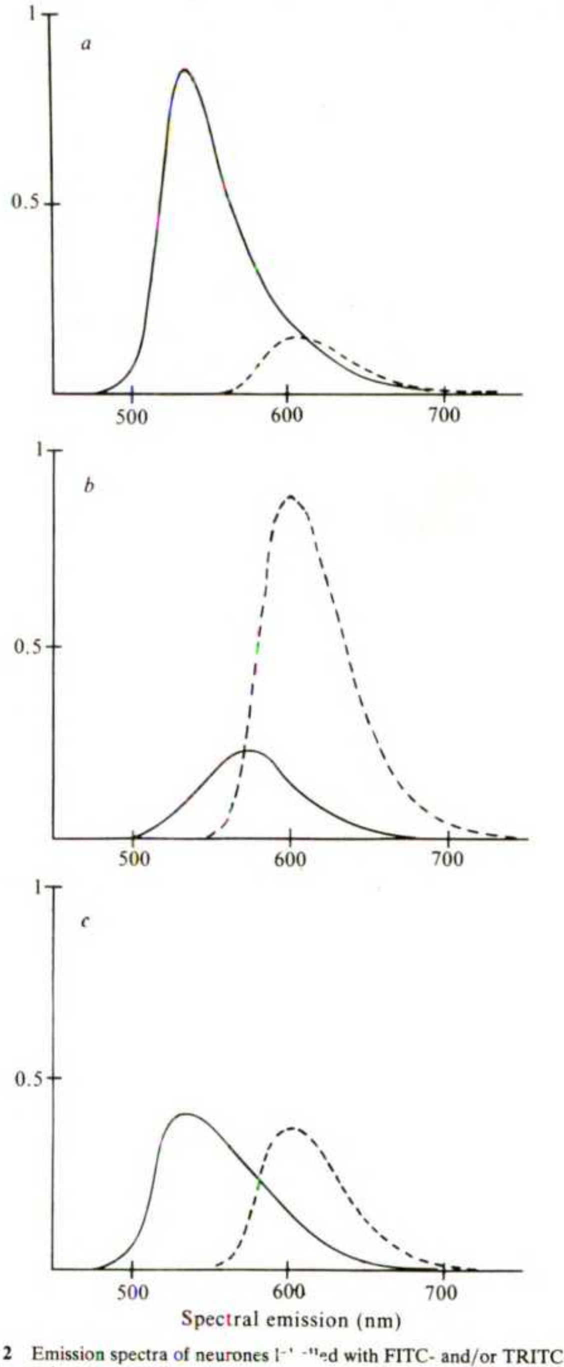

Fig. 2 Emission spectra of neurones labelled with FITC- and/or TRITC-conjugated antisera. Although the wavelength bandpass characteristics of the N cube ensured that FITC fluorescence was not detectable while the tissue was being examined using this cube, TRITC fluorescence was observable through the I cube. Nonetheless, because the TRITC fluorescence seen through the I cube is discernibly reddish while FITC fluorescence is greenish-yellow, true FITC fluorescence can be distinguished from TRITC 'breakthrough'. However, microspectrophotometry (using a Leitz MPV-2 with a B-60 Veril motor-driven filter with output recorded on an HP 2000-A *x*-*y* recorder) was used to confirm that individual neurones appearing to show both FITC and TRITC fluorescence did indeed show peak emissions through the N and I cubes at the wavelengths characteristic of TRITC and FITC, respectively. *a* Shows the spectral emission of a neurone from control series 2 (see text) that showed only FITC labelling (solid line represents emission spectrum through I cube; dashed line represents emission spectrum through N cube). The small emission recorded through the N cube represents nonspecific background binding of the anti-rabbit IgG-conjugated TRITC. *b* Shows the spectral emission of a neurone from control series 3 that showed only TRITC labelling. Note that the peak recorded through the I cube is somewhat displaced to the right of the FITC wavelength peak seen in *a*. This peak represents TRITC breakthrough on the I cube and, as can be seen, has its maximum amplitude in the red range. *c* Shows the emission spectra of the double-labelled ICo neurone shown in Fig. 1. Note that this neurone shows an emission maximum through the N cube at the TRITC peak (see *b*) and an emission maximum through the I cube at the FITC peak (see *a*). The gradations along the *y*-axis represent an arbitrary scale designed to aid comparisons of the intensity of emission at different wavelengths (*x*-axis) for different cells.

tion fluorescence microscopy system in conjunction with an 'I' cube for FITC and an 'N' cube for TRITC (Fig. 2). Control tissue incubations were carried out to confirm the specificity of the individual primary and secondary antisera.

Details of the immunohistochemical procedures used have been described elsewhere[12–14]. Tissue incubations were carried out in a primary antisera 'cocktail' consisting of both SP and L-Enk antisera at 1:1,000 dilutions; subsequently, the tissue was incubated in a secondary antisera cocktail consisting of anti-rabbit IgG-conjugated TRITC at a 1:30 dilution and anti-rat IgG-conjugated FITC at a 1:50 dilution. In some cases, three further series of sections from a given animal were run through separate control procedures: (1) incubation in a SP/L-Enk primary antisera cocktail that also contained synthetic SP and L-Enk, (2) incubation only in SP primary antiserum, and (3) incubation only in L-Enk primary antiserum. All three series of sections were subsequently incubated in the above described secondary antisera cocktail. The results of these control procedures were consistent from case to case. In the first (or blocked control) series, no labelled neurones or fibres were observed in the sections, in the second series only FITC-labelled cells and fibres were observed, and in the third control series only TRITC-labelled cells and fibres were observed (Fig. 2). The results of the first control procedure indicated that the individual primary antisera are specific for SP and L-Enk or structurally similar compounds. The specificity of the SP and L-Enk antisera in avian nervous tissue in our experimental conditions has been routinely and consistently observed in many previous single-label studies in our laboratory[12,13,15–18]. In such studies, as in the present double-label study, no immunoreactivity with either SP antiserum blocked with synthetic SP or L-Enk antiserum blocked with synthetic L-Enk was ever observed in neural regions of interest to the present study. The results of the second and third control procedures show that neither secondary antiserum observably cross-reacts with either opposing primary or secondary antisera. Together, the three control procedures indicate that the immunoreactive substances observed in our double-label experiments are SP and L-Enk or structurally similar compounds. In light of the consistent control results obtained, control procedures were not routinely run with each experimental series.

Separate observations of L-Enk-like and SP-like immunoreactive preganglionic terminal endings in the avian ciliary ganglion[15] suggested that some of the preganglionic terminals within the ciliary ganglion might contain both SP-like and L-Enk-like immunoreactivities, and we have now confirmed this in individual terminal boutons using the double-label techniques described above. Careful examination of double-labelled sections through several levels of the ciliary ganglion indicated that most preganglionic terminal endings in the ciliary ganglion contain both SP-like and L-Enk-like immunoreactivities (Fig. 3), although some terminals contain only a L-Enk-like or SP-like substance. Erichsen *et al.*[16] have shown that lesions of the nucleus of Edinger-Westphal (EW, also known in birds as the accessory oculomotor nucleus) eliminate both the SP-like and L-Enk-like immunoreactivities from the preganglionic terminal endings of the ipsilateral ciliary ganglion, thus indicating that EW contains the cell bodies of origin of the L-Enk-like and SP-like immunoreactive terminal endings in the ciliary ganglion. In birds given a 3 μl injection of colchicine (6 mg μl^{-1}) into the lateral ventricle 48 h before death, examination of the fluorescent labelling of EW neurones indicated the presence of numerous cell bodies containing both SP-like and L-Enk-like immunoreactivities, as well as neurones that showed immunoreactivity for only SP or L-Enk.

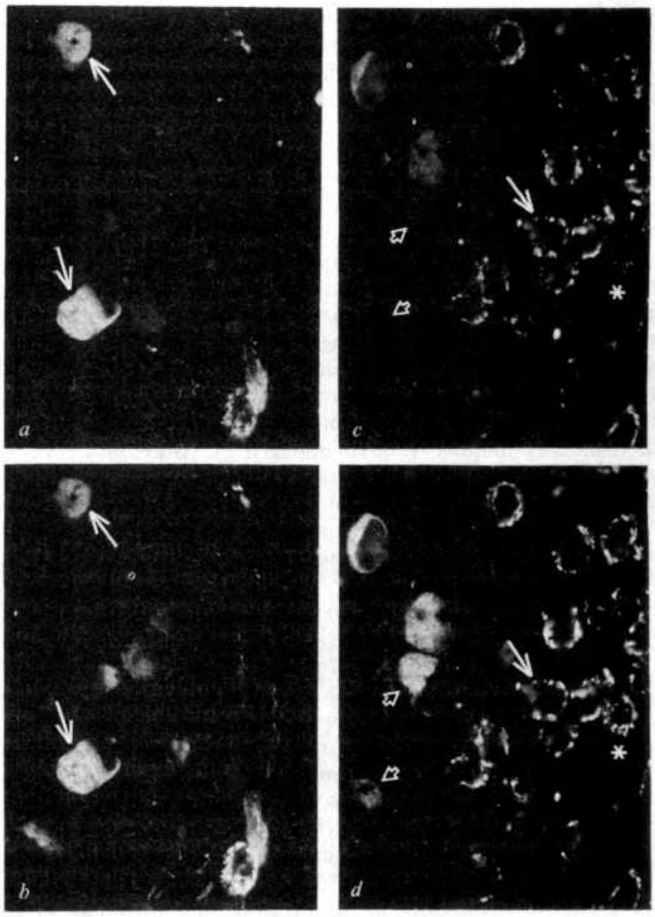

Fig. 3 Photomicrographs of labelled preganglionic terminals in the avian ciliary ganglion. The two types of preganglionic terminals previously described in the avian ciliary ganglion[23] are large cap-like structures that envelop the hilar pole of postganglionic neurones reported to project exclusively to the iris sphincter muscle and the ciliary body and endings characteristically consisting of numerous beaded terminal boutons encircling postganglionic neurones that uniquely project to the smooth musculature of the chorio-capillaris. Both types of terminal endings generally contained both a SP-like substance and a L-Enk-like substance, although the amount of immunofluorescence observed for SP relative to L-Enk varied from terminal to terminal in a given section. *a* And *b* are of the same field of view as seen through an N cube (*a*) and an I cube (*b*). Through the level of the ciliary ganglion shown in *a* and *b*, mostly cap-like endings are present and two of these (indicated by large solid arrows) show both strong TRITC immunofluorescence (indicating the presence of a L-Enk-like substance) and strong FITC immunofluorescence (indicating the presence of a SP-like substance). Several other cap-like endings showing varying amounts of both SP-like and L-Enk-like immunofluorescence are also present in *a* and *b*. One cap-like ending to the lower left in *b* and some fibres to the lower right apparently show only SP-like immunofluorescence. *c* And *d* show the same field of view through the ciliary ganglion as seen through an N cube (*c*) and an I cube (*d*). The level of the ciliary ganglion shown in *c* and *d* contains both cap-like and boutonal terminal endings. Nearly all boutonal endings show both TRITC and FITC immunofluorescence (one such double-labelled terminal ending is indicated by the large solid arrows in *c* and *d*), although variations occur in the relative amounts of TRITC and FITC immunofluorescence (for example, boutonal endings immediately above the asterisk in *c* and *d* show large amounts of SP immunofluorescence but little L-Enk immunofluorescence). The open arrows in *c* and *d* indicate a pair of cap-like endings that both show a large amount of SP-like immunoreactivity (*c*) but little to no observable L-Enk-like immunoreactivity (*d*).

Extensive searches were performed in several other regions of the avian brain known from preliminary observations and published work[17,18] to contain large numbers of neurones showing specific SP-like and specific L-Enk-like immunoreactivities. These were: (1) the small-celled zone of the basal ganglia (comprising the lobus parolfactorius and palaeostriatum augmentatum), (2) the mesencephalic subventricular nucleus intercollicularis (ICo), (3) the hypothalamus and (4) the periaqueductal grey. Immediately rostral to the confluence of the tectal ventricle with the cerebral aqueduct, we observed many ICo neurones that contained both SP-like and L-Enk-like immunoreactivities (Fig. 1). However, no neurones showing the co-existence of a SP-like and L-Enk-like substance were seen at any other level of ICo, although all levels of ICo contained neurones showing only SP-like or only L-Enk-like immunoreactivity. A population comprising neurones whose cell bodies contained both SP-like and L-Enk-like immunoreactivities and also many neurones whose cell bodies showed only SP-like or L-Enk-like immunoreactivity was found in a distinct, round cell group situated dorsally in a portion of the avian hypothalamus (or ventral thalamus) termed the stratum cellulare internum (SCI)[19]. A few neurones in the periaqueductal grey also contained both a SP-like and a L-Enk-like substance, but no such cells were found on examination of ~1,000 FITC-labelled and ~1,000 TRITC-labelled neurones in the basal ganglia.

The present demonstration of the co-existence of a SP-like substance and a L-Enk-like substance in individual neurones and/or fibre terminals in at least five separate regions of the avian nervous system raises the possibility that the co-existence of substance P and an opioid peptide in individual neurones and fibres may be a widespread phenomenon in the nervous system of a variety of vertebrates, including mammals. Consistent with this, a subpopulation of glomus cells of the carotid body of the cat has also recently been found to contain both SP-like and L-Enk-like immunoreactive material (L. Stensaas, personal communication). The functions of SP and L-Enk in neurones and fibres where they co-exist are unclear. In systems studied where they occur singly, SP and L-Enk have opposite actions, the former having excitatory postsynaptic effects and the latter inhibitory postsynaptic effects[20]. Clearly, however, the two need not have the same roles in systems where they co-occur as in those where they occur singly.

As the neurones of EW that project to the ciliary ganglion (a parasympathetic ganglion) are reported to be cholinergic[21,22], the present data suggest the co-existence of SP and L-Enk in a population of cholinergic neurones. Further, our results provide evidence that numerous individual preganglionic terminal boutons of the ciliary ganglion also contain both SP and L-Enk, and presumably acetylcholine. Erichsen *et al.*[15], using electron microscopic immunohistochemical techniques to study separately the ultrastructural localization of SP-like and L-Enk-like immunoreactivities in the preganglionic terminals of the ciliary ganglion, found that both SP-like and L-Enk-like immunoreactivities occurred in the same size class of large dense-core vesicles (85 nm, mean diameter). However, the resolution of the present light microscopic double-label technique was insufficient to determine whether SP-like and L-Enk-like immunoreactivities occurred in the same individual vesicles. Nonetheless, their presence in presumptively cholinergic preganglionic terminal boutons in the ciliary ganglion suggests that all three may have a role in neurotransmission in the ciliary ganglion.

We thank Patricia Lindaman for technical assistance, Dr. Larry Stensaas for discussion and advice during this research, and Drs Ira Cohen, James E. Krause, Thomas G. Sherman and Jeffrey F. McKelvy for their help in the preparation of this manuscript. The research was supported by EY 07039 to J.T.E., NS 15687 to A.R. and NS 12078 to H.J.K.

Received 24 July; accepted 14 October 1981.

1. Chan-Palay, V., Jonsson, G. & Palay, S. L. *Proc. natn. Acad. Sci. U.S.A.* **75**, 1582–1586 (1978).
2. Hokfelt, T. *et al. Neuroscience* **3**, 517–538 (1978).
3. Hokfelt, T. *et al. Nature* **285**, 476–478 (1980).
4. Hokfelt, T. *et al. Neuroscience* **5**, 2093–2124 (1980).
5. Lundberg, J. M. *et al. Neuroscience* **4**, 1539–1559 (1979).
6. Watson, S. J., Akil, H., Richard, C. W. & Barchas, J. D. *Nature* **275**, 226–228 (1978).
7. Schultzberg, M. *et al. Neuroscience* **5**, 689–744 (1980).
8. Hokfelt, T. *et al.* in *Regulation and Function of Neuronal Peptides* (eds Trabucchi, M. & Costa, E.) (Raven, New York, in the press).
9. Hunt, S. P. *et al. Neurosci. Lett.* **21**, 125–130 (1981).
10. Tramu, G., Pillez, A. & Leonardelli, J. *J. Histochem. Cytochem.* **26**, 322–324 (1978).
11. Coons, A. H. in *General Cytochemical Methods* (ed. Danielli, J. F.) 399–422 (Academic, New York, 1958).
12. Brecha, N., Karten, H. J. & Laverack, C. *Proc. natn. Acad. Sci. U.S.A.* **76**, 3010–3014 (1979).
13. Karten, H. J. & Brecha, N. *Nature* **283**, 87–88 (1980).
14. Korte, G. E., Reiner, A. & Karten, H. J. *Neuroscience* **5**, 903–914 (1980).
15. Erichsen, J. T., Karten, H. J., Eldred, W. D. & Brecha, N. C. *J. Neurosci.* (in the press).
16. Erichsen, J. T., Reiner, A., Cabot, J. & Karten, H. J. *Neurosci. Abstr.* **7**, 777 (1981).
17. Davis, B. M., Brecha, N. & Karten, H. J. *Neurosci. Abstr.* **6**, 744 (1980).
18. Reiner, A., Karten, H. J. & Korte, G. E. *Neurosci. Abstr.* **6**, 810 (1980).
19. Karten, H. J. & Hodos, W. *A Stereotaxic Atlas of the Brain of the Pigeon* (*Columba livia*) (Johns Hopkins Press, Baltimore, 1966).
20. Nicoll, R. A., Alger, B. E. & Jahr, C. E. *Proc. R. Soc.* **210**, 133–149 (1980).
21. Martin, A. R. & Pilar, G. *J. Physiol., Lond.* **168**, 443–463 (1963).
22. Martin, A. R. & Pilar, G. *J. Physiol., Lond.* **168**, 464–475 (1963).
23. Hess, A. *J. Cell Biol.* **25**, 1–19 (1965).

Rapid kinetics of single glutamate-receptor channels

S. G. Cull-Candy & I. Parker

Department of Biophysics, University College London,
Gower Street, London WC1E 6BT, UK

Drug-induced ionic channels are known to operate by opening briefly when agonist molecules bind to receptor sites[1-7] to produce rectangular current pulses, the amplitude and lifetime of which can be derived from noise analysis[1-3], or directly recorded using the patch-clamp technique[4-7]. If desensitization is neglected, the distributions of channel open and closed times can generally be fitted by single exponential functions[5-7], suggesting that a simple two-stage reaction scheme is sufficient to account for the observed kinetics[1]. Using patch-clamp recording with an improved time resolution, we have now found that glutamate-activated channels in locust muscle membrane show a large excess of both brief openings and closings over those expected from single exponential distributions. Many events which, with poorer frequency resolution, would have appeared as single openings were found to consist of two or more openings, interspersed with brief (<300 μs) closings. These observations have interesting implications for receptor/channel functioning.

Patch-clamp recordings of single glutamate-activated channels were obtained from the extensor tibiae muscle of the locust (*Schistocerca gregaria*), using techniques similar to those described previously[4,6]. Patch-clamp pipettes contained 200 μM glutamate, which gave a high frequency of channel openings, and muscle fibres were usually voltage-clamped at a potential of −110 mV to increase the size of the single channel currents. Muscles were pretreated with 1 μM concanavalin A to reduce receptor desensitization[5], and recording patches were

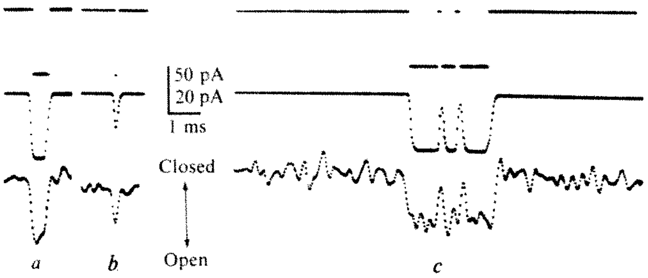

Fig. 1 Patch-clamp recordings of test pulses (*a*, *b*) and single channel currents (*c*) illustrating the time resolution of the recording system and the method of measurement. In each record the lower trace is a computer-digitized signal from the path-clamp amplifier, sampled at 25-μs intervals after sharp cut filtering ($1/f^4$) at 3.2 kHz. The upper traces show computer-generated traces used to help measure the data. A rectangular pulse (upper trace) with a height equivalent to the single channel current was generated and the position and width of this could be altered manually. A smoothing function applied to this pulse approximated the step response function of the recording system and the resultant smoothed pulse (middle trace) was displayed on a screen superimposed on the data. The position and width of the generated rectangular pulse was adjusted so that the smoothed pulse gave the best match to a channel opening and these parameters were then stored. Channel openings in each 512-point data block were fitted sequentially and a display of previously fitted openings was maintained to assist in matching brief channel closings (*c*). After analysis of several hundred data blocks, histograms of open and closed times of the generated rectangular pulses were automatically constructed. *a*, *b*, Lower traces show recordings of rectangular test pulses with durations of 500 and 50 μs respectively. Upper traces are computer-generated pulses fitted to the recordings. Calibrations, 50 pA and 1 ms. *c*, Lower trace shows single channel currents recorded from a membrane patch. Channel openings are shown as downward deflections. Upper trace shows the rectangular current pulses considered to underlie the records, whilst the middle trace shows the expected distortion of these pulses due to the frequency response characteristics of the recording system. Calibrations, 20 pA and 1 ms.

0028-0836/82/050410—03$01.00

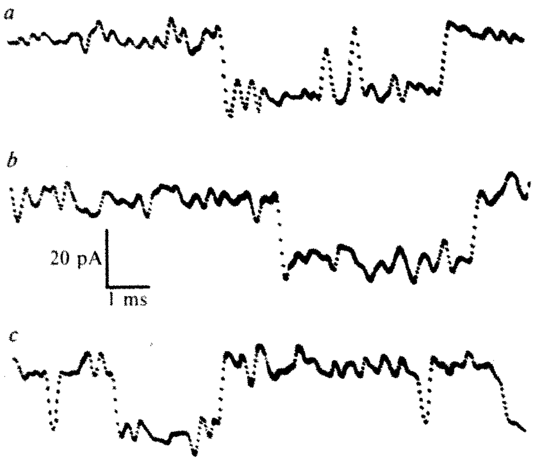

Fig. 2 Examples of single channel currents recorded with high time resolution (d.c. to 3.2 kHz). Channel openings correspond to downward deflections. Same membrane patch and recording parameters as in Fig. 1*c*. Temperature, 23 °C. Calibrations, 20 pA and 1 ms.

selected where only one active channel was present (that is, where no simultaneous openings were observed[6]). The time resolution of the recordings was improved significantly by using a circuit, after the headstage amplifier, which partially compensated for high-frequency roll-off caused by capacitance across the feedback resistor. This gave an overall frequency response of d.c. to ~5 kHz, but records were usually filtered at 3 kHz to reduce noise, before being digitized for computer analysis. Data were sampled in blocks of 512 points, at a digitization rate of 40 or 20 kHz.

The frequency response of the patch clamp was such that test pulses lasting 500 μs could be recorded with little distortion (Fig. 1*a*), whilst 50 μs pulses were detectable but became broadened and attenuated (Fig. 1*b*). The rise and fall times of single channel currents were similar to those of the test pulses (Figs 1*c*, 2), suggesting that the true transition times of the channel were faster than the resolution of the recording system. To permit more accurate measurements of brief channel openings and closings, a computer program was developed which partially compensated for the restricted frequency response of the recordings (see Fig. 1 legend). The ultimate limiting factor in time resolution was then set by the signal-to-noise ratio. We were unable to obtain seal resistances against the muscle membrane of better than 20 MΩ, so noise from this source was high[4], but as large single channel currents (20 pA) can be recorded from locust muscle the problem was not too serious.

A striking feature in our records was that many channel openings were interrupted by one or more brief closings (Figs 1*c*, 2*a*), although some long openings showed no apparent intervening closings (Fig. 2*c*). Also, there seemed to be more brief openings than expected from an exponential distribution (Fig. 2*c*). A quantitative examination was made by forming histograms of open and closed time distributions; Fig. 3 illustrates data from 832 channel openings recorded from one membrane patch. The present results are consistent with previous findings that both the open and closed time distributions of single glutamate channels can be fitted reasonably by single exponentials[5,6] and that open times are exponentially distributed[3], except that at short intervals (<200 μs) there is a considerable excess of both channel openings and closings (Fig. 3*b*, *d*), which are probably too brief to have been detected in previous patch-clamp studies having a narrower frequency range.

Figure 3*a*, *c* shows the distributions of brief openings and closings on an expanded time scale. In both cases an excess of events over a single exponential distribution becomes apparent at intervals of <~300 μs, and increases steeply with shorter intervals, except for a falloff in the shortest histogram bin (0–50 μs). A duration of 50 μs is about the limit of resolution of the recording system, so the falloff in this bin is probably due to very brief events remaining undetected.

We attempted to estimate roughly the total numbers of brief openings and closings by assuming they are distributed exponentially, and fitting the observed distributions by the sum of two exponentials corresponding to the 'brief' and 'normal' events. In the case of channel closings, the data (Fig. 3*c*) can be fitted by exponentials with time constants $\tau_{\text{fast}} = 100$ μs, $\tau_{\text{slow}} = 2$ ms. The predicted total excess of brief closings (=area under fast exponential) is 383, compared with 616 closings fitted by the slow exponential. It is clear therefore that channel openings generally occurred in bursts, with brief intervening closings within bursts and, on average, longer closings between bursts. For the events in Fig. 3 the mean number of closings per burst is

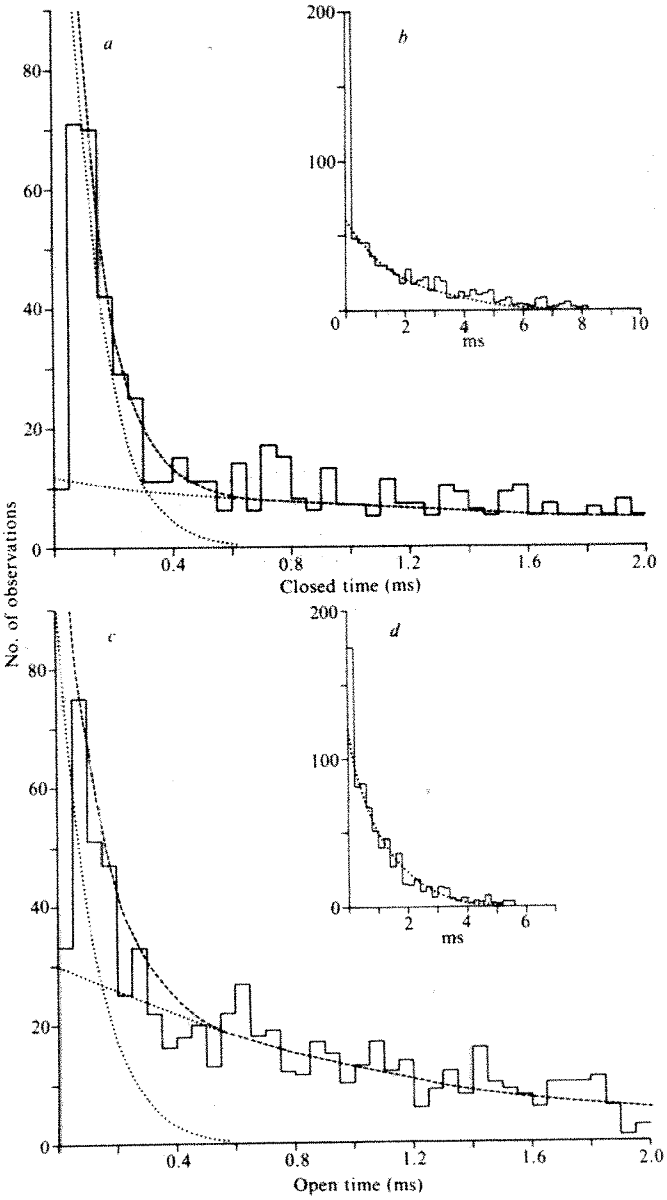

Fig. 3 Histograms of distributions of single channel closed (*a*, *b*) and open (*c*, *d*) times illustrating the excess of brief events. Data are measurements from 832 channel openings recorded from one membrane patch where only one channel appeared to be present. During the entire recording period the channel was in the 'normal' kinetic state[6]. Insets (*b*, *d*) show the same data as the main histograms, but on a different time scale. The distributions in *a* and *c* have been manually fitted by the sum of two exponentials; the component exponentials are indicated by dotted curves and the sum by dashed curves. Only the slow exponentials are shown in the insets. Time constants of the exponentials are: open times, $\tau_{\text{fast}} = 120$ μs, $\tau_{\text{slow}} = 1.5$ ms; closed times, $\tau_{\text{fast}} = 100$ μs, $\tau_{\text{slow}} = 2$ ms. Area under the exponentials are: open time, fast = 220, slow = 717; closed time, fast = 383, slow = 616. In preliminary experiments with different glutamate concentrations, estimated time constants for the closed time were: 100 μM, $\tau_{\text{fast}} = 110$ μs, $\tau_{\text{slow}} = 6.8$ ms; 600 μM, $\tau_{\text{fast}} = 117$ μs, $\tau_{\text{slow}} = 0.86$ ms (mean values from 5–7 patches).

~0.6 and hence the mean number of openings per burst is 1.6. The mean open time per burst can be estimated from the total area under the open time distribution (dashed line in Fig. 3*a*) divided by the number of inter-burst intervals and is 1.64 ms. Hence, the total burst length is ~1.7 ms and the mean duration of the openings within a burst ~1.0 ms. This estimate includes both the fast and slow components of the open time distribution. If the brief intra-burst closings were not detected, the apparent 'channel lifetime' would correspond to the mean burst length, and previous estimates of channel lifetime from noise analysis[3] and patch-clamp recording[5,6] are in reasonable agreement with our estimate of the mean burst length.

Considering next the excess of brief openings, the mean lifetime of this component estimated from the fitted fast exponential is 120 μs, and the predicted number in the recording period is 220, compared with 717 'normal' openings. Thus, about one-quarter of all channel openings were due to the brief component, but because of their short duration they would have carried only ~3% of the total current.

Records from seven other membrane patches (four muscles) using 200 μM glutamate were similar: a mean value of 1.6 ± 0.03 (s.e.) openings per burst, with a mean channel open lifetime of 0.97 ± 0.12 ms. However, in view of possible errors and assumptions in fitting the fast exponential functions to the tails of poorly resolved distributions, these values should be regarded as provisional.

Brief intervening closings during channel openings and an excess of brief openings have been observed from acetylcholine-receptor channels in frog twitch muscle[8] and the existence of intra-burst closings has been inferred from noise analysis in frog slow muscle fibres[9]. It seems likely therefore that these features may be general to most drug-activated channels. One possible mechanism for the intra-burst closings is that the channel is transiently blocked in a manner analogous to the action of local anaesthetics[10,11]. If this blocking resulted from glutamate molecules plugging the channel, then the number of brief closings would be expected to increase directly with glutamate concentration. In preliminary experiments we found that the number of brief closings per millisecond of open time showed little change over a range of glutamate concentrations (100, 200, 400, 600 μM). A more attractive possibility, which has been predicted from model reaction schemes[12,13], is that the intra-burst closings result from re-isomerization of the channel to the open configuration after closing, without dissociation of the bound agonist molecules. A simple two-step model for channel opening is:

$$\mathrm{A}+\mathrm{T} \underset{k_{-1}}{\overset{k_1}{\rightleftharpoons}} \mathrm{AT} \underset{\alpha}{\overset{\beta}{\rightleftharpoons}} \mathrm{AR} \qquad (1)$$

where A = agonist molecule, T = closed channel and R = open channel. In this scheme, intra-burst closings result from the transitions $\mathrm{AR} \rightarrow \mathrm{AT} \rightarrow \mathrm{AR}$, and their mean duration is $1/(\beta + k_{-1})$. For our data $\beta \approx 4 \times 10^3\ \mathrm{s}^{-1}$. Similarly, $\alpha \approx 1/$channel lifetime $\approx 10^3\ \mathrm{s}^{-1}$. The mean number of openings per observed burst $= (1+\beta/k_{-1}) = 1.6$; hence $k_{-1} \approx 6 \times 10^3\ \mathrm{s}^{-1}$. In fact, this two-step model is probably an over-simplification; for example, opening of the glutamate channel seems to involve binding of two or more agonist molecules[6,14]. Such a cooperative model is expected to give rise to a three-component distribution of closed times[13]. The intermediate component (due to brief closings via the singly bound state) may be partially included in our estimated fast component, but calculations based on a cooperative model indicate that the maximum contribution would be smaller than our experimental error. The rough estimates of α, β and k_{-1} are therefore applicable to both cooperative and non-cooperative models.

The origin of the excess brief openings is more mysterious. One possibility, which may be readily discarded, is that two separate channels of different mean lifetimes, were present under the patch pipette. If this were the case, 47 simultaneous openings would have been expected in the record of Fig. 3, and the probability of observing zero simultaneous events is $\approx 10^{-20}$; none was observed. Another possibility, which has been suggested to explain similar brief openings of acetylcholine-receptor channels[8], is that they arise from channel openings when only one agonist molecule is bound. Important clues as to the origins of both the brief openings and closings should be given by their dependence on agonist concentration and species of agonist. It is hoped to explore these possibilities further using internally perfused patch-clamp pipettes[6,14].

We thank the MRC for support.

Received 27 July; accepted 2 December 1981.

1. Katz, B. & Miledi, R. *J. Physiol., Lond.* **224,** 665–700 (1972).
2. Anderson, C. R. & Stevens, C. F. *J. Physiol., Lond.* **235,** 655–692 (1973).
3. Anderson, C. R., Cull-Candy, S. G. & Miledi, R. *J. Physiol., Lond.* **282,** 219–242 (1978).
4. Neher, E., Sakmann, B. & Steinbach, J. H. *Pflügers Arch. ges. Physiol.* **375,** 219–228 (1978).
5. Patlak, J. B., Gration, K. A. F. & Usherwood, P. N. R. *Nature* **278,** 643–645 (1979).
6. Cull-Candy, S. G., Miledi, R. & Parker, I. *J. Physiol., Lond.* **321,** 195–210 (1981).
7. Sakmann, B., Patlak, J. & Neher, E. *Nature* **286,** 71–73 (1980).
8. Colquhoun, D. & Sakmann, B. *Nature* **294,** 464–466 (1981).
9. Dionne, V. E. *J. Physiol., Lond.* **310,** 159–190 (1981).
10. Adams, P. R. *J. Membrane Biol.* **58,** 161–174 (1981).
11. Neher, E. & Steinbach, J. H. *J. Physiol., Lond.* **277,** 153–176 (1978).
12. Colquhoun, D. & Hawkes, A. G. *Proc. R. Soc.* **B199,** 231–262 (1977).
13. Colquhoun, D. & Hawkes, A. G. *Proc. R. Soc.* **B211,** 205–235 (1981).
14. Cull-Candy, S. G., Miledi, R. & Parker, I. *J. Physiol., Lond.* **317,** 3–4P (1981).

T-cell colonies recognize antigen in association with specific epitopes on Ia molecules

Robert B. Clark, Joe Chiba, Stephen E. Zweig & Ethan M. Shevach

Laboratory of Immunology, National Institute of Allergy and
Infectious Diseases, National Institutes of Health, Bethesda,
Maryland 20205, USA

The products of the *I* region of the major histocompatibility complex have a role in many immunological processes and are intimately involved with, if not identical to, the genes controlling specific immune responses (*Ir*). Alloantibodies to *I* region-associated (Ia) antigens have proved extremely useful in defining the relationship between Ia antigens and *Ir* gene product function[1]. We have recently reported data which suggest that monoclonal anti-Ia antibodies interact with different epitopes (antigenic determinants) on macrophage Ia molecules and that distinct epitopes, though on the same Ia molecule, are recognized by T cells in association with different antigens or antigen fragments[2]. We have now used these monoclonal xenogeneic antibodies to guinea pig Ia antigens together with antigen-specific T-cell colonies to analyse further the role of macrophage Ia antigens in T-cell activation. We demonstrate here that the proliferative responses of individual antigen-specific T-cell colonies were often completely inhibited by only one of several anti-Ia monoclonal antibodies. These results strongly support the notion that monoclonal anti-Ia antibodies can be used to define epitopes on Ia molecules that have unique functions in the activation of antigen-specific T cells, and that individual T-cell colonies recognize antigen in association with functionally distinct epitopes on Ia molecules.

Antigen-specific T-cell colonies were prepared from lymph node cells of guinea pigs primed *in vivo*, using a modification of the soft agar cloning technique described elsewhere[3]. Over 80% of the colonies that were picked from the agar could subsequently be expanded to testable numbers of cells, and ~95% of these colonies proliferated specifically when challenged with the soluble protein antigens used to generate the colonies, but not in response to other antigens to which the T-cell donor had been primed (data not shown). Furthermore, it is likely that the initial colonies picked from soft agar represen-

Table 1 Antigen-sepcific MHC-restricted guinea pig T-cell colonies

Colony	T cell	Macrophage used to generate colony	Antigen	Δ c.p.m. ^{3}H-TdR incorporation into test culture Macrophages Strain 2	Strain 13	(2×13)
10	$(2\times13)F_1$	$(2\times13)F_1$	PPD	61	5,705	2,216
31	$(2\times13)F_1$	$(2\times13)F_1$	PPD	319	16,333	13,450
124	$(2\times13)F_1$	$(2\times13)F_1$	OVA	<10	7,301	12,896
126	$(2\times13)F_1$	$(2\times13)F_1$	OVA	3,170	958	4,998
62	$(2\times13)F_1$	Strain 2	PPD	9,126	435	8,582
63	$(2\times13)F_1$	Strain 2	PPD	18,519	<10	13,613
131	$(2\times13)F_1$	Strain 2	PPD	21,070	907	ND
500	Strain 13	Strain 13	PPD	148	9,027	12,537
501	Strain 13	Strain 13	PPD	<10	13,391	13,503

Antigen-specific T-cell colonies were generated from inbred strain 2, strain 13 or $(2\times13)F_1$ regional lymph node nylon wool-purified T cells obtained from animals which had been primed *in vivo* with ovalbumin (OVA) (Miles) in complete Freund's adjuvant (CFA) (Difco). T cells (4×10^6) were cultured with X-ray irradiated (2,500 R) non-immune, unfractionated mineral oil-induced PECs (1×10^6) and 100 μg ml^{-1} PPD (Connaught) or OVA for 4–7 days in 24-well plates (Costar) in RPMI-1640 (Gibco) containing 300 μg ml^{-1} L-glutamine, 100 U ml^{-1} penicillin, 100 μg ml^{-1} streptomycin, 1 μg ml^{-1} 5-fluorocytosine, 5×10^{-5} M 2-mercaptoethanol (complete medium), and 5% heat-inactivated normal guinea pig serum. After this period of liquid culture, the antigen-stimulated T cells were plated onto a double layer of soft agar. The lower layer of agar, prepared 24 h before the upper layer, consisted of 0.5% Noble agar (Difco), 100–300 μg ml^{-1} PPD or OVA, with or without 25% T-cell growth factor (TCGF) and 10% heat-inactivated fetal calf serum (FCS). The TCGF used consisted of crude supernatants of concanavalin A-stimulated guinea pig lymph node cells and always contained 20 mg ml^{-1} α-methylmannoside (Calbiochem-Behring). The upper layer of agar consisted of 0.32% Noble agar, 10% heat-inactivated FCS, fresh PECs (2×10^5) and antigen-stimulated T cells (4–8×10^5). After 3–5 days on agar, colonies consisting of ~50 cells were picked off with a Pasteur pipette and then liquid-cultured in complete medium with 5% heat-inactivated FCS, 100 μg ml^{-1} PPD or OVA, 10^4 PECs and 25% TCGF in 96-well flat-bottomed microtitre plates (Costar). Expanding colonies were transferred to 24-well plates and fed twice weekly with 5×10^5 PECs, 200 μg ml^{-1} PPD or OVA and 25% TCGF. Antigen-induced proliferation of T-cell colonies (10^4) was measured by incubation with 10^5 PECs and 100 μg ml^{-1} PPD or OVA in 0.2 ml of complete medium with 5% heat-inactivated FCS and 10% TCGF in flat-bottomed microtitre wells. After 3 days, the contents of each well were divided into three new flat-bottomed, microtitre plates, each containing 0.2 ml of complete medium with 5% heat-inactivated FCS, 10% TCGF, 100 μg ml^{-1} PPD or OVA and fresh PECs (10^5). After an additional 48 h of culture, 1.0 μCi of tritiated thymidine (^{3}H-TdR: specific activity 6.7 Ci mmol^{-1}; NEN) was added to each well and after 18 h the amount of radioactivity incorporated into the cellular DNA was determined using a semi-automated microharvesting device (Mash II; Microbiological Associates). The results of triplicate cultures are expressed as total c.p.m. with antigen – c.p.m. without antigen (Δ c.p.m.). The s.e.m. of triplicate samples was rarely >10% of the mean, and for simplicity, only the mean of triplicate samples is given. ND, not determined.

ted true T-cell clones and not mixed cell populations because almost all T-cell colonies derived from $(2\times13)F_1$ donors that had been selected and expanded with F_1 peritoneal exudate cells (PECs) demonstrated an antigen-specific proliferative response in the presence of one but not the other parental strain of PEC (Table 1, colonies 10, 31, 124 and 126). $(2\times13)F_1$ T-cell colonies that had been generated and expanded with strain 2 PECs, and T-cell colonies derived from inbred strain 13 T cells that had been expanded with syngeneic PECs, also demonstrated a strict genetic restriction in their proliferative response to the appropriate strain of PEC (Table 1, colonies 62, 63, 131, 500 and 501).

The production and characterization of the murine monoclonal antibodies to guinea pig Ia antigens have been described in detail elsewhere[4]. Both monoclonals 22C4 and 27E7 reacted with all Ia antigens identified by a strain 2 anti-strain 13 serum (anti-Ia 1, 3, 7). However, in sequential immunoprecipitation studies with a strain 13 anti-strain 2 serum (anti-Ia 2, 4), monoclonal 27E7 reacted only with the Ia 2-bearing molecule while monoclonal 22C4 reacted with all the Ia molecules identified by the anti-Ia 2, 4 serum (ref. 4 and S.E.Z. and E.M.S., in preparation). Monoclonal antibodies 25E11 and 13S1 reacted with alloantigenic determinants of strain 2 and strain 13 Ia molecules, respectively.

These monoclonal antibodies were studied for their effects on the proliferative responses of the antigen-specific T-cell colonies; as a control population we used short-term lines of antigen-specific T cells which had been prepared by stimulation with antigen in liquid culture but which had not been separated into distinct colonies on agar. Colonies 62, 63 and 131 are strain 2-restricted, purified protein derivative of tuberculin (PPD)-specific, $(2\times13)F_1$ T-cell colonies. As seen in Table 2, colony 62 was inhibited only by monoclonal antibody 22C4, which is directed against an Ia determinant present on all strain 2 and strain 13 Ia molecules. Colony 63 was inhibited only by monoclonal antibody 25E11, which is directed against a strain 2 alloantigenic determinant. Colony 131 was inhibited by monoclonal antibodies 25E11 and 27E7, the latter being directed against a determinant present on all strain 13 and on some, but not all, strain 2 Ia molecules. Thus, while monoclonal 22C4 reacts with all strain 2 and strain 13 Ia molecules, it inhibits the response of colony 62 but not that of colonies 63 and 131. This indicates that colony 62 recognizes PPD in association with a region or epitope on the restricting Ia element different from that recognized by colonies 63 and 131. It is also likely that the latter colonies recognize PPD in association with distinct epitopes, as colony 63 was blocked only by 25E11 whereas colony 131 was blocked by both 25E11 and 27E7. As competitive binding studies have demonstrated partial inhibition of the binding of 25E11 by 27E7, the determinants identified by these monoclonal antibodies are probably adjacent to each other on the Ia molecule (S.E.Z. and E.M.S., unpublished observations). Thus, colony 131 may react with PPD in association with an epitope of strain 2 Ia located between the sites defined by 25E11

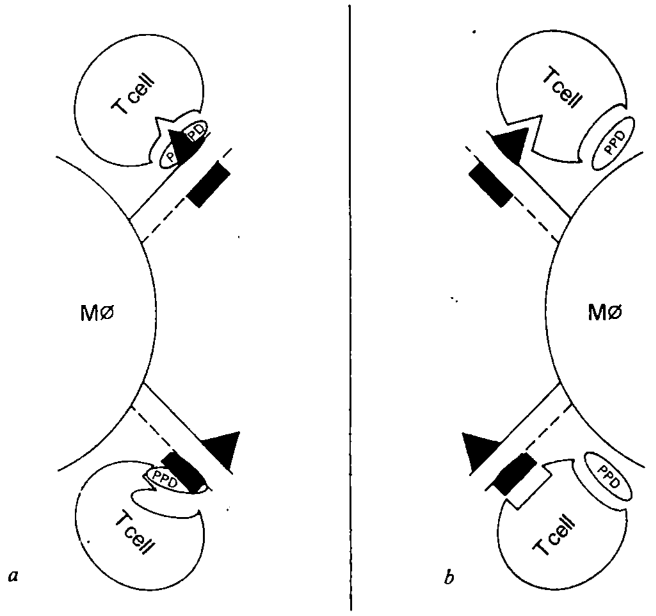

Fig. 1 *a*, Model of antigen presentation in which distinct epitopes on macrophage Ia molecules interact with conventional antigens and determine the orientation of antigenic determinants presented to the responding T cells. *b*, Model of antigen presentation in which distinct epitopes on Ia molecules and conventional antigens are recognized separately by two distinct receptors on responding T cells.

Table 2 Effect of monoclonal anti-Ia antibodies on the antigen-specific proliferative responses of T-cell colonies and T-cell lines

			Δ c.p.m. ^{3}H-TdR incorporation in the presence of monoclonal anti-Ia antibody			
Responder	PPD-pulsed macrophage (MØ)	Control	25E11	27E7	22C4	13S1
Colony 62	Strain 2	2,178	3,906	2,669	643	ND
Colony 63	Strain 2	13,055	863	15,022	12,956	ND
Colony 131	Strain 2	5,785	803	1,089	5,473	ND
T-cell line $(2\times13)F_1$	Strain 2	9,353	4,605	6,184	6,184	6,946
Colony 500	Strain 13	3,190	4,038	182	2,533	2,587
Colony 501	Strain 13	1,361	1,153	795	1,540	19
T-cell line (strain 13)	Strain 13	13,031	13,465	3,105	11,490	1,832

Antigen-specific T-cell colonies were generated as described in Table 1 legend. Short-term T-cell lines were generated as follows: nylon wool column-purified T cells were obtained from regional lymph nodes of inbred strain 13 or $(2\times13)F_1$ guinea pigs which had been primed *in vivo* with OVA in CFA. T cells (4×10^6) and irradiated, non-immune mineral oil-induced PECs (1×10^6) were cultured in complete medium containing 5% heat-inactivated normal guinea pig serum and 100 μg ml^{-1} PPD for 1 week before testing. $(2\times13)F_1$ T cells were cultured with parental strain 2 PECs. Inbred strain 13 T cells were cultured with strain 13 PECs. Antigen-induced proliferation of short-term T-cell lines or antigen-specific T-cell colonies was measured by incubation with antigen-pulsed PECs. For antigen pulsing, unfractionated, mineral oil-induced, non-immune, irradiated PECs $(10\times10^6$ ml$^{-1})$ were incubated in complete medium at 37 °C for 1 h in the presence of 100 μg ml^{-1} PPD. The cells were then washed three times to remove unbound antigen. These antigen-pulsed PECs (1×10^5) were incubated in 0.2 ml of complete medium with 5% heat-inactivated FCS and 5% TCGF, together with cells from T-cell lines or T-cell colonies (2×10^3) for 3 days in a round-bottomed microtitre plate (Linbro Chemical). To measure inhibition of antigen-specific proliferation by the monoclonal anti-Ia antibodies, ascitic fluids produced from the individual hybrid cell lines were added to the above microtitre wells at a final concentration of 1%. As all the monoclonal antibodies used were either of the IgM or IgG1 isotype[4], we used as control ascitic fluid, a hybrid myeloma line (provided by Ms R. Lieberman) which secreted an IgM antibody directed against inulin in addition to the parental IgG1 antibody of the P3×63Ag8 myeloma line. All the ascites containing monoclonal anti-Ia antibody had previously been found to have peak binding or cytotoxicity values when used at 0.1% or 0.01%. ^{3}H-TdR (1.0 μCi) was added to each well after 48 h of culture and 18 h later the amount of radioactivity incorporated into cellular DNA was determined using a semi-automated microharvesting device, Mash II. The results of triplicate cultures are expressed as total c.p.m. with antigen-pulsed PECs plus ascites – total c.p.m. with unpulsed PECs plus ascites (Δ c.p.m.). The s.e.m. of triplicate samples was rarely >10% of the mean, thus for simplicity only the mean of triplicate samples is given. ND, not determined.

and 27E7, while colony 63 reacts with PPD in association with an epitope close or identical to that defined by 25E11. Colonies 500 and 501, both derived from PPD-immune strain 13 T cells, were also inhibited by different monoclonal anti-Ia antibodies (Table 2). Despite the fact that monoclonal 27E7 reacts with a determinant present on all strain 13 Ia molecules, colony 500 was significantly inhibited by 27E7 whereas colony 501 was inhibited significantly only by monoclonal 13S1, which is directed against an alloantigenic determinant on strain 13 Ia molecules.

In contrast to the inhibition profiles of the colonies, the PPD-specific response of the short-term line of $(2\times13)F_1$ T cells was inhibited only moderately by 25E11, 27E7 and 22C4 (Table 2). The short-term line of inbred strain 13 PPD-specific T cells was significantly inhibited by 27E7 and 13S1 (Table 2). Thus, both short-term T-cell lines demonstrated some inhibition by more than one monoclonal antibody. These results are identical to those observed for T cells stimulated directly after being taken from the animal, without previous short-term culture[2].

Our results are consistent with the hypothesis that the monoclonal anti-Ia antibodies inhibit T-cell proliferation by masking individual Ia epitopes and that individual antigen-specific T-cell colonies recognize antigen in association with such distinct epitopes on Ia molecules. In agreement with this hypothesis, the unseparated T-cell lines, containing multiple antigen-specific clones, were inhibited by more than one monoclonal antibody, and this inhibition was often only moderate. We have recently demonstrated similar differential inhibition by these monoclonal antibodies of alloreactive T-cell colonies, thus these results are not unique to antigen-specific T-cell colonies[5]. It is very difficult to exclude the possibility that our results actually represent inhibition of T-cell recognition by masking of the entire Ia molecule rather than by masking of distinct epitopes on the same Ia molecule. However, the former explanation seems unlikely because several of the monoclonal antibodies which recognize determinants present on all guinea pig Ia molecules inhibit the response of only some of the colonies. Similarly, the differential inhibition by monoclonal antibodies that recognize monomorphic Ia determinants makes it unlikely that monoclonal anti-Ia antibodies inhibit T-cell proliferation by a generalized capping and shedding of Ia antigens. We have so far been unable to reclone any of our antigen-specific T-cell colonies, but the significance of our demonstration that individual antigen-specific T-cell colonies show fine differences in genetic restriction at the level of Ia epitope recognition, is not dependent on rigorous proof of the monoclonality of these putative clones.

The results presented here are most consistent with the theories of *Ir* gene function proposed by Rosenthal *et al.*[6] and Benacerraf[7], in which Ia molecules on macrophages interact with antigens and determine the orientation of antigenic determinants presented to the responding T cells. In this case, monoclonal anti-Ia antibodies would selectively inhibit T-cell activation by masking one of the sites of interaction of the Ia molecules with conventional antigen (Fig. 1*a*). However, the results are also compatible with the theories[8] proposing that the T cell has two receptors, one for self-Ia and the other for conventional antigen. In the latter case (Fig. 1*b*), monoclonal anti-Ia antibodies would inhibit T-cell proliferation by masking the recognition of individual Ia epitopes seen by the anti-self-Ia receptor on the T cell.

These results have important implications for the relationship between Ia antigens, *Ir* genes and disease susceptibility. As suggested by Schwartz *et al.*[9], the frequently noted associations between disease susceptibility and HLA antigens in man may, in fact, be associations between disease susceptibility and distinct epitopes on those HLA antigens. Determination of such disease–MHC epitope associations could have great practical and theoretical value by allowing more accurate detection of those individuals at highest risk for developing certain diseases and by furthering our understanding of the relationship between the immune system and disease susceptibility.

We thank Mrs Clare Horton for technical assistance and Ms Shirley Starnes for assistance with the manuscript. S.E.Z. is a Fellow of the Arthritis Foundation.

Received 28 May; accepted 26 November 1981.

1. Shevach, E. M. *Springer Semin. Immunopath.* **1,** 207–234 (1978).
2. Burger, R. & Shevach, E. M. *J. exp. Med.* **152,** 1011–1023 (1980).
3. Sredni, B., Tse, H. Y. & Schwartz, R. H. *Nature* **283,** 581–583 (1980).
4. Burger, R., Clement, L., Schroer, J., Chiba, J. & Shevach, E. M. *J. Immun.* **126,** 32–37 (1981).
5. Malek, T. R., Clark, R. B. & Shevach, E. M. *J. Immun.* **127,** 616–621 (1981).
6. Rosenthal, A. S., Barcinski, M. A. & Blake, J. T. *Nature* **267,** 156–158 (1977).
7. Benacerraf, B. *J. Immun.* **120,** 1809–1812 (1978).
8. Von Boehmer, H., Haas, W. & Jerne, N. K. *Proc. natn. Acad. Sci. U.S.A.* **75,** 2439–2442 (1978).
9. Schwartz, B. D., Luehrman, L. K. & Rodey, G. E. *J. clin. Invest.* **64,** 938–947 (1979).

Progesterone monoclonal antibody blocks pregnancy in mice

L. J. Wright, A. Feinstein, R. B. Heap, J. C. Saunders, R. C. Bennett & M.-Y. Wang

ARC Institute of Animal Physiology, Babraham,
Cambridge CB2 4AT, UK

Production of monoclonal antibodies by hybrid cell lines[1] provides a method potentially superior to conventional techniques for raising antisera[2] in respect of titre and specificity. Many lines have been prepared[3] that secrete antibody to cell-surface and soluble antigens and to viruses, but the products of hybridomas that recognize steroid haptens have not yet been exploited. Progesterone, the hormone of pregnancy, is essential for the establishment and maintenance of gestation in all mammalian species so far studied in detail[4], and we describe here the production and characterization of an anti-progesterone monoclonal antibody which blocks the establishment of pregnancy in mice.

Adult male BALB/c mice from a colony maintained at this Institute were immunized against progesterone-11α-succinyl–bovine serum albumin (BSA) conjugate (molar ratio of steroid to protein, 26:1) prepared using carbodiimide as the coupling agent. The spleen cells from these animals were fused with the mouse myeloma cell line NSI[5,6]. Immediately after fusion the cells were cultured in selection medium containing hypoxanthine–aminopterin–thymidine (HAT) and subsequently HT[5], and the supernatants were screened by a binding assay (see Table 1) for the presence of progesterone-binding antibodies. Vigorous growth of hybrids was observed but the supernatant of only one well displayed marked anti-progesterone activity. Of 14 subcultures established from this well, four remained active and stable over a 5 month period (AA1, BA2, 2A3, AB1). After cloning the hybrid AA1 on soft agar[7], one colony was selected for further study (III A4.1) and was recloned. Seventeen subcultures grew well and anti-progesterone antibody was detected by a high binding activity in the supernatants of all 17 wells. This, together with later evidence, suggests that III A4.1 is a clone. Ascites fluid formed after cells of clone III A4.1 were injected into mice was found to contain a high concentration of anti-progesterone monoclonal antibody (up to 15 mg ml^{-1}) by immunoelectrophoresis and analytical ultracentrifugation. It was also shown to possess precipitating activity against steroid–BSA conjugate, but not against BSA alone. Specific antisera showed it to be of mouse IgG1 sub-class. The results of similar tests on ascites fluid prepared with cells of subculture AA1 were identical. When tested by the binding assay (see Table 1), 50% binding of radioligand was obtained at dilutions of ascites fluid ranging from 1:3,000 to 1:43,000. Anti-progesterone antibody (AA1, ascites fluid) had an association constant of 0.4×10^9 M^{-1} (Scatchard analysis).

The specificity of binding in ascites fluid (AA1 and III A4.1) was compared with that obtained for an antiserum (provided by Dr A. P. F. Flint) raised against the same antigen by the conventional procedure in a sheep. The anti-progesterone monoclonal antibody was less specific than the average of the polyclonal antibodies in antiserum 18.2 (Table 1) as noted by others[8]. However, the high concentration of clonal IgG available in the ascites fluid preparation, its relatively low contamination with other proteins and the preservation of clone III A4.1 in liquid nitrogen provided a long-term reproducible source of a suitable reagent for testing anti-fertility properties.

The anti-implantation properties of the monoclonal antibody (clone III A4) were tested in BALB/c mature virgin mice. Five daily injections of ascites fluid (15 μl) blocked implantation in all animals, whether given intraperitoneally (i.p.) or intravenously (Table 2: route). To determine the time at which the monoclonal antibody blocked pregnancy most effectively, mature virgin BALB/c mice were given a single i.p. injection at 32 and 109–130 h post-coitum (p.c.). Monoclonal antibody blocked implantation in all 13 mice treated at 32 h ($P < 0.001$, Table 2: time) and in a further four mice treated at 65 h p.c. (Table 3). Pregnancy was also blocked in 9 of 11 mice treated 109–130 h p.c. but implantation occurred and pregnancy appeared to progress normally in two animals (Table 2: time). Control ascites fluid from mouse myeloma McPc 1748 had no effect on pregnancy when injected at 32 h p.c., but when given at later stages (109–130 h) reduced fertility (Table 2: time).

In mice receiving five daily injections, the mean concentration of plasma progesterone was higher in the experimental than the control group of animals on day 10 p.c., but the difference was not statistically significant. The high concentration was associated with a marked increase in the amount of ^{3}H-progesterone bound by plasma *in vitro* ($P < 0.001$, Table 3). The number of

Table 1 Cross-reactivity of anti-progesterone monoclonal antibody and anti-progesterone polyclonal antiserum

	% Cross-reaction	
	Monoclonal antibody III A4.1	Polyclonal antiserum 18.2
Progesterone	100	100
11α-Hydroxyprogesterone	310	44
Aetiocholanolone	273	<2
5β-Pregnanedione	82	8
5α-Pregnanedione	58	12
11β-Hydroxyprogesterone	26	14
16α-Hydroxyprogesterone	23	4
5β-Androstanedione	8	<2
Deoxycorticosterone	<2	4
Cortisol	<2	<2
20α-Hydroxyprogesterone	<2	<2
17α-Hydroxyprogesterone	<2	<2
Pregnenolone	<2	<2
17α-Hydroxypregnenolone	<2	<2
Androstenedione	<2	<2
6β-Hydroxyandrostenedione	<2	<2
Testosterone	<2	<2
5α-Dihydrotestosterone	<2	>2
5α-Pregnane-3β,20β-diol	<2	<2
5β-Pregnane-3α,20β-diol	<2	<2
5α-Pregnane-3α,20α-diol	<2	<2
Androsterone	<2	<2
5α-Androstanedione	<2	<2
3-Epiandrosterone	<2	<2
Oestrone	<2	<2
Oestradiol-17β	<2	<2
Oestradiol-17α	<2	<2
Oestriol	<2	<2
16-Epioestriol	<2	<2

Cross-reactivity was determined using monoclonal antibody III A4.1 and polyclonal antiserum 18.2 at a dilution in phosphate buffer of 1:15,500 and 1:1,400 respectively. At this dilution each preparation bound ~50% of the radioligand used in the binding assay. A high concentration of monoclonal antibody was obtained by the injection of cells of clone III A4.1 into BALB/c mice primed with pristane (2,6,10,14-tetramethylpentadecane) 14 days before injection i.p. of $\sim 7 \times 10^6$ cells. The binding assay consisted of 100 μl supernatant incubated overnight at doubling dilutions with 100 μl [1,2,6,7-^{2}H]progesterone (89 Ci mmol^{-1}; 20,000 d.p.m. per 100 μl phosphate buffer; Amersham). For screening purposes, supernatants were diluted 1:1 (v/v) with phosphate buffer. Unbound radioligand was absorbed by the addition of 200 μl dextran-coated charcoal, and 20 min later charcoal-bound radioligand was separated from antibody-bound radioligand by centrifugation. Radioactivity in the supernatants indicative of antibody binding was measured by liquid scintillation spectrometry[15]. The nonspecific binding of the assay (culture medium with no antibody) was 5.2±0.8% (mean±s.e.m.) of the added radioligand. Competitive binding studies were carried out using increasing amounts of the compounds listed (25–25,000 pg in 25 μl buffer) and a constant amount of ^{3}H-progesterone (100 μl buffer containing 20,000 d.p.m.). Incubation conditions and the method of separation of antibody-bound and unbound radioactivity were identical to those used in the binding assay. Cross-reactivity was calculated as the amount of progesterone required to reduce the amount of radioligand bound by one-half, divided by the amount of competing steroid that produced a similar displacement (×100)[16].

0028-0836/82/050415—03$01.00

Table 2 Effect of the route and time of administration (h p.c.) of anti-progesterone monoclonal antibody on blocking of pregnancy in mice

Group		No. pregnant/ no. treated	Total no. of implantations
Route: five daily injections			
Intraperitoneal	Experimental	0/6*	0
	Control	4/6	20
Intravenous	Experimental	0/6*	0
	Control	4/6	39
Time: single injection			
32 h p.c.	Experimental	0/13*	0
	Control	13/14	109
109–130 h p.c.	Experimental	2/11	20
	Control	7/12	75

Route: BALB/c mice were injected daily at ~10.00 h on days 1, 2, 3, 4 and 5 (day 1 = day of copulation plug; coitus ~02.00 h). Injections consisted of 200 µl 0.9% NaCl containing 15 µl ascites fluid (cloned hybrid III A4.1, experimental), 15 µl ascites fluid (mouse myeloma McPc 1748, control) or 15 µl non-immune mouse serum. Ascites fluid from the cloned hybrid III A4.1 diluted 1:42,000 bound 50% of radioligand when incubated with ^{3}H-progesterone (~20,000 d.p.m.). Ascites fluid from McPc 1748 or non-immune serum showed no detectable binding of ^{3}H-progesterone. Autopsy was performed on day 10 p.c. Time: BALB/c mice were given a single injection i.p. at the times shown (0 h = estimated time of coitus, ~02.00 h of the morning when a copulation plug was found, day 1). Injections consisted of 200 µl 0.9% NaCl containing 15 µl ascites fluid (cloned hybrid III A4.1, experimental) or 15 µl ascites fluid (mouse myeloma McPc 1748, control, see above). Autopsy was performed on days 11–15 p.c.

* Difference between experimental and control group was significant ($P<0.001$) when tested after the calculation of exact significance probabilities using the randomization procedure first proposed by Fisher[17].

corpora lutea counted in serial sections of ovaries removed at autopsy was similar in experimental (10.0 ± 0.7, mean ± s.e.m.) and control (9.0 ± 2.0) groups, though the corpora lutea were frequently small and regressed in mice treated with anti-progesterone antibody. Thus the high concentration of progesterone in peripheral plasma was probably due to the retention of antibody-bound steroid in circulation, and the decline of luteal function to a lack of pituitary and/or placental luteotropin arising from the failure of implantation.

Plasma progesterone levels in mice treated with a single dose of anti-progesterone antibody at 32 or 65 h p.c. and killed on day 11–15 p.c. were less than one-half those found in mice treated daily for 5 days, presumably due to the further decline of luteal secretion of progesterone. The mean plasma progesterone concentration in mice injected at 109–130 h p.c. was similar to that in control animals; in two animals that remained pregnant the values were high (64 and 94 ng ml^{-1}) whereas in a further two mice which were not pregnant values were low (2 and 14 ng ml^{-1}). Circulating monoclonal antibody was still present at autopsy in mice injected only once with cross-reacting IgG as judged by the greater amount of radioligand bound by plasma *in vitro* (47.3 ± 2.3%) compared with values obtained in control mice (15.5 ± 1.8%, $P<0.001$, Table 3). The binding observed in plasma from control animals was attributed to corticosteroid-binding globulin[9] as when plasma was heated at 60 °C for 20 min the value was reduced to levels similar to the nonspecific binding values of the assay, whereas in monoclonal-treated animals it was only reduced to 36% due to the presence of anti-progesterone IgG (Table 3).

The results show that anti-progesterone monoclonal antibody given as single or repeated injections during preimplantation will prevent implantation in mice. It was estimated that at equilibrium, anti-progesterone antibody reduced the concentration of readily available progesterone in circulation by >95% during the critical preimplantation stage, when a precise hormonal sequence of progesterone and oestrogens is normally required to sensitize the endometrium for implantation[10] which begins at ~90 h p.c. The finding that a single injection of monoclonal anti-progesterone IgG (200 µg; 10 mg per kg) prevented pregnancy in all 17 mice treated between 32 and 65 h p.c. and that its effect was slightly reduced when it was administered later, may be associated with the limited capacity of antibody to reduce circulating progesterone levels in the face of increasing luteal secretion[11,12]. The results obtained with this monoclonal preparation in mice showed a substantial improvement compared with those obtained with a polyclonal antiserum in rats in which anti-progesterone antiserum (10 mg; 50 mg per kg) delayed implantation by at least 24 h but blocked pregnancy in only 6 of 14 treated animals[13].

The mechanism by which this anti-progesterone monoclonal antibody reduced fertility in mice probably differs according to the time of treatment. When injected at 32 h p.c. transport along the Fallopian tubes may have been affected, whereas when injected 109–130 h p.c. the process of implantation itself seemed to be inhibited. Ligand specificity of the monoclonal anti-progesterone antibody used in this study was relatively inferior to that of a conventional antiserum, certain steroids structurally dissimilar to progesterone (such as aetiocholanolone) competing successfully with progesterone for the monoclonal binding site. Whether or not these cross-reactivities are an essential feature of the anti-implantation efficacy of this antibody remains to be established, but products of suitably selected anti-progesterone clones should prove invaluable for further studies of the regulation of fertility.

We thank Professor E. C. Amoroso, Drs A. P. F. Flint, J. C. Howard and D. E. Walters for help and valuable discussions, and Mrs E. Tredget, Miss M. Hamon, Miss P. Hansford and Mr I. R. Fleet for technical assistance.

Note added in proof: It has been demonstrated that an anti-progesterone monoclonal antibody can be prepared with high specificity[14].

Table 3 Effect of anti-progesterone monoclonal antibody on progesterone levels and binding of progesterone in plasma during pregnancy

Treatment	Group	No. pregnant/ no. treated	Progesterone: Plasma conc. (ng ml^{-1})	Progesterone: % Bound, Before heating	Progesterone: % Bound, After heating
Five daily injections	Experimental	0/6	35.7 ± 12.6 (6)	54 ± 9* (6)	ND
	Control	4/6	11.1 ± 3.8 (4)	10 ± 4 (4)	ND
One injection, 32 h p.c.	Experimental	0/4	16.5 ± 4.1*	45 ± 3* (4)	33 ± 3* (4)
	Control	4/4	38.8 ± 2.3 (4)	19 ± 2 (4)	8 ± 1 (4)
One injection, 65 h p.c.	Experimental	0/4	8.7 ± 5.2 (4)	52 ± 4 (4)	40 ± 2 (4)
	Control	2/4	31, 32 (2)	14, 15 (2)	6, 8 (2)
One injection, 109–130 h p.c.	Experimental	2/4	43.5 ± 21.5	45 ± 6* (4)	ND
	Control	3/4	34.3 ± 3.3 (3)	13 ± 2 (3)	7 ± 1 (3)

Details of treatment are given in Table 2 legend. Blood was collected from mice under ether anaesthesia on days 10–15 and plasma progesterone concentration was measured by radioimmunoassay. Values of % bound were obtained by the addition of a known amount of ^{3}H-progesterone (100 µl phosphate buffer containing 20,000 d.p.m.) to 100 µl plasma diluted 1:10 with phosphate buffer. In selected cases plasma was heated at 60 °C for 20 min to inactivate binding associated with the presence of corticosteroid-binding globulin[9]. Conditions of incubation and the method of preparation of antibody-bound and unbound radioactivity are described in the text. The amount of radioligand bound in plasma was expressed as a percentage of the total amount of ^{3}H-progesterone added. Results are given as mean ± s.e.m.; numbers of animals are shown in parentheses. ND, not determined.

* Difference between experimental and control group was significant ($P<0.001$) using Student's unpaired *t*-test.

Received 26 June; accepted 30 November 1981.

1. Köhler, G. & Milstein, C. *Nature* **256**, 495–497 (1975).
2. Milstein, C., Galfré, G., Secher, D. S. & Springer, T. *Cell Biol. int. Rep.* **3**, 1–16 (1979).
3. Melchers, F., Potter, B. M. & Wagner, N. (eds) *Lymphocyte Hybridomas* (Springer, Berlin, 1978).
4. Heap, R. B., Perry, J. S. & Challis, J. R. G. in *Handbook of Physiology: Endocrinology* Vol. 2, pt 2, 217–260 (American Physiological Society, Washington, 1973).
5. McMaster, R. W. & Williams, A. F. *Eur. J. Immun.* **9**, 426–433 (1979).
6. Galfré, G. & Milstein, C. *Meth. Enzym.* **73**, 3–46 (1981).
7. Cotton, R. G. H., Secher, D. S. & Milstein, C. *Eur. J. Immun.* **3**, 135–140 (1973).
8. Fantl, V. E., Wang, D. Y. & Whitehead, A. S. *J. Steroid Biochem.* **14**, 405–407 (1981).
9. Seal, U. S. & Doe, R. P. in *Steroid Dynamics* (eds Pincus, G., Nakao, T. & Tait, J. F.) 63 (Academic, New York, 1966).
10. Finn, C. A. & McLaren, A. *J. Reprod. Fert.* **13**, 259–267 (1967).
11. McCormack, J. T. & Greenwald, G. S. *J. Endocr.* **62**, 101–107 (1974).
12. Gerber, G. B., Jacquet, P., Léonard, A. & Maes, J. *C.r. Séanc. Soc. Biol.* **173**, 644–649 (1979).
13. Raziano, J., Ferin, M. & Van de Wiele, R. L. *Endocrinology* **90**, 1133–1138 (1972).
14. White, A., Anderson, D. C. & Daly, J. R. *J. clin. Endocr. Metab.* **54** (in the press).
15. Heap, R. B., Holdsworth, R. J., Gadsby, J. E., Laing, J. A. & Walters, D. E. *Br. vet. J.* **132**, 445–464 (1976).
16. Abraham, G. F., Swerdloff, T., Tulchinsky, D. & Odell, N. B. *J. clin. Endocr. Metab.* **32**, 619–624 (1971).
17. Fisher, R. A. *J. R. statist. Soc.* **98**, 39–54 (1935).

Isolation from murine sarcoma cells of novel transforming growth factors potentiated by EGF

A. B. Roberts*, M. A. Anzano*, L. C. Lamb*, J. M. Smith*, C. A. Frolik*, H. Marquardt†, G. J. Todaro† & M. B. Sporn*

Laboratories of *Chemoprevention and †Viral Carcinogenesis,
National Cancer Institute, National Institutes of Health, Bethesda,
Maryland 20205, USA

Polypeptides classified as transforming growth factors (TGFs) have been found in various neoplastic cells and tumour tissues[1–5], and most recently in many non-neoplastic tissues[6]. These TGFs are low-molecular-weight (7,000–20,000) acid-stable polypeptides, which induce anchorage-dependent non-neoplastic indicator cells to form progressively growing colonies in soft agar. Certain extracellular TGFs isolated from conditioned medium derived from both rodent sarcoma virus-transformed cells and several human tumour cell lines have been shown to compete with epidermal growth factor (EGF) for membrane receptors[1,3,4,7]. By direct extraction from Moloney sarcoma virus (MSV)-transformed cells, we have isolated two distinct classes of intracellular TGFs, one of which competes with EGF for receptor binding sites, whereas the other does not. We report here that after purification by HPLC, the colony-forming activity of the TGFs that do not compete with EGF for receptor binding was enhanced 100-fold by the addition of EGF. This ability to enhance the growth-stimulating effects of the TGFs is specific to EGF, as insulin, the insulin-like growth factors, platelet-derived growth factor and nerve growth factor do not show this property. In contrast, the colony-forming activity of TGFs that compete with EGF for receptor binding is not potentiated by EGF.

Direct extraction of MSV-transformed 3T3 cells with acid–ethanol has been shown[2] to yield TGFs which, when chromatographed on Bio-Gel P-30, seem to behave similarly to the extracellular sarcoma growth factor (SGF) isolated from conditioned medium derived from these cells[1]. However, other experiments have shown that the major soft-agar colony-forming activity in the unfractionated acid–ethanol extract of MSV-transformed cells is potentiated by EGF[6]. Using reverse-phase HPLC for further purification, we now demonstrate the heterogeneous nature of these intracellular TGF preparations.

As seen in Fig. 1, the TGF fraction from Bio-Gel P-30 columns (10,000–12,000 molecular weight) can be separated into two major components by HPLC on C_{18} μ Bondapak columns using a linear acetonitrile gradient in 0.1% trifluoroacetic acid. One component, which we term the EGF-potentiated TGF, elutes later (38% acetonitrile) than marker EGF (35% acetonitrile), and together with EGF (2 ng ml^{-1}) results in the formation of large colonies (>3,140 μm^2) in soft agar (Fig. 1*a*). The other component elutes earlier (32% acetonitrile) and induces formation of smaller colonies (>840 μm^2) in soft agar in the absence of added EGF (Fig. 1*b*). Binding competition studies using ^{125}I-labelled EGF showed that only the latter component competes strongly with EGF (Fig. 1*c*); this is designated 'intracellular SGF', as its behaviour is similar biologically to the extracellular SGF of conditioned medium[1,7]. In radioimmunoassays using anti-murine EGF antiserum, all these fractions were shown to be free of native EGF (data not shown). The intracellular SGF peak contained 3.7% of the total recovered absorbance at 280 nm and ~80% of the total colony-forming units assayed in the absence of EGF; the EGF-potentiated TGF peak contained 4.2% of the recovered absorbance units and ~90% of the total colony-forming units assayed in the presence of EGF.

The growth-stimulating effect of EGF and each of the two classes of TGFs on NRK cells, clone 49F (ref. 8), was quantified in the soft-agar system described previously[2]. Cells were stained and analysed for colony formation 1 week after seeding in the presence of TGF and/or EGF. Colony size was determined quantitatively using a Zeiss microscope and Videcon television camera coupled to a Bausch and Lomb Omnicon image analysis system and a data terminal. The field of view was displayed in two dimensions and all parameters were derived from the area

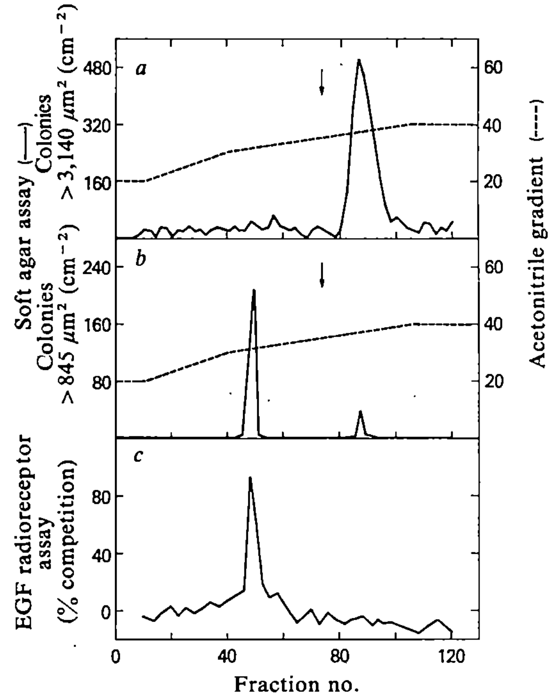

Fig. 1 HPLC purification of TGFs from MSV-transformed 3T3 cells. The acid–ethanol extract of MSV-transformed cells was purified initially on Bio-Gel P-30 in 1 M acetic acid as described elsewhere[2]. EGF was obtained by similar extraction of male mouse salivary glands[6]. The TGF pool (20 mg) was dissolved in 2 ml 0.1% trifluoroacetic acid (TFA), applied to a μ Bondapak C_{18} column (7.8×300 mm; Waters Associates) and eluted at a flow rate of 0.8 ml min^{-1} with a gradient of acetonitrile in 0.1% TFA as shown. Aliquots (40 μl; 5%) were lyophilized and assayed for activity in the soft-agar assay: *a*, in the presence of 2 ng ml^{-1} murine EGF; *b*, without EGF. *c*, Duplicate aliquots (40 μl) were assayed for inhibition of ^{125}I-EGF-receptor binding in mink lung epithelial cells (CCL 64) as described elsewhere[7] (3.5 ng ml^{-1} EGF resulted in 50% competition). Arrow indicates position of elution of marker murine EGF (*a*, *b*).

0028–0836/82/050417—03$01.00

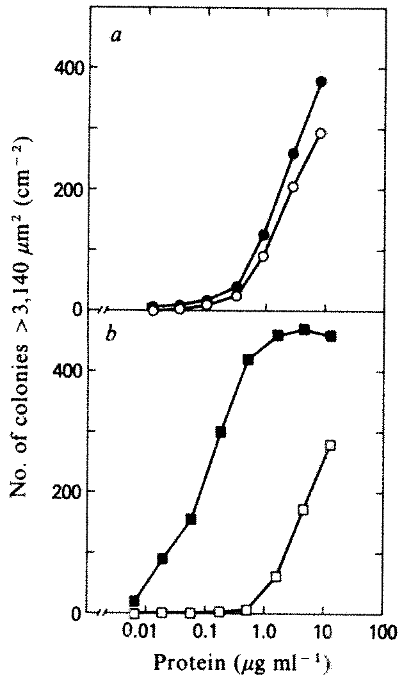

Fig. 2 Effect of EGF on the dose–response curves of the two classes of TGFs. *a*, EGF-independent TGF that competes with EGF for binding (Fig. 1, fractions 49–53) or *b*, EGF-potentiated TGF that does not compete with EGF (Fig. 1, fractions 88–98) was assayed in the absence of EGF (open symbol) or presence of 2 ng ml^{-1} murine EGF (solid symbol). The background level of colonies >3,140 μm^2 (51 per cm^2) that was observed in response to EGF alone has been subtracted. An identical response was seen for EGF prepared by the method of Savage and Cohen[24] and for receptor grade EGF (Collaborative Research).

of the colony cross-section. The system was programmed to size and count colonies >500 μm^2 and to determine the mean colony size from the data obtained for each plate. The effect of EGF on the dose–response curves of the two classes of TGFs is shown in Fig. 2*a*, *b*. If the background of colonies formed in response to EGF alone (2 ng ml^{-1}) is subtracted, it is apparent that there is no enhancement by EGF of the intrinsic colony-forming activity of the intracellular SGF (which competes for EGF receptor binding) (Fig. 2*a*). In contrast, the addition of EGF (2 ng ml^{-1}) to the culture medium caused the NRK cells to be ~100-fold more sensitive to the EGF-potentiated class of TGFs, as measured by the number of colonies >3,140 μm^2 (Fig. 2*b*). In the presence of EGF, soft-agar colony-forming activity was detected in 6 ng ml^{-1} protein from the EGF-potentiated TGF peak after HPLC purification.

The effect on colony size of EGF added to sub-optimal levels of the EGF-potentiated TGF is shown in Fig. 3. EGF alone (2 ng ml^{-1}) induced the NRK cells to form numerous small colonies of mean size 3,300 μm^2, in agreement with the data of Topp *et al.*[9], whereas TGF alone (4.6 μg ml^{-1}) caused the cells to undergo only a few divisions, to give a mean colony size of 1,800 μm^2. The simultaneous addition of EGF and TGF resulted in the formation of a large number of colonies of mean colony size 7,700 μm^2. The numbers of colonies per cm^2 greater than 3,140 μm^2 were 51 and 5, respectively, for EGF and TGF alone, whereas the two factors combined gave 470 colonies, suggesting cooperative effects. The potentiating effect of EGF in the soft-agar assay was optimal at concentrations of 0.4–10 ng ml^{-1}; higher or lower concentrations had less effect. The response of the NRK cells to EGF alone differed from the response to EGF plus EGF-potentiated TGF; colonies reached a plateau of 2,000–3,000 μm^2 mean colony size in the presence of optimal concentrations of EGF alone, whereas colonies formed in response to the two factors combined reached colony sizes of 13,000–19,000 μm^2.

Soft-agar assays (data not shown) in which EGF and/or the EGF-potentiated TGF were added sequentially as an overlay 1 week later showed that the order in which EGF or TGF is added is not important for the potentiation of the colony-forming response of the cells, and that the mean colony size attained after sequential addition is not significantly different from that after simultaneous addition of the two factors. In contrast, cells treated initially with EGF alone were refractory to further EGF added 1 week later, and cells treated initially with TGF responded to a further addition of TGF with only a doubling in mean colony size. Other growth factors were investigated for their ability to amplify the anchorage-independent growth response induced by this TGF. Platelet-derived growth factor, nerve growth factor, insulin and the insulin-like growth factors, each tested over a 1,000-fold concentration range, had little effect on the colony-forming response to sub-optimal levels of the EGF-potentiated TGF. By themselves, these factors caused very few cells to undergo even a single division in the soft-agar medium.

The potentiating effect of EGF is specific for a class of TGFs that do not compete with EGF for receptor binding, possibly implicating interaction of two distinct membrane receptors. In model systems, platelet-derived growth factor and pituitary fibroblast growth factor, while not competing for EGF-receptor sites, can induce a transient down-regulation of the EGF receptor, suggesting co-internalization of the receptors for these hormones[10]. Phorbol ester tumour promoters[11,12] and vasopressin[13] can alter the affinity of EGF receptors, and EGF can alter the response of rat pituitary cells to thyroid hormone and hence alter the hormonal control of growth hormone and prolactin synthesis by these cells[14].

Assuming that anchorage-independent growth correlates with neoplasia[15,16], the results reported here suggest a mechanism for some of the observed promoter-like effects ascribed to EGF. EGF can increase viral transformation of cells[17,18] and promote methylcholanthrene-induced papillomas in mouse skin[19]. It can also increase the anchorage-independent growth of adenovirus-transformed rat embryo cells, as measured by increases in both colony size and number[20]. Each of these effects could be mediated by EGF potentiation of sub-optimal levels of a class of EGF-responsive TGFs resembling those described here.

Results similar to those presented here for the cellular extracts of MSV-transformed mouse cells have also been obtained from both non-neoplastic and neoplastic tissues of man, mouse, chicken and cattle[21]. In every case, the major TGF activity does not compete with EGF for receptor binding but is markedly potentiated by EGF to induce growth of large colonies in soft agar. The presence in these extracts of TGFs that compete with EGF for receptor binding but are not enhanced by EGF in

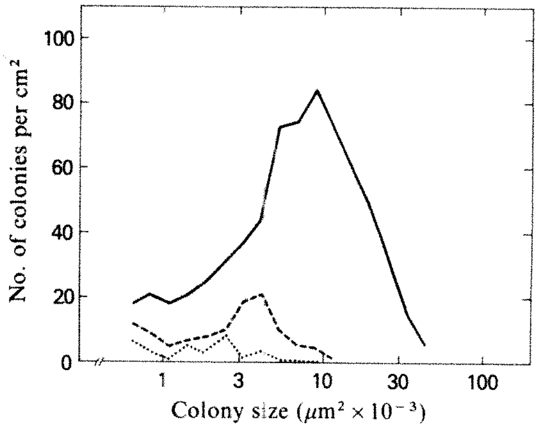

Fig. 3 Size distribution curves of colonies formed in response to EGF and/or sub-optimal concentrations of the EGF-potentiated TGF. The size distribution of colony area, as determined by image analysis, for 4.6 μg TGF (Fig. 2*b*) is represented on a logarithmic scale. · · · ·, TGF alone (4.6 μg ml^{-1}); ——, TGF at the same concentration in the presence of EGF (2 ng ml^{-1}); and - - - -, EGF alone (2 ng ml^{-1}) as a control.

the induction of anchorage-independent growth has not yet been conclusively demonstrated. Recent data of Moses *et al.* on TGF production in chemically transformed cells also demonstrate the existence of several TGFs, only one of which competes for binding to the EGF receptor[5]. The physiological significance of the interaction between EGF and this new class of TGFs is unknown, but it is possible that, in addition to a role in malignant transformation, these factors may function in the natural mechanism of wound repair and in embryogenesis, where both EGF[22] and the TGFs[23] have been postulated to play a part.

We thank Dr P. Nissley for assaying the mouse insulin and insulin-like growth factors, Dr R. Humbel for providing the insulin-like growth factors, Dr H. Antoniades for platelet-derived growth factor, Dr R. Bradshaw for nerve growth factor, Dr J. E. De Larco for helpful discussions, and Ms Ellen Friedman and Ms Ruth Morsillo for typing the manuscript.

Received 21 September; accepted 25 November 1981.

1. De Larco, J. E. & Todaro, G. J. *Proc. natn. Acad. Sci. U.S.A.* **75**, 4001–4005 (1978).
2. Roberts, A. B. *et al. Proc. natn. Acad. Sci. U.S.A.* **77**, 3494–3498 (1980).
3. Todaro, G. J., Fryling, C. & De Larco, J. E. *Proc. natn. Acad. Sci. U.S.A.* **77**, 5258–5262 (1980).
4. Ozanne, B., Fulton, R. J. & Kaplan, P. L. *J. cell. Physiol.* **105**, 163–180 (1980).
5. Moses, H. L., Branum, E. L., Proper, J. A. & Robinson, R. A. *Cancer Res.* **41**, 2842–2848 (1981).
6. Roberts, A. B., Anzano, M. A., Lamb, L. C., Smith, J. M. & Sporn, M. B. *Proc. natn. Acad. Sci. U.S.A.* **78**, 5339–5343 (1981).
7. De Larco, J. E. & Todaro, G. J. *J. cell. Physiol.* **102**, 267–277 (1980).
8. De Larco, J. E. & Todaro, G. J. *J. cell. Physiol.* **94**, 335–342 (1978).
9. Topp, W. C., Rifkin, D., Graessmann, A., Chang, C. M. & Sleigh, M. J. *Cold Spring Harb. Conf. Cell Proliferation* Vol. 6 (eds Sato, G. H. & Ross, R.) 361–370 (1979).
10. Wrann, M., Fox, C. F. & Ross, R. *Science* **210**, 1363–1365 (1980).
11. Shoyab, M., De Larco, J. E. & Todaro, G. J. *Nature* **279**, 387–391 (1979).
12. Magun, B. E., Matrisian, L. M. & Bowden, G. T. *J. biol. Chem.* **255**, 6373–6381 (1980).
13. Rozengurt, E., Brown, K. D. & Pettican, P. *J. biol. Chem.* **256**, 716–722 (1981).
14. Johnson, L. K., Baxter, J. D., Vlodavsky, I. & Gospodarowicz, D. *Proc. natn. Acad. Sci. U.S.A.* **77**, 394–398 (1980).
15. Kahn, P. & Shin, S. *J. Cell Biol.* **82**, 1–16 (1979).
16. Cifone, M. A. & Fidler, I. J. *Proc. natn. Acad. Sci. U.S.A.* **77**, 1039–1043 (1980).
17. Harrison, J. & Auersperg, N. *Science* **213**, 218–219 (1981).
18. Seif, R. *J. Virol.* **36**, 421–428 (1980).
19. Rose, S. P., Stahn, R., Passovoy, D. S. & Herschman, H. *Experientia* **32**, 913–915 (1976).
20. Fisher, P. B., Bozzone, J. H. & Weinstein, I. B. *Cell* **18**, 695–705 (1979).
21. Roberts, A. B., Anzano, M. A., Frolik, C. A. & Sporn, M. B. *Cold Spring Harb. Conf. Cell Proliferation* (in the press).
22. Hollenberg, M. D. *Vitam. Horm.* **37**, 69–110 (1979).
23. Sporn, M. B., Newton, D. L., Roberts, A. B., De Larco, J. E. & Todaro, G. J. in *Molecular Actions and Targets for Cancer Chemotherapeutic Agents* (eds Sartorelli, A. C., Bertino, J. R. & Lazo, J. S.) 541–554 (Academic, New York, 1981).
24. Savage, C. R. & Cohen, S. *J. biol. Chem.* **247**, 7609–7611 (1972).

Stimulation of tyrosine-specific phosphorylation by platelet-derived growth factor

Bo Ek*, Bengt Westermark†, Åke Wasteson* & Carl-Henrik Heldin*

* Institute of Medical and Physiological Chemistry, Biomedical Center, Uppsala University, Uppsala, Sweden
† The Wallenberg Laboratory, Uppsala University, Uppsala, Sweden

Recent studies have shown that tyrosine-specific protein kinases may be involved in both virus transformation and growth stimulation with polypeptide growth factors. Thus, several *onc* gene products possess such kinase activity[1–9] and, further, binding of epidermal growth factor (EGF)[10] to A-431 cells stimulates phosphorylation of tyrosine residues of both membrane and cytoplasmic proteins[11–16]. Platelet-derived growth factor (PDGF), a 30,000 molecular weight (M_r) polypeptide, is the major growth-promoting factor in serum for connective tissue-derived cells and glial cells in culture[17–22]. High-affinity binding of ^{125}I-PDGF to a specific receptor on such cells has recently been demonstrated; thus, human foreskin fibroblasts were found to have some 300,000 PDGF receptors per cell, with an affinity constant of 1 nM (ref. 23). The addition of PDGF to human glial cells and fibroblasts produces various phenotypic changes, similar to those induced by EGF[24] and tumour viruses[25], which include rapid induction of membrane ruffling, reduction in cell adhesion, change in structure of the actin cytoskeleton and increased mitotic activity (B.W. *et al.*, unpublished data). These considerations suggested that PDGF binding to cellular receptors might similarly stimulate kinase activity. The present report demonstrates such an effect: when incubated with plasma membranes from human fibroblasts or glial cells, PDGF induces the phosphorylation of tyrosine residues of membrane proteins with apparent molecular weights of 175,000 and 130,000.

Membranes were prepared from cultured human foreskin fibroblasts or glial cells as described previously[26] and incubated at 0 °C with ^{32}P-ATP and pure PDGF[21]. After 10 min incubation, the resulting phosphoprotein pattern was analysed by SDS-polyacrylamide gel electrophoresis (PAGE).

As Fig. 1 shows, PDGF stimulated the incorporation of ^{32}P into membrane proteins of both fibroblasts (Fig. 1*a*) and glial cells (Fig. 1*b*), promoting, in particular, the phosphorylation of a 175,000-M_r and a 130,000-M_r protein, in comparison with the

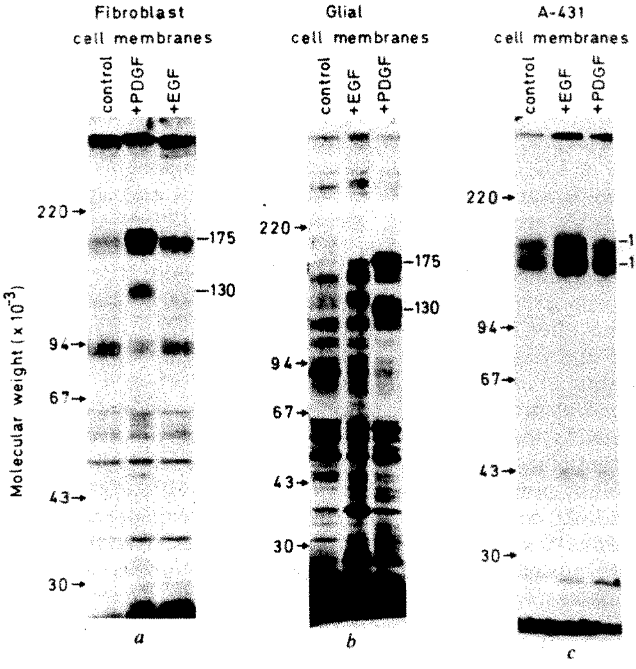

Fig. 1 Effect of PDGF and EGF on the phosphorylation of fibroblast (*a*), glial (*b*) and A-431 (*c*) cell membrane proteins. Cell membranes were prepared from serum-starved cultures of human foreskin fibroblasts (cell line AG 1523, obtained from the Human Genetic Mutant Cell Repository, Institute for Medical Research, Camden, New Jersey), human normal glia-like cells (cell line 1508 CG from our own laboratory) and A-431 cells (obtained from J. E. De Larco, National Cancer Institute, Bethesda, Maryland) according to Thom *et al.*[26] as modified in ref. 12, and were stored in aliquots suspended in 20 mM HEPES *p*H 7.4 at −70 °C for up to 2 months. The phosphorylation reaction was carried out at 0 °C in a final volume of 40 µl containing 40 µg (*a*, *c*) or 10 µg (*b*) of cell membrane protein (determined according to Bradford[31]), 20 mM HEPES *p*H 7.4, 3 mM $MnCl_2$, 0.1% bovine serum albumin, 15 µM (γ-^{32}P]ATP (33.3 kBq (*a*, *c*) or 333 kBq (*b*)) and 100 ng PDGF (76 nM) or 40 ng EGF (167 nM). PDGF was prepared according to Heldin *et al.*[21] and EGF was purchased from Collaborative Research. The cell membranes were preincubated with growth factors at 0 °C for 10 min before the phosphorylation reaction was started by adding ^{32}P-ATP. The reaction was terminated after another 10 min by adding 40 µl of SDS-sample buffer (80 mM Tris-HCl *p*H 8.8, 30% w/v sucrose, 3.6% SDS, 10 mM dithiothreitol and 0.01% bromophenol blue) and heating at 95 °C for 3 min. After alkylation with iodoacetamide the samples were subjected to SDS-PAGE as described elsewhere[32], using polyacrylamide gradients of 5–10% (*a*, *c*) or 3–10% (*b*) and gel dimensions of 170 × 1 mm. Gels were run at a constant current of 15 mA. After fixation in 20% 5-sulphosalicylic acid for 1 h, staining with Coomassie blue, destaining and drying under vacuum, the gels were autoradiographed using intensifying screens (DuPont, Lightning Plus) and pre-exposed Kodak X-Omat AR films[33]. Exposure was at −70 °C for up to 3 days. The following proteins were used as molecular weight standards: fibronectin (220,000), phosphorylase *b* (94,000), bovine serum albumin (67,000), ovalbumin (43,000) and carbonic anhydrase (30,000).

0028-0836/82/050419—02$01.00

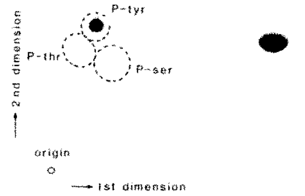

Fig. 2 Phosphoamino acid analysis after PDGF-stimulated phosphorylation. Glial cell membranes (10 µg) were incubated with ^{32}P-ATP and PDGF and the incubation mixture analysed by SDS-PAGE (see Fig. 1 legend). The phosphorylated 175,000-M_r component was localized by autoradiography and the corresponding region of the gel excised. The gel piece was hydrolysed under vacuum in 200 µl 6 M HCl at 110 °C for 2 h. After removal of HCl by evaporation under reduced pressure at 37 °C, the sample was resuspended in 20 µl of acetic acid/formic acid/water (78:25:897) containing 2 mg ml^{-1} each of phosphoserine (Sigma), phosphothreonine (Sigma) and phosphotyrosine (synthesized according to ref. 34). Two-dimensional chromatography was performed on cellulose thin layer plates (20 × 20 cm) as described previously[1], that is, electrophoresis at *p*H 1.9 in acetic acid/formic acid/water (78:25:897) at 1 kV for 3 h (first dimension) followed by ascending chromatography in isobutyric acid/0.5 M ammonia (5:3) (second dimension). Autoradiography was performed as described in Fig. 1 legend. Standards were visualized by ninhydrin staining. Broken lines: ninhydrin staining of phosphoserine (P-Ser), phosphothreonine (P-Thr) and phosphotyrosine (P-Tyr). The unidentified spot with the highest electrophoretic mobility probably consists of inorganic ^{32}P formed during the hydrolysis[1].

control incubation, in which no growth factor was added. Slight effects of PDGF were also seen in other components of the autoradiogram, associated with both increased (for example, a 36,000-M_r protein) and decreased (99,000 M_r) phosphorylation. In a separate experiment to determine the time and dose dependence of the phosphorylation reaction, stimulation of phosphorylation was observed after 1 min at 0 °C and was maximal after 5 min; it was detectable in the presence of 8 nM PDGF and was maximal at 40 nM (not shown).

A similar experiment investigated the effect of EGF on phosphorylation of human fibroblast and glial cell membrane proteins. In the presence of EGF, ^{32}P incorporation increased preferentially in a 170,000-M_r protein of the fibroblast membrane preparation (Fig. 1*a*) and in both a 170,000- and a 150,000-M_r component of the glial cell membrane preparation (Fig. 1*b*). This result is clearly distinct from that obtained with PDGF, indicating that different proteins serve as substrates for the kinases stimulated by the two factors. There is evidence that the EGF receptor proper is phosphorylated after stimulation with EGF[13], but whether PDGF binding induces phosphorylation of the PDGF receptor in an analogous manner remains to be clarified. PDGF seems to be more potent than EGF, producing a higher degree of phosphorylation in fibroblast as well as glial cell membranes. This might be due to the presence of three to five times more PDGF receptors than EGF receptors on both types of cells[23,27].

The epithelial cell line A-431, which has an unusually high number of EGF receptors[28], has been shown to lack high-affinity receptors for PDGF[23]. Membranes from this cell line were therefore incubated with ^{32}P-ATP and PDGF or EGF and the phosphorylation pattern analysed by SDS-PAGE (Fig. 1*c*). After incubation with PDGF the distribution of phosphoproteins was similar to that of the control carried out in the absence of growth factor. As expected, however, EGF was active in this system, increasing the phosphorylation of proteins in the 140,000–160,000-M_r region. The absence of an appreciable effect of PDGF on membranes from this PDGF receptor-negative cell line in conditions where membranes from PDGF receptor-positive cells did respond to PDGF indicates that the response to PDGF was mediated by binding to the PDGF receptor.

We also investigated the specificity of the PDGF-stimulated kinase activity with regard to the type of phospho-accepting amino acid residue involved. Human glial cell membranes were incubated with ^{32}P-ATP in the presence or absence of PDGF and the incubation mixture analysed on SDS-PAGE. The 175,000-M_r component was identified by autoradiography and the corresponding portion of the gel excised. After partial acid hydrolysis the phosphoamino acids were separated on cellulose thin layer plates by electrophoresis at *p*H 1.9 (first direction) and chromatography in isobutyric acid/0.5 M ammonia (5:3) (second direction)[1]. Figure 2 shows an autoradiogram from this experiment, which indicates that the 175,000-M_r component phosphorylated under the influence of PDGF contained only tyrosine-bound phosphate; no labelled phosphoserine or phosphothreonine was detected. An identical result was obtained with the 175,000-M_r ^{32}P-labelled product of fibroblast membranes. Analysis of the 130,000-M_r protein also showed the presence of phosphotyrosine, although some phosphothreonine and phosphoserine were detectable (not shown).

In conclusion, PDGF stimulates tyrosine-specific phosphorylation of two membrane components of human fibroblasts and glial cells with apparent M_rs of 175,000 and 130,000, distinct from the 170,000-M_r component phosphorylated in response to EGF. The precise relationship between the individual members of the growing family of tyrosine-specific protein kinases[9,29,30] remains to be elucidated. As they seem to be involved both in the cellular response to growth factors, like EGF and PDGF, and in tumour-virus induced transformation, including the expression of abnormal growth properties, it is reasonable to believe that this type of enzyme participates in the mediation of growth regulatory signals. Therefore, PDGF and EGF, although they bind to separate cell-surface receptors[23], may function via similar or identical intracellular events, that is, tyrosine-specific phosphorylation of certain growth-controlling proteins. The similarity in some of the phenotypic properties of virus-transformed cells and those of PDGF- or EGF-stimulated cells might then be explained by an overlapping substrate specificity of the respective protein kinases.

This work was supported by grants from the Swedish Cancer Society (55 and 689), the Swedish MRC (4486 and 03X-4) and O. E. and Edla Johansson's Foundation. We thank S. Hermansson, M. Kastemar and A. Magnusson for technical assistance.

Received 21 September; accepted 30 November 1981.

1. Hunter, T. & Sefton, B. *Proc. natn. Acad. Sci. U.S.A.* **77,** 1311–1315 (1980).
2. Witte, O. N., Dasgupta, A. & Baltimore, D. *Nature* **283,** 826–831 (1980).
3. Kawai, S. *et al. Proc. natn. Acad. Sci. U.S.A.* **77,** 6199–6203 (1980).
4. Neil, J. C., Ghysdael, J. & Vogt, P. K. *Virology* **109,** 223–228 (1981).
5. Feldman, R. A., Hanafusa, T. & Hanafusa, H. *Cell* **22,** 8757–8766 (1980).
6. Pawson, T. *et al. Cell* **22,** 767–776 (1980).
7. Beemon, K. *Cell* **24,** 145–153 (1981).
8. Barbacid, M., Beemon, K. & Devare, S. G. *Proc. natn. Acad. Sci. U.S.A.* **77,** 5158–5162 (1980).
9. Hunter, T., Sefton, B. M. & Beemon, K. *ICN–UCLA Symp. molec. cell. Biol.* **18,** 499–514 (1980).
10. Cohen, S. *J. biol. Chem.* **237,** 1555–1562 (1962).
11. Carpenter, G., King, L. E. Jr & Cohen, S. *Nature* **276,** 409–410 (1978).
12. Carpenter, G., King, L. E. Jr & Cohen, S. *J. biol. Chem.* **254,** 4884–4891 (1979).
13. Cohen, S., Carpenter, G. & King, L. E. Jr *J. biol. Chem.* **255,** 4834–4842 (1980).
14. King, L. E. Jr, Carpenter, G. & Cohen, S. *Biochemistry* **19,** 1524–1528 (1980).
15. Ushiro, H. & Cohen, S. *J. biol. Chem.* **255,** 8363–8365 (1980).
16. Hunter, T. & Cooper, J. A. *Cell* **24,** 741–752 (1981).
17. Ross, R. & Vogel, A. *Cell* **14,** 203–210 (1978).
18. Scher, C. D., Shepard, R. C., Antoniades, H. N. & Stiles, C. D. *Biochim. biophys. Acta* **560,** 217–241 (1979).
19. Antoniades, H. N., Scher, C. D. & Stiles, C. D. *Proc. natn. Acad. Sci. U.S.A.* **76,** 1809–1813 (1979).
20. Heldin, C.-H., Westermark, B. & Wasteson, A. *Proc. natn. Acad. Sci. U.S.A.* **76,** 3722–3726 (1979).
21. Heldin, C.-H., Westermark, B. & Wasteson, Å. *Biochem. J.* **193,** 907–913 (1981).
22. Deuel, T. F. *et al. J. biol. Chem.* **256,** 8896–8899 (1981).
23. Heldin, C.-H., Westermark, B. & Wasteson, Å. *Proc. natn. Acad. Sci. U.S.A.* **78,** 3664–3668 (1981).
24. Chinkers, M., McKanna, J. A. & Cohen, S. *J. Cell Biol.* **83,** 260–265 (1979).
25. Wang, E. & Goldberg, A. R. *Proc. natn. Acad. Sci. U.S.A.* **73,** 4065–4069 (1976).
26. Thom, D., Powell, A. J., Lloyd, C. W. & Rees, D. A. *Biochem. J.* **168,** 187–194 (1977).
27. Carpenter, G. & Cohen, S. *A. Rev. Biochem.* **48,** 193–216 (1979).
28. Haigler, H., Ash, J. F., Singer, S. J. & Cohen, S. *Proc. natn. Acad. Sci. U.S.A.* **75,** 3317–3321 (1978).
29. Spector, M., Pepinsky, R. B., Vogt, V. M. & Racker, E. *Cell* **25,** 9–21 (1981).
30. Racker, E. & Spector, M. *Science* **213,** 303–307 (1981).
31. Bradford, M. M. *Analyt. Biochem.* **72,** 248–254 (1976).
32. Blobel, G. & Dobberstein, B. *J. Cell Biol.* **67,** 835–851 (1975).
33. Laskey, R. A. & Mills, A. D. *FEBS Lett.* **82,** 314–316 (1977).
34. Rothenberg, P. G., Harris, T. J. R., Nomoto, A. & Wimmer, E. *Proc. natn. Acad. Sci. U.S.A.* **75,** 4868–4872 (1978).

A hypothesis for the initiation of genetic recombination in eukaryotes

Paul Markham & Harold L. K. Whitehouse

Botany School, University of Cambridge, Downing Street,
Cambridge CB2 3EA, UK

Initiation of genetic recombination at meiosis in Ascomycete fungi is thought to occur from fixed sites, at least in the majority of events. The simplest way to initiate recombination from fixed sites would be if an endonuclease recognized them and cut one strand of the DNA duplex to allow formation of asymmetric hybrid DNA, as proposed in the Meselson–Radding model of recombination[1]. However data from the *Neurospora crassa his-3* gene[2] and the conversion patterns of a mutation in *Schizosaccharomyces pombe*[3] and one in *Sordaria brevicollis*[4], require this idea of initiation to be modified. Here we propose a hypothesis of initiation that will accommodate these experimental observations, which involves the recognition of initiation sites by an endonuclease capable of migrating along a DNA duplex and that cuts in *trans*.

Catcheside and Angel[2] have described a mutation in *N. crassa* in which the distal quarter of the *his-3* gene with respect to the centromere has been transferred from linkage group I to linkage group VII. On crossing a strain carrying this mutation with strains having a complete *his-3* gene, recombination events were observed in the section of the gene proximal to the break point, but which had been initiated from the distal *cog* site (see Fig. 1). From this they have inferred that recombination events initiated at the *cog* site[5], at the distal end of the gene, are capable of migrating down the gene and past the break point, before hybrid DNA formation. These observations require that the mechanism of initiation of recombination from fixed sites allows for the migration of the initiation event before hybrid DNA formation.

The single mutations M26 in the *ade6* gene of *S. pombe*[3] and YS17 in the *buff* gene of *S. brevicollis*[4] are characterized by high conversion frequency, dramatic elevation of levels of interallelic recombination when the alleles are present in a cross and ability to modify recombination polarity. Such behaviour can best be explained if the effect of the mutations has been to introduce fortuitously a site for the initiation of recombination in their respective genes. Both mutations are also converted predominantly to wild type, so that in crosses with wild-type strains, >95% of all aberrant asci produced have three wild-type products of meiosis and one mutant (see Table 1). This observation is clearly at odds with the simple idea of initiation of recombination, which would predict that if M26 and YS17 are initiation sites, they should be recognized by an endonuclease which would cut a single strand of their DNA duplex. This would provide a free single-strand end to invade one of the chromatids of the other parental type, as predicted by the Meselson–Radding model[1], which would result in either correction back to wild type in the invading strand, which would go undetected because it would restore the normal allele ratio, or persistence of the heteroduplex section. Persistence of the uncorrected invading strand would lead to postmeiotic segregation and a three wild-type plus five mutant spored ascus in *S. brevicollis* or an ascus generating one wild-type colony, one sectored colony and two mutant colonies in *S. pombe*. If correction to mutant occurred in the second strand of the invaded chromatid, then a two wild-type plus six mutant spored ascus would result in *S. brevicollis* or a one wild-type plus three mutant spored ascus in *S.*

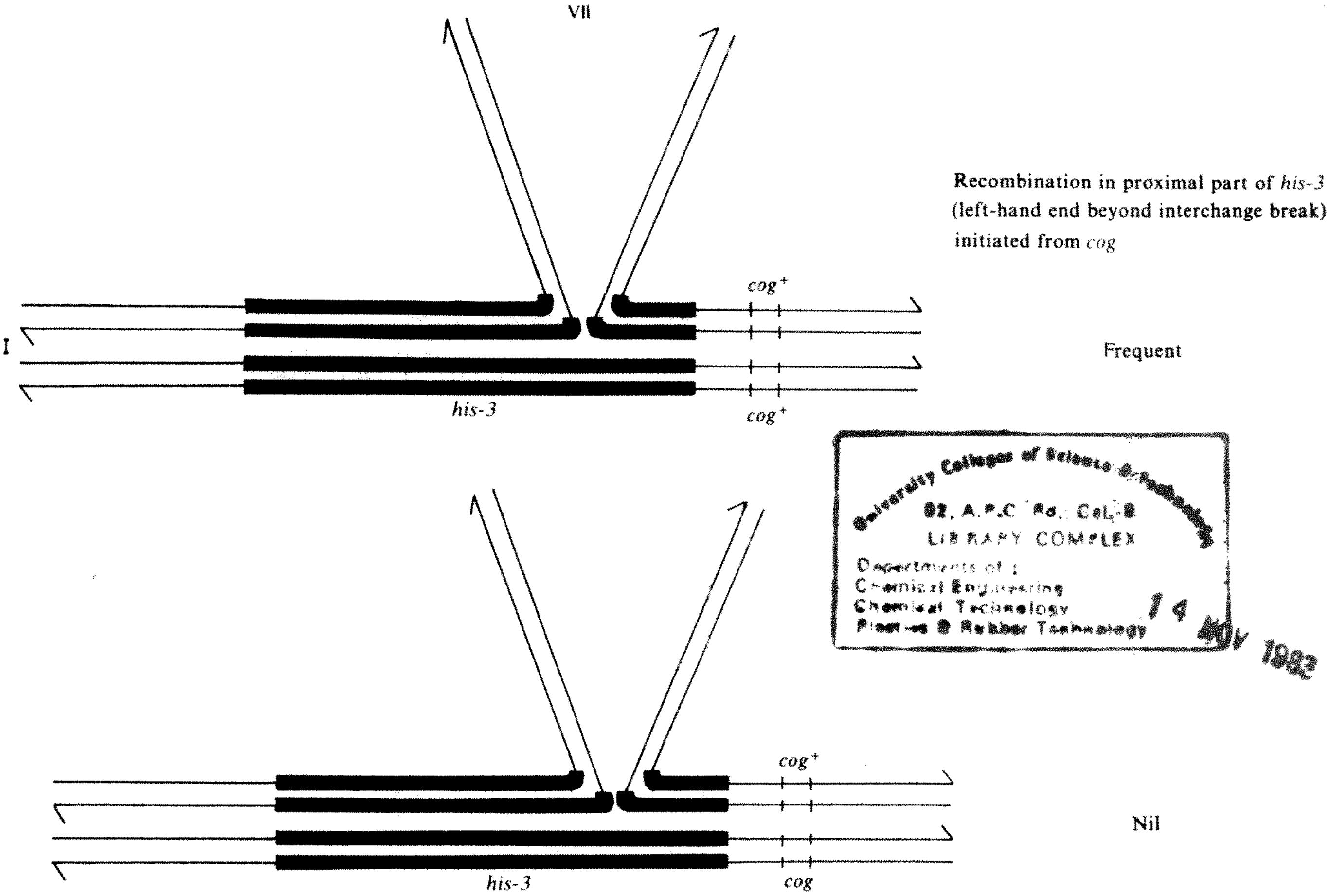
VII
Recombination in proximal part of *his-3* (left-hand end beyond interchange break) initiated from *cog*
cog⁺
I
Frequent
his-3
cog⁺
cog⁺
Nil
his-3
cog

University Colleges of Science & Technology
92, A.P.C. Rd., Cal-9
LIBRARY COMPLEX
Departments of:
Chemical Engineering
Chemical Technology
Plastics & Rubber Technology
14 NOV 1982

Fig. 1 Diagram illustrating results obtained by Catcheside and Angel[2] for recombination in the *his-3* gene (thick lines) of *N. crassa* when heterozygous for a *his-3* structural mutant. Not drawn to scale. I and VII indicate the linkage groups.

0028-0836/82/050421—03$01.00

pombe. This mechanism cannot explain the observed six wild-type plus two mutant spored asci in *S. brevicollis* and three wild-type plus one mutant spored asci in *S. pombe*. This pattern of behaviour is also observed in the *his-3* gene of *N. crassa*. When only one parental strain in a cross carries the more active form of the *cog* site (*cog*$^+$), the other carrying a much less active form (*cog*), then alleles of the *his-3* gene present on the molecule with the *cog*$^+$ site are preferentially converted to wild type with respect to alleles present on chromatids of the other parental type (*cog*), regardless of the normal gene polarity[5] (see Table 1). This therefore requires that the DNA strand carrying the initiation site becomes the recipient of hybrid DNA and not the donor.

To accommodate all these observations, we suggest that initiation of recombination from fixed sites occurs by the following mechanism (see Fig. 2). It is assumed that the two homologous DNA molecules, one from each parent, are closely paired before nuclease action. An enzyme complex with endonuclease activity recognizes the fixed site (Fig. 2*a*) and either cuts a single strand of a chromatid of the other parental type (Fig. 2*b*), or migrates along the duplex that it has recognized before cutting in *trans* at some random position removed from the initiation site (Fig. 2*c*). This provides the single-strand end capable of producing hybrid DNA as described by the Meselson–Radding model[1]. This hypothesis clearly allows for the migratory capacity necessary to explain the results of Catcheside and Angel[2] and also explains the results obtained with M26, YS17 and *cog*$^+$ by allowing for the cutting of a DNA strand of different parental origin from the initiation site. Catcheside and Angel[2] originally explained their observations by postulating that the nick or gap introduced at the initiation site was capable of being moved along the DNA strand by combined exonuclease and polymerase activity before giving rise to hybrid DNA. The migration of the initiating enzyme complex and the ability of a gap or nick to be moved along the DNA strand are not, of course, mutually exclusive, so it is useful to examine the idea of nick or gap movement in the light of our hypothesis. Catcheside and Angel[2] found that the presence of a fully active (*cog*$^+$) site in only one of the *N. crassa* parental strains in a cross involving the *his-3* interchange mutation affected recombination in the part of the gene beyond the break point. Recombination initiated from *cog*$^+$ was observed in this region only when *cog*$^+$ was in the chromosome carrying the complete *his-3* gene and not when it was in the chromosome carrying the interchange (see Fig. 1). This suggests that if the endonuclease does cut in *trans* then either the nick or gap cannot move along the DNA strand or if it does so it is not recombinogenic, and thus any gap or nick introduced into a complete *his-3* chromatid by an endonuclease recognizing a *cog*$^+$ site in a chromatid carrying the interchange cannot result in recombination beyond the interchange point.

The capacity of enzyme systems to carry out the functions required by this hypothesis has been demonstrated in different but closely related systems. Enzyme migration from a recognition site before acting has been postulated for the type I restriction endonucleases of *Escherichia coli* B and *E. coli* K-12[6-12]. A protein in the *recBC* recombination pathway of *E. coli* is believed to recognize a particular nucleotide sequence[13,14]. To account for the ability of this enzyme to promote recombination at a distance from such a hot spot, it has been suggested that the enzyme usually slides away from its binding site before nicking the DNA[15]. The inability of an intervening non-homologous region to lower the recombination frequency showed that the movement from site of recognition to site of action could not involve the second DNA molecule. Diffusion along the DNA has also been proposed for deoxyribonuclease I of *Ustilago maydis*[16]. Cutting in *trans* as a feature of recombination was proposed by Ross and Howard-Flanders[17,18] for repair in *E. coli* of DNA containing cross-links as a result of exposure to psoralen and 360 nm light. An investigation of recombination between phage λ DNA damaged in this way and undamaged prophage λ, showed that the damaged DNA led to cutting in *trans* of the undamaged homologous DNA. Homology of nucleotide sequence between the two

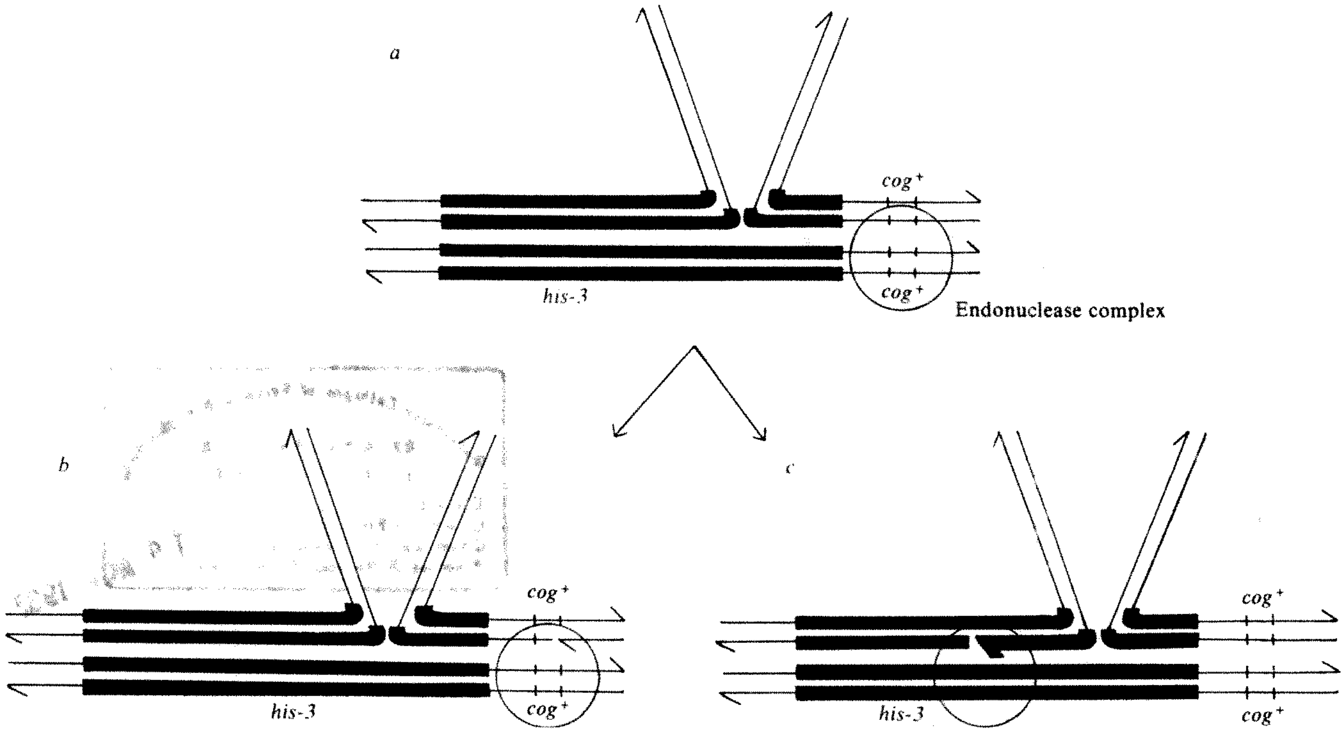

Fig. 2 Diagram illustrating the hypothesis for initiation of recombination. *a*, The endonuclease complex recognizes and binds to the initiation site. Then, either *b*, the endonuclease complex, while still bound to the initiation site, cuts in *trans* one strand of the second chromatid, or *c*, the endonuclease complex migrates along the chromatid which it originally recognized and cuts in *trans* one strand of the second chromatid at a position removed from the initiation site. In this case the enzyme migration leads to a cut being made beyond the interchange break in the second chromatid. After either of these alternative events, invasion of the unbroken chromatid by the free end of the cut strand may lead to hybrid DNA formation. The *his-3* region of *N. crassa* with the interchange break in one chromatid, as illustrated in Fig. 1, is used here to demonstrate the two major features of the hypothesis. The thick lines denote the *his-3* gene. Diagram not drawn to scale.

Table 1 Data from fungal crosses heterozygous for recombination initiation sites

Species and ref.	Parental genotype	Favoured recombinant genotype
Schizosaccharomyces pombe[3]	$\frac{+}{M26}$	+ + + *M26*
Sordaria brevicollis[4]	$\frac{+}{YS17}$	+ + + + + + *YS17* *YS17*
Neurospora crassa[5]	$\frac{M\,his\text{-}3^{a}\,cog^{+}\,N}{m\,his\text{-}3^{b}\,cog\;\;n}$	$M\,his\text{-}3^{+}\,cog^{+}\,N$

M/*m* and *N*/*n* are flanking markers. +, Wild type.

molecules was necessary for the cutting, which required the host *recA* gene function. Subsequently cutting in *trans* was demonstrated *in vitro* using damaged and undamaged molecules of phage $\phi X174$ DNA (replicative form I) and crude *E. coli* extracts[19].

Enzyme migration along the DNA from an initiation site, before hybrid DNA formation, offers an explanation for several features of eukaryotic recombination. First, it could account for the occurrence of crossing-over between the sites of alleles without either site apparently being included in hybrid DNA. Such crossing-over is frequent in some genes[20] but to account for the polarity often observed in recombination it is necessary to postulate initiation of recombination from fixed sites which appear to be outside genes, such as *cog*. Enzyme migration offers a solution to this paradox by allowing initiation from outside a gene to become manifest only within it on some occasions. Second, there is the mutant specificity of crossing-over between alleles (mutants 137 and 277 in series 46 of *Ascobolus immersus*[20] and mutants 4 and 4b at the *g* locus in *Sordaria fimicola*[21–23]). As there is no hybrid DNA at either mutant site with such crossing-over, it was not obvious how the mutant specificity came about. If a mutant had a molecular structure that interfered with heteroduplex formation, selection for recombinants might imply selection for meiotic cells in which enzyme migration had moved hybrid DNA formation beyond the site of the mutation as in the case of the interchange mutation of *his-3* in *N. crassa*. Work with spore colour mutants of *A. immersus* shows that mutations favouring crossing-over with an allele may be deletions. Thus, mutants 1028, 1130 and 49 of series 19 appeared to be deletions because they showed no recombination with two or more closely linked alleles that recombined with one another. They showed frequent crossing-over with more distant alleles[20]. Such multisite mutations might be expected to interfere with hybrid DNA formation. Third, enzyme migration would allow recombination of distal origin to effect conversion at a proximal site and vice versa, which may have some bearing on apparent cases of polarity reversal.

The Meselson–Radding model of recombination is seen as the most likely consequence of these initiation steps because it best explains data on recombination in eukaryotes. Nevertheless there are alternative mechanisms which could give rise to recombination following the proposed method of initiation.

Received 25 July; accepted 9 December 1981.

1. Meselson, M. S. & Radding, C. R. *Proc. natn. Acad. Sci. U.S.A.* **72,** 358–361 (1975).
2. Catcheside, D. G. & Angel, T. *Aust. J. biol. Sci.* **27,** 219–229 (1974).
3. Gutz, H. *Genetics* **69,** 317–337 (1971).
4. MacDonald, M. V. & Whitehouse, H. L. K. *Genet. Res.* **34,** 87–119 (1979).
5. Angel, T., Austin, B. & Catcheside, D. G. *Aust. J. biol. Sci.* **23,** 1229–1240 (1970).
6. Meselson, M. & Yuan, R. *Nature* **217,** 1110–1114 (1968).
7. Horiuchi, K. & Zinder, N. D. *Proc. natn. Acad. Sci. U.S.A.* **69,** 3220–3224 (1972).
8. Horiuchi, K., Vovis, G. F. & Zinder, N. D. *J. biol. Chem.* **249,** 543–552 (1974).
9. Hartman, N. & Zinder, N. D. *J. molec. Biol.* **85,** 345–356 (1974).
10. Brammar, W. J., Murray, N. E. & Winton, S. *J. molec. Biol.* **90,** 633–647 (1974).
11. Linn, S., Lautenberger, J. A., Eskin, B. & Lackey, D. *Fedn Proc.* **33,** 1128–1134 (1974).
12. Rosamond, J., Endlich, B. & Linn, S. *J. molec. Biol.* **129,** 619–635 (1979).
13. Sprague, K. U., Faulds, D. H. & Smith, G. R. *Proc. natn. Acad. Sci. U.S.A.* **75,** 6182–6186 (1978).
14. Schultz, D. W., Swindle, J. & Smith, G. R. *J. molec. Biol.* **146,** 275–286 (1981).
15. Stahl, F. W. & Stahl, M. M. *Molec. gen. Genet.* **140,** 29–37 (1975).
16. Ahmad, A., Holloman, W. K. & Holliday, R. *Nature* **258,** 54–56 (1975).
17. Ross, P. & Howard-Flanders, P. *J. molec. Biol.* **117,** 137–158 (1977).
18. Ross, P. & Howard-Flanders, P. *J. molec. Biol.* **117,** 159–174 (1977).
19. Cassuto, E., Mursalim, J. & Howard-Flanders, P. *Proc. natn. Acad. Sci. U.S.A.* **75,** 620–624 (1978).
20. Lissouba, P., Mousseau, J., Rizet, G. & Rossignol, J-L. *Adv. Genet.* **11,** 343–380 (1962).
21. Kitani, Y. & Olive, L. S. *Genetics* **62,** 23–66 (1969).
22. Kitani, Y. & Whitehouse, H. L. K. *Genet. Res.* **24,** 229–250 (1974).
23. Whitehouse, H. L. K. *Genet. Res.* **24,** 251–279 (1974).

Bacterial expression of an enzymatically active protein encoded by RSV *src* gene

J. P. McGrath & A. D. Levinson

Department of Molecular Biology, Genentech, Inc.,
460 Point San Bruno Boulevard, South San Francisco,
California 94080, USA

Genetic evidence indicates that the oncogenic potential of Rous sarcoma virus (RSV) resides in a single viral gene denoted *src*[1,2]. The product of this gene is a 60,000-molecular weight (M_r) phosphoprotein ($pp60^{src}$)[3–6] which is linked to the plasma membrane of RSV-infected cells[7–9] by an interaction at its amino terminus[10]. This protein is associated with a protein kinase activity[5,11] capable of phosphorylating tyrosine residues in acceptor proteins[12–15]. A closely related protein occurs in uninfected cells from a wide variety of vertebrates[16–18] and is presumably encoded by a cellular gene that is alleged to be the progenitor of *src*[16–19]. Because detailed enzymological characterization of $pp60^{src}$ has been hampered by a lack of sufficient quantities of purified material, we have produced a bacterial plasmid capable of expressing in *Escherichia coli* a protein closely related to $pp60^{src}$. We report here the construction of this vector, which directs the synthesis in *E. coli* of large quantities of a protein having the size and immunological properties characteristic of $pp60^{src}$. In addition, we have demonstrated tyrosine-specific protein kinase activity associated with the bacterially derived protein, an observation which greatly strengthens the claim that the kinase activity previously observed to be associated with $pp60^{src}$ represents a bona fide property of the protein.

The general approach used for the bacterial synthesis of $pp60^{src}$ was to express the protein as a fusion product involving the amino terminus of human growth hormone (HGH) (Fig. 1). HGH has been synthesized directly in *E. coli* under the control of both the *lac* promoter (pHGH107)[20] and the *trp* promoter (pHGH207-1)[21]. To minimize the involvement of HGH sequences while preserving the essential control elements of the plasmid (including promoter, ribosome binding site and start codon), we digested cloned pHGH207-1 DNA with *Pvu*II and *Bam*HI and isolated the 4,350-base pair (bp) fragment which contains pBR322 sequences, the *trp* promoter and the first 23 amino acids of HGH[20]. An *Eco*RI subclone of the Schmidt–Ruppin strain of RSV containing the entire *src* gene (pSRC-RI)[22] was cut with *Hae*II and *Bam*HI, and the 2,334-bp fragment (encoding all of $pp60^{src}$ except the first 14 amino acids) was ligated into the *trp* expression plasmid. From the known sequence of HGH[20] and $pp60^{src}$ (ref. 22), such a construction was expected to join the HGH and $pp60^{src}$ sequences in the proper reading frame; this was verified by DNA sequence analysis across the HGH-src junction (R. Najarian and P. Seeberg, unpublished results). After screening and

0028–0836/82/050423—03$01.00

identification of the appropriate recombinant molecules, one such clone (pSRCex16) was tested for the expression of the 60,000-M_r HGH–src protein (p60) in *E. coli*. Because the *trp* promoter is induced by a lack of tryptophan in the medium, it was expected that p60 would be induced in pSRCex16-transformed cultures as depletion of tryptophan occurred. As a specific test of this, cultures of *E. coli* K12 strain 294 were transformed with either pBR322, pHGH207-1 or pSRCex16 and grown to $A_{550} = 0.25$ or 1.00 in either LB broth (rich medium) or M9 broth (minimal medium). Tryptophan depletion, and consequent activation of the *trp* promoter, have been shown to occur by $A_{550} = 1.0$ in M9 medium[21,23]. Total cellular extracts were then prepared and the proteins visualized by Coomassie blue staining after electrophoresis on SDS-polyacrylamide gels (Fig. 2). As expected, no overall change in the protein profile occurred in cells transformed with pBR322 regardless of the growth state (Fig. 2*a*). However, in the pHGH207-1 extract (Fig. 2*b*), a prominent protein of 22,000-M_r appeared after induction in M9 medium (lanes c, d); this protein was not observed after corresponding times in LB medium, in which tryptophan is abundant (lanes a, b). This protein represents mature HGH when synthesized under *trp* control[21]. Figure 2*c* demonstrates that in bacteria transformed with pSRCex16, a protein of 60,000-M_r was induced in M9 medium; this corresponds to the size of the protein encoded by *src*[22]. The protein appeared selectively during late growth phase in M9 medium in bacteria transformed with pSRCex16 (Fig. 2*c*, lanes c, d), but not in similar cultures grown in rich medium (LB) (lanes a, b), strongly suggesting that it represents the translational product of the *src* gene under the control of the *trp* promoter. We estimate that when induced, this protein represents ~5% of total bacterial protein (170,000 molecules per cell).

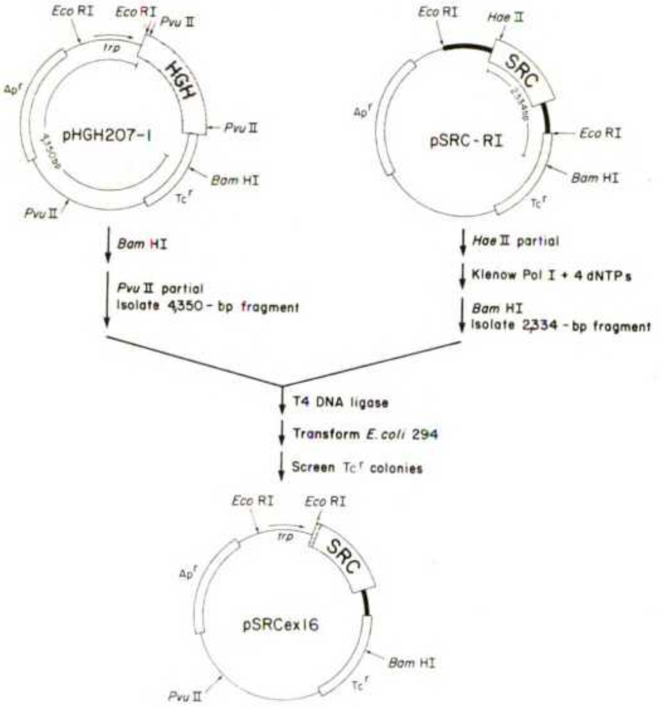

Fig. 1 Construction of a plasmid (pSRCex16) expressing p60. Cloned pGHG207-1 DNA[21] was partially digested with *Pvu*II, then digested to completion with *Bam*HI. The 4,350-bp fragment containing the *trp* promoter, most of pBR322, and the first 69 nucleotides of HGH was isolated from polyacrylamide gels by electroelution[32]. Plasmid pSRC-RI (ref. 22) was partially digested with *Hae*II, and the 3′ single-stranded cohesive termini removed using DNA polymerase I (Klenow fragment) in the presence of four dNTPs. The products were then digested to completion with *Bam*HI, and the 2,334-bp fragment representing 375 base pairs of pBR322 and all but 42 nucleotides of the coding region of pp60^{src} was isolated. The two isolated fragments were ligated to each other using T4 DNA ligase and transformed into *E. coli* 294 (ref. 33). Transformants were selected on LB plates containing 5 $\mu g\ ml^{-1}$ tetracycline (Tc) and screened for recombinant plasmid DNA by digestion with restriction enzymes. (Enzymes were from either New England Biolabs or BRL and were used according to manufacturer's instructions.)

To characterize this protein further, we labelled cultures of *E. coli* transformed with either pBR322 or pSRCex16 with ^{35}S-methionine, and prepared lysates for immunoprecipitation. The specificity and efficacy of this procedure have been well documented[3,5]. Figure 3*a* illustrates that antiserum reactive against pp60^{src} (TBR serum) specifically precipitated a protein of 60,000 M_r from labelled extracts derived from the 294/pSRCex16 culture (lane d). No corresponding protein was seen with control serum, nor was this protein precipitated when TBR serum was used with an extract derived from a 294/pBR322 culture (lane b). As a further test of specificity, we analysed the bacterially derived 60,000-M_r protein by partial hydrolysis with the V8 protease of *Staphylococcus aureus*, according to the procedure of Cleveland *et al.*[24]. The digestion products of bacterially produced p60 are virtually identical to those of RSV-encoded pp60 produced in transformed vertebrate cells, when analysed either by ^{35}S-methionine labelling or by Coomassie blue staining (A.D.L. and Hermann Oppermann, unpublished data).

There is much evidence which suggests that the protein kinase activity observed in preparations of pp60^{src} purified from RSV-transformed vertebrate cells represents an inherent property of the protein[14,15,25]; direct evidence, however, has proved elusive. We therefore assessed the enzymatic activity of bacterially derived p60. We prepared lysates of recombinant *E. coli* strains

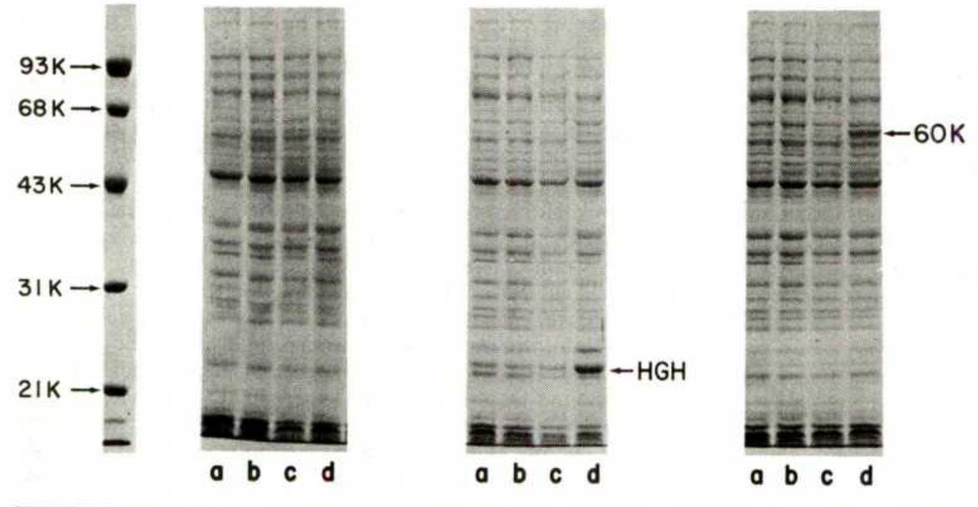

Fig. 2 Analysis of total cellular proteins in *E. coli* transformed with recombinant vectors. *E. coli*, transformed with pBR322 (*a*), pHGH207-1 (*b*), or pSRCex16 (*c*) were grown to $A_{550} = 0.25$ (lanes a, c) or $A_{550} = 1.0$ (lanes b, d) in rich medium (lanes a, b) or minimal medium (lanes c, d) and total cell lysates from 3×10^7 cells were prepared for SDS-gel electrophoresis[34] as described elsewhere[20]. Proteins were visualized by Coomassie blue staining. Molecular weight markers (obtained from BioRad) were electrophoresed in parallel. K represents 1,000 M_r.

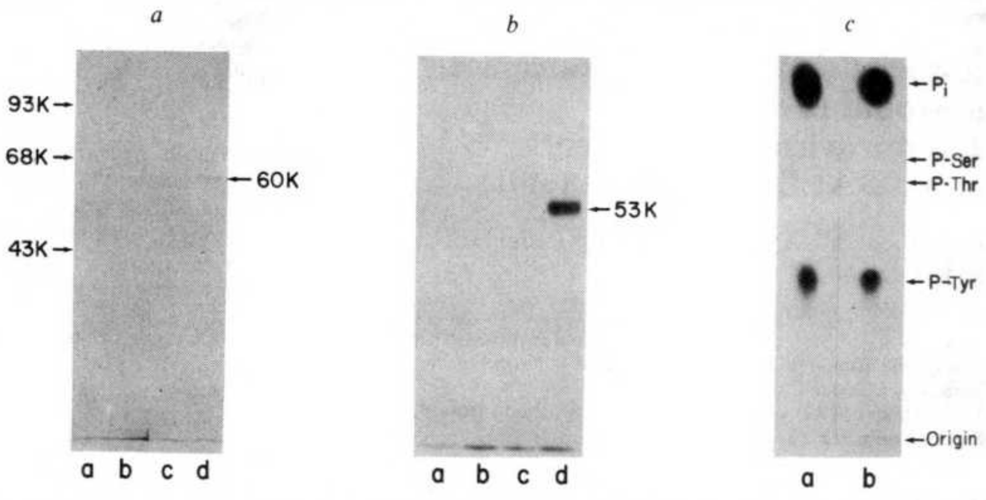

Fig. 3 Analysis of *E. coli* strains transformed with recombinant vectors. *a*, Immunoprecipitation of p60 synthesized by *E. coli*. Cultures (2 ml) of *E. coli* strains transformed with either pBR322 (lanes a, b) or pSRCex16 (lanes c, d) were grown to $A_{550} = 1.0$ in M9 medium (10^9 cells) containing 5 μg ml^{-1} tetracycline, pelleted, washed, re-pelleted and suspended in 2 ml of M9 supplemented with 0.2% glucose, 1 μg ml^{-1} thiamine, 20 μg ml^{-1} standard amino acids (except methionine, which was 2 μg ml^{-1} and tryptophan which was excluded) 5 μg ml^{-1} tetracycline and 20 μCi ml^{-1} ^{35}S-methionine (1,200 Ci mmol^{-1}; NEN). After incubation at 37 °C for 30 min, bacteria were pelleted, resuspended in 0.2 ml 25% sucrose, 50 mM Tris *p*H 8.0. Lysozyme was added to 1 mg m^{-1}. After incubation at 4 °C for 10 min, the extract was adjusted to 0.5% NP-40, 0.4 M NaCl, 5 mM $MgCl_2$ and DNase added to 100 μg ml^{-1} (Worthington). The extract was incubated at 4 °C for 15 min to reduce the viscosity, clarified by centrifugation at 10,000*g* at 4 °C for 5 min, and 10% of the supernatant immunoprecipitated with normal baby rabbit serum (lanes a, c) or TBR serum (lanes b, d) and analysed by electrophoresis in polyacrylamide gels as described elsewhere[5]. The autoradiogram was exposed for 3 h. *b*, Immunoprecipitation of a *src*-specific protein kinase activity from recombinant *E. coli* strains. Cultures (1 ml) of *E. coli* strains transformed with either PBR322 (lanes a, b) or pSRCex16 (lanes c, d) were grown to $A_{550} = 1.0$ in M9 medium containing 5 μg ml^{-1} tetracycline. The bacteria were pelleted and lysates prepared as in *a*. Samples were immunoprecipitated with normal baby rabbit serum (lanes a, c) or TBR serum (lanes b, d) and IgG kinase assays performed and analysed as described elsewhere[17]. *c*, Identification of amino acids phosphorylated by viral pp60^{src} and bacterially derived p60. Immunoglobulin heavy chains phosphorylated by pp60^{src} from RSV-transformed rat cells[15] (lane a) and p60 isolated from *E. coli* (lane b) (see Fig. 2*b*) were isolated, subjected to partial acid hydrolysis and analysed on cellulose thin-layer plates as described elsewhere[12]; 4,500 c.p.m. from each heavy chain were applied to the origin (marked by an arrow). Autoradiography was performed using a fluorescent screen for 8 h. Markers (P-Ser, phosphoserine; P-Thr, phosphothreonine; P-Tyr, phosphotyrosine) were run as internal standards and visualized by ninhydrin staining. (Phosphoserine and phosphothreonine were from Sigma; phosphotyrosine was provided by H. Oppermann.)

harbouring either pBR322 or the p60 expression plasmid (pSRCex16), and kinase activity capable of phosphorylating anti-pp60^{src} antibody was assayed after purification by immunoprecipitation as described elsewhere[5]. Figure 3*b* (lane d) demonstrates that such a protein kinase activity is present in bacteria expressing p60. No activity was present in bacteria not synthesizing p60 (lanes a, b), nor was activity observed in either case when normal serum was used (lanes a, c).

Previous evidence[12–15] has indicated that the kinase activity associated with pp60^{src} phosphorylates acceptor proteins at tyrosine residues rather than at serine and threonine residues, which more typically serve as targets of protein kinase action. To examine the substrate specificity of p60 produced in *E. coli*, we characterized the amino acid on the IgG molecule phosphorylated by bacterially derived preparations of p60. ^{32}P-labelled IgG was isolated and subjected to acid hydrolysis, and the resulting free amino acids separated by TLC[12]. Figure 3*c* reveals that all detectable incorporation of label into antibody occurred at tyrosine residues following reactions using either pp60^{src} derived from RSV-transformed rat cells[15] as a control[12] (lane a), or p60 derived from *E. coli* (lane b). We have attempted to label *E. coli* harbouring the p60 expression plasmid with ^{32}P *in vivo* to identify possible bacterial targets of p60 action, but have so far been unsuccessful. Similarly, we have been unable to detect any 'self' phosphorylation of p60 *in vivo*.

The specificity of the IgG kinase assay has been well documented[5,11,16,17], and has provided the basis for the conclusion that pp60^{src} possesses protein kinase activity. However, the possibility that pp60^{src} specifically interacts with and activates a cellular protein kinase responsible for this activity has not been excluded. Our demonstration that bacterially derived p60 also exhibits protein kinase activity addresses this issue, as given the considerable evolutionary divergence between bacteria and vertebrates, and more specifically the lack of any detectable homology between the *src* gene and DNA from *E. coli*[19], we would expect no specific interaction between the avian gene product (p60) and protein kinases of *E. coli*. Furthermore, *E. coli* has been reported to exhibit no[26–28], or only a very low level[29–31] of protein kinase activity that is specific for phosphorylation at serine and threonine residues[29,30]. We therefore consider that this demonstration of tyrosine-specific protein kinase activity in a highly purified bacterially derived preparation of p60 lends considerable support to the conclusion that this enzymatic activity represents an intrinsic property of the molecule.

We thank J. M. Bishop for providing the pSRC-RI clone and for helpful discussions, H. Opperman for TBR sera and assistance with the phosphoamino acid analysis, F. Fields for technical assistance, D. Goeddel and D. Kleid for advice, and R. Swanson for support and encouragement.

Note added in proof: Since the submission of this letter, similar results have been published by Gilmer and Erikson[35].

Received 30 October; accepted 4 December 1981.

1. Hanafusa, H. in *Comprehensive Virology* Vol. 10, 401–483 (Plenum, New York, 1977).
2. Vogt, P. K. in *Comprehensive Virology* Vol. 10, 341–455 (Plenum, New York, 1977).
3. Brugge, J. S. & Erikson, R. L. *Nature* **269**, 346–348 (1977).
4. Purchio, A. F., Erikson, E., Brugge, J. S. & Erikson, R. L. *Proc. natn. Acad. Sci. U.S.A.* **75**, 1567–1571 (1978).
5. Levinson, A. D., Oppermann, H. O., Levintow, L., Varmus, H. E. & Bishop, J. M. *Cell* **15**, 561–572 (1978).
6. Collett, M. S. *et al. Proc. natn. Acad. Sci. U.S.A.* **76**, 3159–3163 (1979).
7. Willingham, M. C., Jay, G. & Pastan, I. *Cell* **18**, 125–134 (1979).
8. Kruger, J. G., Wang, E. & Goldberg, A. R. *Virology* **101**, 25–49 (1980).
9. Courtneidge, S. A., Levinson, A. D. & Bishop, J. M. *Proc. natn. Acad. Sci. U.S.A.* **77**, 3783–3787 (1980).
10. Levinson, A. D., Courtneidge, S. A. & Bishop, J. M. *Proc. natn. Acad. Sci. U.S.A.* **78**, 1624–1628 (1981).
11. Collett, M. S. & Erikson, R. L. *Proc. natn. Acad. Sci. U.S.A.* **75**, 2021–2024 (1978).
12. Hunter, T. & Sefton, B. M. *Proc. natn. Acad. Sci. U.S.A.* **77**, 1311–1315 (1980).
13. Sefton, B. M., Hunter, T., Beemon, K. & Eckhart, W. *Cell* **20**, 807–816 (1980).
14. Collett, M., Purchio, A. F. & Erikson, R. L. *Nature* **285**, 167–169 (1980).
15. Levinson, A. D., Oppermann, H. O., Varmus, H. E. & Bishop, J. M. *J. biol. Chem.* **255**, 11973–11980 (1980).
16. Collett, M. S., Brugge, J. S. & Erikson, R. L. *Cell* **15**, 1363–1369 (1978).
17. Oppermann, H. O., Levinson, A. D., Varmus, H. E., Levintow, L. & Bishop, J. M. *Proc. natn. Acad. Sci. U.S.A.* **76**, 1804–1808 (1979).
18. Karess, R. E., Hayward, W. S. & Hanafusa, H. *Proc. natn. Acad. Sci. U.S.A.* **76**, 3154–3158 (1979).
19. Spector, D., Varmus, H. E. & Bishop, M. J. *Proc. natn. Acad. Sci. U.S.A.* **75**, 4102–4106 (1978).
20. Goeddel, D. G. *et al. Nature* **281**, 544–548 (1979).
21. De Boer, H. A. *et al.* in *Promoters, Structure and Function* (eds Chamberlain, M. J. & Rodriguez, R.) (Praeger Scientific, 1981).
22. Czernilofsky, A. P. *et al. Nature* **287**, 198–203 (1980).
23. Yanofsky, C. *Nature* **289**, 751–758 (1981).
24. Cleveland, D. W. *et al. J. biol. Chem.* **252**, 1102–1106 (1977).
25. Erikson, R. L., Collett, M. S., Erikson, E. & Purchio, A. F. *Proc. natn. Acad. Sci. U.S.A.* **76**, 6260–6264 (1979).
26. Rubin, C. S. & Rosen, O. M. *A. Rev. Biochem.* **44**, 831–887 (1975).
27. Rahmsdorf, H. J. *et al. Proc. natn. Acad. Sci. U.S.A.* **71**, 586–589 (1974).
28. Khandelwal, R. L., Spearman, T. N. & Hamilton, I. R. *FEBS Lett.* **31**, 246–252 (1973).
29. Wang, J. & Koshland, D. E. *J. biol. Chem.* **253**, 7605–7608 (1978).
30. Garnak, M. & Reeves, H. C. *J. biol. Chem.* **254**, 7915–7920 (1979).
31. Wang, J. & Koshland, D. E. *J. biol. Chem.* **256**, 4640–4648 (1981).
32. Smith, H. *Meth. Enzym.* **65**, 371–380 (1980).
33. Backman, K., Ptashne, M. & Gilbert, W. *Proc. natn. Acad. Sci. U.S.A.* **73**, 4174–4178 (1976).
34. Laemmli, U.K. *Nature* **227**, 680 (1970).
35. Gilmer, T. M. & Erikson, R. L. *Nature* **294**, 771–773 (1981).

Association between a transposed α-globin pseudogene and retrovirus-like elements in the BALB/c mouse genome

Kira Lueders*, Aya Leder†, Philip Leder†‡ & Edward Kuff*

* Laboratory of Biochemistry, National Cancer Institute, and
† Laboratory of Molecular Genetics, National Institute of Child Health and Human Development, National Institutes of Health, Bethesda, Maryland 20205, USA
‡ Department of Genetics, Harvard Medical School, Boston, Massachusetts 02115, USA

Mice have three functional α-globin genes and two closely related pseudogenes[1-5]. In BALB/c mice, the functional genes are known to be clustered on chromosome 11, but the pseudogenes, designated $\alpha\psi3$ and $\alpha\psi4$, are located on chromosomes 15 and 17, respectively[5]. One of the pseudogenes, $\alpha\psi3$, has precisely lost the intervening sequences characteristic of the functional genes[3,4], as if it had been generated from a processed RNA intermediate. It has been suggested that retroviral functions could have been instrumental in the formation of this 'spliceless' pseudogene[6] and its integration at a novel chromosomal locus[5]. We report here that retrovirus-like elements are located on both sides of the $\alpha\psi3$ gene.

The genome of *Mus musculus* contains, in addition to endogenous type B and C retroviral genes, 1,000–2,000 copies of retrovirus-like elements related to the mouse intracisternal type A particle (IAP)[7-10]. The IAP-related sequences are associated with many if not all of the mouse chromosomes[7]. We have isolated multiple examples of IAP genes from BALB/c DNA as recombinants in λ phage Charon 4A[9,10]; a common form is about 7.3 kilobases (kb) long, colinear with the IAP 35S genomic RNA and bounded by 0.3–0.4 kb of terminal repeated sequences (LTRs). Deleted forms of the IAP genetic units have also been observed[8,10].

As IAP genes are abundant and widely distributed throughout the mouse genome, and as integrated retroviruses can have important effects on nearby genetic elements[11], we (K.K.L. and E.L.K.) have been systematically searching for proximities between IAP and other known mouse genes. Originally, we found IAP-related sequences associated with 1% of recombinants in a mouse genomic library consisting of ~15 kb inserts in λ phage[9]. Since then, we have tested 98 recombinants selected because they contained an identifiable mouse gene (unrelated to IAP genes). Five of these clones gave positive reactions when the DNAs were spotted on nitrocellulose membranes and hybridized with ^{32}P-labelled DNA prepared from an isolated IAP gene, MIA14 (refs 9, 10). Among 13 recombinants containing the various α-globin genes and pseudogenes[5], positive reactions were confined to 2 containing the $\alpha\psi3$ sequences. As described below, the spatial relationships between IAP and pseudogene regions were then determined by examining heteroduplexes between these clones and two representative recombinants that contain IAP genes in known orientation and position with respect to the λ arms[9].

Some structural aspects of the recombinants used for heteroduplexing are indicated in Fig. 1*a*, *b*. The IAP isolates do not share flanking sequences and have no known topographical relationship to one another. The two $\alpha\psi3$-containing clones represent overlapping fragments that span about 22 kb of the mouse genome[5]. In $\alpha\psi3$-1, a deletion (Δ) has interrupted the pseudoglobin sequence and brought the truncated gene into juxtaposition with DNA sequences that are located at some distance downstream in the intact genome. In $\alpha\psi3$-2, the original relationships of the $\alpha\psi3$ gene to its flanking sequences have been maintained; this clone shares sequences with $\alpha\psi3$-1 in the region of overlap to the left of the pseudogene (see also Fig. 1*g*).

Representative heteroduplexes are shown in Fig. 1*c*, *d*, while

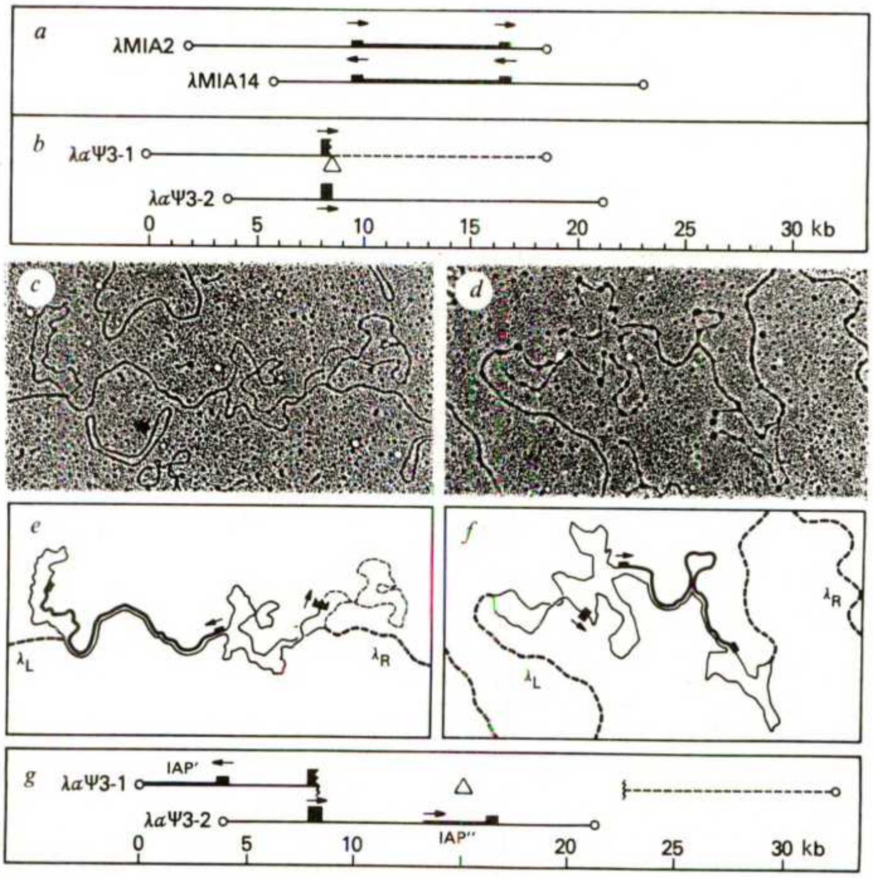

Fig. 1 Heteroduplex mapping of IAP sequences in BALB/c genomic clones containing the pseudo α-globin gene $\alpha\psi3$. The cloned genomic fragments were derived from mouse embryo DNA by partial *Hae*III digestion and inserted into λ Charon 4A via *Eco*RI linkers. All the inserts are shown in the same orientation with respect to the phage arms, that is, with the left arm towards the left of the figure. The 5′–3′ orientations of the genes themselves are indicated by arrows. The λ arms are not shown. The heteroduplexes were prepared and examined as described previously[9,10]. *a*, Diagrams of two previously mapped recombinants[9,10] containing 7.3 kb IAP genes in opposite orientations. The IAP sequences are indicated by heavy lines with thickened ends representing the LTRs. The flanking sequences in the two clones (thin lines) are unrelated. *b*, Two recombinants known[5] to contain $\alpha\psi3$ gene sequences (filled bars) in the indicated locations. The cloned fragments represent overlapping segments from the same region of the mouse genome[5]; however, in $\lambda\psi3$-1, a cloning deletion (Δ) has interrupted the $\alpha\psi3$ gene (jagged edge) and brought it into continuity with more distant downstreams flanking sequences (light broken line). *c*, Typical heteroduplex between $\lambda\alpha\psi3$-1 and λMIA14. A relaxed SV40 DNA molecule (*) provides a 5.2 kb size standard. *d*, Heteroduplex between $\lambda\alpha\psi3$-2 and λMIA2. *e*, *f*, Semi-diagrammatic representations of the heteroduplexes in *c* and *d*, respectively, showing the known positions of the IAP and $\alpha\psi3$ sequences on the individual strands. The λ arms are indicated by heavy broken lines. *g*, The two $\alpha\psi3$-containing clones, showing the positions and orientations of the IAP sequence elements. In $\lambda\alpha\psi3$-1, the presence of the cloning deletion (Δ) is indicated and the right-hand flanking sequences are detached to show that they occupy a position downstream in the intact mouse genome[5].

0028-0836/82/050426—03$01.00

Fig. 1*e*, *f* show the individual strands of each heteroduplex, on which we have indicated the known locations of the IAP and pseudoglobin sequences. In Fig. 1*c*, *e*, the $\lambda\alpha\psi3$-1 strand shows 4 kb of homology with the IAP gene in λMIA14 before being interrupted at the junction with the λ arm. The IAP and $\alpha\psi3$ sequences in this clone have opposed 5'–3' orientations. $\lambda\alpha\psi3$-2 also has a major region of homology with the IAP gene in λMIA2 (Fig. 1*d*, *f*). The IAP sequences in this clone show two major alterations with respect to the complete IAP gene; one involves the loss of 0.8–1 kb of 5' sequence including the 5' LTR; the other represents the deletion of 3 kb of internal sequence. It is unlikely that these deletions are artefacts produced in cloning because deletions of similar size and position have been seen in several other IAP gene isolates[8,10]. In fact, three of the other IAP genes found in association with known mouse genes contained deletions (K.K.L. and E.L.K., unpublished observations). Figure 1*g* summarizes the locations of the IAP and $\alpha\psi3$ sequences in the $\lambda\alpha\psi3$ clones. The structures of the clones as deduced from the heteroduplexes were confirmed by restriction enzyme analysis and hybridization with specific probes derived from selected regions of the IAP gene (data not shown).

Figure 2*a* shows a reconstruction of the genomic region encompassing the $\alpha\psi3$ gene in BALB/c mice. This putative arrangement, in which the gene is bracketed at a distance of ~4 kb on either side by IAP sequences (IAP' and IAP"), was verified by direct restriction analysis of cellular DNA. The individual $\alpha\psi3$-containing clones were first mapped with respect to several restriction endonuclease sites and these sites were positioned on the reconstructed genomic segment (Fig. 2*b*). The predicted restriction fragments were then sought in digests of BALB/c embryo DNA using hybridization probes (see Fig. 3 legend) derived from the 4.7 kb $\alpha\psi3$-containing *Eco*RI fragment shown in Fig. 2*b*. The results (Fig. 3) were entirely consistent with the proposed gene order. The 11.5 kb *Sst*I fragment provided the most direct evidence for this arrangement because it is defined by sites located in the two IAP sequences themselves (Fig. 2). *Sst*I fragments of the same size were detected with the $\alpha\psi3$ probe in the DNAs from several other mouse strains and cell types (livers of AKR/N, C3H, A, C57BL and NIH Swiss mice, BALB/c myeloma and 3T3 fibroblasts), suggesting that the gene order may be a general property of *M. musculus* laboratory strains and is relatively stable in conditions of continued cell division.

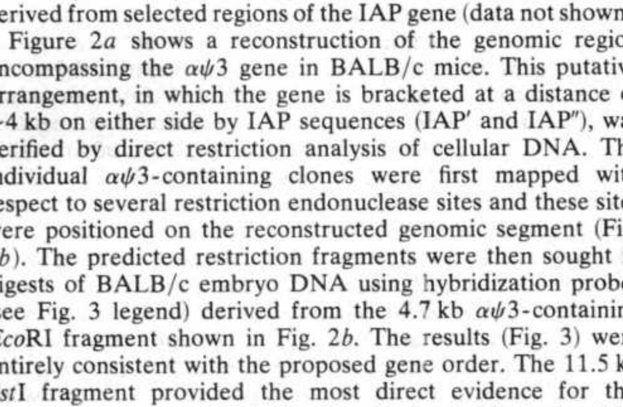

Fig. 2 Putative arrangement of $\alpha\psi3$ and IAP sequences in the BALB/c genome and some restriction endonuclease fragments predicted from this arrangement. *a*, The continuous bar represents a 23 kb segment of genomic DNA reconstructed from the two individual $\alpha\psi3$ clones shown in Fig. 1g. The expanded gene sequences at the top show the positions of the IAP LTRs and the two deletions in IAP". The vertical broken lines in the $\alpha\psi3$ gene indicate the positions of two intervening sequences found in the closely related functional adult α-globin genes but absent in this pseudogene[3]. *b*, Putative locations of *Sst*I, *Pvu*II, *Bst*EII and *Eco*RI restriction endonuclease sites in the regions flanking the $\alpha\psi3$ gene. The individual $\lambda\alpha\psi3$ clones were first mapped with respect to the enzymes, using probes derived from the 4.7 kb $\alpha\psi3$-containing *Eco*RI fragment separately cloned in λgtWES[3]. When these sites were then positioned on the reconstructed genomic region, they yielded the indicated set of predicted fragments.

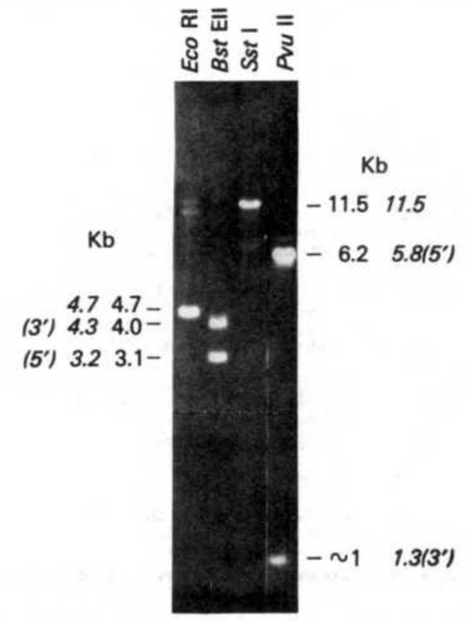

Fig. 3 Comparison of observed genomic restriction endonuclease fragments with those predicted from the sequence arrangement shown in Fig. 2. BALB/c embryo DNA was digested to completion with the indicated enzymes and digests equivalent to 20 μg of DNA were applied to each lane for electrophoresis in 1.2% agarose gels. After transfer to nitrocellulose membranes the fragments were hybridized sequentially with ^{32}P-labelled fragments derived by *Bst*EII cleavage of the 4.7 kb $\alpha\psi3$-containing *Eco*RI fragment (cloned in λgtWES) shown in Fig. 2*b*. The blots were autoradiographed after each hybridization step. In this way, the reactive fragments in the *Bst*EII and *Pvu*II genomic digests were identified in terms of their 5' or 3' position with respect to the $\alpha\psi3$ gene. The observed sizes of the reactive restriction fragments are shown in upright numerals, the predicted sizes in italics.

Retroviruses are known to acquire and transmit cellular genes[6,12,13] and Goff *et al.*[6] have emphasized that such transfer can result in the loss of intervening sequences within the acquired gene after one cycle of virus infection. The topographical relationships shown in Fig. 2 lead us to ask whether IAPs could have had a role in generating the $\alpha\psi3$ gene and/or bringing it to its present location. Because the observed organization of the IAP sequence elements on either side of the $\alpha\psi3$ gene does not permit us to construct a straightforward model for the events in question, it cannot be ruled out that the observed spatial association is fortuitous. On the other hand, although IAPs are not horizontally infectious, they do have several retrovirus-like properties, and their LTRs have a retroviral type of organization[10,14] and contain signal sequences appropriate for the initiation and termination of RNA transcription (L. A. Smith and E. L. Kuff, unpublished observations). In addition, IAPs are expressed in pre-implantation embryos[15–17], that is, at a developmental stage that would facilitate integration of a recombinant provirus into germ-line DNA.

Perhaps the evolutionary aspects of the situation offer the best hope of resolving this problem. It has been estimated that a functional precursor of the α3 pseudogene may have been generated about 24 Myr ago and eventually become inactive as long ago as 17 Myr[18]. Even allowing for major uncertainties inherent in such calculations, these intervals are large with respect to the estimated time of divergence of mouse and rat species from a common ancestral form[19,20]. IAP-related sequences are found not only in these[21,22] but in other more distant rodent species such as gerbil and Syrian hamster[23], so that it is likely that IAP genes or their evolutionary precursors were extant at the time the ancestral α3 pseudogene was formed. Comparative observations using gene libraries prepared from other species may clarify the possible role of IAPs in the evolution of the pseudo α-globin gene.

Note added in proof: Evidence has recently been obtained for the presence of $\alpha\psi3$ genes in the DNAs of other species of *Mus* and of other more distantly related rodents such as rat, gerbil and hamster (R. Taub and A. Leder, unpublished observations).

Received 17 August; accepted 24 November 1981.

1. Leder, P. *et al. Science* **209,** 1336–1342 (1980).
2. Nishioka, Y. & Leder, P. *Cell* **18,** 875–882 (1979).
3. Nishioka, Y., Leder, A. & Leder, P. *Proc. natn. Acad. Sci. U.S.A.* **77,** 2806–2809 (1980).
4. Vanin, E. F., Goldberg, G. I., Tucker, P. W. & Smithies, O. *Nature* **286,** 222–226 (1980).
5. Leder, A., Swan, D., Ruddle, F., E'Eustachio, P. & Leder, P. *Nature* **293,** 196–200 (1981).
6. Goff, S. P., Gilboa, E., Witte, O. N. & Baltimore, D. *Cell* **22,** 777–785 (1980).
7. Lueders, K. K. & Kuff, E. L. *Cell* **12,** 963–972 (1977).
8. Ono, M., Cole, M. D., White, A. T. & Huang, R. C. C. *Cell* **21,** 465–473 (1980).
9. Lueders, K. K. & Kuff, E. L. *Proc. natn. Acad. Sci. U.S.A.* **77,** 3571–3575 (1980).
10. Kuff, E. L., Smith, L. A. & Lueders, K. K. *Molec. cell. Biol.* **1,** 216–227 (1981).
11. Neel, B. G., Hayward, W. S., Robinson, H. L., Fang, J. & Astrin, S. M. *Cell* **23,** 323–334 (1980).
12. Scolnick, E. M. & Parks, W. P. *J. Virol.* **13,** 1211–1219 (1974).
13. Halpern, C. C., Haywood, W. S. & Hanafusa, H. *J. Virol.* **29,** 91–101 (1979).
14. Cole, M. D., Ono, M. & Huang, R. C. C. *J. Virol.* **38,** 680–687 (1981).
15. Biczysko, W., Pienkowski, M., Solter, D. & Koprowski, H. *J. natn. Cancer Inst.* **51,** 1041–1051 (1973).
16. Calarco, P. G. & Szollosi, D. *Nature new Biol.* **243,** 91–93 (1973).
17. Chase, D. G. & Pikó, L. *J. natn. Cancer Inst.* **51,** 1971–1973 (1973).
18. Miyata, T. & Yasunaga, T. *Proc. natn. Acad. Sci. U.S.A.* **78,** 450–453 (1981).
19. Benveniste, R. E., Callahan, R., Sherr, C. J., Chapman, V. & Todaro, G. *J. Virol.* **21,** 849–862 (1977).
20. Callahan, R. & Todaro, G. in *Origins of Inbred Mice* (ed. Morse, H. C. III) 689–713 (Academic, New York, 1978).
21. Kuff, E. L., Lueders, K. K. & Scolnick, E. M. *J. Virol.* **28,** 66–74 (1978).
22. Callahan, R., Kuff, E. L., Lueders, K. K. & Birkenmeier, E. *J. Virol.* **40,** 901–911 (1981).
23. Lueders, K. K. & Kuff, E. L. *Nucleic Acids Res.* **9,** 5917–5930 (1981).

Structural alterations in J regions of mouse immunoglobulin λ genes are associated with differential gene expression

Jim Miller, Erik Selsing & Ursula Storb

Department of Microbiology and Immunology, University of Washington, Seattle, Washington 98195, USA

Immunoglobulin λ light chains in the mouse comprise three types: λ1, λ2 and λ3 (refs 1–3 respectively) and are encoded by three constant region (Cλ) and two variable region (Vλ) genes. The Cλ2 and Cλ3 protein sequences differ at only 5 amino acid positions whereas Cλ1 differs from both by about 30 amino acids. The Cλ1 and Cλ3 genes are closely linked[4], separated by ~3 kilobases (kb) of DNA. The Cλ2 gene is closely linked to a Cλ4 gene, but is an unknown distance from the Cλ3–Cλ1 cluster[4,5]. Although the Cλ4 gene shares homology with Cλ1, we show here that it represents a pseudogene. Only two germ-line V genes appear to be expressed in mouse λ chains: Vλ1 is used in association with either Cλ1 (ref. 1) or Cλ3 (ref. 6), while Vλ2 has only been found with Cλ2 (ref. 2). Differential gene expression is observed in the λ locus. Among mouse serum antibodies, λ1 chains occur 10 times more frequently than λ2 (ref. 7) or λ3 (ref. 3) chains while λ4 chains have not been identified. We have now searched for structural differences between Cλ genes which could explain this differential expression. Our nucleotide sequence analysis indicates that Cλ4 is not expressed due to an inactive RNA splice site. Although no structural defects were found in Cλ2 or Cλ3, substitutions in the rearrangement recognition sequences associated with Jλ2 and Jλ3 segments, together with nearby competing pseudo recognition sequences, may explain the relatively low levels of Cλ2 and Cλ3 gene expression.

Immunoglobulin gene expression requires the recombinational joining of V and C gene segments via a small joining (J) DNA segment[8–11]. J segments characteristically display V–J joining and RNA splicing recognition sequences separated by a short coding sequence (13 amino acids). We have found J segments 1.2–1.4 kb 5′ of each Cλ gene (Fig. 1). In each Jλ segment, sequences showing homology to V–J joining and RNA splice sites are observed (Fig. 2). In the Jλ1, Jλ2 and Jλ3 genes the coding sequences correspond exactly to the J peptide segments in λ1, λ2 and λ3 light chains respectively (refs 2, 12 and H. Eisen, personal communication).

The J region associated with Cλ4 was of particular interest because λ4 proteins have not been observed among mouse light chains; comparison of the Jλ4 sequence with the closely homologous Jλ1 sequence suggests an explanation for this observation (Fig. 2). Relative to Jλ1, Jλ4 has both a deletion of two nucleotides near the beginning of the coding sequence and a nucleotide substitution in a critical position of the RNA splice site. The substitution changes the G-T, found in all 5′ intron sequences[13], to an A-T. Even if this unconventional splice site (*a* in Fig. 2) were used, the 2-base pair (bp) deletion at the beginning of Jλ4 would result in a shortened, and possibly nonfunctional, mRNA. A possible alternative splice site for Jλ4 (*b* in Fig. 2) results in termination codons in all mRNA reading frames, either in Jλ4 (Fig. 2) or in Cλ4 (E.S., J.M., R. Wilson and U.S., in preparation). Apparently, rearranged Vλ2–Jλ4–Cλ4 genes would not result in an active mRNA. Thus, Cλ4 represents a nonfunctional pseudogene.

Although the events leading to the inactivation of the Cλ4 gene cannot be ordered unambiguously, it is possible that, like Jκ3 in the κ gene complex[8,9], Jλ4 initially became inactive due to an alteration in its RNA splice site. Subsequent evolutionary drift could have resulted in the 2-bp deletion.

Mouse κ and H chain C genes are associated with four functional and one nonfunctional J gene segment[8–11]. Known λ protein chains only contain one type of J segment: Jλ1 for λ1, Jλ2 for λ2 and Jλ3 for λ3 (refs 12, 2 and H. Eisen, personal communication, respectively). A corresponding J segment is present 5′ of each of the Cλ genes (Fig. 1). No additional J segments were found in the regions 250–350 bp 3′ of Jλ1, Jλ2, Jλ3 or Jλ4, that is, at the distance J segments are spaced in κ and H chain genes.

However, there is another J-like region 601 nucleotides 3′ from the end of Jλ3 (see Fig. 1). Identified by sequences homologous to V–J recombination and RNA splice sites, this J also contains a potential coding region of the appropriate length, in which all three possible reading frames are open (Fig. 2). Nevertheless, certain characteristics of J regions are missing. First, the recognition sequence contains a poorly matched heptamer. Second, the nucleotides in the potential coding region have little resemblance to those of known J segments. Furthermore, this resemblance is no greater when these nucleotides are translated into amino acids in any of the three open reading frames. We conclude that this is a pseudo J region (ψJλ3). ψJλ3 differs in structure from the recently detected ψJH, which contains in-phase termination codons[10].

Although we find a pseudo J sequence associated with Cλ3, in the analogous position relative to Cλ2 there is no well matched V–J recombination or RNA splice site (d (downstream) Jλ2 in Fig. 2). Sequences similar to V–J joining sites are found 117 and 113 bp 3′ of Jλ1 and Jλ4 (dJλ1 and dJλ4 in Figs 1, 2). It appears possible, therefore, that, like Cκ and CH genes, Cλ genes once had associated multiple Jλ sequences but these have been partially lost during evolution.

Do the primary DNA sequences of λ genes suggest a basis for the differential serum concentrations found for λ1, λ2 and λ3 protein chains? Comparison of Cλ1 and Cλ3 is most straightforward because both are associated with Vλ1 in the respective light chains. As only the very conservative substitutions, Trp–Val in Jλ1 compared with Phe–Ile in Jλ3, are found in the third hypervariable region[14] of germ-line λ1 and λ3 genes (Fig. 2), it seems unlikely that differential expression of λ1 and λ3 results from different affinities for antigen. In addition, we have found normal RNA splicing and translation termination signal sequences associated with Cλ2 and Cλ3 as well as with Cλ1 (the sequencing strategy for the Cλ genes is shown in Fig. 1; data will be presented elsewhere: E.S., J.M., R. Wilson and U.S., in preparation). Thus, the low levels of Cλ2 and Cλ3 proteins in mouse serum are not due to any apparent faulty processing signals associated with the Cλ2 and Cλ3 exons.

Although preferential association of the Cλ1 protein region with CH regions cannot be ruled out, structural features in the DNA sequences flanking the J genes could explain the differential gene expression. All J segments associated with mouse κ[8,9], H[10,11] and λ[15] genes and human κ genes (P. Hieter, J. Maizel and

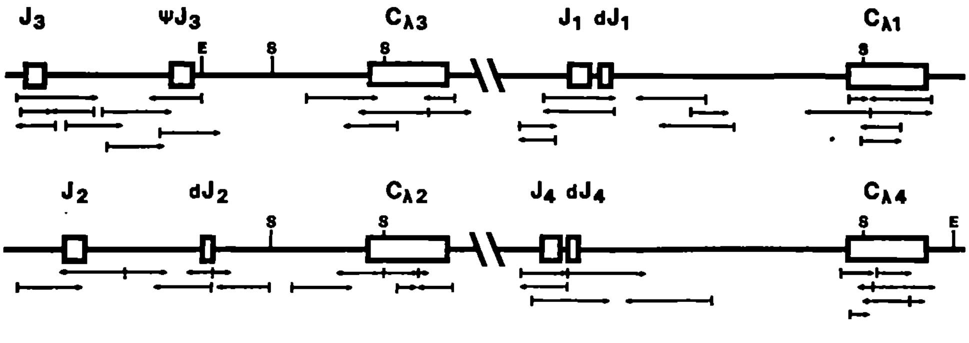

Fig. 1 Organization and sequence analysis of the four Cλ genes. Sequencing strategy of the four Cλ genes and their corresponding J regions (open boxes). Clones containing either the Cλ3–Cλ1 (ref. 4) or the Cλ2–Cλ4 (E.S., J.M., R. Wilson and U.S., in preparation) gene clusters were obtained from a BALB/c kidney DNA library. The distance between Cλ3 and Cλ1 is 3.2 kb, that between Cλ2 and Cλ4 is 3.0 kb. The sequence was determined by the dideoxynucleotide termination method[22] as described previously[23] or in conjunction with M13 cloning vectors[24]. The direction and extent of the sequence determinations are indicated by arrows. The pseudo (ψ) and downstream (d) J regions are described in the text. E, *Eco*RI; S, *Sac*I.

P. Leder, personal communication) are preceded 5′ by two blocks of conserved 'recognition' sequences presumed to be involved in V–J joining: a nanomer with the consensus sequence GGTTTTTGT separated by a spacer of 12 (λ) or 21–24 (κ and H) nucleotides from a heptamer with the consensus sequence CACTGTG. Differences in the Jλ1 and Jλ3 recognition sequences could explain the unequal expression of λ1 and λ3 genes, assuming homology with the consensus recognition sequence determines the frequency of V–J joining. The recognition sequences of both Jλ1 and Jλ3 exhibit three mismatches when compared with the consensus sequence (Fig. 2). However, the mismatches in Jλ3 are all clustered at the 3′ end of the nanomer whereas those in Jλ1 are distributed over both the nanomer and heptamer. No Jκ or JH recognition sequences exhibit multiple mismatches at the 3′ end of the nanomer.

Also striking in the Jλ3 recognition sequence is the presence of 'interfering' nanomers. The ψJλ3 gene possesses a nanomer which shows greater homology to the consensus sequence than does the Jλ3 nanomer. Also, extraneous nanomers occur in the recognition sequence spacers of both Jλ3 and ψJλ3 V–J joining sites (Fig. 2), which are also more homologous with the consensus nanomer than is the functional Jλ3 nanomer. No other JH, Jκ, or Jλ (except Jλ2, see below) exhibits a nanomer sequence in the recognition site spacer. These extra recognition sequences surrounding the Jλ3 region might create substrate competition for putative V–J recombination proteins, which could then interfere with correct recombination to Jλ3, and so decrease the ratio of Vλ1–Jλ3 to Vλ1–Jλ1 rearrangements.

Although it is not known whether λ2 containing immunoglobulins have less affinity for common antigens than those containing λ1, the low level of λ2 expression could result from the same structural defects as in λ3. For example, there are deviations from the consensus sequence clustered at the 3′ end of the Jλ2 nanomer and an interfering nanomer exists in the recognition site spacer which is more closely matched to the consensus than is the Jλ2 nanomer. In addition, Jλ4 and dJλ4 could compete with Jλ2 for Vλ2 rearrangements. As both Jλ4 and dJλ4 lack functional RNA splice sites, any rearrangement into these J regions would lead to a nonfunctional transcription unit. These structural features, in and around Jλ2, could interfere with proper Vλ2–Jλ2 joining and result in decreased expression of λ2.

Jλ1 is also associated with an interfering recognition sequence (dJλ1, see Figs 1, 2). This sequence is not as well matched to the consensus as is Jλ1 and, therefore, less likely to interfere with λ1 expression. Thus, the differential expression of the λ isotypes in normal mouse serum correlates well with the structural integrity of the J region associated with the individual Cλ genes.

The λ gene family not only shows variation in isotype expression, but as a whole represents only 5% of mouse serum immunoglobulin light chains[7,16]. Studies of individual immunoglobulin-producing cells have also indicated that the rearrangement frequency is much lower for λ genes than for κ genes[17,18]. Note that all functional J segments associated with Cλ genes exhibit a 3′-terminal C or G residue in their recognition sequence nanomers. Because this position is invariably a T in all other Jκ and JH segments, it is tempting to speculate that these substitutions might particularly affect the V–J joining rate. However, as several components may differently affect λ and κ genes (such as antigenic selection, specific mechanisms which might rearrange κ genes before λ genes) it would be premature to implicate a specific position in the nanomer sequence. In particular, the ratio of λ and κ rearrangements may only reflect the different numbers of V genes (50–2,000 for κ[19,20] compared

```
                    V-J recombination                                               RNA splice
                    recognition site                                                   site
                     **   **               * ****
Consensus J         GGTTTTTGT                CACTGTG                                      AG|GTRAG

      Jλ1           GTTTTTTGC atgagtctatat  CACAGTG ctgggtgttcggtggaggaaccaaactgactgtcctAG|GTGAG
                                                     TrpValPheGlyGlyGlyThrLysLeuThrValLeuGly

     dJλ1           GCTTTTTGT tgtatactttcc  CTTTCTG tattctgcttcatacctatacttcacactaggtaaagaatttct

      Jλ2           GGTTTTGGG ttgGGTTTTAGT  CATTGTG ttatgttttcggcggtggaaccaaggtcactgtcctAG|GTAAG
                                                     TyrValPheGlyGlyGlyThrLysValThrValLeuGly

     dJλ2           GGATCCCGC tgtttcacatttc CATTGCC agcttctcgttttcctcaaatggcctagtatatgcaggagatca

      Jλ3           GGTTTAGGG ttgGGTTTCAGT  CACTGTG gtttattttcggcagtggaaccaaggtcactgtcctAG|GTAAG
                                                     PheIlePheGlySerGlyThrLysValThrValLeuGly

     ψJλ3           GGATTTTGC tGTTTTGTGTttc CGTTGCC aggttctttttcctcaaatggcctattgtatgcaggAG|GTCAG
                                                    ArgPhePhePheLeuLysTrpProIleValCysArgArg
                                                     GlySerPheSerSerAsnGlyLeuLeuTyrAlaGlyGly
                                                      ValLeuPheProGlnMetAlaTyrCysMetGlnGluVal
                                                                                            a    b
      Jλ4           GTTTTTTGC attagactatat  CAGTGTT gggtgttcggaggtggaaccagattgactgtcctAG|ATGA|GTGAC
                                                    GlyCysSerGluValGluProAspTer
                                                     GlyValArgArgTrpAsnGlnLeuAspCysProArgTer
                                            →         ValPheGlyGlyGlyThrArgLeuThrValLeuAspGlu

     dJλ4           GATTTTTGT tggataatttct  CATTATG tattctacttcatgcctaaacttcactctaggtcgaataatc
```

Fig. 2 Comparison of the λ J region DNA segments. The DNA sequences were obtained as described in Fig. 1 legend. Rearrangement recognition sequences and RNA splice sites are in capital letters. Differences from the consensus sequences (see text) are underlined. *a* And *b* indicate possible RNA splice sites in Jλ4. dJλ1, dJλ2, dJλ4: recognition sequences located 117, 600 and 113 bp respectively 3′ of the beginning of the nanomer preceding Jλ1, Jλ3 and Jλ4. * Indicates positions of the J recognition sequences which are invariant in functional κ and H genes. →, Only reading frame of Jλ4 which, using RNA splice site *a*, would also be open in Cλ4.

with 2 for λ) associated with these families. If recombination occurs equally at λ and κ recognition sites and functional recombinations represent only a portion of these events, then the observed λ/κ rearrangement ratio could merely be a statistical phenomenon. Further investigation will be required to clarify this point.

Our studies suggest that differences in the J regions may have profound effects on the level of immunoglobulin gene expression. In particular, clustering of mismatches at the 3′ end of J gene recognition nanomers and competition by interfering recognition sequences may be important. The degree of alteration of the Jλ regions is well correlated with their respective frequency of expression. Such alterations may also explain the *cis*-dominant defect that results in very low levels of λ1 expression in the SJL mouse strain[21]. In addition, we have found that the J region associated with the Cλ4 gene, whose product has not been found among λ chains, has lost its 3′ RNA splice site by a point mutation. Thus the Jλ4–Cλ4 gene represents a pseudogene. Because each Cλ gene is associated with only a single J region, unlike κ and H chains[8-11], the inactivation of a Jλ region would cause the entire gene to become nonfunctional.

We thank R. Wilson and R. Gelinas for help with M.13 cloning, M. McMullen, P. Engler and J. Voss for the isolation of some of the λ gene containing clones, and B. Arp for some of the DNA sequence. This work was supported by NSF grant PCM78-13205 and NIH grants CA/AI25754 and DE02600. J.M. is supported by NIH training grant GM07270.

Received 9 November; accepted 16 December 1981.

1. Weigert, M. & Riblet, R. *Cold Spring Harb. Symp. quant. Biol.* **41,** 837–846 (1977).
2. Dugan, E.S., Bradshaw, R. A., Simms, E. S. & Eisen, H. N. *Biochemistry* **12,** 5400–5416 (1973).
3. Azuma, T., Steiner, L. & Eisen, H. *Proc. natn. Acad. Sci. U.S.A.* **78,** 569–573 (1981).
4. Miller, J., Bothwell, A. & Storb, U. *Proc. natn. Acad. Sci. U.S.A.* **78,** 3829–3833 (1981).
5. Blomberg, B., Traunecker, A., Eisen, H. & Tonegawa, S. *Proc. natn. Acad. Sci. U.S.A.* **78,** 3765–3769 (1981).
6. Breyer, R., Sauer, R. & Eisen, H. in *ICN-UCLA Symp. molec. cell. Biol.* (eds Janeway *et al.*) (Academic, New York, in the press).
7. Cotner, T. & Eisen, H. N. *J. exp. Med.* **148,** 1388–1399 (1978).
8. Max, E., Seidman, J. & Leder, P. *Proc. natn. Acad. Sci. U.S.A.* **76,** 3450–3454 (1979).
9. Sakano, H., Huppi, K., Heinrich, G. & Tonegawa, S. *Nature* **280,** 288–294 (1979).
10. Gough, N. M. & Bernard, O. *Proc. natn. Acad. Sci. U.S.A.* **78,** 509–513 (1981).
11. Early, P., Huang, H., Davis, M., Calame, K. & Hood, L. *Cell* **19,** 981–992 (1980).
12. Appella, E. *Proc. natn. Acad. Sci. U.S.A.* **68,** 590–594 (1971).
13. Sharp, P. *Cell* **23,** 643–646 (1981).
14. Weigert, M., Gatmaitan, L., Loh, E., Schilling, J. & Hood, L. *Nature* **276,** 785–790 (1978).
15. Bernard, O., Hozumi, N. & Tonegawa, S. *Cell* **15,** 1133–1144 (1978).
16. McIntyre, K. R. & Rouse, M. *Fedn Proc.* **29,** 704 (1970).
17. Hieter, P., Korsmeyer, S., Waldmann, T. & Leder, P. *Nature* **290,** 368–372 (1981).
18. Coleclough, C., Perry, R., Karjalainen, K. & Weigert, M. *Nature* **290,** 372–378 (1981).
19. Cory, S., Tyler, B. & Adams, J. *Molec. appl. Genet.* **1** (in the press).
20. Zeelon, E., Bothwell, A., Kantor, F. & Schechter, J. *Nucleic Acids Res.* **9,** 3809–3820 (1981).
21. Geckler, W., Blomberg, B., dePieval, C. & Cohn, M. *Cold Spring Harb. Symp. quant. Biol.* **41,** 743–748 (1976).
22. Sanger, F., Nicklen, S. & Coulson, A. *Proc. natn. Acad. Sci. U.S.A.* **74,** 5463–5467 (1977).
23. Selsing, E. & Storb, U. *Cell* **25,** 47–58 (1981).
24. Messing, J., Crea, R. & Seeburg, P. *Nucleic Acids Res.* **9,** 309–321 (1981).

Nucleotide sequence of a macronuclear gene for actin in *Oxytricha fallax*

Brian P. Kaine* & Brian B. Speart†

Section of Biological Sciences, Department of Biochemistry,
Molecular and Cell Biology, Northwestern University, Evanston,
Illinois 60201, USA

The hypotrichous ciliated protozoan *Oxytricha fallax* possesses a mechanism for processing its genome into a collection of small, gene-sized, transcriptionally active sections. Macronuclear DNA is arranged as short achromosomal sections, 0.5–22 kilobase pairs (kbp) long, while micronuclear DNA has a typical chromosomal organization[1,2]. Macronuclear DNA is derived from micronuclear DNA by a process of polytene chromosome fragmentation with a resultant decrease in DNA sequence complexity[3,4]. The isolation of intact macronuclear DNA sections enables the study of specific structural units of genetic material that occur naturally in the organism. We have previously described[5] the construction of a recombinant plasmid, pOfACT (1.6), which contains an intact 1.6-kb length of macronuclear DNA (Fig. 1) homologous to a yeast actin gene[6]. We now present the complete nucleotide sequence of the cloned DNA molecule and the derived sequence of the actin protein which it encodes. As the sequence is that of a complete, naturally occurring DNA molecule, it shows all *cis*-active regulatory regions in addition to the coding region. The actin protein encoded differs considerably from other known actins.

The complete nucleotide sequence of the cloned 1.6-kb macronuclear DNA section, determined by the chemical procedure of Maxam and Gilbert[7], is shown in Fig. 2. The overall length of the 1.6-kb insert from plasmid pOfACT(1.6) is 1,561 bp, measured from the *Pst*I cleavage sites which flank the cloned sequence. This length includes the cleavage sites and the polynucleotide tails which were added enzymatically during construction of the plasmid. Incubation of macronuclear DNA with terminal transferase and cloning in *Escherichia coli* added 24 dG bases to the 5′ end and 26 dC bases to the 3′ end of the 1.6-kb section.

DNA sequencing has demonstrated an inverted repeat sequence at both ends of the cloned 1.6-kb macronuclear section. This sequence takes the form of a repeating octanucleotide 3′-GGGGTTTT...5′. Subsequent sequencing of total native macronuclear DNA (A. F. Pluta, B.P.K. and B.B.S., in preparation) has confirmed the presence of this terminal sequence on all macronuclear DNA molecules. Similar sequences have been found at the macronuclear termini of other related species[8,9]. The repeat sequences does not appear at any internal locations in the 1.6-kb clone.

The nucleotide sequence 5′ to the actin-coding region but 3′ to the terminal repeat is 183 bases long. Several possible promoters for RNA polymerase have been identified in this region. Three sequences beginning at positions 8, 137 and 154 (Fig. 2) resemble the 'Hogness box' sequence, TATAAAA. This sequence (or others closely related to it) has been found in 5′ regions flanking numerous eukaryotic genes and is believed to be a transcriptional promoter[10,11]. Surprisingly, the 'Pribnow box' prokaryotic transcriptional promoter sequence, TATGATG[12], occurs at position 20. If this sequence is indeed a functional promoter, it is possible that *O. fallax* possesses an RNA polymerase similar to that of prokaryotic organisms.

A second group of putative regulatory signals resembles the pentanucleotide CCAAT, which has also been implicated in the control of transcription[13]. These sequences occur at positions −2 (beginning with the last two bases of the terminal repeat on the anti-sense strand), 101, 129 and 152 (Fig. 2). A similar sequence, CCAAA, forms part of the terminal repeats upstream from the actin-coding region. The significance, if any, of this sequence occurring in the repeats is unknown.

The DNA sequence 3′ to the termination codon but 5′ to the terminal repeats is 186 bases long. Like the 5′ region, the 3′-flanking region also contains several possible control signals. The pentanucleotide AATAA occurs downstream from the termination codon at positions 1,412 and 1,424. This sequence may be a potential signal for polyadenylation and is commonly found near the end of the 3′-untranslated region of eukaryotic mRNAs[14,15]. A sequence that serves as a transcriptional termination signal for type III genes, TTTT[16], occurs 3′ to the termination codon at position 1,433. This tetranucleotide also occurs as part of the terminal repeats at the 3′ end of the anti-sense strand. As with the CCAAA pentanucleotide in the 5′-terminal repeats, it is unknown whether the TTTT tetranucleotide in the 3′ repeats has an actual role in RNA synthesis.

The 3′-flanking region contains a sequence similar to that

---

* Present address: Department of Genetics and Development, University of Illinois, Urbana, Illinois 61801, USA.

† To whom reprint requests should be addressed.

0028-0836/82/050430—03$01.00

Fig. 1 Restriction map of plasmid pOfACT(1.6). The restriction sites shown are those used in sequencing. ■, *O. fallax* actin-coding sequence; □, *O. fallax* non-coding sequence; ——, pBR322 sequence. Sizes are shown in base pairs.

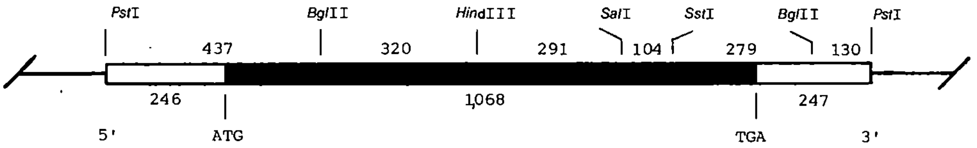

found near the origin of DNA replication on the polyoma virus chromosome. The sequence in *O. fallax*, between positions 1409 and 1436, consists of the palindromic sequence TTTAATAATTT (1,409–1,419) and an adjacent 15-base sequence, AAAATAACTTATTTT (1,422–1,436), capable of forming a self-complementary hairpin loop. The polyoma virus sequence consists of an A+T-rich palindrome located near a 15-base G+C-rich hairpin[17]. Recently, several stretches of DNA referred to as autonomously replicating sequences (ARS) have been isolated[18]. When linked to a bacterial plasmid, these elements are capable of replication in yeast. The sequence of one ARS element contains an 18-base A+T-rich region of perfect symmetry which is capable of forming a hairpin loop[19]. These similarities suggest that the origin of replication of the *O. fallax* macronuclear DNA molecule may be the region 1,409–1,436.

The overall length of the coding region on the 1.6-kb macronuclear DNA molecule is 1,068 bases from the initiation codon ATG (position 184) to the termination codon TGA (position 1,255). The amino acid sequence encoded (see Fig. 3) has 65.4% sequence homology with that of yeast actin[6], calculated as the number of amino acid residues in common divided by the number of co-linear amino acids. Similarly, the nucleotide sequence homology between the yeast and *O. fallax* actin genes is 65.7%. There are no intervening sequences in the *O. fallax* actin gene. However, this does not rule out the possibility of interruptions in the actin-coding sequence as it exists in the micronuclear DNA; such intervening sequences could be removed during macronuclear development.

The *O. fallax* actin sequence is 356 amino acids long whereas actins from other organisms, including yeast, consist of 374 or 375 amino acids. This is due primarily to the absence of 18 amino acids that, in yeast, would occupy the region containing residues 65–82. Restriction mapping has demonstrated that the corresponding 54-bp deletion occurs in macronuclear DNA as well as in pOfACT(1.6) and thus is not an artefact of cloning. The *O. fallax* actin sequence is also one amino acid shorter at the N terminus than yeast and has one additional internal residue (Leu 258).

The macronuclear gene appears to be expressed, rather than being an inactive pseudogene. *O. fallax* RNA, ranging in size from 7 to 15S, was labelled with ^{32}P and hybridized to pOfACT(1.6) that had been cut with *Pst*I. The RNA hybridized strongly to the *O. fallax* actin sequence but not to pBR322 (Fig. 4). The conditions of hybridization were sufficiently stringent so that the actin DNA could bind only to its homologous RNA sequence[5]. Therefore, the 1.6-kb actin sequence must be transcribed, and we presume that it is also translated, as it has a continuous open reading frame.

```
5'
GGGGGGGGGGGGGGG GGGGGGGGGCCCCAA AACCCCAAAACCCCA AAACCCCAAAACCCC ATAAATCTATATTTT
                                                                1            15

GACGTATGATGATAT GAGAAATATAGTTTA AGTCGAGACTGATTA AAAGGGTAGATTGCG GCAAAATATACGCGT
             30              45              60              75              90

TCGTAATTATCAAAT AAGATTTATTAGGGA AAGATATGCAAATTA ATATAATAATTTATT TCCTATAAATCTTTC
            105             120             135             150             165

TATCTACTACTCGTA CATATGTCAGACCAA CAAACTTGCGTTATT GATAACGGTTCAGGA GTCGTCAAGGCTGGT
            180             195             210             225             240

TTCGCCGGTGAGGAT GCTCCAAGAGCTGTA TTCCCATCAATCGTC GGAAGACCCAAGAAC GTCAGCGCTTTGATC
            255             270             285             300             315

CGTGTTGATTCCGCC TCAGAGTACCTCGGA GATGAAGCCCAACAA AAGAGAGGAGTCCTA AAGATCTGGAACCAC
            330             345             360             375             390

ACCTTCTACGTTGAG CTGAGAGTTCAACCC GATGAGCATCCGATT CTCTTGACTGAGGCC CCACTTAGCCCAAAG
            405             420             435             450             465

ACTAACAGAGAAAAG ATGACTCAAATCATG TTCGAGACTTTCAAT GTCCCCGCTCTCTAC GTTGCCATCCAAGCC
            480             495             510             525             540

GTCTTATCTCTCTAC TCCCGCGGCAGAACA ACCGGTATTGTTTGC GATGCTGGTGATGGT GTTACTCACACCGTC
            555             570             585             600             615

CCCATCTATGAAGGT TTCTCAATCCCACAC GCCGTATCAAGAATC CAACTAGCCGGTAGA GACCTTACCACCTTC
            630             645             660             675             690

TTGCCCAAGCTTTTC ACCGAAAGAGGATAC AACTTCACTTCATCT GCTGAGTTGGAAATC GTTAGAGATATTAAG
            705             720             735             750             765

GAAAAGCTCTGCTTC GTTGCTTTGAACTAC GAGAGTGCCCTTAAG CAATCACACGATAGC TCCCAATTCGAGAAG
            780             795             810             825             840

AACTACGAACTTCCA GATGGAAAGGTTATC ACCATTGGAAGCGAG AGATTCAGATGCCCA GAATATCTCTTCAAG
            855             870             885             900             915

CCACTCGAAATGAAC GGAAGAGAACTCGAC TCTATCCAAGACTTG ACCTACAAATCAATC CAAGAGTGCGACGTC
            930             945             960             975             990

GACGTTAGAAGAGAC CTCTATCAAAACATC ATCCTCTCCGGTGGT ACTACCATGTACGAA GGTATCGGTGAGAGA
          1,005           1,020           1,035           1,050           1,065

CTCCTCAAGGAAATT GAGAACAGAGCTCCC AAGTCAATCAACGTT AAAGTTATTGCCAGC CCAGACAGAAGATTC
          1,080           1,095           1,110           1,125           1,140

GCCGTATGGAGAGGT GGTTCTACCCTTACT TCCCTATCAACCTTC GCCAGCATGTGGATC ACTAAAGAAGACTAC
          1,155           1,170           1,185           1,200           1,215

GACGAAAACGGAGCC AGCATCGTTCACAGA AAATGTATCTGAGGA ATCAAATTTAGTTTT AGCATATGAATTATA
          1,230           1,245           1,260           1,275           1,290

AGTGTGCTGGTTAGT CGCCCTTTGTGACTG CGTCTCTTCAATACT GAAACTTAACCAACC GGCTATGGACGGGTT
          1,305           1,320           1,335           1,350           1,365

GAATGAGATCTTTAT AATGTGTGCACAGTC TTAGTATTCTACATT TAATAATTTCAAAAA TAACTTATTTTGATC
          1,380           1,395           1,410           1,425           1,440

GATGGGGTTTTGGGG TTTTGGGGTTTTGGG GTTTTCCCCCCCCCC CCCCCCCCCCCCTGC A
                                                                3'
```

Fig. 2 The complete nucleotide sequence of the 1.6-kb macronuclear DNA insert from plasmid pOfACT(1.6). The sequence shown is that of the anti-sense strand. Directions are assigned with respect to the orientation of the actin-coding sequence on the DNA molecule. Bases are numbered starting with the first base occurring internally to the inverted terminal repeat at the 5′ end of the molecule. Putative regulatory signals are underlined.

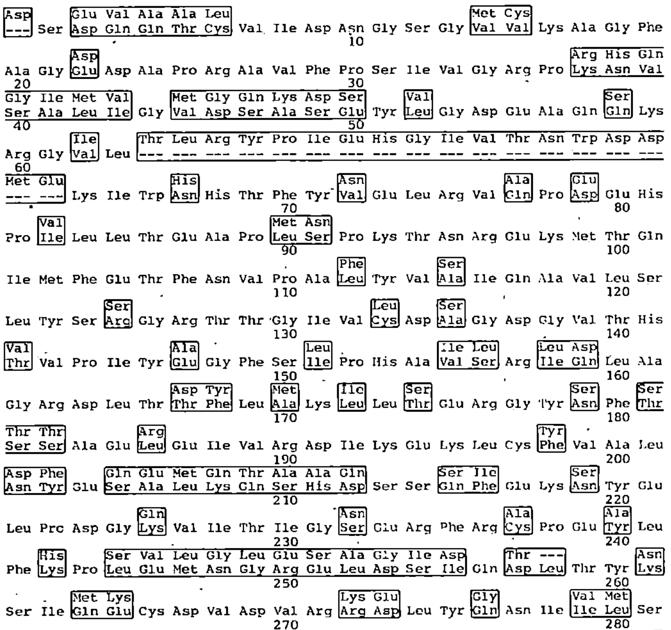

```
Asp     Glu Val Ala Ala Leu                             Met Cys
--- Ser Asp Gln Gln Thr Cys Val Ile Asp Asn Gly Ser Gly Val Val Lys Ala Gly Phe
                                         10

        Asp                                                         Arg His Gln
Ala Gly Glu Asp Ala Pro Arg Ala Val Phe Pro Ser Ile Val Gly Arg Pro Lys Asn Val
 20                                      30

Gly Ile Met Val     Met Gly Gln Lys Asp Ser     Val                     Ser
Ser Ala Leu Ile Gly Val Asp Ser Ala Ser Glu Tyr Leu Gly Asp Glu Ala Gln Gln Lys
 40                                      50

        Ile     Thr Leu Arg Tyr Pro Ile Glu His Gly Ile Val Thr Asn Trp Asp Asp
Arg Gly Val Leu --- --- --- --- --- --- --- --- --- --- --- --- --- --- --- ---
 60

Met Glu             His                 Asn                 Ala     Glu
--- --- Lys Ile Trp Asn His Thr Phe Tyr Val Glu Leu Arg Val Gln Pro Asp Glu His
                                 70                                      80

    Val                         Met Asn
Pro Ile Leu Leu Thr Glu Ala Pro Leu Ser Pro Lys Thr Asn Arg Glu Lys Met Thr Gln
                                 90                                     100

                                        Phe         Ser
Ile Met Phe Glu Thr Phe Asn Val Pro Ala Leu Tyr Val Ala Ile Gln Ala Val Leu Ser
                                110                                     120

            Ser                             Leu     Ser
Leu Tyr Ser Arg Gly Arg Thr Thr Gly Ile Val Cys Asp Ala Gly Asp Gly Val Thr His
                                130                                     140

Val                 Ala             Leu             Ile Leu     Leu Asp
Thr Val Pro Ile Tyr Glu Gly Phe Ser Ile Pro His Ala Val Ser Arg Ile Gln Leu Ala
                                150                                     160

                    Asp Tyr     Met     Ile     Ser                 Ser     Ser
Gly Arg Asp Leu Thr Thr Phe Leu Ala Lys Leu Leu Thr Glu Arg Gly Tyr Asn Phe Thr
                                170                                     180

Thr Thr         Arg                                             Tyr
Ser Ser Ala Glu Leu Glu Ile Val Arg Asp Ile Lys Glu Lys Leu Cys Phe Val Ala Leu
                                190                                     200

Asp Phe     Gln Glu Met Gln Thr Ala Ala Gln         Ser Ile         Ser
Asn Tyr Glu Ser Ala Leu Lys Gln Ser His Asp Ser Ser Gln Phe Glu Lys Asn Tyr Glu
                                210                                     220

                Gln                     Asn                 Ala         Ala
Leu Pro Asp Gly Lys Val Ile Thr Ile Gly Ser Glu Arg Phe Arg Cys Pro Glu Tyr Leu
                                230                                     240

    His     Ser Val Leu Gly Leu Glu Ser Ala Gly Ile Asp     Thr ---         Asn
Phe Lys Pro Leu Glu Met Asn Gly Arg Glu Leu Asp Ser Ile Gln Asp Leu Thr Tyr Lys
                                250                                     260

        Met Lys                         Lys Glu         Gly         Val Met
Ser Ile Gln Glu Cys Asp Val Asp Val Arg Arg Asp Leu Tyr Gln Asn Ile Ile Leu Ser
                                270                                     280

                    Phe Pro Ser     Ala         Met Gln             Thr Ala Leu
Gly Gly Thr Thr Met Tyr Glu Gly Ile Gly Glu Arg Leu Leu Lys Glu Ile Glu Asn Arg
                                290                                     300

        Ser     Met Lys         Ile         Pro     Glu     Lys Tyr Ser
Ala Pro Lys Ser Ile Asn Val Lys Val Ile Ala Ser Pro Asp Arg Arg Phe Ala Val Trp
                                310                                     320

Ile             Ile     Ala         Thr         Gln Gln             Ser     Gln
Arg Gly Gly Ser Thr Leu Thr Ser Leu Ser Thr Phe Ala Ser Met Trp Ile Thr Lys Glu
                                330                                     340

Glu             Ser     Pro                 His         Phe
Asp Tyr Asp Glu Asn Gly Ala Ser Ile Val His Arg Lys Cys Ile
                                350
```

Fig. 3 The amino acid sequence encoded by the cloned 1.6-kb *O. fallax* macronuclear actin gene. Regions differing in homology from the yeast actin sequence[6] are boxed, with the yeast residues given in the upper half of each box. Positions of deleted residues are indicated by broken lines.

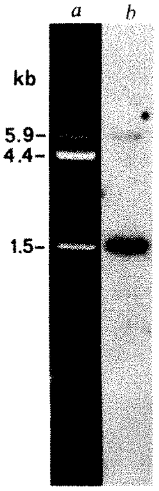

Fig. 4 Hybridization of *O. fallax* RNA to pOfACT(1.6). The plasmid pOfACT(1.6) was digested to near completion with *Pst*I, the fragments were separated by electrophoresis in a 1.2% agarose gel and then blotted on to nitrocellulose. *O. fallax* 7–15S RNA was cleaved by brief alkaline hydrolysis and labelled with ^{32}P using polynucleotide kinase and ^{32}P-ATP. Hybridization was carried out for 42 h at 65 °C with 1 M [Na$^+$] in conditions described previously[5]. The filter was washed in 2×SSC, 0.1% SDS, 0.1% Na-pyrophosphate at 65 °C. The input RNA was shown to be alkaline hydrolysable, thus ruling out DNA–DNA hybridization. *a*, DNA stained with ethidium bromide showin the *O. fallax* actin sequence at 1.5 kb, pBR322 at 4.4 kb and linear plasmid at 5.9 kb. *b*, Hybridization of *O. fallax* RNA.

The actins are a strongly conserved family of eukaryotic proteins. Actin isolated from the slime mold *Physarum polycephalum*, for example, differs from mammalian cytoplasmic actin in only 17 out of 375 amino acid residues—95.5% homology[20]. However, the *O. fallax* actin encoded by the 1.6-kb long macronuclear DNA differs considerably in structure from these proteins. It is possible that the *O. fallax* actin has become highly specialized in function. Ciliated protozoans are complex cells having a highly ordered anatomical structure, including such features as ciliary rows, an oral apparatus and a cytoproct (cell anus)[21]. It would not be unusual for these organisms to have proteins modified for use in such specialized structures.

Ciliate actin has not been well characterized. A protein that co-migrates with muscle actin has been isolated from *Tetrahymena thermophila*[22] but is absent from *Tetrahymena pyriformis* (N. E. Williams, personal communication). Recently, a fibre-forming protein (FFP-38) has been found in both *Tetrahymena* species[23] that co-precipitates with muscle myosin and is found in contractile regions of the cell. However, FFP-38 is smaller than muscle actin and is biochemically and antigenically distinct. It is possible that FFP-38 may be homologous to the *O. fallax* sequence.

A second *O. fallax* macronuclear DNA molecule has been detected that hybridizes to the yeast actin gene[5]. This molecule is 1.4 kb long and differs substantially in nucleotide sequence from pOfACT (1.6). However, the 1.4-kb molecule hybridizes no more readily to the yeast actin sequence than does the 1.6-kb molecule, and the melting temperatures of the hybrids produced are similar. It is unlikely that the 1.4-kb molecule is any more a true actin gene than the 1.6-kb molecule. Rather, we view the actin genes in *O. fallax* as a multigene family, as in most other eukaryotes[24].

The unusual *O. fallax* actin might also reflect a large evolutionary distance between the ciliates and other eukaryotes. Such an interpretation has been supported by other experimental evidence[25–27] and it has been suggested[20] that the ciliates formed a distinct phylogenetic group which may have been the first to separate from the main eukaryotic stem. Our results support this hypothesis.

From the sequence of the *O. fallax* actin gene we conclude that, in hypotrichous ciliates, first, only a small amount of DNA is necessary to make up the noncoding regions of a complete genetic unit, which, in this case is only ~200 bp at each end. Second, the sequenced DNA molecule clearly contains only a single gene. Thus the earlier hypothesis of Prescott and Murti[1] that the macronucleus is a collection of single-gene DNA molecules lacking non-genic spacer sequences seems correct.

Received 4 November; accepted 4 December 1981.

1. Prescott, D. M. & Murti, K. G. *Cold Spring Harb. Symp. quant. Biol.* **38,** 609–618 (1973).
2. Rae, P. M. M. & Spear, B. B. *Proc. natn. Acad. Sci. U.S.A.* **75,** 4992–4996 (1978).
3. Ammermann, D. *Chromosoma (Berl.)* **33,** 209–238 (1971).
4. Lauth, M. R., Spear, B. B., Heumann, J. & Prescott, D. M. *Cell* **7,** 67–74 (1976).
5. Kaine, B. P. & Spear, B. B. *Proc. natn. Acad. Sci. U.S.A.* **77,** 5336–5340 (1980).
6. Ng, R. & Abelson, J. *Proc. natn. Acad. Sci. U.S.A.* **77,** 3912–3916 (1980).
7. Maxam, A. M. & Gilbert, W. *Proc. natn. Acad. Sci. U.S.A.* **74,** 560–564 (1977).
8. Oka, Y., Shiota, S., Nakai, S., Niskida, Y. & Okuba, S. *Gene* **10,** 301–306 (1980).
9. Klobutcher, L. A., Swanton, M. T., Donini, P. & Prescott, D. M. *Proc. natn. Acad. Sci. U.S.A.* **78,** 3015–3019 (1981).
10. Baker, C. C., Herisse, J., Courtois, G., Galibert, E. & Ziff, E. *Cell* **18,** 569–580 (1979).
11. Lewin, B. *Gene Expression* Vol. 2, 2nd edn (Wiley, New York, 1980).
12. Pribnow, D. *Proc. natn. Acad. Sci. U.S.A.* **72,** 784–788 (1975).
13. Efstratiadis, A. *et al. Cell* **21,** 653–668 (1980).
14. Proudfoot, N. J. & Brownlee, G. G. *Nature* **263,** 211–214 (1976).
15. Konkel, D. A., Tilghman, S. M. & Leder, P. *Cell* **15,** 1125–1132 (1978).
16. Korn, L. J. & Brown, D. D. *Cell* **15,** 1145–1156 (1978).
17. Soeda, E., Miura, K., Nakaso, A. & Kimura, G. *FEBS Lett.* **79,** 383–389 (1977).
18. Stinchcomb, D. T., Thomas, M., Kelly, J., Selker, E. & Davis, R. W. *Proc. natn. Acad. Sci. U.S.A.* **77,** 4559–4563 (1980).
19. Tschumper, G. & Carbon, J. *J. supramolec. Struct. Cell Biochem.* Suppl. **5,** 346 (1981).
20. Vanderkerckhove, J. & Weber, K. *J. molec. Biol.* **126,** 783–802 (1978).
21. Nanney, D. L. *Experimental Ciliatology* (Wiley, New York, 1980).
22. Williams, N. E., Vaudaux, P. E. & Skriver, L. *Expl Cell Res.* **123,** 311–320 (1979).
23. Numata, O., Yasuda, T., Hirabayashi, T. & Watanabe, Y. *Expl Cell Res.* **129,** 223–230 (1980).
24. Firtel, R. A. *Cell* **24,** 6–7 (1981).
25. Dayhoff, M. O., McLaughlin, P. J., Barker, W. C. & Hunt, L. T. *Naturwissenschaften* **62,** 154–161 (1975).
26. Ragan, M. A. & Chapman, D. J. *A Biochemical Phylogeny of the Protists* (Academic, New York, 1978).
27. Glover, C. V. C. & Gorovsky, M. A. *Proc. natn. Acad. Sci.* U.S.A. **76,** 585–589 (1979).

Agrobacterium rhizogenes inserts T-DNA into the genomes of the host plant root cells

**Mary-Dell Chilton*, David A. Tepfer, Annik Petit,
Chantal David, Francine Casse-Delbart
& Jacques Tempé**

Station de Génétique et d'Amelioration des Plantes, INRA,
78000 Versailles, France

Agrobacterium rhizogenes, which induces hairy root disease of dicotyledonous plants[1], is closely related to _Agrobacterium tumefaciens_, the causative agent of crown gall disease[1–3]. Virulence in both species is conferred by large plasmids[4–7]. Infected plant tissue synthesizes novel metabolites, opines[8–11], that are not found in normal plant tissues. The pattern of opines synthesized is determined by the type of virulence plasmid in the bacterium, and in general virulence plasmids confer on the host bacterium the ability to catabolize the same opines (refs 8, 12, 13 and A.P. _et al._, in preparation). Opine synthesis persists when the affected plant tissue is cultivated _in vitro_ in the absence of the pathogenic bacterium[9–11,14,15], which in the case of crown gall tumours is a consequence of gene transfer from the pathogen to the plant cells. A small specific part of the tumour-inducing (Ti) plasmid of _A. tumefaciens_, termed T-DNA (transferred DNA), is incorporated into host plant nuclear DNA[16–21] and transcribed into mRNA[18,22–25]. A specific region of T-DNA confers the ability to synthesize the characteristic opine[26,27]. Synthesis of opines is thus a natural example of genetic engineering in which the agent is the Ti plasmid of, _A. tumefaciens_. The discovery of opines in roots induced by _A. rhizogenes_ (ref. 11 and A.P. _et al._, in preparation) suggested that they too might contain T-DNA derived from the virulence plasmid of the pathogen. We report here DNA hybridization studies that confirm this hypothesis.

A. rhizogenes strain 8196 (from Dr J. Lippincott) contains three plasmids, the intermediate-sized one being the virulence plasmid, isolated in transconjugant C58C1 (pRi 8196) (Fig. 1). Similar data have been reported by White and Nester[7] for *A.*

---

* Present address: Department of Biology, Washington University, St Louis, Missouri 63130, USA.

0028-0836/82/050432—03$01.00

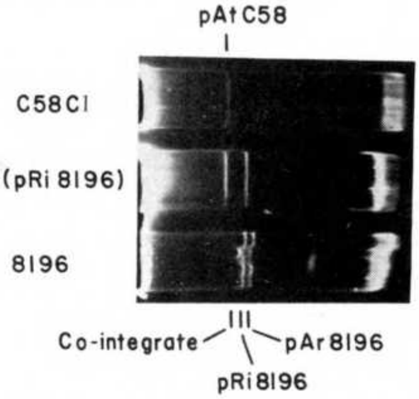

Fig. 1 Eckhardt gel[39] analysis of plasmids of *A. rhizogenes* 8196 and C58C1 (pRi 8196). Transconjugant strain C58C1 (pRi 8196) was obtained by conjugation of *A. rhizogenes* 8196 with *A. tumefaciens* C58C1, a strain cured of its Ti plasmid[4]. The donor strain was grown overnight in AT medium[40] with *N*-(1-mannityl)-glutamic acid ($2\ g^{-1}$)[11] as the sole carbon source; the recipient strain was grown overnight in AT medium with mannitol as sole carbon source. Recipient bacteria (10^8) were spread on AT agar with *N*-(1-mannityl)-glutamic acid as sole carbon source, rifampicin ($100\ \mu g\ ml^{-1}$) and streptomycin ($500\ \mu g\ ml^{-1}$) (drugs to which only the recipient is resistant). Donor bacteria (5×10^7) were applied to the lawn as a drop of liquid culture. Transconjugant colonies were picked after 8 days at 25 °C, and cloned on selective medium. Plasmids were visualized by a modification[41] of the Eckhardt gel technique. Strain 8196 contained three plasmids whose relative amounts varied between experiments. The two smaller plasmids (visible here) were sometimes impoverished and a larger plasmid (almost invisible here) predominant. We presume the larger plasmid to be a co-integrate of the smaller ones, analogous to the plasmids of *A. rhizogenes* strain 15824 (ref. 7). The transconjugant strain possesses the larger of the two small plasmids of the donor strain, and is virulent. It also contains the large cryptic plasmid of strain C58C1 (ref. 42).

rhizogenes 15834. As expected, plasmid DNA isolated[29] from C58C1 (pRi 8196) exhibits only a subset of the *Bam*HI fragments of plasmid from the parent 8196 strain (see Fig. 2). The giant cryptic plasmid of C58C1 (isolated in extremely poor yield because of its size) is present only as a trace contaminant in this preparation of pRi 8196. We propose the designation Ri for root-inducing virulence plasmids[11], analogous to Ti for tumour-inducing plasmids[30,31]. Contour length measurements by Constantino *et al.*[32] have shown pRi 8196 to have a molecular weight (MW) of $137 \pm 2 \times 10^6$.

In our experiments we used carrot disks inoculated with $\sim 10^9$ bacteria in 0.1 ml H_2O. Roots appeared after 2–3 weeks. Terminal pieces 10–15 mm long were excised and planted on Monier medium[11] without hormones, solidified with 1–1.5% agar. Explants were incubated in darkness at 25–27 °C and grew vigorously as roots. Those without visible bacterial contamination were transferred every 2–3 weeks and subcultured in Monier liquid medium without hormones (80 ml per Petri dish). Sterility of the cultures was assessed by plating macerates of the cultures on rich medium[11]. The cultures studied here were derived from single root tips; such cultures could be either cellular clones or chimaeras. Normal root cultures used as controls were established from roots of axenic carrot seedlings.

DNA was isolated from axenic root cultures previously induced by strains 8196 ('8196 root DNA') and C58C1 (pRi 8196) ('8196TC root DNA'), and from normal carrot roots cultivated similarly. The DNA isolation procedure is described in Fig. 3 legend. Southern blot hybridization analysis was performed on these DNA samples to determine the presence of any fragments homologous to the virulence plasmid. Plant DNA samples digested with *Bam*HI, as well as undigested samples, were electrophoresed in horizontal agarose gels. As controls, two parallel lanes were run with a low concentration of pRi 8196 digested to completion with *Bam*HI; the concentration used was calculated to be the amount of plasmid DNA expected per 5 μg of carrot DNA if the transformed roots contained one or three copies of the virulence plasmid per diploid nucleus. A Southern blot of the resulting agarose gel was hybridized with pRi 8196 DNA labelled *in vitro* by nick translation[33]. The autoradiogram of the blot (Fig. 3) shows hybridization bands in the lanes containing digests of transformed root DNA, but not in the lane containing normal carrot DNA. T-DNA was therefore present in the roots transformed by pRi 8196.

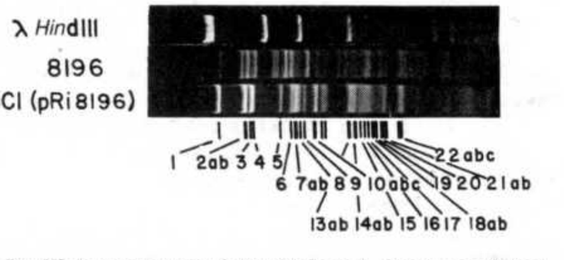

Fig. 2 *Bam*HI cleavage pattern of plasmids from *A. rhizogenes* 8196 and C58C1 (pRi 8196). *Bam*HI digests of plasmid DNA (2 μg samples) were electrophoresed in a horizontal agarose gel (0.7%)[31]. The line drawing indicates our assignment of fragment numbers, which was based in part on other studies in which digests were electrophoresed for longer.

Two prominent hybridization bands in the 8196TC root DNA digest co-migrated with bands 6 and 19 of the pRi 8196 digest and with hybridization bands in the 8196 root DNA digest. We interpret these T-DNA bands as 'internal fragments'[17–21] consisting entirely of pRi 8196 DNA. Six additional faint hybridization bands in 8196TC root DNA have no counterpart in 8196 root DNA, which in turn has four unique bands. We

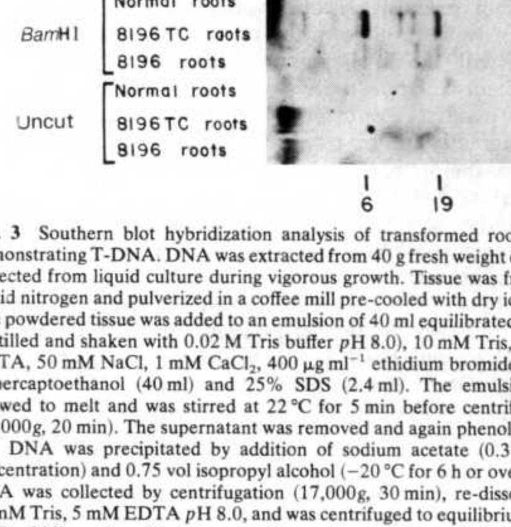

Fig. 3 Southern blot hybridization analysis of transformed root DNA demonstrating T-DNA. DNA was extracted from 40 g fresh weight of roots, collected from liquid culture during vigorous growth. Tissue was frozen in liquid nitrogen and pulverized in a coffee mill pre-cooled with dry ice chips. The powdered tissue was added to an emulsion of 40 ml equilibrated phenol (distilled and shaken with 0.02 M Tris buffer *p*H 8.0), 10 mM Tris, 50 mM EDTA, 50 mM NaCl, 1 mM $CaCl_2$, $400\ \mu g\ ml^{-1}$ ethidium bromide, 5 mM β-mercaptoethanol (40 ml) and 25% SDS (2.4 ml). The emulsion was allowed to melt and was stirred at 22 °C for 5 min before centrifugation (17,000*g*, 20 min). The supernatant was removed and again phenol-extracted. DNA was precipitated by addition of sodium acetate (0.3 M final concentration) and 0.75 vol isopropyl alcohol (−20 °C for 6 h or overnight). DNA was collected by centrifugation (17,000*g*, 30 min), re-dissolved in 10 mM Tris, 5 mM EDTA *p*H 8.0, and was centrifuged to equilibrium in six CsCl–ethidium bromide step gradients in a Spinco SW50.1 rotor (35,000 r.p.m. at 15 °C for 48 h). DNA bands were visualized using long-wavelength UV light and were removed by syringe. After repeated extractions with isopropyl alcohol to remove dye, the DNA solution was diluted with an equal volume of water, adjusted to 0.3 M sodium acetate and precipitated with 0.75 vol isopropyl alcohol. DNA was spooled on a rod, re-dissolved in 10 mM Tris, 1 mM EDTA *p*H 8, then dialysed briefly against the same buffer before restriction endonuclease cleavage. All glassware used for plant DNA isolation was either new or acid-cleaned and/or autoclaved to eliminate accidental contamination of the sample with native bacterial or plasmid DNA. Plant DNA and pRi 8196 were digested to completion with *Bam*HI (Boehringer-Mannheim). Plant DNA (5 μg per well), either digested or undigested, and pRi 8196 plasmid DNA digest (1.6 or $0.5 \times 10^{-3}\ \mu g$) (equivalent to three or one copies, respectively, per diploid carrot DNA equivalent based on a genome of MW 1.2×10^{12} (ref. 43)) were electrophoresed in horizontal 0.8% agarose gels. DNA was blotted on to cellulose nitrate (Schleicher & Schuell)[44] and hybridized with pRi 8196 DNA, labelled to a specific activity of 90×10^6 c.p.m. μg^{-1} by nick with [α-^{32}P]dCTP (Amersham) using a commercial kit (Amersham). Labelled DNA (1 μg) was incubated for 36 h with the Southern blot in 3 × SSC, 5 × Denhardt's solution at 68 °C as described by Thomashow *et al.*[45]. Blots were washed[45] to remove unhybridized probe and were subjected to autoradiography on Kodak RP X-omat film at −80 °C for 8 h with two intensifying screens.

interpret these bands as 'border fragments' analogous to those seen in T-DNA studies of crown gall tumour DNA[17-21], consisting of T-DNA covalently joined to host plant DNA. The six and four border fragments observed in these autoradiograms suggest that the transformed root cultures contained, respectively, three and two copies of T-DNA. The possibility of additional copies is not excluded. The various T-DNA copies may not be contained in the same cell, as the root cultures used here were not cloned from single cells.

Uncleaved DNA from the transformed roots, but not that from normal carrot roots, hybridized to the labelled probe DNA at the position of the high molecular weight plant DNA in the original gel. T-DNA does not migrate as a sharp band on the gel, as expected for a free replicon of fixed size. A very large free replicon would, however, escape detection because of fragmentation during DNA isolation. Our isolation method would certainly have broken covalently closed circular DNA molecules.

When we used the mixture of plasmids from *A. rhizogenes* strain 8196 (Fig. 2) as probe in a similar hybridization to transformed root DNA digests, we detected the same T-DNA fragments (data not shown), which confirms that all T-DNA is situated on pRi 8196.

Roots containing T-DNA can give rise to plantlets via callus and embryogenesis. Root tissue was transferred to Monier medium containing 2,4-D (0.36 μM) and kinetin (0.72 μM) solidified with agar (0.8%). After 4 weeks, the resulting callus tissue was transferred to liquid hormone-free Monier medium and incubated on an orbital shaker (150 r.p.m.) at 22–25 °C. The callus dissociated into suspension culture, and after 1 month embryos differentiated from these suspensions. Embryos were further incubated in Petri dishes containing hormone-free Monier medium where they developed into plantlets. Adventitious embryogenesis was observed on the newly differentiated plantlets, which resulted in the formation of tufts but did not interfere with the development of the plantlets into vigorous plants of normal appearance.

Of 20 plantlets examined, all contained high levels of the opine characteristic of transformed roots, N^2-(1-mannityl)-glutamine (mannopine), which suggests that the transformed roots derived from single root tips may indeed be a cellular clone. Studies of T-DNA in the plants obtained will determine whether each contains the several T-DNA inserts found in the parental root culture.

The results presented here demonstrate that a new family of pathogenic plasmids, the Ri plasmids that induce hairy root disease, share with the Ti plasmids (crown gall agent) the ability to insert T-DNA into the host plant genome. The Ri plasmids studied thus far share little DNA homology with the T-DNA of the Ti plasmids[34,35]; thus they seem to represent separate pathogenic agents. The similarity of the molecular mechanism of plant cell transformation by Ti and Ri plasmids thus extends the T-DNA concept and suggests that additional examples of foreign gene transfer may be found in plant pathogens.

Because of their natural ability to insert T-DNA into plant cells, the Ti plasmids are being extensively investigated as vectors for use in plant genetic engineering[36,37]. Regeneration of complete plants from crown gall tissue has proved extremely difficult[38]. In contrast, the roots containing pRi 8196 T-DNA regenerate reproducibly into plants containing opines, and thus presumably containing T-DNA. The Ri plasmid is thus an attractive alternative to the Ti plasmid as a genetic engineering vector.

This research was funded by CNRS grants ATP and AI 032750 to J.T. and DOE contract ERa0889 and American Cancer Society grant NP194 to M.D.C. M.D.C. received travel and fellowship support from CNRS, DGRST and INRA.

Received 7 October; accepted 8 December 1981.

1. Smith, E. F. *Phytopathology* **1**, 7–11 (1911).
2. New, P. B. & Kerr, A. *J. appl. Bact.* **34**, 233–236 (1971).
3. DeLey, J., Tijtgat, R., De Smedt, J. & Michiels, M. *J. gen. Microbiol.* **78**, 241–252 (1973).
4. Van Larabeke, N. *et al. Nature* **252**, 169–170 (1974).
5. Watson, B., Currier, T. C., Gordon, M. P., Chilton, M.-D. & Nester, E. W. *J. Bact.* **123**, 255–264 (1975).
6. Moore, L., Warren, G. & Strobel, G. *Plasmid* **2**, 617–626 (1979).
7. White, F. F. & Nester, E. W. *J. Bact.* **141**, 1134–1141 (1980).
8. Guyon, P., Chilton, M.-D., Petit, A. & Tempé, J. *Proc. natn. Acad. Sci. U.S.A.* **77**, 2693–2697 (1980).
9. Firmin, J. L. & Fenwick, G. R. *Nature* **276**, 842–844 (1978).
10. Ellis, J. G. & Murphy, P. J. *Molec. gen. Genet.* **181**, 36–43 (1981).
11. Tepfer, D. A. & Tempé, J. C. *Cr. hebd. Séanc. Acad. Sci., Paris* **295**, 153–156 (1981).
12. Bomhoff, G. *et al. Molec. gen. Genet.* **145**, 177–181 (1976).
13. Montoya, A. L., Chilton, M.-D., Gordon, M. P., Sciaky, D. & Nester, E. W. *J. Bact.* **129**, 101–107 (1977).
14. Goldman-Menagé, A. *Annls Sci. nat. Sér. 12* **11**, 223–310 (1971).
15. Petit, A., Delhaye, S., Tempé, J. & Morel, G. *Physiol. Végétale* **8**, 205–213 (1970).
16. Chilton, M.-D. *et al. Cell* **11**, 263–271.
17. Chilton, M.-D., Saiki, R. K., Yadav, N., Gordon, M. P. & Quétier, F. *Proc. natn. Acad. Sci. U.S.A.* **77**, 4060–4064 (1980).
18. Willmitzer, L., De Beuckeleer, M., Lemmers, M., Van Montagu, M. & Schell, J. *Nature* **287**, 359–361 (1980).
19. Zambryski, P. *et al. Science* **209**, 1385–1391 (1980).
20. Yadav, N. S., Postle, K., Saiki, R. K., Thomashow, M. F. & Chilton, M.-D. *Nature* **287**, 458–461 (1980).
21. Thomashow, M. F. *et al. Proc. natn. Acad. Sci. U.S.A.* **77**, 6448–6452 (1980).
22. Drummond, M. H., Gordon, M. P., Nester, E. W. & Chilton, M.-D. *Nature* **269**, 535–536 (1977).
23. Gurley, W. B., Kemp, J. D., Albert, M. J., Sutton, D. W. & Callis, J. *Proc. natn. Acad. Sci. U.S.A.* **76**, 2828–2832 (1979).
24. Yang, F., McPherson, J. C., Gordon, M. P. & Nester, E. W. *Biochem. biophys. Res. Commun.* **92**, 1273–1277 (1980).
25. McPherson, J. C., Nester, E. W. & Gordon, M. P. *Proc. natn. Acad. Sci. U.S.A.* **77**, 2666–2670 (1980).
26. Hernalsteens, J.-P. *et al. Nature* **287**, 654–657 (1980).
27. Schröder, J., Schröder, G., Huisman, H., Schilperoort, R. A. & Schell, J. *FEBS Lett.* **129**, 166–168 (1981).
28. Murai, N. & Kemp, J. D. *Proc. natn. Acad. Sci. U.S.A.* (in the press).
29. Currier, T. C. & Nester, E. W. *Analyt. Biochem.* **66**, 431–441 (1976).
30. Van Larebeke, N. *et al. Nature* **255**, 742–743 (1975).
31. Sciaky, D., Montoya, A. L. & Chilton, M.-D. *Plasmid* **1**, 238–253 (1978).
32. Constantino, P. *et al. Plasmid* **5**, 170–182 (1981).
33. Maniatis, T., Jeffrey, A. & Kleid, D. G. *Proc. natn. Acad. Sci. U.S.A.* **72**, 1184–1188 (1975).
34. White, F. F. & Nester, E. W. *J. Bact.* **144**, 710–720 (1980).
35. Constantino, P., Hooykaas, P. J. J., den Dulk-Ras, H. & Schilperoort, R. A. *Gene* **11**, 79–87 (1980).
36. Chilton, M.-D. in *Genetic Engineering of Osmoregulation* (eds Rains, D. W., Valentine, R. C. & Hollaender, A.) 23–31 (Plenum, New York, 1980).
37. Van Montagu, M. *et al. Proc. R. Soc.* **210**, 351–365 (1980).
38. Wullems, G. J., Molendijk, L., Ooms, G. & Schilperoort, R. A. *Cell* **24**, 719–727 (1981).
39. Eckhardt, T. *Plasmid* **1**, 584–588 (1978).
40. Petit, A. & Tempé, J. *Molec. gen. Genet.* **167**, 147–155 (1978).
41. Rosenberg, C., Casse-Delbart, F., David, M. & Boucher, C. *J. Bact.* (in the press).
42. Casse, F., Boucher, C., Julliot, J. S., Michal, M. & Dénarié, J. *J. gen. Microbiol.* **113**, 229–242 (1978).
43. Bennett, M. D. & Smith, J. B. *Phil. Trans. R. Soc.* **274**, 227–274 (1976).
44. Southern, E. *J. molec. Biol.* **98**, 503–517 (1975).
45. Thomashow, M. F., Nutter, R., Montoya, A. L., Gordon, M. P. & Nester, E. W. *Cell* **19**, 729–739 (1980).

Stratification and terminal differentiation of cultured epidermal cells

Fiona M. Watt*‡ & Howard Green*†

* Department of Biology, Massachusetts Institute of Technology,
Cambridge, Massachusetts 02139, USA
† Department of Physiology and Biophysics, Harvard Medical
School, Boston, Massachusetts 02115, USA

As keratinocytes move from the basal to the outer layers of a stratified squamous epithelium, they enlarge and terminally differentiate. Hence, the stage of terminal differentiation is correlated with both cell size and position. To determine whether position is an important signal in differentiation, we have now grown human keratinocytes in conditions that prevented stratification but not cell enlargement. Involucrin, a marker of terminal differentiation, was synthesized in such a monolayer, but only by large cells. We conclude that the onset of involucrin synthesis, while normally restricted to cells in a non-basal position, does not depend on this position for an essential signal; however, a signal associated with increased cell size is not ruled out. When monolayer cultures were induced to stratify, the large involucrin-containing cells preferentially adopted a suprabasal position, indicating that terminal differentiation is associated with a decrease in substrate adhesiveness. Suprabasal cell position is therefore a consequence rather than a cause of terminal differentiation.

---

‡ Present address: Kennedy Institute of Rheumatology, Hammersmith, London W6 7DW, UK.

0028-0836/82/050434—03$01.00

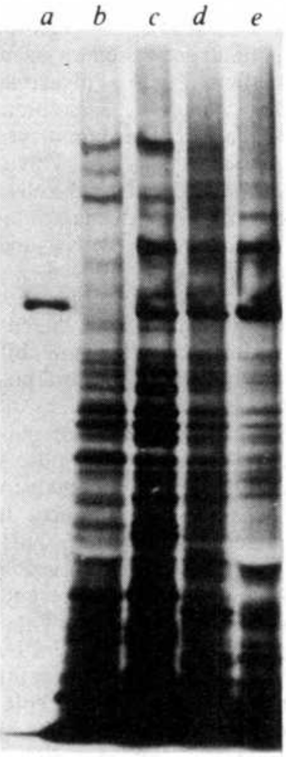

Fig. 1 Presence of involucrin in keratinocyte monolayers grown in low calcium medium. Second to fourth subcultures of human epidermal cells isolated from newborn foreskin were cultured in the presence of irradiated 3T3 feeder layers[9] in Dulbecco–Vogt medium supplemented with 10% fetal calf serum, 0.4 μg ml^{-1} hydrocortisone, 10^{-10} M cholera toxin[10], 5 μg ml^{-1} transferrin, 5 μg ml^{-1} insulin and 2×10^{-11} M tri-iodothyronine[3]. Epidermal growth factor was added to 10 ng ml^{-1} beginning on the third day after subculture[11]. The calcium concentration of control medium, determined by flame photometry, was 1.9 mM. When medium was prepared without calcium and supplemented with fetal calf serum that had either been dialysed against Ca-, Mg-free isotonic phosphate buffer (PBS) or treated with Chelex-100 resin[12], the final concentration of Ca^{2+} in the medium was about 0.1 mM (low calcium medium). Cells were labelled before collection with ~15 μCi ml^{-1} ^{35}S-methionine (Amersham, 600–1,300 Ci mmol^{-1}) for 24 h in medium containing 3 mg l^{-1} methionine. They were collected by scraping and sonicated in 10 mM EDTA, 50 mM Tris, *p*H 7.4. Insoluble material was removed by centrifugation for 2 min at 12,800*g*. *a*, Purified ^{35}S-involucrin marker. *b*, Extract of small cells selected by passage through a Nitex screen. Note the absence of involucrin. Small cells were plated out in control medium (*c*) or low calcium medium (*d*) and collected at confluence. *e*, Cells collected from the medium of a culture in low calcium by gentle aspiration 1 week after confluence. Only cells that were already detached or loosely attached to the monolayer were collected in this way.

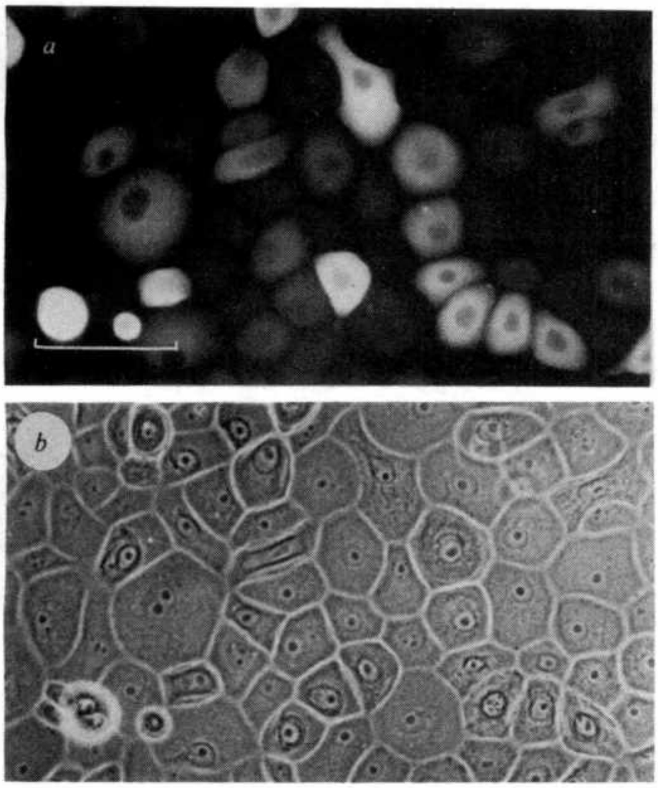

Fig. 2 Identification by immunofluorescence of involucrin-containing cells in keratinocyte monolayers grown in low calcium medium. Keratinocytes grown to confluence in low calcium medium and fixed with 3.7% formaldehyde in PBS (room temperature) for 8 min, in absolute methanol (−20 °C) for 4 min and in absolute acetone (−20 °C) for 2 min. The cells were incubated first with rabbit antiserum to involucrin (1:20 in PBS), then with fluorescein-conjugated goat anti-rabbit IgG (1:16 in PBS) (Miles). *a*, Immunofluorescence image. *b*, Phase image of the same field; scale bar 100 μm. Note mixture of involucrin-positive and -negative cells in the monolayer. Positive cells also seem to have better defined nuclear borders.

Involucrin is a soluble keratinocyte protein that becomes incorporated into the cross-linked envelope during terminal differentiation[1]. It is found in all human stratified squamous epithelia and cell cultures derived from them[2]. We have previously shown that the onset of involucrin synthesis is correlated with an increase in cell size[3] and with cell migration from the basal layer into the outer layers[1,2]. In culture, synthesis begins in the layers immediately suprabasal, while in intact tissues, cells migrate several layers beyond the basal layer before starting to make the protein[1,2]. Hennings *et al.*[4] have shown that cultivation of keratinocytes in medium containing a low concentration of Ca^{2+} prevents stratification by inhibiting desmosome formation, and this allows the relationship between cell position and involucrin synthesis to be tested.

Pre-confluent cultures of human epidermal keratinocytes derived from newborn foreskin were collected and passed through a screen of Nitex nylon monofilament cloth (type HC-3-11, Tetko). Only cells <15 μm in diameter passed through the screen; these cells did not contain involucrin, as judged by immunofluorescence and polyacrylamide gel electrophoresis (ref. 3 and Fig. 1*b*).

The small involucrin-free cells were collected in sterile conditions and plated in the presence of irradiated 3T3 cells in medium containing 0.1 mM Ca^{2+} (low calcium medium), grown into a confluent monolayer, then fixed and stained for indirect immunofluorescence, using antiserum raised in rabbits against purified involucrin[1]. As Figs 2 and 3 show, even though the cells were confined to a monolayer, the proportion of involucrin-positive cells was 30–50%, similar to the proportion found in stratified colonies cultured in control medium[3]. The presence of involucrin was confirmed by polyacrylamide gel electrophoresis of ^{35}S-methionine-labelled cell extracts (Fig. 1, compare *c* and *d*). Thus, terminal differentiation progressed to the stage of involucrin synthesis, even though stratification was prevented by the low Ca^{2+} concentration.

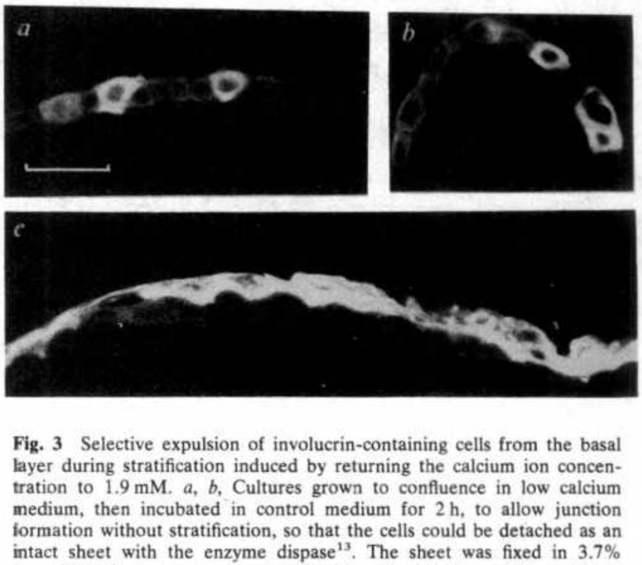

Fig. 3 Selective expulsion of involucrin-containing cells from the basal layer during stratification induced by returning the calcium ion concentration to 1.9 mM. *a*, *b*, Cultures grown to confluence in low calcium medium, then incubated in control medium for 2 h, to allow junction formation without stratification, so that the cells could be detached as an intact sheet with the enzyme dispase[13]. The sheet was fixed in 3.7% formaldehyde at room temperature for 1 h, embedded in paraffin, and 5 μm sections were cut at right angles to the surface of the epithelial sheet. The sections were prepared for immunofluorescence as described in Fig. 2 legend. Note that involucrin-positive and -negative cells are interspersed in the monolayer. *c*, Cells grown to confluence in low calcium medium, and transferred to control medium for 24 h before fixation, to induce stratification. The section was prepared as in *a* and *b*. Note that all the involucrin-positive cells have left the basal layer. *a*, *b*, *c* Are all at the same magnification; scale bar, 50 μm.

In control medium, the modal cell diameter was 12–13 μm and virtually all cells of ≥17 μm synthesized involucrin[3]. Cells grown to confluence in low calcium medium tended to be larger, the modal diameter increasing by 1–2 μm after 1 week in culture. In low calcium medium none of the involucrin-positive

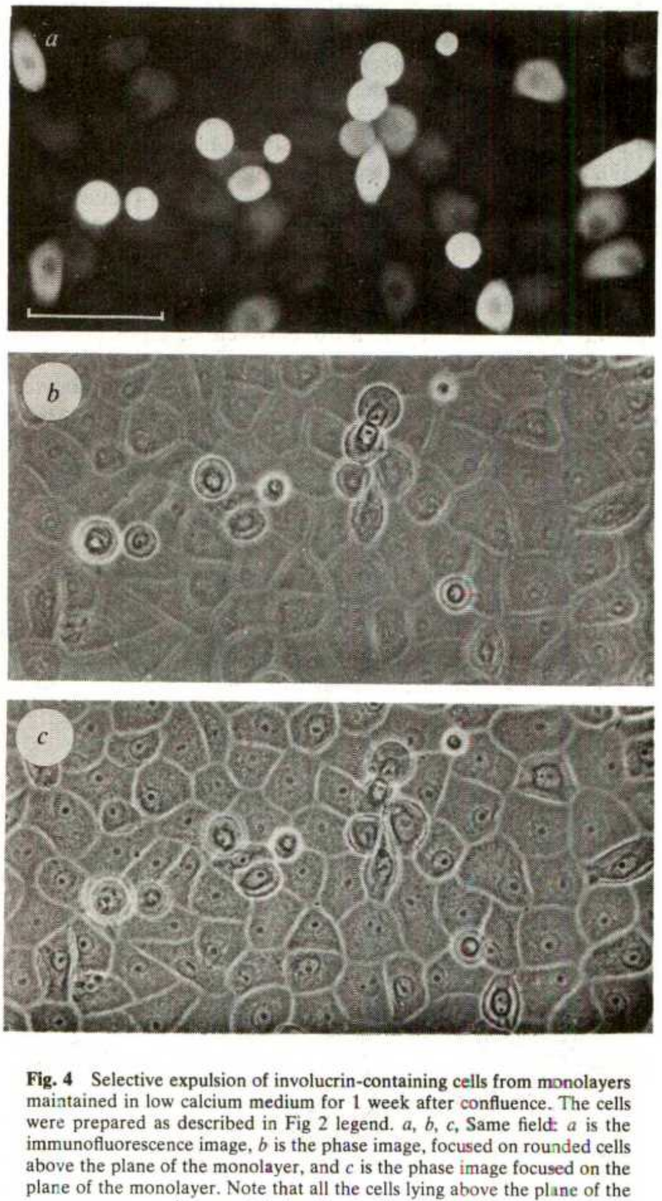

Fig. 4 Selective expulsion of involucrin-containing cells from monolayers maintained in low calcium medium for 1 week after confluence. The cells were prepared as described in Fig 2 legend. *a, b, c,* Same field: *a* is the immunofluorescence image, *b* is the phase image, focused on rounded cells above the plane of the monolayer, and *c* is the phase image focused on the plane of the monolayer. Note that all the cells lying above the plane of the monolayer contain involucrin. Scale bar, 100 μm.

cells was <17 μm in diameter, and 66% of cells >18 μm were positive. Although the absolute size at which involucrin synthesis began depended to some extent on the culture conditions, the onset of synthesis in both monolayer and stratified cultures was correlated with an increase in cell size.

We also investigated the effect of returning the calcium concentration to 1.9 mM, thereby inducing stratification, to see whether the involucrin-positive and -negative cells would distribute randomly between the basal and outer cell layers or whether they would sort out. Within 24 h of raising the calcium concentration, stratification occurred (Fig. 3*c*): all the differentiating, involucrin-positive cells were found in the outer cell layers and the involucrin-negative cells remained in the basal layer. Thus, although the newly stratified cultures were only two to three layers thick, the distribution of involucrin was the same as in cultures grown in control medium[2]. This demonstrates that the cells sufficiently differentiated to synthesize involucrin were selectively expelled from the basal layer.

Monolayers of keratinocytes were also maintained in low calcium medium for 1–2 weeks after reaching confluence. Some cell division continued in the cultures and those cells forced out of the monolayer were rounded and either loosely attached to the surface of the monolayer, or detached into the medium. When such cultures were fixed and stained for immunofluorescence with antiserum to involucrin, it was clear that involucrin was present in all the rounded cells above the plane of the monolayer as well as in most cells detached and free in the medium (Fig. 4). Polyacrylamide gel electrophoresis confirmed that extracts of ^{35}S-methionine-labelled cells detached from the surface of the monolayer by gentle aspiration contained involucrin (Fig. 1*e*). This suggests that the terminal differentiation of epidermal cells is accompanied by a decrease in substrate adhesiveness, which could account for the sorting out of involucrin-positive and -negative cells observed when stratification is induced.

These observations show that cells need not achieve a suprabasal position in the stratified epithelium to synthesize involucrin. Rather, the ability of involucrin-containing cells to sort out shows that cell position in the epithelium depends on properties established by the process of terminal differentiation. Selective expulsion of the more differentiated cells from the basal layer has been postulated to explain the kinetics of thymidine labelling in the superficial layers of intact epidermis[5]. Quantitative differences in adhesiveness are known to be sufficient to produce immiscibility between two cell populations[6]. A continuing gradient of surface adhesiveness linked to terminal differentiation and extending outwards from the basal layer would serve to maintain homogeneity of cells along a given plane in the epithelium by preventing the mixing of cells at different stages of differentiation. This is probably the basis for the ability of mixed epidermal cells at different stages of differentiation to reassemble histotypic structure, either in culture[7] or following their injection into animals[8].

These investigations were aided by NCI grants.

Received 7 October; accepted 14 December 1981.

1. Rice, R. H. & Green, H. *Cell* **18,** 681–694 (1979).
2. Banks-Schlegel, S. & Green, H. *J. Cell Biol.* **90,** 732–737 (1981).
3. Watt, F. M. & Green, H. *J. Cell Biol.* **90,** 738–742 (1981).
4. Hennings, H. *et al. Cell* **19,** 245–254 (1980).
5. Iversen, O. H., Bjerknes, R. & Devik, F. *Cell Tissue Kinet.* **1,** 351–367 (1968).
6. Steinberg, M. *Proc. natn. Acad. Sci. U.S.A.* **48,** 1769–1776 (1962).
7. Moscona, A. *Expl Cell Res.* **22,** 455–475 (1961).
8. Doran, T. I., Vidrich, A. & Sun, T.-T. *Cell* **22,** 17–25 (1980).
9. Rheinwald, J. G. & Green, H. *Cell* **6,** 317–330 (1975).
10. Green, H. *Cell* **15,** 801–811 (1978).
11. Rheinwald, J. G. & Green, H. *Nature* **265,** 421–424 (1977).
12. Brennan, J. K., Mansky, J., Roberts, G. & Lichtman, M. A. *In Vitro* **11,** 354–360 (1975).
13. Green, H., Kehinde, O. & Thomas, J. *Proc. natn. Acad. Sci. U.S.A.* **76,** 5665–5668 (1979).

Unusual interactions of benzodiazepine receptor antagonists

David J. Nutt & Philip J. Cowen

MRC Unit and University Department of Clinical Pharmacology,
Radcliffe Infirmary, Woodstock Road, Oxford OX2 6HE, UK

Hilary J. Little

Department of Pharmacology, Oxford University, South Parks Road,
Oxford OX1 3QT, UK

Two compounds have recently been described which act as potent benzodiazepine (BDZ) antagonists *in vivo* and which, *in vitro*, show high affinity and selectivity for the BDZ receptor of the mammalian central nervous system (CNS). One, ethyl β-carboline-3-carboxylate (β-CCE), was extracted from human urine and may be related to an endogenous ligand for the BDZ receptor[1–3]. It reverses the effects of BDZs *in vivo*[4,5] and *in vitro*[6], but also has intrinsic activity, as it lowers the seizure threshold to drugs antagonistic to the action of γ-aminobutyric acid (GABA)[5,7]. The other compound, an imidazodiazepine (Ro 15-1788), which is also a potent and specific antagonist of

0028-0836/82/050436—03$01.00

BDZ binding *in vivo* and *in vitro*[8], blocked the sedative, hypnotic and anticonvulsant actions of conventional BDZs, without demonstrating any intrinsic activity[9,10]. Because of the different profiles of action of these two BDZ 'antagonists', we have here investigated their interactions in two well established systems for assessing BDZ activity: seizure thresholds *in vivo*[11] and the action of GABA on cervical sympathetic ganglia *in vitro*[12]. We find that Ro 15-1788 not only opposes the actions of BDZs but also is an effective antagonist of β-CCE in both systems. At high doses it has BDZ-like activity, suggesting that it may be a partial agonist at the BDZ receptor site.

Seizure thresholds in rats were determined by measuring the dose of drug, when infused at a constant rate through a tail vein, needed to elicit a seizure (see Table 1 legend), a method known to provide a reliable guide to the activity of certain anticonvulsant drugs[13]. Ro 15-1788 was prepared as a suspension in distilled water (DW) with 1 drop of Tween 40 per 10 ml and was injected intraperitoneally (i.p.) 15 min before infusion. All animals received a volume of 2 ml per kg, controls being given the Tween/DW vehicle.

Table 1 Effect of different doses of Ro 15-1788 on the seizure thresholds to PTZ, bicuculline and strychnine

Dose of Ro 15-1788 (mg per kg)	Seizure thresholds (mg per kg) PTZ	Bicuculline	Strychnine
Vehicle alone	30 ± 4 (5)	0.24 ± 0.02 (4)	2.2 ± 0.4 (5)
1	—	0.25 ± 0.02 (4)	—
10	29 ± 2 (6)	0.26 ± 0.03 (4)	—
50	36 ± 5 (6)*	0.29 ± 0.06 (4)*	2.1 ± 0.3 (6)
100	40 ± 5 (5)†	—	—

Seizure thresholds are expressed as mean ±s.d. with number of animals in parentheses. Rats were given either vehicle or Ro 15-1788 in a volume of 2 mg per kg i.p. and 15 min later convulsant was infused in a tail vein via a 25-gauge cannula, at a rate of 2.22 ml min^{-1}, and the time taken to the first seizure activity was recorded. Using this time and the concentration of infused drug and weight of the animal, the seizure threshold was computed. The concentrations of convulsant solutions used were PTZ 10 mg ml^{-1}, bicuculline 0.05 mg ml^{-1} and strychnine 1 mg ml^{-1}. PTZ and strychnine were dissolved in normal saline; bicuculline was dissolved in saline acidified to *p*H 3 with 0.1 M HCl. Significance was determined by Student's *t*-test: * $P < 0.05$; † $P < 0.01$, as compared with vehicle controls.

When tested alone on seizure thresholds to the GABA antagonist drugs pentylenetetrazol (PTZ) and bicuculline, Ro 15-1788 showed anticonvulsant activity at a dose of ⩾50 mg per kg, with a potency about 1/50th that of diazepam (Table 1). However, even at 50 mg per kg, Ro 15-1788 gave no protection against the seizures produced by the glycine antagonist, strychnine, suggesting that Ro 15-1788's anticonvulsant effect has a similar pharmacological specificity to that of the BDZs[14].

To determine the effect of Ro 15-1788 on the anticonvulsant effect of diazepam, rats were injected with diazepam, 5 mg per kg, and 15 min later with Ro 15-1788, 10 mg per kg (this dose was devoid of agonist effects, see Table 1). When PTZ was infused a further 15 min later the pronounced elevation of seizure threshold produced by diazepam was substantially reduced in the Ro 15-1788-treated group (Table 2).

The selectivity of this effect was determined by giving the same dose of Ro 15-1788 15 min after treatment with anticonvulsants thought to act at sites other than the BDZ receptor. As Table 2 shows, the anticonvulsant activity of phenobarbitone (40 mg per kg, i.p.), sodium valproate (400 mg per kg, i.p.) and progabide (200 mg per kg, i.p.), which raise seizure thresholds to PTZ by mechanisms which may involve GABAergic systems[15-17], was unaffected by Ro 15-1788.

The action of Ro 15-1788 on the previously reported proconvulsant action of β-CCE was evaluated by administering Ro 15-1788, 10 mg per kg, or Tween followed 10 min later by intravenous (i.v.) β-CCE, 1 mg per kg (1 mg ml^{-1} in propylene glycol/ethanol 2 : 1) and 5 min after this by PTZ infusion. The fall in seizure threshold produced by β-CCE was abolished by the Ro 15-1788 pretreatment (Table 2).

In the seizure threshold model, therefore, Ro 15-1788 at a dose of 10 mg per kg i.p. antagonized both the anticonvulsant effects of 5 mg per kg diazepam and the proconvulsant effects of 1 mg per kg β-CCE, without having any detectable effect of its own. This antagonistic effect seems to be selective for drugs acting at the BDZ receptor, as Ro 15-1788 did not reduce the anticonvulsant effects of phenobarbitone, sodium valproate or progabide.

GABA perfusion of the isolated rat cervical sympathetic ganglion induces depolarization which may be blocked by the GABA receptor antagonist, bicuculline. In this preparation the conductance change produced by GABA (an increase in chloride conductance) has been shown to correspond with those produced by GABA in the CNS[18]. Moreover, the binding characteristics of the ganglion and CNS GABA receptors are similar[19]. Figure 1 shows that, in agreement with previous studies[12] with BDZs, the water-soluble BDZ, chlordiazepoxide, increases the amplitude of the responses to GABA in the presence of bicuculline. Treatment of the ganglion with Ro 15-1788 (835 nm) abolished the effect of chlordiazepoxide (Fig. 1),

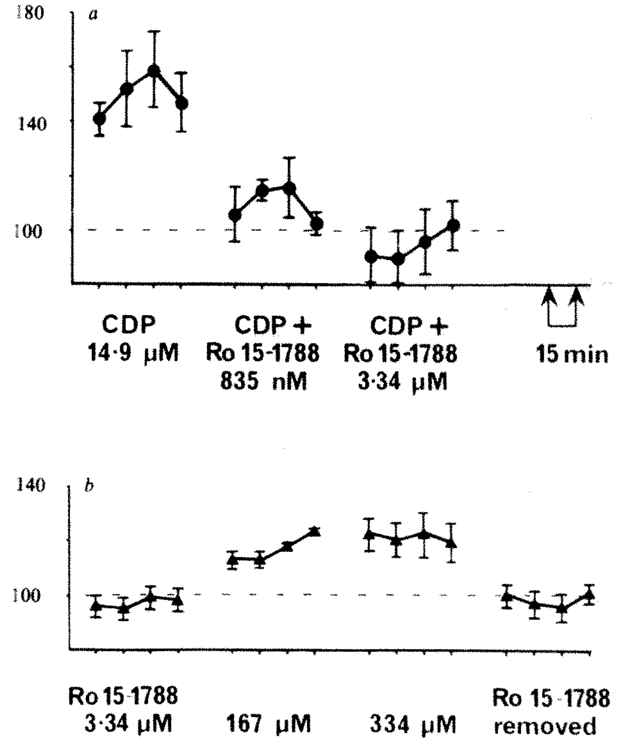

Fig. 1 The method used was that of Brown and Marsh[22] and involves superfusion of the isolated ganglion (1 ml min^{-1}) with extracellular recording of the postsynaptic potential changes. Application of GABA to the perfusion fluid for 2 min every 15 min was found to give steady control responses without desensitization. Four steady control responses to GABA (38.8 μM) were obtained in each experiment before the above treatments were applied. This concentration produces near-maximal responses to GABA in this preparation and the concentration of bicuculline used throughout (27.2 μM) reduced this to approximately half the maximum responses. These concentrations were similar to those used originally by Bowery and Dray[12] and were chosen to demonstrate the optimum changes in response amplitude. The results give the amplitude of the depolarizations produced by application of GABA, expressed as percentages of the mean of the four control values ($n = 5$ throughout). The compounds were added to the perfusion medium 15 min before GABA and were present throughout the treatment periods. Standard errors are included to give an indication of the variation. Analysis of variance performed on the original data showed that Ro 15-1788 (concentrations 835 nM and 3.34 μM) significantly antagonized the effects of chlordiazepoxide (CDP, $P < 0.01$). When applied alone, Ro 15-1788 caused significant increases in amplitude of responses at 167 μM and 334 μM ($P < 0.01$) but not at 3.34 μM. There was no further increase in response amplitude when the Ro 15-1788 concentration was raised to 835 μM. The mean amplitude of the control responses was 211 ± 19 μV. The drugs were made up in the following solutions: GABA and Ro 15-1788 in standard Krebs, chlordiazepoxide in distilled water, β-CCE in 0.03 M HCl, bicuculline in 0.1 M HCl titrated to *p*H 3.

Table 2 Effect of Ro 15-1788 on the changes in seizure threshold produced by diazepam, other anticonvulsants and β-CCE

	Seizure threshold to PTZ (mg per kg)		
Drug treatment	Vehicle (Tween)	Ro 15-1788 (10 mg per kg)	*P* value
Saline	34 ± 2 (5)	35 ± 3 (6)	N/S
β-CCE (1 mg per kg, i.v.)	26 ± 3 (5)	35 ± 3 (6)	<0.001
Diazepam (5 mg per kg, i.p.)	62 ± 14 (7)	39 ± 4 (5)	<0.001
Phenobarbitone (40 mg per kg, i.p.)	52 ± 5 (6)	56 ± 9 (6)	N/S
Valproate (400 mg per kg, i.p.)	57 ± 14 (5)	53 ± 10 (6)	N/S
Progabide (200 mg per kg, i.p.)	50 ± 6 (7)	55 ± 11 (7)	N/S

Diazepam, phenobarbitone, sodium valproate and progabide were given in the doses shown. Concentrations of solutions were diazepam 5 mg ml^{-1} in commercial vehicle (Roche), phenobarbitone 10 mg ml^{-1} and sodium valproate 100 mg ml^{-1} in normal saline, and progabide 100 mg ml^{-1} in Tween. Saline was given in a volume of 4 ml per kg. 15 min later Ro 15-1788, 10 mg per kg, was injected i.p. and a further 15 min later PTZ was infused (see Table 1 legend). With β-CCE, Ro 15-1788, 10 mg per kg in Tween, was given 10 min before an i.v. injection of 1 mg per kg β-CCE (1 mg ml^{-1} solution), with PTZ infused 5 min later. Seizure thresholds were expressed as mean ±s.d. with the number of animals given in parentheses. The *P* value refers to significance of differences between Ro 15-1788 and Tween vehicle-treated animals. There were no differences in seizure threshold between animals pretreated with saline, Tween, β-CCE vehicle or diazepam vehicle. Statistical analysis performed by Student's *t*-test. N/S, not significant.

while higher concentrations of Ro 15-1788 (167–835 μM) showed intrinsic activity in that they increased the responses to GABA (Fig. 1). The ratio of agonist and antagonist doses of Ro 15-1788 in this system was similar to that displayed in the seizure threshold model.

Barbiturates also increase the responses to GABA in the ganglion preparation[12], but as in the seizure threshold model, the effect of phenobarbitone (40% increase in the amplitude of GABA responses at 787 μM) was not antagonized by Ro 15-1788 at either 3.34 or 33.4 μM. These concentrations of Ro 15-1788 alone had no effect on the response to GABA.

When applied to the GABA–bicuculline-pretreated ganglion, 1 μM β-CCE showed opposite actions to BDZs in that it significantly ($P<0.01$) decreased the depolarization produced by GABA, 38.8 μM (results, expressed as in Fig. 1, were 85 ± 3% at 15 min, 78 ± 5% at 30 min, 85 ± 6% at 45 min and 83 ± 7% at 60 min). This effect was antagonized by Ro 15-1788 at the same concentration which blocked the effect of chlordiazepoxide (3.34 μM).

It thus seems that in two experimental systems in which specific BDZ activity may be assessed, β-CCE has the opposite effect to BDZs. Ro 15-1788 seems to be a selective and potent antagonist of both compounds in both systems. Investigations have failed to demonstrate specific binding of either β-CCE[1] or Ro 15-1788 (ref. 8) to CNS sites other than the BDZ receptor. In view of the selective and high-affinity BDZ receptor binding of β-CCE and Ro 15-1788, and the parallels between their binding and pharmacological activity, it is likely that the pharmacological effects observed are due to interaction at the BDZ receptor site.

We suggest three possible explanations for these findings. First, the partial agonist effect of Ro 15-1788 may be sufficient to account for its reversal of the actions of β-CCE. This seems unlikely because the concentrations of Ro 15-1788 that antagonized β-CCE had no agonist action when tested alone. However, it is possible that in the presence of β-CCE the BDZ receptor is altered so that Ro 15-1788 has a greater agonist effect.

The second explanation is that the functional interaction of ligands with the BDZ receptor may be unusual in that specific high-affinity ligands may produce opposite pharmacological effects and yet have a common antagonist. The possible existence of this type of receptor interaction has been predicted from receptor theory (see, for example, ref. 20). The allosteric models of receptor behaviour suggest that receptors exist in equilibrium between two states (which may be termed 'active' and 'inactive') and that this equilibrium is altered by ligand binding. If we apply this theory to our findings, BDZs would be considered to be agonists, binding to the active state, whereas Ro 15-1788 would be a conventional antagonist, binding to both forms without altering the equilibrium. If β-CCE bound preferentially to the receptors in the inactive state it would shift the equilibrium in the opposite direction. This form of antagonism has been predicted but not so far demonstrated.

A third explanation derives from results of ligand binding studies suggesting the existence of subclasses of BDZ receptors. These have identical affinities for the BDZs, including Ro 15-1788 (ref. 8), but differ in their affinities for the β-carbolines[2,21]. The pharmacological actions of the BDZs and β-CCE may thus be exerted through different subpopulations of BDZ receptors, and it is conceivable that the unusual interactions we have described represent a functional consequence of this differential binding.

We thank Dr B. Jones, Glaxo, and Dr Ian Martin, MRC Neurochemical Pharmacology Unit, Cambridge, for β-CCE, Dr W. Haefely, Roche, for Ro 15-1788, Synthelabo (Paris) for progabide, Professors Sir William Paton and D. G. Grahame-Smith and Dr A. R. Green for helpful advice and criticism and Mr C. Howard for technical assistance.

Received 26 August; accepted 16 December 1981.

1. Braestrup, C., Nielsen, M. & Olsen, C. E. *Proc. natn. Acad. Sci. U.S.A.* **77,** 2288–2292 (1980).
2. Nielsen, M. & Braestrup, C. *Nature* **286,** 606–607 (1980).
3. Braestrup, C. & Nielsen, M. *Trends pharmac. Sci.* **1,** 424–427 (1980).
4. Tenen, S. & Hirsch, J. D. *Nature* **288,** 609–610 (1980).
5. Oakley, N. R. & Jones, B. J. *Eur. J. Pharmac.* **68,** 381–382 (1980).
6. Mitchell, R. & Martin, I. *Eur. J. Pharmac.* **68,** 513–514 (1980).
7. Cowen, P. J., Green, A. R., Nutt, D. J. & Martin, I. *Nature* **290,** 54–55 (1981).
8. Möhler, A., Burkard, W. P., Keller, A. H., Richards, J. G. & Haefely, W. *J. Neurochem.* **37,** 714–722 (1981).
9. Hunkeler, W. *et al. Nature* **290,** 514–516 (1981).
10. Darrogh, A. *et al. Lancet* **ii,** 8–10 (1981).
11. Randall, L. O. & Kappell, B. in *The Benzodiazepines* (eds Garattini, S., Mussini, E. & Randall, L. O.) (Raven, New York, 1973).
12. Bowery, N. G. & Dray, A. *Br. J. Pharmac.* **63,** 197–215 (1978).
13. Nutt, D. J., Cowen, P. J. & Green, A. R. *Neuropharmacology* **19,** 1017–1023 (1980); *Eur. J. Pharmac.* **71,** 287–295 (1981).
14. Costa, E., Guidotti, A., Mao, C. C. & Suria, A. *Life Sci.* **17,** 167–176 (1975).
15. Olsen, R. W. *J. Neurochem.* **37,** 1–13 (1981).
16. Kerwin, R. W., Olpe, H-R. & Schmutz, M. *Br. J. Pharmac.* **7,** 545–551 (1980).
17. Lloyd, K. G. *et al. Adv. Biochem. Pharmac.* **26,** 199–206 (1981).
18. Adams, P. R. & Brown, D. A. *J. Physiol., Lond.* **250,** 85–120 (1975).
19. Bowery, N. G. & Brown, D. A. *Br. J. Pharmac.* **50,** 205–218 (1974).
20. Colquhoun, D. in *Drug Receptors* (ed. Rang, H. P.) 149–182 (Macmillan, London, 1975).
21. Ehlert, F. J., Roeske, W. R. & Yamamura, H. I. *Life Sci.* **29,** 235–248 (1981).
22. Brown, D. A. & Marsh, S. *J. Physiol., Lond.* **246,** 24–25P (1974).

Errata

In the *Nature Directory of Biologicals 1982*, on page vi James Manley of Columbia University is incorrectly listed as Michael Manley under the heading 'Scientific Advisory Committees'.

In the letter 'Tree remains in a North York Moors peat profile' by I. G. Simmons & J. B. Innes, *Nature* **294,** 76–77 (1981), Figs 1 and 2 are transposed. Thus Fig. 1 is the pollen diagram shown on page 78.

In the article 'Magma chamber profiles from the Bay of Islands ophiolite complex' by J. F. Casey & J. A. Karson, *Nature* **292,** 295–301 (1981), NAM in Fig. 1 legend stands for North Arm Mountain. The received date for the article should read 29 September 1980.

Corrigendum

In the letter 'Mouse IgG3 antibodies are highly protective against infection with *Streptococcus pneumoniae*' by D. E. Briles *et al., Nature* **294,** 88–90 (1981), the dose of *S. pneumoniae* is given as 100 CFU in Table 2 and 150 in the text. This should read 100 CFU throughout.

BOOK REVIEWS

Tomorrow, the world

Brenda Maddox

Electronic Colonialism: The Future of International Broadcasting and Communication. By Thomas L. McPhail. Pp. 260. Hbk ISBN 0-8039-1602-7; pbk ISBN 0-8039-1603-5. (Sage: 1981.) Hbk $22.50, £15.50; pbk $9.95, £6.50. *Global Talk: The Marriage of the Computer, World Communications and Man.* By Joseph N. Pelton. Pp.336. Hbk ISBN 0-7108-0371-0; pbk ISBN 0-7108-0347-8. (Harvester: 1981.) Hbk £17.95; pbk £7.95.

ANY writer who sits down to try to explain the public policy issues embedded in complicated technology has two contradictory censors inside his head. "Don't get it wrong", demands one. "Don't make it boring", shouts the other. Because the dilemma is so common, a common solution has evolved: to be lofty. Cast the questions in terms of the survival of the race and the future of the planet; the technical experts will thus forgive you for skating over tedious details, while the lay reader will work extra hard and re-read tough pages rather than giving up.

To be sure, Mr McPhail, who teaches mass communication and journalism at Carleton University in Ottawa, has set his chisel to the hardest stone: Unesco and the issue of the New World Information Order. For at least a decade, the countries of the developing world have been demanding a New World Information Order. This fuzzy concept expresses a legitimate grievance — that most of their communication with the developed world flows in one direction only: in. Little news about them of their own choice flows out toward the wider world, and even less entertainment. They fear eventual cultural swamping and, at the present, resent what is seen as constant misinterpretation by Western news agencies.

To right this balance, these countries are using their numerical strength in the United Nations where each country has one vote. Their favourite battleground is Unesco. Unesco's secretariat has so taken up the Third World's campaign for a re-ordering of information (of news-gathering in particular), that it has come up with proposals which to Britain, the United States and other countries committed to a free (well, fairly free) press amount to nothing less than a Unesco endorsement of government control of the media. In 1980 at Unesco's general conference in Belgrade the West reluctantly, with many doubts and qualifications, allowed the barest acknowledgement that something like a New World Information Order may be needed.

All this sets a very demanding exercise for a writer, especially as Unesco obscures its own activities behind dense screens of jargon. Earnestness so permeates Mr McPhail's efforts that it is sad to have to declare that his book does not meet the challenge. For example, what did the West surrender in the way of press freedom at Unesco's general conference in Belgrade in 1980? The Western press tried analysis (duly quoted in Mr McPhail's text) and was hampered by the differing views, even between Britain and the United States, as to what happened. For its part, the developing world is not sure what it has achieved in securing within Unesco the creation of the International Programme for the Development of Communications: a talking shop, a funnel for practical aid or its own power base inside the secretariat? And neither is Mr McPhail. All he can conclude is that the New World Information Order is not going to go away.

For a book on the future of the media, Mr McPhail gets off to a disastrous start. In his very first two words, he spells a man's name wrong — and not just any man, but the legendary Lord Copper, the archetypal Fleet Street press baron of Evelyn Waugh's *Scoop*. Mr McPhail calls him Lord Cooper, somewhat spoiling Waugh's point. He then gets others wrong (President Kekkonen of Finland) but these could be the computer typesetting.

Another device which Mr McPhail's book would have been better without is the use of ponderous lists, with scarcely a verb at all:

> The questions of transnational data flows, computers, data processing, privacy, and computerization effects on the work place and labor are central to policy concerns of several industrialized nations.

The third stylistic flaw which makes the book unreadable is the excessive use of long quotations, with little guide as to how the extracted material furthers the author's argument.

At the start of his book, Joseph Pelton looks like falling into the same traps. *Global Talk,* he declares, "is only my third book on science policy and applications". But it was his hardest — because he says he has tried to be funny, and sophisticated too, without being as tedious as the *New York Times.* What a relief, therefore, to wade in and find that Mr Pelton, an executive of Intelsat, the International Telecommunications Satellite Organization, has assembled much hard-to-get and fascinating information — studies of telecommunications plans and expenditure in developing countries; similar statistical profiles of "the information societies" and on the technical and economic outlook for satellites.

Mr Pelton, too, dips into the slough of the UN conference — specifically the WARCs, the world radio conferences of the International Telecommunications Union. He knows, unlike Mr McPhail, that the "A" in WARC stands for "administrative" and not "administration" and he is, moreover, unafraid to use his own words, instead of quoted material, to draw conclusions. In the case of the 1979 WARC, his judgement is that, for their own purposes, more and more countries are willing to tax the ITU's cumbersome regulatory mechanisms — such as the mammoth WARC conferences — to the maximum, yet he sees this as no cause for despair. In spite of their complexity, the issues of international management of technology are no harder than those which international institutions have dealt with successfully in the earlier part of the century. Not a bold conclusion, perhaps, but a clear one.

In sum, Mr Pelton's grasp of his subject triumphs over his whimsy (although, in some cases, just barely: an excellent chapter on the worsening problem of incompatible international technical standards contains an awful poem, "Electronic Gumbo Stew"), and has allowed him to produce an ambitious and original work of reference. ☐

Brenda Maddox is Home Affairs Editor of The Economist *and Chairman of the Association of British Science Writers. She is author of* Beyond Babel: New Directions in Communications *(1972).*

Tasteless behaviour

Mark Ridley

The Foundations of Ethology. By Konrad Z. Lorenz. Pp.380. ISBN 0-387-81623-2. (Springer-Verlag: 1981.) $21.95.

The Foundations of Ethology, a translation of a book that appeared in German a few years ago, is a monograph of Lorenzian ethology. The text reads well, unlike most translations, although "selfish", which becomes *egoistische* in German, returns in " 'The egoistical gene' has become the popular phrase. . .". All in all there is not much about natural selection in the book, for Lorenz founds ethology in the philosophy of *Gestalt* psychology, in physiology and in embryology. These three fill the main sections of the book: one on philosophy and methods, and two marked by Lorenz's controversial distinction between innate and acquired information. He repeats once again his argument for a fundamental distinction between innate and acquired information, and, in the present environment of debates about "genetic determinism", it is undoubtedly worth repeating. The fact that the behaviour of animals is adapted to their environments means that they must have "information" about their environment; it is this information (not behaviour) which Lorenz dichotomizes into genetic and acquired.

Lorenz could have written a book with the conceptual content of *Foundations of Ethology* 30 years ago. If it had been published then it would have become a classic alongside Tinbergen's *Study of Instinct* (Clarendon, 1951). Coming out now it appears awkwardly antediluvian. In his foreword, T.H. Bullock says that the book is intended as a contribution to the history of ethology. But to write a period textbook is not to write the history of a period. *Foundations of Ethology*, however, is not even simply a period textbook, for Lorenz is far too concerned with defending his concepts against later criticism. The fault with the book can be clarified by an analogy with historiography. By tracing back the pedigree of ideas that are interesting now, it is easy to distort history, because isolated ancestral ideas are rarely representative of contemporary thinking. Lorenz, by tracing forward and defending his ideas, produces an extraordinary futuristic distortion. For example, in his discussion of motivation he defends himself against Robert Hinde's criticisms and even presents an updated hydraulic analogy. But modern work on motivation is established on quite separate foundations, manifesting itself to most of us only as a fascinating and imposing castle, with sheer walls of solid algebra, surrounded by minefields of exegesis.

Lorenz's later books have tended to be increasingly concerned with human beings, but this one is almost entirely about animal behaviour. There is a typically nonconciliatory appendix on the uniqueness of mankind and a stricture or two against the deadly sins of civilized man. Our "innate releasing mechanisms", we are told on p.166, give us an unhealthy liking for chocolate and "even the most complete insight into the workings of our IRMs does not make it easy to avoid suicide by overeating". As a gastronomic experience, *Foundations of Ethology* is not so much suicidal as dry and unappetizing; it rather resembles three full courses of stale bread. Well before I had reached p.166, I had found that it went down best when taken with *religeuses* and *éclairs au chocolat.* ☐

Mark Ridley is a Junior Research Fellow of Oriel College, and a member of the Animal Behaviour Research Group, University of Oxford.

IRCS JOURNALS

Keeping pace with science

IRCS Medical Science
St. Leonard's House
St. Leonardgate,
Lancaster, U.K.
A member of Elsevier Science Publishers

Circle No.04 on Reader Enquiry Card.

Galactic sociology

John D. Barrow

Galactic Astronomy: Structure and Kinematics, 2nd Edn. By Dimitri Mihalas and James Binney. Pp.597. ISBN 0-7167-1280-6. (W.H. Freeman: 1981.) $29.95, £20.70.

THE story is told of a lecturer beginning his address on the structure of stars with the words "Stars appear to be very simple objects", whereupon someone in the audience retorted "You'd look pretty simple too at a distance of a hundred light years!". Because they are a good deal farther away than stars, astronomers used to think that galaxies were even simpler. Until very recently elliptical galaxies were thought to be uncomplicated and understood — just isothermal "gases" of stars whose various degrees of ellipticity were merely reflections of their differing rotation rates. During the past six years this naive picture has been obliterated and replaced by that complexity, masquerading as simplicity, that is the hallmark of all natural phenomena. Ellipticals have been revealed as complicated systems with three-dimensional dynamics that are neither isothermal nor rotating to any significant degree. Their flattening is a consequence of much more subtle dynamical properties.

Surprisingly, there has never been an authoritative advanced textbook on the structure of galaxies. There are indeed several good introductory texts and collections of review articles, either scattered around the literature or gathered into massive review volumes that send a shiver down your cheque book, but no single, detailed and up-to-date guide to all the relevant observational data and theoretical ideas — until now.

Mihalas and Binney have completed the first part of a two-volume treatise on the subject, this book being confined to observations and kinematics. The second volume, to be written by Binney and Tremaine, will be devoted to dynamics. By any standards this first volume is outstanding. Although advertised as a second edition of Mihalas and Routly's book of the same title, do not be misled, this is an entirely new book of more than double the length and considerably more depth than its prototype. After a brief history and introduction to astronomical concepts and vocabulary, it begins with a detailed overview of stellar evolution and the interstellar medium before describing the stellar content and kinematics of external galaxies and the Milky Way. The final chapters provide studies of the hydrogenic content of galaxies and their rotational properties. References to the original literature are always provided, although through a rather cumbersome system, and good tables and diagrams illuminate the text throughout.

This book is essential for any graduate course on galaxies. It is too advanced for undergraduate courses although lecturers and more able students will want to refer to it. Most graduate courses on galaxies divide their time equally between the material covered in this volume and the dynamical theory that will appear in Vol. 2, and together the two books should provide everything such students require. Unfortunately, it is hard to believe that many of them will be willing or able to pay the considerable price of both volumes — one hopes that a paperback edition will soon be available, as all astronomers should own and read this book. Perhaps also the authors and publishers might consider a third volume which would be an abridged combination of the two earlier volumes, with a length and level comparable to the original edition written by Mihalas and Routly.

John Barrow is a Lecturer in Astronomy at the University of Sussex.

Everything e^- can do ν can do better

P.W. Hawkes

Optical Information Processing: Fundamentals. Edited by S.H. Lee. Pp.308. ISBN 3-540-10522-0. (Springer-Verlag: 1981.) DM 99, $42.20.

How is optical information processing getting on? For nearly two decades now, the advantages of light for manipulating data have been attracting more and more attention, although, as Casasent says in this book, "optical processors are somewhat like discrete transistors before the dawn of LSI; they are truly in their infancy". These advantages may be summarized as parallel processing, high throughput and the ability to perform such operations as cross-correlation virtually instantaneously. Such features clearly make optical processors serious potential competitors of digital systems, though, to quote Casasent again, "the shortcomings of one system are the advantages of the other. The two technologies (optical and digital) are actually complementary rather than similar".

The present text, which should be regarded as a companion to an earlier volume in the same Springer series edited by Casasent (*Optical Data Processing: Applications*, 1978), gives an impressively complete account of the degree of sophistication that such optical systems have reached. About a third of the book has been written by the editor, S.H. Lee, who first sets out the basic principles, covering essentially the Fourier transforming properties of lenses and their mathematical implications. His chapter on coherent optical processing then gives an account of filter design and synthesis, including optical feedback, and classifies the various thick and thin filters; a number of more elaborate processor designs are described and clearly illustrated, and the chapter ends with a few words on coherent noise suppression.

The third chapter, by W.T. Rhodes and A.A. Sawchuk, deals with incoherent optical processing, where the advantages of easy input/output, tolerance towards dust and other common imperfections of laboratory equipment and the absence of phase problems is offset by the restriction to real, non-negative signals. This is followed by an extremely important contribution by G.R. Knight on interface devices and memory materials. If the progress described here is maintained, optical processors cannot fail to gain in importance even though an immense amount remains to be done. Some of the problems of purely optical processors can be circumvented by using hybrid systems, as D. Casasent explains in the next chapter. Here, the most powerful features of optical and digital systems are united so that the fast two-dimensional signal handling of the optical unit complements the flexibility of the digital computer. More space might have been given to the achievements of Lohmann's school in Erlangen, which has made many interesting contributions in this field.

The penultimate chapter, by J.W. Goodman, deals with a difficult task on which comparatively little work has been done, linear space-variant optical data processing. Crudely speaking, here we are concerned with integrals that are not in the form of convolutions and hence do not separate conveniently under Fourier transformation. Goodman's clear statement of the problems involved is particularly welcome. The book concludes with a further contribution by the editor, on nonlinear optical processing: "logarithm, exponentiation, intensity level slicing, thresholding, analog-to-digital conversion, logics and bistability", the last four of which are "important toward developing a futuristic digital optical processor".

Applications of these various techniques are only mentioned in passing, as we should expect in a book on "fundamentals", but many are explored in detail in Casasent's earlier volume which contains chapters on optical transforms and systems, enhancement and restoration, synthetic aperture radar (one of the first triumphs of optical processing), photogrammetry, nondestructive testing and metrology, biomedical applications and signal processing. Taken together, the two books give an excellent account of the present state of this field, still young but rapidly maturing. A minor criticism is the under-representation of European work in both works — perhaps this can be rectified in a future volume in the series. Even so, they give the best available account of a mass of new material, written by experts on the various topics. □

P.W. Hawkes is Maître de Recherches at the Laboratoire d'Optique Electronique du CNRS, Toulouse.

Myriapod carnivores

John A. Wallwork

The Biology of Centipedes. By J.G.E. Lewis. Pp.476. ISBN 0-521-23413-1. (Cambridge University Press: 1981.) £33, $69.95.

Few students of the soil fauna can fail to be fascinated by centipedes, although these elusive predators are often overlooked because of their secretive habits. Accounts of their biology have hitherto been widely scattered in the literature, usually in a fragmentary fashion. There has long been a need to gather this information together, stemming from the recognition that these carnivores may regulate the prey populations on which they feed. The prey (mainly Collembola) are principally primary consumers of dead organic material, and predation by centipedes on these "key industry" detritivores may operate to control, indirectly, rates of organic decomposition.

In this book, Dr Lewis does not concern himself with this latter theme to any great extent; indeed, by his own admission, his ecological survey is less than comprehensive. In this, however, he is a victim of circumstances since the integration of centipede ecology with that of the entire soil–litter system is only just beginning. What he has provided is a comprehensive account of centipede biology which soil ecologists will find most useful, and which forms a worthy complement to Eason's earlier taxonomic treatise, *Centipedes of the British Isles* (Warne, 1964). Eason, however, dealt only with British centipedes, and Dr Lewis's experience with temperate and tropical myriapods is reflected in a widely based survey of centipede anatomy, behaviour, physiology, reproduction, life histories, taxonomy and ecology. He devotes as much attention to the mainly tropical Scolopendromorpha as he does to the temperate Lithobiomorpha and the cosmopolitan Geophilomorpha.

As the dust cover of the monograph reminds us, this is primarily a source-book and the way in which Dr Lewis organizes his information — into sections dealing with taxonomic groups — emphasizes the point. Although this device allows the reader easy access to the subject matter, since it is repeated chapter after chapter, the result makes for less than compelling reading; this is a book to inform rather than to be contemplated at leisure. The style is direct, as befits a rather clinical presentation of a catalogue of facts, and the illustrations are numerous but variable in quality, which may reflect the fact that they were taken directly from original sources rather than re-drawn. The reproduction of Manton's (1965) figures are, for example, excellent as might be expected. At the other extreme, the figure of *Lithobius forficatus* eating a fly (Fig. 126) is less than impressive and perhaps unnecessary. Some figures are inadequately labelled (for example, Figs 162a, 203b, 204 and 206). The bibliography is extensive and up to date, and although there is no author index a detailed subject index is provided.

My overall verdict is that the author has succeeded admirably in what he has set out to do. Despite its defects, many of which are unavoidable, the result is a valuable reference book which will be sought by undergraduates and research workers alike. □

John A. Wallwork is Reader in Zoology at Westfield College, University of London.

Everything you wanted to know about protein phosphorylation

P.J. England

Protein Phosphorylation. Cold Spring Harbor Conferences on Cell Proliferation, Vol.8. Edited by Ora M. Rosen and Edwin G. Krebs. Two-volume set, pp.1,421, ISBN 0-87969-140-9. (Cold Spring Harbor Laboratory: 1981.) $140 US, $168 elsewhere.

THE discovery that enzymes could be reversibly phosphorylated, with concomitant changes in activity, was made 25 years ago. For some time after that it appeared that only the enzymes of glycogen metabolism were so regulated, and that protein phosphorylation was a rather special and restricted form of control. However, during the past decade it has become apparent that almost every aspect of eukaryotic cell function is regulated in some way by phosphorylation, and the phenomenon is now known to have implications in many areas of molecular biology. This rapid expansion has made it difficult even for specialists to keep in touch with all aspects of the subject. The publication of these impressive books is thus most welcome; details of almost all of the current research on protein phosphorylation are brought together, so that no one working in this or related areas now has any justification for ignorance.

The books are the result of a five-day conference held in the summer of 1980. It was attended by about 200 people from all the major laboratories working on protein phosphorylation in North America, and a small number from elsewhere. Approximately 100 talks were given, each one of which is represented by a chapter. These individual contributions are grouped into ten sections, the titles of which give a clear idea of the wide range of topics covered in the two volumes — cyclic AMP-dependent protein kinases: structural studies; cyclic nucleotide-dependent and independent protein kinases and protein phosphorylation; glycogen synthetase/phosphoprotein phosphatases; regulation of lipid and carbohydrate metabolism; insulin and growth factor-promoted protein phosphorylation; contractile proteins; protein synthesis; nuclear and cytoskeletal protein phosphorylation; viruses and cell transformation; neural and membrane protein phosphorylation.

Each of the sections contains a wealth of recent results and interpretations from several laboratories. For example, one of the newest areas of interest is that of tyrosine phosphorylation coupled to viral transformation of cells. No less than six chapters are either devoted exclusively to this topic or mention it in detail. There are, overall, some 17 chapters on the role of protein phosphorylation in the control of transcription, translation and cell transformation. However, it should not be thought that some of the more established areas have been neglected; about half of the contents deals with protein kinases, phosphoprotein phosphatases and carbohydrate metabolism. There is now considerable knowledge of the structure and catalytic mechanism of cyclic-AMP-dependent protein kinase, which is discussed at length in several articles. The detailed descriptions of this enzyme at the atomic level contrast strongly with the imperfectly understood role of protein phosphorylation in the imperfectly understood eukaryotic nucleus. The books give the clear impression of a subject with distinct, well-established origins now bursting out in many directions.

Reading either whole sections or individual chapters I found much useful information and many stimulating ideas. Almost all of the chapters give an impression of current work being actively pursued, with little that is dated or incorrect. Excellently produced in the clear, uniform style typical of Cold Spring Harbor publications, the books will be equally useful to those new to protein phosphorylation who wish to discover how it relates to their current research interests, and to those already working in the area who need to be informed of new developments. This is undoubtedly a key reference work which should be in any laboratory working on protein phosphorylation, and in all medical and biological libraries. □

P.J. England is a Lecturer in Biochemistry at the University of Bristol.

Textbook supplement

Next week's issue of *Nature* will include the Textbook Supplement, comprising reviews of over 100 recently published books for undergraduate students.

What can be inferred from exciton lines?

Dennis Dunn

Excitons: Their Properties and Uses. By Donald C. Reynolds and Thomas C. Collins. Pp.291. ISBN 0-12-586580-5. (Academic: 1981.) $36, £33.80.

THE optical absorption of most insulating crystals exhibits a series of sharp lines at frequencies just below the onset of the continuous absorption spectrum. These are the exciton lines. The non-interacting electron theory presented in most solid state physics texts readily accounts for the general features of the continuous absorption spectrum but fails to predict the existence of the exciton lines. These arise as a consequence of the electron-hole correlation induced by the Coulomb interaction.

The aim of *Excitons* is to provide a self-contained review of the theory and experimental properties of excitons and of the information about electronic structure which can be determined by a study of the exciton lines.

The conventional effective-mass theory is presented in Chapter 2, which includes discussion of the effects of electric and magnetic fields (Stark and Zeeman splitting). The highlights of the book are the chapters on the experimental properties of intrinsic and bound excitons. These, of course, are just the areas where the authors have made significant contributions and their mastery of the subject is clearly demonstrated. Set in between — the chapters seem to be randomly ordered — is a brief review of the recent work on the electron-hole liquid, a condensed phase which occurs only if the optical excitation is intense enough to produce a high exciton density.

There are a few surprising omissions from the text. There is no discussion of the theory or experimental properties of the line-shapes. The mass of research on excitons in alkali halides rates only one paragraph, and the rare-gas solids are not mentioned. This is a great pity because research on these materials, which have "deep" excitons, has demonstrated that the effective-mass theory has a far wider range of applicability than was previously thought.

The low-point of the book is the first chapter which tries to lay down the theoretical foundations of exciton theory. Here the authors have been too ambitious and have attempted to present the whole of many-body theory in one brief account: Green function formalism, Bethe–Saltpeter equations, spectral representations all appear and disappear within the space of ten pages.

Excitons is certain to become one of the standards in solid state literature. Physicists who want to initiate their research students into the mysteries of excitons can safely direct them to this book with just one piece of advice: start with Chapter 2. □

Dennis Dunn is a Lecturer in Theoretical Physics at the University of Reading.

BOOKS RECEIVED

Chemistry

BAILEY, R.T., NORTH, A.M. and PETHRICK, R.A. Molecular Motion in High Polymers. Pp.415. ISBN 0-19-851333-X. (Clarendon Press/Oxford University Press: 1981.) £42.50.

BATES, R.B. and BEAVERS, W.A. Carbon-13 NMR Spectral Problems. Organic Chemistry. Pp.259. ISBN 0-89603-010-5. (Humana Press, Clifton, New Jersey:1981.) Hbk $29.50; pbk $12.95.

BURNS, D.T., TOWNSHEND, A. and CARTER, A.H. Inorganic Reaction Chemistry. Vol.2, Reactions of the Elements and Their Compounds. Part B: Osmium to Zirconium. Pp.580. ISBN 0-85312-352-7. (Wiley: 1981.) £27.50, $61.75.

CULLIS, C.F. and HIRSCHLER, M.M. The Combustion of Organic Polymers. Pp.419. ISBN 0-19-851351-8. (Clarendon Press/Oxford University Press: 1981.) £37.50.

FIESER, M., DANHEISER, R.L. and ROUSH, W. Fieser and Fieser's Reagents for Organic Synthesis, Vol.9. Pp.596. ISBN 0-471-05631-6. (Wiley: 1981.) £28, $55. Also available as a 9-Vol. set, £225, $450.

GOLDWHITE, H. Introduction to Phosphorous Chemistry. Pp.113. Hbk ISBN 0-521-22978-2; pbk ISBN 0-521-29757-5. (Cambridge University Press: 1981.) Hbk £12.50; pbk £5.95.

JEFFERY, P.G. and HUTCHISON, D. Chemical Methods of Rock Analysis. 3rd Edn. Pergamon Series in Analytical Chemistry, Vol.4. Pp.379. ISBN 0-08-023806-8. (Pergamon: 1981.) £25, $60.

JENNINGS, K.R. and CUNDALL, R.B. (eds). Progress in Reaction Kinetics, Vol.10. Pp.406. ISBN 0-08-027155-3. (Pergamon: 1981.) £36, $82.50.

MAITLAND, G.C. *et al.* Intermolecular Forces. Their Origin and Determination. Pp.616. ISBN 0-19-855611-X. (Clarendon Press/Oxford University Press: 1981.) £39.50.

MORTIMER, R.G. Mathematics for Physical Chemistry. Pp.403. Pbk ISBN 0-02-384000-5. (Collier Macmillan: 1981.) Pbk £6.95.

SJÖSTRÖM, E. Wood Chemistry. Fundamentals and Applications. Pp.223. ISBN 0-12-647480-X. (Academic: 1981.) $22.

YINON, J. and ZITRIN, S. The Analysis of Explosives. Pergamon Series in Analytical Chemistry, Vol.3. Pp.310. Hbk ISBN 0-08-023846-7; flexi ISBN 0-08-023845-9. (Pergamon: 1981.) Hbk £25; flexi £9.35, $22.50.

Biological Sciences

CLARK, M. Mammal Watching. Pp.176. ISBN 0-7278-2010-9. (Severn House, London: 1981.) £7.95.

CORDELL, G.A. Introduction to Alkaloids. A Biogenetic Approach. Pp.1055. ISBN 0-471-03478-9. (Wiley: 1981.) £92.50, $165.

DAY, C.E. (ed.). High-Density Lipoproteins. Pp.728. ISBN 0-8247-1220-X. (Marcel Dekker: 1981.) SwFr. 185.

DAY, D. The Doomsday Book of Animals. A Unique Natural History of Three Hundred Vanished Species. Pp.288. ISBN 0-85223-183-0. (Ebury Press, London: 1981.) £14.95.

DE LAS HERAS, F.G. and VEGA, S. (eds). Medicinal Chemistry Advances. Proceedings of the 7th International Symposium on Medicinal Chemistry, Torremolinos, Spain, September 1980. Pp.512. ISBN 0-08-025297-4. (Pergamon: 1981.) £33, $80.

DIXON, G.R. Vegetable Crop Diseases. Pp.404. ISBN 0-333-23574-6. (Macmillan Press, London & New York: 1981.) £35.

DOBBS, H.E. Save The Dolphins. Pp.128. ISBN 0-285-62437-7. (Souvenir Press, London: 1981.) £7.95.

DOWNERK, R.G.H. (ed.). Energy Metabolism in Insects. Pp.244. ISBN 0-306-40697-7. (Plenum: 1981.) $32.50.

DuBOW, M.S. (ed.). Bacteriophage Assembly. Progress in Clinical and Biological Research, Vol.64. Proceedings of the 7th Biennial Conference, Asilomar, California, September 1980. Pp.574. ISBN 0-8451-0064-5. (Alan R. Liss, New York: 1981.) £35.50, DM 156.

DUMONT, J.E., GREENGARD, P. and ROBINSON, G.A. (eds). Advances in Cyclic Nucleotide Research, Vol.14. 4th International Conference on Cyclic Nucleotides, Brussels, Belgium, July 1980. Pp.756. ISBN 0-89004-546-1. (Raven: 1981.) $79.

EHRMAN, L. and PARSONS, P.A. Behavior Genetics and Evolution. Pp.450. ISBN 0-07-019276-6. (McGraw-Hill: 1981.) £17.25.

ENOCH, J.M. and TOBEY, F.L. Jr. (eds). Vertebrate Photoreceptor Optics. Springer Series in Optical Sciences, Vol.23. Pp.483. ISBN 3-540-10515-8. (Springer-Verlag: 1981.) DM98, $41.70.

FALCONER, D.S. Introduction to Quantitative Genetics. 2nd Edn. Pp.340. Pbk ISBN 0-582-44195-1. (Longman: 1981.) Pbk £9.95.

FINEAN, J.B. and MICHELL, R.H. (eds). Membrane Structure. New Comprehensive Biochemistry, Vol.1. Pp.275. ISBN 0-444-80304-1. (Elsevier/North-Holland: 1981.)

FISHMAN, M.C. *et al.* Medicine. Pp.464. Pbk ISBN 0-397-50436-5. (J.B. Lippincott, Philadelphia: 1981.) Np.

FRÈRE, J.-M. and GERDAY, C. Les Methodes de Purification et D'Analyse des Protéines. Techniques de Laboratoire' 8. Pp.128. Pbk ISBN 2-225-68850-8. (Editions Masson, Paris: 1981.) Np.

GREAVES, M.F. (Chairman) *et al.* Microenvironments in Haemopoietic and Lymphoid Differentiation. Ciba Foundation Symposium 84 in Honour of Professor John Humphrey, FRS. Pp.348. ISBN 272-79636-0. (Pitman Books: 1981.) £22.50.

GREEP, R.O. (ed.). Recent Progress in Hormone Research. Proceedings of the 1980 Laurentian Hormone Conference, Vol.37. Pp.713. ISBN 0-12-571137-9. (Academic: 1981.) $65.

GROSS, E. and MEIENHOFER, J. (eds).The Peptides: Analysis, Synthesis, Biology. Vol.4, Modern Techniques of Conformational, Structural, and Configurational Analysis. Pp.309. ISBN 0-12-304204-6. (Academic: 1981:) $51.50.

HABER, B., GABAY, S., ISSIDORIDES, M.R. and ALIVISATOS, S.G.A. (eds). Serotonin: Current Aspects of Neurochemistry and Function. Advances in Experimental Medicine and Biology, Vol.133. Proceedings of a Symposium, September 1979, Athens, Greece. Pp.824. ISBN 0-306-40579-2. (Plenum: 1981.) $75.

HALL,D.O. and RAO, K.K. Photosynthesis. 3rd Edn. The Institute of Biology's Studies in Biology, No.37. Pbk ISBN 0-7131-2827-5. (Edward Arnold, London: 1981.) Pbk £2.75.

HALLIDAY, G. and MALLOCH, A. (eds). Wild Flowers: Their Habitats in Britain and Northern Europe. Pp.184. ISBN 0-85654-618-6. (Peter Lowe, London: 1981.) £6.95.

HELMSEN, R.J. *et al.* (eds). Immunology of the Eye. Workshop II: Autoimmune Phenomena and Ocular Disorders (A Special Supplement to Immunology Abstracts.) Pp.200. Flexi ISBN 0-917-000-07-2. (Information Retrieval, Arlington, VA: 1981.) £10, $25.

HOAGLAND, M. Discovery: The Search for DNA's Secrets. Pp.198. ISBN 0-395-30510-1. (Houghton Mifflin: 1981.) $10.95.

HOBBIE, J.E. (ed.). Limnology of Tundra Ponds. Barrow, Alaska. US/IBP Synthesis Series, 13. Pp.514. ISBN 0-87933-386-3. (Academic: 1980.) $29.50.

HOWELL, J.B.L. and TATTERSFIELD, A.E. (eds). Methods in Clinical Pharmacology–Respiratory System. Pp.94. ISBN 0-333-31186-8. (Macmillan Press, London & New York: 1981.) Np.

ISLIKER, H. and SCHÜRCH, B. (eds). The Impact of Malnutrition on Immune Defense in Parasitic Infection. Nestlé Foundation Publication Series, Vol.2. A Nestlé Foundation Workshop, Lutry, Lausanne, September 1980. Pp.199. ISBN 3-456-81110-1. (Hans Huber, Bern, Stuttgart, Vienna: 1981.) Fr.34, DM 37.

KIERNAN, J.A. Histological and Histochemical Methods: Theory and Practice. Pp.344. Hbk ISBN 0-08-024936-1; flexi ISBN 0-08-024935. (Pergamon: 1981.) Hbk £29, $70; flexi £10.50, $22.

LAHUE, R. (ed.). Methods in Neurobiology. Vol.2. Pp.665. ISBN 0-306-40518-0. (Plenum: 1981.) $44.75.

LAMY, J. and LAMY, J. (eds). Invertebrate Oxygen-Binding Proteins. Structures, Active Site and Function. Pp.836. ISBN 0-8247-1243-9. (Marcel Dekker: 1981.) SwFr. 242.

LANGONE, J.J. and VAN VUNAKIS, H. (eds). Immunochemical Techniques Part B. Methods in Enzymology, Vol.73. Pp.739. ISBN 0-12-181793-6. (Academic: 1981.) $59.

LETT, J.T. and ADLER,H. (eds). Advances in Radiation Biology, Vol.9. Pp.473. ISBN 0-12-035409. (Academic: 1981.) $55.

LEVY, S.B., CLOWES, R.C. and KOENIG, E.L. (eds). Molecular Biology, Pathogenicity, and Ecology of Bacterial Plasmids. Proceedings of the International Conference held January 1981 in Santo Domingo, Dominican Republic. Pp.708. ISBN 0-306-40753-1. (Plenum: 1981.) $69.50.

LEWIS, P.J. and O'GRADY, J. (eds). Clinical Pharmacology of Prostacyclin. Pp.274. ISBN 0-89004-591-7. (Raven: 1981.) $29.50.

LEYDHECKER, W. and CRICK, R.P. All About Glaucoma. Questions and Answers for People with Glaucoma. Pp.76. Hbk ISBN 0-571-11764-3; pbk ISBN 0-571-11765-1. (Faber & Faber, London: 1981.) Hbk £4.95; pbk £1.95.

LOWENSTEIN, J.M. (ed.). Lipids Part C. Methods in Enzymology, Vol.71. Pp.857. ISBN 0-12-181971-X. (Academic: 1981.) $65.

MAJDE, J.A. and PERSON, R.J. (eds). Pathophysiological Effects of Endotoxins at the Cellular Level. Progress in Clinical and Biological Research, Vol.62 Proceedings of a Symposium Sponsored by the Office of Naval Research held in Washington, D.C. Pp.204. ISBN 0-8451-0062-9. (Alan R. Liss, New York: 1981.) £21.90, DM 96.

MANGE, A.P. and MANGE, E.J. Genetics: Human Aspects. Pp.675. ISBN 0-03-056751-3. (Saunders College, Philadelphia, Pennsylvania: 1980.) Np.

MANN, T. and LUTWAK-MANN, C. Male Reproductive Function and Semen. Themes and Trends in Physiology, Biochemistry and Investigative Andrology. Pp.495. ISBN 3-540-10383-X. (Springer-Verlag: 1981.) DM 150, $71.40.

MANUILA, A. (ed.). Progress in Medical Terminology. Pp.116. Flexi ISBN 3-8055-2112-X. (Karger, Basel: 1981.) SwFr.79, DM 95, $47.50.

MATSUMOTO, G. and KOTANI, M. Nerve Membrane: Biochemistry and Function of Channel Proteins. Proceedings of the 5th Taniguchi International Symposium, Tsukuba, November 1979. Pp.250. UTP 3045-68658-5149. (University of Tokyo Press/Global Book Resources, London: 1981.) £19.50.

MORRIS, D.R. and MARTON, L.J. (eds). Polyamines in Biology and Medicine. The Biochemistry of Disease, Vol.8. Pp.459. ISBN 0-8247-1342-7. (Marcel Dekker: 1981.) SwFr. 156.

MUGGLETON-HARRIS, A.L. (ed.). International Review of Cytology. Supplement 12, Membrane Research, Classic Origins and Current Concepts. Pp.428. ISBN 0-12-364373-2. (Academic: 1981.) Np.

MULLINS, L.J. Ion Transport in Heart. Pp.144. ISBN 0-89004-645-X. (Raven: 1981.) $16.50.

MUSACCHIA, X.J. and JANSKY, L. (eds). Survival in the Cold. Hibernations and Other Adaptations. Proceedings of the International Symposium, Prague, Czechoslovakia, July 1980. Pp.225. ISBN 0-444-00635-4. (Elsevier/North-Holland: 1981.) $50, Dfl. 133 (U.S.A.) $65 (elsewhere).

OPPENHEIMER, S.B. Introduction to Embryonic Development. Pp.404. ISBN 0-205-07348-4. (Allyn & Bacon: 1980.) Np.

PATE, J.S. and McCOMB, A.J. (eds). The Biology of Australian Plants. Pp.412. Pbk ISBN 0-85564-194-0. (University of Western Australia Press: 1981.) $25.

PERLMAN, D. (ed.). Advances in Applied Microbiology, Vol. 26. Pp.271. ISBN 0-12-002626-0. (Academic: 1980.) $29.50.

POAG, C.W. Ecologic Atlas of Benthic Foraminifera of the Gulf of Mexico. Pp.174. ISBN 0-87933-900-4. (Academic: 1981.) $27.50.

REISFELD, R.A. and FERRONE, S. Current Trends in Histocompatibility. Vol. 1, Immunogenetic and Molecular Profiles. Pp.543. ISBN 0-306-40480-X. (Plenum: 1981.) $36.25.

REISFELD, R.A. and FERRONE, S. (eds). Current Trends in Histocompatibility. Vol. 2, Biological And Clinical Concepts. Pp.311. ISBN 0-306-40481-8. (Plenum: 1981.) $36.25.

RICHARDSON, D.H.S. The Biology of Mosses. Pp.220. Flexi ISBN 0-632-00782-6. (Blackwell Scientific: 1981.) £9.80.

RIDGWAY, S.H. and HARRISON, R.J. (eds). Handbook of Marine Mammals. Vol. 1, The Walrus, Sea Lions, Fur Seals and Sea Otter. Pp.235. ISBN 0-12-588501-6. (Academic: 1981.) £14.60, $35.50.

RIDGWAY, S.H. and HARRISON, R.J. (eds). Handbook of Marine Mammals. Vol. 2, Seals. Pp.350. ISBN 0-12-588502-4. (Academic: 1981.) £20.20, $48.50.

RITZEN, M. *et al.* (eds). The Biology of Normal Human Growth. Transactions of the 1st Karolinska Institute Nobel Conference. Pp.350. ISBN 0-89004-588-7. (Raven: 1981.) $38.50.

ROBERTS, P.J., STORM-MATHISEN, J. and JOHNSTON, G.A.R. (eds). Glutamate: Transmitter in the Central Nervous System. Pp.226. ISBN 0-471-27951-X. (Wiley: 1981.) £16.50.

WATKINS, G.M. (ed.). Compendium of Cotton Diseases. Pp.87. Pbk ISBN 0-89054-031-4. (The American Phytopathological Society, St. Paul, Minnesota: 1981.) Pbk $11.

WEBER, G. (ed.). Advances in Enzyme Regulation, Vol.19. Proceedings of the 19th Symposium on Regulation of Enzyme Activity and Synthesis in Normal and Neoplastic Tissues held at Indiana University School of Medicine, Indianapolis, Indiana, October 1980. Pp.571. ISBN 0-08-027393-9. (Pergamon: 1981.) $125.

WHARTON, C.W. and EISENTHAL, R. Molecular Enzymology: Tertiary Level Biology. Pp.326. ISBN 0-216-91012-9. (Blackie: 1981.) £19.75.

WILLIAMS, E.D., SIEBENMANN, R.E. and SOBIN, L.H. Histological Typing of Endocrine Tumours. International Classification of Tumours, No.23. Pp.69. ISBN 92-4-176023-0. (WHO: 1980.) SwFr.204 (includes set of 146 colour transparencies) book only SwFr.58.

WILLIAMSON, R. (ed.). Genetic Engineering, 2. Pp.204. Pbk ISBN 0-12-270302-2. (Academic: 1981.) Pbk £9.80, $24.

WILLS, C. Genetic Variability. Pp.312. ISBN 0-19-857570-X. (Clarendon Press/Oxford University Press: 1981.) £24.

WINTERBOURN, M.J. and GREGSON, K.L.D. Guide to the Aquatic Insects of New Zealand. Bulletin of the Entomological Society of New Zealand, 5. Pp.80. Pbk ISBN 0-477-06673-9. (Entomological Society of New Zealand, Huia, New Zealand: 1981.) Pbk NZ $9 + postage.

WOLBURG, H. Axonal Transport, Degeneration, and Regeneration in the Visual System of the Goldfish. Advances in Anatomy, Embryology and Cell Biology, Vol.67. Pp.94. Flexi ISBN 3-540-10336-8. (Springer-Verlag: 1981.) DM 48, $25.20.

YASAKA, T. (ed.).Progress in Health Monitoring (AMHTS). Proceedings of the International Conference on Automated Multiphasic Health Testing and Services, Tokyo, October 1980. Pp.545. ISBN 0-444-90198-1. (Excerpta Medica, Amsterdam: 1981.) $95, Dfl.195.

YOUNG, M. *et al.* (eds). Placental Transfer: Methods and Interpretations. Pp.250. ISBN 0-7216-9661-9. (W.B. Saunders: 1981.) Np.

Applied Biological Sciences

BERNER, P., LENZ, G. and WOLF, R. (eds). Current Perspectives in Lithium Prophylaxis. Bibliotheca Psychiatrica, No.161. International Symposium on Aktuelle Perspektiven der Lithiumprophylaxe, Vienna, October 1979. Pp.248. Flexi ISBN 3-8055-1753-X. (Karger, Basel: 1981.) SwFr.88, DM 105, $52.75.

CALIENDO, M.A. Nutrition and Preventive Health Care. Pp.705. ISBN 0-02-318330-6. (Collier Macmillan: 1981.) £12.95.

CARTER, S.K., SAKURAI, Y. and UMEZAWA, H. (eds). New Drugs in Cancer Chemotherapy. Recent Results in Cancer Research, Vol.76. Pp.336. ISBN 3-540-10487-9. (Springer-Verlag: 1981.) DM 98, $46.70.

EMEJUAIWE, S.O., OGUNBI, O. and SANNI, S.O. (eds). GIAM VI. Global Impacts of Applied Microbiology. 6th International Conference. Pp.652. Pbk ISBN 0-12-238280-3. (Academic: 1981.) Pbk £26.80, $49.50.

LAWSON, R.H. National Work Conference on Microbial Collections of Major Importance to Agriculture. Report of the Conference convened at the University of Maryland, College Park, Maryland, March 1980. Pp.52. ISBN 0-89054-044-6. (The American Phytopathological Society, St. Paul, Minnesota: 1981.) $6.50.

LIEBERMAN, H.A. and LACHMAN, L. (eds). Pharmaceutical Dosage Forms, Tablets, Vol.2. In Three Vols. Pp.520. ISBN 0-8247-1269-2. (Marcel Dekker: 1981.) SwFr.165.

NAJEAN, Y., TOGNONI, G. and YUNIS, A.A. (eds). Safety Problems Related to Chloramphenicol and Thiamphenicol Therapy. Pp.118. ISBN 0-89004-547-X. (Raven: 1981.) $13.50.

NINET, L. *et al.* (eds). The Future of Antibiotherapy and Antibiotic Research. Based on the Proceedings of the 2nd Rhône-Poulenc Round Table Conference held in Paris, February 1980. Pp.508. ISBN 0-12-519780-2. (Academic: 1981.) £25, $60.

OREN, O.H. (ed.). Aquaculture of Grey Mullets. International Biological Programme, 26. Pp.507. ISBN 0-521-22926-X. (Cambridge University Press: 1981.) £55.

SHAPIRO, J. Radiation Protection. A Guide for Scientists and Physicians. 2nd Edn. Pp.480. ISBN 0-674-74584-1. (Harvard University Press: 198 Combustion Science, Vol.6. Pp.395. ISBN 0-08-027153-7. (Pergamon: 1981.) £51, $118.

STRAUB, W. (ed.). Current Genetic, Clinical and Morphologic Problems. Developments in Ophthalmology, Vol.3. Pp.218. ISBN 3-8055-2000-X. (Karger, Basel: 1981.) SwFr.157, DM 188, $94.

TESI, M. and DORMANDY, J.A. (eds). Vascular Occlusion: Epidemiological, Pathophysiological and Therapeutic Aspects. Proceedings of the Serono Symposia, Vol.37. Pp.474, ISBN 0-12-685380-0. (Academic: 1981.) £28.80, $69.50.

Sociology

FORSLIN, J., SARAPATA, A. and WHITEHILL, A.M. (eds). Automation and Industrial Workers. A Fifteen Nation Study, Vol.1, Part 1. Pp.249. ISBN 0-08-023339-2; Vol.1, Part 2. Pp.303. ISBN 0-08-024310. (Pergamon: 1981.) £42, $100. 2-Vol. set.

LERNER, M.J. and LERNER, S.C. (eds). The Justice Motive in Social Behavior. Adapting to Times of Scarcity and Change. Pp.494. ISBN 0-306-40675-6. (Plenum: 1981.) $32.50.

LOZOYA, J.A. and BIRGIN, H. (eds). Social and Cultural Issues of the New International Economic Order. Pp.212. ISBN 0-08-025123-4. (Pergamon: 1981.) £10, $20.

MEACHAM, J.A. and SANTILLI, N.R. (eds). Social Development in Youth: Structure and Content. Contributions to Human Development, Vol.5. Pp.186. Flexi ISBN 3-8055-2868-X. (Karger, Basel: 1981.) SwFr. 73, DM 87, $43.75.

WOLF, S. Social Environment and Health. The Jessie and John Danz Lectures. Pp.126. ISBN 0-295-95777-8. (University of Washington Press: 1981.) $8.95.

General

ALEXANDER, J. In Praise of the Common Man. Pp.86. Pbk ISBN 0-931826-02-0. (Sitnalta Press, San Francisco: 1980.) $9.95.

ARNON, I. Modernization of Agriculture in Developing Countries: Resources, Potentials and Problems. Pp.565. ISBN 0-471-279285. (Wiley: 1981). £29.50, $66.50.

BEAL, R.C., DeLEONIBUS, P.S. and KATZ, I. (eds). Spaceborne Synthetic Aperture Radar for Oceanography. Pp.215. ISBN 0-8018-2668-3. (The Johns Hopkins University Press: 1981.) £15.75, $28.10.

BONES, J. Jr. Texas West of the Pecos. Pp.136. ISBN 0-89096-117-4. (Texas A & M University Press: 1981.) $29.95.

BRENNER, M.J. Nuclear Power and Non-proliferation: The Re-making of U.S. Policy. Pp.324. ISBN 0-521-23517-0. (Cambridge University Press: 1981.) £20.

CHAMBERLAIN, M. Old Wives' Tales. Their History, Remedies and Spells. Pp.284. Hbk ISBN 0-86068-015-0; pbk ISBN 0-86068-016-9. (Virago, London: 1981.) Hbk £7.50; pbk £4.50.

COOPER, C. Economic Evaluation and the Environment: A Methodological Discussion With Particular Reference to Developing Countries. Pbk ISBN 0-340-26555-8. (Hodder & Stoughton, Sevenoaks, UK: 1981.) Pbk £8.

DENT, D. and YOUNG, A. Soil Survey and Land Evaluation. Pp.278. Hbk ISBN 0-04-631013-4; pbk ISBN 0-04-631014-2. (Allen & Unwin, London: 1981.) Hbk £15, $35; pbk £7.95, $17.50.

DOLMAN, A.J. Resources, Regimes, World Order. Pp.411. Hbk ISBN 0-08-028080-3; pbk ISBN 0-08-028079-X. (Pergamon: 1981.) Pbk £4.85. (Hbk to be published.)

DOMMEN, E. (ed.). Islands. Special Programme for Least-Developed Land-Lacked and Island Developing Countries UNCTAD, Geneva. Pp.1061. ISBN 0-08-026799-8. (Pergamon: 1981.) £7.50, $18.

DURANT, F.C. III (ed.). Between Sputnik and the Shuttle: New Perspectives on American Astronautics. AAS History Series, Vol.3. Pp.334. Hbk ISBN 0-87703-145-2; pbk ISBN 0-87703-149-5. (American Astronautical Society, California: 1981.) Hbk $40, pbk $30.

EYSENCK, H.J. (ed.). A Model for Personality. Pp.287. ISBN 3-540-10318-X. (Springer-Verlag: 1981.) DM 78, $37.20.

FELIX, R., KAZNER, E. and WEGENER, O.H. (eds). Contrast Media in Computed Tomography. International Workshop, Berlin, January 1981. Pp.302. ISBN 90-219-0502-7. (Excerpta Medica, Amsterdam: 1981.) $51, Dfl. 120.

FEYERABEND, P.K. Problems of Empiricism. Philosophical Papers, Vol.2. Pp.255. ISBN 0-521-23964-8. (Cambridge University Press: 1981.) £17.50.

FREEMAN, H. and PIERONI, G.G. (eds). Map Data Processing. Proceedings of a NATO Advanced Study Institute held in Maratea, Italy, June 1979. Pp.374. ISBN 0-12-267180-5. (Academic: 1980.) $26.

GARCIA, R.V. and SMAGORINSKY, J. Drought and Man. The 1972 Case History. Vol.1, Nature Pleads Not Guilty. Pp.300. ISBN 0-08-025823-9. (Pergamon: 1981.) £25, $60.

GILL, P.E., MURRAY, W. and WRIGHT, M.H. Practical Optimization. Pp.401. ISBN 0-12-283950-1. (Academic: 1981.) £19.20, $46.50.

GLAESER, P.S. (ed.). Data for Science and Technology. Proceedings of the Seventh International CODATA Conference, Kyoto, Japan, October 1980. Pp.615. ISBN 0-08-026201-5. (Pergamon: 1981.) £62.50, $150.

GODWIN, H. The Archives of the Peat Bogs. Pp.229. ISBN 0-521-23784-X. (Cambridge University Press: 1981.) £25.

GOODMAN, G.T., KRISTOFERSON, L.A. and HOLLANDER, J.M. The European Transition From Oil: Societal Impacts and Constraints on Energy Policy. Based on the Proceedings of the 49th Nobel Symposium held by the International Institute for Energy and Human Ecology (Beijer Institute), Royal Swedish Academy of Sciences, Stockholm, Sweden, April 1980. Pp.338. ISBN 0-12-290420-6. (Academic: 1981.) £20.60, $49.50.

GREENE, J.C. Science, Ideology, and World View. Essays in the History of Evolutionary Ideas. Pp.202. ISBN 0-520-04217-4. (University of California Press: 1981.) Hbk £11.50, $20.60; pbk £4, $7.45.

GUYENNE, T.D. and LÉVY, G. (eds). Spacecraft Flight Dynamics. Proceedings of an International Symposium, May 1981, Darmstadt, Germany. Pp.494. Pbk ISSN 039-6566. (ESA, Paris: 1981.) Np.

HAMMOND, J.H. The Camera Obscura: A Chronicle. Pp.182. ISBN 0-85274-451-X. (Adam Hilger, Bristol: 1981.) £13.50.

HAWKINS, A.D. (ed.). Aquarium Systems. Pp.452. ISBN 0-12-333380-6. (Academic: 1981.) £27.80, $67.

nature

4 February 1982

Test-tube babies pilloried again

Physicians' organizations in the United Kingdom are busying themselves with an examination of the ethics of in vitro fertilization and related developments. Why now? And to what end?

The British medical establishment seems bent on making an unpalatable mess of its consideration of the ethical problems occasioned by recent developments in the treatment of human infertility. This week, the ethical committee of the British Medical Association will have held a private but much publicized meeting to brood about the ethical implications of *in vitro* fertilization and the possibility of setting up banks of frozen sperms, oocytes and even embryos. And the Royal College of Obstetricians and Gynaecologists is embarking on a joint exercise with the same objectives. Naturally enough, an army of pundits has joined in the fuss, announcing to an astonished world that a new revolution of technique has suddenly taken place and that a novel set of legal conundrums has been created overnight. Whether or not physicians are enlightened by the work of the committees now hard at work, it is certain that the public will be confused.

The issues provoked by human embryology are by no means novel. For the past fifteen years, Mr Patrick Steptoe and Dr R.G. Edwards have made no secret of their ambitions to use *in vitro* fertilization of oocytes as a means of treating human infertility. The novelty is merely that their techniques are now reproducibly successful, in Britain but also in other places (see R.G. Edwards, *Nature* **293**, 253; 1981). Although first thought of as a technique for treating female infertility, *in vitro* fertilization has also turned out to be a means of arranging for the conception of a live fetus by an oligospermic male partner to a marriage.

Strictly speaking, however, these novel developments occasion no novel ethical or legal problems. So much was made clear in the report in 1974 of a committee of the British Association for the Advancement of Science (see *Our future inheritance: Choice or chance* by Walter Bodmer and Alun Jones, OUP). For it seems generally agreed that conception is preferable to childlessness within a marriage, and that *in vitro* fertilization using a husband's sperm is preferable to fertilization (by artificial insemination) with male gametes from some sperm bank or donor. It may be appropriate (but can hardly be necessary) that physicians should have guidance in advising their patients when one form of treatment or the other may be advisable; they are more likely themselves to be guided by specialists in the field. It is entirely inappropriate that they should be given the false impression that entirely novel issues have been raised.

One particular red herring, wrongly linked with the practice of *in vitro* fertilization because of a recent wave of publicity in Britain, is the fear that there will emerge a new profession of surrogate mothers — people offering uterine hospitality to *in vitro* embryos. The chances of this happening more often now than hitherto are small, while legal precedent suggests that children born in such circumstances would be the children of their host — and that their later disposal would be governed by the law regulating adoption, including the customary strict interdiction against money changing hands.

Superficially at least, sperm banks and frozen embryos are different. That, however, is more illusion than reality. Given that many couples who at present cannot conceive children naturally are driven to AID, what is more natural than that they should seek to make good their disappointment by looking for some genetic authentication of the sperms they eventually use? Such a system would indeed be far preferable to the present amateurish ways of collecting sperms without pedigrees, but it would of course be unacceptable that sperms should be sold at outrageous profit and that the identity of their donors should be advertised or even disclosed. For such reasons, and also because genetic authentication requires supervision, legislation for the licensing of sperm banks is plainly necessary. It goes without saying, however, that sperm banks cannot offer those who use them more than a negative bill of good health; to say that some known genetic defects are absent is not the same as to promise that the particular combination of paternal genes that meiosis had provided in a sperm will be thoroughly welcome.

Similar arguments limit the likely uses of frozen embryos. The bizarre uses of the technique to propagate an endless succession of children from the same parents, often long dead, will run foul of the unwillingness of women to give hospitality to other people's children (and of the long-established unwillingness of physicians to assist them). But the technique might help to avoid maternally transmitted defects, and should for that reason be welcomed in the rare cases in which it is likely to be used. If ethical committees wish to brood about something tangible, they should worry about cloning — still some way off, but no longer out of sight. The trouble is that such a technique may seem to some to offer means of eugenic improvement justifying all kinds of clandestine stratagems — and which are likely, in the end, to be disappointed by the genetic defects well recognized in amphibian cloning. The best safeguard, for the time being at least, is to require that people engaged on such experiments should discuss the implications of their projects with a suitably independent laboratory committee.

Washington Editor, *Nature*

Ms Deborah Shapley has been appointed Washington Editor of *Nature* in succession to Mr David Dickson, who is leaving the journal at the end of March, after four years in the post. Ms Shapley, a graduate of Harvard University, has worked for the MIT alumni journal *Technology Review* (1968–71) and *Science* (1971–79). She is at present Guest Scholar at Resources for the Future Inc. in Washington, DC after three years at the Carnegie Endowment for International Peace; she is completing a book on Antarctica on a project supported by the Carnegie Endowment.

Nature is looking for a second member of staff to join the Washington office, primarily as a reporter and to commission various contributions to the journal. A formal advertisement will appear next week.

Down with airline cartel

The collapse of Laker Airways should provoke an outcry against government interference.

The benefits of a new technology cannot be assessed in the abstract, but only in the marketplace. This is the conventional wisdom. Whatever ingenuity is lavished on, say, the improvement of mousetraps, an innovation can be counted a success only if its performance and price command a sale among those seeking to rid themselves of mice. For mousetraps and similar products, the primacy of the marketplace is well-established. In other fields of technology, however, all governments choose to suspend the rules

0028-0836/82/060445-02$01.00

in their own narrow and political interests. They habitually give national manufacturers preference in much of their own purchasing of technological products, from computers to power stations. The result is that the potential benefits of technological advance, and especially potential reductions of costs to ultimate consumers, are needlessly and often scandalously diluted. And scandal is nowhere more rampant than in the airline business, where the potential benefits of a beneficent aeronautical technology are watered down by the insistence of national governments that the places to which aircraft fly should be decided not by the marketplace but by negotiations among diplomats, and that airline fares should be decided by an international price-fixing cartel organized by the United Nations, the International Air Transport Association (IATA).

The only comfort in the unfortunate financial collapse at the weekend of the independent British airline Laker Airways is that the folly of governments' attempts to regulate the world's airlines may now be more widely recognized. Laker Airways, not a member of IATA, has won its reputation in the past five years by offering cheap fares on various transatlantic routes from the United Kingdom. Its attempts to bust the international cartel on routes between Britain and the rest of Europe were, however, frustrated by the unwillingness of governments other than the British to expose their national airlines to competition. While the airline's collapse is probably as much a consequence of commercial overoptimism as of unrealistic expectations that it would be allowed to continue to expand, the suspicion remains that it would not have run into trouble if the international airline business were, in the commercial sense, a business.

The difficulty lies in the widespread assumption by governments that a soveriegn government without an airline is like a baseball team without a stadium — incomplete and unconvincing. For how would it seem, in the domestic newspapers, if a president or a prime minister were seen alighting in some foreign capital from an aircraft operated by some carrier other than the national airline? Worse still, how could those lined up to receive such a personage be expected to take the visit seriously if he or she were seen to be a mere fare-paying passenger? (The calculation that since many of these journeys are made with the objective of borrowing money, and that ostentatious extravagance might in the circumstances prudently be avoided, is usually overlooked.) One result is that most governments shoulder without too much complaint the direct subsidies their airlines cost (but the United States government provides hidden subsidies instead). Another is that, to ensure that their national airlines have something to do when not transporting dignitaries about the world, governments assume the right to negotiate strictly bilateral agreements with each other to regulate the numbers of flights by national airlines that there should be. Then, to limit the subsidies they must provide, governments agree that their national airlines should rig the prices that they charge.

To be fair, both the British and the United States governments have recently been trying to break free from this pattern. Within the United States, the consequences of substantial deregulation of domestic flights in the past two years have been dramatic, both in providing cheaper fares and in showing which among the competing airlines are the weak and which the strong. In Britain, the government has allowed small and sometimes new independent airlines to operate new routes and has also encouraged independent carriers such as Laker to seek business abroad. Even if, however, a substantial part of the stock in British Airways is eventually sold to the public, the existing apparatus of horsetrading for routes and price-fixing for fares will remain. For, as things are, the restrictive practices now operated by governments and their national airlines serve one practical purpose — they protect governments from themselves and from each other.

So long as most airlines are supported financially by some public and thus supposedly bottomless purse, price-fixing is defensible. Without it, there would be nothing to prevent airlines in collusion with their governments from openly selling airline tickets below the full cost of servicing them, decreasing its own financial loss by making fuller use of its aircraft and, in the process, transferring the loss to some other carrier. The snag, of course, is that those who rig the prices are the national airlines, with no conspicuous interest in competition. Bilateral agreements on which airlines should be allowed to fly which routes should in principle be unnecessary if fares have been fixed correctly, taking full account of the costs of servicing capital as well as of flying aircraft.

Not least from nostalgia for the Laker enterprise (which may yet be rescued), the time has come when this bumbledom should be replaced. Regulations, unfortunately, cannot be entirely set aside, for international air transport is socially and commercially too important to be exposed to the risk of commercial cartelization, potentially as damaging as that now operated by governments. But the present regulation of air transport could and should be replaced by a system consisting of very little more than a set of common rules by which competition is permitted.

The first essential ingredient of such a system is that competition on routes and fares should be freely allowed between airlines provided that they do not enjoy the support of governments, direct or indirect. Common standards of safety would be necessary (as at present), but an airline able to pay its pilots and other people less than its competitors should be entitled to charge lower fares. Arrangements would be necessary to ensure that airlines did not subsidize competitive routes or some categories of passengers at the expense of others, but such tasks are familiar and well within the competence of accountants.

But how, if governments are wedded to the concept of a national airline, can such a state of grace be reached? Fortunately, at least some governments seem now to be disenchanted with the need to hand out subventions every year. Why should they not club together to put the airline business on a rational footing, using the existing apparatus of restriction and pricerigging to regulate their dealings with the airlines of more backward states? Even if only Britain and the United States were able to make a deal along these lines, a telling example would be provided for the others. But the natural place for an agreement is within the European Community, which has been talking about the issue for a decade to no effect.

New budget, no change

Science does well, on paper, in the US budget for 1983. But the promise is paper-thin.

President Ronald Reagan's second budget (or is it his fifth?) is, as predicted, kind to science but, unexpectedly, beastly to the conservative aspirations of the President's supporters. Although there will be many disappointments in the proposals published at the weekend, many of the obvious ways in which economies might have been sought have been avoided. The new (and much delayed) accelerator at Brookhaven is not permanently scrapped but put into suspended animation. The basic research programme supported by the budget of the National Aeronautics and Space Administration survives more robustly than seemed likely only a few months ago, marred only by the folly of the decision that there will be even less support for attempts to make sense of the data existing and new which spacecraft will collect. Similarly, the chief sources of support for research at United States universities — the National Science Foundation and the National Institutes of Health — are to be protected from the consequences of inflation. If only (but see page 449) the Department of Defense can spend some of its extra money in the universities, the research community will be in good shape.

The snags are less easily defined. Cutting back on student support will put more severely to the test than in the past few months the unproven hope that students will, when pushed, work their way through every course of study — and may be disastrous. Even more seriously, the cavalier decision that budgets need not be balanced, with its inflationary and international consequences, may so undermine the economic well-being of the United States that the formal protection of research will count for nothing.

0028-0836/82/060447-01$01.00

DNA panel has second thoughts

Mandatory rules not yet to be abandoned

Washington

Bending to political realities, the Recombinant DNA Advisory Committee (RAC) to the US National Institutes of Health (NIH) has backed away from its support for a proposal that guidelines covering NIH-sponsored research using recombinant DNA techniques should be made voluntary, and that research institutions should no longer be formally required to establish safety committees to ensure that the guidelines are observed.

At its last meeting in September, the members of RAC decided to support the publication for public comment of the proposals for major revisions to the guidelines that would essentially transform them into a voluntary code of conduct.

However, in the light of the comments received — and in particular of warnings that if the guidelines become voluntary states such as California are likely to introduce their own more restrictive regulations — RAC on Monday adopted a compromise formula that would streamline the containment requirements for different types of experiments, but retain their mandatory aspects. Two proposals had been put out for comment. One, a revision of amendments originally proposed by Dr Alan Campbell of Stanford University and Dr David Baltimore of Massachusetts Institute of Technology, would eliminate all the mandatory requirements of the guidelines, including the sanction that noncompliance could lead to a loss of NIH funds.

The alternative proposal, submitted by RAC-member Dr Susan Gottesman of the National Cancer Institute, would retain the guidelines as a required procedure for those receiving NIH grants, including the requirement that certain experiments be reviewed either by RAC or by local Institutional Biosafety Committees (IBCs). The containment classifications, however, would be reorganized, and containment requirements for some classes of experiments would be made less stringent.

The potential consequence of transforming the guidelines into a code of practice for community opinion at local and state levels dominated the discussions.

Most informed scientists who had sent in written comments expressed strong support for making guidelines voluntary, arguing that risks once thought plausible had now been shown to be either remote or non-existent. Dr Paul Berg of Stanford University, for example, one of the three signatories of the original letter suggesting a moratorium on rDNA research, wrote that he believed the guidelines "are now dispensable".

The institutional response, however, has been different. Many local IBCs, those in universities and in private industry, told NIH that they were not experiencing major difficulties in implementing the guidelines as they now stood. Several warned that the absence of mandatory federal guidelines would provide an opportunity for the introduction of a patchwork of individual laws.

The Industrial Biotechnology Association, for example, which represents a number of small biotechnology companies such as Cetus and Genex, wrote that "one significant reason for adherence to a uniform system of federal guidance and overseeing is our belief that such an approach is more compatible with commercial development and the benefits it brings to society than would be a system of varying local requirements".

If there was an unexpected consensus at Monday's meeting that a strong federal presence in regulating rDNA research remains desirable, there was less agreement on whether the potential hazards of such research should be treated differently from related areas of biomedical research.

Some members of the committee, arguing the lack of substantial evidence of additional hazard, suggested that this was a reason for adopting uniform practices by making guidelines voluntary. Others, however, used the same data to urge that the experience of RAC should be used as a basis for encouraging a similar approach to research with other organisms.

After hearing the arguments for both proposed revisions, the members of the committee voted by 17 to 3 to adopt those put forwards by Dr Gottesman as the basis for revising the guidelines, rather than those which had been informally endorsed at the September meeting. It also agreed to set up a small working group to revise the specific recommendations which she had put forward to change the current classifications, and to present its conclusions to the director of the National Institute for Allergic and Infectious Diseases, Dr Richard Krause, who will decide what changes to the guidelines will be introduced.

David Dickson

Budget protection for research

Washington

The United States scientific community has done relatively well out of the budget proposals which President Ronald Reagan submitted to Congress on Monday for the fiscal year 1983, which begins on 1 October.

Overall, the President is requesting an increase of about 10 per cent in expenditure on research and development. With an officially-estimated inflation rate of 6.5 per cent, the Administration is claiming that this would represent a real growth in research and development of about 3.5 per cent. The same pattern of growth is being suggested for the basic research budget, scheduled to increase by 8.8 per cent to a total of $5,821 million.

In both instances, the major contribution to this growth has been increased spending on military research, which rose 25 per cent between 1981 and 1982, and is scheduled for a further growth of 18.9 per cent next year.

Where these increases reflect Mr Reagan's election campaign promises to boost United States military strength, another promise is reflected in moves to reduce substantially federal sponsorship of energy research, on the grounds that this should, where possible, be made the responsibility of the private sector.

The most dramatic reductions are proposed in solar research and other renewable energy sources, such as hydropower and geothermal, scheduled to come

Recommended budget obligations for fiscal year 1983

	Research and development		Basic research	
	Total (million $)	Increase 1982–83(%)	Total (million $)	Increase 1982–83(%)
Department of Defense	24,469	18.9	781	16.0
National Aeronautics and Space Administration	6,513	12.1	682	17.6
Energy Research and Technology Administration*	3,917	-13.3	741	14.5
National Institutes of Health	3,533	3.1	1,897	3.1
National Science Foundation	1,033	7.5	984	7.9
US Department of Agriculture	838	3.8	359	8.1
Environmental Protection Agency	230	- 27.4	10	- 50.0
Other agencies	2,464		367	
Total	42,997	10.7	5,821	8.81

*Previously Department of Energy, intended to become part of the Department of Commerce.

0028-0836/82/060446-02$01.00

down from $248 million in 1982 to $83 million in 1983. Energy conservation research would be reduced even more drastically, from $144 million to $18 million; both proposed cuts are expected to be challenged in Congress.

Another agency which has been the target of criticism from the private sector and which would also see its research budget cut under Mr Reagan's 1983 proposals is the Environmental Protection Agency, down from $317 million to $230 million.

Other research agencies, however, have done quite well, reflecting a broadly-based acceptance within the Administration that strong federal support for research and development is a legitimate claim on the public purse.

The National Science Foundation, for example, is listed for a budget increase of 7.5 per cent, with considerable real growth in areas such as computer research (up 14 per cent) to $29.3 million, earth sciences (up 17.8 per cent) and mechanical engineering (up 13.7 per cent). The Administration has relented slightly in its efforts to cut back support for the social and economic sciences, having initially requested $10 million in the 1982 budget, but now supporting a figure of $17.8 million in 1983, the same level to which the 1982 budget was raised by Congress. However, it is sticking to its previous determination to eliminate virtually all science education activities sponsored by the National Science Foundation, arguing that education at the school level should remain primarily a responsibility of the states and local school boards.

The National Institutes of Health are scheduled for a modest 3.1 per cent increase in its research budget, slightly less than the anticipated rate of inflation. Unlike last year, the Administration is not seeking to eliminate institutional support for research training awards, a move which provoked a major outcry from biomedical research institutions.

Inevitably, budgetary stringencies have caused disappointments. The National Aeronautics and Space Administration, for example, has for the moment abandoned plans to send an orbiting imaging radar to Venus; but the rumoured extinction of the Galileo mission to Jupiter failed to materialize, and space science is scheduled for a healthy increase of almost 20 per cent, including full funding for the gamma-ray observatory, as well as sustained support for the space shuttle.

Dr George (Jay) Keyworth, the President's Science Advisor, said on Monday that he was "delighted" with the budget increase for science. He said that the physical sciences, once in jeopardy, had been spared during the review process to enable increased utilization of existing particle accelerators. "Next year", he said, "there will be more effort to separate the mediocre from the excellent in research."

David Dickson

US budget described in outline

Energy support

Washington

Not unexpectedly, the requested budget for the Energy Research and Technology Agency will contain strong support for the Clinch River liquid metal fast breeder reactor. The design and construction of the fast breeder are described as priorities and will receive $257 million for the initiation of site preparation and continued procurement of parts.

However, work on both the Large Development Plant, started by the Carter Administration as an alternative to Clinch River, and the light water breeder reactor will be phased out, leading to an overall decrease of $108 million from 1982 in spending on breeder reactors.

There will also be reduced support for fusion research, with the focus shifting from the construction of new facilities to what the Office of Management and Budget describes as "resolving key outstanding physics and technology issues". This will delay construction of the tandem mirror test facility at the Lawrence Livermore Laboratory, a decision which has contributed to the resignation of the head of the Department of Energy's fusion programme, Dr Edward Kintner.

Funds for inertial confinement fusion, until recently treated as a major alternative to the magnetic fusion programme, have also been reduced from $209 million in 1982 to $119 million in 1983, again through shifting the focus from the completion of new facilities, such as Lawrence Livermore's Nova device, towards experiments on existing machines.

In contrast to the continued — if slightly reduced — support for research into nuclear fusion and fission, only $315 million is being requested to support research in fossil, solar, biomass and other renewable energy sources, compared with $814 million in 1982.

Unrest on loans

If US universities have been relieved at escaping the prospect of heavy cuts in research spending, there is less consolation in the Reagan Administration's proposals to limit its assistance for students by reducing the support for the Guaranteed Student Loan (GSL) programme.

First introduced in 1965, the programme provides loan guarantees and interest subsidies to states, private lending institutions and eligible students. Under the present plans, federal support would increase from $3,397 million in 1983 to $3,768 by 1987. Tightening up on eligibility requirements and increasing the costs of obtaining a guaranteed loan will result in savings of $912 million in 1983, rising to $2,247 million by 1987.

Loans to about 600,000 graduate students would disappear under plans to reduce by about a third the number of so-called Pell awards. Graduate students would be restricted to raising loans from the less-heavily subsidized GSL auxiliary loan programme, and lending institutions would be required to pay a higher insurance premium to the government.

The Administration claims that the cuts are justified on the grounds that the primary beneficiaries of the guaranteed loans have been "middle and upper income families", which had as a result been able to put their own savings into investment schemes yielding far higher returns. The universities, however, are worried that tightening up the loan conditions could lead to a severe drop in student numbers.

David Dickson

ISABELLE

Construction work on ISABELLE, the 400 × 400 GeV proton–proton accelerator at Brookhaven National Laboratory on Long Island, New York, will be halted under budget plans for the Department of Energy for 1983. However, development work will continue as an accelerator research and development programme on superconducting magnets.

In general, high-energy physics has done well in the budget proposals. Mr Reagan is seeking an increase of 17.5 per cent in funding to $429 million, claiming this will allow increased use of existing research facilities, the completion of both the Energy Saver and the Tevatron I and II at Fermilab, and further research and development at the linear collider being planned by Dr Burton Richter at the Stanford Linear Accelerator Center.

Construction on ISABELLE, which started in 1978 and had been due for completion in 1987, has been held up largely due to difficulties with the magnets. Although these now appear to have been solved, the delays have meant extra expense. Last November, a special panel set up by the Department of Energy's High-Energy Physics Advisory Panel to look at the future of US high-energy physics concluded that ISABELLE was still important, but did not place its completion as a first priority in stringent budget conditions.

According to the Office of Management and Budget, the accelerator research at Brookhaven will be related to a "future high-energy physics accelerator project", and "any decision to proceed with this project will be based on overall scientific potential and budget considerations".

Space science

The Venus Orbiting Imaging Radar (VOIR) has been dropped from the National Aeronautics and Space Administration (NASA)'s list of future planetary exploration missions. However, the agency is discussing with space scientists the possibility of launching a

0028-0836/82/060448-02$01.00

cheaper version of the mission, using real rather than synthetic aperture radar, which could halve the estimated $500 million cost and might still be launched by the end of the decade.

VOIR was initially proposed by the Carter Administration two years ago for a launch from the space shuttle in 1986, with the launch being merely postponed to 1988 by the Reagan Administration last March. It is the major casualty in NASA's space science budget, which otherwise is in a much healthier state than had been widely feared.

Both the Galileo mission to Jupiter and the gamma-ray observatory, which had been threatened by the Office of Management and Budget, have survived. Efforts to cut back substantially on space science seem to have been frustrated by strong pressure from the space science community, and fears that the cuts could have a traumatic effect on NASA's Jet Propulsion Laboratory in Pasadena, California.

NASA will not be providing any money for the development of the Centaur rocket as an upper stage for the space shuttle, previously suggested as an alternative to the delayed Inertial Upper Stage.

One area to be cut will be the analysis of data from other planetary missions, being reduced from $61.8 million in 1981 to a suggested $26.5 million in 1983. NASA officials say that although data will continue to be received and analysed from the Voyager spacecraft, now on their way to the outer planets, it may be necessary to stop tracking or taking data from the Pioneer spacecraft.

Delay for *Explorer*

The National Science Foundation has abandoned plans for a major deep-sea drilling programme aimed at investigating the margins of the continental shelf which was to have been conducted from the converted spy ship, *Glomar Explorer*.

Dr John Slaughter, director of the foundation, announced last Saturday that the Reagan Administration would not be requesting any further funds for the so-called ocean margin drilling programme, which was to have been jointly funded with a number of private oil companies.

According to Dr Slaughter there were two reasons for abandoning the project, first formally proposed by the Carter Administrtion two years ago: a lack of sufficient funding, given general pressures on the federal budget; and the lack of interest by companies in making the type of investment required to convert the *Explorer* and fully equip it.

The proposal has also been a controversial one in the scientific community, since it would have meant curtailing funds for the *Glomar Challenger*. Dr Slaughter said that a decision will be made next summer on whether to refurbish the *Explorer* as a replacement for *Glomar Challenger*. **David Dickson**

US defence research

Signs of doubt

Washington

The Reagan Administration is proposing in its latest budget recommendations to Congress (see p447) that there should be an increase in the amount of university-based research sponsored by the Department of Defense in the fiscal year 1983 beginning on 1 October. But the universities themselves are ambivalent about this promise.

Many universities view Defense Department support as a necessary substitute for other federal funds whose sources are rapidly drying up. However, increased military spending on campuses is beginning to act as a catalyst for protest groups opposed to the Administration's policies.

University administrators seem to have fallen in with recent moves by the Department of Defense to increase support for basic research, while fearing some of the restrictions that this money may bring with it. Although many universities still insist that no classified research is carried out on campus, academic leaders have been quick to reassure Congress that little remains of the anti-military sentiment of the 1960s.

Dr Alan Bromley, for example, professor of physics at Yale University and president of the American Association for the Advancement of Science, told the House of Representatives science and technology subcommittee last week that the time to rebuild bridges between the Pentagon and the university research community was "long overdue".

Yet the enthusiasm for increased military support of university research is far from unanimous and there have already been rumblings of protest:

- 170 people from the University of California were arrested last Monday after demonstrating outside the Lawrence Livermore National Laboratory — run by the university on behalf of the Department of Energy — in protest at the laboratory's research on the design of nuclear weapons.
- At the University of Michigan, the students' union has hired a historian to analyse the Defense Department's support of research in the university and in local companies.
- A demonstration was held last summer at the University of Wisconsin's Madison campus over a visit by army scientists to the university's Mathematics Research Center, sponsored by the Department of Defense, to talk about military needs in mathematics. A group has since been formed to study the university's links with the Department of Defense, and a small organization has been set up to stimulate and coordinate efforts by similar groups elsewhere.
- At the Massachusetts Institute of Technology, about 1,000 people held a demonstration when Vice-President George Bush spoke to the institute's board of trustees. Several study groups have since been holding regular meetings on military topics, and 30 faculty members have just launched a disarmament project for the spring term.
- There have been protests at Rutgers over a statement by its president, Dr Edward J. Bloustein at a congressional hearing last year that he would be prepared to consider lifting the current ban on classified research on the campus.
- Last November, "teach-ins" were held at 148 colleges and universities across the country on the arms race. The meetings were coordinated by the Boston-based Union of Concerned Scientists, which claimed that they had been the largest anti-war demonstrations since the Vietnam era.

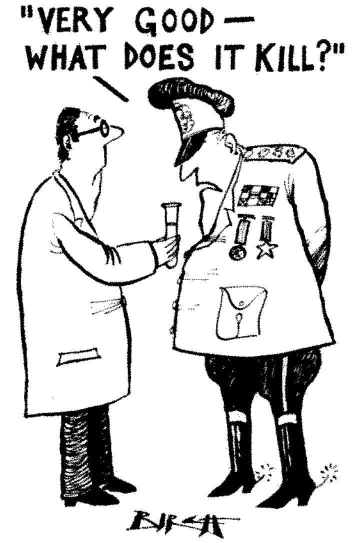
"VERY GOOD — WHAT DOES IT KILL?"

Nobody suggests that these isolated protests represent a significant national movement — at least not yet. Several factors have produced a less fertile environment for protest than the 1960s, ranging from the more conservative outlook of most undergraduates to tight research budgets that can lead to a muting of criticism of the sources of research support.

At the same time, some see as significant the fact that each individual incident has taken place on campuses where there were fierce clashes over military research in the 1960s and early 1970s.

University representatives lobbying the Pentagon for more research funds in Washington tend to play down the potential campus disruption. Even the protesters agree that, although anti-military feeling on campuses has grown rapidly over the past two years, it has yet to coalesce into a major source of opposition.

But the military is still treading warily. When the Defense Communications Agency agreed to sponsor a National Science Center for Communications and Electronics — largely sponsored by the private sector — to stimulate science and engineering education, it chose to concentrate its initial efforts on high schools rather than universities.

Building links with the academic

0028-0836/82/060449-02$01.00

community "could be a very delicate issue" the agency's director and the principal sponsor of the centre, Lt Gen. William Hilsman, said in a recent interview, stating that the schools had been chosen because they were less likely than universities to view the military interest in education as a threat to academic freedom.

Meanwhile the universities themselves are hoping to receive some guidance from a report recently completed by the Defense Science Board for the Department of Defense. The report is expected to recommend the development of clear guidelines to separate basic research from that which may be of a more practical nature — and hence require special protection and treatment. **David Dickson**

British university crisis

Cuts with tears

British universities, still in chaos over how to meet cuts in government income over the next three years, were relieved last week to learn that they are to be compensated for payments made to academics who must lose their jobs. A letter from the University Grants Committee set out the terms under which they will be reimbursed for payments made to redundant staff. Essentially, the compensation scheme is that devised by the Committee of Vice-Chancellors and Principals and blessed by the Secretary of State for Education and Science a week earlier.

The approved scheme allows redundant academic staff below 50 years of age to claim one month's pay for each year of service plus one month's pay for every year of service in excess of five years or after their 30th birthday, whichever is the later. Staff over 50 will be entitled to compensation under the universities' scheme for premature retirement introduced a year ago. The grants committee says that it will not meet claims for compensation that are more generous than those now approved, which begs the question of who will pay if the courts decide that higher awards are just.

The universities' relief will also be tempered by other provisos spelled out in the committee's letter. Full reimbursement willl be made only where universities convince the grants committee that redundancies are made in the interests of economy and that resulting vacancies will not be refilled. Redundancies should also be "consistent with academic planning", a vague phrase thought to give the committee some come-back if universities fail to comply with its advice on general policy.

In the meantime, the end of January deadline by which all universities were to have submitted outlines of how they plan to adapt has passed. Most have sent the numbers of staff they plan to lose by the end of the next academic year, on which basis the grants committee will allocate the £70 million already set aside for helping with restructuring. It seems to be accepted that the sum will be inadequate to settle all claims, although the grants committee has not yet totted up those so far submitted. It is hoped, however, that the government will make more money available by the beginning of the following year.

Only about half the universities have managed to submit returns on how they plan to restructure operations. The grants committee will be looking at the returns later this month, when it will decide whether to reallocate money to those universities that have asked to be reconsidered. The committee is unwilling to say whether the returns suggest that the universities are following its advice, except that one or two of them look "a bit odd".

Some universities seem to have managed to get away with fewer compulsory redundancies than was originally expected. The University of Leicester, for example, plans to make none. The Association of University Teachers claims that success in minimizing compulsory redundancies may reflect the efforts of its members in putting forward alternative strategies for coping with the cuts. **Judy Redfearn**

Correction

In the note in News and Views by Dr R.J. Wilson in last week's *Nature* (4 February, page 369), the third paragraph should, except for a misunderstanding in the *Nature* office, have referred to the work of Professor David Weatherall and his colleagues in the Nuffield Department of Clinical Medicine at the University of Oxford; the article describing this work will be published in *Nature* shortly.

Soviet dissidents

Helpers divided

Scientists campagning for academic freedom and civil and human rights for their less fortunate colleagues cannot confine themselves to a single cause or campaign. This was the consensus of opinion at a one-day seminar at University College, Oxford, on 7 February, organized by the Scientific and Medical Committee for Soviet Jewry.

The main guest was Dr Mark Azbel, from the University of Tel Aviv, himself a former refusnik and convenor of the Moscow Sunday Scientific Seminars for Refusniks, Dar Azbel, like most Soviet Jewish activists believes that a clear distinction should be made between the Jewish emigration movement and the dissident movement in the USSR. Any confusion between the Jews, whose only wish is to leave the Soviet Union, and the dissidents who would prefer to stay there and reform the system from within, is, he believes, dangerous to both movements, allowing the Soviet authorities to accuse the Jews of subversion and dissidents of being agents of international Zionism.

The other participants, however, felt obliged to disagree with him. Professor Paul Kessler from the Collège de France, who spoke on "Visiting Refusniks in the Soviet Union", said that he could not in conscience, while on a vist to Moscow, visit refusniks and refuse to visit dissident scientists who had also, though for other reasons, been expelled from their jobs. Dr Louis Cohen, executive secretary of the Institute of Physics, speaking on "Transnational science as an influence on Soviet science policy", talked not only of the work of his own institute which in 1978 had sponsored the parallel trial in defence of Dr Yurii Orlov, but also the valuable work of the American Association for the Advancement of Science, primarily on behalf of victims of oppression in South America and also for other human rights causes, including the refusniks. Dr Gary Low Beer, who is both head of the Scientific and Medical Committee for Soviet Jewry, and a prominent campaigner against the political misuse of psychiatry, put the point bluntly and pragmatically. One cannot expect one's colleagues to campaign for a human rights cause in which one feels a special interest, if one is unwilling to reciprocate for the causes they favour.

In reply, Dr Azbel explained that he did not want to discourage scientists who wished to campaign for dissidents. Everyone, he said, must choose his own cause. But it was better to campaign for only one person at a time, rather than several in parallel.

His support of this line of action seemed inspired not only by practical considerations but by the Yiddish proverb that to save one life is equivalent to saving all humanity. The seminar particpants, however, applauded him warmly, but clearly still favoured a unified stand by the scientific community as a whole, on all abuses of human rights and academic freedom, wherever they occur. **Vera Rich**

Small growth fund

The fund established by the Association for Research into Restricted Growth as a memorial to Mary Lindley, an assistant editor of *Nature* who died in May 1981, has now reached £700. The group intends to use the money to help young people suffering from restricted growth in problems arising during their early education. Further donations should be sent to the Treasurer, Pam Worsfold, 8 Cotswold Avenue, Chelmsford, Essex.

Polish universities

On hold again

Student protest continues in Poland, in spite of the stern controls on university life imposed by General Jaruzelski's Military Council for National Salvation Plans for the opening of undergraduate courses at the University of Warsaw were shelved again last week, following the widespread distribution of an underground leaflet appealing to students elsewhere to support the Poles' right to academic freedom and the restoration of the banned Independent Students' Association (NZS)

NZS, the leaflet pointed out, was legally recognised by the Lodz accords which concluded five weeks of student protest last spring Almost all the students who held office or played an active part in this legal organization are now, the leaflet said, interned

In Gdansk, the already severe restrictions on student life have apparently been tightened after a 3,000-strong demonstration on 30 January was broken up by riot police The local newspaper, which was only allowed to report the event several days later, said that out of the 205 persons detained, 40 were students and 56 were schoolchildren According to the government's press spokesman, Jerzy Urban, stricter controls have also had to be imposed at Wroclaw Technical University following a student protest march

Wroclaw is a sensitive area, last autumn, when a young mathematics lecturer and Solidarity activist, Kornel Morawiecki, was charged with including provocative and anti-state material in internal union publications, the rector and academic council spoke out strongly in his defence Another Wroclaw mathematician, 68-year old Dr Tadeusz Koszecki, is reported to have died of a heart attack while attempting to protect students during a police raid on 23 December

Expulsions of students and the dismissal of academics unwilling to take the oath imposed by the political "verification" process are reported across the country Unconfirmed reports state that the expulsion rate at the Academy of Mining and Metallurgy in Krakow is as high as 35 per cent — which bodes ill for the future of Poland's two major industries, for which the academy is intended to supply experts and research consultants **Vera Rich**

Euratom treaty

Call for change

Brussels

The Euratom treaty, signed by the European Economic Community's six founder members in 1958, is in urgent need of revision, asserted European Commissioner for Industry and Energy, Vicomte Etienne Davignon, at a press conference on 4 February The Euratom treaty is an instrument setting up a common market for nuclear energy It is intended to guarantee common safety standards and safeguards and to ensure that all nuclear energy users obtain a regular supply of nuclear materials Under the treaty, the European Commission has the exclusive right to conclude supply contracts

The economic advantages of nuclear power are once again argued in this provision policy paper The present 16 per cent of EEC's total electricity production created by nuclear power equalled 56 million tonnes of oil equivalent in 1981 With the planned capacity increase of 69 megawatts by 1990, nuclear energy could supply as much electricity as coal and save imports of 150 million tonnes of oil equivalent

The Commission estimates that electricity from nuclear energy is between 30 and 90 per cent cheaper than that from coal, and compared with petrol nuclear power is 100–150 per cent cheaper Although the investment costs are high, nuclear fuel costs are negligible compared with coal and oil And Davignon considers the nuclear option to have other advantages supplying a bonus in jobs and a high level of technology More detailed economic studies are awaited

In order to boost investment, the Commission wants Euratom loans doubled Credit worth 800 million European currency units (approximately $800 million) has so far been taken up out of the ceiling of 1,000 million fixed in 1977 The new ceiling would then be 2,000 million

More common efforts are called for from the member states in the storage and reprocessing of irradiated waste This could involve the establishment of EEC reprocessing companies In addition, Davignon proposes an end to electricity subsidies, which distort competition among power supplies

The essential element in the new strategy relates to the supply of nuclear materials Here judicial changes to the Euratom treaty are envisaged which might mean dismantling the Commission's exclusive trading rights and leaving Brussels with the task of ensuring that there is discrimination towards purchasing countries By this means, Davignon hopes to stimulate competition among suppliers such as the United States, Canada and Australia with which supply contracts already exist The Community would then only guarantee that the fission materials would be used exclusively for peaceful purposes

To reassure public opinion on nuclear safety, the Commission's proposals provide for a more open policy and more information The system of technical controls and safeguards needs to be updated together with a "concentration of powers" Much the same was recommended in a report by the Belgian Member of the European Parliament, Anne-Marie Lizin (see *Nature* 21 January, p 179)

Jasper Becker

Laboratory animals

Culture sought

A multi-laboratory research programme organized by FRAME (Fund for the Replacement of Animals in Medical Experiments) to investigate alternatives to animal toxicity tests is being backed by several established drugs and cosmetics manufacturers Of the £240,000 needed to support the programme, £180,000 has already been guaranteed The programme involves the collaboration of four laboratories the Huntingdon Research Centre and centres at the University of Surrey, the University of Nottingham and St George's Hospital Medical School in London

Although there have been isolated projects on toxicity testing, this is the first in the United Kingdom to link the work of several laboratories The aim is to scrutinize a common list of chemicals, some toxic, using tissue cultures rather than animals

The programme is the product of a two-year study by FRAME's Toxicity Committee who will assess the feasibility of non-animal methods of toxicity testing and report in November 1982

FRAME's board of trustees numbers only four, of whom two are scientists Dr Michael Balls of the University of Nottingham and Dr Peter Hodges, a senior scientist with Pfizer Although still a small organization, FRAME seems to have acquired some influence since its inception in 1969 A group of 40 Members of Parliament, led by Joan Lester, has pledged itself to promote alternatives to animals in experiments Industrial sponsors for FRAME's research programme include Avon Cosmetics, Rimmel International, Bristol-Myers and Pfizer

FRAME's objectives superficially conflict with the interests of the companies, which at present market their products with a degree of confidence in protection from legal proceedings for negligence because of tests using animals Their support for the new research programme seems to have been stimulated by the cost of animal screening tests and the growth in public concern for the welfare of laboratory animals

Thus Avon Cosmetics, which is supporting one of the four research groups says that its interest in alternative methods of toxicity testing is based on ethical considerations Pfizer says that it has incurred "significant expense" in making senior staff available for internal studies of alternatives to animal laboratory tests, and describes FRAME as its chief British channel for this kind of work

The Royal Society was urged at a recent meeting to set up an "ethical committee" Its *ad hoc* Committee on Animal Experiments is likely to decide on the terms of reference and chairmanship of such a working party later this month

Jane Wynn

0028 0836/82/060451 01$01 00

CORRESPONDENCE

Original life

Sir — David Dickson has quoted (*Nature* 14 January, p 87) from Judge Overton's ruling against the creationists in Arkansas Among these we find "Although the subject of origins of life is within the province of biology, the scientific community does not consider origins of life a part of evolutionary theory" "The theory of evolution assumes the existence of life and is directed to an explanation of *how* life evolved Evolution does not presuppose the absence of a creator or God " Now, these statements show that much of the creationist attack on the synthetic theory of evolution is irrelevant It would be a pity if that short-term goal contributed towards a long-term predisposition in the minds of the scientific community to continue excluding the origin of life from evolutionary theory That would not be in line with the views of some important evolutionists who contributed to both disciplines Nevertheless, a bias against considering origins exists in the minds of many evolutionary biologists — I discovered for example that my textbook *Evolutionary Biology* (Holt, Rinehart & Winston, New York, 1972) was not favoured by some teachers because it has a prominent chapter on the origin of life

The evolutionary process is represented at the molecular level on the one hand and encompasses cosmogony on the other At some point a theoretical framework covering the entire range of that process will become necessary Presumably the evolution of molecular systems leads to the origin of life just as the evolution of living systems leads to the origin of ecological systems Individuals need not become proficient students of all these subjects, but it is quite another argument for an important legal document to declare that part of this subject matter is not considered proper by important exponents of the study of evolution, when that is only the provincial bias of some Such statements are potentially stultifying and to be regretted by those who otherwise rejoice in Judge Overton's document

Stanley N Salthe

Brooklyn College, New York, USA

All in the Book

Sir — That anyone writing from the evolutionists' standpoint is willing to expose such crass ignorance of the creationists' case as does Jon Marks[1] is almost beyond belief It is much to be hoped that the tone, let alone the substance, from any creationist writing about evolution would not expose such hostility

May I answer only the three biblical points raised? *Leviticus* 11 v 19 is not taxonomic but gastronomic, (and very prudent at that) it does not attempt a classification of mammalia *Luke* 23 v 43 has the comma incorrectly placed, a point of punctuation well understood over the past four hundred years *Genesis*, in respect of the fourth day, as taken up by Origen and later by Voltaire, is explained by Wiseman[2] It is, I regret, open to both sides of this argument to accuse the other of fraud and obscurantism, but nothing useful is served thereby

Frank W Cousins

Westminster, London SW1, UK

Workers' union

Sir — The letter from ten Russian scientists (*Nature* 24/31 December, p 688) is in part an approach to the WFSW The federation is indeed concerned with the difficulties that can afflict scientific workers in any country We have been able, in various circumstances, to resolve or prevent serious problems

We have been aware for several months that certain requests for exit visas from the Soviet Union have remained unanswered On 3 November 1981 I wrote to the president of the "Educational and Scientific Workers' Union of the USSR" in Moscow, in conformance with the policy of the federation first to contact our affiliated organization in the country concerned I asked to be informed of the nature of the difficulties relating to these scientists I feel certain that Mme Yanoushkovskaya is making the necessary investigation and that she will soon be able to furnish an explanation

The list of signatories in the letter published by *Nature* is not identical to that in a letter I had earlier received, two names have been dropped and four added I infer that the situation has evolved since last year

J M Legay

World Federation of Scientific Workers, Lyon, France

Reagan's right

Sir — The editorial "Reagan's mistake on Soviet sanctions" (*Nature* 7 January, p 1) is disturbing Science is not now (as it may have been in Davy's time) merely a pastime for scientists It has powerful consequences for humanity in both peaceful and war-like activities If all humankind were one big happy family, then free interchange of science would be both desirable and inevitable But humanity is divided into groups whose objective is not to have cheery little wars with "sweetness and light" in view down the road, but to destroy each other Therefore, free exchange of science cannot be allowed *Nature*'s reasoning resembles that of "pacifists" in the last two Great Wars who helped the enemy and hindered our own war effort because they hated war We all hate war, and we're all for scientific freedom and exchange But that is no reason to give science that we've worked or paid for — our science — to people who will use it directly (in weapons) or indirectly, by improving their efficiency, to destroy other people Poles, Afghanistanis, or us

R G S Bidwell

Dalhousie University, Halifax, Nova Scotia, Canada

An SOS from a Polish scientist

from a correspondent in Poland

Sir — It was not an eruption of anger as in Hungary, nor was it the movement of a rather narrow group of politically mature intelligentsia as in the Czechoslovakian spring It was a vast popular movement, in which men of the arts, literature and science found their usual role as articulaters of popular demands

This cleansing process began a few years ago In 1978 the group *Doswiadczenie i Przysclośc* (DiP, Experience and Future) was formed This small group of scientists and journalists published a number of important reports, their main message being that the country was on the edge of catastrophe and that the very last opportunity of avoiding it by the introduction of essential social reforms had arrived The authors expected that if their voice was not heard the economy of the country would collapse, leading to social turmoil and possibly bloodshed

The wave of strikes before August 1980 proved the accuracy of these predictions, but the decline was halted — or, as we see it now, postponed — by the "social contract" signed in the Gdansk shipyard

Some of those involved in DiP formed an openly acting *Komitet Porozumiewawczy Stowarzyszen Twórczych i Naukowych* (Coordination Committee of Cultural and Scientific Associations) headed by the philosopher Klemens Szaniawski This committee played a leading role in the cultural life of the country, especially in preparing and promoting the new law concerning publications, the law aimed at moderating the omnipotent power of censors

The most spectacular event organized by the committee was the Congress of Culture chaired by the art historian Jan Bialostocki The congress was planned for three days starting 11 December 1981 Martial law was introduced at midnight December 12 and the last session could not be held

Among many important speeches delivered during this meeting the most prophetic was the opening address by the president of the Association of Polish Writers, Jan Jozef Szczepánski He compared the congress to the orchestra on board the *Titanic* This prophecy was soon verified — several of the participants of the congress met during the night in the corridors of Warsaw prisons, and many are there still

At the end of 1980 the process of revival of all scientific establishments began with a few fundamental demands freedom of scientific inquiry, promotion of scientists according to merit, the right of a university to decide on its curricula and a significant role for scientists in formulating the scientific and educational policies of the country The autonomy of universities and of the academy, including election of their officers, was seen as a necessary institutional guarantee of the promotion of these demands and the improvement of scientific activities Autonomy became the keynote of the whole process of change

Of course none of these demands is very clever But it is also not very innovative for citizens to demand to be able to influence the fate of their own country, or to require history, records and information to be truthful and not selected according to the needs of authorities However, these demands coming after many years of the opposite policy sounded heretical And behind this policy there were people still possessing considerable power and by no means ready to resign from it

Continued on page 540

---

[1] Marks, J *Nature* 295, 276 (1982)

[2] Wiseman, P J *Creation Revealed in Six Days The Evidence of Scripture Confirmed by Archaeology*, p 128 (London, 1948)

University College of Science & Technology
92, A.P.C. Rd Cal.-9
LIBRARY COMPLEX
Departments of
Chemical Engineering
Chemical Technology
Plastics & Rubber Technology
19 NOV 1983

Interferon-gamma: success, structure and speculation

from Lois B Epstein

ANOTHER milestone has been reached in the interferon story with the publication in this week's issue of *Nature* of a report by David Goeddel and his colleagues at Genentech and NIH of the first successful identification of an interferon-gamma (IFN-γ) gene and the expression of a cloned cDNA sequence for human IFN-γ in bacterial and monkey cells[1] Since the discovery in 1965 of an 'interferon-like substance' in the supernatants of human leukocyte cultures stimulated with phytohaemagglutinin[2], much progress has been made in defining its cellular origin, range of inducers, physical and chemical properties, actions and methods of purification[3] This substance, originally called type II or immune interferon, is now called IFN-γ to distinguish it from IFN-α and IFN-β which were discovered earlier, and are now known to have different cellular origins, physical properties and antigenic determinants

Lymphocytes produce IFN-γ in response to numerous mitogens, bacterial and viral antigens, allogeneic cells and antisera directed against lymphocyte surface determinants Although the purification of IFN-γ was initially hampered by the relatively low levels induced and considerable loss of activity during the purification procedure, numerous laboratories throughout the world persisted in their efforts To date, preparations having a specific activity of greater than 10^7 units per mg have been attained[4-6], but microsequencing information is not yet available Although at first IFN-γ was thought to be larger than the other interferons with a molecular weight of 35,000-70,000, the most recent report indicates that it can exist in 20,000 and 25,000 molecular weight forms[7]

Initial efforts to define the range of actions of IFN-γ were hampered by the lack of abundant or partially purified material Many investigators were forced to use crude preparations which contained numerous other lymphokines and factors that affected cell function independently of the action of the interferon However, with the development of better methods of purification and the preparation of antisera to IFN-γ[8,9] specific activities could be assigned to IFN-γ in a more rigorous manner It became clear that although IFN-γ differs from IFN-α and IFN-β in its response to low *p*H, antigenic determinants, host range and cellular origin, it still induces the same enzymes[10] and the same peptides[11,12], and shares their ultimate antiviral[11], immunoregulatory[9] and antitumour[13] actions To date no unique function which would distinguish IFN-γ as a separate functional entity from the other interferons has been found

Recently, four laboratories have isolated and translated mRNA for IFN-γ in oocytes[14-17], thus paving the way for future production of IFN-γ by recombinant DNA techniques The latest achievement by Goeddel and his colleagues gives testimony to the tremendous accomplishments now possible with recombinant DNA technology when multiple resources are integrated into an attack on a specific problem If one considers the many methodologies and types of expertise required to accomplish this work it is clear that it could only have been achieved in a large industrial research centre

The cloning of the IFN-γ gene now makes it possible to produce IFN-γ in unlimited quantities and should lead to profound insights into the evolutionary history of IFN-γ, its tertiary structure, the relationship of its primary structure to its function and physical properties, and its genetic control In the report by Goeddel *et al* it is suggested that the gene which codes for IFN-γ contains an intron This is in contrast to the genes which code for IFN-α and IFN-β which contain no introns Conclusive proof of this must await future studies when the genomic sequence of the IFN-γ gene is determined and compared with the present cDNA sequence The results also demonstrate that IFN-γ has a molecular weight of 17,100, consistent with another recent report based on physical measurements[7], and suggest that higher molecular weights observed by other investigators might have been due to multimeric forms of IFN-γ or to the fact that IFN-γ is glycosylated *in vivo*

If the primary amino acid sequences of the various interferons are compared, it is apparent that 80 per cent homology exists within members of the IFN-α family and 30 per cent between IFN-α and IFN-β Goeddel and his colleagues report that their cDNA sequence codes for a polypeptide of 166 amino acids, of which 20 could constitute a signal peptide The authors have looked for sequence homologies between their IFN-γ and IFN-α and IFN-β and indicate that the only homology noted covering more than three consecutive amino acids occurs at amino acids 15-18 in IFN-γ, and these are found in positions 121-124 in two recombinant forms of IFN-α I find it intriguing but strange that although IFN-α, -β and -γ have a common range of biological actions such little apparent homology exists However, in my own comparative examination of the sequence of Goeddel's IFN-γ with that of several recombinant forms of IFN-α I find a definitive pattern of single amino acid homology throughout the entire sequence (see the figure) If one postulates a difference of one amino acid in the length of the IFN-γ sequence between residues 49 and 65 and of the recombinant IFN-α sequence between residues 49 and 66, then 14 positions have identical amino acids and 4 more differ by only the most conservative replacement (Asp for Asn, Leu for Ile, Ile for Leu) Thus there are 12 per cent identical amino acids or most conservative replacements in precise sequence order

	1	41	42	49	65	68	72	78	84	93	94	96	103	116	117	119	131	133
IFN-γ	Cys	Glu	Glu	Gln	Asp	Ser	Ser	Glu	Phe	Asp	Asp	Glu	Val	Leu	Ile	Val	Lys	Lys
IFN-α	Cys	Glu	Glu	Gln	Asn	Ser	Ser	Glu	Phe	Asn	Asp	Glu	Val	Ile	Leu	Val	Lys	Lys
	1	41	42	49	66	69	73	79	85	94	95	97	104	117	118	120	132	134

Fig 1 Sequence homology of recombinant IFN-γ and IFN-α The information is derived from published amino acid sequences for IFN-γ[1] and IFN-α[22]

Lois B Epstein is a Professor in the Department of Pediatrics and Research Associate in the Cancer Research Institute at the University of California, San Francisco, California 94143

0028-0836/82/060453-02$01 00

Even more intriguing is the fact that if one examines the model for the tertiary structure of IFN-α and IFN-β proposed by Sternberg and Cohen[18] virtually all the conserved areas shown in the accompanying figure are clustered in the exposed β sheets linking the four roughly parallel postulated α-helical segments of the molecule or on the exposed surface of one α-helical region

Although chromosome 21 has been shown to control the response to all the interferons[19], recent evidence suggests that the receptors for IFN-γ and the other interferons may be different[20,21] Without knowing how any interferon interacts with its receptor or what part of the molecule induces its subsequent effects, it is not clear where these conserved amino acids fit into the picture of interferon–receptor binding and interferon function I would expect, however, given the probable existence of different receptors, that the various interferons would differ in regions that bind, and that the conserved regions would be important determinants of effector function, in analogy to regulatory and catalytic sites on allosteric enzymes

There is tremendous interest, enthusiasm and expectation for the future of IFN-γ as an antiviral, antitumour, or immune response modifier The issue that has attracted the greatest attention is its potency relative to that of the other interferons In some cases IFN-γ has been shown to be more potent than the other interferons, but there are an equal number of cases which do not substantiate such a difference Resolution of the question of relative potency of IFN-γ depends on its purification to homogeneity so that it can be compared mole for mole with the other interferons with regard to all their known biological effects At present all units used to describe IFN-γ are peculiar to a given laboratory, and as such are arbitrary It is hoped that an international standard for IFN-γ will be available in the near future, which will permit all the IFN-γ preparations to be compared on a common basis

Not only is IFN-γ of considerable intellectual and scientific interest but also of tremendous commercial interest as well This is demonstrated by the large number of commercial, private, or university-based laboratories now devoted to its production in large quantities by conventional or recombinant DNA techniques The object of many such ventures is to prepare enough IFN-γ for future clinical trials on patients with malignant or infectious diseases or with immunological defects However at present the amount of information available on which these trials would be based is very limited

Thus there is much still to be learned about IFN-γ The primary, secondary and tertiary structures of IFN-γ induced by various inducers must be determined to see whether they are the same or different The chromosome which controls the production of IFN-γ, and the nucleotide sequence of the gene on chromosome 21 which controls the response to IFN-γ, must be determined The biochemistry of the action of IFN-γ and its method of induction at the cellular and genetic levels must be defined Abnormalities in IFN-γ production or action in various diseases must be sought, and the range of viruses susceptible to its antiviral activity determined. Finally, concerted efforts must be made to determine the manner and degree to which the growth of various human tumours is affected by IFN-γ so that its maximum therapeutic potential may be realized ☐

---

1 Gray, P W *et al* *Nature* **295**, 503 (1982)
2 Wheelock, E F *Science* **149**, 310 (1965)
3 For a review, see Epstein, L B in *Interferon 1981*, 13 (1981)
4 Yip, Y K *et al* *Proc natn Acad Sci U S A* **78**, 1601 (1981)
5 Koistinen, V & Cantell, K Rep presented at Univ Warwick (1981)
6 Sedmak, J J & Grossberg, S E Personal communication (1981)
7 Yip, Y K *et al* *Science* **215**, 411 (1982)
8 Langford, M P *et al* *J Immun* **126**, 1620 (1981)
9 de Ley, M *et al* *Eur J Immun* **10**, 877 (1980)
10 Hovanessian, A G *et al* *J Interferon Res* **1**, 125 (1980)
11 Rubin, Y & Gupta, S L *Proc natn Acad Sci U S A* **77**, 5928 (1980)
12 Epstein, L B *et al* in *The Biology of the Interferon System* (eds De Maeyer, E , Galasso, G & Schellekens, H) 247 (Elsevier, Amsterdam, 1981)
13 Blalock, J E *et al* *Cell Immun* **49**, 390 (1980)
14 Taniguchi, T *et al* *Proc natn Acad Sci U S A* **78**, 3469 (1981)
15 Wallace, D M *et al* *Biochem biophys Res Commun* **100**, 865 (1981)
16 Falcoff, R *et al* Abstr presented at 2nd a int Congr for Interferon Res (1981)
17 Billiau, A Rep presented at Harden Conf on Interferon (1981)
18 Sternberg, M J E & Cohen, F E *Int J biol Macromolecules* (in the press)
19 Epstein, C J & Epstein, L B *Tex Rep Biol Med* (in the press)
20 Branca, A A & Baglioni, C *Nature* **294**, 768 (1981)
21 Slate, D L *et al* in *Interferon-1981*, 65 (1981)
22 Goeddel, D V *et al* *Nature* **290**, 20 (1981)

Stem cell regulation in erythropoiesis

from P R Harrison

EVER since it was demonstrated using genetically marked cells that all types of blood cells derive from a common progenitor, the haematopoietic stem cell, interest has been focused on trying to define what controls the differentiation of the stem cell into one type of blood cell rather than another and how the relative numbers of blood cells are regulated

Although it has long been known that the tissue environment has an important influence on the differentiation of a stem cell, the way in which it exerts this influence is highly controversial The various mature functional blood cells are all derived from relatively small numbers of stem cells by way of a series of intermediate precursor cells which become progressively more restricted (or committed) in the types of blood cells they can produce, large numbers of mature blood cells are then produced by proliferation and maturation of the appropriate committed precursor cells (see the figure) One view of stem cell differentiation sees the microenvironment as having an instructive or determinative role in causing a stem cell to become committed to one blood cell lineage rather than another[1,2] through mechanisms such as cell–cell interactions or short-range 'inducers' But critics of this hypothesis have shown that the way in which a stem cell proliferates or becomes committed can be explained in terms of a purely random genetic process[3,4], perhaps involving some form of DNA rearrangement or movement of transposons Other strong evidence against an instructive role of the tissue microenvironment at the commitment stage is the finding that in spleen colonies formed after inoculation of bone marrow cells into irradiated mice the relative numbers of the various types of the earliest granulocyte and erythroid committed precursors (CFU-C, BFU-E) are strongly correlated, irrespective of colony size (or morphology)[5] Thus it is argued that the various haematopoietic tissue environments influence the types of blood cells produced purely by facilitating the proliferation of particular kinds of committed precursor cells

The 'instructive microenvironment' hypothesis now seems to have taken another knock with new experiments reported by Magli, Iscove and Odartchenko in this issue of *Nature* (p 527) They used the classic spleen colony assay for stem cells devised by Till and McCulloch[6], where cells of interest are injected into lethally irradiated mice and the presence of haematopoietic stem cells is quantified by counting the number of macroscopic colonies formed on the surface of the spleen After 7 days the spleen colonies consist mainly of erythroblasts, whereas spleen colonies present after 11 days comprise a variety of haematopoietic cell types, including granulocytes and megakaryocytes as well as erythroblasts It has previously been assumed that, since each colony is derived from a single cell, the changes in the local environment as the colony grows and comes into contact with different parts of the spleen are responsible for changes in the differentiation pattern What Magli and her co-workers have now shown is simply that the mixed colonies present after 11 days are not in the same positions as the early erythroid colonies, and that only the

P R Harrison is at The Beatson Institute for Cancer Research, Switchback Road, Bearsden, Glasgow G61 1BD

0028-0836/82/060454-02$01 00

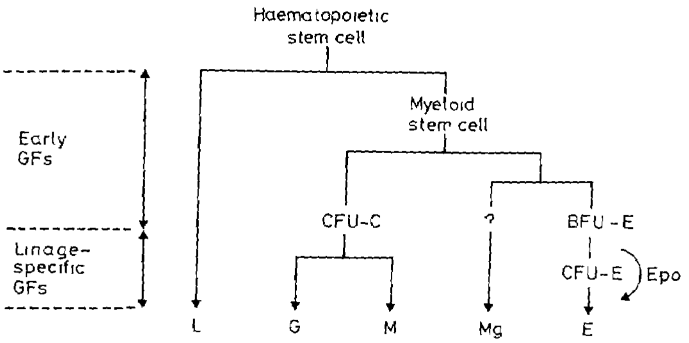

Simplified ontogeny of blood cells L, lymphocytes, G, granulocytes, M, macrophages, Mg, megakaryocytes/platelets, E, erythroblasts/red blood cells, GF, growth factor, Epo, erythropoietin CFU-C, precursor cell giving rise only to granulocytes and macrophages, BFU-E and CFU-E, early and late erythroid precursors respectively, the CFU-E is responsive to erythropoietin Some scientists believe that the B lymphocytes and the myeloid stem cell are derived from a common precursor whereas the T lymphocytes derive from the haematopoietic stem cell independently Others believe T and B lymphocytes derive from a common lymphoid precursor independently of the myeloid stem cell (see ref 7) There is also evidence for a common precursor of erythroid and megakaryocyte lineages

late colonies contain precursors capable of proliferating in culture to form colonies having mixed differentiation patterns (that is, early precursor cells of some kind, although not necessarily haematopoietic stem cells *per se*) This result rather undermines the argument for an influence of the splenic microenvironment on differentiation pattern during colony growth Furthermore, since stem cell assays have traditionally been based on early colony counts, it also means that certain conclusions about stem cells will need to be reassessed

But the question of how the haematopoietic tissue environment facilitates the proliferation and/or differentiation of particular types of committed precursor cells remains open Much of the progress in this direction has resulted from the development of *in vitro* systems capable of supporting the growth of stem cells on bone marrow feeder layers by Dexter and his colleagues in Manchester and of assays for committed precursor cells of various kinds by Metcalf, Johnson, Iscove, Axelrad and others It seems that, in general, both the earliest precursor cells and the various intermediate committed cell precursors require growth factors to sustain their proliferation and differentiation (see the figure, and ref 7 for a recent review) As such factors are often produced by other haematopoietic cells or stromal cells in the tissue environment, then clearly the regulation of haematopoiesis involves complex interacting cell networks

Does the production of these growth factors explain the effects of the tissue macroenvironment on the differentiation of haematopoietic stem cells? The answer is probably not, according to Dexter[8] It appears, for example, that purified growth factors cannot mimic the local effects of the microenvironment if the stem cells are separated from the stromal cells by a thin layer of agar or if they are cultured in diffusion chambers where direct cell–cell contact is prevented So either cellular contacts are involved as well as the circulating growth factors, or the essential factors produced by the stromal cells are extremely labile and therefore act over only very short distances □

---

1 Trentin, J J in *Regulation of Haematopoiesis* Vol 4 (ed Gordon, A S) (Appleton-Century-Crofts, New York, 1970)
2 Wolf, N S *Cell Tissue Kinetics* **11**, 335 (1978)
3 Till, J E , McCulloch, E A & Siminovitch, L *Proc natn Acad Sci U S A* **51**, 29 (1964)
4 Humphries, R K , Eaves, A C & Eaves, C J *Proc natn Acad Sci U S A* **78**, 3629 (1981)
5 Gregory, C J & Henkelman, R M in *Experimental Haematology Today* (eds Baum, S J & Ledney, G D) (Springer, New York, 1977)
6 Till, J E & McCulloch, E A *Radiat Res* **14**, 2131 (1961)
7 Till, J E & McCulloch, E A *Biochim biophys Acta* **605**, 431 (1980)
8 Dexter, T M *J cell Physiol* (in the press)

The nature of immune response gene defects

from Ronald H Schwartz

A NUMBER of recent experiments on immune responses *in vitro* have suggested what will seem to some a revolutionary solution to the conundrum of the antigen-specific genetic defects in immunity that are controlled by the immune response (Ir) genes These genes were discovered in the early 1960s, in the course of experiments on inbred guinea pig and mouse strains immunized with simple synthetic polypeptides[1] The experiments showed that some strains (known as nonresponders) are unable to respond to specific antigens, and that this blind spot is due to a single dominant genetic locus in the major histocompatibility complex (MHC) It is now clear[2-5] that the Ir genes code for Ia molecules — polymorphic two-chain polypeptides expressed, like the other major histocompatibility antigens, on the cell surface The first real clue to how the Ia molecules might influence the immune response lies in the phenomenon of MHC restriction[6] T cells can recognize foreign antigens only in association with products of the MHC — the particular product recognized being dependent on the subset of T cells involved in the response The T cell subset that recognizes Ia molecules is the amplifier T cell subset[7], which among other things cooperates with B cells in the production of antibodies These T cells are believed to be activated by foreign antigens presented in the context of an Ia molecule on the surface of a macrophage

Thus it is clear how in principle an Ia molecule could influence an immune response, but it is not obvious how a particular Ia molecule leads to non-responsiveness only to certain antigens Two solutions to this problem have been proposed One, the so-called determinant selection model, is that different Ia molecules possess different abilities to bind antigens, and that non-responsiveness arises from the failure of the macrophage bearing the nonresponder Ia molecule to bind the antigen for presentation to the T cell[8,9] The alternative is that the T cells specific for a particular combination of antigen and Ia molecule are missing in nonresponder strains[10 12] This could be because of the absence of a gene encoding a T cell receptor with the relevant specificity, or it could be secondary to somatic selection of the T cell repertoire Two kinds of selection have been envisaged One is negative selection, in which T cell clones responding to self determinants are deleted during the generation of tolerance The immune deficiency would then arise because a particular combination of Ia molecule and foreign antigen mimicked a self determinant[10] Alternatively, T cells may be positively selected to produce a repertoire in which antigen recognition is restricted to self MHC In this case, the immune defect would be due to a failure to select for those clones recognizing the nonresponder Ia molecule in association with a specific foreign antigen[11,12] It is to this theoretical controversy that the experiments reported by Ishii and his colleagues in this week's *Nature* (p 531) are addressed

Their experiments were designed to eliminate an ambiguity inherent in the results of earlier experiments on the cellular basis of non-response The usual procedure has been to immunize a hybrid (responder x nonresponder) F_1 animal, and then test its T cells for proliferation in response to antigen plus either responder or nonresponder macrophages *in vitro* In such experiments, the F_1 T cells always respond to the antigen in combination with the responder macrophages, but not in combination with the nonresponder

Ronald H Schwartz is in the Laboratory of Immunology, National Institute of Allergy and Infectious Diseases, National Institutes of Health, Bethesda, Maryland 20205

0028-0836/82/060455-02$01 00

macrophages[13] This has been taken to mean that it is the macrophage and not the T cell that is defective But if the defect were in fact due to the absence of certain T cell clones as a result of somatic selection, then one would expect the F_1 to be unable to respond to antigens presented on nonresponder macrophages Thus the only way to test unambiguously whether tne defect is in the macrophage or the T cell repertoire would be by using fully allogeneic nonresponder macrophages to present the antigen

In order to do this, Ishii *et al* had to overcome a technical difficulty normally, T cells would be expected to mount an immune response to the allogeneic macrophages alone, and this would obscure any proliferative response to the combination of allogeneic Ia and antigen They therefore had first to remove any T cells reactive to the macrophage alloantigens This was accomplished by stimulating the T cell population with the macrophages in the absence of antigen and killing the proliferating alloreactive T cells by exposure to bromodeoxyuridine and light The remaining T cell population was then restimulated with the same nonresponder macrophages, but now in the presence of antigen The interesting result which they obtained was that these T cells could respond to the antigen in association with the nonresponder macrophages Even if the T cells were obtained from one nonresponder strain and thus could not see the antigen in association with their own macrophages, they could respond to the same antigen in association with the macrophages from another nonresponder strain These results suggest that a nonresponder T cell population is only blind to the antigen in the context of its own syngeneic macrophages This in turn argues strongly against several of the theoretical models discussed above First, if T cells exist which can recognize the antigen and nonresponder Ia molecules, then genes must exist in the species which encode for these receptors either as direct products or as somatic variants Second, if T cells can respond to the antigen and nonresponder Ia molecules, then the Ia molecules themselves cannot be defective in binding and presenting the antigen Therefore, these experiments can be interpreted as arguing against determinant selection models and by default supporting the somatic T cell selection models for generating Ir gene defects

This is not the first report of nonresponder macrophages presenting antigen to responder T cells In 1973 Kapp *et al* [14] demonstrated that nonresponder macrophages could stimulate a helper T cell-supported antibody response from responder spleen cell populations However, these experiments were criticized because the investigators did not deplete the responding population in alloreactive cells, which might have produced false positive results through complex interactions between lymphocyte subsets and the release of soluble recruitment molecules (so-called positive allogeneic effects)[15] Even in the experiments reported by Ishii *et al* one has to ask whether the authors have sufficiently depleted the T cell population in alloreactive cells to eliminate all such effects They demonstrate that the nonresponder macrophages alone do not induce a proliferative response, suggesting by the criterion of cell division that alloreactivity has been removed However, given the fact that all the strain combinations reported on in the paper produced a response, one has to worry whether residual alloreactivity, such as the release of recruitment factors, still remains The authors state that they have some negative results using strain combinations with only partial histocompatibility differences, but these combinations might also generate reduced allogeneic effects

Nonetheless, the implications of the findings reported in this paper have been supported by recent results from other laboratories Pierce *et al* [16] reported that responder T cell populations contain cells capable of helping B cells from nonresponders to make antibody, whereas (responder x nonresponder) F_1 populations lacked such T cells Even more striking have been the data obtained with cloned T cell populations Clark and Shevach[17] have isolated several clones from a responder strain of guinea pigs that respond to antigen presented on nonresponder macrophages from a different strain, but not to nonresponder macrophages alone, or to the same antigen presented on responder macrophages This last result is analogous to that of the Ishii experiments The beauty of the cloning experiments is that they totally eliminate the possibility of a false positive allogeneic effect since alloreactive T cells have been entirely removed On the other hand, the problem with the cloning results published so far is that they only describe a few examples These could represent rare phenotypes and thus might not be sufficient to explain Ir gene effects, which require the absence or lack of stimulation of whole families of T cells with similar specificities[7] Overall, however, the data from both types of experiments would seem to complement one another, the clones addressing the doubts about alloreactivity and the Ishii experiments addressing the doubts about population size Thus it would appear that these collective experiments represent a strong challenge to determinant selection models It remains to be seen how and if this challenge will be met □

1 See Benacerraf, B , Green, I & Paul, W E *Cold Spring Harb Symp quant Biol* **32,** 569 (1967)
2 Longo, D L , Matis, L & Schwartz, R H *Crit Rev Immun* **2,** 83 (1981)
3 Rossenwasser, L J & Huber, B T *J exp Med* **153,** 1113 (1981)
4 Michaelides, M *et al J exp Med* **153,** 464 (1981)
5 Lin, C -C S , Rosenthal, A S , Passmore, H C & Hansen, T H *Proc natn Acad Sci U S A* **78,** 6406 (1981)
6 Zinkernagel, R M & Doherty, P C *Adv Immun* **27,** 51 (1979)
7 Schwartz, R H in *Ia Antigens and Their Analogues in Man and Other Animals* (eds Ferrone, S & David, C S) (CRC, Boca Raton, in the press)
8 Rosenthal, A S *Immun Rev* **40,** 136 (1978)
9 Benacerraf, B *J Immun* **120,** 1809 (1978)
10 Schwartz, R H *Scand J Immun* **7,** 3 (1978)
11 Jerne, N *Eur J Immun* **1,** 1 (1971)
12 Langman, R E *Rev Physiol Biochem Pharmac* **81,** (1978)
13 Shevach, E M & Rosenthal, A S *J exp Med* **138,** 1213 (1973)
14 Kapp, J A , Pierce, C W & Benacerraf, B *J exp Med* **138,** 1121 (1973)
15 Katz, D H in *Lymphocyte Differentiation, Recognition, and Regulation* Ch 11 (Academic, New York, 1977)
16 Pierce, S K , Klinman, N R , Maurer, P H & Merryman, C F *J exp Med* **152,** 336 (1980)
17 Clark, R B & Shevach, E M *J exp Med* (in the press)

100 years ago

THE MOVEMENTS OF JUPITER'S ATMOSPHERE

Mr Darwin describes the bands on Jupiter as "due to the trades and anti-trades" set in motion by the action of solar radiation on the solid body of the planet as are the trade-winds of the earth Many other eminent astronomers still appear to accept this time-honoured explanation of the phenomena

Have they reflected on the revelations supplied by the low specific gravity of Jupiter? There is no form of matter with which we are acquainted that could exist at a mean density of about one-fourth of that of the earth, while subject to the enormous pressure due to the mass of Jupiter, unless it were sufficiently hot to render the formation of a solid crust on its surface quite impossible In order to attribute terrestrial solidity to either Jupiter, Saturn, or Neptune we must invent a new kind of matter as infusible as platinum, and far lighter than hydrogen, or endow it with absolute incompressibility

These planets, if composed of any of the chemical elements or compounds known to us, can only retain their low density under the enormous pressure of their masses by the agency of proportionately counteracting heat-repulsion At and about their centres this may be so far overcome by the superincumbent pressure as to produce solid nuclei

Assuming the existence of such a central nucleus of Jupiter surrounded by a great fluid envelope, how will it be affected by the gravitating reaction of the satellite, supposing the compression to give it a specific gravity exceeding the mean specific gravity of its envelope?

It will obviously perform an eccentric rotation, or reeling, within the envelope This motion must be very irregular and complex, owing to the different periods and the varying relative positions of the satellites The effect of such internal reeling upon the surrounding gaseous mass explains far more efficiently than any possibility of solar radiation, the disturbances indicated by the ever-changing belts and spots of this planet

W Mattieu Williams

From *Nature* **25,** 9 February, 338, 1882

Making muonium in vacuum

from C J Batty and G Marshall

MUONIUM is the name given to the simple atomic state consisting of a positively charged muon and an electron For atomic and chemical purposes it is aptly described as a light isotope of hydrogen with only about one-ninth the hydrogen mass However the properties of its 'nucleus' make muonium both interesting and useful in physics and chemistry Two recent papers describe a novel way of forming muonium which will extend its use to measurements in vacuum

The muon, identified in 1936 in cosmic ray studies, was one of the earliest of the elementary particles to be discovered But despite an enormous amount of study and a considerable knowledge of its properties, its existence remains an enigma Like the electron and the positron, negative and positive muons are weakly interacting point-like leptons and are not influenced by the strong interaction felt by hadrons The muon differs from the electron essentially only in its mass, which is 207 times that of the electron

It is relatively simple to produce intense, high-quality muon beams from the decay of pions obtained at some particle accelerators So it has been possible to make a thorough study of the properties of the muon, and then with this knowledge, to use the muon as a tool for measurements in other fields Thus the spin and magnetic moment of the muon, together with the fact that its weak decay (with a mean lifetime of 2 2 μs) into an electron plus two neutrinos is asymmetric or parity violating, have been used to give information on the magnetic fields inside a variety of materials This technique of muon spin rotation, or μSR in analogy with NMR and ESR, is a subject of intense interest at several laboratories throughout the world Another application involves the formation of muonic atoms, in which a negative muon is captured in an atomic orbital, effectively replacing one of the electrons Measurements of the radiation emitted in the subsequent atomic cascade can determine the distribution of charge in the nucleus

The formation of muonium is fundamental to experiments with muons in fields as diverse as quantum electrodynamics, particle physics, solid-state and surface physics, and chemistry For most applications muonium can be formed by arresting a beam of energetic positive muons in a suitable solid, liquid, or gas target, in the same way that hydrogen atoms can be formed by stopping proton beams Near the end of its range, the positive particle loses energy by ionization, and in the low-velocity regime (corresponding to less than about 20 keV for muons) there is a high probability that it will form a neutral muonium atom In general the muon will capture and lose an electron many times before it reaches thermal energies, and if the likelihood for the capture process is large compared with that for electron loss as thermalization becomes complete, muonium will be formed In most chemical and solid-state applications the interaction of muonium with the target material is studied, but this interaction can be a hindrance when studying certain other phenomena It is therefore of interest to develop an alternative method of muonium production so that measurements can be made on the atom in vacuum

A group working at the LAMPF accelerator facility in New Mexico has recently reported the observation of fast ($\sim$10 keV) muonium in vacuum (P R Bolton *et al Phys Rev Lett.* **47**, 1441, 1981) The authors allowed an intense low-energy (4 MeV) muon beam to slow down in a polyethylene degrader before it passed through a thin foil target in vacuum It is predicted, on the basis of proton measurements, that a significant fraction of the muons emerging with energies less than 20 keV will be in the form of muonium

In order to separate the small neutral muonium component from the charged remainder of the beam, a 5 kG magnetic sweeping field is used immediately after the target foil The neutral particles travel 160 cm from the target through the magnetic field to a beam stop The positrons expected from the decay of the muon are detected in an array of scintillation counters and a NaI detector If the e^+ are from the decay of μ^+ then they should have a characteristic energy spectrum with an endpoint energy of 53 MeV

This characteristic energy spectrum, superimposed on a flat background of events due to cosmic rays and dominated at energies below 30 MeV by counts due to the electron contamination in the incident beam, has been observed in the experiment reported The introduction of a few Torr of helium gas into the normally evacuated ($< 5\times10^{-5}$ Torr) apparatus causes the muonium signal to disappear due to the ionizing collisions $\mu^+e^- + \mathrm{He} \rightarrow \mu^+ + e^- + \mathrm{He}$, the μ^+ are then swept away by the magnet, and the background spectrum can be measured The results show that, for the particular muon beam used, the production rate for muonium is about 3×10^{-4} per incident μ^+ regardless of which of several target foils is used The conclusions are consistent with proton beam data and with models of the neutralization process

Estimates of the energies of the muonium atoms indicate that 50 per cent have energies of less than 5 keV and 95 per cent of less than 20 keV

There are two measurements in particular which would benefit from copious quantities of muonium in vacuum One is a sensitive search for the conversion of muonium to antimuonium (μ^-e^+) which can be accommodated in some versions of the electroweak theory The interaction of muonium with matter drastically reduces the expected conversion rate, so that current limits on the process are not particularly restrictive The other is the Lamb shift in muonium, the energy difference between the 2s½ and 2p½ states of the $n = 2$ atomic level Since both the muon and the electron are leptons and thus have no structure, quantum electrodynamics can predict the Lamb shift very accurately, in contrast to the case for atomic hydrogen The fast muonium emerging from the foil in the LAMPF experiment should contain a 2s component of about one-eighth the total muonium intensity

This component was also shown to exist in another recent experiment performed by a group from the TRIUMF meson facility in Vancouver, Canada (C J Oram *et al J Phys* **B14**, L789, 1981) using a similar muon beam and thin foil target Muonium produced in the skin of the foil emerged to pass through two successive sets of parallel plates, used to produce high electric fields at right angles to the direction of motion of the atoms The electric fields will introduce through the Stark effect a 2p component to any 2s state which may be present Decay can then proceed from the 2p to the 1s state by emission of UV light with a lifetime of about 3 ns The light can be detected by a wavelength shifter and photomultiplier system mounted close to the second set of plates A clock is started when a muon is incident on the thin foil and is stopped when an event is recorded by the UV detection system

If voltage is applied only to the second set of plates the time spectrum should show three muon components an exponential decay due to muon-decay positrons incident on the photomultiplier system; a flat background due to uncorrelated events, and a foreground peak, about 150 ns wide, due to muonium in the 2s state decaying in the region of high electric field The foreground peak should largely disappear when an electric field is applied to the first set of plates, as this would cause the 2s state muonium atoms emerging from the foil to decay rapidly to the 1s ground state before they reach the second set of plates and photon detector system

Further experiments are planned to improve the production of muonium in vacuum In this way, the goals of an accurate determination of the Lamb shift and a sensitive search for the conversion of muonium to antimuonium should be achieved □

C J Batty and G Marshall are at the Rutherford Appleton Laboratory, Chilton, Didcot, Oxfordshire OX11 0QX

0028-0836/82/060457 01$01 00

Is amorphous silicon played out?

from J I B Wilson

IN spite of enthusiasm for amorphous silicon as a means of making cheap photovoltaic diodes, the improvement of the performance of these diodes has recently been slow and difficult. So is amorphous silicon destined to be a false trail in the search for a cheap solar cell? Although some Japanese companies (principally Sanyo Electric Co.) have set up production lines for these solar cells, chiefly for use in consumer products such as calculators, large-scale power conversion requires a better efficiency than the present about 7 per cent. The main barrier to further improvement is the poor photocurrent, caused by the high concentration of imperfections in the material. These trap the free charges produced by light and inhibit their collection by the metal contacts.

Scepticism about the potential of amorphous silicon cells is easily justified. It has always been suspected that an amorphous semiconductor will have unavoidably poor electrical characteristics, even when it is passivated with hydrogen produced by the plasma decomposition of silane gas (SiH_4). So is it possible to improve the electrical conductivity of this hydrogenated amorphous silicon (a-Si:H) only by sacrificing the high optical absorption of the amorphous structure? Although the hydrogen will reduce strain in the structure and reduce the number of unsatisfied silicon bonds, it will not necessarily control the concentration of defects, so that hydrogen content is not in itself a measure of the structural disorder.

Indeed, recent papers[1,2] suggest that in a-Si:H the structural disorder rather than the hydrogen content controls the optical absorption, especially below the 'bandgap', even though the removal of hydrogen by heating leads to both a deterioration in semiconducting behaviour and an increase in optical absorption. This suggests that if the optical absorption is to remain high, then the electrical behaviour of devices made with a-Si:H may always be limited by intrinsic structural disorder even if the structure is modified with hydrogen or fluorine. This conflict is already accepted in efforts to develop solar cells, and more complicated structures than a simple metallurgical junction have been suggested as ways of increasing the photocurrent without abandoning the simplicity of the plasma technique of depositing semiconductors.

In spite of theoretical estimates of the position in the energy level scheme of particular defects, such as unsatisfied silicon 'dangling' bonds and those produced by silicon-hydrogen groups, the inverse process of identifying bandgap energy levels with the physical entities to which they correspond has been unsuccessful, largely because of disagreement about the actual distribution of these energy levels within the bandgap. (Only in a pure crystalline semiconductor is this bandgap completely disallowed.)

Since the bandgap levels are those responsible for photoluminescence and photoconductivity, as well as for the control of electrical conduction, it is surprising that there should still be so many uncertainties. One difficulty in the interpretation of experimentally determined distributions is that the surface of the semiconductor (or its interface with an electrical contact) may contribute a substantial number of additional energy levels, perhaps with an energy distribution different from that in the semiconductor bulk. Another is that some experimental techniques are insensitive to any structure in the distribution. Thus field effect measurements (using a metal oxide-semiconductor transistor) give a mid-bandgap density of energy levels of $\sim 10^{17}$ cm^{-3} eV^{-1}, whereas a transient capacitance technique (deep-level transient spectroscopy), which is said to distinguish between bulk and surface effects, has given a surprisingly low value of $\sim 10^{15}$ cm^{-3} eV^{-1}. There is, however, disagreement about the interpretation of this data[3].

Moreover, there is one intriguing electrical conductance phenomenon for which the simple one-electron model of the energy levels due to defects appears to be inadequate — the 'Staebler–Wronski effect'. This consists of photostructural changes when a-Si:H is illuminated with a high flux of visible wavelength photons[4]: the electrical conductivity gradually decreases by a small factor, but the subsequent dark conductivity decreases by up to 10,000 times. These changes can be reversed by annealing the sample at $\sim$ 150°C for some minutes, but there is no distinct temperature threshold. Although similar effects can be produced by adsorption on the surface, this is definitely a bulk effect and is ascribed to a movement of the Fermi level towards the middle of the bandgap. The phenomenon does not occur in heavily doped p- or n-type samples.

An explanation invoking self-trapped excitons has been proposed by Elliot[5], while a more elaborate model due to Adler[6] successfully explains variations of the effect in lightly doped samples as well as other experimental observations. Adler proposes that two adjacent neutral dangling bonds (T_3^0) in the predominantly tetrahedral lattice (for not all dangling bonds are removed by hydrogen) are dehybridized from their usual sp^3 character to the (trigonal) sp^2-p_z form. The transfer of an electron creates a pair of charged centres, an acceptor (T_3^+) and a donor (T_3^-), but their energy levels within the bandgap are thought to be inverted compared with those of the usual substitutional impurity donors and acceptors.

On Adler's model, interconversion is prevented by a potential energy barrier, for the charge centres have different bond angles within the lattice. On this view, the decrease in photoconductivity and the shift in Fermi level observed in the Staebler–Wronski effect are produced by the asymmetric trapping of free charges at these energy levels, with a consequent conversion of neutral donors to acceptors. The increased concentration of acceptors causes the Fermi level to move downwards, giving a lower dark conductivity. Thermal annealing helps the potential barrier to be overcome, assisting a gradual return to the orginal T_3^0 states. (An inverse effect occurs when the initial position of the Fermi level favours the conversion of neutral acceptors to donors.)

Althougn the Staebler–Wronski effect is of little importance for the operation of solar cells (because the photoconductivity changes are too small to have much effect on the cell resistance), it does demonstrate the complexity of the defects in this disordered solid. These must be better understood before it can be told whether their presence is unavoidable. And even as things are, useful solar cells can be made from plasma-deposited amorphous silicon of existing quality, while other devices are not far behind. Further improvements in the material, either during production or by treatment afterwards, should still be possible. ☐

J I B Wilson is in the Department of Physics, Heriot-Watt University, Riccarton, Edinburgh EH1 1HX

---

1. Cody, G D, Tiedje, T, Abeles, B, Brooks, B & Goldstein, Y *Phys Rev Lett* **47**, 1480 (1981)
2. Deneuville, A, Mini, A & Bruyere, J C *J Phys Solid State Phys* **14**, 4531 (1981)
3. Proc 9th int Conf on Amorphous & Liquid Semiconductors, Grenoble, 1981 *J de Physique* **42**, Suppl 10, c-4 (1981)
4. Staebler, D L & Wronski, C R *Appl Phys Lett* **31**, 292 (1977)
5. Elliot, S R *Phil Mag* B39, 349 (1979)
6. Ad'er, D *J de Physique* **42**, Suppl 10, pc4 3 (1981)

Corrigendum *from B T Pickering*

In commenting in these columns on the sequence of the common precursor to vasopressin and its neurophysin I stated that it held no surprises (*Nature* **295**, 280, 1982). However I also stated that the signal sequence is separated from that of vasopressin by a pair of basic residues which re-examination of Fig. 4 in the paper by Land *et al.* (*Nature* **295**, 299, 1982) shows to be incorrect. Indeed, had it been so, this would have been a surprise, since the membrane-associated cleavage of prepeptides is not thought to involve basic residues.

0028-0836/82/060458 01$01 00

TEXTBOOK SUPPLEMENT

What makes a good textbook?

The most warmly welcomed textbooks are new editions of standard works. What lessons should publishers draw?

THAT there is unlikely to be an immediate shortage of new textbooks is well attested by the pages that follow. In spite of the way in which most university systems are at present short of funds, publishers are still prepared to launch new products on student bookshops, while teachers of all kinds appear to have the time to put them together. On the face of things, at least one part of the academic industry is in good shape. Moreover, on the showing of this year's crop of books, there is no reason to suppose that the creationists' complaints about the compilation of textbooks for high schools in the United States, or even the hidden threat engendered by the recent trial in Arkansas, have their counterpart in higher education. Textbooks remain what they have always been — honest attempts to put between two covers (or, sometimes, four) an account of some field of knowledge and, frequently, some means of helping students to be sure that they have come to grips with it. Moreover, some of the fashions of the past few years seem now to be on the decline. The programmed-learning book, for example, seems far less common than a decade ago, partly no doubt because of the high cost usually involved but chiefly because students have apparently voted with their pocket books, and have thus told publishers that they do not like to be so tightly constrained. It is good to have this demonstration that the market functions.

So does it follow that the present offering of textbooks is precisely what the community of students needs? Unfortunately not. Even when it is accepted (as it should be) that students' reading is not confined to the textbooks on their recommended reading lists, even a cursory reading of the reviews that follow will show that the textbooks now available are not uniformly satisfactory, even by the objectives stated by the authors in the introduction. Why should this be? And how does it come about that the three new books on which reviewers have lavished something akin to affection are in their different ways idiosyncratic books? J Z Young's *The Life of Vertebrates* is now a classic, read by people other than students, and has managed to survive more than a decade out of print. Dirac's *The Principles of Quantum Mechanics,* now put into paperback in its fourth edition, has exactly the same status in a very different field and is as much an historical document as a textbook. (Indeed, students should be warned not to trust their conclusions if their arguments are as economical as Dirac's.) Sir Arthur Holmes's *Principles of Physical Geology* (long out of print) was, in its time, in the same mould — it was a robust and almost personal statement of the structure of the Earth which did not, for example, shrink from remarks about the plausibility of continental drift. Textbook writers (and their publishers) should prudently consider why these three volumes, and others like them, have been such great successes, intellectual and no doubt commercial.

The common properties of such volumes are easily listed. First, their authors were practising and enthusiastic teachers. (Though when Dirac's book first appeared, more than half a century ago, he was by no means an experienced teacher.) Second, the enthusiasm has been transferred from the classroom to the page. Third, perhaps as a consequence, the selection of topics and the distribution of emphasis is not what would be recommended by a solemn academic committee brooding about the exact balance of some students' course. Fourth, the sweep of all these books is grand, the reader is left in no doubt that the essence of the field concerned has been fully described, even if a great many details have been omitted, which is most probably why they have all appeared in one edition after another. Finally, the language in which the text is written has an interest of its own. These three books are more than merely literate. Each also has a distinctive and even memorable style that somehow impresses on the reader's mind a sense that he is acquiring not merely information but an imaginative assessment of it.

For publishers, these reflections are no doubt discouraging. If textbooks of distinction require of their authors such a blend of uncommon qualities, the chances of outstanding success must be very small. Fortunately, the prospects are not so gloomy. Often, a group of people may be found collectively to show the qualities of a single talented author. One interesting example among this year's textbooks is *The Principles of Neural Science,* edited by E R Kandel and J L Schwartz but in reality an apparently accurate reflection of the interests and enthusiasms of the strong research group at Columbia University. As the reviewer remarks, readers may learn less about the chemistry of the central nervous system than (at this level) they need to know — and they may also learn more about the motor system than they want to know. But the book, bulky though it is, makes good reading and has a character of its own.

The consequences, for the textbook trade, are straightforward. The principles that apply elsewhere in book publishing are still applicable. The first test that should be satisfied by a textbook proposal is that it should be organized around a clear intellectual objective — and not too much encumbered by extraneous chapters whose function is chiefly to satisfy course requirements in this or that department. Self-conscious attempts to define the content of textbooks by means of curriculum development, which have been valuable and successful in the schools, have not so far been of great value in higher education. The chief but obvious difficulty is that even undergraduate courses are these days bound to be evolving rapidly, while the committees that superintend curriculum projects are bound to dilute the vision of their most imaginative members. By the same test, there are also limits to what can be done, in advance of publication, to ensure that textbooks for use in higher education can be tested by representative groups of the intended users. For the outstanding textbooks are those which, by being available, influence the pattern of what is taught. As elsewhere in the book trade, publishers cannot hope to know in advance whether they have published an outstanding book or a mere potboiler.

Thus the charitable view of the continuing spate of textbooks is that it represents the efforts of publishers and their authors to produce books that will endure, influencing the pattern of teaching in the process. There is, unfortunately, more to be said. The numbers of apparently similar titles, especially in fields in which the scale of teaching is quickly growing, are too great to be explained simply by people's earnest wish to put a potentially worthwhile book to the test of time and the student market. Too often, new textbooks uncannily resemble well-established works. Too often, they reflect the narrow idiosyncracies of individual teachers or departments. And, too often, they leave their student users with the false impression that science is, after all, a dull business.

In Dirac's shadow

R.B. Jones

The Principles of Quantum Mechanics, 4th Edn By P A M Dirac Pp 314 Pbk ISBN 0-19-852011-5 (Oxford University Press 1981) £7 95, $29 50 *Basic Quantum Mechanics* By J L Martin Pp 241 Hbk ISBN 0-19-851815-3, pbk ISBN 0-19-851816-1 (Oxford University Press 1981) Hbk £17 50, $39 50, pbk £7 95, $17 95 *Quantum Mechanics* By Hendrik E Hameka Pp 387 ISBN 0-471-09223-1 (Wiley 1981) £24, $43 25 *Quantum Mechanics For Applied Physics and Engineering* By Albert Thomas Fromhold, Jr Pp 430 ISBN 0-12-26915-4 (Academic 1981) £22 60, $34

It is a malicious fate that sends a new book on quantum mechanics to be reviewed beside that of Dirac It places an inhuman burden of restraint on the reviewer, whose first thoughts of Decline and Fall seem to require the pen of Gibbon or perhaps rather Evelyn Waugh Dirac's classic textbook, *The Principles of Quantum Mechanics,* first appeared in 1930 but it remains incomparably the best book on the fundamentals of quantum theory Here it is freshly reprinted as a paperback from its hardbound fourth edition, incorporating the revisions of 1967 on quantum field theory

For those not yet familiar with it, let me say briefly that starting from the clearest of all accounts of the linear structure of quantum mechanics it proceeds to cover all the standard non-relativistic aspects of quantum mechanics other than variational techniques In addition, the relativistic single electron and the quantum field theory of photons, electrons and positrons are described with masterly clarity and economy Only the section on field theory may be regarded as provisional or seriously incomplete, since there is no hint of the rich development of quantum field theories since 1967 for the description of leptons and hadrons All serious students should read this book but it demands unflagging intellectual courage Moreover, it seems to get better and to yield more insights with increasing experience on the part of the reader For these reasons almost no lecturer dares to use it as a standard textbook

It is doubtless for similar reasons that we have, year after year, yet another crop of new books on quantum mechanics for irascible reviewers to condemn John Martin's *Basic Quantum Mechanics* is meant as an introductory book for physicists His approach is modern and non-historical, and from the beginning he banishes classical thinking in favour of the calculus of probability amplitudes This approach is shown to good effect in his use of the Stern–Gerlach experiment to set up the two-component description of electron spin He treats the standard solvable problems and then covers time-independent and time-dependent perturbation theory through the golden rule and the resonance approximation There is a short account of dipole radiation and finally an introduction to the variational principle Many familiar topics, however, are missing There is very little discussion of the uncertainty principle and no mention of the geometrical shape of wave functions or of the link between nodes and quantum numbers There is no commutation rule treatment of orbital angular momentum eigenvalues, no three-dimensional scattering, no exclusion principle In spite of many such omissions, this is a good, well-written introductory book with a distinctive point of view to justify its existence

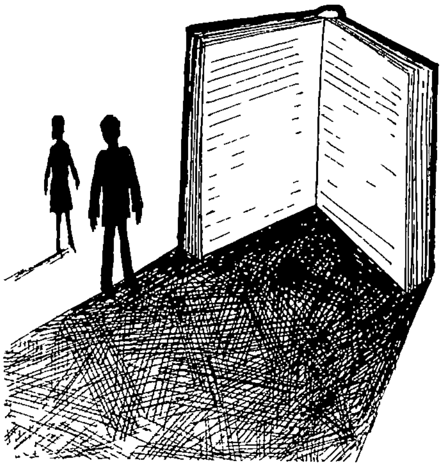

Quantum Mechanics by Hendrik F Hameka is a book written for chemists His approach is historical and primarily wave mechanical, he has made the book self-contained in its mathematical techniques to a degree not necessary for physics students but perhaps helpful to chemists In this respect he over-emphasizes the role of special functions at the expense of matrix mechanics aspects of the subject His treatment of the standard solvable examples is undistinctive and for me the book only came to life with the treatment of approximation methods There is a nice combination of time-independent perturbation theory with variational techniques to include perturbations about approximate eigenfunctions Time-dependent perturbation theory includes an introduction to line widths and lifetimes There is both a semi-classical and a second quantized treatment of atomic radiation Spin and the exclusion principles are discussed, with a clear introduction to Slater determinants and Slater orbitals in the Hartree–Fock treatment of many-electron atoms There is very little on angular momentum addition and no three-dimensional scattering theory This is a reasonable textbook for a course biased towards atomic structure but, while perhaps an attractive book for chemistry students, it will not be a text of first choice for physicists

Albert Thomas Fromhold, Jr, calls his book *Quantum Mechanics for Applied Physics and Engineering* and intends it as a two-year course for technologists working with solid state devices such as tunnel diodes or Josephson junctions It is, in fact, three books in one for he covers elementary quantum mechanics, statistical mechanics of ideal quantum gases and solid state physics — an ambitious venture which does not succeed to my mind because these three subjects appear in unbalanced and piecemeal form Thus in the section on quantum mecnanics the simple harmonic oscillator and the hydrogen atom are omitted, apart from quoting their energy levels, while endless pages are devoted to one-dimensional tunnelling probabilities for square and trapezoidal barriers in WKB approximation One learns about the almost free electron model of metals but nothing serious about phonons or magnetic properties of solids The book is well produced and copiously supplied with problems and illustrations, but I do not think this approach will produce a broadly based or coherent understanding It would not take so much longer to learn these subjects as a physicist would by using the excellent textbooks already available and, incidentally, obtaining a much broader understanding

One last stone remains to be hurled at each of the three books just considered The authors treat mathematics as a subject which will terrify or confound their readers It is in fact the natural language of quantum mechanics, and should be used without comment rather than segregated into separate sections marked "Dangerous" □

R B Jones is a Lecturer in Physics at Queen Mary College, University of London

Variations on cosmology and astrophysics

Joseph Silk

The Physics–Astronomy Frontier By Fred Hoyle and Jayant Narlikar Pp 483 ISBN 0-7167-1160-5 (W H Freeman 1981) £16 60, $23 95 *Relativistic Cosmology An Introduction* By Jean Heidmann Pp 168 ISBN 0-387-10138-1 (Springer-Verlag 1980) DM48, $28 30 *Cosmology*, 2nd Edn By Michael Rowan-Robinson Pp 152 Hbk ISBN 0-19-851857-9, pbk ISBN 0-19-851858-9 (Oxford University Press/Clarendon 1981) Hbk £12 50, $44 50, pbk £5 95, $17 95

IN ANY rapidly developing area of science, the textbook writer should do more than prepare a guide, no matter how thorough, to past accomplishments in his field He must capture some of the excitement of developments in research, of new and tentative discoveries, of competing claims and counterclaims An up-to-date treatment is especially crucial in the field of astrophysics, where the student is confronted in the daily press with a barrage of half-digested reports of new advances

The texts by Jean Heidmann and by Fred Hoyle and Jayant Narlikar are failures by this measure This defect is unfortunate since both books possess refreshingly novel features Heidmann's text is a translation from French, originally published in 1973 Few revisions were made for the English edition, affecting only about five per cent of the text The field of cosmology has developed enormously in the past decade, little of this is reflected in *Relativistic Cosmology* However an unusual feature is the attempt, on the whole successful, to make esoteric topics in differential geometry accessible to the non-specialist

The book begins with a discussion of topics in extragalactic astronomy that are of interest to the aspiring cosmologist, including clustering of galaxies, the expansion of the Universe, and intergalactic matter The text, though, suffers from a lack of modern results Although the intent is for the reader to fill in details by reference to the bibliographies, this will be difficult, since the references, almost without exception, stop at 1978 The section on the differential geometry of curved spaces is lucid and interesting My only quibble is that it is almost irrelevant to the rest of the book The remaining sections consist of a discussion of the Friedmann–Lemaitre cosmological models and of rudimentary observational cosmology While the level of this book is appropriate for a first-year course for an undergraduate with a mathematics and physics background, it is difficult to imagine any course being based on this text without an enormous amount of supplementary material

By way of contrast, *The Physics–Astronomy Frontier* does provide a self-contained account of astrophysics Its aim is to describe astronomy from the perspective of a physicist Consequently, each section begins with a discussion of one of the fundamental forces of nature (electromagnetic, nuclear weak and strong, and gravitational) before moving on to the astronomical phenomena This book is especially interesting on historical developments and anecdotes — such as when Hoyle reminisces about how Walter Baade almost discovered the pulsar in the Crab nebula — and the early years of radio and X-ray astronomy are well covered However, the authors do not mention any observational discoveries of the past five years Consequently, the explosive growth in radio and X-ray astronomy and other fields is ignored This is especially unfortunate in a book that purports to be probing the frontiers of astronomy and physics One notable omission is any discussion of particle physics in the very early stages of the big bang Instead, the reader is offered an exotic cosmological theory, developed, and possibly only taken seriously, by the authors themselves

The Physics–Astronomy Frontier is written for students who possess a strong secondary school science background The text is mostly non-mathematical Does it succeed, as the authors hope, by focusing on the fundamental forces of nature in enabling the reader to actually acquire a physical understanding of astronomical phenomena? Certainly it is far superior in this regard to other astronomy texts at a comparable level However, the astronomical contents are deficient and dated, at best, one might use the Hoyle–Narlikar book to complement a more conventional astronomy text assigned for an undergraduate course for non-specialists

Michael Rowan-Robinson's second edition of *Cosmology* is an updated version of a text originally published in 1975 for first-year mathematics and physics undergraduates It provides a self-contained description of the visible Universe, including both galactic and extragalactic phenomena of interest to the observational cosmologist There are minor omissions, such as any discussion of chemical evolution, but a reasonably thorough basis is established for cosmological theory The meat of the book lies in its discussion of the big bang models and of their observational implications This is a well-written summary of cosmology, which aspires (not without good reason) to be a successor to Hermann Bondi's text of the same title that had such a profound influence on undergraduates two or three decades ago □

Joseph Silk is Professor of Astronomy at the University of California, Berkeley

---

Life of cosmic rays

G.T. Bath

High Energy Astrophysics By M S Longair Pp 412 Hbk ISBN 0-521-23513-8, pbk ISBN 0-521-28013-3 (Cambridge University Press 1982) Hbk £24, $49 95, pbk £8 95, $19 95

IT IS a considerable task of synthesis to show the connections between the main fields of astronomy which have flourished in recent years and at the same time convey the drama of research at the frontiers It must range from the solar wind to clusters of galaxies, from radiation processes in the presence of strong magnetic fields to the space–time structure of black holes This is the ambitious aim of this introductory textbook — to show how astronomers work, how they think and how the subject has developed — by introducing the reader to many of the discoveries of the past 20 years, and by explaining some of the theoretical interpretation that has survived the rigours of criticism and discussion

But this book is not simply an exposition of modern astrophysics The author adopts a quite original approach Taking as his central theme the subject of cosmic rays, their detection and the physics of their interaction with the environment, the presentation derives the necessary basic physics to trace the cosmic ray propagation path through the atmosphere, the magnetosphere, the solar wind, and the interstellar and intergalactic medium, back to the production of high energy particles in galactic and extra-galactic objects The high energy astrophysics of the title refers to these ultimate sources of cosmic rays in the Universe, which are introduced as their peregrinations through the hazards of space are traced back to their birth

The author makes no apology for presenting the material, and referring to it, as a lecture course Indeed his personality and enthusiasm shine through the informal and stimulating style of the writing The depth of discussion varies from subject to subject In a book which introduces cosmic ray physics and detectors, basic astronomy at all wavelengths, stellar evolution and stellar death, the properties of galaxies and clusters of galaxies, and high energy astrophysics, this is not surprising As a stimulating undergraduate introduction to particle propagation at high energies, and the astrophysical environment in which it all takes place, this book gives a broad background without losing contact with the dynamism that created the subject

---

G T Bath is a Research Fellow in the Department of Astrophysics, University of Oxford

Blinded with theory

J.S.A. Green

An Introduction to Atmospheric Physics, 2nd Edn By Robert G Fleagle and Joost A Businger Pp 432 ISBN 0-12-260355-9 (Academic 1980) $29 50, £19 60 *An Introduction to Atmospheric Radiation* By Kuo-Nan Liou Pp 392 ISBN 0-12-451450-2 (Academic 1980) $34 50, £22 80

We live in a world where physics students seem to believe that if a process can be visualized, it must be trivial Thus the really important things to study are theoretical physics, quantum mechanics and nuclear physics A subject such as biophysics becomes more respectable if the object of study is first reduced to a molecular soup, less so if an actual tangible biological entity is involved Meteorology comes somewhere in the middle because, though we have our share of specialized incommunicable topics, the essential feature of the subject is the bringing together of many branches of physics in a way that can lead to understanding the very tangible phenomena presented by the weather

Fleagle and Businger cover aspects of cloud microphysics, scattering and absorption of electromagnetic radiation, fluid dynamics and photochemistry at a level acceptable to a graduate student of physics or mathematics The text is clear, but as in any such collection of work from different specializations notation is a problem and the authors' suffix notation gets out of hand at times Worked problems are used to extend the students' appreciation, though it takes a lot of will power not to cheat and look at the solution straight away Definite improvements to the 1963 edition are the addition of a useful chapter on dynamics and more modern theory of turbulence, with the rather isolated chapter on geomagnetic effects now being omitted

Liou deals with the transfer and detection of solar and terrestrial radiation, aimed perhaps at the student anxious to study data provided by the earth-satellite programme Recommendation is difficult because the book is so carelessly written The text is distinctly oriental at times — cgs and calories are dominant units, rainbows are a consequence of scattering and 1cm = 30 GHz A more conventional explanation of the rainbow is given later and the chapters on Mie theory and multiple scattering are extensive

Something, however, is missing from both books and finally I concluded that it was that there isn't actually any meteorology in them Never do the authors dig you in the ribs and mutter conspiratorially "there — you have seen that phenomenon before, and never realized the beauty of the physics behind it" Thus both books suffer because they do not make use of the students' (or the authors') prior knowledge of what the atmosphere is like For judgement, context and excitement the student would too often have to refer to the original texts, and so, he might as well study quantum mechanics

Most telling to me is that the authors do not use their eyes Liou's three-dimensional diagrams (pp 130 and 222, for example) look as though they were drawn by Escher for purposes other than conveying information about physics Fleagle and Businger's are not much better ☐

John Green is Reader in Physical Climatology at Imperial College, University of London, and runs a course in atmospheric physics

---

Mixed diet for students of climatology

J.P. Palutikof & T.M.L. Wigley

An Introduction to Climate, 5th Edn By Glenn T Trewartha and Lyle H Horn Pp 416 ISBN 0-07-065152-3 (McGraw-Hill 1980) £18 25, $32 95 *Climatology· Selected Applications* By John E Oliver Pp.260 ISBN 0-7131-6303-8 (Edward Arnold/Halsted 1981) £14 95, $34 95 *Mountain Weather and Climate* By Roger G Barry Pp 313 ISBN 0-416-73730-7 (Methuen 1981) £17 50, $33 25

If climatology were breakfast, these three books would be eggs Benedict (Barry), Spanish omelette (Oliver) and rather old porridge (Trewartha and Horn) Barry's book is imaginative and nourishing, but perhaps a little esoteric for everyday tastes, Oliver's, original in concept although not totally successful in execution, is nevertheless full of good things As for Trewartha and Horn, while the book still has some nutritional value, the average breakfast eater would probably choose to eat out

An Introduction to Climate is the fifth edition of a book which was first published in 1937 The style is still reminiscent of the pre-War approach to climatology, although in this edition some effort has been made to give the book a "more modern cast" Unfortunately it needs a completely new script as well as a new cast Much of the book is devoted to the Köppen classification of climates, and little attention is paid to modern developments in climatology One hopes that few lecturers or teachers today would structure an introductory course on climate with this sort of emphasis As an illustration of the old-fashioned approach, the data given in the form of maps, diagrams and tables rarely have any indication of the period represented, the reliability or the source This denies two key issues in modern climatology — the facts that climate *does* change, on all time-scales, and that our knowledge of *global* climate is very meagre The book is at best misleading, at worst wrong; it provides a salutary lesson that a time must come when updating (even if it is done well, which it is not here) is no longer a useful exercise

The stated aim of *Climatology Selected Applications* is to "supply appropriate real-world applications" for basic university courses in climatology The author takes in turn each of the themes which form the content of such courses, summarizes it, and then proceeds to provide case studies of the incidence and impact of the climatological features involved To take one example, Chapter 7 begins with a general description of global circulation patterns, then examines in detail the synoptic patterns of the severe winter of 1976–1977 in the United States and finally considers the impact of this unusual climatic event This is followed by a complementary analysis of the contrasting summers of 1975 (wet) and 1976 (dry) in the US midwest The approach is a new and valuable one, which for many teachers will supply a long-felt need For others, awareness of this text may well provide a new dimension to teaching

The book is likely, therefore, to be widely read and have considerable influence As a first attempt, it must be praised Criticism may be levelled at it for being somewhat shallow, although this can be rectified in subsequent editions when the concept is better established British readers will perhaps think that the concentration on examples from the United States is disappointing, others will find the system of blocking the data analysis sections into separate boxes disrupting to the flow of the text Perhaps the greatest compliment one can give any textbook is that it makes learning interesting and dare we say it, fun In this, Oliver's book certainly succeeds

Barry's *Mountain Weather and Climate* is a unique volume on a special subject He discusses all aspects of the weather and climates of mountainous regions The coverage is global and the framework very general, but the material presented is invariably most detailed and specific As an example of a specialist work it is excellent

ideal as the basis for an upper-level undergraduate or graduate course, and sufficiently detailed and authoritative that it can act as a comprehensive and up-to-date reference work. Since no other publication covers this field, and because the author perceives well the far-reaching implications of the subject matter, it succeeds also as a basic source book for botanists, foresters, glaciologists and hydrologists. The bibliography is most impressive, but unfortunately there is no author index. This is a mere token criticism, however. Although a specialist work, this book should be on the shelf of all climatologists and all those interested in the mountain environment.

Comparing three such different books is an invidious task, one which we shall not attempt. The fact that, in a "small" discipline like climatology, such diversity is possible illustrates the mushrooming growth of the subject in recent years. The different approaches of Trewartha and Horn on the one hand and Oliver on the other are an indication of the extent to which the subject has developed. Both Oliver's and Barry's books show how much climatology impinges on many other disciplines, and are harbingers of future developments. □

J. P. Palutikof and T. M. L. Wigley are in the Climatic Research Unit at the University of East Anglia.

Earthly delights . . .

Keith Bell

Essentials of Earth History: An Introduction to Historical Geology, 4th Edn. By W. Lee Stokes. Pp. 577. ISBN 0-13-285890-8. (Prentice-Hall: 1982.) $25.95, £19.45. *Evolution of the Earth,* 3rd Edn. By Robert H. Dott and Roger L. Batten. Pp. 573. ISBN 0-07-017625-6. (McGraw-Hill: 1981.) $31.50, £17.50.

To write a well-balanced, comprehensive textbook at the introductory level about the history of the Earth, palatable to both arts and science students alike, offers something of a challenge, particularly at the present time. Results of space exploration, as well as new findings in plate tectonics and evolution (dare I mention the word?) must be fitted into one compact volume along with at least some of the basic principles of stratigraphy.

Exciting introductory textbooks are rare. My own favourite used to be the second edition of Arthur Holmes's *Principles of Physical Geology* (Ronald Press, 1965), a book written in a bold, masterly style, brimful of ideas and still retaining a freshness some 20 years later. But what of present-day texts?

Under review are new editions of two books that have been popular in North American universities for some years. Both are well-written, profusely illustrated, accurate and surprisingly similar both in scope and in content. Diverse topics such as the evolution of the Solar System, the origin of life and palaeomagnetism are included, along with a generous serving of historical geology. Both books retain layouts similar to the earlier editions. Stokes's text, however, has been extensively rewritten and many new illustrations either supplement or replace those of the previous work.

Stokes's approach is the more cautious and circumspect of the two. Although *Essentials of Earth History* tends to be written in a dry, somewhat formal style, the book is by no means dull. The well-illustrated volume contains a number of excellent photographs, including some from the recent Pioneer and Viking missions. Most chapters are self-contained (Chapter 7, "Cosmic Beginnings", was particularly enjoyable). And, under the heading "Search for an Ethic" in the final chapter, it was interesting to see at least a token attempt to reconcile present evolutionary theory with religious beliefs. Stokes, throughout most of the book, seems to have the knack of anticipating students' questions and needs, rather than evading contentious issues, the author confronts most of them head on.

The book by Dott and Batten is generally more direct and the reader is led at a fairly brisk pace from start to finish. The diagrams are superb and are among the clearest that can be seen in any introductory textbook. Topics such as geochronology, plate tectonics and the early evolution of the Earth are handled with a minimum of jargon and in a straightforward, concise style. However, I suspect that those chapters dealing with historical geology, mainly of North America, may overwhelm most students, each of them contains too much detail and too many disjointed topics. Although the introduction of many concepts within each chapter was probably meant to challenge, the overall effect may be to daunt all but the most enthusiastic students. Chapter 14, for example, includes discussions about sedimentary cycles, the red-bed problem, the Appalachian Orogeny, the significance of thrust-faulting and Palaeozoic land floras!

Nevertheless, either book would make a good introductory text, though less stratigraphy and a little more about igneous and metamorphic rocks (mentioned but briefly) would certainly extend the scope of both of them. An interesting feature of each book is a glossary of geological terms — to any student just coming into the earth sciences this is particularly useful. □

Keith Bell is Professor of Geology at Carleton University, Ottawa.

. . . heavenly bodies

L. Wilson

Earthlike Planets: Surfaces of Mercury, Venus, Earth, Moon, Mars. By Bruce Murray *et al.* Pp. 387. Hbk ISBN 0-7167-1148-6, pbk ISBN 0-7167-1149-4. (W. H. Freeman: 1981.) Hbk $27.50, £20.40; pbk $15.95, £10.95.

The constant development of the planetary sciences presents problems for the writers of textbooks, since such works are in real danger of being significantly out of date, at least in parts, by the time they are published. This problem is avoided by the authors of *Earthlike Planets* by omitting all mention of the gas giants, Jupiter and Saturn, and their satellites (targets of the most recent planetary probe missions), and confining attention to the more truly Earth-like inner planets — Mercury, Venus, the Moon and Mars. Many aspects of the major stages of evolution of these bodies are now well understood and it is becoming possible to make useful comparisons between these planets and the Earth, both in terms of the histories of their interiors and of the geological, physical and chemical processes which have moulded their surfaces.

Indeed, this book is explicitly committed to the concept of comparative planetology and the first four chapters deal with various aspects of the study of all the inner planets taken as a group: a summary of changing ideas on the ways in which these bodies were formed, a global description of the surfaces and atmospheres, a review of processes modifying planetary surfaces (impact by meteoroids and asteroids, mass movement under gravity and, where appropriate, wind erosion and fluvial action), and a survey of the volcanic and tectonic processes which renew planetary crusts. The next three chapters are explicit attempts to synthesize the planetary history for each of the Moon, Mercury and Mars. Finally, emphasis returns again to comparisons, with a review of those processes which appear to have influenced all of the inner planets to varying degrees — impact modification of the earliest-forming crust, magmatic and tectonic evolution of the interior and, on the planets with atmospheres, climatic change.

Each chapter ends with a well-chosen list of books and papers for further reading, and an excellent guide to sources of planetary photography is included as an appendix before the index. *Earthlike Planets* is probably the best general introduction to planetology available at the moment and will find a place in undergraduate courses at all levels. It is equally suitable as a starting point for a postgraduate student entering the planetary science field. □

L. Wilson is a Lecturer in the Environmental Sciences Department at Lancaster University.

Tectonics as theory, tectonics as history

B.C. Burchfiel

Geology of the Continental Margins By G Boillot Pp 115 ISBN 0-582-30036-3 (Longman 1981) £4 95, $11 95 *Geotectonics* By V V Beloussov Pp 330 ISBN 0-387-09173-4 (Springer-Verlag 1980) DM48, $28 40 *Tectonics and Landforms* By Cliff Ollier Pp 324 Hbk ISBN 0-582-30032-0, pbk ISBN 0-582-30033-9 (Longman 1981) Hbk £20, $55, pbk £9 95, $24

WITH our rapidly increasing understanding of global tectonics, books published on the subject are commonly outdated within a few years of publication Two of the books reviewed here (*Geology of Continental Margins* and *Geotectonics*) are translations of previously published works, which originally appeared several years ago and contain material which is already somewhat out of date *Tectonics and Landforms*, in contrast, promises an interesting approach and in some instances makes excellent use of recent tectonic concepts and their relationship to geomorphology However, books on such broad topics often cannot adequately cover each subject within their scope, and this one is no exception

Geology of Continental Margins is a translation of a book first published in French in 1978 No subject in the earth sciences has evolved more rapidly in the past five years, which renders the book introductory at best and outdated at worst While some of the material presented is still generally valid, recently developed details of continental margin evolution, particularly passive margin evolution, are obviously missing

Instead of focusing on the great wealth of information which now exists about the geology of the continental margins of the world, the book concentrates on plate tectonic models of continental margins and presents little real data, if readers are looking for factual information on particular continental margins, they won't find it in this book I was also surprised to find lengthy discussions of subduction, the deep seismic structure of subduction zones, paired metamorphic belts, geosynclines and collisional tectonics

Although advertisements for the book suggest that some updating has been done for the English edition, it seems to have been minor Some articles published in 1979 have been added to the "further reading" section, but little new data appears in the written part of the text In my view this is a model-orientated, highly simplified presentation of continental margins The emphasis is on the plate tectonic development of continental margins, rather than on what they are really like

Geotectonics is a slightly-updated translation of a book published in Russian in 1976 Some of the data presented were published as recently as 1978 Even so, the book presents a view of the geotectonics of the Earth in the well-known and unique conceptual framework developed by Beloussov himself In the preface it is suggested that the reader should be familiar with the principles of tectonophysics developed in Beloussov's *Structural Geology* (published in 1978, in French) I think this would be advisable, as much of the terminology and some of the conceptual ideas in this work need such a background

Most of the geological examples and figures presented are either from older works — 1960s or earlier — or are Beloussov's reinterpretations of work by other scientists The examples cited, as well as those not presented for the same area, were apparently selected to develop the author's particular view of geotectonics Vertical movement of material in the crust, mantle and core remain the dominant principle of Beloussov's view of the evolution of the Earth, horizontal movements of rocks are considered to be of limited importance Basification of continental crust leads to the formation of ocean crust These and other concepts developed by the author are generally not acceptable to many of us, but deserve publication If we cannot explain more adequately the geotectonic evolution of the Earth, and do not continue to test all reasonable hypotheses, earth science will stagnate

Except for a five-page discussion of plate tectonics near the end of the book and another seven pages of critique, the book is all Beloussovian tectonics and will be of interest to only avid scientists interested in the subject

The purpose of *Tectonics and Landforms* is to relate tectonics and structure to landforms on a scale which ranges from continents and oceans to local surficial features This is truly an admirable purpose and potentially very exciting and interesting With such a broad purpose but abbreviated length, the presentation has some successes, but inevitably some subjects are treated superficially Much of Ollier's presentation focuses on large-scale tectonics, developing the concepts of plate tectonics and its resultant geomorphic features From this basis, a great variety of subjects, such as flow of ice and rock, planation surfaces and drainage patterns are covered in very short sections Not only are modern concepts developed in the book, but reviews of older, historical, and in many cases obsolete, theories are also presented

I was particularly pleased to see that many of the pioneering ideas on tectonics by S W Carey are discussed, but I doubt whether a chapter on the expanding Earth was necessary, particularly when most of the book is devoted to the development of plate tectonics In several places the author gives plate tectonic explanations for various features followed by a disclaimer that other explanations which are incompatible with plate tectonics, such as interpretations based on expanding Earth models, should not be discounted

Tectonics and Landforms is well written, well organized and well illustrated Although the author claims to aim at senior undergraduates, in my opinion the book is too superficial for students at that level Rather, it would be better suited to an introductory audience, but even then offers a rather uneven overview of a great variety of earth science subjects ☐

B C Burchfiel is a Professor in the Department of Earth and Planetary Sciences at the Massachusetts Institute of Technology

Crystal growth

R.A. Howie

Crystallography An Introduction for Earth Science (and Other Solid State) Students By E J W Whittaker Pp 254 Hbk ISBN 0-08-023805-X, pbk ISBN 0-08-023804-1 (Pergamon 1981) Hbk £13 50, $32 50, pbk £8 35, $19 95 *Mineralogy for Students*, 2nd Edn By M H Battey Pp 355 ISBN 0-582-44005-X (Longman 1981) £8 95, $19 95

Crystallography is presented in two evenly-divided parts the first deals with morphological crystallography, symmetry and systems, stereographic projections, and derivation of symmetry and forms in all 32 crystal classes, while Part II covers the fundamental features of X-ray crystallography, the 14 Bravais lattices, the interpretation of powder photographs, X-ray diffraction by single crystals and symmetry in repeating patterns Part I thus somewhat overlaps in coverage with *An Introduction to Crystallography* (4th Edn, Longman, 1971) by F C Phillips and A C Bishop's *An Outline of Crystal Morphology* (Hutchinson, 1967) though, like the former, it aims to be of use not only to geologists and mineralogists but to other students of the solid state

Although both of these older texts (and *Mineralogy for Students*) give relatively brief treatment to X-ray crystallography, Part II of Whittaker's book covers this expanding field in considerable detail and develops a number of novel features in response to the difficulties and attitudes of students who are unlikely to have a primary interest in morphological crystallography There are brief but useful chapters on electron diffraction, the determination of crystal structures and on irregularities in crystals (though here twinning is touched on rather too briefly whether or not we understand why and how twins form they are frequently to be seen under the microscope and may be of considerable relevance) The book concludes with a brief essay on the relationship between morphology and crystal structure Altogether this elegant text should be a worthy successor to that of F C Phillips As Whittaker states in his introduction, mineralogy is merely the first branch of solid state science to be developed, and structural crystallography is equally relevant to all students of the solid state

The format and most of the text of the new edition of *Mineralogy for Students* are identical with that of the first The only fresh feature is the inclusion of a new series of optical orientation diagrams for most of the common rock-forming minerals, but whether this justifies the whole work being labelled as a second edition is, in my opinion, doubtful Nevertheless this was a useful, well-written text when it first appeared in 1972 and is improved by the additional diagrams — though it is a pity that these are not presented at the appropriate places in the section on descriptive mineralogy

The book has some things in common with *Crystallography* in that it deals with the principles of crystal structure, crystal morphology and X-ray diffraction in some 85 pages, a reasonable proportion for an elementary mineralogy course It has the advantage for students of including both the principles and methods in Part I (comprising just under half of the book) and descriptions of minerals in Part II, compared, for example, with the rather more detailed descriptive mineralogy (but without any descriptions of techniques) provided by Deer, Howie and Zussman's *An Introduction to the Rock-Forming Minerals* (Longman, 1966) Dr Battey's text is well illustrated and presented, though surely the formula of chloritoid could be given in a rather simpler fashion than one involving four consecutive brackets, the book will nevertheless continue to be deservedly popular with students ☐

R A Howie is Professor of Mineralogy at King's College, University of London, and Principal Editor of Mineralogical Abstracts

Mixed sediments

R.C. Selley

Sedimentary Petrology An Introduction By M E Tucker Pp 252 ISBN 0-632-00074-0 (Blackwell Scientific/Halsted 1981) £8 50, $24 95 *Sedimentology of Shale Study Guide and Reference Source* By Paul E Potter, J Barry Maynard and Wayne A Pryor Pp 303 ISBN 0-387-90430-1 (Springer-Verlag 1980) DM59 90, $32 80 *Depositional Sedimentary Environments With Reference to Terrigenous Clastics,* 2nd Edn By H -E Reineck and I B Singh Pp 549 ISBN 0-387-10189-6 (Springer-Verlag 1981) DM59, $34 90

THE three books considered in this review all deal with the study of sedimentary rocks but differ widely in subject area, level of assumed knowledge and approach

Tucker's *Sedimentary Petrology* is an excellent textbook for second-year geology students An introduction is followed by chapters dealing with sandstones, shales, carbonates, evaporites, ironstones, phosphates, coal, chert and volcaniclastic sediments, each concluding with a selective reading list There are many clear line drawings and photographs, though some of the latter have suffered from over-reduction

The chapter on sandstones (conglomerates and breccias) also briefly describes sedimentary structures and processes, the textural properties of grains and sediments, and the concept of facies That on limestones (including dolomites) deals adequately with the complex genesis of the various carbonate grains and presents a synthesis of the horrors of carbonate diagenesis

These two chapters make up nearly half of the volume and it is by them that the work as a whole will be largely judged Basically they are excellent introductions which lay the foundation for later, more advanced study Even the concept of porosity is introduced, and there are short sections on the porosity of sandstones and carbonates

The book as a whole is most nearly comparable with Greensmith's *Petrology of the Sedimentary Rocks* (Thomas Murby, 1975) Both deal with sedimentary rocks largely from the microscopic as opposed to the megascopic aspects Tucker's book, however, lacks a chapter on weathering so students may not be too clear on where on Earth all this sediment actually comes from

Sedimentology of Shale is a very different book Until recent years, shale had long played Cinderella to the ugly sisters of sandstone and limestone The advent of modern analytical techniques, however, coupled with the quest for oil shales and oil source rocks, has stimulated interest in the mud rocks The book is subtitled *Study Guide and Reference*

New Text Books from

HEYDEN

An Introduction to Atomic Absorption Spectrometry: A Self-Teaching Approach
L. Ebdon, Plymouth Polytechnic, UK.

Based on the author's well-validated teaching programme, this self-study text will equip the newcomer with a thorough theoretical and practical understanding of the technique Self-assessment questions and revision exercises are provided, keywords are highlighted throughout, and numerous instructional diagrams illustrate the theory
ISBN 0 85501 714 7 138pp 1982
Softcover £9 00 $19 50 DM43 00

The Structure and Properties of Solids: An Introduction to Materials Science
Bruce Chalmers, Harvard University, USA

A clear introduction, using non-mathematical terms, to the fundamental themes of materials science The book describes the characteristic structures of the four major classes of man-made materials - ceramics, metals, polymers, and semiconductors - in terms of the role played by electrons in bonding atoms together to form solids
ISBN 0 85501 721 X 1982
Casebound £9 00 $19 50 DM43 00

Introduction to Electronic Control Engineering
F. Frohr and F. Orttenburger

Only a basic knowledge of mathematics is required to understand this excellent introductory handbook
ISBN 0 85501 290 0 344pp 1981
Casebound £18 00 $39 00 DM85 00
A Siemens/Heyden Co–Publication

Practical Reliability Engineering
P.D.T. O'Connor, British Aerospace UK

" a most comprehensive review of the state-of-the-art in reliability . "
Microelectronics and Reliability
ISBN 0 85501 496 300pp 1982
Casebound £16 00 $35 00 DM76 00
Fully detailed prospectus available on request

Heyden & Son Ltd, Spectrum House, Hillview Gardens, London NW4 2JQ, England Tel 01-203 5171
Heyden & Son Inc, 247 South 41st St, Philadelphia, PA 19104, USA
Tel (215) 382 6673

Circle No 26 on Reader Enquiry Card

Source This must be noted for the work is unconventional in format It contains but three chapters "Overview", "Question Set" (*sic*) and "Annotated and Illustrated Bibliography" Chapter 1 covers the mineralogy and chemistry of clays, but ranges widely from Bouma sequences to ichnofacies The second deals with methods for analysing shales, ranging from descriptions of the measurement of a section to the reflectance of phytoclasts Fifteen colour photomicrographs illustrate various shale microfacies

It is the third chapter that is unconventional This takes up over half of the book and consists of an annotated and illustrated reference list It is divided into sections with headings ranging from "Books, Classics and Classification" to "Shales as Hosts for Metallic Minerals" and "Environmental and Engineering Geology" Within each section the authors have arranged alphabetically references which they deem to be significant

A sentence or, at the most, a paragraph explains the relevance of each reference, and key illustrations are reproduced from the original papers This is a novel and painless way of "writing" a book There may be some customer resistance to buying a volume which is largely an annotated bibliography — many geologists may prefer to use *GeoAbstracts* or a computer-based literature retrieval system For those who do not, *Sedimentology of Shale* will prove to be an essential source book, pity, though, that with three authors "desiccation" is misspelt throughout

Of Reineck and Singh's *Depositional Sedimentary Environments* there is far less to say The first edition appeared in 1973 and rapidly became established as the definitive work on recent terrigenous sedimentary processes, structures and environments The standard of the second edition ensures that it will maintain this position A major re-write has not been attempted, but the book has been updated throughout and sections have been added to each chapter on ancient environments Nonetheless, the main emphasis of the book remains on recent terrigenous sediments ☐

R C Selley is Reader in Petroleum Geology at Imperial College, University of London

---

From the abyss to the lecture theatre

Peter J. Smith

Marine Geology By James P Kennett Pp 813 ISBN 0-13-556936-2 (Prentice-Hall 1982) $34 95, £26 20

No disrespect to Professor Kennett, but in one sense this huge volume is alarming For only three decades ago hardly any of it could have been written Only during the past 20 years or so has the vaguely peripheral topic of marine geology moved to centre stage as Marine Geology — and with such vengeance that it is now possible for Kennett to write a textbook of an astonishing 813 pages at the comparatively lowly undergraduate–early-graduate level

What made the rise of marine geology possible was the development of the appropriate exploration techniques, but what has made it matter is the discovery of the oceanic lithosphere's central role in the plate tectonics story and the consequent realization that the ocean floor's evolution is altogether more complex and interesting than that of a passive sedimentary dumping ground of great antiquity Holism is the keyword here, and despite the need to become expert in a bewildering variety of subdisciplines, Kennett is wise enough not to allow his presentation to disintegrate into its constituent elements

Of course, the parts are important, and in a teaching text it is essential that they be dealt with in some detail Thus well over half of the volume is devoted to the basics of ocean morphology, marine stratigraphy and correlation, the current plate tectonic framework, crustal structure, sea-level changes, ocean margin processes, sediments and their microfossil loads, and so on The extended climax of the book, however, is a long three-chapter section on palaeoceanography — a splendid synthesis of almost everything we know, or think we know, about how the ocean system has evolved

This is the first major textbook on marine geology to appear since the plate tectonics revolution, although others are in progress in what could turn out to be a small publishing growth area during the 1980s Because so much of the material is new and far from all of it has become part of the consensus, the book is necessarily referenced to an extent that undergraduates will find unusual, and perhaps even distracting, but graduates will find helpful On the whole, Kennett has achieved a reasonable compromise between the need to attribute and the desire to find a lucid instructional style The book is clearly intended chiefly for advanced undergraduates in the marine geology courses now springing up in the more forward-looking universities and colleges, but in view of the subject's crucial importance to all geology, it will prove indispensable to earth scientists at much higher levels and of all persuasions Potential competitors will be hard pressed to improve on it ☐

Peter J Smith is Reader in the Department of Earth Sciences at the Open University, Milton Keynes, and editor of Open Earth

---

Soils: their genesis and physics

David Rimmer & Michael Adey

The Soil Resource Origin and Behavior By Hans Jenny Pp 377 ISBN 0-387-90453-X (Springer-Verlag 1981) DM57, $33 70 *Fundamentals of Soil Physics* By Daniel Hillel Pp 430 ISBN 0-12-348560-6 (Academic 1980) $40, £26 40 *Applications of Soil Physics* By Daniel Hillel Pp.385 ISBN 0-12-348580-0 (Academic 1980) $40, £26 40

It is now 40 years since the publication of Hans Jenny's classic monograph *Factors of Soil Formation* (McGraw-Hill, 1941), a book which provided the framework for much subsequent work in soil genesis Now in his eighties, Jenny has written what amounts to a sequel to that earlier work In it he develops his ideas into a broader, ecological view, describing how, by analysis of the "state factors", either whole ecosystems or their separate components — vegetation, animals and soil — evolve with time and vary from place to place This treatment occupies the second half of the book and is preceded by a consideration of the processes of soil genesis (water balance, ion exchange, clay formation, for example)

Jenny draws many of his examples from his own work and that of his students and colleagues His use of the English language is unconventional, for example, he talks of "swarms" of ions around particles, "particle bondage with humus" and words like "porositors" and "depauperizes" appear In addition the editors have purposely retained many of the original drawings which he made for the diagrams and figures, in order "to carry through the artistic touch" So what one gets overall is a very personal, even idiosyncratic, view of the soil resource Although written in a textbook style, and in part intended for students, one would not recommend this as an undergraduate text However the second part of the book particularly will be of interest to the many soil scientists who have been influenced, directly or indirectly, by the ideas of Hans Jenny

In recent years a number of texts on soil physics have been published, rectifying the absence of much choice which had existed for some time *Fundamentals of Soil Physics* together with its companion volume *Applications of Soil Physics* further extends the range of material in a most comprehensive way Whilst each is a separate, self-contained volume, the latter does draw on the former and assumes an appreciation of the basic principles of soil physics Together they cover the broad range of soil physics, providing a welcome integration of basic principles and practical applications

Fundamentals treats the basic static and dynamic properties of the solid, liquid and gaseous phases in turn After an introduction to the general physical characteristics of soils and basic properties of water, the solid phase of soil is studied through a consideration of particle size distributions and specific surface areas, the properties of clays, and structure and aggregation The concept of soil water potential is carefully developed and used in a consideration of both saturated and unsaturated hydraulic conductivity and the movement of solutes The roles of diffusion and respiratory activity in determining the composition of the soil atmosphere are considered and this leads naturally to a chapter on heat flow and temperature Finally, soil strength, consistency and compaction are discussed

The author introduces essential physics where appropriate and is thorough without being overly mathematical Thus care has been taken to use both one- and three-dimensional forms of flow equations Developments of theoretical aspects describing basic processes are complemented by discussion of both laboratory and field methods of measuring important parameters Except, perhaps, for the lack of any coverage of the soil–plant–atmosphere continuum and erosion, this text alone should cover most undergraduate courses

Applications continues the discussion, paying particular attention to the management of the soil environment and the field-water cycle Thus infiltration, drainage, irrigation, evaporation and soil moisture uptake by plants are considered, drawing on the basic principles introduced in the companion volume These themes are elaborated in a second section consisting of five chapters by invited authors who cover further aspects of the field-water cycle and the problems of studying soil heterogeneity These contributions dovetail well with the earlier section and give a useful insight into some of the more advanced realms of soil physics

These two books provide a modern, clear and concise introduction to soil physics They are international in style and content, drawing examples from a wide range of situations Unfortunately the cgs system of units is used, though the metric equivalents are often given (however, the Pascal is not introduced when considering soil water potential) Whilst the texts do introduce an appreciable amount of mathematics, they should not prove too difficult for the careful student and understanding is aided by the excellent sample problems at the end of each chapter Over 400 references (up to 1980) are given at the end of each volume, and provide a good starting point for further work

Together, the two volumes represent an admirable textbook for undergraduates They should certainly be in every library covering soil science ☐

David Rimmer and Michael Adey are Lecturers in the Department of Soil Science at the University of Newcastle upon Tyne

---

Dirty work at the crossroads?

M.J. Kirkby

Soils and Landforms An Integration of Geomorphology and Pedology By A J Gerrard Pp 219 Hbk ISBN 0-04-551048-2, pbk ISBN 0-04-551049-0 (George Allen & Unwin 1981) Hbk £15, $35, pbk £7 95, $16 95

Soil science and geomorphology have borrowed from one another throughout their joint histories and, as with other disciplines, the relationship has been very fruitful Areas of mutual interaction have, however, largely relied on the static properties of soil or sediment, while understanding of process dynamics has followed rather divergent paths in the two disciplines Pedologists have tended to concentrate on the chemistry, physics and biology of the soil, mainly at a micro-scale, while geomorphologists have attempted to understand sediment and solute transfers, generally at a macroscopic to world-wide scale

One very important area of common ground has, I think, been surprisingly neglected At its simplest, it springs from the obvious fact that contemporary soils are the very materials which are moved downhill by current landform processes It follows that the physical and chemical processes by which landforms and soils evolve are substantially identical To develop this theme — and there are signs that it is being increasingly developed — there is an urgent need to collate existing concepts and data, to translate concepts between the two disciplines, and to re-think many of our approaches in a new idiom

John Gerrard's book makes a worthwhile contribution to the first of these three aims, by bringing together work on soil formation, on soil movement and removal, on hillside hydrology and on the catena concept which must be central to any integrative work In reviewing this material there is however little evidence of fresh insights or of the author's own syntheses, so that little headway is made in translating concepts or adding to them

About half of the book then proceeds to consider soils on the basis of the landforms on which they are formed, including soils on erosion surfaces, flood and coastal plains, and glacial deposits In this section, there is the focus on landforms which might be expected from the title, but not enough emphasis on the links with solution and other geomorphological processes The final chapter, "A Pedogeomorphic Synthesis", is very brief and summarizes the general timidity in approaching any conceptual development With other recent books, such as R V Ruhe's *Geomorphology* (Houghton Mifflin, 1975) and P W Birkeland's *Pedology, Weathering and Geomorphological Research* (Oxford University Press, 1974), it will nonetheless be of help to those wishing to begin work on a topic which is, and should be, ripe for considerable development ☐

M J Kirkby is Professor of Physical Geography at The University of Leeds

---

Back to the land

D.L. Dineley

The Stratigraphy of the British Isles, 2nd Edn By Dorothy H Rayner Pp 460 Hbk ISBN 0-521-23452-2, pbk ISBN 0-521-29961-6 (Cambridge University Press 1981) Hbk £32 50, $59 50, pbk £12 50
The Structure of the British Isles, 2nd Edn By J G C Anderson and T R Owen Pp 251 Hbk ISBN 0-08-023998-6, pbk ISBN 0-08-023997-8 (Pergamon 1980) Hbk £13 75, $32, pbk £5 95, $14 50
Methods in Field Geology By Frank Moseley Pp 211 Hbk ISBN 0-7167-1293-8, pbk ISBN 0-7167-1294-6 (W H Freeman 1981) Hbk $29 95, £12 95, pbk £6 95, $14 95

Good "standard" geological texts abound, trying to revise them to keep abreast of new facts and ideas is a daunting task for any author In this trio, the stratigraphy and structure of the British Isles are described in two second editions, while the third text shows how basic field studies may be carried out Whilst the influence of new hypotheses upon the Rayner and the Anderson and Owen books is rather small, Moseley's book is another matter altogether, new ideas have their place there, and in style and content it is very welcome

Since the first edition of Rayner appeared in 1967, the impact of plate tectonic theory upon stratigraphy has prompted intriguing new scenarios explaining the geological evolution of the British Isles and western Europe Dynamic stratigraphy has replaced the classical "static" listing of strata, attention has swung to the relationships between sedimentation, igneous activity and tectonism The first edition was a clear account of the strata found in these islands The second is equally elegant and there is reference to plate tectonic influence upon palaeogeography and the stratigraphic record Such references are, however, so restrained as to seem reluctant Perhaps because we now have so many working hypotheses in this area, Dr Rayner has deliberately avoided them and has confined herself to making few changes to her previous account The individual stratigraphic trees have not lost their identity in the collective crustal evolutionary wood The diagrams are clear and good — many more of the same standard would have been welcome

The teaching of stratigraphy now involves emphasis upon correlation and interrelationships of many different kinds of phenomena, essential in all of this is the use of fossils Without palaeontology stratigraphy will fail, and the reference to biostratigraphy in this text remains far too meagre Lists of strata commonly are as short of meaning as are lists of fossils to most students, but it ought not to be so — here is a missed opportunity to remedy the one substantial criticism that I had of the original edition All in all, however, the book is adequate for the undergraduate "who may have only a general acquaintance with the broad principles of geology"

Structural geology has made some significant strides since the first edition of Anderson and Owen's book was published in 1968, and not only in the field of plate tectonics Ideas about the formation of sedimentary basins and about both shallow and deep geological structures in Britain are changing and debate is lively This text has not gone as far as might have been expected in presenting new ideas and integrating them with previous knowledge It remains an orthodox description of structural units, one by one, grouped as Precambrian, Caledonian, Hercynian and Alpine terrains, Tertiary igneous terrain and with a chapter on "The Seas around Britain" (an unfortunate and inaccurate title) that contains material that should have been integrated into the preceding chapters The geographical distinction between structures on land and those on the submerged continental shelf is, to an increasing extent, untenable

Chapters 2 and 3 deal with the tectonic evolution of the British Isles A simpler outline of palaeogeographical changes might have served better at this stage, with a fuller, more decidedly plate-tectonic-orientated discussion at the end of the book The style of this volume is very dry, the illustrations are generally poor and many are very poor indeed The authors advise that the book should be read with the aid of the appropriate geological maps published by the Institute of Geological Sciences, but there are very few pointers in the text as to which maps should be consulted regarding specific features or terrain The list of references is extensive, but the standard bibliographical abbreviations are not used and several entries are inaccurate The printing, direct from authors' typescript, the errata and the poor diagrams give the book the air of having been compiled in a great hurry One would have expected better

A book to turn students' attention and interest towards how (a local) stratigraphy or structure is discovered, examined and recorded seems doubly welcome in the context of what has been said above Hail, then, Moseley's students' manual of field geology! Principles of geological mapping are nicely stated and readable case histories are provided to illustrate them The latter cover diverse terrains, from Greenland's icy mountains to the seared wastes of Oman, with Cumbria, Andalusia and even a Quaternary torment in between Igneous, metamorphic, sedimentary and surficial geological examples are treated with just about the right level of technicality and with commendable care. The book shows how aerial photographs, field survey and data logging of many kinds are pressed into map-making Abundant and generally excellent illustrations complement the text very well

This is an attractive book and something of a bargain, especially since it seems to capture the essence and spirit of geological exploration Congratulations to author and publisher for a brave new book ☐

D L Dineley is Chaning Wills Professor of Geology and Head of the Department of Geology in the University of Bristol

Geological classics

K.G. Cox

Basalts and Phase Diagrams An Introduction to the Quantitative Use of Phase Diagrams in Igneous Petrology By S A Morse Pp 493 ISBN 0-387-90477-8 (Springer-Verlag 1981) DM62, $36 60

In the teaching of igneous petrology the study of phase diagrams for compositionally-simple synthetic systems occupies an honourable niche similar to that of Latin in the arts subjects It is thought to be good for the soul, though the precise benefits are sometimes difficult to define

Professor Morse's book is probably the most comprehensive survey available for all those systems which are relevant to the study of natural igneous rocks, particularly though not exclusively, basalts It is written with clarity, humour and a loving attention to detail The diligent reader, undergraduate or postgraduate, will acquire a good feel for the way igneous processes work, by absorbing the many, but inevitably rather diffuse, parallels between synthetic and natural systems Our old friends such as Ab–An–Di, Fo–Di–SiO_2, the ternary feldspars and many more, are dealt with in detail, and there are good sections on the effects of volatiles and the interpretation of layered intrusions On the level of simple, every-day problems of how magmas crystallize, fractionate or originate by partial melting, this is an excellent book

I am less happy when the author becomes involved with more major issues of basalt genesis The decision to restrict discussion to synthetic systems means that problems arising from work on natural materials (basalts and peridotites), and no less from geochemistry and field studies, cannot be adequately dealt with In itself this might be acceptable — any author has to decide what to leave out — were it not for the misleading nature of some of the comments which do appear I doubt, for example, if many petrologists really would agree that "the heart of the basalt problem lies in the eruption, often from the same vent, of tholeiitic basalts at one time and alkali basalts at another time" (p 2), though they might have in the mid-1960s. Other examples, which are consistent with this rather dated viewpoint are numerous, and constitute something of a hazard to the incautious reader Nevertheless, as a book on phase diagrams this is first rate — it is only the basalts which should be taken with a pinch of salt ☐

K G Cox is a Lecturer in Petrology at the University of Oxford

Plants of the past...

Keith Allen

Paleobotany. An Introduction to Fossil Plant Biology By Thomas N Taylor Pp 589 ISBN 0-07-062954-4 (McGraw-Hill 1981) $41 25, £22 95

I have awaited this publication with much interest, because it is the first general palaeobotany textbook to be written in the English language for almost 20 years During that time, new discoveries, new interpretations and a much wider use of both stereoscan and transmission electron microscopes have greatly increased knowledge of fossil plant morphology and anatomy Interest in the origins of plant life, the earliest land plants, the evolution of flowering plants, fossil fuels and the palynological correlation of strata has sparked an awareness of palaeobotany which now reaches far beyond university botany departments

In writing a palaeobotany textbook, one must choose either to make it very botanical, giving comprehensive taxonomic coverage throughout the plant kingdom, or to aim for a wider audience, especially amongst geologists, by reducing the morphological information and including details of floras, palaeogeography, palaeoclimatology, fossil fuels and palynology Like most earlier authors, Taylor has chosen the former course

This is a scholarly, well-researched textbook, bringing the reader right up to date on plant groups, from bacteria and fungi through to angiosperms There are also chapters on methods of preservation and techniques for studying fossil plants, on Precambrian biology and a particularly good one on origins and evolution of the seed habit Taylor's own research interests are reflected in a fuller treatment of the Pteridosperms, though all groups are adequately covered In the angiosperm chapter, he has wisely forsaken the taxonomic approach and dealt more broadly with selected topics, including the possibility of pre-Cretaceous angiosperms The bibliography, usefully listed by chapter, contains over 1,000 references

Taylor's research papers are always accompanied by excellent illustrations, and he must be aggrieved at the poor production of many of the photographs in the book, some of which are so ghostly that they fail to show clearly the details intended Also, the positioning of many illustrations leaves unnecessary blank areas which could usefully have been filled with photographs at larger magnification The photographs of "extinct" palaeobotanists add a nice touch, though I would have liked to see Professor Lang in the Hall of Fame, having contributed so much to Devonian floras and in particular to that from the Rhynie Chert

To whom do I recommend this book? Clearly all palaeobotanists will find it valuable in bringing them up to date on groups outside their main fields of interest, for this, I find it excellent Third-year botany students, though perhaps being slightly overwhelmed by the number of genera included, will find it a most useful and readable source of information I cannot, however, recommend it with too much enthusiasm to geologists, who will find the comprehensive morphological approach very hard going However, this informative textbook replaces many of the earlier palaeobotanical books, and should be available in all biological libraries □

Keith Allen is Senior Lecturer in Botany at the University of Bristol

---

. . . and the present

Peter D. Moore

100 Families of Flowering Plants By Michael Hickey and Clive King Pp 567 Hbk ISBN 0-521-23283-X, pbk ISBN 0-521-29891-1 (Cambridge University Press 1981) Hbk £27 50, $66, pbk £9 95, $19 95 *The Study of Plant Structure Principles and Selected Methods* By T P O'Brien and M E McCully Hbk ISBN 0-632-00926-8, pbk ISBN 0-632-00927-6 (Blackwell Scientific 1981) Hbk £20, pbk £12

ATTEMPTS are being made to shed the Victorian image of botany in many universities, sometimes even resulting in radical, but rarely fruitful, alterations in departmental titles in order to attract more students (Plant Science or Plant Biology, for example) Courses offered to plant-orientated students are also changing rapidly, often in the direction of subcellular studies or, at the whole-organism level, towards physiology and ecology Subjects which once occupied a substantial part of the undergraduate curriculum are now becoming neglected, amongst which are classical (structural) taxonomy and anatomy

An unfortunate consequence of this is that we are spawning a generation of ecologists which is incapable of defining the criteria upon which plants are identified in the field, and of physiologists which is often sadly deficient in a knowledge of the anatomical structure of the plants with which they deal In the long term this problem can only be dealt with by a reassertion of balance in undergraduate training, and the two books under review here are designed to encourage the development of such courses

Hickey and King's book, as its title implies, covers 100 plant families, devoting about four pages to each (up to eight pages for more complex families such as Compositae and Gramineae) For each family one is given general information such as distribution (but no maps), general characteristics (most of which are available from a good flora), economic or decorative uses, and taxonomic subdivision Thus far the book is comparable to V H Heywood's *Flowering Plants of the World* (Oxford University Press, 1978), but is more detailed in its coverage of family characteristics and rather less so in dealing with uses

A typical member species of the family (or sometimes more than one for families with a wide spread of structural variation, as in the Rosaceae), chosen for ease of availability for student classes (alternatives are suggested), is then fully described and the descriptions are accompanied by detailed line drawings These will provide valuable aids to students as they dissect the flower and fruit Extensive annotation is provided on the pages opposite these

Optima for Animals
R. McNeill Alexander
Optimization theory is the branch of mathematics concerned with finding those structures and behaviours that are in some sense the best possible, and is therefore a very appropriate tool for trying to discover why animals have evolved in particular ways
£5 approx paper 160 pages
Probable publication April

Plant Growth Curves
A Functional Approach to Plant Growth Analysis
Roderick Hunt
A review of the theory, practice and applications of the use of fitted mathematical functions in plant growth analysis The approach taken is very broad and includes an extended coverage of the philosophical and scientific links between this topic and related fields of activity in plant science
£8 50 approx paper 240 pages
Probable publication April

A Biologist's Guide to Principles and Techniques of Practical Biochemistry
Second Edition
Edited by Bryan L. Williams and Keith Wilson
Contemporary Biology Series
This book aims to make biology students aware of the principles and methodology of those analytical techniques which are fundamental to the development of our understanding of cellular and subcellular processes The second edition has been revised to include new techniques, in particular a new chapter on immunochemical techniques
£8 50 paper 336 pages

Studies in Biology

136 Biotechnology
John E Smith
£2 60 paper 80 pages

Edward Arnold
41 Bedford Square
London WC1B 3DQ

Circle No 32 on Reader Enquiry Card

drawings, but a more helpful approach would have been achieved by adding labels to the diagrams In the seeds of the Violaceae, for example, one can talk of elaiosomes and their function in dispersal, but it would help to have a detailed drawing with an appropriate label The diagrams are, however, generally well chosen and informative, they lack the striking, aesthetic appeal and full vegetative detail of those in Heywood's book, but they make up for this in precision and clarity

This book will become a vital and valued tool to those botanists, both amateur and professional, who wish to look more closely at the structure of easily available flowers

O'Brien and McCully's book is also concerned with observational techniques, but is evidently intended both for teaching and research It is essentially a laboratory manual of microscopic, anatomical and morphological methods, giving both theoretical background and practical instruction It begins from first principles of microscopy and has a "cook-book" approach with some very helpful and informal marginal comments, such as, "If you cannot budge something with finger and thumb before exerting your strength, ASK!" Very clearly aimed at the undergraduate! This chatty style, accompanied by lucid explanations of principle and practice should prove very helpful, especially in such areas as phase contrast and interference contrast microscopy The language used avoids unnecessary jargon and has many hints for trouble-shooting and image improvement Chapters on specimen preparation and microphotography for both light and electron microscopy are included However, the format and sub-heading numbering demand serious criticism, what is otherwise an agreeably usable book is given an unduly forbidding appearance by a complex cross-referencing system and an ugly off-set litho production

Both of these books seek to reach a small, and still shrinking market They will serve this market well, but whether they will succeed in reversing its slow demise is questionable ☐

Peter D Moore is Senior Lecturer in the Department of Plant Sciences, King's College, University of London

---

Panglossian botany

J.L. Harper

Physiological Plant Ecology, 2nd Edn By W Larcher Pp 303 ISBN 0-387-09795-3 (Springer-Verlag 1980) DM59, $34 90 *Environmental Physiology of Plants* By A H Fitter and R K M Hay Pp 355 Hbk ISBN 0-12-257760-4, pbk ISBN 0-12-257762-0 (Academic 1981) Hbk £19 60, $47 50, pbk £7 95, $19 50

"PLANT ecophysiology, a discipline within plant ecology, is concerned fundamentally with the physiology of plants as it is modified by fluctuating external influences" (Larcher) "How do the intricate physiological mechanisms which have been elucidated over the last 100 years by plant physiologists really operate under natural conditions?" (Fitter and Hay) These sentences define the scope of these two books and at the same time relegate the rest of plant physiology (that which is not "eco-") to the study of plants in constant and perhaps irrelevant conditions

It is easy to recognize a text in environmental or eco-physiology by the high frequency of the words "adaptation" and "stress" Counting their occurrences and guessing their meanings in different contexts is a fascinating exercise I suspect that to most ecophysiologists adaptation is that feature of an organism that may be explained away as "a good thing" It is, then, a comfort that the word carries the guesstimate that such properties are the result of all-powerful natural selection which has sought out the optimal solutions to the problems set by nature It then remains the task of the ecophysiologist to demonstrate just how everything about his organisms is for the best in the best of all possible worlds

Stress is, of course, a "bad thing". Sometimes it is a nasty stimulus, sometimes an uncomfortable response Fitter and Hay don't like the word because it lacks the precision given to it in mechanics — yet, use it 22 times on one page (Stress is not in the index, though strain is) To Fitter stress appears to be a stimulus, a force imposed by the environment, but to his co-author the word appears to mean response — a state induced in the organism "Plant cells at a turgor pressure lower than the maximum value are said to be suffering from Water Stress" To Larcher "stress is the exposure to extraordinarily unfavourable conditions" — clearly to him it is a stimulus, not a response and must be extreme I also puzzled about Fitter and Hay's phrase "low light stress" but suppose it is a synonym for "shade stress"!

These two books cover very similar ground — the responses of plants to light, water, nutrients, temperature (and for Fitter and Hay the effect of animals and some microorganisms) Fitter and Hay are more interested in cellular and biochemical processes than Larcher, who is more concerned with the whole plant and its contribution to community processes Fitter and Hay include a section on allelopathy in which they accept uncritically some very dubious evidence

Both books carry an extensive bibliography and between them cite more than 1,500 references, of which only about 50 are quoted in both Together they give a splendid introduction to the literature Fitter and Hay's is a very Anglo-American text (less than 5% of the references are in alien tongues) Larcher's bibliography is international, as befits an author who advises "Despite the difficulties it is worth taking the trouble to read original works in that language in which the author can express himself most precisely" Is this a warning to those who are reading his own book in its excellent translation?

Students could be expected to read and enjoy chapters in Larcher and not become too badly infected with teleology and Panglossian optimism However, as regards Fitter and Hay, I admit to a bias I cannot stomach phrases such as " respiration has a purpose ", " the various mechanisms that have been adopted to fit the species [*sic*] to their environment"; "plants appear to use it [phytochrome] to detect shading", "species [*sic*] may need to maximise plastic responses to permit offspring to colonise a wide range of habitats " I must stint my praise for a book that seems to present biology as a study of purposeful and soothsaying species like football managers planning their future goals ☐

J L Harper is Head of the School of Plant Biology at the University College of North Wales, Bangor

---

Renewed growth of plants

James F. Sutcliffe

Growth and Differentiation in Plants, 3rd Edn By P F Wareing and I D J Phillips Pp 343 Hbk ISBN 0-08-026351-8, pbk ISBN 0-08-026350-X (Pergamon 1981) Hbk £20, $40, pbk £9, $20

THIS popular textbook, which was published first in 1970 and reprinted several times before the second edition appeared in 1978, has now had another face-lift Apart from a shortening of the title — which does not indicate any change in approach — there is a new format with double-column printing on a larger folio size Even the flowering shoot of *Plumbago indica* which continues to decorate the front cover appears to have had a new lease of life The plant has turned green again and several new leaves have appeared

The increase in the size of page has made it possible to achieve a more pleasing layout, and despite the use of a larger typeface and slight expansion of the text, there is a reduction in the number of pages Unfortunately the improved appearance of the book is not enhanced by the photographic reproductions, the quality of some of which (for example Figs 1 10, 3 4 and 6 1) seems to have deteriorated progressively in succeeding editions

The sequence of topics follows closely that of the second edition but the chapters have now been arranged in four sections Structural and morphological aspects of development (Chapters 1 and 2), internal controls in plant development (Chapters 3–6), environmental control of development (Chapters 7–12), and, molecular and general aspects of differentiation (Chapter 13) Each section is prefaced by a short introduction and these serve to link the book together The reading lists at the end of each chapter have been expanded considerably by the inclusion of some recent reviews and research publications

However, much of the text remains unaltered and the claim of the publisher that the book has been "extensively re-written" is hardly justified New material has been added here and there, particularly in the chapter dealing with the biochemistry of growth-regulating substances Despite continuing research we are still a long way from understanding the mechanism of their action In fact, as the authors recognize, the picture instead of becoming clarified seems to be getting more confused — a cause of some embarrassment to those of us who attempt to teach this subject to biologists

Librarians who stocked up recently with copies of the second edition of this book will be relieved to learn that there is no great need to replace them with the new edition Undergraduates who have little choice may begrudge the extra cost, but we will go on recommending the book to our students as the best overall introduction to the physiology of plant growth that is available at present ☐

James F Sutcliffe is Professor of Plant Physiology at the University of Sussex

---

Introducing whom to natural products?

T.W. Goodwin

Secondary Plant Metabolism By Brian Vickery and Margaret L Vickery Pp 335 Hbk ISBN 0-333-27017-7, pbk ISBN 0-333-27018-5 (Macmillan Press, London/University Park Press 1981) Hbk £25, $49 50, £12

It is important not to criticize a book for not being what it was never intended to be This is made difficult in the present instance because neither the authors nor the publishers give any hint of the type of reader the book is aimed at What the book clearly is, is a full and up-to-date descriptive account at a rather simple level of the formation and metabolism of secondary plant products On a slightly lower level, the function, uses, ecological interactions and chemosystematic properties are also discussed

After an introductory chapter, which considers such topics as the differences between secondary and primary metabolites and how biosynthetic pathways are elucidated, the bulk of the book is devoted to essays on families of compounds which arise from basic precursors these are sugars and sugar derivatives arising from the primary product of photosynthesis, considered to be glucose 6-phosphate, the various fatty acids produced from the acetate–malonate pathway and their incorporation into plant lipids and glycerides, polyketides from acetate which are mainly fungal rather than higher plant products, terpenoids derived from mevalonate, shikimic acid derivatives, compounds synthesized from two different fundamental units as exemplified by the flavonoids, porphyrins, purines and pyrimidines, compounds, including alkaloids, which are derived from various amino acids A great deal of ground is covered and one's way about the concentrated information in the book is facilitated by three good indexes

One can make a reasonable guess that this book is aimed at organic chemistry students studying a natural products course in their second year It would be a satisfactory basis for such a course but probably lecturers would nowadays concentrate more on reaction types and reaction mechanisms rather than simply on biogenetic schemes Certainly, stereochemical aspects would be given more prominence than they are afforded in the present text The book would be useful to biochemists for basic information but not as a working text because, as the authors state, enzymology — the ultimate key to the explanation of all biosynthetic activity — is not included In the same way it would be useful as a source book for botanists, agriculturalists and pharmacists

This, then, is a good introductory book on natural products, although there is difficulty in visualizing exactly which academic slot it is intended to fill ☐

T W Goodwin is Johnston Professor of Biochemistry at the University of Liverpool

---

Botany for beginners

Ralph S. Quatrano

Biology of Plants, 3rd Edn By Peter H Raven, Ray F Evert and Helena Curtis Pp 686 ISBN 0-87901-132-7 (Worth 1981) $19 95, £10 50

One of the most widely adopted textbooks for introducing students to the plant sciences over the past several years has been *Biology of Plants* by Raven, Evert and Curtis The new and much improved third edition of this popular text must still be considered as one of the best overall books of general botany

Previous editions were clearly aimed at beginning courses for majors Such courses would form the basis upon which more advanced courses, such as morphology, physiology and ecology, would build The new edition is no exception The depth and breadth are still sufficient for majors and it will be a good source book for any student of the biological sciences However, the detail is not overwhelming and with the continual mention of applied and practical aspects of plant biology, as well as good chapter summaries, appendices for chemistry and classification, and a complete glossary, makes it a possible choice for non-major courses Much of the condensing and rewriting in this edition have also helped to make it an attractive choice for a less rigorous introduction to botany The length of the text, however, may be excessive for such courses, especially in view of the availability of other shorter, good "non-major" texts (see *Nature* **284**, 91, 1980)

Although the sequence of topics presented in the text may not be followed, most botany instructors will find no problem in choosing specific chapters to fit their schedule Several changes for the better in the organization of the third edition include moving the chapter on the chemistry of heredity to the section on genetics and evolution, more emphasis on the Cyanobacteria, and the treatment of the fungi as a group separate from the water and slime moulds (Protista) Several sections have been condensed (for example "Ecology", "Genetics and Evolution") without deleting important concepts, while others have been extensively updated and revised (for example "Growth Regulators", "Uptake and Transport")

The illustrations and diagrams are clear and the inclusion of colour plates for angiosperm anatomy in this edition will be helpful to students in the laboratory The book will undoubtedly maintain its high ranking and competitiveness with other new editions of excellent, popular texts such as the sixth edition of *Botany* by Weier *et al* (Wiley, 1982) ☐

Ralph S Quatrano is Professor of Botany and Instructor in General Botany and Biology Courses at Oregon State University, Corvallis, Oregon

Legacy of tradition in plant geography

Honor C. Prentice

Historical Plant Geography An Introduction By Philip Stott Pp 151 Hbk ISBN 0-04-580010-3, pbk ISBN 0-04-580011-1 (George Allen & Unwin 1981) Hbk £12, $30, pbk £5 95, $14 95

THIS book is an elementary introduction to the traditional subject matter of "plant geography" — species distributions and their interpretation It is concise, very readable, well produced and accessibly priced Care has been taken to make it comprehensible to students with different backgrounds in biology, geography or environmental science There are chapters on taxonomy, maps, distribution patterns, disjunctions, endemism, and geological and historical evidence

I am sceptical, however, about the value of a textbook on plant geography that carefully avoids modern ecological *and* evolutionary concepts Some plaintive remarks on the state of biogeography (Chapter 1) are revealing — if the "ecological tradition" has "flourished and grown out of all proportion" it is surely because of advances in ecological theory!

Classical phytogeography has not made comparable progress, and indeed the same paradoxes and ambiguities that run through the classical literature reappear, unresolved, in Stott's book ("Isoflors are used to locate centres of origin and migratory patterns " — but how?) Pollen analysis is introduced, but its most relevant results — reconstructions of complex Late-Quaternary migrational histories — are not There is no discussion of how taxonomic information may lead to reconstructions of phyletic patterns, cluster analysis and the like are dealt with, but cladistics is not mentioned, despite the impact of cladistic and vicariance concepts on modern evolutionary biogeography For many reasons, then, I find this a disappointing book however well it succeeds in its stated aims ☐

Honor C Prentice is a Visiting Research Fellow in the Department of Biology at the University of Southampton

ATTENTION TECHNICAL INSTRUCTORS!

THE AMERICAN NUCLEAR SOCIETY
OFFERS THIS TEXTBOOK SERIES TO THE EDUCATIONAL COMMUNITY

- *El Wakil* **NUCLEAR ENERGY CONVERSION** 682 pages 6 x 9 hard bound ANS Order No 350001 **$28 60 ea**
- *El Wakil* **NUCLEAR HEAT TRANSPORT** 514 pages 6 x 9 hard bound ANS Order No 350002 **$26 80 ea**
- *Karl Wirtz* **LECTURES ON FAST REACTORS** 310 pages 8½ x 11 softbound ANS Order No 350003 **$18 00 ea**
- *Murray/Cobb* **CONCEPTS AND CONSEQUENCES** 710 pages 7 x 9½ hardbound ANS Order No 350004 **$13 95 ea**

SEND FOR INFORMATION ON HOW TO OBTAIN A DESK COPY

Please take my order for
__________Copies of ANS Order No 350001 $__________
__________Copies of ANS Order No 350002 $__________
__________Copies of ANS Order No 350003 $__________
__________Copies of ANS Order No 350004 $__________
TOTAL $__________

NAME __________
ADDRESS __________
CITY __________
STATE __________
ZIP __________

Send to

AMERICAN NUCLEAR SOCIETY
555 North Kensington Avenue
La Grange Park, IL 60525, USA

Payment enclosed in the amount of $__________
Bill me and I will pay the additional postage and handling charge

7/81

Circle No 42 on Reader Enquiry Card

Ethology: the classic and the *avant-garde*

Peter Marler

An Introduction to Behavioural Ecology By J R Krebs and N B Davies Pp 292 Hbk ISBN 0-632-00666-8, pbk ISBN 0-632-00668-4 (Blackwell Scientific/ Sinauer 1981) Hbk £18, $39 50, pbk £7 50, $16 50 *Modern Ethology The Science of Animal Behaviour* By S A Barnett Pp 705 ISBN 0-19-502780-9 (Oxford University Press 1981) £12 95, $23 95

ETHOLOGY helped the study of animal behaviour off to a good start with a number of simplifying assumptions, one of which was crucial in convincing sceptics that natural behaviour is even studiable Given the right kind of description, it was asserted, behaviour would turn out to be as stereotyped and species-specific as morphology This worked well for a time, but in the 1960s it became obvious that, just as morphology exhibits adaptive variations, so patterns of behaviour vary widely within a species Even small differences in the behaviour of groups of individuals may be so amplified by processes of social interaction that different patterns of social organization are created The theorizing of Lorenz and Tinbergen, primarily reductionistic in its orientation, was ill-suited to guide investigations of the quantitative impact of behavioural variations on animal–environment interactions Counsel was sought from other disciplines such as ecology, population genetics and economics

In the past ten years several subdivisions of ethology have developed to deal with such problems one of which, behavioural ecology, is admirably reviewed in the introductory text by Krebs and Davies The approach is that of the evolutionary biologist, concerned with functional explanations of behaviour at the level of individual and kin selection The book is a pleasure to read Its style is lucid and entertaining, and the illustrations are clear and instructive There are well-balanced reviews of the evolution of alternative social systems and evolutionarily stable strategies, feeding strategies and optimality modelling, fighting and manipulation, altruism and cooperation The pride of place assigned by Kropotkin and Allee to cooperation, however, is now superseded by an emphasis on conflicts of interest, effectively translating the motivational drive conflicts of Tinbergen into the functional domain Instead of collaboration, we have selfishness, spite and calculated exploitation

While arguing their case forcefully, Krebs and Davies are cautious about over-extending their theorizing, much of which, they admit, serves more as description than as predictive theory In that sense, the book also serves well to point the more ambitious student towards new problems awaiting solution In particular, genetic issues raised, such as uncertainties about paternity and how "kin" are actually distributed in natural vertebrate populations, deserve to be tackled by direct observation and experiment as well as at the abstract, theoretical level

Behavioural ecology forms only a part of Barnett's much larger endeavour *Modern Ethology* is more of a "mechanisms" book than that by Krebs and Davies, analysing critically the concepts of classical ethology in the light of recent research, and reviewing an extensive literature in the process It is both a textbook and a serious, scholarly work that grapples with conceptually difficult and controversial issues such as intention, conscious awareness and the role of reductionism in behavioural science Accounts of social behaviour are interwoven with such topics as behavioural endocrinology and learning theory One of the major index entries, habituation, does not appear in the index of Krebs and Davies, though clearly relevant to their subject matter In this sense, the two books complement one another well

Especially salutary are Barnett's discussions of concepts of heritability and aggression Aggression is interpreted with care, especially in the section on human ethology A quotation from W D Hamilton, a founder of sociobiology and behavioural ecology, stating that "vicious and war-like tendencies are natural in man'' sounds a cautionary note Misunderstandings about such issues are bound to arise until we understand the epigenetics of such traits as aggressive behaviour and the points in development at which they are accessible to environmental modification As Barnett indicates, the interaction of nature and nurture is a central problem in biology and those trained in the ethological tradition are especially well placed to deal with it An historic opportunity will be missed if current enthusiasm for behavioural ecology diverts all young ethologists from what has to be the most challenging and momentous issue ethology has yet faced Only when we understand how genes impose adaptive limits on behavioural plasticity will we fully appreciate the pervasiveness of genetic influences on the development of behaviour, whether animal or human ☐

Peter Marler is Professor at the Rockefeller University, New York, and a member of the Rockefeller University Center for Field Research in Ecology and Ethology

Sixty years on?

Michael B. Usher

Elementary Mathematical Ecology By John Vandermeer Pp 294 ISBN 0-471-08131-0 (Wiley 1981) £24 05, $43 25 *Population Systems A General Introduction* By Alan A Berryman Pp 222 ISBN 0-306-40589-X (Plenum 1981) $16 95, £10 71 *Population Ecology A Unified Study of Animals and Plants* By Michael Begon and Martin Mortimer Pp 200 Hbk ISBN 0-632-00812-1, pbk ISBN 0-632-00667-6 (Blackwell Scientific/Sinauer 1981) Hbk £15, $33, pbk £7 90, $16 95

MANY origins of the subject of population dynamics can be traced to the 1920s, when A J Lotka, R Pearl, P F Verhulst, V Volterra and others were publishing relatively simple mathematical models of population growth and interaction During the following half-decade the subject grew slowly, but in the 1970s there was an explosion of research interest It is inevitable that this would eventually manifest itself in teaching and writing textbooks to fill the students' need Three recent examples are considered here

John Vandermeer teaches population dynamics with a programmed text of ten lessons, each of which is designed to take 5 ± 2 hours The explanatory sections of *Elementary Mathematical Ecology* are kept short, and the exercises, for which relatively sketchy but adequate answers are given, are both numerous and essential for understanding the lesson I am reasonably certain that most undergraduates would take considerably longer than the designed time, and in the exercises I found the lack of consistency of rounding intermediate results most confusing (for example, in the first chapter one has $\ln (2\ 25)=0\ 81093$ and $\exp (0\ 83)=2\ 3$)

In *Population Systems,* Alan Berryman has written a more traditional textbook, setting the subject out in only six chapters which contain few exercises and only brief solutions The text itself does not make reference to the ecological literature a series of notes, listed in rather small type at the end of each chapter, provides reviews of a few references and also gives some of the more technical material I found the shuffling between text and notes a rather frustrating aspect of the book's subject presentation

A slight departure from the usual progression from single-species to two-species interactions to communities is a characteristic of Michael Begon and Martin Mortimer's *Population Ecology* Although the first five chapters follow the first two steps in this sequence, the authors conclude the book with three chapters — on life-history strategies, population regulation and community structure — in a section called "Synthesis" Although this makes for interesting, if unexpected, reading, since one is asked to think about migration, costs of reproduction, r- and K-selection, and so on, after reading about interspecific competition and predator–prey relationships, the attempt at synthesis really fails

It is interesting to compare the subject matter of these books All of them include introductions to population growth, interspecific competition, predator–prey relationships, spatial patterns (rather briefly dealt with in *Population Ecology*) and community structure (only sketchily introduced at the end of *Elementary Mathematical Ecology*) A consideration of life tables is the most surprising omission from *Population Systems,* which also lacks an account of matrix models of age-structured populations These, then, are the core topics, but what are the specialities? *Elementary Mathematical Ecology* contains data on island biogeography and species-area relationships, but I wish that the author had not used the ambiguous term "species number" (implying ranking) for the unambiguous "number of species" *Population Systems* takes a systems analysis approach, introduces much of the jargon such as "feedback", which then leads to an extensive consideration of density-dependent effects *Population Ecology* includes chapters dealing with life-history phenomena, key factors and harvesting None of the books contains detailed discussions of genetical aspects of population regulation

The theoretical foundation of 60 years ago is still strongly evident *Population Systems* perhaps diverges most in taking a systems theory point of view But, for teaching, I would certainly recommend the excellent blend of example and theory in *Population Ecology,* and possibly support some areas by the greater theoretical and practical development coming from the 291 exercises in *Elementary Mathematical Ecology* ☐

Michael B Usher is Senior Lecturer in Biology at the University of York

Search for a science

Graham Hoyle

Neuroethology An Introduction to the Neurophysiological Fundamentals of Behavior By Jorg-Peter Ewert Pp 342 ISBN 0-387-09790-2 (Springer-Verlag 1981) DM 49, $29 *Neuroethology An Introduction* By D M Guthrie Pp 221 Pbk ISBN UK 0-632-00303-0, ISBN US 0-471-26993-6 (Blackwell Scientific/Halsted 1981) £8 75, $27 95

THESE two introductory texts, appearing independently at about the same time, offer an insight into viewpoint as well as subject matter Ewert does his research on a backboned animal, the toad, Guthrie on invertebrates Each goes out of his way to offer a fair balance, with extensive examples from the other's group Many of the same studies are reported by both authors, showing that they agree as to what constitutes neuroethology It is remarkable to find such concurrence, since others who consider themselves to be neuroethologists have quite different notions as to what should be included Guthrie has chapters on evolutionary trends and human neuroethology, with illustrations taken directly from textbooks on neuroanatomy, psychology and animal behaviour Ewert avoids such a nebulous search for principles, sticking to observations and hypotheses — although he does manage to squeeze in a section termed "Stress in Human Society"

The Nobel prize-worthy finding of Lorenz and Tinbergen in the name of ethology was a simple generalization complex behavioural acts of animals as different as insects, birds and human beings are handled genetically — and therefore evolutionarily — as wholes This applies especially to acts of territoriality, home-building, prey-capture and courtship They introduced key concepts and clear descriptive terms, notably "fixed action pattern", "releaser", "drive" and "consummatory act" Each of these offers a major challenge to neurobiologists, because each implies a specific kind of underlying neural circuitry and properties Working them out offers a splendid and significant intellectual/laboratory pursuit, but there have been only a very few successes in this new field so far Ewert and Guthrie both cover them, but all too briefly To create a larger body of knowledge, each has padded the relevant data with selected bits of physiology, psychology, sociology and ethology Thus students will be able to learn from either of these books, but only if they also receive lectures and extensive reading assignments, and if they already have a good background in basic neurophysiology Both books are lavishly and attractively illustrated, Ewert's, in particular, is well-endowed with clear diagrams, many of which are original, in two colours Each represents good value for money

Unfortunately, the uninitiated reader is very likely to suffer from a severe attack of mental indigestion because of the highly condensed treatments of diverse sets of data The budding researcher will still have to make a critical choice within some traditional discipline before being able to practise neuroethology, and will be forced to face the difficult decision as to whether to go with backbones, or a "squishy" or "crunchy" invertebrate In effect, this is a choice between going for cellular detail now, or for the prestige and significance automatically associated with vertebrate animals, but which at present show few signs of yielding the information needed for understanding at the level of nerve cells and circuits □

Graham Hoyle is a Professor in the Department of Biology at tne University of Oregon, Eugene

---

Strong-minded neuroscience

Maria Fitzgerald

Principles of Neural Science Edited by Eric R Kandel and James H Schwartz Pp 731 Hbk ISBN 0-7131-4405-X, pbk ISBN 0-7131-4406-8 (Elsevier/North-Holland/Edward Arnold 1981) Hbk £45, $60, pbk £25 50, $32 50

NEUROSCIENCE is one of the most rapidly expanding branches of biology today, the task of putting together a comprehensive textbook on the subject is therefore becoming increasingly difficult Such a book should inform clearly and accurately of the basic scientific facts while giving a balanced account of newer, less substantiated work Ideally it should also convey the excitement of new ideas and the importance of future research *Principles of Neural Science* fulfills all of these requirements It is an excellent book, fun to read yet informative and accurate — a combination rare in scientific literature

The editors believe that it is implicit in most neuroscientists' thinking that "all behaviour is an expression of neural activity" The task, therefore, of the neuroscientist is to explain how the brain and its cells function and so to understand behaviour This view is the underlying theme of the whole book and it contributes greatly to its strength It results in a great emphasis on behaviour, from simple spinal reflexes to the neural basis of emotions It also results in a strong emphasis on disease and mental illness After all, if behaviour is a reflection of brain function, then disorders of affective and cognitive functions must result from disturbances of the brain, and much can be learnt from them Some may disagree with this philosophy and thus with the framework of the book, nevertheless they will still find the contents useful and stimulating

All of the expected chapters are there, from cellular membranes to motor control, plus good, up-to-date sections on topics such as sleep, ageing and CNS development In each section, the relevant regional anatomy is surveyed, which is especially useful in discussions of the brainstem and the limbic system At the end of the book there are several excellent appendices on brain fluids, neuro-ophthalmology and electrical circuit theory with set questions to work through

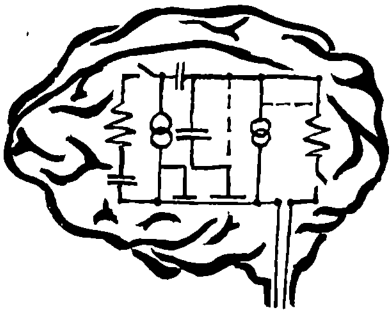

Of course there are shortcomings Neurochemistry, one of the most challenging branches of neuroscience, is inadequately covered The basic, classical information is there but neuropeptides, for example, get only cursory attention The autonomic nervous system is mentioned now and again but should certainly have had its own chapter The index is so short as to be practically useless, although in compensation the chapters are clearly divided by straightforward subheadings These are in the American style of a statement of fact, some are refreshing in this cautious age, some irritating My particular favourite, arbitrarily used in the chapter on diseases of neuromuscular transmission, is "Unsolved problems remain" □

Maria Fitzgerald is a Tutor in Neurosciences and a Research Fellow in the Cerebral Functions Group, Department of Anatomy, University College London

---

Childish thoughts

Albert Yonas

Foundations of Developmental Psychology By R C LaBarba Pp 545 ISBN 0-12-432350-2 (Academic Press 1981) $20 75, £13 20 *Developmental Psychology*, 3rd Edn By R M Liebert and R Wicks-Nelson ISBN 0-13-208256-X Pp 665 (Prentice-Hall· 1981) $21 95, £16 45

I DO NOT know how many students enroll in introductory courses in child psychology each year, but the number must be vast Apparently, every publisher of textbooks feels that it is worthwhile to produce a new book, or at least a new edition of an old one, every two or three years in an attempt to attract part of this huge market Something like 80 to 100 introductory child psychology textbooks are currently available This competition has resulted in some specialization of books, as well as a great deal of homogeneity in the content and organization within each type of book

Ten years ago, many leading texts tried to do everything They were organized by age, beginning with prenatal development and infancy, and describing the child up to adolescence In addition, within each age section, topics such as perceptual and social development were discussed The writing style of many of these books has always reminded me of a sequence of 3" × 5" note cards

In recent years, specialization has led to the creation of a great many texts that do little to introduce students to the scientific discipline of child psychology, rather, their goal is to give the prospective parent or teacher a picture of what the average child is like at each stage of development and to provide information of practical use At the opposite end of the continuum, we have LaBarba's *Foundations of Developmental Psychology* This book is a scholarly and historical introduction to the theoretical issues that have guided developmental researchers It presents empirical studies primarily to illustrate issues and concepts, and makes little attempt to give the reader a picture of what behaviour to expect from a newborn child or to describe the average two-year-old

The book is organized topically, with a heavy emphasis on biological areas such as genetics and human behavioural embryology The behaviour of the neonate apparently is not of sufficient interest to the author to merit inclusion Very little space is given to the development of sensory and perceptual processes, there is no mention, for example, of any sensory modality other than vision

Unlike most introductory books, LaBarba's presents theoretical and empirical work not as fact but as the focus of argument with the opposing point of view This may confuse and depress students, although it does convey the state of the art

The basic problem with this text may be its assumption that a unified discipline of developmental psychology exists with its own explanatory concepts and body of facts that can be presented in an introductory text in the same manner as would a physics text In reality, developmental psychology is an interdisciplinary field, strongly concerned with practical applications It focuses on the description of the course of development, and is still groping towards theoretical concepts which will make explanation possible

Developmental Psychology, by Liebert and Wicks-Nelson, is the third edition of a comprehensive and successful text that should be even more successful in this new version The authors view developmental psychology as a branch of science that is both basic and applied, they believe that students can best understand practical applications in the light of the theory and research on which they are based.

The authors and publisher have responded to competition by producing a book with every pedagogical aid imaginable, from an outline at the beginning and a summary at the end of each chapter, to coloured and italicized marking of important concepts and terms The figures are especially effective

The quality of the writing is probably the book's most outstanding trait It has fewer details, and is more readable, than a similar, widely used book by Hetherington and Parke Students are introduced to basic research with as little pain as possible, interest is gained by discussion of practical topics (for instance, various childbirth methods) The sense of controversy and uncertainty in developmental psychology is almost entirely missing from this book, but this may well be pedagogically necessary

While many teachers may find LaBarba's book full of fascinating information useful in the preparation of lectures, they are more likely to assign Liebert and Wicks-Nelson's book to their students ☐

Albert Yonas is a Professor of Developmental Psychology at the Institute of Child Development, University of Minnesota

Merit in a minefield

B. Burnet

Behavior Genetics and Evolution By Lee Ehrman and Peter A Parsons Pp 450 ISBN 0-07-019276-6 (McGraw-Hill 1981) $31 50, £17 50

As A focus of intellectual excitement, the genetics of behaviour is rivalled only by pursuit of an understanding of the genetics of differentiation and development Since it requires an interdisciplinary approach in integrating biology and genetics with social sciences, it is also a minefield for misunderstanding, and requires a nice balance of scholarship and careful judgement in any who would venture a good textbook for teaching Here is just such a text *Behavior Genetics and Evolution* is a revised and updated edition of *The Genetics of Behavior* published a few years ago by the same authors It gives a comprehensive account of the principles and methods used to study the genetics of behaviour and stresses the point that greater understanding of the genetic architecture of complex behavioural traits necessitates subdividing them into discrete components prior to genetic analysis Separate chapters are devoted to reviewing the genetics of behaviour of human beings, small mammals and fruit flies, together with a range of other organisms including some less familiar invertebrates and domesticated species

The authors give a balanced account of the genetics of human behaviour and, rightly in my opinion, emphasize the need for concentration less on the current obsession with IQ differences than on the genetic analysis of more accessible human sensory, perceptual and motor skills — although, in view of the difficulties inherent in interpreting EEG wave patterns, speculation about their possible significance with regard to deviant or criminal behaviour should be treated with caution Particularly valuable is the discussion of the complications caused by cultural transmission in relation to the inheritance of human behavioural characteristics In the later chapters the special merits of the book emerge in a synthesis discussing the genetic architecture of behaviours in relation to niche breadth of species, habitat selection, population structure and mechanisms of evolution Relatively little attention is given to kin selection and the evolution of altruistic behaviour, which is surprising in view of the widespread current interest in this topic

The book is directed towards undergraduate and postgraduate students in biology and psychology, and should also be valuable to those professionally involved in the social sciences, agriculture or medicine who require a comprehensive treatment of the subject ☐

B Burnet is Reader in Animal Genetics at the University of Sheffield

Two views of evolutionary genetics

J.S. Jones

Basic Population Genetics By Bruce Wallace Pp 688 ISBN 0-231-05042-9 (Columbia University Press· 1981) $26, £12 95 *Introduction to Quantitative Genetics*, 2nd Edn By D S Falconer Pp 340 ISBN 0-582-44195-1. (Longman 1981) £9 95, $23

The old controversies about Darwinism have made their periodic return to the public stage In modern terms, evolution is nothing more than a change in gene frequencies Here are two books dealing with genes in populations, one, that of Wallace, is concerned largely with natural populations, the other mainly with genetic responses of populations in the laboratory or on the farm

Wallace's substantial work surveys many aspects of population genetics After a chapter on the usefulness of models (which are used throughout the book, but always at a level which should be accessible to undergraduates), he considers attempts to measure genetic variation, the effects of migration and assortative mating on population structure, the influence of inbreeding and mutation, and modes of selection in field and laboratory An account of genetic load (a term which has lost much of its earlier prominence) leads into a treatment of heterozygote advantage, which is considered in the context of "hard" natural selection (which depends on the rigid application of environmental challenges) versus "soft" selection (in which fitness depends as much on the frequency of competing genotypes as on the rigours of the environment) The book concludes with a discussion of coadaptation and population differentiation Wallace's treatment is biased towards the familiar laboratory species of *Drosophila* — organisms which are unique in the extent of our knowledge of their genetics and our ignorance of their ecology There is little mention of the classics of ecological genetics such as industrial melanism, mimicry or heavy metal tolerance in plants

In later chapters Wallace enters into speculation and polemic which, although always entertaining, means that in some ways the book belies its title, this text is much more than an account of the basics of evolutionary genetics

Falconer has produced a new edition of a book which has for 20 years been the basis for almost all introductory courses in quantitative genetics His second edition looks as durable as the first It gives a clear and complete account of the inheritance of continuous characters, many of which are of considerable practical importance Falconer does not hesitate to discuss the relevance of research on laboratory populations to cattle milk yield or corn production, so that his book will have a wide audience Two-thirds of the references cited have appeared since the first edition, and the inclusion of so much new work inevitably means that the book has lost some of its earlier clarity and directness, quantitative genetics has, in common with all other aspects of genetics, gained nothing in simplicity as our knowledge has increased. Nevertheless, this new text is unrivalled as an introduction to the subject.

As Wallace points out, there are parallels between the theories of population genetics and those of economics. In both fields there exist impressive and complex models of the process of change, a huge literature, of increasing mathematical sophistication, deals with their most obscure workings, and at the furthest reaches of these great machines small bands of workers labour to improve still further our understanding of the details of the evolutionary or economic universe. Economics and evolution share another remarkable feature, in each there exist two quite different sets of models which, although largely complete within themselves, provide mutually incompatible explanations of the same phenomena.

The present dominance of one economic model means that academics must now assess textbooks as much by price as by content. In population genetics there is an equivalent controversy between the view that most evolution results from the differential action of natural selection on genetic polymorphisms, and the more radical thesis that much evolutionary change — including even changes in the fossil record — arises from the accidents of sampling. Wallace, in particular, is an evolutionary Keynesian, throughout *Basic Population Genetics* he emphasizes the directing influence of gradual natural selection in controlling the course of evolution. Although Falconer does devote a higher proportion of his space to the influence of random events, he too does not give this view the prominence which it now has in much of the population genetics literature. Evolution by random change still awaits its student text. ☐

J S Jones is in the Department of Genetics and Biometry, University College London

---

Mendel meets DNA: the story continued

D.J. Cove

An Introduction to Genetic Analysis, 2nd Edn. By David T. Suzuki, Anthony J. F. Griffiths and Richard C. Lewontin. Pp.911. Hbk ISBN 0-7167-1263-6, pbk ISBN 0-7167-1307-1. (W. H. Freeman: 1981.) Hbk $24.95, £18.50; pbk £11.95.

Genetics: A Molecular Approach. By Laura Livingston Mays. Pp.693. ISBN 0-02-378320-6. (Collier Macmillan/Macmillan, New York: 1981.) £15.95, $23.95.

Genetics: Its Concepts and Implications. By Anna C. Pai and Helen Marcus-Roberts. Pp.711. ISBN 0-13-351007-7. (Prentice-Hall: 1981.) $24.95, £18.70.

LAST year, I reviewed here (*Nature* **289**, 702–704) seven textbooks of genetics, published in 1980, which were primarily intended for use by undergraduates taking introductory genetics courses. In 1981, three more general genetics texts have appeared and so we have moved in the space of only two years from a state of relative famine to what might be judged to be a glut.

In my previous review, I was allowed to devote space to my own views of how genetics should be taught at this level. These have not changed so I will not repeat them here at length, but I believe that the teaching of genetics is not made easier by a rigid adoption of a historical approach nor by the compartmentation of classical and molecular genetics. However, as with almost all of the 1980 textbooks, last year's were again slaves of history. All, for example, introduce Mendelian genetics by considering the pattern of segregation observed when, in a diploid tissue, a character difference is due to a pair of alleles, one dominant to the other. In fact, in all three textbooks, the first segregations described are in the garden pea. Once again, the student is expected to cope with diploidy and dominance at the same time as understanding the principles of segregation. All three texts also adopt a "Mendel before molecules" approach, but Mays manages to deal with meiosis, Mendelism, DNA and even the regulation of gene expression, all in her first chapter. She returns to most of these topics later, where her treatment is, of course, more detailed. There is certainly something to be said for this approach, but in Mays's case its adoption has been accompanied by the sacrifice of rigour.

My review has so far implied that the three textbooks are rather similar and it is therefore time that I should redress the considerable injustice that this impression would cause to Suzuki, Griffiths and Lewontin. Although I was disappointed to find that these authors should have adopted such a conventional approach to the teaching of genetics — and that even they should imply that every gene has only two alleles, one dominant to the other, for about 70 pages of their text — of its kind, this textbook is excellent. It is clearly written, well illustrated and, in particular, as its title implies, puts considerable emphasis on the analytical aspects of genetics. Although it adopts a historical approach, it is up-to-date but, perhaps surprisingly, it is better in this respect on molecular than evolutionary topics. It contains, for example, a clear account of how DNA base sequence can be determined but does not deal with the punctuated equilibria debate. Lewontin's chapters on quantitative, population and evolutionary genetics, although as usual tacked on behind, are just as good as would be expected from a geneticist of his stature. However, most students will find the book's first chapter, which explores the difference between genotype and phenotype, and which was also contributed by Lewontin, difficult and only understandable when they return to it later having acquired some knowledge of the physiology of gene expression.

The book is not without faults, its treatment of the regulation of gene expression in the context of metabolism is weak in so far as it implies that there is much more uniformity of mechanisms than now seems justified and in particular that the operon is universal among prokaryotes and fundamental to gene regulation.

Mays's book, subtitled "A Molecular Approach", attempts to integrate molecular with classical genetics much more than Suzuki, Griffiths and Lewontin. It adopts a descriptive style which therefore neglects the logical rigour which is central to both molecular and Mendelian genetics. It is up-to-date and deals, perhaps in too much detail, with topics such as DNA sequencing. Population, ecological and evolutionary genetics are covered in two chapters, but although one of these is not at the end of the book, there is no greater integration of these topics with the rest of genetics than in most other texts.

Pai and Marcus-Roberts is unfortunately the runt of this litter. Its approach is conventional, very descriptive and where it attempts to explain classical genetical phenomena in physiological or molecular terms, the explanation is often misleading or even wrong. The book is in fact full of errors, some trivial, others more important. *Hemophilus influenza* (*sic*) is said to be a virus, a heterokaryon "a cell with a diploid nucleus", an *E coli* strain developed for safe genetic engineering to have no sites in its DNA "which can be acted on by restriction endonucleases".

All three books contain set problems. Mays contains no answers while Suzuki, Griffiths and Lewontin in their book give answers only to selected problems, although answers to all problems are available in a separate booklet. The answers are as usual rather brief, no doubt publishers will say that space is at a premium but I still believe that very full answers, perhaps to fewer questions, are essential.

Finally, I must compare this year's books with last year's. Suzuki, Griffiths and Lewontin goes straight into my "best buy" category. It is inevitably a little more up-to-date than my last year's choice, Ayala and Kiger's *Modern Genetics* (Benjamin/Cummings, 1980) but I do not think that it is obviously better I prefer Ayala and Kiger's somewhat less historical approach and their greater integration of molecular and Mendelian genetics, although I believe both should be taken much further I still think there is much to be said in favour of Fristrom and Spieth's *Principles of Genetics* (Chiron/Blackwell Scientific, 1980), last year's second choice, which adopts a much less conventional approach to the subject, and so my own list of recommended texts now includes all these three Mays's book is neither good enough nor bad enough to warrant special mention but I am afraid I will have to warn my students off Pai and Marcus-Roberts

D J Cove is Professor in the Department of Genetics at the University of Leeds

Not quite Wilson

Michael Ashburner

Cytogenetics The Chromosome in Division, Inheritance and Evolution, 2nd Edn By Carl P Swanson, Timothy Merz and William J Young Pp 557 ISBN 0-13-196618-9 (Prentice-Hall 1981) $25 95, £19 45 *Cytogenetics· Plants, Animals, Humans* By Jurgen Schulz-Schaeffer Pp 446 ISBN 3-540-90467-0 (Springer-Verlag 1981) DM69, $40 60

A DISTINGUISHED cytologist of my acquaintance never ventures abroad without his copy of the third edition of E B Wilson's *The Cell in Heredity and Development* (Macmillan, 1925) under his arm, carefully preserved from the elements by a wrapping of plain brown paper I fear that neither of the two textbooks of cytogenetics reviewed here will command such devotion 60 years hence Both Swanson, Merz and Young (SMY) and Schulz-Schaeffer have written texts aimed, by and large, at an advanced undergraduate audience, though both hope that their volumes may be of use to more "advanced" researchers

The books are not only similar in purpose, they are similar in the general extent of their coverage, treating such broad topics as the structure and function of chromosomes, the behaviour of chromosomes at mitosis and meiosis, chromosome aberrations and chromosomes in evolution in a reasonably conventional way There is, it is true, a considerable difference in emphasis between SMY and Schulz-Schaeffer, the latter gives the cytogenetics of plants (especially cereals) particularly strong attention, whilst the former devotes more space to a consideration of evolutionary issues It is, perhaps, for this reason that I am more naturally drawn to SMY and approached Schulz-Schaeffer more from the desire to know what new I could glean from it

I began this review with an implicit comparison of these two books with E B Wilson's masterpiece Part of the reason for Wilson's greatness (I speak of both book and man) was the regard and understanding he had of genetics The signal failure of Schulz-Schaeffer stems, in my opinion, from the absence of any true integration of the "cyto-" and the "genetics" This book suffers too from a lack of balance in the presentation of the material and from the author's inability to distinguish between the trivial and the lasting Perhaps I should illustrate these harsh criticisms A very common class of chromosome aberration, both in natural and experimental populations, is the inversion Inversions have the property that, when heterozygous, they suppress genetic recombination The precise mechanisms by which this suppression of recombination is achieved were elucidated by Sturtevant and Beadle in 1936, and their paper (*Genetics* **21**, 554–604) is one of the most elegant in genetics Not only does Schulz-Schaeffer fail to give a summary of this work (let alone reference it) but he wastes his reader's time with such trivia as the "fact" that "twenty seven different autosomal inversions have been reported from three different localities in Bulgaria in the mosquito species *Anopheles messeae*"

A second example of the lack of balance in this book may not be amiss A paragraph (p 294) discussing somatic crossing over includes the statement that "soybean seems to be an ideal object for the study of somatic crossing over" This may well be so, but it is rather an eccentric statement to make when the detailed and sophisticated studies of mitotic crossing over (as it should be called) in both yeast and *Drosophila* have virtually been ignored

The lack of balance that I see in this textbook is serious not only will it mislead the student but it will also undermine the confidence of other readers who might otherwise seek from it new information There is, not surprisingly, much in Schulz-Schaeffer that is new to me, yet I am reluctant to take anything at face value from an author who awards Francis Crick a knighthood (trivial in itself, perhaps, but a minor irritation) and who has, at least on occasion, clearly not consulted his original references His account of parthenogenesis in aphids is but a poor paraphrase of White's review in the third edition of *Animal Cytology and Evolution*, and I see no signs of any attempt to look at the original data or take into account subsequent studies

The second textbook, that by SMY, is far better Although the second edition of a text first published in 1967, it is really the successor of Swanson's *Cytology and Cytogenetics* published by Macmillan ten years before that Not only have SMY made a reasonably successful job of integrating the cytology and genetics (though even here I think Swanson did better in 1957) but they have also stamped upon the whole volume an evolutionary perspective that generates an impression of intellectual coherence There is, however, one area of weakness in this book that is in the various discussions of molecular cytogenetics Not only is this subject treated, to my mind, in a rather oversimplified manner but the authors are too naive, accepting at face value some of the more speculative of models whose very authors, I am sure, would shudder to see exhumed in student text □

Michael Ashburner is a Reader in the Department of Genetics, University of Cambridge

Citron pressé?

P.A. Lawrence

The Genetic Basis of Development By Alistair D Stewart and David M Hunt Pp 221 Hbk ISBN 0-216-91161-3, pbk ISBN 0-216-91160-5 (Blackie/Wiley 1982) Hbk £18 95, $27 95, pbk £8 95

THE genetic approach to developmental biology can be fun and ought to be popular But embryology is traditionally a soft subject that has often been closer to theology than science, while genetics has always been hard and numerological Which may explain why, in the past, practitioners of the two disciplines have understood each other little and have rarely collaborated to solve biological problems This makes no sense at all as genes are there to provide materials and information to construct and maintain animals Genes and their products ought therefore to be at the heart of embryology — which is just where Stewart and Hunt perceive them to be

Their aim was to write a brief embryological text from the geneticist's view point, and the result is a usefully analytical account It is also up to date and breaks with the common practice (especially in embryology) of beating a new textbook out of older ones In short, the authors have used the primary literature as their source This may explain why the book is often tricky — especially for the "advanced undergraduate" for whom it is written And also why it is too much of a review, being strong on lists of experiments and results and weak on explanation A good example is the description of the bithorax complex of *Drosophila* This locus is an illuminating link between genetics and development, as it appears that the elements of the locus are specifically deployed in developing segments

Lewis (*Nature* **276**, 565-570, 1978) has shown that without this gene complex most of the segments develop identically and the result is more like a worm than an insect Unfortunately the account of bithorax by Stewart and Hunt is so replete with facts that this advanced undergraduate found it almost incomprehensible Nevertheless, the original approach of the book makes it refreshing and, as with a cold drink, one can always leave the ice in the glass ☐

Peter Lawrence is at the MRC Laboratory of Molecular Biology, Cambridge

---

Genetics: bottom . . .

Neville Symonds

Bacterial and Bacteriophage Genetics An Introduction By Edward A Birge Pp 359 ISBN 0-387-90504-9 (Springer-Verlag 1981) DM54, $25 70

EDWARD Birge's brief was to produce a book of reasonable size which would serve as a contemporary text for introductory courses in bacterial and phage genetics This has involved starting with a brief treatment of DNA replication and the nature of mutation, proceeding through chapters on phage genetics and the mechanisms underlying transduction, transformation and conjugation, and then bringing the story up to date with further chapters on plasmids, gene regulation, the molecular basis of recombination and gene manipulation

The "historical" chapters on the development of the basic prokaryote genetic systems using the phages T4 and λ and the bacterium K12 as examples are of necessity only sketches of what took place and do not give a balanced idea of the nature of the discoveries involved or the problems which had to be overcome More successful is the chapter on the properties of the less well-known phages which outlines clearly the amazing variation in the strategies which have been adopted in various situations, and there are two well-researched chapters on plasmids which bring together a lot of useful ideas and practical material Transposition and its consequences are treated rather briefly, but there is a clear exposition at the end of the book of how modern techniques in gene manipulation are performed and of the new frontiers which are being opened up by these techniques

Overall the book succeeds in what it sets out to do It is clearly written, the diagrams and format are of a high standard, and it is as up to date as can be expected in such a rapidly expanding field There is no doubt it will be a useful adjunct in teaching introductory courses in molecular genetics ☐

Neville Symonds is Professor of Microbial Genetics at the University of Sussex

---

. . . to top

Dorothy A. Miller

Genetics Human Aspects By Arthur P Mange and Elaine Johansen Mange Pp 675 ISBN 0-03-056751-3 (Holt, Rinehart & Winston 1980) $25 95, £14 95
Human Chromosomes Structure, Behavior, Effects By Eeva Therman Pp 235 ISBN 0-387-90509-X (Springer-Verlag 1981) DM37, $21 80

THE tone of *Genetics Human Aspects* is set by the cover, which has a picture of Adam pondering as he sits alone on the stump of a primitive tree Perhaps he is thinking about the fact that all human beings will arise from him and hence be similar, but never identical, to him This is not to imply that this is a creationist text, but rather one which builds on the assumption that the study of human genetics should be of interest to a student just because he is a human being

Mange and Mange have written a very readable book, indeed It is aimed at those with only a moderate scientific background, not including a general genetics course Hence the authors try to give a comprehensive presentation of genetics in which, whenever possible, concepts are illustrated by human rather than plant or animal examples Simple statistics and chemistry are dealt with in appendices

In addition to the easily understood, not to say sprightly, text, the book has much to recommend it The material is up-to-date and relatively free of errors The line drawings are particularly well conceived and are very effective in simplifying concepts as they are presented in the text The references are well chosen and include some original articles so that the student can appreciate the step by step nature of research The authors refer to numerous areas that still require research, leaving some room for student imagination There are adequate questions at the end of each chapter and the answers are accompanied by explanations

Will the book be suitable for a course? The fast pace that makes the book so enjoyable also means that most areas are not dealt with in depth Hence, the text would be more suitable for undergraduate or adult education courses than for graduate or medical school courses As in any text, the balance of material selected is a matter of personal preference which teachers must assess for themselves They would be well advised to at least examine this text

The material in *Human Chromosomes* by Eeva Therman overlaps about one-fourth of that in *Genetics Human Aspects* because chromosomes play such an important role in human genetics The text covers areas of human cytogenetics that have been studied using the light microscope chromosome structure, mitosis, meiosis, banding, structural and numerical abnormalities, changes in cancer cells and human gene mapping Examples are drawn primarily from human material, but use has been made of plant or animal studies when these provide the best material available The book does not deal with molecular approaches to cytogenetics and includes almost nothing about findings of biophysical, biochemical or electron microscopic studies (for example, nucleosomes are not mentioned)

Therman's writing is clear and her style didactic She includes many definitions and presents the facts that have been established Although she has carried out extensive research on the human X chromosome, her presentation is not research orientated She does not, for example, discuss the way the facts were obtained, nor does she try to entice students into cytogenetics by emphasizing questions that remain to be answered She prefers to cite reviews rather than original articles so that "the reader is encouraged to delve deeper into any question of interest", whether this will have the desired effect is not clear For me it produced a rather static image of an active field

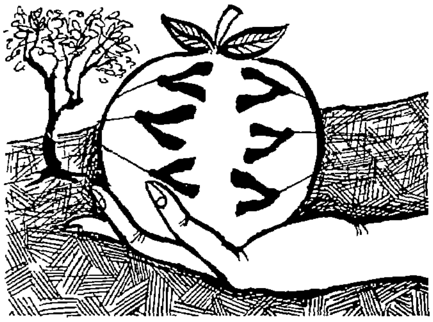

Cytogenetics is a visual science, unfortunately the illustrations of human chromosomes given in the book do not provide a very complete background for the student Full human karyotypes are shown for unbanded Giemsa (two), G- and Q-banded cells, but not for C- or R-banded cells, which are represented by a partial karyotype of C-banded E group chromosomes and a single R-banded number 1 Reciprocal translocation is poorly illustrated by the karyotype of an unbanded endoreduplicated cell, even though the figure legend states the identity of the translocated chromosomes was confirmed with Q This selection of illustrations must have been a matter of choice, rather than space limitation, because a full page is devoted to C-banding of plant chromosomes and another to a G-banded karyotype of the rat

Human Chromosomes is an introductory text suitable for undergraduate or graduate students Since the subject matter is not dealt with in great detail, it should be compared to presentations of the same material in general human genetics texts

Dorothy A Miller is a Senior Research Associate in the Department of Human Genetics and Development at Columbia University

Science or scholarship for students of developmental biology?

D.R. Newth

Patten's Foundations of Embryology, 4th Edn By Bruce Carlson Pp 672 ISBN 0-07-009875-1 (McGraw-Hill 1981) $30 25, £16 25 *Development,* 2nd Edn By Gerald Karp and N J Berrill Pp 692 ISBN 0-07-033340-8 (McGraw-Hill 1981) $32 95, £18 25 *Developmental Biology* By Leon W Browder Pp 602 ISBN 0-03-056748-3 (Holt, Rinehart & Winston 1980) $28 95, £13 95 *Introduction to Embryonic Development* By Steven B Oppenheimer Pp 404 Hbk ISBN 0-205-06899-5, pbk ISBN 0-205-07348-4 (Allyn & Bacon 1981) Hbk $23 95, £16 50, pbk £8 95

THE student of developmental biology, or of its senior component animal embryology, does not lack for possible textbooks However, perhaps paradoxically, only the most elementary can afford to be comprehensive, the more advanced being tempted to specialize in one of two ways They may be restricted systematically, dealing for example, only with animals, only with vertebrates or only with *Xenopus* Or they may be mechanism based and call widely upon prokaryote, unicellular, and plant and animal multicellular systems for illustrations of their themes In either case one senses a certain discomfort in the authors and fears a lack of satisfaction in the student reader

Of the four books now considered, one — Carlson's revision of Patten — is unashamedly selective both systematically and thematically It derives from an earlier book which celebrated the developmental anatomy of chick, pig and man but had little use for other material Dr Carlson has now remodelled the work with the object of narrowing the gap between accounts of formal changes in developing animals and their experimental analysis His main changes have been to stress the morphogenesis of organs that have been important in analytical work, to give an account of limb development that is a genuine integration of the formal and the analytical, and to introduce experimental findings at points where they help to solve anatomical problems

The material is presented clearly and the book is abundantly and effectively illustrated The student will gain from the self-imposed limitation of the treatment in that at the end he or she will feel confident of, and in, what has been accomplished Dr Carlson provides an introduction to laboratory studies on early chick development as a long appendix

Karp and Berrill have produced a very much revised and improved second edition of a fairly ambitious text They cover so much and their treatment is so good in so many ways, that it seems churlish to question the coherence of the picture of development that emerges And yet, after the early chapters in which a developmental story unfolding can be discerned, the book inevitably fragments into sections whose sequence seems arbitrary This, I must emphasize, is not meant as a criticism only as an acknowledgement of the impossibility at the present time of ordering our presentation of developmental problems consistently

Plants apart — and few texts successfully integrate them with animal material — the systematic coverage is catholic, and the emphasis biological That is to say that the biochemical and molecular biological approaches do not predominate, although usefully presented at many points

Karp and Berrill, in my view, offer one of the half-dozen best general texts of developmental biology now available in English They will run to a third edition no doubt, and may then take the opportunity to improve the proof reading, most especially in correcting the spelling of proper names

Browder's *Developmental Biology* is also a large and ambitiously conceived work, but leaning more heavily upon molecular biology, and being somewhat kinder to plants It has the virtue of clarity and is well illustrated, but it too shows that selection of material has been a serious problem It would not be simply an act of piety to include discussion of, say, the development of the immune system and of the origin of antibody diversity in a textbook of developmental biology, especially in one which concentrates on biochemical and cellular matters Yet Browder skates over these and a number of other fields which might have been expected to attract him, amphibian metamorphosis, for example, is given cavalier treatment

Yet his discussions of the matters that he deals with are well balanced and should incite students to explore the original literature Especially in the area of gene control of development, his accounts are among the best available at this level

Oppenheimer's book is the shortest and claims only to be an introduction It is eclectic in coverage, but not very kind to plants It is written with enthusiasm, is sometimes a little careless, but deals with most of its topics in a stimulating way However, as with so many elementary introductions, it does not avoid the danger of unquestioning acceptance of matters which are not quite as certain as all that In a section quaintly headed "Gastulation in Amphibian" *(sic)* is given a not very good account of the process in question, but with no suggestion that it may still have uncertainties or that it may vary from one amphibian species to another Yet it does Nor is bird gastrulation so simple, or so well understood, as the student reading Oppenheimer might believe

These are, of course, complaints of a kind that most elementary texts invite To avoid them is difficult, but the attempt must be made if the reader is to be helped into science rather than into scholarship

The authors of all these books have clearly gone to some trouble with their illustrations Many, especially the scanning electron micrographs, are excellent But publishers will have to take greater pains to ensure that their production methods are equal to the challenge □

D R Newth was formerly Regius Professor of Zoology in the University of Glasgow

---

Biology: broad brush for a large canvas

E.C. Cox & R.M May

A View of Life By Salvador E Luria Stephen J Gould and Sam Singer Pp 806 ISBN 0-8053-6648-2 (Benjamin/Cummings 1981) $26 95, £10 95

THIS introductory biology text aims to concentrate on "the great themes and arguments of biology", rather than to offer the encyclopaedic catalogue that characterizes many of its competitors The result is an interesting and unusual text which in places has a minimalist air to it; this is particularly true in the earlier sections, where a lot of the material is simply set forth without critical examination of the historical or contemporary experiments that compel belief

The broad pattern of organization is the conventional one beginning with the basic chemistry of living things, we progress through genetics, developmental biology and the functioning of organisms to evolutionary biology and ecology The presentation is uniformly lucid, easy to read and backed by first-rate line drawings and other illustrations (along with "boxes" developing special points)

Among the early chapters are some strikingly elegant and careful discussions the structure of water, allosteric effectors (where the models and figures are superb), introductory genetics and gene regulation in bacteria The molecular biology is not as contemporary as one might wish, virtually passing over much of the exciting new work on the gene structure of higher eukaryotes (such as gene inserts, the splicing together of variable and constant regions of the globulin chains, the molecular changes associated with the regulation of mating type in yeast and so on) In short, the early sections are strong on the classic things, but appear a bit dated

The chapters on the functioning of organisms do a good job of covering the major problems faced and solved by higher organisms nutrition and gas exchange, transport, hormone functioning and the like The emphasis is strongly on human biology (again with excellent illustrations), with occasional genuflection toward comparative and evolutionary analyses

The concluding chapters focus on the broad themes of evolutionary thinking the history of the subject, micro- and macroevolution, biogeography and the fossil record No other introductory text treats this material so thoroughly or so well These chapters expound the essential philosophical character of Darwin's theory, and discuss problems associated with it, both past (blending inheritance, Mivart's doubts about the evolution of the incipient stages of useful structures, as instanced by the two reptilian jaw bones that are ear bones in contemporary mammals) and present ("neutral evolution", mechanisms that can maintain heterozygosity in populations, cladist, phenetic and classical evolutionary schools of taxonomy) Given the current misrepresentation of evolutionary thinking by the so-called "scientific" creationists, these chapters are especially valuable They are marred only by an occasional tendency to intrusive editorial comment, and by the misrepresentation of Darwin as holding thât evolution proceeds at a consistently gradual rate, in contrast with contemporary notions about "punctuated equilibrium" As observed by Andrew Huxley in his Presidential Address to the Royal Society last year, Darwin's statement that "each form remains for long periods unaltered, and then again undergoes modification" and

> the periods during which species have been undergoing modification, though very long as measured by years, have probably been short in comparison with the periods during which these same species remained without undergoing any change

effectively makes him a punctuated equilibrist

The treatment of population genetics is brief and not well organized, and that of population biology and ecology is perfunctory

In short, this is a distinctive introductory biology text that all teachers of such courses will profit from reading But we feel it is a bit too thin and quirky to displace the canonical Curtis or Keeton, unless supplemented by extensive additional readings □

Edward C Cox is Chairman of, and Robert M May Professor in, the Biology Department at Princeton University, where they jointly teach an introductory biology course

---

The multifarious questions of evolution

Bentley Glass

Understanding Evolution By Earl D Hanson Pp 556 ISBN 0-19-502784-1 (Oxford University Press 1981) £14 95, $23 95

THE recent flurry of attacks on school textbooks and the teachers of biology who deal with evolution should focus attention on the college textbooks of evolution and the way in which the subject is taught The questions to be asked are multifarious Is organic evolution itself, as distinct from the mechanism of natural selection, a theory or a fact? Is adequate attention given to the gradual change of ideas about a theory, starting in the case of evolution with the first glimmerings of the concept among the Greek philosophers and the ancient and mediaeval belief in spontaneous generation? What of the long debate over the inheritance of acquired characteristics, continuing even today? Just what was Darwin's contribution to the theory of evolution? How does the evolutionary synthesis of today differ from Darwin's own ideas? There are many more

In most respects, the teacher — if not the student — will welcome Hanson's book It is comprehensive and clearly written As might be expected from his earlier books, Hanson emphasizes animal and plant diversity, homologies and relationships But there is a substantial section devoted to Mendelian and modern genetics as the basis of understanding what Darwin always affirmed was the crux of the matter the nature and origin of hereditary variations There is also a detailed treatment of the evidence for relationships that comes from biochemical comparisons of amino acid sequences in proteins and nucleotide sequences in DNA For a course intended to run only for one semester of a college year, there may be far more technical detail here than a student can master, yet better too much than too skimpy a treatment

As for noticeable deficiencies in the book, it seems to me that not enough attention is given to the history of the idea of evolution, to the pre-Darwinian as well as post-Darwinian gropings for an explanation of origins, to the marvellous combination of evidence from every sub-field of biology. I notice also a tendency to deal rather briefly with the evolution of plants, although their speciation by polyploidy, especially allopolyploidy, affords some of the best evidence for the origin of species in recent times The coverage of plant and animal geography in relation to evolution is also somewhat meagre Nevertheless, the classical evolutionary synthesis is well expounded

Finally, in respect to human evolution, in my opinion a fuller development of primate and hominid evolution would be enjoyed by teacher and students alike It is difficult, in this area of knowledge, to keep pace with discovery and choose between conflicting interpretations Hanson has relied heavily on the work of the Leakeys He omits entirely any reference to the breathtaking discovery of "Lucy", the three-million-year-old, erect-walking australopithecine whose complete skeleton is the most magnificent and astounding of all palaeoanthropological discoveries This section of Hanson's book already cries out for revision

The last 200 pages of *Understanding Evolution* are devoted to a phylogenetic survey of plant and animal groups That is clearly the author's own bent Other teachers may wish that those pages had been used for a fuller treatment of some of the matters I have mentioned that have received little attention In particular, there would be a solid advantage in allotting space to an explicit exposé of the assumptions and subterfuges of the "scientific" creationists □

Bentley Glass is Distinguished Professor of Biology Emeritus at the State University of New York, Stony Brook

---

Natural history of vertebrates

Barry Cox

Patterns of Vertebrate Biology By E W Jameson, Jr Pp 477 ISBN 0-387-90520-0 (Springer-Verlag 1981) DM 63, $33 20

THE preface to Jameson's book states that it is concerned with the natural history of vertebrates, and he comments that "the laboratory, however essential and productive, is a departure from the animal's real world" Much of the book is therefore primarily descriptive, made up of a collection of discussions of different aspects of the field biology of vertebrates

However, Jameson commences with chapters concerned with "An Overview of Vertebrate Phylogeny", "Mechanics of Evolution" and "Zoogeography" It is always difficult to know where to draw the line between relevant topics and those which are merely general background, but I thought that none of these contributed significantly to Jameson's main thesis, while the first also revealed an uncertain knowledge and understanding of this topic

The remainder of the book is divided into three parts "Individual Environmental Responses" (with chapters on breathing, food and feeding, thermoregulation and water balance, activity and seasonal dormancy), "Communication" (sensory receptors and perception, signals), and "Population Phenomena" (reproduction, growth, community and population density) Here again, there are sections that have little to do with natural history For example, the details of the structure and ventilation of the bird's lung and airsac system are merely functional anatomy, and only become natural history if comparative data are given on variations in the structure or relative size of the system in different birds, such as penguins, ostriches, humming birds and so on The book is also not without errors for example, hagfish do not have only a single pair of gills (p 104), and the spiracle is not the vestigial *last* gill (p 106)

Nevertheless, those wishing to flesh out structural anatomy with interesting examples of natural history will find many useful examples in this book, and there is an extensive bibliography of well over 1,000 entries ☐

Barry Cox is a Professor of Zoology at King's College, University of London

The welcome return of J.Z. Young

L. Beverly Halstead

The Life of Vertebrates, 3rd Edn By J Z Young Pp 645 Hbk ISBN 0-19-857172-0, pbk ISBN 0-19-857173-9 (Oxford University Press 1981) Hbk £25, $26 95, pbk £14 *The Chordates*, 2nd Edn By R McNeill Alexander Pp 510 Hbk ISBN 0-521-23658-4, pbk ISBN 0-521-28141-5 (Cambridge University Press 1981) Hbk £35, $69 50, pbk £12 50, $24 95 *Lecture Notes on Vertebrate Zoology* By R Pearson and J N Ball Pp 180 Pbk ISBN 0-632-00729-X (Blackwell Scientific/ Halsted 1981) £7 50, $21 95 *Anatomy of the Chordates*, 4th Edn By C K Weichert Pp 814 ISBN 0-07-069007-3 (McGraw-Hill 1981) $37 75, £20 95

IN 1950 J Z Young published *The Life of Vertebrates*, which rapidly came to dominate the teaching of vertebrate zoology at a time when the vertebrates occupied an entire academic year in most zoology degree courses In 1962 the second edition appeared, but by the end of the 1960s and throughout the 1970s there was no J Z and teachers were obliged to look elsewhere Not only that, but vertebrate zoology had to relinquish much of its territory as newer aspects of biology rose to the fore Vertebrate courses became a catalogue of anatomy, with long names to be studied and learnt for no other apparent reason than that it was supposed to do students good The vertebrates tended to be relegated to a smaller and smaller part of the curriculum As this process was underway, by some curious irony advanced texts, monographs and symposium volumes on the group seemed to be constantly pouring out of publishing houses, yet there was nothing remotely suitable in the way of a general textbook

In 1975 there appeared McNeill Alexander's *The Chordates*, a general textbook of vertebrate zoology written by a leading expert in biomechanics, which in many ways fitted the bill Here, the structures of the vertebrates were discussed from the standpoint of their mechanics This approach lent itself especially to practical demonstration of the basic principles involved and was a truly excellent contribution to teaching, though the mathematical aspects tended to intimidate both the students and the less numerate teachers However, this textbook signalled a refreshing new approach that deserved encouragement The publication of a second edition, which has been updated and includes several new topics such as a useful discussion of dinosaur biomechanics, augurs well for the future of vertebrate zoology and the biomechanical approach being promoted by Alexander

The appearance of Pearson and Ball's *Lecture Notes on Vertebrate Zoology* clearly fills a need in the teaching scheme of things It is sad that it should be so This book as far as one can judge sets out to record all the boring bits of the subject, with its emphasis on pure anatomy The authors' aim "to release the teacher from the drudgery of simply reproducing anatomy and to create a platform for profitable expansion on innumerable other topics" Well, here is the drudgery all right but I fear that having created this platform, far from inspiring a prospective student into "profitable expansion" it would convince him that the subject is one of stupefying boredom to be avoided at all cost The illustrations are notable for their variable quality the crude sketch of the structure of a reptile scale (p 93) conveys nothing to me, and I suspect the authors would not have included it had they ever looked at a microscopic section of, say, lizard skin Worse, some of the information is so out of date that it would appear that the authors have cobbled together their material from a selection of older textbooks I suppose a teacher could use the book to instruct students in some basic information but they would be failing in their duty to allow students a glimpse of it This book can only do harm in that it is guaranteed to snuff out any spark of enthusiasm

Last year also saw the appearance of the fourth edition of Weichert's *Anatomy of the Chordates*, a system by system comparison of the chordates — a worthy, albeit rather fusty book, again dating from a time (1951) when the vertebrates formed a larger proportion of the syllabus than today This book, however, can be recommended for all teachers of vertebrate zoology in that it is relatively easy to pick out how, for instance, the vascular system varies from one major structural grade of vertebrate to another This is the kind of book to have to hand as a reference for teaching

For teachers and students of vertebrate zoology the publishing event of 1981 was, however, the long awaited return of J Z Young, with the third edition of *The Life of Vertebrates* It all comes back now, why J Z had such a profound effect on both teachers and students, here he speaks directly to the reader about really fascinating topics It is always possible to complain that the choice of topics is rather too personal but this is surely what gives the book its vitality The notable thing about *The Life of Vertebrates* is that a mass of information is communicated in such a light and easy manner, but, more important, the enthusiasm of youth pervades this book There are odd bits where one cannot help but be irritated because it is either grossly out of date or plain wrong, such as the hopelessly inaccurate diagram of the visceral arches and jaws in early vertebrates One of the greatest surprises is that the current controversies on methods of classification and the arguments over the process of evolution and the fossil record are alluded to and the clear voice of common-sense always characterizes J Z 's overview, not only of current fashions but of the place of zoology in its wider perspective

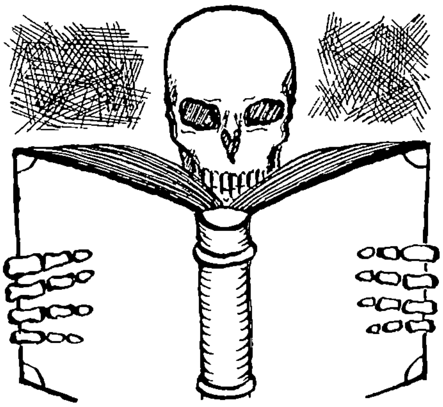

The pre-eminent position of J Z Young as the teacher and enthusiast of the study of the vertebrates is richly deserved This is the best textbook around The occasional lapses can be forgiven, it is the inspiration that he provides that will encourage a new generation to come into vertebrate zoology ☐

L B Halstead is Reader in Geology and Zoology at Reading University and Research Fellow in Anatomy at the Royal Dental Hospital of London

Chicago

Recent paperback editions

Lawrence H Aller & Dean B McLaughlin, eds
Stellar Structures 1965 £21 00
Louis J Battan
Radar Observation of the Atmosphere 1973 £10 50
S A Barnett
The Rat. A Study of Behaviour *revised edition* 1975 £7 70
Jonathan R Cole & Stephen Cole
Social Stratification in Science 1973 £6 30
E J H Corner
The Life of Plants 1964 £6 30
Paul H Barrett, ed
The Collected Papers of Charles Darwin *two volumes in one* 1977 £8 75
Stillman Drake
Galileo at Work: His Scientific Biography 1978 £7 00
Ludwik Fleck *translators Fred Bradley & Thaddeus J Trenn, editors Thaddeus J Trenn & Robert K Merton*
Genesis & Development of a Scientific Fact 1979 £4 90
Carl Gans & Thomas Parsons
A Photographic Atlas of Shark Anatomy The Gross Morphology of *Squalus Acanthias Work Book* 1980 £5 60
Robert Geroch
General Relativity from A to B 1977 £3 50
Gordon M Greenblatt
Cat Musculature A Photographic Atlas *Work Book, second edition 1980* £2 80
Norman Lebovitz, William H Reid & Peter O Vandervoort
Theoretical Principles in Astrophysics & Relativity 1978 £5 95
David C Lindberg
Theories of Vision from Al-Kindi to Kepler 1976 £7 00
Michael Ruse
The Darwinian Revolution Science Red in Tooth & Claw 1979 £7 00
Harald Stumpke (*Gerolf Steiner*) *translator Leigh Chadwick*
The Snouters: Form & Life of the Rhinogrades 1967 £3 50
Robert M Wald
Space, Time, and Gravity· The Theory of the Big Bang and Black Holes 1977 £2 80

coming in 1982

Ginestra Amaldi *Translator Peter Astbury*
The Nature of Matter: Physical Theory from Thales to Fermi 1961/1966
Neal C Gillespie
Charles Darwin & the Problem of Creation 1979
Jeanne Hopkins, compiler & editor
Glossary of Astronomy & Astrophysics *Second edition* 1980
Jean Piaget *translator Terrace A Brown*
Adaptation & Intelligence: Organic Selection and Phenocopy 1980
Joseph J Schwab *edited by Ian Westbury & Neil J Wilkof*
Science, Curriculum, and Liberal Education Selected Essays 1978
G M Dack
Food Poisoning 1956
The University of Chicago Press
126 Buckingham Palace Road
London SW1W 9SD

Chicago

Circle No 35 on Reader Enquiry Card

No bones, but plenty of meat

A.E. Brafield

Invertebrate Zoology, 4th Edn By R D Barnes Pp 1,089 Hbk ISBN 0-03-056-747-5, pbk ISBN 4-8337-001-8 (Holt-Saunders 1980) Hbk £17 95, $27 95, pbk £11 50 *Invertebrate Zoology*, 3rd Edn By J G Engemann and R W Hegner Pp 746 ISBN 0-02-333780-X (Collier Macmillan/Macmillan, New York 1981) £13 95, $20 95 *Invertebrate Respiration* By R M G Wells Pp 72 Pbk ISBN 0-7131-2806-2 (Edward Arnold 1980) £2 60 *Practical Invertebrate Zoology*, 2nd Edn Edited by R P Dales Pp 356 Pbk ISBN 0-632-00755-9 (Blackwell Scientific/Halsted 1981) £9 50, $32 95

A SYSTEMATIC and detailed study of the vast array of invertebrate animals continues to form a substantial part of undergraduate teaching in zoology The problem of striking a satisfactory balance between their anatomy, physiology, ecology and evolutionary relationships has become more acute as our knowledge in these areas has increased A sound and comprehensive textbook to supplement "the invertebrate course" is essential, and two which have built up a considerable reputation have recently appeared in new editions

Invertebrate Zoology, by Barnes, has reached its fourth edition Barnes claims that "there is no way a book of this sort can avoid growing to some extent", which is debatable to say the least, but most of the considerable increase in length of this edition comes from the many new drawings and photographs The new artwork by Mary Ann Nelson is excellent and she has made her drawings from actual specimens (a habit which seems, unfortunately, all too rare) The text is as clear and sound as ever Summaries have been added, a central section of over 40 colour photographs is a new feature, and there is now an interesting chapter on coral reefs Barnes still plays down the insects too much, however, allowing them only about 30 pages in a book of over a thousand The paperback version has a much smaller page size than the hardback and the consequent reduction in the size of typeface and diagrams tends to make the text hard to read and the illustrations less clear, but the paperback, being roughly half the bulk and weight of the hardback, is certainly easier to handle

The third edition of *Invertebrate Zoology* by Engemann and Hegner is also welcome (Engemann's name now precedes that of the late Robert Hegner) It is as concise and well organized as previous editions, with key words in italics and the material arranged in short, headed sections Engemann is a devotee of the "type approach", in which one species is treated in great detail to serve as an example of its group A drawback of this practice, it seems to me, is that every aspect of the selected type is described, whether it happens to be typical of the group or not, at the expense of more information on other members (The crayfish occupies as many pages as all other crustaceans put together, for example) An unusual feature is the new chapter on deep-sea invertebrates, in which the suggestion that these animals tend to be extremely long-lived is critically examined in order to discuss "a broad range of principles" of invertebrate zoology and to encourage the student to think more deeply A worthy aim, which Engemann achieves convincingly

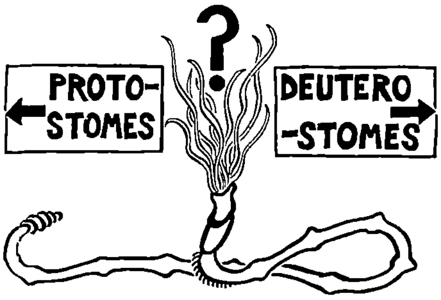

The division of coelomates into protostomes and deuterostomes is coming under some attack nowadays, but it is a convenient and useful concept and both Barnes and Engemann retain it They disagree, however, over many points of classification For example, Barnes puts the pogonophorans among the protostomes, rightly I think, whereas Engemann still lists them among his deuterostome groups (although he acknowledges elsewhere that their position is puzzling) Engemann discusses the problems of protozoan relationships but in the end sticks to the system customarily used by zoologists, whereas Barnes now raises each of the major protozoan groups to the rank of phylum (in the Kingdom Protista) Such disagreements over classification are inevitable, but they can confuse students Barnes has dropped his earlier chapter on phylogeny, and Engemann also avoids, sensibly, a long consideration of possible evolutionary relationships between the phyla

In addition to comprehensive textbooks, there is now a wide variety of smaller works which cover specific aspects of invertebrate zoology *Invertebrate Respiration*, by Wells, is a fine example The author's lively style reflects his great enthusiasm for the subject, and the longest chapter deals effectively with the comparative physiology of blood pigments, Wells's own speciality Zoologists with no great feeling for the physical sciences will find the introductory chapter on the principles of gaseous exchange particularly valuable

Laboratory classes are an indispensable part of invertebrate courses They generally include an intensive study of anatomy (by microscopy and by dissection), demonstrations of specimens to illustrate the range of form within each group, and some simple experiments All these aspects are well served by the second edition of *Practical Invertebrate Zoology,* edited by Dales He and the six other authors are all experienced university teachers and each is an expert on one of the major invertebrate phyla The book is well written and the material sensibly arranged There is too much writing and not enough illustration for a laboratory manual, to my mind, but the book contains a great deal of valuable information The section on general methods, and the numerous suggestions for simple experiments, make the work a useful sourcebook for the teacher as well as the student ☐

Alan Brafield is a Senior Lecturer in the Biology Department of Queen Elizabeth College, University of London

Insects entomed

M.E.G. Evans

The Science of Entomology, 2nd Edn By William S Romoser Pp 575 ISBN 0-02-403410-X (Collier Macmillan/Macmillan, New York 1981) £13 95, $21 95 *Fundamentals of Entomology,* 2nd Edn By Richard J Elzinga Pp 422 ISBN 0-13-338194-3 (Prentice-Hall 1981) $22 95, £17 20 *Insect Physiology* By W Mordue *et al* Pp 108 Pbk ISBN 0-632-00385-5 (Blackwell Scientific/Halsted 1981) £5 75, $16 95

ENTOMOLOGY is one of the few component parts of zoology to be taught as a science in its own right Physiology, parasitology and cytology, for example, are major topics covering the whole of the animal kingdom, the Insecta and Chordata are the only individual groups to merit major topic treatment, and this is reflected by the large number of books concerned with their study One might wonder whether more entomology texts are really necessary — perhaps merely to include recent advances? — but since the fundamentals of insect biology do not change, a sensible solution is to rewrite the better books Two of the three texts reviewed here are second editions of books already established in North America All three are good examples of the recent generation of entomological texts which pack a large amount of information into a single, readable and well-illustrated volume Modern textbooks are not necessarily better than some of their predecessors, but they are often more lucid and are usually more attractive visually, studying is still hard work, but now it may be less painful

Romoser and Elzinga have each written comprehensive accounts which emphasize the general biology of insects rather than their classification or economic importance *The Science of Entomology* is the larger book and is clearly intended for intermediate or advanced courses (second or third years in Britain, for North America, the author suggests a one-semester course) It nas a rather academic approach of the sort found in a good standard text such as Richards and Davies's *Imms' General Textbook of Entomology* (10th Edn, Wiley/Chapman & Hall, 1977) Romoser ranges from morphology and physiology to ecology and evolution, allotting a chapter each to applied entomology and systematics For completeness, an entomology course would need a more extended treatment of systematics based on a text such as Richards and Davies or Borror, DeLong and Triplehorn's *An Introduction to the Study of Insects* (5th Edn, Holt, Rinehart & Winston, 1981) In fact, such back-up is emphasized throughout the book, as demonstrated by the introductory section on entomological literature and by the impressive number of references cited

Fundamentals of Entomology is an introductory-course book which aims to cover the whole of entomology at a more elementary level Again, it is based on general biology, but there is also a lengthy classificatory section with keys to both orders and major families It is profusely illustrated with line drawings and photographs, however, as in many zoological texts, the macrophotographs sometimes lack the clarity of the scanning electron micrographs and the precision of the line drawings Most of the topics have been treated by Elzinga in a compact and readable manner, although it might have been wiser to omit some sections rather than over-reduce them, for instance, it is difficult to explain population dynamics in eight pages

Insect Physiology is a multi-author paperback which deals with only part of a large subject It is a clear exposition of homeostatic problems — from cell metabolism to nerves and muscles — although only about one-fifth of the book deals with behavioural physiology In spite of four authors, the chapters link together well and the diagrams are excellent A few key references are quoted at the end of each chapter to guide the student to the more important literature, I would have preferred a few more in order to reach the most interesting topics more rapidly Although an introductory text, the book has the merit of conveying some of the fascination of recent research in this field

All three books are welcome additions to the field of insect biology Elzinga can be recommended for a short, introductory course, Romoser for a major part of a longer, more advanced course, and Mordue for the up-to-date physiology section of a general entomology course

---

M E G Evans is a Senior Lecturer in Zoology at the University of Manchester

Saline solutions

D.J. Crisp

Elements of Marine Ecology An Introductory Course, 3rd Edn By R V Tait Pp 356 ISBN 0-408-71054-3 (Butterworths 1981) £8 95, $22 50 *The Estuarine Ecosystem* By Donald McLusky Pp 150 Hbk ISBN 0-216-91115-X, pbk ISBN 0-216-91116-8 (Blackie/Wiley 1981) Hbk £12 75, $29 95, pbk £6 25 *The Ecology of Marine Sediments An Introduction to the Structure and Function of Benthic Communities* By John S Gray Pp 185 Hbk ISBN 0-521-23553-7, pbk ISBN 0-521-28027-3 (Cambridge University Press. 1981) Hbk £15, $34 50, pbk £6 95, $16 50

AN ELEMENTARY text should not only provide a clear and comprehensive account of its subject, but it should also stress those areas where there is a consensus of view and give less prominence to more controversial subjects where current research has yet to resolve the pattern In doing so it will provide the reader with an historical perspective, identify the founders of classical works and provide up-to-date reviews

The third edition of Tate's *Elements of Marine Ecology* achieves most of these objectives It differs little in content from earlier editions and fully meets the needs of elementary students of marine biology who seek only the minimum of understanding of chemical and physical oceanography The reference lists have been considerably enlarged and the division into books for general reading and specific references to textual matters has been eliminated Neither of these changes seems particularly beneficial, other than to a reference collector The majority of classical marine biology works are included but so also are a frightening number of minor papers The author therefore has done less than he might in guiding the student towards serious and essential reading Nonetheless, it remains a sound, well-ordered and very useful student text There are no obvious errors, except for the blatant misuse of the word "parameter" in the title of Chapter 4 — alas, a fault now almost sanctioned by usage

The Estuarine Ecosystem is aimed at a more specialized readership The first chapter includes some elementary consideration of the hydrography, sedimentary processes, species composition and food webs of estuaries It is a rather superficial account suffering from false simplification, perhaps on the wrong assumption that students of marine biology should not have to bite on hard science To take a simple example, sinking rates are discussed in relation to the impact law for large particles and Stokes' law for small ones, but the underlying reason behind the different approaches is not explained Neither the bounds over which the equations hold true nor their derivations are given, yet this information is exactly what the intelligent student needs in order to grasp the relevant scientific principles. In the same chapter, hydrographic features of estuaries are not fully discussed in terms of estuary size and salinity fluctuation, while recent work on the importance of rate of change of estuarine variables on the tolerance of animal species is not mentioned. Indeed the diagrams showing species penetration into estuaries are related to "salinity", not even "mean salinity" and certainly without reference to fluctuation.

Insufficient consideration is given to estuarine topography especially the influence of coastal emergence and submergence on estuarine form. The book as a whole deals almost exclusively with British and eastern American coasts, omitting any consideration of Arctic and tropical estuaries. In regard to the historical perspective of the subject, it fails dismally. The names of Bowden, Ketchum and Redfield, and Riley never appear, while in the place of the original figure depicting the mid-estuarine minimum in faunal diversity, given by Alexander *et al.* in their classical paper of 1935, the author quotes only from his own book of 1971.

The book includes a useful accumulation of productivity data for estuaries, with many food web diagrams, but little of novelty or abstracted wisdom which cannot be found elsewhere. The reference lists do not appear to be selective or exhaustive.

John Gray's *Ecology of Marine Sediments,* though less weighty in information, contains the essential material for the author's purpose and a good historical background. It aims to focus the minds of benthic ecologists on the interpretation of data in terms of modern ecological principles. Gray seizes on the linearity of the log–normal distribution of individual numbers in relation to species as a good measure of community equilibrium in the absence of disturbance. One would like to have seen a further extension of the philosophical basis of the idea, with a guess at the ecological meaning of the relevant statistics.

The book contains thoughtful discussions on niches, diversity and faunal stability — ideas that are currently being tested by ecologists in many environments. Finally, the author considers practical means of monitoring benthic communities in respect of long-term effects of pollution or of other factors that may control their structure.

This volume affords good reading for the above-average student of marine ecology who is prepared to sit and reflect, and is essential for those engaged in research on the fauna of sediments. It is a valuable contribution to ecological theory.

D.J. Crisp is Professor of Marine Biology at the Marine Science Laboratories, Menai Bridge, Gwynedd.

Aspects of environmental physiology

J.A. Riegel

Functional Adaptations of Marine Organisms. Edited by F. John Vernberg and Winona B. Vernberg. Pp.347. ISBN 0-12-718280-2. (Academic 1981.) $39.50, £26.20. *Animal Osmoregulation.* By J.C. Rankin and J. Davenport. Pp.202. Hbk ISBN 0-216-91014-5, pbk ISBN 0-216-91015-3. (Blackie/Wiley 1981.) Hbk £17.95, $39.95, pbk £8.95.

THESE two books have one common feature: they represent attempts to relate various aspects of organismal function to environmental variables. That edited by the Vernbergs is a multi-authored treatise whose main use will be as a source of reference. Rankin and Davenport's book is much more didactic in its approach, and it should find a wide audience amongst students and teachers of courses in environmental physiology.

Functional Adaptations of Marine Organisms contains chapters written by specialists on primary production, bacteria, zooplankton, meiofauna, benthic macrofauna, pelagic macrofauna and deep-sea organisms. In addition, the editors have provided an introductory chapter describing the ecological subdivisions of the marine habitat. This is both welcome and necessary for the non-specialist reader. Like most multi-authored works, however, the book's coverage is inadequate. For example, the discussion of zooplankton is confined to copepods, and primary producers are reviewed largely from an ecological viewpoint. Recent discoveries of communities of animals densely clustered around deep-sea, warm-water vents and dependent upon the primary production of chemosynthetic bacteria receive only brief mention. Nevertheless, the major shortcoming of the book is due to the inadequacy of the background data. Although more could have been done to round out the material, this deficiency is not altogether the authors' (or editors') fault — precious little is really known about the functional adaptations of marine organisms, especially those in the less-accessible parts of the sea.

Despite its shortcomings, the book should be a useful reference work for specialists and non-specialists alike. Although no chapter represents an exhaustive review of the literature, most authors have included references to reviews and papers covering aspects of their subjects not discussed extensively in their contributions.

Animal Osmoregulation presents a refreshingly uncluttered overview of not only the basic concepts of the subject, but also most of the currently-active fields of research. The book starts with a consideration of basic principles, the explanations of which should be of sufficient clarity to be understood readily by the average undergraduate. Following this come discussions of the adaptations of animals to various habitats, from the sea to brackish water, fresh water and land. Specialized adaptations of osmoregulatory mechanisms, such as the mammalian kidney, buoyancy and to life in acid and alkaline waters, are also covered. The examples used to illustrate the various adaptations are highly selective and several are drawn from the research of the authors and their associates. Perhaps it is this personal experience of much of the research underlying the material which gives the narrative an admirable lack of dogmatism. Aware of the highly-variable nature of most data, they tend to generalize with caution.

The final chapter of *Animal Osmoregulation* deals with some of the common physiological and behavioural techniques used in studies of osmoregulation. The description of physiological techniques may provide useful background, but the short discussion of behavioural techniques should prove more valuable, especially as the basis of classroom experiments or demonstrations. □

J.A. Riegel is a Reader in Zoology at Westfield College, University of London.

Adaptation to supply and demand

Garth Chapman

Animal Physiology: Adaptations in Function. By F. Reed Hainsworth. Pp.669. ISBN 0-201-03401-8. (Addison-Wesley 1981.) $25.95, £10.95.

HAINSWORTH'S *Animal Physiology* declares itself to be ecological and comparative by its subtitle but only discloses the fact that it is "organized around" an "economic theme for comparative physiology" in the preface. The animal's balance sheet of benefits and costs uses the currency of resources and concludes about joules and survival what Mr Micawber concluded about pence and happiness.

This is certainly an important theme but it becomes a little tedious by reiteration. However heuristically valuable such an approach may be when applied to resources such as oxygen, food, water and salts, it is less directly applicable to that large and distinctive part of animal physiology which is concerned with reception, co-ordination and response. Accordingly, perhaps, the section dealing with these topics is placed at the end of the book Although not neglected, less prominence is given to them and to the current tenets of membrane physiology on which they are based than in some recent texts such as Goldstein's *Introduction to Comparative Physiology* (Holt, Rinehart & Winston, 1977) and Eckert and Randall's *Animal Physiology* (W H Freeman, 1978) where they follow the opening chapters on physical and chemical principles

In style the book is densely and didactically written but the terse generalization is usually supported by example or the brief report of an observation or experiment Nevertheless, I found myself wondering whether an introductory text ought not to lead readers more gently along the path of interest rather than seek to impress them with sheer quantity of information Unlike some bulky and extravagant textbooks, this one is handy and well produced apart from a few gimmicks such as two contents lists, one short and obscure and one detailed and eleven pages in length! There is no indication of part or section in the running headlines, which makes cross-reference difficult since such references are frequently indicated by subdivision and not by page Bibliographical references (not indicated in the text) are divided into annotated, at the end of each part, and "credit" — whatever they may be — at the end of the volume

In short, this seems a somewhat daunting introductory text to read although good indexing increases its value to an industrious student for purposes of reference and study □

Garth Chapman is Professor of Zoology at Queen Elizabeth College, University of London

Enzymology: the general and the specific

R.N. Perham

Understanding Enzymes By Trevor Palmer Pp 405 Hbk ISBN 0-85312-202-4, pbk ISBN 0-85312-307-1 (Ellis Horwood, Chichester/Halsted 1981) Hbk £25, $80 95, pbk £9 50 *Molecular Enzymology* By Christopher W Wharton and Robert Eisenthal Pp 326 ISBN 0-216-91012-9 (Blackie/Wiley 1981) £19 75, $46 95 *Isoenzymes* By C C Rider and C B Taylor Pp 78 Pbk ISBN 0-421-15640-7 (Chapman & Hall/Methuen 1981) £2 45, $5 95 *Enzyme Kinetics The Steady-state Approach*, 2nd Edn By P C Engel Pp 96 Pbk ISBN 0-412-23970-1 (Chapman & Hall/Methuen 1981) £2 45, $5 95

THERE is hardly a corner of biochemistry or molecular biology — not to mention the cognate biological and chemical sciences — where modern ideas of enzymology have not intruded to good effect The study of enzymes is therefore properly an important part of all degree courses in these subjects, and there continues to be no shortage of authors willing to try their hand at providing the necessary textbooks

Dr Palmer's offering, *Understanding Enzymes,* attempts to cover all of the fascinating aspects of enzymes, from their biosynthesis to their structure, chemical mechanisms and kinetics, from their place in metabolism to their use in medicine and industry It is an heroic task but one of dubious practicability — witness how few authors have followed the trail so comprehensively blazed by Dixon and Webb in their classic first edition of *Enzymes,* published by Longman Thus one should not be surprised that in the volume under review, which is furthermore written by a single author, the coverage is uneven and appears to rely heavily on secondary sources It is sad to record that some of those sources are significantly out of date For example, in the short chapter on protein structure nothing published since 1970 is suggested for further reading, the chapter on biosynthesis of proteins (surely now misplaced in a book on enzymes) has no specialist reference later than 1974, and the chapter on metabolic regulation includes a diagram of the cell that places the cisternae of the rough endoplasmic reticulum in unrestricted communication with the extracellular environment The kinetics of enzymes are dealt with more extensively and sympathetically, and the later sections on technological and medical applications of enzymology cover a wide range of topics Each of the 20 chapters concludes with a useful summary of its contents and most carry a set of problems and answers In what I take to be an otherwise commendable attempt to lower costs, many of the illustrations, though clear, appear to have been left as sketches, which adds a slightly makeshift air to the printed page

All in all, I cannot see this book supplanting the more narrowly based texts on which the undergraduate teaching of enzymology normally rests, though the convenience of a broad range of topics falling within a single volume may commend it to those with less stringent needs

A new contender for a place among the more specialized texts is *Molecular Enzymology* by Wharton and Eisenthal, which assumes a basic knowledge of university biochemistry and chemistry The approach is first to tackle the chemical aspects of catalysis and the properties of enzymes as proteins, to develop ideas in enzyme kinetics and then to deal in some depth with the mechanisms of eight or nine selected enzymes as examples The book concludes with a return to the practical problems of studying enzyme kinetics in the laboratory The treatment is clear and conventional, cuts few corners and makes plain the complementarity of the different methods, it should appeal particularly to those with a background in the physical sciences The bibliography is sound and extensive The authors eschew the usual efforts to represent three-dimensional events on paper in favour of a more descriptive turn-by-turn account of the involvement of amino acid side-chains and other functional groups, an approach with which I do not altogether agree And at the risk of a charge of chauvinism, I suggest that any new text on molecular enzymology that largely neglects protein mobility and dynamics, multienzyme systems and multifunctional proteins cannot be regarded as complete These quibbles apart, I found little to quarrel with and expect the book to find an honourable place in university reading lists

Finally, it is a pleasure to notice two further additions to the series of *Outline Studies in Biology* The first, *Enzyme Kinetics* by Engel, is the second edition of his successful account of steady-state kinetics and their contributions to problem-solving in enzymology The second, *Isoenzymes* by Rider and Taylor, describes the importance of isoenzymes in a broad range of biochemical and medical contexts Both are clear, unpretentious and informative, in accord with the general style of this well-known series □

R N Perham is Reader in Biochemistry of Macromolecular Structures at the University of Cambridge, and a Fellow of St John's College, Cambridge

Spanning a bridge

Peter H.W. Butterworth

Biochemistry, 2nd Edn By Lubert Stryer Pp 949 Hbk ISBN 0-7167-1226-1, pbk ISBN 0-7167-1306-3 (W H Freeman 1981) Hbk $32 95, £24 40, pbk £12 95

THERE are a lot of biochemistry textbooks and, as the borders of the subject continue to be extended, there will be more Some adopt a particular emphasis, others attempt a comprehensive approach to the subject Lubert Stryer's text belongs to the latter genre and it is doubtful whether there will be another which will appeal to the student as strongly as this one does When the first edition appeared, immediate reaction was dominated by the impact of the remarkable illustrations and the succinct text Familiarity with the book brings with it the realization of how ingeniously interdependent these facets are the illustrations are not just attractive but they are required and used to support the concise style of the text At the same time, the student is provided with a graphic framework into which complex concepts often seem to sit with comfort

Every author of a basic biochemistry textbook is faced with two decisions first, at what level to pitch the book and second where to begin and end Stryer seems to aim unashamedly for the "early undergraduate", yet the brevity of the text often belies its depth· the author has a unique ability to expound difficult concepts in a few words As biochemistry constitutes a bridge between physical and biological sciences, the limits are difficult to define and, regardless of how far apart the covers are, it would be impossible to satisfy every whim Here the subject matter is very broadly based and the student is required to accumulate background knowledge of the physical sciences, organic chemistry, cell biology and basic molecular genetics from elsewhere Nevertheless, one of the strengths of this textbook is that it can be appreciated before the background is complete

It is not surprising that this second edition is bigger than the first Neither is it surprising that many of the illustrations in the first edition have been updated and many more have been added, a major effort has been made to get across the concept of the integration of metabolic processes and the text has been extended greatly to accommodate major advances in the subject, particularly in the area of molecular biology

Textbooks for major subjects often present a daunting prospect where they should foster the enthusiasm of the student and provide a realistic challenge. The response to Stryer is generally enthusiastic for a textbook, that is an accolade The only penalties for confronting so massive a task may be that the compact style sometimes excludes subtlety and may not leave room for mystery, the solving of which will provide the material for the next edition. □

Peter H W Butterworth is Reader in Biochemistry at University College London

---

Whole chemistry?

Peter Garratt

Chemistry: An Introduction to General, Organic, and Biological Chemistry By Joanne M Widom and Stuart J Edelstein Pp 799. ISBN 0-7167-1224-5 (W H Freeman 1981) $23 95, £16 60 *Atoms, Molecules, and Life: An Introduction to General, Organic, and Biological Chemistry.* By Michael S Matta and Antony C Wilbraham Pp 721 ISBN 0-8053-9640-3 (Benjamin/Cummings 1981) $22.95, £14 95 *Basic Chemistry of Life* By Milton Toporek Pp 521 Pbk ISBN 0-8016-5002-X (C V Mosby 1981) $7 95, £12

THESE three texts are all directed at North American students of the life sciences and each presupposes little previous exposure to chemistry *Chemistry* and *Atoms, Molecules, and Life* (AML) declare the same interest in their mutual subtitle, while the third, *Basic Chemistry of Life* (BCL), intends to provide a base in chemistry on which the student may build an understanding of the complex processes of life

How are they to do this in less (BCL considerably less) than 1,000 pages? Clearly there must be selection and much of the treatment must be superficial For example, atomic structure is treated by BCL in six pages and no student could have any basis for a further understanding of this subject after reading these Both of the other books treat this topic in more detail, *Chemistry* making a valiant attempt to promote the ideas of quantum mechanics, whereas AML is rather cloudy on this issue Chemical bonding is initially introduced in all three texts by "dot formulae", *Chemistry* and AML developing the subject further to indicate the three-dimensional shape of molecules All of the texts attempt to provide a foundation in physical chemistry, with an emphasis on those topics of interest to biologists Electrolytes and non-electrolytes, solubility, osmosis and pH are all discussed in some detail and illustrated with biological examples, thus, for example, osmosis is described by the effect of changes in extracellular salt concentration on the red blood corpuscles Each book includes a substantial section on organic chemistry, starting with methane and ending with nucleic acids and the genetic code Both AML and BCL have extensive sections on biochemistry

Of the three, BCL has the most medically orientated approach, the least basic chemistry and would require considerable elaboration on the part of the lecturer to give the student any real understanding of the subject It virtually ignores the three-dimensional structure of molecules, and conformation is no where introduced The consequences of three-dimensional structure is an area in which none of these texts is consistently satisfactory, thus although AML shows that the steroids are chair structures, it does not indicate how this influences the stereochemistry of the system, whilst *Chemistry,* though clearly indicating the stereochemistry, does not mention the conformational consequences All of the texts use Haworth formulae for the carbohydrates and although *Chemistry* does introduce the conformational formula for glucose it does not exploit it *Chemistry* as its title suggests, is most clearly directed towards the exposition of this science and, starting from the four elements and ending with global biochemical problems, it represents an impressive attempt to encompass both the essential and the exciting new aspects of the subject within a single volume

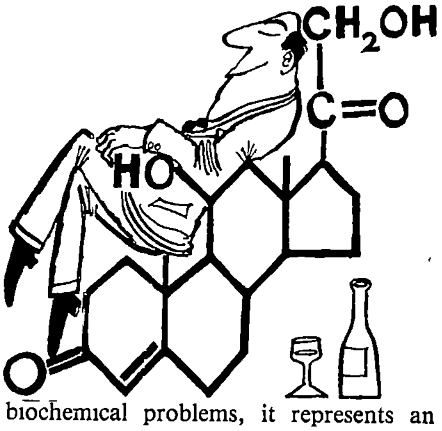

The print of all three books is excellent and chemical structures are clearly illustrated, *Chemistry* and AML in two-tone, BCL in monochrome Each provides problems, often with answers, and *Chemistry* has available both a study guide for the student and a manual for the instructor The latter provides answers for those questions without textual answers, test questions and suggestions for demonstrations □

Peter Garratt is Reader in Chemistry at University College London

---

Beyond description

H. Hassall

Basic Mathematics for Biochemists By Athel Cornish-Bowden Pp 137 Hbk ISBN 0-412-23000-3, pbk ISBN 0-412-23010-0 (Chapman & Hall/ Methuen 1981) Hbk £7 95, $17 95, pbk £3 95, $8 95 *Quantitative Problems in Biochemistry,* 6th Edn By Edwin A Dawes Pp 335 ISBN 0-582-44402-0 (Longman 1980) £13 95, $32 *Biochemistry A Problems Approach* By William B Wood *et al* Pp 498 ISBN 0-8053-9840-6 (Benjamin/Cummings 1980) $14 95, £8 95

YEAR after year, with only one or two exceptions, the questions that are done least well in biochemistry examinations are those involving calculations and data assessment Mass panic ripples through the examination rooms and those painstakingly constructed subtleties of the examiners, the diauxic inflections of the growth curve, the sigmoidicity of the Michaelis–Menten graph or the slight curvature of the Yphantis plot, are either missed or explained as experimental error

If these three books have a common objective, as I believe they have, then it is to encourage a more quantitative treatment of the subject However, each is different in its approach and has something unique to offer

Basic Mathematics for Biochemists is the shortest of the three and has a straightforward aim — to rectify deficiencies in the mathematics needed to understand modern biochemistry It begins reassuringly simply (almost too simply in that one is told that 2^2 means $2\times2=4$) but it does go on to cover integral and differential calculus, matrices and partial differentiation The examples used have a biochemical origin and, taken as a whole, one is impressed by just how much information the author has been able to get into a book of 137 pages Clearly, the students who assimilate its contents would have more than enough mathematics to cope with any first-degree course in biochemistry

The book by Edwin Dawes, *Quantitative Problems in Biochemistry*, should need no introduction It is now in its sixth edition and, coincidentally, in its sixth language At the time of the first edition it must surely have been one of the first books of its kind, and the familiar style and content have altered only little over the years despite some changes in format There is a new and useful chapter on membrane bioenergetics, this addition being balanced by a pruning of the text elsewhere With respect to the problems themselves, the book relies heavily on the presumably well-tried and tested finals examination questions from biochemistry degree courses in British universities Few of these, however, have been updated since the last edition

The third book, ***Biochemistry A Problems Approach,*** has a different emphasis to the others It is really a textbook of biochemistry using data assessment and questions to illustrate the principles, rather than just a book of problems with biochemistry as the source of material The approach, while clearly not new, is refreshing It has a chatty, personal style and although Fluhardy Pharmaceuticals, Dr F Holding Munney and Dr Klassik appear (but only briefly) as the bodies faced with problems, the information that is conveyed is no less valuable, who knows, perhaps interest actually is more readily stimulated this way Most of the questions are particularly searching and are balanced by full explanations in the answers The text is comprehensive, ranging in 21 chapters from the "Clinical Characteristics of Living Matter" through to "Recombinant DNA and Genetic Engineering" The treatment is even, and while the book is not meant to replace standard texts such as Lehninger or Stryer, it complements them well and is good value at the price □

H Hassall is Senior Lecturer in the Department of Biochemistry, University of Leeds

---

Physical chemistry: sugar in the medicine

S.P Spragg

Physical Chemistry With Applications to Biological Systems, 2nd Edn By Raymond Chang Pp 659 Hbk ISBN 0-02-321040-0, pbk ISBN 0-02-978355-0 (Collier Macmillan/Macmillan, New York 1981) Hbk £16 50, $24 95, pbk £10 50 *Physical Chemistry for the Life Sciences,* 2nd Edn By Garry M Barrow Pp 468 ISBN 0-07-003858-9 (McGraw-Hill 1981) $32 95, £18 25

IF ONE consults biological colleagues on what physical concepts they wish they had learnt as students, two extreme views appear there are those who feel they prospered without needing physical chemistry, while others consider that physical chemistry is central to their branch of biology The fact that two extremes are quoted by leaders in their fields confirms the view that some parts of biology can be pursued without an understanding of physical chemical principles, but if one is educating on a broad front then exposure to physical chemistry cannot be a bad thing The question is, should we apply the old adage often used when preparing medicines, namely it must be good because it tastes so bad? Personally, I feel this is not necessary because all principles of physics and biology can be explained attractively and clearly despite their complexity These thoughts were uppermost in my mind when reading the new editions of these two books

Both texts are written in attractive styles and each depends on the working of simple numerical examples to illustrate the principles The contents cover the full range of modern physical chemical ideas, carefully written using the properties of biological molecules for the examples The authors have made considerable improvements over the first editions, mainly by expanding the discussions on thermodynamics Both have rearranged the sequence of topics so that thermodynamics precedes spectroscopy There are also more worked examples in the texts and more problems for the students to tackle (with answers at the end of the book) here Chang differs from Barrow since he has indicated which problems are more advanced Chang has also expanded and moved the mathematical derivations of equations to the end of the appropriate chapters Barrow follows a similar arrangement but unlike Chang he mixes mathematics with the particular applications of the chapter

Both authors have introduced modern views into all topics, and I was particularly pleased to see that they have explained how transition state theory for solutions differs from that for a gas, as well as providing models for diffusion-controlled reaction (Chang is better here) They have also squeezed in descriptions of relaxation methods for studying rates of reactions

As one would expect when comparing the products of two experienced teachers, there are differences in presentation for example, Chang employs more diagrams than Barrow My lasting impression was that Barrow contained more detail than Chang on subjects embraced by hydrodynamics, however, aspects such as wave-mechanics appeared to be more complex in Barrow than Chang Also, I found that Chang's index was not as comprehensive as Barrow's Yet these are details and students are as different as reviewers in their selection of material So, since both books can be recommended, I suggest that prospective buyers dip into each of them before deciding which approach best suits their own personality □

S P Spragg is Senior Lecturer in Physical Chemistry at the University of Birmingham

---

Talking of organic chemistry

John Mann

The Vocabulary of Organic Chemistry By Milton Orchin *et al* Pp 609 ISBN 0-471-04491-1 (Wiley 1980) £18 75, $43 75 *Introduction to Organic Chemistry,* 2nd Edn By Andrew Streitwieser and Clayton H Heathcock Pp 1,258 Hbk ISBN 0-02-418050-5, pbk ISBN 0-02-978310-8 (Collier Macmillan/Macmillan, New York 1981) Hbk £18 95, $28 95, pbk £9 95 *A Guidebook to Mechanism in Organic Chemistry,* 5th Edn By P Sykes ISBN 0-582-44121-8 (Longman 1981) £7 50, $16 95

LINGUISTS have prepared lists of key words and expressions for most languages, but *The Vocabulary of Organic Chemistry* represents the first real attempt to do the same for organic chemistry The intention of the authors was to " identify the fundamental vocabulary of organic chemistry and then to present concise, accurate definitions with examples where appropriate ", and in this they have been eminently successful They define some 1,350 terms and concepts, with entries ranging in length from one line to a page

The compendium is organized into 15 chapters, and commences with a concise introduction to symmetry, followed by a series of mathematical definitions pertaining to wave and quantum mechanics In this second chapter the sections on bonding and orbitals are particularly good Structural aspects of hydrocarbons are covered in Chapter 3, followed by a comprehensive list of organic functional groups, including 35 containing sulphur and 24 containing phosphorus, this chapter thus provides a far better source of such information than any undergraduate textbook on the market

Stereochemistry and conformational analysis appear in Chapter 5, and this compilation of terms is most timely since there is ever-increasing attention paid to the stereochemical aspects of organic chemistry in the research literature In addition, many undergraduates have difficulty distinguishing between terms such as "stereoselective" and "stereospecific", or in understanding the significance of "prochiral hydrogens" and "asymmetric induction", and this chapter provides accurate and easily understood definitions for all of the commonly encountered terms

Polyfunctional compounds are dealt with in Chapter 6, and this includes coverage of sugars and amino acid derivatives Here, I feel too much stress is laid on Fischer projection formulae and there is scant mention of more realistic cyclic structures, also, the amino acid and protein section is too short to be really useful — surprisingly, the terms "enzyme" and "active-site" do not appear Chapter 7 contains a useful collection of terms pertaining to separation techniques, following which there is excellent coverage of ions and electron deficient species This is also timely since there is often confusion over the terms "carbocation", "carbonium ion" and "carbenium ion", and these are all unambiguously defined Essential thermodynamics (Chapter 9) then precedes a classification of organic reaction mechanisms, and this latter chapter should be particularly useful for undergraduates since it also includes 15 pages encompassing topics such as orbital correlation diagrams, the Woodward–Hoffmann rules, and the frontier orbital approach to mechanism It is interesting to note that the same number of pages is given over to these topics in Streitwieser and Heathcock, but the clarity of the coverage is greater in *The Vocabulary*

The outstanding chapter then follows, in which 159 name and type reactions are discussed, with a mechanism given for each of them This would make an excellent 90-page monograph in its own right, it certainly highlights the reason behind the oft-heard lament of the undergraduate "There's too much to learn in organic chemistry" Chapter 12 is entitled "Organometal Chemistry", but contains little of relevance to organometallic chemistry The term "cuprate", for example, does not appear, yet this is much more a part of the vocabulary of modern organic chemistry than are the terms "ligand field theory" and "edge-bridging ligand" Chapter 13 commences with a rather awkward definition of "natural product", and it would perhaps have been better to define the terms "primary metabolite" and "secondary metabolite" This said, however, the chapter has good sections on cofactors and on all of the major biosynthetic pathways and classes of secondary metabolites Finally, there are useful chapters on polymers and industrial processes, mainly those involving fossil fuels

There is perhaps only one major omission in the book (and the authors recognize this), and that is coverage of spectroscopic methods The book is beautifully produced with excellent structures throughout, and includes well-chosen examples and a good index In parts it is reminiscent of a book of revision notes, but this may endear it to undergraduates Overall, it is a unique and very useful reference work, all organic chemists should find something of interest within its pages

Streitwieser and Heathcock have made a number of changes of organization for the second edition of their popular textbook, and the sections on organometallic chemistry, ^{13}C-NMR, and sulphur and phosphorus chemistry have been expanded One omission is the useful appendix on functional group preparations which was popular with undergraduates using the first edition This book and Solomons's *Organic Chemistry* (for review see *Nature* **289**, 721) are two of the most popular organic texts on the market There is little to choose between them, though the two-tone illustrations in Solomons perhaps give it a slight edge

Finally, any book that has reached its fifth edition and been translated into six foreign languages must be rated a success Such is the volume by Peter Sykes — a text that has probably been used by most chemistry undergraduates at one time or another There were major revisions for the fourth edition, and the only important change for this edition is the inclusion of a chapter on linear free energy relationships, which further increases the utility of the book It will be interesting to see if *The Vocabulary* is read as widely and proceeds through as many editions — I see no reason why it should not achieve this distinction □

John Mann is a Lecturer in Organic Chemistry at Reading University

Theory guides, but experiment decides

Gary O. Spessard

Spectral and Chemical Characterization of Organic Compounds A Laboratory Handbook, 2nd Edn By W J Criddle and G P Ellis Pp 115 Hbk ISBN 0-471-27813-0, pbk ISBN 0-471-27812-2 (Wiley 1980) Hbk £13, $30 90, pbk £4 50, $10 70

Operational Organic Chemistry A Laboratory Course By John W Lehman Pp 671 ISBN 0-205-07146-5 (Allyn & Bacon 1981) $24 95, £9 95

THE task of introducing students to the experimental side of organic chemistry can be an awesomely difficult one, not only because of the wide variety of vocational goals and interests one encounters, but also because there are so many aspects of the subject which ought to be considered in any laboratory course These aspects essentially centre on the synthesis and characterization of compounds Criddle and Ellis in their *Spectral and Chemical Characterization of Organic Compounds* address the latter concern, while Lehman's *Operational Organic Chemistry* endeavours to cover both synthesis and characterization

The second edition of Criddle and Ellis's text is only slightly modified from the first which appeared five years ago For example, small additions and modifications appear in the notes explaining the chemical bases for the functional group tests in Chapter 2, in the section on interpretation of spectral data in Chapter 3 and in Chapter 5 where extensive tables of physical data are found Using a step-wise approach, hints on how to interpret the results of chemical and spectral tests in addition to compendia of physical data on compounds and their derivatives are presented in a compact style While concise and informative, the book must be supplemented, as the authors point out, with more comprehensive works on the chemical bases of function group tests, the chemistry of derivatization and practical spectroscopy No mention is made of the use of chromatography in analysing and separating mixtures, and only the briefest reference is given to safety in regard to handling reagents (often quite toxic) typical of the organic "qual" laboratory As long as access to more complete sources of information is possible, this text can usefully serve as a guide for students involved in the qualitative analysis segment of a regular organic laboratory course or in one concerned with characterization alone

Operational Organic Chemistry is another addition to the spate of laboratory manuals currently available The author suggests that working in the laboratory involves performance of a series of operations such as filtration, extraction or spectral analysis from the start to the finish of an experiment The student should gain an appreciation of these operations, described separately in the text, by learning to perform them within a series of preparative and analytical experiments Superb background essays are included which encourage student involvement in the chemistry behind each experiment by suggesting roles (such as working as a chemist for a perfume manufacturer) students may assume while working in the laboratory I especially like the emphasis on pre-laboratory preparation whereby students are directed to read certain text sections and to complete specific exercises *before* working on an experiment

The menu of practical exercises includes many of the "old reliables" as well as several new ones, suggestions for additional work are provided in the form of "minilabs" and "experimental variations" Potentially attractive to students with biologically-related interests is the extensive use of natural products because, as Lehman states, "they often cost less, smell nicer, and are more pleasant to work with than purely synthetic analogs" Safety is treated thoroughly and conscientiously throughout the book I do have reservations, however, about the pedagogical benefits to be gained from the synthesis of azo dyes or the use of toluene-2,4-diisocyanate for polyurethane synthesis in light of the chemical hazards involved The sections in the text on spectral techniques are adequate but not as good as those found in *Introduction to Organic Laboratory Techniques* by Pavia *et al* Nonetheless, in spite of these minor criticisms, the book is rather unique in its approach and one which is well worth considering for adoption ☐

Gary O Spessard is Associate Professor of Chemistry at St Olaf College, Northfield, Minnesota

Atkins anew

Maurice Rigby

Physical Chemistry, 2nd Edn By P W Atkins Pp 1,095 Hbk ISBN 0-19-855150-9, pbk ISBN 0-19-866151-7 (Oxford University Press/W H Freeman 1982) Hbk £25, $29 95; pbk £10 95 *Physical Chemistry* By J Philip Bromberg Pp 882 Hbk ISBN 0-205-06572-4, pbk ISBN 0-205-06867-7 (Allyn & Bacon 1980) Hbk $27 95, £22 25, pbk £9 95

In the past few years several candidates have presented themselves as potential successors to established and widely-used general textbooks of physical chemistry such as W J Moore's *Physical Chemistry* (Longmans/Prentice-Hall, 1972) and G M Barrow's *Physical Chemistry* (McGraw-Hill, 1979) One of the most successful has been that of P W Atkins, first published in 1978 and rapidly followed by a corrected reprint, which now appears in a second edition The first edition of this work was notable for a generally well-judged level of coverage of most aspects of the subject, and for the fresh and accessible presentation of difficult concepts

In the new edition these desirable qualities have been retained, and some omissions and slight imbalances have been rectified There is a completely new chapter dealing with macromolecules — a subject sadly neglected in the first edition — and many figures have been changed, with the introduction of computer graphics In addition the treatment of chemical bonding, which was previously rather brief, has been amplified, and the introductory material on statistical mechanics has been simplified Comparisons between corresponding sections of the two editions reveal numerous small changes, supporting the claim that all sections of the book have been reconsidered My overall impression is of an excellent textbook which has become even better, and which seems sure to enjoy continued popularity in the future Who, in any case, could resist a physical chemistry book which considers (p 103) the musical implications of a dying ocarina player?

Against such competition, yet another general textbook will have to be very good if it is to wean readers away from the established sources J Philip Bromberg has taken up this challenge but has not completely persuaded me The author claims to have aimed to present the subject at the mid-college level, and has consciously reframed from producing an encyclopaedia of physical chemistry For this ambition he should be congratulated — at least one recent text has seemed to be aimed more at the readership of *Annual Reviews of Physical Chemistry* than at an undergraduate audience

The book follows a fairly well-worn path from the gas laws through thermodynamics, statistical mechanics, quantum mechanics and reaction kinetics, giving quite formal and detailed coverage of the necessary theoretical development though not neglecting to draw attention to the practical relevance of the subject, where appropriate It is liberally interspersed with short biographical sketches of notable scientists, which may help to give students some feeling for the development of the subject The overall balance appears to emphasize thermodynamics and quantum mechanics, which are respectively developed classically and axiomatically Electrochemistry and surface chemistry appear as applications of thermodynamics, and there is no mention of catalysis or of non-equilibrium aspects of electrochemistry The treatment of reaction kinetics is short and repeatedly uses a rather laborious analogy with molecular effusion, the merits of which are not immediately apparent In short, although the book has some attractive qualities, and I shall try to arrange for a copy to be available in our college library, I do not believe that it will replace its rivals in a majority of chemistry departments ☐

Maurice Rigby is a Lecturer in Chemistry at Queen Elizabeth College, University of London

NEW

GENETICS AND PROBABILITY IN ANIMAL BREEDING EXPERIMENTS

EARL L. GREEN

Director Emeritus of The Jackson Laboratory, Bar Harbor, Maine
Editor, Biology of the Laboratory Mouse, Second Edition

Contents

Probability and Statistics, Segregation of Alleles, Assortment of Non-Alleles, Linkage, Recombination and Mapping, Mating Systems, Appendix 1 – Mean and Variance of a Binomial Distribution, Appendix 2 – Estimation of a Parameter by the Method of Maximum Likelihood, Appendix 3 – Extensions of the Method of Maximum Likelihood, Appendix 4 – Comparative Efficiency of Matings for Detecting and Measuring Linkage, Appendix 5 – the Fibonacci Sequence, Appendix 6 – Systems of Mating, Appendix 7 – Numbers of Mating and Numbers of Mice per Mating, Appendix 8 – Nomenclature, Appendix 9 – Record Keeping, Appendix 10 – Mouseroom Layout and Procedures, Glossary of Signs, Literature Cited, Index

This book is a primer and reference on probability, segregation, assortment, linkage and mating systems for biomedical scientists who breed and use genetically defined laboratory animals for research

It is organised so as to be useful to 'novices' and 'experts' alike The former will find an orderly development of the probability aspects of transmission tests, segregation analysis, allelism tests, independence tests, linkage analysis and mapping They will see how to design genetic experiments to yield data which can be analysed and they will also find a clear exposition of the theoretical consequences of various breeding systems which will enable them to make rational choices as to the kinds of animals to use in their own research

Experts will find that the most frequently used formulae needed for estimating various genetic parameters and their random sampling variances are assembled in tables or are clearly set forth in the text and that the extensive table of contents and detailed index will enable them to find the necessary formulae quickly

LEVEL Professional, graduate, undergraduate reference

February 1981 £20 00, 256pp, ISBN 0 333 27243 9

RELATED TITLES

FESTING Inbred Strains in Biomedical Research £25 00 1979
FESTING Animal Models of Obesity £17 50 1979
SPARROW Immunodeficient Animals for Cancer Research £20 00 1980

Send your orders, requests for further information etc to Frances Roach, Scientific and Medical Division, Macmillan Publishers, Houndmills, Basingstoke, Hampshire, RG21 2XS, U K

SCIENTIFIC & MEDICAL M MACMILLAN PUBLISHERS

BOOKS RECEIVED

Astronomy

BOK, B J and BOK, P F The Milky Way 5th Edn Pp 356 ISBN 0-674-57503-2 (Harvard University Press 1981) £14

HOYLE, F The Quasar Controversy Resolved Pp 80 Flexi ISBN 0-906449-28-6 (University College Cardiff Press 1981) £3 25

PEEK, B M The Planet Jupiter The Observer's Handbook 2nd Edn Revised by Patrick Moore Pp 240 ISBN 0-571-18026-4 (Faber & Faber 1981) £10

PONNAPERUMA, C (ed) Comets and the Origin of Life Proceedings of the 5th College Park Colloquium, University of Maryland, College Park, Maryland, October 1980 Pp 282 ISBN 90-277-1318-9 (Reidel 1981) Dfl 85, $39 50

WHEELER, J C (ed) Type I Supernovae Proceedings of the Texas Workshop held in Austin, Texas, March 1980 Pp 216 Pbk ISBN 0-9603796-1-4 (University of Texas at Austin 1980) Pbk $5

Physics

EHRENBERG, W and GIBBONS, D J Electron Bombardment Induced Conductivity and Its Applications Pp 448 ISBN 0-12-233350-0 (Academic 1981) £39 80, $96

HAMEKA, H F Quantum Mechanics Pp 387 ISBN 0-471-09223-1 (Wiley 1981) £24, $43 25

HODGSON, P E Growth Points in Nuclear Physics, Vol 3 Pp 261 Hbk ISBN 0-08-026485, flexi ISBN 0-08-02648-0 (Pergamon 1981) Hbk np, flexi £4 70, $10 30

HOWES, M J and MORGAN, D V Large Scale Integration Devices, Circuits, and Systems Pp 346 ISBN 0-471-27988-9 (Wiley 1981) £17 50, $39 50

KUO, T T S and WONG, S S M (eds) Topics in Nuclear Physics, I A Comprehensive Review of Recent Developments Lecture Notes in Physics, Vol 144 Lecture Notes for the International Winter School in Nuclear Physics held at Beijing (Peking), December 1980–January 1981 Pp 567 Flexi ISBN 3-540-10851-3 (Springer-Verlag 1981) DM 59, $26 90

KUO, T T S and WONG, S S M (eds) Topics in Nuclear Physics, II A Comprehensive Review of Recent Developments Lecture Notes in Physics, Vol 145 Lecture Notes for the International Winter School in Nuclear Physics held at Bejing (Peking), December 1980–January 1981 Pp 511 Flexi ISBN 3-540-10853-X (Springer-Verlag 1981) DM 59, $26 90

LOPES, J L Gauge Field Theories An Introduction Pp 484 ISBN 0-08-026501-4 (Pergamon 1981) £17, $37

MARTIN, J L Basic Quantum Mechanics Pp 241 Hbk ISBN 0-19-851815, pbk ISBN 0-19-851816-1 (Clarendon Press/Oxford University Press 1981) Hbk £17 50, pbk £7 95

NEGELE, J W and VOGT, E (eds) Advances in Nuclear Physics, Vol 12 Pp 258 ISBN 0-306-40708-6 (Plenum 1981) $35

NEWTON, R C , NAVROTSKY, A and WOOD, B J (eds) Thermodynamics of Minerals and Melts Advances in Physical Geochemistry, Vol 1 Pp 304 ISBN 3-540-90530-8 (Springer-Verlag 1981) DM 78, $35 50

PERLMUTTER, A (ed) Gauge Theories, Massive Neutrinos, and Proton Decay Studies in the Natural Sciences, Vol 18 Proceedings of Orbis Scientiae 1981, held by the Centre for Theoretical Studies, University of Miami, Coral Gables, Florida, January 1981 Pp 392 ISBN 0-306-40821-X (Plenum 1981) $49 50

VANASSE, G A (ed) Spectrometric Techniques, Vol II Pp 303 ISBN 0-12-710402-X (Academic 1981) $43

ZABOLITZKY, J G *et al* (eds) Recent Progress in Many-Body Theories Lecture Notes in Physics, Vol 142 Proceedings of the 2nd International Conference held at Oaxtepec, Mexico, January 1981 Pp 479 Flexi ISBN 3-540-10710-X (Springer-Verlag 1981) DM 52, $24 80

Chemistry

CAZES, J (ed) Liquid Chromatography of Polymers and Related Materials III Chromatographic Science Series, Vol 19 Pp 312 ISBN 0-8247-1514-4 (Marcel Dekker 1981) SwFr 108

FRIEDLANDER, G *et al* Nuclear and Radiochemistry 3rd Edn Pp 684 Hbk ISBN 0-471-28021-6, pbk ISBN 0-471-86255-X (Wiley 1981) Hbk £31, $55 90, pbk £18 90, $33 95

KAUFFMAN, G B Inorganic Co-ordination Compounds Pp 256 Hbk ISBN 0-85501-683-3, pbk ISBN 0-85501-684-1 (Heyden, London 1981) Hbk £12, pbk £5 50

MANN, B E and TAYLOR, B F ^{13}C NMR Data for Organometallic Compounds Pp 400 ISBN 0-12-469150-1 (Academic 1981) £15 80, $32 50

RAMSAY, O B Stereochemistry Pp 254 Hbk ISBN 0-85501-681-7, pbk ISBN 0-85501-682-5 (Heyden, London 1981) Hbk £12, pbk £5 50

TRENN, T J Transmutation–Natural and Artificial Pp 160 Hbk ISBN 0-85501-685-X, pbk ISBN 0-85501-686-8 (Heyden, London 1981) Hbk £12, pbk £5 50

VON BALLMOOS, R The ^{18}O-Exchange Method in Zeolite Chemistry Synthesis, Characterization and Dealumination of High Silica Zeolites Pp 235 Flexi ISBN 3-7935-5523-2 (Otto Salle Verlag, Frankfurt 1981) Np

Technology

BUTLER, E P and HALE, K F Dynamic Experiments in The Electron Microscope Practical Methods in Electron Microscopy, Vol 9 Pp 457 Hbk ISBN 0-444-80285-1, pbk ISBN 0-444-80286-X (Elsevier/North-Holland Biomedical, Amsterdam 1981) Hbk $95 25, Dfl 195, pbk $45, Dfl 92

DANCKWERTS, P V Insights into Chemical Engineering (Selected Papers of P V Danckwerts) Pp 307 ISBN 0-08-026250-3 (Pergamon 1981) £27, $65

FIECHTER, A (ed) Reactors and Reactions Advances in Biochemical Engineering, Vol 19 Pp 269 ISBN 3-540-10464-X (Springer-Verlag 1981) DM98, $44 60

MIDDLEDITCH, B S (ed) Environmental Effects of Off-shore Oil Production The Buccaneer Gas and Oil Field Study Marine Science, Vol 14 Proceedings of a Symposium held October 1980 during EXPOCHEM '80 in Houston, Texas Pp 446 ISBN 0-306-40826-0 (Plenum 1981) $49 50

MOORE, J G (ed) Scientific Basis for Nuclear Waste Management, Vol 3 Proceedings of the 3rd International Symposium held in Boston, Massachusetts, November 1980 Pp 632 ISBN 0-306-40803-1 (Plenum 1981) $49 50

MORAAL, J and KRAISS, K -F Manned Systems Design Methods, Equipment, and Applications Proceedings of a Conference held September 1980 in Freiburg, West Germany NATO Conference Series III Human Factors, Vol 17 Pp 487 ISBN 0-306-40804-X (Plenum 1981) $35

PICHLER, F R and TRAPPL, R (eds) Progress in Cybernetics and Systems Research Vol VI, Cybernetics in Biology and Medicine Systems Analysis, Systems Engineering Methodology, Mathematical Systems Theory Pp 416 ISBN 0-89116-194-5, ISBN 0-07-049846-6 (Hemisphere, New York/McGraw Hill 1981) $80

PROBSTEIN, R F and HICKS, R E Synthetic Fuels Pp 490 ISBN 0-07-050908-5 (McGraw-Hill 1981) $29 95

VON DER HARDT, P and RÖTTGER, H (eds) Commission of the European Communities Handbook of Materials Testing Reactors and Associated Hot Laboratories in the European Community Nuclear Science and Technology Pp 152 ISBN 90-277-1347-2 (Reidel 1981) Dfl 55, $24

Computer Science

DUFF, M J B and LEVIALDI, S (eds) Languages and Architectures for Image Processing Pp 300 ISBN 0-12-223320-4 (Academic 1981) £16 40, $39 50

HERMAN, G T Image Reconstruction from Projections The Fundamentals of Computerized Tomography Pp 316 ISBN 0-12-342050-4 (Academic 1981) $29 50

KATZ, P Digital Control Using Microprocessors Pp 293 ISBN 0-13-212191-3 (Prentice-Hall 1981) £16 95

LEWIS, R and TAGG, E D (eds) Computer Assisted Learning Scope, Progress and Limits Proceedings of the IFIP TC Working Conference, Roehampton, England, September 1979 Pp 223 ISBN 0-435-77700-9 (Heinnenan Educational, London 1981) £4 95

TANIMOTO, S and KLINGER, A (eds) Structured Computer Vision Machine Perception through Hierarchical Computation Structures Pp 234 ISBN 0-12-683280-3 (Academic 1980) $21

General

HOCKNEY, R W and EASTWOOD, J W Computer Simulation Using Particles Pp 540 ISBN 0-07-029108-X (McGraw-Hill 1981) £27 50

HUECK-VAN DER PLAS E H (ed) Chemosphere Chemistry, Biology and Toxicology as Related to Environmental Problems Special Issue Disposal of Chemical Waste in the Marine Environment Implications of the International Dumping Conventions Pp 505-716 Pbk ISBN 0-08-026289-9 (Pergamon 1981) Pbk £7 25, $16

JAKI, S L Immanuel Kant University Natural History and Theory of the Heavens Pp 302 ISBN 0-7073-0294-3 (Scottish Academic Press, Edinburgh 1981) £12 50

JAKLOVSKY, J Preparation of Nuclear Targets A Comprehensive Bibliography Pp 324 ISBN 0-306-65200-5 (IFI/Plenum 1981) Np

JOHANSSON, T B and STEEN, P Radioactive Waste from Nuclear Power Plants Pp 197 ISBN 0-520-04199-2 (University of California Press 1981) $15 95

KEPLER, J Mysterium Cosmographicum The Secret of the Universe Pp 267 ISBN 0-913870-64-1 (Abaris Books, New York 1981) Np

KUZNETSOV, B V (ed) Russian-English Polytechnical Dictionary About 90,000 terms Pp 723 ISBN 0-08-023609-X (Pergamon 1981) £45, $110

LEARMONTH, A T A (ed) The Geography of Health Pp 262 ISBN 0-08-027434-X (Pergamon 1981) £8 50, $20

LEWIS, G N J (ed) Proceedings of the Seminar, Environmental Quality The Industrial Dimension, held at the Harwell Laboratory, June 1980 Pp 212 (no ISBN) (AERE, Harwell, Oxfordshire 1981) Np

LIKENS, G E (ed) SCOPE 17 Some Perspectives of the Major Biogeochemical Cycles Published on behalf of SCOPE of the ICSU Pp 175 ISBN 0-471-27989-7 (Wiley 1981) £11, $74 95

LOWE, F R Milking Machines A Comprehensive Guide for Farmers, Herdsmen and Students Pp 181 Hbk ISBN 0-8-024381-9, flexi ISBN 0-08-024382-7 (Pergamon 1981) Hbk np, flexi £6 50, $13

MACDONALD, M Mystical Bedlam Madness, Anxiety and Healing in Seventeenth-Century England Pp 323 ISBN 0-521-23170-1 (Cambridge University Press 1981) £27 50

MARTIN, J Telematic Society A Challenge for Tomorrow Pp 244 ISBN 0-13-902460-3 (Prentice-Hall 1981) £9 70

MEYERHOFF, A A The Oil and Gas Potential of the Soviet Far East Pp 176 Flexi ISBN 0-901360-13-9 (The Scientific Press, Beaconsfield, Bucks 1981) Np

MICHAELS, M Stay Healthy with Wine Pp 246 ISBN 0-8037-8139-3 (Columbus Books, London 1981) £6 95

MITCHELL, A W Operation Drake Voyage of Discovery Pp 224 ISBN 0-7278-2007-9 (Severn House, London 1981) £12 95

ARTICLES

Convective growth rates of equatorial features in the jovian atmosphere

Garry E. Hunt, Jan-Peter Müller & Philip Gee

Laboratory for Planetary Atmospheres, Department of Physics and Astronomy, University College London, London WC1E 6BT, UK

The first results of measurements of divergence and vertical velocity of cloud features in the atmosphere of Jupiter are presented from analyses of Voyager images, performed using the interactive planetary imaging processing system at University College London Active equatorial plumes are found to have typical divergences of $\sim(1\text{–}2)\times10^{-5}\,s^{-1}$, *and vertical velocities of* $20\text{–}40$ *cm* s^{-1}, *during the observational periods examined These plumes are considerably more active than the bright albedo features in the turbulent regions of the jovian north and south equatorial belts*

OBSERVATIONS made by the Voyager imaging and IRIS instruments of the equatorial region of Jupiter have shown details of trains of white plume features moving in a westerly direction, with cloud material spreading out behind small bright centres of rising motion[1] The plume centres are positioned at about 9°N A total of 13 features were seen at the time of the Voyager 1 encounter, with four active centres[2] Four months later, in July 1979, at the time of the Voyager 2 encounter, the structure of this region had changed so that only 11 features were evident and three had active centres[3]

It has been suggested[1] that the plumes are mesoscale convective structures, formed as a travelling wave disturbance in a manner similar to that found in the Inter-Tropical Convergence Zone (ITCZ) of the Earth's atmosphere Indeed, there are indications[1,4] that these active plumes cause a major perturbation to the structure of the atmosphere from the cloud tops, throughout the troposphere and into the lower stratosphere This is a distance of at least 20 km, which is approximately the atmospheric scale height for Jupiter at this pressure level A major disturbance to the atmosphere of this type must be associated with rapid vertical motion in the atmospheric levels beneath the visible clouds themselves Furthermore, these plumes will have a significant effect on the energy budget of the equatorial region, through the mass transport of material associated with their morphological changes

We estimate in this article, for the first time, the divergence characteristics of these plumes using Voyager images analysed on the University College London (UCL) interactive planetary image processing system (IPIPS)[5] From this information, we calculate the vertical velocities which relate to the observed changes in the plume head structures These new measurements provide valuable insight into the development and variations in these mesoscale structures, which have an important role in the equatorial meteorology of the jovian atmosphere

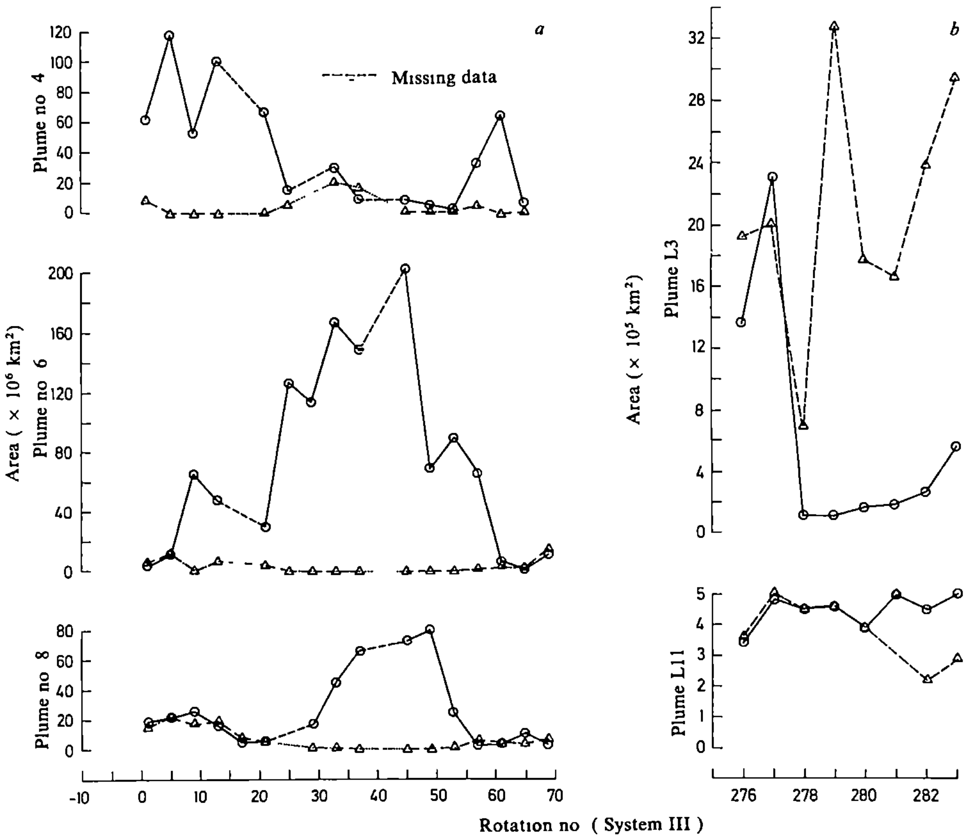

Fig. 1 The variation in the convective area of the three active plumes observed by Voyager 1(*a*) and for the two active plumes observed by Voyager 2(*b*) as a function of the rotation number for a single threshold level of brightness digital number (DN) = 185 (a, Δ) (b, Δ DN = 195) and the 90% contour level (O) of instantaneous maximum brightness

0028-0836/82/060491—04$01 00

Observations and data analysis

Observations obtained by the Voyager imaging system every 72° long (System III) during the observatory phases of each spacecraft encounter were used as a basis for this study The measurements for this investigation were taken from blue filter Mercator projection mosaics made from rotation periods 1–70 (6 January–2 February 1979) for Voyager 1, when the spatial resolution was 438 km per pixel with a temporal resolution of four rotation periods The rotation periods covered by Voyager 2 were 276–283 (24–28 May 1979), for which the spatial resolution was 138 46 km per line pixel, and the temporal resolution was every rotation period The images used were violet filter cylindrical map projection mosaics The rotation period reference system refers to the number of jovian days in System III longitude beginning with the first observations by the Voyager 1 spacecraft and continuing throughout the mission, concluding with the final measurements by Voyager 2 This is therefore a convenient scheme to represent the time variation of the observations during the 1979 Jupiter encounter

To remove the effects of the spacecraft viewing geometry and the illumination conditions, the full disk images were first radiometrically decalibrated and then map projected for the Voyager 2 observations The differences between these projections is negligible in the equatorial regions of Jupiter, where our analyses are performed The Sun angle illumination effects were removed at the Jet Propulsion Laboratory from these images using a Lambert function for Voyager 1, and a Hapke function for the Voyager 2 images (see, for example, ref 6) Then these photometrically decalibrated images were constructed into a mosaic to form sequential image maps of the entire planet for a full rotational period

With the observations in this format, we can carry out the meteorological investigations using the analysis techniques developed and carried out at UCL The bright albedo structures in the equatorial region certainly represent mesoscale convective structure[1] In the terrestrial atmosphere, Sikdar *et al*[7] and Sikdar and Suomi[8] have shown that the time variation of the visible brightness of a cloud anvil may be used to derive cloud-top divergences

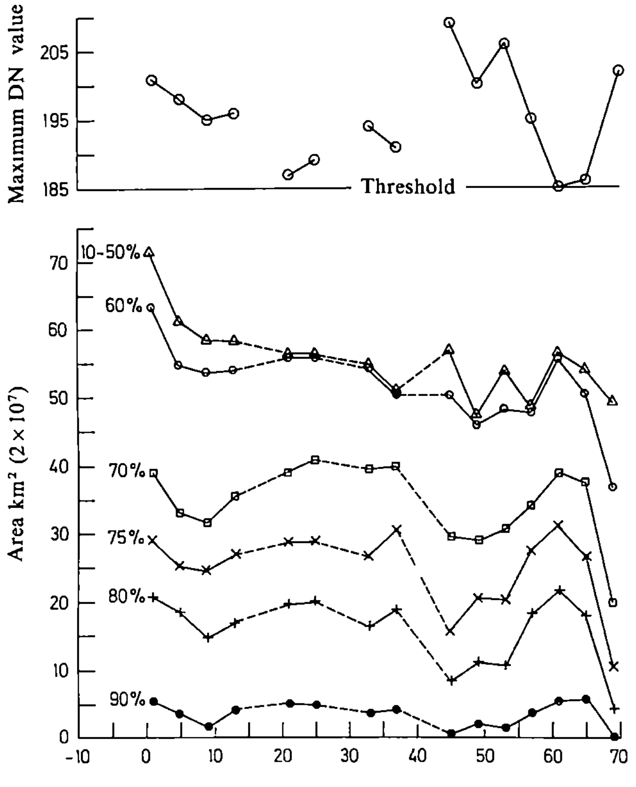

Fig. 2 The variation in the area of the bright albedo features in the turbulent region of the north equatorial belt (NEB) of Jupiter Individual contours are shown separately for areas calculated at 10–90% of the maximum brightness level for each rotation period, together with the value of the instantaneous maximum DN level

From the continuity equation, the rate of change of horizontal area, *A*, which represents the cross-section of the visible cloud system, is equal to the horizontal divergence This may be written as

$$\frac{1}{A}\frac{\mathrm{d}A}{\mathrm{d}T} = \mathrm{div_h}\,V \qquad (1)$$

Where $\mathrm{div_h}\,V = \partial u/\partial x + \partial v/\partial y$, and u, v are the x, y components of velocity[9,10] Then the time and area averaged divergence, $\mathrm{div_h}\,V$, is given by the expression

$$\frac{\ln(A_2/A_1)}{\Delta t} = \mathrm{div_h}\,V \quad \mathrm{s}^{-1} \qquad (2)$$

where the area of the layer of outflow has increased from A_1 to A_2 during the time interval $\Delta t = t_2 - t_1$

If we now use a scale analysis argument (see ref 10) and assume that the vertical motion in the layer of outflow takes place over less than or equal to a scale height *D*, then the vertical velocity required to produce the observed divergence field is given by

$$w \leq D\,\mathrm{div_h}\,V = \frac{D\ln(A_2/A_1)}{\Delta t} \quad \mathrm{ms}^{-1} \qquad (3)$$

We consider the measurement of the time rate of change of area of the ammonia cirrus anvil above the region of the updraft to be representative of the layer of outflow for the convective storm system and subsequently referred to as the 'convective area' Hunt *et al*[1] suggest that the main driving mechanism for the equatorial plume systems is provided by the latent heat released in the layers of water clouds that are thought to exist up to three scale heights beneath the visible ammonia clouds The depth of the total convective structure would therefore need to be a factor of two larger than terrestrial tropical cyclones

Fraedrich *et al*[9] showed that for tropical cloud clusters, the area of the convectively active region of a cloud system may be calculated using two methods Either (1) the brightness threshold remains constant throughout the sequence, or (2) the brightness threshold varies relative to the instantaneous maximum brightness in the cloud cluster We have examined these two procedures for the Voyager plumes using the IPIPS image processing facility[5] and find that procedure (1) is unsuitable for these studies Thus we have used procedure (2) to obtain divergence and vertical velocity estimates, as it was demonstrated to be more sensitive to the changes of the area of the convective core and not to gross brightness variations which were a function of the photometric decalibration, the mosaic image 'overlap' area of the errors inherent in the radiometric decalibration (see ref 6)

Results

We have studied the three active convective structures visible in the equatorial zone in the Voyager 1 sequence Figure 1*a* shows the considerable variation in the growth and dissipation of these active features Over the 70 rotation periods observed, two of these features changed in area by a factor of 40 The two sets of curves refer to the calculated areas for a threshold of 185 (on a maximum grey scale of 255) and the 90% of maximum brightness contour level The 90% contour level clearly shows the most active region of the convective structure, while the threshold reflects only gross brightness changes There were apparently less active plumes observed during the time period studied in the second Voyager encounter[1] We have measured two active plumes, shown in Fig 1*b*, and the 90% level seems again more representative of the areal changes in the convective area of these features than the threshold of 195 Once more, the rapid increase and decrease in the active areas is noticeable on relatively short time scales From the resolution of the images

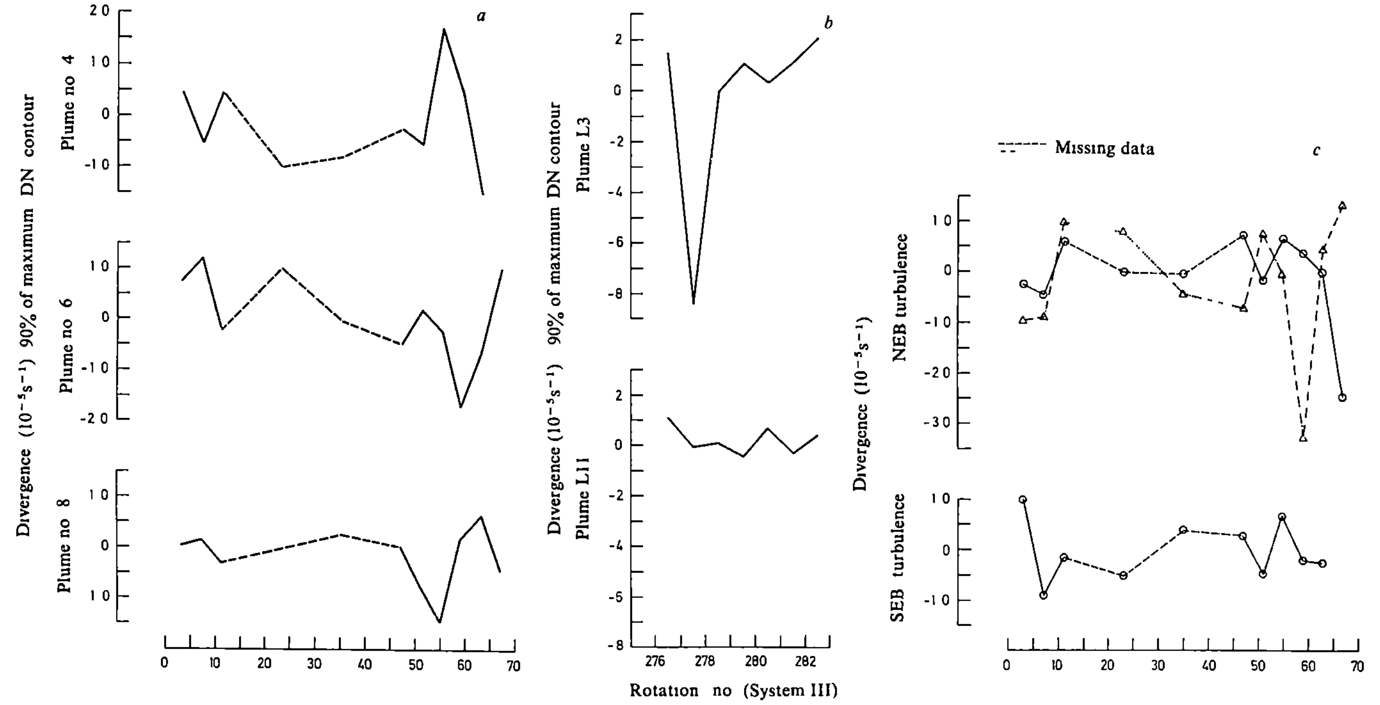

Fig. 3 The variation of divergence (10^{-5} s^{-1}) as a function of rotation number for *a*, the three active plumes observed by Voyager 1, *b*, the two active plumes observed by Voyager 2, *c*, the bright albedo features in the turbulent regions of north and south equatorial belts ○, 90% maximum DN contour, △, DN = 185 contour

used in this study the smallest area that may be resolved corresponds to ~4×10^4 km^2. This is ~10^{-2}% of the area of a whole plume. Smaller scale structure, such as the core of the 'convective area' cannot be resolved with this data set.

There are also regions of rapidly changing small-scale bright albedo features in the north and south equatorial belts of Jupiter (see, for example, refs 2, 3). To determine whether the variations of these features have any similarity with the plumes, we have analysed them using the same procedures. Figure 2 illustrates the changes in area of these active regions of the north equatorial belt. We show the variation in area for various percentages of the brightness maximum of the region along with the maximum brightness and the threshold level of 185 used. Although the actual areas are similar in magnitude (~10^7 km^2 for the 90% level) to the plume feature, there is a smaller variation in the area of the north equatorial belt. A similar situation is apparent from our analysis of the features in the south equatorial belt.

These changes in the convective areas of the plumes and features in the north and south equatorial belts may then be used to calculate the divergence from equation (2). Figure 3*a* shows the divergence variation for the three active plumes observed by Voyager 1. The maximum divergences are not in phase with one another and their values are not identical: the maximum value for plume 4 is 1.75×10^{-5} s^{-1} at rotation 55, while for plumes 6 and 8 the values are 1.25×10^{-5} s^{-1} at rotation 67, and 0.7×10^{-5} s^{-1} at rotation 63, respectively. The features observed during the Voyager 2 encounter have divergences of about $(1–2)\times10^{-5}$ s^{-1}. On rotation 1, the 'active' centres of plumes 4, 6 and 8 were located at approximately 138°, 197° and 267° long (System III). On rotation 276 the 'active' centres of plumes L3 and L11 were located at 317° and 131° long (System III).

The negative values of divergence which appear in Fig 3*a*, do not correspond to convergences, but to evaporation at the edges of the plume heads.

The analyses by Hunt *et al*[1] and Conrath *et al*[4] have shown that the plumes are mesoscale disturbances that cause a significant perturbation to the vertical temperature structure throughout the jovian troposphere above the visible clouds and into the lower stratosphere. It is possible that the entire region from 50 to 1,000 mbar may contain clouds of ammonia condensates of varying opacities as Sato and Hansen[11] suggest. The clouds which constitute the plumes, would therefore be contained in a larger portion of this region and may extend more than 40 km from the base of the water cloud to the base levels of the ammonia cirrus anvil. The anvil cloud itself will extend at least a further 20 km which is consistent with jovian cloud models[12]. The outflow from the convective disturbance which we see in the Voyager images as the plume tail is more than 500 times the possible vertical depth of the plumes. The jovian plume then closely resembles the terrestrial large scale convective cloud system, but on a much greater scale.

We therefore scale the measured divergence values by the minimum depth of the convective flow, which we estimate to be about 20 km. With this value, we see that the larger vertical velocities are about 20–40 cm^{-1}. These values represent the vertical motion of an area of the plumes whose cross-section is several thousand kilometres and certainly consistent with the values found in terrestrial convective storms (see for example, ref 10). Note that Adler and Fenn (see ref 12) showed that the maximum updraft may be as much as two orders of magnitude greater than that implied by the scaling argument used here. Our derived values may therefore be an underestimate of the true vertical motions. Furthermore, the magnitude of vertical motions, associated with individual cloud turrets in the convective area, would certainly be large enough to create 'horizontal' gravity waves downstream of the convective activity, as was observed[13] in the tail of one of these active plumes.

The major driving mechanism for these features must come from the latent heat released by condensation of water in the cloud layer, located some three density scale heights beneath the visible convective area[12]. The modelled top of the ice cloud was shown to be at a temperature of around 210 K (ref 12). Hunten *et al*[14] have modelled the observed IR opacities and produced a vertical temperature profile which shows that at this temperature the pressure is at ~2.5 bar. In addition, their calculations show that the dominant heating up to the 2 bar level is solar. At higher pressures, internal heating is the only possible source for triggering convective activity. It has been suggested[15] that only small amounts of internal heating anomalies are required to produce vertically propagating gravity waves which may trigger convective activity This may lead to further sub-cloud convergence due to the convective environment initiating in a wave-mean flow interaction This could then provide the necessary criteria for setting up an equatorially travelling-wave disturbance

Conclusions

We have measured for the first time the growth rate of convective cloud features in the equatorial region of the jovian atmosphere The equatorial plumes seem to possess many of the characteristics of the large-scale convective cloud systems observed in the Earth's tropical regions The vertical velocities associated with these features are similar in magnitude to the terrestrial systems However, the jovian clouds occupy a much larger spatial scale

The disturbances seen in the turbulent regions of the north and south equatorial belts are much less active than the equatorial features It is possible therefore that these features are shallower in this region of the atmosphere Furthermore, this situation may also be related to their shorter lifetime

In both situations, the convective activity seems to be generated from travelling wave disturbances in the jovian atmosphere The intensity of the convection in the equatorial plumes and the magnitude of the divergence and vertical velocities derived for these features is consistent with them being generated by large-scale convergence in deep cloud layers beneath the visible surface of the planet

We thank Glenn Garneau, Erik Korsmo and Gary Yagi for assistance This research is supported by the UK Science and Engineering Research Council

Received 28 April, accepted 8 December 1981

1 Hunt, G E, Conrath, B J & Pirraglia, J A *J geophys Res* **86**, 8777–8783 (1981)
2 Smith, B A *et al Science* **204**, 951–972 (1979)
3 Smith, B A *et al Science* **206**, 927–950 (1979)
4 Conrath, B J, Flasar, F M, Pirraglia, J A, Gierasch, P J & Hunt, G E *J geophys Res* **86**, 8769–8776 (1981)
5 Hunt, G E *et al Phil Trans R Soc* (in the press)
6 Jepson, P *et al J Br interplanet Soc* **33**, 315–320 (1980)
7 Sikdar, D N, Suomi, V E & Anderson, C E *Tellus* **22**, 521–532 (1970)
8 Sikdar, D N & Suomi, V E *J atmos Sci* **28**, 170–180 (1971)
9 Fraedrich, K, Ruprecht, E & Trunte, U *J appl Met* **15**, 1312–1316 (1976)
10 Holton, J *An Introduction to Dynamical Meteorology* (Academic, New York, 1973)
11 Sato, M & Hansen, J E *J atmos Sci* **36**, 1133–1167 (1979)
12 Lewis, J *Icarus* **10**, 365–378 (1969)
13 Hunt, G E & Muller, J-P, *Nature* **280**, 725–804 (1979)
14 Hunten, D M, Tomasko, M & Wallace, L *Icarus* **43**, 143–152 (1980)
15 Muller, P & Hunt, G E *Pap at the COSPAR Meet* Innsbruck (1980)
16 Lindzen, R S *J atmos Sci* **31**, 156–179 (1974)

Glacial to interglacial contrasts in the northern Indian Ocean

J. C. Duplessy
Centre des Faibles Radioactivités, Laboratoire mixte CNRS–CEA, 91190 Gif sur Yvette, France

Differences between the ^{18}O/^{16}O ratios of planktonic foraminifera deposited during the last glacial maximum, about 18,000 yr ago, and those deposited during the Holocene show that in the Indian Ocean, the south-west monsoon was weaker than today but that the north-east monsoon was stronger The upwelling observed in modern conditions along the southern coast of Arabia had disappeared because of the low speed of the southwestern winds during glacial summers. The reduction in rainfall and runoff over the continent caused a reduction of the salinity gradient in the Bay of Bengal and along the western coast of India Increased precipitation fell on the sea south of 10° N, while strong evaporation over the northernmost Arabian Sea produced an enhanced salinity gradient in that area

THE seasonally varying monsoon circulations associated with the annual heating and cooling of the Asian continent are important aspects of the general circulation of the atmosphere During the summer, as solar radiation warms the land and the ocean, the overlaying air is heated by conduction and expands because the land heats faster than the ocean The warmer air over the land rises and is replaced by denser ocean air which carries moisture evaporated from the ocean When the moist air moves inland, it too rises and its water vapour condenses causing heavy rain over the continent The circulation of the monsoon winds is deflected by the rotation of the Earth through the Coriolis force, which deflects winds to the right in the Northern Hemisphere so that summer monsoon winds essentially blow from the south-west With the onset of winter, both the land and the ocean lose heat by radiation to space The greater heat capacity of the ocean results in a greater cooling over the continent than over the ocean so that dry winds blow from the continent to the ocean Due to the rotation of the Earth, winter winds blow from the north-east The north-east monsoon continues in a steady state until solar heating of the spring dissipates the temperature gradient that powers the winter monsoon

This monsoon climate that prevails over the northern Indian Ocean produces large salinity gradients in surface waters, although sea-surface temperatures, which are largely determined by the amount of radiation received from the Sun, are much less variable As freshwater is depleted in the heavy isotopes of oxygen compared with seawater, the modern salinity pattern for surface waters is closely matched by the oxygen isotopic composition of recent Holocene calcitic tests of surface dwelling foraminifera such as *Globigerinoides ruber* During the

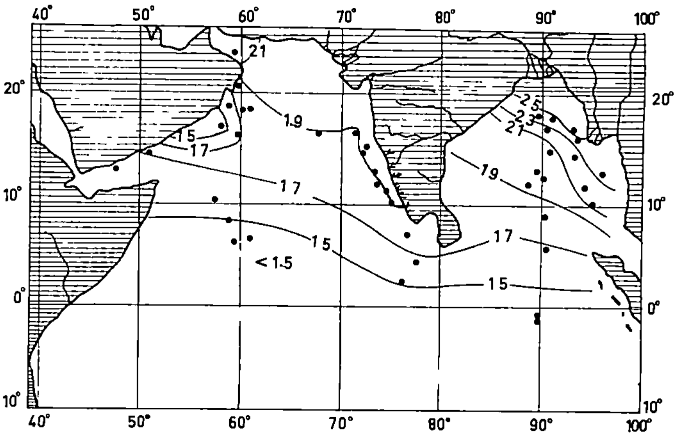

Fig. 1 *a*, Map of mean annual sea-surface salinity in modern times computed from monthly data collected by Wyrtki[3] *b*, Map of *G ruber* δ^{18}O values during Holocene time ●, Location of deep-sea core samples *, Location of trigger weight core-top samples *c*, Map of *G ruber* δ^{18}O values at the last glacial maximum iso-δ^{18}O lines have been drawn by hand by interpolating between the control points

0028-0836/82/060494—05$01 00

last ice age, which reached its maximum ~18,000 yr ago[1,2] only small changes in the northern Indian Ocean temperature pattern have been recorded[2–4], but important variations in the precipitation pattern over the surrounding continents have been evident[5–7]. I now reconstruct the major hydrological trends, essentially that of salinity, in the northern Indian Ocean during the last glacial maximum by comparing maps of the oxygen isotopic composition (δ^{18}O) of planktonic foraminifera that lived in surficial waters during the Holocene and at the last glacial maximum.

Modern hydrological setting

Today, the northern Indian Ocean is characterized by a strong salinity contrast between its two major basins, the Arabian Sea and the Bay of Bengal[8]. The heavy summer monsoon rain above the south-west Asian continent is collected by major rivers (Ganges, Brahmaputra, Irrawaddy and Salween) which drain into the northern end of the Bay of Bengal and the Andaman Sea. Because this area receives a large excess of direct precipitation, its low salinity surface water contrasts sharply with high salinity surface water of the Arabian Sea where evaporation is high (Fig. 1*a*). Due to this general pattern of evaporation–precipitation, isohalynes show generally east–west trends, but along the western coast of India they turn north–south. This local pattern is due to two major freshwater inflows[9]. The first is the heavy rain which falls above the western flank of the Dekkan Mountains during the summer monsoon and is drained to the sea along the coast of Kerala, south-west India, by a dense net of mountain rivers. The second is the transport of low-salinity water from the Bay of Bengal into the eastern Arabian Sea during the north-east monsoon. Thus low-salinity water is found along the coast from July to February[10], and means that the general pattern of mean annual sea-surface salinity in the northern Indian Ocean is closely related to the monsoon circulations.

The sea-surface temperature gradient is much weaker than that of salinity. During the north-east monsoon, a rather gentle phenomenon, the oceanic circulation is only moderately strong[8]. No striking upwelling areas develop and the sea-surface temperature pattern is essentially zonal, with temperature decreasing progressively towards the north[10]. The more vigorous atmospheric and oceanic circulation during the south-west monsoon causes intense upwelling along the coast of Arabia. This upwelling which brings cool, nutrient-rich deep water in the surface, is characterized by a strong drop of sea-surface temperature which falls below 24 °C in the proximity of the coast of Arabia north of 15° N (ref. 11). This produces a strong temperature gradient perpendicular to that coast. As the upwelling is restricted to the summer period, when the winds blow parallel to the coast, the sea-surface temperature gradient linked with the coastal upwelling is another good indicator of the intensity of the south-west monsoon circulation.

Isotopic strategy

The modern hydrological setting of the northern Indian Ocean is closely related to the monsoon. Therefore, the reconstruction of historical geographical variations of sea-surface salinity and upwelling areas should be an effective way of estimating the intensity of the south-west monsoon in climatic conditions different from those of today. Present palaeooceanographic reconstructions of the Arabian Sea and the Bay of Bengal essentially deal with sea-surface temperature[2–4], which show upwelling variations during the last climatic cycle[2,3,12], but past sea-surface salinity has been estimated along only one north–south transect in the Bay of Bengal[13]. We have mapped the geographical distribution of the oxygen isotopic composition (δ^{18}O) of planktonic foraminifera that lived in surficial waters during Holocene time and at the last glacial maximum. Planktonic foraminiferal δ^{18}O is controlled in a complex way by sea-surface water δ^{18}O and temperature[14–17]. In upwelling areas, the δ^{18}O variations should mainly reflect the sea surface temperature gradient, the slope of which is linked to the intensity of upwelling and the wind strength. Except for the Arabian coast, upwelling is not significant in the northern Indian Ocean, and temperature gradients are small in modern conditions[10], and have remained small during the Upper Quaternary while the global climate varied[1,2,4]. Hence geographical variations of planktonic foraminifera δ^{18}O in the northern Indian Ocean should essentially reflect the sea-surface water δ^{18}O.

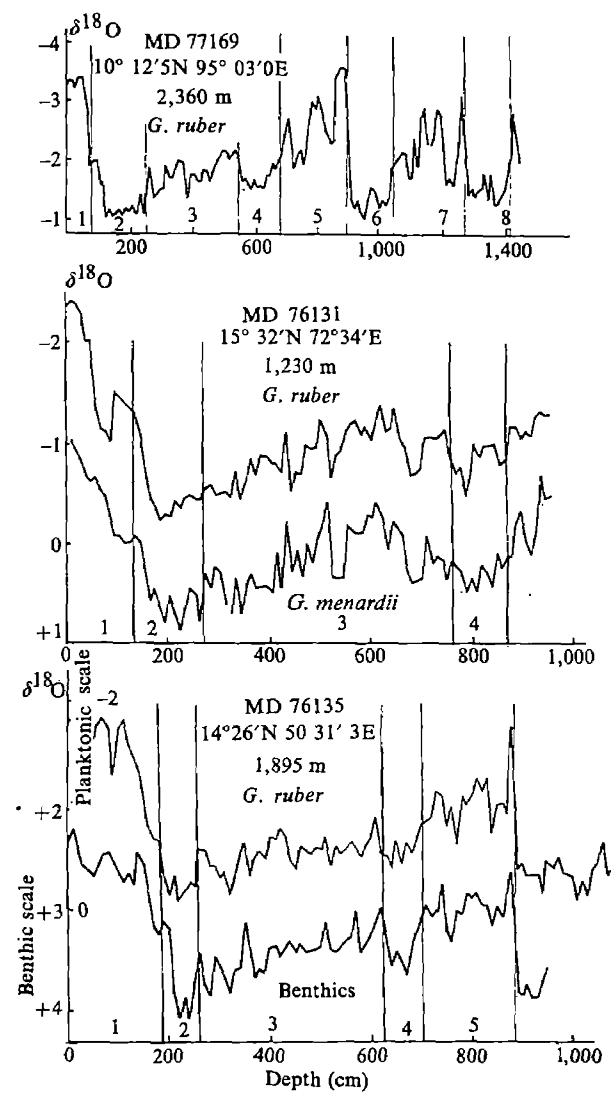

Fig. 2 Isotopic record of three cores from the northern Indian Ocean: cores MD 77169 (the Andaman Sea), MD 76131 (the Eastern Arabian Sea) and MD76135 (the Gulf of Aden). Odd and even numbers refer to interglacial and glacial stages as defined by Emiliani[27]. *Globorotalia menardii* is a deep foraminifera which, like benthic foraminifera, is not sensitive to the variations of temperature and salinity in the euphotic zone[14].

Surface waters of the oceans have widely different δ^{18}O which are related to salinity[17–20]. In general, tropical waters have a high salinity and are isotopically heavy, owing to the preferential loss of the isotopically light molecule $H_2{}^{16}O$ and the concentration of the isotopically heavy molecule $H_2{}^{18}O$ in the residual sea-surface water. In the atmosphere, cooling of the vapour causes condensation and precipitation. The oxygen isotopic composition of the first condensed rain will be enriched in ^{18}O compared with the atmospheric water vapour, but its δ^{18}O will be slightly lower than that of surficial sea water[21] due to the low condensation temperature and the relative humidity of the atmosphere which is far from saturation[18]. A further ^{18}O depletion in rain falling over the continent can be explained by considering the formation of precipitation as a Rayleigh process, whereby with continuing precipitation from an air mass the remaining water vapour is progressively depleted in ^{18}O (refs 18, 21).

Hence a linear relationship between sea-surface salinity and $\delta^{18}O$ is observed locally. The gradient of the isotope–salinity relationship depends on the mode of formation of the freshwater arriving into the sea: it is small for a first condensation rain falling over the ocean, whereas it is much larger for the outflow of rivers fed by rain falling over cold mountains[18,21,22]. This slope can be determined experimentally in modern conditions, but we have no way to determine it accurately in the past. Hence I consider only a qualitative discussion.

Data base

The oxygen isotopic composition of the foraminiferal species *G. ruber* was measured in 41 piston cores and 36 core-top samples from the Arabian Sea, the Bay of Bengal and the Andaman Sea, of which 12 are from ref. 3. This species was chosen because it secretes most of its carbonate in the surficial mixed layer[17]. About 30–40 shells were separated for each stable isotope analysis. The shells were roasted under vacuum at 50 °C and evolved CO_2 was analysed in a VG Micromass mass spectrometer[23,24].

Downcore analyses were performed every 10 cm to obtain an accurate stratigraphy for the deep-sea sediments. Isotopic stratigraphy is based on the demonstration that downcore variations in the oxygen isotope composition of foraminiferal shells reflect primarily variations in the continental ice volume[23,25,26]. Because these variations are synchronous within the mixing time of the world ocean, sediment deposited during the last glacial maximum can be recognized by the youngest $\delta^{18}O$ maximum in the isotopic record. Variations in local factors, such as temperature, evaporation–precipitation pattern and continental runoff, also affect the isotopic composition of planktonic foraminifera living in the most surficial water. This is the case for *G. ruber*. The pattern of isotopic changes in the northern Indian Ocean for this species was therefore checked to show that it was similar to that of the rest of the world ocean. First, for a few cores, downcore analyses were extended beyond the last climatic cycle. The isotopic records closely correlate with the standard sequence of stages defined by Emiliani[27], an indication that local effects in the northern Indian Ocean did not modify the generalized pattern of isotopic change during the Upper Quaternary (Fig. 2). Second, the isotopic record of *G. ruber* was compared with that of benthic or deep dwelling planktonic foraminifera. Although the amplitude of the *G. ruber* record was generally much larger than that of deep species (Fig. 2), the general trends of the records are similar. Therefore the last glacial maximum level in

Table 1 Location of piston cores used for the Holocene and last glacial maximum reconstructions

Core	Lat.	Long. E	Depth (m)	$\delta^{18}O$ Holocene	$\delta^{18}O$ Glacial
MD 76127	12°05′ N	75°54′	1,610	−2.17	−0.54
MD 76128	13°08′ N	73°19′	1,712	−2.44	−0.46
MD 76129	15°00′ N	72°20′	1,954	−2.28	−0.35
MD 76131	15°32′ N	72°34′	1,230	−2.38	−0.26
MD 76132	17°00′ N	71°31′	1,430	−2.13	−0.24
MD 76135	14°27′ N	50°31′	1,895	−1.90	−0.18
MD 76136	12°52′ N	46°49′	1,649	−1.81	−0.28
MD 77169	10°13′ N	95°03′	2,360	−3.14	−1.02
MD 77171	11°46′ N	94°09′	1,760	−3.24	−0.99
MD 77176	14°31′ N	93°08′	1,375	−3.18	−1.17
MD 77177	16°25′ N	93°24′	2,284	−3.41	−1.02
MD 77178	17°12′ N	93°05′	2,459	−3.70	−1.12
MD 77179	18°22′ N	91°01′	1,986	−3.50	−1.02
MD 77180	18°28′ N	89°51′	1,986	−3.41	−0.90
MD 77181	17°24′ N	90°29′	2,271	−3.34	−0.99
MD 77191	07°30′ N	76°43′	1,254	−2.61	−0.84
MD 77194	10°28′ N	75°14′	1,222	−2.56	−0.68
MD 77195	11°30′ N	74°32′	1,426	−2.55	−0.57
MD 77200	16°33′ N	67°54′	2,910	−1.77	+0.13
MD 77202	19°13′ N	60°41′	2,427	−1.92	−0.08
MD 77203	20°42′ N	59°34′	2,442	−1.79	+0.07
MD 77204	19°18′ N	58°26′	1,430	−1.71	−0.13
ORKS 08	23°28′ N	59°11′	2,700	−1.58	+0.55
ORKL 10	17°29′ N	37°30′	2,390	−1.71	−0.30
RC 9 162	19°05′ N	60°25′	3,092	−1.94	−0.17
RC 12 339	09°08′ N	90°02′	3,010	−2.65	−0.93
RC 12 340	12°42′ N	90°01′	3,012	−2.84	−1.04
RC 12 341	13°03′ N	89°35′	2,988	−2.71	−0.75
RC 12 343	15°10′ N	90°34′	2,666	−2.84	−1.04
RC 12 344	12°46′ N	96°04′	2,140	−3.28	−0.88
RC 14 35	00°50′ S	89°57′	3,021	−2.25	−0.51
RC 14 36	00°28′ S	90°00′	3,076	−2.25	−0.93
RC 14 39	05°51′ N	90°31′	2,952	−2.64	−0.94
V 14 101	08°39′ N	58°34′	2,849	−2.10	−0.54
V 14 102	10°15′ N	57°11′	3,915	—	−0.67
V 19 185	06°42′ N	59°20′	2,867	−2.16	−0.70†
V 19 188	06°52′ N	60°40′	3,356	−1.82	−0.55
V 29 15	11°57′ N	88°44′	3,173	−2.68	−0.74
V 29 29	05°07′ N	77°35′	2,673	−2.36	−0.68
V 29 30	03°05′ N	76°15′	3,651	−2.34	−0.81
V 34 88	16°31′ N	59°32′	2,120	−1.94	−0.27

The oxygen isotopic composition of *G. ruber* for Holocene and glacial times are reported as $\delta^{18}O$ versus PDB.

† Value taken from ref. 2.

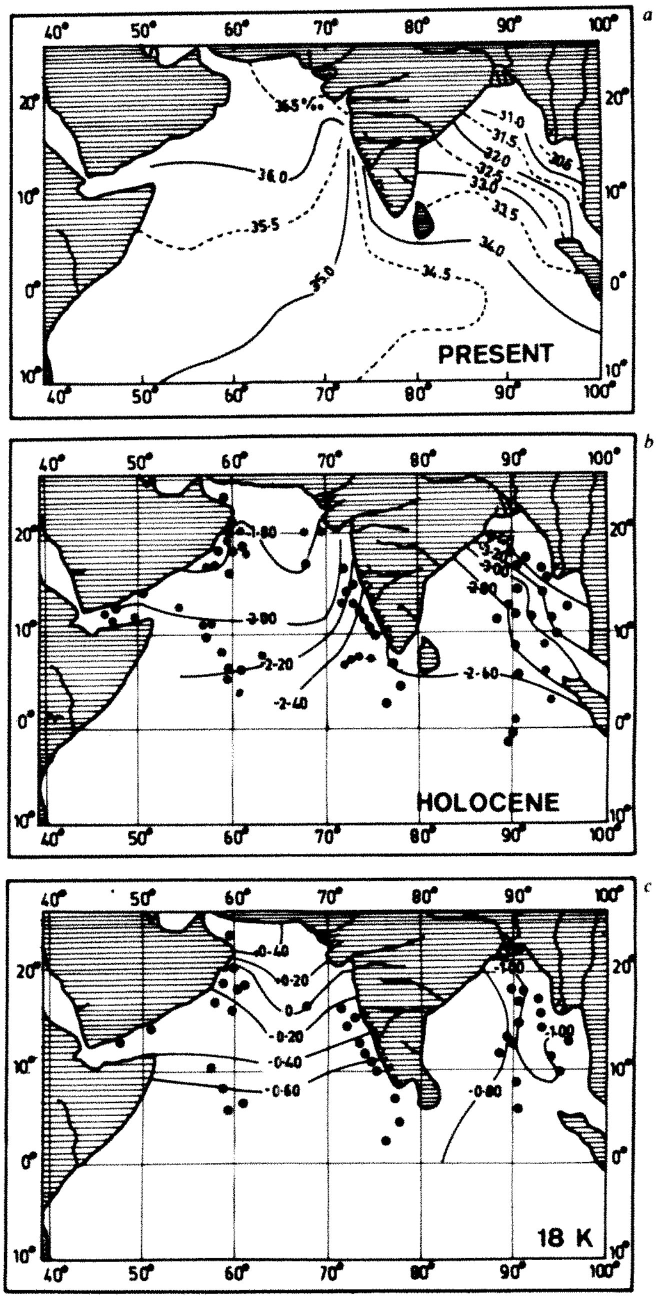

Fig. 3 Amplitude of $\delta^{18}O$ variations between the last glacial maximum (Isotope Stage 2) and the Holocene (Stage 1).

the sediment cores can be recognized from the planktonic record as well as from the benthic record.

The synchrony of the Indian Ocean isotopic records was recently checked by ^{14}C dating in six cores[2]. The mean age of the maximum glaciation was $\sim$18,000 yr BP with a standard deviation of 1,500 yr. If the climate and the global ice volume were changing rapidly around 18,000 yr BP, there might be serious inaccuracies in the estimates of the $\delta^{18}O$ value at the last glacial maximum. However, high sedimentation rate deep sea cores suggest that the interval 22,000–15,000 yr BP was characterized by relatively stable conditions[24,27–29].

Holocene reconstruction

The data used to construct the Holocene map (Fig. 1*b*) represent the mean value of Holocene levels for each piston core: digital values are reported in Table 1. In four cores, the uppermost levels show evidence of strong dissolution and a correlative $\delta^{18}O$ increase during the end of the Holocene. Such an increase can be explained by the preferential removal through dissolution of fragile individuals[31,32] whose tests were not overlain by a thick calcitic crust deposited during gametogenesis. As gametogenetic calcification occurs at great depth, below the euphotic zone, and in cold water, the tests under the thicker crust are also isotopically heavier[33]. Hence the fossil population remaining in a deeply dissolved sediment is isotopically heavier than the undissolved fauna. Such a $\delta^{18}O$ increase is not evidenced in other nearby cores that are free from dissolution. Therefore the enriched levels were rejected in calculating the mean Holocene $\delta^{18}O$ value. Core top samples were also used to complete the Holocene map but stratigraphical control for those samples is not available and some scatter is inevitable in such a data set. Nine core-tops were rejected because their $\delta^{18}O$ did not fall within the range of values for nearby core that were verified by oxygen isotope stratigraphy. These samples were collected from the 90° E ridge and from the central Arabian Sea, where sedimentation rates are very low, and probably did not represent the most recent sediment. Consequently, iso-$\delta^{18}O$ map for the Holocene (Fig. 1*b*) is based on measurements of *G. ruber* $\delta^{18}O$ from 68 locations. The standard deviation of a single analysis is 0.07‰ (ref. 24). Although most $\delta^{18}O$ values were calculated as mean value of several intervals, variations of 0.1‰ were not considered significant and iso-$\delta^{18}O$ lines have been drawn separated by 0.2‰.

The map of *G. ruber* $\delta^{18}O$ in the northern Indian Ocean during the Holocene (Fig. 1*b*) reveals the major features of the mean annual salinity in modern conditions. In the Bay of Bengal, the $\delta^{18}O$ values decrease progressively towards the mouth of the Ganges, Brahmaputra, Irrawaddy, Salween River system, clearly reflecting the salinity pattern. The low-salinity waters along the southwestern coast of India are also well recorded in the *G. ruber* $\delta^{18}O$ values that are $\sim$0.5‰ isotopically lighter than values from the same latitude in the central and western Arabian Sea. The general north–south $\delta^{18}O$ increase in the Arabian Sea also fits the salinity pattern and reflects the strong evaporation excess in this basin. The only misfit between the salinity and $\delta^{18}O$ patterns is observed in the western Arabian Sea along the coast of Arabia. As the oxygen isotopic composition of the foraminifera shells depends on the seawater temperature, the observed *G. ruber* $\delta^{18}O$ increase reflects the strong temperature drop due to coastal upwelling which brings cool, nutrient-rich deep waters in the surface[38]. To summarize the Holocene pattern, from south to north, *G. ruber* $\delta^{18}O$ values decrease by 1.1‰ in the Bay of Bengal and increase by 0.8‰ in the Arabian Sea whereas mean annual sea-surface salinity decreases by 3‰ in the Bay of Bengal and increases by 1.5‰ in the Arabian Sea. The proportionality coefficient between $\delta^{18}O$ and salinity is not the same in the two basins because the mechanisms which produce the isotopic changes are different: dilution with freshwater in the Bay of Bengal and evaporation in the Arabian Sea.

Isotopic pattern during the last glacial maximum

$\delta^{18}O$ values for the last glacial maximum (Fig. 1*c*) were calculated as mean values of the isotopic stage 2 maximum and are reported in Tables 1 and 2. Dissolution was systematically lower during glacial time than during Holocene time and no sample was rejected for dissolution bias, so that iso-$\delta^{18}O$ map for glacial conditions is based on measurements of *G. ruber* $\delta^{18}O$ for 41 locations.

Glacial *G. ruber* $\delta^{18}O$ values are significantly heavier than those of Holocene time. This strong isotope enrichment primarily reflects the waxing of large continental ice-sheets, depleted in ^{18}O, and which extensively covered northern Europe and North America[1,25,26]. The amplitude of this glacial effect is $\sim$1.6‰ (refs 24, 28, 34), the remaining part of the ^{18}O enrichment is due to local surface seawater salinity and temperature changes. Temperature changes have been rather small in the northern Indian Ocean during the past 25,000 yr (ref. 2). At the last glacial maximum, mean annual sea-surface temperatures for the Bay of Bengal were $\sim$1 °C lower than modern values, while those from the Arabian Sea were almost the same or warmer than those of today. Geographical variations of *G. ruber* $\delta^{18}O$ values at the last glacial maximum will therefore mainly reflect the mean annual sea-surface salinity pattern.

The ice-age *G. ruber* $\delta^{18}O$ map (Fig. 1*c*) reveals striking differences with the modern pattern.

(1) A marked reduction in the $\delta^{18}O$ gradient observed in the Bay of Bengal and the Andaman Sea is probably associated with

Table 2 Location of core-tops and oxygen isotopic composition of *G. ruber* used for the Holocene reconstruction

Core	Lat. N	Long. E	Depth (m)	$\delta^{18}O$ Holocene
A 15585	20°09′	69°26′	216	−1.85*
A 15586	20°07′	67°55′	3,047	−1.87*
A 15591	21°00′	59°33′	1,267	−1.48*
A 15592	20°50′	61°01′	2,628	−1.55*
A 15596	18°56′	61°23′	3,694	−1.80*
A 15597	17°26′	57°11′	1,805	−1.50*
A 15612	13°35′	71°34′	1,697	−1.95*
Dodo 204	03°09′	94°06′	2,150	−2.57
MD 77164	06°05′7	93°37′3	2,140	−2.89
MD 77185	12°24′	92°03′7	1,461	−3.07
MD 77197	13°11′	73°26′	1,260	−2.46
RC 9 155	07°24′	72°48′	1,765	−2.57
RC 9 161	19°34′	59°36′	3,332	−1.61*
RC 12328	03°57′	60°36′	3,087	−2.33
RC 12347	09°20′	93°20′	1,533	−2.78
RC 14 37	01°28′	90°10′	2,226	−2.86
RC 17126	07°—	72°—	1,723	−2.47
V 14103	11°27′	56°14′	4,232	−2.00
V 14104	13°26′	53°27′	2,670	−1.98
V 14106	12°52′	48°25′	2,144	−2.17
V 14107	11°51′	46°45′	1,608	−2.23
V 14108	12°37′	45°38′	1,176	−2.41
V 19177	07°35′	74°13′	2,770	−2.37
V 19178	08°07′	73°15′	2,188	−2.49/−2.58*
V 19183	08°07′	62°47′	4,451	−2.09
V 34 80	06°07′	59°26′	3,292	−1.85
V 34 85	11°48′	57°37′	3,190	−1.86
A 15558	08°59′	51°44′	3,985	−1.44†
Dodo 197	02°58′	88°51′	4,017	−1.73†
Dodo 200	02°55′	91°03′	3,472	−2.15†
Dodo 201	02°59′	91°41′	4,131	−2.26†
RC 12329	02°59′	65°12′	3,864	−1.09†
RC 12331	02°30′	69°52′	3,941	−1.44†
RC 14 39	05°51′	90°31′	2,952	−2.42†
V 19176	07°07′	76°33′	1,773	−2.34†
V 19184	07°26′	61°04′	3,471	−0.58†

* Value taken from ref. 3.

† Rejected value.

a decrease in river discharge into the northern end of this basin. The isotopic result supports independent sea-surface salinity estimates deduced from faunal analysis[13]. The shape of the tongue of low salinity water (marked by the line $\delta^{18}O = -1‰$) suggests that in the Bay of Bengal the clockwise circulation linked to the north-east monsoon[35] dominates the mean annual water circulation. The occurrence of a strong north-east monsoon during glacial conditions is supported by independent pollen evidence[30].

(2) The glacial *G. ruber* $\delta^{18}O$ pattern for the Arabian Sea is much more zonal than the modern one because within the same latitudinal belt, *G. ruber* $\delta^{18}O$ values are similar. This uniform latitudinal distribution is related to the disappearance of both the low salinity–low $\delta^{18}O$ area along the southwestern coast of India and the cool-high $\delta^{18}O$ upwelling area along the coast of Arabia[3]. Both trends are likely to be associated with a reduction of the south-west monsoon wind regime.

(3) A marked increase in the *G. ruber* $\delta^{18}O$ gradient is observed in the Arabian Sea. This strong glacial isotope gradient which is larger than 1‰ (compare with the modern one which is only 0.8‰) is not related to the geographical distribution of the sea-surface temperatures which have been shown to be more uniform than today[24] but indicates a strong salinity increase from south to north. The map of the amplitude of $\delta^{18}O$ change between the last glacial maximum and the Holocene (Fig. 3) shows marked latitudinal variations. In the Arabian Sea, this amplitude is lower than the ice volume effect alone (1.6‰) south of 10° N. Such a low amplitude is not due to bioturbation as it is found in cores with sedimentation rates larger than 2–3 cm kyr^{-1} (core V 19 188; V 2930). Because no major rivers outflow south of 10° N in the northern Indian Ocean, this low amplitude would reflect a marked precipitation increase over oceanic regions south of 10° N. Towards the north, the glacial–interglacial $\delta^{18}O$ amplitude increases. In the Bay of Bengal, this pattern clearly reflects the low river discharge during glacial conditions. In the Arabian Sea, it reflects stronger evaporation over its northernmost area and the Gulf of Oman. This stronger evaporation is probably linked to reinforced dry northeastern winds which blew from the continent to the ocean and to the warming of the Arabian Sea resulting from the reduction of the upwelling along the coast of Arabia which is clearly marked in Fig. 3 by an area of reduced $\delta^{18}O$ amplitude.

Conclusions

The isotopic reconstruction of the last ice age for the northern Indian Ocean indicates a weaker south-west monsoon. This would cause less precipitation over the Indian subcontinent, much of the Himalayas, the eastern and southern Tibetan uplands and Bangladesh which are drained by the Ganges, Brahmaputra, Irrawaddy and Salween rivers. This pattern is confirmed by continental evidence which shows that, at this time, the Persian Gulf region[36] and the Rajasthan[37] were dry, the Zagros Mountains in the north were drier than they are today[38] and strong loess storms occurred in the cold sand deserts of Inner Asia[39–41]. This result is consistent with the widespread aridity in tropical Africa[5,6,42,43] and dune activity in Arabia and northwestern India[41]. Continental aridity contrasted sharply with heavy oceanic precipitation south of 10° N, a pattern which supports the simulation of the tropical climate of the last ice age made with the GFDL general circulation model of the atmosphere[44]. The oceanic reconstruction provides weak indications that the north-east monsoon was stronger than today in glacial conditions. The occurrence of strong north-east dry winds is supported by the large influx of pollen from the Irano–Turanian steppe of the north and north-east[30] and the higher percentage of quartz[45] in Arabian Sea sediments.

In the glacial world, the contrast between a weak south-west monsoon and a strong north-east monsoon is probably related to the environmental conditions prevailing over the Asian continent. In modern conditions, the central and southeastern Tibetan plateau which remains free of snow throughout the year, seems to accelerate the onset of the Asian monsoon and to increase its ultimate intensity because it must be rapidly heated during the spring in the Northern Hemisphere[46]. During the last ice age, these mountains were covered with glaciers[47,48]. This permanent ice coverage would have prevented any marked warming of the Asian continent at high altitude during the summer. Thus, the pressure difference between the Asian continent and the Indian Ocean would be smaller than today and the south-west monsoon weaker. By contrast, during winter, the presence of permanent ice would have helped to maintain a continent much cooler than today in the vicinity of a warm ocean, a mechanism that would have enhanced the north-east monsoon.

I thank J. Labeyrie, C. Lalou, A. W. H. Bé, W. Dudley and W. Prell for discussions, W. Prell and C. H. Hendy for a careful review. Cores for this study were collected during cruises OSIRIS II and III of the French M/S *Marion Dufresne* sponsored by TAAF or came from Lamont Doherty Geological Observatory collections. J. Antignac and B. Le Coat helped for the analyses. Financial support by CEA, CNRS and DGRST is acknowledged.

Received 10 August; accepted 26 November 1981.

1. Climap Project *Science* **191,** 1131–1137 (1976).
2. Prell, W. L. *et al. Quat. Res.* **14,** 309–336 (1980).
3. Prell, W. L. & Curry, W. B. *Oceanol. Acta* **4,** 91–98 (1981).
4. Prell, W. L. & Hutson, W. H. *Science* **206,** 454–456 (1979).
5. Street, F. A. & Grove, A. T. *Nature* **261,** 385–390 (1979).
6. Delibrias, G., Gasse, F. & Rognon, P. *C.r. Acad. hebd Séanc. Sci., Paris* D**277,** 2633–2636 (1973).
7. McClure, H. A. *Nature* **263,** 755–756 (1976).
8. Wyrtki, K. in *The Biology of the Indian Ocean* (ed. Zeitschel, B.) 18–36 (Springer, New York, 1973).
9. Darbyshire, M. *Deep Sea Res.* **14,** 295–320 (1967).
10. Wyrtki, K. *Oceanographic Atlas of the International Indian Ocean Expedition* (NSF,Washington DC, 1971).
11. Currie, R. I., Fisher, A. E. & Hargreaves, P. M. in *The Biology of the Indian Ocean* (ed. Zeitschel, B.) 37–52 (Springer, New York, 1973).
12. Prell, W. L. in *Evolution des Atmosphères Planétaires et Climatologie de la Terre*, 149–156 (CNES, Paris, 1979).
13. Cullen, J. L. *Palaeogeogr. Palaeoclimatol. Palaeoecol.* **35,** 315–356 (1981).
14. Emiliani, C. *Am. J. Sci.* **252,** 149–158 (1954).
15. Epstein, S., Buchsbaum, R., Lowenstam, H. & Urey, H. C. *Bull. geol. Soc. Am.* **64,** 1315–1326 (1953).
16. Shackleton, N. J. & Vincent, E. *Mar. Micropaleontol.* **3,** 1–13 (1978).
17. Duplessy, J. C., Bé, A. W. H. & Blanc, P. L. *Palaeogeogr. Palaeoclimatol. Palaeoecol.* **33,** 9–46 (1981).
18. Craig, H. & Gordon, T. L. in *Stable Isotopes in Oceanographic Studies and Paleotemperatures* (ed. Tongiorgi, E.) 9–130 (CNR, Pisa, 1965).
19. Duplessy, J. C. *C.r. Acad. hebd. Séanc. Sci., Paris* D**271,** 1075–1078 (1970).
20. Epstein, S. & Mayeda, T. *Geochim. cosmochim. Acta* **4,** 213–224 (1953).
21. Dansgaard, W. *Tellus* **16,** 436–468 (1964).
22. Siegenthaler, V. & Oeschger, H. *Nature* **285,** 314–317 (1980).
23. Shackleton, N. J. *Colloq. int. CNRS* No. 219, 203–209 (1974).
24. Duplessy, J. C. in *Climatic Change* (ed. Gribbin, J.) 46–67 (Cambridge University Press, 1978).
25. Shackleton, N. J. & Opdyke, N. *Quat. Res.* **3,** 39–55 (1973).
26. Duplessy, J. C., Lalou, C. & Vinot, A. C. *Science* **168,** 250–251 (1970).
27. Emiliani, C. *J. Geol.* **631,** 538–578 (1955).
28. Ninkovich, D. & Shackleton, N. J. *Earth Planet. Sci. Lett.* **27,** 20–34 (1975).
29. Duplessy, J. C., Delibrias, G., Turon, J. L., Pujol, C. & Duprat, J. *Palaeogeogr. Palaeoclimatol. Palaeoecol.* **35,** 121–144 (1981).
30. Van Campo, E., Duplessy, J. C. & Rossignol-Strick, M. *Nature* (in the press).
31. Berger, W. H. & Killingley, J. S. *Science* **197,** 563–566 (1977).
32. Erez, J. *Nature* **281,** 535–538 (1979).
33. Duplessy, J. C., Blanc, P. L. & Bé, A. W. H. *Science* **213,** 1247–1250 (1981).
34. Duplessy, J. C., Moyes, J. & Pujol, C. *Nature* **286,** 479–482 (1980).
35. La Fond, E. C. & La Fond, K. G. *Bull. natn. Inst. Sci. India* **38,** 164–183 (1968).
36. Sarntheim, M. & Diester-Hass, L. *J. Sedim. Petrol.* **47,** 868–889 (1977).
37. Bryson, R. A. & Swain, A. M. *Quat. Res.* **16,** 135–145 (1981).
38. Zeist, W. van *Paleobotan. Palynol.* **2,** 301–311 (1967).
39. Pias, J. *Rev. Géogr. Phys. Géol. Dyn.* **4,** 39–52 (1974).
40. Huang, Y. C. in *Loess deposits in China* (ed. Fairbridge, R. W.) 63–76 (1973).
41. Sarntheim, M. *Nature* **272,** 43–46 (1978).
42. Pastouret, L., Chamley, H., Delibrias, G., Duplessy, J. C. & Thiede, J. *Oceanol. Acta* **1,** 217–231 (1978).
43. Gasse, F. *Nature* **265,** 42–45 (1977).
44. Manabe, S. & Hahn, D. G. *J. geophys. Res.* **82,** 3889–3911 (1977).
45. Kolla, V. & Biscaye, P. E. *J. Sedim. Petrol.* **47,** 642–649 (1977).
46. The Monsoon Experiment *GARP Publ. Ser.* No. 18 (WMO, 1976).
47. Flint, R. F. *Glacial and Quaternary Geology*, 892 (Wiley, New York, 1971).
48. Singh, G. & Agrawal, D. P. *Nature* **260,** 232 (1976).

Protochordate allorecognition is controlled by a MHC-like gene system

V. L. Scofield, J. M. Schlumpberger, L. A. West[*] & I. L. Weissman

Laboratory of Experimental Oncology, Department of Pathology, Stanford University School of Medicine, Stanford, California 94305, USA and Hopkins Marine Station of Stanford University, Pacific Grove, California 93950, USA

Colonial tunicates, unlike vertebrates, undergo transplantation in nature. Rejection or acceptance between colonies of Botryllus *is controlled by a single gene locus with multiple alleles. The same genetic region apparently maintains this polymorphism by preventing fertilization between gametes sharing alleles. The* Botryllus *histocompatibility system may reflect the original adaptive function of ancestral MHC genes.*

In vertebrates, immune recognition of tissue antigens is responsible for rejection of transplanted allogeneic organs, tissues and cells[1]. Prompt rejection of allotransplants by the cell-mediated immune system usually occurs when donor and host differ genetically at the major histocompatibility complex (MHC)[2,3]. It appears that all vertebrate species may have MHC genes and the capacity for response to MHC-disparate antigens[4], but the extent to which the MHC and adaptive immunity are found in invertebrate metazoans is unclear[5]. While vertebrate species exist normally as individuals which encounter foreign transplantation antigens only as a consequence of experimental transplantation, some members of invertebrate phyla allow the coexistence or fusion of individuals (or of groups of individuals, or of newly budded offspring to their parents) to form colonies. In fact, colonial forms are found in virtually all metazoan branches leading to the vertebrates. Recent studies have established the capacity for tissue transplant histocompatibility discrimination in both solitary and colonial members of diverse invertebrate animal phyla[6,7]. Because of their phylogenetic position as the most primitive chordates, certain colonial tunicates provide a very interesting example of colony specificity, where fusion of neighbouring individuals or colonies is under strict genetic control[8–10], and where, by contrast to the vertebrate situation, transplant rejection may be essential for survival. We set out to test the hypothesis that allorecognition in colonial tunicates is controlled by genes of an ancestral MHC gene complex[7].

Botryllus colonies are usually clones of individuals (zooids) sharing a common vascular network and covered by a gelatinous tunic. Colonies grow by budding from a founder individual (oozooid), which arises by metamorphosis from a swimming tadpole-like larva. Production of new buds, resorption of old individuals, ovulation and sperm release occur synchronously for all individuals in a colony and are apparently controlled by blood elements[11,12]. In the natural environment, ovulation occurs immediately on 'takeover' by a new generation of buds. Eggs are fertilized by sperm which enter from the surrounding seawater when the siphons of the new buds open. Embryonic development is phase-locked to the budding cycle, so that developed tadpoles hatch and swim away shortly before their parent zooids are resorbed and replaced by the next generation of buds. The hatched tadpoles, in turn, settle and metamorphose to become oozooids, and begin budding to produce new colonies.

Studies of the genetic control of intercolony fusibility by Watanabe and Oka[9] performed with cut pieces from grown *Botryllus* colonies have established (for *Botryllus primigenus*) that each colony gathered from the marine environment is heterozygotic at a single fusibility gene locus represented in natural populations by many codominant alleles, and that two colonies must share one allele in order to fuse[9,10]. The fusion itself involves apposition of two colonies, dissolution of the intervening tunic, contact between extracorporeal blood vessel termini (ampullae) and fusion (or nonfusion) of the contacted blood vessels to form a multi-individual chimaeric colony with a common blood circulation[13,14]. In this study we have developed a rapid fusion microassay which uses pairs of newly metamorphosed individual oozooids from *in vivo* or *in vitro*[12] crosses. *Botryllus* oozooids possess eight vascular microampullae which are involved in fusion or rejection reactions identical in appearance and time course to those described for ampullae from growing edges of adult colonies (refs 13, 14; Fig. 1). Our results show that allorecognition and control of fertilization, two phenomena characteristic of the murine MHC-bearing chromosome 17, are present as linked characters in two species of the colonial tunicate *Botryllus*.

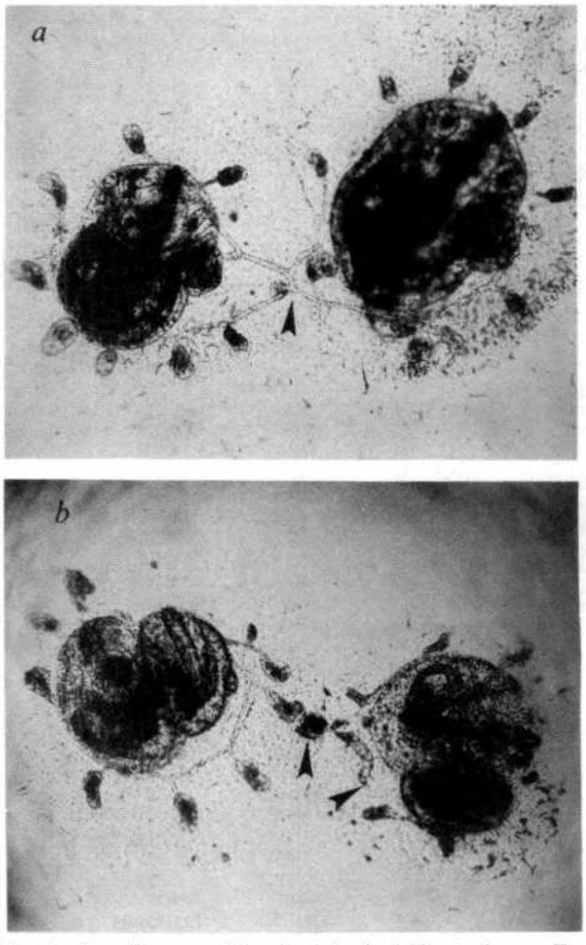

Fig. 1 *Botryllus* oozooids paired for fusibility testing. *a*, Fused oozooids; arrow points to new vascular connection. *b*, Rejected oozooids; arrow points to necrotic zone and detached vascular ampullae. ×240.

---

[*] Present address: Department of Zoology, Oregon State University, Corvallis, Oregon 97331, USA.

0028–0836/82/060499—04$01.00

Colony fusion is controlled by a single, highly polymorphic genetic region

To examine the suitability of this microfusion assay for genetic studies and to determine whether genetic control of fusibility in Monterey *Botryllus* is similar to that described for *Botryllus schlosseri*[10], we first examined fusibility frequencies for pairs of oozooids hatched from colonies fertilized in the natural environment. If colonies are heterozygotic at one locus determining fusibility (that is, *AB*; Fig. 2) at which there are many codominant alleles (*A*, *B*, *C*, *D*...) and if they are fertilized by sperm carrying a large number of (unknown) fusibility alleles (designated x_1, or x_2, or $x_3 \ldots y$), then 25% of random pairs of oozooids hatched from this wild-fertilized colony will be composed of Ax_1, or Ax_2, or $Ax_3 \ldots Ay$ (designated $Ax \ldots y$), all of which will fuse with each other due to sharing of the *A* allele; another 25% of random pairs will be composed of Bx_1, or Bx_2, or $Bx_3 \ldots By$ (designated $Bx \ldots y$), all of which will fuse with each other due to sharing of the *B* allele; and 50% of the random pairs will be $Ax \ldots y$ paired with $Bx \ldots y$, none of which will fuse with each other due to non-sharing of *A* or *B* alleles, and non-sharing of the $x \ldots y$ alleles if a large number of distinct sperm donors ($x \ldots y$) are involved in the fertilization.

Table 1 Fusion frequencies for *a*, oozooid pairs from single wild-fertilized *Botryllus* colonies, and *b*, oozooid pairs from single wild-fertilized *Botryllus* colonies from crowded locations

Colony no.				
a				
Botryllus sp.				
(Monterey)	*n*	Fusions (%)	Rejections (%)	
1	32	17(53)	15(47)	
2	25	11(44)	14(56)	
3	14	6(43)	8(57)	
4	35	15(43)	20(57)	
5	18	5(28)	13(72)	
6	25	10(40)	15(60)	
7	44	23(52)	21(48)	
8	38	20(53)	18(47)	
9	28	15(54)	13(46)	
10	28	15(54)	13(46)	
11	53	29(55)	24(45)	
12	8	6(75)	2(25)	
13	19	10(53)	9(47)	
Total	367	182(50)	185(50)	$P > 0.8$*
B. schlosseri				
(Woods Hole)				
1	13	5(38)	8(62)	
2	24	13(54)	11(46)	
3	12	9(75)	3(25)	
4	11	5(45)	6(55)	
5	16	7(44)	9(56)	
6	13	5(38)	8(62)	
7	13	7(54)	6(46)	
8	15	8(53)	7(47)	
9	46	21(46)	25(54)	
10	16	10(63)	6(37)	
11	16	8(50)	8(50)	
Total	195	98(50)	97(50)	$P > 0.5$*
b				
Botryllus sp.				
(Monterey)				
1	11	7(64)	4(36)	
2	46	31(67)	15(33)	
3	11	8(73)	3(27)	
4	19	12(63)	7(37)	
5	6	4(67)	2(37)	
6	7	5(71)	2(29)	
7	78	47(60)	31(40)	
8.	22	14(64)	8(36)	
9	7	6(86)	1(14)	
10	26	17(65)	9(35)	
11	18	13(72)	5(28)	
12	39	30(77)	9(23)	
13	14	12(86)	2(14)	
14	37	20(54)	17(46)	
15	28	13(46)	15(54)	
16	10	5(50)	5(50)	
17	29	19(66)	10(34)	
18	40	32(80)	8(20)	
19	12	8(66)	4(33)	
20	6	3(50)	3(50)	
21	15	11(73)	4(27)	
22	37	29(78)	8(22)	
23	9	6(67)	3(33)	
Total	527	352(67)	175(33)	

*After data from different colonies in each of the studies were found to be homogeneous, χ^2 was computed and the *P* value determined. χ^2 for each study was calculated from individual samples as $\chi^2 = -2\Sigma \ln P$, where *P* is the *P* value corresponding to the value of χ^2 (for goodness of fit) for individual experiments.

Colonies of *Botryllus* were collected from the Monterey Marina (designated *Botryllus* sp.) or from the Green Pond at Falmouth or the Eel Pond at Woods Hole, Massachusetts (*B. schlosseri*). Embryonic development of wild-fertilized eggs was completed in the laboratory, and progeny oozooids were paired immediately after hatching and scored for fusion or rejection 48 h later. In both studies, colonies gathered from scattered locations consistently yielded oozooid progeny with a fusion frequency of ~50% (Table 1). This system thus gives results which parallel those obtained by other methods[9,10].

If fusibility in Monterey *Botryllus* is controlled by a single polymorphic gene locus, and one shared allele is required for fusion, then crosses between any two colonies collected from different locations (represented by *AB* × *CD*) will provide progeny oozooids which are *AC*, *AD*, *BC* and *BD* at the fusion locus, and 75% of random pairs of the hybrid oozooids should fuse; this was the case with crosses at *Botryllus* colonies from both locations (Table 2*a*). Late in the growing season (February), many *Botryllus* colonies are crowded together and fertilizing sperm come predominantly from one or a few neighbouring colonies. One would thus expect newly hatched oozooids from these matings to give fusibility frequencies of 50–75%; in fact, fusion frequencies of 60–80% were obtained in such cases (Table 1*b*).

Fusibility alleles are not homozygous lethals

In no case did sampled colonies from East and West coast collecting sites give fusibility frequencies significantly above

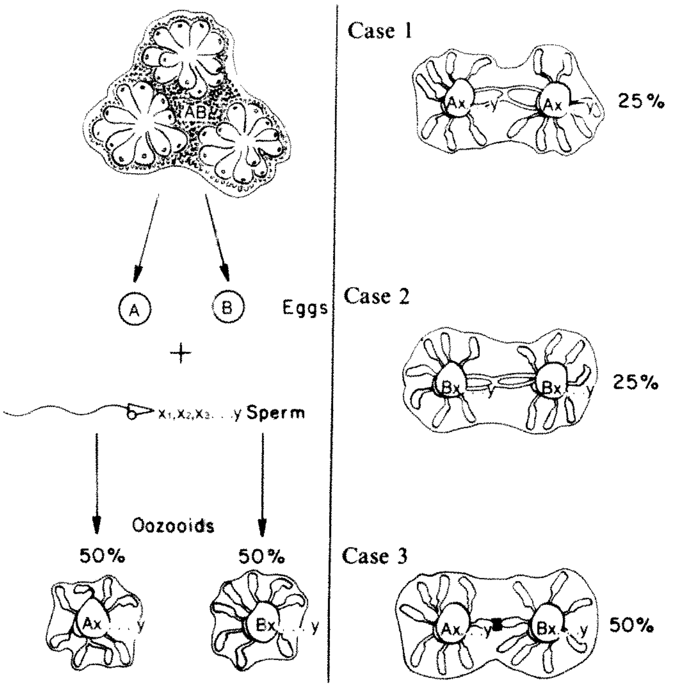

Fig. 2 Testing of the one locus, multiple-allele model for genetic control of colony specificity using the oozooid microassay. Paired oozooids for any crossed *Botryllus* colony will show at least 50% fusions, regardless of the number of alleles involved in the fertilization (above). As the number of sperm alleles participating in the fertilization is decreased, the probability that any two pairs will share a paternal allele increases, and fusibility frequency approaches the 75% frequency for a defined cross (*AB* × *CD*, see text and Table 2).

50–75% (Table 1), so we conclude that homozygotes at the fusibility locus may be rare or nonexistent in natural populations of both North American *Botryllus* species, as may be the case for *B. primigenus* in Japan[9]. Although they are hermaphroditic, colonies of *B. primigenus* have been claimed to be incapable of self-fertilization[9] despite simultaneous ovulation and sperm release. In the two *Botryllus* species studied here, ovulation and fertilization by exogenous sperm occur before endogenous sperm release (protogyny), thus limiting self-fertilization in natural conditions (ref. 15, and V.L.S., unpublished results). When protogyny is circumvented by crossing between separated pieces of the same colony which have been phase-separated by temperature, self-fertilization does occur, but a large proportion of the resulting embryos undergo developmental arrest, or fail to complete metamorphosis after hatching[15].

To test whether embryonic maldevelopment which occurs in the progeny of self-crosses in *B. schlosseri*[15] and Monterey *Botryllus* (V.L.S. and J.M.S., unpublished) replaces the self-sterility operating in *B. primigenus*, we isolated seven colonies, allowed them to self-cross ($AB \times AB$) and counted the fusion frequencies of the few surviving oozooids. If homozygotes (AA and BB) fail to develop, all the survivors should be identical (AB) and the fusion frequency should be 100%. However, none of the self-crosses gave this result (Table 2*b*). Thus, although it is possible that the fusion locus causes late maturation and differentiation effects in homozygotes[15], the fusibility locus cannot be the major determinant in inbreeding depression. It was, therefore, necessary to find another explanation for the puzzling absence of homozygotes in the two *Botryllus* populations studied.

Fusibility locus affects self-fertilization by sperm–egg incompatibility

We have observed that in Monterey *Botryllus*, as in *B. schlosseri*[15], self-fertilizations do not occur synchronously and immediately after ovulation as do cross-fertilizations; in colonies isolated for selfing, the cleavages begin at scattered times and some eggs are never fertilized. We therefore designed experiments to test the hypothesis that there is a gametic barrier to fertilization which breaks down in time to allow self-fertilization in laboratory conditions of isolation. At Woods Hole, 18 colonies of *B. schlosseri* were isolated, 5 of which were early ovulating and fertilized by exogenous sperm brought in from the collection site. In these 5 colonies fertilizations were synchronous, and gave large hatches of oozooids whose fusibility frequency was ~50%. The other 13 late-ovulating colonies were placed *in vitro* in conditions allowing self-fertilization. In these conditions early embryonic cleavages were scattered in colonies whose eggs were ovulated after 2 days of isolation, and 7/13 of these colonies showed delays of 2–4 days after ovulation before the first fertilizations occurred. This occurred despite sperm-producing testes being present in each colony from 1 day after ovulation onwards (data not shown). It seems likely that *Botryllus* eggs resist fertilization by sperm from the same colony for varying periods of time after ovulation.

To extend this observation to the Monterey species, paired colonies at ovulation were divided in half, with one of the subcolonies (A_1 and B_1) from each pair placed in isolation and the others (A_2 and B_2) placed together. In all experiments, cross-fertilization (A_2/B_2) occurred between the paired pieces 1–2 days before self-fertilization (A_1/A_1 and B_1/B_1) occurred in the isolated controls (data not shown), indicating that sperm-producing testes and fertilization-competent eggs are present in both colonies at a time when self-fertilization cannot occur.

To determine whether this barrier to self-fertilization is controlled by the fusibility locus, colonies from the same algal blade were crossed. Our sampling data for colonies with contacted borders indicate that, in these conditions, >20% of such defined crosses should be between sibling colonies sharing at least one fusibility allele. We expected for such semiallogeneic crosses ($AB \times BC$) that sperm carrying the shared allele (B)

Table 2 Fusion frequencies for F_1 oozooid pairs from defined crosses

a, Cross-fertilizations Colony no.	*n*	Fusions(%)	Rejections(%)	
Botryllus sp. (Monterey)				
1	10	7(70)	3(30)	
2	17	12(71)	5(29)	
3	35	23(66)	12(34)	
4	14	10(71)	4(29)	
5	6	4(67)	2(33)	
6	5	3(60)	2(40)	
7	29	22(76)	7(24)	
8	52	37(71)	15(29)	
9	9	8(89)	1(11)	
10	7	6(86)	1(14)	
11	4	3(75)	1(25)	
12	17	13(76)	4(24)	
13	7	5(71)	2(29)	
14	13	10(77)	3(23)	
15	26	20(77)	6(23)	
16	6	4(67)	2(33)	
17	22	16(73)	6(27)	
18	8	7(88)	1(12)	
19	9	8(89)	1(11)	
20	67	49(73)	18(27)	
Total	363	267(74)	96(26)	$P=0.9$*
B. schlosseri (Woods Hole)				
1	8	6(75)	2(25)	
2	29	18(62)	11(38)	
3	20	13(65)	7(35)	
4	5	4(80)	1(20)	
Total	62	41(67)	21(33)	$P=0.5$*
b, Self-fertilizations				
Botryllus sp. (Monterey)				
1	8	6(75)	2(25)	
2	15	13(87)	2(13)	
3	5	4(80)	1(20)	
4	4	3(75)	1(25)	
Total	32	26(81)	6(19)	
B. schlosseri (Woods Hole)				
1	5	4(80)	1(20)	
2	4	3(75)	1(25)	
3	3	2(67)	1(33)	
Total	12	9(75)	3(25)	

When two colonies are crossed ($AB \times CD$), not only is the maternal allele shared in 50% of the oozooid pairs (above), but the paternal allele is also shared in 50% of the pairs (half of which are pairs not sharing a maternal allele); thus the fusibility frequency for these oozooids is 75% (Table 2*a*). All oozooid pairs hatched from a self-fertilization (except the 1/8 which are composed of two homozygotes for opposite alleles—AA to BB) share at least one allele; thus 87.5% will fuse (Table 2*b*).

*Data were analysed as described in Table 1 legend.

Table 3 Fusion frequencies for oozooid pairs from colonies crossed with potential siblings

Colony no.	*n*	Fusions(%)		Rejections(%)
1	43	35(81)		8(19)
2	17	13(76)		4(24)
3	22		22(100)	0
4	11	6(55)		5(45)
5	25	17(68)		8(32)
6	30	20(67)		10(33)
7	6		6(100)	0
8	18	12(67)		6(33)
9	8		8(100)	0
10	8	6(75)		2(25)
11	10	8(80)		2(10)
12	14	9(64)		5(36)
13	18		18(100)	0
14	13	10(77)		3(23)
15a Reciprocal	19		19(100)	0
15b crosses	113		113(100)	0
16	6	5(83)		1(17)
17	14		14(100)	0
Total	281 (195)	141(72)		54(28)
			86(100)	

For all data, $\chi_1^2 = 17.58$ ($P = 0.005$); thus we reject the null hypothesis that no gametic barrier to fertilizations by sperm carrying the shared allele exists between crossed sibling colonies (see text).

Table 4 Fusibility frequencies for F_2 oozooids

Cross	*n*	Fusions	Rejections	% Fusions
1	27	27	—	100
2a	13	13	—	100
2b	11	11	—	100
3a	49	49	—	100
3b	40	40	—	100
4	10	9	1	90
6	47	47	—	100
7	7	7	—	100
8	29	20	9	69
9	21	18	3	86

From an *AB* × *CD* defined cross, four classes of offspring, present in equal numbers, are expected: *AC*, *AD*, *BC* and *BD*. Random crossings of the grown progeny colonies from such a cross were expected to be of three kinds: (1) one-half should be crosses where one fusibility allele is shared, and only sperm carrying the non-shared allele can fertilize the eggs, giving offspring which are 100% fusible with one another; (2) one-quarter should be crosses where both fusibility alleles are shared, giving oozooid progeny which are 87.5% fusible (Table 2*b*) and small hatches because fertilization is delayed for 24–48 h until the gametic barrier has broken down; (3) one-quarter should be crosses where no alleles are shared, giving the expected 7.5% fusible progeny (Table 2*a*). 'a' And 'b' notations denote reciprocal crossings between the same two colonies.

should not fertilize any of the eggs of the crossing partner, thus allowing all eggs to be fertilized by the sperm carrying the nonshared allele (all by *A* or all by *C*, depending on which colony serves as a sperm donor). All offspring from such a cross should share a fusibility allele. Table 3 shows the results of fusion analysis of oozooids from the 17 crosses performed in this study. Although 11 of the 17 crosses produced oozooids whose fusion frequencies were close to those expected for cross-fertilizations (75%), 6/17 gave frequencies of 100% (Table 3). The above data are most consistent with a model for self-sterility in which the haploid expression of fusibility allele patterns by sperm is recognized by the diploid, maternally derived egg envelopes[9], resulting in selective fertilization by sperm bearing new fusibility alleles.

To test these findings further, sibling *B. schlosseri* colonies, grown from the F_1 oozooid progeny of a defined cross (*AB* × *CD*) were crossed with one another. Two of the eight crosses performed produced F_2 oozooids whose pairs gave fusibility frequencies close to 75% (Table 4). This is consistent with the expectation that 25% of such crosses will involve no shared alleles (this is the proportion of the grown colonies which would not have fused as oozooids; Table 2*a*). Paired oozooids hatched from all but one of the remaining six crosses (a frequency consistent with that proportion of defined-cross F_1 oozooids which fuse; Table 2*a*) gave fusibility frequencies of 100%. Fertilizations between colonies sharing both fusibility alleles (which should comprise 25% of the crosses between sibling colonies in this experiment) can occur only after the selfing barrier has broken down, after which scattered, asynchronous fertilizations lead to small hatches (Table 2*b*). The expected fusibility frequency for such oozooids is 87.5% (Table 2*b*). Very small hatches, giving fusibility frequencies of 90%, 100%, and 100% respectively (Table 4), resulted from three of the eight crosses in this experiment (Table 4). On the other hand, fertilizations between colonies sharing one fusibility allele, a group which should comprise one-half of the crossings between F_1 progeny of a defined cross, should yield oozooids whose pairs give 100% fusions, as was found in three of the eight defined crosses between sibling colonies shown in Table 4. These data support our hypothesis for genetic control of colony specificity tested in other experiments (Tables 1, 2) and, with the results shown in Table 3, confirm the prediction by Watanabe and Oka[9] of a gametic barrier to fertilization by sperm carrying shared fusibility alleles.

Discussion

The *Botryllus* fusibility gene locus shows the same degree of polymorphism as the genes of the vertebrate MHC[14] and the self-incompatibility systems of plants[16,17]. Because *Botryllus* histocompatibility genes control both somatic tissue recognition and response, as does the vertebrate MHC, and gamete behaviour at fertilization, as does the Ss system in the angiosperms, our findings support hypotheses[16,18,19] that vertebrate histocompatibility genes evolved from gametic self–nonself recognition systems which prevented self-fertilization in hermaphroditic organisms. It seems likely that self–nonself discrimination in *Botryllus* may represent the evolutionary precursor(s) to the MHC[7]. Polymorphism at the *Botryllus* and vertebrate loci may be maintained through linkage of histocompatibility genes with elements which enforce the heterozygous condition through control of fertilization[20–22] or development[22–24].

Despite the similarities between the vertebrate MHC and the *Botryllus* fusion systems, several major differences have yet to be reconciled. For example, fusion is allowed between ampullae of *Botryllus* colonies sharing one allele. In vertebrate allorecognition, by contrast, lymphocyte clones recognize and eliminate cells carrying non-shared histocompatibility antigens, even in the presence of one shared allele. However, events subsequent to a fusion between semiallogeneic *Botryllus* oozooids or colonies (that is *AB* fused to *BC*) frequently lead to the complete resorption of one member of a fused oozooid pair (V.L.S., in preparation) or to the disappearance of germ cells of one of two fused colonies (A. Sabbadin, personal communication). Further studies of these delayed (or induced) responses to contact between semiallogeneic cells may therefore disclose even more similarities between both the native immune reactivities (for example colony specificity and the natural killer cell reactivities of mammals) and the induced allogeneic recognition responses in these two chordate systems. For these purposes, it will be important to determine whether *Botryllus* allorecognition is a capacity possessed by all cells, or only by ampullar and blood cells[13,14].

We thank D. P. Abbott for advice and editorial assistance, D. Epel, C. Pittendrigh, C. Nottenburg and E. Pillemer for critical reading of the manuscript, C. Lambert and G. Freeman for valuable discussions, and C. Patton for photography. Part of this study was completed while V.L.S. was an investigator at the Marine Biological Laboratory, Woods Hole. This work was supported by NSF grant PCM78-10345 and by NIH grant GM 25902. V.L.S. is a NIH Postdoctoral Fellow.

Received 7 May; accepted 16 December 1981.

1. Medawar, P. B. *J. Anat.* **78,** 176–199 (1944).
2. Snell, G. D. *Folia biol., Praha* **14,** 335–358 (1968).
3. Gorer, P. A. *J. Path. Bact.* **47,** 231–252 (1938).
4. Klein, J. *Biology of the Mouse Histocompatibility-2 Complex* (Springer, New York, 1975).
5. Hildemann, W. H., Clark, E. A. & Raison, R. L. *Comprehensive Immunogenetics* (Elsevier, New York, 1981).
6. Hildemann, W. H. *Transplantation* **27,** 1–3 (1979).
7. Scofield, V. L. & Weissman, I. L. *Devl comp. Immun.* **5,** 23–28 (1981).
8. Bancroft, R. W. *Proc. Calif. Acad. Sci.* **3,** 137–187 (1903).
9. Oka, H. & Watanabe, H. *Proc. Japan Acad.* **33,** 657–659 (1957).
10. Sabbadin, A. *Rc. Accad. naz. XL* **32,** 1031–1035 (1962).
11. Sabbadin, A. in *Marine Organisms: Genetics, Ecology, and Evolution* (eds Battaglia, B. & Beardmore, B. A.) 195–209 (Plenum, New York, 1979).
12. Milkman, R. *Biol. Bull.* **132,** 229 (1967).
13. Tanaka, K. & Watanabe, H. *Cell. Immun.* **7,** 410–426 (1973).
14. Tanaka, K. *Cell. Immun.* **7,** 427–443 (1973).
15. Sabbadin, A. *Devl Biol.* **24,** 379–391 (1971).
16. Burnet, F. M. *Nature* **230,** 232–235 (1971).
17. Heslop-Harrison, J. *Cellular Recognition Systems in Plants* (Arnold, London, 1978).
18. Bennett, D., Boyse, E. A. & Old, L. J. in *3rd Lepetit Colloq.* 247263 (North Holland, Amsterdam, 1972).
19. Monroy, A. & Rosati, F. *Nature* **27,** 165–166 (1979).
20. Hedrick, P., Jain, S. & Holden, L. in *Evolutionary Biology* Vol. 11 (eds Hecht, M. K., Steere, W. C. & Wallace, B.) 104–184 (Plenum, New York, 1978).
21. Hammerberg, C. & Klein, J. *Nature* **258,** 296–299 (1975).
22. Lyon, M. F., Evans, E. P., Karvos, S. E. & Sayer, I. *Nature* **279,** 38–42 (1979).
23. Sabbadin, A. Cited in Scofield, V. L. & Weissman, I. L. *Devl comp. Immun.* **5,** 23–28 (1981).
24. Bennett, D. *Cell* **6,** 441–454 (1975).

Expression of human immune interferon cDNA in *E. coli* and monkey cells

Patrick W. Gray, David W. Leung, Diane Pennica, Elizabeth Yelverton, Richard Najarian, Christian C. Simonsen, Rik Derynck, Pamela J. Sherwood, Donald M. Wallace*, Shelby L. Berger*, Arthur D. Levinson & David V. Goeddel

Department of Molecular Biology, Genentech, Inc., 460 Point San Bruno Boulevard, South San Francisco, California 94080, USA
* Laboratory of Pathophysiology, National Cancer Institute, Bethesda, Maryland 20205, USA

A cDNA sequence coding for human immune interferon (IFN-γ) has been identified in a cDNA library prepared from gel-fractionated IFN-γ mRNA. The DNA sequence codes for a polypeptide of 166 amino acids, 20 of which could constitute a signal peptide. The polypeptide produced through expression of this DNA sequence in Escherichia coli *or cultured monkey cells had properties characteristic of authentic human IFN-γ.*

INTERFERONS (IFNs) are secreted proteins which induce an antiviral state in their target cells, and which have immunomodulatory and antitumour properties[1]. On the basis of antigenicity and biological and chemical properties, human interferons have been grouped into three major classes: IFN-α (leukocyte), IFN-β (fibroblast) and IFN-γ (immune)[2]. Considerable information has accumulated on the structures and properties of the virus-induced acid-stable interferons (IFN-α and -β). These have been purified to homogeneity and partial amino acid sequences determined[3–7]. Analyses of cloned cDNA and gene sequences for IFN-β_1 (refs 8–10) and the IFN-α multigene family[11–16] have permitted the deduction of the complete amino acid sequences of many of these interferons. In addition, efficient synthesis of IFN-β_1 (ref. 10) and several IFN-αs[13,16] in *Escherichia coli* and IFN-α_1 in yeast[17] have now made possible the purification of large quantities of these proteins in biologically active form.

Much less data are available concerning the structure and properties of IFN-γ. IFN-γ is generally produced in cultures of lymphocytes exposed to various mitogenic stimuli, is acid labile and does not cross-react with antisera prepared against IFN-α or IFN-β (ref. 1). Molecular weights ranging from 35,000 to 70,000 have been reported for IFN-γ (refs 18–21). Recently, a quite extensive, but still partial, purification of IFN-γ has been reported[20], and IFN-γ mRNA has been isolated and translated in *Xenopus laevis* oocytes[22,23]. A broad range of biological activities have been attributed to IFN-γ, including potentiation of the antiviral activities of IFN-α and -β (ref. 24), and it differs from these interferons in its virus and cell specificities and in the antiviral mechanisms it induces[25]. However, *in vitro* studies performed with crude preparations suggest that the primary function of IFN-γ may be as an immunoregulatory agent[26]. The antiproliferative effect of IFN-γ on transformed cells has been reported to be 10–100-fold greater than that of IFN-α or -β (refs 25, 27), suggesting a potential use in the treatment of neoplasia. Indeed, murine IFN-γ preparations have been shown to have significant antitumour activity against mouse sarcomas[28]. However, the poor availability of purified IFN-γ has precluded the unambiguous determination of its physicochemical and biological properties.

We describe here the first isolation and characterization of a recombinant plasmid containing a cDNA sequence coding for human IFN-γ. Expression of this sequence in *E. coli* and cultured monkey cells gives rise to a polypeptide having the properties of authentic human IFN-γ.

Construction and identification of bacterial clones containing induced cDNA sequences

Human peripheral blood lymphocytes (PBLs) from healthy donors were stimulated to produce IFN-γ by treatment with staphylococcal enterotoxin B (SEB) and desacetylthymosin α_1 as described by Svedersky *et al.*[29]. Cell cultures from individual donors were collected 48 h after induction and used to prepare polyadenylated RNA[30,31] which was fractionated by electrophoresis through denaturing agarose gels[32,33]. Interferon mRNA activity was determined by injecting aliquots of each fraction into *X. laevis* oocytes[34–37] and after 24 h assaying the incubation medium for antiviral activity[36,37]. One peak of activity was consistently observed which co-migrated with 18S RNA (Fig. 1). Using different procedures for sucrose density gradient centrifugation, Wallace *et al.*[22] and Taniguchi *et al.*[23] have reported single peaks of IFN-γ mRNA activity sedimenting at 18S and 15S respectively. RNA from our most active 18S gel fraction (600 units ml^{-1} when 0.5 μg was injected into 15 oocytes at a concentration of $0.5\ \mu\mathrm{g}\ \mu\mathrm{l}^{-1}$) was used to prepare double-stranded cDNA by standard procedures[38,39]. The cDNA was fractionated according to size and material longer than 800 base pairs (bp) was extended with deoxy(C) residues, annealed to deoxy(G)-tailed *Pst*I-cleaved pBR322 and used to transform *E. coli* K-12 strain 294 (ref. 40) as described previously[13,19].

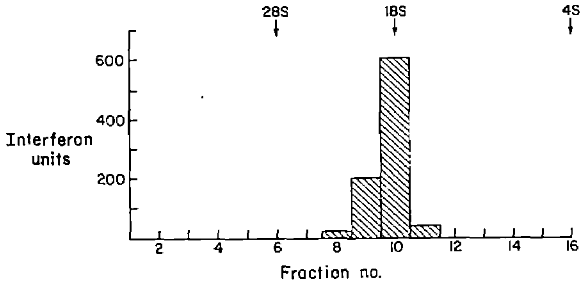

Fig. 1 Gel electrophoresis of induced lymphocyte polyadenylated RNA. Peripheral blood lymphocytes (PBLs) derived from individual human donors by lymphophoresis were purified by centrifugation on a Ficoll–Hypaque gradient and induced for IFN-γ production with staphlococcal enterotoxin B ($1\ \mu\mathrm{g\ ml}^{-1}$) and desacetylthymosin-$\alpha_1$ ($0.1\ \mu\mathrm{g\ ml}^{-1}$)[29]. Total RNA was extracted[30] from PBL cultures and poly(A)-containing RNA was purified by oligo(dT) cellulose chromatography[31]. 200 μg of mRNA was fractionated by electrophoresis through a denaturing agarose gel (1.75% agarose, 0.025 M sodium citrate (*p*H 3.8) and 6 M urea) for 7 h at 25 mA and 4 °C (refs 32, 33). The slab gel was sectioned with a razor blade and individual slices were melted at 70 °C and extracted twice with phenol and once with chloroform. Fractions were precipitated with ethanol and subsequently assayed for IFN-γ mRNA by injection into *X. laevis* oocytes[34–37] at a concentration of $0.5\ \mu\mathrm{g}\ \mu\mathrm{l}^{-1}$. After 24 h incubation at room temperature the antiviral activity of the translation products in the incubation medium was determined by the cytopathic effect (CPE) inhibition assay using vesicular stomatitis virus or encephalomyocarditis virus on WISH (human amnion) cells[1]. All IFN-γ units are expressed with reference to the NIH IFN-α standard (G-023-901-527), because no internationally accepted IFN-γ standard was available. In this assay system 0.2 units of the standard results in a 50% reduction in cytopathogenic effect. A single peak of activity was observed which co-migrated with 18S ribosomal RNA. The positions of ribosomal RNA markers which were electrophoresed in an adjacent lane and visualized by ethidium bromide staining are labelled above the activity profile. The activity seems to be due to IFN-γ, as no activity was observed when the same fractions were assayed on a bovine cell line (MDBK) which is not protected by IFN-γ (ref. 29). Both IFN-α activity and IFN)-β activity would have been easily detectable with the MDBK assay[10].

0028-0836/82/060503—06$01.00

We screened 8,300 bacterial clones from the cDNA library for the presence of specifically induced cDNA sequences by the following procedure. Two copies of the colony library were grown up on nitrocellulose filters and DNA was fixed to the filters for *in situ* colony hybridization[41,42]. One set of filters was hybridized with a ^{32}P-labelled cDNA probe prepared using the same 18S gel-fractionated mRNA (induced) used to prepare the colony library. The second set of filters was hybridized with ^{32}P-labelled cDNA prepared using 18S gel-fractionated poly(A) RNA isolated from unstimulated PBLs. The hybridization intensity of each colony with the two probes was compared, as IFN-γ sequences should only hybridize with the induced probe. 124 colonies hybridized with the induced probe but undetectably or weakly with the uninduced probe (see Fig. 2). Plasmid DNA was isolated from each of these colonies[43], bound to nitrocellulose filters[44] and hybridized with the same induced and uninduced probes. DNA from 22 colonies hybridized specifically with the induced probe in this rescreening.

The cDNA inserts from several of these 'induced' colonies were mapped using restriction endonucleases and found to contain common *Dde*I, *Hin*cII and *Rsa*I sites (Fig. 3*a*). A ^{32}P-labelled DNA probe was prepared[45] from one of the plasmids using two internal *Dde*I fragments (130 and 600 bp) and hybridized to DNA from the 124 colonies selected in the first round of screening. Only the 22 induced clones were found to hybridize with this probe, establishing their relatedness. Subsequent rescreening[41,42] of the cDNA library with this same probe revealed that approximately 1 in 120 *E. coli* clones contained related sequences. Digestion of plasmid DNA from these clones with *Pst*I showed that clone 69 contained the largest cDNA sequence (~1,250 bp).

Induced ^{32}P-cDNA probe

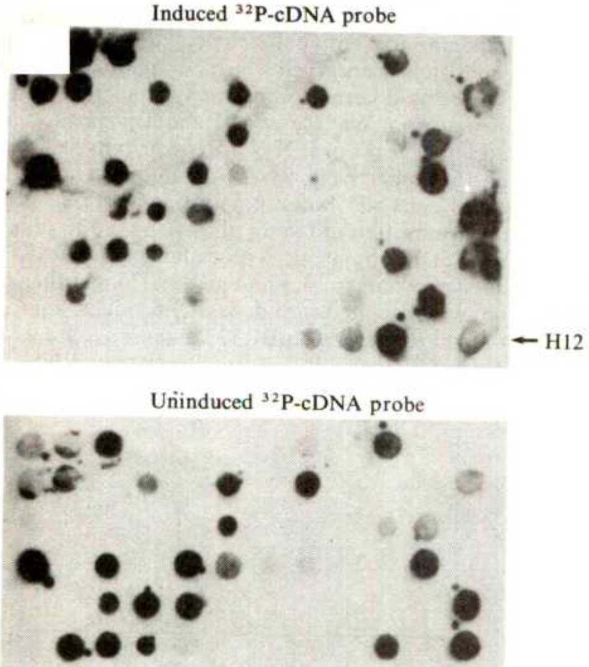

Uninduced ^{32}P-cDNA probe

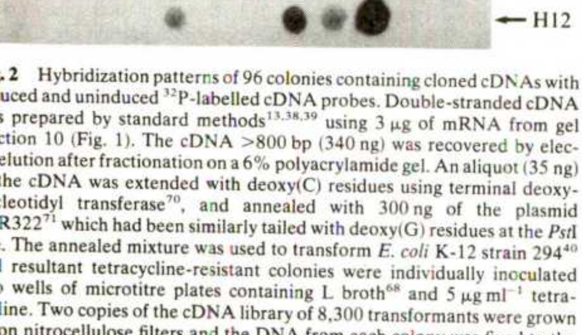

Fig. 2 Hybridization patterns of 96 colonies containing cloned cDNAs with induced and uninduced ^{32}P-labelled cDNA probes. Double-stranded cDNA was prepared by standard methods[13,38,39] using 3 μg of mRNA from gel fraction 10 (Fig. 1). The cDNA >800 bp (340 ng) was recovered by electroelution after fractionation on a 6% polyacrylamide gel. An aliquot (35 ng) of the cDNA was extended with deoxy(C) residues using terminal deoxynucleotidyl transferase[70], and annealed with 300 ng of the plasmid pBR322[71] which had been similarly tailed with deoxy(G) residues at the *Pst*I site. The annealed mixture was used to transform *E. coli* K-12 strain 294[40] and resultant tetracycline-resistant colonies were individually inoculated into wells of microtitre plates containing L broth[68] and 5 μg ml^{-1} tetracycline. Two copies of the cDNA library of 8,300 transformants were grown up on nitrocellulose filters and the DNA from each colony was fixed to the filter[41,42]. ^{32}P-labelled cDNA probes were prepared from 18S size gel-fractionated mRNA from induced and uninduced PBL cultures. Oligo(dT)$_{12-18}$ was used as a primer and reaction conditions have been previously described[13]. One set of 86 filters (96 colonies per filter) containing the entire cDNA library was hybridized[72] to 2×10^7 c.p.m. of the induced ^{32}P-cDNA. The duplicate set of filters was hybridized with 2×10^7 c.p.m. of uninduced ^{32}P-cDNA. After 16 h at 45 °C, filters were washed extensively[72] and exposed to X-ray film. The two filters shown here are representative of 86 such sets: approximately half the colonies hybridize with both probes, while half fail to hybridize with either probe, and ~1% hybridize with only the induced probe. An example of an 'induced' clone is labelled as H12.

Sequence analysis of the cDNA insert of plasmid p69

The complete nucleotide sequence of the *Pst*I insert from plasmid p69 was determined by the Maxam–Gilbert chemical procedure[46] and by the dideoxynucleotide chain termination method[47] after subcloning fragments into the M13 vector mp7 (ref. 48). The presence of 19 consecutive A residues corresponding to the 3' poly(A) terminus of the mRNA permitted us to orient the 1,200 nucleotide long sequence as shown in Fig. 3*b*. As IFN-γ mRNA co-migrates with 18S ribosomal RNA (>2,000 nucleotides) on denaturing agarose gels, it was important to see whether the 1,200 bp insert of p69 represented a full-length copy of its respective mRNA. To measure the length of this mRNA the synthetic tridecanucleotide dTCGTTTCCGAGAG, complementary to nucleotides 98–110 of the p69 insert (Fig. 3*b*), was chemically synthesized[49], 5' ^{32}P-labelled and used to prime the reverse transcription of induced lymphocyte poly(A) RNA into single-stranded ^{32}P-cDNA. The cDNA product was sized on a polyacrylamide–urea gel[46] and found to be 125–130 nucleotides long (unpublished results), indicating that the cDNA insert of p69 lacks only about 15–20 nucleotides of 5' mRNA sequence. Induced poly(A) mRNA was also fractionated on a denaturing agarose gel[33,34], transferred to nitrocellulose paper[50] and hybridized with ^{32}P-labelled cDNA insert from p69. A single hybridizing band, with the same mobility as 18S rRNA, was observed. Therefore, the mRNA corresponding to the p69 cDNA insert co-migrates with IFN-γ mRNA activity.

The DNA sequence of the p69 cDNA insert contains a single large open reading frame, beginning with the ATG codon at nucleotides 110–112 from the 5' end. This ATG is followed, 166 codons later, by a TAA termination triplet at nucleotides 608–610. This ATG is the first one encountered, consistent with the observation that the first ATG codon from the 5' end of mRNA usually serves as the site of translation initiation in eukaryotes[51]. The 3'-untranslated region of 587 nucleotides contains the hexanucleotide AATAAA (position 1,173–1,178) which precedes the site of polyadenylation in many eukaryotic mRNAs[52]. The 20 N-terminal amino acids encoded by the cDNA insert of p69 may constitute a signal peptide which is involved in the secretion of the mature polypeptide from lymphocytes. This putative signal sequence is strongly hydrophobic, having features common to eukaryotic secretory protein signal peptides in general[53,54] and more specifically to the IFN-αs for which DNA sequences have been determined[11–16]. It has the same potential cleavage site (Gly-Cys) that is likely to be the signal peptide cleavage sequence common to all IFN-αs[14]. Furthermore, the three amino acids (Ser-Leu-Gly) preceding this potential cleavage site are identical to those encoded by 10 of the 11 IFN-α genes sequenced to date[11–16].

The only other homology between this potential IFN-γ sequence and IFN-α or IFN-β covering more than three consecutive amino acids occurs at amino acids 15–18 (Lys-Lys-Tyr-Phe). These same four amino acids are found at positions 121–124 of two IFN-αs (IFN-αD and -αF; ref. 14). The 146 amino acid polypeptide estimated to constitute the mature protein has a calculated molecular weight of 17,110, much smaller than the molecular weights reported previously for IFN-γ (refs 18–21). The reasons for this discrepancy are not clear, but it should be noted that the molecular weights reported previously represent the size of the undenatured active species, which could exist as a multimer of individual subunits. Addi-

Table 1 Characterization of IFN-γ produced by *E. coli* and monkey cells

	Antiviral activity (U ml^{-1})				
Treatment	IFN-α standard	IFN-β standard	IFN-γ standard	*E. coli* W3110/pIFN-γtrp48 extract	COS-7 cell/pSVγ69 culture medium
Untreated	375	125	250	250	62.5
*p*H 2	375	125	<6	<12	<4
0.1% SDS	375	—	<4	<8	≤4
Rabbit anti-IFN-α	<8	125	250	250	62.5
Rabbit anti-IFN-β	375	<8	187	250	62.5
Rabbit anti-IFN-γ	375	125	<4	<8	<4

An overnight culture of *E. coli* W3110/pIFN-γtrp48 in Luria broth[68] containing 5 μg ml^{-1} tetracycline was diluted 1 : 100 in M9 medium[68] containing 0.2% glucose, 0.5% casamino acids and 5 μg ml^{-1} tetracycline at a 1 : 100 dilution. Indole acrylic acid was added to a final concentration of 20 μg ml^{-1} when A_{550} was 0.1–0.2. Samples (10 ml) were collected by centrifugation at A_{550} = 1.0 (~3.5 × 10^8 cells ml^{-1}) and resuspended immediately in 1 ml phosphate-buffered saline containing 1 mg bovine serum albumin (PBS–BSA). Cells were opened by sonication and cleared of debris by centrifugation. The supernatants were stored at 4 °C until assay. The plasmid pSVγ69 was introduced in COS-7 cells[62] using a modification of the DEAE-dextran technique[69]. Fresh monolayers of COS-7 cells in 6-cm diameter plates were transfected with 1 μg of pSVγ69 in 1.5 ml of Dulbecco's minimal essential medium (DMEM; Gibco), 200 μg ml^{-1} DEAE-dextran (500,000 molecular weight; Pharmacia), 0.05 M Tris-HCl (*p*H 7.5). After 16 h at 37 °C, the plates were washed twice with DMEM, and 1.5 ml of fresh DMEM supplemented with 10% fetal bovine serum, 2 mM glutamine, 50 μg ml^{-1} penicillin G and 50 mg ml^{-1} streptomycin was added to each plate. The medium was replaced the following day with serum-free DMEM. Fresh serum-free medium was then added every day. The collected media were stored at 4 °C until assayed. IFN-α and IFN-β control samples were NIH reference standards. The IFN-γ control was partially purified (~10^6 units per mg) from induced PBLs. The anti-IFN-α and -β were obtained from the National Institute of Allergy and Infectious Diseases. The anti-IFN-γ antisera was prepared using authentic IFN-γ (5–20% purity) purified from stimulated PBLs. Samples for antibody neutralizations were diluted, if necessary, then incubated for 2 h at 4 °C with 1 : 20 dilutions of rabbit anti-human leukocyte, fibroblast or immune interferon antisera. Samples were centrifuged for 3 min at 12,000*g* before assay. To test *p*H 2 stability, samples were adjusted to *p*H 2 by addition of 1 M HCl, incubated for 2 h at 4 °C and neutralized by addition of 1 M NaOH before assay. To test SDS sensitivity, samples were incubated with an equal volume of 0.2% SDS for 2 h at 4 °C before assay. The IFN assay was performed as described in Fig. 1 legend.

tionally, IFN-γ is glycosylated *in vivo*[20,21,55], which could affect molecular weight estimates. Consistent with this observation is the presence of two potential *N*-glycosylation sites[56] in the predicted protein sequence, at amino acids 28–30 (Asn-Gly-Thr) and 100–102 (Asn-Tyr-Ser). As the only two cysteines present in the deduced amino acid sequence occur at positions 1 and 3, the tertiary structure of the polypeptide is probably not dependent on intramolecular disulphide bonds. This is in agreement with the finding that, in contrast to IFN-α and IFN-β, disulphide linkages are not critical for the antiviral activity of IFN-γ (ref. 21). The mature protein sequence shown in Fig. 3*b* is quite basic in character, having 27 basic amino acids (Arg+Lys) and 19 acidic residues (Asp+Glu). This is consistent with the observation of Yip *et al.*[20] that IFN-γ has a high isoelectric point (*p*I = 8.6–8.7), whereas IFN-α and IFN-β have been shown to have distinctly lower *p*Is[20,57].

Synthesis of IFN-γ in *E. coli* and monkey cells

As IFN-γ has not been purified to homogeneity, nothing is known directly about its amino acid sequence. Therefore, the only direct means of proving that the cDNA sequence of p69 actually codes for IFN-γ is by demonstrating that the polypeptide obtained through expression of this cloned gene has the properties of natural IFN-γ. Two independent expression systems involving *E. coli* and monkey cells were used for this purpose. The *E. coli* system was selected because it has been used to produce biologically active IFN-αs and IFN-β (refs 10, 13). The mammalian cell system was chosen because, unlike *E. coli*, it should be able to perform specific processing (for example, glycosylation) which might be required for the expression of a biologically active product.

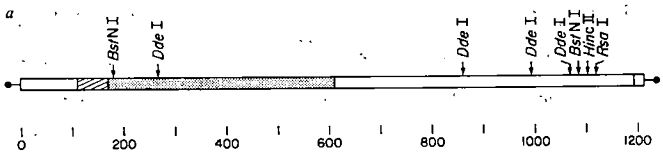

```
b
5'                                                                                               S1
                                                                                                 met lys tyr
CTGAAGATCAGCTATTAGAAGAGAAAGATCAGTTAAGTCCTTTGGACCTGATCAGCTTGATACAAGAACTACTGATTTCAACTTCTTTGGCTTAATTCTCTCGGAAACG ATG AAA TAT
                                                  50                                                  100

                        S10                                     S20  1                                  10
thr ser tyr ile leu ala phe gln leu cys ile val leu gly ser leu gly CYS TYR CYS GLN ASP PRO TYR VAL LYS GLU ALA GLU ASN
ACA AGT TAT ATC TTG GCT TTT CAG CTC TGC ATC GTT TTG GGT TCT CTT GGC TGT TAC TGC CAG GAC CCA TAT GTA AAA GAA GCA GAA AAC
                                        150                                                                 200

                        20                                      30                                      40
LEU LYS LYS TYR PHE ASN ALA GLY HIS SER ASP VAL ALA ASP ASN GLY THR LEU PHE LEU GLY ILE LEU LYS ASN TRP LYS GLU GLU SER
CTT AAG AAA TAT TTT AAT GCA GGT CAT TCA GAT GTA GCG GAT AAT GGA ACT CTT TTC TTA GGC ATT TTG AAG AAT TGG AAA GAG GAG AGT
                                                    250

                        50                                      60                                      70
ASP ARG LYS ILE MET GLN SER GLN ILE VAL SER PHE TYR PHE LYS LEU PHE LYS ASN PHE LYS ASP ASP GLN SER ILE GLN LYS SER VAL
GAC AGA AAA ATA ATG CAG AGC CAA ATT GTC TCC TTT TAC TTC AAA CTT TTT AAA AAC TTT AAA GAT GAC CAG AGC ATC CAA AAG AGT GTG
300                                                                 350

                        80                                      90                                      100
GLU THR ILE LYS GLU ASP MET ASN VAL LYS PHE PHE ASN SER ASN LYS LYS LYS ARG ASP ASP PHE GLU LYS LEU THR ASN TYR SER VAL
GAG ACC ATC AAG GAA GAC ATG AAT GTC AAG TTT TTC AAT AGC AAC AAA AAG AAA CGA GAT GAC TTC GAA AAG CTG ACT AAT TAT TCG GTA
            400                                                                 450

                        110                                     120                                     130
THR ASP LEU ASN VAL GLN ARG LYS ALA ILE HIS GLU LEU ILE GLN VAL MET ALA GLU LEU SER PRO ALA ALA LYS THR GLY LYS ARG LYS
ACT GAC TTG AAT GTC CAA CGC AAA GCA ATA CAT GAA CTC ATC CAA GTG ATG GCT GAA CTG TCG CCA GCA GCT AAA ACA GGG AAG CGA AAA
                            500                                                                 550

                        140                         146 STOP
ARG SER GLN MET LEU PHE GLN GLY ARG ARG ALA SER GLN
AGG AGT CAG ATG CTG TTT CAA GGT CGA AGA GCA TCC CAG TAA TGGTTGTCCTGCCTGCAATATTTGAATTTTAAATCTAAATCTATTTATTAATATTTAACATTA
                                        600                                                                 650

TTTATATGGGGAATATATTTTTAGACTCATCAATCAAATAAGTATTTATAATAGCAACTTTTGTGTAATGAAAATGAATATCTATTAATATATGTATTATTTATAATTCCTATATCCTG
                          700                                                   750

TGACTGTCTCACTTAATCCTTTGTTTTCTGACTAATTAGGCAAGGCTATGTGATTACAAGGCTTTATCTCAGGGGCCAACTAGGCAGCCAACCTAAGCAAGATCCCATGGGTTGTGTGT
    800                                                850                                                        900

TTATTTCACTTGATGATACAATGAACACTTATAAGTGAAGTGATACTATCCAGTTACTGCCGGTTTGAAAATATGCCTGCAATCTGAGCCAGTGCTTTAATGGCATGTCAGACAGAACT
                                      950                                                  1000

TGAATGTGTCAGGTGACCCTGATGAAAACATAGCATCTCAGGAGATTTCATGCCTGGTGCTTCCAAATATTGTTGACAACTGTGACTGTACCCAAATGGAAAGTAACTCATTTGTTAAA
                  1050                                                  1100

ATTATCAATATCTAATATATATGAATAAAGTGTAAGTTCACAACTAAAAAAAAAAAAAAAAAAAAA
1150                                            1200
                                                             3'
```

Fig. 3 *a*, Restriction endonuclease map of the cDNA insert of p69. The cDNA insert is bounded by *Pst*I sites (dots at both ends) and poly(dG-dC) tails (single lines). The number and size of fragments produced by restriction nuclease cleavage were estimated by electrophoresis through 6% polyacrylamide gels. Positions of sites were confirmed by nucleic acid sequencing (presented below). The shaded region indicates the coding sequences of the putative mature protein, the cross-hatched region represents the putative 20 residue signal peptide coding sequence, and the open regions show the 3'- and 5'-noncoding sequences. *b*, Nucleotide sequence and deduced amino acid sequence of plasmid p69 cDNA insert. The putative signal sequence is represented by the residues labelled S1 to S20. The entire sequence was determined by both the dideoxynucleotide chain termination method[47] after subcloning fragments into the M13 vector mp7[48] and the chemical method of Maxam and Gilbert[46]. Numbers above each line refer to amino acid position (S refers to presumed signal peptide) and numbers below each line to nucleotide position.

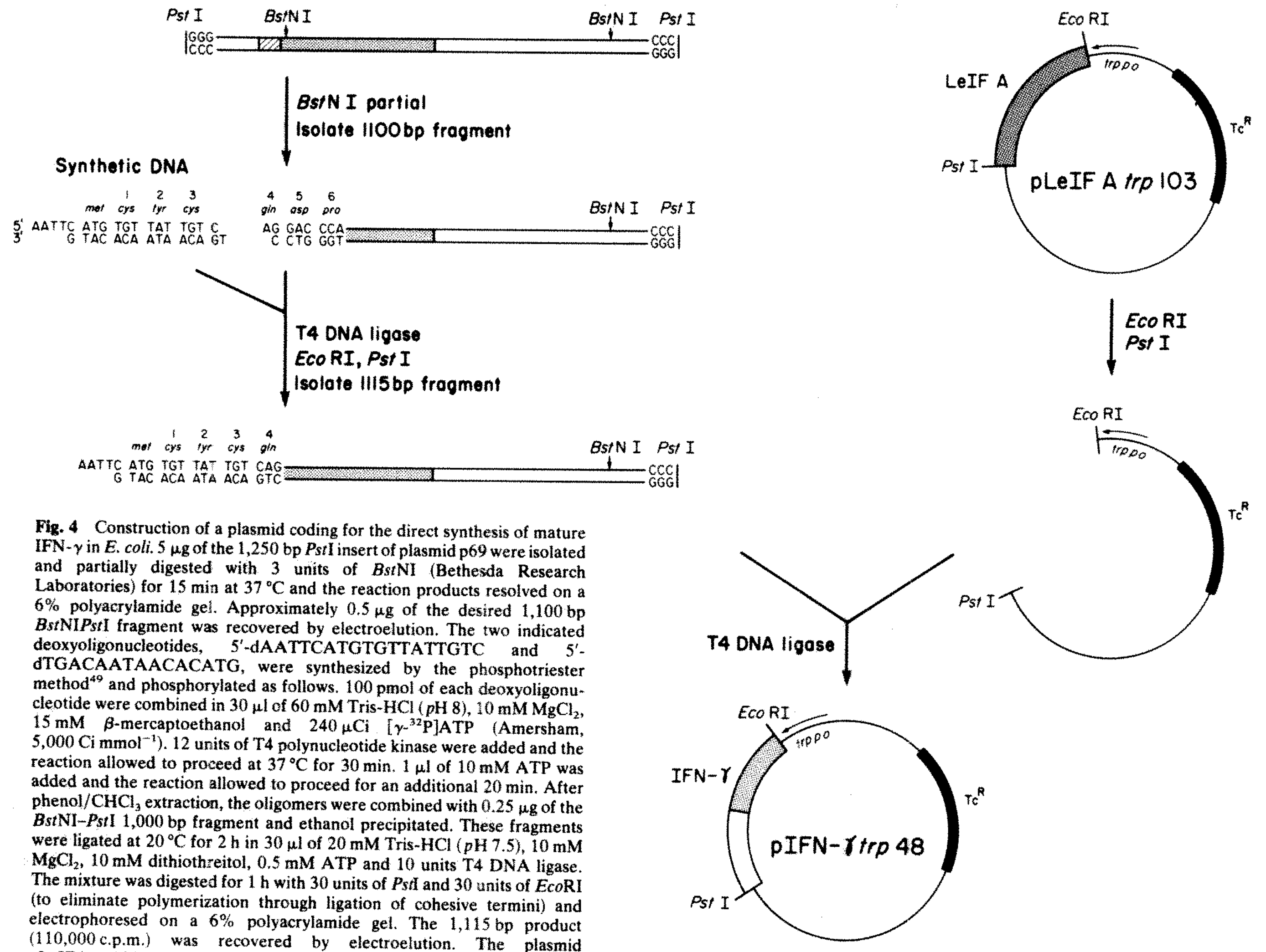

Fig. 4 Construction of a plasmid coding for the direct synthesis of mature IFN-γ in *E. coli*. 5 μg of the 1,250 bp *Pst*I insert of plasmid p69 were isolated and partially digested with 3 units of *Bst*NI (Bethesda Research Laboratories) for 15 min at 37 °C and the reaction products resolved on a 6% polyacrylamide gel. Approximately 0.5 μg of the desired 1,100 bp *Bst*NI*Pst*I fragment was recovered by electroelution. The two indicated deoxyoligonucleotides, 5′-dAATTCATGTGTTATTGTC and 5′-dTGACAATAACACATG, were synthesized by the phosphotriester method[49] and phosphorylated as follows. 100 pmol of each deoxyoligonucleotide were combined in 30 μl of 60 mM Tris-HCl (*p*H 8), 10 mM $MgCl_2$, 15 mM β-mercaptoethanol and 240 μCi [γ-^{32}P]ATP (Amersham, 5,000 Ci $mmol^{-1}$). 12 units of T4 polynucleotide kinase were added and the reaction allowed to proceed at 37 °C for 30 min. 1 μl of 10 mM ATP was added and the reaction allowed to proceed for an additional 20 min. After phenol/$CHCl_3$ extraction, the oligomers were combined with 0.25 μg of the *Bst*NI–*Pst*I 1,000 bp fragment and ethanol precipitated. These fragments were ligated at 20 °C for 2 h in 30 μl of 20 mM Tris-HCl (*p*H 7.5), 10 mM $MgCl_2$, 10 mM dithiothreitol, 0.5 mM ATP and 10 units T4 DNA ligase. The mixture was digested for 1 h with 30 units of *Pst*I and 30 units of *Eco*RI (to eliminate polymerization through ligation of cohesive termini) and electrophoresed on a 6% polyacrylamide gel. The 1,115 bp product (110,000 c.p.m.) was recovered by electroelution. The plasmid pLeIFAtrp103 is a derivative of the plasmid pLeIFA25 (ref. 13) in which the *Eco*RI site distal to the LeIF A gene has been removed. 3 μg of pLeIFAtrp103 were digested with 20 units of *Eco*RI and 20 units of *Pst*I for 90 min at 37 °C and electrophoresed on a 6% polyacrylamide gel. The large (~3,900 bp) vector fragment was recovered by electroelution and the 1,115 bp *Eco*RI–*Pst*I IFN-γ DNA fragment ligated into 0.15 μg of this prepared vector. Transformation of *E. coli* K-12 strain 294[40] gave 120 tetracycline-resistant colonies. Plasmid DNA was prepared from 60 of these transformants and digested with *Eco*RI and *Pst*I. Three of these plasmids contained the desired 1,115 bp *Eco*RI-*Pst*I fragment. DNA sequence analysis verified that these plasmids had the desired nucleotide sequence at the junctions between the *trp* promoter, synthetic DNA and cDNA. One of these plasmids, pIFN-γtrp48, was chosen for additional study.

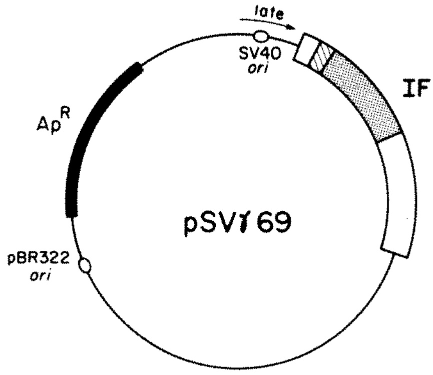

Fig. 5 Plasmid constructed for the expression of IFN-γ in monkey cells. The 342 bp *Hin*dIII–*Pvu*II fragment encompassing the SV40 replication origin[60] was converted to a fragment bounded by *Eco*RI restriction sites. The *Hin*dIII site was converted to an *Eco*RI site by addition of a synthetic oligomer (5′dAGCTGAATTC) and the *Pvu*II site was converted by ligation to an *Eco*RI site which had been filled-in using DNA polymerase I (Klenow fragment). The *Eco*RI fragment containing the SV40 origin was ligated into the *Eco*RI site of pML-1[59]. The resulting expression vector was chosen which contained the SV40 late promoter oriented to read away from the ampicillin-resistance gene of pML-1. The *Eco*RI site nearest the ampicillin-resistance gene was destroyed by partial *Eco*RI digestion, filling in with the Klenow fragment of DNA polymerase I, and subsequent ligation (as outlined in ref. 73). The 1,250 bp *Pst*I insert of p69 was converted to a fragment bounded by *Eco*RI sites by insertion in the *Pst*I site of pNCV[13], as the *Pst*I site of pNCV is flanked by *Eco*RI sites. The *Eco*RI-flanked cDNA insert was ligated into the single *Eco*RI site of the pML-SV40 expression vector to give the plasmid shown.

The procedure followed to express the cDNA insert of p69 directly in *E. coli* was similar to that used previously for human growth hormone[39], IFN-β (ref. 10) and several IFN-αs[13,16], and is outlined in Fig. 4. A *Bst*NI restriction site located at codon 4 of the presumed mature coding sequence was used to remove the signal peptide coding region. Two synthetic deoxyoligonucleotides were designed which restore the codons for amino acids 1–4, incorporate an ATG translational initiation codon and create an *Eco*RI cohesive terminus. These two oligomers were ligated to the remainder of the cDNA insert to construct a 1,115 bp synthetic–natural hybrid gene coding for a polypeptide of 147 amino acids and bounded by *Eco*RI and *Pst*I sites. This gene was inserted into the plasmid pLeIFAtrp103 (a derivative of pLeIFA25 (ref. 13) in which the *Eco*RI site distal to the LeIF *A* gene was destroyed) between the *Eco*RI and *Pst*I sites to give the expression plasmid pIFN-*γtrp48*. In this plasmid the cloned gene is transcribed under the control of a 300 bp fragment of the *E. coli trp* operon[13]. This fragment contains the *trp* promoter, operator and the Shine–Dalgarno sequence of the *trp* leader peptide[58], but lacks the ATG sequence for initiation of translation of the leader peptide. *E. coli* W3110 strains transformed with either pIFN-γtrp48 or p69 were grown and extracted for interferon assay (see Table 1). Extracts from cultures of W3110/pIFN-γtrp48 exhibited definite interferon activity (~250 units per ml of extract), whereas no activity (<3 units per ml) was detected in extracts of W3110/p69.

To express the putative IFN-γ coding sequence of p69 in mammalian cell culture, the expression vector pSVγ69 (Fig. 5)

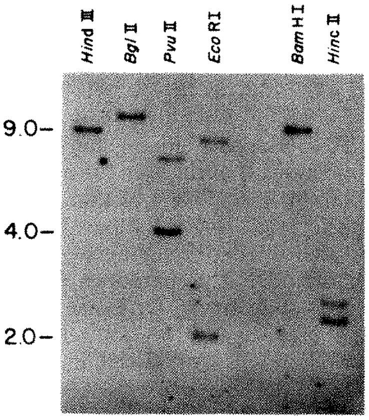

Fig. 6 Hybridization of human genomic DNA with a ^{32}P-labelled cDNA probe from plasmid p69. High molecular weight human lymphocyte DNA (5 μg) prepared by the procedure of Blin and Stafford[74] was digested to completion with various restriction endonucleases, electrophoresed on 1.0% agarose gels and blotted to a nitrocellulose filter[67]. The ^{32}P-labelled DNA probe was prepared from a 594 bp *Dde*I fragment (nucleotides 266–860 of Fig. 3*b*) of the cDNA insert of p69 as described previously[45]. 1 × 10^7 c.p.m. of the probe were hybridized with the filter for 16 h and then washed as described elsewhere[14]. Two hybridizing DNA fragments were observed with three endonuclease digests: *Pvu*II (6.7 and 4.0 kbp), *Eco*RI (8.8 and 2.0 kbp) and *Hinc*II (2.5 and 2.2 kbp). Three endonuclease digestion patterns provide only one hybridizing DNA fragment: *Hin*dIII (9.0 kbp), *Bgl*II (11.5 kbp) and *Bam*HI (9.5 kbp).

was constructed from the following three components: (1) the plasmid pML-1 (pML-1 is a derivative of pBR322 in which sequences known to inhibit the replication of SV40–pBR322 recombinants in simian cells have been deleted, but which still contains the ampicillin-resistance selectable marker and an *E. coli* replication origin[59]); (2) a 342 bp *Pvu*II–*Hin*dIII fragment of SV40 virus providing the replication origin of SV40[60] and which is thought to encompass the promoter for both the early and late SV40 transcriptional units[61]; and (3) the entire cDNA insert from plasmid p69.

The cDNA insert and the SV40 origin region were oriented in pSVγ69 such that the interferon structural gene should be transcribed from the promoter for the late transcriptional unit (Fig. 5). This vector was introduced by DNA transfection into the transformed monkey cell line COS-7 (ref. 62). COS-7 endogeneously expresses SV40 large T antigen and has been shown to permit the propagation of recombinant plasmids containing pML-1 and SV40 origin sequences[59,60]. Cell media from transfected cultures were assayed daily for the presence of interferon activity. Yields of 50–100 units per ml were obtained 3 or 4 days after transfection, indicating that the interferon was being secreted into the culture medium by the COS-7 cells. No interferon activity was observed in the media from cells transfected with plasmids in which the cDNA coding region was inserted in the opposite orientation to that shown in Fig. 5 (data not shown).

Characterization of interferon activity produced by *E. coli* and monkey cells

The properties of the interferon activity present in extracts of *E. coli* W3110/pIFN-γtrp48 and secreted from COS-7/pSVγ69 cells were compared with authentic human IFN-γ produced by stimulated PBLs and with authentic IFN-α and IFN-β. Distinguishing characteristics of IFN-γ include *p*H 2 lability and lack of neutralization by antisera prepared against human IFN-α or IFN-β (ref. 2). As indicated in Table 1, the interferon produced by *E. coli* and monkey cells, like the IFN-γ produced by SEB/desacetylthymosin α_1-stimulated PBLs, was not neutralized by antisera to either IFN-α or IFN-β, although these antisera were effective in neutralizing authentic IFN-α or IFN-β. Antisera prepared against partially purified PBL-produced IFN-γ (E. Rinderknecht and V. Anicetti, unpublished results) completely neutralized the interferon activity synthesized by *E. coli* and monkey cells while having no effect on the activity of IFN-α and IFN-β (Table 1). Furthermore, the complete loss of activity observed when these interferon preparations were treated with *p*H 2 or 0.1% SDS is characteristic of IFN-γ, and distinct from IFN-α and IFN-β. Therefore, the polypeptide encoded by the cloned cDNA sequence of p69 has the same immunological and chemical properties as authentic IFN-γ.

A single gene for IFN-γ

The human interferon gene family comprises 12 or more distinct IFN-α genes having 80–95% DNA sequence homology[11–16,63] and at least one IFN-β gene (IFN-β_1; refs 64–66) which is 40–50% homologous with the IFN-α genes. To estimate the number of related IFN-γ genes in the human genome, human DNA of one individual was digested with several restriction enzymes, electrophoresed through agarose gels, transferred to nitrocellulose paper[67] and hybridized to a ^{32}P-labelled IFN-γ cDNA probe (Fig. 6). *Hinc*II is the only one of the six restriction enzymes used that cleaves the IFN-γ cDNA sequence, but the *Hinc*II site is not located in the DNA fragment which was used as probe. A unique, intronless gene would thus have appeared as a single hybridizing DNA fragment in each lane of the gel. Instead, two hybridizing DNA fragments were observed for three of the endonuclease digestions (*Pvu*II, *Eco*RI, *Hinc*II) and single hybridizing fragments of about 9 kilobase pairs (kbp) each were found for the other digestions (*Hin*dIII, *Bgl*II, *Bam*HI). Similar genomic blots using DNA from other individuals gave the same hybridization patterns. There are two possible explanations for these results: first, there are two homologous and closely linked (<8 kbp apart) IFN-γ genes separated by *Pvu*II, *Eco*RI and *Hinc*II sites, and second, there is a single IFN-γ gene which contains one or more introns containing *Eco*RI, *Pvu*II and *Hinc*II sites. This second possibility was supported by repeating the hybridizations with a ^{32}P-labelled probe prepared from the 3′-untranslated region of IFN-γ cDNA. In this experiment only single *Pvu*II, *Eco*RI and *Hinc*II fragments hybridized to the probe (data not shown). The gene structure of IFN-γ is therefore distinctly different from that of IFN-α and IFN-β, which contain no introns[15,63–66].

Discussion

Poly(A) mRNA from human lymphocytes producing IFN-γ was fractionated on a denaturing agarose gel. The 18S size fraction was used to prepare a cDNA library in *E. coli*. Twenty-two bacterial clones containing potential IFN-γ sequences were identified by specific hybridization to ^{32}P-cDNA probes prepared using mRNA from induced lymphocytes and failure to hybridize to similar probes prepared from uninduced mRNA. Restriction mapping and DNA hybridization experiments revealed that all 22 induced cDNA clones were related and that the frequency of these clones in the cDNA library was about 1:120. Therefore, the frequency of IFN-γ mRNA in our most active poly(A) RNA preparation is ~1:2,400 because the mRNA used to prepare this cDNA library had been enriched about 20-fold in IFN-γ sequence by the agarose gel fractionation procedure.

The 1,194 bp cDNA insert (excluding poly(A) sequence and dG·dC tails) of p69 codes for a polypeptide of 166 amino acids, 20 of which are probably cleaved during the process of secretion of mature IFN-γ from lymphocytes. The encoded amino acid sequence, which bears little resemblance to those of IFN-α or IFN-β, has two potential glycosylation sites and is quite basic in character. Identification of this sequence as IFN-γ was obtained by expression of the cDNA sequence of p69 in bacterial and mammalian cells. In both systems the expression product was shown to have antiviral activity which was immunologically indistinguishable from that of the IFN-γ produced by stimulated human lymphocytes. Additionally, the SDS and *p*H 2 sensitivity observed for the IFN-γ produced by bacteria and monkey cells are distinguishing features of authentic IFN-γ (refs 2, 18–21).

The amounts of antiviral activity recovered from *E. coli* producing IFN-γ are significantly lower than those obtained for IFN-α or IFN-β using similar expression vectors[10,13,16]. If a specific activity range of 10^8–10^9 units per mg is assumed for IFN-γ (ref. 20), between 8 and 80 active molecules are present per cell. However, if the specific activity of the interferon depends to some degree on its state of glycosylation, considerably more interferon molecules could be present per cell. Additionally, if we were incorrect in our assumptions about which amino acids constitute the signal peptide, the molecule expressed in *E. coli* may not exhibit the same specific activity as natural IFN-γ. If one assumes that authentic mature IFN-γ is a 146-amino acid polypeptide, its molecular weight, minus carbohydrate, would be 17,110. The difference between this value and the published molecular weights of 35,000–70,000 for IFN-γ probably cannot be accounted for by glycosylation alone. It is conceivable that authentic IFN-γ is associated with carrier proteins in serum or exists as a multimer of identical subunits. The purification and sizing of IFN-γ synthesized by *E. coli* and monkey cells should help resolve this discrepancy in molecular weight.

The human IFN-γ gene corresponding to the cDNA sequence described here seems to contain at least one intron and to have no additional genomic homologues. It remains to be determined, however, whether additional nonhomologous genes exist which code for proteins meeting the criteria required for classification as IFN-γ (refs 1, 2).

We thank Dr Lloyd Svedersky and Anna Hui for processing PBLs, Eileen Cunningham for performing *Xenopus* oocyte injections, Laurie May for interferon assays, Dr Nowell Stebbing for his support of those aspects of the work which were performed in the Biology Department at Genentech, Mark Vasser for deoxyoligonucleotide synthesis, Shirley Norton for plasmid DNA preparations, Dr Peter Seeburg for help with the DNA sequencing, Dr Ernst Rinderknecht and Vince Anicetti for preparing IFN-γ antiserum and Dr Yakov Gluzman for providing the COS-7 cell line.

Received 16 November; accepted 7 December 1981.

1. Stewart, W. E. II *The Interferon System* (Springer, Berlin, 1979).
2. Stewart, W. E. II *et al. Nature* **286,** 110 (1980).
3. Zoon, K. C. *et al. Science* **207,** 527–528 (1980).
4. Knight, E. Jr, Hunkapillar, M. W., Korant, B. D., Hardy, R. W. F. & Hood, L. E. *Science* **207,** 525–526 (1980).
5. Allen, G. & Fantes, K. H. *Nature* **287,** 408–411 (1980).
6. Levy, W. P., Shively, J., Rubenstein, M., Del Valle, U. & Pestka, S. *Proc. natn. Acad. Sci. U.S.A.* **77,** 5102–5104 (1980).
7. Stein, S. *et al. Proc. natn. Acad. Sci. U.S.A.* **77,** 5716–5719 (1980).
8. Taniguchi, T., Ohno, S., Fujii-Kuriyama, Y. & Muramatsu, M. *Gene* **10,** 11–15 (1980).
9. Derynck, R. *et al. Nature* **285,** 542–547 (1980).
10. Goeddel, D. V. *et al. Nucleic Acids Res.* **8,** 4057–4073 (1980).
11. Mantei, N. *et al. Gene* **10,** 1–10 (1980).
12. Streuli, M., Nagata, S. & Weissmann, C. *Science* **209,** 1343–1347 (1980).
13. Goeddel, D. V. *et al. Nature* **287,** 411–416 (1980).
14. Goeddel, D. V. *et al. Nature* **290,** 20–26 (1981).
15. Lawn, R. M. *et al. Science* **212,** 1159–1162 (1981).
16. Yelverton, E., Leung, D., Weck, P., Gray, P. W. & Goeddel, D. V. *Nucleic Acids Res.* **9,** 731–741 (1981).
17. Hitzeman, R. *et al. Nature* **293,** 717–722 (1981).
18. Langford, M. P., Georgiades, J. A., Stanton, G. J., Dianzani, F. & Johnson, H. M. *Infect. Immun.* **26,** 36–41 (1979).
19. de Ley, M. *et al. Eur. J. Immun.* **10,** 877–883 (1980).
20. Yip, Y. K., Pang, R. H. L., Urban, C. & Vilcek, J. *Proc. natn. Acad. Sci. U.S.A.* **78,** 1601–1605 (1981).
21. Nathan, I., Groopman, J. E., Quan, S. G., Gersch, N. & Golde, D. W. *Nature* **292,** 842–844 (1981).
22. Wallace, D. M., Hitchcock, M. J. M., Reber, S. B. & Berger, S. L. *Biochem. biophys. Res. Commun.* **100,** 865–871 (1981).
23. Taniguchi, T., Pang, R. H. L., Yip, Y. K., Henriksen, D. & Vilcek, J. *Proc. natn. Acad. Sci. U.S.A.* **78,** 3469–3472 (1981).
24. Fleishmann, W. R., Georgiades, J. A., Osborne, L. L. & Johnson, H. M. *Infect. Immun.* **26,** 248–253 (1979).
25. Rubin, B. Y. & Gupta, S. L. *Proc. natn. Acad. Sci. U.S.A.* **77,** 5928–5932 (1980).
26. Sonnenfeld, G., Mandel, A. D. & Merigan, T. C. *Cell. Immun.* **40,** 285–293 (1978).
27. Blalock, J. E., Georgiades, J. A., Langford, M. P. & Johnson, H. M. *Cell. Immun.* **49,** 390–394 (1980).
28. Crane, J. L. Jr, Glasgow, L. A., Kern, E. R. & Youngner, J. S. *J. natn. Cancer Inst.* **61,** 871–874 (1978).
29. Svedersky, L. P., Hui, A., May, L., McKay, P. & Stebbing, N. *Proc. 3rd int. Symp. Human Lymphokines* (Academic, New York, in the press).
30. Berger, S. B. & Birkenmeier, C. S. *Biochemistry* **18,** 5143–5149 (1979).
31. Aviv, H. & Leder, P. *Proc. natn. Acad. Sci. U.S.A.* **69,** 1408–1412 (1972).
32. Lehrach, H., Diamond, D., Wozney, J. M. & Boedtker, H. *Biochemistry* **16,** 4743–4751 (1977).
33. Lynch, K. R., Pennica, D., Ennis, H. L. & Cohen, P. S. *Virology* **98,** 251–254 (1979).
34. Gurdon, J. B., Lane, C. D., Woodland, H. R. & Marbaix, G. *Nature* **233,** 177–182 (1971).
35. Cavalieri, R. L., Havell, E. A., Vilcek, J. & Pestka, S. *Proc. natn. Acad. Sci. U.S.A.* **74,** 3287–3291 (1977).
36. Colman, A. & Morser, J. *Cell* **17,** 517–526 (1979).
37. Berger, S. L. *et al. J. biol. Chem.* **255,** 2955–2961 (1980).
38. Wickens, M. P., Buell, G. N. & Schimke, R. T. *J. biol. Chem.* **253,** 2483–2495 (1978).
39. Goeddel, D. V. *et al. Nature* **281,** 544–548 (1979).
40. Backman, K., Ptashne, M. & Gilbert, W. *Proc. natn. Acad. Sci. U.S.A.* **73,** 4174–4178 (1976).
41. Grunstein, M. & Hogness, D. S. *Proc. natn. Acad. Sci. U.S.A.* **72,** 3961–3965 (1975).
42. Hanahan, D. & Meselson, M. *Gene* **10,** 63–67 (1980).
43. Birnboim, H. C. & Doly, J. *Nucleic Acids Res.* **7,** 1513–1523 (1979).
44. Kafatos, F. C., Jones, C. W. & Efstratiadis, A. *Nucleic Acids Res.* **7,** 1541–1552 (1979).
45. Taylor, J. M., Illmensee, R. & Summers, S. *Biochim. biophys. Acta* **442,** 324–330 (1976).
46. Maxam, A. M. & Gilbert, W. *Meth. Enzym.* **65,** 499–560 (1980).
47. Smith, A. J. H. *Meth. Enzym.* **65,** 560–580 (1980).
48. Messing, J., Crea, R. & Seeburg, P. H. *Nucleic Acids Res.* **9,** 309 (1981).
49. Crea, R., Kraszewski, A., Hirose, T. & Itakura, K. *Proc. natn. Acad. Sci. U.S.A.* **75,** 5765–5769 (1978).
50. Thomas, P. S. *Proc. natn. Acad. Sci. U.S.A.* **77,** 5201–5205 (1980).
51. Kozak, M. *Cell* **15,** 1109–1123 (1978).
52. Proudfoot, N. J. & Brownlee, G. G. *Nature* **263,** 211–214 (1976).
53. Blobel, G. *et al. Symp. Soc. exp. Med.* **33,** 9–36 (1979).
54. Davis, B. D. & Tai, P. C. *Nature* **283,** 422–438 (1980).
55. Mizrahi, A. *et al. J. biol. Chem.* **253,** 7612–7615 (1978).
56. Winzler, R. J. in *Hormonal Proteins and Peptides* (ed. Li, C. H.) 1–15 (Academic, New York, 1973).
57. Havell, E. A., Yip, Y. K. & Vilcek, J. *Archs Virol.* **55,** 121–129 (1977).
58. Miozzari, G. F. & Yanofsky, C. *J. Bact.* **133,** 1457–1466 (1978).
59. Lusky, M. & Botchan, M. *Nature* **293,** 79–81 (1981).
60. Myers, R. M. & Tjian, R. *Proc. natn. Acad. Sci. U.S.A.* **77,** 6491–6495 (1980).
61. Griffin, B. in *DNA Tumor Viruses* 2nd edn (ed. Tooze, J.) 61–123 (Cold Spring Harbor Laboratory, New York, 1980).
62. Gluzman, Y. *Cell* **23,** 175–182 (1981).
63. Nagata, S., Mantei, N. & Weissmann, C. *Nature* **287,** 401–408 (1980).
64. Houghton, M. *et al. Nucleic Acids Res.* **9,** 247–266 (1981).
65. Tavernier, J. *et al. Nucleic Acids Res.* **9,** 461–471 (1981).
66. Lawn, R. M. *et al. Nucleic Acids Res.* **9,** 1045–1052 (1981).
67. Southern, E. M. *J. molec. Biol.* **98,** 503–517 (1975).
68. Miller, J. *Experiments in Molecular Genetics*, 431–433 (Cold Spring Harbor Laboratory, New York, 1972).
69. McCutchan *et al. J. natn. Cancer Inst.* **41,** 351 (1968).
70. Chang, A. C. Y. *et al. Nature* **275,** 617–624 (1978).
71. Bolivar, F. *et al. Gene* **2,** 95–113 (1977).
72. Fritsch, E. F., Lawn, R. M. & Maniatis, T. *Cell* **19,** 959–972 (1980).
73. Itakura *et al. Science* **198,** 1056 (1977).
74. Blin, N. & Stafford, D. W. *Nucleic Acids Res.* **3,** 2303–2308 (1976).

LETTERS TO NATURE

Is the remnant of SN1006 composed of iron?

A. C. Fabian & G. C. Stewart

Institute of Astronomy, Madingley Road, Cambridge CB3 0HA, UK

W. Brinkmann

MPI für Extraterrestrische Physik, D-8046 Garching bei München, FRG

The remnant of the supernova explosion of AD 1006 (the brightest in recorded history) has a shell-like appearance at both radio and X-ray wavelengths. Einstein X-ray observations by Pye *et al.*[1] show a soft (photon energy $\varepsilon \leqslant \frac{1}{4}$ keV) filled interior surrounded by a harder ($\varepsilon \geqslant 1$ keV) unresolved ring of emission of radius ~15 arc min. Superficially it appears to be similar to most supernova remnants for which many studies have shown that the X-ray emission is thermal radiation from gas shock-heated by high-velocity ejecta. The spectrum[2] of parts of the edge of the remnant in the range $0.75 \leqslant \varepsilon \leqslant 10$ keV shows, however, no evidence for line emission. The spectral shape is consistent with a power-law perhaps due to a non-thermal mechanism. Moreover, the total mass of gas[1] required exceeds ~10 $M_\odot$ if it is of normal cosmic abundance. This is much greater than that expected for a remnant several hundred parsecs above the galactic plane. As no pulsar (or Crab-like morphology) is evident in the remnant of SN1006, Reynolds and Chevalier[3] have proposed that relativistic particles are being efficiently accelerated in shocked gas, and provide the major source of X rays through synchrotron emission. SN1006 is then an important region for the study of such acceleration processes. Here we reinvestigate a thermal interpretation and show that the element abundances associated with a Type I supernova[4–7] may provide an alternative explanation.

First we note that the observed lack of line emission from the edge of the remnant requires that sulphur, silicon and iron be at less than half their cosmic value relative to hydrogen[2]. We suggest that SN1006 was a Type I supernova of a few solar masses exploding into its own stellar wind (outer density $\rho \propto$

0028-0836/82/060508—02$01.00

r^{-2}). If the progenitor star was a pop II object (appropriate for its galactic position) then it is quite reasonable to suppose that the metal abundances are lower than the cosmic values. It is also possible that most of the metals are in the form of grains, which have not yet had time to combine with the hot gas. The stellar wind may have been associated with a red-giant phase (compare with the formation of planetary nebulae) or mass-transfer from a binary companion. The unresolved outer ring of emission[1] is then due to the shocked wind material. Gas shocked earlier (and closer to the contact discontinuity) is now denser and cooler than gas that is now just being shocked and swept up. Bremsstrahlung from a range of densities and temperatures in the shocked wind can then mimic a power-law spectrum.

The mass of the interior region has been estimated[1] as $\sim 6M_{\odot}$, if due to a gas of cosmic abundance (the temperature is $\sim 10^6$ K). Most of the emission is strongly peaked below 0.25 keV and could be completely due to lines. (The spectral resolution of the detector used for these observations is ~100% at these energies.) It has been widely suggested[4-7] that $\sim 1M_{\odot}$ of ^{56}Fe is ejected in a Type I supernova explosion. Line emission from such material can easily provide the interior X-ray flux from SN1006 if it has a distance of ~1 kpc. Interstellar absorption corresponding to a column density of $N_{\rm H} \approx 5 \times 10^{20}$ cm^{-2} is required to make this hypothesis consistent. One clear prediction is the possibility of detecting coronal line emission from the interior of the remnant in the optical. We expect a flux of $\approx 2 \times 10^{-7}$ erg s^{-1} cm^{-2} sr^{-1}.

The overall 0.2–2.5 keV spectrum[8] of SN1006, after subtraction of a contribution due to the Lupus Loop, does show evidence of an emission feature at ~0.6 keV. This is identified in ref. 8 as oxygen line emission, but we note that line emission due to calcium, which is also likely to be produced in a Type I outburst, occurs at a similar energy.

One major problem with any thermal interpretation of the X-ray observations lies in maintaining the interior of the remnant at 10^6 K. Adiabatic cooling on the expansion time scale erases all memory of the initial phase of expansion of the remnant. All but large scale velocity inhomogeneities should have decayed and the effects of radioactivity will have died away. We propose that a reverse shock[6] propagated back through the material at an age of a few hundred years. This requires the ejecta to have collided with roughly its own mass in that time. Perhaps the pre-supernova was surrounded by a wind with $\rho \propto r^{-2}$ at large radii ($R \leqslant 10^{18}$ cm), but with ρ constant (and total mass $\sim 1\,M_{\odot}$) at small radii (the wind velocity may have decreased and $\dot{M}$ increased) just before the supernova explosion. We have verified that present-day interior temperatures of $\sim 10^6$ K and reasonable luminosities are obtainable from such a situation by numerical computation of a spherically-symmetric explosion. The remnant is now freely expanding. No definite conclusion may be drawn, although the structure of young remnants depends strongly on the initial conditions in the ejecta and surrounding material. We consider that a complex structure is quite likely and that the appearance of young supernova remnants may be quite variable. The unusual properties of SN1006 discussed here may be partly due to its galactic location. The low temperature interior can be easily detected as the line-of-sight column density is low, and the expected low density of the surrounding interstellar medium allows a stellar wind to propagate freely to relatively large radii.

Optical confirmation that the interior of SN1006 is mostly composed of iron would strongly support the ^{56}Ni–^{56}Co–^{56}Fe radioactive interpretation of Type I light curves[4-7] and the related theoretical interpretation of the explosion itself. It would also make a more detailed discussion of the above admittedly *ad hoc* picture worthwhile. As discussed earlier, any more-normal abundance of a thermal gas requires that the progenitor was $>10\,M_{\odot}$, although it is out of the galactic plane by several hundred pc. This seems most unlikely and suggests that failure to detect coronal lines will provide support for rapid and efficient acceleration of cosmic rays in shocks (see ref. 3).

We conclude by considering the cup-shape appearance of the remnant of SN1006, as it appears in the X ray[1]. This could partly be due to the exploding star having been a member of a close binary system. The flow and subsequent shocks surrounding the companion could well have slowed the ejecta down in one direction, provided that the ejecta was roughly at its final velocity by the time it had crossed the binary orbit (say $\sim 10^{11}$ cm).

A.C.F. acknowledges the Radcliffe Trust for support.

Received 15 September; accepted 7 December 1981.

1. Pye, J. P. *et al. Mon. Not. R. astr. Soc.* **194,** 569 (1981).
2. Becker, R. H. *et al. Astrophys. J. Lett.* **240,** 33 (1980).
3. Reynolds, S. P. & Chevalier, R. A. *Astrophys. J.* **245,** 912 (1981).
4. Truran, J. W., Arnett, W. D. & Cameron, A. G. W. *Can. J. Phys.* **45,** 2315 (1967).
5. Arnett, W. D. *Astrophys. Space Sci.* **5,** 180 (1969).
6. Colgate, S. A. & McKee, C. *Astrophys. J.* **157,** 623 (1969).
7. Wheeler, J. C. *Proc. Texas Wkshp. on Type I SN* (1980).
8. Galas, C. M. F., Venkatesan, D. & Garmire, G. Preprint (University of Calgary, 1981).
9. McKee, C. F. *Astrophys. J.* **188,** 335 (1974).
10. Gull, S. F. *Mon. Not. R. astr. Soc.* **171,** 263 (1975).

Asymmetric Balmer line profiles in Seyfert galaxies

A. Lawrence*

Center for Space Research, Massachusetts Institute of Technology,
Cambridge, Massachusetts 02139, USA

The profiles of the broad Balmer emission lines in Seyfert galaxies are often asymmetrical in the sense that the red wing extends further than the blue wing[1]. Explanations of the observed asymmetry have involved relativistic effects[2,3], infalling clouds immersed in an absorbing medium[4], and radially expanding clouds that are bright only on the side facing the ionizing source[4,5]. In all these hypotheses, the fact that only some galaxies have asymmetric emission lines was not considered important. Here I present evidence that both the degree of asymmetry and the difference between Hα and Hβ profiles are correlated with the overall line width. I also argue that current evidence is most compatible with an expanding system of optically thick clouds, in which the thickest clouds are moving fastest.

In his study of 36 Seyfert galaxies, Osterbrock[1] classified each Hβ profile as either symmetric, slightly asymmetric, or asymmetric. Figure 1 shows that all the 'asymmetric' objects have large values of the full width at zero intensity (FWZI) of Hα. There is a large overlap between the 'symmetric' and 'slightly asymmetric' populations, but in a probabilistic sense the 'slightly asymmetric' objects have values of FWZI (Hα) intermediate between the 'symmetric' and the 'asymmetric objects'. The profiles were not corrected for the instrumental resolution of the Lick scanner. As the instrumental profile[1] has FWZI ~2,000 km s^{-1} at Hβ, it is clear that the narrowest lines would always appear symmetric. However, most of the lines concerned are well resolved, and some of the observed asymmetries are very strong; the resolution effect cannot explain the proposed correlation.

Osterbrock[1] noted that an apparent asymmetry may actually be due to the broad weak feature Fe II λ4,924 appearing in the red wing of Hβ. I considered the strength of the well observed feature Fe II λ4,570, assuming it to correlate with Fe II λ4,924. There is no significant difference between the three populations (symmetric, slightly asymmetric, and asymmetric) for their distributions of the value of Fe II λ4,570/Hβ (not shown). Thus, an apparent asymmetry is probably not caused by FeII emission dominating the wings of Hβ. Of course, some extra, as yet undetected, component could appear redward of Hβ, and thus also increase the apparent overall line width. The FWZI is very difficult to measure, so that there may be important unknown systematic errors. However, I shall assume that the asymmetry, and its dependence on line width, is a real feature of the Balmer line profiles, and attempt to explain it in terms of the properties of the emission line cloud system as a whole. Let us reconsider the three categories of explanation mentioned above in the context of a dependency on line width.

---

* Present address: Royal Greenwich Observatory, Herstmonceux Castle, Hailsham, East Sussex BN27 1RP, UK.

(1) Objects with extremely broad lines must contain emission line gas moving at mildly relativistic velocities. Furthermore, if the clouds are bound to a massive central object and have virialized velocities, those moving fastest also have the largest gravitational redshift, and transverse Doppler shift (also always a redshift). We need not assume, as did Netzer[2] that the clouds are rotating in a disk, but only that typical velocities at each radius are comparable with the orbital velocity at that radius. These assumptions do predict that excess redward emission is increasingly important for objects with very fast moving clouds. Unfortunately, however, the effect is probably too small to explain at least some asymmetries. For clouds orbiting a massive body at ~15,000 km s^{-1}, we would expect that the red wing may extend ~10% further than the blue wing, whereas in some cases the red wing actually extends twice as far as the blue wing (see, for example, the profile of MKN374 reproduced in Fig. 1 of ref. 4, or the profile of PHL1093 reproduced in Fig. 1 of ref. 3). For instance, the profile of PHL1093 extends to −5,000 km s^{-1} and +10,000 km s^{-1}. This would require that clouds exist within 30 Schwarzchild radii of the massive central object, but move slower than the corresponding orbital velocity by a factor of 7.

(2) A consensus is forming that the anomalous ratios of Lα/Hα/Hβ observed in QSOs and Seyfert galaxies imply that the broad line emitting clouds are optically thick to the Balmer lines[5-12]. This means that the inner, ionized face of the cloud (that closest to the nucleus) will be brighter in the Balmer lines than the outer face. Most Balmer line photons detected by the observer will thus have originated in clouds on the far side of the ionizing source. A red excess then implies that the clouds on the far side are moving away from us; that is, the system is expanding radially outward[4,5]. The correlation found here between the degree of asymmetry and FWZI (Hα) (Fig. 1), further requires that faster moving clouds have a larger contrast in brightness between inner and outer faces, and thus presumably a larger Balmer line optical thickness (see Fig. 1 of ref. 5).

(3) Alternatively, one may consider isotropically emitting clouds immersed in an obscuring medium (for example, dust). Clouds on the far side of the system are seen through a larger column of the obscuring material, and are thus fainter. A fainter blue wing then means that clouds on the far side are moving towards us; that is the system is moving radially inward. The correlation between asymmetry and line width would then imply that objects with very wide lines have a larger overall amount of obscuring material. However, where those 'asymmetric' galaxies (all except MKN374) have been measured in X rays, they are all as luminous as, or more luminous than, the average Type 1 Seyfert galaxy[13,14]. By contrast, much evidence now suggests that only low luminosity Seyfert galaxies have appreciable amounts of obscuring material[15].

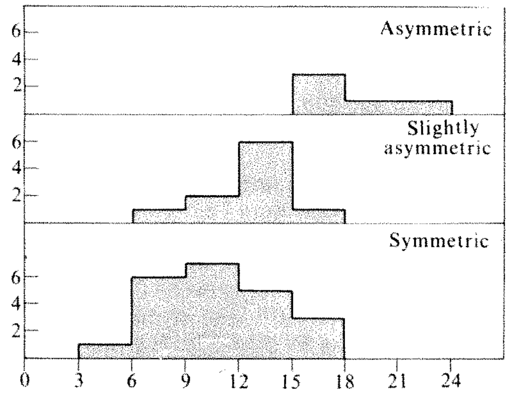

Fig. 1 Distribution of the values of the full width at zero intensity of Hα for the three different profile symmetry classes defined by Osterbrock[1].

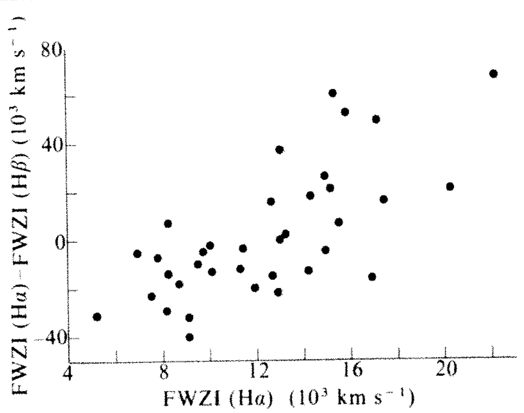

Fig. 2 The difference in full width at zero intensity between Hα and Hβ as a function of the full width at zero intensity of Hα. Values are from ref. 1.

There is further evidence that supports model (2). Figure 2 shows that the line-width difference, FWZI (Hα) − FWZI (Hβ), is an increasing function of FWZI (Hα). Such a correlation must be treated cautiously, as FWZI is difficult to measure. The value of FWHM is less ambiguous, but will be dominated by the relative strength of the narrow component of the emission line, which will have little bearing on the dynamics of the region forming the broad lines.

Line profiles have been described as 'logarithmic'[4] or 'triangular'[16]. In the latter case, FWZI is a better defined quantity than in the former case; but in general one may suspect that the measured value of FWZI is as much a function of the signal-to-noise ratio as intrinsic line width. In this situation FWZI could correlate with line strength; a strong line may be traced out further from the line centre. The difference in FWZI between Hα and Hβ could then correlate with the ratio of line strengths. However, from Osterbrock's data, there is no correlation between $I(\text{H}\alpha)/I(\text{H}\beta)$ and FWZI (Hα) − FWZI (Hβ) (not shown). Such signal-to-noise effects may still cause a correlation of line width difference with overall line width if, regardless of the total line intensities, Hα 'fades out' more slowly far from the line centre than does Hβ; that is to say, if the Balmer decrement is a function of cloud velocity. This suggests that, in general, different objects all have the same 'potential' profile; it is just a question of how much of the 'iceberg' is above water.

A consistent physical picture is that clouds are moving outward; that faster moving clouds are optically thicker; and that therefore they have a larger brightness contrast between inner and outer faces, and larger values of Hα/Hβ. Examination of these questions at higher resolution and sensitivity is desirable, as is examination of other spectral lines.

Received 28 September; accepted 22 December 1981.

1. Osterbrock, D. E. *Astrophys. J* **215**, 733 (1977).
2. Netzer, H., *Mon. Not. R. astr. Soc.* **181**, 89P (1977).
3. Anderson, K. S. *Astrophys. J.* **246**, 13 (1981).
4. Capriotti, E., Foltz, C. F. & Byard, P. *Astrophys. J.* **230**, 681 (1979).
5. Ferland, G. J., Netzer, H. & Shields, G. A. *Astrophys. J.* **232**, 382 (1979).
6. Capriotti, E. R. *Astrophys. J.* **139**, 225 (1964).
7. Anderson, K. S. *Astrophys. J.* **162**, 743 (1970).
8. Netzer, H. *Mon. Not. R. astr. Soc.* **171**, 395 (1975).
9. Netzer, H. *Mon. Not. R. astr. Soc.* **178**, 489 (1977).
10. Krolik, J. H. & McKee, C. F. *Astrophys J. Suppl.* **37**, 459 (1978).
11. Kwan, J. & Krolik, J. H. *Astrophys. J. Lett.* **233**, L91 (1979).
12. Ferland, G. J. & Netzer, H. *Astrophys. J.* **229**, 274 (1979).
13. Elvis, M. *et al. Mon. Not. R. astr. Soc.* **183**, 159 (1978).
14. Kriss, G. A., Canizares, C. R. & Ricker, G. R. *Astrophys. J.* **242**, 492 (1980).
15. Lawrence, A. & Elvis, M. *Astrophys. J.* (in the press).
16. Davidsen, K. & Netzer, H. *Rev. Mod. Phys.* **51**, 715 (1979).

A molecular interpretation of stress corrosion in silica

Terry A. Michalske* & Stephen W. Freiman

Fracture and Deformation Division, National Bureau of Standards,
Washington DC 20234, USA

The mechanical strength of many glasses and ceramic materials decreases with time under static loading and ambient environments. This strength loss is associated with slow growth of pre-existing surface flaws due to a stress-corrosion process. To make long-term strength predictions for ceramic components, it is important to understand the stress-corrosion mechanism. We have studied stress corrosion in vitreous silica exposed to water and several non-aqueous environments and report here that environments which enhance stress corrosion are composed of molecular groups with electron donor sites on one end and proton donor sites at the other. These results suggest a detailed chemical model for the interaction of the environment with mechanically strained bonds in the solid at the tip of a crack. The proposed model also has implications for the long-term strength behaviour of a wide variety of brittle materials.

Several generalized mechanisms have been proposed to explain the effect of water-containing environments on crack growth in glass, for example, surface energy reduction[1], stress-enhanced dissolution[2], or dielectric charge compensation[3]. None of these models attempts to explain why water is such an effective stress-corrosion agent for glasses and ceramics nor does any suggest a specific stress-enhanced reaction. We now describe, on a molecular scale, a specific chemical reaction between strained bonds in vitreous silica and water, which can be used to explain environmentally enhanced crack growth. Experimental support of this model will be presented.

Previously published results[4] have shown that slow extension ($<10^{-2}$ m s^{-1}) of a crack in vitreous silica is facilitated by water in the environment. In the present study, crack growth data were taken in N_2 gas containing a small amount of water as well as in liquid water and other environments. Crack velocities were obtained by visual observation of crack extension in a double cantilever beam specimen[5], and the data plotted as crack velocity (V) versus stress intensity factor (K_I), where K_I is a measure of the stress field at the crack tip (Fig. 1). The important features are:

(1) In a water-free environment such as vacuum, spontaneous failure is observed when K_I reaches a critical value[4] (shown as a vertical line in Fig. 1).

(2) When small amounts of water vapour are present (moist N_2 gas), crack growth in the low velocity regime is enhanced (curve is shifted to lower K_I and V is a measurable function of K_I).

(3) A plateau in crack velocity is observed in water-containing environments (such as moist N_2). This plateau has been linked to crack growth limited by the rate of water transport to the tip of the moving crack[6]. At sufficiently high V, the plateau behaviour ends and rapid fracture is observed.

(4) Liquid water enhances crack growth over the entire range of crack velocity (10^{-9}–10^{-2} m s^{-1}).

Highly concentrated tensile stress fields are produced at a crack tip in a stressed brittle solid. Continuum approximations indicate that the bridging Si—O bond experiences strains >20%. The effect of this strain on the bonding molecular orbitals is not easy to predict but can be discussed in terms of a decrease in the overlap between atomic orbitals, thus increasing their availability for bonding with other species.

The molecular structure of water is the key to its ability to cause stress corrosion in vitreous silica. Oxygen atomic orbitals 2s, $2p_x$, and $2p_y$ form three hybrid orbitals—two of which σ-bond with hydrogen atoms. The remaining lone pair orbitals (one hybrid and the remaining p_z) are directed away from the hydrogen atoms. This arrangement results in a positive charge centre at the hydrogen end of the water molecule and a negative charge centre on the opposite end of the molecule where the lone pair orbitals are located.

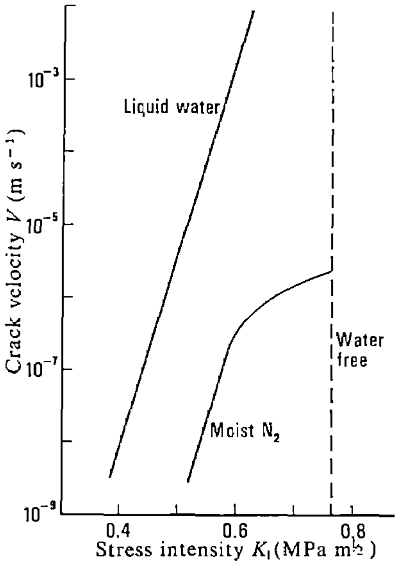

Fig. 1 Effect of water on slow crack growth in vitreous silica (curves represent best fit to experimental data).

Interaction between strained bridging bonds at a crack tip in silica and water from the environment can be represented by a three-step process (see Fig. 2).

Step 1—a water molecule from the environment attaches to a bridging Si—O—Si bond at the crack tip. The water molecule is aligned by: (1) formation of a hydrogen bond with the O_{br} atom; and (2) interaction of the lone pair orbitals from O_w with the Si atom. The lone pair orbital interaction may involve either Van der Waals attraction or some covalent bonding with unoccupied d orbitals of Si.

Step 2—a concerted reaction occurs in which proton transfer to the O_{br} is accomplished simultaneously with electron transfer from the O_w to the Si atom. As a result of this reaction, two new bonds are formed (one between O_w and Si and one between hydrogen and O_{br}; the original bridging bond (between O_{br} and Si) is destroyed.

Step 3—rupture of the hydrogen bond between O_w and transferred hydrogen occurs to yield surface Si—O—H groups on each fracture surface. As the hydrogen bond is weak, this step is expected to occur immediately after proton transfer. (Budd[7] has proposed a similar mechanism for the dissolution of silica in water; however, note that the present model for crack growth is not contingent on the removal of material from the fracture surface.)

Reaction rate theory[8] can be used to show how the proposed mechanism for bond rupture leads to enhanced crack growth rates. In vacuum, the entire energy of the bridging bond must be overcome before bond rupture can occur. (This energy is supplied in part by mechanical strain as well as by thermal contributions.) When water is present, the height of the energy barrier to bond rupture is reduced because charge transfer (step 2) provides an alternative, lower energy, reaction path. As the rate of a chemical reaction (in this case bond rupture) is reciprocally dependent on the exponent of the energy barrier, mechanisms that provide a lower energy activated state will enhance crack growth rates. We have omitted factors resulting from changes in the energy of the Si—O—Si bond due to adsorbed water (step 1) and the energy of the reaction products (step 3); these terms are not critical to this discussion.

---

*Present address: Sandia National Laboratories Albuquerque, New Mexico 87185, USA.

0028-0836/82/060511—02$01.00

Experimentally, the role of the concerted reaction (simultaneous electron and proton transfer) as the rate of limiting step to fracture can be borne out through isotopic effects. Results of fracture experiments performed in deuterated water produced crack velocities consistently lower than those attained in normal water. This result can be analysed in terms of the different ground state vibrational energies of deuterium and protium resulting in different activation barriers for the two isotopes. The lower crack velocities measured in deuterated water agree with the larger energy barrier expected for deuteron transfer[9].

This model for chemical bond rupture presents some interesting implications. First, it suggests that environments other than water should enhance cracking in silica glass, if the species possess structural and bonding features similar to water, that is proton donor sites at one end of the molecule (or group) and lone pair orbitals at the other. The environmental molecule must also fit between the Si—O bond ($\approx$1.63 Å). To test this hypothesis, crack growth studies were conducted in vitreous silica exposed to gaseous ammonia (NH_3). Ammonia has a structure similar to water except that it has three orbitals σ-bonded to hydrogens leaving one lone pair orbital directed away from the hydrogen atoms (the N—H bond length is 0.94 Å). Figure 3 shows that NH_3 enhanced crack growth over the entire velocity range. When evaluating such data, it is important to be aware that small amounts of water in an inert carrier (N_2) can have large effects on crack growth rates. However, the enhancement due to small amounts of water is limited in velocity. As the NH_3 gas used in this experiment contained less H_2O than the N_2+H_2O gas mixture, the absence of a plateau indicates that the NH_3 was controlling the fracture behaviour. Crack growth experiments in hydrazine (N_2H_4) and formamide (CH_3NO) showed that these environments also controlled crack growth over the entire velocity range (Fig. 3). However, these environments were less effective (V–K_I curve shifted to higher K_I) then either water or ammonia, possibly due to steric hindrance and/or delocalization of lone pair orbitals. Note also that other non-aqueous environments such as carbon monoxide (contains lone pair orbital but no proton donor site) or acetonitrile (has high dipole moment, 3.92 D, but no localized lone pair orbital) have no measurable effect on crack growth rates.

This chemical model and its supporting experimental data represent an important step in the understanding of stress corrosion and the mechanical durability of materials. First, knowing that an effective stress-corrosion environment must have an electron donor site as well as a proton donor site allows for qualitative predictions of those environments which will decrease the long term strength of silica. As the structural bonds in the solid must also engage in the stress-corrosion reaction, qualitative predictions of the susceptibility of a range of solids to stress corrosion are also possible, that is the more covalent the solid the less susceptible it is to stress corrosion. This is supported by experimental evidence that single crystal silicon shows little, if any, susceptibility to stress corrosion with water (E. R. Fuller, personal communication). The ability to make such qualitative predictions is an advance over previous models which were intended only to explain stress corrosion in water.

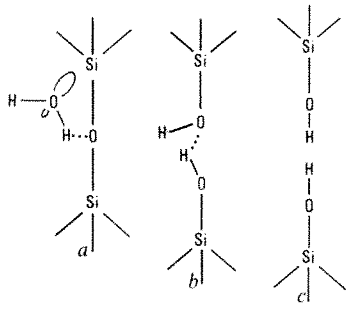

Fig. 2 Representation of the proposed reaction between water and a strained Si—O—Si bond at the crack tip. Reaction steps involve; (*a*) adsorption of water to Si—O bond, (*b*) concerted reaction involving simultaneous proton and electron transfer, and (*c*) formation of surface hydroxyls.

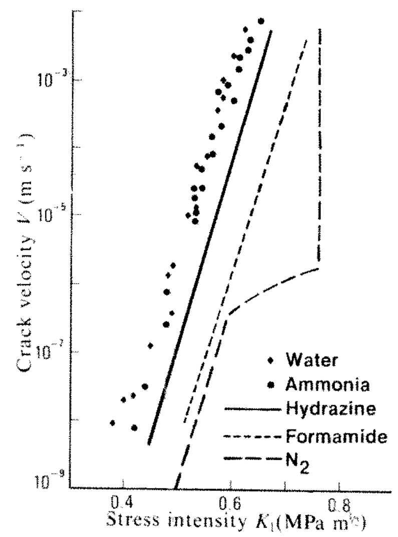

Fig. 3 Comparison of the effects of various environments on slow crack growth in vitreous silica at room temperature.

Second, this attempt at analysing the molecular interaction involved in the stress-corrosion process opens the door for detailed molecular calculations. Results of such calculations could allow quantitative predictions of the response of any solid material with any particular stress-corrosion environment.

This work was carried out at the National Bureau of Standards. We thank J. Houston for helpful discussions and the Office of Naval Research for partial support of this work.

Received 26 May; accepted 14 December 1981.

1. Orowan, E. *Nature* **154,** 341 (1944).
2. Hillig, W. B. & Charles, R. J. in *High Strength Materials* (ed. Zackay, V. F.) 682 (Wiley, New York, 1965).
3. Wiederhorn, S. M., Fuller, E. R. Jr & Thomson, R. *Metal Sci.* **14,** 450 (1980).
4. Wiederhorn, S. M. & Bolz, C. H. *J. Am. ceram. Soc.* **53,** 543 (1970).
5. Freiman, S. W., Mulville, D. R. & Mast, P. W. *J. mater. Sci.* **8,** 1527–1533 (1973).
6. Wiederhorn, S. M. in *Fracture Mechanics of Ceramics* Vol. 4 (eds Bradt, R. C., Hasselman, D. P. H. & Lange, F. F.) 549 (Plenum, New York, 1978).
7. Budd, S. M. *Phys. chem. Glass* **2,** 111 (1961).
8. Laidler, K. J. *Theories of Chemical Reaction Rates* (McGraw-Hill, New York, 1969).
9. Melander, L. & Saunders, W. H. *Reaction Rates of Isotopic Molecules* (Wiley, New York, 1980).

Errors and resolution of thermal techniques for obtaining the geomagnetic intensity

D. Walton*

Physics Department, McMaster University, Hamilton, Ontario,
Canada L85 4L8

Techniques designed to obtain the intensity of the geomagnetic field by thermal demagnetization are subject to error due to differences between the ancient and laboratory cooling rate[1–3] and alteration in the physical and chemical properties of the magnetic grains which can lead to a systematic overestimate of the field by as much as 50%. A new technique is proposed here which uses the change in moment with time at a fixed temperature in conjunction with the magnetization acquired on cooling to determine the ancient field and ancient cooling rate. This new technique also appears to be able to detect alteration with greater sensitivity.

---

* Present address: Bullard Laboratories, Madingley Rise, Madingley Road, Cambridge CB3 0EZ, UK.

0028-0836/82/060512—04$01.00

It has been found that the magnitude of both the above errors increases with temperature. Alteration often begins at relatively low temperatures, and increases smoothly as the temperature increases. The cooling rate correction in effect also increases with temperature. If alteration results in a decrease in magnetization the result is an accelerating decrease in moment with increasing temperature. Consequently the abrupt change in the slope of a natural remanent magnetism (NRM)/palaeothermal remanent magnetism (PTRM) plot which has been used to signal the onset of alteration is not always present. This will result in an accelerating apparent increase in the intensity of the ancient field. An extreme example of this behaviour is shown in Fig. 1: while the NRM/PTRM plot settles down to a straight line above 300 °C the grains involved have probably undergone alteration. Thus the reliability of using the slope of the straight line portion is questionable.

The technique described here not only corrects for the difference between laboratory and ancient cooling rates, but enables the ancient cooling rate to be estimated. Preliminary results indicate that the ancient cooling rate could vary by more than an order of magnitude. Thus the error due to differences in cooling rate can be random even for pottery. These results will also reveal that alteration begins to appear at surprisingly low temperatures.

As derived in ref. 1, the moment produced on cooling is

$$M = H_A \int_{v_1}^{v_2} \frac{J_B J}{3kT_B} v^2 N(v)\,\mathrm{d}v \qquad (1)$$

where H_A is the ancient field, J_B the saturation magnetization at the blocking temperature T_B, v is the grain volume, $N(v)$ the grain size distribution and v_2 and v_1 the volumes of grains blocked at the higher temperature and lower temperature respectively.

The quantities J_B and T_B depend on the rate of cooling[1]. Let a variable α be defined as

$$\alpha = \frac{\mathrm{d}}{\mathrm{d}t}\left(\frac{K}{T}\right) \qquad (2)$$

where K is the anisotropy constant.

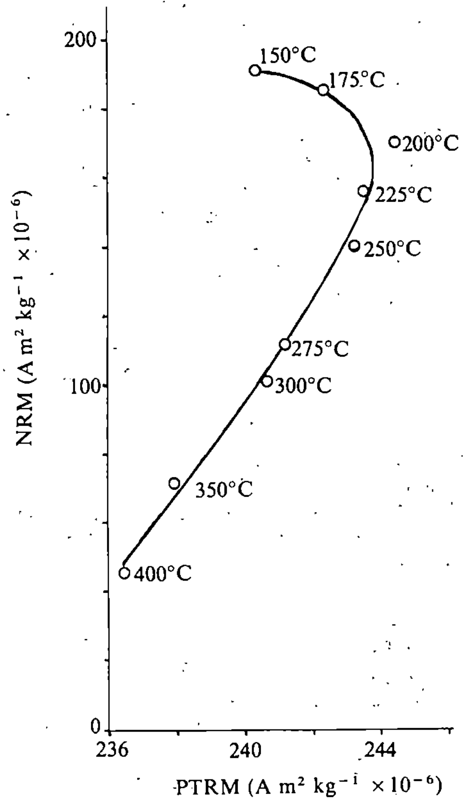

Fig. 1 The change in moment of a sample of Attic pottery after successive heatings to the temperatures (O). Two coolings are performed from each temperature, the first in a field of 70 μT, the second in zero field to establish the loss of the NRM.

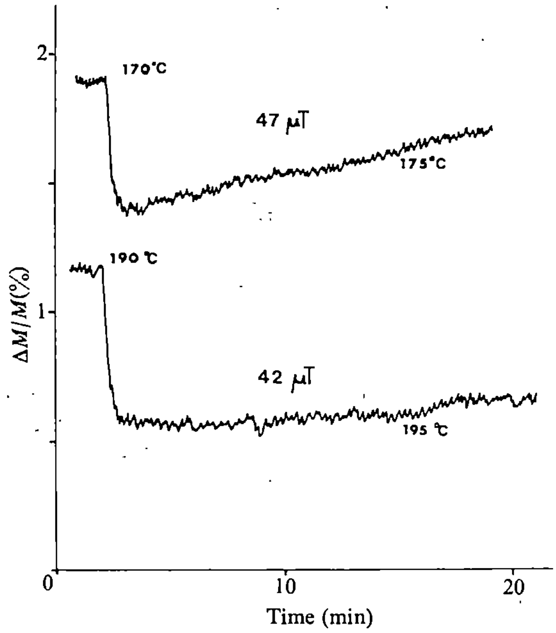

Fig. 2 The change in moment, M, with time of a sample of Attic pottery on heating by 5 °C from two temperatures at two different fields. The zero level for both curves has been shifted by an arbitrary amount.

The moment is then proportional to $(\ln ck/v\alpha)^n$ where c is a frequency factor.

A cooling time constant τ can be defined as

$$\tau = \frac{k}{v\alpha} \qquad (3)$$

In general τ is temperature dependent. In particular if the sample cools according to Newton's law of cooling, τ decreases as the temperature increases.

The coefficient n results from approximating the temperature dependence of J as

$$J = J_0(1 - T/T_c)^n \qquad (4)$$

For magnetite $n \cong \frac{1}{2}$ while for haematite it is $\frac{1}{4}$.

The thermal techniques for obtaining the ancient field pioneered by Thellier, involve comparing a moment introduced on cooling in the laboratory field with that removed on heating to successively higher temperatures. A knowledge of the ancient cooling rate is necessary for an accurate determination of the ancient field intensity. This knowledge need only be approximate because the function $(\ln c\tau)^n$ is only weakly dependent on τ.

Assuming that the sample is heated rapidly from a temperature T_0 to a higher temperature T, when the sample reaches T part of the magnetic moment will reside in grains whose blocking temperatures are both above and below T. Those grains whose blocking temperatures are lowest will first come to equilibrium with the applied magnetic field. But the approach to equilibrium of grains whose blocking temperatures are less than T will result in a loss of moment; this produces a decrease in moment followed by an increase when the distributions of those grains with blocking temperatures higher than T begin to reach equilibrium.

The rate of change of the moment[1] with ln ct is

$$\frac{\partial M}{\partial \ln ct} = \frac{\pi\sqrt{2}}{e}(n_0 - n_{\mathrm{eq}})J\left(\frac{kT}{K}\right)^2(\ln ct)\left[N\left(\frac{kT}{k}\ln ct\right)\right] \qquad (5)$$

n_0 is determined by the moment distribution produced on cooling and is

$$n_0 = \frac{J_B v H_A}{3kT_B} \tag{6}$$

and

$$n_{eq} = \frac{J^v H_L}{3kT} \tag{7}$$

where H_L is the laboratory field.

As the sample is held at the temperature T, initially smaller grains will come to equilibrium followed by grains of increasingly larger volume. Initially, then, the distribution of the grains with low blocking temperature come to equilibrium followed by grains which blocked at higher temperatures. Since T_B increases and J_B decreases as v increases, n_0 will decrease with time. On the other hand, n_{eq} increases with time as v increases.

Now $\partial M/\partial \ln ct$ will be zero when $n_{eq} = n_0$, when

$$\frac{H_A}{H_l} = \frac{JT_B}{J_B T} \tag{8}$$

Now

$$\frac{\bar{K}_B v}{3kT_B} = \ln c\tau \quad \text{and} \quad \frac{\bar{K} v}{3kT} = \ln ct \tag{9}$$

where t is the time at which $\partial M/\partial \ln ct = 0$ and $\bar{K}_B$ is the anisotropy constant evaluated at the blocking temperature.

So if

$$\bar{K} = aJ^p \tag{10}$$

$$\frac{J}{J_B} = \left(\frac{T \ln ct}{T_B \ln c\tau}\right)^{1/p} \tag{11}$$

Using equation (4)

$$\frac{J_B}{J} = \left(\frac{1 - T_B/T_c}{1 - T/T_c}\right)^n = \left(1 + \frac{T - T_B}{T_c - T}\right)^n$$

Bearing in mind that T_B is close to T this equation may be expanded. After some algebra equation (8) becomes

$$H_A \ln c\tau_A = H_L \ln ct\left\{1 + \left[\frac{(p-1)n}{(pn-1) + T/Tc}\right] \times [\ln (t/\tau_A)/\ln c\tau_A]\right\} \tag{12}$$

where τ_A is the ancient cooling time constant.

Figure 2 displays the moment as a function of time for a sample of Attic pottery. The data were obtained with a highly sensitive magnetometer capable of obtaining moments, while the sample is held at an elevated temperature, with an accuracy of better than 0.1%. It will be described in detail elsewhere.

Since there are two values for H and two values of t, an approximate value for c may be deduced, if the second term in the brackets in equation (12) is neglected, c is $\sim 7 \times 10^7\ \mathrm{s}^{-1}$.

It is impossible to obtain the ancient field unless τ_A is known, although it need not be known precisely because it enters equation (12) as $\ln c\tau_A$. This requires another relation which can be obtained from the dependence of the moment on the laboratory cooling rate, as the moment gain on cooling is proportional to $(\ln c\tau_L)^n$. For example, on further heating to 250 °C the sample revealed a decrease in moment when cooled to 190 °C relative to that observed after it had been cooled from 195 °C. On decreasing the cooling rate by an order of magnitude (increasing τ_L by a factor of 10) half the lost moment was recovered. Thus a two order of magnitude increase in τ_L would be required to restore completely the moment lost between 195 and 250 °C. As shown in ref. 1 the moment introduced on cooling is proportional to $H_L(\ln c\tau_L)^n$. Hence,

$$H_A(\ln c\tau_A)^n = H_L(\ln c\tau'_L)^n \tag{13}$$

where $\tau' L$ is that cooling time constant that would be required to restore completely the moment lost by heating to 250 °C.

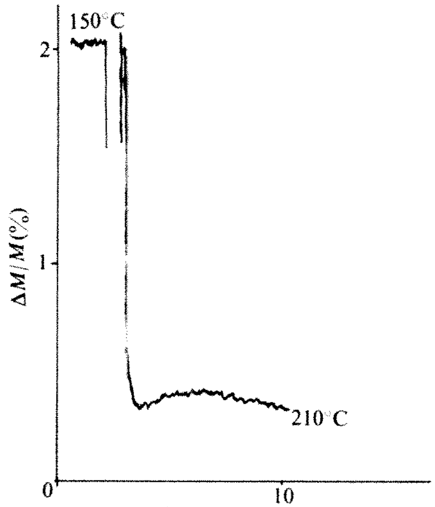

Fig. 3 The change in moment, M, with time of a sample of Attic pottery on heating to 210 from 150 °C. The zero is arbitrary, and two changes of zero suppression were made to keep the recorder pen on scale. The decrease in moment apparent after about 7 min is due to alteration of the magnetic constituents.

Using equation (12), and taking $n = \frac{1}{2}$ which is appropriate for magnetite, $\tau_A \sim 100$ s—a rather low value. Other samples of Attic pottery yielded values about an order of magnitude higher. Typically τ_A appears to be of the order of 1,000 s for this pottery.

H_A for this sample is 46 μT. The modified Thellier method used for a previous determination yielded $H_A = 63$ μT for a sample from the same sherd. The difference is rather more than can be accounted for by differences in cooling rate. Alteration probably affected the old result.

This technique consists of holding the sample at an elevated temperature and monitoring the change in its moment with time. If the laboratory field is within ~10% of the ancient field the moment will show a characteristic decrease followed by an increase. The time at which the inflection occurs yields the product $H_A \ln c\tau_A$. The values for $\ln c\tau_A$ and H_A can be separated by obtaining the laboratory cooling rate for which no change in moment occurs on cooling to a fixed temperature in the chosen laboratory field.

With this particular material the onset of mineral alteration seems to result in a net loss of moment by the grains. This has manifested itself by an anomalously large τ_L. Thus in the second step of the method either a proportionally greater decrease in rate or a larger H_L is necessary to restore the lost moment. Further heating again requires either a further increase in τ_L or an increase in H_L.

It is possible for alteration to result in an increase in moment; in that event H_L or τ_L must be continually decreased. If when alteration is in progress the moment should decrease with time it can sometimes be identified as follows: if H_L is chosen so that the moment shows the characteristic decrease followed by an increase when alteration is absent at lower temperatures, the moment will decrease when alteration begins. Then it is possible for the moment to decrease then increase and then decrease again, due to alteration. An example of this behaviour is shown in Fig. 3.

Probably the most surprising aspect of the alteration is that it has manifested itself at temperatures as low as 210 °C. Also, of 18 samples of Attic pottery 15 showed evidence of alteration at temperatures below 250 °C.

Most investigators obtain the ratio of the ancient to laboratory fields from the slope of a 'best' straight line drawn through the points in a plot of the natural remanent moment against the moment introduced by a laboratory field at successively higher temperatures. Unfortunately, in most cases it is difficult to demagnetize the sample sufficiently to draw a meaningful line unless temperatures above 300 °C are used, where the present results indicate that alteration may be present. In the event that those points are displaced from their true positions by increasing amounts the slope will be wrong.

The effect of cooling rate has been thought to introduce a correction which would be a constant fraction of the ancient field, assuming that the ancient cooling rate was within a factor of 2 or 3 for all pottery (at least those fired in the same area). Unfortunately the preliminary results obtained with Attic pottery indicate rather more variability. One advantage of the present technique is that measurements at low temperatures yield the ancient field. Thus, provided alteration does not begin before all viscous moments are removed, a value for H_A can always be obtained. If an accurate value of H_A is not required it is possible to assume a value for τ_A, in which case one, or at most two, temperatures are all that is necessary.

Finally, the previous measurements[4] on Attic pottery should be repeated, as they use values obtained above 300 °C. These measurements are in progress, and the results will be published in due course. Preliminary results indicate that the shape of the curve of intensity plotted against time has not changed radically, but that the values of intensity have decreased by ~15–25%.

I thank the National Science and Engineering Research Council of Canada for support.

Received 28 September; accepted 3 December 1981.

1. Walton, D. *Nature* **286**, 245–247 (1980).
2. Fox, J. M. W. & Aitken, M. J. *Nature* **283**, 462–463 (1980).
3. Dodson, M. H. & McLelland Brown, E. J. *J. geophys. Res.* **85**, 2625 (1980).
4. Walton, D. *Nature* **277**, 643–644 (1979).

Sm–Nd dating and cooling history of Scourian granulites, Sutherland

F. J. Humphries & R. A. Cliff

Department of Earth Sciences, The University of Leeds,
Leeds LS2 9JT, UK

The Scourian gneisses of the Lewisian complex of north-west Scotland have been the subject of many geochronological investigations. Sm–Nd whole-rock measurements suggest that the protoliths of the Lewisian complex differentiated 2.92±0.05 Gyr ago from an approximately chrondritic mantle[1]. Rb–Sr and Pb–Pb whole-rock ages between ~2.8 and 2.6 Gyr reflect subsequent depletion in Rb and U (refs 2, 3) which has generally been associated with granulite facies metamorphism. Zircons which are thought to have crystallized during this metamorphism have also given U–Pb ages of 2.66 Gyr (ref. 4). This granulite facies metamorphism, involving pressures in excess of 10 kbar and peak temperatures estimated between 820±50 °C (ref. 5) and 1,250 °C (refs 6, 7), affects a terrain including supracrustal rocks[7] and thus implies a major tectonic event. We report here the first geochronological data measured on mineral assemblages that have also provided estimates of the conditions of metamorphism. Such measurements are possible because the major minerals of granulite facies assemblages show an unusually favourable spread in Sm/Nd ratios; garnet, especially, is strongly enriched in Sm (ref. 8). Data for three garnetiferous basic gneiss assemblages suggest that closure of the Sm–Nd system occurred significantly later than the peak of the metamorphism.

The textures of Scourian basic gneisses are complex and it has been suggested that three stages of granulite facies mineral growth can be recognized[6,9]. The earliest assemblage consists of garnet and clinopyroxene with minor plagioclase and hornblende. During the second stage garnet broke down to form coronas of plagioclase, orthopyroxene and magnetite. Subsequently regrowth of garnet, especially rimming grains of orthopyroxene and magnetite, occurred. Locally, much coarser (up to 150 mm) aggregates of garnet and clinopyroxene occur within the garnetiferous basic gneisses; it has been suggested that these are the result of exsolution from an Fe–Al rich amphibole[10]. Sample 3966 'coarse' is an example of these aggregates, occurring in a typical basic gneiss represented by 3966 'fine'. There is a sharp contact between the two assemblages. The third sample, 40117, is also a typical garnetiferous basic gneiss. All three assemblages show, to varying degrees, the three stages of mineral growth noted above.

The results of the isotopic analyses are given in Table 1 and are plotted on Sm–Nd isochron diagrams in Fig. 1. In each case the data show some scatter in excess of analytical error but the three calculated ages are similar. 40117 gives an age of 2.49 ± 0.12 Gyr with an initial $^{143}Nd/^{144}Nd$ ratio of 0.50944 ± 0.00016, 3966 'fine' gives 2.49 ± 0.03 Gyr with an initial ratio of 0.50949 ± 0.00009 and 3966 'coarse' gives 2.49 ± 0.03 Gyr with an initial ratio of 0.50973 ± 0.00008. The garnet and clinopyroxene in the analysed mineral separates are from the earliest stage of mineral growth whereas the other analysed mineral separates also include grains from the later stages. The isotopic relationships between the minerals show that the different stages of mineral growth cannot be resolved with the present data. Moreover, the earliest formed minerals, garnet and clinopyroxene, systematically give ages that are up to 0.05 Gyr younger, rather than older, than those calculated for the complete mineral assemblage; thus the excess scatter in the calculated errorchrons does not simply reflect differences in the age of formation of the various minerals.

The consistency of the ages from all three samples may reflect a relatively short overall duration for the granulite facies metamorphism, or they may date closure of the Sm–Nd system at some stage in the post-metamorphic cooling. The latter is strongly supported by the interpretation of the 2.66-Gyr zircon age as the result of zircon growth during granulite facies metamorphism[4], and by 2.56 Gyr Rb–Sr ages on pegmatites[11] which intruded the basic gneisses after the granulite facies metamorphism[12]. Theoretical closure temperatures can be calculated from experimentally determined diffusion coefficients[13], but such data are only available for Sm in grossular and pyrope at temperatures between 1,100 and 1,500 °C (see ref. 14 and

Table 1 Sm–Nd isotopic analyses of minerals from three samples of garnetiferous basic gneiss

Mineral	Sm (p.p.m.)	Nd (p.p.m.)	$^{147}Sm/^{144}Nd$ $\pm 2\sigma$	$^{143}Nd/^{144}Nd$ $\pm 2\sigma$
40117, Scourie Mhor (GR 142442)				
GT	1.64	0.94	1.0696 ± 20	0.52690 ± 22
	1.68	0.98	1.0529 ± 134	0.52694 ± 3
CPX	3.47	11.65	0.1833 ± 3	0.51279 ± 15
OPX	0.15	0.61	0.1516 ± 40	0.51210 ± 8
PLAG	0.21	1.44	0.0889 ± 1	0.51096 ± 5
MT	0.44	1.50	0.1824 ± 1	0.51239 ± 3
	0.47	1.64	0.1748 ± 1	0.51262 ± 6
HB	6.91	23.98	0.1772 ± 1	0.51233 ± 3
3966 'coarse', north Scourie Bay (GR 152452)				
GT	1.70	1.31	0.7960 ± 19	0.52277 ± 7
	1.75	1.36	0.7932 ± 4	0.52273 ± 5
CPX	0.63	2.36	0.1647 ± 7	0.51247 ± 3
PLAG	3.11	19.11	0.1000 ± 3	0.51131 ± 4
MT	0.25	1.90	0.0826 ± 4	0.51157 ± 34
3966 'fine', north Scourie Bay (GR 152452)				
GT	1.91	1.52	0.7696 ± 5	0.52215 ± 3
	1.97	1.59	0.7614 ± 4	0.52202 ± 5
CPX	4.11	15.33	0.1650 ± 13	0.51224 ± 3
	4.02	14.89	0.1661 ± 2	0.51231 ± 5
PLAG	0.39	2.96	0.0813 ± 5	0.51092 ± 3
HB	7.40	29.87	0.1523 ± 6	0.51193 ± 2

GT, garnet; CPX, clinopyroxene; OPX, orthopyroxene; PLAG, plagioclase; MT, magnetite; HB, hornblende. Most of the analytical uncertainty on the $^{147}Sm/^{144}Nd$ ratio is from isotope dilution analysis of the Sm. For many of these analyses, Sm was run on a single Ta filament. Greater precision (± 0.05%) has since been obtained by running Sm on a triple filament assembly with a central Re and side Ta filament. The high concentrations in plagioglase from sample 3966 'coarse' reflect the presence of small discrete grains of apatite within the sample.

0028–0836/82/060515—03$01.00

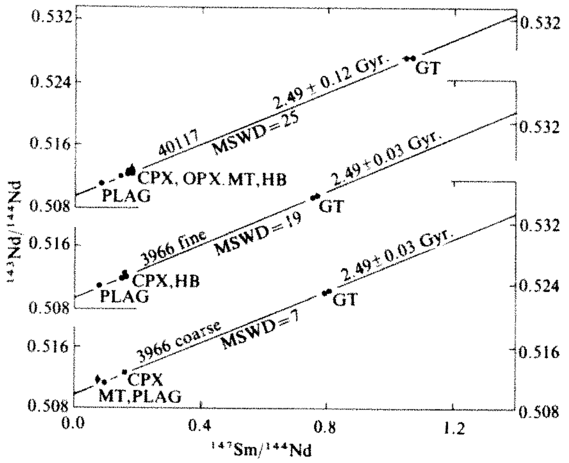

Fig. 1 Sm–Nd diagrams. $\lambda^{147}\text{Sm} = 6.54 \times 10^{-12}\,\text{yr}^{-1}$. The regression errors have been multiplied by $\sqrt{\text{MSWD}}$ to make allowance for the excess scatter. The magnetite (MT) data were omitted from the regression analysis of sample 3966 'coarse'.

Table 2). To apply these data to Nd isotopes it must be assumed that (1) the diffusion behaviour of Nd is similar to that of Sm, (2) extrapolation from the experimental to geological temperature ranges using the Arrhenius equation is valid, and (3) the difference in diffusion coefficients between pure grossular and pure pyrope encompasses the value appropriate to the dated garnets ($\text{Alm}_{1.6}\text{Pyr}_{0.9}\text{Gross}_{0.5}$). Consideration of anion porosity[15] suggests that Sm diffusion coefficients should increase systematically across the solid solution series from pyrope to grossular and for the end members this is confirmed by the experimental data (Table 2). Because of the variation in activation energy with composition, at the temperatures of interest it is expected that D_{pyrope} will be greater than $D_{\text{grossular}}$; closure temperatures based on these values should bracket the closure temperature for the analysed garnets.

Calculated closure temperatures are given in Table 2. The result for pyrope does not exceed 600 °C even in conditions of very rapid cooling (100 °C Myr^{-1}); for grossular the corresponding value is 775 °C. In each case a slower cooling rate reduces the calculated closure temperatures. These temperatures are below even the lowest estimated conditions at the peak of the granulite facies metamorphism (820 °C)[5] so that the available diffusion data also suggest that the measured ages should be interpreted as cooling ages.

While the concordant Sm–Nd ages indicate a close approach to isotopic equilibrium within the individual assemblages, that is between grains of 1–5 mm diameter, the initial ratios for the two assemblages from 3966 are significantly different, thus showing that the scale of diffusion 2.49 Gyr ago was ≪ 100 mm. The higher initial ratio of 3966 'coarse' also shows that the higher bulk Sm/Nd ratio of this assemblage was established appreciably earlier than 2.49 Gyr. Figure 2 shows the evolution of ^{143}Nd/^{144}Nd with time for 3966. Because 3966 'coarse' contributes insignificantly to the Sm–Nd mass balance for the whole sample, the pre-metamorphic evolution of this sample is approximately represented by the growth line for 3966 'fine'. The fact that this line intersects the error ellipse for the Lewisian whole-rock suite[1] supports this interpretation. During metamorphism at ~2.62 ± 0.12 Gyr, 3966 'coarse' was formed as an isolated sub-system with higher Sm/Nd and its ^{143}Nd/^{144}Nd began to grow at a correspondingly faster rate. In view of the difficulties in estimating modes in coarse-grained rocks, this estimate of the time of segregation is very tentative, although the intersection age agrees well with the 2.66 Gyr age of metamorphic zircons[4].

Table 2 Diffusion in garnet

Mineral	Species	D_0 (m^2 s^{-1})	E (kJ mol^{-1})	Ref.	T_c*
Pyrope	Sm	2.6×10^{-12}	140	14	480
Grossular	Sm	4.3×10^{-4}	331	14	700
Almandine-pyrope	Fe–Mg inter-diffusion	6.11×10^{-4}	344	17	725

Diffusion rate, D, at temperature T is given by the Arrhenius relationship:

$$D = D_0 \exp(-E/RT)$$

where R is the gas constant. Theoretical closure temperature, T_c is related to the cooling rate $\dot{T}$ by:

$$E/RT_c = \ln(-AD_0RT_c^2/E\dot{T}a^2) \qquad \text{(ref. 13 equation (11))}$$

where a is the radius of the grain; A is a geometric factor, equal to 55 for radial diffusion in a sphere.

* Closure temperature calculated for a cooling rate of 5 °C Myr^{-1}.

The relation between the isotopic ages and the temperature history based on conventional geothermometry is not as clear as the above discussion would suggest. Temperature estimates for the metamorphic peak have been based on feldspar thermometry[6], pyroxene exsolution[6,7] and Fe–Mg binary exchange equilibrium between garnet and clinopyroxene[5]. In conditions of slow cooling, these reactions are also likely to continue after the metamorphic peak, like diffusion of Nd isotopes, until the relevant closure temperature is reached and the compositions of the minerals are frozen in. Realistic closure temperatures for the metamorphic reactions are difficult to estimate as the commonly used reactions involve major components whose diffusion rates may be strongly coupled with diffusion of other major components which do not directly participate in the reaction[16].

For binary exchange reactions there may be further problems where the two minerals involved have different closure temperatures. Consider the Fe–Mg exchange between garnet and clinopyroxene. Apparent equilibration temperatures for this reaction in rocks from Scourie are typically between 750 and 850 °C (refs 5, 10, and F.J.H. unpublished data on the dated samples). Experimental data on the interdiffusion of Fe and Mg in garnet[17] (Table 2) indicate a closure temperature of 725 ± 30 °C for 5 °C Myr^{-1} cooling rate. Diffusion is likely to be slower in clinopyroxene which would therefore close at a higher temperature than garnet. Below the closure temperature of clinopyroxene, garnet may potentially exchange with other Fe–Mg minerals, for example orthopyroxene in the coronas around garnets. This would result in a more Fe-rich garnet and lead to erroneously low temperature estimates. The consistency of temperatures calculated from garnet–clinopyroxene pairs and

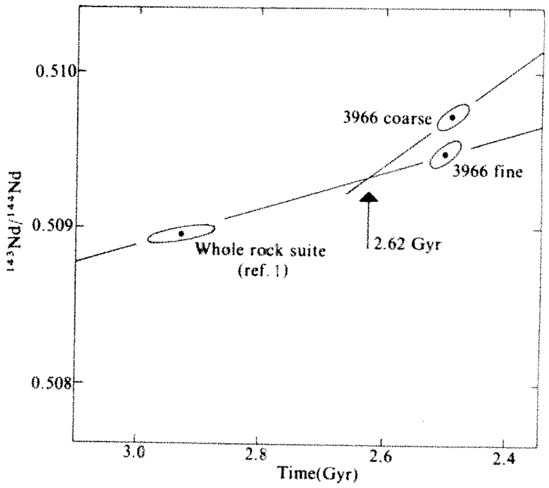

Fig. 2 Nd isotopic evolution in sample 3966. The data points for 3966 'coarse' and 3966 'fine' are the ages and initial ratios of the respective mineral isochrons. The data point for Lewisian whole rocks is the age and initial ratio of the whole-rock isochron from ref. 1. The 95% confidence ellipses were calculated following ref. 18. The lines representing the growth of ^{143}Nd/^{144}Nd with time were calculated from estimated 'whole-rock' Sm/Nd ratios for 3966 'coarse' and 3966 'fine', based on modal analyses and the Sm and Nd contents of the analysed minerals.

likely closure temperatures perhaps indicates that this is not a major problem in the rocks considered here, although it may explain some of the lower temperatures that have been reported[5]. From the above discussion we know that binary exchange thermometers will not record the peak metamorphic temperatures if the relevant closure temperatures are exceeded. Thus neither the estimate of 820 °C based on such reactions[5] nor the higher estimate of 1,250 °C (refs 6, 7), which was criticized on other grounds by Rollinson[5], are well founded and the peak conditions of Scourian metamorphism remain uncertain.

From the estimated closure temperatures for Nd and Fe-Mg in garnet it is suggested that the temperatures recorded by the garnet–clinopyroxene geothermometer date from a time before 2.49 Gyr. After the metamorphic peak close to 2.66 Gyr, the Scourian complex cooled at such a rate that temperatures did not drop below ~600 °C until after 2.49 Gyr.

Our data confirm the potential of Sm–Nd dating in basic granulites and the ability to determine metamorphic conditions and isotopic ages on the same samples. However, diffusion of rare earth elements between mineral grains is sufficiently rapid in granulite facies conditions to prevent the preservation of Sm–Nd crystallization ages. Also the uncertain relationships between closure of different geochemical systems is a fundamental limitation on our ability to determine metamorphic conditions.

Isotope geochemical research at Leeds is supported by the NERC. F.J.H. acknowledges receipt of a NERC research studentship. We thank Professor M. J. O'Hara for sample 3966, and Dr M. H. Dodson for constructive criticisms.

Received 26 October; accepted 10 December 1981.

1. Hamilton, P. J., Evensen, N. M., O'Nions, R. K. & Tarney, J. *Nature* **277**, 25–28 (1979).
2. Chapman, H. J. thesis, Oxford Univ. (1978).
3. Chapman, H. J. & Moorbath, S. *Nature* **268**, 41–42 (1977).
4. Pidgeon, R. T. & Bowes, D. R. *Geol. Mag.* **109**, 247–258 (1972).
5. Rollinson, H. R. *Lithos* **14**, 225–238 (1981).
6. O'Hara, M. J. & Yarwood, G. *Phil. Trans. R. Soc.* **A288**, 441–456 (1978).
7. Barnicoat, A. C. & O'Hara, M. J. *Miner. Mag.* **43**, 371–375 (1979).
8. van Breemen, O. & Hawkesworth, C. J. *Trans. R. Soc. Edinb.* **71**, 97–102 (1980).
9. Savage, D. thesis, London Univ. (1979).
10. Barnicoat, A. C. & O'Hara, M. J. *J. geol. Soc. Lond.* **138**, 637 (1981).
11. Evans, C. R. & Lambert, R. St. J. *J. geol. Soc. Lond.* **130**, 125–150 (1974).
12. Sutton, J. & Watson, J. *Q. Jl geol. Soc. Lond.* **106**, 241–307 (1951).
13. Dodson, M. H. *Nature* **259**, 551–553 (1976).
14. Harrison, W. J. & Wood, B. J. *Contr. Miner. Petrol.* **72**, 145–155 (1980).
15. Dowty, E. *Am. Miner.* **65**, 174–182 (1980).
16. Loomis, T. P. *Am. J. Sci.* **278**, 1099–1137 (1978).
17. Freer, R. *Contr. Miner. Petrol.* **76**, 440–454 (1981).
18. Grauert, B., Hänny, R. & Soptrajanova, G. *Contr. Miner. Petrol.* **45**, 37–63 (1974).

Asphalt in carbon-14-dated archaeological samples from Terqa, Syria

Mahalakshmi I. Venkatesan*, Timothy W. Linick†, Hans E. Suess*† & Giorgio Buccellati‡

Institutes of *Geophysics and Planetary Physics and ‡Archeology, University of California, Los Angeles, California 90024, USA
† Department of Chemistry, University of California, San Diego, La Jolla, California 92093, USA

The presence of fossil fuel compounds in archaeological samples giving ages much higher than expected has long been suspected but never proved by appropriate chemical analyses. An excessively high conventional ^{14}C age was found in an archaeological charcoal sample from Terqa, Syria[1] (S313, Table 1). Its ^{14}C age of 28,700 yr BP was at variance with the archaeological context, and with the ^{14}C age of several other samples[1] (such as S283, Table 1) obtained from the same area and expected to date from ~3000 BC or younger. The inconsistency can be explained by assuming contamination with geologically old material—either industrial petroleum products or ancient asphalt. We report here organic geochemical investigations of the sample S313 and of sample S267, which gave a ^{14}C age ~2,000 yr too old. A third charcoal sample (S283) from the same area, whose ^{14}C age was consistent with its known historical age, and an asphalt sample found stuck to the bottom of a goblet from another site in the area dated at 1700 BC on typological grounds, were also analysed. Similar studies of used crankcase oils from motor vehicles, weathered 0–2 yr, and of hydraulic transmission fluid show that modern motor oil cannot be the contaminant at this excavation site. Our data clearly indicate that ancient asphalt must be the source of contamination. Caution should be exercised, therefore, in interpreting ^{14}C dates of archaeological samples from areas containing asphalt or other fossil fuel deposits.

Fine charcoal samples were collected by D. Berry from and around an ancient dumpsite outside the ancient city wall of Terqa, Syria and stored in glass jars (see ref. 1 for details). Obvious extraneous matter, such as rootlets, was removed; the samples were converted to acetylene via lithium carbide[2] and counted in stainless-steel gas proportional β-detectors for ^{14}C (Table 1).

The samples were Soxhlet-extracted successively with methanol and toluene/methanol (3 : 7 v/v) for 100 h. The extract was separated into hexane-insoluble (asphaltenes) and hexane-soluble (lipid or bitumen) fractions. The latter was fractionated into aliphatic and aromatic hydrocarbons and resins by silica gel column chromatography[4]. Samples S313 and S267 had asphaltenes and S267 also had traces of elemental sulphur (Table 1). Sample S283 had no asphaltenes, but a considerable amount of elemental sulphur and resinous material characteristic of wood. The fractions were analysed by gas chromatography (GC) and GC–mass spectrometry. Sample S313 was ^{14}C tested again after exhaustive extraction with toluene methanol (3 : 7 v/v) and methylene chloride. After rinsing with 1 l of acetone to remove other organic solvents, the material was analysed for ^{14}C measurements[2]. The ^{14}C age determined was not significantly different from that found previously for the unextracted sample (Table 1).

The gravimetric (Table 1) and GC analyses revealed that the greater the discrepancy in age, the larger is the content of asphaltenes and hydrocarbons. The alkane profile of the control sample (S283) with correct ^{14}C age was very different from those of the other two samples (Fig. 1, S267 not shown).

The normal alkanes in sample S283 ranged from C_{15} to C_{31} overlying a broad unresolved complex mixture (Fig. 1). Pristane and phytane are almost equally abundant. The carbon preference index (CPI) is ~2.0, indicative of immature hydrocarbons derived from higher plant waxes[5]. Triterpanes are present in minor amounts and are mainly 17α(H), 21β(H)-hopanes. The lipids in this charcoal sample appear to be of mixed secondary origin from biogenic sources and traces of petroleum-like products seem to have been leached into the area by water over thousands of years. The presence of a few pyrolytic arenes[6] is consistent with such an input. The alkanes in samples S313 and S267 are predominantly cyclic triterpanes with minor amounts of steranes. Normal alkanes are found only in trace amounts (much less than in crude oils). The triterpanes consist mainly of a homologous series of 17α(H), 21β(H)-hopanes and the extended hopanes ($\geq C_{31}$) occur as their two diastereomers (*R* and *S* at position 22) in approximately equal abundance[7]. In fact, the ratio of the first eluting epimer (22*S*) to the second eluting epimer (22*R*) in the C_{31}–C_{35} hopane series is ~1.4 (measured with baseline GC resolution), consistent with mature ancient bitumen[8]. The aromatic fraction exhibits an unresolved hump over the entire boiling range, indicating heavy weathering of the lipid fraction. The low *n*-alkane content, such as that found in sample S283, could be masked in the other two samples which contain relatively higher concentrations of triterpanes from the presumed (fossil fuel) contamination.

Possible sources of oil contamination in the area are crankcase oil from motor vehicles, although the samples were retrieved from a depth of 2 m below the surface of an area with little or no

0028–0836/82/060517—03$01.00

Table 1 Organic geochemical results for archaeological samples from Terqa, Syria

Sample	Conventional ^{14}C age (BP)	Elemental sulphur* (μg per g)	Asphaltenes* (μg per g)	Hexane -soluble lipids* (μg per g)	Aliphatic fraction* (μg per g)	Aromatic fraction* (μg per g)	Asphaltenes H/C	Asphaltenes $\delta^{13}C$ (‰ PDB)	Asphaltenes $\delta^{18}O$ PDB	Asphaltenes δD (‰ SMOW)
Charcoal S283	4,110±70	~15	—	144	41	53	—	—	—	—
Charcoal S267	5,700±100	Trace	900	1,440	260	86	1.27	−27.61	−15.58	−60.9
Charcoal S313	28,700±1,100 28,200±1,300†	—	5,300	14,560	2,790	1,820	1.03	−27.61	−15.88	Lost
Asphalt from goblet	—	—	104,000	43,000	4,860	2,410	1.23	−27.95	−15.58	−60.0

1σ statistical counting errors are given for the conventional BP dates. The calibrated dates in centuries can be obtained using the table in ref 3. The age of the charcoal samples expected from stratigraphy is 3000 BC. PDB, Peedee belemnite. SMOW, standard mean ocean water. La Jolla Laboratory numbers in sequence of increasing ^{14}C are: LJ 5052, LJ 4823 and LJ 5031.

* Gravimetric determination. † After exhaustive extraction with organic solvents.

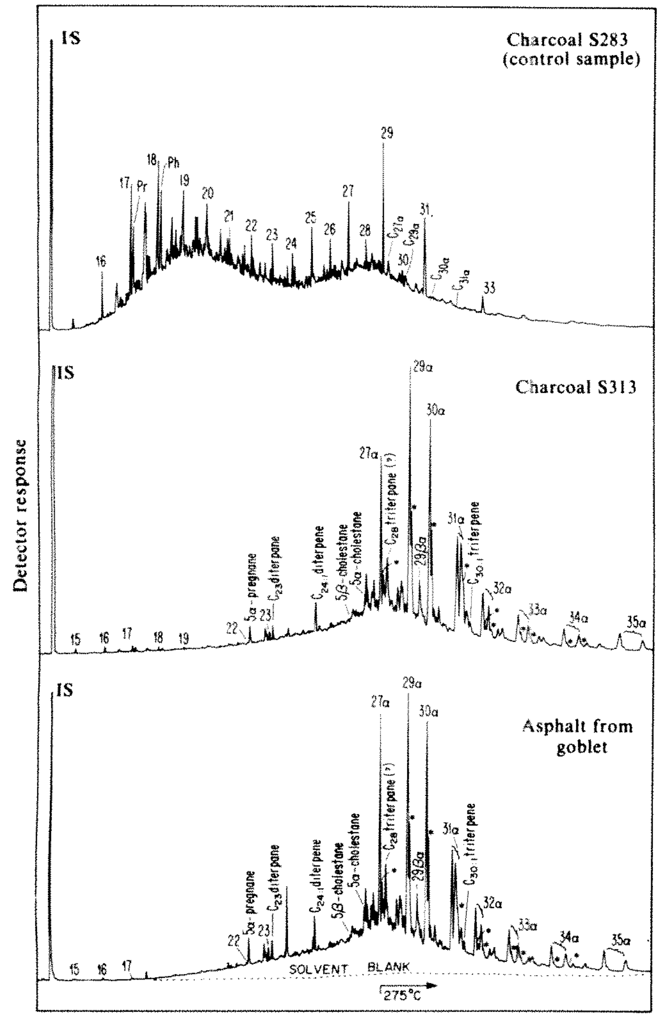

Fig. 1 Gas chromatograms of aliphatic fraction from charcoal and asphalt samples from Terqa, Syria. A Hewlett-Packard 5840A gas chromatograph equipped with a fused silica capillary column (SP-2100, 25 m, 0.2 mm i.d.) was used. The column was temperature-programmed for 35–275 $°C_{iso}$ at 4 °C per min. A 30 m, SE-54 (J&W) column of the same specifications was used for GC–MS analysis on a Finnigan model 4000 quadrupole mass spectrometer interfaced with a Finnigan Model 9610 gas chromatograph. The mass spectra data were processed with a Finnigan Incos Model 2300 data system. *n*-Alkanes were identified by their retention times. Di- and triterpenoids were identified from m/z 191 mass chromatograms. Triterpanes $\geq C_{31}$ occur as *R* and *S* diastereomers. IS, internal standard (hexamethylbenzene); numbers (except when followed by α or β) refer to *n*-alkanes; Pr, pristane; 27α, 29α, and so on refer to 17α(H), 21β(H)-hopanes with the designated carbon numbers; 29βα is a C_{29} moretane (17β(H), 21α(H)). * Refers to the homologous series of methylated hopanes. Charcoal sample S267 had the same GC profile as S313 and therefore is not shown here.

traffic until a few years ago, and ancient asphalt. The area on the Euphrates in Syria contains asphalt[9].

We analysed the hydrocarbon fractions of fresh hydraulic fluid and crankcase oil, fresh and weathered for ~1 month to 2 yr. The crankcase oil was collected from underneath impounded cars and the period of weathering of the spilled oil from the cars is documented. The GC profiles of the hydrocarbons in the oils (Fig. 2) have a major unresolved hump at C_{20}–C_{30} with a homologous series of *n*-alkanes and branched and cyclic hydrocarbons, in contrast to the contaminated charcoal samples which are depleted in *n*-alkanes. If the contaminant were crankcase oil weathered only since cars began operating in this region (20–40 yr), then almost total degradation of *n*-alkanes would be impossible. This can be surmised if we compare the fresh oil to the one weathered over two years (also heated to a certain extent in the car). The maximum temperature to which crankcase oil is normally heated is ~205 °C (250 °C in diesel engines, D. Godfrey, personal communication), which may not be high enough to pyrolyse all the *n*-alkanes[10,11] in the time during which the oil is heated in the car. Also, the stratigraphy at the sample locations showed no streaks of spilled oil from the surface to the 2 m depth of the samples. These observations preclude automobile oil from being the contaminant.

The only other possible source seems to be ancient, indigenous asphalt. Modern asphalt seems an unlikely candidate as there were no paved roads near the excavation site. An asphalt sample from a goblet in the area had the same *n*-alkane (trace amounts) and triterpenoidal distributions as did the two contaminated samples (Fig. 1). The H/C ratio and $\delta^{13}C$ data of the asphaltenes from the samples (Table 1) are typical of data reported for asphalts[12–14]. The close agreement in the stable isotopic data (of carbon, oxygen and hydrogen obtained according to ref. 15) of the asphaltenes also suggests a common source of asphalt in the contaminated samples and the asphalt from the goblet, that is, indigenous asphalt.

The nonextractable residue, after exhaustive solvent extraction, gave almost the same ^{14}C age as the original sample (Table 1), suggesting that the unusually old age is largely due to the insoluble pyrobitumen[16] that could have originated from the asphalt. (Modern motor oil would probably be completely extracted by organic solvents used on sample S313, in which case the residue should have given a comparable age to that of other syngenetic samples in the area.)

In the third millennium in Syria, the asphalt used for sealing cracks in ceramic vessels[17] and fastening tool heads onto wooden handles[9] was probably melted by heating[18,19]. Frequent reheating, coupled with weathering, might have altered most of the asphalt into pyrobitumen. The residual asphalt which did not undergo complete thermal alteration could contain a triterpenoidal profile similar to the one reported here. At elevated temperatures (~375 °C) straight-chain alkanes decompose[10], whereas tricyclic diterpanes and pentacyclic triterpanes survive[20]. Indeed, the triterpenoidal distribution in the contaminated samples and asphalt are very similar to those of pyrolysates from kerogen matrices[20]. These pyrolysates have lesser amounts of steranes and moretanes compared with triterpanes and the $C_{29}\alpha$ hopane is more abundant than the $C_{30}\alpha$ homologue, as is observed here (Fig. 1). A minor series with m/z 205, analogous to the major hopane series, is also present, indicating an extra methyl group in the A or B ring. 3-Methylhopanes have been detected in bacteria[21] and the presence of the methylated hopanes implies microbial residues probably involved in the synthesis of petroleum hopanes[22]. Water washing and biodegradation of crude oil in reservoirs also could remove n-alkanes and isoprenoids and lead to a similar distribution of triterpenoids in the resultant asphalt[23] as these compounds do not seem to be significantly affected by bacterial degradation[23,24]. It is not surprising, therefore, to see the biomarker steranes and di- and triterpanes (derived from the thermally altered and probably biodegraded indigenous asphalt) in the charcoal samples.

A broken storage pot of asphalt dumped in refuse could easily have contaminated some of the charcoal samples excavated from the ancient dumpsite. It is also feasible, that some of the native asphalt might have undergone thermal alteration by its proximity to the fireplace from which the charcoal samples could have originated. It is not known whether the asphalt was used as a fuel.

According to the ^{14}C data, pyrobitumen from ancient asphalt has contributed as much as 95.5% and 18% to the total carbon in samples S313 and S267 respectively. This large amount explains why, after removing the solvent solubles, a younger ^{14}C age was not observed for S313. The extractable material was much lower in concentration relative to the non-extractables.

This is the first organic geochemical study to verify contamination in ^{14}C dated archaeological samples, which could account for much older apparent ages than expected. Chronologies based on ^{14}C dates of archaeological materials containing fossil organic carbon in the absence of confirmatory molecular analysis should be accepted with caution. Similar organic geochemical analyses of a few samples (^{14}C dated) from Jericho and Jarmo (northern Iraq) where traces of asphalt have been found on ancient stone tools[18] are in progress.

We thank I. R. Kaplan for encouragment and advice, B. R. T. Simoneit, R. Eganhouse and I. R. Kaplan for reviewing the manuscript, E. Ruth for GC–MS analyses and D. Winter for helping in the stable isotope analyses. H.E.S. greatly appreciates the opportunity to spend the winter quarter (1981) with the IGPP at UCLA. Support for organic geochemical work (M.I.V.) was provided by NASA grant NGR-05-007-221. Excavations at Terqa were carried out with grants from the Ahmanson Foundation, the Ambassador International Cultural Foundation, the Samuel H. Kress Foundation and the Chancellor's Office at UCLA. This is contribution no. 2163 of the Institute of Geophysics and Planetary Physics, University of California, Los Angeles.

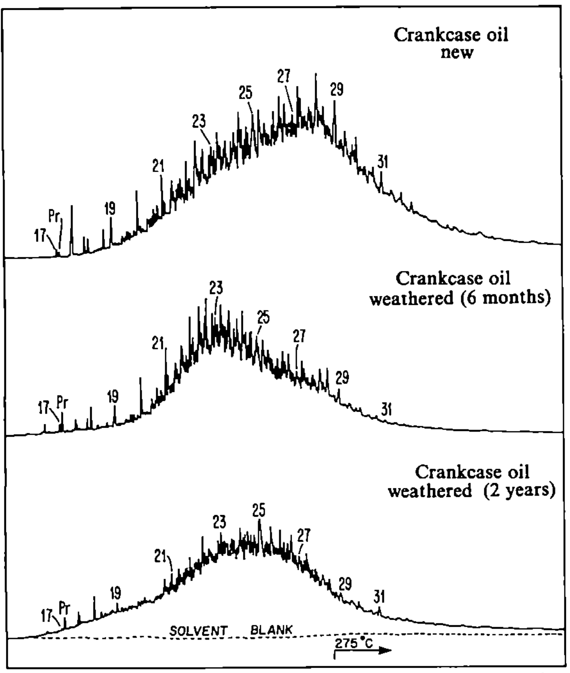

Fig. 2 Gas chromatograms of aliphatic fraction from crankcase oils. Experimental details as for Fig. 1. Numbers refer to n-alkanes; Pr, pristane.

Received 15 June; accepted 7 December 1981.

1. Buccellati, G., Kelly-Buccellati, M. & Knudstad, J. in *Terqa Preliminary Reports*, No. 10 (ed. Buccellati, G.) 42–86 (Undena, Malibu, California, 1979).
2. Linick, T. W. *Radiocarbon* **19**, 19–20 (1977).
3. Suess, H E. in *Radiocarbon Dating* (eds Berger, R. & Suess, H. E.) 777–784 (University of California Press, 1979).
4. Venkatesan, M. I., Brenner, S., Ruth, E., Bonilla, J. & Kaplan, I. R. *Geochim. cosmochim. Acta* **44**, 789–802 (1980).
5. Simoneit, B. R. T. thesis, Univ. Bristol (1975).
6. Youngblood, W. W. & Blumer, M. *Geochim. cosmochim. Acta* **39**, 1303–1314 (1975).
7. Dastillung, M. & Albrecht, P. *Mar. Pollut. Bull.* **7**, 13–15 (1976).
8. Seifert, W. K. & Moldowan, J. M. *Adv. org. Geochem.* **12**, 229–237 (1979).
9. Marschner, R. F. & Wright, H. T. in *Archaeol. Chem. II, Adv. Chem. Ser. 1977* (ed. Carter, G. F.) 151–171 (American Chemical Society, 1978).
10. Henderson, W., Eglinton, G., Simmonds, P. & Lovelock, J. E. *Nature* **219**, 1012–1016 (1968).
11. Abelson, P. H. in *Researches in Geochemistry* (ed. Abelson, P. H.) 79–103 (Wiley, New York, 1959).
12. Tissot, B. P. & Welte, D. H. in *Petroleum Formation and Occurrence* (eds Tissot, B. P. & Welte, D. H.) 362 (Springer, New York, 1978).
13. Grizzle, P. L., Coleman, H. J., Sweeney, R. E. & Kaplan, I. R. in *Chem. Congr. Am. chem. Soc. and chem. Soc. Japan*, 39–50 (Division of Petroleum Chemistry Inc., American Chemical Society, Honoloulu, Hawaii, 1979).
14. Stahl, W. J. *Chem. Geol.* **20**, 121–149 (1977).
15. Stuermer, D. H., Peters, K. E. & Kaplan, I. R. *Geochim. cosmochim. Acta* **42**, 989–997 (1978).
16. Connan, J., LeTran, K. & Van Der Weide, B. *Proc. 9th Wld Petrol. Congr.* **2**, 171–178 (Applied Science, Tokyo, 1977).
17. Buccellati, G. & Kelly-Buccellati, M. in *New Archaeological Harvests from Syria*, 1–8 (Ambassador College, California, 1977).
18. Marschner, J. F., Duffy, L. J. & Wright, H. T. *Paleorient* **4**, 97–112 (1978).
19. Gutman, T. E. *J. New World Archaeol.* **3**, 232–243 (1979).
20. Seifert, W. K. *Geochim. cosmochim. Acta* **42**, 473–484 (1978).
21. Rohmer, M. & Ourisson, G. *Tetrahedron Lett.* **40**, 3641–3644 (1976).
22. Ensminger, A., Van Dorsselaer, A., Spyckerelle, C., Albrecht, P & Ourisson, G. in *Advances in organic Geochemistry* (eds Tissot, B& Bienner, F.) 245–260 (Editions Technip. Paris 1973).
23. Connan, J, Restle, A. & Albrecht, P. *Adv. org. Geochem.* **12**, 1–17 (1979).
24. Rubinstein, I., Strausz, O. P., Spyckerelle, C., Crawford, R. J. & Westlake, D. W. S. *Geochim cosmochim. Acta* **41**, 1341–1353 (1977).

O-sulphated Leu-enkephalin in brain

C. D. Unsworth & John Hughes*

Department of Biochemistry, Imperial College of Science and Technology, London SW7 2AZ, UK

J. S. Morley

Pharmaceutical Division, ICI Ltd, Alderley Park, Cheshire, UK

The enkephalins appear to share a common precursor which is distinct from pro-opiocortin[1,2]. The adrenal proenkephalins have molecular weights (M_rs) in the range 5,000–30,000 with the largest species containing six copies of Met-enkephalin to one of Leu-enkephalin[3]. The brain proenkephalins appear to differ in that the molecular weights are in the range 5,000–90,000 and digestion of the largest protein with trypsin and carboxypeptidase B generates approximately equal proportions of Met- and Leu-enkephalin[4]. During our studies of brain proenkephalin we noted the generation of enkephalin-immunoreactive species that were chromatographically distinct from Met- and Leu-enkephalin. Here we identify one of these species as *O*-sulphated Leu-enkephalin and suggest possible roles for sulphation in the metabolism of opioid peptides.

Digestion of the striatal proenkephalin fraction ($M_r > 5{,}000$) with trypsin yielded a mixture of enkephalin-like immunoreactive and bioactive opioid species; these were separated by

---

*To whom reprint requests should be addressed.

0028-0836/82/060519—04$01.00

high-voltage paper electrophoresis (HVPE) at *p*H 6.5 into basic, neutral and acidic species. The neutral peptides were analysed by reverse-phase HPLC using antisera directed against Met- and Leu-enkephalin, which showed that the two peptides were present in a ratio of 2 : 1. The precursor pool therefore contains extreme C-terminal enkephalin sequences with the Leu-enkephalin form predominating. Treatment of the basic peptide fraction with carboxypeptidase B yielded a further mixture of Met- and Leu-enkephalin with the former predominating although we were unable to determine an absolute ratio because of the presence of other unidentified immunoreactive species. Treatment of the acidic fraction with carboxypeptidase B resulted in an increase in Leu-enkephalin immunoreactivity but this activity still moved towards the anode at *p*H 6.5 and was found to possess a negative charge even at *p*H 1.9. Isoelectrophoretic analysis confirmed the presence of immunoreactive and bioactive opioid peptides with *p*I values of 3.5 to <2.5, that is, beyond the range of our ampholyte system. The peptides derived from trypsin and carboxypeptidase B digestion were subjected to HVPE both before and after treatment with neuraminidase, phosphatase and arylsulphatase. Treatment with the first two enzymes had no discernible effect on the mobility or immunoreactivity of the acidic fraction; however, arylsulphatase treatment caused a marked increase in Leu-enkephalin immunoreactivity which now co-migrated with marker enkephalin. When the acidic peptide fraction derived from trypsin digestion alone was reacted with arylsulphatase, the products were found to carry a positive charge at *p*H 6.5.

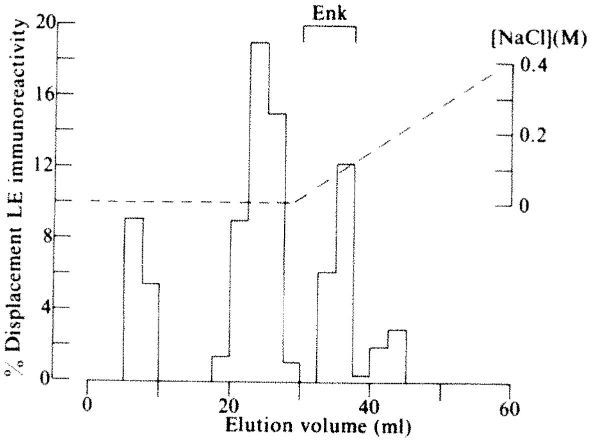

Fig. 1 Separation of tryptic opioid peptides by DEAE-ion-exchange chromatography. Mouse striatum was extracted with $10\ \mathrm{ml\ g^{-1}}$ of 1M acetic acid adjusted to *p*H 1.9 with HCl. The soluble proteins were passed through a Sephadex-G25 column and the excluded volume was collected and lyophilized. This protein fraction was dissolved in 50 mM Tris-HCl *p*H 8, incubated with trypsin (1 mg per 100 mg protein) for 4 h, then passed through a 400 mg Poropak-Q column and after a water wash the absorbed peptides were eluted with ethanol. The dried ethanol eluate was dissolved in 50 mM Tris-HCl, *p*H 9.25 and applied to a 20 × 0.7 cm DEAE-Sephadex (A-25) column. The column was first developed with 28 ml of 50 mM Tris-HCl *p*H 7.3, at which point a linear salt gradient was started. Aliquots of each 2.5-ml fraction, corresponding to 3 mg of starting tissue, were immunoassayed with both anti-Leu-enkephalin-antisera (LE1, 5% cross-reactivity with Met-enkephalin) and anti-Met-enkephalin-antisera (ME-T1, $<0.1\%$ cross-reactivity with Leu-enkephalin). The first two peaks, 0.6 and 1.2 pmol Met-enkephalin-equivalents, represent basic peptide fractions and only reacted with ME-T1. The third peak (0.33 pmol) corresponds to the elution position of authentic enkephalin and contained Leu- and Met-enkephalin in a 2 : 1 ratio. The fourth peak (0.11 pmol Leu-enkephalin (LE) equivalents) only reacted with LE1 and carried a negative charge at *p*H 6.5. Treatment of this peak with carboxypeptidase B gave a slight increase in immunoreactive material carrying a negative charge at *p*H 1.9. (Note that cross-reactivity of LE1 with Arg or Lys C-terminal-extended Leu-enkephalin is only slightly less than that of *O*-sulphated-Leu-enkephalin.)

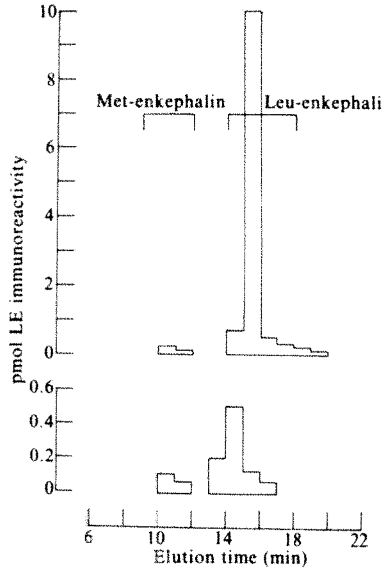

Fig. 2 Reverse-phase HPLC analysis of acidic Leu-enkephalin (LE)-immunoreactive peptide. Sheep striatum (70 mg protein) was extracted and treated with trypsin as in Fig. 1 and the acidic Leu-enkephalin-immunoreactive peak isolated by DEAE chromatography. This material was incubated at 37 °C for 2 h with 10 µg of carboxypeptidase B in 50 mM Tris-HCl, *p*H 8. One half of the sample was then incubated with arylsulphatase (0.5 unit) from *Patella vulgata* (200 mM sodium acetate, *p*H 5 for 2 h). The products of these digestions were absorbed on Poropak-Q and then chromatographed on a 250 × 4 mm Partisil-10-ODS-2 column in isocratic conditions (100 ethanol/250 water/3.5 acetic acid by vol) at $0.8\ \mathrm{ml\ min^{-1}}$. The lower panel shows the elution profile of LE1 immunoreactivity after trypsin and carboxypeptidase treatment, the upper panel after the additional arylsulphatase treatment.

Gradient elution of the tryptic digest on Sephadex-DEAE revealed the presence of four peaks of immunoreactivity (Fig. 1). Peaks 1 and 2 reacted strongly with anti-Met-enkephalin antibodies and were strongly basic. Peak 3 corresponded to the elution position of authentic Met- and Leu-enkephalin, the greater affinity for anti-Leu-enkephalin antisera reflecting the preponderance of Leu-enkephalin generation after trypsin digestion. Peak 4 corresponds to the acidic fraction detected by HVPE and showed a much greater affinity for anti-Leu- rather than for anti-Met-enkephalin antisera. Peak 4 was divided and one fraction treated with carboxypeptidase B, the other with carboxypeptidase B and arylsulphatase. These fractions were chromatographed on a Partisil-10-ODS (octadecyl silane) HPLC column (Fig. 2). Immunoassay of the effluent revealed the presence of a small Leu-enkephalin-immunoreactive peak in the carboxypeptidase B-treated fraction, this peak being close to, but not coincident with, an authentic Leu-enkephalin sample. The arylsulphatase-treated fraction yielded a much larger Leu-enkephalin-immunoreactive peak coincident with authentic Leu-enkephalin. Identical results were obtained with protein extracts of both mouse and sheep striatum.

These results indicated the presence in our protein fraction of a sulphated Leu-enkephalin sequence flanked by basic amino acids. Trypsin digestion alone should liberate a sulphated Leu-enkephalin sequence containing C-terminal Arg or Lys residues and carrying an overall negative charge due to the presence of *O*-sulphate. Treatment with arylsulphatase should change the overall charge to +1 due to the loss of sulphate while treatment with carboxypeptidase B and arylsulphatase yields a Leu-enkephalin-like peptide having no overall charge at *p*H 6.5. We cannot exclude the possibility that some sulphated Leu-enkephalin sequences might exist at the extreme C-terminal of proenkephalin but the above evidence supports an internal location for most of the material.

In view of the small amounts of natural material available, the *O*-sulphate ester of Leu-enkephalin (LES) was prepared and its properties compared with those of the material derived from enzymatic digestion of striatal proenkephalin. LES was prepared by coupling *N-t*-butoxycarbonyl-l-tyrosine-*O*-sulphate barium salt with glycylglycyl-l-phenylalanyl-l-leucine *t*-butyl ester. The final purified product was homogeneous in five TLC and two HPLC systems and gave amino acid ratios, after aminopeptidase M digestion, of Tyr(SO_3H) (1): Gly (1.99): Phe (0.97): Leu (1): Tyr (0), (J.S.M. and C. F. Hayward in preparation). LES caused a dose-dependent, naloxone-reversible inhibition of both the mouse vas deferens and guinea pig ileum but had only 0.0001 times the activity of Leu-enkephalin in these assays. Its cross-reactivity with our anti-Met- and anti-Leu-enkephalin antisera was <0.1% and 5% respectively. LES has no intrinsic opiate receptor activity as a small proportion can undergo desulphation during bioassay. Incubation of LES with arylsulphatase for 2–4 h caused a maximal conversion of 20–30% of the material to Leu-enkephalin within 2 h. An alternative method of desulphation was developed based on the observation that exposure of LES to anhydrous trifluoroacetic acid (TFA) during its synthesis causes a rapid loss of the sulphate moiety. Incubation of dried samples of LES with anhydrous TFA (50 μg LES in 500 μl TFA) at 37 °C resulted in complete conversion to Leu-enkephalin within 80 min as judged by HPLC. No other product was detected by HPLC nor was there any alteration of Leu-enkephalin activity.

Synthetic LES and our acidic Leu-enkephalin-immunoreactive fraction had identical mobilities in several chromatographic systems including silica-gel TLC, Partisil-10–anion-exchange HPLC and reverse-phase HPLC. Synthetic LES eluted between Met- and Leu-enkephalin on the Partisil-10–ODS system with overlap between Leu-enkephalin and LES. This was consistent with the result obtained before the synthetic material was available (Fig. 2). Complete separation of LES from the enkephalins was achieved by gradient elution on a μ-Bondepak C18 column (Fig. 3). Several peaks of immunoreactivity were observed in this separation but only those fractions co-eluting with authentic LES showed a marked increase in immunoreactivity after treatment with TFA or arylsulphatase (Fig. 3).

LES was also detected in the free form as part of the endogenous peptide pool in brain extracts. Material having the chromatographic properties of LES was detected by immunoassay or by bioassay after TFA treatment in several systems including silica-gel TLC, reverse-phase and cation- and anion-exchange HPLC. In Fig. 4*a*, material eluting at the position of synthetic LES was bioassayed before and after TFA treatment of the eluate fractions. Naloxone-reversible activity (~45 pmol) was detected in one fraction before TFA treatment. However, ~200 pmol of activity were detected in the same fraction after TFA treatment. As LES is only bioactive at nanomolar concentrations it was unlikely that the activity detected before TFA treatment was due to LES. Support for the existence of both LES and another intrinsically active opioid in this sample was obtained by chromatography of an identical sample on the same column after treatment with TFA. There were two peaks of activity, one (~120 pmol) corresponding to Leu-enkephalin arising from the desulphation of LES and the other, earlier peak (~40 pmol) eluting close to but slightly later than marker LES (Fig. 4*b*). The bioactivity detected in Fig. 4*a* before desulphation was quantitatively the same as that detected in Fig. 4*b* close to the LES elution point; the increase in bioactivity (Fig. 4*a*) after TFA was also quantitatively similar to the amount of Leu-enkephalin detected in Fig. 4*b*.

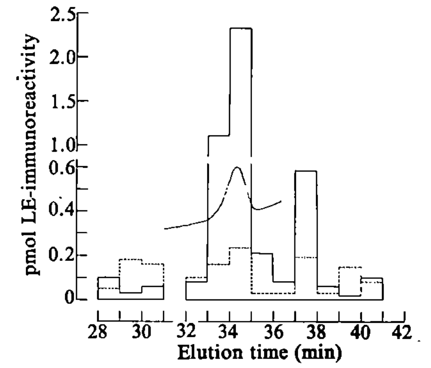

Fig. 3 Identification of the sulphate ester of Leu-enkephalin from mouse striated protein. The acidic fraction of a tryptic digest was isolated as described in Fig. 1 legend and then treated with carboxypeptidase B. The final digested sample was chromatographed on a μ-Bondepak C18 reverse-phase column (0.78 × 30 cm). The initial conditions were 5% acetic acid/propranol (90/10 v/v) with a 30-min concave gradient to give final proportions of 60/40 (v/v) and this was continued for a further 15 min. Fractions (1 ml) were collected and aliquots divided, one half being immunoassayed directly with LE1 antisera (dotted lines), and the other half treated with TFA before immunoassay (solid lines). The values correspond to 20 mg wet weight of mouse striatum. Several small peaks of Leu-enkephalin immunoreactivity were detected before TFA treatment, but only fractions 33–34, corresponding to the elution position of LES (superimposed UV absorption trace), showed a marked increase after TFA. A threefold increase in immunoreactivity was also seen with fraction 37.

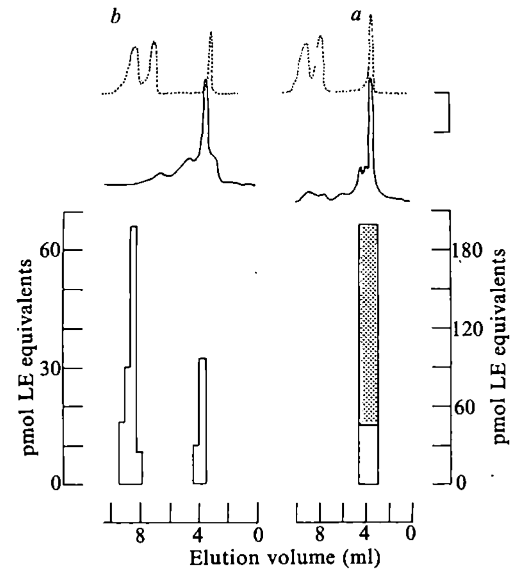

Fig. 4 Detection of endogenous acidic opioid peptides. Mouse striata were extracted as described in Fig. 1 legend and the peptide fraction separated from protein on Sephadex G-25. Acidic peptides were isolated by DEAE–Sephadex chromatography. The acidic peptides were chromatographed on a 250 × 4 mm Partisil-10–SCX column in isocratic conditions (10 mM NaH_2PO_4/H_3PO_4 *p*H 2.4; 0.5 and 0.4 ml min^{-1} for traces *a* and *b* respectively). Samples equivalent to 480 mg of starting tissue were used. *a*, Elution profile of an untreated sample. *b*, Chromatogram obtained for a sample that had been incubated with TFA for 80 min. In *a*, 2 min samples were collected and divided, one half being bioassayed directly on the mouse vas deferens for naloxone-reversible activity and the other half being treated with TFA before bioassay (shaded column). One fraction in *a* contained 45 pmol of intrinsic activity; treatment of this sample with TFA increased the activity to 198 pmol. In contrast, the other fractions contained no activity either before or after TFA treatment. In *b*, 1 min fractions were collected and bioassayed directly; opiate activity was detected in a peak emerging just after the position of authentic LES and coincident with authentic Leu-enkephalin. Activity is expressed in pmol Leu-enkephalin (LE) equivalents. The upper traces are the 206 nm absorption traces for the tissue samples and the broken traces those of marker peptides. Order of elution (right to left): LES, Met- and Leu-enkephalin.

The intrinsically active acid opioid peptide fraction, LES, the enkephalins and more basic endogenous opioid peptides were also separated and detected by isoelectrophoresis (Table 1). We demonstrated the existence of basic opioids which migrated to the cathode (*p*I >7.5), the enkephalins (*p*I 5.0–5.5) and a more acidic fraction (*p*I 2.9–3.1). None of the fractions showed any

Table 1 Isoelectrophoretic separation of rat brain opioid peptides

*p*I	Leu-enkephalin equivalent activity (pmol) Untreated eluate	 TFA-treated eluate
>7.5	110	120
4.9–5.5	460	425
2.9–3.2	60	48
<2.5	0	80

Three whole rat brains were homogenized in 5% TCA (10 ml per g tissue) and the solubilized peptides were absorbed on 200 mg of Poropak-Q; after a water wash the peptides were eluted with 5 ml of methanol. The methanol eluate was divided and dried. Isoelectric focusing was carried out on horizontal slab gels of Ultradex (prepared as recommended by LKB). Two runs were made with *p*H gradients of 5–8 and 2.5–4.0 respectively (2% Ampholines (LKB); 8 W constant power at 10 °C for 12 h). At the end of each run the gels were sliced and the peptides eluted with 2 ml distilled water. The samples were then absorbed on to Poropak-Q which was washed thoroughly with water to remove ampholines, then eluted with methanol. The dried methanol eluates were bioassayed directly on the mouse vas deferens and after TFA treatment. Trace amounts of ^{3}H-labelled enkephalins added to the original samples were also used to establish the isoelectric points of these peptides: Leu-enkephalin = 5.4 (5.2–5.5); Met-enkephalin = 5.2 (4.9–5.3).

enhancement of activity after TFA treatment except material from the anode where LES would be expected to migrate with a *p*I of <2.0.

We have detected the presence of protein-incorporated LES in sheep, mouse and guinea pig striatum. The free peptide, which is also present in these species and the rat, appears to constitute 10–20% of the total free pool of Leu-enkephalin. The proportion of LES in the proenkephalin fraction may be much higher, initial studies indicating that as much as 50% of protein-incorporated Leu-enkephalin may be sulphated. We have also detected LES in the high-molecular weight proenkephalin[4] and thus sulphation may occur early in peptide biogenesis, possibly at the nascent peptide stage. The sulphate ester of Met-enkephalin has not been detected although we cannot exclude completely its occurrence.

The significance of these findings is unknown. Sulphation may represent an inactivation mechanism, a signal for selective precursor cleavage or a means for conferring novel non-opiate activities on opioid peptides. The brain contains several endogenous enkephalin-related peptides including α-neo-endorphin[5], dynorphin[6], Met^5-enkephalinylarginylphenylalanine[7] as well as Met- and Leu-enkephalin[8]. At present we do not know if they share common biosynthetic pathways but it will be of considerable interest to determine whether any of these other peptides undergo sulphation. In the pro-opiomelanocortin system, *N*-acetylation[9] can lead to the activation of melanotropin and inactivation of β-endorphin, thus providing a flexible system for determining the nature of active products generated by a common precursor. It remains to be determined whether sulphation has a similar role in the proenkephalin system.

We thank Professor H. R. Morris, Dr G. Taylor, Dr C. F. Hayward, Mr A. Etienne, Ava Singh and Miss B. Birchmore for their help and advice. This work was supported by grants from the MRC and Nuffield Trust to J.H. C.D.U. is an MRC scholar.

Received 18 September; accepted 16 December 1981.

1. Lewis, R. V. *et al. Biochem. biophys. Res. Commun.* **89,** 822–829 (1979).
2. Hughes, J. *et al. J. exp. Biol.* **89,** 239–255 (1980).
3. Lewis, R. V. *et al. Science* **208,** 1459–1461 (1980).
4. Beaumont, A., Fuentes, J. A., Hughes, J. & Metters, K. M. *FEBS Lett.* **122,** 135–137 (1980).
5. Kangawa, K. *et al. Biochem. biophys. Res. Commun.* **99,** 871–878 (1981).
6. Goldstein, A. *et al. Proc. natn. Acad. Sci. U.S.A.* **76,** 6666–6670 (1979).
7. Stern, S. *et al. Proc. natn. Acad. Sci. U.S.A.* **77,** 1681–1685 (1980).
8. Hughes, J. *et al. Nature* **258,** 577–579 (1975).
9. Smyth, D. G., Massey, D. E., Zakarian, S. & Finnie, M. *Nature* **299,** 352–354 (1979).

Molecular size of benzodiazepine receptor in rat brain *in situ*: evidence for a functional dimer?

A. Doble & L. L. Iversen

MRC Neurochemical Pharmacology Unit, MRC Centre, Medical School, Hills Road, Cambridge CB2 2QH, UK

Benzodiazepine tranquillizers such as diazepam and chlordiazepoxide interact with high-affinity binding sites in nervous tissue[1,2]. The correlation between the affinities of various benzodiazepines for these sites with their clinical potencies and activity in behavioural and electrophysiological tests in animals suggests that the sites represent the functional 'receptor' whereby benzodiazepines exert their effects[3]. The intimate involvement of benzodiazepines with γ-aminobutyric acid (GABA) and chloride channels raised the possibility that the benzodiazepine binding site (BDZ-R) may be a protein in the GABA receptor–effector complex[4,5]. GABA agonists enhance the affinity of BDZ-R for benzodiazepines[6], although BDZ-R is distinct from the GABA receptor itself[3]. However, electrophysiological evidence suggests that the action of benzodiazepines is chloride channel, rather than receptor, directed[7–10]. Several attempts have been made to measure the molecular weight (M_r) of BDZ-R after solubilization from brain membranes: treatment with 1% Triton X-100 followed by assay of binding activity in solute fractions separated according to molecular weight suggested[11] a value of ~200,000, photoaffinity labelling of BDZ-R with ^{3}H-flunitrazepam (^{3}H-FNZ) followed by more rigorous solubilization and gel chromatography indicated[12,13] an apparent M_r of ~55,000 and a third approach[14] a value of ~100,000. The measured molecular weight seems to depend critically on the solubilization procedure used. Chang *et al.*[15] recently described the use of radiation inactivation to determine the size of BDZ-R *in situ* in calf brain membranes, and estimated a M_r of 216,000. We have also used this approach; the results reported here indicate a M_r of between 90,000 and 100,000, but this is reduced to 60,000–63,000 in membranes pretreated with GABA, suggesting the disaggregation of a normally dimeric form.

Radiation inactivation has been widely used to obtain the molecular weights of enzymes and other soluble macromolecules, and the technique has also been applied to membrane-bound proteins such as the (Na$^+$ + K$^+$)ATPase in erythrocytes, the tetrodotoxin binding site in neuronal membranes and the glucagon-stimulated adenlyate cyclase in hepatocytes[16]. The method has the great attraction of allowing size determinations to be made on functionally defined membrane proteins *in situ*. High-energy particles can inactivate biological macromolecules according to classical target theory: thus, if inactivation is considered an all-or-none event, the relationship between degree of inactivation and radiation dose will be an exponential one, whose decay constant will be solely a function of molecular size. This can be computed from the dose of radiation in megarads required to reduce biological activity by a factor of $1/e$ (the D_{37}) using a conversion constant which has been derived both theoretically and empirically[17]

$$M_r = 6.4 \times 10^5 / D_{37}$$

The radiation dose delivered was independently monitored by assaying an endogenous membrane marker of known molecular weight (acetylcholinesterase); the measurements indicated a M_r of 65,000 for the enzyme, in good agreement with previously determined values[17].

In the present study we irradiated *in vacuo* lyophilized neuronal membranes from rat brain with electrons accelerated through 16 MeV by the linear accelerator at Addenbrooke's Hospital, Cambridge for various times at a rate of 2 Mrad min^{-1}.

0028-0836/82/060522—02$01.00

Table 1 Affinity (K_D) and capacity (B_{max}) of ^{3}H-FNZ binding sites determined by Scatchard analysis

	K_d (nM)	B_{max} (pmol per g protein)	
Fresh membranes	2.5±0.3	282±11	($n = 3$)
Lyophilized membranes	2.3	270	
Irradiated membranes	2.0	90	

Values are compared in freshly prepared membranes, lyophilized and reconstituted membranes, and lyophilized membranes irradiated with 10 Mrad high-energy electrons before reconstitution. Each determination used data from triplicate determinations of specific binding at eight ^{3}H-FNZ concentrations between 0.1 and 10 nM. For K_d values, regression analysis of the slopes of Scatchard plots revealed no significant difference between experimental groups.

The residual BDZ-R activity was measured using a conventional ^{3}H-FNZ radiolabelling assay and compared with non-irradiated controls. The binding properties of lyophilized membranes were not significantly different from freshly prepared membranes (Table 1); by contrast the increase in GABA receptor affinity on freezing is well documented[18].

Figure 1 demonstrates that electron bombardment inactivated BDZ-R and the linear nature of the logarithmic transform suggests loss of a single component of homogeneous size; further experiments show that this linearity is preserved up to doses inactivating >90% of BDZ-R activity. Irradiation produced no change in the nonspecific ^{3}H-FNZ binding. Scatchard analysis shows that loss of activity reflected a loss of binding sites rather than a change in binding characteristics—as might be expected if the inactivation were not all-or-none (Table 1). The radiation-sensitive M_r calculated from these data is 89,000±15,000.

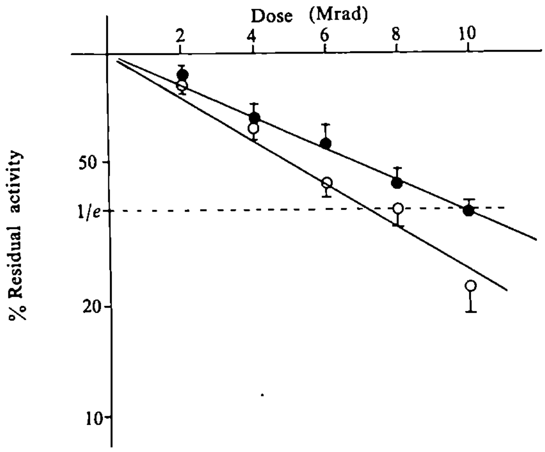

Fig. 1 Inactivation of ^{3}H-FNZ binding sites in rat neuronal membranes by high-energy electrons in the absence (○) and presence (●) of GABA. Membranes were prepared by homogenization of whole brain tissue 1:40 (w/v) in 50 mM Tris-citrate buffer *p*H 7.1, followed by 20 min centrifugation at 50,000*g*. The pellet obtained was resuspended and centrifuged a further four times before use. Pellets were suspended in distilled water with or without 10^{-4}M GABA and aliquots lyophilized in 5 ml glass centrifuge tubes. The tubes were evacuated and irradiated at 2 Mrad min^{-1}; during irradiation they were cooled by a stream of air that had passed through dry ice to maintain the temperature below 60 °C; this heating had no effect on the binding properties. Following irradiation, the samples were suspended in Tris-citrate buffer at a concentration of ~3 mg protein per ml, and the amount of ^{3}H-FNZ binding assessed: 500-μl aliquots were incubated at 4 °C for 30 min with 0.5 nM ^{3}H-FNZ and the binding terminated by filtration. 'Specific' binding was defined as the component displaceable by excess (2 μM) FNZ, and represents ~95% of total binding in control samples. Each sample was assayed in triplicate, and the data represent mean±s.e.m. of six independent experiments. Residual ^{3}H-FNZ binding is expressed as the percentage of that seen in non-irradiated controls. In these controls, specific binding represented 18.8±0.7 pmol per g protein, which was significantly increased ($P < 0.05$) in the presence of 10^{-4}M GABA to 22.4±1.5 pmol per g protein. The data were plotted as a semi-log transform, and the exponential decay lines of best fit computed by linear regression analysis. Intercept values (1/*e*) were 7.2 (5.8–8.6; 95% confidence limits) Mrad and 10.1 (9.1–11.1) Mrad, without and with GABA respectively. The dose of irradiation was monitored by measuring current flow to Earth from a Faraday cup before which the samples were mounted. The current flux was regularly calibrated by reference to absorbance change in clear Perspex HX mounted in place of the samples[22]. The dosimetry was independently confirmed by monitoring the acetylcholinesterase activity in aliquots of the brain membranes by the colorimetric method of Ellman *et al.*[23].

We also studied the molecular size of the BDZ-R in membranes treated before lyophilization with 10^{-4}M GABA, a concentration sufficient to cause a maximum increase in BDZ-R binding affinity[6]. In these membranes, the radiation-sensitive size was significantly ($P < 0.05$) decreased to 63,000±7,000. Values obtained from a further series of five experiments were 102,000 and 60,000 without and with GABA respectively; these values are not significantly different from the original values. The simplest explanation of this effect of GABA is that BDZ-R may exist as a dimer whose disaggregation is triggered by GABA receptor activation. If, as discussed above, BDZ-R is related to the chloride ion channel, then it is possible that GABA receptor activation causes the separation of two transmembrane proteins, thus opening a chloride ion channel; the open channel (BDZ-R monomer) would have a higher affinity for the benzodiazepines than the closed channel (BDZ-R dimer). A similar model of protein transformation in a receptor–ionophore complex has been postulated for GABA on physicochemical grounds[19], and parallels current models for the nicotinic acetylcholine receptor[20].

The apparent molecular size reported here for BDZ-R, between 90,000 and 100,000, is not significantly different from the value obtained by Braestrup *et al.*[14]. The more rigorous purification of photoaffinity-labelled BDZ-R which yields a weight of 55,000 may produce the 'monomeric' BDZ-R we have postulated above. The 200,000-M_r moiety labelled after solubilization[11] is still sensitive to GABA[21] and co-chromatographs with ^{3}H-labelled receptors[11], thus may represent the GABA receptor–ionophore complex, rather than independent BDZ-R. It is not clear why Chang *et al.*[15] found a value of ~200,000, using a similar radiation inactivation technique. However, they used a different species (ox) and treated the brain membranes with Triton X-100, which may affect the state of aggregation of membrane proteins.

The present study demonstrates the feasibility of using radiation inactivation not only to measure the size of membrane-bound receptors, but also to analyse physicochemically the effects of interactions between transmitters, receptors and effectors on their molecular properties.

We thank Dr J. C. Ellory for useful discussion, Mr R. Gouldstone and his staff in the Radiotherapeutics Department, Addenbrooke's Hospital, Cambridge for operating the linear accelerator and Mrs I. Anderson for typing assistance. A. D. is a MRC scholar.

Received 8 June; accepted 16 December 1981.

1. Squires, R. F. & Braestrup, C. *Nature* **266**, 732–734 (1977).
2. Mohler, H. & Okada, T. *Life Sci.* **20**, 2101–2110 (1977).
3. Braestrup, C. & Squires, R. F. *Br. J. Psychiat.* **133**, 249–260 (1978).
4. Tallman, J. F., Paul, S. M., Skolnick, P. & Gallagher, D. W. *Science* **207**, 274–281 (1980).
5. Mazzari, S., Massotti, M., Guidotti, A. & Costa, E. *Adv. biochem. Psychopharmac.* **26**, 1–8 (1981).
6. Martin, I. L. & Candy, J. M. *Neuropharmacology* **17**, 993–998 (1978).
7. Simmonds, M. A. *Nature* **284**, 558–560 (1980).
8. Ticku, M. K., Van Ness, P. C., Haycock, J. W., Levy, W. B. & Olsen, R. W. *Brain Res.* **150**, 642–647 (1978).
9. Doble, A. & Turnbull, M. J. *J. Pharm. Pharmac.* **33**, 267–268 (1981).
10. Costa, T., Rodbard, D. & Pert, C. B. *Nature* **286**, 285–287 (1980).
11. Asano, T. & Ogasawara, N. *Life Sci.* **26**, 1131–1137 (1980).
12. Mohler, H., Battersby, M. K. & Richards, J. G. *Proc. natn. Acad. Sci. U.S.A.* **77**, 1666–1670 (1980).
13. Steghart, W. & Karobath, M. *Nature* **286**, 285–287 (1980).
14. Braestrup, C., Nielsen, M., Skovberg, H. & Gredal, O. *Adv. biochem. Psychopharmac.* **26**, 147–156 (1981).
15. Chang, L-R., Barnard, E. A., Lo, M. S. S. & Dolly, J. O. *FEBS Lett.* **126**, 309–312 (1981).
16. Ellory, C. *Trends biochem. Sci.* **4**, 99–100 (1979).
17. Kepner, G. R. & Macey, R. I. *Biochim. biophys. Acta* **163**, 188–203 (1968).
18. Enna, S. J. & Snyder, S. H. *Molec. Pharmac.* **13**, 442–453 (1977).
19. Van Gelder, N. M. *Can. J. Physiol. Pharmac.* **49**, 513–519 (1971).
20. Heidmann, T. & Changeux, J.-P. *Adv. Biochem.* **47**, 317–357 (1978).
21. Gavish, M. & Snyder, S. H. *Life Sci.* **26**, 579–582 (1980).
22. Berry, R. J. & Marshall, C. H. *Phys. med. Biol.* **14**, 585–596 (1969).
23. Ellman, G., Courtney, D., Andres, V. & Featherstone, R. M. *Biochem. Pharmac.* **7**, 88–95 (1961).

Use of carboxyfluorescein diacetate to study formation of permeable channels between mouse blastomeres

H. Goodall & M. H. Johnson

Department of Anatomy, Downing Street, Cambridge
CB2 3DY, UK

The transmission of signals between cells of the early preimplantation embryo may be important in the recognition of relative cell position, thereby influencing the direction of cell differentiation[1-5]. Gap junctional (water-permeable) channels may provide one route for such signal transmission[6]. A previous report[7], in which intact, zona-free mouse embryos were impaled by microelectrodes, demonstrated that gap junction-mediated dye transfer and electrical continuity were absent between blastomeres of two- and four-cell embryos but appeared during the eight-cell stage. It is at the eight-cell stage that compaction occurs, during which cells polarize[3], flatten on each other[3,8] and show the first morphological evidence of intercellular junctions[9,10]. We report here the use of a simple, non-iontophoretic method to detect the passage of a low-molecular-weight dye between aggregated blastomeres of the early preimplantation mouse embryo. Cells are incubated in the nonfluorescent, non-polar reagent, 6-carboxyfluorescein diacetate (CFDA)[11,12], which enters the cell freely, where it becomes entrapped following enzymatic conversion[13] to the hydrophilic fluorophore 6-carboxyfluorescein (CF; molecular weight 370). The labelled cells may then be aggregated with unlabelled cells and the formation of communicating channels between cells is revealed by the passage of dye from labelled to unlabelled blastomeres. CFDA provides better results than previously used fluorescein esters[14,15], which hydrolyse to a much less hydrophilic fluorophore that leaks from the cell relatively quickly[11,15]. Using CFDA we have confirmed that the capacity to form channels is lacking at all stages from the mature oocyte to the four-cell embryo but appears during the first 6 h of the eight-cell stage, preceding the fully compacted state.

In preliminary experiments, it was established that CFDA (derived from a 10 mg ml^{-1} stock solution in acetone) at concentrations of 4–40 μg ml^{-1} in phosphate-buffered medium (PB1)[16] labelled cells brightly, with no detectable effects on viability or subsequent division. The dye was distributed evenly throughout the cytoplasm (Fig. 1), leaked only slowly from two-, four- or eight-cell blastomeres, as reported for the lymphocyte[11], although somewhat faster from unfertilized or fertilized eggs, and was not taken up in detectable quantity by unlabelled blastomeres co-cultured with labelled blastomeres. Free transfer of dye was detected only between aggregated blastomeres from the eight-cell embryo (Figs 1, 2).

The first sign of dye transmission was the appearance of a weak fluorescence in the unlabelled blastomeres, which subsequently increased, concomitant with a decline in the fluorescence of the labelled blastomeres, until all blastomeres fluoresced with similar intensity (Fig. 1). No dye was transferred between aggregated pairs of unfertilized eggs (Fig. 3*a*, *b*; 43 pairs observed at 15–17 h following injection of human chorionic gonadotropin [hCG]), consistent with earlier studies[17], or between one-cell embryos (18 pairs observed at 20 h post-hCG). Blastomeres from two- and four-cell embryos were not able to transmit dye (68 and 20 pairs examined respectively), even when cultured for up to 5 h (Figs 2, 3). A similar result was obtained from all pairings between cells of different embryonic stages from mature oocyte to eight-cell embryo (229 aggregates examined in various combinations), even when one cell of the aggregated pair was from a population proved capable of transmitting dye within itself (Fig. 3).

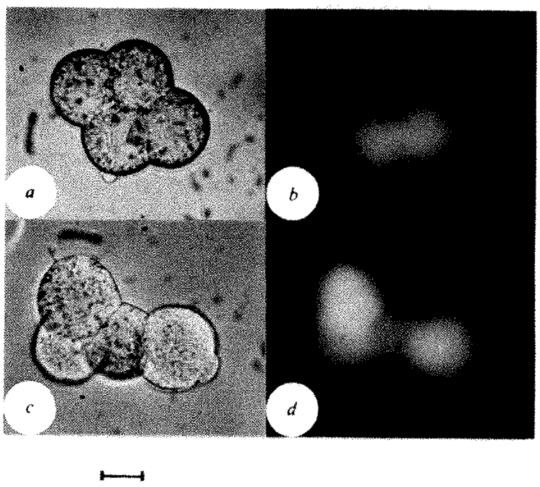

Fig. 1 Passage of CF between blastomeres derived from eight-cell mouse embryos. Female CFLP mice (Hacking and Churchill) were superovulated by intraperitoneal injection of 5 IU (international units) pregnant mare serum (PMS; Folligon) and 5 IU human chorionic gonadotropin (hCG) (Chorulon) 44–48 h later. Mice were mated, and compacted eight-cell embryos (~70 h post-hCG) were recovered, their zonae pellucidae removed and they were then disaggregated to either single cells (1/8) or pairs of cells, according to established procedures[3]. Blastomeres were then taken through four changes of CFDA (4 μg ml^{-1}) in phosphate-buffered medium (PB1)[16] without protein, and incubated in suspension in the final change of labelling medium for 2 min and then rinsed three times in PB1 containing 4 mg m^{-1} bovine serum albumin (BSA). Labelled cells were then aggregated to unlabelled cells using phytohaemagglutinin (Gibco Biocult) (5% v/v of stock solution in Ca^{2+}-deficient medium 16 + 6 mg ml^{-1} BSA), shown previously to have no obvious effect on development[3,19], rinsed in PB1 + BSA and cultured as described previously[3] in drops of medium 16 + 4 mg ml^{-1} BSA at 37 °C in 5% CO_2 in air, under oil in plastic cell culture dishes (Sterilin). After 3 h, the aggregates were mounted in PB1 + BSA on a tissue typing plate (Baird and Tatlock) and viewed with a Zeiss photomicroscope (filter set 48 77 09 with incident source HBO 200 for epifluorescence [*b*, *d*] and transmission optics for brightfield [*a*, *c*]). Photographs were taken on Kodak Tri-X 35 mm film. Fluorescence exposures were of 2 min duration. *a*, *b*, No transfer of CF between a labelled and unlabelled pair of blastomeres has yet occurred. *c*, *d*, Complete exchange of dye has occurred between the labelled pair and the unlabelled pair. Scale bar, 10 μm.

To measure the time taken to establish water-permeable channels between cells with an existing capability to transfer, individual blastomeres from compacted, late eight-cell embryos were labelled and aggregated with similar, unlabelled cells. Couplets were analysed at various times after aggregation for evidence of dye transmission (Fig. 2, left-hand curve). Four hours elapsed before all the pairs showed complete dye transmission, although this had occurred in some pairs within the first hour. Whether these early transmitting pairs resulted from assembly of pre-existing proteins or the synthesis *de novo* of gap-junctional proteins is not known, although in Cl-1d cells the minimum time required for synthesis and construction of permeable channels has been estimated to be 4–6 h (ref. 18).

To determine the time at which an eight-cell blastomere first develops the capacity to transmit dye, labelled 2/8 pairs were aggregated at a known time after their formation by division of 1/4 blastomeres, with unlabelled 2/8 pairs of the same age, and cultured for 3 h before analysis. The results are shown in the right-hand curve of Fig. 2; the slope of the curve is similar to that on the left, and presumably reflects the variability in time required to assemble functional junctions and transmit dye. However, the whole curve is shifted to the right by 2–3 h; it seems that ~2–3 h must elapse before a newly formed 1/8 blastomere becomes competent to assemble channels and transmit the dye. Junction formation, therefore, is a relatively early event in the life of the eight-cell embryo, coinciding with the induction of polarity[19] and preceding cell flattening[3].

This conclusion is further supported by experiments in which complete eight-cell embryos were aggregated and assayed for transfer of CF (Fig. 4). Transmission of dye occurred when both embryos were in a precompact state at the time of aggregation

0028-0836/82/060524—03$01.00

(Fig. 4*a*, *b*), suggesting that the competence to form water-permeable channels must precede complete cell flattening. However, when both embryos were compacted at aggregation, no transfer occurred (Fig. 4*c*, *d*), despite the proven ability of individual blastomeres isolated from compacted embryos to transmit the dye (Fig. 4*e*, *f*). Presumably, in compact embryos, the completely microvillous outer surfaces[20–22] of the cells either lacked gap-junctional proteins or were unable to assemble them in the time available to form functional channels.

The use of CFDA provides a simple technique for studying gap-junctional communication between small groups of cells. Moreover, many observations can be made within a short period. The results reported here confirm and extend previous observations using conventional iontophoretic techniques[7]. Thus the capacity to assemble functional gap-junctional channels does not develop until the early eight-cell stage when they form rapidly, due either to the insertion of gap-junctional proteins or to reorganization of existing gap-junctional proteins within the membrane[23]. It will be important to establish whether gap junction formation is required for the coordination of events resulting in polarization and cell flattening and if so, whether such coordination depends on the evening out of metabolic potential[24] or the passage of specific signalling molecules[6] between cells. The available evidence does not suggest that gap junctions are involved in the induction of polarity because two- and four-cell blastomeres can induce polarity in eight-cell blastomeres[19], yet cannot transmit to them. It remains to be determined, however, to what degree junctions are involved in subsequent events of early mouse development.

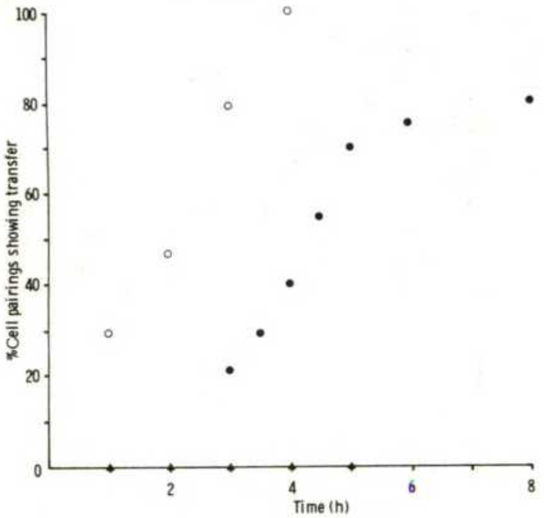

Fig. 2 Capacity of blastomeres to transmit CF. ○, Compact eight-cell embryos were disaggregated to single cells, some of which were labelled with CF and reaggregated with unlabelled cells. Couplets were examined for dye transfer at 1, 2, 3 or 4 h (67 couplets examined). For comparison, results with blastomeres derived from two-cell embryos (41 h post-hCG) and treated similarly are shown (Δ; 68 couplets examined). The horizontal axis represents time (in h) after aggregation at which aggregates were examined for dye transmission. ●, Four-cell embryos were disaggregated to 1/4 blastomeres, which were cultured *in vitro* and examined at 1/2 h intervals. Any cells dividing to 2/8 were collected[3], and the couplets were cultured for 0–5 h. At 0, 0.5, 1, 1.5, 2, 3 and 5 h, some couplets were labelled and aggregated to unlabelled couplets of the same age post-division. The aggregates were then cultured for 3 h and analysed for dye transmission as described in Fig. 1 legend. Fifty-nine pairs of couplets were examined in total. The horizontal axis represents total time (in h) elapsed since division to 2/8 had occurred and includes in each case the 3 h between labelling plus aggregation and examination for dye transmission. In all cases controls were prepared consisting of co-incubated, but unpaired, labelled and unlabelled cells that had been subjected to otherwise identical experimental conditions to the paired cells. The failure of 100% of paired cells to transmit merely reflects the choice of a 3-h transfer period (see the left-hand curve in which only 80% of pairs showed transmission after 3 h).

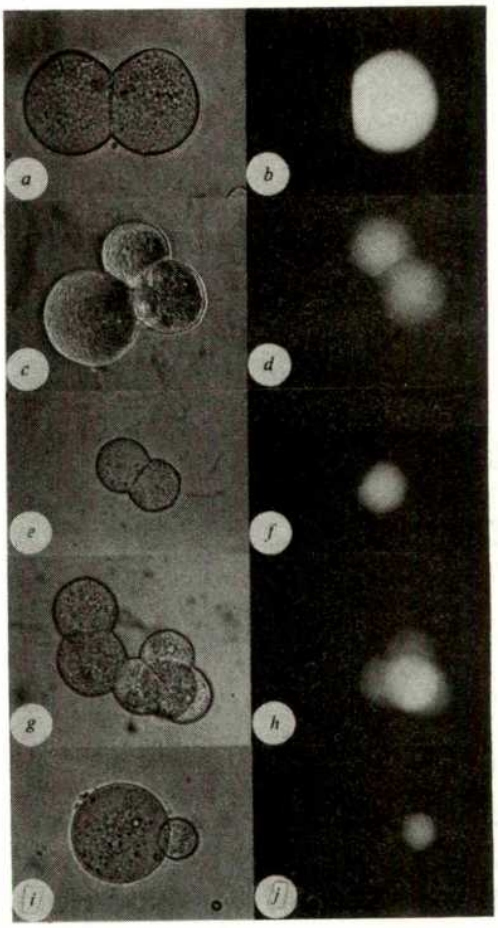

Fig. 3 Failure of CF to pass between cells taken from embryos at different stages of early development. Individual blastomeres were labelled with CF, incubated and photographed as described in Fig. 1 legend, whilst whole embryos were labelled within their zonae for 10 min, their zonae removed and then similarly treated. All aggregates were cultured for at least 3 h before examination. Phase-contrast (*a*, *c*, *e*, *g*, *i*) and fluorescence (*b*, *d*, *f*, *h*, *j*) images of the following couplets are shown: *a*, *b*, unfertilized egg + unfertilized egg; *c*, *d*, fertilized egg + two-cell embryo; *e*, *f*, 1/4 + 1/4 blastomeres; *g*, *h*, two-cell + four-cell embryos; and *i*, *j*, unfertilized egg + 1/8 blastomere. (No transfer was apparent even when the egg was labelled; thus failure to detect transfer did not result from dilution of CF.) Scale bar, 50 μm.

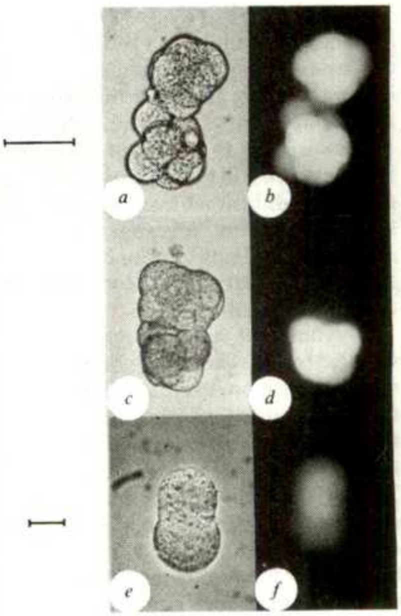

Fig. 4 CF transfer between intact eight-cell embryos after 3 h incubation. Late two-cell embryos were recovered and incubated *in vitro* for 16 h (ref. 3), by which time some had become precompact eight-cells. Some of these were labelled with CF and aggregated with unlabelled precompact eight-cell embryos immediately, whilst others were cultured further until compaction was complete and then were either similarly treated or disaggregated into 1/8 cells and then assayed for dye transfer. Phase-contrast (*a*, *c*, *e*) and fluorescence (*b*, *d*, *f*) images are shown. *a*, *b*, The transmission of CF between embryos that were precompact at time of labelling and aggregation. *c*, *d*, No transmission of CF between embryos that were compacted at labelling and aggregation. *e*, *f*, For comparison, the transmission of dye between 1/8 cells isolated from compacted eight-cell embryos. Scale bar: *a*–*d*, 50 μm; *e*, *f*, 10 μm.

The carboxyfluorescein diacetate was a gift from Dr J. W. Bruning via Dr A. J. Munro. It is now available from Molecular Probes Inc., Texas. We acknowledge the advice and criticism of Alan Munro, who suggested this new approach, and thank Hilary MacQueen, Carol Ziomek, Hester Pratt and John Reeve for criticism of the manuscript; Gin Flach, Ian Edgar, Mike Parr and John Bashford for help; and Tim Crane for preparation of photographic material. The work was supported by grants to M.H.J. from Cancer Research Campaign, MRC and Ford Foundation.

Received 7 September; accepted 17 November 1981.

1. Tarkowski, A. K. & Wroblewska, J. *J. Embryol. exp. Morph.* **18,** 155–180 (1967).
2. Hillman, N., Sherman, M. I. & Graham, C. F. *J. Embryol. exp. Morph.* **28,** 263–278 (1972).
3. Ziomek, C. A. & Johnson, M. H. *Cell* **21,** 935–942 (1980).
4. Gardner, R. L. *J. Embryol. exp. Morph.* **28,** 279–312 (1972).
5. Rossant, J. *J. Embryol. exp. Morph.* **33,** 991–1001 (1975).
6. Lo, C. W. in *Development in Mammals* Vol. 4 (ed. Johnson, M. H.) 39–80 (Elsevier, Amsterdam, 1980).
7. Lo, C. W. & Gilula, N. B. *Cell* **18,** 399–409 (1979).
8. Lehtonen, E. *J. Embryol. exp. Morph.* **58,** 231–249 (1980).
9. Ducibella, T., Albertini, D. F., Anderson, E. & Biggers, J. D. *Devl Biol.* **45,** 231–250 (1975).
10. Magnuson, T., Jacobson, J. B. & Stackpole, C. W. *Devl Biol.* **67,** 214–224 (1978).
11. Bruning, J. W., Kardol, M. J. & Arentzen, R. *J. immun. Meth.* **33,** 33–44 (1980).
12. Van der Poel, J. J., Kardol, M. H., Goulmy, E., Blokland, E. & Bruning, J. W. *Immun. Lett.* **2,** 187–193 (1981).
13. Rotmann, B. & Papermaster, B. W. *Proc. natn. Acad. Sci. U.S.A.* **55,** 134–141 (1966).
14. Sellin, D. *et al. Eur. J. Immun.* **4,** 189–193 (1974).
15. Loewenstein, W. R. *Biochim. biophys. Acta* **560,** 1–65 (1979).
16. Whittingham, D. B. & Wales, R. G. *Aust. J. biol. Sci.* **22,** 1065–1068 (1969).
17. Gilula, N. B., Epstein, M. L. & Beers, W. H. *J. Cell Biol.* **78,** 58–75 (1978).
18. Dahl, G., Azarnia, R. & Werner, R. *Nature* **289,** 683–685 (1981).
19. Johnson, M. H. & Ziomek, C. A. *J. Cell Biol.* **91,** 303–308 (1981).
20. Calarco, P. G. & Epstein, C. J. *Devl Biol.* **32,** 208–213 (1973).
21. Ducibella, T. & Anderson, E. *Devl Biol.* **47,** 45–58 (1975).
22. Reeve, W. J. D. & Ziomek, C. A. *J. Embryol. exp. Morph.* **62,** 339–350 (1981).
23. Pratt, H. P. M. in *Development in Mammals* Vol. 3 (ed. Johnson, M. H.) 83–129 (Elsevier, Amsterdam, 1978).
24. Sheridan, J. D., Finbow, M. E. & Pitts, J. D. *Expl Cell Res.* **123,** 111–117 (1979).

Crystal structure of a polyfunctional macrocyclic K^+ complex provides a solid-state model of a K^+ channel

Jean-Paul Behr & Jean-Marie Lehn

Institut Le Bel, Université Louis Pasteur, 4 rue Blaise Pascal,
67000 Strasbourg, France

Ann-Catherine Dock & Dino Moras

IBMC du CNRS, 15 rue Descartes, 67084 Strasbourg Cédex, France

Molecular channels are thought to be important in ion exchange processes across membranes, and biophysical and physiological data point to the existence of ion-specific Na^+ and K^+ pores (see, for example, refs 1, 2). The nature and structure of these entities, as well as the molecular mechanism of ion flow through channels, are still largely unknown, whereas cation transport via facilitated diffusion by natural or synthetic carrier molecules has been extensively investigated in both natural and model membrane systems[3–5]. The formation of transmembrane cation channels has been studied mainly with linear peptides (gramicidin A, alamethicin; refs 3, 7, and refs 6, 8 and refs therein). The cylindrical macrotricyclic molecules are suitable model species for investigating both the synthetic construction of molecular channel subunits and their cation binding properties as they form cation inclusion complexes of cryptate type and undergo intramolecular cation jump processes[9–11]. We report here the crystal structure of the potassium complex (1, 1.5 KBr, 3.5 H_2O) of the chiral macrocyclic tetracarboxamide 1, a member of a group of functionalized macrocyclic polyethers[12,13] which strongly bind alkali and ammonium cations[14]. This structure presents a solid-state model of a molecular channel, in which the macrocyclic units are organized in a polymolecular stack and the K^+ cations are located alternatively inside and on top of successive macrocycles, as in a frozen picture of potassium ion propagation through the stack.

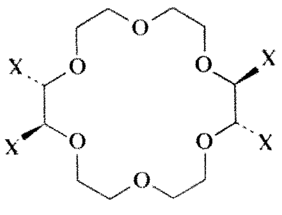

1 X = CONMe$_2$

Figure 1 shows the molecular crystal packing of the above complex along the [110] axis. The structure contains a polymolecular organic unit resulting from the repetition of a stacked dimeric asymmetric unit $[(\mathbf{1}, K)_2(H_2O)_3]^{2+}$, and is stabilized by hydrogen bonding of the water molecules with each other (O···O length 2.63 Å) and with six amide carbonyl groups (O···O length 2.50–2.95 Å), as well as by one ion dipole interaction (K_2^+···O 2.83 Å). The counterions are located in a polymeric chain $[KBr_3(H_2O)_4]^{2-}$ parallel to the organic one, made of alternating water-bridged KBr and BrBr fragments (Br···O 3.3–3.45 Å). The stability of the crystal packing is completed by Br···CH_3 van der Waals' interactions (3.68–3.76 Å) between the cationic and anionic chains.

The organic part of this structure has many attractive features. (1) The solid-state stacking of the macrocyclic units builds up an intermolecular arrangement clearly suggestive of a channel structure. The mean planes of the macrocycles are parallel to

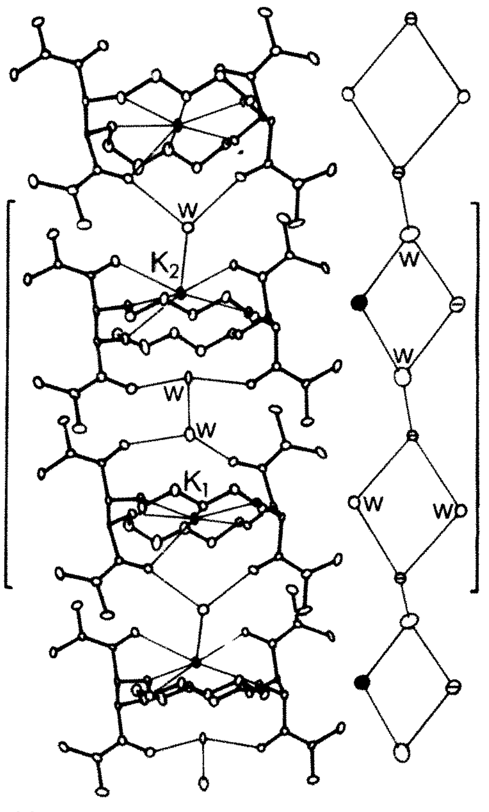

Fig. 1 Molecular packing of the complex $[(\mathbf{1}, K)_2, 3H_2O]^{2+} \cdot [KBr_3, 4H_2O]^{2-}$ down the [110] vector. Intermolecular contacts between the oxygen atoms of water molecules (W), and K^+ (●) or Br^- (⊖) ions are visualized by thin lines. Crystals belonging to the triclinic space group P1 were obtained by slow evaporation of an equimolecular solution of **1** and KBr in $CHCl_3/MeOH/H_2O$ ($a = 10.73$ Å, $b = 11.27$ Å, $c = 15.78$ Å; $\alpha = 109.85°$, $\beta = 99.35°$, $\gamma = 92.18°$). The crystal used had a size of $(0.4)^3$ mm^3. 6669 significant ($I > \sigma(I)$) reflections were collected up to $2\theta = 140°$ on an automated Nonius CAD4 diffractometer, using nickel-filtered Cu Kα radiation. The structure was solved by the standard heavy atom method followed by Fourier syntheses; final refinement by full-matrix least squares with anisotropic temperature factors for all non-hydrogen atoms led to an R factor of 0.096 for 799 variables. Atomic coordinates are available on request and will be deposited in the Cambridge Crystallographic Data Centre.

0028-0836/82/060526—02$01.00

each other and two neighbouring units are slightly shifted in a staircase-like fashion, due to steric hindrance between the lateral appendages.

(2) Both the macrocycles composing the asymmetric unit are in a relaxed conformation, similar to that found in other 18-crown-6-type complexes[15,16].

(3) The side chains $-CON(CH_3)_2$ are in an axial conformation, on both sides of the macrocyclic ring and direct their polar amide carbonyl groups into the internal space of the ligand.

(4) As a result of features (2) and (3) all apolar groups (methyl and methylene) of the macrocyclic units are on the outside. The previously determined structures of related compounds having secondary amide residues as lateral branches ($X = CONHR$ in **1**)[15] had already shown a *trans*-diaxial arrangement of the branches, but the carbonyl groups were directed outwards, with formation of an intramolecular $N-H\cdots O$ hydrogen bond between the CONH residues and the nearest ring ether oxygen atom. Consequently, the simple interconversion between secondary and tertiary amide functions allows a conformational control of the orientation of the polar groups towards the exterior or the interior of the structure respectively. This feature is of considerable interest for designing receptor molecules built on the basic macrocyclic unit **1**.

(5) There are two distinct K^+-binding schemes. In one complex of the asymmetric unit, the cation (K_1^+, Fig. 1) is located inside the macrocyclic ring, 0.25 Å from its mean plane; the receptor site includes all six ether oxygen atoms ($K_1^+\cdots O$ length 2.80 Å; $\sigma = 0.05$) and one carbonyl group ($K_1^+\cdots O{=}C$ length 2.76 Å). The other potassium ion (K_2^+, Fig. 1) is located on top of the macrocycle, at 1.13 Å from its mean plane; it is bound to only three ring oxygen atoms ($K_2^+\cdots O$ length 2.85 Å; $\sigma = 0.06$), to two amide carbonyl groups ($K_2^+\cdots O{=}C$ lengths 2.69, 2.89 Å) and to the oxygen of a water molecule ($K_2^+\cdots O$ 2.83 Å). These two modes of K^+ binding may be considered as two steps in a hopping mechanism of cation flow through the pore-like structure. Enniatins form sandwich complexes[17] like the RbNCS complex of enniatin B, in which every Rb^+ ion is bound to carbonyl oxygens of two ligand molecules[18].

(6) The polar interior of this solid-state channel contains three water molecules per asymmetric unit. They solvate the K^+ and amide groups, and provide H-bonding links between successive macrocyclic units.

In conclusion, the present structure possesses three main features which are expected to have a role in ion flow through membrane protein channels: a chain of cation binding units; polar inside/apolar outside orientation of residues; and mixed-site cation binding. It may therefore be considered a solid-state model of a molecular channel with cation propagation through the channel from one binding site to the next. The stepwise connection of macrocyclic units (Fig. 1) by their lateral appendages would allow the construction of a true artificial molecular channel, whose properties depend on the choice of the basic unit and of the linking branches. Synthetic work along these lines is in progress.

Received 2 November; accepted 14 December 1981.

1. Klingenberg, M. *Nature* **290,** 449–454 (1981).
2. Neher, E. & Sakmann, B. *Nature* **260,** 799–802 (1976).
3. Pressman, B. C. *A. Rev. Biochem.* **45,** 501–530 (1976).
4. Ovchinnikov, Y. A., Ivanov, V. T. & Shkrob, A. M. *Membrane-active Complexones*, BBA Library Vol. 12 (Elsevier, New York, 1974).
5. Lehn, J. M. *Pure appl. Chem.* **51,** 979–997 (1979).
6. Bradley, R. J., Urry, D. W., Okamoto, K. & Rapaka, R. *Science* **200,** 435–437 (1978).
7. Bramberg, E. *et al. Fedn Proc.* **37,** 2633–2638 (1978).
8. Fringeli, U. P. & Fringeli, M. *Proc. natn. Acad. Sci. U.S.A.* **76,** 3852–3856 (1979).
9. Lehn, J. M. *Accts chem. Res.* **11,** 49–57 (1978).
10. Lehn, J. M. & Simon, J. *Helv. chim. Acta* **60,** 141–151 (1977).
11. Lehn, J. M. & Stubbs, M. E. *J. Am. Chem. Soc.* **96,** 4011–4012 (1974).
12. Girodeau, J. M., Lehn, J. M. & Sauvage, J. P. *Angew. Chem.* **87,** 813–814 (1975); *Angew. Chem., int. Edn. Engl.* **14,** 764–765 (1975).
13. Behr, J. P., Girodeau, J. M., Hayward, R. C., Lehn, J. M. & Sauvage, J. P. *Helv. Chim. Acta* **63,** 2096–2111 (1980).
14. Behr, J. P., Lehn, J. M. & Vierling, P. *J. Chem. Soc. chem. Commun.* 621–623 (1976).
15. Behr, J. P., Lehn, J. M., Moras, D. & Thierry, J. C. *J. Am Chem. Soc.* **103,** 701–703 (1981).
16. Daly, J. J., Schönholzer, P., Behr, J. P. & Lehn, J. M. *Helv. Chim. Acta* **64,** 1444–1451 (1981).
17. Ivanov, V. T. *et al. FEBS Lett.* **36,** 65–71 (1973).
18. Tishchenko, G. N. & Karimov, Z. *Kristallografiya* **23,** 729–742 (1978).

Transient nature of early haematopoietic spleen colonies

M. C. Magli*, N. N. Iscove† & N. Odartchenko*

* Swiss Cancer Research Institute, Épalinges-sur-Lausanne CH-1066, Switzerland
† Basel Institute for Immunology, Basel CH-4005, Switzerland

Certain cells (CFU-S) in the haematopoietic tissues of mice are able to form macroscopic nodules in the spleen 7–14 days after injection in heavily irradiated recipient mice[1]. At 7–9 days, most of the spleen colonies contain recognizable cells of one predominant haematopoietic lineage[2], and do not contain cells capable of spleen colony formation on injection in secondary hosts[3]. However, by 14 days most of the spleen colonies do contain cells of more than one line of haematopoietic differentiation[2], as well as precursor cells capable of again generating similar multilineal spleen colonies on retransplantation[3]. These observations have led to the widely accepted conclusion that most spleen colonies are derived from pluripotential 'stem' cells[3], and to the suggestion that the apparent transformation in character of spleen colonies from unilineal at early times to mixed later on reflects the local operation of 'instructive' differentiative signals in the splenic environment[2]. The reasoning behind these suggestions implicitly assumed that late colonies simply represented a further stage in the development of the same colonies observable at earlier times. Here, we present direct evidence against this assumption. Our data indicate that most spleen colonies identified as surface nodules at days 7–8 are neither multipotential nor self-maintaining, but rather are destined to disappear from the spleen within 72 h. The observations set limits on the validity of the spleen colony method as an assay for self-maintaining pluripotential progenitor cells, and give cause for reassessment of the data on which widely accepted views concerning the regulation of such cells are based.

Initial experiments compared individual spleen colonies at early and late times in their development in terms of their content of cells capable of growth in culture. Such data would provide two kinds of information concerning the character of a spleen colony. First, the presence or absence of 'primitive' haematopoietic precursors capable of extended proliferation in culture would indicate the potential of the spleen colony for further growth. Second, the number of different kinds of cells growing in the cultures would supply information on the differentiative potential of the original spleen colony-forming cell.

Adult mouse bone marrow cells were injected into heavily γ-irradiated syngeneic recipients, and after varying time intervals, the recipient spleens were excised and examined at ×11 magnification for surface colonies. A total of 156 consecutively identified colonies were dissected out from spleens containing 9 or fewer surface nodules. Particular care was taken to exclude the occasional colonies whose geometry suggested possible confluence of more than one colony. Single cell suspensions were prepared from each colony. Most of the cells were plated in methylcellulose cultures to assay for haematopoietic precursor cells, and the remaining cells were centrifuged onto glass slides for morphological evaluation. From the culture results, spleen colonies were classified as P^+ or P^- according to whether or not they contained any relatively 'primitive' precursor cells, defined as cells capable of forming mixed myeloid/erythroid clones in culture containing at least 1,000 cells, or clones containing at least 50 mononuclear or granulocytic cells, or at least 200 erythroid cells. Almost all spleen colonies which contained *in vitro* clonable mononuclear or granulocytic precursors also contained erythroid precursors. The proportion of each colony plated was such that the absence of growth in culture signified

0028–0836/82/060527—03$01.00

the presence within the spleen colony of fewer than eight clonable precursors in the case of large spleen colonies, and fewer than one or two in the case of spleen colonies consisting of $\leq$200,000 cells.

Figure 1*a* shows the results for 7–8-day spleen colonies. Most colonies consisted predominantly of recognizable erythroblasts and contained no 'primitive' precursors. Although devoid of primitive cells clonable *in vitro*, these P^- colonies did contain high numbers (up to 25% of the cells) of relatively mature erythroid precursors (CFU-E) capable of forming small clones of 8–60 erythroblasts in culture. Few spleen colonies contained >20% of morphologically unrecognizable cells. The frequency of such cells correlated neither with the predominant morphological type nor with the presence of primitive precursors.

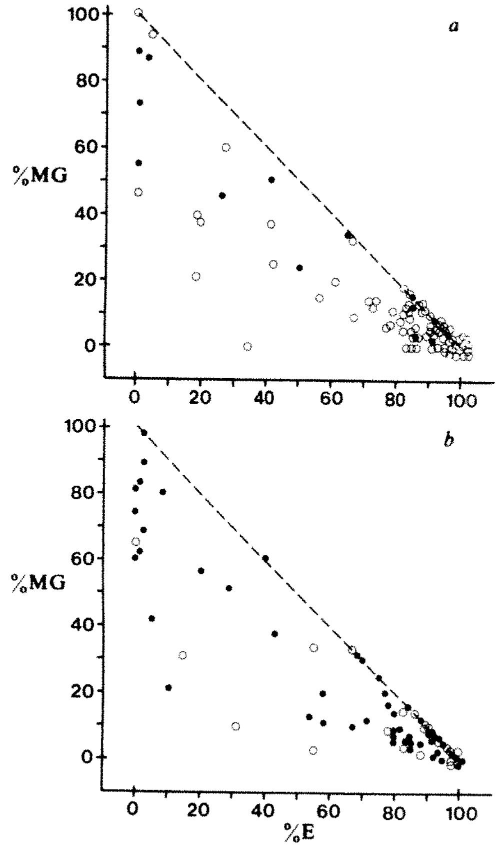

Fig. 1 Distribution of spleen colonies according to the character of their constituent cells. Each point represents one spleen colony, indicating presence (●) or absence (○) of primitive precursors capable of proliferating in culture, and the percentage of the cells identifiable morphologically as erythroid (E) or mononuclear/granulocytic (MG). *a*, Composition of spleen colonies after 7–8 days of growth in the spleen; *b*, after 9–12 days. Total numbers of spleen colonies examined were 37, 49, 14, 30, 17 and 9 on days 7–12, respectively. Female 8–12-week old BALB/c mice were γ-irradiated (800 R, ^{137}Cs) and injected intravenously with 1 or 3×10^4 nucleated syngeneic bone marrow cells suspended in IMDM[8] with 5% fetal calf serum (FCS). Controls injected with cell-free suspending medium had <1 colony per 20 spleens. Spleen colonies were dissected out and gently dispersed into single cell suspensions in IMDM containing 50% FCS. Some of the cells were cytocentrifuged onto glass slides, fixed in methanol and stained with Gurr's Giemsa. Cells were assigned to erythroid, mononuclear, granulocytic or megakaryocytic lineages on the basis of nuclear size, form, degree of condensation and presence of nucleoli, nuclear/cytoplasmic ratio, and cytoplasmic basophilia and granulation, according to classical morphological criteria. Cells were cultured at a maximum density of 10^5 per ml in IMDM containing α-thioglycerol, methylcellulose, bovine serum albumin, 15% FCS, iron-saturated transferrin, lecithin, oleic acid, cholesterol, 1 IU ml^{-1} human urinary erythropoietin (all as detailed elsewhere[8]) and 10% conditioned medium from WEHI-3 cells[9] as a source of erythroid burst-promoting activity[5] and of granulocyte/macrophage colony-stimulating activity. Small erythroid colonies from CFU-E were counted after 2 days of culture, and larger erythroid or mixed myeloid/erythroid bursts and granulocyte/macrophage colonies were counted on days 7, 10 and 14.

Figure 1*b* shows pooled results from spleen colonies analysed at later times of development (days 9–12). Three-quarters of the colonies now contained primitive precursors, a proportion consistent with earlier observations[3] on CFU-S in later spleen colonies but higher than that reported by Gregory and Henkelman in 11–12-day spleen colonies[4], possibly because of the addition to our cultures of a controlled concentration of 'burst-promoting activity'[5]. Half of our P^+ colonies showed mixed differentiation morphologically. Most P^- colonies again consisted predominantly of recognizable erythroblasts.

The relationship between early and late spleen colonies was then examined directly as follows. On days 7 or 8 after irradiation and marrow injection, recipient mice were anaesthetized and a small abdominal incision was made over the spleen. Each spleen was carefully inspected at ×11 magnification without excision and a topographical sketch made. The incision was then closed and splenic colony development permitted to continue for an additional 2 to 5 days before the mice were killed, and their spleens excised and again mapped topographically. Control experiments using irradiated mice which had not received bone marrow indicated that the surgical procedure did not itself induce the appearance of endogenous spleen colonies. The accuracy of the topographical sketches was confirmed in most cases by direct photography of the spleens. Figure 2 shows a typical result. Two of five colonies present on the spleen at day 8 are no longer visible at day 10, while, conversely, two of five colonies visible on day 10 were not visible at day 8. The aggregate results of the mapping experiments are presented in Table 1. Of the surface colonies visible on days 7 or 8, only half were still visible on day 10, whereas only one-third of colonies visible on day 10 had visible antecedents on days 7 or 8. In a separate experiment on a smaller scale, 80% of colonies visible at day 7 had vanished by day 12.

These results show spleen colonies to be divisible into two major categories. The first colony type (P^-) grows rapidly to achieve macroscopic dimensions at the spleen surface within 7–8 days and typically consists almost entirely of erythroid cells. Devoid of primitive cells capable of sustaining their growth, the P^- colonies soon vanish from the spleen, presumably as their cells differentiate terminally into erythrocytes and enter the circulation. A second colony type (P^+) grows more slowly in the first week, and at 7 days few can be indentified grossly at the spleen surface. Because their growth is sustained well beyond day 9 by the continuous presence of primitive cells, these P^+ colonies gradually become the predominant colony type as the P^- colonies recede and disappear.

These findings provide a fresh context for interpreting the significance of the 'transient endogenous erythroid spleen colonies' reported earlier[6,10,11]. Our observations and interpretations are also consistent with those of Hodgson and Bradley[7] on late-appearing spleen colony formation by fluorouracil-resistant precursors. Our results imply that the spleen colony method provides a measure of pluripotential cells

Table 1 Number of surface spleen colonies visible at ×11 magnification

	Days 7–8	Day 10
Transient	51	0
Persistent	50	50
Delayed in appearance	0	97
Total	101	147
	Day 7	Day 12
Transient	19	0
Persistent	5	5
Delayed in appearance	0	44
Total	24	49

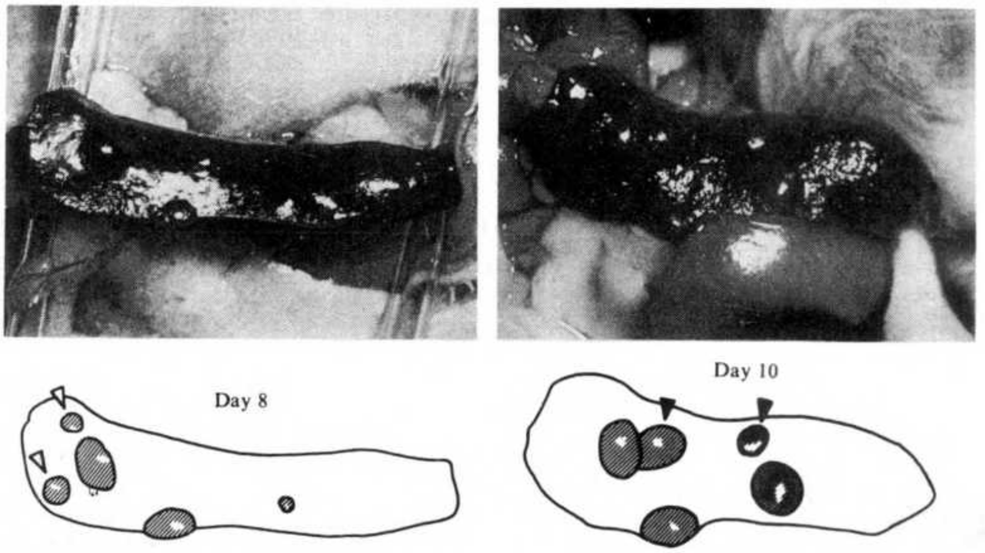

Fig. 2 The same spleen photographed after 8 (left) and 10 (right) days of spleen colony development. Drawings indicate the locations of the colonies. Colonies marked ▽ disappeared in this time interval; those marked ▼ were delayed in appearance.

capable of extensive proliferation only where macroscopic colonies are scored at 11 days or later. When spleen colonies are scored earlier than this, as has been done in almost the entire literature on the subject, the method appears to detect a population of cells more closely akin to the cells (BFU-E) which form large erythroid colonies after a similar length of time in semi-solid tissue culture[4,5]. Finally, our observations show that late multilineal P^+ spleen colonies are not derived from the unilineal P^- colonies visible at earlier times, and therefore remove a key supporting element from earlier arguments for 'instructive' local environmental control of self-renewal and determination at the level of multipotential progenitors.

We thank P. Barba and M. Bonzon for technical assistance, and N. Williams and C. Paige for critical readings of the manuscript. The work was supported by a Long Term Fellowship from the European Molecular Biology Organization, by the Swiss National Foundation for Scientific Research, and by the Swiss Cancer League. The Basel Institute for Immunology was founded and is supported by F. Hoffmann-LaRoche and Co., Basel, Switzerland.

Received 15 September; accepted 9 December 1981.

1. Till, J. E. & McCulloch, E. A. *Radiat. Res.* **14,** 213 (1961).
2. Curry, J. L. & Trentin, J. J. *Devl Biol.* **15,** 395 (1967).
3. Siminovitch, L., McCulloch, E. A. & Till, J. E. *J. cell. comp. Physiol.* **62,** 327 (1963).
4. Gregory, C. J. & Henkelman, R. M. in *Experimental Hematology Today* (eds Baum, S. J. & Ledney, G. D.) 93 (Springer, New York, 1977).
5. Iscove, N. N. in *Hematopoietic Cell Differentiation* (eds Golde, D. W., Cline, M. J., Metcalf, D. & Fox, C. F.) 37 (Academic, New York, 1978).
6. Gregory, C. J., McCulloch, E. A. & Till, J. E. *J. cell Physiol* **86,** 1 (1975).
7. Hodgson, G. S. & Bradley, T. R. *Nature* **281,** 381 (1979).
8. Iscove, N. N., Guilbert, L. J. & Weyman, C. *Expl Cell Res.* **126,** 121 (1980).
9. Ralph, P. & Nakoinz, I. *Cancer Res.* **37,** 546 (1977).
10. Robinson, C. V. *Proc. Soc. exp. Biol. Med.* **124,** 118 (1967).
11. Boggs, S. S., Chervenick, P. A. & Boggs, D. R. *Blood* **40,** 375 (1972).

Isolation of membrane components associated with human red cell antigens Rh(D), (c̄), (E) and $\mathrm{Fy^a}$

Stephen Moore, Christina F. Woodrow
& D. Brian L. McClelland

South-east Scotland Regional Blood Transfusion Service,
The Royal Infirmary, Edinburgh EH3 9HB, UK

The isolation of human red cell membrane components associated with Rhesus (Rh) and Duffy (Fy) blood group antigen expression has been largely frustrated due to the small quantities in the membrane[1–5] and their probable integral membrane nature requiring lipid for optimum antigen expression[6–10]. The disadvantage of reported immunoaffinity techniques for investigating Rh(D) has been non-specific adsorption which complicates identification of antigen-associated components[11,12]. Thus, Rh(D) has been attributed to a 7,000 molecular weight (MW) fraction[11] and a subpopulation of band 3 (ref. 13; MW ~90,000)[12]. We report here a technique, with negligible non-specific adsorption, for the isolation of blood group antigen–antibody complexes and their analysis by SDS-polyacrylamide gel electrophoresis (PAGE). Radiolabelling techniques facilitated identification of antigen-associated membrane components. We found that expression of Rh(D), (c̄) and (E) was associated with a component(s) of 28,500 apparent MW, with additional 50,000- and 68,000-MW components associated with Rh(D). In contrast, $\mathrm{Fy^a}$ is associated with 39,500- (possibly PAS 2), 64,000- and 88,000-MW components, the latter having a similar mobility in SDS-PAGE to band 3.

The demonstration of stable Rh(D)–^{14}C-anti-Rh(D) complexes in detergent solution[10] together with the known affinity of protein A for the Fc region of IgG[14] suggested a rapid and generally applicable technique for the isolation of detergent-solubilized immune complexes of blood group antigen with the corresponding IgG antibody by adsorption to protein A–Sepharose (Pharmacia). The observation[10] that the optimum expression of Rh(D) occurs only in the native membrane environment suggested that it was advisable to form immune complexes by incubating antibody with the intact red cell.

^{125}I surface-labelled red cells were incubated (sensitized) with an appropriate IgG antibody and, following solubilization of the membrane in non-ionic detergent, the immune complexes isolated by adsorption to protein A–Sepharose. The complexes were eluted with SDS and analysed, in reducing conditions, by SDS-PAGE. The presence of ^{125}I label which indicated membrane components exposed on the outer surface of the red cell, a prerequisite for implication in expression of blood group antigen activity, was detected by autoradiography of the dried SDS-PAGE gels.

The total radioactivity present in complexes isolated from cells sensitized with anti-Rh(D), anti-Rh(c̄), anti-Rh(E) and anti-$\mathrm{Fy^a}$ antibodies is shown in Table 1. When compared with the negative controls, all complexes contained significant levels of ^{125}I, indicating the presence of surface exposed membrane components. The results obtained with anti-Rh(D) show, in particular, the effect of antigen dosage. The rare cells of genotype *-D-/-D-* ('super D') have ~2.5–5 times the amount of surface-exposed Rh(D) antigen compared with cells homozygous for Rh(D), such as $\bar{c}DE/\bar{c}DE$ (R_2R_2) cells[3]. The increased levels of ^{125}I in complexes from super D cells is consistent with this observation and is evidence for the specific association of the labelled component with Rh(D) antigen.

0028–0836/82/060529—03$01.00

Table 1 Adsorption, using protein A–Sepharose, of immune complexes present in Triton X-100 extracts of ghosts prepared from ^{125}I-labelled human erythrocytes sensitized with blood group antibody IgG and their elution with SDS

Cell genotype	Antibody specificity used*	Immune complex on protein A–Sepharose (1) (c.p.m.)	Protein A–Sepharose residue (post SDS elution) (2) (c.p.m.)	SDS eluate of protein A–Sepharose (1 − 2) (c.p.m.)
-D-/-D- (super D)	anti-Rh(D) (1:1,028, 10 ml)	211,490	8,402	203,088 (*n*)
c̄DE/c̄DE (R_2R_2)	anti-Rh(D) (1:1,028, 10 ml)	72,298	4,989	67,309 (*a*)
c̄de/c̄de (rr)	anti-Rh(D) (1:1,028, 10 ml)	4,978	2,202	2,776 (*b*)
c̄DE/c̄DE	anti-Rh(c̄) (1:512, 25 ml)	26,919	1,634	25,285 (*c*)
CDe/CDe (R_1R_1)	anti-Rh(c̄) (1:512, 25 ml)	4,189	1,700	2,489 (*d*)
c̄DE/c̄DE	anti-Rh(E) (1:128, 25 ml)	23,656	1,604	22,052 (*e*)
CDe/CDe	anti-Rh(E) (1:128, 25 ml)	5,083	571	4,512 (*f*)
Fy(a + b−)†	anti-Fy^a (1:128, 25 ml)	23,912	1,530	22,382 (*g*)
Fy(a − b+)†	anti-Fy^a (1:128, 25 ml)	4,060	1,258	2,802 (*h*)

Washed human erythrocytes were surface-labelled with ^{125}I using the procedure of Reichstein and Blostein[18]: packed cells (1 ml) were incubated (37 °C, 90 min) with 20 ml of incubation buffer and washed (2 × 20 ml) with phosphate-buffered saline (PBS), *p*H 7.4. Packed cells were incubated (37 °C, 15 min) with 0.7 ml PBS, lactoperoxidase (EC1.11.1.7; Calbiochem grade B; 13 µl, 2.5 mg ml^{-1} in PBS), *β*-D-glucose oxidase (EC1.1.3.4; Sigma type V; 40 µl of 1:100 dilution in PBS), Na^{125}I (100 mCi ml^{-1}; Amersham; 10 µl (100 µCi) of 1:10 dilution in 0.01 M NaOH) and *α*-D-glucose (0.22 ml, 18 mg ml^{-1} in PBS prepared 24 h before use to allow mutarotation to occur), and washed with PBS (4 × 20 ml). The use of fresh batches of ^{125}I was critical to the success of the procedure. Old batches of ^{125}I did not significantly label Rhesus antigen-associated components, possibly due to oxidation of iodide by admitted air during storage. Packed, labelled (~30 µCi per ml packed cells) cells were incubated (37 °C, 60 min) with blood group antibody (whole human serum containing IgG blood group antibody of known specificity was obtained from volunteer donors and the titre determined by manual indirect antiglobulin test[19]), washed with PBS (3 × 20 ml) and the ghosts isolated[22] (1 ml of packed cells plus 40 ml of 5 mM NaH_2PO_4/Na_2HPO_4, *p*H 7.4 (4 °C), mix, centrifuge (48,000*g*, 15 min, 4 °C) repeat wash). Ghosts were incubated (15 min, room temperature) with 6 ml of PBS-Triton (PBS containing 1% (w/v) Triton X-100; BDH, scintillation grade), centrifuged (48,000*g*, 15 min, 4 °C) and the supernatant carefully aspirated. Immune complexes were adsorbed from the PBS-Triton extract (contained in a 10 ml, conical, plastic centrifuge tube) with 0.5 ml of a 10% (v/v) suspension of protein A–Sepharose in PBS-Triton and the mixture incubated (30 min, room temperature) with continuous roller mixing. The protein A–Sepharose beads were washed (4 × 10 ml) with PBS-Triton, counted for ^{125}I, washed with distilled H_2O (10 ml) and the packed beads resuspended in 1% SDS (1 ml) and incubated at 37 °C for 30 min. The supernatant was lyophilized by vacuum centrifugation[23] and reconstituted in 0.15 ml of electrophoresis sample buffer (0.0625 M Tris-HCl, *p*H 6.8, 8 M urea, 0.5 mM EDTA, 0.001% (w/v) Bromophenol blue, 5% (v/v) 2-mercaptoethanol) and stored at −40 °C. *a–h*, *n* Cross-refer to Fig. 1.

* Values for antibody titres and the volume used are given in parentheses.

† 2 ml packed cells used.

Figure 1 shows the results of SDS-PAGE analysis. In preliminary experiments (not shown) we could not obtain discrete electrophoretic separation of ^{125}I-labelled bands using the standard Laemmli sample buffer because the labelled material did not penetrate the stacking gel. Inclusion of 8 M urea in the sample buffer was essential to obtain discrete separation, thus suggesting the hydrophobic nature of these components.

Figure 1 shows that non-specific binding in negative controls (Fig. 1*b*, *d*, *f*, *h*) was not a problem in our procedure. The ^{125}I activity detected in negative controls (Table 1) was not detected by autoradiography and presumably represents low molecular weight, non-specifically adsorbed material not retained in the gel during fixation as autoradiography readily detects this level of activity[15,16]. The complexes isolated from cells sensitized with anti-Rh(D), anti-Rh(c̄) and anti-Rh(E) antibodies gave similar patterns of Coomassie brilliant blue (CBB) staining. In addition to IgG heavy (H) and light (L) chains, all contained CBB-stained components migrating in the band 3 region. This is of interest because recent reports suggest that band 3 is associated with the expression of Rh(D) activity[12,17]. However we did not detect any radioactivity in these components, suggesting that either these are not of band 3 origin (it is known that band 3 is labelled by the procedure used in this work[18]) or they are composed of an unlabelled band 3 subpopulation. We cannot completely exclude the possibility that these bands are derived from IgG.

Marked differences were observed in the radiolabelled components present in the various immune complexes which we isolated; for example compare the anti-Rh(D) complex pattern with that of anti-Fy^a complex (Fig. 1*j* and *i* respectively), and the patterns of the anti-Rh(c̄) and anti-Rh(E) complexes (Fig. 1*c* and *e* respectively). Differences were also observed in the Rhesus system; thus anti-Rh(D) complexes contained in addition to the 28,500-MW component (A28 in Fig. 1) common to all Rhesus complexes, bands of 50,000 and 68,000 MW which together accounted for ~20% of the radioactivity in the anti-Rh(D) complex. The presence of these extra bands was not influenced by sample loading (compare Fig. 1*a* with *j*). The possibility of qualitative differences between Rh(D)-associated components on *-D-/-D-* and *c̄DE/c̄DE* cells was investigated. Anti-Rh(D) complexes from these cells were qualitatively identical (Fig. 1*n*, *o*). However, we observed an increase in a component with similar mobility to A28 when comparing Triton extracts of *-D-/-D-* (Fig. 1*k*) and *c̄DE/c̄DE* (Fig. 1*l*) cells. This component is probably A28 because there is increased expression of Rh(D) on *-D-/-D-* cells. The A28 bands were the most prominent feature in the three Rhesus complexes tested and therefore most likely to carry the majority of the antigen sites on the cell surface. The ratio of ^{125}I activity to observed CBB staining intensity for A28 was much higher in anti-Rh(D) complexes. There are two possible explanations: (1) Rh(D) may be associated with a different population of A28 molecules which contain a higher number of iodination sites, and (2) the increased ratio of label to CBB stain may reflect a greater exposure on the red cell surface. The latter possibility is intriguing because it is well documented that Rh(D) is by far the most immunogenic of the Rhesus antigens[19,20].

The lower quantity of IgG H and L chains observed in anti-Fy^a complexes (Fig. 1*g*) may reflect the smaller number of Fy^a sites per cell compared with Rhesus antigens[5]. We concluded from Fig. 1*g*, *m* that expression of Fy^a activity is associated with a radiolabelled band of 39,500 MW showing similar mobility to PAS 2 (compare Fig. 1*l* with *m*). Labelled bands of 64,000 and 88,000 MW were also seen with counterparts in Triton extracts of labelled membranes (Fig. 1*k*, *l*, *p*). The 88,000-MW component had a similar mobility to PAS 1 and band 3. The possibility that Fy^a is carried by a fraction of the major red cell membrane sialoglycoprotein and band 3 requires further investigation. The 50,000-MW component (Fig. 1*i*) with an apparent similarity to the 50,000-MW component associated with Rh(D) (Fig. 1*j*) was not always observed in anti-Fy^a complexes (see Fig. 1*m*). The identity of this component is therefore obscure.

The molecular composition of the Rhesus and Duffy native antigens remains unclear. Folkerd *et al.*[21] have measured a value of 174,000 ± 10,000 for the *in situ* molecular weight of Rh(D) by radiation inactivation, which suggests that A28 is a subunit of a larger molecule or that degradation has occurred during immune complex isolation. Degradation due to radiolabelling or proteolysis was not detected in our procedure. Identical CBB staining of Rh complexes isolated from labelled and unlabelled cells was seen in SDS-PAGE. Identical CBB staining and autoradiographic profile were also seen when 1 mM phenyl-

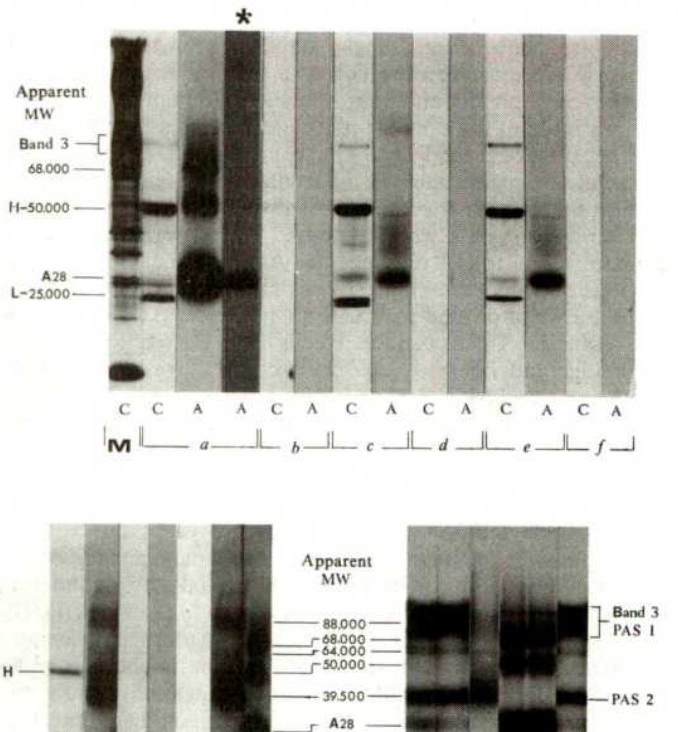

Fig. 1 SDS-PAGE of immune complexes eluted from protein A-Sepharose (see Table 1). Electrophoresis was performed at 35 mA (stacking) and 100 mA (running) on 7.5–15% polyacrylamide gradient gels ($180\times140\times0.27$ cm; Pharmacia GE2/4LS vertical apparatus) with a 5% polyacrylamide stacking gel using the discontinuous system of Laemmli[24]. Gels were stained with CBB and autoradiography of dried gels performed at −75 °C using Kodak XS-1 X-ray film and Cronex Lighting Plus intensifying screens[15,16]. Films were developed and fixed with Kodak DX-80 and FX-40 respectively, according to the manufacturers instructions. Samples were incubated overnight at 37 °C before electrophoresis. Samples *a–h* (see Table 1) were applied to gels in their entirety. *i*, *j*, Comparison of autoradiographs of anti-Fy^a (*i*) and anti-Rh(D) (*j*) immune complexes, 20,000 c.p.m. per sample. *k–p*, Autoradiographic comparison of anti-Rh(D) complexes from *-D-/-D-* (*n*) and *c̄DE/c̄DE* (*o*) cells with anti-Fy^a complexes (*m*; separate experiments to *g*, *i*), and with Triton-soluble membrane fractions sampled before protein A-Sepharose addition and diluted with 9 vol of electrophoresis sample buffer plus 5% SDS; *k*, *-D-/-D-* cells; *l*, *p*, *c̄DE/c̄DE*, Fy(a+) cells. 50,000 c.p.m. were applied for samples *k*, *l*, *n–p*; 16,000 c.p.m. for *m*. Average c.p.m. for total Triton soluble fraction (7 ml) $\approx 4\times10^7$. Autoradiograph exposure times: *a–j*, *m*, 60 h; *k*, *l*, *n–p*, 3.6 h. H, L, H and L chains of IgG; A, autoradiograph; C, CBB stained. *, Short exposure of Kodak XR-1 film to demonstrate the centre of the radiolabelled band. M, red cell ghosts solubilized in sample buffer plus 5% SDS.

methylsulphonyl fluoride, 2 mM *N*-ethylmaleimide and 0.5 mM EDTA were included in cell lysis and membrane solubilization buffers to inhibit proteolysis. The possibility that A28 and the 68,000-MW component in Rh(D) complexes (Fig. 1*a*, *j*, *n*, *o*) are the band 3 degradation products reported to bind IgG non-specifically[12] can be discounted as these were absent in Fy^a complexes (Fig. 1*i*, *m*).

In conclusion, the advantages of our procedure are its simplicity, lack of non-specific interference and the ease with which membrane components exposed on the outer surface of the red cell can be identified. Coupled with the potential for preparative isolation of immune complexes we consider this technique to be of value for future work on the structure of red cell antigens.

This work was supported by grant K/MRS/50/206 from the Biomedical Research Committee of the Scottish Home and Health Department. We thank Mr A. McGowan and Mr G. Neill for supplying the necessary antisera and the South London Blood Transfusion Service for the gift of *-D-/-D-* cells.

Received 29 September; accepted 15 December 1981.

1. Rochna, E. & Hughes-Jones, N. C. *Vox Sang.* **10,** 675–686 (1965).
2. Masouredis, S. P., Sudora, E. J., Mahan, L. & Victoria, E. J. *Transfusion* **16,** 94–106 (1976).
3. Hughes-Jones, N. C., Gardner, B. & Lincoln, P. J. *Vox Sang.* **21,** 210–216 (1971).
4. Skov, V. & Hughes-Jones, N. C. *Vox Sang.* **33,** 170–174 (1977).
5. Masouredis, S. P., Sudora, E., Mahan, L. & Victoria, E. J. *Blood* **56,** 969–977 (1980).
6. Green, F. A. *J. biol. Chem.* **243,** 5519–5524 (1968).
7. Green, F. A. *J. biol. Chem.* **247,** 881–887 (1972).
8. Plapp, F. V., Kowalski, M. M., Evans, J. P., Tilzer, L. L. & Chiga, M. *Proc. Soc. exp. Biol. Med.* **164,** 561–568 (1980).
9. Hughes-Jones, N. C., Green, E. J. & Hunt, V. A. M. *Vox Sang.* **29,** 184–191 (1975).
10. Lorusso, D. J., Binette, J. P. & Green, F. A. *Immunochemistry* **14,** 503–508 (1977).
11. Plapp, F. V. *et al. Proc. natn. Acad. Sci. U.S.A.* **76,** 2964–2968 (1979).
12. Victoria, E. J., Mahan, L. C. & Masouredis, S. P. *Proc. natn. Acad. Sci. U.S.A.* **78,** 2898–2902 (1981).
13. Steck, T. L. *J. Cell Biol.* **62,** 1–19 (1974).
14. Forsgren, A. & Sjöquist, J. *J. Immun.* **97,** 822–827 (1966).
15. Laskey, R. A. & Mills, A. D. *FEBS Lett.* **82,** 314–316 (1977).
16. Swanstrom, R. & Shank, P. R. *Analyt. Biochem.* **86,** 184–192 (1978).
17. Anstee, D. J. & Edwards, P. A. W. in *Book of Abstracts of the Joint Meeting of the ISH and 16th Congress of the ISBT,* Abstr. 1479 (1980).
18. Reichstein, E. & Blostein, R. *J. biol. Chem.* **250,** 6256–6263 (1975).
19. Mollison, P. L. in *Blood Transfusion in Clinical Medicine* 6th edn, 292–352, 448–455 (Blackwell, Oxford, 1979).
20. Issitt, P. D. in *Serology and Genetics of the Rhesus Blood Group System,* 12–43 (Montgomery, 1979).
21. Folkerd, E. J., Ellory, J. C. & Hughes-Jones, N. C. *Immunochemistry* **14,** 529–531 (1977).
22. Dodge, J. T., Mitchell, C. & Hanahan, D. J. *Archs Biochem. Biophys.* **100,** 119–130 (1963).
23. Pepper, D. S. *Lab. Pract.* **22,** 538–539 (1973).
24. Laemmli, U. K. *Nature* **227,** 680–685 (1970).

Absence of *Ir* gene control of T cells recognizing foreign antigen in the context of allogeneic MHC molecules

Norihisa Ishii*, Zoltan A. Nagy & Jan Klein

Max-Planck-Institut für Biologie, Abteilung Immungenetik,
Corrensstrasse 42, 7400 Tübingen, FRG

The major histocompatibility complex (MHC)-linked immune response (*Ir*) genes confer high responsiveness on some MHC haplotypes and low or no responsiveness to certain antigens on other haplotypes (for review see ref. 1). The cause of nonresponsiveness is thought to be a failure of T cells to be stimulated by a given combination of antigen and MHC molecules, which can, in principle, arise in two ways: either the antigen-presenting cells (APCs or macrophages) of the nonresponder haplotypes are incapable of presenting the foreign antigen to T cells in an immunogenic form[2,3] or the T-cell repertoire of nonresponder haplotypes lacks clones recognizing the antigen in the context of a given MHC[4]. We have recently shown that APCs from nonresponder strains can in fact present antigen to allogeneic responder T cells, depleted of alloreactivity against the APCs themselves[5], which indicates that the mechanism of nonresponsiveness is not a failure of APC function. Using the same experimental system, we show here that responses of T cells to antigen presented on allogeneic APCs do not depend on the Ir phenotype of either the T cell or the APC: *Ir* gene control is completely absent from these responses. The results strongly suggest that *Ir* gene-controlled nonresponsiveness is associated with the adjustment of the T-cell repertoire to self-MHC antigens.

Recently we have developed an assay system for measuring the proliferative response of T cells to antigens presented by allogeneic APCs[5]. T cells were prepared by nylon wool-column separation of nucleated spleen cells from unprimed mice, and adherent cells obtained from peritoneal washing served as APCs. The T cells were first cultured with allogeneic APCs and alloreactive T cells were removed by treatment with 5-bromo-2′-deoxyuridine (BUdR) and light on day 3 (ref. 6). The surviving T cells were then primed *in vitro* using fresh allogeneic APCs and an antigen, the response to which is under *Ir* gene control. After an additional 7 days in culture, T cells were collected, distributed into flat-bottomed microtitre plates and tested for

---

[*] Permanent address: Department of Dermatology, Yokohama City University, School of Medicine, Urafune-cho 3-46, Minami-ku, 232 Yokohama, Japan.

0028-0836/82/060531—03$01.00

Table 1 *Ir* gene-controlled secondary proliferation of T cells primed *in vitro* with GA on syngeneic APCs

T cell					
Strain	*H–2* haplotype	Responder status	APC	Δ c.p.m.	SI
C57BL/10	*b*	R	C57BL/10	7,467	45.7
BALB/c	*d*	R	BALB/c	8,308	3.6
B10.D2	*d*	R	B10.D2	7,733	23.6
B10.P	*p*	NR	B10.P	112	1.2
C3H.NB	*p*	NR	C3H.NB	243	1.4
B10.Q	*q*	NR	B10.Q	89	1.2
DBA/1	*q*	NR	DBA/1	43	1.1
A.SW	*s*	NR	A.SW	−113	0.7
$(B10.A(5R)F_1 \times B10.P)$	*i5* × *p*	R×NR	F_1	25,363	28.9
$(B10.A(5R)F_1 \times B10.P)$	*i5* × *p*	R×NR	B10.A(5R)	36,679	32.6
$(B10.A(5R)F_1 \times B10.P)$	*i5* × *p*	R×NR	B10.P	416	1.5

Proliferation of *in vitro* primed T cells (1×10^5) in the presence of 1×10^5 APCs and 40 μg ml^{-1} GA was measured by ^{3}H-thymidine incorporation[7]. The results are expressed as Δ c.p.m., that is, c.p.m. in cultures with GA and APC −c.p.m. in cultures with APC and without GA; and stimulation index (SI), that is, c.p.m. in cultures with GA and APC divided by c.p.m. in cultures with APC but without GA. The background c.p.m. in cultures without antigen were in the range 167–3,224. The culture and assay conditions were identical (including preculturing of T cells with APCs alone, followed by BUdR and light treatment) to those used for allogeneic T cell–APC combinations[5]. R, responder; NR, nonresponder.

secondary proliferative response to the priming antigen and fresh APCs in a 3-day assay[7]. In this system, allogeneic APCs alone did not induce appreciable specific T-cell proliferation. Using the antigens poly($Glu^{40}Ala^{60}$) (GA), poly($Glu^{51}Lys^{34}Tyr^{15}$) (GLT) and lactate dehydrogenase B (LDH-B), secondary T-cell proliferation was induced only by the priming antigen presented on the priming allogeneic APC. Furthermore, proliferation was inhibited by monoclonal antibodies raised against Ia antigens on the APCs, but was not affected by antibodies to Ia antigens present on the T cells (ref. 5 and N.I., unpublished results). Thus, the secondary proliferation *in vitro* of T cells is antigen specific, and is restricted by Ia antigens of the allogeneic APCs.

This study was undertaken to determine the possible influence of the Ir phenotype of T cells and APCs on the secondary response *in vitro*. We used GA as a test antigen because the number of responder and nonresponder *H–2* haplotypes to this antigen is about the same[7]; this allowed us to assemble a large number of allogeneic T cell–APC combinations with strains of different responder status. To ascertain that our *in vitro* system is subject to the same *Ir* gene control as the *in vitro* response of T cells primed *in vivo*, we first studied the responses of T cells primed *in vitro* to GA on syngeneic APCs. The data in Table 1 demonstrate that responder T cells can mount a proliferative response when primed with GA on syngeneic APCs, whereas nonresponder T cells cannot. T cells from F_1 hybrids between responder and nonresponder mice can only respond to GA when presented by F_1 APCs, or APCs of the responder parent. Thus we conclude that the *Ir* gene control of the *in vitro* secondary T-cell response is identical to that observed after priming *in vivo*[7,8]. We then tested the anti-GA response in a large number of allogeneic T cell–APC combinations. The combinations fell into four groups: (1) responder T cell–responder APC, (2) nonresponder T cell–nonresponder APC, (3) nonresponder T cell–responder APC, and (4) responder T cell–nonresponder APC. The results (Table 2) show that T-cell proliferation to GA was readily induced in all four types of strain combination. The rate of success of our experiments was 83% (for a total of 108 tests), and the occasional negative results were never reproducible. The data therefore establish that the response of T cells to antigen presented by fully allogeneic APCs is not under *Ir* gene control.

However, note that we did observe nonresponsiveness in partially allogeneic T cell–APC combinations. For example, of several strain combinations where the genetic difference between the T cells and APCs consisted of non-expression as opposed to expression of the I-E molecule (such as B10.A(4R)–B10.A(2R) and B10.S(7R)–(B10.S(9R)), some combinations were consistently found to respond, whereas others were nonresponders, to the antigen GLT. The detailed results of these experiments and their interpretation will be published elsewhere (N.I., Z.A.N. and J.K., in preparation).

Table 2 Lack of *Ir* gene control of the proliferative response of T cells to GA presented by allogeneic APCs

T cell			APC				
Strain	*H–2* haplotype	Responder status	Strain	*H–2* haplotype	Responder status	Δ c.p.m.	SI
C57BL/10	*b*	R	BALB/c	*d*	R	17,534	23.0
C57BL/10	*b*	R	CBA	*k*	R	22,773	74.7
B10.D2	*d*	R	BALB.B	*b*	R	45,163	34.3
BALB/c	*d*	R	B10.BR	*k*	R	14,829	13.3
B10.BR	*k*	R	BALB/c	*d*	R	8,701	17.9
B10.BR	*k*	R	A.CA	*f*	R	40,848	16.6
C3H.NB	*p*	NR	B10.WB	*j*	NR	22,678	9.0
C3H.NB	*p*	NR	DBA/1	*q*	NR	17,600	7.0
C3H.NB	*p*	NR	B10.RIII	*r*	NR	17,251	7.3
C3H.NB	*p*	NR	B10.PL	*u*	NR	24,215	6.9
B10.P	*p*	NR	B10.PL	*u*	NR	20,735	10.5
DBA/1	*q*	NR	C3H.NB	*p*	NR	11,490	5.5
DBA/1	*q*	NR	A.SW	*s*	NR	32,857	15.3
DBA/1	*q*	NR	B10.SM	*v*	NR	15,490	13.3
A.SW	*s*	NR	B10.Q	*q*	NR	26,465	18.1
C3H.NB	*p*	NR	BALB.B	*b*	R	38,224	13.5
C3H.NB	*p*	NR	BALB/c	*d*	R	36,833	35.6
C3H.NB	*p*	NR	A.CA	*f*	R	27,180	11.0
DBA/1	*q*	NR	BALB.B	*b*	R	9,039	4.7
DBA/1	*q*	NR	DBA/2	*d*	R	7,398	4.1
DBA/1	*q*	NR	B10.M	*f*	R	18,971	26.8
A.SW	*s*	NR	BALB/c	*d*	R	11,121	29.2
C57BL/10	*b*	R	B10.Q	*q*	NR	11,338	8.4
C57BL/10	*b*	R	B10.S	*s*	NR	15,566	36.0
BALB/c	*d*	R	B10.P	*p*	NR	17,479	7.8
BALB/c	*d*	R	B10.Q	*q*	NR	22,407	14.2
BALB/c	*d*	R	B10.RIII	*r*	NR	13,514	6.3
BALB/c	*d*	R	B10.SM	*v*	NR	13.039	9.8
A.CA	*f*	R	B10.Q	*q*	NR	12,332	9.9

The assay conditions and calculations of Δ c.p.m. and SI were as described in Table 1 legend. Background c.p.m. (cultures with allogeneic APCs but without GA) were in the range 445–4,263.

The lack of *Ir* gene control in allogeneic T cell–APC interactions is best explained by assuming that the T-cell repertoire of each individual consists of (at least) two different compartments: one that recognizes foreign antigen in the context of self-MHC antigens[9–13], and another that uses all allogeneic MHC antigens of the species for antigen recognition. The self-restricted part of the repertoire is incomplete, that is, it exhibits *Ir* gene-controlled nonresponsiveness, whereas the allogeneic MHC-restricted part appears to be complete. Nonresponsiveness probably arises by functional or physical elimination of autoaggressive T-cell clones from the self-restricted repertoire[14]. This elimination process should not affect the allogeneic MHC-restricted part of the repertoire. The physiological significance of T cells restricted by allogeneic MHC is unclear. There are two possible explanations: either these cells are irrelevant for the individual or allogeneic restriction represents cross-reactivity of T cells normally recognizing another foreign antigen together with self-MHC molecules.

This work was supported in part by grants Wa 139/10/AI.5 and Na 135/1-1 from the Deutsche Forschungsgemeinschaft.

Received 12 August; accepted 24 November 1981.

1. Krco, C. J. & David, C. S. *Crit. Rev. Immun.* **1,** 211–257 (1981).
2. Rosenthal, A. S. *Immun. Rev.* **40,** 136–152 (1978).
3. Benacerraf, B. *J. Immun.* **120,** 1809–1812 (1978).
4. von Boehmer, H., Haas, W. & Jerne, N. K. *Proc. natn. Acad. Sci. U.S.A.* **75,** 2439–2442 (1978).
5. Ishii, N., Baxevanis, C. N., Nagy, Z. A. & Klein, J. *J. exp. Med.* **154,** 978–982 (1981).
6. Thomas, D. W. & Shevach, E. M. *Proc. natn. Acad. Sci. U.S.A.* **74,** 2104–2108 (1977).
7. Baxevanis, C. N., Wernet, D., Nagy, Z. A., Maurer, P. H. & Klein, J. *Immunogenetics* **11,** 617–628 (1980).
8. Shevach, E. M., Green, I. & Paul, W. E. *J. exp. Med.* **139,** 679–695 (1974).
9. Kindred, B. & Shreffler, D. C. *J. Immun.* **109,** 940–943 (1972).
10. Zinkernagel, R. M. & Doherty, P. C. *Nature* **248,** 701–702 (1974).
11. Shearer, G. M., Rehn, T. G. & Garbarino, C. A. *J. exp. Med.* **141,** 1348–1364 (1975).
12. Bevan, M. J. *J. exp. Med.* **142,** 1349–1364 (1975).
13. Sprent, J. *J. exp. Med.* **147,** 1159–1174 (1978).
14. Schwartz, R. H. *Scand. J. Immun.* **7,** 3–10 (1978).

---

tRNA precursor transcribed from a mutant human gene inserted into a SV40 vector is processed incorrectly

Michael Zasloff*, Tomas Santos* & Dean H. Hamer†

* Genetics and Biochemistry Branch, National Institute of Arthritis, Diabetes, Digestive and Kidney Diseases, and † Laboratory of Biochemistry, National Cancer Institute, National Institutes of Health, Bethesda, Maryland 20205, USA

We have identified 12 initiator methionine tRNA ($\mathrm{tRNA}_i^{\mathrm{Met}}$) genes in the haploid human genome[1]. One gene, cloned from a recombinant phage library of human fetal liver DNA, contained a base substitution at position 56 in the mature eukaryotic initiator tRNA sequence. The substitution, a G replaced by a T, should generate a tRNA species having a U at a sequence position not observed in any of 178 sequenced prokaryotic and eukaryotic tRNAs[2]. Recently, we have demonstrated[3] that this variant tRNA gene is efficiently transcribed in an homologous *in vitro* system derived from KB cells. However, the precursor RNA species of the variant gene, unlike that of the normal one, is not fully processed to a mature sequence in these cell-free extracts. Although the three nucleotides of the 5′ leader sequence are efficiently trimmed, the 13-nucleotide 3′ trailer is not processed, resulting in the accumulation of an 87-nucleotide precursor. In this report we assay the functional properties of the human variant initiator tRNA gene within an intact cell by studying its transcription from a simian virus 40 (SV40) recombinant during lytic infection of African green monkey kidney (AGMK) cells. We demonstrate that the variant gene is efficiently transcribed when inserted in the SV40 chromosome but, as *in vitro*, the precursor tRNA is not processed to a mature tRNA species.

The SV40 vector used for this study has been described in detail elsewhere[4]. The structure of the SV40–$\mathrm{tRNA}_i^{\mathrm{Met}}$ recombinant (SVtm) is shown in Fig. 1. It contains a 1.15-kilobase (kb) fragment of human genomic DNA harbouring a single $\mathrm{tRNA}_i^{\mathrm{Met}}$ gene. This fragment is inserted in an SV40 vector that contains the origin of replication, the entire viral early region, and the extreme 5′ and 3′ termini of the viral late region. The $\mathrm{tRNA}_i^{\mathrm{Met}}$ gene is oriented such that its polarity of transcription is opposed to that of the viral late promoters. AGMK cells were infected with a mixture of SVtm DNA and the temperature-sensitive helper, SV40tsA239 (ref. 5), and the resulting viral stocks were used in the following studies.

Confluent flasks of AGMK cells were infected with an innoculum of the viral stock prepared as described above, or with a control preparation consisting of a SV40 recombinant containing murine α-fetoprotein DNA sequences[6]. After 60 h of infection at 39.5 °C, the cells were placed in low phosphate medium containing 100 μCi ml^{-1} of ^{32}P$_i$, and cultured for an additional 6 h. Restriction analysis of the DNA recovered from one such infection showed that SVtm represented ~60% of the viral molecules and SV40tsA239 the remainder.

Total cytoplasmic and nuclear RNA were recovered from the infected cells and analysed by electrophoresis in 10% polyacrylamide gels in 7 M urea[7]. An autoradiograph of one such product analysis is shown in Fig. 2. Both the cytoplasmic and nuclear fractions from SVtm-infected cells contain a single low-molecular weight species, absent from the control samples, that is ~89 nucleotides long, compared with the 90-nucleotide primary transcript observed *in vitro*[3]. This RNA species represents ~30% of the newly synthesized tRNA species resolved on the gel. The relative intensities of the other low-molecular weight RNA species observed do not appreciably differ between the SVtm and control infections. For example, with respect to the intensity of the 5S RNA species, the amounts of labelled 4.5S and total tRNA do not differ between the SVtm- and control-infected cells.

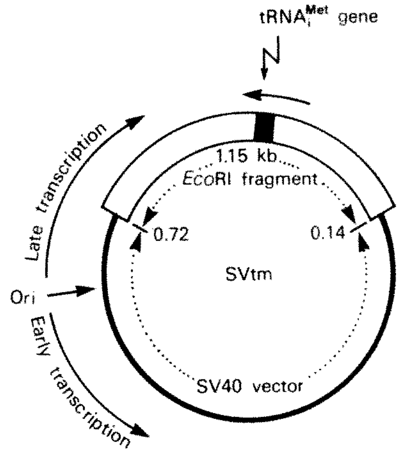

Fig. 1 SV40 recombinant containing the 1.15-kb fragment of human DNA bearing the variant $\mathrm{tRNA}_i^{\mathrm{Met}}$ gene. A 3.1-kb fragment of SV40 DNA, extending from 0.72 to 0.14 on the circular map and containing the early region, was cloned in pBR322 at the *Eco*RI site as described previously[4]. The pBR322–SV40 vector was linearized by partial *Eco*RI digestion and recovered after agarose gel electrophoresis. The linear vector was ligated to the 1.15-kb fragment bearing the variant $\mathrm{tRNA}_i^{\mathrm{Met}}$ gene[1], and the ligation mixture used to transform *Escherichia coli* strain LE392 (ref. 18). Clones bearing the 1.15-kb insert were identified by colony hybridization[19], and one containing the $\mathrm{tRNA}_i^{\mathrm{Met}}$ in an orientation opposite to that of the late viral promoter was propagated. Plasmid DNA from this clone was isolated[20] and digested partially with *Eco*RI, releasing a 4.25-kb fragment consisting of the 3.1-kb viral sequence and the 1.15-kb fragment. Following purification by gel electrophoresis, the fragment was recovered and circularized with T4 DNA ligase[4]. Ori, origin of viral replication; ■, schematic location of the $\mathrm{tRNA}_i^{\mathrm{Met}}$ gene within the chromosomal insert, with arrow above indicating direction of transcription from the tRNA promoter.

0028–0836/82/060533—03$01.00

The RNA species accumulating in the SVtm infection was recovered from the gel and analysed by classical fingerprinting techniques[8,9]. A fingerprint of a T1 digest of this RNA is shown in Fig. 3 and the complete sequence is presented in Fig. 4. The numbered spots were identified by secondary complete pancreatic RNase digestion and product analysis. Absolute identification was aided by knowledge of the sequence and previous fingerprint analysis of *in vitro* transcripts of this gene[3]. The point critical to this discussion is that the transcript is clearly a precursor of the variant tRNA$_{\mathrm{i}}^{\mathrm{Met}}$. The base substitution at position 56 eliminates an AUCG oligonucleotide and results in the appearance of the long oligonucleotide AUCUAAACCAUCCUCUG (spots 12, 13), representing the loop 4 region of the tRNA. The 3'-terminal sequence CUUU is present, along with the oligonucleotide CUAAAG, which lies within the 3' trailer. Digestion of the precursor with T1 generates a pUUAG arising from position −2 in the DNA sequence. Analysis of a total T2 digest by two-dimensional TLC fails to reveal any pppGp.

We have performed only a preliminary analysis of base modification within the precursor. 1-Methylation of adenosine at position 57, adjacent to the base substitution at 56, occurs in ~70% of the precursor. The adenosine at position 36, adjacent to the anticodon, and normally modified in tRNA$_{\mathrm{i}}^{\mathrm{Met}}$ to N^6-(threoninocarbonyl)adenosine is unmodified in the precursor (data not shown). Analysis of total modified nucleosides by the TLC methods of Nishimura[10] demonstrated some 5,6-dihydrouridine, 5-methylcytidine (position 47) and G-methylation, but the full extent of these, and specific positions, have not been determined.

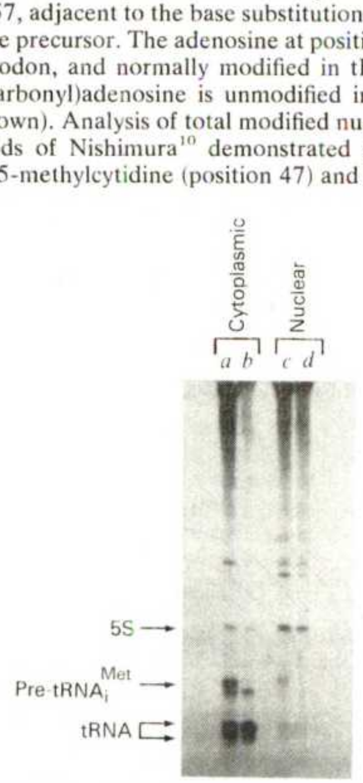

Fig. 2 Electrophoretic analysis of ^{32}P-labelled RNA isolated from AGMK cells during late phase of SVtm infection. SVtm, described in Fig. 1, was encapsidated by transfection of AGMK cells with 0.5 μg of SVtm DNA and 0.2 μg SV40 tsA239 helper DNA, as described elsewhere[4]; 2.5 ml of the resulting lysate was added to a monolayer of 2×10^7 AGMK cells and incubated at 39.5 °C for 64 h. Media was replaced with minimal essential medium without phosphate but containing 5% dialysed fetal calf serum. Carrier-free ^{32}P (New England Nuclear) was added to 100 μCi ml^{-1}, and the cells were incubated at 39.5 °C for an additional 6 h. The flasks were washed several times with Dulbecco's phosphate-buffered saline (PBS) (without added magnesium and calcium) and then scraped free with a rubber policeman. After several washes with PBS the cells were washed once in TKM buffer containing 50 mM Tris-HCl *p*H 7.6, 80mM KCl, 5mM magnesium chloride, collected by centrifugation, and lysed by suspension in 1 ml of TKM containing 0.2% NP-40. Nuclei were removed by centrifugation at 10,000*g* for 10 min. The post-nuclear supernatant was collected, made 0.2% in SDS and extracted twice with 1 vol of phenol, 1/2 vol chloroform/isoamyl alcohol (24:1). Nuclear RNA was extracted by the hot acid-phenol method[21]. A control infection, using the identical SV40 vector ligated to a 2.5-kb fragment containing the murine α-fetoprotein gene sequences[6] was carried through all corresponding steps. Samples of RNA were loaded onto a 1 mm-thick, 25 cm-long 10% acrylamide gel in TBE buffer[7] containing 7M urea and electrophoresed at 700 V for 4 h. The gels were autoradiographed against Kodak XR2 film at −20 °C for 20 min. Lanes *a*, *c*, ^{32}P-RNA from cells infected with SVtm; lanes *b*, *d*, RNA from cells infected with SV40 vector containing murine α-fetoprotein genomic insert. Arrows indicate mobilities of 5S RNA, tRNA and tRNA$_{\mathrm{i}}^{\mathrm{Met}}$ precursor.

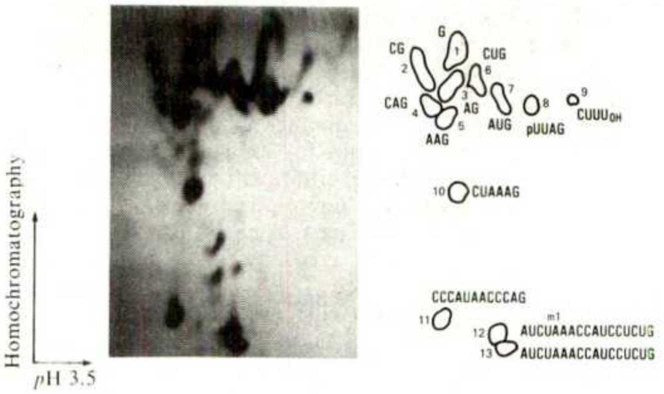

Fig. 3 Fingerprint analysis of the 89-nucleotide RNA accumulating during late infection with SVtm. The major species migrating in the pre-tRNA region, as shown in Fig. 2*a*, was recovered from the gel[22] (10^5 d.p.m.), digested to completion with T1 RNase and fingerprinted as described elsewhere[8,9] using iontophoresis on cellulose acetate at *p*H 3.5 in the first dimension; and homochromatography on DEAE-cellulose TLC plates in the second dimension. Secondary digestions of selected oligonucleotides were done using pancreatic RNase, followed by electrophoresis on DEAE-cellulose paper, to confirm oligonucleotide assignment. 1-Methyladenosine was identified by secondary digestion of oligonucleotide 12 with RNase T2, followed by two-dimensional TLC[10].

As the precursor represents ~30% of the total newly synthesized RNA in the tRNA population, we would expect that efficient processing of this species should result in the accumulation of tRNA$_{\mathrm{i}}^{\mathrm{Met}}$ as a major RNA species in the cell. However, hybridization of equal amounts of gel-purified tRNA from SVtm and control infections to filter-bound tRNA$_{\mathrm{i}}^{\mathrm{Met}}$ DNA occurred at approximately equal rates and reached a maximum level of hybridization of ~1% of the input radioactivity in each case (data not shown). We conclude that conversion of the mutant precursor to mature tRNA does not occur with any significant efficiency.

Conclusions concerning the *in vivo* activity of the human variant tRNA$_{\mathrm{i}}^{\mathrm{Met}}$ gene are based on the assumption that transcription of the gene occurs from the tRNA$_{\mathrm{i}}^{\mathrm{Met}}$ promoter. Several observations lead us to believe that this is the case. The tRNA$_{\mathrm{i}}^{\mathrm{Met}}$ is most likely transcribed from the recombinant SV40 chromosome by RNA polymerase III, based on the 3'-terminal sequence of the tRNA$_{\mathrm{i}}^{\mathrm{Met}}$ precursor, GCUUU. The polymerase responsible appears to have recognized accurately the termination signal of the gene, GCTTTTT . . . , a property, as far as we know, unique to RNA polymerase III[11]. Although the major intermediate lacks a 5'-terminal triphosphate, and thus is not an intact initial transcript, it is shorter by only one nucleotide than the primary transcript observed during transcription *in vitro* of the variant tRNA$_{\mathrm{i}}^{\mathrm{Met}}$ gene. We presume that some nibbling of the 5' end has occurred in the system, similar to that observed during the biosynthesis of tRNA$^{\mathrm{Tyr}}$ following injection of the gene into the intact *Xenopus laevis* oocyte[12]. Although it is possible that the 89-nucleotide intermediate represents the product of previous cleavage of a longer RNA species initiated upstream, we believe there is no strong evidence to support this possibility. No RNA polymerase III promoter has been demonstrated on the 1.15-kb chromosomal fragment inserted in SV40, except for the tRNA$_{\mathrm{i}}^{\mathrm{Met}}$ gene, in *in vitro* systems using KB cells and *X. laevis* ovarian extracts[3]. Initiation from within a viral sequence is unlikely as no functional RNA polymerase III transcription unit having activity comparable with that observed on the SVtm recombinant has been identified on SV40[13]. Furthermore, the level of expression is much higher than would be expected from the viral early promoter, which is oriented in the same polarity as the tRNA gene, representing no more than 0.01% of total RNA synthesized late in lytic infections[14].

Although the variant human tRNA$_{\mathrm{i}}^{\mathrm{Met}}$ gene is transcribed *in*

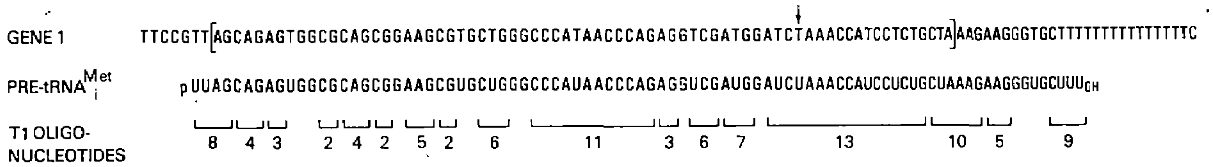
GENE 1
TTCCGTT[AGCAGAGTGGCGCAGCGGAAGCGTGCTGGGCCCATAACCCAGAGGTCGATGGATCTAAACCATCCTCTGCTA]AAGAAGGGTGCTTTTTTTTTTTTTTTC
PRE-tRNA$_i^{Met}$
pUUAGCAGAGUGGCGCAGCGGAAGCGUGCUGGGCCCAUAACCCAGAGGUCGAUGGAUCUAAACCAUCCUCUGCUAAAGAAGGGUGCUUU$_{OH}$
T1 OLIGO-NUCLEOTIDES
8 4 3 2 4 2 5 2 6 11 3 6 7 13 10 5 9

Fig. 4 Sequence of the variant tRNA$_i^{Met}$ transcript and the corresponding gene. Arrow denotes the base transversion at position 56 in the tRNA$_i^{Met}$ sequence. Brackets indicate mature termini of the tRNA. Numbered oligonucleotides correspond to those noted in Fig. 3. The sequence of the gene and flanking regions was determined previously[1].

vitro to about the same extent as the normal gene, the significance of this is rather clouded in that the template is not, in conditions of cell-free transcription, organized into chromatin, the structure it assumes physiologically. By using the SV40 vector, however, we can demonstrate that the mutant tRNA gene is indeed functional when present in the nucleus as a supercoiled, chromatin-packaged structure.

Our finding that the variant human tRNA$_i^{Met}$ gene is transcribed in an intact cell but that the precursor is not efficiently processed to a mature tRNA suggests that mutations within eukaryotic tRNA genes may be more prevalent than assumed from the limited sequence variation observed in mature tRNA species. We suggest that nucleolytic processing of tRNA precursors, which in the case of the human tRNA$_i^{Met}$ gene transcript involves excision of a 5′ leader and 3′ trailer, provides a 'proof-reading' function resulting from stringent sequence or structural requirements of cellular processing endonucleases. Note that the absence of any significant conversion of the variant precursor to mature tRNA$_i^{Met}$ also argues against the presence of an activity in the intact cell, such as a purine 'insertase'[15], which might efficiently correct mutations at a post-transcriptional step.

Although it is clear that the variant tRNA$_i^{Met}$ gene is expressed on the SV40 vector, it does not necessarily follow that the gene is active in the human genome. Foreign genes inserted into SV40 are generally expressed regardless of the state of transcriptional activity of the gene in the infected cell[16]. We do not yet know the functional state of the variant tRNA$_i^{Met}$ locus in human somatic cells, although several studies probing the nuclease sensitivity[17] of the locus are in progress.

We thank Dr Schumperli for help with the RNA sequence analysis and Mrs Joan Glass for helping to prepare the manuscript.

Received 21 September; accepted 7 December 1981.

1. Santos, T. & Zasloff, M. *Cell* **23**, 699–709 (1981).
2. Singhal, R. P. & Fallis, P. A. M. *Prog. Nucleic Acid Res. molec. Biol.* **23**, 228–290 (1979).
3. Zasloff, M., Santos, T., Romeo, P. H. & Rosenberg, M. *J biol. Chem.* (submitted).
4. Hamer, D. H., Kaehler, M. & Leder, P. *Cell* **21**, 697–708 (1980).
5. Hamer, D. & Leder, P. *Nature* **281**, 36–40 (1979).
6. Gorin, M. B. & Tilghman, S. M. *Proc. natn. Acad. Sci. U.S.A.* **72**, 1351–1355 (1980).
7. Telford, J. *et al. Proc. natn. Acad. Sci. U.S.A.* **76**, 2590–2594 (1979).
8. Brownlee, G. G. & Sanger, F. *Eur. J. Biochem.* **11**, 395–415 (1969).
9. Barrel, B. G. in *Procedures in Nucleic Acid Research* Vol. 2 (eds Cantoni, G. L. & Davies, D. R.) 751–799 (Harper and Row, New York, 1971).
10. Nishimura, S. *Prog. Nucleic Acid Res. molec. Biol.* **12**, 49–85 (1972).
11. Bogenhagen, D. F. & Brown, D. D. *Cell* **24**, 261–270, (1981).
12. DeRobertis, E. M. & Olson, M. V. *Nature* **278**, 137–143, (1979).
13. Ziff, E. B. *Nature* **287**, 491–499 (1980).
14. Ferdinand, F., Brown, M. & Khoury, G. *Virology* **78**, 150–161 (1977).
15. Okado, J. *Nucleic Acids Res.* **3**, 2593–2603 (1978).
16. Hamer, D. H. in *Genetic Engineering* Vol. 2 (eds Setlow, J. & Hollaender, A.) 83–101 (Plenum, New York, 1980).
17. Zasloff, M. & Camerini-Otero, R. *Proc. natn. Acad. Sci. U.S.A.* **77**, 1907–1911 (1980).
18. Dagert, H. & Ehrlich, S. D. *Gene* **6**, 23–28 (1979).
19. Grunstein, M. & Hogness, D. *Proc. natn. Acad. Sci. U.S.A.* **72**, 3961–3965 (1975).
20. Zasloff, M., Ginder, G. & Felsenfeld, G. *Nucleic Acids Res.* **5**, 1139–1151 (1978).
21. Scherrer, K. in *Fundamental Techniques in Virology* (eds Habel, K. & Salzman, N. P.) 413–432 (Academic, New York, 1969).
22. Maxam, A. & Gilbert, W. *Proc. natn. Acad. Sci. U.S.A.* **74**, 560–564 (1977).

Stereochemistry of iron in deoxyhaemoglobin

M. F. Perutz*, S. Samar Hasnain†, P. J. Duke†, J. L. Sessler‡ & J. E. Hahn‡

* MRC Laboratory of Molecular Biology, Cambridge CB2 2QH, UK
† Daresbury Laboratory, Warrington WA4 4AD, UK
‡ Department of Chemistry, Stanford University, Stanford, California 94305, USA

X-ray crystallography has shown that in deoxyhaemoglobin the iron atoms are displaced by 0.56±0.03 Å from the mean porphyrin plane, whereas in liganded haemoglobins they lie either in or close to that plane[1,2]. Perutz[3] proposed this shift as one principal factor responsible for haem–haem interaction. Eisenberger *et al.* used extended X-ray absorption fine structure (EXAFS) to measure the Fe–N distance in deoxyhaemoglobin and concluded that the irons lie only 0.2 $^{+0.1}_{-0.2}$ Å from the plane of the porphyrin nitrogens and that the mechanism of Perutz is therefore invalid[4]. We have now compared the EXAFS of deoxyhaemoglobin with that of the ferrous 'picket fence' 2-methylimidazole complex in which the displacement of the iron from the plane of the porphyrin nitrogens is known to be 0.399±0.004 and 0.426±0.004 Å from the mean porphyrin plane (ref. 5). The two EXAFS spectra are very similar, consistent with similar displacements of the irons. We find the same Fe–N distance of 2.06±0.01 Å in deoxyhaemoglobin as Eisenberger *et al.*, but show that the displacement of the iron cannot be calculated from that distance.

The samples were prepared as follows. A 15 mM solution of human deoxyhaemoglobin was prepared from a red cell lysate by pressure dialysis followed by deoxygenation and addition of neutral $Na_2S_2O_4$ in an oxygen-free glove box. A drop of this solution was mounted in a hole 5 mm wide in a 1 mm-thick copper strip, sealed between thin mylar films and kept under nitrogen before use. The crystalline picket fence complex (2-methylimidazole-*meso*-tetra(*α*,*α*,*α*,*α*-*O*-pivamidophenyl)porphyrinatoiron-(II)-ethanol [Fe^{2+}(T piv PP)-(2-MeIm).EtOH] was prepared in oxygen-free conditions as described in ref. 5. In the first of the two independent EXAFS experiments, 2 mm-wide thin-walled glass capillaries were filled with the sample and sealed with bees' wax. In the second, the complex was diluted by mixing with boron nitride (~1 : 1 by wt) and then formed into a pellet 0.4 mm thick by pressing between two Mylar sheets separated by an aluminium spacer. After the EXAFS experiment, the sample was extracted from the pellet with toluene and checked spectrophotometrically to ensure that neither oxygenation nor oxidation has occurred.

EXAFS associated with the Fe K-edge was recorded both in fluorescence and transmission modes at the Stanford Radiation Laboratory. Five spectra of deoxyhaemoglobin collected at 10K (three scans), 44K (one scan) and 110K (one scan) were averaged to give a good-quality spectrum. For the first picket fence sample a single spectrum was recorded at 100K; for the second sample three spectra were recorded at 300K. No appreciable difference was found between these spectra at $E < 150$ eV. The spectrum analysed in detail at Daresbury was that recorded at 100K; those recorded at 300K were analysed at Stanford.

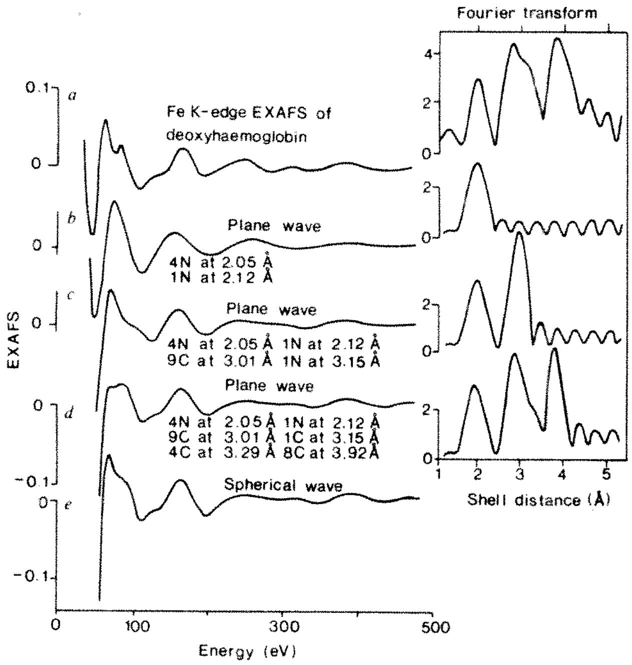

Fig. 1 EXAFS and Fourier transforms of human deoxyhaemoglobin. *a*, Experimental curve and transform derived from it. *b*, Calculated curves taking into account scattering from nearest neighbours only (first shell); *c*, same for first and second shell; *d*, same for first three shells; *b*–*d* were calculated using the plane wave method. *e*, EXAFS curve calculated for first three shells using spherical wave method. Best-fitting distances of carbon and nitrogen atoms from the iron are listed in Table 1. Fourier transforms have been multiplied by R^2 to obtain the radial intensity distributions of the atoms surrounding the iron.

We have used the atomic coordinates of the picket fence model[5] to calculate the distances of carbon and nitrogen atoms up to 4 Å from the Fe atom. For data manipulation and the calculation of theoretical spectra at the Daresbury Laboratory we used the procedures and programs described in refs 6 and 7 and for our interpretation we relied on Lee and Pendry's theoretical approach[8,9].

Phase shifts were calculated using the MUFPOT program, by constructing a complex muffin-tin potential following the standard Matheiss prescription, and making use of the Clementi–Roetti wave functions for carbon and nitrogen atoms in the neutral state. The excited iron atom was approximated by the wave functions of the Co atom with one electron from the 1 s orbital removed. The EXAFS spectra of deoxyhaemoglobin and the picket fence are shown in Figs 1–3. They show a close resemblance: each contains several beat regions at 40–90, 100–180 and 200–300 eV, indicating similarities in the distances and nature of the atoms surrounding the Fe atom. The large number of beats suggests that the complex EXAFS profile arises from the interference of several back-reflected waves. This is evident from the Fourier transforms which show strong contributions from scattering distances of up to 4 Å.

The theoretical and experimental EXAFS spectra were converted into k space defined by $k = \sqrt{2(E - E_0)}$ where E is the energy of the incident beam and E_0 the energy of the beam at the absorption edge of iron. Fourier transforms were then calculated with respect to $\exp(-i2kR)$ where R is the radial distance of an atom from the Fe atom. The problems of secondary maxima and changes in peak positions induced by phase shifts were dealt with by correcting the spectrum for the back-scattering factor of the nearest shell and by multiplying the EXAFS spectrum with a gaussian function, $\exp[-0.1(k - k_0)]$ with k_0 at the centre of the available range. Instead of using a Fourier filtering technique and isolating individual shells (peaks) we preferred to identify the contribution of individual shells to the EXAFS spectrum and to the Fourier transforms. This approach has recently been applied successfully to Cu-Zn superoxide dismutase and its various substituents[7]. EXAFS simulations were performed with both the raw and the splined data.

The following parameters were used to calculate the EXAFS: (1) the distances of the shells from the central Fe atom; (2) the kinds and numbers of atoms in each shell; (3) their thermal and structural disorder; and (4) the shift in energy of the X-ray absorption edge (E_0). Parameters (1) and (2) determine the phase and amplitude over the whole energy range; (3) influences the amplitude at energies >200 eV; and (4) linearly shifts the experimental spectrum. Parameters (2) are known. The crystallographic distances in the picket fence[5] were used as the starting distances for both deoxyhaemoglobin and the picket fence. Parameters (1) and (3) were optimized individually for each shell by visual inspection of (*a*) the agreement between the experimental and theoretical EXAFS; (*b*) the agreement between their respective Fourier transforms; (*c*) by considering the major features of the Fourier transform of the difference between the experimental and theoretical EXAFS; and (*d*) by monitoring the difference function $[0.15(\chi_{exp} - \chi_{theo})]^2$. Once the theoretical EXAFS resembled the experimental one, an edge shift of 15 eV was applied and then parameters (1) and (3) were further refined, again using criteria (*a*)–(*d*).

Figure 1 shows the uniqueness of the EXAFS spectrum and its Fourier transform with the contributions to them by the individual shells of atoms. The three beat regions could be simulated only by including all the atoms lying within 4 Å of the Fe atom. Figure 2 shows two theoretical spectra and two theoretical transforms, one set calculated with the optimized Fe–$N_{porphyrin}$ distance of 2.05 Å and the other with a distance of 2.07 Å. The longer distance makes the theoretical curve in the first beat region narrower than the experimental curve and makes the first shell peak of the Fourier transform appear at a longer distance than the experimental one. Figure 3 shows the EXAFS spectrum of the picket fence and its theoretical simulation together with their respective transforms. Table 1 lists the distances and Debye–Waller terms used for the simulations. The most important parameter is the distance from the Fe atom to the porphyrin nitrogens, Fe–$N_{porphyrin}$. That distance measured by EXAFS at ≤110K is 2.05 (±0.01) Å for deoxyhaemoglobin and 2.06±0.02 Å for the picket fence; at 300K a distance of 2.10±0.04 Å was measured for the picket fence: also at 300K a

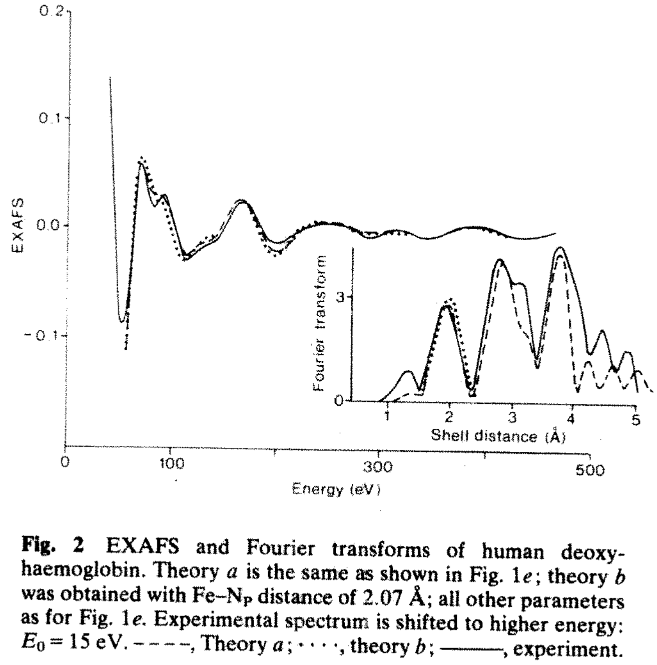

Fig. 2 EXAFS and Fourier transforms of human deoxyhaemoglobin. Theory *a* is the same as shown in Fig. 1*e*; theory *b* was obtained with Fe–N_P distance of 2.07 Å; all other parameters as for Fig. 1*e*. Experimental spectrum is shifted to higher energy: $E_0 = 15$ eV. ----, Theory *a*; ····, theory *b*; ——, experiment.

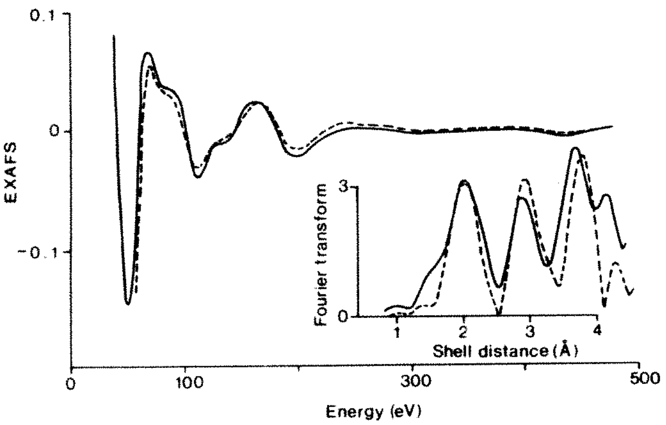

Fig. 3 EXAFS and Fourier transform of oxygen-free picket fence complex (first samples, 100K). Curves were calculated by the spherical wave method. Experimental spectrum is shifted to higher energy: $E_0 = 15$ eV.

distance of 2.072 ± 0.005 Å was found by single crystal X-ray analysis[5]. Thermal expansion between 100K and 300K would lengthen the Fe–N bond by ~0.01 Å. All the values therefore agree within the error limits. For the next three shells the agreement between the picket fence EXAFS and crystallographic data is also good, but for the distant shells 4C (3.45 Å) and 8C (4.3 Å), EXAFS gives shorter distances than the crystallographic analysis. A similar apparent shortening of distances was found in the Cu–Zn superoxide dismutase for both the enzyme systems and the well characterized chemical system $Cu(imid)_4(NO_3)_2$ (ref. 7). The reasons for this discrepancy were not well understood, but multiple scattering and shadowing effects may become important for distances >3.2 Å. The application of EXAFS to this well characterized model of deoxyhaemoglobin provides confidence that the theory can be used reliably for determining the distances of atoms within 3.2 Å from the Fe atom; beyond this EXAFS may underestimate them.

Before comparing the EXAFS results with the crystallographic data for deoxyhaemoglobin[1] and the picket-fence model[5], we must consider the powers and limitations inherent in the different methods of structural analysis. EXAFS gives the distances of atoms from a central metal atom with a standard error of ≤0.02 Å, but no data on the distribution of these atoms in space. Refinement of X-ray data obtained from single crystals of the picket fence at high resolution using Mo K_α radiation gives the positions of the central Fe atom with a standard error of 0.001 Å and of the carbon and nitrogen atoms with a standard error of 0.01 Å. The distance of the Fe from the plane of the porphyrin nitrogens can be determined with a standard error of 0.004 Å (ref. 5). The electron density maps of human deoxyhaemoglobin at 2.5 Å resolution obtained by multiple isomorphous replacement, allow the positions of the Fe atoms to be determined with a standard error of 0.05 Å. By fitting a planar model of protoporphyrin IX to the map, the positions of the porphyrin nitrogens and carbons in that plane can be determined with a standard error of 0.14 Å and the distance of the Fe from the porphyrin plane with a standard error of 0.03 Å (refs 1 and 10). All three analyses rely on computer algorithms that render the results fairly free from human bias.

Table 1 Parameters used to simulate the EXAFS associated with the Fe K-edge of deoxyhaemoglobin and deoxy picket fence complex

	Deoxyhaemoglobin		Deoxy 'picket fence'		Single crystal X-ray analysis[5]
Atom	σ^2 (Å^2)	R (Å)	σ^2 (Å^2)	R (Å)	
4N	0.004	2.05	0.006	2.06	2.07
1N	0.006	2.12	0.006	2.11	2.10
9C	0.003	3.01	0.011	3.01	3.09
1C	0.003	3.15	0.003	3.15	3.14
4C*	0.003	3.29	0.008	3.34	3.45
8C*	0.003	3.92	0.006	3.89	4.30

R denotes the distance of the atom from the Fe atom. σ^2 is a Debye Waller factor and is equivalent to ΔR^2. $E_0 = 15$ eV. The difference in Debye Waller factors of the 9 carbon atoms is significant and derives from a difference of EXAFS at ~300 eV and of the amplitudes of the Fourier terms at ~3 Å (Figs 2, 3).

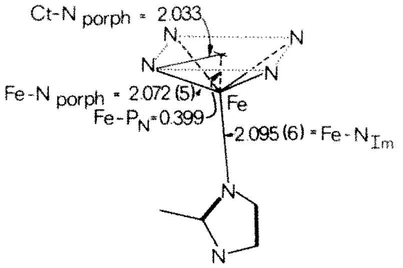

Fig. 4 Stereochemistry of iron coordination in the oxygen-free picket fence complex[5]. Distances in ångströms; numbers in parentheses give the standard error in 0.001 Å.

In the picket fence the four pyrrol rings are domed slightly towards the Fe which lies 0.399 Å from the plane of the porphyrin nitrogens and 0.426 Å from the mean plane of the 24 porphyrin nitrogens and carbons (Fig. 4). In deoxyhaemoglobin the resolution is insufficient to determine whether the pyrrol rings are domed. The distance of the Fe from the planar skeleton of 32 nitrogens and carbons that Fermi fitted to the electron density was 0.56 Å in both the α and β subunits[1]. Our EXAFS results are consistent with Fermi's finding as they show that the distances from the Fe atom to the nitrogens and carbons are similar in the picket fence and in deoxyhaemoglobin. Our EXAFS spectrum and $Fe–N_{porph}$ distances agree with those of Eisenberger *et al.*[4]; we wondered, therefore, what led them to conclude that the iron in deoxyhaemoglobin was only 0.2 Å from the porphyrin plane.

Eisenberger *et al.* obtained this value by triangulation. They used their EXAFS distance of 2.055 Å from the Fe to the porphyrin nitrogens ($Fe–N_{porph}$) in deoxyhaemoglobin as the base of a right-angled triangle; for one of its sides they used the distance of 2.045 Å of the porphyrin nitrogens from the centre of the porphyrin ring ($Ct–N_{porph}$) found in a single crystal study of model compound $Fe^{2+}(TPP)(2\text{-}MeIm).EtOH$ (D. A. Buckingham, quoted in ref. 14). This makes the other side of the triangle $Fe–P_N = \sqrt{(2.055)^2 - (2.045)^2} = 0.2$ Å. Eisenberger *et al.* also compared the EXAFS of deoxyhaemoglobin with that of a deoxygenated picket fence complex having a water molecule weakly coordinated to the sixth position at the Fe atom. This has $Fe–N_{porph} = 2.068 \pm 0.014$ Å, the same as the picket fence we have used, but due to the sixth ligand the displacement of the Fe from the plane of the porphyrin nitrogens is reduced to 0.28 Å (ref. 12).

Table 2 Parameters of five-coordinated high-spin iron porphyrins from single crystal X-ray analyses

Complex	Fe–P_N (Å)	Fe–N_{porph} (Å)	Ct–N_{porph}	Δ	Fe–P_{CN}
O[Fe^{3+}(diMeOEP)]$_2$	0.512	2.065	1.995	0.018	0.535
O[Fe^{3+}(TPP)]$_2$	0.496	2.087	2.027	0.044	0.532
Fe^{3+}(TPP)(Br)	0.489	2.069	1.992	0.070	0.539
Fe^{3+}(TPP)(NCS)	0.485	2.065	2.007	0.068	0.541
Fe^{3+}(TPP)(I)	0.480	2.066	1.996	0.068	0.537
Fe^{3+}(Protoporph)Cl	0.474	2.062	2.007	0.080	0.541
Fe^{3+}(Meso-DME)(OCH_3)	0.456	2.073	2.022	0.034	0.484
Fe^{3+}(Proto-DME)(SR)	0.434	2.064	2.015	0.015	0.446
Fe^{2+}(TPP)(2-MeIm)	0.418	2.086	2.043	0.134	0.530
Fe^{2+}(Tpiv PP)(2-MeIm)	0.399	2.072	2.033	0.027	0.505
Fe^{3+}(TPP)Cl	0.404	2.063	2.023	−0.015	0.392
Mean	0.457	2.070	2.015	0.052	0.507

P_N, mean plane of porphyrin nitrogens; P_C, mean plane of conjugated carbons; P_{CN}, mean plane of nitrogens and carbons. Δ is the doming parameter, giving the difference between the plane of the nitrogens and carbons ($=P_C-P_N$). For details of these structures see ref. 15, except Fe^{2+}(TpivPP)(2-MeIm) EtOH which is described in ref. 5.

Table 2 summarizes structural parameters for various high-spin iron porphyrins determined by X-ray analysis of single crystals at high resolution. In no case is Fe–$P_N < 0.4$ Å. If the displacement in deoxyhaemoglobin were only 0.2 Å, as Eisenberger *et al.* proposed, then its stereochemistry would be unique among five-coordinated high-spin iron porphyrins. The triangulation of Eisenberger *et al.* relies on taking the root of the difference of two squares of nearly equal value. A change in Fe–N_{porph} or Ct–N_{porph} of only 0.01 Å therefore changes Fe–P_N by ~0.05 Å. Eisenberger *et al.*'s value of Fe–P_N = 0.2 Å was derived by using Fe–N_{porph} and Ct–N_{porph} values from two different haem complexes. Because calculation shows that $\delta(\text{Fe–}P_N)/\delta(\text{Ct–}N_{porph}) = 5$, an accurate value of Fe–P_N could be obtained by this method only if Ct–N_{porph} distances were invariant among five-coordinated high-spin haems and a direct correlation therefore existed between Fe–N_{porph} and Fe–P_N; but this is not the case (Table 2 and Fig. 5). The structures of five-coordinated high-spin iron porphyrins determined by X-ray analysis of single crystals at high resolution show that the value of Fe–N_{porph} from one compound cannot be combined with that of Ct–N_{porph} from another to derive a reliable value for Fe–P_N, because the individual distances are too variable and there is no correlation between the two parameters. We conclude that it is impossible to infer from EXAFS the displacement of the iron from the porphyrin plane unless multiple scattering theory can be applied to the near-edge structure[13]; it has to be measured directly by single crystal X-ray analysis.

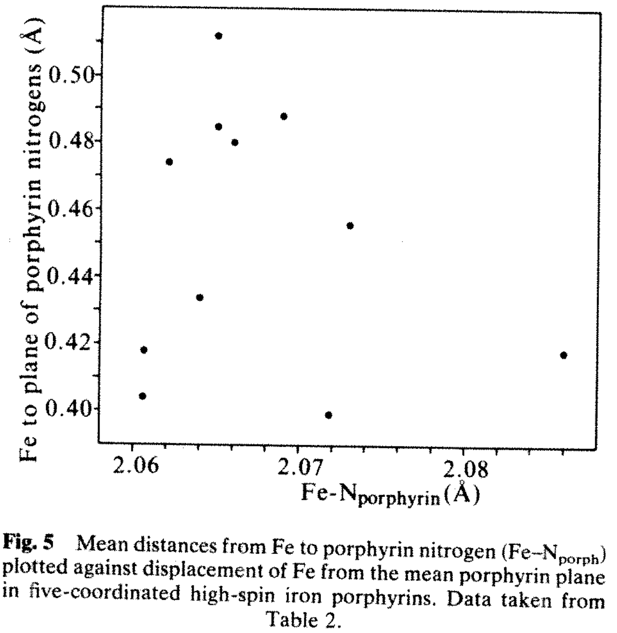

Fig. 5 Mean distances from Fe to porphyrin nitrogen (Fe–N_{porph}) plotted against displacement of Fe from the mean porphyrin plane in five-coordinated high-spin iron porphyrins. Data taken from Table 2.

When M.F.P. first proposed his stereochemical mechanism of haem–haem interaction, he believed the displacement of the Fe from the porphyrin plane in deoxyhaemoglobin to be due entirely to the increase in iron radius on going from its low-spin in oxyhaemoglobin to its high-spin form in deoxyhaemoglobin. Warshel[13] and Eisenberger *et al.*[4] have pointed out that this was an oversimplication. In reality, a mixture of electronic factors (repulsion of the occupied $d_{x^2-y^2}$ orbitals of the Fe by the π orbital of the porphyrin) and steric factors (van der Waals' repulsion of the proximal histidine by the porphyrin nitrogens) conspire to push the Fe out of the porphyrin plane and dome the pyrrols towards the Fe, so that the Fe atoms and the proximal histidines in deoxyhaemoglobin are further from the mean porphyrin planes than in liganded haemoglobins. However, from the mechanistic point of view, the causes of the displacements do not matter: what matters is that they do occur. Hopfield[14] predicted that the free energy of haem–haem interaction may be directly proportional to the sum of those displacements. Many other observations point to the crucial part played by the movement of the iron and the proximal histidine relative to the porphyrin and the general dominance of stereochemical factors in the mechanism of cooperativity.

We acknowledge the support of NSF grant DMR77-27489 and NIH grant RR-01209 in cooperation with the Stanford Linear Accelerator Center and the US Department of Energy. J.L.S. thanks the NIH for partial support (grant 6M17880) and J.E.H. thanks the NSF for post-doctoral fellowship. M.F.P. thanks J. P. Collman and the Director of the Stanford Linear Accelerator Center for their hospitality.

Received 22 September; accepted 4 December 1981.

1. Fermi, G., Perutz, M. F., Dickinson, L. C. & Chien, J. C. W. *J. molec. Biol.* (in the press).
2. Perutz, M. F. *A. Rev. Biochem.* **48,** 327–386 (1979).
3. Perutz, M. F. *Nature* **228,** 726–739 (1970).
4. Eisenberger, P., Shulman, R. G., Kincaid, B. M., Brown, G. S. & Ogawa, S. *Nature* **274,** 30–34 (1978).
5. Jameson, G. B. *et al. J. Am. chem. Soc.* **102,** 3224–3237 (1980).
6. Bordas, J., Bray, R. C., Garner, C. D., Gutteridge, S. & Hasnain, S. S. *Biochem. J.* **191,** 499–508 (1980).
7. Hasnain, S. S. *et al. J. Am. chem. Soc.* (submitted).
8. Lee, P. A. & Pendry, J. B. *Phys. Rev.* **11B,** 2795 (1975).
9. Pendry, J. B. in *EXAFS for Inorganic Systems* (eds Garner, C. D. & Hasnain, S. S.) 5 (Proc. Daresbury Study Weekend, 1981).
10. Fermi, G. *J. molec. Biol.* **114,** 412–413 (1977).
11. Jameson, G. B., Robinson, W. T., Collman, J. P. & Sorrell, T. N. *Inorg. Chem.* **17,** 858–864 (1978).
12. Greaves, G. N., Durham, P. J., Deakun, D. P. & Quinn, P. D. *Nature* **294,** 139–142 (1981).
13. Warshel, A. *Proc. natn. Acad. Sci. U.S.A.* **74,** 1789–1793 (1977).
14. Hopfield, J. J. *J. molec. Biol.* **77,** 202–222 (1973).
15. Hoard, J. L. in *Porphyrins and Metalloporphyrins* (ed. Smith, K. M.) 318–380 (Elsevier, Amsterdam, 1975).

ANNOUNCEMENTS

Awards

The National Academy of Sciences awards for 1982 include: James Murray Luck Prize to **Victor A. McKusick,** (The Johns Hopkins School of Medicine); Award in Chemical Sciences to **Gilbert Stork** (Columbia University); Award for Initiatives in Research to **Kerry E. Sieh** (California Institute of Technology); Public, Welfare Medal to **Paul G. Rogers** (formerly of the House Subcommittee on Health and the Environment); Gilbert Morgan Smith Medal to **Luigi Provasoli** (Yale University); Mary Clark Thompson Medal to **William A. Berggren** (Woods Hole Oceanographic Institution); US Steel Foundation Award in Molecular Biology to **Joan A. Steitz** (Yale University); Selman A. Waksman Award to **I.C. Gunsalus** (University of Illinois); Charles Doolittle Walcott Medal to **Martin F. Glaessner** (University of Adelaide); G.K. Warren Prize to **John T. Hack** (The Geroge Washington University); James Craign Watson Medal to **Stanton J. Peale** (University of California).

Dr Theodore Brewster Taylor (Appropriate Solar Technology Institute, Inc.) is the recipient of The Boris Pregel Award for Applied Science and Technology.

Professor William Trager (Rockefeller University) has been awarded the First Rameshwardas Birla Triennial International Award in tropical medicine by the Medical Research Centre of the Bombay Hospital Trust.

Nineteen Prize Fellow selected by D. and Catherine T. MacArthur Foundation will receive unrestricted awards of $24,000 to $60,000 annually for five years: **Dr Hugh John Cairns** (Cancer research; microbiology); **Joel E. Cohen** (Mathematics & demography; public health); **Richard P. Critchfield** (Journalism); **Howard E. Gardner** (Developmental psychology; clinician); **John P. Gaventa** (Political science; social activism); **David Hawkins** (Philosophy; education); **John P. Holdren** (Physics; energy and environment); **Ada Louise Huxtable** (Architecture criticism); **Robert W. Kates** (Geography; natural hazards research); **Dr Raphael C. Lee** (Surgery; biomedical engineering); **Cormac McCarthy** (Novels); **Richard C. Mulligan** (Cancer research; biochemistry); **Elaine H. Pagels** (History of religion); **David Pingree** (History of science); **Paul G. Richards** (Theoretical seismology); **Richard M. Rorty** (Philosophy); **Joseph H. Taylor** (Radio astronomy; astrophysics); **Michael Woodford** (Economics; legal theory); **George Zweig** (Physics; neurobiology). In addition Barbara McClintock, 79, a geneticist, has been selected as the Foundation's first Prize Fellow Laureate — assuring her of $60,000 annually.

Dr Nien-Chu C. Yang (University of Chicago) is the recipient of The Gregory and Freda Halpern Award in Photochemistry sponsored by the Polychrome Corporation.

The Institute of Physics Award for 1982 are: Charles Vernon Boys Prize to **Dr B.J. Isherwood** (GEC Hirst Research Centre); Duddell Medal and Prize to **S. van der Meer** (CERN); Glazebrook Medal and Prize to **Professor J.M.A. Lenihan** (West of Scotland Health Boards); Guthrie Medal and Prize to **Sir Charles Frank** (University of Bristol); Maxwell Medal and Prize to **Dr J.R. Ellis** (CERN); Rutherford Medal and Prize to **Dr D.M. Brink** (University of Oxford); Prizes for the 1981 Graduateship Examination of the Institute to **D.J. Pointer** and **T.J. Mays** (Bristol Polytechnic).

The Paul-Martini-Prize for promoting the development of scientific methods for the evaluation in the clinical pharmacological and therapeutical fields will be confered by the Paul-Martini-Foundation which is sponsored by the Medizinisch Pharmazeutische Studiengesellschaft (Mainz, FRG). Papers must be self-contained not older than two years. They should be sumbitted either in English or German with six copies to the Medizinisch Pharmazeutische Studiengesellschaft e.V., Bilhildisstraße 2, Postfach 3048, D-6500 Mainz, FRG before 30 April 1982.

An open competition in geometry for an award of $2,500 is being sponsored by Science Software Systems, Inc. The award will be presented to the competitor who submits the most complete solution to the problem: What geometrical properties of dissimilar inversion loci are consequences of the property of self-inversion of a basis curve at angles other than 0° or 180°? For further information send a stamped self-addressed envelope to Science Software Systems, Inc., 11899 W. Pico Boulevard, Los Angeles, California 90064, USA.

The Trustees of the Lady Tata Memorial Trust invite applications for Awards for personal support for research on leukaemia, in the Academic Year beginning 1 October 1982. Candidates with programmes of research on any aspect of malignant disease which may throw light on problems of leukaemia will be eligible for consideration. Awards are open to suitably qualified investigators of any nationality, working either in their own institutions or in other centres abroad. Further particulars from the Secretary of the (European) Scientific Advisory Committee, Lady Tata Memorial Trust, MRC Leukaemia Unit, Royal Postgraduate Medical School, Du Cane Road, London W12, UK.

The Eli Lilly Fellowship in diabetes in children has been established by the British Diabetic Association. It will be funded by Eli Lilly & Company. This fellowship will be for a doctor of registrar status and will last for two years. The research into diabetes in children will be carried out at the hospital of the successful candidate. Application forms from the assistant secretary, British Diabetic Association, 10 Queen Anne Street, London W1, UK.

The L.S.B. Leakey Trust is now able to award research grants to scholars in the fields of human palaeontology, archaeology and primate behaviour. Contact: Miss Anne Turner, The L.S.B. Leakey Trust, 10 St George's Mansions, Vauxhall Bridge Road, London SW1, UK.

Appointments

Mr J.W. Bundy (Agricultural General Manager of Birds Eye Foods Limited) has been elected by the Council of the National Institute of Agricultural Botany to be their Chairman for 1982–83.

Professor C.S. Holling (University of British Columbia in Vancouver) will be the new director of the International Institute for Applied Systems Analysis in Laxenburg near Vienna, Austria.

Meetings

1-4 March, **Mobility and Function in Proteins and Nucleic Acids,** London (The Ciba Foundation, 41 Portland Place, London W1, UK).

4 March, **Developments in Low-temperature Biochemistry and Biology,** London (The Royal Society, 6 Carlton House Terrace, London SW1, UK).

15-17 March, **Energy and Feedstocks for the European Chemical Industry,** Belgium (Society of Chemical Industry, 14-15 Belgrave Square, London SW1, UK).

15-23 March, **Introduction of Utramicrotomy,** Seefelder (Reichert-Jung UK, 820 Yeovil Rd, Slough, UK).

18 March, **The "Simple Surface"**, London (Conference Secretary, IEETE, 2 Savoy Hill, London WC2, UK).

19, March, **Wind and its Effects on Man,** Plants and Animals, Edinburgh (The Royal Society of Edinburgh, 29 Queen St, Edinburgh, UK).

22 March, **European Symposium on the CANDU Reactor,** London (Scientific and Technical Studies, Norwich House, Norwich St, London EC4, UK.

24 March, **Concrete for Durability,** London (The Concrete Society, Terminal House, Grosvenor Gardens, London SW1, UK).

CORRESPONDENCE

Continued from page 452

During a relatively short period, many of the above demands were introduced practically although not by law. In particular the presidium of the academy and the chancellors and deans in almost all universities were chosen in a truly democratic way.

It is significant that most of those elected were politically inactive before 1980 and of moderate views, and gained their authority solely on the basis of their scientific achievements. Thus the elected people can be seen as truly representative of a scientific community which is not heroic but truthful, which follows directives but recognizes that the political direction of science has damaging effects.

It can be argued that a similar attitude is typical of "normal" scientific communities. But the Polish one is not "normal". Its older members endured the Nazi holocaust or harsh life in remote Soviet provinces; their students started their careers during the period of the Stalin cult with its brainwashing machinery. This community suffered the wave of repressions and purges in 1968 followed by the liquidation of the remnants of academic freedoms. It was corrupted during the past ten years of mild but effective "sovietization". Thus it was encouraging to see that the old ideals of scientific freedom, so often declared to be outdated, are so deeply rooted in the bulk of this community and that it is ready to support democratic changes.

Surely the power of the reformers of the scientific establishment rested not only, and not even mainly, on the social forces in their own home but on the forces of an awakening society.

Perhaps much more could have been achieved. There were too many useless meetings, endless and inconclusive discussions about the new structure of science or about formulations of new constitutions. We were drunk after taking too large a draught of democracy and were not yet ready to use it effectively.

Most of the staff of the academy and universities joined Solidarity. But surprisingly, during 1980–81, students were less eager to follow this movement, although a large number of new student organizations appeared. Even the most influential of these, *Niezalezne Zrzeszenie Studentów* (NZS, Independent Student Association) was joined by fewer than 20 per cent of the students.

The main action of NZS was the proclamation in October 1981 of a general strike in protest at the halting of legislative procedures concerned with the new progressive law of higher education and in support of the protest of the Radom branch of NZS and Solidarity against the way the rector of Radom Polytechnic had been elected. This strike was joined by a most of the schools of higher education in the country. In spite of the efforts of Solidarity, the Church and the Council of Chancellors of the Polish Schools of Higher Education, this strike was continued after the strikers' first demand was conceded. A few days before martial law was declared the strike broke down. In January 1982 NZS was dissolved by the authorities.

The era of Solidarity — understood here not as a name of this particular organization with its achievements and follies but as synonymous with the greatest all-national movement in our history — is over. Solidarity is for the time being defeated. But it should be underlined that to the same or an even larger extent the communists who ruled the country for more than 35 years have also been defeated. The political regime proved itself to be not only ineffective and acting against the will of the people, but irreparable and wholly dependent on external powers. In a sense only the Russians won the battle, by finding a way of solving the problem without needing to use their own troops.

The battle is lost, the war is not. It is still the common belief that something very important happened which will influence our future, and perhaps not only ours. I have in mind not only economic and social changes but the changes of spirit of those who rule and those who are ruled — these changes are not as abstract as the word spirit suggests.

Just after the declaration of martial law there was a wave of protests. This wave did not bypass scientific institutions. As yet we do not have a full account of what happened, but we know about the strikes of a few institutes of the academy in the Staszic Palace in the centre of Warsaw which were terminated by force; about a letter of protest signed by more than 300 scientists in the Institute of Chemical Physics; about the strike in the Institute of Nuclear Research in Swierk near Warsaw followed by arrests and trials of several scientists.

The work of all schools of higher education was immediately suspended, but there was a protest of teachers and students in Wroclaw Technical University where several people including the vice-chancellor were badly beaten. We know about strikes in the Warsaw Agricultural Academy, the Mining Academy in Krakow, and the University of Lublin. The senate of the oldest Polish University, the Jagiellonian University in Kraków, sent a letter of protest with a demand for the release of the arrested people.

The number of students and staff arrested is not known. In the University of Warsaw more than 40 people were either interned or arrested. An overall estimate based on this figure might be misleading because the University of Warsaw has been under the special care of the authorities for many years.

Young people, those between 18 and 25, seem likely to be the main losers: they will lose if they decide to fight, because there is no chance of winning; they will lose if they decide to give up, because of the devastating effects of conformity. The generation gap between them and us, already felt during their strike, seems to be widening. The students prefer to follow the heroic pattern of the young generation duing World War II and do not want to give up the only experience they have gained by their own efforts, the experience of the past year.

As yet almost nothing of importance has been changed in scientific institutions by martial law. True, in all universities, as well as in all schools and in most institutes, there are military commissars who are acting not directly but through the existing administration.

But we are only at the beginning of the new road. It seems almost certain that many teachers at all levels will lose their jobs. In secondary schools and in all institutions of public administration the authorities have already demanded written declarations of loyalty, and those who refuse to sign are fired. A similar type of verification of staff and students is expected in the universities, and it will lead to the replacement of all elected bodies by nominees. Many scientists will probably lose the opportunity to continue their scientific work, as happened in Czechoslovakia.

The outlook is not optimistic. We may expect the worst members of the scientific community to move to the front of the scene. It is a well established tradition to ignore such people; but in the present situation this should not be followed. Scientists who try to abolish what has been achieved should be named and ostracized by the scientific community all over the world. And those who suffer for the defence of scientific freedom should feel the moral, and perhaps also material, support of all their friends and colleagues, first of all here in Poland, but also abroad. If we fail to condemn the former and to provide effective support for the latter our defeat may become a catastrophe.

Not the baron

SIR — Sir Peter Medawar asks in a book review (*Nature* 28 January, p.351) "was it not Cuvier who named a fossil ichthyosaurus *Homo diluvii testis* . . .?". It was not: the fossil (now on display in the Teyler Museum, Haarlem) was so called by J.J. Scheuchzer (1726)[1]. Scheuchzer also describes the fossil in a letter published in *Philosophical Transactions of the Royal Society of London*[2]. Baron Cuvier, visiting the Netherlands as a member of a commission sent by Napoleon, confirmed his own identification of the fossil as a giant salamander by carefully removing some of the matrix to reveal the forelimbs (illustrated in Cuvier, 1824)[3].

JULIE HAMILTON
University of Oxford, UK

1. Scheuchzer, J.J. *Homo Diluvii Testis et theoskopos.* (Tiguri 1726).
2. Scheuchzer, J.J. *Phil. Trans. R. Soc.* **24**, 38–39 (1726–27).
3. Cuvier, G. *Recherches sur les Ossemens Fossiles* 1st Edn, Vol. V, 431–434 and Plate XXVI (Paris, 1824).

US spoken

SIR — The editor's leftist leanings have been quite evident of late, but isn't the sentence (*Nature* 14 January, p.86), "*United States users* of the telephone will most immediately discover that it costs them more to use the local telephone service as if it were unmetered water" (italics mine), not only lacking in lucidity but also bending a bit too far left when it employs "United States" as a general adjective? We are Americans, by God!, not "United Statesers" — and the adjective is *American*! I and others proud of America deplore your emasculation of our rightful name, especially when it is to indulge the arrogance of leftists in Nicaragua, Mexico, or wherever, who never refer to themselves as "Americans", but at the same time, with a malevolent dog-in-the-manger attitude, wish to deny us that distinctive title.

EDWIN E. ROSENBLUM
New York, America

What about the Canadians? *Editor*

nature

18 February 1982

University Colleges of Science & Technology
92, A.P.C. Rd., Cal.-9
LIBRARY COMPLEX
Departments of
Chemical Engineering
Chemical Technology
14 NOV 199

What universities should aim at

The die may not be finally cast on British university policy. The universities should quickly propose a reform of the system of student maintenance grants.

For the past several weeks, there has been a curious lull in the storm about the future of the British universities. The belief that the British government could not seriously intend the beastliness it first advertised fifteen months ago has in most places been dispelled, and universities have dutifully set about making the self-inflicted wounds that their reduced budgets require. Most of them have been spurred on by the knowledge that they may not be able to share in the £220 million with which the University Grants Committee has been provided to compensate redundant academics unless their claims are staked about now. Temporarily at least, however, the lull has now been unexpectedly broken by no less a person than Sir Keith Joseph, Secretary of State for Education and Science, in a long letter to the London *Times* last week. Inevitably, his intervention will tempt some to hope that all is not yet lost. Is there a chance that, even at this late stage, the British government might be persuaded to change its mind?

The circumstances which have provoked this public statement are significant. The minister had apparently been stung by the pointed criticism of Dr Robin Marris, professor of economics at Birkbeck College in London, whose complaints appear to have been all the more forceful because they acknowledged that there is an economic need for the British government to contain economic expenditure. This is a point that the universities should have conceded, more generously, at the outset of their long wrangle with the government. That would have enabled them more strenously now to complain that, as things have turned out, the university system is likely to become less and not more efficient.

The planned reduction of student numbers is likely to be proportionately less than the reduction of the teaching force, so that the ratios of students to teachers at many universities will be "improved". There is, however, a high chance that the teachers who will volunteer to leave their jobs in the next few months will include many of those whose departure can least be afforded. Similarly, as teaching departments shrink, teaching staffs will be less able to cover the ground expected of them, while buildings and other equipment will be less than fully used. One glimmer of hope in last week's public statement is the promise that the University Grants Committee will be allowed some room for manoeuvre. Moreover, Sir Keith has now agreed that if academics nationally agree to salary increases which are less than four per cent, the money thus saved could be used for other purposes, and that the University Grants Committee will similarly behave leniently towards individual universities. So far, however, there is no sign that the government will allow a relaxation of the principle from which the most absurd diseconomies spring — its insistence that the numbers of students taught at British universities should now decline.

The ceilings on the numbers of home students which have been set, nationally and for individual universities, are absurd for several reasons. They are diseconomies in the sense that they prevent the full utilization of a well developed university system. They are inequitable, and an arbitrary infringement of academic freedom and university autonomy, in that they limit the right of universities to decide for themselves what to teach, and to whom. The quotas are certain needlessly to deprive young men and women leaving British schools of a university education. So why should the government perversely persist with its support for student quotas (technically, it is true, devised by the University Grants Committee)? Sir Keith Joseph had two comments on this issue last week. Letting universities decide for themselves their responses to shrunken budgets is unacceptable because the universities depend on the public purse and because "planning" is necessary for universities as for the other sectors of higher education. Then, more to the point, student numbers entail a hidden cost to the public purse because of the government's commitment to reimburse local authorities required by legislation to pay maintenance grants to students following first degree courses anywhere in the system of higher education. For the past year, the government has been muttering that these arrangements provide the universities with a blank cheque on its resources. Student quotas conveniently give an upper limit to the annual bill.

The government's preoccupation with the supposed blank cheque is irrational. In 1979–80, local authorities in England and Wales spent £192 million on maintenance grants to university students, when the recurrent budget of the University Grants Committee (for the whole of the United Kingdom) was £801 million. In that year, the average cost of maintenance grants was just over £1,000 a student — less than the maximum amount because individual awards are means-tested on the basis of parental income. In the same year, local authorities paid university fees of £137 million on behalf of their students, an amount that will be reduced from next September by the simple device of reducing by a half the notional cost of university fees for students from the United Kingdom (thus penalizing universities that have taken in extra students in the past two years). In happier times, the social value of this system was not seriously questioned. The system has, for example, partially ensured that students are not discouraged from going on to higher education because of the economic circumstances of their families. But the system is also wasteful. British students make only the smallest contributions towards the cost of their maintenance, and are tempted by the system to seek university places far from their homes, increasing the cost of student housing on university campuses.

These circumstances offer the basis for a better deal between the government and the universities than that now being implemented. In impoverished Britain, the simple abolition of the system of maintenance grants would have the effect of putting university education beyond the reach of a large and important section of the school-leaving population. But why not substitute for the present system of mandatory awards a system of scholarships awarded on merit to some tens of thousands of potential students each year? One result would be that the government would know the extent of its commitment each year. Another is that, by a suitable choice of numbers, students would have an incentive to opt for the most economical education they could find. Finally, provided that university fees were not driven sky-high by government decree, universities would have an incentive to educate as many young people as their resources (determined by the University Grants Committee on the government's behalf) would allow. The result of that would be far-reaching and important. For in such a system, universities would find they had an incentive towards diversity — not, as at present, a common ambition to ape the Oxbridge model. Given last week's evidence, flimsy though it is, that Sir Keith Joseph's mind is not finally closed, the universities should seize the chance to advocate some such scheme.

0028-0836/82/070541-01$01.00

Doves in false garb

The claim by the anti-nuclear movement of professional support is mostly a sham.

Professional societies have now lost most of the characteristics of the mediaeval guilds from which they sprang. A little like trades unions, from which they are often indistinguishable, they are naturally defensive of the interests of those who happen to belong to them. On many issues, they are often at odds with the communities in which they are embedded. So how, and in what circumstances, should professional organizations set out to influence events on a wider canvas than that with which they are professionally concerned? These are some of the questions provoked by last week's meeting in London (see page 544) at which a number of informal groups set out to stimulate professional interest in the problems of nuclear disarmament. It is important, not least for professional people themselves, that the questions should be answered clearly.

In modern circumstances, professional societies have become anachronisms. The days have long since gone when they could automatically assume responsibility for deciding which individuals should be licensed to carry out professional tasks. Even in Britain, only the two halves of the legal professional retain an absolute right to determine entry into a profession; the professional registration of physicians has long since been the responsibility of the General Medical Council, while the analogous functions of the engineering institutions are about to be transferred to a more public central body (as recommended by Finniston two years ago). Other professional organizations, the Royal Institute of British Architects for example, have found it convenient to offer the public service of a means by which disappointed clients may settle claims against professional people, often as an antidote for some restrictive practice such as the enforcement of minimum fees. Others have chosen to shoulder the public burden of defining technical standards of performance, as the Institute of Electrical and Electronics Engineers does for much of the electronic equipment introduced in the United States and thus, by extension, internationally. However truncated their roles, however, most professional organizations remain valuable as learned societies and also rightly function as legitimate and beneficial pressure groups. Physicians' organizations usually have something to say about public policy on smoking and fluoridation, for example. Science, it will be remarked, is for the most part too new to have been tarred with the mediaeval brush.

But if the professional societies have been liberated from most of their statutory functions of deciding who is and is not entitled to practise as a professional, is it not all the easier for them to speak out on wider issues, military policy for example? This was the implicit assumption of last week's conference in London. The simple answer is that the expectation is over-simple. Even as things are, professional organizations are needlessly indifferent to important public issues well within the spheres in which their professional competence would command respect. Physicians have been consistently indifferent to the quality of health care (in Britain) and its cost (in the United States). In the past thirty years, members of teachers' organizations in many places have officiated at the rapid transformation of teaching practice without drawing attention to the serious social consequences that may accompany the intended benefits. Yet these are questions on which the opinions of quasi-professional organizations might be influential, even welcome. And, in their absence, opinions on wider issues, even if they could be arrived at without violence to the views of dissenting members, would cut no ice.

This is why much of last week's discussion was misplaced. The claim that the professions as such have a responsibility to alert the general public to the great issues that confront society, inflation and unemployment just as much as nuclear armaments, is unwarranted and impractical. But there is a sense in which professional people, acting individually, may be held to shoulder an extra responsibility for giving wider currency to their conclusions about important issues on which they have some special knowledge. Professional people have in the past been too mealy-mouthed on many important questions. Even if the question is necessarily as contentious as a nation's defence policy, they should not be afraid to say so. But professional people are mistaken to suppose that the task can be done respectably under titles such as those paraded at last week's conference. What other justification is there for the Medical Campaign against Nuclear Weapons except that physicians prefer hobnobbing with other physicians than with the hoi polloi? Or can they waywardly suppose that they may be able to capture something of the now-vanished mediaeval mystique by pretending that they are part of such an organization? The truth is that they are not, and that their attempts to invest their legitimate causes with spurious authority are a deceit, and a counter-productive one at that. If architects, physicians, teachers and scientists claim a special right to speak for their professions on nuclear weapons, they should take their courage in their hands and join Lords Brockway and Noel Baker on the hustings.

Up and over the top

The United States seems not to appreciate the damage that will be done by last week's budget.

When the United States began in the 1960s to pay for the Vietnam war by printing dollar bills, several years went by before people elsewhere fully appreciated what was happening. The result was that inflation had firmly taken hold throughout the industrialized world before governments (including that of the United States) began to take remedial action — by which time the oil-producing states had devised their own way of penalizing fiscal self-indulgence. Now the shoe is on the other foot. Thanks to the tight coupling between the major industrial markets ironically engendered by institutions such as the Eurodollar market created during the last bout of inflation exported from the United States, economies other than the American are now, if possible, almost hypersensitive to what Washington is planning. That is the simple reason why administrations elsewhere are busily planning for the inevitable rise of interest rates in the coming year; their financial markets are discounting the consequences as quickly as their courage will allow.

Even those who sympathize with the Administration's present objectives are dismayed by what is happening. In round numbers, President Ronald Reagan has asked Congress for authority to spend something like $100,000 million more than his Administration will collect in taxes. While some of his more contentious demands may be moderated in the long months that lie ahead, he must know as well as the rest of the world that Congress will also declare itself strongly against some of the sharp curtailments of welfare expenditure now planned. So it is natural that people should already be anticipating with varying degrees of gloom the prospect of a United States deficit greater than the total revenue of any other government in the West.

But why should this matter? And how can the scientific enterprise be affected? Why should not honest researchers persist in the pursuit of understanding, confident that in the end some productive use will have been made of their findings? The snag is that it will not and cannot be so easy. The Administration must soon settle for some blend of the only two ways of dealing with the crisis it has wished upon itself — it can use higher interest rates to persuade citizens of the United States to lend their earnings to the Treasury rather than to spend them, in which case there will be a slump. Or it can print dollar bills to make up the difference between what it spends and what it collects, in which case there will certainly be high interest rates, but the slump may be avoided at the expense of established institutions — universities, foundations and the like. Mr Paul Volker at the Federal Reserve Board would prefer the first course. Most politicians would prefer the second. Other people, other institutions and the research enterprise as a whole will suffer either way.

0028-0836/82/070542-01$01.00

Cancer Institute withholds grant

Straus denies fresh charges of impropriety

Washington

The running battle between the US National Cancer Institute (NCI) and research scientist Dr Mark Straus of the New York Medical College (NYMC) in Valhalla, New York State, entered a new round last week when the institute announced it was suspending part of Dr Straus's current grant because of failure to comply with federal rules on the use of human subjects in research.

Dr Vincent DeVita, the director of NCI, has also informed the medical college that the final part of the three-year, $910,000 grant is being withheld from the beginning of March on the basis of a site-visit team's report that there has been "minimal progress" in the research into the application of cell kinetics to chemotherapy.

Dr Straus has angrily denied both the charges. On the first, he argues that his work with human cancer patients has involved only conventional radiotherapy and chemotherapy, and is therefore not covered by federal research rules. On the second, he argues that the conclusions of the visiting team are at variance with reports prepared by three previous visiting teams which each claimed that progress in the research was satisfactory.

Four years ago, Dr Straus was relieved of his position as chief of the oncology department at Boston University after the discovery that patients' records had been falsified in part of a broad survey of cancer treatment, supported by NCI, for which he had been the principal investigator.

Dr Straus, who has denied allegations that he was responsible for the forged data, has since moved to NYMC where he is professor of medicine and chief of the department of oncology. In 1979 he was awarded a three-year grant, beginning in March 1980, to continue his research into cell kinetics following what Dr DeVita has described as a "very good" score by scientific reviewers of his grant application.

Disagreements between Dr Straus and NCI emerged last summer, when NCI was accused by members of the Senate's Labor and Human Resources Committee of failing to take stricter action against him in the light of the Boston allegations. Several senators were especially critical of the fact that Dr Straus had been awarded a new NCI grant even though his previous activities were under investigation.

Dr DeVita defended the grant on the basis of the high marks it had received from reviewers but said that support for the clinical trials proposed in the application had not been provided. After the Senate hearing, at which he received some harsh criticism from the committee's chairman, Senator Orrin Hatch of Utah, Dr DeVita received a strong public vote of confidence from the cancer research community.

The new disagreement between NCI and Dr Straus seems to focus on his treatment of cancer patients with a combination of radiation and the drug 5-fluorouracil (5-FU), which was approved by the Food and Drug Agency as an anti-cancer agent several years ago and is widely used by physicians and clinical oncologists.

NCI contends that even though it was not part of the NCI grant, Dr Straus's use of such treatment was experimental, and that a research protocol should therefore have been submitted to the medical college's institutional review board under new federal regulations.

Since this was not done, Dr DeVita said in a letter last month to NYMC president Dr John Connolly, the result has been a "material failure to comply with the terms of the grant". The clinical portion of the grant has therefore been suspended "until the matter is resolved to NCI's satisfaction or until the grant is terminated", as required by federal regulations.

Asked to explain how funding for the "clinical portions" of the grant could be suspended if Dr DeVita had previously assured the Senate committee that no clinical work was covered by the grant, NIH officials admitted last week that this had caused some unfortunate confusion. "The statement made last summer should have said that the approved grant did not involve therapeutic research, rather than

Amersham International floats

Amersham International, the supplier of radioactive chemicals being sold off this week by the British government, seems likely to cause a minor sensation on the London Stock Exchange. On Monday this week, the financial community was persuaded that the 50 million shares could have been successfully offered for sale at a higher price than £1.42 each, thus recouping a larger sum for British taxpayers and providing the company with a larger stock of working capital than the £5 million it now expects. As things are, the offer for sale was expected to be heavily oversubscribed.

The sale of Amersham has been on the cards for the past two years, and is broadly welcomed by the management of the company. Arrangements have been made to give each employee £50 worth of shares, and there are also arrangements whereby employees may buy further shares, now and in the future, which will be held in trust for them.

The argument that Amersham is being sold too cheaply derives from the company's rapid growth in recent years and from the relatively high profit (£8.0 million) before tax forecast for the current year. But some in the financial community point out that the offer price is 18.9 times the expected profit after tax, a largeish ratio for conventional businesses but by no means as great as the price of shares in other high-technology companies, electronics for example.

In such circumstances, shares are preferably sold by tender, with the highest bidders being given preference. On this occasion, however, the merchant banks handling the sale of shares appear to have persuaded the British Treasury that a sale by tender would have been too complicated for many would-be investors.

The Treasury seems also to have devised an ingenious device for assuring the future independence of the company. The government will retain a single "special rights preference share" that will allow it to prevent either a substantial disposal of the assets of the company or a significant change in the pattern of share ownership that might compromise independence.

That Amersham is attractive to investors at this point in its history is easily understood. The company's new plant at Cardiff has come into production within the past year, while the weakening of sterling in relation to the dollar within the past year has necessarily increased the profits of the company, which earns 80 per cent of its revenue outside the United Kingdom. (The prospectus estimates that a five per cent change in the value of sterling implies a ten per cent change in profit.)

Amersham's interest in genetic manipulation through its sale of labelled nucleotides and other materials used in genetic manipulation, at least at the research bench, seems not to have been widely appreciated by the financial press, which may moderate the embarrassment caused to the company's merchant banks by an even more heavily oversubscribed offer than that now in prospect.

The prospectus for the public sale of shares explains that Amersham International owes its existence to a business established in 1940 to refine radium used in the manufacture of self-luminous components for navigational aids. The company employs just over 2,000 people, three-quarters of them in the United Kingdom and most of the remainder in North America and West Germany. In recent years, Amersham has been spending seven per cent of its revenue on research and development. The City of London is impressed; others wonder whether it is enough.

0028-0836/82/070543-02$01.00

clinical research", an NIH spokesman said, adding that biopsy analysis had been included.

Describing the NCI charges as "outrageous", a research colleague of Dr Straus, Dr Jeffrey Ambinder, insisted last week that only conventional treatment had been used. He read a statement from Dr Straus, who was not available for comment, comparing NCI's claims to a situation in which, if a cancer patient is given an aspirin and then finds the cancer has gone away, "then it should have been submitted to a review board".

NYMC has already set up a subcommittee of its Institutional Review Board to investigate whether the treatment should have been submitted for its approval. Although the subcommittee was established before the site visit by the NCI team, it will now have to decide whether to concur with the visiting team's conclusion that the treatment should have been classified as experimental, or to accept Dr Straus's argument that prior approval was not required.

NCI itself has referred the matter to its Office of Protection from Research Risks to see if any further action should be taken. The institute's verdict on the progress of Dr Straus's research is also likely to generate controversy, since the decision to withhold the third year of the grant — amounting to about $300,000 — can be taken to appeal by Dr Straus and/or the medical college.

Explaining his actions in the letter to Dr Connolly, Dr DeVita says the decision to withhold the grant followed the visiting team's conclusion that "minimal progress had been made on both the pre-clinical and the clinical cytogenetic studies".

Dr Straus, described by Dr Ambinder as a "brilliant scientist" whose "ethics are beyond reproach", says in his statement that the criticism is incorrect, and that his group had not been supported to carry out the studies which the visiting team says should have been done. Dr Ambinder also defended the research group's use of tritiated thymine, to study the kinetics of cancer cells, which he says had been approved of by the three previous visiting teams but criticized by the last team which visited in November.

Dr Straus is already suing five of his former research colleagues at Boston University for $33 million, denying the allegations that he had been responsible for the falsified data in the earlier study. Last week he and his lawyer, Andrew Good, were taking depositions from witnesses to establish the basis for his charges of conspiracy.

A full report on the Boston incident is expected to be completed shortly by the Department of Health and Human Services. Meanwhile, staff members of the Senate Health Committee, which was strongly criticized for its treatment of Dr DeVita last summer, said last week that the committee had no further action planned, but was watching events. **David Dickson**

Polish students

Workers help

Help is urgently needed for Polish students penalized under the martial law regulations, according to a clandestine Solidarity bulletin from the Krakow region. The dissolution last month of the Independent Students' Association (NZS) has left the students without any organization to defend them, just when the new rules of conduct for the universities make such protection more necessary than ever. Several former NZS activists have already received prison sentences for allegedly organizing resistance to the military takeover; scores or hundreds more are in internment camps. Those who sign the necessary oath of loyalty and return to their studies face penalties ranging from compulsory "socially useful work" to expulsion and military service even for such minor infractions as cutting lectures or being on campus after hours.

The bulletin notes that the staff of the University of Warsaw have already organized a system of financial and legal aid for students, and are also trying to provide accommodation for those students who have been expelled from their hostels. A similar initiative seems to be under way in Poznan. There, on the declaration of martial law, the deans and deputy deans of the various faculties apparently resigned as a body, but had returned to their posts last week, apparently for the sake of the students, in advance of the riots at the end of the week.

The Krakow bulletin marks an important new development in the Polish democratic movement. Before 1976, there were protests by workers and by intellectuals (including students) but for different causes and on different occasions. After the food-price demonstrations of June 1976, however, intellectuals and students organized legal and material aid to those affected by the wave of police repressions, and were themselves frequently heavily penalized for doing so. This is the first time, however, that a workers' organization has spoken out in defence of intellectuals and students.

The bulletin, which describes the victimized students as "our best young people", coincides with a major propaganda offensive designed to break the ties between workers and intellectuals which developed after 1976 and which are consolidated by Solidarity. At the end of January, Michal Hebda, the rector of Radom Engineering College, whose "undemocratic" appointment triggered the nationwide student strikes last autumn, said on Warsaw radio that the combination of student and worker protests showed that it must have been organized from abroad. Many intellectuals in internment have been creamed off from the general camps and transferred to somewhat more comfortable accommodation.

Most surprising of all is the remark attributed to deputy prime minister Mieczyslaw Rakowski, editor in chief of the weekly *Polityka*, which is due to resume publication shortly. He is reported to have told a staff briefing conference that in his opinion the intellectuals in Solidarity were directly responsible for the imposition of martial law. What finally tipped the balance, he claimed, was the declaration by the Conference of University Rectors that its members should have the right to vote for the Minister of Science, Higher Education and Technology. **Vera Rich**

British anti-nuclear campaign

Pros not all con

The two British veterans of disarmament, Lords Brockway and Noel-Baker, gave their blessing last weekend to a campaign to mobilize British professional opinion against nuclear arms. But the conference at Imperial College, London on 12 February, planned by the World Disarmament Campaign, demonstrated that only the anti-nuclear profession is sure of where it stands.

The theme of the conference was that professional people and even professional organizations have a responsibility to inform the general population of the present danger from the accumulation of nuclear weapons, calculated by Dr Frank Barnaby, until recently director of the Stockholm International Peace Research Institute, as the equivalent of 3 tonnes of TNT per head of the world's population.

British professional organizations were not formally represented at the conference, although Mr Jack Chambers, president of the National Union of Teachers, claimed the backing of an organization with 250,000 members for his demand for a place in the school curriculum for the "teaching of peace". In passing, he protested at the complaints from newspapers that teachers were guilty of "political indoctrination" by telling their students of their "profound distaste for the present levels of armaments" and of the British government's "scandalous support for the United States government on El Salvador".

Dr John Dawson, head of the division responsible for professional questions at the British Medical Association, gave a more temperate account of the association's study of the effects of a nuclear attack on Britain, which should be complete in about a year. He explained that the association's objective was to enable members of the medical profession to make up their own minds. He provoked cries of "Shame!" from some among the audience by saying that the British Medical Association had "no policy" on nuclear weapons, and the ridicule of a psychiatrist from the north of England who asked what purpose could be served by a solemn study of the effects of nuclear weapons on the

0028-0836/82/070544-02$01.00

British water supply if the recent cold weather had caused water to be rationed in some places.

The association's study has in part been occasioned by a resolution passed at last year's annual representative conference. That circumstance is counted as a success for the Medical Campaign against Nuclear Weapons, which now claims 1,400 members, perhaps 2 per cent of registered physicians in Britain. Other professional anti-nuclear groups may follow this example.

Architects for Peace has similarly taken the initiative by asking the professional organization whether architects can ethically help with building missile sites or underground bunkers, while both the physicians and the Nursing Campaign against Nuclear Weapons intend to make fun of the plans worked out by central and local government for dealing with the consequences of a nuclear attack.

Mr Michael Walsh, chairman of the nurses' organization, produced a scathing criticism of the official British policy that medical personnel should be dispersed to rural areas if there should be advance warning of a nuclear attack, and that the urban population should rely on "self-help". One participant at the conference contributed the intelligence that a local authority plan for dealing with the aftermath of a nuclear attack on the north of England has prudently qualified the advice that the dean of the local medical school should be consulted with the phrase "or his representative".

"IT WAS DESIGNED BY ARCHITECTS FOR PEACE."
BIFF

The surprise of the conference was the declaration by General Michael Harbottle, now secretary-general of the World Disarmament Campaign, that there are now almost enough ex-military men like himself to form an organization called "Generals for Peace". More predictable was the steady undertone of criticism of the British and American governments, accused by Ms Norma Turner ("Journalists against Nuclear Extermination") of assailing the media with "anti-Soviet pro-nuclear propaganda". Several speakers considered that the meeting early in June of the NATO council that President Ronald Reagan will attend had been arranged to distract attention from the Second Special Assembly of the United Nations on disarmament, while General Harbottle thought it possible that Queen Elizabeth II's political independence had been compromised by her invitation to the president to dine at Windsor Castle on 10 June.

The conference was attended by 430 people, more than a third of them from the medical professions. About ten per cent of the participants were scientists, among whom Dr Tom Kibble, professor of physics at Imperial College and vice-chairman of "Scientists against Nuclear Arms", raised the provoking (and unanswered) question of how and when to raise with students, "very often the military technicians of tomorrow", the propriety of taking jobs in military research.

Rights on DNA

Brussels

A move to widen the scope of the European Human Rights Convention to include the dangers of genetic engineering provides further evidence of the unease which recombinant DNA work still arouses in Europe. A report adopted by the assembly of the Council of Europe in Strasbourg on 26 January included eight recommendations on the legal, ethical and social issues raised by the prospect of interference with human genetic inheritance. The rapporteurs, Lennart Petterson (Social Democrat, Sweden) and Bjorn Elmquist (Liberal, Denmark), based their recommendations on the findings of a public parliamentary hearing last May.

The right to a genetic inheritance free from any form of engineering should be included in the European Human Rights Convention, say the Strasbourg legislators. Exceptions include the treatment of genes to eliminate genetically transmitted diseases but this must only be done with the consent of those concerned or, for children or a fetus, the consent of the parents.

The recommendations also stress the need to monitor the harmonization of safety regulations applied to recombinant DNA research in Europe, and suggest that this should be done by the European Science Foundation. EEC's draft legislation on the registration of DNA research should also be examined to see whether it should be applied throughout Europe. Finally, the Council of Europe proposes to study how microorganisms which have been modified by recombinant DNA techniques can be patented.

Jasper Becker

Chemical warfare

Protest plans

Washington

Twenty-five religious, environmental and arms control groups have formed a coalition to lobby against the Reagan Administration's plans to resume the production of chemical weapons after a 13-year moratorium.

The coalition, being organized by the Washington-based Council for a Livable World, was announced last week, just after President Reagan had removed the last remaining legal barrier to resumed production by declaring that the production of nerve gas weapons was "essential" to the national security of the United States.

This in turn coincided with a request from the Reagan Administration for a budget of $705 million for chemical warfare activities conducted by the Department of Defense for the 1983 fiscal year, which begins on 1 October. $77 million is also being added to the budget for the current year, which will now total $532 million — and compares with the $111 million being spent only four years ago.

Included in the 1983 request, most of which will be spent on improving defensive equipment and apparatus, is $30 million which will be used to produce "binary weapons" at the Pine Bluff Arsenal in Arkansas. Congress has already agreed to spend $20 million to build the production facilities, which are now expected to be completed by mid-1983.

According to Defense Secretary Caspar Weinberger, two types of chemical weapons will be produced: 155 mm artillery shells and Big-Eye bombs. Both will be based on the binary concept, in which two non-lethal chemicals are stored separately.

President Reagan's announcement had been widely expected, following pressure from the US military to replace the existing stockpile of chemical weapons, and widespread claims about Soviet superiority in chemical weapons as well as the alleged use of "yellow rain" in South-East Asia. (*Nature* **293**, 327; 1981).

Two years ago, the Pentagon's Defense Science Board, chaired by Dr John Deutch of the Massachusetts Institute of Technology, recommended a start on the production of binary weapons and that the Department of Defense should prepare for a major increase in its chemical warfare programmes. The department is said to be planning to spend about $1,400 million in 1984, and even more later.

Supporters of the chemical weapons programme argue that it is necessary to persuade the Soviet Union to speed up the chemical disarmament treaty, which the United States and the Soviet Union have been discussing in Geneva since 1975.

In a letter to the leader of the House of Representatives, Mr Tip O'Neill, President Reagan argued that the resumption of production, which had been banned by

0028-0836/82/070545-02$01.00

President Nixon in 1969, would "provide strong leverage towards negotiating a verifiable agreement banning chemical weapons." He added: "Considering the current world situation, particularly the absence of a verifiable ban . . . the United States must also deter chemical warfare by denying a significant military advantage to any possible initiator."

Opposition to the Administration's plans is expected to focus on two main lines of argument. The first is the technical discussion about whether an increased chemical capability would, in fact, act as a deterrent to the Soviet Union, or whether — given some of the inherent limitations of binary weapons — it would make more sense to modernize existing stockpiles by more conventional means.

The second argument focuses on the opposition which is already developing in Western Europe, where the chemical weapons would have to be stored if, as expected, their main use was to be in a European theatre of war. According to critics of the Administration from both the left and the right, this opposition could lead to a destabilizing of the Atlantic Alliance which would, in itself, be an additional threat to national security.

Last year, the Administration's plans to build the production facility were approved by the Senate only by two votes in contrast in the House of Representatives there was a strong majority in favour of the new facility. This year the critics hope that the combination of a stringent budget outlook and forthcoming congressional elections will give them the votes needed to defeat the proposal to resume production; but with both the Defense Department and the White House apparently determined to push the proposal through, those trying to head it off recognize that they face a tough uphill task.

David Dickson

Deep-sea mining

Fairer shares

Brussels

A recent European Commission policy paper is urging that, when the world's developed and developing countries meet again in March at the International Conference on the Law of the Sea, to renew their fight over the mineral spoils of the deep seabeds, the EEC's member states should vote together in favour of a better deal for the mining consortia.

Europe, the Commission points out, is almost totally dependent on outside supplies of the minerals in question. Nearly all of Europe's cobalt, copper, manganese and nickel requirements are mined in the developing world, mostly in countries marked by political instability and a poor investment record.

Added to this are the national interests of the six consortia at present in the queue for mining licences. France is represented by the Association d'Etude et de Recherche des Nodules Polymetalliques (AFERNOD), which includes CNEXO (National Centre for the Exploration of the Oceans), the Le Nickel company and the atomic energy commissariat. Britain is represented by the Kennecott Copper Corporation, which is controlled by British Petroleum. Italy's ENI and Belgium's Union Minière Belge have interests in Ocean Mining Associates. Three German companies are partners in Ocean Management Incorporated and Holland's Bos Kalis is a member of the Ocean Mineral Company.

Although they have obvious interests in common, the member states have largely acted independently of one another. However, both the European Commission and the European Parliament would like the conference to decide on a joint EEC policy on raw materials. For the forthcoming round of negotiations the Commission recommends that the Ten should concentrate on ensuring that the mining consortia are not burdened to the point of non-profitability by restrictions and levies.

Mining permission by the proposed authority should be given impartially and there should, the Commission considers, be a way of appealing against decisions. However, the Commission rejects the idea that the authority should be funded by taxes levied in the mining consortia, pointing out that the financial risks of investing an estimated $1,000 or 1,500 million to mine a site of 3 million tonnes are well above those required to extract the same amount of metal in a developing country. To counterbalance this, the Commission wants the law to guarantee that production levels as well as access to the markets can be maintained for the duration of a licence.

The developing countries see the problem as ensuring that their own mineral resources are not cut out of the market by competition from seabed mining. In addition, they are pressing for a transfer of technology and joint ventures, and hence a share of mining profits. The Commission is doubtful about how this would work out in practice and wants developing countries to share more of the risks involved.

Sources at the Commission suggest that since the conference ended last March little has happened to alter the negotiating positions of the opposing camps of developed and developing countries which are likely to remain at loggerheads this coming March.

Jasper Becker

Small growth fund

The address of the Treasurer of the Association for Research into Restricted Growth was given incorrectly in *Nature* 11 February. The following is the correct address: Pam Worsfold, 8 Cotswold Avenue, Rayleigh, Essex.

German academics

Tenure vanishes

Hannover

Since its inception 10 years ago, the policy of *Berufsverbot*, the exclusion of "political activists" from employment in West Germany's civil service, has meant not so much the dismissal of persons considered "extremist" but rather the blocking of their entry into public employment. In academic circles, therefore, the principal victims were young graduates who had formerly been members of (quite legal) left-wing student societies, and found themselves barred from an academic career.

But the recent "Campaign against *Berufsverbot*" conference in Hannover met under the shadow of a new threat, which has arisen as a result of the case of post office official Hans Peter, sacked for his political views after 30 years of service. After a vociferous campaign Peter's appeal was finally dismissed by the federal court last October.

The significance of the Peter case is that this is the first time a tenured official (*Beamte*) has been dismissed for his political views. West German employment policy recognizes three categories of employed person: "worker", "employee" and "*Beamte*". In return for job tenure for life, *Beamte* employees are expected to swear an oath to uphold the constitution. Anti-*Berufsverbot* campaigners explain that those barred from state employment for being activists are fully prepared to uphold the constitution (which guarantees freedom of conscience and opinion). What they are not always willing to do is to equate their loyalty to the constitution with unqualified support of specific government policies.

During the past 10 years, the spectrum of victims of *Berufsverbot* (the campaign lists some 5,000 cases of exclusion throughout the Federal Republic) has gradually widened from communists to socialists, to liberals, to the peace movement and — most recently — to the ecology lobby.

The immediate threat of *Berufsverbot* policy to academics is indirect. Although the Peter case threatens any tenured position, during the past few years a tacit agreement has grown up in the universities that a scholar at risk would formally hold a non-tenured post, but would in other respects be treated as if fully tenured. However, recent cut-backs in university funding in West Germany have meant the abolition of a large number of non-tenured posts. Academics who have been at risk of *Berufsverbot* are thus being eliminated from the universities without the direct intervention of political considerations. With the scope of the screening process apparently becoming ever wider, and unemployment figures soaring, their prospect of finding other jobs seems bleak.

Vera Rich

0028-0836/82/070546-01$01.00

Scientific exchanges

DoD retreat

Washington

Following a series of protests from the academic community, the US State Department has backed away from its previous insistence that rigid restrictions be placed on the topics that a Soviet computer scientist will be allowed to discuss with American scientists during his visit to various research universities later this year.

Last month Stanford University told the State Department that it was not prepared to accept limitations on a visit to its department of mechanical engineering by Dr Nickolay V. Umnov, a robotics specialist. In particular, the university objected to the requirement that Dr Umnov should only be shown research results that have already appeared in the open literature, only discuss theoretical aspects of the research and not be shown details of robot control units or programming techniques.

Stanford's dean of research, Dr Gerald Liebermann, said the university was not prepared to police Dr Umnov's visit, either on or off the campus. He also expressed surprise that the State Department's restrictions had been forwarded without comment by the National Academy of Sciences (NAS), which is arranging Dr Umnov's visit as part of its conventional scientific exchange programme.

NAS president Dr Frank Press subsequently announced that the academy was suspending the automatic transmission of such instructions until the matter had been discussed in detail with the State Department. And last week, Stanford announced that the department had "clarified" its instructions, producing a revised form of the restrictions which the university would now be able to accept.

In particular, Dr Umnov would be able to discuss any research that either has been or is about to be published in scientific papers, and also be given access to details about the control units and programming techniques. In addition, Stanford would no longer be responsible for ensuring that he did not visit local industrial research facilities, another restriction included in the earlier letter.

After the State Department's clarification, the University of Wisconsin, which had previously withdrawn an invitation to Dr Umnov in the wake of Stanford's protest, also announced that it found the new conditions acceptable and Dr Umnov could now visit the university.

The softening of the State Department's line follows intense discussions involving both Stanford and the National Academy of Sciences. It also reflects a split within the Administration on the advantages to be gained from the strict control of university-based research, given the disruption of the free flow of scientific information that would result.

Critics in both Congress and the Administration have identified scientific exchange programmes as vehicles by which the Soviet Union is able to gain access to technical data which it is then able to use to bolster its own military efforts. In response, universities such as Stanford argue that this is a small price to pay for the advantages of open communication in the scientific community.

Dr Jay Keyworth, President Reagan's science adviser, said in an interview last week that he thought the tightening up of the restrictions applied to visiting Soviet scientists was more a reflection of the efforts by President Reagan to make access for the Soviet Union to US technology more difficult after recent events in Poland than a specific attempt to restrict the export of technical data on robotics.

Although Stanford has now said that it is prepared to accept Dr Umnov's visit under the revised restrictions from the State Department, the department itself has yet to give formal approval to the visit. The university has described the National Academy as acting as an "honest broker" between itself and the department.

The academy's position will be discussed at a meeting of its governing board and of the National Research Council which takes place in Washington next week. Academy officials are still hoping to set up a committee to examine the tensions between national security and academic freedom in greater depth. Meanwhile, Stanford president Dr Donald Kennedy, one of the public leaders of the academic community's campaign against excessive government restrictions on research, has agreed to act as chairman with Dr Richard DeLauer, Under-Secretary of Defense for research and development, of a committee being established by the Association of American Universities, to address the same topic.

David Dickson

Lister Institute

End of the road

At the end of May, the Lister Institute of Preventive Medicine will announce the results of applications for five newly created research fellowships thus marking the fundamental change in its status that has now been accomplished. Inflation and escalating costs over the past ten years have defeated the institute's struggle to support a research programme with its investments and production facilities. The laboratories at Elstree and Chelsea have been sold and the interest from the institute's capital of £6 million will now be used for the fellowships.

The Lister Institute was the first major medical research body in Britain, predating the Medical Research Council by 30 years, and in its early days ranked with institutes such as the Pasteur and the Rockefeller. When established in 1891, the institute had a dual function — the production of vaccines and antitoxins and medical research. In spite of passionate opposition from anti-vivisectionists, the institute enlisted the sympathy of the first Lord Iveagh, who after his stableman was bitten by a rabid dog and was sent to Pasteur in Paris because no treatment could be procured in England, gave it £250,000. (The stableman lived to the ripe old age of 89.) In its early decades, the Lister Institute flourished as a private research organization with endowments and income from the sale of biomedical products.

By 1952, the institute encompassed twelve departments. Research was concentrated at the Chelsea laboratory, which closed in 1975 and is now being developed as a hospital. The sale of biomedical products contributed greatly to the income of the institute but Elstree laboratories, the production centre, was finally sold in 1978. From 1896, when the first diphtheria antitoxin used in Britain was prepared, Elstree manufactured vaccines against tetanus, whooping cough, typhoid, plague and cholera and was the main British supplier of smallpox vaccine. Elstree also developed the dried smallpox vaccine widely used in the WHO smallpox eradication programme.

The fate of the institute reflects the difficulties of a privately funded research organization in times of inflation. The institute repeatedly failed to obtain government support, but its Blood Products Laboratory and Blood Group Reference Laboratory have been handed over to the North West Thames Regional Health Authority.

The institute has now been reduced to a small governing body under the chairmanship of Professor Albert Neuberger, a small secretariat and a Scientific Advisory Committee chaired by Professor Geoffrey Dawes, director of the Nuffield Institute for Medical Research at Oxford. The fellowships now to be offered are aimed at promising young scientists who, in the present economic climate, may find it difficult to obtain financial backing for their research. The institute is encouraged by the response to its first advertisement — "It takes only one to make a breakthrough, after all".

Jane Wynn

0028-0836/82/070547-01$01.00

CORRESPONDENCE

Aircraft evolution

SIR — Hoyle (*Nature*, 12 November 1981, p.105) was echoed by Wickramasinghe, as reported in newspapers on 17 December 1981 during the Arkansas trial, and is quoted by Sluyser (*Nature* 21 January, p.184), as saying that "for higher life forms to have evolved by chance is comparable with the chance that a tornado sweeping through a junkyard might assemble a Boeing 747 from the materials therein". The simile is glib, meretricious and deceptive. No evolutionist has suggested that higher life forms are assembled by chance from debris.

However, the inept comparison provokes memories of the actual evolution of the Boeing 747, starting a mere 80 years ago with primitive flying machines that indeed looked like products of junkyards. As in biology, but almost infinitely more rapidly, aeronautics proceeded from the simple to the complex. The inventions of the Wright brothers and Santos Dumont led to Blériot's 1909 monoplane and a host of larger aircraft within the next decade. Boeing planes started to cross the oceans in 1934 and the 74-passenger Boeing Clipper was in trans-Pacific service in 1937. Preceded by the British Comet, Boeing 707s brought in the jet age of travel in 1959. They were the evolutionary predecessors of the 747. The brief history of aircraft technology is filled with branching processes, phylogeny and extinctions that are a striking counterpart of three billion years of biological evolution.

Instead of misleading newspaper reporters with attacks on evolution and fables about 'flu bugs in comet tails, Hoyle and Wickramasinghe should note that protein molecules evolve by elongation of small polypeptides and that living organisms acquire ever-increasing complexity from gene duplication as now revealed in DNA sequences. Also, that wide-bodied jets evolved from small contraptions made in bicycle shops. Or in junkyards.

THOMAS H. JUKES

University of California,
Berkeley, California, USA

Brought to Book

SIR — Jon Marks's letter about Creationism (*Nature* 28 January, p.276) is obviously either a parody or a hoax. No other explanation is possible of such a farrago of perversity and farce.

The inerrancy of the Bible may well be a risible Aunt Sally, but even so it is not to be knocked down by the ineptly aimed brickbats lobbed at it by Mr Marks. His paraphrase of St Luke's account of Jesus and the repentant thief is inaccurate, and his comment upon it ludicrously, if not wilfully, naive; his gibe at *Leviticus*'s classification of bats with birds would strike home only if "bird" had always had the same narrow meaning as it has today, which, of course, is not the case. And as for Origen's mockery of the proposition that "the first three days existed without Sun, Moon and stars", I suspect that most modern cosmologists would prefer to side with *Genesis*! If one wishes to confute Fundamentalism, is it not best merely to point to the Bible's self-contradictions? These, after all, are many: for example, the discrepancy between the genealogies of Jesus offered in *Matthew* 1 and in *Luke* 3.

Fallible the Bible certainly is, but I cannot agree with Mr Marks that its myth has even more rivals, let alone any superiors. The wealth of the Bible's wisdom, the beauty of its story, the power of its images are vast, unexampled, seemingly inexhaustible: if proof were needed, the Bible is the source of some of the greatest works of some of our greatest artists — the *Divina Commedia*, the *St Matthew Passion*, the Sistine frescoes, *Paradise Lost*, the *Last Supper*, *Messiah*. Where are the fruits of the *Kalevala*, or the *Elder Edda*, or the *Odyssey*?

That the Bible is not "original", everyone admits: but that is far from being a failing: in literature, as in ethics, "originality" is the prerogative of cranks, and the "original" usually monstrous — and, like most monsters, sterile. No great story — be it the *Morte d'Arthur* or the tale of Noah's Flood — is *sui generis*. Indeed, to trace the resemblances between the biblical myth and those of other books is to play straight into the Christians' hands, for it is part of the Christian thesis that among the pagan legends there may be "good dreams" sent from Heaven: blurred, poetic visions of what, in the New Testament, became concrete, prosaic fact.

It is sad that Mr Marks thinks that a Creator of 750,000 species of insect would have to be a "cosmic bore", but the blame for boredom usually lies with the bored: Mr Marks's remark tells us more about Mr Marks than it does about God. Yawns are not admissible as philosophical arguments.

But Mr Marks is quite correct, I believe, when he says that the existence of God is "irrelevant" to evolution; perhaps one might broaden his observation, and say that the existence of God is irrelevant to science generally. The supernatural, if it exists, is by definition intrinsically unknowable to "natural" science (except in the very limited sense that Shakespeare is knowable to literary criticism). Worse still, even if the supernatural not only existed but also operated upon nature, science would certainly find those operations all but impossible to assimilate: for the price that science pays for relying ultimately upon repeatable experiments is that science finds it enormously difficult to incorporate irreproducible phenomena, especially when such phenomena do not seem to accord with current scientific theory. There is a perennial temptation to reject odd phenomena as "impossible". "Improbable" they may be, but "impossible" they most definitely are not. To label any observation, however bizarre, as "impossible", is profoundly to misunderstand the provisional nature of scientific law. Those who jeer at the Bible's reports of miracles commit precisely the same philosophical error as those old astronomers who, we recall, were frightfully amused by the quaint bucolic fantasy that stones sometimes fell from the sky.

In conclusion, then, Christian apologists should regard science neither with fear nor with hope: science is not, and never can be, an arbiter of theology: no experiment in any laboratory will ever verify or falsify the resurrection of Jesus Christ. Similarly scientists must have the honesty and the humility to concede that science's methods of inquiry are radically limited in scope. We cannot vivisect God.

Though, in our way, we tried.

A.J. HOLLIN

London SW15, UK

Losers all

SIR — Your report that the Medical Research Council will not accept grant applications from British university departments inadequately equipped for the proposed research (*Nature* 19 November 1981, p.201) invites comparison with the analogous situation in the United States. In both countries, a system of "dual support" prevails for government-sponsored academic research. Government agencies, accepting that discipline-oriented university research yields fundamental findings of profound cultural value and of potential benefit for society, and the major — but by no means only — investors in these activities. As a condition of making limited grants to departments or individuals, the government expects the universities to supply the remaining research necessities. (In Britain, the university's resulting relative share is much higher than in the United States.)

Here, the two systems diverge in nature. The British university's general funds come from the same exchequer as do research grants. The same austerity mood that leads a research council to emphasize that it will withhold funding unless the laboratory involved is "well found" also leads to the tightening of general university support from which the university is expected to equip laboratories. Without other resources for this type of research, the institution makes painful choices to sustain part of the research "duet".

In the United States, the federal government pays less than total direct and total indirect costs of sponsored faculty projects (regardless of method of reimbursement). The universities receive no general federal support but must meet the balance of federal project costs by drawing on their own general funds for instruction and other activities. These come principally from state governments (for state universities) and student tuition and, to a lesser extent, from alumni, foundations, industry and endowment. Admittedly, American universities have a more diversified financial base than do most British institutions. Yet, non-federal sources of funds have their own views on research and are not eager to make up the difference on federal projects.

Here, some similarities can perhaps be suggested. In Britain, departments receiving inadequate university funding may be denied research council support. In the United States, the university may be forced to make up the balance, on federal projects, with funds it would otherwise use for promising research by graduate students or young faculty members. In this zero-sum situation, these faculty and graduates are not only the immediate losers but also involuntary co-sponsors of the public interest research that *does* receive their university's funds. Ultimately, as you observe, "the rest of us" are the losers.

KATHRYN SMUL ARNOW

Brussels, Belgium

Breaking the 600 metre barrier

from the Scientific Party, DSDP Leg 83

In the 12 years' existence of the *Glomar Challenger*, deep-sea drilling in more than 600 holes has repeatedly failed to penetrate deeper than 582 m into the pillow lava sequence at the top of the crust. A myth had thus arisen among geologists that deeper drilling in the oceanic basement is prohibited with current technology. Now the mythical 600 m barrier has been broken. Leg 83 of the Deep-Sea Drilling Project has deepened, by 514 m, Hole 504B in the 6.2 Myr crust on the southern flank of the Costa Rica Rift, and penetrated to 1,076 m of basalt. The hole penetrates almost twice as deep into the oceanic crust as any other and has been used for making an extensive set of geophysical experiments, utilizing the borehole as a natural 'window' into the crust.

A consensus has steadily arisen over the past several years that the best model of the structure and composition of the oceanic crust is provided by ophiolites on land. An ophiolite is a layered tectonic sequence progressing, top to bottom, from marine deep-water sediments to pillow basalts, then to a sheeted, nearly vertical dike complex. Beneath the dikes are the cooled remains of what was once a magma chamber, gabbros and layered cumulates. Ultramafics lie beneath the gabbros across a transition thought to be the MOHO. With depth the entire sequence is altered to successively higher-temperature metamorphic rock: first zeolite facies in the pillows, then greenschist facies in the pillows and dikes, and finally amphibolite facies in the lower dikes and gabbros. Ophiolites are thought to represent old oceanic crust generated at a mid-ocean ridge spreading centre and somehow 'obducted' onto land during collisions of the gigantic plates moving over the Earth's surface.

Leg 83 goes a long way towards validating the ophiolite model, although it exposes a few inconsistencies that will require re-examination of the ophiolites. First, Leg 83 penetrated through the pillow lavas, and at about 700 m it broke through into a sheeted dike complex. The transition occurred sharply, over a depth range of about 50 m, in every geophysical log and experiment run in the hole. The figure shows that seismic velocity, density and thermal conductivity of samples, as well as *in situ* electrical resistivity, sonic velocity and reflectivity from a downhole sonic televiewer (showing rock hardness), all increased in a step-like fashion. By contrast the porosity, degree of fracturing, amount of alteration minerals, and magnetic intensity and susceptibility all fell while *in situ* permeability decreased by three orders of magnitude below the boundary.

Marine seismology has provided evidence of a layered structure of the oceanic crust in which surficial low-velocity pillows are referred to as layers 2A and 2B, a deeper dike layer as layer 2C and the deeper gabbros as layer 3. Leg 83 drilled into layer 2C and measured *in situ* 'layer 2C-type' seismic velocities in the sheeted dike sequence.

Above the dikes, Leg 83 found an extensively altered pillow and breccia layer, with a stockwork of iron, zinc and probably copper sulphides in hydrothermal silicate veins. In the ophiolites, massive sulphide ore bodies of economically important metals have been mined, whose 'feeders' are stockworks strikingly similar to that found in the Leg 83 drill hole. Above this layer, alteration dropped off in extent and grade, and a highly permeable layer 2A was found.

In 1979, Legs 69 and 70 had drilled 562 m into the same area of oceanic crust and had discovered an underpressured aquifer. Leg 83 verified that this aquifer was still

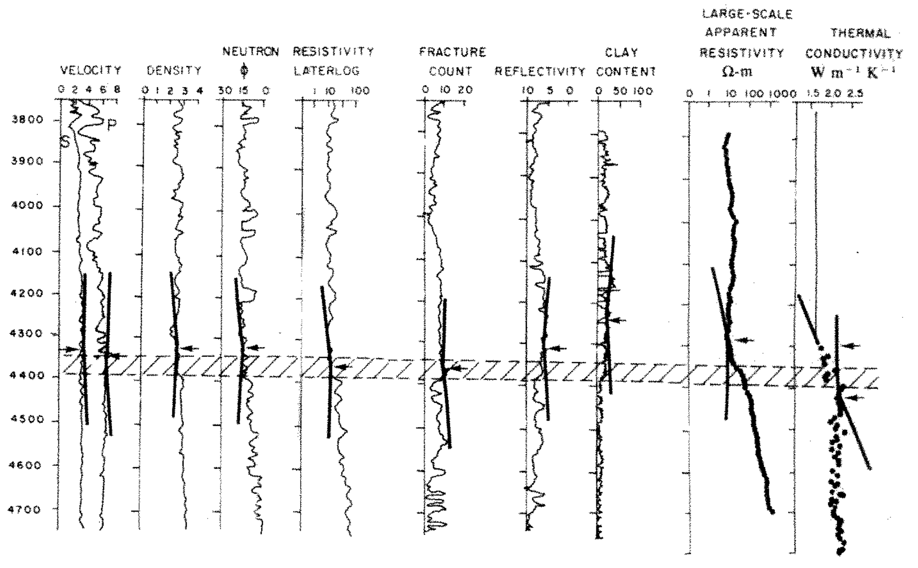

Geophysical logs from Leg 83, Hole 504B. Hatched line is base of transition between seismic layers 2B and 2C. Below are predominantly dikes; above pillows. Arrows and solid lines are changes in gradients near this transition. Each log shows this transition. Velocities are from sonic log, density from active-source γ-ray log, fracture count and reflectivity are from Borehole Televiewer log, clay hydroxyl content from a cross-correlation between neutron porosity, which measures porosity plus hydroxyls in formation, and density which measures only porosity. Thermal conductivities are measured from cores on board ship and are the only measurements not done *in situ*.

Scientists aboard D/V Glomar Challenger for Leg 83 were Roger Anderson and Jose Honnorez (Co-Chief Scientists), A.C. Adamson, J.C. Alt, K. Becker, R. Emmerman, P.K. Kempten, H. Kinoshita, C. Laverne, M.J. Mottl, R. Newmark and E. Tual.

0028-0836/82/070549-02$01.00

drawing ocean bottom water downwards into the oceanic crust, but at a slower rate — $1,500\ \mathrm{l\ h^{-1}}$ compared with $6,000\ \mathrm{l\ h^{-1}}$. In the two year period, 50×10^6 kg of sea water have been drawn into the crust.

An apparent discrepancy between the Leg 83 findings and the ophiolite model did turn up, however. According to the literature ophiolite rocks appear to have generally re-equilibrated under increasing temperature metamorphic facies, Leg 83 basalts display only partial recrystallization, showing they have not reached equilibrium. Also Leg 83 rocks do not grade with increasing depth into increasingly higher-temperature facies. Some of the minerals of lowest-temperature alteration and the least altered rocks were found in the middle cores of the dikes complex.

The sequence of alteration has not yet been resolved by analysis on board the *Challenger*. Recovered rocks show the effects of at least two stages of alteration: a greenschist facies (hotter) event depositing actinolite, chlorite and epidote into veins and actinolite, chlorite, sphene and albite throughout the rock matrix, and a zeolite facies (lower temperature) event, characterized by laumontite, epidote, chlorite and smectite. Anhydrite seems to occur with both facies mineral pargenesis in veins and appears to be a late forming mineral. It is not clear whether the stockwork metallogenesis belongs with the hotter or the cooler event. The question still unresolved is whether both events took place at the ridge axis or whether the cooler event is occurring now on the flank of the ridge. Significantly, water in formation pores has the composition predicted to be in equilibrium with currently occurring alteration in the rock. Formation waters therefore do not reflect the greenschist facies (hot) type of event.

This is an important geophysical issue as well, for the plumbing system of the dikes and lower pillows is clearly plugged up by alteration, whereas the top of the crust (layer 2A) is obviously open to aquifer-type flow. Closer to the ridge, was layer 2A thicker and convection more pervasive? Or has convection — even at the ridge axis — always been limited to the upper 500 m of the oceanic crust now at Hole 504B?

Shore-based analysis of Leg 83 results promises much excitement. In any event, the myth of not being able to drill deep in the oceanic crust has been proved to be just that. Leg 83 left Hole 504B clean and ready for even deeper drilling on a possible future leg — layer 3 or bust! ☐

Ocean floor conductivity measured

from T.J.G. Francis

A WIDE range of electrical methods has been used for several decades over land to measure the conductivity of the underlying rocks. But whereas the study of the electrical properties of rocks has become the most important method of geophysical exploration for metal ore bodies, the application of these techniques to the sea bed, even in the shallow waters of continental shelves, has been severely restricted by the high conductivity of seawater. Much effort has been directed to getting round this difficulty and in *Geophysical Research Letters*, P.D. Young and C.S. Cox have now described an active-source electromagnetic sounding experiment carried out on the ocean floor[1]. The technique offers new possibilities for studying the geology of the oceanic crust.

Magnetotelluric sounding, in which the horizontal magnetic and electric fields of naturally occurring electromagnetic signals are observed, has been carried out on the ocean floor since 1965 (ref.2). The conductivity of the ocean eliminates frequencies above about 10 c.p.h. (0.003 Hz) however, so that the method is suitable only for studying the conductivity of the mantle on a scale of hundreds of kilometres and is thus insensitive to the conductivity structure of the crust and uppermost mantle. Using an array towed at the sea surface behind a ship to measure the resistivity of the sea bed on the continental shelf[3], it has been possible to distinguish between unconsolidated sediments and hard rock and to detect the presence of a sulphide ore body, but this method is not thought practicable in oceanic depths.

In the novel active-source electromagnetic sounding experiment of Young and Cox[1], low-frequency signals of 0.25–2.25 Hz were detected at a range of 19 km close to the axis of the East Pacific Rise at 21°N. The transmitting antenna, lowered from a ship, consisted of an 800 m long insulated wire through the ends of which 70 A peak alternating current was passed into the sea. The freely deployed receiver measured the electric field at two 9 m long crossed antennas and at the end of the experiment floated back to the surface for recovery. The observations have been modelled to yield a conductivity structure of the crust and upper mantle to a depth of 30 km beneath the sea floor.

The important thing about the work of Young and Cox is not so much their results, fascinating though they are, as the potential which the technique may have for future studies of the geology of the ocean floor. Our present knowledge of the deeper geological structure of the ocean crust has been obtained largely by seismic methods. Reflection methods have told us most about the structure of the sedimentary layers and refraction about the underlying basement. However, the translation of velocity structures into geology is ambiguous and compressional wave velocities are insensitive to many of the properties of the ocean crust which now interest earth scientists. By contrast, the electrical conductivity of a rock is extremely sensitive to the presence of cracks filled with seawater, to even smaller amounts of partial melting and to the presence of sulphide ore minerals. All have the capacity to increase the conductivity of a rock by two or more orders of magnitude.

The extent to which seawater penetrates newly formed oceanic crust has been a subject of considerable interest ever since it was first demonstrated by Lister a decade ago[4]. Now Young and Cox have demonstrated that close to the East Pacific Rise, the high-conductivity ($0.1\ \mathrm{S\ m^{-1}}$) basalts penetrated with seawater are no more than 1.4 km thick. This result has already received support from large-scale resistivity measurements made on Leg 83 of the Deep-Sea Drilling Project in Hole 504B on the Costa Rica Rift[5] (see previous article). Seawater may penetrate much more deeply into the crust of slowly spreading ridges and active-source electromagnetic sounding is probably the best method for measuring it.

This technique may also provide the means of finding magma chambers beneath the axes of mid-oceanic ridges. The existence of such magma chambers has long been postulated, but finding them has proved difficult, particularly on slowly spreading ridges where seismic refraction experiments have produced negative results[6].

Finally, sulphide ore bodies are now thought to exist in the upper levels of the oceanic crust at a frequency of one ore body of horizontal area 0.1 km^2 per 20 km^2 (ref.7). Attempting to find such ore bodies by drilling would be futile, since on the average it would take 200 holes to discover one ore body. Deep penetration logging of the bore holes could improve these odds, but only by a factor of about four. Active-source electromagnetic sounding is certainly the best available means of finding such bodies once they have become buried by pillow lavas and sediment.

Thus Young and Cox have demonstrated a technique which, if widely deployed, possibly using other frequencies and source–receiver configurations, could provide answers to many of the problems which have eluded solution by more conventional marine geophysical techniques. ☐

T.J.G. Francis is Head of Geophysics at the Institute of Oceanographic Sciences, Wormley, Godalming, Surrey GU8 5UB.

1. Young, P.D. & Cox, C.S. *Geophys. Res. Lett.* **8**, 1043 (1981).
2. Filloux, J.H. *Nature* **269**, 297 (1977).
3. Francis, T.J.G. *Rep. Inst. geol. Sci.* No. **77/4** (1977).
4. Lister, C.R.B. *Geophys. J.R. astr. Soc.* **26**, 515 (1972).
5. Becker, K. Personal communication (1982).
6. Fowler, C.M.R. *Geophys. J.R. astr. Soc.* **47**, 459 (1976).
7. Cann, J.R. *J. geol. Soc. Lond.* **137**, 381 (1980).

0028-0836/82/070550-01$01.00

Fifty years of substance P

from T.M. Jessell

SUBSTANCE P, the doyen of the common peptides[1], is now 50 years old and on the verge of achieving respectability as a neurotransmitter. Yet by comparison with many other peptides of inferior pedigree, the physiological functions of substance P have remained obscure. Some of the reasons for the slow progress are easy to find. Although many of the peripheral actions and chemical properties were established by von Euler and Gaddum, it took 40 years before substance P was eventually isolated and its amino acid sequence determined. But even with the availability of synthetic material, advances in the chemistry of substance P have been disappointingly slow. Simple modifications in the native amino acid sequence did not immediately generate receptor antagonists or more potent agonists. More fundamental perhaps, the behaviour elicited by the central or peripheral application of substance P has been less easily interpretable than, for example, the elevation of pain threshold associated with administration of opioid peptides or the modification of feeding and drinking behaviour elicited by cholecystokinin and angiotensin.

At a recent CIBA Foundation symposium* there were encouraging signs that some of these obstacles have been, or are about to be, overcome. In particular, it is now apparent that modifications of the C-terminal sequence of substance P can generate receptor antagonists, stable agonists and analogues that are selective for substance P receptor subtypes within the central (CNS) and peripheral nervous systems (see Table 1). By substituting d-amino acids at residues 7 and 9, Rosell (Karolinska Institute) and colleagues have synthesized a peptide analogue that antagonizes the spasmogenic activity of substance P on intestinal smooth muscle and the vasodilatory actions on peripheral vessels. At present, effective blockade of substance P responses can be achieved only at relatively high antagonist concentrations (10^{-5} -10^{-4}M) and partial agonist activity has also been observed in some bioassav systems[2]. However, more potent and specific antagonists can now be anticipated and their availability will undoubtedly prove crucial for evaluating many of the postulated physiological functions of substance P.

Attaching a methyl group to the nitrogen atom in the peptide bonds at residues 8 and 9 and deleting the N-terminal tetrapeptide (Lee, Johns Hopkins Medical School) results in an analogue (termed Di Me C7) which is biologically active and completely resistant to degradation by a membrane-bound endopeptidase that inactivates substance P[3]. Whether the endopeptidase isolated by Lee, or any other enzyme for which substance P can act as a substrate, is actually involved in the inactivation of neuronally released substance P is still unclear. It is conceivable that diffusion alone could effectively terminate the actions of substance P. However, injection of Di Me C7 into the ventral tegmental area of rats (Iversen, University of Cambridge) produces a spectrum of behavioural responses that resembles, but greatly outlasts, the response elicited by substance P itself. The prolonged duration of action of Di Me C7 *in vivo* provides the first indication that substance P-inactivating enzymes may in fact function physiologically.

Comparison of the potency of substance P and its analogues on a battery of different bioassay systems is beginning to generate a pattern of activity which may reflect the existence of at least two subclasses of substance P receptors. The clearest demonstration of this derives from studies with the tachykinins, a family of naturally occurring peptides isolated from amphibian skin, which share a common C-terminal amino acid sequence with substance P[4]. For example, substance P is five times more potent than the tachykinin kassinin as a spasmogen in the guinea pig ileum, but is 100–1,000 times less active than kassinin in potentiating the electrically evoked contraction of the rat vas deferens. Iversen and Hanley (MRC Neurochemical Pharmacology Unit) have now extended this analysis to synthetic substance P analogues, including the methyl ester of substance P, which is 10,000 times less active than kassinin on the rat vas deferens but equipotent on the guinea pig ileum[5]. Iversen and Hanley have consequently introduced the terminology SP-P and SP-E receptors to represent these two extremes of biological activity. SP-P receptors predominate in the guinea pig ileum and exhibit greatest selectivity for the methyl ester of substance P and the tachykinin physalaemin. SP-E receptors are present in the rat vas deferens and are activated most potently by the tachykinins eledoisin and kassinin. Synthetic substance P analogues exhibiting specificity for CNS receptors may also exist. Iversen reported that extension of the C-terminal amide group produces an analogue that is ten times more potent than substance P itself in displacing ^{3}H-labelled substance P binding to rat brain membranes but has only one-thousandth its potency on peripheral bioassay systems (Table 1).

The existence of mammalian receptor subtypes that exhibit selectivity for peptides of amphibian or arthropod origin raises the possibility that similar tachykinins may also exist in mammalian species. In fact, Lazarus *et al.* have recently reported low amounts of physalaemin-like peptide in rat brain and intestine[6]. In addition, Keen (University of Bristol) has observed that rat dorsal root ganglia incubated with ^{35}S-methionine can synthesize authentic substance P and also a peptide that is immunoprecipitated by C-terminal- but not N-terminal-specific anti-substance P antisera[7]. Although the identity of this peptide is unknown, these findings suggest that there may be a second

T.M. Jessell is in the Department of Neurobiology, Harvard Medical School, 25 Shattuck Street, Boston, Massachusetts 02115.

---

*CIBA Foundation Symposium no.91 'Substance P in the Nervous System', organized by Dr Ruth Porter and chaired by Sir Arnold Burgen, was held at the CIBA Foundation 30 November — 3 December 1981 and followed by a one day meeting organized by the Centre for Neuroscience at University College London.

---

100 years ago

NOTES ABOUT SNAKES

A serpent's first instinctive impulse of self-preservation, like that of every other animal, lies in escape; probably a more nervous creature does not exist. If surprised suddenly, or brought to bay at close quarters, it may be too terror-stricken to attempt flight; then it *bites*, following a curious general rule which seems to obtain throughout nearly the whole animal world, from a passionate child downward, no matter what the natural weapons of offence may be. Young *Felidæ* will keep their talons sheathed until they have exterted all possible force with their soft milk-teeth, and a lizard will seize the hand which restrains it with its insignificant little jaws, when its tail or claws might inflict far more injury. The *Boidæ* never use their constrictive powers in self-defence (unless they are gripped), and it seems probable that if a venomous snake's fangs lay in its tail, it would use its teeth *first* when attacked before bringing them into play.

I was walking in the Botanical Gardens of Rio de Janeiro some time ago, when I found myself literally upon an immense green tree-snake, at least nine or ten feet long. This serpent, of course, was harmless, so that there would have been no danger in grasping it; but it emitted a curious sound in its terror, such as I have never heard before or since. It *screamed*, and so loudly, that some people near, who saw nothing of what was going on, thought they heard a child cry. Serpants make all sorts of noises besides hissing, according to their different kinds; Crotali spring their rattles; the carpet-viper (*Echis carinata*) rubs the imbricated scales of its adjacent coils together; the fer-de-lance (*Trigonocephalus lanceolatus*) is said in St. Lucia to give out a series of little taps with its horny extremity; and many others — such as the rat-snake (*Spilotes variabilis*) of South America — certainly indicate their presence when angry by quivering their tails against the ground; but a crying snake would have been a decided novelty in one's collection.

ARTHUR STRADLING

From *Nature* **25**, 16 February, 377, 1882.

0028-0836/82/070551 03$01.00

tachykinin-like peptide within primary sensory neurones. The presence in mammalian species of peptides that may be structurally related to substance P once again emphasizes the need for caution in interpreting immunoassay and immunocytochemical data and justifies the use of such caveats as 'radioimmunoassayable substance P-like immunoreactivity'.

The availability of stable and selective agonists and antagonists is likely to reinforce the existing evidence that substance P is a neurotransmitter in some mammalian sympathetic ganglia. A series of elegant experiments have been performed on the guinea pig inferior mesenteric ganglion (Otsuka, Tokyo Medical and Dental University). In this preparation the organization of preganglionic inputs makes it possible to elicit a pure cholinergic excitatory postsynaptic potential (e.p.s.p.) in postganglionic neurones, by stimulation of preganglionic fibres in the ventral root, whereas stimulation of the dorsal root produces only a slow, non-cholinergic e.p.s.p. (see the figure). Otsuka has shown that the depolarization and changes of membrane resistance that accompany the slow e.p.s.p. can be mimicked by application of substance P[8]. Ultrastructural studies (Cuello, University of Oxford) demonstrated that substance P-immunoreactive fibres in the inferior mesenteric ganglion exhibit classical synaptic specializations at their contacts with the sympathetic neurones. Moreover, there is convincing evidence that these substance P terminals are almost exclusively sensory in origin. When the fluorescent dye, true blue, was injected into the inferior mesenteric ganglion (Höfelt, Karolinska Institute) it was transported retrogradely to sensory neurone cell bodies in the dorsal root ganglion that also contain substance P[9]. The sensory nature of the intraganglionic substance P fibres has been confirmed by Otsuka in electrophysiological studies. Application of capsaicin, which is thought to act selectively on sensory neurones, elicits a slow depolarization of post-ganglionic neurones that is probably mediated by the release of substance P from sensory endings in the ganglion. Furthermore, prolonged application of capsaicin abolishes the non-cholinergic slow e.p.s.p. but does not affect the cholinergic potential or the response to bath application of substance P.

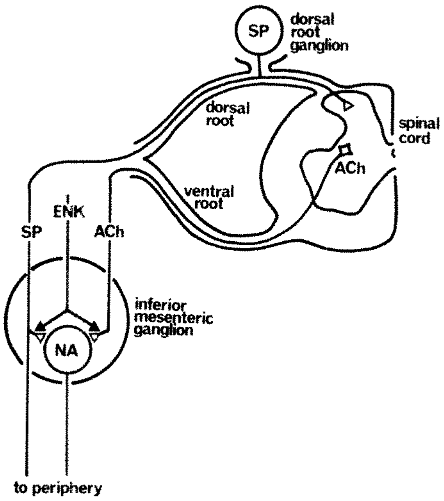

Diagram showing the organization of substance P (SP), acetylcholine (ACh) and enkephalin (ENK) inputs to the guinea pig inferior mesenteric ganglion. Details are given in refs. 8 and 9.

Otsuka also presented evidence that both the fast cholinergic e.p.s.p. and the non-cholinergic slow e.p.s.p. are depressed presynaptically by opioid peptides and that the release of substance P from the ganglion is suppressed by enkephalin[8]. The pharmacological properties of substance P-containing sensory collaterals within the inferior mesenteric ganglion are therefore remarkably similar to those of central sensory terminals in the dorsal horn of the spinal cord, which are also sensitive to capsaicin and opiates. Whether the peripheral processes of the same sensory neurones, which Lembeck (University of Graz) and others reported to be sensitive to capsaicin also respond to opiates is not known.

While substance P in the guinea pig inferior mesenteric ganglion clearly derives from sensory ganglia, the origin of substance P in the rat superior cervical ganglion may be quite different (Black, Cornell University Medical College). When the superior cervical ganglion (SCG) from neonatal rats is removed and maintained in explant culture there is a rapid and dramatic increase in substance P levels within the ganglion[10]. Under these conditions many principal sympathetic neurones exhibit substance P-like immunofluorescence. This is in contrast to the innervated adult SCG where only immunoreactive fibres can be observed, and these are of unknown origin. The increase in ganglionic substance P content in explant culture can be prevented by veratridine, which presumably depolarizes the neurones and releases substance P. Black has, therefore, proposed that in addition to the well established activity-dependent regulation of adrenergic activity in sympathetic ganglia, the peptide content of sympathetic neurones may be modified by activity. However, since decentralization of the SCG *in vivo* results in a very much smaller increase in substance P, other factors must contribute to the enormous increase observed after explantation of immature ganglia.

If substance P can act as a transmitter of slow potentials at synapses formed by sensory terminals in the inferior mesenteric ganglion it may be reasonable to anticipate a similar role for substance P at the central terminals of the same neurones in the dorsal horn. Excitation of dorsal horn neurones following iontophoretic application of substance P (Henry, McGill University) is of a similar duration to that observed by Otsuka in sympathetic ganglia. In a more accessible preparation of spinal neurones in culture, a slow depolarization in response to substance P occurs that may result from a decrease in potassium conductance[11]. While substance P is present in and released from the central terminals of primary afferents in the superficial dorsal horn, physiological evidence

Table 1 Chemical modifications in substance P structure and consequent changes in biological activity

	N-terminal									C-terminal			
	1	2	3	4	5	6	7	8	9	10	11		Reference
Substance P	ARG -	PRO -	LYS -	PRO -	GLN -	GLN -	PHE -	PHE -	GLY -	LEU -	MET -	NH_2	
Antagonist	.	**D**-PRO	.	.	.	.	**D**-TRYP	.	**D**-TRYP	.	.	.	2
Stable agonist					< GLU	.	.	$N-CH_3$ PHE	$N-CH_3$ GLY	.	.	.	3
SP-P agonist	.	.	.	.	.	.	.	.	.	.	.	$COOCH_3$	4
SP-E agonist (kassinin)	ASP - VAL	.	.	SER - ASP		.	.	VAL	.	.	.	.	4,5
CNS agonist	.	.	.	.	.	.	.	.	.	.	.	$NH(CH_2)_2NH_3^+$	4

for a sensory transmitter role for substance P has been more difficult to obtain. In fact, the lack of change in C fibre-evoked responses of dorsal horn neurones, after substance P depletion induced by peripheral nerve section, led Wall (University College, London) to question the entire concept that substance P might be a sensory transmitter[12]. Although it seems clear that substance P does decrease substantially in central sensory terminals after peripheral nerve lesions with little immediate change in response to C fibre input, it is not known whether enough substance P remains in the central terminals to maintain a small but releasable pool that is sufficient to exert a postsynaptic action. Given the relatively slow time course of action of substance P on sympathetic and spinal neurones, any depletion of substance P probably leads to gradual and prolonged changes in the excitability of dorsal horn neurones that might be difficult to detect with extracellular recording techniques. Furthermore, as somatostatin will probably also be depleted by peripheral nerve section and inhibits those dorsal horn neurones that are excited by substance P, the net change in postsynaptic response may be even more subtle. It is, however, important to emphasize that the evidence in favour of substance P as an afferent transmitter in the dorsal horn is still tenuous — although at present there are no compelling suggestions for alternative roles. By analogy with the inferior mesenteric ganglion, it is possible that substance P acts on dorsal horn neurones that also receive input from primary afferents releasing a more rapidly acting sensory transmitter. Once again, an effective receptor antagonist would go some way to resolving these problems.

Finally, in any symposium devoted to a single peptide, there is the danger of becoming a little myopic. Recent immunocytochemical studies on the retina and on enteric neurones, for example, have revealed that substance P is found in only about 10 per cent of the total population of peptide-containing neurones, in similar or the same classes of cell that are often functionally indistinguishable. In these systems the appreciation of a specific function for substance P may still be some way off. It is more encouraging to reflect that many of the chemical probes necessary for analysing substance P system will at least be available by that time. □

1. Pearse, A.G.E. in *Centrally Acting Peptides* (ed. Hughes, J.) 49 (Macmillan, London, 1978).
2. Leander, S. *et al. Nature* 294, 467 (1981).
3. Sandberg, B.E. *et al. Eur. J. Biochem.* 114, 329 (1981).
4. Erspamer, V. *Trends in Neurosci.* 4, 267 (1981).
5. Iversen, L.L. *et al. Br. J. Pharmac.* (in the press).
6. Lazarus, L.H. *et al. Nature* 287, 555 (1980).
7. Harmar, A, Schofield, J.G. & Keen, P. *Neuroscience* 6, 1917 (1981).
8. Konishi, S. *et al. Biomed. Res.* 1, 528 (1980).
9. Dalsgaard, C.J. *et al. Soc. Neurosci. Abstr.*, 101 (1981).
10. Kessler, J.A. *et al. Science* 214, 335 (1981).
11. MacDonald, R.L. & Nowak, L.M. *Adv. Biochem. Psychopharmac.* 28, 159 (1981).
12. Wall, P.D., Fitzgerald, M. & Gibson, S.J. *Neuroscience* 6, 2205 (1981).

The unregenerate nervous system

from Miranda Robertson

CUT the optic nerve of a frog, or the spinal cord of a fish, and within weeks the frog will see and the fish will swim again; the same lesions in a man will cause irreversible blindness and paraplegia. Must man, in common with other mammals, accept the loss, or can the regenerative capacity of his central neurones be reawakened? This question was the chief common focus of participants at a recent meeting in Berlin*, where neurobiologists discussed with clinical neurologists individual interests ranging from the control of development in intact invertebrate nervous systems to the control of oedema in damaged human ones.

The central problems have not changed since the time of Cajal, who in the 1920s clearly perceived that the two prerequisites for effective repair in the central nervous system of higher vertebrates were signals for axon growth and signals for axon guidance, both apparently lost at maturity. In this the mammalian central nervous system differs not only from the central nervous system of lower vertebrates, but from the mammalian peripheral nervous system, in which cut nerves do regrow. The question is, why? Interest very early focused on the differences between central and peripheral glial cells: whereas peripheral glia tend to form a tunnel through which a growing axon may extend, central glia at the site of a lesion form an apparently impenetrable scar. This observation led Tello, working in Cajal's laboratory in 1911, to test the effect of inserting a segment of sciatic nerve containing healthy proliferating glia into a deep incision in the cerebral cortex of a rabbit. This procedure induced vigorous sprouting of the ordinarily recalcitrant central neurones into the grafted nerve, even across glial scar tissue of central origin[1].

The excitement evidently felt by Cajal at this discovery found an echo 70 years later in Berlin, where A. Aguayo (Montreal General Hospital) aroused considerable interest with reports of his own recent work, identical in principle with Tello's but with some important technical refinements. Foremost of these has been the use of horseradish peroxidase to establish unequivocally the central origin of the regenerating fibres, and thus eliminate the possibility — later raised in connection with Tello's results — that they derived from the sympathetic nerves innervating cerebral blood vessels. Aguayo and his colleagues have thus been able to show that grafts of sciatic nerve in spinal cord[2], brainstem[3] and cortex[4] can induce sprouting of adult neurones for up to 2 cm, which is probably more than most central axons ever attain in normal development. The importance of this finding, as Cajal recognized, is that it clearly shows that the capacity for axon growth is not irretrievably lost in differentiated central neurones, and that the behaviour of adult neurones, like that of embryonic ones, may still be influenced by their environment.

Indeed, the identification of the environmental tropic factors that determine the developmental fate of neurones has become one of the major preoccupations of neurobiology. So far, the only factor to have been purified and characterized is nerve growth factor (NGF), which is required for the growth and development of sensory and sympathetic neurones and has been implicated in the regeneration of some nerves[5]. It has, however, proved technically difficult to demonstrate NGF in the nervous system, although the presence of specific NGF receptors has been shown on several types of neurone (H. Theonen, Max-Planck-Institut, Martinsreid).

It is notorious that NGF would probably have remained undiscovered to this day but for the series of lucky accidents and inspired guesswork that led R. Levi-Montalcini to the male mouse salivary gland which, for reasons that are still entirely opaque, is full of it. In the absence of an equivalent fortuitous source, it should not be surprising that other factors, identified through their effects on cultured cells, have remained largely elusive. A new one, which may have some bearing on the influence of the glial environment, has been discovered by Thoenen in a crude extract of pig brain. It seems to be a basic protein with two interesting effects on dorsal root ganglion cells *in vitro*: it enhances their survival, and it substantially reduces their ability to bind NGF. The glial origin of the factor is inferred from the correlation between the proportion of glial tissue in the brain and the relative amount of factor that can be extracted from it. The existence of a factor that enhances neuronal survival could clearly be of considerable interest, particularly since it is specific for a subpopulation of cells whose survival is not enhanced by NGF. But it is not yet known whether it acts *in vivo*.

The effect of the factor on NGF receptors may be of even greater interest: it is still not clear how far changes in neuronal behaviour with maturity are due to the disappearance of growth signals, and how far to the loss of receptors for the signalling molecules. While it has now been shown that adult central axons can be induced to

---

Miranda Robertson is associate editor of Nature.

0028-0836/82/070553-02$01.00

grow, it has not yet been demonstrated that they can be guided to the appropriate targets, and it remains possible that those factors that drive them to terminal differentiation also blind them for ever to the signals that directed their earlier growth.

To unleash the extension of such undirected axons would, as Aguayo acknowledged and R.W. Gilliatt (Institute of Neurology, London) repeatedly emphasized, be to invite consequences far more hideous than paraplegia. Gilliatt's experience is with peripheral nerve injuries. Although peripheral nerves regrow, they seldom do so perfectly: a patient with damage to the brachial plexus in the shoulder, for example, will never regain the full use of his hand. And even where the damage is more limited, aberrant reinnervation — or worse, correct reinnervation accompanied by aberrant collateral innervation — may cause pain and malfunction more serious than the original loss. Hence the need to know not only what induces the growth of fibres but what guides them to their targets and determines what they do when they arrive.

The most resplendent example of functional reinnervation after injury is probably that of the amphibian optic nerve, which is able to regenerate to a topologically precise array of connections on the optic tectum. If such precise reconnection can be induced in a frog, might if not in principle be inducible in man? E. Frank (Harvard University) argued that the limiting factor might be size: morphogenetic signals that can operate efficiently in embryos and frogs might have too short a range to work properly in adult man. But while this is a perfectly reasonable supposition, it is quite inadequate to account for the differences in the regenerative capacities of different species. Mice, which are tiny, are as badly off as we are, whereas bullfrogs (S.S. Easter, University of Michigan, pointed out), can be enormous but can still re-establish accurate connections.

In fact, it is becoming increasingly clear that there can be profound differences in the morphogenetic flexibility even of the embryos of different species. These differences first came to light as discrepancies in the data on the specification of retino-tectal connections in chicks on the one hand and amphibia on the other. Broadly speaking, if the eye of a frog or a kitten is damaged early enough, nerve fibres from the undamaged tissue will spread out to innervate the vacant space. In chicks, however, no such adjustment takes place; the space remains vacant and the denervated neurones die. More recent data, reported by J.K.S. Jansen (University of Oslo), provide further evidence that this reflects a real difference in the developmental plasticity of the different species. Jansen has tested the monosynaptic reflexes of chicks after removal of a small segment of the neural crest that supplies the sensory component of the reflex, and finds permanent sensory denervation of the target muscle[6].

In an equivalent experiment on the developing frog, Frank removed the single dorsal root ganglion that supplies the sensory innervation of the forelimb, and found by contrast that the mature frog had normal monosynaptic reflexes. He also found that the ganglion adjacent to the ablated one was enlarged, and concluded that sensory neurones in the enlarged ganglion had established both the central and the peripheral connections appropriate to the forelimb[7]. Plainly the larval frog nervous system retains a plasticity that is lost at a much earlier stage of development in the chick.

There may, however, be insuperable obstacles to the recapitulation of the processes leading to functional reinnervation in a similarly damaged adult. The obstacles lie in the probable mechanisms of developmental specificity. Frank, for example, offers two explanations for his results. One possibility is that the enlarged ganglion at the time of the lesion still contains undetermined cells which proliferate and adopt the specification of the missing cells. The other is that cells with the appropriate specification were already present in the ganglion, where they would ordinarily have been eliminated in competition with the existing correct ganglion cells. In either case, the replacement cells would no longer be available in an adult.

There is already evidence in other systems that specificity of neuronal connections is brought about by competitive and other interactions between cells whose initial specification may be relatively coarse and graded rather than precise and discrete. One case in point seems to be the specification of the spinal nerves innervating the sympathetic ganglia of guinea pigs[8]. Thoracic or lumbar ganglia transplanted into the normal site of the superior cervical ganglion will attract innervation from a far higher proportion of more caudal roots than would normally innervate cells at the level of the superior cervical ganglion. J.R. Sanes (Washington University) has recently shown a similar gradient in the reinnervation of intercostal muscle transplanted from two different levels of the thorax to the level of the superior cervical ganglion: while both grafts attracted a broad spectrum of innervation, the main source was significantly more caudal for the more caudal graft.

The gradients of overlapping specificities implicit in these results, however, are seldom characteristic of the innervation pattern of nerves at their final destinations. Developing motor nerves arriving at the periphery undergo ruthless pruning that involves the death of some cells and the withdrawal of many terminals; central nerves arriving at the visual cortex of binocular mammals segregate into a pattern of alternating stripes representing the input from the two eyes. In both cases, there is compelling evidence that the patterning depends on activity in the nerves. If all the neuromuscular junctions in a chick embryo are silenced with curare or α-cobra-toxin, the normal process of selective motor neurone death does not occur at the usual time; and conversely, it can be accelerated by electrical stimulation of the limb[10]. In the visual cortex, the segregation of the inputs from the two eyes fails if the optic nerves are silenced with tetrodotoxin[11]. Exactly how activity determines the pattern of connections is not known; but plainly where cell death is involved it is unlikely that regeneration will be capable of reproducing the specificity of the original. (On the other hand, a regenerating peripheral nerve may have the advantage of indelible footprints left by its predecessor. In particular, the Schwann cell sheath round the distal stump of a severed axon may guide the regenerating fibre in the general direction of its target, and there is now a great deal of evidence that the re-establishment of neuromuscular junctions is directed by molecules inserted in the basal lamina of the muscle at the site of the synapse[12].)

In general, however, if cell death is a part of development then cell growth may be a necessary part of perfect regeneration. It is probably significant that in those species in which central nerves regenerate, the neural tissues continue to grow in adult life. The retina of the frog and fish, for example, continue to recruit new cells indefinitely. It may also be significant that animals whose central nervous systems regenerate never make very sophisticated use of them. If a frog's eye is inverted before it is allowed to rejoin to the tectum, the frog never learns to adjust to the rotated image. A man, similarly handicapped by means of inverting lenses, can — at least up to a point. Possibly the loss of developmental plasticity is the price mammals have paid for the synaptic plasticity that enables us to learn. Why such a loss should be the concomitant of an increase in synaptic plasticity, however, we shall be unable to guess at until we understand learning. In the meantime, we are left with Cajal's verdict of more than half a century ago: ". . . in adult centres the nerve paths are something fixed, ended, immutable. Everything may die, nothing may be regenerated. It is for the science of the future to change, if possible, this harsh decree." □

---

1. Cajal, R. *Degeneration and Regeneration of the Nervous System*, 738 (Oxford University Press, 1928).
2. Richardson, D.M. McGuinness, U.M. & Aguayo, A.J. *Nature* **284**, 264 (1980).
3. David, S. & Aguayo, A.J. *Science* **214**, 931 (1981)
4. Aguayo, A.J. & Benfy, M. *Nature* (in the press).
5. Turner, J.E. Delaney, M.K. & Johnson, J.E. *Brain Res.* **204**, 283 (1981).
6. Eide, A.L. Jansen, J.K.S. & Ribchester, R.R. *J. Physiol. Lond.* (in the press).
7. Frank, E. & Westerfield, M. *J. Physiol.* (in the press).
8. Purves, D. Thompson, W. & Yip, J.W. *J. Physiol. Lond.* **313**, 49 (1981).
9. Pitman, R. & Oppenheim, R.W. *Nature* **271**, 364 (1978)
10. Oppenheim, R.W. & Minnez, R. *Nature* (in the press).
11. Stryker, M. *Neurosci. Abstr.* **7**, 842 (1981).
12. Sanes, J.R. Marshall, L.M. & McMahan, U.J. *J. Cell Biol.* **78**, 176 (1978).

0028-0836/82/070554-02$01.00

What role for autologous marrow transplantation in cancer therapy?

from Rainer Storb

Toxicity to the marrow is a serious limitation of cancer therapy due to the vulnerability of the rapidly dividing haematopoietic stem cells to the anti-cancer agents. Higher — and potentially curative — doses of chemoradiotherapy may be possible when they are given in conjunction with replacement of the marrow by transplantation. However, because the donor marrow must be free of all tumour cells the graft has had to come from a separate, healthy individual — raising all the problems of immunological compatibility and restricting treatment to those with suitable donors, either an identical twin or a histocompatible sibling. A way round this restriction would be possible if marrow could be taken from the affected individual before chemoradio therapy and cleared of tumour cells without destroying the haematopoietic cells. In this issue of *Nature* Krolick and his colleagues report some preliminary successes in mice using an antibody–toxin conjugate to purge marrow of tumour cells.

In general, for marrow grafting to be effective, two requirements must be fulfilled. First, tumours must be responsive to a short burst of high-dose therapy. Candidate tumours are leukemias and lymphomas, oat cell carcinoma of the lung, carcinoma of the breast, testis and ovary, soft-tissue sarcomas and pediatric malignancies such as neuroblastoma and Wilm's tumour. Second, as pointed out above, the infused marrow must be free of clonogenic tumour, for otherwise, tumour would recur from cells transferred with the marrow even when the body burden of tumour has been eradicated.

Much has been learned about tumour responsiveness from aggressive high-dose chemoradiotherapy of haematological malignancies using 'rescue' with healthy marrow either from an identical twin — a syngeneic graft — or from a sibling identical at the major histocompatibility complex — an HLA-identical allogeneic graft[1-5]. Success has been most impressive in patients with acute nonlymphoblastic leukaemia (ANL) grafted in first remission, with a long-term disease-free survival rate of 55–60 per cent and relapse rates of 10 per cent after allogeneic grafts. The survival rate in patients with ANL grafted in relapse or second remission has been 25 per cent, with a relapse rate of 50 per cent. These rates compare with a survival rate of 20 per cent and a relapse rate of 70–80 per cent in patients with acute lymphoblastic leukaemia (ALL) grafted in relapse or second remission. Results in non-Hodgkin's lymphoma are limited, but perhaps 50 per cent disease-free survival can be achieved. Relapse rates were significantly lower after allogeneic than after syngeneic grafts, perhaps because graft-versus-host disease contributed an antileukaemic effect[6]. Relapses originated almost exclusively in cells of host origin. Clearly, the problem of eradicating leukaemia has not yet been solved.

Nevertheless, the relative success of syngeneic and allogeneic marrow transplantation and the availability of effective cryopreservation techniques have stimulated research in autologous transplantation[7] — transplantation of bone marrow within the individual. The major limitation in syngeneic and allogeneic transplantation is that only 25–40 per cent of all patients have suitable donors. The use of autologous marrow would extend high-dose therapy to larger groups of patients and avoid graft-versus-host disease.

To achieve results with autologous marrow grafting comparable to those with syngeneic or allogeneic grafts the marrow must be cleaned of contaminating tumour cells without destroying haematopoietic stem cells. A number of laboratories have shown that this can be accomplished in certain rodent tumours using *in vitro* treatment with cytotoxic drugs or immune reagents. The latter have usually been absorbed antisera from a different species cytotoxic to the tumour but not to haematopoietic stem cells. In most experiments, haematopoietic cells were first contaminated with syngeneic tumour cells and then incubated with antibody and complement before infusion into a lethally irradiated syngeneic recipient. Successful elimination of murine T cell AKR/J leukaemia and of, 6C3HED lymphoma with haematological restoration of the recipients have been reported[8,9]. Initial attempts have been described to apply *in vitro* treatment with antibody and complement to autologous human marrow grafts for common ALL[10].

Unfortunately, cell killing by antibody and complement is incomplete, and 5–10 per cent of tumour cells can be predicted to survive. Moreover, the quality of complement is variable. These problems with the conventional antibody plus complement approach emphasize the importance of the report by Krolick *et al.* (p.604) on the selective killing of leukaemia cells of the murine B-cell tumour, BCL$_1$, by antibody–toxin conjugates. They have treated $1\text{–}10 \times 10^5$ spleen cells from mice-bearing BCL$_1$, 80 per cent of which were estimated to be tumour cells, with rabbit anti-mouse immunoglobulin antibody coupled with the A chain of the natural toxin ricin. From studies of cell transfers, they conclude that less than ten viable tumour cells remain in the spleen cell inocula. They then showed that antibody–ricin treatment could be used to 'purge' marrow from BCL$_1$ tumour cells. Transplanted mice observed for 6 weeks did not show tumour although haematopoiesis was restored.

Encouraging as these results are, they must be interpreted with caution. First, the observation period of six weeks is short not only by human but also by murine standards. Leukaemic relapse has been seen as late as three and a half years after allogeneic human marrow grafting. Second, as the authors themselves point out, the BCL$_1$ tumour consists almost entirely of cells expressing surface immunoglobulin and does not possess a major pre-B cell component, a quality perhaps not shared by human leukaemias.

Experimental animal tumours may be more mature because they are often perpetuated by way of passaging. In contrast, spontaneous human leukaemias may originate from stem cells closely resembling normal haematopoietic stem cells and not expressing the differentiation antigens characteristic of their leukaemic progeny. Indeed, studies using the marker glucose-6-phosphate dehydrogenase have suggested that ANL may involve stem cells capable of differentiating into granulocytes–monocytes, platelets and erythrocytes[11]. Thus, despite complete removal of recognizable leukaemic cells from a marrow inoculum by antibody–ricin conjugate, leukaemia might recur from infused leukaemic stem cells.

Despite these reservations, clinical studies should be undertaken. Monoclonal and polyvalent antibodies are now available that react with a variety of human tumour cells, including non-T cell ALL, T cell ALL, non-Hodgkin's lymphoma and ANL[12]. The results of syngeneic and allogeneic marrow transplantation will serve as the yardstick by which the potential of autologous transplantation can be measured. ☐

Rainer Storb is at the Fred Hutchinson Cancer Research Center, Seattle, Washington 98104.

1. Thomas, E.D. *et al. New Engl. J. Med.* **301,** 597 (1979).
2. Johnson, F.L. *et al. New Engl. J. Med.* **305,** 846 (1981).
3. Fefer, A. *et al. Blood* **57,** 421 (1981).
4. Appelbaum, F.R. *et al. Blood* **58,** 509 (1981).
5. Thomas, E.D. *et al. New Engl. J. Med.* **292,** 832–895 (1975).
6. Weiden, P.L. *et al. New Engl. J. Med.* **300,** 1068 (1979).
7. Keystone Conf. on Autologous Bone Marrow Transplantation *Expl. Hemat.* **7,** Suppl.5 (1979).
8. Thierfelder, S., Rodt, H. & Netzel, B. *Transplantation* **23,** 459 (1977).
9. Economou, J.S., Shin, H.S., Kaizer, H., Santos, G.W. & Schron, D.S. *Proc. Soc. exp. Biol. Med.* **158,** 449 (1978).
10. Netzel, B., Haas, R.J., Rodt, H., Kolb, H.J. & Thierfelder, S. *Lancet* **i,** 1330 (1980).
11. Fialkow, P.J. *et al. Blood* **57,** 1068 (1981).
12. Ritz, J. & Schlossman, S.F. *Blood* **59,** 1 (1981).

0028-0836/82/070555-01$01.00

Quasars resolved?

from M.G. Edmunds

SOME controversies seem to go on for ever, but the quasar redshift debate must surely soon come to an end. During the past year the arguments for interpreting the redshifts as an indicator of large distances to the quasars have grown stronger, despite a spirited rearguard action by the main champion of a non-cosmological interpretation.

In a recent paper in the *Astrophysical Journal*[1], Arp reports the discovery of several new quasars which lie in directions close to galaxies not very far away in space from our own Galaxy. Arp has maintained that there is evidence for a considerable excess in the number of quasars per unit area of sky around nearby galaxies (as seen from Earth), compared with regions away from obvious galaxies. He has suggested that this supports the idea that quasars are objects ejected by the galaxies, since the conventional 'cosmological' interpretation of redshifts would require an approximately random distribution of quasars on the sky. Arp's latest claim is that around a sample of galaxies which are companions to large nearby spiral galaxies, the observed density of quasars is so high that the probability of the configurations occurring by a chance fluctuation in a random distribution would be an astounding 10^{-17}. If this statistic were right, a cosmological interpretation would be very hard to justify — but the estimate does not stand up to closer examination.

Arp has performed a useful survey in looking at some 34 areas of sky and, although it is unfortunate that he does not give details of the exact area searched in each case, we may use his results to discuss the statistical significance of association. His analysis is to assign a probability of occurrence individually to each association he finds, and then combine these together to obtain an overall likelihood. A rather simpler (and probably preferable) approach is to ask what the expected number of associations would be, given a random distribution and a search of the 34 areas, and compare this with the observed numbers. In his analysed sample Arp finds 13 quasars at an angle of less than 300 arc s from the 34 companion galaxies, and all the quasars are brighter than about 20th magnitude on his magnitude scale. If we assume the search for these objects is complete out to at least 300 s, then if there are on average *n* quasars per square degree the expected number within 300 s of any one galaxy will be of order

$$\pi \times \left(\frac{300}{60 \times 60}\right)^2 \times n,$$

and 34 times this for the total of 34 galaxies sampled. The total predicted is thus $0.74n$. The problem comes in the choice of *n*.

Arp initially assumes 10 per square degree down to 20th magnitude, giving a predicted number of 7 against an observed 13, which is perhaps a larger fluctuation than could reasonably be ascribed to chance (although not a fluctuation with as small a chance as 10^{-17}). But it is not obvious that 10 is the correct value to take for *n*. By assuming instead 18 per square degree down to 20th magnitude observed and predicted values can be made to agree, and as emphasized by Véron and Véron[2], a reconsideration of all available data on quasar densities shows that such an assumption is not unreasonable. Osmer[3] found 14 per square degree down to 19.75 magnitude. Véron and Véron suggest that the major problem in the comparison of the various estimates of surface density is the variation of magnitude scales between different observers. Since the observed numbers are a very sensitive function of limiting magnitude, a difference between magnitude estimates propagates very strongly into a difference in surface density. A problem with Arp's statistics is emphasized when he claims that even if *n* were as high as 100, the probability of the associations he observed occuring by change would still be only 10^{-5}, and we note that in this case he should have discovered about 74 quasars within 300 arc s of the galaxies — and indeed the chances of discovering just 13 are very small, but the result would then imply anti-association!

These kinds of statistical argument cannot be considered satisfactory until reasonably large areas of sky have been surveyed completely to a consistent magnitude limit. Arp could fairly argue that most of the quasars he finds are substantially brighter than 20th magnitude (by up to 0.5 magnitude), but again the difficulty arises over variation of magnitude scales — an exactly similar search in 34 areas not centred on companion galaxies would be a useful control sample in setting the relevant (inevitably observer-dependent) value of *n*. Further, neither Arp nor this discussion have taken account of possible enhancement of the surface density of quasars by the brightening of distant quasars by the gravitational lens if the galaxies have massive haloes of stellar mass objects[4].

Strong evidence that most quasars are at the cosmological distances implied by their redshifts has come from the work of two groups, one Canadian[5], the other from the United States and Germany[6]. By definition quasars are 'quasi-stellar' and hence have unresolved circular images on direct photographic plates, although some spatial structure has been recognized in a few cases. What these groups have done is to look carefully at the images of some two dozen low redshift (that is, not too distant) quasars, including the classic 3C273. By scanning both quasars and star images with an accurate measuring machine, they have been able to 'resolve' the quasars by demonstrating that in nearly every case the images of the quasars are more extended than those of stars. The light distribution of these extended images is consistent with their being galaxies — although the data cannot reliably distinguish between the light distribution of a spiral and an elliptical galaxy. Furthermore, the apparent size of the extended image decreases with increasing redshift of the quasar in just the way expected if the underlying galaxies were all of comparable size and the redshift were an indicator of distance.

These results support the idea that what we see as quasars are just the very bright active nuclei of some galaxies. This is not to say that the underlying galaxies are completely normal — the intense radiation source at the centre undoubtedly has some influence on the morphology and evolution of the system. A few of the quasar images are extended into huge jets (as in the case of 3C273) of comparable size to the underlying galaxy — a phenomenon not seen on anything like this scale in normal galaxies — and for a few quasars, the nebulosity around the centre has previously been shown to have the characteristics of highly excited gas.

It must be conceded to Arp that it remains possible that a subset of quasars could have a non-cosmological component to their redshift, although the apparent similarity of nearly all quasar spectra might then be surprising. Apparent alignments of quasar groups on the sky could be interpreted as evidence for physical association of quasars of very different redshifts, and this would be impossible if the redshifts were true distance indicators. However, the statistical simulations of Zuiderwijk[7] confirm previous suggestions that such alignments as are observed are quite likely to arise by chance juxtaposition on the sky, with no physical association.

It was the very considerable spread in the intrinsic luminosity of quasars which vitiated the plotting of a simple magnitude-redshift Hubble diagram that would long ago have settled doubts about their distance. The new information of angular diameter versus redshift of Wyckoff *et al.* must, however, considerably strengthen the cosmological distance interpretation of quasar redshifts. □

M.G. Edmunds is in the Department of Applied Mathematics and Astronomy, University College, PO Box 78, Cardiff CF1 1XL.

Erratum: The Flavells

The article *The mystery of the mouse* α-globin pseudogene (*Nature* **295**, 370; 1982) was written by Andrew Flavell of the Imperial Cancer Research Fund Laboratories, Mill Hill, London. We regret that we erroneously attributed authorship to his brother R.A. Flavell of the National Institute of Medical Research, Mill Hill, London.

0028-0836/82/070556-01$01.00

ARTICLES

Molecular effects in pion capture in complex materials

Daphne F. Jackson, C. A. Lewis* & K. O'Leary
Department of Physics, University of Surrey, Guildford GU2 5XH, UK

G. K. Y. Lam
Batho Biomedical Facility, TRIUMF, Vancouver, Canada

Intensities of X rays from pionic atoms in various materials determine the pion capture ratio in carbon and oxygen. A molecular model with transfer from hydrogen has the features necessary to fit the data whereas the Fermi–Teller law (Z-law) fails. Implications for pion dosimetry and radiotherapy and for studies of molecular structure are noted.

A NEGATIVE pion is a strongly interacting particle, 273 times heavier than an electron. Like any other heavy charged particle, it travels in an almost straight line through material, losing energy by excitation and ionization, and stops at a certain depth which depends on the properties of the material and the incident energy of the pion. Little is known about the capture of stopping pions from the continuum into excited states ofa pionic atom or molecule[1], as this process is simple only in metals when the pion can give up its energy to the conduction electrons[2]. In an isolated pionic atom, the captured pion falls from a highly excited state to lower states by electromagnetic Auger and X-ray processes which are well understood[3].

The influence of the material in which the pionic atom is formed is manifested in several ways. Because the binding energy of a pion is proportional to Z^2, where Z is the atomic number of the nucleus, a pion captured by hydrogen may be transferred to a more tightly bound orbit around a nucleus of higher Z. This means that deexcitation of pionic hydrogen by electromagnetic processes and subsequent nuclear capture of the pion by the proton are in competition with the transfer process. Experimental studies[4,5] have shown that transfer of pions does occur in chemical compounds, mixtures of compounds and gas mixtures. Chemical and physical effects have been observed[5–7] by measuring the intensities of X-ray lines emitted from selected elements in various compounds and mixtures and comparing the ratios of the summed intensities of a series for the same pair of elements in different materials or by comparing the relative intensities of the lines in a series for the same element in different materials.

When a pion reaches the lowest atomic orbits, its distribution overlaps with that of the nucleus. A nuclear interaction can then take place, causing disintegration of the nucleus and emission of short-range charged particles and longer-range neutrons and γ rays[8]. The charged particles are heavily ionizing and their energy is deposited on top of the pion Bragg peak. The neutron spectra produced by pion interactions in carbon and oxygen nuclei are rather similar[9] but the number of charged particles produced by captures on oxygen is less than in captures on carbon and the mean energies are lower[10]. It is therefore important for pion radiotherapy to know accurately the atomic capture probabilities for negative pions on carbon and oxygen atoms. The work by Fowler and Mayes[11] and subsequent dose estimates have assumed the validity of the Fermi–Teller law[2] which predicts that the probability of capture on an atom in a chemical compound is proportional to Z (Z-law). This rule has been shown experimentally to fail quite dramatically in inorganic materials[12,13].

Mesomolecular model

A mesomolecular model of the pion capture process has recently been developed[12–14]. Its essential feature is that the pion may be captured directly into an atomic orbit or may be captured first into a molecular orbit in the vicinity of the valence electrons and subsequently deexcite to an atomic orbit. We have extended the model to include the transfer process from hydrogen[15].

The ratio per molecule of captures on atoms Z_1 to captures on atoms Z_2 is given by[14,15]

$$R=\frac{N_1[n_1+2\nu_1\omega_1+h_1\delta_1 a]}{N_2[n_2+2\nu_2\omega_2+h_2\delta_2 a]} \qquad (1)$$

where N_i is the number of atoms of type i in the molecule, n_i is the number of core electrons, ν_i is the number of valence electrons, ω_i is the probability of de-excitation from the molecular orbit to an atomic orbit of atom Z_i, N_ih_i is the number of hydrogen atoms which are nearest neighbour to (bonded to) a

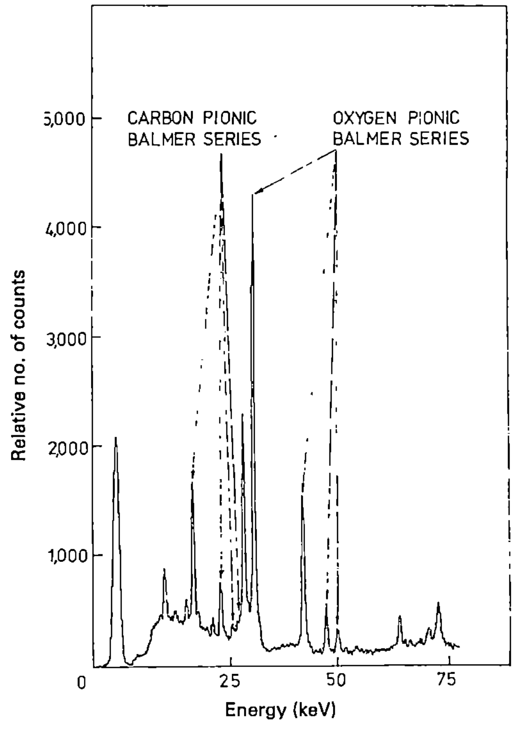

Fig. 1 A typical X-ray spectrum for organic molecules. This example is for malonic acid.

---

*Present address: Department of Physics, Mount Vernon Hospital, Northwood, Middlesex HA6 2RN, UK.

0028-0836/82/070557—04$01.00

heavier atom Z_i, δ_i is the number of electrons participating in the transfer process and a is the probability per electron of transfer. (This treatment of the core and valence electrons is a simplification, valid for light atoms, of that given in ref. 14.) We have considered $\delta_i = 1$ and $\delta_i = 2\nu_i - 1$ as extreme pictures[15] of the involvement of the valence electrons in the transfer process.

When $a = 0$ and $\omega_1 = \omega_2 = 0.5$, equation (1) yields the Z-law, because $n_i + \nu_i = Z_i$. When $a = 0$ and ω_1, ω_2 are the same for all molecules containing atoms Z_1, Z_2, equation (1) predicts that the relationship between R and N_1/N_2 is a straight line passing through the origin. However, if hydrogen transfer is important or if ω depends on molecular structure, or both, discrepancies from a straight line relationship will be seen. When many different molecules are contained in the material, the values of N_i are determined by dividing the proportion by weight of element i by its atomic weight.

For non-polar chemical bonds the mesomolecular model yields[14]

$$\omega_i = Z_i^2/\Sigma Z_i^2 \qquad (2)$$

and for molecules containing only carbon, oxygen and hydrogen this gives $\omega_C \simeq 0.36$, $\omega_O \simeq 0.64$, $\omega_H \simeq 0$. Because the electronegativity, which is the power of an atom to attract electrons to itself, is different for different atoms, covalent bonds may have a polar character. It has been suggested[14] that this effect will give rise to localization of the pion in the molecular orbital near the most electronegative atom. For a bond Z_1–Z_2, the localization parameters are defined as $p_1 = \frac{1}{2}(1-\sigma)$, $p_2 = \frac{1}{2}(1+\sigma)$, where Z_2 is the most electronegative atom and 100σ is the percentage ionic character of the bond. The probability of capture from a mesomolecular orbit to an atomic orbit of atom Z_i is then given by[14]

$$\omega_i = p_i Z_i^2/\Sigma p_i Z_i^2 \qquad (3)$$

Thus the effect of polarity is to reduce the capture probability for the least electronegative atom and increase it for the most electronegative one.

Outline of the experiment

We have measured the relative intensities of lines in the Balmer series emitted by pionic atoms of carbon and oxygen in a range of materials[15,16]. For some materials we have also measured the intensities of the Balmer series in nitrogen. It is not feasible to study the pionic Lyman series because of the very considerable broadening of the atomic 1s level due to the nuclear absorption of pions from this level. For these light elements the nuclear shifts and widths of the 2p and higher levels are negligible[3], and so is the effect of electron screening.

The experiment was performed with the biomedical pion channel[17] at the TRIUMF Laboratory, Vancouver, using a conventional plastic scintillator counter telescope to detect pions stopping in the target. An additional coincidence was obtained between the stopping signal in the counter telescope and a pion time-of-flight signal to reduce false triggers due to muon or electron contamination or scattered events. X-ray photons emitted from the target were detected using a carefully shielded HPGe detector. Signals from the HPGe detector were accumulated on a 1,024 channel analyser which was calibrated over the range 6–140 keV. Measurements of detector efficiency and resolution were performed over the same range.

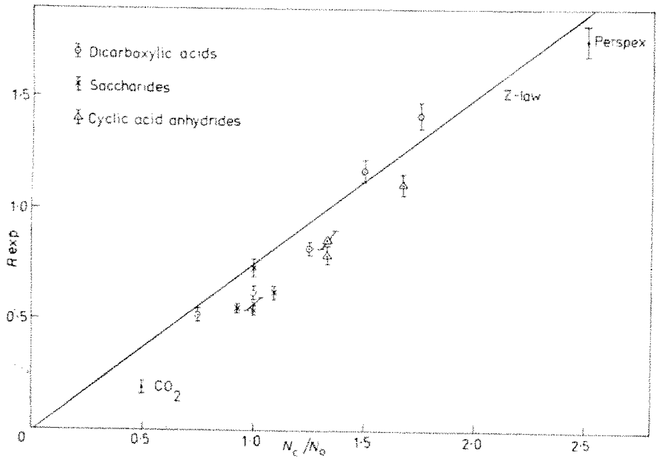

Fig. 2 Experimental results for the C/O capture ratio R plotted against the ratio N_C/N_O of the number of carbon atoms to the number of oxygen atoms.

Table 1 Chemical composition of target materials

Dicarboxylic acids	$COOH(CH_2)_nCOOH$
Malonic acid	$n = 1$
Succinic acid	$n = 2$
Glutaric acid	$n = 3$
Adipic acid	$n = 4$
Pimelic acid	$n = 5$
Cyclic acid anhydrides	
Maleic anhydride	$C_4H_2O_3$
Succinic anhydride	$C_4H_4O_3$
Glutaric anhydride	$C_5H_6O_3$
Saccharides	
D(+) Xylose	$C_5H_{10}O_5$
D(+) Glucose	$C_6H_{12}O_6$
D(+) Mannose	$C_6H_{12}O_6$
Sucrose	$C_{12}H_{22}O_{11}$
D(+) Trehalose dihydrate	$C_{12}H_{22}O_{11} \cdot 2H_2O$
Carbon dioxide (dry ice)	CO_2
Amino acids	$NH_3^+ \cdot CHR.COO^-$
Glycine	R = —H
DL-α-Alanine	$R = —CH_3$
DL-Valine	$R = —CH(CH_3)_2$
DL-Serine	$R = —CH_2OH$
L-Cysteine	$R = —CH_2SH$
Tissue equivalent materials	
Perspex (polymethylmethacrylate)	$(C_5H_8O_2)_n$
Tissue equivalent liquid [19]	Water, glycerol, urea
Tissue equivalent plastic (A150) [19]	Nylon, polymethylene, carbon, calcium fluoride

A typical spectrum is shown in Fig. 1. The principal source of uncertainty in the analysis arose from the determination of the peak areas under the pion lines which were determined using a version of the γ-ray analysis code SAMP O[18]. The main factors influencing the accuracy were the magnitude of the peak intensities and the complexity of the spectrum. In general, the percentage errors in the total intensities for each element, as calculated by SAMP O, were 4–7%. No background subtractions, other than those performed by SAMP O, were needed. The total intensities for nitrogen were subject to much larger errors because the nitrogen content was low and the principal nitrogen line overlapped with a carbon line. It was particularly important to correct the individual X-ray intensities for self-absorption in the target, but the uncertainties introduced by this correction was <1%. The errors shown in Fig. 2 are the standard deviations arising from all sources.

It is assumed that the summed intensities of the lines in the Balmer series is proportional to the atomic capture probability. The validity of this assumption is discussed below.

Choice of target materials

Table 1 lists the target materials and their chemical composition. The rather difficult measurement with dry ice was attempted because it was important to study a molecule containing carbon and oxygen but no hydrogen. However, the main emphasis of the experiment was on the ratio of captures in carbon and oxygen and the effect of hydrogen transfer, and therefore most of the samples consisted of molecules of carbon, oxygen and hydrogen. These molecules were chosen because of their biological importance and also to vary the C/O ratio and the number of OH and CH bonds. The character of the amino acids is strongly influenced by the side-chain R; the form of R for the chosen amino acids is given in Table 1. Certain amino acids and saccharides are strongly lyoluminescent, that is, they emit light when dissolved after irradiation in the dry state, and this property has potential applications in dosimetry. Because of the importance of the results for the pion radiotherapy programme, several targets composed of animal tissues were irradiated. The targets comprised fat, muscle, brain, kidney, liver and lung from a freshly killed pig and samples of fat and muscle from a second pig. The elemental composition of these samples was obtained by chemical analysis before and after irradiation. No significant changes due to irradiation were noted. Several tissue equivalent materials used as muscle substitutes[19], such as perspex, tissue equivalent liquid and tissue equivalent (A150) plastic, were also used. The special features of this part of the experiment are described eleswhere[16].

Results

The experimental ratio R of captures in carbon to captures in oxygen is plotted in Fig. 2 against the ratio N_C/N_O of the number of carbon atoms to the number of oxygen atoms in each molecule, for those molecules containing only C, O and H. It is evident that although the expected trend of increasing capture ratio with increasing N_C/N_O is present, the results do not fall on the same straight line. The Z-law is clearly inadequate. The largest discrepancy is an overestimate of 95% for carbon dioxide. For most, but by no means all, the organic molecules the Z-law gives discrepancies of 20–25%.

The result for carbon dioxide is particularly important because the question of hydrogen transfer does not arise. Using equation (1) with $h_C = h_O = 0$, we find the best value of ω_C to be $\omega_C = 0.19 \pm 0.06$, with the restriction that $\omega_C + \omega_O = 1$. This result is very important as it suggests that equation (2) is not appropriate. The explanation for this result can be found by using the value of the ionicity of the carbon–oxygen bond to obtain the localization factors. For a single bond $\sigma = 0.22$ (ref. 20), which yields $p_C = 0.39$, $p_O = 0.61$ and $\omega_C = 0.26$. But because carbon dioxide contains double bonds, it may be more appropriate to take $\sigma = 0.44$, which yields $p_C = 0.28$, $p_O = 0.72$ and hence $\omega_C = 0.21$. Thus the downward shift of ω_C is a clear indication of the influence of the polarity of the bonds and the sensitivity of the atomic capture ratio to the electronic distribution in the molecule.

Inclusion of hydrogen transfer is not straightforward because we have as yet only plausible pictures of the process and no quantitative theory which predicts the values of the parameters. We have made χ^2 fits to the data, for each group of similar molecules and for the whole set. The parameters were constrained so that $0 \leq \omega_C \leq 1$, $0 \leq a \leq 1$, $\omega_C + \omega_O = 1$. This yields the parameters given in Table 2, with $\delta = 2\nu - 1$. When $(\omega_C + \omega_O)$ is allowed to fall below unity, to allow for a significant value of ω_H, there is no significant change in the results. When $\delta = 1$, the agreement with the data is comparable but in all cases $\omega_C \geq 0.36$ so that this model would not yield agreement with the result for carbon dioxide. If, however, we allow $a > 1$ an overall description can be obtained with a lower value of ω_C. This can be seen from the last line of Table 2 where $\delta_C a_C = \delta_O a_O = 1.77$.

Table 2 Values of ω_C, a_C and a_O obtained by fitting the data and assuming that $\omega_C + \omega_O = 1$, $\delta = 2\nu - 1$

	ω_C	a_C	a_O	χ^2
Acid anhydrides	0.25	0.258	*	0.98
	0.335	0.130	*	0.00
Dicarboxylic acids	0.25	0.340	0.340	2.90
	0.306	0.256	0.256	2.75
	0.325	0.265	0.513	2.75
Saccharides	0.25	0.192	0.192	4.03
	0.375	0.00	0.00	4.00
	0.415	0.00	0.285	3.98
All the above	0.25	0.266	0.266	5.40
	0.263	0.247	0.247	5.39
	0.290	0.254	0.591	4.85

The first row for each group corresponds to the constraints $\omega_C = 0.25$, $a_C = a_O$ and the second row corresponds to the constraint $a_C = a_O$ with ω_C varied. For the third row, all three parameters are varied.

*No transfer occurs to oxygen.

Table 3 Values of R_{exp} divided by R_{theory} for capture ratios in the amino acids

Amino acid target	C/O capture ratio $R_{exp}/R_{Z\text{-law}}$ ($\omega_O = \omega_C = 0.5$, $a = 0$)	$R_{exp}/R_{\text{molecular model}}$ ($\omega_C = 0.25$, $\omega_O = 0.38$, $a_C = 0.16$, $a_O = 0.24$)
Glycine	0.77 ± 0.04	0.85 ± 0.05
Serine	0.77 ± 0.05	1.00 ± 0.06
Cysteine	0.95 ± 0.10	0.97 ± 0.12
Alanine	1.01 ± 0.05	1.04 ± 0.06
Valine	1.11 ± 0.06	1.08 ± 0.06
	N/O capture ratio ($\omega_O = \omega_N = 0.5$, $a = 0$)	($\omega_N = 0.37$, $\omega_O = 0.38$, $a_N = 0.066$)
Glycine	0.95 ± 0.26	0.86 ± 0.23
Serine	1.07 ± 0.28	1.00 ± 0.23
Cysteine	1.59 ± 0.45	—
Alanine	1.21 ± 0.27	1.10 ± 0.25
Valine	1.07 ± 0.23	1.00 ± 0.21

The results for perspex and TE liquid can be reproduced exactly with $\omega_C = 0.25$, $a_C = a_O = 0.21$, whereas the Z-law prediction is too high in both cases. The values $\omega_C = 0.25$, $a_C = 0.266$ give excellent agreement[21] with experimental results for cellulose acetate and mylar obtained at SIN, Zurich[22].

For the amino acids, we have used the value $\omega_C = 0.25$ deduced as an average value for other molecules (see Table 2). Quite good agreement for the C/O capture ratio is then obtained with $\omega_O = 0.38$, $a_C = 0.16$, $a_O = 0.24$, as can be seen from Table 3. Assuming that $\sum_i \omega_i = 1$, we infer that $\omega_N = 0.37$ for the amino acids containing C, N, O, and H only (excluding cysteine). This yields excellent agreement with the data for the N/O capture ratios, with $a_N = 0.066$.

The results for the C/O capture ratio in the muscle samples from the two pigs are in very good agreement. The results for the fat samples are quite different because the samples represent different kinds of fat from different parts of the animal. The sample of subcutaneous fat, which may contain muscle fragments, gave results consistent with the other tissues[16]. Taking the average of the C/O capture ratios for the tissue samples, we obtain

$$R_{exp} \simeq 0.58 R_{Z\text{-law}}.$$

Inserting this value into equation (1), neglecting hydrogen transfer and assuming $\omega_C + \omega_O \simeq 1$ (the nitrogen content is low), we obtain $\omega_C = 0.23 \pm 0.04$ which is in good agreement with the results for the organic molecules. The tissue equivalent materials give quite different results for the C/O capture ratio in the sense that $R_{exp}/R_{Z\text{-law}}$ is 0.82 (TE liquid), 0.96 (perspex) and 1.66 (TE plastic).

The large deviations from the Z-law for cysteine, TE plastic and pig tissues are almost certainly due to the presence of additional elements, such as S(cysteine), F, Ca (TE plastic), minor and trace elements (tissues).

Comparison with muon data

Similar measurements have previously been made with muons[8,12,13,23,24] and also show significant departures from the Z-law. Because muons are not strongly interacting, the data are generally easier to interpret. However, there are reasons why the capture ratios for pions and muons may not be identical. We have assumed that the summed intensity of the Balmer series is proportional to the total capture probability for a particular element, while for muons it is assumed that the same is true for the Lyman series. Both assumptions will be valid if the cascade process leads to a low population of the 2s state and higher np states ($n > 2$). Cascade calculations for isolated atoms confirm that this is indeed the case, but formation of molecular orbitals could change the selection rules at the beginning of the cascade.

(Theoretical investigation of this point is in progress.) But to produce any significant error in our assumption, the effect would need to be significantly different in carbon and oxygen and there is experimental evidence that this is not the case for pions (H. Koch, personal communication quoted in ref. 22). There is also the more important possibility that direct nuclear capture of pions by hydrogen can occur from highly excited molecular states[12,13]. The contribution of transfer of pions from hydrogen to heavier atoms would then be reduced in comparison to transfer of muons.

From previous measurements[23] of muon capture in tissues and tissue equivalent materials we have taken the concept of transfer from hydrogen to the nearest heavier atom but the particular model used, with $\delta = 1$, does not give the best description of our data. Furthermore, there is a factor of three discrepancy between the muon results reported for pig fat[23,24]. A detailed comparion with the pion and muon data, including muon measurements made as part of our experiment, are given elsewhere[16] and indicate that there are sufficient differences to make this detailed study of pion data necessary.

Discussion

The results for tissues and tissue equivalent materials are of considerable practical importance because the ratio of captures in carbon to captures in oxygen in real tissues is very much less than has hitherto been assumed. Our results confirm the suggestion[25] that materials which are tissue equivalent to X rays, electrons and neutrons are not tissue equivalent for pions. This is clearly due to major differences in molecular structure. Hitherto, only atomic and nuclear properties, such as electron density, effective atomic number and neutron cross-section, have been taken into account in defining tissue equivalence.

The Z-law, and its variations, fail to fit the data. The mesomolecular model contains an essential new feature[13]—the redistribution of the contribution of the valence electrons—because in general $n_i + 2\nu_1\omega_1 \neq Z_i$. The probability ω for atomic capture from the molecular orbit is not proportional to Z^2; instead it seems that ω is sensitive to the electronic structure of the molecule in a manner which relates to the localization of the mesomolecular orbital near to atoms of high electronegativity.

Hydrogen transfer is essential for a quantitative description of the data. The choice $\delta = 2\nu - 1$ may be preferred and different transfer parameters for CH and OH bonds may be indicated. Clearly the transfer parameter a is very sensitive to molecular structure but further work will be needed to give complete understanding of the transfer mechanism.

It had been suggested that muonic X-ray analysis can be used for bulk elemental analysis[23]. Our results suggest, in contrast, that pion capture (and probably also muon capture) is a sensitive means of probing molecular structure in complex materials. It should be very sensitive to changes brought about by substitution of one atom by another of a different element or when bonds are broken, for example, by radiation damage.

We thank the SRC for support to C.A.L. and K. O'L. and for visits by the Surrey team to Vancouver. We thank the director and staff of the TRIUMF Laboratory and the Batho Biomedical Facility, Vancouver, for the facilities and assistance provided, and particularly R. W. Harrison. We also thank the muon physics group of the University of Victoria, Canada, for the loan of equipment.

Received 17 August; accepted 30 December 1981.

1. Gershtein, S. S. & Ponomarev, L. I. *Muon Physics* Vol. 3, Ch. 7 (Academic, New York, 1975).
2. Fermi, E. & Teller, E. *Phys. Rev.* **72,** 399 (1974).
3. Barrett, R. C. & Jackson, D. F. *Nuclear Sizes and Structure,* Chs 4, 9 (Clarendon, Oxford, 1977).
4. Petruhkin, V. I., Risin, V. E. & Suvorov, V. M. *Soviet J. nucl. Phys.* **19,** 317 (1974).
5. Petruhkin, V. I., Risin, V. E., Samenkova, I. F. & Suvorov, V. M. *Soviet Phys. JETP* **42,** 955 (1976).
6. Tauscher, L. *et al. Phys. Lett.* **27**A, 581 (1968).
7. Grin, G. A. & Kunselman, R. *Phys. Lett.* **31**B, 116 (1970).
8. Jackson, D. F. & Brenner, D. F. *Progress in Particle and Nuclear Physics* Vol. 5, Ch. 4 (Pergamon, Oxford, 1981).
9. Klein, U. *et al. Nucl. Phys.* A**329,** 339 (1979).
10. Mechtersheimer, G. *et al. Nucl. Phys.* A**324,** 379 (1979).
11. Fowler, P. H. & Mayes, V. *Proc. phys. Soc.* **92,** 377 (1967).
12. Ponomarev, L. I. *A. Rev. nucl. Sci.* **23,** 395 (1973).
13. Schneuwly, H. *Int. School of Physics of Exotic Atoms*, 255 (1977).
14. Schneuwly, H., Pokrovsky, V. I. & Ponomarev, L. I. *Nucl. Phys.* A**312,** 419 (1978).
15. Jackson, D. F., Lewis, C. A. & O'Leary, K. *Phys. Rev.* (in the press).
16. Lewis, C. A., O'Leary, K., Jackson, D. F. & Lam, G. K. Y. *Phys. med. Biol.* (in the press).
17. Henkelman, R. M., Skarsgaard, L. D., Lam, G. K. Y., Harrison, R. W. & Palcic, B. *Int. J. Radiat. Oncol. biol. Phys.* **2,** 123 (1977).
18. Routti, J. & Prussin, S. G. *Nucl. Instrum. Meth.* **72,** 125 (1969).
19. The Hospital Physicists' Association *Scient. Rep. Ser.* 420 (1977).
20. Stark, J. G. & Wallace, H. G. *Chemistry Data Book* (Murray, London, 1971).
21. Jackson, D. F. *Phys. med. Biol.* (in the press).
22. Münchmeyer, D. *KfK Rep.* 2786B (Diplomarbeit Universität Karlsruhe, 1979).
23. Reidy, J. J., Hutson, R. L. & Springer, K. *IEEE Trans. nucl. Sci.* **NS-22,** 1780 (1975).
24. Daniel, H., Pfeiffer, H.-J. & Springer, K. *Biomed. Technik* **18,** 222 (1973).
25. Dicello, J. F., Fessenden, P. & Henkelman, R. M. *Int. J. Radiat. Oncol. biol. Phys.* **3,** 299 (1977).

How honey bees use landmarks to guide their return to a food source

B. A. Cartwright & T. S. Collett
School of Biological Sciences, University of Sussex, Brighton BN1 9QG, UK

Bees trained to forage at a place specified by landmarks do not construct a cartesian map of the arrangement of landmarks and food source. Instead they store something like a two-dimensional snapshot of their surroundings taken from the food source. To return there, bees move so as to reduce discrepancies between the snapshot and their current retinal image. A computational model embodying these principles mimics the bees' behaviour.

HONEY BEES can learn the position of a source of sugar by reference to nearby landmarks (reviewed in ref. 1). We describe here what bees seem to learn about the spatial layout of landmarks and how this information might guide their approach to the source. Our experimental results strongly support earlier proposals[1-4] that to identify a place to which it will return an insect learns no more than the appearance of the landmarks viewed from that spot—just as though it takes and stores a panoramic snapshot of the landmarks from that position. Then, to find its way back, it compares the image on its retina with the stored snapshot and moves until the two match. It is not immediately obvious that this hypothesis can work, and we have therefore developed a computational model to show that it does.

Bee tests

Single marked bees were trained to fly through an open window into an experimental room (floor area 4 m × 4 m) to collect sugar

0028-0836/82/070560—05$01.00

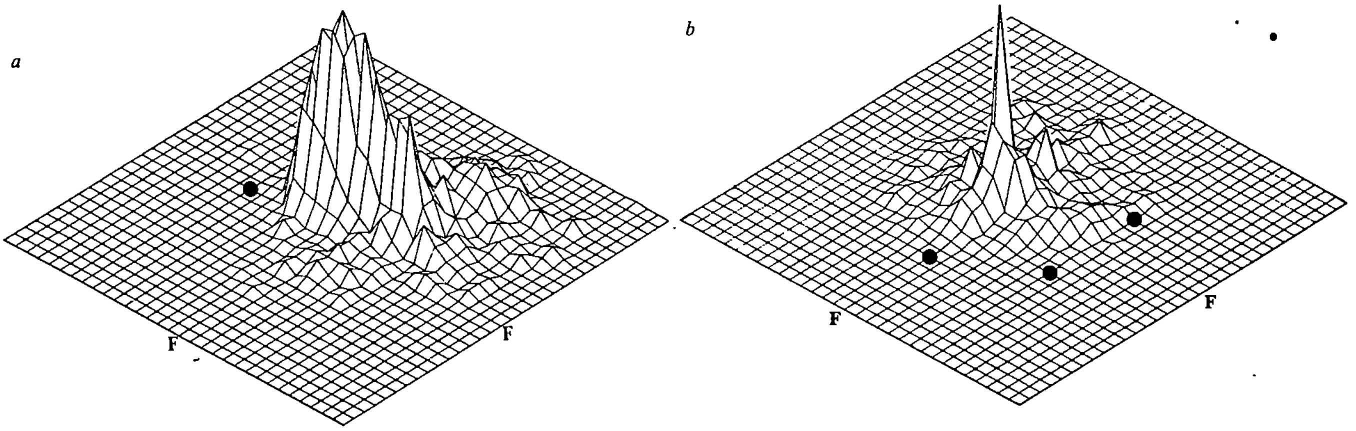

Fig. 1 *a*, Distribution of a single bee's flight time within the area surveyed by the camera when trained to a food source 50 cm from a single cylindrical landmark and tested with the same-sized landmark (4 cm diameter and 40 cm high). The position of the food source during training is marked by 'F' on the *x* and *y* axes. The position of the base of the landmark is indicated by filled circles. Height shows relative times spent in different regions of the testing area. Lines on grid are 8.7 cm apart. *b*, Distribution of bee's flight time when trained and tested with three landmarks in the standard array described in Fig. 2.

solution from a small reservoir (diameter 1.5 cm) on the floor. The room was painted entirely white, except for random green markings on the floor to help the bee stabilize its flight, and the window was covered by white sheeting. The location of the reservoir was indicated by the position of one or three matt black cylindrical landmarks standing upright on the floor. The bee returned to the room every 5 to 10 minutes. To encourage the bee to associate the food source with the landmarks, between visits the whole arrangement of cylinders and reservoir was shifted in register to a new position, without changing its orientation.

After a day of training with a standard array, tests were conducted at ~40-min intervals. The food source was then removed and the flight path of the bee recorded for 2 min by an overhead video camera suspended on runners fixed to the ceiling. The camera surveyed an area of floor 2.7 m×2.7 m centred on the position of the missing reservoir, and the testing site was varied systematically within the room. Sometimes the size, number or spatial arrangement of landmarks was altered between training and the subsequent test. An individual bee was given several types of test, each replicated 5–10 times. Each type of test was conducted on at least two bees.

The position of a bee was recorded every 100 ms from the video tape and the results from 5–10 tests of the same type are combined to show in Figs 1 and 2 how an individual bee distributed its time in the vicinity of the landmark array. Our aim was to infer from the bee's searching pattern where it thought the reservoir was to be found, and from this to deduce what it knew about the arrangement of landmarks.

When a bee was trained to a food source at a constant distance from a single cylindrical landmark, and then tested with the food source removed, it searched roughly where it had previously foraged with respect to the landmark (Fig. 1*a*). Although a radially symmetrical landmark does not define direction, the bee does not fly in a circle around the landmark, implying that some other cue (possibly the window) must specify in which direction from the landmark the food lay. Tests with single landmarks smaller (or larger) than the training size result in a search area shifted closer to (or further from) the landmark (ref. 5 and B.A.C. and T.S.C., in preparation). This suggests that the bee has not learnt the distance between landmark and food source but rather how large the landmark appears when viewed from the food source, and also that to find the reservoir the bee flies to where the image of the landmark on the retina is of the right size.

Experiments using three landmarks, when the search area is rather more sharply defined (Fig. 1*b*), reinforce these conclusions. If a bee is trained to a particular configuration of landmarks and then tested with a different spatial arrangement of those same landmarks, it always searches in an area where the inter-landmark angles (as shown in Fig. 2) are the same as when seen from the food source. The actual distances of the landmarks from each other or from the search area are of minor importance.

Figure 2*a*, *b* shows a bee's search area when it was confronted with an array in which the distances between landmarks differed from those with which it was trained. The bee spent most of its time where the inter-landmark angles matched those experienced during training. Furthermore, if the test configuration was such that a bee could search where either the distances from the landmarks or the inter-landmark angles were correct, it chose to do the latter (Fig. 2*c*).

A bee tested with cylinders that were larger or smaller than the ones used in training also searched where the inter-landmark angle was approximately correct. Figure 2*d* illustrates that this behaviour persists for very dramatic changes of landmark shape and size, when cubes with 30-cm edges were substituted for the training cylinders (4 cm diameter, 40 cm height). We conclude that to a bee the most important feature of the landmark array is the retinal position of the landmarks as seen from the food source.

At first sight, the bees' neglect of landmark size would seem to conflict with their behaviour when they are trained to a single landmark and its size is changed. However, whatever the size of a single test landmark, a bee can always find a position where there is a perfect match between its 'snapshot' and the retinal image of the test landmark. But with three landmarks both their sizes and the distances between them must be changed in a coordinated way for a position to exist where retinal image and snapshot are congruent. If just one of these parameters is varied, then wherever the bee searches there will be some degree of mismatch. Simple geometry suggests that in this case the retinal sizes of landmarks should carry less weight than the angles between them, because the inter-landmark angles are much larger than the angle subtended by the landmark itself. Thus, were the bee to station itself where the angle subtended by one of the landmarks is correct, the positions of the other landmarks on its retina would be very wrong.

It seems, then, that a bee will search within a circumscribed area without requiring a perfect match between its postulated snapshot and its current retinal image. This can be shown in another way by testing bees with landmarks added to or taken away from the training array. Figure 2*e* shows that with two extra landmarks the bee's search area, although slightly larger than normal, is roughly in its usual position. When a bee was tested with any of the three landmarks removed, it still spent most of its time looking where the inter-landmark angle formed by the remaining two landmarks was the same as it was during training (not illustrated). This test also demonstrates that the bee must learn the sizes of the landmarks, for it is only their size that tells the bee whether or not the two remaining landmarks are neighbours and whether the inter-landmark angle should be 60 or 120°.

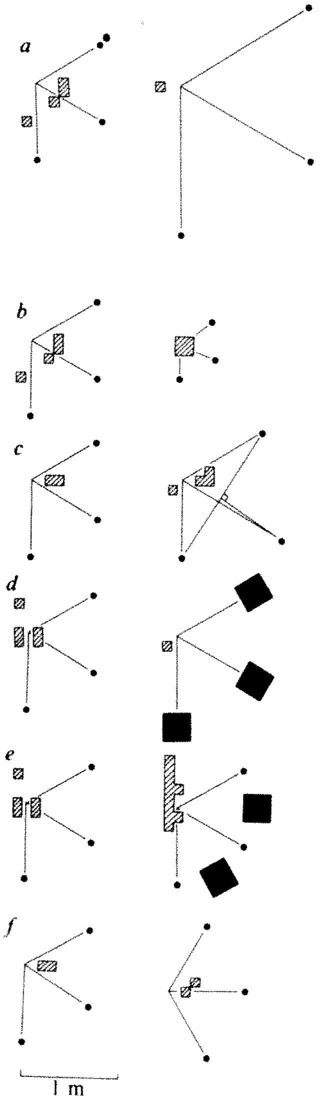

Fig. 2 Tests with three landmarks. The training configuration is shown in plan view in the left-hand column. The food source was placed 76 cm from each landmark at the intersection of the three lines drawn from the landmarks. Inter-landmark angles refer to the angles between these lines. In *a* and *b*, the cylinders were 5 cm in diameter and 50 cm high. In *c* to *f* they were 4 cm × 40 cm. Each row of the figure presents a pair of test arrays. The left half shows where a single bee searched when presented with the training array. On the right is the same bee's search area when presented with a variant of the training array. The hatching represents the search area defined as those squares within the test area (as in Fig. 1) that are at least 80% as high as the peak value. *a*, Distance between landmarks doubled; *b*, distance halved; *c*, landmarks arranged so that bee could search either where the inter-landmark angles or where the distances from the landmarks were the same as during training; *d*, cubes substituted for cylinders; *e*, cubes added to landmark array; *f*, landmark array rotated through 30° from training orientation. The point of intersection of the lines in the right-hand column show where the bee would need to search to see the same inter-landmark angles that it experienced when foraging at the food source. This is generally where the bee spends most of its time.

The snapshot model

All the above findings argue that the representation of landmarks in the bee's memory can be described in terms of a snapshot taken from the food source (see also ref. 1 for somewhat similar experiments on desert ants). The bee does not seem to be equipped with anything akin to a floor plan or cartesian map. We have therefore explored how well a model bee can guide itself using a representation of this kind. The basic idea is that the direction in which the bee moves at any moment is governed by the discrepancy between the snapshot and its current retinal image (Fig. 3).

To construct such a model we must make assumptions about the way images are coded in the visual system and the snapshot. In part these are arbitary. However, we have some evidence that the most important features of the retinal image are the edges between the dark landmarks and the light ground (B.A.C. and T.S.C., in preparation). Accordingly, in the model the retinal image consists of edges lying on a circular retina and the snapshot is represented in a compatible way (Fig. 3). The positions of the edges on both retina and snapshot are defined as compass bearings with respect to Earth-based coordinates. This assumption is supported by several experimental results. First, the tests with single landmarks (Fig. 1*a*) imply that cues external to the landmark specify the direction of the food source from the landmark. Second, when bees were tested with a three-landmark array rotated by 90° from the training orientation, the search area shifted away from the position predicted by the inter-landmark angles experienced during training. Third, bees find it difficult to use landmarks if, during training, the array is rotated between each of the bee's foraging visits. The simplest way to picture how edges in the snapshot can be given Earth-based coordinates is to suppose that the snapshot is fixed in the bee's head and that the bee always maintains the same orientation. This is not in fact so, and one needs to assume that as the bee turns, the snapshot counter-rotates.

Algorithms for calculating flight direction

We have examined two algorithms for generating the bee's direction of flight. These were programmed in Basic and run on a PDP8/a computer. The first, the simplest we could devise, fails to mimic all the bee's behaviour, but the second and more elaborate version performs very much as real bees do.

In the first algorithm (Fig. 4*a*) a unit vector is associated with each edge in the snapshot. The direction of the vector depends on the bearing of the closest edge of the same sign (that is, dark–light or light–dark) on its retina. Imagine each edge in the snapshot putting out an extensible arm to reach the nearest retinal edge. Once the edge is located, a unit vector is generated lying perpendicularly to the bearing of the retinal edge and pointing away from the paired edge in the snapshot, tending thus to align the two edges. These unit vectors are then summed, in the conventional way for adding vectors, to give the bee's flight direction. As the bee moves through the field of landmarks, it will continually update its direction as the edges shift over its retina. Note that it is not necessary for all edges in the retina to be matched to partners in the snapshot. Some may have more than one partner and others none at all. Furthermore, the bee is not required to assess the goodness of fit between its snapshot and the retinal image.

Figure 4*b* shows the computed vector directions for different points within the field of landmarks for a bee which is trained and tested with the same array of three landmarks. If the algorithm is to be successful, then from any starting point the vectors must lead the bee to the food source. The extent to which this is the case is shown in Fig. 4*c*. For most starting points the

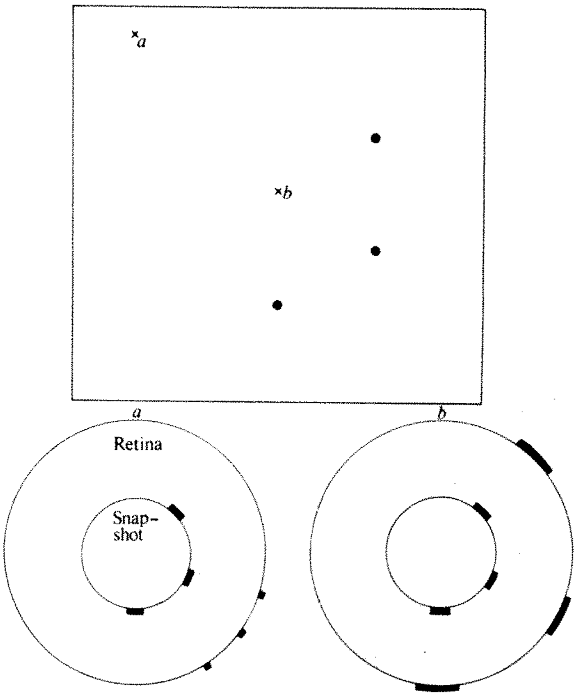

Fig. 3 The snapshot model. Positions of images of landmarks on circular retina (outer circle) and in snapshot (inner circle) viewed from two points within the landmark array as shown by crosses. *a*, Distance from food source; *b*, at food source, where snapshot and retinal image match. The aim of the model is to move the insect from *a* to *b* using the discrepancy between retinal image and snapshot as a guiding cue. Note that positions of edges on the circular snapshot and retina are compass bearings with respect to external coordinates. Frame round landmark array shows area viewed by video camera.

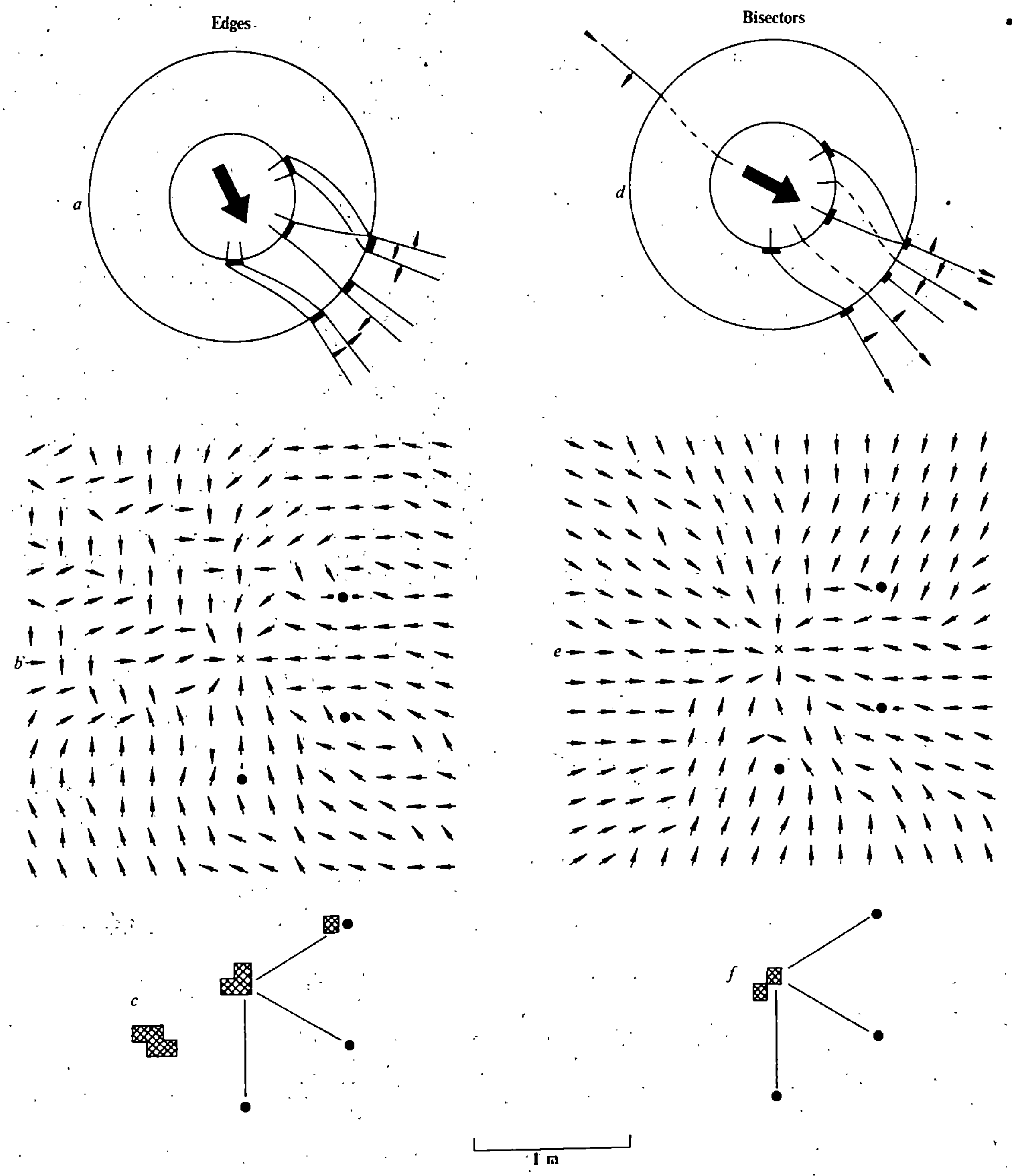

Fig. 4 Two algorithms for transforming retinal image to snapshot. *a*, Edge algorithm. Each edge in snapshot paired with closest edge on retina. Unit vector, shown by arrows around outer circle, is associated with each pair and lies perpendicularly to edge on retina, pointing away from edge in snapshot. Larger arrow in centre of circle shows flight direction of bee obtained by summing the unit vectors. *b*, The flight direction for different positions of the bee within landmark field, computed as outlined in *a*. Model bee trained and tested with landmark configuration of Fig. 3. *c*, Positions of end points are shown by cross-hatching. The bee is started at different positions within the landmark field and it follows the vectors as shown in *b* until it stops. *d*, Bisector algorithm. Unit vectors of positional component shown by arrows lying tangentially to outer circle, those of angular component by radially aligned arrows (details in text). *e*, Vector field for bisector algorithm. *f*, Position of end points for bisector algorithm.

bee does indeed end up at the food source. However, there are mishaps which arise because partial matches exist. There is one position within the field, for instance, where the two outer landmarks form an inter-landmark angle of 60°. The bee is trapped there because within a region on either side the vectors have opposite directions, pointing towards the partial match. Real bees do not make this mistake. The algorithm's performance can be improved if it takes into account the amplitude of the summed vectors. However, it still does not work in all the situations we have tested. In particular it fails if the array of landmarks is rotated by 30° from the orientation to which the bee was trained—a situation with which the bee can cope (Fig. 2*f*). Because the algorithm depends on the positions of edges defined with respect to external coordinates, a changed orientation of the landmark array will generate several points in the field where the edges of two landmarks can be roughly matched with edges in the snapshot, but none where all edges can be correctly matched.

To overcome these problems the second algorithm requires the bee to assess not only the position of each edge, but also the angular distance between them (Fig. 4*d*). Its first step is to decide on the basis of the signs of neighbouring edges whether the angles between them are dark or light. It then measures the size of each dark and light angle in the snapshot and on the retina, and locates the positions of their bisectors. Next, each bisector in the snapshot searches out the closest bisector on the retina with the same sign (dark or light), so pairing angles in the snapshot with angles on the retina. As in the first algorithm, a unit vector (the positional component) is associated with each pair, tending to move the bee perpendicularly to the bearing of the bisector on the retina, pointing away from the bisector in the snapshot (or toward it if the retinal angle is greater than 180°). The additional feature of this algorithm is a second unit vector (an angular component) which depends on the differences between the sizes of the paired angles. This vector faces centripetally along the bisector on the retina if the angle in the snapshot is the smaller, and centrifugally if it is the larger. It thus takes the bee away from retinal angles that are too big and towards those that are too small. All the component vectors are then summed to determine the bee's flight direction, which is shown by the arrow in the centre of Fig. 4*d*.

Figure 4*e* illustrates the directions of the summed vectors within the standard three-landmark array. The improvement over the first algorithm is obvious: there are paths from all points to the food source, and when the bee is flown from different starting points it now always finishes there (Fig. 4*f*). It is easy to see that neither the positional nor the angular component of the summed vector would by itself be sufficient to locate a food source specified by a single landmark, although either can do so when there are three landmarks. With one landmark the positional component defines direction but not distance, so that the bee would search along a line originating at the landmark and passing through the food source. The angular component, on the other hand, only specifies distances and would leave the bee flying in an annulus centred on the landmark. The two acting together are needed to identify the intersecting point.

This algorithm copes with all the one- and three-landmark tests we have tried, including those with landmarks added or deleted. The 30° rotation of the three-landmark configuration on which the first algorithm founders is taken care of by the angular component. However, to prevent aberrant solutions, the angular component must be given a greater weighting than the positional one (3:1), a weighting which works in all situations. When the landmark array was rotated through 90° from the training orientation, the search area was displaced for the model, as it was for real bees.

The algorithm will not only move bees to the right position within an array of landmarks, but it will also bring a bee successfully to a foraging position in the centre of a ring of eight landmarks from points well outside the circle, as in tests with real bees[6].

The model does not specify how directional information is abstracted. The information is assumed to be provided by an independent system. We have attempted, but failed, to generate a simple alternative model in which direction can be automatically obtained from an array of close and distant landmarks.

Despite the success of the model in our artificial environment, it is rash to conclude that this is how bees operate in the real world. For a start, sensory processing is undoubtedly more complicated than we have allowed it to be here. However, what does seem to be certain is that bees do not need a three-dimensional representation of their immediate surroundings in order to use nearby landmarks to locate a food source. A much simpler model will work: one in which the bee is not required to identify landmarks as such, or even to separate figures from the background. There is, of course, a price to be paid for simplifying one's visual world in the way the experiments suggest that the bee has done. It is that the bee can only use the information provided by its snapshot of the landmarks to return to the food source. The snapshot provides it with no means of navigating to anywhere else within the array of landmarks.

We thank David Blest, Mike Land, Christopher Longuett-Higgins, Peter Slater and Geoff Sullivan for their comments and Jo Harper for typing. Financial support came from SRC.

Received 24 June; accepted 16 October 1981.

1. Wehner, R. in *Handbook of Sensory Physiology* Vol. VII/6C (ed. Autrum, H. J.) (Springer, Berlin, 1981).
2. Collett, T. S. & Land, M. F. *J. comp. Physiol.* **100,** 59–84 (1975).
3. Wehner, R. & Räber, F. *Experientia* **35,** 1569–1571 (1979).
4. Hölldobler, B. *Science* **210,** 86–88 (1980).
5. Cartwright, B. A. & Collett, T. S. *J. exp. Biol.* **82,** 367–372 (1979).
6. Anderson, A. M. *J. comp. Physiol.* **114,** 335–355 (1977).

Rate of turnover of structural variants in the rDNA gene family of *Drosophila melanogaster*

Enrico S. Coen, John M. Thoday & Gabriel Dover
Department of Genetics, University of Cambridge, Cambridge CB2 3EH, UK

A high degree of polymorphism for the length and copy number of rDNA spacers, in both the X and Y chromosome clusters, has been found in a wild population of Drosophila melanogaster. *The genetic behaviour of rDNA structural variants in separate and mixed populations derived from isofemale lines suggests that they are not subject to strong selection and are stable for over 1,000 generations. The high structural variability suggests an evolutionary rapid process of turnover in the family which could partly explain widespread sequence homogeneity (concerted evolution) of rDNA within a species.*

SEVERAL studies on the evolution of tandem and interspersed repeated DNA families have revealed an unexpected greater family homogeneity within than between species. This phenomenon is known as concerted evolution and has been observed in a wide variety of genic and non-genic families.

The degree and extent of homogeneity in each species cannot easily be understood solely in terms of natural selection and drift, and is more probably the result of molecular mechanisms of homogenization (see refs 1–3 for reviews). Smith[4] and Ohta[5] have described the possible dynamics of homogenization in tandem arrays based on the mechanism of unequal exchange; and others[6–8] have discussed the potential of gene conversion for homogenizing tandem and interspersed families. Mechanisms of homogenization probably have a significant role in shaping the evolutionary progress of a family of genes and it is important to understand the extent and rates of these mechanisms.

Unequal chromatid exchange has been shown to be taking place in the arrays of sequences coding for ribosomal RNA (rDNA) of yeast[9,10] and *Drosophila*[11–13] (for reviews see refs 1, 14–16). In the rDNA of *Xenopus*[15] and *Drosophila*[12], unequal exchange in and between the spacers generates variation in length and copy number of these regions. Using such structural

0028–0836/82/070564—05$01.00

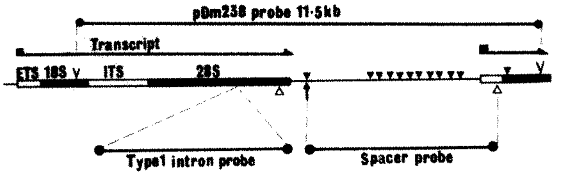

Fig. 1 Map of a repeating unit of ribosomal genes in *D. melanogaster* (see ref. 16 for review). 18S and 28S code for RNAs. ETS and ITS are external and internal transcribed spacers respectively. The nontranscribed spacer (NTS) appears as a line. About 50–60% of rDNA repeats of the X chromosomes have type 1 insertion sequences in the 28S gene. The length and direction of the primary transcript is shown by an arrow. The pDm238 probe is an *Eco*RI fragment cloned into the plasmid pBR322 and was a kind gift of D. Glober[32]. The type 1 intron probe, pC225, contains 5 kb of the type 1 insertion cloned into pBR322 and was constructed by S. Kidd[33]. The spacer probe, pDm103HH2, is a *Hin*dIII/*Hae*III fragment subcloned from cDm103[34] into the plasmid pAT153. The restriction sites are: V, *Eco*RI; Δ, *Hae*III; ↑ *Hin*dIII; ▼, *Alu*I. The position of only those sites in, or flanking, the NTS are shown for *Hae*III, *Hin*dIII and *Alu*I.

features it is possible to assess the rate of unequal exchange and the stability of its products by examining rDNA structural polymorphism in genetically defined populations. Here we present the data on natural variation within and between individual X and Y chromosome rDNA clusters from a population of *D. melanogaster* flies, collected from a single watermelon. We have also examined the genetic progress of each X and Y rDNA type of organization in separate and mixed populations derived from the wild-type founders.

Nontranscribed spacer length and copy number polymorphism in a wild population

In *D. melanogaster* the 18S and 28S rRNA genes are present in 250 tandem repeats in each nucleolus organizer (NO) of the X and Y chromosomes. The organization of the repeating unit is shown in Fig. 1.

The isofemale lines of *D. melanogaster* used in this study are derived from females collected in 1970 from around a single watermelon in Oklahoma (OK. lines)[17]. The first laboratory generation from each female was divided into two sublines—a and b. Analysis of rDNA from females in OK. lines 1 and 19 in 1978 showed differences in restriction pattern between the lines[18].

To examine the full extent of the natural variation we have analysed rDNA organization after 230 generations in each subline for OK. lines 1–10. Variation in length and copy number of the nontranscribed spacer (NTS) was investigated by probing *Hae*III-digested DNA with a NTS cloned probe pDm103HH2 (Fig. 1). *Hae*III restriction of pDm238 produces a 5.1 kilobase (kb) fragment containing an intact NTS together with a small part of the 28S gene and part of the external transcribed spacer (ETS) (Fig. 1). To ensure that only a single NO cluster from each line was being examined, XO male rDNA was analysed by mating single males from the OK. lines to $\hat{X}X/O$ females and collecting the male progeny. *Hae*III digests of XO male DNA from each subline of OK. lines 1–10, probed with NTS clone pDm103HH2, reveal extensive variation between the lines (Fig. 2).

Independent extraction and analysis of XO males derived from the same XY male parent always produced the same *Hae*III pattern, confirming that the variation is not an artefact of partial digestion. *Hin*dIII and *Eco*RI digests suggest that the *Hae*III fragment length variation is due to changes in NTS length (data not shown).

DNA from diploid tissue of larval brains of OK. lines 1a, 2a, 3a and 5a was digested with *Hae*III and probed with the NTS clone. The pattern characteristic of the adults from each line could be identified. Differences between rDNA arrays are not therefore due to differences in polytenization of rDNA units of the sort described by Endow[19].

The contribution of intron-containing repeats to the variation in rDNA organization was investigated by probing *Eco*RI digests with a type I intron clone pC225 (see Fig. 1). Only comparatively small differences were revealed between the OK. lines (data not shown), confirming changes in NTS length and abundance as the major source of polymorphism.

To examine the molecular basis for NTS number and length heterogeneity, a repetitive sequence region in the NTS was investigated by digesting DNA from XO males, carrying the same X chromosomes as analysed in Fig. 2, with *Alu*I (Fig. 1) and hybridizing them to the NTS probe. This experiment revealed the expected 250 base pair (bp) *Alu*I band plus a 1.4 kb band corresponding to the right-hand fragment, and several higher molecular weight bands, presumably from the left of the repetitious *Alu*I region (Fig. 3). The hybridization patterns clearly show that the most abundant lengths of the left- and right-hand flanking sequences fall between 1.4 and 2.4 kb. However, the *Hae*III digests of these chromosomes show that the rDNA from lines 1a, 4a and 9a have some NTS fragments >9 kb long (Fig. 2). The absence of any large right- or left-hand *Alu*I fragments flanking the internal 250 bp repetition in these

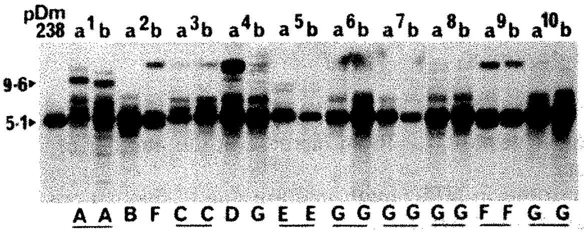

Fig. 2 Hybridization patterns of X chromosome rDNA from the a and b sublines of Oklahoma lines 1–10 in an autoradiograph of *Hae*III digests of XO male DNA that have been fractionated on agarose gels, transferred to nitrocellulose and hybridized to a ^{32}P-labelled clone, pDm103HH2, containing the NTS. Each track contains the DNA of four XO male progeny from a cross between an OK male and an $\hat{X}X/O$ female. The various hybridization patterns have been classified into seven types (A–G). Indistinguishable sublines are underlined. *Hae*III-digested pDm238 hybridized to the same probe is shown on the left for comparison. XO males were constructed by mating OK. males with females from a C(1)A, y/O/Y^{s}XY^{L}, In(1)EN, B y stock obtained from M. Ashburner. Progeny were checked to ensure that all females had a yellow and males a wild-type body colour. Some of the males were also checked for sterility. The remaining males were collected and stored frozen at −70°C for up to 6 months. In all cases DNA was extracted from the flies by a modification of the method of D. Ish-Horowicz (personal communication). Four flies were gently homogenized in a 1.5 ml microfuge tube containing 100 μl of 10 mM Tris, 60 mM NaCl, 5% sucrose, 10 mM EDTA, *p*H 7.5. 100 μl of 1.25% SDS, 0.3 M Tris, 0.1 M EDTA, 5% sucrose, 0.8% diethyl pyrocarbonate (freshly mixed), *p*H 9 were then added. After a 30 min incubation at 65 °C, 30 μl of 8M potassium acetate were added and the mixture kept on ice for 45 min. The precipitate was spun down for 5 min in an Eppendorf centrifuge 5412 and the supernatant added to 2 vol of ethanol. After standing for 5 min at room temperature the ethanol precipitate was spun down for 10 min in the Eppendorf centrifuge and the supernatant discarded. The pellet was resuspended in 100 μl of 0.1 × SSC, 0.2% diethyl pyrocarbonate (freshly mixed) and left to stand at room temperature for 30 min; three volumes of ethanol were then added and the mixture left at room temperature for a further 5 min. The DNA was spun down for 10 min in the Eppendorf centrifuge and washed with 70% ethanol. Residual ethanol was removed by drying the precipitate in a dessicator for 30 min and the DNA was dissolved in 15 μl of 5 mM Tris-HCl, *p*H 7.5, at room temperature overnight. The DNA was digested in a final volume of 25 μl with restriction endonuclease *Hae*III (BRL) after adding 0.2 μg of M13 DNA as a marker and 2 μl of RNase A (Sigma) at 1 mg ml^{-1} (preboiled for 10 min). *Hae*III digests were in 50 mM Tris-HCl, *p*H 7.6, 5 mM MgCl$_2$, 1 mM dithiothreitol. Digestion was with 2–3 U of enzyme for 2 h at 37 °C, followed by 10 min at 65 °C to inactivate the endonuclease. Digests were fractionated on 1% agarose gels using a Tris-borate buffer (Tris 89 mM, boric acid 89 mM, Na$_2$ EDTA 2.5 mM). Gels were stained with ethidium bromide to ensure that digests were complete, and the DNA was transferred to nitrocellulose filters as described elsewhere[35]. Cloned DNA was nick-translated[36] with α-^{32}P-labelled dATP to a specific activity of 10^{8} c.p.m. μg^{-1}. Filters were hybridized with 15 ml of hybridization mixture containing 10^{7} c.p.m. of ^{32}P-labelled cloned DNA after it had been denatured at 100 °C for 10 min. Hybridization conditions were 5 × SSC, 50% formamide, 0.5% SDS at 42 °C overnight with gentle agitation. After hybridization, filters were washed extensively in 3 mM Tris base (unneutralized), dried and autoradiographed.

Table 1 Frequencies of rDNA types in the OK. lines and OK. mixed populations

rDNA type	Frequency in OK. lines	Frequency in OK. mixed	No. of OK. mixed populations 'fixed'
A	0.075	0.03	1
B	0.075	0.13	4
C	0.1	0.10	4
D	0.075	0.13	5
E	0.1	0.16	4
F	0.125	0.07	1
G	0.45	0.26	6
H	0	0.06	1
I	0	0.02	0
J	0	0.03	1
6-PGDH: Slow	0.20	0.23	7

The left column shows the frequency of each rDNA type based on two samples of XO males and averaged over all OK. lines (see text). The second column gives the frequencies in the OK. mixed populations based on about three XO males sampled from each population and averaged over all 38 populations. The right column shows the number of OK. mixed populations in which the particular rDNA type was the only one found. The bottom row shows frequencies for the 6-phosphogluconate dehydrogenase (6-PGDH) slow allozyme. The average 6-PGDH allozyme frequencies for the OK. lines are taken from Downes[27]. The methods used for constructing XO males and for DNA extraction, restriction, transfer and hybridization are the same as described in Fig. 2 legend except that the DNA was fractionated on 0.8% agarose gels. The 6-PGDH allozyme carried by each XO male was determined by homogenizing the fly in a drop of water followed by electrophoresis of the extract in a 12.5% starch gel and staining the gel for 6-PGDH. The conditions used for electrophoresis and subsequent staining were as described by Downes[27].

lines suggests that the larger *Hae*III fragment lengths in these chromosomes are due to an increase in the number of 250 bp repeats.

Variations in NTS length that are due to fluctuations in the lengths of the fragment to the left of the *Alu*I region occur in OK. lines 2a and 9a, as both have a major fragment ~250 bp below the common 1.9 kb size (Fig. 3). This is also reflected in the *Hae*III digests which show a prominent band ~250 bp below the common 5.1 kb length (Fig. 2). As both the *Alu*I repetitive region and the *Alu*I fragment to the left of it lie entirely within the NTS, these results confirm that the length variation of the *Hae*III NTS fragment is due primarily to changes in the length of the NTS itself and not to changes in the 28S gene or ETS.

Variation in NTS length in rDNA clusters of the Y chromosome

To analyse the rDNA variation between individual Y chromosomes, males from the OK. lines were mated to C(1)DX/Y females. The C(1)DX/Y progeny contain rDNA mainly from the Y chromosome because the C(1)DX chromosome contains no detectable amounts of rDNA[20]. *Hae*III digests of DNA from C(1)DX/Y females containing Y chromosomes, sampled in 1979, from eight of the OK. lines were probed with the NTS clone and revealed 10 different rDNA patterns (Fig. 4).

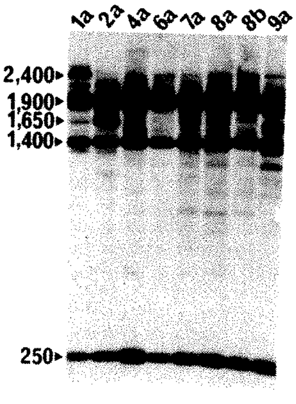

Fig. 3 Autoradiographs of total DNA of XO males after digestion with *Alu*I and hybridization to ^{32}P-labelled NTS clone pDm103HH2. Each track contains the DNA of four XO male progeny from a cross between an OK. male and an XX/O female (see Fig. 2 legend for details). The source of the OK. male parent is indicated above each track. In each case DNA was extracted from the same XO male progeny as used in the corresponding track of Fig. 2. Arrows on the left indicate fragment sizes in base pairs. *Alu*I digests were in 6 mM Tris-HCl *p*H 7.6, 6 mM $MgCl_2$, 1 mM dithiothreitol and DNA was electrophoresed in a 2% agarose gel. The methods used for DNA extraction, transfer and hybridization are the same as described in Fig. 2 legend.

The internal repetitive structure of Y chromosome NTSs from five different OK. sublines was investigated using *Alu*I and the NTS probe (data not shown). As with the X chromosomes, major bands are seen at 250 bp and 1.4 kb. However, the 1.9 kb band, corresponding to the fragment left of the *Alu*I region in X chromosomes (Fig. 1), is not prominent in any subline. Instead, a new major band is revealed at either 1.2 or 1.65 kb. A greater similarity between different Y chromosomes than between Y and X chromosomes, as found for the organization of rDNA repeats, has been found for other rDNA characteristics[21,22] and may be a result of the genetic isolation of the NOs on the X and Y chromosomes. Interestingly, the isolation has been sufficient for a particular character (the presence or absence of the 1.9 kb band in this case) to spread to a high proportion of the rDNA repeats of the NO.

High correlations for rDNA patterns between sublines separated for over 200 generations

By comparing the different X chromosome *Hae*III patterns in the OK. lines it is possible to classify them into seven types—A to G (Fig. 2). For 8 of the 10 cases, the rDNA patterns of the chromosomes sampled are indistinguishable between the a and b sublines, showing that the variation between lines is due to a polymorphism in the original Oklahoma population. When the XO male progeny derived from a different set of OK. line XY males were analysed, the same patterns as before were obtained, except for OK. lines 1a, which had pattern D, and 2b, which had pattern B. The a/b correlation in this sample of chromosomes is, however, the same as before, as sublines 2a and 2b are identical and 1a and 1b different.

Similarly, 10 Y chromosome rDNA patterns can be classified (M to W; Fig. 4). In four cases the a and b sublines are identical and in OK. line 5 they differed by only one band, possibly due to slight partial digestion. That differences between a pair of a and b sublines may be due to double insemination of the ancestral Oklahoma females leading to the introduction of two Y chromosomes in the subsequent progeny is consistent with an estimated frequency of ~50% for double insemination in a wild population of *D. melanogaster*[23]. An alternative explanation is that the a/b differences are due to variation generated during the 9 yr of laboratory maintenance.

Discontinuous variation of NTS length and copy number

One of the most striking features of the NTS length variation is that, despite the large fluctuations in copy number of many of the different lengths of NTS, a prominent 5.1 kb *Hae*III NTS length is common to most of the X and Y chromosomes (Figs 2, 4), which may reflect either a preference for this length by the mechanism producing the variation or its conservation due to natural selection. NTS length is usually confined to between 3 and 6 kb in the *D. melanogaster* sibling species subgroup[12] and *D. hydei*[24], *D. virilis*[25] and other Dipterans (such as *Calliphora erythrocephala*[26]).

An interesting feature of the NTS length variation is the differential abundance of many of the NTS lengths other than 5.1 kb. For example, the 9.6 kb *Hae*III NTS fragment of the X chromosome of OK. line 1 represents ~10% of the total repeats (estimated by microdensitometry and accounting for length), but no more than 1.5% in other X chromosomes from the Oklahoma stocks (Fig. 2). Assuming there are 250 copies of the rDNA repeats on the X chromosomes, these percentages represent 25 and 4 repeats respectively. Thus repeats in an array do not evolve independently, rather variants somehow spread in the array.

What mechanism might underlie the latter process? The data can be explained by unequal exchange occurring at two different levels. First, unequal staggers at the level of the region of repetition in the NTS (see Fig. 1) would generate NTS length heterogeneity. Second, unequal staggers at the level of the total rDNA units would generate the differences in copy number of each NTS length.

Continual unequal exchange at these two levels would contribute to the amplification or elimination of one or other of the rDNA lengths and hence explain the observed discontinuities in copy number of lengths. In addition, a continual turnover of rDNA by unequal exchange could explain the homogeneity within a species for variant sequences in regions of rDNA, that is, concerted evolution[1,12] (see below). Homogenization of a rDNA variant facilitates the expediency with which natural selection accepts or rejects, if need be, the variant in question. It is improbable that a single variant member of a multigene family of 400 members would have sufficient effect on the phenotype to be recognized by natural selection. However, a mechanism which amplifies or reduces the copy number of a variant to different degrees on different chromosomes will increase its contribution to phenotypic variance and hence the effectiveness with which natural selection may act on it.

Behaviour of rDNA types in mixed laboratory populations

To investigate the important question of the degree to which natural selection may be acting on the variation at the rDNA locus, we analysed populations derived from mixtures of flies from the OK. lines. In 1974 10 replicate populations were set up, each with 10 males and 10 females from each of the 20 OK. sublines, 1a–10b. After the first generation each population was divided into four sub-populations, each of which was subsequently maintained on fly medium containing a different species of yeast as food. After 6 yr (~150 generations) several males were sampled from 38 of these 40 OK. mixed populations and mated to $\hat{X}X/O$ females to produce XO male progeny. Restriction enzyme analysis of the XO male DNA with *Hae*III and probing with the NTS clone showed that all the original rDNA types found in OK. lines 1–10 were also present in the OK. mixed populations and that, in addition, three new types of rDNA pattern could be identified (H, I, J in Fig. 5). At least two (usually three) X chromosomes were analysed from each population and classified.

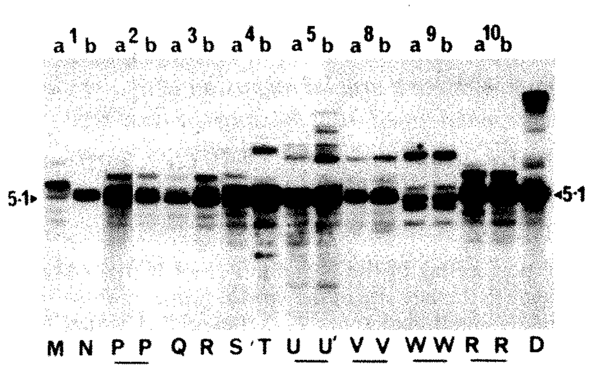

Fig. 4 Autoradiographs of total DNA of individual $\hat{X}X_{-NO}/Y$ males after digestion with *Hae*III and hybridization to ^{32}P-labelled NTS clone pDm103HH2. Y chromosomes were derived from males sampled from the sublines of OK. lines 1–5, 8–10 in 1980. The various hybridization patterns have been classified into 10 types (M–W). Subline 5b has been labelled U' because it differs by only one minor band from 5a (see text). Those lines in which the sublines show similar patterns are underlined. The rightmost track is an OK. mixed XO male with pattern D (see Fig. 5) run on the same gel for comparison. Arrows indicate sizes of fragments in kilobases. The $\hat{X}X_{-NO}/Y$ females were constructed by mating an OK. male with females from a mal/C(1)DX, y f stock. Progeny were checked to ensure that all females had a yellow and all males a wild-type body colour. Yellow females were collected and stored frozen at −70 °C for up to 6 months. The methods used for DNA extraction, restriction, transfer and hybridization are the same as for Fig. 2 except that a 0.8% agarose gel was used.

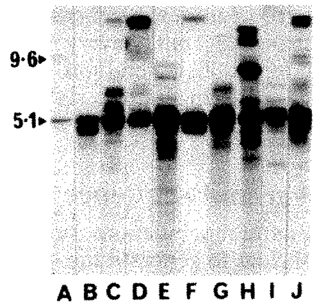

Fig. 5 Autoradiographs of total DNA of XO males after digestion with *Hae*III and hybridization to ^{32}P-labelled NTS clone pDm103HH2. Each track contains the DNA of four XO male progeny from a cross between an OK. mixed male and an $\hat{X}X/O$ female (see Fig. 2 legend for details). Tracks have been chosen to represent all the types of rDNA pattern found in the OK. mixed lines investigated. Types A–G are the same as those found in the OK. lines (Fig. 2) and three new types, H, I and J, are shown. Arrows on the left indicate fragment sizes in kilobases. The methods used for DNA extraction, restriction, transfer and hybridization are the same as for Fig. 2 except that the DNA was fractionated on 0.8% agarose gels.

The frequencies of the rDNA patterns showed no statistically significant correlation with any yeast species; thus the populations may be treated as 38 replicates. The frequency of each rDNA type, averaged over all 38 populations, was not significantly different from its frequency in the OK. lines, indicating that there has been no strong selection in these conditions for or against any particular type of rDNA (Table 1). However, there might be strong selection in each population maintaining the original rDNA type frequencies. On this basis, it might be expected that the frequencies in each population would show some resistance to genetic drift and remain relatively unaltered. That 27 out of 38 populations contained only one rDNA type, detected in average sample sizes of three, clearly shows the final populations are more homogeneous than expected from the overall initial frequencies, probably due to genetic drift. This conclusion is supported by studies[27] on autosomal allozyme frequencies of the same mixed populations which indicate an average population size of ~90–400. Additionally, the XO males used for the rDNA analysis have been assayed for the X-linked allozyme variant 6-phosphogluconate dehydrogenase which is 65 map units away from *bobbed*[28]. The degree of 'fixation' of this variant in the populations is similar to that of rDNA type G which has a comparable overall frequency calculated from all the populations combined (Table 1). Thus both the overall frequencies and the frequencies within populations indicate that there has been no strong selection of rDNA variants in these circumstances.

Stability of rDNA types in the laboratory

The data from the separate OK. lines and the OK. mixed populations show that the rDNA types of the X chromosomes have been stable in the laboratory. In the OK. lines no rDNA pattern has been found which is restricted to only one subline when all X chromosome replicate samples are taken into account. As at the time of analysis each a/b subline had been separate for over 200 generations, then the probability that a pattern remained unchanged in both sublines is $(1-m)^{400}$, where m is the rate of detectable change per generation. The probability that no unique type would be sampled in any of the 10 pairs of lines is therefore $(1-m)^{4,000}$. If m were $\frac{1}{1,250}$, this would give a probability of 0.05. The data therefore suggest that the rate of detectable change in the laboratory is <1 in 1,250 generations.

Analysis of the OK. mixed populations revealed only three rDNA types not found in the OK. lines. One of these, H, is present in more than one population and could have been present when the OK. mixed populations were established. The other two types, I and J, could either be newly generated variants, or were left undetected in the OK. lines. If we assume that these types have been newly generated, then this would indicate a rate of change of 2 out of every 38 populations in 150 generations, or 1 in 3,000 generations. Such estimates are consistent with rates of change at the rDNA locus of 3×10^{-4} estimated by analysis of bristle selection lines[29].

Family turnover and sequence fixation

When considering natural populations, such mutation rates are quite high and sufficient to generate the very extensive rDNA polymorphism observed in effective population sizes of 10^4–10^5 with no selection. If the high polymorphism is indeed a result of a high rate of unequal exchange which can amplify or reduce the copy number of variant repeats, then on an evolutionary time scale the rDNA family would be in a continual state of turnover. The rate of turnover would influence the extent to which an array becomes homogeneous for a variant rDNA unit[4]; and the breeding size of a population would influence the extent to which a variant array becomes fixed in a population[5]. Natural selection would interact with these processes depending on the variant in question.

Our calculations, however, of the extent to which the above assessments of the rate of turnover and stability of rDNA types can explain the concerted evolution of rDNA sequence variants in the *melanogaster* subgroup suggest that additional forces might be necessary to drive specific variants to fixation[1,12]. Observations that continual homogenization is occurring in families on different sex chromosomes (such as the rDNA arrays) or on many different chromosomes[8,30,31] suggest that mechanisms of non-reciprocal interchromosome transfer and 'conversion' of sequences are involved with fixation[1,3,8]. We discuss elsewhere[1] the extent and significance of such a process of molecular drive in the evolution of multigene families.

We thank Nick Barton, Steve Brown, John Dallas, Steve Downes, Tom Strachan and Martin Trick. This research was supported in part by SRC grant GR/A/65379 to G.A.D. and GR/A/3758.1 to J.M.T. E.S.C. acknowledges receipt of a SRC studentship.

Received 27 July; accepted 16 December 1981.

1. Dover, G. A. *et al.* in *Genome Evolution* (eds Dover, G. A. & Flavell, R. B.) 343–374 (Academic, London, 1982).
2. Jeffreys, A. in *Genome Evolution* (eds Dover, G. A. & Flavell, R. B.) 157–176 (Academic, London, 1982).
3. Dover, G. A. & Coen, E. S. *Nature* **290,** 731–732 (1981).
4. Smith, G. P. *Cold Spring Harb. Symp. quant. Biol.* **38,** 507–513 (1974).
5. Otha, T. *Evolution and Variation of Multigene Families* (Springer, New York, 1980).
6. Klein, H. L. & Petes, T. D. *Nature* **289,** 144–148 (1981).
7. Scherer, S. & Davis, R. W. *Science* **209,** 1380–1384 (1980).
8. Brown, S. D. M. & Dover, G. A. *J. molec. Biol.* **150,** 441–466 (1981).
9. Petes, T. D. *Cell* **19,** 765–774 (1980).
10. Szostak, J. W. & Wu, R. *Nature* **284,** 426–430 (1980).
11. Tartof, K. *Cold Spring Harb. Symp. quant. Biol.* **38,** 491–500 (1974).
12. Coen, E. S., Strachan, T. & Dover, G. A. *J. molec. Biol.* (in the press).
13. Schalet, A. *Genetics* **63,** 133–153 (1969).
14. Ritossa, F. in *The Genetics and Biology of Drosophila* Vol. 1b (eds Ashburner, M. & Novitski, E.) 801–846 (Academic, New York, 1976).
15. Federoff, N. *Cell* **16,** 697–710 (1979).
16. Long, E. O. & Dawid, I. B. *A. Rev. Biochem.* **49,** 727–764 (1980).
17. Woodruff, R. C. & Thompson, J. N. Jr *Heredity* **38,** 291–307 (1977).
18. Endow, S. A. & Glover, D. M. *Cell* **17,** 597–605 (1979).
19. Endow, S. A. *Cell* **22,** 149–155 (1980).
20. Ritossa, F., Malva, C., Boncinelli, E., Graziani, F. & Polito, L. *Proc. natn. Acad. Sci. U.S.A.* **68,** 1580–1584 (1971).
21. Tartof, K. D. & Dawid, I. P. *Nature* **263,** 27–30 (1976).
22. Yagura, T., Yagura, M. & Muramatsu, M. *J. molec. Biol.* **133,** 533–547 (1979).
23. Milkman, R. & Zeitler, R. R. *Genetics* **78,** 1191–1193 (1974).
24. Renkawitz-Pohl, R., Glatzer, K. H. & Kuntz, W. *Nucleic Acids Res.* **8,** 4593–4611 (1981).
25. Rae, P. M. M., Barnett, T. & Murtif, V. L. *Chromosoma* (*Berl.*) **82,** 637–655 (1981).
26. Schafer, M., Wyman, A. R. & White, R. *J. molec. Biol.* **146,** 179–200 (1981).
27. Downes, S. P. thesis, Univ. Cambridge (1981).
28. Gerasimova, T. I. & Ananjev, E. V. *Drosoph. Inf. Serv.* **48,** 93 (1972).
29. Frankham, R., Briscoe, D. A. & Nurthen, R. K. *Genetics* **95,** 727–742 (1980).
30. Strachan, T., Coen, E. S., Webb, D. A. & Dover, G. A. *J. molec. Biol.* (in the press).
31. Arnheim, N. *et al. Proc. natn. Acad. Sci. U.S.A.* **77,** 7323–7327 (1980).
32. Roiha, H., Miller, R. M., Woods, L. C. & Glover, D. M. *Nature* **290,** 749–753 (1981).
33. Roiha, H. & Glover, D. M. *J. molec. Biol.* **140,** 341–355 (1980).
34. Glover, D. M. & Hogness, D. S. *Cell* **10,** 167–176 (1977).
35. Wahl, G. M., Stern, M. & Stark, G. R. *Proc. natn. Acad. Sci. U.S.A.* **76,** 3683–3687 (1979).
36. Rigby, P. W. J., Dieckmann, M., Rhodes, C. & Berg, P. *J. molec. Biol.* **113,** 237–251 (1977).

Activation of SV40 genome by 72-base pair tandem repeats of Moloney sarcoma virus

Barbara Levinson, George Khoury, George Vande Woude & Peter Gruss

Laboratory of Molecular Virology, National Cancer Institute, National Institutes of Health, Bethesda, Maryland 20205, USA

The simian virus 40 (SV40) 72-base pair (bp) tandem-repeated sequences have a crucial role as an activator element in viral gene expression. We replaced the SV40 72-bp repeat with a 72-bp repeat derived from the long terminal repeat (LTR) of cloned Moloney murine sarcoma virus (MSV) DNA. Although there is no detectable sequence homology to SV40, the MSV repeats can substitute functionally for the SV40 repeats and generate a viable virus in monkey kidney cells.

THE identification of nucleotide signals directing the initiation of transcription should provide an insight into the complex regulatory mechanisms controlling the activity of eukaryotic genes. In this regard, the DNA tumour viruses such as SV40 probably represent the best studied model systems. Experimental approaches using SV40 have been facilitated by the detailed information available concerning viral genetics, together with a knowledge of the entire nucleotide sequence of the small circular genome and the 5′ termini of the mRNAs (see ref. 1 for review).

Various control elements have been localized to the region around the origin of SV40 DNA replication. Besides binding sites for the multifunctional early gene product, the large T-antigen[2–6], a Goldberg–Hogness (G–H) box precedes the most abundant early mRNA cap sites by ~25 nucleotides[7,8]. Recent data[9–12] suggest that the G–H box is dispensable for *in vivo* expression of the SV40 early genes but is apparently involved in precise positioning of the 5′ termini of early mRNAs. Further upstream (to the late site of the viral genome) are several sets of tandem-repeated sequences[7,8,13], the role of which has been investigated by constructing deletion mutants. Although little is known about the function of the 21-bp repeat, several sets of mutants have focused on the function of the 72-bp tandem repeat. Removal of precisely one 72-bp repeat does not affect viability of the viral genome[13–16], but if the deletion is extended into the second 72-bp repeat, the genome becomes nonviable[16]. Similar conclusions have been drawn from parallel experiments using constructed plasmids[10]. On the basis of these data, we concluded that the 72-bp repeat is essential for the expression of the early SV40 genes.

Several other viral systems have elements which bear a structural resemblance to the 72-bp repeat and possibly express related activities[16,17]. Although no significant sequence homology to the SV40 72-bp repeat has been detected[17,18],

0028-0836/82/070568—05$01.00

studies on the LTRs of cloned MSV revealed putative transcriptional control elements and a 72-bp tandem repeat preceding by ~180 nucleotides the 5′ end of all the major mRNAs[18]. Furthermore, it was demonstrated in DNA transfection–transformation assays that the viral LTR provides all the necessary functions for activation of transforming genes[19–21], including the SV40 T-antigen (M. Krigler and M. Botchan, and M. McGeady *et al.*, personal communications).

Based on these observations, we decided to investigate the possibility that other sequences from nonhomologous sources (like MSV) might replace the functional activity of the SV40 repeats, and whether tandem-repeated elements might be involved in host range. Here we demonstrate that although the nucleotide sequence of the MSV 72-bp repeat differs from that of SV40, it has similar functional activity and can rescue the *cis*-defective SV40 deletion mutant, thus generating a viable recombinant virus. This recombinant virus can express early SV40 genes in monkey kidney cells and in mouse cells.

Construction of the recombinant

The construction of the SV40 recombinant carrying the 72-bp tandem repeat from MSV is illustrated in Fig. 1. In the protocol used, we first cloned a recombinant plasmid harbouring the entire SV40 genome except for the 72-bp tandem repeats. For this purpose, we removed from the DNA of a viable SV40 variant bearing a second *Bam*HI site, the *Sph*I–*Bam*HI region (218 bp) comprising almost all nucleotide sequences from both 72-bp repeats plus some flanking sequences from the end of the repeat to the *Bam*HI site (nucleotide 348 (ref. 13), the former *Hpa*II site). A pBR322 derivative (pA10) was constructed which contained a short stretch of nucleotides with the *Eco*RI, *Xba*I and *Bam*HI restriction enzyme sites. The pA10 plasmid was cleaved with *Sph*I and *Bam*HI and the larger fragment was ligated to the *Sph*I–*Bam*HI SV40 fragment lacking the two 72-bp repeats. This cloned recombinant plasmid pSV-r$^-$ served as the recipient for the insertion of the 72-bp repeats from the LTR of cloned Moloney murine sarcoma viral DNA. A convenient 199-bp fragment containing primarily the two 72-bp MSV repeats was generated using *Xba*I and *Sau*3A (an isoschizomer of *Mbo*I which cleaves G$^{\text{Me}}$ATC as well as GATC). For ligation, the plasmid recipient pSV-r$^-$ was partially cleaved with *Bam*HI to generate mainly single-cut linear molecules and the purified linear molecules were cleaved to completion with *Xba*I. The large fragment was ligated to the *Sau*3A–*Xba*I fragment derived from the MSV LTR (*Bam*HI and *Sau*3A have identical cohesive ends). Polar insertion of the MSV repeat was achieved because both fragments contained two non-identical termini. The polarity of the MSV repeat in the recombinant was the same as that of the 72-bp repeat in the SV40 wild-type (wt) genome. After cloning of this plasmid (pSV-r$^{\text{MSV}}$) in *Escherichia coli* HB101, the viral sequences were separated from the plasmid sequences by cleavage with *Sph*I and *Xba*I (see Fig. 1).

Biological activity of SV-r$^{\text{MSV}}$

To assay the functional activity of the MSV 72-bp repeat, we transfected the linear SV40–MSV recombinant (SV-r$^{\text{MSV}}$) into African green monkey kidney (AGMK) cells using DEAE-dextran as a facilitating agent. As a control, the *Xba*I–*Sph*I linear molecules that did not contain the MSV 72-bp repeats (SV-r$^-$) were transfected in parallel. After ~10 days, a SV40 cytopathic effect (CPE) was seen on dishes transfected with SV-r$^{\text{MSV}}$ DNA, whereas no vacuolization was seen in control plates. Sixteen to eighteen days after transfection, the cells which received SV-r$^{\text{MSV}}$ DNA were completely lysed, whereas there was no CPE apparent on the control plates. To demonstrate infectious virus, the lysate was filtered through a nitrocellulose filter (Millipore, 0.45 μm pore size) and subsequently used to reinfect AGMK cells; CPE was observed 3–4 days after infection and complete cell lysis occurred after ~7–10 days. No CPE was observed on the control plates infected with SV-r$^-$ lacking the MSV repeats.

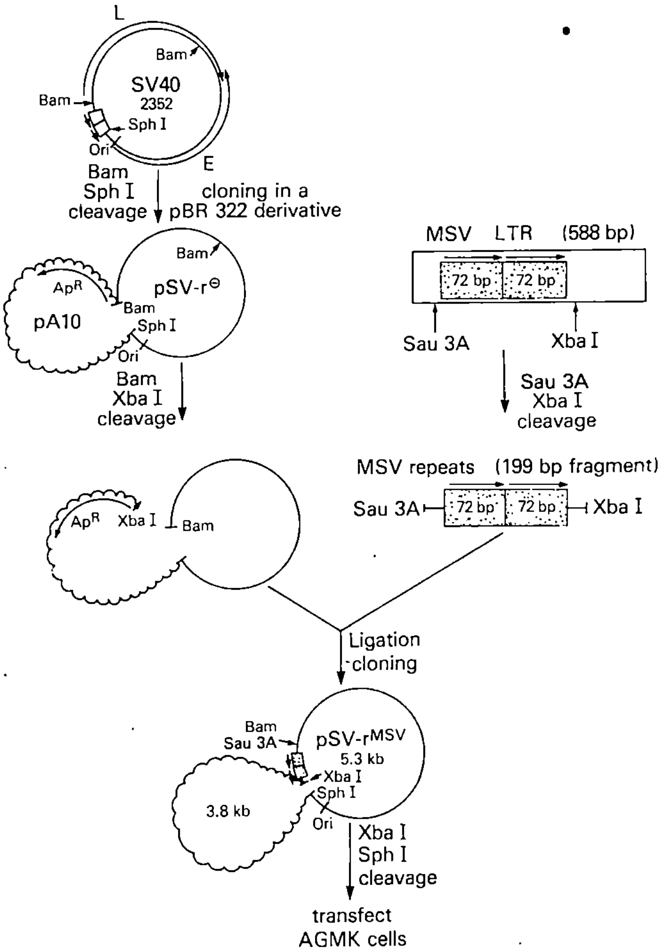

Fig. 1 Construction of SV-r$^{\text{MSV}}$ recombinants. A viable variant of SV40 (2352) carrying a second *Bam*HI site at the *Hpa*II site (P.G., unpublished results) was partially cleaved with *Bam*HI and unit-length molecules isolated after electrophoresis in 1.4% agarose gels[33]. These linear molecules were cleaved to completion with *Sph*I to remove a fragment (218 bp) constituting the majority of the SV40 72-bp repeats (plus sequences from the end of the repeat to the *Bam*HI–*Hpa*II site). This SV40 repeat-minus deletion mutant (SV-r$^-$) resembling our recently reported *cis*-defective SV40 deletion mutant 2356 (ref. 16), was cloned in a pBR322 derivative (pA10). pA10 differs from pBR322 (ref. 34) primarily in the presence of a polylinker *Eco*RI, *Xba*I and *Bam*HI. In addition, it carries a deletion in the tetracycline-resistance (Tc$^{\text{r}}$) gene (from *Eco*RI to *Bam*HI). This was achieved by deletion of the small *Eco*RI–*Bam*HI fragment from pBR322. Subsequently, the protruding 5′ ends of the remaining larger fragment were filled using T4 polymerase[35], and *Xba*I linkers were ligated to the blunt ends. The pA10 plasmid was restricted with *Bam*HI and *Sph*I and the larger fragment isolated by electrophoresis in a 1.4% agarose gel. This fragment was ligated[33] to the *Bam*HI, *Sph*I-cleaved SV40 DNA fragment and cloned in *E. coli* HB101[36,37]. After isolation[38,39], the superhelical recombinant plasmid DNA (pSV-r$^-$) was partially cleaved with *Bam*HI and the unit-length recombinant plasmid purified by agarose gel electrophoresis. The linear pSV-r$^-$ DNA was subsequently cleaved to completion with *Xba*I and the large fragment again purified by agarose gel electrophoresis. In parallel, the recombinant plasmid carrying the cloned MSV LTR sequences[21] was cleaved with *Sau*3A and *Xba*I and a 199-bp fragment isolated by polyacrylamide gel electrophoresis[33]. This fragment was ligated to the pSV-r$^-$ plasmid and cloned in *E. coli* HB 101[36,37]. Cloned plasmids were identified by restriction enzyme analysis using *Xba*I and *Eco*RI followed by blotting[22], then hybridized with ^{32}P-labelled MSV LTR DNA probe. Only the predicted fragment had homology to this probe. One of the recombinants carrying the MSV 72-bp repeats, pSV-r$^{\text{MSV}}$, was subsequently cleaved to completion with *Xba*I and *Sph*I, releasing the viral recombinant from the plasmid sequences, and 5 μg of DNA transfected on to 1×10^6 secondary AGMK cells using DEAE-dextran as facilitating agent[16]. As a control, 5 μg of the plasmid pSV-r$^-$DNA, cleaved with *Xba*I and *Sph*I, was similarly transfected.

Analysis of SV-r$^{\text{MSV}}$ recombinant DNA

Having tentatively established the presence of an infectious virus in the cell lysate, we then had to characterize the structure of the recombinant viral DNA molecules. AGMK cells were inoculated in parallel with wild-type SV40 or the SV-r$^{\text{MSV}}$ virus stock. Superhelical DNA was isolated from infected cells

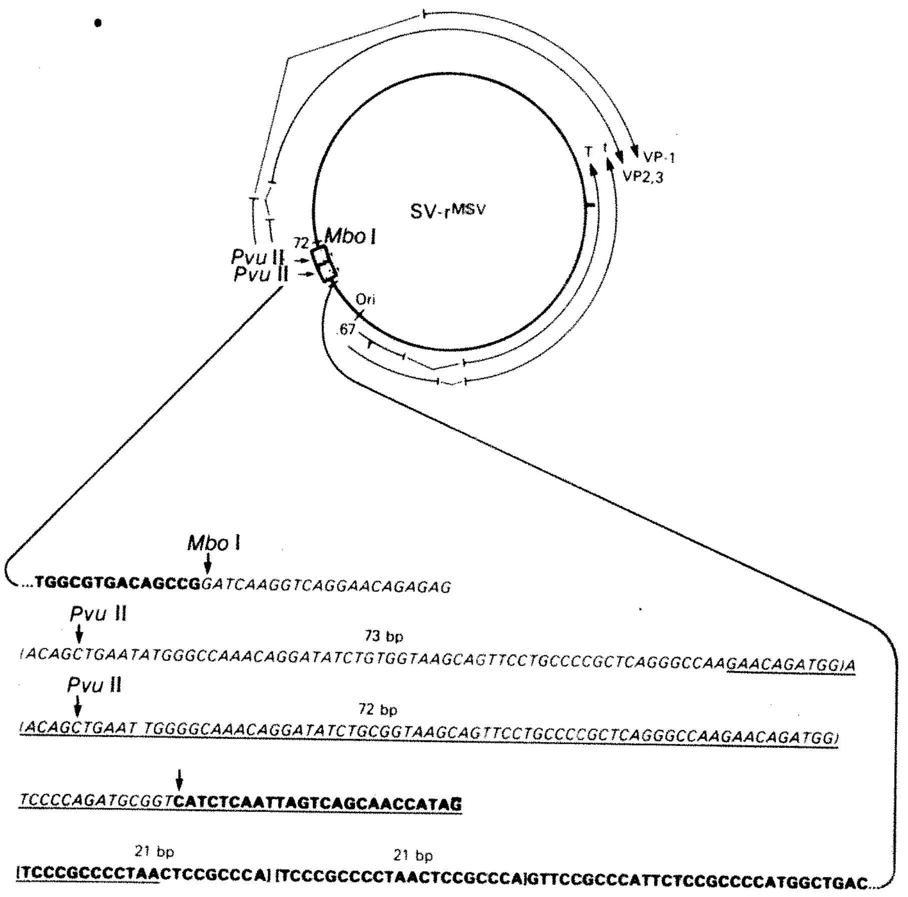
VP-1
VP2,3
T
t
SV-rMSV
72
Mbo I
Pvu II
Pvu II
Ori
.67
Mbo I
...TGGCGTGACAGCCGGATCAAGGTCAGGAACAGAGAG
Pvu II
73 bp
(ACAGCTGAATATGGGCCAAACAGGATATCTGTGGTAAGCAGTTCCTGCCCCGCTCAGGGCCAAGAACAGATGG)A
Pvu II
72 bp
(ACAGCTGAAT TGGGGCAAACAGGATATCTGCGGTAAGCAGTTCCTGCCCCGCTCAGGGCCAAGAACAGATGG)
TCCCCAGATGCGGTCATCTCAATTAGTCAGCAACCATAG
21 bp
21 bp
[TCCCGCCCCTAACTCCGCCCA] [TCCCGCCCCTAACTCCGCCCA]GTTCCGCCCATTCTCCGCCCCATGGCTGAC...

Fig. 2 DNA sequence analysis of the SV-r^{MSV} recombinant. Ten flasks (150 cm^2) of secondary AGMK cells were infected with 1 ml each of SV-r^{MSV} and superhelical viral DNA was collected 4 days after infection[40]. The viral DNA (20 μg) was cleaved to completion with *Mbo*I and the enzyme removed by phenol extraction. DNA fragments were terminally labelled with [γ-^{32}P]ATP[24] and separated in a 4% polyacrylamide gel[31]. A fragment of 844 bp was isolated, the DNA was electroeluted and re-cleaved with *Bgl*I. The smaller fragment (307 bp) was purified by 4% acrylamide gel electrophoresis and sequenced using the forward-backward method[25]. Nucleotides read from the 6% polyacrylamide-urea gel are underlined; the others were deduced from the construction (see Fig. 1) and from the published sequences of SV40[7,8,13] and MSV[18].

labelled with ^{32}P. To test for the presence of MSV sequences in the recombinant virus, we hybridized the labelled DNA to a Southern blot[22] containing a DNA fragment from the cloned MSV LTR[23]. Only SV-r^{MSV} DNA, and not control SV40 wt DNA showed homology to the MSV LTR sequences (data not shown). Furthermore, the restriction enzyme pattern of SV-r^{MSV} DNA followed exactly the predicted structure. The presence of the acquired *Sau*3A (*Mbo*I) site used for ligation (see Fig. 1), and *Pvu*II sites present in each MSV 72-bp repeat, further clarifies the physical structure of SV-r^{MSV} recombinants. As expected, the *Sph*I site present in the SV40 72-bp repeat was missing (Fig. 2).

As linear molecules were used for the initial transfection of AGMK cells, it is likely that during circularization by cellular enzymes, several nucleotides were removed from each terminus. To determine more precisely the structure of the recombinant, we analysed the nucleotide sequence in the region encompassing the junction between SV40 and MSV sequences. An *Mbo*I fragment (844 bp) containing the entire MSV insert joined to SV40 sequences around the origin of replication was isolated, terminally labelled[24], re-cleaved with *Bgl*I and the smaller fragment (307 bp) purified by gel electropohoresis. A recently described dideoxy sequencing method was used[25]; the physical structure and nucleotide sequence around the recombinant junction are outlined in Fig. 2. Both MSV repeats were found to be present. As deduced from the restriction enzyme analysis, 22 nucleotides precede the first repeat. Although the SV-r^{MSV} linear molecule used for infection of AGMK cells had ~36 bp flanking the terminus of the second repeat, 20 nucleotides (including the terminal *Xba*I site) were deleted, presumably through the action of cellular nucleases. This left 14 nucleotides of MSV sequence after the second repeat and before the SV40 junction (atgcggtÇATCTCA·). Three nucleotides were deleted from the SV40 sequence, including those of the *Sph*I site (the Ç at the junction may derive either from MSV or SV40). As very few nucleotides were deleted from SV40, both SV40 21-bp repeats were preserved. The third binding site for T-antigen, which has been localized to the 21-bp repeats[26], was also present in the recombinant virus.

Analysis of mRNAs transcribed from SV-r^{MSV} recombinants

To analyse the mRNAs transcribed from the recombinant genome, AGMK cells were infected in parallel with either wt SV40 or the SV-r^{MSV} recombinant. Poly(A)-containing cytoplasmic RNA was isolated and analysed by the nuclease S$_1$ technique[27,28]. Using an SV40 DNA probe uniformly labelled *in vivo*, both early and late transcripts were detected in cells infected with SV-r^{MSV} recombinant virus (Fig. 3*a*). No difference was observed in the spliced bodies compared with SV40 early or late (19S, 16S) mRNA. As SV-r^{MSV} recombinants do not retain the nucleotide sequences coding for the 5′ ends of the most abundant late transcripts, it was of interest to investigate further the structure of the late mRNAs. For this analysis, we used a uniformly labelled *Hpa*II–*Bam*HI fragment B. The results (Fig. 3*b*) indicate that the 5′ ends of the SV-r^{MSV} late transcripts are located further upstream towards the origin of replication than the *Hpa*II end of the DNA probe. This suggests the presence of novel 5′ ends located probably in MSV sequences. The 5′ termini of the early mRNAs seem identical to those of wt SV40 (data not shown).

Protein induced by the SV-r^{MSV} recombinants

As the overall structure of early and late mRNAs of SV-r^{MSV} were very similar to transcripts of SV40 wt RNA, it seemed likely that the translational products also would be similar. To confirm this, AGMK cells were infected in parallel with wt SV40 virus or the SV-r^{MSV} recombinant stock. About 72 h after infection, cells were labelled with ^{35}S-methionine for 2 h. Proteins were extracted and immunoprecipitated either with a hamster antiserum recognizing both the early T-antigen and late VP-1 capsid protein or with normal hamster antiserum, then analysed by gel electrophoresis (Fig. 4). Both T-antigen and

VP-1 co-migrate with the SV40 wt markers. These data establish the physical integrity and functional activity of SV-r$^{\rm MSV}$ recombinants.

Conclusion

In previous studies[10,16] we and others have defined sets of repeated sequences to the late side of the SV40 replication origin as being essential for the transcription of viral gene sequences. Unlike the so-called Goldberg–Hogness sequence, which seems to be responsible for setting the 5′ end of eukaryotic transcripts[9-12], these repeated sequences appear to contribute to the transcriptional activity of genes located in their general vicinity. Thus, we designated them 'activator' elements. Presumably these SV40 activator elements enhance the expression of heterologous genes introduced into eukaryotic cells in a variety of cDNA transfection experiments (ref. 29 and V. B. Reddy and W. Schaffner, personal communications). Studies are now being directed at determining what part the position and orientation of such sequences play in contributing to gene activity.

At first glance, the striking feature of the SV40 activator element is its repetitive nature, although one copy is sufficient for its functional activity[13-16]. In searching for similar sequences among other eukaryotic genes and viral genomes, we focused on the 72-bp repeats in the MSV LTR. The position of the repeat within the LTR (a set of ~600 nucleotides which had previously been shown capable of restoring transforming activity to viral and cellular sarcoma virus genes[19-21]) indicated that it might have an analogous role in the regulation of retrovirus gene activity. The MSV 72-bp repeat sequence was therefore used to demonstrate similar functional activity by reactivating an SV40 deletion mutant lacking the SV40 72-bp repeats. As mentioned above and elsewhere[17,18], this heterologous set of nucleotides bears little if any resemblance to the original SV40 sequence. Restriction endonuclease analysis and DNA sequencing methodology has established the physical structure of a recombinant virus which retains the SV40 21-bp repeat elements and carries a 167-bp insert, most of which represents the MSV 72-bp repeats. This recombinant virus induced the synthesis of polypeptides indistinguishable from those of wt SV40. The structures of the viral RNAs were similar to those of SV40, except for the 5′ ends of late mRNAs, most of which probably reside in the acquired MSV sequences. This result is expected as the nucleotide sequence encoding the most common 5′ ends of late SV40 mRNAs has been deleted from the SV-r$^{\rm MSV}$ recombinants. In addition, alterations representing either deletion mutants[30] or recombinant viral genomes[31] in this region of SV40 frequently generate novel 5′ termini of the late SV40 mRNA species. That the activator function of the mutant virus resides in the MSV 72-bp sequences and is not simply dependent on a 'spacer' function has been demonstrated in part by previous experiments. Studies in which plasmid sequences were substituted for the SV40 72-bp repeats (ref. 10 and our unpublished results) did not lead to the activation of early SV40 functions.

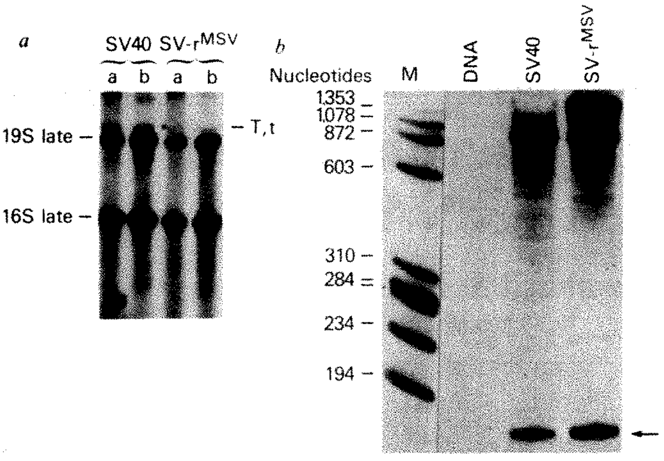

Fig. 3 Analysis of SV-r$^{\rm MSV}$ RNA. Cytoplasmic poly(A)-containing RNA was isolated[41] 72 h after infection of secondary AGMK cells with SV-r$^{\rm MSV}$ and SV40 wt viral stock. The RNA was analysed using the nuclease S$_1$ procedure[27,28]. *In vivo* ^{32}P-labelled SV40 wt DNA (specific activity 1×10^6 c.p.m. per μg DNA) was used as probe. *a*, S$_1$ analysis in a 1.4% alkaline agarose gel of SV-r$^{\rm MSV}$ RNA and control SV40 RNA annealed with the uniformly labelled SV40 wt DNA, linearized at the *Hpa*II site. RNA was prepared from 6×10^6 cells (a) or 2.5×10^7 cells (b) infected with SV-r$^{\rm MSV}$ from 1×10^6 (a) or 6×10^6 cells (b) infected with wt SV40. *b*, Analysis of SV-r$^{\rm MSV}$ RNA (from. 2.5×10^7 cells), SV40 wt RNA (from 1×10^6 cells) and no RNA (DNA control) in an 8% polyacrylamide-urea gel[24]. In this experiment, SV40 wt *Hpa*II–*Bam*HI fragment B was used as a probe representing the late region of the genome. M represents terminally labelled fragments of ΦX 174 DNA.

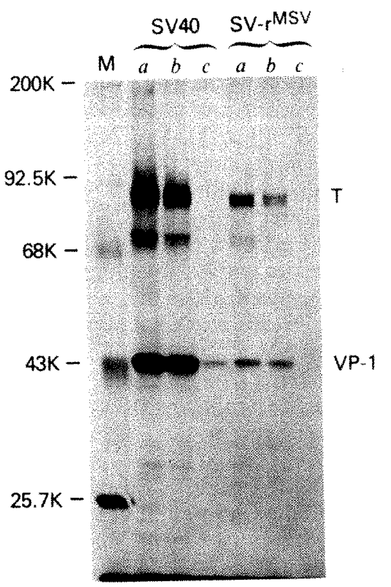

Fig. 4 Analysis of SV-r$^{\rm MSV}$ proteins. One flask of secondary AGMK cells (2×10^7 cells) was infected with 1 ml of either SV-r$^{\rm MSV}$ or wt SV40 (control). At 40 h post-infection, each culture was starved for 1 h in methionine-free medium and labelled for 2 h with ^{35}S-methionine (35 μCi ml^{-1}) in methionine-free medium. Viral proteins were extracted by treating the cells with 2 ml each of lysis buffer (0.01 M Tris *p*H 8.1, 0.1 M NaCl, 0.1% NP-40, 1 mM dithiothreitol, 2mM phenylmethylsulphonyl fluoride, 100 μg ml^{-1} tosylphenylethylchloromethylketone). The insoluble fraction was removed by centrifugation in a Beckman 50TI rotor at 40,000 r.p.m. for 30 min. Viral proteins were immunoprecipitated[42,43] with a hamster antiserum recognizing both tumour(T)-antigen-specific and protein (VP-1)-specific imunodeterminants (*a*, *b*) or with normal hamster serum (*c*). The SDS/polyacrylamide gel system used was that of Laemmli[44]. Radiolabelled protein bands on the gel were detected by fluorography[45]. *a*, Protein extract from 3.75×10^6 cells; *b*, protein from 1.25×10^6 cells. K represents a molecular weight of 1,000.

Given a lack of sequence homology between the 72-bp repeats of SV40 and MSV, it is remarkable that the recombinant virus is viable. If these so-called activator elements are required to interact with a well defined set of host cell macromolecules (for example, proteins or nucleic acids), it is conceivable that they bear a nucleotide sequence homology to one another that is difficult to recognize. Perhaps this homology resides in an interrupted or irregularly distributed pattern of the critical nucleotides. In this respect, we have also considered the possibility that the repeat unit might form a secondary or tertiary structure which is important for its biological function. We found that the SV40, BKV and MSV repeat units can form extensive stem and loop structures (unpublished observations). Alternatively, it is possible that a number of unrelated sequences can provide a similar activating function in host cells by performing parallel functions with an analogous set of host macromolecules. BKV, a human papovavirus, contains three copies of a 68-bp sequence to the late side of its replication origin[32]. This putative activator, which functions in both human and AGMK cells, has no obvious nucleotide sequence homology to the activators of SV40 or MSV. In fact, the late repeated sequences represent the region of the papovavirus BKV genome that has the least sequence homology to SV40[13,17,32].

As we have suggested previously[16,17], activator sequences may have been acquired from host cellular DNA. If this is the case, one might speculate that such sequences could in some way influence the host range of viruses. In this regard, it is of interest that we were unable to detect normal plaques after inoculation of AGMK cells with SV-r^{MSV}, although minute plaques may have been overlooked. One possible explanation for the reduced growth of the recombinant virus on monkey cells is the absence of sequences between the second SV40 72-bp repeat and the converted *Hpa*II (*Bam*HI) site (see Fig. 1). A number of SV40 mutants having deletions in this region grow slowly (J. Mertz, personal communication and our unpublished results). On the other hand, the MSV repeats may function at a lower level in AGMK cells than in mouse cells, which is suggested by preliminary studies comparing T-antigen synthesis in mouse and monkey cells infected with either SV40 or the SV-r^{MSV} recombinant genome.

It is clear that an insight into the role of sequence specificity in activator elements will require a broader understanding of the function of these sequences in activating transcription from specific promoters. It may be that these elements provide viral genomes with a competitive advantage for growth in eukaryotic cells. Nevertheless, we suggest that not only viral genes but eukaryotic genes are regulated by the presence of activator elements, and experiments to identify such sequences in cellular DNA are now in progress.

We thank Monika König and L. Greenbaum for technical assistance; G. Jay, D. Cosman, N. Rosenthal and T. Wood for helpful discussions; and D. Little for preparing the manuscript. These experiments were conducted in accordance with the NIH Guidelines for Recombinant DNA. Studies with the recombinant virus stock in eukaryotic cells were conducted at the P3 containment level.

Received 27 September; accepted 2 December 1981.

1. Tooze, J. *DNA Tumor Viruses, Molecular Biology of Tumor Viruses* Pt 2 (Cold Spring Harbor Laboratory, New York, in the press).
2. Reed, S. I., Ferguson, J., Davis, R. W. & Stark, G. *Proc. natn. Acad. Sci. U.S.A.* **72,** 1605–1609 (1975).
3. Tjian, R. *Cell* **13,** 165–179 (1978).
4. Shortle, D., Margolskee, R. F. & Nathans, D. *Proc. natn. Acad. Sci. U.S.A.* **76,** 6128–6131 (1979).
5. Shalloway, D., Kleinberger, T. & Livingston, D. M. *Cell* **20,** 411–422 (1980).
6. McKay, R. & DiMaio, D. *Nature* **289,** 810–812 (1981).
7. Reddy, V. B. *et al. Science* **200,** 494–502 (1978).
8. Fiers, W. *et al. Nature* **273,** 113–120 (1978).
9. Ghosh, P. K., Lebowitz, P., Frisque, R. J. & Gluzman, Y. *Proc. natn. Acad. Sci. U.S.A.* **78,** 100–104 (1981).
10. Benoist, C. & Chambon, P. *Nature* **290,** 304–310 (1981).
11. Grosschedl, R. & Birnstiel, M. L. *Proc. natn. Acad. Sci. U.S.A.* **77,** 1432–1436 (1980).
12. Mathis, D. J. & Chambon, P. *Nature* **290,** 310–315 (1981).
13. Van Heuverswyn, H. & Fiers, W. *Eur. J. Biochem.* **100,** 51–60 (1979).
14. Waldeck, W. & Sauer, G. *FEBS Lett.* **71,** 313–315 (1976).
15. Subramanian, K. N. & Shenk, T. *Nucleic Acids Res.* **5,** 3635–3642 (1978).
16. Gruss, P., Dhar, R. & Khoury, G. *Proc. natn. Acad. Sci. U.S.A.* **78,** 943–947 (1981).
17. Gruss, P., Dhar, R., Maizel, J. & Khoury, G. in *Genes and Tumor Genes* (eds Schoene, H. H. & Winnacker, E.)(Raven, New York, in the press).
18. Dhar, R., McClements, W. L., Enquist, L. W. G. & Vande Woude, G. *Proc. natn. Acad. Sci. U.S.A.* **77,** 3937–3941 (1980).
19. Blair, D. G., McClements, W. L., Oskarsson, M. K., Fischinger, P. J. & Vande Woude, G. *Proc. natn. Acad. Sci. U.S.A.* **77,** 3504–3508 (1980).
20. Chang, E. H., Ellis, R. W., Scolnick, E. M. & Lowy, D. R. *Science* **210,** 1249–1251 (1980).
21. Blair, D. G. *et al. Science* **212,** 941–943 (1981).
22. Southern, E. M. *J. molec. Biol.* **98,** 503–517 (1975).
23. McClements, W. L., Enquist, L. W., Oskarsson, M., Sullivan, M. & Vande Woude, G. F. *J. Virol.* **35,** 488–497 (1980).
24. Maxam, A. M. & Gilbert, W. *Meth. Enym.* **65,** 499–599 (1980).
25. Seif, I., Khoury, G. & Dhar, R. *Nucleic Acids Res.* **6,** 3387–3398 (1979).
26. Myers, R. M. & Tjian, R. *Proc. natn. Acad. Sci. U.S.A.* **77,** 6491–6495 (1980).
27. Berk, A. J. & Sharp, P. A. *Proc. natn. Acad. Sci. U.S.A.* **75,** 1274–1278 (1978).
28. Berk, A. J. & Sharp, P. A. *Cell* **12,** 721–732 (1977).
29. Capecchi, M. R. *Cell* **22,** 479–488 (1980).
30. Ghosh, P. K. *et al. Proc. natn. Acad. Sci. U.S.A.* **78,** 1386–1390 (1981).
31. Gruss, P., Efstratiadis, A., Karathanasis, S., Konig, M. & Khoury, G. *Proc. natn. Acad. Sci. U.S.A.* **78,** 6091–6095 (1981).
32. Seif, I., Khoury, G. & Dhar, R. *Cell* **18,** 963–977 (1979).
33. Gruss, P. & Khoury, G. *Proc. natn. Acad. Sci. U.S.A.* **78,** 133–137 (1981).
34. Sutcliff, J. G. *Cold Spring Harb. Symp. quant. Biol.* **43,** 77–90 (1979).
35. Morris, C. F., Hama-Inaba, H., Mace, D., Sinha, N. F. & Alberts, B. *J. biol. Chem.* **254,** 6787–6796 (1979).
36. Dugaiczyk, A., Boyer, H. W. & Goodman, H. M. *J. molec. Biol.* **96,** 174–184 (1975).
37. Hutchinson, K. W. & Havlorson, H. O. *Gene* **8,** 267–278 (1980).
38. Clewell, D. B. *J. Bact.* **110,** 667–676 (1972).
39. Wesnik, P. C., Finnegan, D. J., Donelson, J. E. & Hogness, D. S. *Cell* **3,** 315–325 (1974).
40. Hirt, B. *J. molec. Biol.* **26,** 365–369 (1967).
41. Penman, S. *J. molec. Biol.* **17,** 117–130 (1966).
42. Gruss, P., Lai, C.-J., Dhar, R. & Khoury, G. *Proc. natn. Acad. Sci. U.S.A.* **76,** 4317–4321 (1979).
43. Simmons, D. T. & Martin, M. A. *Proc. natn. Acad. Sci. U.S.A.* **75,** 1131–1135 (1978).
44. Laemmli, U. *Nature* **227,** 680–685 (1970).
45. Laskey, R. A. & Mills, A. D. *Eur. J. Biochem.* **56,** 335–341 (1975).

Intracellular transport of microinjected 5S and small nuclear RNAs

Eddy M. De Robertis, Susanne Lienhard & Ruth F. Parisot
Biocenter, University of Basel, Klingelbergstrasse 70, 4056 Basel, Switzerland

The mechanism by which some RNAs are segregated in the cell nucleus was analysed by microinjecting ^{32}P-labelled total RNA from HeLa cells into the cytoplasm of Xenopus *oocytes. Small nuclear RNAs (U1, U2, U4, U5 and U6) migrated into the cell nucleus, where they became 30–60 fold more concentrated than in the cytoplasm. Other RNAs, such as tRNA and 7S RNA, remained in the cytoplasm, while 5S RNA became concentrated in the nucleolus. Studies with lupus erythematosus antibodies showed that the migrating RNAs become associated with oocyte RNA-binding proteins.*

SOME types of RNA are normally located in the nucleus of eukaryotic cells, including heterogeneous nuclear RNA (hnRNA)[1,2], small nuclear RNAs (sn RNAs)[3,4] and tRNA precursors. However the mechanism by which these molecules become segregated is unknown. We became interested in this problem when studies with cloned tRNA genes microinjected into the nucleus of frog oocytes showed that they are transcribed initially into precursor RNAs containing 5′-leader and 3′-trailer sequences[5–8] which do not leave the oocyte nucleus[7,8]. As tRNA precursors with very short extra sequences (of $\sim$5 nucleotides) at the termini are retained in the nucleus, it did not seem likely that the nuclear segregation could result simply from the precursor tRNAs being too bulky to traverse the pores in the nuclear envelope. An alternative possibility is that the precursor RNAs might bind to other intranuclear molecules (such as processing enzymes) which could block nuclear exit either because of size or because they might have an intrinsic affinity for the nucleus, as is known to be the case for many nuclear proteins (see below).

Although other models could explain why some RNAs are located in the nucleus, the binding hypothesis has the advantage that it can be tested using available techniques. Indeed, it

0028–0836/82/070572—06$01.00

predicts that if naked RNA of nuclear origin were injected into the cytoplasm it should be able to diffuse within the cell and eventually accumulate in the nucleus, provided that the nuclear membrane did not block the free diffusion of RNA. This experiment, reported here, was carried out with snRNAs because they provide a convenient source of stable RNAs of nuclear origin.

A large variety of nuclear proteins migrate and accumulate in the nucleus after microinjection into the cytoplasm of frog oocytes[9–13], amoebae[14] or cultured cells[15]. Transient precursors are not involved and thus mature nuclear proteins accumulate in the nucleus, which they normally must re-enter at each mitotic division. The mechanism of accumulation is not yet certain, but on the basis of experiments involving damage of the nuclear membrane[16,17] and saturation with competing proteins[18] it is thought that nuclear proteins may bind inside the nucleus to a non-diffusible nucleoplasmic component(s). If some of the proteins with nuclear affinity were also RNA-binding proteins, then this could provide a mechanism for the intracellular segregation of RNAs.

In the present study we injected labelled RNAs extracted from HeLa cells into the cytoplasm of frog oocytes. The results show that snRNAs migrate into the nucleus, that 5S RNA enters the nucleus and becomes localized in the nucleolus, and that other RNAs (tRNA, 7S RNA) remain in the cytoplasm. The migrating snRNAs bind to oocyte proteins after microinjection, as shown by studies with lupus erythematosus antibodies.

Cellular distribution of microinjected HeLa ^{32}P-RNAs

HeLa cells were chosen as the source of RNA for these experiments because their small RNAs are well characterized[19–21] and are known to be highly conserved throughout evolution. Figure 1, lane *a*, shows the electrophoretic pattern of total RNAs extracted from HeLa cells labelled for 18 h with ^{32}P-orthophosphate. Previous observations[19–21] (which we confirmed, data not shown), relevant to our subsequent experiments, are: (1) some RNAs—tRNAs and 7S RNA (which is complementary to the Alu family of repeated genes)[21]—are preferentially cytoplasmic; (2) other RNAs are preferentially nuclear (U1–U6 snRNAs); and (3) 5S RNA and 5.8S RNA, although preferentially cytoplasmic, are also present in the nuclear fraction after labelling for 18 h, presumably reflecting the time course of assembly of the large ribosomal subunit of which they are part.

Figure 1 shows the results of two experiments in which total HeLa ^{32}P-RNA was injected into the cytoplasm of *Xenopus* oocytes, which were then incubated for 18 h and subsequently manually separated into nucleus and cytoplasm. Most of the injected low-molecular-weight RNAs (lane *a*) are stable after microinjection into oocytes (lane *b*). (An unequal number of counts were loaded in lanes *a* and *b*, but other experiments have shown that the degradation of most small RNAs is negligible.) Exceptions are U3 snRNA (a nucleolar snRNA[3]), which is to a large extent specifically degraded in the oocyte cytoplasm (Fig. 1, lane *b*), and 5.8S, 18S and 28S RNAs (not shown) which seem to diminish in amount relative to other RNAs. Comparison of the labelled RNAs present in the cytoplasm (Fig. 1, lanes *c*, *e*) and in the nucleus (Fig. 1, lanes *d*, *f*) of injected oocytes shows that: (1) the tRNAs and the 7S transcript remain in the cytoplasm (their normal cellular location) as well as 5.8S RNA (which has a complex biogenesis); (2) U1 and U2 snRNAs become more concentrated in the nucleus, although a part still remains in the cytoplasm; and (3) 5S RNA, although predominantly cytoplasmic, also enters the nucleus (but clearly to a lesser degree than U1 or U2).

The microinjected U1 and U2 RNAs concentrate in the nucleus to a remarkable extent. As the nucleus is much smaller than the cytoplasm (about 20 times by volume, 10 times if one assumes that one-half of the cytoplasm is occupied by yolk platelets[18]), and one cytoplasm and one nucleus from individual oocytes were analysed in the lanes of Fig. 1, the amounts of U1 and U2 snRNAs present in the nuclei (lanes *d*, *f*) should be multiplied by a factor of 10–20 to visualize the difference in terms of concentration. Despite slight variations (compare lanes *c*, *d* with lanes *e*, *f* in Fig. 1), generally at least three times as

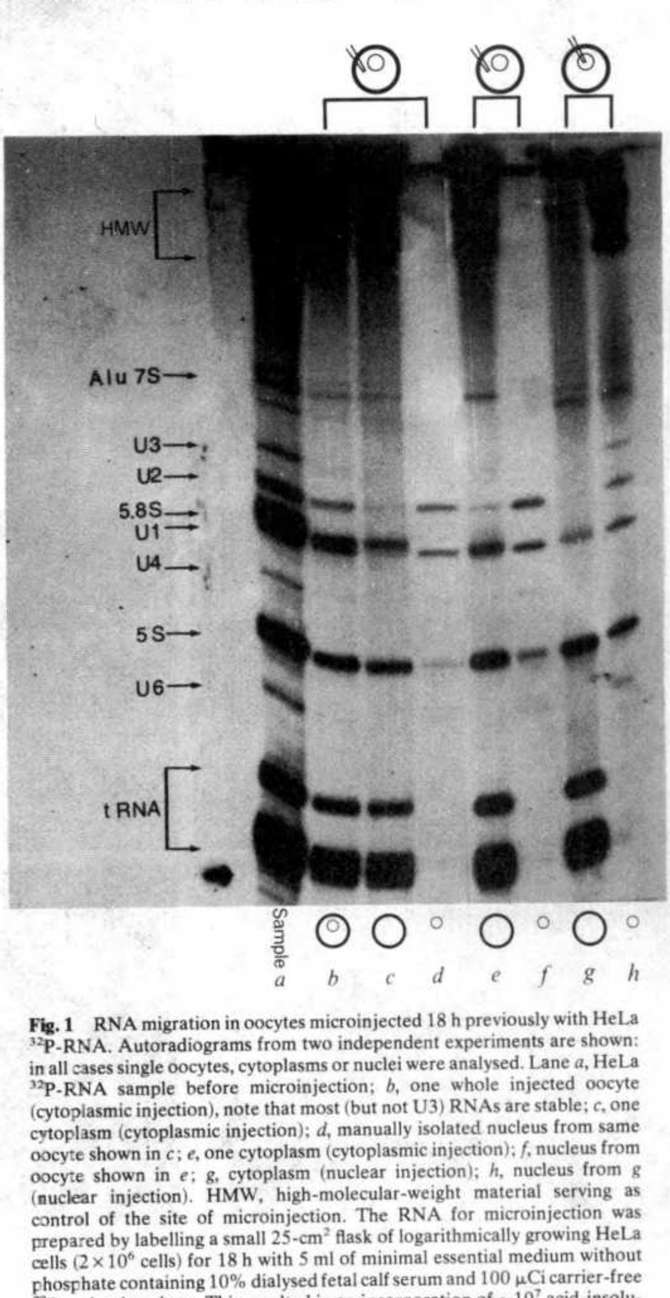

Fig. 1 RNA migration in oocytes microinjected 18 h previously with HeLa ^{32}P-RNA. Autoradiograms from two independent experiments are shown: in all cases single oocytes, cytoplasms or nuclei were analysed. Lane *a*, HeLa ^{32}P-RNA sample before microinjection; *b*, one whole injected oocyte (cytoplasmic injection), note that most (but not U3) RNAs are stable; *c*, one cytoplasm (cytoplasmic injection); *d*, manually isolated nucleus from same oocyte shown in *c*; *e*, one cytoplasm (cytoplasmic injection); *f*, nucleus from oocyte shown in *e*; *g*, cytoplasm (nuclear injection); *h*, nucleus from *g* (nuclear injection). HMW, high-molecular-weight material serving as control of the site of microinjection. The RNA for microinjection was prepared by labelling a small 25-cm^2 flask of logarithmically growing HeLa cells (2×10^6 cells) for 18 h with 5 ml of minimal essential medium without phosphate containing 10% dialysed fetal calf serum and 100 μCi carrier-free ^{32}P-orthophosphate. This resulted in an incorporation of $\sim10^7$ acid-insoluble c.p.m. per flask. Total nucleic acid was prepared by trypsinizing cells, washing in phosphate-buffered saline (PBS: 130 mM NaCl, 20 mM Na phosphate, *p*H 7.3), and lysing cells by vortexing in 1.5 ml of proteinase K–SDS solution (1.7% SDS, 300 mM NaCl, 2 mg ml^{-1} proteinase K, 40 mM Tris-HCl, *p*H 7.5). After phenol–chloroform extraction and addition of 2 vol of ethanol, the high-molecular-weight DNA was carefully spooled with a sealed 5 μl 'micropet' capillary (which very effectively reduces the viscosity thus allowing subsequent microinjection) and the remaining nucleic acids precipitated overnight at −20 °C, washed with 70% ethanol and the pellet finally redissolved in distilled water. Thirty nl of ^{32}P-RNA were injected into fully grown *Xenopus* oocytes and incubated overnight at 19 °C (ref. 39) before manual separation into nucleus and cytoplasm in J-buffer[40]. Samples were homogenized in proteinase K–SDS buffer, and the extracted nucleic acids[41] dissolved in 10 μl of loading buffer (95% formamide, 0.01% SDS containing Bromophenol blue and xylene cyanol) and electrophoresed in 8% polyacrylamide/7M urea thin (0.35 mm) 40 cm gels as previously described[5,6], except that 0.5X TBE buffer and faster runs (20 mA, electrophoresis completed in 1.75 h) were utilized. Each oocyte was injected with the RNA extracted from 500 HeLa cells. The cytoplasmic injection experiment shown here is highly reproducible, and was repeated in more than 10 independent experiments using oocytes from different frogs. It was also carried out successfully by the undergraduate biology students of the Biocenter in a practical course, showing that the manipulations involved are not excessively difficult.

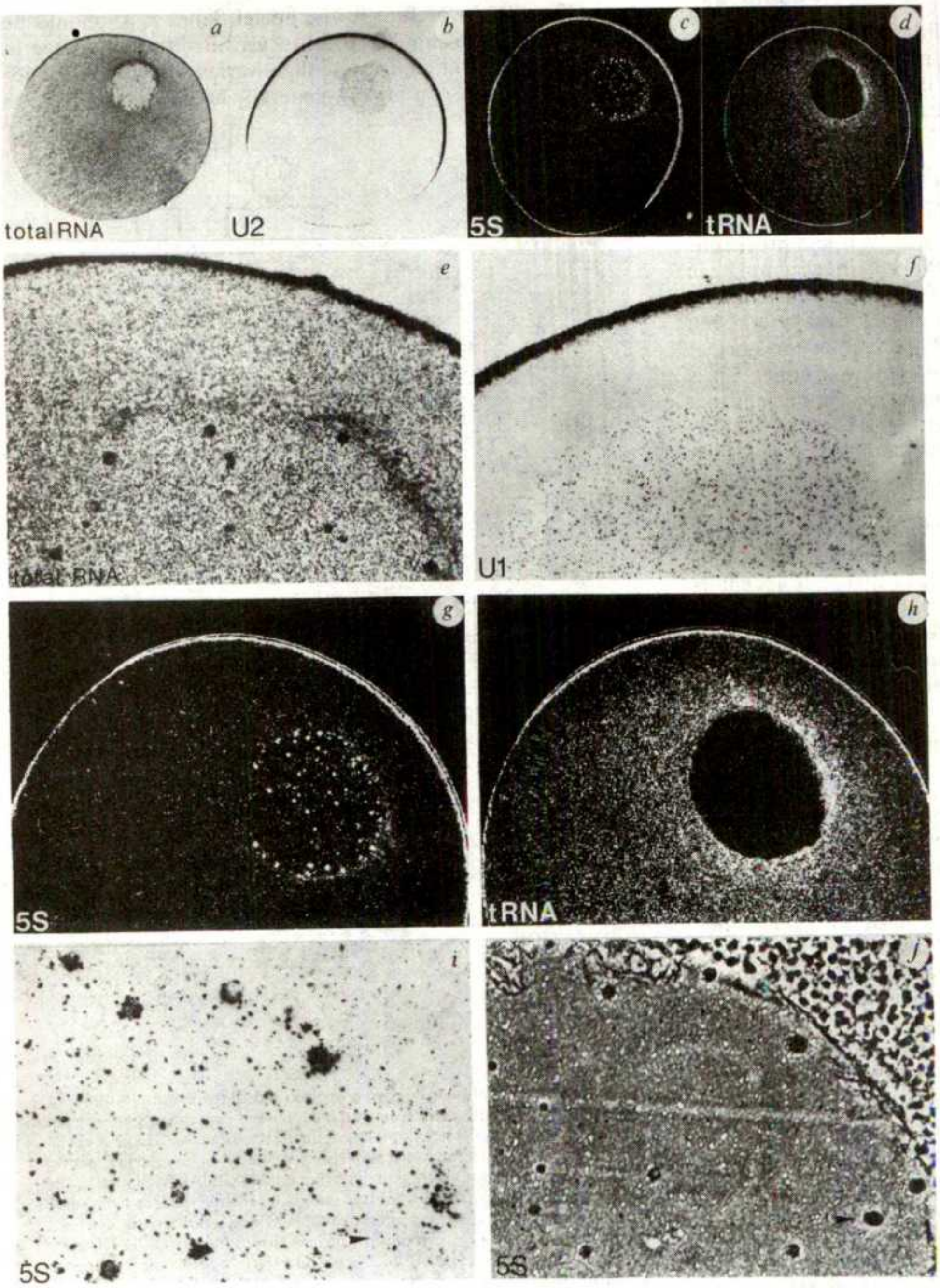

Fig. 2 Intracellular distribution of ^{3}H-RNAs from HeLa cells microinjected into the cytoplasm of frog oocytes. Total or individual RNAs (eluted from polyacrylamide gels[6]) were localized by autoradiography of sections of fixed oocytes. *a*, Total RNA; *b*, U2 RNA; *c*, 5S RNA (dark field); *d*, tRNA (dark field); *e*, total RNA; *f*, U1 RNA; *g*, 5S RNA (dark field); *h*, tRNA (dark field); *i*, 5S (transmission microscopy); *j*, same field as *i* but in phase contrast. Oocytes were fixed in San Felice fixative, embedded in paraffin, sectioned and dipped for autoradiography according to standard histological practice[39]. The radioactivity can be seen as dark grains. The black material on the oocyte periphery is pigment, present mostly in the animal hemisphere of frog oocytes. Some sections (for example *h*) show more grains in the juxtanuclear region because this part of the oocyte frequently does not contain yolk platelets (and thus effectively has more cytoplasm). Each oocyte has a diameter of ~1.2 mm. Individual nucleoli differ considerably in the extent of 5S RNA migration, as can be seen by comparing Fig. 4, *i* and *j*. A nucleolus that is not labelled at all is arrowed in Fig. 4*i*, which may correlate with the variability known to exist in the transcriptional activity of individual nucleoli in fully grown frog oocytes[42].

much U1 and U2 RNA is present in the nucleus as in the cytoplasm (determined by densitometry of autoradiograms) in individual oocytes, indicating that they are 30–60 times more concentrated in the nuclear fraction. Other less abundant snRNAs (U4, U5, U6) also migrate to the nucleus but longer exposures are required to visualize them (see Fig. 3, lane *d*). In most of the experiments reported here, samples were analysed 18–24 h after microinjection, but in time course tests a half-maximal nuclear concentration of snRNAs was already achieved by 3–4 h.

In the experiment described above, the HeLa RNAs were deposited in the oocyte cytoplasm. It could be argued, however, that this is a very artificial situation, for these RNAs are normally synthesized in the nucleus. We therefore compared the RNA distribution after injection into either the cytoplasm (Fig. 1, lanes *e*, *f*) or the nucleus (Fig. 1, lanes g, *h*). The results show that essentially the same distribution is achieved regardless of the site where the RNA was deposited, except in the case of U3 RNA, which is stable when injected into the nucleus (Fig. 1, lane *h*) but largely degraded when injected into the cytoplasm. The control indicating that the RNA was indeed injected in the oocyte nucleus is provided by high-molecular-weight material (presumably containing 18S RNA, ribosomal RNA degradation products and DNA) that runs near the top of the gel, which does not migrate and remains at the site of the injection (either in the cytoplasm, Fig. 1, lane *e*, or in the nucleus, Fig. 1, lane *h*). This control is essential because there is often reflux of material into the cytoplasm during nuclear injection[22]. When we analysed a series of 20 individual oocytes injected into the nucleus, only two presented negligible leakage into the cytoplasmic fraction (although some material had been introduced into the nucleus in 80% of the attempts). This type of experiment is technically difficult and requires analysis of many single oocytes, but it is interesting that it can be done at all, for this opens new possibilities in the study of RNA transport (such as, can a mature mRNA without intervening sequences be transported out of the nucleus?). In fact, the experiment shown in Fig. 1, lanes *g*, *h*, suggests that the transport of tRNA from nucleus to cytoplasm does not depend on the simultaneous processing of longer precursor tRNAs.

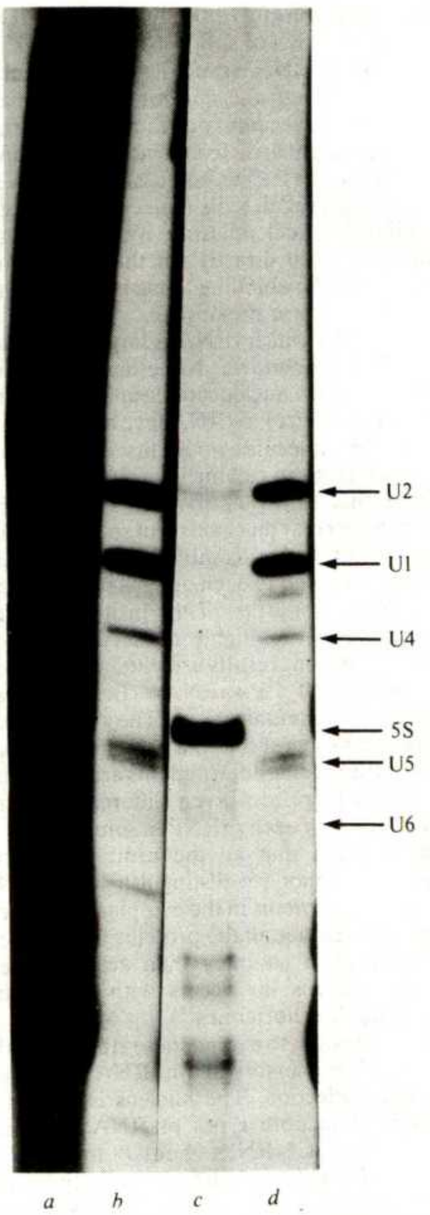

Fig. 3 Immunoprecipitation of microinjected HeLa ^{32}P-RNAs with anti-Sm lupus erythematosus antibodies. The antibodies do not react with naked RNA and therefore immunoprecipitation reflects association with oocyte proteins. Lane *a*, immunosupernatant of 8 injected oocytes; *b*, immunoprecipitate from *a*; *c*, immunosupernatant of 10 manually isolated nuclei from microinjected oocytes; *d*, immunoprecipitate from the 10 oocyte nuclei. Note that essentially all the snRNA that migrates into the nucleus is bound by the lupus antibodies. The oocyte cytoplasm contains nucleases which degraded the RNA in sample *a* during the immunoprecipitation procedure. The protein-bound snRNAs seem to be less sensitive to degradation. The nucleases are not present in the oocyte nucleus (lane *c*). For immunoprecipitation, 20 μl of serum were bound to 40 μl of a suspension containing one part staphyllococcal protein A–Sepharose beads (Pharmacia) and three parts Ipp buffer (0.5 M NaCl, 0.1% NP-40, 10 mM Tris-HCl, *p*H 8.0) in 1.5 ml Eppendorph tubes for 2 h at room temperature with end-over-end rotation, washed three times with 1 ml of Ipp buffer and then incubated with oocyte extract (nuclei isolated and homogenized in 0.5 ml PBS) for 2 h. After three 10-min washes with Ipp buffer the beads were digested for 20 min at 37 °C with 1.5 ml of proteinase K-SDS buffer and the RNAs extracted as for Fig. 1. Note that, in lane *d*, the less abundant snRNAs (U4, U5, U6) also migrate into the nucleus and bind to oocyte proteins.

Concentration of microinjected 5S RNA in the nucleoli

The cytological location of the injected RNAs was analysed by injecting ^{3}H-uridine-labelled HeLa RNAs into the cytoplasm of oocytes which 24 h later were fixed, embedded in paraffin, sectioned and autoradiographed. When oocytes injected with total HeLa RNA were examined (Fig. 2*a*, *e*) autoradiographic grains were found in both the nucleus and cytoplasm, as expected from the electrophoresis results, but the nucleoli also were intensely labelled. Analysis of the distribution of individual RNAs purified by elution from polyacrylamide gels showed that U1 (Fig. 2*f*) and U2 (Fig. 2*b*) snRNAs became concentrated uniformly in the nucleoplasm, whereas tRNA remained predominantly in the cytoplasm as expected (Fig. 2*d*, *h*). Purified 5S RNA, in addition to labelling uniformly in cytoplasm and nucleoplasm, clearly accumulated in the nucleoli (Fig. 2*c*, *g*).

The nucleolar migration of 5S RNA is not entirely surprising. In *Xenopus* oocytes the genes for 18S, 28S and 5.8S ribosomal RNAs are amplified early in oogenesis[23,24] and stored in about 1,000 extrachromosomal nucleoli, where they are transcribed. The 5S genes, on the other hand, are not located in the nucleoli but in the telomeres of most *Xenopus* chromosomes[25]. As ribosomes are known to be assembled at the nucleoli, 5S RNA must somehow migrate through the nucleoplasm before being incorporated into the immature ribosomal subunits at the nucleolus. In the nucleolus, the 5S RNA was located in the most external part (barely recognizable in some of the nucleoli shown in Fig. 2*i*, but clearly visible under the microscope), which in amphibian oocytes is known to contain the maturing ribosomal subunits which give this 'granular zone' its electron microscopic morphology[26]. Thus it is conceivable—but by no means proved—that the injected 5S RNA may become incorporated into nascent ribosomes.

Microinjected snRNAs associate with oocyte proteins

Investigation of whether snRNAs bind to oocyte components after microinjection was greatly facilitated by the discovery[27–29] that human autoantibodies from some patients with lupus erythematosus react with small nuclear ribonucleoproteins (snRNPs) but not with the naked snRNAs. We screened a collection of human sera with antinuclear antibodies (L. Mather, T. Nyffenegger, R.F.P. and E.D.R., in preparation) and obtained antisera with anti-Sm (which precipitates U1, U2, U4, U5 and U6 snRNPs) and anti-U1-RNP (which reacts only with U1-RNPs). Lanes *b* and *d* of Fig. 3 show that U1, U2, U4, U5 and U6 snRNAs are immunoprecipitable by anti-Sm antibodies after microinjection, and U1-RNA by anti-U1-RNP (not shown). Thus the HeLa RNAs bind to oocyte proteins. Essentially all the snRNAs that migrate into the nucleus are bound to oocyte proteins, whereas the nuclear-migrating 5S RNA is not recognized by this particular type of antibody (compare lanes *c* and *d* of Fig. 3).

Having established that the microinjected snRNAs accumulate in the nucleus in a ribonucleoprotein form, we then investigated whether the proteins bind to them in the nucleus or the cytoplasm, using *Xenopus* oocytes which can be manually enucleated and then microinjected in the surviving cytoplasm[30]. Figure 4 shows that about the same amount of snRNA is precipitated by anti-Sm antibodies after microinjection into nucleated or enucleated oocytes. Similar results were obtained with anti-U1-RNP antibodies. Thus the injected RNAs can bind to at least some of the snRNA binding proteins in the cytoplasm before entering the nucleus.

Small nuclear RNAs injected into enucleated oocytes together with 5 mg ml^{-1} cycloheximide (known to inhibit protein synthesis by >95%)[31] were precipitated equally well by lupus antibodies, suggesting that the cytoplasm contains an excess of pre-existing free RNA-binding proteins. Although these proteins have not been titrated, a minimum estimate is that they are sufficient to saturate the snRNAs extracted from 1,000 HeLa cells (amount of RNA microinjected per oocyte in Fig. 4).

Conclusions and prospects

The results show that microinjected snRNAs can migrate from the cytoplasm into the nucleus, where they become concentrated 30–60 fold. A similar distribution is attained irrespective of whether the material is injected into the cytoplasm or the

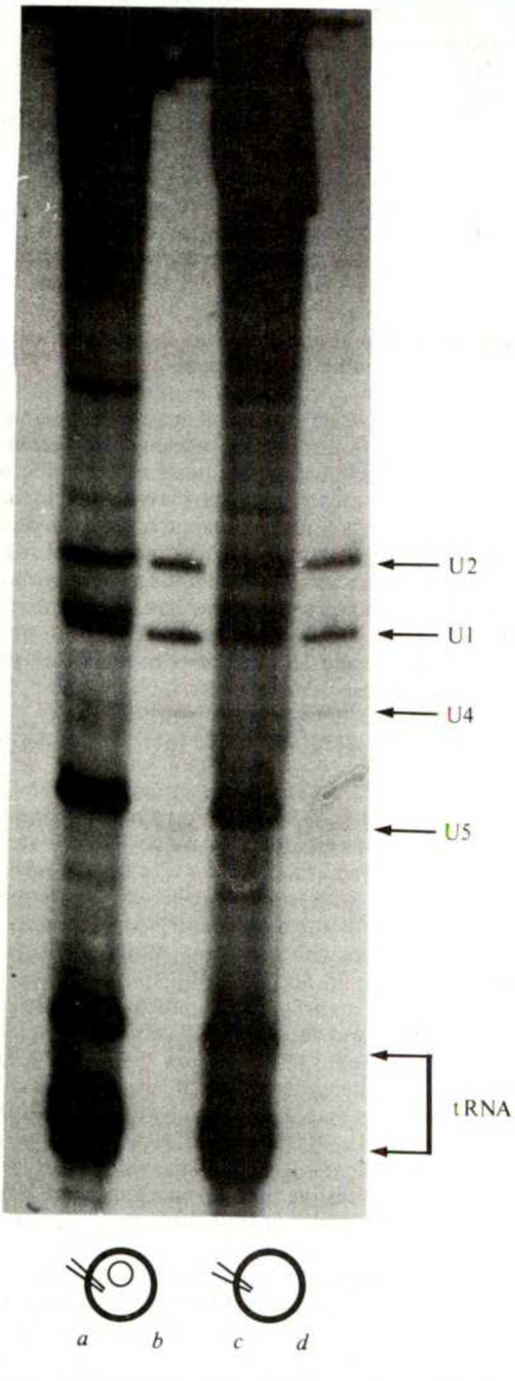

Fig. 4 Immunoprecipitation of HeLa ^{32}P-RNAs after microinjection into nucleated (*a*, *b*) or enucleated (*c*, *d*) frog oocytes with lupus anti-Sm antibodies. Ten oocytes of each type were injected and incubated for 6 h at 19 °C in enucleation 'healing buffer'[30], after which they were homogenized in PBS, and one half immediately extracted with phenol/chloroform (*a*, *c*) and the other half immunoprecipitated (*b*, *d*) with lupus antibodies. U4, U5 and U6 snRNAs were also detected in lanes *b* and *d* after longer exposure of this gel.

nucleus. Thus the nuclear membrane does not seem to be an obstacle for the movement of at least some low-molecular-weight RNAs. The nuclear affinity of snRNAs resembles that displayed by a variety of nuclear-migrating proteins (described in the introduction). Previous work with pulse-labelled cultured cells has demonstrated that newly synthesized snRNAs are not tightly bound to the nuclear fraction[19,32,33], and in *Amoeba proteus* transplanted with ^{3}H-uridine-labelled nuclei, the labelled material can migrate into the host nucleus[14,34]; these are probably manifestations of the phenomenon described here for frog oocytes. The oocyte system, however, differs in that purified, naked, RNA molecules can be introduced, and therefore it could provide a useful test system with which to determine the biological function(s) of snRNAs.

Microinjected 5S RNA accumulates in the nucleoli. It is interesting that although the nucleolus is not enveloped by a membrane, 5S RNA accumulates there. It is perhaps easy to conceive how this might arise from binding to specific sites (such as maturing ribosomes). One could similarly envisage how a whole nucleus might regulate its molecular exchanges via binding to non-diffusible nucleoplasmic components; however our experiments do not test directly whether nuclear migration of snRNAs is controlled by binding to intranuclear components or at the level of the nuclear membrane.

The mechanism by which tRNA is largely excluded from the nucleus (Fig. 2*h*) is unknown. Nonetheless, the behaviour of tRNA illustrates how nucleocytoplasmic transport could be important for gene control: if tRNA levels were to regulate their own synthesis, the molecules would first have to gain access to the genes by entering the cell nucleus.

It is hoped that lupus antibodies[29] will facilitate future analyses of the molecular mechanism of snRNA accumulation in nuclei. That a heterologous combination of human RNAs and frog proteins should bind to each other is not surprising because both the antigenic properties of the proteins and the snRNA nucleotide sequences are highly conserved in evolution[20,35]. Furthermore, equivalent results are obtained by microinjecting *Xenopus* cultured cell ^{32}P-snRNAs (E. Ackermann and J. Gurdon, personal communication). The results obtained with enucleated oocytes suggest that the proteins responsible for the Sm and U1-RNP antigenic determinants are stored in the oocyte cytoplasm, but as there are seven different proteins and one molecule of U-RNA in each snRNP in somatic cells[27], this does not necessarily mean that all the proteins are cytoplasmic. Consequently we cannot yet distinguish whether the injected snRNAs bind some proteins in the cytoplasm and then to others in the nucleus, or whether all the proteins bind in the cytoplasm and the RNA–protein complex then acquires the ability to migrate to the nucleus (as occurs with cytoplasmic steroid receptors after binding hormones[36]).

It would be interesting to extend these studies to other nuclear RNAs, like tRNA precursors and hnRNA, provided they are stable after microinjection. The nucleus is known to contain proteins that bind to both types of RNA[8,37,38] and hnRNA probably also has U1-RNPs bound to the intervening sequences[20], all of which could provide affinity for the nucleus. In the meantime, it is encouraging that at least some aspects of the transport of snRNA and 5S RNA against a concentration gradient can be approached in injected living cells.

We thank Dr L. Matter and his patients for generous gifts of antisera, Dr Georges Köhler for suggesting the immunoprecipitation method, W. Gehring, R. White, E. Ackerman, J. B. Gurdon and R. Zeller for comments on the manuscript and Mirjam Bollag for help in its preparation.

Received 28 September; accepted 7 December 1981.

1. Perry, R. P. *J. Cell Biol.* (in the press).
2. Schibler, V., Marcu, K. B. & Perry R. P. *Cell* **15,** 1495–1509 (1978).
3. Ro-Choi, T. S. & Busch, H. in *The Cell Nucleus* Vol. 1 (ed. Busch, H.) 151–208 (Academic, New York, 1974).
4. Zieve, G. W. *Cell* **25,** 296–297 (1981).
5. De Robertis, E. M. & Olson, M. V. *Nature* **278,** 137–143 (1979).
6. Nishikura, K. & De Robertis, E. M. *J. molec. Biol.* **145,** 405–420 (1981).
7. Melton, D. A. & Cortese, R. *Cell* **18,** 1165–1172 (1979).
8. Melton, D. A., De Robertis, E. M. & Cortese, R. *Nature* **284,** 143–148 (1980).
9. Gurdon, J. B. *Proc. R. Soc.* B**176,** 303–314 (1970).
10. Bonner, W. M. *J. Cell. Biol.* **64,** 421–430 (1975).
11. Bonner, W. M. *J. Cell Biol.* **64,** 431–437 (1975).
12. De Robertis, E. M., Longthorne, R. & Gurdon, J. B. *Nature* **272,** 254–256 (1978).
13. Mills, A. D., Laskey, R. A., Black, P. & De Robertis, E. M. *J. molec. Biol.* **139,** 561–568 (1980).
14. Goldstein, L. in *The Cell Nucleus* Vol. 1 (ed. Bush, H.) 387–437 (Academic, New York, 1974).
15. Rechsteiner, M. & Kuehl, L. *Cell* **16,** 901–908 (1979).
16. Feldherr, C. M. & Pomerantz, J. *J. Cell Biol.* **78,** 168–175 (1978).
17. Feldherr, C. M. & Ogburn, J. A. *J. Cell Biol.* **87,** 589–593 (1980).
18. Bonner, W. M. in *The Cell Nucleus* Vol. 4 (ed. Bush, H.) 97–148 (Academic, New York, 1978).
19. Zieve, G. & Penman, S. *Cell* **8,** 19–31 (1976).
20. Lerner, M. R., Boyle, J. A., Mount, S. M., Wolin, S. L. & Steitz, J. A. *Nature* **283,** 220–224 (1980).

21. Weiner, A. M. *Cell* **22,** 209–218 (1980).
22. Wyllie, A. H., Gurdon, J. B. & Price, J. *Nature* **268,** 150–152 (1977).
23. Brown, D. D. & Dawid, I. B. *Science* **160,** 272–277 (1968).
24. Gall, J. G. *Proc. natn. Acad. Sci. U.S.A.* **60,** 553–558 (1968).
25. Pardue, M. L., Brown, D. D. & Birnstiel, M. L. *Chromosoma* **42,** 191–198 (1973).
26. Miller, D. L. *Handbook of Molecular Cytology* (ed. Lima-de-Faria, A.) (North Holland, Amsterdam, 1969).
27. Lerner, M. R. & Steitz, J. A. *Proc. natn. Acad. Sci. U.S.A.* **11,** 5495–5499 (1979).
28. Lerner, E. A., Lerner, M. R., Janeway, C. A. Jr & Steitz, J. A. *Proc. natn. Acad. Sci. U.S.A.* **78,** 2737–2741 (1981).
29. Lerner, M. R. & Steitz, J. A. *Cell* **25,** 298–300 (1981).
30. Ford, C. C. & Gurdon, J. B. *J. Embryol. exp. Morph.* **37,** 203–209 (1977).
31. Harland, R. M. & Laskey, R. A. *Cell* **21,** 761–771 (1980).
32. Eliceiri, G. *Cell* **3,** 11–14 (1974).
33. Eliceiri, G. L. & Sayavedra, M. S. *Cell* **72,** 507–512 (1976).
34. Goldstein, L. & Ko, C. *Cell* **2,** 259–269 (1974).
35. Busch, H., Reddy, R., Henning, D. & Epstein, P. in *International Cell Biology 1980–1981* (ed. Schweiger, H. G.) 47–52 (Springer, Berlin, 1981).
36. Yamamoto, K. R. & Alberts, B. M. *A. Rev. Biochem.* **45,** 721–746 (1976).
37. Beyer, A. L., Christensen, M. E., Walker, B. W. & Le Stourgeon, W. M. *Cell* **11,** 127–138 (1977).
38. Martin, T. E. & Okamura, C. S. *International Cell Biology 1980–1981* (ed. Schweiger, H. G.) 77–84 (Springer, Berlin, 1981).
39. Gurdon, J. B. *J. Embryol. exp. Morph.* **36,** 523–540 (1976).
40. De Robertis, E. M., Black, P. & Nishikura, K. *Cell* **23,** 89–93 (1981).
41. Wickens, M. P., Woo, S., O'Malley, B. W. & Gurdon, J. B. *Nature* **285,** 628–634 (1980).
42. Trendelenburg, M. F. & McKinnell, R. G. *Differentiation* **15,** 73–95 (1979).

LETTERS TO NATURE

Alignment of randomly distributed objects

E. J. Zuiderwijk

Royal Greenwich Observatory, Herstmonceux Castle, Hailsham, Sussex BN27 1RP, UK

Recently, Edmunds and George[1] discussed alignments of randomly distributed quasars, following the discovery by Arp and Hazard[2] of several conspicuously aligned 'triplets' of quasars with widely disparate redshifts. If the probability of such alignments occurring by chance is very small, a physical association between the objects could be suspected[2], implying a non-cosmological component in some of the quasar redshifts. A similar problem concerning supposed alignments of megalithic sites[3] has prompted substantial analysis of the statistics of such colinearities in random sets of objects[3,4]. Here I use the angular definition of alignment to estimate the significance of the quasar triplets and confirm the results of computer simulations[1], showing that it is not improbable for these alignments to occur by chance.

The angular criterion to define alignment of three points was first used systematically by Broadbent[3]: two points I and J somewhere in an area A (Fig. 1) are said to be aligned within a small acceptance angle ε on a third point P if the angle between the lines connecting P and I, and P and J is between $\pi-\varepsilon$ and $\pi+\varepsilon$. This definition is more suitable for analysis than one in terms of the distance of P to the line connecting I and J being small[1], because the probability of finding an alignment does not depend on the dimensions of the area, and is therefore independent of the surface density of points, as long as their number is kept constant. Furthermore, the present definition ensures that three points can represent only one alignment (I and P are not aligned on J). It is easily envisaged how the probability of alignment can be computed: two points, for example, I and P, define two fan-shaped areas each with top angle 2ε. The condition for alignment will be satisfied if a third point is located somewhere in this area. Of course, we have to consider many possible separations of I and P, each defining a different area of the fans.

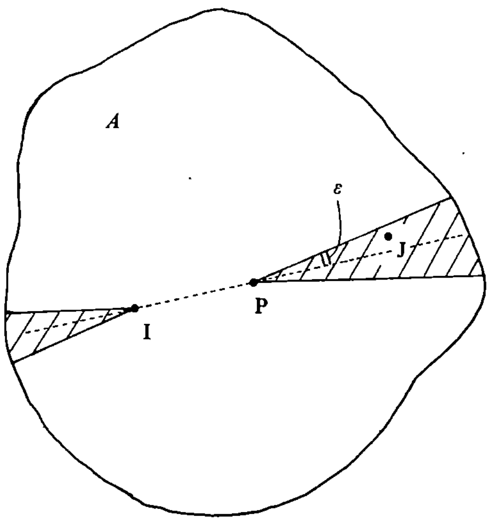

Fig. 1 Geometry of alignment for randomly distributed objects in area A. I and J are aligned on P within an angle ε.

A preliminary estimate of the probability P_ε of having an alignment of three randomly distributed points within angle ε can be obtained as follows. The average distance of the two randomly distributed points I and P is roughly half the typical diameter of the area A: two fans with $\varepsilon=90.0°$ will cover on average about half the surface. Consequently $P_\varepsilon \sim 0.5\,\varepsilon/90$, which for $\varepsilon=1°$ yields $P_{1°} \sim 1/180 = 0.00556$. Note that although the size of the area considered does not affect the value of P_ε, its shape does. This can be understood by comparing, for example, a square region with a very long but narrow area; randomly distributed objects in the latter case are bound to have a much higher chance to form an alignment. Kendall and Kendall[4] give exact values for probabilities of alignment on the 1° acceptance criterion of $1/180=0.005556$ (0.00554) and $1/180\times\pi/3=0.005818$ (0.00580) for a circular and square area respectively (numbers between parentheses indicate the probabilities as measured from 10^6 trial fields, each with three randomly distributed points). For small angles, P_ε is proportional[4] to ε. The quasar field studied by Arp and Hazard[2] is rectangular and measures about 40×50 arc min. In this case the probabilities for a square field have to be multiplied by the Broadbent coefficient[3,4] $\frac{1}{2}(s+1/s)$ with $s=40/50$, which results in $P_{1°}=0.005960$ (0.00596).

We now want to determine the probabilities of multiple alignments for N objects present in the area. Given the value of P_ε, the probabilities $P(N,K,P_\varepsilon)$ to find K alignments within an angle ε in N randomly distributed objects can be expressed in the form $P(N-1,K,P_\varepsilon)$:

$$P(N,K,P_\varepsilon)=\sum_{L=0}^{K} P(N-1,L,P_\varepsilon)\cdot B\left[\binom{N-1}{2},K-L,P_\varepsilon\right]$$

$$K\leqslant\binom{N}{3},\qquad N>3$$

The coefficients B represent the probability of finding $K-L$ alignments out of the $\binom{N-1}{2}$ combinations between two of the $N-1$ objects and the newly added Nth object. Assuming that all combinations are independent, while each combination has probability P_ε to be an alignment, B is given by the binomial distribution:

$$B(I,J,P_\varepsilon)=\binom{I}{J}P_\varepsilon^{J}(1-P_\varepsilon)^{I-J}$$

All probabilities can now be computed because by definition:

$$P(3,0,P_\varepsilon)=1.0-P_\varepsilon \quad\text{and}\quad P(3,1,P_\varepsilon)=P_\varepsilon$$

N points on a straight line represent $\binom{N}{3}$ alignments, which is

0028–0836/82/070577—02$01.00

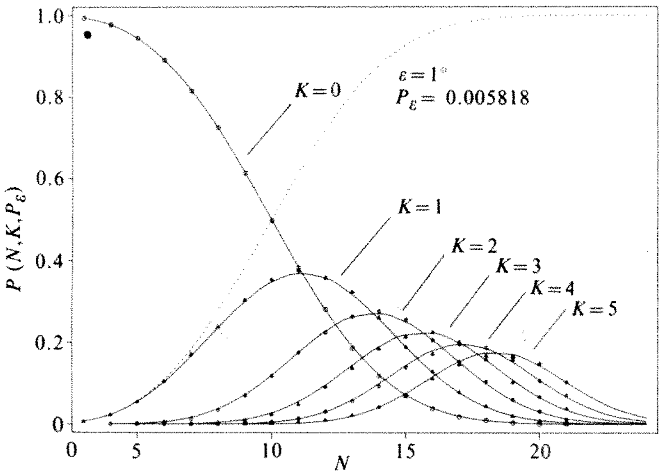

Fig. 2 Theoretical probabilities for K alignments within an angle of 1° in N randomly distributed points, here shown as smooth curves. Symbols along the curves indicate the probabilities as measured from simulations of random fields. The dashed curve represents the probability to find at least one alignment as a function of N. The presence of alignments within 1° is expected in every other field with 10 objects (the expected number of triplets per 10 points[4] is 0.698).

therefore the maximum value that K can attain. The average (expected) number of alignments equals $\binom{N}{3}P_\varepsilon$ (ref. 4). Figure 2 shows predicted probabilities for up to five alignments as a function of N. The decrease in likelihood after the initial increase with N is due to the growing chance of finding one more alignment. Computer simulations were performed using 40,000 trial random fields for N up to 10; in view of the rapid increase with N of processing time per field, the number of trials was gradually reduced to 5,000 for $N=20$.

To estimate the probability of having two aligned triplets of quasars in the field studied by Arp and Hazard[2] we have to establish the alignment angles ε. Because the exact positions of these quasars have not been previously published, they were measured on a glass copy of the ESO QB sky survey, using the RGO Coradograph and standard astrometry reduction methods (Table 1). Alignment of angles of 0.48° ± 0.14° and 0.56° ± 0.20° are easily computed in spherical trigonometry. The probability of having two alignments within 0.56° is $P(6,2,P_{0.56°})=2.0\times10^{-3}$. Because for small N and ε the distribution of the number of colinear triplets is close to the poissonian (see ref. 3), a rough estimate of the probability of obtaining two alignments can be made in this case by using the expected number of alignments ($0.00596\times0.56\times\binom{6}{3}=0.0668$); the chance of getting two from a Poisson variable with that expectation is 2.08×10^{-3}. Thus the occurrence of these aligned triplets by chance is not at all unlikely when it is realized that this particular field is part of a survey of about 5,000 quasars covering an area of ~500 square degrees (C. Hazard, personal communication). Moreover, we would expect many similar configurations to exist on the sky; the presence of two more alignments[2] in the area at 11 h 46 min + 11° with nine objects is not surprising as $P(9,2,P_{1°})=0.074$.

Table 1 Positions, accurate to about 0.8″, of quasars[2] in two aligned triplets at 11 h 30 min + 11°, and alignment angles ε

	α (1950)	δ (1950)	ε
X	11 h 31 min 00.78 s	11° 14′ 53.0″	
Y	11 30 54.97	11 08 58.2	0.48° ± 0.14°
Z	11 30 44.22	10 58 24.3	
A	11 30 24.19	10 40 16.3	
B	11 30 30.26	10 42 53.1	0.56° ± 0·20°
C	11 30 09.37	10 33 44.1	

I thank Ann Pocock for the position measurements. Professor D. G. Kendall brought refs 3 and 4 to my attention and provided valuable comments. Computations described in this paper were performed on the RGO/Starlink Vax 11 computer system.

Received 23 October 1981; accepted 6 January 1982.

1. Edmunds, M. G. & George, G. H. *Nature* **290,** 481–483 (1981).
2. Arp, H. C. & Hazard, C. *Astrophys. J.* **240,** 726–736 (1980).
3. Broadbent, S. R. *J. R. statist. Soc.* A**143**, 109–140 (1980).
4. Kendall, D. G. & Kendall, W. S. *Adv, appl. Prob.* **12,** 380–424 (1980).

Oxygen evolution on tantalum–polypyrrole–platinum anodes

Gerald Cooper, Rommel Noufi*, Arthur J. Frank & Arthur J. Nozik

Photoconversion Research Branch and * Photovoltaic Program
Office, Solar Energy Research Institute, Golden,
Colorado 80401, USA

Electrically conducting polymer films of polypyrrole were previously reported[1–6] to provide greatly enhanced stability against the photodegradation of semiconductor photoanodes in electrochemical photovoltaic cells. To determine the feasibility of protecting photoanodes with polypyrrole in photoelectrolysis cells where O_2 is evolved some basic questions had to be answered. To achieve this we have performed experiments using polypyrrole films as protective coatings on Ta metal electrodes; Ta is known to form insulating oxides that prevent O_2 evolution from aqueous solution. We found that polypyrrole is stable in the presence of O_2; that while polypyrrole itself is a poor electrocatalyst for O_2 evolution, metal catalysts can be deposited on its surface to enhance O_2 evolution; and that Ta–polypyrrole–Pt electrode structures are electrochemically indistinguishable from naked Pt electrodes with respect to O_2 evolution.

Recent research[1–6] has shown that electrically conducting polypyrrole films can be easily electrodeposited on n-type semiconductor electrodes, thereby imparting to the electrode greatly enhanced stability against anodic photodegradation in photoelectrochemical cells. This effect has been demonstrated[1–6] for n-type Si, GaAs, CdS, CdSe, and CdTe electrodes operating in contact with aqueous electrolyte in photovoltaic-type photoelectrochemical cells. In those experiments, electroactive redox couples, such as Fe^{3+}/Fe^{2+} or $Fe(CN)_6{}^{3-}/Fe(CN)_6{}^{4-}$, are added to the aqueous electrolyte to facilitate positive hole transfer to the electrolyte to inhibit self-oxidation of the semiconductor electrode; the net product of such cells is electrical power[7–11].

A more difficult application of conducting polymer-coated semiconductor electrodes is in the photoelectrolysis-type of photoelectrochemical cell. Here, the polymer film must protect the n-type semiconductor electrode against photooxidation in the presence of the oxygen evolution reaction in aqueous electrolyte. The oxidation of water to oxygen is a relatively difficult four-electron reaction and therefore requires positive holes with a rather positive redox potential. Holes created and utilized at such high positive potentials in photoexcited semiconductor electrodes generally result in oxidation of the semiconductor itself in addition to, or even to the exclusion of, the oxidation of water. A few large band-gap oxide semiconductors (such as TiO_2, $SrTiO_3$ and Fe_2O_3) show exceptions to this behaviour. The role of the polypyrrole film in photoelectrolysis cells would therefore be to channel preferentially the photogenerated holes in smaller band-gap and non-oxide semiconductors to the H_2O/O_2 redox couple at a rate that is much faster than the self-oxidation rate of the semiconductor.

Before the above application of polypyrrole films can be realized, the following questions must be answered. (1) Is poly-

0028-0836/82/070578—03$01.00

pyrrole itself stable in O_2-evolving conditions? (2) Can the water oxidation reaction be confined to the outermost polypyrrole–liquid interface so that physical destruction of the film by internal gas evolution can be prevented? (3) Can polypyrrole act as a sufficiently good electrocatalyst for O_2 evolution, and if not can a catalytic agent be deposited on the film surface to achieve good O_2 evolution rates?

Affirmative answers to these questions have been obtained from studies of polypyrrole films deposited on tantalum metal electrodes. Normally, Ta electrodes do not evolve O_2 because of the spontaneous development of thick tantalum oxide layers on the surface at potentials less positive than the H_2O/O_2 redox potential. Ta electrodes therefore provide a good system for testing the ability of polypyrrole to prevent substrate oxidation and to answer the above three problems.

Polypyrrole films were electrochemically deposited in a three-electrode, potentiostatically controlled cell containing a deaerated, aqueous solution of about 1 M pyrrole with 2.0 M LiCl supporting electrolyte at pH ~0.5. Rapid deposition of the polymer on the Ta substrate occurred at a potential of about +0.7 V (versus SCE). Below this potential the rapid, initial growth rate would decrease quickly to almost zero, probably because of competitive oxide film growth. At about +0.7 V (SCE) or higher, the growth rate appeared to be diffusion controlled only.

The Ta substrates were freshly ground with 600 grit SiC paper (scratch depth ~0.25 μm) before deposition to remove the insulating oxide layer and to provide for excellent film adhesion. Films grown on polished Ta surfaces readily peeled off whereas they stuck tenaciously to rougher surfaces. The area exposed to solution during film polymerization was 1.3 cm^2; this resulted in a circular spot of polypyrrole 1.3 cm in diameter at the centre of a 2.5 × 2.5 cm square Ta sample.

In some experiments, Pt was ion-beam sputtered onto the polypyrrole disk using an Ar ion beam. In these cases, a mask was used with a hole having a smaller diameter than the polypyrrole film. This ensured that no direct electrical contact was possible between the Pt and the Ta. The ion beam deposition rate for Pt was calculated by measuring the thickness of a thick Pt sputtered film with an interferometer and dividing by the sputter time. Pt film thicknesses used in subsequent experiments were then calculated from this sputter rate and the sputter time.

Electrochemical measurements were performed on the electrodes in 2 M phosphate buffer (pH = 6.7); the thermodynamic potential for water oxidation at this pH is +0.60 V (SCE). The working electrode area was defined by a pressure seal having a diameter less than the Pt film diameter; this ensured that only the Pt coated polypyrrole was in contact with the solution.

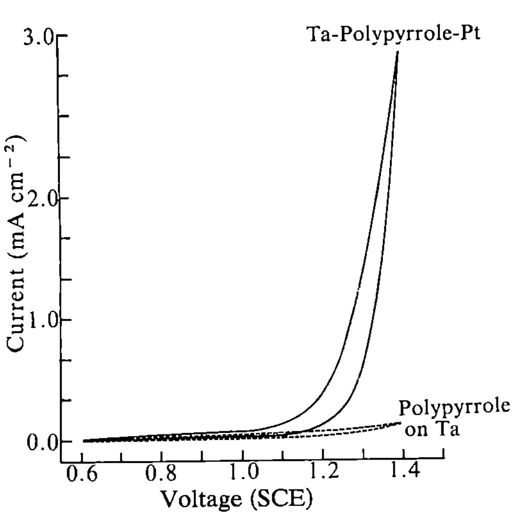

Fig. 1 Dashed line is the current–voltage characteristic of a 2.5 μm polypyrrole film on tantalum. The solid line is the current–voltage characteristic of a Pt-coated (72 Å) polypyrrole film (5 μm) on tantalum. In both cases data are shown for the sample after it was cycled 15 times from 0.6 to 1.0 V (SCE). These latter data are indistinguishable from those for a naked Pt electrode. A Ta electrode showed essentially zero current (after the oxide formed) out to 1.4 V (SCE) and beyond.

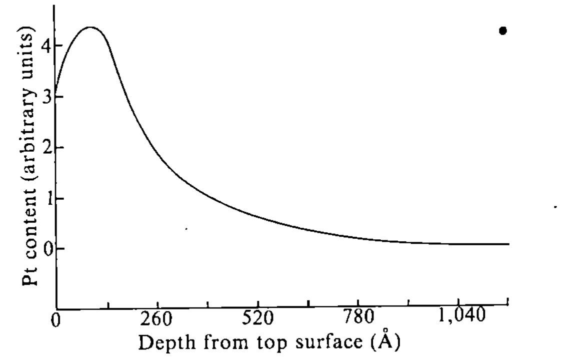

Fig. 2 Auger depth profile analysis for Pt for a Pt-coated (45 Å) polypyrrole film (12.5 μm) on tantalum. The Pt is mainly confined to the outer 100 Å, and decays to zero at ~800–900 Å.

Experiments with Ta electrodes and with just polypyrrole on Ta showed that O_2 could not be evolved from Ta metal and that polypyrrole is a poor catalytic surface for H_2O oxidation. As seen in Fig. 1, O_2 could not be readily evolved from a polypolypyrrole surface even at 1.4 V (SCE); the data represented by the dashed lines in Fig. 1 are for a 2.5 μm polypyrrole film on Ta. Initially the electrode was cycled between +0.6 and 1.0 V (SCE) 15 times to oxidize completely the polypyrrole film and thus eliminate interferring anodic current arising from polypyrrole oxidation; fully oxidized polypyrrole is required for high film conductivity.[12–14]. The sample was then cycled from +0.6 to +1.4 V (SCE); the maximum generated current density in these conditions was <0.2 mA cm^{-2}. In contrast to this behaviour, a smooth, naked Pt electrode (formed by ion-beam sputtering) developed a current density of ~1 mA cm^{-2} at 1.3 V (SCE); this is about the minimum current density necessary to observe the formation of O_2 bubbles. At 1.4 V (SCE) the current density increased to about 3 mA cm^{-2}.

When a thin film of Pt (~72 Å) was sputter-deposited on the surface of polypyrrole-coated Ta, O_2 evolution occurred (confirmed by observing bubbles) at the same potential that it appeared on the naked Pt electrode and at approximately the same current density (1.3 mA cm^{-2}). Figure 1 (solid lines) shows a typical current versus voltage curve for the Ta–polypyrrole–Pt electrodes we studied. Cyclic sweeps between +0.6 and +1.1 V (SCE) were performed before O_2 evolution for the same reasons given above. Inspection of Fig. 1 and comparison of current versus time plots for naked Pt and Ta–polypyrrole–Pt samples indicate that the electrochemical behaviour of the Ta–polypyrrole–Pt electrode is indistinguishable from that of the naked Pt electrode with respect to O_2 evolution.

The polypyrrole film thicknesses studied ranged from 0.45 to 12.5 μm; they all showed O_2 evolution on Ta substrates. Despite these relatively thick films, the question could be raised concerning Pt penetrating through the polypyrrole film and reaching the Ta surface thereby short circuiting the polypyrrole (Pt deposited on Ta also behaves as a naked Pt electrode with respect to O_2 evolution). To rule out this possibility, a Ta electrode with a 6.2 μm polypyrrole film and with about 45 Å of Pt sputtered onto the surface was examined using Auger spectroscopy to determine the elemental profile perpendicular to the surface. In this technique a 1-mm diameter Ar ion-beam drills a hole into the sample while a 1/8 mm electron beam simultaneously impinges on the walls of the hole. The Pt profile, determined by the peak-to-peak amplitude of the characteristic 1970 eV Auger electron signal of Pt, has a maximum at ~100 Å and then decays to background noise levels at ~800–900 Å depth below the surface (see Fig. 2). The fact that a peak exists at 100 Å and that Pt is detected down to ~800–900 Å below the surface is probably due to entrainment of Pt atoms by the polymer matrix due to collisions with the Ar ion-beam, and momentum transfer in the forward beam direction. In any event, Pt clearly cannot short out any of the films studied.

It was also observed that the thinner polypyrrole films (0.45 μm) were more physically stable than the thicker films. The latter tended to blister after the passage of about 1 C of charge. The thin films showed no visible deterioration after the passage of several coulombs and were very adherent and scratch resistant.

We conclude that an electrochemically deposited polypyrrole film can be used to protect a metal surface from self-oxidation in conditions where O_2 is being evolved and where the metal would normally form an insulating oxide layer. Because of its high conductivity, the film can efficiently transfer charge over large distances (12.5 μm). We have thus shown that the electrochemical production of O_2 on Ta–polypyrrole–Pt electrodes is almost indistinguishable from naked Pt electrodes. Polypyrrole itself cannot evolve O_2 because it is a poor electrocatalyst for the O_2 evolution reaction. However, an electrocatalyst, such as Pt, can be deposited on the surface to ease O_2 evolution. The O_2 evolution reaction can be confined to the outermost polypyrrole–water interface, and the film is rather stable both physically and chemically in O_2-evolving conditions; this is especially true for thin polypyrrole films. The results are encouraging with respect to the potential application of polypyrrole films to stabilize small band gap and non-oxide n-type semiconductors for O_2 evolution in photoelectrolysis cells.

We thank Terence M. Thomas for the Auger depth-profile analyses. This work was supported by the Office of Basic Energy Sciences, Division of Chemical Sciences, US Department of Energy, under contract EG-77-C-01-4042.

Received 8 October; accepted 10 December 1981.

1. Noufi, R. Frank, A. J. & Nozik, A. J. *J. Am. chem. Soc.* **103,** 1849 (1981).
2. Noufi, R. Tench, D. & Warren, L. F. Warren, *J. electrochem. Soc.* **127,** 2310 (1980).
3. Noufi, R. Tench, D. & Warren, L. F. *J. electrochem. Soc.* (in the press).
4. Fan, F. R. F. Wheeler, B., Bard, A. J. & Noufi, R. *J. electrochem. Soc.* **128,** 2042 (1981).
5. Skotheim, T., Lundstrom, I. & Prejza, J. *J. electrochem. Soc.* **128,** 1625 (1981).
6. Frank, A. J. in *Molecular Crystals and Liquid Crystals* (eds Conwell, E. M. & Epstein, A. J.) (Gordon & Breach, New York, in the press).
7. Nozik, A. J. *A. Rev. phys. Chem.* **29,** 189 (1978).
8. Wrighton, M. S. *Accts chem. Res.* **12,** 303 (1979).
9. Bard, A. J. *Science* **207,** 139 (1979).
10. Heller, A. *Accts chem. Res.* **14,** 154 (1981).
11. Harris L. A. & Wilson, R. H. *A. Rev. Mater. Sci.* **8,** 99 (1978).
12. Diaz, A. F. Kanasawa, K. K. & Gardini, G. P. *JCS Chem. Commun.* 635 (1979).
13. Diaz, A. F. & Castillo J. I. *JCS Chem Commun.* 397 (1980).
14. Diaz, A. F. & Logan, J. A. *J. electroanalyt. Chem.* **111,** 111 (1980).

Penetration of water into hot rock boundaries of magma at Grímsvötn

H. Björnsson, S. Björnsson & Th. Sigurgeirsson

Science Institute, University of Iceland, Dunhaga 3, 107 Reykjavík, Iceland

The Grímsvötn geothermal area is located within one of the most active caldera volcanoes in Iceland in the interior of the ice cap Vatnajökull at an altitude of 1,400 m (Fig. 1). Its setting offers unique conditions for calorimetric measurement of the heat release from the subglacial geothermal system. The melting of ice due to the geothermal activity creates a depression in the surface of the ice cap. Ice and water are diverted towards the depression from a 300 km² drainage basin. The meltwater accumulates in a 30 km² subglacial lake. Periodic outbursts of water (jökulhlaups) drain the lake subglacially down to the Skeidarársandur plain. We propose here that penetration of water into hot rock is the primary reason for the intense heat release (5,000 MW thermal) of the subglacial Grimsvötn geothermal area. Injection of water into boundary rocks of magma should be considered as a method of heat exploitation.

The history of Grímsvötn has been studied extensively[1] and the first report on a jökulhlaup dates back to AD 1332. From 1600 until 1934 about one jökulhlaup occurred each decade with an estimated discharge of 6–7 km^3 of water, but since 1934 there have been two outbursts per decade and the observed volume correspondingly smaller, 3–3.5 km^3 (refs 1,2). A long-term mass balance of the drainage basin has been given elsewhere[3]. The average accumulation in the form of ice is equivalent to 2,200 mm yr^{-1} of water and the surface ablation amounts to 500 mm yr^{-1}. A long-term steady-state model for the drainage basin proves to be a valid approximation[3]. The water added to the lake is 6.6×10^{11} kg yr^{-1}. About 1.5×10^{11} kg yr^{-1} are melted at the glacier surface by meteorological processes, but the difference, about 5×10^{11} kg yr^{-1} is melted by geothermal heat within the drainage basin. The heat flux required to melt this ice is ~5,000 MW (thermal). The geothermal activity responsible for the melting of the ice is not limited to the lake but scattered over a large area, estimated to be up to 100 km^2. If the heat released at Grimsvötn is averaged over 100 km^2 we obtain an average heat flux density of 50 W m^{-2} or some 1,200 h.f.u. To illustrate the dimension of this heat flux, note that it is equivalent to the average global heat flow through an area of 80,000 km^2 or nearly the whole area of Iceland.

Magma is commonly assumed to be the source of heat for high-temperature geothermal systems. A heat output of 5,000 MW is equivalent to the heat released by solidification and cooling of $\sim5\times10^7$ m^3 yr^{-1} of magma down to a temperature of 400 °C. A magma volume of at least 20 km^3 is required to maintain the present heat output at Grímsvötn over the 400 yr of reported jökulhlaups. Given a magmatic source of this size the extraction of heat at the observed rate is still problematic. A conducting wall separating stagnant magma and a hydrothermal system could supply the observed heat flux for a short period after intrusion of the magma, but the wall would soon thicken as magma solidified and the flux would decline below the observed rate.

The difficulty of explaining the thermal output of high temperature systems by conduction from a magmatic source has been recognized[4–6]: Banwell[5] considered steam released from convecting magma to act as a heat carrier. Water could penetrate to the magma through a few deep faults, and diffuse into the magma, but be released when it had circulated to some higher level where the pressure is lower.

White[6] proposed alternatives for the Steamboat Springs systems, either a convection within a magma chamber maintaining magmatic temperatures near the base of the hydrothermal circulation or a fissure system controlling the circulating water and gradually extending deeper into the batholith, as stored heat was removed at higher levels by circulating water. Irvine[7] described a convective process in a magma body where crystals accumulate in the lower part of the intrusion but the temperature near the top remains close to, or above, the liquidus temperature of the magma. This process allows higher rate of heat loss and solidification than would occur if the crystals were frozen to the roof of the magma chamber. Bodvarsson[4] favoured penetration of water into the hot rock boundary of intrusions to compensate for the increased thickness of the solidifying rock that insulated the molten lava from the hydrothermal system. Lister[8] has presented a conceptual model of the downward penetration of water into hot rocks by a process of cooling, thermal contraction and cracking. The cracks enable the water to penetrate to the horizon of solidification, although the horizon proceeds downwards. Thermal insulation of the rock is no longer an effective barrier for heat removal as the water is steadily penetrating into new, hot rock and carrying its heat away by convection.

Models of a replenished chamber of convecting magma or steam released from convecting magma, might explain the heat output at Grímsvötn. Recent field evidence obtained by watering of a molten lava flow, however, suggests that the process of penetration of water into hot rock is most likely to be respon-

0028-0836/82/070580—02$01.00

sible for the heat extraction at Grímsvötn. During the Heimaey eruption in Iceland in 1973 water was pumped onto the molten lava in attempts to impede the flow and divert it away from the town. A flow of 100 kg of water per second, applied in one place, spread over some 7,000 m^2 of lava, which was engulfed in steam. Drillholes revealed that after two weeks of watering the solidification of the lava had progressed to a depth of ~12 m, leaving the solidified lava at the temperature of saturated steam, that is 100 °C. Temperature logs of the holes indicated that the transition layer, where the temperature rose from 100 to 1,050 °C, was only a fraction of a metre thick during watering. Excavation of lava after the eruption revealed that the structure of water-cooled lava was greatly different from the structure of large jointed blocks where no water had been applied during the solidification. The water-cooled rock was intensely fractured and broken into pieces commonly 10–20 cm across. The structure resembled entablature lava, a formation frequently found in river beds and canyons, where a lava flow has solidified under floods of river water, dammed up by the lava flow[9]. Each cubic metre of lava which solidifies and cools down to 100 °C releases sufficient heat to evaporate 1.4 m^3 of water. To evaporate 100 kg s^{-1} of water spread over 7,000 m^2 of lava the heat flux density must have been ~40 kW m^{-2}.

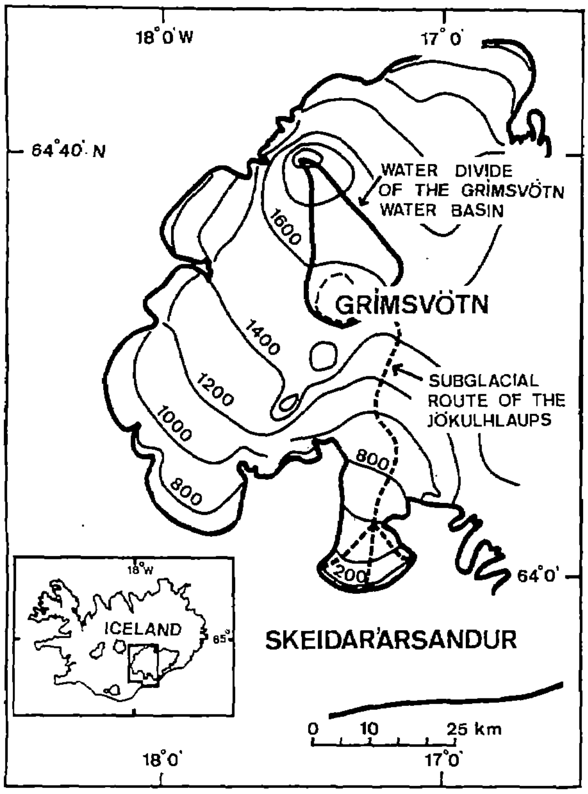

Fig. 1 Location of Grimsvötn geothermal area within the Vatnajökull ice cap in Iceland.

The propagation rate of the front of solidification was 12 m in 14 days or 0.9 m per day. In model calculations one may view this process as stationary, seen from the solidification boundary. Instead of considering the boundary progressing downward at a constant rate, one may, in calculations, assume that the boundary is fixed, but the lava is moving upwards and solidifying as it passes the fixed boundary. Just above the boundary there is a thin transition layer of solid, uncracked rock, where the heat flux is carried by the moving rock and by conduction. The first cracks which appear above this layer are narrow and filled with superheated steam but the bulk of the rock above has shrunk by cooling and developed cracks wide enough to admit percolation of a mixture of water and saturated steam. Simple calculations based on this model give 0.1 m for the thickness of the conductive transition layer.

There is every possibility that the effective extraction of heat by watering of hot rock at Heimaey can also take place at the boundaries of magma bodies or intrusions at a depth of several kilometres, if water is readily available. The process acts in hot rocks close to solidus temperature, irrespective of whether the heat source is a regular confined magma chamber or a swarm of magma sheets, completely or partially molten. There are, however, two reasons to expect lower heat flux densities than in the surface lava. First, due to higher overburden pressure at depth the cracks will open up at a lower temperature. Second, the heat is transported upwards by a one-phase fluid at pressures exceeding the critical pressure of water[8].

Returning to the problem of heat transfer from the Grímsvötn caldera, a magmatic source of heat must be inferred, but its size and depth has not been investigated. Observations of S-wave shadows at the Krafla caldera in the Northern Volcanic Zone of Iceland suggest a magma body at 3–7 km depth beneath that caldera[10]. Its horizontal extent is ~8 km^2. Assuming 10 km^2 for a similar body under Grímsvötn, water penetrating into that body would have to propagate at an average rate of 5 m yr^{-1} to yield the observed flux of 5,000 MW. At the deep end of the geothermal system, where the temperature may be near 400 °C, a mass flux of 2,400 kg s^{-1} of water is required to transport the extracted heat up to the bottom of the glacier. Vertical permeability is likely to be favourable near the ring fractures of the caldera. A special feature at Grímsvötn is the cyclic loading of the caldera by accumulation of meltwater for 5 yr and a drop of the water level of the lake by 100 m in one week during jökulhlaups. This sudden drop in pressure might help to keep fractures open and it has even been suggested that it could excite magma and lead to eruptions, which sometimes have been observed to coincide with jökulhlaups[1].

The above considerations have important implications for the exploitation of geothermal systems which derive heat from an underlying magma body. Drilling of wells for injection of water into the hot rock boundary might accelerate the heat extraction and aid in the generation of steam, where water is deficient, or the access of water to the magma body is hindered by an impermeable barrier. Controlled injection of water might even be used to establish reservoir conditions in temperature, pressure and fluid saturation which are optimal for the exploitation. There are some indications that the Krafla geothermal system[11] in Iceland might be a water-deficient system of this kind. On the other hand, abundant supply of water might explain the fact that geothermal systems with the highest natural heat output in Iceland are found in subglacial areas[12–14].

We thank I.B. Fridleifsson and S. Thorarinsson for constructive comments and G. Bodvarsson, G. Foulger, K. Grönvold and V. Stefánsson for criticism of an early version of this paper.

Received 21 October; accepted 7 December 1981.

1. Thorarinsson, S. *J. Glaciol.* **14,** 267–275 (1953); *The Swift Flowing Rivers* (Bókaútgáfa Menningarsjóðs, Reykjavík 1974).
2. Rist, S. *Jökull* **5,** 30–36 (1955); **23,** 55–60 (1973).
3. Björnsson, H. *Jökull* **24,** 1–26 (1974).
4. Bodvarsson, G. *Tímarit V.F.I.* **36,** 1–48 (1951); *Jökull* **11,** 29–38 (1961).
5. Banwell, C. J. *DSIR* (*Wellington*) *Bull.* **123,** (1957); *N.Z.J: Geol. Geophys.* **6,** 52–69 (1963).
6. White, D. E. *Bull geol. Soc. Am.* **68,** 1637–1658 (1957); *U.S. geol. Surv. Prof. Pap.* **458–C** (1968).
7. Irvine, T. N. *Can. J. Earth Sci.* **7,** 1031–1061 (1970).
8. Lister, C. R. B. *Geophys. J. R. astr. Soc.* **39,** 465–509 (1974); *Proc. 2nd U.N. Symp. Dev. and Use of Geothermal Resources,* 459–463 (1976); *Tectonophysics* **37,** 203–218 (1977); *A. Rev. Earth planet. Sci.* **8,** 95–117 (1980).
9. Saemundsson, K. *Jökull* **20,** 62–77 (1970).
10. Einarsson, P. *Bull. volcan.* **41,** 1–9 (1978).
11. Stefánsson, V. in *Geothermal Systems and Case Histories* (eds Rybach, L. & Muffler, L.J.P.) 273–294 (Wiley, New York, 1981).
12. Björnsson, H. *Jökull* **24,** 1–26 (1974); **27,** 71–78 (1977).
13. Friedman, J. D., Williams, R. S. Jr, Thorarinsson, S. & Pálmason, G. *Jökull* **22,** 27–43 (1972).
14. Bodvarsson, G. *Jökull* **11,** 29–38 (1961).

Handling and measurement techniques for anoxic interstitial waters

W. Davison & C. Woof

Freshwater Biological Association, Windermere Laboratory,
Ambleside, Cumbria LA22 0LP, UK

D. R. Turner

Marine Biological Association of the United Kingdom,
The Laboratory, Citadel Hill, Plymouth PL1 2PB, UK

Reports on problems associated with sampling, handling and measuring interstitial waters[1–5] have led to a refinement in methodology, but apart from the introduction of *in situ* sampling, techniques have not fundamental changed. The *in situ* techniques include a hydraulically operated device for filtering samples at pre-selected sediment depths on the ocean floor[6,7], and the insertion of dialysis membranes into sediments where they are left to equilibrate[8,9]. The former method requires specialized unwieldy equipment, and the latter necessitates a return to the sampling site. We report here a new method for measuring Fe (II), Mn (II) and sulphide ions in the interstitial waters of anoxic sediments which have been sampled using a simple corer. Rapid filtration directly into a polarographic vessel permits the extraction of interstitial water and the measurement of all three components <5 min after subsampling the sediment. The non-destructive polarographic measurement is able to assess the extent of contamination by oxygen and to study subsequent reactions in the interstitial water.

Previous workers[4,5] have noted that Fe(II) in interstitial water can be readily oxidized which can lead to erroneously low results for Fe(II) determinations. Scavenging by the freshly formed Fe(III) species can distort the analysis of trace metals, silica and phosphate[5]. Recommendations for handling in oxygen-free conditions have therefore been made[4,5] but glove box techniques can be laborious and monitoring oxidation which occurs during handling is difficult. Complications are introduced by the need either to squeeze under high pressure or to centrifuge to obtain sufficient sample for analysis. Observations in our laboratory have shown that equilibration using dialysis membranes is unsuitable for sediment rich in iron and sulphide, because FeS may precipitate inside the membrane and so total analysis for iron and sulphide does not give equilibrium concentrations in solution. Polarography unambiguously measures, on as little as 1 ml of sample, solution species of unique oxidation state[10]. Such a small volume may be obtained by simple hand filtration and refinements, such as small filter pore sizes, are unnecessary because the technique distinguishes the soluble component. Moreover, the technique functions best in the oxygen-free conditions which these waters provide.

Jenkin cores[11] of the sediment–water interface were taken from Esthwaite Water[12] and Rostherne Mere[13], both seasonally anoxic lakes with organic-rich fine sediments, using core tubes with pre-drilled 3 mm diameter holes at 5 mm depth intervals and sealed with polythene tape. A 20 ml disposable syringe fitted with a 7.5 cm 12 G stainless-steel needle was flushed several times with N_2 and then used to remove a 10 ml subsample of sediment. A 47 mm Swin-Lok (Nucleopore) filter holder, containing a Whatmans GF/C glass fibre filter, was fitted with 10 cm of 0.5 mm bore polythene tubing which led to the bottom of a standard Metrohm EA-800-5 polarographic cell assembly containing three electrodes: hanging mercury drop, platinum wire and calomel. The cell was flushed with a controlled gas mixture of Ar and CO_2 and the filter holder was flushed with N_2. Immediately the N_2 stream was disconnected from the filter assembly the syringe of sediment was attached. 1–2 minutes of hand pressure on the syringe provided the necessary 1–5 ml of sample for measurement. A polarographic scan from 0 to 1.7 V was immediately initiated while the Ar–CO_2 mixture was flushed over the surface of the liquid. Trials with various filter assemblies indicated that a unit with a large dead volume, in this case 3–4 ml, was needed because the wide passages prevented constriction and allowed rapid movement of slurry and also ensured that there was sufficient volume to accommodate the particulate material in proximity to the filter. It was possible to use Whatmans GF/F or Millipore 0.45 µm filters if the filtration time was extended.

Figure 1 shows typical polarographic scans of the overlying water and interstitial water. The polarography of anoxic lake water has been well documented[14,15] and measurements on interstitial waters have recently been reported[16]. The named peaks in Fig. 1 have been well characterized and the pre-wave at −1.1V has been attributed to interactions between Fe^{2+} and sulphide[14]. Determination of sulphide, Fe (II) and Mn (II) in a single scan is particularly useful because iron and manganese reflect the redox conditions of the sediments and are often major components in the interstitial waters[17]. Ferrous sulphide is usually a controlling solid phase. Figure 1 indicates that iron is dominant and sulphide is restricted to undetectable (<0.3 µmol l^{-1}) levels in the interstitial waters of Esthwaite Water, whereas in Rostherne Mere sediments the higher sulphate concentration of the overlying water (0.58 mmol l^{-1} compared with 0.13 mmol l^{-1} for Esthwaite Water) allows sulphide to dominate and suppress the iron. Respective concentrations (in µmol l^{-1}) of sulphide, Fe (II) and Mn (II) taken from Fig. 1 are: for overlying Esthwaite Water 4, 110 and 42; for interstitial Esthwaite Water <0.3, 550 and 53; and for interstitial Rostherne Mere 15, 1.7 and 370. Measurement of the *p*H of interstitial Esthwaite Water

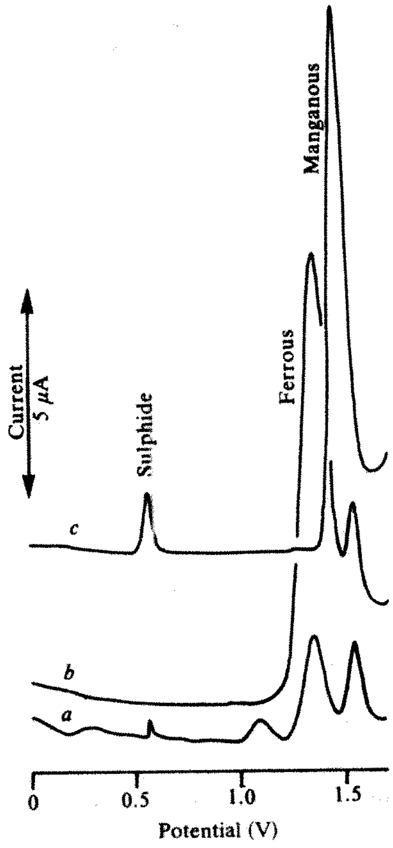

Fig. 1 Differential pulse polarograms (current versus potential) of *a*, the overlying lake water of Esthwaite Water; *b*, interstitial water of Esthwaite Water; and *c*, interstitial water of Rostherne Mere. The interstitial water samples were from a sediment depth of 3–4 cm. Samples *a* and *b* are for 8 September 1981 and sample *c* for 30 September 1981.

0028-0836/82/070582—02$01.00

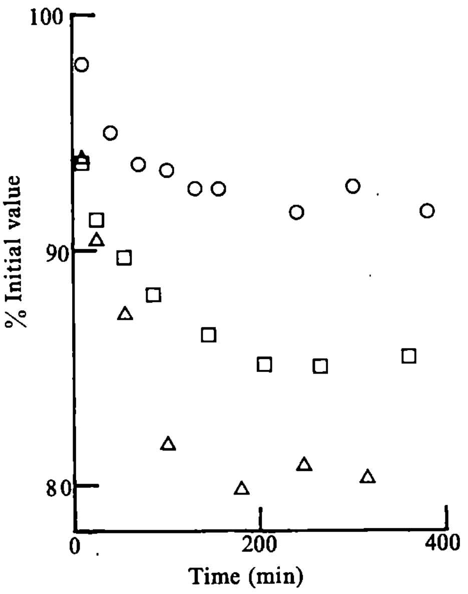

Fig. 2 Decay of Fe (II) with time. ○, No stirring, sampled on 23 September 1981; △, bubbling with $Ar–Co_2$, sampled on 24 September 1981; □, with magnetic stirring, sampled on 29 September 1981. All samples are from Esthwaite Water sediment at a depth of 4–5 cm.

by inserting an electrode into a filtered sample and extrapolating to zero time gives a value of 6.94 which agrees well with the value of 6.88 from an electrode inserted directly into the sediment. For Rostherne Mere, however, values from analogous measurements differ and are 7.1 (extracted) and 6.8 (direct). The overlying water is known to have a pH of 7.13 (10 °C)[18]. Therefore the solubility product, $pK_{sp}^{NBS} = a_{Fe^{2+}} \cdot a_{HS^-}/(H^+)$, can be calculated using documented activity coefficients[19] to be 2.71 for overlying Esthwaite Water, >3.45–3.55 for Esthwaite interstitial water and 4.05–4.55 for Rostherne Mere interstitial water. The result for the overlying water is in good agreement with previous work[18,19]. Both interstitial waters seem to exhibit a reduced solubility and, because the solid phase has more opportunity to age in the sediment than in the anoxic waters of the lake, support is given to the supposition that the ageing solid phase controls the interstitial water concentrations[19,20]. This result, and the small Mn (II) gradient and large Fe (II) gradient across the sediment–water interface, which agrees with previous water column measurements[12], show how useful is this simple handling technique. The method should be applicable to organic-rich marine sediments, although the Fe (II) and Mn (II) peaks will be closer together[21,22]. Because anodic stripping voltammetry uses the same equipment this simple procedure could be used to measure trace metals in interstitial water.

Changes in the concentration of pore water components after extraction from the sediment have previously been noted[4]. Because polarography is a non-destructive technique any change may be continuously monitored on the same sample. Figure 2 shows the change in Fe (II), as a percentage of the initial measured value, with time, for a quiescent solution, one stirred with a magnetic flea and one bubbled with an $Ar–CO_2$ mixture with, in order to preserve a constant pH of 6.94, the same partial pressure of CO_2 as that in the pore water (corrections for loss by volatilization have been made). Ferrous iron decays to a new lower equilibrium value when the solution is stirred. This result cannot be readily attributed to an oxidation effect because bubbling with the inert gases results in a lower equilibrium value and Mn (II), which has much slower oxidation kinetics[23], also shows an initial decay. In all solutions Mn (II) was reduced to 95% of the initial signal after 10 min and thereafter remained constant. Moreover the polarographic technique is able to measure oxygen directly in the sample[15] and show that it was never initially greater than 4 μmol l^{-1}. This introduced oxygen was quickly consumed (<5 min) by the solution to undetectable quantities, but it would be insufficient to account for >100 μmol l^{-1} of Fe (II) which were removed after 200 min (Fig. 2). It must be concluded that once pore water is extracted a re-equilibrium occurs which, contrary to previous conclusions[4,5], need not be linked to oxidation, loss of CO_2 or changes in pH.

We thank the NERC for financial support.

Received 13 October; accepted 18 December 1981.

1. Mangelsdorf, P. C., Wilson, T. R. S. & Daniell, E. *Science* **165**, 171–174 (1969).
2. Bischoff, J. L., Greer, R. E. & Luistro, A. D. *Science* **167**, 1245–1247 (1970).
3. Fanning, K. A. & Pilson, M. E. Q. *Science* **173**, 1228–1230 (1971).
4. Troup, B. N., Bricker, O. P. & Bray, J. T. *Nature* **249**, 237–239 (1974).
5. Loder, T. C., Lyons, W. B., Murray, S. & McGuinness, H. D. *Nature* **273**, 373–374 (1978).
6. Sayles, F. L., Wilson, T. R. S., Hume, D. N. & Mangelsdorf, P. C. *Science* **181**, 154–156 (1973).
7. Sayles, F. L., Mangelsdorf, P. C., Wilson, T. R. S. & Hume, D. N. *Deep Sea Res.* **23**, 259–264 (1976).
8. Mayer, L. M. *Limnol. Oceanogr.* **21**, 909–912 (1976).
9. Hesslein, R. H. *Limnol. Oceanogr.* **21**, 912–914 (1976).
10. Davison, W. *J. electroanalyt. Chem.* **87**, 395–404 (1978).
11. Mortimer, C. H. *Limnol. Oceanogr.* **16**, 387–404 (1971).
12. Davison, W. *Nature* **290**, 241–243 (1981).
13. Reynolds, C. S. *Field Studies* **5**, 93–173 (1979).
14. Davison, W. *Limnol. Oceanogr.* **22**, 746–753 (1977).
15. Davison, W. *Freshwat. Biol.* **7**, 393–401 (1977).
16. Nembrini, G. P., Garcia, J., Capobianco, J. A. & Jaquet, J. M. Pap. *2nd int. Symp. on the Interactions between Sediments and Freshwater*, Kingston (1981).
17. Berner, R. A. *Early Diagenesis* (Princeton University Press, 1980).
18. Davison, W. & Heaney, S. I. *Limnol. Oceanogr.* **23**, 1194–1200 (1978).
19. Davison, W. *Geochim. cosmochim. Acta* **44**, 803–808 (1980).
20. Doyle, R. W. *Am. J. Sci.* **266**, 980–994 (1968).
21. Davison, W. & Heaney, S. I. *Limnol. Oceanogr.* **25**, 153–156 (1980).
22. Knox, S. & Turner, D. R. *Estuar. Coastal mar. Sci.* **10**, 317–324 (1980).
23. Stumm, W. & Morgan, J. J. *Aquatic Chemistry* 2nd edn (Wiley, New York, 1981).

Radiation-induced dissolution of colloidal haematite

George V. Buxton & Trevor Rhodes

The University of Leeds, Cookridge Radiation Research Centre,
Cookridge Hospital, Leeds LS16 6QB, UK

Robin M. Sellers

Central Electricity Generating Board, Berkeley Nuclear
Laboratories, Berkeley, Gloucestershire GL13 9PB, UK

The dissolution of metal oxides that are normally insoluble in aqueous solution is an important process in the transport of corrosion products around the circuits of water-cooled nuclear reactors[1], and in reactor decontamination[2,3]. It has recently been shown[4–6] that one-electron reducing agents dissolve iron (III) oxides, often at much faster rates than the more conventional reagents such as chelating agents and strong acids. In appropriate conditions the products of water radiolysis can be used to generate the one-electron reducing reagents in the form of free radicals. We report here our preliminary results on the radiation-induced dissolution of colloidal Fe_2O_3 by propan-2-ol radicals, $Me_2\dot{C}OH$, in acidic aqueous solution.

Colloidal Fe_2O_3 was prepared by the method of Matijevic *et al.*[7]. Aqueous solutions containing 3×10^{-2} mol dm^{-3} $FeCl_3$ and 5×10^{-3} mol dm^{-3} HCl were refluxed for 2 weeks at 100 °C. The colloidal particles were spherical, with diameters of 0.5–1.5 μm as shown by electron microscopy of the dry material and by particle sizing of the colloidal solution. The latter measurements showed that the mean diameter of the particles was 0.9 μm and the FWHM of the diameter distribution 0.6 μm. These parameters changed little from one preparation to another.

Irradiations were carried out using ^{60}Co γ rays at dose rates of 0.15–0.8 krad min^{-1} on solutions at pH 2.2 containing $\sim 10^{-13}$ mol dm^{-3} Fe_2O_3 particles and 10^{-1} mol dm^{-3} propan-2-ol, saturated with N_2O. In these conditions the following sequence

0028–0836/82/070583—03$01.00

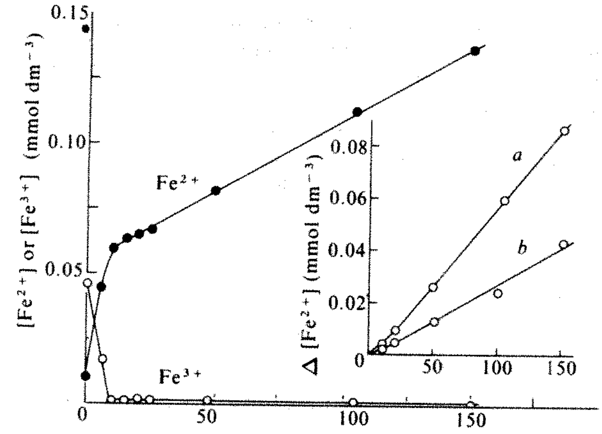

Fig. 1 Fe^{2+} formed in the reduction of Fe^{3+} and colloidal Fe_2O_3 by $Me_2\dot{C}OH$. Inset: effect of dose rate on the rate of formation of Fe^{2+} from Fe_2O_3. *a*, 0.17 krad min^{-1}; *b*, 0.82 krad min^{-1}.

of reactions generates propan-2-ol radicals with $G(Me_2\dot{C}OH) = 7$, where G is the radiation chemical yield in molecules $(100\ eV)^{-1}$.

$$H_2O \rightsquigarrow e^-_{aq}, H, OH, H_2, H_2O_2 \tag{1}$$

$$e^-_{aq} + N_2O \rightarrow N_2 + O^-(\xrightarrow{H_2O} OH + OH^-) \tag{2}$$

$$OH \text{ or } H + Me_2CHOH \rightarrow Me_2\dot{C}OH + H_2O \text{ or } H_2 \tag{3}$$

After an irradiation the remaining colloidal Fe_2O_3 was removed by centrifuging and the dissolved iron was measured as Fe(II) using *o*-phenanthroline, either as Fe(II) alone or as total iron after reducing Fe(III) with hydroxylamine.

Figure 1 summarizes the results. The high initial yield of Fe^{2+} is due to the reduction (reaction (4)) of Fe^{3+} present in the colloidal preparation ($\sim 6 \times 10^{-5}$ mol dm^{-3}), and the lower yield represents the reduction of Fe(III) in the colloidal particles. On the basis that the competing reactions involving $Me_2\dot{C}OH$ after the initial Fe^{3+} has been reduced are (5) and (6), the observed dose rate effect (Fig. 1 inset) is consistent with reaction (5) being diffusion controlled.

$$Me_2\dot{C}OH + Fe^{3+} \rightarrow Fe^{2+} + Me_2CO + H^+ \tag{4}$$

$$Me_2\dot{C}OH + Fe(III)_{colloid} \rightarrow Fe^{2+} + Me_2CO + H^+ \tag{5}$$

$$2\ Me_2\dot{C}OH \rightarrow Me_2CO + Me_2CHOH \tag{6}$$

Experiments in the absence of propan-2-ol and N_2O show that hydrogen atoms formed in reactions (1) and (7) also bring about dissolution of Fe_2O_3

$$e^-_{aq} + H^+ \rightarrow H \tag{7}$$

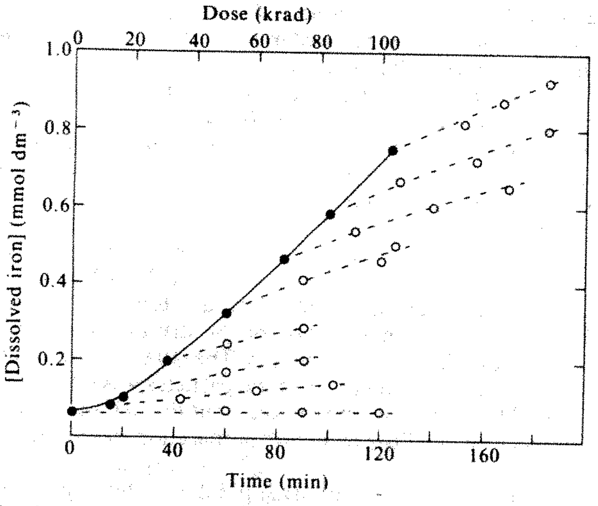

Fig. 2 Radiation-induced (●) and thermal (○) dissolution of colloidal Fe_2O_3 by Fe(II)–EDTA.

Reaction (6) competes favourably with reaction (5) because of the low concentration of colloidal particles ($\sim 10^{-13}$ mol dm^{-3}) and this is a limiting factor to the rates of dissolution which can be achieved. However, this problem can be overcome by adding EDTA to the system, as shown by Fig. 2. In the presence of 10^{-3} mol dm^{-3} EDTA the rate of radiation-induced dissolution is greatly enhanced and when the irradiation is stopped the dissolution process continues at a rate which depends on the radiation dose. The explanation for these effects is that dissolved Fe^{2+} complexes with EDTA to form Fe(II)–EDTA which undergoes reaction (8) with the colloidal Fe_2O_3 and $Me_2\dot{C}OH$ now reduces Fe(III)–EDTA in reaction (9)

$$Fe(II)\text{–}EDTA + Fe(III)_{colloid} \rightarrow Fe^{2+} + Fe(III)\text{–}EDTA \tag{8}$$

$$Me_2\dot{C}OH + Fe(III)\text{–}EDTA \rightarrow Fe(II)\text{–}EDTA + Me_2CO + H^+ \tag{9}$$

Because reaction (9) occurs in the bulk solution and [Fe(III)–EDTA] ≫ $[Me_2\dot{C}OH]$, reaction (6) cannot compete with it. From the measured rates of thermal dissolution we calculate $k_8 = 2 \times 10^9\ dm^3\ mol^{-1}\ s^{-1}$, indicating that reaction (8) is $\sim 10^3$-fold slower than diffusion controlled.

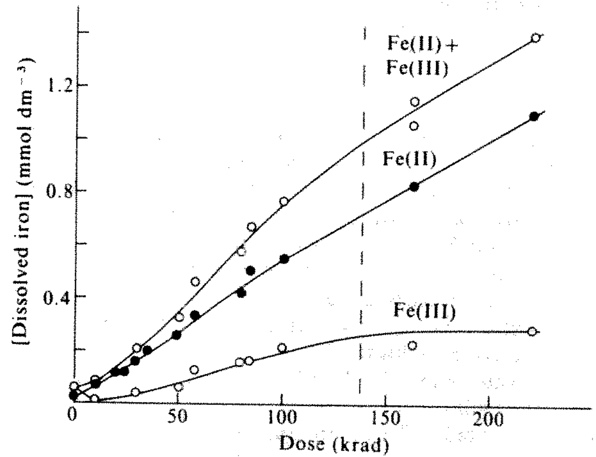

Fig. 3 Radiation-induced dissolution of Fe_2O_3 by Fe(II)–EDTA. The vertical broken line shows the dose at which no uncomplexed EDTA remains.

Ultimately, sufficient dissolved iron is produced to complex all the EDTA. When this state is reached the rate of dissolution of the colloid will be limited by the rate of reaction (9) provided sufficient Fe(III)–EDTA remains in solution (see Fig. 3). However, $G(Fe^{2+}) \sim 5$ instead of 7 ($= G(Me_2\dot{C}OH)$ as expected. This discrepancy is attributed to a reaction of $Me_2\dot{C}OH$ with the EDTA or an impurity introduced with it, because G(Fe(II)) from solutions of Fe(III)–EDTA in the absence of Fe_2O_3 followed a similar pattern. $G(Me_2CO) = 7.7$ was obtained in both cases, which is the expected result if all $Me_2\dot{C}OH$ is oxidized because $G(H_2O_2)$ (see reaction (1)) is 0.7 and H_2O_2 also generates $Me_2\dot{C}OH$ through reactions (10) and (3)

$$H_2O_2 + Fe(II) \rightarrow Fe(III) + OH + OH^- \tag{10}$$

Two points of wider implications emerge from this work. First, water radiolysis leading to the generation of reducing free radicals may bring about dissolution of corrosion products in the reactor core. There is growing evidence[8,9] that radiolysis enhances the corrosion rates of certain materials and, although several other factors are involved, there is good reason to believe that the intermediacy of species such as the hydrated electron will increase the rate of release of iron from corroded surfaces in radiation zones. The second point is the potentially important part played by complexes of iron(II), such as Fe(II)–EDTA, in reactor decontamination. Many commercial reactor decontaminating reagents are composed of mixtures of organic acids and complexants. These alone tend to be poor at effecting the dissolution of iron (III)-containing oxides, although some dissolution may occur, for instance, by corrosion of the underlying metal to give Fe^{2+} in solution. We suggest that complexes of this ferrous ion give rise to a further, and possibly much more rapid, autocatalytic dissolution. Recent experiments show the dissolution of haematite powder by oxalic acid to occur by an autocatalytic process of this type (R.M.S., unpublished data).

T.R. thanks the SERC for a CASE studentship and R.M.S. thanks the Central Electricity Generating Board for permission to publish this paper.

Received 13 November; accepted 21 December 1981.

1. Taylor, N. K. *Rev. Coatings Corr.* **2,** 261–321 (1978).
2. Ayres, J. A. *Decontamination of Nuclear Reactors and Equipments* (Ronald, New York, 1970).
3. Osterhout, M. M. *Decontamination and Decommisioning of Nuclear Facilities* (Plenum, New York, 1980).
4. Segal, M. G. & Sellers, R. M. *JCS Chem. Commun.*, 991–992 (1980).
5. Segal, M. G. & Sellers, R. M. *JCS Faraday Trans. I* (in the press).
6. Bradbury, D., Segal, M. G., Sellers, R. M., Swan, T. & Wood, C. J. *Water Chemistry of Nuclear Reactor Systems* Vol. 2, 403–408 (British Nuclear Energy Society, London, 1981).
7. Matijevic, E. & Scheiner, P. *J. Colloid Interface Sci.* **63,** 509–524 (1978).
8. Ishigure, K., Kawaguchi, M., Oshoma, K. & Fujita, N. *Water Chemistry of Nuclear Reactor Systems* Vol. 2, 293–298 (British Nuclear Energy Society, London, 1981).
9. Christensen, J. *Radiat. phys. Chem.* **18,** 147–158 (1981).

Uranium–lead system in fragments of a single zircon grain

Urs Schärer & Claude J. Allègre

Laboratoire de Géochimie et Cosmochimie, Institut de Physique du Globe et Département des Sciences de la Terre, Universités Paris VI et VII, 4 place Jussieu, 75230 Paris Cedex 5, France

Since the demonstration that U–Pb analyses of zircon fractions[1] (from a few grains up to several thousand grains or fragments of grains[2]) or single zircon grains[3,4] yield reliable radiometric age data, this method has been widely applied to igneous, metamorphic and sedimentary rocks. The present investigation of U–Pb systems for a suite of distinct fragments of a single zircon grain from a 1,093$\pm^{21}_{18}$-Myr old syenite of the Pikes Peak batholith (Colorado, USA) demonstrates that uranium is heterogeneously distributed in this zircon crystal. Most parts of the grain suffered various degrees of lead loss, the others show a closed-system behaviour. We show that degrees of lead loss are not correlated with uranium concentrations of the fragments.

In contrast to other U-bearing minerals such as monazite and sphene, zircons often show an open-system behaviour for lead defining discordant age patterns (^{206}Pb/^{238}U age < ^{207}Pb/^{235}U age < ^{207}Pb/^{206}Pb age). The most common presentation of U–Pb age data is as the Concordia diagram[5] in which ^{206}Pb/^{238}U is plotted against ^{207}Pb/^{235}U (with reference to the Concordia curve). The perturbations of the U–Pb systems creating the discordancies in zircon are interpreted as being mainly due to either continuous lead diffusion[6,7], or episodic lead loss[5,8]. In many cases a combined diffusion–episodic model[9,10] or a multi-stage episodic lead loss model[9,10] is needed to explain the data. Uranium gain[11] has also been suggested as an important cause of discordant U–Pb ages.

Our main aim was to elucidate the U–Pb systematics in a single zircon grain. In contrast with previous work which was based on zircon fraction—or single—grain measurements, the present study focused on distinct fragments within a single zircon grain. For comparison, a grain by grain U–Pb dating of zircon and coexisting allanite/chevkinite was carried out. Both minerals were extracted from a quartz–fayalite–syenite body (B65D) from the central part of the Pikes Peak batholith. The mineralogy, petrology, major/minor element chemistry and genesis of this batholith has been extensively studied by Barker and co-workers[12,13]. For the genesis of the quartz–fayalite–syenite they conclude on an alkali olivine basaltic magma which reacts with a lower crust of granulite facies. Previous K–Ar and Rb–Sr mica ages[14–19] from different lithological variants of the batholith yield ages between 930 and 1,060 Myr (recalculated for the conventional decay constants[20]). Rb–Sr whole rock isochrons determine ages of ~1,008 Myr (ref. 13) and 1,019 ± 13 Myr (ref. 14) for the emplacement of the batholith.

The zircon population of the quartz–fayalite–syenite consists of slightly coloured, transparent to yellow-brown, translucent euhedral prisms with a pronounced concentric zoning. The length-to-width ratios vary from about 1/1 to 10/1. Small grains are mainly free of microscopically visible inclusions whereas coarser crystals frequently contain different inclusions—mostly opaque phases. The analysed allanite/chevkinite are dark-red glassy subhedral grains. To verify the mineralogical composition of zircon, a series of grains was analysed for major and trace elements on the CAMECA IMS 3F ion microprobe. Tracing of profiles in single crystals showed that all grains consist of at least 98% of Zr-silicate. Therefore an intergrowth of zircon with other U-bearing mineral phases such as xenotime can be excluded. The chemical compositions (major elements and a few trace elements) of three opaque inclusions in zircon were also determined. The analyses show that the inclusions consist of Al, Fe, Ca-silicate phases with U and Th concentrations of the order of 1‰. The allanite/chevkinite grains represent a Ca, Ti, Ce, Fe-silicate as revealed by electron-microprobe analysis.

U–Pb results of the grain by grain analyses for both minerals are shown in Fig. 1 and listed in Table 1. The analysed zircon grains are free of microscopically visible inclusions. Grains 1, 2 and 7 (see Table 1 and Fig. 1) are transparent prisms with width-to-length ratios of about 1/3, whereas grains 3 and 4 show identical habits but a higher degree of radioactive damage. Crystals 5 and 6 are translucent short prisms with length-to-width ratios of ~1/1 and zircon 10 is a translucent long prismatic grain. Zircons 8 and 9 are surface-rich almost spherical transparent crystals with a well developed concentric zoning.

A regression line[21] (Fig. 1) including the data from the 10 measured zircon grains and the allanite/chevkinite grain intersects the Concordia curve at 1,097$^{+68}_{-47}$ Myr and 109 ± 150 Myr. The upper intercept age can be interpreted as the time of crystallization of zircon. The lower intercept age could be

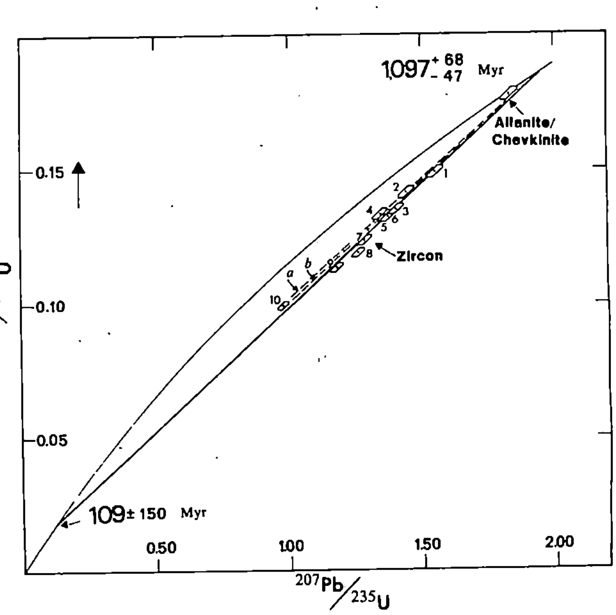

Fig. 1 Concordia diagram for U–Pb grain by grain analyses of zircon and allanite/chevkinite from a quartz–fayalite–syenite body within the Pikes Peak batholith (Colorado, USA).

Table 1 U–Pb results of the grain by grain and zircon fragment analysis

		U and Pb concentrations (p.p.m.)				Radiogenic lead (atomic %)			Atomic ratios			Apparent gas (Myr)		
Sample	Weight in 10^{-6} g	U*	Pb_{rad}†	Pb_c‡	$^{206}Pb/^{204}Pb$ measured	^{206}Pb	^{207}Pb	^{208}Pb	$\frac{^{206}Pb}{^{238}U}$	$\frac{^{207}Pb}{^{235}U}$	$\frac{^{207}Pb}{^{206}Pb}$	$\frac{^{206}Pb}{^{238}U}$	$\frac{^{207}Pb}{^{235}U}$	$\frac{^{207}Pb}{^{206}Pb}$
Grain by grain analyses												Errors (approx.)		
Zircon												±15	±14	±34
1	ND			—§	815	77.4	5.9	16.7	0.1489	1.555	0.07579	895	953	1,090
2	37.4±0.2	766	109	7.5	435	85.4	6.3	8.3	0.1413	1.443	0.07409	852	907	1,044
3	ND			—	689	82.7	6.2	11.1	0.1350	1.407	0.07558	816	892	1,084
4	ND			—	112	82.1	6.0	11.9	0.1332	1.348	0.07340	806	867	1,025
5	ND			—	770	80.5	6.0	13.5	0.1326	1.368	0.07482	803	876	1,064
6	80.0±10.0	660	90	—	2,400	82.0	6.2	11.8	0.1322	1.378	0.07558	800	880	1,084
7	100.0±10.0	400	50	—	866	79.8	6.0	14.2	0.1234	1.287	0.07564	750	840	1,086
8	47.8±0.2	350	44	—	110	82.1	6.3	11.6	0.1190	1.266	0.07720	725	831	1,126
9	44.0±0.2	715	86	3.5	420	81.3	6.1	12.6	0.1133	1.182	0.07570	692	792	1,085
10	140.0±10.0	1,930	203	32.0	352	81.1	5.8	13.1	0.09968	0.9808	0.07137	613	694	968
Allanite/chevkinite														
	56.0±0.2	240	463	19.5	146	8.0	0.6	91.4	0.1773	1.832	0.07493	1,052	1,057	1,067
Zircon fragment analyses														
F_1	101.3±0.2	958	153	12.5	381	56.6	4.0	39.5	0.1049	1.014	0.07012	643	711	932
F_2	46.6±0.2	1,181	345	2.0	1,170	52.1	3.9	44.0	0.1767	1.823	0.07483	1,049	1,054	1,064
F_3	30.0±0.2	207	38	—	501	77.9	5.8	16.4	0.1653	1.698	0.07450	986	1,008	1,055
F_4	21.9±0.2	657	134	—	603	73.3	5.5	21.2	0.1757	1.823	0.07528	1,043	1,054	1,076
F_5	13.8±0.2	473	99	—	200	71.1	5.4	23.5	0.1737	1.831	0.07644	1,033	1,057	1,107
F_6	14.3±0.2	838	183	—	234	65.2	4.9	29.9	0.1649	1.714	0.07541	984	1,014	1,080
F_7	23.6±0.2	518	81	235	35	75.8	5.7	18.5	0.1501	1.556	0.07520	902	953	1,074
F_8	37.6±0.2	2,274	361	32.0	396	64.3	4.7	31.0	0.1188	1.189	0.07256	724	795	1,002
F_9	14.7±0.2	561	73	14.0	112	75.4	5.5	19.1	0.1146	1.153	0.07301	699	779	1,014
F_{10}	6.7±0.2	663	96	—	203	82.1	6.2	11.7	0.1383	1.443	0.07567	835	907	1,086
F_{11a}	40.0±10.0	1,120	335	—	1,373	53.0	3.9	43.1	0.1836	1.900	0.07508	1,086	1,081	1,071
F_{11b}	50.0±10.0	950	220	6.5	648	58.4	4.4	37.2	0.1578	1.627	0.07483	944	981	1,064

Decay constants and atomic ratios were used according to the recommendation of IUGS[20]. After dissolution of zircon[24], element separation and purification[25] the atomic compositions and concentrations have been determined by isotopic dilution (^{205}Pb–^{233}U mixed-spike) in a Thomson THN 206 mass spectrometer. The samples were loaded with H_3PO_4 and silica gel on Re single filaments. The isotopic composition of blank common lead was determined to: 17.98±0.10 (2σ errors) for $^{206}Pb/^{204}Pb$, 15.45±0.10 for $^{207}Pb/^{204}Pb$ and 37.28±0.20 for $^{208}Pb/^{204}Pb$. The blank amount for lead varies between 40×10^{-12} g and 280×10^{-12} g with an average value of $\sim140\times10^{-12}$ g whereas the U blank lies at $\sim20\times10^{-12}$ g (the lead-blank consists of 20–40×10^{-12} g introduced by the chemical procedure and 20–260×10^{-12} g extracted from the Teflon bombs in which the zircons are dissolved; the uranium blank is mainly due to memory effects in the Teflon bombs). Taking into account the observed isotopic variation of blank common lead as well as the precisions of Pb and U measurements, the accuracies are: 1.5% for $^{206}Pb/^{238}U$, 2.0% for $^{207}Pb/^{235}U$ and 1.7% for $^{207}Pb/^{206}Pb$. The 2σ errors of the Concordia intercept ages are computed from the intersections of the asymptotes to the hyperboles that limit the confidence interval of the regression lines[21].

ND, not determined.

* Corrected for a U-blank of 20×10^{-12} g.

† Radiogenic lead corrected for blank common lead and where present (see Pb_c) corrected for incorporated common lead with: $^{206}Pb/^{204}Pb$ of 16.64, $^{207}Pb/^{204}Pb$ of 15.35 and $^{208}Pb/^{204}Pb$ of 36.58.

‡ Incorporated common lead, calculated for maximal blank common lead amount. The given values are therefore minimum concentrations.

§ No incorporated common lead detectable.

explained by different models: (1) diffusive lead loss; (2) combined diffusive–epidodic lead loss; and (3) epidodic lead loss. Previous K–Ar and Rb–Sr data[13-19] do not indicate any episodic event postdating the intrusion of the batholith, thus favouring an interpretation by a continuous lead diffusion[6,7] (Fig. 1, line *a*: volume-dependent diffusion[6], and line *b*: time-dependent diffusion[7]). On the other hand, several episodes of Tertiary volcanism[22,23] (~20–70 Myr ago) are known in areas south of the batholith, so an episodic or combined episodic –diffusion lead loss of zircon cannot be excluded. An episodic lead loss would mean that the U–Pb system in zircon is more sensitive to moderate heating than the Rb–Sr system in minerals. However, exactly discordant age pattern cannot be determined.

The concordant allanite/chevkinite grain does not plot on the regression line yielding a slightly younger age of ~1,060 Myr (upper intercept age being ~1,097 Myr). This disagreement on age could be due either to a real age difference reflecting the cooling history of the pluton or to an incorrect common lead correction. As this mineral contains a large amount of common lead (~20 p.p.m., see Table 1), the isotopic composition of which is not known, the apparent younger age could be caused by this uncertainty. The deviations of zircons 2, 4, 8 and 10 from the regression line can also be explained by an incorrect common lead correction due to unknown lead in zircon. Grains 2 and 10 with common lead concentrations of 7.5 p.p.m. and 32 p.p.m. respectively (see Table 1) are the best illustration of this observation of incorporated lead in zircon. The lead could be either primary common lead absorbed during growth of the crystal or younger common lead which diffused from the intergranular phases into zircon. Such a mechanism might take place in fissures or highly metamict parts of the grain.

The primary lead, included during growth of zircon and allanite, can be (1) common lead from an uncontaminated mantle magma, (2) common lead from a contaminating older crust, or (3) inherited radiogenic lead from U-bearing minerals from an older crust. The latter two types of lead would yield too high $^{207}Pb/^{206}Pb$ ages with respect to the real crystallization age of zircon and allanite. A weak indication for such an older lead is given by grain 8 ($^{207}Pb/^{206}Pb$ age 1,126; Table 1).

None of the deviations from the regression line can be fully explained by uncertainties of the isotopic composition of lead introduced during analysis (blank common lead, Table 1).

A zircon weighing ~0.5 mg was broken into 11 distinct fragments. The yellow-brown translucent grain showed a microscopically clearly visible igneous zoning. The fragment edges crosscut these heterogeneities and therefore the zircon parts analyses do not reflect the different growth stages of the crystal. Figure 2 shows the location of the various fragments (F_1–F_{11}) in the zircon grain. The fragments were obtained by selective breaking in an agate mortar filled with alcohol. The zircon was first broken in two parts almost equal in size (fragment F_1–F_6 and F_7–F_{11} respectively), then the upper part (F_1–F_6) was broken into three pieces, F_1, F_2 and a remaining part (F_3–F_6) which was then divided. Fragments F_7–F_{10} were separated in the same way from the other half of the crystal. In contrast with the well defined fragments F_1–F_{10}, F_{11} consisted of small splinters and therefore this fragment was analysed through two series (F_{11a} and F_{11b}) of such small pieces. Except for F_3, F_4, F_{10} (centre domains) and F_{11a} and F_{11b}, all fragments crosscut the whole crystal. The centre domains reach only to about two-thirds of the

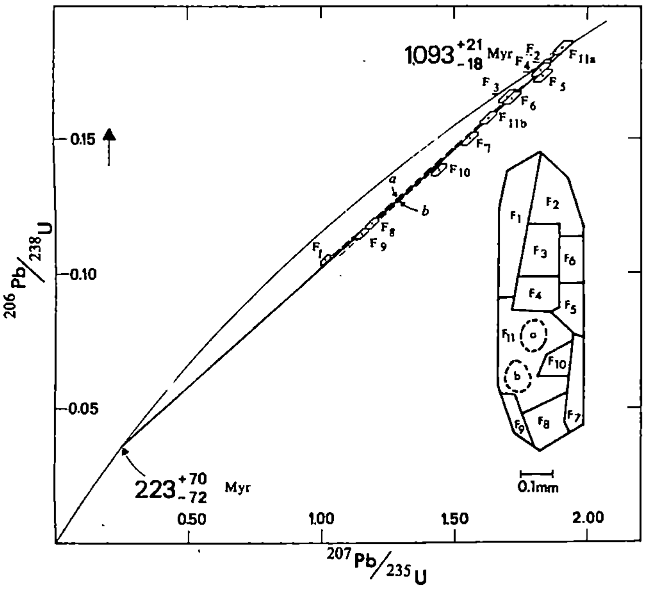

Fig. 2 Concordia diagram for U–Pb zircon fragment analyses of a single grain from a quartz–fayalite–syenite body within the Pikes Peak batholith (Colorado, USA).

depth of the crystal. The three-dimensional relationship of F_{11a} and F_{11b} is not known.

Figure 2 represents the Concordia diagram for the U–Pb fragment results (Table 1). The most remarkable observation from the fragment analyses are the concordant fragments: no concordant grains could be found. Additionally, the spread of degree of lead loss is larger than among single grains. The coexistence of concordant and strongly discordant fragments demonstrates that the U–Pb system remained closed for some crystal parts while others suffered a strong lead loss. This difference in behaviour occurs at a very small scale (<0.1 mm) as is best shown by the most discordant fragment F_1 and the adjacent concordant fragment F_2.

The concordant fragments, together with the large spread of degrees of discordance permit, for this zircon population, a more precise age determination than the grain by grain analysis. A regression line including all fragment data (Fig. 1) defines an age of $1,093^{+21}_{-18}$ Myr for the crystallization of the zircon grain (grain by grain analysis: $1,097^{+68}_{-47}$ Myr). The deviation of fragment F_5 and F_{10} could again be ascribed to an incorrect common lead correction due to small, not detectable incorporated lead in zircon.

The different degrees of lead loss are not correlated with the U concentrations of the fragments nor with their location within the grain. The most discordant fragment F_1 with a U concentration of 958 p.p.m. and the adjacent concordant fragment F_2 with a higher U concentration of 1,181 p.p.m. support these observations which strongly contrast with the other pattern observed from zircon fraction analyses (thousand of grains) which shows a positive correlation between increasing U concentrations and degree of lead loss. The most discordant grains 9 and 10 (Fig. 1) and the most discordant fragments F_1, F_8 and F_9 (Fig. 2) are characterized by unusually high common lead contents (Table 1). This observation could indicate a relationship between loss of radiogenic lead and gain of common lead.

These results suggest that the discordancy phenomenon should be discussed in terms of domains within a single grain and not in terms of grain dimensions or volume diffusion relative to grain size. Our cutting techniques do not allow us to determine domain geometry or size—further research is necessary. The variability of the common lead contents in the fragments suggests that we should consider lead loss as an exchange with the surroundings rather than as a one way process.

As the regression line coincides within analytical error to a volume-dependent[6] as well as a time-dependent[7] continuous lead diffusion model (Fig. 2, line *a* and *b* respectively), continuous lead diffusion appears to be the most plausible interpretation for the discordant U–Pb ages of the zircon fragments. However, the relatively large errors do not allow us to resolve definitively whether or not a subordinate episodic lead loss occurred. On the other hand, an episodic lead loss alone, related to the Tertiary volcanism[22,23] in the adjacent areas ~20–70 Myr ago, cannot explain the lower intercept age of 223^{+70}_{-72} Myr.

This study of one grain shows that the lead loss mechanism is more complex than generally thought and in particular probably occurs at the domain side. Thus the degree of discordancy varies through a single zircon grain and permits an accurate dating.

The age of $1,093^{+21}_{-18}$ Myr of the quartz–fayalite–syenite is significantly older than the previous Rb–Sr whole rock age[14] for the Pikes Peak batholith (1,019 ± 13 Myr). This difference could be explained in two ways: (1) the lithological variants of the Pikes Peak batholith crystallized in a time range of ~70 Myr; or (2) the Rb–Sr system in whole rocks remained open for ~70 Myr while the U–Pb system in zircon was closed from the very first moment of crystallization of the pluton. As there is no indication for a metamorphism in this rock[12,13] interpreting the younger Rb–Sr age as a reopening of the system is difficult.

We thank F. Barker and the USGS for supplying zircon and allanite, G. Manhes and D. Ben Othman for useful discussions, A. Pierre for ion probe analyses, and O. Krebs for calculating the lead diffusion lines. This is IPGP contribution NS/535.

Received 16 June; accepted 7 December 1981.

1. Silver, R. T. & Deutsch, S. *J. Geol.* **71**, 747–758 (1963).
2. Krogh, T. E. & Davis, G. L. *Yb. Carnegie Instn Wash.* **73**, 601–605 (1973).
3. Lancelot, J., Michard-Vitrac, A. & Allègre, C. J. *Earth planet. Sci. Lett.* **29**, 357–366 (1976).
4. Michard-Vitrac, A., Lancelot, J. R. & Allègre, C. J. *Earth planet. Sci. Lett.* **35**, 449–453 (1977).
5. Wetherill, G. S. *Geochim. cosmochim. Acta* **9**, 290–292 (1956).
6. Tilton, G. R. *J. geophys. Res.* **65**, 2933–2945 (1960).
7. Wasserburg, G. J. *J. geophys. Res.* **68**, 4823–4846 (1963).
8. Wetherill, G. S. *Am. geophys. Un.* **37**, 320–326 (1956).
9. Wetherill, G. S. *J. geophys. Res.* **68**, 2957–2965 (1963).
10. Allègre, C. J., Albarède, F., Grünenfelder, M. & Köppel, V. *Contr. Miner. Petrol.* **43**, 163–194 (1974).
11. Davis, G. L., Hart, S. R. & Tilton, G. R. *Earth planet. Sci. Lett.* **5**, 27–34 (1968).
12. Barker, F., Wones, D. R., Sharp, W. N. & Desborough, G. A. *Precambr. Res.* **2**, 97–160 (1975).
13. Barker, F., Hedge, C. E., Millard, H. T. Jr & O'Neil, J. R. *Prof. Contr. Colorado School of Mines* **8**, 44–55 (1976).
14. Hedge, G. E. *U.S. Survey Prof. Pap.* **700-B** B86–B89 (1970).
15. Aldrich, L. T., Wetherill, G. W., Davis, G. L. & Tilton, G. R. *EOS* **39**, 1124–1134 (1958).
16. Griffin, C. E. & Kulp, J. L. *Bull. geol. Soc. Am.* **71**, 219–222 (1960).
17. Hutchinson, R. M. & Hedge, C. E. *Rocky Mountain Guidebook* (Geological Society of America, 1967).
18. Gross, E. B. & Heinrich, E. W. *Am. Miner.* **51**, 299–323 (1966).
19. Hawley, C. C., Huffman, C. Jr, Hamilton, J. C. & Rader, L. F. *U.S. geol. Survey Prof. Pap.* **550-C**, C138–C147 (1966).
20. Steiger, R. H. & Jäger, E. *Earth planet. Sci. Lett.* **36**, 359–362 (1977).
21. York, D. *Can. J. Phys.* **44**, 1079–1086 (1966).
22. Dickinson, R. G., Leopold, E. B. & Marvin, R. *Colorado School Mines Quart.* **63**, 125–148 (1968).
23. Lipman, P. W., Doe, B. R., Hedge, C. E. & Steven, T. A. *Bull. geol. Soc. Am.* **89**, 59–82 (1978).
24. Krogh, T. E. *Geochim. cosmochim. Acta* **37**, 485–494 (1973).
25. Manhes, G., Minster, J. F. & Allègre, C. J. *Earth planet. Sci. Lett.* **39**, 14–24 (1978).

Thermal stresses in subducting lithosphere can explain double seismic zones

L. S. House*† & K. H. Jacob*

*Lamont-Doherty Geological Observatory and
† Department of Geological Sciences, Columbia University,
Palisades, New York 10964, USA

The discovery of double-planed zones of intermediate-depth seismicity associated with subducting oceanic lithosphere (refs 1–7 and L.S.H. and K.H.J., in preparation) has generated much interest in the origin and distribution of stresses in descending plates. Several mechanisms have been proposed to explain why double zones occur[8]. Here we investigate the role of thermal stresses for the state of stress in a descending plate and test whether they can account for the observed characteristics of double seismic zones. By modelling the descending slab as a thin elastic plate and using the temperatures in the slab estimated by

0028–0836/82/070587—03$01.00

Toksöz *et al.*[9], we find that the polarities of thermally generated stresses agree with those obtained from the focal mechanisms of earthquakes in the two zones. Thermal stresses also can explain the separation between the two zones of seismicity at shallow depths and their gradual merging at greater depth.

The best studied double seismic zone is that beneath North-east Honshu, Japan (Fig. 1). Note that the double zone of seismicity occurs in a portion of the downgoing plate that appears to be straight. We sought to evaluate whether the thermal stresses that result from the warming of the plate as it descends into the mantle could produce the prominent features of most double seismic zones, as exemplified by that beneath North-east Honshu.

Toksöz *et al.*[9] have computed several physically reasonable models of temperatures in subducting slabs, from which we have chosen one that does not include the effects of shear heating, phase changes, or heat sources internal to the slab. Temperatures from this model should produce minimum estimates of thermoelastic stresses, because heating of the slab occurs only by adiabatic compression and conduction from the surrounding asthenosphere. The model in Fig. 2 assumes an 80 km thick slab which dips at 45° and subducts at a rate of 8 cm yr^{-1}.

The temperatures selected, $T(x, y)$, are at 10 km intervals along 20 profiles oriented normal to the slab and spaced at equal downdip (x) intervals of 20 km. After smoothing temperatures in the x direction, we obtain differential temperatures, $\Delta T(x + \Delta x, y) = T(x + \Delta x, y) - T(x, y)$, from successive profiles.

For initial calculations of thermal stresses we assume that the entire 80 km thickness of the plate remains elastic. Later computations modify this assumption to allow for relaxation by high temperature creep. Incremental profiles of thermoelastic stress are computed from the differential temperatures using the formulation of ref. 10, which is appropriate for a thin elastic plate free of external force or moment. As downgoing lithospheric plates have lateral dimensions at least several times their thickness, a thin-plate approximation seems reasonable. The method assumes complete relief of thermal strains in the direction normal to the plate (y; Fig. 2), thus σ_{yy} (thermal) $= 0$. Thermal stresses in the downdip (σ_{xx}) and along the strike (σ_{zz}) directions are equal and obey the relationship[10]:

$$\sigma_{xx} = [1/(1-\nu)]\left[-\alpha \Delta T E + 1/(2C) \int_{-C}^{+C} \alpha \Delta T E \,\mathrm{d}y + (3y/2C^3) \int_{-C}^{+C} \alpha \Delta T E y \,\mathrm{d}y\right] \quad (1)$$

in which ν is Poisson's ratio (0.25); α is the linear coefficient of thermal expansion, about one-third of the volumetric coefficient[11], and chosen to be 3.6×10^{-5} °C^{-1}, an average value for olivine at 800 °C (ref. 12); for E, Young's modulus, we chose a value of 9×10^5 bar, slightly less than that of olivine quoted by Birch[13]; $2C$ is the thickness of the plate. Results of the initial stress computations are shown in Figs 2 and 3*a*.

On a time scale of 10^5–10^6 yr, not all the thickness of the lithosphere will remain elastic[14]; high temperature creep may relax strains in the remainder of the plate. Experimental work[15] has suggested the following relationship for steady-state creep at differential stresses of <2 kbar:

$$\dot{\varepsilon}(\mathrm{s}^{-1}) = 70\sigma^3 \exp(-Q_\mathrm{p}(RT)^{-1}) \quad (2)$$

where σ is $\sigma_1 - \sigma_3$ (bar); Q_p is the activation energy, 122 kcal mol^{-1}; R is the gas constant, 1.986 cal K^{-1} mol^{-1}; and T is the temperature in Kelvin. The second set of computations allows for relaxation of thermal strains by creep; when the creep rate at a sample point exceeds the thermal strain rate ($\approx 10^{-17}$–10^{-18} s^{-1}), we assume that that portion of the descending plate has relaxed. We reduce the thickness of the plate ($2C$) by the amount that has relaxed, and calculate thermal stresses in the remaining portion of the plate from equation (1). The equation is not strictly applicable to a plate of variable thickness, but probably is still sufficiently accurate for the results (Fig. 3b) to be representative.

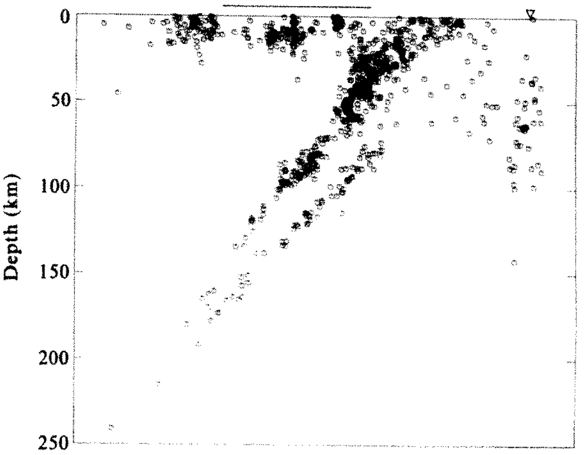

Fig. 1 Double seismic zone benaeath North-east Honshu, Japan[5]. The main features are: (1) microearthquakes between depths of ~60 and 180 km define two subparallel zones of seismicity (a down-dip length of 210 km); (2) at the shallow end, the two zones are ~40 km apart, and gradually merge at depth; (3) Hasegawa *et al.*[5] find composite focal mechanisms that indicate reverse faulting and down-dip-directed P axes for events in the upper zone, while those in the lower zone have down-dip-directed T axes. Note the 2:1 vertical exaggeration in the figure. The horizontal bar at the top of the figure is the projection of the island of Honshu; ∇ marks the position of the Japan Trench.

Stresses computed with an 80 km thick elastic slab (Fig. 3*a*) show good agreement with the characteristic features of the double seismic zone shown in Fig. 1. Stresses in individual profiles reach magnitudes of ~500 bar, which are consistent with observed stress drops of earthquakes at intermediate depths (refs 16, 17 and J. Mori, unpublished results). At shallow depths maximum tensional stresses are reached ~40 km below

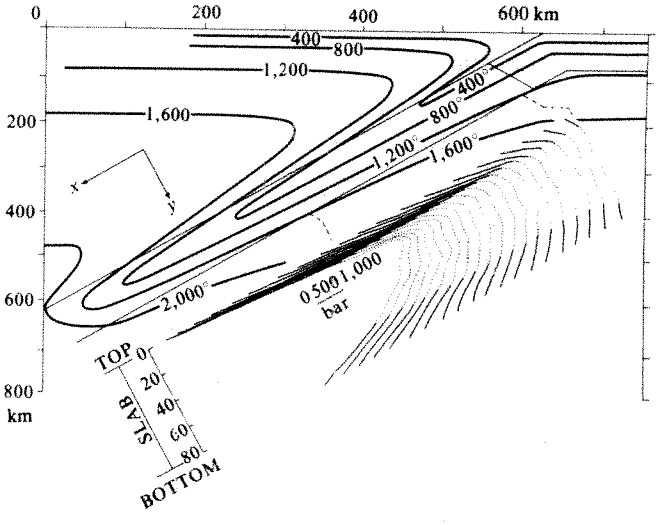

Fig. 2 Thermal model of the descending lithospheric slab and cumulative thermoelastic stresses obtained from it. Isotherms (in °C) are derived from numerical modelling of an 80 km thick slab that dips at 45° and subducts at a rate of 8 cm yr^{-1} (after ref. 9). The coordinate system used appears in the inset, upper left; $y = 0$ at the centre of the slab; the z axis points out the page (along the strike of the slab). Cumulative thermoelastic stresses calculated for the 80 km thick slab model (no relaxation) are inset in the lower right. Each successively deeper profile is the sum of the stresses from the previous profile, plus the increment of stresses developed between the profiles. Note the difference in the y scale from the main figure. Tensional stresses are indicated by the dotted portions; compressional by the solid lines. Note that cumulative tensional stresses of >2 kbar are reached only ~20 km inside the slab from where cumulative compressional stresses of 6 kbar have developed. A grid spacing of 10 km in the y direction was used in the computations; details with a comparable wavelength are unreliable. Note the horizontal exaggeration of ~1.7 in the main figure.

the plane of maximum compressional stress, which is located at the upper surface of the descending plate. The loci of maximum tension and compression appear to converge at greater depth although they do not actually merge. Cumulative stress profiles (Fig. 2) obtained by summing the successive down-dip profiles of Fig. 3*a* show similar features; note that cumulative thermal stresses reach ~6 kbar. Stress profiles obtained by allowing for relaxation (Fig. 3*b*) show loci of maximum compression and tension separated by only ~10 km. This proximity results in part from the thinness of the unrelaxed portion of the plate. High temperature creep, as calculated for Fig. 3*b*, assumes steady-state creep rates, but establishment of the latter may require strains as large as[15] 1–2%. As thermal strains are generally <0.5%, the thickness of lithosphere depicted as relaxed in Fig. 3*b* may be overestimated.

Models explaining double seismic zones by invoking phase changes[2] and unbending of the plate[3,4,6] have difficulties in explaining some of the observed seismic features, notably the downdip length over which double zones are observed[8] (see Fig. 1). Previous studies found agreement between the polarities of thermoelastic stresses and those inferred from earthquake focal mechanisms[18] and of the separation between the zones of maximum thermal tension and compression and that observed from earthquakes[19]. Our results further demonstrate that thermoelastic stresses can account for the gradual merging of the two seismic zones at depth, and that stresses resulting from unbending or phase changes in the plate are probably generated in small volumes in the downdip direction. Once relaxed (for example, by creep or fracture) such stresses are irrevocably dissipated. In contrast, thermoelastic stresses are continuously induced as the temperature increases in the plate during subduction.

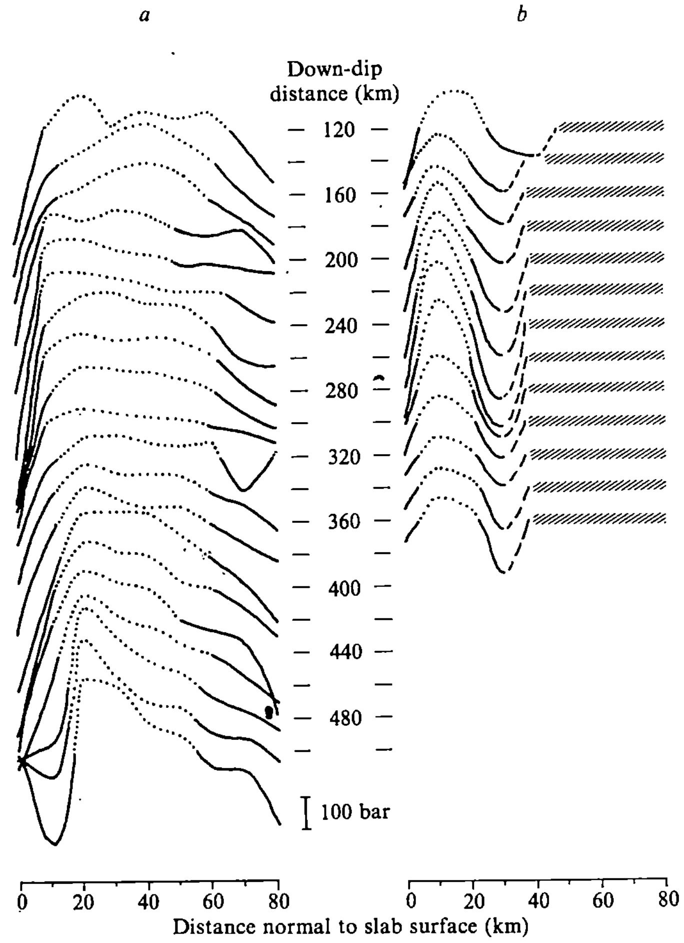

Fig. 3. *a*, Incremental thermoelastic stress profiles calculated with an 80 km thick elastic slab. As in Fig. 2, the dotted portions of each profile are tensional, the solid portions compressional. Features with a wavelength comparable with or smaller than the grid spacing (10 km) are unreliably determined. Note the narrowing of the separation between the maximum tension and compression towards the lower profiles. *b*, As *a*, except that relaxation by high temperature creep (see text) is allowed to reduce the effective elastic thickness of the slab, when relaxation approximately equals or exceeds the thermal strain rates ($\approx 10^{-18}\,s^{-1}$). Portions of the slab where relaxation has occurred are shaded. Dashed portions of the stress profiles indicate regions of transition between elastic and relaxed portions of the slab. Stress profiles are omitted below a down-dip length of 360 km; only a 20 km thickness of the lithosphere remains elastic and as temperatures are sampled at 10 km intervals, computed stresses would be unreliable.

We emphasize that the state of stress in a descending plate probably results from many factors (see refs 20–22 for example). Strain rates due to thermal effects ($\approx 10^{-17}$–$10^{-18}\,s^{-1}$) are much smaller than those resulting from bending or unbending of the downgoing plate where it undergoes maximum curvature ($\approx 10^{-15}\,s^{-1}$; in Fig. 1, maximum curvature occurs at a depth of <50 km). In the apparently straight portion of the downgoing plate, where Fig. 1 shows a double seismic zone, strain rates resulting from slight bending or unbending could be comparable with, or smaller than, those due to thermal effects. Although unbending occurs in most descending plates, double seismic zones do not[8]. Hence, double seismic zones may result from stresses of relatively small magnitude that are easily overprinted. Double seismic zones are observed only in the downgoing plates that are not strongly in either down-dip tension or compression[8].

The thermal model used above is very simple. It does not consider, for example, the effects of frictional heating[23], dehydration[24], or interactions between the downgoing plate and a convecting asthenosphere[25]. Nevertheless, the major features obtained from the model should be reliable enough to evaluate the validity of the thermal stress hypothesis.

Thermoelastic stresses seem to account for many of the major features of almost all the double seismic zones identified so far. A notable exception is the double zone beneath the Shumagin Islands region of the eastern Aleutians where there is a stress polarity in an upper seismic zone opposite to that found elsewhere—down-dip tension[7]. This is interpreted as a temporary feature related to a great earthquake that is expected to occur in the Shumagin Seismic Gap[26] in the near future and so does not necessarily contradict the model presented here.

In conclusion, we suggest that thermal stresses may strongly influence the state of stress in descending slabs of lithosphere that are not otherwise dominated by tension or compression.

This work was supported by the US Department of Energy (contract DE-ASO2-76ERO-3134). We thank W. Menke and J. Bodine for helpful discussions, and J. T. Engelder, P. G. Richards, C. H. Scholz, L. R. Sykes and A. B. Watts for critical reviews of the manuscript. L-DGO number 3276.

Received 4 September; accepted 9 December 1981.

1. Sykes, L. R. *J. geophys. Res.* **71,** 2981–3006 (1966).
2. Veith, K. F. thesis, Southern Methodist Univ. (1974); *EOS* **58,** 1232 (1977).
3. Isacks, B. L. & Barazangi, M. *Island Arcs, Deep Sea Trenches and Back-Arc Basins* Vol. 1, 99–114 (American Geophysical Union, Washington DC 1977).
4. Engdahl, E. R. & Scholz, C. H. *Geophys. Res. Lett.* **4,** 473–476 (1977).
5. Hasegawa, A., Umino, N. & Takagi, A. *Tectonophysics* **47,** 43–58 (1978).
6. Samowitz, I. & Forsyth, D. *J. geophys. Res.* **86,** 7013–7021 (1981).
7. Reyners, M. & Coles, K. *J. geophys. Res.* **87,** 356–366 (1982).
8. Fujita, K. & Kanamori, H. *Geophys. J. R. astr. Soc.* **66,** 131–156 (1981).
9. Toksöz, M. N., Minear, J. W. & Julian, B. R. *J. geophys. Res.* **76,** 1113–1138 (1971).
10. Timoshenko, S. P. & Goodier, J. N. *Theory of Elasticity* 3rd edn, 435–436 (McGraw-Hill, New York, 1970).
11. Resnick, R. & Halliday, D. *Physics* Vol. 1, 543 (Wiley, New York, 1966).
12. Skinner, B. J. *Mem. geol. Soc. Am.* **97,** 78–96 (1966).
13. Birch, F. *Mem. geol. Soc. Am.* **97,** 107–173 (1966).
14. Bodine, J. H., Steckler, M. S. & Watts, A. B. *J. geophys. Res.* **86,** 3695–3707 (1981).
15. Goetze, C. *Phil. Trans. R. Soc.* **A288,** 99–119 (1978).
16. Wyss, M. & Molnar, P. *Phys. Earth planet. Inter.* **6,** 279–292 (1972).
17. Chung, W.-Y. & Kanamori, H. *Phys. Earth planet. Inter.* **23,** 134–159 (1980).
18. Yang, M., Toksöz, M. N. & Smith, A. T. *EOS* **58,** 1233–1234 (1977).
19. Hamaguchi, H., Goto, K. & Suzuki, Z. *IASPEI 21st Assembly*, Pap. A4.26 (Department of Geophysics, University of W. Ontario, London, Ontario 1981).
20. Richter, F. & McKenzie, D. *J. Geophys.* **44,** 441–471 (1978).
21. Sleep, N. H. *J. geophys. Res.* **84,** 4565–4571 (1979).
22. Davies, G. F. *J. geophys. Res.* **85,** 6304–6318 (1980).
23. Turcotte, D. L. & Schubert, G. *J. geophys. Res.* **78,** 5876–5886 (1973).
24. Anderson, R. N. DeLong, S. E. & Schwarz, W. M. *J. Geol.* **88,** 445–451 (1980).
25. Hsui, A. T. & Toksöz, M. N. *Tectonophysics* **60,** 43–60 (1979).
26. Davies J., Sykes, L. House, L. & Jacob, K. *J. geophys. Res.* **86,** 3821–3855 (1981).

New dates for the Tata, Hungary archaeological site

H. P. Schwarcz

Department of Geology, McMaster University, Hamilton, Ontario, Canada L8S 4M1

I. Skoflek

Tata Museum, Tata, Hungary

The archaeological site at Tata, 70 km WNW of Budapest, has yielded a Mousterian lithic industry of small artefacts chipped from chert pebbles, with affinity to the Quina type[1]. However, the two best known artefacts from the site are a 'churinga' carved from a piece of a mammoth tooth (Fig. 1), and an amulet with an inscribed cross, made on a polished nummulite fossil. Marshack (personal communication), who examined both the churinga and nummulite, observed that one or both arms of the cross 'engraved' on the nummulite are in fact natural fractures that penetrate through the stone. However, the ivory plaque appears to have been carefully separated from a compound molar tooth of a mammoth, shaped and bevelled, and then coloured red by rubbing with ochre. The age of this site was first determined by ^{14}C analysis of charcoal from the cultural layer[2]. The age of 55 ± 2.5 kyr led Bordes to assign the cultural material to the middle Mousterian. However, palaeontological data[3] indicate that this site was occupied towards the end of the last interglacial. Also, two single determinations of Th/U ages on travertines from the site yielded dates of 116 ± 16 kyr (ref. 4) and 70 ± 20 kyr (ref. 5), both of which are more consistent with present estimates of the time interval corresponding to the last interglacial (125–90 kyr). We report here new uranium series dates on the travertine which show that the site was occupied at ~100 kyr BP. This confirms that the amulet from this site is one of the oldest decorative artefacts known, and was presumably created by *Homo sapiens neanderthalensis*.

The cultural material of this site is all contained within lenses of loess, 1 m or less in thickness, which lie within a mound-like accumulation of spring deposited travertines. Such travertines can be dated by the Th/U method if they are relatively free of clastic impurities[6]. However, some travertines of this sequence, and in particular, those immediately over- and underlying the cultural layer, contained significant amounts of detrital contaminants. This results in the presence at the time of deposition of significant amounts of thorium, including ^{230}Th, which can interfere with the age determination. The presence of this 'common' thorium is monitored by the activity ratio ^{230}Th/^{232}Th. If this ratio is <20, then some correction is necessary to obtain a reliable estimate of the age.

Travertine samples were taken from above and below the culture layer, and aliquots were dissolved in acid; any insoluble material was discarded. Uranium and thorium were then chemically separated from the solution, plated onto steel disks, and their α activity was counted. Radiochemical data are given in Table 1. Sample 21, with a high ^{230}Th/^{232}Th value, defines a maximum age for the culture layer of 116 ± 5 kyr, for a layer of travertine ~3 m below the culture layer. Sample 40 from a layer 1 m above the culture layer, also had a high thorium ratio, and gives a minimum age for the culture layer of 78 ± 5 kyr. However, the remaining samples, which were collected immediately above and below the culture layer, all had high detrital contamination, as evidence by ^{230}Th/^{232}Th ratios <10, and abundant insoluble residues. Estimates of their ages, assuming an initial ^{230}Th/^{232}Th ratio of 1.5, are shown in Table 1, column 7, and suggest a mean age of 118 ± 37 kyr, which is not much more informative than the estimate based on the over- and underlying samples.

An alternative method of treating such highly contaminated samples is to plot ^{230}Th/^{232}Th against ^{234}U/^{232}Th for each sample[6]. If these travertines had all formed at approximately the same time from mixtures of a homogenous, pure, chemically precipitated calcite, admixed with a single detrital component with a uniform ^{230}Th/^{232}Th ratio, then they should lie on a line with a slope equal to the ^{230}Th/^{234}U ratio of the chemically precipitated carbonate, and a ^{230}Th/^{232}Th intercept equal to the value for the detrital component today (or $e^{-\lambda_0 t}$ times the value of the initial ^{230}Th/^{232}Th ratio, where λ_0 = decay constant of ^{230}Th).

Figure 2 shows a graph of the analyses of the contaminated samples. They define a line with a slope of 0.5850 ± 0.0002; this taken together with the average ^{234}U/^{238}U ratios of the samples yields an apparent age of 99.4 ± 0.1 kyr. The error of this age estimate was evaluated by comparing regression lines through the points, taking each variable in turn as independent. Clearly the accuracy of such an age determination cannot be as great as implied by the variance of the regression line. No account has been taken of the errors of the individual analyses, and to some extent the accuracy of the age also depends on the validity of the assumptions given above, namely that all samples were mixtures of two uniform end-members (calcite and detritus). Until the validity of this method of collective age analysis has been established in a wider range of circumstances (see, for example, ref. 7) we cannot properly evaluate an error for the calculated age, although it is presumably comparable to the average error of the individual dated samples, about ±8%.

The initial ^{230}Th/^{232}Th ratio of 1.6 obtained from this regression analysis is close to the value commonly encountered in

Table 1 Radiometric data for samples from Tata travertine mound

Stratigraphic layer*	Level height from base (m)†	Sample no.	^{234}U/^{238}U	^{230}Th/^{234}U	^{230}Th/^{232}Th	Age (kyr)	[U] (p.p.m.)
T1i	11.5	40	0.769 ± 0.026	0.497 ± 0.022	34.7 ± 5.3	78 ± 5	0.50
T1i	10.5	23	0.871 ± 0.077	0.746 ± 0.070	2.5 ± 0.2	$88 \pm^{44}_{31}$‡	0.48
			0.859 ± 0.034	0.866 ± 0.036	2.2 ± 0.1	$172 \pm^{70}_{43}$‡	0.43
T1h	10		Culture layer			99.4 ± 0.1§	
T1g	9.5	22	0.795 ± 0.028	0.629 ± 0.034	8.5 ± 0.9	101 ± 12‡	0.57
T1g	9.5	45	0.805 ± 0.023	0.664 ± 0.034	6.1 ± 0.5	109 ± 15‡	0.36
T1d	7	21	0.816 ± 0.013	0.627 ± 0.016	88 ± 23	113 ± 5	0.70
			0.810 ± 0.013	0.646 ± 0.018	56 ± 10	120 ± 6	0.67

* From ref. 9, Beilage 3.

† Estimated from ref. 9 and field observations.

‡ Corrected assuming initial ^{230}Th/^{232}Th = 1.5.

§ Obtained by interpolation of samples 22, 23, 45; see text.

0028–0836/82/070590—02$01.00

detrital contaminants. In fact this is very close to the value of 1.5 which was used to obtain 'corrected' ages for the highly contaminated samples (Table 1). Nevertheless, at least one of those corrected dates (for sample 23) is still far from our new collective estimate for the age of the archaeological layer. This is because for samples with such low ^{230}Th/^{232}Th ratios the corrected age is very sensitive to the choice of initial ^{230}Th/^{232}Th ratios, while the value of that ratio in an individual sample may have differed significantly from the estimate obtained by regression from the complete set of samples. This discrepancy in ages emphasizes the value of the correlation method shown in Fig. 2 for obtaining a collective age.

The ^{234}U/^{238}U ratios of all the travertines analysed here are strikingly low. Correcting for the age of the deposit, they correspond to initial ratios of from 0.799 to 0.712, average = 0.738 ± 0.028. They are similar to the values obtained by Cherdyntsev at this site (0.80 ± 0.01), and indicate that the uranium in the spring water feeding the travertine deposits was derived from a source that was intensely leached, such as a deep soil profile. Such low ratios are rarely encountered in groundwaters or in carbonates precipitated from them.

The estimate of the age of the cultural layer obtained by the regression analysis lies midway between the ages of the over- and underlying layers and is consistent with a fairly constant rate of accumulation of travertine at between 0.007 and 0.018 cm yr^{-1}. The culture layer itself is described by Vértes[8] as having formed during a hiatus in the deposition of travertine, at least locally, and a period of relatively rapid deposition of aeolian detritus, first sand and then loessic silt.

This age estimate of the culture layer agrees well with the palaeontological estimates of palaeoclimate and thus of timing relative to glacial chronology. Kretzoi and Vértes[9] conclude that the site was occupied sometime after the thermal optimum of the last interglacial but considerably before the onset of the next glaciation. The climate at the site was estimated by them to have been "somewhat cooler and more continental then at present"; based on the associated mammalian fauna an average July temperature of 19 °C is estimated. These characteristics would be consistent with a point in the last interglacial when climate began to deteriorate in advance of an ensuing glacial stage such as isotope stage 5a, which occurred at about 90–100 kyr (ref. 10).

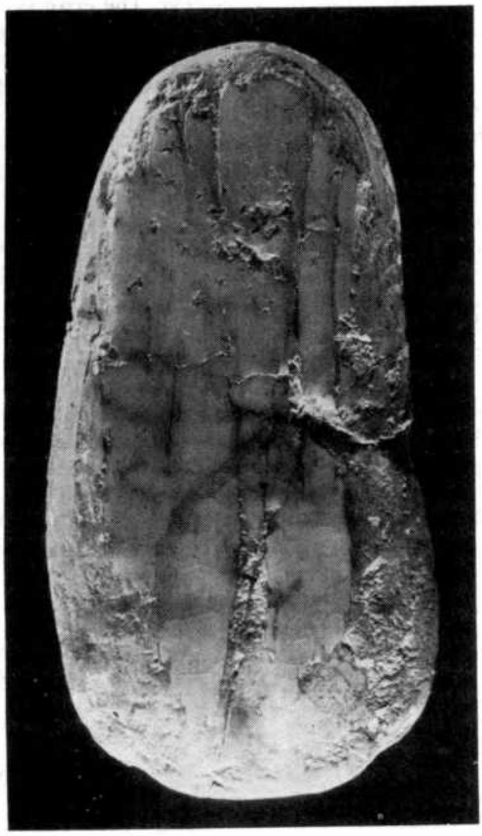

Fig. 1 Ivory plaque, made from piece of a mammoth's molar tooth, and rubbed with ochre (churinga). Photograph courtesy of A. Marshack. Plaque is 10.8 cm long.

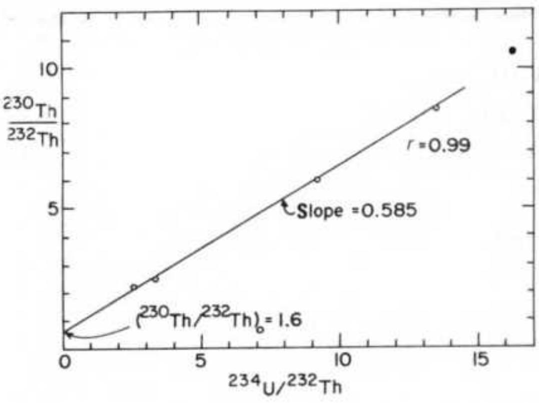

Fig. 2 Correlation between ^{230}Th/^{232}Th and ^{234}U/^{232}Th for radiometric analyses of contaminated travertines above and below the cultural layer of Tata. Slope of line gives estimate of ^{230}Th/^{234}U ratio of authigenic calcite component of travertine, from which age may be computed. Intercept gives ^{230}Th/^{232}Th ratio of detrital component.

We conclude that hominids who were utilizing a Mousterian tool assemblage occupied this site about 100 kyr BP., and created at least one purely decorative artefact. From what is known about the association between cultural remains and hominid skeletal remains at other Eastern European sites, we may infer that the makers of these artefacts were of the subspecies *H. s. neanderthalensis*. This is also consistent with our limited knowledge of timing of the appearance of *H. s. sapiens* and the disappearance of Neanderthal man. Eventually, through dating of other artefactual and hominid skeletal sites such as La Chaise[11] we hope to be able to reconstruct a complete chronology of the various stages in the cultural and biological evolution of the middle and upper Pleistocene.

This study was supported by funds from the National Geographic Society, the Social Sciences and Humanities Research Council of Canada and the Natural Sciences and Engineering Research Council of Canada. We thank A. Dixon and M. M. Russell for analytical assistance and A. Marshack for discussions on the nature of the decorative artefacts and for permission to use his photographs of them. McMaster Isotope and Nuclear Geochemical Contribution Number 124. This paper is dedicated to the memory of Dr Skoflek who died in an accident on 6 August 1981.

Received 9 August; accepted 11 December 1981.

1. Bordes, F. *The Old Stone Age*, 110 (New York, McGraw Hill, 1972).
2. de Vries, H. & de Waard, H. *Arch. Hungarica* **43**, 35–36 (1964).
3. Kretzoi, M. *Arch. Hungarica* **43**, 105–128 (1964).
4. Cherdyntsev, V., Kazachevskii, I. V. & Kuzmina, E. A. *Geochem. Int.* **2**, 794–801 (1965).
5. Pecsi, M. *Földr. Közl.* **2**, 109–119 (1973).
6. Schwarcz, H. P. *Archaeometry* **22**, 3–24 (1980).
7. Szabo, B. J., Carr, W. J. & Gottschall, W. C. *U.S. Geol. Survey, Open-File Rep* 81–119 (1981).
8. Vértes, L. *Arch. Hungarica* **43**,133–249 (1964).
9. Kretzoi, M. & Vértes, L. *Arch. Hungarica* **43**, 251–256 (1964).
10. Shackleton, N. & Opdyke, N. J. *Geol. Soc. Am. Mem.* **145**, 449–464 (1976).
11. Schwarcz, H. & Debénath, A. *C. r. hebd. Acad. Sci., Paris* **288**, 1155–1157 (1979).

Proline content does not influence pest and disease susceptibility of barley

S. W. J. Bright*, P. J. Lea*, J. S. H. Kueh*, C. Woodcock†, D. W. Hollomon† & G. C. Scott†

Departments of *Biochemistry and †Insecticides and Fungicides,
Rothamsted Experimental Station, Harpenden,
Hertfordshire AL5 2JQ, UK

The genetic engineering of crop plants for specific desired characters is of potential importance in agriculture[1]. Serious consideration must therefore be given to undesirable side effects of particular modifications. The soluble nitrogen content of leaves is important in the relationship between plants and their insect predators and increases during periods of environmental stress[2,3]. Soluble proline increases markedly during water stress in a wide range of plant species including barley[4,5] and it has been suggested that plants selected for higher proline content may be more tolerant of drought stress[6]. However, proline is phagostimulatory to locusts when presented on an inert matrix[7] and this work has been extended by Haglund[8] to suggest that proline (or valine) may be a cue detected by grasshoppers to lead them to drought-stressed nitrogen-enriched plants. Plants selected for a higher content of free proline in an attempt to increase their tolerance of drought stress might therefore prove more attractive to insect predators. To test this hypothesis we have now compared the responses of locusts, slugs, aphids and a mildew fungus to normal barley and a barley mutant[9] which has up to six times the normal content of free proline in the leaves. We find no evidence that the mutant is more susceptible than its parent to damage by any of these organisms.

Unstressed leaves of the mutant R5201 were found to contain up to six times the soluble proline of the parent line in the first three leaves over a 16-day period (Table 1). We examined two aspects of pest attack: whether locusts or slugs would choose preferentially to attack and consume mutant plants and whether growth and reproduction of aphids or mildew were greater on the mutant than the wild type. All four organisms are economically important and include a major pest and an important disease of barley.

Locust plagues have been correlated with periods of environmental stress[3] and locusts might therefore be expected to detect the higher proline content of the mutant. Locusts from two separate genera (*Schistocerca gregaria* and *Locusta migratoria*) were allowed to feed for 48 h until ~50% of the shoot fresh weight had been consumed. Observation every 8 h of the order in which plants were attacked, and measurement of the weight of material eaten (Table 2) gave no evidence for preference of mutant over parent plants by either species of locust (differences not significant at $P < 0.05$).

Proline has been reported to be a feeding attractant for snails[10]. Slugs damage cereals either by attacking seeds or by shredding young leaves. We therefore examined the possibility that slugs could distinguish between the high proline mutant, its parent cultivar and a further cultivar, Bomi, included as an extra control. In this case (Table 3), although there was no significant preferential shredding of the leaves of R5201 compared with the parent, the slugs did not attack Bomi to the same extent as the other two lines.

Table 1 Proline content of the first three leaves of two lines of barley

Leaf no. from germination	Age (days)	Proline content (nmol per g fresh wt ± s.e.) Maris Mink	R5201
1	6	70±4	259±31*
	10	72±9	346±39*
	16	71±6	224±23*
2	10	79±8	493±69*
	16	73±6	207±11*
3	16	38±7	164±25*

Seeds of Maris Mink and R5201 were grown in Eff compost (Eff Products) in a controlled environment chamber (temperature 20°/16 °C, 16 h day, with light 11,000 lx from fluorescent plus tungsten light). On day 6, plants were transferred from seed trays to 4-inch pots (two per pot). Three samples each of three leaves were analysed. The entire leaf blade or that which had emerged from the sheath was taken. Leaves were ground in 3% w/v sulphosalicylic acid and assayed for proline content by the acid–ninhydrin method[9,17].

* Significant difference from Mink values at $P < 0.01$ by *t*-test.

Because aphids are vectors of virus diseases their control is of major importance in cereal farming[11]. Aphids are known to be able to detect some amino acids[12]. We therefore compared the multiplication rates of the cereal aphid (*Sitobion avenae*) on the three test lines of barley, and found that the aphids multiplied rapidly on all the lines tested (Table 4), and that there was no significant difference between the numbers of young on the leaves.

Powdery mildew (*Erysiphe graminis*) is also of considerable economic importance in British agriculture[11]. In a standard leaf bioassay, growth of mildew was the same on Maris Mink and R5201 3 days after inoculation (Table 4) and visual inspection at 14 days revealed no differences in disease development on any line.

A complicating factor in these experiments was that mutant plants were somewhat larger than controls (Table 2). It is unclear whether this is caused by a pleiotropic effect of the gene for proline accumulation, other mutated genes or a physiological difference in the seed samples used. Both water content[13] and plant age[14] can contribute to palatability of plant diets and might confound any effect of proline content. However, the absence of any observed preference for mutant or parent by the four tested organisms suggests that in this case these effects are small. These points can only be settled by reselection of mutant lines after backcrossing to normal types, a programme now being undertaken.

The use of a mutant with a single gene change leading to proline accumulation in a background substantially isogenic

Table 2 Preference of locusts for feeding on two lines of barley

Locust	Test plant	Fresh wt per plant (mg ± s.e.) Control	+ Locusts	Estimated consumption	Fraction consumed (% ± s.e.)
Schistocera gregaria	Maris Mink	292±7	120±15	172	59±5
	R5201	348±9	187±13	161	46±4 (NS)
Locusta migratoria	Maris Mink	173±7	100±12	73	42±7
	R5201	230±8	169±14	61	27±6 (NS)

Seeds were grown for 6–7 days as in Table 1, and 24 plants per treatment were transplanted to a 22 × 16 cm seed tray in a 2 × 2 Latin square. After a further 2 days' growth, the tray was placed at the bottom of a glass side cage 67 × 64 × 24 cm, fitted with a 100-W light bulb directly over the centre of the square. Mature adult locusts were purchased from Larujon locust suppliers, Colwyn Bay. Two male locusts were introduced into the cage and left for 24 h at 20 °C, when they were replaced with two female locusts for a further 24 h. The shoots were individually weighed after 48 h and compared with the weight of shoots in an identical tray in the absence of locusts. Essentially similar data were obtained in replicate experiments carried out with both locust types. NS, not significantly different from Maris Mink value at $P < 0.05$ by *t*-test.

Table 3 Susceptibility of three lines of barley to damage by slugs

Test plants	% Of plant shredded Expt no. 1	2	3	4	Grand mean ± s.e.
Maris Mink	40	60	50	38	47 ± 4.3
R5201	28	26	65	38	39 ± 6.1
Bomi	10	10	16	18	13 ± 1.6*

Seeds were grown in a glasshouse in rows of seven or eight plants in plastic trays with Eff compost. After 11 days 10 slugs (adult *Derocerus reticulatum*) that had been starved for 5 days were placed equidistant from the three rows. The trays were kept in a slug rearing room (12 h day 15 °C, night 5 °C) for 7 days. Two independent observers then estimated the percentage of plants that had been shredded. The values quoted are the means for the two observers in the four different experiments.

* Significantly different from other values at $P < 0.01$ by t-test.

Table 4 Growth and multiplication of aphids and mildew on three lines of barley

Organism	Test plant	Growth No. of young
Aphid	Maris Mink	17.5 ± 1.5
	R5201	18.1 ± 1.3
	Bomi	23.6 ± 3.2
		Colony length (μm ± s.e.)
Mildew	Maris Mink	112 ± 4
	R5021	121 ± 6
	Bomi	91 ± 5*

Seeds were grown in a glasshouse. For the growth of aphids, plants at 12 days were enclosed in a cylinder of dialysis tubing sealed at the top with cotton wool. Five adults or large nymphs of the cereal aphid (brown *Sitobion avenae*) were introduced onto each plant. After 7 days the number of young aphids was counted in 12 replicates of each test plant. Growth of barley powdery mildew (*Erysiphe graminis* f.sp *hordei* isolate 23D5) on intact 11-day plants was assessed using leaf segments removed 72 h after inoculation (1,000 conidia per cm^2). Segments were stained and cleared in trypan blue in lactophenol[18] and the length of at least 25 colonies measured.

* Significantly different from other values at $P < 0.01$ by t-test. All aphid values not significantly different at $P < 0.05$.

with the parent cultivar provides a strong, if limited, test of Haglund's hypothesis[8] that proline may be detected by grasshoppers to lead them to leaves enriched with nitrogen. The mutant, which accumulates proline within the leaf, has allowed us to test this hypothesis without external application of amino acid solutions, with its attendant disadvantages of plant or microbial degradation and dilution or run off during the test period. The third method of increasing internal proline by the application of water stress is also inferior because there may be associated increases in other nitrogenous compounds such as asparagine, glutamine and glycine betaine[4,15], and alterations in hormone levels[16]. Our experiments always showed greater differences between the two control barley varieties than between the mutant R5201 and its parental variety. Any possible differences are therefore small compared with acceptable varietal differences. Furthermore, the tests we have used are capable of discriminating between varieties and are therefore not biased to give a negative result. Our results therefore do not support the hypothesis that any of the tested organisms preferentially feed on, detect or multiply faster on barley plants with a sixfold increase in soluble proline. It thus seems unlikely that such increases in proline content will increase the risk of pest and disease development, so that we can now proceed to investigate the effects of leaf proline content on the ability to resist environmental stress.

We thank Mrs C. Lea for facilities for the locust experiments, Mr J. Franklin for growing the barley and Dr B. J. Miflin for helpful discussions.

Received 16 July; accepted 16 December 1981.

1. Day, P. R. *Trends biochem. Sci.* **6**, 1–2 (1981).
2. McNeil, S. & Southwood, T. R. E. *Biochemical Aspects of Plant and Animal Coevolution* (ed. Harbone, J. B.) 77–98 (Academic, London, 1978).
3. White, T. C. R. *Oecologia, Berl.* **22**, 119–134 (1976).
4. Stewart, G. R. & Larher, F. *The Biochemistry of Plants* Vol. 5 (ed. Miflin, B. J.) 609–635 (Academic, New York, 1980).
5. Singh, T. N. *et al. Aust. J. biol. Sci.* **26**, 65–76 (1973).
6. Singh, T. N. *et al. Nature new Biol.* **236**, 188–190 (1972).
7. Cook, A. G. *Ecol. Ent.* **2**, 113–121 (1977).
8. Haglund, B. M. *Nature* **288**, 697–698 (1980).
9. Kueh, J. S. H. & Bright, S. W. J. *Planta* **153**, 166–171 (1981).
10. Uhazy, L. S. *et al. Science* **201**, 924–926 (1978).
11. Graham-Bryce, I. J. *et al. J. R. agric. Soc. Engl.* **140**, 131–139 (1979).
12. Van Emden, H. F. *Symp. R. ent. Soc.*, London (1972).
13. McKinlay, K. S. *Can. Ent.* **113**, 5–8 (1981).
14. Bernays, E. A. *et al. Bull. ent. Res.* **64**, 413–420 (1974).
15. Wyn Jones, R. G. & Storey, R. *Aust. J. Pl. Physiol.* **5**, 817–829 (1978).
16. Stewart, C. R. *Pl. Physiol.* **66**, 230–233 (1980).
17. Bates, L. S. *et al. Pl. Soil* **39**, 205–207 (1973).
18. Hollomon, D. W. *Crop Protection Agents: Their Biological Evaluation* (ed. McFarlane, N. R.) 505–515 (Academic, New York, 1972).

Identification of a β-endorphin-like peptide in cultured human placental cells

Anthony S. Liotta, Richard Houghten & Dorothy T. Krieger

Department of Medicine, Mount Sinai School of Medicine,
New York City, New York 10029, USA

In the pituitary, adrenocorticotropic hormone (ACTH)- and β-endorphin-related peptides are post-translationally derived from a common precursor glycoprotein[1,2]. ACTH- and β-endorphin-like peptides have been demonstrated in human placental extracts by radioimmunoassay (RIA), bioassay and opioid radioreceptor assay[3–7]. Recently, we have shown that short-term cultured human placental trophoblastic cells synthesize a high molecular weight glycoprotein(s) physicochemically similar to the pituitary common precursor molecule; ACTH(9–15)- and β-endorphin(1–9)-like fragments were detected in a tryptic digest of this precursor. Pulse-chase experiments revealed that radiolabel disappeared from the molecule and accumulated in smaller molecular species having either ACTH or β-endorphin antigenic determinants[8]. We now report the use of reverse-phase HPLC to resolve the tryptic fragments of one component of β-endorphin-like peptide synthesized in placental cells, and show that it is comparable to synthetic human β-endorphin. The two reverse-phase HPLC systems used resolved all tryptic fragments of human β-endorphin (β_h-endorphin) with differing selectivities, thus providing two unique 'fingerprints', in analogy to conventional two-dimensional peptide analysis. The fact that identical maps were obtained for β_h-endorphin and the placental peptide in both systems, provides strong evidence that they are structurally identical.

Human term trophoblastic cells were prepared and maintained in tissue culture as previously described[8]. On day 3 of culture, cells were incubated for 6 h in the presence of ^3H-lysine (SA, 112 Ci $mmol^{-1}$; 100 μM). Cells were homogenized in 0.2 M HCl/1 M formic acid containing 10 mM dithiothreitol (DTT), centrifuged (18,000g at 10 °C for 30 min) and the supernatant submitted to molecular sieve chromatography[8]. Material that eluted with a K_{av} similar to β_h-endorphin was pooled and lyophilized. After reconstitution, the sample was applied to a microcolumn packed with affinity-purified anti-β-endorphin antiserum covalently linked to Sepharose 4B[8]. The anti-β-endorphin immunoglobulin recognizes determinants within the β-endorphin(20–28) sequence and reacts with β_h-lipotropin on a nearly equimolar basis, while not reacting at all with human (h)ACTH(1–39). Specifically retained material was eluted with 25 μg synthetic β_h-endorphin dissolved in 500 μl 10 mM Tris-HCl pH 7.5, containing 10 mM DTT and 0.01% bovine serum albumin (BSA)[8,9]. The eluate was diluted with 1.25 ml 0.05 M HCl/2 M CH_3COOH and subjected to cation-exchange chromatography[10]. The elution position of the synthetic β-endorphin was located by β-endorphin RIA[10].

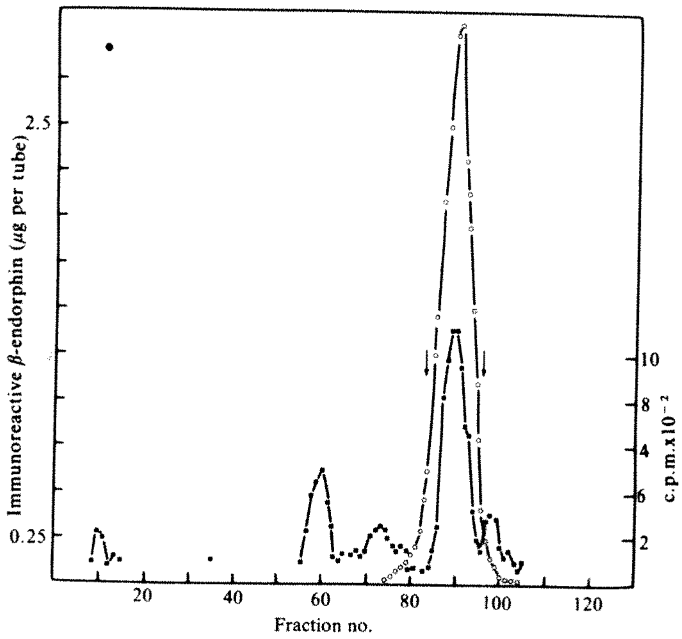

Fig. 1 Cation-exchange chromatography of the immune affinity-purified placental β-endorphin-like material. After incubation of placental cells with ^{3}H-lysine, an extract was prepared and chromatographed on a Sephadex G-50 superfine column (1 × 60 cm; eluent, 0.2 M HCl/1 M formic acid, containing 0.01% human serum albumin; flow rate 10 ml h^{-1}). Material eluting with a K_{av} similar to authentic β_h-endorphin was pooled, lyophilized, and further purified by immune affinity chromatography (see text). ^{3}H-labelled immunoreactive β-endorphin was eluted with 25 μg synthetic β_h-endorphin. The eluate was applied to a 0.9 × 15 cm SP-Sephadex C-25 column equilibrated with 5 mM HCl/1.8 M CH_3COOH. Elution was performed with a linear gradient of NaCl (0.5 M NaCl achieved after 100 1-ml fractions were collected). All fractions were assayed in the β-endorphin radioimmunoassay to locate the synthetic β_h-endorphin peak (○) and aliquots (100 μl) of fractions were removed for liquid scintillation counting (■; activity <10 c.p.m. above background, not plotted). Fractions containing most of the synthetic β_h-endorphin (fractions 83–96, defined by vertical arrows) were pooled for reverse-phase HPLC (see Fig. 2). As the purpose of this study was to determine if any of the ^{3}H-labelled β-endorphin-like material was physicochemically similar to β_h-endorphin, the remaining fractions were stored for future analysis.

Aliquots of the appropriate fractions were removed for liquid scintillation counting and the remaining portions pooled and analysed by reverse-phase HPLC using the triethylammonium phosphate/CH_3CN solvent system of Rivier[11]. About 9.3 × 10^7 d.p.m. per mg protein was incorporated into trichloroacetic acid-precipitable protein; an average of 6.12 × 10^3 d.p.m. per mg protein of β-endorphin-like material was specifically eluted from the immune-affinity microcolumn. Cation-exchange chromatography revealed that ~47% of this ^{3}H-labelled material co-eluted with synthetic β_h-endorphin (Fig. 1) and ~88% of this ^{3}H-labelled material showed a retention time identical to that of synthetic β-endorphin after reverse-phase HPLC (Fig. 2). Of the synthetic β_h-endorphin added to the placental sample at the affinity column elution step, 91% was recovered after reverse-phase HPLC. We do not attribute any physiological significance to either the absolute amount of ^{3}H incorporated into β-endorphin-like material or the relative amount compared to TCA-precipitable ^{3}H-labelled products, as different tissue culture conditions significantly alter biosynthetic capacity of the tissues. In addition, we do not know how much *in vitro* synthesized β-endorphin-related material was released into the medium during the labelling procedure.

The HPLC-purified sample was then trypsinized and the digest analysed by reverse-phase HPLC in two different chromatographic conditions (see Fig. 3 for details). Five major UV-absorbing peptide peaks were detectable in each system, indicating the positions of the fragments generated from the synthetic β-endorphin. β-Endorphin contains five lysyl residues (but no arginine residues) at positions 9, 19, 24, 28 and 29; the Lys^{29}-Gly^{30} bond was not significantly cleaved in the conditions used. Hence all tryptic fragments of β_h-endorphin contain a lysyl residue, and all tryptic fragments of the placental peptide should be ^{3}H-labelled if the placental peptide is structurally identical to β_h-endorphin. Five major ^{3}H-labelled peaks exhibiting the same retention times as the synthetic fragments were indeed detected in both systems (Fig. 3). Further evidence for the identity of the ^{3}H-labelled fragments with the synthetic tryptic peptides was obtained by exopeptidase digestion studies. In all cases, ^{3}H-lysine was released in conditions that released lysine from the synthetic fragment. Carboxypeptidase B digestion rapidly released ^{3}H-lysine from the ^{3}H-labelled β-endorphin(1–9)-, (10–19)-, (20–24)- and (25–28)-like moieties. The ^{3}H-labelled β-endorphin(29–31)-like fragment was completely resistant to carboxypeptidase B action; aminopeptidase M, however, did release ^{3}H-lysine (lysine is located at the N terminus of authentic β-endorphin(29–31)). Lysine was identified by the pre-column *o*-phthaldialdehyde derivatization/reverse-phase HPLC system described by Jones *et al.*[12] (data not shown).

In contrast to these findings, Julliard *et al.*[13] recently reported that high molecular weight precursor β-endorphin-like material in extracts of human placenta is a fragment of IgG. Using a commercially prepared extract derived from whole-term placentae and sequestered postpartum blood (placentae are used solely as a source of blood; an average of 24 g haemoglobin is extractable per placenta, indicating ~200 ml of blood per placenta)[14,15] and a purification procedure which included an

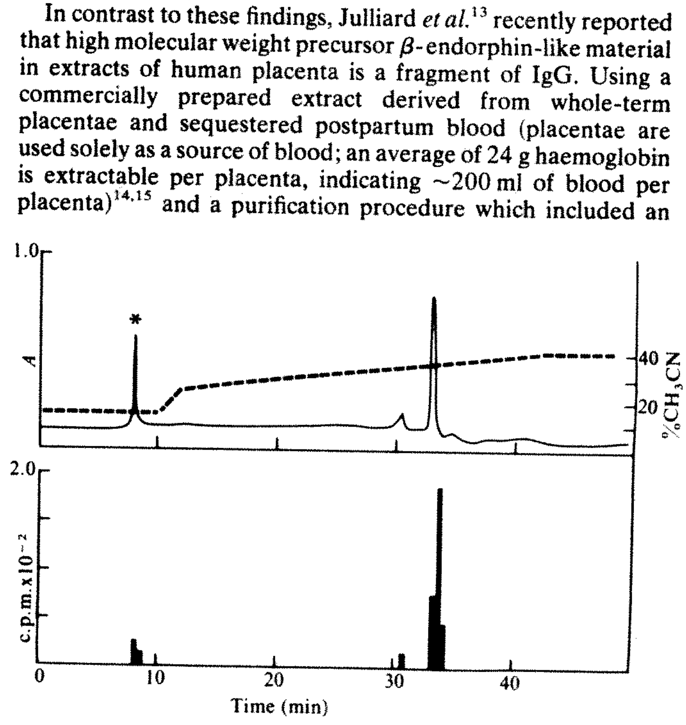

Fig. 2 Reverse-phase HPLC of synthetic β-endorphin and co-eluted ^{3}H-labelled immunoreactive β-endorphin resolved by cation-exchange chromatography (see Fig. 1). Fractions were pooled, desalted on a Sep-Pak C18 cartridge (Waters Associates)[10] (99% recovery of immunoassayable β-endorphin; 91% recovery of ^{3}H-labelled material) and analysed by reverse-phase HPLC (Ultrasphere ODS column, 0.46 × 25 cm) using the triethylammonium solvent system described by Rivier[11] (solvent A, 0.12 M H_3PO_4, adjusted to pH 3.0 with triethylamine; solvent B, H_3PO_4/triethylamine containing 70% acetonitrile). Flow rate was 0.5 ml min^{-1}; the CH_3CN gradient is indicated by the broken line. Upper panel, synthetic β-endorphin peak was detected by UV absorbance at 210 nm (continuous trace, 1.0 absorbance units full scale (AUFS)); the appropriate fractions were also assayed by β-endorphin RIA to confirm the elution position and calculate recovery (data not shown). Lower panel, aliquots (50 μl) were removed for liquid scintillation counting (see Fig. 3 for counting details). Peak marked by * on the UV trace represents an injection artefact. A small peak (upper and lower panels) is detected eluting with the retention time of the Met(O) form of β_h-endorphin. The nature of the ^{3}H-labelled peak eluting at 8.5 min is unknown. Material detected by UV monitor reached the fraction collector 0.72 min after passing through flow cell; data shown are not corrected for this difference.

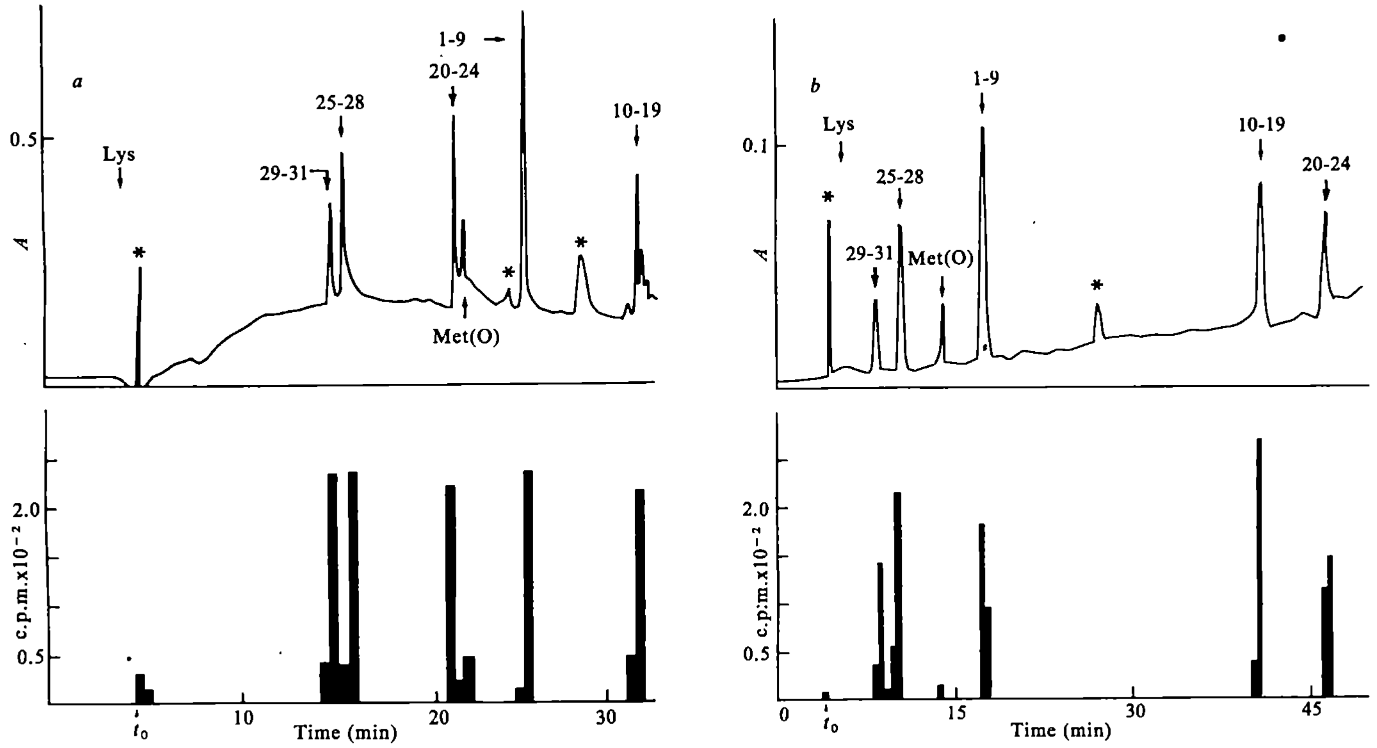

Fig. 3 Comparative HPLC tryptic peptide maps of synthetic humanβ-endorphin and purified ^{3}H-labelled placental β-endorphin-like peptide. Fractions containing the HPLC-purified placental peptide (see Fig. 2) were pooled and concentrated on a Sep-Pak C18 cartridge (Waters Associates). The cartridge was washed to remove H_3PO_4 and salts, and the retained peptides were eluted with 80% CH_3CN in 0.01 M HCl. The CH_3CN was removed with a gentle stream of N_2 and the aqueous phase lyophilized. The sample was then reconstituted in a minimum volume of 2 M DTT, incubated at 60 °C for 8 h (to reduce any Met(O) or Met(O_2) forms present) and trypsinized (25 °C for 8 h; tosylphenylethylchloromethylketone (TPCK)–trypsin to protein weight ratio of 1:1,000, *p*H 7.5). The sample was diluted to 525 µl with 0.01 M trifluoroacetic acid (TFA) and equal aliquots (250 µl) analysed in two separate gradient reverse-phase HPLC systems. *a*, Altex ultrasphere ODS column (0.46 × 25 cm, 5 µm) was equilibrated with 0.01 M TFA (Bennett *et al.*[16] have suggested the use of perfluorinated carboxylic acids for reverse-phase HPLC of peptides) containing 4% CH_3CN and the sample was injected onto the column using a 250 µl Altex sample loop. Elution was performed for 2 min at 4% CH_3CN/0.01 M TFA, followed by a 25-min linear gradient of 4–64% CH_3CN in 0.01 M TFA. Flow rate was 0.5 ml min^{-1} and 0.25 ml fractions were collected. Column effluent was continuously monitored at 210 nm (0.5 AUFS). *b*, Lichrosorb RP-18 column (0.46 × 25 cm, 10 µm) was equilibrated with 2% isopropanol in 0.015 M ammonium acetate, *p*H 4.1). Elution was performed for 5 min with the equilibration buffer, followed by a 45-min linear gradient of 2–50% isopropanol in 0.015 M ammonium acetate. Column effluent was continuously monitored at 220 nm (0.1 AUFS). All samples were evaporated in counting vials, dissolved in 200 µl 0.02% SDS, and then 15 ml Aquasol-2 was added to each vial before liquid scintillation counting. Arrows indicate the elution positions of synthetic β_h-endorphin(1–9), (10–19), (20–24), (25–28) and (29–31). These marker peptides were obtained by trypsinization of synthetic β_h-endorphin and identified by amino acid analysis of the resolved fragments. In addition, the elution position of lysine and the methionine sulphoxide [Met(O)] form of β-endorphin(1–9) are shown. Peaks marked by * on the UV trace are inherent to the baseline trace and not components of the peptide profile. The nature of the small radioactive peaks eluting at the retention time of a completely unretained compound (t_0) is unknown. Upper panels, UV absorbance profiles; lower panels, ^{3}H-labelled profiles. Material arrived at the fraction collector 0.72 min after passing though the UV monitor flow cell; the comparative maps shown are corrected for this time factor.

immune-affinity chromatographic step (that is, Sepharose-immobilized anti-β-endorphin antiserum), they isolated 269 mg of a glycoprotein (molecular weight (M_r) = 48,500) that contained the antigenic determinants of both ACTH and β-endorphin. Structural analysis demonstrated this protein to be the heavy chain of the IgG1 class. The protein cross-reacted 0.039% and 0.0064% (by weight), respectively, with the specific β-endorphin and ACTH antisera used. Inspection of the IgG1 heavy chain revealed that sequences 364–377 and 9–22 had 40% and 36% homologies, respectively, with the antigenic determinants of β-endorphin and ACTH. We believe these results can be reconciled with our findings by considering the starting material used in the previous study, that is, the precipitate formed when whole-term placentae and entrapped blood are frozen, thawed, homogenized in 0.9% NaCl and brought to 25% ethanol. Such an homogenate exhibits a broad range of proteolytic activities. We have been unable to recover significant amounts either of highly purified rat pituitary precursor ACTH/β-endorphin, synthetic β_h-endorphin, or hACTH(1–39) when we added these to a similarly prepared placental homogenate (~25 pmol of each added per placenta). In addition, as Julliard *et al.*[13] performed an affinity chromatographic purification step, using anti-β-endorphin antiserum coupled to Sepharose, any authentic precursor ACTH/β-endorphin material present would have had to compete with a very large molar excess of the IgG1 heavy chain (haemoglobin and β- and γ-globulins comprise most of the proteins precipitated at 25% ethanol) for column binding sites, and hence, even if bound, would comprise a minor component.

Our results further demonstrate synthesis in cultured human placental cells of a peptide that is structurally similar to human pituitary β-endorphin. Moreover, these data, together with previous results[8], suggest that, analogous to the pituitary, the placental β-endorphin-like moiety is contained within a larger precursor molecule and is derived from it by post-translational proteolytic cleavage.

Received 21 October; accepted 17 December 1981.

1. Eipper, B. A. & Mains, R. E. *Endocrine Rev. U.S.A.* **1,** 1–27 (1980).
2. Herbert, E. *et al. Front. Neuroendocr.* **6,** 67–102 (1979).
3. Rees, L. H., Burke, C. W., Chard, T., Evans, S. W. & Letchworth, A. T. *Nature* **254,** 620 (1975).
4. Fraioli, F. & Genazzani, A. R. *Gynec. Obstet. Invest.* **11,** 37–44 (1980).
5. Liotta, A. S., Osathanondh, R., Ryan, K. J. & Krieger, D. T. *Endocrinology* **101,** 1552–1558 (1977).
6. Nakai, Y., Nakao, K., Oki, S. & Imura, H. *Life Sci.* **23,** 2013–2018 (1978).
7. Odagiri, E. D., Sherrell, B. J., Mount, C. D., Nicholson, W. E. & Orth, D. N. *Proc. natn. Acad. Sci. U.S.A.* **76,** 2027–2031 (1979).
8. Liotta, A. S. & Krieger, D. T. *Endocrinology* **106,** 1504–1511 (1980).
9. Liotta, A. S., Li, C. H., Schussler, G. & Krieger, D. T. *Life Sci.* **23,** 2323–2330 (1978).
10. Liotta, A. S., Yamaguchi, H. & Krieger, D. T. *J. J. Neurosci.* **1,** 585–595 (1981).
11 Rivier, J. *J. Liquid Chromatogr.* **1,** 347 (1978).
12. Jones, B. N., Paabo, S. & Stein, S. *J. Liquid Chromatogr.* **4,** 565–586 (1981).
13. Julliard, J. H., Shibasaki, T., Ling, N. & Guillemin, R. *Science* **208,** 183–185 (1980).
14. Liautaud, J. *et al. Devl Biol.* **27,** 115 (1974).
15. Taylor, H. L., Bloom, F. C., McCall, K. B. & Hyndman, L. A. *J. Am. chem. Soc.* **78,** 1353–1355 (1956).
16. Bennett, H. P. J., Browne, C. A. & Solomon, S. *J. Liquid Chromatogr.* **3,** 1353–1365 (1980).

Averaged evoked responses and psychometric intelligence

S. F. Blinkhorn* & D. E. Hendrickson†

* Psychology Department, Hatfield Polytechnic, PO Box 109, Hatfield AL10 9AB, Hertfordshire, UK
† Psychology Department, Institute of Psychiatry, DeCrespigny Park, London SE5 8AF, UK

Attempts to establish correlations between psychometrically defined and measured intelligence and brain electrical activity have met with limited success. For example, as in the work of Ertl[1], the latency of components of averaged evoked potentials (a.e.ps) has been adopted as the EEG measure most likely to correspond to intelligence quotient (IQ). Although correlations as high as 0.35 have been reported on samples unselected for IQ, the sign of the correlation seems to depend on the stimulus modality used, which suggests that a straightforward identification of intelligence with 'mental speed', for which read 'short a.e.p. component latencies', is inappropriate. Hendrickson and Hendrickson[2] have proposed both a novel a.e.p. measure and a theory to account for individual differences in scores based on this measure, claiming remarkably high correlations with IQ, of the order of 0.7–0.8. We report here a study using highly selected subjects which supports these claims.

The Hendricksons' theory[2] proposes that higher intelligence is a function of low error rates in the central nervous system and that as a result of the way in which information is coded and transmitted in the brain, the effect of error is to reduce both the number and amplitude of excursions of the a.e.p. trace. Therefore, differences in IQ should be manifested in a.e.p. traces as differences in complexity, which can be determined simply by measuring the length of the trace over a standard epoch. This measure we refer to as the 'string' measure, as in effect one treats an a.e.p. trace like a piece of string and measures its straightened length.

The principal psychometric measure used was Raven's Advanced Progressive Matrices (APM) 1962 edition, a test with a substantial reputation as a culture-reduced measure of general intelligence with low achievement loading, routinely used in the selection of psychology undergraduates at the Hatfield Polytechnic, UK. Test scores had been obtained previously and were unknown to D.E.H. who analysed the EEG recordings made.

Thirty-six subjects were tested initially. Of these, three were not used in further experiments because of technical problems with their EEG records. Of those remaining, 17 were male and 16 female, with an age range of 18–36 yr. (All subjects were or had been undergraduate psychology students at the Hatfield Polytechnic.) Subjects scored between 17 and 35 on the APM (mean score ±s.d. = 26.03±4.33). The APM manual gives the estimated mean and standard deviation for university students as 21 and 4.0 respectively, and for adult students 'of more than average intellectual capacity' as 10.06 and 8.95 at a first testing and 13.95 and 9.38 on re-testing. (These values take into account the changes between the 1947 and 1962 editions). Furthermore, in the table of estimated norms, the 95th percentile point is given as 23–24 for 20–30-yr olds. In the absence of a more detailed calibration of APM scores in IQ terms, these and other indications in the manual suggest that the mean score in the group being studied corresponds to an IQ of ~128–130, with a standard deviation of between 5 and 7.5.

EEG recordings were carried out with the subject seated in a comfortable chair in a darkened, sound-attenuated room. Silver/silver chloride electrodes were attached using collodion to the scalp at the vertex and both mastoids. The subject was presented with a train of 100 tones through stereophonic headphones and asked to relax, listen to the tones and keep his eyes closed throughout the presentation. The background EEG was recorded from a bipolar derivation with the active electrode at the vertex and the reference electrode at the left mastoid. The output of the electrodes was amplified 10,000 times with virtually no high-frequency attenuation using a portable PTT4 EEG amplifier. Background EEG was recorded on one channel of a Yasec CD 1000 instrumentation tape recorder with stimulus markers recorded on a second channel for later analysis of the stimulus-initiated EEG activity. Auditory stimuli consisted of 1,000-Hz tones, 30 ms in duration, switched at the zero-crossing point (to minimize harmonic content) and presented binaurally at 85 dB. The inter-stimulus interval was randomly selected and varied between 1 and 8 s. The tone was generated and timed by a custom-built stimulus generator.

A PDP11/04 was used to average the post-stimulus 512 ms epochs from analog tape in the first instance. Three averaging passes were made: the first using 90 unselected epochs; the second, 64 epochs with eye movement and other obvious artefacts removed; and a third pass of 32 epochs. There were two records which had fewer than 64 'good' epochs because of recording difficulties, but all had at least 32. Variance was calculated for each of the three averaging passes. The process of averaging involved digitizing each 512-ms epoch at 1,024 points, thus the averaged waveform was based on 0.5 ms resolution.

Subsequently, as a control, unstimulated EEG was averaged. Specifically, the 256 ms immediately before stimulus onset were averaged for 90 unselected epochs, and 256-ms post-stimulus epochs were also averaged for comparison. As the shortest inter-stimulus interval used was 1 s, a 256-ms epoch was adopted for this control analysis to avoid residual evoked activity which might have contaminated 512-ms unstimulated string calculations. Mean unstimulated string score was 184.4±50.7 (±s.d). Mean string score over 90 post-stimulus 256-ms epochs was 278.2±133.4 (±s.d.). Units are arbitrary, but constant. The correlation between unstimulated string and APM was 0.127, which is not significantly different from zero. However, the correlation between post-stimulus 256-ms string and APM was 0.538, which is significantly different from zero at the $P<0.001$ level. The three original 512-ms string measures gave correlation coefficients of 0.530, 0.362 and 0.452 with APM for 90, 64 and 32 epoch passes, respectively, with significance levels of $P<0.001$, 0.02 and 0.005. None of the variance measures from the various data passes correlated significantly with APM. The highest scoring subject on the APM (35 correct out of 36) also had the highest scores for both the 90-epoch post-stimulus string measures, although the unstimulated string was unremarkable. Reducing these scores to those of the next highest scorer on the 256- and 512-ms 90-epoch string measures reduced the correlations between these and APM to 0.499 and 0.530, respectively.

In considering these correlations, it should be borne in mind that the various post-stimulus string measures were derived from repeated passes over the same data and not from independent observations. Thus, the correlations should be considered as different estimates of the same underlying correlation, and not as replications.

For 25 of the subjects in this study, scores in various other psychometric tests had been recorded previously. These were all verbal tests, and thus may be expected to be considerably more achievement-loaded than the APM. They included NIIP GT90A, a high-speed, conventional verbal measure; Verbal Concepts and Verbal Critical Reasoning, two tests developed for closed circulation emphasizing, respectively, verbal analogies and detection of fallacies; and various so-called 'divergent thinking' tests—uses of objects, meanings of words, etc. None of these tests correlated significantly with any of the EEG measures.

The principal feature of these results, therefore, is that despite the severe restriction of range on the IQ measure adopted, EEG–IQ correlations were at least as large as those found by other investigators using unselected subjects. This implies that

---

* Present address: Psychology Department, Stanford University, Stanford, California 94305, USA.

0028-0836/82/070596—02$01.00

over the full range of IQ the correlation would be substantially higher. Taking a value of 0.45 as a mid-range estimate from the various string–APM correlations, a s.d. of 7.5 or 5.0 IQ points for this sample would give a corrected correlation of 0.71 or 0.84, respectively.

Given the relatively small sample size, it is pointless to attempt great accuracy in estimating the underlying correlation between the string measure and IQ. However, unless the 'normal' data in the APM manual are substantially inaccurate or out of date, the data presented here suggest a correlation approaching the reliabilities typical of group tests of intelligence.

Correlations of this magnitude between measures which apparently have little in common are very rare. On the one hand psychometric tests involve the individual in problem-solving activities of a kind which might be thought amenable to the sort of analysis undertaken by cognitive psychologists. On the other hand, the string measurement procedure involves the subject in no decisions, makes no apparent demands on memory, involves no difficult perceptual discriminations, and uses stimulus intensities much greater than threshold. In this respect it differs from the procedure of Nettelbeck and Lally[3]. Furthermore, the effect obviously occurs in the first 256 ms after presentation of the stimulus, in a task which can perhaps best be described as mindless.

These results, and comparable results reported elsewhere[4] using similar techniques on a large sample of school children, suggest the possibility of identifying sources of individual differences in measured intelligence distinct from the quality of cognitive strategies and processes involved in intelligent performance, which might ultimately resolve several of the outstanding issues in differential psychology.

D.E.H. was supported by a grant from the Social Science Research Council.

Received 16 July; accepted 15 December 1981.

1. Ertl, J. & Schafer, E. W. P. *Nature* **223,** 422–423 (1969).
2. Hendrickson, D. E. & Hendrickson, A. E. *J. Personality Individual Differences* **1,** 3–33 (1980).
3. Nettelbeck, T. & Lally, M. *Br. J. Psychol.* **67,** 17–22 (1976).
4. Hendrickson, D. E. in *Models of Intelligence* (ed. Eysenck, H. J.) (Springer, Heidleberg, in the press).

Motilin in the Purkinje cell of the cerebellum

Gajanan Nilaver*, Richard Defendini*, Earl A. Zimmerman*, Margery C. Beinfeld† & Thomas L. O'Donohue‡

* Departments of Neurology and Neuropathology, College of Physicians and Surgeons, Columbia University, New York, New York 10032, USA
† Department of Pharmacology, St Louis University Medical School, St Louis, Missouri 63104, USA
‡ Laboratory of Clinical Sciences, National Institute of Mental Health, Bethesda, Maryland 20205, USA

None of the brain peptides has been demonstrated to be present in significant amounts in the cerebellum[1,2]. The only effector substance known in the Purkinje cell, whose axon carries the integrated output of the cerebellar cortex, is the decarboxylated residue of glutamic acid[3–6]. An antiserum raised against synthetic porcine gut motilin and directed at the midportion and carboxyl end of the 22-amino acid polypeptide[7] shows, in anatomically intact rat, mouse and human cerebellum, that most Purkinje cells contain motilin or a closely related substance[8]. We report here that motilin-absorbable immunoreactivity is evident from the spines of tertiary dendrites, through the cell body and axon, to nerve endings terminating, as expected, in the deep cerebellar nuclei and, unexpectedly, on nerve cells of some brain stem nuclei. In addition to its obvious functional implications, motilin is thus an important marker with which to re-examine the organization and projections of Purkinje cells, their ontogeny and their response to injury.

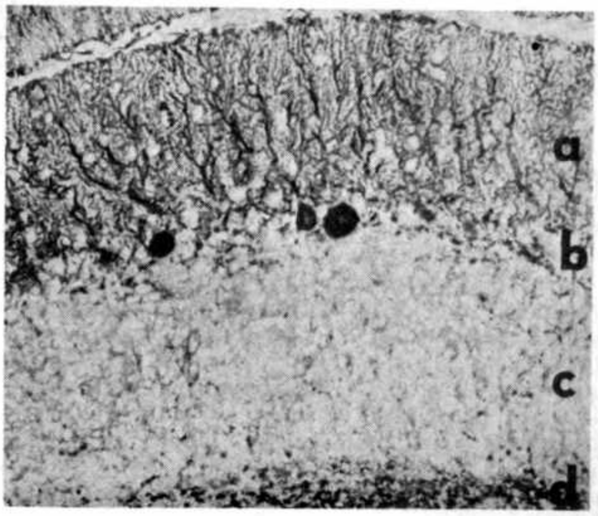

Fig. 1 Flocculus of rat cerebellum showing motilin immunoreactivity in dendritic tree of Purkinje cells in the molecular layer (a); three Purkinje cell bodies in the Purkinje layer (b); occasional beaded axons coursing through the granule cell layer (c); and gathering axons in the subcortical white matter (d).

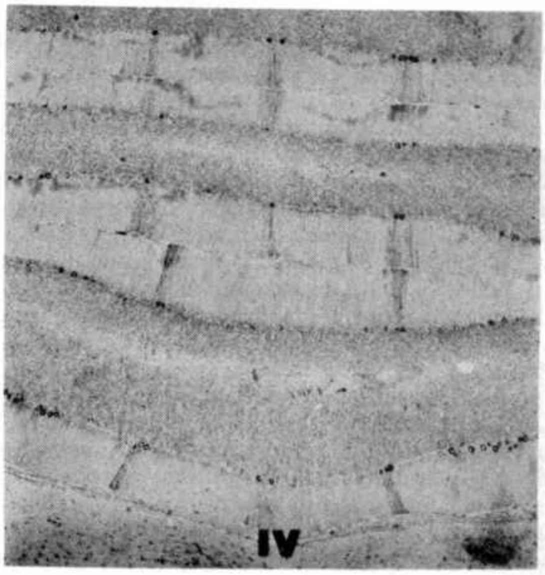

Fig. 2 Coronal section of rat cerebellar vermis and subjacent medulla. The symmetry of motilin-immunoreactive Purkinje cells and their dendrites between (1) the right and left sides, (2) opposite sides of the same folium, and (3) opposite surfaces of adjacent folia produces a palisading effect. (The pattern is best appreciated in sections, such as this one, in which < 50% of cells are reactive.) IV, Fourth ventricle, midline.

We examined the brains of 10 Long Evans rats and 10 Swiss albino mice, and the cerebellum of five human adults. Four of the rats were injected with 60 μg of colchicine in the lateral ventricle 48 h before killing. Animals were killed under pentobarbital anaesthesia by cardiac perfusion with isotonic saline, then 10% buffered formalin; brain fixation was completed by immersion in formalin overnight. Blocks of human cerebellum dissected at autopsy were fixed by immersion in 10% formalin for 48 h. The blocks were embedded in paraffin[9], and 6 μm serial sections were cut in the coronal or sagittal plane.

Rabbit anti-motilin antiserum was generated against synthetic porcine gut motilin conjugated to bovine thyroglobulin by the glutaraldehyde method[10] after multiple intradermal injection[11] of 500 μg of the immunogen emulsified in 1 ml of complete Freund's adjuvant and, 3 and 6 weeks later, further administration by the same route of 100 and 50 μg of the immunogen in incomplete adjuvant.

Immunocytochemistry was carried out by the indirect peroxidase method of Sternberger[12]. Deparaffinized tissue sections were reacted in sequence with the antiserum to motilin (1:800) at 4 °C overnight, goat anti-rabbit globulin (1:100) at room temperature for 30 min and rabbit peroxidase–antiperoxidase complex (1:400) at room temperature for 60 min. Reaction products were visualized with 3,3′-diaminobenzidine tetrahydrochloride[9]. Negative specificity controls included replacement of the primary antiserum with the rabbit's pre-immune serum and solid-phase preabsorption of the primary antiserum with 200 μg of synthetic porcine motilin bound covalently to cyanogen bromide-activated Sepharose beads[13].

The following forebrain structures were motilin immunoreactive in the rat and mouse: (1) clusters of pituitary cells in the pars distalis and, in the rat, also the pars intermedia; (2) a few nerve cell perikarya in the ventrolateral hypothalamus; (3) a few nerve cell bodies in the arcuate nucleus of rat only after colchicine treatment; and (4) bundles of fibres confined to the zona externa in the lateral recesses of the median eminence. None of the hypophysial or hypothalamic reaction products was seen after incubation of the primary antiserum with synthetic motilin.

The high concentration of motilin found in the cerebellum by radioimmunoassay of homogenized tissue extracts[7] is readily explained by the presence of immunoreactive products in most Purkinje cells, which often fill the soma of the cell, its dendritic arbor as far as the spiny tertiary branches, the length of its axon through the internal granule cell layer and white matter (Fig. 1), and its terminals on nerve cell bodies of the deep cerebellar nuclei Fig. 3. The other types of nerve cell in the molecular and granular layers of the cortex, as well as the nerve cells of the deep cerebellar nuclei themselves, are not reactive. In the rodent species examined, 90% of Purkinje somata in the hemispheres and the flocculus were labelled, whereas only one-half were reactive in the vermis. In the human vermis, the proportion of labelled Purkinje cells was much greater than in the rodents. Colchicine pretreatment in the rat intensified somatic staining, but did not alter the proportion of reactive cells.

In the rodent vermis, short and long runs of motilin-reactive Purkinje neurones alternate with runs of unreactive ones. The grouping is not random, as reactive groups often occupy the same position on either side of a folium and in adjacent folia (Fig. 2). The symmetrical palisades of reactive cells are continuous in serial sections in the coronal plane, running rostrocaudally in the sagittal plane. This pattern, which is analogous to the longitudinal organization of cortical efferents and afferents described by Voogd[14], suggests that the substance detected is intimately related to the functional organization of the Purkinje cell system.

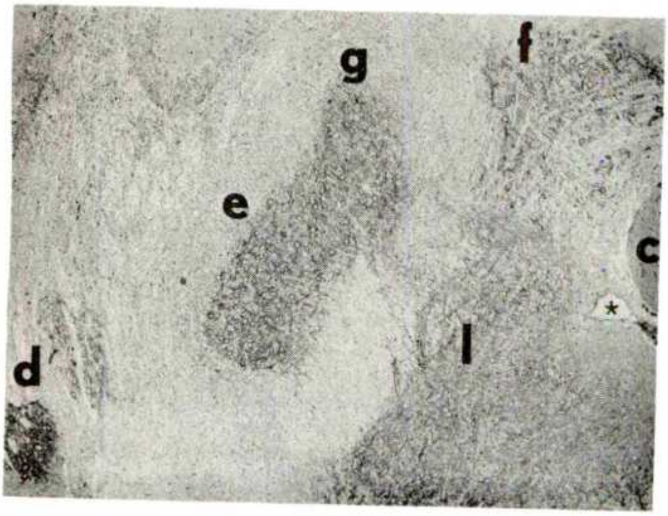

Fig. 3 Rat cerebellum. Numerous nerve cells in dentate (d), emboliform (e), globose (g) and fastigial (f) nuclei are outlined by motilin-immunoreactive axons and nerve terminals. The lateral vestibular nucleus (l) is also innervated. Fourth ventricle (★); vermal cortex (c).

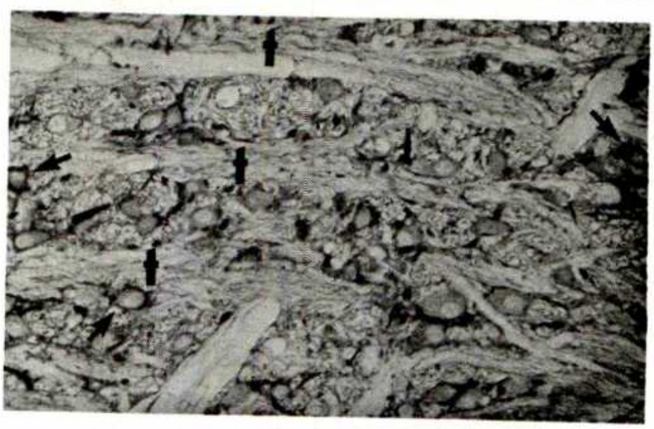

Fig. 4 Rat basis pontis. The bands of nerve cells lie between bundles (t) of transverse pontine (pontocerebellar) fibres. Several nerve cells are outlined by motilin-immunoreactive nerve terminals (arrows).

Most nerve cell bodies in the rodent cerebellar nuclei were surrounded by punctate immunoreactive products (Fig. 3) interpreted as axon terminals making synaptic contact with the cells. The vestibular nuclei presented a similar pattern. In addition, nerve cells in several other brain stem nuclei (spinal and motor fifth, basis pontis, medial parabrachial, dorsal tegmental, reticular gigantocellular, accessory superior olive, trapezoid, facial, prepositus, abducens and lateral lemniscus) were surrounded by motilin-absorbable immunoreactive terminals. As we found no reactive cells or axons in the brain stem, spinal cord, or dorsal root ganglia, the reactive terminals in these brain stem nuclei raise the possibility of previously unknown direct projections to the brain stem from the cerebellar cortex. Preliminary results of unilateral cerebellar leukotomy between the cortex and deep nuclei demonstrated a substantial diminution of reactive terminals in the brain stem, predominantly on the same side. Innervation of the nucleus basis pontis (Fig. 4), the precerebellar relay nucleus in the multi-station circuit between the cerebellar and cerebral cortices, suggests feedback modulation from the terminal Purkinje cell to its afferent station in the pons.

Electrophysiological studies of motilin report an excitatory effect in cerebral cortex[15]. The cellular distribution of motilin in the cerebellum described here supports a neurotransmitter role. Differential immunohistological studies in progress are expected to elucidate the relative distribution of motilin and γ-aminobutyric acid in the Purkinje cell population. Motilin immunoreactivity as a marker of Purkinje cell processes and nerve terminals, in conjunction with ablation, tracer, and radiolabel uptake experiments, provides a major new tool to study the organization of the cerebellar cortex.

We thank Ms Judith A. Mulhern for technical assistance. This work was supported by a Parkinson's Disease Foundation grant to Columbia University.

Received 14 September; accepted 15 December 1981.

1. Zetler, G. *Adv. biochem. Psychopharmac.* **18,** 1–21 (1978).
2. Hökfelt, T., Joohansson, O., Łungdahl, A. & Schultzberg, M. *Nature* **284,** 515–521 (1980).
3. Barber, R. & Saito, K. in *GABA in Nervous System Function* (eds Roberts, E. Chase, T. N. & Tower, D. B.) 113–132 (Raven, New York, 1976).
4. Chan-Palay, V. *Cerebellar Dentate Nucleus, Organization, Cytology and Transmitters* (Springer, Berlin, 1977).
5. Chan-Palay, V. *Proc. natn. Acad. Sci. U.S.A.* **75,** 1024–1028 (1978).
6. Chan-Palay, V., Wu, J.-Y. & Palay, S. L. *Proc. natn. Acad. Sci. U.S.A.* **76,** 2067–2071 (1979).
7. O'Donohue, T. L. *et al. Peptides* (in the press).
8. Nilaver, G., Defendini, R., Zimmerman, E. A., Beinfeld, M. C. & O'Donohue, T. L. *Soc. Neurosci.* **7,** 99 (1981).
9. Nilaver, G. *et al. J. Cell Biol.* **81,** 50–58 (1979).
10. Avrameas, S. & Ternynck, T. *Immunochemistry* **6,** 53 (1969).
11. Vaitukaitis, J. L., Ross, G. T., Pierce, J. G., Cornell, J. S. & Reichert, L. E. *J. clin. Endocr. Metab.* **37,** 653–659 (1973).
12. Sternberger, L. A. *Immunocytochemistry* (Prentice-Hall, New Jersey, 1974).
13. Sato, N. & Cargille, C. M. *Endocrinology* **90,** 302–306 (1976).
14. Voogd, V. in *Neurobiology of Cerebellar Evolution and Development* (ed. Llinas, R.) 493–514 (AMA-ERF Institute for Biomedical Research, Chicago, 1969).
15. Phillis, J. W. & Kirkpatrick, J. R. *Eur. J. Pharmac.* **58,** 469–472 (1979).

Closure of membrane channels gated by glutamate receptors may be a two-step process

K. A. F. Gration*, J. J. Lambert*, R. L. Ramsey, R. P. Rand* & P. N. R. Usherwood†

Department of Zoology, University of Nottingham, University Park,
Nottingham NG7 2RD, UK

Measurements of currents through individual receptor-gated ion channels using the patch clamp technique have shown that each open channel contributes a square pulse of current and has a constant conductance, and that transitions between open and closed states are rapid[1]. To increase the signal-to-noise ratio of patch clamp recordings of glutamate channels in locust muscle, the bandwidth of the patch clamp amplifier has usually been restricted by a low pass filter (3 dB point, nominally 1 kHz with an 18 dB per octave slope). With concentrations of L-glutamate $\leq 5\times10^{-5}$ M, we previously found that frequency histograms of channel lifetimes, constructed from data recorded with a 1 kHz bandwidth, could be fitted by single exponentials using the least-squares method[2,3]. Mean channel lifetimes estimated from the exponentials agree reasonably well with values obtained by 'noise' analysis of locust neuromuscular junctions[4] and with mean values calculated directly by averaging the open times of single channel events[5]. However, the histograms are deficient in the region 0–1 ms because of the limited high-frequency response of the recording system. We have now recorded glutamate-gated channels in locust muscle membrane with signal-to-noise ratios of 3 : 1 or better and a recording bandwidth of d.c. to 10 kHz, and report lifetimes as brief as 50 µs. Frequency distribution histograms constructed from data recorded at 10 kHz suggest that the lifetime of the glutamate channel in extrajunctional membrane of locust muscle is governed by at least two exponential time-dependent processes, one of which has the effect of delaying channel closure.

Experiments were performed on the extrajunctional membrane of innervated extensor tibiae muscles from the metathoracic legs of adult (female) locusts (*Locusta migratoria* and *Schistocerca gregaria*) pretreated with concanavalin A (Con A) to block receptor desensitization[6]. The outsides of Pyrex (borosilicate) patch electrodes were coated with a film of nitrate cellulose dope before being filled with saline containing either glutamate or agonist. Recordings with clear signal resolution (signal-to-noise >3:1) are best obtained with a 10 kHz amplifier if the patch electrode seal resistance is >20 MΩ and the muscle fibre membrane is clamped[7] at potentials (such as −125 mV) more negative than the resting potential (about −60 mV). At −125 mV single channel currents often exceed 18 pA (Fig. 1).

The activity of single glutamate channels was recorded on a FM tape recorder with a bandwidth of >10 kHz for later analysis. To increase the objectivity of our measurements we have automated our measuring procedures. Recorded analog data are played back through a window comparator which produces a square pulse having a duration equal to the channel open time. The analog input signal and the upper and lower window levels are multiplexed and can, therefore, be displayed on the same beam of an oscilloscope, allowing the comparator levels to be easily adjusted. The input signal must fall through the window, that is the input signal must first cross the upper comparator level and then cross the lower level to initiate the digital output pulse. To terminate this pulse the input signal must rise above the window by crossing both comparator levels. (Crossings of only one comparator level are, therefore, ignored.) The duration of the square pulse (open time) and the intervals between square pulses (closed times) are then measured by a PDP11/34A computer. To validate this method the same channels were measured by hand and using the window comparator. The results obtained using the two methods showed very close agreement (>99%).

Three calibration techniques have been used to define the resolution of our system for recording and measuring single channel data. (1) Square current pulses, with rise and fall times of <1 µs, mixed with bandwidth limited noise, were injected into the front end of the patch amplifier. The noise and pulse amplitudes were adjusted to match channel data recorded using this amplifier and then analysed in the same way as comparable channel data. (2) Square voltage pulses, also with rise and fall times <1 µs, were injected into the bath containing the locust nerve–muscle preparation through a saline-filled microelectrode placed close to a patch electrode sealed onto the extrajunctional membrane of a muscle fibre. (3) A.c.-coupled triangular voltage pulses were injected into the bath adjacent to the patch electrode, sealed onto the surface membrane of a muscle fibre and recorded as square current pulses[8]. All three techniques produced essentially similar results and indicate that the rise and the fall time of our recording system is <100 µs. To check the efficiency (number of pulses injected per pulse recovered) of our recording system for collecting injected pulses of different durations, it was necessary either to locate the patch electrode on membrane which did not exhibit channel activity or to fill the patch electrode with glutamate-free saline. Otherwise

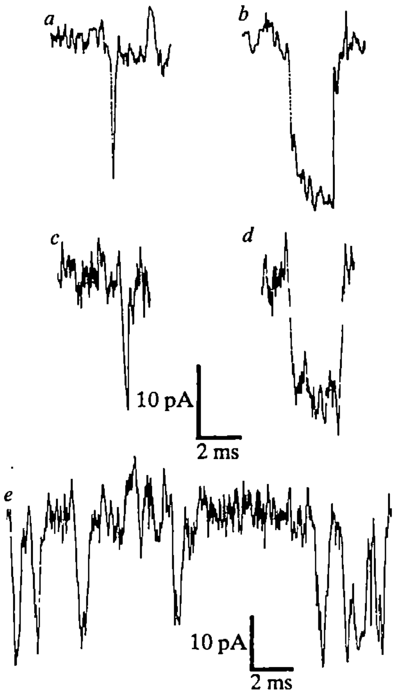

Fig. 1 Calibration pulses and single glutamate channels of locust extrajunctional muscle membrane recorded at a bandwidth of d.c. to 10 kHz. The square calibration pulses of rise time ~1 µs were injected from a saline-filled micropipette (resistance <1 M) into the bath containing a muscle preparation. The micropipette was placed to within 100 µm of a patch electrode sealed onto extrajunctional muscle membrane (see text). *a*, *b*, Typical recordings for a 65 µs and a 1.25 ms calibration pulse, respectively. *c* and *d* show single glutamate channels of comparable durations to the calibration pulses in *a* and *b*. Note that the amplitudes of the channels in *c* and *d* are approximately equal. *e*, Typical example of single channel activity with channel lifetimes ranging from ~50 µs to 1 ms. Records *c*–*e* were obtained in the presence of 5×10^{-5} M L-glutamate from a voltage-clamped muscle fibre (clamp potential −125 mV). *c* and *d* were obtained from the same site and *e* from a different site on the same muscle fibre. Temperature ~20 °C. Time and current calibrations were the same for *a*–*d*.

---

* Present addresses: Agricultural Biology Research Department, Pfizer Ltd, Sandwich, Kent CT13 9NJ, UK (K.A.T.G.); Department of Pharmacology and Therapeutics, University of Dundee, Ninewells Hospital, Dundee DD1 9SY, UK (J.J.L.); Department of Biological Sciences, Brock University, Ontario, Canada L2S 3A1 (R.P.R.).

† To whom correspondence and reprint requests should be addressed.

0028-0836/82/070599—03$01.00

it was sufficient to use low (such as 10^{-5} M) concentrations of L-glutamate in the patch electrode, thereby generating only a low frequency of channel events to ensure that the time courses of at least some of the calibration pulses were not influenced by accompanying glutamate channels. There is close agreement between the duration of the square pulse injected into the bath and the recovered pulse as measured by the computer. For example, with an input pulse of mean duration 65 ± 0.01 μs (±s.d.), an output pulse of mean duration 70 ± 0.04 μs was obtained. Note that a square pulse, which has its rise and fall times limited, appears as an inverted triangle or trapezoid (Fig. 1*a*). In our system, a 100 μs pulse appears at the output as a triangle with its amplitude approximately equal to that of the injected square pulse but with the base of the triangle ~200 μs long. With close attention to the setting of the comparator level during measurement of channel lifetimes, we can reliably detect at least 90% of channel openings and closings of 50–100 μs duration. In addition, our calibration technique indicates that the measured durations for channel openings and closings are within 20% of their true value for events between 50 and 100 μs. As we obtained excellent agreement between recovered durations and input durations for calibration pulses of duration >100 μs, we are confident that our recording and analysis techniques give accurate information on channel openings and closings >100 μs.

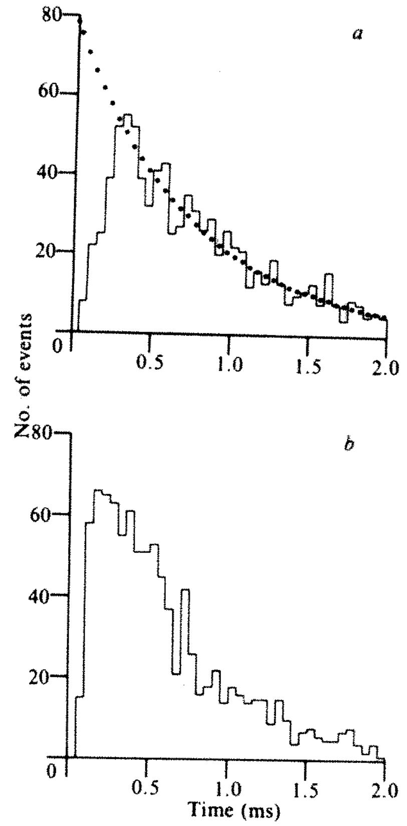

Fig. 2 Frequency distributions of glutamate channel lifetimes. *a*, Lifetime distribution for single glutamate channels recorded from an extrajunctional site with 5×10^{-5} M L-glutamate in the patch electrode. The data were obtained from a voltage-clamped muscle fibre (clamp potential −125 mV) and at a recording bandwidth of d.c. to 10 kHz. The peak in the lifetime distribution occurs at ~325 μs (bin no. 7). The dotted line, which is the best fit exponential to the falling phase of the distribution, was fitted by the least-squares method using the data in bins 6–40 (0.275–1.975 ms). The time constant of the exponential (τ_{open}) is 0.8 ms. Note the discrepancy between the observed number of short (≤250 μs) lifetimes and the number of events predicted by an exponential distribution of lifetimes. All recordings were obtained at a temperature of ~20 °C. *b*, Frequency distribution of channel lifetimes recorded in the presence of 10^{-3} M L-cysteate. Note that although the recording conditions were identical to those described for recording the glutamate channels (*a*), the peak in the cysteate channel distribution occurs at ~175 μs (bin no. 3) compared with ~325 μs (bin no. 7) for L-glutamate.

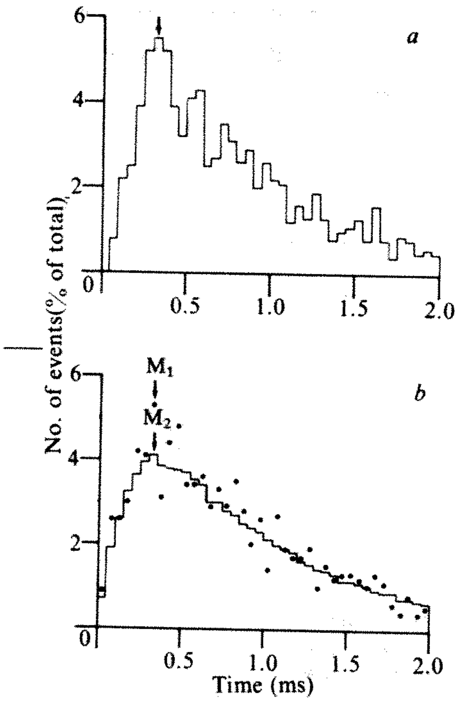

Fig. 3 Comparison of the distribution of glutamate channel lifetimes with a computer-simulated distribution. *a*, Frequency distribution of glutamate channel lifetimes recorded in the presence of 5×10^{-5} M L-glutamate (see Fig. 2*a* legend for description of recording procedure). The peak in the distribution (G) occurs at ~325 μs. *b*, Simulated frequency histograms constructed using the procedure described in the text. Two simulations are plotted, constructed from 1,000 (●) and, 100,000 (—) events. Both simulations were constructed using exponential time constants. $\tau_1 = 0.2$ ms for the first time-dependent process (state A) and $\tau_2 = 0.8$ ms for the second process (state B). The peaks (M_1 and M_2) occur at ~325 μs, coincident with the peak (see arrows) in the frequency distribution for glutamate channel lifetimes.

It is possible to monitor activity of an individual channel at a single site on a locust muscle fibre for long periods (for example 30 min) and, therefore, with an appropriate concentration of L-glutamate in the patch electrode, to collect information on a large number (for example, 1,000) of channel openings. Thus we have been able to construct histograms of channel openings using narrow (50 μs) bin widths. (Average lifetimes for quartiles of the recording period were not significantly different, indicating stationarity.) Figure 2*a* is a typical frequency histogram of lifetimes constructed from 1,000 open events recorded from a single site in the presence of 5×10^{-5} M L-glutamate. The dotted line is the best fit exponential to the falling phase of the distribution. Similar histograms have been obtained for lifetimes of channels recorded from many other preparations and with other agonists, such as L-cysteate (Fig. 2*b*). It is clear that despite the increased frequency response, our recording system histograms are still deficient in brief channel openings (of duration <250 μs), that is, the distributions are not exponential but exhibit a peak. As this deficiency could be explained only in part by the limitations of the recording system, the distributions suggest that two (or possibly more) processes may be involved in channel closure.

The open–close kinetics of desensitizing channels—bursts of channel openings separated by relatively long quiet periods[3,9,10]—make it difficult to obtain the large number of events needed to construct reliable histograms of channel lifetimes in the absence of Con A. We cannot be certain, therefore, that this lectin does not influence the lifetime of the glutamate channel, although the measured mean lifetimes of channels gated by extrajunctional receptors in Con A-treated and untreated muscle preparations are not significantly different when determined from data recorded using a 1 kHz low pass filter[5]. In addition, the measured mean channel lifetime of channels recorded with a 10 kHz amplifier, and with 5×10^{-5} M glutamate in the patch electrode, is ~1 ms—significantly shorter than the measured mean lifetimes of the glutamate channel (2–2.5 ms) reported previously using an amplifier with a more restricted bandwidth[5].

As a first approximation, the frequency distributions of lifetimes for locust glutamate receptors with 5×10^{-5} M glutamate can be described by two exponentials, the process characterized by one exponential having the effect of delaying the observed event of channel closure which is characterized by the other exponential. To test this idea we have attempted to simulate the frequency histograms of channel openings in the following way. A random number was selected from an exponential distribution with a mean corresponding to the estimated time constant of the first time-dependent process (transition from first open state [state A] to second open state [state B]). This assumes that transition from state B to state A has a low probability ($k_3 \gg k_{-3}$, see model below). A second random number was selected from another exponential distribution with a mean corresponding to the estimated time constant of the second time-dependent process (transition from open state B to closed state). The two random numbers were summed to produce a simulated channel opening. Figure 3*b* illustrates two frequency histograms, one constructed from 1,000 such events, the other from 100,000 simulated events. Initially the two time constants were estimated from the frequency histograms of real data and then refined by trial and error until the simulated histogram matched that for the real data. There is close agreement between the simulated distributions of channel lifetimes and the real data for the glutamate channel illustrated in Fig. 2*a*, suggesting that if channel closure is a two-step process, then in the case of the glutamate channel the rate of decay of state A is about four times faster than that of state B.

Cyclic kinetic schemes containing two open states have been proposed[11,12] for channels gated by acetylcholine receptors on vertebrate skeletal muscle but the three-state sequential model of Del Castillo and Katz[13] with two closed states is generally favoured for this system, that is,

$$\begin{array}{ccccc} nA+R & \underset{k_{-1}}{\overset{k_1}{\rightleftharpoons}} & A_nR & \underset{k_{-2}}{\overset{k_2}{\rightleftharpoons}} & A_nR^* \\ \text{closed} & & \text{closed} & & \text{open} \end{array}$$

This scheme describes the binding of an undefined number (n) of agonist molecules to the receptor (R) to form an intermediate closed state, A_nR, which then makes the transition to the open channel state A_nR^*. Obviously the model does not adequately describe the data for locust glutamate receptors because it implies that histograms of channel lifetimes should be fitted by a single exponential function. Instead we propose that the following cyclic model, modified from the desensitization scheme developed by Katz and Thesleff[14] for the acetylcholine receptor, is a reasonable working hypothesis for the operation of glutamate-gated channels in locust muscle:

$$\begin{tikzcd}
\text{closed} & \text{closed} \\
nA+R \arrow[r, shift left, "k_1"] & A_nR \arrow[l, shift left, "k_{-1}"] \arrow[d, "k_2"] \\
nA+R^* \arrow[u, "k_4"] \arrow[r, shift left, "k_{-3}"] & A_nR^* \arrow[l, shift left, "k_3"] \\
\text{(state B) open} & \text{open (state A)}
\end{tikzcd}$$

This model includes the two open states anticipated by our lifetime data. Because the scheme includes two irreversible steps (k_2, k_4), an energy supply would be required to maintain the steady state[14,15]. Its advantage is that it provides a mechanism for dependence of channel lifetime on agonist concentration which does not require multiple binding sites for the agonist[5] because the back reaction described by k_{-3} depends on the concentration of agonist.

We thank Mr A. Tivey for technical assistance and Dr T. F. Palmer for helpful discussions. This work was supported by SERC grants to P.N.R.U. R.P.R. was a SERC Senior Visiting Fellow.

Received 21 March; accepted 22 December 1981.

1. Neher, E., Sakmann, B. & Steinbach, J. H. *Pflügers Arch. ges. Physiol.* **375**, 219–228 (1978).
2. Patlak, J. B., Gration, K. A. F. & Usherwood, P. N. R. *Nature* **278**, 643–645 (1979).
3. Gration, K. A. F. & Usherwood, P. N. R. *Verlaufb. dt. zool. Ges.* **73**, 122–132 (1980).
4. Anderson, C. R., Cull-Candy, S. G. & Miledi, R. *J. Physiol., Lond.* **282**, 219–242 (1978).
5. Gration, K. A. F., Lambert, J. J., Ramsey, R. & Usherwood, P. N. R. *Nature* **291**, 423–425 (1981).
6. Mathers, D. A. & Usherwood, P. N. R. *Nature* **259**, 409–411 (1976).
7. Anwyl, R. & Usherwood, P. N. R. *Nature* **252**, 591–593 (1974).
8. Hamill, O. P., Marty, A., Neher, E., Sakmann, B. & Sigworth, F. J. *Pflügers Arch. ges. Physiol.* **391**, 85–100 (1981).
9. Gration, K. A. F., Lambert, J. J. & Usherwood, P. N. R. *J. Physiol., Lond.* **310**, 49P (1980).
10. Gration, K. A. F., Lambert, J. J. & Usherwood, P. N. R. *Adv. physiol. Sci.* **20**, 377–383 (1981).
11. Rang, H. P. *Neurosci. Res. Prog. Bull.* **11**, 220–224 (1973).
12. Dionne, V. E. *J. Physiol., Lond.* **310**, 159–190 (1981).
13. Del Castillo, J. & Katz, B. *J. Physiol., Lond.* **125**, 546–565 (1954).
14. Katz, B. & Thesleff, S. *J. Physiol., Lond.* **138**, 63–80 (1957).
15. Rang, H. P. & Ritter, J. M. *Molec. Pharmac.* **6**, 357–382 (1970).

Similar mode of action of pyrethroids and DDT on sodium channel gating in myelinated nerves

Henk P. M. Vijverberg, Johan M. van der Zalm & Joep van den Bercken

Department of Veterinary Pharmacology, Pharmacy and Toxicology,
University of Utrecht, Biltstraat 172, 3572 BP Utrecht,
The Netherlands

Synthetic pyrethroids are a new class of highly active insecticides with great potential for practical application[1]. They are generally recognized as neurotoxicants that act directly on excitable membranes[2,3]. Previous studies have shown that the effect of the pyrethroid allethrin closely resembles that of the classical insecticide dichlorodiphenyl trichloroethane (DDT) in the peripheral nervous system of *Xenopus laevis*[4,5]. Both compounds induce intense repetitive activity in sense organs and in myelinated nerve fibres. In the lateral-line sense organ this repetitive activity increases with cooling, a phenomenon that may be related to the negative temperature coefficient of toxicity of DDT[6] and pyrethroids[7] in insects. In frog node of Ranvier, DDT slows the closing of sodium channels that open during depolarization[8,9] so that a prolonged sodium tail current persists after the membrane has been repolarized. We have recently found that the pyrethroid allethrin[10] causes a similar sodium tail current in the nodal membrane of *Xenopus*. Pyrethroids[11,12] and DDT[13,14] are also known to cause prolongation of the sodium current together with repetitive activity in nerve fibres of invertebrates. The prolonged sodium current is thought to be directly responsible for this repetitive activity[3,15], and it has been suggested that the sodium channel in the nerve membrane is the major target site of pyrethroids and DDT-like compounds[10,12]. We have now investigated the mechanism by which pyrethroids and DDT prolong the sodium current in *Xenopus* nodal membrane. Our results show that these compounds—despite marked differences in chemical structure—modify sodium channel gating in a strikingly similar way and reduce selectively the rate of closing of the activation gate.

The experiments were carried out on voltage-clamped[16] myelinated nerve fibres from the sciatic nerve of *X. laevis* at 15 °C. Potassium currents were eliminated by applying tetraethylammonium (TEA) and by substituting Cs^+ for K^+. Allethrin ((±)-*cis*, *trans*-(±)-allethrin), permethrin ((±)-*cis*, *trans*-permethrin) and DDT (*p,p'*-DDT) were first dissolved in ethanol and then suspended in the external solution so that the

0028-0836/82/070601—03$01.00

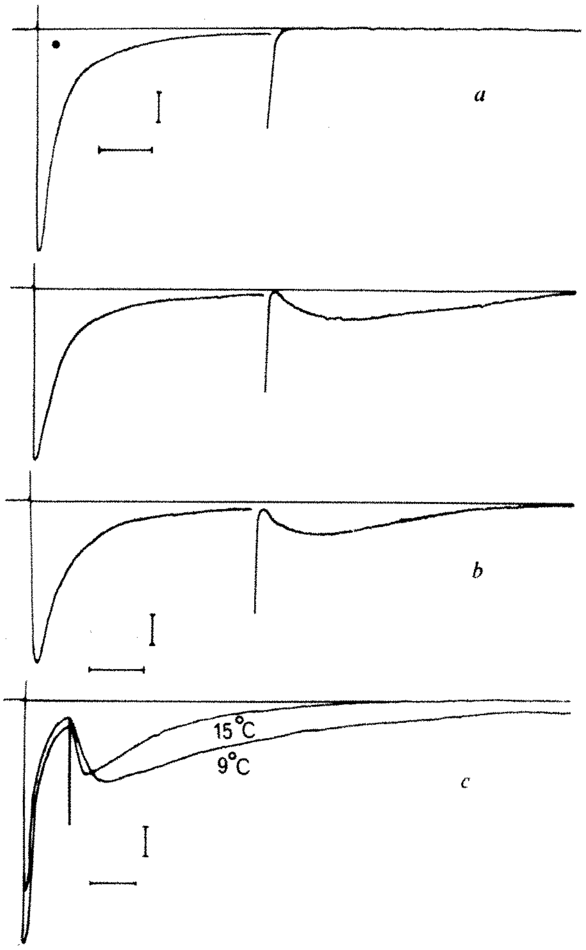

Fig. 1 Modification of sodium currents by pyrethroids and DDT. Recordings of sodium currents elicited by a depolarizing test pulse together with baseline level. Temperature 15 °C. *a*, Before (upper trace) and after (lower trace) exposure to 20 μM allethrin. *b*, After exposure to 40 μM DDT. *c*, After exposure to 10 μM permethrin. In *c* two traces are superimposed, recorded at the temperatures indicated. Test pulse amplitude: 60 mV (*a*), 70 mV (*b*, *c*). The insecticides were applied by a single perfusion of three to six times the volume of the pool bathing the node. The membrane was held at the potential at which $h_\infty = 0.70$ (−70 mV). Test pulses were preceded by a 100-ms conditioning prepulse to −120 mV to remove resting sodium inactivation. Linear parts of capacitive and leakage currents were electronically subtracted. Sodium currents were filtered at 5 kHz by an active two pole low-pass filter. Time constants of tail currents were calculated using a least squares algorithm. The external solution contained (in mM): Na^+ 104.4, Cs^+ 2.2, Ca^{2+} 1.8, TEA^+ 12, Cl^- 122.2 and HEPES 2.7; *p*H was adjusted to 7.3 with approximately 1.5 mM NaOH. The ends of the fibre were cut in 120 mM CsCl. Vertical bars, 1 nA; horizontal bar, 2 ms (*a*, *b*), 10 ms (*c*).

final nominal concentration was 10–40 μM. The amount of ethanol in the final solution was below 0.5% (v/v), which was found to be without effect in control experiments.

Allethrin and permethrin only slightly affected sodium currents during step depolarizations of the membrane. Peak sodium current amplitude was slightly reduced and the declining phase was slightly prolonged, but the rate of rise remained unaffected. The effect of allethrin and permethrin was most marked after the membrane was repolarized to holding potential. In untreated nodes the sodium current was always rapidly turned off by repolarization, whereas in the pyrethroid-treated nodes a large sodium tail current persisted (Fig. 1*a*,*c*). DDT also induced a sodium tail current after repolarization without seriously affecting sodium currents during depolarization (Fig. 1*b*), as previously reported[8,9]. The rate of decay of the tail current was independent of the amplitude and duration of the depolarizing test pulse. The decaying phase of the tail current was fitted by a single exponential with a time constant of 9.8 ± 1.2 ms (mean ± s.d., number of nodes *n* = 6) for allethrin, 17.4 ± 0.3 ms (*n* = 3) for permethrin and 3.7 ± 1.6 ms (*n* = 3) for DDT. At lower temperatures the exponential decay of the tail currents was markedly slowed, as illustrated in Fig. 1*c* for permethrin.

In pyrethroid- as well as DDT-treated nodes the membrane conductance during the tail was proportional to the degree of sodium activation during the test pulse (Fig. 2*a*). When the sodium current during the test pulse was inactivated to various degrees by varying the prepulse potential, the tail current amplitude was reduced proportionally (Fig. 2*b*). The potential dependence of sodium activation and sodium inactivation was not significantly affected by the insecticides. The magnitude of the tail current also depended on the duration of depolarization. After very short test pulses there was almost no tail current; with increasing duration of test pulse the amplitude of the tail current rapidly increased, reached a maximum and slowly declined with longer depolarizations. These results show that in pyrethroid- as well as DDT-treated nodes the number of sodium channels activated during the tail was always proportional to the number of sodium channels which had opened during depolarization, suggesting a precursor–product relationship[8] between open sodium channels and sodium channels affected by the insecticides and indicating that pyrethroids and DDT preferentially interact with open sodium channels.

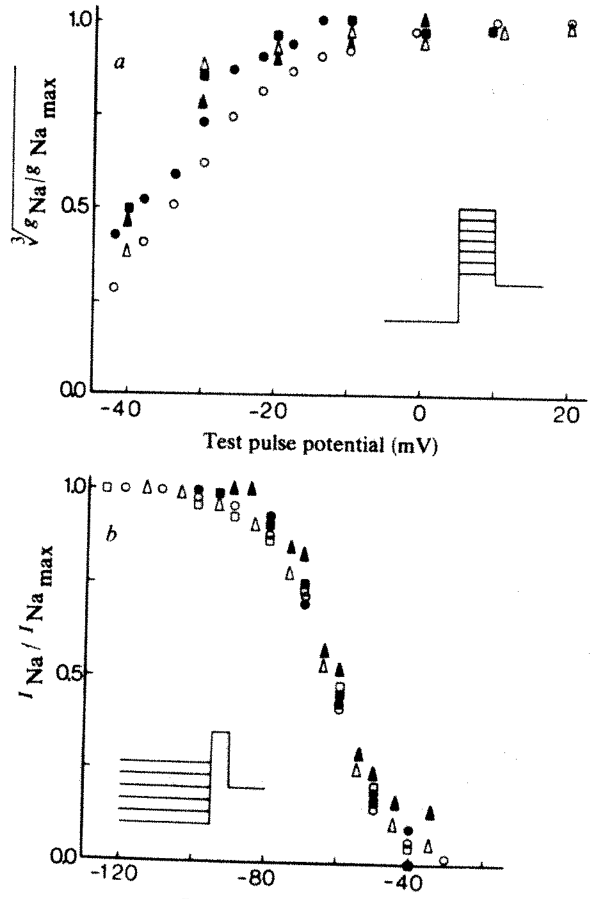

Fig. 2 *a*, Dependence of tail current amplitude on sodium activation. Sodium currents were elicited by 8-ms depolarizing test pulses of various amplitudes. Tail currents were extrapolated to the moment of repolarization and tail conductance (closed symbols) was normalized according to the procedure commonly used for sodium conductance[24] (open symbols). *b*, Dependence of tail current amplitude on sodium inactivation. Sodium currents were elicited by a standard test pulse (60 mV, 3 ms) following 100-ms conditioning prepulses of various amplitudes. Open symbols, sodium current during test pulse; closed symbols, tail current. Nodes treated with allethrin (triangles), permethrin (squares) or DDT (circles). Temperature 15 °C. Insets indicate voltage steps.

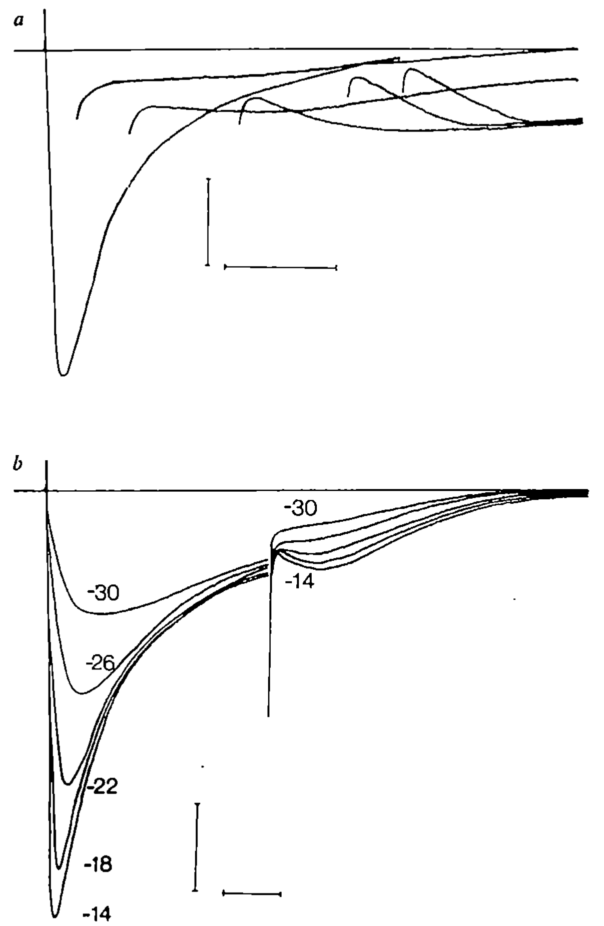

Fig. 3 Influence of duration and amplitude of depolarization on the shape of the tail current. Temperature 15 °C. *a*, Five superimposed traces of sodium currents elicited by 60-mV test pulses of 0.5, 1.5, 3.5, 5 and 6 ms, respectively, together with baseline level in a node treated with 20 μM allethrin. Following short test pulses the decay of the tail current was monotonic, whereas after longer test pulses an initial increase of the tail current gradually developed. *b*, Five superimposed traces of sodium currents elicited by 8-ms test pulses to the membrane potentials indicated together with baseline level in a node treated with 40 μM DDT. The initial increase of the tail current gradually developed with increasing amplitude of depolarization. Vertical bar, 0.5 (*a*) and 1 (*b*) nA; horizontal bars, 2 ms.

It was also found that the shape of the initial phase of tail current strongly depended on amplitude and duration of depolarization, with essentially the same results for all three insecticides. After small or short test pulses the decay of the tail current was always monotonic. With increasing amplitude and also with increasing duration of test pulse, however, the tail showed a marked initial rise before the exponential decay (Fig. 3*a*,*b*). Apparently the shape of the tail current depends on the degree of sodium inactivation at the moment of repolarization. In terms of the classical Hodgkin–Huxley model of sodium channel gating[17] this can be most readily explained by postulating that pyrethroids and DDT selectively reduce the rate of closing of the activation (m) gate in a fraction of the sodium channels that open during depolarization. After test pulses producing little inactivation, sodium channels which are not affected close as rapidly as normal, but those modified by the insecticides will close more slowly and a slowly decaying tail current will remain. Modified sodium channels are still subject to inactivation (see Fig. 3*a*) and at the end of test pulses that cause almost complete inactivation, most h-gates will be closed. On repolarization to holding potential, h-gates will start to reopen, causing modified channels to become conductant again because the closing of their m-gate is delayed. This mechanism adequately accounts for the development of a hooked tail current with increasing duration and amplitude of depolarization.

Some nodes treated with the pyrethroids or DDT failed to show an initial increase in the tail current, even after large depolarizations lasting for up to 50 ms. These nodes behaved identically to the other nodes in every respect except that they had a high degree of slow sodium inactivation[18]. Thus at the moment of repolarization many sodium channels are still open and the initial increase in the tail current will be masked by a large instantaneous sodium current.

Our hypothesis that these insecticides selectively reduce the rate of closing of the activation gate of the sodium channel is fully supported by the observation that in DDT-treated frog nodes the off-response of asymmetrical displacement currents was slowed down, while the on-response was not altered[19]. The similarity between the action of DDT and pyrethroids predicts that pyrethroids will have qualitatively similar effects on nodal displacement currents. Recently we have found that other pyrethroid insecticides, including some cyanophenoxybenzyl pyrethroids, also induce a persistent sodium tail current in *Xenopus* node of Ranvier (ref. 20 and H.P.M.V. and J.v.d.B., unpublished observations), indicating that the mechanism described here may apply to pyrethroids in general. An additional argument in favour of a similar mode of action of pyrethroids and DDT and its analogues is the existence of a high degree of non-metabolic cross-resistance in the housefly to these two classes of insecticide due to a common genetic factor (*kdr*) that presumably leads to nerve insensitivity[21,22].

The present results suggest that pyrethroids as well as DDT[8] interact with sodium channels having both the m-gate and h-gate open, and thereby stabilize the open configuration of the m-gate. On repolarization the sodium channel changes state[23] and the tail current slowly decays to zero level with a single exponential time course which is independent of tail current amplitude. This indicates that the relaxation of the m-gate of the modified sodium channels is determined by an apparent unimolecular first-order process. Differences in rate of decay of the tail current induced by the three compounds can be accounted for by differences in rate of this relaxation process. Furthermore, the marked prolongation of the tail current on cooling indicates that the relaxation process has a positive temperature coefficient which may underly the reversed temperature dependency of repetitive activity[4,5] caused by pyrethroids and DDT. Whether pyrethroids and DDT compete for the same site in the nerve membrane remains to be elucidated.

This work was supported by the Foundation for Medical Research FUNGO/ZWO and by Shell Internationale Research Mij.

Received 10 August; accepted 8 December 1981.

1. Elliott, M., Janes, N. F. & Potter, C. *A. Rev. Ent.* **23**, 443–469 (1978).
2. Narahashi, T. in *Insecticide Biochemistry and Physiology* (ed. Wilkinson, C. F.) 327–352 (Plenum, New York, 1976).
3. Wouters, W. & van den Bercken, J. *Gen. Pharmac.* **9**, 387–398 (1978).
4. van den Bercken, J., Akkermans, L. M. A. & van der Zalm, J. M. *Eur. J. Pharmac.* **21**, 95–106 (1973).
5. van den Bercken, J., Kroese, A. B. A. & Akkermans, L. M. A. in *Neurotoxicology of Insecticides and Pheromones* (ed. Narahashi, T.) 183–210 (Plenum, New York, 1979).
6. Eaton, J. L. & Sternburg, J. *J. Insect Physiol.* **10**, 471–485 (1964).
7. Harris, C. R. & Kinoshita, G. B. *J. econ. Ent.* **70**, 215–218 (1977).
8. Hille, B. *J. gen. Physiol.* **51**, 199–219 (1968).
9. Årnhem, P. & Frankenhaeuser, B. *Acta physiol. scand.* **91**, 502–511 (1974).
10. van den Bercken, J. & Vijverberg, H. P. M. in *Insect Neurobiology and Pesticide Action*, 79–85 (Society of Chemical Industry, London, 1980).
11. Narahashi, T. *Pestic. Sci.* **7**, 267–272 (1976).
12. Narahashi, T. & Lund, A. E. in *Insect Neurobiology and Pesticide Action*, 497–505 (Society of Chemical Industry, London, 1980).
13. Narahashi, T. & Haas, H. G. *J. gen. Physiol.* **51**, 177–198 (1968).
14. Pichon, Y. & Boistel, J. *J. Physiol., Paris* **61**, 373–374 (1969).
15. van den Bercken, J. *Eur. J. Pharmac.* **20**, 205–214 (1972).
16. Dodge, F. A. & Frankenhaeuser, B. *J. Physiol., Lond.* **143**, 76–90 (1958).
17. Hodgkin, A. L. & Huxley, A. F. *J. Physiol., Lond.* **116**, 500–544 (1952).
18. Chiu, S. Y. *J. Physiol., Lond.* **273**, 573–596 (1977).
19. Dubois, J. M. & Bergman, C. *Nature* **266**, 741–742 (1977).
20. Vijverberg, H. P. M. & van den Bercken, J. *Eur. J. Pharmac.* **58**, 501–504 (1979).
21. Farnham, A. W. *Pestic. Sci.* **8**, 631–636 (1977).
22. Sawicki, R. M. *Nature* **275**, 443–444 (1978).
23. Hille, B. *J. gen. Physiol.* **69**, 497–515 (1977).
24. Dodge, F. A. thesis, Rockefeller Inst. (1963).

Selective killing of leukaemia cells by antibody–toxin conjugates: implications for autologous bone marrow transplantation

Keith A. Krolick, Jonathan W. Uhr & Ellen S. Vitetta

Department of Microbiology, University of Texas Southwestern Medical School, Dallas, Texas 75235, USA

The recent development of tumour-reactive monoclonal antibodies has stimulated interest in their use in targeting toxic agents to tumour cells. One such approach involves the covalent coupling of tumour-reactive antibodies to the toxic peptide of the plant toxin, ricin. Such conjugates are highly effective in killing various tumour cells *in vitro*[1–6]. Here we have used the murine B-cell tumour, BCL$_1$, in an adoptive transfer system capable of detecting 1–10 tumour cells, to demonstrate the effectiveness and specificity of an anti-immunoglobulin(Ig)–ricin A chain conjugate in deleting tumour cells from infiltrated murine bone marrow. We report that the transferred cells were able to repopulate the haematopoietic system of lethally irradiated mice and that in most mice the tumour did not recur. We discuss the implications of this approach for autologous bone marrow transplantation following supralethal tumour therapy.

The murine BCL$_1$ tumour is in many respects similar to the prolymphocytic variant of human chronic lymphocytic leukaemia (CLL)[7–9]. The malignant cells are of B-cell origin and carry immunoglobulin on their surface. BCL$_1$ grows primarily in the spleen and blood of recipient mice with invasion of the bone marrow occurring only later in the course of the disease[7]. Depending on the number of tumour cells injected, recipient mice survive for 3–5 months. We have shown previously that if tumour cells are treated *in vitro* with an antibody specific for the variable region of the surface immunoglobulin molecules (anti-idiotype antibody) covalently coupled to the A chain of ricin, protein synthesis is irreversibly inhibited and the cells are killed[1]. In such experiments, inhibition of protein synthesis correlated well with the percentage of tumour cells in the treated population. However, as injection of only 10 BCL$_1$ cells into normal BALB/c mice will induce tumour formation[10], the adoptive transfer assay represents a more sensitive measurement of the number of residual viable tumour cells in a treated cell population. The extent of tumour cell death is particularly important when comparing this technique with other procedures which eliminate tumour cells bearing specific markers.

The antibody used in the present studies was an affinity-purified polyvalent rabbit anti-mouse immunoglobulin (RαMIg) which binds to surface immunoglobulin on both BCL$_1$ tumour cells and normal B cells[11]. An affinity-purified rabbit anti-ovalbumin (RαOVA) antibody was used as a control. As described previously[1], the antibodies were covalently coupled to the A chain of ricin using the heterobifunctional cross-linker *N*-succinimidyl-3-(3-pyridyldithio)propionate (Pharmacia). The preservation of antibody activity and the presence of A chain in the conjugate were established by solid-phase radioimmunoassay. Antibody–A chain conjugates were reacted with antigen (mouse immunoglobulin or OVA) and the presence of antibody or A chain was subsequently demonstrated by binding of radiolabelled antibodies directed against rabbit immunoglobulin or ricin A chain. It was confirmed that the conjugates could kill BCL$_1$ cells *in vitro*.

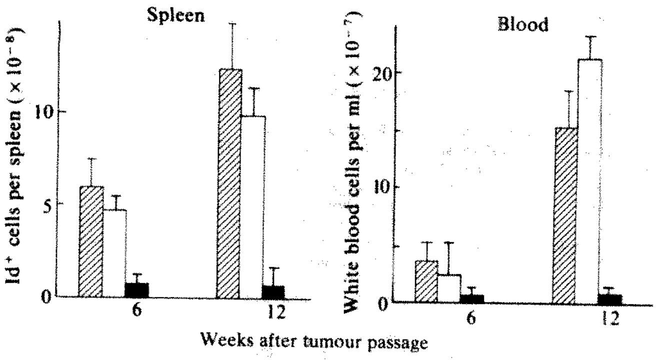

Fig. 1 Adoptive transfer of spleen cells treated with RαMIg–A chain from BCL$_1$-bearing mice. 10^7 spleen cells, containing 8×10^6 tumour cells, were treated at 4 °C for 15 min with 1 μg ml^{-1} of either RαMIg–A chain (■) or RαOVA–A chain (□). Treated cells, as well as untreated cells (▨), were washed and injected i.v. into groups of five normal BALB/c mice (10^4 cells per mouse). At 6 and 12 weeks after adoptive transfer, recipient mice were killed and examined for Id$^+$ (tumour) cells in the spleen, and for leukaemia.

Spleen cells ($1–10 \times 10^5$) from BCL$_1$-bearing mice were treated at 4 °C for 15 min with an optimal concentration of the specific (RαMIg–A) or control (RαOVA–A) antibody conjugate. Approximately 80% of the spleen cells in the populations used were tumour cells, as judged by immunofluorescent analysis after staining with anti-BCL$_1$ idiotype and by morphology. After treatment, 10^4 cells were injected into normal BALB/c mice. A group of mice also received untreated cells. At 6 and 12 weeks after adoptive transfer, recipient mice were killed and examined for presence of tumour cells in the spleen and for leukaemia. As shown in Fig. 1, untreated cells or cells treated with the control conjugate induced significant tumour formation. Animals receiving cells treated with RαMIg–A chain showed a concentration of Id$^+$ cells just above the level of control staining (5–10%) and this number did not increase between 6 and 12 weeks. Furthermore, white blood cells in RαMIg–A chain-treated mice never exceeded levels observed in normal mice ($5–10 \times 10^6$ ml^{-1}). Therefore, it is probable that treated animals contained no viable tumour cells, but we cannot exclude the possibility that there was a small number of tumour cells whose growth was inhibited by an immune response transferred with the treated splenocytes. To determine how many viable tumour cells would have been necessary to induce tumour formation at 12 weeks, additional experiments were performed using *untreated* tumour cells. In these experiments, groups of 35 mice received 1, 10 or 100 BCL$_1$ tumour cells and the time at which hepatosplenomegaly became apparent was noted. At 12 weeks after transfer of tumour cells, 95% of the animals receiving 10 tumour cells and 43% of those receiving 1 tumour cell had overt tumour (Table 1). Based on these experiments, we estimate that animals injected with spleen cells treated with RαMIg–A chain (Fig. 1) received <10 viable tumour cells. Thus, by using an inoculum of 10^4 tumour cells, we eliminated at least 99.9% of the cells.

One treatment of patients with disseminated neoplasia involves vigorous chemotherapy/radiotherapy with autologous bone marrow rescue[12]; bone marrow is removed before the patient is treated with supralethal chemotherapy and/or radiotherapy to kill all tumour cells. The autologous bone marrow is then injected into the patient to reconstitute the haematopoietic system. One major problem with this approach is that the bone marrow may contain tumour cells. We therefore applied the antibody-A chain technique to treat marrow cells from BCL$_1$-bearing mice (10–20% BCL$_1$ cells) with antibody–A chain

Table 1 Time required for small doses of tumour cells to induce hepatosplenomegaly in BALB/c recipients

No. of BCL$_1$ cells injected	Weeks after transfer	% Tumour-positive mice*
100	9	94
	12	100
10	9	69
	12	94
1	9	17
	12	43

The appearance of hepatosplenomegaly corresponds to plateau levels of Id$^+$ cells in the spleen, and mild leukaemia.

* 35 mice per group.

0028-0836/82/070604—02$01.00

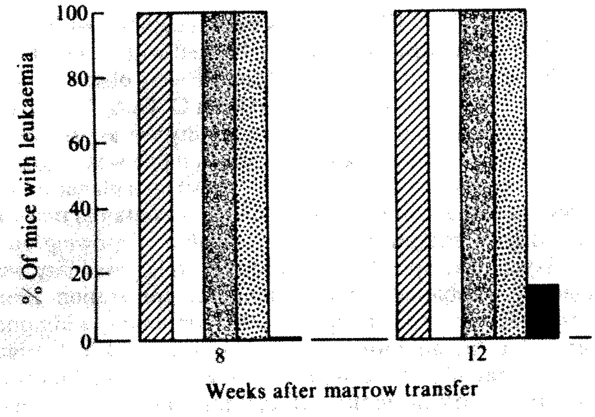

Fig. 2 Adoptive transfer of bone marrow cells treated with RαMIg–A chain from BCL$_1$-bearing mice into lethally irradiated recipients. 10^6 bone marrow cells, containing $1–2\times10^5$ tumour cells, were left untreated (▨), or were treated with RαMIg (▩), RαMIg plus C′ (▦), RαMIg–A chain (■), or RαOVA–A chain (□). Groups of 20 mice received 10^6 marrow cells per mouse. Every 2 weeks after adoptive transfer, mice were examined for leukaemia.

conjugates to eliminate tumour cells, but not stem cells, from the marrow. Preliminary experiments showed that such lethally irradiated mice could be rescued with an intravenous injection (i.v.) of 10^6, but not 10^5, normal bone marrow cells. Therefore, 10^6 marrow cells treated with specific or control conjugates or specific antibody and complement (C′) were injected into lethally irradiated (750 rad) mice.

Although all mice were rescued with 10^6 marrow cells, only those animals receiving marrow treated with RαMIg–A were leukaemia-free 8 weeks later (Fig. 2). However, 12 weeks after marrow transfer, 3/20 of the mice receiving RαMIg–A-treated marrow were leukaemic. Based on the number of animals which became leukaemic and the length of time necessary to achieve a leukaemic state (see Table 1), it was estimated that 1–10 tumour cells remained in the RαMIg–A chain-treated marrow. Thus, as the original 10^6 marrow cells injected contained 10^5 tumour cells, we estimate that the specific conjugate eliminated 99.9% of the tumour cells while preserving sufficient numbers of stem cells to repopulate the mice. Moreover, other experiments (not shown) have demonstrated that the repopulated tumour-free mice contain normal numbers of T and B cells in their spleens.

Note that the treatment of marrow with RαMIg plus C′ required 250 times more antibody for optimal cytotoxicity (20%) than treatment with RαMIg–A chain. Although the RαMIg plus C′ eliminated an estimated 90–95% of the tumour cells from the treated marrow, the recipient mice rapidly developed leukaemia, emphasizing the advantage of using antibody–A chain compared with C′-mediated cytotoxicity.

These results indicate that: (1) almost all (>99.9%) BCL$_1$ tumour cells bear surface immunoglobulin, that is, the BCL$_1$ tumour does not have a major pre-B cell component; (2) treatment with RαMIg–A chain conjugate eliminates Ig$^+$ tumour cells from the marrow of most mice but leaves sufficient numbers of stem cells intact; (3) neoplastic B cells can be eliminated by a conjugate using an antibody that is not tumour-specific. Thus, the above approach to autologous bone marrow transplantation, requires only a tumour-reactive, stem cell-non-reactive antibody.

Further experiments are needed to determine whether all BCL$_1$ tumour cells can be killed by the above approach. We emphasize that spontaneous B-cell leukaemias in man could have malignant pre-B cells[13], that is, surface Ig$^-$ in addition to surface Ig$^+$ leukaemic cells. Elimination of Ig$^-$ leukaemic cells would require treatment with a monoclonal antibody to a differentiation antigen that is expressed on pre-B cells and not stem cells.

We thank Ms B. Huber, Ms M. Bagby-Wyatt, Ms L. Trahan and Mr Y. Chinn for technical assistance, and Ms D. Marcoulides and Ms G. A. Cheek for secretarial help. This work was supported by NIH grants AI-11851, AI-12789, CA-28149 and CA-23115.

Received 14 September; accepted 9 December 1981.

1. Krolick, K. A., Villemez, C., Isakson, P. C., Uhr, J. W. & Vitetta, E. S. *Proc. natn. Acad. Sci. U.S.A.* **77,** 5419 (1980).
2. Krolick, K. A., Isakson, P. C., Uhr, J. W. & Vitetta, E. S. *J. Immun.* **123,** 1928 (1979a).
3. Gilliland, D. G. *et al. Proc. natn. Acad. Sci. U.S.A.* **77,** 4539 (1980).
4. Raso, V. & Griffin, T. *J. Immun.* **125,** 2610 (1980).
5. Musuho, Y. & Hara, T. *Gann* **71,** 759 (1980).
6. Blythman, H. E. *et al. Nature* **290,** 145–146 (1981).
7. Krolick, K. A., Isakson, P. C., Uhr, J. W. & Vitetta, E. S. *Immun. Rev.* **48,** 81 (1979).
8. Muirhead, M. J., Holbert, J. M. Jr, Uhr, J. W. & Vitetta, E. S. *Am. J. Path.* (in the press).
9. Galton, D. A. G. *et al. Br. J. Haemat.* **27,** 7 (1974).
10. Slavin, S. & Strober, S. *Nature* **272,** 624–626 (1977).
11. Pure, E. & Vitetta, E. *J. Immun.* **125,** 1240 (1980).
12. Gale, R. P. *J. Am. med. Assoc.* **243,** 540 (1980).
13. Vogler, L. B. *et al. Nature* **290,** 339–341 (1981).

Mitochondrial transformation of mammalian cells

Mike A. Clark & Jerry W. Shay*

Department of Cell Biology, The University of Texas Health Science
Center at Dallas, 5323 Harry Hines Boulevard, Dallas,
Texas 75235, USA

Resistance to the antibiotics chloramphenicol (CAP$^{\rm r}$) and efrapeptin (EF$^{\rm r}$) in mammalian cells is cytoplasmically inherited[1,2]. We demonstrate here that purified mitochondria obtained from CAP$^{\rm r}$ and EF$^{\rm r}$ cells are taken up by endocytosis and transfer antibiotic resistance to chloramphenicol-(CAP$^{\rm s}$) and efrapeptin-(EF$^{\rm s}$) sensitive cells. The resultant cells, termed mitochondrial transformants, are stably resistant to the antibiotics and are produced with high efficiency. The ability to transfer antibiotic resistance using mitochondria supports the notion that CAP$^{\rm r}$ is due to a mutation of the mitochondrial DNA[3]. This technique of mitochondrial-mediated transfer of antibiotic resistance may provide a novel means for studying mitochondrial genetics in mammalian cells.

The antibiotics chloramphenicol and efrapeptin inhibit mitochondrial protein synthesis and ATPase, respectively, thereby killing sensitive (wild-type) mammalian cells. Various mutant cell lines have been isolated[2,4] which are resistant to these drugs; we used these mutants to investigate the ability of isolated mitochondria[5] to transfer resistance to the antibiotics. In these experiments we produced antibiotic-resistant cells by mixing purified resistant mitochondria with sensitive (wild-type) intact cells and selecting the transformants by using antibiotics. The following are evidence that we were able to transfer antibiotic resistance via isolated mitochondria: (1) mitochondria obtained from antibiotic-resistant cells previously incubated with the vital non-toxic laser dye rhodamine 123, which specifically stains mitochondria[6], accumulated in wild-type cells by endocytosis; (2) transfer of antibiotic resistance was stable even in the absence of antibiotic selection; (3) contaminating resistant parental cells were not responsible for these observations, as wild-type recipent cells had specific nuclear markers allowing positive identification of cell types; (4) the transfer was cytoplasmically determined because mitochondrial transformants were used as donors to transfer antibiotic resistance by enucleation and cybridization; (5) this transfer was UV light sensitive and appeared to be species specific; (6) there was a high cotransfer frequency of both CAP$^{\rm r}$ and EF$^{\rm r}$.

Y-1 and PCC$_4$ wild-type (CAP$^{\rm s}$ and EF$^{\rm s}$) cells (respectively obtained from the American Type Culture Collection, Maryland, and W. E. Wright, UTHSCD, Texas), plated out in medium containing 50 μg ml^{-1} CAP or 0.1 μg ml^{-1} EF, were

---

[*] To whom correspondence should be addressed.

able to attach to the substrate. After 4–5 days the cells became vacuolated, developed pycnotic nuclei and eventually detached from the substrate (Fig. 1*b*, *c*). The incidence of spontaneous resistance to CAP or EF in these cell lines was below our level of detection ($<10^{-8}$). When CAP^s EF^s Y-1 cells were incubated with CAP^r EF^s AMT mitochondria and then challenged in CAP or EF for 2 weeks, it was observed that many CAP^r colonies, but no EF^r colonies, were produced (Fig. 1*d*, *e*). (The AMT cells were obtained from Dr N. Wivel, NIH, Maryland, and the antibiotic stability was as previously described[4].) The plating efficiency of this cell line was ~28% in the condition described.

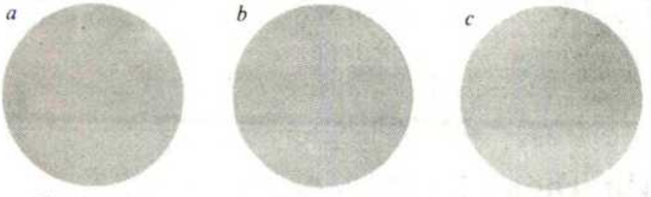

Mitochondria alone

Y-1 cells in Ef

Y-1 cells in Cap

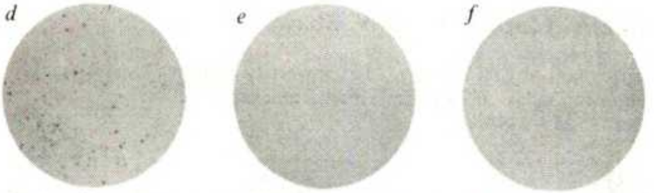

Y-1 cells + AMT mitochondria in CAP

Y-1 cells + AMT mitochondria in Ef

Y-1 cells + P815 mitochondria in Cap

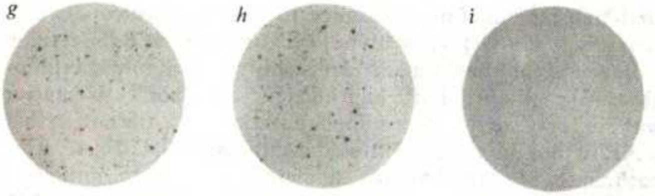

Y-1 cells + TL-1 mitochondria in Cap

Y-1 cells + TL-1 mitochondria in Ef

Y-1 cells + P815 mitochondria in Ef

Fig. 1 Mitochondria were obtained by homogenizing AMT (CAP^r EF^s) or TL-1 (CAP^r, EF^r) cells and removing nuclei and whole cells by low speed centrifugation (500*g*, 5 min). Mitochondria were then pelleted (20,000*g*, 20 min) and further purified on a discontinuous sucrose gradient (75,000*g*, 30 min), The mitochondria were removed from the 1.0–1.5 M sucrose interface[5]; this fraction was found to be free of nuclei and whole cells after ultrastructural examination. The DNA content of this fraction, determined by reading the absorption at 260 nm (ε, 1 mg = 27 o.d.), was found to average 1–2 μg of DNA recovered from 10^9 cells. In addition, there was no growth when purified mitchondria isolated from 2×10^6 cells were placed in culture for 2 weeks (dish *a*), suggesting that this mitochondrial fraction did not contain viable cells. Y-1 cells (EF^s, CAP^s) do not grow when challenged with 0.1 μg ml^{-1} EF or 50 μg ml^{-1} CAP (*b*, *c*, respectively). Cells to be transformed were placed in a 98-well dish (3×10^4 cells per well) with purified mitochondria. 12 h later the cells were washed and re-plated at 10^3 cells per 100 mm dish in medium containing 50 μg ml^{-1} CAP or 0.1 μg ml^{-1} EF. After 2 weeks of growth the dishes shown in the figure were fixed in methanol/acetic acid (3:1) and Giemsa-stained. Because *p*H, cell density and glucose concentration are important factors in the expression of the CAP^r phenotype, they were kept the same for all experiments. All cells were grown in Dulbecco's modified medium with 1 mg ml^{-1} glucose (with pyruvate) and 10% fetal bovine serum in an atmosphere containing 5% CO_2, *p*H 7.2. In each of the dishes shown except *a*, mitochondria (obtained from 2×10^6 cells) were incubated with 3×10^4 wild-type Y-1 cells. Y-1 cells incubated with CAP^r EF^s AMT mitochondria produced many CAP^r clones of Y-1 cells (*d*). The surviving cells were shown to be Y-1 and not AMT cells by their ability to round up and secrete steroids in response to ACTH[7]. Although the AMT mitochondria were able to confer CAP resistance, they were unable to confer EF resistance (*e*). In control experiments, CAP^s EF^s mitochondria obtained from P815 mastocytoma cells were incubated with Y-1 cells; these mitochondria were unable to confer either CAP or EF resistance (*f*, *i*, respectively). If CAP^r EF^r TL-1 mitochondria were used, both CAP-resistant (*g*) and EF-resistant (*h*) Y-1 clones grew. Similar results were obtained using PCC_4 Aza-1 wild-type recipient cells (Table 1). In these experients the PCC_4 cells have a specific nuclear marker (resistance to 8-azaguanine) allowing positive identification of cell types.

However, if the CAP^s EF^s Y-1 cells were incubated with CAP^r EF^r TL-1 mitochondria and then challenged with CAP or EF, many colonies resistant to both CAP and EF were observed (Fig. 1*g*, *h*). (The TL-1 cells were obtained from G. Getz, University of Chicago, Illinois, and the antibiotic stability was as previously described[2].) The plating efficiency of this cell line was ~30% in the cloning conditions described. One possible explanation for these results is that antibiotic-resistant cells contaminated the mitochondrial preparation and were capable of growing on a 'feeder' layer of recipient cells. However, this possibility was excluded by incubating the mitochondrial preparation alone (Fig. 1*a*) and by using recipient cells containing additional markers. That the antibiotic-resistant cells were of Y-1 origin was demonstrated by treating the cells with 100 milliunits of adrenocorticotropic hormone (ACTH) for 30 min[7]. A mean of 49 out of 50 CAP^r colonies and 47 out of 50 EF^r colonies in three separate experiments were responsive to ACTH by morphological analysis (rounding up) and fluorimetric analysis (increased steroid secretion). This result indicated that the surviving antibiotic-resistant cells were not intact AMT or TL-1 cells, which might have contaminated the mitochondrial preparation, since the AMT and TL-1 cells were fibroblasts and thus not responsive to ACTH. Similar results were obtained with the PCC_4 cell line. In these experiments, CAP^r and EF^r transformed cells were demonstrated to be PCC_4 cells by their resistance to 8-azaguanine; a nuclear mutation (HGPRT$^-$) allows the PCC_4 cells, but not AMT or TL-1 cells, to proliferate in the presence of 8-azaguanine. Mitochondria isolated from antibiotic-sensitive (wild-type) P815 cells were unable to confer CAP^r or EF^r on either Y-1 or PCC_4 cells (Fig. 1*f*, *i*). (P815 cells were obtained from W. T. Garrard, University of Texas Health Science Center, Texas.)

The production of mitochondrial transformants was dependent on the number of mitochondria added to the Y-1 or PCC_4 cells (see Table 1). It was observed that the AMT mitochondria conferred resistance to CAP but not to EF on both cell lines used, while the TL-1 mitochondria conferred CAP and EF resistance with similar frequencies. In control experiments, mitochondria obtained from CAP^s EF^s P815 cells conferred neither CAp nor EF resistance. In these experiments we observed no spontaneous mutants that were able to grow in CAP or EF in either the Y-1 or PCC_4 cells when plated at 3×10^4 cells per 10-cm dish. In addition, even if plated at higher density ($>10^6$ cells per 10-cm dish), we were unable to isolate any spontaneous stable antibiotic-resistant revertants.

If mitochondria were responsible for the transfer of antibiotic resistance, then extracts depleted of mitochondria or UV-inactivated mitochondrial preparations should be less efficient in transformation. Supernatants from the differential centrifugation which contained very few mitochondria (as determined by electron microscopy) were ~80-fold reduced in their ability to transform cells. Exposure of mitochondria to UV light also resulted in a reduction in their ability to transform antibiotic-

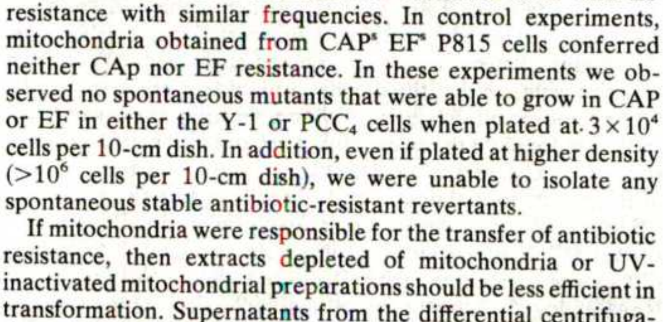

Fig. 2 AMT cells were grown in 1 μg ml^{-1} of R123 (Kodak, New York) for 30 min before homogenization. The resulting R123-stained mitochondria were then incubated with unstained Y-1 cells for 2 h before observation by fluorescence microscopy. *a*, Fluorescence and *b*, phase-contrast micrograph of the same field of cells. About 40% of all Y-1 cells contained varying numbers of fluorescent mitochondria. However, there were many cells which did not appear to incorporate any R123 mitochondria (arrow). Scale bar, 10 μm.

Table 1 No. of CAP^r or EF^r clones observed after 2 weeks of growth in antibiotics for varying numbers of mitochondria used in transformation

Source of mitochondria	No. of antibiotic-resistant colonies (>50 cells) observed 2 weeks after transformation AMT (CAP^{r}EF^s)				TL-1 (CAP^r EF^r)				P815 (CAP^s EF^s)			
Antibiotic challenge	CAP	CAP	EF	EF	CAP	CAP	EF	EF	CAP	CAP	EF	EF
Recipient cell line	Y-1	PCC$_4$	Y-1	PCC$_4$	Y-1	PCC$_4$	Y-1	PCC$_4$	Y-1	PCC$_4$	Y-1	PCC$_4$
Mitochondrial equivalents												
0	0	0	0	0	0	0	0	0	0	0	0	0
4×10^4	1	0	0	0	0	0	0	0	0	0	0	0
1.5×10^5	7	110	0	0	2	49	11	30	0	0	0	0
6×10^5	18	318	0	0	31	178	19	157	0	0	0	0
2.5×10^6	112	307	0	0	106	276	143	241	0	0	0	0

Mitochondria were isolated from the CAP^r EF^s AMT, CAP^r EF^r TL-1 and CAP^s EF^s P815 cell lines and incubated with the CAP^s EF^s Y-1 and PCC$_4$ cell lines as described in the text. Values are the average number (three experiments) of CAP^r or EF^r clones observed after 2 weeks of growth in either CAP or EF when varying numbers of mitochondria (1 mitochondrial equivalent = the number of mitochondria recovered from 1 cell) were incubated with a constant number (3×10^4) of Y-1 or PCC$_4$ cells. (10^6 mitochondrial equivalents contain 2.5 ng of DNA.)

sensitive cells (Table 2 shows the results as average of three experiments). A constant number of mitochondria obtained from 10^9 AMT cells were diluted into aliquots, each aliquot containing a number of mitochondria equivalent to that obtained from 10^6 cells. These aliquots were then incubated with 3×10^4 Y-1 cells. Control mitochondria that had not been exposed to UV light were able to confer CAP^r at a frequency of $\sim1.5\times10^{-3}$. However, aliquots of mitochondria that had been exposed to UV light (Sylvania germicidal UV light (G15T8) at a distance of 10 cm) showed a much reduced transformation frequency.

We then tested the stability of antibiotic resistance in the mitochondrial transformants. Twelve clones were chosen at random (six from CAP^r and six from EF^r colonies) that had been grown for 3 weeks in the presence of the antibiotic. These clones were transferred to antibiotic-free medium for 2 weeks (12–14 cell doublings) before being retested with CAP or EF; all 12 clones retained equal resistance to both antibiotics. The per cent of cells retaining their antibiotic resistance and the plating efficiencies of the transformed cells were the same as those of the parental drug-resistant strains. Furthermore, we maintained these clones for over 12 weeks in the presence of the antibiotics and all clones were stable in their transformation. There was no decrease in plating efficiency between the initial testing and after 12–14 population doublings in the absence of antibiotics.

In addition to the antibiotic resistance originally selected, other information was transferred in the mitochondrial genome to the recipient cells. After incubation of CAP^s EF^s Y-1 cells with CAP^r EF^r TL-1 mitochondria, one half of the cells were plated in dishes containing CAP and the other half in EF. Five random clones of CAP^r Y-1 cells and six clones of EF^r cells were isolated and tested for their ability to grow in the reciprocal antibiotic. All 11 clones were resitant to both antibiotics. This is in agreement with the observations of Wigler *et al.*[8], who demonstrated a high incidence of co-transfer of genetic material using purified nuclear DNA. The high antibiotic co-transfer frequency may result from incorporation of intact mitochondria into the recipient cells. This hypothesis was tested by isolating mitochondria from cells which had been treated previously with rhodamine 123 (R123), a vital dye which specifically stains mitochondria[6]. When R123-stained mitochondria were incubated with unstained Y-1 cells, uptake of the stained mitochondria was observed by fluorescence microscopy (Fig. 2).

If mitochondria were responsible for the stable transfer of antibiotic resistance, then mitochondrial transformants could be used as antibiotic-resistant donors in cybridization experiments. CAP^r and EF^r mitochondrial transformants were enucleated using cytochalasin B[9] and their cytoplasts fused to CAP^s and EF^s Y-1 cells. The rationale for producing cybrids, rather than a second generation of mitochondrial transformants, was that fewer (5×10^5) cells were needed in each experiment. These experiments demonstrated that two out of eight clones of transformants were able, in turn, to transfer antibiotic resistance, which indicated that the TL-1 and AMT transforming material was incorporated into the cytoplasm.

Not all cell lines were equally capable of acting as recipients for transformation by purified mitochondria. Murine CAP^r and EF^r mitochondria were unable to confer either CAP or EF resistance on human Lesch Nyhan cells. This result was consistent with previously published cybrid data[10] which demonstrated that CAP resistance could not be transferred between species. In addition, not all murine cell lines were equally capable of transformation. After repeated attempts, we have been unsuccessful in conferring either CAP or EF resistance to the murine C17-S1-D-T984 cell line, originally derived from a teratoma. It is not understood why there is such variability in the efficiency of mitochondrial transformation, but the above observation is consistent with previous findings which indicated that murine cell lines differ widely in their ability to incorporate isolated nuclear DNA[8]. In addition, the C17-S1-D-T984 cell line was markedly reduced in R123–labelled mitochondria uptake when compared with the Y-1 and PCC$_4$ cells, suggesting that differences in endocytosis may be important in mitochondrial-mediated transfer of antibiotic resistance.

Thus, we have used isolated mitochondria to confer CAP and EF resistance with high efficiency. There was a high co-transfer frequency and transformed cells were stable even in the absence of antibiotic selection pressure. After enucleation of mitochondrial transformants, antibiotic resistance was subsequently transferred cytoplasmically. These results suggest that either the antibiotic resistance was transferred by recombination with the recipient cell mitchondrial genome or that the recipient cell incorporated intact antibiotic-resistant mitochondria (or both). Experiments are now in progress to determine whether isolated mitochondrial DNA can also transfer antibiotic resistance.

We thank Drs Brown, Butow, Cuthbert, Garrard, Martin, Reudelhuber and Wright for helpful discussions. This work was supported by NIH grants GM-29261, HL00422, and NSF grant PCM-8023070 (to J.W.S.).

Received 13 August; accepted 4 December 1981.

1. Bunn, C. L., Wallace, D. C. & Eisenstadt, J. M. *Proc. natn. Acad. Sci. U.S.A.* **71**, 1681–1685 (1974).
2. Lichtor, T. & Getz, G. *Proc. natn. Acad. Sci. U.S.A.* **75**, 324 (1978).
3. Kearsey, S. E. & Craig, I. W. *Nature* **290**, 607–608 (1981).
4. Malech, H. L. & Wivel, N. A. *Cell* **9**, 383–391 (1976).
5. Bogenhagen, D. & Clayton, D. A. *J. biol. Chem.* **249**, 7991–7995 (1974).
6. Johnson, L. V., Walsh, M. L. & Chen, L. B. *Proc. natn. Acad. Sci. U.S.A.* **77**, 990–994 (1980).
7. Clark, M. A. & Shay, J. W. *Scanning Electron Microsc.* **3**, 527–535 (1979).
8. Wigler, M. *et al. Proc. natn. Acad. Sci. U.S.A.* **77**, 3567–3570 (1980).
9. Shay, J. W. & Clark, M. A. *J. supramolec. Struct.* **11**, 33–49 (1979).
10. Wallace, D. C. & Eisenstadt, J. M. *Somat. Cell Genet.* **5**, 373–396 (1979).

Table 2 UV inactivation of mitochondria

	No. of CAP^r clones	Transformation frequency
Control	47	1.5×10^{-3}
30 min UV treatment	17	5.66×10^{-4}
60 min UV treatment	3	1.00×10^{-4}

^{31}P NMR examination of two patients with NADH-CoQ reductase deficiency

G. K. Radda*, P. J. Bore†, D. G. Gadian*, B. D. Ross‡, P. Styles†, D. J. Taylor† & J. Morgan-Hughes§

*Department of Biochemistry, University of Oxford, South Parks Road, Oxford OX1 3QU, UK
†Clinical Magnetic Resonance Laboratory, Radcliffe Infirmary, Oxford OX2 6DH, UK
‡Nuffield Department of Clinical Medicine, John Radcliffe Hospital, Headington, Oxford OX3 9DU, UK
§Institute of Neurology, National Hospital, Queen's Square, London WC1N 3BG, UK

Mitochondrial myopathies are becoming increasingly recognized as uncommon causes of muscular disorders[1] characterized by weakness and severe exercise intolerance. Electron micrographs of the muscle show gross abnormality of the mitochondrial structure. Such defects are expected to affect the energy metabolism of muscle but investigations in human subjects have necessarily been limited by the need for biopsy material. Following extensive phosphorus nuclear magnetic resonance (^{31}P NMR) measurements on isolated organs, tissues and selected parts of live animals (see ref. 2 for review), it has become possible to observe non-invasively the energy metabolism of human muscle *in vivo*[3–5]. Here, we report abnormal recovery of phosphocreatine (PCr) and *p*H after exercise of the forearm in two sisters, one of whom has been shown to have a mitochondrial NADH-coenzyme Q reductase deficiency and the other presumed to have the same defect on the basis of clinical symptoms, histology and biochemical studies of blood constituents[6]. Our results, together with studies on normal subjects and patients with impaired glycogen metabolism, allow the assessment of the relative importance of oxidative and glycolytic regeneration of high-energy phosphates during exercise and recovery.

The results of the clinical, biochemical and histological examination of the two patients have been reported previously[6]. Case 1 (L.O.), 28 yr old, was normal at birth but since early childhood has been unable to run more than a few paces. Muscular weakness has often been accompanied by nausea and sickness; the worst attack, which led to her admission and diagnosis, was precipitated by a small intake of alcohol. On that admission she had severe lactic acidosis (17.8 mM). Biopsy evidence showed structurally abnormal mitochondria with paracrystalline inclusions, and the biochemical studies established inability to oxidize NAD-linked substrates, while succinate was oxidized normally.

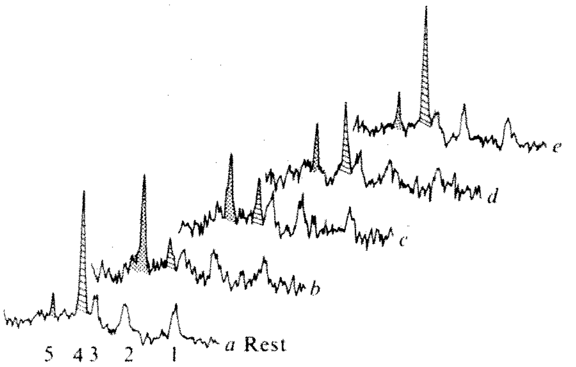

Fig. 1 ^{31}P NMR spectra of one of the patients (R.O.), taken at rest, during exercise and recovery. The signals are assigned as follows: 1, 2 and 3, the β, α and γ phosphates of ATP; 4, phosphocreatine; 5, inorganic phosphate. The inorganic phosphate and phosphocreatine signals are shaded for clarity. All spectra were accumulated at 32.5 MHz using a train of radiofrequency pulses applied at intervals of 2 s; the number of pulses was 128 for spectrum *a*, 32 for spectra *b–d*, and 64 for spectrum *e*. Spectrum *a* was recorded at rest immediately before exercise. Spectrum *b* was recorded during the last minute of aerobic exercise, and spectra *c–e* were recorded during the recovery period at 5, 9.5 and 37 min, respectively, after the end of exercise.

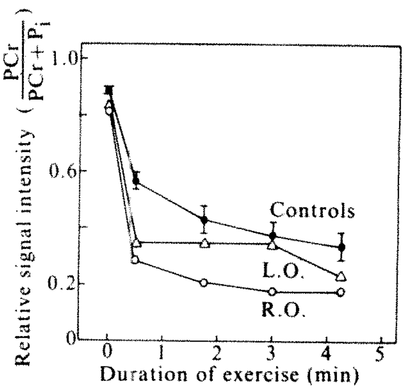

Fig. 2 Change in PCr concentration (expressed as a ratio to PCr + P$_i$) during aerobic exercise. Exercise was carried out by opening and closing the fist (L.O. and R.O.) or squeezing a rubber bulb to a pressure of 100 mmHg (controls) every 2 s for 5 min. Controls (five males and five females) were aged 22–37 yr. Values are given as ± s.e.m.

Case 2 (R.O.), 2 yr younger, with a similar medical history and more severe exercise intolerance, has a resting lactic acid concentration in blood of 4.7–7.9 mM (normal 1 mM). Biopsy showed the same histological abnormality of mitochondria as for L.O., but no biochemical studies of biopsies were undertaken in this patient. She was assumed to have the same metabolic defect as patient 1.

For the ^{31}P NMR examination, a circular radiofrequency surface coil of diameter 2.5 cm was positioned adjacent to the flexor digitorum superficialis of the right forearm. Five to ten minutes after the arm had been placed in the bore of the superconducting magnet, three spectra were collected. This procedure took about 10 min, during which time the arm remained at rest. The spectra from both patients contained the normally observed metabolites inorganic phosphate (P$_i$), PCr and ATP (Fig. 1). However, they differed quantitatively from the spectra of control subjects obtained at rest in that during the 10 min, the ratio PCr : P$_i$ gradually increased from abnormally low values (R.O., 2.3; L.O., 3.5) to nearer normal values (R.O., 4.9; L.O., 5.8; normals, 9.3 ± 2.0 (s.d.), $n = 21$). In R.O. and L.O., the intracellular *p*H at rest, measured from the frequency of P$_i$ resonance, was 7.04 ± 0.01 and 6.96 ± 0.02 (three measurements, ± s.d.), respectively, compared with a value of 7.04 ± 0.03 observed for 20 control subjects.

Light exercise was begun (opening and closing the fist every 2 s for 5 min). Spectra were collected every 75 s throughout exercise and during 30–40 min of recovery following exercise. The patients' metabolic response to exercise and their subsequent recovery were markedly abnormal. During the first minute of the very light exercise regime, the concentration of PCr decreased and that of P$_i$ increased more rapidly than in normal controls doing considerably more work (Fig. 2). By the second minute of exercise, 65–75% of the PCr had been consumed and the *p*H had fallen to 6.56 (L.O.) and 6.73 (R.O.). This change in *p*H relative to PCr consumption is normal but was achieved at much lower work loads than in control subjects. No change in the ATP concentration was detected during exercise, but with the available signal-to-noise ratio, changes of less than 20% would not be detected.

The most marked abnormality which was observed in both patients was the extremely slow return, following exercise, of the PCr and P$_i$ to their initial concentrations. Normal subjects recovered >90% of the resting PCr/(PCr + P$_i$) in less than 3 min, while in the two patients this level of recovery was not reached until 30 min or more (Fig. 3). Because the recovery process is so lengthy, the muscle may not have been at 'rest'

0028–0836/82/070608—02$01.00

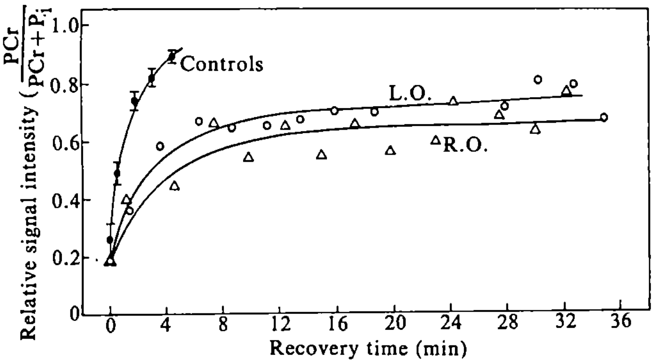

Fig. 3 Recovery of PCr/(PCr+P_i) following exercise. Exercise was carried out by opening and closing the fist every 2 s for 5 min (R.O. and L.O.), or squeezing a rubber bulb to a pressure of 100–300 mm Hg every 2 s for 7.5–21 min. Resting values of PCr/(PCr+P_i) were 0.83 (L.O.), 0.84 (R.O.) and 0.90±0.01 (controls, ±s.e.m.). Control values were obtained from four female and four male subjects aged 22–37 yr. Values are ±s.e.m.

when the first spectra were obtained, and this may account for the low PCr:P_i ratio observed before the start of exercise. Interestingly, the intracellular *p*H returned to the original level 2.5–3.5 min after the cessation of exercise (Fig. 4). The initial rate of *p*H increase was ~0.25 *p*H units min^{-1}. In eight normal individuals whose muscle *p*H in exercise decreased to an average value of 6.4, the recovery time was >9 min and the *p*H change was linear for 9 min, with a rate of 0.07 *p*H units min^{-1}.

In patients with glycogen phosphorylase deficiency the recovery of PCr results predominantly from oxidative phosphorylation. In the three such patients that we have investigated, the rate of recovery is the same as in control subjects[5]. Thus, we conclude that the recovery phase is largely governed by the rate of mitochondrial ATP synthesis ($t_{1/2}\sim 1$ min). The slow rate of PCr recovery in our two patients is consistent with a decreased rate of oxidative metabolism. In patient 1 the rate of oxidation of NAD-linked substrates in isolated mitochondria is six to seven times slower than in control subjects[6]. Interestingly, the rate of oxidative PCr recovery *in vivo* is also about six times slower in the two patients than in controls. The importance of oxidative processes in recovery is confirmed by studies in which four control subjects have undergone 1 min of exercise during ischaemia followed by 6 min of rest during which ischaemia was maintained. At the end of exercise, the PCr decreased to 50% or less of the initial value, but there was no detectable recovery of PCr during the subsequent 6 min of ischaemia. In addition, the *p*H varied by less than 0.15 *p*H units in the ischaemic rest period. On resumption of blood flow, the metabolic recovery was very rapid, the PCr returning to >90% of its control value within 2–5 min. This suggests that glycogenolysis is switched off at the end of exercise, possibly because Ca^{2+} ions are taken up by the sarcoplasmic reticulum.

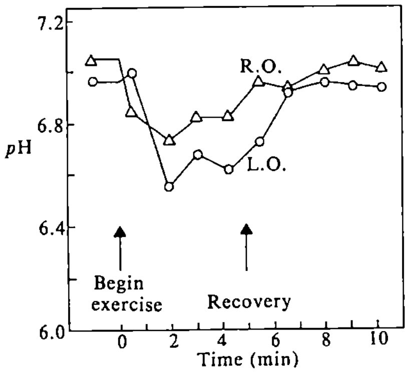

Fig. 4 Intracellular *p*H during exercise and recovery in the patients. *p*H was obtained from the chemical shift of P_i with reference to PCr as described previously[5].

In view of the high blood lactate levels that have been observed in one of the patients, the changes in intracellular *p*H on exercise are perhaps milder than might have been expected. A similar observation has been made in another patient with a mitochondrial myopathy[7]. It is possible that such people have an adaptive mechanism for removing intracellular lactate into the bloodstream. This would be consistent with the rapid recovery of intracellular *p*H following exercise.

^{31}P NMR examination of patients with muscle disease offers an objective means of assessing therapy. The patients described here have in the past received sporadic and largely ineffective treatment with menadione. It is now intended to repeat this trial of therapy with objective measurement of the response from NMR determination of the rate of rephosphorylation of creatine to PCr.

This work was supported by the MRC, the British Heart Foundation and the SRC. We thank Miss Judith Harley and Mrs Yvonne Green for technical assistance.

Received 25 November 1981; accepted 12 January 1982.

1. Morgan Hughes, J. A. *Recent Advances in Neurology* Vol. 3 (eds Matthews, W. B. & Glaser, G. H.) 1–46 (1982).
2. Gadian, D. G. & Radda, G. K. *A. Rev. Biochem.* **50,** 69–83 (1981).
3. Cresshull, I. D. *et al. Bull. magn. Resonance* **2,** 426 (1981).
4. Cresshull, I. D. *et al. J. Physiol., Lond.* **317,** 18P (1981).
5. Ross, B. D. *et al. New Engl. J. Med.* **304,** 1338–1342 (1981).
6. Morgan-Hughes, J. A., Darveniza, P., Landon, D. N., Land, J. M. & Clark, J. B. *J. neurol. Sci.* **43,** 27–46 (1979).
7. Gadian, D. G. *et al. Lancet* **ii,** 774–775 (1981).

Simulated cross-bridge patterns corresponding to ciliary beating in *Paramecium*

Kazuyuki Sugino & Yutaka Naitoh

Institute of Biological Sciences, University of Tsukuba,
Ibaraki 305, Japan

It is generally accepted that bending of a cilium is caused by active sliding between outer doublets in the cilium produced by ATP-driven activation of their dynein–tubulin cross-bridges[1–3]. Changes with time in the location and extent of the active sliding regions in the outer doublets are thought to be primarily responsible for the changing shape of a beating cilium. However, using conventional techniques of biochemistry and electron microscopy, it is difficult to identify the regions on the outer doublets where active sliding occurs[4]. Here we have used computer simulation of the beating of a cilium to investigate changes in the distribution of activated cross-bridges, and hence of active sliding, in the nine outer doublets. Hereafter, the pattern of this distribution will be termed 'cross-bridge pattern'. Published data have indicated that there is a periodically changing series of cross-bridge patterns in the nine outer doublets. On this assumption, the computer mimicked relatively well the beating of a cilium of *Paramecium* in media of both normal and high viscosity. The computer also simulated flagellar-type beating[5], in which the cross-bridge patterns were modified slightly.

We used a ACOS-800 II (Nippon Electric, Tokyo) computer for simulation[6], and made the following basic assumptions: (1) active sliding occurs between adjacent outer doublets[1]. (2) The *n*th outer doublet drives its adjacent $(n+1)$th outer doublet up towards the tip when activated[7]. (3) In given chemical conditions within the cilium, the sliding velocity between adjacent doublets is constant, independent of the location and extent of the active region in a doublet pair[8,9]. (4) In given chemical conditions the stiffness of the cilium is almost constant[10] and sufficient to maintain overall spatial arrangement of the doublets during beating. (5) Sliding between the doublets is restrained only at the basal region. Therefore, bending of the doublets occurs in the region between the base and the actively sliding region[11]. (6) A

0028–0836/82/070609—03$01.00

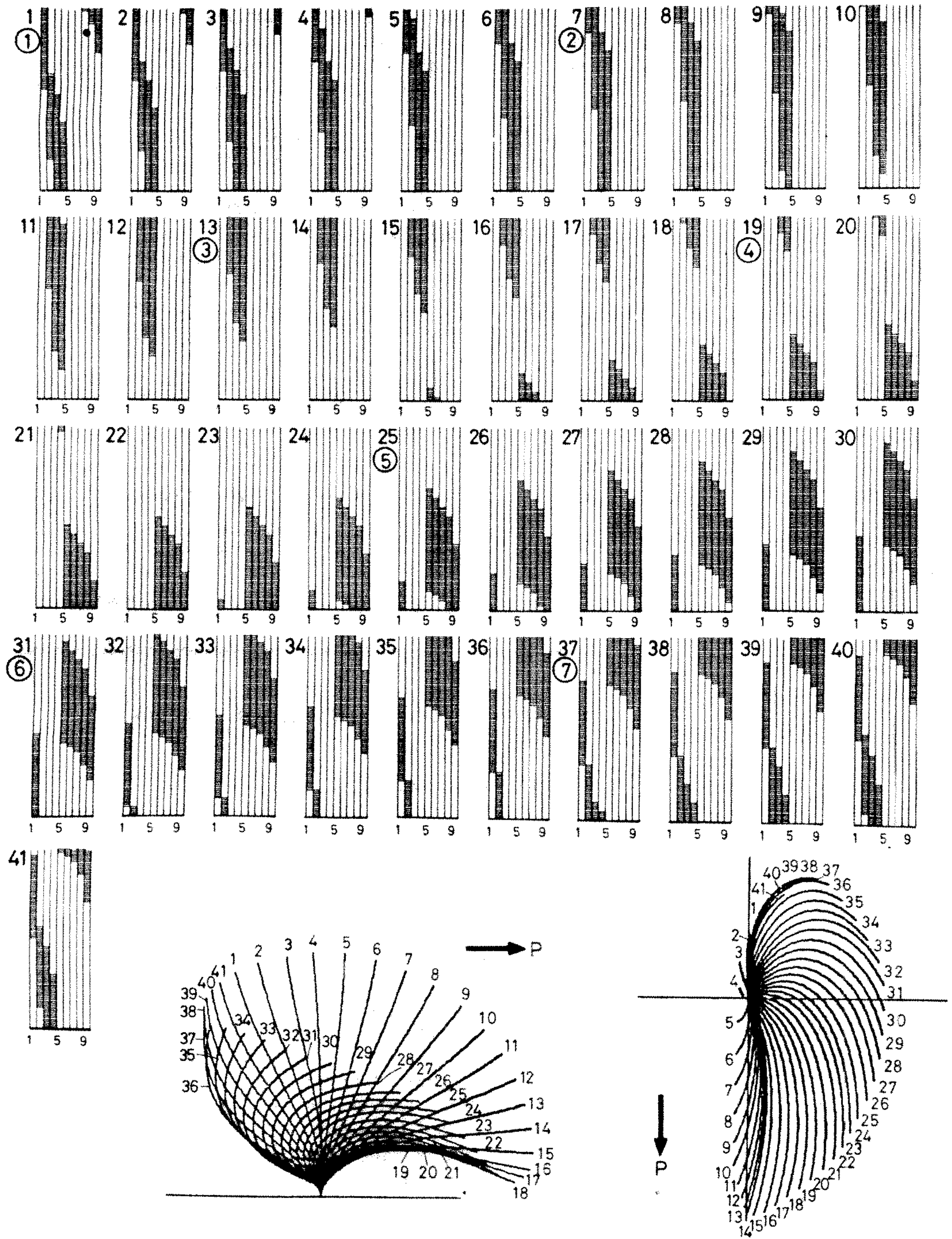

Fig. 1 Upper part, computer-estimated changes with time in the distribution pattern of the actively sliding regions in the nine outer doublets of a cilium (cross-bridge pattern) in *Paramecium* during a single beat cycle. The nine doublets are shown schematically in a plane as ten vertical lines numbered at their bases (1, 5 and 9) according to Bradfield–Afzelius[18,19]. Lines 1 and 10 correspond to doublet no. 1 (note that doublets are arranged sequentially about the circumference of the cilium). Shaded areas between the vertical lines represent the actively sliding regions. (Each small horizontal line does not necessarily indicate activated dynein–tubulin cross-bridges.) Time interval between each successive pattern was kept constant at 1/41 of the period of a single beat cycle. Lower part, computer-simulated change in the shape of a cilium of *Paramecium* during a single beat cycle. Each shape is simulated according to each cross-bridge pattern with the corresponding number in the upper part of the figure. Left, side view; right, top view. Arrows labelled P indecate posterior end of *Paramecium*.

region of active sliding between two doublets is not necessarily straight, and may be bent by forces generated by sliding between another pair of doublets. (7) Bending moment of a cilium appears as a vector sum of bending moments generated by sliding in each pair of doublets. (8) Elastic backforce exerted by a cilium when it is bent is negligible. (9) External viscosity restricts ciliary movement according to Stokes' law, that is, each element on a cilium has a viscous resistance proportional to the length and velocity of the element. (10) Bending moment of a cilium is always balanced by a moment produced by viscous resistance during ciliary beating, which causes a drag on the beating. (11) No twisting of a cilium occurs around its longitudinal axis during bending.

We introduced to the model by trial and error a successively changing cross-bridge pattern together with some degree of viscosity restriction of the cilium, until it mimicked beating of a cilium of *Paramecium*. Thus we finally estimated a periodic change in the cross-bridge pattern corresponding to ciliary beating. Figure 1 shows 41 successive changes in the cross-bridge pattern (upper part) and the corresponding successive changes in the shape of a cilium (lower part) during a single beat cycle. There is striking similarity between the simulated and the actual beating forms shown in Fig. 2. The active sliding is localized in each pair of the doublets (Fig. 1). In a single pair of the doublets, the local activation starts at the basal end, travelling up along the doublets, then disappears at the tip. In the nine pairs of doublets, the activation is transmitted from one pair clockwise to the adjacent pair ($n \rightarrow n+1$). There is an exceptionally long interval between the start of activation in the 4–5 pair (pattern no. 37) and that in the 5–6 pair (pattern no. 15). This indicates that the cyclic activation of the dynein–tubulin cross-bridges originates in the 5–6 pair and terminates at the 4–5 pair. Initiation of activation in the 5–6 pair corresponds to the start of the recovery stroke. Therefore, we propose that in a single beat cycle the recovery stroke precedes the effective stroke, which is consistent with the observation that when cilia of *Paramecium* are inhibited by Ni^{2-} ions and stop, they assume a position which corresponds to the final position of the effective stroke[12–14]. Similarly, a large abfrontal cilium of *Mytilus* gill rests exclusively at the end of the effective stroke[15].

Our simulated patterns are consistent with the proposal of Satir and co-workers[7,16] that activation in the 6–9 doublets

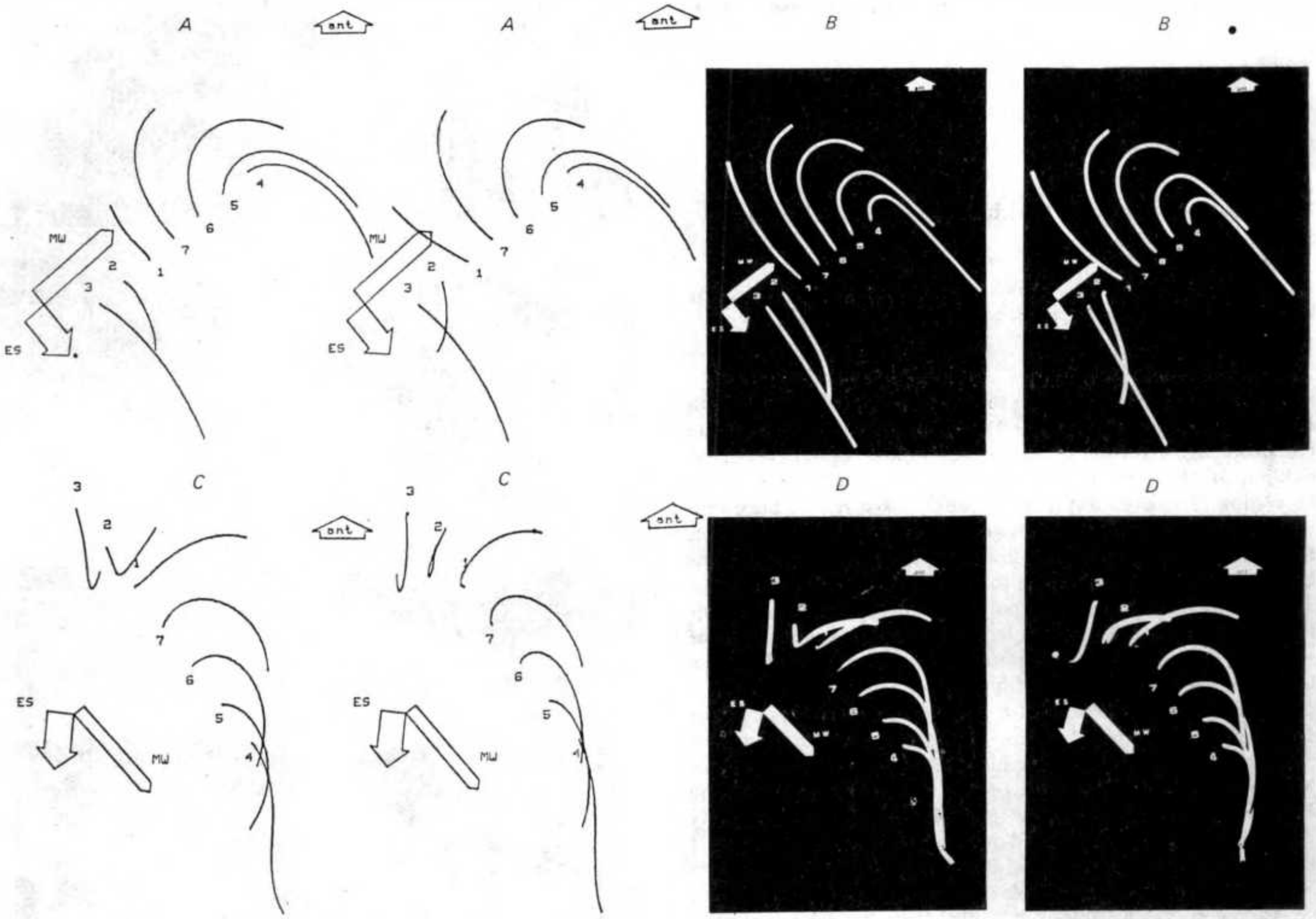

Fig. 2 Stereoscopic displays of seven successive changes in the shape of a cilium from *Paramecium* during a single beat cycle. *A*, *C*, stereoscopic display of computer-simulated beating forms. Each ciliary shape is simulated according to each cross-bridge pattern having corresponding numbers encircled in Fig. 1. Those on the left were viewed from just above, and those on the right were viewed 10° from the right. *B*, *D*, stereophotographs of metal wire models of cilia. Seven pieces of metal wire were shaped and arranged according to Machemer[20,21] based on his photographs of free-swimming *Paramecium*. The computer displays (*A* and *C*) also follow Machemer's arrangement of the wire models. *A*, *B*, beating forms in normal solution; *C*, *D*, beating forms in viscous medium (viscosity 40 times greater than that of normal solution). Arrows labelled 'ant' indicate the anterior end of *Paramecium*. Arrows labelled 'ES' indicate the direction in which the cilium points at the end of effective stroke. Arrows labelled 'MW' indicate the direction of movement of the metachronal wave of cilia. The seven successive ciliary shapes are aligned in the direction of the metachronal wave. Time interval between each successive ciliary shape was kept constant at 1/7 of the period of a single beat cycle.

corresponds to the recovery stroke, that in the 1–4 doublets to the effective stroke. A long time interval is also observed between activation in the 1–2 pair (pattern 23) and that in the 2–3 pair (pattern 32), although it is shorter than the activation time interval between the 4–5 pair and the 5–6 pair. These two time intervals in doublet activation observed in our simulated patterns, one at the start of the effective stroke and the other at the start of the recovery stroke, strongly suggest the presence of two switching mechanisms for the activation in a single beat cycle of a cilium, as suggested by Wais-Steider and Satir[16] based on inhibition experiments on mussel gill cilia by vanadate and calcium.

Note that when viscous restriction 40 times larger than that used for the simulation of the beating in normal medium was introduced into the model, the simulated form was strikingly similar to a cilium of *Paramecium* swimming in a medium of viscosity 40 times greater than that of normal medium (compare Fig. 2*C* with *D*). This strongly supports our idea that computer-estimated cross-bridge patterns closely resemble those of an actual cilium during beating. Computer-assisted estimation of the distribution of the actively sliding regions in a cilium may elucidate the molecular mechanisms underlying ciliary movement.

Parts of this work were presented at the 2nd IBS Symposium on cell motility (held in March 1980 at Okazaki, Japan) and at the 53rd annual meeting of the Zoological Society of Japan (October 1980, Shizuoka, Japan)[17]. The work was supported by the Mitsubishi Foundation and the Ministry of Education of Japan (Y.N.) (grants 144006, 411802, 411808, 510902, 511201). We thank Drs K. Nakayama, Y. Fujiwara, K. Ikeda and their colleagues in the Computer Center at the University of Tsukuba for discussions. We also thank Drs S. Ishizaka and R. Le Brasseur for reading the manuscript and Mrs K. Fujiwara for help with the graphic display.

Received 10 August; accepted 23 December 1981.

1. Satir, P. *J. Cell Biol.* **26,** 805–834 (1965).
2. Satir, P. *J. Cell Biol.* **39,** 77–94 (1968).
3. Summers, K. E. & Gibbons, I. R. *Proc. natn. Acad. Sci. U.S.A.* **68,** 3092–3096 (1971).
4. Omoto, C. K. & Kung, C. *J. Cell Biol.* **87,** 33–46 (1980).
5. Kuznizki, L., Jahn, T. L. & Fonseca, J. R. *J. Protozool.* **17,** 16–24 (1970).
6. Ikeda, K., Nishihara, S., Isohama, K. & Nakayama, K. *J. Inf. Processing* **2,** 231 (1980).
7. Sale, W. S. & Satir, P. *Proc. natn. Acad. Sci. U.S.A.* **74,** 2045–2049 (1977).
8. Yano, Y. & Miki-Noumura, T. *J. Cell Sci.* **44,** 169–186 (1980).
9. Kamimura, S. & Takahashi, K. *Zool. Mag, Tokyo* **88,** 513 (1979).
10. Lindemann, C. B., Rudd, W. G. & Rikmenspoel, R. *Biophys. J.* **13,** 437–448 (1973).
11. Shingyoji, C., Murakami, A. & Takahashi, K. *Nature* **265,** 269–270 (1977).
12. Kuznicki, L. *Acta protozool.* **1,** 301–312 (1963).
13. Naitoh, Y. *Science* **154,** 660–662 (1966).
14. Eckert, R. & Naitoh, Y. *J. gen. Physiol.* **55,** 467–483 (1970).
15. Gray, J. *Ciliary Movement* (Cambridge University Press, 1928).
16. Wais-Steider, J. & Satir, P. *J. supramolec. Struct.* **11,** 339–347 (1979).
17. Sugino, K. & Naitoh, Y. *Zool Mag, Tokyo* **89,** 444 (1980).
18. Bradfield, J. R. G. *Symp. Soc. exp. Biol.* **9,** 306–334 (1955).
19. Afzelius, B. *J. biophys. biochem. Cytol.* **5,** 269–281 (1959).
20. Machemer, H. *Acta protozool.* **11,** 295–300 (1970).
21. Machemer, H. *J. exp. Biol.* **57,** 239–259 (1972).

Release of spectrin-free spicules on reoxygenation of sickled erythrocytes

David Allan, Anthony R. Limbrick*, Paul Thomas & Maxwell P. Westerman†

Department of Experimental Pathology, University College London, School of Medicine, University Street, London WC1E 6JJ, UK

It has long been suspected that the erythrocytes of patients with sickle cell disease gradually shed part of their plasma membrane either through a normal ageing process or as a result of repeated sickling, and that this membrane loss may be associated with the formation of irreversibly sickled cells[1–3]. We report here that when sickled HbS erythrocytes are unsickled by reoxygenation, the cells lose ~2–3% of their lipid as spectrin-free haeomoglobin-containing spicules in the form of rods and microspheres. The rods, which still contain polymerized haemoglobin, eventually degrade to chains of microvesicles having diameters of ~0.1 μm. Similar spicular material has been found in the untreated blood of patients with sickle cell disease.

Blood from patients with homozygous sickle cell disease was collected in heparinized tubes; red cells were sedimented at 2,000 r.p.m. for 5 min and the plasma was retained. Cells were washed four times with 10 vol of 0.15 M NaCl containing 10 mM HEPES–NaOH buffer *p*H 7.4, with removal of buffy coat. They were resuspended in the same medium to 10% haematocrit and deoxygenated by incubation at 37 °C under a N_2 atmosphere for 1 h. In these conditions, at least 90% of the cells showed the characteristic sickled form, with long spicules protruding from the cell surfaces (Fig. 1*a*). Cells were sedimented at 1,500 r.p.m. for 5 min and after removal of the supernatant, they were resuspended in the same volume of the original medium. Reoxygenation and restoration of the original diskoid shape of the cells (see Fig. 1*d*) was achieved by exposure to air for 30 min at 37 °C, then the cells were again sedimented at 1,500 r.p.m. for 5 min. The resulting opalescent supernatant was centrifuged at 16,000 r.p.m. for 10 min, giving a small red pellet, sometimes overlain by a filmy deposit of ghosts which was removed during aspiration of the supernatant. Cell lysis after reoxygenation was <1%. The red pellet was resuspended in 8 ml HEPES-buffered saline, centrifuged at 1,500 r.p.m. for 5 min to remove any contaminating cells, then sedimented again at 16,000 r.p.m. for 10 min. The final red pellet was resuspended in 0.5 ml HEPES-buffered saline and samples were taken for electron microscopy and polyacrylamide gel electrophoresis and for determination of lipid and haemoglobin.

Light and electron microscopy revealed that this material consisted largely of rod-like elements similar in size (up to 15 μm long) and shape to the spicules seen protruding from the original deoxygenated cells. The material released probably corresponded to the distal portions of the spicules on the original N_2-treated cells, as subsequent exposure of the reoxygenated cells to N_2 yielded cells with less extreme spiculation (Fig. 1*b*). However, in addition to the rod-like elements in the high-speed pellet, there were many spherical bodies of ~0.5 μm diameter. Some of this fraction evidently sedimented at lower speed than the rod-like spicules as it was present together with intact cells in a low-speed fraction derived from the original high-speed pellet (Fig. 1*d*). In some cases, it appeared that these small spherical components were still being released from the reoxygenated cells (arrows, Fig. 1*d*).

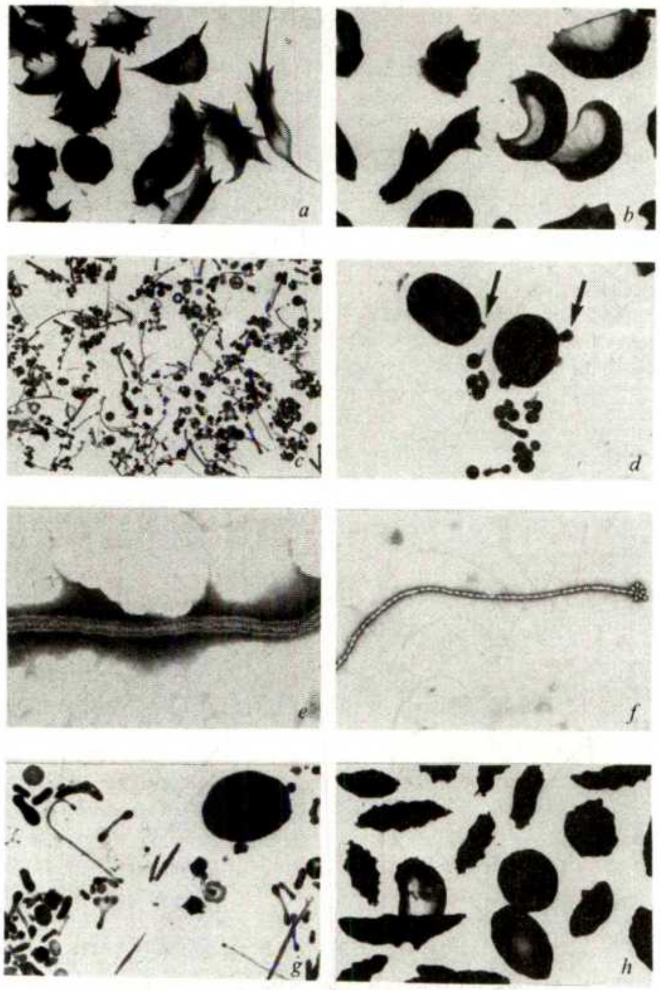

Fig. 1 Electron micrographs of sickle red cells and free spicules. *a*, Sickle cells incubated under N_2 for 1 h (×1,200). *b*, Sickle cells subjected to three doxygenation–oxygenation cycles, then reincubated under N_2 for 1 h (×1,200). *c*, Free spicules isolated after reoxygenation of deoxygenated sickle cells (purified fraction remaining after removal of fraction shown in *d*) (×1,200). *d*, Low-speed (1,500 r.p.m.) sediment from crude spicule fraction (×1,200). *e*, Rod-like spicule (×16,000). *f*, Free spicule after incubation of sample *c* at 20 °C for 2 h (×5,000). *g*, Free spicules isolated from plasma of patient P.R. with sickle cell disease. Fresh plasma was centrifuged at 16,000 r.p.m. for 10 min. The pellet was resuspended, decanted from clumped platelets and centrifuged again at 16,000*g* to give a small red pellet (×1,200). *h*, Red cells of patient R.E. with a high level (50%) of irreversibly sickled cells (×1,200). Specimens were fixed in 2% glutaraldehyde in 0.1 M cacodylate buffer *p*H 7.4 for 1 h then washed in buffer several times. For negative staining, a drop of the suspension of fixed specimen was placed on a carbon-coated copper grid and after 2 min, excess buffer was removed with filter paper. Samples were then stained for 2 min with 1% phosphotungstate, *p*H 7.0. Excess stain was removed with filter paper and the preparation was air-dried. All specimens were examined using a JEOL 100CX microscope.

The rod-like forms appeared under the light microscope to be rigid structures, suggesting that the sickle haemoglobin present within the rods was still in a polymerized form even after oxygenation. This interpretation was confirmed by electron microscopy of negatively-stained specimens which often showed an internal structure resembling a helical continuous filament ~30 nm thick and of ~120 nm pitch (Fig. 1*e*). These dimensions are consistent with those observed previously for the helical polymer of pure haemoglobin S[4]. After several hours at room temperature, it was apparent that the rod-like spicules became 'floppy' and tended to break down into chains of tiny vesicles with diameters of ~0.1 μm (Fig. 1*f*). There was then no visible

---

* Department of Biophysics, University College London, Gower Street, London WC1E 6BT, UK.

† Permanent address: Department of Medicine, Mount Sinai Hospital Medical Center, 15th St. & California Avenue, Chicago, Illinois 60608, USA.

0028-0836/82/070612—02$01.00

evidence of internal structure, suggesting that the haemoglobin had finally depolymerized, perhaps thus allowing membrane fusion to occur along the length of the rods.

When cells were subjected to several cycles of deoxygenation–oxygenation, ~2–3% of the total cell phospholipid and 0.2–0.3% of the total haemoglobin were released as free spicules (Table 1). Incubation under N_2 alone released negligible amounts of material and 80–90% of the release occurred after the first reoxygenation. Neither N_2 treatment nor reoxygenation produced a significant change in cell volume. No measurable release was observed from normal (HbA) erythrocytes which were treated similarly. Release of free spicules from sickle erythrocytes was unaffected by incubation in medium to which was added either 10 mM glucose, 5 mM iodoacetamide and 1 mM deoxyglucose (which reduced intracellular ATP to <10% of normal), 1 mM Ca^{2+} or 1 mM EGTA, or by substitution of autologous plasma for the normal HEPES-buffered saline medium. Incubation in the presence of protease inhibitors (diisopropylfluorophosphate, TLCK) did not alter the production of free spicules.

Figure 2 and Table 1 demonstrate that the composition of the released material resembles that of microvesicles released from normal cells aged *in vitro*[5,6] or treated with Ca^{2+} ionophore[7–9], and from sickle cells incubated *in vitro* with Ca^{2+} or EGTA.[3] No reproducible differences in lipid composition were observed between the free spicules and the cells themselves.

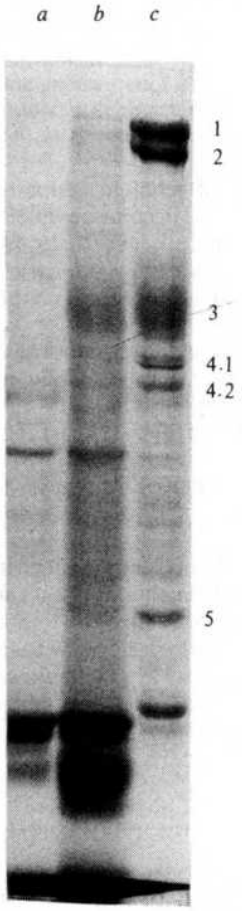

Fig. 2 Polyacrylamide gel electrophoresis of cell fractions. Cytosol (*a*) and membranes (*c*) from sickle cells were prepared as described previously[3]. Free spicular material (*b*) was prepared as described in the text. Samples containing ~20 nmol phospholipid (membranes and spicules) or 500 μg protein (cytosolic fraction) were analysed by polyacrylamide gel electrophoresis on 7.5% gels[15]. Gels were stained with Coomassie blue. Bands are numbered according to the nomenclature of Steck[16].

Table 1 Composition of sickle cells and of free spicules •

	Cells	Free spicules produced by reoxygenation or anerobic cells	Free spicules from plasma (determinations on two patients)
Phospholipid (nmol per mg haemoglobin)	19±1 (10)	233±43 (12)	179, 210
Cholesterol (mol per mol phospholipid	0.70±0.06 (29)	0.53±0.14 (17)	0.51, 057
Acetylcholinesterase activity (μmol min^{-1} per μmol phospholipid)	4.3±1.0 (20)	3.6±1.2 (6)	3.0, 2.5

The mean yield of free spicules produced *in vitro* was 2.3±0.4% (5) of the total red cell lipid. The yield of spicules *in vivo* (plasma) was 0.5±0.2% (3) of total red cell lipid in a given volume of blood. Results are derived from studies of 12 patients and are expressed as mean±s.d. Number of determinations is shown in parentheses. Assays were carried out as in ref. 9.

The most striking feature of the free spicules was their almost complete lack of the membrane cytoskeletal polypeptides spectrin (bands 1, 2), ankyrin (band 2.1), band 4.1 and actin (band 5). This implies that the spicules observed on the cells before reoxygenation similarly lacked these cytoskeletal proteins and that the spicules were produced by polymerization of HbS through gaps in the actin–spectrin framework, causing a herniation of the lipid bilayer part of the membrane only. Release of the rod-like spicules following reoxygenation may depend on the failure of HbS in the spicules to depolymerize (perhaps because of its close association with membrane[10,11]) in conditions where HbS in the cell body does depolymerize, allowing membrane fusion to occur only around the 'necks' of the spicules.

Loss of spicules from sickle cells may also occur during the deoxygenation–oxygenation cycling which occurs naturally *in vivo*, as spicular material similar to that prepared *in vitro* has been found in the untreated plasma of sickle cell patients (Fig. 1*g*) but is completely absent from the blood of normal individuals. The composition of this material resembled that of the free spicules *in vitro* (Table 1) and the yield was equivalent to ~0.5% of the total red cell lipid in a given volume of blood.

The clinical significance and eventual fate of the *in vivo* spicules is unknown, but it seems possible that these particles, particularly those with rigid rod-like structures, might contribute to the vaso-occlusive events associated with sickle cell disease[12]. Loss of spicular material from sickle cells *in vivo* may also contribute to the production of irreversibly sickled cells, which appear to have reduced membrane content[13] and show much less surface spiculation than do reversibly sickled cells[14] (Fig. 1*h*). Preliminary data suggest that patients with higher levels of irreversibly sickled cells also have more free spicules in their plasma.

M.P.W. was the recipient of a Research Travel Grant from the Burroughs Wellcome Fund. We thank Professors E. J. Huehns and J. M. White for providing samples of blood from their patients. We also thank the MRC for supporting this work.

Received 25 November 1981; accepted 11 January 1982.

1. Bessis, M. D., Bricka, E. E., Breton-Gorius, J. & Tabius, J. *Blood* **9,** 39–45 (1954).
2. Padilla, F., Bromberg, P. A. & Jensen, W. N. *Blood* **41,** 653–660 (1973).
3. Allan, D., Limbrick, A. R., Thomas, P. & Westerman, M. P. *Br. J. Haemat.* **47,** 383–390 (1981).
4. Maugh, T. H. *Science* **211,** 265–267 (1981).
5. Rumsby, R. H., Trotter, J., Allan, D. & Michell, R. H. *Biochem. Soc. Trans.* **5,** 126–127 (1977).
6. Lutz, H. V. *J. supramolec. Struct.* **8,** 375–389 (1978).
7. Allan, D., Billah, M. M., Finean, J. B. & Michell, R. H. *Nature* **261,** 58–60 (1976).
8. Shukla, S. D., Berriman, J., Coleman, R., Finean, J. B. & Michell, R. H. *FEBS Lett.* **90,** 289–291 (1978).
9. Allan, D., Thomas, P. & Limbrick, A. R. *Biochem. J.* **188,** 881–887 (1980).
10. Lessin, L. S., Kurantsin-Mills, J., Wallas, C. & Weems, H. *J. supramolec. Struct.* **9,** 537–554 (1978).
11. Shaklai, N., Sharma, V. S. & Ranney, H. M. *Proc. natn. Acad. Sci. U.S.A.* **78,** 65–68 (1981).
12. Chui, D., Lubin, B., Roelofsen, B. & van Deenen, L. L. M. *Blood* **58,** 398–401 (1981).
13. Westerman, M. P., Diloy-Puray, M. & Streczyn, M. *Biochim. biophys. Acta* **557**, 149–155 (1979).
14. Bertles, J. F. & Döbler, J. *Blood* **33,** 884–898 (1969).
15. Laemmli, U. K. *Nature* **277,** 680–685 (1970).
16. Steck, T. L. *J. Cell Biol.* **62,** 1–19 (1974).

A non-collagenous glycoprotein from elastic tissue acts as substratum for growth of cells *in vitro*

P. Knox*, P. Wells† & A. Serafini-Fracassini‡

* Department of Biochemistry, St. George's Hospital Medical School, Cranmer Terrace, London SW17 0RE, UK
† Department of Dental Biochemistry, Royal Dental Hospital of London School of Dental Surgery, St. George's Hospital Medical School, Cranmer Terrace, London SW17 0RE, UK
‡ Department of Microbiology and Biochemistry, University of St Andrews, St Andrews, Fife, UK

***In vivo*, cells are in intimate contact with an extracellular matrix, one of the components of which is collagen; the adhesion of cells to collagen *in vitro* has been extensively studied (for review, see ref. 1). In several connective tissue matrices, collagen fibres are replaced to a variable extent by elastin fibres which, under the electron microscope, appear to be composed of an elastin core surrounded by a network of fibrils ~11 nm in diameter, usually referred to as the microfibrillin component. These fibrils have been implicated, on morphological grounds, in the biosynthesis of elastin fibres. A glycoprotein referred to as structural glycoprotein (SGP)[2], which has a molecular weight (*M_r*) of 34,000 and aggregates to form cylindrical tactoids having a uniform diameter of 11 nm, has been isolated from bovine ligamentum nuchae[3]. SGP was found to have amine oxidase activity, thus it seems to be functionally related to other peptidylysine oxidases involved in the biosynthesis of the elastin cross-links[4–6]. Here we show that SGP acts as a substratum for fibroblasts and other cell types with fibronectin mediating the attachment and spreading of the cells. These results suggest that SGP may have a role in wound healing, morphogenetic movement and development of elastic tissues.**

SGP was isolated from ligamentum nuchae as described elsewhere[2]. Briefly, the microfibrils found in elastic tissue were dissociated by treatment with 5 M guanidine HCl containing a disulphide bond reducing agent[3], and purified by preparative gel electrophoresis[2]. In the absence of chaotropic and reducing agents, and in the presence of Cu^{2+} ions, the purified SGP aggregates as described previously[2]. We have used this property to prepare SGP aggregates for assays of cell adhesion and growth *in vitro*. This was achieved by forming discrete areas of aggregated SGP by precipitation on to bacteriological grade Petri dishes. The dishes are made of untreated polystyrene with negligible surface charge and as already described[7] have only a limited capacity to support cell adhesion. Using a single Petri dish it is therefore possible to compare cell attachment, spreading and proliferation of cells on an SGP substratum with that on areas of untreated polystyrene.

When an established cell line BHK 21 was subcultured on to these Petri dishes, the cells attached and spread rapidly on the SGP. In contrast, there was little attachment to the untreated polystyrene, and after 6 h no spreading had occurred. Figure 1 shows the kinetics of attachment and spreading. Cells on the SGP areas proliferate and become completely confluent. On the untreated areas, some cells eventually assume a fibroblastic morphology, but most cells grow as loose clumps[7]. After 2 days, little or no proliferation had occurred on the untreated surfaces.

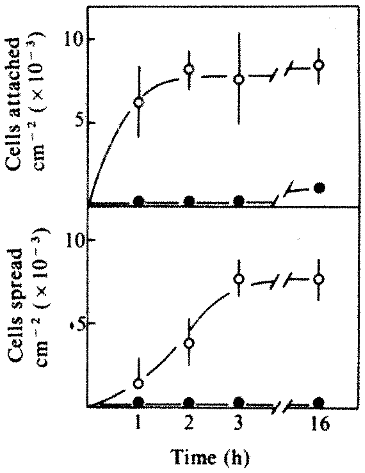

Fig. 1 Attachment and spreading of cells on SGP. Petri dishes containing SGP spots were prepared as follows: purified SGP was dissolved under nitrogen in 8 M urea containing 3% mercaptoethanol. Several 6-µl droplets of this solution were placed on bacteriological grade Petri dishes (three or four spots per dish) to which were immediately added 6-µl drops of copper sulphate solution providing a 400 M excess of Cu^{2+} ions. The Petri dishes were dried over P_2O_5 *in vacuo* for 24 h, then washed exhaustively with distilled water and finally dried. Confluent cultures of BHK 21 cells (Flow) were trypsinized (0.05% trypsin/0.02% EDTA; Flow) and resuspended at a density of 5×10^4 ml^{-1} in Ham's F10 medium supplemented with 7.5% newborn calf serum (Flow). Cell suspension (10 ml) was poured into each Petri dish containing SGP spots and then incubated at 37 °C in a humidified 5% CO_2 atmosphere. At intervals the dishes were examined using an inverted microscope. The numbers of attached and/or spread cells were counted for six random areas of SGP substrata (○) and control polystyrene substrata (●). The criteria for spreading are that a cell exhibits polarity and the nucleus and nucleoli are clearly visible. Results are expressed as the mean ± s.d. for the six areas.

We have tested other proteins for activity as substrata. Albumin, fibrinogen, γ-globulin and ovalbumin do not support attachment when they are either dried on to bacteriological polystyrene or precipitated with Cu^{2+} or Cu^{2+} plus mercaptoethanol. The only proteins, apart from SGP, that are completely effective as substrata are collagen or fibrin. Fibronectin is only partially effective on bacteriological polystyrene; possibly the low surface charge does not allow suitable binding of the glycoprotein.

The technique used for coating bacteriological plastic with SGP is only suitable for smaller areas; it cannot be used to coat whole Petri dishes. To determine the total number of cells able to attach to SGP, bacteriological plastic coated with SGP was cut into circles that would just fit into multiwell plates, and these

Table 1 Fibronectin mediates cell attachment and spreading on SGP

	Cells attached per cm^2 $\times 10^{-3}$				Cells spread per per cm^2 $\times 10^{-3}$			
	Native polystyrene	Tissue culture plastic	Collagen	SGP	Native polystyrene	Tissue culture plastic	Collagen	SGP
No protein	0	9.8 ± 0.1	3.2 ± 1.7	2.0 ± 0.7	0	0	0	0
Newborn calf serum (1%)	0	9.5 ± 1.6	8.6 ± 1.9	9.3 ± 2.1	0	9.3 ± 2.2	8.1 ± 0.9	8.9 ± 2.7
Fibronectin (25 µg ml^{-1})	0.6 ± 0.4	10.0 ± 1.2	9.4 ± 2.4	9.6 ± 1.8	0	9.8 ± 1.1	8.9 ± 0.9	9.6 ± 1.6

Fibronectin was prepared from fresh human plasma as described elsewhere[14], but using chaotropic elution buffers[15]. BHK cells were suspended as described in Fig. 1 legend in Ham's F10 medium containing 1% newborn calf serum or 25 µg ml^{-1} fibronectin, or no protein supplement. Cell suspensions were poured into bacteriological grade Petri dishes containing SGP spots and incubated at 37 °C for 4 h. At this time cell attachment and spreading on SGP was assessed as described in Fig. 1 legend.

0028-0836/82/070614—02$01.00

were secured in place with Araldite. BHK cell suspensions were poured into the multiwells and it was found that >96% of cells were able to adhere to the SGP.

Primary cultures derived from chick embryo also proliferate on SGP; Fig. 2*a* shows a Petri dish fixed and stained at 72 h. The SGP spots were clearly visible because of the high cell density in these areas. The spots have discrete edges and cells appear to remain on the SGP rather than migrate on to areas of untreated polystyrene. Harris[8] has previously shown that cells will preferentially migrate on to areas of suitable charge density. Figure 2*b* shows cells at the edge of an SGP spot.

We have repeated these experiments and found that various cell types including 3T3 and a virally transformed derivative, a human osteosarcoma cell line, human skin fibroblasts and primary cultures derived from neonatal rat all attach to and proliferate on SGP, but not on untreated polystyrene. Compared with established cell lines, primary cell cultures display a more fastidious requirement for a suitable substratum. Thus some epithelial cells show a specific requirement for collagen type IV[1]. Similarly, myogenic cultures will only differentiate on layers of collagen (or gelatin)[9]; in this case the collagen seems to aid alignment of myoblasts before their fusion to form multinucleate myotubes. We derived cell suspensions from embryonic chicken muscle and plated these on to Petri dishes containing discrete spots of SGP. When the cultures were fixed and stained 4 days later, cells were found only on the SGP spots. Multinucleate myotubes were present but were located only on the upper surfaces of other cells, presumably fibroblasts. The morphology of these cultures is in marked contrast to control cultures grown on collagen, where myotubes were found in the monolayer. Cultures grown on tissue culture plastic showed few myotubes and all cells were present as a monolayer. Myogenic cultures consist predominantly of fibroblasts and myoblasts. The above results indicate that fibroblasts adhere to SGP but myoblasts cannot. However, fibroblasts synthesize collagen and it is to this substrate that the myoblasts adhere and on which they subsequently differentiate. This explains why the cultures were bilayers rather than monolayers, and why the myotubes were found almost exclusively in the upper layer. In contrast to these cultures on SGP, both myoblasts and fibroblasts adhere to collagen or to tissue culture plastic, and hence in both cases only monolayer cultures result.

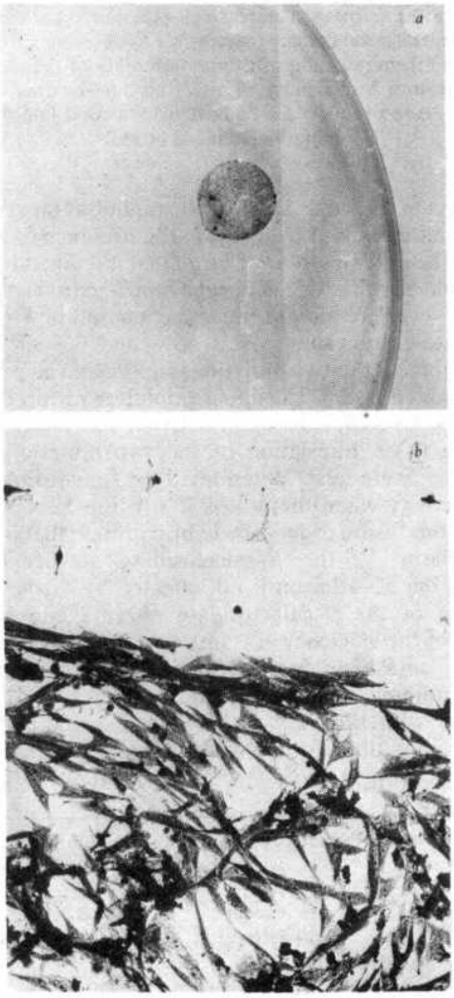

Fig. 2 Primary cultures on SGP substrata. Cell suspensions were derived from chick embryos as described elsewhere[16], and suspended at a density of 10^5 cells ml^{-1} in Ham's F10 medium containing 10% fetal calf serum (Flow). Cells were plated in bacteriological grade Petri dishes containing SGP spots and incubated at 37 °C in a humidified 5% CO_2 atmosphere. Cultures were refed after 24 h, then incubated for a further 48 h. Dishes were then rinsed with phosphate-buffered saline, fixed with 3% glutaraldehyde and stained with 1% filtered Giemsa. *a*, SGP spots are clearly visible because of the density of cells staining with Giemsa. *b*, Photomicrograph showing cells forming a discrete boundary at the edge of a SGP spot. ×70.

Cells require specific proteins for their attachment to a substratum. We have investigated the requirement for adhesion to SGP using fibronectin prepared from human plasma. Table 1 shows the attachment and spreading of cells in the presence and absence of fibronectin on SGP, collagen and tissue culture or bacteriological grade plastic. It is clear that fibronectin is able to mediate spreading on SGP surfaces, the concentration of fibronectin necessary to promote maximal attachment to SGP or to collagen being $<1\ \mu g\ ml^{-1}$. However, to achieve maximal spreading, according to our criteria, the concentration has to be $>5\ \mu g\ ml^{-1}$.

We have demonstrated that the microfibrillary glycoprotein referred to as SGP acts as a solid substratum *in vitro* and supports the attachment, spreading and growth of various cell types. Certain synthetic agents including tissue culture plastic, glass[10] and resins[11] also have this property. However, SGP is a physiological glycoprotein and it is therefore possible that, like collagen, and to a lesser extent fibrin, there is a physiological role for this adhesive property. We, and others[12] have shown that other proteins do not act as suitable substrata for cell adhesion and growth. The adhesion of cells to SGP is clearly analogous to that of the attachment of cells to collagen[1], and indeed to fibrin[13]. In all these cases fibronectin appears to mediate at least part of the adhesive process. (This in contrast to the attachment of epithelial cells to collagen type IV which is mediated by laminin[1].)

Microfibrillary SGP is particularly abundant during fetal development[14], thus it is possible that SGP may, by providing a pathway for morphogenetic movement, play a part in the genesis of vascular and other tissues requiring an elastic stroma. During wound repair of vascular tissue, SGP may also have a role in directing the movement of endothelial fibroblasts.

It has been suggested that SGP plays a part in the elaboration of elastin and we are now investigating the possibility that the adhesion of certain fibroblasts to SGP in some way acts as a signal for elastin synthesis.

We thank Mrs Salma Siddiqui and Miss Sheila Griffiths for technical assistance.

Received 13 November; accepted 18 December 1981.

1. Kleinman, H. K., Klebe, R. J. & Martin, G. R. *J. Cell Biol.* **88,** 473–485, (1981).
2. Serafini-Fracassini, A. *et al. Biochemistry* **20,** 5424–5429 (1981).
3. Ross, R. & Bornstein, P. *J. Cell Biol.* **40,** 366–381 (1969).
4. Siegel, R. C. *Int. Rev. Connective Tissue Res.* **8,** 73–118 (1979).
5. Jordan, R. E., Milbury, P., Sullivan, K. A., Trackman, P. C. & Kagan, H. M. *Adv. exp. Med. Biol.* **73,** 531–542 (1977).
6. Kagan, H. M., Hewitt, N. A., Salcedo, L. L. & Franzblau, C. *Biochem. J.* **177,** 203–214 (1979).
7. Martin, G. R. & Rubin, H. *Expl Cell Res.* **20,** 319–333 (1960).
8. Harris, A. *Expl Cell Res.* **77,** 285–297 (1973).
9. Hauschka, S. D. & Konigsberg, I. R. *Proc. natn. Acad. Sci. U.S.A.* **55,** 119–126 (1966).
10. Rappaport, C., Poole, J. P. & Rappaport, H. P. *Expl Cell Res.* **20,** 465–510 (1960).
11. Grinnell, F., Tobleman, M. Q. & Hackenbroch, C. R. *J. Cell Biol.* **70,** 707–713 (1976).
12. Taylor, A. C. *Expl Cell Res.* Suppl. **8,** 154–173 (1961).
13. Grinnell, F., Feld, M. & Minter, D. *Cell* **19,** 517–525 (1980).
14. Ruoslahti, E. & Engvall, E. *Biochim. biophys. Acta* **631,** 350–358 (1980).
15. Klebe, R. J., Bentley, K. L., Sasser, P. J. & Schoen, R. C. *Expl Cell Res.* **130,** 111–117 (1980).
16. Knox, P. & Wells, P. *J. Cell Sci.* **40,** 77–88 (1979).

A role for mRNA secondary structure in the control of translation initiation

Michael N. Hall*, Joëlle Gabay, Michel Débarbouillé & Maxime Schwartz

Unité de Génétique Moléculaire, Institut Pasteur, 25 rue du Dr Roux, 75724 Paris Cedex 15, France

A role for messenger RNA (mRNA) secondary structure in the control of translation initiation has been assumed for many years[1-3]. Strong additional evidence supporting this notion is now provided by work on the *lamB* gene of *Escherichia coli*, which codes for a major outer membrane protein that functions both as a receptor for phages λ, K-10 and TP1, and as a component of the maltose and maltodextrin transport system[4-9]. Mutations that affect translation initiation of the *lamB* mRNA have been described previously[10]. DNA sequence analysis indicated that one such mutation, *lamB* 701, is located two nucleotides promoter-proximal to the *lamB* Shine–Dalgarno sequence. A second mutation, *lamB* 708, is located in the sixth codon of the *lamB* gene (see Fig. 1). Schwartz *et al.*[10] suggested that these two point mutations affect translation initiation by favouring the formation of a base-paired hairpin structure in the *lamB* transcript which makes the Shine–Dalgarno sequence[11] inaccessible to ribosomes (see Fig. 2). This suggestion was genetically testable because it predicted that the translation initiation defect caused by either of the two mutations alone would be suppressed in a *lamB* 701–708 double mutant (see Fig. 2). Here we demonstrate that the 701 and 708 mutations do indeed suppress each other, as predicted by an effect attributable to mRNA secondary structure.

The 701–708 double mutant was constructed *in vivo* by homologous recombination within the 26 base pairs (bp) that separate the two mutations. The strategy used in this construction, described in Fig. 3 legend, involved three steps. First, a λ transducing phage carrying the *lamB–lacZ* hybrid gene 52–4 (refs 12, 13) containing the 701 mutation (Fig. 3*a*) was constructed. This phage was then used to lysogenize a strain containing the 708 mutation such that the integrative recombination event occurred between the sites of the two mutations. The last step consisted of curing the prophage, the cured strain containing both 701 and 708 *cis* to an otherwise wild-type *lamB* gene. The eventual double mutation construct (Fig. 3*c*) was verified by DNA sequence analysis using the Maxam–Gilbert method[14,15].

The effects of 701 and 708, individually and in combination, were measured by two independent methods (Table 1). One consisted of assaying λ receptor protein present in the outer membrane of the single and double mutants. The second method exploited the availability of *lamB–lacZ* hybrid genes to measure translational activity initiated at the *lamB* initiation codon.

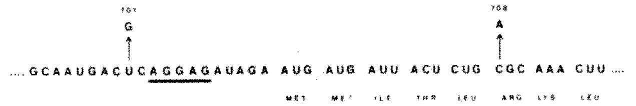
701
G
708
A
....GCAAUGACUCAGGAGAUAGA AUG AUG AUU ACU CUG CGC AAA CUU....
MET MET ILE THR LEU ARG LYS LEU

Fig. 1 The *lamB* mRNA Shine–Dalgarno and surrounding sequences. The Shine–Dalgarno sequence is underlined. The nucleotide changes resulting from the 701 and 708 mutations are indicated. The 708 mutation causes an arginine to serine change in the sixth codon of the *lamB* gene. The *lamB* gene is the promoter-distal gene of the maltose-inducible *malK–lamB* operon.

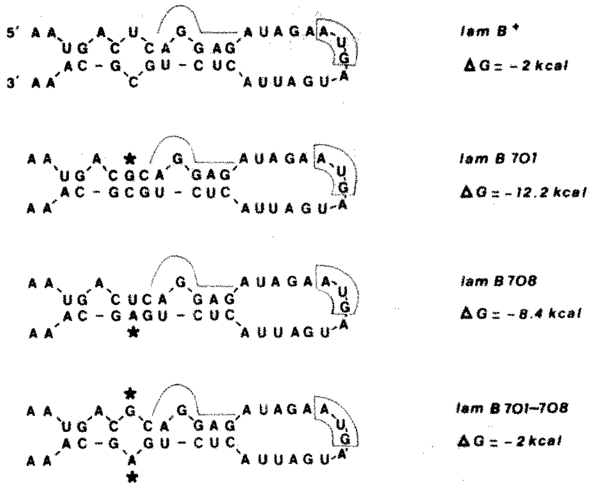

Fig. 2 Possible hairpin structure and corresponding thermodynamic stabilities of *lamB* mRNA containing a wild-type sequence, the 701 mutation, the 708 mutation or the 701–708 double mutation. The thermodynamic stabilities are calculated according to Tinoco *et al.*[26], and are expressed as the free energy (ΔG) of the structure. The two single mutations thermodynamically favour the hairpin structure which would be assumed to render the Shine–Dalgarno domain inaccessible to ribosomes. The double mutation regenerates the wild-type instability of the hairpin and should restore accessibility of the ribosome-binding site. The Shine-Dalgarno sequence is indicated by a solid line; the *lamB* initiation codon is boxed.

The effect of the single and double mutations on gene expression was first measured by assaying the presence of λ receptor activity in the outer membrane of cells containing the mutations of interest in an otherwise wild-type *lamB* gene. The mutations individually were found to reduce the amount of λ receptor to approximately equivalent levels—5% and 8% of wild type. When combined, the two mutations suppressed each other, but only to a limited extent. The double mutation restored only 25% of wild-type levels of λ receptor activity.

The effects on translation of the two mutations and the combination were also determined by measuring β-galactosidase activity when these were *cis* to the 52-4 *lamB–lacZ* fusion. As this fusion codes for a hybrid protein that is located in the cytoplasm[12,13], the β-galactosidase activity of strains containing the 52-4 fusion is not affected by extracytoplasmic localization of the β-galactosidase enzyme and is a direct indication of the efficiency of translation initiating at the beginning of the *lamB* gene. In the case of 701 and 708 individually, strains containing either one of the two mutant alleles were lysogenized with the 52-4 fusion phage containing the corresponding mutation. For the wild-type control, a *lamB*$^+$ strain was lysogenized with a wild-type 52-4 fusion phage. In the case

Table 1 Effect of mutations 701 and 708, individually and combined, on *lamB* expression.

	% λ receptor activity	% β-galactosidase activity
lamB$^+$	100	100
lamB 701	8	4
lamB 708	5	28
lamB 701–708	25	81

Values are expressed as per cent of wild type. The λ receptor value indicates the effect of mutation in an otherwise wild-type *lamB* gene; β-galactosidase value indicates effect of mutation when *cis* to a *lamB–lacZ* hybrid gene. The λ receptor activity was assayed as described previously[4,24] with the following modifications. Outer membranes were solubilized in 10 mM Tris-HCl *p*H 7.5, 5 mM EDTA, 3% Triton X-100 and incubated for 1 h at 37 °C. Phage λ inactivating ability was then assayed directly, and β-galactosidase activity was assayed as described elsewhere[25].

---

* Present address: Department of Biochemistry and Biophysics, University of California, San Francisco, California 94143, USA.

0028–0836/82/070616—03$01.00

of the double mutation, an appropriate strain was constructed (Fig. 4). In contrast to the results obtained by measuring λ receptor activity, showing a similar effect of 701 and 708 individually and a low level of suppression in the double mutant, β-galactosidase assays indicated that the effects of 701 and 708 individually are quantitatively different, 708 being significantly more leaky than 701. Essentially full suppression is observed in the 701–708 double mutant.

These results indicate three facts. (1) The 701 and 708 mutations do indeed suppress each other, suggesting that their effect is attributable to mRNA secondary structure (see Fig. 2). (2) The relative effects of the two mutations on translation initiation can be correlated with their effect on the thermodynamic stability of the predicted mRNA secondary structure. (3) The phenotype of a strain containing the 708 mutation in an otherwise wild-type *lamB* gene is a superimposition of defects in both translation initiation of the *lamB* message and localization of the *lamB* gene product to the outer membrane.

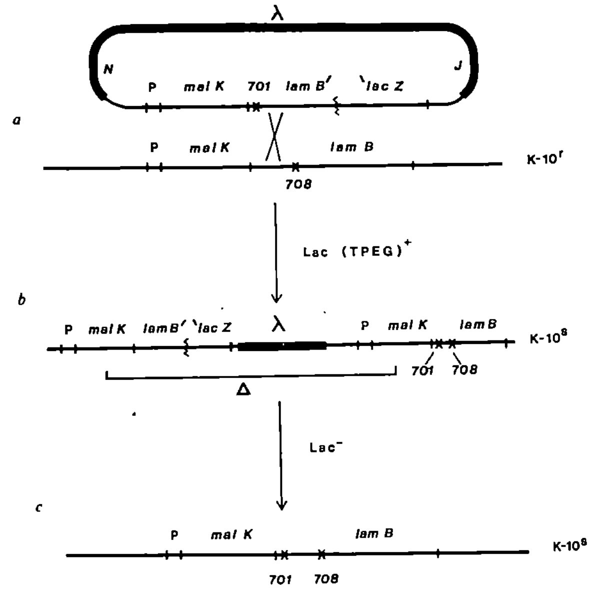

Fig. 3 Construction of the 701–708 double mutant, *in vivo*, by homologous recombination between the 701 and 708 mutations. A λ transducing phage carrying the 701 mutation recombined into the *lamB* portion of the 52-4 *lamB–lacZ* gene fusion was first constructed. The 52-4 fusion codes for a hybrid protein consisting of the NH_2-terminal 39 amino acids from LamB (including the signal sequence) and a COOH terminus of active β-galactosidase[12]. Expression of β-galactosidase activity by the 52-4 hybrid gene relies on translation initiated at the *lamB* initiation codon. The 701 and 708 mutations both reduce initiation of translation of a *lamB* transcript such that these confer resistance to phage K-10 (K-10ʳ) when *cis* to a wild-type *lamB* gene or elicit low levels of β-galactosidase activity when *cis* to a *lamB–lacZ* fusion. To recombine the 701 mutation into the 52-4 hybrid gene, the λ transducing phage carrying this gene was used to infect a *lamB* 701 strain. A phage carrying both the 701 mutation and the fusion was subsequently obtained by plating on Lac indicator media and a Lac⁻ host, the phage being spontaneously released from the resultant lysogen. The desired phage was detected by a Lac⁻ plaque phenotype. *a*, The transducing phage bearing the 52-4 fusion and the 701 mutation was used to infect the 708 mutant. *a*, *b*, A Lac⁺ phenotype in the presence of 10^{-3} M phenylethyl-β-D-thiogalactoside (TPEG) was selected. TPEG, a competitive inhibitor of β-galactosidase[27], was required to increase the stringency of the leaky Lac⁻ phenotype conferred by the 701 and 708 mutations when *cis* to the 52-4 *lamB–lacZ* fusion. A Lac⁺ selection stipulated integration of the phage such that a wild-type sequence was generated *cis* to the fusion, placing the 701 and 708 mutations *cis* to the wild-type *lamB* gene. This scheme avoided exerting selective pressure on the gene bearing the double mutation. Assuming that the K-10 resistant phenotype of either one of the single mutants would be suppressed in the double mutant, Lac⁺ colonies were picked and screened for sensitivity to the phage K-10. K-10ˢ strains were obtained. *c*, A K-10ˢ Lac⁺ lysogen was cured of the prophage. Spontaneous loss of the prophage was detected by a Lac⁻ phenotype. 'P' indicates the promoter of the *malK–lamB* operon. Primes, as in *lamB'* or *lacZ*, indicate that the DNA for the genetic region referred to is deleted on the side the prime is written.

The 701–708 double mutation was constructed and placed *cis* to a *lamB–lacZ* fusion, thereby allowing direct determination of the effect of the combined mutations on *lamB* translation. The observed suppression of 701 and 708 by each other argues strongly that mRNA conformation does have a role in the effect of these two mutations on translation initiation.

The levels of β-galactosidase activity in strains containing the 701 and 708 mutations individually *cis* to a *lamB–lacZ* fusion indicate that whereas the 701 mutation reduces *lamB* translation to 4% of wild type, 708 reduces it to only 28%. This difference is consistent with the different predicted thermodynamic stabilities of the *lamB* mRNA hairpin structure in strains containing one of these mutations (see Fig. 2). Whereas the 701 mutation creates a G-C pairing in the hairpin stem, the 708 mutation creates a less stable U-A pairing. The relatively leaky effect of the 708 mutation can therefore be explained by a less stable hairpin structure and a consequently more accessible ribosome-binding site. This provides additional evidence that mRNA conformation can control relative levels of translational expression, which is particularly relevant to situations where proteins are known to be produced in vastly different amounts from a single transcript, such as in the case of the λ morphogenetic proteins[16–18].

The amount of λ receptor present in the outer membrane of strains containing either the 708 mutation or the 701–708 double mutation is much less than that predicted by the effect of these mutations on translational initiation as measured by β-galactosidase assays (see Table 1). This discrepancy can be explained by the fact that the 708 mutation has two effects: it not only allows base-pairing to occur, thereby affecting translation initiation as described above, but it also creates an arginine to serine change at the sixth position of the λ receptor signal sequence. We believe that this alteration of a charged amino acid to a neutral residue in the early hydrophilic portion of the signal sequence[19] reduces localization of the λ receptor protein to the outer membrane. The amount of λ receptor activity in the outer membrane therefore reflects a compound effect of the 708 mutation whereas cytoplasmic β-galactosidase activity reflects only the effect on translation initiation. The 701 mutation, which resides outside the *lamB* structural gene, has a similar effect as measured by either β-galactosidase or receptor activity. The 708 alteration in the early hydrophilic portion of the λ receptor

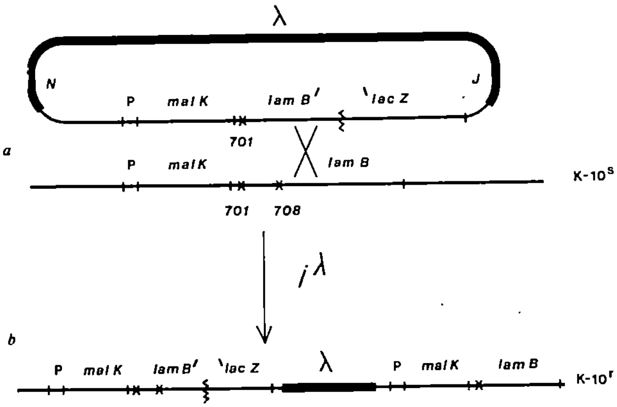

Fig. 4 Construction of strain for assaying suppression of translation initiation defect. *a*, The λ transducing phage carrying the 52-4 *lamB–lacZ* fusion containing the 701 mutation was used to infect the 701–708 mutant. Lysogens were selected by λ immunity. *b*, Integration of the transducing phage such that the double mutation was located *cis* to the *lamB–lacZ* fusion placed the 701 mutation *cis* to the otherwise wild-type *lamB* gene. The resultant strain was resistant to phage K-10, and was detected as such. The level of translation initiated at the *lamB* initiation codon flanked by the 701 and 708 mutations was determined by assay of *lacZ* expression—β-galactosidase activity.

signal sequence is a novel type of signal sequence mutation[20-22]. The unique properties of this signal sequence mutation in protein localization are described elsewhere (ref. 23 and M.N.H., M.D., J.G. and M.S., in preparation).

We thank Agnès Ullmann for suggesting use of phenylethyl-β-D-thiogalactoside, and Olivier Raibaud for helpful discussions. This work was supported by grants from the CNRS (LA 270) and DGRST (80-70182). M.N.H. was the recipient of an ADIP Fellowship from the Institut Pasteur.

Received 1 September; accepted 18 December 1981.

1. Gold, L. *et al. A. Rev. Microbiol.* **35,** 365–403 (1981).
2. Queen, C. & Rosenberg, M. *Cell* **25,** 241–249 (1981).
3. Merril, C. R., Gottesman, M. E. & Adhya, S. L. *J. Bact.* **147,** 875–887 (1981).
4. Randall-Hazelbauer, L. & Schwartz, M. *J. Bact.* **116,** 1436–1446 (1973).
5. Roa, M. *J. Bact.* **140,** 680–686 (1979).
6. Wandersman, C. & Schwartz, M. *Proc. natn. Acad. Sci. U.S.A.* **75,** 5636–5639 (1978).
7. Szmelcman, S. & Hofnung, M. *J. Bact.* **124,** 112–118 (1975).
8. Wandersman, C., Schwartz, M. & Ferenci, T. *J. Bact.* **140,** 1–13 (1979).
9. Ferenci, T. & Boos, W. *J. supramolec. Struct.* **13,** 101–116 (1980).
10. Schwartz, M., Roa, M. & Débarbouillé, M. *Proc. natn. Acad. Sci. U.S.A.* **78,** 2937–2941 (1981).
11. Shine, J. & Dalgarno, L. *Nature* **254,** 34–38 (1975).
12. Moreno, F. *et al. Nature* **286,** 356–359 (1980).
13. Hall, M. N., Schwartz, M. & Silhavy, T. J. *J. molec. Biol.* (in the press).
14. Maxam, A. M. & Gilbert, W. *Proc. natn. Acad. Sci. U.S.A.* **74,** 560–564 (1977).
15. Roa, M. & Clément, J. M. *FEBS Lett.* **121,** 127–129 (1980).
16. Ray, P. N. & Pearson, M. L. *J. molec. Biol.* **85,** 163–175 (1974).
17. Ray, P. N. & Pearson, M. L. *Nature* **253,** 647–650 (1975).
18. Ray, P. N. & Pearson, M. L. *Virology* **73,** 381–388 (1976).
19. Hedgepeth, J., Clément, J. M., Marchal, C., Perrin, D. & Hofnung, M. *Proc. natn. Acad. Sci. U.S.A.* **77,** 2621–2625 (1980).
20. Emr, S. D., Schwartz, M. & Silhavy, T. J. *Proc. natn. Acad. Sci. U.S.A.* **75,** 5802–5806 (1978).
21. Emr, S. D., Hall, M. N. & Silhavy, T. J. *J. Cell Biol.* **86,** 701–711 (1980).
22. Hall, M. N. & Silhavy, T. J. *A. Rev. Genet.* **15,** 91–142 (1981).
23. Hall, M. N. & Schwartz, M. *Ann. Microbiol.*, Institut Pasteur, **133**A, 123–127 (1982).
24. Gabay, J. & Yasunaka, K. *Eur. J. Biochem.* **104,** 13–18 (1980).
25. Miller, J. H. *Experiments in Molecular Genetics* (Cold Spring Harbor Laboratory, New York, 1972).
26. Tinoco, I. Jr *et al. Nature new Biol.* **246,** 40–41 (1973).
27. Jacob, F. & Monod, J. *J. molec. Biol.* **3,** 318–356 (1961).

Partial sequence of 16S ribosomal RNA and the phylogeny of *Prochloron*

Elke Seewaldt & Erko Stackebrandt

Lehrstuhl für Mikrobiologie, Technische Universität München,
Arcisstrasse 21, 8000 München 2, FRG

***Prochloron*, a symbiont of colonial ascidians, is a unicellular prokaryote, containing chlorophylls *a* and *b* and lacking phycobiliproteins[1], thus differing from all other prokaryotes found, and resembling the chloroplasts of Euglenaphyceae, Chlorophyceae and those of higher plants in respect of their photosynthetic pigments. Some workers in the field of endosymbiosis already favour the idea that the green algal chloroplasts may have arisen by the uptake of prochlorons as symbionts[2-5]. Partial sequence analysis of 16S ribosomal RNA of *Prochloron* in fact assigns this organism to the cyanobacteria-chloroplast line of descent[6-8]. However, we report here that a comparison of 16S ribosomal RNA sequences detects no specific relationship between *Prochloron* and the chloroplasts of the green algae *Euglena gracilis* and *Chlamydomonas reinhardii*, nor between *Prochloron* and the chloroplasts of higher plants, represented by *Lemna* and *Zea mays*. On the contrary, *Prochloron* shows the highest sequence homology with *Nostoc*, *Fischerella*, *Agmenellum*, *Aphanocapsa* and *Synechococcus*. These results question the significance of *Prochloron* in the current view of the origin of chloroplasts.**

All attempts to date to cultivate *Prochloron* in the laboratory have failed[9]. To study *Prochloron*, it is therefore necessary either to work with freeze-dried material collected in the field, or to isolate the molecule of choice in the field. Because previous attempts to isolate 16S rRNA from freeze-dried material were unsuccessful, one of us (E.St.) joined the 6th International Prochlorophyta Expedition to Palau, Micronesia. *Prochloron* was isolated from its host animal, *Lissoclinum patella*, simply by squeezing the host colonies, and its identity checked microscopically and by the photospectroscopic determination of chlorophylls *a* and *b* in acetone extracts. Samples of *Prochloron* were found to be free of host cells and bacterial contamination, a fact proved later by a clean 16S rRNA oligonucleotide fingerprint.

The ribonuclease T_1-resistant oligonucleotides of *Prochloron* ribosomal 16S RNA were then investigated by the method introduced by Woese and collaborators[10]. For the isolation of the RNA, cells were opened by French Press, the lysate was phenolized and the nucleic acids separated by one-dimensional polyacrylamide gel electrophoresis. Sequencing involved the digestion of the 16S rRNA by RNase T_1, dephosphorylation of 5′-terminated phosphates, *in vitro* labelling of the oligonucleotides with [γ-^{32}P]ATP and polynucleotide kinase, and resolution of the labelled fragments in two dimensions using a combination of high-voltage electrophoresis and gradient TLC[11]. The sequences of the isolated oligonucleotides ($\geq$6 nucleotides) were determined by controlled alkali cleavage, followed by separation of the products by combined high-voltage electrophoresis and homochromatography[11]. Table 1 shows the oligonucleotides $\geq$6 nucleotides long of the *Prochloron* 16S rRNA. Also indicated are any oligonucleotides of identical sequence found in the catalogues of various cyanobacteria and chloroplasts characterized previously, such as *Nostoc* (strain MAC)[6,12], *Fischerella ambigua*[6,12], *Agmenellum quadruplicatum*[6], *Synechococcus* strains 6301[6,13] and 7502[6], *Aphanocapsa* strains 6701 and 6714[6,14], and the chloroplasts of *Porphyridium creuntum*[6,15], *Z. mays*[16], *E. gracilis* strain Z[6,17] and *C. reinhardii* strain II/32–90 (our unpublished data).

Prochloron 16S rRNA has most oligonucleotides in common with *Agmenellum* (37), *Nostoc* (34), *Fischerella* (35) and *Aphanocapsa* (31 with strain 6701 and 32 with strain 6714). *Prochloron* and *Synechococcus* strains 7502 and 6301 are found to have 26 and 25, respectively, in common. The chloroplasts of *Porphyridium* and *Zea* have, respectively, 26 and 24 fragments in common with *Prochloron*, while *Prochloron* shares only 18 and 16 fragments with the chloroplasts of *Chlamydomonas* and *Euglena*, respectively.

The binary matching coefficients (S_{AB}) give a more detailed picture of the overall similarity between the catalogues of two organisms, because the total number of common nucleotides in all identical fragments is used to calculate relatedness between organisms. Table 2 shows the S_{AB} values of all pairwise comparisons between any two RNAs *A* and *B*. Figure 1 is a dendrogram of the relationship derived by average linkage clustering among the merged groups. S_{AB} values for *Prochloron*

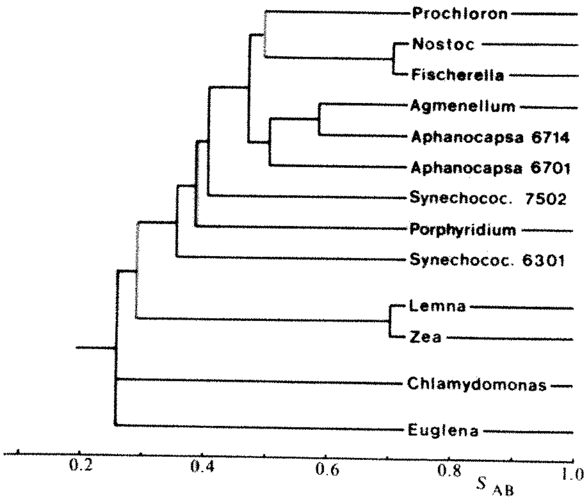

Fig. 1 Dendrogram of relationship, derived by average linkage clustering using a Dice-type similarity coefficient[20].

0028-0836/82/070618—03$01.00

Table 1 Oligonucleotide catalogue of *Prochloron* 16S rRNA

Oligonucleotide sequence in *Prochloron*	Occurrence in										
	Nostoc	*Fischerella*	*Aphanocapsa* 6701	*Agmenellum*	*Aphanocapsa* 6714	*Synechococcus* 7502	*Synechococcus* 6301	*Porphyridium*	*Z. mays*	*Euglena*	*Chlamydomonas*
6-*mers*											
CCACAG	0	0	0	0	0	0	0	0	0	0	0
CCAAAG	0	0	0	0	0	0	0	0	0	0	0
CACAAG	1	1	1	1	1	1	1	1	1	1	1
ACACAG	1	0	0	0	0	0	0	0	1	1	0
AAACCG	0	1	0	0	0	0	0	0	0	0	0
ACAAAG	0	1	1	1	0	1	0	0	1	0	0
AAAAAG	0	0	0	0	0	0	0	0	0	0	0
CUAACG	1	1	0	1	1	1	0	1	1	0	1
CAACUG	1	1	0	0	0	0	0	0	0	0	0
ACACUG	1	1	1	1	1	0	0	1	1	0	1
UAAACG	1	1	1	1	1	1	1	1	1	0	1
AAACUG	0	0	1	1	1	1	1	0	0	0	1
UAAAAG	1	0	1	0	0	1	0	0	0	0	0
UUCCCG	1	1	1	1	1	1	1	1	1	0	1
CCUUCG	1	1	0	1	0	1	0	0	0	0	0
UACCUG	1	1	0	1	1	1	1	1	0	0	0
AUCCUG	1	1	1	1	1	1	1	1	1	0	1
UAAUCG	0	0	1	1	1	1	1	1	1	1	1
UUAAAG	1	1	0	0	1	1	0	1	0	1	0
UCUUAG	0	0	0	1	0	1	0	1	0	0	0
AUAUUG	0	0	0	1	1	1	0	1	0	0	0
UCUUUG	0	0	0	1	0	0	0	0	0	0	0
CUUUUG	0	0	0	0	0	0	0	0	0	0	0
7-*mers*											
ACACACG	0	0	0	0	0	0	0	0	0	1	0
AACACAG	1	1	1	1	1	0	0	0	0	0	1
ACAACAG†	1	1	1	1	1	0	0	0	0	0	0
CAACUCG	1	1	0	1	1	1	1	0	1	0	1
AAUAAAG	0	0	0	0	0	0	0	0	0	0	0
UAUCCCG	1	1	1	1	1	0	0	1	1	1	1
CAUACUG	1	1	1	1	0	0	1	0	0	0	0
UACAAUG	0	0	0	0	0	0	0	0	0	0	0
UAAUACG	1	1	1	1	1	0	1	1	0	1	0
AUACUAG	1	1	1	1	1	0	0	1	1	0	0
UACUUAG	0	1	0	0	0	0	0	0	0	0	0
UUAUAAG	0	0	0	0	0	0	0	0	0	0	0
U*AACAAG	1	1	1	1	1	1	1	1	1	1	1

Oligonucleotide sequence in *Prochloron*	Occurrence in										
	Nostoc	*Fischerella*	*Aphanocapsa* 6701	*Agmenellum*	*Aphanocapsa* 6714	*Synechococcus* 7502	*Synechococcus* 6301	*Porphyridium*	*Z. mays*	*Euglena*	*Chlamydomonas*
8-*mers*											
CCACACUG	1	1	1	1	1	0	1	1	1	1	1
CAAUACCG	1	1	1	1	1	1	0	1	0	1	0
CAAACUCG	0	0	0	0	0	0	0	0	0	0	0
ACAACUCG	0	0	0	0	0	0	0	0	0	0	0
CACUCUAG	1	0	0	1	1	1	1	0	0	0	0
AAUCAUUG	0	0	1	0	0	0	0	0	0	0	0
AUUUAUUG	0	0	0	0	0	0	0	0	0	0	0
9-*mers*											
UACACACCG	1	1	1	1	1	1	1	1	1	1	1
CAACCCUCG	1	1	1	1	1	0	0	0	1	0	1
CCUACCAAG	0	0	0	0	0	0	1	0	0	0	0
CCCCUUACG	1	1	1	0	1	1	0	1	0	0	0
CUAACUCCG	1	1	1	1	1	1	0	1	0	0	0
ACUCCUACG	1	1	1	1	1	1	1	1	1	0	1
AUACCCCUG	0	0	1	1	1	0	1	0	0	0	0
AAUCCUCCG	0	0	0	0	0	0	0	0	0	0	0
CUCUACUAG	0	0	0	0	0	0	0	0	0	0	0
AACUCUUCG	0	0	0	0	0	0	0	0	0	0	0
AAUUUUCCG	1	1	1	1	1	1	1	1	1	1	0
UUUAAUUCG	1	1	1	1	1	0	1	0	1	1	0
10-*mers*											
AAACUCAAAG	1	1	1	1	1	1	1	1	1	1	1
CUAAUACCCG	0	0	0	1	0	0	0	0	0	0	0
CUAAACUCCG	0	0	0	0	0	0	0	0	0	0	0
UACUACAAUG	1	1	1	1	1	0	1	0	0	0	0
UCAC*ACCAUG	1	1	1	1	1	0	1	0	0	1	0
11-*mers*											
AACCUUACCAG	0	1	0	0	0	0	1	1	1	1	1
CUUAACACAUG	1	1	1	0	0	1	1	1	1	1	1
CCAAUAUUAAG	0	0	0	0	0	0	0	0	0	0	0
13-*mers*											
UUACCCUAACCCG	0	0	0	0	0	0	0	0	0	0	0
AAUCUACCUCAAG	0	0	0	0	0	0	0	0	0	0	0
UAAACCUCUUUUG	0	0	0	0	0	0	0	0	0	0	0
17-*mers*											
ACUCUCAUCAAACCCAG	0	0	0	0	0	0	0	0	0	0	0
3′ *terminus*											
AUCACCUCCUX$_{OH}$	a	a	a	a	a	a	a	a	a	0	a

The table lists the oligonucleotide sequences in the 16S rRNA of *Prochloron* from *L. patella* and indicates which of these are also present in the 16S RNAs from cyanobacteria[6,12–14] and the 16S chloroplast rRNAs from *Porphyridium*[6,15], *Euglena*[6,17], *C. reinhardii* and *Z. mays*[16]. The catalogues of the 16S rRNA of *Lemna* and *Chlamydomonas* are unpublished: The position of *Lemna* chloroplast in the dendrogram of relationship is taken from ref. 8. 1, Sequence present; 0, sequence not present; *, modified nucleotide. Sequence C$_{4-5}$UUACC[6] is listed as CCCCUUACG, because the shorter version is more likely to be the accurate one (C. R. Woese, personal communication). a, For S_{AB} calculation all 3′ termini (except that of *Euglena* chloroplast) are treated as identical[6].

† Listed as AAC, AC, AG by Bonen *et al.*[6].

and the cyanobacteria *Nostoc*, *Fischerella*, *Agmenellum* and *Aphanocapsa* strains are as high (0.42–0.51) as those found for *Nostoc* and *Fischerella* on the one hand and *Aphanocapsa* and *Agmenellum* on the other (0.46–0.50) (*Nostoc* and *Fischerella* exhibit a high S_{AB} value of 0.69). *Synechococcus* strains show less rRNA sequence homology with *Prochloron*, and with the other cyanobacteria (0.34–0.45). Chloroplasts from *Porphyridium*, *Zea* and *Lemna* exhibit similar low S_{AB} values to *Prochloron* (0.31–0.35) (chloroplasts of *Lemna* and *Zea* are themselves highly related: 0.71)[8]. Chloroplasts of *Euglena* and *Chlamydomonas* show even less RNA homology with *Prochloron* (0.26 and 0.23 respectively), having S_{AB} values similar to those found for *Prochloron*, *Escherichia coli* (0.21)[10] and *Bacillus subtilis* (0.24)[18].

The comparative analysis of the 16S ribosomal RNA shows *Prochloron* definitely to be a member of the cyanobacteria–chloroplast line of descent. However, as *Prochloron* does not show the same, low S_{AB} value as all members of this line, it cannot be regarded as a direct and independent descendent of the ancient cell that gave rise to the line. Furthermore, although *Prochloron* resembles the chloroplasts of green algae and plants in respect of pigment composition and the topography of the thylakoids, it is phylogenetically not specifically related to them; this would have resulted in specifically higher S_{AB} values to the chloroplast in question.

The degree of relatedness found between *Prochloron* and the chloroplast of *Lemna* and *Zea* is only remote, while that to the chloroplasts of *Euglena* and *Chlamydomonas* is even more distant (note that the 16S rRNA catalogues of the algal chloroplasts lack some of the universal oligonucleotides found in almost all other members of this cluster; (see Table 1). This may indicate that these chloroplasts have a 'fast clock'[8], resulting in deeper apparent than true branching. A striking example of this is seen in the very low S_{AB} value between the chloroplasts of *Euglena* and *Chlamydomonas* (0.16). The inclusion of the missing oligonucleotides would raise the S_{AB} values of the *Euglena* and *Chlamydomonas* chloroplasts to *Prochloron*, *Nostoc* and relatives (to ~0.30).

The high similarity coefficient between *Prochloron* and the cyanobacteria indicates that, phlogenetically, *Prochloron* is a member of the cyanobacteria. The RNA of *Prochloron* is more similar to that of *Nostoc* and its relatives than to the RNA of *Synechococcus* strains. The deep branching point of *Synechococcus* strain 6301 in the phylogenetic tree is definitely not due to a 'fast clock' of its 16S rRNA (C. R. Woese, personal communication).

Table 2 Binary comparison among the 16S rRNA catalogues

Organism	1	2	3	4	5	6	7	8	9	10	11	12	13
1 *Prochloron*	—	256	266	234	275	233	199	199	197	168	171	140	130
2 *Nostoc*	0.48	—	360	268	253	264	206	227	216	157	154	136	141
3 *Fischerella*	0.50	0.69	—	253	245	247	214	207	221	168	171	147	146
4 *Aphanocapsa* 6714	0.42	0.49	0.46	—	314	286	226	256	251	148	161	131	140
5 *Agmenellum*	0.51	0.48	0.46	0.57	—	254	218	230	214	160	163	131	146
6 *Aphanocapsa* 6701	0.43	0.50	0.46	0.52	0.48	—	200	207	222	138	157	137	142
7 *Synechococcus* 6301	0.34	0.36	0.37	0.38	0.38	0.34	—	200	171	135	132	139	168
8 *Synechoccus* 7502	0.36	0.42	0.38	0.45	0.42	0.38	0.34	—	218	138	139	133	139
9 *Porphyridium* (chloroplast)	0.35	0.39	0.39	0.43	0.38	0.39	0.28	0.38	—	161	168	153	179
10 *Zea* (chloroplast)	0.31	0.30	0.32	0.27	0.30	0.26	0.23	0.25	0.29	—	379	143	143
11 *Lemna* (chloroplast)	0.32	0.29	0.32	0.29	0.31	0.29	0.23	0.25	0.30	0.70	—	140	147
12 *Chlamydomonas* (chloroplast)	0.26	0.26	0.28	0.23	0.24	0.25	0.24	0.24	0.27	0.27	0.26	—	91
13 *Euglena* (chloroplast)	0.23	0.25	0.26	0.24	0.26	0.25	0.27	0.24	0.30	0.25	0.26	0.16	—

Triangle above the diagonal: number of bases in sequences common to each pair of catalogues (for hexamers and larger). Bottom triangle: S_{AB} values for each pair of catalogues. Calculations were done as described in ref. 20; only those oligonucleotides which were comprehensively published previously[6] are used for S_{AB} calculation. Due to the omission of pentamers in the calculation, similarity coefficients for cyanobacteria and chloroplasts are lower than the published ones[6], resulting in lower branching points of the evolutionary lines in the dendrogram of relationship (Fig. 1) compared with those published[6,8].

It is generally believed that chlorophyll *b* is an extraordinarily conserved molecule. If this is the case, *Prochloron* actually is the direct descendent of the common ancestor of the chloroplasts and the cyanobacteria; but it seems that chlorophyll *b* was lost more than once in the chloroplast–cyanobacteria line of descent. An alternative explanation may be that *Prochloron* is an offshoot of the cyanobacteria that 're-invented' chlorophyll *b* and, as a result, could afford to lose its phycobiliproteins. The possibility of a co-occurrence of chlorophylls *a* and *b* in Cyanophyta, together with the resulting taxonomic problems, have already been discussed[19].

Our results do not exclude the possibility that the common ancestor of chloroplasts and cyanobacteria was a *Prochloron*-type organism, but it seems unlikely that the direct ancestor of the *Prochloron* we investigated played this part.

We thank Drs Lanna Cheng and Ralph A. Lewin for help in collecting and identifying *Prochloron*. This work was supported by the Deutsche Forschungsgemeinschaft.

Received 25 August; accepted 15 December 1981.

1. Lewin, R. A. *Phycologica* **16,** 217 (1977).
2. Stanier, R. Y. & Cohen-Bazire, G. *A. Rev. Microbiol.* **31,** 225–274 (1977).
3. Taylor, F. J. R. in *Endocytobiology, Endosymbiosis and Cell Biology*, 917–942 (De Gruyter, Berlin, 1980).
4. Gibbs, S. P. & Gillott, M. A. *Endocytobiology, Endosymbiosis and Cell Biology*, 737–743 (De Gruyter, Berlin, 1980).
5. Whatley, J. M., John, P. & Whatley, F. R. *Proc. R. Soc.* B**204,** 165–187 (1979).
6. Bonen, L., Doolittle, W. F. & Fox, G. E. *Can. J. Biochem.* **57,** 879–888 (1979).
7. Fox, G. E. *et al. Science* **209,** 457–463 (1980).
8. Stackebrandt, E. & Woese, C. R. *Molecular and Cellular Aspects of Microbial Evolution*, 1–31 (Cambridge University Press, 1981).
9. Lewin, R. A. *Ann. N. Y. Acad. Sci.* **361,** 325–329 (1981).
10. Uchida, T. *et al. J. molec. Evol.* **3,** 63–77 (1974).
11. Stackebrandt, E., Ludwig, W., Schleifer, K. H. & Gross, H. J. *J. molec. Evol.* **17,** 227–236 (1981).
12. Bonen, L. & Doolittle, W. F. *J. molec. Evol.* **10,** 283–291 (1978).
13. Doolittle, W. F., Woese, C. R., Sogin, L., Bonen, L. & Stahl, D. *J. molec. Evol.* **4,** 307–315 (1975).
14. Bonen, L. & Doolittle, W. F. *Nature* **261,** 669–673 (1976).
15. Bonen, L. & Doolittle, W. F. *Proc. natn. Acad. Sci. U.S.A.* **72,** 2310–2314 (1975).
16. Schwarz, A. & Kössel, H. *Nature* **283,** 739–742 (1980).
17. Zablen, L. B., Kissil, M. S., Woese, C. R. & Buetow, D. E. *Proc. natn. Acad. Sci. U.S.A.* **72,** 2418–2422 (1975).
18. Woese, C. R., Sogin, M., Stahl, D., Lewis, B. J. & Bonen, L. *J. molec. Evol.* **7,** 197–213 (1976).
19. Antia, N. J. *Br. Phycol. J.* **12,** 271–276 (1977).
20. Fox, G. E., Pechman, K. R. & Woese, C. R. *Int. J. Syst. Bact.* **27,** 44–57 (1977).

Substrate and sequence specificity of a eukaryotic DNA methylase

Yosef Gruenbaum, Howard Cedar & Aharon Razin

Department of Cellular Biochemistry, The Hebrew University–Hadassah Medical School, Jerusalem, Israel 91010

In eukaryotic DNA, 50–90% of the dinucleotide sequence C-G is methylated. Most methylated sites are apparently placed at fixed locations in the genome and this methylation pattern is faithfully inherited from generation to generation[1]. Holliday and Pugh[2] and Riggs[3] have suggested that methyl moieties are inherited in a semi-conservative fashion during DNA replication, and this model has been confirmed by experiments in which methylated DNA was integrated into mouse L-cells following DNA-mediated gene transfer[4–6]. For this mechanism to operate, two basic requirements must be satisfied: (1) methyl moieties must be symmetrically placed on both strands of the DNA[7,8] and (2) the cellular methylase should be specific for the hemi-methylated substrate present during DNA replication. Here we demonstrate conclusively that the preferred substrate *in vitro* for the mouse ascites DNA methylase is indeed hemi-methylated DNA. Furthermore, this enzyme seems to methylate exclusively cytosine residues located at the dinucleotide C-G.

The lack of a suitable substrate for the eukaryotic methylase has hampered the study of its activity and sequence specificity. Preliminary results have suggested that the preferred substrate for this enzyme may be hemi-methylated DNA[9]. To test this hypothesis we have prepared hemi-methylated ΦX DNA *in vitro* using primed repair synthesis with single-stranded ΦX DNA as template in the presence of the nucleotides dATP, dGTP, dTTP and 5-methyl-dCTP. The product of this reaction is a covalently closed circular duplex ΦX DNA (RFI) in which the complementary strand is methylated at every cytosine residue (all sequences are in the 5′→3′ direction). This hemi-methylated molecule is a very efficient substrate for DNA methylation *in vitro*, having an initial rate of methylation 100-fold greater than that of either single-stranded or double-stranded ΦX DNA molecules (Fig. 1). Using excess enzyme, we determined that the maximum methylation obtainable for hemi-methylated ΦX DNA is 70 pmol methyl per μg DNA, which is consistent with a methylation level of ~100%, assuming that only C-G residues, representing 4.5% of the ΦX dinucleotide content[10], undergo modification.

It has been shown that when hemi-methylated ΦX DNA is inserted into mouse L-cells by DNA-mediated gene transfer, only methylation at C-G residues is inherited from generation to generation[5]. This selectivity is presumably determined by the enzymatic specificity of the cell methylase. This hypothesis was tested by methylating duplex hemi-methylated ΦX DNA by the ascites tumour cell methylase *in vitro* and analysing the sequence specificity of the reaction. Modified nearest-neighbour analysis[11] of *in vitro* methylated ΦX DNA indicated that 95% of the C-G residues were indeed modified. However, this technique is unsuitable for studying specificity because it detects methyl groups on the *in vitro* synthesized fully methylated complementary strand as well as those added onto the viral strand by the ascites methylase *in vitro*. We therefore used the restriction enzyme *Hae*III to develop a method for measuring only those

0028-0836/82/070620—03$01.00

methylations inserted enzymatically. Although *Hae*III will not cleave hemi-methylated ΦX DNA, this enzyme does produce nicks in the unmethylated strand at its restriction site[12]. Thus, when hemi-methylated ΦX DNA is nick-translated using *Hae*III as the nicking agent, labelled nucleotides are incorporated exclusively into the unmethylated strand. Following eukaryotic methylation *in vitro*, the locations of the enzymatically introduced methyl moieties could be determined by nearest-neighbour analysis (Fig. 2)[11]. This experiment showed that the dinucleotide C-G undergoes extensive modification while other cytosine-containing sequences are not recognized to any appreciable degree by this animal cell enzyme. These results do not completely rule out methylation at other sites but indicate that in the reaction conditions used, the major site of methylation is the sequence C-G.

The results presented here show conclusively that hemi-methylated DNA is the preferred substrate for DNA methylation *in vitro* by the animal cell methylase. This property of the enzyme is consistent with the proposed model of methylation inheritance whereby methylation occurs on nascent DNA immediately following DNA synthesis during replication or repair. Assuming specificity for hemi-methylated sites, this mechanism guarantees that the modification will be inherited at previously methylated sites, while unmethylated sites will remain unmethylated. The process requires the presence of symmetrical cytosine residues on both strands of the DNA. In animal cells symmetry is provided by the dinucleotide sequence C-G. Any other cytosine-containing dinucleotide cannot serve as a template for methylation because it would lack a methylatable cytosine residue in the opposite strand. In fact, as shown here, the animal methylase recognizes only the sequence C-G. Note that higher plant DNA is methylated at C-X-G residues as well as the expected C-G sites[13]. This is in keeping with the strand symmetry of cytosine residues required for methylation inheritance. These sites cannot, however, be methylated by the animal cell enzyme either *in vivo*[5] or *in vitro* (present study).

Although >95% of all animal DNA methylation occurs at the sequence C-G[11], several reports have indicated methylation at C-C residues[14–16]. In particular, specific *Msp*I (CCGG) sites located in the 5′-flanking region of the human γ-globin genes are modified at the external cytosine. These unusual methyl moieties also seem to be faithfully inherited by almost all cells during cell differentiation[14,15]. Although this external cytosine of the *Msp*I site does not undergo methylation either *in vivo*[5] or *in vitro* (this study), we cannot rule out the possibility that such methylation can occur in special conditions either by the cell

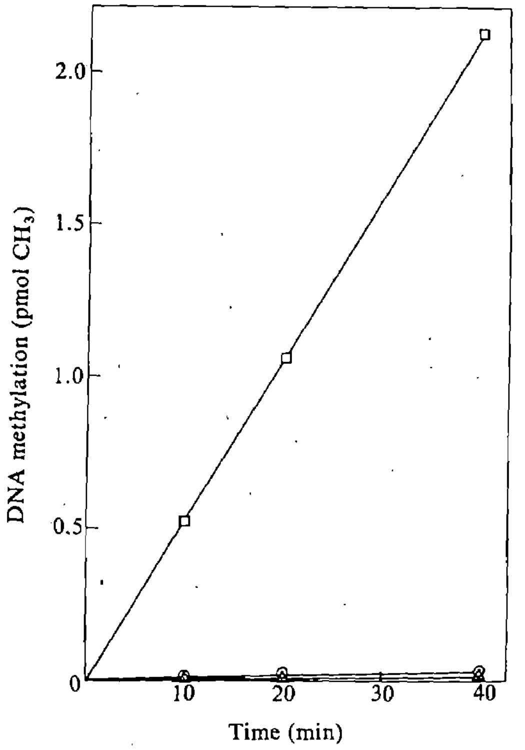

Fig. 1 Substrate specificity of DNA methylase from mouse ascites tumour cells. DNA of the bacteriophage ΦX174: single-stranded, double-stranded (RF) and *in vitro* synthesized hemi-methylated duplex were prepared as previously described[12]. The methylase preparation was a partially purified fraction III from mouse ascites tumour cells[9]. The methylation reaction was carried out at 37 °C in a 25 μl volume containing 0.2 mM dithiothreitol, 10 mM EDTA, 10 mM Tris-HCl (pH 7.9), 30 mM NaCl, 15% (v/v) glycerol, 16 μM *S*[Me-^{3}H]adenosylmethionine (Amersham, 15 Ci mmol^{-1}), 0.07 μg single-stranded or double-stranded phage DNA or 0.14 μg hemi-methylated DNA and enzyme (10 μg protein). The reaction was terminated at various times and DNA purified and analysed for the incorporation of radioactive methyl moieties as described elsewhere[11]. This reaction was found to be linear for at least 2 h. Using higher levels of enzyme, the reaction reached saturation at a level of ~9.5 pmol methyl incorporation. The initial rate of methylation, as calculated from this curve and other experiments, was 3.7 pmol h^{-1} for hemi-methylated DNA (□), 0.05 pmol h^{-1} for single-stranded DNA (○) and 0.03 pmol h^{-1} for double-stranded DNA (△). Note that 0.14 μg hemi-methylated DNA corresponds to 0.07 μg of substrate available for methylation. The rate of reaction using hemi-methylated DNA was also shown to be 100-fold greater than for other DNA substrates in additional experiments using various substrate and enzyme concentrations.

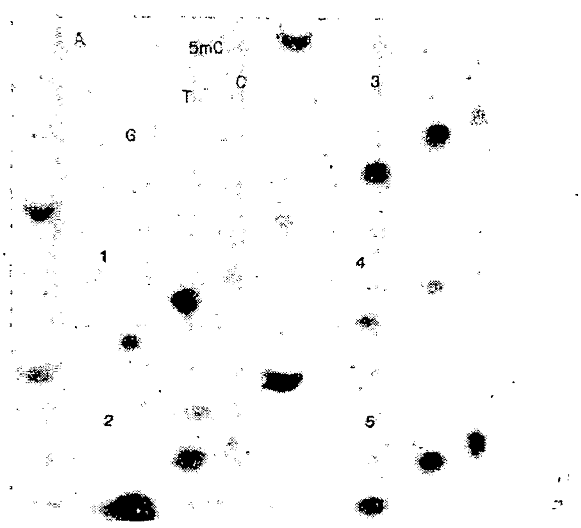

Fig. 2 Sequence specificity of the ascites DNA methylase. Hemi-methylated ΦX174 DNA[12] (0.3 μg) was incubated with 16 U *Hae*III (Biolabs) for 3 h at 37 °C in a 20 μl incubation mixture as recommended by the enzyme manufacturer. The reaction was terminated by incubation for 10 min at 60 °C. This solution of nicked DNA was brought to a volume of 50 μl containing 66 mM Tris-HCl pH 7.4, 6.6 mM MgCl$_2$, 10 mM dithiothreitol, 1 μM of one [α-^{32}P]dNTP (670 Ci mmol^{-1}, NEN) and 50 μM of the other three unlabelled dNTPs and incubated with 30 U *Escherichia coli* DNA polymerase I (Biolabs) to replace ~10% of the unmethylated strand. *In vitro* methylation was carried out on one half of this DNA for 3 h at 37 °C in a volume of 125 μl containing 10 mM EDTA; 16 μM *S*[Me-^{3}H]adenosylmethionine, 0.1 μg nick-translated DNA and 35 μl partially purified ascites DNA methylase (fraction III, 45 μg protein)[11]. The other half of the nick-translated DNA sample served as a non-methylated control. Methylated and non-methylated DNA were digested to deoxynucleoside 3′-monophosphates by micrococcal nuclease and spleen phosphodiesterase and the nucleotides separated by TLC as described previously (bottom to top, 1st dimension; left to right, 2nd dimension)[11]. Autoradiographs of such chromatograms are as follows: (1) DNA before enzymatic methylation, nick-translated with [α-^{32}P]dGTP. (2) DNA after enzymatic methylation, nick-translated with [α-^{32}P]dGTP. (3) DNA after enzymatic methylation, nick-translated with [α-^{32}P]dCTP. (4) DNA after enzymatic methylation, nick-translated with [α-^{32}P]dTTP. (5) DNA after enzymatic methylation, nick-translated with [α-^{32}P]dATP. Following autoradiography the spots were scraped and the amount of radioactivity in each spot was determined by scintillation counting. In this experiment, when DNA, after enzymatic methylation, was labelled with [α-^{32}P]dGTP, 60% of the cytosine was found to be methylated. When DNA was labelled with other radioactive nucleotides, less than 0.5% of the cytosine was in 5mC. The ratio of counts for all the nucleotides on each TLC plate was found to be consistent with the nearest-neighbour frequencies of the ΦX viral strand[10]. In frame 2 the spot corresponding to dGMP is seen to be stronger than expected from the nearest-neighbour frequencies. This was seen only in the *in vitro* methylated sample labelled with [α-^{32}P]dGTP and seems to be an artefact of the preparation and purification of the DNA following methylation, as the ratios of intensities of the other spots on this chromatogram are appropriate. Abbreviations used: A, dAMP; C, dCMP; T, dTMP; 5mC, 5methyl-dCMP.

maintenance enzyme itself or by some other enzymatic activity *in vivo*.

Whereas most somatic cellular methylation is carried out by a maintenance enzyme recognizing hemi-methylated DNA, *de novo* methylation has occasionally been observed in virus-transformed cells[17,18]. Although the enzyme examined here carried out inefficient *de novo* methylation on double-stranded or single-stranded DNA, this same enzyme may operate *in vivo* in special conditions to produce new methylated sites. Recent studies have shown that specific genes may be undermethylated in certain somatic cells as compared with germ-line DNA[19,20]. This change presumably occurs during differentiation by a process of demethylation achieved by DNA replication in the absence of concomitant methylation[1]. Thus, the control of the cellular DNA methylase may be an important factor in the regulation of gene activity.

This work was supported by NIH grant GM 20483 and Israel–US Binational Science Foundation grant 2333. We thank Dr G. Felsenfeld for his gift of 5methyl-dCTP.

Received 6 October 1981; accepted 6 January 1982.

1. Razin, A. & Riggs, A. D. *Science* **210,** 604–610 (1980).
2. Holliday, R. & Pugh, J. E. *Science* **187,** 226–232 (1975).
3. Riggs, A. D. *Cytogenet. Cell Genet.* **14,** 9–14 (1975).
4. Pollack, Y., Stein, R., Razin, A. & Cedar, H. *Proc. natn. Acad. Sci. U.S.A.* **77,** 6463–6467 (1980).
5. Stein, R., Gruenbaum, Y., Pollack, Y., Razin, A. & Cedar, H. *Proc. natn. Acad. Sci. U.S.A.* **79,** 61–65 (1982).
6. Wigler, M., Levy, D. & Perucho, M. *Cell* **24,** 33–40 (1981).
7. Bird, A. P. *J. molec. Biol.* **118,** 49–60 (1978).
8. Cedar, H., Solage, A., Glaser, G. & Razin, A. *Nucleic Acids Res.* **6,** 2125–2132 (1979).
9. Adams, R. L. P., McKay, E. L., Craig, L. M. & Burdon, R. H. *Biochem. biophys. Acta* **561,** 345–357 (1979).
10. Setlow, P. *CRC Handb. Biochem. molec. Biol.* **2,** 312–318 (1976).
11. Gruenbaum, Y., Stein, R., Cedar, H. & Razin, A. *FEBS Lett.* **142,** 67–71 (1981).
12. Gruenbaum, Y., Cedar, H. & Razin, A. *Nucleic Acids Res.* **9,** 2509–2515 (1981).
13. Gruenbaum, Y., Naveh-Many, T., Cedar, H. & Razin, A. *Nature* **292,** 860–862 (1981).
14. van der Ploeg, L. H. T. & Flavell, R. A. *Cell* **19,** 947–958 (1980).
15. van der Ploeg, L. H. T., Graften, J. & Flavell, R. A. *Nucleic Acids Res.* **8,** 4563–4574 (1980).
16. Sneider, T. W. *Nucleic Acids Res.* **8,** 3829–3840 (1980).
17. Sutter, D. & Doerfler, W. *Proc. natn. Acad. Sci. U.S.A.* **77,** 253–256 (1980).
18. Desrosiers, R. C., Mulder, C. & Fleckenstein, B. *Proc. natn. Acad. Sci. U.S.A.* **76,** 3839–3843 (1979).
19. Waalwijk, C. & Flavell, R. A. *Nucleic Acids Res.* **5,** 4631–4641 (1978).
20. Mandel, J. L. & Chambon, P. *Nucleic Acids Res.* **7,** 2081–2090 (1979).

Long terminal repeats of endogenous mouse mammary tumour virus contain a long open reading frame which extends into adjacent sequences

Nick Kennedy, Gudrun Knedlitschek, Bernd Groner, Nancy E. Hynes, Peter Herrlich, Rob Michalides* & Albert J. J. van Ooyen*

Kernforschungszentrum Karlsruhe, Institut für Genetik und Toxikologie von Spaltstoffen, Postfach 3640,
D7500 Karlsruhe 1, FRG
* Antoni van Leeuwenhoekhuis, The Netherlands Cancer Institute, Plesmanlaan 121, 1066 CX Amsterdam, The Netherlands

The integrated DNA copies (proviruses) of RNA tumour virus genomes are flanked by long terminal repeat (LTR) sequences, which are generated by the duplication of segments present at both ends of the viral RNA[1]. LTRs vary in length from 330 (ref. 2) to 1,328 (this paper) base pairs (bp). The primary viral transcript starts in the left LTR (L-LTR) and terminates in the right LTR (R-LTR)[3]. We have now sequenced both LTRs from an inherited (endogenous) mouse mammary tumour virus (MMTV) of the GR strain. This provirus, which is one of five present in the haploid genome of GR mice[4], does not produce virus[5] and is not identical with the exogenous MMTV of GR mice[6]. The provirus (GR40) could nevertheless be transcribed and its transcription hormonally regulated after cloning and transfection into mouse L cells[7]. The LTRs are identical and exhibit the following features: a terminal inverted 6-bp repeat, a Goldberg–Hogness (TATAAA) sequence, sequences which have been implicated in polyadenylation and the termination of transcription, and an open reading frame. The open reading frame of the R-LTR starts at the *env*/LTR junction and encodes a 36,700-molecular weight (M_r) protein. The open reading frame of the L-LTR extends into the adjacent mouse sequence. A host sequence of 6 bp at the site of integration into the mouse chromosome is directly repeated.

The MMTV proviral fragment in λ clone GR40 is shown schematically in Fig. 1*a*. To sequence the LTRs we adopted the strategy described in ref. 8 (Fig. 1*b–e*). DNA subfragments were cloned into pBR322 and a series of staggered deletions made. All the deletions extended from a unique restriction enzyme site in pBR322. Sequencing from this site resulted in an overlapping series of sequences which could then be used to reconstitute that of the subcloned fragment. The sequence extending from the *Pst*I site at the 5′ end of the L-LTR and into the adjacent mouse region was obtained in two ways. A *Pst*I restriction fragment covering the left junction was end-labelled and sequenced by the base modification method[9]. To confirm the sequence across the *Pst*I site we subcloned *Hae*III and *Alu*I fragments into the single-strand bacteriophage M13mp7 (ref. 10) and subjected appropriate clones to the chain termination sequencing method[11].

The LTRs at the ends of the GR40 provirus have the same sequence (shown as a single line numbered 1–1328 in Fig. 2). The following findings suggest that positions 1 and 1,328 represent the limits of the proviral LTR. (1) The flanking sequences of both LTRs diverge beyond these points. (2) Six nucleotides at the ends of the repeated sequence form an inverted repeat (underlined at positions 1–6 and 1,323–1,328 in Fig. 2). The inverted repeats are the same as those found at the termini of other MMTV LTR junctions sequenced[12,13]. Inverted terminal repeats 3–23 bp long are common to all retroviruses[14], insertion sequences (IS elements) and most transposons[15]. In the latter cases they are required for integration[16]. (3) Six nucleotides in the host DNA adjacent to the LTRs are directly repeated (underlined at positions −6 to −1 and 1,329 to 1,334 in mouse flanking sequences). Such direct repeats are also a common feature among LTRs, IS elements and transposons[15], and apparently result from the duplication of a 3–6 bp host sequence during integration[17–19]. Integration is also thought to be accompanied by the loss of 2 bp from both ends of the linear DNA intermediate[12,13,19]. In GR40 they can be tentatively identified by reference to the internal LTR junctions. The 2 bp lost from the 5′ end of the linear DNA would correspond with the A-A at positions −1 and −2 of the R-LTR. Similarly the 2 bp lost from the 3′ end would correspond with the G-C at positions 1,329–1,330 of the L-LTR. (4) The proviral DNA sequence left of the R-LTR at positions −1 to −9 (dotted in Fig. 2) is identical to the corresponding sequence in avian sarcoma virus and thought to be part of the site involved in the initiation of plus-strand DNA[20]. (5) The primer for minus-strand DNA[21] is $tRNA_3^{Lys}$. A 16 bp sequence in the proviral DNA right of the L-LTR (positions 1,331–1,345, dotted in Fig. 2) matches the 3′-terminal end of the primer.

The identical nature of the LTRs of GR40 was not necessarily expected. As the endogenous provirus is genetically transmitted and silent, there is probably no selection against sequence alterations. The identity of the GR40 LTRs, and their ability to direct specific and hormonally regulated transcription[7], imply that its entry into the germ line was a recent event in evolutionary terms. In contrast, there is a large difference between the endogenous sequence presented here and that of an exogenous LTR from the C3H mouse[13], there being 93 base changes between the two. This suggests that the endogenous GR40 provirus and the exogenous virus of the C3H mouse have evolved separately[22,23].

Several sequences thought to be transcriptional control signals are present in the LTRs. A Goldberg–Hogness

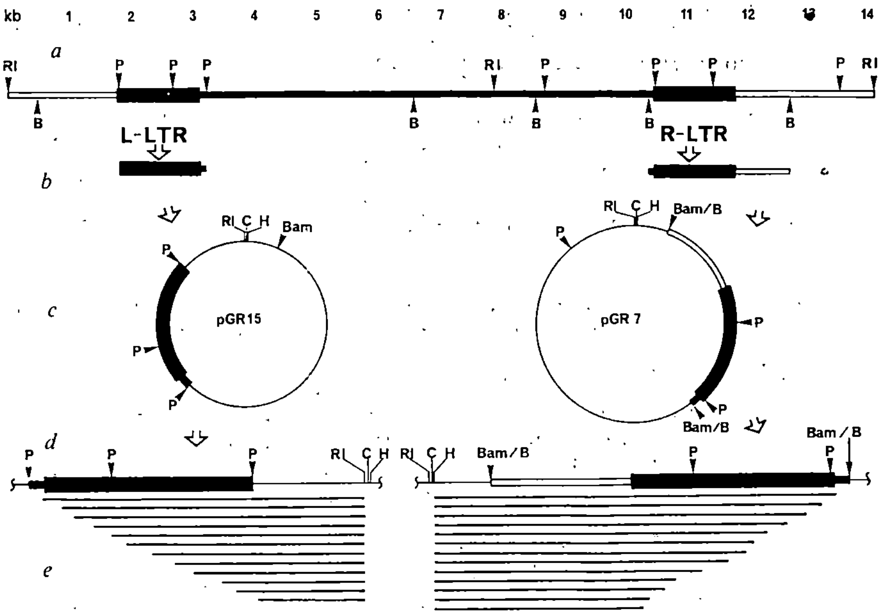

Fig. 1 *a*, Restriction map of the insert in recombinant λ phage Charon 4a/GR40[1]. The solid black region represents the provirus with the LTRs shown thicker; the rest is mouse flanking DNA. Restriction endonuclease sites: Bam, *Bam*HI; B, *Bgl*II; C, *Cla*I; H, *Hin*dIII; P, *Pst*I; RI, *Eco*RI. The two *Eco*RI fragments of the insert were subcloned into pBR322 (not shown). *b*, A 1.4 kb *Pst*I fragment contains all but 11 bp of the L-LTR, and a 2.2 kb *Bgl*II fragment contains all of the R-LTR. *c*, These fragments were introduced into the *Pst*I and *Bam*HI sites respectively of pBR322, in the orientations shown. From the two resulting plasmids, pGR15 and pGR7, two sets of deletions were produced using the method described elsewhere[8]. Briefly, *Eco*RI linkers were ligated onto pGR15 molecules which had been randomly linearized by treatment with DNase I. Digestion with *Eco*RI and size fractionation on a low-gelling temperature agarose gel were followed by re-ligation and the transformation of Ca^{2+}-treated *Escherichia coli* cells. Deletions in pGR7 were created in an analogous way, but using *Hin*dIII linkers. *d*, The LTR regions of the two plasmids are shown relative to the *Eco*RI, *Cla*I and *Hin*dIII sites of pBR322. *e*, The deleted DNA is represented by lines which correspond in size and position to the map in *d*. Each member of a set differs in length by ~100 bp from the next. Sequencing by the method of Maxam and Gilbert[9] into the LTR from each deletion endpoint produced an overlapping series from which the sequence of the whole LTR could then be reconstituted. *Hin*dIII digestion of pGR7 followed by 5′ end-labelling with [γ-^{32}P]ATP and T4 polynucleotide kinase produces linear molecules labelled at both ends. Subsequent digestion with *Cla*I cleaves off a 5 bp pBR322 terminal fragment and the mixture of fragments may be sequenced directly with no further separation necessary. In the case of pGR15, a terminal 26 bp fragment may be similarly removed by *Cla*I from end-labelled *Eco*RI-digested molecules. As the two sets of deletions enter the LTRs from opposite ends, opposite strands of the LTR are sequenced. The 11 bp missing from the 5′ end of the L-LTR were determined by sequencing from the *Pst*I site at map position 1.8 in *a*. The sequence across the *Pst*I site was confirmed by chain termination sequencing[11] using fragments cloned into the single-stranded DNA bacteriophage M13mp7 (ref. 10).

```
                                                                                              >
                                                             MOUSE (flanking L-LTR) - - - 5' TAATTATGTGACAAGAAGATTGTCTTT

                                                                                                                   >
                                                  MMTV (flanking left end of R-LTR) - - - 5' CCAACCACGATGCGTCCGGCGTAGACC
                                                                                                  -60       -50

(mouse)                     M  L  L  V  L      LTR
TCTGGTCCCATTTATTTTGTGTTCTATATGCTTCTTGTAC
                        <               M  P  R  L  Q  Q  K  W  L  N  S  R  E  C  P  T  L  R  R  E  A  A  K  G  L  F  P
                                        TGCCGCGCCTGCAGCAGAAATGGTTGAACTCCCGAGAGTGTCCTACACTTAGGAGAGAAGCAGCCAAGGGGTTGTTTCCC
(mmtv)             >           .........  G  R  R  C  C  F  H  N  F  E  R  S  H  G  V  S  L  L  S  A  A  L  P  N  N  G
ATCTTAACGTGCTTCTTTTAAAAAAGAAAAAAGGGGGAAA        10        20        30        40        50        60        70        80
                  <  F  L  F  F  P  S  I
        -30       -20       -10        -1

 T  L  D  D  P  S  A  C  T  R  M  S  P  S  D  K  D  I  L  I  L  C  C  K  L  G  I  A  L  L  C  L  G  L  L  G  E  V  A  V
ACCAAGGACGACCCGTCTGCGTGCACGCGGATGAGCCCATCAGACAAAGACATACTCATTCTCTGCTGCAAACTTGGCATAGCTCTGCTTTGCCTGGGGCTATTGGGGGAAGTTGCGGTT
V  L  S  S  G  D  A  H  V  R  I  L  G  D  S  L  S  M  S  M  R  Q  Q  L  S  P  M        170       180       190       200
        90       100       110       120       130       140       150       160

 R  A  R  R  A  L  T  L  D  S  F  N  N  S  S  V  Q  D  Y  N  L  N  N  S  E  N  S  T  F  L  L  G  Q  G  P  Q  P  T  S  S
CGTGCTCGCAGGGCTCTCACCCTTGATTCTTTTAATAACTCTTCTGTGCAAGATTACAATCTAAACAATTCGGAGAACTCGACCTTCCTCCTGGGGCAAGGACCACAGCCAACTTCCTCT
       210       220       230       240       250 <     260       270       280       290       300       310       320

 Y  K  P  H  R  L  C  P  S  E  I  E  I  R  M  L  A  K  N  Y  I  F  T  N  K  T  N  P  I  G  R  L  L  I  M  M  L  R  N  E
TACAAGCCACACCGACTTTGTCCTTCAGAAATAGAAATAAGAATGCTTGCTAAAAATTATATTTTTACCAATAAGACCAATCCAATAGGTCGATTATTAATCATGATGTTAAGAAATGAA
       330       340       350       360       370       380       390       400       410       420       430       440

 S  L  S  F  S  T  I  F  T  Q  I  Q  R  L  E  M  G  I  E  N  R  K  R  R  S  T  S  V  E  E  Q  V  Q  G  L  R  A  S  G  L
TCTTTGTCTTTTAGCACTATATTTACTCAAATTCAAAGGTTAGAAATGGGAATAGAAAATAGAAAGAGACGCTCAACCTCAGTTGAAGAACAGGTGCAAGGACTAAGGGCCTCAGGCCTA
       450       460       470       480       490       500       510       520       530       540       550       560

 E  V  K  R  G  K  R  S  T  L  V  K  I  G  D  R  W  W  Q  P  G  T  Y  R  G  P  Y  I  Y  R  P  T  D  A  P  L  P  Y  T  G
GAAGTAAAAAGGGGAAAGAGGAGTACGCTTGTCAAAATAGGAGACAGGTGGTGGCAACCAGGGACTTATAGGGGACCTTACATCTACAGACCAACAGACGCCCCGCTACCATATACAGGA
       570       580       590       600       610       620       630       640       650       660       670       680

 R  Y  D  L  N  F  D  R  W  V  T  V  N  G  Y  L  V  L  Y  R  S  L  P  F  R  E  R  L  A  R  A  R  P  P  W  C  V  L  T  Q
AGATACGATTTAAATTTTGATAGGTGGGTCACAGTCAACGGCTATAAAGTGTTGTACAGATCCCTCCCCTTTCGTGAAAGACTCGCCAGAGCTAGACCTCCTTGGTGTGTGTTAACTCAG
       690       700       710       720       730       740       750       760       770       780       790       800

 E  E  K  D  D  I  K  Q  Q  V  H  D  Y  I  Y  L  G  T  G  M  N  V  W  G  K  I  F  H  Y  T  K  E  G  A  V  A  R  Q  L  E
GAAGAAAAAGACGACATAAAACAACAGGTACATGATTATATTTATCTAGGAACTGGAATGAACGTTTGGGGAAAGATTTTTCATTATACCAAGGAGGGGGCAGTGGCTAGACAATTAGAA
       810       820       830       840       850       860       870       880       890       900       910       920

 H  I  S  A  D  T  F  G  M  S  Y  N  G  >
CACATTTCTGCAGATACTTTTGGCATGAGCTATAATGGATAACCTTTATGAGCCCAACCTTGCGGTTCCCAAGGTTTAAGTAAGTTCAGGGTCACAAACTGTTCTTAAAACAAGGATGTG
       930       940       950       960       970       980       990      1000      1010      1020      1030      1040

AGACAAGTGGTTTCCTGACTTGGTTTGGTATCAAATGTTTTGATCTAAGCTCTGAGTGTTCTATTCTCCTATGTTCTTTTGGAACTTATCCAAGTCTTATGTAAATGCTTATGTAAACCA
      1050      1060      1070      1080      1090      1100      1110      1120      1130      1140      1150      1160

                  ---------U3-------|           |-------U5--------
                                    |-----R-----|
TGATATAAAAGAGTGCTGATTTTTTGAGTAAACTTGCAACAGTCCTAACATTCACCTCTCGTGTGTTTGTGTCTGTTCGCCATCCCGTCTCCGCTCGTCACTTATCCTTCACTTTCCAGA
      1170      1180      1190      1200      1210      1220      1230      1240      1250      1260      1270      1280

                                                  .................
                                     LTR        GCTGGCGCCCGAACAGGGCCCTCGGATA 3' - - - MMTV (flanking right end of L-LTR)

GGGTCCCCCCGCAGACCCCGGTGACCCTCAGGTCAGCCGACTGCGGCA
      1290      1300      1310   <  1320
                                                TTGTACCTTAATGTCCATCTCTTTATTA 3' - - - MOUSE (flanking R-LTR)
                                              1330      1340      1350
```

Fig. 2 The identical nucleotide sequences of the GR40 LTRs are written as a single line numbered 1–1,328. L-LTR flanking regions are presented above those of the R-LTR. Sequences left of the LTRs are numbered negatively. Amino acid sequences generated by the open reading frames are given in the single-letter code. The orf sequence, and its alternative N-terminal peptide, are written above the corresponding nucleotides. The translation of the reading frame in the opposite strand is shown below the appropriate DNA sequence. Stop codons flanking open reading frames are indicated by arrow heads pointing in the direction in which they are to be read. Underlined sequences are referred to in the text. U3, R and U5 represent the unique 3′ terminally repeated and unique 5′ sequences of MMTV genomic RNA respectively; the corresponding proviral regions are delimited by vertical lines. The R sequence is defined at its left and right ends by the positions at which transcription starts and stops. Nucleotides associated with the initiation of synthesis of the plus and minus DNA strands are marked by dots.

(TATAAA) sequence[24] is present at positions 1,164–1,169. The MMTV mRNA cap site is probably at position 1,196 (ref. 10 and our unpublished S_1 mapping data). Direct sequencing of the viral RNA[25] shows that its 3′ end corresponds with position 1,206. The sequence AGTAAA, an analogue of the sequence AATAAA which may be a signal for polyadenylation[26], is present (underlined at positions 1,187–1,192) 17 bp upstream from this site. Another sequence associated with transcription termination, TTTG[27], is present (underlined at positions 1,225–1,228) 20 bp downstream from the 3′ end of the viral RNA, and flanked by alternating T and G residues.

The LTR sequence possesses an open reading frame, in the direction of viral transcription, with coding potential for a basic 36,700-M_r protein. A similar open reading frame has been found in the exogenous MMTV LTR of the GR mouse (N. Fasel, K. Pearson, E. Buetti and H. Diggelmann, personal communication), and in the exogenous and endogenous MMTV LTRs of the C3H mouse[28]. Dickson and co-workers[29,30] have described the synthesis *in vitro* of a 36,000-M_r protein (orf) from templates containing LTR sequences. In addition, an open reading frame for a 6,600-M_r protein exists in the opposite strand, extending from position 160 to −20 in the MMTV *env* region, to −14 in the mouse flanking sequence, or, when read from the circular DNA intermediate, to 1,316 in the R-LTR.

An interesting feature of the *orf* open reading frame is that the first AUG codon is composed of an A, which is the last nucleotide of the *env* region, and a T-G representing the first two nucleotides of the R-LTR. At the 5′ end of the provirus, integration has replaced the A with a C in the AUG codon, thereby creating a CUG (lysine) codon. Another start codon, in phase with the open reading frame, occurs by chance in the mouse DNA at positions −11 to −13. Note that in both cases the open reading frame is preceded by a stop codon in phase. Furthermore the open reading frame is contained within the unique 3′ sequence of the genomic RNA, and ends at position 959, well before the 3′ end of the RNA at position 1,206.

The corresponding RNAs for these hypothetical proteins have not yet been found. Rightward transcription of the integrated L-LTR would have to start in the flanking mouse sequence. Transcription of the R-LTR might start from an internal promoter or from the L-LTR. A further possibility is that *orf* mRNA is transcribed from the L-LTR in circular DNA intermediates containing two copies of the LTR in tandem[31]. In this configuration the GC which we suppose to be present at the 3′ end of the linear DNA intermediate would be juxtaposed with the A-A at its 5′ end[13], resulting in the AUG codon at the beginning of the L-LTR being retained and its *orf* coding region brought under the influence of the R-LTR promoter. No AUG codons intervene between the R-LTR Goldberg–Hogness (TATAAA) sequence and the appended L-LTR *orf* coding sequence. Transcription in this case would generate an *orf* mRNA of unit LTR length.

The extra length of the LTR of MMTV as compared with other retroviruses can be accounted for by the open reading frame. Whether this difference is associated with another special feature of MMTV—its hormonally mediated transcription—may be answered by testing after transfection[7] the biological properties of the deletion mutants described here.

We thank R. Staden for computer programs used in DNA sequence analysis.

Received 2 November 1981; accepted 8 January 1982.

1. Gilboa, E., Mitra, S. W., Goff, S. & Baltimore, D. *Cell* **18,** 93–100 (1979).
2. Swanstrom, R., DeLorbe, W. J., Bishop, J. M. & Varmus, H. E. *Proc. natn. Acad. Sci. U.S.A.* **78,** 124–128 (1981).
3. Yamamoto, T., de Crombrugghe, B. & Pastan, I. *Cell* **22,** 789–797 (1980).
4. Groner, B. & Hynes, N. E. *J. Virol.* **33,** 1013–1025 (1980).
5. Michalides, R., van Nie, R., Nusse, R., Hynes, N. E. & Groner, B. *Cell* **23,** 165–173 (1981).
6. Herrlich, P. *et al. Nucleic Acids Res.* **9,** 4981–4995 (1981).
7. Hynes, N. E., Kennedy, N., Rahmsdorf, U. & Groner, B. *Proc. natn. Acad. Sci. U.S.A.* **78,** 2038–2042 (1981).
8. Frischauf, A. M., Garoff, H. & Lehrach, H. *Nucleic Acids Res.* **8,** 5541–5549 (1980).
9. Maxam, A. L. & Gilbert, W. *Meth. Enzym.* **65,** 499–559 (1980).
10. Messing, J., Crea, R. & Seeburg, P. *Nucleic Acids Res.* **9,** 309–321 (1981).
11. Sanger, F., Nicklen, S. & Coulson, A. R. *Proc. natn. Acad. Sci. U.S.A.* **74,** 5463–5467 (1977).
12. Majors, J. E. & Varmus, H. E. *Nature* **289,** 253–258 (1981).
13. Donehower, L. A., Huang, A. L. & Hager, G. *J. Virol.* **37,** 226–238 (1981).
14. Hishinuma, F., DeBona, P. J., Astin, S. & Skalka, A. M. *Cell* **23,** 155–164 (1981).
15. Calos, M. P. & Miller, J. H. *Cell* **20,** 579–595 (1980).
16. Ohtsubo, H., Ohmori, H. & Ohtsubo, E. *Cold Spring Harb. Symp. quant. Biol.* **43,** 1269–1277 (1979).
17. Shimotohno, K. & Temin, H. M. *Cold Spring Harb. Symp. quant. Biol.* **45,** 719–732 (1981).
18. McClements, W. L., Enquist, L. W., Oskarsson, M., Sullivan, M. & Vande Woude, G. F. *J. Virol.* **35,** 488–497 (1980).
19. Shoemaker, C. *et al. Cold Spring Harb. Symp. quant. Biol.* **45,** 711–717 (1981).
20. Czernilofsky, A. B. *et al. Nucleic Acids Res.* **8,** 2967–2984 (1980).
21. Peters, G. & Glover, C. C. *J. Virol.* **35,** 31–40 (1980).
22. Cohen, J. C. & Varmus, H. E. *Nature* **278,** 418–423 (1979).
23. Cohen, J. C., Majors, J. E. & Varmus, H. E. *J. Virol.* **32,** 483–496 (1979).
24. Benoist, C., O'Hare, K., Breathnach, R. & Chambon, P. *Nucleic Acids Res.* **8,** 127–142 (1980).
25. Klemenz, R., Reinhardt, M. & Diggelmann, H. *Molec. Biol. Rep.* **7,** 123–126 (1981).
26. Proudfoot, N. J. & Brownlee, G. G. *Nature* **252,** 357–362 (1974).
27. Lai, E. C. *et al. Cell* **18,** 829–842 (1979).
28. Donehower, L. A., Fleurdelys, B. & Hager, G. L. *J. Virol.* (in the press).
29. Dickson, C. & Peters, G. *J. Virol.* **37,** 36–47 (1981).
30. Dickson, C., Smith, R. & Peters, G. *Nature* **291,** 511–513 (1981).
31. Shank, R. S., Cohen, J. C., Varmus, H. E., Yamamoto, K. R. & Ringold, G. *Proc. natn. Acad. Sci. U.S.A.* **75,** 2112–2116 (1978).

Expression of human *hprt* gene on the inactive X chromosome after DNA-mediated gene transfer

A.J.R. de Jonge*, P. J. Abrahams†, A. Westerveld* & D. Bootsma*

* Department of Cell Biology and Genetics, Erasmus University, Rotterdam, The Netherlands
† Laboratory of Physiological Chemistry, Sylvius Laboratory, Leiden, The Netherlands

The paternal or maternal mammalian X chromosome is inactivated ('lyonization') at random early in the development of the female embryo[1,2]. Once established, the inactivation of the chromosome is maintained in the cell and in all its descendants. However, spontaneous local reactivation of the inactive X chromosome is found at low frequency in human–mouse hybrid cells[3,4]. So far only the X_g locus[5,6] and the locus for microsomal steroid sulphatase (*sts*)[7] (both assigned to the short arm of the X chromosome), have been shown to escape inactivation. The locus for hypoxanthine phosphoribosyltransferase (*hprt*) is susceptible to inactivation[8] and humans heterozygous for HPRT deficiency (the Lesch–Nyhan syndrome, L–N)[9], show a mosaic pattern of HPRT activity in their cultured fibroblasts[8]. To investigate the molecular basis of X inactivation, we have used DNA isolated from each of the two subpopulations of a L–N heterozygote, to transform cultured HPRT-deficient mouse fibroblasts. Transformation of the mouse cells with the inactivated human *hprt*$^+$ gene occurred with essentially the same efficiency as with the active human *hprt*$^+$ gene. Thus, reactivation of the lyonized human *hprt* locus is possible after interspecific DNA-mediated gene transfer.

To obtain sufficient cells of only the HPRT$^+$ or only the HPRT$^-$ subpopulation, primary fibroblasts of the L–N heterozygote (cell strain 79RD19) were transformed using the *ori*$^-$ simian virus 40 (SV40) mutant originally isolated by Gluzman *et al.*[10] and various of these transformed clones were tested for HPRT expression. One HPRT$^-$ clone, SV1 (the inactivated X chromosome carries the *hprt*$^+$ allele) and one HPRT$^+$ clone, SV3 (the active X chromosome carries the *hprt*$^+$ allele) were expanded for DNA isolation. Immediately before collection, the cells were checked again for HPRT$^+$ or HPRT$^-$ phenotype by measuring ^{3}H-hypoxanthine incorporation and also by a growth test in two selective media. Cells (10^7) of each clonal cell line were plated in medium selecting either for (hypoxanthine–aminopterin–thymidine (HAT) medium[11]) or against (medium containing 6 μg ml^{-1} 6-thioguanine, 6-TG) the expression of HPRT in the cells. Cells having a phenotype which differed from that expected were not observed in either test.

Table 1 Transformation of LTH1 and LTK⁻ with HeLa, SV1 and SV3 DNA

	LTH1 Selection for HPRT⁺			LTK⁻ Selection for TK⁺		
DNA donor	Plates with clones/total plates	No. of clones	Transfer frequency	Plates with clones/total plates	No. of clones	Transfer frequency
No DNA	0/25	0	0	0/7	0	0
HeLa	5/15	7	0.2×10^{-6}	4/4	18	2×10^{-6}
SV1	6/10	11	0.5×10^{-6}	3/3	26	4.5×10^{-6}
SV3	9/10	21	1×10^{-6}	3/3	17	3×10^{-6}

DNA was isolated using a modification of a previously described method[26]. DNA–calcium phosphate precipitate was produced by slowly adding DNA, dissolved at 40 μg ml^{-1} in 10 mM Tris-HCl *p*H 7.6, 1 mM EDTA, 250 mM $CaCl_2$ to an equal volume of HEBS buffer[27], with agitation. After 30–45 min, 1 ml of the fine precipitate was added to the medium over 2×10^6 cells in a 10-cm cell culture dish. Control dishes received calcium phosphate precipitate without DNA. Post-treatment with 10% dimethyl sulphoxide[28] was given 3.5–4 h after addition of precipitate. Selective medium (LTH1, HAS medium[13]; LTK⁻, HAT medium[11]) was added 24 h later and changed initially every second or third day, later every fifth to seventh day. Clones appeared after 2–4 weeks and were isolated using glass cloning cylinders. The plates were then fixed and stained to detect other clones. The medium used in all cell culture procedures was a 1 : 1 mixture of Ham's F10 and Dulbecco's minimal essential medium (MEM; Flow) containing 5% fetal and 5% newborn calf serum and antibiotics, gassed with 5% CO_2.

Furthermore, the presence of an inactive X chromosome was verified in these cell lines by staining the Barr body in interphase nuclei (Fig. 1).

DNA isolated from SV1 or SV3 was used to transform mouse LTH1 cells. LTH1 is an HPRT-deficient subline of LTK⁻ (ref. 12), which we have isolated after selection for a spontaneous mutant by culturing in 6-TG medium. Reversion of LTH1 to an HPRT⁺ phenotype was $<2\times10^{-8}$ when tested by culturing cells in medium containing hypoxanthine as the exogenous purine source and azaserine to block the *de novo* biosynthesis of purines (HAS medium[13]). We have tested HPRT-deficient cell lines of different origins in transformation experiments with human HeLa DNA and found the highest transformation frequency of the HPRT⁺ phenotype using LTH1 cells as DNA recipients (our unpublished results). The results of DNA-mediated gene transfer of the *hprt* locus into LTH1 cells are shown in Table 1. For comparison, we also selected for transfer of the thymidine kinase (*tk*) locus into LTK⁻ cells using the same DNA–calcium phosphate precipitates.

The *hprt* gene was transformed by SV1 DNA at a frequency intermediate between those obtained using HeLa and SV3 DNA. In addition, the transformation frequency of the *tk* locus in SV1 DNA was not significantly different from the frequencies obtained with the other DNAs used although for each DNA, transfer of the *hprt* locus into LTH1 cells occurred at a lower frequency than transfer of the *tk* locus into LTK⁻ cells. Evidently there were no significant differences in transformation capacity between the different DNA preparations for either the *tk* or *hprt* locus. From LTH1 cells treated with HeLa, SV1 and SV3 DNA, respectively, 2, 9 and 15 transformed clones were isolated.

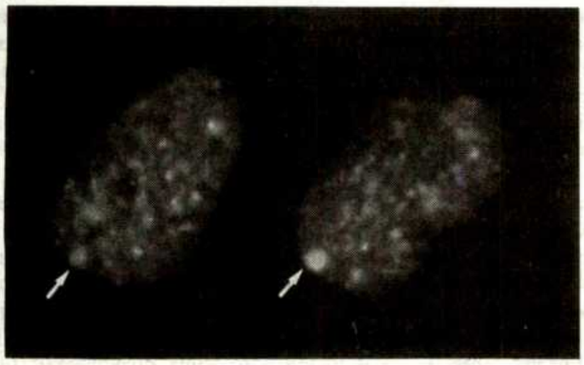

Fig. 1 Barr body in SV1 cells. After fixation in methanol/acetic acid (3 : 1) the cells, grown on coverslips, were air-dried and stained for 10 min in a 0.5% atebrin solution in methanol. After rinsing and mounting in 0.07 M phosphate buffer *p*H 6.5, the cells were examined by fluorescence microscopy and photographed. The Barr body is indicated by an arrow.

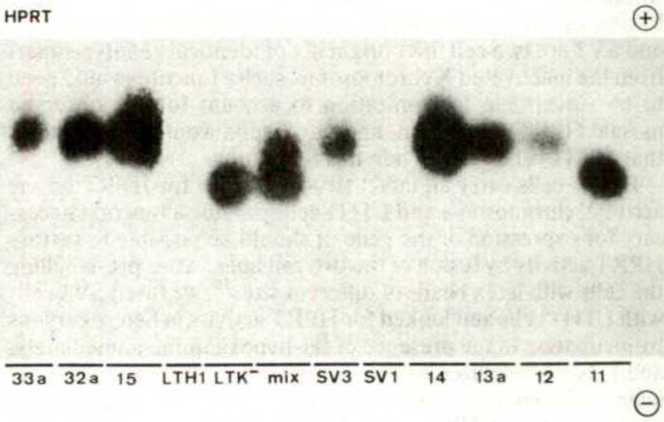

Fig. 2 Cellogel electrophoresis of HPRT. Cell lysates were produced by sonication and electrophoresis was carried out according to Meera Khan[14]. Enzyme activity was visualized by incubation with ^{14}C-hypoxanthine and autoradiography[15]. For an explanation of SV1, SV3, LTH1 and LTK⁻, see text. Clones 12, 13a, 14 and 15 are independent transformant clones isolated after treatment of LTH1 cells with SV1 DNA. Clone 11 appears to be a revertant. Clones 32a and 33a are independent clones isolated after treatment of LTH1 cells with SV3 DNA. Mix is an artificial mixture of extract from LTK⁻ and SV3 cells.

In a number of independent transformed cell lines isolated from different culture dishes, we identified the HPRT and glucose-6-phosphate dehydrogenase (G-6-PD) activities by electrophoresis on Cellogel[14,15] (Table 2). Figure 2 shows the electrophoretic mobility of human (SV3) and murine (LTK⁻) HPRT. In extracts of SV1 and LTH1 cells, HPRT was not detectable, while in transformants isolated from LTH1 cells treated with SV1 DNA, human HPRT was synthesized. One cell line (clone 11) showed HPRT of murine electrophoretic mobility and was assumed to be a revertant. In all the transformants tested, only the murine G-6-PD was present.

The results are most readily explained by a reactivation of the lyonized *hprt* locus after interspecific DNA transformation. A simple reversion of the *hprt* mutation on the active X chromosome in the donor strain SV1 appears unlikely because of the equal transformation frequencies obtained with DNA isolated from SV1 and SV3, and from results of the tests performed on the cells immediately before DNA isolation. An alternative explanation is that in the cells of the particular L–N heterozygote used, the HPRT deficiency was not due to a mutation in the structural gene for HPRT, but due to a defect in some other function necessary for expression of the gene. This

Table 2 Identification of HPRT and G-6-PD activities in cell lysates of independent transformant clones

DNA donor	Transformant	Electrophoretic mobility of HPRT	G-6-PD
HeLa	95.1-1	H	M
	95.1-2	H	M
SV1	96.1-11	M	M
	96.1-12	H	M
	96.1-13a	H	M
	96.1-14	H	M
	96.1-15	H	M
SV3	96.1-31a	H	M
	96.1-32a	H	M
	96.1-33a	H	M
	96.1-34	H	M
	96.1-36	H	M

H represents human, M murine electrophoretic mobility.

would render the SV1 cells phenotypically HPRT$^-$ despite their having an intact *hprt* gene on the active X chromosome. As SV1 and SV3 are two cell lines originally of identical genotype apart from the inactivated X chromosome, such a function would need to be susceptible to lyonization to account for the observed mosaic HPRT expression, and our results would then indicate that LTH1 cells can provide this function.

If SV1 cells carry an intact structural gene for HPRT on the active X chromosome and LTH1 cells provide a function necessary for expression of the gene, it should be possible to restore HPRT activity by fusion of the two cell lines. After pre-labelling the cells with latex beads of different sizes[16], we fused SV1 cells with LTH1 cells and looked for HPRT activity in heterokaryons by incubation in the presence of ^{3}H-hypoxanthine immediately, and 1,2 or 3 days after fusion. At each time point we examined at least 1,000 heterokaryons having 2–10 nuclei per cell, but found no restoration of HPRT activity. It is thus highly unlikely that SV1 cells have an active X chromosome carrying an intact structural gene for HPRT which can become expressed in LTH1 cells as a result of some murine function. These results agree with data reported elsewhere[17,18] which suggest that in cells obtained from L–N patients, the mutation has affected the structural gene for HPRT.

Several mechanisms proposed for X inactivation agree with our results. (1) Taking the human X chromosome to be 2×10^5 kilobase pairs (kbp) (1/23 of the haploid genome) and the average length of the isolated DNA molecules to be 100 kbp (estimated by agarose gel electrophoresis), one isolated DNA molecule could represent, on average, only 0.05% of the X chromosome. If there are one or a few 'inactivation centres'[19] from which inactivation of the X chromosome is maintained, our procedure could have caused an uncoupling of such a centre from the *hprt* locus, resulting in expression of the gene. (2) Recently, evidence has been obtained that DNA methylation could be involved in X-chromosome inactivation[20]. Also, almost total, random methylation of a DNA sequence inhibits the expression of that sequence after DNA transformation[21]. We have shown here that the *hprt* locus, kept inactive in human cells, can be efficiently expressed in rodent cells. Taken together, these findings indicate that the inactive state of the X chromosome is maintained by a species-specific methylation pattern, the human pattern not being recognized as a lyonization signal in the rodent cells. In this respect, it is interesting that Liskay and Evans[22] have not found reactivation in experiments similar to ours, but they performed transfers between rodent cells only. (3) As purified DNA was used in our experiments it is possible that the inactivated state is maintained by non-DNA components of the X chromosome[23].

Our results do not support models based on differences in DNA base sequence being responsible for lyonization[24,25].

The system using the two L–N heterozygote subpopulations as a source of active and inactive X-chromosomal material should enable us to investigate further the possibilities of X-chromosome reactivation, for example after chromosome-mediated gene transfer, or in intraspecific transfer experiments.

The assistance of Dr W. J. Kleijer and Mrs S. de Smit and W. Keijzer is gratefully acknowledged. This work was supported by FUNGO, Foundation of Medical Scientific Research in The Netherlands and by EURATOM contract BIO-E-404-NL (G).

Received 12 August; accepted 4 December 1981.

1. Lyon, M. F. *Nature* **190,** 372–373 (1961).
2. Gartler, S. M. & Andina, R. J. *Adv. hum. Genet.* **7,** 99–140 (1976).
3. Kahan, B. & DeMars, R. *Proc. natn. Acad. Sci. U.S.A.* **72,** 1510–1514 (1975).
4. Hellkuhl, B. & Grzeschik, K.-H. *Cytogenet. Cell Genet.* **22,** 527–530 (1978).
5. Race, R. R. & Sanger, R. *Blood Groups in Man*, 578–639 (Blackwell, London, 1975).
6. Fialkow, P. J. *Am. J. hum. Genet.* **22,** 460–463 (1970).
7. Mohandas, T., Sparkes, R. S., Hellkuhl, B., Grzeschik, K.-H. & Shapiro, L. J. *Proc. natn. Acad. Sci. U.S.A.* **77,** 6759–6763 (1980).
8. Rosenbloom, F. M., Kelley, W. N., Henderson, J. F. & Seegmiller, J. E. *Lancet* **ii,** 305–306 (1967).
9. Lesch, M. & Nyhan, W. L. *Am. J. Med.* **36,** 561–570 (1964).
10. Gluzman, Y., Frisque, R. J. & Sambrook, J. *Cold Spring Harb. Symp. quant. Biol.* **44,** 293–299 (1980).
11. Littlefield, J. W. *Science* **145,** 709–710 (1964).
12. Kit, S., Dubbs, D. R. , Piekarski, L. J. & Hsu, T. C. *Expl Cell Res.* **31,** 297–312 (1963).
13. Graf, L. H. Jr, Urlaub, G. & Chasin, L. A. *Somat. Cell Genet.* **5,** 1031–1044 (1979).
14. Meera Khan, P. *Archs Biochem. Biophys.* **145,** 470–483 (1971).
15. Shin, S., Meera Khan, P. & Cook P. R. *Biochem. Genet.* **5,** 91–100 (1971).
16. Matsukuma, S., Zelle, B., Keijzer, W., Berends, F. & Bootsma, D. *Expl Cell Res.* **134,** 103–112 (1981).
17. Fujimoto, W. Y. & Seegmiller, J. E. *Proc. natn. Acad. Sci. U.S.A.* **65,** 577–584 (1970).
18. Ghangas, G. S. & Milman, G. *Proc. natn. Acad. Sci. U.S.A.* **72,** 4147–4150 (1975).
19. Kahan, B. & DeMars, R. *Somat. Cell Genet.* **6,** 309–323 (1980).
20. Mohandas, T., Sparkes, R. S. & Shapiro, L. J. *Science* **211,** 393–396 (1981).
21. Wigler, M., Levy, D. & Perucho, M. *Cell* **24,** 33–40 (1981).
22. Liskay, R. M. & Evans, R. J. *Proc. natn. Acad. Sci. U.S.A.* **77,** 4895–4898 (1980).
23. Cook, P. R. *Biol. Rev.* **49,** 51–84 (1974).
24. Brown, S. W. & Chandra, H. S. *Proc. natn. Acad. Sci. U.S.A.* **70,** 195–199 (1973).
25. Davidson, E. H. & Britten, R. J. *Science* **204,** 1052–1059 (1979).
26. Wigler, M., Pellicer, A., Silverstein, S. & Axel R. *Cell* **14,** 725–731 (1978).
27. Graham, F. L. & van der Eb, A. J. *Virology* **52,** 456–467 (1973).
28. Miller, C. L. & Ruddle, F. H. *Proc. natn. Acad. Sci. U.S.A.* **75,** 3346–3350 (1978).

Inter-replicon transposition of Tn*1*/*3* occurs in two sequential genetically separable steps

Paul A. Kitts, Angus Lamond & David J. Sherratt

Department of Genetics, University of Glasgow,
Glasgow G11 5JS, UK

The 4,957-base pair (bp) transposon Tn*3* encodes three polypeptides, two of which are needed for normal inter-replicon transposition and one, β-lactamase, which is responsible for the transposon's ampicillin resistance (Ap^r)[1,2]. The closely related transposon Tn*1* specifies three interchangeable polypeptides of identical function. The 1,015-amino acid *tnp*A protein is essential for transposition, whereas the 185-residue *tnp*R protein regulates the rate of transposition[3,4] and is required for the generation of normal end products of inter-replicon transposition[5,6]. Here we report the inter-replicon transposition properties of *tnp*A$^-$ *tnp*R$^-$ derivatives of both Tn*1* and Tn*3*. We show that the *tnp*A product is sufficient to generate a transpositional co-integrate intermediate in which the donor and recipient replicons become fused between two directly repeated copies of the transposon. In the absence or presence of *tnp*A product, such co-integrates are efficiently converted to normal transposition end products in the presence of *tnp*R protein. Two amber mutants selected because of their derepressed *tnp*R-mediated control of transposition are also unable to resolve co-integrate intermediates in a Sup^0 (suppressor minus) background. For each mutant, both mutant phenotypes are suppressed by *Sup*D and *Sup*E but not by *Sup*F, confirming that the *tnp*R coding sequence specifies a single protein having both functions.

0028–0836/82/070626—03$01.00

To test whether *tnp*A and *tnp*R products act independently, we constructed *tnp*A$^-$ *tnp*R$^-$ derivatives of both Tn*1* and Tn*3* (Tn*1031* and Tn*3651* respectively). The structures of the parental plasmids and their deleted derivatives are indicated in Fig. 1. Note that both *tnp*A$^-$ *tnp*R$^-$ derivatives retain the transposon ends and the internal site (*res*) at which *tnp*R-mediated site-specific recombination occurs during resolution of transpositional co-integrates[5,7]. Therefore provision of both *tnp*A and *tnp*R proteins in *trans* by complementation should allow normal transposition of these transposons. Similarly, provision of these gene products separately should allow their individual roles in transposition to be determined.

Our inter-replicon transposition assay depends on the fact that the multicopy plasmids pMB9 (tetracycline resistant, Tc^{r})[8] and pACYC184 (Tc^{r} and chloramphenicol resistant, Cm^{r})[9] are not mobilized during conjugation promoted by the *Inc*W conjugative plasmid R388 (trimethoprim resistant; Tp^{r})[10]. Transposition from transposon-containing derivatives of pMB9 and pACYC184 into non-essential regions of R388 can be simply assayed by crossing out the R388 plasmids and assaying the fraction that contains the transposon. Table 1 summarizes the data from such experiments. *tnp*A$^-$ derivatives of either Tn*1* or Tn*3* fail to complement transposition of the *tnp*A$^-$ *tnp*R$^-$ transposons. In the absence of *tnp*R protein, provision of either Tn*1* or Tn*3* *tnp*A protein results in a high frequency of transposition and a similar high frequency of co-integrate formation. When individual R388::Tn*3651* transconjugant clones were examined, 98% were found to contain the donor plasmid marker. Thus *tnp*A protein results in the generation of stable co-integrates as the sole transposition product (Fig. 1*C*). The structures of these co-integrates were confirmed by both restriction enzyme digestion (Fig. 2) and their resolution patterns (Fig. 3), and are in agreement with the co-integrate structures reported previously[5,11]. In the presence of both *tnp*A

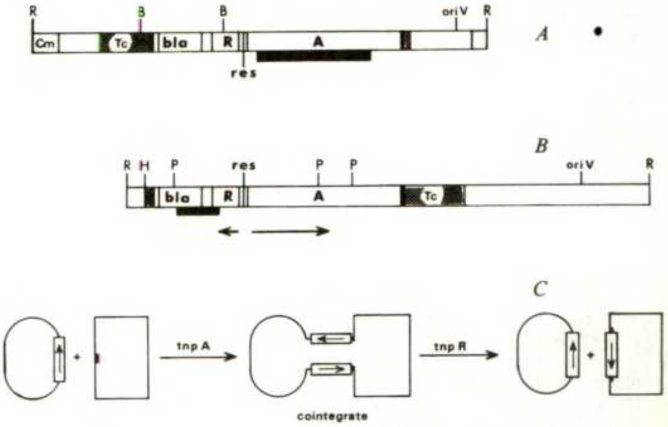

Fig. 1 Construction of *tnp*A$^-$ *tnp*R$^-$ derivatives of Tn*1* and Tn*3*. *A*, Map of pACYC184::Tn*3* and its deleted derivative pACYC184::Tn*365*. The deletion in *tnp*A is indicated by a thick black bar. pACYC184::Tn*3651* (*tnp*A$^-$ *tnp*R$^-$) was constructed by inserting a 1,150-bp *Bgl*II fragment from plasmid F (a gift from Dr R. Thompson) into the *Bam*HI site of the *tnp*R gene. *B*, Map of pMB9::Tn*1* and its deleted derivative pMB9::Tn*103*. The deletion in *tnp*R and the β-lactamase gene (*bla*) is indicated by a thick black bar. A Tn*1* *tnp*A$^-$ *tnp*R$^-$ derivative (pMB9::Tn*1031*) was constructed from pMB9::Tn*103* by deleting the *Pst*I fragment within the *tnp*A gene. In this plasmid, expression of Tc^{r} is under *tnp*R gene control and is coordinately expressed with *tnp*A protein; that is, this plasmid confers Tc^{r} in a *tnp*R$^-$ cell but Tc^{s} in a *tnp*R$^+$ cell. R, *Eco*RI site; B, *Bam*HI site; H, *Hin*dIII site; P, *Pst*I site. oriV indicates origin of plasmid replication. Thick vertical bars indicate transposon boundaries; res (resolution site) indicates the site of action of *tnp*R. Divergent transcription from the *res* region is indicated in Fig. 1*B*. *C*, transposition pathway of Tn*1/3*. Circle, donor replicon; rectangle, recipient replicon; ⇥, transposon.

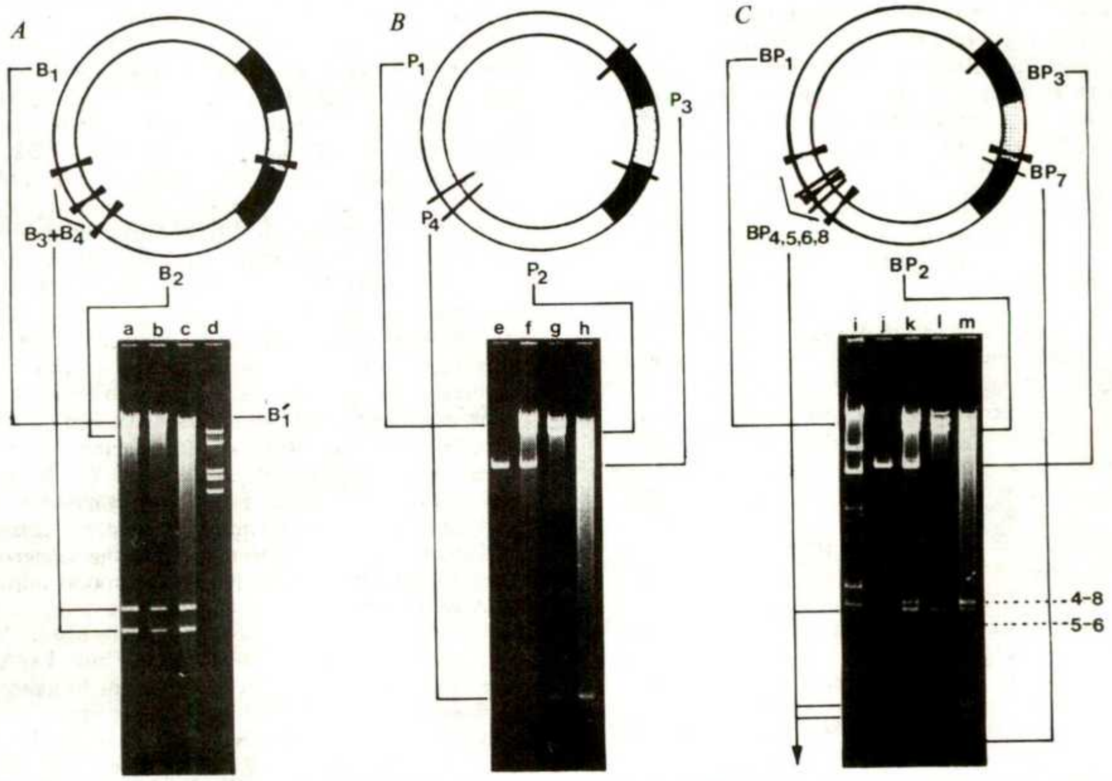

Fig. 2 Restriction analysis of a R388::TN*3651*::pACYC184 co-integrate. *A*, *Bam*HI restriction map of the R388::Tn*3651*::pACYC184 co-integrate (44 kilobases) and *Bam*HI digests of: *a*, R388::Tn*3651*::pACYC184 DNA; *b*, R388::Tn*3651* DNA; *c*, R388 DNA; *d*, λCI*857Sam*7 DNA. *B*, *Pst*I restriction map of the R388::Tn*3651*::pACYC184 co-integrate and *Pst*I digests of: *e*, pACY184::Tn*3651* DNA; *f*, R388::Tn*3651*::pACYC184 DNA; *g*, R388::Tn*3651* DNA; *h*, R388 DNA. *C*, *Bam*HI and *Pst*I restriction map of the R388::Tn*3651*::pACYC184 co-integrate and *Bam*HI–*Pst*I double digests of: *j*, pACYC184::Tn*3651* DNA; *k*, R388::Tn*3651*::pACYC184 DNA; *l*, R388::Tn*3651* DNA; *m*, R388 DNA. Track *i*, λCI*857Sam*7 DNA digested with *Hin*dIII. R388::Tn*3651* was derived from the R388::Tn*3651*::pACYC184 co-integrate by recombination across the two copies of Tn*3651*. It has a single copy of Tn*3651* and no pACYC184 sequences. Digestion with *Bam*HI produces the novel B'_1 fragment. ■, Tn*3651* sequences; □, pACYC184 sequences; □, R388 sequences; ▮, *Bam*HI site; ▮, *Pst*I site.

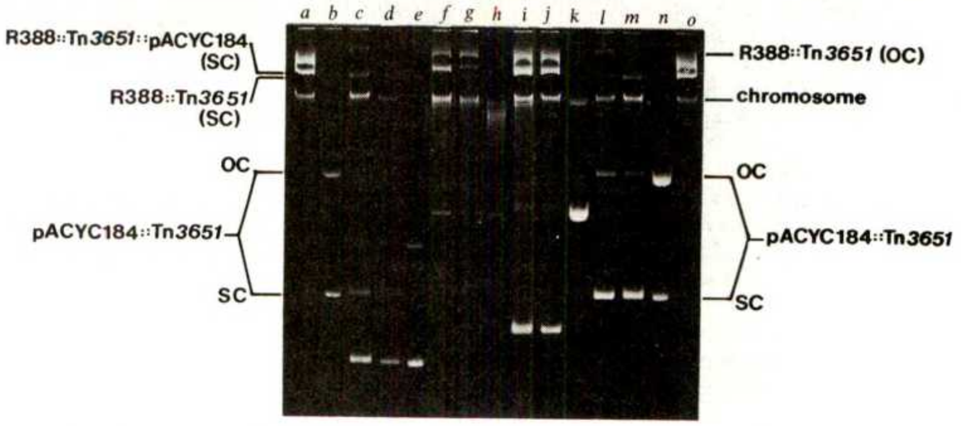

Fig. 3 Resolution of a co-integrate between pACYC184::Tn*3651* and R388, formed by transposition in a *tnp*A$^+$ *tnp*R$^-$ cell. Lanes *a*, *o*, R388::Tn*3651*::pACYC184 co-integrate-containing strain; *b*, pACYC184::Tn*3651* plasmid DNA; *c*, *d*, co-integrate strain + *tnp*A$^-$ *tnp*R$^+$ derivative of pMB8::Tn*3*; *e*, pMB8::Tn*3* *tnp*A$^-$ *tnp*R$^+$ plasmid DNA; *f*, *g*, co-integrate strain + *tnp*A$^+$ *tnp*R$^-$ derivative of ColE1::Tn*3*; *h*, ColE1::Tn*3* *tnp*A$^+$ *tnp*R$^-$ plasmid DNA; *i*, *j*, co-integrate strain + *tnp*A$^-$ *tnp*R$^-$ derivative of pMB8::Tn*3*; *k*, pMB8::Tn*3*; *tnp*A$^-$ *tnp*R$^-$ plasmid DNA; *l*, and *m*, co-integrate strain − *tnp*A$^+$ *tnp*R$^+$ pMB8::Tn*3*; *n*, pMB8::Tn*3* plasmid DNA. The plasmid DNA content of cells derived from a single colony was analysed by electrophoresis through 0.8% agarose gels. Cells were lysed by resuspension in electrophoresis buffer containing 2% Ficoll and 1% SDS. After centrifugation (18,000*g* for 15 min) to remove chromosomal DNA and cell debris, the supernatants were loaded directly on to gels. Open circle (OC) and supercoil (SC) bands of the co-integrate and of the resolution products, pACYC184::Tn*3651* and R388::Tn*3651*, are indicated. Note that in tracks *a*, *f*, *g*, *i*, *j* and *o*, the R388 co-integrate copy number is higher than in the tracks containing R388::Tn*3651*. This is because co-integrate replication occurs from the multicopy origin of pACYC184. In tracks *l* and *m*, pACYC184::Tn*3651* and pMB8::Tn*3* co-migrate. The presence and identity of all Tn*3651* derivatives were confirmed after DNA transformation or conjugation.

and *tnp*R proteins, transposition frequencies are generally some 10 times lower than in *tnp*A$^+$ *tnp*R$^-$ cells, with co-integrates occurring between 10^2 and 10^4 times less frequently. In these cases the major transposition end product is a simple transposon insertion into the recipient replicon (Fig. 1*C*), demonstrating that the *tnp*R gene product is involved in conversion of co-integrates to normal transposition end products. That the *tnp*R protein alone is sufficient to mediate this resolution was demonstrated by introducing complementing transposon derivatives into cells carrying *tnp*A$^-$ *tnp*R$^-$ co-integrates (Fig. 3). Providing *tnp*R protein alone (Fig. 3*c*,*d*) or in the presence of *tnp*A protein (Fig. 3*l*,*m*) brings about a rapid resolution of the co-integrates into the normal end products of transposition (Fig. 1*C*). However, the co-integrates are stable in the presence of *tnp*A protein alone (Fig. 3*f*,*g*). Both Tn*1* and Tn*3* *tnp*R gene products act efficiently to resolve co-integrates formed by the Tn*1* *tnp*A$^-$ *tnp*R$^-$ derivative (data not shown). Thus Tn*1* and Tn*3* gene products are completely interchangeable in the two steps of transposition.

Table 1 Complemented transposition of *tnp*A$^-$ *tnp*R$^-$ derivatives of Tn*1* and Tn*3*

Donor transposon type (*tnp*A$^-$ *tnp*R$^-$)	Complementing transposon	Frequency of transposition*	Frequency of stable co-integrate formation†
Tn*3*	—	$<1\times10^{-7}$	$<1\times10^{-7}$
Tn*3*	A$^-$R$^-$ Tn*3*	$<2\times10^{-7}$	$<2\times10^{-7}$
Tn*3*	A$^-$R$^+$ Tn*3*	8×10^{-7}	$<2\times10^{-7}$
Tn*3*	A$^+$R$^-$ Tn*3*	1.6×10^{-2}	1.5×10^{-2}
Tn*3*	A$^+$R$^+$ Tn*3*	3.5×10^{-3}	4×10^{-5}
Tn*3*	—	$<2\times10^{-7}$	$<2\times10^{-7}$
Tn*3*	A$^-$R$^+$ Tn*1*	$<1\times10^{-7}$	$<1\times10^{-7}$
Tn*3*	A$^+$R$^-$ Tn*1*	6.6×10^{-3}	7.3×10^{-3}
Tn*1*	—	ND	$<1\times10^{-6}$
Tn*1*	A$^-$R$^+$ Tn*1*	ND	$<1\times10^{-6}$
Tn*1*	A$^+$R$^-$ Tn*1*	ND	1.3×10^{-4}

Transposition into R388(Tp^r) was measured by mating *rec*A$^-$ donor strains containing R388, either pACYC184::Tn*3651* (*tnp*A$^-$ *tnp*R$^-$ Tn*3*) or pMB9::Tn*1031* (*tnp*A$^-$ *tnp*R$^-$ Tn*1*) and where indicated a third compatible plasmid carrying the complementing Tn*1* or Tn*3*, with a *rec*A$^-$ plasmid-free recipient strain.

* Fraction of Tp^r transconjugants receiving the transposon marker Ap^r; this include co-integrates and complete transposition products (Fig. 1*C*). (In all cases, except for the *tnp*A$^+$ *tnp*R$^+$ Tn*3* plasmid, the complementing plasmid was unable to transpose Ap^r.) We do not believe that the value of 8×10^{-7} in line 3 represents true transposition.

† Fraction of Tp^r transconjugants receiving the plasmid marker (Cm^r for pACYC184::Tn*3651* or Tc^r for pMB9::Tn*1031*).

That the same product from the *tnp*R region of Tn*1* and Tn*3* mediates both site-specific recombination at *res*, and repression of *tnp*A/*tnp*R expression, presumably by binding at or close to *res*, was confirmed by selecting *tnp*R$^-$ mutants derepressed for *tnp*A expression, which could then be tested for co-integrate resolution activity. Cells containing a R388::Tn*1031*::pMB9 co-integrate are Tc^r by virtue of derepressed expression of the Tc^r gene from the *tnp*A promoter (see Fig. 1*B*). Such cells were therefore transformed with hydroxylamine-mutagenized plasmid DNA (pDS4153; an Ap^r *tnp*A$^-$ *tnp*R$^+$ ColK::Tn*1* derivative). Ap^r transformants receiving unmutagenized DNA become Tc^s by virtue of *tnp*R-mediated repression whereas Ap^r transformants inheriting a *tnp*R$^-$ mutant of pDS4153 should remain Tc^r. About 10^{-3} of the Ap^r transformants remained Tc^r. Two of these were analysed in detail: plasmids the size of R388::Tn*1031*::pMB9 co-integrates and pDS4153 were observed. Isolation and subsequent characterization of the pDS4153-sized plasmids (designated pDS41531 and pDS41532) showed that the two mutants failed both to repress Tc^r and to resolve Tn*1031*-containing co-integrates in a *Sup*^{0} strain (that is, they appeared to be *tnp*R$^-$, by their inability both to repress *tnp*A-driven expression and to resolve co-integrates). In *Sup*D and *Sup*E strains, both mutant phenotypes were suppressed (to give Tc^s and co-integrate resolution) for each plasmid, whereas in a *Sup*F strain, no significant suppression of either Tc^r or co-integrate non-resolution was observed for either plasmid.

This provides further evidence that a single polypeptide from the *tnp*R region mediates both site-specific recombination and repression of *tnp*A/*tnp*R expression. We have previously suggested that *tnp*R protein could simply mediate both properties by binding at *res* if *res* contains promoters for *tnp*A and *tnp*R expression; sequence information and the known *in vitro* properties of the related $\gamma\delta$ *tnp*R protein support this idea[12,13].

P.A.K. is supported by a MRC studentship.

Received 29 October 1981; accepted 8 January 1982.

1. Gill, R. E., Heffron, F. & Falkow, S. *Nature* **282,** 797–801 (1979).
2. Heffron, F., McCarthy, B. J., Ohtsubo, H. & Ohtsubo, E. *Cell* **18,** 1153–1163 (1979).
3. Chou, J., Casadaban, M. J., Lemaux, P. G. & Cohen, S. N. *Proc. natn. Acad. Sci. U.S.A.* **76,** 4020–4024 (1979).
4. Chou, J., Lemaux, P. G., Casadaban, M. J. & Cohen, S. N. *Nature* **282,** 801–806 (1979).
5. Arthur, A. & Sherratt, D. J. *Molec. gen. Genet.* **175,** 267–274 (1979).
6. Sherratt, D., Arthur, A. & Burke, M. *Cold Spring Harb. Symp. quant. Biol.* **45,** 275–284 (1981).
7. Reed, R. R. *Proc. natn. Acad. Sci. U.S.A.* **78,** 3428–3432 (1981).
8. Bolivar, F. *Life Sci.* **25,** 807–817 (1979).
9. Chang, A. C. Y. & Cohen, S. N. *J. Bact.* **134,** 1141–1156 (1978).
10. Datta, N. & Hedges, R. W. *J. gen. Microbiol.* **72,** 349–355 (1972).
11. Gill, R., Heffron, F., Dougan, G. & Falkow, S. *J. Bact.* **136,** 742–756 (1978).
12. Reed, R. R. *Cell* **25,** 713–719 (1981).
13. Reed, R. R. & Grindley, N. D. F. *Cell* **25,** 721–728 (1981).

MATTERS ARISING

Two major genes, linked to HLA and Gm, control susceptibility to Graves' disease

WE are pleased that Uno *et al.*[1] have extended to family material the finding[2] that variation in 'immunological networks', identified by HLA and Gm allotypes, contributes to Graves' disease susceptibility in a more than additive manner.

However, like Welsh[3] we regret the uncertainty created by the unspecific but clearly extensive selection of the families analysed by these workers. For example, if as they suggest two dominant alleles are involved, general offspring–parent correspondence between markers and disease, as in the family illustrated[1] is expected, but not reported. There is evidence that HLA-associated genetic susceptibility to Graves' disease is not dominant but involves the participation of two parental haplotypes[4], and in a series of 28 affected sib pairs, 68, 25 and 7% shared respectively two, one and no HLA haplotypes, more compatible with recessive or intermediate than dominant action of HLA-associated susceptibility[5]. In one large family having several cases of Graves' disease, HLA patterns were consistent with a dominant association[6] but Gm patterns (which have not been reported) are not. Generalization from small numbers of selected families regarding the genetic component in susceptibility to Graves' disease, and possibilities for predictions of risk to relatives[3], are inappropriate. In Caucasians, the associated HLA and Gm markers are found in 23 and 80%, respectively of the general population, but only ~1% of the general population and 5% of sibs of affected persons develop Graves' disease.

We are intrigued with the lack of association between specific allotypes and Graves' disease found by ourselves in Caucasians[7] and by Nakao *et al*[8] in Japanese individuals, although admittedly different allotypes were involved in the case of the Japanese and were less closely associated with the disease.

Sasazuki's laboratory previously reported[9] a strong association between Graves' disease and HLA-Dw12 (previously DHO), but now report instead an increase in HLA-DR5. This is rather surprising because DR5 seems slightly reduced in Caucasian patients with Graves' disease, and is instead associated with goitrous thyroiditis[5]. Moreover, HLA-DR5 does not exhibit cross-reactivity with HLA-Dw12-positive cells[10]. The authors need to resolve this discrepancy.

In contrast to the mouse, in which idiotypic determinants have been shown to be linked to C_H allotypic markers, no such evidence have been provided for humans, whose allotypic markers are located further down the Fc region[11]. Further work may reveal such an association; meanwhile it is worth considering the possibility that allotype- or isotype-specific networks of immunoregulatory cells may be involved in disease susceptibility[5]. Indeed, immunoglobulin subclass and allotypic restriction of the thyroid stimulating antibody have been demonstrated[12,13].

NADIR R. FARID
JOHN C. BEAR

Faculty of Medicine,
Memorial University of Newfoundland
Health Sciences Centre,
St John's, Newfoundland,
Canada A1B 3V6

1. Uno, H., Sasazuki, T., Tamai, H. & Matsumoto, H. *Nature* **292,** 768–780 (1981).
2. Farid, N. R., Newton, R. M., Noel, E. P., Barnard, J. M. & Marshall, W. H. *Tissue Antigens* **12,** 205–211 (1978).
3. Welsh, K. *Nature* **292,** 673–674 (1981)
4. Farid, N. R. *et al. Tissue Antigens* **15,** 492–500 (1980).
5. Farid, N. R. & Bear, J. C. in *Autoimmune Endocrine Disease* (Ed Davies, T. F.) (Wiley, New York, in the press).
6. Farid, N. R., Barnard, J. M., Marshall, W. H., Woolfrey, I. & O'Driscoll, R. F. *J. clin. Endocr. Metab.* **45,** 1165–1172 (1977).
7. Farid, N. R., Newton, R. M., Noel, E. P. & Marshall, W. H. *J. Immunogenet.* **4,** 429–432 (1977).
8. Nakao, Y. *et al. Clin. exp. Immun.* **42,** 20–26 (1980).
9. Sasazuki, T. *et al. New Engl. J. Med.* **298,** 630–631 (1978).
10. Terasaki, P. I. (ed.) *Histocompatibility Testing* 1980 (UCLA Tissue Typing Laboratory, Los Angeles, 1980).
11. Weigert, T., Potter, M. & Sachs, D. *Immunogenetics* **1,** 511–523 (1975).
12. Pepper, B., Noel, E. P. & Farid, N. R. *J. Immunogenet.* **8,** 89–100 (1981).
13. Zakarija, M. *Horm. Res.* **13,** 1–15 (1980).

SASAZUKI AND UNO REPLY—We reported that two major genes, linked to HLA and Gm, control susceptibility to Graves' disease[1]. Of 30 Japanese families in which more than two first degree relatives were affected, only 15 families had at least two affected siblings, which we could analyse by the sib-pair method[2]. We did not conclude in any way that an HLA-linked disease susceptibility gene for Graves' disease was dominant. Recently we proposed[3] two genetic models for Graves' disease by analysing the same families using the affected sib-pair method[4]: (1) an HLA-linked recessive gene (gene frequency (gf) = 0.30) plus a Gm-linked recessive gene (gf = 0.10) with penetrance >0.60; (2) an HLA-linked dominant gene (gf = 0.08) plus a Gm-linked recessive gene (gf = 0.10) with penetrance >0.50. Due to the small number of affected sib-pairs, we could not distinguish between a dominant and recessive model for an HLA-linked Graves' disease gene. However, we can reject a dominant model if we analyse our data together with those of Farid and Bear[5]: of 43 affected sib-pairs, 27 shared two, 14 shared one and two shared zero HLA haplotypes.

There was not significant association between 30 probands with Graves' disease and Gm 1,2,21 (*a,x,z*) halotype which was reported[6] to be associated with Graves' disease. Rather in our study this haplotype was decreased in frequency (0.0860) compared with that in the Japanese population (haplotype frequency = 0.1575). Similarly, the present patient group did not show any association with Bw35(w5), which was reported to be associated with Graves' disease in the Japanese patients[7], where increased frequency of DW12(DHO) was also observed[8]. The present patients under study were selected from multiple case families whereas our previous study and that of Nakao *et al.* used unselected patients. This may partly explain the discrepancies observed for the statistical association of Graves' disease with the genetic markers, HLA and Gm, between our present study and those of Nakao *et al.*[6], Grumet *et al.*[7] and ourselves. This may also explain the observed discrepancy in the frequency of HLA-DR5 between our study and the report of Farid and Bear[5].

In any event, there are two distinct genes which have a major effect on susceptibility to Graves' disease and which are clearly identified by the genetic markers, HLA and Gm. Clarification of the immunological mechanisms controlled by these major genes awaits elucidation of the environmental factors which are crucial in triggering Graves' disease.

TAKEHIKO SASAZUKI
HISAMITSU UNO

Department of Human Genetics,
Medical Research Institute,
Tokyo Medical and Dental University,
Tokyo 113, Japan

1. Uno, H., Sasazuki, T., Tamai, H. & Matsumoto, H. *Nature* **292,** 768–770 (1981).
2. Penrose, L. S. *Ann. Eugen.* **6,** 133–138 (1935).
3. Sasazuki, T., Uno, H., Yasuda, N., Tamai, H. & Matsumoto, H. in *6th int. Congr. of Human Genetics* (Liss, New York, in the press).
4. Thomson, G. & Bodmer, W. F. in *Measuring Selection in National Populations* (eds Christiansen, T. B. & Fenchel, T. M.) 545–546 (Springer, Berlin, 1977).
5. Farid, N. R. & Bear, J. C. in *Autoimmune Endocrine Disease* (Ed. Davies, T. F.) (Wiley, New York, in the press).
6. Nakao, Y. *et al. Clin. exp. Immun.* **42,** 20–26 (1980).
7. Grumet, F. C., Payne, R. O., Konishi, J., Mori, T. & Kriss, J. P. *Tissue Antigens* **6,** 347–352 (1975).
8. Sasazuki, T. *et al. New Engl. J. Med.* **298,** 630–631 (1978).

0028–0836/82/070629—02$01.00

Positive selection causes purifying selection

IN their support of the neutral mutation hypothesis of molecular evolution, Li *et al.*[1] oversimplify the views of selectionists and use a specious logic that should not go unchallenged. They assert after Clark[2] and Milkman[3] that "selectionists believe that most nucleotide substitutions are caused by positive darwinian selection" and then using King and Jukes[4,5] as their authorities argue "in which case the rate of nucleotide substitution in functionally unimportant genes or parts of genes is expected to be relatively lower because the mutations in these regions of DNA would not produce any significant selective advantages".

I believe that the assertion of Li *et al.*[1] is an oversimplication. There are molecular evolutionists who are selectionists because they consider natural selection to be a driving force steering protein evolution[6-8]; however, such proponents of darwinian evolution of proteins are quite willing to have neutral substitutions occur at a high rate in pseudogenes, in the third position of the codons when the base changes do not cause amino acid changes[8], and in general in functionally less important regions of DNA.

The argument of Li *et al.*[1] is specious because it ignores two factors: (1) the time span for molecular evolution above the species level is in millions of years, not hundreds; and (2) the selection, which is positive darwinian selection when it increases the frequency of an allele in an evolving lineage, becomes stabilizing (=purifying or negative) selection after the allele replaces all others in that lineage. When these two factors are considered it follows that the nucleotide substitutions in functionally important parts of genes, as measured in distant pairwise comparisons such as those of Li *et al.*[1], could be primarily adaptive substitutions and still yield a slower evolutionary rate per nucleotide position than the neutral substitutions in functionally less important genes or parts of genes. For the short time span that an adaptive mutation is being fixed in a lineage by the positive darwinian form of natural selection, there could follow a very long time span during which the fixed mutation was maintained by the stabilizing form of natural selection. Thus over the total time span of many millions of years, the average evolutionary rate for such adaptive mutations could be relatively small. Nevertheless, the findings of Li *et al.*[1] on pseudogenes do not exclude the possibility that for certain important categories of base substitutions, for example, those that change amino acids, a relatively large proportion were fixed by selection rather than random drift.

MORRIS GOODMAN
Department of Anatomy,
Wayne State University
School of Medicine,
Detroit, Michigan 48201, USA

1. Li, W-H, Gojobori, T. & Nei, M. *Nature* **292,** 237–239 (1981).
2. Clark, B. *Science* **168,** 1009–1011 (1970).
3. Milkman, R. *Trends Biochem. Sci.* **1,** N152–N154 (1976).
4. King, J. L. & Jukes, T. H. *Science* **164,** 788–798 (1969).
5. Jukes, T. H. & King, J. L. *Nature* **231,** 114–115 (1971).
6. Goodman, M., Moore, G. W. & Matsuda, G. *Nature* **253,** 603–608 (1975).
7. Goodman, M. & Czelusniak, J. *Protein Biol. Fluids* **28,** 57–60 (1980).
8. Goodman, M. *Prog. Biophys. molec. Biol.* **38,** 105–164 (1981).

LI *ET AL.* REPLY—Goodman accepts our view that random fixation of neutral alleles occurs at a high rate in such unimportant genes as pseudogenes or in general in functionally less important regions of DNA, but believes that natural selection is a driving force steering protein evolution. He suggests that a large proportion of amino acid substitutions in proteins are caused by natural selection. It is known, however, that the rate of amino acid substitution is also higher in functionally less important proteins or parts of proteins, as in the case of nucleotide substitution in DNA[1,2]. For example, fibrinopeptides A and B, which apparently do not have any biological function except for holding other polypeptides that later form a protein, show a rate of nucleotide (amino acid) substitution as high as that of pseudogenes[3,4]. The fact that amino acid sequence apparently does not affect appreciably fibrinopeptide function, and the mutation rate per nucleotide site is presumably the same for these peptides and pseudogenes, strongly suggests that the amino acid substitutions in fibrinopeptides are mainly due to random fixation of neutral alleles.

In functionally important proteins or parts of proteins, the rate of amino acid substitution is much lower than that in fibrinopeptides[1,2]. The neutralist's explanation for this is that these proteins have strong functional constraints, which cause many new mutations to be eliminated from the population, and only those mutations (amino acid sequences) that are functionally equivalent are incorporated into the genome[2]. In the neutral theory, therefore, the entire set of substitution data from pseudogenes to highly conserved proteins such as histone can be explained by the simple and realistic assumption that the mutation rate is the same for all segments of DNA (genes or parts of genes) but the proportion of fresh mutations eliminated varies with DNA segment and the higher this proportion, the slower the rate of gene substitution. Available data support this view, that is, fresh mutations are known to occur almost at random in the entire coding region of haemoglobin DNA[5], and any amino acid substitutions generally occur between two amino acids having similar biochemical properties[6,7]. However, if natural selection is the driving force for protein evolution, it would be difficult to explain the inverse relationship between the functional importance of genes and the rate of gene substitution[4]. Note that the rate of gene substitution due to darwinian selection depends not only on the mutation rate but also on the selection coefficient and population size[8]. In any theory based on selection these three factors must be considered.

Goodman's statement that we have ignored the two factors mentioned by him is unfounded. Our conclusion is based on a study of evolutionary change of genes for 80 Myr and on a due consideration of the effects of mutation, selection and random genetic drift. Note also that neutralists believe that adaptive evolution occurs by positive darwinian selection but a small proportion of gene substitutions is sufficient for this[9].

WEN-HSIUNG LI
TAKASHI GOJOBORI
MASATOSHI NEI

Center for Demographic and
Population Genetics,
University of Texas at Houston,
Houston, Texas 77030,
USA

1. King, J. L. & Jukes, T. H. *Science* **164,** 788–798 (1969).
2. Kimura, M. & Ohta, T. *Proc. natn. Acad. Sci. U.S.A.* **71,** 2848–2852 (1974).
3. Kafatos, F. C. *et al. Proc. natn. Acad. Sci. U.S.A.* **74,** 5618–5622 (1977).
4. Li, W.-H., Gojobori, T. & Nei, M. *Nature* **292,** 237–239 (1981).
5. Vogel, F. *J. molec. Evol.* **1,** 334–367 (1972).
6. Jukes, T. H. & King, J. L. *Nature* **231,** 114–115 (1971).
7. Grantham, R. *Science* **185,** 862–864 (1974).
8. Kimura, M. & Ohta, T. *Theoretical Aspects of Population Genetics* (Princeton University Press, Princeton, 1971).
9. Nei, M. *Molecular Population Genetics and Evolution* (North Holland, Amsterdam, 1975).

Matters Arising

Matters Arising is meant as a vehicle for comment and discussion about papers that appear in *Nature*. The originator of a Matters Arising contribution should initially send his manuscript to the author of the original paper and both parties should, wherever possible, agree on what is to be submitted. Neither contribution nor reply (if one is necessary) should be longer than 300 words and the briefest of replies, to the effect that a point is taken, should be considered.

0028-0836/82/070630—01$01.00

BOOK REVIEWS

Evolution, sex and ideology

University Colleges of Science & Technology
92, A.P.C. Rd., Cal.-9
LIBRARY COMPLEX
Departments of:
Chemical Engineering
Chemical Technology
Plastics & Rubber Technology

Jon Beckwith

MICHAEL Ruse's collection of ten essays covers a number of important issues in biology, biomedical science and the philosophy of biology. However, only one of these essays, 25 pages long, deals with the title question, is science sexist? Further, as I will consider later, his discussion of it misrepresents an important controversy over science and values. Let me follow this complaint with some praise for the author — this is probably the most accessible and lively writing by a philosopher of science I have come across. The book is entertaining, if often wrong-headed, and does present in clear fashion arguments on such issues as evolutionary theory, the recombinant DNA debate, genetic screening and medical views of homosexuality.

However, there is a current of reductionist thought which permeates most of these essays. For instance, in the first few chapters Ruse presents one of the most persuasive arguments in support of evolutionary theory — arguments which are particularly pertinent today with the attack on the teaching of evolution by creationists in the United States. (Ruse recently testified on behalf of the evolutionists in the Arkansas court case.) Yet he is so enamoured of the adaptationist explanation for biological phenomena that his arguments almost begin to turn against themselves. He describes lucidly how the "founder effect" accounts for the variations seen in Darwin's finches in the Galapagos Archipelago. (The founder effect refers to situations in which a small number of individuals of a species become geographically isolated from the rest and "founds" a new variant of the species with its own peculiar gene pool.) Yet the founder effect (among many other factors) could well lead to a number of variations which are not themselves a product of natural selection. If an adaptationist explanation is available for a phenomenon, it is presented as if it were almost proof of the explanation itself.

To take a strict adaptationist view trivializes evolutionary theory and turns it into a sterile enterprise. In fact, we are entering a rich period in the study of evolution as a result of advances in many areas of science, including protein chemistry, molecular genetics and palaeontology. This progress does not in any way lead to a rejection of the fundamentals of Darwin's theory, but vitalizes it with variations and new mechanisms some of which could not even be conceived of until recently.

Is Science Sexist? And Other Problems in the Biological Sciences. By Michael Ruse. Pp.299. Hbk ISBN 90-277-1249-2; pbk ISBN 90-277-1250-6. (Reidel: 1981.) Hbk Dfl.80, $42; pbk Dfl.32.50, $14.95.

Ruse also deals with the validity of Darwinian evolution as a genuine scientific theory using the criteria of Karl Popper. While I have no qualms about evolutionary theory, I do not feel that the defence in Popperian terms is very successful. As I will describe later, the use of falsifiability is problematic as many philosophers of science have recognized.

After covering some issues of interest to philosophers concerning the relationship between molecular genetics and Mendelian genetics, Ruse passes on to a discussion of genetic screening and its implications. By and large I found myself in agreement with the perspective in this essay. The fallacies of cost-benefit analysis of genetic screening programmes, the dangers of categorizing social and ethical problems as medical ones, the potential for discrimination against minority groups and the dangers of broadening the definition of genetic disease to include social behaviours such as homosexuality are pointed out. This is an excellent account for everyone working in the area of genetic screening. One complaint, however, which perhaps relates to the reductionist streak in this book: Ruse repeats the now discredited myth that XYY males exhibit antisocial behaviour, citing as his source a review by Borgaonkar and Shah, which apparently he has not read. For, in fact, these authors concluded that "The frequency of antisocial behaviour of the XYY male is probably not very different from non-XYY persons of similar background and social class".

Ruse's analysis of many of the issues in the recombinant DNA debate hits the mark, but his prejudice for reductionist science shows up again in such comments as "scientists [working with recombinant DNA] are finding out in the most basic way, precisely what makes the world work. . . .". Recombinant DNA is not a field of research; it is a tool for studying *certain* biological problems which are approachable at the level of the gene or of DNA structure. Because of its enormous power in studying these questions, this new tool has had a distorting influence on priorities in biological research. First, the study of genes in isolation from their general environment and from the cells and organisms in which they function provides answers to only a very limited number of questions. Further, most of the areas of biology which have to do with "what makes the world work" are ones to which recombinant DNA may not make major contributions. Can Ruse's attraction to "recombinant DNA research" be connected with his obvious interest in the explanations at the level of the gene found in sociobiology?

It is the arguments on the issue of sociobiology that seem the most strained in these essays. Ruse tries to put sociobiology on the same plane as evolutionary theory using analogous arguments about testability and falsifiability. Here the problems with falsifiability become clearer. Many might have thought that Marshall Sahlins's descriptions of the enormous variations in kinship systems in various cultures which counter predictions of sociobiology would have been a falsification of kin selection as applied to human societies. Instead, Sahlins's examples are either ignored or explained away by sociobiologists as due to unusual circumstances or to genetically aberrant societies, or *ad hoc* hypotheses are devised to incorporate them into sociobiology. What becomes clear is that a falsification to one person is an irrelevancy to another. Ruse is aware of this when he points out that just because "some people will not let a theory be falsified does not mean that the theory itself is unfalsifiable . . . ". But who decides when a theory has been falsified? To my mind, the conclusion that a particular set of data does or does not falsify sociobiology is a reflection of one's general stance on the issue rather than on some objective truth. In this light, Popper's concept of falsifiability seems vacuous.

While in earlier chapters Ruse points out the alternatives to evolutionary theory and convincingly dismisses them, in his discussion of sociobiology he barely mentions cultural explanations for human social behaviour. Again in contrast to the discussion of evolution, he does not indicate how one would go about distinguishing between the two explanations. It is simply his attraction to the adaptationist scheme which leads him to favour the genetic explanation. However, for complex human social behaviours, the environmental and genetic factors are so intertwined and so difficult to distinguish that I cannot imagine how this distinction can be achieved in the foreseeable future. Until that time the claims for evidence for the genetic model must be considered as no more than an indication of the biases of the scientists (and philosophers) who put forth the claims.

These arguments apply, of course, to the question of sex roles which Ruse discusses in his penultimate chapter. According to Ruse, one is not a sexist if one values positively the role of the female human being. This extraordinarily naive position ignores the broad cultural and institutional forms of power in society which perpetuate male domination. Sociobiologists place a heavy emphasis on sexual selection and on sex role division of labour and its evolutionary basis. These points are essential to the theory. The sexism of sociobiology does not lie in its conclusions, as Ruse would have us believe the critics have charged. Rather, the conclusions are a natural consequence of the fundamental assumptions which underly the whole sociobiological enterprise. For example, basic to E.O. Wilson's explanation of sex roles as they exist today is a reconstruction of human prehistory which describes the male as a hunter from early evolutionary times. He accepts the arguments of popularizers of palaeontology such as Ardrey and ignores the bulk of evidence which suggests that, for most of hominid evolution, we were vegetarians and fruit eaters. There are numerous similar examples in sociobiology where a social bias leads to the choice of explanation or of data which, in turn, are determinants of the conclusions of the theory. One has only to read Kropotkin's *Mutal Aid* to see that a different social perspective leads to a choice of different examples and thus to a totally different view of human nature.

This is a strange, contradictory and provocative book. While admitting that "one should [not] try to pretend that science can proceed divorced from ideology", Michael Ruse ignores the pervasive ideological influences on those attempts to use the biological sciences to explain human social behaviour. □

Jon Beckwith is in the Department of Microbiology and Molecular Genetics at Harvard Medical School.

Putting the environment back in genetics

Lindon J. Eaves

Cultural Transmission and Evolution: A Quantitative Approach. By L.L. Cavalli-Sforza and M.W. Feldman. Pp.388. Hbk ISBN 0-691-08280-4; pbk ISBN 0-691-08283-9. (Princeton University Press: 1981.) Hbk $25, £17.70; pbk $10.50, £7.50.

IN MANY applications of quantitative methods to human genetics it has been assumed, by default, that transmission is biological in spite of repeated criticism that environmental factors may simulate Mendelian inheritance. Historians and philosophers of science may wonder why the genetic theory of human differences has proved so powerful. Some of the credit must be given to the fact that the consequences of genetic inheritance found a precise mathematical form very early, in the work of such pioneers as Fisher and Wright. By contrast, environmental transmission models were inexplicit and devised to explain rather than predict.

The past ten years have seen a number of critical developments which have gone far to redress the imbalance of theory. Sociobiology arose because existing evolutionary theory seemed to run counter to those very human characteristics that evolution had established. Much of this work has been conservative, retaining at its centre the genetic basis of information transfer and attempting to show how such characteristics of higher organisms as sex, altruism, parental care, social organization and mate selection could evolve in a Darwinian universe.

Cavalli-Sforza and Feldman begin from a radically different position. They take the human capacity for learning and social interaction for granted and examine the many ways in which the dynamics and equilibria of human populations are modified when the rules of transmission are freed from their Mendelian straitjacket. Their work is a pleasing balance of theory and colourful examples.

They examine a number of ways in which cultural transmission may differ from genetic inheritance. In the simplest case, transmission may involve a single dimorphic cultural state passed from parent to child without the constraints which accompany Mendelian segregation. Such "vertical transmission" may often be confused with Mendelian inheritance but can generate a far wider range of dynamics and equilibria. The authors show, for example, the conditions under which cultural states may oscillate between generations if children react against the values of their parents. The theory is developed mathematically using assumptions and methods largely familiar to population geneticists. Cultural parallels of mutation, migration, selection and drift are examined, together with some models of assortative mating. Later chapters consider multi-state and continuous traits.

Cavalli-Sforza and Feldman recognize that transmission is not confined to the nuclear family. Information may be passed from teachers in the parental generation ("oblique" transmission) or in the same generation ("horizontal" transmission). In such cases only the type of social organization and communication network restrict the number of people influenced by a new idea, so the rates of evolutionary change increase dramatically. One possible consequence is the rapid spread of an innovation which has an adverse effect on fitness.

The authors are the first to admit that there is an element of unreality in treating cultural transmission independently of genetic inheritance, and there are other workers who have considered the joint effects of genetic factors and social interactions on the resemblance between relatives. Perhaps the only weakness of the present book is a failure to integrate the theory with other contemporary work in human quantitative genetics, much of which is just as concerned with the environment.

Part of the richness of *Cultural Transmission and Evolution* stems from the inclusion of illustrative examples, ranging from national differences in pronunciation, through the familial transmission of Buddhism, to the distribution of surnames. Data are used by Cavalli-Sforza and Feldman very much as they were used a century ago by Galton and Pearson, to illustrate rather than prove. There is little attempt to test and exclude alternative genetic hypotheses.

The long-term value of the book is likely to stem not from the data, however, but from the authors' ability to crystallize the elements of cultural transmission in a mathematical model which starts with a few simple assumptions. It offers, to biologists and behavioural scientists alike, an attractive demonstration of the heuristic value of model-building as a way of drawing together the more haphazard intuitions of the past and may make clinical and behavioural geneticists more sensitive to the ambiguities of their data. □

Lindon J. Eaves is Distinguished Professor of Human Genetics at the Medical College of Virginia, Richmond.

Supergiant behaviour

J.B. Hutchings

The Brightest Stars. Geophysics and Astrophysics Monographs, 19. By Cornelis De Jager. Pp.456. Hbk ISBN 90-277-1109-7; pbk ISBN 90-277-1110-0. (Reidel: 1981.) Hbk Dfl.140, $73.50; pbk Dfl.60, $31.50.

IN attempting to cover our current knowledge of the most luminous stars in nine self-contained chapters, Dr De Jager has set himself a formidable task. The recent pace of research has expanded the frontiers of this subject to an extent that no one volume can fully encompass. What the book does is cover, with examples and illustrative theory, the behaviour of all types of supergiant stars. Slightly surprisingly, it also sets out to deal with novae and supernovae.

The subject matter includes data from all wavelengths between X-ray and radio, on stars of all possible temperatures. Considerable space is given to describing observations and derived quantities typical of subgroups such as Of, Be, W-R, P Cygni stars and ζ Aur stars. Evolution, atmospheric structure and mass-loss are described in separate chapters, and the largest section deals with chromospheric, coronal and circumstellar dust phenomena.

It is perhaps too easy for one familiar with the subject to look for deficiencies or omissions. My main personal regrets were the lack of summarizing tables in many sections, the lack of coherence between some of the chapters and the omission of many of the observational details and uncertainties. A good bibliography of more specialized books, conference proceedings and reviews would also have been welcome.

Nonetheless, the book is fairly thorough in its coverage and it is hard to find much of importance that is left out. Theoretical sections accompany all descriptions of data, but are mostly given at the physical concept level; the book is not a reference source for applying or deriving rigorous models. The chapter on atmospheres is perhaps the exception here and is an excellent introduction to recent work. However some other topics are belaboured to the point of my wondering how important they really are.

The author has clearly made extensive use of other published material and diagrams. While this tends to override any particular bias, it leads to a somewhat variable depth in the treatment of different topics. Diagrams are generally reproduced from other work and often contain symbols or features not explained in the captions. There is a sprinkling of typos and grammatical curiosities, which do not detract seriously from the book's impact — one which occurs regularly is "criterium". I also spent some time looking for the fifth type of nova.

The most luminous stars are important as they are responsible for most of the X-rays, supernovae, enrichment of the ISM, star formation and optical radiation in a galaxy, but they are rare and constitute a small fraction of its mass. They are often the only individual objects we can study in other galaxies, and it is clear that we need to understand them more fully. This book provides a good background and overall description of their properties at a time when many new facts are being learned about them. ☐

J.B. Hutchings is a Research Scientist at the Dominion Astrophysical Observatory, Victoria, British Columbia.

Coming out on top

D.H. Everett

Chemistry in Two Dimensions: Surfaces. By Gabor A. Somorjai. Pp.575. ISBN 0-8014-1179-3. (Cornell University Press: 1981.) $48.50, £29.

THE George Fisher Baker Lectures at Cornell University have long had a reputation for excellence, and those which have subsequently appeared in print have been important milestones in the development of chemistry: they include the books of Alfred Stock, Monteath Robertson, Linus Pauling, C.K. Ingold, G. Herzberg, Paul Flory, Jack Dunitz, Herbert Brown and R.P. Bell. This volume by Gabor Somorjai will prove to be no exception.

The past 20 years have seen an explosive development of surface physics and surface chemistry, brought about as so often happens by major developments in experimental techniques. Today the tools of the surface scientist are represented by a bewildering and annually increasing number of acronyms. In this book, after an introductory chapter, some 20 such techniques are explained, and their application to the characterization of solid surfaces is outlined. The results of experimental work on the surface composition of alloys are then described and their theoretical interpretation discussed. Enrichment of the surface of alloys by one preferentially adsorbed component follows a pattern familiar in work on liquid–vapour and solid–liquid interfaces, and it is perhaps a pity that the opportunity was missed here to draw attention to the underlying unity of various branches of surface science. Thus the theories of the surface enrichment of alloys, published in the mid-1970s and presented in the book, are essentially identical with those of adsorption at the liquid–vapour interface originally developed for ideal systems by Butler in 1932 and for regular solutions by Schuchowitsky and Guggenheim in the 1940s, and applied in the 1960s to adsorption at the solid–liquid interface. The unfortunate impression left by the present account is that the theories described are recent developments aimed specifically at the solid–vacuum interface.

Two chapters on the structure of clean surfaces and of adsorbed monolayers on solids provide full and authoritative accounts of the voluminous literature on the subject. A discussion of the surface chemical bond and of energy transfer in gas–surface interactions provides a valuable introduction to the last third of the book, which is concerned with catalysed chemical reactions at surfaces. A general account of heterogeneous catalysis includes extensive and valuable tables of kinetic parameters characterizing the catalysis by metal surfaces of the hydrogenolysis of ethane, propane, *n*-butane, isobutane, the isomeric pentanes, several hexane isomers, *n*-heptane, benzene and a number of other hydrocarbons. Also tabulated are kinetic data on the ring opening of cycloalkanes, toluene hydrodealkylation and hydrogenolysis, the hydrogenation of olefins and aromatics, and the isomerization and dehydrocyclization of alkanes. These tables in themselves make the book an essential part of the literature on heterogeneous catalysis. Particular attention is then given to hydrocarbon conversion on platinum and to the catalytic hydrogenation of carbon monoxide; and a brief final chapter deals with photochemical surface reactions.

Gabor Somorjai has contributed much distinguished research to surface science. His enthusiasm and the authoritative position he commands in this field are apparent throughout this book. It cannot fail to become a classical text, the value of which will not be diminished by the rapid developments which will surely ensue in the future. Both as a wide survey of surface science, and as a source of critically assessed kinetic data on heterogeneous catalysis on metals, the book is most strongly recommended. ☐

D.H. Everett is Leverhulme Professor of Physical Chemistry at the University of Bristol.

Seminal secrets

R.J. Aitken

Male Reproductive Function and Semen: Themes and Trends in Physiology, Biochemistry and Investigative Andrology. By Thaddeus Mann and Celia Lutwak-Mann. Pp.495. ISBN 0-387-10383-X. (Springer-Verlag: 1981.) DM150, £32.

IN *Male Reproductive Function and Semen*, Mann and Lutwak-Mann have produced a highly authoritative treatment of a vast volume of literature relating to the production, composition and function of semen. The book is a sequel to the successful *Biochemistry of Semen and of the Male Reproductive Tract*, published by Methuen in 1964, and summarizes the important advances that have taken place in the field since that time.

There should be something in the text for any student, clinician or scientist interested in this subject. For the student, there is an extensive bibliography and a comparative approach which provides a fascinating insight into the diversity of reproductive strategies employed by different groups of animals.

For the clinician and scientist no page of this book should really remain unturned. Of particular interest to the former are sections on such topics as the assessment of semen quality, the cryostorage of spermatozoa and the biochemistry of seminal plasma in relation to andrological practice. For the research worker there are excellent, well-referenced methodological sections dealing with the logistics of experimentation in the male reproductive sciences.

To all proud possessors of a Y chromosome the final chapter on the influence of environmental factors on spermatogenesis and sperm function should be of special interest. The chapter covers a wide range of interactions, including those between addictive drugs, therapeutic agents, food additives, industrial chemicals and pesticides. The list of compounds interfering with male reproductive function is indeed alarmingly long and may go some way towards explaining the apparent progressive decline in the sperm densities encountered in normal fertile men from a mean of 100×10^6 cells per millilitre twenty years ago to a value of 50×10^6 at the present time. The role of such environmental hazards in the aetiology of male infertility is obviously in urgent need of assessment.

The emphasis of the book is clearly a reflection of the interests of the authors. Thaddeus Mann's contribution to our understanding of the biochemistry and function of semen has been universally acknowledged and his work has inspired a generation of scientists, including myself. One consequence of this interest in semen, however, is that the behaviour of spermatozoa once they have escaped from the seminal plasma and initiated their quest for the female gamete(s) is not given the same depth of treatment. The abilities of spermatozoa to migrate through the female reproductive tract and engage in the process of fertilization are of critical importance to the definition of fertility, yet neither of these important properties can be accurately predicted from the behaviour in sperm in seminal plasma.

A related problem is that the population of spermatozoa participating in fertilization *in vivo* spend a majority of their lifespan in a state of so-called capacitation. In contrast, a significant proportion of the studies reviewed in the extensive chapter on sperm biochemistry have been carried out on spermatozoa of uncertain physiological status suspended in simple, artificial media. The authors are obviously aware of this problem but conclude that it in no way detracts from the value and biological significance of the results. I wish I could share their confidence.

The layout of the book is excellent, although certain passages might have benefited from more extensive illustration, and I wish there had been a concluding chapter in which the authors' knowledge and experience could have been used to highlight the most significant recent developments. Nonetheless this is a major work by two highly distinguished authors; it should find a home on the bookshelves of anyone professing an interest in male reproductive physiology. □

R.J. Aitken is a Research Scientist at the MRC Unit of Reproductive Biology, Edinburgh.

Favourite recipes for the macrophage chef

S. Gordon

Manual of Macrophage Methodology: Collection, Characterization, and Function. Edited by H.B. Herscowitz *et al.* Pp.514. ISBN 0-8274-1222-6. (Dekker: 1981.) SwFr. 185, $65.

METCHNIKOFF drew attention to the specialized phagocytic capability of macrophages a century ago. Apart from their role in immunity against many important intracellular pathogenic organisms, the macrophages distributed throughout the body secrete numerous products responsible for inflammation, repair and injury. In addition, these cells retain differentiated traits *in vitro* and thus provide ideal material to study growth, membrane traffic, destruction of tumour cells and many other topics of interest to both cell biologists and immunologists.

Description of methods for studying the macrophage has traditionally been relegated to immunology texts, but several attempts are now under way to produce a separate, specific manual. This volume has arrived early and does contain much useful information, but is badly flawed by lack of a proper sense of where macrophage research is heading. Although sound prescriptions are given for the isolation of macrophages and study of some of their activities, exciting areas like H_2O_2 production and surface antigens are overlooked. Individual authors often turn to outmoded methods of cell characterization and elimination, by silica for example, rather than coming to grips with the problem of adherent cell heterogeneity. Thus, the implications of the discovery of the potent "antigen presenting" activity of dendritic cells, a minor contaminant of most macrophage populations, are not confronted. Other points of emphasis are irregular; interleukin-1 is well covered, but not CSF; the recovery of macrophages from spleen by enzyme digestion, a difficult but important procedure, is neglected; pinocytosis mediated by specific receptors is ignored; and so on.

Some authors give workmanlike assessments of procedures otherwise scattered in research papers. These include a catalogue of permanent cell lines with macrophage markers, culture methods for bone marrow precursors, cytochemical procedures for the light microscope, and the ever-useful detailing of Fc and complement receptor assays. Nevertheless, there are too many descriptions of everyone's favourite assay for microbicidal/cytocidal activity of activated macrophages and not enough assessment of their value. Readers will therefore find this book only moderately useful, and not sufficiently critical, integrated or comprehensive. □

In celebration of its fiftieth anniversary the American Institute of Physics has published a handbook for physicists of all persuasions, the *Physics Vade Mecum*. The book consists of 22 chapters containing useful formulae, numerical data, definitions and references pertinent to various fields, and is available from AIP Marketing Services, 335 East 45 Street, New York, price $25.

S. Gordon is Reader in Experimental Pathology at the Sir William Dunn School of Pathology, University of Oxford.

Chemical dynamics

J.N. Murrell

Potential Energy Surfaces and Dynamics Calculations for Chemical Reactions and Molecular Energy Transfer. Edited by Donald G. Truhlar. Pp.866. ISBN 0-306-40755-8. (Plenum: 1981.) $85, £53.55.

IN A rapidly developing area of science it is usually necessary to go to the primary literature to obtain details about the currently active experimental or theoretical techniques. The reason for this is not just that textbooks take some time to be published, but that authors have difficulty in deciding the opportune moment to write them. This book consists of a collection of original papers that were given at a symposium in August 1980. In that respect it provides an up-to-date perspective on this field and, in my view, a broadly balanced one.

Researchers interested in potential surfaces and molecular dynamics are concerned with understanding and predicting the results of collisions between simple molecules. The equations necessary for these predictions are well established but it is only in recent years that computational techniques have reached the level of providing, in many cases, reliable predictions. There are two stages in the calculation, both of which have seen recent advances: first, it is necessary to have accurate potential functions, and second they must be used for accurate dynamics.

There are three papers in the volume which give an overview of particular aspects of the field. These are on unimolecular dynamics, reactive scattering and non-reactive scattering. In addition there are 33 papers which deal largely with particular molecular systems. The contributions are generally of good quality and by respected authors, and thus I can thoroughly recommend the book for purchase by libraries and by active research workers in the field. □

J.N. Murrell is a Professor in the School of Chemistry and Molecular Sciences, University of Sussex.

nature

25 February 1982

University College ... Dr. A.P.C. ... LIBRARY COMPLEX
Department of :
Chemical Engineering
Chemical Technology
NOV 1982

What to tell the White House

The new White House Science Council is only a pale shadow of the old President's Science Advisory Committee; it should stay that way.

The King is dead; long live the King (or the Queen as the case may be)! Can this declaration, much cherished by historians keen to demonstrate the repetitivity of events, be applied to that curious political animal in the United States — the President's Science Advisory Committee? The committee (PSAC, pronounced *pea-sack*) was abolished in 1973 by President Nixon, as legend has it because it had become too uppish. Although many in the then administration, including even the Secretary of State, Dr Henry Kissinger, agreed with PSAC's most talkative members that anti-ballistic missile systems were then technically backward and always likely to be strategically ineffectual (and, for that reason, dangerous), the administration plainly did not want its negotiating position compromised by a bunch of fast and independently-talking academics, among whom members of PSAC were prominent. But now, after a decent interval, there is to be a science advisory council in the White House again (see page 637). PSAC having ceased to exist, it seems as if it has been necessary to reinvent it as the White House Science Council. Appearances, however, are misleading.

In its heyday, perhaps until the mid-1960s, PSAC was a remarkable institution. In many ways, it was a continuation into peacetime (made to seem threatening by the arrival of the first sputnik) of the camaraderie of the veterans of technological wars — the people who had set up radiation laboratories, Manhattan Projects and the like. PSAC in its early days was immensely influential because its members were influential, both in the academic community and with the government. PSAC seemed merely to have to wave its wand, and the federal government would agree that there should be a programme of curriculum development aimed at the improvement of science teaching in high schools, for example — ironically, the programme now finally dismantled in the Administration's budget for 1983. On other occasions, the committee lent powerful support, from outside the White House, to the executive functions of the Science Advisor as, for example, in the early 1960s when Dr Jerome Wiesner was battling with Mr McGeorge Bundy for an influence over United States policy on disarmament (and defence). Unlike most other advisory committees, PSAC seems not to have bothered to wait for a request for advice but would offer its opinions gratuitously, sometimes to people who did not want to hear. Always, PSAC gave the technical community in the United States the sense, but also the illusion, that there was an effective and publicly constituted channel by means of which account could be taken of raw technical opinion. What went wrong?

The doctrine that everything that President Nixon did must by definition be mistaken is a poor guide to the truth. While the Nixon administration may have been more afflicted by public disagreement about arms control policy than previous administrations, there is also something in the view that the virtues that made PSAC seem to the technical community to be exceedingly important were precisely those calculated to be a thorn in the flesh of the White House. The dilemma has been neatly described by Dr Edward J. Burger in his book *Science at the White House*, published last year. (For Professor Harvey Brooks's review, see *Nature*, 290, 635; 1981). Because many of the committee's pronouncements were unsolicited, they were not assured of the welcome they might otherwise have had. But when asked for its advice, PSAC would often provide its masters with an opinion which, even if entirely correct, could only seem to the embattled administrators to be unhelpful and even self-serving. Burger tells how the White House of 1970, anxious to do "something big" about public health but unsure of what, was disconcerted by a PSAC panel's view that a rapid growth of the force of practising physicians was unnecessary but that more money should be spent on biomedical research. The question remains unanswered whether a more pointed commentary on the options before the administration might have headed off President Nixon's "war" on cancer.

Administratively, Dr Keyworth's latter-day version of PSAC may be an improvement on the original. Even from the narrow view of the technical community, there is a balance to be struck between the prestige and independence of the old committee and the possibility that its successor may be listened to more attentively. The "bring back PSAC" campaign of the past nine years has been unreflective about this point. And even if, in the months immediately ahead, the chief function of the new science council is to strengthen Dr Keyworth's own position in the White House, that in the long run can do no harm. It may also help that the President's Science Advisor will be the sole channel for communication between the new council and the Administration. He, no doubt, is likely to be best placed to judge when this or that study can most effectively be put into circulation — and which had better be kept in a drawer. The other side of the coin is that the new council will not become a focus for the attention of the technical community, a legitimized whispering tube, and that even the members of the new council may from time to time suspect that they are being used.

The field of operations for the new council is less certain. From some remarks let slip in London last week, Dr Keyworth seems to think of the new council as a means of helping him solve some awkward administrative problems — making different uses of well-established national laboratories for example. But how? A high-level survey of the resources and capabilities of the national laboratories would benefit the whole technical community, even outside the United States, but Dr Keyworth seems to have more particular goals in mind. Does he want the committee to be his hatchet-man? Or, more machiavellian, does he hope that a committee which includes Dr Harold Agnew (once director at Los Alamos) and Dr Edward Teller (closely identified with Livermore) is bound to resolve the ancient dilemma of deciding which laboratory should go? The most obvious danger is that if the committee is too much used as a means of confirming administrative decisions, or as a means of sanctifying prejudices about what the national laboratories can and cannot accomplish, its reputation in the technical community will be unenviable.

Even without a single meeting to its credit, the composition of the new council cannot fail to excite prurient speculation. For the first time in almost a decade, the White House now has a science adviser who is not afraid to confess his enthusiasm for high-energy physics, and many of the members of the new council can be counted on the back him up. But should not Dr Keyworth be mixing in wider circles? The appointment of Dr Edward Teller to the council is similarly disconcerting. Nobody disputes Dr Teller's ingenuity or his zeal. That he should be thought of as a hawk is beside the point. But his inconsistency and intellectual impulsiveness are hardly assets for a new committee.

0028-0836/82/080635-01$01.00

A strategy for coal

The belief that indigenous coal production is strategically essential neglects lost opportunity.

Sir Derek Ezra, the chairman of the National Coal Board, is understandably cross to have been told (*Nature* 21 January) that the industry that he runs with such distinction should go out of business. His letter on page 642 makes a number of points that can readily be conceded. British coal-miners have indeed become more productive; output per man has increased by more than 50 per cent in the past 30 years, consonant with the further increase of three per cent in 1981. Many of the difficulties of the British coal industry can indeed be blamed on backward technology and inadequate investment over a substantial period of time; these were, after all, some of the reasons why the British coal industry was nationalized in 1947. It is also true that the Commission on Energy and the Environment, whose chairman is Lord Flowers, in its report last year supported the understanding between the coal industry and the British government that there should be a long-term programme of investment in British mines; the commission's report, *Coal and the Environment,* would no doubt have been more widely read and thus more influential if it had not been priced out of the market (at £23.00, from Her Majesty's Stationery Office) and then not distributed, on the grounds of cost, to those who might have reviewed it. But neither these arguments nor all the social and thus political arguments that attend coal-mining (not merely in Britain) are sufficient reasons for not asking whether Britain can afford its coal industry.

The central issue is the assumption that not merely coal, but British-mined coal, is strategically necessary now and in the future. The question arose earlier this year with the prospect (now happily averted) that the coal board's final offer to British miners on pay for 1982, widely advertised as the most it could afford, would nevertheless be scorned and some part of British industry once more brought to a halt. This annual tussle between the miners and the board, bodies otherwise entirely in concert in their conviction that public investment in British coal mines must be sustained, has in recent years been emphasized by the discovery that the cost of importing coal into Britain even from Australia is frequently less than that of the home-produced product. Sir Derek Ezra rightly argues that the price of job-lots of coal bought at the depths of a slump are not representative of the prices likely to be charged for it on the open market when prosperity returns again. This point was conceded, but perhaps too grudgingly, in the article now complained of. But who can suppose that if and when international prosperity returns, it will be possible to moderate miners' demands on the size of the British share that should come their way?

None of this implies that British miners are more grasping than miners elsewhere, or that miners as such are a cupiditous lot. The reality is rather that coal-mining is a dirty and dangerous job, especially in deep mines. Many people who do not work in deep mines say they would never do so. Some, perhaps many, who do work there would prefer to work elsewhere, given half a chance. Nobody blames them. Nobody should. So it seems probable that if and when prosperity returns, not merely will cheap job-lots of coal be harder to come by but so will miners — as in the mid-1960s, when Sir Derek's predecessor, Sir Alf (now Lord) Robens laid the foundations of the now conventional wisdom that British coal production at about the present rate (a third down since 1950) is a fixed point in the compass of the future. But mining, however well mechanized, remains labour-intensive, so that the return of prosperity to Britain (there are no mines worth speaking of in Northern Ireland, so that the nomenclature is permissible) will herald either the flight of miners from the mines or their demand to be paid even more above the odds or, more probably, both. To anticipate this is not to slander an honourable group of men but, rather, is to acknowledge their wit and their good sense.

The argument can even be turned around. In the tight communities of mining Britain, miners are acknowledged to be resourceful as well as stubborn. They do not cut the figures of people who are especially well paid. How could it be otherwise? Even if coal could be sold at the pithead for £100 a tonne (roughly the equivalent of the landed cost of oil in Britain), which is mercifully out of sight, coal-miners would still be producing less wealth than most of those who work in old-fashioned modern industries — motor-car manufacturing, for example. Their capacity individually to create as much wealth as those who work in truly modern industries — the design of microcircuits for example — is certain always to be small. So why not consider what the circumstances would be like if the part of the British work force that rightly prides itself on its special skill was working in a really productive industry? The hidden costs of the conventional British assumption that coal is strategically necessary, reflected not only in subsidies by taxpayers but in needlessly high prices, are certainly high. The opportunity costs of employing such large numbers of talented people on work characterized by its rigours and its hazards hardly seems wise. (The Commission on Energy and the Environment, no doubt because of its terms of reference, does not take up this question.) So why not follow some different strategy — buy fuel on the open market, or buy less labour-intensive ways of generating energys nuclear power stations for example. And none of this is new — W. Stanley Jevons argued, more than a century ago, that the time would come when coal-mining would no longer be competitive in Britain.

Mercury handcuffed

Liberalizing British telecommunications is uphill work because it goes against the grain.

All concerned seem to be making heavy weather of the attempt in the United Kingdom to liberate the telecommunications industry from the monopoly of the British Post Office (now known in this guise as British Telecom). For the best part of two years, the government was struggling with the unfamiliar problems of how in the abstract to define the conditions under which others than the public monopoly might be allowed to compete with it in the market place. Now, with the Telecommunications Act on the statute book, it is possible to buy telephone handsets retail in British shops without breaking the law. The instruments are those to which the monopoly has agreed to recommend that a licence can safely be given, on technical grounds. It has, by all accounts, been less easily persuaded that it should also fall in with the proposals by Cable and Wireless and Barclays Bank to set up an independent trunk telephone system. Called Mercury, the new system was announced last summer as the commercial alternative to British Telecom.

Only this week has an agreement been reached by the Department of Industry, the Mercury consortium and British Telecom. For some unaccountable reason, the parliamentary draughtsman of the bill supposedly ending the monopoly foresaw the possibility that British Telecom's network might at some point be used by communicators other than itself, but failed to provide that those licensed to communicate electromagnetic circuits to each other might use the public network if that were convenient. The public monopoly has therefore been legally within its rights, in the past few weeks, to agree that the alternative network could go ahead but that it would not be allowed to use its own interconnections, domestically (which is less important) and internationally. The trouble, for the monopoly, is that this legally valid position was politically untenable. The Department of Industry could not have lived with such an impasse. So, in the end, all three parties have compromised. British Telecom agrees that Mercury can use its connections, Mercury has agreed to pay a royalty to the monopoly — and the Department of Industry is probably in a mood to proclaim that competition is not the universal boon it is cracked up to be. What it should have done is to have defined the rules of competition and then to have deligated their interpretation to some regulatory body or the courts.

0028-0836/82/080636-01$01.00

New White House science council

Physics looms large on advisory panel

Washington

Dr Jay Keyworth, President Reagan's Science Advisor, announced last week that he is setting up a new White House Science Council to advise him on "science and technology issues of national concern" and of "changing perspectives in the science and technology communities".

The thirteen members of the new council will carry out tasks similar to those of the President's Science Advisory Committee (PSAC), which was abolished by President Nixon in 1973. However, unlike PSAC, which reported directly to the president, the council will report to Dr Keyworth as director of the Office of Science and Technology Policy.

Dr Keyworth in turn reports to the president's chief-of-staff in the White House, Mr Edwin Meese, implying a lower status to the Science Advisor's job than in previous administrations. So the Science Council, which is also distinct from the commission proposed by Congress in the Science and Technology Policy Act of 1976, will probably enhance Dr Keyworth's position on key policy issues.

The council, already being referred to as WHSC (or "wissick"), will therefore perform many of the functions of the President's Science Advisory Committee, established by President Eisenhower in 1957 in response to the launching of the Russian sputnik, and abolished by President Nixon in 1973 when some of its members took a public stand against his policies on anti-ballistic missiles and supersonic aircraft. But officials at the Office of Science and Technology Policy (OSTP) emphasize that whereas the committee formally reported directly to the president, WHSC will report to Dr Keyworth, OSTP's director.

There was no official comment on the balance of academic interests of the members of the new council, with its heavy emphasis on physics and the "hard sciences", and, apart from Dr Donald Fredrickson, the former director of the National Institutes of Health, no expert from the life or social sciences.

It was stressed, however, that individuals had been selected as much for their broad perspective and judgement on science policy questions as for their particular areas of expertise, and that each member had been hand-picked by Dr Keyworth "after a considerable amount of deliberation".

"We were concerned to have persons who can deal with the range of issues that we understand to be the greatest interest to this office," said OSTP staff member Dr Thomas H. Johnson, who will act as the executive director of the new council.

The chairman of the council will be Dr Solomon J. Buchsbaum, executive vice-president of Bell Laboratories in New Jersey. Dr Buchsbaum is a plasma physicist by training, and is an experienced governmental science adviser, having acted as chairman of the Defense Science Board under President Ford, and chairman of the Department of Energy's Energy Research Advisory Board under President Carter.

Vice-chairman will be Dr Edward Frieman, also a plasma physicist and a vice-president of the La Jolla-based consulting firm Science Applications Inc. Dr Frieman served as director of the Department of Energy's Office of Energy Research during the second half of the Carter Administration, and before that was deputy director of the Plasma Physics Laboratory at Princeton University.

Like Dr Buchsbaum and several other members of the new council, Dr Frieman has worked extensively as a scientific consultant to the Department of Defense. The military connection is also illustrated by the links which several members have with the Department of Energy's Los Alamos National Laboratory in New Mexico, where Dr Keyworth spent most of his professional career as a physicist before going to Washington last May.

Dr Harold Agnew, for example, was a member of the original Manhattan Project team that worked on the atomic bomb at Los Alamos. He joined the laboratory in 1942, became a director in 1970, and left to become president of General Atomic in 1978.

Dr Edward Teller, now emeritus professor of physics at the University of California and widely known as "the father of the hydrogen bomb", also worked at Los Alamos between 1943 and 1946, and acted as assistant director of the laboratory between 1949 and 1953. Dr George Cowan, a senior fellow at the laboratory, is a radiochemist specializing in nuclear reactions who, like Teller, worked at the University of Chicago before moving to Los Alamos in 1949.

According to a formal notice which appeared in last Thursday's edition of the *Federal Register*, the council will have a

Keyworth irked by national labs

One of the first jobs for the White House Science Council will be to hammer out a policy for the national laboratories supported by a federal government. And, according to Dr George A. Keyworth, President Reagan's Science Advisor, the national laboratories must be reorganized so as to provide more support for universities on the one hand and for United States industry on the other.

Dr Keyworth was speaking in London at the annual lunch of the Parliamentary and Scientific Committee, a regular event in the social calendar frequently used by British politicians to make promises or threats to their own scientific community. Dr Keyworth's irritation with the US national laboratories, made conspicuous by the blandness of the remainder of his speech, may cause managers of similar laboratories in Britain to fear that their own paymasters would follow Dr Keyworth's hint.

Dr Keyworth said that the original missions of United States national laboratories are frequently outdated, and that the "many billions of dollars" they receive from the federal government are not all used to "further fundamental knowledge or to address technologies pertinent to our national goals". He said that the laboratories have been "subject only superficially to external review" and that their missions had only rarely been reexamined.

Yet, according to Dr Keyworth, the national laboratories have a logical role as centres for cooperative research involving universities and could even help to make good shortages of teachers of engineering and computer science. He also wants the national laboratories to help reduce the present "unacceptably high resistance" to the application of research.

For the rest, Dr Keyworth gave his somewhat bemused audience a self-congratulatory account of how research and development, and federal support for basic research in particular, were second only to defence in the protection they had enjoyed in the two Reagan budgets. Nevertheless, he said, the scientific community would have to accept a greater degree of discrimination — and more responsibility for making discriminatory judgements.

On international collaboration, Dr Keyworth said that the United States had come to realize the limitations of what it could accomplish on its own, and the opportunities for collaboration with Europe and Japan. He thought that the next generation of high-energy accelerators would have to be built collaboratively, and that there were already opportunities for broadening the base of thermonuclear research programmes, at present too exclusively dependent on tokamak designs.

Although Dr Keyworth did at one point emphasize that he was not to be mistaken for Mr David Stockman, director of the Office of Management and Budget, he left many of his audience with the impression of a man still preoccupied with the small print of resource allocation. ●

0028-0836/82/080637-02$01.00

maximum of fifteen members, and will hold regular meetings up to six times a year. Some of the council's discussions may take place in public, since Dr Keyworth has said that he will comply with the requirements of the Federal Advisory Committee Act, which requires federal advisory committees to hold open meetings unless there is a specific reason that the meeting should be closed.

In addition to the members of the council, OSTP is compiling a list of about 100 other outside consultants from the scientific and industrial community who are expected to be called upon on an *ad hoc* basis to carry out specific studies.

Although both the apparent "military-industrial" bias, and the lack of social scientists — and women — have already received a certain amount of comment in the scientific community, reaction to the announcement of the new council has generally been favourable.

Mr William Golden, a New York banker who is treasurer of the American Association for the Advancement of Science, said last week that although the Science Council was "not as good as a presidentially-appointed group would be", it was better than none. He added that the individual members of the council were "first class", and that the new council should help strengthen Dr Keyworth's standing in the White House, since at present he was "not very high on the totem pole".

David Dickson

Council's members

Solomon J. Buchsbaum (chairman). Executive vice-president, Bell Laboratories

Edward Frieman (vice-chairman). Vice-president, Science Applications Inc.

Harold M. Agnew. President, General Atomic Company

John Bardeen. Emeritus Professor of Electrical Engineering and Physics, University of Illinois, Urbana

D. Allan Bromley. Henry Ford II Professor of Physics, Yale University

George A. Cowan. Laboratory Senior Fellow, Los Alamos National Laboratory

Edward E. David. President, Exxon Research and Engineering Company

Donald S. Fredrickson. Fellow-in-residence, National Academy of Sciences

Paul E. Gray. President, Massachusetts Institute of Technology

Robert O. Hunter Jr. President, Western Research Company

Arthur K. Kerman. Director, Center of Theoretical Physics, Massachusetts Institute of Technology

David Packard. Chairman of the Board, Hewlett-Packard Company

Edward Teller. Senior Research Fellow, Hoover Institution, Stanford University.

Turkish civil rights

Trials ahead

Dr Yeter Ögelman, a Turkish specialist in thermoluminescence and a lecturer in physics at Cukorova University, Adana, until her arrest and imprisonment on 16 May 1981, has now been released on bail. Her trial for helping to organize a women's rights group between 1975 and 1977 will, however, be resumed on 10 March. The prosecution is asking for a prison sentence of between 8 and 15 years.

Dr Ögelman's plight was exemplified some weeks ago when an article submitted for publication in *Nature* recorded her change of address and relocation in prison. The article will be published very shortly.

According to the Turkish authorities, Dr Ögelman's arrest and prosecution fall under the terms of article 141 of the Turkish criminal code. This lays down that those administering societies "with the purpose of establishing domination of a social class or overthrowing any of the established basic economic or social orders of the country shall be punished by heavy imprisonment from eight to fifteen years".

The code has already been used to ban the Turkish communist party. However, Dr Ögelman protests that, contrary to the authorities' accusations, neither she nor the "Progressive Women's Organization" was associated with the communist party. She says the women's organization was formed to campaign for women's rights and for improved education for women in Turkey.

Amnesty International has taken up Dr Ögelman's case, and says that her arrest contravenes the European Convention of Human Rights, of which Turkey is a signatory. That convention guarantees the right to freedom of expression and of association with others, although those rights may be prescribed by law "in the interests of national security or public safety". The Turkish authorities have denied that Dr Ögelman's arrest contravenes the convention.

Dr Ögelman was one of more than 170 people brought before the courts on 15 January, and was one of the lucky fifteen released on bail. Most of those on trial were allegedly members of the left-wing schoolteachers' association. Teachers' unions were banned nearly ten years ago, while the association was banned after General Evren's coup in 1980.

A number of academics have been arrested since the coup, and Amnesty International is unsure of their fate. A more general worry facing Turkish higher education is the bill announced last November that will further circumscribe university autonomy — for example, by giving the state control of senior appointments. The government's stated intention is to reduce the universities' tendency to act as foci for political disruption and violence.

Philip Campbell

European Space Agency

Peace declared

There is a new cheerfulness among the delegates to the European Space Agency (ESA). One sign of this, at last week's council meeting, is that the member governments have agreed on a resource budget for the next five years. The practical result is that it should now be possible to settle the annual science budget without waiting for unanimous agreement.

The council agreed to maintain the mandatory budget, which covers both science and the agency's basic running costs, at more or less its present level. Hence about 900 million accounting units (£540 million) will be spent over the next five years. But the director-general has promised to shift the balance in favour of science by making savings on the agency's overheads and by diverting interest earned on capital into the science programme. During the next three or four years, the science budget is expected to increase by about three per cent in real terms.

The increase is unlikely to make a substantial difference to the scientific community, which typically has to wait up to ten years for a particular kind of satellite. But the extra money may help ESA out of some of its difficulties.

The council's agreement is nevertheless something of an achievement. The level of the science budget has been hotly disputed for at least the past year, with some member states struggling to maintain their existing commitments and others, in particular France and Germany, arguing forcefully for a substantial increase. At the end of last year, agreement seemed beyond reach, largely because of Germany's wish to spend 20 per cent more on science after 1983. That would have involved all other member states increasing their contributions proportionately. In the event, Germany agreed to the five-year resource level with the proviso that discussions on the level of the science budget start again in 1984.

Last week's council meeting was notable for the formal announcement that Britain has joined the Ariane launcher programme as a fully-fledged member. Until now, Britain has contributed just over 2 per cent of Ariane's development costs through a bilateral agreement with France. The decision to contribute 3.5 per cent of the cost and to enter the programme proper is a recognition of the early promise of Ariane — and also of the diplomatic need to participate in other member' projects.

The quarrels of early last year seem thus to have receded. Then the British hankering after telecommunications and the French after the development of launchers polarized discussion of a ten-year plan for the agency proposed by Erik Quistgaard, the new director-general. The agency then had insufficient new applications programmes to fill the gap left when Ariane and Spacelab end development. During the past year, however, things have changed. Several new programmes have been approved including Ariane IV, the next stage of Ariane development; a Spacelab follow-on programme; L-sat, the heavy telecommunication satellite; and a microgravity programme. Pressure of work has taken precedence over the ten-year plan. But when the delegates next turn to the long-term strategy they may well find that the events of the past year have ironed out some of their earlier differences.

Judy Redfearn

Agricultural Research Council

Cuts tempered

The Agricultural Research Council is having second thoughts about its intended reorganization of agricultural research. The livestock industry may have persuaded the council to cut the Animal Breeding Research Organization at Edinburgh by a half, not four-fifths as originally intended. But the proposal to halve the cost of the Long Ashton Research Station at Bristol is to stand. The future of the two stations was the topic of a meeting last week between the council and representatives of the laboratories; final decisions will be taken at the end of March.

If the Edinburgh institute is partly reprieved, other council institutes will be on their guard. The council had hoped to save £3 million on its budget for 1983–84 by economies at the two establishments. Now, it will be £1 million short of its targets, and a call has gone to other institutes for self-imposed economies.

With the next financial year upon it, the council seems just now especially anxious to protect its interests in academic research. Last year, central government provided for only a 6 per cent rise on the wages bill but salaries rose by 7.5 per cent, leaving a shortfall of £0.8 million. As the council spends 95 per cent of its budget in its own institutes and units, and two-thirds of that on salaries, research budgets became unacceptably squeezed.

The council expects a more intense squeeze in coming years and fears a shortfall of £3–6 million in 1984–85. As grants to researchers in universities are to be protected and even increased, savings are being sought in institutes.

The council has nevertheless set its face against closing any institute that relies on commissions from the agriculture ministries for more than half its income. Other criteria used to decide which institutes to cut include the level of recent capital expenditure, future needs for facilities, overhead costs and the chances of successfully transferring work.

The proposal to cut the Animal Breeding Research Organization was based largely on internal assessments that had questioned the value of long-term animal breeding experiments. Originally, the council proposed to reduce the organization to only fundamental work, in particular on animal genetics. Representations from the livestock industry, however, seem to have rescued some breeding experiments, and the cattle blood-typing service may also now be retained.

Research on fruit is over-subscribed due to historical accident, according to the council — hence its decision to abandon pomology (apple-work) at Long Ashton and to transfer other work to the East Malling Research Station. Representations from strawberry, plum and mutant-apple growers, however, will now probably ensure some provision for research in these areas.

The council estimates that it will lose £0.5–1 million earned from ministry commissions. Other costs of the closures, including redundancy payments to approximately 220 staff, will initially increase the burden on the council's income. But much will depend on how many staff required to be mobile under the terms of their contracts can be redeployed in other institutes.

Judy Redfearn

Spain back to fold

The European Centre for Nuclear Physics (CERN) near Geneva has been in a pleasant spin for the past few weeks deciding how to react to an advance from the Spanish government. Spain wishes to rejoin (after a brief membership between 1961 and 1968) but there are few people at CERN who remember how such things are done.

In fact the last time a country joined CERN was 21 years ago, when the new adherent was Spain again. But they were early days for CERN, which is now an enormous institution with some 6,000 researchers and staff, massive experimental facilities for elementary particle physics and a £177 million annual budget to match. No official figures are available yet, but accession could cost Spain of the order of £10 million a year, something approaching a quarter of the present Spanish science budget.

The precise price which Spain must pay will be a matter for negotiation. Although members must pay in proportion to their gross national product, and Spain's is moderately high, it might be possible to negotiate step-by-step entry. However, all 12 members of the CERN council must agree to the terms, and there is an argument that Spain should pay entry fee in addition to the annual rate, to account for the fact that it will become part owner of the CERN accelerators. The lawyers are working on that, a spokesman said this week.

Robert Walgate

Polish universities

Trouble in store

Further clashes between Polish university students and the representatives of the ruling Military Council for National Salvation are feared in the near future, according to a Warsaw Radio broadcast last Sunday. In one of the regular morning briefings on the state of the country, an unidentified speaker said that classes have resumed just when the anniversary of the "so-called March events" is approaching.

The speaker was referring to the expulsion on political grounds of two Warsaw university students, by a decision of the then Minister of Education and Enlightenment, now president, Henryk Jablonski (5 March 1968). Three days later, a mass protest was held in the university grounds, claiming that the expulsion was contrary to university regulations since it had not been made by the rector. The students and some sympathetic academics were forcibly dispersed, but the incident triggered similar protests at universities throughout Poland — and ultimately resulted in mass dismissals and expulsions of students and staff, and the closure of several university departments.

Last year, the March anniversary was marked by a rally of students and academics in Warsaw, and by the formal rehabilitation of the "victims of 1968", including the philosopher, Dr Leszek Kolakowski. Even in the relatively liberal climate of 1981, the commemorations did not take place unopposed; the new "Grunwald Patriotic Association" was set up to hold a counter-meeting to praise government action in 1968.

Last Sunday's broadcast pinpointed growing official fears that young people have not yet accepted the changed situation in Poland and, in particular, the outlawing of the Independent Students Association (NZS). Formally, all protests are attributed to manipulation by hostile elements and political provocateurs. A government leaflet addressed to young people urges them not to be duped into involving the country in a civil war which would be a "tragedy for millions". There are hints in the media of attempts to defuse the tense situation by suggesting that all is not lost. An article in the daily *Zycie Warszawy* on the reopening of the University of Warsaw said that so far, no student had been expelled as a result of martial law — not even those at present interned. At the same time, the danger of taking part in demonstrations is stressed; a Gdansk commentator noted that those students arrested in the demonstration of 30 January would "have to say goodbye to their studies, at least for some considerable time".

Significantly, the announced agenda for the session of the Sejm (parliament), next Friday and Saturday, makes no mention of the new higher education bill.

Vera Rich

0028-0836/82/080639-02$01.00

US student loans

Lean prospects

Washington

Students from across the United States are planning to converge on Washington next Monday for a mass demonstration on Capitol Hill against cuts proposed in federal support for student loans. The demonstration is part of an intense, nationwide lobbying campaign by both students and university administrators aimed at persuading Congress to reject the Reagan Administration's cuts.

The Administration points to the escalating costs of the loan support programme, largely a result of recent increases in US interest rates to record high levels, and is seeking to reduce federal subsidies from an estimated $3,000 million in 1980 to $1,600 million by 1983.

Graduate students will be among those heavily affected by the cuts. Under the government's Guaranteed Student Loan (GSL) programme, graduates qualify for loans at a fixed 9 per cent interest rate; under new proposals from the Department of Education, they would now be allowed to borrow only from an auxiliary loan programme at significantly higher costs, with an interest rate of 14 per cent.

The result, according to figures prepared by the American Council on Education (ACE), is that a student who borrows $8,000 a year on top of previous undergraduate loans to make his or her way through graduate school could be paying off the money at a rate of about $500 a month for the succeeding ten years.

The presidents of almost all the nation's universities and colleges have loudly denounced the proposed cuts, claiming that by discouraging students from entering graduate training unless their sources of income are secure, the Administration is discriminating against groups who lack this security and undermining the long-term economic health of the nation.

Many feel that they had accepted last year's 20–25 per cent cuts in student loan support as their appropriate share of broader efforts to reduce federal spending. The new cuts, which in some cases would reduce federal subsidies by up to 50 per cent, have provoked the feeling that students are being asked to carry an unfair burden of Mr Reagan's economic policies.

The Reagan Administration's proposals are a mixture of economic pragmatism and ideological conviction that federal subsidies should be confined to the "truly needy". At present, under the GSL programme the government pays the 9 per cent interest on loans for both undergraduate and graduate students while they are at college, and also pays the difference between 9 per cent and the current interest rate for the remaining period of the loan.

Mr Terrel H. Bell, the Education Secretary, said in Washington soon after the budget proposals were announced that, as a result of soaring interest rates, the cost of administering the guaranteed loans, $367 million in 1977, is expected to rise to $3,400 million in 1983.

Reducing the eligibility requirements for the guaranteed loans and shifting the graduate students to the auxiliary loan programme would, claims the Administration, not only ensure that the available loans go to those most in need, but that the total costs to the federal government would be decreased by more than $2,000 million by 1987.

Many of the leading research universities, however, claim that such cuts would have a devastating impact. Dr Edward J. Bloustein, president of Rutgers Univesity in New Jersey, believes they would eliminate more than $12 million in aid received by about half of the 4,000 graduate students at his university.

According to figures produced by ACE, about 600,000 graduate students — half of those at present enrolled in US universities — are borrowing money under the GSL programme, in many cases close to the limit of $5,000 a year. At some of the nation's leading private research universities, the cost of graduate education, including living and tuition expenses, can be as much as $13,000 a year and university officials argue that, if they are forced to seek the more expensive loans, many students will either give up or delay their graduate education.

Given the extent of popular support for the student loan programme, the proposed reductions are expected to be strongly opposed by Congress.

In their defence, Administration officials reply that the present loan programme "encourages students to borrow regardless of financial need from their first year at school and can needlessly cause students to amass high levels of debt" which in turn allows "decreased reliance on family savings and student work". They also point to other initiatives, such as the efforts by the National Science Foundation to support graduate students in science and engineering, as proof that the government is prepared to continue support where it feels it to be necessary and appropriate.

David Dickson

Indian Antarctic expedition

Going for good

New Delhi

The Indian government, which sent its first expedition to Antarctica last month, is now actively considering the establishment of a permanent Antarctic base by 1985 or even earlier. Until then, the government intends to operate an unmanned weather station that will be linked via the polar Sun-synchronous satellite that India hopes to launch next year. The automatic solar powered weather station left behind by the recent expedition team will function for six months. It will be replaced in October, when it is hoped that a second team will arrive for a three-month stay.

Plans are also under way to set up an Antarctic Research Centre in India for training manpower, developing research programmes and working out the logistics of base support with the help of air force planes. The Department of Ocean Development is also planning to buy a ship for Antarctic work. One vessel under consideration is the 3,600 tonne *HMS Endurance,* the British Antarctic patrol ship, now for sale at a price of £1.5 million.

There are several reasons for India's new-found interest in Antarctica. Politically India does not want to be left behind China, which is planning to set up a manned station this year. The Antarctic programme is also considered essential to raise India's prestige among littoral states and to give it more weight in international forums on Indian Ocean affairs.

Although many of the Antarctic treaty powers have welcomed India to their club, India does not intend to sign the treaty immediately. It is, however, likely to stake territorial claims if the treaty members do not adopt the common heritage principle.

The Indian expedition was not advertised in advance for fear of adverse reactions from Antarctic treaty members. But, as it turned out, the reaction was quite favourable. The Indian team on board the chartered Norwegian ship *Polarsirkel* not only received weather reports from bases in Antarctica but also navigational help from the Japanese icebreaker *Fuji.*

The 21-member team led by Dr S. Z. Qasim landed on 9 January at a location 70° 3'S and 40° 7'E — an abandoned Soviet campsite. The Indians named the place "Dakshin (South) Gangotri". (Gangotri is the source of the River Ganges in the Himalayas.) The team left Antarctica after camping for 10 days, bringing back a tonne of rocks, several samples of ice and aerosols. One notable observation by the team was an unrecorded undersea mount in the Indian Ocean which has now been named Mt Indira after the Indian Prime Minister.

K. S. Jayaraman

0028-0836/82/080640-01$01.00

Acid rain

Swedes persist

Brussels

Sweden is yet again to hold a major ministerial conference in an attempt to persuade its European neighbours to take the country's acid rain problem seriously. In June a two-week conference is to be held in Stockholm attended by 15 environment ministers from East and West — the sole country not being represented at a ministerial level being the United Kingdom. The first week of the conference will be devoted to examining the scientific evidence, and a political debate will follow.

It will be hard to separate science from politics. Many of the political arguments rely on demonstrating convincingly the direct link between sulphur dioxide emissions from the coal and oil burning industrial centres in Europe and the increase in the acidity and the presence of heavy metals in surface water in Scandinavia.

At a recent meeting in Brussels, organized by the European Environmental Bureau, many experts admitted that nobody was entirely clear about the precise mechanism between the cause and effect of acid rain. The evidence was there, though, to show that dramatic changes have taken place in the forests and lakes of Scandinavia even in the past two years. Research is now revealing evidence that sulphur dioxide emissions may also be linked to acidity in fresh water in Belgium and damage to forests in Germany.

While much of continental Europe is far richer in limestone than Scandinavia and is, therefore, less vulnerable to increases in the acidity of fresh water, the effect of the acid precipitation is nonetheless becoming apparent. The problem, the environmentalists argue is not just a Scandinavian one, and is already too serious to allow scientists the luxury of building up irrefutable evidence about the mechanisms involved before action is taken.

The political and economic opposition facing the Swedes seem unsurmountable. Eastern Europe is the source of much of the pollution — notably East Germany and Czechoslovakia. Each provides per capita sulphur emissions of more than 100 kg per year, well above that from West European states. The poor economic situation and energy problems of Comecon countries make it unlikely that they would consider investing money in costly anti-pollution equipment.

The 1979 Geneva Convention on long-range transboundary air pollution merely binds signatory states to "using the best available technology which is economically feasible". The Geneva Convention is still not in force, although 34 countries have initialled it. In the European Community. Greece, Belgium and Italy have so far failed to ratify.

Sweden's attempts to create the political momentum needed for change include the UN conference in Stockholm in 1972, the Helsinki meeting in 1975 and last year's acid rain conference in Gothenburg, but these initiatives have so far produced few concrete actions. Despite the ammunition provided by a study by the Organization for Economic Cooperation and Development, the European Commission has also remained far from convinced that there is a need to do anything more than monitor the situation. Many member states, like the United Kingdom, remain openly sceptical about the cause and effect of acid rain. **Jasper Becker**

Dutch elm disease

Northern drift

The British battle against Dutch elm disease has been virtually lost in the south of England and Wales, while the chances of success in northern Britain are slim, according to last week's annual review of the state of the disease by the Forestry Commission. In the south, perhaps 20 million of an estimated 29 million elm trees have been killed. And in the north, where beetles of the Scolytidae family have already crossed the north–south divide, the fight against the fungus carried by the beetle seems likely to be hampered by straitened local authority budgets.

The battle strategy recommended for the north of England is one which has failed in the south: sanitation felling. The objective is to cut down trees infected with the fungus *Ceratocystis ulmi* at an early stage and to burn the bark. The Forestry Commission holds out little hope for alternative control strategies now being tested — the "tree trap" technique that uses cacodylic acid (a tree-killing herbicide) to attract the beetles, artificial pheromones in conjunction with sticky traps and the fungicide Ceratotect, which can cure lightly infected elms. These techniques, the commission says, are only supplementary to sanitation felling, and are expensive.

So the labour-intensive technique of sanitation felling is recommended to continue in lightly affected areas. But local authorities must decide on what scale to battle. While control over the movement of elm wood is maintained by the Forestry Commission, the decision to divert funds to a felling campaign rests entirely with local authorities.

Where the elm population is isolated, active sanitation has proved highly effective. East Sussex County Council began its campaign in 1973, when signs of the disease first showed. Losses there have declined since 1979 and the worst may well be over. In Brighton, the casualty rate is down to 10 per cent. An important factor in the success of the campaign here was luck. The region is isolated and a good distance from the sources of infection — the docks of London, Bristol and the south. The council sees no reason to give up its campaign, and its budget for 1982 — £97,000 — will also cover planting costs.

East Sussex, however, is only a small pocket on a map of devastation. Authorities in the western counties have long since given up the fight and the area, with its dead elms and broken stumps, is described as looking like the Somme 65 years ago. The area to the north of Merseyside and the Wash, where conditions and species of elm are different, is described as "lightly affected", with as few as one per cent of elms lost each year. But the 5 million elms in the north of England, mostly wych elm (*Ulmus glabra*) have an important amenity value and constitute 10 per cent of total northern tree population. A majority of local authorities in the border regions of Scotland and northern England have ceased to exercise their powers of direct felling, some as long ago as 1977.

The problem is twofold. Once the disease takes hold, it is impossible to eradicate. Moreover, the elm bark beetle is no respector of regional boundaries and so far local authority programmes have been piecemeal. But the cost of sanitation felling falls entirely on local authority funds. Until 1979, the Countryside Commission for England and Wales supported local programmes, but has now been told that there is no prospect of diverting any substantial part of its funds to assist felling campaigns.

Support from central government has been equally unforthcoming. The Department of the Environment has its eyes set firmly over the horizon and describes the present problem as being on a "back burner", pointing to the Tree Council as the body maintaining a watching brief. The Tree Council, however, has been wholly independent, financially as well as administratively, since 1978. Hope for the future, as far as the Department of the Environment is concerned, lies in the development of elms resistant to the disease. Japanese elms are being planted in the royal parks.

The irony is that in seeking to avoid present costs, local authorities may well incur higher future costs. Merseyside County Council is having to spend nearly £250,000 to fell dead and dying elms that pose a danger to public safety. **Jane Wynn**

0028-0836/82/080641-01$01.00

CORRESPONDENCE

Coal as Britain's security

From the Chairman of the National Coal Board

SIR — Your uncustomarily superficial and misleading article (21 January 1982, p.177) accuses the National Coal Board and the Government of being "in collusion to make water run uphill".

What, in fact, the NCB, the trade unions and the Government are jointly involved in is to ensure the security of future energy supplies for Britain by developing new and reconstructed collieries so that sufficient coal continues to flow to power stations, industry and homes and the country can continue, progressively, to diminish its dependence on oil.

Throughout the 1960s the coal industry was starved of capital when the policy of successive governments was to rely on plentiful supplies of cheap Middle East oil. Since the Middle East crisis of 1973–74 which changed that shortsighted strategy, investment in new and replacement mining capacity — essential to ensure continuity of production in an extractive industry like coalmining — has totalled £3 billion and continues at the level of more than £700 million per year. Because it takes about 10 years to develop a major new colliery, there is an obvious short-term financial burden of meeting heavy interest charges before coal production begins. That is one of the main problems the coal industry faces today and it is the legacy of earlier years of strategic neglect.

Your article scarcely recognizes the industry's considerable achievements. The coal we supply today is about two-thirds the price of oil and meets nearly 40 per cent of Britain's entire energy needs. Productivity in 1981–82 has so far risen by 5 per cent at the coal face and more than 3 per cent overall. After a previous period of decline, output at long-life collieries has increased by more than 7 million tonnes in the past three years. Exports have doubled for the third year running, and will reach about 10 million tonnes of coal and coke, which — with the addition of machinery exports by the manufacturing companies and mining consultancy services — will earn for Britain over £500 million in foreign currency.

Particularly in these times of continuing recession the British economy benefits from major purchases of goods and services from the National Coal Board — totalling £983 million in 1980–81 and having an overseas content of only £26 million (2.6 per cent).

It is astonishing to find you now repeating the same question that was asked in the 1960s of whether Britain needs a coal industry. An independent answer was recently given by the report of the Commission on Energy and the Environment which supported the coal indsutry's continuing large-scale investment. The Commission, whose chairman was Lord Flowers, stated that: "In both the energy and the environmental interest, we consider that greater stability of long-term planning is the essential pre-condition of successful modernization of the industry".

The Commission's conclusions on coal imports will also interest your readers: "We believe that most western governments will continue to find it sensible to favour indigenous coal supplies, and to be unwilling to jeopardize sensible long-run developments by allowing customers to play the market by allowing short bursts of low-cost imports of coal during temporary recessions. Most importantly, we recognize the social unacceptability of repeating in the last decades of the century the sequence of creation and then destruction of mining communities."

DEREK EZRA

National Coal Board,
London SW1, UK

Commercial risk

SIR — There is surprisingly little discussion about the ways in which the practice of the biological sciences is changing as a result of the massive commercial investment in biotechnology. While some, like myself, may find the growing commercialization of bioscience depressing, there seems little one can do to stop its spread. But there is one aspect of the process that is an outrage, and bioscientists and the public agencies that fund them should unite to prevent its continuing.

Increasing numbers of scientists are giving their monoclonal-antibody-producing hybridoma cell lines to commercial companies and are then refusing to provide the antibodies and/or the cells to their colleagues. It can be argued that by relieving scientists of the time-consuming task of sending materials around the world, commercial distribution aids rather than hinders the distribution process. But in many cases the cell lines themselves are not made available and the cost of the antibodies is prohibitive if they are needed in large amounts.

The withholding of cells and antibodies for financial gain (or even worse, for selfish scientific advantage) is especially outrageous when these have been developed using public funds. Since it is the granting agencies that must ultimately pay for reagents that would otherwise be free and must endure the slowed pace of scientific advance resulting from the restricted exchange of materials, they should be leading the fight against such anti-science practices. Instead, it has been left to a few enlightened journals, such as *Cell* and *Immunogenetics*, to take up the cause and make free availability of cell (and DNA) clones and antibodies a condition of publication. Is it not time that the granting agencies followed suit and made free availability a condition of financial support?

The American Type Culture Collection was set up to provide a free cell banking and distribution service and has recently taken over the cell bank previously located at the Salk Institute, which contains a number of monoclonal-antibody-producing hybridomas. It would be helpful if this admirable facility were extended to include the distribution of those DNA clones and antibodies that are in especially heavy demand. There could then be no legitimate excuse for scientists not making their clones and antibodies freely available to their colleagues.

Free exchange between scientists is too important to be given up without a struggle. Without it, not only is efficiency sacrificed, but much of the joy of science will be lost as well.

MARTIN RAFF

Zoology Department,
University College London,
London, UK

Spacecraft in orbit

SIR — The suggestion put forward by David Hughes[1] that the number of objects in near-Earth orbit has recently been decreasing, thus lowering the probability of spacecraft collisions, is seriously outdated. The data he presents, which stop at the end of 1980, show a small decrease in the number of objects in orbit from a peak in early 1978 until the end of 1980. However, during 1981 the number of objects in orbit rose rapidly, to an all-time high of 4,740 objects in October 1981 (NASA Satellite Situation Reports). From December 1980 to October 1981 the net increase of objects in orbit was 319. Most of these new objects resulted from two events. Early in 1981, 137 new objects associated with the US Landsat 3 satellite, launched in 1978, were detected. If this is another case of an exploding rocket motor, it indicates that the problem may not yet be solved. Another 118 objects associated with the USSR's Cosmos 1275 were identified shortly after its 4 June 1981 launch. If this rate of increase of objects in orbit continues, the first collision between satellites would be expected in the next 10–15 years according to calculations by Kessler and Cour-Palais[2]. A reversal of this trend is required to prevent a serious hazard to orbiting satellites in the twenty-first century.

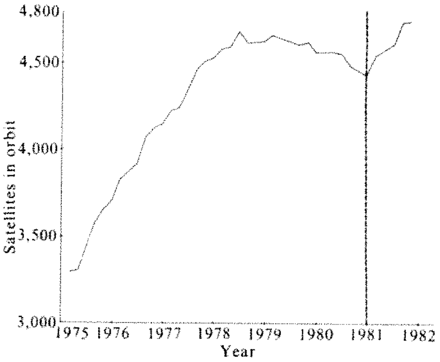

Data from NASA satellite situation reports. The previous chart[1] finished where the dashed line indicates.

GEORGE J. FLYNN

Washington University,
St Louis,
Missouri, USA

1. Hughes, D.W. *Nature* **295**, 100 (1982).
2. Kessler, D.J. & Cour-Palais, B.G. *J. geophys. Res.* **86** 2637 (1978).

NEWS AND VIEWS

Whence so much ^{15}N?

from John F. Kerridge

An intriguing puzzle is emerging in cosmochemistry about the isotopic composition of nitrogen in the mixture of gas and dust from which the Solar System formed. Recent analyses of meteorite and lunar samples reveal enormous variations in the ratio of the stable nitrogen isotopes, ^{15}N and ^{14}N. The question at issue is whether the variations are due to nuclear processes in the Solar System, mass-dependent isotopic fractionation or mixing of 'solar' nitrogen with one or more alien components — material that has experienced different nucleosynthetic processing from the bulk of Solar System matter. Addition of alien material at levels up to about 5% is already well established from meteorite analyses[1]; but the nitrogen data, if the result of nucleosynthetic heterogeneity, could imply much greater levels of alien additions.

Observational data bearing on this issue are numerous and come from a wide variety of sources; a comprehensive review by Geiss and Bochsler will be published shortly[2]. I shall focus here on models advanced to account for those data, addressing specifically the value of protosolar ^{15}N/^{14}N inherent in each model. Isotopic components will be identified by their percentage depletion or enrichment in ^{15}N relative to the terrestrial atmospheric standard value, ^{15}N/^{14}N = 3.66×10^{-3}.

Geiss and Bochsler[2] propose that the dominant nitrogen component in the protosolar nebula had a value of +12%; virtually all natural samples could then be explained by admixture of a minor ^{15}N-depleted alien component, possibly pure ^{14}N. Occasional meteorites, such as Renazzo and Al Rais, with values up to +17%, are interpreted as containing interstellar molecules enriched in ^{15}N by ion–molecule reactions at temperatures below 100K in molecular clouds. Such reactions have been identified as the causes of the enormous fractionations observed for the hydrogen isotopes in interstellar molecular clouds, but little corresponding astrophysical evidence exists for nitrogen and it is debatable whether adequate ionization of nitrogen-bearing species occurs in the interstellar medium. The secular increase from <-21% to +12% observed in nitrogen trapped during the past 3–4 Gyr in lunar surface samples is ascribed to mixing of solar wind characterized by a constant nitrogen value of +12% with an outgassed lunar component rich in alien ^{14}N, whose mixing ratio decreased with time. There is strong evidence from the analysis of lunar samples, however, against the presence of such a hypothetical non-solar wind nitrogen component, and, furthermore, indigenous lunar nitrogen appears to have a composition close to zero rather than <-21% as predicted.

A recent analysis of nitrogen in the Allende carbonaceous meteorite, by Thiemens and Clayton[3], has been interpreted in terms of a major protosolar value of -3% and a minor alien component of -9%. A -3% component is also observed in meteorites known as enstatite chondrites, which many believe to contain nitrogen condensed directly from the nebula at relatively high temperatures with minimal isotopic fractionation. It must be stressed, however, that no host phase for nitrogen in any meteorite has been firmly identified with relict nebular material, so the possibility of secondary fractionation is always present. The alien nature of the -9% component is supported by correlations with an alien xenon component recently identified by Frick and Pepin[4]. Thiemens and Clayton interpret meteoritic values up to about +4% as due to mass fractionation during nebular condensation, and the <-21% lunar value as due to fractionation of the -3% component in an early solar wind. The apparent secular increase recorded by the lunar surface samples is ascribed to nuclear reactions, that is, production of ^{15}N, in the solar wind reservoir. Problems concerning production of ^{15}N in the Sun will be discussed later; specific difficulties of the Thiemens and Clayton model are its failure to account for for the +17% meteoritic values and the lack of evidence that mass fractionation in the solar wind could reduce a value of -3% to <-21%.

My own model[5] of this process which yields a protosolar ^{15}N/^{14}N of <-21%, assumes that the earliest apparent solar wind value characterized the solar convective zone at that time, thereby establishing an upper limit to the protosolar value. The apparent secular increase in the solar wind value is ascribed to nuclear production of ^{15}N in surface regions of the Sun; meteoritic and planetary values are attributed to mass fractionation during formation of condensed species at very low temperatures, though addition of ^{15}N-enriched alien material is a reasonable alternative. The main difficulty with this model, and the preceding one, stems from the considerable body of observational evidence constraining nuclear production of ^{15}N in the Sun.

The present γ-ray flux from the Sun indicates a level of nuclear activity far too low to generate adequate ^{15}N; the lack of evidence for significantly greater solar flare activity in the past similarly precludes greater ^{15}N production then; and certain other nuclides, whose production would accompany that of ^{15}N, are not observed. Another problem concerns the temperatures at which adequate isotopic fractionation could occur to explain the meteoritic and planetary data; at such low temperatures reaction or exchange between neutral species, as customarily invoked for nebular condensation, is implausible. Ion–molecule reactions can again be invoked, but with the same reservations as discussed earlier. As an alternative to fractionation, addition of alien ^{15}N-rich matter cannot be ruled out but the scarcity of ^{15}N in the interstellar medium reduces the plausibility of such a component.

John F. Kerridge is in the Institute of Geophysics and Planetary Physics, University of California, Los Angeles, California 90024.

0028-0836/82/080643-02$01.00

Finally, there is a class of models based, like the previous one, on solar wind data, but which ascribes the apparent secular change to 'contamination' of the Sun's convective zone by interstellar matter. The most detailed of these models[6] proposes an early addition of material from a planetary nebula rich in ^{14}N to a proto-Solar System consisting initially of +17‰ material. This would have resulted in a value of <−21‰ for the solar convective zone which has subsequently evolved towards the bulk solar value of +17‰ as underlying material replaced ejected solar wind. Meteoritic and planetary compositions may be interpreted as in the Geiss and Bochsler model. A general problem with 'contamination' models is the large apparent size of the actual convective zone; this would require massive additions of alien material for which evidence should be, but is not, found elsewhere.

A potential weakness of models relying on solar wind data lies in the identification of solar wind composition with that of the solar convective zone. Persuasive arguments have been advanced by Geiss and others (see, for example, ref. 7) that such equivalence does exist, but recent spacecraft measurements of solar flare composition suggest otherwise. Mewaldt and co-workers[8] have reported an isotopic composition of solar flare neon which is distinctly different from that in the solar wind, and they also argue against mass fractionation in the flare as an explanation of the difference. Arguments against fractionation in the solar wind are equally strong, but the flare measurements are at least a warning against identifying solar wind composition with that in the convective zone.

Clearly, an unequivocal estimate of protosolar $^{15}N/^{14}N$ is not yet in sight. Indeed, the observations discussed above may signify isotopic heterogeneity for this element in nebulae. It is equally clear that the apparent secular change in solar wind $^{15}N/^{14}N$ lacks a satisfactory explanation. The issue of protosolar $^{15}N/^{14}N$ may soon be resolved by the Galileo mission to Jupiter. No net fractionation should have accompanied accretion of nitrogen by Jupiter, and all nitrogen should now be present as ammonia; this simplifies the interpretation of the mass spectrometric data that will be gathered. It is to be hoped that the mission will not succumb to the budget-cutting zeal of the present US administration. If not Galileo, who? If not now, when? □

---

1. Begemann, F. *Rep. Prog. Phys.* **43**, 1309 (1980).
2. Geiss, J. & Bochsler, P. *Geochim. cosmochim. Acta* (in the press).
3. Thiemens, M.H. & Clayton, R.N. *Earth planet. Sci. Lett.* **55**, 363 (1981).
4. Frick, U. & Pepin, R.O. *Earth planet. Sci. Lett.* **56**, 64 (1981).
5. Kerridge, J.F. *Nature* **283**, 183 (1980).
6. Ray, J. & Heymann, D. *Proc. Conf. Ancient Sun*, 491 (Pergamon, Oxford, 1980).
7. Geiss, J. *Proc. 13th int. Cosmic Ray Conf.*, 3375 (1973).
8. Mewaldt, R.A. Spalding, J.D. Stone, E.C. & Vogt, R.E. *Astrophys. J. Lett.* **231**, L97 (1979).

The Vredefort structure still not understood

from Richard A.F. Grieve

THE recognition that impact cratering was a fundamental geological process in the evolution of early planetary crusts[1], together with recent suggestions that faunal extinctions at the Cretaceous–Tertiary boundary may be linked to a major impact event[2], have heightened interest in the terrestrial record of impact cratering. Approximately 100 known terrestrial structures larger than 1 km in diameter are considered to be of impact origin. One criterion for their recognition as such is the occurrence of shatter cones — cone-and-cup structures, with striated surfaces radiating from parasitic horse tail-like half cones on the face of a master cone and varying in size from less than 1 cm to as much as 10 m (see the figure). These cones, as well as microscopic planar deformation lamellae in minerals, solid-state glasses and high-pressure mineral polymorphs, are characteristic of shock metamorphism. They have been reproduced in shock experiments and in nuclear explosions, occur at small terrestrial craters with meteorite fragments, and have also been observed in meteorite and lunar samples. In a recent issue of the *Journal of Geophysical Research*, there are six papers dealing with various aspects of the geology and geochemistry of the Vredefort 'Dome', south of Johannesburg, South Africa, which is considered to be one of the largest terrestrial impact structures. One of the papers, by Simpson[3], interprets the occurrence and orientations of some shatter cones at Vredefort as precluding an impact origin.

The principal morphological elements of Vredefort are a central core of Archaean basement with an 18 km radius, a 17 km wide 'collar' of steeply dipping or overturned sedimentary and volcanic rocks of the Witwatersrand and Transvaal Supergroups, and a 20–30 km wide outer synclinorium containing members of the uppermost unit of the Transvaal Supergroup. If an impact feature, Vredefort would correspond to what is known as a complex structure, where the original excavated cavity has been modified by uplift in the centre, producing the central core, the penetration and overturning of the stratigraphically higher strata of the 'collar' rocks and the downdropping of the outermost regions to give the peripheral synclinorium. Simpson, however, points to two localities which suggest that at least some shatter cones appear to post-date the overturning of the 'collar' rocks. Such an interpretation conflicts with predictions of an impact model, in which shatter-coning occurs during passage of the shock wave, before uplift of the core and overturning of the 'collar' rocks.

At the first locality, about 40 km west of the centre of the structure, shatter cones are developed in both overturned and right-way-up Daspoort quartzite, a unit of the Transvaal Supergroup. The direction and plunge of the cone striae indicate that the master cone axes have nearly equivalent

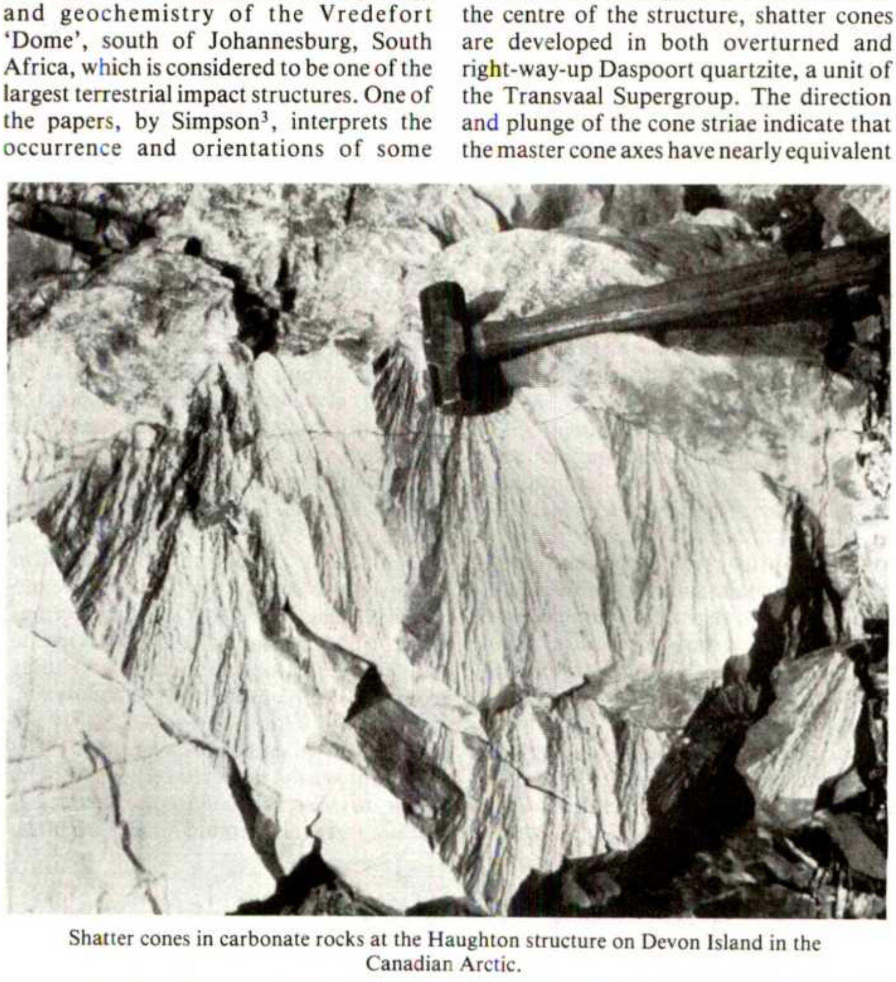

Shatter cones in carbonate rocks at the Haughton structure on Devon Island in the Canadian Arctic.

0028-0836/82/080644-02$01.00

vertical orientations, regardless of bedding orientation. The overturned and right-way-up beds are separated by a fault, which strikes radially towards the centre. If, as suggested, this fault is related to the uplift of the central core, then the similar orientations of the master cone axes indicate that at least one generation of shatter-coning took place after the overturning of the 'collar' rocks.

At the second locality, shatter cones occur in an indurated fault breccia, which lies 40 km north of the centre in a fault zone that is part of a series of faults which downthrow overturned Daspoort quartzite beds. As there is no evidence of shatter-coned clasts in a non-shatter-coned matrix, shatter-coning took place after breccia formation. Furthermore, the faulting is thought to have occurred simultaneously with or after the overturning of the beds, so the shatter-coning is post overturning. Simpson's interpretations of these shatter-coned localities are at odds with an impact origin for Vredefort and, by implication, they cast doubt on shatter cones and other shock features as criteria for the recognition of impact structures.

What then are the alternatives? Simpson suggests the cones resulted from shock waves produced by internal tectonic processes. But the problem with such an explanation is that experimental data indicate that shock features are formed only at pressures of tens to hundreds of kilobars. Shatter cones, in particular, appear to require pressures of 20-60 kbar[4]. Even if such pressures could be maintained in the Earth's crust, how could they be produced? Mechanisms involving a deep internal explosion fail to generate such pressures, because the mechanical coupling efficiency between shock waves in a gaseous medium and rock is low (probably less than 1 per cent).

Previous measurements at about 50 sites by Manton[5] indicated that virtually all shatter cones, when restored to their pre-overturning position, point to the centre of Vredefort and define a focus, or point of origin, for the shock wave some 13.5 km above the base of the Witwatersrand. This corresponds roughly to ground zero at the time of cone formation. Perhaps these two new occurrences are exceptions. Rare cases of cones which do not point to the centre are known from other structures and the formation of occasional inverted cones is predicted in one hypothesis of cone formation involving differential shock impedance of strata. The occurrence of cones in a fault breccia and not in the associated quartzite is certainly unusual. Shatter cones are generally best developed in fine-grained, structurally homogeneous rocks such as carbonates and quartzites and not in inhomogeneous rocks such as breccias. The interpretation of the relative timing of the faulting in the two areas with respect to core uplift is critical. In considering the preservation of coesite and stishovite, high-pressure polymorphs of quartz, in psuedotachylite, Martini[6] noted that some deformation associated with Vredefort is related not to impact but to earlier and normal tectonic action. The injection of psuedotachylite veins into the fault breccia at the second shatter cone locality could be interpreted to indicate that at least some of the faulting predates the shock event.

Whatever the explanation, the bulk of the shatter cone evidence from Vredefort still appears to favour an impact origin. It has taken some twenty years of documentation, experiment and theory to establish the impact origin of shock-metamorphosed structures and to appreciate the complexities of the impact process. The new evidence from Vredefort is enigmatic. It must be weighed against the wealth of other evidence and, in the present author's opinion, is insufficient to invalidate the interpretation of Vredefort as an impact structure and the use of shatter cones and other shock features as indicators of meteorite impact. □

Richard A.F. Grieve is a Research Scientist at the Earth Physics Branch, Department of Energy, Mines and Resources, Ottawa, Canada. He is currently a Visiting Professor at Brown University, Providence, Rhode Island 02912.

---

1. Grieve, R.A.F. & Head, J.W. *Episodes* **2**, 3 (1981).
2. Alvarez, L.W. *et al. Science* **280**, 1095 (1980).
3. Simpson, C. *J. geophys. Res.* **86**, 10701 (1981).
4. Roddy, D.J. & Davis, L.K. *Impact and Explosion Cratering*, 715 (Pergamon, Oxford, 1977).
5. Manton, W.I. *Ann. N.Y. Acad. Sci.* **123**, 1017 (1965).
6. Martini, J.E.J. *Nature* **272**, 715 (1978).

Carbon dioxide and climate: has a signal been observed yet?

from Starley L. Thompson and Stephen H. Schneider

In a recent paper Kukla and Gavin of the Lamont-Doherty Geological Observatory[1] examine recent and historical data on the extent of polar ice and snow, hoping to detect changes that might be a signal of warming caused by the build-up of CO_2 in the atmosphere. This and other new work which looks not only at the effects of changing carbon dioxide levels but also at other gases capable of creating a 'greenhouse effect', make it necessary to consider seriously whether the question posed in the title can now be answered in the affirmative.

Kukla and Gavin compiled recent data for sea ice in the Southern Hemisphere for the period 1973–1980 from weekly charts prepared using satellite IR, visible and microwave observations, as well as conventional surface observations. They selected the late spring and summer periods for examination, for the energy balance model of Ramanathan *et al.*[2] suggests that the largest CO_2-induced changes would occur then (though the model was actually based on snow cover rather than sea ice change). They found that the mean extent of the summer ice decreased from 8.2×10^6 km^2 in 1973 to 5.7×10^6 km^2 in 1980. However, as sea ice varies naturally to a comparable degree the decrease is not necessarily indicative of CO_2-induced warming. Indeed Kukla and Gavin note that the area of ice increased in 1981.

Several atlases published before 1970 report the extent of Southern Hemisphere sea ice to have been greater than that observed during the 1970s. However, as Kukla and Gavin carefully explain, the historical and the recent sets of data are not necessarily comparable as the extent of the ice recorded in the atlases was taken from relatively few surface observations. Observational biases could exist which would give the false appearance of a long-term trend.

Arctic data are even more equivocal. Kukla and Gavin do not find that similar observations of Northern Hemisphere sea ice indicate that there was less ice now than in the 1930s. Satellite-derived records of summer snow-cover do not show a decrease either, although recent positive surface temperature anomalies at 'selected latitudes' in the north have been associated with the belt of melting snow in spring and summer, and are thus 'consistent with' the Ramanathan *et al.* model predictions for CO_2 increase.

Kukla and Gavin suggest that "highly variable components of the climate system such as snow and pack ice fields" be given priority in the search for early signs of a CO_2 effect on climate, a conclusion consistent with Manabe and Stouffer's model[3], whose sensitivity to CO_2 depends heavily on concomitant sea ice changes. Although high variability of some climatic component may imply high sensitivity to external forcing (for example, increased CO_2), such variability unfortunately also makes it difficult to detect a CO_2 signal — even a large one — because high variability usually implies a high noise level as well. The best 'precursor indicators' are, of course, those having a large signal-to-noise ratio.

Chlorofluorocarbons (CFCs)[4], methane

Starley L. Thompson is based at the Department of Atmospheric Sciences, AK-40, University of Washington, Seattle, Washington 98195. At present, he is with Stephen H. Schneider at the National Science Foundation sponsored National Center for Atmospheric Research PO Box 3000, Boulder, Colorado 80307.*

*Any opinions, findings and conclusions or recommendations expressed herein are those of the author and do not reflect the views of the National Science Foundation.

0028-0836/82/080645-02$01.00

and nitrous oxide[5] are, like CO_2, effective absorbers of IR radiation and thus could also help to create a greenhouse effect.

The sum of all trace greenhouse gases has even been referred to as 'virtual CO_2 concentration[6]'. Lacis *et al.*[7] at NASA's Goddard Institute for Space Studies (GISS) recently used a one-dimensional, radiative–convective model to estimate the global equilibrium and transient warmings expected from trace gas increases between 1970 and 1980. Interestingly, the computed equilibrium warming from CH_4, N_2O and CFCs combined was 0.1 °C, nearly as large as the 0.14 °C warming computed from the CO_2 increase during the same decade. There remains, of course, some uncertainty, even in the purely radiative calculations. For example, the equilibrium sensitivity of the Lacis *et al.* model to a 2 p.p.b. (parts per 10^{12}) increase in CFCs was 30 per cent more than that in a calculation published by GISS scientists only two months earlier[8]. The more recent result, +0.65 °C, now agrees more closely with Ramanathan's[4] calculation of +0.9 °C but the above discrepancies remain to be resolved. By allowing for the transient effects from thermal inertia of the oceans[9,10], Lacis *et al.* reduced their calculated equilibrium expected warming during the 1970s by about one-half.

The GISS group results come from a mathematical climate model which has an equilibrium global surface temperature sensitivity of about 3 °C for a doubling of CO_2 concentration. This is within the present 'consensus' estimates (1.5–4.5 °C)[11]. Some still believe that these estimates are much too high[12,13]. Idso, in particular, strongly believes that 'natural experiments' yield an 'empirical response function' some orders of magnitude smaller than the consensus models although he may have neglected some categories of energy flows and storages. In our opinion, it has been convincingly shown[11,14] that the neglect of horizontal heat flux, heat storage and total atmosphere/surface energy budget has caused Idso's low estimates of global, equilibrium sensitivity to a doubling of CO_2. We do, however, agree that tentative model assumptions demand empirical verification, but such comparisons between models and observations must be properly applied.

An example of empirical verification of a climate model is given in a recent study by Hansen *et al.*[8]. A simulation using CO_2 forcing was compared with the historical temperature record to give a 'direct' verification of the CO_2 sensitivity of the model. One difficulty with this approach is distinguishing what is still a small CO_2 signal from background noise. In addition, their model was based on assumed solar and volcanic forcings whose combined effects were matched to the observed temperature record by adjusting empirical coefficients. This 'tuning process' can engender confidence when the results are statistically significant, but this has yet to be shown. Another direct verification approach would be to compare palaeoclimatic temperature proxy data with the results of a model forced with observations — actually reconstructions — of natural long-term CO_2 variations. Such variations have recently been confirmed by Neftel *et al.*[15] to have occurred over at least the past 40,000 yr. Problems with this approach include estimates of global temperature and CO_2 concentration which are subject to large errors and the necessity of accurately accounting for additional climatic forcing factors such as surface albedo changes.

Empirical verification may also be 'indirect' — model performance may be compared with a surrogate 'geophysical experiment' not involving CO_2 change, such as the annual cycles of solar radiation and temperature[3,16]. Difficulty remains in evaluating the extent to which a surrogate experiment is applicable to the CO_2 forcing case. Both of these empirical methods of verification need to be, and have been[11], used to test the 'consensus models'.

The average standard deviation of annual global temperatures within individual decades over the last century is about 0.1 °C. For this reason the estimate of warming during the 1970s given by Lacis *et al.*, despite being comparable with that observed, is too small to engender real confidence in the model results. However, Lacis *et al.* believe that, by 1990, temperature rise signal from the *combined* trace greenhouse gases should stand out clearly from the background of natural climatic variability. This belief assumes, of course, that current trends in CO_2 and other trace gas concentrations continue, and that the sensitivity of present climate models to such increases is reasonably correct. A global warming of 0.2–0.3 °C during the 1980s, as Lacis *et al.* predict, would have a fairly small probability of chance occurrence, although it is not unprecedented. An increase of this magnitude occurred in the 1920s (for example, see Fig. 3 of ref. 8), which presumably was not a CO_2-related event. Furthermore, extrapolations of present trends of trace gas increases past the year 2000, particularly those for CO_2 based on the assumption of large coal use, have been strongly challenged on economic grounds[17,18]. Thus, because a doubling of CO_2 from massive coal use in the near future is questionable, but a further 25–50 per cent increase from petroleum and natural gas combustion is possible, we feel even more strongly[9] that emphasis for research on CO_2-induced climatic effects should be on the transient response over the next fifty years.

The problem of estimating the transient climatic response also has a bearing on the selection of potential 'precursor indicators' of a CO_2 warming. Many of these suggested indicators tend to be regional in extent, such as the sea ice changes examined by Kukla and Gavin. This is significant because it has recently become apparent that different regions will probably respond at different rates to the continuous CO_2 build-up. For example, a simulation performed with a detailed coupled atmosphere/ocean model published recently by Bryan *et al.*[19] shows sea surface temperatures in near-polar latitudes responding relatively slowly to a stepfunction CO_2 increase compared with the global mean response. Thus, for the purpose of highlighting the most promising regional precursor indicators it is questionable whether one should put much confidence in regional climatic perturbations derived from steady-state simulations in which a CO_2 increase is held fixed[20]. A better way of identifying regional climatic changes with potentially good signal-to-noise ratios would be to search for these in the results of detailed time-dependent simulations performed with a coupled atmosphere/ocean model using realistic geography and plausible CO_2 increase scenarios[10].

In summary, then, the recent sea ice observations of Kukla and Gavin and the model versus observed surface temperature trend comparisons of the GISS group are at least consistent with consensus modellers' expectations for a climatic signal from increasing 'greenhouse' gases. We believe, however, that the statistical significance of these results is simply too small and the number of unverified modelling assumptions too large to allow one to proclaim 'detection'. But if Lacis *et al.* are right, then *this* decade, not the often cited year 2000, is when a clear warming signal is due. Verification of model predictions by the real atmosphere, of course, takes time; the recent results strongly suggest that the time is closer at hand than previously believed.

---

1. Kukla, G. & Gavin, J. *Science* **214**, 497 (1981).
2. Ramanathan, V., Lian, M.S. & Cess, R.D. *J. geophys. Res.* **84**, 4040 (1979).
3. Manabe, S. & Stouffer, R.J. *J. geophys. Res.* **85**, 5529 (1980).
4. Ramanathan, V. *Science* **190**, 50 (1975).
5. Ellingson, R.G. & Gille, J.C. *J. atmos. Sci.* **35**, 523 (1978).
6. Flohn, H. *Possible Climatic Consequences of a Man-Made Global Warming* (International Institute for Applied Systems Analysis, Laxenburg, Austria, 1980).
7. Lacis, A., Hansen, J., Lee, P., Mitchell, T. & Lebedeff, S. *Geophys. Res. Lett.* **8**, 1035 (1981).
8. Hansen, J. *et al. Science* **213**, 957 (1981).
9. Thompson, S.L. & Schneider, S.H. *Nature* **290**, 9 (1981).
10. Schneider, S.H. & Thompson, S.L. *J. geophys. Res.* **86**, 3135 (1981).
11. The CO_2/Climate Review Panel of the Joint Climate Board/Committee on Atmospheric Sciences, Climate Research Committee *Carbon Dioxide and Climate: A Second Assessment* (National Academy of Sciences, Washington DC, in the press).
12. Newell, R.E. & Dopplick, T.G. *J. appl. Met.* **18**, 822 (1979).
13. Idso, S.B. *New Scient.* **92**, 444 (1981).
14. Ramanathan, V. *J. atmos. Sci.* **38**, 918 (1981).
15. Neftel, A., Oeschger, H., Schwander, J., Stauffer, B. & Zumbrunn, R. *Nature* **295**, 220 (1982).
16. Schneider, S.H. & Thompson, S.L. *Icarus* **41**, 456 (1980).
17. Lovins, A., Lovins, H., Krause, F. & Bach, W. *Least-Cost Energy: Solving the CO_2 Problem* (Brick House, Andover, Massachusetts, in the press).
18. Ausubel, J.H. *Climate Change and the Carbon Wealth of Nations*, IIASA Working Paper WP-80-75 (1980).
19. Bryan, K., Komro, F.G., Manabe, S. & Spelman, M.J. *Science* **215**, 56 (1982).
20. An example being the mid-latitude, summer 'dry zone' in the simulations of Manabe, S., Wetherald, R.T. & Stouffer, R.J. *Climatic Change* **3**, 345 (1981).

Evolution of photosynthetic pathways in flowering plants

from Peter D. Moore

THE metabolic and anatomical characteristics of plants that possess either Crassulacean Acid Metabolism (CAM) or the C_4 photosynthetic pathway have long interested physiologists and have even begun to stir the imagination of ecologists[1], but relatively few people have applied themselves to the problems associated with the evolution of these mechanisms, beyond the cataloguing of their taxonomic distribution. Briefly, both CAM and C_4 plants have a 4-carbon atom molecule (oxaloacetate) as the first product of photosynthetic carbon fixation, though in the former this process occurs only in the dark. Both have low carbon dioxide compensation points (the CO_2 concentration below which a plant takes up less CO_2 by photosynthesis than it gives out by respiration), are insensitive to atmospheric oxygen concentration and lack photorespiration, by which glycollate is formed and subsequently degraded, thus releasing carbon dioxide. CAM and C_4 plants differ both structurally and ecologically: whereas C_4 plants have the so-called 'Kranz' (literally 'garland') anatomy with modified vascular bundle sheath cells to which the Calvin–Benson cycle carbon fixation system is spatially limited, CAM plants lack Kranz anatomy and the products of carbon fixation are not moved to specialized sites before liberation and fixation. Both types of photosynthesis are characteristically more frequent in hot, often (though not necessarily for CAM) arid regions, where the stomatal control possible with these modifications may be one of their greatest strategic advantages.

Wide-ranging surveys of the plant kingdom by physiologists and anatomists have resulted in a very considerable list of species in which the CAM and C_4 strategies have been found. Most are flowering plants, but at least one gymnosperm[2] and two pteridophytes[3] are reported to be CAM plants. The figure displays the taxonomic distribution of recorded CAM and C_4 species of flowering plants in a form that makes clear the presumed evolutionary development of the two systems. Two major points emerge: first, both CAM and the C_4 mechanism are widespread in the plant kingdom; yet, second, neither is found in what are considered to be the most primitive orders, such as the Magnoliales, Laurales and Ranunculales (that is, those orders close to the supposed 'ancestral complex' (A), within which the angiosperms originated). Perhaps the most primitive orders in which the pathways are found are the Sapindales (with C_4 representatives) and the Rosales (with CAM members). These observations lead to two logical conclusions: that the C_3 system is primitive in the angiosperms[4,5] and that both CAM and C_4 have originated independently and on many occasions during the evolution of flowering plants[6].

The polyphyletic origin of both mechanisms leads one to suppose that the genetic modifications involved in the adoption of either strategy are relatively small; indeed, the major enzymes required are already available in C_3 plants. One obvious way of investigating further this aspect of the subject is to seek and study plants which are intermediate between, say, C_3 and C_4 in character, either in wild populations of plants or as a result of breeding experiments in the laboratory. Rathnam[7] has now collated the information derived from such studies, but finds that natural hybridization has been recorded in only four genera of plants. The laboratory crossing of C_3 and C_4 plants, particularly the work of Björkman with *Atriplex*, has not produced a simple picture, even though individuals with intermediate characters have resulted. Rathnam concludes that the likelihood of introducing the C_4 mechanism to C_3 plants by genetic manipulation is not strong.

Peter D. Moore is a Senior Lecturer in the Department of Plant Sciences, University of London King's College, 68 Half Moon Lane, London SE24 9JF.

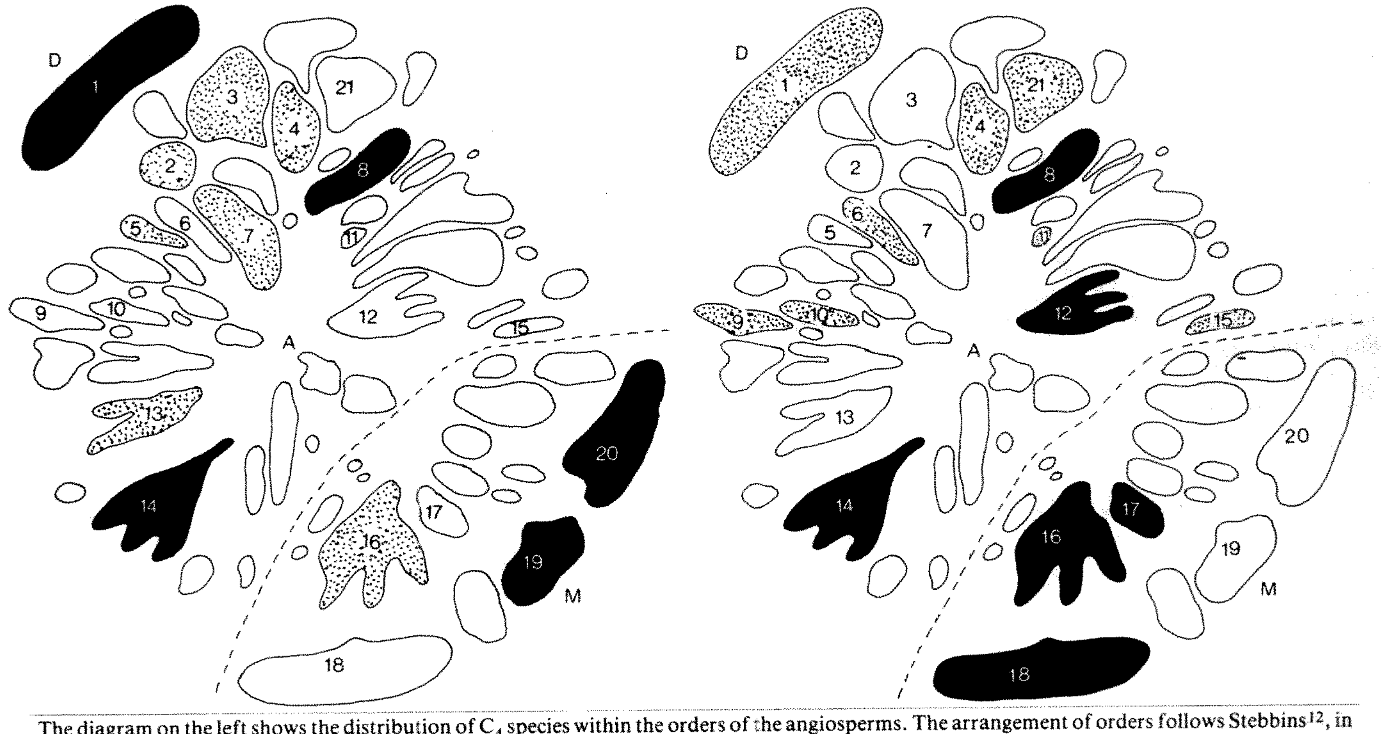

The diagram on the left shows the distribution of C_4 species within the orders of the angiosperms. The arrangement of orders follows Stebbins[12], in which they are shown to radiate from a proposed ancestral complex 'A'. Stippled orders contain fewer than 30 species with C_4 characteristics, shaded orders contain more than 30 species. Kranz anatomy is taken here to be an adequate criterion for C_4 designation, which may be questionable[9]. D, dicotyledons; M, monocotyledons. On the right is the distribution of CAM species among the angiosperms. Symbols as above. The data given in both diagrams are derived from refs 13–16. The numbered orders of flowering plants contain C_4 or CAM species: 1, Asterales; 2, Polemoniales; 3, Scrophulariales; 4, Gentianales; 5, Polygalales; 6, Geraniales; 7, Sapindales; 8, Euphorbiales; 9, Passiflorales; 10, Violales; 11, Rhamnales; 12, Rosales; 13, Capparales; 14, Caryophyllales; 15, Piperales; 16, Liliales; 17, Bromeliales; 18, Orchidales; 19, Cyperales; 20, Poales (Graminea); 21, Lamiales.

0028-0836/82/080647-02$01.00

Perhaps the most satisfying result to emerge from these studies is Rathnam's own work on the millet grass genus ***Panicum*** and in particular *P. milioides*[8]. This plant has a higher than expected phosphoenolpyruvate (PEP) carboxylase activity and an increased affinity for CO_2, which suggest C_4 tendencies. It has Kranz anatomy, an intermediate CO_2 compensation point of 16 μl l^{-1} (40–60 for C_3 and 0–5 for C_4) and is less sensitive to O_2 inhibition of apparent photosynthesis than a C_3 species, but more so than a C_4 species. Rathnam proposes that both photosynthetic pathways are operative within the leaf mesophyll of *P. milioides*, the C_3 system being unconfined and not limited to the bundle sheath cells as in the typical C_4 plant. Although the development of the C_4 pathway is incomplete, it would still provide the plant with the selective advantage of being able to concentrate CO_2 at the bundle sheath and thereby reduce photorespiration. On the basis of these findings, Rathnam proposes that the evolutionary development of Kranz anatomy precedes the metabolic modifications involved in the C_4 pathway, in which case Kranz anatomy is not a reliable indication of the C_4 capacity of a plant[9].

Fortunately, a resolution of these difficulties is suggested by this hypothesis recently put forward by Cockburn[10], who focuses on the mode of operation of the stomatal guard cell. Here, malate (one of the 4-carbon atom molecules involved in both CAM and C_4 metabolism) is known to play an important part and to accumulate in the guard cell during its opening[11]. The malate is fixed from CO_2 using PEP carboxylase, the precise method found in both CAM and C_3 plants. According to Cockburn, "all the essentials of CAM are represented in stomatal guard cell metabolism". Becoming a CAM plant *sensu stricto* simply involves the expression of these characteristics not only in the stomatal guard cells, but in other cells as well. The development of true C_4 metabolism would therefore appear to be a somewhat more complex series of modifications involving the development of Kranz anatomy and the use of malate as a mobile carbon resource.

The polyphyletic origin of both CAM and C_4 is thus easy to explain. The question that remains is which came first, the vascular sheath garland, or the extension of the guard cell malate system? The answer will probably depend on where one looks for it. ☐

---

1. See Moore, P.D. *Nature* **280**, 193 (1979).
2. Kluge, M. & Ting, I.P. *Crassulacean Acid Metabolism* (Springer, Berlin, 1978).
3. Wong, S.C. & Hew, C.S. *Am. Fern J.* **66**, 121 (1976).
4. Evans, L.T. in *Photosynthesis and Photorespiration* (eds Hatch, M.D., Osmond, C.B. & Slatyer, R.O.) 130 (Wiley, New York, 1971).
5. Raghavendra, A.S. *Photosynthetica* **14**, 271 (1980).
6. Smith, B.N. & Robbins, M.J. *Proc. 3rd int. Congr. Photosynthesis* **2**, 1579 (1974).
7. Rathnam, C.K.M. *What's New in Pl. Physiol.* **12** (6), 1 (1980).
8. Rathnam, C.K.M. & Chollet, R. *Progr. Phytochem.* **6**, 1 (1980).
9. Hegde, B.A. & Patil, T.M. *Photosynthetica* **15**, 1 (1981).
10. Cockburn, W. *Plant, Cell Environ.* **4**, 417 (1971).
11. Travis, A.J. & Mansfield, T.A. *New Phytol.* **78**, 541 (1977).
12. Stebbins, G.L. *Flowering Plants — Evolution above the Species Level* (Edward Arnold, London, 1974).
13. Downtown, W.J.S. *Photosynthetica* **9**, 96 (1975).
14. Raghavendra, A.S. & Das, V.S.R. *Photosynthetica* **12**, 200 (1978).
15. Szarek, S.R. & Ting, I.P. *Photosynthetica* **11**, 330 (1977).
16. Szarek, S.R. & *Photosynthetica* **13**, 467 (1979).

Dynein in the spindle?

from Jeremy Hyams

MITOSIS typically involves two distinct phases of chromosome separation: the movement of chromosomes to the spindle poles (usually referred to as anaphase A) followed by the separation of the poles due to spindle elongation (anaphase B). Although the mechanisms of mitosis remain unknown, the most attractive models envisage that force for chromosome movement is generated by an active sliding displacement between spindle microtubules coupled to controlled changes in their lengths[1,2]. Motility based on sliding is now well established for ciliary and flagellar beating, another form of movement involving microtubules. In this case, the active component is the ATPase protein dynein which reversibly interconnects the nine outer doublet microtubules of the ciliary or flagellar axoneme[3]. Crucial to establishing the role of dynein was the demonstration that demembranated sea urchin sperm flagella would resume normal beating movements when supplied with exogenous ATP[4].

The development of a similar, simple *in vitro* model for studying spindle function has, however, proved to be a far less tractable problem. Spindles are notoriously labile and, in general, may be isolated only in the presence of stabilizing agents, which, by definition, alter the characteristics of the organelle. The best alternative has been to use whole cells made permeable to added reagents by treatment with detergent. Most studies of this type have used a cultured cell line derived from the rat kangaroo called PtK_1. If extracted at the start of anaphase, PtK_1 chromosomes continue to move in an apparently normal fashion as long as the lysis solution contains ATP[5]. More recent studies of the permeabilized cell model have shown that anaphase A and B are physiologically distinct. Whilst the basis of anaphase A remains uncertain, ionic conditions required to maintain anaphase B closely parallel those which support flagellar beating. Chromosome separation is specific for ATP as an added nucleotide, is inhibited by non-hydrolysable ATP analogues and sulphydryl poisons and reversibly arrested by vanadate, a potent inhibitor of dynein ATPase activity[6,7].

Jeremy Hyams is in the Department of Botany and Microbiology, University College London, Gower Street, London WC1E 6BT.

In this issue of *Nature* (p.700) Cande reports further evidence for the dynein-like nature of the anaphase B chromosome motor, on the basis of its sensitivity to erythro-9-[3-(2-hydroxynonyl)]adenine (EHNA) which, like vanadate, specifically inhibits flagellar beating and dynein ATPase activity. This physiological evidence for the involvement of dynein in mitosis is supported by the identification in isolated sea urchin spindles of an ATPase which has a subunit molecular weight and ionic and nucleotide characteristics closely resembling flagellar dynein[8]. Although there have been suggestions based on immunological cross-reactivity that the same molecule is involved in both forms of motility[9], the likelihood is that, if the spindle dynein really does exist, it is distinct from its flagellar counterpart.

The organization of microtubules in the two situations is, for a start, quite different. In the axoneme, dynein molecules form cross-bridges between microtubules which all arise from the basal body and hence are parallel in their orientation. In the spindle, on the other hand, interaction is between microtubules originating from opposite poles and so having opposed polarities[10]. Mutants of the green alga *Chlamydomonas* in which the flagella lack the paired dynein arms divide normally[11]. Likewise human patients in which these structures are missing due to genetic defects suffer only from symptoms associated with ciliary paralysis and are otherwise normal[12]. More directly, however, antiserum raised against dynein from mammalian sperm failed to recognize the corresponding proteins in either cytoplasmic extracts or spindles of mammalian cells[13].

At this point the reader might be forgiven for concluding that a unified, and, better still, experimentally testable view of mitosis is at last starting to emerge. Other evidence, however, suggests that the situation is just as uncertain as ever. Particularly fascinating is a recent report from Aist and Berns[14] involving a more primitive organism, the fungus *Fusarium solani*. These workers used a laser microbeam to sever the region of the spindle between the retreating chromosomes. Surprisingly, chromosome separation in these nuclei did not cease but rather proceeded three times faster than in the undamaged controls. By contrast,

0028-0836/82/080648-02$01.00

irradiation of the cytoplasm adjacent to one of the spindle poles caused the chromosomes to move more slowly. Far from supporting a model in which active sliding between microtubules drives chromosome movement, these data are consistent with the spindle acting as a mechanical governor, maintaining a counterforce which resists the pull of some, as yet unidentified, extranuclear component.

It would be quite wrong to conclude that either of the two diametrically opposed views of spindle function presented here is incorrect. On the contrary, mitosis may well involve several distinct mechanisms which are expressed to different degrees in different organisms[15]. The new probes of dynein activity such as vanadate and EHNA may well prove valuable in assessing the contribution of sliding in different cell types. Indeed their value may extend way beyond the world of mitosis. In this issue of *Nature* (p.701), Beckerle and Porter further report that both reagents inhibit particle transport along microtubules in fish chromatophores. It may well be that dynein will be shown to be as ubiquitous a feature of microtubule-based motility systems as myosin is of actin-based ones.

---

1. McIntosh *et al. Nature* **224**, 659 (1969).
2. Margolis *et al. Nature* **272**, 450 (1978).
3. Satir *et al. Cell Motility* **1**, 303 (1981).
4. Gibbons & Gibbons *J. Cell Biol.* **54**, 75 (1972).
5. Cande *et al. Proc. natn. Acad. Sci. U.S.A.* **71**, 1559 (1974).
6. Cande & Wolniak *J. Cell Biol.* **79**, 573 (1978).
7. Cande *Cell* **28**, 15 (1982).
8. Pratt *et al. J. Cell Biol.* **86**, 738 (1980).
9. Mohri *et al. Devl Growth Differ.* **18**, 391 (1976).
10. McDonald *et al. J. Cell Biol.* **83**, 443 (1979).
11. Huang *et al. J. cell. biol. Chem.* **254**, 3091 (1979).
12. Afzelius *et al. J. Cell Biol.* **66**, 225 (1975).
13. Zieve & McIntosh *J. Cell Sci.* **48**, 241 (1981).
14. Aist & Berns *J. Cell Biol.* **91**, 446 (1981).
15. Pickett-Heaps & Bajer *Cytobios* **19**, 171 (1977).

Intracellular membrane traffic

from M.J. Geisow

GEORGE PALADE (Yale University), in opening the 92nd Ciba Foundation Symposium* on membrane recycling, reminded participants of a fundamental problem of cell economics. To grow, cells must maintain fluid membranes at ambient temperature. This requirement is purchased at the expense of high molecular diffusion rates (1–60 μm min^{-1}) which, unless controlled, would lead to randomization of membrane components. When it is realized that animal cells contain up to 10 distinct membranes with characteristic proteins and lipids and that extensive transport occurs between them (the macrophage recycles its 780μm^2 of membrane in 30 min), the full nature of the problem can be appreciated. Nature's

Nature's general solution appears to have been the development of membrane components which can self-assemble to form micro-domains. Within such domains, lateral diffusion rates are very much less than in bulk membrane. Well known examples are the specialized intercellular junctions and clathrin-coated pits. It was from the basis of this generalization, that cells can maintain anisotropic membranes, that the symposium considered how transport between occurs and by what routes.

Cells constitutively internalize their plasma membranes by endocytosis. Two routes of entry of membrane — through coated pits and uncoated invaginations — lead to coat-free, often irregular vesicular bodies in the peripheral cytoplasm of the cell. To designate this poorly characterized compartment, the terms endosome or pre-lysosome have been used, although in the specific case of receptor-mediated uptake initially occurring in coated pits, Ira Pastan and co-workers (NIH) coined the word 'receptosome'[1]. It is the ultimate fate of the endosome to fuse with a lysosome.

Clathrin-coated pits are probably micro-domains specializing in membrane protein selection. Mark Bretscher (University of Cambridge) showed some time ago that certain cell surface antigens, including Thy-1, are excluded from coated pits[2]. Surface receptors, by contrast, are sometimes present at relatively high surface density in coated pits. Clustering of receptors for low-density lipoprotein[3], α_2-macroglobulin[4] and galactose receptor[5] does not even require the presence of specific ligands and can be explained only by a relatively high affinity of pit for receptor protein. Unfortunately, the basis of this interaction is unknown, because structural analysis of coated membrane has not yet probed the organization within the lipid region under the clathrin cytoskeleton.

Immediately after uptake, receptor and ligand are present in coated vesicles, but within 1–5 min they are in uncoated endosomes. The intermediate coated vesicle, in cultured cells at least, must be a very transient transport element. One good reason for the short lifetime of the coat *in vivo* may be the need for partial or complete uncoating before fusion of the underlying membrane with another organelle. At the Ciba Symposium, James Rothman (Stanford University) described a timely uncoating activity in cytosol, which requires ATP.

Recent work has permitted closer biochemical definition of endosomes. They are not like classical secondary lysosomes, since cytochemistry demonstrates the absence of acid hydrolases. Nevertheless, endosomes may have relatively acidic contents. Spectroscopic studies[6,7] point to rapid acidification of endocytosed ligands. A clever confirmation of the low *p*H in the endosome has followed the observation that the fusion of Semliki Forest virions with lipid bilayers only occurs at or below *p*H 6.0. Viral infection *in vivo* necessitates the fusion of enveloped viruses, taken up via coated pits, with the endosome membrane. Ari Helenius (Yale University) has now shown that this fusion is prevented by weak bases such as amantadine which increase endosome *p*H (ref.8). Cells can be 'rescued' from irreversible infection only by supplying

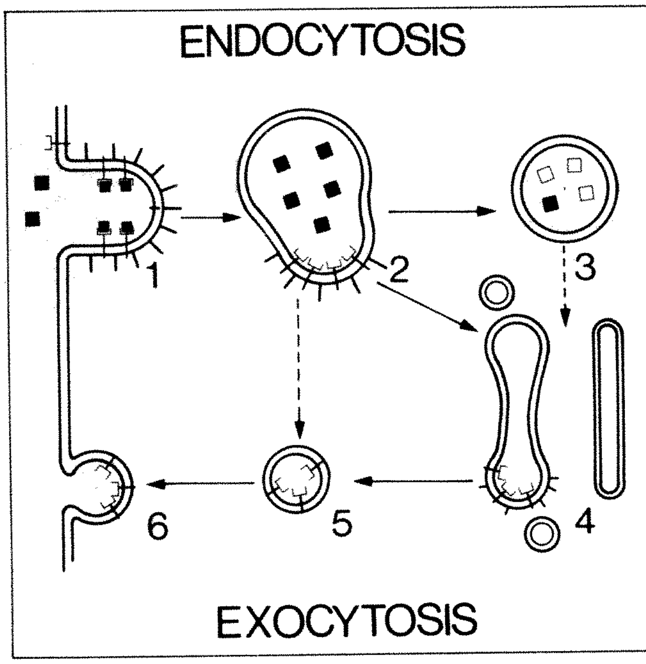

Suggested sequence of intracellular receptor movements. Ligands (■) bind to receptors (┬) and are internalised through coated pits (1), where they are transferred to smooth-membraned structures (endosome, receptorsome 2.) Conditions within this compartment lead to ligand dissociation allowing receptors and ligands to follow different routes. The latter enter secondary lysosomes (3). Receptors may be conveyed to the Golgi (4) or a secretory vesicle (5) and return to the cell surface (not necessarily the same surface in epithelial cells) by exocytosis (6).

The existence of transport vesicles (not illustrated) which shuttle between these organelles is inferred. The nature of these and the topography of the receptors is unknown.

M.J. Geisow is in the Biophysics Division at the National Institute for Medical Research, The Ridgeway, Mill Hill, London NW7 1AA.

---

*The Ciba Symposium on 'Membrane Recycling' was held in London on 19–21 January 1982.

0028-0836/82/080649-02$01.00

the weak base within 4 min of warming cells with adherent virus to 37°C.

The low *p*H of endosomes may bring about dissociation of ligand and receptor protein. In experiments reported by Anne Hubbard (Johns Hopkins University), liver galactose receptor–ligand complexes are endocytosed at 16°C, a temperature at which endosome–lysosome fusion is impaired[5]. However, ligands still dissociate from receptors and the latter return to the cell surface, despite the absence of ligand degradation. It may be that these endosomes represent the elusive sites of receptor recovery — an acid wash through which regular 'preening' of the cell surface can be achieved.

The fate of the ligands and soluble content of endosomes is clearer — they are transferred to secondary lysosomes and degraded, which for them is a one-way trip. Exceptionally, certain receptors, for epidermal growth factor or the Fc portion of immunoglobulin, also enter lysosomes. Whether this is because their affinity for ligands is unaffected by the low *p*H in the endosome or because of intrinsic differences in the molecular structures of such receptors, remains an open question.

Equally enigmatic is the direction taken by the receptors which do recycle following the dissociation of their ligands or their normal recovery during membrane recycling in the absence of a specific ligand. Specific labels are lost at this stage and anti-receptor immunocytochemistry can only demonstrate the total cellular distribution, not the pathways of recycling. However, the endocytosis of cationized ferritin (CF), a positively charged, electron-dense marker which binds tightly and non-specifically to membranes, has provided some indirect evidence of how receptors recycle.

Kinetic studies of the endocytosis of CF by pituitary cells and lymphocytes made over a number of years by Marilyn Farquhar[9,10] show that after its appearance in endosomes, CF enters the trans elements of the Golgi stacks. After 30 min, CF appears on the inner membrane of secretion granules and therefore on the exocytotic leg of its journey through the cell. Autoradiography of iodinated surface membrane proteins suggests essentially the same route — although slow techniques such as conventional fixation and electron microscopy provide images which reflect rate-determining stages in the flux through a cell, so this picture may be incomplete.

In at least one case there is good evidence that CF follows the same route as receptors. Richard Rodewald (University of Virginia) has described transcytosis or diacytosis (passage through a cell) of maternal IgG across the intestinal epithelium of new-born rats[11]. The immunoglobulin is bound by Fc receptors at the gut lumen and is discharged into the neonatal circulation. Efficient segregation of IgG–Fc receptor complexes from soluble markers occurs in the endosomes near the sites of absorption (coated pits). The integrity of the receptor–ligand complex may be favoured in this case by low *p*H, since the neutral *p*H of the neonatal blood affects dissociation of the complex when it appears at the basolateral cell surface. CF accompanies the ligand through the same pathway and is exocytosed, still in membrane-bound form, at the sites of IgG release.

Considerable advances have been made in this popular area of cell biology, to which an increasingly 'molecular' approach is being applied. There remain, of course, major problems. We still need to account for the fast recycling times of cell membrane (seconds in the neuromuscular junction) and certain receptors (a minute or less for low-density lipoprotein receptor). Do these membrane components have time to follow the pathways described above? The relationship between endocytosis of membrane components through coated and uncoated regions is also unclear. Most telling of all, however, is the degree of our ignorance of the nature of the signals which direct this extensive traffic of receptor proteins and orchestrate the flow of cellular membrane. To understand these, we need techniques which allow us to observe the membranes from within the cell itself. □

1. Willingham, M.C. & Pastan, I. *Cell* **21**, 67 (1980).
2. Bretscher, M.S., Thomson, J.N. & Pearse, B.M.F. *Proc. natn. Acad. Sci. U.S.A.* **77**, 4156 (1980).
3. Goldstein, J.L., Anderson, R.G.W. & Brown, M.S. *Nature* **279**, 679 (1979).
4. Willingham, M.C. & Pastan, I.H. *Cell* **21**, 67 (1980).
5. Wall, D.A. & Hubbard, A.L. *J. Cell Biol.* **90**, 687 (1981).
6. Geisow, M.J., Hart, P., D'Arcy & Young, M.R. *J. Cell Biol.* **89**, 645 (1981).
7. Maxfield, F.R. & Tycko, R. *J. Cell. Biol.* **91**, 212a (1981).
8. White, J., Matlin, K. & Helenius, A. *J. Cell Biol.* **89**, 674 (1981).
9. Farquhar, M.G. *J. Cell Biol.* **77**, R35 (1978).
10. Ottensen, P.D., Courtoy, P.J. & Farquhar, M.G. *J. exp. Med.* **152**, 1 (1980).
11. Rodewald, R.D. & Abrahamson, D.R. *J. Cell Biol.* **91**, 270 (1981).

100 years ago

Amongst the batrachians exhibited at the Zoological Society are several species of gigantic size when compared with their puny representatives in this country, such as the Agua Toad (*Bufo agua*) of Brazil and the Ocellated Bladder-Frog (*Cystignathus ocellatus*) of Buenos Ayres. But by far the most remarkable of these forms in the series is the Adorned Ceratophrys, or "Esquerzo" of the natives of the Argentine Republic — a large toad of brilliant colours and extraordinary form, of which a figure (Fig 16) is now given, taken from a water-colour sketch prepared by Mr Ernest Griset.

The Esquerzo was discovered by Mr Darwin during the celebrated voyage of H.M.S. *Beagle*, and first described by the late Prof. Bell in the "Zoology of the Voyage of the *Beagle*." This monster inhabits the pampas of Buenos Ayres, and is said to feed chiefly on its smaller brethren of the same class. Mr Ernest William White, F.Z.S., to whom the Society is indebted for one of the two specimens now in the Gardens, specially mentions it in his lately-published "Cameos from the Silver-Land" as one of the characteristic forms of the grassy plains of the Argentine Republic. "In the damp grass," he says, may often be perceived the leering eyes and mottled black and green body of the huge Esquerzo (*Ceratophrys ornata*), whose gaping mouth crammed with the body of an unfortunate sapo (toad), and surmounted by threatening horns, inspires terror. This said Esquerzo bears an awfully spiteful character, and is credited with the deaths of many children.

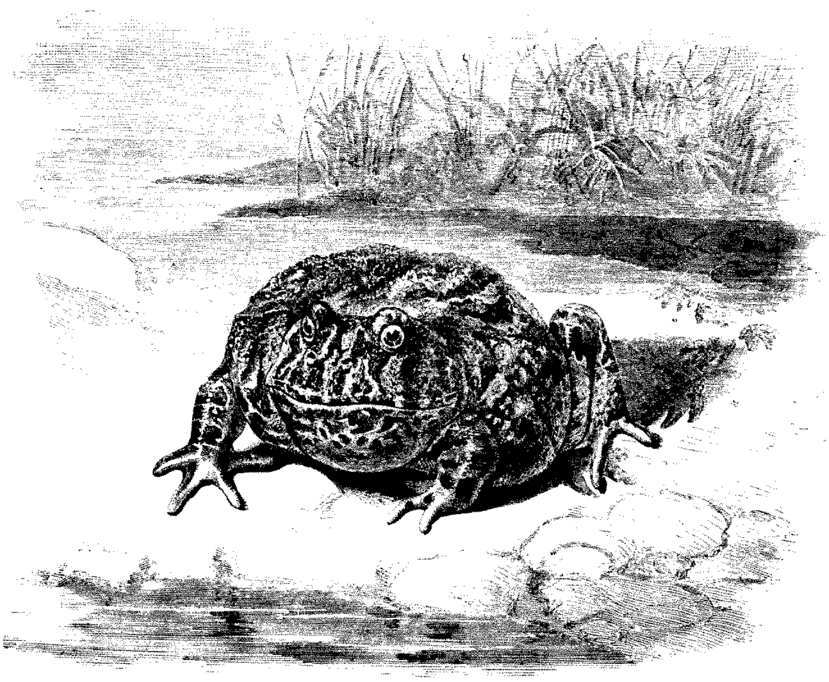

THE ESQUERZO, OR BARKING TOAD

From *Nature* **25**, 393; February 23 (1882).

REVIEW ARTICLE

Very large ground-based telescopes for optical and IR astronomy

J. R. P. Angel

Steward Observatory, University of Arizona, Tucson, Arizona 85721, USA

Optical and IR astronomers are taking a hard look at their ground-based facilities and devising new ways of making more economic, bigger and better telescopes. Features of instruments of the 15-m class are likely to include servo control to compensate for atmospheric wavefront errors as well as structural deformation, large honeycomb mirror blanks and mirror surfaces produced by economical techniques developed for aspherics.

WHILE detectors and instrumentation have improved enormously during the past 50 yr, the size of the largest optical telescopes has not increased significantly. Detectors have now reached close to the fundamental noise limit set by photon statistics and techniques have been developed to observe simultaneously many objects in the telescope's field of view. Further progress in many problems of astrophysics now requires an order of magnitude increase in light grasp.

The main purpose of increasing telescope aperture is to reach fainter objects and to improve accuracy of measurement. The quantum nature of light means that to measure intensity, spectrum or polarization to a certain accuracy, even with ideal detectors and optics, requires the collection of a certain minimum amount of energy. For other types of measurements in which detector noise is dominant, the rate of collecting energy is an additional factor, and gives an added advantage to the large telescope. Given that on average only a few hours each day meet all the requirements for observing, and that the largest telescopes must serve a broad community of observers, it is not practical to integrate for more than around 20 h in a season the light from even an object of exceptional importance. For a given collecting aperture this sets a limit to faintness or accuracy.

The qualitative advantages to larger apertures arise from the improved limit to angular resolution set by diffraction. At long IR wavelengths, where image quality is limited by diffraction, high spatial resolution is achieved directly. At shorter wavelengths various interferometric techniques allow the recovery of information on spatial structure at the diffraction limit. This is <10 m arc s in visible light for the telescopes I now consider.

In the US a programme has been started to develop the critical technology for a national telescope with a collecting area equivalent to 15 m diameter. Closely linked projects for smaller telescopes for California and Texas are under way. Meanwhile, in Arizona, the Multiple Mirror Telescope (MMT), a joint research facility of the University of Arizona and the Smithsonian Institution, is a working prototype of many aspects of the new technology. Most ideas for very large telescopes involve multiple primary mirror elements, and the MMT, the first of this type, has six mirrors of 1.8 m diameter all bringing light to a common focus (Fig. 1).

Why ground-based?

The Earth's atmosphere limits the value of ground-based telescopes in various ways. It is completely opaque to wavelengths below 0.3 μm while the IR spectrum is broken up by molecular absorption bands, being completely blocked over the range 40–300 μm. Background radiation from air scattering of sunlight and moonlight, and from thermal emission in the IR interferes with the observation of faint objects. Refractive index changes caused by thermal gradients in the air prevent one achieving diffraction limited images at shorter wavelengths, and the uncertainty of weather means one cannot be sure of any particular observing period.

These limitations are removed for telescopes above the atmosphere. The Space Telescope, scheduled for launch in 1985, will overcome many of these problems. However, its aperture of 2.4 m diameter has only 1/40 the area of a 15-m telescope, while its cost is an order of magnitude larger. Although technology may become so advanced that one could afford very large telescopes to realize the potential of space, our present needs for huge light grasp can only be met by building on the ground.

In fact, many of the observations that need large aperture can be done efficiently through the atmosphere provided that the design, siting and scheduling of the telescope are optimized. Spectroscopy will be the major application for a very large telescope. Provided the atmospheric background is kept to the minimum, the dominant noise source for this work will often be photon shot noise of the signal itself, or detector noise in IR spectroscopy—these noise sources are not reduced by going to space.

Image quality

The factor that most strongly drives cost is the need for excellent image quality. This is required not so much to resolve detail in extended objects but to minimize the background underlying faint unresolved objects. A giant light bucket with indifferent images would be of relatively little value. If, for example, the spectrograph entrance aperture has to be increased in diameter to capture the light of a degraded image, then the increased background may overwhelm the signal. For the faintest objects doubling the telescope diameter is of no advantage if the image diameter is also doubled.

Our intention of achieving good images is likely to have far-reaching consequences for telescope design. Recent experiments and studies demonstrate that some degree of active correction for atmospheric distortion is generally possible, with potentially very large gains for giant telescopes in the IR. If the means to implement such corrections are an integral part of the telescope design, then they may also be used to correct for slight distortion of the optics which would be intolerable otherwise. Large cost savings may be possible if a correction system were to relax the normal tolerance for accuracy, rigidity and stability, especially if the optics are extremely large.

The distortion at the atmosphere can be thought of in terms of the corrugation of a wavefront that was perfectly plane when incident at the top of the atmosphere. It has ripples and waves on all scales, which can be modelled by random turbulence[1]. (Note, however, that turbulence inside the telescope housing has only small scales, and causes separate problems discussed separately below.) The random wavefront deviation δ in micrometres between points separated by d across the wave is given by

$$\delta(\mu) \simeq (d/d_0)^{5/6} \qquad (1)$$

0028–0836/82/080651—07$01.00

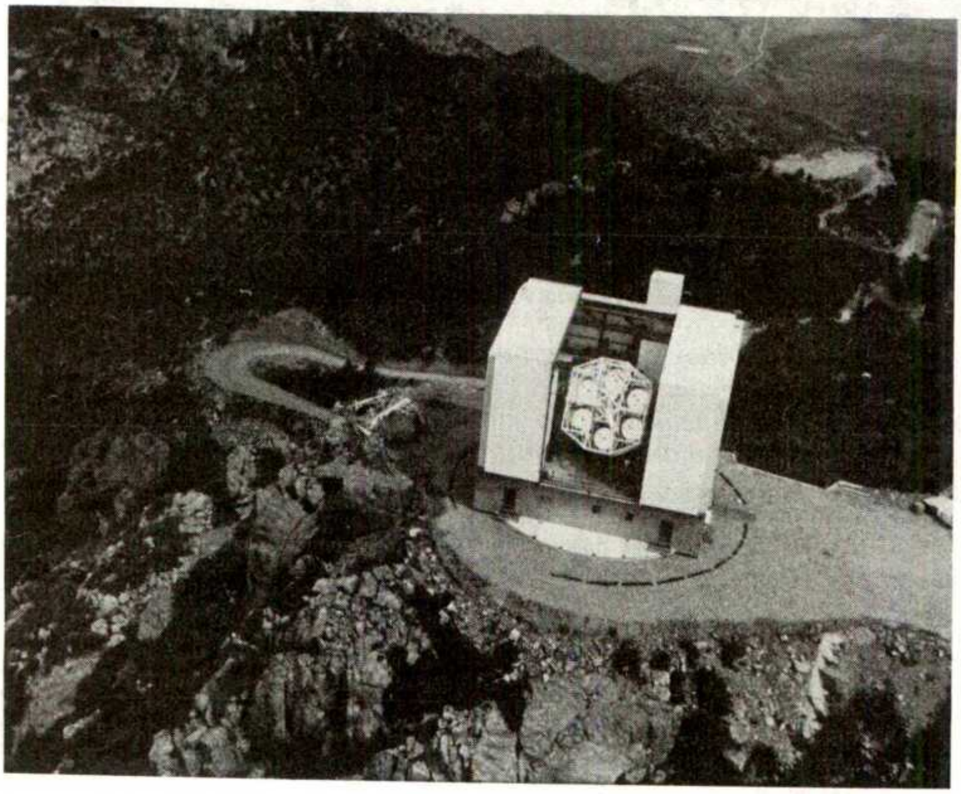

Fig. 1 An aerial view of the Multiple Mirror Telescope in Arizona. The location on top of a sharp, high peak, gives favourable conditions for sharp images. The MMT is jointly owned and operated by the University of Arizona and the Smithsonian Institution.

where d_0 is a measure of the seeing quality and in good conditions may be as large as several metres. The corrugations move at about the wind speed, so that large-amplitude deviations over a scale of 10 m change on a time scale of 1 s, while ripples on a scale of 10 cm vary 100 times faster.

If a true diffraction limited image is to be obtained at any given wavelength, then the deviations across the telescope aperture must not exceed about $\lambda/10$ (see ref. 2). For visible light, the task of correcting the wavefront of a large telescope to this tolerance is extremely difficult. The length scale of ripples with amplitude $>\lambda/10$ is 10–20 cm at best and the time scale is short. Compensation has to be made at an optical surface that can mimic all these rapidly changing small-scale ripples. Considerable progress in making such 'rubber' mirrors has been made by Hardy[3]. Apart from engineering difficulties, however, a fundamental limitation to achieving complete correction of the visible light wavefront is that of deriving the information needed to make the correction. This requires that the source being observed should be bright, or that there should be a bright source no more than a few arc seconds away whose wavefront, similarly distorted, can be used to derive corrections.

Although full correction of the wavefront is generally not possible, correction of the errors on a scale of metres is. Faint field stars within a couple of arc minutes of a target are adequate to provide the necessary much reduced amount of information. From equation (1) we see that the wavefront tilts δ/d are almost as big at large scales as at small, varying only as $d^{-1/5}$, so significant improvement of visible image quality can be expected. Woolf[4] has analysed in detail the improvements that can be made in various conditions: typically, 20–30% reduction in image size can be expected in visible light[4,55]. The better the seeing, the greater the improvement to be made.

In the IR, there is dramatic potential for high quality imaging with large telescopes. At 10 μm, for example, the small-scale ripples that do most damage to visible images are below the $\lambda/10$ threshold, and are not noticed. The seeing disk, resulting only from large-scale waves, will be only a little more than half that of visible light. Woolf has pointed out, though, that if the large-scale errors can be measured and continually corrected with the aid of a nearby visible star, fully diffraction limited performance at 10 μm is achieved in reasonably good seeing conditions. For a filled aperture of 15 m diameter the FWHM of the Airy disk is 0.16 arc s. Because almost every source of interest at 10 μm is fainter than sky background, the advantage of operating a large telescope at this high resolution is enormous.

Thermal control

The frequency of occurrence of different degrees of atmospheric turbulence and hence wavefront distortion has been measured with small, low level, test telescopes by Walker[5]. The results show little difference between the good test sites. From these data and balloon observations of turbulence by Barletti *et al.*[6],

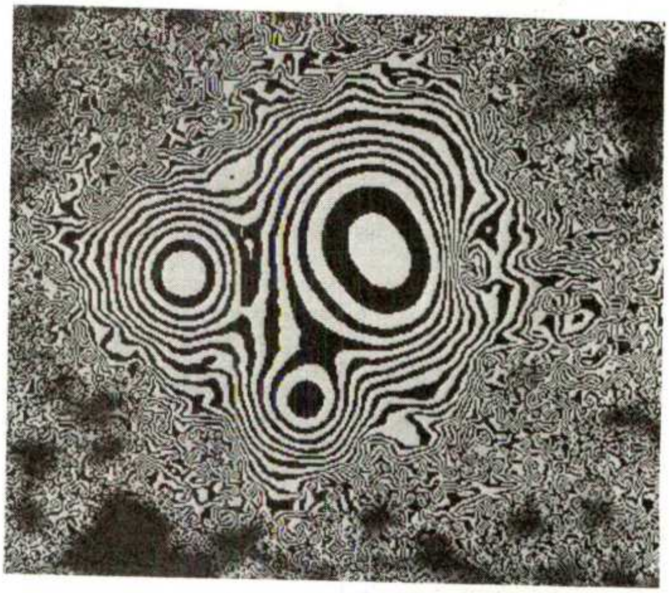

Fig. 2 An example of high resolution imaging from the ground, the QSO PG1115+08. It shows multiple components because of gravitational bending of light rays by an intervening galaxy. The two unresolved round images, separated by 2 arc s, have FWHM of 0.6 arc s. The brightest, elongated image is shown by speckle interferometry to be a double with 0.5 arc s separation[54]. This figure, courtesy of E. K. Hege, was made by Doug Tody at Kitt Peak National Observatory using the IPPS facility with contours space logarithmically by factors of two.

Woolf[7] has derived probability distributions for long exposure (time averaged) image size. He finds the diameter containing half the energy of a point source should be 0.7 arc s at the 50th percentile, 0.3 arc s at the 10th percentile.

The images that are actually recorded at most large telescopes are rarely as good as this, mostly because of thermal disturbance of the air near the telescope and enclosure. The increased size and thermal inertia of a giant telescope means we must be especially careful to understand and control these local effects. Adiabatic effects of turbulence on refractive index are not significant at normal wind speeds, but heating and cooling by convection and radiation are. The sensitivity to heat can be appreciated when we realize that light passing through a single bubble of air with a temperature difference of only 1 °C from its surroundings is spread into a cone of 0.5 arc s diameter. Turbulent thermal boundary layers can cause acute problems.

Local thermal gradients are potentially worse at high desert sites where diurnal changes of air temperature are large, and where radiation cooling at night is strong. The effects of an observatory building on image quality stem both from heat sources within the building and from failure of external surfaces to accommodate the changes in the ambient temperature. In the MMT building, exposed surfaces were of low thermal mass and were backed by good insulation, and the telescope chamber was small and well ventilated[8]. Beckers[9] reports a series of measurements at the MMT of temperature made with thermometers and a 10-μm TV camera, and of internal seeing measured with laser beams in the dome. The use of insulation and surfaces with low emissivity at 10 μm on the telescope and mount as well as the building, means that very good thermal equilibrium with the ambient air is achieved.

The one part of any telescope that cannot be insulated is the mirror. Seeing generated by mirrors has been studied by Lowne[10], who finds experimentally a seeing disk of 0.5 T arc s for a mirror temperature T °C hotter than ambient. Conventional large solid mirrors have time constants of many hours, and so are generally likely to be out of equilibrium by at least 1 °C from the changing night-time air, even if refrigeration is used during the day to set some anticipated mean operating temperature. Mirror seeing will thus frequently spoil potential sub-arc second seeing, unless the thermal time constant is kept to an hour or less. This goal can be achieved using metal mirrors or glass with faceplates no more than a few centimetres thick and air circulated behind. The fact that the MMT has thin-faced honeycomb mirrors may account in part for its frequently excellent seeing, despite substantial diurnal temperature variation at its high site. The image shown in Fig. 2 of the 'triple' QSO, having high resolution of 0.6 arc s, was obtained with one of the MMT honeycomb mirrors, with correction every 1 s for low frequency image motion caused by large scale wavefront tilts[11].

Ideas for very large telescopes

Traditionally telescopes have a single primary mirror made from a rigid massive disk of glass. Mirror supports for optical telescopes are based on the principle that perfect support against gravitational distortion of an elastic solid at any orientation is given by floating it in a liquid of the same density. Mirror cells arrange for the gravity balancing force to be distributed over the mirror back and sides, simulating flotation as far as possible. Thermal distortion of modern mirrors is effectively eliminated through the use of very low expansion materials having coefficient of $<10^{-7}$ per °C. Stiffness is such that the mirror figure is not significantly disturbed by wind in the telescope enclosure.

Mirrors of 4-m diameter are probably the limiting size for an economical telescope using these principles. Considerable increase should be practical if lightweight (thin or honeycomb) blanks are used together with some active compensation for mirror deformation and resultant wavefront distortion. Lewis[12] finds that on site manufacturing of a 10-m blank of 20 cm thickness out of fused silica or ultra low expansion (ULE) glass is practical. Studies of stiffness and designs for supports of thin meniscus mirrors of ULE or Zerodur in the 7–10 m range have been made by Epps *et al.*[13], Mack[14] and Pearson[15]. Pyrex honeycomb mirrors in this size range that would be considerably stiffer and potentially less expensive are under development[16,17]. Flotation support alone of large thin mirrors is unlikely to yield a surface precision much better than 1 arc s, particularly when one considers that wind forces in reasonable size domes will be large. However, with the aid of servo controls, as we have considered above for wavefront correction, slight errors in figure may not be a serious drawback.

The goal of a 15-m diameter primary aperture, which I adopt as representative of a very large telescope, is probably too large to be handled practically if made from a single piece of glass. Certainly the technology would have to be proved in smaller sizes before one could consider seriously such an approach. I thus consider designs that involve several or many separate mirror sections. For nearly all optical observations other than interferometry these separate elements could be in the form of separate telescopes, with data from separate instruments added to yield all the signal-to-noise advantage of the full aperture. Disney[18] has pointed out the advantages of such an array, in which fairly high spectroscopic resolution can be obtained with silicon CCD detectors without reaching the detector noise limit. Heterodyne IR interferometry would be possible with such an array[1], but direct interferometry and those IR observations which need all the light at a single focus[19] are almost impossible to achieve if the telescopes are on fixed separate mounts[20].

The most obvious route to a single focus is to figure all the elements as parts of a single parabolic surface. These must be mounted in a supporting structure as stiff as possible, and a scheme must be devised to manipulate the segments (or smaller elements reflecting images of the segments) to maintain correct orientation and phase. Such an approach has been studied by astronomers at the University of California. Nelson[21,22] and his collaborators are developing methods to prepare separately and bring together 25 off-axis hexagonal elements, to make an approximately hexagonal parabolic surface 10 m across. Angel *et al.*[23] have considered a design of six identical circular off-axis mirrors, each 6-m in diameter.

The MMT[24] takes an intermediate approach between separate telescopes and a segmented single reflecting surface. The experience of this working prototype has led to proposals[4] for much larger versions. A design for a 15-m telescope now being studied in some detail incorporates four 7.5-m honeycomb glass primaries co-aligned in a single telescope mount. Many optical observations would be done with relatively small instruments at the four separate foci but, as in the MMT, auxiliary mirrors would be arranged to bring the light to a combined and phase focus when needed. In this concept structural deformation and wavefront errors could be compensated in the small secondary optics or the primary mirrors.

Both the single-surface concept and the multiple telescope concept have the potential of yielding a telescope which can optimize images yet is versatile enough to undertake optical, thermal IR or interferometric observations. These approaches are being considered for the United States national 15-m telescope by a consortium of the Universities of Arizona, California and Texas with Kitt Peak National Observatory. This effort is concentrating on the key areas of technology that need development, bearing in mind a target cost of around $100 million.

Other concepts for very large telescopes which have received considerable attention are generally less versatile, but may have an important part to play for special tasks. Designs based on the Arecibo radio telescope with a fixed spherical bowl and moving secondary optics[25–28], solve the problems of gravitation distortion of a moving primary surface. Spherical segments of the surface could be produced inexpensively and spherical figure can be maintained easily against thermal deformation by laser metrology from the centre of curvature. However, performance

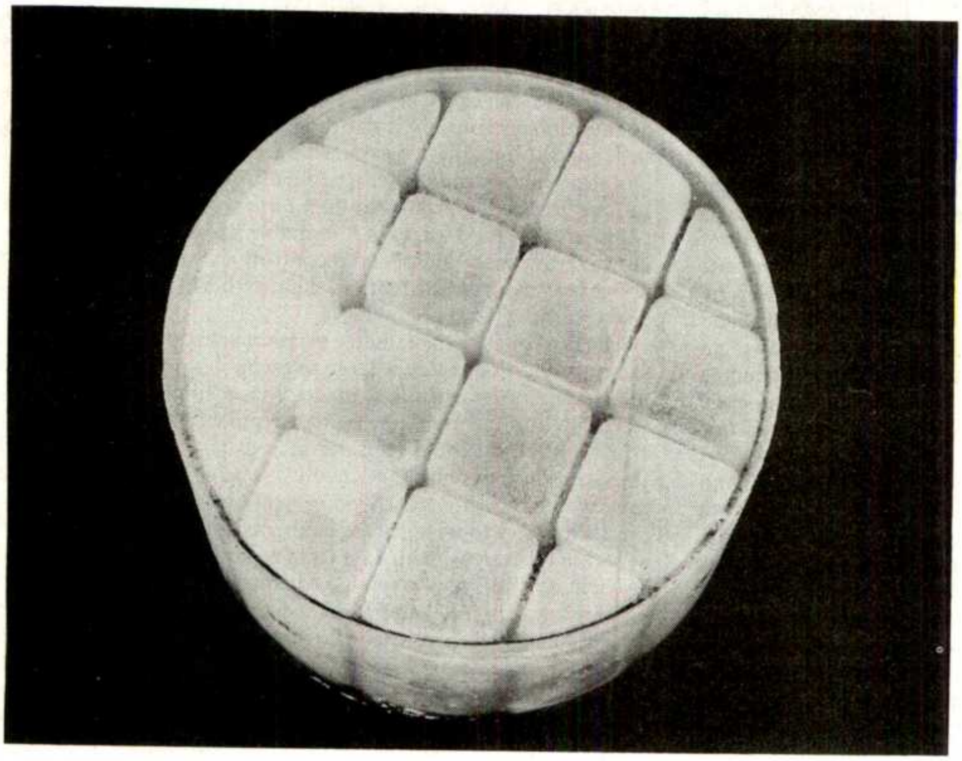

Fig. 3 A honeycomb–faceplate sandwich mirror blank cast from borosilicate glass as a single piece[14]: it is 60 cm in diameter and 35 cm thick, with ribs 6 mm thick on 15-cm squares.

in the thermal IR would be poor because of varying background as the detector tracks across different parts of the sphere. Also sky coverage is limited and it is difficult to correct spherical abberation over a large field of view. Furthermore, it would be expensive to raise such a telescope above the turbulent thermal boundary of the ground. A valuable application for this type of telescope would be for multiple object spectroscopy, in which a small corrector would be used for each point object under study, and many such correctors would be tracked at once across a limited spherical focal surface of some 20–30° (ref. 29). Multiple object spectroscopy is, of course, an important application of any of the giant telescopes discussed here.

A large telescope configuration that might become very important, with more experience with interferometry, has been suggested by Low[30]. Several telescopes would move on circular tracks, so as to remain in a line perpendicular to the object under study. If individual lightweight and stabilized telescopes of 5 m or more in diameter could be moved in this way, then the array would also be a good general purpose telescope. A fundamental question is the image quality that can be achieved in telescopes close to flat ground with no domes.

Making mirror elements

A central issue of any plan for a very large telescope must be a technique to fabricate the huge reflecting surface at acceptable cost and in a reasonable period of time. Without new ideas, mirror costs could take up most of the entire budget. If very low expansion materials are to be used then any structures other than solid sheets are probably ruled out because of very expensive fabrication costs. Costs for material alone are in the range \$50–100 kg^{-1}.

Borosilicate glass honeycomb is an attractive alternative for large mirror elements. The raw material is inexpensive and can be easily fabricated into complex structures by casting at relatively low temperatures. Figure distortion is a problem in solid borosilicate glass mirrors because temperature gradients persist for a long time, but will not be significant in a structure that can rapidly be made isothermal. The Palomar 5-m, the Lick 3-m and the KPNO 2.1-m mirrors are ribbed Pyrex structures with thickness of faceplate and ribs of ~10 cm. Thermal distortion of these mirrors is generally below the 1 arc s level[31]. At Steward Observatory we have undertaken to make large blanks consisting of 3-cm faceplates and still thinner wall honeycomb sandwiched between. These will be ventilated internally with air at ambient temperature, so equilibration will be rapid. A fundamental advantage is that mirror seeing, discussed earlier, will be eliminated. Two 60-cm test mirrors have been made from borosilicate glass: one has a slotted strut type of construction[32] and has been figured to a $\lambda/8$ r.m.s. sphere. The other, a similar honeycomb sandwich but made by a single casting in a complex mould, is shown in Fig. 3. Thermal relaxation and structural properties of both mirrors are being investigated by interferometry. Efforts are now directed towards casting in one piece

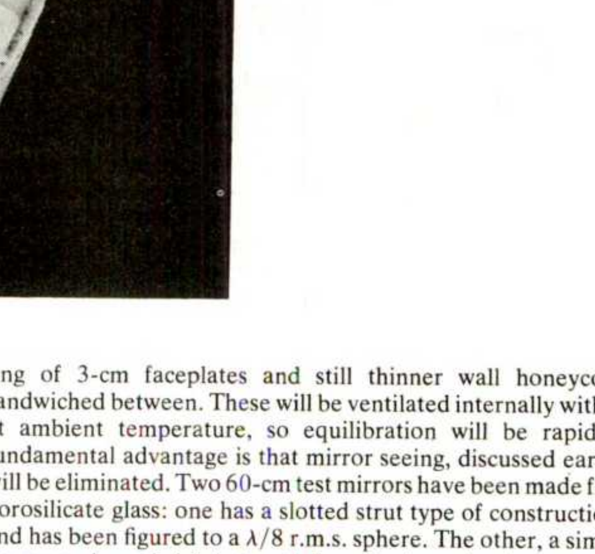

Fig. 4 Atmospheric-induced motion in one coordinate of two stars close to the North Pole separated by 50 arc s. Each data point gives the centre of gravity of an image integrated for 1/6 s. The r.m.s. fluctuation of the difference in positions is 0.11 arc s (ref. 41).

a honeycomb–faceplate sandwich mirror 1.8 m in diameter that will be figured as a parabola and tested alongside the fused silica mirrors in the MMT. We hope to work up to a 7.5-m blank over the next few years.

Ideas for reducing cost are needed in optical figuring. Traditional methods of grinding and polishing are time consuming and expensive for aspherics. One solution was devised by Schmidt, to make the aspheric corrector plates for his camera. A glass blank is polished spherical by conventional methods while being stressed in such a way that on release it takes up the required figure. Lemaitre[33] has demonstrated this method for making on-axis paraboids, making a diffraction limited $f/2$ parabola of 40 cm diameter. Nelson *et al.*[22] have extended the technique to make a precise off-axis parabola 35 cm in diameter, stressing the blank during manufacture with levers at the edge. The major effort of Kitt Peak National Observatory in the field of large telescopes is directed towards making matched off-axis elements 2m in diameter by the same method[34]. Precise tolerance in curvature ($\sim$1 in 10^5) is needed if a large parabola is to be made from separately figured segments. Another area of concern[35] is how these elements are to be made hexagonal, so they can be fitted together to make a nearly seamless surface of low thermal emission. Trimming a large thin circular mirror could disturb its figure as strain is relieved.

Traditional methods of figuring glass are based on the fact that two rigid blocks rubbed against each other with abrasive between will develop surfaces that are very accurately spherical. Machines to do the rubbing need not have any great precision, they only have to drag one piece across the other in a suitable pattern. A different approach is used in the production of optical surfaces by diamond turning of metal substrates. This is done with an extremely accurate lathe, and a single diamond tool of large radius advanced gradually so as to leave a mirror-like finish with only very shallow grooves. Optical elements up to a metre or so with surface accuracy of the order of micrometres have been produced by this method. Polishing can then give surfaces with better than a wave accuracy and remove the small-scale structure[36].

Unfortunately, metal substrates have not yet been demonstrated that can withstand the repeated temperature cycling of mountain top observatories without gradually losing their shape. Glass, while stable, cannot be finished like metals with a single diamond, but precision direct machining is possible with an abrasive diamond grinding wheel. This can again bring the surface to within a micrometre or so of the final figure, minimizing the work to be done in polishing. Large mirrors or segments would be turned on an air bearing about a vertical axis, and the tool moved across the surface as in Leighton's[37] method of making precision radio telescopes. Parks and Angel[38] have worked out a scheme to make mirror segments in which the grinding tool moves on an arm turned about an axis inclined to the vertical, yielding naturally a very close approximation to a parabola.

Electronic image stabilization

Despite the electronic sophistication available, large telescopes are being built which rely exclusively on massive rigid optics and supports to maintain image quality: only the MMT has used active control to replace force rigidity. The potential for achieving very large collecting areas by this technique at relatively low cost is enormous: the MMT has been built for about one-quarter the cost of its rigid equivalent.

There are various ways that active correction might be made. For single-mirror telescopes (or individual elements of a bigger telescope) we can alter the forces that support the primary, or leave it alone and devise a mechanism to distort the secondary or subsequent mirrors. For high frequency control, Hardy's scheme[3] uses piezo-electric actuators acting on the back of a thin mirror. Merkle *et al.* have demonstrated[39] an electrostatic force system. Magnetic actuators could be used for correction on a less rapid time scale.

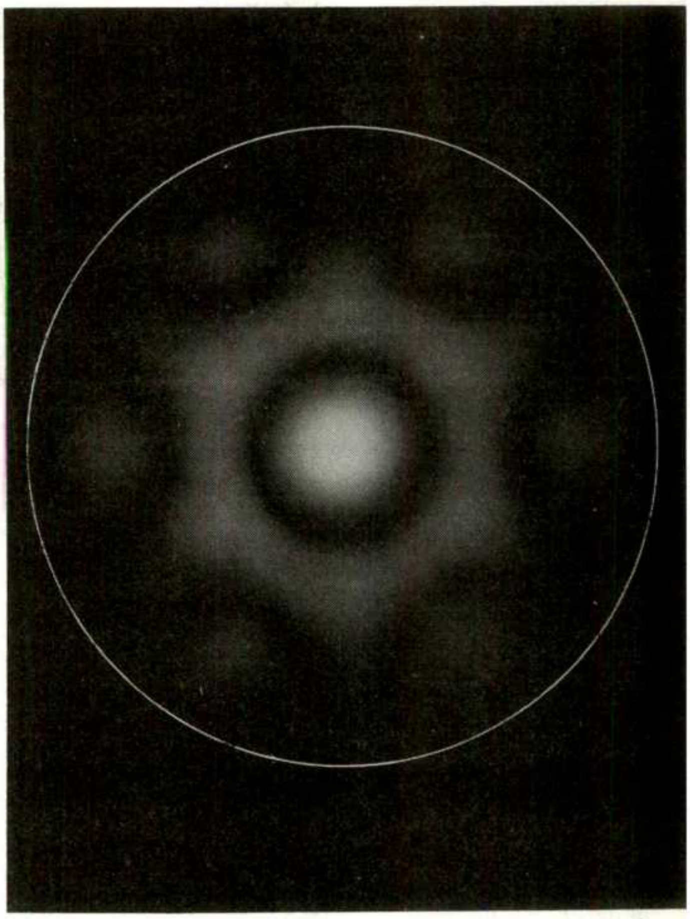

Fig. 5 The diffraction pattern computed by Meinel *et al.* for a phased circular array of six mirrors separated by 0.15% of their diameter. 40% of the total energy is within the first dark ring. The peaks in the continuous hexagonal ring reach 0.11 the intensity of the central peak, the six isolated peaks 0.06. The Airy pattern of one individual mirror, with a first dark ring of diameter shown by the white circle, has a resolution nearly four times poorer then that of the phased pattern.

To achieve a single focus in telescopes that have more than one collecting mirror we need to sense and correct the alignment of each mirror. In the MMT the tilt of individual secondary mirrors is controlled by micrometers driven by stepper motors, giving single steps of 0.05 arc s at the combined focus. Gabor[40] has demonstrated a ball screw actuator suitable for tilting 2-m primary elements with even higher angular precision.

How do we derive the information necessary to make corrections? Elastic deflections arising from differing orientation with respect to the gravitational field are repeatable, and tables of corrections necessary for their compensation can be stored in the control computer. There will remain unpredictable errors, such as wind forces, uncompensated thermal gradients in the structure, and friction in mirror supports, and in the MMT these residual effects amount to about 1 arc s in image motion[9] and a few tens of micrometres in pathlength error as the telescope is moved to different parts of the sky[30]. The residuals which might be achieved in a 15-m class instrument, probably not much worse than in the MMT, are comparable with the random wavefront error already present from atmospheric turbulence.

To realize fully the potential of active optics, one must determine how rays from a star illuminating different parts of the reflecting surface come together at the focus, and feed back corrections to the active elements. This will correct both the structural errors and the large-scale wavefront errors, if done with a frequency response of a few hertz. One method is by

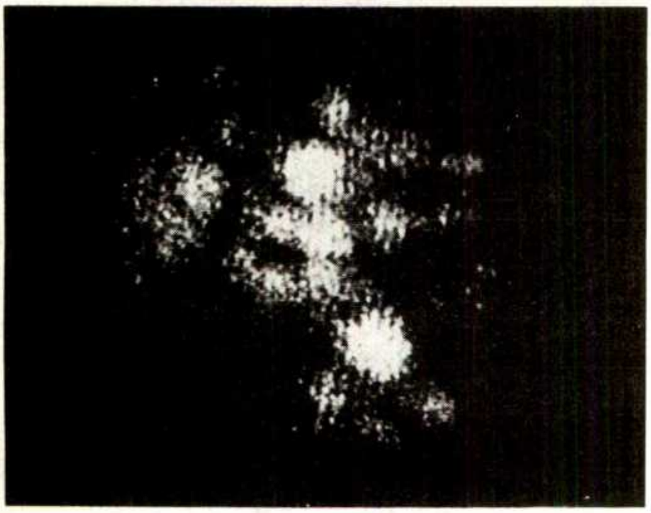

Fig. 6 Interference fringes spaced by 30 m arc s in the highly magnified image of an unresolved star. The image was formed by two of the 1.8-m mirrors of the MMT, with a centre-to-centre spacing of 5 m. (Courtesy of E. K. Hege and P. A. Strittmatter.)

automating the knife edge test: in its basic form the star image is focused on a sharp edge, such as a razor blade, and an auxiliary lens is used behind the edge to form an image of the primary mirror. A tilt of the wavefront in a particular region will then show as a bright or dark patch in the image. Hardy[41] has used a scheme in which an oscillating grating cuts across the star image, and the pupil is imaged on a bank of photomultipliers. Phases of the signals from each photomultiplier then give the tilt error of each part of the pupil. A variant of this idea is where the reference star is imaged on a sharp four-sided pyramid, and each reflected beam passes through a Fabry lens to image the pupil on one of the four sensitive imaging detectors[4]. A complete map across the pupil of tilt of the wavefront in both directions is obtained by intercomparison of the four pupil images. An alternative method that does not use a knife edge uses a lens placed after the combined focus to image the pupil on an array of tilted mirrors. Each mirror directs light from a part of the pupil to a field reimaging lens, and imaging detectors monitor the full field image from each pupil segment. Image locations relative to a reference dot in the combined focal plane then give the tilt of each pupil segment. In both these schemes the problem of maintaining co-alignment of a multiple element telescope reduces to the same problem addressed by offset guiders in today's single element telescopes. An automated system has to be reproduced for each section of the primary that will be independently corrected.

For the wavefront error correction to work, one must either use part of the light from the program star itself, or use a field star close enough for it to share the same large-scale wavefront errors. The angular separation α of shared motion is approximately d/h, where d is the scale of the wavefront error and h is the effective height of the wavefront disturbance. For $d = 2$ m and $h = 4$ km (ref. 42), α is about 2 arc min. Well correlated motion of two stars 50 arc s apart observed with a 1.8 m aperture in conditions of reasonably good seeing (1.2 arc s) is shown in Fig. 4 (ref. 43).

Because much of the work of a large telescope will be with faint objects giving no useful signal for electronic stabilization, the capability for continuous fine tuning of the image relies on finding a guide star within the field of common motion. Fortunately, the development of CCD detectors of excellent red sensitivity means that adequate signals can be obtained. Consider, for example, stars of R magnitude <16, which with a red filter would stand out clearly even in full moonlight. At the sparsest regions near the galactic poles these have a density of 382 per square degree[42], and will thus be found with 75% probability within a 2 arc min radius. The light from such a star collected by a 2-m element will give a signal of 8000 electrons s^{-1} in a CCD, adequate to implement the schemes outlined above with a frequency response of a few hertz.

When rapid wavefront tilt corrections are made to a telescope with continuous primary and secondary surfaces then instantaneous large-scale phase errors are also removed. As discussed earlier, this should allow diffraction-limited performance to be achieved in the IR. Even if the full collecting aperture is made from separate elements it should still be possible to maintain correct phasing from tilt measurement provided that the elements are close to each other, and that no steps are allowed to develop in the wavefront going from element to element. Relative phases between elements can be established by occasional observations of broad band interference in an unresolved reference source[30]. For a system of adjacent segments making a single surface, capacitive sensors such as those developed by Gabor[40] can be used to maintain accurately steps between adjacent mirrors.

The diffraction pattern of MMT type telescopes when multiple circular apertures are combined perfectly in phase has been explored elsewhere[25,45,46]. The intensity at the central maximum of the pattern depends only on the total collecting area; at this point all the radiation is added in phase no matter where it was collected. The width of the central peak depends on the diameter of the full array. An exact calculation of a typical diffraction pattern is shown in Fig. 5. This is for a circular array of six mirrors, separated by 0.15% of their diameter. Such a close array could potentially be maintained in phase from tilt sensing. The power of such a telescope for IR imaging is realized when we consider the potential resolution at 10 μm. Equation (1) shows that the phase errors over individual 6-m mirrors will get to $\lambda/10$ or less in good seeing. An MMT configuration of six such mirrors with active correction of phase differences between mirrors would give images close to the diffraction limit of Fig. 5, that is 0.11 arc s FWHM of the central peak, the same as for a filled aperture of 22-m diameter.

Although active wavefront correction to achieve directly diffraction limited images for visible light is not generally possible, various interferometric techniques can be used to study spatial structures at the diffraction limit. Very large single mount telescopes will allow resolution of ~5 m arc s at 0.5 μm. An example of interferometry between the full surface of two of the 1.8-m mirrors of the MMT is shown in Fig. 6. The centres of the mirrors are separated by 5 m, giving a fringe spacing of 30 m arc s at the observed wavelength of 0.75 μm. A specialized interferometric telescope array, such as Labeyrie is building, will give longer baseline and higher resolution than any single large telescope, but the latter will be able to reach considerably fainter objects[47].

Instrumentation and operation

We have focused on current ideas for making the large telescopes which, nevertheless, have excellent images; it is beyond our scope to review other characteristics, but we can indicate some of the challenges.

The sensitivity of present large telescopes in the wavelength range below 1 μm is being brought close to the theoretical maximum using silicon arrays. CCDs have near unit quantum efficiency and negligible noise for nearly all applications. We must also plan to use these detectors in very large telescopes: the challenge is to handle the inevitably large detector area. Because optics of present telescopes and spectrographs are close to the fastest practical speeds, increases in detector area proportional to the primary collecting area are inevitable. Detector areas from 10 to 1,000 cm^2 will be needed, depending on the number of spatial and/or spectral resolution elements to be resolved in a single exposure. Just as we will probably make large collecting areas from more than one piece of glass, we will probably need to make the detector from more than one piece of silicon. Many options exist for arranging detector chips in close mosaics, or in multiple smaller instruments. Some of the factors are discussed in ref. 18.

Another challenge is to maintain a sizeable field of view for a very large telescope. With good detectors there will be an important role for precise photometry and objective spectroscopy[48] of many thousands of objects at once in a wide field. With fibres automatically positioned in the focal plane and feeding the light along the slit of a spectrograph, dozens of objects can be observed over a wide field at once, with high spectral resolution if required[49,50]. If the primary focal ratio is made very fast to keep down tube length and dome size in a single-surface telescope, difficulties can arise in obtaining a wide field. However, two-element reflecting correctors offer a remarkable opportunity of obtaining a large corrected field with a fast primary. An optimized design[23] of the Baker–Paul type[51,52], explored in detail by ray tracing has an $f/1$ primary and an $f/2$ corrected focus. The achromatic images are no worse than 0.2 arc s over a 1° field.

The third challenge in a giant telescope is to maximize the operational efficiency. The best use is to match the type of observations to the conditions prevailing. Moonlight and twilight are obvious factors but there are also unpredictable changes in transparency, seeing, water vapour, wind and clouds. Ideally one needs several complementary instruments, ready for use with only a few minutes time lost for interchanging. Astronomers need not be present at the site for observations with standard equipment: they could be called to a local data terminal when their observations were to be made. Experiments in this type of operation have already begun at Kitt Peak National Observatory[53].

Multiple detectors, automated multiple object probes, automatic interchange of instruments, resident observing staff and communication with remotely located astronomers are expensive. When we consider, though, the capital investment in a 15-m class telescope, the costs of development, construction and operation of these instruments will not be disproportionate.

Conclusion

We are seeing the beginning of a new generation of large telescopes for optical astronomy, characterized by innovative methods of mirror fabrication and active feedback to maintain image quality. Large, rigid mirror substrates of honeycombed glass are being developed, along with techniques for inexpensive manufacture of precision aspheric surfaces. Advances in sensors and data processing now make it practical to measure continuously atmospheric distortion and make rapid corrections to the wavefront to improve image quality. Very large telescopes incorporating these mirrors and active control should work better and cost less than if built by conventional means. Remarkable advances over current levels of performance, beyond simply collecting more photons, now seem within reach. A 15-m telescope can potentially, with a modest degree of wavefront correction, give images at 10 μm approaching 0.1 arc s in diameter. This is comparable to the diffraction-limited resolution of the space telescope in visible light. Interferometry with the 15-m telescope at visible wavelengths will allow the exploration of structures in faint objects at 5 m arc s resolution, approaching the resolution achieved at radio wavelengths with interferometry over intercontinental baselines.

These unique advantages for higher spatial resolution argue that the first of the very large instruments should be a phasable design. However, when several very large telescopes are to be built it may be advantageous to design different complementary specialized types. For example, a very large telescope directed towards spectroscopy at shorter wavelengths might take the form of an array of independent smaller telescopes, or of a fixed spherical dish with tracking foci, and could be conveniently located on a lower mountain. Telescopes for thermal IR and submillimetre work need to be as high as possible for low water vapour and put a premium on the largest possible phased aperture. Again, for high resolution interferometry widely spaced large telescope elements are needed that move smoothly along the ground. Each type has a place.

This review has benefited from discussions with colleagues at the University of Arizona and the Smithsonian Institution. In particular, Nick Woolf inspired the discussion of atmospheric effects and has made many suggestions for improving the manuscript. I also thank Jacques Beckers and his staff at the MMT, for it is at this telescope that we are working out many of the basic new ideas common to proposed advanced telescopes. Work was supported by the NSF under grant AST 78-22714 and NASA NAGW-121.

1. Townes, C. *Optical and Infrared Telescopes for the 1990's* (ed. Hewitt, A.) 797 (Kitt Peak National Observatory, Tucson, 1980).
2. Born, M. & Wolf, E. *Principles of Optics* 5th edn (Pergamon, Oxford, 1975).
3. Hardy, J. W. *Optical and Infrared Telescopes for the 1990's* (ed. Hewitt, A.) 535 (Kitt Peak National Observatory, Tucson, 1980).
4. Woolf, N. J. & Angel, J. R. P. *Optical and Infrared Telescopes for the 1990's* (ed. Hewitt, A.) 1062 (Kitt Peak National Observatory, Tucson, 1980).
5. Walker, M. F. *P.A.S.P.* **83**, 401 (1971); *Trans. IAU* XVI A, Pt 1, 219 (1972).
6. Barletti, R., Cepatelli, G., Paterno, L., Righini, A. & Speroni, N. *J. opt. Soc. Am.* **66**, 1380 (1976).
7. Woolf, N. J. *A. Rev. Astr. Astrophys.* **20** (in the press).
8. Carleton, N. P. in *The MMT and the Future of Ground Based Astronomy*', 37 (ed. Weekes, T. C.) (SAO Spec. Rep. No. 385, 1979).
9. Beckers, J. *MMT tech. Rep. No.* 10. 10 (1981).
10. Lowne, C. M. *Mon. Not. R. astr. Soc.* **188**, 249 (1979).
11. Hege, E. K., Angel, J. R. P., Weymann, R. J. & Hubbard, E. N. *Nature* **287**, 416 (1980).
12. Lewis, W. C. *Workshop on Optical Fabrication and Testing*, Tucson, 5 (Optical Society of America, 1979).
13. Epps, H., Rank, D. & Wampler, J. *Report to the Director of Lick Observatory on the Choice of Primary Mirror for the UC Ten Meter Telescope* (1979).
14. Mack, B. *The Observatory* **101**, 135 (1981).
15. Pearson, E. Internal Rep. Univ. Texas (1981).
16. Angel, J. R. P. & Hill, J. *Proc. ESO Conf.* (1981)
17. Angel, J. R. P., Arganbright, D., Harmonson, L., Hill, J. M. & Woolf, N. *Proc. IAU Colloq.* No. 67 (1981).
18. Disney, M. *Optical and Infrared Telescope for the 1990's* (ed. Hewitt, A.) 649 (Kitt Peak National Observatory, Tucson, 1980).
19. Gillette, F. *Optical and Infrared Telescopes for the 1990's* (ed. Hewitt, A.) 293 (Kitt Peak National Observatory, Tucson, 1980).
20. Learner, R. C. M. *The Observatory* **101**, 137 (1981).
21. Nelson, J. *Optical and Infrared Telescopes for the 1990's* (ed. Hewitt, A.) 11 (Kitt Peak National Observatory, Tucson, 1980).
22. Nelson, J., Gabor, G., Hunt, L., Lubliner, J. & Mast, T. *Appl. Opt.* **19**, 2341 (1980).
23. Angel, J. R. P., Woolf, N. J. & Epps H. *Pap. S. P. I. E. Meet. Advanced Technology Optical Telescopes* Tucson (1982).
24. Beckers, J. *et al. Telescopes of the* 1980'*s* (Annual Reviews Monograph, 1981).
25. Meinel, A. *IAU Symp. No.* 27, 611 (1965).
26. Drake, F. *Optical and Infrared Telescope for the 1990's*, (ed. Hewitt, A.) 649 (Kitt Peak National Observatory, Tucson, 1980).
27. Mertz, L. *Optical and Infrared Telescopes for the 1990's* (ed. Hewitt, A.) 957 (Kitt Peak National Observatory, Tucson, 1980).
28. Aikens, R. *et al. NGT Rep.* No. 2, (Kitt Peak National Observatory, Tucson, 1977).
29. Angel, J. R. P. *Proc. IAU Colloq. No.* 67, (1981).
30. Low, F. J. *Optical and Infrared Telescopes for the 1990's* (ed. Hewitt, A.) 825 (Kitt Peak National Observatory, Tucson, 1980).
31. Bowen, I. *IAU Symp. No.* 27, 1313 (1965).
32. Loytty, E. Y. & DeVoe, C. F. *I.E.E.E. Trans. Aerospace Electron. Syst.* **5**, 300 (1969).
33. Lemaitre, G. *Optical and Infrared Telescopes for the 1990's* (ed. Hewitt, A.) 896 (Kitt Peak National Observatory, Tucson, 1980).
34. Ghozeil, I. *Optical and Infrared Telescope for the 1990's* (ed. Hewitt, A.) 616 (Kitt Peak National Observatory, Tucson, 1980).
35. Brown, D. *Meet. New Techniques and Telescopes in Optical Astronomy* (Royal Astronomical Society, London, 1980).
36. Parks, R. E. *Workshop on Optical Fabrication and Testing*, Tucson (Optical Society of America, 1979).
38. Parks, R. and Angel, J. R. P. *Paper S.P.I.E. Meet. Instrumentation in Astronomy-IV*, Tucson (1982).
37. Leighton, R. B. *Final Techn. Rep. NSF Proj.* AST 73-04908; *Astrophys. J.* **230**, 149 (1978).
39. Merkle, F., Freischlad, K. & Bille, J. in *Scientific Importance of High Angular Resolution at Infrared and Optical Wavelengths*, Munich (1981).
40. Gabor, G. *S.P.I.E. Proc. Instrumentation in Astronomy III* **172**, (1979).
41. Hardy, J. W. *Proc. ESO Conf. on Optical Telescopes of the Future*, Geneva, 455 (1977).
42. Young, A. T. *Astrophys J.* **189**, 587 (1974).
43. Angel, J. R. P. *Proc. ESO Conf. Scientific Importance of High Angular Resolution at Infrared and Optical Wavelengths*, Munich (1981).
44. Bahcall, J. & Soneira, R. M. Preprint (Princeton Univ., 1981).
45. Meinel, A. B., Meinel, M. & Woolf, N. J. *Appl. Opt. opt. Engng* **9** (in the press).
46. Sanger, G. thesis, Univ. Arizona (1978).
47. Roddier, F. in *Scientific Importance of High Angular Resolution at Infrared Optical Wavelengths* (eds Ulrich, & Kjar,) (ESO, 1981).
48. Hoag, A. A. & Schroeder, D. J. *P. A. S. P.* **82**, 1141 (1970).
49. Hill, J. M., Angel, J. R. P., Scott, J. S., Lindley, D. & Hintzen, P. *Astrophys. J. Lett.* 242 L69 (1980).
50. Angel, J. R. P. in *The MMT and the Future of Ground-Based Astronomy* (ed. Weekes, T. C.) (SAO Special Report No. 385, 1979).
51. Paul, M. *Rev. Opt.* **14**, 169 (1935).
52. Baker, J. G. *I.E.E.E. Trans. Aerospace Electron. Syst.* **5**, 261 (1969).
53. Janes, C., Robinson, W. & Shechter, P. *KPNO tech. Rep.* (in preparation.).
54. Hege, E. K., Hubbard, E. N., Strittmatter, P. A. & Worden, S. P. *Astrophys. J. Lett.* **248**, L1 (1981).
55. Woolf, N. J., Angel, J. R. P., Antebi, J., Carleton, N. & Barr, L. D. *Paper S. P. I. E. Meet. Advanced Technology of Optical Telescopes*, Tucson (1982).

Simulating silicate structures and the structural chemistry of pyroxenoids

C. R. A. Catlow*, J. M. Thomas†, S. C. Parker* & D. A. Jefferson†

* Department of Chemistry, University College London, 20 Gordon Street, London WC1H 0AJ, UK
† Department of Physical Chemistry, University of Cambridge, Lensfield Road, Cambridge CB2 1EP, UK

Chain silicates, both naturally-occurring and synthetic, exhibit 'backbone repeat' patterns of corner-linked SiO_4 tetrahedra. The extent to which these repeats may be interpreted or predicted, as a function of the associated cation M^{2+} (in the general formula $MSiO_3$), is discussed, and the broader issues involved in the theoretical simulation of the structures of inorganic silicates are considered.

NATURALLY-occurring and synthetic silicates display an extensive range of structural types including isolated anions, chains, rings, sheets and various kinds of framework, all based on SiO_4^{4-} tetrahedra[1-3]. The diversity of structural types is exceptional, being matched only by the borates, where both trigonally and tetrahedrally bonded atoms may occur[4]. Even so, the total number of known silicate structures is substantially less than that theoretically predicted on simple topological arguments. Several attempts[5,6] have been made recently to rationalize and interrelate the structures of the silicates using largely qualitative solid-state, chemical principles. We have pursued a quantitative approach with the hope, ultimately, of predicting the behaviour of many different kinds of novel silicates. Such computations also offer an attractive method of assimilating new structural information brought to light[7-11] by real-space crystallography, using high-resolution electron microscopy (HREM). In particular, we have sought to interpret the structure composition relationships that have emerged from HREM studies of the so-called pyroxenoid silicates[12,13].

The pyroxenoids possess a general formula $MSiO_3$ ($M \equiv Ca^{2+}$, Fe^{2+}, Mn^{2+}, Mg^{2+} and so on). They display intriguing variability in their structural types and inter-relationships. The difference between individual members of this family manifests itself in the backbone repeat patterns of the single chain of corner-sharing SiO_4^{4-} tetrahedra.

Nature of the experimental facts

Figure 1 shows the various kinds of backbone repeat patterns characteristic of the diopside ($CaMg(SiO_3)_2$), wollastonite ($CaSiO_3$), rhodonite ($(Mn, Ca)SiO_3$) and pyroxmangite ($(Mn, Fe, Ca, Mg)SiO_3$) structures. In wollastonite, three SiO_4^{4-} tetrahedra constitute the unit (7.3 Å in length); in rhodonite, the five-unit repeat runs to 12.5 Å; whereas in pyroxmangite the seven-unit repeat is 17.4 Å. Diopside, with a two-unit repeat (5.2 Å), is an archetypal member of the pyroxene family of chain silicates: the other three are pyroxenoids.

X-ray studies of naturally-occurring and synthetic analogues of pyroxenoids are fraught with difficulties principally because of the occurrence of complicated intergrowths of various members of the pyroxenoid range of structures. Great headway can, however, be made[14-17] by real-space direct methods (HREM) as may be seen in Fig. 2. Although it is difficult to be sure that equilibrium states have been reached, certain preferences for given pyroxenoid structures can be noted for given cations (or stoichiometric ratio of cations). Thus, as the synthetic pyroxenoid of formula $Mn_3MgSi_4O_{12}$, emerges from the glassy state, the pyroxene structural type is first seen to predominate, with embryonic regions (a few unit cells in width) of various other pyroxenoids (Fig. 2*a*). Eventually (after prolonged annealing at 800 °C) a marked propensity for the pyroxmangite structural type prevails (Fig. 2*c*); but an intermediate stage (Fig. 2*b*) may be detected by HREM in which strips of wollastonite are inserted regularly to produce small regions of pyroxmangite.

Likewise the synthetic pyroxenoid of formula $MnFeSi_2O_6$ first displays some individual strips of nine-unit backbone repeats (that is the ferrosilite III structure which has a unit length of 22.7 Å) interspersed amongst pyroxmangite and rhodonite structural types (Fig. 3*a*). Gradually (Fig. 3*b*), five-unit repeats gain ascendancy, and a well-ordered rhodonite (five-unit repeat) ultimately prevails.

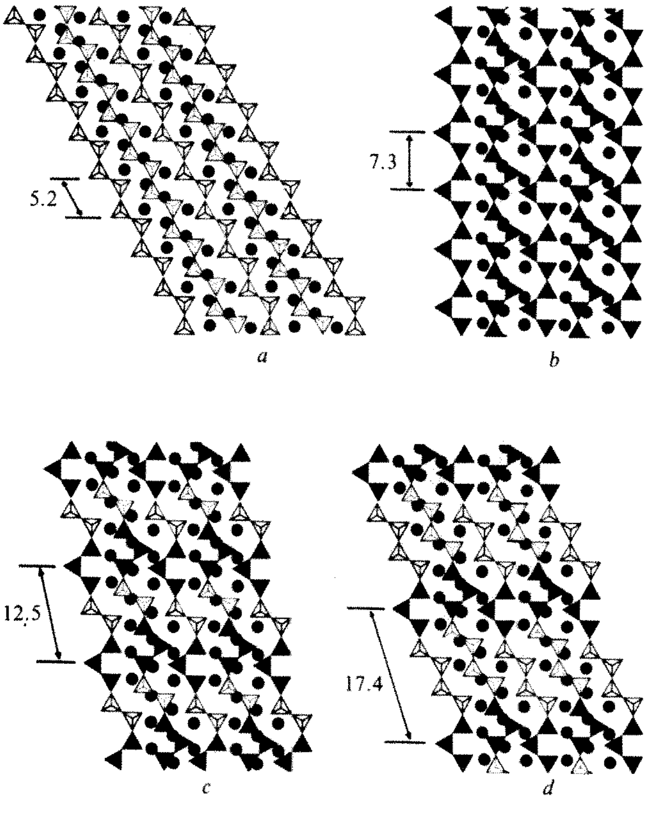

Fig. 1 Illustration of the pyroxenoid structures referred to in the text. *a*, Diopside (two unit repeat); *b*, wollastonite (three unit); *c*, rhodonite (five unit); *d*, pyroxmangite (seven unit).

0028-0836/82/080658—05$01.00

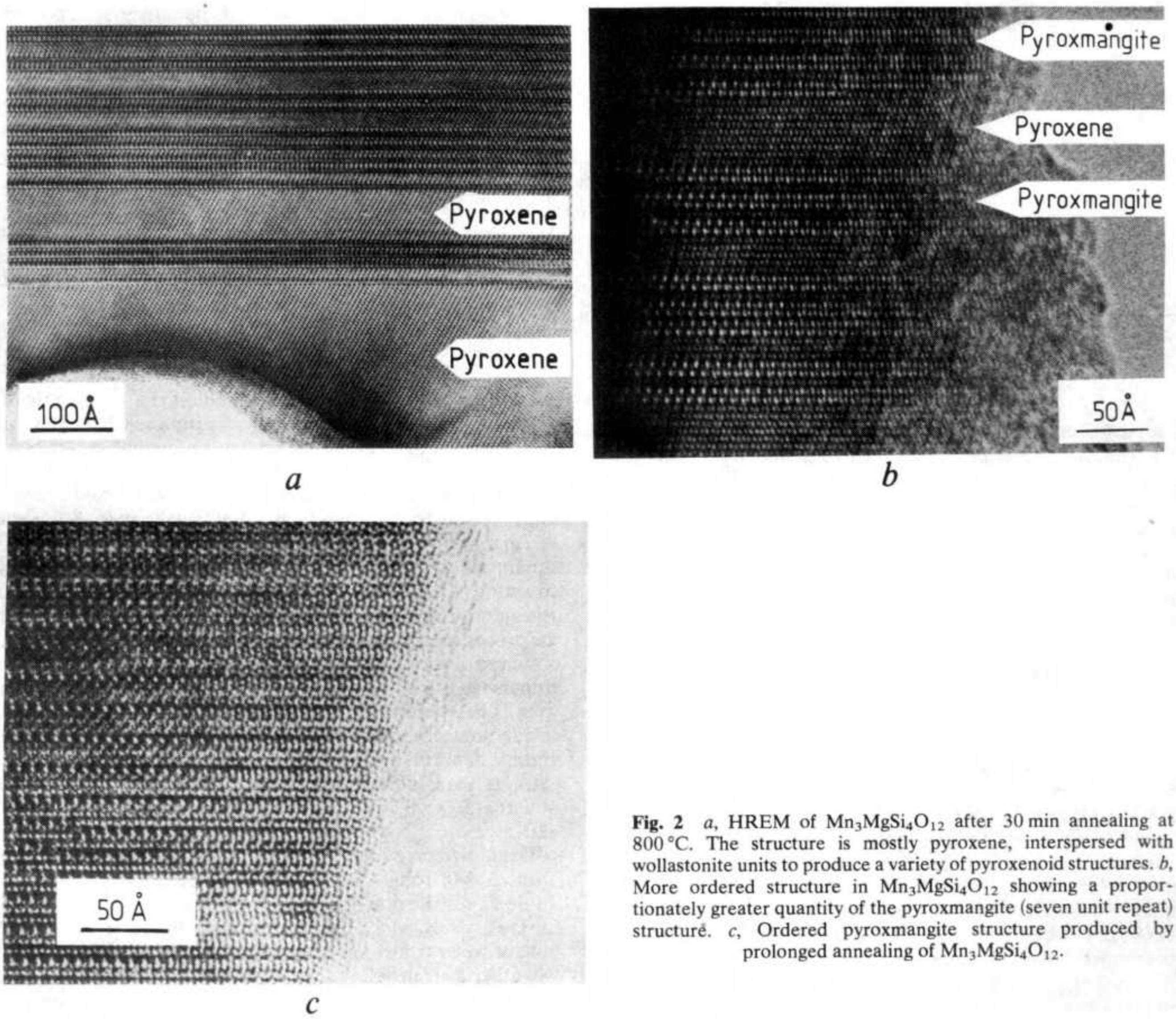

Fig. 2 *a*, HREM of $Mn_3MgSi_4O_{12}$ after 30 min annealing at 800 °C. The structure is mostly pyroxene, interspersed with wollastonite units to produce a variety of pyroxenoid structures. *b*, More ordered structure in $Mn_3MgSi_4O_{12}$ showing a proportionately greater quantity of the pyroxmangite (seven unit repeat) structure. *c*, Ordered pyroxmangite structure produced by prolonged annealing of $Mn_3MgSi_4O_{12}$.

One key question to which our simulation studies are addressed is which structural type is preferred for a particular cationic sublattice? A related question raises the issue of whether mixed cations (ordered or disordered?) can tilt preference from one structural type to another?

Knowing the success that procedures using pair potentials have achieved in interpreting the behaviour of molecular crystals, and organic solid-state chemistry[18–21], it seemed appropriate to evolve computationally more advanced procedures that could cope with the demanding set of circumstances associated with the silicates. Fortunately, the techniques developed by C.R.A.C. and Norgett[22–25], which have proved successful in the study of non-stoichiometry, extended defects and superionic conductivity, have considerable value in the present context and promise much more extensive interpretive scope in silicate chemistry. It has been shown[22–32] that simulation techniques can elucidate the nature of the complex defect aggregation modes in heavily defective systems such as $Fe_{1-x}O$ (ref. 26) and UO_{2+x} (ref. 27), and identify the factors that determine whether compositional variation is accommodated by extended rather than by point defects[28,29].

The simulation procedure

The methods are, at least conceptually, simple. A potential model is used to describe the interactions between the ions in the crystal; the energy of the crystal is then minimized with respect to all structural parameters. [The methods do not explicitly include the effects of thermal motion. However, this omission is unlikely to affect seriously the use of the methods for structural predictions.] In contrast to this conceptual simplicity the actual computational techniques are sophisticated. This relates first to the handling of the summation procedures, where we have developed procedures available in the PLUTO lattice simulation code[26] to evaluate the long-range electrostatic interactions. (Our methods are based on the Ewald transformation which replaces a slowly convergent summation in real space with a rapidly convergent reciprocal space sum). Second, efficient minimization methods are vital if we are to cope with large unit cells. Earlier work showed the advantages of Newton–Raphson procedures which result in rapid and stable convergence[30]. Special problems arise when the minimization procedure adjusts unit cell dimensions in addition to ion coordinates—an essential feature in the simulation of silicates.

Application of the techniques to silicates requires first, development of adequate potential models for these materials and second, adaptation of minimization procedures to handle the complex structural problems posed by these systems.

Potential models for the silicates

Successful simulation studies of transition metal and actinide oxides have been based on ionic model potentials with two-body, short range potentials described by a simple analytic function (generally of the Born–Mayer or Buckingham form). Although the ionic model is clearly an approximate description of the bonding in these oxides, there is growing evidence (which includes the success of the calculations) that the approximation

Table 1 Short-range parameters

$V(r) = A \exp(-r/\rho) - C/r^6$

	A (eV)	ρ (Å)	C (eV Å^6)
a			
O^{2-}–O^{2-}*	2,2764.3	0.1490	27.88
Mg^{2+}–O^{2-}†	2,214.39	0.2756	4.45
Ca^{2+}–O^{2-}†	1,996.35	0.3189	26.57
Sr^{2+}–O^{2-}†	2,187.61	0.3377	64.08
Mn^{2+}–O^{2-}†	2,618.35	0.3033	27.46
Fe^{2+}–O^{2-}†	2,886.3	0.2973	29.73
b			
Si^{4+}–O^{2-}	998.98	0.3455	0.0

* See refs 27, 39.
† See ref. 44.

is good for materials such as TiO_2 (ref. 31) NiO (ref. 32) and UO_2 (ref. 27). To what extent, however, has the model any validity when applied to quartz and to silicates? To answer this question we must first consider the meaning and implication of the term ionicity.

Following Cochran[33] we note that there are two distinct (although related) operational definitions of this concept. The first concerns the distribution of valence shell electron density, and although we have no definite evidence, use of this criterion would almost certainly suggest the inapplicability of the ionic model to silicates. The second criterion, which has much greater relevance to the present study, is in terms of interatomic forces and the response of the crystal to external perturbations (elastic or electrostatic) or internal structural modifications (such as the formation of defects or the introduction of impurity ions). In this context a solid is regarded as ionic if a description of the lattice based on ions can correctly predict (1) the lattice energetics of the solid, (2) its elastic and dielectric properties and (3) the formation energies of defects and structural response of the lattice to the introduction of disorder. This latter criterion is equally valid to, but distinct from, the former. It is essentially a definition in terms of forces rather than charge distribution. In the context of the debate on the extent of ionicity in solids, it is important that this distinction in the connotation of the term should be appreciated. We shall show below that the ionic model forms a reasonable basis for the simulation of silicates.

We have therefore developed ionic model potentials which are generally applicable to ring and chain silicates. Our procedure differs from that adopted in earlier studies of simpler inorganic oxides[27,29,32] where variable parameters in a general potential model were adjusted so as to give the best fit to experimental elastic and dielectric data. Such data are in general unavailable for minerals. However, the structures of complex low symmetry crystals are themselves a rich source of interatomic potentials, because, in such crystals a given type of interaction potential (say silicon···oxygen) is generally sampled over a wide range of separations. (This fact has already been successfully exploited[34], in developing a potential model for ZrO_2 from the low temperature, low symmetry structure.) We have, therefore, used the structural data available on a range of chain and ring silicates to develop our generalized potential model for these systems.

The precise procedure is as follows. First, we define the form of our potential model which has two main features: (1) the crystal is simulated by point entities of integral charge; and (2) short-range forces are included for the Si···O and O···O interactions (we discovered that inclusion of Si···Si interactions over short-range was not necessary in order to reproduce structural data on ring and chain silicates—a result which is apparently at variance with recent suggestions[5,35–38] concerning the dominance of these interactions in determining the structures of minerals.) The short-range forces are described by a potential of the form:

$$V(r) = A\, e^{-r}/\rho - Cr^{-6}$$

For the O···O interaction we took parameters (reported in Table 1*a*) which were derived from a quantum mechanical calculation of the interactions between two O^{2-} ions[27,39]. For the interaction between the metal cations and oxygen in the minerals studied, we used parameters obtained for the appropriate metal oxide. All metal–oxygen parameters used are listed in Table 1*a*. Interactions between metal and Si^{4+} ions were ignored, as these are negligible at the interatomic spacings in silicates. The parameters A, ρ and C for the Si···O interactions were taken as variables and were fitted to the structural data. This procedure involves adjusting the parameters until the forces acting on all atoms in the unit cell are zero, and the unit cell itself is in equilibrium with its observed dimensions. This is achieved by a second application of the PLUTO program, which, given a specified structure and potential, calculates both the forces acting on the individual atoms in the cell and forces of dilation or contraction acting on the unit cell as a whole. The program is linked with a least-squares routine which minimizes these forces with respect to the variable potential parameters. In practice, for relatively simple potentials of the type we have used, it is not possible to derive a fully strain-free potential. Thus, to check that our final fitted potential is in adequate agreement with the structural data, we allow the structure to equilibrate (that is achieve its minimum energy configuration by adjusting all structural parameters) using the potential. Our criterion for the acceptability of the fitted potential was that in the process of equilibration no atom should be displaced from its observed position by more than 0.25 Å. In general the discrepancies were much smaller than this figure (typical values were 0.1 Å). However, the neglect of thermal motions by our calculations when combined with the errors in the crystallographic data could lead to a discrepancy of this magnitude in an extreme case, although in general we would expect a good potential to give better agreement with high quality structural data.

The above procedure was applied to the six silicates listed in Table 2. We found that a single set of parameters listed in Table 1*b* for the potential could fit the observed structural data for the crystals, which include structures based on isolated SiO_4 units as well as rings and chains. On the basis of the second of the two criteria given below, the result supports the suitability of the ionic model for describing the bonding in these systems. The model yields correct structures for those crystals in which there is a considerable range of structural variation. The implication is that the forces in the silicate lattice are being described correctly, and this conclusion is supported by calculations of the lattice energies. Studies of silicates have been reported using ionic model potentials[40–43]; and the work of Jenkins *et al.*[41,42] has clearly demonstrated the accuracy of lattice energy calculations using these potentials We should note, however, that it is much more difficult to derive potentials which satisfactorily model structural data on more condensed silicate systems, that is layer and framework structures. Investigation of more sophisticated models for these systems is continuing.

We should emphasize the important differences between the approach adopted here and that used in earlier theoretical studies of mineral systems. First our approach is fully quantitative including representations of short range as well as

Table 2 Mineral structures used in calculating short-range parameters for silicon–oxygen interaction

Name	Formula unit	Ref.
Monticellite	$CaMgSiO_4$	45
Sillimanite	Al_2SiO_5	46
Sphene	$Ca(TiO)SiO_4$	47
Benitoite	$BaTi(SiO_3)_3$	48
Diopside	$CaMg(SiO_3)_2$	49
Jadeite	$NaAl(SiO_3)_2$	49
β-Wollastonite	$CaSiO_3$	50

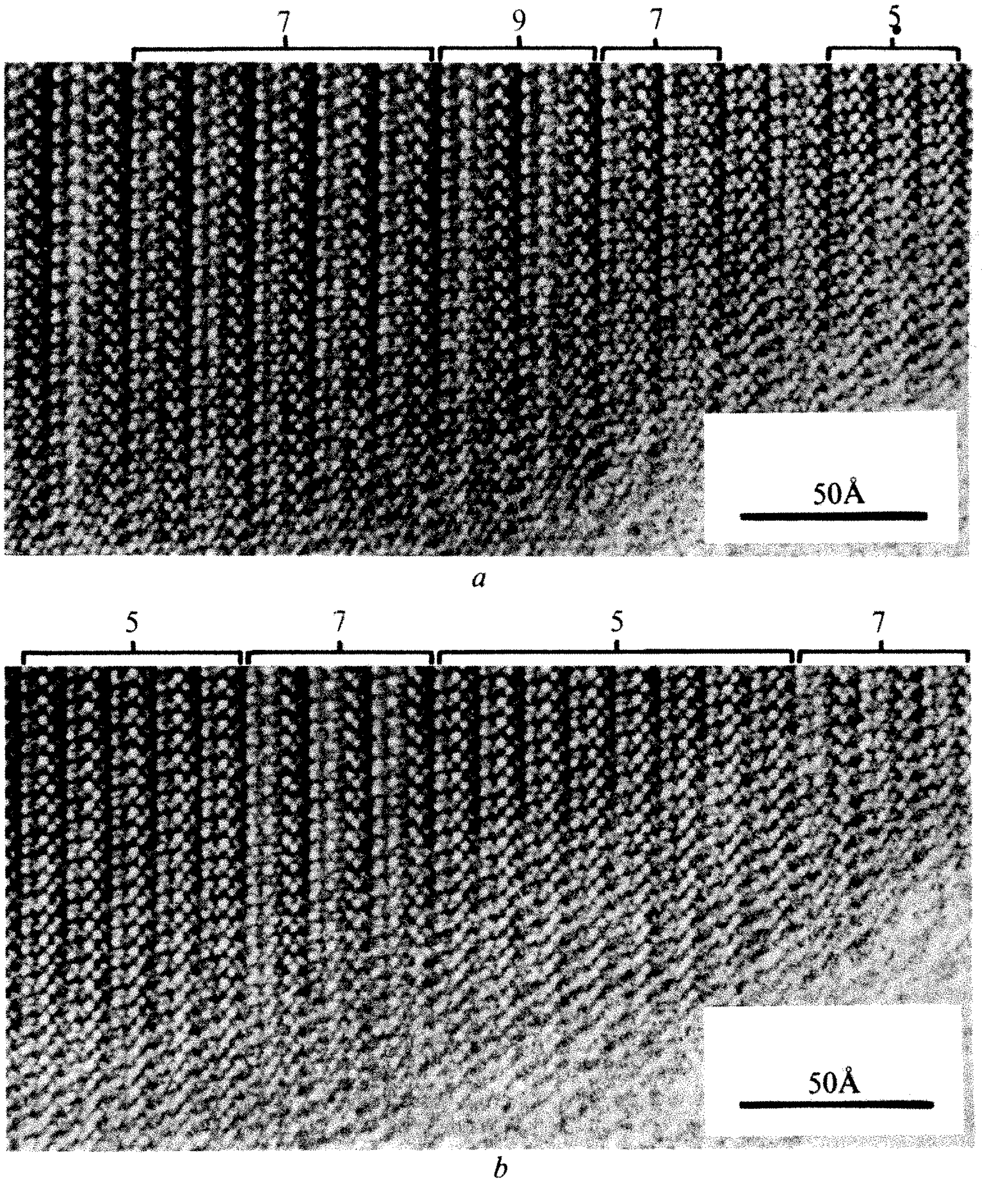

Fig. 3 *a*, Disordered pyroxenoid structure produced by annealing a glass of composition $MnFeSi_2O_6$. (The nine-unit repeat has the so-called ferrosilite(III) structure.) *b*, Ordered rhodonite (eight five-unit repeat) structure predominating after annealing of $MnFeSi_2O_6$.

electrostatic terms (which are the sole terms considered in several previous studies[41,43]). Second, structural data are used as a source of interatomic potentials. Third, energy minimization is used in predicting structural properties.

Further information on the viability of our parameterized potential will follow from the study of the structural effects of the variation of the divalent cation present in chain-structured systems. Before presenting the results of such calculations the problem of energy minimization must, however, be considered.

Minimization methods

Two points are of general importance to the simulation of complex crystal structures. The first concerns the adjustment of unit cell dimensions in such calculations. We found that, for example, on varying the nature of the divalent cation present in a pyroxenoid silicate it was inadequate merely to adjust the coordinates of the ions surrounding the divalent cation. It was also necessary to include dilation (or contraction) of the unit cell; and, moreover, the dilation must be allowed to be anisotropic. Indeed, failure to include anisotropic dilation may lead to qualitatively inconsistent results.

The second point concerns the question of the precise minimization techniques. Our general approach was to modify the unit cell dimensions followed by an iterative adjustment of the atomic coordinates until these are in equilibrium with respect to the new cell. Subsequent cycles then effect further variation of the cell dimension and the procedure continued until a structure is attained which is in equilibrium with respect to both unit cell parameters and atomic coordinates. Note that in adjusting unit cell dimensions it is very important to vary the angle between the axes of the cell as well as the lengths of the cell edges. Failure to include this feature will drastically reduce the efficiency of the minimizations. We should also note that the equilibrated cell

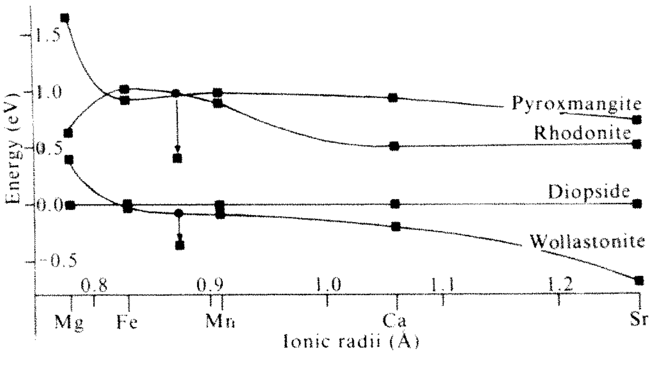

Fig. 4 Plot of energy (per mol SiO_3) relative to that of diopside as a function of radius of the cation M^{2+}. The arrow (↓) indicates stabilization arising from the mixed cation effect in Mn_3Mg; ●, result calculated for average cation radius.

dimensions were within 2% of observed values for all compounds for which crystallographic data are available.

Results and discussion

Calculations were performed on the four pyroxenoid structures, diopside, wollastonite, rhodonite and pyroxmangite. In each case the structures were investigated with the five cations Mg^{2+}, Ca^{2+}, Fe^{2+}, Mn^{2+}, and Sr^{2+}; a full minimization was performed both with respect to the unit cell dimensions and the ion coordinates. The results are summarized in Table 3, where we give the lattice energy of the equilibrated structures per Si atom; and Fig. 4 displays the calculated energies relative to that obtained for the diopside structure.

The following conclusions may be drawn from these calculations: (1) The pyroxmangite and rhodonite structures are never energetically favoured with respect to the diopside and wollastonite structures. (2) Pyroxmangite and rhodonite have very similar lattice energies especially for Fe^{2+} and Mn^{2+}. (3) The most energetically favoured structure is found to be wollastonite for all ions except Mg^{2+} for which diopside is preferred. The energetic preference for the wollastonite structure increases with the radius of the cation.

The first of the above conclusions does not apparently accord with the experimental data as stable rhodonite and pyroxmangite structures are observed. However, in most cases these are found with mixtures of divalent cations, for example, the structural pyroxenoid $Mn_3Mg(SiO_3)_4$, mentioned earlier, which has the pyroxmangite structure (Fig. 2). We investigated whether these structures could be stabilized by the presence of several, rather than one type of divalent cation. In practice, such calculations could be more conveniently performed on the rhodonite structure with 3/4 Mn^{2+} and 1/4 Mg^{2+} cations. (The Mg^{2+} cations were allocated to the smallest cation sites in the crystal.) The result was compared with that for a crystal in which all the divalent cations are the same with a potential taken as a weighted average of that for Mn···O and Mg···O interactions. The former was more stable, relative to the diopside structure, by 0.6 eV, than the latter, which gives an estimate of the magnitude of the 'mixed-cation' effect in this structure.

The wollastonite structures were stabilized by only 0.2 eV by this mixed cation effect, when this was calculated in an analogous fashion. Thus, although the relative stabilization of the rhodonite structure by the mixed cation distributed is insufficient in this particular case to render this structure more energetically favourable than wollastonite, the effect is clearly large and may be decisive in certain cases. One situation for which this appears to be so is $CaMg(SiO_3)_2$, which when an 'average' potential is used, is calculated to be more stable in the wollastonite structure, but when a proper mixed cation distribution is used is found to have greater stability (by 0.6 eV per Si) in the diopside structure as is observed experimentally.

Table 3 Calculated lattice energy of $MSiO_3$ per Si atom

Cation (M^{2+})	Structure Diopside (eV)	Wollastonite (eV)	Rhodonite (eV)	Pyroxmangite (eV)
Mg	163.534	163.133	162.909	161.888
Fe	159.673	159.682	158.582	158.754
Mn	159.204	159.285	158.311	158.232
Ca	158.424	158.622	157.921	157.496
Sr	156.081	156.725	155.564	155.359
Mn_3Mg	159.754	160.137	159.431	—
(Mn_3Mg) composite*	160.216	160.126	159.254	—
CaMg	161.139	160.683	160.130	—
(CaMg) composite*	160.958	160.778	159.926	—

Lattice energies are all calculated as negative quantities; the modulus is given in the table.

* (M_1 M_2) indicates a hypothetical ion with anionic radius equal to the mean of M_1 and M_2.

The results for $CaMg(SiO_3)_2$ and $CaSiO_3$ are thus most encouraging. Each is correctly predicted to have the structure that is observed experimentally. Moreover, the trend in the variation with ionic radius of the relative energies of the wollastonite and diopside structures is in accord with experiment. It remains an open question as to whether rhodonite and pyroxmangite structures are ever thermodynamically stable with respect to the wollastonite structure. On the basis of our results we suggest that pyroxenoids are metastable when they crystallize exclusively into either the rhodonite or pyroxmangite structures. Our computations also show that both structures may be stabilized if there is a mixed cation sublattice of the kind discussed above.

We shall show elsewhere that computations of the kind presented here also reveal much valuable information, pertaining to the behaviour of aluminosilicates such as zeolites. In particular the energetics associated with various possible Si, Al, ordering schemes[51,52] are assessed; and it transpires that the total energy of the aluminosilicates can be a sensitive function of cation position.

We thank the SRC for support and AERE Harwell for generous provision of computer time.

Received 17 July; accepted 29 December 1981.

1. Bragg, W. L. & Claringbull, G. F. *Crystal Structures of Minerals* (Bell, London, 1965).
2. Belov, N. V. *Crystal Chemistry of Large-Cation Silicates* (Consultants Bureau, New York, 1963).
3. Liebau, F. *Handbook of Geochemistry* Vol. 2, Ch. 14 (Springer, Berlin, 1971).
4. Waugh, J. L. T. in *Structural Chemistry and Molecular Biology* (eds Rich, A. & Davidson, N.) 731 (Freeman, San Francisco, 1968).
5. O'Keefe, M. & Hyde, B. G. *Acta crystallogr.* B**34,** 27 (1978).
6. Dent Glasser, L. S. *Chem. Br.* **18,** 33 (1982).
7. Alario Franco, M. A., Jefferson, D. A., Pugh, N. J., Thomas, J. M. & Bishop, A. C. *Mater. Res. Bull.* **15,** 73 (1980).
8. Thomas, J. M., Jefferson, D. A., Mallinson, L. G., Smith, D. J. & Crawford, E. S. *Chem. Scr.* **14,** 1677 (1978–79).
9. Jefferson, D. A., Thomas, J. M., Alario Franco, M. A. & Pugh, N. J. *Acta crystallogr.* A**36,** 1058 (1980).
10. Jefferson, D. A. & Pugh, N. J. *Acta crystallogr.* A**37,** 281 (1981).
11. Thomas, J. M. & Jefferson, D. A. *Endeavour, New Ser.* **2,** 127 (1978).
12. Thomas, J. M. *New Scient.* 580 (21 August 1980).
13. Shu-Lin Wen, Jefferson, D. A. & Thomas, J. M. *Mater. Res. Bull.* **15,** 1643 (1980); *JCS Chem. Commun.* (in the press).
14. Jefferson, D. A. *et al. Nature* **281,** 51 (1979).
15. Tilley, R. J. D. *R. Soc. Chem. Spec. Per. Rep.* **8,** 121 (1980).
16. Bursill, L. A. *Chem. Scr.* **14,** 83 (1978–79).
17. Thomas, J. M., Millward, G. R. & Bursill, L. A. *Phil. Trans. R. Soc.* A**300,** 43 (1981).
18. Kitaigorodsky, A. I. *Chem. Soc. Rev.* **7,** 133 (1978).
19. Williams, D. E. *J. chem. Phys.* **45,** 3770 (1966).
20. Ramdas, S. & Thomas, J. M. *R. Soc. Chem. Spec. Per. Rep.* (*Chem. Phys. Solids and Surfaces*) **7,** 31 (1978).
21. Grammaccioli, C. M. *et al. JCS Faraday Trans II.* **76,** 1336 (1980).
22. Catlow, C. R. A. & Norgett, M. J. *UKAEA Rep.* M2936 (1978).
23. Norgett, M. J. *UKAEA Rep. AERE* (*Harwell*) R.7650 (1974).
24. Catlow, C. R. A. *J. Phys.* C6–53 (1980).
25. Catlow, C. R. A. & Mackrodt, W. C. (eds) in *Lecture Notes in Physics* (Springer, Berlin, 1982).
26. Catlow, C. R. A. & Fender, B. E. F. *J. Phys.* **C8,** 3267 (1975).
27. Catlow, C. R. A. *Proc. R. Soc.* A**353,** 533 (1977).
28. Catlow, C. R. A. & James, R. *Nature* **272,** 602 (1978).
29. Catlow, C. R. A. & James, R. *R. Soc. Chem. Spec. Per. Rep.* (*Chem. Phys. Solids and Surfaces*) **8,** 108 (1980).
30. Norgett, M. J. & Fletcher, R. *J. Phys.* C**3,** L190 (1970).
31. Catlow, C. R. A. & James, R *Proc. R. Soc.* (submitted).
32. Catlow, C. R. A., Mackrodt, W. C., Norgett, M. J. & Stoneham, A. M. *Phil. Mag.* A**40,** 162 (1979).
33. Cochran, W. *Nature* **191,** 60 (1961).
34. Butler, V., Catlow, C. R. A. & Fender, B. E. F. *Solid State Ionics* **2,** 245–251 (1981).
35. O'Keefe, M. & Hyde, B. G. *Acta crystallogr* B**32,** 2923 (1976).
36. Glidewell, C. *Inorg. Nucl. Chem. Lett.* **11,** 353 (1975).
37. Glidewell, C. *Inorg. Nucl. Chem. Lett.* **38,** 669 (1976).
38. Glidewell, C., *Inorg. Nucl. Chem. Lett.* **13,** 65 (1977).
39. Catlow, C. R. A. thesis, Oxford Univ. (also available as UKAEA Rep. TP566 (1974).
40. Baur, W. H. *Am. Miner.* **57,** 709 (1972).
41. Jenkins, H. D. B. & Hartman, P., *Phil. Trans. R. Soc.* A**293,** 169 (1979).
42. Jenkins, H. D. B. & Pratt, K. F. *JCS Faraday II,* **74,** 968 (1978).
43. Alberti, A. & Vezzalini, G. *Z. Krist.* **147,** 167 (1978).
44. MacKrodt, W. C. & Stewart, R. F. *J. Phys.* C**12,** 431 (1979).
45. Lager, G. A. & Meagher, E. P. *Am. Miner.* **63,** 365 (1978).
46. Winter, J. K. & Ghose, S. *Am. Miner.* **64,** 573 (1979).
47. Wyckoff, R. W. G. *Crystal Structures* 2nd edn (Interscience, New York, 1968).
48. Fischer, K. *Z. Krist.* **129,** 222 (1969).
49. Cameron, M., Sueno, S., Prewitt, C. T. & Papike, J. J. *Am. Miner.* **58,** 594 (1973).
50. Ito, T., Sadanga, R., Takeuchi, Y. & Tokonami, M. *Proc. Jap. Acad.* **45,** 913 (1969).
51. Ramdas, S., Thomas, J. M., Klinowski, J., Fyfe, C. A. & Hartman, J. S. *Nature* **292,** 228 (1981).
52. Bursill, L. A., Lodge, E. A. & Thomas, J. M. *Nature* **286,** 111 (1980).

Primary structure of the human Met- and Leu-enkephalin precursor and its mRNA

Michael Comb*, Peter H. Seeburg†, John Adelman†, Lee Eiden‡ & Edward Herbert*

* University of Oregon, Eugene, Oregon 97403, USA
† Genentech Corporation, 460 Point San Bruno Boulevard, San Francisco, California 94080, USA
‡ National Institutes of Health, Bethesda, Maryland 20205, USA

The nucleotide sequence of a complete cDNA copy of enkephalin precursor mRNA from human phaeochromocytoma is reported. The corresponding amino acid sequence shows that the precursor is 267 amino acids long and contains six interspersed Met-enkephalin sequences and one Leu-enkephalin sequence. Five of the seven enkephalins are flanked on both sides by pairs of basic amino acid residues. The precursor does not contain the sequences of the opioid peptides, dynorphin, α-neo-endorphin or β-endorphin.

A NUMBER of peptides have been isolated in the past 6 years that exhibit opioid activity. The simplest of these are methionine (Met)- and leucine (Leu)-enkephalin first identified in brain tissue in 1975 (ref. 1)[1]. The other opioid peptides are C-terminal extensions of either Leu-enkephalin or Met-enkephalin. For example, β-endorphin is a C-terminal extension of Met-enkephalin[2,3], and dynorphin[4] and α-neo-endorphin[5] are C-terminal extensions of Leu-enkephalin (Fig. 1).

Because of the structural similarities of these peptides it was postulated that β-endorphin is the precursor of Met-enkephalin and that dynorphin (or α-neo-endorphin) is the precursor of Leu-enkephalin. However, in the past 2 years it has become clear that the enkephalins are derived from a different gene product than β-endorphin, and that β-endorphin is synthesized from a protein, pro-opiomelanocortin (POMC), that contains sequences of adrenocorticotropic (ACTH) and melanocyte stimulating (MSH) hormones[6-8]. The source of the enkephalins has been elucidated recently by studying the biosynthesis of these peptides in bovine adrenal medulla[9,10]. Enkephalin peptides are abundant in adrenal medulla and can be released by neurotransmitters specific for that tissue. Several enkephalin-containing peptides have been purified from chromaffin granules of the bovine adrenal medulla and shown by sequence analysis to contain more than one enkephalin sequence[9,10]. These studies suggest that a precursor protein exists which contains multiple copies of the enkephalins and that the enkephalins can be released from this protein by digestion with trypsin-like enzymes[9,10].

Enkephalins are also abundant in human phaeochromocytoma, a tumour derived from the adrenal medulla. The RNA from this tumour contains a high level of enkephalin mRNA sequences as demonstrated by cell-free translation studies[11]. Therefore, we have used human phaeochromocytoma as a source of human proenkephalin mRNA for the preparation and cloning of human enkephalin cDNA.

We have previously shown that a synthetic oligodeoxynucleotide probe pool complementary to a mRNA sequence that codes for Met-enkephalin can be used to detect a proenkephalin mRNA species in bovine adrenal and human phaeochromocytoma by the Northern blot procedure[12]. These species of RNA are between 1,400 and 1,500 bases long. In the present study we have used the same probe to identify transformants containing recombinant plasmids with inserts of human proenkephalin cDNA. In this manner we have been able to derive the nucleotide sequence of DNA complementary to the entire human proenkephalin mRNA sequence.

Isolation of cDNA clones

Poly(A) RNA was isolated from human phaeochromocytoma tissue as previously described[12]. Northern blot analysis of this RNA, using an enkephalin pentadecamer pool ($5'\cdots\text{CAT}\genfrac{}{}{0pt}{}{\text{A}}{\text{G}}\text{AAGCCGCC}\genfrac{}{}{0pt}{}{\text{A}}{\text{G}}\text{TA}\cdots 3'$) containing two possible mismatches with the enkephalin-coding mRNA sequence, revealed that proenkephalin mRNA constitutes ~0.1% of the total poly(A) RNA from this tissue[12]. A four- to fivefold enrichment of enkephalin mRNA was achieved by density gradient sedimentation (Fig. 2). A clone bank of 15,000 tetracycline-resistant transformants was made from cDNA copies of the enriched enkephalin mRNA.

To screen and maintain the phaeochromocytoma clone bank, 7,000 transformants were picked and grown in 96-well microtitre plates. All cultures were transferred in ordered arrays to nitrocellulose for *in situ* hybridization with ^{32}P-labelled Met-enkephalin pentadecamer probe pool. Seventeen colonies hybridized strongly with the pool (Fig. 3). Plasmid DNA was isolated from the corresponding cultures and the size of cDNA inserts examined after endo *Pst*I cleavage by polyacrylamide gel electrophoresis. Most of the plasmids were found to contain both a 410 and a 600 base pair (bp) fragment. Several plasmids contained a third fragment of varying size. Two of the latter plasmids with the biggest inserts were selected for nucleotide sequencing together with the 600 and 410 bp fragments.

Sequencing strategy

To determine the nucleotide sequence of the cDNA inserts, recombinant plasmid DNA was cleaved with endo *Pst*I and the DNA fragments were cloned into the *Pst*I site of the bacteriophage vector M13mp7 RF-DNA. The single-stranded DNA prepared from recombinant phage served as a template for enzymatic sequencing reactions in the presence of chain terminators[13] using a synthetic oligomer as universal primer[14]. Figure 4 shows the entire nucleotide sequence of preproenkephalin mRNA as derived from sequencing the cDNA inserts of two separate clones. One insert contained the entire 5′ portion of the mRNA and ended ~20 nucleotides after the termination codon. The other had the entire 3′ end but did not

	1	2	3	4	5	6	7	8	9	10	11	12	13
β-endorphin β(61-91)LPH	Tyr	Gly	Gly	Phe	Met	Thr	Ser	Glu	Lys	Ser	Gln	Thr	Pro
Met-enkephalin	Tyr	Gly	Gly	Phe	Met								
Leu-enkephalin	Tyr	Gly	Gly	Phe	Leu								
Dynorphin	Tyr	Gly	Gly	Phe	Leu	Arg	Arg	Ile	Arg	Pro	Lys	Leu	Lys
α-neo-endorphin	Tyr	Gly	Gly	Phe	Leu	Arg	Lys	Pro	(Gly, Tyr^2, Lys^2, Arg)				

Fig. 1 Structure of the opioid peptides. Only a partial structure of β-endorphin is shown. LPH, lipotropin.

0028-0836/82/080663—04$01.00

contain the region corresponding to the 5′-untranslated region of the mRNA and the portion coding for the signal peptide (leader or presequence).

Primary structure of enkephalin precursor mRNA

The mRNA coding for Met- and Leu-enkephalin is 1,350 nucleotides long (Fig. 4), close to the size of 1,400 nucleotides observed in Fig. 2*b*. The 5′-untranslated region is remarkable for being >200 nucleotides long. We do not know how many nucleotides are missing from the capped 5′ end of the mRNA. As artefacts can occur in the cDNA corresponding to the 5′ end of the mRNA, we cannot rule out that the actual mRNA sequence is different in this region[15]. The 5′ end features several stretches of homo-oligomeric pyrimidines, especially runs of UMP. The coding region starts with the first AUG and consists of 267 triplets with seven interspersed small repeat units corresponding to the enkephalin sequences. The 3′-untranslated region is 320 nucleotides long and is rich in UMP with several homo-oligomeric pyrimidine stretches towards the 5′ end. An AAUAAA sequence common to most mRNA species[16] is found 19 nucleotides before the poly(A) tail. It is curious that another such sequence occurs 20 nucleotides upstream. With both sequences represented in the chromosomal gene, it is possible that two populations of mRNA exist which contain either one or both sequences.

Primary structure of enkephalin precursor protein

The first 24 amino acids of the precursor protein have the characteristics of a leader sequence containing many hydrophobic amino acids, particularly Leu (Fig. 4). As Ala is the most common amino acid preceding the cleavage site of leader sequences[17], we tentatively conclude that the leader sequence ends after Ala 24, as indicated in Fig. 5, although Ala 20 is another possible termination site. The N-terminal one-third of the mature proenkephalin molecule does not contain any enkephalin sequences but consists of a 73 amino acid peptide (residues 25–97 in Fig. 4) containing all six Cys residues in the protein. A proper folding for efficient processing is probably ensured by the formation of disulphide bridges in this part of the precursor.

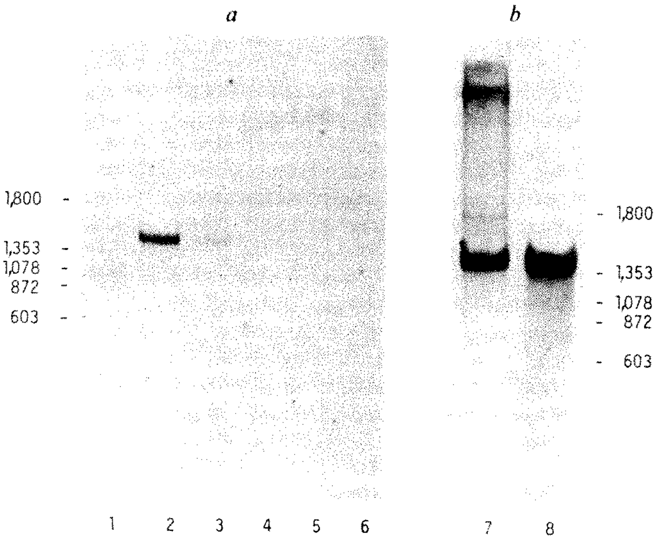

Fig. 2 Northern hybridization analysis of human phaeochromocytoma poly(A) RNA using enkephalin probes. *a*, Fifty µg of human phaeochromocytoma poly(A) RNA was fractionated on a 5–35% linear sucrose gradient at 4 °C for 16 h in a Beckman SW41 rotor at 35,000 r.p.m. Fractions from the gradient were precipitated and washed with EtOH and the pellets were resuspended in 10 µl of H_2O. Two µl aliquots from alternate fractions (0.8 µg) were denatured with glyoxal and electrophoresed in a 1.75% agarose gel for 3 h at 100 V. RNA was transferred from the gel to nitrocellulose[25]. The RNA blot was hybridized with 6×10^7 c.p.m. of ^{32}P-labelled pentadecamer probe pool (5×10^6 c.p.m. pmol^{-1}) in 5 ml of 4×SSC, 1× Denhardts, 0.1% SDS and 100 µg ml^{-1} yeast tRNA at 30 °C for 2 days. Hybridization and washing of blots was done as described previously[12]. Autoradiography was for 16 h at −70 °C using Dupont lightning plus intensifying screens. The top of the gradient is at the left hand side of the chart. *b*, Five µg of human phaeochromocytoma poly(A) RNA was hybridized with 1×10^7 c.p.m. pentadecamer probe pool (5×10^6 c.p.m. pmol^{-1}; lane 7) and 3×10^6 c.p.m. of nick translated pHPE 41 containing a nearly full-length proenkephalin cDNA insert (4×10^8 c.p.m. µg^{-1}; lane 8). The length scale (number of nucleotides) was constructed by running glyoxal-denatured DNA fragments of *Hae*III digests of phase ΦX174 RF-DNA and *Hin*dIII digests of phage λ DNA on adjacent lanes of the gel.

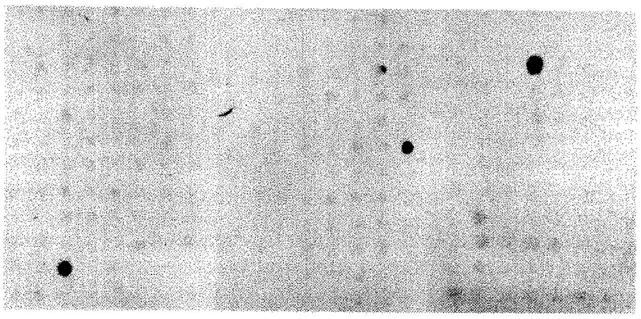

Fig. 3 *In situ* colony screening of a human phaeochromocytoma cDNA library using ^{32}P-labelled enkephalin pentadecamer pool. Sucrose gradient fractions containing enkephalin mRNA (Fig. 2, lane 2) were pooled and used to direct the synthesis of single-stranded cDNA using reverse transcriptase and oligo(dT) as primer. Double-stranded cDNA was prepared using the large fragment of DNA polymerase I (Boehringer Mannheim), and the hairpin loops were cleaved with S_1 nuclease (Miles). Double-stranded S_1-treated cDNA was fractionated on a 10% polyacrylamide gel and cDNA 600–2,000 bases long was eluted. Forty ng of size-fractionated cDNA were obtained from 2 µg of enriched poly(A) RNA. Poly(dC) homopolymeric extensions were added to the 3′ end using terminal transferase (PL Biochemicals). A clone bank of human phaeochromocytoma cDNA was prepared by annealing the poly(dC)-tailed cDNA to endo *Pst*I-cleaved plasmid pBR322 DNA tailed with dGMP[26], and the mixture used to transform competent *Escherichia coli* 294 cells. Approximately 15,000 tetracycline-resistant transformants were obtained from which <3% were ampicillin resistant. Seven thousand tetracycline-resistant colonies were picked and grown in 96-well microtitre plates. Colonies were transferred from the microtitre plates to nitrocellulose filters placed on 15 cm LB Petri plates containing 5 µg ml^{-1} tetracycline using a 96-prong stainless-steel stamp. Colonies were grown on the filters for 6 h at 37 °C after which the filters were transferred to Petri plates containing LB with 12.5 µg ml^{-1} chloramphenicol, and amplified overnight. Filters were lysed, neutralized and prepared for hybridization as described in ref. 27. Prehybridization of filters was for 6 h at 30 °C in 4× SSC, 2× Denhardts, 40 mM $NaPO_4$, *p*H 7.8, and 300 µg ml^{-1} heat-denatured herring sperm DNA. The pentadecamers were phosphorylated using T_4 polynucleotide kinase (New England Biolabs) and (γ-^{32}P]ATP (NEN) to a specific activity of 2×10^6 c.p.m. pmol^{-1}. ^{32}P-labelled probe pool was purified by chromotography on 10 ml Sephadex G-50 columns. Each 15×7 cm filter was hybridized in 2 ml of the above hybridization mixture at 30 °C for 20 h containing 4×10^6 c.p.m. pentadecamers. Filters were washed for 15 min, once at 25 °C and twice at 30 °C, in 4× SSC, 0.1% SDS, dried and exposed to X-ray film. Autoradiography was at −70 °C for 2 h using intensifier screens. Results are shown above for several filters containing positive signals.

It is tempting to speculate that the occurrence of multiple enkephalin sequences in the same molecule is due to duplication events of one small genetic unit in the distant past. If so, sequence changes dictated by diversified functional and processing requirements may have erased most of the supporting evidence, as can be seen by analysing the structure of the regions that separate the enkephalin units. The length of these 'spacer' regions ranges from 2 amino acids (between units 1 and 2) to 41 (between units 3 and 4). Four of these spacer regions contain highly hydrophilic sequences with several Glu and Asp residues in a row. The spacer peptide that separates Met-enkephalin unit 5 from Leu-enkephalin is missing this hydrophilic feature. It is interesting to note that this peptide (peptide E) is totally conserved in the bovine and human enkephalin precursors and is a more potent opioid agent than the enkephalins[10]. Perhaps processing of the hydrophobic spacer is less efficient than processing of the hydrophilic spacers. The hydrophobic spacer might ensure that peptide E is released intact from the precursor to serve as an opioid agent or another kind of regulator.

```
HUMAN PREPROENKEPHALIN mRNA

5' - CUGGGGCCUGGGGGCCACCAGUGGGAAAAGAUAUUAAAAUCUCAUAAAUCCUCCGUAUCUUUUUCCAUUUCAGGAACUUCUUUGGAGUAACUUUCGCCUUCUUCG

UCGGAGGCAGAGCCCCGCAGCCUGGCCCGUGACCCCGCAGAGACGCUGAGGACCGCGACGAGUCGUGUCUGAACCCGGCUUUUCCAAUUGGCCUGCUCCAUCCGAACAGCGUCAACUCC


1                                   10                                      20                                       30
AUG GCG CGG UUC CUG ACA CUU UGC ACU UGG CUG CUG UUG CUC GGC CCC GGG CUC CUG GCG ACC GUG CGG GCC GAA UGC AGC CAG GAU UGC
met ala arg phe leu thr leu cys thr trp leu leu leu leu gly pro gly leu leu ala thr val arg ala glu cys ser gln asp cys

                                    40                                      50                                       60
GCG ACG UGC AGC UAC CGC CUA GUG CGC CCG GCC GAC AUC AAC UUC CUG GCU UGC GUA AUG GAA UGU GAA GGU AAA CUG CCU UCU CUG AAA
ala thr cys ser tyr arg leu val arg pro ala asp ile asn phe leu ala cys val met glu cys glu gly lys leu pro ser leu lys

                                    70                                      80                                       90
AUU UGG GAA ACC UGC AAG GAG CUC CUG CAG CUG UCC AAA CCA GAG CUU CCU CAA GAU GGC ACC AGC ACC CUC AGA GAA AAU AGC AAA CCG
ile trp glu thr cys lys glu leu leu gln leu ser lys pro glu leu pro gln asp gly thr ser thr leu arg glu asn ser lys pro

                                    100                                     110                                      120
GAA GAA AGC CAU UUG CUA GCC|AAA AGG|UAU GGG GGC UUC AUG|AAA AGG|UAU GGA GGC UUC AUG|AAG AAA|AUG GAU GAG CUU UAU CCC AUG
glu glu ser his leu leu ala|lys arg|tyr gly gly phe met|lys arg|tyr gly gly phe met|lys lys|met asp glu leu tyr pro met

                                    130                                     140                                      150
GAG CCA GAA GAA GAG GCC AAU GGA AGU GAG AUC CUC GCC|AAG CGG|UAU GGG GGC UUC AUG|AAG AAG|GAU GCA GAG GAG GAC GAC UCG CUG
glu pro glu glu glu ala asn gly ser glu ile leu ala|lys arg|tyr gly gly phe met|lys lys|asp ala glu glu asp asp ser leu

                                    160                                     170                                      180
GCC AAU UCC UCA GAC CUG CUA AAA GAG CUU CUG GAA ACA GGG GAC AAC CGA GAG CGU AGC CAC CAC CAG GAU GGC AGU GAU AAU GAG GAA
ala asn ser ser asp leu leu lys glu leu leu glu thr gly asp asn arg glu arg ser his his gln asp gly ser asp asn glu glu

                                    190                                     200                                      210
GAA GUG AGC|AAG AGA|UAU GGG GGC UUC AUG AGA GGC UUA|AAG AGA|AGC CCC CAA CUG GAA GAU GAA GCC AAA GAG CUG CAG|AAG CGA|UAU
glu val ser|lys arg|tyr gly gly phe met arg gly leu|lys arg|ser pro gln leu glu asp glu ala lys glu leu gln|lys arg|tyr

                                    220                                     230                                      240
GGG GGC UUC AUG|AGA AGA|GUA GGU CGU CCA GAG UGG UGG AUG GAC UAC CAG|AAA CGG|UAU GGA GGU UUC CUG|AAG CGC|UUU GCC GAG GCU
gly gly phe met|arg arg|val gly arg pro glu trp trp met asp tyr gln|lys arg|tyr gly gly phe leu|lys arg|phe ala glu ala

                                    250                                     260
CUG CCC UCC GAC GAA GAA GGC GAA AGU UAC UCC AAA GAA GUU CCU GAA AUG GAA|AAA AGA|UAC GGA GGA UUU AUG AGA UUU UAA
leu pro ser asp glu glu gly glu ser tyr ser lys glu val pro glu met glu|lys arg|tyr gly gly phe met arg phe end


UAUCUUUUCCCACUAGUGGCCCCCAGGCCCCAGCAAGCCUCCCUCCAUCCUCCAGUGGGAAACUGUUGAUGGUGUUUUAUUGUCAUGUGUUGCUUGCCUUGUAUAGUUGACUUCAUUGU

CUGGAUAACUAUACAACCUGAAAACUGUCAUUUCAGGUUCUGUGCUCUUUUUGGAGUCUUUAAGCUCAGUAUUAGUCUAUUGCAGCUAUCUCGUUUUUCAUGCUAAAAAUAGUUUUUUG

UUAUCUUGUCUCUUAUUUUUUGACAAACAUCCAAUAAAUGCUUACUUGUAUAUAGAGAUAAUAAACCUGUUACCCCAAGUGCAUAAAAAAA - 3'
```

Fig. 4 Primary structure of human Met- and Leu-enkephalin in precursor mRNA and protein. Plasmid DNA was isolated by mini-screen procedure from 5 ml of overnight cultures and digested to completion with endo *Pst*I (New England Biolabs). Digested DNA was ligated to 10 ng of *Pst*I-cleaved M13mp7 RF-DNA in 20 µl containing 50 mM Tris-HCl, *p*H 8, 0.1 mM EDTA, 7 mM $MgCl_2$, 10 mM dithiothreitol, 500 µM rATP and 0.2 U of T_4 DNA ligase (New England Biolabs) for 1 h at room temperature. The mixture was used to transform competent *E. coli* JM103 cells and transformed cells were plated with top agar in the presence of isopropyl-tgio-β-D-galactoside and 5-bromo-4-chloro-3-indolyl-β-D-galactoside. After a 10 h incubation at 37 °C, colourless plaques were transferred to 1.5 ml 2× yeast-tryptone broth. Bacteria were sedimented from grown cultures by centrifugation and phage were precipitated from the supernatant with polyethylene glycol-6000 (3%) and NaCl (0.5 M). DNA was isolated by phenol–$CHCl_3$ extraction, precipitated with ethanol and redissolved in 10 µl of H_2O. DNA templates were sorted by single-lane tracking to avoid redundancy and non-productive sequencing generated by the empty phage DNA or poly(dG)-tailed sequences at the insertion site. For the final sequence determination, six templates were chosen which originated from two different cDNA clones. Sequencing reactions were done for 15 min at 25 °C in 4 µl of 10 mM Tris, *p*H 8, 0.1 mM EDTA, 7 mM $MgCl_2$ and 1 mM dithiothreitol containing about 100 ng of template DNA, 0.2 pmol of primer, 0.2 U *E. coli* DNA Polymerase I (Klenow fragment; Boehringer Mannheim), 5 µCi of [α-^{32}P]dCTP (Amersham, 400 Ci $mmol^{-1}$) and deoxy- and dideoxynucleoside triphosphates in the proper concentrations. A chase was performed for 15 min by adding 1 µl of a 2 mM solution of each of the deoxyribonucleoside triphosphates and reactions were stopped by adding 10 µl of a formamide–dye mixture. After heating the reaction mixtures to 100 °C for 3 min, 1 µl aliquots were electrophoresed on thin 40 cm long 5% polyacrylamide–8 M urea gels for 2–6 h at 25 mA. Gels were dried onto Whatman 3 mm paper and exposed to X-ray film overnight.

The molecular weight of the precursor calculated from the sequence in Fig. 4 is the same as that determined by Dandekar *et al.* for bovine adrenal medulla (31,000)[18] but much smaller than those reported for bovine adrenal medulla (50,000)[19], guinea pig striatum (92,000)[20] or human phaeochromocytoma (70,000–180,000)[11]. The estimates by Dandekar *et al.*[18] on the adrenal precursor and by Beaumont *et al.*[20] on the striatum precursor were made by SDS-polyacrylamide gel electrophoresis while the other estimate[11] was made by gel-filtration.

Special features of the human enkephalin precursor and possible cleavage products

Some of the special features of the enkephalin precursor are presented in Fig. 5. Five of the seven enkephalin moieties are flanked on both sides by pairs of basic amino acid residues (enkephalin moieties 1–3, 5 and 6, Figs 4 and 5), suggesting that they are cleaved out of the precursor by the combined action of a trypsin-like enzyme and a carboxypeptidase. Action of these

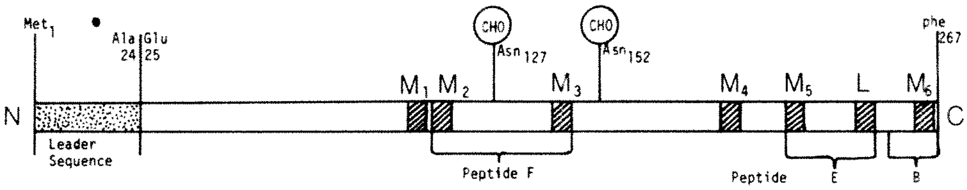

Fig. 5 Low-resolution model of enkephalin precursor showing the distribution of Met-enkephalin sequences (M_1, M_2, M_3 and so on) and Leu-enkephalin (L). The position of potential carbohydrate (CHO) attachment sites and the sequences corresponding to peptides F, E and B of bovine adrenal medulla[10] are depicted.

enzymes would also be expected to generate Met-enkephalin-Arg-Gly-Leu from enkephalin sequence 4 and Met-enkephalin-Arg-Phe from the carboxy-terminal region of the protein. Met-enkephalin-Arg-Phe has actually been observed in bovine adrenal medulla[9].

The biologically active domains of other prohormones, such as proinsulin[21] and POMC[22], are also flanked on both sides by pairs of basic amino acid residues, suggesting that similar trypsin-like enzymes are involved in processing of these prohormones. The amino acid sequence in Fig. 4 also reveals the existence of two potential glycosylation sites in the precursor at Asn 127 and Asn 152. The sequence Asn-X-Ser or Asn-X-Thr is required to attach carbohydrate to an Asn in a protein[23]. However, as not all Asn residues in such a sequence are glycosylated, it is not possible to predict whether the enkephalin precursor contains Asn-linked oligosaccharides[23].

Comparison of human pro-enkephalin- and bovine enkephalin-containing peptides

Kilpatrick *et al.*[10] have sequenced several large enkephalin-containing peptides isolated from chromaffin granules of bovine adrenal medulla. Comparison of the sequence of three of these peptides with the sequence of human proenkephalin shows that all three are contained within the human precursor. The sequence of bovine peptide B corresponds to amino acid residues 238–267 (the C terminus of the protein) of the human precursor with at least one amino acid substitution at residue 240 (a Pro in the bovine peptide for Ala in the human)[10]. The sequence of peptide E (a more potent opioid than the enkephalins)[10], which contains both a Met- and a Leu-enkephalin moiety, corresponds exactly to the sequence of residues 210–235 in the human enkephalin precursor. The sequence of peptide F (34 amino acids long) corresponds to the sequence of residues 107–140 in the human precursor with five amino acid substitutions. The amino acid substitutions in human peptide F are (human for bovine) in positions 120 (Met for Leu), 122 (Pro for Val), 129 (Ser for Gly), 131 (Leu for Val) and 133 (Ala for Gly). It is interesting that peptides E and F have pairs of basic amino acid residues flanking both sides of the enkephalin sequences they contain. As pairs of basic amino acid residues are potential tryptic cleavage sites, this finding suggests that peptides E and F are processing intermediates in the formation of enkephalins. Yet the high potency of peptide E as an opiate and the complete conservation of sequence between human and bovine peptides indicate that this peptide is an important opiate compound in itself.

Enkephalin-like immunoreactivity has been observed not only in several areas of the brain but also in sympathetic ganglia, nerve plexuses in the intestine and nerve fibres in adrenal medulla and phaeochromocytoma. It would be very interesting to know whether the same array of opioid peptides is produced in these tissues as in adrenal medulla. Tissue-specific use of enkephalin peptides could occur by differential processing of the precursor molecule or by selective expression of one or more of a family of enkephalin genes in different tissues. Isolation and characterization of enkephalin genes will be an important step in attempting to answer this question.

Close examination of the structure of the human enkephalin precursor reveals that it does not contain the sequence of any of the other opioid peptides, β-endorphin, dynorphin or α-neo-endorphin. Hence, at least three of the four types of opioid peptides are derived from different primary gene products.

The complete sequences of the precursors to β-endorphin (POMC) and enkephalins are now known. In both precursors there is repetition of a sequence that is flanked on both sides by pairs of basic amino acid residues. POMC has three copies of the MSH sequence[22] and the enkephalin precursor has seven copies of the enkephalin sequence. J. Kurjan and I. Herskowitz have recently discovered that α-factor, a peptide pheromone 13 amino acids long that promotes sexual union of yeast gametes, is synthesized from a precursor containing four copies of the peptide in an evenly spaced arrangement (personal communication). The α-factor sequences are flanked on only one side by a pair of basic amino acid residues indicating that the proteolytic processing of the precursor is different from that of proenkephalin and POMC.

Thus widely diverse organisms make use of the multivalent precursor for the synthesis of important regulatory peptides. In the case of POMC, peptides from different regions of the precursor (MSH, ACTH and endorphin) may act as agonists or antagonists in coordinating a behavioural response such as the response to stress[24]. The function of the multi-enkephalin precursor is less clear.

This work was supported by National Institutes of Health Grants AM-16879 and GM07759. We also thank R. Swanson for his support.

Note added in proof: While this paper was in press two papers appeared in the 21 January issue of *Nature* on the structure of the enkephalin precursor in bovine adrenal gland[28,29]. The distribution of enkephalin sequences in the human precursor is very similar to that in the bovine precursor.

Received 28 December 1981; accepted 15 January 1982.

1. Hughes, J. *et al. Nature* **258**, 577–579 (1975).
2. Li, C. H. & Chung, D. *Proc. natn. Acad. Sci. U.S.A.* **73**, 1145–1148 (1976).
3. Bradbury, A. F., Smyth, P. G., Snell, C. R., Birdsall, N. J. M. & Hulme, E. C. *Nature* **260**, 793–795 (1976).
4. Goldstein, A., Tachibay, A. S., Lowney, L. I., Hunkapiller, R. M. & Hood, L. *Proc. natn. Acad. Sci. U.S.A.* **76**, 6666–6670 (1979).
5. Kangawa, K., Matsuo, H. & Igarashi, M. *Biochem. biophys. Res. Commun.* **86**, 153–160 (1979).
6. Mains, R. E., Eipper, B. A. & Ling, N. *Proc. natn. Acad. Sci. U.S.A.* **74**, 3014–3018 (1977).
7. Roberts, J. L. & Herbert, E. *Proc. natn. Acad. Sci. U.S.A.* **74**, 4826–4830 (1977).
8. Roberts, J. L. & Herbert, E. *Proc. natn. Acad. Sci. U.S.A.* **74**, 5300–5304 (1977).
9. Stern, A. S. *et al. Biosynthesis, Modification and Processing of Cellular and Viral Proteins* (eds Koch, G. & Richter, D. (Academic, New York, 1980).
10. Kilpatrick, D. L. *et al. Proc. natn. Acad. Sci. U.S.A.* **78**, 3265–3268 (1981).
11. Giraud, P. & Eiden, L. E. *Biochem. biophys. Res. Commun.* **99**, 969–975 (1981).
12. Comb, M. & Herbert, E. *Proc. natn. Acad. Sci. U.S.A.* (in the press).
13. Sanger, F., Nickleu, S. & Coulson, A. R. *Proc. natn. Acad. Sci. U.S.A.* **74**, 5463–5467 (1977).
14. Messing, J., Crea, R. & Seeburg, P. H. *Nucleic Acids Res.* **9**, 309–321 (1981).
15. Richard, R. I., Shine, J., Ullrich, A., Wells, J. R. E. & Goodman, H. M. *Nucleic Acids Res.* **7**, 1137–1146 (1979).
16. Proudfoot, N. J. & Brownlee, G. G. *Nature* **263**, 211–214 (1976).
17. Steiner, D. F., Quinn, P. S., Shu, J. C., March, J. & Tager, H. S. *Ann. N.Y. Acad. Sci.* **343**, 1–16 (1980).
18. Dandekar, S. & Sabol, S. L. *Proc. natn. Acad. Sci. U.S.A.* (in the press).
19. Lewis, R. V., Stern, A. S., Rossier, J., Stern, S. & Udenfriend, S. *Science* **208**, 1459–1561 (1980).
20. Beaumont, A., Feuntes, J. A., Hughes, J. & Metters, K. M. *FEBS Lett.* **122**, 135–137 (1980).
21. Steiner, D. F., Cunningham, D., Spiegelman, L. & Aton, D. *Science* **157**, 697–701 (1967).
22. Nakanishi, S. *et al. Nature* **278**, 423–427 (1979).
23. Marshall, R. D. *A Rev. Biochem.* **41**, 673–702 (1972).
24. Pedersen, R. C. & Brownie, A. C. *Proc. natn. Acad. Sci. U.S.A.* **77**, 2239–2243 (1980).
25. Thomas, P. S. *Proc. natn. Acad. Sci. U.S.A.* **77**, 5201–5205 (1980).
26. Deng, G. & Wu, R. *Nucleic Acids Res.* **9**, 4173–4188 (1981).
27. Grunstein, M. & Hogness, D. S. *Proc. natn. Acad. Sci. U.S.A.* **72**, 3961–3965 (1975).
28. Noda, M. *et al. Nature* **295**, 202–206 (1982).
29. Gubler, U., Seeburg, P., Hoffman, B. J., Gage, L. P. & Udenfriend, S. *Nature* **295**, 206–209 (1982).

Studies of X chromosome DNA methylation in normal human cells

Stanley F. Wolf & Barbara R. Migeon

Department of Pediatrics, The Johns Hopkins University School of Medicine, Baltimore, Maryland 21205, USA

Studies of methylation along 28 kilobases of X-chromosome DNA, assayed by Southern blot analysis using cloned X-chromosome-specific probes, indicates that X DNA methylation in normal human cells changes with replication, is not correlated with number of X chromosomes or transcriptional activity, and is less stable and more prevalent than when the human X is in the foreign environment of mouse–human hybrid cells. In contrast with observations of others in heteroploid cells, we observed no derepression of the inactive X in clonal populations of normal human fibroblasts treated with 5-azacytidine. This may reflect the differences in stability of the methylation of the human X in a foreign environment. Our observations preclude ubiquitous methylation differences as the molecular basis for X-chromosome inactivation.

DNA METHYLATION has frequently been proposed to be responsible for the regulation of developmental processes[1–3]. These differentiation events include that resulting in the inactivation of all but one X chromosome in somatic cells of mammals[4]. Riggs[3] proposed that DNA methylation was responsible for initiation and maintenance of mammalian X inactivation, invoking the presence of sequence methylases with preference for half-methylated sites. Methylation has been implicated in X-chromosome inactivation on the basis of indirect evidence: the ubiquity of 5-methylcytosine, the existence of sequence-specific methylases and tissue-specific differences in methylation of differentiated genes[5,6]. There is some evidence that a gene on the inactive X remains incapable of expression even when protein superstructures are removed[7], implying that the DNA of the inactive X has undergone a permanent modification. The tissue-specific association of undermethylation with gene activity[8–17] and abundant methylation in the early embryo[15] has led to speculation that the inactive X chromosome might be highly methylated[14,15]. Recent studies of interspecies cell hybrids have shown that 5-azacytidine (5-azaC) can induce local derepression of the inactive X chromosome, presumably because the cytidine analogue has blocked methylation at relevant sites on the inactive X[18].

We have identified two cloned DNA fragments unique to the X chromosome[19] that provide a more direct means of looking for methylation differences between inactive and active X chromosomes. Using these probes, we have compared DNA methylation in placentas and skin fibroblasts from males and females. Furthermore, we have carried out direct experiments testing the ability of 5-azaC to induce reactivation of the silent X in normal human cells having enzyme markers that distinguish active from inactive X. Our results show no significant sex differences in methylation of X sequences. Moreover, studies of clonal populations of normal human cells demonstrate that the pattern of DNA methylation is not faithfully transmitted.

X-chromosome DNA methylation studies

X-chromosome-specific DNA probes provide a direct means of testing the hypothesis that the inactive X chromosome is highly methylated. The restriction enzymes *Hpa*II and *Msp*I recognize the sequence CCGG but *Hpa*II cannot cut if the internal C is methylated[20]. If DNA methylation of active and inactive X chromosomes differs significantly, the restriction fragments generated by digestion with *Hpa*II and hybridization with a labelled X-specific probe should differ between DNA of male cells with a single active X and that of female cells that have an inactive X as well.

The plasmids 0307 and 0604 contain sequences specific to the human X chromosome[19]. By means of mouse–human hybrids, the insert segments in the 0307 and 0604 plasmids have been mapped to the region on the long arm between Xq13 and Xq25. Mapping was carried out using a series of hybrids derived from mouse cells (Sv-tfm or A9) and human cells with balanced X/autosome translocation that have been used to map other X-linked genes[21,22]. The 0307 plasmid contains DNA that is transcribed as it hybridizes to total RNA extracted from normal human fibroblasts and this hybridization is RNase sensitive (Fig. 1). The 3.4-kilobase (kb) insert is a single copy sequence based on (1) analysis of reassociating kinetics using human genomic DNA[19], (2) intensity of hybridization to genomic DNA in Southern blots, relative to that obtained with a γ-globin probe[19] and (3) identification of a *Pst*I polymorphism within the sequence that behaves as expected for a single copy sequence. (Southern blot analysis of human lymphocyte DNA digested with *Pst*I and probed with 0307 usually results in bands at 7.4 and 1.0 kb. In one male with a *Pst*I restriction site polymorphism, the 7.4-kb band has been replaced by a 4.2-kb band. If the 0307 sequence were present more than once on the X, one would expect a new band in addition to the original ones.)

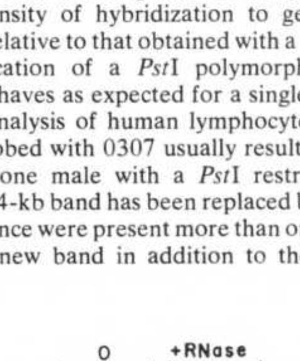

Fig. 1 Hybridization of 0307 DNA to cultured human fibroblast RNA. Total RNA, purified using hot phenol–SDS[30], was aliquoted precisely into two tubes. Pancreatic RNase A (Sigma: 5×crystallized, boiled 10 min) was added to one tube ($100\ \mu g\ ml^{-1}$) and incubated (37 °C, 2 h); the second tube was untreated. The RNA in serial dilutions was dotted onto nitrocellulose filters[16] and the filter was hybridized to 0307 labelled with ^{32}P by nick translation[19]. The final wash was at 60 °C, 0.1 SET and exposed to Kodak XAR5 X-ray film (−70 °C, 6 days). Hybridization did not occur in the absence of RNA. Parallel filters hybridized with γ-globin cDNA probe showed hybridization only to the 20-μg dots and no RNase sensitivity.

0028-0836/82/080667—05$01.00

Because the X-chromosome DNA sequence in the plasmid 0307 contains no *Hpa*II site, 0307 is a probe for methylation of *Hpa*II sites in neighbouring DNA. The 7.5-kb insert in plasmid 0604 includes a single *Hpa*II site.

Methylation patterns in male and female placentas and uncloned fibroblast cultures

Figure 2 shows the results of *Hpa*II and *Msp*I analysis of placentas (chorionic villi) and uncloned fibroblasts using probe 0307. The probe hybridizes to a single band (4.6 kb) in each of the DNA samples digested with *Msp*I (Fig. 2, lanes 1–6) so that the distance between *Hpa*II sites which span the 0307 sequence is the same in all cells. In *Hpa*II digests of male and female specimens (Fig. 2, lanes 7–12) the 0307 probe hybridizes to multiple fragments, ≥4.6 kb. Hybridization to fragments larger than 4.6 kb indicates that the internal C in the *Hpa*II recognition sequence is methylated in site(s) flanking the 0307 sequence.

The multiple bands observed in *Hpa*II digests probed with 0307 are unlikely to be the result of partial digestion. Samples were digested with excess enzyme for up to 20 h (see figure legends for details). Moreover, the number and relative intensity of bands, although variable in DNA from different individuals, are highly reproducible in repeat assays of DNA from the same individual. Furthermore, a recombinant λ phage with a 15-kb human DNA insert that includes the 0307 sequence has the *Hpa*II sites necessary to produce the multiple bands we observe. (We have identified and purified a recombinant phage containing the 0307 sequence from a *Hae*III-*Alu*I human genomic DNA library[24]. Southern blots of the recombinant phage DNA, partially digested with *Msp*I and probed with 0307, show the same 4.6–13-kb bands seen in blots of genomic DNA digested with *Hpa*II.)

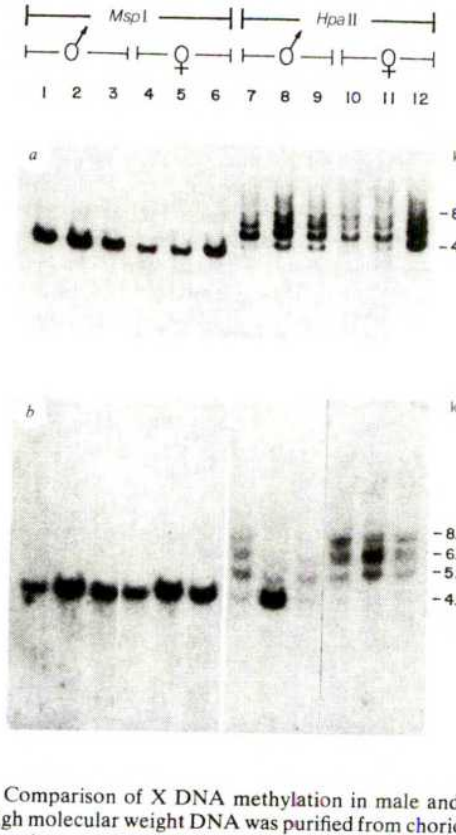

Fig. 2 Comparison of X DNA methylation in male and female cells. High molecular weight DNA was purified from chorionic villi of human placentas (*a*) and cultured human diploid fibroblasts (*b*). Southern blots[31] of enzyme-digested DNA, fractionated on 0.8% agarose gels, were hybridized with the X-specific DNA probe 0307. Digestions were carried out for 16 h with 24 U *Msp*I or *Hpa*II per μg of DNA in conditions recommended by the manufacturer. Filters washed at 65 °C in 0.1 SET were exposed to X-ray film (−70 °C, 5 days).

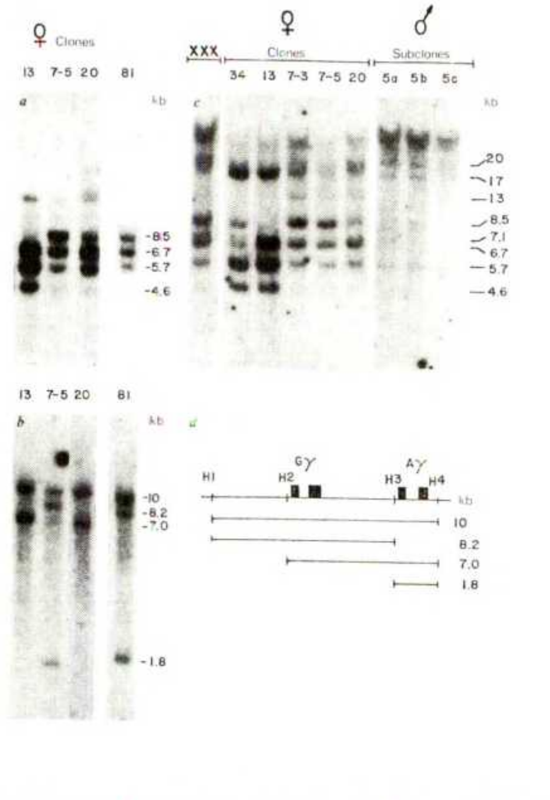

Fig. 3 DNA methylation in cloned human fibroblasts. *a*, DNA of fibroblast clones independently isolated from a culture of 46XX female cells (see text) was digested with *Hpa*II (20 U per μg DNA, 16 h). The filter was hybridized with ^{32}P-labelled 0307, washed at 55 °C in 0.1 SET and exposed to X-ray film (−70 °C, 5 days). *b*, Hybridized probe was removed from the filter used in *a* by washing (70 °C, 70% formamide, 0.1 SET). The filter was hybridized with ^{32}P-labelled γ-globin cDNA insert of plasmid JW151[33]. After a final wash (65 °C, 0.1 SET), the filter was exposed to X-ray film (−70 °C, 12 days). *c*, DNA from clones of female fibroblasts and subclones of male origin (son of the source of female clones) was digested with *Hpa*II (10 U per μg DNA for 16 h when a further 3 U enzyme per μg DNA was added and the incubation continued for 4 h). Electrophoresis was longer than in Figs 1 or 2*a* and DNA was transferred for 48 h to enhance the resolution and transfer of high molecular weight fragments. The filter was hybridized with the 0307 X DNA probe, washed (55 °C, 0.1 SET) and exposed to X-ray film (−70 °C, 5 days). Lane 1, DNA from 47XXX fibroblasts; lanes 2–4, 6, DNA from clones of the same female as in *a*; lane 5, DNA from the same clone as in lane 4, purified after five further population doublings; lanes 7–9, independent subclones derived from a single clone of male fibroblasts. *d*, *Hpa*II restriction site map of human γ-globin loci[11].

Because the 0307 sequence is single copy, yet hybridizes to multiple restriction fragments in *Hpa*II digests, the region around the 0307 sequence must be methylated differently from cell to cell. Similar studies with the second X-specific cloned DNA (0604) as probe indicate that the methylation of the single internal *Hpa*II site is also variable in both male and female fibroblasts (data not shown). The complexity of the banding pattern is not obviously related to the number of X chromosomes in the cell, as some cultures from females have as many bands as those found in trisomic cells with three X chromosomes (including two inactive ones) (Fig. 3*a*, lane 1).

Therefore, DNA methylation in the regions probed by both X-specific sequences is characterized by variability and we observe no consistent sex differences in placentas or fibroblasts.

DNA methylation in clonal populations of fibroblasts

The multiple bands we observed in chorionic villi and uncloned fibroblast cultures might be attributed to a mixed population of cells, each with a fixed but different methylation pattern. To test this hypothesis, we examined methylation in clonal populations derived from dermal fibroblasts of a female heterozygous for the X-linked marker glucose 6-phosphate dehydrogenase (G6PD) A. Clones were obtained by plating 10 cells per 60-mm dish and clonal cultures established by picking well isolated colonies, using cloning cylinders[25] to ensure that all cells in each clonal culture were progeny of a single cell. Furthermore, purity could be monitored on the basis that each clone, although of heterozygous genotype, expressed only a single G6PD isozyme, the one coded by the active X chromosome[4]. DNA was also purified from clonal populations of fibroblasts from a male, as well as derivative subclones to ensure that each colony was of homogeneous composition. The Southern blots of DNA from these clonal cultures generated by *Hpa*II digestion and hybridization with the 0307 probe show multiple bands (Fig. 3*a*, *c*) similar to those observed in uncloned cultures.

Hybridization to more than one restriction fragment in DNA from clonal populations of male cells or more than two in DNA from clones of female cells indicates that during the 20 generations required for these clonal populations to proliferate, the methylation of *Hpa*II sites in the DNA adjacent to the 0307 sequence was not fixed. Methylation in the vicinity of the γ-globin loci in the same clones is also heterogeneous, as at least two patterns were observed when the same filters were hybridized with a γ-globin cDNA probe (Fig. 3*b*).

Although the methylation of *Hpa*II sites in X DNA differs among progeny of single cells, the relative intensities of the various *Hpa*II bands generated indicate that the changes are not random. No clone produced all possible bands (compare uncloned fibroblasts in Fig. 3*c*, lane 1, with others). Moreover, the banding pattern (relative intensity and size of restriction fragments) for each clone is characteristic of that clone and is relatively stable. For example, the pattern of multiple bands produced by clone 7 remained the same after six further cell doublings (Fig. 3*c*, lanes 4, 5).

Methylation of human X chromosomes in male subclones

The difference in the banding patterns between various clones of female fibroblasts more probably reflects the unique origin of each clone. We know that clones 13 and 20 originated from different skin fibroblasts of this female because each expresses a different G6PD allele, and the other clones, as they were derived from a heterogeneous uncloned culture, may also have a unique origin.

On the other hand, subclones obtained from the homogeneous cloned population in the male are all progeny of the same cell. Therefore, our observation that three of these subclones have restriction fragments of identical size and relative intensity (Fig. 3*c*, lanes 7–9) indicates that the pattern as a whole is conserved over at least 20 population doublings. It seems that methylation of individual *Hpa*II sites is not stably inherited, but the probability that a site will be methylated is heritable.

Methylation of human X chromosomes in mouse–human hybrid cells

Although the methylation at *Hpa*II sites around the 0307 sequence is not fixed in cultured human diploid fibroblasts, methylation at these sites is more stable when the human X chromosome is present in a mouse–human hybrid cell. Figure 4 shows the Southern blot analysis of DNA from four independently derived hybrid clones (each with a different active human X) digested with *Hpa*II and probed with 0307.

The hybrid clones produced bands of the same size as those in DNA from normal human male cells, so that the sites of methylation are the same for active X DNA in either cell. However, the striking predominance of one band in each hybrid clone is evidence for greater stability of methylation of the human X in the foreign environment of the mouse–human hybrid, than in its normal habitat.

It is notable that none of the four mouse–human hybrid cells generated bands >6.7 kb. While the absence of longer bands could be mearly fortuitous, it may be that the human X chromosome in hybrid cells is in fact less methylated than in human cells.

Relationship of methylation to X-chromosome activity

One might expect that the banding pattern would be identical for clones of cells derived from the same culture, each with the same active X chromosome. However, clones 7, 13 and 34 from cultures of a heterozygous female have the same active X (maternal X), as they express the G6PD A allele, but have different banding patterns; patterns also differ for clones 81 and 20, which express the G6PD B allele (paternal X is active; Fig. 3*a*, *c*).

The presence of both active and inactive X chromosomes in these female cells may obscure specific banding patterns associated with the functional state of the chromosome. It is clear, however, that female cells do not have large *Hpa*II X DNA fragments that are not present in males. In fact, the single active X chromosome in male fibroblasts can be highly methylated in the 0307 region, as indicated by the presence of very large fragments in *Hpa*II-digested DNA from some male cells (Fig. 3*c*, lanes 7–9). However, the same sites in X chromosomes of other male cells are not methylated (Figs 2, 3*c*, lanes 7–9). The predominant band from the single active human X in various mouse–human hybrid cells can also differ in size, but tends to be of lower molecular weight, compatible with less methylation of these active X chromosomes (Fig. 4). Thus, no consistent methylation differences can be seen with respect to X-chromosome activity.

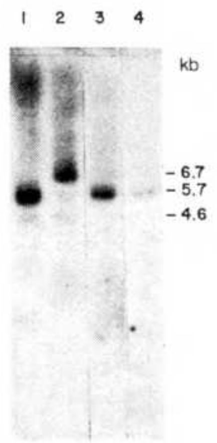

Fig. 4 Methylation in the single active human X chromosome of mouse–human hybrid cells. Purified DNA was digested with *Hpa*II (20 U per μg, 16 h). Hybridization was with labelled 0307 X DNA probe. Final wash: 55 °C, 0.1 SET; exposure: −70 °C, 5 days. Lanes 1, Sv-tfm × Kop (clone 4a)[22]; 2, Sv-tfm × 297 (clone 1)[22]; 3, A9 × Gm 1322 (clone 9-1b)[19]; 4, A9 × clone 81 (clone 6a).

Table 1 Effect of 5-azacytidine on X chromosomal phenotype

Expt	Cells per dish ($\times 10^4$)	5-azaC (μM)	Exposure (h)	Recovery (days)	Cells analysed ($\times 10^5$)	HPRT phenotype HAT^r colonies	HPRT phenotype Labelled cells	G6PD phenotype
1	20	3	24	5–6	20.0		0	
	20–40	3–10	24–48	1–14	120.0			A
2	0.4–2.0	2–5	68	0	1.1	0		
	14	5	68	6	20.0	0		
3	0.2–0.5	2–3	24	1–4	3.2	0		
4	4	2	48	0	20.0	1		A
	40	2	48	4	20.0	0		
	40	2	48	6	40.0		0	
	40	2	48	12–14	100.0			A

Effect of 5-azacytidine on X-chromosome activity and methylation

Studies were carried out to determine if 5-azaC could derepress the inactive X chromosome in normal human skin fibroblasts. The two X chromosomes in female cells used for this study differ with respect to alleles at two loci, being heterozygous for G6PD A as well as for hypoxanthine phosphoribosyl transferase (HPRT) deficiency (G6PD A/B; HPRT −/+). For these experiments we treated clonal populations of cells that expressed G6PD A and HPRT deficiency (the alleles coupled on the active X). The phenotypic changes expected if 5-azaC were effective in derepressing the X were the re-expression of G6PD B and the wild-type HPRT alleles on the inactive X chromosome.

Four experiments were carried out, essentially similar but differing in the conditions of exposure to 5-azaC (see Table 1). Cells were plated at densities of 2×10^3–2×10^5 cells per dish in normal growth medium (minimal essential medium + 15% fetal calf serum, Gibco), and treated 24 h later with a fresh solution of 1–10 μM 5-azaC for 24–72 h. Cells were analysed for evidence of reactivation of the inactive X by: (1) hypoxanthine/aminopterin/thymidine (HAT) selection for cells that had acquired HPRT activity, (2) autoradiography of cells exposed to ^{3}H-hypoxanthine, or (3) G6PD electrophoresis to detect cells expressing the G6PD B allele on the inactive X.

More than 1.7×10^7 cells were treated with 5-azaC; of the 6.4×10^6 cells selected in HAT medium, we observed only one subclone that had undergone a phenotypic change. That colony (HAT^r-5-azaC-1) was able to proliferate in HAT medium, having acquired HPRT activity, but it expressed only G6PD A. Studies of mouse–human hybrids derived from this clone suggest that the change is at the HPRT locus on the active X chromosome (Fig. 5).

Although the lack of HAT^r subclones might be related to poor proliferation of cells in which derepression had occurred at the HPRT locus, the cloning efficiency for treated cells (Table 2) was sufficient to reveal reactivants if they occurred with 10^{-3} frequencies reported for mouse cells[18].

To circumvent the problem of cell proliferation, a further 6×10^6 cells were examined by autoradiography. Cells in nonselective medium were exposed to ^{3}H-hypoxanthine (NEN, 3.6-10C/M, 10 μCi ml^{-1} for 18 h); the dishes were then washed, fixed and treated with 5% trichloroacetic acid. In some cases, the cells were replated following recovery so that cell density in autoradiographs did not exceed 10^6 cells per dish. The dishes were emulsed in Kodak NTB-2, developed 1 week later, and screened microscopically for the presence of labelled cells. The assay is sensitive enough to detect individual cells that have acquired HPRT activity and only 10% normal activity is necessary for a cell to be labelled in the conditions used; however, no labelled cells were observed.

Finally, more than 20 cultures of cells totalling 3.6×10^7 cells were examined for G6PD phenotype on cellulose acetate[25] in conditions sensitive enough to detect an admixture of enzyme where the minor component is as little as 5%. However, the G6PD B allele on the inactive X was never observed.

The experimental conditions that were used induced a decrease in cloning efficiency (Table 2) similar to that reported for phenotypically altered mouse cells[26,27]. Furthermore, we observed changes in methylation at CCGG sites with both X DNA and γ-globin probes (Fig. 6); namely, a relatively greater intensity of small *Hpa*II bands with 0307 probe and the appearance of a 5.2-kb band with γ-globin probe (see Fig. 3*d*). This hypomethylation, although more subtle than that reported from more indirect observations in mouse cells[27], is compatible with changes seen in retroviral sequences from transformed chicken cells[16]. We observed an effect of treatment only in DNA from cells treated with 2 μM 5-azaC 7 days previously; none was apparent directly after treatment (Fig. 6) or with 5–10 μM 5-azaC at any time (data not shown).

Therefore, despite the use of conditions able to induce methylation changes and toxicity, we have obtained no compelling evidence that 5-azaC can derepress HPRT or G6PD loci on the inactive X chromosome in normal human cells carrying suitable markers.

Implications

The rationale for implicating DNA methylation as a mechanism for regulating gene activity is based on the presumption that, as in bacterial systems, the methylation pattern of specific DNA sequences is stably transmitted from progenitor to progeny. Our studies of clonal populations of normal diploid fibroblasts demonstrate that, in fact, methylation of the *Hpa*II sites we examined is not stably transmitted in newly replicated X DNA. There is other evidence that methylation may not be stably inherited. Methylation of the chicken thymidine kinase gene changes during propagation of the recipient mouse cells[14]. In addition, 5-azaC-induced expression of the metallothionein I gene in mouse thymoma cells, attributed to undermethylation, is unstable within five cell generations[17]. In these cases, the instability might be attributed to the foreign environment, experimental manipulation or heteroploidy. However, our results indicate that methylation is unstable in entirely normal euploid cells.

Our observations are limited to an examination of *Hpa*II sites around the two X-chromosome DNA probes that have not been characterized with regard to translation. However, we have

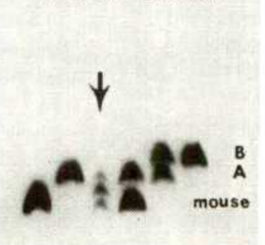

Fig. 5 G6PD electrophoresis of mouse–human hybrid showing G6PD A and heterodimer (arrow). The 5-azaC-induced HAT^r clone was hybridized to A9 mouse cell and hybrids selected in HAT[25]. Because the HPRT activity in clone HAT^r 5-azaC-1 was significantly less than that of a wild-type allele (10–20% of control), hybrids proliferated poorly and only one was able to produce sufficient cells for analysis. This hybrid clone expressed human G6PD A, mouse G6PD and the heterodimer, so that the chromosome contributing HPRT activity was that with the G6PD A allele and therefore the active X. Lanes: 1, A9; 2, HAT^r 5-azaC-1; 3, hybrid; 4, mixture of parental cells; 5, mixture of G6PD B and G6PD A fibroblasts; 6, G6PD B control.

explored a significant portion of the human X chromosome. Based on the total number of *Hpa*II fragments and the size of the largest band (see Fig. 3*c*), we estimate that with probe 0307 we have examined the methylation of at least eight *Hpa*II sites in a segment of ~20 kb in the middle of the long arm of the X. With probe 0604, we have examined another site within a 7.5-kb sequence at Xq13–25. Evidence from DNA transfer experiments and observations of local derepression at X loci suggest that modifications of DNA associated with inactivity are likely to be numerous and occur over relatively small regions of the chromosome[7,28].

Because there are no large 0307-specific *Hpa*II fragments unique to female cells, we can exclude the possibility that ubiquitous methylation accounts for inactivity of the silent X. The failure of hypomethylation, induced by 5-azaC, to reactivate alleles on the inactive X chromosome provides further evidence that X-chromosome inactivity in normal human cells is not influenced by the state of methylation at all sites along the chromosome. It is conceivable that phenotypic changes observed in transformed mouse and chick cells treated with 5-azaC[16–18,26,27,29] are not attributable to direct effects on DNA methylation. The HAT^r clone we obtained probably reflects reversion at the HPRT locus on the active X and other evidence that 5-azaC can induce mutation has been reported[29].

On the other hand, our observations do not preclude a relationship between X-chromosome methylation and transcriptional activity. The instability of methylation at individual *Hpa*II sites and the different methylation patterns observed for the active X chromosome in male cells indicate that many arrays of methylation along the X chromosome are compatible with X-chromosome activity (some highly methylated). Similarly, many methylation patterns may be compatible with X-chromosome inactivity. It is clear that several patterns of methylation at *Hpa*II sites surrounding γ-globin sequences are associated with inactivity at these loci in clonal populations of fibroblasts (Fig. 3*b*, *d*).

Table 2 Effect of 5-azaC on proliferation of fibroblast clones (expt 4, Table 1)

5-azaC (μM)	Length of exposure (h)	Clones per cells plated	Cloning efficiency	Relative cloning efficiency (%)
0		60/150	0.40	100
2	24	34/150	0.23	57.5
	48	41/150	0.27	67.6
5	24	14/150	0.09	22.5

The variety and instability of X DNA methylation patterns observed in normal human cells may explain our inability to reactivate loci on the inactive X chromosome with 5-azaC. Because 5-azaC did not induce extensive demethylation and because methylation of *Hpa*II sites seems to occur spontaneously in these cells, we may not have achieved sufficient demethylation at critical sites for X-chromosome reactivation. It is significant that the human X chromosome in the foreign environment of the mouse–human hybrid cell is probably less methylated than in normal human cells, and that the pattern is more stably transmitted. Therefore, it is not surprising that all 5-azaC-induced reactivation events have occurred in transformed mouse and chick cells[16–18,26,27], where the demethylation would be more extensive and more stable.

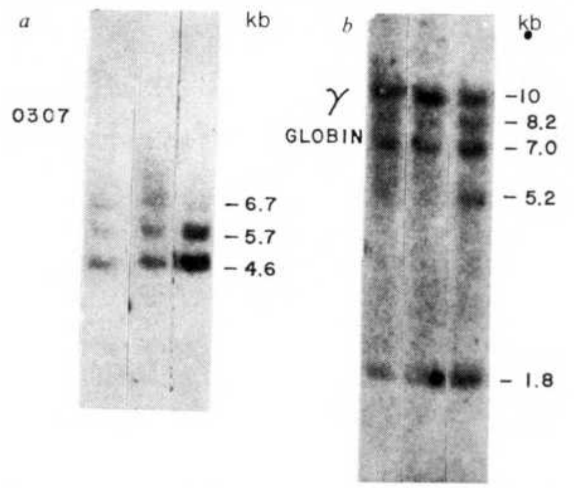

Fig. 6 Methylation of *Hpa*II restriction sites in human diploid fibroblasts treated with 5-azaC. Lanes: 1, untreated; 2, 2 μM, 48 h; 3, 2 μM, 48 h, recovery 7 days. *a*, DNA was digested with *Hpa*II (20 U per μg DNA, 16 h) and Southern blots were hybridized to the labelled 0307 probe. Final wash: 55 °C, 0.1 SET; exposure: −70 °C, 4 days. *b*, after autoradiography, the X probe was removed and the filters rehybridized with a γ-globin cDNA probe as described in Fig. 3*b* legend. Exposure: −70 °C, 7 days.

Even if methylation is involved in maintaining X-chromosome inactivity, it may be only one of several components influencing transcriptional activity. For example, the accessibility of DNA to methylases and the subsequent methylation at particular sites may depend on chromatin structure. The identical *Hpa*II-generated banding pattern seen in male subclones suggests a stable higher order determinant of DNA methylation. Similarly, the more stable methylation pattern for the human X in interspecies hybrid cells may reflect changes in the chromatin structure attributable to a foreign environment or associated with transformation (for example, acquisition of immortality, heteroploidy). Chromatin differences of this kind might explain the extensive variability in amount and distribution of 5-methylcytosine between species[5]. Further evidence for more than one level of regulation underlying X-chromosome activity are recent observations that alleles on the inactive X in normal human cells, when derepressed, produce less enzyme than those on the active X[32]. The precise relationship between X inactivation and DNA methylation remains unknown.

We thank Joyce Axelman for assistance with the azacytidine studies and Joseph B. Wiley for assistance with purification and identification of recombinant phage. This work was supported by NIH grant HD 05465.

Received 16 September; accepted 17 December 1981.

1. Holliday, R. & Pugh, J. E. *Science* **187**, 227–232 (1975).
2. Sager, R. & Kitchin, R. *Science* **184**, 426–433 (1978).
3. Riggs, A. D. *Cytogenet Cell Genet.* **14**, 9–25 (1975).
4. Lyon, Mary F. *Biol. Rev.* **47**, 1–35 (1972).
5. Ehrlich, M. & Wang, R. Y-H. *Science* **212**, 1350–1357 (1981).
6. Razin, A. & Riggs, A. D. *Science* **210**, 604–610 (1980).
7. Liskay, R. M. & Evans, R. J. *Proc. natn. Acad. Sci. U.S.A.* **77**, 4895–4898 (1980).
8. Comings, D. C. *Expl Cell Res.* **74**, 383–390 (1972).
9. McGhee, J. D. & Ginder, G. D. *Nature* **280**, 419–420 (1979).
10. Mandel, J. L. & Chambon, P. *Nucleic Acids Res.* **7**, 2081–2103 (1979).
11. van der Ploeg, L. H. T. & Flavell, R. A. *Cell* **19**, 947–958 (1980).
12. Shen, C. K. J. & Maniatis, T. *Proc. natn. Acad. Sci. U.S.A.* **77**, 6634–6638 (1980).
13. Pollock, Y., Stein, R., Ragin, A. & Cedar, H. *Proc. natn. Acad. Sci. U.S.A.* **77**, 6463–6467 (1980).
14. Wigler, M., Levy, D. & Perucho, M. *Cell* **24**, 33–40 (1981).
15. Singer, J., Roberts-Ems, J., Luthardt, F. W. & Riggs, A. D. *Nucleic Acids Res.* **7**, 2369–2385 (1979).
16. Groudine, M., Eisenman, R. & Weintraub, H. *Nature* **292**, 311–317 (1981).
17. Compere, S. J. & Palmiter, R. D. *Cell* **25**, 233–240 (1981).
18. Mohandas, T., Sparkes, R. S. & Shapiro, L. J. *Science* **211**, 393–396 (1980).
19. Wolf, S. F., Mareni, C. E. & Migeon, B. R. *Cell* **21**, 95–102 (1980).
20. Waalwijk, C. & Flavell, R. A. *Nucleic Acids Res.* **12**, 4631–4641 (1978).
21. Scott, A. F., Phillips, J. A. & Migeon, B. R. *Proc. natn. Acad. Sci. U.S.A.* **76**, 4563–4565 (1979).
22. Migeon, B. R., Brown, T., Axelman, J. & Migeon, C. J. *Proc. natn. Acad. Sci. U.S.A.* **78**, 6339–6343 (1981).
23. Benton, D. W. & Davis, R. W. *Science* **196**, 1980–1982 (1977).
24. Lawn, R. M. *et al. Cell* **15**, 1157–1174 (1978).
25. Migeon, B. R., Sprenkle, J. A. & Do, T. T. *Cell* **18**, 637–641 (1979).
26. Taylor, S. M. & Jones, P. A. *Cell* **17**, 771–779 (1979).
27. Jones, P. A. & Taylor, S. M. *Cell* **20**, 85–93 (1980).
28. Kahan, B. & DeMars, R. *Proc. natn. Acad. Sci. U.S.A.* **72**, 1510–1514 (1975).
29. Clough, W. D. & Davidson, R. L. *Science* (in the press).
30. Wolf, S. F. & Schlessinger, D. *Biochemistry* **16**, 2783–2791 (1977).
31. Southern, E. M. *J. molec. Biol.* **98**, 503–517 (1975).
32. Migeon, B. R., Wolf, S. F., Mareni, C. E. & Axelman, J. (in preparation).
33. Wilson, J. T. *et al. Nucleic Acids Res.* **5**, 563–581 (1978).

Vitamin A and pattern formation in the regenerating limb

M. Maden

Division of Developmental Biology, National Institute for Medical Research, Mill Hill, London NW7 1AA, UK

Vitamin A and its derivatives, the retinoids, cause specific alterations in the proximo-distal pattern of regenerating axolotl limbs. In some cases complete limbs grow from carpal level amputations. If retinoids are responsible for changing the positional information of limb cells, these compounds may represent valuable probes for investigating the molecular basis of pattern formation.

VARIOUS experimental approaches have been used to study pattern formation. The original approach, begun in the last century, is to alter the spatial relationships of the system under study by transplanting tissue to different sites and observing the resultant disruption of the pattern. In the limb, the system studied here, this approach has revealed organizing regions such as the zone of polarizing activity[1,2], the polarizing zone[3] and the apical ectodermal ridge[1,4], and the beginnings of a theoretical framework into which the phenomena can be fitted[5]. An alternative approach is to search for substances which alter pattern formation in specific ways, for example, the effect of lithium on early development[6]. Unfortunately, in this case subsequent investigations did not prove particularly valuable in advancing our understanding of the molecular basis of pattern formation. Here I report that vitamin A and its derivatives, the retinoids, alter pattern formation specifically in the proximo-distal axis of regenerating axolotl limbs. If these effects are due to changes in the positional information of limb cells caused by retinoids, these compounds may be used in future research to elucidate the molecular nature of positional information.

Niazi and Saxena[7] studied the effects of retinol palmitate on hindlimb bud regeneration of *Bufo* tadpoles. In addition to its inhibitory properties, they found several cases of duplicated or triplicated regenerates, some of which consisted of more than those distal parts of the limb removed by amputation. These results seemed not only to contradict the rule of distal transformation[8], but also were unique in increasing the potency of blastemal cells as all other substances which have been administered to regenerating limbs have caused deficiencies[9,10]. Thus I decided to investigate further this phenomenon in the regenerating limbs of larval axolotls, *Ambystoma mexicanum*, an animal commonly used for regeneration studies.

Effect of vitamin A

To confirm the existence of the effect described by Niazi and Saxena, I amputated the forelimbs of 14 animals through the mid-radius and ulna. The animals were immediately placed in a solution of retinol palmitate (15 IU ml^{-1}, made up in tap water) for 12 days and then transferred to normal water. An equal number of control animals were allowed to regenerate in pure tap water. After 1 month the limbs were fixed and stained. In contrast to the high mortality caused by hypervitaminosis A in *Bufo* tadpoles[7] (and confirmed by my own results on *Rana* tadpoles), axolotls seemed immune. All experimental animals survived and seemed even healthier than normal.

In control limbs, all the elements removed by amputation were regenerated (Fig. 1*a*), whereas after retinol palmitate treatment, every limb (28 in all) was abnormal in the proximo-distal sequence of regenerated elements. The severity of the effect varied and could be separated into four classes (Table 1). The least severely affected were those limbs in which there was an extra row of carpals (Fig. 1*b*). In the next group an additional length of radius and ulna had been intercalated, which fused with the stump radius and ulna resulting in an abnormally long segment (Fig. 1*c*). The third class comprised limbs in which a complete additional radius and ulna had been intercalated, resulting in a tandem repeat of that segment (Fig. 1*d*). The most severe effect was the additional presence of the distal part of the humerus (Fig. 1*e*). Most of the abnormalities observed (46%; Table 1, top row) consisted of extra carpals, the least severe effect.

In all other aspects, however, these experimental regenerates were normal: the digits were in the normal sequence with the

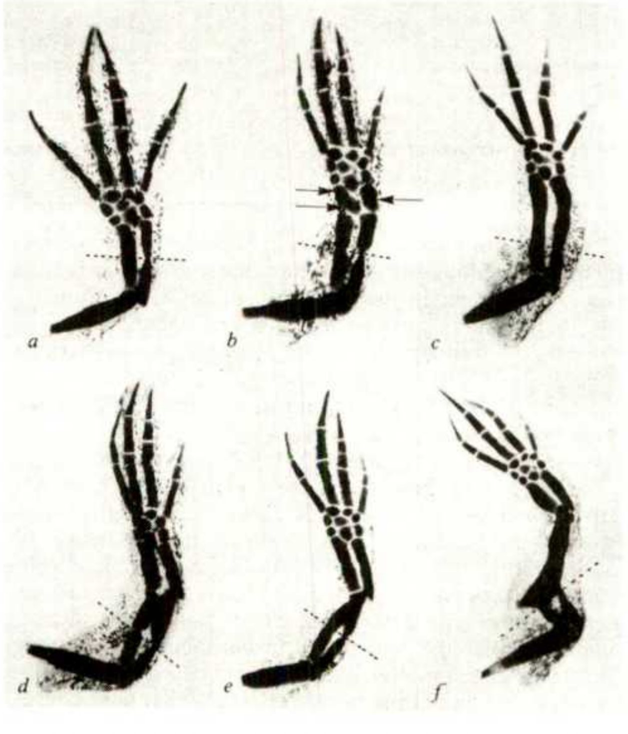

Fig. 1 Cleared whole mounts of regenerated limbs stained with Victoria blue. All limbs were amputated through the mid-radius and ulna, the broken line marking the amputation plane. *a*, Control. The elements removed by amputation (distal radius and ulna, 8 carpals and 4 digits) have been replaced. *b–e*, Limbs treated with 15 IU ml^{-1} retinol palmitate for 12 days. *b*, Three extra cartilages (arrows) have been produced which resemble carpals. *c*, An abnormal length of radius and ulna has been regenerated making this segment grossly out of proportion. *d*, A complete extra radius and ulna has been produced in tandem. *e*, The radius and ulna have fused into the distal end of the humerus with a perfect elbow joint followed by a complete radius and ulna and hand. *f*, A limb regenerated after 15 days in 75 IU ml^{-1} retinol palmitate; here a complete limb has been produced distal to the amputation plane. Magnifications: *a*, ×9; *b*, ×8; *c*, ×7.6; *d*, ×7.6; *e*, ×7; *f*, ×6.

0028–0836/82/080672—04$01.00

Table 1 Effects of varying concentrations and lengths of exposure to vitamin A (retinol palmitate) after forelimb amputation through the mid-radius and ulna

Length of exposure (days)	Concentration of vitamin A (IU ml^{-1})	No. of cases	Type of regenerate: Normal (Fig. 1*a*)	Extra carpals (Fig. 1*b*)	Extra part radius and ulna (Fig. 1*c*)	Extra full radius and ulna (Fig. 1*d*)	Extra part humerus (Fig. 1*e*)	Extra full humerus (Fig. 1*f*)
12	15	28	0	13(46%)	7(25%)	5(18%)	3(11%)	0
10	30	10	0	0	7(70%)	3(30%)	0	0
15	30	8	0	0	1(13%)	2(25%)	6(62%)	0
10	75	10	0	0	0	5(50%)	5(50%)	0
15	75	8	0	0	0	0	1(13%)	7(87%)

Length of exposure is from the day of amputation. The types of regenerate are exemplified in Figs 1, 2 and described in more detail in the text.

correct phalangeal number, there were no alterations in the anteroposterior axis (compare Fig. 1*a* and *b–e*) nor any duplications or triplications as found in *Bufo* tadpoles[7], and serial sections of four limbs revealed normal muscle patterns in the extra segments. Thus only the proximo-distal sequence of elements seemed to be affected in that varying lengths of extra pattern were intercalated between the amputation plane and the appropriate distal level.

Effect of increasing concentration and length of exposure

Four groups of five animals each had their forelimbs amputated as before, and were placed in 2× concentration (30 IU ml^{-1}) or 5× concentration (75 IU ml^{-1}) of retinol palmitate for 10 or 15 days. Neither concentration caused increased mortality and the effects of these treatments on pattern formation are shown in Table 1. Increasing the concentration caused a greater amount of pattern to be intercalated between the amputation plane and the appropriate distal level (compare rows 1, 2 and 4) such that after 10 days in 75 IU ml^{-1}, half the limbs had tandem repeats of the radius and ulna as well as the distal humerus. Similarly, increasing the time of exposure caused more pattern to be intercalated so that after 15 days in 75 IU ml^{-1}, a new class of abnormality appeared (Table 1, bottom row)—a complete limb regrew from the amputation plane, resulting in a proximo-distal sequence of elements of humerus, proximal radius and ulna (stump), full humerus, radius and ulna, carpals and digits (Fig. 1*f*).

Thus by increasing the concentration of retinol palmitate and the length of exposure, the level at which the limb was repeated became more and more proximal, finally resulting in a complete limb being regenerated from the distal amputation plane.

Morphological observations

While observing the animals during these experiments it became apparent that retinol palmitate was inhibiting the rate of regeneration. Normal regeneration in control animals progressed rapidly—cone stage on day 10, notch stage by day 12 and by day 18 four digits were present in outline. In the presence of retinol palmitate a progressive retardation of regeneration with increasing concentration was revealed and in 75 IU ml^{-1}, there were no external signs of regeneration. Immediately after removal to pure water, blastema formation commenced, consistent with the known inhibitory effects of retinoids on cell division. However, during the period in which there was no blastema development, preparations for the dramatic changes in pattern formation must, nevertheless, have been occurring.

Other amputation levels

The above experiments were repeated in animals whose forelimbs had been amputated either through the mid-humerus or through the carpals.

Amputation through the humerus (56 cases in all) gave the same results as those described above, that is, increasing the concentration of and length of exposure to retinol palmitate caused the level at which the limb was repeated to become more proximal. For example, after 12 days at the lowest concentration (15 IU ml^{-1}) the regenerates had abnormally long humeri, whereas after 15 days in 30 or 75 IU ml^{-1}, 67% and 87% respectively of the cases regenerated a complete new limb from the amputation plane (Fig. 2*a*).

After amputation through the carpals (46 cases in all), many regenerates had digital deficiencies such as missing or fused digits at the lower concentrations. This was the only series of experiments in which these abnormalities occurred consistently. At 15 and 30 IU ml^{-1} the only other effect on regeneration was the production of an extra row of carpals (for example, see Fig. 1*b*). However, at 75 IU ml^{-1}, six out of eight limbs regenerated complete limbs from the carpals (Fig. 2*b*). Furthermore, in two of these cases the most proximal element regenerated was not just the proximal epiphysis of the humerus, but also the glenoid cavity and part of the scapula (Fig. 2*c*).

By comparing the regenerates obtained from these three amputation levels of the forelimb, one further conclusion was drawn. The concentration of retinol palmitate needed to induce the regeneration of a complete limb decreased as the amputation plane became more proximal, that is, only the longest time at the highest concentration (75 IU ml^{-1}) led to regeneration of complete limbs from the carpal level, whereas 30 IU ml^{-1} produced the same result from amputations at the humerus level.

Effect on hindlimbs

The whole range of experiments was repeated on a total of 133 hindlimbs. At high concentrations of retinol palmitate, complete limbs were regenerated from amputations through the mid-femur or mid-tibia and fibula (Fig. 3*a*) and with lower concentrations and shorter exposure times the extent of serial repetition decreased. In the cases where whole limbs regenerated, not only was there a complete femur, but also a

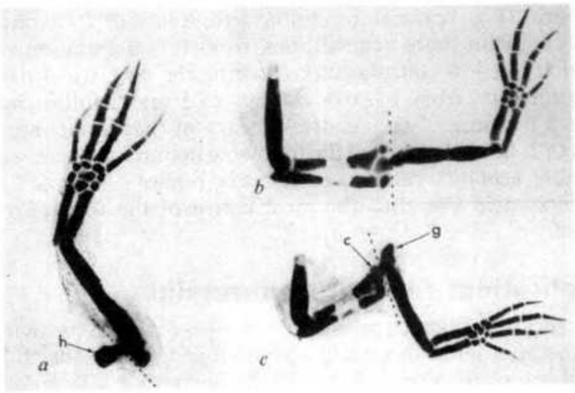

Fig. 2 Forelimbs placed in retinol palmitate (75 IU ml^{-1}) for 15 days. Broken lines mark the amputation planes. *a*, Proximal to the amputation plane is the remaining small part of the original humerus (h). Distally a complete limb has regenerated. *b*, Amputation through the carpals. Three carpals remain in the stump (radiale, intermedium and ulnare) and distally a complete limb has regenerated. *c*, Same as *b* but in this case part of the pectoral girdle (g) including the glenoid cavity has also been produced. Magnifications: *a*, ×6; *b*, ×5; *c*, ×5.

Table 2 Effects of 15-day exposure to various retinoids after amputation through the mid-radius and ulna or tibia and fibula

			Type of regenerate						
Compound		No. of cases	Normal	Extra carpals	Extra part radius and ulna	Extra full radius and ulna	Extra part humerus	Extra full humerus	Relative effectiveness
Retinol palmitate	(0.6 mM)	20	3(15%)	0	3(15%)	8(40%)	6(30%)	0	54
Retinol acetate	(0.6 mM)	13	0	0	12(92%)	0	1(8%)	0	43
Retinol palmitate	(0.12 mM)	20	15(75%)	0	5(25%)	0	0	0	10
Retinol acetate	(0.12 mM)	20	18(90%)	0	2(10%)	0	0	0	4
Retinol	(0.12 mM)	16	0	0	4(25%)	3(19%)	8(50%)	1(6%)	68
Retinoic acid	(0.12 mM)	15	0	0	0	3(20%)	9(60%)	3(20%)	80

Same classes of abnormalities as in Table 1. All compounds were obtained from Sigma. Retinol palmitate, retinol acetate and retinoic acid were dissolved in water, retinol in dimethyl sulphoxide.

socket, acetabulum and what appeared to be a small part of the pelvic girdle (Fig. 3*a*, *b*). Complete limbs were not regenerated from tarsal level amputations even at 75 IU ml^{-1} as in the case of forelimbs. Subsequent experiments revealed that a concentration of 150 IU ml^{-1} was needed for this to occur (Fig. 3*b*). This confirmed a trend which was apparent from a comparison of fore- and hindlimb experiments, that any one concentration and time had a greater effect (that is, caused regeneration to commence from a more proximal level) in the forelimb than in the hindlimb.

Effectiveness of other retinoids

I tested retinol palmitate, retinol acetate, retinol and retinoic acid to determine their comparative efficacy in inducing pattern abnormalities. Two concentrations were used: 0.6 mM (equivalent to 75 IU ml^{-1} retinol palmitate) and 0.12 mM (equivalent to 15 IU ml^{-1} retinol palmitate). Five animals whose fore- and hindlimbs had been amputated through the radius and ulna or tibia and fibula were immersed in each of the test solutions for 15 days (a total of 160 limbs). At the highest concentration, all the animals kept in retinol died, as did three out of five in retinoic acid with the remaining two not regenerating. One animal in retinol acetate died. Thus only retinol palmitate and retinol acetate could be compared in this experiment (Table 2). In 0.6 mM retinol palmitate, as before there was a spread of abnormalities, with most producing an extra radius and ulna in tandem (Fig. 1*d*) or an extra humerus also (Fig. 1*e*). The effects of retinol acetate were less severe, most consisting of an abnormally long radius and ulna (Fig. 1*c*).

At the lower concentration (0.12 mM; Table 2, rows 3–6), retinol palmitate had only minor effects; most of the regenerates were normal and the remainder had an abnormally long radius and ulna. Again retinol acetate was less effective. However, in 0.12 mM retinol the majority of limbs had an extra part humerus (Fig. 1*e*), and in retinoic acid, a further 20% of cases had complete limbs regenerating from the amputation plane even at this low concentration. Scoring the severity of pattern abnormalities from 1 (extra carpals) to 5 (extra full humerus) gave a measure of the relative efficacy of these four retinoids (Table 2, last column) and the following heirarchy was revealed: retinol acetate < retinol palmitate < retinol < retinoic acid. Retinoic acid was thus the most active of the four retinoids tested.

Implications for pattern formation

The most obvious conclusion from these results is that the regenerated limbs described above all contravene the 'rule of distal transformation'[8]. It has been shown that cells from any one level can only generate more distal limb levels during intercalary regeneration[11,12] or regeneration from a reversed stump[13,14] nor can they be forced to transform proximally in normal conditions[12]. However, it is now clear that if conditions are changed by the addition of retinoids this rule no longer applies.

As the profound changes brought about by retinoids occur while blastemal development and presumably cell division is inhibited, it follows that changes in pattern do not necessarily require cell division. They can be totally independent of growth, although subsequent proliferation is needed to manifest any alterations that have occurred. Thus pattern formation and growth control may be specified by different mechanisms. I have argued elsewhere[15] that limb regeneration consists of two phases, an early morphallactic phase during which positional values are reassigned without cell division, followed by a period of growth when the remaining discrepancies are evened out. This scheme agrees in all respects with the results reported here.

One possible explanation of the results is that the time delay itself is responsible for the extra pattern generated. However, a similar retardation occurs after amputated limbs have been denervated, a procedure which removes the source of neurotrophic factor and inhibits cell division[16], but in contrast to retinoid treatment, when nerves are allowed to regrow into such limbs, only those elements that were removed by amputation are regenerated[17]. Therefore time delays *per se* do not cause changes in pattern.

Possible mode of action of retinoids

Research into the cellular effects of retinoids has mainly involved mammalian tissues and even within this constraint many contradictory results have been reported. Thus extrapolation to amphibian tissues is of limited value, but perhaps two effects are noteworthy. One is the blocking of cell communication by gap junctions[18] (although an increase in gap junction formation has also been noted[19]). Cellular communication must surely have a vital role in the normal process of

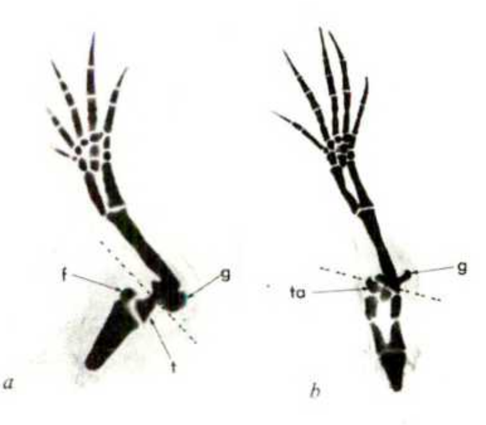

Fig. 3 Hindlimbs regenerated after vitamin A treatment. Broken lines mark the amputation planes. *a*, Retinol palmitate (75 IU ml^{-1}) for 15 days. The remaining parts of the tibia (t) and fibula (f) can be seen and not only has a whole limb been produced distally but also part of the pelvic girdle, the acetabulum (g). *b*, Amputation through the tarsals and retinol palmitate (150 IU ml^{-1}) for 15 days. The remaining tarsals (ta) can be seen and a complete new hindlimb including part of the girdle (g) has regenerated distally. Magnifications: *a*, ×6; *b*, ×6.

regeneration and any interference could cause pattern abnormalities. The other concerns speculations on the role of the cell surface in pattern formation. It has been suggested that positional information is encoded in the lengths of sugar chains on surface glycoproteins[20] and retinol does indeed act as a sugar donor in glycosyl transfer reactions[21]. In the nearest experimental system to that described here, that is, chick or mouse limb bud mesenchyme, retinoids cause specific alterations in cell-surface glycoproteins[22,23]. These speculations must await further research, but hopefully we now have a probe for investigating the molecular nature of positional information during pattern formation, at least in the limb.

I thank Katriye Mustafa for technical assistance in all aspects of this work.

Received 12 October 1981; accepted 18 January 1982.

1. Saunders, J. W. & Gasseling, M. T. in *Epithelial–Mesenchymal Interactions* (eds Fleischmajer, R. & Billingham, R. E.) 78–97 (Williams & Wilkins, Baltimore, 1968).
2. Tickle, C., Summerbell, D. & Wolpert, L. *Nature* **254,** 199–202 (1975).
3. Slack, J. M. W. *Nature* **261,** 44–46 (1976).
4. Stocum, D. L. *Differentiation* **3,** 167–182 (1975).
5. Wolpert, L. *J. theor. Biol.* **25,** 1–47 (1969).
6. Lallier, R. *Adv. Morph.* **3,** 147–196 (1964).
7. Niazi, I. A. & Saxena, S. *Folio biol., Kraków* **26,** 1–8 (1978).
8. Rose, S. M. in *Regeneration* 20th Growth Symp. (ed. Rudnick, D.) 153–176 (Ronald, New York, 1962).
9. Dearlove, G. E., Lopez, S. & Dresden, M. H. *J. exp. Zool.* **194,** 413–428 (1975).
10. Bazzoli, A. S., Manson, J., Scott, W. J. & Wilson, J. G. *J. Embryol. exp. Morph.* **41,** 125–135 (1977).
11. Stocum, D. L. *Devl Biol.* **45,** 112–136 (1975).
12. Maden, M. *J. Embryol. exp. Morph.* **56,** 201–209 (1980).
13. Butler, E. G. *J. Morph.* **96,** 265–281 (1955).
14. Wallace, H. *J. Embryol. exp. Morph.* **56,** 309–317 (1980).
15. Maden, M. *J. theor. Biol.* **69,** 735–753 (1977).
16. Singer, M. *Am. Zool.* **18,** 829–841 (1978).
17. Schotté, O. E. & Butler, E. G. *J. exp. Zool.* **97,** 95–121 (1944).
18. Pitts, J. D., Burk, R. R. & Murphy, J. P. *Cell Biol. int. Rep.* Suppl. A **5,** 45 (1981).
19. Elias, P. M., Grayson, S., Caldwell, T. M. & McNutt, N. S. *Lab. Invest.* **42,** 469–474 (1980).
20. Slack, J. M. W. *J. theor. Biol.* **82,** 105–140 (1980).
21. Lotan, R. *Biochim. biophys. Acta* **605,** 33–91 (1980).
22. Hassell, J. R., Pennypacker, J. P., Yamada, K. M. & Pratt, R. M. *Ann. N.Y. Acad. Sci.* **312,** 406–409 (1978).
23. Pennypacker, J. P., Lewis, C. A. & Hassell, J. R. *Archs Biochem. Biophys.* **186,** 351–358 (1978).

LETTERS TO NATURE

X-ray observations of the 1980 Cygnus X-1 'high state'

Y. Ogawara*, K. Mitsuda*, K. Masai†, J. V. Vallerga‡, L. R. Cominsky‡, J. M. Grunsfeld‡, J. S. Kruper‡ & G. R. Ricker‡

*Institute for Space and Astronautical Science, 4-6-1 Komaba, Meguro-ku, Tokyo, Japan
†Department of Astrophysics, Nagoya University, Chikusa-ku, Nagoya, Japan
‡Department of Physics and Center for Space Research, Massachusetts Institute of Technology, Cambridge, Massachusetts 02139, USA

Observations of intensity transitions in the X-ray emission from the black-hole candidate Cygnus X-1 (see ref. 1 and refs therein) were made by the Hakucho satellite[2] during the summer of 1980 and are reported here. In addition, we report the results of hard (20–120 keV) X-ray observations of Cyg X-1. These data were obtained during the 'high' intensity state by balloon-borne mercuric iodide detectors, and are compared with data obtained at similar energies approximately 1 month earlier (A. Sheepmaker *et al.*, in preparation) during the 'low' intensity state.

Cyg X-1 was observed to be in a 'high' state by the Uhuru satellite[3] from December 1970 (its first observation of the source) to April 1971 and again during 1975 by the Ariel V (refs 4–6), and OSO-8 instruments[7], as well as the Astronomical Netherlands Satellite[8]. Subsequent observations at many different X-ray energies have indicated that Cyg X-1 has been in an extended 'low' state since early 1976. In his review of Cyg X-1 (ref. 1), Oda has summarized the light curves and spectral information which were published up to 1977. During the transition to a 'high' state, the soft (< 10 keV) and hard (> 10 keV) X-ray intensities seem to be anticorrelated, that is, a 'high' state below 10 keV is associated with a substantial decrease in the X-ray intensity above 10 keV.

For the work reported here, soft X-ray observations (1–30 keV) were made with the scanning y-axis detectors on board the Hakucho satellite. The y-axis detector system consists of a pair of Xenon-filled proportional counters (SFX-VI and SFX-V2) with a 1.7° × 32° FWHM field of view. Each of the two counters has an effective area of 32 cm^2. Only the SFX-V1 data were used in this analysis as the SFX-V2 field of view contained Cyg X-3 during most of the observations. The satellite spins at 6 r.p.m., so that 3,000 transits of a given source are available during the five daily 10-min passes above the tracking station at Uchinora, Japan. The source transits are superposed and corrected for aspect transmission and Earth occultation. Background is also subtracted. (For further details on the Hakucho satellite see ref. 9.)

Figure 1 shows part of the X-ray light curve obtained with the Hakucho y-axis detectors during 1980. Each point represents the daily average X-ray intensity from Cyg X-1. Two 'high' states are clear: the first lasted at least 15 days, and was followed by a decrease over ~25 days to the pre-transition level; a second increase was observed ~4 months later. This transient event resulted in the highest measured intensity shown in Fig. 1 and began after JD 2444551.66 but before JD 244553.56 (binary phase 0.05 and 0.39 respectively). Thus the rise time was less than 1.9 days. This increase was quite brief, with the 'high' state persisting for only 2 days. The erratic variability seen during the 1980 observations is similar to that observed in 1975 and reported by Holt *et al.* using the Ariel V All Sky Monitor[6].

Also indicated in Fig. 1 are the dates when hard X-ray (20–200 keV) balloon observations of Cyg X-1 took place. The 'low' state observations (8 May 1980) were performed by the MIT/Leiden Balloon Group and will be reported separately (A. Scheepmaker *et al.* in preparation). The 'high' state observations (28 June 1980) constituted the first use of a mercuric iodide X-ray detector[17] in an astronomical experiment. The detector consisted of 11 HgI_2 crystals with a total effective area of 7.6 cm^2. The detector assembly (crystals and preamps) was enclosed within a cylindrical NaI scintillator well (active anticoincidence shield) which rejected charged particles and γ rays. The preflight energy resolution of the detectors ranged from 2–6 keV FWHM at 60 keV and remained stable during the 13-h flight from Palestine, Texas. The gondola containing the detector was

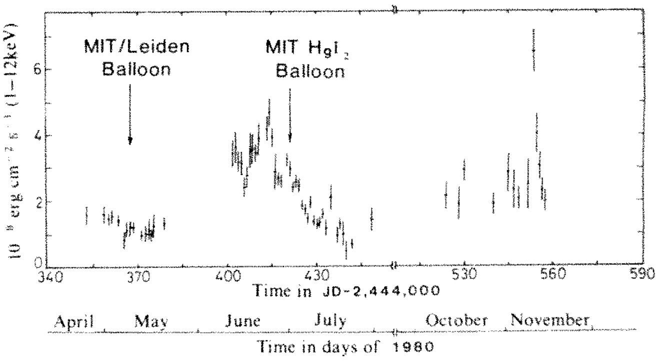

Fig. 1 Soft X-ray (1–12 keV) light curve of Cyg X-1 obtained with the Hakucho satellite. Two 'high' states are evident. The first began before 10 June 1980 and the second transient event occurred in November 1980. Also shown are the dates of simultaneous observations in hard X-rays by balloon-borne instruments.

0028–0836/82/080675—02$01.00

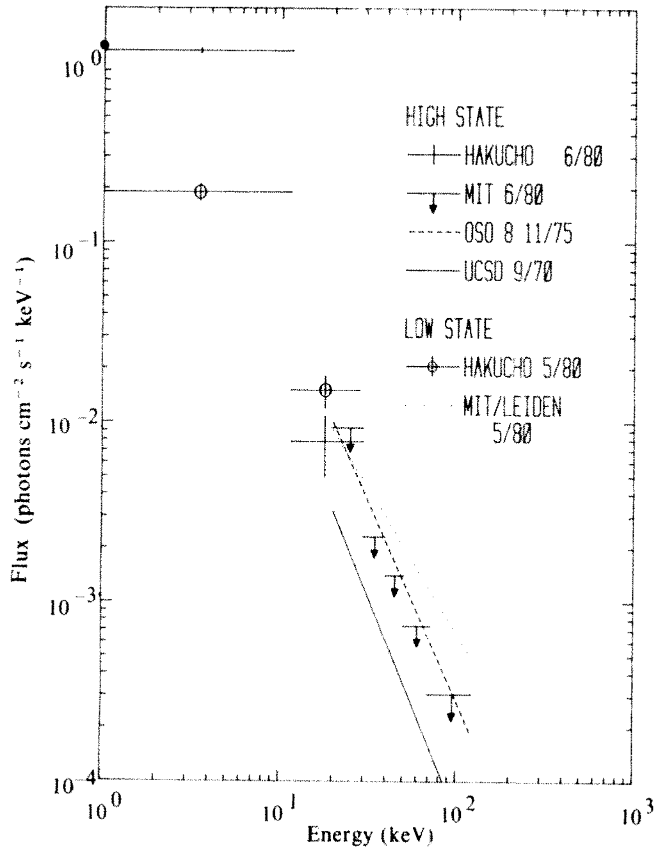

Fig. 2 X-ray spectra taken before and after the 'high' state transition of Cyg X-1 in late May/early June 1980. Data were obtained with the Hakucho satellite and with balloon-borne hard X-ray detectors. The Hakucho data points for high and low states are averages for 12–30 June 1980 and 1–19 May 1980, respectively. Also included are representative hard X-ray spectra taken during previous high states[7,11].

launched on an 11×10^6 ft^3 balloon at 00.15 UT on 28 June 1980 and floated west for 13 h at an average altitude of 40 km (~ 2.9 g cm^{-2}). Maximum exposure to Cyg X-1 occurred at 08.30 UT 28 June 1980. The detectors were calibrated using an on-board ^{241}Am source for 2 min out of every hour. The counts for each separate HgI$_2$ detector were binned in 64-s intervals in coarse energy channels, 10 keV wide. The detector counts were then summed to give the total counts per energy channel per 64 s.

Total exposure to the X-ray source was calculated as a function of time, taking into account aspect (azimuth, latitude, sidereal time, and field of view of individual HgI$_2$ detectors), atmosphere and detector window transmission, detector efficiency, and dead time. The maximum exposure to Cyg X-1 at transit was 37% over the 50–70 keV energy range. For each energy channel, an effective time on source, $t_{\text{eff}} = \sum_i t_i \varepsilon_i$, was calculated and used to convert observed counts to a photon flux at the top of the atmosphere. Here, t_i refers to an individual time bin and ε_i is the total exposure, including atmospheric and aspect corrections as discussed above. There was less than a 2σ detection in all energy bands.

Cygnus X-1 passed through the field of view in 95 min resulting in 83 min of 'on source' data (that is, 5 min were occupied by calibrations and 7 min were lost due to telemetry dropouts); 40 min before and after this period were averaged and used as background.

Figure 2 shows the 2σ upper limits derived for the hard X-ray spectrum during the 28 June 1980 Cyg X-1 'high' state observation. Also indicated are the results from the 8 May 1980 hard X-ray observations by Scheepmaker *et al.* (in preparation) which were obtained when Cyg X-1 was in the 'low' state, as well as representative hard X-ray measurements during the 1971 and 1975 'high' states. The 1–12 keV and 12–30 keV X-ray intensities from the Hakucho observations have been averaged over the high state and the low state separately. As can be seen in Fig. 2, the hard X-ray intensity is anticorrelated with the soft X-ray intensity; the pivot point occurs for an energy below 30 keV. The best fit power law for the Hakucho measurements gives a photon number spectral index of 1.5 ± 0.1 for the low state and 2.7 ± 0.2 for the high state. Using detectors on HEAO 3, Ling *et al.* (ref. 10 and personal communication) also recorded a continuous decrease in the hard X-ray intensity (48–183 keV) from 19 May 1980 until at least 2 June. The spectral anticorrelation reported here was also observed in previous low to high state transitions[7,11] and seems to be a consistent feature of the bimodal behaviour of Cyg X-1.

Previous observations have established that the spectrum varies with time during the different intensity states and is not well represented by a simple relation (for example, power law or exponential). This has led to the idea that the soft component of the spectrum may originate in the outer optically thick region of an accretion disk surrounding the central compact object, whereas the hard component arises in an optically thin, hot inner region[12]. The observed time scales for the transition to, and decay from, a 'high' state are consistent with theoretical calculations for the evolution of a standard accretion disk[13], and suggest fluctuations in the accreted stellar wind or changes in the optical depth of the gas at the outer edge of the disk (see refs 1, 14 and refs therein). Spectral anticorrelation has also been used to explain the energy dependence of the short term variability (milliseconds to seconds)[15]. A numerical model proposed by Ichimaru[16] shows that two physically distinct states can exist in the accretion disk depending on whether the radiative loss is smaller or larger than the viscous heating near the outer boundary (that is, a transition is expected to occur for $\dot{M}/T^2 \sim 5 \times 10^3$ g s^{-1} K^{-2} where $\dot{M}$ is the accretion rate and T is the gas temperature at the outer edge of the disk). Thus, the middle part of the disk may become optically thick (high state) or optically thin (low state).

We conclude that Cygnus X-1 returned to its high state in 1980 after an apparent 4.5-yr interval in the low state. Note that this time period is similar to the 4-yr interval between the first and second observed transitions[3,4]. We have established that the soft and hard X-ray intensities are anticorrelated in the transition between the two distinct states and we believe that any theoretical model of the bimodal behaviour of Cyg X-1 must account for this spectral anticorrelation.

We thank all the members of the Hakucho team for their contributions to the observations; Drs H. Inoue, K. Makishima and T. Murakami for help in the data analysis and preparation of the manuscript; Robert Kubara and the launch crew at the National Center for Atmospheric Research; and Dick Lynn, Carol Ortale, Wayne Schnepple and John Warren for assistance. A. Scheepmaker provided data from the MIT/Leiden 1980 balloon flight before publication. L.R.C. acknowledges support from Zonta International during part of this work. This research was sponsored in part by NASA under grants NAGW-14 and NSG7339.

Received 23 October; accepted 7 December 1981.

1. Oda, M. *Space Sci. Rev.* **20,** 757–813 (1977).
2. Oda, M. & Hakucho Team *IAU Circ.* No. 3491 (1980).
3. Tananbaum, H. *et al. Astrophys. J. Lett.* **177,** L5–L10 (1972).
4. Holt, S. S., Boldt, E. A., Kaluzienski & Serlemitsos, P. J. *Nature* **256,** 108–109 (1975).
5. Sanford, P., Ives, J. C., Bell Burnell, S. J., Mason, K. O. & Murdin, P. *Nature* **256,** 109–111 (1975).
6. Holt, S. S., Kaluzienski, Boldt, E. A. & Serlemitsos, P. J. *Nature* **261,** 213–215 (1976).
7. Dolan, J. F., Crannell, L. J., Dennis, B. R., Frost, K. J. & Orwig, L. E. *Nature* **267,** 813–815 (1977).
8. Heise, J. *et al. Nature* **256,** 107–108 (1975).
9. Kondo, I. *et al. Space Sci. Instrum* **5,** 211 (1981).
10. Ling, J. C., Mahoney, W. A., Riegler, G. R., Wheaton, W. A. & Jacobson, A. S. *Bull. Am. astr. Soc.* **13,** 549 (1981).
11. Matteson, J. L., Mushotzky, R. F., Paciesas, W. S. & Laros, J. G. in *X-Ray Binaries* (eds Boldt, E. & Kondo, Y.) 407–424 (NASA SP-389, 1975).
12. Thorne, K. S. & Price, R. H. *Astrophys. J. Lett.* **195,** L101–L105 (1975).
13. Lightman, A. P. *Astrophys. J.* **194,** 419–427 (1974).
14. Eardley, D. M., Lightman, A. P., Shakura, N. I., Shapiro, S. L. & Sunyaev, R. A. *Comments Astrophys.* **7**(5), 151–160 (1978).
15. Doi, K. *Nature* **287,** 210–212 (1980).
16. Ichimaru, S. *Astrophys. J.* **214,** 840–855 (1977).
17. Vallerga, J. V., Ricker, G. R., Schnepple, W. & Ortale, C. *IEEE Trans. Nucl. Sci. NS-29* (1982).

Quantum conformal fluctuations in a singular space–time

T. Padmanabhan & J. V. Narlikar

Tata Institute of Fundamental Research, Bombay 400 005, India

The cosmological solutions of Einstein's general relativistic equations lead inevitably to space–time singularities[1]. However, general relativity is only an approximation to a fully quantized theory of gravity and we need to consider whether singularity persists in the quantum domain. Although a full quantum theory of gravity has not yet been developed, we show here that the above question can be tackled in a simplified model where only the conformal degree of freedom is quantized. Previous applications of this technique had shown that in specific cases the quantum conformal fluctuations (QCF) from the classical solutions diverge at the classical singularity, thus rendering the classical solution physically meaningless[2,3]. Recently one of us (J.V.N. ref. 4) has generalized this result to cover all dust cosmologies. Here we show that this conclusion is applicable to even more general types of cosmological singularities.

To arrive at this result we draw on the mathematical details of previous work; in particular, we make extensive use of the formalism developed in ref. 4.

Classical equations of general relativity are derived from the variation of the action S given by

$$S=\frac{1}{16\pi}\int R\sqrt{-g}\,\mathrm{d}^4x+\int \mathscr{L}_{\mathrm{m}}\sqrt{-g}\,\mathrm{d}^4x \qquad (1)$$

We have taken $c=1$ and $G=1$. As we are discussing quantum phenomena we will also take $\hbar=1$, thus making the Planck length the basic unit. $\mathscr{L}_{\mathrm{m}}$ is the lagrangian density for matter.

In the thin sandwich problem[5] of classical gravity, if data are given on initial and final hypersurfaces Σ_1 and Σ_2, $\delta S=0$ determine the geometry of the space–time sandwiched between Σ_1 and Σ_2. The initial and final data are specified by 3-geometries ${}^{(3)}\mathscr{G}_1$ and ${}^{(3)}\mathscr{G}_2$. In the quantum problem there is no unique sequence of 3-geometries leading from Σ_1 to Σ_2. Instead we have a probability amplitude $K[{}^{(3)}\mathscr{G}_2, \Sigma_2; {}^{(3)}\mathscr{G}_1, \Sigma_1]$ for the system to have the specified initial and final data. The kernel K is formally written as the Feynman functional integral

$$K[{}^{(3)}\mathscr{G}_2, \Sigma_2; {}^{(3)}\mathscr{G}_1, \Sigma_1]=\int \exp iS[\mathscr{G}]\mathscr{D}\mathscr{G} \qquad (2)$$

where $S[\mathscr{G}]$ is the action for an arbitrary geometry $\mathscr{G}$ which satisfies the given boundary conditions. If we are considering only the conformal degrees of freedom we have to take all geometries given by the metrics

$$g_{ik}=\Omega^2\bar{g}_{ik} \qquad (3)$$

where Ω is a function of space and time ($i=0,1,2,3$), while $\bar{g}_{ik}$ is the metric tensor describing the solution of the classical problem (all physical quantities pertaining to the classical solution carry an overbar).

Using a time coordinate t to label the spacelike hypersurfaces Σ_1, Σ_2 as t_1, t_2 we may rewrite equation (2) as

$$K[\Omega_2, t_2; \Omega_1, t_1]=\int \exp iS[\Omega]\mathscr{D}\Omega \qquad (4)$$

with

$$S[\Omega]=\frac{1}{16\pi}\int(\bar{R}\Omega^2-6\Omega_i\Omega^i)\sqrt{-\bar{g}}\,\mathrm{d}^4x+\int\mathscr{L}_{\mathrm{m}}\sqrt{-g}\,\mathrm{d}^4x \qquad (5)$$

The lack of a unique space–time geometry in the quantum regime may also be expressed through a wavefunction Ψ which 'propagates' with the kernel K:

$$\psi(\Omega_2, t_2)=\int K[\Omega_2, t_2; \Omega_1, t_1]\psi(\Omega_1, t_1)\mathscr{D}\Omega_1 \qquad (6)$$

A physical interpretation can be given to the above relation by choosing a Gaussian wavepacket form for $\psi(\Omega_1, t_1)$ and then studying its dispersion as the final hypersurface Σ_2 approaches the singularity. For the examples discussed in refs 2 and 3, it was shown that while the 'mean' of the wavepacket stays on the classical solution $\Omega=1$, its dispersion diverges as the classical singularity is approached.

It was shown in ref. 4 that the above results were in fact part of a general result which was valid for all singular space–times containing only dust. By a similar analysis it can be shown that whenever $S[\Omega]$ is a quadratic functional in Ω and its derivatives, the kernel can be writtten as

$$K[\Omega_2, t_2; \Omega_1, t_1]=F(t_2, t_1)\exp[i\bar{S}] \qquad (7)$$

where $F(t_2, t_1)$ depends only on t_2 and t_1, and

$$\bar{S}=\sum_{P=1}^{2}\sum_{Q=1}^{2}\frac{3}{8\pi}\iint A_{PQ}(\mathbf{x}_P, t_P; \mathbf{x}'_Q, t'_Q)\times\Omega_P(\mathbf{x}_P)\Omega_Q(\mathbf{x}'_Q)\,\mathrm{d}^3\mathbf{x}_P\,\mathrm{d}^3\mathbf{x}'_Q \qquad (8)$$

The coefficients A_{11} and A_{22} are given by certain integrals involving the retarded Green's function $G(\mathbf{x}_2, t_2; \mathbf{x}_1, t_1)$ of a scalar wave equation determined by the background classical geometry and the source. In the dust case discussed in ref. 4, the scalar wave operator is simply $\bar{\Box}+\bar{R}/6$.

The interesting part of $\bar{S}$ in equation (8) is, however, the cross term containing A_{12}, which retains the memory of the initial wavefunction at $t=t_1$. The coefficient A_{12} is given by

$$A_{21}(\mathbf{x}_2, t_2; \mathbf{x}_1, t_1)=A_{12}(\mathbf{x}, t_1; \mathbf{x}_2, t_2)=[G(\mathbf{x}_2, t_2; \mathbf{x}_1, t_1)]^{-1} \qquad (9)$$

Suppose now that G diverges as the space–time singularity is approached. We then have $A_{12}\to 0$ and a decoupling of the final wavefunction from the initial one. This is precisely the state of complete uncertainty of the final state represented in the wavepacket case by infinite dispersion.

In ref. 4 the divergence of G at the singularity was deduced from the conformal invariance of the operator $\bar{\Box}+\bar{R}/6$. However, the result also seems to be valid for other cases. For example, it was shown recently[6] that the QCF diverge for a Robertson–Walker universe containing a massless scalar field. The QCF also diverge at the singularity of the empty Kasner universe[7]. These results suggest that we should look for a proof of the divergence of G in a fairly general scenario as follows.

Belinskii *et al.*[8] argued that a general approach to the space–time singularity can be described by a succession of Kasner type solutions, in which the Universe contracts along two axes and expands along the third. (We have reversed the direction of time so that $t\leq 0$ and the final singular state is described by $t=0$.) Without going into detail we will simply accept the claim that number, 8, of arbitrary functions in the Belinskii *et al.*[8] solution makes it a general solution of Einstein's equations.

Belinskii *et al.*[8] have argued that near the space–time singularity the contributions from $\mathscr{L}_{\mathrm{m}}$ can be neglected and the wave operator for our Green's function then becomes simply $\bar{\Box}$. We therefore have to show that in the space–time of their model the Green's function of the wave equation

$$\bar{\Box}\bar{G}(\mathbf{x}_2, t_2; \mathbf{x}_1, t_1)=[-\bar{g}(\mathbf{x}_1, t_1)]^{-1/2}\delta_4(\mathbf{x}_2, t_2; \mathbf{x}_1, t_1) \qquad (10)$$

diverges as $t_2\to 0$.

The line element of the Belinskii *et al.* model is given by

$$\mathrm{d}s^2=\mathrm{d}t^2-\gamma_{\alpha\beta}\mathrm{d}x^\alpha\,\mathrm{d}x^\beta, \quad \alpha,\beta=1,2,3 \qquad (11)$$

$$\gamma_{\alpha\beta}=\sum_{\mu=1}^{3}|t|^{2p_\mu}l_{\mu\alpha}l_{\mu\beta} \qquad (12)$$

where p_μ, $l_{\mu\alpha}$ are functions of space coordinates. As in the Kasner universe, the p_μ satisfy

$$\sum_{\mu=1}^{3}p_\mu=\sum_{\mu=1}^{3}p_\mu^2=1 \qquad (13)$$

Simple algebra shows that close to the singularity the Green's function is given by

$$G(\mathbf{x}_2, t_2; \mathbf{x}_1, t_1)\cong\frac{\delta_3(\mathbf{x}_2, \mathbf{x}_1)}{f(\mathbf{x}_2)}\ln\left|\frac{t_1}{t_2}\right| \quad 0>t_2>t_1 \qquad (14)$$

0028-0836/82/080677—02$01.00

while $G = 0$ otherwise. The function f depends on the space coordinates. We are interested in the behaviour of the Green's function as $t_2 \rightarrow 0$, the singular epoch.

From equation (14) we have $G \rightarrow \infty$ logarithmically as $t_2 \rightarrow 0$, leading to divergence of QCF. Matter terms are unimportant in the final stages of the Belinskii *et al.* solution so our conclusion should hold for general distributions of matter and energy.

Although we have quantized only the conformal degree of freedom, the fact that the QCF diverge at the classical singularity is sufficient to demonstrate that quantum uncertainty becomes so large near the classical singular epoch that the classical singularity ceases to have any significance. In analogy with the example of the hydrogen atom can we therefore expect explicit examples of quantum behaviour in the very early Universe? Recent investigations[9,10] have shown that closed Friedmann models have stationaty states and that the Planck length sets the lower limit to the 'size' of the Universe. Whether this is a general feature of quantum cosmology remains to be seen.

Received 2 November 1981; accepted 6 January 1982.

1. Hawking, S. W. & Ellis, G. F. R. *The Large Scale Structure of Space-time* (Cambridge University Press, 1973).
2. Narlikar, J. V. *Nature* **269**, 129 (1977).
3. Narlikar, J. V. *G. R. G. J.* **10**, 883 (1979).
4. Narlikar, J. V. *Foundn. Phys.* **11**, 473 (1981).
5. Misner, C. W., Thorne, K. S. & Wheeler, J. A. *Gravitation* (Freeman, San Francisco, 1973).
6. Padmanabhan, T. *Phys. Rev.* D (in the press).
7. Padmanabhan, T. Preprint (Tata Institute of Fundamental Research, Bombay, 1981).
8. Belinskii, V. A., Khalatnikov, I. M. & Lifshitz, E. M. *Adv. Phys.* **19**, 525 (1970).
9. Padmanabhan, T. & Narlikar, J. V. *Phys. Letts.* A**84**, 361 (1981).
10. Padmanabhan, T. Preprint (Tata Institute of Fundamental Research, Bombay, 1981).

Individual electrons detected after the interaction of ionizing radiation with gases

O. H. W. Siegmund, J. L. Culhane, I. M. Mason & P. W. Sanford

Mullard Space Science Laboratory, University College London,
Dorking, Surrey RH5 6NT, UK

The interaction of ionizing radiation (X rays or high-energy particles) with gases results in the creation of electron-ion pairs. For low-energy X rays a small cluster of primary ionization is produced close to the point of the initial photoionization. High-energy particles, however, lose a small fraction of their energy in each of a number of ionizing collisions resulting in a long track composed of clusters of ionization. We report here that the light signals emitted by a parallel-plate proportional counter are fast enough to allow the individual electrons in the ionization clusters to be resolved. By counting the number of electrons for low energy X ray events we demonstrate an improvement in energy resolution of more than a factor of two over conventional proportional counters.

The mean number of electrons, $\bar{n}$, created by the photoelectric absorption of X rays in a gas is a function of the X-ray energy, E, and the mean energy required to create an ion pair, W, such that $\bar{n} = E/W$ (where $W \sim 26$ eV in Ar). In conventional gas proportional counters the electrons produced are accelerated by a strong electric field such that a Townsend charge avalanche results. At a constant mean charge gain, $\bar{A}$, the charge signal from the proportional counter is directly proportional to the X-ray energy. The charge signal pulse amplitude distribution which is observed results from the variation in n and in A. Fano[1] pointed out that the standard deviation in n is $\sigma_n = (F\bar{n})^{1/2}$, where F (the Fano factor) is ~0.17 for Ar. The total fractional deviation in the charge pulse amplitude, $\sigma_N/\bar{N}$, is given by,

$$\frac{\sigma_N}{\bar{N}} = \left[\left(\frac{\sigma_n}{\bar{n}}\right)^2 + \frac{1}{\bar{n}}\left(\frac{\sigma_A}{\bar{A}}\right)^2\right]^{1/2} \qquad (1)$$

where $\bar{N}$ is the mean number of final electron-ion pairs, and

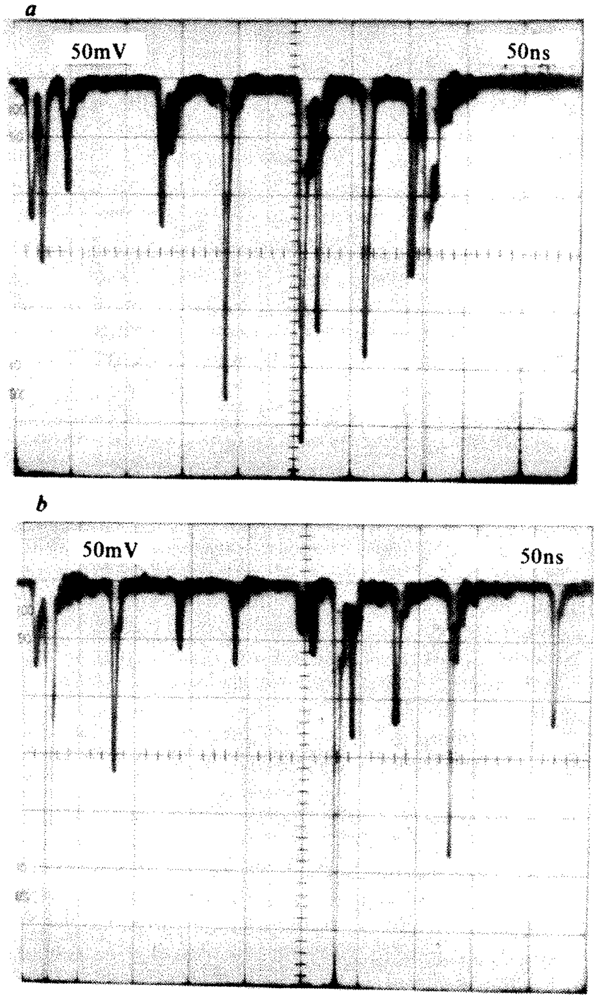

Fig. 1 Traces of the light pulses for two C-K X-ray events. The individual peaks correspond to avalanches initiated by single electrons. The gas used was Ar-CH_4(5%)-CO_2(5%)-N_2(7.5%), with a drift region field strength of ~10 V cm^{-1} and a gas gain of 10^6.

$\sigma_A/\bar{A}$ is the fractional deviation in the charge gain. We may write $f = (\sigma_A/\bar{A})^2$ for the variance in A (f is typically[2] 0.6–0.7 when $A = 10^4$–10^5). Rewriting equation (1) in the form $\sigma_N/\bar{N} = [(F+f)W/E]^{1/2}$, it is clear that the elimination of f would result in a factor of more than two improvement in energy resolution. This is accomplished in the gas scintillation proportional counter[3,4]. The same result may be achieved by counting the individual initial electrons.

In the approach described here the light pulses emitted by Townsend avalanches in a parallel plate proportional counter[5] are detected by a fast photomultiplier tube (PMT, EMI 9818 QBM, ~2 ns rise time). The PMT views the 1 mm-deep avalanche region through an optically transparent anode deposited on a fibre optic substrate[5,6]. The gas mixture used was Ar-CH_4(5%)-CO_2(5%)-N_2(7.5%) at a pressure of 760 torr. Ar and N_2 in the mixture are responsible for the light emission. Ar emits in the range 7,000–8,000 Å and N_2 emits in the range 3,000–4,000 Å (from the second positive band of N_2), with an optimum light emission attained for of the order of 10% N_2 (ref. 6). CH_4 and CO_2 are used in the gas mixture to inhibit secondary electron emission processes, thus enabling high charge gains to be achieved, and to reduce the lateral diffusion of the electron cluster so that acceptable position resolution may be obtained in applications requiring imaging[5,7]. Addition of CO_2 also reduces the electron drift velocity[8] (A. J. F. Den Boggende and C. J. Schrijver, personal communication). Fairly low concentrations (5%) of CH_4 and CO_2 were used as these gases also suppress the light emission[6].

For an X-ray event the overall duration of the light signal is set by the time taken for the initial electron cluster to cross the grid

0028-0836/82/080678—02$01.00

which separates the drift and avalanche regions of the counter. Because each electron initiates an avalanche the overall light signal is composed of a number of light pulses (n). The ability to resolve the light pulses attributable to individual electrons depends on the number of electrons, the overall duration of the light signal and the width of the individual light pulses. As the electron velocities in the avalanche region are high the excitation time, and hence the rise time, of the individual light pulses is fast (~1 ns). It has also been found that the light pulse decay time is fast (~1 ns) because CO_2 and CH_4 heavily quench the excited states responsible for light emission by collisional de-excitation[7]. This time scale compares with a resolution of ~20 ns obtained by Walenta[8] with the charge signal from a time expansion drift chamber. Walenta[8] was able to resolve the ionization clusters for high energy charged particle events, but was not able to resolve individual electrons for 5.9-keV X-ray events, although this might have been possible if low energy (<1 keV) X rays and very low electron drift velocities had been used. Light pulses from a counter of similar geometry to that used in this work were studied by Charpak *et al.*[9] and show some structure for ^{55}Fe events, but the detector gas and operating conditions were not optimized for high time resolution.

In this study the overall duration of the light signal, required to be able to resolve the light pulses initiated individual electrons, was established by using a low field strength (10 V cm^{-1}) in the drift region of the counter, giving a low electron drift velocity ($\sim 1.5 \times 10^5$ cm s^{-1})[7]. However, this field strength is substantially less than that required for optimum position resolution (>100 V cm^{-1})[7] and results in an increase of a factor of ~3 in the lateral size of the electron cluster.

Figure 1 demonstrates the resolution of C–K X rays into several single electron events (the signals were displayed on a Tektronix 1 GHz oscilloscope). It is estimated (from the data in ref. 2) that for the gas mixture used $F \sim 0.17$ and $W \sim 26.5$ eV so the theoretical number of initial electrons is 10.6 ± 1.3. This compares with an experimental value of 11 ± 1.6, deduced by counting the number of light pulses which comprise each individual C–K X-ray event. For C–K X rays this method results in an energy resolution of ~34% FWHM, compared with a value of ~85% FWHM for typical proportional counters. For B–K (0.18 keV) X rays we obtain a value of 7 ± 1.5 electrons compared with a theoretical value of 7 ± 1.1. This gives an experimental energy resolution of ~50% FWHM at B–K compared with ~105% FWHM for conventional counters. The energy resolution for the electron counting technique is compared with the energy resolution of a conventional proportional counter in Fig. 2.

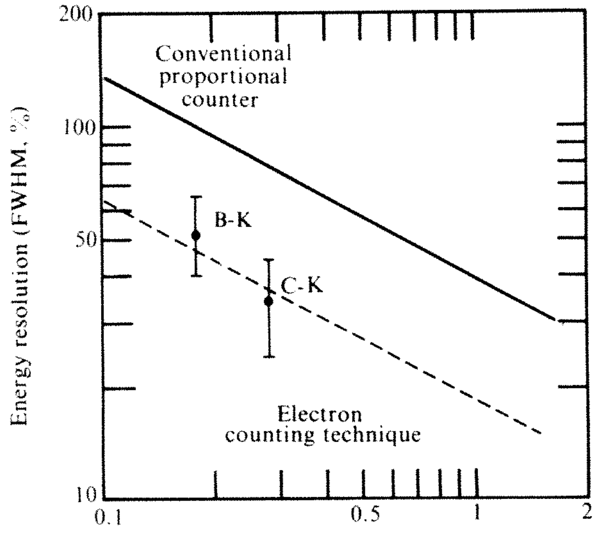

Fig. 2 Comparison of the FWHM energy resolution as a function of X-ray energy for a proportional counter with the predicted energy resolution for counting individual initial electrons, derived from measurements with C–K and B–K X rays.

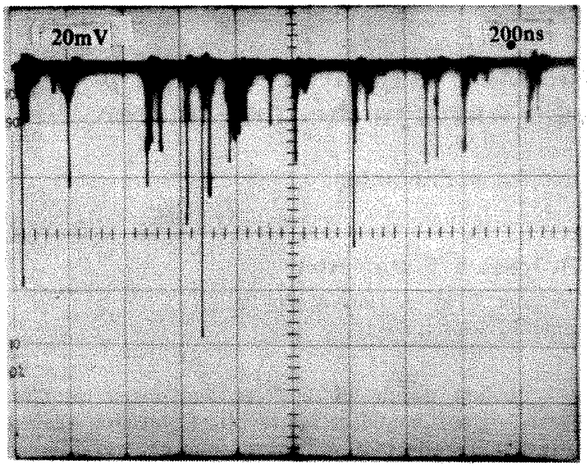

Fig. 3 Trace of the light pulse emitted for a ^{60}Co event showing the resolution into clumps of ionization, which are made up of a number of peaks corresponding to individual electrons.

^{60}Co (~1.2 MeV) γ rays were also observed with the detector. γ rays interact mainly with the walls, resulting in the ejection of high-energy electrons. These electrons are mostly within a factor of two of being minimum ionizing. The ionization tracks produced extend across the 3.5-mm deep drift region of the counter, therefore the overall light signals lasts about four times longer than for X-ray events, which produce small electron clouds. Figure 3 shows the structure of a typical ^{60}Co event in which ionization clusters may be discerned, each composed of several electrons.

In X-ray detection the increased light signal duration for high energy particle events allows identification and rejection of the latter. This ability has already been demonstrated with the integrated light signal[5,6]. Background rejection may be accomplished more efficiently, however, by setting upper limits to the number of single electron avalanches and the duration of the light pulse train.

The practical realization of electron avalanche counting will require suitable pulse counting circuits. Although the theoretical limiting resolution, as determined by the Fano factor, is ~37% (B–K) and ~30% (C–K) it is anticipated that counting errors due to closely spaced single electron events will degrade the resolution achievable in practice. Results obtained with fast logic devices indicate that electronic counting can be at least as efficient as the technique used here. Therefore it seems possible that improvements in energy resolution of at least a factor of two over current proportional counters may be attained.

This improvement in energy resolution for a parallel plate proportional counter should find applications in low energy X-ray astronomy, where both high energy resolution and high spatial resolution are desirable[6]. The ability to count individual electrons, as demonstrated here, makes it possible to determine Fano factors for gases, as was suggested by Walenta[8]. The increased time resolution may also enable improved ionization cluster counting efficiency to be achieved for applications in high-energy charged particle physics.

We thank Professor R. L. F. Boyd for his encouragement. This work was supported by the SERC.

Received 4 November 1981; accepted 11 January 1982.

1. Fano, U. *Phys. Rev.* **72,** 26–29 (1947).
2. Alkhazov, G. D., Komar, A. P. & Vorob'ev, A. A. *Nucl. Instrum. Meth.* **48,** 1–12 (1967).
3. Alice, M., Alves, F., Policarpo, A. J. P. L. & Salete, M. *IEEE. Trans. nucl. Sci.* NS-**22,** 107–115 (1975).
4. Inoue, H., Koyama, K., Matsuoka, M., Tanaka, Y. & Tsunemi, H. *Nucl. Instrum. Meth.* **157,** 295–300 (1978).
5. Siegmund, O. H. W., Sanford, P. W., Mason, I. M., Culhane, J. L. & Cockshott, R. *Nature* **287,** 808–810 (1980).
6. Siegmund, O. H. W. *et al. IEEE. Trans. nucl. Sci.* NS-**28,** 478–482 (1981).
7. Siegmund, O. H. W. thesis, Univ. London (1981).
8. Walenta, A. H *IEEE. Trans. nucl. Sci.* NS-**26,** 73–80 (1979).
9. Charpak, G., Majewski, S. & Sauli, F. *Nucl. Instrum. Meth.* **126,** 381–389 (1975).

Nonlinear reflectivity of high-power radio waves in the ionosphere

H. Kopka & P. Stubbe

Max-Planck-Institute für Aeronomie, 3411 Katlenburg-Lindau 3, FRG

T. B. Jones & T. Robinson

Department of Physics, University of Leicester,
Leicester LE1 7RH, UK

An important result of earlier ionospheric modification experiments performed at Platteville, Colorado, was the discovery that the reflectivity of the ionosphere was greatly reduced in the reflection region of a high-power radio (pump) wave[1]. Because the reflectivity of low-power diagnostic waves passing through the modified region with frequencies from just below the pump wave frequency up to the F region critical frequency were reduced, the phenomenon was termed wide-band absorption (WBA). Subsequent experimental and theoretical work (for review see ref. 2) has led to the conclusion that WBA is due to the scattering of radio waves from field-aligned irregularities into plasma waves. These irregularities are generated by the interaction of the pump wave and the ionospheric plasma but the mechanism by which this occurs is not completely understood. It is evident, however, that in the process the pump wave itself undergoes WBA. In a recent campaign using the Max-Planck Institute ionospheric modification facility at Ramfjordmoen, near Tromso, Norway, the existence of WBA at high latitudes was confirmed by experiments using low-power diagnostic waves passing through the reflection region of the high-power radio wave[3,4]. As we report here, during an experiment to measure the effect of WBA on the pump wave itself, the essentially nonlinear nature of the interaction between the high-power radio waves and the ionosphere was demonstrated in a new and striking way.

The experiment consisted of measuring the amplitude of the reflected 5.423-MHz pump wave at a receiver about 40 km south of the transmitter while the effective radiated power (ERP) of the pump wave was being changed. The changes in ERP consisted of 40 steps of 6.5-MW increases from 0 to 260 MW (full power) and then 40 incremental decreases of 6.5 MW down to 0 MW, the steps being made at 9-s intervals. One cycle was thus completed within 12 min and was repeated several times.

Figure 1 shows a record of the reflected pump signal during this experiment. The reflected signal increases suddenly during the first step from 0 to 6.5 MW ERP and then continues to increase but less rapidly, during successive increases in ERP. This behaviour is a result of the usual WBA effect and persists up to ~40–50% of full power. However, further increases in power produce a completely new type of behaviour in which the reflected signal decreases with increasing ERP.

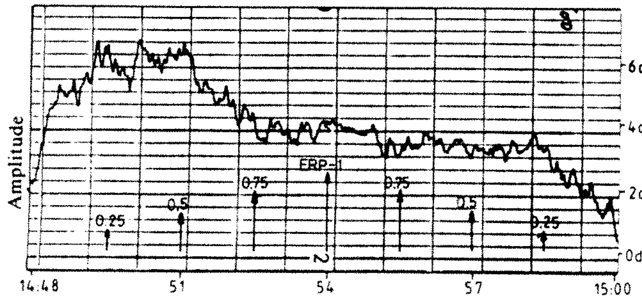

Fig. 1 Record of reflected pump wave amplitude during one 12-min cycle.

This result is a direct consequence of the dependence of the reflectivity of the ionosphere on the amplitude E_0 of the pump wave. If the absorption coefficient of the ionosphere under the influence of the pump wave is $\chi(E_0)$, the reflected amplitude E_R after the wave has travelled twice through a thickness L_0 of modified ionosphere is

$$E_R = E_0\, e^{-2L_0\chi(E_0)} \qquad (1)$$

from which it can be seen that

$$\partial E_R/\partial E_0 = e^{-2L_0\chi(E_0)}\,(1 - 2L_0E_0\partial\chi/\partial E_0) \qquad (2)$$

Thus, as long as χ is an increasing function of E_0 (which theory predicts to be the case), then expression (2) shows that E_R will increase with E_0 when E_0 is less than a critical value, E_c, but that E_R will decrease with increasing E_0 when E_0 exceeds E_c, where E_c is given by

$$E_c = 1/(2L_0\partial\chi/\partial E_0) \qquad (3)$$

This result may have far-reaching practical implications, especially in the field of telecommunications. It is normally assumed that in a broadcasting system, the signal amplitude at a remote receiver can be increased by increasing the radiated power of the transmitter. The present results suggest that a certain optimum power exists above which the signal received via the ionosphere at a remote site will be reduced.

Received 23 November; accepted 23 December 1981.

1. Cohen, R. & Whitehead, J. D. *J. geophys. Res.* **75,** 6439–6445 (1970).
2. Fejer, J. A. *Rev. Geophys. Space Phys.* **17,** 135–153 (1979).
3. Jones, T. B., Robinson, T., Kopka, H. & Stubbe, P. *J. geophys. Res.* (in the press).
4. Stubbe, P., Kopka, H., Jones, T. B. & Robinson, T. *J. geophys. Res.* (in the press).

Unusual luminescence behaviour of terbium phosphate glasses

David J. Cronin, Douglas H. Blackburn & Wolfgang K. Haller

National Bureau of Standards, Washington, DC 20234, USA

While preparing a terbium-containing phosphate glass, an intense emission of green light was observed when the melt was poured into a metal mould. This emission was easily visible to the naked eye and was only observed on quenching of the melts. To our knowledge this phenomenon, termed 'cooling-induced luminescence (CIL)', has not previously been reported. Experimental evidence suggests that the CIL may be related to a thermally induced shift in the oxidation-reduction balance in the melt. A similar phenomenon was also observed with europium phosphate melts.

To determine the exact nature of the emission, a series of spectra was recorded using a quartz prism spectrometer, taking successive photographic film exposures, as the melt cooled. Figure 1 shows the emission spectra obtained during the cooling of a melt of terbium metaphosphate, $Tb(PO_3)_3$, and the emission spectrum obtained by exciting the glass, at room temperature, with an UV light source fitted with a 'black light' filter. The CIL peaks agree well with the UV-excited peaks and correspond to the known fluorescence spectrum of Tb^{3+}. The peaks at 412 and 436 nm in the spectrum taken at 1,284 °C also correspond to known terbium emissive transitions, even though they were not observed in the UV-excited spectra. The spectra in Fig. 1 obviously represent a superposition of the terbium fluorescence lines and the thermal emission continuum of the hot melt. Figure 2 shows the thermal emission continuum of a metaphosphate melt, $La(PO_3)_3$, which does not contain an ion exhibiting fluorescence.

Quenching of the melt was required to observe CIL. Table 1 summarizes the effect of cooling history and rate for $Tb(PO_3)_3$. If

0028–0836/82/080680—03$01.00

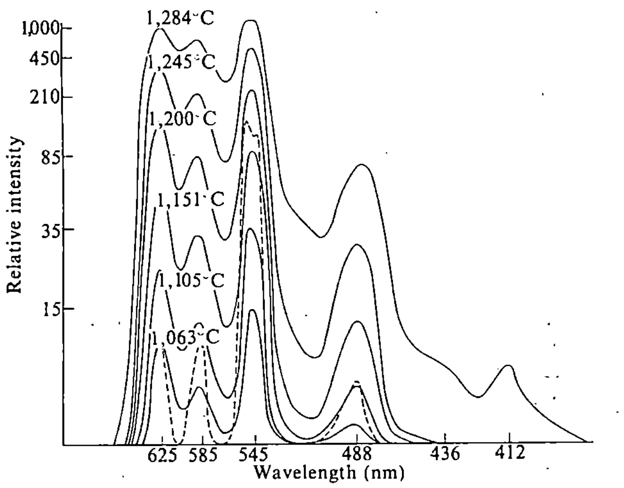

Fig. 1 Spectra obtained on cooling of $Tb(PO_3)_3$. ---, UV-excited spectrum of $Tb(PO_3)_3$.

the melt was allowed to cool freely in air in its crucible, a cooling rate of ≤ 2 °C s^{-1}, no emission was observed. On casting from an initial melt temperature of 1,400 °C, the centre temperature of the cast piece showed a cooling rate of ~10 °C s^{-1} and the emission for a 100 g melt was visible for ~20 s. In another set of experiments small solid glass samples were heated to up to 1,100 °C and then quenched. If the samples were allowed to cool in air the initial cooling rate was ~100 °C s^{-1} but no CIL was observed. However, if the samples were taken from the heat source and immediately placed in water, giving an initial cooling rate of ~500 °C s^{-1}, CIL was observed for samples having an initial temperature of 850 °C or higher. No CIL was observed in cases where the initial temperature was <850 °C. These results indicate that a certain quench rate is needed to observe CIL and that this quench rate is related to the initial temperature of the glass.

Several melts were made by melting a mixture of Tb_4O_7 and $NH_4H_2PO_4$ to determine the composition range over which the CIL effect could be observed. Additions, if any, were in the form of oxides, except in the case of sodium where the carbonate was used. The melts were carried out at 1,400 °C in Al_2O_3 crucibles after an initial preheating to drive off most of the NH_3 and H_2O and preheat the crucible before placing it in the melt furnace. The melts were generally cast after 1 h at the melting temperature.

In binary terbium phosphates, CIL was observed over a composition range of 16–25 mol % Tb_2O_3. No melts were made with >25 mol % Tb_2O_3. Various oxides were added to the $Tb(PO_3)_3$ composition, at 5 mol %, to determine their effect on the CIL. Individual additions of MgO, Na_2O, and Al_2O_3 did not seriously affect the emissions. However, additions of oxides with variable valency states, such as Sb_2O_3 or CeO_2, completely quenched the CIL effect, although UV-excited fluorescence was observed.

As an alternative to introducing the P_2O_5 as $NH_4H_2PO_4$, other melts were prepared from material formed by mixing H_3PO_4 and Tb nitrate solution. The terbium nitrate was made by digesting terbium oxide in concentrated nitric acid. The material was dried at ~100 °C before placing it in the melt crucible. Melting was carried out in an Al_2O_3 crucible at 1,400 °C for 1 h, as with the other melts, and resulted in a clear fluid melt which cooled to a clear glass. Although it showed only a very faint indication of CIL on pouring, UV-excited fluorescence was observed.

Table 1 Effect of thermal history on CIL in $Tb(PO_3)_3$

Initial temperature (°C)	Cooling rate (°C s^{-1}) CIL observed	CIL not observed
1,400	10	2.5
1,100–850	500	100
$\leq$800	—	500

The intensity of the CIL in these melts could be increased greatly, to the level of the original glasses, by bubbling NH_3 or CO gas through the melts at 1,400 °C. The CIL could be quenched again by bubbling O_2 gas through the melt.

During melting of the various compositions, it was noted that holding time at temperature also affected the CIL. The Na_2O-containing glass, which originally exhibited CIL, did not show CIL after an additional 3 h of melting. The Al_2O_3-containing glass also showed a significant decrease in intensity of the CIL in similar conditions, as did $Tb(PO_3)_3$, particularly at long melting times, up to 22 h. The ability of oxygen to quench the CIL indicates that the decrease in intensity may be due to the slow oxidation of the melt from prolonged heating in air.

CIL was also photographically recorded for a europium metaphosphate melt, though the luminescence is in the red portion of the spectrum and therefore difficult to distinguish visually from the black body radiation.

Our results identify the emissions involved in the CIL as the normal Tb^{3+} fluorescence transitions, and provide some indication of the nature of the excitation process. One obvious possibility is excitation by the thermal black-body radiation. However, if the mechanism was a simple excitation by the UV portion of the continuum, a steady-state emission would be expected while holding the glass at elevated temperatures, and none is observed. Another possibility is a stress-induced triboluminnescence. However, the CIL occurs at temperatures where the melt is still quite fluid and no stress could be developed.

The need for quenching to observe the CIL, and the dependency of high quench rates on starting temperature, indicate that the emission is the result of the decay of a temperature-dependent excited state. The fact that the cooling rate necessary to observe the CIL depends on starting temperature may indicate that the decay process is always radiative but during slow cooling the emission cannot be observed because of the relative magnitude of the background. The other possibility is a competition between radiative and nonradiative decay with the radiative process being favoured in rapid cooling conditions and the nonradiative process in slow cooling conditions.

One possible temperature-dependent mechanism is a valency change of the terbium. Only terbium oxide is known to show a large change in Tb^{4+}/Tb^{3+} ratio as a function of temperature[1], and many other multivalent ions, such as iron[2] and cerium[3], show similar changes even when incorporated in a glassy matrix. That oxidation of the melt, by batch additions (such as Sb_2O_3, CeO_2) or by bubbling O_2 gas, quenches the CIL and reduction of the melt, by CO_2 or NH_3 gas, can revitalize the CIL indicates the sensitivity of the effect to the overall redox balance of the

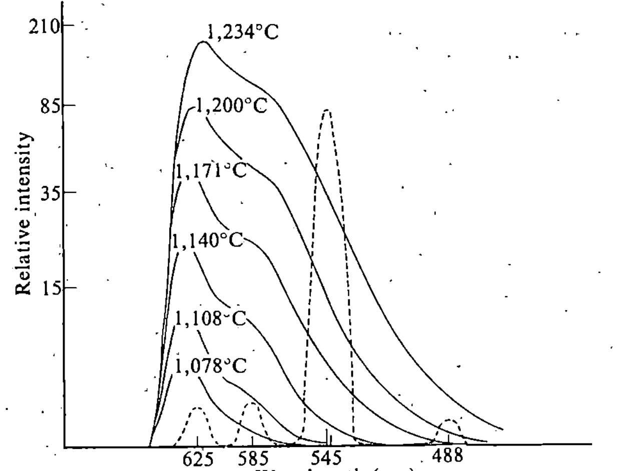

Fig. 2 Spectra obtained on cooling of $La(PO_3)_3$. ---, UV-excited spectrum of $Tb(PO_3)_3$.

system. Therefore a temperature-dependent valency change may indeed contribute to the CIL effect. However, the intensity of the Tb^{3+} fluorescence in UV irradiation was essentially the same, for terbium phosphate glasses, regardless of whether CIL was observed or not, implying that the Tb^{3+} content of the glasses, at room temperature, was not greatly different, thus indicating that the redox changes are more complicated than a simple shift in Tb^{4+}/Tb^{3+} ratio. It also is not clear from our results whether the quenching of the CIL by oxidation prevents formation of the excited state or shifts the decay process to a non-radiative path.

In conclusion, a unique form of luminescence was observed which was quite sensitive to the overall oxidation reduction balance of the melt and the rate of cooling of the melt. The experimental evidence indicates that the excitation mechanism requires species of a particular valence and may be due to a thermally induced shift in the oxidation reduction balance in the melt which results in the observed terbium luminescence. This may involve the terbium directly or may involve the phosphorus with the energy released being transferred to the terbium to produce the fluorescence.

Received 10 September; accepted 15 December 1981.

1. Lowe, A. T. & Eyring, L. *J. Solid State Chem.* **14**, 383–384 (1975).
2. Johnston, W. D. *J. Am. ceram. Soc.* **47**(4), 198–201 (1964).
3. Gottardi, V. *et al.* in *Advances in Glass Technology*, Proc. 6th int. Glass Congress, Washington, DC (Plenum, New York, 1962).

Slope anomaly in the vapour pressure curve of Hg

S. R. Hubbard

Lowestoft College of Further Education, St Peters Street,
Lowestoft NR32 2NB, UK

R. G. Ross

School of Mathematics and Physics, University of East Anglia,
Norwich NR4 7TJ, UK

The investigation of normally-metallic fluids at reduced densities has created considerable experimental and theoretical interest. Hensel[1] has presented evidence for transitions, related to electronic properties, in both the liquid and vapour phases of Hg, and predicted that these would affect the liquid–vapour transition. We present here evidence that the vapour pressure curve of Hg, $p(T)$, has an unusual and probably unique form in that the $\ln p$ against $1/T$ plot showed a sharp change of slope at temperature $T = T' = 1{,}361$ K and saturated liquid density $\rho_L = 10.7\ \mathrm{g\,cm^{-3}}$. The latter is about the density at which Hensel[1] deduced that the electronic mean free path equalled the mean interatomic spacing, and which he took to be associated with the electronic-property related transition in the liquid phase.

Our experiments were made using an internally-heated pressure vessel pressurized with argon gas. The sample of Hg was contained in a closed cell, fabricated largely of Mo, which entered the internal furnace of the pressure vessel and which was also connected by means of high-pressure capillary tubing to a strain gauge type of pressure transducer outside of the pressure vessel. This transducer was used to measure the vapour pressure. The argon pressure in the pressure vessel was adjusted so as to be approximately equal to the measured vapour pressure of the Hg to prevent deformation of the cell under stress. The pressure transducer was calibrated using a dead-weight tester, and we estimate the inaccuracy in p as ±0.4 MPa. The temperature was measured using several Pt/Pt13Rh thermocouples in close contact with the hot part of the cell where the liquid–vapour meniscus was located. Users of internally-heated pressure vessels are familiar with systematic errors in temperature measurement arising from convection in the pressure-transmitting medium, here argon gas. To correct for such error, we adjusted our temperatures so that, at 929 K, our data agreed with the relatively accurate, low-temperature vapour pressure data of Sugawara *et al.*[2]. The required adjustment of temperature varied from 0 to 20 K in the various runs which were made.

We fitted our data to several different equations using a least-squares procedure. The simplest form of equation was $\ln p = A/T + B$. To obtain a good fit to our data, we needed different values of A and B above and below a temperature of 1,361 K where we observed a change of slope (Fig. 1). At low temperatures, our data in the range 742–1,271 K yielded

$$\ln (p/\mathrm{MPa}) = -7{,}148(\mathrm{K}/T) + 9.064 \qquad (1)$$

Using the same procedure, the data of Sugawara *et al.*[2] in the temperature range 602–929 K yielded

$$\ln (p/\mathrm{MPa}) = -7{,}132(\mathrm{K}/T) + 9.038 \qquad (2)$$

From the agreement of the corresponding parameters in equations (1) and (2), in particular that corresponding to the slope, we inferred that systematic error in temperature measurement in our experiments was constant, essentially independent of temperature, in any given run. Over the temperature range 742–929 K, where there was data overlap between our experiments and those of Sugawara *et al.*[2], pressures calculated using equations (1) and (2) differed at most by 0.88%.

The same fitting procedure and form of equation when applied to our data in the temperature range 1,389–1,719 K yielded

$$\ln (p/\mathrm{MPa}) = -8{,}180(\mathrm{K}/T) + 9.822 \qquad (3)$$

To confirm the validity of our data at the higher temperatures, we used the most recent and reliable values of critical temperature, T_c, and critical pressure, p_c, obtained independently

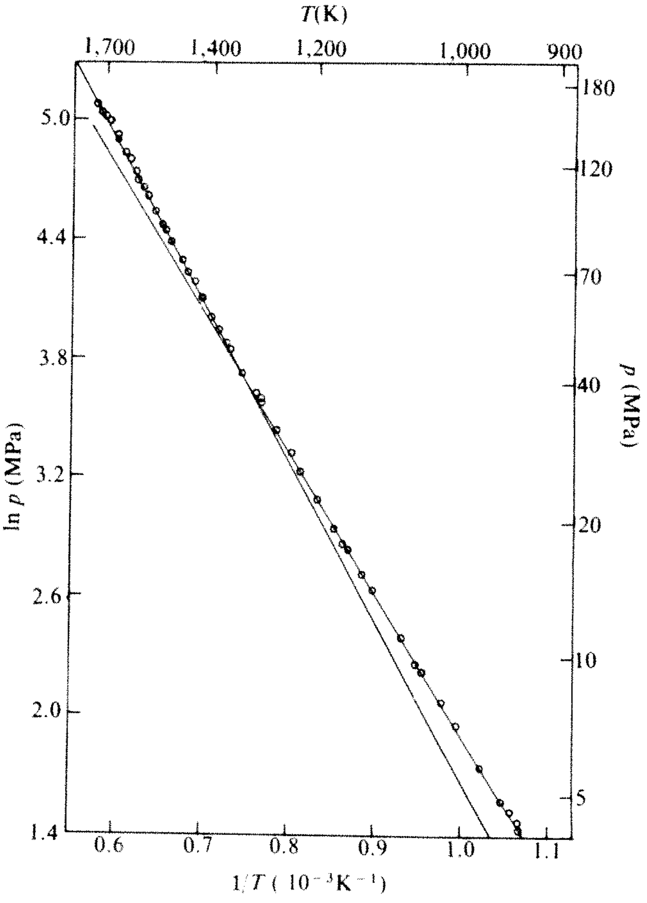

Fig. 1 Vapour pressure of Hg.

0028-0836/82/080682—02$01.00

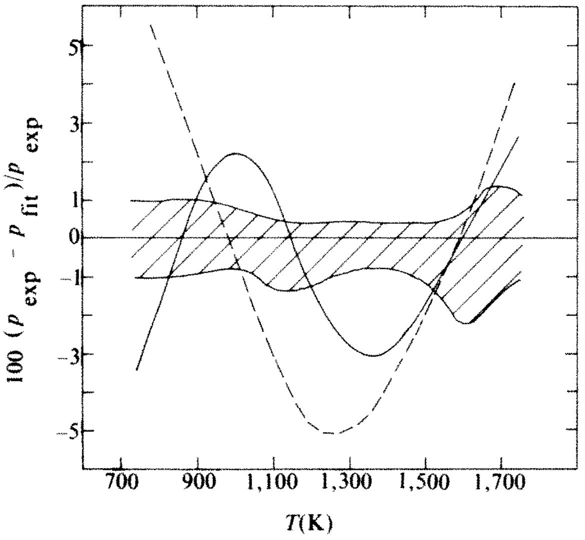

Fig. 2 Deviation between experimental and fitted values for vapour pressure of Hg: solid line, $\ln p = A/T + B + C \ln T$; broken line, $\ln p = A/T + B$; cross-hatched region, deviations scattered within this region both for Frost–Kalkwarf[6] equation $\ln p = A/T + B + C \ln T + Dp/T^2$, and for equations (1) and (3) of the present work.

by other workers. Experiments by Neale and Cusack[3] and Schönherr and Hensel[4] yielded an experimental value $p_c = 170$ MPa, obtained by averaging 167.5 and 172 MPa. Substitution in equation (3) of values of T_c obtained by these workers yielded an average predicted value $p_c = 179$ MPa, that is, 9 MPa higher. Alternatively, substitution of the same values of T_c in equation (1) yielded an average predicted value $p_c = 151$ MPa, that is, 19 MPa lower than the average experimental value obtained independently. From such comparisons we inferred: (1) that our predicted value of p_c from equation (3) was in reasonable agreement with other work, (2) that our values of vapour pressure near p_c were not subject to serious unsuspected systematic error and (3) that linear extrapolation of low temperature data in a $\ln p$ against $1/T$ plot (equation (1)) yielded an improbably low predicted value of p_c. As we have found reasonable agreement of our data with that of other workers[3,4] at $T = T_c$, and good agreement of the slope with the data of Sugawara *et al.*[2] at low temperatures, it follows that the $\ln p$ against $1/T$ plot must bend upward at intermediate temperatures.

The typical results shown in Fig. 1 were reproducible both on heating and cooling and for a range of different total Hg masses in the cell. The temperature at which the change of slope occurred (T') we estimated as 1,361 ± 30 K.

We also attempted to fit other forms of equation to our data; the results are shown in Fig. 2. A single equation of form $\ln p = A/T + B$, or the Kirchhoff equation $\ln p = A/T + B + C \ln T$, evidently yielded poor fits. The latter has been used successfully[5] to fit high-temperature vapour pressure data for Cs, which showed only a slight curvature in a $\ln p$ against $1/T$ plot, concave towards the $1/T$ axis. The four-parameter implicit equation, $\ln p = A/T + B + C \ln T + Dp/T^2$, due to Frost and Kalkwarf[6], gave as good a fit as two equations of form $\ln p = A/T + B$, and thus these two possibilities cannot be distinguished on numerical grounds.

Whatever the form of equation(s) used, the data shown in Fig. 1 clearly indicate a rapid change of slope at a temperature ~1,361 K. As already suggested by Hensel[1], liquid–vapour equilibrium would be expected to be affected by an electronic 'transition' in the liquid phase or vapour phase, or both. By using our value for T' together with well-established coexistence curve data[7], we obtained a value $\rho_L = 10.7 \pm 0.3\ \mathrm{g\,cm^{-3}}$ for the corresponding liquid phase density. This is about the density which has been taken[1,8] to be that by which the electron mean free path has been reduced to about the mean interatomic spacing, and which marks the beginning of a rapid reduction in the density of states at the Fermi level ($N(E_F)$) for lower densities. The latter densities have been referred to as corresponding to the strong scattering region. As the density of states should affect the thermodynamic properties, we conclude that the reduction of $N(E_F)$ with volumetric expansion of the liquid phase in the strong scattering region is the most likely cause of the different slope of the vapour pressure curve which we have found for temperatures greater than 1,361 K.

S.R.H. acknowledges financial support from the Suffolk County Council. We thank F. Hensel for a preprint.

Received 14 October 1981; accepted 18 January 1982.

1. Hensel, F. in *Proc. 8th Symp. on Thermophysical Properties*, Gaithersburg, (in the press).
2. Sugawara, S., Sato, T. & Minamiyama, T. *Bull. Jap. Soc. mech. Engr* **5**, 711–718 (1962).
3. Neale, F. E. & Cusack, N. E. *J. Phys. F: Metal Phys.* **9**, 85–94 (1979).
4. Schönherr, G. & Hensel, F. *Ber. Bunsenges. Phys. Chem.* **85**, 361–367 (1981).
5. Ewing, C. T. *et al. J. Chem. Engng Data* **15**, 508–510 (1970).
6. Frost, A. A. & Kalkwarf, D. R. *J. chem. Phys.* **21**, 264–267 (1953).
7. Ross, R. G. & Greenwood, D. A. *Prog. Mater. Sci.* **14**, 175–242 (1969).
8. Cusack, N. E. in *The Metal Non-metal Transition in Disordered Systems* (eds Friedman, L. R. & Tunstall, D. P.) 455–490 (Scottish Universities Summer School in Physics, Edinburgh, 1978).

Factors controlling the acidity of natural rainwater

R. J. Charlson* & H. Rodhe

Department of Meteorology, University of Stockholm, Arrhenius Laboratory, S-106 91 Stockholm, Sweden

It is often assumed[1–4] that the *p*H of natural rainwater is controlled by the dissociation of dissolved CO_2, has a value of 5.6, and that decreases below this are due to the addition of acidic components by human activity. However, decreases could be due to the removal by rainwater of naturally occurring acids from the air (notably H_2SO_4 in the natural portion of the sulphur cycle). Consideration of the cycling of water and sulphate through the atmosphere and the amount and composition of sulphate aerosol expected to be scavenged by a given amount of cloud water in remote locations indicates that, in the absence of basic materials (such as NH_3 and $CaCO_3$), average *p*H values of ~5 are expected to occur in pristine locations. This value must vary considerably due to variability in scavenging efficiencies as well as geographical patchiness of the sulphur, nitrogen and water cycles. Thus, *p*H values might range from 4.5 to 5.6 due to variability of the sulphur cycle alone. Because of widespread concern regarding the acidification of rain, it is important to understand the factors controlling the *p*H and composition of natural rainwater. We suggest here that there are integral constraints imposed by (1) the requirement for mass continuity in each elemental cycle and (2) the relative concentrations of soluble species and liquid water in cloudy air; these factors must be mutually consistent.

Although the NH_3/NH_4^+ part of the nitrogen cycle is important (NH_3 being the dominant atmospheric gaseous base) it is not yet possible to consider it quantitatively. Similarly, the $NO/NO_2/HNO_3$ cycle is inadequately measured. However, HNO_3 will always add to the acidity of rainwater due to H_2SO_4. We can make a preliminary estimate of the concentrations of strong acids in rain in remote locations by first studying the sulphur cycle alone. The maximum or potential acidity thus estimated neglects neutralization by bases such as NH_3 or $CaCO_3$ which will increase *p*H. However, as both NH_3 and basic dust concentrations are often low (such as in maritime air) this approach has actual application.

Estimates of the natural flux of sulphur through the atmosphere have been based on indirect arguments: for example, using river run-off data[5], and more direct measurements of deposition by precipitation[6], of emissions of sulphur-containing gases from the ocean surface[7], coastal sediments[8], or volcanoes[9]. The global total of such fluxes—disregarding anthropogenic emissions and those associated with the formation of sea spray—is still uncertain but recent estimates[6,10] are in the range $35-110\times10^{12}$ g S yr^{-1}, which is comparable with the present anthropogenic emissions[11] of $\sim100\times10^{12}$ g yr^{-1}. For illustrative purposes we may assume a value of 60×10^{12} g yr^{-1} for the global emission of natural, non-sea spray sulphur, but it is uncertain by at least a factor of two in either direction. If this sulphur were evenly distributed over the globe and one-half of it were deposited as sulphate in precipitation[12], the resulting pH would be ~5.2 (assuming the remaining sulphur is present as H_2SO_4 in the rainwater).

---

*Present address: Environmental Engineering and Science Program, Department of Civil Engineering, University of Washington, Seattle, Washington 98195, USA.

Note that the 'global sulphur cycle' is far from global. Because of the limited residence time in the atmosphere of the major sulphur-bearing compounds (H_2S, $(CH_3)_2S$, SO_2 and SO_4^{2-})[12] and an uneven geographical and temporal distribution of sources and sinks, the sulphur cycle will exhibit large variations in space and time. Examples include volcanic emissions of SO_2; production of $(CH_3)_2S$ in the surface water of the oceans and its subsequent release to the atmosphere that is likely to be coupled to the biological productivity of the ocean water and therefore vary with it; and the possibility of enhanced sulphur emissions in coastal areas (see, for example, ref. 13). (OCS, while important in terms of concentration, is assumed to be less important in this context due to a smaller flux.) Consequently, the global averages need not be very representative for any particular location. As a first step towards examining the factors controlling this variability, the cycle can be evaluated over spatial scales compatible with the average residence time in the atmosphere of the important sulphur compounds, that is, a few hundred to a few thousand kilometres[14]. Studies of regional sulphur budgets have already been attempted for regions with very large industrial emissions[15,16].

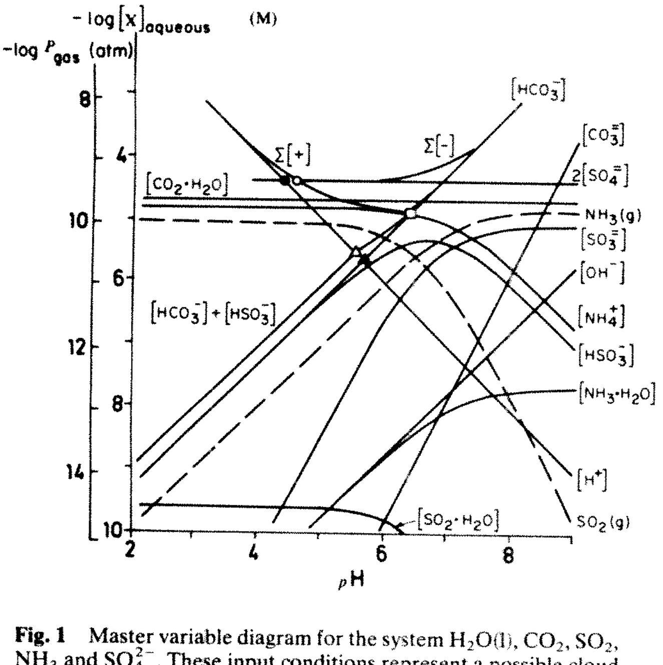

Fig. 1 Master variable diagram for the system H_2O(l), CO_2, SO_2, NH_3 and SO_4^{2-}. These input conditions represent a possible cloud in a remote, unpolluted area. Assumptions: $T=5$ °C; $L=0.5$ g m^{-3} liquid cloud water; $CO_2=340$ p.p.m.v.; $SO_2=100$ p.p.t.v.; $(NH_3+NH_4^+)=0.13$ μg m^{-3} as NH_3; $(SO_4^{2-})_{aerosol}=1.0$ μg m^{-3}, all dissolved in cloud. Charge balances: ○, pH 4.6 for whole system; ●, pH 4.4 in absence of NH_3 (and NH_4^+); □, pH 6.2 in absence of SO_4^{2-}; △, pH 5.5 in absence of both NH_3 and SO_4^{2-}; ▲, pH 5.6 in absence of NH_3, SO_4^{2-} and SO_2. [X] denotes aqueous concentration (M). SO_2(g) and NH_3(g) represent the gas phase (----). Equations and equilibrium constants have been taken from refs 17, 35.

Table 1 Potential acidity (pH) of atmospheric liquid water: effects of dissolved aerosol SO_4^{2-} and liquid water content of cloud

SO_4^{2-}	L (g m^{-3})		
(μg m^{-3})	0.1	0.5	2.5
0.04	5.1	5.4	5.5
0.2	4.4	5.1	5.4
1.0	3.7	4.4	5.1

Concentrations of CO_2 and SO_2 are assumed to be constant and equal to 340 p.p.m.v. and 100 p.p.t.v. respectively. Total $NH_3=0$.

We conclude that substantial variations around the global average value of the potential acidity attributable to naturally circulating sulphur should be expected. The absolute magnitude of such variations is hard to estimate without a better understanding of the characteristics of the regional sulphur cycles, but variation by a factor of five either way seems possible. The corresponding pH values would then lie in the range 4.5–5.6. If the natural part of the atmospheric sulphur cycle is not spatially uniform by even a factor of two, then the pH of rainwater unaffected by human activity could be <5.0 in some regions. (Note that the concentration of hydrogen ion in rainwater will be influenced by other compounds as well; for example, the NH_3/NH_4^+ cycle may be as variable as the sulphur cycle, and probably not in phase with it.)

Another approach to estimating the composition of rainwater is to utilize existing data on aerosol composition and liquid water content of clouds. Although the degree to which the composition thus calculated may reflect that of rain itself is not known precisely, the composition of rainwater, cloud water and the aerosol and trace gases that went into the cloud must be related.

Equilibria exist in clouds among several trace gases, their respective dissolved species and liquid water, and there are further inputs of aerosols containing sulphates, soil-derived dust and sea salt to cloud droplets. The sulphate aerosols are of particular interest because they often occur as H_2SO_4 partly neutralized by NH_3 (ref. 17). An approximate empirical formula of NH_4HSO_4 exists in remote, maritime submicrometre aerosols[18] and, as such particles can be incorporated into cloud droplets, sulphate aerosols are potentially important sources of strong acid in rain. If we neglect the soil dust and sea salt, given the 3 Henry's law expressions for NH_3, SO_2 and CO_2, 6 equilibria for dissociation of these and water, 3 mass conservation equations for NH_3 and NH_4^+, S(IV) and carbonate species and one equation of charge balance, a system of 13 equations can be solved for the equilibrium conditions[17]. Figure 1 is a Sillén or master variable diagram[19] for the system NH_3, SO_2, CO_2, H_2SO_4 and H_2O(l) in a pristine cloud, in which the concentration of each dissolved species and the partial pressure of the trace gases are given as functions of pH. When the 9 equilibrium statements are combined with the conservation equations, 12 separate curves result, portraying the concentration of each of the species. In addition, $[SO_4^{2-}]$ is given as pH independent at $p\text{H}>3$, while CO_2(g) is omitted and the sum of $[HSO_3^-]+[HCO_3^-]$ is included. The charge balance then is given at the pH where the sums of positive and of negative charges are equal ($\Sigma[+]=\Sigma[-]$). For this set of conditions (see Fig. 1 legend), at $p\text{H}=4.6$ there is charge neutrality (open circle in Fig. 1) and sulphate is the dominant anion; $[NH_4^+]$ is slightly $<[H^+]$, $[HCO_3^-]\cong[HSO_3^-]\cong10^{-6.8}$ and $\ll[SO_4^{2-}]$. Also, the partial pressure scale is set so that the curves for SO_2(g) and NH_3(g) have the same limiting ordinate value as $[SO_3^{2-}]$ and $[NH_4^+]$ respectively. Thus the mass continuity expressions for these two can also be followed graphically as functions of pH, showing that if $p\text{H}<5.5$, most S(IV) is SO_2(g) while NH_4^+ is the dominant ammonia species.

This plot can also be used to show what equilibrium pH would occur in the absence of various components. Only in the absence of NH_3, SO_2 and SO_4^{2-} does pH equal 5.6; higher values occur with the absence of SO_4^{2-} alone, while pH decreases if NH_3 is removed. Increasing CO_2 slightly decreases the pH in those cases where SO_4^{2-} is low. (Doubling CO_2 causes at most a decrease in pH of 0.15.) Decreasing SO_4^{2-} or increasing NH_4^+ by even small amounts increases the pH significantly. Complete oxidation of all the SO_2 in the cloud would raise $[SO_4^{2-}]$ to 2.8×10^{-5} M and decrease the equilibrium pH to 4.4, with all other variables constant. Thus, although these input conditions were selected as possible in a remote, unpolluted area, they are clearly variables to which pH is very sensitive.

To study further the relationship between the chemical compositions of aerosols, cloud water and rainwater and to estimate the effect of their variability on pH, consider the simplest case of in-cloud scavenging of a pre-existing sulphate aerosol with no in-cloud SO_2 oxidation. The cloud water composition is then given by[20]

$$[SO_4^{2-}]_{\mathrm{cloud}} = \frac{\varepsilon(SO_4^{2-})_{\mathrm{aerosol}}}{96L} \qquad (1)$$

where $[SO_4^{2-}]$ cloud is the molar sulphate concentration in cloud water, 96 is the molecular mass of SO_4^{2-}, $(SO_4^{2-})_{\mathrm{aerosol}}$ is the mass concentration of sulphate aerosol in air ($\mathrm{g\,m^{-3}}$), ε is the scavenging efficiency for sulphate aerosol particles in the cloud and L is the liquid water content ($\mathrm{l\,m^{-3}}$) of the cloud. For soluble particles of 0.1–1.0 μm radius, ε is expected to be[20] 0.5–1.0.

Allowing for dilution (D) and evaporation (E) of the cloud and rainwater, the sulphate concentration in rainwater becomes:

$$[SO_4^{2-}]_{\mathrm{rain}} = (SO_4^{2-})_{\mathrm{aerosol}}\frac{\varepsilon DE}{96L} \qquad (2)$$

Data from the OECD study on long-range transport of air pollutants[21] indicate a value of $\varepsilon DE/L$ in the range $(0.6\text{–}1.6)\times 10^3\ \mathrm{m^3\,kg^{-1}}$. If ε, D and E were unity, this would correspond to a liquid water content of $\sim 1\ \mathrm{g\,m^{-3}}$, a value which is reasonable compared with observations of the liquid water content of precipitating clouds[22] and consistent with other published values of washout ratios[23,24].

Table 1 lists values of expected pH of rain as a function of $(SO_4^{2-})_{\mathrm{aerosol}}$ and L for $\varepsilon\times D\times E=1$. The effects on pH of compounds other than CO_2 and a background concentration of SO_2 of 100 p.p.t.v. (parts per 10^{12} by vol.)[25] are disregarded. For simplicity, SO_2 is assumed not to react. The L values used embrace most measured values of the liquid water content of clouds[22]. Generally, the lower values may be more representative of fogs and stratiform clouds[26] and the higher values of convective clouds, especially the rain-producing ones. Data from remote locations on the concentration of aerosol sulphate (excluding the contribution from sea spray) are sparse but values vary from $\sim 0.05\ \mu\mathrm{g}\ SO_4^{2-}\ \mathrm{m^{-3}}$ in remote parts of South America[27] to of the order of $1\ \mu\mathrm{g}\ SO_4^{2-}\ \mathrm{m^{-3}}$ in the marine boundary layer[28,29]. The range of sulphate values used in the Table evidently covers most of the observed data. Although it might have been logical to vary SO_2 with the concentrations of sulphate, dissolved SO_2 itself only slightly affects pH (see Fig. 1), and we did not want to complicate the picture with further variations. Clearly a raining cloud low in both basic materials and L might be quite acidic. It is not possible to construct a frequency-of-occurrence histogram from these computations, the above discussion indicates that pH values well below 5 might occur in pristine areas.

Considerable spatial and temporal variations in the acidity should be expected with lowest pH values occurring in situations with high concentrations of non-sea spray sulphate in aerosols, low concentrations of basic constituents (such as ammonia gas, $CaCO_3$) and low liquid water content in the clouds. As the sources of these basic constituents are mainly in continental areas whereas substantial emissions of sulphur compounds take place over the oceans, rain is likely to be more acidic in marine environments than over the continents. It is therefore not appropriate to use $p\mathrm{H}=5.6$ as a reference value against which human influences should be judged. We believe that, generally, pH alone is a poor indicator of departure from the natural composition of rain and cloud water, mainly because of its large natural variability and the difficulty of measuring it accurately.

To assess man-made acidification it is necessary to study in detail the cycles—particularly of sulphur and nitrogen—that influence the acidity of atmospheric water, in different regions of the world, and the degree to which the cycles have been affected. Long-term (decades) programmes for monitoring the chemical composition of air and precipitation should be supplemented by direct estimates of emission fluxes from different types of sources potentially affecting the monitoring sites. A large number of variables must be studied simultaneously to define clearly natural and perturbed conditions.

Note that the present pH values in precipitation in the heavily industrialized regions are significantly affected by anthropogenic emissions. In Northern Europe and eastern parts of North America[4,30,31], annual average pH values of 4.3 are common. At a typical station in rural parts of southern Sweden (Forshult; lat. 60.15 N long. 13.78 E) 50% of the monthly precipitation samples during the period 1975 to 1980 had a pH value in the range 4.1–4.6, due primarily to H_2SO_4 and secondarily to HNO_3 (ref. 32). Annual sulphur deposition as SO_4^{2-} is typically 2–3 $\mathrm{g\,m^{-2}}$, resulting in substantial ecological effects[31]. Clearly the sulphur and nitrogen cycles in these regions are much perturbed[15,21] and if all industrial emissions of SO_2 and NO_x were stopped—emissions of NH_3 remaining the same—the pH would increase to >5. Note that low pH values reported for rainwater in remote locations[33,34] need not be interpreted as due exclusively by natural processes. The possibility of long-range as well as local anthropogenic influences should be investigated. However, natural factors exist which can cause variable and significant decreases of pH from that expected from pure carbonic acid equilibrium.

Contribution No. 448 from International Meteorological Institute, Stockholm, Sweden.

Received 23 October; accepted 16 December 1981.

1. Garrels, R. M. & MacKenzie, F. T. *Evolution of Sedimentary Rocks* (Norton, New York, 1971).
2. Galloway, J. N., Likens, G. E. & Edgerton, E. S. *Science* **194**, 722–724 (1976).
3. Likens, G. E. & Bormann, F. H. *Science* **184**, 1176–1179 (1974).
4. Likens, G. E., Bormann, F. H. & Johnson, N. M. in *Some Perspectives of the Major Biogeochemical Cycles* SCOPE Rep. 17 (ed. Likens, G. E.) (Wiley, Chichester, 1981).
5. Hallberg, R. O. in *Nitrogen, Phosphorus and Sulphur—Global Cycles* SCOPE Rep. 7, (eds Svensson, B. H. & Söderlund, R.) 93–101 (Swedish Natural Science Research Council, 1976).
6. Granat, L. in *Nitrogen, Phosphorus and Sulphur—Global Cycles* SCOPE Rep. 7 (eds Svensson, B. H. and Söderlund, R.) 102–122 (1976).
7. Nguyen, B. C., Gaudry, A., Bonsang, B. & Lambert, G. *Nature* **275**, 637–639 (1978).
8. Hansen, M. H., Ingvorsen, K. & Jørgensen, B. B. *Limnol. Oceanogr.* **23**, 68–76 (1978).
9. Cadle. R. D. *J. geophys. Res.* **80**, 1650–1652 (1975).
10. Friend, J. P. in *Chemistry of the Lower Atmosphere* (ed. Rasool, S. I.) 177–201 (Plenum, New York, 1973).
11. Cullis, C. F. & Hirschler, M. M. *Atmos. Envir.* **14**, 1263–1278 (1980).
12. Rodhe, H. & Isaksen, I. *J. geophys. Res.* **85**, 7401–7409 (1980).
13. Eriksson, E. *Tellus* **12**, 63–109 (1960).
14. Rodhe, H. *Atmos. Envir.* **12**, 671–680 (1978).
15. Rodhe, H. in *Nitrogen, Phosphorus and Sulphur—Global Cycles* SCOPE Rep. 7 (eds Svensson, B. H. & Söderlund, R.) 123–128 (Swedish Natural Science Research Council, 1976).
16. Galloway, J. N. & Whelpdale, D. M. *Atmos. Envir.* **14**, 409–418 (1980).
17. Taylor, G. S., Baker, M. B. & Charlson, R. J. in *Interaction of the Biogeochemical Cycles* (eds Bolin, B. & Cook, R.) (Wiley, London, 1982).
18. Duce, R. A. *Biogeochemical Cycles and the Air/Sea Exchange of Aerosols* (Wiley, London, 1982).
19. Sillén, L. G. in *Equilibrium Concepts in Natural Water Systems* Adv. Chem. Ser. no. 67, 45–56 (American Chemical Society, Washington DC, 1967).
20. Junge, C. E. *Air Chemistry and Radioactivity* (Academic, New York, 1963).
21. OECD. *The OECD Programme on Long Range Transport of Air Pollutants, Measurements and Findings* (Organization for Economic Cooperation and Development, Paris, 1977).
22. Fletcher, N. H. *The Physics of Rain Clouds* (Cambridge University Press, 1962).
23. Slinn, W. G. N. *et al. Atmos. Envir.* **12**, 2055–2087 (1978).
24. Scott, B. C. *J. appl. Met.* **20**, 619–625 (1981).
25. Maroulis, P. J., Torres, A. L., Goldberg, A. B. & Bandy, A. R. *J. geophys. Res.* **85**, 7345–7349 (1980).
26. Garland, J. A. *Q. J. R. met. Soc.* **97**, 483 (1971).
27. Lawson, D. R. & Winchester, J. W. *Science* **205**, 1267–1269 (1979).
28. Huebert, B. J. & Lazrus, A. L. *J. geophys. Res.* **85**, 7337–7344 (1980).
29. Bonsang, B., Nguyen, B. C., Gaudry, A. & Lambert, G. *J. geophys. Res.* **85**, 7410–7416 (1980).
30. Bolin, B. *et al. Air Pollution Across National Boundaries; The Impact on the Environment of Sulfur in Air and Precipitation* (Royal Ministry for Foreign Affairs, Stockholm, 1971).
31. Drabløs, D. & Tollan, A. *Ecological Impact of Acid Precipitation*; Proceedings of an International Conference (SNSF, Ås, Norway, 1980).
32. Granat, L. *Atmos. Envir.* **12**, 413–424 (1978).
33. NOAA. *Geophysical Monitoring for Climatic Change* No. 7 (National Oceanic and Atmospheric Administration, Boulder, Colorado, 1979).
34. Kerr, R. A. *Science* **212**, 1014 (1981).
35. Larsen, T. V. & Harrison, H. *Atmos. Envir.* **11**, 1133–1141 (1977).

Mesozoic magnetic anomalies in the southern Natal Valley

S. W. Goodlad*, A. K. Martin* & C. J. H. Hartnady†

* Marine Geoscience Unit and † Precambrian Research Unit,
Department of Geology, University of Cape Town, Rondebosch,
South Africa

The recognition of Mesozoic magnetic anomalies M0–M12 within the submarine Natal Valley (south-west Indian Ocean) provides a further constraint on the relative motion between South America (Falkland Plateau) and Africa during the early opening phase of West Gondwanaland (Fig. 1). Colinear with M12, magnetic anomaly *G* (ref. 1) is delineated north of the South Tugela Ridge[2], an acoustic basement high which is suspected to have been emplaced within continental crust immediately north of the continental–oceanic crust boundary (COB) during the initial rifting phase. Starting from a revised West Gondwana reconstruction[3] and using palaeo-poles of rotation[1,3], the Falkland Plateau can be rotated into the Natal Valley superposing the corresponding Georgia Basin and Natal Valley magnetic anomalies. This achieves an optimum continuity of inter-continental structural lineaments[3] by overlapping of an anomaly intermediate to M10 and M11 (~M10N[4]). This suggests that the Natal Valley COB is located between anomalies M10 and M11, implying that in this zone of south-west Gondwana, seafloor spreading commenced at ~125 Myr.

Previous confirmation of the continental nature of the Falkland Plateau[5-7], necessitates its inclusion in recent reconstructions of south-west Gondwana[3,7,8]. In these reconstructions it fits into the gap between south-east Africa and the Mozambique Ridge (Fig. 1). During the West Gondwana drift phase, the Falkland Plateau moved past Africa constrained by the orientation of the Agulhas/Falkland Fracture Zone[9,10]. Recognition of magnetic anomalies on conjugate margins of the southern South Atlantic has helped to define the seafloor spreading history of South America and Africa[1] north of the Agulhas/Falkland Fracture Zone. In contrast, to the south of this fracture zone, the Natal Valley has been largely ignored as a prospective source of geophysical data for testing reconstruction of West Gondwana. The distant location (~40°) from the early pole of rotation[1,3] suggests that seafloor spreading in the Natal Valley may have advanced at a fast rate and thus resultant magnetic anomalies should be widely spaced and easy to recognize. Magnetic anomaly lineations present in the Natal Valley should be aligned approximately perpendicular to the Agulhas Fracture Zone.

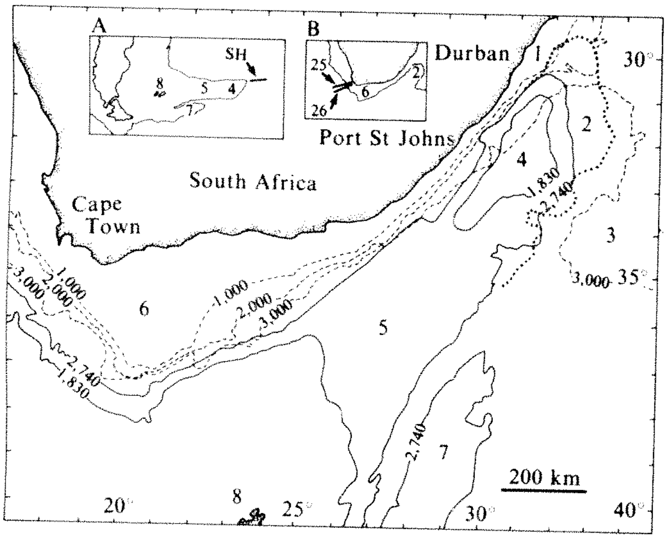

Fig. 1 Reconstruction of south-west Gondwana after Martin *et al.*[3] depicting the close contiguity of the Falkland Plateau and Natal Valley physiographic features. Dashed line, South African bathymetry[2,17] (1,000, 2,000 and 3,000 m). Solid line, South American/Falkland Plateau bathymetry[18] (1,830 and 2,740 m); conversion factor 1 fathom = 1.83 m. Alternative position for north-east apex of the Falkland Plateau (2,740 m isobath) in reconstruction using Rabinowitz and LaBrecque[1] rotation parameters dotted. Physiographic zones: 1, Tugela Cone; 2, Natal Valley; 3, Mozambique Ridge; 4, Maurice Ewing Bank; 5, Falkland Plateau Basin; 6, Agulhas Bank (Outeniqua Basin); 7, Burdwood Bank; 8, Falkland Islands. A, The location of magnetic profile Shackleton[11] (SH) in the Georgia Basin east of the Falkland Plateau apex. B, Locations of magnetic profiles 25 and 26 (ref. 1) from the Cape Basin, south-west of South Africa.

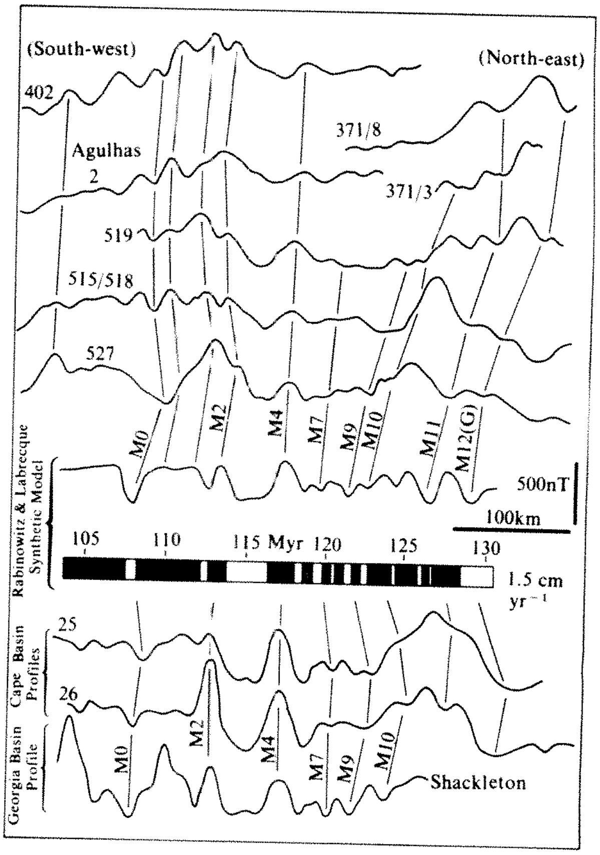

Fig. 2 Natal Valley magnetic profiles geographically aligned and correlated with respect to the magnetic block model of Rabinowitz and LaBrecque[1]. The model was generated by using a half spreading rate of 1.5 cm yr^{-1} for the Mesozoic reversal time scale of Larson and Hilde[4]. Profiles 402 (PR 2a), 371/8, 371/3, Agulhas 2, 519 (PR 3), 515/518 (PR 4) and 527 (PR 5) trend south-west–north-east within the Natal Valley sub-parallel to the Agulhas Fracture Zone. Notation in brackets refers to profile numbers used by du Plessis[10]. Profiles 25 and 26 (after ref. 1) from the Cape Basin and profile Shackleton (after ref. 11) from the Georgia Basin (immediately east of the Falkland Plateau) are included to show their general similarity to the Natal Valley traverses. Profile Shackleton is depicted as a mirror-image. Locations of profiles 25, 26 and Shackleton are shown in Fig. 1 insets.

Four previously published magnetic traverses[10] reassessed in conjunction with newly acquired data reveal a Mesozoic magnetic anomaly lineation pattern (Cape Sequence) within the southern Natal Valley (Fig. 2). Du Plessis[10] recognized magnetic lineations normal to the coast but did not correlate these with any published Mesozoic anomaly models[1,4]. The reinterpreted profiles (527, 515/518, 519, 371/3, 371/8, Agulhas 2 and 402) are geographically aligned and compared with the Mesozoic anomaly sequence of Rabinowitz and LaBrecque[1] in Fig. 2. Inter-profile correlation and correspondence to the synthetic model is good. The slight disparity of profile 527 with respect to the synthetic is suspected to be due to navigational inaccuracy. The Natal Valley and Cape Basin magnetic signatures parallel to the spreading direction show similarities (Fig. 2), confirming correct anomaly sequence identification.

We recognize anomalies M12 to M0 with correlation being particularly good for M4 to M0 (Fig. 2). Anomaly M4 is prominent in all profiles as a broad positive anomaly 250 nT in amplitude while the M2–M0 composite anomaly is conspicuous as a positive triple peak some 200–500 nT in amplitude. Lineations defining M11, M9 and M7 are less distinct but still considered valid (Fig. 2). However, identification of the Mesozoic Cape Sequence rests primarily on recognition of anomalies M4–M0.

The observed profiles provide a reasonable fit to the model[1] presented in Fig. 2 and thus 1.5 cm yr^{-1} is proposed as an average Mesozoic half-spreading rate for the Natal Valley. In detail, however, the M4–M0 rate appears slightly slower than the 1.5 cm yr^{-1} model (the anomalies are more compressed) while a slightly faster spreading rate (~1.7 cm yr^{-1}) may be appropriate to the M11–M4 sequence. These velocities are comparable with those calculated for crust immediately east of the Falkland Plateau in the Georgia Basin[11].

An areal plot of the magnetic traverses (Fig. 3) show the anomalies to be in sub-parallel alignment with a strike trend normal to the Agulhas Fracture Zone (defined here by the Cape Slope Anomaly[12]). Oceanic crust that was created directly east of the Falkland Plateau in the Georgia Basin should theoretically generate mirror images of Natal Valley magnetic profiles although these may now be distorted by differing ambient field declination, inclination and skewness. A profile from the Georgia Basin[11], plotted in reverse in Fig. 2, exhibits a degree of similarity to Natal Valley anomalies.

Recently, Martin *et al.*[3] proposed a revised fit of South America and South Central Africa (Fig. 1) primarily based on cross-continent alignment of three major pre-drift tectonic features: (1) the eastern and western boundaries of the submarine Jurassic Outeniqua Basin (Agulhas Bank) and the Falkland Plateau Basin; (2) the northern tectonic limit of the Triassic Cape Fold Belt (South Africa) and a closely contiguous major morphological feature on the Falkland Plateau; and (3) the late Precambrian transcurrent fault and mylonite belts of Pernambuco (Brazil) and Foumban (West Africa).

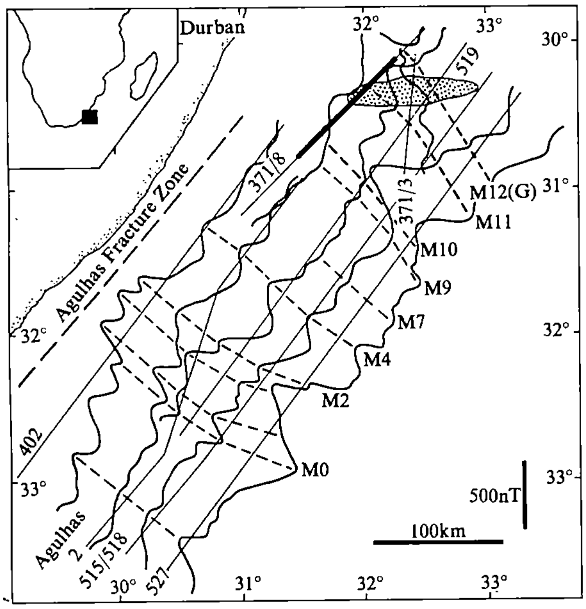

Fig. 3 Magnetic anomaly profiles plotted perpendicular to ship's tracks. Lines 402, 515/518, 519, 527, 371/3 and 371/8 were run between 1971 and 1977 on the *RV Thomas B. Davie*. Track Agulhas 2 was run on the *MV S A Agulhas* in August 1978. Inter-profile correlation identifying the Mesozoic anomaly sequence M12 (*G*) to M0 picked out by short dashed lines. Disparity of traverse 527 is suspected to be due to navigational inaccuracy. Note that the anomaly sequence trends normal to the Agulhas Fracture Zone (heavy dashed line adjacent to the coast). Enhanced portion of traverse 371/8 indicates location of the continuous seismic reflection profile depicted in Fig. 4. Dotted zone demarcates the seismically-defined extent of the South Tugela Ridge. Inset shows the study area in relation to southern Africa and Madagascar.

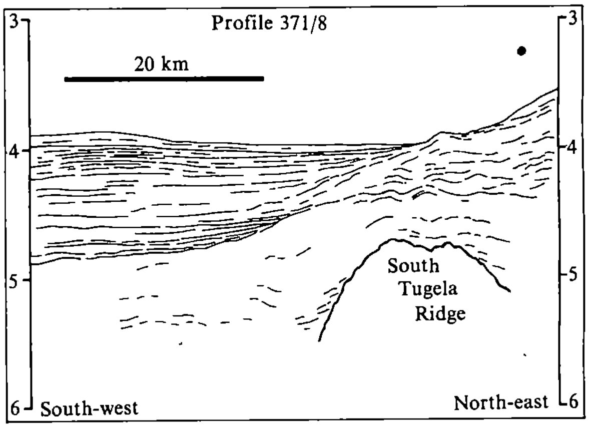

Fig. 4 Line tracing of continuous seismic reflection profile (371/8) showing the acoustic signature of the South Tugela Ridge. Profile location is shown in Fig. 3. Vertical scale is in seconds of two-way travel time.

This revised reconstruction[3] (total pole of rotation 46.75° N, 32.65° W; rotation angle 56.4°) is close to the refit of Rabinowitz and LaBrecque[1] but does not so tightly juxtapose conjugate margins of the Natal Valley and Falkland Plateau (see Fig. 1). This looser reconstruction[3] therefore removes suspected continental basement overlap in the Natal Valley and Precambrian basement overlap in the Gulf of Benin (West Africa)[3].

Seismic profiling surveys have delineated an approximately east–west oriented, deeply buried, basement ridge—the South Tugela Ridge (Fig. 4) underlying or immediately south of the steep Tugela Cone southern flank. The ridge location is depicted in Fig. 3. Significantly, in the revised reconstruction of Martin *et al.*[3], the South Tugela Ridge becomes juxtaposed to the continental–oceanic crust boundary (COB) of the Falkland Plateau as approximated by the 2,740 m isobath on seismic refraction results[5]. Independent geological–geophysical evidence therefore suggests that the South Tugela Ridge may be situated just north of the Natal Valley COB and is probably a result of initial rift volcanics intercalating with splintered continental blocks.

Within the Natal Valley, the oldest correlative magnetic anomaly is identified as M12 (Figs 2 and 3) and corresponds in character to anomaly *G* of Rabinowitz and LaBrecque[1,13]. Magnetic anomaly *G*, first mapped along the west coast of Africa[1,13], has been interpreted as a magnetic edge effect separating continental from oceanic basement. Reinforced by isostatic gravity modelling, Rabinowitz and LaBrecque use anomaly *G* to demarcate the COB. However, the west coast Africa magnetic lineation *G*, to which Rabinowitz and LaBrecque[1] assign an M12 age, has previously been dated as M13 by Larson and Ladd[14] using the same raw data; thus dating of this anomaly is not unambiguous.

The revised fit of Martin *et al.*[3] suggests that the south-west Africa COB may be sited ~40 km seaward of magnetic anomaly *G*, but still positioned within the landward gradient of the isostatic gravity anomaly. On the basis of reconstruction evidence[3], the Natal Valley COB is suspected to be located south of the South Tugela Ridge implying that anomaly *G* is placed on continental crust.

Utilizing the new palaeo-spreading pole of Martin *et al.*[3], the rotation of South America towards Africa achieves precise juxtaposition of Mesozoic anomalies (M0, M2, M4 and M10) in areas both south and north of the Agulhas/Falkland Fracture Zone. Thus, using only one set of rotation parameters, abutment of Cape and Argentine Basin anomalies[1] is simultaneous to abutment of the equivalent Natal Valley and Georgia Basin anomalies[11]. Complete kinematic description of the early spreading history will be more fully considered elsewhere. However, back-rotation to M10N (an anomaly intermediate to M10 and M11)[4] accomplishes optimum contiguity of the intercontinental structural lineaments previously described. We therefore postulate that opening of the South Atlantic commenced at ~125 Myr (M10N using the time scale of Larson and Hilde[4]).

Accepting this looser reconstruction as compared to that of Rabinowitz and LaBrecque[1] (see Fig. 1), it is necessary to explain the existence of recognizable magnetic lineaments (M11 and M12) landward of M10N (approximate COB) as demarcated in Figs 2 and 3. A possible explanation may be that before final separation, crustal rifting allowed extensive intrusion of volcanic lavas which were magnetized in the Earth's ambient field. This mechanism, with possible interference from basement topography and non-magnetized slivers of continental crust, may explain the poorer M11 and M12 correlation with the modelled profile (Fig. 2) and severe anomaly distension on several profiles. Larson and Ladd[14] likewise attribute poor correlation between anomalies older than M7 along the south-west Africa continental margin to disruption of the lineation pattern by the initial rifting phenomenon. Basement topography certainly induces modulation of the ambient field in this zone with high amplitude positive anomalies plotting over the South Tugela Ridge (Fig. 3, profiles 371/8, 371/3 and 519).

The collection of multichannel seismic data off the continental margin of south-west Africa[15,16] has cast additional doubt on the 'anomaly *G*' refit[1] of South America and Africa. In particular, Uchupi and Austin[15] locate their southwestern Africa COB at or closely seaward of the 3,000 m isobath. This placement is in general agreement with the reconstruction of Martin *et al.*[3] which likewise corroborates the new magnetic evidence presented here. Although the south-west Africa COB of Gerrard and Smith[16] is located even further seaward, constraints on data quality allow for some ambiguity in exact positioning (I. Gerrard, personal communication, 1981). These new multichannel data also imply that extensive intracontinental stretching took place along the passive margin of south-west Africa[15] during the early opening phase of the South Atlantic. However, the reconstruction of Martin *et al.*[3] in combination with the magnetic data outlined in this study suggests that post-breakup continental crust stretching may not have been active over the Falkland Plateau/Natal Valley zone.

We thank R. V. Dingle for a critical review, D. Murray and the CSIR for access to unpublished Agulhas 2 magnetic data, the Director of the Geological Survey for funding the project and permission to publish, and Mrs M. C. Hollander for typing the script.

Received 30 April; accepted 30 October 1981.

1. Rabinowitz, P. D. & LaBrecque, J. L. *J. geophys. Res.* **84,** 5973–6002 (1979).
2. Goodlad, S. W. thesis, Univ. Cape Town (in preparation).
3. Martin, A. K., Hartnady, C. J. H. & Goodlad, S. W. *Earth planet. Sci. Lett.* **54,** 293–305 (1981).
4. Larson, R. L. & Hilde, T. W. C. *J. geophys. Res.* **80,** 2586–2594 (1975).
5. Ewing, J. I., Ludwig, W. J., Ewing, M. & Eittreim, S. C. *J. geophys. Res.* **76,** 7118–7137 (1971).
6. Rabinowitz, P. D., Cande, S. C. & LaBrecque, J. L. *Ann. Acad. Brasil. Cienc.* **48,** 241–251 (1976).
7. Barker, P. F. *et al. Init. Rep. DSDP* Leg **36,** 933–1014 (1977).
8. Norton, I. O. & Sclater, J. G. *J. geophys. Res.* **84,** 6803–6830 (1979).
9. Francheteau, J. & Le Pichon, X. *Bull. Am. Ass. petrol. Geol.* **56,** 991–1007 (1972).
10. du Plessis, A. *Nature* **270,** 719–721 (1977).
11. Barker, P. F. *Geophys. J.R. astr. Soc.* **59,** 131–145 (1979).
12. du Plessis, A. & Simpson, E. S. W. *Mar. geophys. Res.* **2,** 99–110 (1974).
13. Rabinowitz, P. D. *Bull. geol. Soc. Am.* **87,** 1643–1653 (1976).
14. Larson, R. L. & Ladd, J. W. *Nature* **246,** 209–212 (1973).
15. Uchupi, E. & Austin, J. A. *EOS* **62,** 407 (1981).
16. Gerrard, I. & Smith, G. C. *Paper presented at the Hedberg Research Conf. on Continental Margins*, Galveston (1981).
17. Simpson, E. S. W. *Geol. Soc. S. Afr.* **80,** Annexure 1–15 (1977).
18. Lonardi, A. G. & Ewing, M. *Phys. Chem. Earth* **8,** 79–121 (1971).

Magnetic granulometry results for intrusive rock samples

G. S. Murthy & R. R. Pätzold

Geomagnetic Research Laboratory, Physics Department,
Memorial University of Newfoundland, St John's, Newfoundland,
Canada A1B 3X7

'Magnetic granulometry' techniques have been developed[1–4] to infer the domain state of magnetic minerals contained in rocks. Such techniques include study of the development of hysteresis of samples in fields of the order of 10 Oe (Rayleigh loops), study of hysteresis in high fields both at room temperature and at liquid nitrogen temperatures, and study of variation of magnetic susceptibility with temperature from −196 °C to 700 °C. These methods enable the magnetic properties to be quickly determined and so give an idea of the bulk magnetic behaviour of the rock sample. Although the usefulness of such methods for palaeomagnetic studies is limited because the remanent magnetic behaviour can be quite distinct from the bulk magnetic behaviour[5], in general, the granulometry method is a good supplement to regular experimental methods in palaeomagnetism. The study of several thousands of basalt samples by this method[6,7] has revealed insights into the magnetic behaviour of rocks. However, as part of the interpretive procedure of the method, the presence of low-field hysteresis loops has been considered a diagnostic feature of predominant superparamagnetic bulk behaviour of the rock sample. As we report here, we have observed, for the first time, low-field hysteresis loops associated with confirmed multi-domain magnetic grains, a possibility originally suggested on theoretical grounds by Néel[8].

Although the interpretation of results from granulometric experiments is controversial[7], there is agreement on the following basic points:

(1) A sample with multi-domain pure magnetite as the magnetic mineral will generally show $J_r/J_{\max} \sim 0.2$ with approximate doubling of coercivity as the temperature of the sample is changed from room temperature (25 °C) to liquid nitrogen temperature (−196 °C), a phenomenon consistent with earlier work[9,10]. As the magnetocrystalline anisotropy is more dominant than the shape anisotropy for multi-domain magnetic grains, magnetic susceptibility for this class of samples will be a function of the magnetocrystalline anisotropy constants K_1 and K_2. Because K_1 and K_2 change sign at approximately −150 °C (refs 11, 12), an isotropic point with resultant susceptibility peak occurs close to that temperature. Low-field hysteresis loops for this class of samples have not previously been observed, and Fig. 1*a*, *d*, *g* shows their characteristics.

(2) A sample with single-domain magnetite as the magnetic mineral will have $J_r/J_{\max} = 0.5$ at room temperature, increasing to 0.8 at −196 °C, with a corresponding increase in coercivity. For this class of samples, due to the dominance of shape anisotropy over magnetocrystalline and/or stress anisotropy, the susceptibility peak at the isotropic point would be suppressed and a monotonic susceptibility decrease is usually observed as the temperature is lowered from 25 °C to −196 °C. This class of samples does not exhibit Rayleigh loops. Typical results are shown in Fig. 1*b*, *e*, *h*.

(3) In the class III samples, which were interpreted as being due to the predominantly superparamagnetic bulk behaviour of the sample, Rayleigh loops would be observed[13,14], due to the interaction of clusters of superparamagnetic grains. The high-field hysteresis would show $J_r/J_{\max} \sim 0.2$ at 25 °C, increasing to >0.80 at −196 °C, with a substantial increase in coercivity due to grains which are superparamagnetic at room temperature becoming effectively single-domain at −196 °C because of the lowering of the thermal energy. The susceptibility–temperature

0028–0836/82/080688—03$01.00

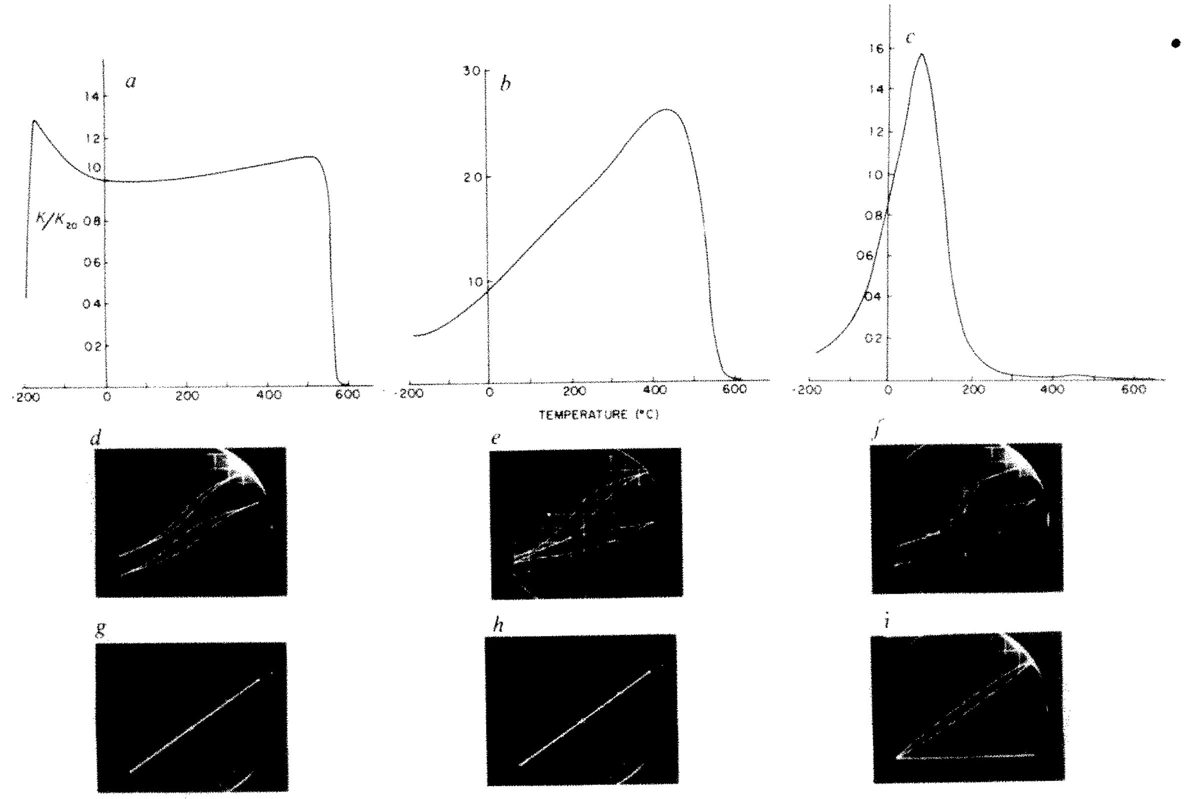

Fig. 1 Basis for interpretation of magnetic granulometry. *a–c*, Normalized susceptibility versus temperature; *d–f*, magnetic hysteresis in a field of 1,200 Oe at room temperature (upper trace) and at −196 °C (bottom trace); *g–i*, Rayleigh loops in a field of 10 Oe. *a*, *d*, *g* are typical responses for class I behaviour (multi-domain) as obtained on G215C, a dolerite dyke sample from Newfoundland; *b*, *e*, *h* are typical responses for class II behaviour (single domain) as obtained on a basalt sample from a DSDP drill hole; *c*, *f*, *i* are typical responses for class III behaviour (superparamagnetic) as obtained on a basalt sample from a DSDP drill hole.

curve would show a decrease in normalized susceptibility to ~0.2 at −196 °C and a location of the peak which differs in different samples, but which is nearly always at temperatures <300 °C, followed by a long tail. Figure 1*c*, *f*, *i* shows typical results exhibited by a member of this class of samples. Class III and class II behaviours were previously designated type 1 and type 2[15,16].

The most controversial aspect of this interpretation is the inference of superparamagnetic grains from the presence of Rayleigh loops and the typical susceptibility–temperature curves of the class III type. The observed grain sizes in most rocks exhibiting this behaviour are of the order of hundreds of micrometres, and for the grains to behave like superparamagnetics, they must be effectively subdivided into SP sizes. The question arises of why the observed Rayleigh loops are not due to multi-domain grains. Néel[8] alluded to the possibility of multi-domain grains exhibiting hysteresis in low fields. The BH_c/A parameter (where B and A are the quadratic and linear coefficients of Rayleigh relation and H_c is the bulk coercive force) for such loops will be of the order of 0.05, while the value for this quantity for the observed loops[13,15] is of the order of 10. The reason cited by Néel for the smaller BH_c/A for multi-domains is that the demagnetizing factor is to be taken into account for multi-domains. In all the thousands of measurements conducted to date, all confined to basalt samples, a Rayleigh loop was never found associated with K–T curves and hysteresis loops of the class I type. Due to the observed association of the susceptibility–temperature variation for the multi-domain samples, well established in theory and experiment, with the corresponding 'absence' of Rayleigh loops for such samples, the established granulometric interpretation was that Rayleigh loops exhibited by multi-domain samples cannot be seen. In particular, it was noted[15] that on the present Rayleigh loop tracer, a multi-domain Rayleigh loop, with its low BH_c/A value, would not be wider than the thickness of the oscilloscope trace itself.

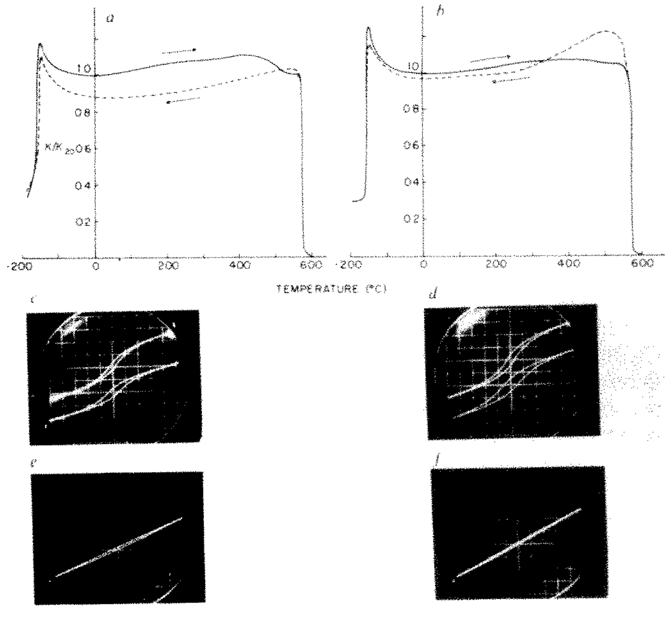

Fig. 2 Magnetic granulometry results: *a*, *c*, *e*, for GR353C, a dolerite dyke sample from the Grenville Province of the Canadian Shield; *b*, *d*, *f*, for N-69.1, an anorthosite sample from Nain, Labrador; *a*, *b*, normalized susceptibility versus temperature; *c*, *d*, magnetic hysteresis in a field of 1,200 Oe at 25 °C (upper trace) and at −196 °C (bottom trace); *e*, *f*, Rayleigh loops in a field of 10 Oe.

We extended the granulometric studies to older intrusive rocks (dolerite dykes, anorthosites and gabbros). Samples studied include the Grenville dykes, Indian Head and Nain anorthosites, and gabbros from Newfoundland. Earlier palaeomagnetic studies of these rock units revealed that their remanent magnetism is extremely stable (Koengsberger ratios ~10) and that their remanence, particularly for the anorthosites, resided in elongated magnetite grains exsolved within the silicates. The present systematic studies include: (1) magnetic susceptibility variation from −196 °C to 700 °C; (2) hysteresis loops at −196 °C and at room temperature in a field of 1,200 Oe (note that a 1,200-Oe field may not always result in saturation of the sample); (3) Rayleigh loops in a field of 10 Oe.

Most samples are class I type; class II and III types are virtually absent. This confirms the earlier conclusions[6] that most 'old' rocks are predominantly multi-domain in nature and that superparamagnetic behaviour is virtually absent in the 'old' rocks. However, many samples exhibited a new type of behaviour—a Rayleigh loop at low fields, associated with class I type hysteresis and K–T curves. Typical examples of results for this behaviour are shown in Fig. 2 for two samples, a dolerite dyke and an anorthosite. These samples do not fall into the three classes discussed earlier. Whereas the presence of Rayleigh loops suggests SP behaviour, the K–T curves and the high-field hysteresis strongly favour the multi-domain state. An explanation in terms of mixtures[3] does not hold here, as experiments lead to different inferences according to the previous interpretation (Fig. 1). Further, an SP component in a mixture should have modified the K–T curve from what is now a 'pure' multi-domain curve. Therefore, there is no doubt that the bulk magnetic properties of these samples, including their Rayleigh loops (Fig. 2*c*, *f*) are caused by magnetite in the multi-domain state. The value of the BH_c/A parameter for these loops is similar to some of the lower values in previously observed loops inferred as being due to effectively superparamagnetic grains.

It is possible that the observed Rayleigh loops reported here are due to a highly conducting nature of the samples (C. Radhakrishnamurty, personal communication) and the resulting eddy currents. Although the conductivity of these samples is of the same order as that of other intrusive rocks of the type studied by us, we tested for this possibility by crushing some of the samples to fine (<50 μm) sizes and remeasuring the Rayleigh loops. The Rayleigh loops were still present, although in slightly diminished thicknesses. We conclude that the observed Rayleigh loops for our samples are real and are not due to eddy current effects. This leads to the following possibilities. (1) With the K–T curve being the main diagnostic feature of multi-domain nature of a magnetic grain (class I type), two types of multi-domain behaviour exist: those samples that do not exhibit a Rayleigh loop and those that do show a Rayleigh loop. (2) Rayleigh loops associated with class III type K–T curves may be interpreted as due to magnetic grains being in a superparamagnetic state. (3) Exhibition of Rayleigh loops is a necessary condition for SP behaviour but is not a sufficient diagnostic feature. Further work is required to clarify these possibilities.

We thank Dr C. Radhakrishnamurty for discussions and advice on various aspects of this observation, and Professor E. R. Deutsch for a critical review of the manuscript. This work was supported by a Natural Sciences and Engineering Research Council of Canada operating grant to G.S.M.

Received 14 July; accepted 30 December 1981.

1. Radhakrishnamurty, C., Raja, P. K. S., Likhite, S. D. & Sahasrabudhe, P. W. *Pure appl. Geophys.* **93,** 129–140 (1972).
2. Radhakrishnamurty, C. & Deutsch, E. R. *J. Geophys.* **40,** 453–465 (1974).
3. Radhakrishnamurty, C., Likhite, S. D. & Sahasrabudhe, P. W. *Phys. Earth planet. Inter.* **13,** 289–300 (1977).
4. Radhakrishnamurty, C., Deutsch, E. R. & Murthy, G. S. *J. Geophys.* **45,** 433–446 (1979).
5. Murthy, G. S., Pätzold, R. & Brown, C. *Phys. Earth planet. Inter.* **26,** 72–80 (1981).
6. Radhakrishnamurty, C., Likhite, S. D., Deutsch, E. R. & Murthy, G. S. *Proc. Ind. Acad. Sci.* A**87,** 235–243 (1978).
7. Senanayake, W. E. & McElhinny, M. W. *Phys. Earth planet. Inter.* **26,** 47–55 (1981).
8. Neel, L. *Adv. Phys.* **4,** 191–243 (1955).
9. Morrish, A. H. & Watt, L. A. K. *J. appl. Phys.* **29,** 1029–1033 (1958).
10. Bean, C. P. *J. appl. Phys.* **26,** 1381–1383 (1955).
11. Bickford, L. R. *Phys. Rev.* **78,** 449–457 (1950).
12. Syono, Y. & Ishikawa, Y. *J. phys. Soc. Jap.* **18,** 1230–1232 (1963).
13. Radhakrishnamurty, C. & Sastry, N. P. *Proc. Ind. Acad. Sci.* A**72,** 94–102 (1970).
14. Néel, L. *C.r. hebd. Séanc. Acad. Sci., Paris* **270,** 1125–1130 (1970).
15. Deutsch, E. R. & Pätzold, R. R. *J. geophys. Res.* **81,** 4188–4198 (1976).
16. Dunlop, D. J. & Hale, C. J. *Can. J. Earth Sci.* **14,** 716–744 (1977).

Explicit dialogue between left and right half-systems of split brains

D. M. MacKay & Valerie MacKay

Department of Communication and Neuroscience,
University of Keele, Keele, Staffordshire ST5 5BG, UK

Much debate has surrounded the interpretation of the well known 'split brain' syndrome, produced by section of the corpus callosum in man [for useful surveys of early studies of the effects of callosal damage (for example by Liepmann (1900), Goldstein (1908) and Bonhoeffer (1914)) see refs 1–3]. On the basis of the observation that left and right half-systems can find themselves in conflict when disparate instructions are flashed to left and right visual hemifields, Sperry[4] has described such patients as having "two free wills inside the same cranial vault". MacKay[7–9], among others, has argued for a more parsimonious interpretation of the available evidence, suggesting that it demonstrates duality only at the 'executive' level where continuous goal-pursuit is administered, rather than at the 'normative' supervisory level where the agent's priorities and criteria of evaluation are themselves subject to evaluation and revision. We report here some experiments in which a split-brain patient showed considerable capacity for explicit interhemispheric exchange of information and instructions, yet gave no sign of the duality of supervisory initiative that might have been expected on the hypothesis of 'two free wills'.

Gazzaniga and co-workers[6,10] have shown both in monkey and man that each hemisphere can apply disparate criteria of evaluation to the same stimulus, as well as expressing disparate preferences in the same situation. This indicates convincingly that both evaluative and organizing systems are split at the executive level, but it falls short of proof that the brain in such patients embodies two independent systems for evaluating priorities themselves—the characteristic human activity with which the term 'will' is associated.

One relevant question is whether, and if so to what extent, one 'half-system' in these cases can be induced to demonstrate any recognition of the other half-system as 'another person', Through the generous cooperation of R. W. Sperry and M. S. Gazzaniga, we have recently contrived a number of laboratory situations designed to give systematic opportunities for such 'interpersonal' types of interaction. Some of these have been described elsewhere[9]. In the case described here our strategy was to train each 'half' in turn to engage in interpersonal exchanges with an experimenter in a simple competitive guessing game, and then to encourage each to use its acquired symbolic skills to engage the other 'half' in the same manner. The question was whether we would see any signs of simultaneous conscious evaluation of priorities from disparate standpoints, such as would be shown by two conscious human agents in a bargaining situation.

The patient (J.W.) was a right-handed 27 yr-old man who had had his corpus callosum, but not his anterior commissure, sectioned in 1977 to help prevent the spread of epileptic seizures from one hemisphere to the other[11]. Apart from side effects of anticonvulsant medication he was in good health, and cooperated with enthusiasm in the experiment. Preliminary tests confirmed observations by Sidtis *et al.*[12] that he was unable to report vocally any visual stimuli flashed to the left of his fixation point, although his left hand could correctly point to or retrieve objects represented by these stimuli. A single numeral randomly selected from the range 0 to 9 was flashed for 150 ms at an eccentricity of 4° to the left of the fixation point, simultaneously with a distractor (one or more letters of the alphabet) flashed at a similar eccentricity to the right. J.W. reported vocally that he saw only the distractor. Both vocal and right-manual responses were normal for stimuli flashed to the right half-field.

0028–0836/82/080690—02$01.00

Each half-system in turn was then trained to participate (on opposite sides) in a guessing game of the '20 questions' type in dialogue with one experimenter (E).

(1) E first assumed the role of 'guesser', attempting to name a 'mystery number' written by the second experimenter on a piece of paper in free view of J.W. E invited J.W. to use his left hand to point to appropriate answers on a card also in free view, bearing the words 'go up', 'go down', 'OK'. The left hand proved immediately capable of providing reliable feedback in this mode.

(2) E then invited J.W. to "guess a number between 0 and 9 which I have been shown". In response to each guess by J.W., E pointed mutely to one of the three messages on the card. J.W. quickly learned to adapt his vocal guesses so as to home in on the correct answer under this mute feedback from E.

(3) Finally, single digits between 0 and 9 were flashed as before to J.W.'s left half-field, with distractors to the right; and E proposed that J.W. should fulfil both roles, using his mouth to make guesses and his left hand to offer feedback by way of the card. J.W. found no apparent difficulty in fulfilling this dual role, although it was notable that all his guesses were addressed to E, who invariably had to ask the left hand to answer. He proved well able to 'talk himself down' on to the correct target each time, frequently showing satisfaction by a smile when the target was finally named. A useful check that he was not just play-acting (which seemed in any case improbable) was provided by an episode when his mouth guessed '1' and his left hand pointed to 'go down'. J.W. complained vocally that there were "no more numbers down there", and had to be reminded of the possibility of '0' (which was the correct answer).

These results make clear that symbolic information-exchange by question and answer can be sustained between left and right half-systems of a split-brain patient. Various forms of cross-cueing have, of course, been known and studied in such patients for many years[13]. Sidtis *et al.*[12] have also shown that a '20 questions' guessing procedure on the part of an experimenter could help a patient with a partially sectioned corpus callosum to 'home in on' the name of a stimulus flashed to the left half-field; but it was by no means obvious that J.W.'s two half-systems could use a public symbolic system of this kind to engage in systematic dialogue with one another.

However, we are still left with the vexed question of whether the two half-systems here embodied 'two free wills' in the sense in which, say, two normal human players on opposite sides of a guessing game have independence of will. An ideal demonstration of such 'duality of will' would be the capacity to bargain: that is, to struggle to induce changes in one another's evaluative criteria or priorities as distinct from merely struggling physically in pursuit of conflicting goals[8,9].

Accordingly, E next proposed to J.W. that "the left hand (LH) should be paid by the right hand (RH) for each item of information". RH was provided with an open box containing a limited supply of tokens, and instructed to pay one token into a similar box on the left for each correct answer by LH. RH was rewarded (with additional tokens) in inverse proportion to the number of guesses required to identify each flashed numeral. Any occasional mistakes made by LH were penalized by repaying three tokens per mistake to RH.

As elaboration of the game in this way proved congenial to J.W., we next introduced the possibility of evaluative conflict by proposing to "ask the left hand whether it would like to be paid more for each answer". LH was asked to reply by pointing to a card representing one, two and three tokens; and it immediately indicated 'three tokens'. As this soon had the (foreseeable) effect of rendering RH bankrupt and halting the game, E then said "Let's ask the left hand whether it would settle for less". LH immediately pointed to 'two tokens'; but at the same time, and apparently as an integral part of the action, J.W.'s mouth said "Sure, make it two tokens". This was typical of the impression conveyed throughout this second phase of the experiment—that although J.W.'s LH and RH were substantially separate at the cognitive level, their priorities gave no evidence of being under the supervision of two independent normative systems[7–9].

It is, of course, impossible to draw firm conclusions from such negative evidence. One can always explain absence of conflict by postulating suppressive (internal) influences from one half-system on normative processes in the other that would otherwise be independent; alternatively, it could be argued that the two half-systems perceived the rewards as jointly shared, and thus had no incentive to quarrel (M. S. Gazzaniga, personal communication). Our evidence is consistent, however, with the null hypothesis that at the higher levels of supervisory evaluation J.W. has not two half-systems but one undivided system, presumably associated with deep neural structures not surgically separated. This null hypothesis is strengthened by the well known fact[5,6] that emotive stimuli to the mute hemisphere can elicit signs of corresponding emotion in the speaking subject. At least, the onus of proof seems now to rest on anyone who would claim that patients like J.W. have, nevertheless, 'two free wills'. Perhaps his own spontaneous comment, offered more than once, is illuminating: "Are you guys trying to make two people out of me?"

These experiments were possible only through the generous cooperation of Dr M. S. Gazzaniga and his colleagues, particularly Drs Jeffrey Holtzman, John Sidtis and Bruce Volpe, in the Division of Cognitive Neuroscience at Cornell University Medical College in New York City. We also thank J.W. for his willing participation. Financial support was received from a Sloan Foundation Grant to Dr Gazzaniga, from the University of Keele to D.M.M. and from the Wellcome Trust to V.M.

Received 20 October 1981; accepted 19 January 1982.

1. Geschwind, N. *Brain* **88,** 584–644 (1965).
2. Zangwill, O. L. in *Hemisphere Function in the Human Brain* (eds Dimond S. J. & Beaumont, J. G.) (Eleck Science, London, 1974).
3. Joynt, R. J. in *Hemispheric Disconnection & Cerebral Function* (eds Kinsbourne, M. & Smith W. L.) (Thomas, Springfield, 1974).
4. Sperry, R. W. in *Brain & Conscious Experience* (ed. Eccles, J. C.) 293–313 (Springer, New York, 1966).
5. Gazzaniga, M. S. *The Bisected Brain* (Appleton-Century-Crofts, New York, 1970).
6. Gazzaniga, M. S. & LeDoux, J. E. *The Integrated Mind* (Plenum, New York, 1978).
7. MacKay, D. M. in *Brain & Conscious Experience* (ed. Eccles, J. C.) 312–313 (Springer, New York, 1966).
8. MacKay, D. M. in *Consciousness and the Physical World* (eds Josephson, B. D. & Ramachandran, V. S.) 95–113 (Pergamon, Oxford, 1980).
9. MacKay, D. M. *Neural Communication and Control* (eds Székely, G., Lábos, E. & Damjanovich, S.) 315–332 (Pergamon, Oxford and Akadémiai Kiado, Budapest, 1981).
10. Gazzaniga, M. S. *Am. Scient.* **60,** 311–317 (1972).
11. Wilson, D. H., Reeves, A. & Gazzaniga, M. S. *Neurology* **28,** 649 (1978).
12. Sidtis, J. J., Volpe, B. T., Holtzman, J. D., Wilson, D. H. & Gazzaniga, M. S. *Science* **212,** 344–346 (1981).
13. Gazzaniga, M. S. *Scient. Am.* **217,** 24–29 (1967).

Somatotopic maps are disorganized in adult rodents treated neonatally with capsaicin

P. D. Wall*, M. Fitzgerald*, J. C. Nussbaumer†, H. Van der Loos† & M. Devor‡

* Cerebral Functions Research Group, Department of Anatomy, University College London, London WC1E 6BT, UK
† Institute of Anatomy, University of Lausanne, CH-1011 Lausanne, Switzerland
‡ Institute of Life Sciences, Hebrew University, Jerusalem, Israel

The somatosensory system is characterized at each stage of the projection pathways by the presence of maps formed by an orderly arrangement of cells and of the incoming fibres. Each cell responds to a definite area of skin, its receptive field (RF). If cell locations and their RFs are plotted side by side, they make up a continuous map of the body surface. Given the stability and repeatability of these maps, it was of interest to find that lesions which destroyed the input to one part of the map of the spinal cord in adults were followed by a readjustment of the RFs of cells which had lost their normal input[1]. It was more surprising to discover in adult cats and rats that peripheral nerve lesions which do not produce an anatomical destruction of spinal cord afferents were followed by the appearance of novel RFs in cells

0028–0836/82/080691—03$01.00

deprived of their normal physiological input[2,3]. Capsaicin given to neonatal mice or rats destroys unmyelinated afferents. We report here that this is followed by an expansion of the normal receptive fields supplied by myelinated afferents[2,3]. Our results suggest that unmyelinated fibres may be involved in controlling the connectivity of myelinated afferents with first central cells.

Experiments in rats show that the foot and toe representation is present in the medial two-thirds of the dorsal horn of segments L4 and L5 of the spinal cord. If this region is searched to a depth of 1 mm with fluid-filled microelectrodes in intact adult rats anaesthetized with Nembutal, an average of five cells responding to the foot or toes are isolated in each track. As the RFs remain stable over many hours of recording and since the maps are accurately repeated from animal to animal, it is reasonable to expect that abolition of a particular input would silence the cells which are normally dominated by that input. We therefore searched the same region with a total of 51 tracks in 13 animals in which the sciatic and saphenous nerves that supply the foot had been cut on the day of the experiment, and found only 0.1 responding cells per track; these few RFs were on the leg. The same virtual absence of responding cells was observed in six animals 2 and 3 days[3] after the nerves had been cut. However, in 13 animals with a total of 69 tracks surviving 4–8 days after nerve section, the value rose to 3.2 cells per track. All these RFs were on the upper leg and pelvis and were supplied by intact nerves[3]. Similar results have been seen in the cat following peripheral nerve section[2]. These new RFs in the foot region could not have been supplied by sprouts growing from the nerve sectioned 4–8 days earlier because resectioning of the nerve on the day of the experiment produced no change in the recordings.

Lesions of nerves in the hind legs, unlike root lesions, produce no frank degeneration of central afferent terminals in the spinal cord for at least 2 weeks after the lesion[2,3], but they do interrupt impulse and chemical transport from the periphery to the spinal cord. We suspected that the component of the peripheral nerve responsible for signalling to the spinal cord that the peripheral nerve was cut might be the unmyelinated C fibres, as anatomical and chemical changes have been reported in their spinal cord terminals and not in the terminals of myelinated afferents following peripheral nerve section[4–6].

Capsaicin, the hot compound in paprika, produces rapid, substantial and permanent destruction of C fibre sensory afferents in dorsal roots and in the trigeminal nerve if injected into neonates[7–10]. This effect seems to be remarkably specific. Ultrastructural studies of cord and trigeminal nuclei show only degeneration of the terminals of fine afferents on laminae I and II[11,12]. Immunochemistry reveals depletion of substance P only in dorsal horn, trigeminal nuclei, nerves and roots, with no depletion in ventral horn or elsewhere in the brain[12–14]. The drug has no effect on enzymes and peptides intrinsic to the dorsal horn: neurotensin, glutamic acid decarboxylase and catecholamine amine transferase[12,15]. Unlike capsaicin given systemically to adults, there is no evidence that neonatal capsaicin produces hypothalamic damage[16]. In our hands the peripheral lesion seems to be limited to the unmyelinated afferents[9], but others have reported a small and variable loss of some myelinated fibres with high doses[8,10].

Litters of Sabra and Wistar rats under ether anaesthesia were injected with capsaicin (50 mg per kg intraperitoneally) dissolved in 10% Tween 80, 10% ethanol in saline on the second and fourth day of life. Littermates were injected with the vehicle. The animals were returned to their mothers and allowed to grow to adults weighing over 200 g. They were apparently healthy, with normal sleeping, eating and grooming behaviour and no deficit in motor activity.

The effectiveness of the drug was tested in three ways. First, the peripheral C compound action potential was measured by stimulating the dorsal root (5 mA, 500 μs) and recording from the sural nerve at the beginning of each experiment. A C wave was never recorded in capsaicin-treated animals from dorsal root stimulation ($n = 4$) whereas in vehicle-treated animals and untreated controls a clear C compound action potential was evoked. Second, the spinal cords were removed from four animals and stained for immunoreactive substance P. Substance P is normally highly concentrated in the region of small fibre terminals in the dorsal horn[17] and in all the tested cords it was substantially depleted. Finally, cords from three rats were stained for fluoride-resistant acid phosphatase[4]. Again, there was substantial depletion of the enzyme from the dorsal horn terminals. Four vehicle control littermates were also tested by these three methods and the measurements were normal. It therefore appeared that the rats treated neonatally with capsaicin had lost a substantial number of their peripheral C fibres.

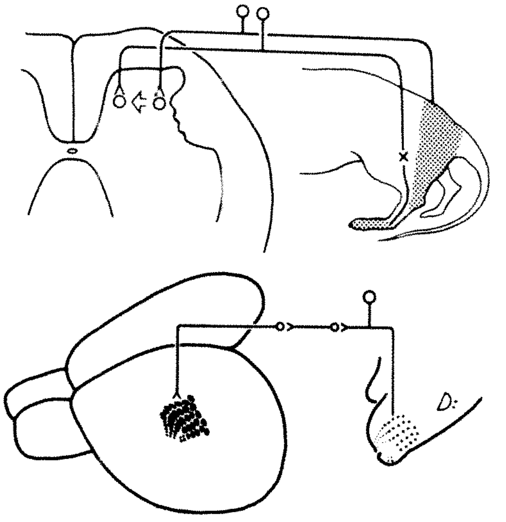

Fig. 1 Above: In the normal rat, the nerves from the foot and toes project to the medial part of the lumbar dorsal horn. The proximal parts of the leg project to the lateral cells in the dorsal horn. If the nerves to the foot are cut in normal animals, most of the medial cells fail to respond to peripheral stimulation for a period of 0–3 days after the cut. During the period 4–8 days after nerve section, many medial cells begin to respond to stimulation of proximal leg. In animals treated neonatally with capsaicin, medial cells respond to the upper leg immediately after peripheral nerves to the foot have been cut. Below: In the normal mouse, each individual large whisker projects by way of the trigeminal nerve, the trigeminal sensory nuclei and the thalamus to the cortex. In the parietal cortex there are barrels of cells in which each cell responds to the movement of one whisker only. Almost all responding cells in an individual barrel respond to the same single whisker. In mice treated with capsaicin soon after birth, the barrels and whiskers are present in their normal arrangement but no cell was encountered which responded to only one whisker. All recorded cells responded to 2–7 whiskers (average 3.8).

The spinal cord maps of 10 neonatally capsaicin-treated rats, 6 vehicle-treated and 4 untreated control animals were then examined. Low-thoracic spinalized preparations were used to increase the excitability of the cord and therefore reveal any aberrant cells in control animals. The rats were either anaesthetized with Nembutal or decerebrated under short-acting Althesin anaesthesia. The saphenous and sciatic nerves were cut acutely at knee level on the day of the experiment and the medial dorsal horn of segments L4 and L5 searched with electrode tracks for cells that responded to skin stimulation on the upper leg above the knee.

In normal and vehicle controls under Nembutal anaesthesia, 0.9 cells were found per track ($n = 43$). Decerebrate controls showed 1.8 responding cells per track ($n = 31$). This region was therefore clearly largely silenced by acute denervation of the lower limb, the actual number of responding cells being somewhat dependent on the excitability of the cord in different preparations. In capsaicin-treated animals with acute deafferentation of the foot, 2.6 cells per track ($n = 64$) were found in six Nembutal-low spinal animals. In the decerebrate preparations, the four treated animals had 6.7 cells per track ($n = 15$). The number of aberrant RFs in the foot area was significantly greater in the capsaicin-treated animals than in controls ($P<0.001$, t-test). The receptive fields were on the upper leg and in some cases (1.2 cells per track) extended to the tail and over to the contralateral limb. The responses were induced by firm pressure or pinch and often also by light touch. Thus, the capsaicin-treated animals have the same type of distorted somatotopic cord map after acute peripheral nerve section as occurs in normal rats after chronic nerve section.

The somatotopic map of spinal cord is not as detailed as that in the somatosensory cortex. A particularly precise and extensively investigated projection is that of the whisker follicles mapped on the parietal cortex of the mouse, in which an anatomical correlation is established between individual whiskers and discrete cytoarchitectonic units in the parietal neocortex, the barrels[18]. Furthermore, Van der Loos and Woolsey[19] showed that limited neonatal lesions of particular whiskers resulted in failure of development of the corresponding barrels. It was later shown that the occasional appearance of an extra whisker is associated with an extra barrel in the topologically equivalent cortical locus[20]. Following previous studies on cortical physiology of whisker responses[21,22], Nussbaumer (manuscript in preparation) has examined the details of the physiological aspect of this tight anatomical mapping in mice and has found an extraordinary specificity of both anatomical and physiological correlation between the periphery and its cortical representation. In penthrane/nitrous oxide-anaesthetized mice, 117/121 tracks through layer IV of these cortical barrels revealed cells responding to only one whisker. In the remaining four tracks, the cells responded to two neighbouring whiskers. In view of this finding, it was obvious that we should test the effect of neonatal capsaicin. Two litters of mice (CBA/CA and ICR) were treated on the second and fifth day of life with 50 mg capsaicin per kg in the same manner as the rats. Littermates were treated with the vehicle alone. The animals were returned to their mothers, allowed to grow to adulthood and examined after more than 4 months.

In two vehicle-treated controls the cortex showed the same results as in normal mice in that five marked penetrations into layer IV of the barrelfield revealed cells responding to only one whisker. In the capsaicin-treated mice of both strains, the cortical anatomy as observed in Nissl preparations showed normal barrelfields. The size and distribution of whiskers were also normal. However, on penetrating the cortex, the recordings were strikingly abnormal. In two CBA and three ICR mice examined with a total of 18 penetrations, each penetration yielded one or more responding cells. No recording sites showed cells responding to only one whisker. The number of whiskers that could excite a cell varied from 2 to 7 (average 3.8). Invariably the whisker producing the most intense excitation was that which would normally have monopolized the barrel within which the recording was being made.

These experiments show that the RFs of some cells in rat spinal cord and in mouse cortex are greatly expanded in adults treated neonatally with capsaicin (Fig. 1). In spinal cord, it has been shown by electrical stimulation of the skin that many of the cells with expanded RFs are excited monosynaptically by myelinated afferents[2,3]. The abnormal RFs of these cord cells may therefore be produced by abnormal coupling of myelinated afferents to central cells. For the mouse cortex cells with expanded RFs, a similar explanation would apply if trigeminal myelinated afferents establish abnormal contacts with cells in the trigeminal sensory nuclei.

These results suggest a testable hypothesis that the normal receptive fields of cord and medulla cells excited by myelinated sensory afferents require the presence of unmyelinated afferents. We propose that the effect of neonatal capsaicin is limited to its destruction of afferent fibres in the periphery. This is supported by the absence of signs of direct central destruction[11,12,16], and by results to be reported elsewhere[23] that local application of capsaicin to a single nerve in the adult also results in abnormal expanded receptive fields limited to cells supplied by the treated nerve. Although it is possible that the toxin has produced some subtle undetected change in the myelinated afferents, in the case of single nerve lesions it is evident that the novel receptive fields are supplied by myelinated afferents which were not touched by the lesion. We therefore propose that unmyelinated afferents have a role in the establishment of ordered connections between myelinated afferents and the first central cells.

Received 17 November; accepted 22 December 1981.

1. Wall, P. D. *Phil. Trans. R. Soc.* **B278**, 361–372 (1977).
2. Devor, M. & Wall, P. D. *J. comp. Neurol.* **199**, 277–291 (1981).
3. Devor, M. & Wall, P. D. *J. Neurosci.* **1**, 679–684 (1981).
4. Devor, M. & Claman, D. *Brain Res.* **190**, 17–28 (1980).
5. Barbut, D., Polak, J. M. & Wall, P. D. *Brain Res.* **205**, 289–298 (1981).
6. Csillik, B. & Knyihar, E. *Prog. Neurobiol.* **10**, 203–230 (1978).
7. Jancso, G., Kiraly, E. & Jancso-Gabor, A. *Nature* **270**, 741–743 (1977).
8. Lawson, S. N. & Nickels, S. M. *J. Physiol., Lond.* **303**, 12P (1980).
9. Scadding, J. W. *J. Anat.* **131**, 473–484 (1980).
10. Nagy, J. I., Hunt, S. P., Iversen, L. L. & Emson, P. C. *Neuroscience* **6**, 1923–1934 (1981).
11. Jancso, G. & Kiraly, E. *J. comp. Neurol.* **190**, 781–792 (1980).
12. Nagy, J. I. *et al. Brain Res.* **186**, 435–444 (1980).
13. Gamse, R., Holzer, P. & Lembeck, F. *Br. J. Pharmac.* **68**, 207–213 (1980).
14. Helke, C. H., Dimico, J. A., Jacobowitz, D. M. & Kopin, I. J. *Brain Res.* **222**, 428–431 (1981).
15. Gamse, R., Leeman, S. E., Holzer, P. & Lembeck, F. N. S. *Archs Pharmac.* **317**, 140–148 (1981).
16. Jancso, G. & Jancso-Gabor, A. N. S. *Archs Pharmac.* **311**, 285–288 (1980).
17. Gibson, S. J., Polak, J. M., Wall, P. D. & Bloom, S. R. *J. comp. Neurol.* **201**, 65–79 (1981).
18. Woolsey, T. A. & Van der Loos, H. *Brain Res.* **17**, 205–242 (1970).
19. Van der Loos, H. & Woolsey, T. A. *Science* **179**, 395–398 (1973).
20. Van der Loos, H. & Dörfl, J. *Neurosci. Lett.* **7**, 23–30 (1978).
21. Welker, C. *J. comp. Neurol.* **166**, 173–189 (1976).
22. Simons, D. J. *J. Neurophysiol.* **41**, 798–820 (1978).
23. Fitzgerald, M. *Brain Res.* (in the press).

Neural cell adhesion molecule is on embryonic muscle cells and mediates adhesion to nerve cells *in vitro*

Martin Grumet, Urs Rutishauser
& Gerald M. Edelman

Department of Molecular and Developmental Biology,
The Rockefeller University, 1230 York Avenue, New York,
New York 10021, USA

The interaction of nerves with muscles, particularly at neuromuscular junctions, is one of the most extensively studied areas of neurophysiology. From the point of view of developmental biology, however, little is known about the cellular and molecular events that lead to formation of these junctions[1,2]. In previous investigations of cell–cell adhesion in the chick embryo, we identified a molecule on the surface of essentially all nerve cells, called neural cell adhesion molecule (N-CAM)[3,4], that appears to be a ligand in the formation of cell–cell bonds[5]. N-CAM is involved in a variety of developmental processes including neurite fasciculation and the formation of plexiform and cell layers in retinal tissue[6–8]. We report here that N-CAM antigenic determinants are also present on chick embryo skeletal muscle cells. This observation raised the possibility that N-CAM is involved in adhesion between nerve and muscle cells. In model systems set up to explore this possibility, we observed that myoblasts will adhere *in vitro* to nerve cells from retina, and that this adhesion can be inhibited by F(ab′) fragments of antibodies against N-CAM. In addition, membrane vesicles obtained from chick embryo brain or artificial vesicles[5] reconstituted from lipid and affinity-purified N-CAM[9] bound to the surface of myoblasts and myotubes; this binding was also blocked by anti-N-CAM F(ab′). These results suggest that the N-CAM adhesion system can facilitate nerve–muscle as well as nerve–nerve interactions *in vitro*.

Immunocytological studies carried out to determine the distribution of N-CAM in chick embryos revealed that the molecule is associated with nerve tissues; however, light staining was also observed in muscle[6]. As shown in Fig. 1, rabbit anti-N-CAM antibodies that had been affinity-purified on N-CAM–Sepharose[5], bound to the surface membrane of cultured skeletal myoblasts and myotubes but not to fibroblasts in the same

0028-0836/82/080693—03$01.00

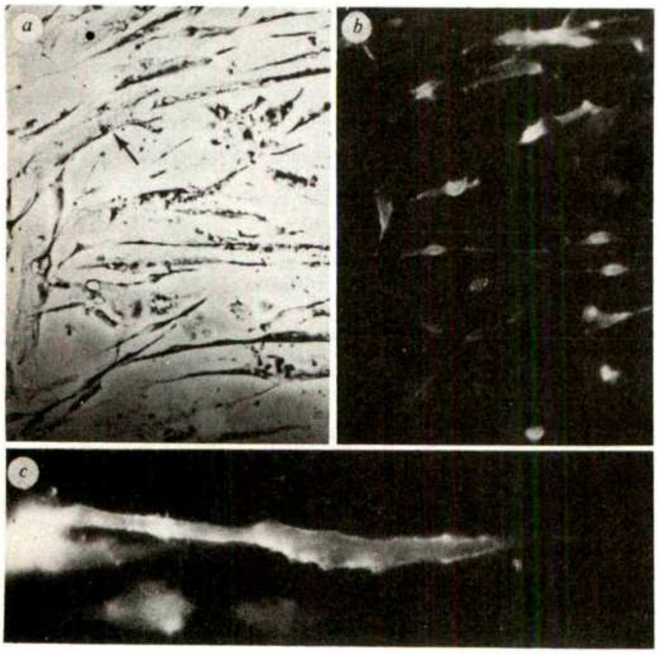

Fig. 1 Immunofluorescence staining of skeletal muscle cells with antibodies to N-CAM. *a*, Phase-contrast micrography of myoblasts and early myotubes (×264), and *b*, fluorescence micrograph of the same field. *c*, Fluorescence micrograph of a myotube. ×880. A fibroblastic cell which is not stained is indicated with an arrow. Muscle cells were obtained from 11–12-day White Leghorn chick embryo legs by trypsinization (0.1%, 30 min, 37 °C) and trituration, and partially separated from fibroblasts by differential adhesion to culture dishes; the nonadherent cells were cultured on collagen-coated substrates for 2 days in Eagle's modified essential medium containing 10% horse serum and 5% chick embryo extract. For staining, the cultures were treated sequentially with 3.7% formaldehyde, 0.1 M glycine, 4% goat serum, affinity-purified rabbit anti-N-CAM IgG and fluorescein-labelled goat anti-rabbit IgG (Miles-Yeda). All reagents were prepared in phosphate-buffered saline; each antibody treatment was followed by four washes with buffer.

cultures. The staining of the muscle cells, which had been prefixed with formaldehyde, was mostly diffuse and lower in intensity than that seen previously on neurones[6]. Immunoglobulin from unimmunized rabbits did not give detectable staining.

The presence of N-CAM antigenic determinants on muscle cells suggested that at some stage of their development they might adhere to nerve cells through this molecule. This possibility was examined by studies of the adhesion of skeletal muscle myoblasts in suspension to monolayers[10] of retinal nerve cells, of the co-aggregation of these cells in rotation–suspension cultures and of the binding of membrane vesicles containing N-CAM to myoblasts in suspension and to myotube monolayers. Although these assays represent highly simplified model systems for the analysis of cell–cell interactions in developing tissues, they have been useful in revealing and quantifying specific adhesion events, in particular for studying their molecular basis[3,10,11]. The use of retina and brain for these studies reflects the requirement for substantial numbers of cells in the binding assays. Although retinal cells can establish a weak and transient synaptic connectivity with muscle *in vitro*[12], this system is of limited use in evaluating nerve–muscle interactions *in vivo*. Nevertheless, spinal cord cells are known to express N-CAM[6], and the results obtained here will provide the necessary background to interpret more complex studies, such as the effects of anti-N-CAM antibody on cultures of muscle cells with spinal cord explants.

Adhesion between nerve cells has been measured previously using a cell suspension–cell monolayer binding assay[10]. In the present studies, myoblasts in suspension also bound to a retinal nerve cell monolayer, the level of binding during a 20-min incubation being about one-half that observed between nerve cells (Table 1). This binding was inhibited by anti-N-CAM F(ab′) and did not require the presence of Ca^{2+}; by these criteria it is distinguishable from the calcium-dependent mechanism of nerve cell adhesion[13]. Fibroblasts, which lack N-CAM[6], did not bind in significant numbers to the retinal nerve cell monolayer.

Further evidence for nerve–muscle adhesion was obtained by incubating retinal and muscle cells together in suspension at 70 r.p.m. and 37 °C for 20 min; in these conditions large aggregates were formed that contained both cell types (Fig. 2). Similarly, fluorescein-labelled membrane vesicles obtained from brain tissue bound to myoblasts and myotubes (Table 2, Fig. 3), although less strongly than to retinal neurones (Table 2). In each case, the interaction was inhibited by anti-N-CAM F(ab′); fibroblasts were included as a control and did not bind the vesicles. Table 2 and Fig. 3 show the binding to muscle cells of vesicles reconstituted from brain lipids and purified N-CAM. This adhesion was almost completely inhibited by anti-N-CAM antibody; vesicles containing lipids alone bound only in small numbers to a few cells. Binding was also observed between the N-CAM vesicles and cells obtained from heart muscle of 9-day embryos by trypsinization as described for the retinal cells. This suggests that N-CAM-mediated interactions may take place in a variety of muscle tissues of different origins.

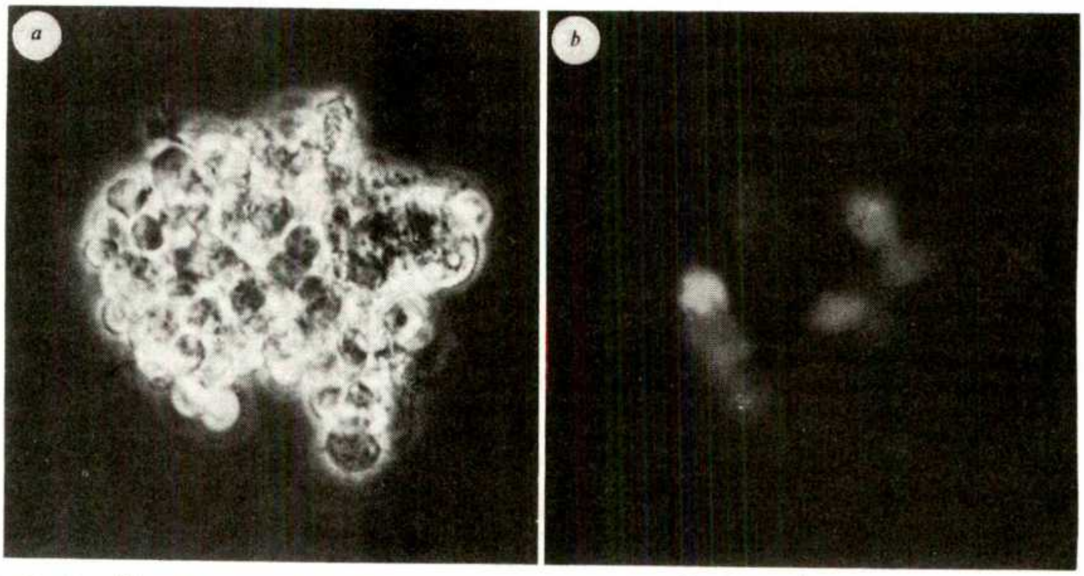

Fig. 2 Co-aggregation of retinal nerve cells with fluorescein-labelled myoblasts. *a*, Phase-contrast micrograph, and *b*, fluorescence micrograph of the same field, ×840. Cells (2.5×10^6 of each type) were incubated in 1 ml Eagle's minimal essential medium with spinner salts (SME medium) for 20 min at 37 °C with rotary shaking at 70 r.p.m. Myoblasts were prepared as described in Fig. 1 legend, cultured in suspension for 4 h and further fractionated by density gradient centrifugation in Ficoll to yield a cell population consisting of about two-thirds myoblasts, the remaining cells probably being fibroblasts[14]. Myoblasts were internally labelled with diacetyl fluorescein[10]. Nerve cells were obtained from retina of 10-day chick embryos by mild trypsinization (0.002%, 15 min, 37 °C)[13].

We have shown previously[5] that the adhesive specificity and the properties of the reconstituted N-CAM vesicles closely resemble those of intact nerve cells and have obtained evidence suggesting that cell–cell binding may involve interactions between N-CAM molecules on different cells. The fact that both muscle and nerve cells have N-CAM on their surfaces is consistent with this hypothesis. It also raises the possibility that muscle cells could bind to each other in part by the N-CAM mechanism. In preliminary studies, however, anti-N-CAM F(ab′) reduced the binding of myoblasts to myoblasts or myotubes by only ~20%, which may indicate that other adhesion mechanisms and molecules are also involved, including those leading to the muscle-specific fusion of plasma membranes to form myotubes.

We conclude that N-CAM (or a similar molecule) is present on the plasma membrane of developing skeletal muscle cells, and that nerve cells can bind to muscle cells via the calcium-independent[13] adhesion mechanism involving N-CAM. The presence of N-CAM on a cell type of mesenchymal origin as well as in ectodermally derived nerve tissue raises the possibility that N-CAM expression on cells is more a reflection of functions required for morphogenesis than of cell lineage. In view of this possibility, it will be of particular interest to test for the presence and localization of N-CAM in embryos at earlier stages of development.

Table 1 Binding of neural and muscle cells to retinal nerve cell monolayers

Cell binding to monolayer	F(ab′) present during binding*	No. of cells bound to monolayer (1 mm^2)	% Inhibition by anti-N-CAM F(ab′)
Myoblasts	Nonimmune	174	—
Myoblasts	Anti-N-CAM	64	63
Retinal neurones	Nonimmune	389	—
Retinal neurones	Anti-N-CAM	105	73
Fibroblasts	—	30	—

Myoblasts and retinal nerve cells were prepared as described in Fig. 2 legend. Fibroblasts were dissociated from skin of 11-day chick embryos with 0.1% trypsin and grown in Dulbecco's modified Eagle's medium containing 10% fetal calf serum. At confluence, fibroblasts were removed from culture dishes with trypsin, cultured in suspension for 4 h and internally labelled with diacetyl fluorescein. As described previously[10], monolayers of retinal cells were prepared on waxbean agglutinin-coated 35-mm culture dishes, incubated for 20 min at 25 °C with a suspension of cells internally labelled with fluorescein and scored for binding by fluorescence microscopy. Retinal nerve cells in suspension also bound to monolayers of myoblasts or myotubes, but only ~20% of this binding was inhibited by anti-N-CAM F(ab′). We have previously observed that inhibition of heterotypic binding by F(ab′) is sometimes affected when the cell types in the suspension and monolayer are reversed[13]. Although the cause of this effect is not understood, binding of vesicles to myotubes in monolayers or to myoblasts in suspension was strongly inhibited by F(ab′) (Table 2).

*20 μg ml^{-1} of affinity-purified F(ab′) or nonimmune F(ab′) were added to the incubation medium.

Table 2 Binding of vesicles containing N-CAM to cells

Cells	Source of vesicles	% Of cells binding vesicles With nonimmune F(ab′)	With anti-N-CAM F(ab′)
Myoblasts*	Brain tissue	69	18
Retinal neurones	Brain tissue	75	26
Fibroblasts	Brain tissue	0	—
Myoblasts	N-CAM + lipid	60	5
Myoblasts	Lipid	6	—

Myoblasts and retinal nerve cells were prepared as for Fig. 2, and fibroblasts as for Table 1, except without the internal fluorescent label. Vesicles containing N-CAM and carboxyfluorescein were isolated as described in Fig. 3 legend, and lipid vesicles were prepared as described but in the absence of N-CAM. Binding was scored by fluorescence microscopy (see Fig. 3 legend) after incubating 20 μl of vesicles with 5×10^6 cells in 1 ml SME medium for 20 min at 37 °C in the presence of 10 μg ml^{-1} of F(ab′).

*60–70% of cells scored were myoblasts[14].

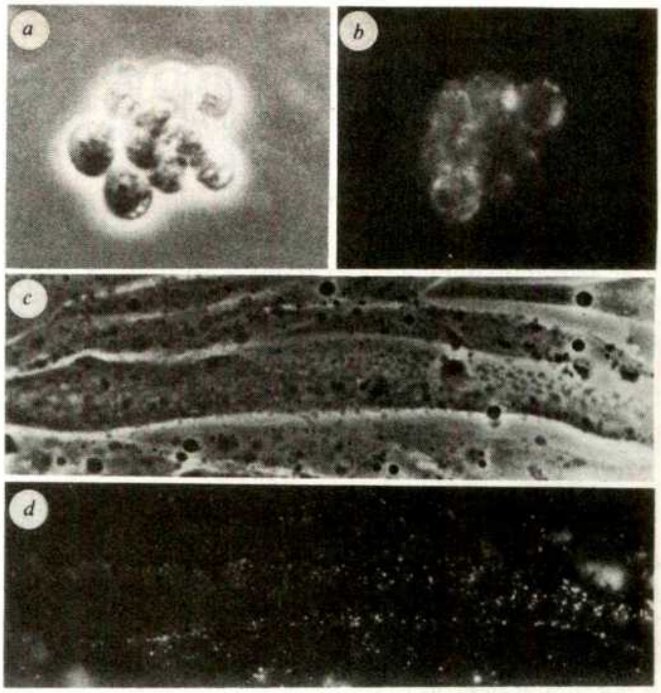

Fig. 3 Binding of brain tissue vesicles to myoblasts (*a*, *b*), and binding of reconstituted vesicles containing lipid and affinity-purified N-CAM to myotubes (*c*, *d*). *a* And *c* are phase contrast micrographs at ×570 and ×375 respectively; *b* and *d* are fluorescence micrographs of the same fields. Myoblasts were prepared as described in Fig. 2 legend, and myotubes as described in Fig. 1 legend. Fluorescent N-CAM vesicles were prepared by removal of detergent from a solution containing 6 mg ml^{-1} of lipids extracted from chick brain, 0.2 mg ml^{-1} of affinity-purified N-CAM and 5 mg ml^{-1} 6-carboxyfluorescein[5]. Membrane vesicles were prepared from 14-day embryo brains by homogenization of the tissue in the presence of 5 mg ml^{-1} 6-carboxyfluorescein, isolated by sucrose density centrifugation and washed with phosphate-buffered saline. Binding of vesicles to cells was carried out by incubation of 20 μl of vesicles with 5×10^6 cells in SME medium in a 1-ml suspension, or with myotubes on coverslips for 20 min at 37 °C with gentle shaking. Unbound vesicles were removed by differential centrifugation of the myoblasts or washing of myotube monolayers.

We thank Ms Helvi Hjelt for technical assistance. This work was supported by NIH grants (HD-09635, AI-11378, AM-04256) and a post-doctoral fellowship to M.G. (AI-06414).

Received 5 October 1981; accepted 11 January 1982.

1. Nelson, P. G. *Physiol. Rev.* **55,** 1–61 (1975).
2. Landmesser, L. T. *A. Rev. Neurosci.* **3,** 279–302 (1980).
3. Brackenbury, R., Thiery, J.-P., Rutishauser, U. & Edelman, G. M. *J. biol. Chem.* **252,** 6835–6840 (1977).
4. Thiery, J.-P., Brackenbury, R., Rutishauser, U. & Edelman, G. M. *J. biol. Chem.* **252,** 6841–6845 (1977).
5. Rutishauser, U., Hoffman, S. & Edelman, G. M. *Proc. natn. Acad. Sci. U.S.A.* **79,** 685–689 (1982).
6. Rutishauser, U., Thiery, J.-P., Brackenbury, R. & Edelman, G. M. *J. Cell Biol.* **79,** 371–381 (1978).
7. Rutishauser, U., Gall, W. E. & Edelman, G. M. *J. Cell Biol.* **79,** 382–393 (1978).
8. Buskirk, D. R., Thiery, J.-P., Brackenbury, R. & Edelman, G. M. *Nature* **285,** 488–489 (1980).
9. Hoffman, S. *et al. J. biol. Chem.* (submitted).
10. Rutishauser, U., Thiery, J.-P., Brackenbury, R., Sela, B.-A. & Edelman, G. M. *Proc. natn. Acad. Sci. U.S.A.* **73,** 577–581 (1976).
11. Frazier, W. & Glaser, L. *A. Rev. Biochem.* **48,** 491–523 (1979).
12. Paro, D. G., De Mello, F. G. & Nirenberg, M. *Proc. natn. Acad. Sci. U.S.A.* **74,** 4977–4981 (1977).
13. Brackenbury, R., Rutishauser, U. & Edelman, G. M. *Proc. natn. Acad. Sci. U.S.A.* **78,** 387–391 (1981).
14. Turner, D. C. *Differentiation* **10,** 81–93 (1978).

Non-dopaminergic fibres may regulate dopamine-sensitive adenylate cyclase in the prefrontal cortex and nucleus accumbens

J. P. Tassin*, H. Simon†, D. Hervé*, G. Blanc*, M. Le Moal†, J. Glowinski* & J. Bockaert‡

* Groupe NB, INSERM U 114, and ‡ Laboratoire de Physiologie cellulaire, Collège de France, 11 place Marcelin Berthelot, 75231 Paris Cedex 05, France

† Laboratoire de Neurobiologie des comportements, Université de Bordeaux II, 33076 Bordeaux, France

The dopaminergic (DA) innervation of the prefrontal cortex in rat originates from neurones distributed in the anterior medial part of the ventral tegmental area (VTA)[1]. Biochemical[2,3] and electrophysiological[4] studies have demonstrated that these mesocortico-prefrontal neurones are distinct from others located in the VTA which project to subcortical structures such as the nucleus accumbens. DA receptors coupled to an adenylate cyclase (D-1 receptors) are present in the prefrontal cortex and their topographical distribution closely resembles that of DA nerve terminals[5–7]. We have now further analysed the properties of the cortical D-1 receptors and compared them with those of a subcortical limbic structure examining, in the rat, the effects on DA-sensitive adenylate cyclase activity in the prefrontal cortex and the nucleus accumbens of (1) bilateral 6-hydroxydopamine (6-OHDA) microinjections in the VTA and (2) bilateral electrolytic lesions of the VTA. The results suggest that regulation of D-1 receptors is not solely dependent on the presynaptic DA innervation and that other non-DA fibres may contribute to it.

Male Sprague–Dawley rats (180–250 g) were lesioned bilaterally in the VTA either by 6-OHDA (4 μg in 1 μl) microinjections or by electrocoagulation as described previously[8,9]. In some cases, animals were pretreated with desipramine (DMI; 25 mg per kg intraperitoneally, i.p.) 30 min before the 6-OHDA microinjections. Sham-operated rats were used as controls. All animals were killed between 11 a.m. and 1 p.m., 40–60 days after the lesions. Brains were rapidly removed, their rostral halves fixed with sodium chloride (0.9%) on a Leitz Kryomat[10] and caudal parts kept for histological control. Using cylindrical tubes (1.4 and 0.9 mm diameter for the prefrontal cortex and the nucleus accumbens respectively), microdisks of tissues were punched out bilaterally on successive 500-μm-thick coronal slices from the ventral part of the prefrontal cortex[7] (planes 11,300 and 10,800 μm according to the atlas of König and Klippel[11]; four microdisks; 310 μg protein) or the nucleus accumbens (planes 9,600 and 9,100 μm; six microdisks; 190 μg protein). Tissues from individual animals were then treated to estimate DA-sensitive adenylate cyclase activity as previously described (refs 6, 7; Fig. 2 legend), and DA and noradrenaline levels in each sample were determined radioenzymatically[12].

As expected, a marked decrease in DA levels was observed in both the prefrontal cortex and the nucleus accumbens in rats with bilateral 6-OHDA lesions (Fig. 1). However, surprisingly, there was no change in the DA-sensitive adenylate cyclase activity in these structures despite the nearly complete destruction of their DA innervation (Fig. 1).

Similarly, in most of the animals with bilateral electrolytic lesions (10 out of the 14 lesioned rats) there was a significant reduction of DA levels in both the prefrontal cortex and the nucleus accumbens. In these rats, the DA-sensitive adenylate cyclase activity was significantly increased in the prefrontal cortex (+62 ± 6%; Fig. 1) when compared with results obtained in corresponding sham-operated animals. This effect resulted from an increase in the maximal DA stimulation and not from a change in the apparent affinity of DA for its receptor, suggesting that the number of D-1 receptors coupled to the adenylate cyclase was enhanced (Fig. 2). In contrast, at a DA concentration (10^{-4} M) which induced the effect in the prefrontal cortex, no significant change in the DA-sensitive adenylate cyclase activity was observed in the nucleus accumbens (Fig. 1). This lack of effect was even seen in three animals in which the electrolytic lesions reduced DA levels by >95% (data not shown). These results seem to contradict those of Rosenfeld *et al.*[13] who reported that unilateral electrolytic lesion of the VTA increases the DA-sensitive adenylate cyclase activity in the ipsilateral nucleus accumbens. However, they did not take into account the presence of high levels of DA in nucleus accumbens homogenates from the non-lesioned side. Indeed, a Lineweaver–Burk plot of their data reveals a difference in the affinity but no change in the maximal stimulation of the DA-sensitive adenylate cyclase activity in the denervated nucleus accumbens.

The difference in the effects of the 6-OHDA and electrolytic lesions on cortical noradrenergic (NA) levels might help to explain the lack of development of supersensitivity of the cortical D-1 receptors in the 6-OHDA lesioned rats. Indeed, in most cases, electrolytic VTA lesions did not destroy the ascending NA fibres projecting to the prefrontal cortex (Table 1). On the contrary, probably due to the neurotoxin diffusion, 6-OHDA microinjections also severely affected all ascending fibres of the NA dorsal bundle which pass near the VTA (Table 1). In another experiment designed to test further the eventual

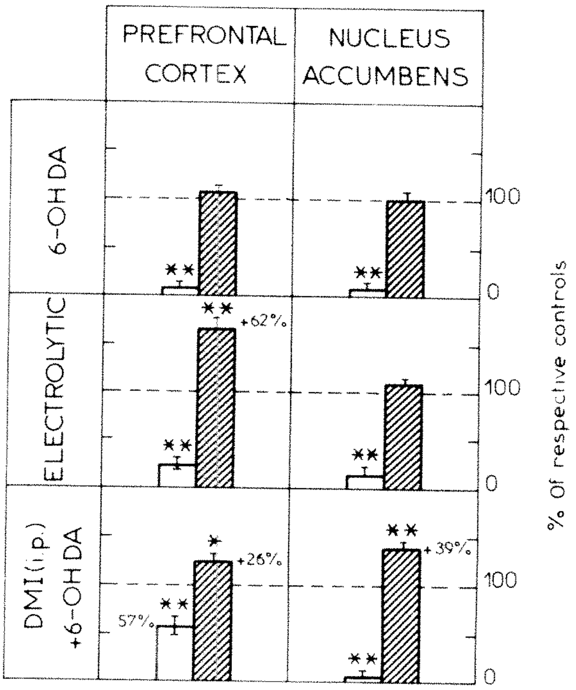

Fig. 1 Effects of different VTA lesions on DA levels and DA-sensitive adenylate cyclase activity in the prefrontal cortex and the nucleus accumbens. Rats were killed 40–60 days after each type of lesion and microdisks of tissue were punched out from the prefrontal cortex and the nucleus accumbens. After homogenization aliquots were taken for the estimation of DA levels and DA-sensitive adenylate cyclase activity. Results are the mean ±s.e.m. of data obtained with groups of 5–10 rats. Mean values ±s.e.m. of sham-operated animals were, respectively, in the prefrontal cortex and the nucleus accumbens: DA levels, 1.2 ± 0.1 and 75 ± 6 ng per mg protein; basal adenylate cyclase activities, 32 ± 1 and 38 ± 2 pmoles cyclic AMP per min per mg protein; DA (10^{-4} M)-stimulated adenylate cyclase activity, 63 ± 3 and 151 ± 12 pmoles cyclic AMP per min per mg protein. The basal adenylate cyclase activity in the lesioned animals was not affected in either the prefrontal cortex or the nucleus accumbens. $* P < 0.05$ and $** P < 0.01$ (Student's *t*-test) when compared with respective values obtained in sham-operated animals. □, DA levels; ▨, DA-sensitive adenylate cyclase activity.

0028-0836/82/080696—03$01.00

Table 1 Effects of different VTA lesions on NA levels in the prefrontal cortex

VTA lesion	Noradrenaline (ng per mg protein)	% Change compared with control
Sham	2.80 ± 0.20 (10)	
6-OHDA	0.10 ± 0.05 (10)	−96*
Electrolytic	2.29 ± 0.25 (10)	−18
DMI (i.p.) + 6-OHDA	1.85 ± 0.19 (8)	−34†

Forty to sixty days after each type of VTA lesion, rats were killed and, after sampling and homogenization of the prefrontal cortex tissues, NA levels were estimated radioenzymatically[12]. Numbers in parentheses correspond to the size of each group. Values are mean ±s.e.m.

* $P < 0.001$ and † $P < 0.01$ when compared with sham-operated animals.

influence of the NA fibres on the regulation of cortical D-1 receptors, animals were treated with DMI before the microinjections of 6-OHDA in the VTA. As expected, this treatment markedly reduced the 6-OHDA neurotoxic effect on NA fibres but allowed the complete destruction of DA neurones projecting to the nucleus accumbens. Curiously, for an unknown reason, the cortical DA innervation was partially preserved because DA levels were only reduced by 43% in the prefrontal cortex. In these conditions, DA-sensitive adenylate cyclase activity was significantly increased in both the prefrontal cortex and the nucleus accumbens, the effect being more pronounced in the latter structure (Fig. 1).

A supersensitivity of D-1 receptors has already been shown in the striatum after electrolytically or 6-OHDA-induced degeneration of the nigro-striatal DA system[14,15]. The results reported here—the marked increase in the DA-sensitive adenylate cyclase activity in the prefrontal cortex after electrolytic destruction of the mesocortico-prefrontal DA neurones—extend these observations. As already discussed, this effect probably results from an enhanced number of D-1 receptors. Its amplitude depends on the extent of DA denervation—in animals with electrolytic lesions a correlation was found between the increase in cortical DA-sensitive adenylate cyclase activity and the degree of the reduction in cortical DA levels (data not shown). It is thus not surprising that the increase in the cortical DA-sensitive adenylate cyclase activity was less pronounced after the partial destruction of the mesocortico-prefrontal DA neurones induced by the 6-OHDA lesion in DMI-pretreated rats. An interesting finding was that the presence of NA fibres seems necessary for the appearance of the increased cortical DA-sensitive adenylate cyclase activity; changes in the regulation of the cortical D-1 receptors were only seen when cortical NA fibres were only slightly or not affected by the lesion (electrolytic, 6-OHDA in DMI-pretreated rats). In contrast, in rats injected with 6-OHDA alone the concomitant destruction of the NA fibres prevented the increase in DA-sensitive adenylate cyclase activity despite the pronounced degeneration of the DA neurones innervating the prefrontal cortex. It is therefore possible that the cortical NA fibres exert a permissive role on the development of the cortical D-1 receptors supersensitivity. Of relevance in this context is the observation that there is a population of cells in the rat prefrontal cortex which responds to both DA and NA[16].

Because NA accounts for ~2% of DA levels in the nucleus accumbens, it was not possible to estimate precisely the effect of 6-OHDA lesions on NA levels in this structure. However, changes in cortical NA levels can be used as an index of the destruction of ascending NA fibres which pass near or through the nucleus accumbens. In any case the development of the D-1 receptors' supersensitivity in the nucleus accumbens does not seem to depend on the presence of ascending NA fibres as there was no change in DA-sensitive adenylate cyclase activity in this structure either when NA fibres were not destroyed (electrolytic lesion) or when they were markedly affected (6-OHDA lesions). Although all types of lesion made induced a pronounced degeneration of the nucleus accumbens DA innervation, the only one which resulted in a significant increase in the DA-sensitive adenylate cyclase activity in this structure was the 6-OHDA lesion made in DMI-pretreated rats. As this lesion was also the only one which partially prevented the destruction of the mesocortico-prefrontal DA neurones, we suggest that the presence of the mesocortico-prefrontal DA neurones is required for the development of D-1 receptors supersensitivity in the DA-denervated nucleus accumbens. Neurones originating in the prefrontal cortex are known to project into the nucleus accumbens[17], and Pycock *et al.*[18] have recently shown that the specific destruction of DA terminals in the prefrontal cortex induced several biochemical changes in various subcortical structures, including an enhanced rate of DA utilization in the nucleus accumbens and the striatum. By their effect on cortical efferent pathways, the mesocortico-prefrontal DA neurons may contribute not only to the regulation of DA transmission in subcortical structures such as the nucleus accumbens, but also to the control of the activity of the target cells on which D-1 receptors are located. In other words, changes in the activity of cortical neurones projecting to the nucleus accumbens could be involved in the regulation of the DA-sensitive adenylate cyclase activity in this structure.

Several electrophysiological studies have demonstrated that the sensitivity of a receptor for a given transmitter can be modified by the action of another transmitter on the same cell[19,20]. Moreover, sustained changes in cell responsiveness to non-monoaminergic transmitters have been shown after denervation of monoaminergic systems in the central nervous system[21]. Our biochemical results provide a novel example of a regulatory process which could intervene in the control of receptor sensitivity: we have shown that the expected increase in the DA-sensitive adenylate cyclase activity after DA denervation can be modulated or even prevented in situations in

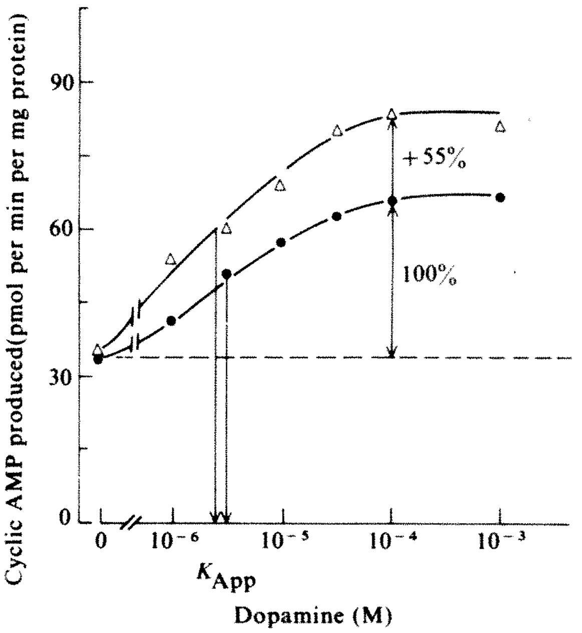

Fig. 2 Effect of bilateral electrolytic lesions of the VTA on the activity of the DA-sensitive adenylate cyclase in the prefrontal cortex. Eight microdisks of tissue (1.4 mm diameter) were punched out bilaterally in the ventral part of the frontal cortex[7] (11,300 μm and 10,800 μm slices following the atlas of König and Klippel[11]). Samples were homogenized in 200 μl of a 2 mM Tris-maleate, *p*H 7.2, 2 mM EGTA, 300 mM sucrose solution. Aliquots were taken to measure DA-sensitive adenylate cyclase activity[6,7] and to estimate dopamine and noradrenaline levels[12]. Each point corresponds to the mean of three determinations; extreme values did not differ by >5%. Variation of values obtained in 10 different sham-operated animals were within 8%. △, Electrolytic VTA lesion; ●, control.

which the target cells are simultaneously deprived or exposed to other significant signals. Such mechanisms may explain the variations observed[14,15,22] in receptor supersensitivity, which may depend on the selectivity of the procedure used to destroy the afferent fibres. Although further evidence is required for such regulation of receptor sensitivity, the phenomenon may be functionally significant and should be taken into consideration when evaluating the efficacy of a given transmission.

This research was supported by grants from DRET (81050), INSERM (CRL 7953626) and Rhône Poulenc S.A.

Received 6 July 1981; accepted 12 January 1982.

1. Fuxe, K. *et al. Brain Res.* **82,** 349–355 (1974).
2. Hervé, D. *et al. Neurosci. Lett.* **15,** 127–133 (1979).
3. Lisoprawski, A., Hervé, D., Blanc, G., Glowinski, J. & Tassin, J. P. *Brain Res.* **183,** 229–234 (1980).
4. Deniau, J. M., Thierry, A. M. & Féger, J. *Brain Res.* **189,** 315–326 (1980).
5. Von Hungen, K. & Roberts, S. *Eur. J. Biochem.* **36,** 391–401 (1973).
6. Bockaert, J., Tassin, J. P., Thierry, A. M., Glowinski, J. & Prémont, J. *Brain Res.* **122,** 71–86 (1977).
7. Tassin, J. P. *et al. Brain Res.* **154,** 241–251 (1978).
8. Le Moal, M., Cardo, B. & Stinus, L. *Physiol. Behav.* **4,** 567–573 (1969).
9. Galey, D., Simon, M. & Le Moal, M. *Brain Res.* **124,** 83–97 (1977).
10. Tassin, J. P. *et al. Brain Res.* **141,** 267–281 (1978).
11. König, J. H. R. & Klippel, R. A. *A Stereotaxic Atlas of the Forebrain and Lower Parts of the Brain Stem* (William and Wilkins, Baltimore, 1963).
12. Gauchy, C., Tassin, J. P., Glowinski, J. & Cheramy, A. *J. Neurochem.* **26,** 471–480 (1976).
13. Rosenfeld, M. R., Seeger, T. F., Sharpless, N. S., Gardner, E. L. & Makman, M. H. *Brain Res.* **173,** 572–576 (1979).
14. Mishra, R. K., Gardner, E. L., Katzman, R. & Makman, M. H. *Proc. natn. Acad. Sci. U.S.A.* **71,** 3883–3887 (1974).
15. Prémont, J., Tassin, J. P., Thierry, A. M. & Glowinski, J. *Expl Brain Res.* **23,** Suppl. 165 (1975).
16. Bunney, B. S. & Aghajanian, G. K. *Life Sci.* **19,** 1783–1792 (1976).
17. Becksteadt, R. M. *J. comp. Neurol.* **184,** 42–43 (1979).
18. Pycock, C. J., Carter, C. J. & Kerwin, R. W. *J. Neurochem.* **34,** 91–99 (1980).
19. Ferron, A., Descarries, L. & Reader, T. A. *Brain Res.* **231,** 93–108 (1982).
20. Moises, H. C., Woodward, D. J., Hoffer, B. J. & Freedman, T. *Expl. Neurol.* **64,** 493–515 (1979).
21. Wang, R. Y., De Montigny, C., Gold, B. I., Roth, R. H. & Aghajanian, G. K. *Brain Res.* **178,** 479–497 (1979).
22. Krueger, B. K., Forn, J., Walters, J. R., Roth, R. H. & Greengard, P. *Molec. Pharmac.* **12,** 639–648 (1976).

Importance of amino acid uptake and decarboxylation in gastrin release from isolated G cells

Lenard M. Lichtenberger, Remi Delansorne & Lynne A. Graziani

Department of Physiology and Cell Biology, University of Texas Medical School at Houston, Houston, Texas 77025, USA

Studies of various species have demonstrated that the post-prandial rise in serum gastrin levels is primarily attributable to the proteinaceous substances ingested[1-5]. Although it is generally assumed that dietary amino acids are the primary stimulants of gastrin release, evidence supporting this notion based on experiments *in vivo* has been conflicting and unconvincing[6-10]. We have investigated the role of amino acids as stimulants of gastrin release using a preparation of isolated rodent gastrin-containing G cells[11,12]. We report here that the ability of an amino acid to stimulate gastrin release *in vitro* is directly correlated with its lipid solubility, the aromatic and long chain aliphatic amino acids being the most potent. In addition, we provide evidence that amino acid decarboxylation may be a necessary step in gastrin release as inhibitors of decarboxylase activity abolished amino acid-induced gastrin release, and amines, the decarboxylated derivatives of amino acids, were potent stimulants of hormone secretion *in vitro*. Thus, the uptake and decarboxylation of amine precursors may be a functionally important property of cells belonging to the APUD (amine precursor uptake and decarboxylation) class of endocrine cells.

We investigated the effects of amino acids and their metabolites on gastrin release *in vitro* using a preparation of enriched G cells isolated according to a modification of a procedure described elsewhere[11,12] (see Fig. 1 legend). Initially we compared the ability of various amino acids to stimulate gastrin release *in vitro*. We included one or more of the amino acids from each of the major classes. The results (see Table 1) indicate that both charged amino acid residues and simple neutral aliphatic amino acid residues having a 1–3 carbon backbone failed to induce gastrin release from isolated G cells. In contrast, the more nonpolar molecules, the aliphatic amino acids having four or more carbon atoms, and the aromatic amino acids, stimulated gastrin release into the medium.

The effectiveness of an amino acid in stimulating gastrin release correlated significantly ($r < 0.001$) with the relative hydrophobicity of its side chain (Fig. 1). This relationship between the lipid solubility of an amino acid and its efficacy in stimulating gastrin release *in vitro* suggests that hormone secretion may depend on the ability of the amino acid to diffuse from the lumen into the interior of the G cell. This notion is supported by reports that amino acids and related compounds are transported into the gastric epithelium by a passive transport process[13]. The intracellular mechanism by which amino acid uptake is coupled to gastrin secretion, however, has yet to be characterized.

Table 1 Effect of amino acids and amines on gastrin release *in vitro*

Amino acids $NH_2\text{–}\overset{\overset{R}{\vert}}{C}H\text{–}COOH$	Gastrin release (% basal)	Amines $NH_2\text{–}\overset{\overset{R}{\vert}}{C}H_2$	Gastrin release (% of basal)
Aliphatic			
Glycine	98 ± 22(4)	Methylamine	350 ± 77(5)*†
Alanine	76 ± 20(4)	Ethylamine	455 ± 98(5)*†
Valine	101 ± 11(10)	Isobutylamine	306 ± 30(10)*†
Leucine	134 ± 5(4)*		
Isoleucine	176 ± 49(4)		
Hydroxy			
Serine	87 ± 6(5)		
Aromatic			
Phenylalanine	186 ± 26(5)*	Methylbenzylamine	252 ± 46(5)*
Tryptophan	212 ± 23(5)*		
Charged			
Arginine	99 ± 27(4)		
Ornithine	65 ± 15(5)		
Glutamine	109 ± 6(4)		
Cysteine	89 ± 10(9)	Cysteamine	200 ± 25(10)*†
Glutamic Acid	87 ± 7.3(4)	δ-Aminobutyric acid	126 ± 24(5)
Imino			
Proline	143 ± 24(4)		

An isolated and enriched preparation of rodent antral G cells was prepared using a modification of a procedure described elsewhere[11,12]. Strips of antral tissue were incubated for 90 min in enriched KRB (Krebs-Ringer bicarbonate) buffer containing pronase E(0.125%; EM Laboratories,) with shaking in water bath at 37 °C in an atmosphere of 95% O_2/5% CO_2 at 105 cycles min^{-1}. At the end of this period the remaining tissue was vigorously shaken by hand (~2,000 cycles min^{-1}) in pronase-containing medium, and then lightly scraped with a glass slide. This combination of selective pronase digestion followed by high shearing forces results in the removal of cells from the basal elements of the antral gland. The exfoliated cells and tissue were then incubated in enriched KRB buffer containing 20 $\mu g\ ml^{-1}$ of DNase I for 30 min, followed by gentle filtration (70 μm pore size) to disrupt the cell aggregates. The resulting cell suspension was washed several times in fresh enzyme-free KRB, and counted using a haemocytometer. Gastrin secretory testing was initiated by injecting the cells ($50\text{–}150 \times 10^3$ per tube) into a siliconized tube containing amino acid-free KRB with and without (control) the test agent. All test agents were used at a final concentration of 10 mM. The cells were incubated with shaking in a water bath at 37 °C in an atmosphere of 95% O_2/5% CO_2 for 10 min. The cells and medium were separated by filtration, and the filtrate was heat extracted at 96 °C for 10 min (ref. 2). The medium samples were then stored at −20 °C before radioimmunoassay of the medium gastrin concentration. Gastrin concentration was determined by a modification of the technique of Yalow and Berson[19]. Purified human gastrin G-17 I was iodinated by the chloramine T method and purified by the method of Stadil and Rehfeld[20]. Antibody 1296, which recognizes all known molecular forms of gastrin[21], was used in all assays. Numbers in parentheses are number of tubes per group.

* Represents a statistically significant difference ($P < 0.05$) compared with medium gastrin concentration of cells incubated in control medium.

† Represents a statistically significant difference ($P < 0.05$) compared with medium gastrin concentration for cells incubated in medium containing the respective amino acid (carboxylated derivative of the amine).

0028-0836/82/080698—03$01.00

Pearse initially proposed the APUD hypothesis[14]. He demonstrated that many endocrine cells, like neural tissue, are able to decarboxylate amine precursors to form the parent amine. Many endocrine cells of the gastrointestinal tract, including the G cell, have been demonstrated histochemically to be members of the APUD family of endocrine cells. Although the importance of the decarboxylase enzymes has been established neurophysiologically, their functional role in endocrine cells remains to be elucidated fully.

We have also demonstrated (see Table 1) that many amines, products of amino acid decarboxylation, are highly efficient in stimulating gastrin release *in vitro*. Note that without exception, amines induced a greater stimulation of hormone secretion than the respective amino acids from which they are derived. These findings are not totally unexpected as previous studies have demonstrated that certain aromatic and aliphatic amines (the catecholamines and cysteamine) are potent stimulants of gastrin release *in vivo*[23-25]. Subsequent experiments have indicated that certain biogenic amines, (serotonin, histamine, spermine and taurine) are unable to stimulate gastrin release *in vitro*. These results suggest that amine-stimulated gastrin release is not a nonspecific G cell response to amines in general, but is a specific response to certain molecular species of this class of compounds.

We then investigated whether the ability of an amino acid to stimulate gastrin release *in vitro* could be modulated in parallel with the decarboxylase activity of the endocrine cell. To test this possibility, glandular cells of the antrum were incubated in medium containing the stimulatory aromatic amino acid, phenylalanine, with or without the addition of the decarboxylase inhibitors, α-methyl-L-dopa (specific L-aromatic amino acid decarboxylase inhibitor), 4-deoxypyridoxine and aminooxyacetic acid (nonspecific decarboxylase inhibitors)[15,16]. Subsequent studies revealed that all three agents significantly reduced the L-aromatic amino acid decarboxylase activity of isolated intact antral glandular cells when [1-alanine-^{14}C]DL-dopa was used as substrate (unpublished results). Figure 2 shows that all three inhibitors significantly blocked phenylalanine-induced gastrin release. In addition, this abolition of amino acid-induced hormone release could not be attributed to a general depression of cell function, as the decarboxylated derivative of phenylalanine, methylbenzylamine, was still capable of stimulating gastrin release in the presence of deoxypyridoxine. Note also that subsequent experiments demonstrated that these inhibitors of cellular decarboxylase activity had minimal affect on basal gastrin release, and effectively abolished the stimulatory actions of other aromatic amino acids (such as tryptophan) on gastrin release *in vitro*.

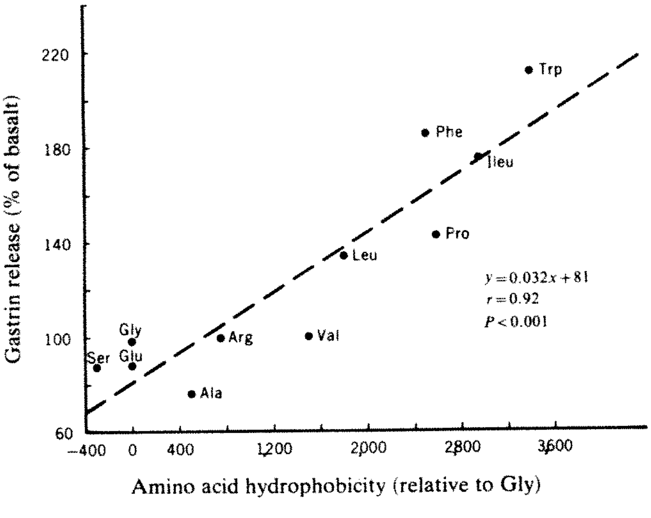

Fig. 1 Relationship between the ability of an amino acid to stimulate gastrin release *in vitro* and the hydrophobic properties of its side chain. The data points were limited to those amino acids whose relative hydrophobicity were estimated by Bigelow and Channon[22]. There is a statistically significant linear relationship between the two properties ($r = 0.92$; $P < 0.001$).

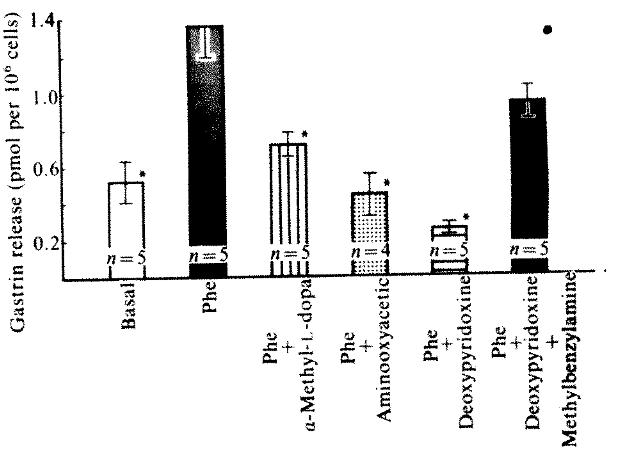

Fig. 2 Effect of decarboxylase inhibitors on phenylalanine-induced gastrin release *in vitro*. The isolated and enriched G cells were prepared and studied as described in Table 1 legend. In addition to cells incubated in amino acid-free KRB alone (basal), cells were incubated in phenylalanine-containing medium (10 mM) in the absence and presence of the following inhibitors of decarboxylase activity: α-methyl-L-DOPA (0.01 mM); aminooxyacetic acid (1 mM); 4-deoxypyridoxine (1 mM) alone, and together with the stimulatory amine, methylbenzylamine (10 mM). * Represents a statistically significant difference ($P < 0.05$) compared with the medium gastrin levels of cells incubated with phenylalanine alone. † Represents a statistically significant difference ($P < 0.001$) compared with the medium gastrin levels of cells incubated with phenylalanine and deoxypyridoxine.

These results suggest that gastrin release, which is triggered by the ingestion of a meal containing protein, may depend in part on the passive transport of amino acids into the G cell, followed by their intracellular decarboxylation. This notion is further supported by autoradiographic evidence[17,18] that the DOPA decarboxylase activity of the G cell resides anatomically in close proximity to the gastrin-containing secretory granules. However, the mechanism by which the amine product is coupled to hormone release remains to be determined. Further experiments will ascertain whether the decarboxylase enzymes have a similar role in mediating the amino acid-induced release of hormones from other endocrine cells possessing the APUD facility.

We thank Mr William Vargo for technical assistance and Drs Morton I. Grossman and John H. Walsh (CURE) for donating purified human gastrin G-171 and antibody 1296 which were used in the radioimmunoassays. This work was supported by NIH grant AM 20686. R.D. performed this work as a visiting student from Ecole Nationale Veterinaire D'Alfort.

Received 31 August; accepted 23 December 1981.

1. Saint-Hilaire, S., Lavers, M. K., Kennedy, J. & Code, C. F. *Gastroenterology* **39**, 1–11 (1960).
2. Debas, H. T., Csendes, A., Walsh, J. H. & Grossman, M. I. in *Endocrinology of the Gut* (eds Chey, W. Y. & Brooks, S. P.) 222–232 (Charles B. Slack, New Jersey, 1974).
3. Debas, H. T., Walsh, J. H. & Grossman, M. I. in *Gastrointestinal Hormones* (ed. Thompson, J. C.) 425–435 (University of Texas Press, Texas 1975).
4. Richardson, C. T., Walsh, J. H., Hicks, J. I. & Fordtran, J. S. *J. clin. Invest.* **58**, 623–631 (1976).
5. Walsh, J. H. *Fedn. Proc.* **36**, 1948–1951 (1976).
6. Walsh, J. H. & Grossman, M. I. *N. Engl. J. Med.* **292**, 1377–1384 (1975).
7. Elwin, C. E. & Uvnas, B. in *Gastrin* (ed. Grossman, M. I.) 69–82 (UCLA Press, Los Angeles 1966).
8. Elwin, C. E. *Scand. J. Gastroent.* **9**, 239–247 (1974).
9. Konturek, S. J., Tasler, J., Cieszkowski, M., Dobrzanska, M. & Wunsch, E. *Am. J. Physiol.* **233**, 170–174 (1977).
10. Strunz, U. T., Walsh, J. H. & Grossman, M. I. *Proc. Soc. exp. Biol. Med.* **157**, 440–441 (1978).
11. Forssmann, W. G., Lichtenberger, L. M., Helmstaedter, V. & Ito, S. *Cell Tissue Res.* **200**, 163–177 (1979).
12. Lichtenberger, L. M., Forssmann, W. G. & Ito, S. *Gastroenterology* **79**, 447–459 (1980).
13. Schanker, L. S. *J. Mednl pharm. Chem.* **2**, 343–359 (1960).
14. Pearse, A. G. E. *J. Histochem. Cytochem.* **17**, 303–313 (1969).
15. Holtz, P. & Palm, D. *Pharmac. Rev.* **16**, 113–178 (1964).

16. Lovenberg, W., Weisback, H. & Udenfriend, S. *J. biol. Chem.* **237,** 89–93 (1962).
17. Kobayashi, S. *Archs Histol. Jap.* **37,** 313 (1975).
18. Rubin, W. & Schwartz, B. *Gastroenterology* **81,** 311–320 (1981).
19. *Yalow, R. S. & Berson, S. A. Gastroenterology* **58,** 1–14 (1970).
20. Stadil, F. W. & Rehfeld, J. F. *Scand. J. clin. Invest.* **30,** 361–368 (1972).
21. Dockray, G. J. & Walsh, J. H. *Gastroenterology* **68,** 222–230 (1975).
22. Bigelow, C. C. & Channon, M. in *Handbook of Biochemistry and Molecular Biology* 3rd edn (ed. Fasmann, G. D.) 209 (CRC, Ohio 1976).
23. Stadil, F. & Rehfeld, J. F. *Gastroenterology* **66,** 7–15 (1974).
24. Hayes, J. R., Ardill, J., Kennedy, L., Buchanan, K. D. & Shanks, R. G. *Lancet* **i,** 819–821 (1972).
25. Lichtenberger, L. M., Szabo, S. & Trier, J. S. *Gastorenterology* **73,** 1305–1308 (1977).

Inhibition of spindle elongation in permeabilized mitotic cells by erythro-9-[3-(2-hydroxynonyl)] adenine

W. Zacheus Cande

Department of Botany, University of California, Berkeley,
California 94720, USA

Studies using living cells[1,2] and experimental manipulation of permeabilized mitotic cells[3,4] demonstrate that the movement of anaphase chromosomes consists of two physiologically distinct events: chromosome movement to the spindle poles (anaphase A) and separation of the poles via spindle elongation (anaphase B). Shortening of kinetochore-attached microtubules is associated with anaphase A and rearrangement and lengthening of the polar microtubules, especially those found in the spindle midzone, with anaphase B[5,6]. It has been suggested that interactions between microtubules, mediated by dynein-like cross-bridges similar to those found in flagella, may be the mechanochemical system responsible for anaphases A and B[7,8]. Recently Bouchard *et al.*[9] have demonstrated that erythro-9-[3-(2-hydroxynonyl)]adenine (EHNA), a protein carboxylmethylation inhibitor, is a specific inhibitor of flagellar beat and dynein ATPase activity. I have now investigated the possibility that dynein-like ATPases have a role in anaphase by adding EHNA to permeabilized cell models in conditions compatible with maintenance of anaphases A and B after lysis[3,4]. I find that EHNA blocks anaphase B but not anaphase A. These results are consistent with the involvement of a dynein-like ATPase in spindle elongation.

Mitotic PtK_1 cells (a kidney epithelial line derived from the rat kangaroo) continue to undergo anaphase after permeabilization of the cell with the nonionic detergent Brij 58 (Fig. 1, step 1, and ref. 3) provided polyethylene glycol is added to the medium 1–2 min after lysis (Fig. 1, step 2). After lysis the dividing cells are permeable to ions, nucleotides, dyes and proteins[3,4]. The rate and extent of spindle elongation (Fig. 1*a*, ●) in lysed mitotic cells depend on the ATP concentration in the medium[4]. In contrast, chromosome-to-pole movement in the permeabilized cell (Fig. 1*a*, △) does not require Mg^{2+}-ATP and is not affected by the presence of sulphydryl reagents, vanadate (a flagellar dynein ATPase inhibitor) and non-hydrolysable ATP analogues in the lysis medium[4].

EHNA, at concentrations that block movement of native rat and sea urchin spermatozoa[9], does not block anaphase when added to intact PtK_1 cells during prometaphase.

After lysis, EHNA preferentially blocks spindle elongation in dividing cells (Fig. 1*b*, Table 1) but does not reduce the rate of chromosome-to-pole movement. Inhibition of anaphase B by EHNA can be prevented by increasing the level of ATP in the lysis medium (Table 1). This result is consistent with the observation that EHNA is a weak mixed competitive inhibitor of dynein ATPase activity[9]. The relative concentration of EHNA required for 75% inhibition of anaphase B (0.2 mM ATP, 0.5 mM EHNA; Table 1) is similar to that required for 50% inhibition of dynein ATPase activity (0.1 mM ATP, 0.23 mM EHNA)[9] and reactivation of demembranated sea urchin spermatozoa (0.2 mM ATP, ~0.75 mM EHNA)[9].

Table 1 Effect of EHNA on chromosome movement

Treatment	No. of experiments	Rates of movement (μm min^{-1}) Chromosome separation	Spindle elongation	Chromosome-to-pole movement
0.2 mM ATP	14	0.55±0.15	0.26±0.10	0.15±0.07
+0.1 mM EHNA	6	0.55±0.16	0.19±0.14	0.18±0.05
+0.5 mM EHNA	9	0.46±0.15	0.06±0.10	0.19±0.06
+2.0 mM EHNA	13	0.32±0.11	0.04±0.06	0.14±0.05
+2.0 mM EHNA and 1.25 mM ATP	5	0.59±0.14	0.33±0.06	0.14±0.04

Rates of movement were estimated by measuring the slopes of the graphs (Fig. 1) of chromosome–chromosome and pole–pole distances from the moment of addition of the step 2 medium (see Fig. 1 legend) to the position of maximum displacement of chromosomes or poles. The rate of chromosome-to-pole movement was calculated as one-half the difference between the rates of chromosome separation and spindle elongation[3]. Values are given with standard deviations.

EHNA was originally described as a potent inhibitor of protein carboxylmethylation because it increases the intracellular concentration of *S*-adenosyl-L-homocysteine through inhibition of adenosine deaminase[9–11]. To study whether EHNA blocked anaphase by this mechanism, PtK_1 cells were lysed in *S*-adenosyl-L-homocysteine, adenosine and cycloleucine, which are known to inhibit protein carboxylmethylation[9–11], and in *S*-adenosyl-L-methionine, a donor of methyl groups[11]. As *S*-adenosyl-L-homocysteine and adenosine are almost as effective as EHNA in retarding spindle elongation (Table 2), we cannot rule out the possibility that protein carboxylmethylation is somehow involved in this process. However, the concentration of these drugs required to inhibit anaphase B are 10^2–10^3-fold higher than that required to inhibit protein carboxylmethylation *in vivo* or *in vitro*[9–11]. Cycloleucine, another inhibitor, does not block anaphase B (Table 2), and *S*-adenosyl-L-methionine, which should promote protein carboxylmethylation *in vitro*, inhibits anaphase B (Table 2) in the permeabilized cell. In addition, inhibition of spindle elongation by EHNA and adenosine depends on the ATP concentration in the lysis medium (Tables 1, 2). These results suggest that EHNA, *S*-adenosyl-L-homocysteine and adenosine all inhibit spindle elongation due to a common property other than their ability to inhibit protein carboxylmethylation. In this regard, spindle elongation differs from flagellar movement, because dynein ATPase activity and flagellar beat are not inhibited by adenosine[9].

It has been suggested that actomyosin may help to generate the forces required for anaphase chromosome movement[12]. As described previously[13], skeletal myosin ATPase activity is unaffected by millimolar concentrations of EHNA, and glycerinated myofibril contraction continues in concentrations of ATP and EHNA that block anaphase B (W.Z.C., unpublished data). To study the effect of EHNA on a process in lysed cells known to involve actomyosin, 1–2 mM EHNA was added to permeabilized PtK_1 cells undergoing cytokinesis. Cleavage furrow constriction continues for several minutes after lysis using

Table 2 Effect of carboxyl transmethylation inhibitors on chromosome movement

Treatment	No. of experiments	Rates of movement (μm min^{-1}) Chromosome separation	Spindle elongation	Chromosome-to-pole movement
0.2 mM ATP	5	0.56±0.08	0.24±0.09	0.16±0.02
+0.5 mM *S*-adenosyl-L-homocysteine	5	0.37±0.15	0.11±0.16	0.13±0.03
+0.5 mM *S*-adenosyl-L-methionine	5	0.43±0.10	0.09±0.08	0.18±0.06
+12 mM cycloleucine	5	0.61±0.10	0.21±0.11	0.19±0.06
+0.5 mM adenosine	5	0.39±0.09	0.14±0.16	0.13±0.04
+2.0 mM adenosine and 1.25 mM ATP	3	0.62±0.20	0.33±0.12	0.15±0.04

0028-0836/82/080700—02$01.00

the procedure described in Fig. 1 legend (see ref. 3) and EHNA does not alter the rate or extent of cleavage (W.Z.C., unpublished data).

As microtubule polymerization may have a role in spindle elongation (reviewed in refs 2, 5), the effect of EHNA on *in vitro* polymerization of neurotubulin was followed spectrophotometrically by monitoring changes in turbidity[14]. Extracts containing 3–5 mg ml^{-1} twice-cycled neurotubulin[3] were warmed to 37 °C in medium containing 100 mM PIPES, *p*H 6.94, 1 mM $MgSO_4$, 1 mM EGTA and either 0.5 mM GTP and 2 mM EHNA or 1 mM GTP and 5 mM EHNA. No change in rate or extent of microtubule polymerization in the presence of four- to fivefold more EHNA than nucleotide was detected.

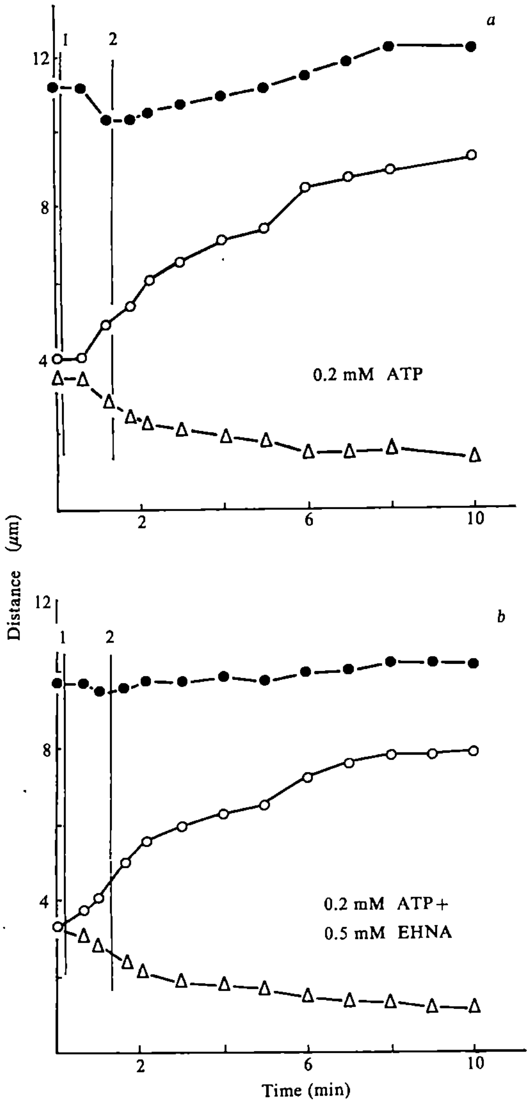

Fig. 1 Effect of EHNA on chromosome movements in permeabilized cells. Separation of spindle poles (●), sister chromatids (○) and chromosome-to-pole movement in one half spindle (△) when cells are lysed in a medium containing 0.2 mM ATP (*a*) or 0.2 mM ATP and 0.5 mM EHNA (*b*). PtK$_1$ cells were used in all experiments and were maintained and handled for light microscopy as described in ref. 3. Coverslips were mounted on slides with coverslip fragments as spacers. Anaphase cells were lysed by flushing solutions under the coverslip in a two-step lysis procedure: step 1 medium contained 85 mM PIPES, 0.08% Brij 58, equimillimolar nucleotide or EHNA (Burroughs-Wellcome) and $MgSO_4$, 10^{-7} M free Ca^{2+} and 1 mM free Mg^{2+}. Step 2, which followed 70–90 s after step 1, used a similar medium that included in addition 2.5% polyethylene glycol (molecular weight 20,000) and 0.1% Brij 58. The composition of the Ca^{2+}-EGTA buffer system was determined using a computer program provided by R. Steinhardt. Using a stability constant of 10.7 at *p*H 6.94 and 10 mM EGTA as a buffer, 1.51 mM $CaCl_2$ and 1.28 mM $MgSO_4$ were added to the lysis medium.

Thus EHNA inhibition of anaphase B is consistent with the argument that a dynein-like ATPase is responsible for generating the forces required for spindle elongation[7,8] and that anaphases A and B are physiologically distinct processes that can be uncoupled by the appropriate experimental manipulation[1,3,4].

I thank Susan Elliger for technical assistance, Carl Elliger and Kent McDonald for helpful discussions, and Steve Penningroth for preprints describing the specificity of EHNA inhibition of dynein ATPase activity and helpful discussions concerning the mechanism of EHNA inhibition. This research was supported by grants from NIH, American Cancer Society and the University of California Cancer Research Coordinating Committee.

Received 10 August; accepted 21 December 1981.

1. Ris, H. *Biol. Bull.* **96,** 90–106 (1949).
2. Inoué, S. & Ritter, H. in *Molecules and Cell Movement* (eds Inoué, S. & Stephens, R. E.) 3–30 (Raven, New York, 1975).
3. Cande, W. Z., McDonald, K. & Meeusen, R. L. *J. Cell Biol.* **88,** 618–629 (1981).
4. Cande, W. Z. *Cell* (in the press).
5. Fuge, H. *Int. Rev. Cytol.,* Suppl. **6,** 1–58 (1977).
6. McDonald, K., Pickett-Heaps, J. D., McIntosh, J. R. & Tippet, D. H. *J. Cell Biol.* **74,** 377–388 (1977).
7. McIntosh, J. R., Hepler, P. K. & van Wie, D. G. *Nature* **224,** 659–663 (1969).
8. Margolis, R. L., Wilson, L. & Kiefer, B. I. *Nature* **272,** 450–452 (1978).
9. Bouchard, P., Penningroth, S. M., Cheung, A., Gagnon, C. & Bardin, C. W. *Proc. natn. Acad. Sci. U.S.A.* **78,** 1033–1036 (1981).
10. Berthelsen, S. & Pettinger, W. A. *Life Sci.* **21,** 595–606 (1977).
11. O'Dea, R. F., Viveros, O. H., Diliberto, E. J. Jr *Biochem. Pharmac.* **30,** 1163–1168 (1981).
12. Forer, A. in *Nuclear Division in the Fungi* (ed. Heath, I. B.) 21–68 (Academic, New York, 1978).
13. Penningroth, S. M., Cheung, A., Bouchard, P., Gagnon, C. & Bardin, C. W. *Biochem. biophys. Res. Commun.* (in the press).
14. Gaskins, F. & Cantor, C. R. *J. molec. Biol.* **89,** 737–758 (1974).

Inhibitors of dynein activity block intracellular transport in erythrophores

Mary C. Beckerle & Keith R. Porter

Department of Molecular, Cellular and Developmental Biology,
University of Colorado, Campus Box 347, Boulder,
Colorado 80309, USA

Erythrophores, cells capable of translocating pigment granules along a radially arrayed cytoskeletal framework, provide an excellent model system for studying intracellular particle transport. Numerous examples of intracellular motility are based on microtubules[1] and all available evidence indicates that organized pigment granule transport in erythrophores depends on these structures[2]. The best studied microtubule-based motility system is the flagellum. As it relies on a dynein–microtubule interaction to generate motive force[3], we have investigated the effects of dynein ATPase inhibitors on pigment granule transport. Vanadate is a potent inhibitor of dynein ATPase activity *in vitro*[4–6] and has been shown to inhibit microtubule-based motility in cilia[4], flagella[4] and the mitotic spindle[7]. Recently, another dynein inhibitor, erythro-9-3-(2-hydroxynonyl)adenine (EHNA), has been described[8]. We report here that both microinjected vanadate and exogenously applied EHNA block saltatory movement of pigment granules in isolated squirrelfish erythrophores. The vanadate and EHNA sensitivities of directed pigment motion suggest that a dynein-like molecule may be an essential component of the erythrophore intracellular motility system.

Erythrophores isolated from the scales of the squirrelfish (*Holocentrus ascensionis*) and cultured on glass coverslips retain their capacity to translocate pigment granules[9]. Mass aggregative movement of the pigment towards the cell centre is rapid and of uniform velocity, while dispersive radial movements are

0028-0836/82/080701—03$01.00

slow and faltering. When the cell is in the dispersed state, the granules shuttle to and fro in short radial jumps or 'saltations'[9,10].

Pressure microinjection[11] of erythrophores with $\sim 7 \times 10^{-14}$ l ($\sim$7% of the cell volume) of a 10% sucrose solution at *p*H 7, containing fluorescein isothiocyanate-labelled bovine serum albumin (5–10 mg ml^{-1}) results in an initial aggregation of the pigment followed, within 1 min, by a return of normal granule movements. In contrast, the saltatory intracellular motility of erythrophores is rapidly inhibited when the cells are injected with vanadate (>50 μM) in the V(V) oxidation state (Table 1). Microinjection of vanadate at a concentration of 250 μM causes the pigment granules to freeze transiently and then disperse slightly, perhaps because of vanadate enhancement of adenylate cyclase activity[12]; chromatophores characteristically respond to increased intracellular cyclic AMP by dispersing their pigment[13,14]. Once this initial dispersion has occurred, the shuttling of granules ceases, and the pigment will no longer aggregate, as it usually would, in response to touch by the microinjection needle. Adjacent cells which pulsed in synchrony with the experimental cell before injection will, however, respond by aggregating their pigment when the injected cell is touched (Fig. 1). This result suggests that the injected cell is receiving the stimulus to aggregate and is communicating it to nearby cells, but is incapable of translocating its own pigment in response to the stimulus. Erythrophores injected with 50 or 100 μM V(V) exhibit all the above characteristics except they can occasionally aggregate their pigment in response to touch by the micropipette. However, this aggregation is much slower than that in coupled or control cells and is generally less complete.

When the concentration of vanadate in the injection buffer is increased to 500 μM, a cell immediately adjacent to the injected cell often loses its ability to translocate pigment granules, but touching either of these incapacitated cells results in aggregation of other cells previously observed to be coupled to the injected cell. It seems likely that the excess vanadate is passing through the same junctions that serve to couple the cells electrically; the $H_2VO_4^-$ form of V(V) which exists in aqueous solution at neutral *p*H[12,15] should pass readily through gap junctions because it is both small and negatively charged. The fact that an uninjected cell is inhibited in its motility illustrates that the injection procedure itself is not responsible for the effects on granule movement noted here. Moreover, as depolarization of the cell membrane is probably the primary signal to aggregate the pigment[16], the immobilized, injected cell must remain alive in order to communicate the aggregation stimulus to adjacent cells.

When the concentration of injected vanadate is decreased to 10 μM, an intermediate inhibitory effect is observed. The pigment translocation ceases in 32% of the cells injected while the remainder are affected either transiently or not at all. If the concentration of injected material is decreased to 1 μM, all injected cells remain competent to move their pigment.

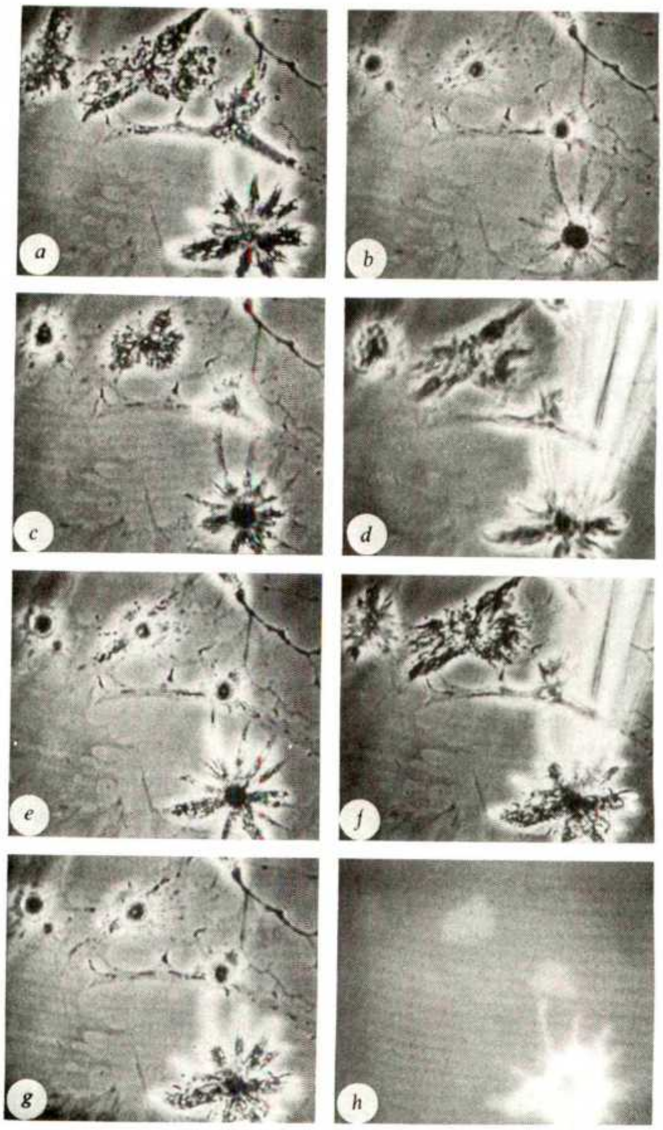

Fig. 1 Phase-contrast micrographs of four erythrophores in culture. The cells are coupled, that is, they disperse (*a*), aggregate (*b*) and redisperse (*c*) their pigment granules in synchrony. In *d*, the cells are in the dispersed state and one cell is microinjected with vanadate (250 μM) in injection buffer containing fluorescein-labelled bovine serum albumin. The injected cell is rapidly inhibited in its intracellular transport function whereas the three other cells continue to aggregate and disperse their pigment (*e*, *f*). Touching the microinjected cell with the micropipette (*f*) results in aggregation of the three coupled, uninjected cells, but the vanadate-injected cell does not respond to the stimulus with pigment movement (*g*). A fluorescence image (*h*) of the four cells illustrates that the cell on the lower right has been successfully injected. Slight autofluorescence of the pigment granules can be seen in the other erythrophores.

Kinetic analyses of the effect of vanadate on dynein *in vitro* have demonstrated that its inhibition of the ATPase activity is noncompetitive[5,6]. Vanadate inhibition of myosin[17] and the $(Na^+ + K^+)$ATPase[18,19], on the other hand, is competitive with substrate binding. Injection of a large excess of MgATP (up to 2.5 mM) together with 250 μM vanadate fails to prevent or slow the vanadate effects on pigment granule migration *in vivo*, suggesting that vanadate inhibition of granule motility is probably not due to an effect on any of the numerous ATPases[6] known to be competitively inhibited by vanadate.

Table 1 The effect of vanadate on pigment granule migration

Concentration of vanadate in micropipette (μM)	Approximate intracellular concentration* (μM)	No. of cells injected	Inhibition of transport (no. of cells; % inhibited)
500	37	55	55; 100
250	18.5	29	28; 97
100	7.3	21	21; 100
50	3.7	31	31; 100
10	0.73	22	7;32
1	0.073	42	0; 0

* Microinjection needles were calibrated by measuring the volume of oil droplets injected into erythrophores.

Incubation of erythrophores with another dynein inhibitor, EHNA, at a concentration of 4×10^{-3} M, in culture medium for 20 min also results in cessation of saltatory shuttling of pigment granules. At 10^{-3} M EHNA, a 60–90-min exposure is required before motility is inhibited. The dispersed cells appear to be frozen with regard to particle translocation. Although there is some brownian movement of the pigment granules, they do not shuttle and no spontaneous aggregation–dispersion cycles occur. Exogenous application of adrenaline stimulates the cells to aggregate their pigment granules, although the response is slowed relative to untreated cells.

EHNA has also been reported to inhibit protein carboxyl-methylase activity by increasing the intracellular concentration of *S*-adenosyl homocysteine[20]. In view of the fact that calcium appears to be the intracellular signal for aggregation of pigment granules[21] and calmodulin can be methylated[22], we examined the possibility that EHNA inhibition of pigment saltation was due to the inhibition of carboxyl-methylase rather than dynein ATPase. Microinjection of *S*-adenosyl homocysteine at concentrations up to 100 μM yielded no inhibition of pigment granule shuttling or aggregation and dispersion even after 60 min. As EHNA-induced inhibition of monocyte chemotaxis occurs rapidly when intracellular *S*-adenosyl homocysteine reaches $\sim 6\times 10^{-18}$ g per cell[20], the high concentration injected into erythrophores ($\sim 3\times 10^{-15}$ g per cell) should have readily inhibited pigment motion if it relied on carboxyl-methylase activity.

It seems unlikely that either vanadate or EHNA is simply interfering with the general ATP metabolism of the cells because co-injection of vanadate and ATP affects cells in the same manner as vanadate alone, and the cells treated with either vanadate or EHNA do not ultimately aggregate their pigment as do cells treated with various inhibitors of oxidative phosphorylation[10].

Dynein-like ATPase activity has been isolated from numerous microtubule-based motility systems, from sources as diverse as the sea urchin mitotic apparatus[23], *Saccinobaculus* axostyle[24] and human sperm[25]. Probes for dynein activity have been shown to inhibit anaphase chromosome movement[7,26], flagellar beat[4,8], microtubule-associated particle transport in fibroblasts[27] and, now, erythrophore pigment movement. Taken together these observations suggest that a dynein-like protein is a force-transducing molecule in microtubule-dependent intracellular motility in general.

This work was supported by a grant from the Muscular Dystrophy Association of America to K.R.P. and a Danforth Fellowship to M.C.B. M.C.B. thanks M. Zavortink for encouragement and instruction in microinjection and M. McNiven for care of the squirrelfish. We thank J. R. McIntosh and his team for many helpful discussions and generosity with equipment.

Received 1 November 1981; accepted 15 January 1982.

1. Hyams, J. S. & Stebbings, H. in *Microtubules* (ed. Hyams, J. S.) (Academic, New York, 1979).
2. Schliwa, M. in *International Cell Biology, 1980–1981* (ed. Schweiger, H. G.) 275–285 (Springer, Berlin, 1981).
3. Satir, P. *et al. Cell Motility* **1,** 303–327 (1981).
4. Gibbons, I. R. *et al. Proc. natn. Acad. Sci. U.S.A.* **75,** 2220–2224 (1978).
5. Kobayashi, T. *et al. Biochem. biophys. Res. Commun.* **81,** 1313–1318 (1978).
6. Shimizu, T. *Biochemistry* **20,** 4347–4354 (1981).
7. Cande, W. Z. & Wolniak, S. M. *J. Cell Biol.* **79,** 573–580 (1978).
8. Bouchard, P., Penningroth, S. M., Cheung, A., Gagnon, C. & Bardin, C. W. *Proc. natn. Acad. Sci. U.S.A.* **78,** 1033–1036 (1981).
9. Byers, H. R. & Porter, K. R. *J. Cell Biol.* **75,** 541–558 (1977).
10. Luby, K. J. & Porter, K. R. *Cell* **21,** 13–23 (1980).
11. Graessmann, M. & Graessmann, A. *Proc. natn. Acad. Sci. U.S.A.* **73,** 366–370 (1976).
12. Simons, T. J. B. *Nature* **281,** 337–338 (1979).
13. Geschwind, I. I. *et al. J. Cell Biol.* **74,** 928–939 (1977).
14. Beckerle, M. C. & Porter, K. R. *J. Cell Biol.* **91,** 302a (1981).
15. Cantley, L. C. *et al. J. biol. Chem.* **252,** 7421–7423 (1977).
16. Parker, G. H. *Animal Colour Changes and their Neurohumours,* 122–134 (Cambridge University Press, 1948).
17. Goodno, C. C. *Proc. natn. Acad. Sci. U.S.A.* **76,** 2620–2624 (1979).
18. Hansen, O. *Biochim. biophys. Acta* **568,** 265–269 (1979).
19. Jorgensen, P. L. & Anner, B. M. *Biochim. biophys. Acta* **555,** 485–492 (1979).
20. Pike, M. C., Kredich, N. M. & Snyderman, R. *Proc. natn. Acad. Sci. U.S.A.* **75,** 3928–3932 (1978).
21. Luby, K. J. *Eur. J. Cell Biol.* **22,** 352a (1980).
22. Gagnon, C. *Nature* **291,** 515–516 (1981).
23. Pratt, M. M., Otter, T. & Salmon, E. D. *J. Cell Biol.* **86,** 738–745 (1980).
24. Mooseker, M. S. & Tilney, L. G. *J. Cell Biol.* **56,** 13–26 (1973).
25. Baccetti, A. *et al. J. Cell Biol.* **88,** 102–107 (1981).
26. Cande, W. Z. *J. Cell Biol.* **91,** 320a (1981).
27. Forman, D. S. *J. Cell Biol.* **91,** 414a (1981).

Cyclic AMP induces maturation of trout sperm axoneme to initiate motility

Masaaki Morisawa

Laboratory of Physiology, Ocean Research Institute,
University of Tokyo, Nakano, Tokyo 164, Japan

Makoto Okuno

Department of Biology, University of Tokyo, Komaba, Meguro,
Tokyo 153, Japan

Cyclic AMP has long been implicated as an activator of sperm motility[1–5]. From more recent experiments using demembranated mammalian and sea urchin spermatozoa[6,7], it was concluded that cyclic AMP only increases the motility of the axoneme after it has been initiated by MgATP^{2-}. We have now carried out similar experiments using spermatozoa collected from the rainbow trout and demembranated by treatment with the detergent Triton X-100. Our results suggest that in this species, cyclic AMP is required before MgATP^{2-} to trigger maturation of the nonmotile axoneme. Subsequent addition of an energy source then induces motility.

Semen was collected from mature rainbow trout, *Salmo gairdneri*, by inserting a pipette into the sperm duct. The plasma membrane and mitochondria of the sperm were then removed (confirmed in electron micrographs) by mixing at room temperature 1 volume of semen with 20 volumes of the extracting medium containing 0.15 M KCl, 0.5 mM MgSO$_4$, 5 mM CaCl$_2$, 0.5 mM EDTA, 1 mM dithiothreitol (DTT), 2 mM Tris buffer, *p*H 8.2, and 0.04% Triton X-100 for 30 s in the presence or absence of 0.5 mM cyclic AMP. Removal of the plasma membrane and mitochondria, elimination of the energy supply, and the dispersal of the components essential for axonemal movement in the extracting medium resulted in immotility of the axoneme. Reactivation of axonemal movement was then attempted using the modified method of Gibbons and Gibbons[8]: the demembranated sperm were resuspended in reactivating medium containing 0.15 M KCl, 2 mM MgSO$_4$, 0.5 mM CaCl$_2$, 2 mM EGTA, 1 mM DTT, 20 mM Tris buffer, *p*H 8.2, and 1 mM ATP again in the presence or absence of 0.5 mM cyclic AMP, and were observed by dark-field microscopy with stroboscopic mercury illumination at a magnification of ×200.

During demembranation rainbow trout spermatozoa remain quiescent due to the presence of K$^+$ in the seminal plasma[9] or KCl in the extracting medium. When cyclic AMP was absent from both the demembranating and reactivating media, no axonemal movement was observed (Fig. 1*a*). However, when the demembranated sperm were suspended in reactivating medium containing MgATP^{2-} and cyclic AMP, axonemal movement occurred (Fig. 1*b*), causing the reactivated sperm to swim at a speed of 103 ± 12 μm s^{-1} ($n = 8$). In contrast, motility of demembranated mammalian and sea urchin sperm is restored in the presence of MgATP^{2-}, with no requirement for cyclic AMP[6–8]. These results suggest that whereas the axoneme of mammalian and sea urchin sperm is already functionally mature and requires only an energy supply to initiate motility, the axoneme of rainbow trout sperm is functionally immature and is converted to the mature state by exposure to cyclic AMP.

When trout spermatozoa were demembranated in the extracting medium (always ATP free) containing cyclic AMP and then

0028–0836/82/080703—02$01.00

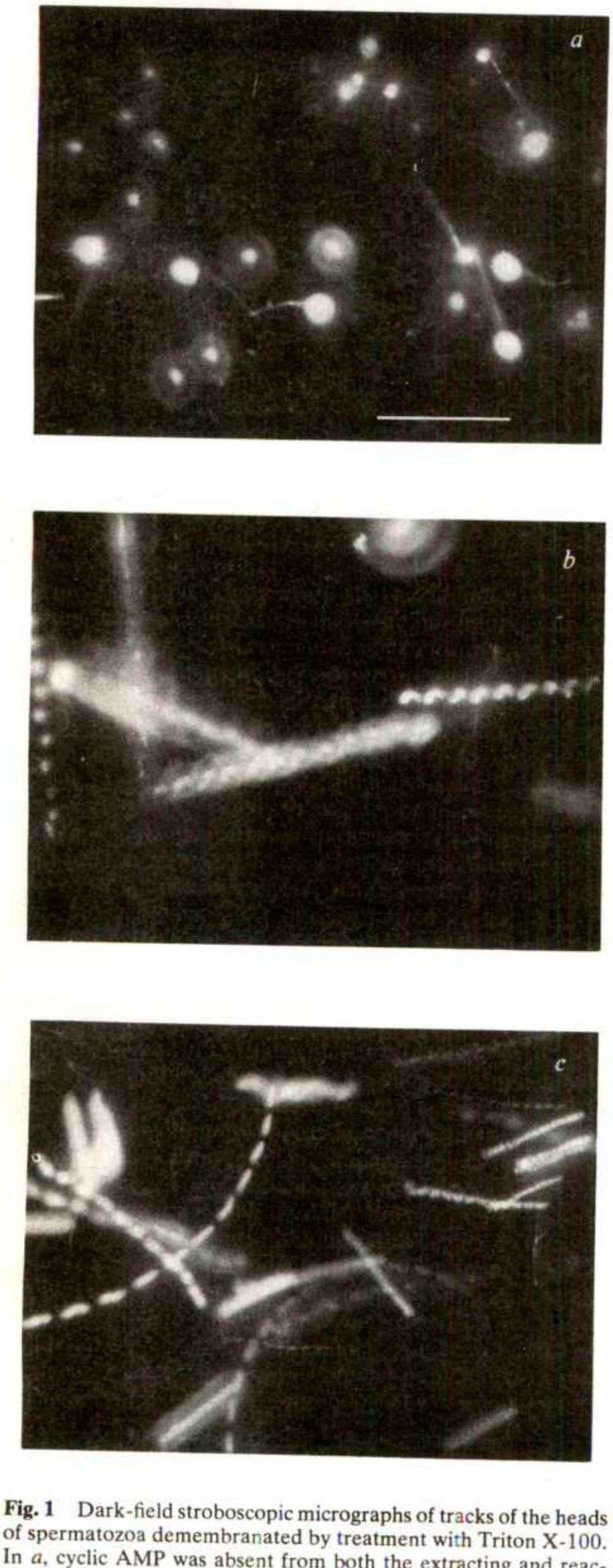

Fig. 1 Dark-field stroboscopic micrographs of tracks of the heads of spermatozoa demembranated by treatment with Triton X-100. In *a*, cyclic AMP was absent from both the extracting and reactivating media; semen was directly immersed in the extracting medium and demembranated; no evidence of movement. In *b*, cyclic AMP was present in the reactivating medium; demembranation of sperm was performed by the same method as in *a*; movement is evident. In *c*, cyclic AMP was absent from both the extracting and reactivating media; semen was diluted in 100 mM NaCl for 30 s and then spermatozoa were demembranated; movement is evident. In *a*, demembranated sperm are immotile; rounded heads and slender axoneme projected from heads are observed. In *b*, *c*, demembranated sperm are motile; the image of tracks of heads which are driven by axonemal movement are observed as a dotted line under stroboscopic illumination; all preparations exhibit straight or curved lines, no rounded heads are present, indicating 100% motility of axonemes. Bar in *a* indicates 50 μm.

placed in reactivating medium containing MgATP^{2-} but no additional cyclic AMP, axonemal movement occurred to give a speed of 78 ± 9 μm s^{-1} ($n = 4$). This can be explained if cyclic AMP becomes bound to the axoneme during the demembranated procedure, and induces its maturation. Axonemal movement can then occur with the addition of the energy source, MgATP^{2-} alone.

In the above experiments Ca^{2+} concentration was ~5 mM in the extracting medium and 10^{-9} M in the reactivating medium (buffered with EGTA). Even when CaCl$_2$ was eliminated from both media, axonemal movement occurred, suggesting that Ca^{2+} did not affect the maturation in motility of the axoneme.

During natural spawning, seminal K$^+$, which inhibits motility of salmonid sperm in the sperm duct, is diluted by fresh water, allowing sperm motility to occur[10]. In the present experiments, the mature axoneme deprived of plasma membrane and mitochondria always displayed motility in reactivating medium containing 0.15 M KCl, suggesting that K$^+$ ions inhibit the motility of intact (functionally mature) sperm through metabolic or membrane effects, and do not directly inhibit axonemal maturation. When an appropriate volume of semen was diluted to 100 vol in K$^+$-free 100 mM NaCl for 30 s (the duration of intact sperm motility of rainbow trout) and then a volume of the sperm suspension was extracted in the absence of cyclic AMP, axonemal movement occurred to give a speed of 100 ± 32 μm s^{-1} ($n = 11$) in reactivating medium containing MgATP^{2-}, again in the absence of cyclic AMP (Fig. 1*c*). This result offers an explanation for normal initiation of trout sperm motility: the reduction of external K$^+$ at spawning may affect metabolic or membrane-mediated processes in the intact sperm and thus induce an increase in intraflagellar cyclic AMP concentration. The endogenous cyclic AMP then induces axonemal maturation (as described above; Fig. 1*b*), and the matured axoneme conveys motility to the sperm, using energy provided by the mitochondria.

Components of the cyclic AMP system, including cyclic AMP, adenylate cyclase, phosphodiesterase, cyclic AMP-dependent protein kinase which phosphorylates the motile apparatus[11], and phosphoprotein phosphatase, occur in motile cells, including spermatozoa[12], cilia[11] and muscle[13], of many animals. The ability to isolate an immature motile apparatus from trout sperm provides a useful model for investigating cell motility, especially the molecular site of cyclic AMP action and phosphorylation in sperm motility and the chemistry of interaction between the cyclic AMP system and the motile apparatus in initiation of cell motility generally.

Independently of our present study, activation of demembranated spermatozoa of a tunicate *Ciona* by cyclic AMP has been described[14].

We thank H. A. Bern and C. J. Brokaw for critical evaluation of the manuscript, H. Mohri for encouragement, and the director and staff of Kumagaya Branch of Saitama Fisheries Experiment Station for providing the materials. This work was supported in part by a grant-in-aid from the Japanese Ministry of Education and Itō Foundation for the Advancement of Ichthyology to M. M.

Received 27 October; accepted 21 December 1981.

1. Garbers, D. L., Lust, W. D., First, N. L. & Lardy, H. A. *Biochemistry* **10,** 1825–1831 (1971).
2. Morton, B., Harringam-Lum, J., Albagli, L. & Jooss, T. *Biochem. biophys. Res. Commun.* **56,** 372–379 (1974).
3. Hoskins, D. D., Hall, M. L. & Munsterman, D. *Biol. Reprod.* **13,** 168–176 (1975).
4. Wyker, R. & Howard, R. S. *Fert. Steril.* **28,** 108–112 (1977).
5. Hoskins, D. D., Brandt, H. & Acott, T. S. *Fedn Proc.* **37,** 2534–2542 (1978).
6. Lindemann, C. B. *Cell* **13,** 9–18 (1978).
7. Mohri, H. & Yanagimachi, R. *Expl Cell Res.* **127,** 191–196 (1980).
8. Gibbons, B. H. & Gibbons, I. R. *J. Cell Biol.* **54,** 75–97 (1972).
9. Schlenk, W. Jr & Kahmann, H. *Biochem. Z.* **295,** 283–301 (1938).
10. Morisawa, M. & Suzuki, K. *Science* **210,** 1145–1147 (1980).
11. Mohri, H. *Biochim. biophys. Acta* **456,** 85–127 (1976).
12. Garbers, D. L., Watkins, H. E., Tubb, D. J. & Kopf, G. S. *Adv. Cyclic Nucleotide Res.* **9,** 583–595 (1978).
13. Adelstein, R. S. & Eisenberg, E. *A. Rev. Biochem.* **49,** 921–956 (1980).
14. Brokaw, C. J. *Cell Motility* (in the press).

Different mRNAs from the transforming region of highly oncogenic and non-oncogenic human adenoviruses

Anders Virtanen & Ulf Pettersson

Department of Microbiology, The Biomedical Centre, University of Uppsala, Box 581, S-751 23 Uppsala, Sweden

Jean Michel Le Moullec, Pierre Tiollais & Michel Perricaudet

Unité de Recombinaison et Expression Génétique, Institut Pasteur, 28 rue du Dr Roux, 75724 Paris Cedex 15, France

Only a fraction of the genome of adenovirus, a DNA tumour virus, is required for transformation *in vitro*[1-4]. The leftmost 11% of the genome, including the two transcription units E1A and E1B, appear to be sufficient for transformation of rat embryo cells in tissue culture for highly, weakly and non-oncogenic adenovirus serotypes[5,6]. Various spliced mRNAs, orginating from the transforming region, have been identified[7-11] and in some cases the corresponding protein products found[12-14] but it is unknown what renders some serotypes highly oncogenic for baby hamsters compared with others that are non-oncogenic although able to transform cells *in vitro*. We have studied the mRNAs from the transforming region of the highly oncogenic serotype 12 (Ad12) in the hope of finding novel mRNAs which could account for the oncogenic properties of the virus. We have previously failed to find any differences between the spliced mRNAs in the transcription unit of the E1A region of Ad12 and the corresponding mRNAs from the non-oncogenic type 2 (Ad2)[15]. Here we have extended our analysis to the E1B region and show that the highly oncogenic Ad12 encodes mRNAs which have different structures from those encoded by Ad2.

We isolated mRNA from Ad12-infected cells and prepared cDNA copies which were inserted into the pBR322 vector. RNA was extracted[16] from infected A549 cells (a cell line derived from a human oat-cell carcinoma) either 8 h after infection in the presence of 25 μg ml^{-1} cycloheximide or 16 h post-infection in the absence of drug. To study the temporal expression of genes in the transforming region we prepared ^{32}P-labelled cDNA copies from the two mRNA preparations, and hybridized[17] these to restriction enzyme fragments of Ad12 DNA. The results (Fig. 1) show that the RNA from the cycloheximide-treated cells hybridized only to the *Acc*I H fragment which covers the E1A region of Ad12 (ref. 18). In contrast, RNA prepared 16 h post-infection in the absence of cycloheximide hybridized also to the *Acc*I F fragment and to two small fragments that are specific for region E1B (Fig. 1).

Double-stranded cDNA copies of late (16 h) poly(A)-containing RNA were prepared as described elsewhere[10] and inserted in the *Pst*I cleavage site of the pBR322 plasmid. Clones having sequences from the E1 region were identified by screening 50,000 colonies by hybridization[19] using ^{32}P-labelled *Eco*RI C fragment as probe. To distinguish between clones from regions E1A and E1B, the *Acc*I restriction fragments, 1, 2 and 3 (see Fig. 1) of the *Eco*RI C fragment were used and 38 E1B-specific clones were identified. Characterization of the clones by cleavage with endonucleases *Hin*dIII, *Sal*I, *Xba*I and *Pvu*II, which cleave the Ad12 DNA within region E1B (Fig. 2), showed that they correspond to three classes of spliced mRNA.

The structures of these classes were determined by sequencing parts of representative clones and comparing the results with

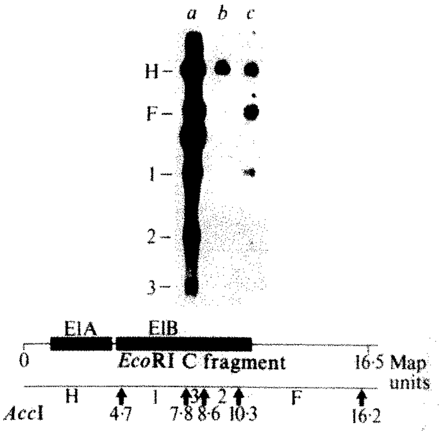

Fig. 1 Kinetic analysis of mRNA expression from the transforming region of Ad12. For this experiment we used a cloned *Eco*RI C fragment of Ad12 DNA comprising the leftmost 16% (M.P., unpublished data). *Acc*I cleavage of the cloned fragment results in five fragments of viral DNA which can be used to discriminate between regions E1A and E1B of Ad12. The lower panel shows a restriction enzyme cleavage map for endonuclease *Acc*I. Only the leftmost 16.5 map units are included and the fragments are indicated by numbers and letters. The top panel shows hybridization between *Acc*I fragments of Ad12 DNA and ^{32}P-labelled cDNA, prepared using AMV polymerase with oligo(dT) as primer. RNA extracted 8 h after infection (*b*) and 16 h after infection in the absence of drug (*c*) was tested. For the analysis a clone containing the *Eco*RI C fragment of Ad12 DNA (0–16.5 map units) was cleaved with *Acc*I and the resulting fragments separated on a 1.4% agarose gel before transfer to nitrocellulose[17]. ^{32}P-labelled Ad12 DNA was hybridized to a separate filter strip to visualize all fragments containing viral DNA (*a*). The band labelled H in the upper panel, contains the *Acc*I H fragment of Ad12 plus flanking sequences from the pBR322 plasmid.

the nucleotide sequence determined for the E1B region of Ad12 DNA (ref. 20 and K. Fujinaga *et al.*, personal communication). We thus established the way in which the three mRNA classes are spliced; mRNAs belonging to class I are spliced between nucleotides 3,295 and 3,369 and resemble closely the 22S mRNA from the E1B region of subgroup C adenoviruses[21]. RNA species belonging to class II have two introns; one is identical to the small intron in class I mRNAs, the second is large and located between nucleotides 2,046 and 3,163 in the sequence of Bos *et al.*[20]. Class III mRNAs also have two introns; one is large and identical to the large intron in class II mRNAs whereas the second is short and located between nucleotides 3,295 and 3,444. Thus the same donor site but different acceptor sites are used for splicing the small intervening sequences present in class II and III mRNAs. All 38 clones in our collection contained the *Xba*I cleavage site at map position 8.9, suggesting that no Ad12 mRNA has the same structure as the 13S mRNA of region E1B in Ad5 (ref. 21), which contains a single large intron.

S$_1$ nuclease analysis has identified a common poly(A) addition site both for the Ad12 E1B mRNAs[11], and the Ad5 E1B

Table 1 Characterization of 38 clones containing sequences from region E1B of Ad12

No. of clones	mRNA species*
4	I
8	II
4	III
22	Unclassified†

* As defined in Fig. 2.

† These clones contained severely truncated cDNA inserts and thus could not be classified unambiguously; most belong to class II and II mRNAs.

0028-0836/82/080705—03$01.00

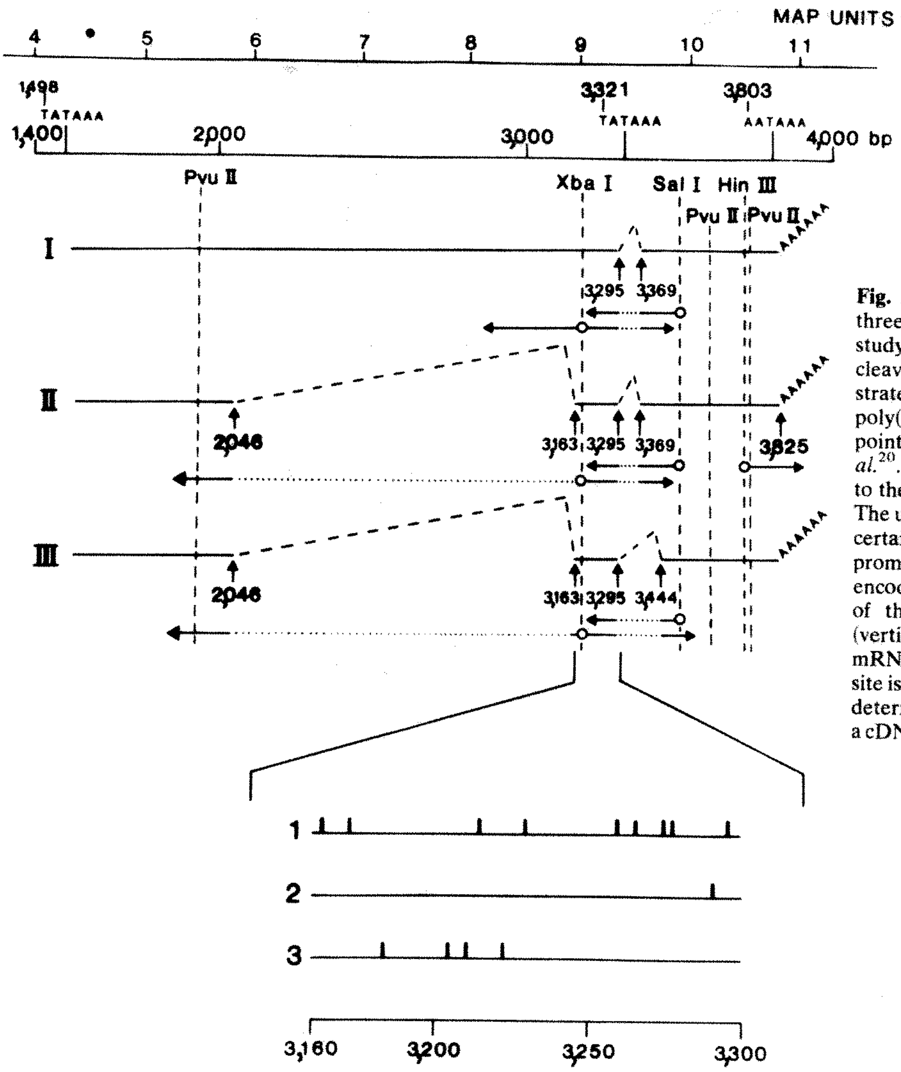

Fig. 2 Schematic drawing of the structure of the three classes of mRNA identified in the present study. The positions of selected restriction enzyme cleavage sites are indicated and the arrows demonstrate how the sequence was determined[28] at the poly(A) addition site and at the different splice points. The sequence is indexed according to Bos *et al.*[20]. The numbers at the exon/intron junctions refer to the first or last nucleotide of the respective exon. The upper part of the figure indicates the positions of certain sequences: TATAAA at position 3,321 is a promoter-like sequence which preceds the sequence encoding the Ad12 polypeptide IX. The lower part of the figure illustrates the termination codons (vertical bars) in the second exon of class II and III mRNAs (data from ref. 20). The poly(A) addition site is located immediately to the left of the sequence determined by Bos *et al.*[20] and was determined from a cDNA clone. Nucleotide 3,825 is the first A residue in the poly(A) tail. bp, Base pairs.

mRNAs[7,8]. By sequencing the ends of a cDNA insert (Fig. 2), the poly(A) addition site in region E1B of Ad12 was located at nucleotide 3,824. It is preceded by the hexanucleotide sequence AAUAAA, which is almost invariably adjacent to poly(A) addition sites in eukaryotic mRNAs[22].

The 5′ ends of the mRNAs belonging to the three classes cannot be determined from the present study. However, results of S_1 nuclease analysis suggest that all mRNAs from region E1B of Ad12 have a common 5′ end located around nucleotide 1,525 in the Ad12 sequence[11]. There are extensive sequence homologies between this region in Ad12 and the known E1B cap site in the Ad5 genome; furthermore, the sequence TATAAA (the 'Goldberg-Hogness box') lies between nucleotides 1,498 and 1,503.

The coding potential of the three classes of Ad12 mRNA can be predicted if it is assumed that they have common 5′ ends around nucleotide 1,525. Bos *et al.*[12] have shown that the E1B region of Ad12 has three major open translational reading frames. One very long reading frame starts with an ATG triplet at position 1,846 and ends with a UGA termination codon at position 3,292 (Fig. 3). This open reading frame has a theoretical coding capacity of molecular weight 54,000 (54 K) and could be used in its entirety only in the long mRNA (class I) with a single splice. When translated from this mRNA the protein would terminate immediately before the splice. The second long open translational reading frame starts with an ATG triplet at position 1,541 and ends at position 2,030 (Fig. 3). From the deduced mRNA structures it is apparent that the latter reading frame can theoretically be used in mRNAs belonging to all three classes (Fig. 3). Class I mRNAs are consequently polycistronic with two uninterrupted reading frames, possibly encoding two completely different polypeptide chains as has been proposed previously[20]. These would have molecular weights of 54 K, and 19 K, which roughly correspond to the molecular weights of two

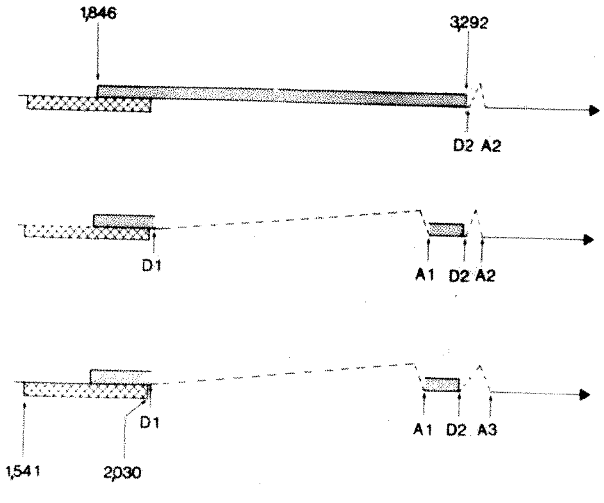

Fig. 3 The two major open translational reading frames in Ad12 as defined by Bos *et al.*[20] and their relationship to the structures of the Ad12 E1B mRNAs. The different acceptor (A) and donor (D) sites used to splice E1B mRNAs are indicated.

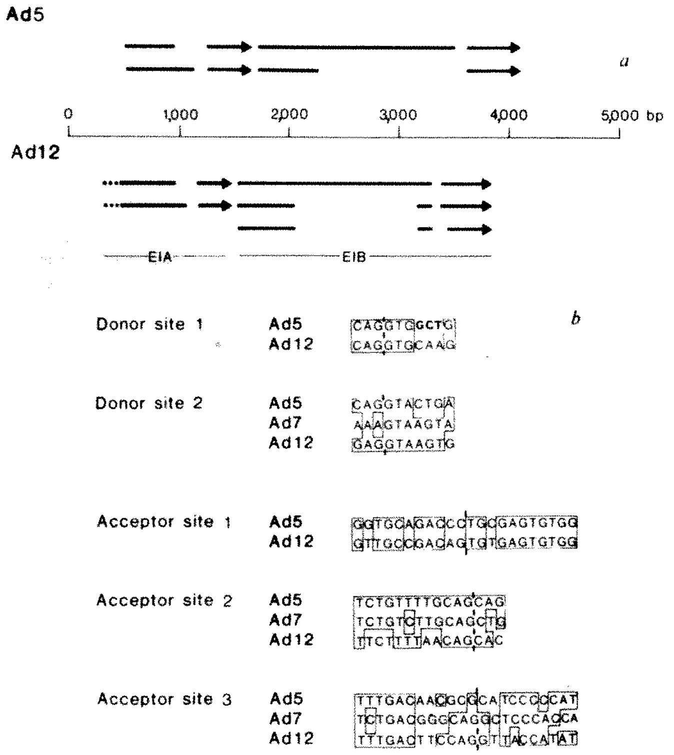

Fig. 4 Comparison of the transforming regions of highly oncogenic and non-oncogenic adenoviruses. *a*, Comparison of the major spliced mRNAs, transcribed from the transforming region of Ad5 and Ad12. *b*, Comparison of nucleotide sequences at different splice junctions in Ad5, Ad7 and Ad12. The donor sites D1 and D2, and the acceptor sites A1, A2 and A3, are defined in Fig. 3. Data for Ad12, Ad5 and Ad7 are from ref. 20, refs 29 and 30, and ref. 26 respectively.

polypeptides identified by translation *in vitro*[23]. If translation were initiated at the ATG triplet which precedes the long open reading frame (at position 1,846) in class II and III mRNAs, a polypeptide would be translated from sequences on both sides of the large splice present in these mRNAs (Fig. 3). The product would be a 12 K polypeptide, related to the 54 K polypeptide but lacking 372 internal amino acids. The third open reading frame in region E1B corresponds to polypeptide IX which is translated from an unspliced mRNA[20].

The existence of two alternative small introns in class II and III mRNAs is puzzling. Table 1 shows that both types are frequent and hence not the result of occasional incorrect splicing events. As the small exon in class II and III mRNAs contains stop codons in all three possible reading frames (Fig. 2), the coding capacity of class II and III mRNAs is the same.

Figure 4*a* outlines the mRNAs encoded by the transforming regions of Ad5 and Ad12. The most striking descrepancy between the highly oncogenic Ad12 and the non-oncogenic Ad5 is the existence in the former of two RNA species from region E1B which have a large and a small intron. No equivalent mRNA species have yet been reported from region E1B of subgroup C adenoviruses. The two alternative splices in class II and III mRNAs of Ad12 are both located in the 3′-noncoding part of the mRNA, which is very unusual. Introns in the 3′-noncoding region of cellular mRNAs have been rarely encountered previously[24], the only known example besides the E1B mRNAs being the splice present in the mRNA for the small T antigen of simian virus 40 (ref. 25). There are two ways in which the two small splices could influence the properties of class I and II mRNAs: either the structure of the 3′-noncoding region predetermines by some unknown mechanism which of the two possible initiation codons is chosen, thereby generating completely different polypeptides from class II and III mRNAs, or the different 3′-noncoding regions in class II and III mRNAs alter the stability or rate of transport of the mRNAs. Provided that the difference between oncogenic and non-oncogenic viruses is quantitative rather than qualitative, the unique 3′-noncoding parts of the Ad12 mRNAs could have a decisive role in determining the oncogenic potential of the virus. It should be possible to eliminate specifically the splice which generates the class III mRNAs by site-specific mutagenesis and thus test directly the hypothesis.

The results, summarized in Fig. 4 together with corresponding data from subgroup B and C adenoviruses, make it possible to compare directly nucleotide sequences at the positions where splicing occurs in region E1B of different adenoviruses. Two donor sites, D1 and D2, and three acceptor sites, A1, A2 and A3, for splicing can be identified in the three classes of Ad12 E1B mRNA (see Fig. 3). Figure 4*b* compares the sequences at the donor and acceptor sites in region E1B of Ad12 with the corresponding sequences in Ad5 and Ad7. The results show that the donor site D1 is well conserved and apparently used to generate a large splice in both Ad5 and Ad12. In addition the second donor site, D2, is well conserved and apparently used to generate a small splice in Ad5, Ad7 (ref. 26) and Ad12. This is in contrast to the leftmost acceptor site A1 which in Ad12 generates the middle splice, not found in Ad5 mRNAs. Sequence homology is observed around the splice site but the A-G dinucleotide is altered in Ad5, which presumably makes it non-functional[27]. The acceptor site A2 is, as expected, conserved in all three serotypes in contrast to the third acceptor site A3 which is unique for serotypes 7 and 12. Although there is no direct evidence, we can predict from sequence similarities that the E1B mRNAs of Ad7 resemble those of Ad12. The similarity between Ad7 and Ad12 with regard to acceptor and donor sites in region E1B supports the idea that, as was recently proposed[15], the highly and weakly oncogenic adenoviruses have evolved together.

We thank Elsy Johnsen for technical assistance and Marianne Gustafson for secretarial help. The gift of reverse transcriptase from Dr J. Beard is also acknowledged. This investigation was supported by grants from the Swedish MRC, the Swedish Cancer Society, CNRS, INSERM, and Fondatione pour la Recherche Medicale.

Received 13 October; accepted 18 December 1981.

1. Sharp, P. A., Petterson, U. & Sambrook, J. *J. molec. Biol.* **86**, 709–726 (1974).
2. Gallimore, P., Sharp, P. A. & Sambrook, J. *J. molec. Biol.* **89**, 49–72 (1974).
3. Graham, F. L. *et al. Cold Spring Harb. Symp. quant. Biol.* **39**, 637–650 (1974).
4. Van der Eb, A. J. *et al. Cold Spring Harb. Symp. quant. Biol.* **44**, 383–399 (1979).
5. Van der Eb, A. J., Mulder, C., Graham, F. L. & Houweling, A. *Gene* **2**, 115–132 (1977).
6. Shiroki, K., Shimojo, H., Sawada, Y., Uemizu, Y. & Fujinaga, K. *Virology* **95**, 127–136 (1979).
7. Berk, A. J. & Sharp, P. A. *Cell* **14**, 695–711 (1978).
8. Chow, L. T., Broker, T. R. & Lewis, J. B. *J. molec. Biol.* **134**, 265–303 (1979).
9. Kitchingman, G. R. & Westphal, H. *J. molec. Biol.* **137**, 23–48 (1980).
10. Perricaudet, M., Akusjärvi, G., Virtanen, A. & Pettersson, U. *Nature* **281**, 694–696 (1979).
11. Sawada, Y. & Fujinaga, K. *J. Virol.* **36**, 639–651 (1980).
12. Halbert, D. W., Spector, D. J. & Raskas, H. J. *J. Virol.* **31**, 621–629 (1979).
13. Esche, H., Mathews, M. B. & Lewis, J. B. *J. molec. Biol.* **142**, 399–417 (1980).
14. Johansson, K. *et al. J. Virol.* **27**, 628–639 (1978).
15. Perricaudet, M., Le Moullec, J. -M., Tiollais, P. & Pettersson, U. *Nature* **288**, 174–176 (1980).
16. Brawermann, G., Mendecki, I. & Lee, S. Y. *Biochemistry* **11**, 637–641 (1976).
17. Southern, E. *J. molec. Biol.* **98**, 503–518 (1975).
18. Sugisaki, H. *et al. Cell* **20**, 777–786 (1980).
19. Grunstein, N. & Hogness, D. *Proc. natn. Acad. Sci. U.S.A.* **72**, 3961–3964 (1975).
20. Bos, J. L. *et al. Cell* **27**, 121–131 (1981).
21. Perricaudet, M., Le Moullec, J. -M. & Pettersson, U. *Proc. natn. Acad. Sci. U.S.A.* **77**, 3778–3782 (1980).
22. Proudfoot, N. J. & Brownlee, G. G. *Nature* **263**, 211–214 (1976).
23. Jochemsen, H., Daniels, G. S. G., Lupker, J. H. & van der Eb. A. J. *Virology* **105**, 551–563 (1980).
24. Breathnach, R. & Chambon, P. *A. Rev. Biochem.* **50**, 349–383 (1981).
25. Reddy, V. B., Gosh, P. K., Lebowitz, P., Piatak, M. & Weissman, S. M. *J. Virol.* **30**, 279–296 (1979).
26. Dijkema, R., Maat, J., Dekker, B. M. M., van Ormondt, H. & Boyer, H. W. *Gene* **13**, 375–385 (1981).
27. Breathnach, R., Benoist, C., O'Hare, K., Gannon, G. & Chambon, P. *Proc. natn. Acad. Sci. U.S.A.* **75**, 4853–4857 (1978).
28. Maxam, A. M. & Gilbert, W. *Meth. Enzym.* **65**, 499–560 (1980).
29. Maat, J., Van Beveren, C. P. & Van Ormondt, H. *Gene* **10**, 27–38 (1980).
30. Maat, J. & van Ormondt, H. *Gene* **6**, 75–90 (1980).

Site-specific mutagenesis by error-directed DNA synthesis

Richard A. Zakour & Lawrence A. Loeb*

The Joseph Gottstein Memorial Cancer Research Laboratory,
University of Washington, Department of Pathology SM-30, Seattle,
Washington 98195, USA

An important experimental strategy for defining functional regions of a DNA sequence involves deleting or mutating particular sequences *in vitro* and observing the effects of the changes in a functional assay. We have approached the problem of making specific changes at defined sites in a nucleotide sequence by attempting to make use of the mistakes made by DNA polymerase enzymes while copying a sequence. Our approach is to initiate DNA synthesis from an isolated restriction fragment, and to elongate the fragment to a designated position by sequentially adding complementary nucleotides, then to incorporate the non-complementary nucleotide using an error-prone DNA polymerase followed by continuation of faithful synthesis. Here we demonstrate by DNA sequence analysis that both transitions and transversions can be produced at a designated position on the DNA template using this method.

DNA polymerases from prokaryotes contain a proofreading $3'\rightarrow5'$ exonuclease activity that enhances their accuracy in catalysis[1]. This associated exonuclease excises any non-complementary nucleotides at a primer terminus before continuing polymerization. In contrast, DNA polymerases from RNA tumour viruses and eukaryotes incorporate non-complementary nucleotides at higher frequency during copying of synthetic polynucleotides[2] and natural DNA[3]. The non-complementary nucleotides incorporated are invariably found to be present as single-base substitutions. Because the frequency of misincorporation by DNA polymerases is proportional to the ratio of non-complementary to complementary nucleotides in the reaction mixture, it should be possible to force a particular non-complementary nucleotide to be incorporated by carrying out the reaction in the presence of only that deoxynucleoside triphosphate. Incorporation of a series of non-complementary nucleotides is unlikely, as it would result in separation of the primer terminus from the template and diminish further synthesis.

To study the feasibility of using nucleotide misincorporation during *in vitro* DNA synthesis for site-specific mutagenesis, we chose to copy single-stranded bacteriophage ΦX174 circular DNA template containing an amber mutation. The frequency of mutagenesis can be determined from the reversion frequency of the copied DNA in transfection assays and the specificity of mutagenesis can be documented by sequence analysis[4,5].

Restriction endonuclease cleavage fragment, *Hpa*I 2 (ΦX174 positions 31–1,294)[6] from ΦX174 RF DNA, was hybridized to ΦX174 amber (*am*)18 template DNA. The 3′ OH terminus of this restriction fragment is located seven nucleotides from the change that causes the amber 18 mutation (*am*18 contains a T in place of C at ΦX174 position 23)[7]. We first elongated the 3′ OH terminus of the restriction fragment primer using *Escherichia coli* DNA polymerase I (Pol I) with only dATP and dCTP. These nucleotides are complementary to the first three template positions beyond the 3′ OH primer terminus (Fig. 1). After isolating template containing the elongated primer, a second series of reactions was carried out using avian myeloblastosis virus (AMV) DNA polymerase. Three different combinations of deoxynucleoside triphosphates were used (Fig. 1). After incubation of the reaction mixtures for 5 min at 37 °C in the presence of the specified nucleotides, all four deoxynucleoside triphosphates were added. Synthesis was allowed to proceed for an additional 5 min, so that any misincorporated nucleotides on termini would be protected from excision by the subsequent incorporation of the next complementary nucleotide. EDTA was added to stop synthesis, and the copied DNA was transfected into *E. coli* spheroplasts. Synthesis was completed by the *E. coli* replicating complex *in vivo*. We determined the reversion frequency of the *am*18 mutation by measuring the number of infective centres[4,8,9].

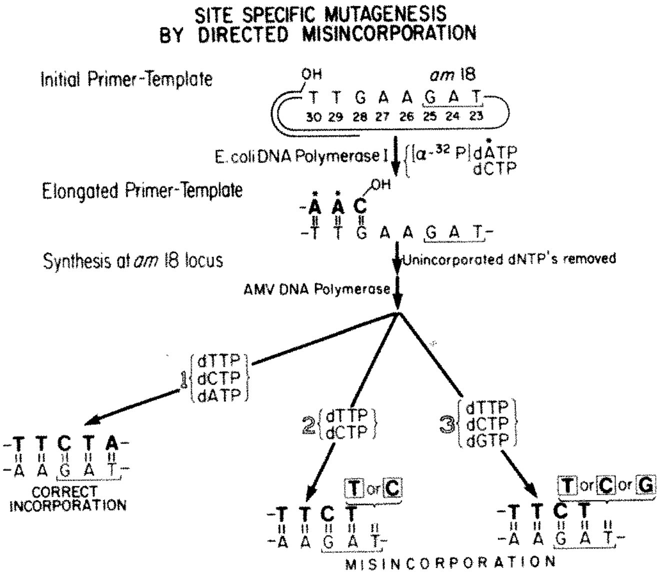

Fig. 1 Steps involved in primer elongation and site-specific mutagenesis. Primer elongation with complementary nucleotides: *Hpa*I 2 restriction endonuclease fragment was hybridized to single-stranded ΦX174 *am*18 DNA. Limited elongation of the 3′ OH terminus of the primer was carried out with Pol I. The reaction contained 3 μg of primed template, 5 μg of Pol I, 1 μM [α-^{32}P]dATP, 1 μM dCTP, 5 mM $MgCl_2$, 2 mM dithiothreitol and 20 mM Tris-HCl (*p*H 8.0) in a volume of 100 μl. Incubation was at 37 °C for 5 min. The reaction was stopped by adding EDTA to a final concentration of 10 mM; the mixtures were heated to 65 °C for 10 min and extracted once with an equal volume of redistilled phenol equilibrated with 20 mM Tris-HCl (*p*H 8.1) containing 1 mM EDTA and 100 mM NaCl. To separate the DNA from the unincorporated nucleotides, the aqueous phase was loaded onto a Sephadex G-100 column (1 × 60 cm) and the column eluted with 0.15 mM KCl, 50 mM Tris-HCl (*p*H 7.8). Fractions (1 ml) were collected and aliquots (20 μl) processed for determination of acid-insoluble radioactivity. The peak fractions were pooled, 1/10th volume of 3 M sodium acetate was added, and the DNA was precipitated with EtOH. The DNA was pelleted, washed and resuspended in 100 μl of 10 mM Tris-HCl (*p*H 8.0) containing 0.1 mM EDTA. Synthesis at *am*18 locus: A second series of *in vitro* DNA reaction mixtures each contained 0.1 μg *am*18 ΦX174 DNA primed with the elongated *Hpa*I 2 restriction fragment, 1 U of AMV DNA polymerase, 50 mM Tris-HCl (*p*H 8.0), 5 mM $MgCl_2$ and 2 mM dithiothreitol in a volume of 50 μl; they were incubated at 37 °C for 5 min. All reaction mixtures contained 10 μM dTTP and dCTP to elongate the primer correctly to position 23 of the *am*18 locus. Various combinations of the other deoxynucleoside triphosphates, each at a concentration of 10 μM, were included in individual reactions as indicated. (1) Correct incorporation is achieved by including the three nucleotides complementary to the *am*18 locus, dTTP, dCTP and dATP. (2) The presence of only dTTP and dCTP during directed misincorporation synthesis will allow the misinsertion of either T or C at position 23 of the *am*18 locus. (3) By including dTTP, dCTP and dGTP during directed misincorporation synthesis, it should be possible to obtain T, C, or G misinsertion at position 23. In experiments performed in this manner, G substitution at position 23 was the only change observed among seven revertants (Table 2). Synthesis with AMV DNA polymerase was followed by *in vitro* DNA synthesis with all four deoxynucleoside triphosphates present to seal the misincorporated nucleotide into the newly replicated DNA. Reactions were stopped by adding 0.1 vol of 100 μM EDTA.

When dATP, the nucleotide complementary to position 23 in the *am*18 region, was present in addition to dCTP and dTTP during DNA synthesis using AMV DNA polymerase, the reversion frequency of the newly synthesized DNA product in the transfection assay was fourfold higher than that of the

---

* To whom correspondence should be addressed.

0028–0836/82/0807[illegible]—03$01.00

uncopied primed template (Table 1, lines 1, 2). This increase, which is a function of the error-prone nature of AMV DNA polymerase[2], provides the background reversion frequency (4×10^{-4}). In both the nucleotide substrate combinations studied (Table 1, lines 3, 4), in which dATP was excluded from the reaction, the reversion frequencies were increased 100-fold. These higher reversion frequencies were presumably due to the substitution by AMV DNA polymerase during the *in vitro* synthesis of one of the non-complementary nucleotides for the missing complementary dATP.

To determine more precisely the efficiency of non-complementary nucleotide misinsertion, we measured the reversion frequency of a population that included only copied DNA molecules. Following mutagenesis with AMV DNA polymerase, synthesis was allowed to continue completely around the ΦX174 template using all four deoxynucleoside triphosphates, and a double-stranded closed circular molecule was formed using DNA ligase; nuclease S_1 was then used to hydrolyse the single-stranded molecules. In initial experiments, the reversion frequency of molecules copied past the *am*18 locus with dCTP, dGTP and dTTP (Table 1, line 4) was increased to 33%. Thus, enrichment for copied DNA molecules should provide designated mutants, even in the absence of a biological procedure for mutant selection.

To show that the increased reversion frequencies were a result of single-base substitutions, we sequenced the DNA of individual revertants. The nucleotide in position 23 of the minus strand was confirmed to be G in wild-type DNA and A in *am*18 DNA (Table 2, line I). In six spontaneous revertants, G substituted for A at position 23. Among the eight revertant DNAs, from reactions in which only dCTP and dTTP were present, seven contained cytosine and one contained thymidine at position 23 (Table 2, line II-1). These changes were probably a result of T-C and T-T mispairings during *in vitro* DNA synthesis. When dGTP was included in the synthesis reaction with dCTP and dTTP, all seven of the revertant DNAs contained G at position 23 (Table 2, line II-2), indicating a T-G mispairing. Thus, all three misincorporations occurred opposite this template thymidine during the *in vitro* DNA synthesis. The substitutions at ΦX174 position 23 were the only changes that we observed in the DNA sequence analysis. This observation suggests that the reaction conditions yielded misinsertions predominantly at the predetermined template position, the first template position the polymerase encountered that lacked a complementary nucleotide.

The patterns of nucleotide misinsertion observed in these experiments indicate that AMV DNA polymerase is capable of catalysing pyrimidine–pyrimidine as well as purine–pyrimidine mispairings. Based on the revertant DNAs that we screened, when dATP was the only nucleotide deleted during synthesis, the presence of dGTP resulted in only T→C transitions, produced by T-G mispairing during synthesis. Despite the presence of both dCTP and dTTP, we observed no transversions in DNAs derived from these copying conditions, even though we have observed that substitutions of these nucleotides at position 23 are genetically viable. Thus, it seems that T-G mispairing may be more likely to occur than either T-T or T-C mispairing. This observation agrees with investigations by others in suggesting that purine–pyrimidine mispairing should be favoured over pyrimidine–pyrimidine mispairing[10,11].

Table 2 DNA sequence analysis of revertants obtained from copying *am*18 DNA with AMV DNA polymerase in the presence of defined deoxynucleoside triphosphate substrates

	Sequence at position [minus (copied) strand] 25	24	23	No. of DNAs sequenced
I. Controls				
1. Wild type	C	T	G	2
2. *am*18	C	T	A	2
3. Spontaneous revertants	C	T	G	6
II. Revertants, added dNTPs				
1. dTTP, dCTP	C	T	C	7
	C	T	T	1
2. dTTP, dCTP, dGTP	C	T	G	7
	C	T	C	0
	C	T	T	0

Viral template DNA which was wild type for *am*18 was isolated from *am*3 ΦX174 bacteriophage (a gift of J. Weiner and A. Kornberg) and DNA from *am*18 was isolated from ΦX174 *am*18 bacteriophage (a gift of P. Weisbeek) as previously described[4,8]. Spontaneous *am*18 revertants were derived from non-permissive infective centres obtained from transfection of uncopied *am*18 molecules. Revertant DNAs were isolated from plaque-purified non-permissive infective centres obtained from *am*18 DNAs copied with AMV DNA polymerase as described in Table 1 legend. Isolation of revertant phage and preparation of viral template DNA for sequencing were performed as described elsewhere[5]. The DNA sequence from ΦX174 positions 1–26 of wild type, *am*18 and revertants of *am*18 were determined by the chain terminator method of Sanger *et al.*[23]. A preparation containing all three fragments from a *Hpa*I restriction digest of ΦX174 RF DNA was used to prime each single-stranded template at a ratio of 1 : 1. The sequencing reactions contained *E. coli* DNA polymerase I at an enzyme to template ratio of 10 : 1 and dideoxy- to deoxynucleotides at a ratio of 200 : 1. After completing the polymerization reactions, restriction endonuclease *Taq*I was added at a ratio of 1 unit per µg of DNA and the sample was incubated at 65 °C for 60 min. The products of the sequencing reaction were displayed on a 12% polyacrylamide gel. The DNA sequence in the *am*18 region (ΦX174 position 23–25) can be unambiguously read because all synthesis initiated at the other *Hpa*I restriction fragment primers are in larger *Taq*I digestion fragments that do not migrate into the readable portion of the gel.

Table 1 Reversion frequency of *am*18 DNA copied by AMV DNA polymerase in the presence of various combinations of deoxynucleoside triphosphate substrates

Added dNTPs	Non-permissive infective centres ($\times 10^1$) (revertants)	Total infective centres ($\times 10^5$)	Reversion frequency ($\times 10^{-4}$)
1. None	3.5	3.41	1
2. dTTP, dCTP, dATP	3.5	0.79	4
3. dTTP, dCTP	291	0.76	383
4. dTTP, dCTP, dGTP	182	0.45	404

The *am*18 template DNA with an elongated *Hpa*I2 primer was copied with AMV DNA polymerase as described in Fig. 1 legend in the presence of the indicated deoxynucleoside triphosphates. The transfection procedure for determining the number of infective centres and the reversion frequency has been described previously[4,8].

From these experiments, we propose that a general method for site-specific mutagenesis can be developed using directed misincorporation during DNA polymerization. The most direct application is with single-stranded or gapped DNA templates. Site-specific mutagenesis of double-stranded DNA can also be performed by this method when cloned into a bacteriophage M13 single-stranded vector. The first step of the procedure is to elongate a primer terminus to reach a pre-selected site by using a prokaryotic. DNA polymerase and different nucleotide combinations. This can be done in a series of reactions to achieve any required degree of elongation[12]. Pol I is particularly suitable for the elongation steps because it is highly accurate with natural DNA templates, the error rate being about 1 in 10^6 (ref. 5). For incorporation of a single non-complementary nucleotide, AMV DNA polymerase offers several advantages. First, it lacks a 3′→5′ exonuclease activity and is thus unable to excise a non-complementary nucleotide once incorporated[13]. Second, because AMV DNA polymerase can add complementary nucleotides into terminal single-base mismatches, misinsertions are sealed in place by subsequent correct nucleotide incorporations. Most importantly, in the presence of all complementary nucleotides, the frequency of misincorporation by AMV DNA polymerase is much higher than by polymerases containing proofreading activities[2,9]. Thus, in copying a natural DNA template, AMV DNA polymerase can be forced to be even more error prone by omitting any complementary nucleotide substrate (that is, an 'infinite pool bias') from the *in vitro* synthesis reaction. An alternative approach is to use Pol I in the presence of only a designated non-complementary deoxynucleoside thiotriphosphate. This analogue is incorporated with normal base-pairing properties but not excised by the 3′→5′ activity of the polymerase[14].

Site-specific mutagenesis at a predetermined position on a DNA molecule has become more feasible with the accumulation of DNA sequence information from a variety of genes. To date, three methods have been used to introduce specific base mutations into DNA. The first requires the chemical or enzymatic synthesis of an oligonucleotide that contains a designated single-base change[15–17]. The oligonucleotide is hybridized onto a template and extended into a biologically active molecule by *in vitro* DNA synthesis. Even though this may be the most exacting method of site-specific mutagenesis, each different substitution requires a unique oligonucleotide of sufficient length to form a stable hybrid with a specific region of the template[15,16,18]. In the second approach, nucleotides in a DNA template are modified to promote mispairing during *in vitro* gap repair synthesis. For example, sodium bisulphite has been used to deaminate specific template cytosines which thereafter will pair with adenine instead of guanine during DNA synthesis to produce C:G→T:A transitions[19,20]. With the third method, base substitutions are produced by misincorporation of a nucleotide analogue in place of a complementary nucleotide during *in vitro* nick translation. For example, by substituting N^4-hydroxy-dCTP for dTTP, A:T→G:C transitions were produced[21,22]. These latter two approaches are restricted to a single type of base substitution. Moreover, it is difficult to introduce the substitution only at a single designated site.

In addition to incorporating a non-complementary nucleotide at a particular site, the method outlined here can be used to generate a 'library' of mutations at a particular region. A restriction endonuclease fragment can be sequentially elongated to produce a new set of fragments of increasing length that can be isolated from a polyacrylamide gel. Each elongated restriction endonuclease fragment can then be used as primer for incorporating a non-complementary nucleotide. A set of elongated fragments isolated from a single gel could be used to produce a series of substitutions throughout a specific region of a gene.

We thank Drs T. A. Kunkel, R. Monnat and R. M. Schaaper for useful discussions and E. James for technical assistance. The procedure for isolating only copied ΦX174 DNA molecules was provided by T. A. Kunkel before publication. This investigation was supported by NIH grants CA-24845 and CA-24998 and NSF grant PCM 76-80439. R.A.Z. is a postdoctoral fellow of the National Institute of General Medical Sciences (GM-07115).

Received 20 October 1981; accepted 8 January 1982.

1. Brutlag, D. & Kornberg, A. *J. biol. Chem.* **247,** 241–248 (1972).
2. Battula, N. & Loeb, L. A. *J. biol. Chem.* **249,** 4086–4093 (1974).
3. Kunkel, T. A. & Loeb, L. A. *Science* **213,** 765–766 (1981).
4. Kunkel, T. A. & Loeb, L. A. *J. biol. Chem.* **254,** 5718–5725 (1979).
5. Kunkel, T. A. & Loeb, L. A. *J. biol. Chem.* **255,** 9961–9966 (1980).
6. Sanger, F. *et al. J. molec. Biol.* **125,** 225–246 (1978).
7. Smith, M., Brown, N. L., Air, G. M., Barrell, B. G. & Coulson, A. R. *Nature* **265,** 702–705 (1977).
8. Weymouth, L. A. & Loeb, L. A. *Proc. natn. Acad. Sci. U.S.A.* **75,** 1924–1928 (1978).
9. Gopinathan, K. P., Weymouth, L. A., Kunkel, T. A. & Loeb, L. A. *Nature* **278,** 857–859 (1979).
10. Topal, M. D. & Fresco, J. R. *Nature* **263,** 285–289 (1976).
11. Fersht, A. R. & Knill-Jones, J. W. *Proc. natn. Acad. Sci. U.S.A.* **78,** 4251–4255 (1981).
12. Donelson, J. E. & Wu, R. *J. biol. Chem.* **247,** 4654–4660 (1972).
13. Battula, N. & Loeb, L. A. *J. biol. Chem.* **251,** 982–986 (1976).
14. Kunkel, T. A., Eckstein, F., Mildvan, A. S., Koplitz, R. M. & Loeb, L. A. *Proc. natn. Acad. Sci. U.S.A.* **78,** 6734–6738 (1981).
15. Hutchison, C. A. *et al. J. biol. Chem.* **253,** 6551–6560 (1978).
16. Razin, A., Hirose, T., Itakura, K. & Riggs, A. D. *Proc. natn. Acad. Sci. U.S.A.* **75,** 4268–4270 (1978).
17. Bhanot, O. S., Kahn, S. A. & Chambers, R. W. *J. biol. Chem.* **254,** 12684–12693 (1979).
18. Astell, C. R. & Smith, M. *Biochemistry* **11,** 4114–4120 (1972).
19. Shortle, D. & Nathans, D. *Proc. natn. Acad. Sci. U.S.A.* **75,** 2170–2174 (1978).
20. Shortle, D., Pipas, J., Lazarowitz, S., DiMaio, D. & Nathans, D. in *Genetic Engineering, Principles and Methods* Vol. 1 (eds Setlow, J. K. & Hollaender, A.) 73–92 (Plenum, New York, 1979).
21. Müller, W., Weber, H., Meyer, F. & Weissmann, C. *J. molec. Biol.* **124,** 343–358 (1978).
22. Weissmann, C., Nagata, S., Taniguchi, T., Weber, H. & Meyer, F. in *Genetic Engineering, Principles and Methods* Vol. 1 (eds Setlow, J. K. & Hollaender, A.) 133–150 (Plenum, New York, 1979).
23. Sanger, F., Nicklen, S. & Coulson, A. R. *Proc. natn. Acad. Sci. U.S.A.* **74,** 5463–5467 (1977).

0028–0836/82/080710—03$01.00

No evidence for 'stress' α-globin genes in chicken

Walter Knöchel*, Burghardt Wittig*, Stephanie Wittig*, Maliyakal E. John*, Ulrich Grundmann*, Walter Oberthür†, Jasminka Godovac† & Gerhard Braunitzer†

* Institut für Molekularbiologie und Biochemie,
Freie Universität Berlin, D-1000 Berlin 33, Arnimallee 22, FRG
† Max-Planck-Institut für Biochemie, Abteilung Proteinchemie,
D-8033 Martinsried bei München, FRG

Phenylhydrazine-induced anaemia in goats and certain sheep carrying a β^A-globin gene, leads to a switch from adult β^A-globin mRNA to β^C mRNA synthesis[1]. The β^C globin chains are also transiently produced late in fetal life. The nucleotide sequence of selected fragments of cloned goat β^C globin gene[2] corresponds to the amino acid sequence determined some years ago[3]. A similar reactivation of globin genes has been reported for the baboon, *Papio cynocephelus*, where anaemic stress also leads to the production of fetal haemoglobin[4]. In the case of anaemic chicken, results of cDNA cloning and nucleotide sequencing experiments suggested that a novel type of α-globin gene, the 'stress' gene, is expressed[5]. The existence of such a gene was mainly supported by the fact that the cDNA nucleotide sequence did not agree with any known chicken α-globin chain amino acid sequence. In contrast, we now report results, including a reinvestigation of the α^A-globin amino acid sequence, which reveal that in the anaemic chicken, the α^A gene is expressed, and there is no evidence for a specific stress α-globin gene.

Reactivation of genes due to physiological stress, such as induction of anaemia, is an important concept in the regulation of gene activity. The difference between the stress gene reported in chicken and the fetal genes of animals mentioned above is that the protein product of the stress gene could not be identified among the adult (α^A, α^D and β) or embryonic (π, π′, α^A, α^D, ε and ρ) globin chains[6]. Therefore, this switch seems not to represent a reactivation of a fetal-type gene. For further analysis of globin-coding sequences expressed in anaemic chicken, globin mRNA was isolated from polychromatic erythrocytes, transcribed into cDNA and cloned in bacterial plasmids[7]. Hybrid arrested cell-free translation from nine randomly selected clones demonstrated that six clones contain sequences coding for α chains and three sequences coding for β chains. The integrated sequence of one of the plasmids containing an α-globin sequence (pα^A HG3), which is 581 nucleotides long, was cleaved by *Pst*I, and after digestion with different restriction enzymes (see Fig. 1) the various fragments were submitted to

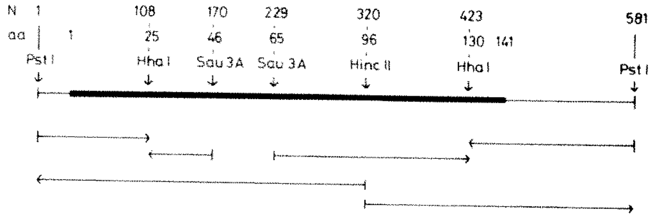

Fig. 1 Restriction map and sequencing strategy of the cloned nucleotide sequence cleared by *Pst*I from plasmid pα^A HG3. N refers to the number of nucleotides and aa to the number of amino acids, after which cleavage by restriction endonucleases occurs. The ends of the cloned sequence are tailed by ~20 G-C base pairs, originating from the G-C insertion technique in plasmid pBR322[7]. Restriction fragments, as shown by arrows, were subjected to sequence analysis (see Fig. 3).

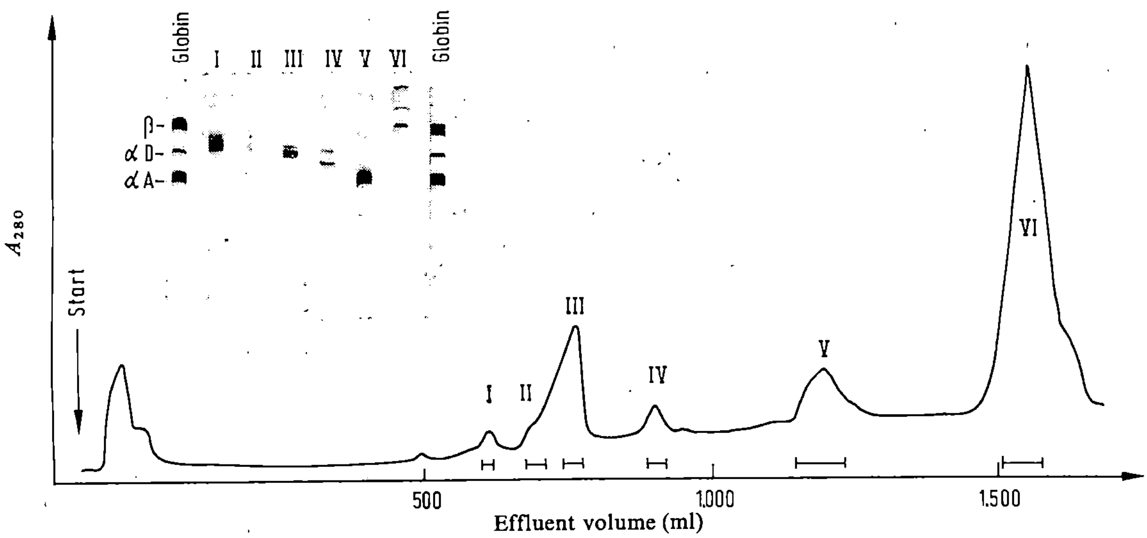

Fig. 2 Carboxymethyl-cellulose chromatography and Triton X-100 electrophoresis of chicken globin chains. Globin chains were isolated from erythrocyte lysates by precipitation of the 100,000*g* supernatant with acidic acetone and submitted to CM-cellulose (CM 52, Whatman) chromatography[15]. The eluting material was further analysed by Triton X-100 polyacrylamide gel electrophoresis[16] (inset).

nucleotide sequence analysis. The resulting nucleotide sequence includes the entire protein-coding region (see Fig. 3) and is very similar to sequences previously reported independently by three other groups[8–10]. The amino acid sequence derived from our cloned structural α-globin gene is identical with that of one of these three groups[9], although there are variations in the third bases of six codons. Our sequence differs at amino acid positions 110 and 121 or at positions 92, 93, 94 and 120, respectively, from the sequences published by the other two groups[8,10]. Although the origin of these differences is not known, it is concluded that our cloned sequence, as well as those reported by the above groups[8–10], represent the processed transcripts of the same gene coding for the major α-globin chain component of polychromatic erythrocytes in anaemic chicken.

A comparison of the amino acid sequence derived from our nucleotide sequence showed differences from embryonic π or π′ chains[11] at 60 positions, from the adult α^D chain[12] at 61 positions and from the adult α^A chain[13] at 22 positions. Thus it seemed that the cloned globin-coding sequence from anaemic chicken differs from the structural genes coding for these α-type chains. However, we re-examined the data for the α^A chain because (1) amino acid composition data[6,14] correspond better to our nucleotide-derived sequence than to the published sequence[13], and (2) a comparison of this α^A chain with the amino acid sequence of the major α-chain component of phylogenetically related animals, such as pheasant (see Fig. 3), revealed a rather large number of 21 exchanges.

For this reinvestigation, the native globin of adult chicken was separated by CM-cellulose (CM 52) chromatography[15], and the different peaks were further analysed by Triton X-100 polyacrylamide gel electrophoresis[16] (Fig. 2). Peak V was identified as the major α component, α^A. The relatively small absorbance can be explained by the fact that the α^A chains contain no tryptophan in contrast to four in the β chains[17] and one in the α^D chains[12]. The CM elution profiles and the electrophoretic patterns of globin chains from mature and immature cells were identical (data not shown). Amino acid analysis was performed on complete chains, tryptic peptides and the C-terminal fragment generated by acidic hydrolysis of the Asp–Pro peptide bond[18] using a Beckman model 121 C amino acid analyser. The chains and peptides were degraded automatically in a Beckman 890 B sequenator or in a Beckman 890 C sequenator with programs as reported elsewhere[15]. The phenylthiohydantoin derivatives of the amino acids were identified by TLC and HPLC[19].

There were no differences in the peptide patterns, amino acid analysis of chains and peptides as well in the sequences of few peptides that reportedly differ in α^A and stress gene products, regardless of whether α chains were isolated from mature or immature blood cells. Figure 3 shows the sequence, which corresponds to that derived from the nucleotides. Moreover, it is obviously homologous to the major α-chain component of the closely related species pheasant (only five differences at positions α28, α34, α38, α70 and α77), thus supporting the validity of our results. Our sequence data differ at 22 amino acid residues from that reported more than 10 years ago[13]. We are unable to identify such a chain in normal or anaemic chicken.

These findings demonstrate that the cloned sequence actually represents the structural gene sequence of the chicken α^A-globin chain. There is no reason to postulate a specific type of α-globin gene which is expressed during anaemic stress[5]. There was also no evidence of such a stress gene when the genomic arrangement of the complex α-globin gene family was investigated[20]. Moreover, a direct comparison of α chains from erythrocytes of uninduced animals and from polychromatic erythrocytes of anaemic animals (7 days after first phenylhydrazine injection) revealed no differences. Whether anaemia for longer periods induces reactivation of embryonic genes similar to that found in sheep and goats[1] cannot be excluded and remains to be elucidated. However, it is clear that the cloned α-globin cDNA

```
No. aa           1   2   3   4   5   6   7   8   9  10  11  12  13  14  15  16  17  18  19  20  21  22  23
a     AACC AUG GUG CUG UCC GCU GCU GAC AAG AAC AAC GUC AAG GGC AUC UUC ACC AAA AUC GCC GGC CAU GCU GAG GAG
b              VAL LEU SER ALA ALA ASP LYS ASN ASN VAL LYS GLY ILE PHE THR LYS ILE ALA GLY HIS ALA GLU GLU
c              VAL LEU SER ALA ALA ASP LYS ASN ASN VAL LYS GLY ILE PHE THR LYS ILE ALA GLY HIS ALA GLU GLU

       24  25  26  27  28  29  30  31  32  33  34  35  36  37  38  39  40  41  42  43  44  45  46  47  48
a      UAU GGC GCC GAG ACC CUA GAA AGG AUG UUC ACC ACC UAC CCC CCA ACC AAG ACC UAC UUC CCC CAC UUC GAU CUG
b      TYR GLY ALA GLU THR LEU GLU ARG MET PHE THR THR TYR PRO PRO THR LYS THR TYR PHE PRO HIS PHE ASP LEU
c      TYR GLY ALA GLU ALA LEU GLU ARG MET PHE ILE THR TYR PRO SER THR LYS THR TYR PHE PRO HIS PHE ASP LEU

       49  50  51  52  53  54  55  56  57  58  59  60  61  62  63  64  65  66  67  68  69  70  71  72  73
a      UCA CAC GGC UCC GCU CAA AUC AAG GGG CAC GGC AAG AAG GUA GUG GCU GCC UUG AUC GAG GCU GCC AAC CAC AUU
b      SER HIS GLY SER ALA GLN ILE LYS GLY HIS GLY LYS LYS VAL VAL ALA ALA LEU ILE GLU ALA ALA ASN HIS ILE
c      SER HIS GLY SER ALA GLN ILE LYS GLY HIS GLY LYS LYS VAL VAL ALA ALA LEU ILE GLU ALA VAL ASN HIS ILE

       74  75  76  77  78  79  80  81  82  83  84  85  86  87  88  89  90  91  92  93  94  95  96  97  98
a      GAU GAC AUC GCG GGC ACC CUC UCC AAG CUC AGC GAC CUC CAU GCC CAC AAG CUC CGC GUG GAC CCU GUC AAC UUC
b      ASP ASP ILE ALA GLY THR LEU SER LYS LEU SER ASP LEU HIS ALA HIS LYS LEU ARG VAL ASP PRO VAL ASN PHE
c      ASP ASP ILE THR GLY THR LEU SER LYS LEU SER ASP LEU HIS ALA HIS LYS LEU ARG VAL ASP PRO VAL ASN PHE

       99 100 101 102 103 104 105 106 107 108 109 110 111 112 113 114 115 116 117 118 119 120 121 122 123
a      AAA CUC CUG GGC CAA UGC UUC CUG GUG GUG GUG GCC AUC CAC CAC CCU GCC GCU CUC ACC CCG GAG GUC CAU GCU
b      LYS LEU LEU GLY GLN CYS PHE LEU VAL VAL VAL ALA ILE HIS HIS PRO ALA ALA LEU THR PRO GLU VAL HIS ALA
c      LYS LEU LEU GLY GLN CYS PHE LEU VAL VAL VAL ALA ILE HIS HIS PRO ALA ALA LEU THR PRO GLU VAL HIS ALA

      124 125 126 127 128 129 130 131 132 133 134 135 136 137 138 139 140 141
a      UCC CUG GAC AAG UUC UUG UGC GCC GUG GGC ACU GUG CUG ACC GCC AAG UAC CGU UAA GACGGCACGGUGGCUAGAGCUGG
b      SER LEU ASP LYS PHE LEU CYS ALA VAL GLY THR VAL LEU THR ALA LYS TYR ARG
c      SER LEU ASP LYS PHE LEU CYS ALA VAL GLY THR VAL LEU THR ALA LYS TYR ARG


a      GGCCAACCCAUCGCCAGCCCUCCGACAGCGAGCAGCCAAAUGAGAUGAAAUAAAACUGUUGCAUUUGUGCUCCA
```

Fig. 3 *a*, Nucleotide sequence of the structural globin gene cloned in pα^A HG3 (see Fig. 1); *b*, amino acid (aa) sequence of chicken α^A-globin chain; *c*, amino acid sequence of the major α-chain component of pheasant.

sequence derived from globin mRNA of phenylhydrazine-induced anaemic chicken does not code for a novel type of globin chain but for the adult α^A-globin chain that is expressed in normal chicken.

Since submission of this work, others[21] have reported that they were unable to detect an anaemic shock α-globin gene by investigation of the genomic α-globin gene family in adult chicken.

We thank Professor H. Tiedemann for his continuous interest and generous support, and acknowledge the technical assistance of Miss E. Müller.

Received 22 October 1981; accepted 6 January 1982.

1. Nienhuis, A. W. & Anderson, W. F. *Proc. natn. Acad. Sci. U.S.A.* **69,** 2184–2188 (1972).
2. Haynes, J. R. *et al. J. biol. Chem.* **255,** 6355–6367 (1980).
3. Dayhoff, M. O. & Eck, R. V. *Atlas of Protein Sequence and Structure,* 154–158 (The National Biomedical Research Foundation, Maryland, 1968).
4. Nienhuis, A. W. & Stamatoyannopoulos, G. *Cell* **15,** 307–315 (1978).
5. Cummings, I. W., Liu, A. Y. & Salser, W. A. *Nature* **276,** 418–419 (1978).
6. Brown, J. L. & Ingram, V. M. *J. biol. Chem.* **249,** 3960–3972 (1974).
7. Knöchel, W., Lange, D. & Grundmann, U. *Molec. Biol. Rep.* (in the press).
8. Deacon, N. J., Shine, J. & Naora, H. *Nucleic Acids Res.* **8,** 1187–1199 (1980).
9. Richards, R. I. & Wells, J. R. E. *J. biol. Chem.* **255,** 9306–9311 (1980).
10. Liu, A. Y. & Salser, W. *Gene* **13,** 409–415 (1981).
11. Chapman, B. S., Tobin, A. J. & Hood, L. E. *J. biol. Chem.* **255,** 9051–9059 (1980).
12. Takei, H., Ota, Y., Wu, K. C., Kiyohara, T. & Matsuda, G. *J. Biochem.* **77,** 1345–1347 (1975).
13. Matsuda, G., Takei, H., Wu, K. C. & Shiozawa, T. *Int. J. Protein Res.* **3,** 173–174 (1971).
14. Moss, B. A. & Thompson, E. O. P. *Aust. J. biol. Sci.* **22,** 1455–1471 (1969).
15. Oberthür, W., Braunitzer, G. & Kalas, S. *Hoppe-Seyler's Z. physiol. Chem.* **362,** 1101–1112 (1981).
16. Alter, B. P., Goff, S. C., Efremov, G. D., Gravely, M. E. & Huisman, T. H. J. *Br. J. Haemat.* **44,** 527–534 (1980).
17. Matsuda, G., Maita, T., Mizuno, K. & Ota, H. *Nature new Biol.* **244,** 244 (1973).
18. Jauregui-Adell, J. & Marti, J. *Analyt. Biochem.* **69,** 468–473 (1975).
19. Zimmermann, C. L. & Pisano, J. *Meth. Enzym.* **47,** 45–51 (1977).
20. Engel, J. D. & Dodgson, J. B. *Proc. natn. Acad. Sci. U.S.A.* **77,** 2596–2600 (1980).
21. Dodgson, J. B., McCune, K. C., Rusling, D. J., Krust, A. & Engel, J. D. *Proc. natn. Acad. Sci. U.S.A.* **78,** 5998–6002 (1981).

Univalent antibodies kill tumour cells *in vitro* and *in vivo*

M. J. Glennie* & G. T. Stevenson

Lymphoma Research Unit, Tenovus Laboratory, Southampton
General Hospital, Southampton SO9 4XY, UK

Antibody molecules are bivalent, or less often multivalent, with each antibody site within a single molecule having the same specificity. Bivalency must enhance the tenacity of antibody attachment to cell surfaces, as dissociation will require simultaneous release at both sites. However, the bivalency of the antibody sometimes induces a target cell to undergo antigenic modulation[1–3], thereby offering the cell a means of evading complement and the various effector cells recruited by the antibody. We have investigated the attack by univalent antibodies, which, despite removal of one antibody site, retain their Fc zones and hence their ability to recruit the killing agents, on neoplastic B lymphocytes of the guinea pig L_2C line. Rabbit antibodies raised against surface immunoglobulin of these cells were partially digested with papain to yield the univalent Fab/c derivatives[4,5]. We report here that these derivatives showed enhanced cell killing both *in vitro* and *in vivo*, and that this enhancement appeared to derive from avoiding antigenic modulation.

The L_2C lymphocytic leukaemia arose spontaneously around the year 1950 in a female guinea pig of the inbred strain 2, and has since been maintained by passaging *in vivo*; the line maintained in our laboratory was obtained in 1972 from Drs I. Green and E. Shevach (NIH). Blood from near-terminal animals was obtained by cardiac puncture and yielded L_2C preparations[6] of >95% viability with <2% contaminating leukocytes. The cells are lymphoblastic and exhibit surface immunoglobulin M (IgM), ~50,000 molecules per cell, of light chain class λ[7].

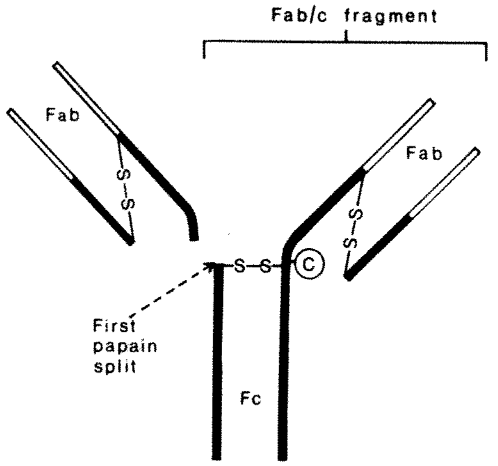

Fig. 1 Preparation of Fab/c from rabbit IgG antibody. The A12 allotypic variant of IgG[17], apparently more common than the allelic A11, possesses a threonine residue on each heavy chain immediately N-terminal to the hinge-region disulphide. An oligosaccharide unit © is attached to the threonine, but on one chain only, rendering this chain relatively resistant to enzymatic cleavage in the vicinity[18]. The chain lacking the oligosaccharide unit is cleaved as shown by brief exposure to papain, yielding the Fab/c fragment.

Here we used two IgG antibodies raised in rabbits to study attack on L_2C cells. Antibody reacting with constant determinants on the λ chain of L_2C surface immunoglobulin (anti-λ) was used for studies *in vitro*; the antibody was raised against serum $F(ab')_2$ $\gamma\lambda$ and prepared as pure IgG antibody by elution from λ chains coupled to immunosorbent[8]. Antibody specific for idiotypic determinants of the surface immunoglobulin (anti-Id) was used for studies *in vitro* and, because it is effectively tumour specific, for therapy *in vivo*[9]. It was raised against Fab μ isolated from the surface IgM[9], rendered specific for idiotypic determinants by absorption with guinea pig normal immunoglobulin, and used in the form of total IgG isolated from the absorbed antiserum.

The Fab/c derivatives of anti-λ and anti-Id, in which the antibody molecule is rendered univalent by removal of just one Fab arm[4,5] (Fig. 1), were prepared by digesting IgG antibody with thiol-free papain (0.8 mg ml^{-1}) at 37 °C for 4 h, *p*H 7.4. The products of digestion were fractionated by recycling chromatography on Ultrogel AcA44. To remove any contaminating $F(ab')_2$, the Fab/c was purified further by elution from an anti-Fc immunosorbent. In subsequent work we have used more limited exposure to papain (0.01 mg ml^{-1} at 37 °C for 30 min) in the presence of dithiothreitol (1 mM), and have been able to omit the immunosorptive step; after removing the thiol the hinge-region disulphide of Fab/c, possibly required for efficient activation of complement[10,11], can re-form by oxidation. Fab/c emerged from AcA44 columns in a zone corresponding to a molecular weight of ~100,000, and was obtained with a yield of 10–20% of the starting IgG. It was shown by precipitin analysis on Ouchterlony plates to possess both Fab and Fc determinants; and by gel chromatography of reduced material in 1 M propionic acid to comprise one light chain, one heavy chain and one-half of a heavy chain.

Previous work[3] has shown that both anti-λ and anti-Id induce rapid antigenic modulation *in vitro*: exposure of the L_2C cells to antibody at 37 °C for 2 min or longer confers resistance to lysis when they are subsequently exposed to antibody plus complement. In contrast to an earlier report describing the mouse TL system[12], bivalency of the antibody was found to be essential for induction of this modulation. It seems therefore that the redistribution of cell surface immunoglobulin induced when it is tethered by bivalent antibody—leading to patching, capping and endocytosis of the antigen–antibody complexes[13]—underlies the modulation of this antigen, although the extent of redistribution required is not clear.

---

* Present address: ARC Institute of Animal Physiology, Babraham, Cambridge CB2 4AT, UK.

0028-0836/82/080712–03$01.00

Fab/c derivatives of both anti-λ and anti-Id were shown by indirect immunofluorescence to bind to the surfaces of L_2C cells. However, in contrast to the parent antibodies, there was no tendency for the Fab/c to undergo redistribution and endocytosis when attached to viable cells incubated at 37 °C for 30 min: subsequent staining by fluorescein-labelled sheep anti-rabbit IgG at 0 °C showed the Fab/c to be distributed uniformly over the cell surfaces.

The Fab/c derivatives retained the ability to invoke complement-mediated lysis of target cells, whether by guinea pig or rabbit complement. Moreover they showed no tendency to induce antigenic modulation. Figure 2*a*, *b* shows the levels of cytotoxicity induced by IgG and Fab/c of anti-λ specificity for a range of concentrations. Preincubation at 37 °C with the IgG, but not with the Fab/c, induced modulation. Note also that Fab/c induced higher levels of cytotoxicity than IgG even in experiments lacking the modulating preincubation. This difference was more marked when guinea pig comlement was used, and is consistent with other evidence[3] that some modulation can occur when cells are confronted simultaneously by IgG antibody and complement at 37 °C.

The findings using IgG and Fab/c from anti-Id (Fig. 2*c*, *d*) were similar. However, note that modulation by the IgG for rabbit complement was less effective than in the case of anti-λ; that IgG antibody titred out further for rabbit complement than did Fab/c; and that the superiority of Fab/c over IgG for lysis by guinea pig complement was again apparent.

The therapeutic efficacies of IgG and Fab/c from anti-Id serum were assessed by inoculating strain 2 guinea pigs with L_2C leukaemia, then injecting them once with the test substance 24 h later, and observing survival (Fig. 3). Our tumour line has a doubling time *in vivo* of ~19 h, thus a simple kinetic model suggests that 50% killing of the tumour will prolong life by this time period. The complexity of events occurring *in vivo* introduces considerable uncertainty, but evidently the greater the cell kill from a single therapeutic event, the greater the subsequent average survival, with the duration of survival permitting some tentative inferences about the extent of killing. By increasing average survival by 10 days Fab/c was much more effective than the parent IgG (3.2 days), and in fact much more effective than any of our previous attempts at antibody therapy.

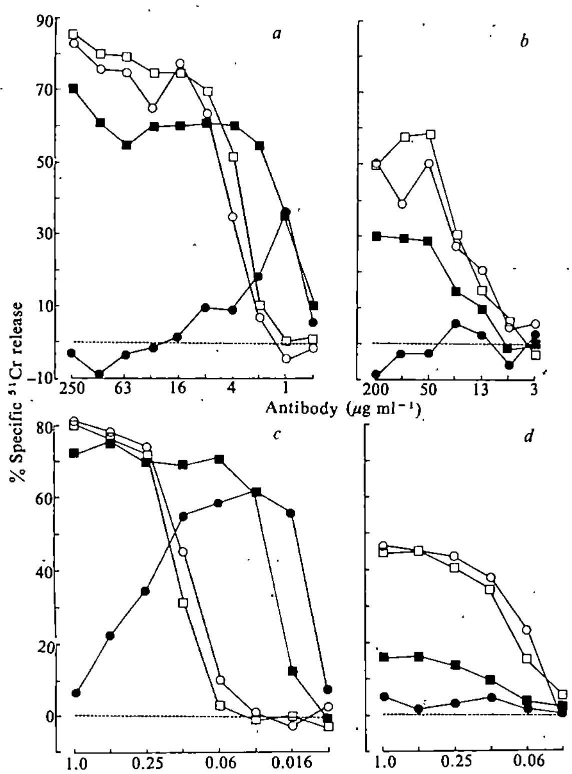

Fig. 2 Complement lysis of L_2C cells invoked by Fab/c (○, □) or IgG (●, ■) from purified anti-λ(*a*, *b*) or anti-Id serum (*c*, *d*). Complement was from rabbit (*a*, *c*) or strain 2 guinea pig (*b*, *d*). First the cells were labelled with ^{51}Cr and washed. To permit modulation they were incubated at $5\times10^5\ ml^{-1}$ with antibody derivatives at the indicated concentrations at 37 °C for 15 min (○, ●); control incubations were at 0 °C (□, ■). All suspensions were placed in an ice bath; 1.5 vol of a 1:2 dilution of fresh serum was added as a source of complement, and the temperature was raised to 37 °C for 30 min to promote complement activity. Finally the suspensions were chilled and the supernatants separated for assay of released ^{51}Cr. Methods are described in detail in ref. 19.

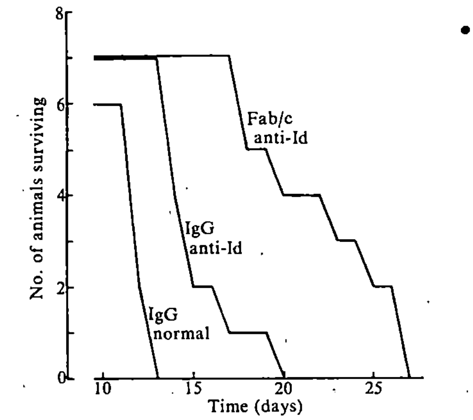

Fig. 3 Immunotherapy with Fab/c or IgG from anti-Id serum. Groups of guinea pigs were inoculated intraperitoneally (i.p.) with 10^5 L_2C cells (day 0). After 24 h they were injected i.p. with 10 mg IgG from normal sheep serum (6 animals), 10 mg IgG from anti-Id serum (7 animals), or 10 mg Fab/c derivative of the anti-Id IgG (7 animals). Animals treated with IgG (anti-Id) survived longer than those treated with IgG (normal), as did those treated with Fab/c (anti-Id) compared with IgG (anti-Id)-treated animals ($P<0.005$, χ^2 test[20]).

We have not yet defined the relative involvements of the classical and alternative complement pathways in the cell lysis invoked by IgG and Fab/c. Activation of the classical pathway by Fab/c would be further evidence against the possibility that steric changes in the IgG molecule consequent on both Fab arms being engaged are necessary for the binding and activation of complement component 1 (C1) (reviewed in ref. 14). The alternative pathway acts as an amplifier after activation of the classical pathway, and apparently acts independently in the lysis of certain virus-infected cells by antibody and complement[15]. The fact that bivalent antibody was required in the latter studies makes it unlikely that Fab/c invokes a similar mechanism.

The clear superiority of Fab/c over IgG antibody in invoking lysis by homologous (guinea pig) complement confirms the importance of antibody bivalency in permitting mammalian cells to escape from antibody-mediated destruction. Eluding this escape mechanism appears to offer a surprisingly simple means of enhancing the attack of antibodies on tumour cells. We are now evaluating Fab/c and similar derivatives of anti-idiotype antibody in the treatment of human chronic lymphocytic leukaemia, where the cells show some susceptibility to cytotoxic atack by anti-idiotype IgG[16].

This work was supported by the Cancer Research Campaign, the MRC and Tenovus.

Received 7 September 1981; accepted 15 January 1982.

1. Boyse, E. A. & Old, L. J. *A. Rev. Genet.* **3**, 269–290 (1969).
2. Stackpole, C. W., Jacobson, J. B. & Lardis, M. P. *J. exp. Med.* **140**, 939–953 (1974).
3. Gordon, J. & Stevenson, G. T. *Immunology* **42**, 13–17 (1981).
4. Goodman, J. W. *Biochemistry* **4**, 2350–2357 (1965).
5. Michaelsen, T. E. & Natvig, J. B. *Scand. J. Immun.* 1255–1268 (1972).
6. Stevenson, G. T., Eady, R. P., Hough, D. W., Jurd, R. D. & Stevenson, F. K. *Immunology* **28**, 807–820 (1975).

7. Hough, D. W., Chapple, J. C., Stevenson, F. K. & Stevenson, G. T. *Immunology* **34,** 889–899 (1978).
8. Stevenson, F. K., Elliott, E. V. & Stevenson, G. T. *Immunology* **32,** 549–557 (1977).
9. Stevenson, G. T., Elliott, E. V. & Stevenson, F. K. *Fedn Proc.* **36,** 2268–2271 (1977).
10. Press, E. M. *Biochem. J.* **149,** 285–288 (1975).
11. Isenman, D. E., Dorrington, K. J. & Painter, R. H. *J. Immun.* **114,** 1726–1729 (1975).
12. Lamm, M. E., Boyse, E. A., Old, L. J., Lisowska-Bernstein, B. & Stockert, E. *J. Immun.* **101,** 99–103 (1968).
13. Taylor, R. B., Duffus, P. H., Raff, M. C. & de Petris, S. *Nature new Biol.* **233,** 225–227 (1971).
14. Metzger, H. *Contemp. Topics molec. Immun.* **8,** 119–152 (1978).
15. Sissons, J. G. P. *et al. J. exp. Med.* **150,** 445–454 (1979).
16. Hamblin, T. J., Abdul-Ahad, A. K., Gordon, J., Stevenson, F. K. & Stevenson, G. T. *Br. J. Cancer* **42,** 495–502 (1980).
17. Prahl, J. W., Mandy, W. J. & Todd, C. W. *Biochemistry* **8,** 4935–4940 (1970).
18. Fanger, M. W. & Smyth, D. G. *Biochem. J.* **127,** 767–774 (1972).
19. Gordon, J., Robinson, D. S. F. & Stevenson, G. T. *Immunology* **42,** 7–12 (1981).
20. Peto, R. *Br. J. Cancer* **29,** 101–105 (1974).

Homocopolymer sequences in the spacer of a sea urchin histone gene repeat are sensitive to S_1 nuclease

Christopher C. Hentschel*

Institut fur Molekularbiologie II der Universitat Zurich,
Honggerberg, 8093 Zurich, Switzerland

The concept of specific functional elements in genes comprising localized or transient structural discontinuities, such as Z-DNA or cruciforms, is becoming increasingly plausible[1–6]. Cruciforms were first detected as supercoil-dependent single-strand nuclease (S_1)-sensitive sites characterized by hyphenated inverted repeat DNA sequences[2,3]. Here I describe examples of a novel type of S_1 nuclease site found in a sea urchin histone gene repeat and characterized by homocopolymer sequences. Endonucleolytic cleavage within these sequences does not depend on supercoiling, is highly sensitive to the salt concentration and shows a reproducible pattern of maxima and minima. This type of S_1 sensitivity may reflect the potential for out-of-register DNA slippage in such sequences and I speculate that related slippage events *in vivo* could lead to their acting as foci for recombinational events.

Recombinant plasmids containing either one copy of the 6.25 kilobase (kb) *Psammechinus miliaris* histone gene repeat h22 (refs 7, 8) inserted in the *Hin*dIII site of pBR322 (ref. 9; pBRh22/3), or a head-to-tail dimer of the repeat (pBRh22/4) similarly inserted, were digested with low levels of the single-strand-specific endonuclease[10] S_1 in conditions which linearized supercoiled pBR322 alone[2,3]. Surprisingly these plasmids were not only linearized but yielded discrete excision products indicating the presence of at least one supercoil-independent S_1 site (Fig. 1 *a*, *b*). In addition, the pattern of excision products bore no relation to A+T-rich stretches or inverted repeats in the DNA sequence. Previous studies have only detected specific S_1 sites in 'duplex' DNA, either at inverted repeats in supercoiled molecules[2–4], or in conditions which partially denature A+T-rich regions (for reviews, see refs 5, 6).

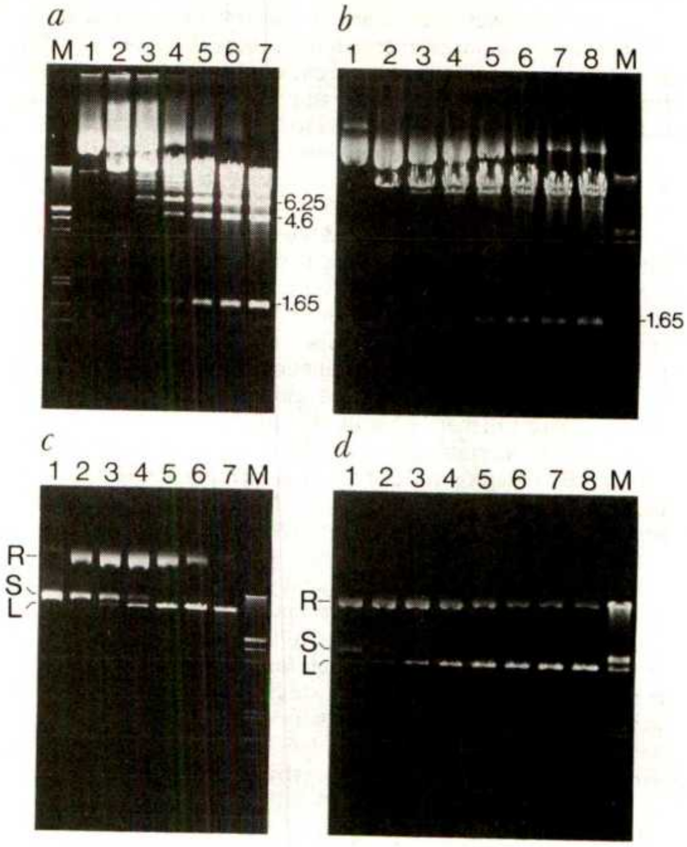

Fig. 1 Effect of S_1 nuclease on four plasmids analysed by 1% agarose gel electrophoresis; *a*, pBRh22/4, a recombinant containing a head-to-tail dimer of the 6.25 kb *Hin*dIII-cut histone repeat h22[7], inserted into the *Hin*dIII site of pBR322[9]; *b*, pBRh22/3, identical to pBRh22/4 but with only one histone repeat; *c*, a derivative of pBRh22/3 lacking the *Hpa*I fragment indicated by a thick line in Fig. 2*c*; *d*, pBR322. Lanes marked M are λ/*Hin*dIII/*Eco*RI size markers[26]. Other lanes are time points of S_1 nuclease digestion (lanes 1–8, respectively, 0, 2, 4, 8, 16, 32, 64 and 132 min). S_1 nuclease, prepared according to Vogt[10], was used at a concentration of 50 Vogt units per ml in 30 mM NaAc *p*H 4.6, 30 mM NaCl, 1 mM ZnCl at 37 °C. Electrophoresis buffer was 100 mM Na/glycine *p*H 8.5 containing 0.5 μg ml^{-1} ethidium bromide for UV photography[27]. For the smaller plasmids (*c*, *d*), the supercoiled (S), relaxed or nicked (R) and linear (L) forms are indicated. Sizes are in kb.

At the S_1 nuclease concentration used (see Fig. 1 legend), there was little background smear from random cleavage at A+T-rich regions but only 'partials' of the specific cleavage reactions were produced. It is nevertheless clear that whether one or two copies of the histone gene repeat is present, a 1.6 kb fragment is always excised. A 6.25 kb repeat length fragment and a 4.6 kb fragment (which together with the 1.65 kb fragment sums to the repeat length) appear only with the dimer insert (Fig. 1*a*). These results are consistent with the presence of only two major S_1 sites in the histone repeat sequence, 1.65 kb apart. Furthermore, as no excision products resulted from identical S_1 digestion of a 'mutant' plasmid lacking the *Hpa*I fragment spanning the H2A coding region and the H2A–H1 spacer (Fig. 1*c* and map in Fig. 2), one of the sites was tentatively located within this region of the histone gene repeat. The mutant plasmid was linearized at the second histone repeat site faster than pBR322 alone (Fig. 1*d*; mapping data not shown).

To locate exactly the two major S_1 sites on h22, S_1-cut pBRh22/3 and pBRh22/4 were secondarily restricted with several enzymes. These double digests mapped the S_1 sites in the spacers flanking the H1 gene. As anticipated, one of the sites lay within the *Hpa*I fragment and the other 1.65 kb downstream (see map in Fig. 2); this was confirmed by purifying the 1.65 kb S_1 excision product and restricting it with either *Bam*HI, yielding 900 and 750 base pair (bp) fragments, or *Bgl*I, yielding 850 and 800 bp fragments (Fig. 2*a*). These fragments are less clearly defined on the gel than the marker restriction fragments, suggesting that the S_1 cut ends are heterogeneous. Such heterogeneity is perhaps not surprising because the DNA sequences to which they map comprise the simple repeat motifs 5′(CA)10(CT)22 [site S_1 (a) in Fig. 2; P. Bucher, unpublished results] and 5′(GA)16 [site S_1(b) in Fig. 2; ref. 7]. The S_1(b) site is so close to the *Hin*dIII site downstream of the H1 gene (Fig. 2*c*) that when the *Hin*dIII-excised repeat is S_1-cleaved again, cutting at this site is not easily discernible, although it does take

---

* Present address: Department of Molecular Genetics, Celltech Limited, 250 Bath Road, Slough SL1 4DY, UK.

0028-0836/82/080714—03$01.00

place at a significant level (data not shown). However, partial cleavage at the S_1(a) site within this linear molecule is easily demonstrable and results in the production of 1.75 and 4.5 kb fragments (Fig. 2*b*). Thus cutting at either S_1(a) or (b) does not strictly depend on supercoiling, although an effect on the cutting rate has not been excluded. Moreover the larger S_1(a) site seems to be inherently more S_1 sensitive, at least in linear molecules (Fig. 2*b* and data not shown).

The observation that the homocopolymers flanking the H1 gene constitute novel S_1-sensitive sites prompted an examination of the possible mechanism involved. Because the S_1 activity is independent of DNA supercoiling, models based on the formation of unpaired regions in structures such as cruciforms[2–4], stabilized by torsional stresses, can be excluded. Moreover, unlike supercoil-dependent S_1 sites[2], the S_1 cleavage at the homocopolymers is highly sensitive to salt concentration: excision of the 1.65 kb fragment is strongly inhibited at 120 mM Na^+, close to the optimum salt conditions for S_1 activity, and is all but abolished at 300 mM, a concentration at which most of the intrinsic S_1 activity still remains[10,11] (Fig. 3). As duplex stability is directly proportional to the logarithm of total salt concentration[12], this result strongly implies that the S_1 sensitivity of the homocopolymers reflects a pre-melting phenomenon specifically associated with such simple repeated sequences[13].

A possible explanation, based on studies with pure homocopolymer preparations[13], is out-of-register DNA slippage with the production of single-strand loops flanking the slipped segment. Such structures would be expected to exist transiently. This notion is supported by examination of the distribution of nucleolytic cleavage within the homocopolymer sequences. For Fig. 4*a*, S_1-cut, ^{32}P-end-labelled pBRh22/4 was secondarily cleaved either with *Bam*HI (as a control to establish that label was incorporated in the anticipated 900 and 750 base fragments adjacent to the two S_1 sites; lane 1), or with the frequent cutting enzymes *Hae*III (lane 2), *Alu*I (lane 3) or *Taq*I (lane 4). The fragments were displayed on a sequencing gel and autoradiographic examination of the gel reveals the double digestion products expected from the S_1 site map (Fig. 2*c*) and the restriction map[1]. Note that the gel fails to resolve the terminal heterogeneity of the S_1-cleaved ends of the larger fragment but the smaller (≤200 bp) fragments are clearly resolved in a manner reflecting the nucleolytic cleavage pattern within the homocopolymers. Thus for the S_1(b) site, this pattern is bimodal and cutting is largely restricted to within a stretch of ~20 nucleotides (bracketed in Fig. 4). Figure 4*c* shows the sequence around S_1(b) with the relevant restriction sites and the deduced pattern of S_1 cleavage within the 5′(GA)16 motif. Thus, for example, *Taq*I restriction (Fig. 4*a*, lane 4) produces only one group of small terminal fragments (65–85 bases long), which can be seen to map from the *Taq*I site (■; Fig. 4*c*); similarly the *Alu*I site (●) maps the 95–115 base fragments. In fact all the bands shown in Fig. 4*a* can be mapped from an appropriate restriction site to either S_1(b) or S_1(a), although in the latter case the fragments are generally larger due to the paucity of restriction sites in the H2A–H1 spacer[1] (sequence not shown).

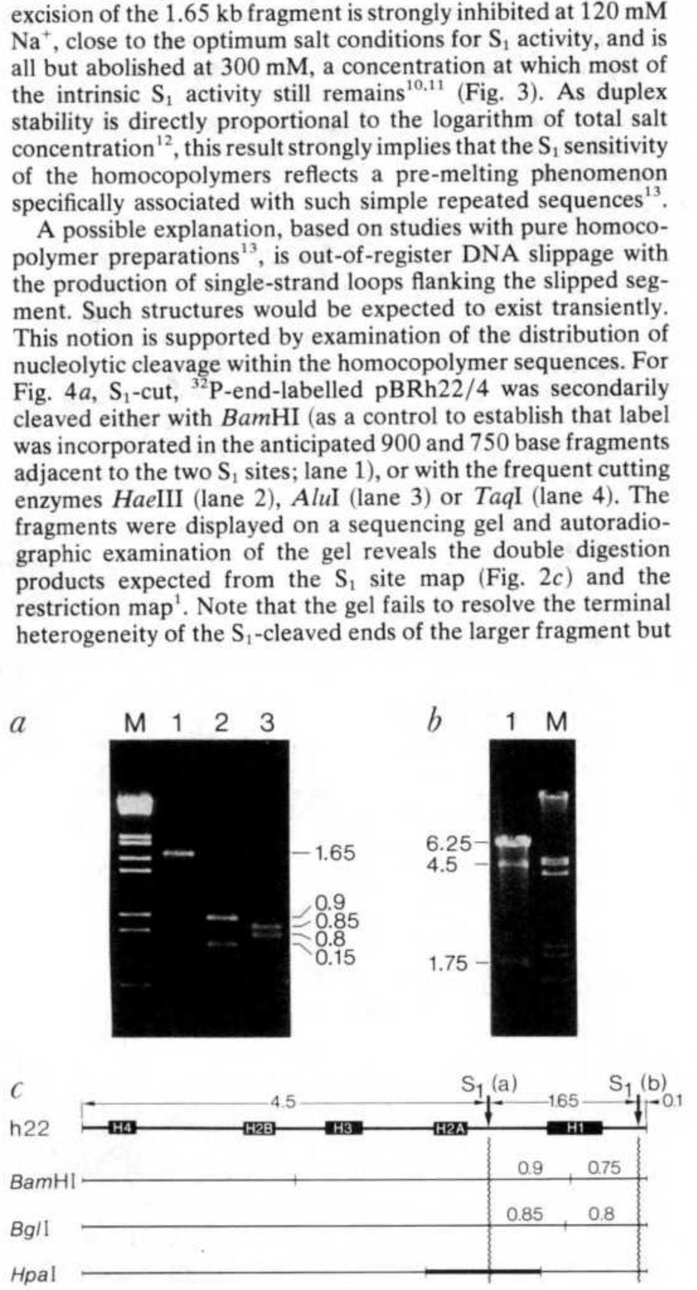

Fig. 2 Restriction enzyme mapping of S_1 cleavage sites. *a*: Lane 1, purified 1.65 kb S_1 excision fragment; 2, *Bam*HI restriction products of the 1.65 kb fragment; 3, *Bgl*I restriction products of the 1.65 kb fragment. *b*: Partial cleavage of *Hin*dIII repeat of h22 with S_1 nuclease using the conditions described in Fig. 1 legend with digestion for 1 h. The electrophoretic analyses were as for Fig. 1 except that for *a*, 2% agarose was used. *c* Is a map of the h22 repeat showing the deduced S1 site map relative to the restriction map[1].

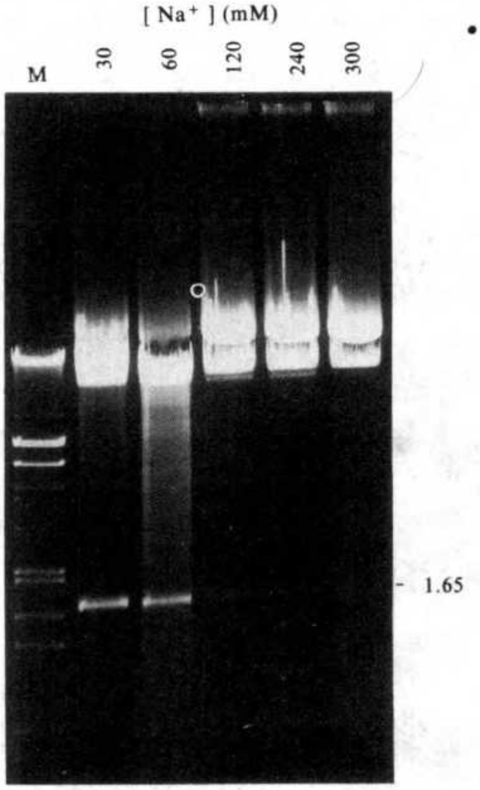

Fig. 3 Salt sensitivity of S_1 cleavage. pBh22/3 was digested with S_1 for 32 min with conditions and electrophoretic analysis as for Fig. 1 except that the NaCl concentration was adjusted to bring the total Na^+ concentration to the values indicated. The degree of S_1 cleavage can be judged by the production of the 1.65 kb excision product.

A bimodal cleavage pattern would be expected from a single predominant type of DNA slip as this creates two single-strand loops adjacent to the slip, each a potential S_1 target. This seems to be compatible with the S_1(b) pattern where the site comprises a simple homocopolymer. The cleavage fragments mapping to the S_1(a) site show a more complex pattern, approximately trimodal with a predominant central cleavage region covering ~40 nucleotides (flanked by a wavy line in Fig. 4). This greater length and complexity may be a time-averaged reflection of the many slipping modes possible within a long dual homocopolymer such as the S_1(a) site (5′(CA)10(CT)22). Figure 4*b* illustrates an alternative 'fine mapping' strategy. The purified 1.65 kb S_1-excised fragment was ^{32}P-end-labelled[14] and the derived *Bam*HI fragments (Fig. 2*a*) subjected to total chemical cleavage at either pyrimidine (lanes 1, 3) or purine (lanes 2, 4) nucleotides. Since the 5′-end-label lies almost exclusively in C-T runs for both *Bam*HI fragments, pyrimidine cleavage yielded no oligonucleotides when analysed on a 20% acrylamide gel (Fig. 4*b*, lanes 1, 3). In contrast, purinolysis mapped the S_1 cleavage pattern from neighbouring purine nucleotides (Fig. 4*b*, lanes

2, 4). Figure 4*b* reproduces almost exactly the complex multimodal pattern previously seen for the S_1(a) site extending over about 40 nucleotides, and the bimodal pattern for S_1(b) extending over about 20 nucleotides (cf. Fig. 4*a*). Note also that these map identically on the sequence (the purines from which to map the S_2(b) pattern are complementary to the 5′TT in Fig. 4*c*).

Whatever the physical basis for the S_1 nuclease sensitivity of the homocopolymers flanking the H1 gene of the h22 histone gene repeat, it is tempting to speculate about the possible biological significance of the localized DNA unpairing implied by these results. Homocopolymer sequences are found not only in the h22 repeat, but also adjacent to histone genes in several species (not necessarily the H1 gene)[8], the sequence 5′(CA)31 has been found ~300 bases downstream of the coding sequence of two immunoglobulin genes[15], and 5′(TG)17 has recently been found in an evolutionarily conserved repeat family in, for example, the 'spacer' separating the human δ- and β-globin genes[16].

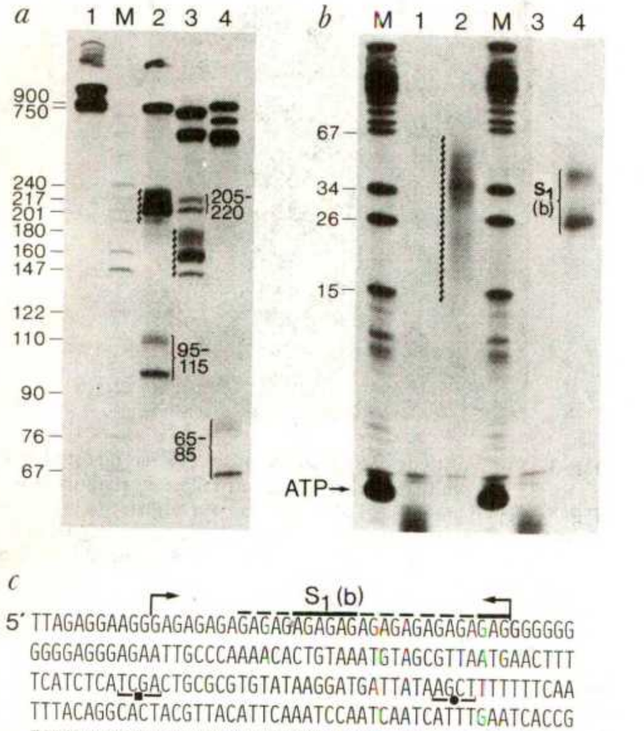
a
1 M 2 3 4
900
750
240
217
201
180
160
147
122
110
90
76
67
205-
220
95-
115
65-
85
b
M 1 2 M 3 4
67
34
26
15
S1
(b)
ATP→
c
S1 (b)
5′ TTAGAGGAAGGGAGAGAGAGAGAGAGAGAGAGAGAGAGAGAGGGGGGG
GGGGAGGGAGAATTGCCCAAAACACTGTAAATGTAGCGTTAATGAACTTT
TCATCTCATCGACTGCGCGTGTATAAGGATGATTATAAGCTTTTTTTCAA
TTTACAGGCACTACGTTACATTCAAATCCAATCAATCATTTGAATCACCG
TCGCAAAAGGCAGATGTAAACTGTCAAGTTGTCAGATTGTGTGCGCGGCC 3′

Fig. 4 Fine mapping of nucleolytic cleavage sites. *a*: Autoradiograph of 8% acrylamide/urea gel[28] of fragments derived by secondarily cutting S_1-digested 5′ ^{32}P-end-labelled pBh22/4 (ref. 14) with the following enzymes: lane 1, *Bam*HI; lane 2, *Hae*III; lane 3, *Alu*I; lane 4, *Taq*I. The size marker (in bp; M) is a *Hpa*II-cut derivative of pBR322 (ref. 29). Note that in these experiments there are eight labelled ends which would be expected to yield four predominant labelled fragments assuming that nearly all the initial S_1 cleavage occurred as indicated in Fig. 2. Thus *Bam*HI should yield fragments 750 and 900 bases long (barely resolved in lane 1) and 2.1 and 2.3 kb (not resolved; see Fig. 2*c*). All the radioactivity is in the expected region of the gel and the sizes were confirmed on an agarose gel (not shown); most important, however, no 'unexpected' low molecular weight fragments are present, thus the heterogeneous bands in lanes 2–4 must derive from the anticipated double digestions. The heterogeneous fragments derived from cleavage at S_1(b) are shown bracketed, while those from S_1(a) are flanked by a wavy line. *c* Shows the sequence for the S_1(b) site in 50 base blocks with the relevant restriction sites (for *Taq*I, *Alu*I *Hae*III) and the deduced regions of maximal cleavage indicated by overlining. *b* Shows an alternative 'fine mapping' strategy. An aliquot of the same purified 1.65 kb fragment shown in Fig. 2*a* was 5′ ^{32}P-end-labelled[14], and the derived *Bam*HI fragments (Fig. 2*a*, lane 2) purified. Each fragment was divided into two aliquots which were either totally hydrolysed at purine nucleotides with formic acid/diphenylamine reagent (lanes 2, 4) or at pyrimidine nucleotides by hydrazinolysis (lanes 1, 3), and then purified as for sequencing reactions[14]. The purified products were analysed by autoradiography following electrophoresis on a 20% acrylamide/urea gel[14]. The products from the 900 bp fragment mapping the S_1(a) sites are in lanes 1 and 2, while those from the 750 bp fragment mapping the S_1(b) site are in lanes 3 and 4. Size marker as in *a*.

The homocopolymer sequences of the histone genes are located in spacer regions not known to have a direct effect on the expression of the genes[8], but which have been strongly implicated in evolutionary behaviour[17]. Although histone genes are usually clustered or tandemly repeated, the copy number, order and polarity of the genes vary widely between species and, in some cases, even within a single genome. Where the copy number is high, as in sea urchins or *Drosophila*, tandem repetition is the norm but escaped 'orphon' histone genes arise with a high frequency[18]. Subtypes of H1 genes arise at a particularly high frequency (see reviews in refs 8, 17, 19, 20, 13–15 and refs therein). All these facts suggest that mechanisms exist which allow occasional histone genes (and in particular H1 genes) to transpose, replicate and diverge independently. Could *in vivo* excision events at homocopolymers be involved in such mechanisms?

The rectification mechanism maintaining the homogeneity of tandemly repeated histone genes may also involve the homocopolymers because they could provide foci for unequal crossover or gene conversion events[17]. Although the exact nature of such recombinations is unknown, they would probably be facilitated by a potential for localized unpairing in these sequences. Moreover, the possibility that such unpairing reflects DNA slippage and that similar slippage may occur *in vivo* is supported by the fact that several biological phenomena are best explained by this mechanism: frequent frameshift mutations in the T4 lysozyme gene[21], mutational hotspots in the *Lac*I gene of *Escherichia coli*[22] and small deletions in human globin genes[23]. In addition, other specific recombinational events, such as globin gene conversion[24] or immunoglobulin class switching[25], are also thought to occur at simple repeated sequences. All these events could be related to a fundamental tendency for DNA slippage at such sequences.

I thank Professor Max Birnstiel for initially suggesting the DNA slippage mechanism, Bill Folk and Mary Bendig for discussion and critical reading of the manuscript, and Fritz Ochsenbein, Bonnie Bryan and Jackie Hardwick for help in its preparation. This work was supported by a grant from the State of Zurich and by Swiss NRF grant 3/257.077.

Received 2 October 1981; accepted 8 January 1982.

1. Nordheim, A. *et al. Nature* **294,** 417–422
2. Lilley, D. M. J. *Proc. natn. Acad. Sci. U.S.A.* **77,** 6468–6472 (1980).
3. Panayotatos, N. & Wells, R. D. *Nature* **289,** 466–470 (1981).
4. Lilley, D. M. J. *Nucleic Acids Res.* **9,** 1271–1289 (1981).
5. Wells, R. D. *et al. Prog. Nucleic Acid Res. molec. Biol.* **24,** 167–267 (1980).
6. Cantor, C. R. *Cell* **25,** 293–295 (1981).
7. Schaffner, W. *et al. Cell* **14,** 655–671 (1978).
8. Hentschel, C. C. & Birnstiel, M. L. *Cell* **25,** 301–313 (1981).
9. Sutcliffe, J. G. *Nucleic Acids Res.* **5,** 2727 (1978).
10. Vogt, V. *Eur. J. Biochem.* **33,** 192–200 (1973).
11. Sutton, W. D. *Biochim. biophys. Acta* **240,** 522 (1971).
12. Schildkraut, C. & Lifson, S. *Biopolymers* **3,** 195 (1968).
13. Cantor, C. R. & Schimmel P. R. in *Biophysical Chemistry* Vol. 3, Ch. 22 (Freeman, San Francisco).
14. Maxam, A. M. & Gilbert, W. *Meth. Enzym.* **65,** 499–560 (1980).
15. Nishioka, Z. & Leder, P. *J. biol. Chem.* **255,** 3691–3694 (1980).
16. Miesfeld, R., Krystal, M. & Arnheim, N. *Nucleic Acids Res.* **9,** 5931–5947 (1981).
17. Kedes, L. H. *An. Rev. Biochem.* **48,** 837–870 (1979).
18. Childs, G., Maxson, R., Cohn, R. & Kedes, L. H. *Cell* **23,** 651–663 (1981).
19. Isenberg, I. *A. Rev. Biochem.* **48,** 159–191 (1979).
20. Hohmann, P. *Int. Rev. Cytol.* **71,** 41–93 (1971).
21. Streisinger, G. *et al. Cold Spring Harb. Symp. quant. Biol.* **31,** 77–84 (1966).
22. Farabaugh, P. J., Schmeissner, U., Hofer, M. & Miller, J. H. *J. molec. Biol.* **126,** 847–863 (1978).
23. Efstratiadis, A. *et al. Cell* **21,** 653–668 (1980).
24. Slightom, J. L., Blech, A. E. & Smithies, O. *Cell* **21,** 627–638 (1980).
25. Nikaido, T., Nakai, S. & Hongo, T. *Nature* **292,** 845–848 (1981).
26. Southern, E. *Meth. Enzym.* **68,** 152–176 (1979).
27. Sharp, P. A., Sugden, B. & Sambrook, J. *Biochemistry* **12,** 3055–3063 (1973).
28. Sanger, F. & Coulson, A. R. *FEBS Lett.* **87,** 107 (1978).
29. Hofstetter, H., Kressmann, A. & Birnstiel, M. L. *Cell* **24,** 573–585 (1981).

MATTERS ARISING

Magma chamber profiles from Bay of Islands ophiolite complex

CASEY and Karson[1] have presented a model for the shape and size of magma chambers underlying mid-ocean ridges, based on observations of the Bay of Islands ophiolite They show that igneous layering in rocks of the plutonic complex is oriented up to 90° oblique to the palinspastic horizontal, and they use this, and other evidence, to infer that nucleation and growth of crystals occurred *in situ* on the chamber walls, without the need for settling of crystals

The magma chamber model of Casey and Karson (Figs 4 and 5 of ref 1) shows a curious, unexplained and yet crucial feature, namely that while ultramafic rocks were forming along the sides of the chamber near its base, mafic rocks were forming along the sides at higher levels Neither the effect of pressure nor that of volatile content on crystallization of the magma can be responsible for this difference If the ultramafic and the mafic rocks indeed formed in the same magma chamber, and if Casey and Karson are correct in saying that crystallization occurred only along the chamber walls, then the magma must have been stratified, with more mafic magma lying below less mafic magma, the 'Unit 2' rocks of the plutonic complex (interlayered mafic and ultramafic rocks) would then represent the junction between the two magma types, that is a zone of mixing

This inference that the magma was compositionally stratified agrees with that reached by Sparks *et al*[2] on the basis of the density variation in mid-ocean-ridge basalts

C H DONALDSON
Department of Geology,
St Andrews University,
Fife KY16 9ST, UK

1 Casey J F & Karson J A *Nature* **292,** 295–301 (1981)
2 Sparks, R S J Meyer, P & Sigurdsson, H *Earth planet Sci Lett* **46,** 419–430 (1980)

CASEY AND KARSON REPLY—Donaldson's comment that we have inferred the existence of chemical heterogeneity along the margin of the magma chamber which formed the plutonic complex of the Bay of Islands Ophiolite is perhaps an understatement We categorically stated that "the lack of lateral continuity of the fine-scale layering must be interpreted as the result of fairly significant changes in physico-chemical conditions on a scale approximated by the lateral continuity of the layering (~⩽50 m)" We also stated that "significant chemical zonation in the magma chamber" was reflected by the fact "that fine scale igneous layers (which define isochronous planes) strike obliquely across the contacts between major lithologic subdivisions of the plutonic section"

Donaldson has also suggested that this interpretation of chemical zonation is consistent with the work of Sparks *et al*[1] (and presumably Huppert and Sparks[2,3]) He has further postulated that the transition zone ('Unit 2') of the plutonic complex can be interpreted as a mixing zone between two distinct magma types Certainly, Sparks and his co-workers have clearly shown the weaknesses inherent in the arguments which lead to the emphatic statements that mafic magma chambers cannot become chemically zoned because of continuous convective overturn Based on the extent of lateral continuity of layering throughout the plutonic complex and other factors treated in the original paper, however, we do not believe that one can simply categorize two magma types The overall chemical and mineralogical zonation of the crystallization products within the plutonic complex seems to span the entire thickness of the plutonic section Previous geochemical studies[4–6] and unpublished data collected by us indicate that there is no sharp break in mineral compositions identified at the transition zone These data seem to indicate that at any single time, the margin of the chamber was in contact with magma of numerous and highly variable compositions The compositional range seems to depend on stratigraphic height within the plutonic section The transition zone simply marks the first appearance of plagioclase as a major phase within the plutonic section

Detailed mineral chemistry studies by our group will attempt to characterize the scale and degree of chemical variations along a single magma chamber profile Until such time, however, it is premature to suggest a simple model having just two magma types and a single mixing zone The chamber could be multiply stratified on a fine scale and consist of multiple mixing zones that need not have a steady-state position within the chamber The dimension of the chamber might also be conducive to local chaotic and laterally discontinuous chemical stratification These possibilities have not yet been tested by Sparks and co-workers because they have initiated their studies using simple two liquid models It is also not clear that pressure and volatile content of the magma should be overlooked or discarded as a possible cause for at least part of the chemical and mineralogical zonation until further work, especially trace element and isotopic studies, has been completed At present there is little evidence to substantiate Donaldson's simplistic model of just two magma types, field and geochemical evidence seems to favour a more complex multiple stratified model

J F CASEY
Department of Geology,
University of Houston,
Central Campus,
Houston, Texas 77004, USA

J A KARSON
Department of Geology and Geophysics,
Woods Hole Oceanographic Institution,
Woods Hole,
Massachusetts 02543, USA

1 Sparks, R S J , Meyer P & Sigurdsson, H *Earth planet Sci Lett* **46,** 419–430 (1980)
2 Huppert, H E & Sparks, R S J *Contr Miner Petrol* **75,** 279–289 (1980)
3 Huppert, H E & Sparks, R S J *Nature* **286,** 5768, 46–48 (1980)
4 Irvine, J N & Findley, T C *Publ Earth Phys Br Dept of Energy Mines Resources Can* **42,** 97–128 (1972)
5 Church, W R & Riccio, L *Can J Earth Sci* **14,** 1156–1165 (1977)
6 Malpas, J thesis, Memorial Univ Newfoundland (1976)

K^+ depletion and Na^+ pump density

IT has been shown[1] that the skeletal muscles of K^+-depleted rats lose large quantities of K^+, gain Na^+, and many have fewer ouabain binding sites than normal, this is in contrast to the findings of Chan and Sanslone[2] and Erdman, Bolte and Luderitz[3] for red blood cells (RBCs) and heart muscle, respectively, of K^+-depleted rats and in cultured human cells grown in low-K^+ medium[4,5]

In our original experiments we showed[4] that more pumps were produced in cells when the internal Na^+ concentration ($[Na^+]_i$) was allowed to rise to 20–60 mM, with a corresponding drop in $[K^+]_i$ In recent experiments we have found that very large increases in $[Na]_i$ (and correspondingly large reductions in $[K^+]_i$) lead to a large loss of ouabain binding sites and transport capacity in HeLa cells (Table 1) These losses in ouabain binding sites are greater than can be accounted for by cessation of the normal insertion rate of new pumps (1 5% h^{-1})[6] and imply that an accelerated removal of pumps is occurring

Our results show that HeLa cells can be made to produce either a greater or lesser density of pumps than normal, apparently depending on the ion concentrations within the cells, they therefore mimic RBCs and heart or skeletal muscles of K^+-depleted rats We suspect that two processes are occurring (1) as $[Na]_i$ rises, the rate of insertion of new pumps increases, and (2) if $[K]_i$ falls below a critical level, the synthesis of new pumps stops (because K^+ is required as a cofactor by most enzymes[7]) and pumps are

Table 1 Effect of changes in extracellular K^+ on the intracellular Na^+ and K^+ concentrations and on the specific ouabain binding of HeLa cells

Expt	$[K]_0$	$[Na]_i$ (mmol per 1 H_2O)	$[K]_i$	Specific ouabain binding as % of control
Ref 4	0 4→0 6	24	145	159
1	0 1→0 3	70	122	136
2	0 2→0 4	87	122	96
1	0 1→0 2	111	35	83
3	0 2→0 3	97	46	55
4	0 04→?	165	50	17

removed from the membrane (by affecting the anchoring process?)

It is possible that the mechanism controlling the density of Na^+ pumps in skeletal muscle is no different from that in other cells, but that the ion concentrations achieved by any reduction of serum $[K^+]$ differ This could be investigated further by looking at the effects of smaller reductions of serum $[K^+]$ on the ouabain binding and $(Na^+ + K^+)$ATPase of rat skeletal muscle

Control cells had a $[Na]_i$ of 16 mmol l^{-1} and a $[K]_i$ of 179 mmol l^{-1} The $[K]_0$ values are the initial and final values (where measured)

J F Lamb
J F Aiton
Pat Ogden

Department of Physiology
and Pharmacology,
Bute Medical Buildings, St Andrews,
Fife KY16 9TS, UK

1 Nørgaard, A , Kjeldsen K & Clausen, T *Nature* **293**, 739–741 (1981)
2 Chan P C & Sanslone W R *Archs Biochem Biophys* **134**, 48–52 (1969)
3 Erdman, E Bolte, H -D & Luderitz, B *Archs Biochem Biophys* **145**, 121–125 (1971)
4 Boardman, L Huett, M , Lamb J F , Newton, J P & Polson, J M *J Physiol , Lond* **241**, 771–794 (1974)
5 Pollack, L R Tate, E H & Cook, J S *J cell Physiol* **106**, 85–97 (1981)
6 Lamb, J F & Ogden, P *Q Jl exp Physiol* **67**, 105–119 (1982)
7 Baker, P F *Endeavour* **25**, 166 (1966)

NØRGAARD *ET AL* REPLY—Our observation that K^+-depletion in mice and rats leads to a progressive decrease in the number of ^3H-ouabain binding sites in skeletal muscle[1], does not agree with the results of previous investigators, who found that K^+ depletion increases $(Na^+ + K^+)$ATPase and the number of ^3H-ouabain binding sites in erythrocytes[2,3] as well as $(Na^+ + K^+)$ATPase activity in guinea pig hearts[4,5] Our observation that erythrocytes of K^+-depleted rats maintain normal K^+-contents even after weeks of exposure to the low plasma K^+ values agrees with the existence of a compensatory rise in their number of $(Na^+ + K^+)$ATPase units The reported measurements[4,5] of $(Na^+ + K^+)$ATPase activity in hearts used a sediment obtained by centrifugation of homogenates, and as this may contain only a minor fraction of the total $(Na^+ + K^+)$ATPase activity present in the starting material (for discussion, see ref 6), the results depend on the recovery being the same for hearts from normal and K^+-depleted animals

To explore this problem further, we have recently measured the binding of ^3H-ouabain to rat heart ventricles *in vivo* In the controls we found 276± 8 pmol per g wet wt, and 157± 18 pmol per g in the K^+-depleted rats ($P < 0\ 001$) This decrease (43%) is smaller than that found in skeletal muscle, which agrees with the observation that the loss of K^+ was not so pronounced in the heart Measurements of the ^3H activity in the plasma after intraperitoneal injection of ^3H-ouabain gave 77% higher values in the K^+-depleted rats than in the controls This also suggests that the peripheral binding capacity for ^3H-ouabain is reduced and that in the K^+-depleted state the heart may be exposed to a higher concentration of digitalis glycosides

At variance with the results obtained using HeLa cells[7], even modest K^+ loss (and a corresponding rise in intracellular Na^+) is associated with a decrease in the number of ^3H-ouabain binding sites in rat skeletal muscle (see Figs 1, 2 of ref 1) This suggests that the synthesis of new $(Na^+ + K^+)$ATPase units has ceased, and we are now investigating the possibility that this results from a general impairment of enzyme activity or protein synthesis

Despite our original expectations, we have been unable to detect any rise in the number of ^3H-ouabain binding sites in the muscles of K^+-depleted mice or rats It seems that skeletal and heart muscle cells differ from cultured cells, perhaps due to central regulatory mechanisms triggered by the drop in plasma K^+ seen a few days after the onset of the K^+-depleting regime The decreased capacity for active $Na^+ + K^+$ transport in muscle may prevent any further reduction in plasma K^+ and delay the development of the muscle paralysis which is the final outcome of prolonged K^+ depletion

Aage Nørgaard
Keld Kjeldsen
Torben Clausen

Institute of Physiology,
Aarhus University,
DK-8000 Aarhus C, Denmark

1 Nørgaard, Aa , Kjeldsen, K & Clausen, T *Nature* **293**, 739–741 (1981)
2 Chan P C & Sanslone W R *Archs Biochem Biophys* **134**, 48–52 (1969)
3 Erdmann, E & Krawietz, W *Acta biol med germ* **36**, 879–883 (1977)
4 Erdmann, E , Bolte, H -D & Luderitz, B *Archs Biochem Biopnys* **145**, 121–125 (1971)
5 Bluschke V , Bonn, R & Greeff, K *Eur J Pharmac* **37**, 189–195 (1976)
6 Clausen, T , Hansen O & Larsson, L -I *Eur J Pharmac* **72**, 331–335 (1981)
7 Boardman, L , Huett, M & Lamb J F *J Physiol , Lond* **241**, 771–794 (1974)

The active radio galaxy 1413+135

BEICHMAN *et al*[1] and Bregman *et al*[2] present interesting IR and high-frequency radio (4 8–14 5 GHz) results on 1413+135 The latter also give an optical spectrum which suggests that it is a galaxy of redshift $z = 0\ 26$, no emission features were seen Curiously Beichman *et al*[1] imply that it was an 'empty field' until discovered as an IR source by Rieke *et al*[3]

The radio source was identified by Hoskins *et al*[4] with a 20 mag galaxy on the Palomar Sky Survey, and a finding chart was given The identification was based on 408-MHz measurements at Molonglo Condon *et al*[5] obtained an accurate radio position which agrees to 1 arc s with the optical position of Hoskins *et al*[4] This confirmed the identification but as Bregman *et al*[2] point out, the finding chart of Condon *et al*[5] is faulty Their positional offsets are also misleading Bregman *et al*[2] reconfirm the identification of Hoskins *et al*[4] but mistakenly refer to this as a 'PKS identification'

A radio spectrum covering the range 178–2,695 MHz is given by Murdoch and Hoskins[6] The low-frequency spectrum peaks at 3 Jy at ~300 MHz falling to 1 9 Jy at 178 MHz and 0 67 Jy at 2,695 MHz (in 1971) Bregman *et al*[2] report a strong and variable rise at 4 8 GHz and above and Beichman *et al*[2] show that the intensity peaks at ~100 GHz In addition to the highly compact component implied by these results, there is evidently a moderately compact component shown by the low-frequency radio data The overall radio spectrum is quite typical of BL Lac objects and highly variable QSOs The object would appear to be a galaxy with a BL Lac object in its nucleus

H S Murdoch

The Astrophysical Department,
School of Physics,
University of Sydney,
New South Wales 2006,
Australia

1 Beichman, C A *et al* *Nature* **293**, 711 (1981)
2 Bregman J N *et al* *Nature* **293**, 714 (1981)
3 Rieke, G H Lebofsky, M J & Kinman, T D *Astrophys J Lett* **232**, L151 (1979)
4 Hoskins, D G Murdoch, H S , Hazard, C & Jauncey, D L *Aust J Phys* **25**, 559 (1972)
5 Condon J J Hicks, P D & Jauncey, D L *Astr J* **82**, 692 (1977)
6 Murdoch H S & Hoskins, D G *Aust J Phys* **26**, 867 (1973)

0028–0836/82/080718—01S01 00

BOOK REVIEWS

…sity Colleges of Science & Technology
…P.C Rd Cal.-9
LIBRARY COMPLEX
Departments of
Chemical Engineering
Chemical Technology
Plastics & Rubber Technology

The ontogeny of phylogeny

David L. Hull

The Development of Darwin's Theory Natural History, Natural Theology, and Natural Selection, 1838–1859. By Dov Ospovat. Pp. 301. ISBN 0-521-23818-8. (Cambridge University Press: 1981.) £20, $39.50.

PUBLICATION is an unnatural event in the life of a scientific theory. Prior to publishing, a scientist can work in relative privacy, changing his views as he sees fit. After publication, however, the process is made more difficult by the critical stare of the scientific community. Darwin worked on his theory of biological evolution from 1837 until his death 45 years later. Historians have charted his intellectual voyage month by month, sometimes day by day — the *Beagle,* his decision to develop a theory of transmutation, his reading Malthus, the Sketch of 1842, the Essay of 1844, the receipt of Wallace's paper, the hurried publication of the *Origin,* and the trials and tribulations that followed. Ospovat retraces familiar ground in Darwin's story from 1838 to 1844 and then fills in the last gap — the period between 1844 and 1859.

Historians have ignored this period primarily because nothing much of any interest seems to have happened during these years. By 1844 Darwin had already decided that species evolve by chance variation and natural selection. The essentials of his theory were complete. Ospovat argues to the contrary that Darwin made several fundamental changes in his theory some time in the second half of 1856. Prior to that date, Darwin thought that every species is perfectly adapted to its environment, a belief that he carried over from natural theology. He considered that significant amounts of variation occur only in response to intermittent changes in the environment. As a result, evolution for Darwin at this stage in his development was "punctuational". However, in 1856 Darwin formulated his principle of divergence, a principle that he thought was as important as that of natural selection. According to this principle, variation exists within species at all times, allowing them to adapt to variations within their range, including the presence of other organisms. By a sort of "division of labour", species become subdivided into varieties, and these varieties are incipient species. From the beginning Darwin believed that evolution is in some sense progressive, but only after 1856 could he explain why the biosphere tended to become increasingly complex.

In 1855 A. R. Wallace published a paper on the law which regulates the introduction of new species, a paper that both Charles Lyell and Edward Blyth brought to Darwin's attention. Lyell urged Darwin once again to publish lest he be forestalled, and Darwin began his projected multi-volume *Natural Selection.* In 1857 Darwin and Wallace exchanged letters on Wallace's 1855 paper. Then Wallace's paper "On the Tendency of Varieties to Depart Indefinitely from the Original Type" (1858) arrived, not exactly like a "bolt out of the blue". What if Wallace's first paper had prompted Darwin to publish an "abstract" of his views in 1855? What if Wallace's 1858 paper had not caused Darwin to publish the *Origin?* What if Darwin had instead doggedly persisted in his original plan for his Big Book? Answers to such contrary-to-fact questions in history are extremely risky. Even so, Ospovat suggests that the *Origin* would have been a very different book had Darwin published it before formulating his principle of divergence. Instead of making the principle an integral part of his theory as first presented, Darwin would have been forced to introduce it later as an emendation. Similarly, he might have quietly passed on Wallace's paper for publication instead of agreeing to publish a short piece of his own along with it. If he had, I think that very little would have changed except later commentators would have been precluded from going on at such interminable length about Darwin's churlish behaviour. Darwin would still be viewed as the founder of the modern theory of evolution. The Darwin–Wallace papers of 1858 caused hardly a stir, Wallace's paper published alone is unlikely to have engendered more interest. But what of intellectual justice? From this perspective, Wallace still loses out, but this time to Patrick Matthew who had anticipated both Darwin and Wallace as early as 1831.

Although Ospovat makes the requisite passing remarks about the social, political and religious sources of Darwin's scientific views and concludes with a chapter on the development of Darwin's theory as a social process, his book is almost entirely an internalist history of the very best sort. Ospovat not only chronicles Darwin's conceptual development but also presents plausible reconstructions of the factors that led him to adopt the views he did. Not all of these factors are narrowly "scientific". For example, the tenacity with which Darwin held on to his belief in perfect adaptation stems at least in part from considerations that anyone, both then and now, would count as theological. Darwin was also influenced by prudential considerations of the sort that play a central role in the politics of science. For example, Ospovat argues that Darwin understates the progressive nature of evolution in the *Origin* for fear of offending Lyell and Huxley. But he does not repeat the usual facile claims about the direct translation of sociopolitical interests into the content of science.

Under normal circumstances, I would conclude this review by remarking that the appearance of *The Development of Darwin's Theory* portends a brilliant career for its author. Sadly, however, shortly after the completion of this manuscript, Dov Ospovat died at the age of thirty three. ☐

David L. Hull is a Distinguished Professor in the Department of Philosophy at the University of Wisconsin–Milwaukee.

Red for green

H. McAllister

The Biological Aspects of Rare Plant Conservation. Edited by Hugh Synge. Pp. 558. ISBN 0-471-28004-6. (Wiley: 1981.) £30, $84.

DESPITE its title, most of this multi-authored book is very usefully devoted to the ways in which botanists in different nations work out which species and communities are in need of conservation in their own countries. As a result, the differences in the scale of the problem between the impoverished but well-known floras of north-western Europe, the rich, less well-known floras of such countries as South Africa, Australia and India, and the very rich, little-known tropical rain forest floras, are clearly brought out.

In north-west Europe the distribution and frequency of occurrence of most species is fairly well documented, so it is usually obvious which species are rare and in need of conservation The habitat requirements of such species are mostly known and several chapters deal with how sufficient autecological information has been obtained to devise successful conservation programmes

The conservation problems of north-west Europe pale into insignificance in comparison with those of such species-rich areas as the Cape of Good Hope with 1,244 threatened plant species Very few of these have been studied in any detail and the two species discussed exemplify the difficulties Field work undertaken to promote their conservation has demonstrated the importance of fire in stimulating germination, but, at least in the case of *Staavia dodii*, all attempts to germinate seed outside the natural field environment — including artificial fire — have failed, making garden cultivation impractical as a conservation measure The concentration of the few remaining populations of so many species in a small area poses serious management problems when so little is known of their autecology

However, by far the most critical situation exists in the tropical rain forests where a fair proportion of the species are still undescribed It can be reliably stated that if the present rate of destruction continues, and it is likely to, many species will become extinct before they can be described There is no doubt that this is the vegetation type in which most extinctions are taking place and that this is a loss not just to biological diversity but to the resources of the world of value to mankind The four chapters in Section 2 of the book, "Tropical Forests — The Conservation Priority", are an excellent statement of the problem and how it should be tackled The only sensible approach is to try to conserve areas of great species diversity and hope thereby to protect the maximum number of species Quite large areas may be required, as a typical tree species may have an average density of 1 per 5 hectares and be dioecious — though sometimes facultatively apomictic Dransfield's paper describes how controlled cropping can be compatible with conservation

One chapter, discussing the conservation of lower plants, points to the similarities with the situation in tropical rain forests — a lack of floras and lack of knowledge of species distributions, most species not being amenable to cultivation, meaning that conservation in their native habitats is the only hope for their survival

The varied topics covered make this work an excellent and much-needed world picture of the present state of plant conservation, although the quality of the individual contributions is very variable Unfortunately the book promises a bleak future, both environmentally and economically, if there is no improvement. □

H McAllister is the Assistant Director of the Botanic Gardens, University of Liverpool

---

Slimmer tracts for gut physiologists

G.J. Dockray

Physiology of the Gastrointestinal Tract, Vols 1 and 2 Edited by Leonard R Johnson Pp 1,492 ISBN 0-89004-440-6 (Raven 1981) Two-volume set $165

WHEN the American Physiological Society devoted a section of their *Handbook of Physiology* to the gut in the late 1960s, it needed five volumes containing well over 100 chapters to produce a comprehensive account of the subject After a period of unprecedented expansion in our knowledge of gut function it comes as a pleasant surprise to find that the present work consists of two volumes and less than half the number of chapters needed over a decade ago Unfortunately, the feeling of relief is tempered by the fact that this brevity has been partly achieved by a selective approach There is, for instance, relatively little attention given to the liver, salivary glands, comparative and evolutionary aspects, and control of nutrient intake The omissions are regrettable, not least because they are inimical to the editors' objective of producing a definitive treatise

This is not to say, however, that there are not good reasons to justify a relatively economical approach in reviewing the present state of gastrointestinal physiology Recent advances in this field have dealt very largely with the elucidation of events at the cellular and sub-cellular levels The present volumes both reflect the recent areas of progress and illustrate how it is possible to explain fundamental aspects of organization in a way that readily reconciles fragmentary and even contradictory work from the past

A series of chapters at the start of the first volume, and at the end of the second, deals with general aspects of digestive physiology and related topics The major gut functions — secretion, motility and absorption — are covered in separate sections In each case there are contributions dealing with functional morphology and molecular mechanisms, and these serve to provide a context for chapters dealing with the integrative aspects of each system The treatment works well, and in particular makes it easy to see how physiological mechanisms of the gut can be related to the functions of other organ systems Indeed, it is worth noting that a significant part of our understanding of such basic cellular mechanisms as membrane transport and secretion have been derived from studies on the alimentary tract and associated organs For this reason these two volumes will be of interest and value to many whose main concerns lie outside the gut, but who nevertheless wish to understand recent developments in gut physiology The gut chauvinist should not, however, feel neglected since there are, for example, chapters dealing with such singularly digestive subjects as dietary fibre and gut gas

The contributors are nearly all well-recognized authorities in their fields and most have taken the opportunity to produce a comprehensive assessment of the present state of their subject This, as much as anything, should serve to ensure the success and value of the work as a whole, since it is likely to be some time before such a strong team will again feel tempted to review their topics at length and in unison In the present climate of recession and austerity it would be surprising if there were many who felt inclined to buy this work for themselves, they need feel no guilt, however, about persuading their librarians to make the investment □

G J Dockray is Reader in Physiology at the University of Liverpool

---

Cladistics clarified

Alan J. Charig

Phylogenetics The Theory and Practice of Phylogenetic Systematics By E O Wiley Pp 439 ISBN 0-471-05975-7 (Wiley 1981) £27 75, $49 90

WILLI Hennig is rightly regarded as the father of phylogenetic systematics, his book, *Phylogenetic Systematics* (University of Illinois Press, 1966) is the fundamental source of this important approach towards the reconstruction of evolutionary history and the classification of living organisms It is therefore appropriate that Wiley's new book on this subject should use a photograph of Hennig as its frontispiece During the last decade of Hennig's life (he died in 1976) the school of thought which he had founded — now loosely referred to as "cladistics" — attracted an ever-increasing volume of attention and comment

Within the last couple of years, however, the Hennigian school has sprouted the new, very different and even more controversial offshoot, "transformed cladistics" ("natural order systematics" in my terminology) The works of Popper on the philosophy of science undoubtedly exerted a major influence upon this schismatic development during its prolonged gestation, but Popper himself seems to have rejected it subsequently Indeed, were Father Hennig still alive today he too would have rejected it wholeheartedly, his arch-opponents would have been, not Mayr and Simpson, but leading transformed cladists like Nelson and Patterson

The approach of the transformed cladists is essentially typological, they maintain that there is a "natural order" in living things, manifesting itself in their aggregate similarity and not requiring to be interpreted as the result of evolution. They believe that time, evolution, genealogical relationships, the fossil record and the possibility of homoplasy have no part to play in systematics. Thus their philosophy is the absolute antithesis of Hennig's or Wiley's, in which — as is implied by the name phylogenetic systematics — phylogeny occupies a central position. Nothing could be more misleading than the recent pronouncement of a transformed cladist that Hennigian cladistics is merely "transformed cladistics with an evolutionary veneer". Contrary to general belief, the battle today is not between cladists and non-cladists but between transformed cladists on the one hand and, on the other, all those — be they followers of Hennig or of Mayr and Simpson — who maintain that the classification of living organisms should be based, wholly or at least in considerable part, upon the phylogeny.

Wiley is unashamedly an evolutionary or Hennigian cladist, he does not even mention transformed cladistics, for the very good reason that he must have written his book just before the new development made its overt appearance. On p. 98 he makes brief reference to the ideas of some workers, *circa* 1977, which foreshadowed the emergence of the new school, there is nothing more. Thus the volume reviewed here, unlike so much recent publication on the subject of cladistics, is concerned solely with Hennigian, i.e. evolutionary or phylogenetic cladistics.

Within that unavoidable limitation the book is first-class and might well be described as the evolutionary cladist's vade-mecum. The central part of the text is organized into five chapters — "Species and Speciation", "Supraspecific Taxa", "Phylogenetic Trees", "Characters and Reconstruction of Phylogenies" and "Phylogenetic Classification". The introduction which precedes it includes a great number of useful definitions clearly explained (although I myself do not agree with all of them) and discusses briefly the relationship of philosophy to systematics and the various approaches to scientific reasoning. Of the later chapters in the book, the first deals critically with the other major systems of taxonomy, the remainder are concerned with biogeography, specimens and curation (even a few pages on field-work and a couple of paragraphs on computer cataloguing), characters and their quantitative analysis, and publication and the Rules of Nomenclature. Bibliography and index run to over 18 pages each, the former providing an invaluable entrée into the literature.

The whole is arranged, set out and written with admirable clarity in excellent English. Compared with Hennig's exposition, Wiley's book is easy to find one's way around in; a remarkable amount of information and commentary on a comprehensive range of subjects is skilfully compressed into a limited amount of space, yet the author still manages to illustrate and emphasize his points by the extensive use of practical examples. Typographical errors are few. The book, nevertheless, is not without its faults. Thus the important aspect of cladistic analysis which everyone else (as far as I know) refers to as "polarity" is never called by that name and it took me a long time to track it down under the heading "Auxiliary criteria of phylogenetic apomorphy". Certain sections of the book with a mathematical flavour (for example those on Wagner algorithms and quantitative character analysis) were virtually incomprehensible to me, but that surely reflects my own innumeracy rather than any failing on the part of the author.

One of the most refreshing aspects of the book is that Wiley, although obviously a committed evolutionary cladist himself, does not assume the quasi-evangelical attitude so often adopted by his fellow cladists. (Just for the record, I myself am a firm believer in the rigour of a cladistic approach to phylogeny reconstruction but am strongly opposed to a purely cladistic classification.) Further, even more than the many other cladists who show healthy divergences of opinion on various points of doctrine, Wiley is no slavish follower of the majority, he shows a sturdy independence of thought, sometimes going so far as to recant on earlier statements of his own. Thus, unusually, he now accepts not only the postulation of ancestral species but also the possibility of occasionally recognizing them and of testing their hypothesized relationships.

I could make dozens of comments on this book, many of them highly favourable, but here are three of the other sort. First, perhaps because I am a palaeontologist, I deplore Wiley's uncompromising rejection of phyletic speciation into palaeospecies (allochronous speciation) and his consequent acceptance of each entire lineage as one species, irrespective of the amount of anagenetic change. (I note with pleasure, however, that Wiley — unlike Hennig — does not insist that the next dichotomy must inevitably terminate the species.) Secondly, I think it a great pity that he missed this opportunity to sort out the fearful confusion regarding the terms monophyly, polyphyly, holophyly and paraphyly once and for all — it is really so simple. And thirdly, I disagree with him profoundly on the alleged weaknesses of "evolutionary" (i.e. Simpsonian) taxonomy.

Notwithstanding such comments, I still feel that if a systematist were to be allowed only one work of reference on his desert island, he could not do better than choose Wiley's *Phylogenetics*. ☐

Alan Charig is Chief Curator of Fossil Amphibians, Reptiles and Birds at the British Museum (Natural History).

The Basel network

J.H. Humphrey

The Immune System, Vols 1 and 2. Edited by C. M. Steinberg and I. Lefkovits. Vol. 1 *Past and Future*, pp. 440, ISBN 3-8055-3407-8; Vol. 2 *The Present*, pp. 472, ISBN 3-8055-3408-6. (Karger: 1981.) Vol. 1 DM 297, SwFr 248, $148.50; Vol. 2 DM 321, SwFr 268, $160.50.

THESE two volumes comprise 125 essays written as a *Festschrift* for Niels Kai Jerne. They are a tribute not only to his seventieth birthday but also to his directorship of the Basel Institute of Immunology during its first ten years. The essays range from philosophical consideration of neurological processes and of art, through critical examinations of various current and earlier immunological hypotheses, to summaries of new experimental findings, mainly discussed in relation to their bearing on Jerne's own theories. Some are written by old friends and colleagues from his days in Copenhagen, Pasadena, Geneva, Pittsburgh and Freiburg, before he came to Basel, but the great majority are by colleagues who were members, students, visitors or even advisers at the Basel Institute.

The attraction of working at Basel was very great, since Jerne's policy was to have only a small core of permanent members but a much larger number of able, mostly young immunologists from all over the world for anything from six months to five years. He had a flair for choosing persons with talent who would return to work in lively departments elsewhere, and thus the list of contributors to the books reads rather like a selection from an immunological *Who's Who*. Most of them evidently felt challenged to write something original which would amuse or interest Jerne himself as well as any potential readership.

The outcome is as much as anything a view of the immune system as seen from Basel. Here the focus has been on the basic problems of how the immune system recognizes self from not-self, and how there arises the immense variety of different antibodies and receptors on T-lymphocytes which a frog or a mouse or a human being can make. This has involved study of the structure of monoclonal antibodies (initially from myelomas but later from hybridomas also) and of the mechanisms of their assembly and secretion, development of greatly improved culture methods, which made it possible to measure the number of lymphocytes able to respond to any given antigen, or to make immunoglobulin (Ig) in response to polyclonal mitogens, and, when cloning of DNA and DNA sequence studies became possible, comparison of the genes controlling the synthesis of specific antibodies with each other and with corresponding genes in the fetus, which led in Basel and elsewhere to the recognition of three separate genes controlling the variable region of Ig Since similar studies on the receptors of T-lymphocytes are frustrated by the difficulty of identifying, let alone purifying T-cell receptors, the variety of T-cells had to be approached by functional assays *in vitro* (mainly the generation of cytotoxic cells but also of helper and suppressor cells) using the improved culture methods developed in Basel to permit enumeration of single cells by limiting dilution assays Faith and hope are now being pinned on T-cell clones, with recognizable specificities, as a source of receptors which can be isolated and sequenced, with the aim of eventually identifying the genes controlling them and so discovering their relationship to the genes controlling Ig and the Ir region of the major histocompatibility complex

When, in 1974, Niels Jerne put forward the network hypothesis (which states that for every specific antibody or T-cell receptor which has a distinct combining site (idiotype), the immune system is likely to contain cells able to recognize that idiotype and, in principle, to respond by making more anti-idiotype — which in turn can stimulate cells making anti-anti-idiotype etc , and so establish an infinite network of interactions), some of his colleagues put it to the test. They found that in the special circumstance when mice respond to a bacterial antigen by making antibodies with predominantly a single idiotype, specific anti-idiotype antibodies could either stimulate or suppress antibody formation against the original antigen The network hypothesis was thus shown to have at least one real mesh, subsequent work on idiotypes has established several more, and a fair amount of the work going on in Basel (and of the more speculative essays in these volumes) is orientated towards the network hypothesis However since the Institute has a horizontal structure, in the sense that in principle no scientist can tell any other scientist what to do, aspects of immunology which profoundly affect the practical outcome of antigenic stimulation — such as lymphocyte recirculation and the role of macrophages — are also studied there, even though Jerne thought them irrelevant to the basic questions which he hoped to see answered

The volumes contain essays on all of these subjects, and even some rather good ones on non-specific factors, such as complement, by scientific advisers who reckoned that Jerne should recognize that they also are important The more speculative essays, with few or even no references, are included in the first volume and the harder science in the second

It may reasonably be asked what a collection of this nature has to offer to persons outside the charmed circle of Jerne's associates Since the contributors felt challenged to write something original, and since free speculation was encouraged and the personalities of the authors show through in their writing, the collection provides enough stimulation to satisfy any reasonably knowledgeable immunologist It would take a keen seeker after enlightenment to read through all of the 900 odd pages, but since the editors have grouped the essays under subject headings, selective browsing is quite possible I would expect to recognize the striking dust jacket (by Jean Tinguely) on train and aeroplane journeys, and even at the bedside □

J H Humphrey is a Professor in the Department of Medicine at the Royal Postgraduate Medical School, University of London

The second volume of *Elsevier's Dictionary of Botany*, edited by Paul Macura, has recently been published by Elsevier Scientific (For review of Vol I, *Plant Names*, see *Nature* **284**, 382, 1980) Volume II, *General Terms*, contains some 10,000 entries of English, French and German terms used in botany and associated disciplines, and includes French, German and two Russian indexes, one numerical and the other alphabetical The book costs Dfl 260, $110 75

Down and beyond the composite particle

M.G. Albrow

Jets of Hadrons. By W Hofmann Pp 210 ISBN 3-540-10625-1/0-387-10625-1 (Springer-Verlag 1981) DM 62, $28 20

THE study of strongly interacting particles (protons, neutrons, pions etc) and the forces between them is no longer frontier physics We have passed beyond and down to the next layer It has become established beyond any reasonable doubt that these so-called particles are not elementary at all, but composites of more fundamental constituents The main effort in high-energy physics is now directed towards studying these constituents and the forces between *them* A vast amount of experimental information is all consistent with a theoretical framework describing these constituents as fractionally charged quarks and antiquarks which bind together by exchanging electrically neutral gluons These entities seem to be at the same level of elementarity as electrons, muons, neutrinos and photons, yet the latter are freely observed unlike quarks and gluons One can do an experiment (for example scatter a high-energy muon through a known large angle on a proton) which should produce a quark with a known energy and direction No quark is seen, always a shower of normal composite particles (hadrons) such as pions, kaons and so on Try harder by increasing, to the limit of present accelerators, the energy of the muon or the angle of scatter, and the showers become more collimated They are known as jets of hadrons

Our theoretical outlook has changed so much and the amount of experimental information has grown so rapidly in recent years that Hofmann's review of the field is extremely welcome To illustrate this rapid development most of the 400 papers in the reference list have been published in the past four years In such a situation the author must of course take the risk that the book becomes quickly dated If it does, I suspect that it will be due to the availability of more (and more precise) experimental data rather than to the concepts and the formalism becoming outdated

The book "is intended to give an introductory review to the phenomenon of jets in hadronic final states ", and the author succeeds admirably in fulfilling this intention Starting from the simplest situation of e^+e^- annihilation (where the massive virtual photon produced by the annihilation transforms to a $q\bar{q}$-pair, which in turn materializes as two jets), he leads the reader through jets in parton models and their development as quantum chromodynamics (the theory of quark–gluon forces) to the more complicated processes of hadron–hadron collisions A chapter on the old "uncorrelated jet model" and one on "soft" hadronic collisions are useful reminders of the importance of phase space effects and four momentum conservation, and also that while theory has a long way to go in describing the most common collisions there is encouraging progress in that direction

It is a pity that the author was not prepared to address the question of future developments Now that proton–antiproton collisions are being studied at CERN at energies nearly ten times higher than previously available at the ISR, and that LEP has received approval to study high-energy electron–positron collisions, a discussion of expectations for future experiments would have been a useful addition Nonetheless, this review is sufficiently detailed and complete that theorists working in the field will find it a valuable guide to the existing experimental data, and experimentalists will appreciate the exposition of the theoretical ideas It is, however, written at a level such that graduate students in high-energy physics should not find it too heavy-going, and it will familiarize them with what may well remain a major topic in the subject over the next decade □

M G Albrow, currently at CERN, is a Research Physicist at the Rutherford Appleton Laboratory, Chilton, Oxfordshire

nature

Author Index for Volume 293

November — December 1981

Issue no	Issue date	Page nos
5836	5 November	1–98
5837	12 November	99–196
5838	19 November	197–294
5839	26 November	295–388
5840	3 December	389–502
5841	10 December	503–598
5842	17 December	599–680
5843	24/31 December	681–786

Abramowicz M A Innermost parts of accretion disks are thermally and secularly stable **294,** 235
Ackers G K *see under* Johnson A D , **294,** 217
Adams C J Migration of late Cenozoic volcanism in the South Island of New Zealand and the Campbell Plateau **294,** 153
Adams J F Room for Anon *correspondence* **294,** 204
Adelstein R S Calcium and calmodulin in Kyoto, *news and views* **294,** 693
Agris P *see under* Munz P **294,** 187
Akagi T *see under* Miyoshi I **294,** 770
Albrecht P *see under* Hussler G **294,** 556
Aldissi M *see under* Rolland M **294,** 60
Allegre C J *see under* Dupre B **294,** 552
Allègre C J , Provost A and Jaupart C Oscillatory zoning a pathological case of crystal growth **294,** 223
Allen D A and Wickramasinghe D T Diffuse interstellar absorption bands between 2 9 and 4 0 μm **294,** 239
Aller H D *see under* Mutel R L **294,** 236
Alvarez W and Lowrie W Upper Cretaceous to Eocene pelagic limestones of the Scaglia Rossa are not Miocene turbidites, **294,** 246
Ambler R P *book review of* Biochemical Evolution, (Gutfreund H *editor*) **294,** 382
Anderson T F and Steinmetz J C Isotopic and biostratigraphical records of calcareous nannofossils in a Pleistocene core, **294,** 741
Anderton R Lower Palaeozoic oceans and Wilson cycles—Reply, *matters arising* **294,** 289
Andrews J *book review of* Countryside Conservation The Protection and Management of Amenity Ecosystems (Green B) **294,** 40
  book review of Estuary Birds of Britain and Ireland (Prater A J) **294,** 500
  book review of Farming and Wildlife (Mellanby K) **294,** 40
  book review of Introduced Birds of the World (Long J) **294,** 500
  book review of The Bird Seeker's Guide (Gooder J) **294,** 500
  book review of The Birdwatcher's Dictionary (Weaver P) **294,** 500
Andrieux J *see under* Tapponnier P **294,** 405
Angus J A and Korner P I Presence and physiological role of presynaptic inhibitory α adrenoreceptors in guinea pig atria—Reply *matters arising* **294,** 671
Anilionis A , Wunner W H and Curtis P J Structure of the glycoprotein gene in rabies virus **294,** 275
Armijo R *see under* Tapponnier P , **294,** 405
  see under Tapponnier P **294,** 410
Arnheiter H , Thomas R M , Leist T , Fountoulakis M and Gutte B Physicochemical and antigenic properties of synthetic fragments of human leukocyte interferon **294,** 278
Arnold F Solvated electrons in the upper atmosphere **294,** 732
  see under McCrumb J L , **294,** 136
Arp B *see under* Storb U **294,** 90
Arthur A *see under* Sherratt D , **294,** 608
Ashby E. *book review of* Reflections on Science and the Media, (Goodfield J) **294,** 33
  What did you read during 1981? **294,** 483
Asimov I What did you read during 1981? **294,** 484
Atkins P W The Creation *book review by* Barrow J D **294,** 595
Aubouin J , Stephan J F , Renard V , Roump J and Lonsdale P Subduction of the Cocos plate in the Mid America Trench **294,** 146
Bach F H *see under* Widmer M B **294,** 750
Baglioni C *see under* Branca A A **294,** 768
Bailey M E and Hale C J Anomalous magnetic directions recorded by laboratory induced chemical remanent magnetization, **294,** 739
Ball I R *book review of* Systematics and Biogeography Cladistics and Vicariance (Nelson G and Platnick N) **294,** 675
  book review of Vicariance Biogeography A Critique, (Nelson G and Rosen D E *editors*) **294,** 675
Baltimore D *see under* Ross A H **294,** 654
Barbee T W Jr *see under* Underwood J H , **294,** 429
Barnes P *book review of* Intermolecular Forces Their Origin and Determination (Maitland G C Rigby M , Smith E B , Wakeham W A) **294,** 384
Baron R L *see under* Elliot J L , **294,** 526
Barraclough D R The 1980 geomagnetic reference field, *news and views* **294,** 14
Barrett J C *see under* Parry J M , **294,** 263
Barrow J D *book review of* The Creation, (Atkins P W) **294,** 595
Bassani L. and Dean A J Absorption of γ rays in active galaxies as a test of the jet hypothesis **294,** 332
Bassoullet J P *see under* Tapponnier P , **294,** 405
Batten D J., Brown P E , Dawes P R , Higgins A K , Koch B E , Parsons I and Soper N J Peralkaline volcanicity on the Eurasia Basin margin **294,** 150
Battey J F *see under* Porter J W , **294,** 249
Beatty J K *et al* *Editors* The New Solar System, *book review by* Hughes D W **294,** 21
Beavan R J *see under* McNutt S R , **294,** 615
Beazley M and Simon & Schuster The International Book of the Forest *book review by* Mitchell A **294,** 496
Beddard G S , Doust T and Hudales J Structural features in ethanol–water mixtures revealed by picosecond fluorescence anisotropy **294,** 145
Bedini S A *book review of* Collecting Microscopes, (Turner G L 'E) **294,** 492
  book review of The Camera Obscura A Chronicle (Hammond J H) **294,** 492
Belintsev B N *see under* Gagua A V , **294,** 662
Bentzel C J *see under* Duffey M E , **294,** 451
Berg P *see under* Lee F , **294,** 228
Bernier P *see under* Rolland M **294,** 60
Bertram B *book review of* Saving the Tiger, (Mountfort G) **294,** 42
Bevan M J *see under* Hunig T **294,** 460
Beverley P C L. *see under* Fischer A **294,** 166
Bevins R E *see under* Green H S , **294,** 707
Beynon J L. *see under* Buchanan-Wollaston V , **294,** 776
Bickle T A *see under* Iida S , **294,** 374
Bienz M and Kubli E Wild type tRNA$_{G}^{Tyr}$ reads the TMV RNA stop codon but Q base modified tRNA$_{Q}^{Tyr}$ does not **294,** 188
Birnstiel M L *see under* Galli G , **294,** 626
  see under Grosschedl R , **294,** 178
Bitensky M W *see under* Rasenick M M , **294,** 560
Blacksell M and Gilg A W The Countryside Planning and Change, *book review by* Williams D G T **294,** 677
Blakeley A G H , Brown D A , Cunnane T C , French A M , McGrath J C and Scott N C Effects of nifedipine on electrical and mechanical responses of rat and guinea pig vas deferens **294,** 759
Blinkhorn S *book review of* Straight Talk about Mental Tests (Jensen A R) **294,** 501
Bloemendal H *Editor*, Molecular and cellular biology of the eye lens, *book review by* Slingsby C **294,** 782
Blumenthal R *see under* Dragsten P R , **294,** 718
Bode H R *see under* Fraser S E , **294,** 356
Boedtker H *see under* Wozney J **294,** 129
Boggs D H *see under* Jones W L , **294,** 704
Boland J N and Duba A Solid-state reduction of iron in olivine planetary and meteoritic evolution, **294,** 142
Bolle B Barometers, *book review by* Hackmann W D **294,** 491
Bond M *see under* Somlyo A V , **294,** 567
Borchers R *see under* Fabian P , **294,** 733
Borthwick J *see under* McNaughton N J , **294,** 639
Bowery N G *see under* Wilkin G P , **294,** 584
Bracalente E M *see under* Jones W L , **294,** 704
Braddick O *book review of* Direct Perception, (Michaels C F and Carello C) **294,** 598
Braestrup C and Nielsen M GABA reduces binding of ^{3}H-methyl β-carboline-3-carboxylate to brain benzodiazepine receptors, **294,** 472
Bramwell M E *see under* White M K **294,** 232
Branca A A and Baglioni C Evidence that types I and II interferons have different receptors, **294,** 768
Brandenburger A , Godson G N , Radman M , Glickman B W , van Sluis C A and Doubleday O P Radiation-induced base substitution mutagenesis in single stranded DNA phage M13, **294,** 180
Brent P Charles Darwin A man of Enlarged Curiosity, *book review by* Cain A J **294,** 781
Bricker O P *see under* Olsen C R **294,** 242
Briles D E , Claflin J L., Schroer K and Forman C Mouse IgG3 antibodies are highly protective against infection with *Streptococcus pneumoniae*, **294,** 88
Brimacombe R Secondary structure and evolution of ribosomal RNA *news and views* **294,** 209
Brittain A *see under* Folsome C E , **294,** 64
Brodhead M J *see under* Cutright P R , **294,** 497
Brokie K Wildlife Sketchbook *book review by* Halliday T R **294,** 502
Brookes J R V *book review of* Petroleum geology of the Continental Shelf of North-West Europe, 1981, (Illing L V and Hobson G D *editors*) **294,** 782
Brooks C K *see under* Koul S L **294,** 347
Brooks D E *see under* Larsen F L **294,** 667
Brosius J *see under* Talmadge K , **294,** 176
Broster M G *see under* Manchee R J , **294,** 254
Brown D A *see under* Blakeley A G H , **294,** 759
Brown J W S *see under* Matthews J A **294,** 175
Brown P E *see under* Batten D J , **294,** 150
Brown R A *see under* Jones W L , **294,** 704
Bruce-Chwatt L J Malaria debated, *correspondence* **294,** 302
Brunel M *see under* Tapponnier P , **294,** 405
Bryant P E *book review of* Hans Eysenck The Man and His Work (Gibson H B) **294,** 44
Buchanan-Wollaston V , Cannon M C , Beynon J L. and Cannon F C Role of the *nifA* gene product in the regulation of *nif* expression in *Klebsiella pneumoniae*, **294,** 776
Buckerman B Extraterrestrials — where are they? *news and views* **294,** 10
Bull P *see under* Green H S **294,** 707
Bunn P A *see under* Kalyanaraman V S , **294,** 271
Burg J P *see under* Tapponnier P **294,** 405
Burgess D D A spectrum of achievements *news and views* **294,** 111
Burl A Rites of the Gods, *book review by* Piggott S **294,** 487
Burridge K Are stress fibres contractile? *news and views* **294,** 691
Burridge K and Feramisco J R Non muscle α-actinins are calcium-sensitive actin-binding proteins, **294,** 565
Burrough P A Fractal dimensions of landscapes and other environmental data, **294,** 240
Busath D and Szabo G Gramicidin forms multi-state rectifying channels, **294,** 371
Businger J A *see under* Guymer T H , **294,** 735
Butler T M *see under* Somlyo A V **294,** 567
Byfield J E and Calabro-Jones P M Carrier-dependent and carrier-independent transport of anti cancer alkylating agents, **294,** 281
Bynum W F *book review of* The Doctrine of the Nerves Chapters in the History of Neurology, (Spillane J D) **294,** 381
Bynum W F *et al* *Editors*, Dictionary of the History of Science *book review by* Cardwell D **294,** 493
Cadene M *see under* Rolland M **294,** 60
Cain A J *book review of* Charles Darwin A man of Enlarged Curiosity, (Brent P) **294,** 781
  book review of The Roving Naturalist Travel Letters of Theodosius Dobzhansky, (Glass B *editor*) **294,** 43
Calabro-Jones P M *see under* Byfield J E , **294,** 281
Campbell C L. The Fischer–Smith Controversy Are There Bacterial Diseases of Plants? *book review by* Heathcote G D **294,** 37
Campbell P Mars, *news and views leading article* **294,** 303
Campbell P N *Editor*, Biology in Profile A Guide to Many Branches of Biology, *book review by* Scott P R **294,** 496
Cann J R Which direction for ocean drilling? *news and views* **294,** 613
Cannon F C *see under* Buchanan-Wollaston V , **294,** 776
Cannon M C *see under* Buchanan-Wollaston V , **294,** 776
Capco D G and Jeffery W R Regional accumulation of vegetal pole poly(A)$^{+}$RNA injected into fertilized *Xenopus* eggs **294,** 255
Cardwell D *book review of* Dictionary of the History of Science (Bynum W F *et al* *editors*) **294,** 493
Carello C *see under* Michaels C F , **294,** 598
Carlock L and Jones N C Synthesis of an unspliced cytoplasmic message by an adenovirus 5 deletion mutant, **294,** 572
Carr M H Martian geology, *news and views* **294,** 307
Cartica R J *see under* Tjepkema J D , **294,** 445
Casimir H B G *book review of* The Physicists, (Snow C P) **294,** 26
Cassuto E *see under* West S C , **294,** 659
Cavalieri L F The Double-Edged Helix, *book review by* Stent G S **294,** 30
Celâl Sengor A M The geological exploration of Tibet *news and views* **294,** 403
Cesareni G *see under* Lacatena R M **294,** 623
Chadderton L T *see under* Koul S L **294,** 347
Chaisson E Cosmic Dawn The Origins of Matter and Life,

book review by Noble Wilford J **294,** 491
Chambon P *see under* Grosschedl R , **294,** 178
Chang S *see under* Folsome C E , **294,** 64
Chapin G *see under* Wasserstrom R , **294,** 388
Chappe B *see under* Hussler G **294,** 556
Chelton D B., Hussey K J and Parke M E Global satellite measurements of water vapour, wind speed and wave height, **294,** 529
Chen K K *see under* Rice-Ficht A C , **294,** 53
Chen R and Kirsh Y Analysis of Thermally Stimulated Processes, *book review by* Garlick G F J **294,** 294
Chenfa C *see under* Tapponnier P , **294,** 405
Cheung D W Pulmonary vein as an ectopic focus in digitalis-induced arrhythmia, **294,** 582
Christiansen P J *see under* Horne R B , **294,** 338
see under Ronnmark K , **294,** 335
Claflin J L. *see under* Briles D E , **294,** 88
Clark D A new view of supernova remnants in the Magellanic clouds *news and views* **294,** 690
Clark D H *see under* Murdin P **294,** 543
Clark J D *book review of* A Short History of Archaeology, (Daniel G) **294,** 45
book review of Antiquity and Man Essays in Honour of Glyn Daniel, (Evans J D *et al editors*) **294,** 45
Clausen H B *see under* Risbo T , **294,** 637
Clifford P *see under* Knowlton N , **294,** 251
Cobbold P H *see under* Cuthbertson K S R , **294,** 754
Cocchia D , Michetti F and Donato R Immunochemical and immunocytochemical localization of S-100 antigen in normal human skin, **294,** 85
Cohen M In Quest of Telescopes, *book review by* Maran S P **294,** 490
Cohen S , Knoll B J , Little J W and Mount D W Preferential cleavage of phage λ repressor monomers by *recA* protease, **294,** 182
Colchen M *see under* Tapponnier P , **294,** 405
Cole G T and Kendrick B ***Editors,*** Biology of conidial fungi, *book review by* Ingold C T **294,** 784
Coleman W *book review of* The Founders of Science at the British Museum, 1753–1900, (Gunther A E) **294,** 18
book review of The Natural History Museum at South Kensington A History of the British Museum (Natural History) 1753–1980, (Stearn W T) **294,** 18
Coles L S *see under* Harvey R P , **294,** 49
Collcutt S N *see under* Green H S , **294,** 707
Collins P Q Gold standard, *correspondence* **294,** 8
Colquhoun D , Neher E , Reuter H and Stevens C F Inward current channels activated by intracellular Ca in cultured cardiac cells, **294,** 752
Colquhoun D and Sakmann B Fluctuations in the microsecond time range of the current through single acetylcholine receptor ion channels, **294,** 464
Compston W *see under* McCulloch M T , **294,** 322
Condeelis J S *see under* Salisbury J L , **294,** 163
Conway R G , Davis R J , Foley A R and Ray T P Radio jet of 3C273, **294,** 540
Cook C *see under* Whittle T , **294,** 494
Cook N G W Geomechanics in the laboratory, *news and views* **294,** 213
Cooke R Stress does not alter the conformation of a domain of the myosin cross bridge in rigor muscle fibres, **294,** 570
Cornell J The First Stargazers, *book review by* Ruggles C **294,** 485
Costantini F and Lacy E. Introduction of rabbit β-globin gene into the mouse germ line, **294,** 92
Cottam D A *see under* Proctor J , **294,** 245
Cowey A *see under* Somogyi P , **294,** 761
Cowley C R and Rice J B HR 465 returning to rare-earth-maximum phase, **294,** 636
Cox B *book review of* The Terrestrial Environment and the Origin of Land Vertebrates, (Panchen A L *editor*) **294,** 194
Cox F E G Hybridoma technology identifies protective malaria antigens, *news and views* **294,** 612
Parasites affect behaviour of mice, *news and views* **294,** 515
Craddock V M Environmental nitrosamines and cancer, *news and views* **294,** 694
Craig I J D and McClymont A N Are coronal loops stable? **294,** 333
Creeth J M *book review of* Protein-Protein Interactions, (Frieden C and Nichol L W *editors*) **294,** 384
Crittenden L. B *see under* Noori-Daloii M R **294,** 574
Croce C M *see under* Erikson J , **294,** 173
Crowson R A The Biology of the Coleoptera, *book review by* Evans M E G **294,** 597
Cruz Y P A sterile defender morph in a polyembryonic hymenopterous parasite, **294,** 446
Cunnane T C *see under* Blakeley A G H **294,** 759
Currant A P *see under* Gascoyne M , **294,** 652
see under Green H S **294,** 707
Curtis C F Malaria debated, *correspondence* **294,** 388
Curtis P J *see under* Anilionis A , **294,** 275
Cuthbertson K S R , Whittingham D G and Cobbold P H Free Ca^{2+} increases in exponential phases during mouse oocyte activation **294,** 754
Cutright P R and Brodhead M J Elliott Coues Naturalist and Frontier Historian *book review by* White C M **294,** 497
Cutshall N H *see under* Olsen C R , **294,** 242
Dalla Favera R *see under* Wong-Staal F , **294,** 273
Dallmeyer D G *see under* Porter J W **294,** 249
Daniel G A Short History of Archaeology, *book review by* Clark J D **294,** 45
What did you read during 1981? **294,** 483
Darnbrough C H , Goddard J P and Stevely W S Creationism *correspondence* **294,** 302
Daune M P *see under* Fuchs R P P , **294,** 657
Davies D *book review of* Cosmos and Creator, (Jaki S L) **294,** 677
Davies P The Edge of Infinity, *book review by* Press W H **294,** 488
What did you read during 1981? **294,** 483
Davis R J *see under* Conway R G , **294,** 540
Dawes P R. *see under* Batten D J , **294,** 150
Day D The Doomsday Book of Animals A Natural History of Vanished Species *book review by* Turner B D **294,** 499
De Mey J *see under* Probert L , **294,** 470
Dean A J *see under* Bassani L , **294,** 332
Dean D *see under* Yates J L , **294,** 190
Debenham N *see under* Green H S , **294,** 707
Dellinger E. P *see under* Welch R A , **294,** 665
Demaille J G *see under* Huchon D , **294,** 358
Denman K L and Gower J F R Satellite sensed turbulent ocean structure—Reply, *matters arising* **294,** 673
Derry R The Art of Robert Bateman *book review by* Halliday T R **294,** 502
Diakun G *see under* Greaves G N , **294,** 139
Dickin A P Hydrothermal leaching of rhyolite glass in the environment has implications for nuclear waste disposal, **294,** 342
Dikii L A., Freiman G A , Freidlin M I , Irlin I S , Vasilevsky A L., Reitman M I , Katz S A , Medvedkov Ya V , Godyak V A and Soyfer V N Voices from a wilderness *correspondence* **294,** 688
Diringer H *see under* Museteanu C , **294,** 360
Dixon D After Man A Zoology of the Future, *book review by* Turner B D **294,** 499
Dlouhá H *see under* Fyskočil F , **294,** 288
Domingo D L. *see under* Trowbridge I S , **294,** 171
Donato R *see under* Cocchia D **294,** 85
Donelson J E *see under* Rice-Ficht A C , **294,** 53
Donoghue J F *see under* Olsen C R , **294,** 242
Doty P *see under* Wozney J , **294,** 129
Doubleday O P *see under* Brandenburger A , **294,** 180
Doust T *see under* Beddard G S , **294,** 145
Dragsten P R , Blumenthal R and Handler J S Membrane asymmetry in epithelia is the tight junction a barrier to diffusion in the plasma membrane? **294,** 718
Drazin P G and Reid W H Hydrodynamic Stability *book review by* Roberts P H **294,** 196
Drummond J R and Mutlow C T Satellite measurements of H_2O fluorescence in the mesosphere, **294,** 431
Duba A *see under* Boland J N , **294,** 142
Duffey M E , Hainau B , Ho S and Bentzel C J Regulation of epithelial tight junction permeability by cyclic AMP **294,** 451
Dunham E *see under* Elliot J L , **294,** 526
Dupre B *see under* Nicolas A , **294,** 414
see under Tapponnier P , **294,** 405
Dupre B , Lambret B , Rousseau D and Allègre C J Limitations on the scale of mantle heterogeneities under oceanic ridges, **294,** 552
Durham P J *see under* Greaves G N , **294,** 139
D'Urso M *see under* Persico M G , **294,** 778
Dwyer F G *see under* Schlenker J L , **294,** 340
Dyer J The Penguin Guide to Prehistoric England and Wales *book review by* Whitehouse R D **294,** 486
Dyson P *see under* Sherratt D , **294,** 608
Eastwood J W *see under* Hockney R W **294,** 293
Edwards D Postdocs in Canada, *correspondence* **294,** 396
Edwards R G Conception in the human female *book review by* Short R V **294,** 784
Egelman E Problem of light piping in immunofluorescence studies, *matters arising* **294,** 674
Ehrlich A *see under* Ehrlich P , **294,** 41
Ehrlich P and Ehrlich A Extinction The Causes and Consequences of the Disappearance of Species *book review by* Mellanby K **294,** 41
Eiferman F A., Young P R , Scott R W and Tilghman S M Intragenic amplification and divergence in the mouse α-fetoprotein gene **294,** 713
Eisen H N *see under* Ross A H , **294,** 654
Elias J H *see under* Elliot J L , **294,** 526
Elliot J L , Mink D J , Elias J H , Baron R L , Dunham E , Pingree J E , French R G , Liller W , Nicholson P D , Jones T J and Franz O G No evidence of rings around Neptune **294,** 526
Elliott S R Order or disorder in the structures of glass? *news and views* **294,** 692
Embleton C *see under* Green H S , **294,** 707
Emmerson P T *see under* Hickson I D , **294,** 578
Epstein C J *see under* Sawicki J A , **294,** 450
Erdman E , Krawietz W , Hackbarth I , Schmitz W and Scholz H Importance of cardiac cell membranes in vanadate induced NADH oxidation, *matters arising* **294,** 288
Erikson J , Martinis J and Croce C M Assignment of the genes for human λ immunoglobulin chains to chromosome 22, **294,** 173
Erikson R L *see under* Gilmer T M , **294,** 771
Etters R D *see under* Raich J C , **294,** 513
Evans D S *book review of* Cosmic Discovery The Search, Scope, and Heritage of Astronomy, (Harwit M) **294,** 22
Evans J D ***et al Editors,*** Antiquity and Man Essays in Honour of Glyn Daniel, *book review by* Clark J D **294,** 45
Evans M E G *book review of* The Biology of the Coleoptera (Crowson R A) **294,** 597
Fabian P , Borchers R , Penkett S A and Prosser N J D Halocarbons in the stratosphere, **294,** 733
Fairhurst A and Soothill E Blandford Guide to Trees of the British Countryside, *book review by* Mitchell A **294,** 495
Falk G *see under* Shiells R A **294,** 592
Falkow S *see under* Welch R A , **294,** 665
Fallick A E *see under* McNaughton N J , **294,** 639
Fanale F P Mars climate change where are the petroglyphs? *news and views* **298,** 308
Farlow J O Estimates of dinosaur speeds from a new trackway site in Texas, **294,** 747
Farquhar M *see under* Partridge L , **294,** 580
Feild J A *see under* Ruscetti S K , **294,** 663
Feldmann M *see under* Fischer A , **294,** 166
Feramisco J R *see under* Burridge K , **294,** 565
Fieldman G Psychological slip, *correspondence* **294,** 510
Fink G Has corticotropin-releasing factor finally been found? *news and views* **294,** 511
Fischer A , Beverley P C L and Feldmann M Long-term human T-helper lines producing specific helper factor reactive to influenza virus, **294,** 166
Fishel R A , James A A and Kolodner R *recA* independent general genetic recombination of plasmids, **294,** 184
Fisher L M DNA supercoiling by DNA gyrase, *news and views,* **294,** 607
Fitzgerald K *see under* Reinherz E L , **294,** 168
Foley A R *see under* Conway R G , **294,** 540
Folkers K *see under* Leander S , **294,** 467
Folsome C E , Brittain A , Smith A and Chang S Hydrazines and carbohydrazides produced from oxidized carbon in Earth's primitive environment, **294,** 64
Ford R J , Mehta S R , Franzini D , Montagna R , Lachman L B and Maizel A L Soluble factor activation of human B lymphocytes **294,** 261
Forman C *see under* Briles D E , **294,** 88
Forno I W *see under* Room P M **294,** 78
Fountoulakis M *see under* Arnheiter H , **294,** 278
Fox R *book review of* Gentlemen of Science Early Years of the British Association for the Advancement of Science (Morrell J and Thackray A) **294,** 19
Fox S W An acid test *correspondence* **294,** 688
Frank L. Leave links open *correspondence* **294,** 396
Franks F Polywater, *book review by* Ubell R **294,** 28
Franz O G *see under* Elliot J L , **294,** 526
Franzini D *see under* Ford R J , **294,** 261
Fraser S E and Bode H R Epithelial cells of *Hydra* are dye coupled, **294,** 356
Free S J *see under* Selker E U , **294,** 576
Freeman R R *see under* Holder A A , **294,** 361
Freidlin M I *see under* Dikii L A , **294,** 688
Freiman G A *see under* Dikii L A , **294,** 688
French A M *see under* Blakeley A G H , **294,** 759
French R G *see under* Elliot J L , **294,** 526
Freund T F *see under* Somogyi P , **294,** 761
Frieden C and Nichol L W ***Editors*** Protein-Protein Interactions, *book review by* Creeth J M **294,** 384
Friend C R L Charnockite and granite formation and influx of CO_2 at Kabbaldurga, **294,** 550
Fuchs R P P , Schwartz N and Daune M P Hot spots of frameshift mutations induced by the ultimate carcinogen *N* acetoxy-*N*-2-acetylaminofluorene, **294,** 657
Fujino K *see under* Ohtani E **294,** 62
Fukida J , Kameyama M and Yamaguchi K Breakdown of cytoskeletal filaments selectively reduces Na and Ca spikes in cultured mammal neurones **294,** 82
Fukushima Y Single channel potassium currents of the anomalous rectifier, **294,** 368
Fuxing W Sinian microfossils from south-west China **294,** 74
Fyskočil F , Dlouha H and Teisinger J Importance of cardiac cell membranes in vanadate induced NADH oxidation—Reply, *matters arising* **294,** 288
Gagua A V , Belintsev B N and Lyubchnko Y L Effect of base-pair stability on the melting of superhelical DNA, **294,** 662
Galli G , Hofstetter H and Birnstiel M L Two conserved sequence blocks within eukaryotic tRNA genes are major promoter elements, **294,** 626
Gallo R C *see under* Kalyanaraman V S **294,** 271
see under Poiesz B J , **294,** 268
see under Wong Staal F , **294,** 273
Galwey A K and Poppl L The role of liquid halogen in the reaction of crystalline KBr with gaseous Cl_2, **294,** 434
Gardner R. C *see under* Gronenborn B **294,** 773
Garfield E What did you read during 1981? **294,** 484
Garlick G F J *book review of* Analysis of Thermally Stimulated Processes (Chen R and Kirsh Y) **294,** 294
Gartland W J Jr NIH guidelines, *correspondence* **294,** 606
Gascoyne M , Currant A P and Lord T C Ipswichian fauna of Victoria Cave and the marine palaeoclimatic record **294,** 652
Geisow M J and Mas-Oliva J Receptors, channels and whole body NMR in Mexico *news and views* **294,** 400
Gelfand I M *see under* Vasiliev J M , **294,** 292
Gelmann E. P *see under* Wong-Staal F **294,** 273
Gerstl S A. W , Zardecki A and Wiser H L Biologically damaging radiation amplified by ozone depletions **294,** 352
Gibson H B Hans Eysenck The Man and His Work, *book review by* Bryant P E **294,** 44
Gilbert W *see under* Talmadge K **294,** 176
Gilg A W *see under* Blacksell M , **294,** 677
Gillmor R ***Editors,*** Sketches of Bird Life *book review by* Halliday T R **294,** 502
Gilmer T M and Erikson R L Rous sarcoma virus transforming protein, p60^{src}, expressed in *E coli*, functions as a protein kinase **294,** 771
Girardeau J *see under* Nicolas A , **294,** 414
see under Tapponnier P **294,** 405
Giuliano J A Lab animals, *correspondence* **294,** 8
Glass B ***Editor,*** The Roving Naturalist Travel Letters of Theodosius Dobzhansky, *book review by* Cain A J **294,** 43
Glickman B W *see under* Brandenburger A **294,** 180
Goddard J P *see under* Darnbrough C H **294,** 302
Godson G N *see under* Brandenburger A **294,** 180
Godyak V A *see under* Dikii L A **294,** 688
Goeddel D V *see under* Shepard H M **294,** 563
Goh K M *see under* Wilson M A , **294,** 648
Golden W T What did you read during 1981? **294,** 484
Goode A D T *see under* Gray C M **294,** 155
Gooder J The Bird Seeker s Guide *book review by* Andrews J **294,** 500
Goodfield J Reflections on Science and the Media, *book review by* Ashby E **294,** 33
What did you read during 1981? **294,** 484
Gough M P *see under* Horne R B , **294,** 338
Gould J Birds, *book review by* Halliday T R **294,** 502
Gower J F R *see under* Denman K L , **294,** 673
Gowlett J A J , Harris J W K , Walton D and Wood B A Early archaeological sites, hominid remains and traces of fire from Chesowanja, Kenya, **294,** 125
Goyert S M and Silver J Isolation of I–A subregion-like molecules from subhuman primates and man, **294,** 266
Gozes I and Sweadner K J Multiple tubulin forms are expressed by a single neurone **294,** 477
Gramsch C *see under* Schulz R **294** 757
Grankvist K , Marklund S and Taljedal I -B Superoxide dismutase is a prophylactic against alloxan diabetes, **294,** 158
Grant D M *see under* Wilson M A , **294,** 648
Gray C M and Goode A D T Strontium isotopic resolution of magma dynamics in a layered intrusion, **294,** 155
Greaves G N , Durham P J , Diakun G and Quinn P Near-edge X-ray absorption spectra for metallic Cu and Mn **294,** 139
Green A G *see under* Mair J A **294,** 439
Green B Countryside Conservation The Protection and Management of Amenity Ecosystems, *book review by* Andrews J **294,** 40
Green H S., Stringer C B , Collcutt S N , Currant A P , Huxtable J , Schwarcz H P , Debenham N , Embleton C , Bull P , Molleson T I and Bevins R E Pontnewydd Cave in Wales — a new Middle Pleistocene hominid site, **294,** 707
Gregory J Middle atmosphere dynamics, *news and views,* **294,**

519
Gregory R L Mind in Science A History of Explanations in Psychology and Physics *book review by* Michie D **294,** 291
Gribbin J Genesis The Origins of Man and the Universe, *book review by* Noble Wilford J **294,** 491
Grobstein C From Chance to Purpose An Appraisal of External Human Fertilization, *book review by* Short R V **294,** 38
Gronenborn B , Gardner R C , Schaefer S and Shepherd R J Propagation of foreign DNA in plants using cauliflower mosaic virus as vector, **294,** 773
Grosschedl R , Wasylyk B , Chambon P and Birnstiel M L Point mutation in the TATA box curtails expression of sea urchin H2A histone gene *in vivo* **294,** 178
Guangcen L *see under* Tapponnier P **294,** 405
Guest J E *see under* Wadge G **294,** 548
Guggenheim K Y Nutrition and Nutritional Diseases The Evolution of Concepts, *book review by* Rivers J **294,** 39
Gunther A E The Founders of Science at the British Museum 1753–1900, *book review by* Coleman W **294,** 18
Guoming C *see under* Tapponnier P **294,** 405
Gutfreund H *Editor* Biochemical Evolution *book review by* Ambler R P **294,** 382
Gutte B *see under* Arnheiter H **294,** 278
Guymer T H *see under* Jones W L **294,** 704
Guymer T H , Businger J A , Jones W L and Stewart R H Anomalous wind estimates from the Seasat scatterometer **294,** 735
Hackbarth I *see under* Erdman E **294,** 288
Hackmann W D *book review of* Barometers (Bolle B) **294,** 491
  book review of Early Scientific Instruments (Hawkes N) **294,** 491
Hainau B *see under* Duffey M E **294,** 451
Haixiang Z *see under* Nicolas A **294,** 414
  see under Tapponnier P **294,** 405
Håkanson R *see under* Leander S , **294,** 467
Halasz N *see under* Somogyi P **294,** 761
Hale C J *see under* Bailey M E **294,** 739
Halie L M *see under* Hol W G J **294,** 532
Hall E R The Mammals of North America *book review by* McKenna M C **294,** 597
Hall T C *see under* Matthews J A **294,** 175
Hallam A What did you read during 1981? **294,** 484
Halliday T R *book review of* Birds, (Gould J) **294,** 502
  book review of British Birds (Morris F O) **294,** 502
  book review of Sketches of Bird Life (Gillmor R *editors*) **294,** 502
  book review of The Art of Robert Bateman, (Derry R) **294,** 502
  book review of Thorburn s Landscape (Southern J) **294,** 502
  book review of Wildlife Sketchbook (Brokie K) **294,** 502
Halstead L B What did you read during 1981? **294,** 484
Hamill O P and Sakmann B Multiple conductance states of single acetylcholine receptor channels in embryonic muscle cells **294,** 462
Hammond J H The Camera Obscura A Chronicle *book review by* Bedini S A **294,** 492
Hanahan D *see under* Wozney J **294,** 129
Handler J S *see under* Dragsten P R , **294,** 718
Harley K L S *see under* Room P M **294,** 78
Harris E *see under* Harris J , **294,** 496
Harris H *see under* White M K , **294,** 232
Harris J H Good as gold, *correspondence* **294,** 106
Harris J and Harris E The Guinness Book of Trees *book review by* Mitchell A **294,** 496
Harris J R *see under* O'Brien G W **294,** 442
Harris J W K *see under* Gowlett J A J **294,** 125
Hart H S *see under* Palka J , **294,** 447
Harvey R P , Krieg P A , Robins A J , Coles L S and Wells J R E Non-tandem arrangement and divergent transcription of chicken histone genes **294,** 49
Harvey S C and McCammon J A Intramolecular flexibility in phenylalanine transfer RNA **294,** 286
Harwit M Cosmic Discovery The Search Scope and Heritage of Astronomy *book review by* Evans D S **294,** 22
Hassan F A Demographic Archaeology *book review by* Renfrew C **294,** 678
Hawkes N Early Scientific Instruments, *book review by* Hackmann W D **294,** 491
Hay A New pathways for chlorinated dioxins, *news and views* **294,** 514
  see under Murphy S , **294,** 204
Head J W III Volcanism on Mars *news and views* **294,** 305
Heathcote G D *book review of* The Fischer–Smith Controversy Are There Bacterial Diseases of Plants? (Campbell C L) **294,** 37
Hemond H F *see under* Tjepkema J D **294,** 445
Heng S *see under* Wilson M A , **294,** 648
Henrey B *book review of* The Shaping of Cambridge Botany, (Walters S M) **294,** 495
Henstridge R M *see under* Manchee R J , **294,** 254
Herz A *see under* Schulz R **294** 757
Heusser C J , Streeter S S and Stuiver M Temperature and precipitation record in southern Chile extended to ~ 43 000 yr ago **294,** 65
Hickson I D and Emmerson P T Identification of the *Escherichia coli recB* and *recC* gene products **294,** 578
Hieter P A , Hollis G F , Korsmeyer S J , Waldmann T A and Leder P Clustered arrangement of immunoglobulin λ constant region genes in man **294,** 536
Higgins A K *see under* Batten D J **294,** 150
Hill A *book review of* On Becoming Human, (Tanner N M) **294,** 500
Hill D R *see under* Wilkin G P , **294,** 584
Hinuma Y *see under* Miyoshi I **294,** 770
Ho B T *see under* Silverman P B , **294,** 475
Ho S *see under* Duffey M E , **294,** 451
Hobson G D *see under* Illing L V , **294,** 782
Hockney R W and Eastwood J W Computer Simulation Using Particles *book review by* James F **294,** 293
Hoffman K A Palaeomagnetic excursions, aborted reversals and transitional fields, **294,** 67
Hofstetter H *see under* Galli G **294,** 626
Hogan B and Williams J Integration of foreign genes into the mammalian germ line genetic engineering enters a new era *news and views* **294,** 9
Hol W G J , Halie L M and Sander C Dipoles of the α-helix and β-sheet their role in protein folding, **294,** 532
Holder A A and Freeman R R Immunization against blood-stage rodent malaria using purified parasite antigens, **294,** 361
Hollands C Lab Animals, *correspondence* **294,** 8
Hollis G F *see under* Hieter P A , **294,** 536
Hongrong Q *see under* Tapponnier P , **294,** 405
Hora B *Editor*, The Oxford Encyclopedia of Trees of the World, *book review by* Howard R **294,** 496
Horne R B , Christiansen P J , Gough M P , Ronnmark K G , Johnson J F E , Sojka J and Wrenn G L Amplitude variations of electron cyclotron harmonic waves **294,** 338
Howard R *book review of* The Oxford Encyclopedia of Trees of the World, (Hora B *editor*) **294,** 496
Howard-Flanders P *see under* West S C , **294,** 659
Hoyle F and Wickramasinghe C Evolution from Space, *book review by* Tyrrell D A J **294,** 489
Hrdy S B The Woman That Never Evolved, *book review by* Zihlman A L **294,** 42
Huaibin S *see under* Tapponnier P , **294,** 405
Huchon D , Ozon R and Demaille J G Protein phosphatase-1 is involved in *Xenopus* oocyte maturation, **294,** 358
Hudales J *see under* Beddard G S , **294,** 145
Hudson A L *see under* Wilkin G P **294,** 584
Hudson L , Rossi J and Landy A Dual function transcripts specifying tRNA and mRNA, **294,** 422
Hughes D W *book review of* Daytime Star The Story of Our Sun, (Mitton S) **294,** 21
  book review of Orbiting the Sun Planets and Satellites of the Solar System (Whipple F L) **294,** 21
  The gassiest comet? *news and views* **294,** 696
  book review of The Moon, (Moore P) **294,** 487
  book review of The New Solar System (Beatty J K *et al editors*) **294,** 21
  book review of The Planet Jupiter The Observer's Handbook (Moore P and Hunt G) **294,** 487
Humphries C , Press J R and Sutton D A The Hamlyn Guide to Trees of Britain and Europe, *book review by* Mitchell A **294,** 495
Hunig T and Bevan M J Specificity of T-cell clones illustrates altered self hypothesis, **294,** 460
Hunt G *see under* Moore P **294,** 487
Husebye E S *see under* Troitskiy P **294,** 618
Hussey K J *see under* Chelton D B , **294,** 529
Hussey R E *see under* Reinherz E L , **294,** 168
Hussler G , Chappe B , Wehrung P and Albrecht P C_{27}–$C^{2}{}_{29}$ ring A monoaromatic steroids in Cretaceous black shales, **294,** 556
Hutchison R and Pillinger C T Meteoritics — more facts, more complexity, *news and views* **294,** 15
Huxtable J *see under* Green H S **294,** 707
Hyde R *book review of* Dynamics of the upper atmosphere, (Kato S) **294,** 782
Ifediba T and Vanderberg J P Complete *in vitro* maturation of *Plasmodium falciparum* gametocytes, **294,** 364
Iida S , Marcoli R and Bickle T A Variant insertion element *Is1* generates 8-base pair duplications of the target sequence, **294,** 374
Illing L V and Hobson G D *Editors*, Petroleum geology of the Continental Shelf of North-West Europe 1981, *book review by* Brookes J R V **294,** 782
Ingle R and Jennings A Science in Schools Which Way Now? *book review by* Mott N **294,** 35
Ingold C T *book review of* Biology of conidial fungi (Cole G T and Kendrick B *editors*) **294,** 784
Innes J B *see under* Simmons I G , **294,** 76
Irifune T *see under* Ohtani E **294,** 62
Irlin I S *see under* Dikii L A , **294,** 688
Israel M , Lesbats B and Manaranche R ACh release from osmotically shocked synaptosomes refilled with transmitter **294,** 474
Jaki S L Cosmos and Creator, *book review by* Davies D **294,** 677
James A A *see under* Fishel R A **294,** 184
James F *book review of* Computer Simulation Using Particles, (Hockney R W and Eastwood J W) **294,** 293
Jande S S , Maler L and Lawson D E M Immunohistochemical mapping of vitamin D-dependent calcium-binding protein in brain, **294** 765
Jaupart C *see under* Allegre C J , **294,** 223
Jay Gould S What did you read during 1981? **294,** 483
Jeffery W R *see under* Capco D G **294,** 255
Jenkins E E *see under* Schlenker J L , **294,** 340
Jenks B G *see under* Martens G J M , **294,** 558
Jennings A *see under* Ingle R **294,** 35
Jensen A R Straight Talk about Mental Tests *book review by* Blinkhorn S **294,** 501
Ji Z *see under* Tapponnier P **294,** 405
  see under Tapponnier P , **294,** 410
Johnson A D , Poteete A R , Lauer G , Sauer R T , Ackers G K and Ptashne M λ Repressor and cro—components of an efficient molecular switch, *review article* **294,** 217
Johnson J F E *see under* Horne R B , **294,** 338
Johnston W R *see under* Proctor J , **294,** 245
Johnstone A A plasma wake for Mars' satellite Deimos *news and views* **294,** 610
Jones B J T *book review of* The Isotropic Universe (Raine D J) **294,** 383
Jones D First remote sensing of the plasmapause by terrestrial myriametric radiation, **294,** 728
Jones N C *see under* Carlock L , **294,** 572
Jones R V *book review of* James Clerk Maxwell A Biography, (Tolstoy I) **294,** 24
Jones T J *see under* Elliot J L , **294,** 526
Jones W L *see under* Guymer T H , **294,** 735
Jones W L , Boggs D H , Bracalente E M , Brown R A , Guymer T H , Shelton D and Schroeder L C Evaluation of the Seasat wind scatterometer **294,** 704
Josephs S F *see under* Wong-Staal F **294,** 273
Kacinski B M and Rupp W D *E coli uvrB* protein binds to DNA in the presence of *uvrA* protein **294,** 480
Kalyanaraman V S *see under* Poiesz B J , **294,** 268
Kalyanaraman V S , Sarngadharan M G , Bunn P A , Minna J D and Gallo R C Antibodies in human sera reactive against an internal structural protein of human T-cell lymphoma virus, **294,** 271
Kameyama M *see under* Fukida J , **294,** 82
Karpen G H and Schubiger G Extensive regulatory capabilities of a *Drosophila* imaginal disk blastema, **294,** 744
Kato S Dynamics of the upper atmosphere, *book review by* Hyde R **294,** 782
Katsaros K B *see under* Taylor P K , **294,** 737
Katz K and Keller J Comb-layering in carbonatite dykes, **294,** 350
Katz S *see under* Larsen F L **294,** 667
Katz S A *see under* Dikii L A , **294,** 688
Kay R How cells live together, *news and views* **294,** 108
Keast A *Editor*, Ecological biogeography of Australia *book review by* Moore P D **294,** 783
Keays R R , Sewell D K B and Mitchell R H Platinum and palladium minerals in upper mantle-derived lherzolites, **294,** 646
Kebabian J W *see under* Stoof J C , **294,** 366
Keck O Fast breeder reactors can we learn from experience? *review article* **294,** 205
Kedes L and Maxson R Histone gene organization paradigm lost, *news and views* **294,** 11
Keller J *see under* Katz K **294,** 350
Kendrick B *see under* Cole G T , **294,** 784
Kennedy A R and Weichselbaum R R Effects of dexamethasone and cortisone with X-ray irradiation on transformation of C3H 10T½ cells, **294,** 97
King R The Temple of Flora, *book review by* Walters S M **294,** 493
King R W *see under* Langley R B **294,** 730
Kintner C and Sugden B Identification of antigenic determinants unique to the surfaces of cells transformed by Epstein–Barr virus, **294,** 458
Kirsh Y *see under* Chen R , **294,** 294
Kitamura Y and Yokoyama M Spleen colony-forming cell as common precursor of tissue mast cells and granulocytes—Reply, *matters arising* **294,** 290
Klein G The role of gene dosage and genetic transpositions in carcinogenesis, *review article* **294,** 313
Knoll B J *see under* Cohen S , **294,** 182
Knowlton N , Lang J C , Rooney M C and Clifford P Evidence for delayed mortality in hurricane-damaged Jamaican staghorn corals, **294,** 251
Koch B E *see under* Batten D J , **294,** 150
Kohli J *see under* Munz P , **294,** 187
Kokotailo G T *see under* Schlenker J L , **294,** 340
Kolb E W and Turner M S The early Universe, *review article* **294,** 521
Kolodner R *see under* Fishel R A , **294,** 184
Konishi S , Tsunoo A and Otsuka M Enkephalin as a transmitter for presynaptic inhibition in sympathetic ganglia, **294,** 80
Konovalenko A A and Sodin L G The 26 13 MHz absorption line in the direction of Cassiopeia A, **294,** 135
Kornberg H *book review of* Otto Warburg Cell Physiologist, Biochemist and Eccentric, (Krebs H) **294,** 595
Korner P I *see under* Angus J A **294,** 671
Korsmeyer S *see under* Siebenlist U , **294,** 631
Korsmeyer S J *see under* Hieter P A , **294,** 536
Koul S L , Chadderton L T and Brooks C K Fission track dating of zeolites, **294,** 347
Krawietz W *see under* Erdman E , **294,** 288
Krebs H Otto Warburg Cell Physiologist, Biochemist and Eccentric *book review by* Kornberg H **294,** 595
Krieg P A *see under* Harvey R P **294,** 49
Krolik J H A particularly anomalous Seyfert galaxy *news and views* **294,** 13
Kroopnick P *see under* Smith S V **294,** 252
Kubli E *see under* Bienz M , **294,** 188
Kubonishi I *see under* Miyoshi I , **294,** 770
Kuhar M J *see under* Palacios J M , **294,** 587
Kuhs W F and Lehmann M S Bond-lengths, bond angles and transition barrier in ice Ih by neutron scattering **294,** 432
Kung H -J *see under* Noori-Daloii M R , **294,** 574
Lacatena R M and Cesareni G Base pairing of RNA I with its complementary sequence in the primer precursor inhibits ColE1 replication, **294,** 623
Lachman L B *see under* Ford R J , **294,** 261
Lacy E *see under* Costantini F **294,** 92
Lafer E M *see under* Nordheim A **294,** 417
Laggner P Lateral diffusion of lipids in sarcoplasmic reticulum membranes is area limited, **294,** 373
Lambret B *see under* Dupre B , **294,** 552
Landy A *see under* Hudson L , **294,** 422
Lang J C *see under* Knowlton N , **294,** 251
Langer S Z Presence and physiological role of presynaptic inhibitory α-adrenoreceptors in guinea pig atria, *matters arising* **294,** 671
Langley R B , King R W , Shapiro I I , Rosen R D and Salstein D A Atmospheric angular momentum and the length of day a common fluctuation with a period near 50 days, **294,** 730
Larsen F L , Katz S , Roufogalis B D and Brooks D E Physiological shear stresses enhance the Ca^{2+} permeability of human erythrocytes, **294,** 667
Larsen I L *see under* Olsen C R , **294,** 242
Larsen J A The Boreal Ecosystem, *book review by* Shetler S G **294,** 382
Lauer G *see under* Johnson A D , **294,** 217
Law R *book review of* Theoretical Ecology Principles and Applications, (May R M *editor*) **294,** 294
Lawrence C *book review of* Matter, Life and Generation Eighteenth-century Embryology and the Haller–Wolff Debate, (Roe S A) **294,** 37
Lawson D E M *see under* Jande S S , **294,** 765
Le Bas M J *see under* Silva L C **294,** 644
Leander S , Håkanson R , Rosell S , Folkers K , Sundler F and Tornqvist K A specific substance P antagonist blocks smooth muscle contractions induced by non cholinergic, non-adrenergic nerve stimulation, **294,** 467
Lebofsky L A *see under* Rieke G H , **294,** 59
Lebofsky M J *see under* Rieke G H , **294,** 59
  see under Stocke J T , **294,** 319
Ledbetter M T Palaeooceanographic significance of bottom-current fluctuations in the Southern Ocean **294,** 554
Leder P *see under* Hieter P A , **294,** 536
  see under Siebenlist U , **294,** 631
Lee A G Movement in membranes *news and views* **294,** 695
Lee F , Mulligan R , Berg P and Ringold G Glucocorticoids regulate expression of dihydrofolate reductase cDNA in mouse mammary tumour virus chimaeric plasmids **294,** 228
Lehmann M S *see under* Kuhs W F **294,** 432

Leist T *see under* Arnheiter H , **294,** 278
Leovy C B The martian lower atmosphere, *news and views,* **294,** 310
Lesbats B *see under* Israël M , **294,** 474
Lesieur M and Sadourny R Satellite-sensed turbulent ocean structure, *matters arising* **294,** 673
Lester H A A potpourri of plucked patches, *news and views* **294,** 398
Leung D *see under* Shepard H M , **294,** 563
Leupold U *see under* Munz P , **294,** 187
Levitt M Molecular dynamics of hydrogen bonds in bovine pancreatic trypsin inhibitor protein, **294,** 379
Lewin W H G *see under* Pedersen H , **294,** 725
Lewry J F Lower Proterozoic arc–microcontinent collisional tectonics in the western Churchill Province, **294,** 69
Liller W *see under* Elliot J L , **294,** 526
Lilley S Discovering Relativity for Yourself, *book review by* Raine D J **294,** 23
Lipes R G *see under* Taylor P K , **294,** 737
Lipschultz F , Zafiriou O C , Wofsy S C , McElroy M B , Valois F W and Watson S W Production of NO and N_2O by soil nitrifying bacteria, **294,** 641
Little J W *see under* Cohen S , **294,** 182
Lloyd C Intrinsic variations of the double quasar 0957+56 AB **294,** 727
Long J Introduced Birds of the World, *book review by* Andrews J **294,** 500
Longuet-Higgins H C *book review of* Chemistry, Quantum Mechanics and Reductionism, (Primas H) **294,** 194
Lonsdale P *see under* Aubouin J , **294,** 146
Lord T C *see under* Gascoyne M , **294,** 652
Lother H and Messer W Promoters in the *E coli* replication origin, **294,** 376
Loutit J F , Peters J and Stevens J Spleen colony forming cell as common precursor of tissue mast cells and granulocytes, *matters arising* **294,** 290
Lovell B Emerging Cosmology, *book review by* Silk J **294,** 21
Lowrie W *see under* Alvarez W , **294,** 246
Luzzatto L *see under* Persico M G , **294,** 778
Lyubchnko Y L *see under* Gagua A V , **294,** 662
McCammon J A *see under* Harvey S C , **294,** 286
McClymont A N *see under* Craig I J D **294,** 333
McCrumb J L and Arnold F High-sensitivity detection of negative ions in the stratosphere **294,** 136
McCulloch M T and Compston W Sm–Nd age of Kambalda and Kanowna greenstones and heterogeneity in the Archaean mantle, **294,** 322
McDougall I ^{40}Ar/^{39}Ar age spectra from the KBS Tuff, Koobi Fora Formation, **294,** 120
McElroy M B *see under* Lipschultz F , **294,** 641
McFarland D *Editor,* The Oxford Companion to Animal Behaviour *book review by* McGill T E **294,** 501
McGill T E *book review of* The Oxford Companion to Animal Behaviour, (McFarland D *editor*) **294,** 501
McGrath J C *see under* Blakeley A G H , **294,** 759
McKenna M C *book review of* The Mammals of North America, (Hall E R) **294,** 597
McMillan F M The Chain Straighteners Fruitful Innovation The Discovery of Linear and Stereoregular Polymers *book review by* Mark H **294,** 29
McNaughton N J , Borthwick J , Fallick A E and Pillinger C T Deuterium/hydrogen ratios in unequilibrated ordinary chondrites, **294,** 639
McNutt S R and Beavan R J Volcanic earthquakes at Pavlof Volcano correlated with the solid earth tide, **294,** 615
Madore B F *book review of* A Revised Shapley–Ames Catalog of Bright Galaxies, (Sandage A and Tammann G A) **294,** 676
Magnuson T *see under* Sawicki J A **294,** 450
Maihle N J *see under* Salisbury J L , **294,** 163
Mair J A and Green A G High-resolution seismic reflection profiles reveal fracture zones within a 'homogeneous' granite batholith, **294,** 439
Maitland G C , Rigby M , Smith E B and Wakeham W A Intermolecular Forces Their Origin and Determination *book review by* Barnes P **294,** 384
Maizel A L *see under* Ford R J **294,** 261
Maler L *see under* Jande S S **294,** 765
Maliga P *see under* Sidorov V , **294,** 87
Manaranche R *see under* Israël M , **294,** 474
Manchee R J , Broster M G , Melling J , Henstridge R M and Stagg A J *Bacillus anthracis* on Gruinard Island, **294,** 254
Manzari V *see under* Wong-Staal F **294,** 273
Maran S P *book review of* In Quest of Telescopes (Cohen M) **294,** 490
Marcoli R *see under* Iida S **294,** 374
Marcoux J *see under* Nicolas A , **294,** 414
see under Tapponnier P **294,** 405
Mark H *book review of* The Chain Straighteners Fruitful Innovation The Discovery of Linear and Stereoregular Polymers, (McMillan F M) **294,** 29
Marklund S *see under* Grankvist K , **294,** 158
Martens G J M , Jenks B G and van Overbeeke A P $N\alpha$-acetylation is linked to α MSH release from pars intermedia of the amphibian pituitary gland **294,** 558
Martin J B Open relations, *correspondence* **294,** 396
Martinis J *see under* Erikson J , **294,** 173
Mascle G *see under* Tapponnier P , **294,** 405
Maskill H To *trans trans trans*-tricyclo [7,3,1,O$^{5\ 13}$] tridecane, *correspondence* **294,** 606
Mas-Oliva J *see under* Geisow M J , **294,** 400
Matsumoto L H Enrichment of satellite DNA on the nuclear matrix of bovine cells, **294,** 481
Matte P *see under* Tapponnier P , **294,** 405
Matthews J A , Brown J W S and Hall T C Phaseolin mRNA is translated to yield glycosylated polypeptides in *Xenopus* oocytes, **294,** 175
Maurer R A Transcriptional regulation of the prolactin gene by ergocryptine and cyclic AMP, **294,** 94
Maxson R *see under* Kedes L , **294,** 11
May R M *Editor,* Theoretical Ecology Principles and Applications, *book review by* Law R **294,** 294
Useful tropical legumes, *news and views* **294,** 516
Medawar P B *book review of* A History of the Study of Human Growth, (Tanner J M) **294,** 34
What did you read during 1981? **294,** 484
Medvedkov Ya V *see under* Dikii L A , **294,** 688
Mehta S R *see under* Ford R J , **294,** 261
Meier W M *see under* Schlenker J L , **294,** 340
Meikle D B and Vessey S H Nepotism among rhesus monkey brothers, **294,** 160
Mellanby K *book review of* Extinction The Causes and Consequences of the Disappearance of Species, (Ehrlich P and Ehrlich A) **294,** 41
Farming and Wildlife, *book review by* Andrews J **294,** 40
Mellen S L W The Evolution of Love, *book review by* Zihlman A L **294,** 42
Melling J *see under* Manchee R J **294,** 254
Menczel L *see under* Sidorov V , **294,** 87
Mercier J L *see under* Tapponnier P , **294,** 405
see under Tapponnier P , **294,** 410
Mertenf G Literary anarchy, *correspondence* **294,** 688
Mertin J and Steckpoole A Anti-PGE antibodies inhibit *in vivo* development of cell mediated immunity, **294,** 456
Messer W *see under* Lother H , **294,** 376
Metzenberg R L *see under* Selker E U , **294,** 576
Meyer P Clues for the origin of cosmic rays, *news and views* **294,** 518
Michaels C F and Carello C Direct Perception, *book review by* Braddick O **294,** 598
Michetti F *see under* Cocchia D , **294,** 85
Michie D *book review of* Mind in Science A History of Explanations in Psychology and Physics, (Gregory R L) **294,** 291
Milnes A R *see under* O'Brien G W , **294,** 442
Mink D J *see under* Elliot J L , **294,** 526
Minna J D *see under* Kalyanaraman V S , **294,** 271
Minshew B *see under* Welch R A **294,** 665
Mitchell A *book review of* Blandford Guide to Trees of the British Countryside (Fairhurst A and Soothill E) **294,** 495
book review of The Guinness Book of Trees, (Harris J and Harris E) **294,** 496
book review of The Hamlyn Guide to Trees of Britain and Europe, (Humphries C , Press J R , Sutton D A) **294,** 495
book review of The International Book of the Forest, (Beazley M and Simon & Schuster) **294,** 496
book review of The Reader's Digest Field Guide to the Trees and Shrubs of Britain, (Reader s Digest Association) **294,** 496
Mitchell R H *see under* Keays R R **294,** 646
Mitsuoka T *see under* Suzuki K , **294,** 453
Mitton S Daytime Star The Story of Our Sun, *book review by* Hughes D W **294,** 21
Miyoshi I , Kubonishi I , Yoshimoto S , Akagi T , Ohtsuki Y , Shiraishi Y , Nagata K and Hinuma Y Type C virus particles in a cord T-cell line derived by co-cultivating normal human cord leukocytes and human leukaemic T cells, **294,** 770
Moffat K *see under* Szebenyi D M E , **294,** 327
Mohler H and Richards J G Agonist and antagonist benzodiazepine receptor interaction *in vitro,* **294,** 763
Moller A *see under* Nordheim A , **294,** 417
Molleson T I *see under* Green H S , **294,** 707
Montagna R *see under* Ford R J , **294,** 261
Montagu A What did you read during 1981? **294,** 483
Montgomery E F *see under* Rieke G H , **294,** 59
Moore P *book review of* A Complete Manual of Amateur Astronomy, (Sherrod P C) **294,** 488
The Moon, *book review by* Hughes D W **294,** 487
book review of The Practical Astronomer, (Ronan C A) **294,** 488
Moore P D *book review of* Ecological biogeography of Australia, (Keast A *editor*) **294,** 783
Life seen from a medieval latrine *news and views* **294,** 614
Poznan Polish palaeohydrology presented *news and views* **294,** 12
Moore P and Hunt G The Planet Jupiter The Observer's Handbook, *book review by* Hughes D W **294,** 487
Morita K *see under* Tokimasa T , **294,** 162
Morrell J and Thackray A Gentlemen of Science Early Years of the British Association for the Advancement of Science *book review by* Fox R **294,** 19
Morris F O British Birds, *book review by* Halliday T R **294,** 502
Mott N *book review of* Science in Schools Which Way Now? (Ingle R and Jennings A) **294,** 35
What did you read during 1981? **294,** 483
Mount D W *see under* Cohen S , **294,** 182
Mountfort G Saving the Tiger, *book review by* Bertram B **294,** 42
Mulligan R *see under* Lee F , **294,** 228
Mulvey J H *Editor,* The Nature of Matter, *book review by* Panofsky W K H **294,** 596
Munz P , Leupold U , Agris P and Kohli J *In vivo* decoding rules in *Schizosaccharomyces pombe* are at variance with *in vitro* data, **294,** 187
Murdin P and Clark D H Halo around the Crab Nebula **294,** 543
Murphy S , Hay A and Robinson J P On chemical war, *correspondence* **294,** 204
Museteanu C and Diringer H Perivascular infiltrates of leukocytes in brains of scrapie-infected mice, **294,** 360
Mutel R L , Aller H D and Phillips R B Milliarcsecond structure of BL Lac during outburst, **294,** 236
Mutlow C T *see under* Drummond J R , **294,** 431
Nadeau P H and Reynolds R C Jr Volcanic components in pelitic sediments, **294,** 72
Nagata K *see under* Miyoshi I , **294,** 770
Naghshineh S *see under* Shiells R A , **294,** 592
Nagy A F *see under* Russell C T , **294,** 311
Naiwen W *see under* Tapponnier P , **294,** 405
Narayanan M S and Rao B M Detection of monsoon inversion by TIROS-N satellite, **294,** 546
Neher E *see under* Colquhoun D , **294,** 752
Neigel J E *see under* Porter J W , **294,** 249
Nelson G and Platnick N Systematics and Biogeography Cladistics and Vicariance, *book review by* Ball I R **294,** 675
Nelson G and Rosen D E *Editors* Vicariance Biogeography A Critique, *book review by* Ball I R **294,** 675
Nevanlinna H *see under* Pesonen L J , **294,** 436
Newcomer M *book review of* Life History of a Fossil An Introduction to Taphonomy and Paleoecology, (Shipman P) **294,** 598
Newth D R *book review of* A New Science of Life The Hypothesis of Formative Causation, (Sheldrake R) **294,** 32
Nichol L W *see under* Frieden C , **294,** 384
Nicholson P D *see under* Elliot J L , **294,** 526
Nicolas A *see under* Tapponnier P , **294,** 405
Nicolas A , Girardeau J , Marcoux J , Dupre B , Xibin W , Yougong C , Haixiang Z and Xuchang X The Xigaze ophiolite (Tibet) a peculiar oceanic lithosphere **294,** 414
Nielsen M *see under* Braestrup C , **294,** 472
Nikolaev A *see under* Troitskiy P , **294,** 618
Nobile C *see under* Persico M G , **294,** 778
Noble Wilford J *book review of* Cosmic Dawn The Origins of Matter and Life, (Chaisson E) **294,** 491
book review of Genesis The Origins of Man and the Universe, (Gribbin J) **294,** 491
Nomura M *see under* Yates J L , **294,** 190
Noori-Dalou M R Swift R A , Kung H -J , Crittenden L B and Witter R L Specific integration of REV proviruses in avian bursal lymphomas, **294,** 574
Nordheim A , Pardue M L , Lafer E M , Moller A , Stollar B D and Rich A Antibodies to left-handed Z-DNA bind to interband regions of *Drosophila* polytene chromosomes, **294,** 417
North A *see under* Tokimasa T , **294,** 162
Oakley B W SERC's plans, *correspondence* **294,** 688
Obendorf S K *see under* Szebenyi D M E , **294,** 327
O'Brien G W , Harris J R , Milnes A R and Veeh H H Bacterial origin of East Australian continental margin phosphorites **294,** 442
O'Grady R T Question of faiths, *correspondence* **294,** 510
Ohtani E , Irifune T and Fujino K Fusion of pyrope at high pressures and rapid crystal growth from the pyrope melt, **294** 62
Ohtsuki Y *see under* Miyoshi I **294,** 770
Okamoto H *see under* Yamamoto H , **294** 284
Okamoto S *see under* Wakabayashi S , **294,** 748
Olsen C R , Larsen I L , Cutshall N H , Donoghue J F , Bricker O P and Simpson H J Reactor-released radionuclides in Susquehanna River sediments **294,** 242
O'Neill G K *book review of* Are We Alone? The Possibility of Extraterrestrial Civilizations (Rood R T and Tefil J S) **294** 25
O'Riordan T and Sewell W R D *Editors* Project Appraisal and Policy Review *book review by* Pearce D **294,** 381
Otsuka M *see under* Konishi S **294,** 80
Ozima M The Earth Its Birth & Growth *book review by* Smith P J **294,** 490
Ozon R *see under* Huchon D , **294,** 358
Paetkau V Lymphokines on the move, *news and views* **294,** 689
Palacios J M and Kuhar M J Neurotensin receptors are located on dopamine-containing neurones in rat midbrain **294,** 587
Palka J , Schubiger M and Hart H S The path of axons in *Drosophila* wings in relation to compartment boundaries **294** 447
Panchen A L *Editor,* The Terrestrial Environment and the Origin of Land Vertebrates *book review by* Cox B **294,** 194
Panofsky W K H *book review of* The Nature of Matter, (Mulvey J H *editor*) **294,** 596
Paoyu L *see under* Tapponnier P , **294,** 405
Paradijs J van *see under* Pedersen H , **294,** 725
Pardue M L *see under* Nordheim A **294,** 417
Parke M E *see under* Chelton D B **294,** 529
Parry E M *see under* Parry J M , **294,** 263
Parry J M , Parry E M and Barrett J C Tumour promoters induce mitotic aneuploidy in yeast, **294,** 263
Parsons I *see under* Batten D J , **294,** 150
Partridge L and Farquhar M Sexual activity reduces lifespan of male fruitflies, **294,** 580
Patel Y C *see under* Srikant C B **294,** 259
Paul W E , Sredni B and Schwartz R H Long term growth and cloning of non transformed lymphocytes *review article* **294,** 697
Paulinyi E I Brazilian funds *correspondence* **294,** 8
Pearce D *book review of* Environmental Impact Assessment **294** 381
book review of Project Appraisal and Policy Review, (O Riordan T and Sewell W R D *editors*) **294,** 381
Pedersen H , Paradijs J van and Lewin W H G A four-hour orbital period of the X-ray burster 4U/MXB1636-53, **294,** 725
Peel D A On Antarctic glaciology Ice sheets and ice cores, *news and views* **294,** 211
Pellegrino R *see under* Ritchie J M **294,** 257
Pendry J B Tripping the light fantastic *news and views* **294,** 109
Penkett S A *see under* Fabian P , **294,** 733
Perkins D N The Mind's Best Work *book review by* Sutherland S **294,** 193
Persico M G , Toniolo D , Nobile C , D'Urso M and Luzzatto L cDNA sequences of human glucose 6 phosphate dehydrogenase cloned in pBR322 **294,** 778
Pesonen L J and Nevanlinna H Late Precambrian Keweenawan asymmetric reversals **294,** 436
Peters J *see under* Loutit J F **294,** 290
Phillips R B *see under* Mutel R L , **294,** 236
Piggott S *book review of* Rites of the Gods (Burl A) **294,** 487
Pillinger C Small minded — the characterization of interplanetary dust by electron microscopy, *news and views* **294** 517
Pillinger C T *see under* Hutchison R , **294,** 15
see under McNaughton N J , **294,** 639
Pingree J E *see under* Elliot J L **294,** 526
Pirke K M *see under* Schulz R , **294** 757
Platnick N *see under* Nelson G **294,** 675
Poiesz B J , Ruscetti F W , Reitz M S Kalyanaraman V S and Gallo R C Isolation of a new type C retrovirus (HTLV) in primary uncultured cells of a patient with Sezary T-cell leukaemia, **294,** 268
Polak J M *see under* Probert L , **294,** 470
Polkinghorne J *book review of* Divine and Contingent Order (Torrance T F) **294,** 27
Poppl L *see under* Galwey A K , **294,** 434
Porcas R W Superluminal quasar 3C179 with double radio lobes, **294,** 47
Porter J W , Woodley J D , Smith G J , Neigel J E , Battey J F and Dallmeyer D G Population trends among Jamaican reef corals, **294,** 249

Poteete A R *see under* Johnson A D **294,** 217
Prater A J Estuary Birds of Britain and Ireland *book review by* Andrews J **294,** 500
Presley R Alisphenoid equivalents in placentals marsupials, monotremes and fossils **294,** 668
Press J R *see under* Humphries C **294,** 495
Press W H *book review of* The Edge of Infinity, (Davies P) **294,** 488
Primas H Chemistry, Quantum Mechanics and Reductionism *book review by* Longuet-Higgins H C **294,** 194
Probert L., De Mey J and Polak J M Distinct subpopulations of enteric p-type neurones contain substance P and vasoactive intestinal polypeptide **294,** 470
Proctor J., Johnston W R , Cottam D A and Wilson A B Field-capacity water extracts from serpentine soils **294,** 245
Prosser N J D *see under* Fabian P , **294,** 733
Proust F *see under* Tapponnier P **294,** 405
Provost A *see under* Allegre C J , **294,** 223
Ptashne M *see under* Johnson A D , **294,** 217
Pugmire R J *see under* Wilson M A **294,** 648
Pye K Marshrock formed by iron sulphide and siderite cementation in saltmarsh sediments **294,** 650
Quinn P *see under* Greaves G N , **294,** 139
Radman M *see under* Brandenburger A , **294,** 180
Raich J C and Etters R D New low temperature phases of H_2 and D_2 at ultrahigh pressure *news and views* **294,** 513
Raine D J *book review of* Discovering Relativity for Yourself (Lilley S) **294,** 23
  The Isotropic Universe, *book review by* Jones B J T **294,** 383
Rampino M R *see under* Self S **294,** 699
Rang H P *see under* Ritchie J M **294,** 257
Rao B M *see under* Narayanan M S , **294,** 546
Raphael S *book review of* Curtis s Flower Garden Displayed (Whittle T and Cook C) **294,** 494
  book review of The Art of the Botanist, (Rix M) **294,** 494
Rasenick M M , Stein P J and Bitensky M W The regulatory subunit of adenylate cyclase interacts with cytoskeletal components **294,** 560
Rasmussen K L. *see under* Risbo T **294,** 637
Ravetch J V *see under* Siebenlist U **294,** 631
Ray T P *see under* Conway R G , **294,** 540
Reader's Digest Association The Reader s Digest Field Guide to the Trees and Shrubs of Britain *book review by* Mitchell A **294,** 496
Reid W H *see under* Drazin P G **294,** 196
Reinherz E L , Hussey R E , Fitzgerald K , Snow P , Terhorst C and Schlossman S F Antibody directed at a surface structure inhibits cytolytic but not suppressor function of human T lymphocytes **294,** 168
Reitman M I *see under* Dikii L A **294,** 688
Reitz M S *see under* Poiesz B J **294,** 268
Renard V *see under* Aubouin J , **294,** 146
Renfrew C *book review of* Demographic Archaeology (Hassan F A) **294,** 678
Reuter H *see under* Colquhoun D **294,** 752
Reynolds R C Jr *see under* Nadeau P H **294,** 72
Rice J B *see under* Cowley C R , **294,** 636
Rice-Ficht A C , Chen K K and Donelson J E Sequence homologies near the C termini of the variable surface glycoproteins of *Trypanosoma brucei* **294,** 53
Rich A *see under* Nordheim A **294,** 417
Richards G Rules for chemical reactions, *news and views* **294,** 114
Richards J G *see under* Mohler H **294,** 763
Rieke G H *see under* Stocke J T , **294,** 319
Rieke G H , Lebofsky L A , Lebofsky M J and Montgomery E F Unidentified features in the spectrum of Triton **294** 59
Rifkin D *book review of* Neoplastic and Normal Cells in Culture (Vasiliev J M and Gelfand I M) **294,** 292
Rigby M *see under* Maitland G C **294,** 384
Ringold G *see under* Lee F **294,** 228
Risbo T , Clausen H B and Rasmussen K L Supernovae and nitrate in the Greenland Ice Sheet **294,** 637
Ritchie J M , Rang H P and Pellegrino R Sodium and potassium channels in demyelinated and remyelinated mammalian nerve **294,** 257
Rivers J *book review of* Nutrition and Nutritional Diseases The Evolution of Concepts (Guggenheim K Y) **294,** 39
  book review of Nutrition and Food Science Present Knowledge and Utilization (Santos W J *et al editors*) **294,** 196
Rix M The Art of the Botanist *book review by* Raphael S **294,** 494
Roberts P H *book review of* Hydrodynamic Stability (Drazin P G and Reid W H) **294,** 196
Robertson A H F *see under* Silva L C **294,** 644
Robins A J *see under* Harvey R P , **294,** 49
Robinson J P *see under* Murphy S **294,** 204
Robson D W Is a bi-stable beam responsible for the complex radio structure of 3C133? **294,** 57
Roe S A Matter Life and Generation Eighteenth century Embryology and the Haller–Wolff Debate *book review by* Lawrence C **294,** 37
Rohrbaugh W J *see under* Schlenker J L **294,** 340
Rolland M , Aldissi M , Bernier P , Cadene M and Schue F Morphology of iodine-doped polyacetylene **294,** 60
Ronan C A The Practical Astronomer *book review by* Moore P **294,** 488
Ronnmark K and Christiansen P J Dayside electron cyclotron harmonic emissions **294,** 335
Ronnmark K G *see under* Horne R B , **294,** 338
Rood R T and Tefil J S Are We Alone? The Possibility of Extraterrestrial Civilizations *book review by* O'Neill G K **294,** 25
Room P M , Harley K L S , Forno I W and Sands D P A Successful biological control of the floating weed salviria, **294,** 78
Rooney M C *see under* Knowlton N , **294,** 251
Rosell S *see under* Leander S **294,** 467
Rosen D E *see under* Nelson G **294,** 675
Rosen R D *see under* Langley R B **294,** 730
Rosner R Thermal instability of solar loop structures *news and views* **294,** 611
Ross A H , Baltimore D and Eisen H N Phosphotyrosine containing proteins isolated by affinity chromatography with antibodies to a synthetic hapten **294,** 654
Rossi J *see under* Hudson L , **294,** 422
Roufogalis B D *see under* Larsen F L , **294,** 667
Roump J *see under* Aubouin J , **294,** 146
Rousseau D *see under* Dupre B , **294,** 552
Rout A E Hoyle on life *correspondence* **294,** 396
Rowsell H C Animal committees, *correspondence* **294,** 204
Ruddle F H A new era in mammalian gene mapping somatic cell genetics and recombinant DNA methodologies, *review article* **294,** 115 *Corrigendum* **294,** 670
Ruggles C *book review of* The First Stargazers, (Cornell J) **294,** 485
Rupp W D *see under* Kacinski B M , **294,** 480
Ruscetti F W *see under* Poiesz B J , **294,** 268
Ruscetti S K , Feild J A and Scolnick E. M Polycythaemia- and anaemia-inducing strains of spleen focus forming virus differ in post-translational processing of envelope-related glycoproteins, **294,** 663
Russell C T and Nagy A F Exploration of the upper atmosphere and ionosphere of Mars, *news and views* **294,** 311
Sadourny R *see under* Lesieur M **294,** 673
Sakmann B *see under* Colquhoun D **294,** 464
  see under Hamill O P **294,** 462
Salisbury J L , Condeelis J S , Maihle N J and Satir P Calmodulin localization during capping and receptor-mediated endocytosis, **294,** 163
Salstein D A *see under* Langley R B , **294,** 730
Sandage A and Tammann G A A Revised Shapley–Ames Catalog of Bright Galaxies, *book review by* Madore B F **294,** 676
Sander C *see under* Hol W G J **294,** 532
Sanders R H Recurrent Seyfert activity in spiral galaxy nuclei **294,** 427
Sands D P A *see under* Room P M , **294,** 78
Santos W J *et al Editors* Nutrition and Food Science Present Knowledge and Utilization *book review by* Rivers J **294,** 196
Sarngadharan M G *see under* Kalyanaraman V S **294,** 271
Satir P *see under* Salisbury J L , **294,** 163
Sauer R T *see under* Johnson A D , **294,** 217
Sawicki J A , Magnuson T and Epstein C J Evidence for expression of the paternal genome in the two-cell mouse embryo **294,** 450
Sawkins F J *book review of* Economic Geology and Geotectonics (Tarling D H *editor*) **294,** 292
Schaefer B E Probable optical counterpart of a γ ray burster **294,** 722
Schaefer S *see under* Gronenborn B **294,** 773
Schlenker J L , Dwyer F G , Jenkins E. E , Rohrbaugh W J , Kokotailo G T and Meier W M Crys'al structure of a synthetic high silica zeolite — ZSM-39, **294,** 340
Schlossman S F *see under* Reinherz E L **294,** 168
Schmitz W *see under* Erdman E , **294,** 288
Scholz H *see under* Erdman E **294,** 288
Schoonmaker R C *see under* Spencer N D , **294,** 643
Schroeder L C *see under* Jones W L **294,** 704
Schroer K *see under* Briles D E **294,** 88
Schubiger G *see under* Karpen G H , **294,** 744
Schubiger M *see under* Palka J , **294,** 447
Schue F *see under* Rolland M **294,** 60
Schulz R , Wilhelm A , Pirke K M , Gramsch C and Herz A β Endorphin and dynorphin control serum luteinizing hormone level in immature female rats, **294** 757
Schwarcz H P *see under* Green H S **294,** 707
Schwartz N *see under* Fuchs R P P **294,** 657
Schwartz R H *see under* Paul W E **294,** 697
Schwartz T W and Tager H S Isolation and biogenesis of a new peptide from pancreatic islets **294,** 589
Scolnick E M *see under* Ruscetti S K , **294,** 663
Scott N C *see under* Blakeley A G H , **294,** 759
Scott P R *book review of* Biology in Profile A Guide to Many Branches of Biology, (Campbell P N *editor*) **294,** 496
Scott R W *see under* Eiferman F A **294,** 713
Self S and Rampino M R The 1883 eruption of Krakatau **294,** 699
Selker E U , Free S J , Metzenberg R L and Yanofsky C An isolated pseudogene related to the 5S RNA genes in *Neurospora crassa*, **294,** 576
Sewell D K B *see under* Keays R R , **294,** 646
Sewell W R D *see under* O'Riordan T **294,** 381
Shapiro I I *see under* Langley R B , **294,** 730
Sheail J Rural Conservation in Inter War Britain, *book review by* Williams D G T **294,** 677
Sheldrake R A New Science of Life The Hypothesis of Formative Causation, *book review by* Newth D R **294,** 32
Shelton D *see under* Jones W L , **294** 704
Shepard H M , Leung D , Stebbing N and Goeddel D V A single amino acid change in IFN β_1 abolishes its antiviral activity **294,** 563
Shepherd R J *see under* Gronenborn B , **294,** 773
Sherratt D , Arthur A and Dyson P Site-specific recombination *news and views* **294,** 608
Sherrod P C A Complete Manual of Amateur Astronomy *book review by* Moore P **294,** 488
Shetler S G *book review of* The Boreal Ecosystem (Larsen J A) **294,** 382
Shiells R A , Falk G and Naghshineh S Action of glutamate and aspartate analogues on rod horizontal and bipolar cells **294,** 592
Shipman P Life History of a Fossil An Introduction to Taphonomy and Paleoecology *book review by* Newcomer M **294,** 598
Shiraishi Y *see under* Miyoshi I , **294,** 770
Short R V *book review of* Conception in the human female (Edwards R G) **294,** 784
  book review of From Chance to Purpose An Appraisal of External Human Fertilization (Grobstein C) **294,** 38
Sidorov V , Menczel L and Maliga P Isoleucine-requiring *Nicotiana* plant deficient in threonine deaminase **294,** 87
Siebenlist U , Ravetch J V , Korsmeyer S , Waldmann T and Leder P Human immunoglobulin D segments encoded in tandem multigenic families **294,** 631
Silk J *book review of* Emerging Cosmology (Lovell B) **294,** 21
Silva L C , Le Bas M J and Robertson A H F An oceanic carbonatite volcano on Santiago Cape Verde Islands **294,** 644
Silver J *see under* Goyert S M , **294,** 266
Silverman P B and Ho B T Persistent behavioural effect of apomorphine in 6-hydroxydopamine-lesioned rats **294,** 475
Simmons I G and Innes J B Tree remains in a North York Moors peat profile, **294,** 76
Simon & Schuster *see under* Beazley M , **294,** 496
Simons K Life out there, *correspondence* **294,** 396
Simpson H J *see under* Olsen C R , **294,** 242
Slingsby C *book review of* Molecular and cellular biology of the eye lens (Bloemendal H *editor*) **294,** 782
Smith A *see under* Folsome C E **294,** 64
Smith D J *book review of* Experimental High resolution Electron Microscopy (Spence J C H) **294,** 195
Smith E B *see under* Maitland G C , **294,** 384
Smith G J *see under* Porter J W **294,** 249
Smith P J *book review of* The Earth Its Birth & Growth (Ozima M) **294,** 490
Smith S V and Kroopnick P Carbon-13 isotopic fractionation as a measure of aquatic metabolism, **294,** 252
Snow C P The Physicists *book review by* Casimir H B G **294,** 26
Snow P *see under* Reinherz E L , **294,** 168
Sodin L G *see under* Konovalenko A A **294,** 135
Sojka J *see under* Horne R B , **294,** 338
Solomon S C The geophysics of Mars whence the Tharsis plateau? *news and views* **294,** 304
Somlyo A P *see under* Somlyo A V , **294,** 567
Somlyo A V , Butler T M , Bond M and Somlyo A P Myosin filaments have non-phosphorylated light chains in relaxed smooth muscle, **294,** 567
Somogyi P , Cowey A , Halasz N and Freund T F Vertical organization of neurones accumulating ^{3}H-GABA in visual cortex of rhesus monkey, **294,** 761
Somorjai G A *see under* Spencer N D , **294,** 643
Soothill E *see under* Fairhurst A , **294,** 495
Soper N J *see under* Batten D J **294,** 150
Southern J Thorburn's Landscape *book review by* Halliday T R **294,** 502
Southward A J Life on an oily wave, *news and views* **294,** 215
Soyfer V N *see under* Dikii L A , **294,** 688
Spence J C H Experimental High-resolution Electron Microscopy, *book review by* Smith D J **294,** 195
Spencer N D , Schoonmaker R C and Somorjai G A Structure sensitivity in the iron single crystal catalysed synthesis of ammonia, **294,** 643
Spillane J D The Doctrine of the Nerves Chapters in the History of Neurology, *book review by* Bynum W F **294,** 381
Sredni B *see under* Paul W E , **294,** 697
Srikant C B and Patel Y C Receptor binding of somatostatin-28 is tissue specific **294,** 259
Stackpoole A *see under* Mertin J **294,** 456
Stagg A J *see under* Manchee R J **294,** 254
Stearn W T The Natural History Museum at South Kensington A History of the British Museum (Natural History) 1753–1980, *book review by* Coleman W **294,** 18
Stebbing N *see under* Shepard H M , **294,** 563
Stein P J *see under* Rasenick M M , **294,** 560
Steinmetz J C *see under* Anderson T F **294,** 741
Stent G S *book review of* The Double-Edged Helix, (Cavalieri L F) **294,** 30
Stephan J F *see under* Aubouin J **294,** 146
Stevely W S *see under* Darnbrough C H **294,** 302
Stevens C F *see under* Colquhoun D **294,** 752
Stevens J *see under* Loutit J F , **294,** 290
Stewart R H *see under* Guymer T H , **294,** 735
Stocke J T , Rieke G H and Lebofsky M J New observational constraints on the M87 jet **294,** 319
Stollar B D *see under* Nordheim A , **294,** 417
Stoof J C and Kebabian J W Opposing roles for D 1 and D-2 dopamine receptors in efflux of cyclic AMP from rat neostriatum, **294,** 366
Storb U , Arp B and Wilson R The switch region associated with immunoglobulin C_μ genes is DNase I hypersensitive in T lymphocytes, **294,** 90
Streeter S S *see under* Heusser C J **294,** 65
Stringer C B *see under* Green H S **294,** 707
Strycharz W A *see under* Yates J L **294,** 190
Stuiver M *see under* Heusser C J **294,** 65
Stumpke H The Snouters Form and Life of the Rhinogrades, *book review by* Turner B D **294,** 499
Sugden B *see under* Kintner C **294,** 458
Sundler F *see under* Leander S , **294,** 467
Sutherland S *book review of* The Mind s Best Work (Perkins D N) **294,** 193
  What did you read during 1981? **294,** 483
Sutton D A *see under* Humphries C , **294,** 495
Suzuki K and Mitsuoka T Increase in faecal nitrosamines in Japanese individuals given a Western diet, **294,** 453
Sweadner K J *see under* Gozes I , **294,** 477
Swift R A *see under* Noori-Dalou M R , **294,** 574
Syka P Not cricket either *correspondence* **294,** 396
Szabo G *see under* Busath D **294,** 371
Szala S *see under* Wong-Staal F **294,** 273
Szebenyi D M E , Obendorf S K and Moffat K Structure of vitamin D dependent calcium-binding protein from bovine intestine **294,** 327
Tabin C Species difference, *correspondence* **294,** 510
Tager H S *see under* Schwartz T W **294,** 589
Taljedal I -B *see under* Grankvist K **294,** 158
Talmadge K , Brosius J and Gilbert W An 'internal' signal sequence directs secretion and processing of proinsulin in bacteria **294,** 176
Tammann G A *see under* Sandage A , **294,** 676
Taniguchi M *see under* Wakabayashi S , **294,** 748
Tanner J M A History of the Study of Human Growth, *book review by* Medawar P B **294,** 34
Tanner N M On Becoming Human, *book review by* Hill A **294,** 500
Tapponnier P , Mercier J L., Armijo R , Tonglin H and Ji Z Field evidence for active normal faulting in Tibet **294,** 410
Tapponnier P , Mercier J L , Proust F , Andrieux J , Armijo R , Bassoullet J P , Brunel M , Burg J P , Colchen M , Dupre B , Girardeau J , Marcoux J , Mascle G , Matte P , Nicolas A , Tingdong L , Xuchang X , Chenfa C , Paoyu L., Guangcen L , Naiwen W , Guoming C , Tonglin H , Xibin W , Wanming D , Haixiang Z , Huaibin S , Yongong C , Ji Z and Hongrong Q The Tibetan side of the India–Eurasia collision, **294,** 405
Tarling D H *Editor*, Economic Geology and Geotectonics *book review by* Sawkins F J **294,** 292
Tate V *see under* Wozney J **294,** 129
Taylor P K , Katsaros K B and Lipes R G Determinations by

Seasat of atmospheric water and synoptic fronts, **294**, 737
Tefil J S *see under* Rood R T **294**, 25
Teisinger J *see under* Fyskočil F , **294**, 288
Terhorst C *see under* Reinherz E L **294**, 168
Thackray A *see under* Morrell J , **294**, 19
Thomas L What did you read during 1981? **294**, 484
Thomas R M *see under* Arnheiter H , **294**, 278
Tilghman S M *see under* Eiferman F A , **294**, 713
Tingdong L *see under* Tapponnier P **294**, 405
Tjepkema J D , Cartica R J and Hemond H F Atmospheric concentration of ammonia in Massachusetts and deposition on vegetation **294**, 445
Tokimasa T , Morita K and North A Opiates and clonidine prolong calcium-dependent after-hyperpolarizations, **294**, 162
Tokuhisa T *see under* Wakabayashi S , **294**, 748
Tolstoy I James Clerk Maxwell A Biography, *book review by* Jones R V **294**, 24
Tomioka H *see under* Wakabayashi S , **294**, 748
Tonglin H *see under* Tapponnier P , **294**, 405
see under Tapponnier P , **294**, 410
Toniolo D *see under* Persico M G **294**, 778
Tornqvist K *see under* Leander S , **294**, 467
Torrance T F Divine and Contingent Order, *book review by* Polkinghorne J **294**, 27
Travers A Control of a mixed tRNA–protein operon, *news and views* **294**, 402
Trevarthen C Hemispheric modes of consciousness in the human brain, *news and views* **294**, 112
Trigg G L Page charges, *correspondence* **294**, 106
Troitskiy P , Husebye E S and Nikolaev A Lithospheric studies based on holographic principles, **294**, 618
Trowbridge I S Cancer monoclonals, *correspondence* **294**, 204
Trowbridge I S and Domingo D L Anti-transferrin receptor monoclonal antibody and toxin–antibody conjugates affect growth of human tumour cells, **294**, 171
Tsunoo A *see under* Konishi S , **294**, 80
Tunnicliffe V High species diversity and abundance of the epibenthic community in an oxygen-deficient basin **294**, 354
Turner B D *book review of* After Man A Zoology of the Future (Dixon D) **294**, 499
book review of The Doomsday Book of Animals A Natural History of Vanished Species, (Day D) **294**, 499
book review of The Snouters Form and Life of the Rhinogrades, (Stumpke H) **294**, 499
Turner G L'E Collecting Microscopes *book review by* Bedini S A **294**, 492
Turner M S *see under* Kolb E W **294**, 521
Tyrrell D A J *book review of* Evolution from Space (Hoyle F and Wickramasinghe C) **294**, 489
Ubell R *book review of* Polywater, (Franks F) **294**, 28
Uchigata Y *see under* Yamamoto H **294**, 284
Underwood J H and Barbee T W Jr Soft X-ray imaging with a normal incidence mirror **294**, 429
Valois F W *see under* Lipschultz F **294**, 641
van Andel T H Consider the incompleteness of the geological record, *news and views* **294**, 397
van den Damme R Belgium's power, *correspondence* **294**, 106
Van Gelder R G *book review of* Harper & Row's Complete Field Guide to North American Wildlife (Whitaker J O) **294**, 498
book review of The Audubon Society Field Guide to North American Mammals (Whitaker J O) **294**, 498
van Overbeeke A P *see under* Martens G J M , **294**, 558
van Sluis C A *see under* Brandenburger A , **294**, 180
Vanderberg J P *see under* Ifediba T **294**, 364
Vasilevsky A L *see under* Dikii L A , **294**, 688
Vasiliev J M and Gelfand I M Neoplastic and Normal Cells in Culture *book review by* Rifkin D **294**, 292
Vasudeva Rao K Harsh words, *correspondence* **294**, 106
Veeh H H *see under* O'Brien G W , **294**, 442
Vessey S H *see under* Meikle D B , **294**, 160
Wadge G and Guest J E Steady-state magma discharge at Etna 1971–81 **294**, 548
Wakabayashi S , Taniguchi M , Tokuhisa T , Tomioka H and Okamoto S Cytotoxic T lymphocytes induced by syngeneic mouse melanoma cells recognize human melanomas, **294**, 748
Wakeham W A *see under* Maitland G C **294**, 384
Waldmann T *see under* Siebenlist U , **294**, 631
Waldmann T A *see under* Hieter P A **294**, 536
Walgate R High energy physics grows tenfold, *news and views* **294**, 107
Walters S M The Shaping of Cambridge Botany, *book review by* Henrey B **294**, 495
book review of The Temple of Flora, (King R) **294**, 493
Walton D *see under* Gowlett J A J , **294**, 125
Wanming D *see under* Tapponnier P , **294**, 405
Wasserstrom R and Chapin G Malaria debated—A reply *correspondence* **294**, 388
Wasylyk B *see under* Grosschedl R , **294**, 178
Watson S W *see under* Lipschultz F , **294**, 641
Watts A Protein–lipid interactions do the spectroscopists now agree? *news and views* **294**, 512
Weaver P The Birdwatcher's Dictionary, *book review by* Andrews J **294**, 500
Weertman J On Antarctic glaciology Ice sheets *news and views* **294**, 210
Wehrung P *see under* Hussler G , **294**, 556
Weichselbaum R R *see under* Kennedy A R **294**, 97
Weiss R A virus associated with human adult T-cell leukaemia, *news and views* **294**, 212
Welch R A Dellinger E P , Minshew B and Falkow S Haemolysin contributes to virulence of extra-intestinal *E coli* infections, **294**, 665
Wells J R E *see under* Harvey R P , **294**, 49
West S C , Cassuto E and Howard-Flanders P Mechanism of *E coli* RecA protein directed strand exchanges in post-replication repair of DNA, **294**, 659
Westing A H Laotian postscript, *correspondence* **294**, 606
Wezel F C Upper Cretaceous to Eocene pelagic limestones of the Scaglia Rossa are not Miocene turbidites—Reply, **294**, 248
Wheeler J C Progress on accretion disks *news and views* **294**, 213
Whipple F L Orbiting the Sun Planets and Satellites of the Solar System, *book review by* Hughes D W **294**, 21
Whitaker J O Harper & Row's Complete Field Guide to North American Wildlife *book review by* Van Gelder R G **294**, 498
The Audubon Society Field Guide to North American Mammals *book review by* Van Gelder R G **294**, 498
White B Shallowing-upward cycles in the Middle Proterozoic Altyn Formation **294**, 157
White C M *book review of* Elliott Coues Naturalist and Frontier Historian, (Cutright P R and Brodhead M J) **294**, 497
White M K , Bramwell M E and Harris H Hexose transport in hybrids between malignant and normal cells **294**, 232
Whitehouse R D *book review of* The Penguin Guide to Prehistoric England and Wales, (Dyer J) **294**, 486
Whitteridge D Visual machinery of the brain *news and views* **294**, 113
Whittingham D G *see under* Cuthbertson K S R , **294**, 754
Whittle T and Cook C Curtis's Flower Garden Displayed, *book review by* Raphael S **294**, 494
Wickramasinghe C *see under* Hoyle F , **294**, 489
Wickramasinghe D T *see under* Allen D A , **294**, 239
Widmer M B and Bach F H Antigen driven helper cell-independent cloned cytolytic T lymphocytes, **294**, 750
Wilhelm A *see under* Schulz R , **294** 757
Wilkin G P , Hudson A L , Hill D R and Bowery N G Autoradiographic localization of GABA$_B$ receptors in rat cerebellum **294**, 584
Williams D G T *book review of* Rural Conservation in Inter War Britain, (Sheail J) **294**, 677
book review of The Countryside Planning and Change (Blacksell M and Gilg A W) **294**, 677
Williams J *see under* Hogan B **294**, 9
Williams N T lymphocytes repertoire and recognition, *news and views* **294**, 399
Williamson P G Morphological stasis and developmental constraint real problems for neo Darwinism, *news and views* **294**, 214
Willmott N Alchemy in cancer *correspondence* **294**, 302
Wilson A B *see under* Proctor J , **294**, 245
Wilson M A , Pugmire R J , Zilm K W , Goh K M , Heng S and Grant D M Cross-polarization ^{13}C-NMR spectroscopy with 'magic angle' spinning characterizes organic matter in whole soils, **294**, 648
Wilson R *see under* Storb U **294**, 90
Wiser H L *see under* Gerstl S A W , **294**, 352
Witter R L *see under* Noori-Daloii M R **294**, 574
Wofsy S C *see under* Lipschultz F **294**, 641
Wong-Staal F , Dalla Favera R , Gelmann E P , Manzari V., Szala S , Josephs S F and Gallo R C The *v-sis* transforming gene of simian sarcoma virus is a new *onc* gene of primate origin **294**, 273
Wood B A *see under* Gowlett J A J **294**, 125
Woodley J D *see under* Porter J W **294**, 249
Wozney J , Hanahan D , Tate V , Boedtker H and Doty P Structure of the pro α2(I) collagen gene **294**, 129
Wrenn G L *see under* Horne R B **294**, 338
Wright A E Lower Palaeozoic oceans and Wilson cycles *matters arising* **294**, 289
Wunner W H *see under* Anilionis A **294**, 275
Xibin W *see under* Nicolas A **294**, 414
see under Tapponnier P **294**, 405
Xuchang X *see under* Nicolas A , **294**, 414
see under Tapponnier P **294**, 405
Yamaguchi K *see under* Fukida J **294**, 82
Yamamoto H , Uchigata Y and Okamoto H Streptozotocin and alloxan induce DNA strand breaks and poly(ADP-ribose) synthetase in pancreatic islets, **294**, 284
Yanofsky C *see under* Selker E U **294**, 576
Yates J L , Dean D , Strycharz W A and Nomura M *E coli* ribosomal protein L10 inhibits translation of L10 and L7/L12 mRNAs by acting at a single site **294**, 190
Yokoyama M *see under* Kitamura Y , **294**, 290
Yongong C *see under* Tapponnier P **294**, 405
Yoshimoto S *see under* Miyoshi I , **294**, 770
Yougong C *see under* Nicolas A , **294**, 414
Young J Z What did you read during 1981? **294**, 484
Young P R *see under* Eiferman F A **294**, 713
Zafiriou O C *see under* Lipschultz F , **294**, 641
Zardecki A *see under* Gerstl S A W , **294**, 352
Zeilinger A Spin directions of interfering beams in quantum interferometry **294**, 544
Zihlman A L *book review of* The Evolution of Love (Mellen S L W) **294**, 42
book review of The Woman That Never Evolved (Hrdy S B) **294**, 42
Zilm K W *see under* Wilson M A , **294**, 648

nature
is available in Microform.

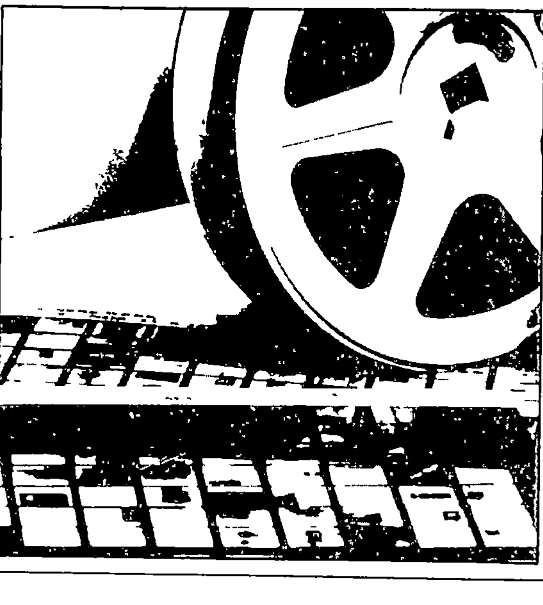

University
Microfilms
International

Please send additional information
for ______________________
(name of publication)
Name______________________
Institution______________________
Street______________________
City______________________
State__________ Zip__________

300 North Zeeb Road
Dept P R
Ann Arbor, Mi 48106

BOOKS RECEIVED

Earth Sciences

HALLAM, A Facies Interpretation and the Stratigraphic Record Pp 316 ISBN 0-7167-1291-1 (W H Freeman 1981) £10 95

HOLMES, S C A Geology of the Country Around Faversham Geological Survey of Great Britain, England and Wales Memoir for 1 50 000 Geological Sheet 273 Pp 117 ISBN 0-11-884141-6 (Institute of Geological Sciences, London 1981) Np

MENARD, H W (Director) The Mississippian and Pennsylvanian (Carboniferous) Systems in the United States Geological Survey, Professional Paper 1110-M-DD Pp 572 (No ISBN) Government Printing Office, Washington 1981) Pbk np

MERRIAM, D F (ed) Computer Applications in the Earth Sciences An Update of the 70s Series Proceedings of the 8th Geochautauqua held October 1979 at Syracuse University, the Division of Marine Geology and Geophysics at the University of Miami, and The International Association for Mathematical Geology Pp 385 ISBN 0-306-40409-0 (Plenum 1981) $45

MOORE, W G The Penguin Dictionary of Geography Definition and Explanations of Terms used in Physical Geography 6th Edn Pp 256 Pbk ISBN 0-14-051-002-8 (Penguin 1981) Pbk £1 95

OLIVER, J E Climatology Selected Applications Pp 260 ISBN 0-7131-6303-8 (Edward Arnold, London 1981) £14 95

OZIMA, O The Earth Its Birth and Growth Pp 117 Hbk ISBN 0-521-23500-6, pbk ISBN 0-521-28005-2 (Cambridge University Press 1981) Hbk £10 50, pbk £3 95

RUDLOFF, W World-Climates with Tables of Climatic Data and Practical Suggestions Pp 632 ISBN 3-8047-0509-X (Wissenschaftliche Verlaggsgesellschaft MBH, Stuttgart 1981) DM 180

SMITH, C D and PARRY, M (eds) Consequences of Climatic Change Pp 143 Pbk ISBN 0-85358-022-7 (University of Nottingham 1981) £3 50, $10

SONNENFELD, P (ed) Tethys The Ancestral Mediterranean Benchmark Papers in Geology, Vol 53 Pp 331 ISBN 0-87933-355-3 (Academic 1981) $40

STOKES, W L Essentials of Earth History An Introduction to Historical Geology 4th Edn Pp 577 ISBN 0 13-285890-8 (Prentice-Hall 1982) $22 95

WILLIAMS, G E Megacycles Long-Term Episodicity in Earth and Planetary History Benchmark Papers in Geology, Vol 57 Pp 434 ISBN 0-87933-366-9 (Academic 1981) $49

Biological Sciences

ADAMS, R L P *et al* The Biochemistry of the Nucleic Acids 9th Edn Pp 517 Hbk ISBN 0-412-22680-4, pbk ISBN 0-412-22690-1 (Chapman & Hall 1981) Hbk np, pbk £8 50

BALABAN, M (ed) Structural Aspects of Recognition and Assembly in Biological Macromolecules Vol 1, Proteins and Protein Complexes, Fibrous Proteins Proceedings of the 7th Aharon Katzir–Katchalsky Conference, The Weizmann Institute of Science, Rehovot and Kibbutz Nof Ginossar, February 1980 Pp 485 ISBN 0-86689-002-5 (Balaban International Science Services, Rehovot/Philadelphia 1981) Np

BALABAN, M Structural Aspects of Recognition and Assembly in Biological Macromolecules Vol 2, Nucleic Acids and Nucleic Acid Complexes, Viruses Proceedings of the 7th Aharon Katzir–Katchalsky Conference, The Weizmann Institute of Science, Rehovot and Kibbutz Nof Ginossar, February 1980 Pp 961 ISBN 0-86689-004-1 (Balaban International Science Services, Rehovot/Philadelphia 1981) Np

BENSON, L and DARROW, R A Trees and Shrubs of the Southwestern Deserts 3rd Edn Pp 416 ISBN 0-8165-0591 (University of Arizona Press 1981) $49 50

BERLINER, L J and REUBEN, J (eds) Biological Magnetic Resonance, Vol 3 Pp 268 ISBN 0-306-38981-9 (Plenum 1981) $35

BERRIDGE, M J , TREHERNE, J E and WIGGLESWORTH, V B (eds) Advances in Insect Physiology, Vol 15 Pp 624 ISBN 0-12-024215 (Academic 1981) $96

BLOOM, A D and JAMES, L S (eds) The Fetus and the Newborn Annual Review of Birth Defects, 1980 March of Dimes Birth Defects Foundation Birth Defects Original Article Series, Vol XVII, Number 1, 1981 Pp 276 ISBN 0-8451-1041-1 (Alan R Liss, New York 1981) £24 60, DM 108

BOLLACK, C and CLAVERT, A (eds) Epididymis and Fertility Biology and Pathology Progress in Reproductive Biology, Vol 8 International Colloquium, Strasbourg, October 1980 Pp 174 ISBN 3-8055-2157-X (Karger, Basel 1981) SwFr 119, DM 143, $71 25

BONTING, S L and DE PONT, J J H H M (eds) Membrane Transport New Comprehensive Biochemistry, Vol 2 Pp 380 ISBN 0-444-80307-6 (Elsevier/North-Holland 1981) $59 50, Dfl 140

BOOTH, P The Life of Plants Biology for the Individual Book 11 Pp 75 Pbk ISBN 0-435-59769-8 (Heinemann Educational, London 1981) Pbk £1 95

BRADBURY, E M , MACLEAN, N and MATTHEWS, H R DNA Chromatin and Chromosomes Pp 281 Flexi ISBN 0-632-00554-8 (Blackwell Scientific 1981) £9 80

BUCKLEY, J P , FERRARIO, C M and LOKHANDWALA, M F (eds) Central Nervous System Mechanisms in Hypertension Perspectives in Cardiovascular Research, Vol 6 Pp 434 ISBN 0-89004-545-3 (Raven 1981) $39 50

CAGAN, R H and KARE, M R (eds) Biochemistry of Taste and Olfaction Pp 539 ISBN 0-12-154450-8 (Academic 1981) S38 50

CARLSON, N R Physiology of Behaviour 2nd Edn Pp 748 ISBN 0-205-07262-3 (Allyn & Bacon 1981) Np

CAUSTON, D R and VENUS, J C The Biometry of Plant Growth Pp 307 ISBN 0-7131-2812-7 (Edward Arnold, London 1981) £25

CHEUNG, W Y (ed) Calcium and Cell Function Vol 1, Calmodulin Pp 395 ISBN-0-12-171401-2 (Academic 1981) $46 50

GUGHES, D T D and EMPEY, D W Lung Function for the Clinician Pp 100 Flexi ISBN 0-12-792078, 0-8089-1369-7 (Academic/Grune & Stratton, New York 1981) £6 80, $16 50

HUMPHREYS, L R Environmental Adaptation of Tropical Pasture Plants Pp 261 ISBN 0-333-26820-2 (Macmillan Press, London and New York 1981)

JAMES C C M and LASSMAN, L P Spina Bifida Occulta Orthopaedic, Radiological and Neurosurgical Aspects Pp 200 ISBN 0-12-792162-1 (Academic 1981) £20, $48

KOELLA, W P (ed) Sleep 1980 Circadian Rhythms, Dreams, Noise and Sleep Neurophysiology, Therapy 5th European Congress, Amsterdam, September 1980 Pp 466 ISBN 3-8055-2045-X (Karger, Basel 1981) SwFr 248, DM 297, $148 50

LAHUE, R (ed) Methods in Neurobiology, Vol 1 Pp 600 ISBN 0-306-40517-2 (Plenum 1981) $42 75

MARTIN, D W , MAYES, P A , RODWELL, D W *et al* Harper's Review of Biochemistry 18th Edn Former title Review of Physiological Chemistry Pp 614 Flexi ISBN 0-87041-036-9 (Lange Medical Publications, Los Altos, California 1981) $8

MORAWETZ, H and STEINBERG, I Z (eds) Annals of the New York Academy of Sciences, Vol 366 Luminescence from Biological and Synthetic Macromolecules, 8th Katzir Conference Pp 413 Hbk ISBN 0-89766-123-0, pbk ISBN 0-89766-124-9 (The New York Academy of Sciences 1981) Hbk $80, pbk np

NAIMAN, R J and SOLTZ, D L (eds) Fishes in North American Deserts Pp 552 ISBN 0-471-08523-5 (Wiley 1981) £29 75, $56 50

NICOLAU, C and PARAF, A (eds) Liposomes, Drugs and Immunocompetent Cell Functions Proceedings of a Conference, September 1980, Grignon, France Pp 194 ISBN 0-12-518660-6 (Academic 1981) £14, $34

PIERS, H Frog and Water Shrew Pp 42 ISBN 0-7226-5731-5 (Kestrel Books, Penguin 1981) £4 25

POWELL, J A and HOGUE, C L California Insects California Natural History Guides, 44 Pp 388 Flexi ISBN 0-520 03782-0 (University of California Press 1981) £5 35, $9 95

RANSOM, R Computers and Embryos Models in Developmental Biology Pp 212 ISBN 0-471-09972-4 (Wiley 1981) £14, $35

RAVEN, P H , EVERT, R F and CURTIS, H Biology of Plants 3rd Edn Pp 686 ISBN 0-87901-132-7 (Worth, New York 1981) $19 95

SCHLESSINGER, D (ed) Microbiology, 1981 Pp 424 ISBN 0-914826-31-X (American Society for Microbiology, 1913 I St N W Washington, DC 20006 1981) $22

SEELEY, H W Jr and VAN DEMARK, P J Microbes in Action A Laboratory Manual of Microbiology 3rd Edn Pp 385 Pbk ISBN 0 7167-1259-8 (W H Freeman 1981) Pbk £6 80

SEELEY, H W Jr and VAN DEMARK, P J Selected Exercises from Microbes in Action A Laboratory Manual of Microbiology 3rd Edn Pp 148 Pbk ISBN 0-7167-1260-1 (W H Freeman 1981) Pbk £5 80

SINCLAIR, J D The Rest Principle A Neurophysiological Theory of Behavior Pp 232 ISBN 0-89859-065-5 (Lawrence Erlbaum, London 1981) £14 95

STALDER, G and FLIEGEL, C P (Herausgeber des Bandes) Präventive Aspekte in der Pädiatrie Pädiatrische Fortbildungskurse für die Praxis Pp 182 Flexi ISBN 3-8055-1980-X (Karger, Basel 1981) SwFr /DM 89, $53 50

STEINBEREITHNER, K and LIST, W F (Bandherausgeber) Infusionstherapie mit Dextranen Beiträge zu Infusionstherapie und klinische Ernährung-Forschung und Praxis, Band 8 Ein aktueller Uberlick Symposium in Krems, Mai 1980 Pp 112 Flexi ISBN 3-8055-2840-X (Karger, Basel 1981) SwFr/ DM 25, $15

STRAUB, W (ed) Metabolic Disorders, Methods of Examination Developments in Ophthalmology, Vol 4 Pp 228 ISBN 3-8055-2014-X (Karger, Basel 1981) SwFr 166, DM 199, $99 50

STRINGER, C B (ed) Aspects of Human Evolution Symposia of the Society for the Study of Human Biology, Vol XXI Pp 233 ISBN 0-85066-209-5 (Taylor & Francis, London 1981) £14

SYNGE, H (ed) The Biological Aspects of Rare Plant Conservation Proceedings of an International Conference held at King's College, Cambridge, England, July 1980 Pp 558 ISBN 0-471-28004-6 (Wiley 1981) £30, $84

TANAKA, K and FUJITA, T (eds) Scanning Electron Microscopy in Cell Biology and Medicine Proceedings of the International Symposium, Kyoto, May 1981 Pp 499 ISBN 90-219-0477-2 (Excerpta Medica, Amsterdam 1981) $97 50, Dfl 200

TURIAN, G and HOHL, H R The Fungal Spore Morphogenetic Controls Proceedings of the 3rd International Fungal Spore Symposium (3IFSS) held August 1980 at Gwatt near Thun, Switzerland Pp 670 ISBN 0-12-703680-0 (Academic 1981) £27 80, $67

TURK, V and VITALE, L (eds) Proteinases and Their Inhibitors Structure, Function and Applied Aspects Proceedings of the International Symposium, Portoroz, Yugoslavia, September–October 1980 Pp 386 ISBN 0-08 027377-7 (Pergamon 1981) £33, $80

VIDRIO, E A *et al* (eds) Biological Rhythms in Structure and Function Progress in Clinical and Biological Research, Vol 59 11th International Congress of Anatomy, Part C Proceedings, Mexico City, Mexico, August 1980 Pp 244 ISBN 0-8451-0059-9 (Alan R Liss, New York 1981) £16 40, DM 72

WALZ, D A and McCOY, L E (eds) Annals of the New York Academy of Sciences, Vol 370 Contributions to Hemostasis Pp 856 Hbk ISBN 0-89766-X, pbk ISBN 0-89766-130-3 (The New York Academy of Sciences 1981) Hbk $159, pbk np

Applied Biological Sciences

CONSTANTINIDES, A , VIETH, W R and VENKATASUBRAMANIAN (eds) Annals of the New York Academy of Sciences, Vol 369 Biochemical Engineering II Pp 384 Hbk ISBN 0-89766-127-3, pbk ISBN 0-89766-128-1 (The New York Academy of Sciences 1981) Hbk $73, pbk np

HAYAT, M A X-Ray Microanalysis in Biology Pp 488 ISBN 0-333-32355-6 (Macmillan Press, London and New York 1981) £30

MALI, J W H (ed) Some Fundamental Approaches in Skin Research Current Problems in Dermatology, Vol 9 Pp 152 Flexi ISBN 3-8055-3080-3 (Karger, Basel 1981) SwFr 98, DM 177, $58 75

McKERNS, K W (ed) Reproductive Processes and Contraception Pp 731 ISBN 0-306-40534-2 (Plenum 1981) $65

METTLIN, C and MURPHY, G P (eds) Progress in Cancer Control Progress in Clinical and Biological Research, Vol 57 Proceedings of the 1st Conference in Progress in Cancer Control held in Buffalo, September 1980 Pp 236 ISBN 0-8451-0057-2 (Alan R Liss, New York 1981) £19 10, DM 84

OLWENY, C L M , HUTT, M S R and OWOR, R (eds) Kaposi's Sarcoma Antibiotics and Chemotherapy, Vol 29 Pp 104 ISBN 3-8055-2076-X (Karger, Basel 1981) SwFr 89, DM 107, $53 50

SALTON, M R J and SHOCKMAN, G D (eds) β-Lactam Antibiotics Mode of Action, New Developments, and Future Prospects Proceedings of a Symposium held at The New York University School of Medicine, September–October 1980 Pp 604 ISBN 0-12-616050-3 (Academic 1981) Np

SELL, K W and MILLER, W V (eds) The Lymphocyte Progress in Clinical and Biological Research, Vol 58 The American Red Cross 12th Annual Scientific Symposium, Washington, D C Pp 228 ISBN 0-8451-0058-0 (Alan R Liss, New York 1981) £23 20, DM 102

TSANG, R C and NICHOLS, B L Jr (eds) Nutrition and Child Health–Perspectives for the 1980s Progress in Clinical and Biological Research, Vol 61 Proceedings of the 21st Annual Meeting of the American College of Nutrition held in Bethesda, Maryland, September 1980 Pp 224 ISBN 0-8451-0061-0 (Alan R Liss, New York 1981) £15, DM 66

Psychology

ANDERSON, J R (ed) Cognitive Skills and Their Acquisition Pp 386 ISBN 0-89859-093-0 (Lawrence Erlbaum Associates, Hillsdale, New Jersey 1981) £14 95

ASHER, S R and GOTTMAN, J M (eds) The Development of Children's Friendships Pp 347 Hbk ISBN 0-521-23103-5, pbk ISBN 0-521-29806-7 (Cambridge University Press 1981) Hbk £20, pbk £7 50

BLOCK, N (ed) Readings in Philosophy of Psychology, Vol 2 Pp 366 ISBN 0416-746004 (Methuen 1981) £12 95

BONARIUS, H , HOLLAND, R and ROSENBERG, S Personal Construct Psychology Recent Advances in Theory and Practice Pp 286 ISBN 0-333-30687-2 (Macmillan Press, London and New York 1981) £30

COLARUSSO, C A and NEMIROFF, R A Adult Development A New Dimension in Psychodynamic Theory and Practice Pp 290 ISBN 0-306-40619-5 (Plenum 1981) $22 50

GLESER, G C , GREEN, G L and WINGET, C Prolonged Psychosocial Effects of Disaster A Study of Buffalo Creek Pp 176 ISBN 0-12-286260-0 (Academic 1981) $19

HOFER, M A The Roots of Human Behavior An Introduction to the Psychobiology of Early Development Pp 331 Hbk ISBN 0-7167-1277-6, pbk ISBN 0-7167-1278-4 (W H Freeman 1981) Hbk £14 10, pbk £6 70

MAYER, R E The Promise of Cognitive Psychology Pp 120 Hbk ISBN 0-7167-1275-X, pbk ISBN 0-7167-1276-8 (W H Freeman 1981) Hbk £8, pbk £3 70

Sociology

AL-FARUQI, I R and NASEEF, A O (eds) Social and Natural Sciences The Islamic Perspective Pp 177 ISBN 0-340-23613-2 (Hodder & Stoughton, Sevenoaks, U K 1981) £6 95

CHAMPION, D J Basic Statistics for Social Research 2nd Edn Pp 452 ISBN 0-02-320600-4 (Collier Macmillan 1981) £12 50

MACKLIN, R and GAYLIN, W Mental Retardation and Sterilization A Problem of Competency and Paternalism Pp 247 ISBN 0-306-40689-6 (Plenum 1981) $19 50

WOLF, S Social Environment and Health Pp 113 ISBN 0-295-95777-8 (University of Washington Press 1981) £5 40

History of Science

BALDWIN, R S The Fungus Fighters Two Women Scientists and Their Discovery Pp 212 ISBN 0-8014-1355-9 (Cornell University Press 1981) £9

ENGSTRAND, I H W Spanish Scientists in the New World The Eighteenth-Century Expeditions Pp 220 ISBN 0-295-95764-6 (University of Washington Press 1981) £15

GOLDSTINE, H H A History of the Calculus of Variations From the 17th Through the 19th Century Studies in the History of Mathematics and Physical Sciences, Vol 5 Pp 410 ISBN 3-540-90521-9 (Springer-Verlag 1980) DM 88, $51 80

WOOLF, H (ed) The Analytic Spirit Essays in the History of Science In Honor of Henry Guerlac Pp 363 ISBN 0-8014-1350-8 (Cornell University Press 1981) £15, $31 25

General

ADRIAN, M Alcoholism & Drug Addiction Research Foundation Statistical Supplement to the Annual Report 1979-1980 Pp 274 Pbk ISBN 0-88868-059-7 (Addiction Research Foundation, Toronto 1981) Pbk np

ANDREWS, J and VON HAHN, H P (eds) Geriatrics for Everyday Practice A Concise Compendium Pp 220 Flexi ISBN 3-8055-1803-X (Karger, Basel 1981) SwFr 39, DM 47, $23 50

BANERJI, B K Towards Quiescence and Immortality Pp 137 ISBN 8022-2366-4 (Philosophical Library, New York 1981) $10

BATTISTA, O A Olympiad of Knowledge–1984 Pp 94 Pbk ISBN 0-915074-09-5 (R S C Publishers, Fort Worth, Texas 1981) $9 95

BEADLE, N C W The Vegetation of Australia Pp 690 ISBN 0-521-24195-2 (Cambridge University Press 1981) £50

BELMAKER, R H and VAN PRAAG, H M (eds) Mania An Evolving Concept Pp 403 ISBN 0-85200-538-5 (MTP, Lancaster, U K 1981) £18 95

BOALCH, G T (ed) Essays on the Exe Estuary The Devonshire Association for the Advancement of Science, Literature and Art, Special Vol No 2 Pp 185 (No ISBN) (The Devonshire Association, Exeter 1981) Pbk £7 50

BURGER, E J Jr Science at the White House A Political Liability Pp 180 ISBN 0-8018-2433-8 (The Johns Hopkins University Press 1981) £9

CANTOR, H N and HODGE, M J S Conceptions of Ether Studies in the Theory of Ether Theories 1740-1900 Pp 351 ISBN 0-521-22430-6 (Cambridge University Press 1981) £30

CUTRIGHT, P R and BRODHEAD, M J Elliott Coues, Naturalist and Frontier Historian Pp 509 ISBN 0-252-00802-2 (University of Illinois Press 1981) £17 10

GRAESSER, A C Prose Comprehension Beyond the Word Pp 310 ISBN 3-540-90544-8 (Springer-Verlag 1981) DM 56, $29 40

HART, J and RICHARDSON, D The Theory and Practice of Homosexuality Pp 206 Pbk ISBN 0-7100-0838-4 (Routledge and Kegan Paul 1981) Pbk £4 95

HAWTHORN, J Foundations of Food Science Pp 207 Hbk ISBN 0-7167-1295-4, pbk ISBN 0-7167-1296-2 (W H Freeman 1981) Hbk £10, pbk £4 95

HAYES, J R The Complete Problem Solver Pp 263 ISBN 0-89168-028-4 (The Franklin Institute Press, Philadelphia 1981) $19 50

JENKINS, C and SHERMAN, B The Leisure Shock Pp 185 Hbk ISBN 0-413-48200-6, pbk ISBN 0-413-48210-3 (Eyre Methuen, London 1981) Hbk np, pbk £4 50

JOHANNES, R E Words of the Lagoon Fishing and Marine Lore in the Palau District of Micronesia Pp 245 ISBN 0-520-03929-7 (University of California Press 1981) £15, $31 20

KARGER, S (ed) The Manuscript Guidelines for the Preparation of Manuscripts and Bibliographies of Scientific Papers With a List of Title Abbreviations for Selected Medical and Related Journals Pp 52 Pbk ISBN 3-8055-2563-X (Karger, Basel 1981) Pbk SwFr 15, DM 18, $9

LANDSBERG, H E The Urban Climate Vol 28, International Geophysics Series Pp 275 ISBN 0-12-435960 (Academic 1981) $29 50

LASZLO, E and KEYS, D (eds) Disarmament The Human Factor Proceedings of a Colloquium on the Societal Context for Disarmament, held at the United Nations, New York Pp 164 Hbk ISBN 0-08-024703-2, flexi ISBN 0-08-028129-X (Pergamon 1981) Hbk np, flexi £5 25

LAUFMAN, H (ed) Hospital Special-Care Facilities Planning for User Needs Pp 533 ISBN 0-12-437740-8 (Academic 1981) $49 50

MAULE, H G and WEINER, J S Design for Work and Use Ergonomic Case Studies, Vol II Pp 147 ISBN 0-85066-208-7 (Taylor & Francis, London 1981) £12

MERCER, R (ed) Farming Practice in British Prehistory Pp 245 Pbk ISBN 0-85224-414-2 (Edinburgh University Press 1981) Pbk £9 50

MILLER, G A Language and Speech Pp 150 Hbk ISBN 0-7167-1297-0, pbk ISBN 0-7167-1298-9 (W H Freeman 1981) Hbk £8 20, pbk £3 50

NIWA, M (Director) Mitsubishi–Kasei Institute of Life Sciences, Annual Report 1980 (No 9) Pp 163 (No ISBN) (Mitsubishi–Kasei Institute of Life Sciences, 11 Minamiooya, Machida-shi, Tokyo 194, Japan 1981) Pbk np

PORTER, D A and EASTERLING, K E Phase Transformations in Metals and Alloys Pp 446 Hbk ISBN 0-442-30439-0, pbk ISBN 0-442-30440-4 (Van Nostrand Reinhold 1981) Hbk £18, pbk £8 95

PRAST, W G Securing U S Energy Supplies The Private Sector as an Instrument of Public Policy Pp 111 ISBN 0-669-03305-7 (Lexington Books, Gower Publishing Company, Aldershot, Hampshire 1981) £10 50

PROPOI, A and ZIMIN, I Dynamic Linear Programming Models of Energy, Resource and Economic Development Systems Pp 60 Flexi ISBN 3-7045-0010-0 (IIASA, Schloss Laxenburg, Austria 1981) $7

REEVES, H Patience Dans L'Azur L'Evolution Cosmique Pp 259 Pbk ISBN 2-02-005924-X (Éditions Du Seuil, Paris 1981) Pbk np

ROSENBERG, B L (ed) Annals of the New York Academy of Sciences, Vol 368 Papers in Science and Public Policy I Pp 235 Hbk ISBN 0-89766-125-7, pbk ISBN 0-89766-126-5 (The New York Academy of Sciences 1981) Hbk $48, pbk np

SIMON, J L The Ultimate Resource Pp 415 ISBN 0-691-09389-X (Princeton University Press 1981) $14 50

SMITH, C S A Search for Structure Selected Essays on Science, Art, and History Pp 410 ISBN 0-262-19191-1 (MIT Press 1981) £21

TALMOR, S Glanvill The Uses and Abuses of Scepticism Pp 102 ISBN 0-08-027407-2 (Pergamon 1981) £8

TANNER, N M On Becoming Human Pp 373 Hbk ISBN 0-521-23554-5, pbk ISBN 0-521-28028-1 (Cambridge University Press 1981) Hbk £20, pbk £6 95

THENIUS, E Versteinerte Urkunden Verstandliche Wissenschaft Band 81 Die Palaontologie als Wissenschaft vom Leben in der Vorzeit Seiten 202 Pbk ISBN 3-540-10674-X (Springer-Verlag 1981) DM 15, $9 60

nature

Author Index for Volume 295

January — February 1982

Issue no	Issue date	Page nos
5844	7 January	1–84
5845	14 January	85–176
5846	21 January	177–268
5847	28 January	269–354
5848	4 February	355–444
5849	11 February	445–540
5850	18 February	541–634
5851	25 February	635–722

Aaronson S A *see under* Eva A 295, 116
Abrahams P J *see under* de Jonge A J R, 295, 624
Acheson E D Data on dioxin, *correspondence* 295, 92
Adamson M G, Aitken E A and Vaidyanathan S Synergistic tellurium–caesium embrittlement of Type 316 stainless steel, 295, 49
Adelman J *see under* Comb M, 295, 663
Adey M *see under* Rimmer D, 295, 466
 see under Rimmer D 295, 466
 see under Rimmer D, 295, 466
Adinolfi M, Akle C A, McColl I, Fensom A H, Tansley L, Connolly P, Hsi B-L., Faulk W P, Travers P and Bodmer W F Expression of HLA antigens β-microglobulin and enzymes by human amniotic epithelial cells, 295, 325
Adler W H *see under* Saxena R K 295, 240
Agrawal D P *see under* Singhvi A K 295, 313
Aitken E A *see under* Adamson M G, 295, 49
Aitken R J *book review of* Male Reproductive Function and Semen Themes and Trends in Physiology Biochemistry and Investigative Andrology, (Mann T and Lutwak-Mann C) 295, 633
Aiton J F *see under* Lamb J F 295, 717
Ajello J M *see under* Pang K D, 295, 43
Akasofu S-I and Aspnes J D Auroral effects on power transmission line systems 295, 136
Akle C A *see under* Adinolfi M, 295, 325
Albrow M G *book review of* Jets of Hadrons, (Hofmann W) 295, 722
Alcock C Gravitational lenses *news and views* 295, 284
Alderton J M *see under* Steinhardt R A, 295, 154
Alexander P Prostaglandins and cancer, *news and views* 295, 188
Alexander R M The Chordates, *book review by* Halstead L B 295, 481
Allan D, Limbrick A R, Thomas P and Westerman M P Release of spectrin free spicules on reoxygenation of sickled erythrocytes 295, 612
Allègre C J *see under* Scharer U 295, 583
Allen D A *see under* Carter D, 295, 126
Allen G C, Tempest P A and Tyler J W Coordination model for the defect structure of hyperstoichiometric UO_{2+x} and U_4O_9 295, 48
Allen K *book review of* Paleobotany An Introduction to Fossil Plant Biology (Taylor T N) 295, 468
Allison J *see under* Craig R K 295, 345
Allison M L. *see under* Parmentier E M 295, 290
Andersen P R *see under* Eva A 295, 116
Anderson J G C and Owen T R The Structure of the British Isles, *book review by* Dineley D L 295, 467
Anderson R N *see under* Zoback M D 295, 375
Andrews P Hominoid evolution, *news and views* 295, 185
Andrews P W *see under* Goodfellow P N 295, 11
Angel J R P Very large ground-based telescopes for optical and IR astronomy, *review article* 295, 651
Antel J *see under* Oger J 295, 66
Anzano M A *see under* Roberts A B 295, 417
Araki K *see under* Tachibana S 295, 339
Arnason B G W *see under* Oger J, 295, 66
 see under Stefansson K, 295, 63
Arnow K S Losers all *correspondence* 295, 548
Ashburner M *book review of* Cytogenetics The Chromosome in Division, Inheritance and Evolution, (Swanson C P, Merz T, Young W J) 295, 477
 book review of Cytogenetics Plants, Animals Humans (Schulz-Schaeffer J) 295, 477
Ashby E *book review of* Science and Technology Policy Priorities of Governments (Tisdell C A) 295, 81
Askonas B A *see under* Morris A G, 295, 150
Aspnes J D *see under* Akasofu S-I, 295, 136
Atkins P W Physical Chemistry, *book review by* Rigby M 295, 489
Baertschi A J, Beny J-L. and Gahwiler B Hypothalamic paraventricular nucleus is a privileged site for brain pituitary interaction in long-term tissue culture, 295, 145
Baker T S *see under* Rayment I, 295, 110
Ball J N *see under* Pearson R, 295, 481
Banaszak L J and Ohlendorf D H Lipoprotein assembly in *Xenopus* yolk-platelet crystals, *matters arising* 295, 264
Barnes R D Invertebrate Zoology *book review by* Brafield A E 295, 482
Barnett S A Modern Ethology The Science of Animal Behaviour *book review by* Marler P 295, 472
Barrow G M Physical Chemistry for the Life Sciences *book review by* Spragg S P 295, 487
Barrow J D *book review of* Galactic Astronomy Structure and Kinematics (Mihalas D and Binney J) 295 440
Barry R G Mountain Weather and Climate *book review by* Palutikof J P, Wigley T M L 295, 462
Bartfai T *see under* Lundberg J M, 295, 147
Bateson P Preferences for cousins in Japanese quail, 295, 236
Bath G T *book review of* High Energy Astrophysics, (Longair M S) 295, 461
Batten R L *see under* Dott R H, 295, 463
Battey M H Mineralogy for Students *book review by* Howie R A 295, 464
Batty C J and Marshall G Making muonium in vacuum *news and views* 295, 457
Baunack E *see under* Gartner K, 295, 172
Bear J C *see under* Farid N R, 295, 629
Beattie D H *see under* Lee T J, 295, 214
Beckerle M C and Porter K R Inhibitors of dynein activity block intracellular transport in erythrophores, 295, 701
Beckwith J *book review of* Is Science Sexist? And Other Problems in the Biological Sciences (Ruse M) 295, 631
Begelman M C *see under* Rees M J, 295, 17
Begon M and Mortimer M Population Ecology A Unified Study of Animals and Plants, *book review by* Usher M B 295, 473
Behr J-P, Lehn J-M, Dock A-C and Moras D Crystal structure of a polyfunctional macrocyclic K^+ complex provides a solid-state model of a K^+ channel, 295, 526
Beinfeld M C *see under* Nilaver G, 295, 597
Bell G I, Selby M J and Rutter W J The highly polymorphic region near the human insulin gene is composed of simple tandemly repeating sequences, 295, 31
Bell K *book review of* Essentials of Earth History An Introduction to Historical Geology (Stokes W L) 295, 463
 book review of Evolution of the Earth, (Dott R H and Batten R L) 295, 463
Bell M B, Feldman P A, Kwok S and Matthews H E Detection of $HC_{11}N$ in IRC+10°216, 295, 389
Bell W J *see under* Tobin T R 295, 263
Beloussov V V Geotectonics *book review by* Burchfiel B C 295, 464
Bennett R C *see under* Wright L J, 295, 415
Benson H, Lehmann J W, Malhotra M S., Goldman R F, Hopkins J and Epstein M D Body temperature changes during the practice of g Tum-mo yoga, 295, 234
Beny J-L *see under* Baertschi A J, 295, 145
Berger S L *see under* Gray P W 295, 503
Berk A J *see under* Montell C, 295, 380
Berrill N J *see under* Karp G 295, 479
Berryman A A Population Systems A General Introduction *book review by* Usher M B 295, 473
Bidwell R G S Reagan's right, *correspondence* 295, 452
Binetruy B *see under* Rassoulzadegan M 295, 257
Binford L R Bones Ancient Men and Modern Myths, *book review by* Brain C K 295, 82
Binney J *see under* Mihalas D, 295, 440
Birge E A Bacterial and Bacteriophage Genetics An Introduction, *book review by* Symonds N 295, 478
Bishop J M *see under* Payne G S, 295, 209
Bjornsson H, Bjornsson S and Sigurgeirsson Th Penetration of water into hot rock boundaries of magma at Grimsvotn 295, 580
Bjornsson S *see under* Bjornsson H 295, 580
Blackburn D H *see under* Cronin D J, 295, 680
Blanc G *see under* Tassin J P 295, 696
Blandford R D *see under* Rees M J 295, 17
Blinkhorn S F and Hendrickson D E Averaged evoked responses and psychometric intelligence, 295, 596
Blitz L *see under* Mark J W-K, 295, 263
Boast S *see under* Lania L, 295, 349
Bockaert J *see under* Tassin J P, 295, 696
Bodmer W F *see under* Adinolfi M 295, 325
Bogue S W and Coe R S Successive palaeomagnetic reversal records from Kauai 295, 399
Boillot G Geology of the Continental Margins *book review by* Burchfiel B C 295, 464
Bootsma D *see under* de Jonge A J R, 295, 624
Bore P J *see under* Radda G K, 295, 608
Bornens M *see under* Maro B, 295 334
Boulter D *see under* Croy R R D 295, 76
Boyce J M *see under* Plescia J B 295, 285
Brafield A E *book review of* Invertebrate Zoology (Barnes R D) 295, 482
 book review of Invertebrate Zoology, (Engemann J G and Hegner R W) 295, 482
 book review of Invertebrate Respiration, (Wells R M G) 295, 482
 book review of Practical Invertebrate Zoology' (Dales R P *editor*) 295, 482
Brain C K *book review of* Bones Ancient Men and Modern Myths, (Binford L R) 295, 82
Brand P W J L *see under* Lee T J, 295, 214
Brandeis L *see under* Pearson J 295, 61
Braunitzer G *see under* Knöchel W, 295, 710
Brazier S *see under* Sparks R S J 295, 218
Brent L., Chandler P, Fierz W, Medawar P B, Rayfield L. S and Simpson E Further studies on supposed lamarckian inheritance of immunological tolerance, 295, 242
Breznik T and Cohen J C Altered methylation of endogenous viral promoter sequences during mammary carcinogenesis, 295, 255
Bright S W J, Lea P J, Kueh J S H, Woodcock C., Hollomon D W and Scott G C Proline content does not influence pest and disease susceptibility of barley, 295, 592
Brinkmann W *see under* Fabian A C 295, 508
Bromberg J P Physical Chemistry *book review by*, Rigby M 295, 489
Brooks C *see under* Machado N 295, 226
Browand F K *see under* Hopfinger E J, 295, 393
Browder L W Developmental Biology, *book review by* Newth D R 295, 479
Brower D L. *see under* Lawrence P A, 295, 55
Brown N *see under* Heston L 295, 160
Brownstein M J *see under* Hook V Y H, 295, 341
Brugge J S and Darrow D Rous sarcoma virus-induced phosphorylation of a 50,000-molecular weight cellular protein 295, 250
Buccellati G *see under* Venkatesan M I 295, 517
Burchfiel B C *book review of* Geology of the Continental Margins (Boillot G) 295, 464
 book review of Geotectonics, (Beloussov V V) 295, 464
 book review of Tectonics and Landforms, (Ollier C) 295, 464
Burnet B *book review of* Behavior Genetics and Evolution, (Erhman L and Parsons P A) 295, 475
Burns W G, Hughes A E, Marples J A C, Nelson R S and Stoneham A M Radiation effects and the leach rates of vitrified radioactive waste, 295, 130
Businger J A *see under* Fleagle R G, 295, 462
Butterworth B E *see under* Mirsalis J C, 295, 322
Butterworth P H W *book review of* Biochemistry (Stryer L) 295, 485
Buxton G B, Rhodes T and Sellers R M Radiation-induced dissolution of colloidal haematite, 295, 583
Campbell A K *see under* Hallett M B 295, 155
Cande W Z Inhibition of spindle elongation in permeabilized mitotic cells by erythro-9-[3-(2-hydroxynonyl)] adenine 295, 700
Carlisle D B No change in RE, *correspondence* 295, 362
Carlson B Patten's Foundations of Embryology *book review by* Newth D R 295, 479
Carter D, Allen D A and Malin D F Nature of the shells of NGC1344 295, 126
Cartwright B A and Collett T S How honey bees use landmarks to guide their return to a food source, 295, 560
Caruthers M H *see under* Montell C 295, 380
Casey J F and Karson J A Magma chamber profiles from Bay of Islands ophiolite complex—Reply 295, 717 *matters arising*
Caspar D L D *see under* Rayment I 295, 110
Casse-Delbart F *see under* Chilton M-D, 295, 432
Catlow C R A, Thomas J M, Parker S C and Jefferson D A Simulating silicate structures and the structural chemistry of pyroxenoids 295, 658
Cavalier-Smith T *book review of* Symbiosis in Cell Evolution Life and its Environment on the Early Earth (Margulis L) 295, 353
Cavalli-Sforza L. L. and Feldman M W Cultural Transmission and Evolution A Quantitative Approach *book review by* Eaves L J 295, 632
Cedar H *see under* Gruenbaum Y 295, 620
Chandler P *see under* Brent L 295, 242
Chang R Physical Chemistry With Applications to Biological Systems *book review by* Spragg S P 295, 487
Chapman G *book review of* Animal Physiology Adaptations in

Function (Hainsworth F R) **295**, 484

Charig A J *book review of* Phylogenetics The Theory and Practice of Phylogenetic Systematics, (Wiley E O) **295**, 720

Charlson R J and Rodhe H Factors controlling the acidity of natural rainwater, **295**, 683

Chatterjee S Phylogeny and classification of thecodontian reptiles, **295**, 317

Chattopadhyay S K , Cloyd M W , Linemeyer D L., Lander M R , Rands E and Lowy D R Cellular origin and role of mink cell focus-forming viruses in murine thymic lymphomas, **295**, 25

Chiba J *see under* Clark R B **295**, 412

Chilton M -D , Tepfer D A , Petit A , David C , Casse-Delbart F and Tempe J *Agrobacterium rhizogenes* inserts T-DNA into the genomes of the host plant root cells, **295**, 432

Chun S F S *see under* Pang K D , **295**, 43

Clapp J F *see under* Zanjani E D , **295**, 244

Clark M A and Shay J W Mitochondrial transformation of mammalian cells, **295**, 605

Clark R B , Chiba J., Zweig S E and Shevach E M T-cell colonies recognize antigen in association with specific epitopes in Ia molecules, **295**, 412

Clausen T *see under* Nørgaard A , **295**, 717

Clegg K B and Piko L RNA synthesis and cytoplasmic polyadenylation in the one-cell mouse embryo, **295**, 342

Cliff R A *see under* Humphries F J , **295**, 515

Cloyd M W *see under* Chattopadhyay S K , **295**, 25

Coe R S *see under* Bogue S W , **295**, 399

Coen E. S , Thoday J M and Dover G Rate of turnover of structural variants in the rDNA gene family of *Drosophila melanogaster*, **295**, 564

Cohen J C *see under* Breznik T **295**, 255

Collett T S *see under* Cartwright B A , **295**, 560

Collins T C *see under* Reynolds D C , **295**, 442

Colombo G and Cook A F *see under* Franklin F A , **295**, 128

Comb M , Seeburg P H , Adelman J , Eiden L and Herbert E Primary structure of the human Met- and Leu-enkephalin precursor and its mRNA, **295**, 663

Comfort A Morphic field sports, *correspondence* **295**, 92

Cominsky L. R *see under* Ogawara Y , **295**, 675

Conner B N , Takano T , Tanaka S , Itakura K and Dickerson R E. The molecular structure of d(^{I}CpCpGpG), a fragment of right-handed double helical A-DNA, **295**, 294

Connolly P *see under* Adinolfi M , **295**, 325

Conway D H T *Vide* the Latin, *correspondence*, **295**, 184

Cooper G , Noufi R , Frank A J and Nozik A J Oxygen evolution on tantalum-polypyrrole-platinum anodes, **295**, 578

Cornish-Bowden A Basic Mathematics for Biochemists, *book review by* Hassall H **295**, 486

Cosman D , Khoury G and Jay G Three classes of mouse H–2 messenger RNA distinguished by analysis of cDNA clones, **295**, 73

Cousins F W All in the Book, *correspondence* **295**, 452

Cove D J *book review of* An Introduction to Genetic Analysis, (Suzuki D T , Griffiths A J F , Lewontin R C) **295**, 476
  book review of Genetics A Molecular Approach, (Livingston Mays L) **295**, 476
  book review of Genetics Its Concepts and Implications, (Pai A C and Marcus-Roberts H) **295**, 476

Coward M P , Jan M Q , Rex D , Tarney J , Thirlwall M and Windley B F Structural evolution of a crustal section in the western Himalaya, **295**, 22

Cowen P J *see under* Nutt D J , **295**, 436

Cowley S W H Substorms and the growth phase problem, *news and views* **295**, 365

Cox B *book review of* Patterns of Vertebrate Biology, (Jameson E W) **295**, 480

Cox E C and May R M *book review of* A View of Life, (Luria S E , Gould S J , Singer S) **295**, 479

Cox F E G Cell mediated immunity in theileriosis, *news and views*, **295**, 14

Cox K G *book review of* Basalts and Phase Diagrams An Introduction to the Quantitative Use of Phase Diagrams in Igneous Petrology, (Morse S A) **295**, 468

Craig R K , Hall L , Edbrooke M R , Allison J and MacIntyre I Partial nucleotide sequence of human calcitonin precursor mRNA identifies flanking cryptic peptides, **295**, 345

Criddle W J and Ellis G P Spectral and Chemical Characterization of Organic Compounds A Laboratory Handbook, *book review by* Spessard G O **295**, 488

Crisp D J *book review of* Elements of Marine Ecology An Introductory Course, (Tait R V) **295**, 483
  book review of The Ecology of Marine Sediments An Introduction to the Structure and Function of Benthic Communities, (Gray J S) **295**, 483
  book review of The Estuarine Ecosystem, (McLusky D) **295**, 483

Cronin D J , Blackburn D H and Haller W K Unusual luminescence behaviour of terbium phosphate glasses, **295**, 680

Croy R R D , Lycett G W , Gatehouse J A , Yarwood J N and Boulter D Cloning and analysis of cDNAS encoding plant storage protein precursors, **295**, 76

Csaba G Ontogeny and Phylogeny of Hormone Receptors *book review by* DeSombre E R **295**, 354

Cuello A C *see under* Pearson J , **295**, 61

Culhane J L. *see under* Siegmund O H W , **295**, 678

Cull-Candy S G and Parker I Rapid kinetics of single glutamate-receptor channels, **295**, 410

Curtis H *see under* Raven P H , **295**, 471

Cuzin F *see under* Rassoulzadegan M , **295**, 257

Czeizel A *see under* Thomas H F , **295**, 276

Dahlen S -E *see under* Smedegård G , **295**, 327

Dales R P *Editor*, Practical Invertebrate Zoology, *book review by* Brafield A E **295**, 482

Darbre A *book review of* Amino Acid Analysis (Rattenbury J M *editor*) **295**, 176

Darrow D *see under* Brugge J S , **295**, 250

DasGupta C and Radding C M Lower fidelity of RecA protein catalysed homologous pairing with a superhelical substrate **295**, 71

Davenport J *see under* Rankin J C , **295**, 484

David C *see under* Chilton M -D , **295**, 432

Davies N B *see under* Krebs J R , **295**, 472

Davison W , Woof C and Turner D R Handling and measurement techniques for anoxic interstitial waters, **295**, 582

Dawes E A Quantitative Problems in Biochemistry, *book review by* Hassall H **295**, 486

de Bie R A The ultimate question *correspondence* **295**, 8

de Boer E *see under* Grosveld G C , **295**, 120

De Jager C The Brightest Stars, *book review by* Hutchings J B **295**, 632

de Jonge A J R , Abrahams P J , Westerveld A and Bootsma D Expression of human *hprt* gene on the inactive X chromosome after DNA-mediated gene transfer **295**, 624

De Robertis E M , Lienhard S and Parisot R F Intracellular transport of microinjected 5S and small nuclear RNAs, **295**, 572

Debarbouille M *see under* Hall M N , **295**, 616

Defendini R *see under* Nilaver G , **295**, 597

Delansorne R *see under* Lichtenberger L M , **295**, 698

Derrick K S *see under* French R C , **295**, 259

Derynck R *see under* Gray P W , **295**, 503

DeSombre E R *book review of* Ontogeny and Phylogeny of Hormone Receptors, (Csaba G) **295**, 354

Devor M *see under* Wall P D , **295**, 691

Diamond J M How eggs breathe while avoiding desiccation and drowning, *news and views* **295**, 10
  Mammary gland as an endocrine organ implications for mastectomy *news and views* **295**, 191
  Mirror-image navigational errors in migrating birds, *news and views* **295**, 277

Dickerson R E *see under* Conner B N , **295**, 294

Dickson R R , Gould W J , Garbutt P A and Killworth P D A seasonal signal in ocean currents to abyssal depths, **295**, 193

Dineley D L. *book review of* Methods in Field Geology (Moseley F) **295**, 467
  book review of The Stratigraphy of the British Isles, (Rayner D H) **295**, 467
  book review of The Structure of the British Isles, (Anderson J G C and Owen T R) **295**, 467

Dirac P A M The Principles of Quantum Mechanics, *book review by* Jones R B **295**, 460

Doble A and Iversen L L Molecular size of benzodiazepine receptor in rat brain *in situ* evidence for a functional dimer? **295**, 522

Dock A -C *see under* Behr J -P , **295**, 526

Dockray G J *book review of* Physiology of the Gastrointestinal Tract, (Johnson L R *editor*) **295**, 720

Donaldson C H Magma chamber profiles from Bay of Islands ophiolite complex, *matters arising* **295**, 717

Doolittle W F *see under* Sapienza C **295**, 384

Dorsch-Häsler K *see under* Mayer A , **295**, 253

Dott R H and Batten R L Evolution of the Earth, *book review by* Bell K **295**, 463

Dover G *see under* Coen E S , **295**, 564

Dreesman G R , Sanchez Y , Ionescu-Matiu I , Sparrow J T , Six H R , Peterson D L , Hollinger F B and Melnick J L Antibody to hepatitis B surface antigen after a single inoculation of uncoupled synthetic HBsAg peptides, **295**, 158

DSDP Scientific Party Breaking the 600 metre barrier, *news and views* **295**, 549

Dudeney J R , Jarvis M J , Kressman R I , Pinnock M , Rodger A S and Wright K H Ionospheric troughs in Antarctica, **295**, 307

Duke P J *see under* Perutz M F , **295**, 535

Dunn D *book review of* Excitons Their Properties and Uses (Reynolds D C and Collins T C) **295**, 442

Duplessy J C Glacial to interglacial contrasts in the northern Indian Ocean, **295**, 494

Eaves L J *book review of* Cultural Transmission and Evolution A Quantitative Approach (Cavalli Sforza L L and Feldman M W) **295**, 632

Edbrooke M R *see under* Craig R K , **295**, 345

Edelman G M *see under* Grumet M , **295**, 693

Edelstein S J *see under* Widom J M , **295**, 486

Edmunds M G Quasars resolved? *news and views* **295**, 556

Eichler D On the reported detection of sub GeV antiprotons in galactic cosmic rays **295**, 391

Eiden L *see under* Comb M , **295**, 663

Eiden L E *see under* Hook V Y H **295**, 341

Eisenberg D A problem for the theory of biological structure *news and views* **295**, 99

Eisenthal R *see under* Wharton C W , **295**, 485

Ek B , Westermark B , Wasteson Å and Heldin C -H Stimulation of tyrosine-specific phosphorylation by platelet derived growth factor, **295**, 419

Elder J Geothermal Systems, *book review by* England P **295**, 82

Ellis G P *see under* Criddle W J , **295**, 488

Ellmore N W *see under* Eva A , **295**, 116

Elson E *see under* Jacobson K , **295**, 283

Elzinga R J Fundamentals of Entomology, *book review by* Evans M E G **295**, 483

Engel P C Enzyme Kinetics The Steady-state Approach *book review by* Perham R N **295**, 485

Engemann J G and Hegner R W Invertebrate Zoology, *book review by* Brafield A E **295**, 482

England P *book review of* Geothermal Resources An Energy Alternative (Gupta H K) **295**, 82
  book review of Geothermal Systems Principles and Case Histories (Rybach L and Muffler L J P *editors*) **295**, 82
  book review of Geothermal Systems, (Elder J) **295**, 82
  book review of Geysers and Geothermal Energy, (Rinehart J S) **295**, 82

England P J *book review of* Protein Phosphorylation, (Rosen O M and Krebs E G *editors*) **295**, 442

Epstein L B Interferon gamma success, structure and speculation, *news and views* **295**, 453

Epstein M D *see under* Benson H , **295**, 234

Erhman L and Parsons P A Behavior Genetics and Evolution, *book review by* Burnet B **295**, 475

Erichsen J T , Reiner A and Karten H J Co-occurrence of substance P-like and Leu enkephalin-like immunoreactivities in neurones and fibres of avian nervous system, **295**, 407

Esterly S D *see under* Knudsen E I , **295**, 238

Eva A , Robbins K C , Andersen P R , Srinivasan A , Tronick S R , Reddy E. P , Ellmore N W , Galen A T , Lautenberger J A , Papas T S , Westin E H , Wong-Staal F , Gallo R C and Aaronson S A Cellular genes analogous to retroviral *onc* genes are transcribed in human tumour cells, **295**, 116

Evans E A and Skalak R Mechanics and Thermodynamics of Biomembranes *book review by* Silberberg A **295**, 84

Evans G A *see under* Margulies D H , **295**, 168

Evans M E G *book review of* Fundamentals of Entomology, (Elzinga R J) **295**, 483
  book review of Insect Physiology (Mordue W *et al*) **295**, 483
  book review of The Science of Entomology (Romoser W S) **295**, 483

Everett D H *book review of* Chemistry in Two Dimensions Surfaces, (Somorjai G A) **295**, 633

Evert R F *see under* Raven P H **295**, 471

Ewert J -P Neuroethology An Introduction to the Neurophysiological Fundamentals of Behavior, *book review by* Hoyle G **295**, 473

Ezra D Coal as Britain's security *correspondence* **295**, 642

Fabian A C , Stewart G C and Brinkmann W Is the remnant of SN1006 composed of iron? **295**, 508

Falconer D S Introduction of Quantitative Genetics, *book review by* Jones J S **295**, 475

Farid N R and Bear J C Two major genes, linked to HLA and Gm, control susceptibility to Graves disease **295**, 629 *matters arising*

Faulk W P *see under* Adinolfi M , **295**, 325

Feinstein A *see under* Wright L J **295**, 415

Feldman M W *see under* Cavalli-Sforza L L , **295**, 632

Feldman P A *see under* Bell M B , **295**, 389

Fensom A H *see under* Adinolfi M **295**, 325

Ferris S D , Sage R D and Wilson A C Evidence from mtDNA sequences that common laboratory strains of inbred mice are descended from a single female, **295**, 163

Festing M F W Do all laboratory mice trace back to a single female? *news and views* **295**, 94

Fiers W *see under* Kastelein R A , **295**, 35

Fierz W *see under* Brent L **295**, 242

Filkin D L *see under* Steed J M , **295**, 308

Finerty M P More repeats, *correspondence* **295**, 362

Fisher D *see under* Koerner R M., **295**, 137

Fisher E F *see under* Montell C **295**, 380

Fitter A H and Hay R K M Environmental Physiology of Plants *book review by* Harper J L **295**, 470

Fitzgerald M *book review of* Principles of Neural Science (Kandel E R and Schwartz J H *editors*) **295**, 474
  see under Wall P D **295**, 691

Flaherty L. *see under* Margulies D H , **295**, 168

Flavell R A The mystery of the mouse α-globin pseudogene, *news and views* **295**, 370 *Erratum* **295**, 556
  see under Grosveld G C , **295**, 120

Fleagle R G and Businger J A An Introduction to Atmospheric Physics *book review by* Green J S A **295**, 462

Flynn G J Spacecraft in orbit, *correspondence* **295**, 642

Fowler V M and Pollard H B Chromaffin granule membrane–F-actin interactions are calcium sensitive **295**, 336

Francis T J G Ocean floor conductivity measured *news and views* **295**, 550

Frank A J *see under* Cooper G , **295**, 578

Franklin F A , Colombo G and Cook A F A possible link between the rotation of Saturn and its ring structure **295**, 128

Fraser H Neuronal spread of scrapie agent and targeting of lesions within the retino-tectal pathway **295**, 149

Freiman S W *see under* Michalske T A , **295**, 511

French R C , Price M A and Derrick K S Circular double-stranded RNA in potato spindle tuber viroid-infected tomatoes **295**, 259

Fried M *see under* Lania L , **295**, 349

Frolik C. A *see under* Roberts A B **295**, 417

Fromhold A T Jr Quantum Mechanics For Applied Physics and Engineering, *book review by* Jones R B **295**, 460

Furutani Y *see under* Noda M , **295**, 202

Gabay J *see under* Hall M N , **295**, 616

Gadian D G *see under* Radda G K , **295**, 608

Gage L P *see under* Gubler U , **295**, 206

Gagosian R B *see under* Repeta D J **295**, 51

Gähwiler B *see under* Baertschi A J **295**, 145

Galen A T *see under* Eva A **295**, 116

Gallagher D L *see under* Reinleitner L A **295**, 46

Gallo R C. *see under* Eva A **295**, 116

Garbutt P A *see under* Dickson R R **295**, 193

Gardner M Science Good, Bad and Bogus *book review by* Medawar P B **295**, 351

Garratt P *book review of* Atoms, Molecules and Life An Introduction to General, Organic and Biological Chemistry (Matta M S and Wilbraham A C) **295**, 486
  book review of Chemistry An Introduction to General Organic, and Biological Chemistry (Widom J M and Edelstein S J) **295**, 486

Gartner K and Baunack E Are monozygotic twins similar due to genetic factors alone?—Reply, *matters arising* **295**, 172

Gatehouse J A *see under* Croy R R D , **295**, 76

Gatler I *see under* Lee T J **295**, 214

Gautier F DNA and Europe, *correspondence* **295**, 184

Gee P *see under* Hunt G E **295**, 491

Geisow M J Intracellular membrane traffic, *news and views* **295**, 649

Gelderblom H *see under* Tischer I , **295**, 64

Gerrard A J Soils and Landforms An Integration of Geomorphology and Pedology *book review by* Kirkby M J **295**, 467

Gilmore G The nature of galactic shells *news and views* **295**, 97

Gingerich P D Is this a record? *correspondence* **295**, 8

Glass B *book review of* Understanding Evolution (Hanson E D) **295**, 480

Glassley W Fluid evolution and graphite genesis in the deep continental crust **295**, 229

Glennie M J and Stevenson G T Univalent antibodies kill tumour cells *in vitro* and *in vivo* **295**, 712

Glowinski J *see under* Tassin J P , **295**, 696

Godovac J *see under* Knochel W , **295**, 710

Goeddel D V *see under* Gray P W , **295**, 503

Gojobori T *see under* Li W -H , **295**, 630

Goldman R F *see under* Benson H **295**, 234

Goodall H and Johnson M H Use of carboxyfluorescein diacetate to study formation of permeable channels between mouse blastomeres **295**, 524

Goodbody A E *see under* Trayhurn P , **295**, 323

Goodfellow P N and Andrews P W Sexual differentiation and H Y antigen *news and views* **295**, 11

Goodlad S W , Martin A K and Hartnady C J H Mesozoic magnetic anomalies in the southern Natal Valley **295**, 686

Goodman M Positive selection causes purifying selection, **295** *matters arising* 630
Goodwin T W *book review of* Secondary Plant Metabolism (Vickery B and Vickery M L) **295,** 471
Gordon S *book review of* Manual of Macrophage Methodology Collection Characterization, and Function, (Herschowitz H B *et al editors*) **295,** 634
Gott J R III Creation of open universes from de Sitter space **295,** 304
Goudie A *Editor*, Geomorphological Techniques, *book review by* Kidson C **295,** 175
Gould S J *see under* Luria S E , **295,** 479
Gould W J New measurements near the Gulf Stream, *news and views* **295,** 364
see under Dickson R R **295,** 193
Graneau P Electromagnetic jet-propulsion in the direction o˜ current flow **295,** 311
***Gration* K A F, Lambert J J, Ramsey R L, Rand R P and Usherwood P N R** Closure of membrane channels gated by glutamate receptors may be a two step process **295,** 599
Gratzer W *book review of* The Nobel Duel (Wade N) **295,** 266
Gray J S The Ecology of Marine Sediments An Introduction to the Structure and Function of Benthic Communities, *book review by* Crisp D J **295,** 483
Gray P W, Leung D W, Pennica D, Yelverton E, Najarian R, Simonsen C C, Derynck R, Sherwood P J, Wallace D M, Berger S L, Levinson A D and Goeddel D V Expression of human immune interferon cDNA in *E coli* and monkey cells **295,** 503
Graziani L A *see under* Lichtenberger L M , **295,** 698
Green H *see under* Watt F M **295,** 434
Green J S A *book review of* An Introduction to Atmospheric Physics (Fleagle R G and Businger J A) **295,** 462
book review of An Introduction to Atmospheric Radiation, (Liou K -N) **295,** 462
Greenland D J and Hayes M H B *Editors*, The Chemistry of Soil Processes, *book review by* West T S **295,** 352
Gregory J *book review of* Zeta Potential in Colloid Science Theory and Application, (Hunter R J) **295,** 267
Grieve R A F The Vredefort structure still not understooc *news and views* **295,** 644
Griffiths A J F *see under* Suzuki D T , **295,** 476
Groner B *see under* Kennedy N , **295,** 622
Grosveld G C, de Boer E, Shewmaker C K and Flavell R A DNA sequences necessary for transcription of the rabbit β-globin gene *in vivo*, **295,** 120
Gruenbaum Y, Cedar H and Razin A Substrate and sequence specificity of a eukaryotic DNA methylase **295,** 620
Grumet M, Rutishauser U and Edelman G M Neural cell adhesion molecule is on embryonic muscle cells and mediates adhesion to nerve cells *in vitro*, **295,** 693
Grundmann U *see under* Knochel W **295,** 710
Grunsfeld J M *see under* Ogawara Y , **295,** 675
Gruss P *see under* Levinson B , **295,** 568
Gubbins D Magnetic messages from the Earth's core, *news and views* **295,** 15
Gubler U, Seeburg P, Hoffman B J, Gage L P and Udenfriend S Molecular cloning establishes proenkephalin as precursor of enkephalin-containing peptides **295,** 206
Gupta H K Geothermal Resources An Energy Alternative *book review by* England P **295,** 82
Gurnett D A *see under* Reinleitner L A **295,** 46
Guthrie D M Neuroethology An Introduction *book review by* Hoyle G **295,** 473
Haddon M Dead end theory *correspondence* **295,** 92
Hahn J E *see under* Perutz M F , **295,** 535
Hainsworth F R Animal Physiology Adaptations in Function *book review by* Chapman G **295,** 484
Haley C S *see under* Jinks J L , **295,** 172
Hall L *see under* Craig R K , **295,** 345
Hall M N, Gabay J, Debarbouille M and Schwartz M A role for mRNA secondary structure in the control of translation initiation, **295,** 616
Hall Z W *see under* Silberstein L **295,** 143
Haller W K *see under* Cronin D J , **295,** 680
Hallett M B and Campbell A K Measurement of changes in cytoplasmic free Ca^{2+} in fused cell hybrids, **295,** 155
Halstead L B *book review of* Anatomy of the Chordates, (Weichert C K) **295,** 481
book review of Lecture Notes on Vertebrate Zoology, (Pearson R and Ball J N) **295,** 481
book review of The Chordates (Alexander R M) **295,** 481
book review of The Life of Vertebrates, (Young J Z) **295,** 481
Hameka H E *Quantum Mechanics*, *book review by* Jones R B **295,** 460
Hamer D H *see under* Zasloff M , **295,** 533
Hamilton J Not the baron *correspondence* **295,** 540
Hamm T E Jr *see under* Mirsalis J C **295,** 322
Hammarstrom S *see under* Smedegård G **295,** 327
Hanson E D Understanding Evolution, *book review by* Glass B **295,** 480
Harper J L *book review of* Environmental Physiology of Plants, (Fitter A H and Hay R K M) **295,** 470
book review of Physiological Plant Ecology, (Larcher W) **295,** 470
Harrison P R Stem cell regulation in erythropoiesis, *news and views* **295,** 454
Hartnady C J H *see under* Goodlad S W , **295,** 686
Hasnain S S *see under* Perutz M F , **295,** 535
Hassall H *book review of* Basic Mathematics for Biochemists (Cornish-Bowden A) **295,** 486
book review of Biochemistry A Problems Approach, (Wood W B *et al*) **295,** 486
book review of Quantitative Problems in Biochemistry, (Dawes E A) **295,** 486
Hawkes P W *book review of* Optical Information Processing Fundamentals, (Lee S H *editor*) **295,** 441
Hawthorne J N Is phosphatidylinositol now out of the calcium gate? *news and views* **295,** 281
Hay R K M *see under* Fitter A H , **295,** 470
Hayakawa K *see under* Herzenberg L A , **295,** 329
Hayashida H *see under* Miyata T **295,** 165
Hayes M H B *see under* Greenland D J , **295,** 352
Head J W *see under* Parmentier E M **295,** 290
Heap R B *see under* Wright L J **295,** 415
Heathcock C H *see under* Streitwieser A **295,** 487
Hedlund B *see under* Lundberg J M **295,** 147
Hedqvist P *see under* Smedegard G , **295,** 327
Hegner R W *see under* Engemann J G , **295,** 482
Heidmann J Relativistic Cosmology An Introduction, *book review by* Silk J **295,** 461
Heisenberg M *see under* Technau G , **295,** 405
Heldin C -H *see under* Ek B , **295,** 419
Hendrickson D E *see under* Blinkhorn S F **295,** 596
Hentschel C C Homocopolymer sequences in the spacer of a sea urchin histone gene repeat are sensitive to S1 nuclease, **295,** 714
Herbert E *see under* Comb M , **295,** 663
Herrlich P *see under* Kennedy N **295,** 622
Herschowitz H B *et al Editors*, Manual of Macrophage Methodology Collection, Characterization and Function, *book review by* Gordon S **295,** 634
Herve D *see under* Tassin J P **295,** 696
Herzenberg L A *see under* Herzenberg L A **295,** 329
Herzenberg L A, Tokuhisa T, Hayakawa K and Herzenberg L A Lack of immune response gene control for induction of epitope-specific suppression by TGAL antigen, **295,** 329
Heston L, Rabson M, Brown N and Miller G New Epstein–Barr virus variants from cellular subclones of P3J-HR-1 Burkitt lymphoma, **295,** 160
Hickey M and King C 100 Families of Flowering Plants *book review by* Moore P D **295,** 469
Hillel D Fundamentals of Soil Physics *book review by* Rimmer D , Adey M **295,** 466
Applications of Soil Physics *book review by* Rimmer D , Adey M **295,** 466
Hirose T *see under* Noda M , **295,** 202
Hirschhorn H H Niche work, *correspondence* **295** 92
Hobbs W Porter R *Editor* The Earth Generated and Anatomized An Early Eighteenth Century Theory of the Earth, *book review by* Sutton J **295,** 352
Hoffman B J *see under* Gubler U **295,** 206
Hofmann A W *see under* White W M , **295,** 363
Hofmann W Jets of Hadrons, *book review by* Albrow M G **295,** 722
Holland C H *Editor* A Geology of Ireland, *book review by* McKerrow W S **295,** 174
Editor Lower Palaeozoic of the Middle East, Eastern and Southern Africa, and Antarctica With Essays on Lower Palaeozoic Trace Fossils of Africa and Lower Palaeozoic Palaeoclimatology *book review by* Watson J V **295,** 268
Hollin A J Brought to Book *correspondence* **295,** 548
Hollinger F B *see under* Dreesman G R , **295,** 158
Hollomon D W *see under* Bright S W J , **295,** 592
Hook V Y H, Eiden L E and Brownstein M J A carboxypeptidase processing enzyme for enkephalin precursors **295,** 341
Hopfinger E J and Browand F K Vortex solitary waves in a rotating, turbulent flow, **295,** 393
Hopkins J *see under* Benson H , **295,** 234
Hoppe M M and Russell C T Particle acceleration at planetary bow shock waves, **295,** 41
Horn L H *see under* Trewartha G T , **295,** 462
Houghten R *see under* Liotta A S , **295,** 593
House L S and Jacob K H Thermal stresses in subducting lithosphere can explain double seismic zones, **295,** 587
Howie R A *book review of* Crystallography An Introduction for Earth Science (and Other Solid State) Students (Whittaker E J W) **295,** 464
book review of Mineralogy for Students, (Battey M H) **295,** 464
Hoyle F and Narlikar J The Physics–Astronomy Frontier, *book review by* Silk J **295,** 461
Hoyle G *book review of* Neuroethology An Introduction to the Neurophysiological Fundamentals of Behavior (Ewert J -P) **295,** 473
book review of Neuroethology An Introduction, (Guthrie D M) **295,** 473
Hsi B -L *see under* Adinolfi M **295,** 325
Hubbard S R and Ross R G Slope anomaly in the vapour pressure curve of Hg, **295,** 682
Hughes A E *see under* Burns W G **295,** 130
Hughes D W Meteorite erosion and cosmic ray variations *news and views* **295,** 279
Spacecraft collisions *news and views* **295,** 100
Hughes J *see under* Unsworth C D , **295,** 519
Hull D L *book review of* The Development of Darwin's Theory Natural History Natural Theology, and Natural Selection, 1838–1859, (Ospovat D) **295,** 719
Humphrey J H *book review of* The Immune System, (Steinberg C M and Lefkovits I *editors*) **295,** 721
Humphries F J and Cliff R A Sm–Nd dating and cooling history of Scourian granulites Sutherland, **295,** 515
Hunt D M *see under* Stewart A D , **295,** 477
Hunt G E, Muller J -P and Gee P Convective growth rates of equatorial features in the jovian atmosphere **295,** 491
Hunter R J Zeta Potential in Colloid Science Theory and Application *book review by* Gregory J **295,** 267
Hutchings J B *book review of* The Brightest Stars (De Jager C) **295,** 632
Hyams J Dynein in the spindle? *news and views* **295,** 648
Hyland A R *see under* Lee T J , **295,** 214
Hynes N E *see under* Kennedy N , **295,** 622
Inayama S *see under* Noda M , **295,** 202
Inestrosa N C *see under* Silberstein L , **295,** 143
Ionescu-Matiu I *see under* Dreesman G R , **295,** 158
Iscove N N *see under* Magli M C **295,** 527
Ishii N, Nagy Z A and Klein J Absence of *Ir* gene control of T cells recognizing foreign antigen in the context of allogeneic MHC molecules, **295,** 531
Itakura K *see under* Conner B N **295,** 294
Itô Y Comparative Ecology *book review by* Lawton J **295,** 83
Iversen L L *see under* Doble A **295,** 522
Izant J G, Weatherbee J A and McIntosh J R A microtubule-associated protein in the mitotic spindle and the interphase nucleus, **295,** 248
Jackson D F, Lewis C A, O'Leary K and Lam G K Y Molecular effects in pion capture in complex materials, **295,** 557
Jacob K H *see under* House L S , **295,** 587
Jacobson K, Elson E, Koppel D and Webb W Fluorescence photobleaching in cell biology, *news and views* **295,** 283
Jaffe E A, Leung L L K, Nachman R L, Levin R I and Mosher D F Thrombospondin is the endogenous lectin of human platelets, **295,** 246
Jahoda M *book review of* The DNA Story A Documentary History of Gene Cloning, (Watson J D and Tooze J) **295,** 173
James M N G *see under* Sawyer L , **295,** 79
Jameson E W Patterns of Vertebrate Biology, *book review by* Cox B **295,** 480
Jan M Q *see under* Coward M P , **295,** 22
Jarvis M J *see under* Dudeney J R , **295,** 307
Jay G *see under* Cosman D , **295,** 73
Jefferson D A *see under* Catlow C R A , **295,** 658
Jenny H The Soil Resource Origin and Behavior *book review by* Rimmer D Adey M **295,** 466
Jessell T M Fifty years of substance P, *news and views* **295,** 551
Jesson J P *see under* Steed J M , **295,** 308
Jinks J L, Haley C S and Last K A Are monozygotic twins similar due to genetic factors alone? *matters arising* **295,** 172
Johansen Mange E *see under* Mange A P , **295,** 478
John M E *see under* Knochel W **295,** 710
Johnson L R *Editor*, Physiology of the Gastrointestinal Tract, *book review by* Dockray G J **295,** 720
Johnson M H *see under* Goodall H , **295,** 524
Johnson P E Grain alignment in the galactic magnetic field, *review article* **295,** 371
Jones J S *book review of* Basic Population Genetics (Wallace B) **295,** 475
book review of Introduction of Quantitative Genetics (Falconer D S) **295,** 475
Jones P M *see under* Trayhurn P **295,** 323
Jones R B *book review of* Basic Quantum Mechanics, (Martin J L) **295,** 460
book review of Quantum Mechanics, (Hameka H E) **295,** 460
book review of Quantum Mechanics For Applied Physics and Engineering, (Fromhold A T Jr) **295,** 460
book review of The Principles of Quantum Mechanics, (Dirac P A M) **295,** 460
Jones R J *see under* Sutherst R W , **295,** 320
Jones T *see under* Lee T J , **295,** 214
Jones T B *see under* Kopka H , **295,** 680
Jukes T H Aircraft evolution, *correspondence* **295,** 548
Kai-Kai M A *see under* Pentreath V W **295,** 59
Kaine B P and Spear B B Nucleotide sequence of a macronuclear gene for actin in *Oxytricha fallax*, **295,** 430
Kandel E R and Schwartz J H *Editors*, Principles of Neural Science *book review by* Fitzgerald M **295,** 474
Karp G and Berrill N J Development, *book review by* Newth D R **295,** 479
Karson J A *see under* Casey J F , **295,** 717
Karten H J *see under* Erichsen J T , **295,** 407
Kastelein R A, Remaut E, Fiers W and van Duin J Lysis gene expression of RNA phage MS2 depends on a frameshift during translation of the overlapping coat protein gene, **295,** 35
Kejzlarova-Lepesant J *see under* Moreau J , **295,** 260
Kennedy J S, Ludlow A R, and Sanders C J Guidance system for pheromone orientation in moths—Reply, *matters arising* **295,** 263
Kennedy N, Knedlitschek G, Groner B, Hynes N E, Herrlich P, Michalides R and van Ooyen A J J Long terminal repeats of endogenous mouse mammary tumour virus contain a long open reading frame which extends into adjacent sequences **295,** 622
Kenneth J P Marine Geology, *book review by* Smith P J **295,** 466
Kerridge J F Whence so much ^{15}N? *news and views* **295,** 643
Key M H *book review of* Laser Interaction and Related Plasma Phenomena, (Schwarz H J *et al editors*) **295,** 84
Khoury G *see under* Cosman D , **295,** 73
see under Levinson B , **295,** 568
Kidson C *book review of* Geomorphological Techniques, (Goudie A *editor*) **295,** 175
Killick H J Soviet sanctions *correspondence* **295,** 362
Killworth P D *see under* Dickson R R , **295,** 193
King C *see under* Hickey M , **295,** 469
Kirby R and Parker W R A suspended sediment front in the Severn Estuary, **295,** 396
Kirkby M J *book review of* Soils and Landforms An Integration of Geomorphology and Pedology, (Gerrard A J) **295,** 467
Kitts P A, Lamond A and Sherratt D J Inter-replicon transposition of Tn*1/3* occurs in two sequential genetically separable steps, **295,** 626
Kjeldsen K *see under* Nørgaard A , **295,** 717
Klein J *see under* Ishii N , **295,** 531
Klinman N R *see under* Owen J A **295,** 347
Knedlitschek G *see under* Kennedy N , **295,** 622
Knight P Exciting Rydberg atoms in cavities, *news and views* **295,** 192
Knochel W, Wittig B, Wittig S, *John M E, Grundmann U*, Oberthur W, Godovac J and Braunitzer G No evidence for stress α globin genes in chicken, **295,** 710
Knox P, Wells P and Serafini-Fracassini A A non-collagenous glycoprotein from elastic tissue acts as substratum for growth of cells *in vitro* **295,** 614
Knudsen E I, Knudsen P F and Esterly S D Early auditory experience modifies sound localization in barn owls, **295,** 238
Knudsen P F *see under* Knudsen E I , **295,** 238
Koch G L E *book review of* Towards Understanding Receptors Current Reviews in Biomedicine, (Lamble J W *editor*) **295,** 352
Koch M A *see under* Tischer I , **295,** 64
Koerner R M and Fisher D Acid snow in the Canadian high Arctic, **295,** 137
Kopka H, Stubbe P, Jones T B and Robinson T Nonlinear reflectivity of high-power radio waves in the ionosphere, **295,** 680
Koppel D *see under* Jacobson K , **295,** 283
Korn L J Transcription of *Xenopus* 5S ribosomal RNA genes, *review article* **295,** 101
Krebs E G *see under* Rosen O M , **295,** 442
Krebs J R and Davies N B An Introduction to Behavioural Ecology, *book review by* Marler P **295,** 472
Kressman R I *see under* Dudeney J R , **295,** 307
Krieger D T *see under* Liotta A S , **295,** 593
Krolick K A, Uhr J W and Vitetta E S Selective killing of leukaemia cells by antibody–toxin conjugates implications for autologous bone marrow transplantation **295,** 604

Kruper J S *see under* Ogawara Y , 295, 675
Kryszewski M Semiconducting Polymers, *book review by* Mark H 295, 176
Ku T L *see under* Reyss J L 295, 401
Kueh J S H *see under* Bright S W J , 295, 592
Kuff E *see under* Lueders K , 295, 426
Kwok S *see under* Bell M B , 295, 389
LaBarba R C Foundations of Developmental Psychology *book review by* Yonas A 295, 474
Lam G K Y *see under* Jackson D F , 295, 557
Lamb J F , Aiton J F and Ogden P K^+ depletion and Na^+ pump density *matters arising* 295, 717
Lamb L C *see under* Roberts A B , 295, 417
Lamb N A *see under* Mackenzie A S , 295, 223
Lambert J J *see under* Gration K A F , 295, 599
Lamble J W *Editor*, Towards Understanding Receptors Current Reviews in Biomedicine, *book review by* Koch G L E 295, 352
Lamond A *see under* Kitts P A , 295, 626
Land H , Schutz G , Schmale H and Richter D Nucleotide sequence of cloned cDNA encoding bovine arginine vasopressin–neurophysin II precursor 295, 299 *Corrigendum* 295, 458
Lander M R *see under* Chattopadhyay S K , 295, 25
Lange R H Lipoprotein assembly in *Xenopus* yolk-platelet crystals—Reply *matters arising* 295, 264
Lania L , Boast S and Fried M Excision of polyoma virus genomes from chromosomal DNA by homologous recombination 295, 349
Larcher W Physiological Plant Ecology, *book review by* Harper J L 295, 470
Last K A *see under* Jinks J L , 295, 172
Lautenberger J A *see under* Eva A 295, 116
Lawrence A Asymmetric Balmer line profiles in Seyfert galaxies, 295, 509
Lawrence P A *book review of* The Genetic Basis of Development (Stewart A D and Hunt D M) 295, 477
Lawrence P A and Brower D L Myoblasts from *Drosophila* wing disks can contribute to developing muscles through out the fly 295, 55
Lawton J *book review of* Comparative Ecology (Ito Y) 295, 83
Le Moal M *see under* Tassin J P , 295, 696
Le Moullec J M *see under* Virtanen A , 295, 705
Lea D J and Sheppeard H Referees unmasked? *correspondence* 295, 184
Lea P J *see under* Bright S W J , 295, 592
Leder A *see under* Lueders K , 295, 426
Leder P *see under* Lueders K , 295, 426
Lee S H *Editor*, Optical Information Processing Fundamentals *book review by* Hawkes P W 295, 441
Lee T J , Beattie D H , Gatley I , Brand P W J L, Jones T and Hyland A R Occurrence of the 3 3 μm feature in galaxies, 295, 214
Lefkovits I *see under* Steinberg C M 295, 721
Legay J M Workers' union, *correspondence* 295, 452
Lehman J W Operational Organic Chemistry A Laboratory Course, *book review by* Spessard G O 295, 488
Lehmann J W *see under* Benson H 295, 234
Lehn J -M *see under* Behr J -P , 295, 526
Lepesant J -A *see under* Moreau J , 295, 260
Leung D W *see under* Gray P W , 295, 503
Leung L L K *see under* Jaffe E A , 295, 246
Levin R I *see under* Jaffe E A 295, 246
Levinson A D *see under* Gray P W , 295, 503
  see under McGrath J P 295, 423
Levinson B , Khoury G , Vande Woude G and Gruss P Activation of SV40 genome by 72-base pair tandem repeats of Moloney sarcoma virus, 295, 568
Lewis C A *see under* Jackson D F , 295, 557
Lewis J G E The Biology of Centipedes, *book review by* Wallwork J A 295, 441
Lewontin R C *see under* Suzuki D T , 295, 476
Li W -H , Gojobori T and Nei M Positive selection causes purifying selection—Reply, *matters arising* 295, 630
Lichtenberger L M , Delansorne R and Graziani L A Importance of amino acid uptake and decarboxylation in gastrin release from isolated G cells, 295, 698
Liebert R M and Wicks-Nelson R Developmental Psychology, *book review by* Yonas A 295, 474
Lienhard S *see under* De Robertis E M , 295, 572
Lim G *see under* Zanjani E D , 295, 244
Limbrick A R *see under* Allan D , 295, 612
Lin Y L *see under* Morris A G , 295, 150
Linemeyer D L *see under* Chattopadhyay S K 295, 25
Linick T W *see under* Venkatesan M I 295, 517
Liotta A S , Houghten R and Krieger D T Identification of a β-endorphin-like peptide in cultured human placental cells 295, 593
Liou K -N An Introduction to Atmospheric Radiation *book review by* Green J S A 295, 462
Little H J *see under* Nutt D J , 295, 436
Livingston Mays L Genetics A Molecular Approach *book review by* Cove D J 295, 476
Loeb L A *see under* Zakour R A , 295, 708
Longair M S High Energy Astrophysics, *book review by* Bath G T 295, 461
Lonsdale P F *see under* Simoneit B R T 295, 198
Lorenz K Z The Foundations of Ethology, *book review by* Ridley M 295, 439
Love F G *see under* Wharton R A Jr 295, 403
Lowy D R *see under* Chattopadhyay S K , 295, 25
Ludden J N *see under* Machado N 295, 226
Ludlow A R *see under* Kennedy J S 295, 263
Lueders K , Leder A , Leder P and Kuff E Association between a transposed α-globin pseudogene and retrovirus like elements in the BALB/c mouse genome 295, 426
Lundberg J M , Hedlund B and Bartfai T Vasoactive intestinal polypeptide enhances muscarinic ligand binding in cat submandibular salivary gland 295, 147
Luria S E , Gould S J and Singer S A View of Life *book review by* Cox E C May R M 295, 479
Lutwak-Mann C *see under* Mann T 295, 633
Lycett G W *see under* Croy R R D , 295, 76
McAllister H *book review of* The Biological Aspects of Rare Plant Conservation, (Synge H *editor*) 295, 719
McClelland D B L *see under* Moore S 295, 529
McColl I *see under* Adinolfi M , 295, 325
McCully M E *see under* O'Brien T P , 295, 469
McGlave P B *see under* Zanjani E D 295, 244
McGrath J P and Levinson A D Bacterial expression of an enzymatically active protein encoded by RSV *src* gene, 295, 423
McGuckin M M *see under* Trayhurn P , 295, 323
Machado N , Ludden J N., Brooks C and Thompson G Fine-scale isotopic heterogeneity in the sub-Atlantic mantle, 295, 226
McIntosh J R *see under* Izant J G 295, 248
MacIntyre I *see under* Craig R K , 295, 345
MacKay D M and MacKay V Explicit dialogue between left and right half systems of split brains, 295, 690
MacKay V *see under* MacKay D M , 295, 690
Mackenzie A S Lamb N A and Maxwell J R Steroid hydrocarbons and the thermal history of sediments 295, 223
McKerrow W S *book review of* A Geology of Ireland, (Holland C H *editor*) 295, 174
McLusky D The Estuarine Ecosystem, *book review by* Crisp D J 295, 483
McPhail T L Electronic Colonialism The Future of International Broadcasting and Communication, *book review by* Maddox B 295, 439
Maddox B *book review of* Electronic Colonialism The Future of International Broadcasting and Communication, (McPhail T L) 295, 439
  book review of Global Talk The Marriage of the Computer World Communications and Man, (Pelton J N) 295, 439
Maden M Vitamin A and pattern formation in the regenerating limb, 295, 672
Magli M C , Iscove N N and Odartchenko N Transient nature of early haematopoietic spleen colonies, 295, 527
Malhotra M S *see under* Benson H , 295, 234
Malin D F *see under* Carter D , 295, 126
Mange A P and Johansen Mange E Genetics Human Aspects *book review by* Miller D A 295, 478
Mann J *book review of* Guidebook to Mechanism in Organic Chemistry (Sykes P) 295, 487
  book review of Introduction to Organic Chemistry, (Streitwieser A and Heathcock C H) 295, 487
  book review of The Vocabulary of Organic Chemistry, (Orchin M *et al*) 295, 487
Mann L I *see under* Zanjani E D , 295, 244
Mann T and Lutwak-Mann C Male Reproductive Function and Semen Themes and Trends in Physiology, Biochemistry and Investigative Andrology, *book review by* Aitken R J 295, 633
Marcaud L *see under* Moreau J , 295, 260
Marchig V *see under* Reyss J L , 295, 401
Marcus-Roberts H *see under* Pai A C , 295, 476
Margulies D H , Evans G A , Flaherty L and Seidman J G *H–2*-like genes in the *Tla* region of mouse chromosome, 295, 168
Margulis L Symbiosis in Cell Evolution Life and its Environment on the Early Earth, *book review by* Cavalier Smith T 295, 353
Mark H *book review of* Semiconducting Polymers, (Kryszewski M) 295, 176
Mark J W -K and Blitz L Tilt of the central gas disk of the Galaxy—Reply, *matters arising* 295, 263
Markham P and Whitehouse H L K A hypothesis for the initiation of genetic recombination in eukaryotes, 295, 421
Marks J All in The Book, *correspondence* 295, 276
Marler P *book review of* An Introduction to Behavioural Ecology, (Krebs J R and Davies N B) 295, 472
  book review of Modern Ethology The Science of Animal Behaviour, (Barnett S A) 295, 472
Maro B and Bornens M Reorganization of HeLa cell cytoskeleton induced by an uncoupler of oxidative phosphorylation, 295, 334
Marples J A C *see under* Burns W G , 295, 130
Marquardt H *see under* Roberts A B 295, 417
Marshall G *see under* Batty C J , 295, 457
Martin A K *see under* Goodlad S W , 295, 686
Martin J L Basic Quantum Mechanics, *book review by* Jones R B 295, 460
Masai K *see under* Ogawara Y , 295, 675
Maschat F *see under* Moreau J , 295, 260
Mason I M *see under* Siegmund O H W 295, 678
Matta M S and Wilbraham A C Atoms Molecules, and Life An Introduction to General Organic, and Biological Chemistry, *book review by* Garratt P 295, 486
Matthews H E *see under* Bell M B , 295, 389
Mattis D C The Theory of Magnetism I Statics and Dynamics, *book review by* Sherrington D 295, 354
Maxwell J R *see under* Mackenzie A S , 295, 223
May R M *see under* Cox E C , 295, 479
Mayer A and Dorsch-Hasler K Endogenous MuLV infection does not contribute to onset of radiation- or carcinogen-induced murine thymoma, 295, 253
Maynard J B *see under* Potter P E , 295, 465
Medawar P B *book review of* Science Good, Bad and Bogus, (Gardner M) 295, 351
  see under Brent L 295, 242
Mellars P *book review of* The Lower and Middle Palaeolithic Periods in Britain (Roe D A) 295, 268
Melnick J L *see under* Dreesman G R , 295, 158
Merz T *see under* Swanson C P , 295, 477
Michalides R *see under* Kennedy N , 295, 622
Michalske T A and Freiman S W A molecular interpretation of stress corrosion in silica 295, 511
Migeon B R *see under* Wolf S F 295, 667
Mihalas D and Binney J Galactic Astronomy Structure and Kinematics *book review by* Barrow J D 295, 440
Miller C *see under* Steed J M , 295, 308
Miller D A *book review of* Genetics Human Aspects, (Mange A P and Johansen Mange E) 295, 478
  book review of Human Chromosomes Structure, Behavior, Effects, (Therman E) 295, 478
Miller G *see under* Heston L , 295, 160
Miller J , Selsing E and Storb U Structural alterations in J regions of mouse immunoglobulin λ genes are associated with differential gene expression, 295, 428
Miller K R Base mettle *correspondence* 295, 8
Minji L *see under* Pang K D , 295, 43
Mirsalis J C , Hamm T E Jr, Sherrill J M and Butterworth B E Role of gut flora in the genotoxicity of dinitrotoluene, 295, 322
Mitsuda K *see under* Ogawara Y , 295, 675
Miyata T and Hayashida H Recent divergence from a common ancestor of human IFN α genes, 295, 165
Model P Oddities in the initiation of translation, *news and views*, 295, 15
Montell C., Fisher E F , Caruthers M H and Berk A J Resolving the functions of overlapping viral genes by site-specific mutagenesis at a mRNA splice site, 295, 380
Moore B W *see under* Stefansson K , 295, 63
Moore P D *book review of* 100 Families of Flowering Plants, (Hickey M and King C) 295, 469
  A new British flower, *news and views* 295, 189
  Evolution of photosynthetic pathways in flowering plants, *news and views* 295, 647
  book review of The Study of Plant Structure Principles and Selected Methods (O'Brien T P and McCully M E) 295, 469
Moore S , Woodrow C F and McClelland D B L Isolation of membrane components associated with human red cell antigens Rh(D), ($\bar{c}$), (E) and Fy^a, 295, 529
Moras D *see under* Behr J -P , 295, 526
Mordue W *et al* Insect Physiology, *book review by* Evans M E G 295, 483
Moreau J , Marcaud L , Maschat F , Kejzlarova-Lepesant J , Lepesant J -A and Scherrer K A+T rich linkers define functional domains in eukaryotic DNA, 295, 260
Morgan-Hughes J *see under* Radda G K , 295, 608
Morisawa M and Okuno M Cyclic AMP induces maturation of trout sperm axoneme to initiate motility, 295, 703
Morley J S *see under* Unsworth C D , 295, 519
Morrell G Another contender, *correspondence* 295, 8
Morris A G , Lin Y L and Askonas B A Immune interferon release when a cloned cytotoxic T-cell line meets its correct influenza-infected target cell, 295, 150
Morse S A Basalts and Phase Diagrams An Introduction to the Quantitative Use of Phase Diagrams in Igneous Petrology, *book review by* Cox K G 295, 468
Mortimer M *see under* Begon M , 295, 473
Moseley F Methods in Field Geology *book review by* Dineley D L 295, 467
Mosher D F *see under* Jaffe E A , 295, 246
Muffler L J P *see under* Rybach L , 295, 82
Muller J -P *see under* Hunt G E , 295, 491
Muller R A How black is the Universe? *news and views* 295, 95
Murakami W T *see under* Rayment I 295, 110
Murdoch H S The active radio galaxy 1413+135, *matters arising* 295, 718
Murray B *et al* Earthlike Planets Surfaces of Mercury Venus, Earth Moon, Mars *book review by* Wilson L 295, 463
Murrell J N *book review of* Potential Energy Surfaces and Dynamics Calculations for Chemical Reactions and Molecular Energy Transfer, (Truhlar D G *editor*) 295, 634
Murthy G S and Patzold R R Magnetic granulometry results for intrusive rock samples, 295, 688
Nachman R L *see under* Jaffe E A , 295, 246
Nagy Z A *see under* Ishii N , 295, 531
Naitoh Y *see under* Sugino K , 295, 609
Najarian R *see under* Gray P W , 295, 503
Nakanishi S *see under* Noda M , 295, 202
Nakato Y , Takamori N and Tsubomura H A composite semiconductor photoanode for water electrolysis, 295, 312
Nansheng Z *see under* Pang K D , 295, 43
Narlikar J *see under* Hoyle F , 295, 461
Narlikar J V *see under* Padmanabhan T 295, 677
Neftel A , Oeschger H , Schwander J , Stauffer B and Zumbrunn R Ice core sample measurements give atmospheric CO_2 content during the past 40 000 yr, 295, 220
Nei M *see under* Li W -H , 295, 630
Nelson A H Tilt of the central gas disk of the Galaxy *matters arising* 295, 263
Nelson R S *see under* Burns W G , 295, 130
Nesteroff W *see under* Rossignol-Strick M , 295, 105
Newth D R *book review of* Development, (Karp G and Berrill N J) 295, 479
  book review of Developmental Biology (Browder L W) 295, 479
  book review of Introduction to Embryonic Development, (Oppenheimer S B) 295, 479
  book review of Patten's Foundations of Embryology (Carlson B) 295, 479
Nilaver G , Defendini R , Zimmerman E A , Beinfeld M C and O'Donohue T L Motilin in the Purkinje cell of the cerebellum, 295, 597
Noda M , Furutani Y , Takahashi H , Toyosato M , Hirose T , Inayama S , Nakanishi S and Numa S Cloning and sequence analysis of cDNA for bovine adrenal preproenkephalin, 295, 202
Norwood T H *see under* Zanjani E D , 295, 244
Noufi R *see under* Cooper G , 295, 578
Nozik A J *see under* Cooper G , 295, 578
Nørgaard A , Kjeldsen K and Clausen T K^+ depletion and Na^+ pump density—Reply, *matters arising* 295, 717
Numa S *see under* Noda M , 295, 202
Nuñez B *see under* Oppenheim R W 295, 57
Nussbaumer J C *see under* Wall P D , 295, 691
Nutt D J , Cowen P J and Little H J Unusual interactions of benzodiazepine receptor antagonists, 295, 436
Oberthur W *see under* Knöchel W , 295, 710
O'Brien T P and McCully M E The Study of Plant Structure Principles and Selected Methods, *book review by* Moore P D 295, 469
Odartchenko N *see under* Magli M C 295, 527
O'Donohue T L *see under* Nilaver G , 295, 597
Oeschger H *see under* Neftel A 295, 220
Ogawara Y., Mitsuda K , Masai K , Vallerga J V , Cominsky L R , Grunsfeld J M , Kruper J S and Ricker G R X-ray observations of the 1980 Cygnus X-1 high state' 295, 675
Ogden P *see under* Lamb J F 295, 717
Oger J , Szuchet S , Antel J and Arnason B G W A monoclonal antibody against human T suppressor lymphocytes binds specifically to the surface of cultured oligodendrocytes 295, 66
Ohlendorf D H *see under* Banaszak L J 295, 264
Ohya S *see under* Tachibana S , 295, 339
Okuno M *see under* Morisawa M , 295, 703
O'Leary K *see under* Jackson D F , 295, 557
Olive P *see under* Rossignol Strick M , 295, 105
Oliver J E Climatology Selected Applications *book review by* Palutikof J P Wigley T M L 295, 462

Ollier C Tectonics and Landforms, *book review by* Burchfiel B C **295,** 464
Oppenheim R W **and Nuñez R** *Electrical stimulation of hind-limb increases neuronal cell death in chick embryo,* **295,** 57
Oppenheimer S B Introduction to Embryonic Development, *book review by* Newth D R **295,** 479
Orchin M *et al* The Vocabulary of Organic Chemistry *book review by* Mann J **295,** 487
Ospovat D The Development of Darwin's Theory Natural History Natural Theology, and Natural Selectios 1838–1859, *book review by* Hull D L **295,** 719
Owen J A, Sigal N H and Klinman N R Heterogeneity of the BALB/c IgM anti-phosphorylcholine antibody response, **295,** 347
Owen T R *see under* Anderson J G C, **295,** 467
Owens A J *see under* Steed J M, **295,** 308
Padmanabhan T and Narlikar J V Quantum conformal fluctuations in a singular space–time, **295,** 677
Pai A C and Marcus-Roberts H *Genetics Its Concepts and* Implications, *book review by* Cove D J **295,** 476
Palmer T Understanding Enzymes *book review by* Perham R N **295,** 485
Palutikof J P and Wigley T M L *book review of* An Introduction to Climate, (Trewartha G T and Horn L H) **295,** 462
  book review of Climatology Selected Applications, (Oliver J E) **295,** 462
  book review of Mountain Weather and Climate, (Barry R G) **295,** 462
Pang K D, Chun S F S, Ajello J M, Nansheng Z and Minji L Organic and inorganic interpretations of the martian UV–IR *reflectance spectrum,* **295,** 43
Papas T S *see under* Eva A, **295,** 116
Parisot R F *see under* De Robertis E M, **295,** 572
Parker B C *see under* Wharton R A Jr, **295,** 403
Parker I *see under* Cull Candy S G, **295,** 410
Parker S C *see under* Catlow C R A **295,** 658
Parker W R *see under* Kirby R, **295,** 396
Parmentier E M, Squyres S W, Head J W and Allison M L The tectonics of Ganymede, **295,** 290
Parsons P A *see under* Erhman L, **295,** 475
Pàtzold R R *see under* Murthy G S **295,** 688
Payne G S, Bishop J M and Varmus H E Multiple arrangements of viral DNA and an activated host oncogene in bursal lymphomas **295,** 209
Pearse A G E Islet cell precursors are neurones, *news and views* **295,** 96
Pearson J, **Brandeis L and Cuello A C** Depletion of substance P-containing axons in substantia gelatinosa of patients with diminished pain sensitivity **295,** 61
Pearson R and Ball J N Lecture Notes on Vertebrate Zoology, *book review by* Halstead L B **295,** 481
Pelton J N Global Talk The Marriage of the Computer, World Communications and Man, *book review by* Maddox B **295,** 439
Pennica D *see under* Gray P W, **295,** 503
Pentreath V W and Kai-Kai M A Significance of the potassium signal from neurones to glial cells **295,** 59
Perham R N *book review of* Enzyme Kinetics The Steady-state Approach, (Engel P C) **295,** 485
  book review of Molecular Enzymology (*Wharton C W and* Eisenthal R) **295,** 485
  book review of Understanding Enzymes, (Palmer T) **295,** 485
Perricaudet M *see under* Virtanen A **295,** 705
Perutz M F, Hasnain S S, Duke P J, Sessler J L and Hahn J E Stereochemistry of iron in deoxyhaemoglobin **295,** 535
Peterson D L *see under* Dreesman G R, **295,** 158
Petit A *see under* Chilton M -D, **295,** 432
Pettersson U *see under* Virtanen A, **295,** 705
Phillips I D J *see under* Wareing P F, **295,** 470
Phinney E S *see under* Rees M J **295,** 17
Pickering B T Prohormones for vasopressin, *news and views* **295,** 280 *Corrigendum* **295,** 258
Pickles H G Ethnic journal, *correspondence* **295,** 362
Piko L *see under* Clegg K B, **295,** 342
Pilbeam D New hominoid skull material from the Miocene of Pakistan, **295,** 232
Pinnock M *see under* Dudeney J R, **295,** 307
Plescia J B and Boyce J M Crater densities and geological histories of Rhea Dione Mimas and Tethys, **295,** 285
Pollard H B *see under* Fowler V M, **295,** 336
Poo M -m Rapid lateral diffusion of functional ACh receptors in embryonic muscle cell membrane, **295,** 332
Porter K R *see under* Beckerle M C, **295,** 701
Potter P E, Maynard J B and Pryor W A *Sedimentology of* Shale Study Guide and Reference Source, *book review by* Selley R C **295,** 465
Pozzan T *see under* Tsien R Y **295,** 68
Prasad S S *see under* Zipf E C, **295,** 133
Prentice H C *book review of* Historical Plant Geography An Introduction (Stott P) **295,** 472
Price M A *see under* French R C, **295,** 259
Pryor W A *see under* Potter P E, **295,** 465
Quatrano R S *book review of* Biology of Plants (Raven P H, Evert R F, Curtis H) **295,** 471
Rabson M *see under* Heston L, **295,** 160
Radda G K, Bore P J, Gadian D G, Ross B D, Styles P, Taylor D J and Morgan-Hughes J ^{31}P NMR examination of two patients with NADH-CoQ reductase deficiency, **295,** 608
Radding C M *see under* DasGupta C, **295,** 71
Raff M Commercial risk *correspondence* **295,** 642
Ramsey R L *see under* Gration K A F, **295,** 599
Rand R P *see under* Gration K A F **295,** 599
Rands E *see under* Chattopadhyay S K, **295,** 25
Rankin J C and Davenport J Animal Osmoregulation, *book review by* Riegel J A **295,** 484
Rassoulzadegan M, Binetruy B and Cuzin F High frequency of gene transfer after fusion between bacteria and eukaryotic cells, **295,** 257
Rattenbury J M *Editor* Amino Acid Analysis, *book review by* Darbre A **295,** 176
Raven P H, Evert R F and Curtis H Biology of Plants *book review by* Quatrano R S **295,** 471
Rayfield L S *see under* Brent L, **295,** 242
Rayment I, Baker T S, Caspar D L D and Murakami W T Polyoma virus capsid structure at 22 5 Å resolution, **295,** 110
Raymond J C A new model for giant H II shells, *news and views* **295,** 282
Rayner D H The Stratigraphy of the British Isles, *book review by* Dineley D L **295,** 467
Razin A *see under* Gruenbaum Y **295,** 620
Reddy E P *see under* Eva A, **295,** 116
Rees M J, Begelman M C, Blandford R D and Phinney E S Ion-supported tori and the origin of radio jets, **295,** 17
Reineck H -E and Singh I B Depositional Sedimentary Environments With Reference to Terrigenous Clastics, *book review by* Selley R C **295,** 465
Reiner A *see under* Erichsen J T, **295,** 407
Reingold N *Editor*, The Papers of Joseph Henry, Vol 4 January 1838–December 1840, The Princeton Years, *book review by Russell C* **295,** *175*
Reinleitner L A, Gurnett D A and Gallagher D L Chorus-related electrostatic bursts in the Earth's outer magnetosphere, **295,** 46
Remaut E *see under* Kastelein R A, **295,** 35
Repeta D J and Gagosian R B Carotenoid transformations in coastal marine waters **295,** 51
Revenäs B *see under* Smedegård G, **295,** 327
Rex D *see under* Coward M P **295,** 22
Reynolds D C and Collins T C Excitons Their Properties and Uses, *book review by* Dunn D **295,** 442
Reyss J L, Marchig V and Ku T L Rapid growth of a deep-sea manganese nodule, **295,** 401
Rhodes T *see under* Buxton G B, **295,** 583
Richards G W and Vita-Finzi C Marine deutxny 35 000–25,000 years old in the Chott el Djerid southern *Tunisia* **295,** 54
Richter D *see under* Land H **295,** 299
Ricker G R *see under* Ogawara Y, **295,** 675
Ridley M *book review of* The Foundations of Ethology, (Lorenz K Z) **295,** 439
Riegel J A *book review of* Animal Osmoregulation (Rankin J C and Davenport J) **295,** 484
  book review of Functional Adaptations of Marine Organisms (Vernberg F J and Vernberg W B *editors*) **295,** 484
Rigby M *book review of* Physical Chemistry (Atkins P W) **295,** 489
  book review of Physical Chemistry, (Bromberg J P) **295,** 489
Rimmer D and Adey M *book review of* Applications of Soil Physics, (Hillel D) **295,** 466
  book review of Fundamentals of Soil Physics, (Hillel D) **295,** 466
  book review of The Soil Resource Origin and Behavior, (Jenny H) **295,** 466
Rinehart J S Geysers and Geothermal Energy *book review by* England P **295,** 82
Rink T J *see under* Tsien R Y, **295,** 68
Rishbeth H Europe probes the auroral atmosphere *news and views* **295,** 93
Robbins K C *see under* Eva A **295,** 116
Roberts A B, Anzano M A, Lamb L C, Smith J M, Frolik C A, Marquardt H, Todaro G J and Sporn M B Isolation from murine sarcoma cells of novel transforming growth factors potentiated by EGF, **295,** 417
Robertson M *The unregenerate nervous system, news and views* **295,** 553
Robinson T *see under* Kopka H, **295,** 680
Rodger A S *see under* Dudeney J R, **295,** 307
Rodhe H *see under* Charlson R J, **295,** 683
Roe D A The Lower and Middle Palaeolithic Periods in Britain *book review by* Mellars P **295,** 268
Romoser W S The Science of Entomology *book review by* Evans M E G **295,** 483
Rosen O M and Krebs E G *Editors* Protein Phosphorylation, *book review by* England P J **295,** 442
Rosenblum E E US spoken, *correspondence* **295,** 540
Ross B D *see under* Radda G K, **295,** 608
Ross R G *see under* Hubbard S R, **295,** 682
Rossignol-Strick M, Nesteroff W, Olive P and Vergnaud-Grazzini C After the deluge Mediterranean stagnation and sapropel formation, **295,** 105
Rowan-Robinson M Cosmology, *book review by* Silk J **295,** 461
Ruse M Is Science Sexist? And Other Problems in the Biological Sciences, *book review by* Beckwith J **295,** 631
Russell C *book review of* The Papers of Joseph Henry, Vol 4 January 1838–December 1840, The Princeton Years, (Reingold N *editor*) **295,** 175
Russell C T *see under* Hoppe M M, **295,** 41
Rutishauser U *see under* Grumet M, **295,** 693
Rutter W J *see under* Bell G I, **295,** 31
Rybach L and Muffler L J P *Editors*, Geothermal Systems Principles and Case Histories *book review by* England P **295,** 82
Rycroft M J Analysing atmospheric carbon dioxide levels, *news and views* **295,** 190
Sage R D *see under* Ferris S D **295,** 163
Salthe S N Original life *correspondence* **295,** 452
Sameulsson B *see under* Smedegård G **295,** 327
Sanchez Y *see under* Dreesman G R **295,** 158
Sanders C J *see under* Kennedy J S, **295,** 263
Sanford P W *see under* Siegmund O H W, **295,** 678
Santos T *see under* Zasloff M, **295,** 533
Sapienza C and *Doolittle* **W F** *Unusual physical organization* of the *Halobacterium* genome, **295,** 384
Sasazuki T and Uno H Two major genes, linked to HLA and Gm, control susceptibility to Graves' disease—Reply, *matters arising* **295,** 629
Saunders J C *see under* Wright L J **295,** 415
Sawyer L and James M N G Carboxyl–carboxylate interactions in proteins, **295,** 79
Saxena Q B *see under* Saxena R K, **295,** 240
Saxena R K, Saxena Q B and Adler W H Defective T-cell response in beige mutant mice, **295,** 240
Scharer U and Allègre C J Uranium-lead system in fragments of a single zircon grain, **295,** 583
Scherrer K *see under* Moreau J, **295,** 260
Schlumpberger J M *see under* Scofield V L, **295,** 499
Schmale H *see under* Land H, **295,** 299
Schneider S H *see under* Thompson S L, **295,** 645
Schnitzerling H J *see under* Sutherst R W **295,** 320
Schoell M and Wellmer F W Anomalous ^{13}C depletion in Precambrian organic carbon—Reply, *matters arising* **295,** 172
Schulz-Schaeffer J Cytogenetics Plants, Animals, Humans, *book review by* Ashburner M **295,** 477
Schutz G *see under* Land H, **295,** 299
Schwander J *see under* Neftel A, **295,** 220
Schwarcz H P and Skoflek I New dates for the Tata, Hungary archaeological site, **295,** 590
Schwartz J H *see under* Kandel E R, **295,** 474
Schwartz M *see under* Hall M N, **295,** 616
Schwartz R H The nature of immune response gene defects, *news and views* **295,** 455
Schwarz H J *et al* *Editors,* Laser Interaction and Related Plasma Phenomena, *book review by* Key M H **295,** 84
Scofield V L, Schlumpberger J M, West L A and Weissman I L Protochordate allorecognition is controlled by a MHC-like gene system, **295,** 499
Scott G C *see under* Bright S W J **295,** 592
Seaburg K G *see under* Wharton R A Jr, **295,** 403
Seeburg P *see under* Gubler U **295,** 206
Seeburg P H *see under* Comb M, **295,** 663
Seewaldt E and Stackebrandt E Partial sequence of 16S ribosomal RNA and the phylogeny of *Prochloron* **295,** 618
Seidman J G *see under* Margulies D H **295,** 168
Selby M J *see under* Bell G I **295,** 31
Sellers R M *see under* Buxton G B **295,** 583
Selley R C *book review of* Depositional Sedimentary Environments With Reference to Terrigenous Clastics, (Reineck H -E and Singh I B) **295,** 465
  book review of Sedimentary Petrology An Introduction (Tucker M E) **295,** 465
  book review of Sedimentology of Shale Study Guide and Reference Source, (Potter P E Maynard J B Pryor W A) **295,** 465
Selsing E *see under* Miller J, **295,** 428
Serafini-Fracassini A *see under* Knox P, **295,** 614
Sessler J L *see under* Perutz M F **295,** 535
Shabad A E and Usov V V γ-Quanta capture by magnetic field and pair creation suppression in pulsars, **295,** 215
Sharma Y P *see under* Singhvi A K, **295,** 313
Shay J W *see under* Clark M A **295,** 605
Sheppeard H *see under* Lea D J **295,** 184
Sherratt D J *see under* Kitts P A **295,** 626
Sherrill J M *see under* Mirsalis J C, **295,** 322
Sherrington D *book review of* The Theory of Magnetism I *Statics and Dynamics, (Mattis D C)* **295,** 354
Sherwood P J *see under* Gray P W, **295,** 503
Shevach E M *see under* Clark R B, **295,** 412
Shewmaker C K *see under* Grosveld G C, **295,** 120
Shoyab M, Warren T C and Todaro G J Phorbol-12, 13-diester 12-ester hydrolase may prevent tumour promotion by phorbol diesters in skin **295,** 152
Siegmund O H W, Culhane J L, Mason I M and Sanford P W Individual electrons detected after the interaction of ionizing radiation with gases, **295,** 678
Sigal N H *see under* Owen J A, **295,** 347
Sigurgeirsson Th *see under* Bjornsson H **295,** 580
Silberberg A *book review of* Mechanics and Thermodynamics *of Biomembranes (Evans E A and Skalak R)* **295,** *84*
Silberstein L, Inestrosa N C and Hall Z W Aneural muscle cell cultures make synaptic basal lamina components **295,** 143
Silk J *book review of* Cosmology, (Rowan-Robinson M) **295,** 461
  Great voids in the Universe, *news and views* **295,** 367
  book review of Relativistic Cosmology An Introduction, (Heidmann J) **295,** 461
  book review of The Physics–Astronomy Frontier, (Hoyle F and Narlikar J) **295,** 461
Simmons G M Jr *see under* Wharton R A Jr, **295,** 403
Simon H *see under* Tassin J P, **295,** 696
Simoneit B R T *and Lonsdale P F Hydrothermal petroleum* in mineralized mounds at the seabed of Guaymas Basin, **295,** 198
Simonsen C C *see under* Gray P W **295,** 503
Simpson E T cell function Ly phenotype and the MHC, *news and views* **295,** 366
  see under Brent L, **295,** 242
Singer S *see under* Luria S E, **295,** 479
Singh I B *see under* Reineck H -E, **295,** 465
Singhvi A K, Sharma Y P and Agrawal D P Thermoluminescence dating of sand dunes in Rajasthan, India, **295,** 313
Six H R *see under* Dreesman G R **295,** 158
Skalak R *see under* Evans E A **295,** 84
Skoflek I *see under* Schwarcz H P, **295,** 590
Sluyser M Brief encounter *correspondence* **295,** 184
Smalley I Migration fund? *correspondence* **295,** 184
Smedegård G, Hedqvist P, Dahlen S-E, Revenäs B, Hammarstrom S and Sameulsson B Leukotriene C_4 affects pulmonary and cardiovascular dynamics in monkey, **295,** 327
Smith G R Animal disease and conservation, *news and views* **295,** 16
Smith J M *see under* Roberts A B **295,** 417
Smith P J *book review of* Marine Geology (Kenneth J P) **295,** 466
  Reservoirs and the triggering of earthquakes *news and views* **295,** 9
Somorjai G A Chemistry in Two Dimensions Surfaces, *book review by* Everett D H **295,** 633
Sparks R S J and Brazier S New evidence for degassing processes during explosive eruptions, **295,** 218
Sparrow J T *see under* Dreesman G R **295,** 158
Spear B B *see under* Kaine B P, **295,** 430
Spessard G O *book review of* Operational Organic Chemistry A Laboratory Course, (Lehman J W) **295,** 488
  book review of Spectral and Chemical Characterization of Organic Compounds A Laboratory Handbook, (Criddle W J and Ellis G P) **295,** 488
Sporn M B *see under* Roberts A B, **295,** 417
Spragg S P *book review of* Physical Chemistry With Applications to Biological Systems (Chang R) **295,** 487
  book review of Physical Chemistry for the Life Sciences, (Barrow G M) **295,** 487
Squyres S W *see under* Parmentier E M **295,** 290
Srinivasan A *see under* Eva A **295,** 116
Stackebrandt E *see under* Seewaldt E **295,** 618
Stamatoyannopoulos G *see under* Zanjani E D, **295,** 244
Stauffer B *see under* Neftel A **295,** 220

Steed J M, Owens A J, Miller C, Filkin D L and Jesson J P Two-dimensional modelling of potential ozone perturbation by chlorofluorocarbons, **295**, 308
Stefansson K, Wollmann R L, Moore B W and Arnason B G W S-100 protein in human chondrocytes, **295**, 63
Steinberg C M and Lefkovits I *Editors*, The Immune System *book review by* Humphrey J H **295**, 721
Steinhardt R A and Alderton J M Calmodulin confers calcium sensitivity on secretory exocytosis, **295**, 154
Sterne M Anthrax island, *correspondence* **295**, 362
Stevenson G T *see under* Glennie M J, **295**, 712
Stewart A D and Hunt D M The Genetic Basis of Development, *book review by* Lawrence P A **295**, 477
Stewart G C *see under* Fabian A C, **295**, 508
Stokes W L Essentials of Earth History An Introduction to Historical Geology, *book review by* Bell K **295**, 463
Stoneham A M *see under* Burns W G, **295**, 130
Storb R What role for autologous marrow transplantation in cancer therapy? *news and views* **295**, 555
Storb U *see under* Miller J, **295**, 428
Stott P Historical Plant Geography An Introduction, *book review by* Prentice H C **295**, 472
Streitwieser A and Heathcock C H Introduction to Organic Chemistry, *book review by* Mann J **295**, 487
Stryer L Biochemistry, *book review by* Butterworth P H W **295**, 485
Stubbe P *see under* Kopka H, **295**, 680
Styles P *see under* Radda G K, **295**, 608
Suess H E *see under* Venkatesan M I, **295**, 517
Sugino K and Naitoh Y Simulated cross bridge patterns corresponding to ciliary beating in *Paramecium*, **295**, 609
Sutcliffe J F *book review of* Growth and Differentiation in Plants, (Wareing P F and Phillips I D J) **295**, 470
Sutherst R W, Jones R J and Schnitzerling H J Tropical legumes of the genus *Stylosanthes* immobilize and kill cattle ticks, **295**, 320
Sutton J *book review of* The Earth Generated and Anatomized An Early Eighteenth Century Theory of the Earth (Hobbs W Porter R *editor*) **295**, 352
Suzuki D T, Griffiths A J F and Lewontin R C An Introduction to Genetic Analysis, *book review by* Cove D J **295**, 476
Swanson C P, Merz T and Young W J Cytogenetics The Chromosome in Division, Inheritance and Evolution, *book review by* Ashburner M **295**, 477
Sykes P Guidebook to Mechanism in Organic Chemistry, *book review by* Mann J **295**, 487
Symonds N *book review of* Bacterial and Bacteriophage Genetics An Introduction, (Birge E A) **295**, 478
Synge H *Editor*, The Biological Aspects of Rare Plant Conservation, *book review by* McAllister H **295**, 719
Szuchet S *see under* Oger J **295**, 66
Tachibana S, Araki K, Ohya S and Yoshida S Isolation and structure of dynorphin, an opioid peptide from porcine duodenum, **295**, 339
Tait R V Elements of Marine Ecology An Introductory Course, *book review by* Crisp D J **295**, 483
Takahashi H *see under* Noda M, **295**, 202
Takamori N *see under* Nakato Y, **295**, 312
Takano T *see under* Conner B N **295**, 294
Tanaka S *see under* Conner B N, **295**, 294
Tansley L *see under* Adinolfi M, **295**, 325
Tarney J *see under* Coward M P, **295**, 22
Tassin J P, Simon H, Herve D, Blanc G, Le Moal M, Glowinski J and Bockaert J Non-dopaminergic fibres may regulate dopamine sensitive adenylate cyclase in the prefrontal cortex and nucleus accumbens, **295**, 696
Taylor D J *see under* Radda G K, **295**, 608
Taylor T N Paleobotany An Introduction to Fossil Plant Biology, *book review by* Allen K **295**, 468
Technau G and Heisenberg M Neural reorganization during metamorphosis of the corpora pedunculata in *Drosophila melanogaster*, **295**, 405
Tempe J *see under* Chilton M-D, **295**, 432
Tempest P A *see under* Allen G C **295**, 48
Tepfer D A *see under* Chilton M-D, **295**, 432
Therman E Human Chromosomes Structure, Behavior, Effects *book review by* Miller D A **295**, 478
Thirlwall M *see under* Coward M P, **295**, 22
Thoday J M *see under* Coen E S, **295**, 564
Thomas H F and Czeizel A Safe as 2,4,5-T? **295**, 276
Thomas J M *see under* Catlow C R A, **295**, 658
Thomas P *see under* Allan D **295**, 612
Thompson G *see under* Machado N, **295**, 226
Thompson S L and Schneider S H Carbon dioxide and climate has a signal been observed yet? *news and views* **295**, 645
Thornton J M Electrostatic interactions in proteins *news and views* **295**, 13
Tiollais P *see under* Virtanen A, **295**, 705
Tischer I, Gelderblom H, Vettermann W and Koch M A A very small porcine virus with circular single stranded DNA, **295**, 64
Tisdell C A Science and Technology Policy Priorities of Governments, *book review by* Ashby E **295**, 81
Tobin T R and Bell W J Guidance system for pheromone orientation in moths, *matters arising* **295**, 263
Todaro G J *see under* Roberts A B, **295**, 417
  see under Shoyab M, **295**, 152
Tokuhisa T *see under* Herzenberg L A, **295**, 329
Tooze J *see under* Watson J D, **295**, 173
Towe K M Anomalous ^{13}C depletion in Precambrian organic carbon, *matters arising* **295**, 171
Toyosato M *see under* Noda M **295**, 202
Travers P *see under* Adinolfi M, **295**, 325
Trayhurn P, Jones P M, McGuckin M M and Goodbody A E Effects of overfeeding on energy balance and brown fat thermogenesis in obese (*ob/ob*) mice **295**, 323
Trewartha G T and Horn L H An Introduction to Climate, *book review by* Palutikof J P, Wigley T M L **295**, 462
Tronick S R *see under* Eva A **295**, 116
Truhlar D G *Editor*, Potential Energy Surfaces and Dynamics Calculations for Chemical Reactions and Molecular Energy Transfer *book review by* Murrell J N **295**, 634
Tsien R Y, Pozzan T and Rink T J T-cell mitogens cause early changes in cytoplasmic free Ca^{2+} and membrane potential in lymphocytes, **295**, 68
Tsubomura H *see under* Nakato Y, **295**, 312
Tucker M E Sedimentary Petrology An Introduction *book review by* Selley R C **295**, 465
Turner D R *see under* Davison W, **295**, 582
Tyler J W *see under* Allen G C, **295**, 48
Udenfriend S *see under* Gubler U, **295**, 206
Uhr J W *see under* Krolick K A, **295**, 604
Uno H *see under* Sasazuki T, **295**, 629
Unsworth C D, Hughes J and Morley J S *O*-sulphated Leu-enkephalin in brain, **295**, 519
Usher M B *book review of* Elementary Mathematical Ecology, (Vandermeer J) **295**, 473
  book review of Population Systems A General Introduction, (Berryman A A) **295**, 473
  book review of Population Ecology A Unified Study of Animals and Plants, (Begon M and Mortimer M) **295**, 473
Usherwood P N R *see under* Gration K A F, **295**, 599
Usov V V *see under* Shabad A E **295**, 215
Vaeck S V Areas of neglect, *correspondence* **295**, 184
Vaidyanathan S *see under* Adamson M G, **295**, 49
Vallerga J V *see under* Ogawara Y, **295**, 675
van den Bercken J *see under* Vijverberg H P M, **295**, 601
Van der Loos H *see under* Wall P D, **295**, 691
van der Zalm J M *see under* Vijverberg H P M, **295**, 601
van Duin J *see under* Kastelein R A, **295**, 35
van Ooyen A J J *see under* Kennedy N, **295**, 622
Van Valen L M A pitfall in random sampling, *matters arising* **295**, 171
Vande Woude G *see under* Levinson B, **295**, 568
Vandermeer J Elementary Mathematical Ecology, *book review by* Usher M B **295**, 473
Varmus H E *see under* Payne G S, **295**, 209
Veevers J J Australian–Antarctic depression from the mid-ocean ridge to adjacent continents, **295**, 315
Venkatesan M I, Linick T W, Suess H E and Buccellati G Asphalt in carbon-14 dated archaeological samples from Terqa Syria, **295**, 517
Vergnaud-Grazzini C *see under* Rossignol-Strick M, **295**, 105
Vernberg F J and Vernberg W B *Editors*, Functional Adaptations of Marine Organisms, *book review by* Riegel J A **295**, 484
Vernberg W B *see under* Vernberg F J, **295**, 484
Vettermann W *see under* Tischer I, **295**, 64
Vickery B and Vickery M L Secondary Plant Metabolism, *book review by* Goodwin T W **295**, 471
Vickery M L *see under* Vickery B, **295**, 471
Vijverberg H P M, van der Zalm J M and van den Bercken J Similar mode of action of pyrethroids and DDT on sodium channel gating in myelinated nerves **295**, 601
Virtanen A, Pettersson U, Le Moullec J M, Tiollais P and Perricaudet M Different mRNAs from the transforming region of highly oncogenic and non-oncogenic human adenoviruses **295**, 705
Vita-Finzi C *see under* Richards G W, **295**, 54
Vitetta E S *see under* Krolick K A, **295**, 604
Wade N The Nobel Duel, *book review by* Gratzer W **295**, 266
Wall P D, Fitzgerald M, Nussbaumer J C, Van der Loos H and Devor M Somatotopic maps are disorganized in adult rodents treated neonatally with capsaicin **295**, 691
Wallace B Basic Population Genetics, *book review by* Jones J S **295**, 475
Wallace D M *see under* Gray P W, **295**, 503
Wallwork J A *book review of* The Biology of Centipedes, (Lewis J G E) **295**, 441
Walton D Errors and resolution of thermal techniques for obtaining the geomagnetic intensity, **295**, 512
Wang M-Y *see under* Wright L J, **295**, 415
Wareing P F and Phillips I D J Growth and Differentiation in Plants, *book review by* Sutcliffe J F **295**, 470
Warren T C *see under* Shoyab M, **295**, 152
Wasteson Å *see under* Ek B, **295**, 419
Watson J D and Tooze J The DNA Story A Documentary History of Gene Cloning, *book review by* Jahoda M **295**, 173
Watson J V *book review of* Lower Palaeozoic of the Middle East, Eastern and Southern Africa, and Antarctica With Essays on Lower Palaeozoic Trace Fossils of Africa and Lower Palaeozoic Palaeoclimatology, (Holland C H *editor*) **295**, 268
Watt F M and Green H Stratification and terminal differentiation of cultured epidermal cells, **295**, 434
Weatherbee J A *see under* Izant J G, **295**, 248
Webb W *see under* Jacobson K **295**, 283
Weichert C K Anatomy of the Chordates, *book review by* Halstead L B **295**, 481
Weissman I L *see under* Scofield V L, **295**, 499
Wellmer F W *see under* Schoell M, **295**, 172
Wells P *see under* Knox P, **295**, 614
Wells R M G Invertebrate Respiration *book review by* Brafield A E **295**, 482
West L A *see under* Scofield V L, **295**, 499
West T S *book review of* The Chemistry of Soil Processes (Greenland D J and Hayes M H B *editors*) **295**, 352
Westerman M P *see under* Allan D **295**, 612
Westermark B *see under* Ek B, **295**, 419
Westerveld A *see under* de Jonge A J R **295**, 624
Westfall R S *book review of* The Mathematical Papers of Isaac Newton Vol VIII, 1697–1722, (Whiteside D T *editor*) **295**, 265
Westin E H *see under* Eva A, **295**, 116
Wharton C W and Eisenthal R Molecular Enzymology, *book review by* Perham R N **295**, 485
Wharton R A Jr, Parker B C, Simmons G M Jr, Seaburg K G and Love F G Biogenic calcite structures forming in Lake Fryxell, Antarctica **295**, 403
White W M and Hofmann A W Mantle heterogeneity and isotopes in oceanic basalts, *news and views* **295**, 363
Whitehouse H L K *see under* Markham P **295**, 421
Whiteside D T *Editor*, The Mathematical Papers of Isaac Newton Vol VIII, 1697–1722, *book review by* Westfall R S **295**, 265
Whittaker E J W Crystallography An Introduction for Earth Science (and Other Solid State) Students, *book review by* Howie R A **295**, 464
Wicks-Nelson R *see under* Liebert R M **295**, 474
Widom J M and Edelstein S J Chemistry An Introduction to General Organic, and Biological Chemistry, *book review by* Garratt P **295**, 486
Wigley T M L *see under* Palutikof J P, **295**, 462
  see under Palutikof J P, **295**, 462
  see under Palutikof J P, **295**, 462
Wilbraham A C *see under* Matta M S, **295**, 486
Wiley E O Phylogenetics The Theory and Practice of Phylogenetic Systematics, *book review by* Charig A J **295**, 720
Wilkinson P C Beat the clock, *correspondence* **295**, 92
Williamson P G Molluscan biostratigraphy of the Koobi Fora hominid-bearing deposits, **295**, 140
Wilson A C *see under* Ferris S D, **295**, 163
Wilson J I B Is amorphous silicon played out? *news and views* **295**, 458
Wilson L *book review of* Earthlike Planets Surfaces of Mercury, Venus, Earth, Moon, Mars, (Murray B *et al*) **295**, 463
Wilson R J How the malarial parasite enters the red blood cell, *news and views* **295**, 368
Windley B F *see under* Coward M P, **295**, 22
Wittig B *see under* Knöchel W, **295**, 710
Wittig S *see under* Knöchel W, **295**, 710
Wolf S F and Migeon B R Studies of X chromosome DNA methylation in normal human cells **295**, 667
Wollmann R L *see under* Stefansson K, **295**, 63
Wong-Staal F *see under* Eva A, **295**, 116
Wood W B *et al* Biochemistry A Problems Approach, *book review by* Hassall H **295**, 486
Woodcock C *see under* Bright S W J, **295**, 592
Woodrow C F *see under* Moore S, **295**, 529
Woof C *see under* Davison W, **295**, 582
Wright K H *see under* Dudeney J R, **295**, 307
Wright L J, Feinstein A, Heap R B, Saunders J C, Bennett R C and Wang M-Y Progesterone monoclonal antibody blocks pregnancy in mice, **295**, 415
Yarwood J N *see under* Croy R R D, **295**, 76
Yelverton E *see under* Gray P W, **295**, 503
Yonas A *book review of* Developmental Psychology (Liebert R M and Wicks-Nelson R) **295**, 474
  book review of Foundations of Developmental Psychology, (LaBarba R C) **295**, 474
Yoshida S *see under* Tachibana S, **295**, 339
Young J Z The Life of Vertebrates, *book review by* Halstead L B **295**, 481
Young W J *see under* Swanson C P, **295**, 477
Zakour R A and Loeb L A Site-specific mutagenesis by error-directed DNA synthesis, **295**, 708
Zanjani E D, Lim G, McGlave P B, Clapp J F, Mann L I, Norwood T H and Stamatoyannopoulos G Adult haematopoietic cells transplanted to sheep fetuses continue to produce adult globins, **295**, 244
Zasloff M, Santos T and Hamer D H tRNA precursor transcribed from a mutant human gene inserted into a SV40 vector is processed incorrectly, **295**, 533
Zimmerman E A *see under* Nilaver G, **295**, 597
Zipf E C and Prasad S S A mesospheric source of nitrous oxide, **295**, 133
Zoback M D and Anderson R N Ultrasonic borehole televiewer investigation of oceanic crustal layer 2A Costa Rica Rift, **295**, 375
Zuckerman A J Developing synthetic vaccines, *news and views* **295**, 98
Zuiderwijk E J Alignment of randomly distributed objects **295**, 577
Zumbrunn R *see under* Neftel A, **295**, 220
Zweig S E *see under* Clark R B **295**, 412

BOOKS RECEIVED

Mathematics

BARNETT, V (ed) Interpreting Multivariate Data Proceedings of the Conference "Looking at Multivariate Data" held in the University of Sheffield, U K , March 1980 Pp 374 ISBN 0-471-28039-9 (Wiley 1981) £21, $49 50

BARRA, J -R Mathematical Basis of Statistics Probability and Mathematical Statistics Pp 249 ISBN 0-12-079240-0 (Academic 1981) $39 50

BREMAUD, P Point Processes and Queues Martingale Dynamics Pp 354 ISBN 3-540-90536-7 (Springer-Verlag 1981) DM 88, $41

GARNETT, J B Bounded Analytic Functions Pp 467 ISBN 0-12-276150 (Academic 1981) Np

GRIFFEL, D H Applied Functional Analysis Pp 386 ISBN 0-85312-226-1 (Ellis Horwood, Chichester 1981) Hbk £25, $54 75, pbk £6 50, $18 60

HAGEMAN, L A and YOUNG, D M Applied Iterative Methods Pp 386 ISBN 0-12-313340-8 (Academic 1981) $39 50

HIORNS, R W and COOKE, D (eds) The Mathematical Theory of the Dynamics of Biological Populations II Based on the Proceedings of a Conference, Oxford, July 1980 Pp 328 ISBN 0-12-348780-3 (Academic 1981) £14 50, $35

ROHLF, F J and SOKAL, R R Statistical Tables 2nd Edn Pp 219 Hbk ISBN 0-7167-1257-1, pbk ISBN 0-7167-1258-X (W H Freeman 1981) Hbk £15 20, pbk £6 50

SENETA, E Non-negative Matrices and Markov Chains 2nd Edn Pp 279 ISBN 3-540-90598-7 (Springer-Verlag 1981) DM 69 90, $32 60

STRĂTILĂ, S-V Modular Theory in Operator Algebras Pp 492 ISBN 0-85626-190-4 (Abacus Press, Tunbridge Wells, Kent 1981) £33

Astronomy

COUTEAU, P Observing Visual Double Stars Pp 257 ISBN 0-262-03077-2 (MIT Press 1981) £14

CRONIN, V The View from Planet Earth Man Looks at the Cosmos Pp 348 ISBN 0-00-211397-X (Collins 1981) £12 50

MIHALAS, D and BINNEY, J Galactic Astronomy Structure and Kinematics 2nd Edn Pp 597 ISBN 0-7167-1280 6 (W H Freeman 1981) £19 50

Physics

ABRAHAMS, K , ALLAART, K and DIEPERINK, A E L (eds) NATO Advanced Study Institutes Series, Vol 67 Proceedings of the Netherlands Physical Society 1980 International Summer School on Nuclear Structure, held August 1980 in Dronten, The Netherlands Pp 432 ISBN 0-306-40728-0 (Plenum 1981) $49 50

ABRAMSON, N The Making and Evaluation of Holograms Pp 326 ISBN 0-12-042820-2 (Academic 1981) £23 40, $48

ADAMS, M J An Introduction to Optical Waveguides Pp 401 ISBN 0-471-27969-2 (Wiley 1981) £21 50, $48 50

ANDERSON, H L (ed) AIP 50th Anniversary Physics Vade Mecum Pp 330 Pbk ISBN 0-88318-289-0 (American Institute of Physics, New York 1981) Pbk np

BREVARD, C and GRANGER, P Handbook of High Resolution Multinuclear NMR Pp 229 ISBN 0-471-06323-1 (Wiley 1981) £18 15, $32 60

CENCE, R J and ROBERTS, A (eds) Neutrino 81 Proceedings of the 1981 International Conference, Maui, Hawaii, July 1981 Pp Vol I 509, pp Vol II 512 (no ISBN) (Dept of Physics and Astronomy, University of Hawaii 1981) Pbk np

COWLEY, J M Diffraction Physics 2nd revised Edn Pp 425 ISBN 0-444-86121-1 (North-Holland 1981) $65 75, Dfl 135

DEVREESE, J T *et al* (eds) Recent Developments in Condensed Matter Physics Vol 2 Metals, Disordered Systems, Surfaces and Interfaces Papers Presented at the 1st Conference of the Condensed Matter Division of the European Physical Society, held April 1980 at the University of Antwerp, Belgium Pp 477 ISBN 0-306-40647-0 (Plenum 1981) $59 50

DEVREESE, J T *et al* (eds) Recent Developments in Condensed Matter Physics Vol 3 Impurities, Excitons, Polarons, and Polaritons Pp 420 ISBN 0-306-40648-9 (Plenum 1981) $55

EBERT, K H , DEUFLHARD, P and JAGER, W (eds) Modelling of Chemical Reaction Systems Proceedings of an International Workshop, Heidelberg, Germany, September 1980 Springer Series in Chemical Physics, Vol 18 Pp 389 ISBN 3-540-10983-8 (Springer-Verlag 1981) DM 72, $33 60

HUKINS, D W L X-ray Diffraction by Disordered and Ordered Systems Pp 164 ISBN 0-08-023976-5 (Pergamon 1981) £11 95, $28 75

IACHELLO, F (ed) Interacting Bose-Fermi Systems in Nuclei Proceedings of the 2nd Specialized Seminar on Interacting Bose-Fermi Systems in Nuclei, held June 1980 in Erice, Sicily Pp 406 ISBN 0-306-40733-7 (Plenum 1981) $49 50

McKELLAR, A R W , OKA, T and STOICHEFF, B P (eds) Laser Spectroscopy V Proceedings of the 5th International Conference, Jasper Park Lodge, Alberta, Canada, June–July 1981 Springer Series in Optical Sciences, Vol 30 Pp 495 ISBN 3-540-10914-5 (Springer-Verlag 1981) DM 70, $32 60

MESSER, J Temperature Dependent Thomas-Fermi Theory Lecture Notes in Physics, Vol 147 Pp 131 Flexi ISBN 3-540-10875-0 (Springer-Verlag 1981) DM 18, $7 70

OONK, H A J Phase Theory The Thermodynamics of Heterogeneous Equilibria Studies in Modern Thermodynamics, 3 ISBN 0-444-42019-3 (Elsevier Scientific 1981) $59 50, Dfl 140

THYAGARAJAN, K and GHATAK, A K Lasers–Theory and Applications Pp 431 ISBN 0-306-40598-9 (Plenum 1981) $39 50

VELO, G and WIGHTMAN, A S (eds) Rigorous Atomic and Molecular Physics Proceedings of the 4th International Schoo of Mathematical Physics held June 1980 in Erice, Sicily, Italy Pp 495 ISBN 0-306-40829-5 (Plenum 1981) $59 50

WEST, B J On the Simpler Aspects of Nonlinear Fluctuating Deep Water Gravity Waves (Weak Interaction Theory) Lecture Notes in Physics, Vol 146 Pp 341 Flexi ISBN 3-540-10852-1 (Springer-Verlag 1981) DM 33, $15

WINDSOR, C G Pulsed Neutron Scattering Pp 432 ISBN 0-85066-195-1 (Taylor & Francis, London 1981) £25

YAO, Y L Irreversible Thermodynamics Pp 343 ISBN 0-442-20074-9 (Van Nostrand Reinhold 1981) £25 10

Chemistry

BARNES, A J *et al* (eds) Matrix Isolation Spectroscopy A Book Based on the NATO Advanced Study Institute held at the Université des Sciences et Techniques du Languedoc, Montpellier, France, July 1980 Pp 616 ISBN 90-277-1328-6 (Riedel 1981) Dfl 160, $69 50

BATES, R B and BEAVERS, W A Carbon-13 NMR Spectral Problems Organic Chemistry Pp 259 Hbk ISBN 0-89603-010-5, pbk ISBN 0-89603-016-4 (The Humana Press, New Jersey 1981) £11 50, $20 50

DAY, P (ed) Emission and Scattering Techniques Studies of Inorganic Molecules, Solids and Surfaces Proceedings of the NATO Advanced Study Institute held at Alghero, Sardinia, Italy, September 1980 Pp 400 ISBN 90-277-1317-0 (Riedel 1981) Dfl 110, $48

DE JONG, F and REINHOUDT, D N Stability and Reactivity of Crown-Ether Complexes Pp 164 Pbk ISBN 0-12-208780-1 (Academic 1981) Pbk £12 80, $31

DHAR, D N The Chemistry of Chalcones and Related Compounds Pp 285 ISBN 0-471-08007-1 (Wiley 1981) £28 50, $50

FREI, R W and LAWRENCE, J F (eds) Chemical Derivatization in Analytical Chemistry Vol 1 Chromatography Pp 344 ISBN 0-306-40608-X (Plenum 1981) $39 50

JACQUES, J , COLLET, A and WILEN, S H Enantiomers, Racemates, and Resolutions Pp 447 ISBN 0-471-08058-6 (Wiley 1981) £38 75, $69 85

JOHNSON, W M and MAXWELL, J A Rock and Mineral Analysis 2nd Edn Chemical Analysis, A Series of Monographs on Analytical Chemistry and its Applications, Vol 27 Pp 489 ISBN 0-471-02743-X (Wiley 1981) £38 85, $69 85

KAYE, B H Direct Characterization of Fineparticles Chemical Analysis A Series of Monographs on Analytical Chemistry and its Applications, Vol 61 Pp 398 ISBN 0-471-46150 (Wiley 1981) £44 40, $75

MÉSZAROS, E Atmospheric Chemistry Fundamental Aspects Studies in Environmental Science, 11 Pp 190 ISBN 0-444-99753-9 (Elsevier Scientific 1981) $41 50, Dfl 85

PRICE, D and TODD, J F J (eds) Dynamic Mass Spectrometry, Vol 5 Pp 242 ISBN 0-85501-143-2 (Heyden, London 1981) £30 30, DM 67

PULLMAN, B (ed) Intermolecular Forces Proceedings of the 14th Jerusalem Symposium, Jerusalem, Israel, April 1981 Pp 567 ISBN 90-277-1326-X (Riedel 1981) Dfl 175, $76

SEYMOUR, R B Conductive Polymers Polymer Science and Technology, Vol 15 Proceedings of a Symposium held August 1980 at the 2nd Chemical Congress of the North American Continent in Las Vegas, Nevada Pp 237 ISBN 0-306-40805-8 (Plenum 1981) $35

WADE, L G Jr and O'DONNELL, M J (eds) Annual Reports in Organic Synthesis — 1980 Pp 456 Pbk ISBN 0-12-040811-2 (Academic 1981) Pbk $24

WEHRY, E L (ed) Modern Fluorescence Spectroscopy Vol 3, Modern Analytical Chemistry Series Pp 354 ISBN 0-306-40690-X (Plenum 1981) $39 50

WEHRY, E L Modern Fluorescence Spectroscopy, Vol 4 Pp 282 ISBN 0-306-40691-8 (Plenum 1981) $35

Technology

BRIGGS, D E *et al* Malting and Brewing Science Vol I, Malt and Sweet Wort 2nd Edn Pp 387 ISBN 0-412-16580-5 (Chapman & Hall 1981) £17 50

CARDON, F , GOMES, W P and DEKEYSER, W (eds) Photovoltaic and Photoelectrochemical Solar Energy Conversion Proceedings of a NATO Advanced Study Institute held August–September 1980 at Gent, Belgium Pp 422 ISBN 0-306-40800-7 (Plenum 1981) $49 50

FRADIN, F Y (ed) Electronic Structure and Properties Treatise on Materials Science and Technology, Vol 21 Pp 447 ISBN 0-12-341821-6 (Academic 1981) $51

HEWITT, G F , DELHAYE, J M and ZUBER, N (eds) Multiphase Science and Technology, Vol 1 Pp 513 ISBN 0-89116-222-4 (Hemisphere Publishing 1981) $49 75

KAKAC, S , BERGLES, A E and MAYINGER, F (eds) Heat Exchangers Thermal-Hydraulic Fundamentals and Design Pp 1131 ISBN 0-07-033284-3 (Hemisphere Publishing 1981) $95

PRATT, A W Heat Transmission in Buildings Pp 308 ISBN 0-471-27971-4 (Wiley 1981) £21 80, $49 90

SAHAL, D Patterns of Technological Innovation Pp 381 ISBN 0-201-06630-0 (Addison-Wesley 1981) $34 50

Computer Science

BOURNE, J R Laboratory Minicomputing Notes and Reports in Computer Science and Applied Mathematics, Vol 1 Pp 297 ISBN 0-12-119080-3 (Academic 1981)

KOGGE, P M The Architecture of Pipelined Computers Pp 334 ISBN 0-07-035237-2 (Hemisphere Publishing 1981) $28

RUDALL, B H Computers and Cybernetics Pp 188 ISBN 0-85626-173-4 (Abacus, Tunbridge Wells, U K 1981) £15

East African Mammals

An Atlas of Evolution in Africa

Jonathan Kingdon

Volume III Part B — Large Mammals
1979, viii+476pp, £55 00 (UK only)/$132.00, 0 12 408343 9
Volume III Part A — Carnivores
1978, viii+476pp, £41 80 (UK only)/$100 50, 0 12 408303 X
Volume II Part B — Hares and Rodents
1975, x+420pp, £29 20 (UK only)/$70 50, 0 12 408302 1
Volume I — Primates, Hyraxes, Pangolins, Protoungulates and Sirenians
1971, x+446pp, £29 20 (UK only)/$70 50, 0 12 408301 3
Volumes IIIC and IIID — Bovids — Complete this Classic Treatise
March 1982, x+394pp, £49 95 (UK only)/$99 50, 0 12 408344 7
March 1982, vi+352pp, £49 95 (UK only)/$99.50. 0 12 408345 5

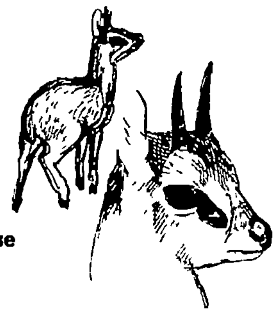

For fifteen years Jonathan Kingdon studied and portrayed the wildlife of Kenya, Uganda and Tanzania Since 1971 his work has been published in a series that has gained international acclaim as one of the most remarkable zoogeographical studies of our time — *East African Mammals* In successive volumes the primates, small mammals, and latterly large mammals, have been subjected to the exhaustive scrutiny of a dedicated observer Details of behaviour and anatomy undetected by the camera have been captured in exquisite and vital line drawings and sketches A wealth of information on physiology, distribution, social systems, habitat, ecology and evolution has been encapsulated in a penetrating and commanding text Taken individually, the volumes of *East African Mammals* provide the most comprehensive guides available for their particular subjects taken together they make up a treatise of immeasurable value, which is now complete with a two-part volume on the bovids

Please direct your enquiries to the Publisher at the appropriate address below

Academic Press
A Subsidiary of Harcourt Brace Jovanovich, Publishers
London New York Paris San Diego San Francisco Sao Paulo Sydney Tokyo Toronto
Academic Press Inc. (London) Ltd: 24-28 Oval Road, London NW1 7DX, England
Academic Press Inc: 111 Fifth Avenue, New York, NY 10003, USA
Academic Press Canada: 55 Barber Greene Road, Don Mills, Ontario M3C 2A1, Canada
Academic Press Australia: PO Box 300, North Ryde, NSW 2113, Australia

Circle No 06 on Reader Enquiry Card

104

British Journal of CLINICAL PHARMACOLOGY

ESSENTIAL INFORMATION AT YOUR FINGERTIPS EVERY MONTH!

Published monthly on behalf of the British Pharmacological Society, *British Journal of Clinical Pharmacology* is as fast-moving as the area of science it examines

Bridging the gap between medical professions, clinical research and the pharmaceutical industry

Containing papers and reports on all aspects of drug action in man, in both health and disease

Providing free copies of the proceedings of selected symposia on new methods, new drugs and new approaches to treatment, to all subscribers

To keep up-to-date in this fast-moving area of science why not join the ever-increasing number of clinical pharmacologists all over the world who rely on the *British Journal of Clinical Pharmacology* as their professional journal

ANNUAL SUBSCRIPTIONS

UK £90
USA/Canada US$225
Rest of the world £110

Orders should be accompanied by remittance, cheques made payable to Macmillan Journals Ltd Subscription Department, Brunel Road, Basingstoke, Hampshire, RG21 2XS, England

Sample copies are also available from the same address

Circle No 27 on Reader Enquiry Card